BNL-100766-2013

RIKEN/RBRC Workshop
Jet Quenching at RHIC vs LHC in Light of Recent dAu vs pPb Controls
April 15-17, 2013

Proceedings of RIKEN BNL Research Center Workshop

Volume 115

RBRC
RIKEN BNL Research Center

Disclaimer

This work was prepared as an account of work sponsored by an agency of the United States Government. Neither the United States Government nor any agency thereof, nor any of their employees, nor any of their contractors, subcontractors or their employees, makes any warranty, express or implied, or assumes any legal liability or responsibility for the accuracy, completeness, or any third party's use or the results of such use of any information, apparatus, product, or process disclosed, or represents that its use would not infringe privately owned rights. Reference herein to any specific commercial product, process, or service by trade name, trademark, manufacturer, or otherwise, does not necessarily constitute or imply its endorsement, recommendation, or favoring by the United States Government or any agency thereof or its contractors or subcontractors. The views and opinions of authors expressed herein do not necessarily state or reflect those of the United States Government or any agency thereof.

Notice: This manuscript has been authored by employees of Brookhaven Science Associates, LLC under Contract No. DE-AC02-98CH10886 with the U.S. Department of Energy. The publisher by accepting the manuscript for publication acknowledges that the United States Government retains a non-exclusive, paid-up, irrevocable, world-wide license to publish or reproduce the published form of this manuscript, or allow others to do so, for United States Government purposes.

Preface to the Series

The RIKEN BNL Research Center (RBRC) was established in April 1997 at Brookhaven National Laboratory. It is funded by the "Rikagaku Kenkyusho" (RIKEN, The Institute of Physical and Chemical Research) of Japan. The Memorandum of Understanding between RIKEN and BNL, initiated in 1997, has been renewed in 2002, 2007 and again in 2012. The Center is dedicated to the study of strong interactions, including spin physics, lattice QCD, and RHIC physics through the nurturing of a new generation of young physicists.

The RBRC has both a theory and experimental component. The RBRC Theory Group and the RBRC Experimental Group consists of a total of 25-30 researchers. Positions include the following: full time RBRC Fellow, half-time RHIC Physics Fellow, and full-time post-doctoral Research Associate. The RHIC Physics Fellows hold joint appointments with RBRC and other institutions and have tenure track positions at their respective universities or BNL. To date, RBRC has over 95 graduates (Fellows and Post-docs) of which approximately 40 theorists and 20 experimenters have already attained tenure positions at major institutions worldwide.

Beginning in 2001 a new RIKEN Spin Program (RSP) category was implemented at RBRC. These appointments are joint positions of RBRC and RIKEN and include the following positions in theory and experiment: RSP Researchers, RSP Research Associates and Young Researchers, who are mentored by senior RBRC Scientists. A number of RIKEN Jr. Research Associates and Visiting Scientists also contribute to the physics program at the Center.

RBRC has an active workshop program on strong interaction physics with each workshop focused on a specific physics problem. In most cases all the talks are made available on the RBRC website. In addition, highlights to each speaker's presentation are collected to form proceedings which can therefore be made available within a short time after the workshop. To date there are over one hundred proceeding volumes available.

A 10 teraflops RBRC QCDOC computer funded by RIKEN, Japan, was unveiled at a dedication ceremony at BNL on May 26, 2005. This supercomputer was designed and built by individuals from Columbia University, IBM, BNL, RBRC, and the University of Edinburgh, with the U.S. D.O.E. Office of Science providing infrastructure support at BNL. Physics results were reported at the RBRC QCDOC Symposium following the dedication. QCDSP, a 0.6 teraflops parallel processor, dedicated to lattice QCD, was begun at the Center on February 19, 1998, was completed on August 28, 1998, and was decommissioned in 2006. It was awarded the Gordon Bell Prize for price performance in 1998. QCDOC was decommissioned in May 2012. The next generation computer in this sequence, QCDCQ (600 Teraflops), is currently operational and is expected to produce many more interesting discoveries in the future.

N. P. Samios, Director
March 2013

*Work performed under the auspices of U.S.D.O.E. Contract No. DE-AC02-98CH10886.

Introduction

In the last decade of the RHIC physics program, studies of jet quenching has played an important role in the discovery and detailed characterization of the strongly interacting Quark-Gluon Plasma. However, these studies also generated several critical puzzles, such as the azimuthal anisotropy of jet quenching, heavy flavor energy loss and initial state suppression, hinting at missing ingredients in our current understanding of jet quenching. Now only two years into the data taking, LHC has produced new measurements on a variety of existing and new jet quenching observables, over a much broader kinematic range.

In addition, in April 2013 new initial state control data via p+A collisions have become available from both RHIC and LHC. With these fresh RHIC and LHC inputs combined, we will be poised to achieve a much better understanding of the hard probes for the quark-gluon matter (such as initial state saturation effects, effective jet medium couplings and tomographic structures) and the implication of these observables about the evolving properties of the Quark-Gluon Plasma from RHIC to LHC.

The purpose of this Workshop was to critically review the recent progress on the theory and phenomenology of jet quenching including both RHIC and LHC data, to develop a consistent unifed picture of jet quenching from RHIC to LHC, and to formulate new research efforts for the future.

Specific topics addressed included:

- To what extent do we achieve control over initial state effects in light of the new dAu and pPb data?
- How do the medium properties change from RHIC to LHC?
- Can we achieve precision by combining the vast amount of data from RHIC and LHC?
- How does the jet quenching response to fluctuating initial geometry (jet tomography) evolve from RHIC to LHC?

Workshop Organizers:

Miklos Gyulassy (Columbia University)
Jiangyong Jia (BNL)
Jinfeng Liao (IU/RBRC)

Contents

Presentations:

Elke Aschenauer..... eRHIC: As the future
Gergely Barnafoldi..... Cronin & shadowing in pA
Barbara Betz ..... Raa and high p_t azimuthal anisotropy (presented by Miklos Gyulassy)
Jean Paul Blaizot ..... In-medium QCD cascade: democratic branching and wave turbulence
Piotr Bozek..... Ridge correlations in pp/pPb: hydro perspective
Wit Busza..... pA studies 1972 – 2013 reminiscences
Alessandro Buzzatti..... Flavor tomography
Helen Caines..... Jet quenching & initial geometry/conditions from the RHIC BES
Brian Cole..... Jet quenching II: or What do we know, and how well do we know it?
Andrea Dainesee..... Experimental status of flavour tomography
Gabor David..... Updates/puzzles of dAu at RHIC
Adrian Dumitru ..... Small-x physics and pA control measurements
Wolfram Fischer..... Future pA: RHIC machine perspective
Ulrich Heinz..... Fluctuations, flow and viscosity in the Little Bang
Boris Kopeliovich..... Nuclear effects in pA
Yuri Kovchegov..... Long range rapidity correlations in heavy-light ion collisions
Alex Kovner..... CGC 2013 – A perspective
Roy Lacey..... Combined analysis of RHIC to LHC suppression & geometry
Jinfeng Liao..... Opaqueness evolution from color liberation
Constantin Loizides ..... Recent results from pPb collisions at the LHC
Frasher Loshaj..... Jet quenching and fragmentation from an exactly soluble model
Abhijit Majumder..... Jet modification in A-A, p-A and D-A at RHIC and LHC (within HT scheme)
Soumya Mohapatra..... Event-by-event flow and initial geometry from LHC
Denes Molnar ..... Hard and soft responses from parton transport
Joern Putschke..... RHIC/LHC complementarity
Gunther Roland ..... CMS results on jet quenching and pPb collisions
Bjorn Schenke..... Initial conditions in A+A, p+A, d+A, and p+p collisions
Edward Shuryak ..... High multiplicity pp & pA: explosive stringy pomeron and hydrodynamics at its edge
Anne Sickles ..... Jet quenching at RHIC: present and future
Vladimir Skokov ..... Suppression of energy loss from partially ionized color
Peter Steinberg..... The ridge at RHIC & the LHC
Raju Venugopalan..... Large ridges in small systems: gluon entanglement in the glasma
Fuqiang Wang..... Particle correlations at RHIC: present & future
Xilin Zhang..... Harmonic jet tomography at RHIC+LHC

Discussions:

Jiangyong Jia.1..... Workshop summary
Jiangyong Jia.2..... Two issues in interpreting the p+Pb ridge
Giorgio Torrieri..... Some simple and provocative comments about v2
Fuqiang Wang..... d+Au ridge at RHIC

Agenda
List of Registered Participants
Additional RIKEN BNL Research Center Proceeding Volumes

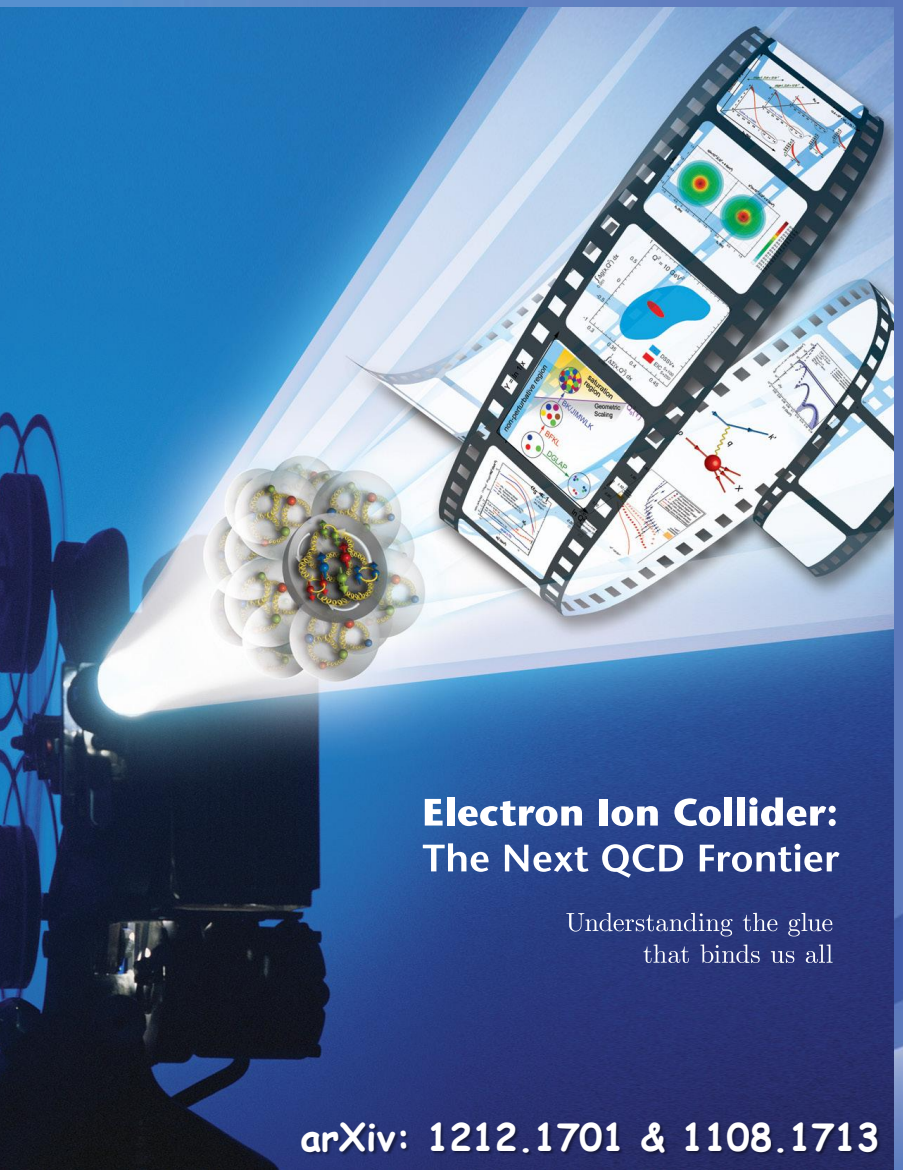

eRHIC:

AS THE FUTURE

THANKS TO
BNL EIC-TASKFORCE
and eRHIC -CAD-TEAM

BROOKHAVEN
NATIONAL LABORATORY

a passion for discovery

U.S. DEPARTMENT OF ENERGY | Office of Science

WHAT IS eRHIC

Electron accelerator

to be build

Unpolarized and polarized leptons
5-20 (30) GeV

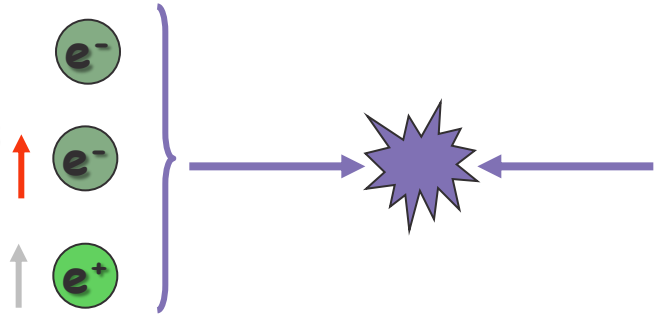

70% e^- beam polarization goal
polarized positrons?

RHIC

Existing = $2B

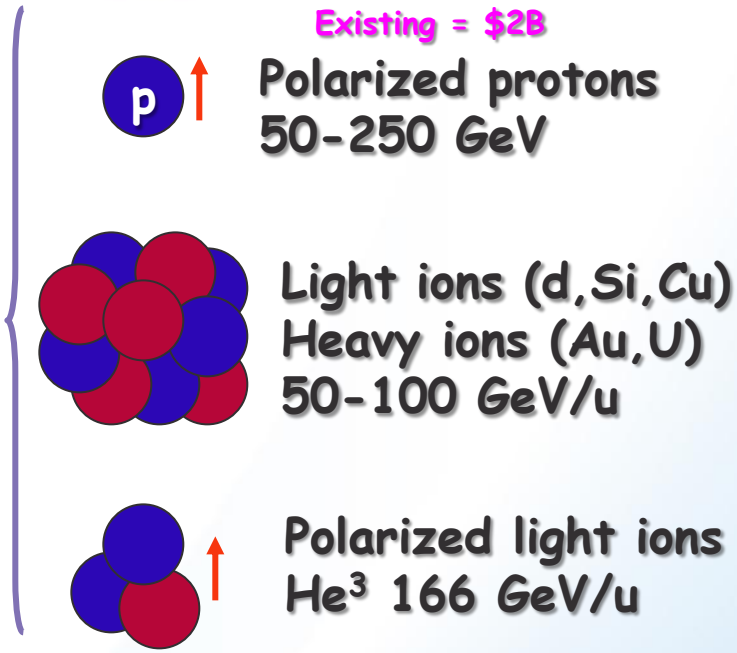

Polarized protons
50-250 GeV

Light ions (d,Si,Cu)
Heavy ions (Au,U)
50-100 GeV/u

Polarized light ions
He^3 166 GeV/u

Center mass energy range: $\sqrt{s}$=30-200 GeV; L~100-1000xHera
longitudinal and transverse polarization for p/He^3 possible

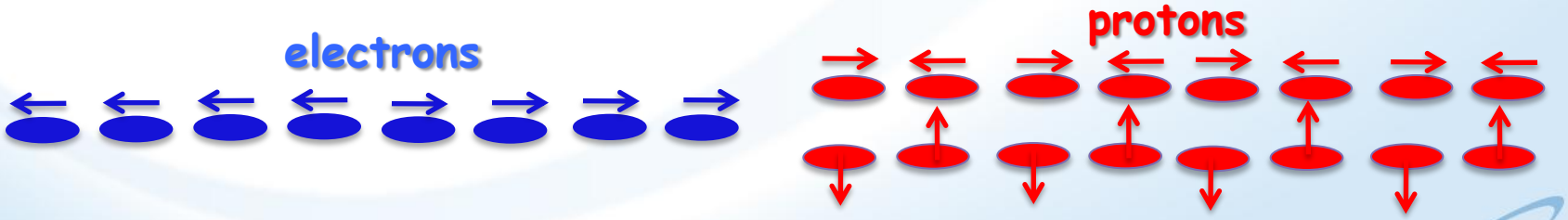

ELECTRON BEAM EVOLUTION IN eRHIC'S ERL

All energies scale proportionally by adding SRF cavities to the injector

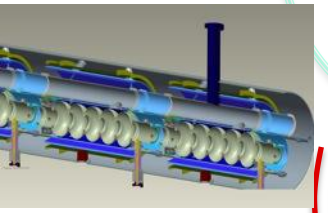

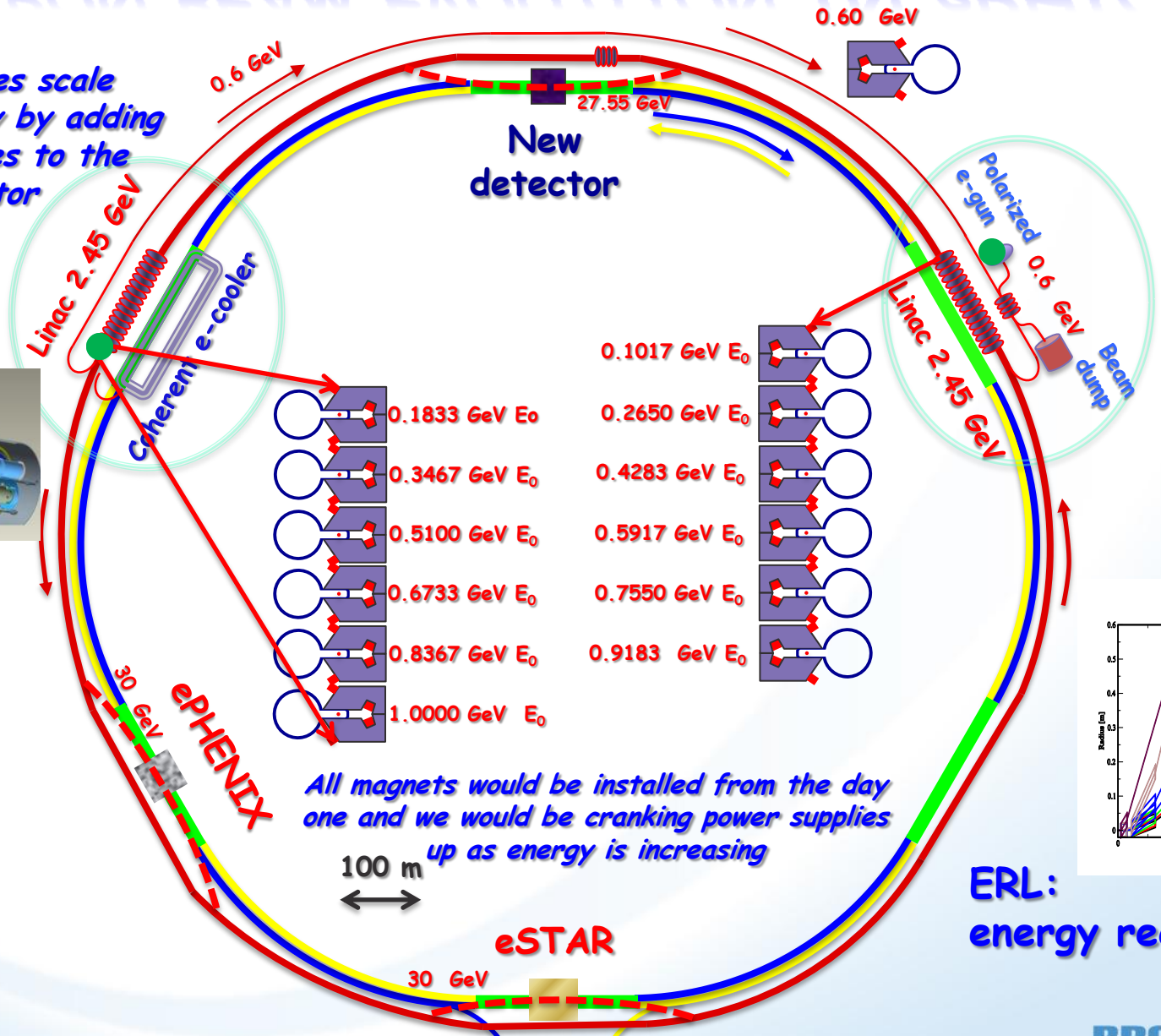

All magnets would be installed from the day one and we would be cranking power supplies up as energy is increasing

E/Eo
0.0200
0.1017
0.1833
0.2650
0.3467
0.4283
0.5100
0.5917
0.6733
0.7550
0.8367
0.9183
1.0000

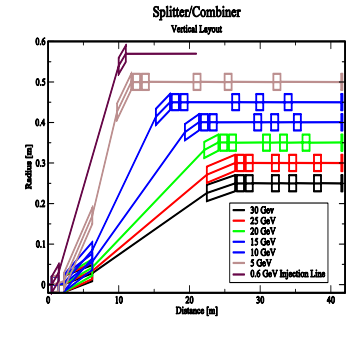

ERL: energy recovery linac

Animation is by N. Tsoupas

eRHIC R&D HIGHLIGHTS AND LUMINOSITY

Challenge	Increase/reduction beyond the state of the art
Polarized electron gun	10 x
Coherent Electron Cooling	New
Multi-pass SRF ERL	5 x incre 30 x incr
Crab crossing	New for h
Understanding beam-beam effects	New typ
β*=5 cm	5x r
Multi-pass SRF ERL	2-3 x in
Feedback for kink instability suppression	Nove
Space charge effect compensation	Nove

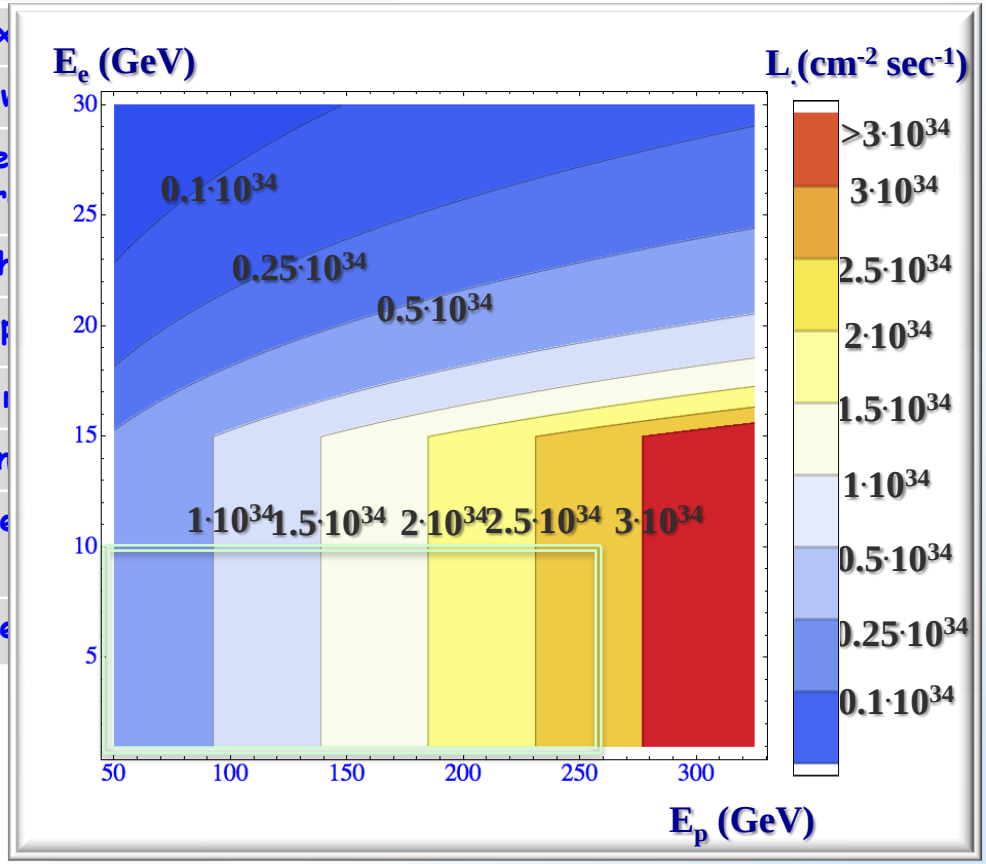

- Hourglass the pinch effects are included. Space charge effects are compensated.
- Energy of electrons can be selected at any desirable value at or below 30 GeV
- The luminosity does not depend on the electron beam energy below or at 20 GeV
- The luminosity falls as E_e^{-4} at energies above 20 GeV
- The luminosity is proportional to the hadron beam energy: $L \sim E_h/E_{top}$

eRHIC: HIGH-LUMINOSITY IR

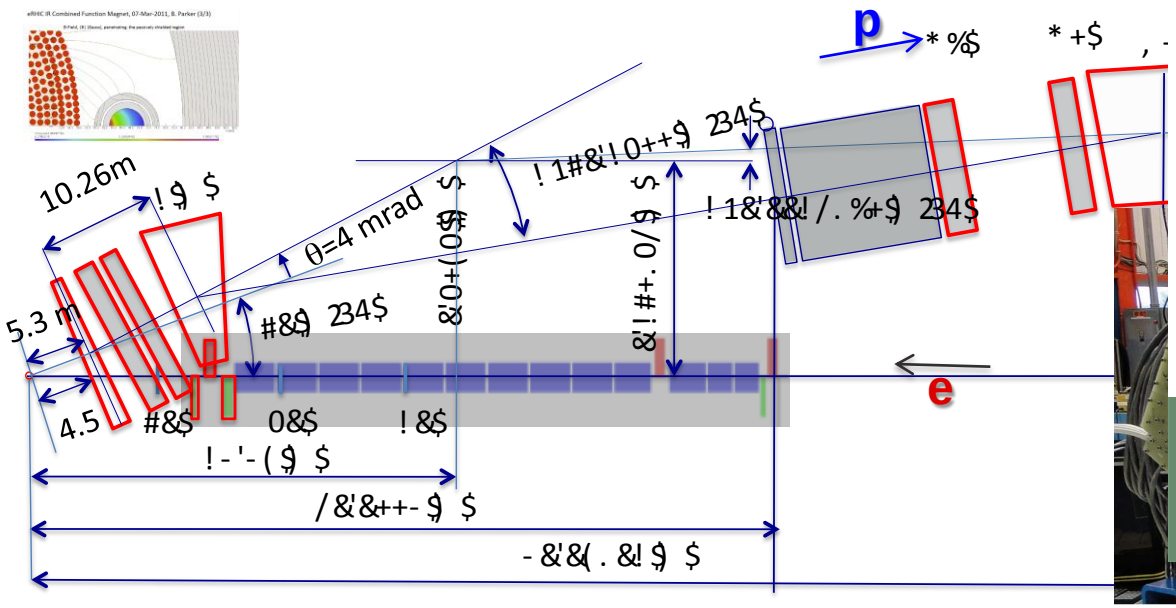

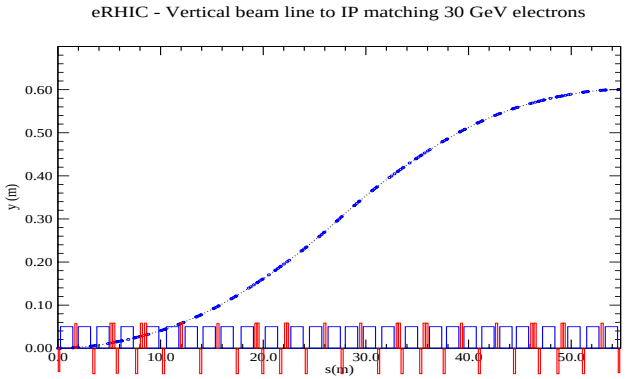

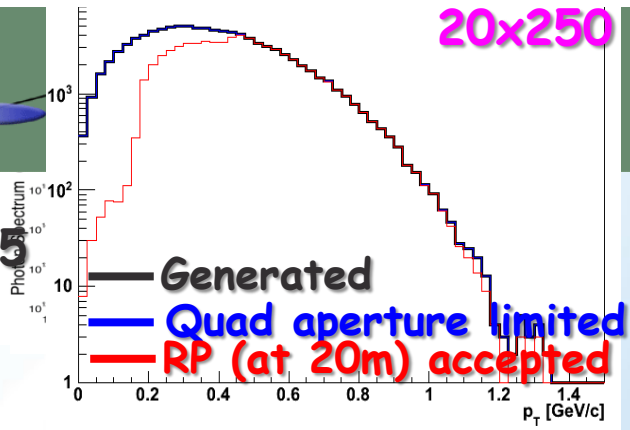

eRHIC - Geometry high-lumi IR with β*=5 cm, l*=4.5 and 10 mrad crossing angle → 10^{34} cm^{-2} s^{-1}

- 10 mrad crossing angle and crab-crossing
- High gradient (200 T/m) large aperture Nb_3Sn focusing magnets
- Arranged free-field electron pass through the hadron triplet magnets
- Integration with the detector: efficient separation and registration of low angle collision products
- Gentle bending of the electrons to avoid SR impact in the detector

© D.Trbojevic, B.Parker, S. Tepikian, J. Beebe-Wang

BNL: 1ST DETECTOR DESIGN CONCEPT

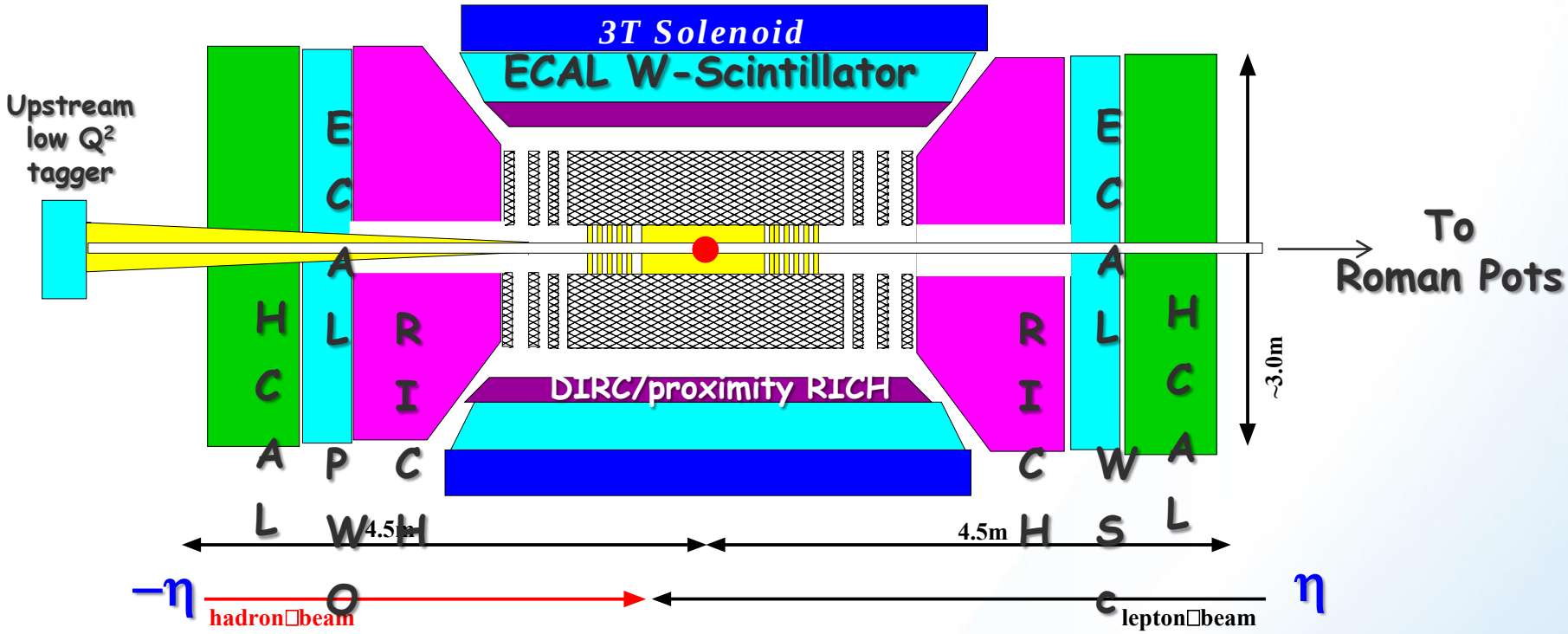

PID:

-1<η<1: DIRC or proximity focusing Aerogel-RICH

1<|η|<3: RICH

Lepton-ID:

-3 <η< 3: e/p

1<|η|<3: in addition Hcal response & γ suppression via tracking

|η|>3: ECal+Hcal response & γ suppression via tracking

-5<η<5: Tracking (TPC+GEM+MAPS)

VIBRANT DETECTOR R&D PROGRAM

- Calorimetry
  - W-Scintillator & W-Si
    - compact and high resolution
  - Crystal calorimeters PbW & BGO

BNL, Indiana University, Penn State Univ., UCLA, USTC, TAM

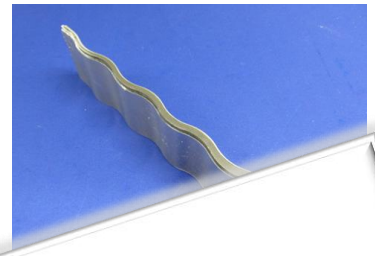

- Pre-Shower
  - W-Si
  - LYSO pixel array with readout via X-Y WLS fi

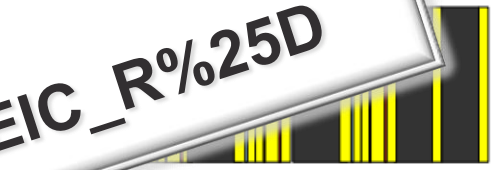

W plates, ~500μ Si pads

Univ. Tecnica Valparaiso

- PID via Cerenk
  - DIR

ution, South Carolina, JLab, GSI

readout

based TRD → eSTAR

diana Univ., USTC, VECC, ANL

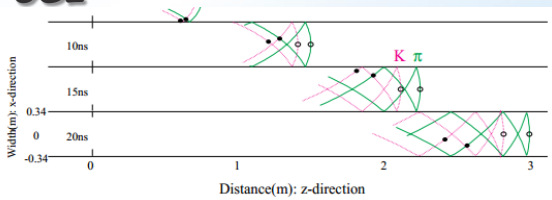

- Tracking

BNL, Florida Inst. Of Technology, Iowa State, LBNL, MIT, Stony Brook, Temple, Jlab, Virginia, Yale

  - μ-Vertex: central and forward based on MAPS
  - Central: TPC/HBD provides low mass, good momentum, dE/dx, eID
    Fast Layer: μ-Megas or PImMS
  - Forward: Planar GEM detectors

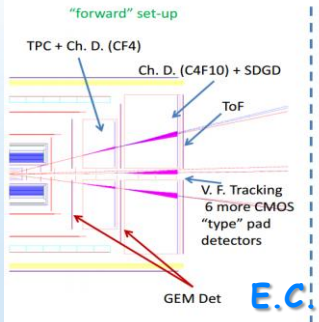

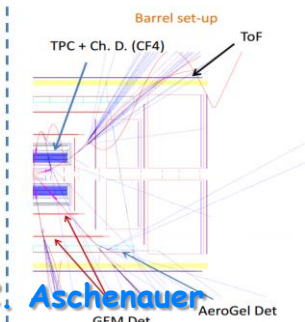

More Info on EIC-Detector R&D:
https://wiki.bnl.gov/conferences/index.php/EIC_R%25D

MOST COMPELLING EIC SCIENCE QUESTIONS

How are sea quarks and gluons and their spin distributed in space and momentum inside the nucleon?

- How are these quark and gluon distributions correlated with the over all nucleon properties, such as spin direction?
- What is the role of the motion of sea quarks and gluons in building the nucleon spin?

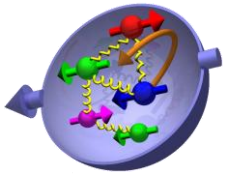

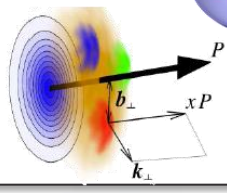

How does the nuclear environment affect the distribution of quarks and gluons and their interaction in nuclei?

- How does the transverse spatial distribution of gluons compare to that in the nucleon?
- How does matter respond to fast moving color charge passing through it? Is this response different for light and heavy quarks?

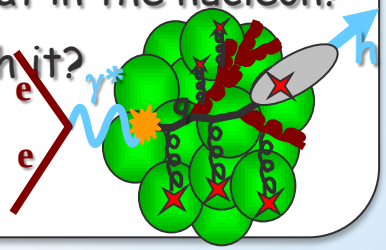

Where does the saturation of gluon densities set in?

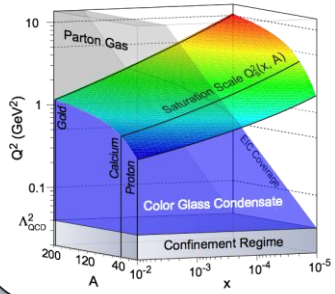

- Is there a simple boundary that separates the region from the more dilute quark gluon matter? If so how do the distributions of quarks and gluons change as one crosses the boundary?
- Does this saturation produce matter of universal properties in the nucleon and all nuclei viewed at nearly the speed of light?

WHAT DO WE KNOW

$$\frac{d^2\sigma^{NC}_{e^\mp p}}{dxdQ^2} = \frac{2\pi\alpha^2_{em}Y_+}{xQ^4}\left(F_2 - \frac{y^2}{Y_+}F_L \pm \frac{Y_-}{Y_+}xF_3\right)$$

$q(x,Q^2)+\bar{q}(x,Q^2)$ quark density

$g(x,Q^2)$ gluon density

$q(x,Q^2)-\bar{q}(x,Q^2)$ valence quarks

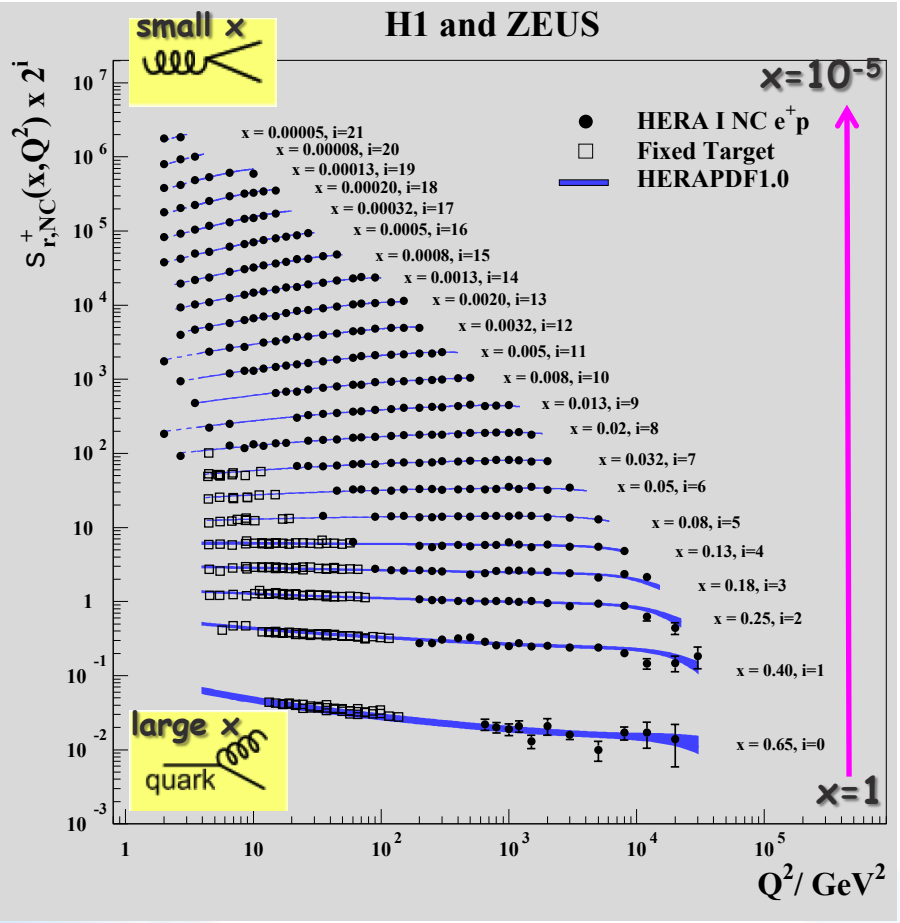

Obse **Gluon density dominates** tions

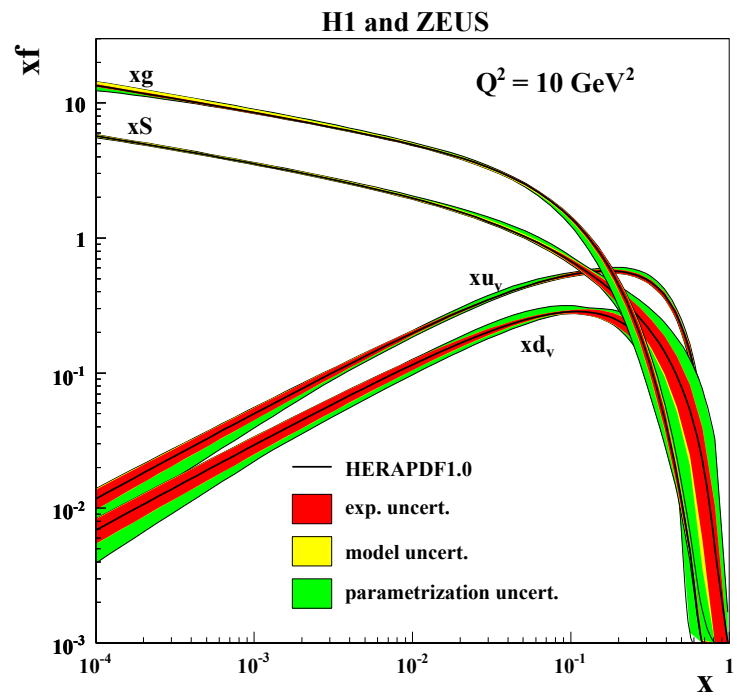

DEEP INELASTIC SCATTERING

Kinematics:

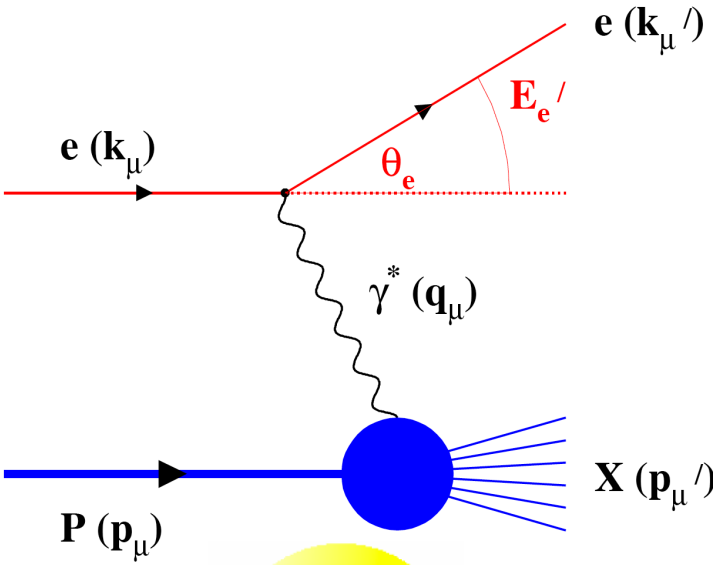

$$Q^2 = -q^2 = -(k_\mu - k'_\mu)^2$$

$$Q^2 = 2E_e E'_e(1 - \cos\Theta_{e'})$$

Measure of resolution power

$$y = \frac{pq}{pk} = 1 - \frac{E'_e}{E_e}\cos^2\left(\frac{\theta'_e}{2}\right)$$

Measure of inelasticity

$$x = \frac{Q^2}{2pq} = \frac{Q^2}{sy}$$

Measure of momentum fraction of struck quark

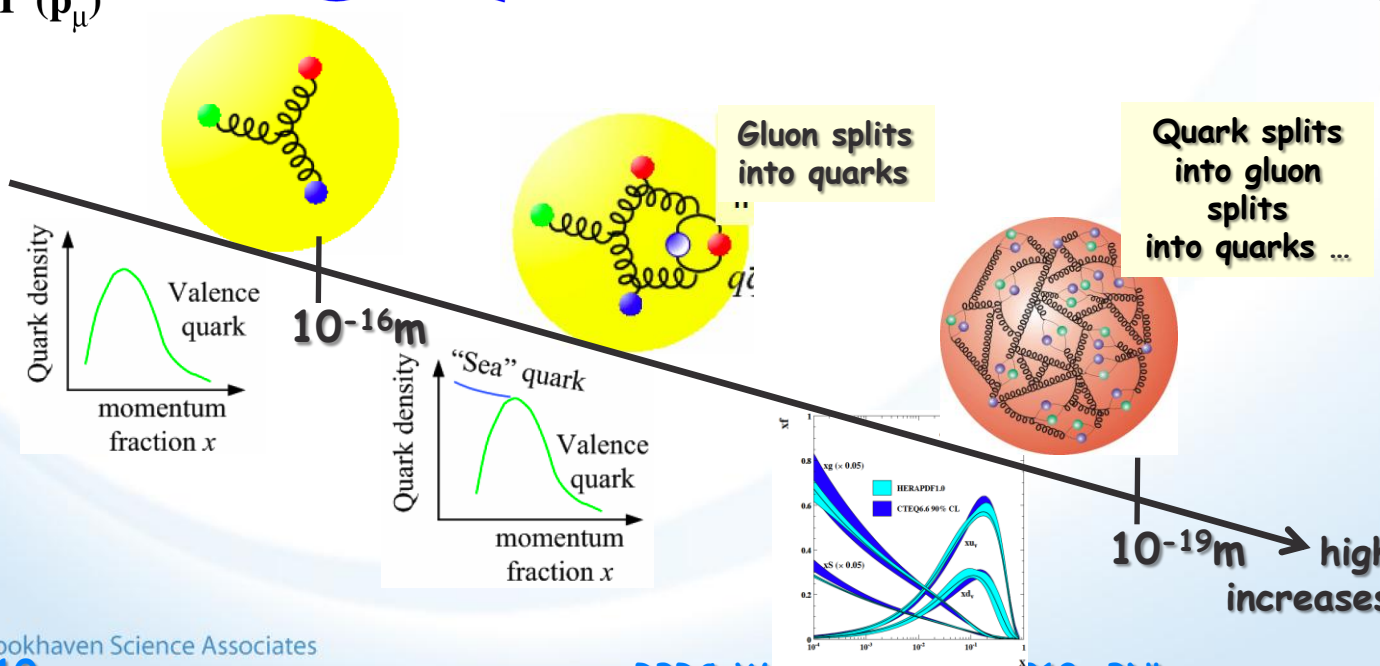

THE PATH TO IMAGING QUARKS AND GLUONS

- PDFs do not resolve transverse momenta or positions in the nucleon
- fast moving nucleon turns into a `pizza' but transverse size remains about 1 fm

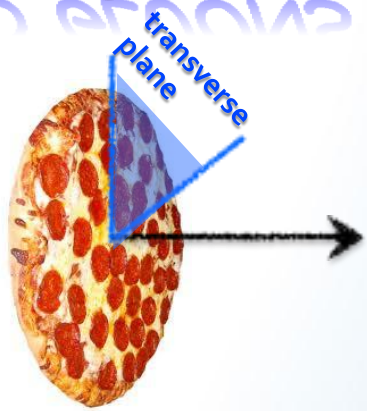

compelling questions

- how are quarks and gluons spatially distributed
- how do they move in the transverse plane
- do they orbit and do we have access to spin-orbit correlations

→ required set of measurements & theoretical concepts

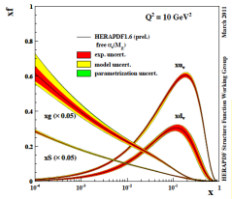

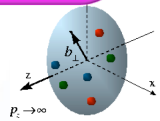

1-D

$\mathbf{f(x)}$ parton densities

$\mathbf{F(t)}$ form factor

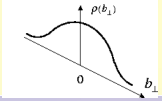

$\int d^2k_T$ $\int d^2b_T$ $\int dx$

$\mathbf{f(x,k_T)}$ transv. mom. dep. PDF ↔ not related by Fourier transf. ↔ $\mathbf{f(x,b_T)}$ impact par. dep. PDF ↔ $\mathbf{b \leftrightarrow t}$ $\mathbf{H(x,0,t)}$ ← $\xi \to 0$ $\mathbf{H(x,\xi,t)}$ generalized PDF

2+1-D

semi-inclusive DIS

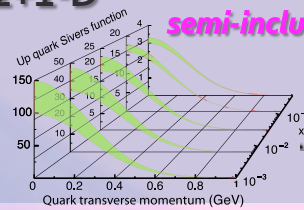

$\int d^2b_T$ $\int d^2k_T$

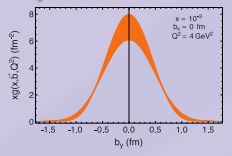

exclusive processes

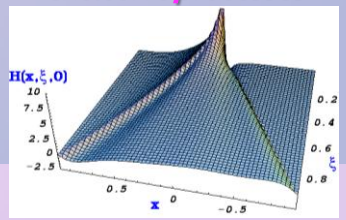

4+1-D

Wigner function

$\mathbf{W(x,k_T,b_T)}$

high-level connection

measurable ?

important in other branches of Physics

BEYOND FORM FACTORS AND QUARK DISTRIBUTIONS

Generalized Parton Distributions

X. Ji, D. Mueller, A. Radyushkin (1994-1997)

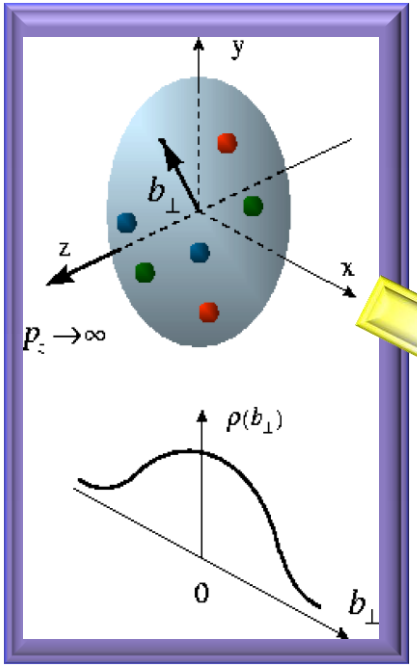

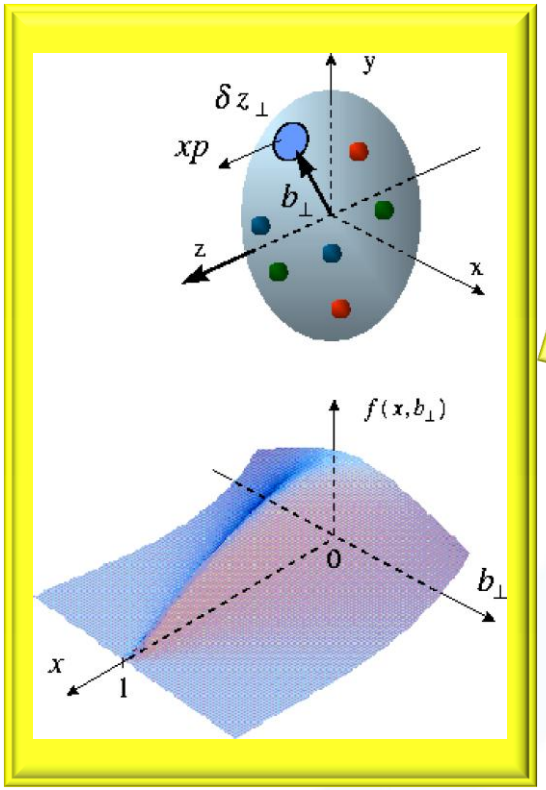

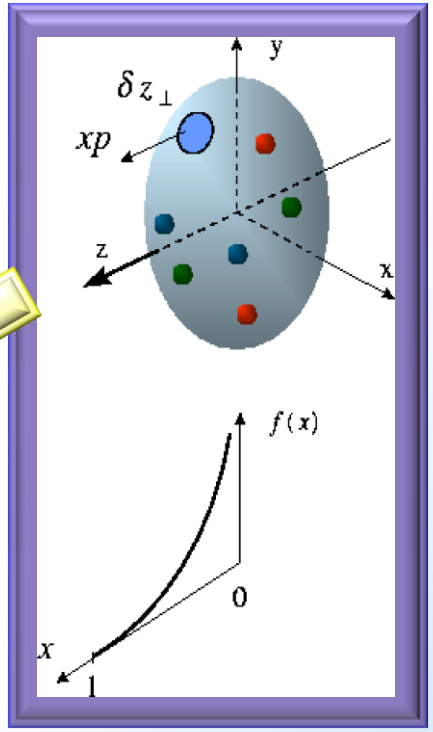

Proton form factors, transverse charge & current densities

Correlated quark momentum and helicity distributions in transverse space - GPDs

Structure functions, quark longitudinal momentum & helicity distributions

How are GPDs characterized?

unpolarized	polarized	
$H^q(x,\xi,t)$	$\tilde{H}^q(x,\xi,t)$	conserve nucleon helicity $H^q(x,0,0)=q,\ \tilde{H}^q(x,0,0)=\Delta q$
$E^q(x,\xi,t)$	$\tilde{E}^q(x,\xi,t)$	flip nucleon helicity not accessible in DIS

quantum … fferent GPD

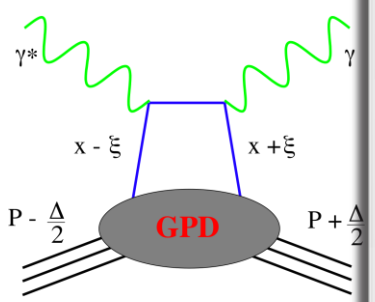

DVCS

H^q E^q $\tilde{H}^q$ $\tilde{E}$

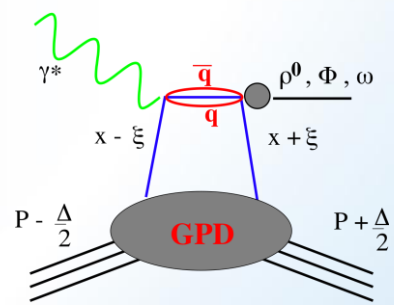

vector mesons

H^q, E^q

Spin-Sum-Rule in PRF:

from g_1

$$\frac{1}{2}=J_q^z+J_g^z=\frac{1}{2}\sum_q \Delta q+\sum_q \mathcal{L}_q^z+J_g^z$$

$$J_q^z=\frac{1}{2}\sum_q \Delta q+\sum_q L_q^z$$

$$J_{q,g}^z=\frac{1}{2}\left(\int_{-1}^{1} x\,dx\left(H^{q,g}+E^{q,q}\right)\right)_{t\to 0}$$

- $Q^2 = 2E_eE_e'(1-\cos\theta$
- $x_B = Q^2/2M\nu$ $\nu=E$

- $x+\xi$, $x-\xi$ long. mom. fract.
- $t = (p-p')^2$
- $\xi \cong x_B/(2-x_B)$

ρ^0	2u+d, 9g/4
ω	2u-d, 3g/4
ϕ	s, g
ρ^+	u-d
J/ψ	g

THE DVCS PHASE SPACE

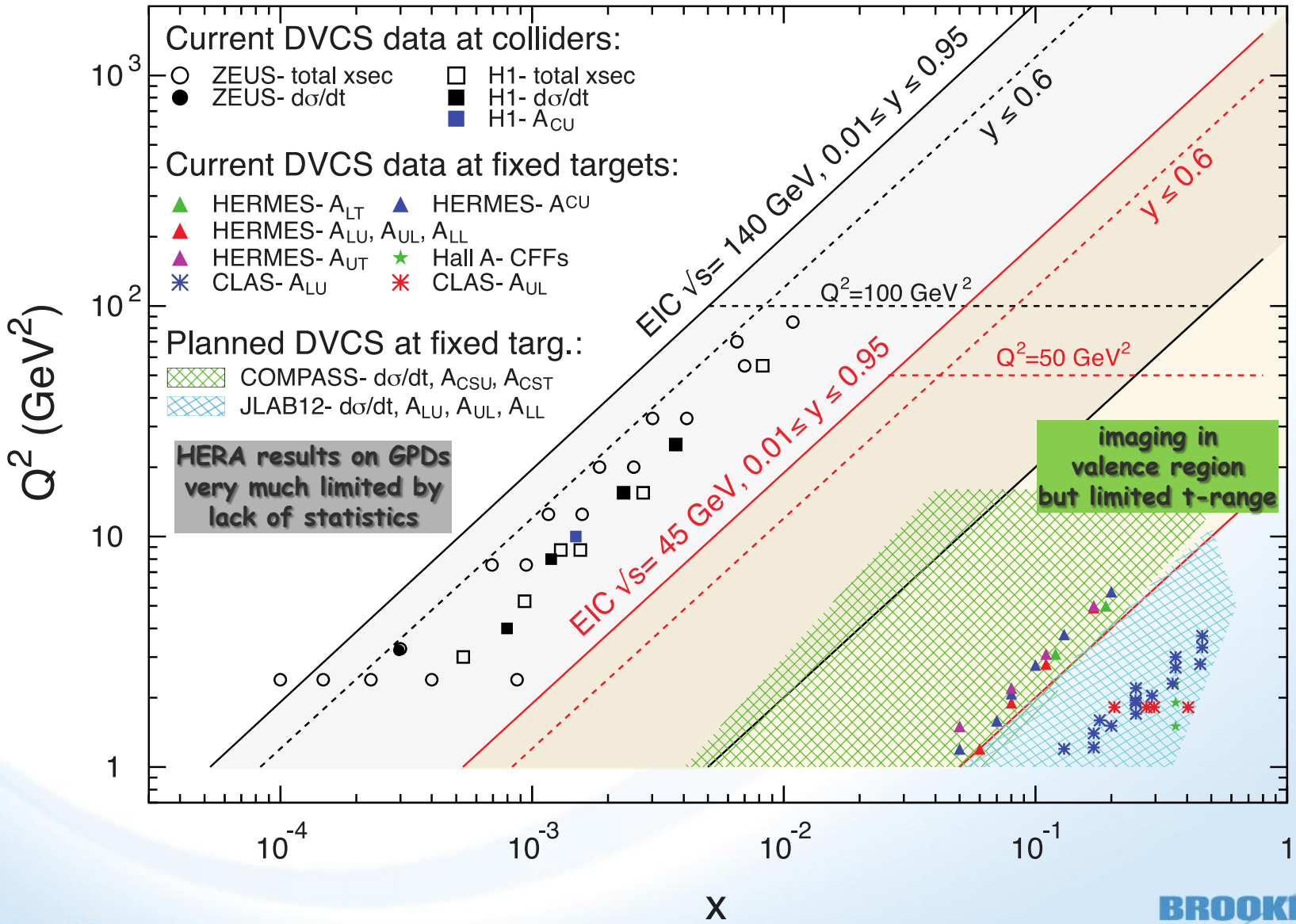

DVCS AT eRHIC

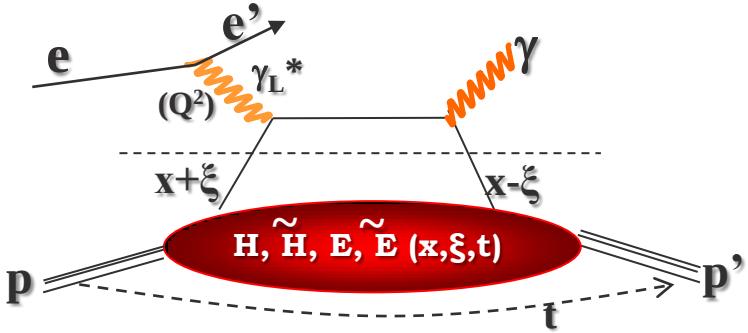

DVCS: Golden channel
theoretically clean
wide range of observables
(σ, A_{UT}, A_{LU}, A_{UL}, A_C)
to disentangle different GPDs

DVCS data at end of HERA

D. Mueller, K. Kumericki
S. Fazio, and ECA
arXiv:1304.0077

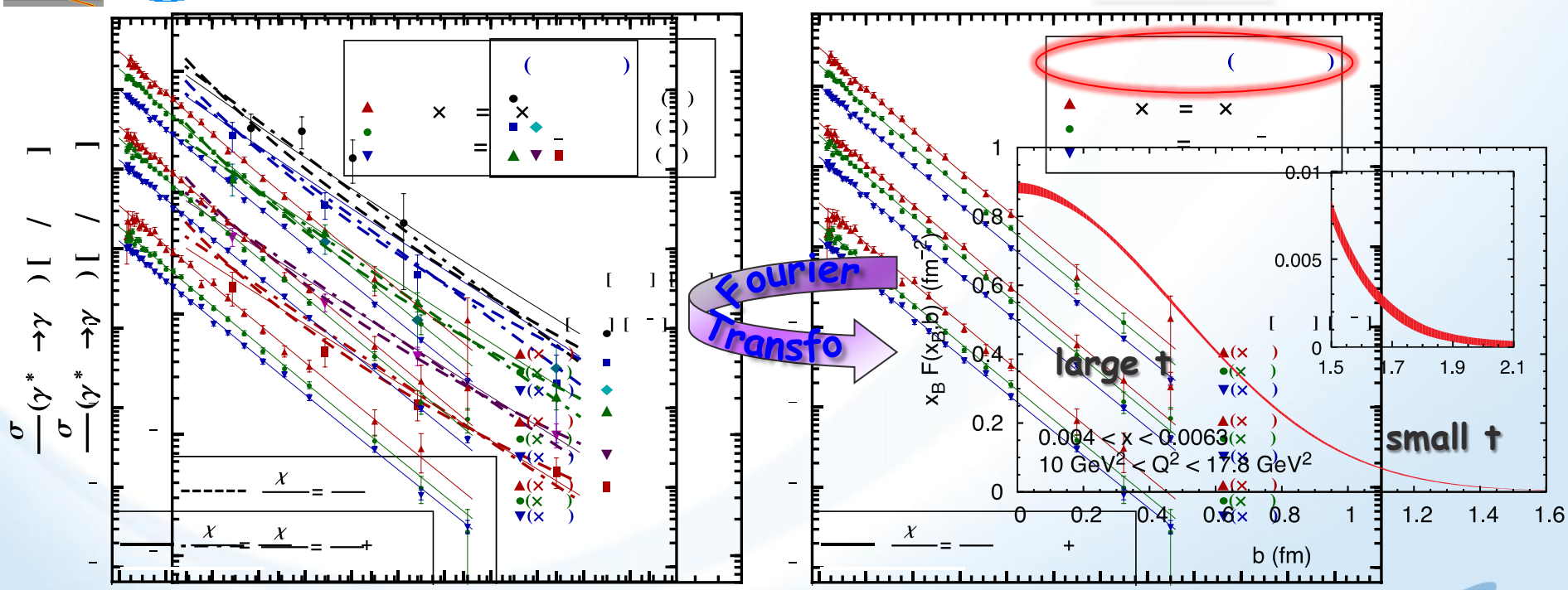

WHAT WILL WE LEARN ABOUT 2D+1 STRUCTURE OF THE PROTON

GPD H and E as function of t, x and Q^2

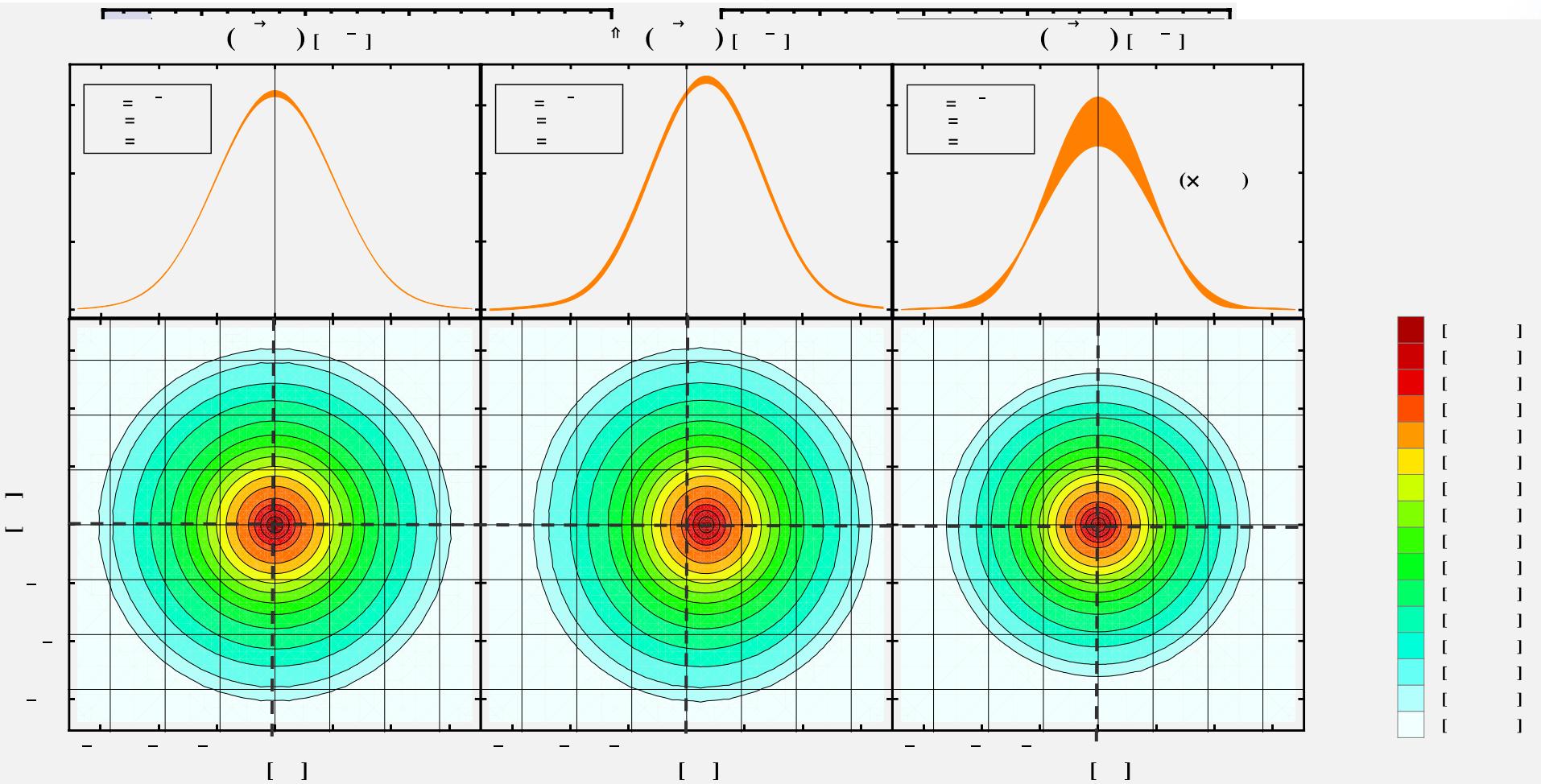

GPD H and E 2d+1 structure for sea-quarks and gluons

- Excellent reconstruction of H^{sea}, H^{s} and good reconstruction of H^{g} (from $d\sigma/dt$)

GPD H: J/Ψ

M. Diehl & ECA

To improve imaging on gluons add J/ψ observables

- cross section
- A_{UT}
- ……

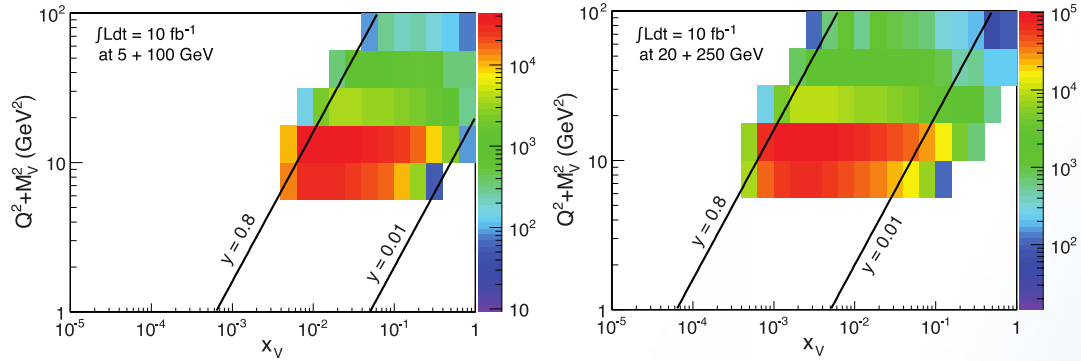

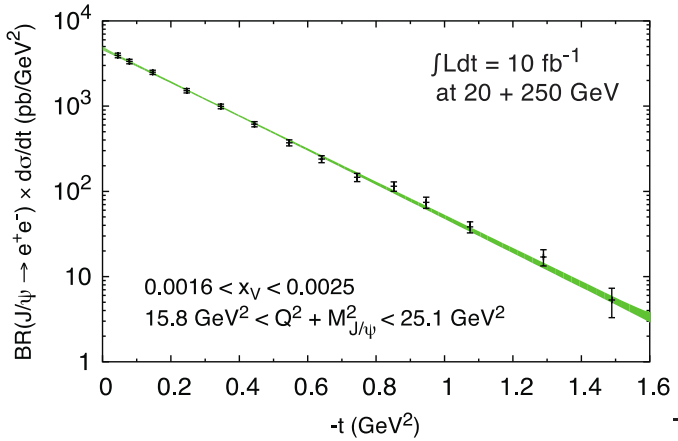

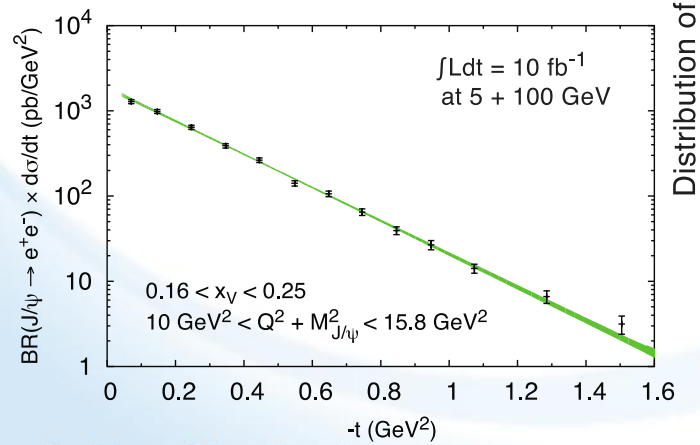

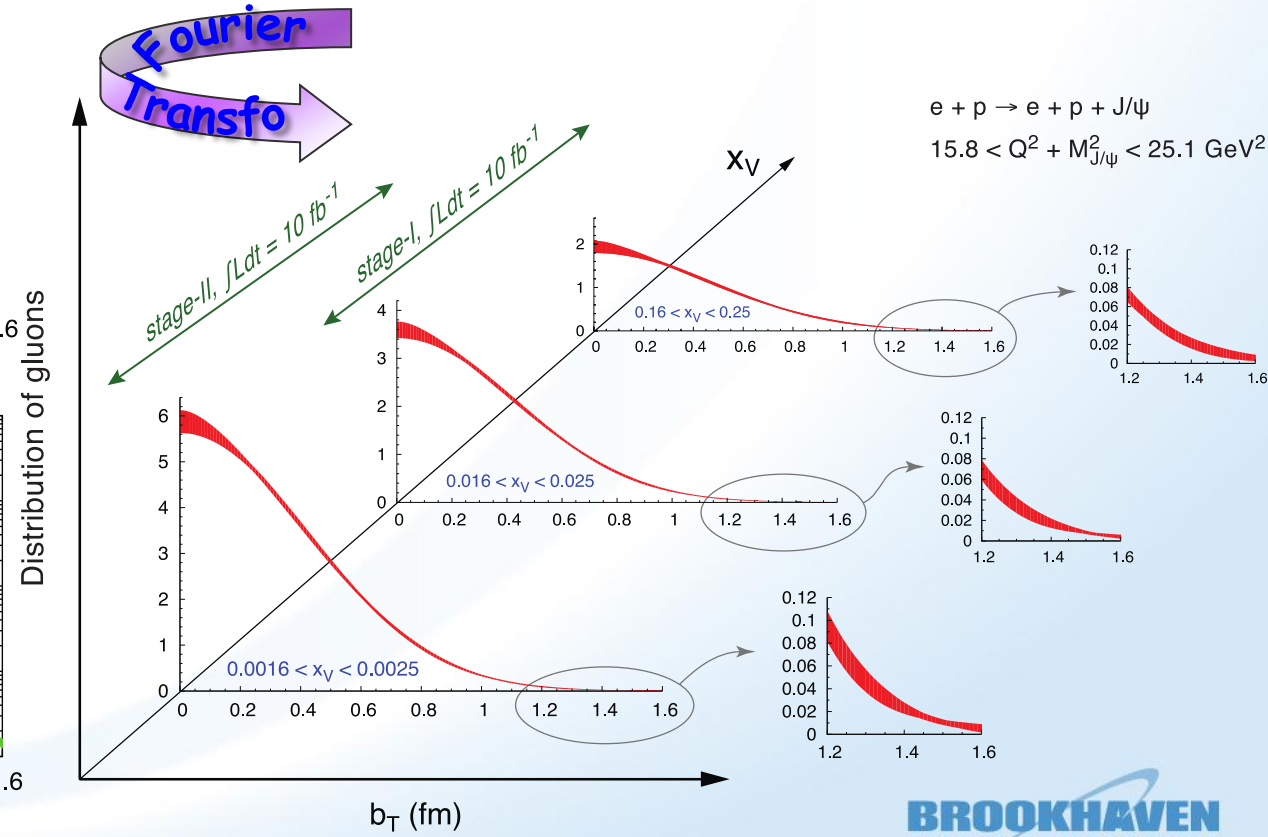

THE eA PHYSICS PROGRAM

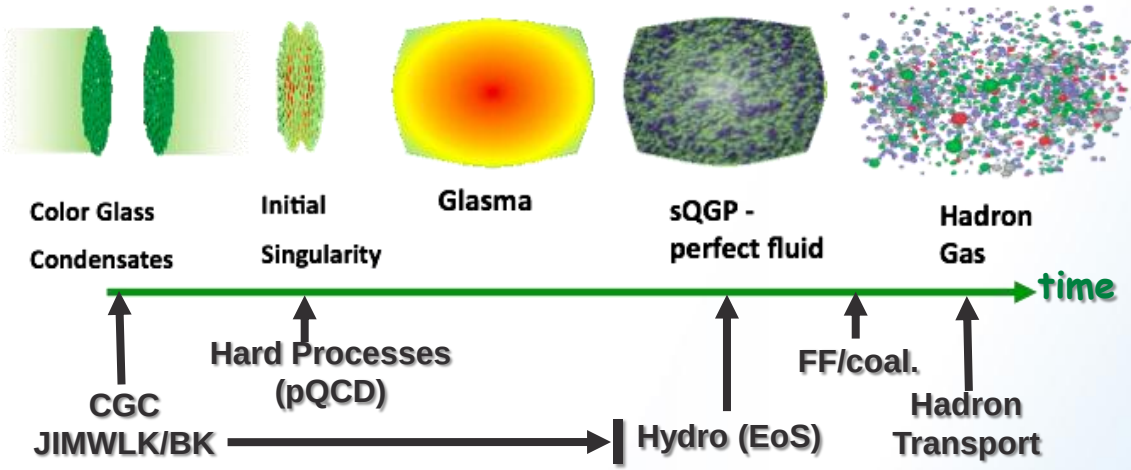

Our understanding of some fundamental properties of the Glasma, sQGP and Hadron Gas depend strongly on our knowledge of the initial state!

3 conundrums of the initial state:

1. What is the spatial transverse distributions of nucleons and gluons?
2. How much does the spatial distribution fluctuate? Lumpiness, hot-spots etc.
3. How saturated is the initial state of the nucleus?

WHAT DO WE KNOW ABOUT xG IN NUCLEI?

Fractional contribution to cross-section

Oth
G(x
Key

$R_L($

Measurements with A ≥ 56 (Fe):

- eA/μA DIS (E-139, E-665, EMC, NMC)
- νA DIS (CCFR, CDHSW, CHORUS, NuTeV)
- DY (E772, E866)

EIC √s = 90 GeV, 0.01 ≤ y ≤ 0.95

EIC √s = 45 GeV, 0.01 ≤ y ≤ 0.95

$Q^2_{s,quark}$ Au, median b

Ca, median b

p, median b

Q^2 (GeV^2)

10^3, 10^2, 10, 1, 0.1

10^{-4}, 10^{-3}, 10^{-2}, 10^{-1}, 1

x

HOW MANY GLUONS HAVE SPACE IN A PROTON?

- at small x linear evolution gives strongly rising g(x)
  - cannot go on forever
- BK/JIMWLK non-linear evolution includes recombination effects → saturation
  - Dynamically generated scale
    Saturation Scale: $Q^2_s(x)$
    - Increases with energy or decreasing x
  - Scale with $Q^2/Q^2_s(x)$ instead of x and Q^2

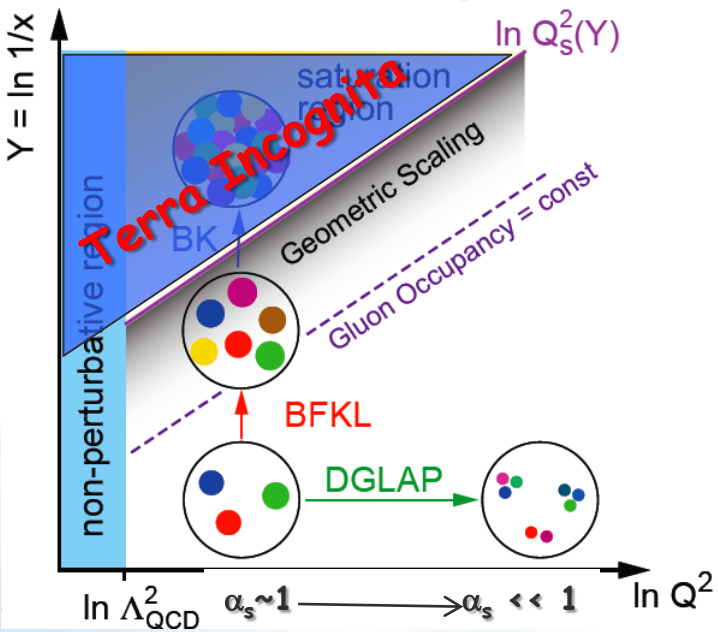

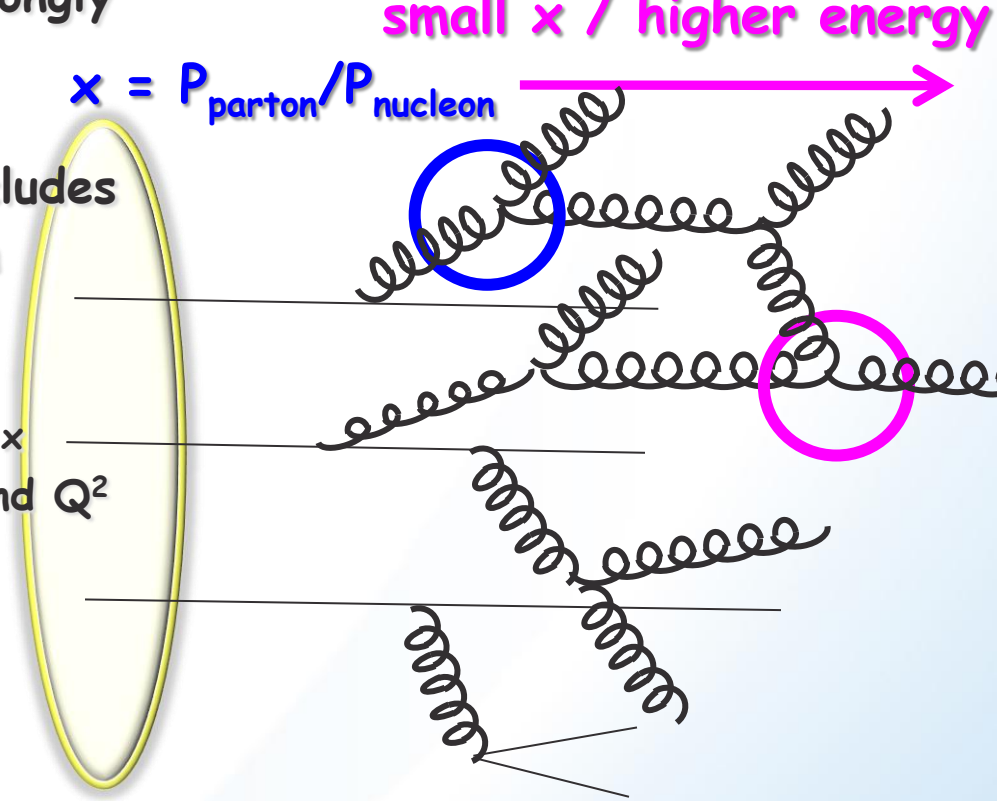

Bremsstrahlung $\sim \alpha_s \ln(1/x)$

Recombination $\sim \alpha_s \rho$

Saturation must set in at low x → high occupancy

eRHIC: REACHING THE SATURATION REGION

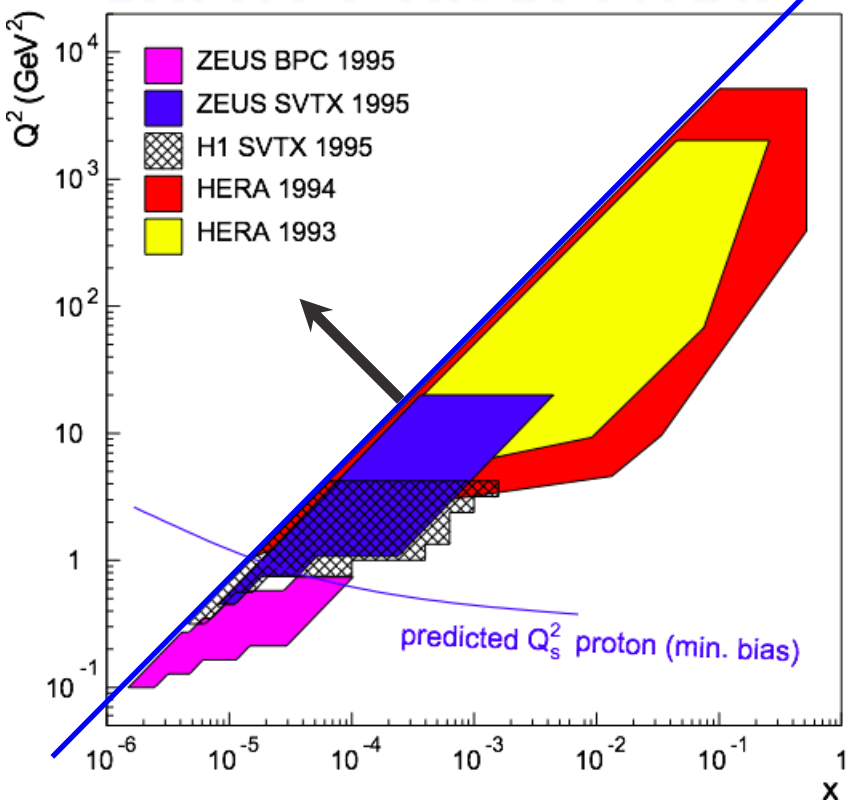

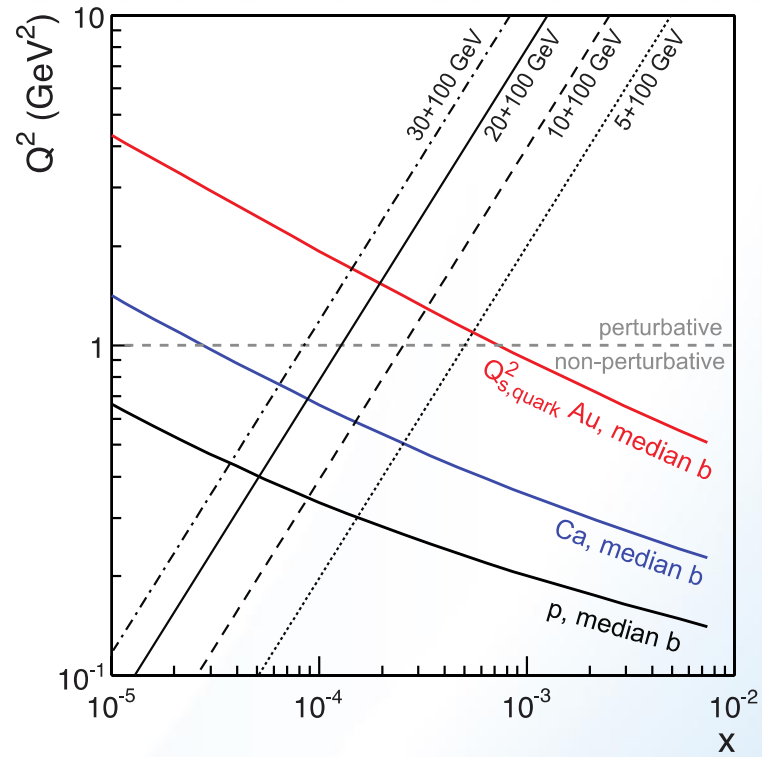

HERA (ep):

Despite high energy range:

- F_2, $G_p(x, Q^2)$ outside the saturation regime
- Need also Q^2 lever arm!
- Only way in ep is to increase $\sqrt{s}$
- Would require an ep collider at $\sqrt{s}$ ~ 1-2 TeV → LHeC

eRHIC (eA):

$$(Q_s^A)^2 \sim c Q_o^2 \left(\frac{A}{x}\right)^{1/3}$$

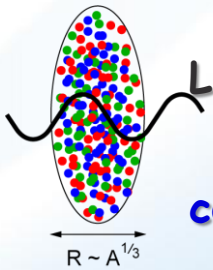

$L \sim (2m_N x)^{-1} > 2 R_A \sim A^{1/3}$

Probe interacts coherently with all nucleons

Gold: 197 times smaller effective x !

INCLUSIVE DIS IN EA: NUCLEAR PDFS

$$\frac{d^2\sigma^{eA\to eX}}{dx\,dQ^2} = \frac{4\pi\alpha^2}{xQ^4}\left[\left(1 - y - \frac{y^2}{2}\right)F_2(x,Q^2) - \frac{y^2}{2}F_L(x,Q^2)\right]$$

quark+anti-quark gluon

- Expect strong non-linear effects in F_L

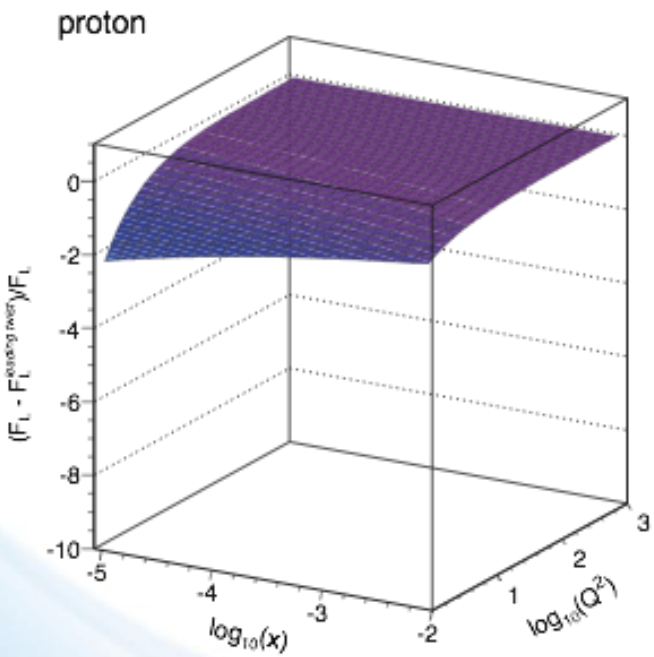

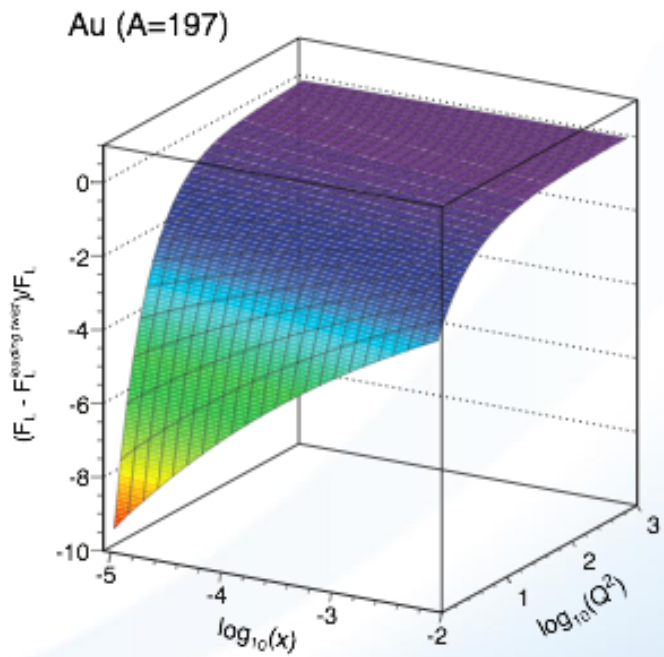

Relative contributions of higher twist effects to F_L amplified in eA

Dipole model (J. Bartels et al.)

INCLUSIVE DIS IN EA: NUCLEAR PDFS

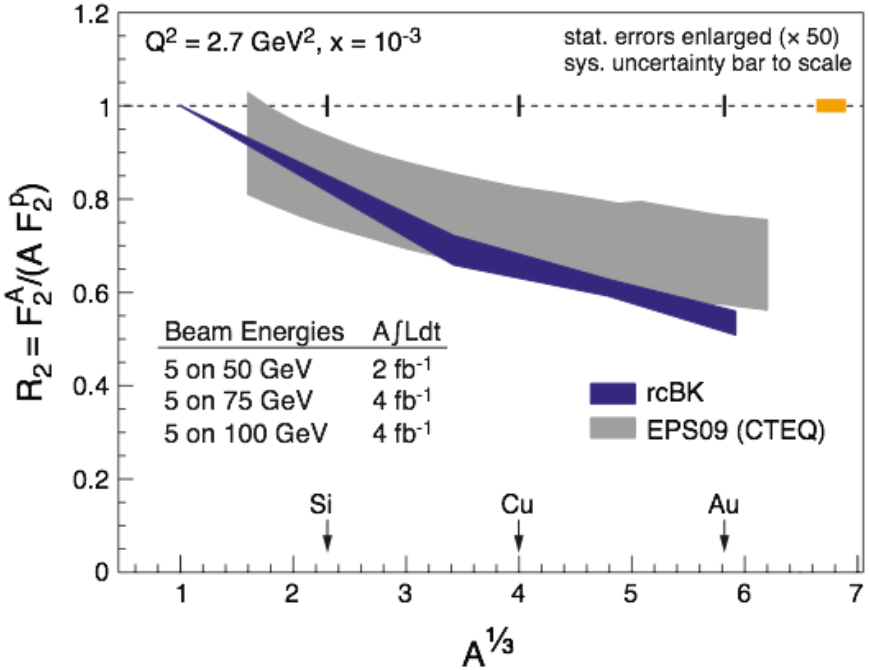

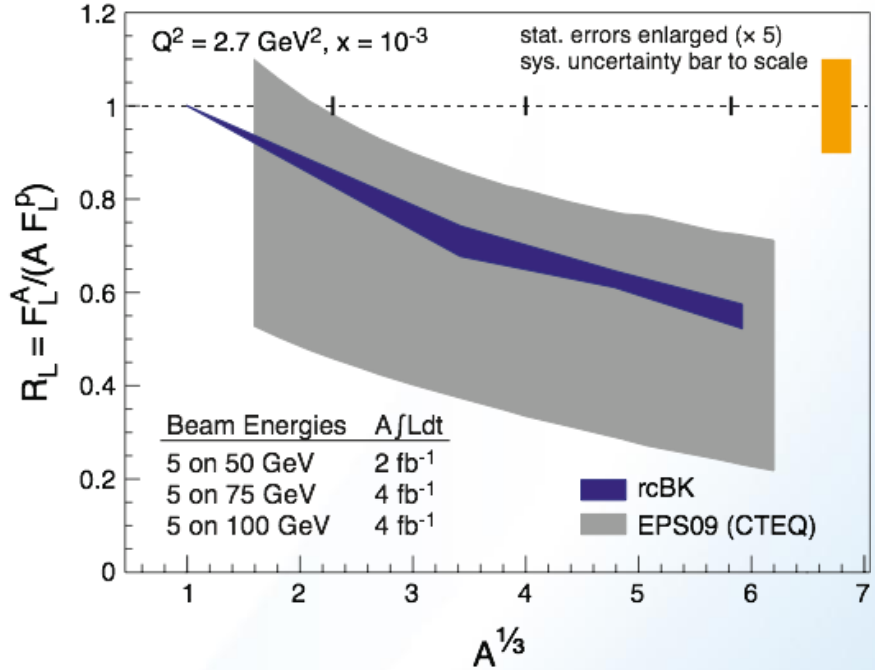

- measurement of F_L requires running at different □s
- F_2, F_L: negligible stat. error, systematics dominated
- A dependence helps to discriminate between linear and non-linear (saturation) models
- Precision nPDF: Huge impact on pA, AA programs

h-h FORWARD CORRELATION IN p(d)A AT RHIC

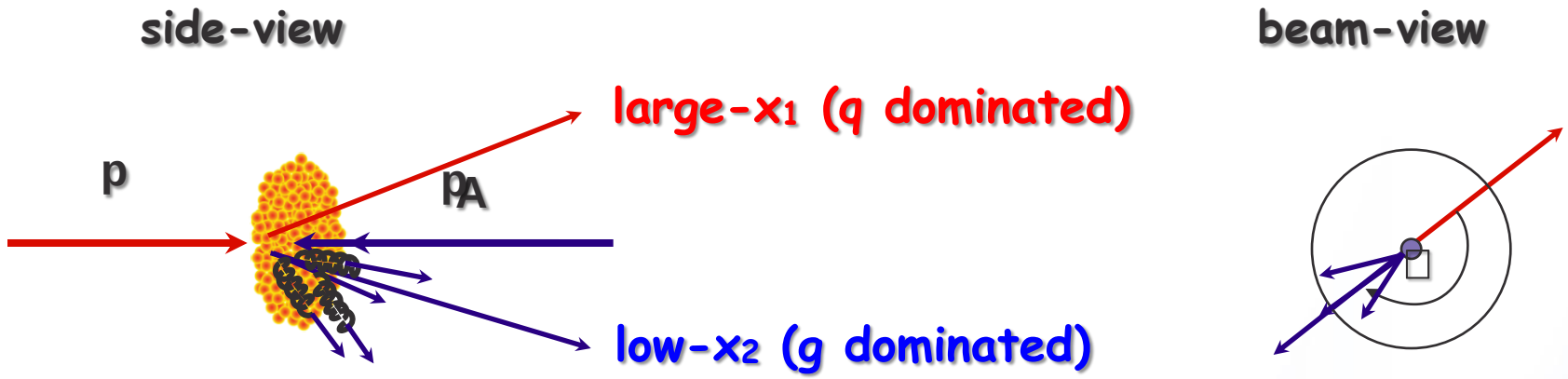

Low gluon density (pp):
pQCD predicts 2→2 process
⇒ back-to-back di-jet

High gluon density (pA):
2 → many process
⇒ expect broadening of away-side

- Small-x evolution ↔ multiple emissions
- Multiple emissions → broadening
- Back-to-back jets (here leading hadrons) may get broadening in p_T with a spread of the order of Q_S

First prediction by: C. Marquet ('07)
Latest review: Stasto, Xiao, Yuan arXiv:1109.1817 (Sep. '11)

FORWARD CORRELATIONS IN dA AT RHIC

1 question, 2 answers

Initial state saturation model

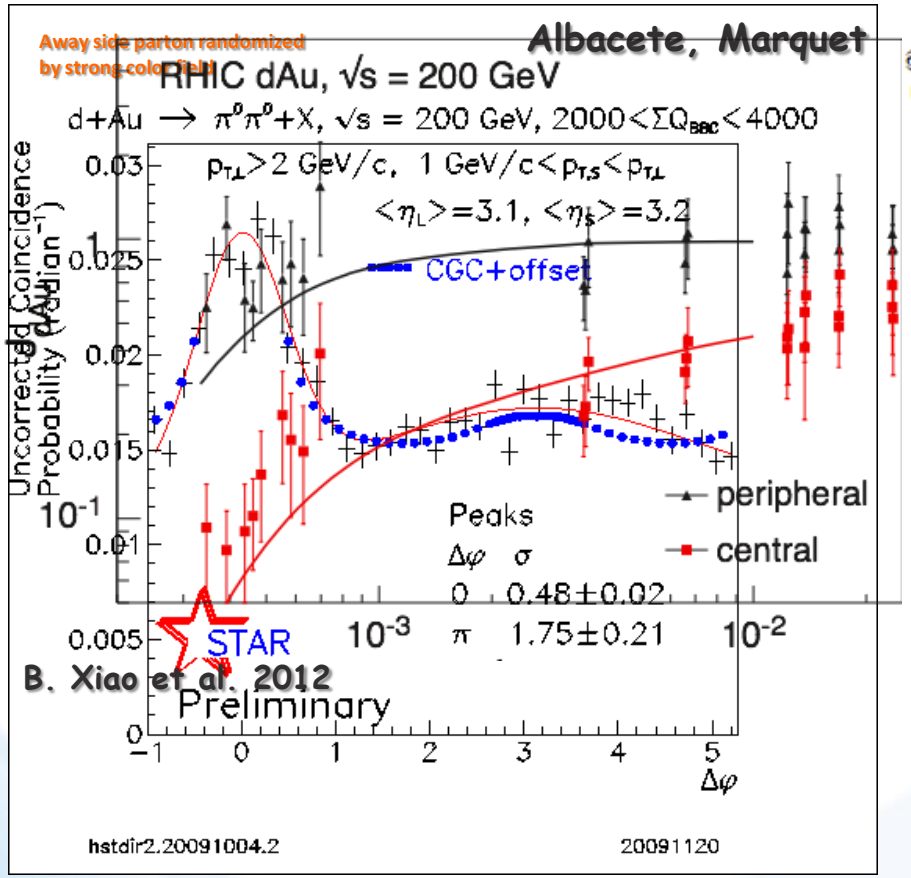

B. Xiao et al. 2012

"Non-initial state" shadowing model

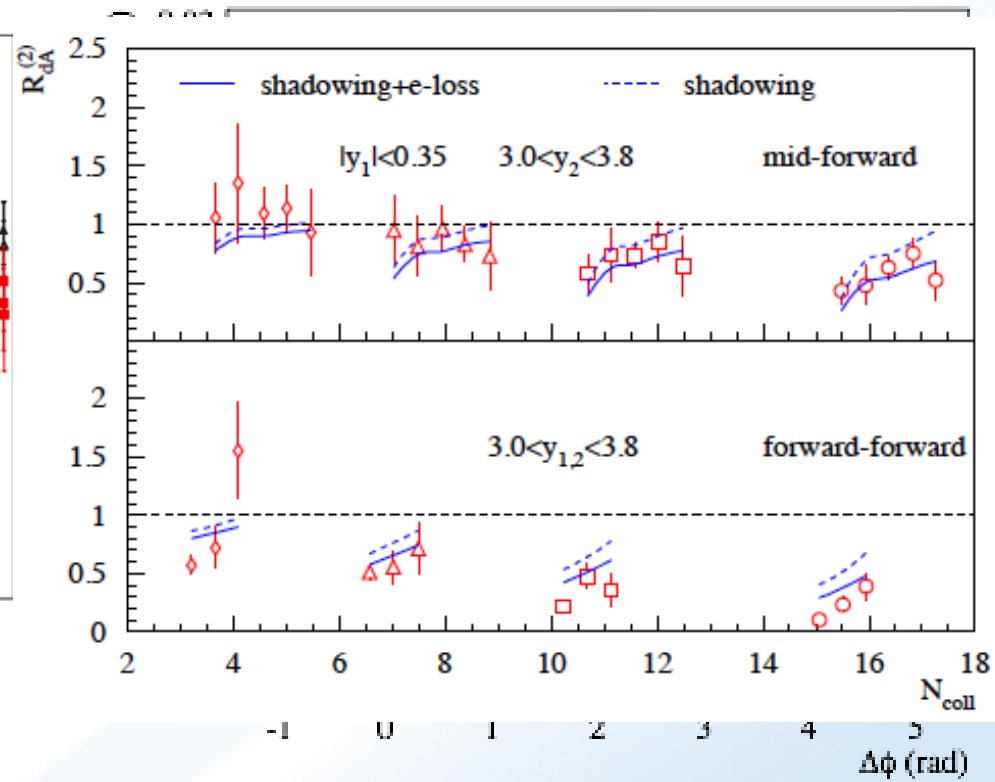

$$\langle q_\perp^2 \rangle_{dAu} = \langle q_\perp^2 \rangle_{pp} + \Delta \langle q_\perp^2 \rangle$$

How saturated is the initial state?

DIHADRON CORRELATIONS IN eA AT EIC

EIC:

- Extract the spatial multi-gluon correlations and study their non-linear evolution
  - essential for understanding the transition from a deconfined into a confined state.

Advantage over p(d)A:

- eA experimentally much cleaner
  - no "spectator" background to subtract
  - Access to the exact kinematics of the DIS process (x, Q^2)

Perfect saturation signature:

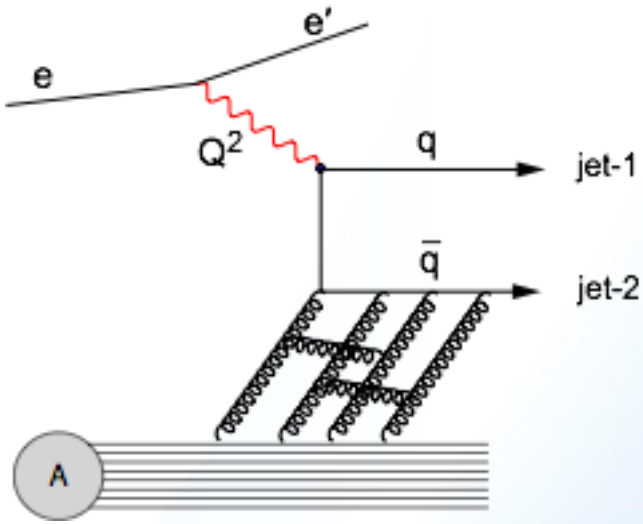

Either jets or use leading hadrons from jets (dihadrons)

EIC: eA DIHADRON CORRELATIONS STUDIES

Theory: Saturation

Dominguez, Xiao, Yuan, Lee, Zheng '11/12

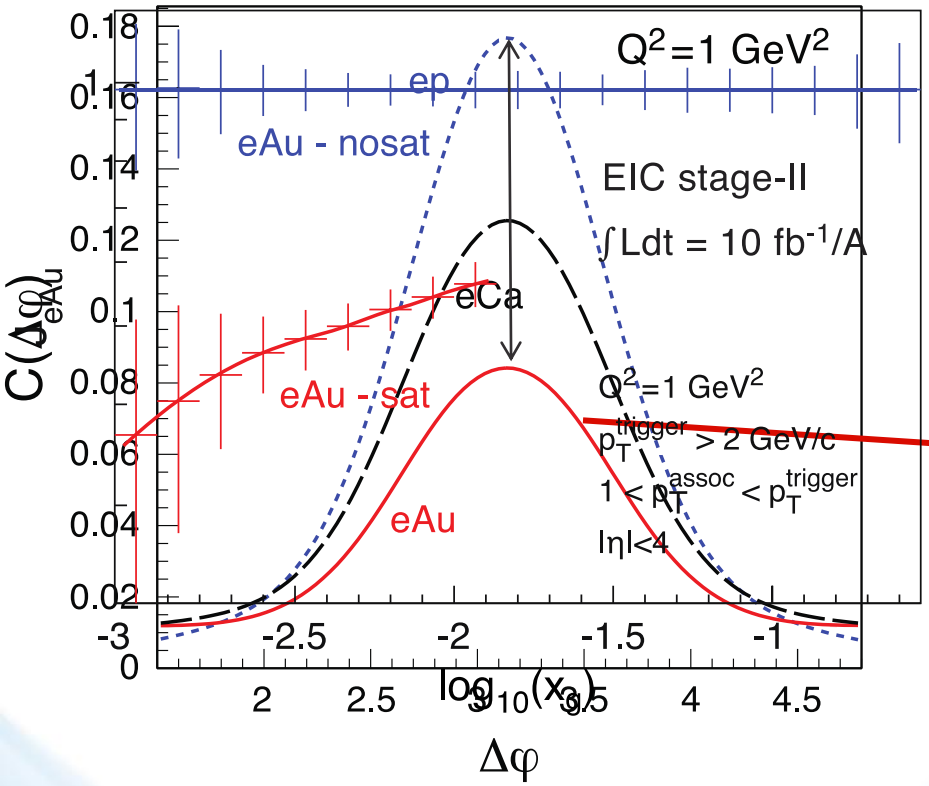

Exp: Saturation versus "conventional" scenario

J.H. Lee, L. Zheng (CCNU) '11/12

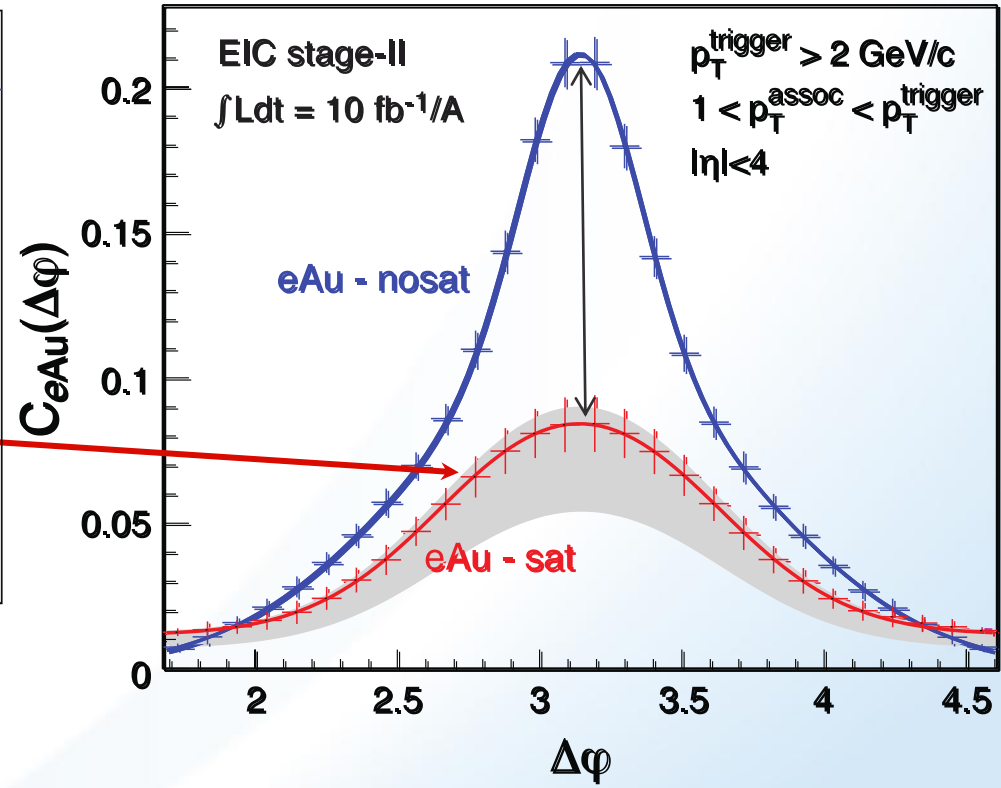

- eA-MC: Pythia6.4 + nPDF (EPS09) + nuclear geometry from DPMJetIII without PS
- Here for 10 fb^{-1}/A (~ 20 weeks), std. experimental cuts
- Clear signal, pronounced differences between sat and no-sat

HARD DIFFRACTION IN DIS AT SMALL X

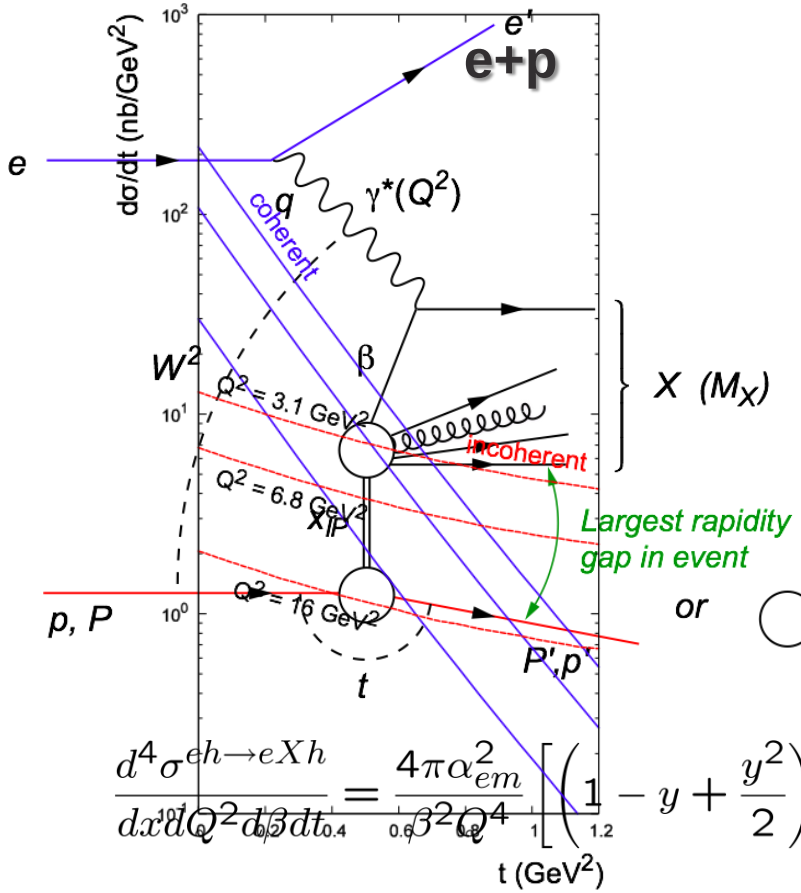

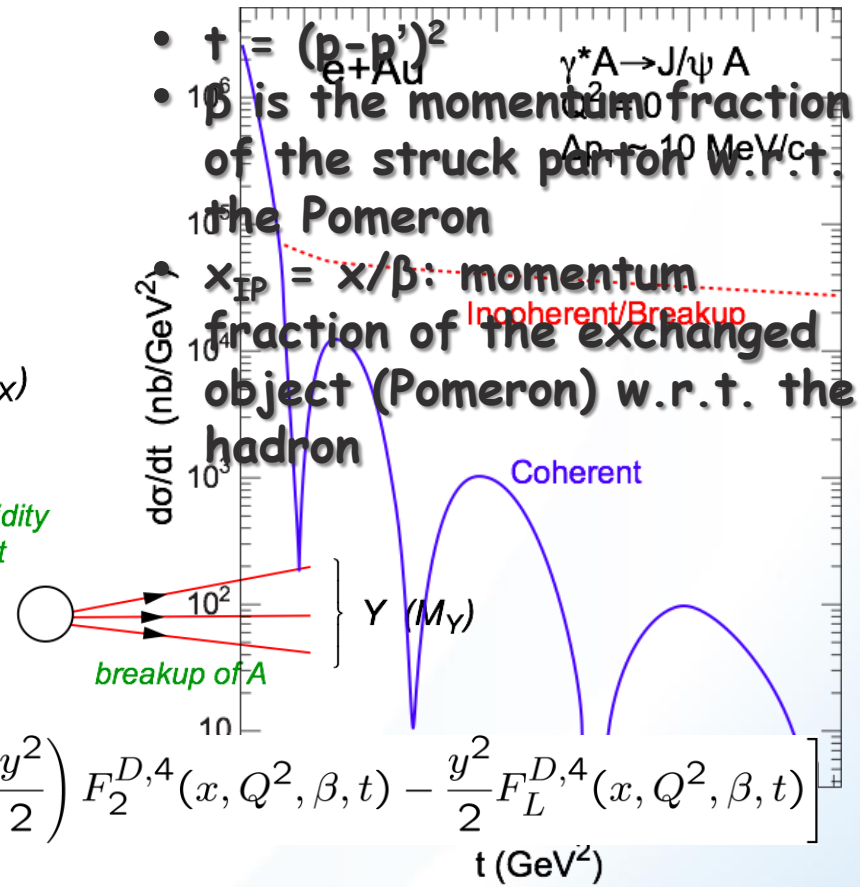

- $t = (p-p')^2$
- β is the momentum fraction of the struck parton w.r.t. the Pomeron
- $x_{IP} = x/\beta$: momentum fraction of the exchanged object (Pomeron) w.r.t. the hadron

$$\frac{d^4\sigma^{eh\to eXh}}{dx\,dQ^2\,d\beta\,dt} = \frac{4\pi\alpha_{em}^2}{\beta^2 Q^4}\left[\left(1-y+\frac{y^2}{2}\right)F_2^{D,4}(x,Q^2,\beta,t) - \frac{y^2}{2}F_L^{D,4}(x,Q^2,\beta,t)\right]$$

- Diffraction in e+p:
  - coherent ⇔ p intact
  - incoherent ⇔ breakup of p
  - HERA: 15% of all events are hard diffractive
- Diffraction in e+A:
  - coherent diffraction (nuclei intact)
  - breakup into nucleons (nucleons intact)
  - incoherent diffraction
  - Predictions: $\sigma_{diff}/\sigma_{tot}$ in e+A ~25-40%

WHY IS DIFFRACTION SO IMPORTANT

- Sensitive to spatial gluon distribution

$$\frac{d\sigma}{dt} \circ \frac{\text{Fourier Transformation}}{\text{of Source Density } r_g(b)}$$

  - Hot topic:
    - Lumpiness?
    - Just Wood-Saxon+nucleon g(b)
  - Incoherent case: measure fluctuations/lumpiness in $g_A(b)$

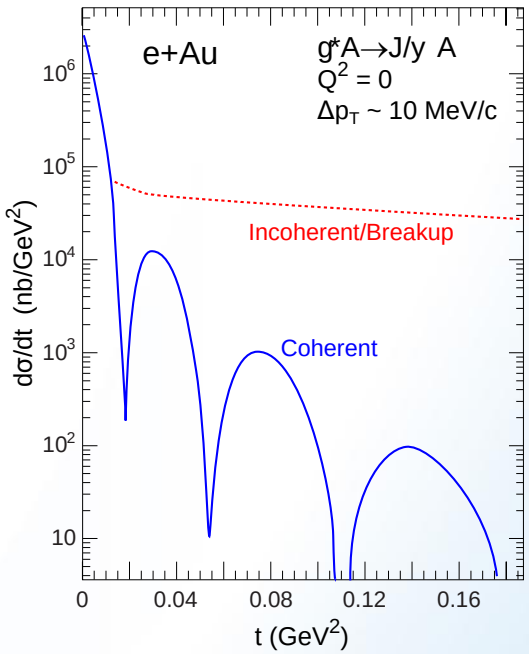

- Sensitive to gluon momentum distributions
  - $\sigma \sim g(x,Q^2)^2$

$$\frac{d\sigma^{\gamma^* p \to pV}}{dt} \sim \left| \int \Psi_V^* \frac{d\sigma_{q\bar{q}}}{d^2b} \Psi e^{-ib\Delta} \right|^2$$

$$\frac{d\sigma_{q\bar{q}}}{d^2b} \sim r^2 \alpha_s x g(x,\mu^2) T(b)$$

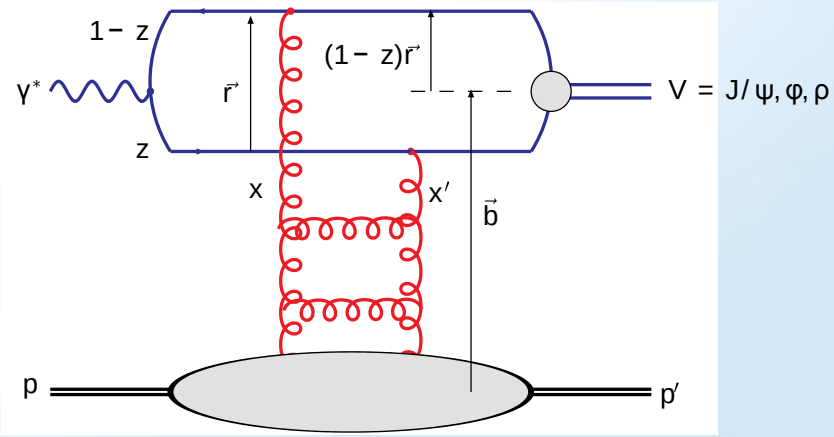

RATIO OF DIFFRACTIVE TO TOTAL CROSS-SECTION

- Black disc limit characterized by $\sigma_{diff}/\sigma_{tot}$ = 1/2 (Hera sees 1/7)
- Large fraction of diffractive event is unambiguous signature for reaching the saturated limit

Fraction of low-mass coherent diffraction in ep and eA at EIC:

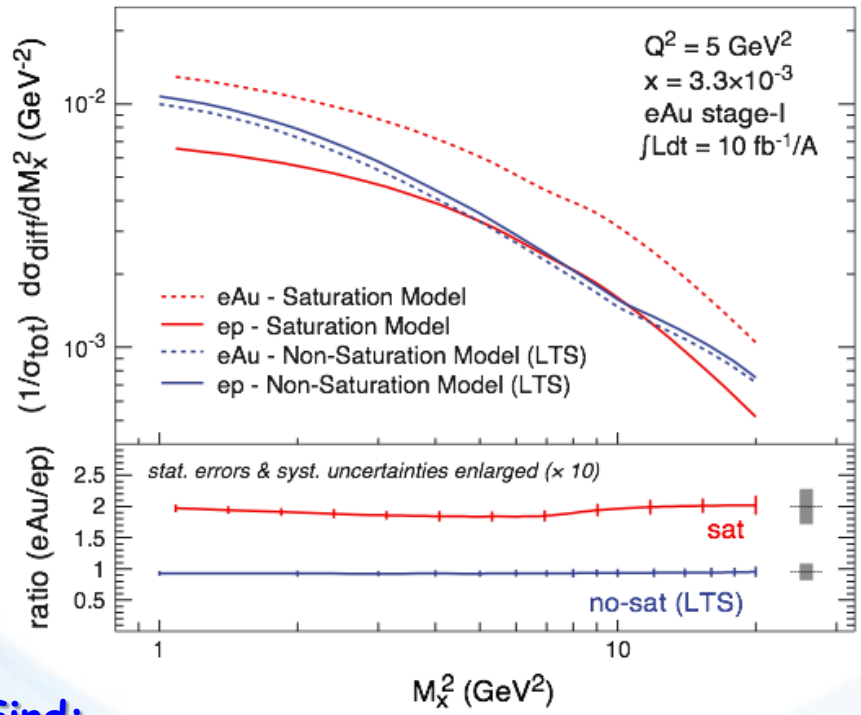

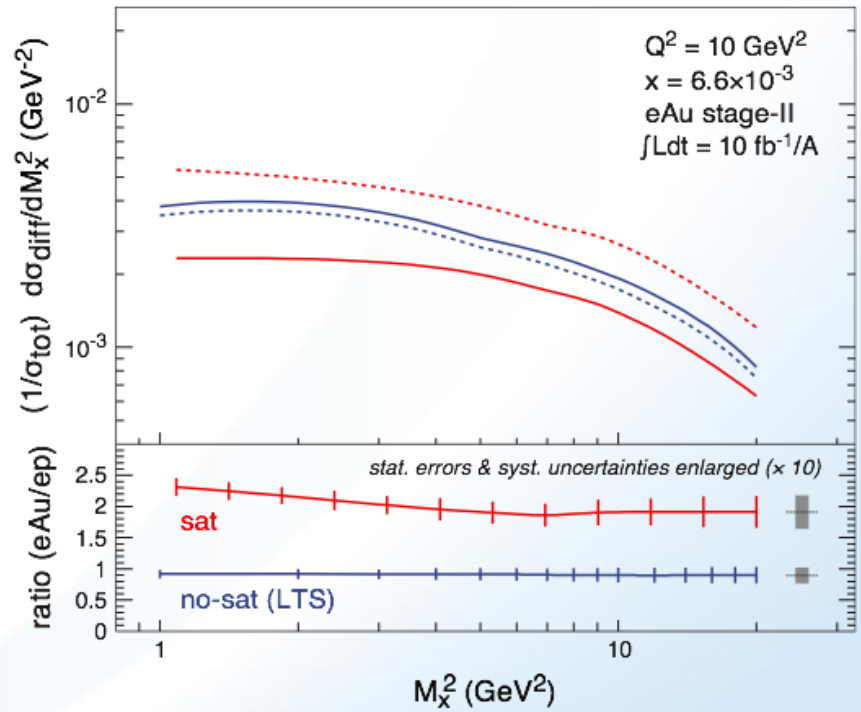

Find:

- w/o non-linear effects eA/ep ratio stays roughly one
- non-linear effects enhance σ_{diff} in eA scattering

Day-1 signature for Saturation

EXCLUSIVE VECTOR MESON PRODUCTION

- Unique probe - allows to measure momentum transfer t in eA diffraction
  - → in general, one cannot detect the outgoing nucleus and its momentum

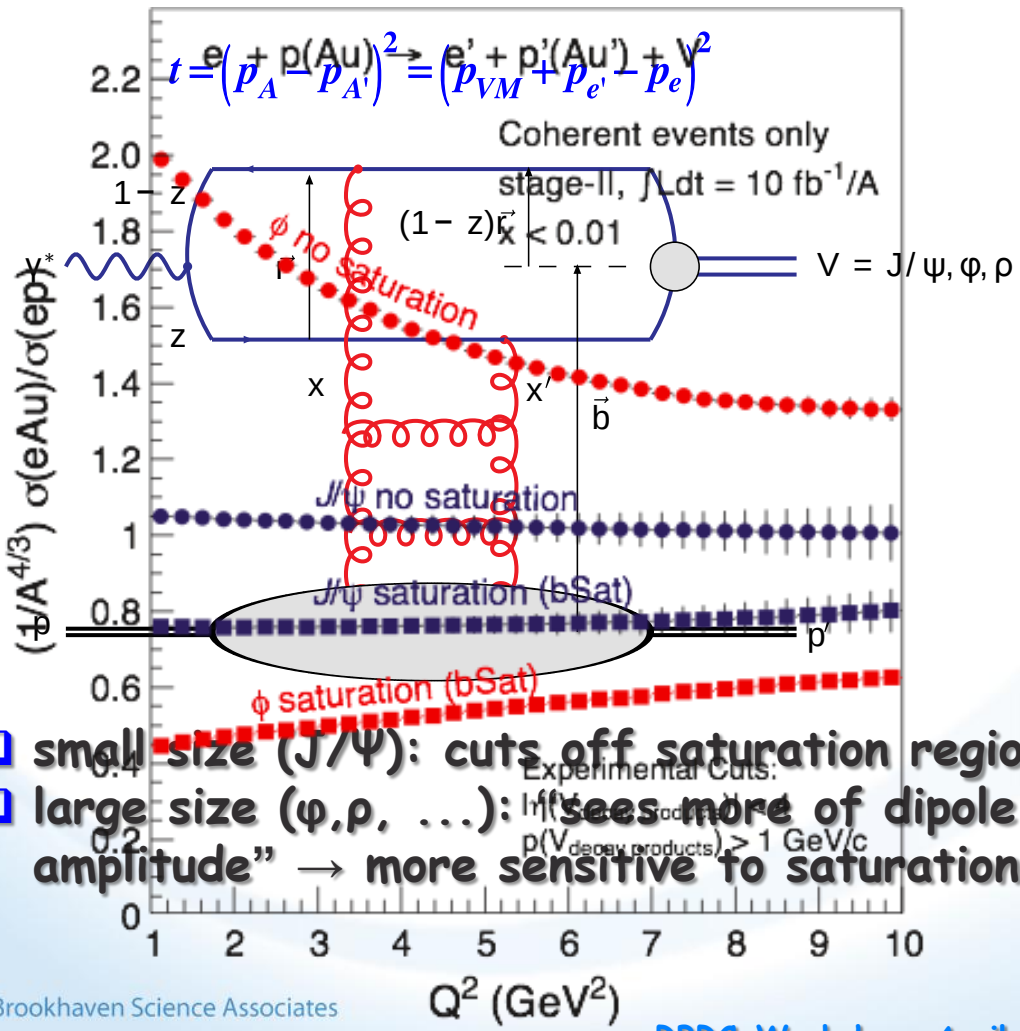

- small size (J/Ψ): cuts off saturation region
- large size (φ,ρ, ...): "sees more of dipole amplitude" → more sensitive to saturation

Dipole Cross-Section:

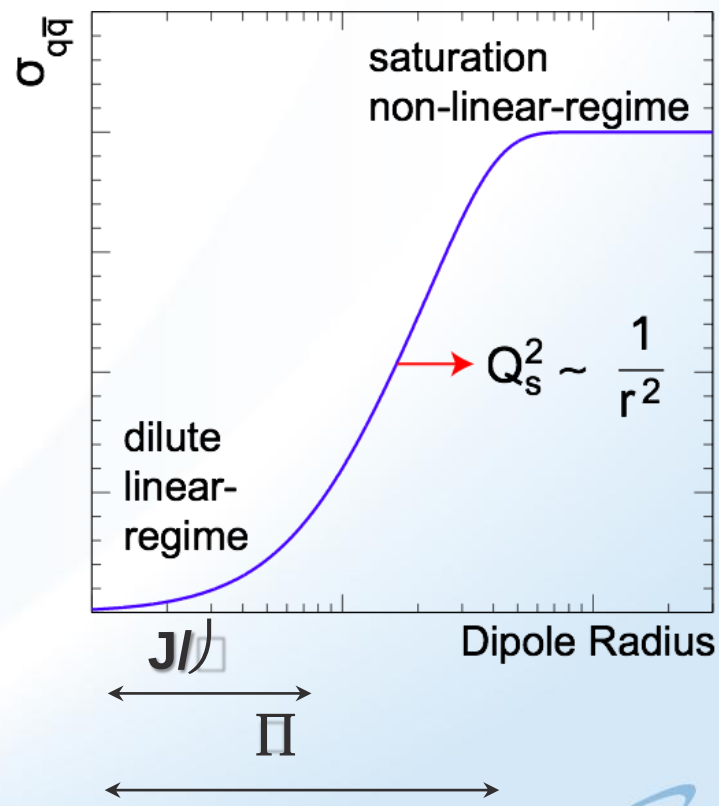

SPATIAL GLUON DISTRIBUTION THROUGH DIFFRACTION

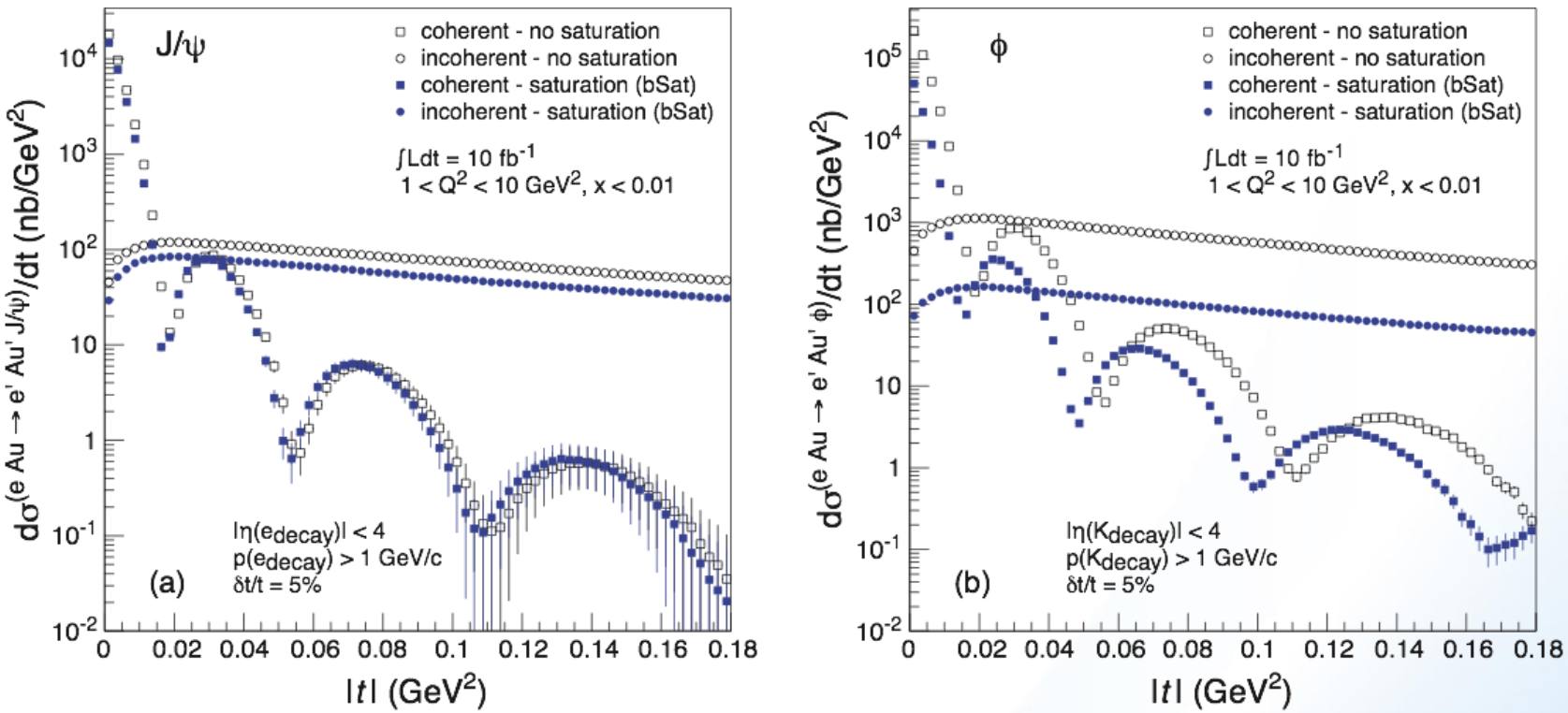

- Goal: going after the source distribution of gluons through Fourier transform of dσ/dt
- Find: Typical diffractive pattern for coherent (non-breakup) part
- As expected: J/Ψ less sensitive to saturation effects than larger Φ-meson

SPATIAL GLUON DISTRIBUTION THROUGH DIFFRACTION

- Idea: momentum transfer t conjugate to transverse position (b_T)
  - coherent part probes "shape of black disc"
  - incoherent part (dominant at large t) sensitive to "lumpiness" of the source (fluctuations, hot spots, ...)

Spatial source distribution: $F(b) \sim \frac{1}{2\pi}\int_0^\infty d\Delta \Delta J_o(\Delta b)\sqrt{\frac{d\sigma}{dt}}$

$t = \Delta^2/(1-x) \approx \Delta^2$ (for small x)

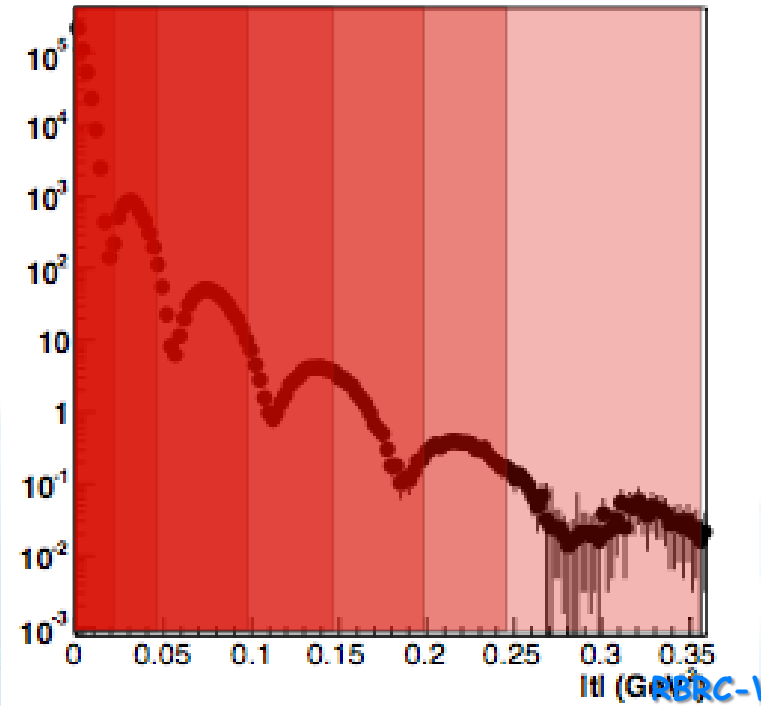

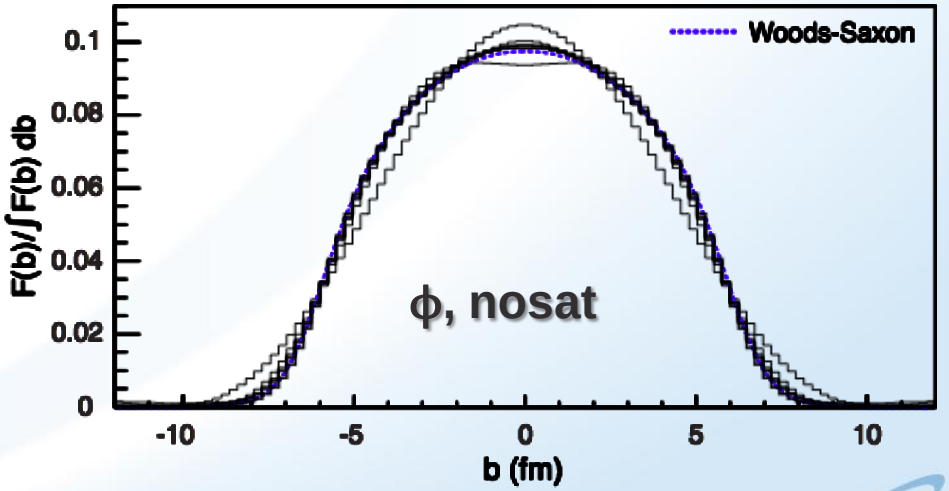

Golden eA measurement for EIC

DEEP INELASTIC SCATTERING - VACUUM

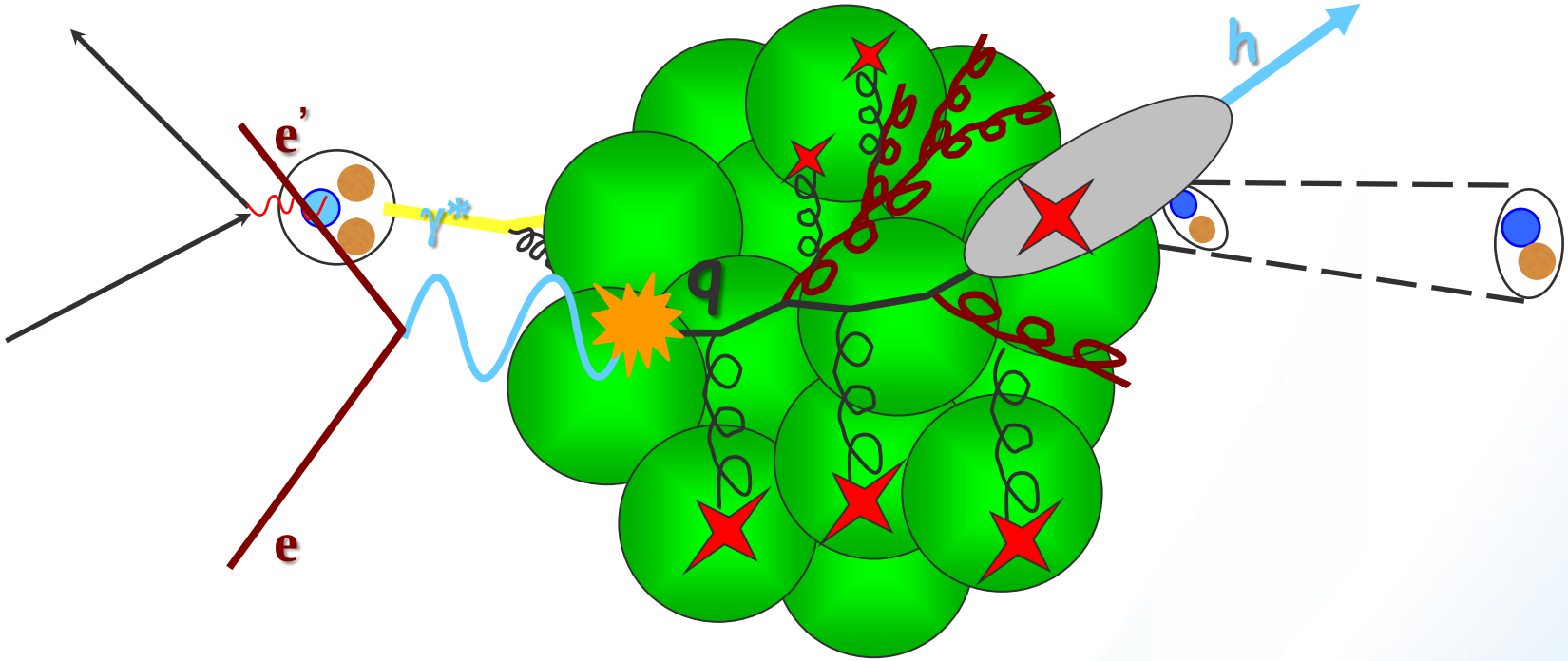

What happens if we add a nuclear medium

Observables:

Broadening: Δp_t^2 linked directly with saturation scale $\Delta p_t^2 = \langle p_t^2 \rangle_A - \langle p_t^2 \rangle_p$

Attenuation: ratio of hadron production in A to d modifications of nPDF cancel out $R_A^h(Q^2, x, z, p_t, Q)$

WHAT DO WE KNOW AND WHAT CAN EIC DO

Hermes:

E_e = 27 GeV → $\sqrt{s}$ = 7.2 G

E_h = 2-15 GeV

Unprecedented precision to distinguish between different models

large ν range

→ hadronization in and out of nucleus

→ first time for charm

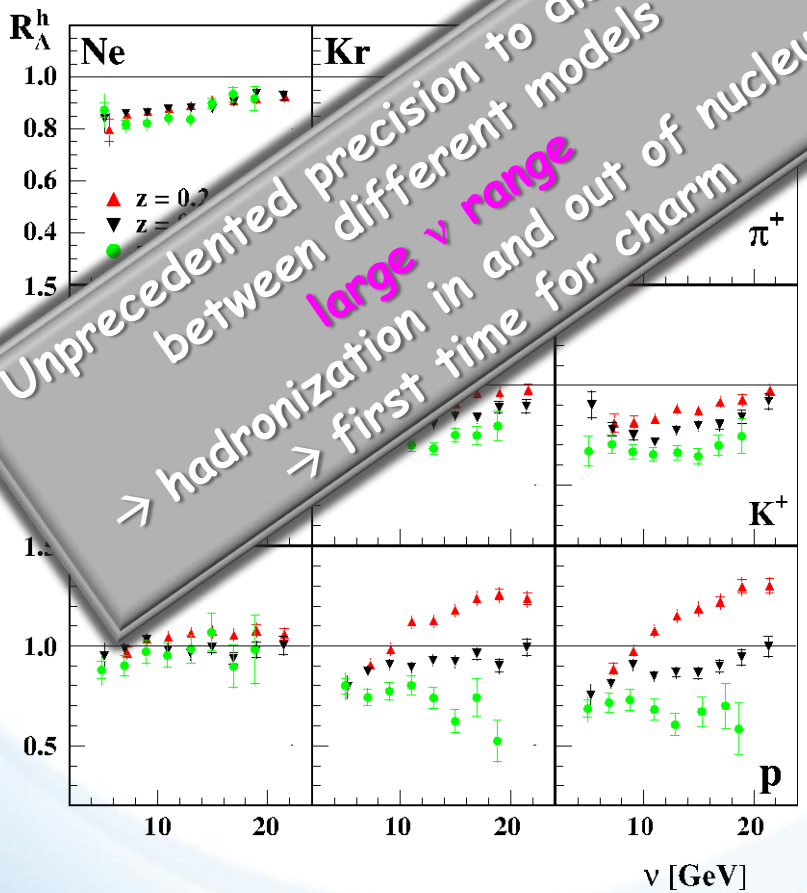

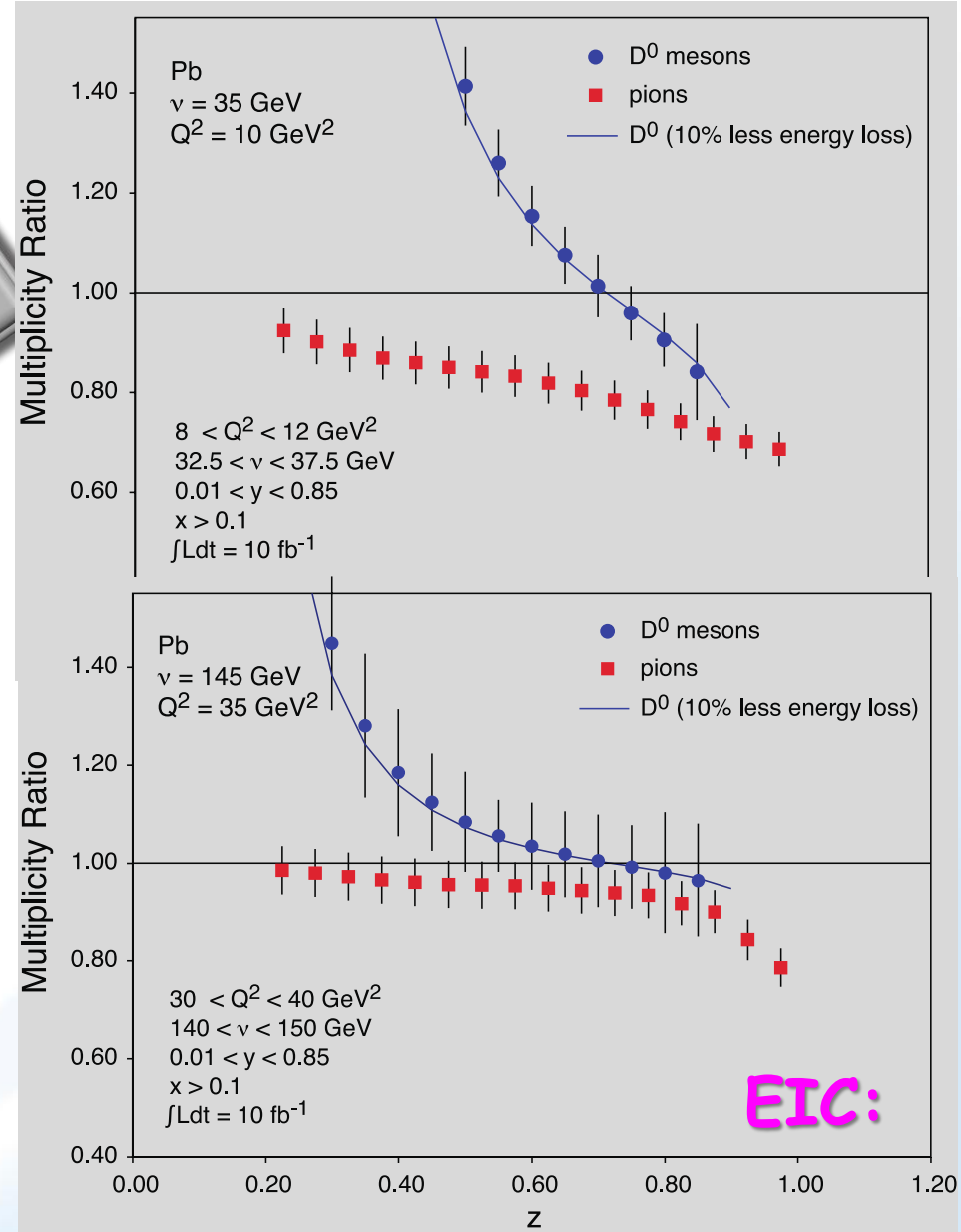

TAKE AWAY MESSAGE

The EIC will profoundly impact our understanding of QCD with its high energy, high luminosity eA and polarized ep collisions

ACHIEVED if eR[illegible] is built

entire science program uniquely tied to a future high energy electron ion collider never been measured before & never without

- **ep:** precision studies [illegible] TMDs, and GPDs will [illegible] nucleon ever [illegible] structure
- [illegible] study of matter in [illegible] regime where physics is not described by "ordinary" QCD: non-linear QCD/saturation/higher twist effects, properties of glue (momentum & space-time), understand how fast partons interact as they traverse nuclear matter, new insight into fragmentation processes, clarification of the nature of pomerons.

BROOKHAVEN NATIONAL LABORATORY

E.C. Aschenauer

BACKUP

POSSIBLE SCHEDULE TO REALIZE eRHIC

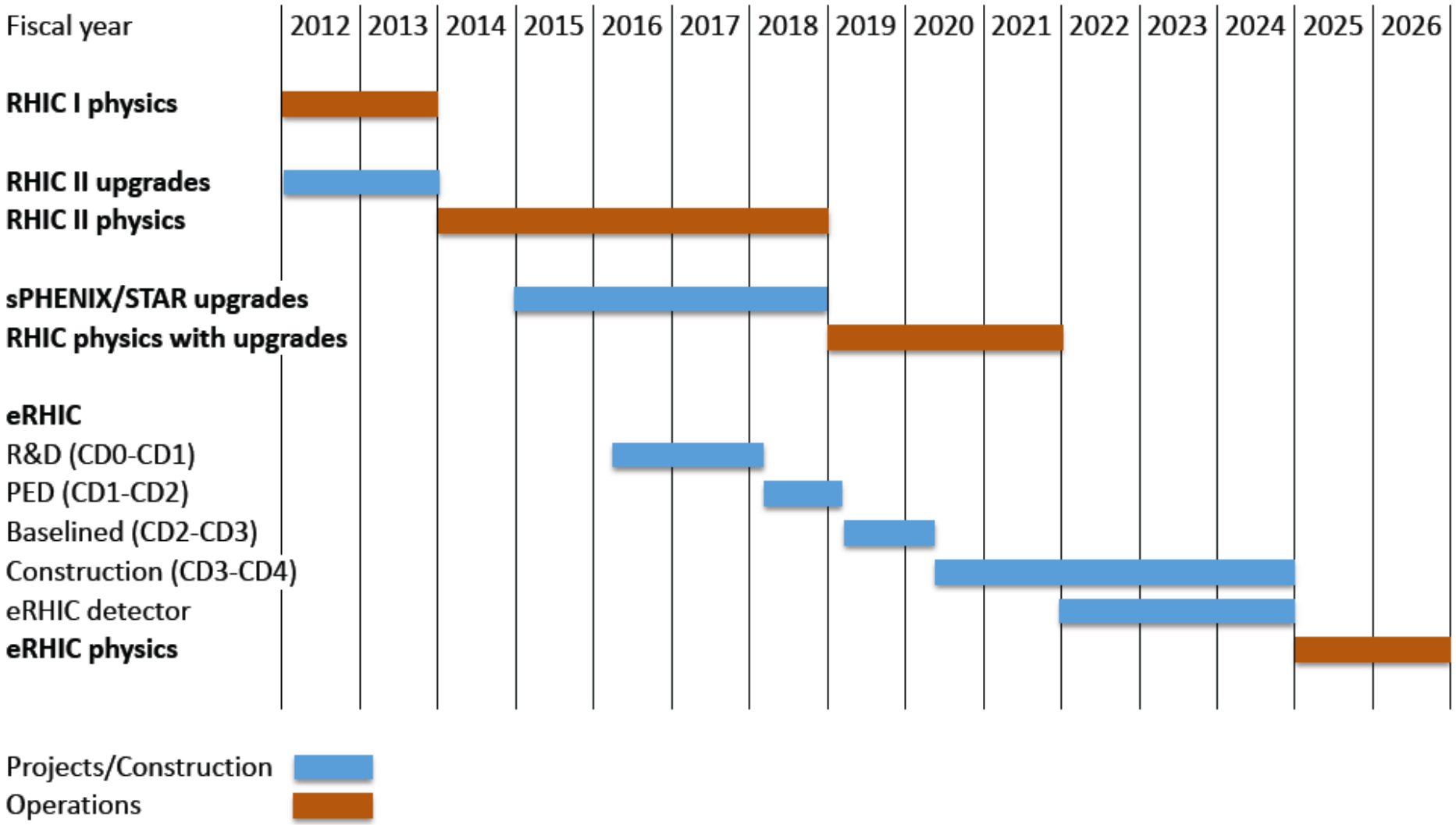

INTERNATIONAL CONTEXT

Electron-"Ion" colliders in the past and future:

	HERA@DESY	LHeC@CERN	eRHIC@BNL	MEIC@JLab	HIAF@CAS	ENC@GSI
E_{CM} (GeV)	320	800-1300	45-175	12-140	12 → 65	14
proton x_{min}	1×10^{-5}	5×10^{-7}	3×10^{-5}	5×10^{-5}	7×10^{-3} $\rightarrow 3 \times 10^{-4}$	5×10^{-3}
ion	p	p to Pb	p to U	p to Pb	p to U	p to ~ ^{40}Ca
polarization	-	-	p, ^{3}He	p, d, ^{3}He (^{6}Li)	p, d, ^{3}He	p,d
L [$cm^{-2}\ s^{-1}$]	2×10^{31}	10^{33}	10^{33-34}	10^{33-34}	$10^{32-33} \rightarrow 10^{35}$	10^{32}
IP	2	1	2+	2+	1	1
Year	1992-2007	2022 (?)	2022	Post-12 GeV	2019 → 2030	upgrade to FAIR

AN ELECTRON ION COLLIDER IN THE US

Requirements:

- High Luminosity > 10^{33} $cm^{-2}s^{-1}$
- Flexible center of mass energies
- Electrons and protons/light nuclei polarised
- Wide range of nuclear beams
- a wide acceptance detector with good PID (e/h and π, K, p)
- wide acceptance for protons from elastic reactions and neutrons from nuclear breakup

eRHIC: design luminosity

	e	p	$^{2}He^{3}$	$^{79}Au^{197}$	$^{92}U^{238}$
Energy, GeV	20	250	167	100	100
CM energy, GeV		100	82	63	63
Number of bunches/distance between bunches	107 nsec	111	111	111	111
Bunch intensity (nucleons) ,10^{11}	0.36	4	6	6	6
Bunch charge, nC	5.8	64	60	39	40
Beam current, mA	50	556	556	335	338
Normalized emittance of hadrons , 95% , mm mrad		1.2	1.2	1.2	1.2
Normalized emittance of electrons, rms, mm mrad		16	24	40	40
Polarization, %	80	70	70	none	none
rms bunch length, cm	0.2	5	5	5	5
β^*, cm	5	5	5	5	5
Luminosity per nucleon, x 10^{34} $cm^{-2}s^{-1}$		2.7	2.7	1.6	1.7

Hourglass the pinch effects are included. Space charge effects are compensated.
Energy of electrons can be selected at any desirable value at or below 30 GeV
The luminosity does not depend on the electron beam energy below or at 20 GeV
The luminosity falls as E_e^{-4} at energies above 20 GeV
The luminosity is proportional to the hadron beam energy: $L \sim E_h/E_{top}$

MODELING THE DETECTOR IN GEANT

μ-vertex detector:

- 6 layers with [30..160] mm radius
- 0.37% X_0 in acceptance per layer simulated precisely;
- digitization: single discrete pixels, one-to-one from MC points

Forward/b

- 3+5+3 sili
- N sectors
- digitizatio

TPC

- ~2m lo
- 1.2% X_0
- digitiza nd 1x5 mm GE

Forward t

- 3 disks behind the TPC endcap
- rather precise START FGT design implemente
- digitization: 100 μm resolution in X&Y; gaussi

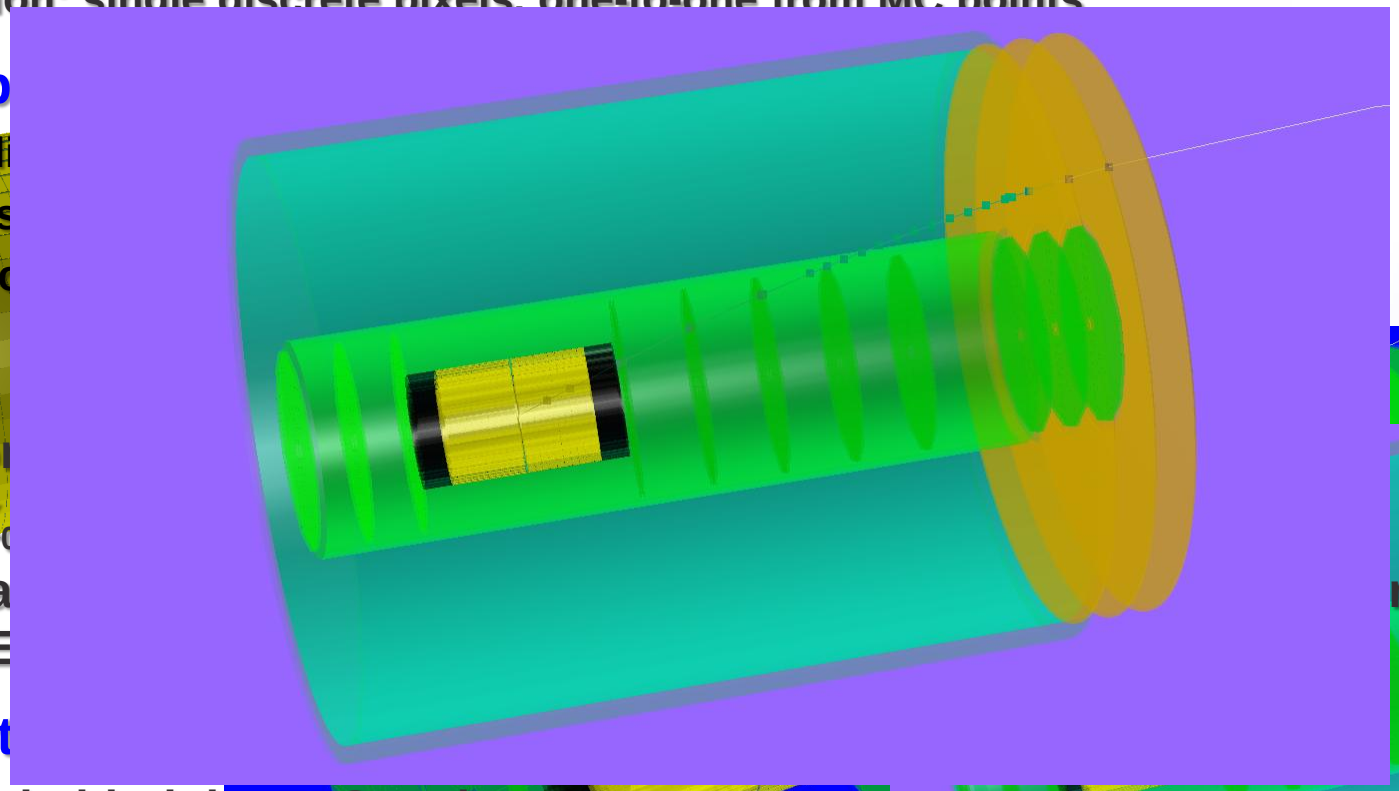

THE PILLARS OF THE eRHIC PHYSICS PROGRAM

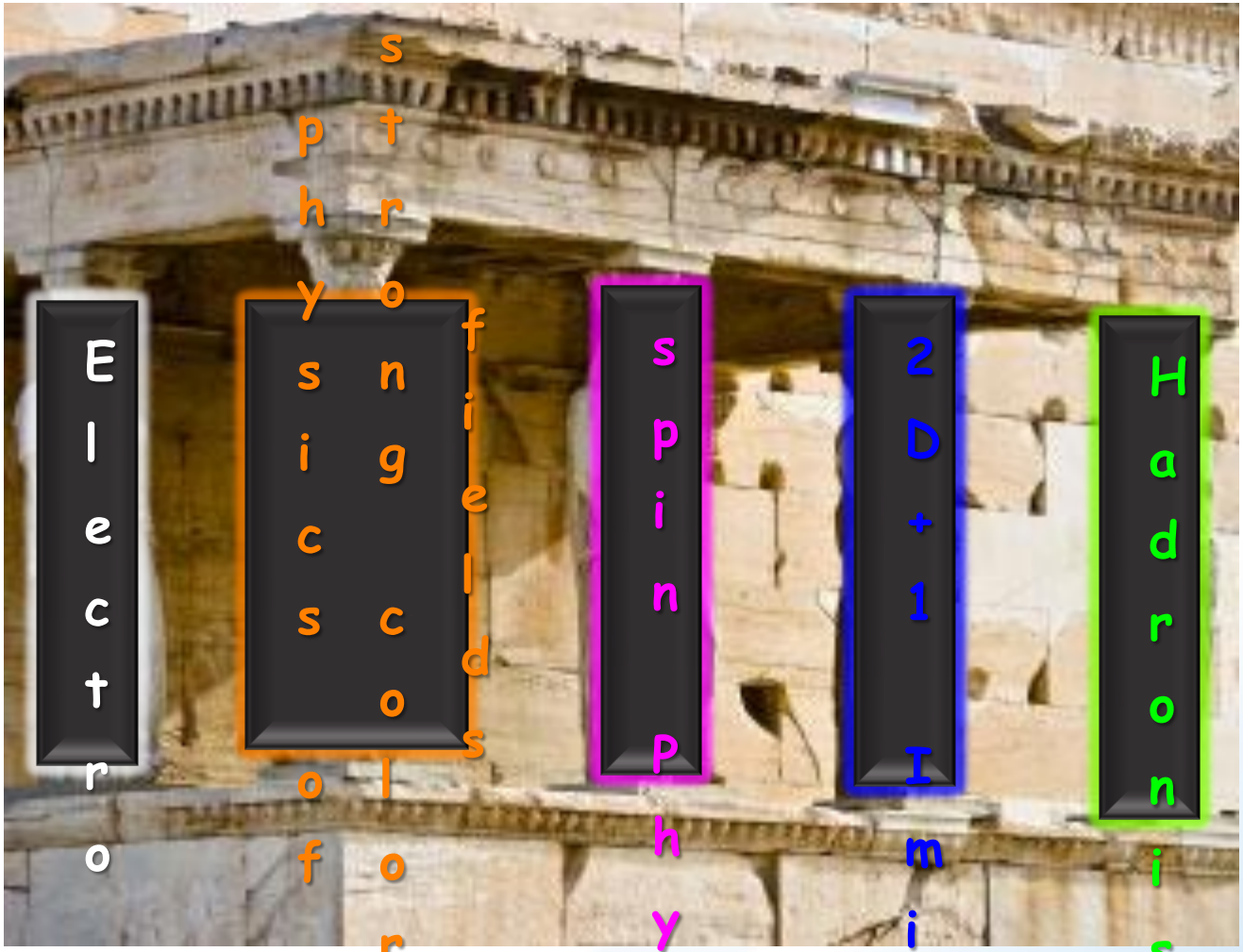

Wide physics program with high requirements on detector and machine performance

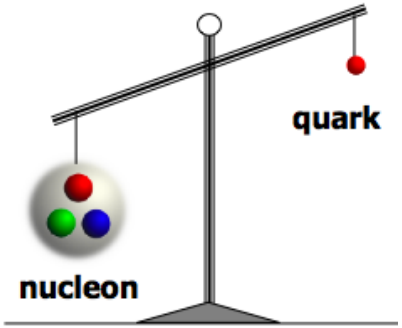

THE HADRONIC MASS PUZZLE

- In QCD, all "constants" of quantum mechanics are actually strongly momentum dependent: couplings, number density, mass, etc.
- So, a quark's mass depends on its momentum.
- Mass function can calculated and is depicted here.

in agreement: the vast bulk of the light-quark mass comes from a cloud of gluons, dragged along by the quark as it propagates.

- Continuum- and Lattice-QCD
- Running gluon mass
  - Gluon is massless in UV, in agreement with pQCD
  - Massive in infrared
    - $m_G(0) = 0.67\text{-}0.81$ GeV
    - $m_G(m_G^2) = 0.53\text{-}0.64$ GeV
- DSE prediction confirmed by numerical simulations of lattice-regularised QCD

C.D. Roberts, Prog. Part. Nucl. Phys. 61 (2008) 50
M. Bhagwat & P.C. Tandy, AIP Conf.Proc. 842 (2006) 225-227

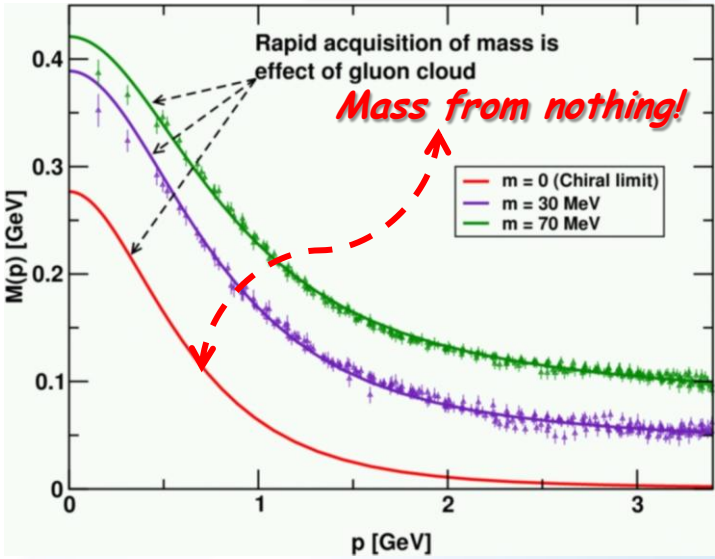

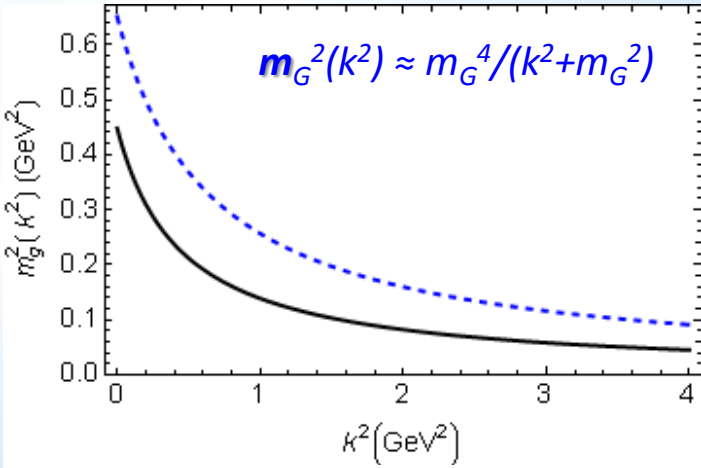

Qin et al., Phys. Rev. C 84 042202 (Rapid Comm.)

CONSTRAIN J_q VIA GPD E

observables sensitive to E:

(J_q input parameter in ansatz for E)

- DVCS A_{UT} : HERMES
- nDVCS A_{LU} : Hall A

Hermes DVCS-TTSA [arXiv: 0802.2499]:

$$A_{UT}^{\sin(\phi-\phi_T)\cos\phi} \sim \mathrm{Im}(F_2 H - F_1 E)$$

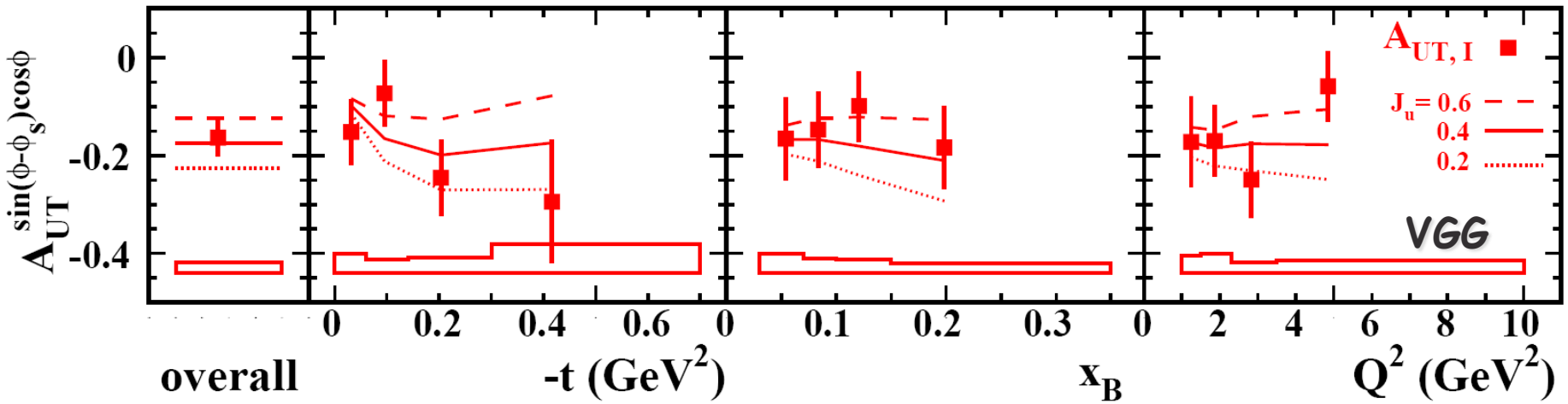

eRHIC:
HERMES like A_{UT}
20 GeV x 250 GeV
Lumi: 2x50fb^{-1}

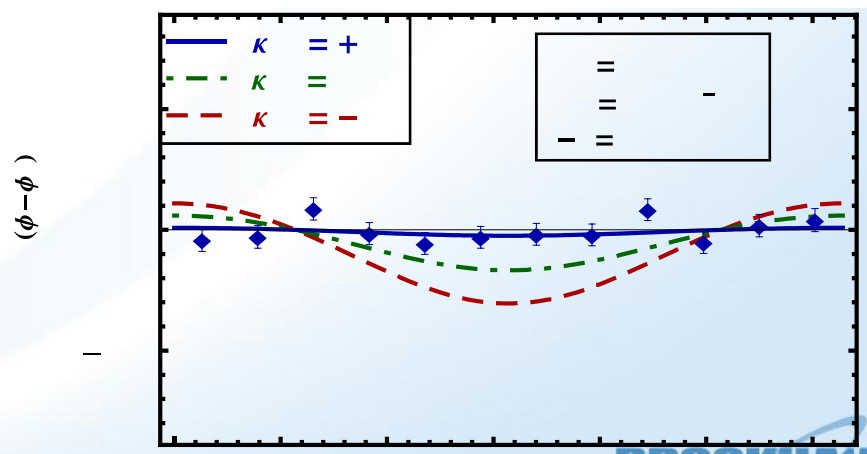

DIFFERENT DVCS ASYMMETRIES

arXiv:1304.0077

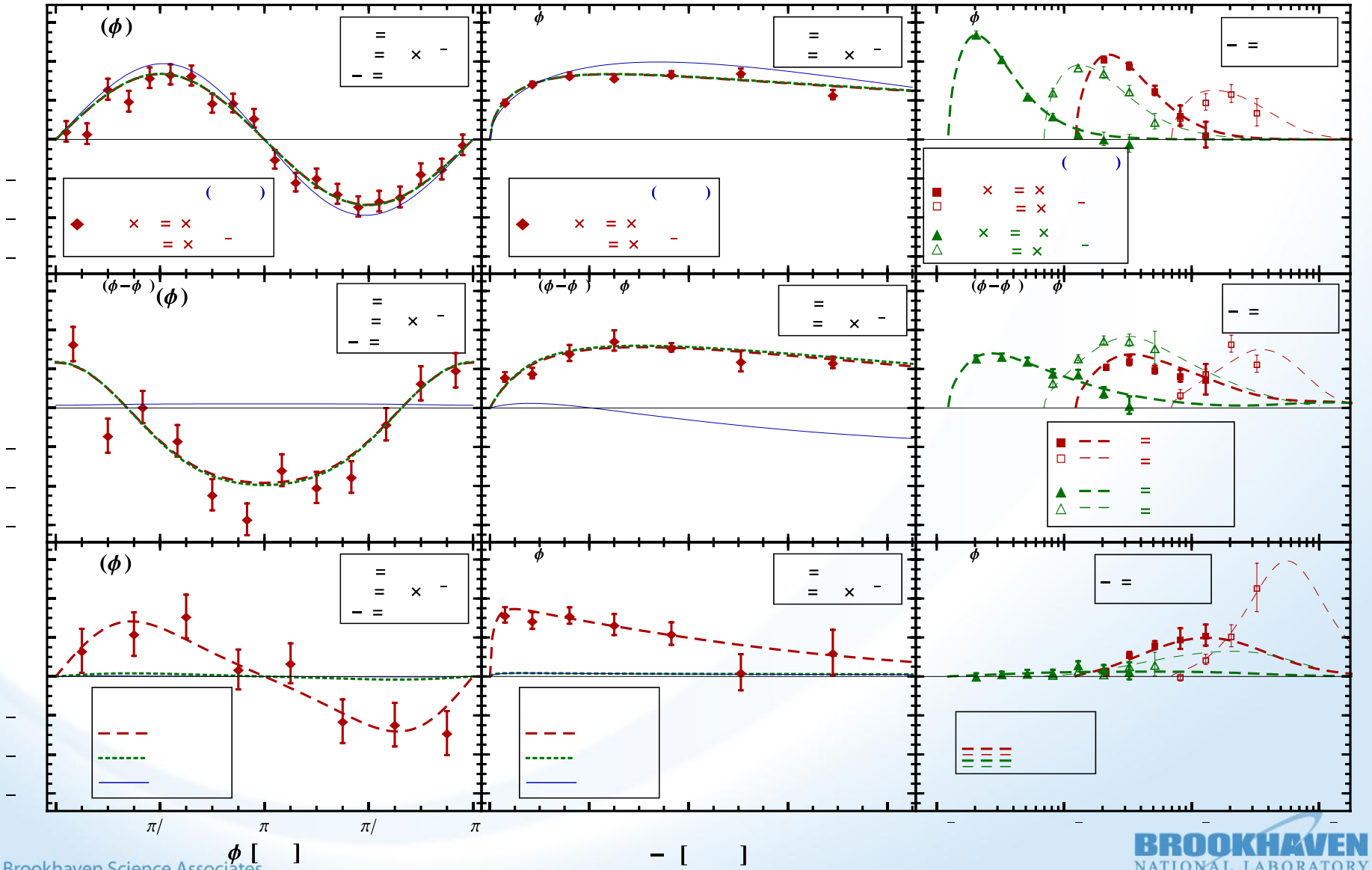

HARD DIFFRACTION IN DIS AT SMALL X

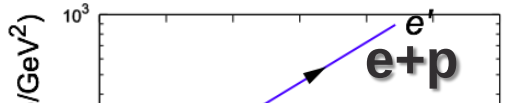

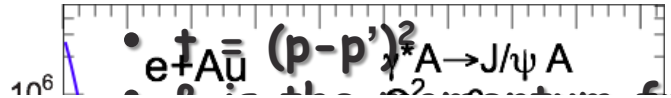

Diffraction Analogy: plane monochromatic wave incident on a circular screen of radius R

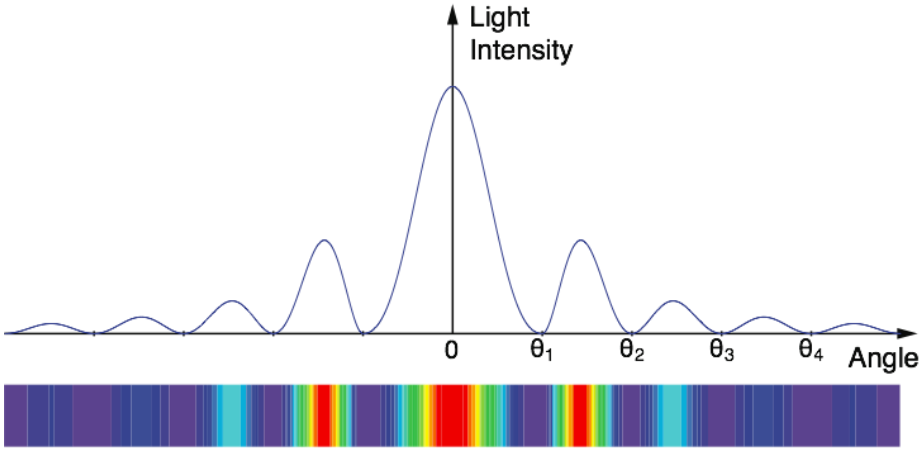

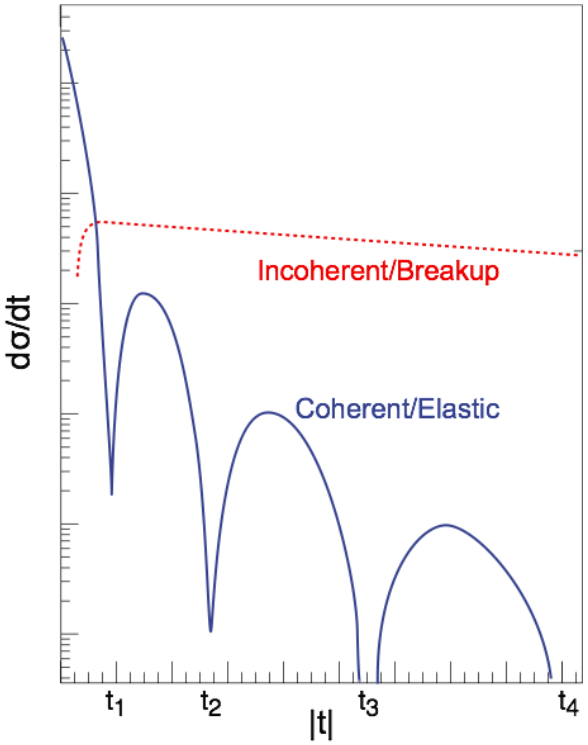

- incoherent ⇔ breakup of p
- HERA: 15% of all events are hard diffractive

- breakup into nucleons (nucleons intact)
- incoherent diffraction
- Predictions: $\sigma_{diff}/\sigma_{tot}$ in e+A ~25-40%

LARGE RAPIDITY GAP METHOD (LRG)

- Identify **Most Forward Going Particle (MFP)**
  - Works at HERA but at higher √s
  - EIC smaller beam rapidities

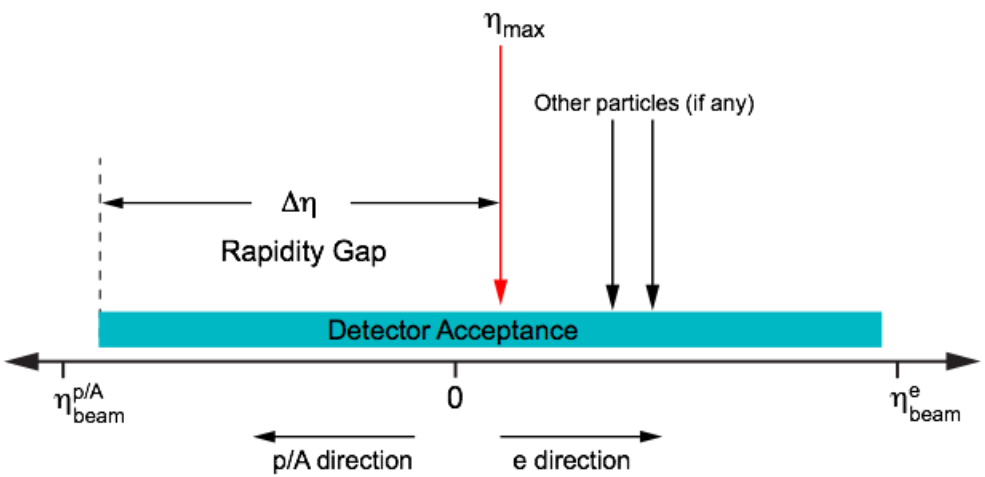

Hermeticity requirement:

- needs just to detector presence
- does not need momentum or PID
- simulations: √s not a show stopper for EIC (can achieve 1% contamination, 80% efficiency)

Diffractive ρ^0 production at EIC: **η of MFP**

M. Lamont '10

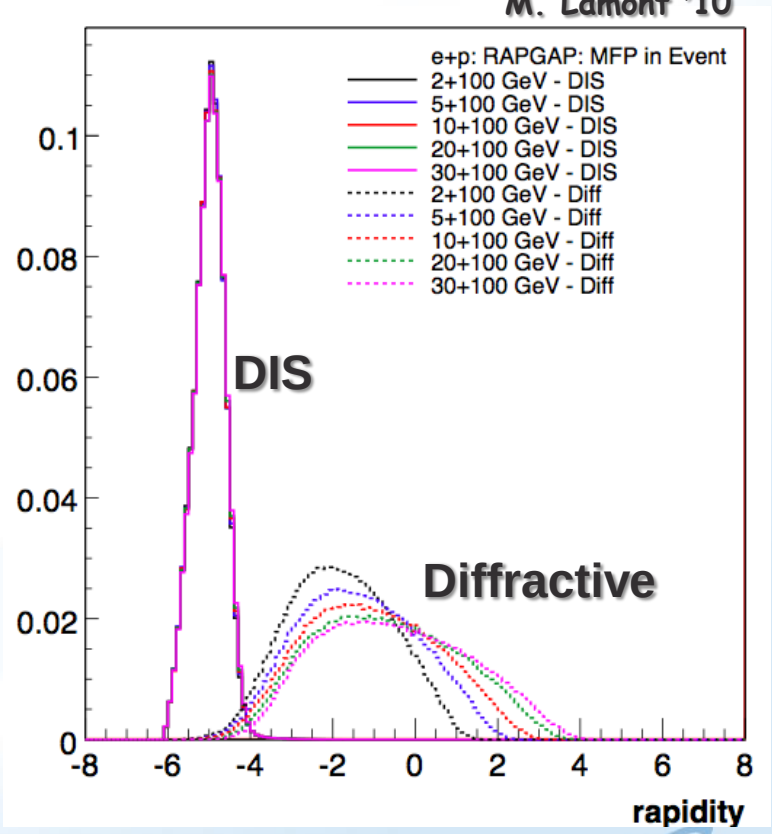

BEST KNOWLEDGE OF Q_S IN eA

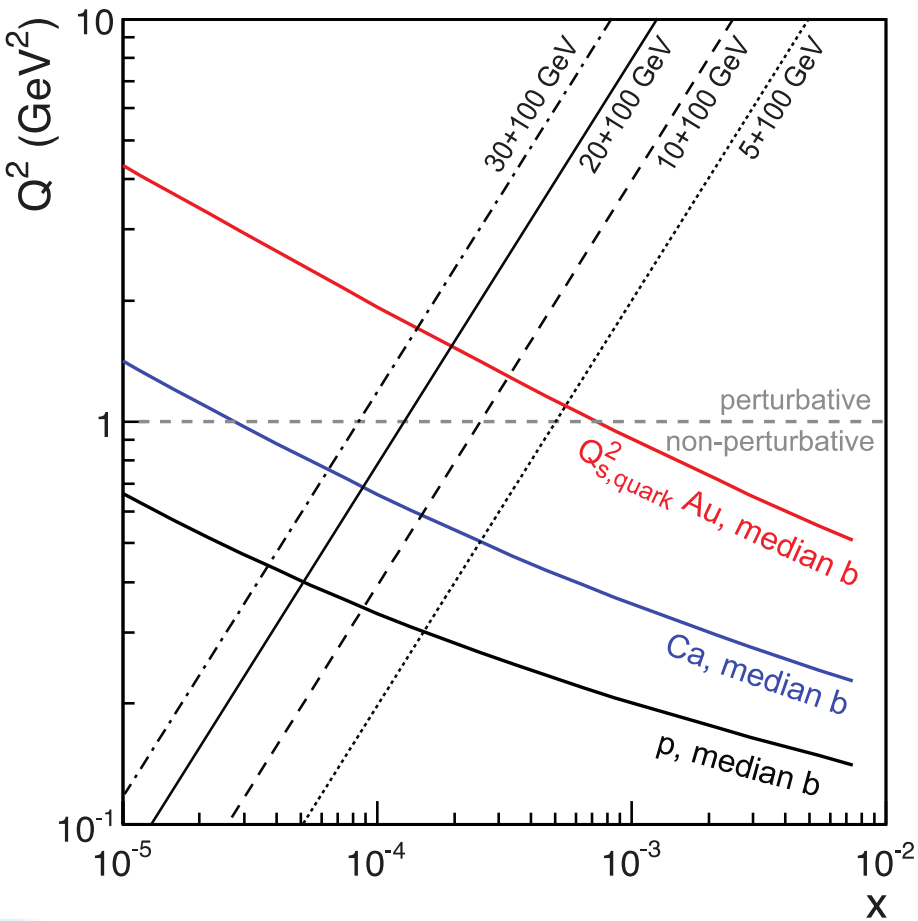

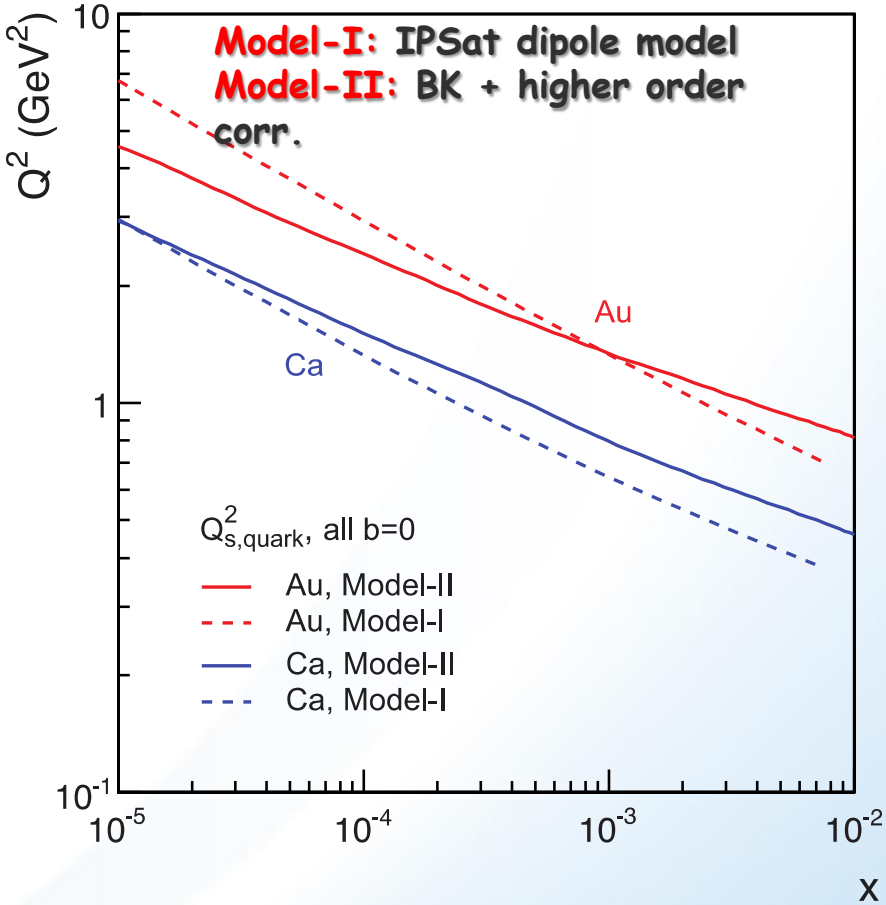

Enhancement of Q_S with A

⇒ saturation regime reached at significantly lower energy in nuclei

MEASURING F_L WITH THE EIC (I)

$$\frac{d^2\sigma^{ep\to eX}}{dxdQ^2} = \frac{4\pi\alpha^2_{e.m.}}{xQ^4}\left[\left(1-y+\frac{y^2}{2}\right)F_2(x,Q^2) - \frac{y^2}{2}F_L(x,Q^2)\right]$$

quark+anti-quark momentum distributions

gluon momentum distribution

In practice use reduced cross-section:

$$\sigma_r = \left(\frac{d^2\sigma}{dxdQ^2}\right)\frac{xQ^4}{2\pi\alpha^2[1+(1-y)^2]} = F_2(x,Q^2) - \frac{y^2}{1+(1-y)^2}F_L(x,Q^2)$$

$$= F_2(x,Q^2) - \frac{y^2}{Y^+}F_L(x,Q^2)$$

- **How to extract F_L**
  - Need different values of y^2/Y^+
  - F_L slope of σ_r vs y^2/Y^+
  - F_2 intercept of σ_r vs y^2/Y^+ with y-axis

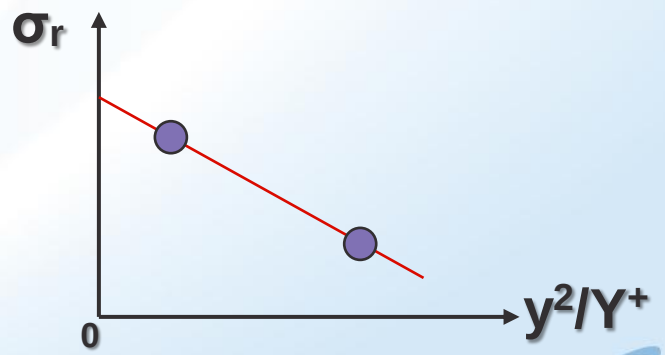

MEASURING F_L WITH THE EIC (II)

In order to extract F_L one needs **at least two measurements** of the inclusive cross section with "wide" span in inelasticity parameter y ($Q^2 = sxy$)

F_L requires runs at various $\sqrt{s}$ ⇒ longer program

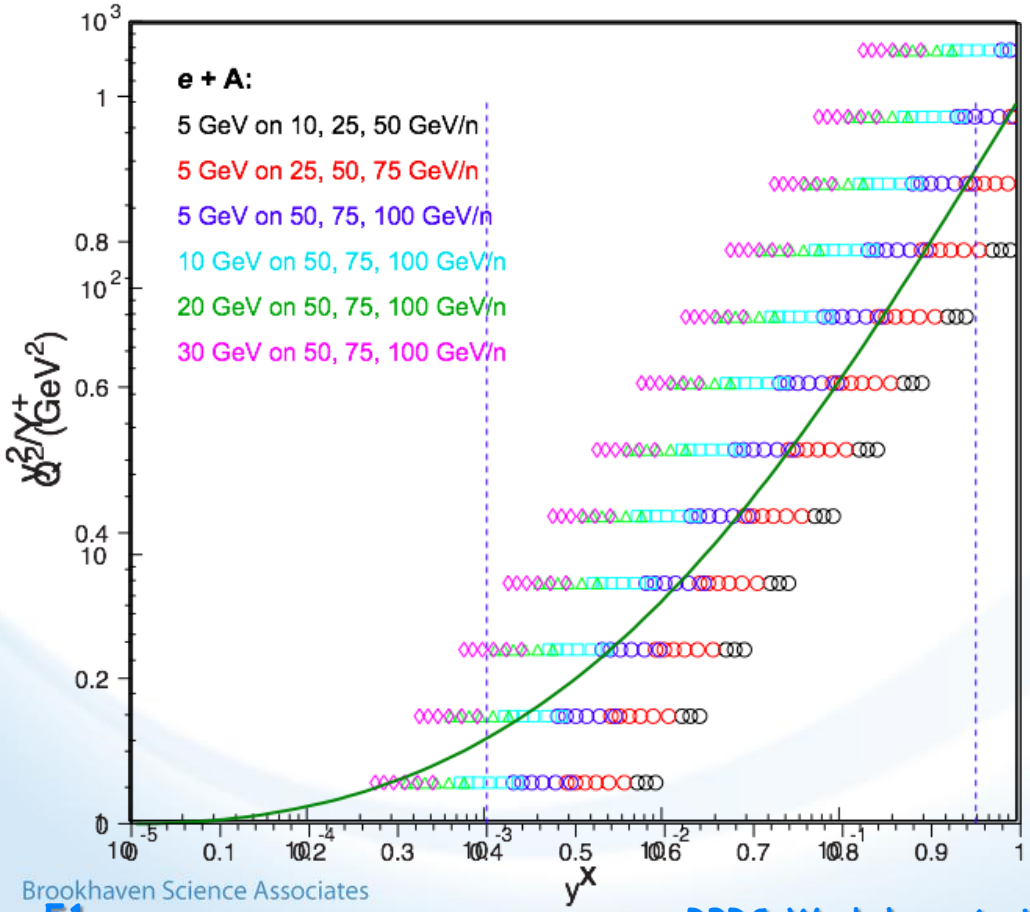

EIC studies:

- Statistical error is negligible in essentially whole range
- Systematical Error
  - Calibration
  - Normalization
  - Experiment
  - Radiative Corrections

PREPARATION OF DIS AND SIDIS MOCK DATA

- PEPSI MC to generate σ^{++} and σ^{+-} with LO GRSV PDFs

DIS

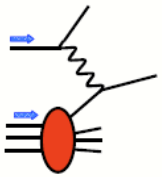

inclusive final-state

SIDIS

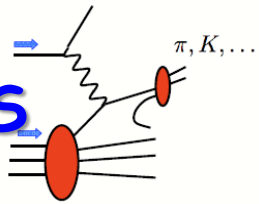

identified charged pions and kaons

assume modest $10\ fb^{-1}$ for each energy, 70% beam polarizations

$Q^2 > 1\ GeV^2$, $0.01 < y < 0.95$, invariant mass $W^2 > 10\ GeV^2$

depolarization factor of virtual photon $D(y,Q^2) > 0.1$ (cuts on small y)

scattered lepton: $1^o < \theta_{elec} < 179^o$ and $p_{elec} > 0.5\ GeV$

hadron: $p_{hadr} > 1\ GeV$, $0.2 < z < 0.9$,
$1^0 < \theta_{hadr} < 179^o$

- use rel. uncertainties of data to generate mock data by randomizing around DSSV+ by 1-σ
- SIDIS: incl. typical 5% (10%) uncertainty for pion (kaon) frag. fcts (from DSS analysis)

SCALING VIOLATIONS AT SMALL X

rough small-x approximation to Q^2-evolution:

$$\frac{dg_1}{d\log(Q^2)} \propto -\Delta g(x,Q^2)$$

spread in $\Delta g(x,Q^2)$ translates into spread of scaling violations for $g_1(x,Q^2)$

- need x-bins with a least two Q^2 values to compute derivative (limits x reach somewhat)

smallest x bins require 20 x 250 GeV 5 x 250 starts here

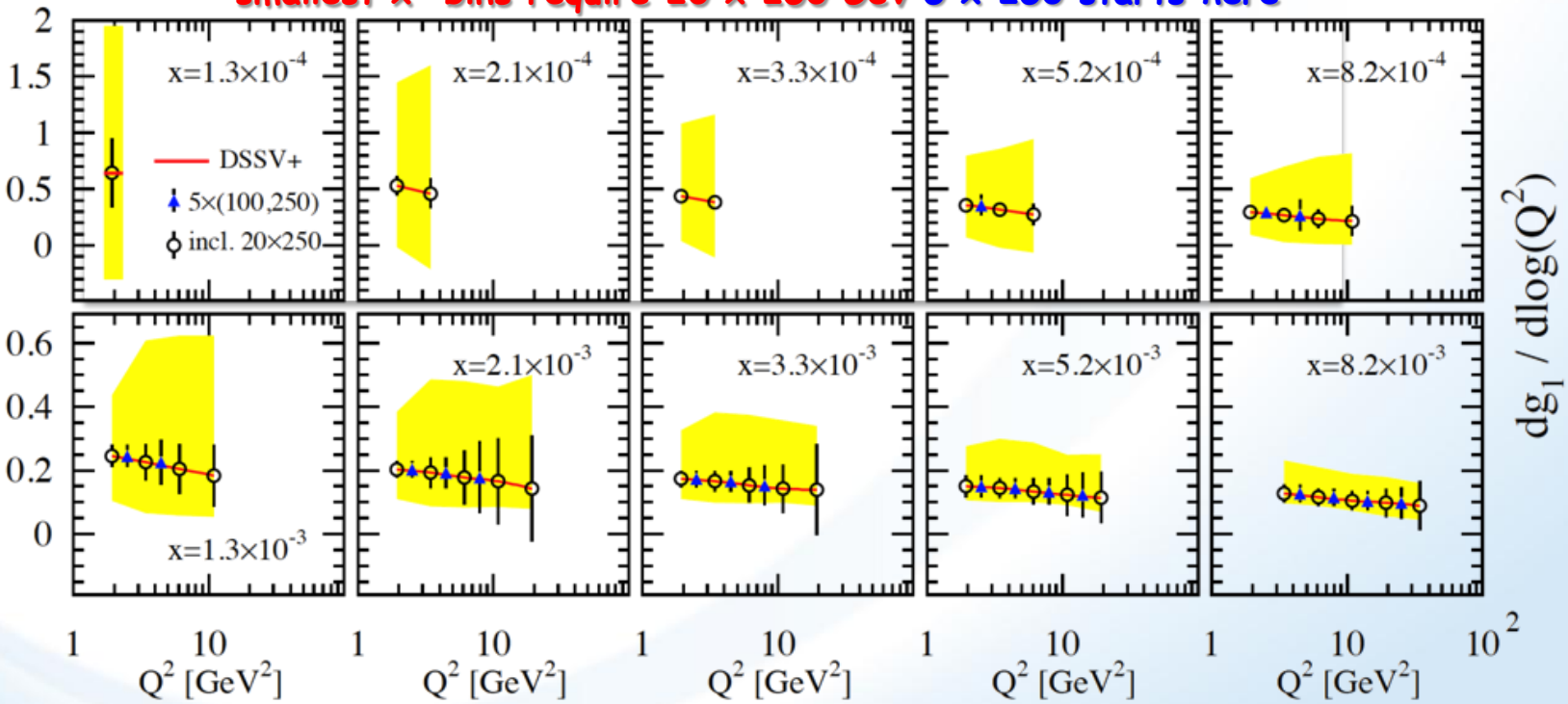

- error bars for moderate $10fb^{-1}$ per c.m.s. energy; bands parameterize current DSSV+ uncertainties

DVCS ASYMMETRIES

$$d\sigma \sim \left(\tau^*_{BH}\tau_{DVCS} + \tau^*_{DVCS}\tau_{BH}\right) + |\tau_{BH}|^2 + |\tau_{DVCS}|^2$$

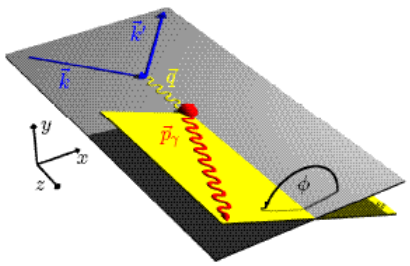

→ different charges: e^+ e^-:

$$\Delta\sigma_C \sim \cos\phi \cdot \mathrm{Re}\{ H + \cancel{\xi\tilde{H}} + \ldots \} \Rightarrow H$$

→ polarization observables:

$$\Delta\sigma_{LU} \sim \sin\phi \cdot \mathrm{Im}\{H + \cancel{\xi\tilde{H}} + \cancel{kE}\} \Rightarrow H$$

$$\Delta\sigma_{UL} \sim \sin\phi \cdot \mathrm{Im}\{\tilde{H} + \cancel{\xi H} + \ldots\} \Rightarrow \tilde{H}$$

$$\Delta\sigma_{UT} \sim \sin\phi \cdot \mathrm{Im}\{k(H - E) \cancel{+} \ldots \} \Rightarrow H, E$$

$\Delta\sigma_{UT}$ → beam, target

$\xi = x_B/(2-x_B)$ $k = t/4M^2$ kinematically suppressed

BH FRACTION

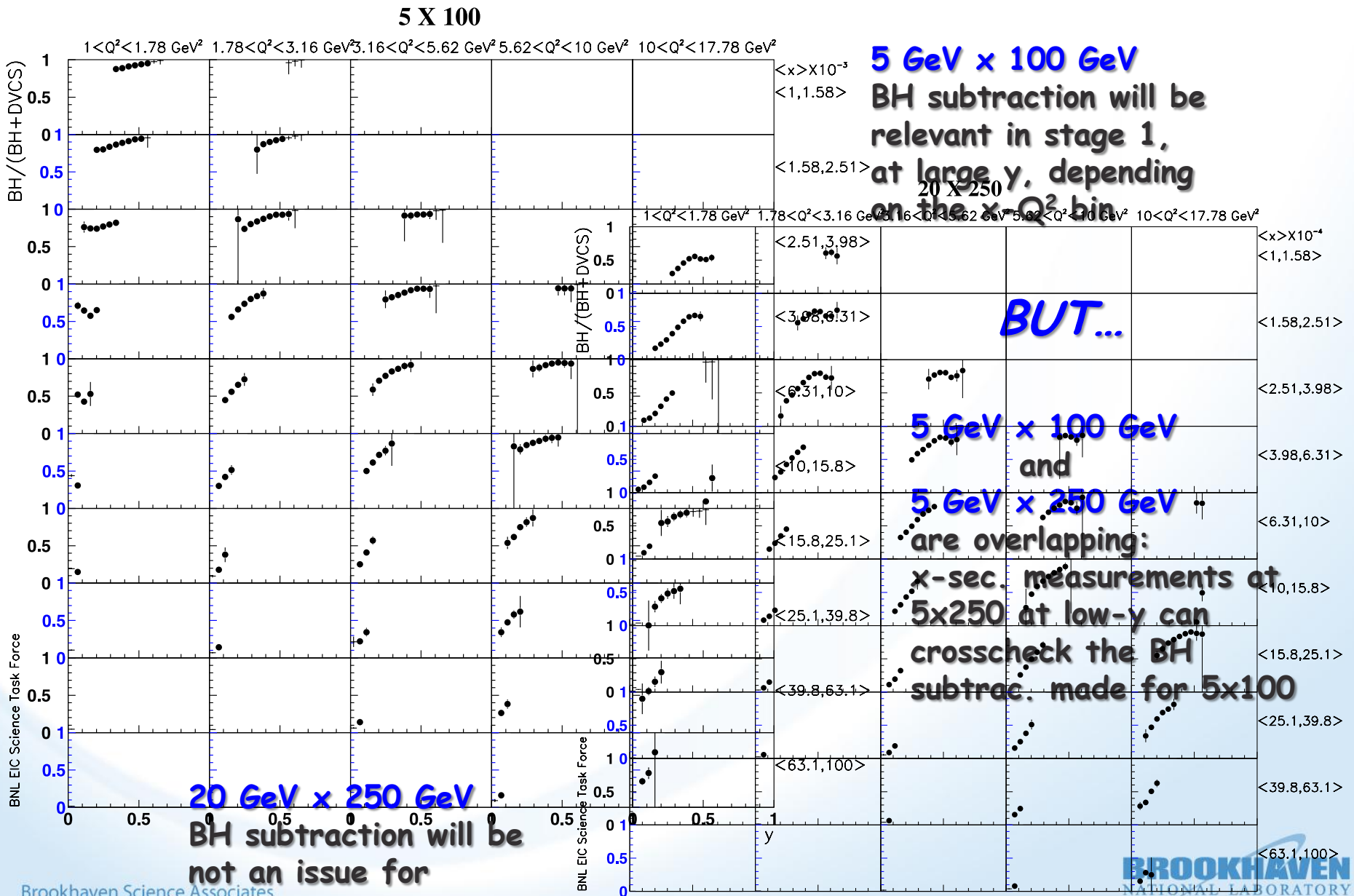

5 GeV x 100 GeV
BH subtraction will be relevant in stage 1, at large y, depending on the x-Q^2 bin

BUT…

5 GeV x 100 GeV and **5 GeV x 250 GeV** are overlapping: x-sec. measurements at 5x250 at low-y can crosscheck the BH subtrac. made for 5x100

20 GeV x 250 GeV
BH subtraction will be not an issue for y<0.6

KINEMATICS OF BREAKUP NEUTRONS

Results from GEMINI++ for 50 GeV Au

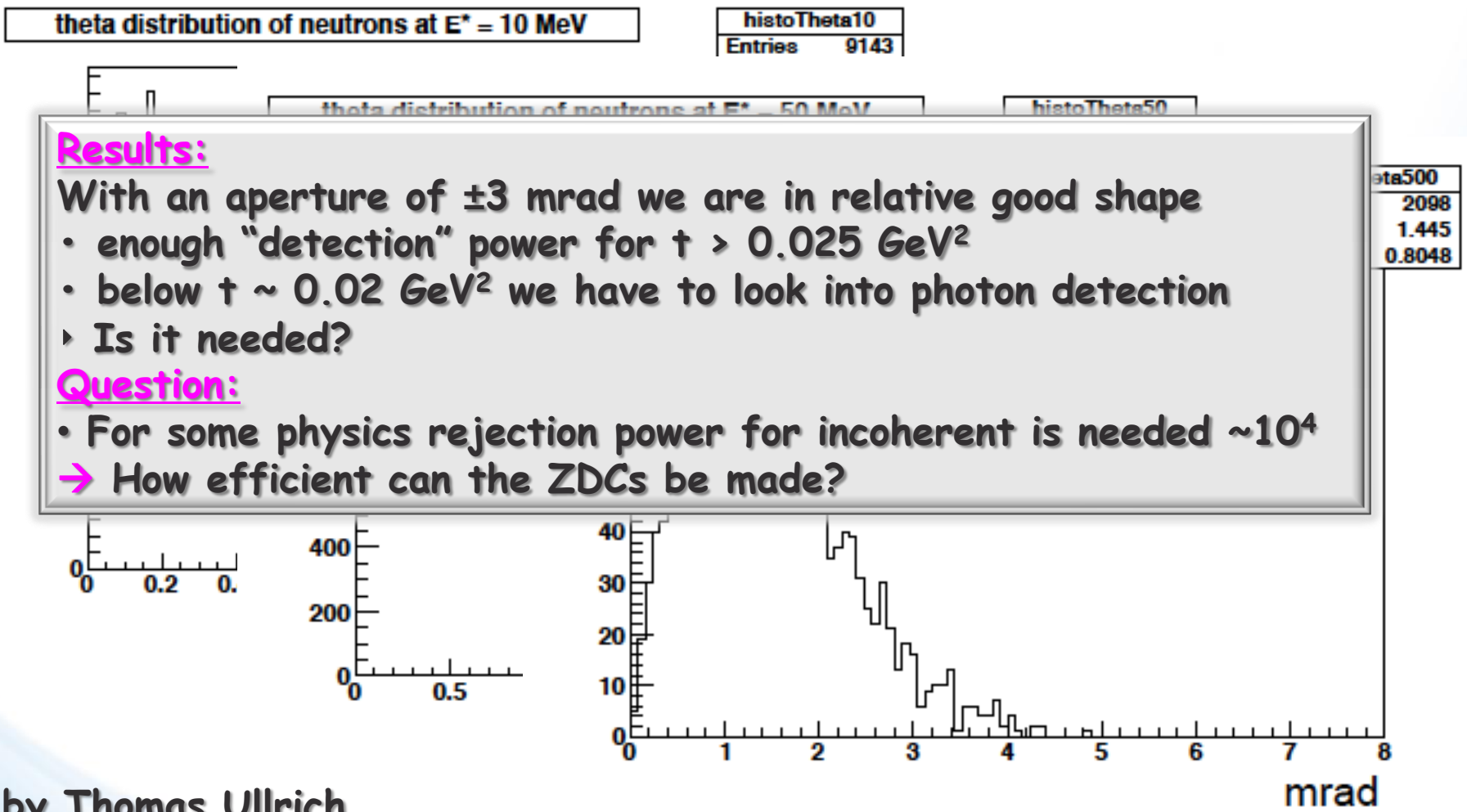

Results:

With an aperture of ±3 mrad we are in relative good shape

- enough "detection" power for t > 0.025 GeV^2
- below t ~ 0.02 GeV^2 we have to look into photon detection
- Is it needed?

Question:

- For some physics rejection power for incoherent is needed ~10^4

→ How efficient can the ZDCs be made?

by Thomas Ullrich

+/-5mrad acceptance seems sufficient

DIFFRACTIVE PHYSICS: P' KINEMATICS

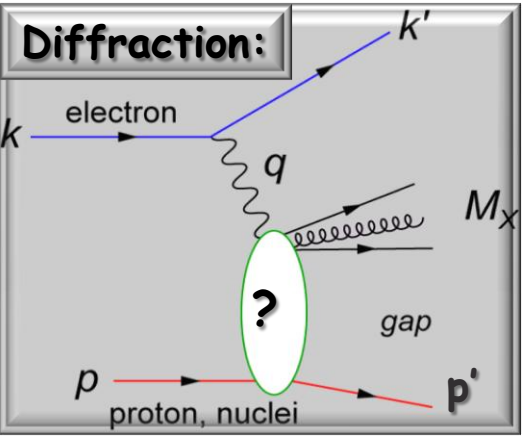

$$t=(p_4-p_2)^2 = 2[(m_p^{in}.m_p^{out})-(E^{in}E^{out} - p_z^{in}p_z^{out})]$$

→ " Roman Pots" acceptance studies see later

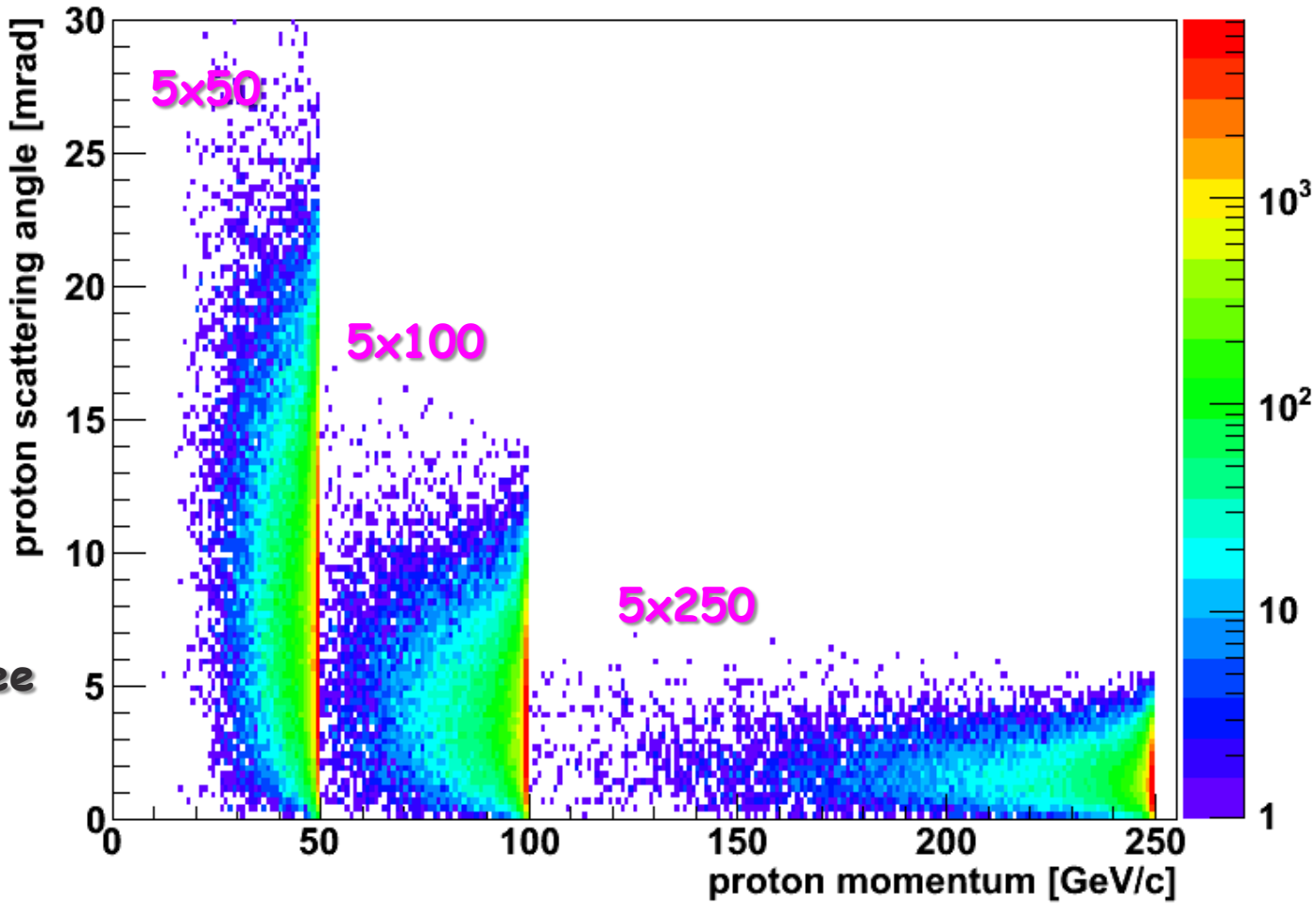

Simulations by J.H Lee

PROTON DISTRIBUTION IN Y VS X AT S=20 M

without quadrupole aperture limit

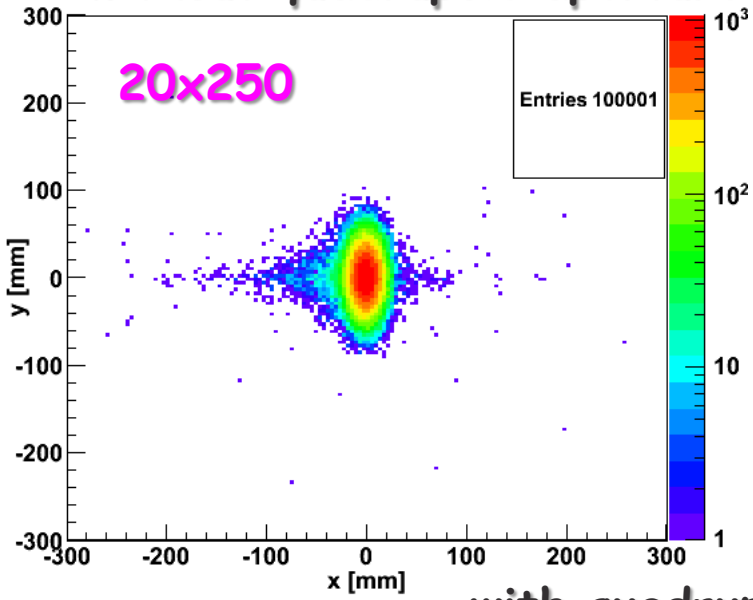

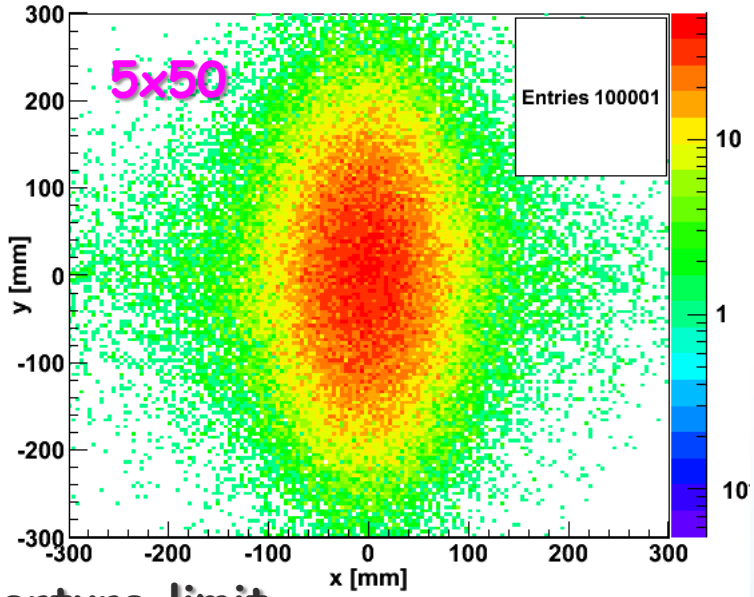

with quadrupole aperture limit

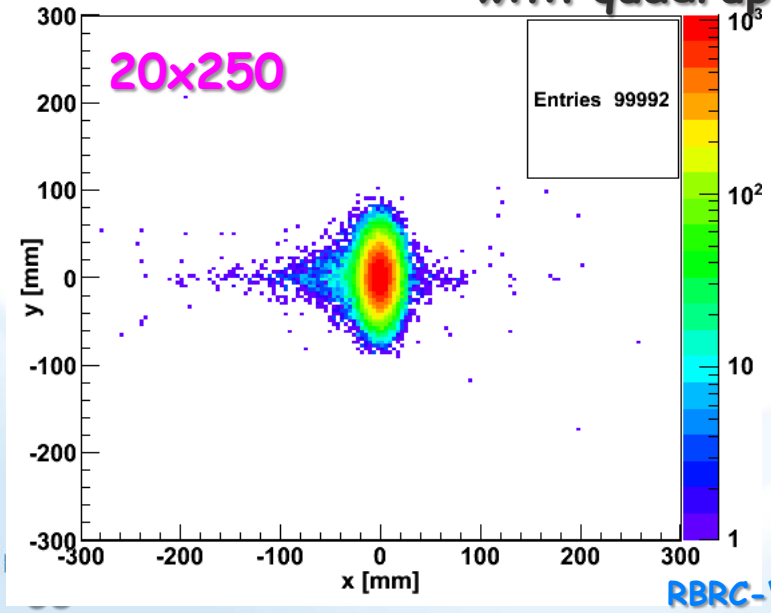

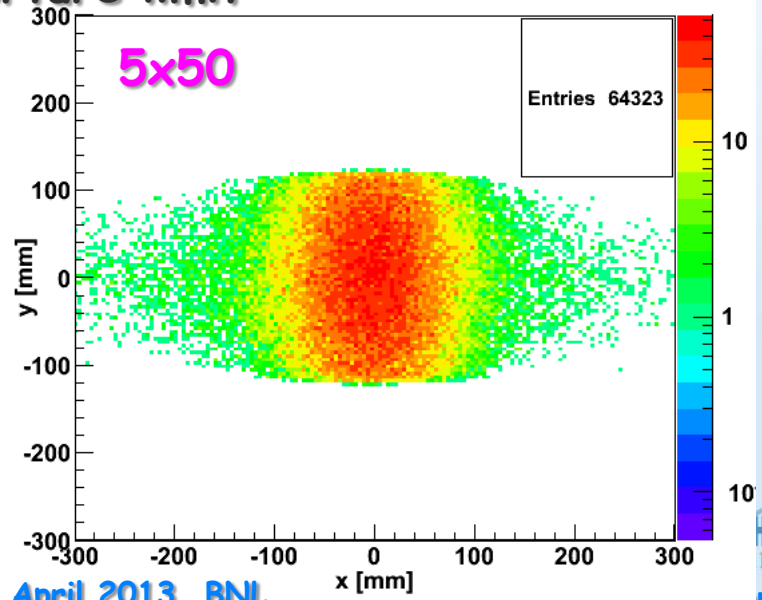

ACCEPTED IN "ROMAN POT" (EXAMPLE) AT S=20M

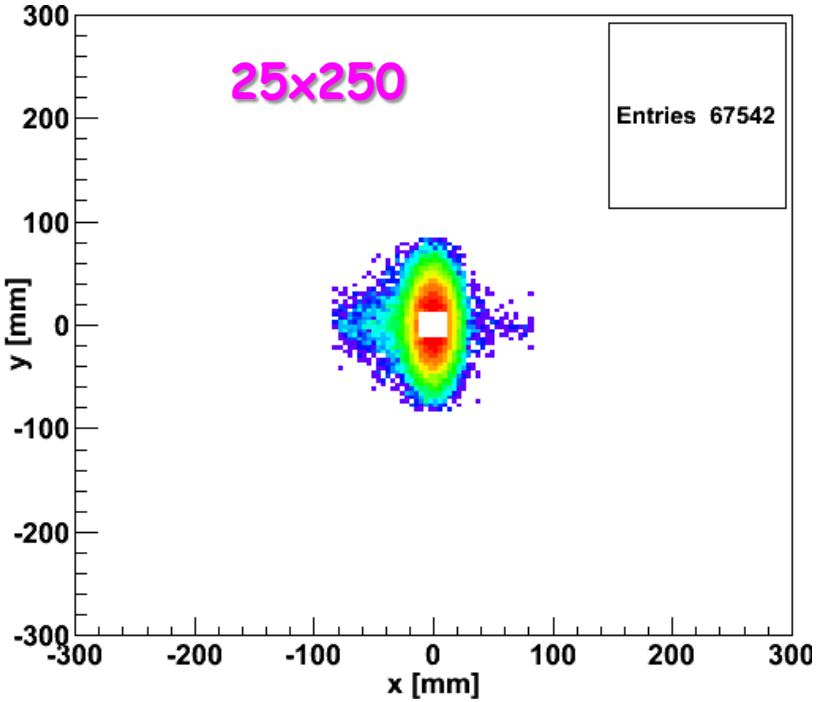

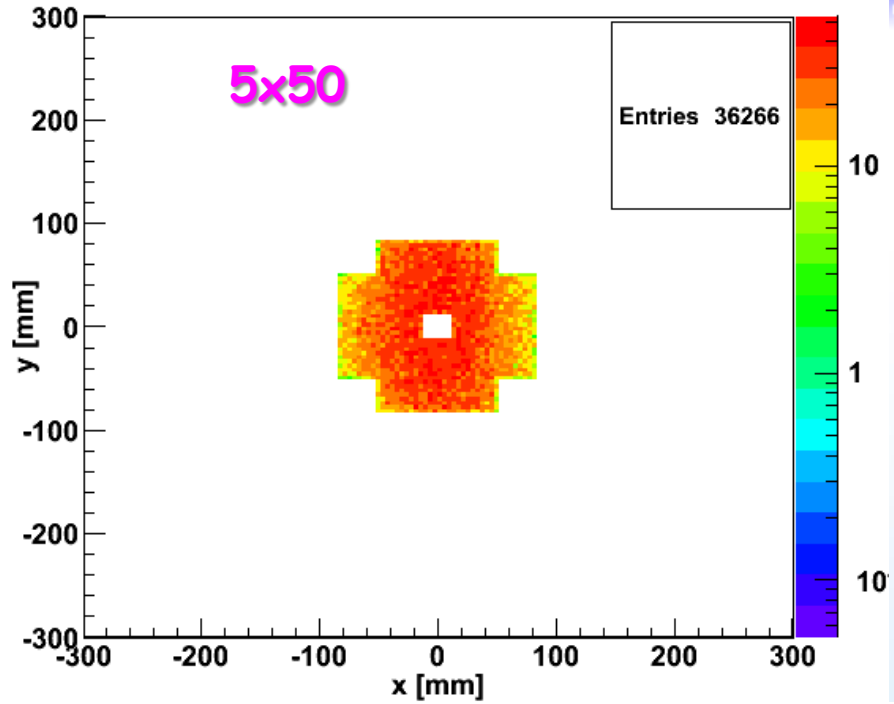

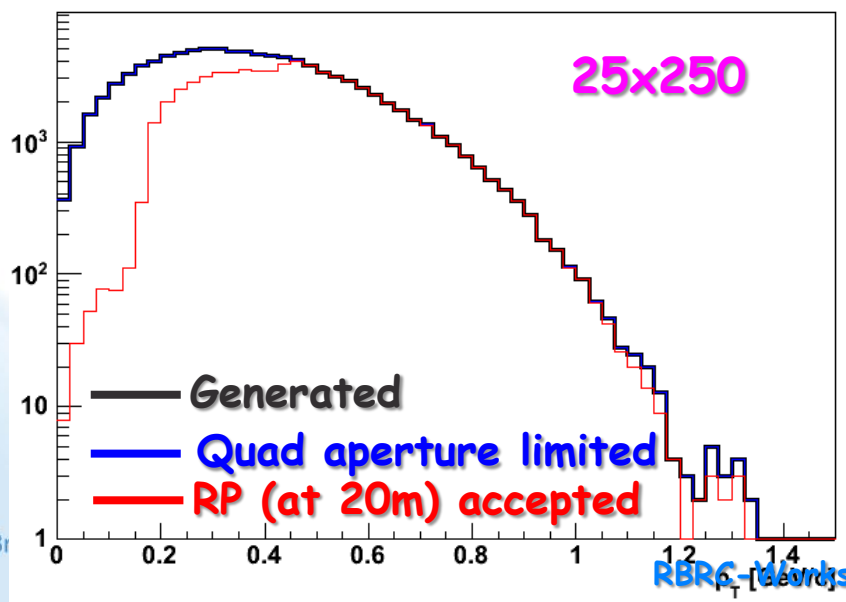

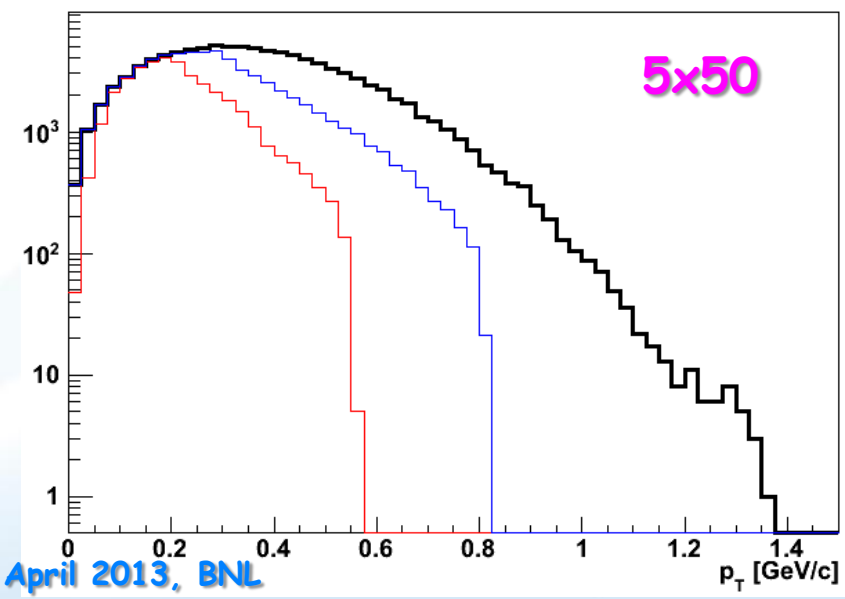

Cronin and Shadowing in *pA*

(PRC80 014903 2009; PRC85, 024903, 2012)

Gergely Gábor Barnaföldi, J. Barrette, M. Gyulassy,

Sz. Harangozó, P. Lévai, G. Papp, V. Topor Pop

Wigner RCP RMI of the HAS, Eötvös Loránd University,

Columbia University, Mc Gill University

O U T L I N E

- Motivation for *pA/dAu* collisions
  - pA/dAu collisions from 30 AGeV to 5 ATeV
  - How latest results fit into the picture.
  - What phenomenology have we leart by the 'Cronin effect' so far?
- Nuclear shadowing
  - Suppression at low-x
  - High-p_T nuclear effects @ midrapidity & large y
- Cronin effect
  - Enhancement in pA
  - Saturated Glauber picture and the Cronin effect

M O T I V A T I O N

- Cronin effect at SPS energies

Brown et al: PRD11 (1975) 3105, Ric.Sci.Edu.Perm Suppl. 122 (2003) 541

40%

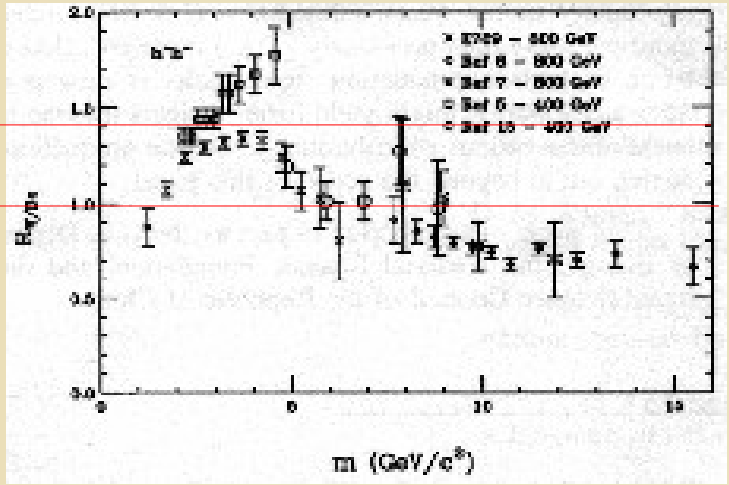

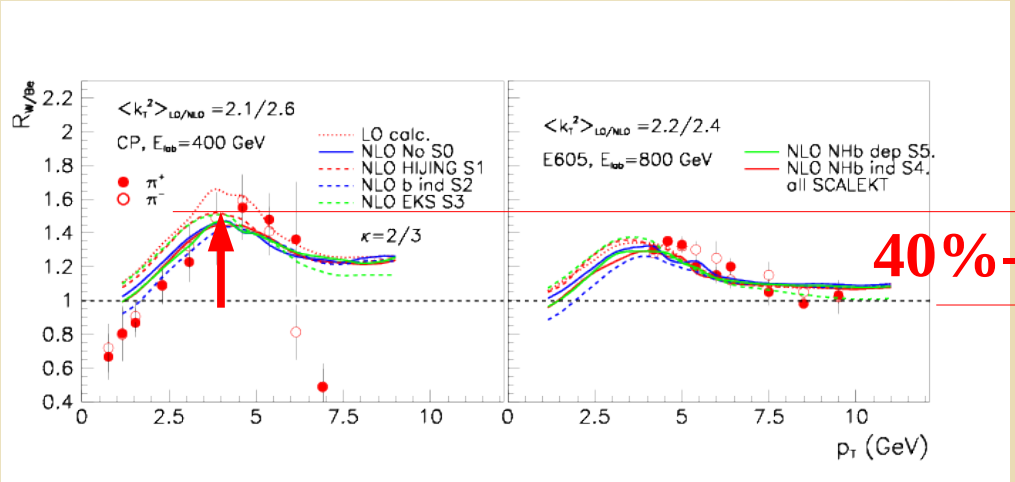

40%-50%

- RHIC analysis on dAu and AuAu

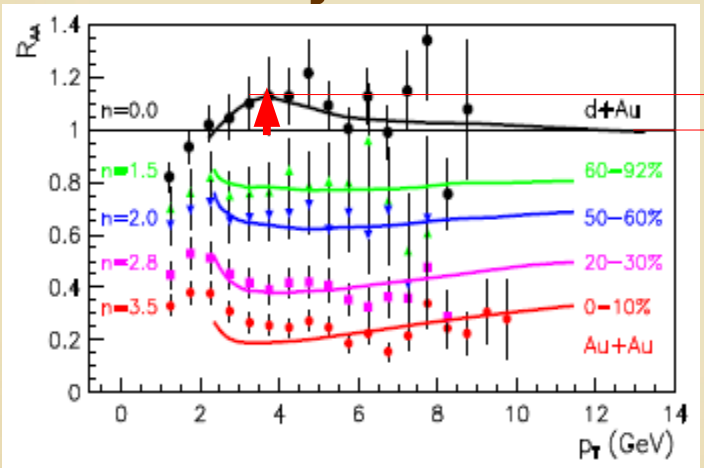

10%

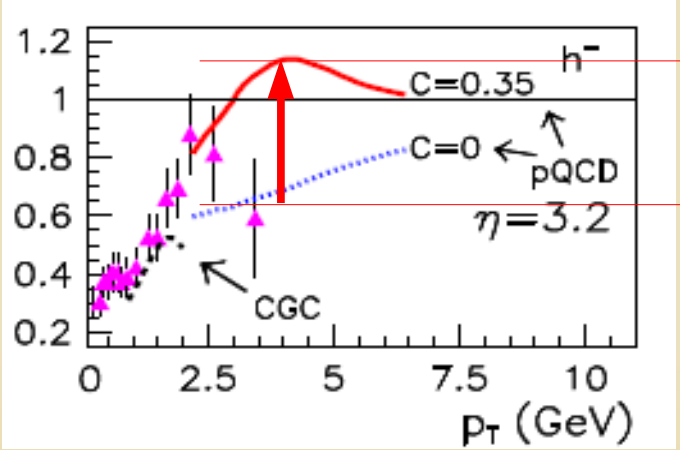

????

M O T I V A T I O N

- Motivation for *pPb/dAu* collisions

Preliminary dAu data from PHENIX@QM12 (B. Sahlmueller)

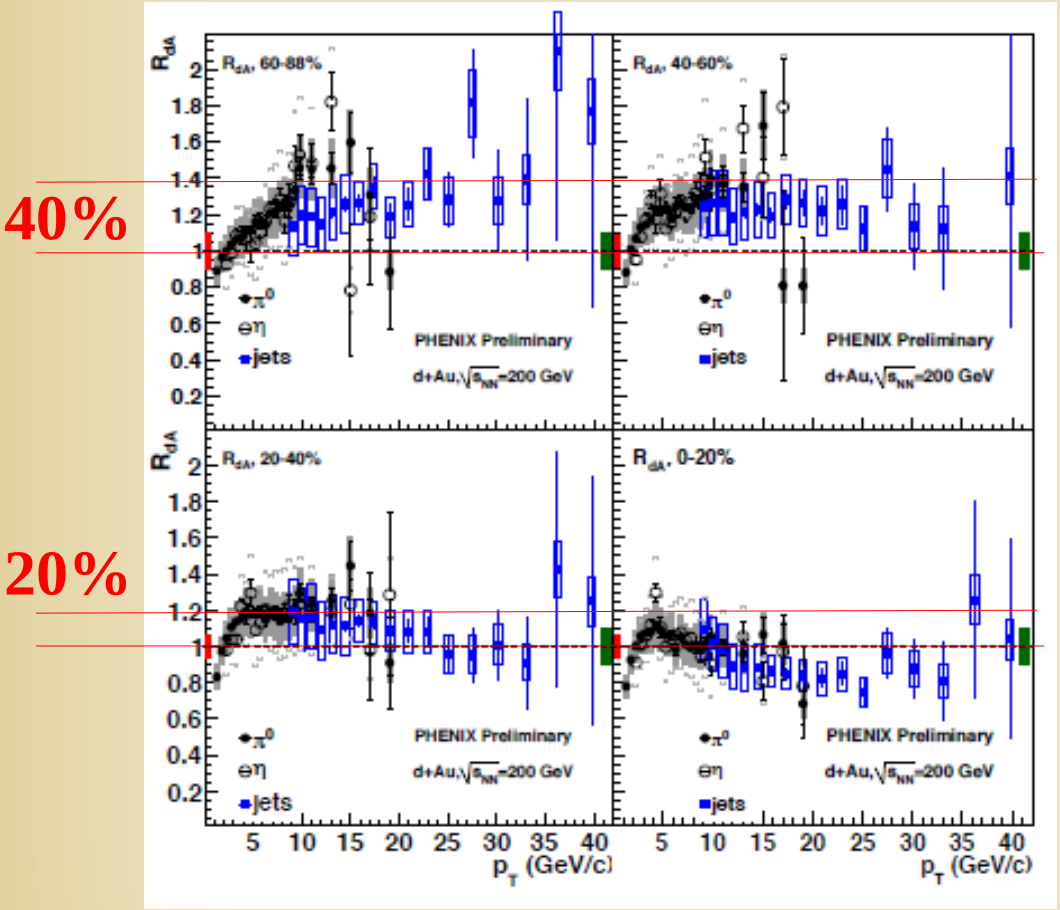

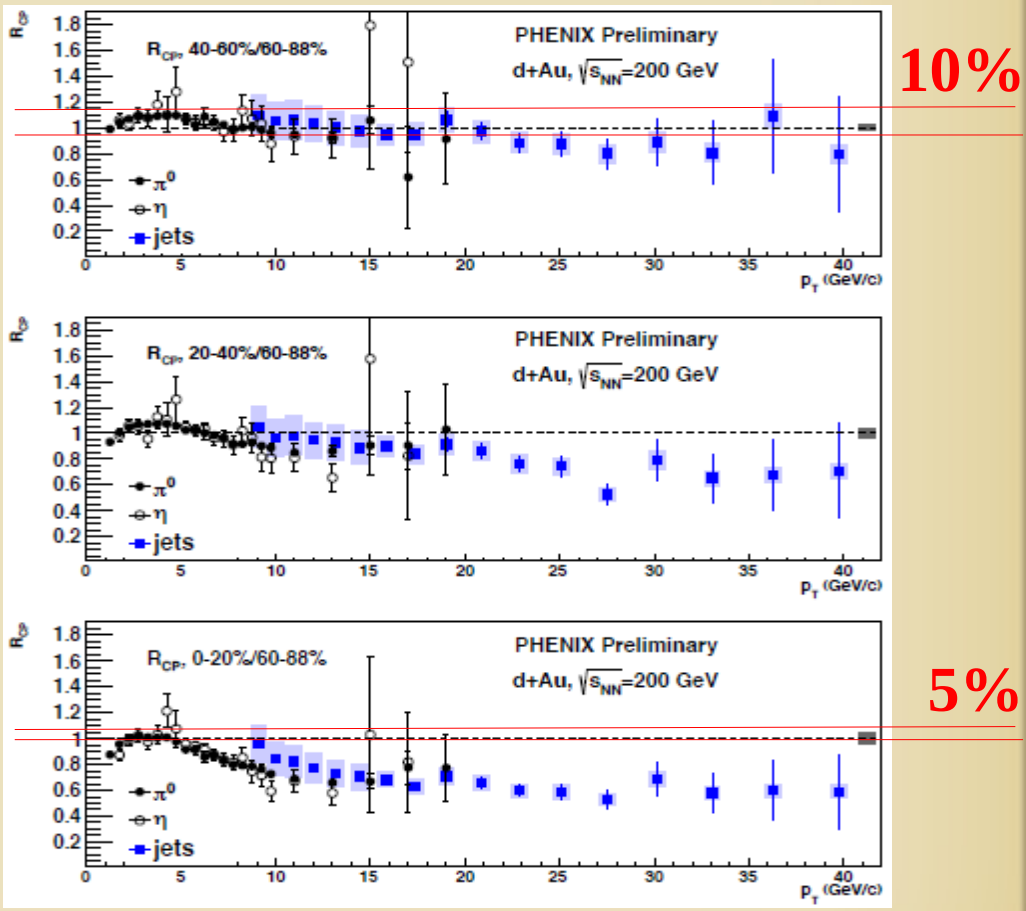

M O T I V A T I O N

- Motivation for *pPb/dAu* collisions

R_{dAu} (y=0, p_T) > R_{CP} (y=0, p_T), seems OK, but strong...

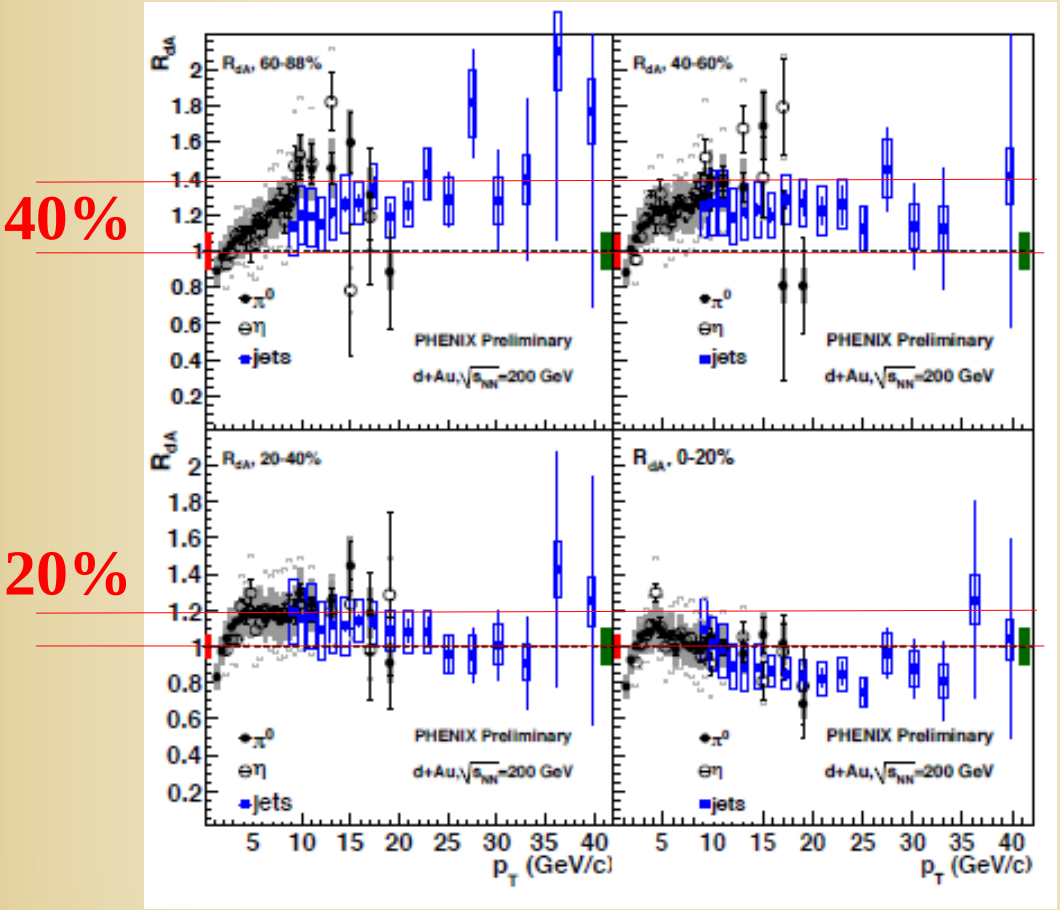

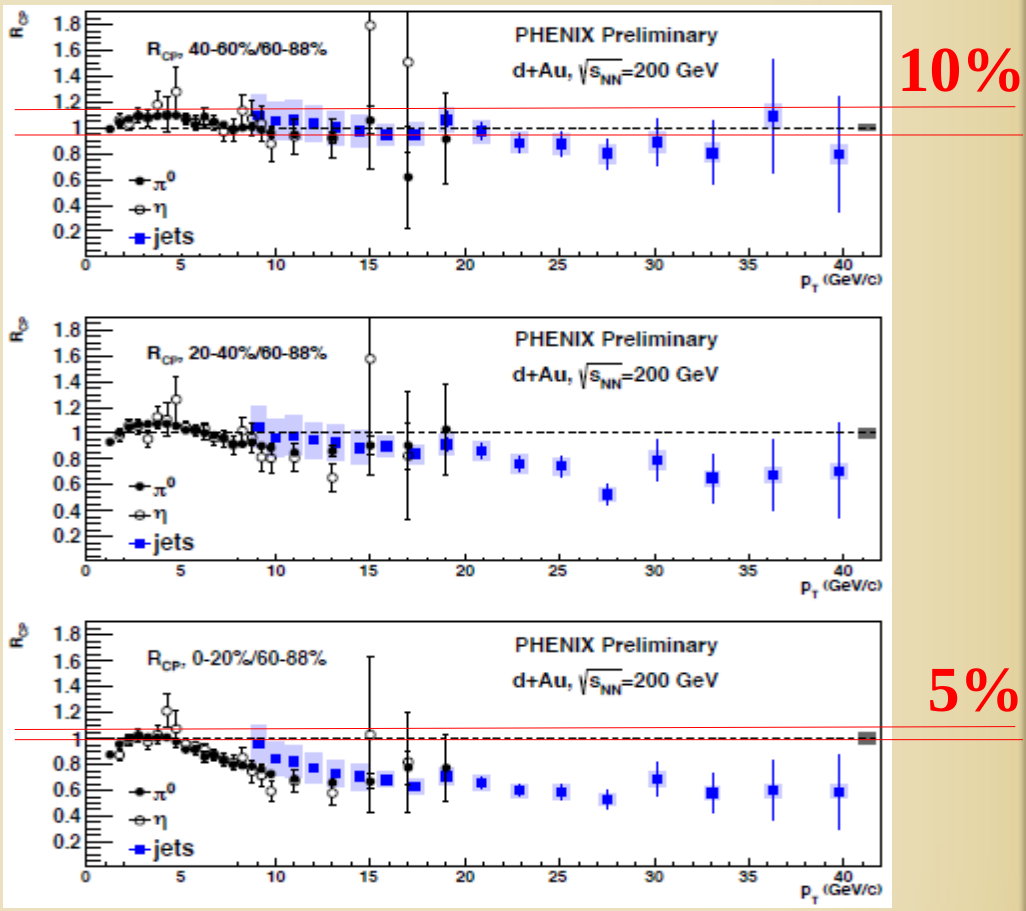

MOTIVATION

- Motivation for *pPb/dAu* collisions

  Preliminary dAu data from PHENIX@QM12 (B. Sahlmueller)

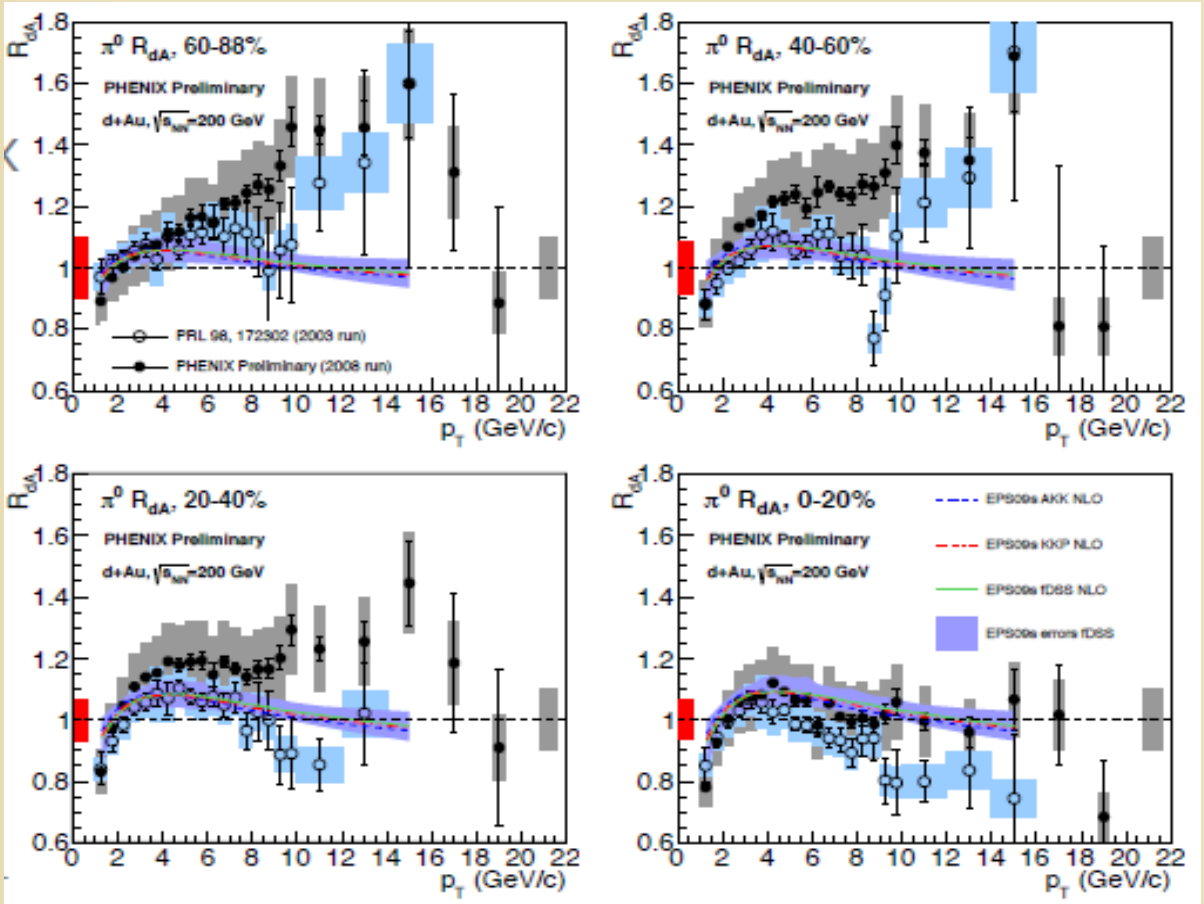

2008 data is not final, but differ at p_T>6 GeV/c in all centralities from data taken in 2003

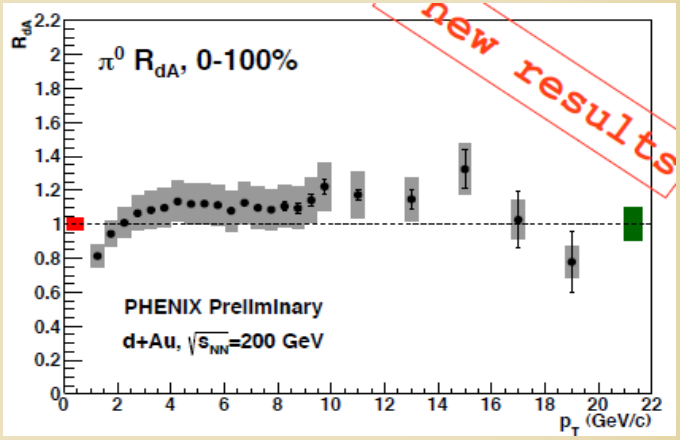

M O T I V A T I O N

- Motivation for *pPb/dAu* collisions

The RHIC MB is similar to the ALICE LHC MB data

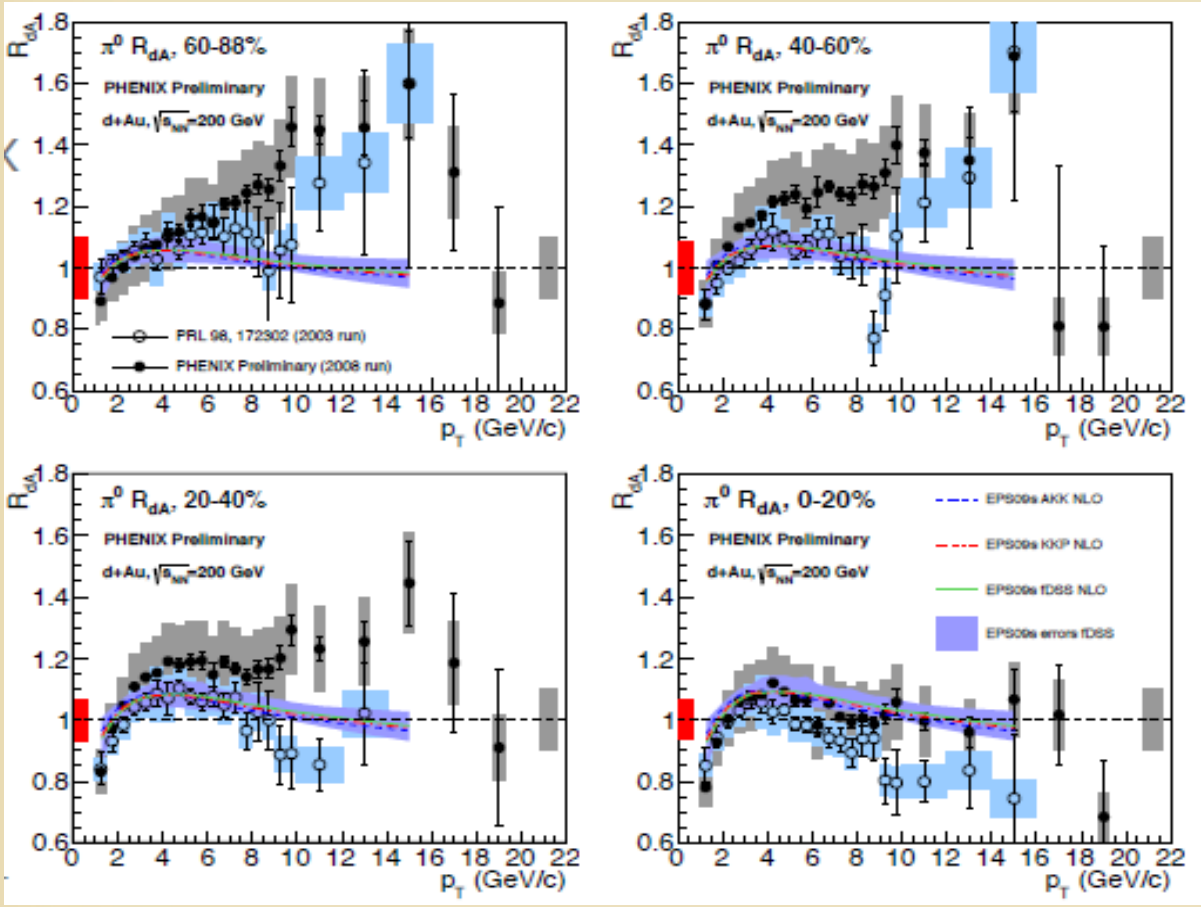

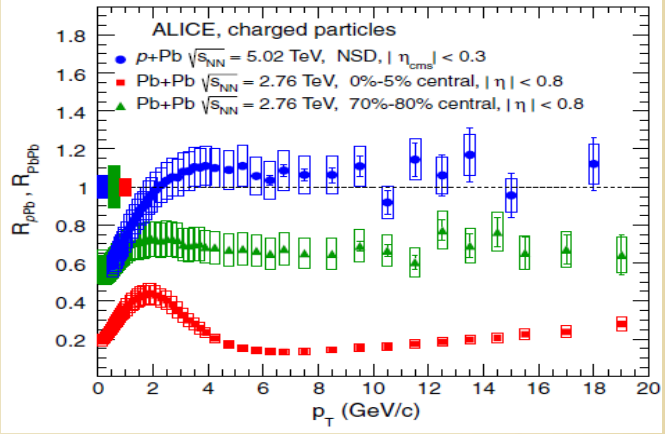

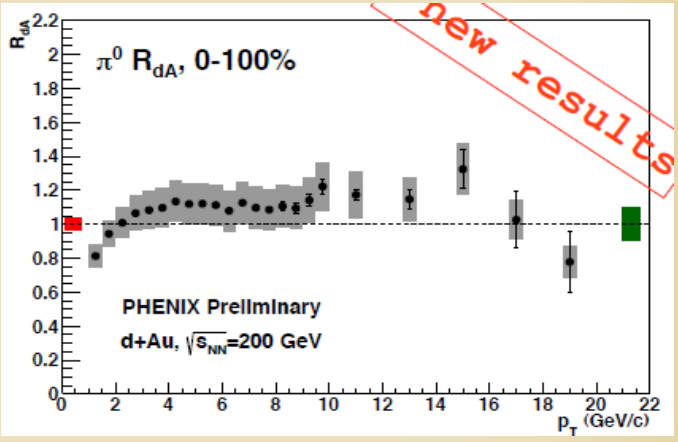

What have we learnt about Cronin so far?

- Overall properties of MB case:

  CM energy dependence: Higher the sqrt(s) lower the peak

  No relevant change in the place of the peak

  Shape is similar, but hard to say anything on width

C.M. Energy [GeV]	Peak' s place p_T [GeV/c]	Max effect. [%]	Type
27.4	4	50%	pW/pBe
38.8	4	40%	pW/pBe
200	4	10-15%	dAu/pp
5020	4	10%	pPb/pp

- Centrality & Rapidity dependence

  Anomalous increase in pheripheral collisions

  Suppression of the peak in forward (y>0): less or no peak

  No measurement in the backward (y<0): ????

What have we learnt about Cronin so far?

- Overall properties of MB case:

  CM energy dependence: Higher the sqrt(s) lower the peak

  No relevant change in the place of the peak

  Shape is similar, but hard to say anything on width

C.M. Energy [GeV]	Peak' s place p_T [GeV/c]	Max effect. [%]	Type	Peak in x
27.4	4	50%	pW/pBe	0.3
38.8	4	40%	pW/pBe	0.2
200	4	10-15%	dAu/pp	0.04
5020	4	10%	pPb/pp	0.002

Shadowing

- Centrality & Rapidity dependence

  Anomalous increase in pheripheral collisions

  Suppression of the peak in forward (y>0): less or no peak

  No measurement in the backward (y<0): ????

What have we learnt about Cronin so far?

- Overall properties of MB case:

  CM energy dependence: Higher the sqrt(s) lower the peak

  No relevant change in the place of the peak

  Shape is similar, but hard to say anything on width

C.M. Energy [GeV]	Peak' s place p_T [GeV/c]	Max effect. [%]	Type	Peak in x
27.4	4	50%	pW/pBe	0.3
38.8	4	40%	pW/pBe	0.2
200	4	10-15%	dAu/pp	0.04
5020	4	10%	pPb/pp	0.002

Geometry & Multiple Scattering

- Centrality & Rapidity dependence

  Anomalous increase in pheripheral collisions

  Suppression of the peak in forward (y>0): less or no peak

  No measurement in the backward (y<0): ????

Models & Parameters

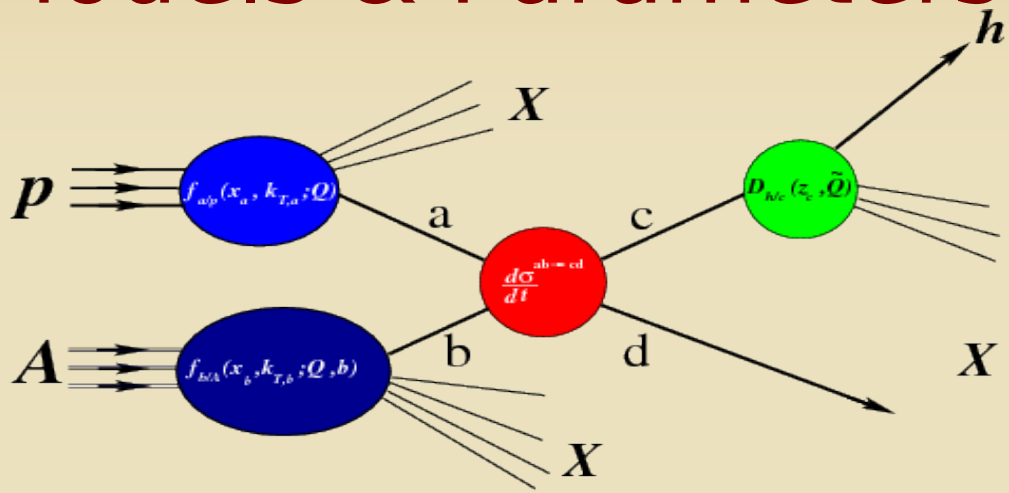

HIJING B/B 2.0

PRC83 024902, PRC84 022002 (2010)

Modified version of HIJING 2.0

Minijet cutoff: p_0=3.1 GeV/c

$$p_0(s,A) = 0.416\ \sqrt{s}^{0.191}\ A^{0.128}\ \mathrm{GeV}/c$$

String tension: κ =2.9 GeV/fm

$$\kappa(s,A) = \kappa_0\ (s/s0)^{0.06}\ A^{0.167}\ \mathrm{GeV/fm}.$$

PDF: GRV+ HIJING shadowing

FF: PYTHIA + minijet

kTpQCD_v2.0

PRC65 (2002)034903

NLO pQCD based parton model with intrinsic-k_T, k_T-broadening, and various shadowing parametrization.

$$E_\pi \frac{\mathrm{d}\sigma_\pi^{dAu}}{\mathrm{d}^3 p_\pi} = f_{a/d}(x_a, Q^2; \mathbf{k}_{Ta}) \otimes f_{b/Au}(x_b, Q^2; \mathbf{k}_{Tb}) \otimes \frac{\mathrm{d}\sigma^{ab\to cd}}{\mathrm{d}\hat{t}} \otimes \frac{D_{\pi/c}(z_c, \hat{Q}^2)}{\pi z_c^2}, \quad (1)$$

PDF:GRV/MRST+Shad, FF:KKP

on the Shadowing

aka suppression

Multiple Scattering in kTpQCD_v2.0

- What experiment gives... :

  No relevant change in the place of the peak

  Shape is similar, but hard to say anything on width

  Anomalous increase in pheripheral collisions

  Suppression of the peak in forward (y>0): less or no peak

  No measurement in the backward (y<0): ????

- you just take into account in a theory...

  Peak does not move or very slowly: assume no or log(s) dependence, and not follows x.

  MB agrees with models: integrated values are constraints

  Geometry matters: shadowing, nuclear size/density, rapidity, asymmetry, correlations, etc

The Spectra and $R_{pPb}(p_T)$ for $|\eta|<0.35$ & 0.3

Predictions by kTpQCD_2.0 @ 5.02 ATeV & 0.2 AGeV

Shadowing:

$$f_{a/A}(x,Q^2) = S_{a/A}(x,Q^2) f_{a/N}(x,Q^2)$$

b-dependent part

$$s_a(b) = s_a \frac{5}{3}\left(1 - \frac{b^2}{R_A^2}\right)$$

with

$$R_A = 1.12 A^{1/3}$$

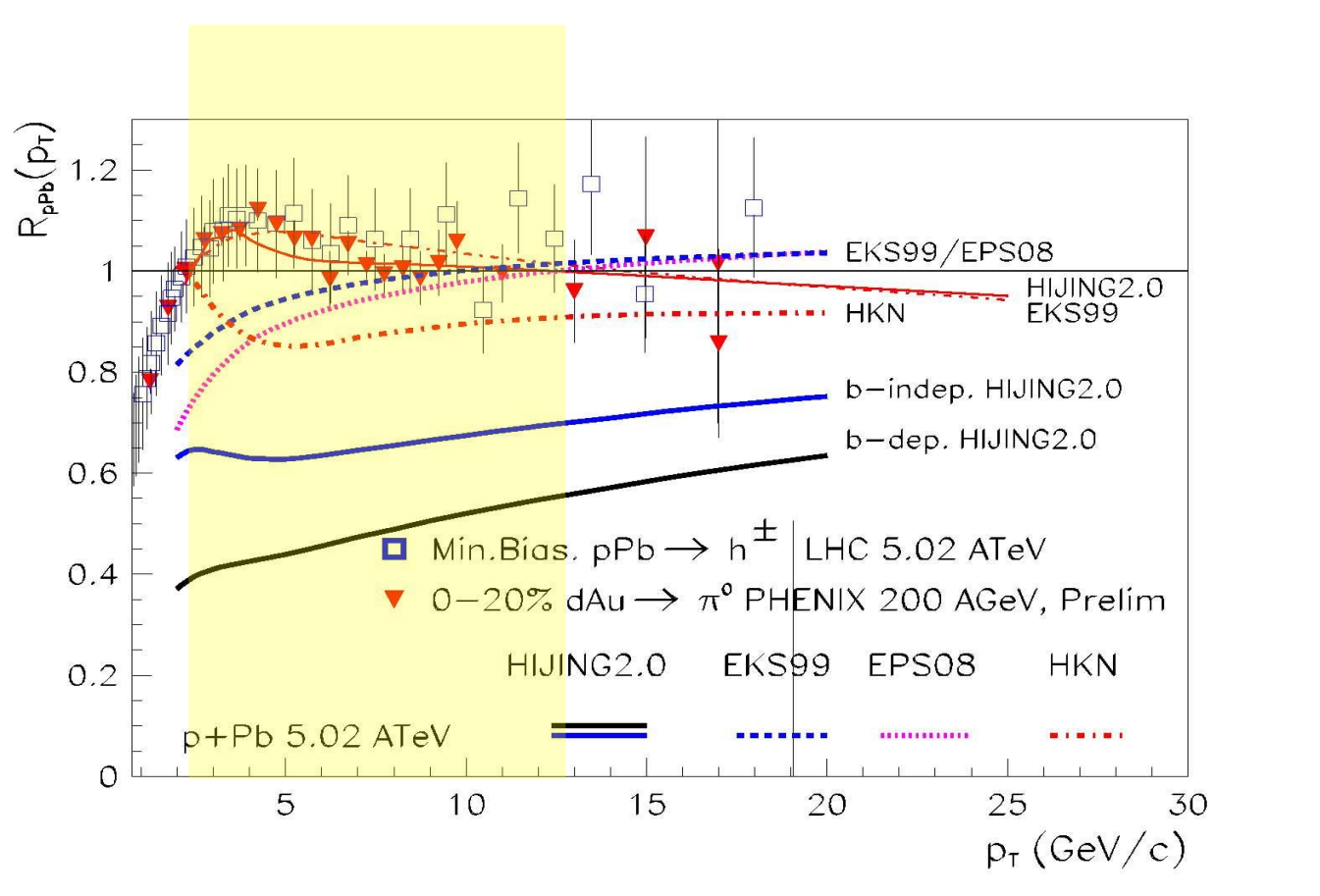

GGB, J. Barrette, M. Gyulassy, P. Lévai, V. Topor Pop: PRC 024903 (2012), arXiv:1211.2256, Int. Mod. Phys E22 1330007 (2013)

The Spectra and $R_{pPb}(p_T)$ for $|\eta|<0.35$ & 0.3

Predictions by kTpQCD_2.0 @ 5.02 ATeV

Shadowing:

$$f_{a/A}(x,Q^2) = S_{a/A}(x,Q^2) f_{a/N}(x,Q^2)$$

b-dependent part

$$s_a(b) = s_a \frac{5}{3}\left(1 - \frac{b^2}{R_A^2}\right)$$

with

$$R_A = 1.12 A^{1/3}$$

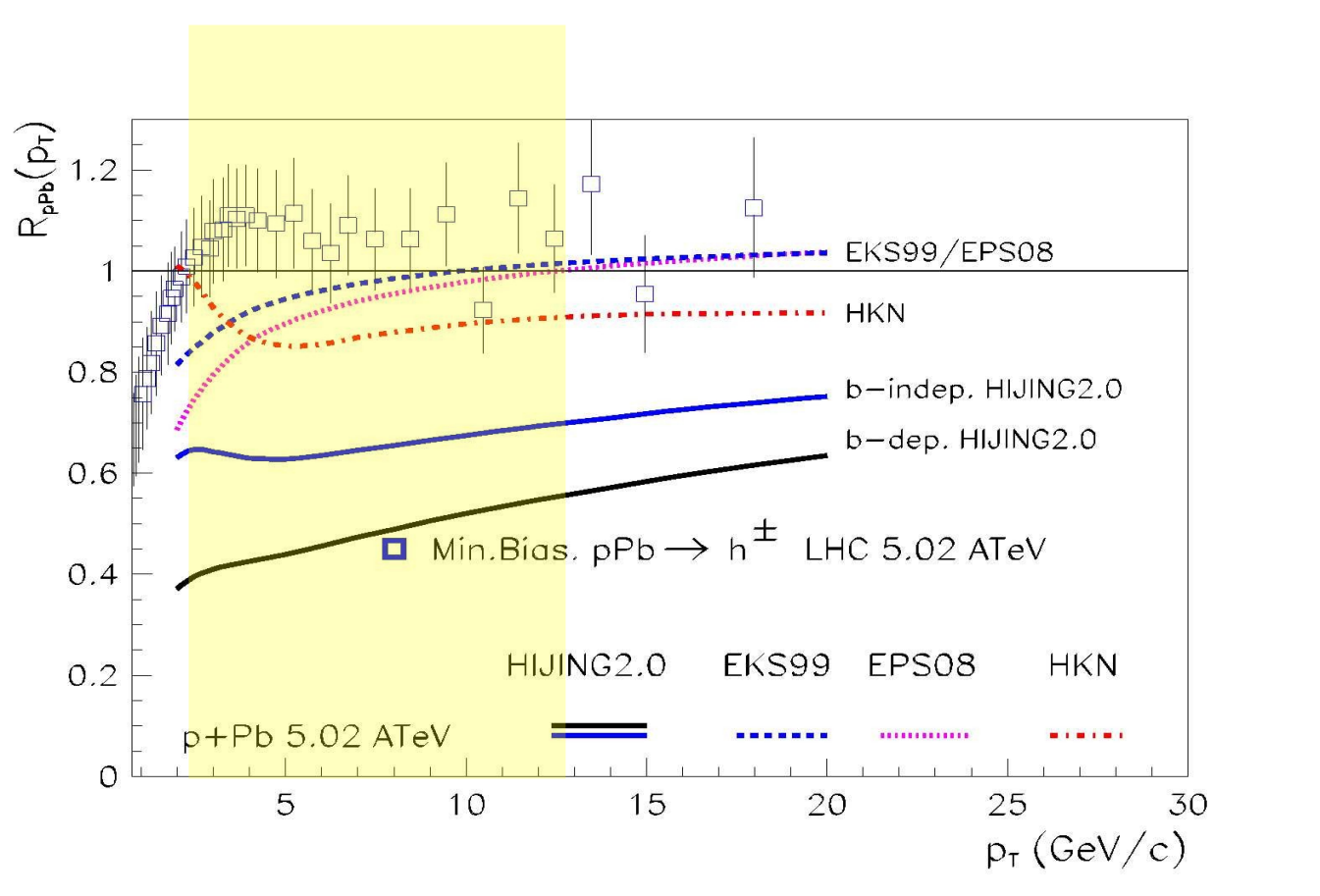

GGB, J. Barrette, M. Gyulassy, P. Lévai, V. Topor Pop: PRC 024903 (2012), arXiv:1211.2256, Int. Mod. Phys E22 1330007 (2013)

The Spectra and $R_{pPb}(p_T)$ for $|\eta|<0.8$

Charged hadron production with HIJING 2.0 @ 4.4 ATeV

$R_{pA} \sim 0.7$

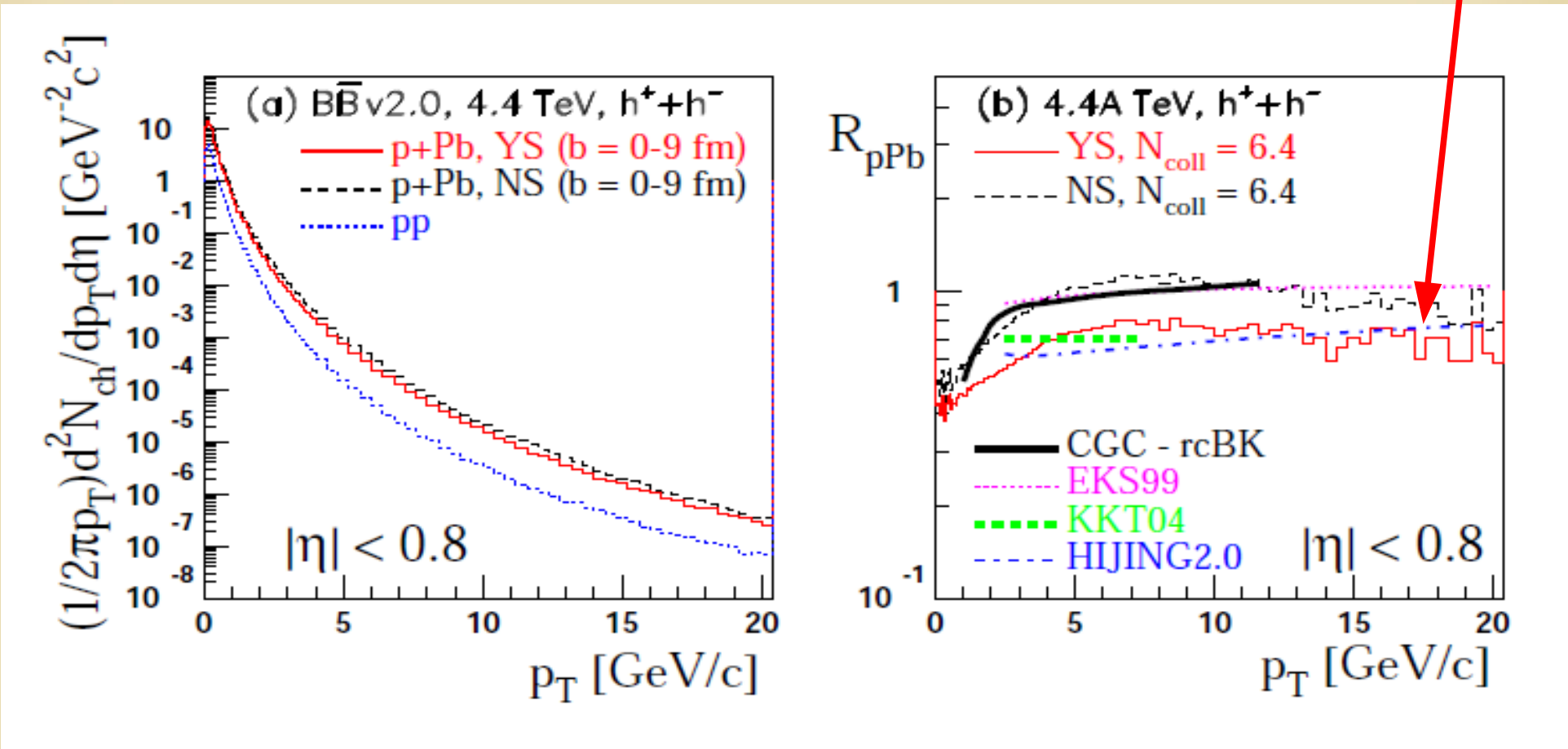

GGB, J. Barrette, M. Gyulassy, P. Lévai, V. Topor Pop PRC85 024903 (2012)

Forward $R_{pPb}(p_T)$ at $|\eta| < 0.8$ & $\eta = 6.0$

Charged hadron production with HIJING 2.0 @ 4.4 ATeV

$R_{pA} \sim 0.35$

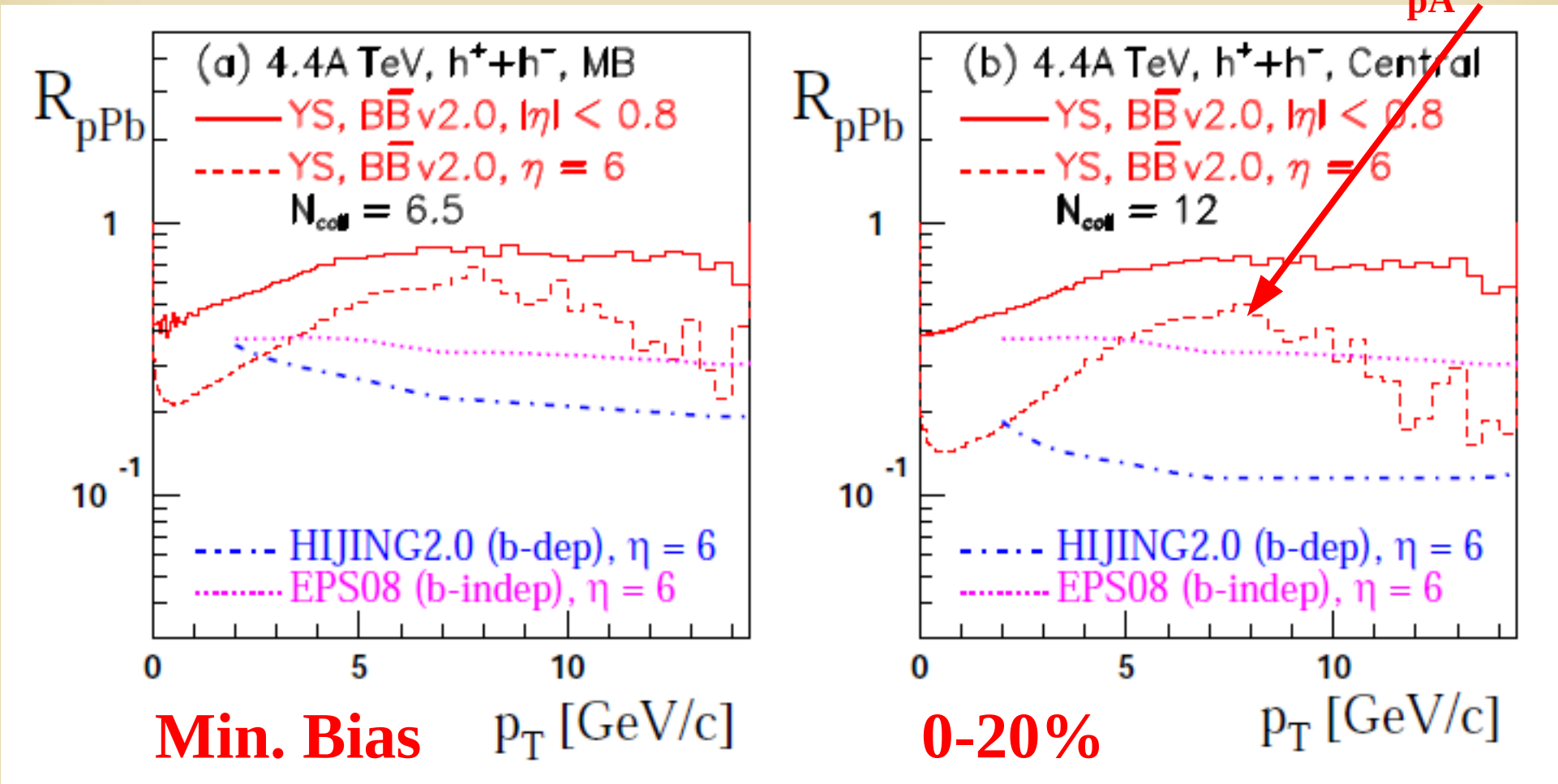

GGB, J. Barrette, M. Gyulassy, P. Lévai, V. Topor Pop PRC85 024903 (2012)

HIJINGB/B 2.0: Rapidity distribution for pp & pPb

Charged hadron production with HIJING 2.0 @ 5.02 ATeV (0-20%)

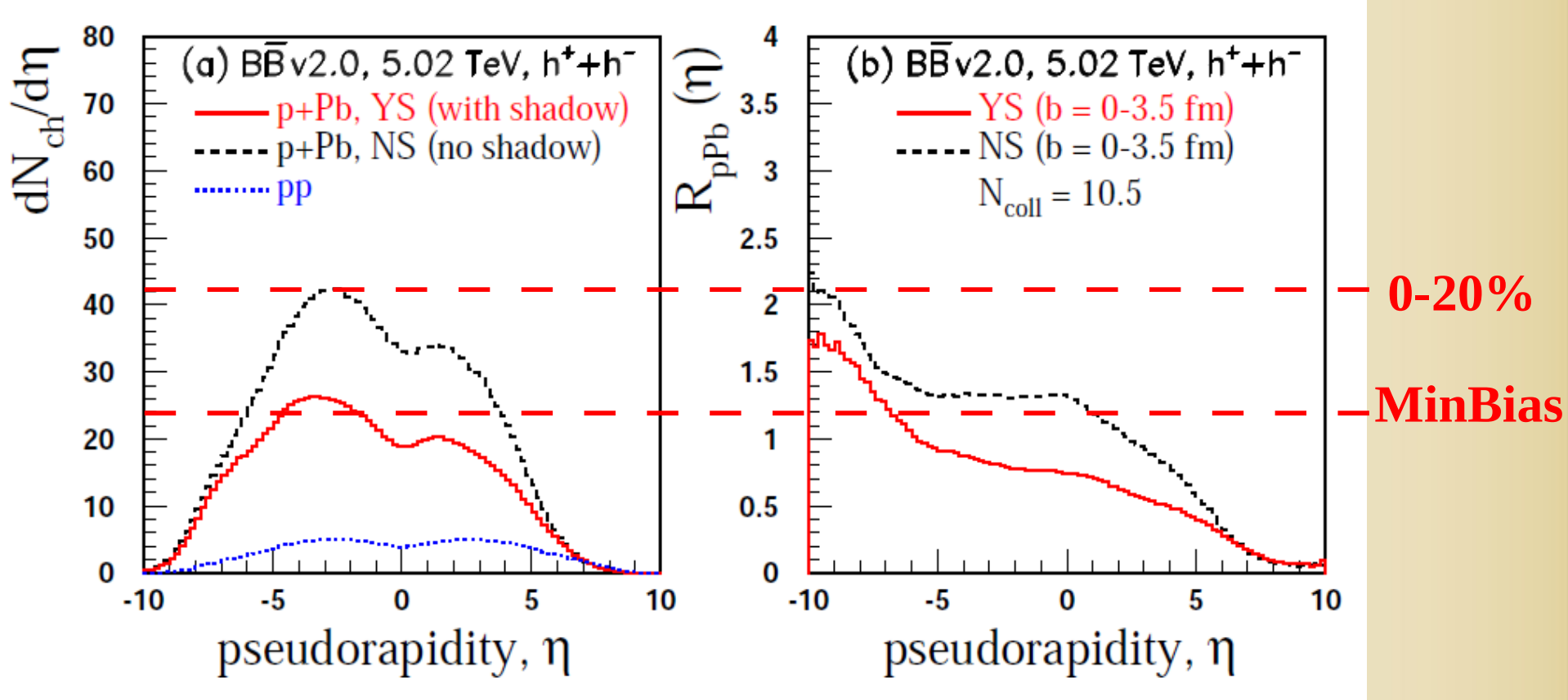

GGB, J. Barret, M. Gyulassy, P. Lévai, V. Topor Pop (in preparation 2012)

Shadowing effects on $R_{dAu}(p_T)$ for $|\eta| < 0.35$

Extreme high-p_T Pion production with kTpQCD @ 200 AGeV

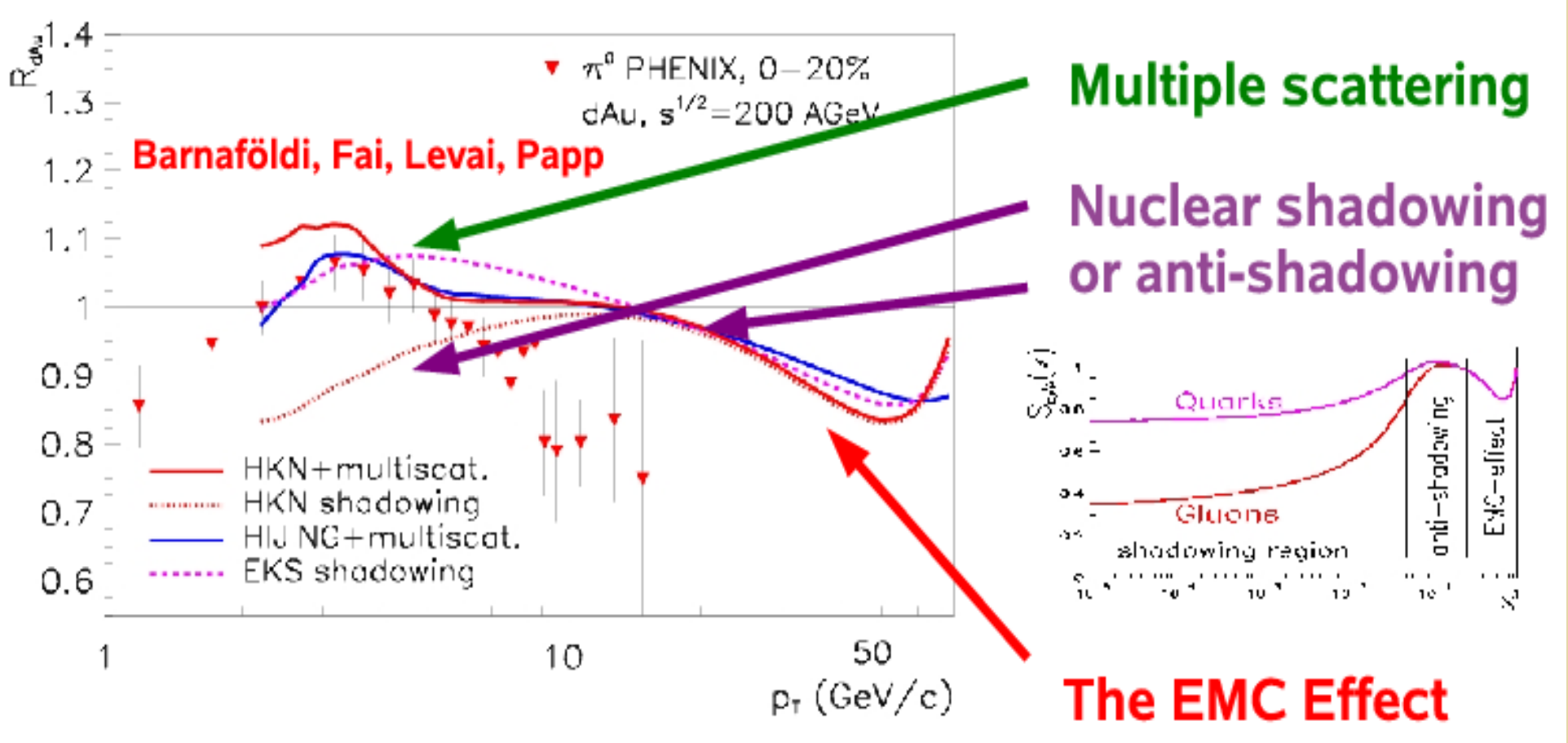

BA Cole, GGB, G. Fai, P. Lévai, G. Papp, arXiv:08073384 (2007)

Shadowing effects on $R_{dAu}(p_T)$ for $|\eta| < 0.35$

Slopes & values are OK with new dAu 0-20% data @ 200 AGeV

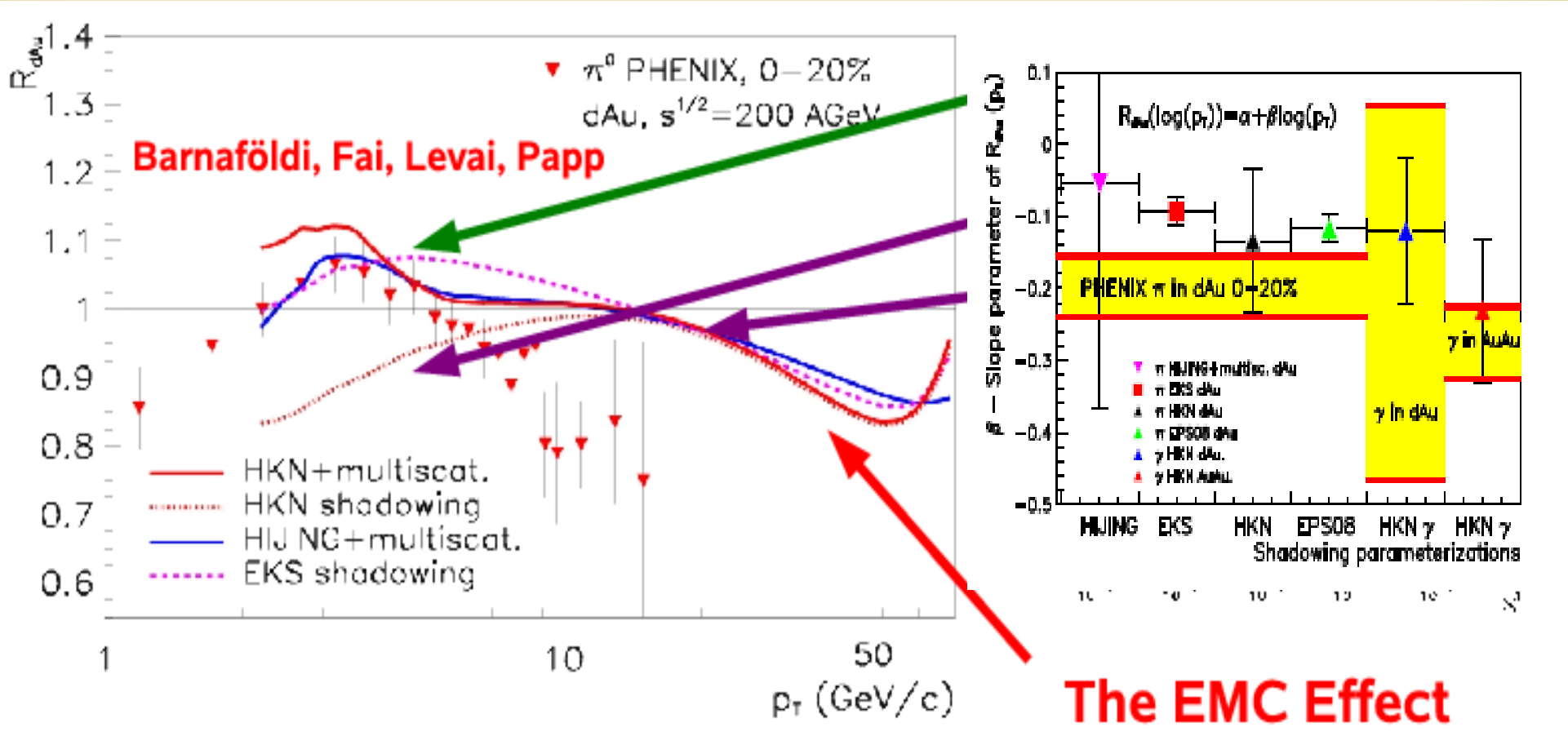

BA Cole, GGB, G. Fai, P. Lévai, G. Papp, arXiv:08073384 (2007)

on the Multiple Scattering

aka the enhacement

Multiple Scattering in kTpQCD_v2.0

Intrinsic k_T from theory & pp experiments

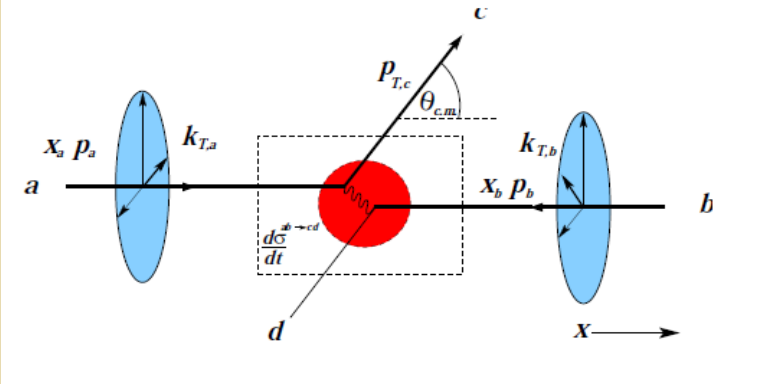

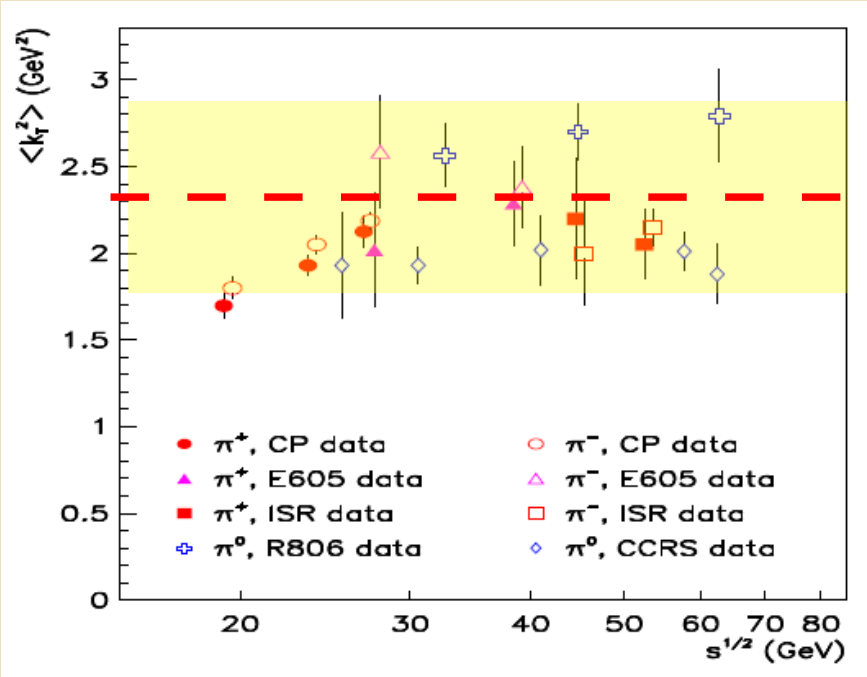

k_T-broadening:

$$f_{a/p}(x_a, \mathbf{k}_{Ta}, Q^2) = f_{a/p}(x_a, Q^2) \cdot g_{a/p}(\mathbf{k}_{Ta})$$

$$g_{a/n}(\mathbf{k}_T) := \frac{1}{\pi \langle k_T^2 \rangle} e^{-\mathbf{k}_T^2/\langle k_T^2 \rangle}$$

$$\langle k_T^2 \rangle_{pp} = \langle p_T \rangle_{pair}^2 / \pi$$

Y. Zhang, GGB, G. Fai, P. Lévai, G. Papp, PRC65 034903 (2002)

Multiple Scattering in kTpQCD_v2.0

Intrinsic k_T from theory & pp experiments

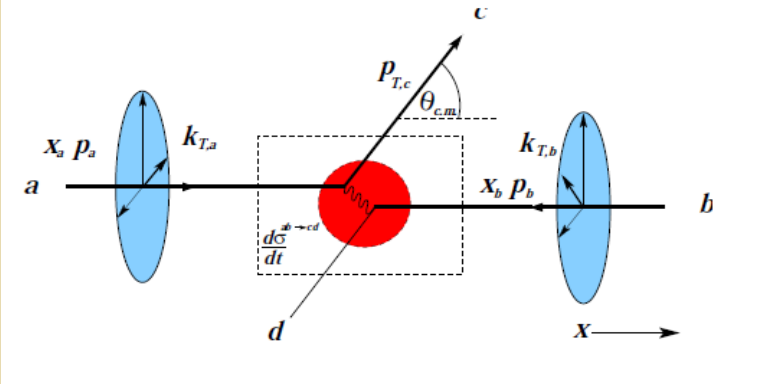

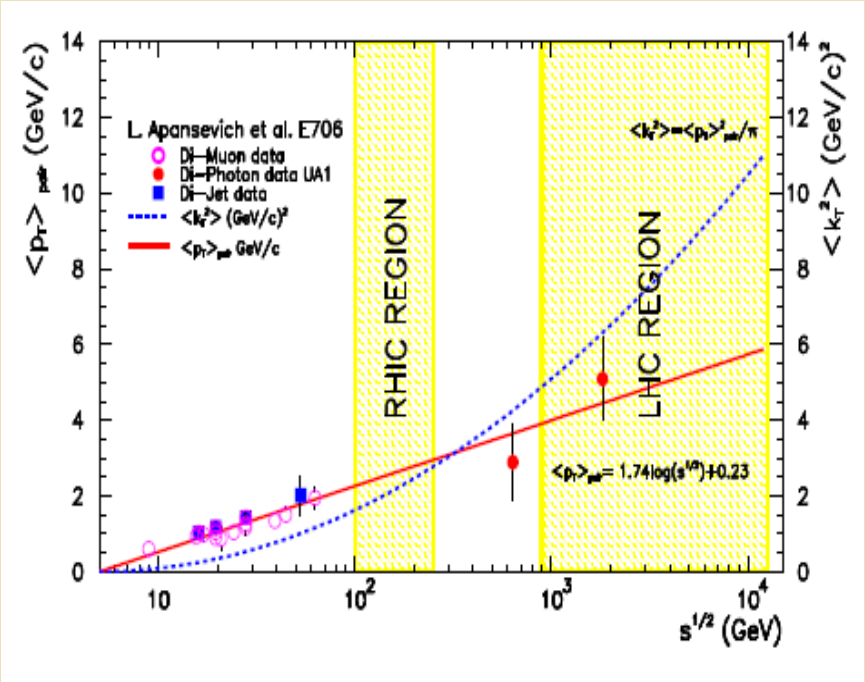

k_T-broadening:

$$f_{a/p}(x_a, \mathbf{k}_{Ta}, Q^2) \;=\; f_{a/p}(x_a, Q^2)\cdot g_{a/p}(\mathbf{k}_{Ta})$$

$$g_{a/n}(\mathbf{k}_T) \;:=\; \frac{1}{\pi\langle k_T^2\rangle} e^{-\mathbf{k}_T^2/\langle k_T^2\rangle}$$

$$\langle k_T^2\rangle_{pp} = \langle p_T\rangle^2_{pair}/\pi$$

BA Cole, GGB, G. Fai, P. Lévai, G. Papp, arXiv:08073384 (2007)

Multiple Scattering in kTpQCD_v2.0

Intrinsic k_T from theory & pp experiments

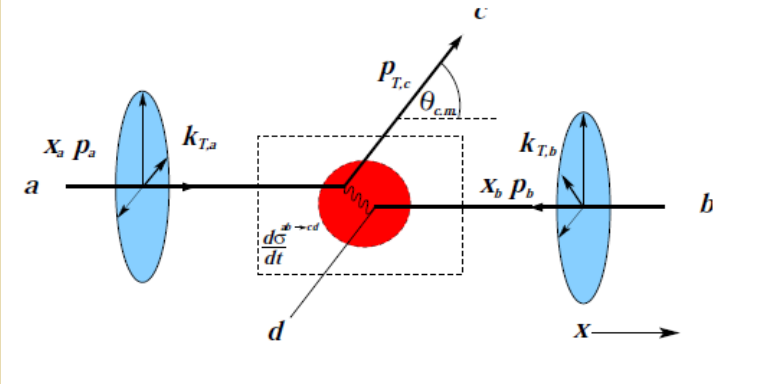

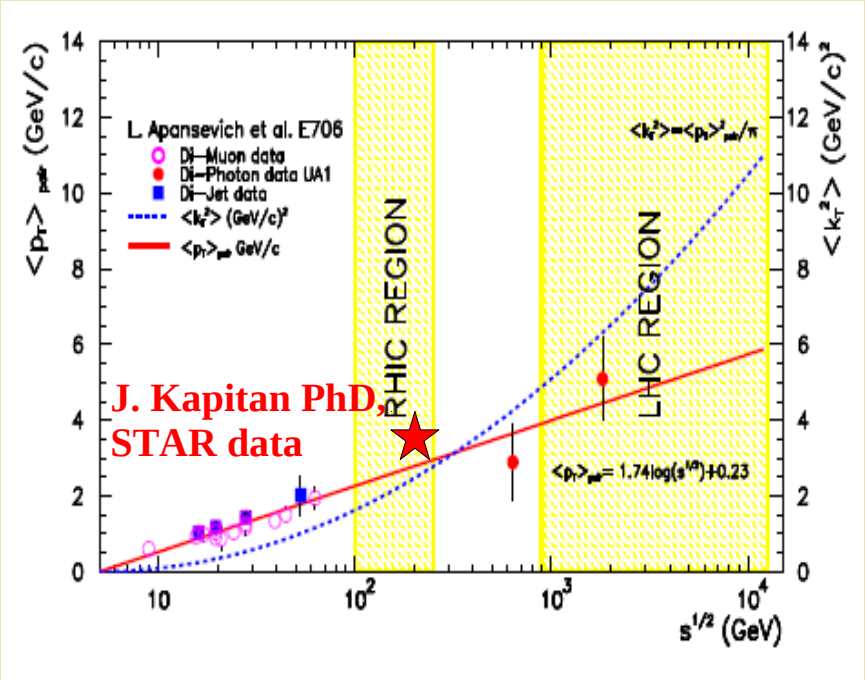

k_T-broadening:

$$f_{a/p}(x_a, \mathbf{k}_{Ta}, Q^2) \;=\; f_{a/p}(x_a, Q^2)\cdot g_{a/p}(\mathbf{k}_{Ta})$$

$$g_{a/n}(\mathbf{k}_T) \;:=\; \frac{1}{\pi\langle k_T^2\rangle} e^{-\mathbf{k}_T^2/\langle k_T^2\rangle}$$

$$\langle k_T^2\rangle_{pp} = \langle p_T\rangle^2_{pair}/\pi$$

BA Cole, GGB, G. Fai, P. Lévai, G. Papp, arXiv:08073384 (2007)

J. Kapitan, PhD Thesis, 2011

Multiple Scattering in kTpQCD_v2.0

Glauber model

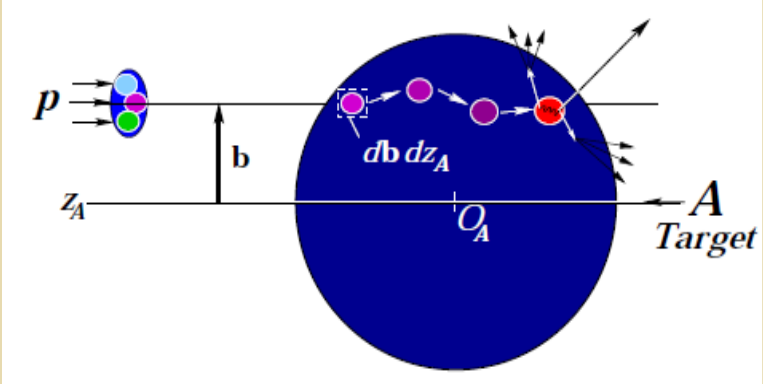

$$\int_0^{b_{max}} t_A(\mathrm{b})\,\mathrm{d}^2\mathrm{b} = \int_0^{b_{max}} \mathrm{d}^2\mathrm{b} \int \mathrm{d}z\rho(\mathrm{b},z) = A$$

with nuclear density:

$$\rho(r) = \frac{\rho_0}{1+\mathrm{e}^{\frac{r-r_0}{c}}}$$

There must be 1 hard and, further semi-hard collisions (number of NN collisions):

$$\nu_A(b) = \sigma_{NN}^{in} \cdot t_A(b)$$

NN-like collisions followed by enhancement of intrinsic k_T

PA: Gaussian broadening

$$g_{a/p}(\mathrm{k}_{T,a}, b) := \frac{1}{\pi \langle k_{Ta}^2(b)\rangle_{pA}} \mathrm{e}^{-\frac{\mathrm{k}_{T,a}^2}{\langle k_{T,a}^2(b)\rangle_{pA}}}$$

BA Cole, GGB, G. Fai, P. Lévai, G. Papp, arXiv:08073384 (2007)

Multiple Scattering in kTpQCD_v2.0

Phenomenological determination of the broadening

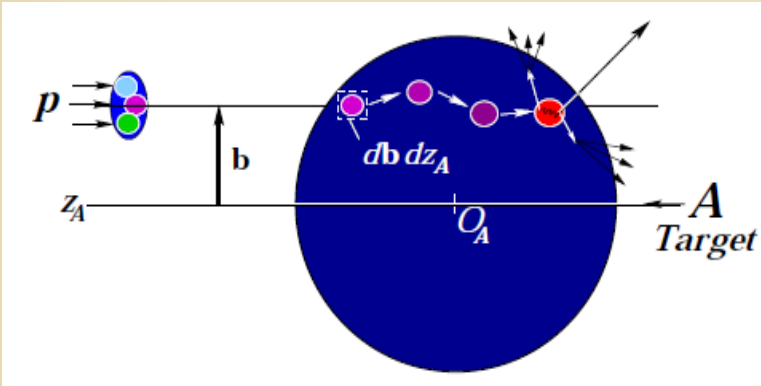

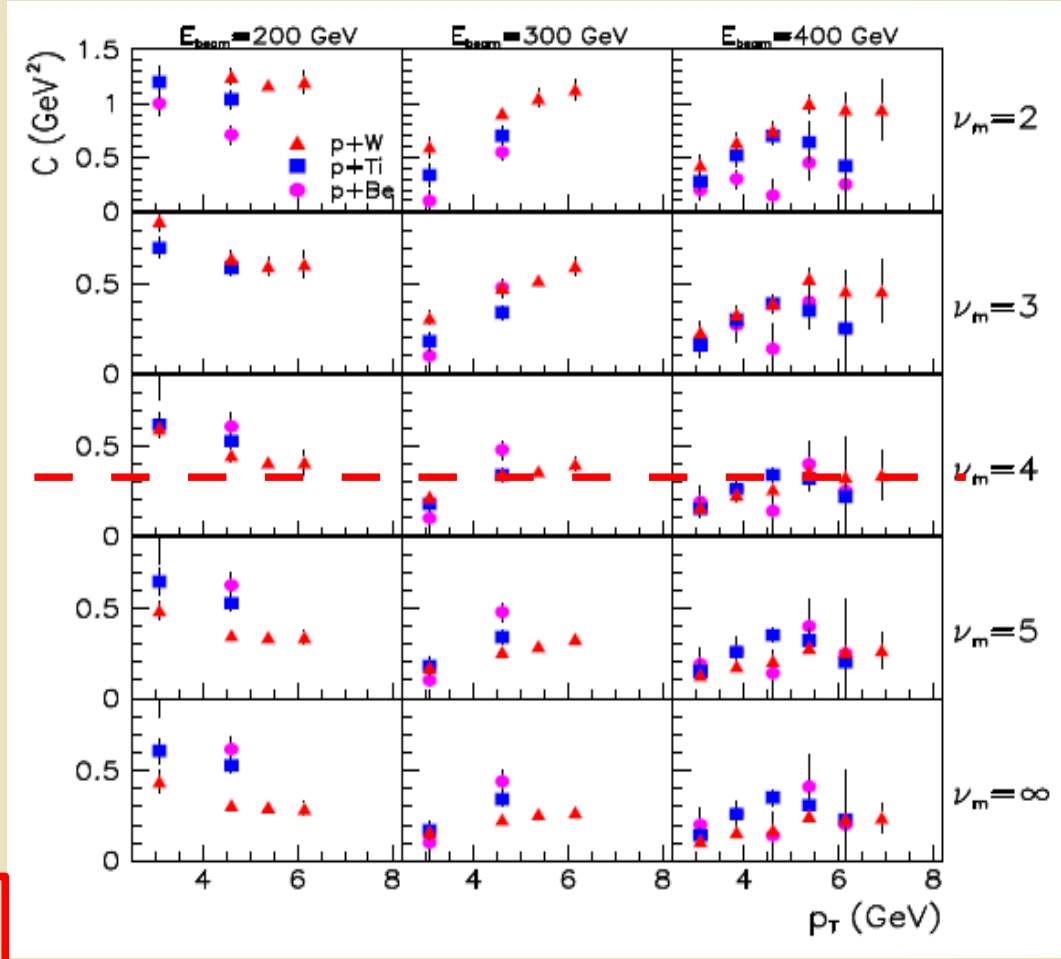

k_T-broadening:

$$g_{a/p}\left(\mathbf{k}_{T,a}, b\right) := \frac{1}{\pi \left\langle k_{Ta}^2(b)\right\rangle_{pA}} \mathrm{e}^{-\frac{\mathbf{k}_{T,a}^2}{\left\langle k_{T,a}^2(b)\right\rangle_{pA}}}$$

$$\left\langle k_T^2(b)\right\rangle_{pA} := \left\langle k_T^2\right\rangle_{pp} + C_{pA}^{sat} \cdot h_{pA}^{sat}(b)$$

$$C_{pA}^{sat} \approx 0.35 \pm 0,05 \ \mathrm{GeV}^2 \qquad \nu_{max} = 3 - 4$$

BA Cole, GGB, G. Fai, P. Lévai, G. Papp, arXiv:08073384 (2007)

Multiple Scattering in kTpQCD_v2.0

Intrinsic k_T from theory & pA experiment

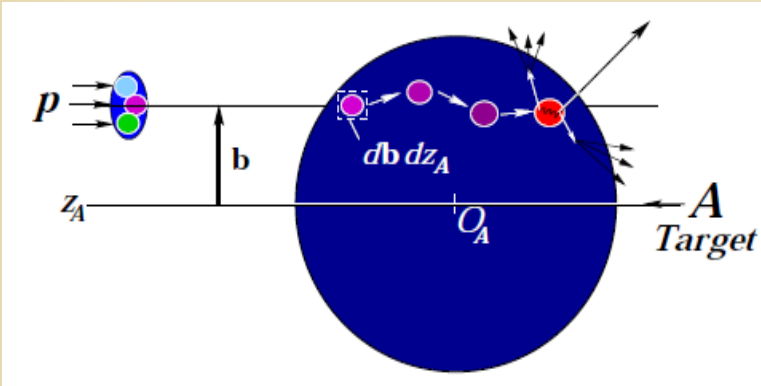

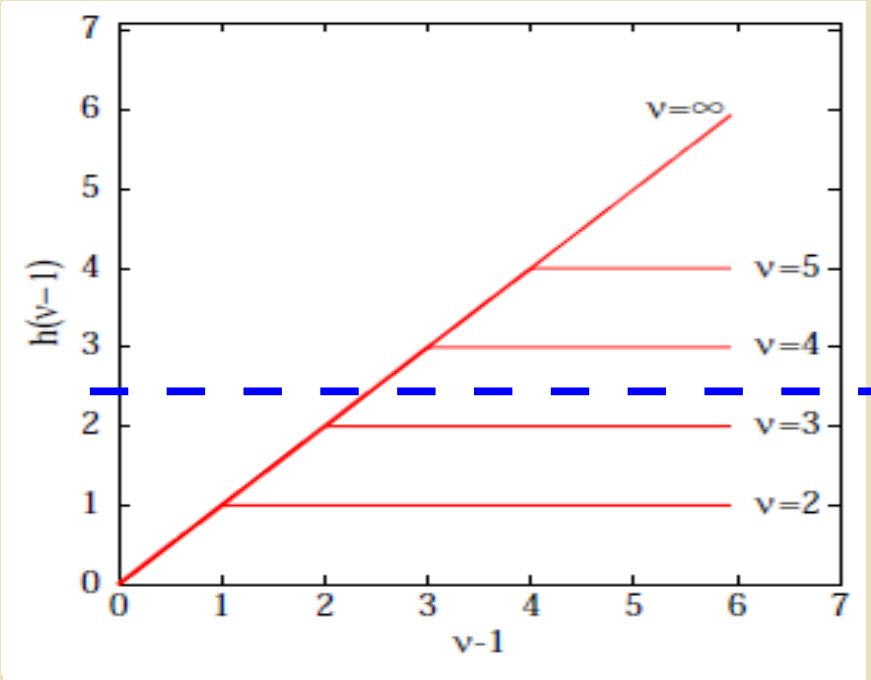

k_T-broadening:

$$g_{a/p}\left(\mathbf{k}_{T,a}, b\right) := \frac{1}{\pi \left\langle k_{Ta}^2(b)\right\rangle_{pA}} \mathrm{e}^{-\frac{\mathbf{k}_{T,a}^2}{\left\langle k_{T,a}^2(b)\right\rangle_{pA}}}$$

$$\left\langle k_T^2(b)\right\rangle_{pA} := \left\langle k_T^2\right\rangle_{pp} + C_{pA}^{sat} \cdot h_{pA}^{sat}(b)$$

Staurated Glauber model:

$$h_{pA}^{sat}(b) = \begin{cases} 0 & \text{ha} \quad \nu_A(b) < 1 \\ \nu_A(b) - 1 & \text{ha} \quad 1 \le \nu_A(b) < 4 \\ 3 & \text{ha} \quad \nu_A(b) \ge 4 \end{cases}$$

BA Cole, GGB, G. Fai, P. Lévai, G. Papp, arXiv:08073384 (2007)

Multiple Scattering in kTpQCD_v2.0

Intrinsic k_T from theory & pp/dAu experiments

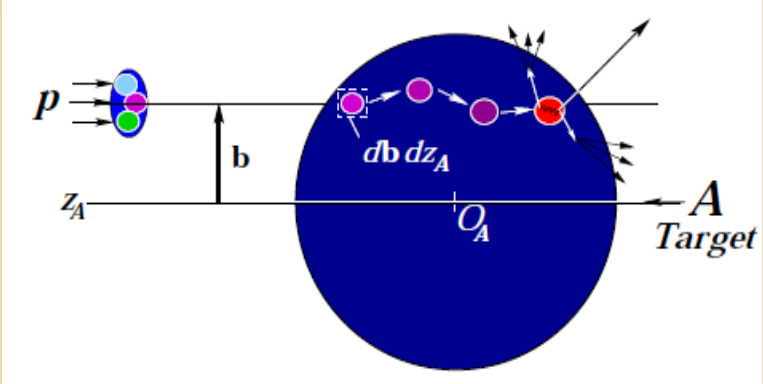

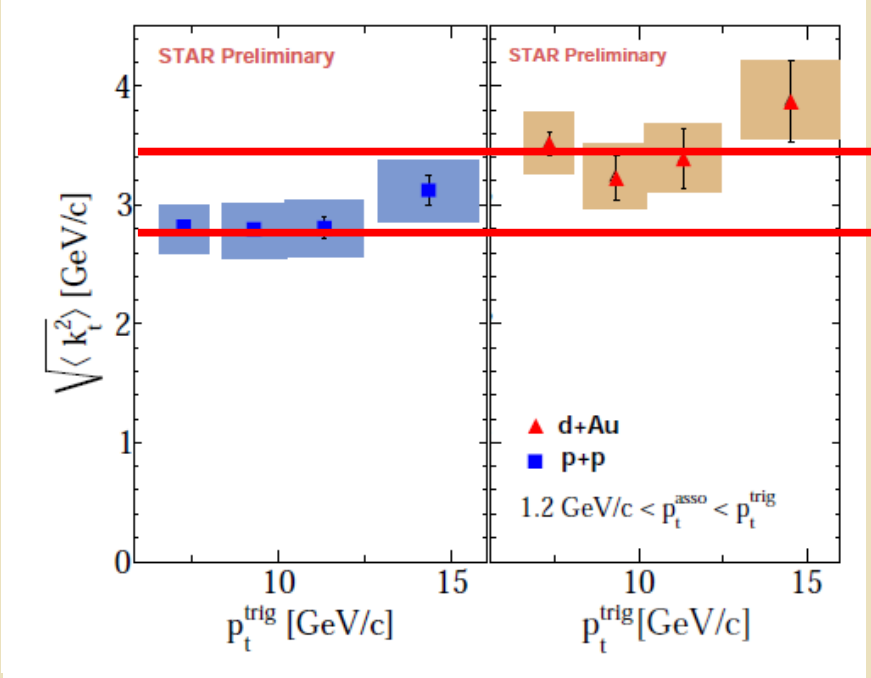

k_T-broadening:

$$g_{a/p}(\mathbf{k}_{T,a}, b) := \frac{1}{\pi \langle k_{Ta}^2(b) \rangle_{pA}} e^{-\frac{\mathbf{k}_{T,a}^2}{\langle k_{T,a}^2(b) \rangle_{pA}}}$$

$$\langle k_T^2(b) \rangle_{pA} := \langle k_T^2 \rangle_{pp} + C_{pA}^{sat} \cdot h_{pA}^{sat}(b)$$

$$\langle k_T^2 \rangle_{pp} = \langle p_T \rangle_{pair}^2 / \pi$$

- p+p collisions: $\sigma_{kT,raw} = 2.80 \pm 0.05(\text{stat.})^{+0.17}_{-0.29}(\text{syst.})$ GeV/c
- 0-20% d+Au col.: $\sigma_{kT,raw} = 3.00 \pm 0.07(\text{stat.})^{+0.18}_{-0.15}(\text{syst.})$ GeV/c

BA Cole, GGB, G. Fai, P. Lévai, G. Papp, arXiv:08073384 (2007)

Multiple Scattering in kTpQCD_v2.0

A proposed effect of saturated Cronin effect on NMF

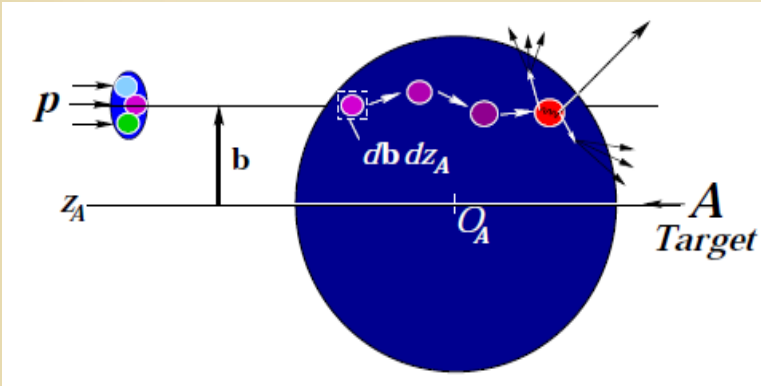

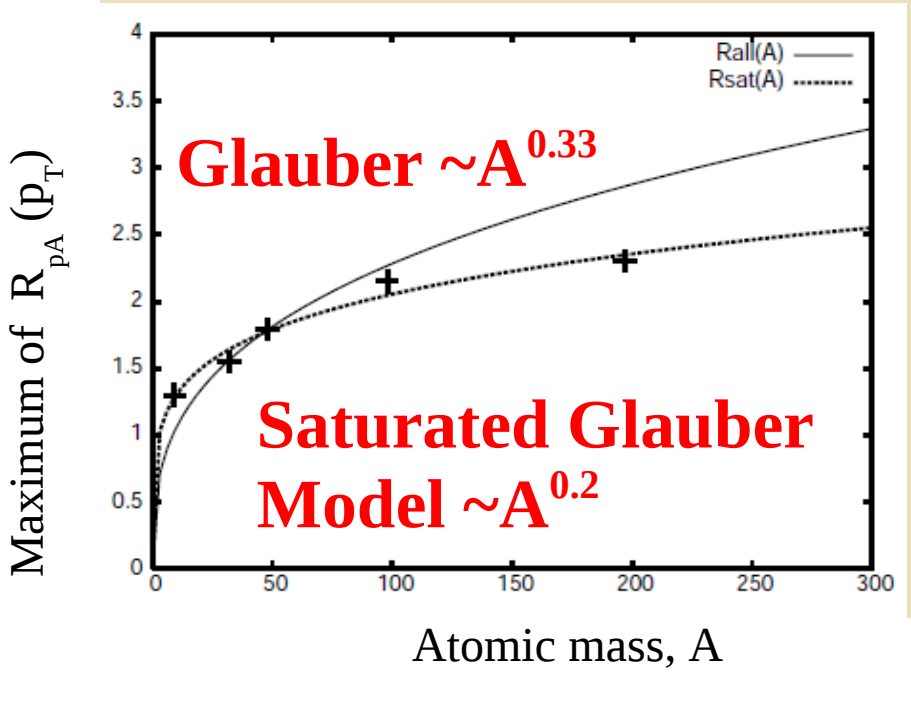

NMF as we know:

$$R^h_{pA}(p_T) := \frac{1}{\langle N_{bin}\rangle_A} \cdot \frac{\mathrm{d}^3\sigma^h_{pA}/\,\mathrm{d}^3p_T}{\mathrm{d}^3\sigma^h_{pp}/\,\mathrm{d}^3p_T}$$

As it was in the beginning, for MB (see e.g. W. Busza's talk)

$$\frac{\mathrm{d}^3\sigma^h_{pA}/\,\mathrm{d}^3p_T}{\mathrm{d}^3\sigma^h_{pp}/\,\mathrm{d}^3p_T} \sim A^{\alpha(p_T)} \longrightarrow R^h_{pA} \sim A^{\alpha(p_T)-1}$$

G. Fai, P. Lévai, G. Papp, PRC61 (2000) 021902,

GGB PhD Thesis, 2006

Multiple Scattering in kTpQCD_v2.0

A proposed effect of saturated Cronin effect on NMF

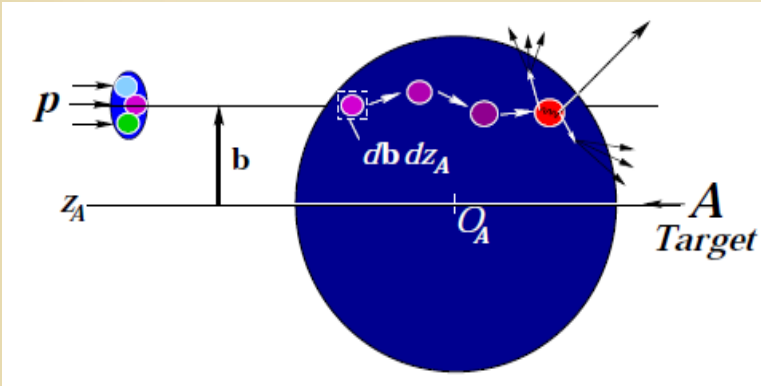

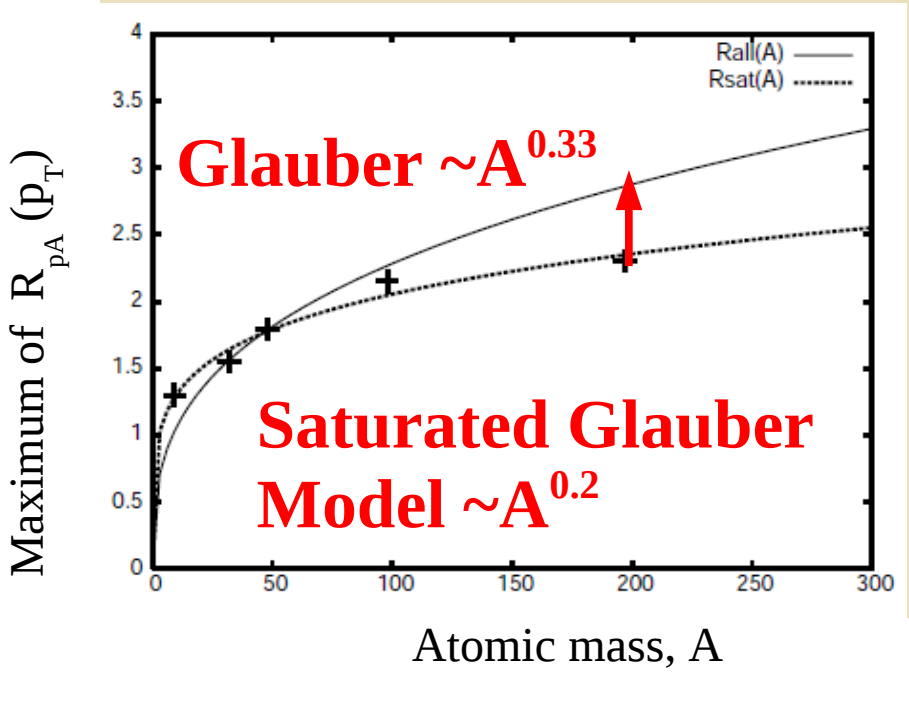

NMF as we know:

$$R^h_{pA}(p_T) := \frac{1}{\langle N_{bin}\rangle_A} \cdot \frac{\mathrm{d}^3\sigma^h_{pA}/\,\mathrm{d}^3p_T}{\mathrm{d}^3\sigma^h_{pp}/\,\mathrm{d}^3p_T}$$

As it was in the beginning, for MB (see e.g. W. Busza's talk)

$$\frac{\mathrm{d}^3\sigma^h_{pA}/\,\mathrm{d}^3p_T}{\mathrm{d}^3\sigma^h_{pp}/\,\mathrm{d}^3p_T} \sim A^{\alpha(p_T)} \longrightarrow R^h_{pA} \sim A^{\alpha(p_T)-1}$$

20% effect for large A

G. Fai, P. Lévai, G. Papp, PRC61 (2000) 021902,

GGB PhD Thesis, 2006

Suggestion for take away...

It is high time to understand the Cronin effect!

- High precision experimental data are available!
  - Handle with care
  - Make consistent physical picture (10 AGeV to 10 ATeV)
  - We have tools to test it (energy, geometry, etc.)
  - Universal description requires solid baseline :-)
  - Suggest a pA study experiment....

- Can we test the Saturated Glauber picture?
  - Test of geometry and scalings.
  - Large rapidities (forward & backward)
  - Correlations

B A C K U P

Rapidity asymmetry for *pBe* at FNAL

Pion production with kTpQCD for pPb@ 5.02 ATeV |η| [0.3:0.8]

$$Y^h_{Asym}(p_T) = E_h \frac{d^3\sigma^h_{AB}}{d^3p_T}\bigg|_{\eta<0} \Big/ E_h \frac{d^3\sigma^h_{AB}}{d^3p_T}\bigg|_{\eta>0}$$

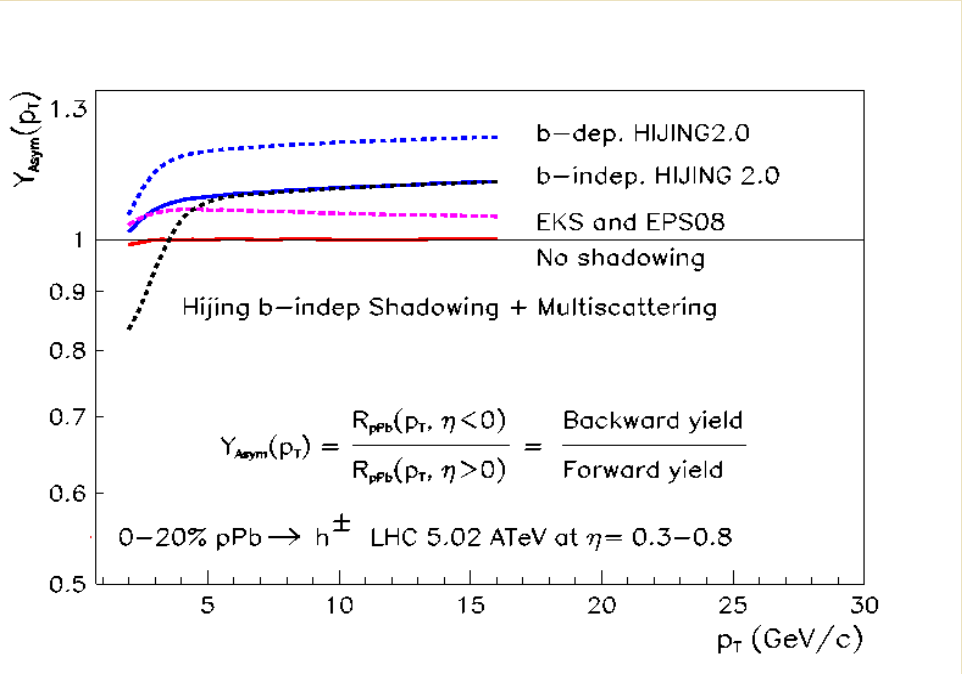

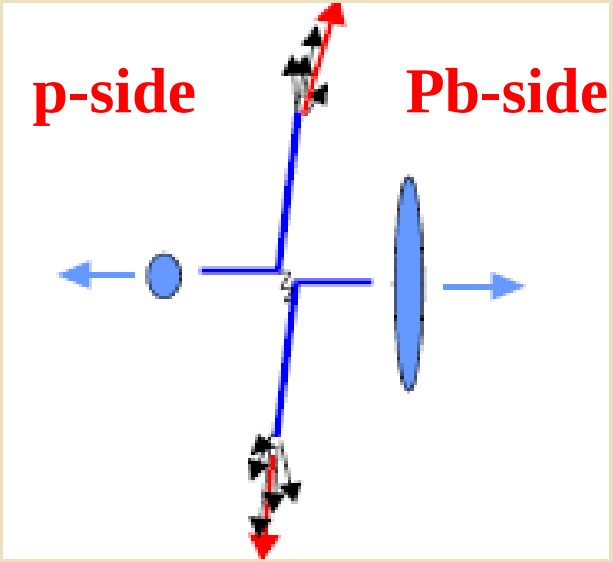

GGB, J. Barret, M. Gyulassy, P. Lévai, V. Topor Pop (in preparation 2012)

Rapidity asymmetry for *dPb* at LHC

Pion production with kTpQCD @ 8.8 ATeV

$$Y^h_{Asym}(p_T) = E_h \frac{d^3\sigma^h_{AB}}{d^3p_T}\bigg|_{\eta<0} \bigg/ E_h \frac{d^3\sigma^h_{AB}}{d^3p_T}\bigg|_{\eta>0}$$

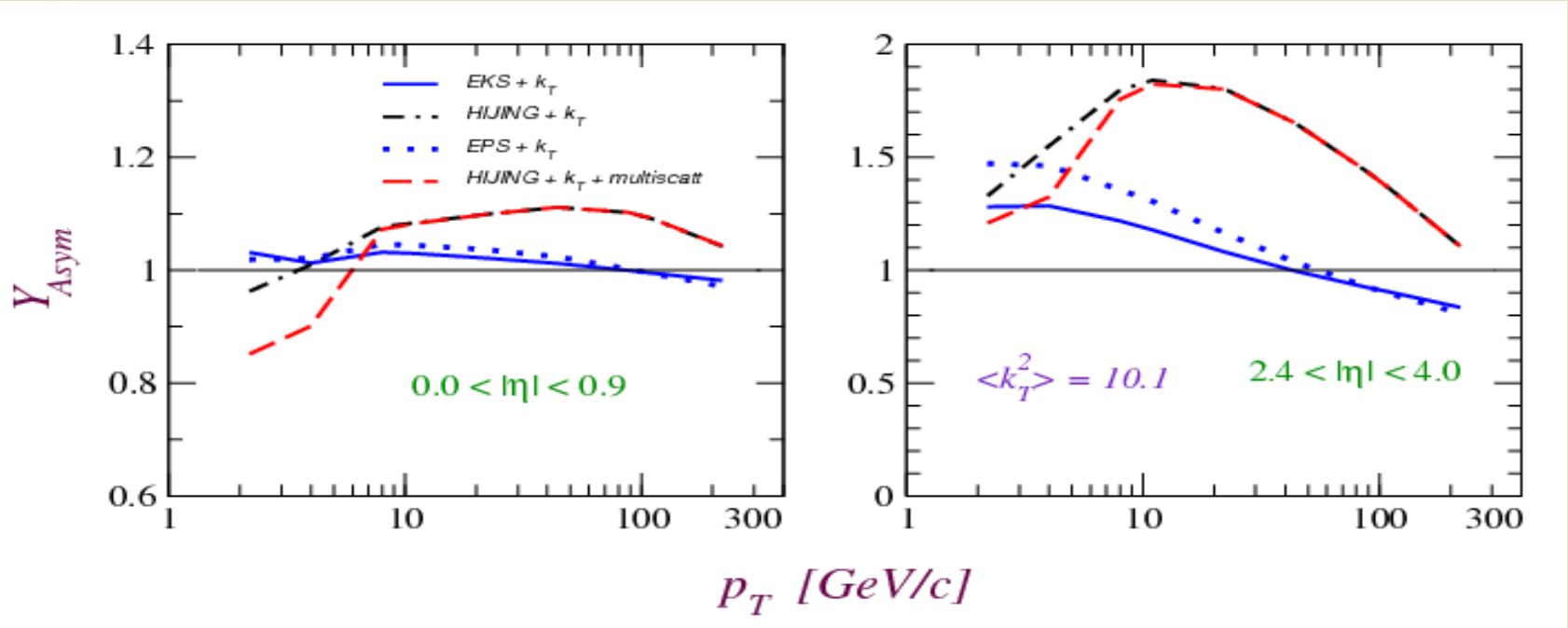

A. Adeluy, GGB, G. Fai, P. Lévai, PRC80 (2009) 014903

Rapidity asymmetry for *dAu* at RHIC

Pion production with kTpQCD @ 200 AGeV

Rapidity asymmatry

$$Y^h_{Asym}(p_T) = E_h \frac{d^3\sigma^h_{AB}}{d^3p_T}\bigg|_{\eta<0} \bigg/ E_h \frac{d^3\sigma^h_{AB}}{d^3p_T}\bigg|_{\eta>0}$$

Relation to NMF

$$Y^h_{Asym}(p_T) = R^h_\eta(p_T) = \frac{R^h_{dAu}(p_T, \eta < 0)}{R^h_{dAu}(p_T, \eta > 0)}$$

X-scaling is OK,
Multiscattering changes *Y(η)*

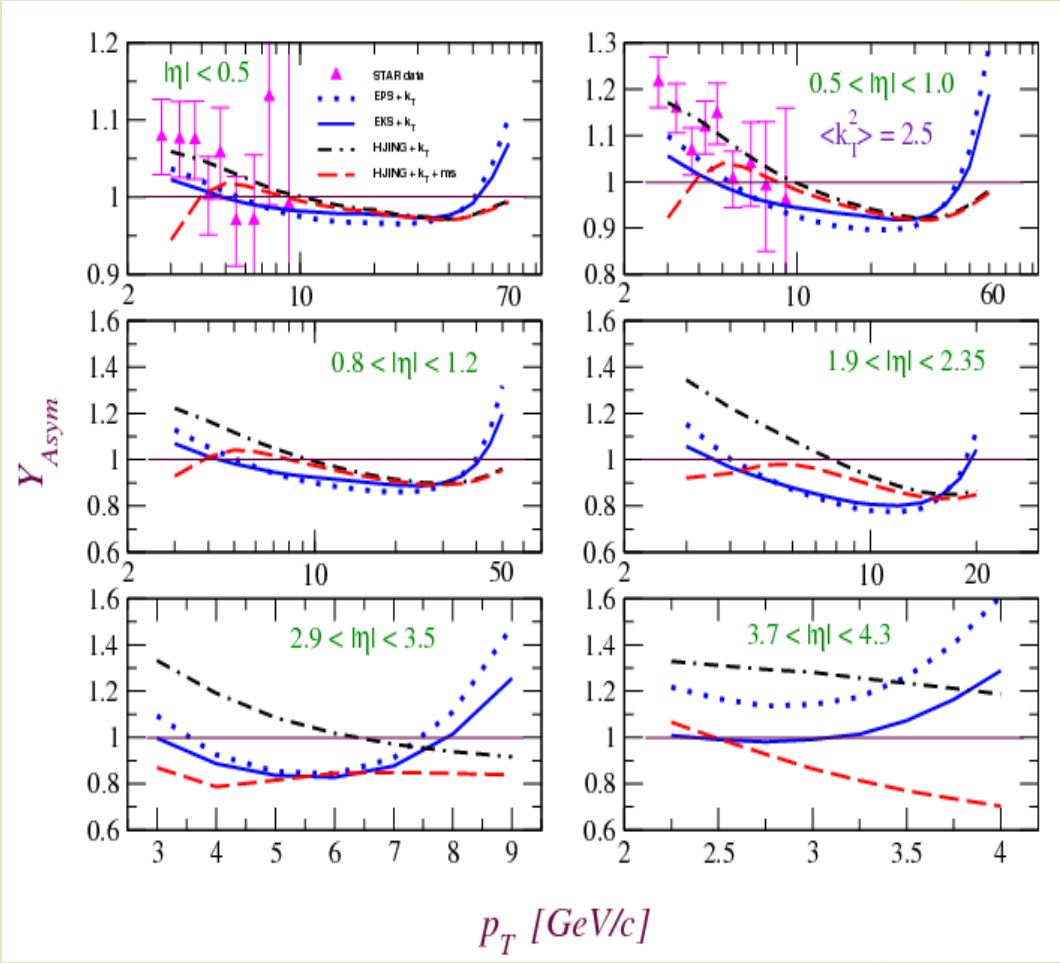

A. Adeluy, GGB, G. Fai, P. Lévai, PRC80 (2009) 014903

Rapidity asymmetry for *pBe* at FNAL

Pion production with kTpQCD @ 30.7 GeV

$$Y^h_{Asym}(p_T) = E_h \frac{d^3\sigma^h_{AB}}{d^3p_T}\bigg|_{\eta<0} \Big/ E_h \frac{d^3\sigma^h_{AB}}{d^3p_T}\bigg|_{\eta>0}$$

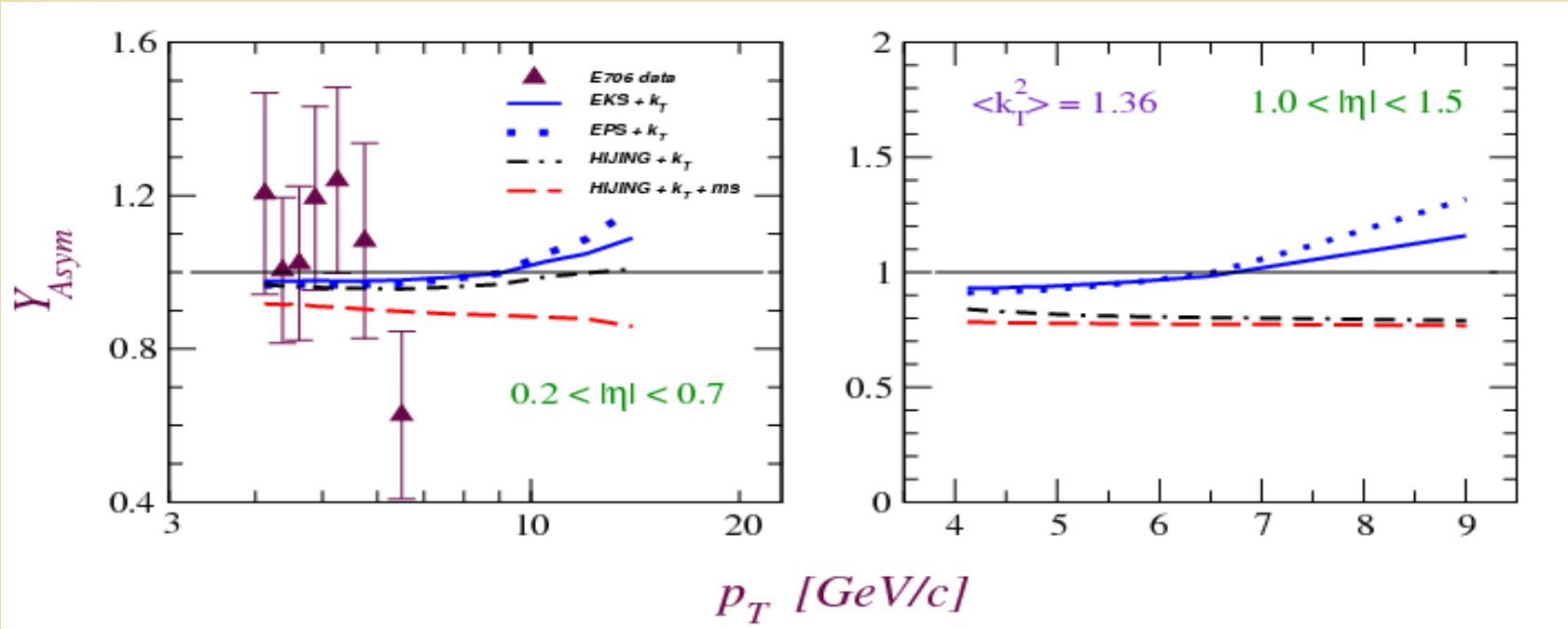

A. Adeluy, GGB, G. Fai, P. Lévai, PRC80 (2009) 014903

Midrapidity $R_{dA}(x_T)$ for $|\eta| < 0.35$

Pion production with HIJING shadowing kTpQCD @ 0.2 & 8.8 ATeV

HIJING Shadowing

x-scaling

DGLAP evolution

Need for additional multiple scattering

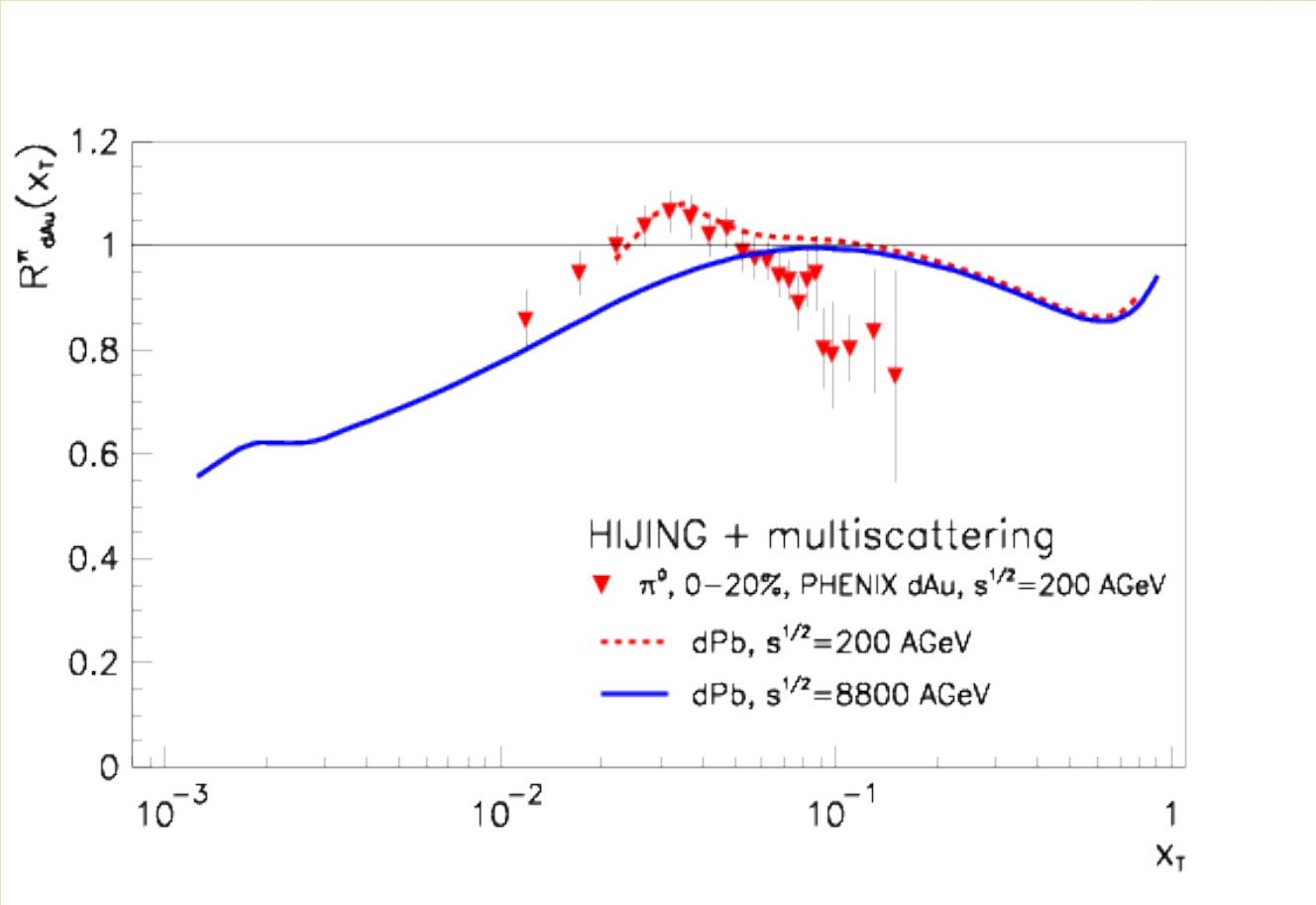

GGB, G. Fai, P. Lévai, BA Cole, G. Papp, Indian J.Phys. 84 (2010) 1721-1725

Midrapidity $R_{dA}(x_T)$ for $|\eta| < 0.35$

Pion production with EKS shadowing kTpQCD @ 0.2 & 8.8 ATeV

EKS Shadowing

x-scaling

DGLAP evolution

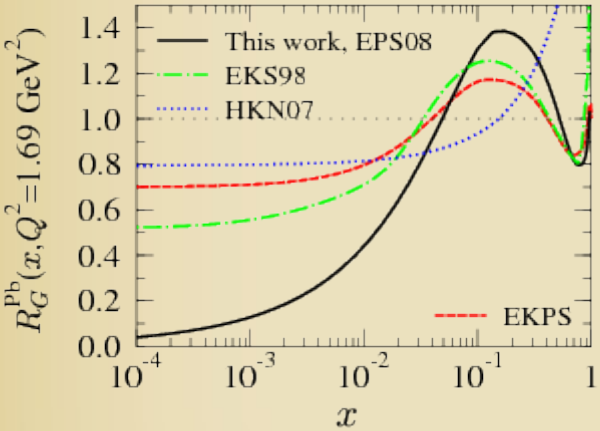

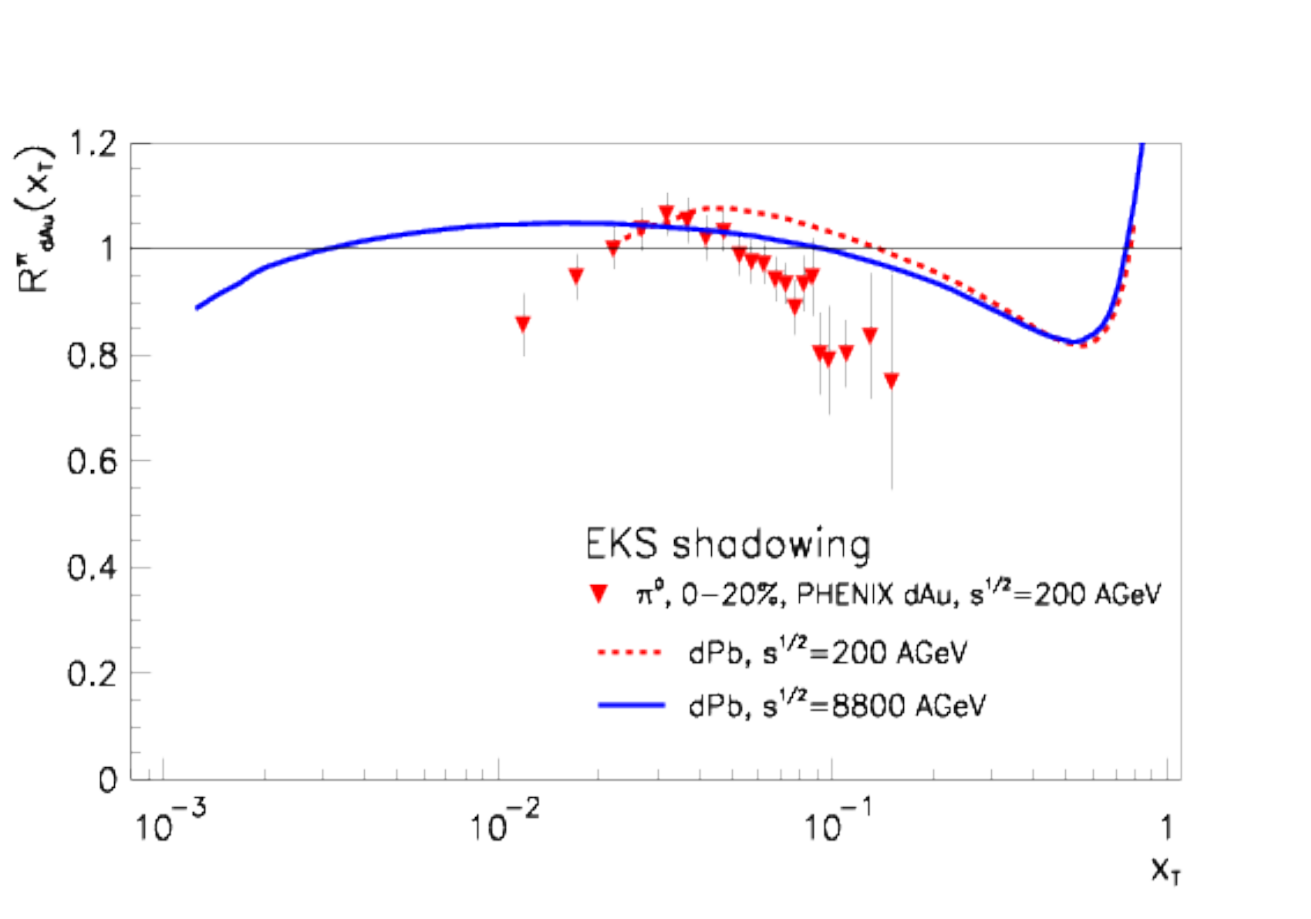

GGB, G. Fai, P. Lévai, BA Cole, G. Papp, Indian J.Phys. 84 (2010) 1721-1725

Midrapidity $R_{dA}(x_T)$ for $|\eta| < 0.35$

Pion production with EPS shadowing kTpQCD @ 0.2 & 8.8 ATeV

EPS Shadowing

x-scaling

DGLAP evolution

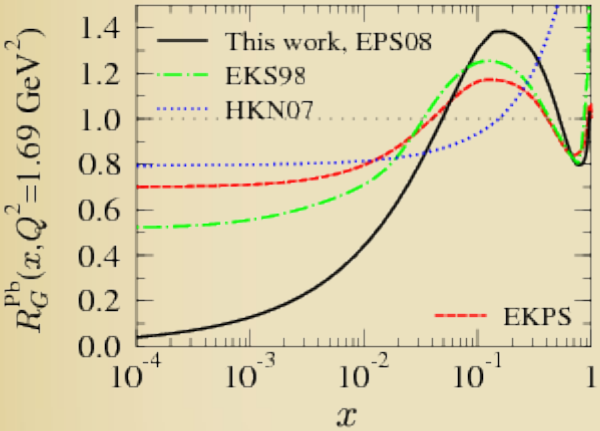

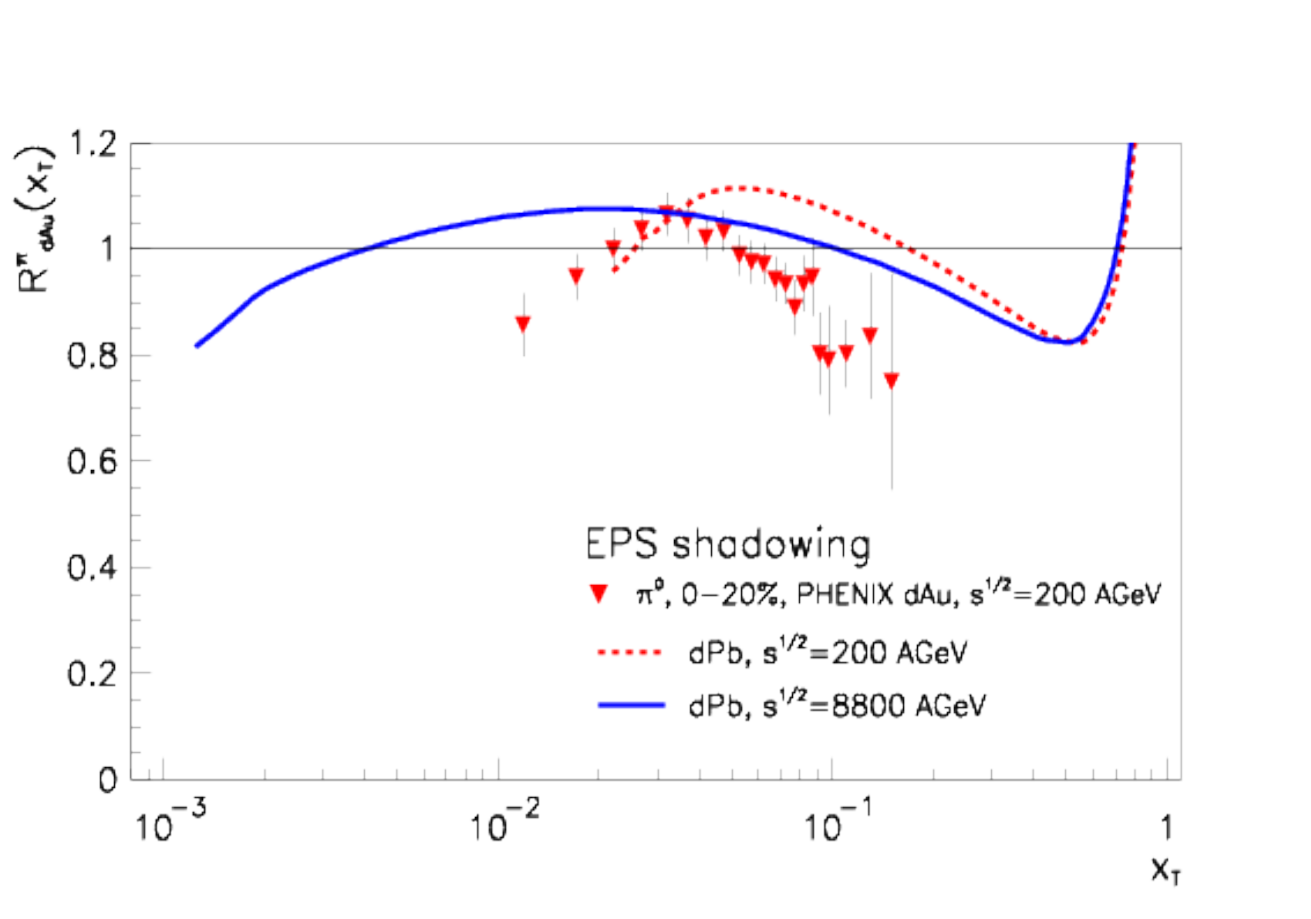

GGB, G. Fai, P. Lévai, BA Cole, G. Papp, Indian J.Phys. 84 (2010) 1721-1725

Midrapidity $R_{dA}(x_T)$ for $|\eta| < 0.35$

Pion production with HKN shadowing kTpQCD @ 0.2 & 8.8 ATeV

HKN Shadowing

x-scaling

DGLAP evolution

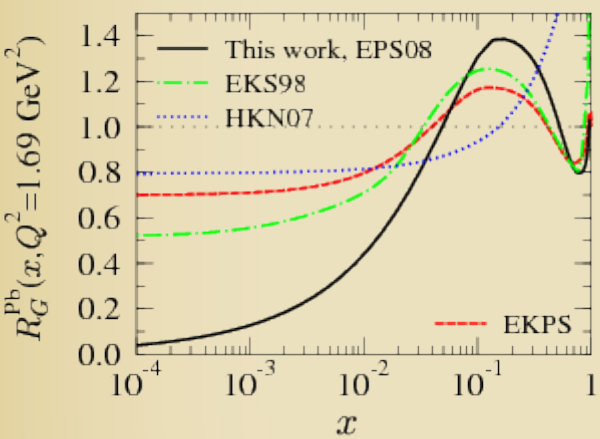

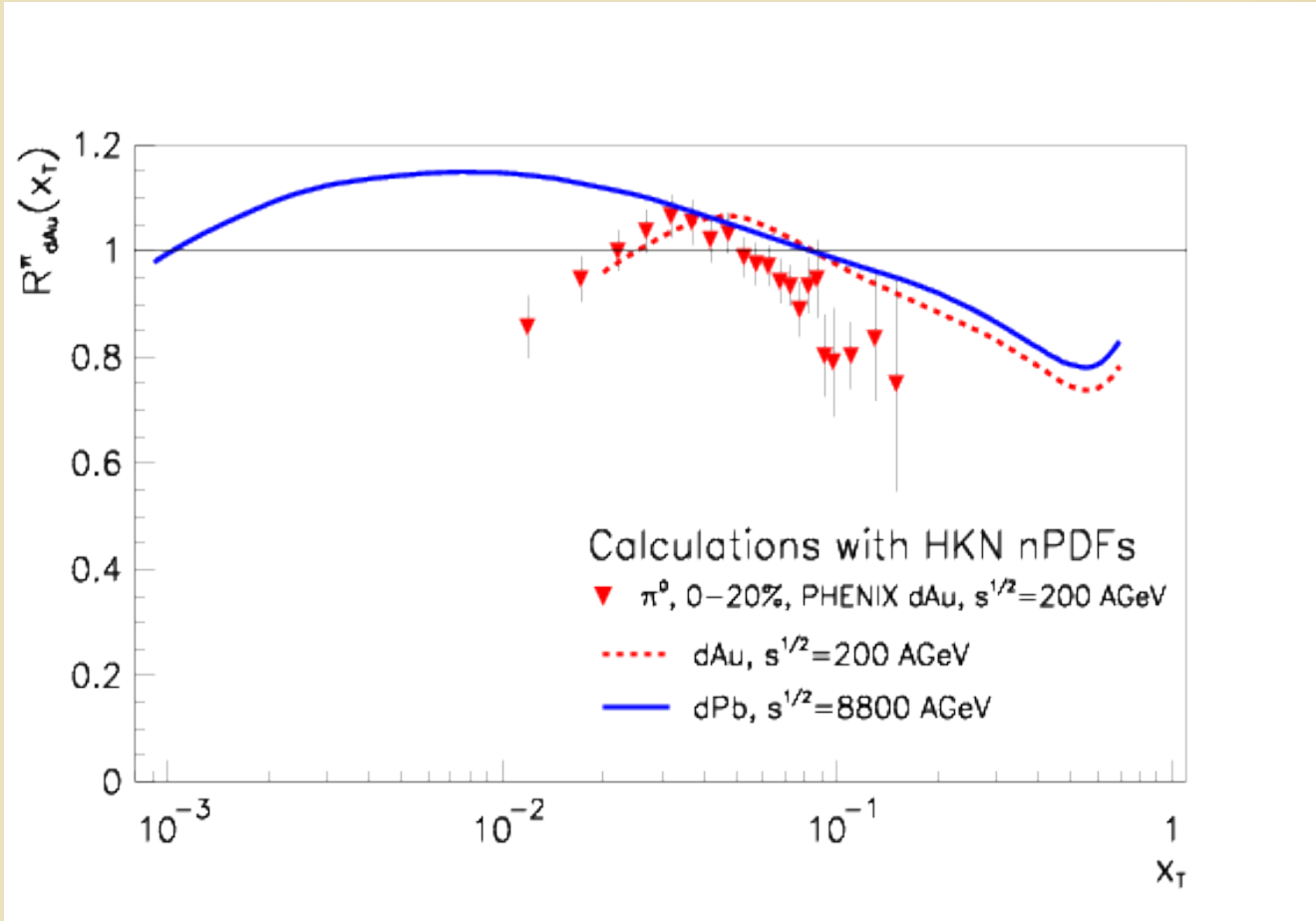

BA Cole, GGB, G. Fai, P. Lévai, G. Papp, arXiv:08073384 (2007)

The Nuclear Modification Factor, R_{pA}

- Measuring nuclear effects 'precisely'

  ratio of the hadron spectra

$$R_{dAu} \equiv \frac{1}{\langle N_{coll} \rangle} \frac{d^2N^{d+Au}/dp_T d\eta}{d^2N^{p+p}_{inel}/dp_T d\eta}.$$

$$R_{AA}(p_T) = \frac{d^2N^{AA}_{ch}/dp_T d\eta}{\langle T_{AA} \rangle \, d^2\sigma^{NN}_{ch}/dp_T d\eta}$$

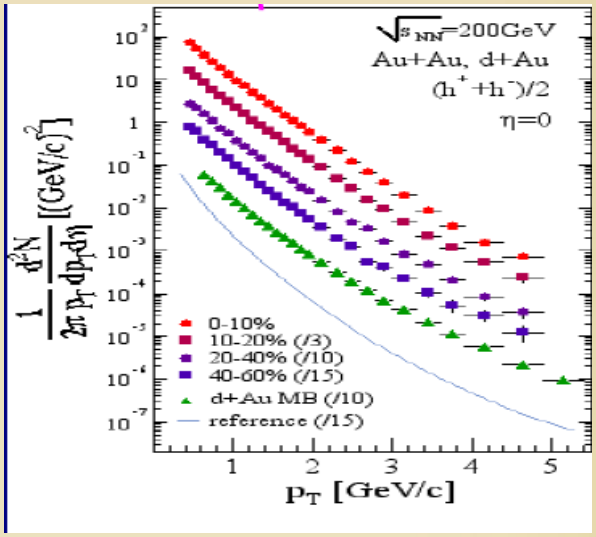

- Collisions:

  proton-nucleus (pA) or nucleus-nucleus (AA, AA')

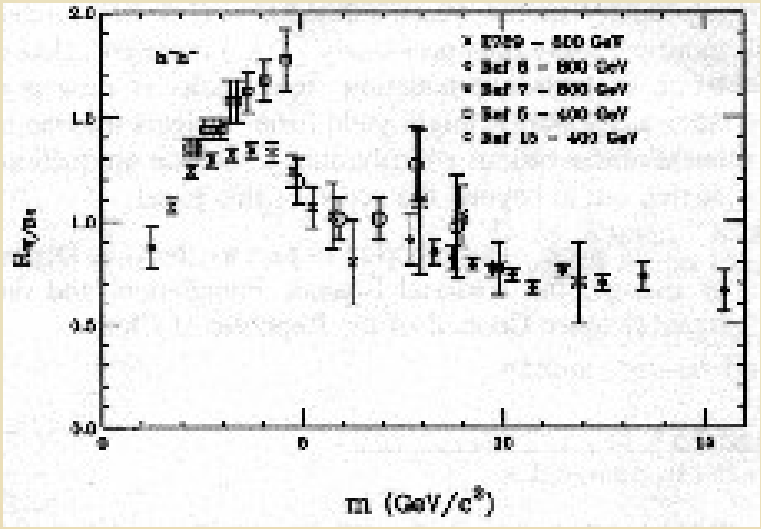

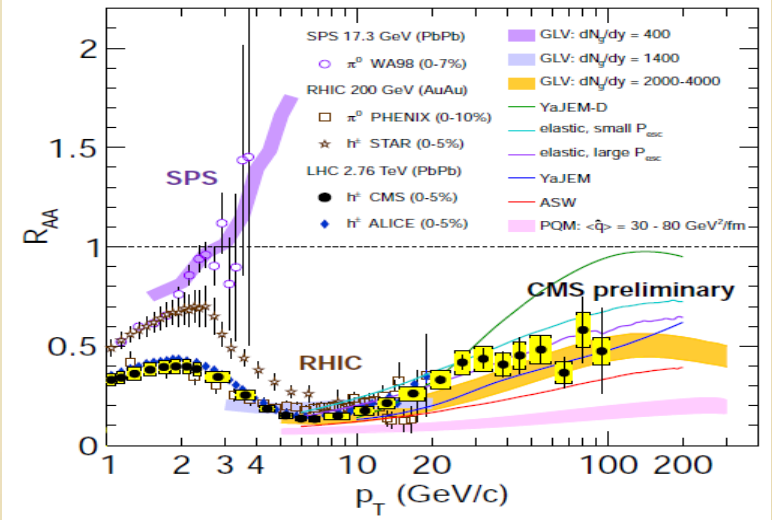

Midrapidity $R_{dA}(p_T)$ fot LHC – Summary

Extreme high-p_T Pion production kTpQCD @ 0.2, 0.9, & 8.8 ATeV

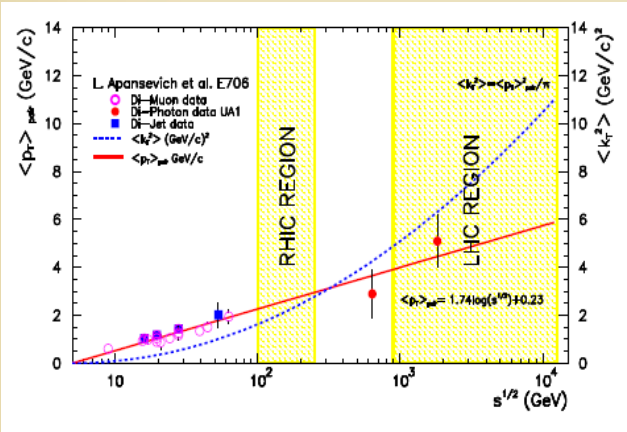

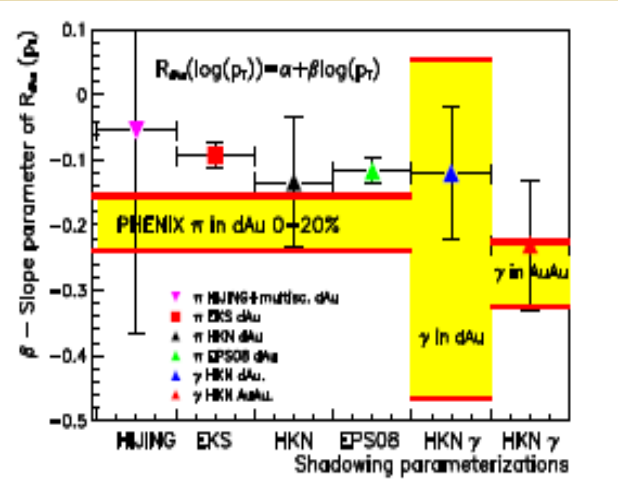

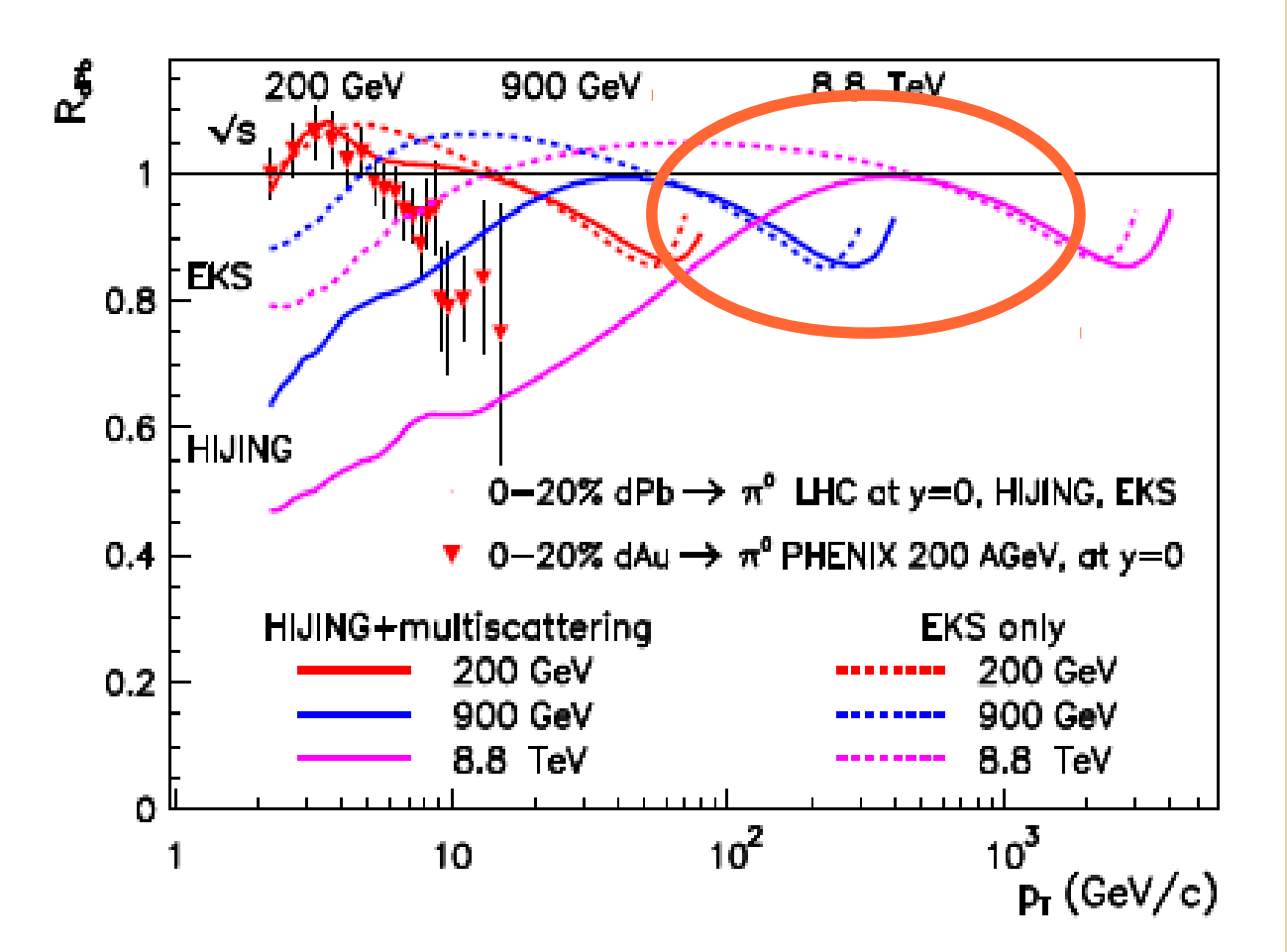

BA Cole, GGB, G. Fai, P. Lévai, G. Papp, arXiv:08073384 (2007)

M O T I V A T I O N

- Motivation for *pPb/dAu* collisions

Preliminary dAu data from PHENIX@QM12 (B. Sahlmueller)

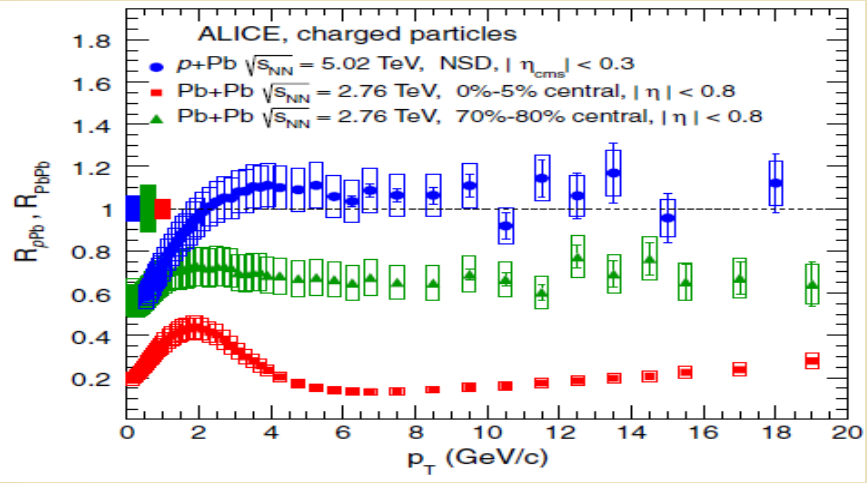

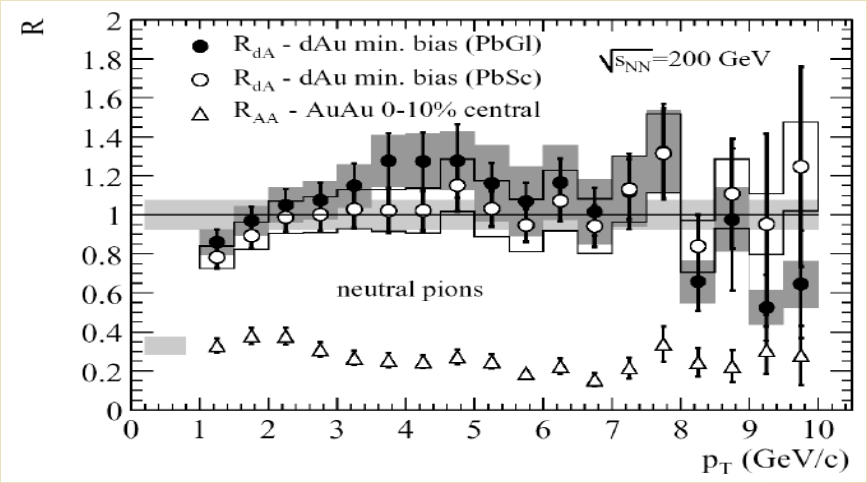

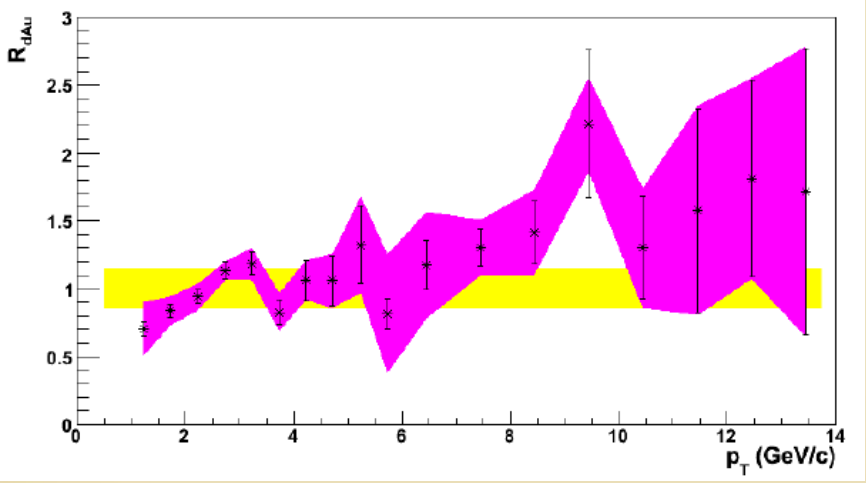

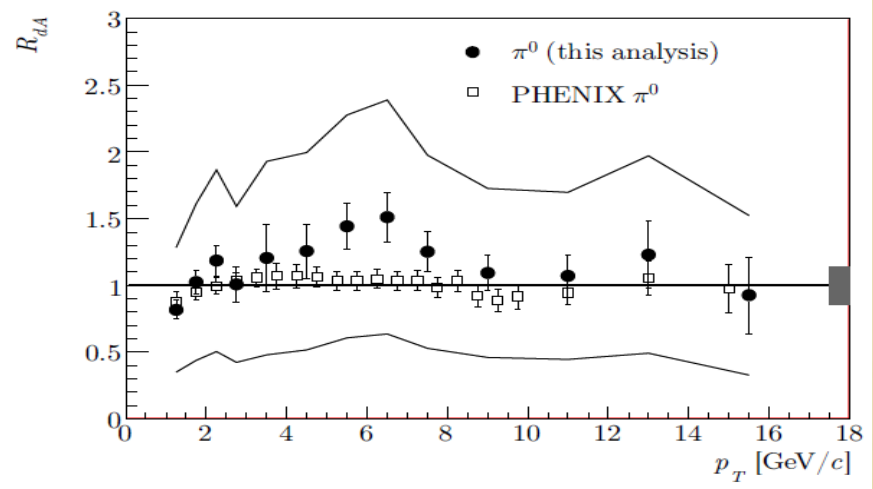

HIJINGB/B 2.0: Rapidity distribution for pp & pPb

Charged hadron production with HIJING 2.0 @ 5.02 ATeV MinBias

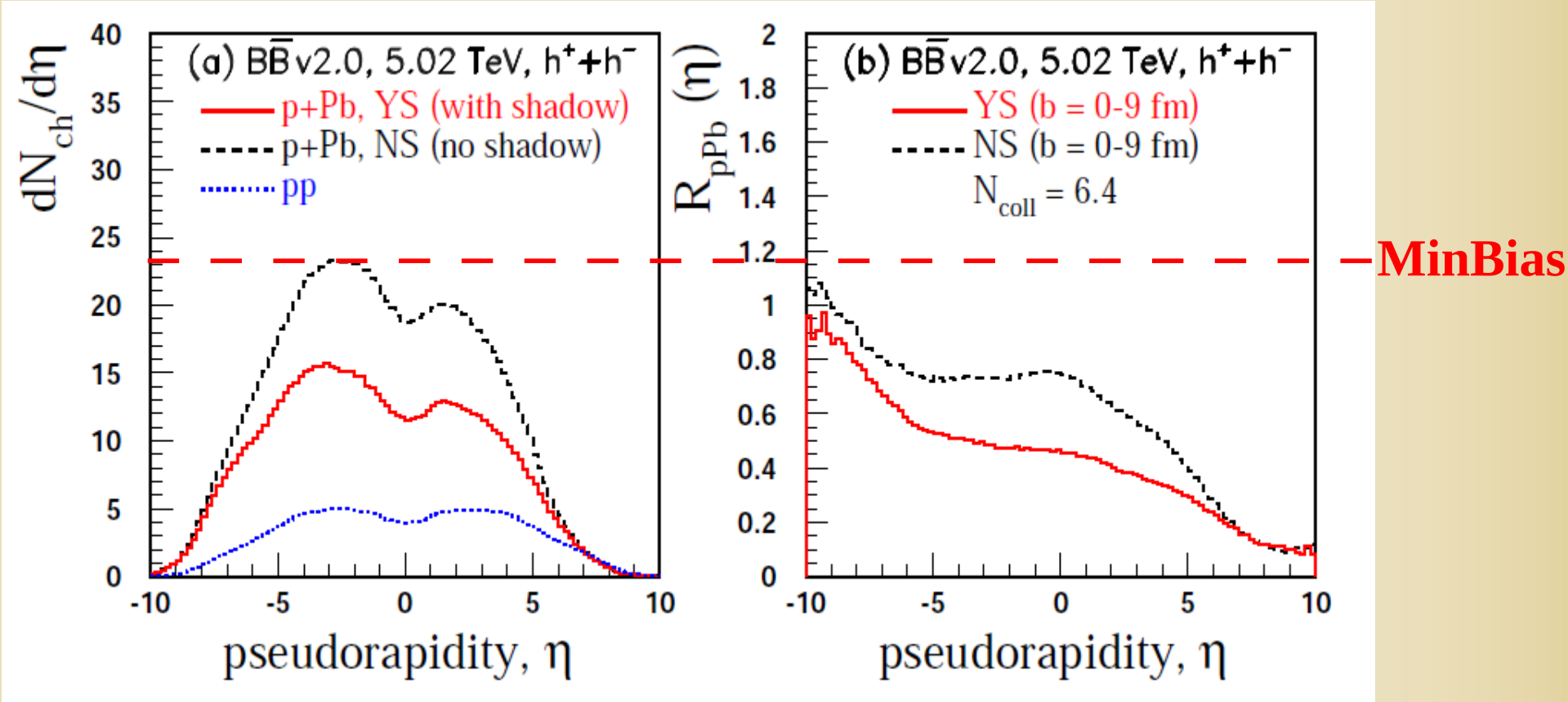

GGB, J. Barret, M. Gyulassy, P. Lévai, V. Topor Pop (in preparation 2012)

The Collection of pA/dAu Data

CP [23, 24]	p	d, Be, Ti, W	$19,4;\ 23,7;\ 27,4$	≈ 0	$[0,77; 6,91]$	$\pi^{\pm}, K^{\pm}, p^{\pm}, d^{\pm}$
ITA [115]	p	C, W	$p_{inc} = 50 - 275$	$[0,7; 1,0]$	$[0,2; 2,35]$	$\pi^{\pm}, K^{\pm}, p^{\pm}$
FNAL [119]	n	Be, Al, C, Sn, Pb	$27,4$	$[4,0; 8,0]$	$[0,1; 1,7]$	$h^{\pm}, \pi^{+}, p$
FNAL [116]	p	Be, W	$19,4;\ 23,7;\ 27,4$	≈ 0	$[0,2; 4,5]$	$\pi^{\pm}, K^{\pm}, p^{\pm}, h^{\pm}$
CP [118]	π^{-}	p, Be, Cu, W	$19,4;\ 23,7$	≈ 0	$[0,8; 5,78]$	$\pi^{\pm}, K^{\pm}, p^{\pm}$
E577/E672 [117]	p	p, Be, C, Al, Cu, Pb	$38,8$	$[-0,75; 0,75]$	$[0,6; 11,5]$	$h^{\pm}$
E605/E789 [114]	p	Be, W	$38,8$	≈ 0	$[0,5; 11,5]$	$h^{\pm}$
E605 [69, 70]	p	d, Be, W	$38,8$	≈ 0	$[0,5; 11,0]$	$\pi^{\pm}, K^{\pm}, p^{\pm}$
E706 [59]	p	Be	$31,6;\ 38,8$	$[-0,75; 0,75]$	$[1,0; 12,0]$	π^{0}, η
E706 [113]	p, π^{-}	Be, Cu	$30,7$	$[-0,7; 0,7]$	$[3,5; 10,0]$	π^{0}, γ
WA80 [144]	S	S, Au	$19,4$	$[2,1; 2,9]$	$[0,3; 3,9]$	π^{0}, γ
WA98 [140]	Pb	Pb, Nb	$17,3$	$[2,3; 4,4]$	$[0,3; 3,7]$	π^{0}, γ
CERES [126]	Pb	Au	$17,3$	$[2,1; 2,6]$	$[1,5; 3,3]$	$\pi^{\pm}$
PHENIX [122, 123]	p, Au	p, d, Au	$130, 200$	$\lvert\eta\rvert \leq 0,35; 2,0$	$[0,5; 10,0]$	$\pi^{0}, h^{\pm}, \gamma$
BRAHMS [127, 128]	p, Au	p, d, Au	$130, 200$	$0,0;\ 1,0;\ 2,2;\ 3,2$	$[0,5; 6,0]$	$\pi^{0}, h^{\pm}$
STAR [129, 130]	p, Au	p, d, Au	$130, 200$	$\lvert\eta\rvert \leq 0,5; 2,0$	$[0,2; 5,5]$	$\pi^{0}, h^{\pm}, \Lambda, K, \gamma$
PHOBOS [132, 133]	p, Au	p, d, Au	$62,4;\ 130;\ 200$	$0,4;\ 0,8;\ 1,2$	$[0,5; 3,5]$	$K^{\pm}, p^{\pm}\pi^{0}, h^{\pm}$

Raa and High pT azimuthal anisotropy

(in light of recent p+A and D+A (un)Control)

Mklz Gyulassy, alias Barbara Betz

High pT nuclear modification of jets in and out of reaction plane at RHIC and LHC
B.Betz, MG, in preparation

Examining a reduced jet-medium coupling in Pb+Pb collisions at the LHC,
B.Betz, MG PRC86 (2012)

Fourier Harmonics of High-pT Particles Probing the Fluctuating Intitial Condition Geometries in Heavy-Ion Collisions, B.Betz, MG, G.Torrieri, PRC84 (2011)

Part 1: Jet Quenching prior to 2012

Part 2: D+Au and p+Pb Shock Waves QM12 and RBRC13

Part 3: Azimuthal Tomography (ignoring part 2)

High-p_T Tomography of d + Au and Au + Au at SPS, RHIC, and LHC

Ivan Vitev[1,2] and Miklos Gyulassy[1]

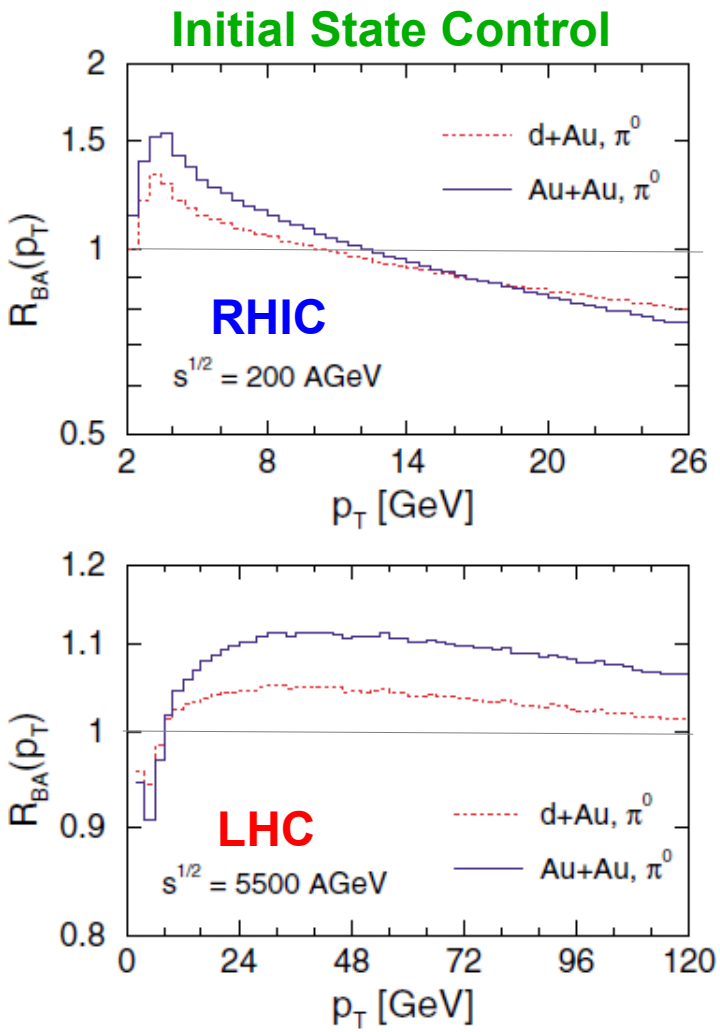

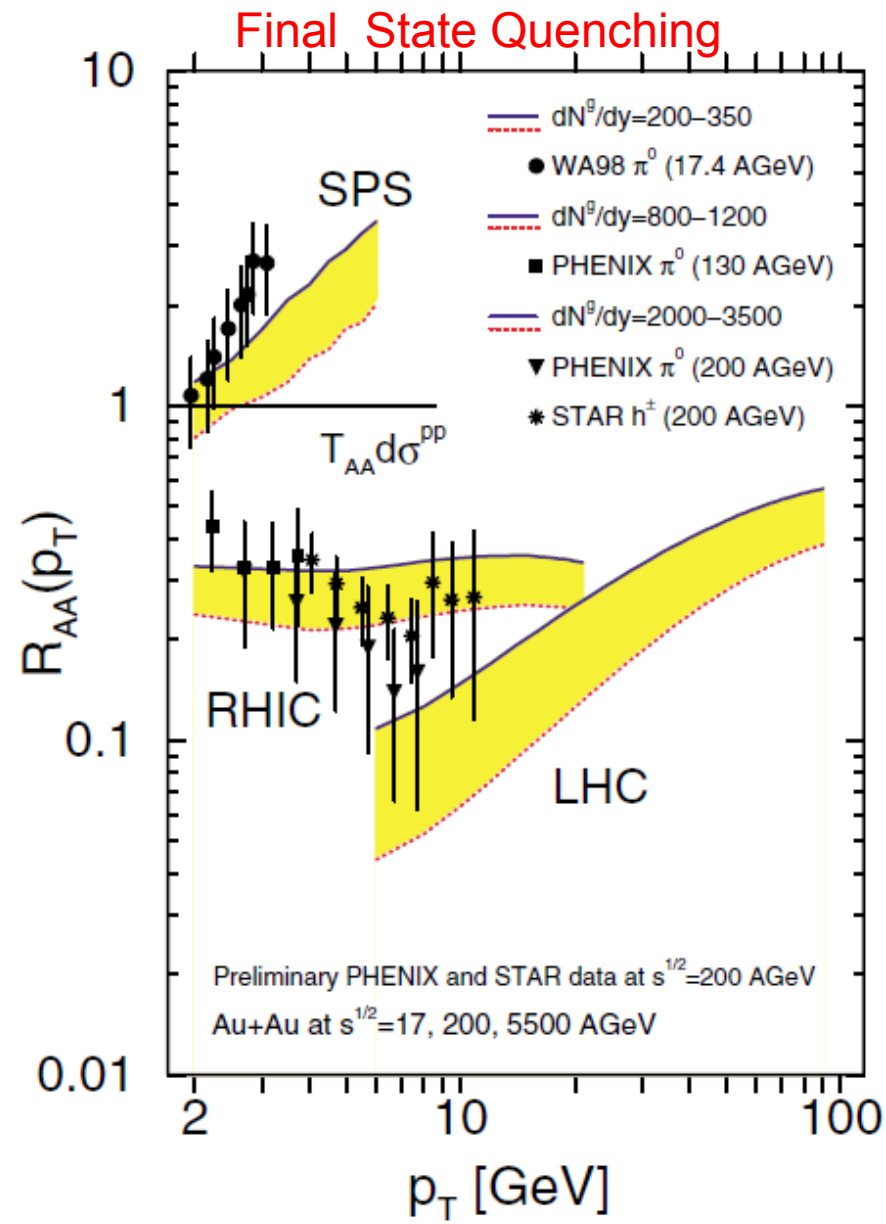

FIG. 2 (color online). The nuclear modification $R_{BA}(p_T)$ due to Cronin effect and shadowing (but not energy loss) for π^0 in d + Au ($B = d, A$ = Au) and central Au + Au ($B = A$ = Au) reactions at $\sqrt{s_{NN}}$ = 17, 200, and 5500 GeV.

M

In the beginning…

Gabor David RBRC13

STAR, PRL 91 (2003) 072304

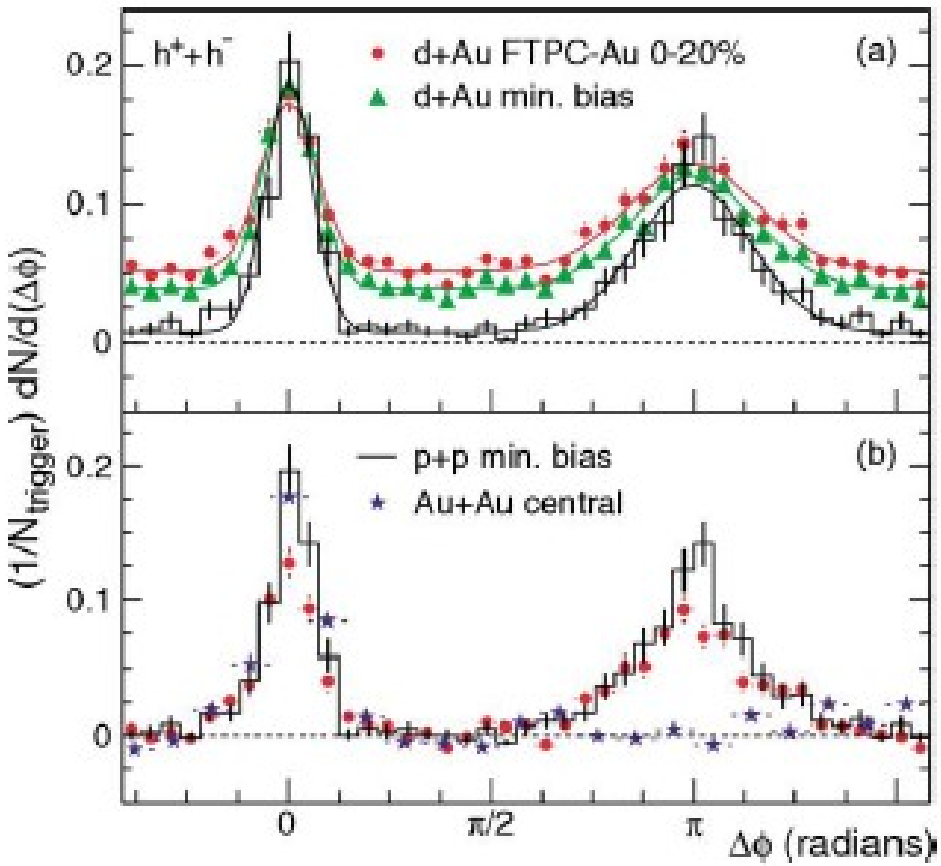

PHENIX, PRL 91 (2003) 072303

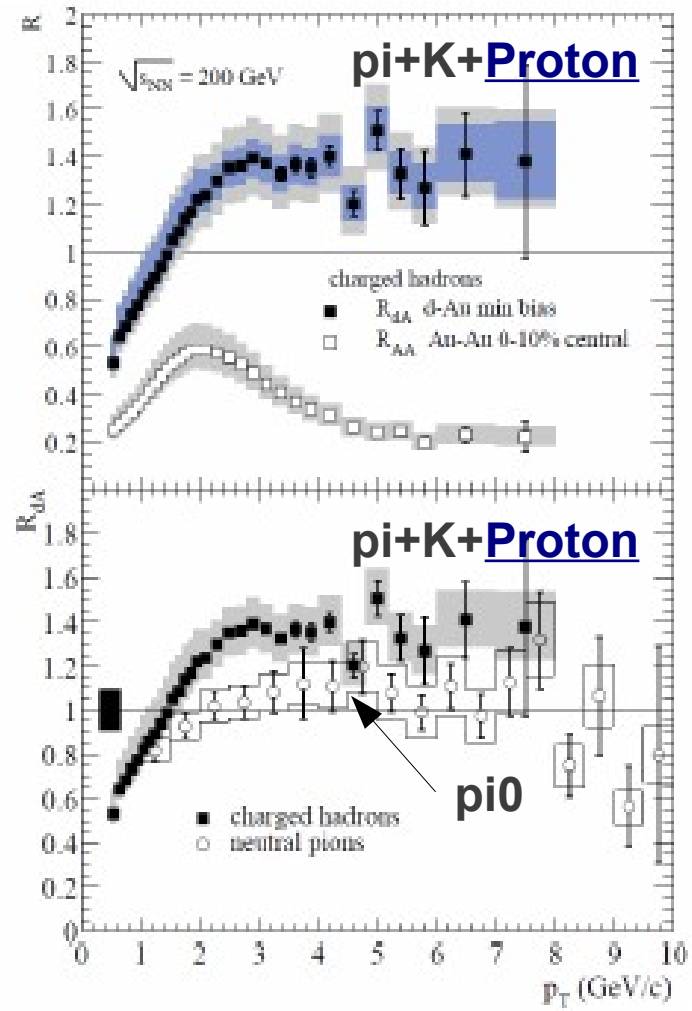

STAR: back-to-back jets reappear in d+Au
PHENIX: large suppression in Au+Au,
no suppression in d+Au
→ ***final state effect (as of 2003)***

Null-Control D+Au → Direct Photon N_{coll} scaling works!

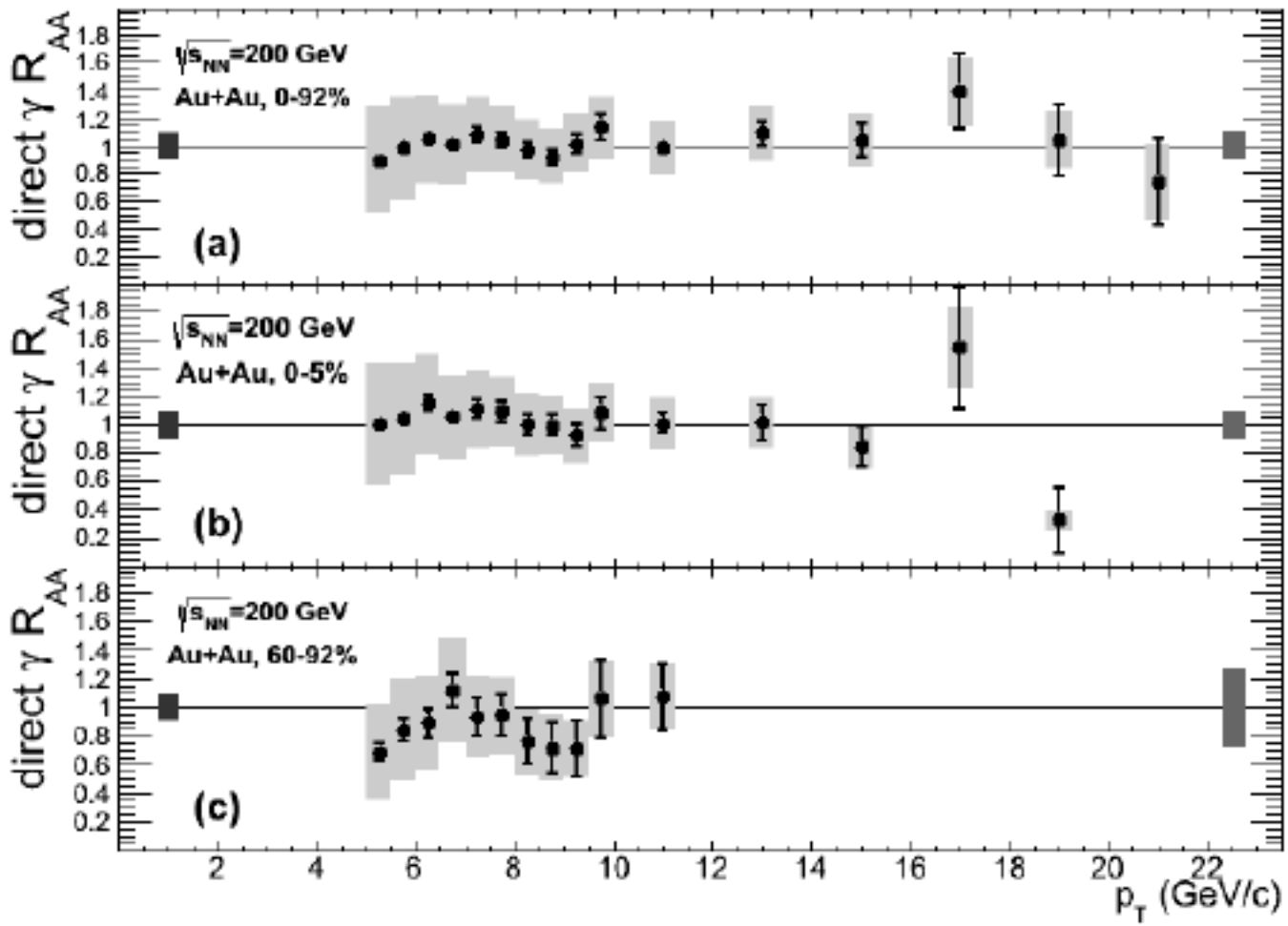

PHENIX, PRL 109, 152302 (2012)

High-p_T Tomography of d + Au and Au + Au at SPS, RHIC, and LHC

Ivan Vitev[1,2] and Miklos Gyulassy[1]

ALICE 2012 pPb 1210.4520v1
Initial State modifications in min bias are small ~10% at y=0 even at 5 ATeV

Predicted Cronin+ EKS98
R(pPb LHC) ~ 1.05

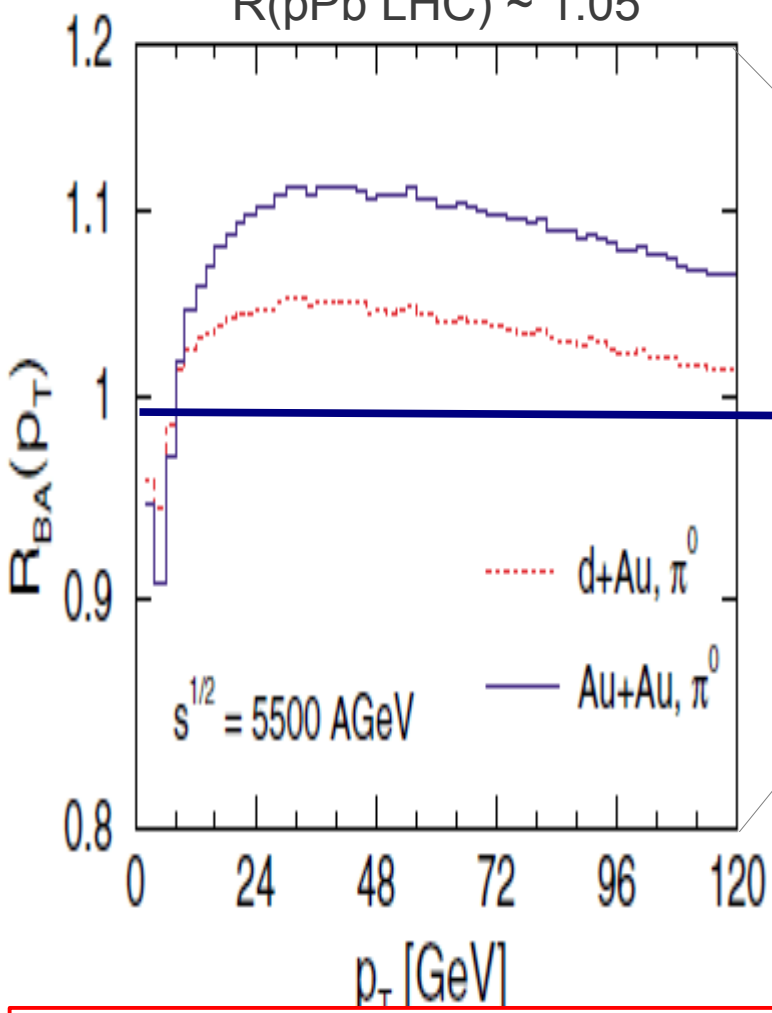

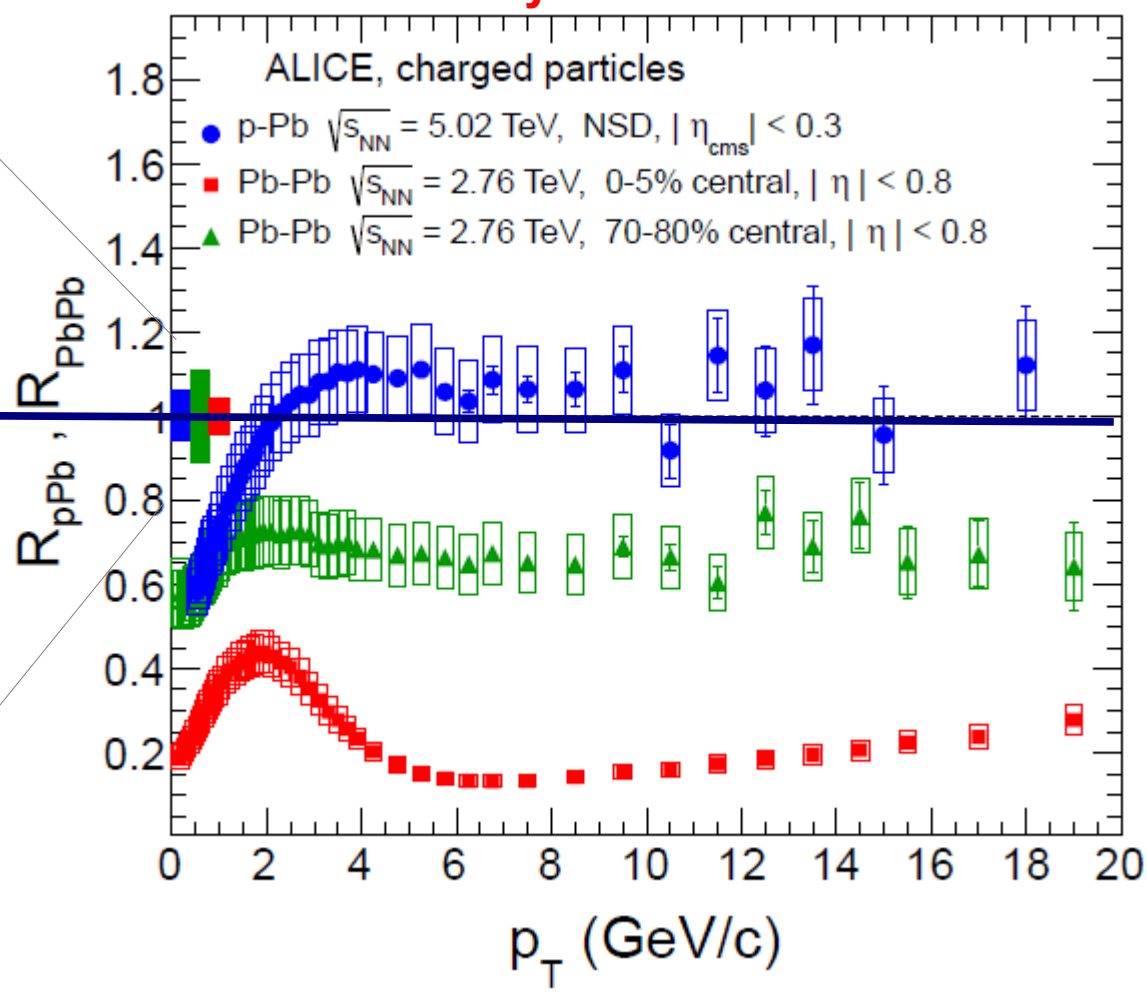

We can safely calculate RPbPb(y=0, pT>4, LHC) *neglecting* initial state interactions

W.Busza, RBRC 4/15/2004

N_{part} scaling for asymmetric collisions:

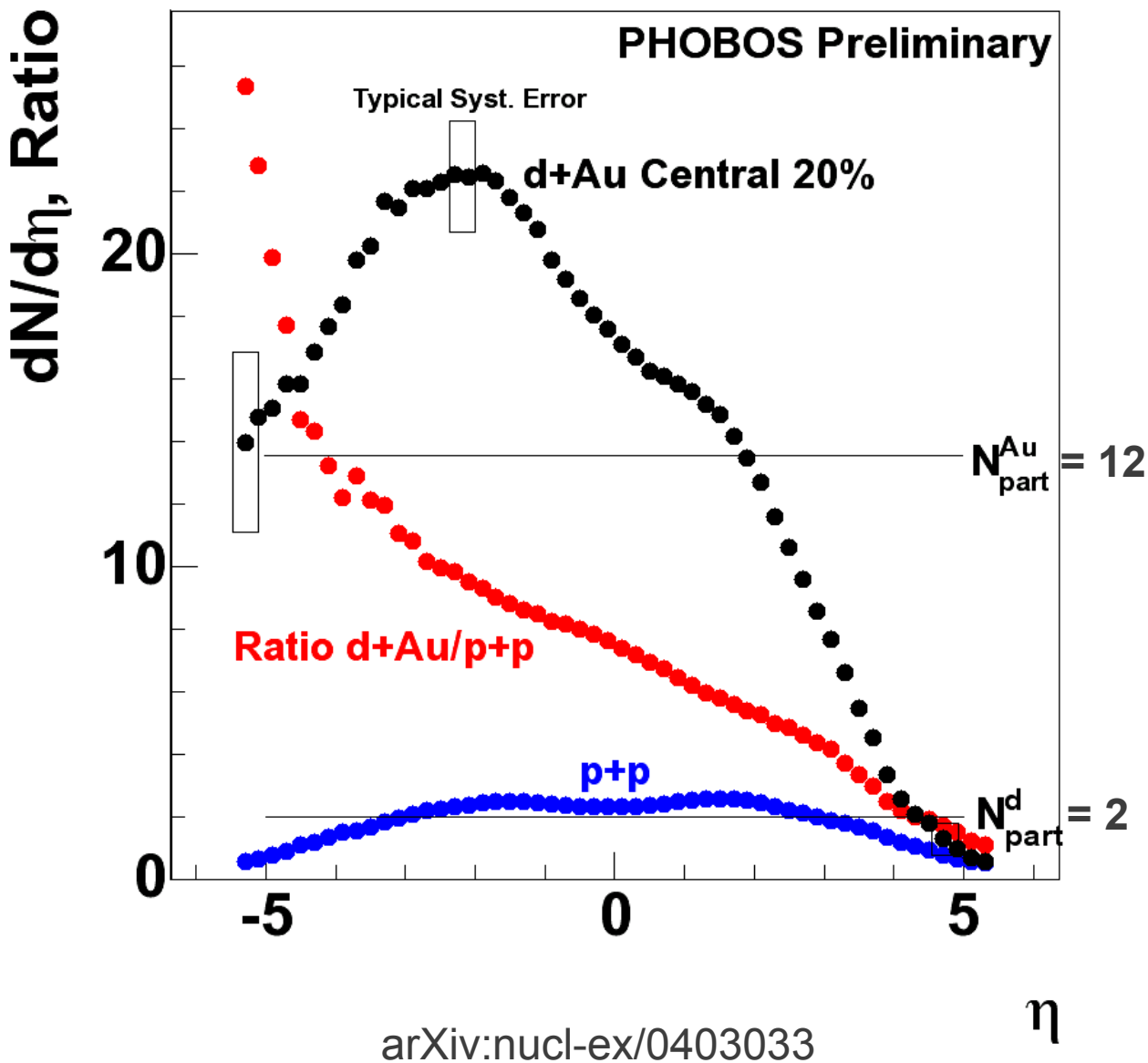

arXiv:nucl-ex/0403033

Busza p+A/p+p dNdy Triangle well described at RHIC via HIJING

- Lund model ***beam jet*** flux tubes (as encoded in HIJING) account well for RHIC data and reproduced the basic BGK77 triangle form of the ratio p+A/p+p, as well as the absolute magnitudes dNch/deta

- Except in target frag region y< -3 where FSI enhance nch yields

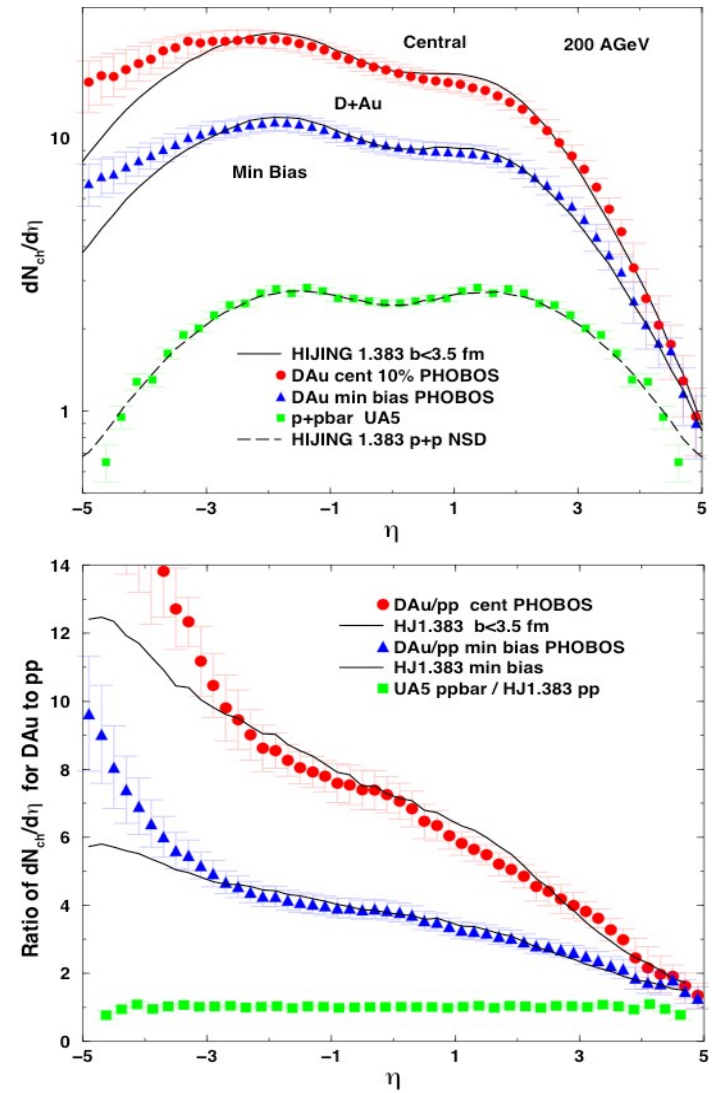

A.Adil, MG, PRC 72 (2005) 034907

In 2003 Three Lines of Data Seemed to Converged to QGP at RHIC

Null Control

Three Legs Stable even if unequal

Bulk P_{QCD}

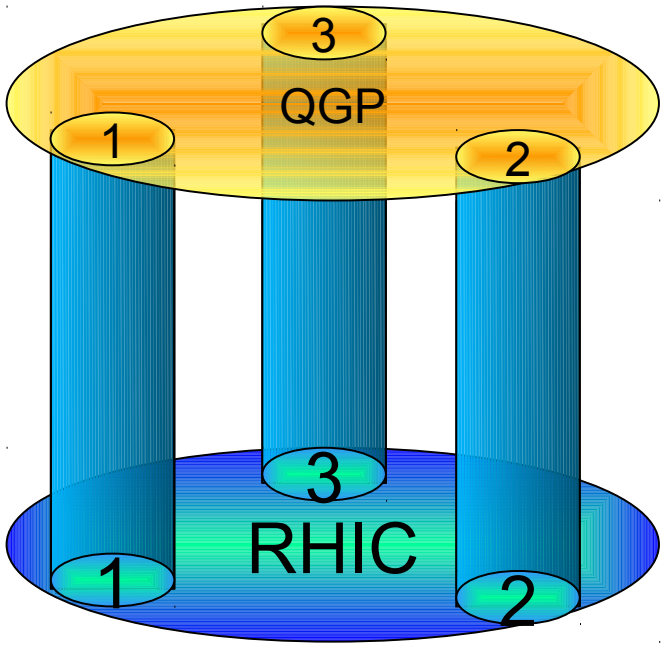

Parton pQCD

1. Bulk P_{QCD} Collective Elliptic Flow v2 √
2. Parton pQCD Jet Quenching RAA √
3. p+p Calibration and d+A Null Control √ √

$$\mathbf{QGP = P_{QCD} + pQCD + dA = v_2 + (R_{AA} + I_{AA}) + R_{dA}}$$

(MG,Nato School, Kemer, Turkey 5/23/03)

Part 1: Jet Quenching prior to 2012

Part 2: D+Au and p+Pb Shock Waves QM12 and RBRC13

Part 3: Azimuthal Tomography (ignoring part 2)

My Summary of QM12

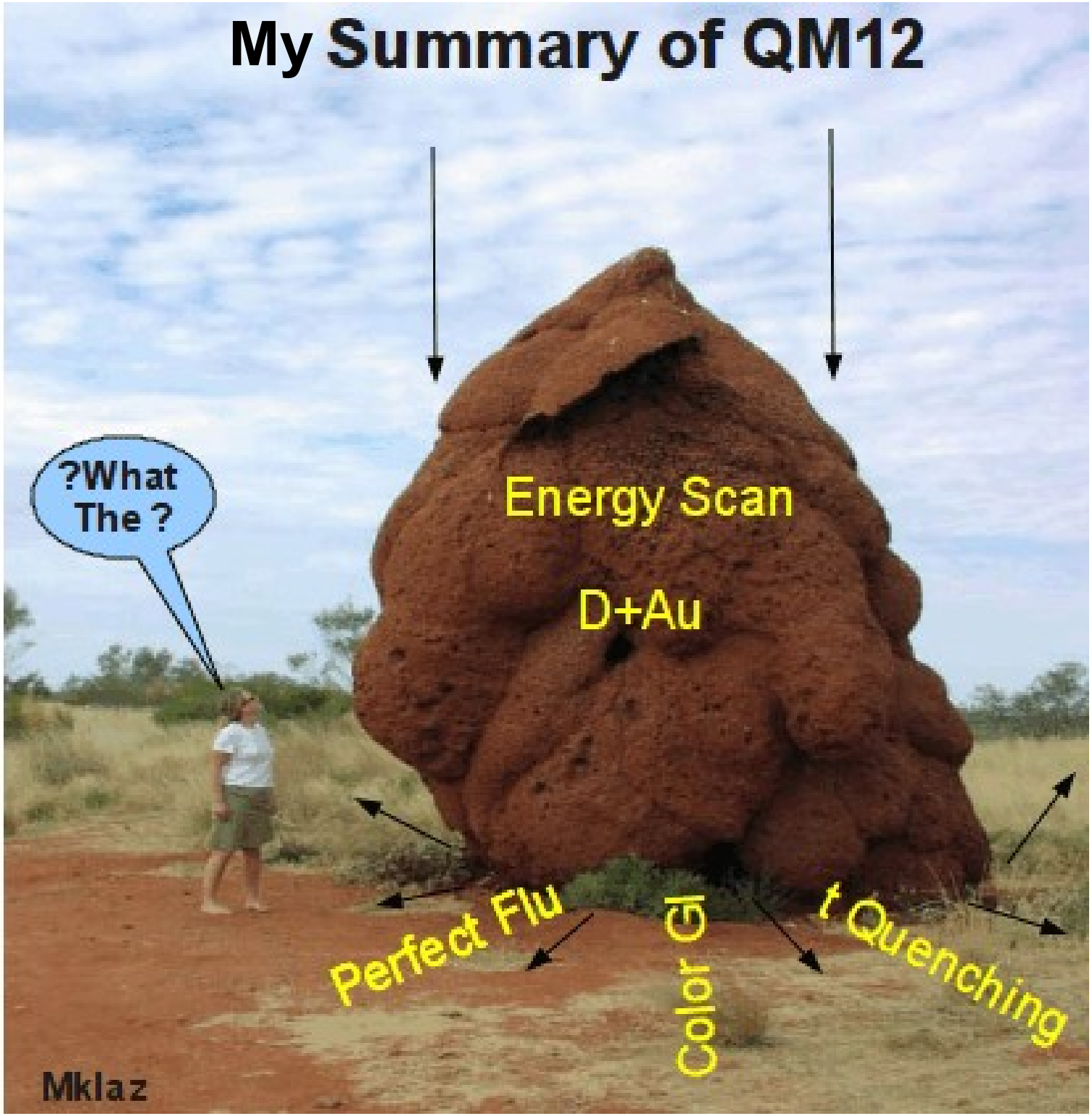

In

QM12 PHENIX story: (same as STAR BES story)

Ecm dependence of vn{Ψn} for charged hadrons

R.Pack, 2012 RHIC & AGS Annual Users' Meeting

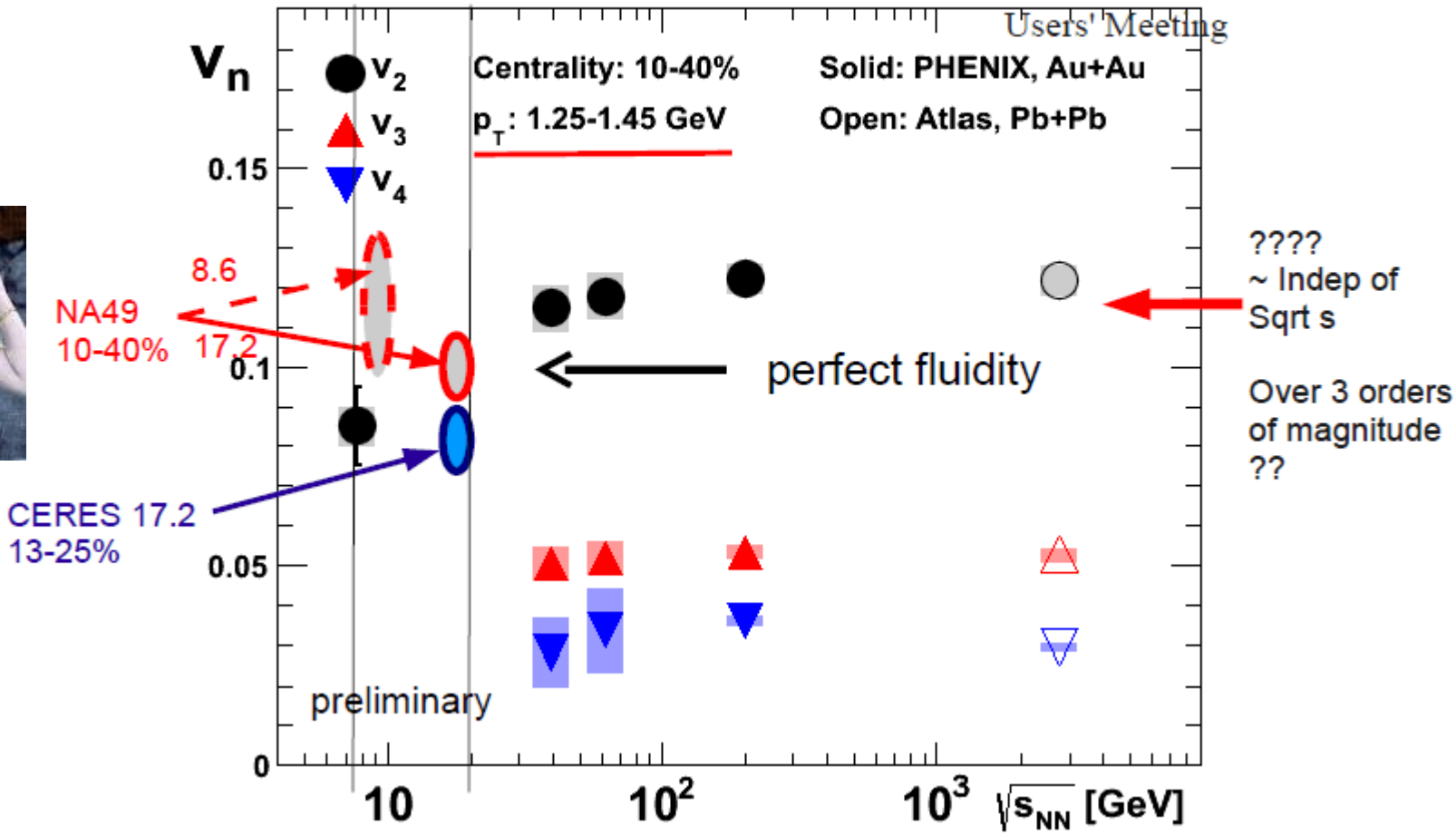

The (Bevalac, AGS, SPS, RHIC 200) Perfect Fluid QGP Core + Lousy HRG Corona Was Crushed: vn(pt) shows no sign of LOUSY HRG Corona down to AGS!!!

more

Now some results to lose sleep over

PHENIX preliminary, QM'12

2008 (high) statistics d+Au data, nuclear modification factors vs centrality

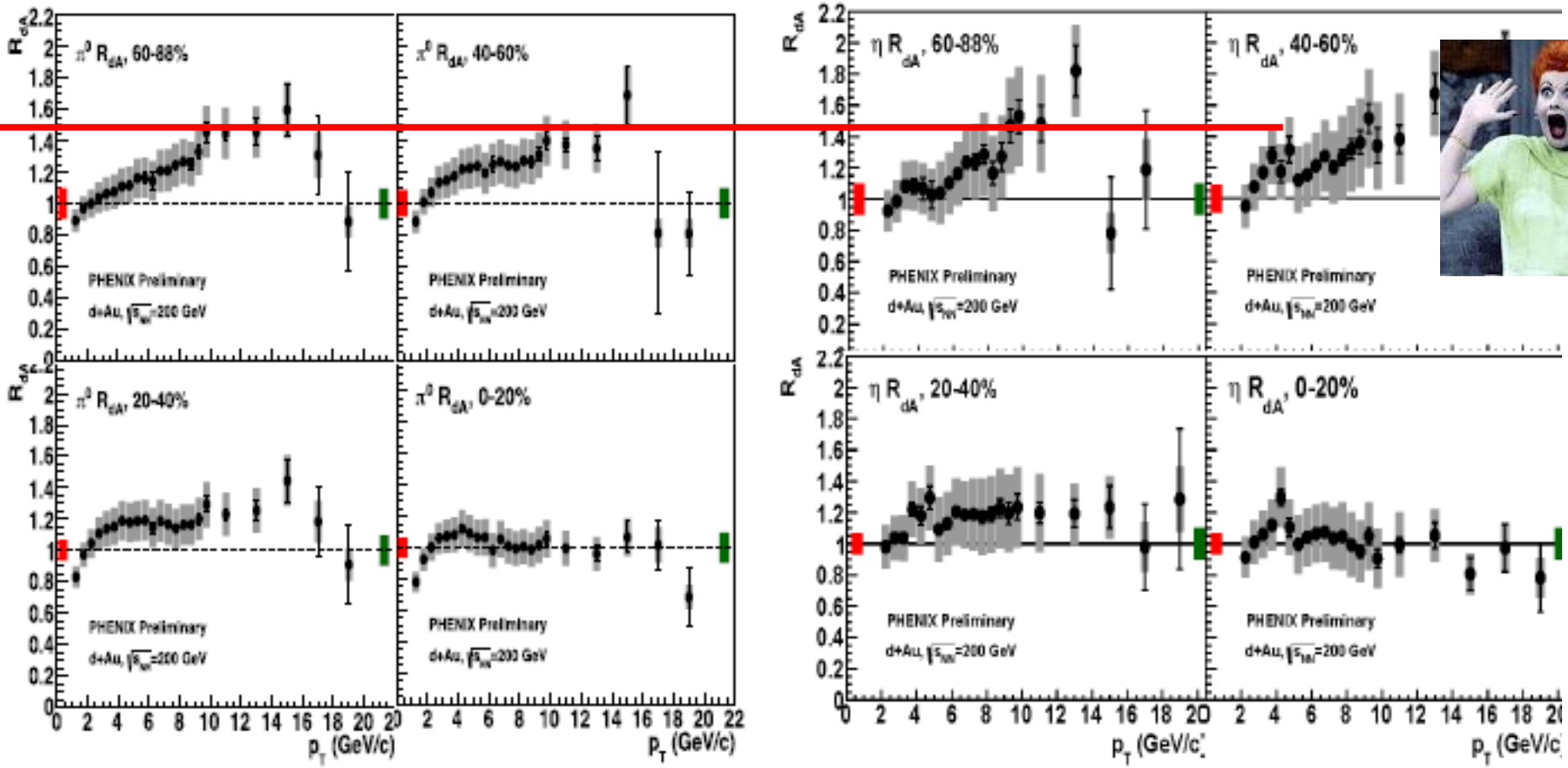

Is it possible that π_0, η production at high p_T in peripherals is enhanced???

v_3 in pPb and PbPb

RBRC13 CMS SHOCK waves from super central pPb @ LHC

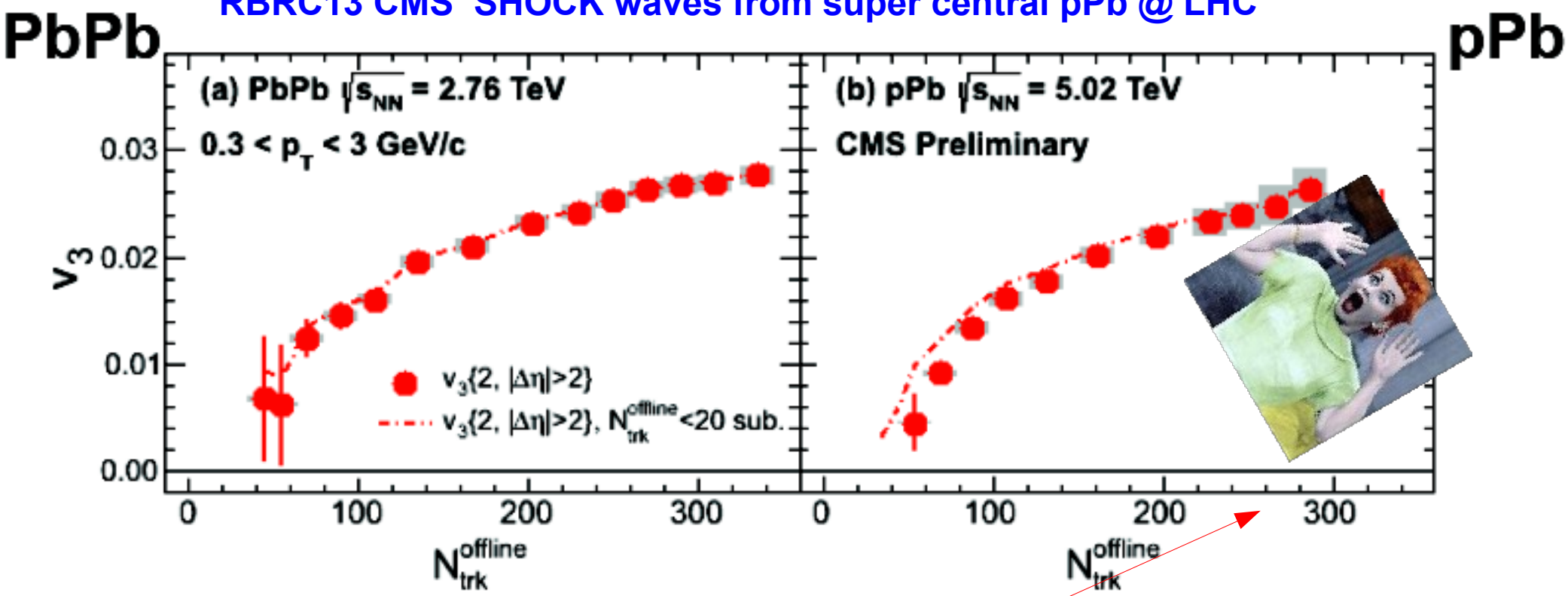

v_3 shows similar shape in pPb and PbPb; magnitude comparable

very rare events
1/ 1,000,000

v_3 in pPb and PbPb

PbPb

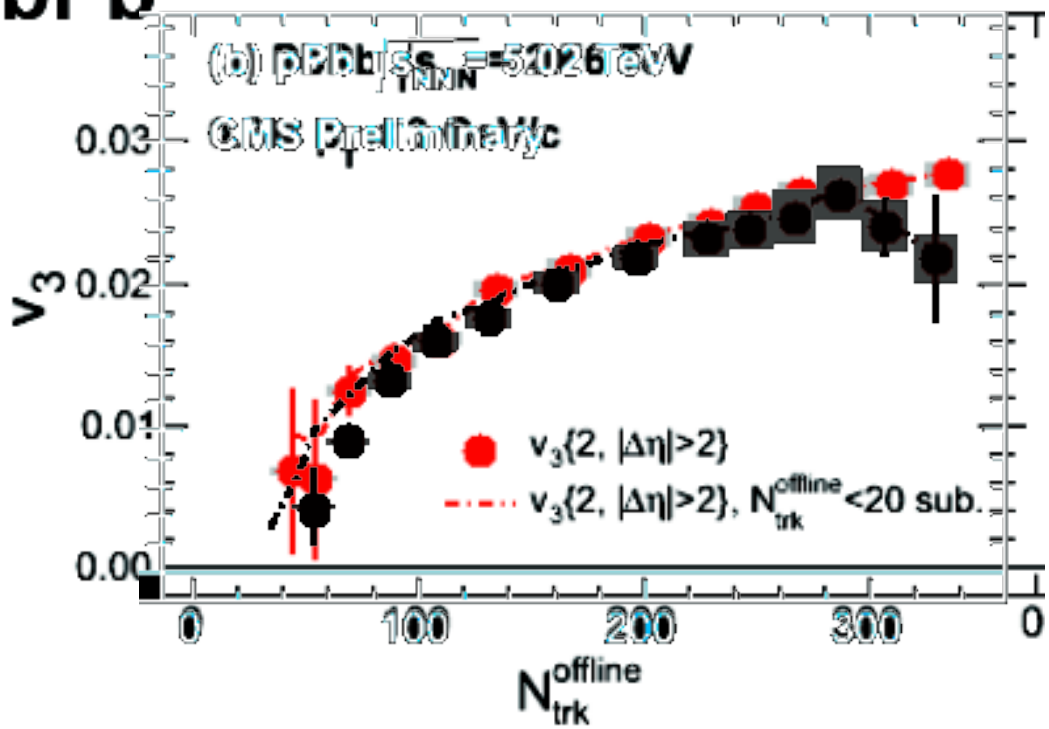

|eta|<2.4

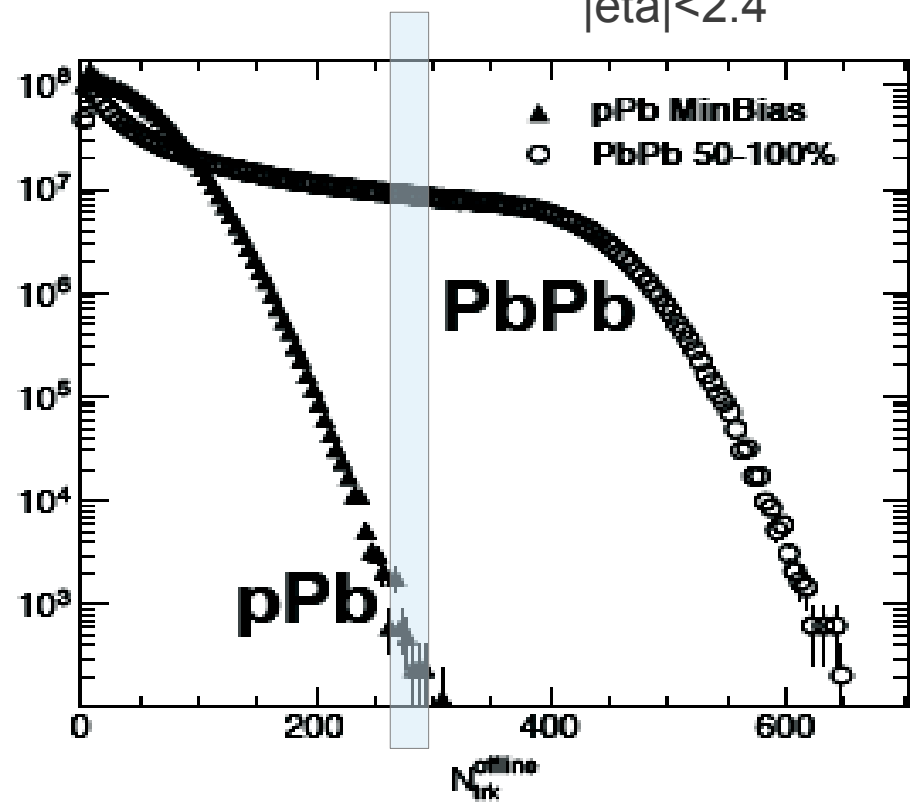

v_3 shows ~~similar~~ shape in pPb and PbPb; magnitude ~~comparable~~

same ***same***

Data seem to falsify "Apples ≠ Oranges" theorem

But dN/deta shapes could differ a lot
(Or it could be multi jetty)

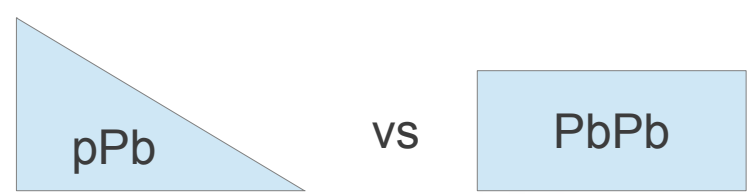

Recall old BGK p+A "Rapidity Triangle"

- Multiple independent wee parton dx/x collisions produce ~uniform in rapidity color charges between valence p and valence wounded A.
- Color neutralizes via pair production between wee and valence partons
-
- Leaving a stack in 10% of
- $A^{1/3}$ ~ 10 Target beam jets
- For rare Ntr~300 maybe 30 Pb nucleons line up
- There is 1 Projectile beam jet
-
- Y *Slope* δ = Ntr / log(s)
- RHIC δ ~ 2 x LHC δ

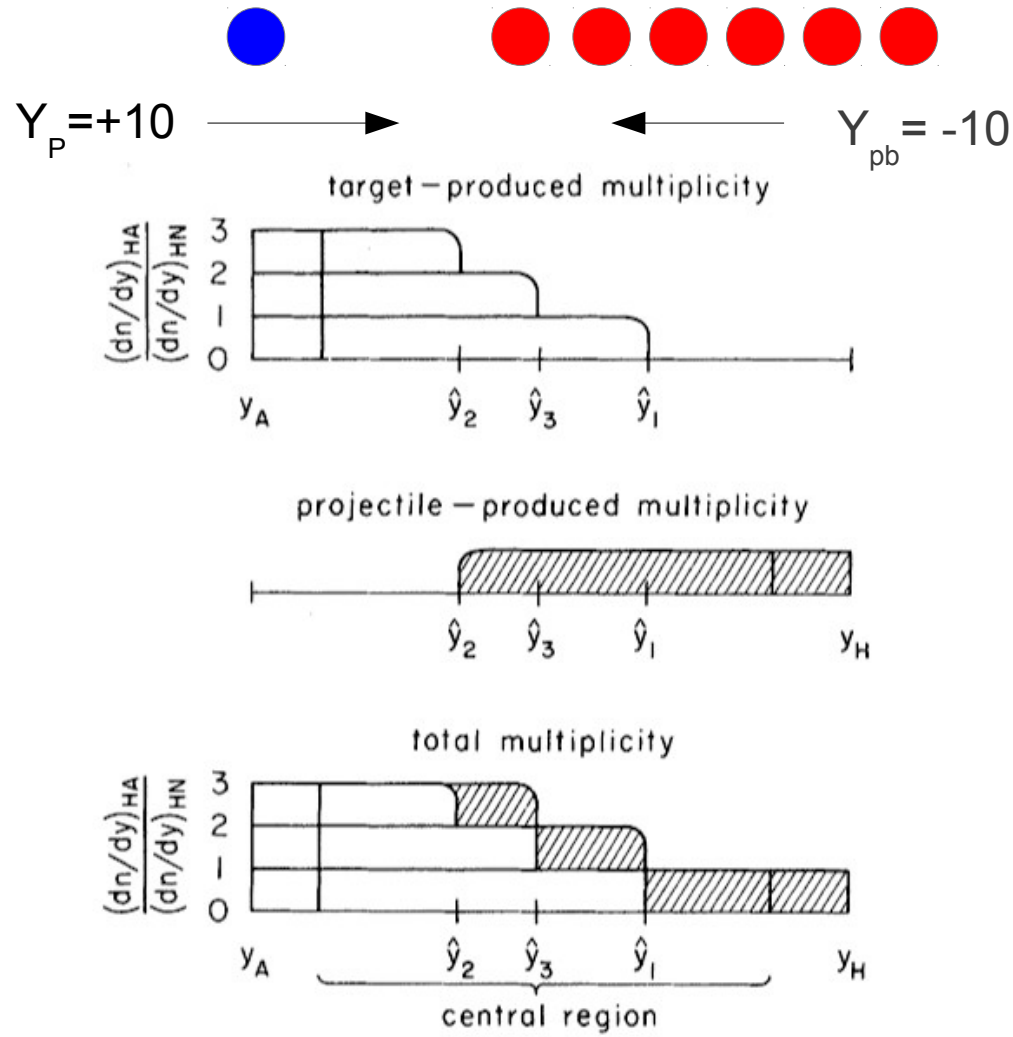

Figure from Brodsky, Gunion, Kuhn 1977

Can sQGP survive the RBRC 2013 D+Au and p+Pb tsunami?

<u>BES , D+Au and p+Pb uncalibrated our v2 Barometer of sQGP</u>
<u>D+Au (and ? soon p+Pb) uncalibrated our RAA opacity meter</u>

One or No Legged Tables are *Unstable!*

D+Au Broke P_{QCD} Flow?

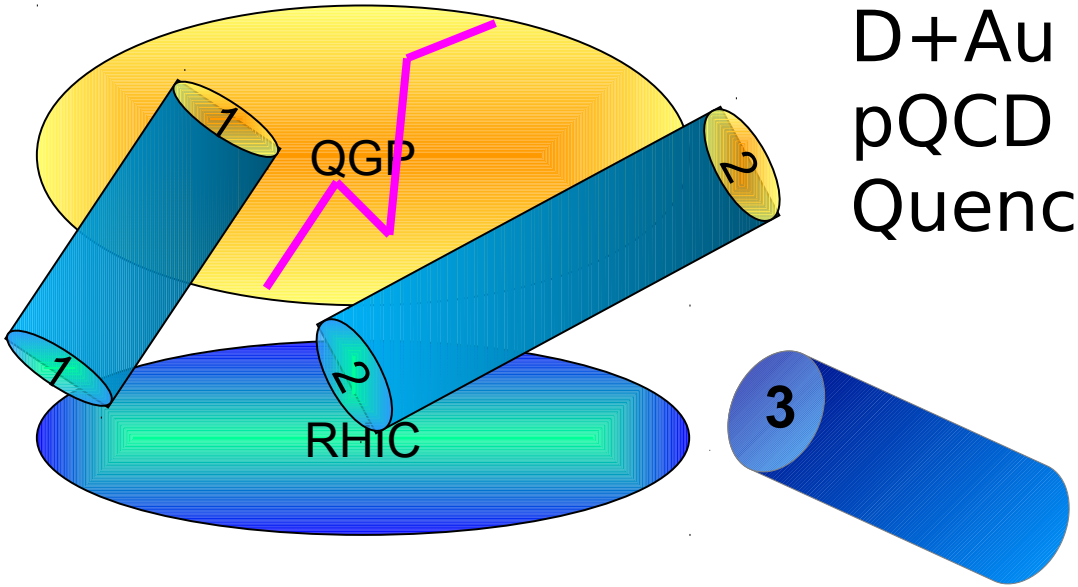

D+Au Broke pQCD Quenching?

R(DAu) ≠ 1 ??

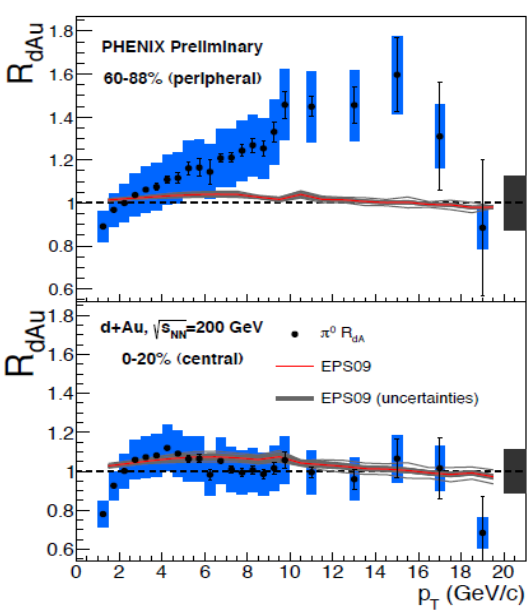

v2(DAu) = v2(AuAu) ??

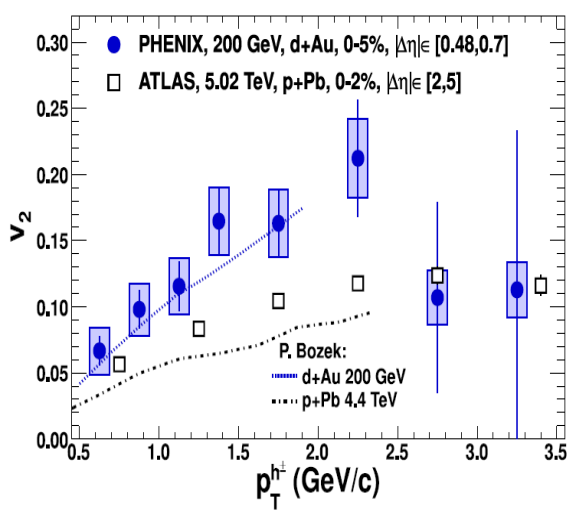

Have we lost our pA Control ?

Maybe v2(DAu , 5%) = v2(AuAu, 30%) is just coincidence bad luck ??

Maybe QM12 BES is also just coincidence ?

v2(AuAu, 7 AGeV) ~ v2(AuAu,200 AGeV) ~ v2(PbPb,2800 AGeV) ??

Should we ignore the "peripheral" R_{DAu}(15 GeV) ~1.5 anomaly and rely instead only on Null Control direct gammas

R_{DA}(gamma) ~ R_{AuAu}(gamma) ~ 1

We need global data on dN/dy, dET/dy, and dN/dydpT at both RHIC and LHC on rare p + A processes

Entropy has been produced (Clausius is happy) but we need to step back and reassess which of our (many) Geomtric and dynamical assumptions may fail in very rare pA and DA processes.

Maybe v2(DAu , 5%) = v2(AuAu, 30%) is just coincidence bad luck ??

Maybe QM12 BES is also just coincidence ?

v2(AuAu, 7 AGeV) ~ v2(AuAu,200 AGeV) ~ v2(PbPb,2800 AGeV) ??

Should we ignore the "peripheral" R_{DAu}(15 GeV) ~1.5 anomaly and rely instead only on Null Control direct gammas

R_{DA}(gamma) ~ R_{AuAu}(gamma) ~ 1

We need global data on dN/dy, dET/dy, and dN/dydpT at both RHIC and LHC on rare p + A processes

Entropy has been produced (Clausius is happy) but we need to step back and reassess which of our (many) Geomtric and dynamical assumptions may fail in very rare pA and DA processes.

Part 3:

The High pT azimuthal asymmetry v2(pT, Ecm)

In the **IM 2 < pT <10** and the deep **UV pT>10**

Puzzling Status update

The *Deep* UV Band pT>10 GeV seemed to agree with pQCD tomography @LHC
Unlike the intermediate IM Band 2 < pT <10 interpolating between IR and UV bands

WAHorowitz, MG, JPG G38 (2011) QM11

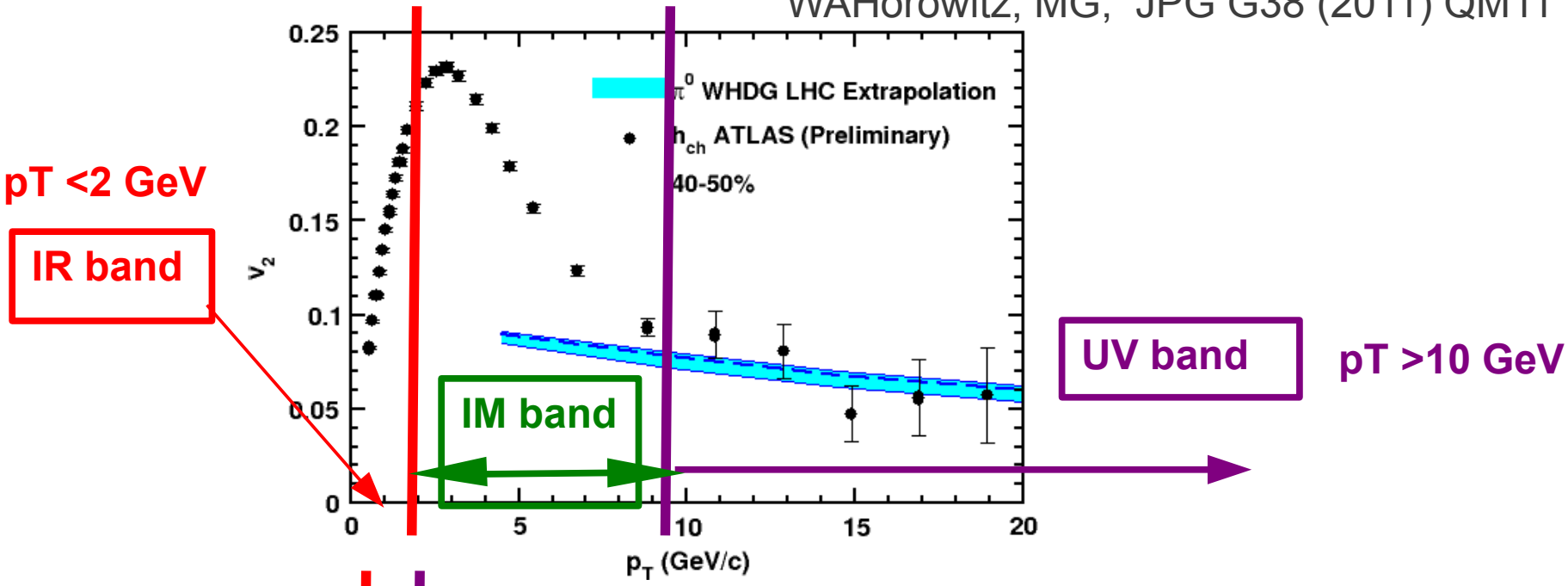

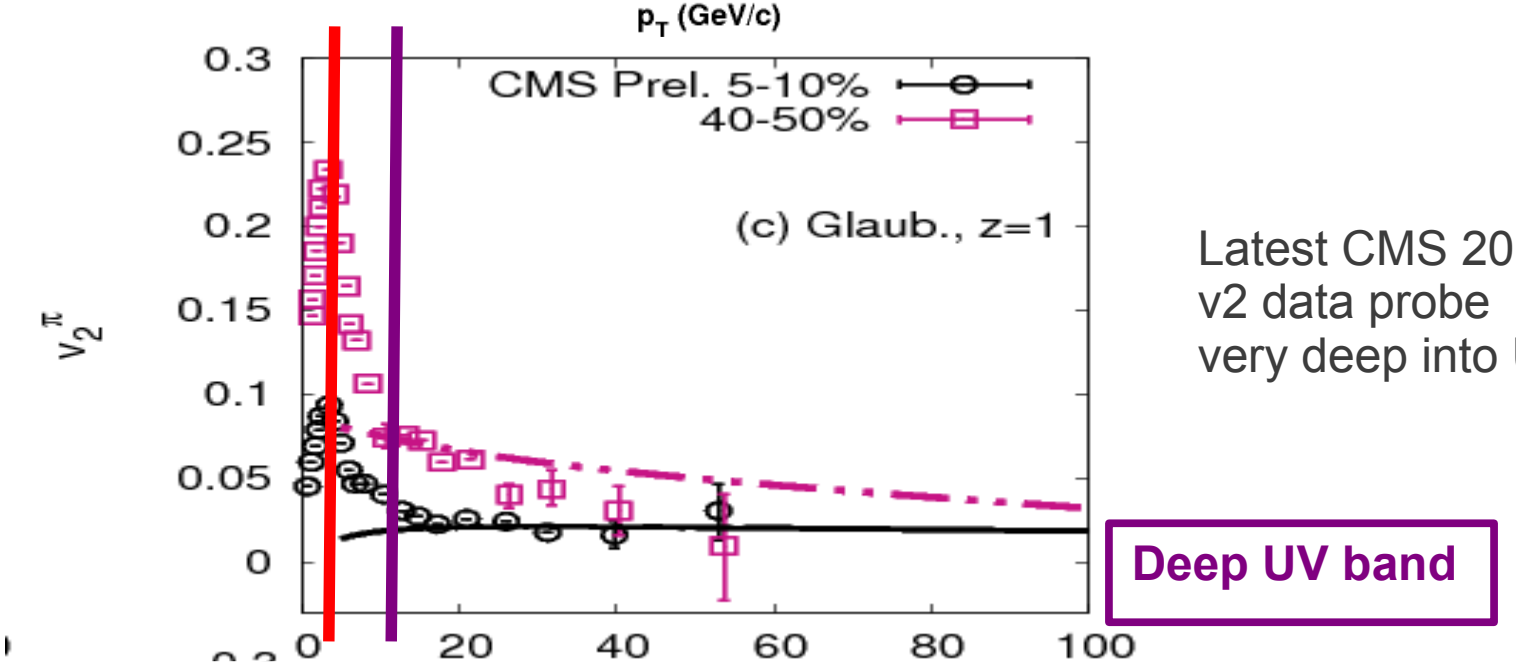

Latest CMS 2012
v2 data probe
very deep into UV ~ 60 GeV !

B.Betz, MG PRCC86 (2012) 024903

Denes Molnar, Deke Sun, QM12 used MPC bulk evolution to evaluate GLV En Loss

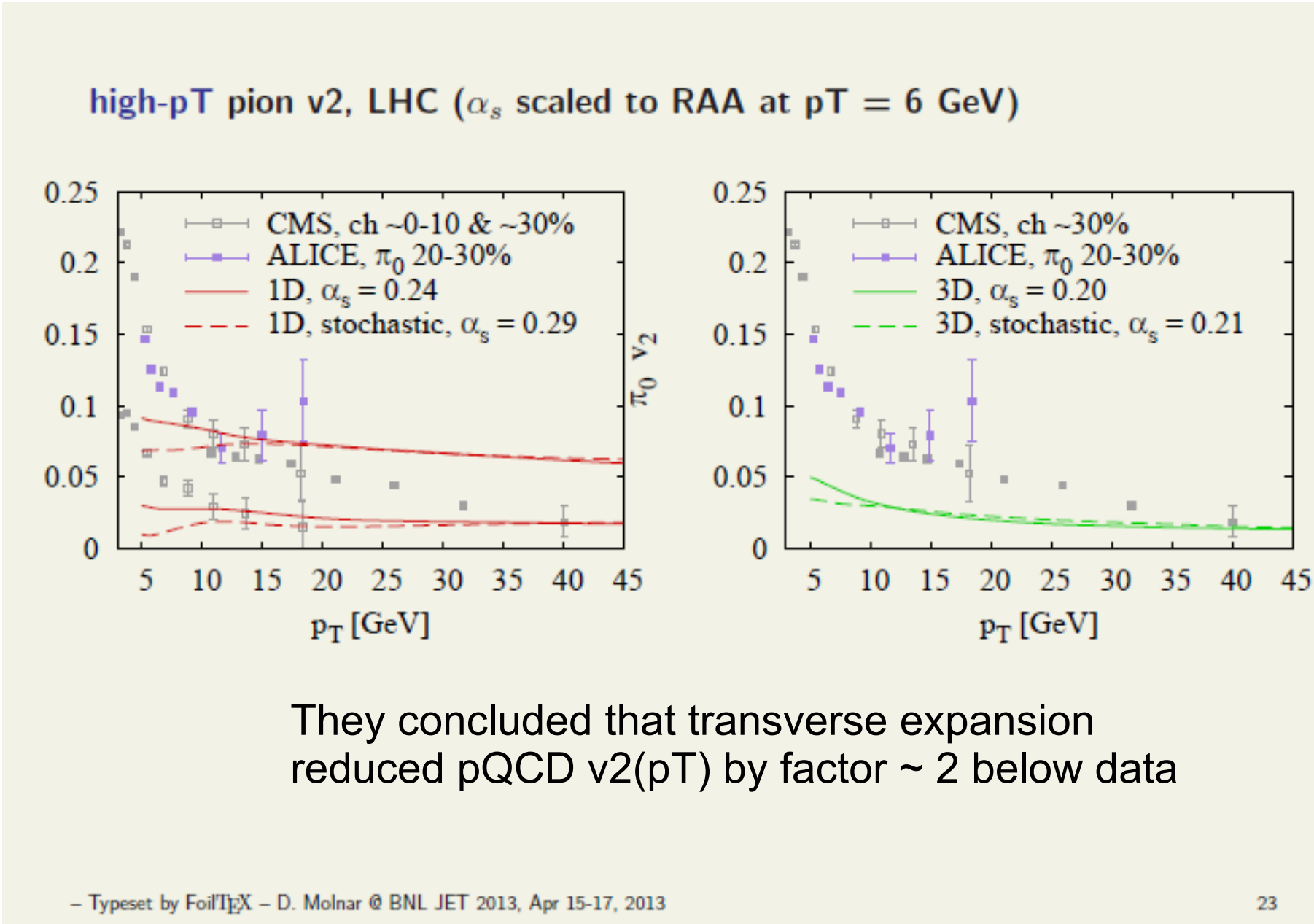

Denes Molnar, Deke Sun, QM12 used MPC bulk evolution to evaluate GLV En Loss

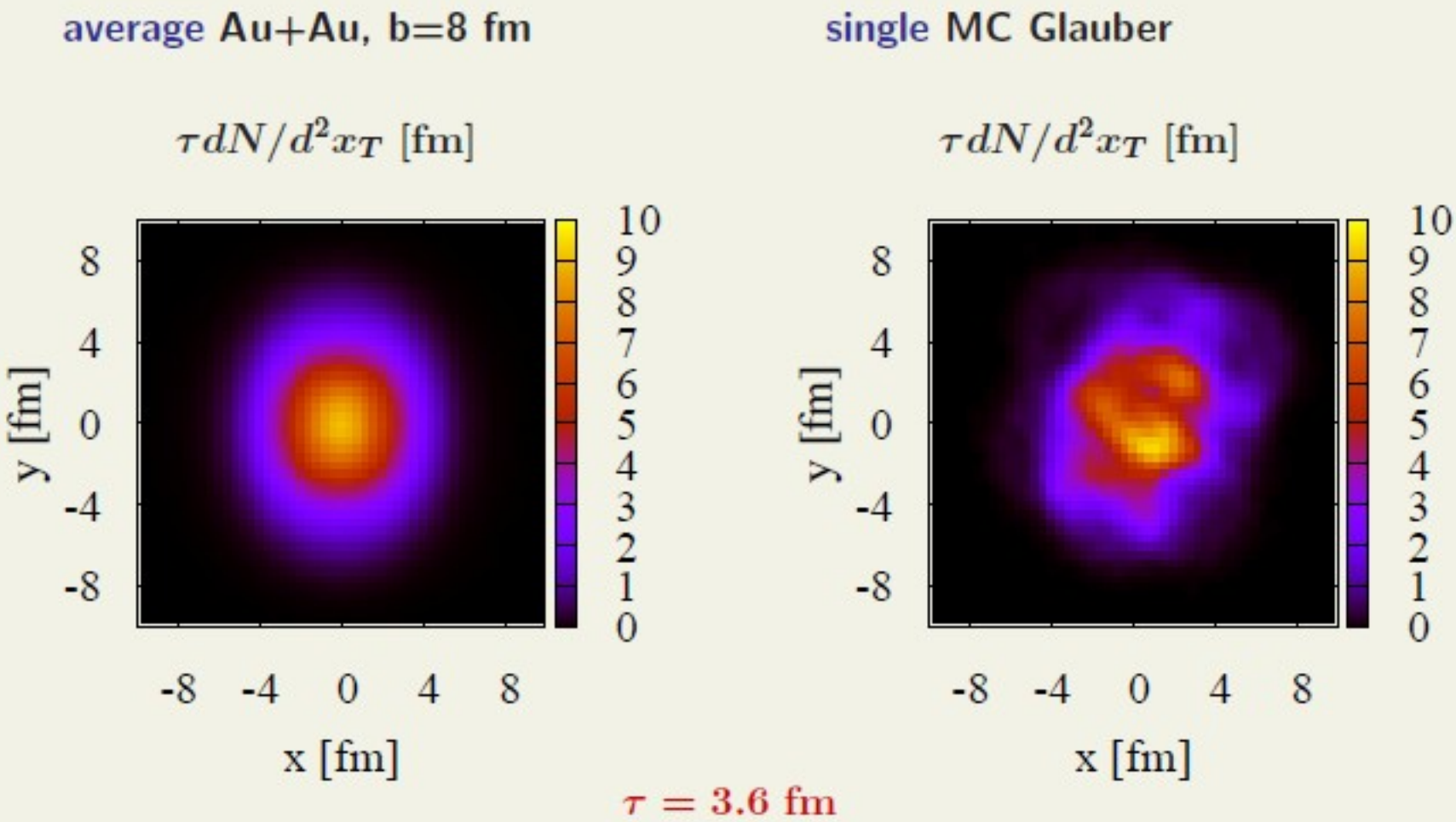

– Typeset by FoilTEX – D. Molnar @ BNL JET 2013, Apr 15-17, 2013 29

Denes Molnar, Deke Sun, QM12 used MPC bulk evolution to evaluate GLV En Loss

Similar to the Ed's 1999 “Nutcracker” scenario bulk hydro like evolution

With rapid decrease of eccentricity to negative values for t>R

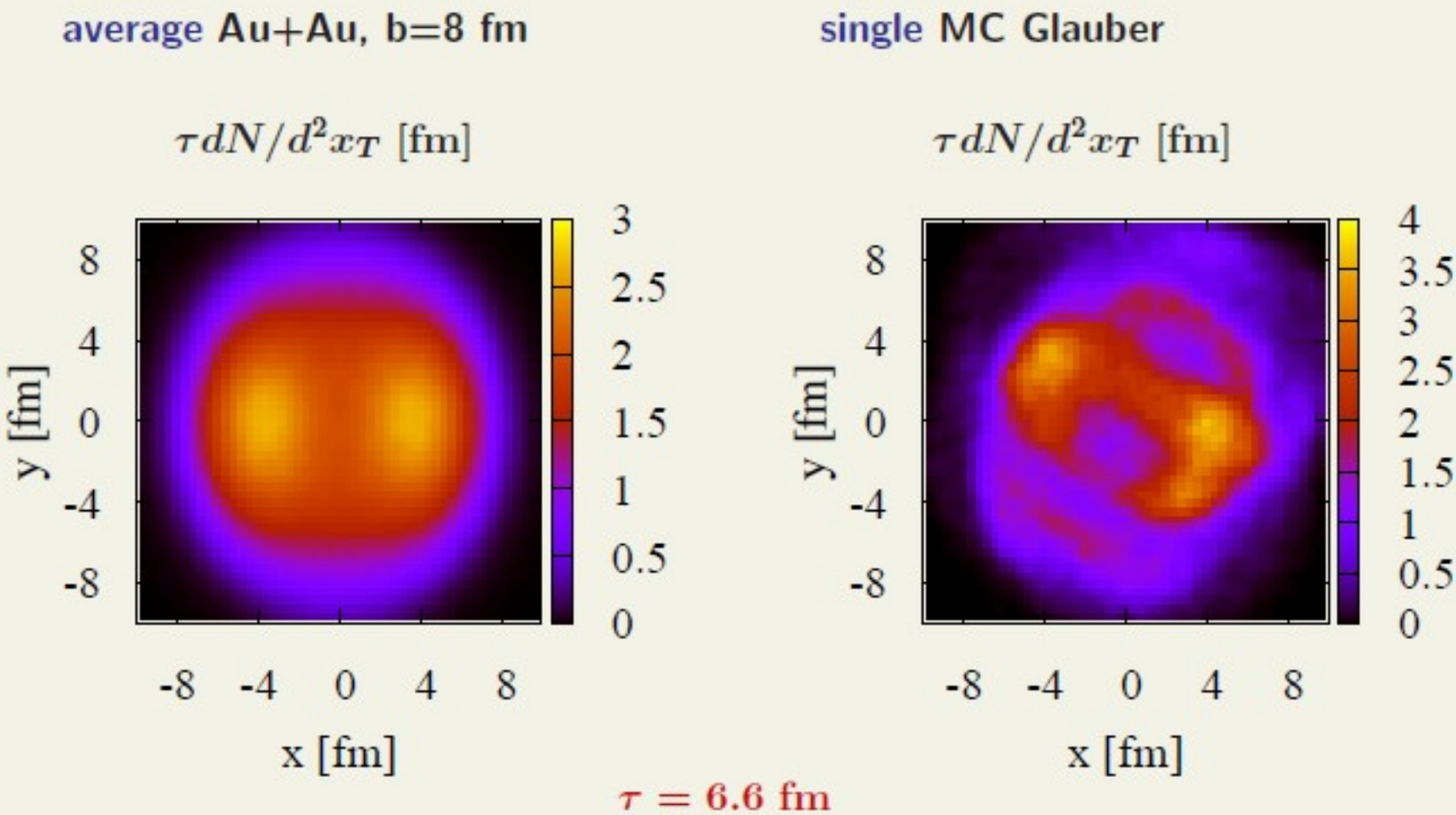

– Typeset by FoilTEX – D. Molnar @ BNL JET 2013, Apr 15-17, 2013 30

PHENIX $R_{AA}^{in} = R_{AA}(1+2v_2)$ vs $R_{AA}^{out} = R_{AA}(1-2v_2)$

A. Adare et al., arXiv:1208.2254

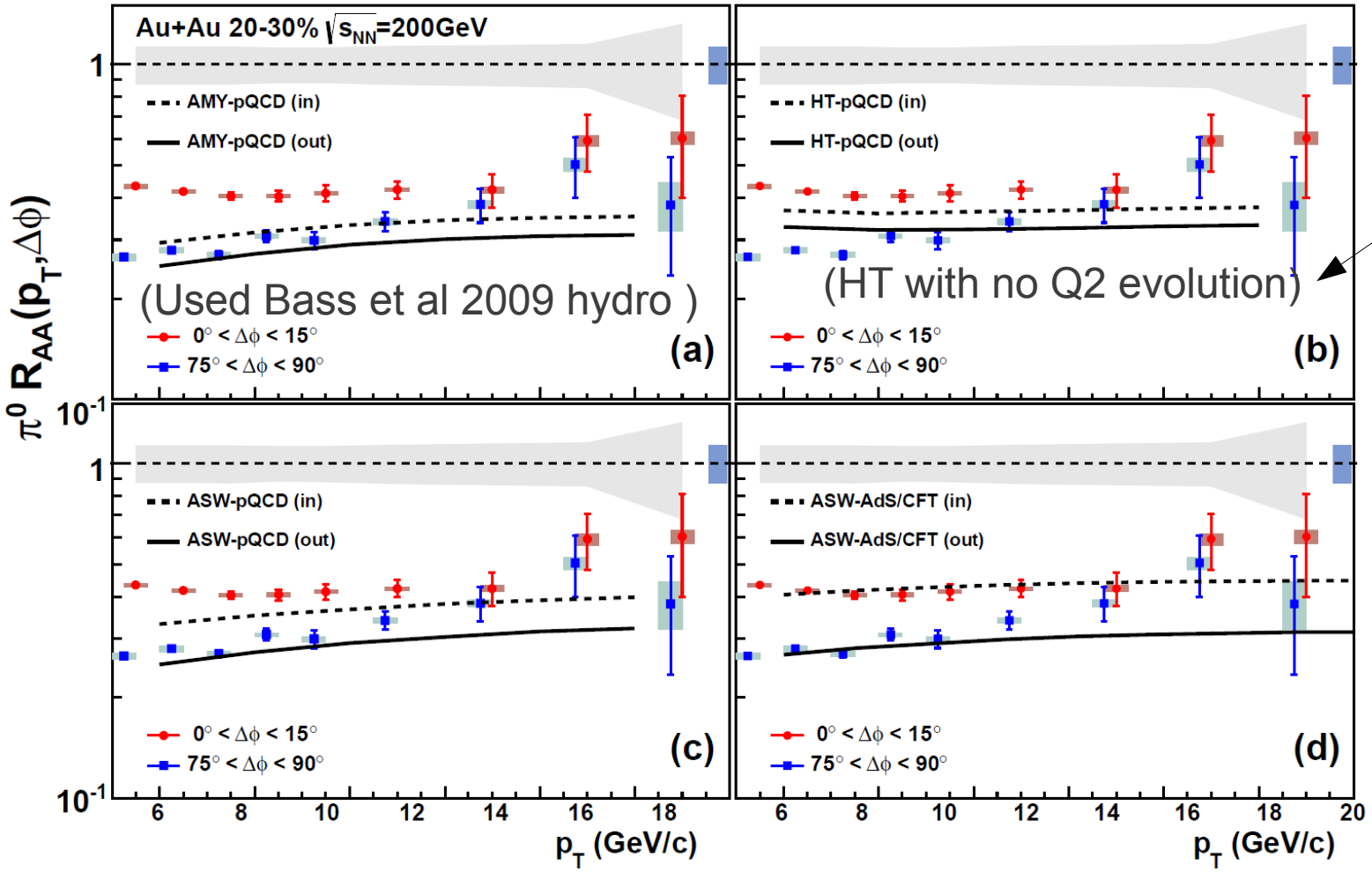

See A. Majumder RBRC13 update

E^0 L^2 En loss

→ PHENIX Concluded: Only Schematic ASW-AdS/CFT can fit both $R_{AA\ in/out}$ for a 3d expanding medium. PQCD based dedx underestimate

→

Provide information about both R_{AA} and v_2

abc Model of Jet Energy Loss and RAA

For pQCD
a ~ 1/3 , b~1

$$\frac{dP}{d\tau} = -\kappa P^a \tau^b T^{2-a+b}(x(\tau),\tau)$$

For Holographic Falling Strings (Chesler Yaffe)
Lstop ~ $E^{1/3}$
=> a = 1/3 , b=1
OR a = 0 , b=2

$$P_0(P_f) = \left[P_f^{1-a} + K\int_{\tau_0}^{\tau_f} \tau^z T^c[\vec{x}_\perp(\tau),\tau]d\tau\right]^{\frac{1}{1-a}},$$

For Holographic String Drag (Gubser, Herzog)
a = 1 . b=0

$$R_{AA}(p_f;s,A) = \frac{\partial p_0}{\partial p_f}\frac{d\sigma(p_0(p_f))/dp}{d\sigma(p_f)/dp}$$

Spectral index From pQCD

For Bj Brick $\approx \left(1+\kappa'\frac{(dN/dy)^{(2-a+b)/3}}{(Lp_f)^{1-a}}\right)^{\frac{a-n(p_f)}{1-a}}$

Fix κ' by fit to one RHIC R(pf=10 GeV ,dNdy=1000) reference point.

Horowitz,MG, NPA872(2011); B.Betz, MG, Torrieri PRC84(11), PRC86(12)

„Magnetic Monopole“ scenario of Liao,Shuryak

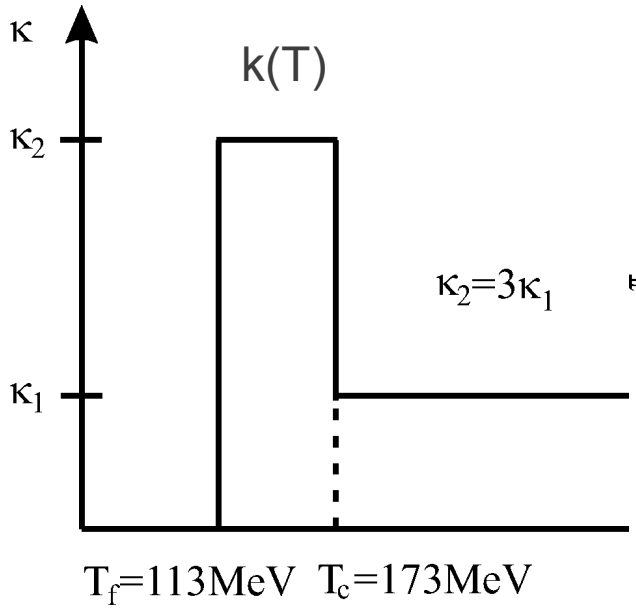

J.Liao et al,. PRL **102** (2009) 202302

$$\zeta = \kappa_1 / \kappa_2$$

→ Apply same $\kappa(T)$ at RHIC and LHC

Original SL, RAA was independent of pT

B.Betz et al., in preparation

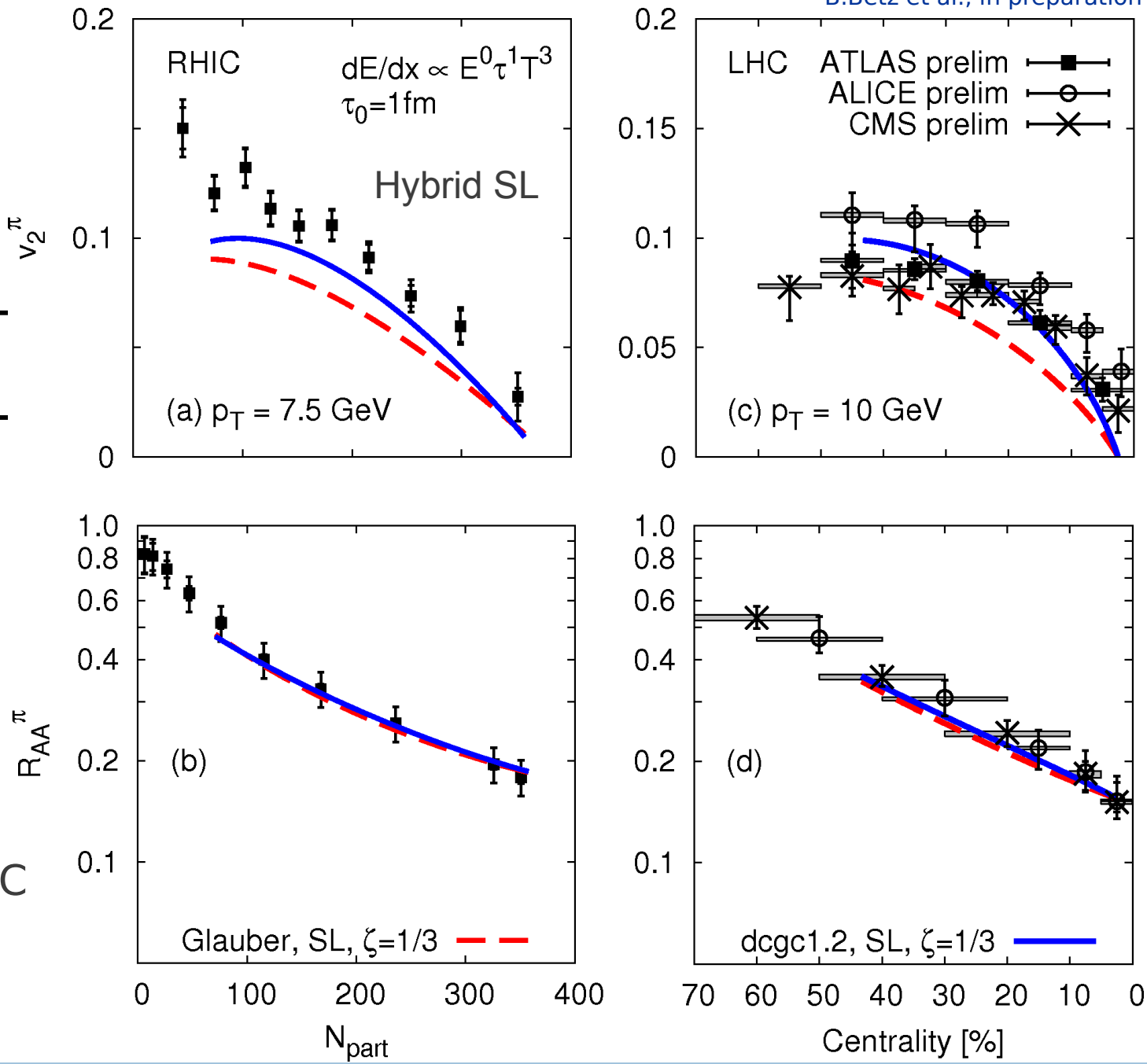

(a=0,b=2,c=4) is like Renk's “AdS” model
(a=0,b=1,c=3) is like Liao's “SL” mag.mono. model

B.Betz.MG 2013

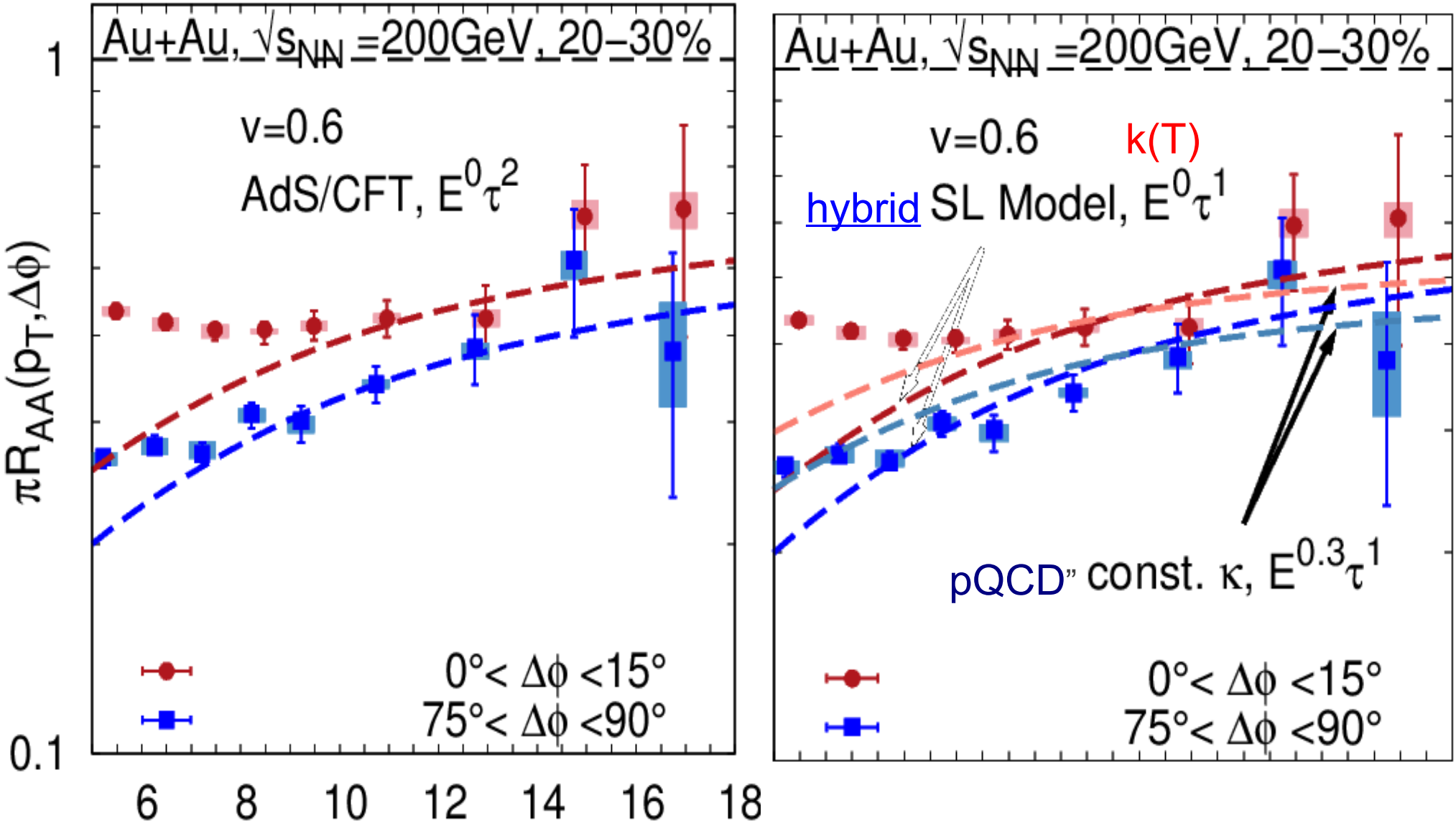

Including transverse flown UV pT>10 GeV, pQCD or “AdS” are adequate within errors
None of the models pQCD, SL, or AdS reproduce in and out in IM pT<10 range
(B.Betz, MG, to be published)

Compare 4 dEdx models using Romatschke hydro or Bj+ radial flow v=0.6 bulk models

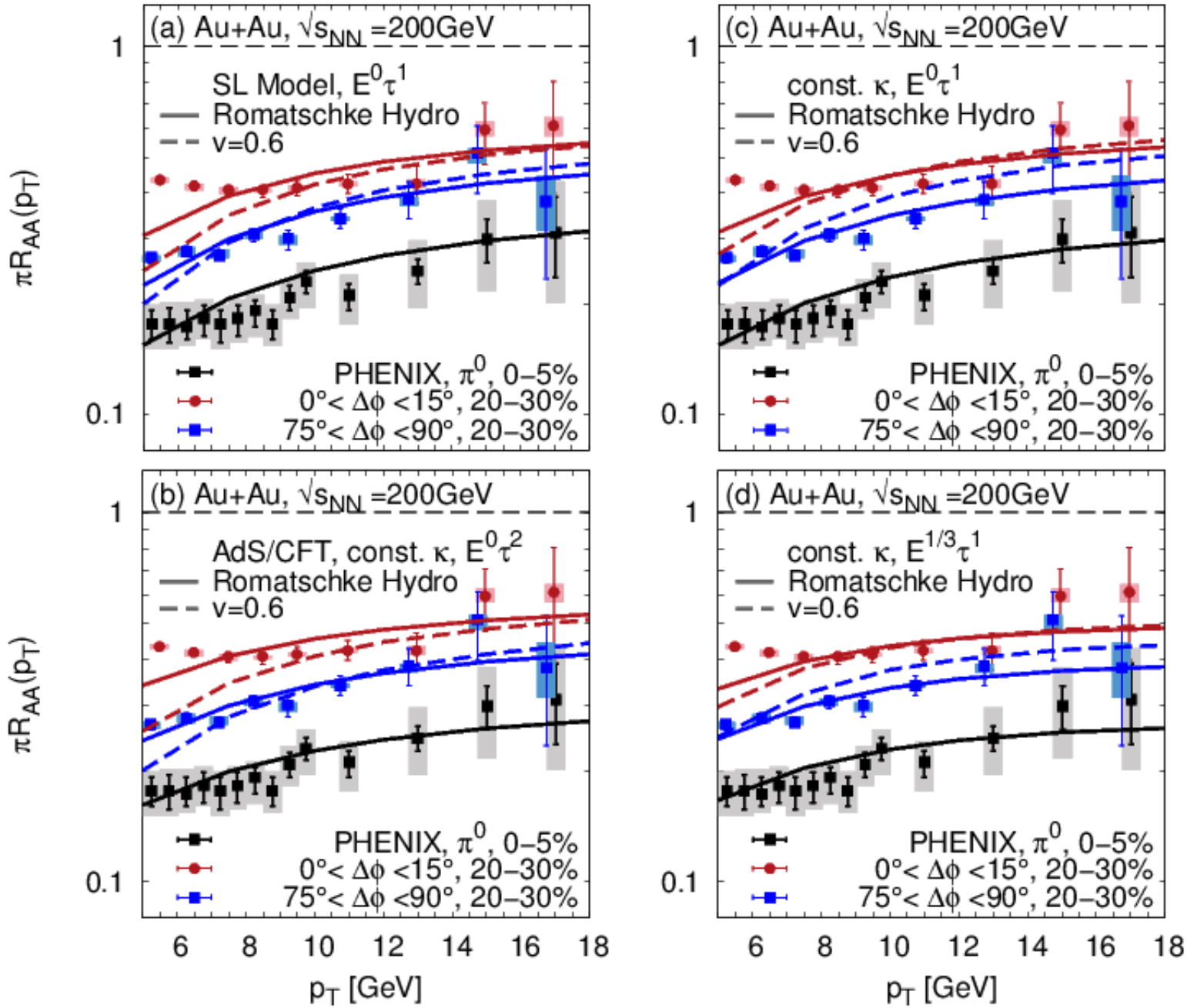

None of 8 scenarios appears preferred within current errors at RHIC
B.Betz, MG (13)

8 Scenarios
Extrapolated
to
LHC

Sensitivity
To dEdx (abc)
and kappa(T)
is weaker
than at RHIC
because
spectral shapes
are harder

Large
Sensitivity of
RAAin/out
To bulk flow
Evolution

(as per Renk 11)

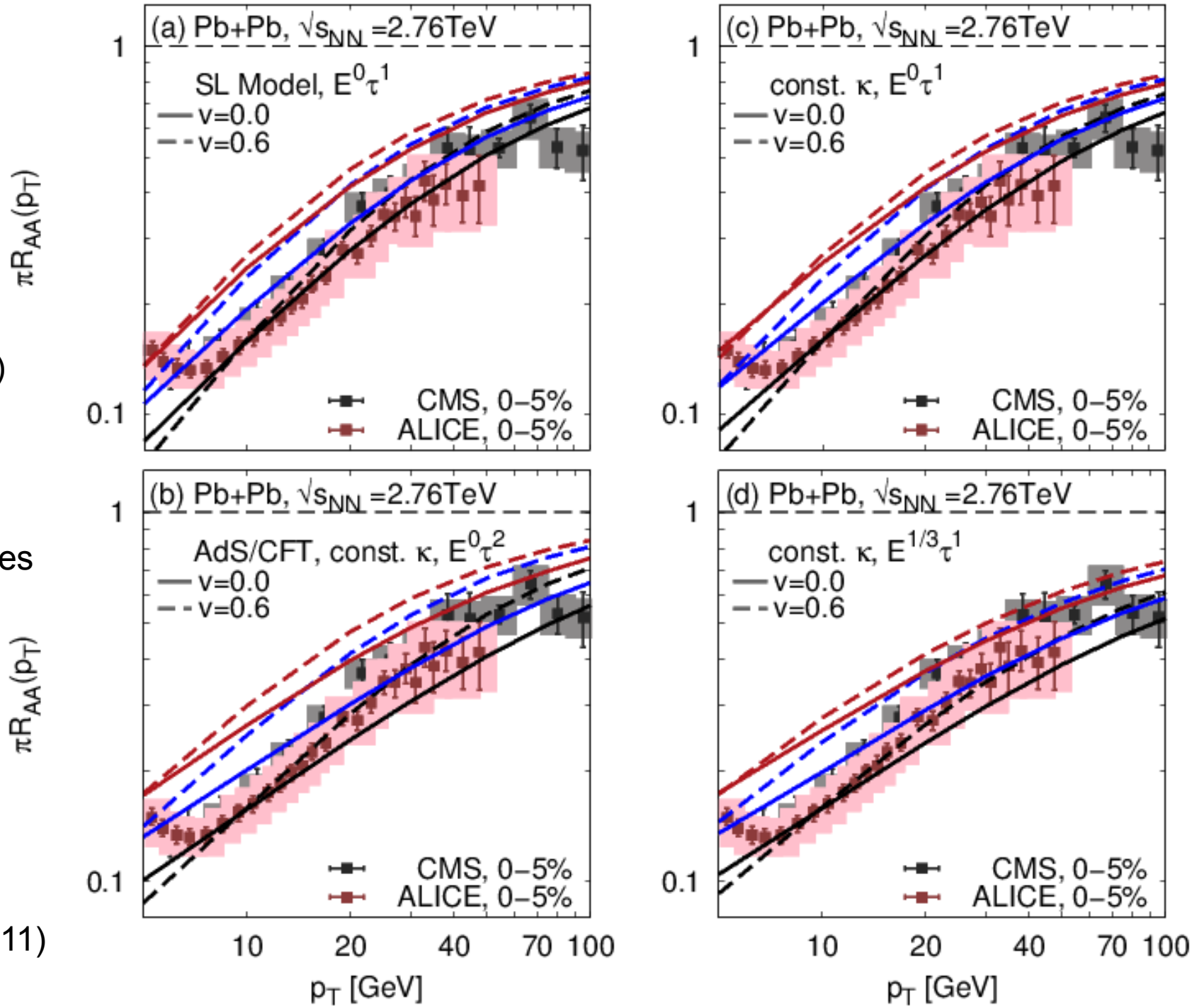

Final remarks :

1) Azimuthal tomography is sensitive to details of the bulk flow T(x,t) and u(x,t) field evolutions that is complementary to low pT vn systematics. This is the good news.

2) However sensitivity is weak more precise RAAin/out(pT) needed to resolve current array of (pQCD, SL, and AdS dEdx models) times the array bulk flow models (Bass, Heinz, Romat, MPC)

3) Different jet asymmetry using Romat hydro and Bass hydro flow fields needs to be clarified.

4) Meanwhile, the new QM12 and RBRC13 p+A and D+A data on bulk vn and anomalous jet modification "discoveries" severely challenge our entire framework of A+A analysis.

Our homework now is to try to regain the lost Null-Controls !

The p-A/p+p "Rapidity Triangle"- BGK Model

- Multiple independent wee parton dx/x collisions produce uniform in rapidity color charges between valence p and and valence wounded A.
- Color neutralizes via pair production between wee and valence partons
-
- Leaving a stack of
- ~ $A^{1/3}$ Target beam jets
-
- and 1 Projectile beam jet
- $\nu_A(b) \approx \sigma_{in} T_A(b)$
- Y Slope $\delta = O(A^{1/3}/\log(s))$
- RHIC $\delta \sim 0.45$, LHC ~ δ 0.28

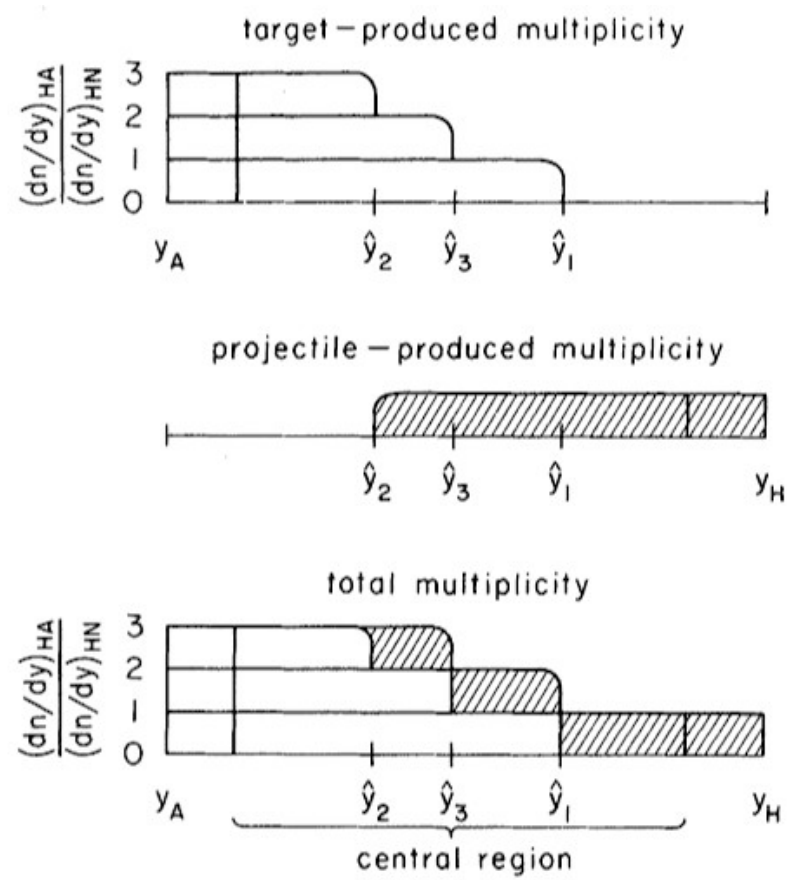

Figure from Brodsky, Gunion, Kuhn 1977

VOLUME 68, NUMBER 10 PHYSICAL REVIEW LETTERS 9 MARCH 1992

XN Wang, MG

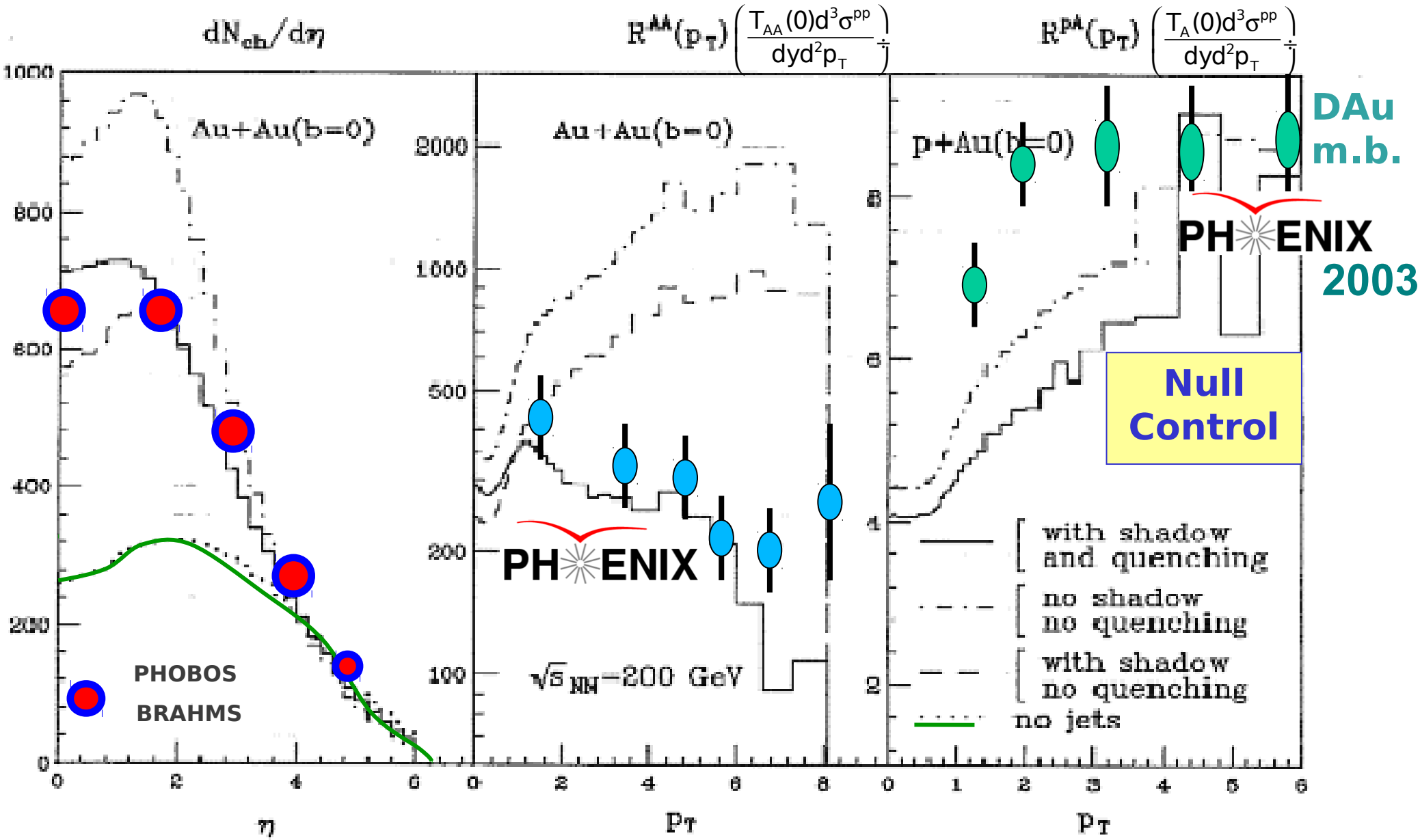

Null Control with p+A @ RHIC was critical to prove that RAA~0.2

Was due to final state jet quenching (not to initial state shadow)

Evidence from the suppression of high-p_T particles:

[in central AA but not in D+A]

W.Busza, RBRC 4/15/2004

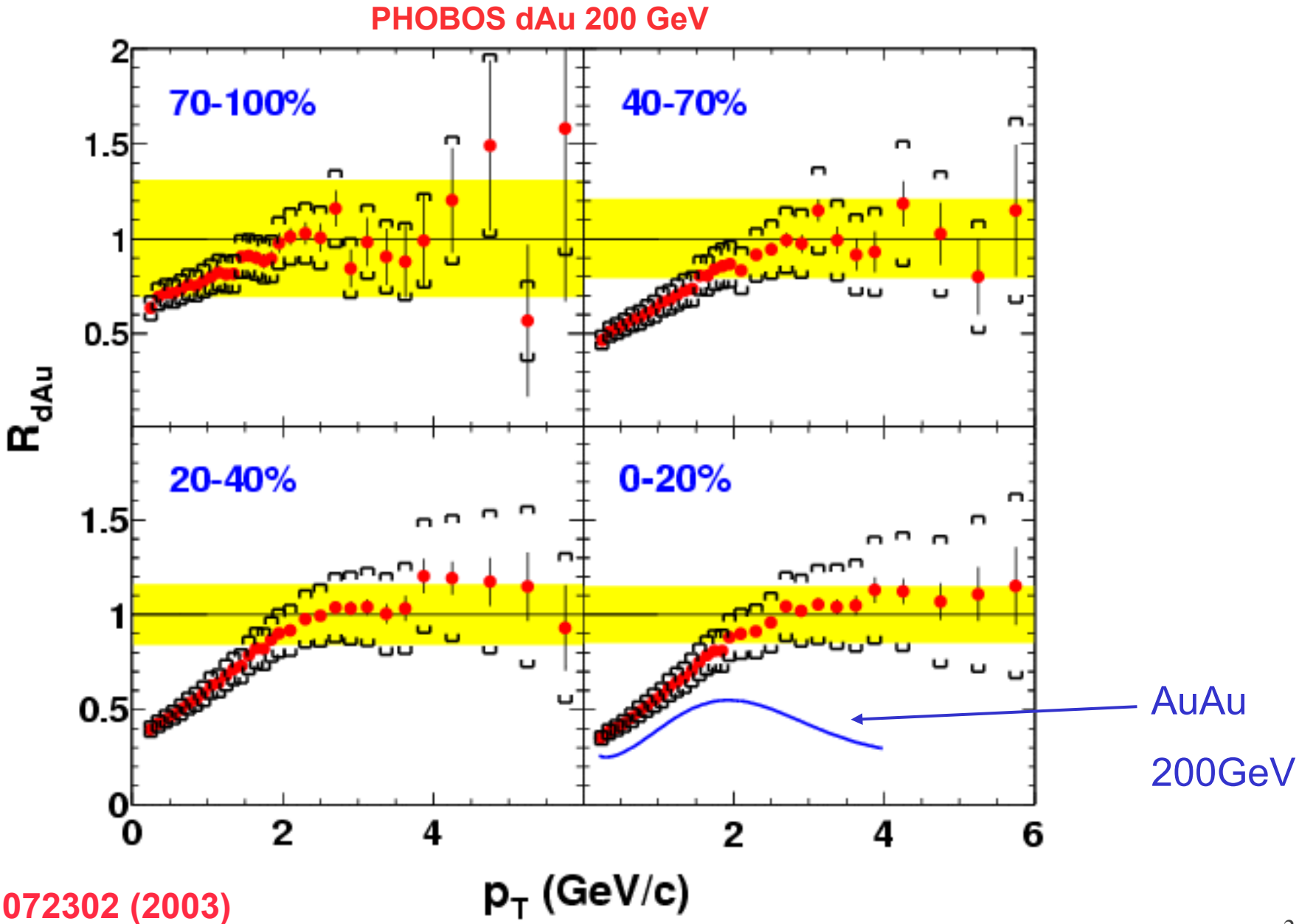

PRL 91, 072302 (2003)

In-medium QCD cascade: democratic branching and wave turbulence

Jet Quenching at RHIC vs LHC
BNL
April 17, 2013

Jean-Paul Blaizot, IPhT- Saclay

erc European Research Council

Outline

- Phenomenological motivations
- In-medium gluon branching (BDMPSZ mechanism)
- Multiple branching, (de)coherence, in-medium cascade
- In-medium cascade, turbulent flow
- Relevance to di-jet asymmetry
- Conclusion

Work done in collaboration with F. Dominguez, E. Iancu and Y. Mehtar-Tani (arXiv:1209.4585, 1301.6102)

Phenomenological motivations

Di-jet asymmetry

there is more to it than just 'jet quenching'...

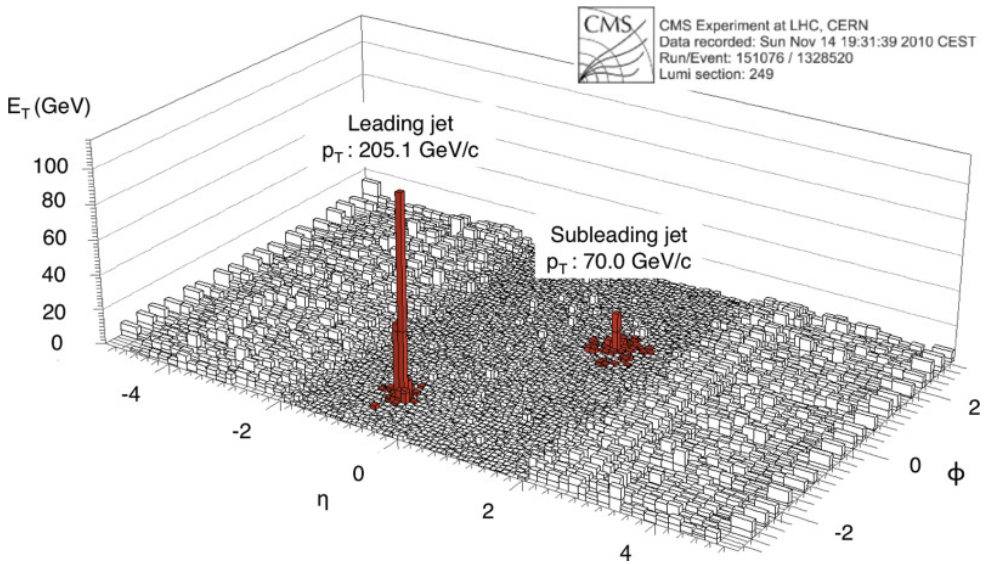

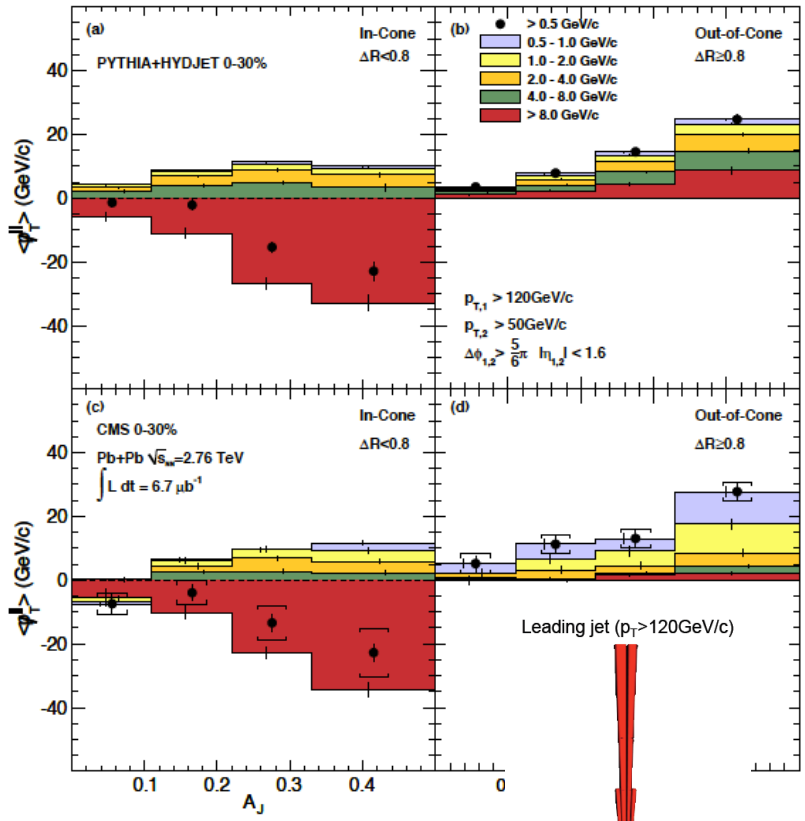

Missing energy is associated with additional radiation of many soft quanta at large angles

Perhaps reflecting a genuine feature of the in-medium QCD cascade (JPB, E. Iancu and Y. Mehtar-Tani, arXiv: 1301.6102)

In-medium parton branching
BDMPSZ mechanism

(Baier, Dokshitzer, Mueller, Peigné, Schiff; Zakharov ~ 1996)

The BDMPSZ mechanism for in-medium branching

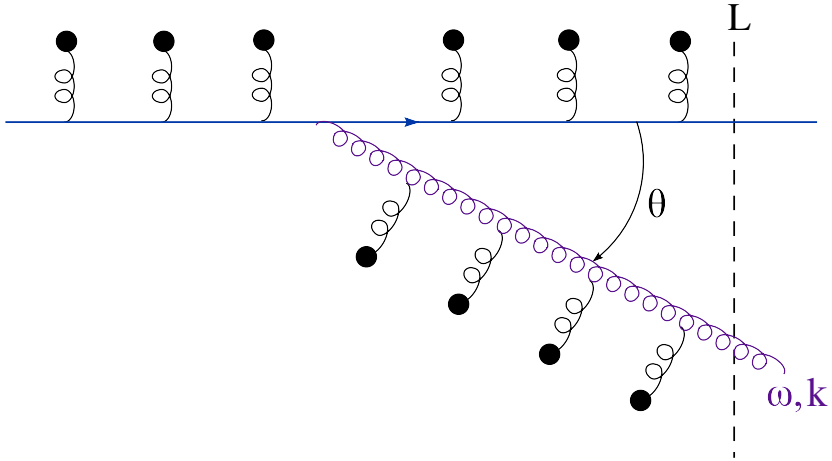

Gluon emission is linked to momentum broadening

$$\frac{1}{\tau_{\rm f}} \sim \frac{k_\perp^2}{2\omega} \qquad \Delta k_\perp^2 = \hat{q}\Delta t$$

Time scale for the branching process $\tau_{\rm br}(\omega) \sim \sqrt{\frac{2\omega}{\hat{q}}}$

Medium of finite extent $\tau_{\rm br} \lesssim L \Rightarrow \omega \lesssim \omega_c \qquad \omega_c \sim \hat{q}L^2$

Formation time and emission angle

Typical branching kT and angle

$$k_{\rm br}^2 = \hat{q}\tau_{\rm br}$$

$$\theta_{\rm br} \sim k_{\rm br}/\omega \sim \left(\hat{q}/\omega^3\right)^{1/4}$$

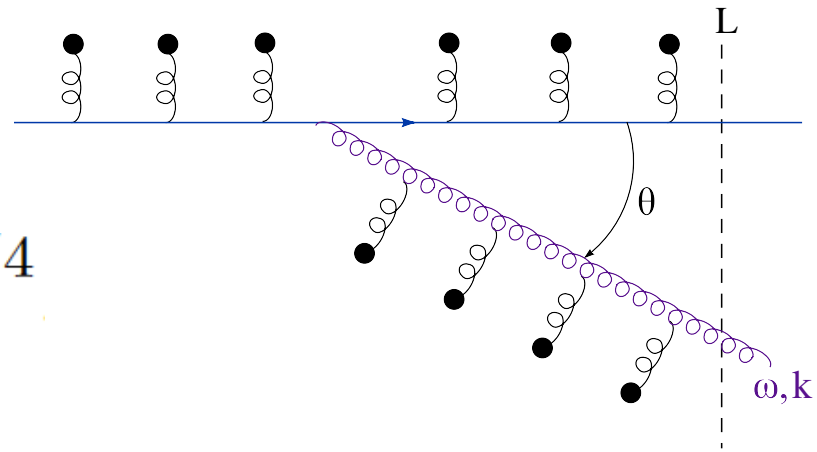

Hard gluon: small angle, long time

$$\tau_{\rm br} \lesssim L \qquad \omega \lesssim \omega_c \qquad \theta_{\rm br} \gtrsim \theta_c$$

Soft gluon: large angle, short time

$$\tau_{\rm br} \ll L \qquad \omega \ll \omega_c \qquad \theta_{\rm br} \gg \theta_c$$

BDMPSZ spectrum

$$\omega \frac{\mathrm{d}N}{\mathrm{d}\omega} \simeq \frac{\alpha_s N_c}{\pi} \sqrt{\frac{\omega_c}{\omega}} \equiv \bar{\alpha} \sqrt{\frac{\omega_c}{\omega}} = \bar{\alpha} \frac{L}{\tau_{\mathrm{br}}(\omega)}$$

Hard emissions

- rare events, with probability $\sim \mathcal{O}(\alpha_s)$
- dominate energy loss: $E_{\mathrm{hard}} \sim \alpha_s \omega_c$
- small angle, not important for di-jet asymmetry

Soft emissions

- frequent, with probability $\sim \mathcal{O}(1)$
- weaker energy loss: $E_{\mathrm{soft}} \sim \alpha_s^2 \omega_c$
- but arbitrary large angles: control di-jet asymmetry

large angles emissions are dominated by soft multiple branchings

Multiple branchings (de)-coherence in-medium cascade

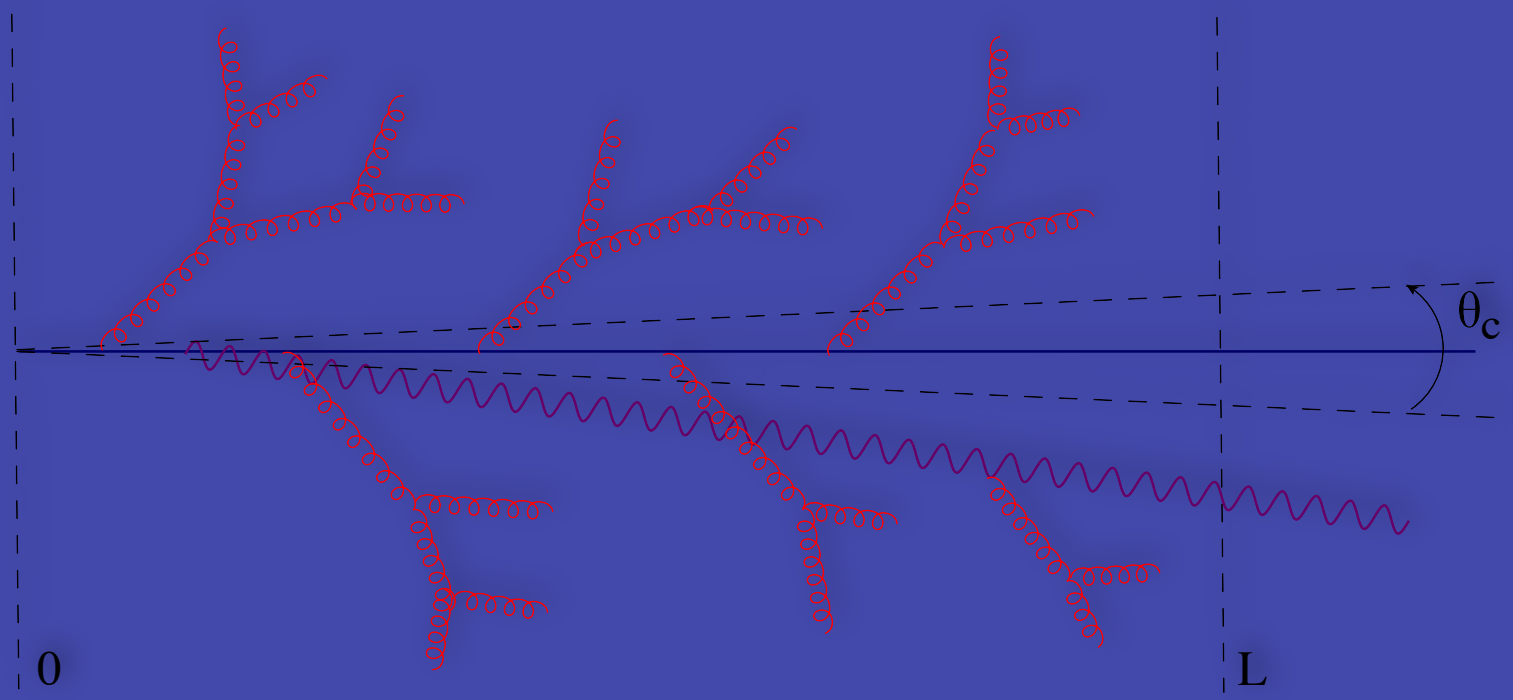

Multiple emissions

A priori complicated by interferences

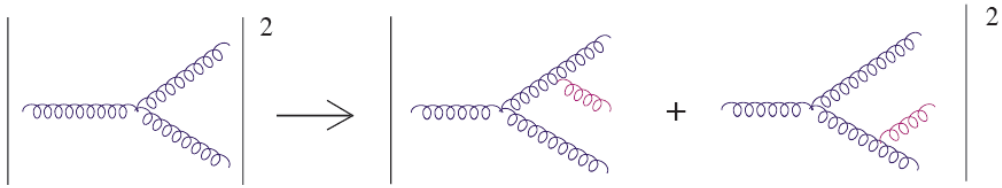

In vacuum, these interferences lead to angular ordering

In medium color coherence is rapidly lost via rescattering

Mehtar-Tani, Salgado, Tywoniuk (1009.2965; 1102.4317)
Iancu, Casalderey-Solana (1106.3864)

In medium, interference effects are subleading

Independent emissions are enhanced by a factor L/τ_f

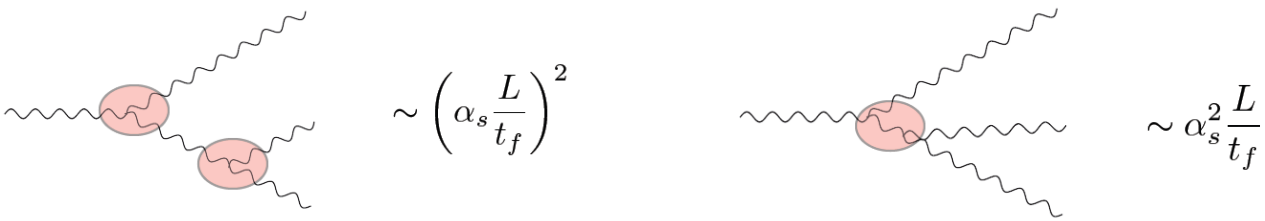

JPB, F. Dominguez, E. Iancu, Y. Mehtar-Tani, arXiv: 1209.4585

Resumming the leading terms

When $\bar{\alpha}L/\tau_{br} \sim 1$ all powers of $\bar{\alpha}L/\tau_{br} \sim 1$ need to be resummed.

Since independent emissions dominate, the leading order resummation is equivalent to a probabilistic cascade, with nearly local branchings

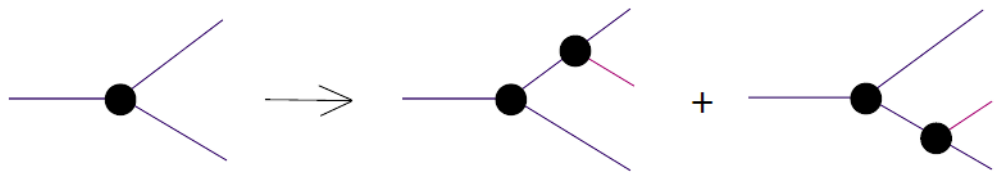

Blob: BDMPSZ spectrum

Line: momentum broadening

JPB, Dominguez, Iancu and Mehtar-Tani (arXiv:1209.4585)

Note: already implemented in Monte Carlo codes

MARTINI (Jeon, Gale, Schenke)
Q_Pythia (Armesto, Salgado et al)
Stachel, Wiedemann, Zapp

Evolution equation for the gluon spectrum

(after integration over kT)

$$D(x,\tau) = x\frac{dN}{dx} \qquad x = \frac{\omega}{E}$$

Probabilistic equation ('gain-loss')

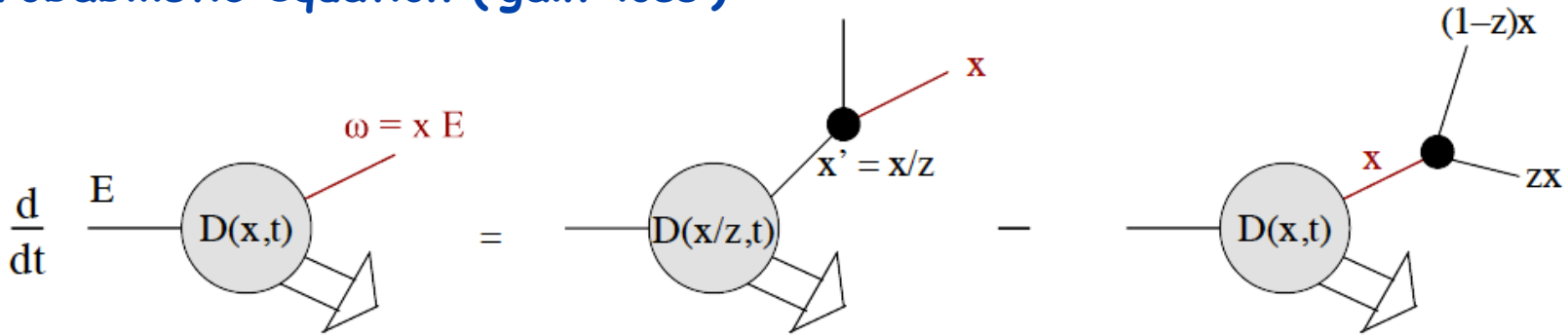

$$\frac{\partial D(x,\tau)}{\partial \tau} = \int \mathrm{d}z\, \mathcal{K}(z) \left[\sqrt{\frac{z}{x}} D\left(\frac{x}{z},\tau\right) - \frac{z}{\sqrt{x}} D(x,\tau)\right]$$

$$\mathcal{K}(z) = \frac{\bar{\alpha}}{2}\frac{f(z)}{[z(1-z)]^{3/2}}, \qquad f(z) = \left[1 - z(1-z)\right]^{5/2}$$

Formally analogous to DGLAP. But very different kernel... and physics.

→ **A QCD cascade of a new type**

In-medium QCD cascade
Turbulent flow at small x

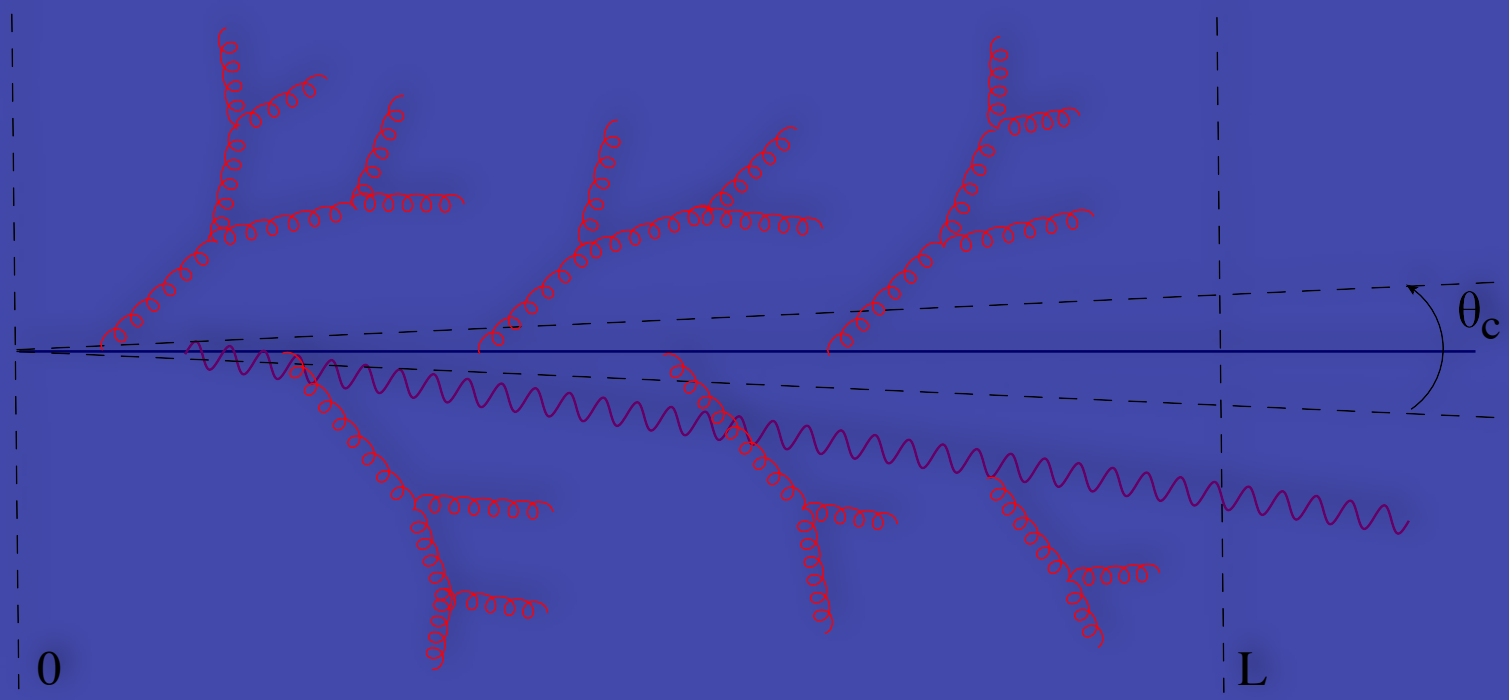

Short times

$$\frac{\partial D(x,\tau)}{\partial \tau} = \int \mathrm{d}z\, \mathcal{K}(z) \left[\sqrt{\frac{z}{x}} D\left(\frac{x}{z},\tau\right) - \frac{z}{\sqrt{x}} D(x,\tau) \right]$$

At short time, single emission by the leading particle $(D_0(\tau=0,x)=\delta(x-1))$

D is the BDMSZ spectrum

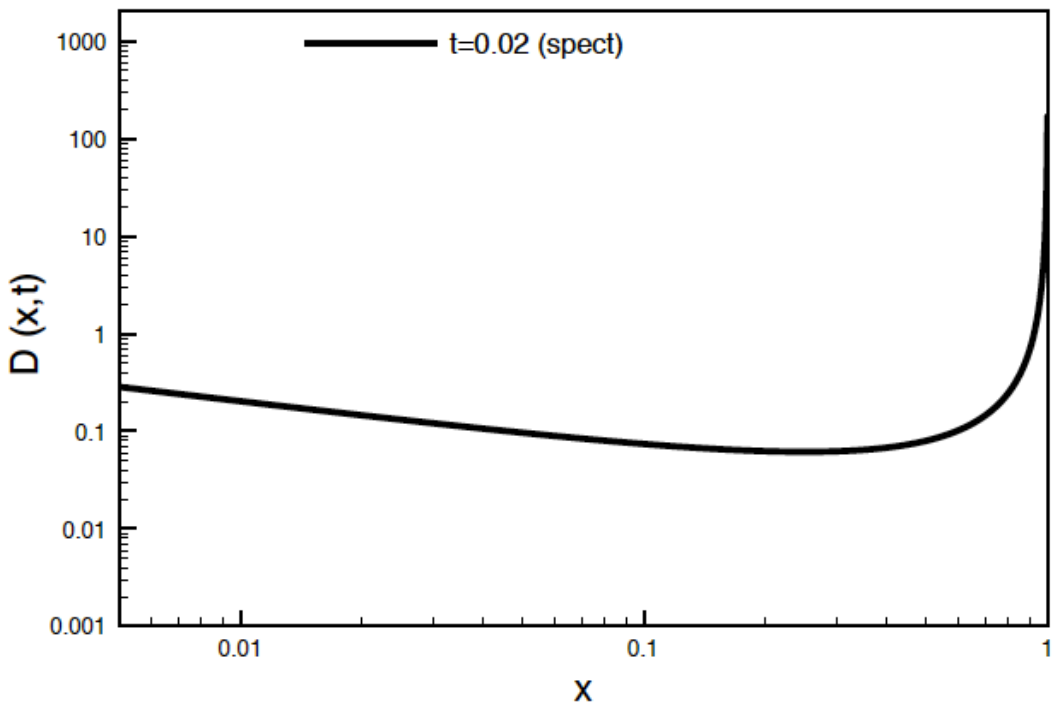

How do multiple branchings affect this spectrum ?

Naively, we could expect the spectrum to be depleted at large x and to increase rapidly at small x, so as to keep the total energy constant

$$\int_0^1 \mathrm{d}x\, D(\tau, x) = 1$$

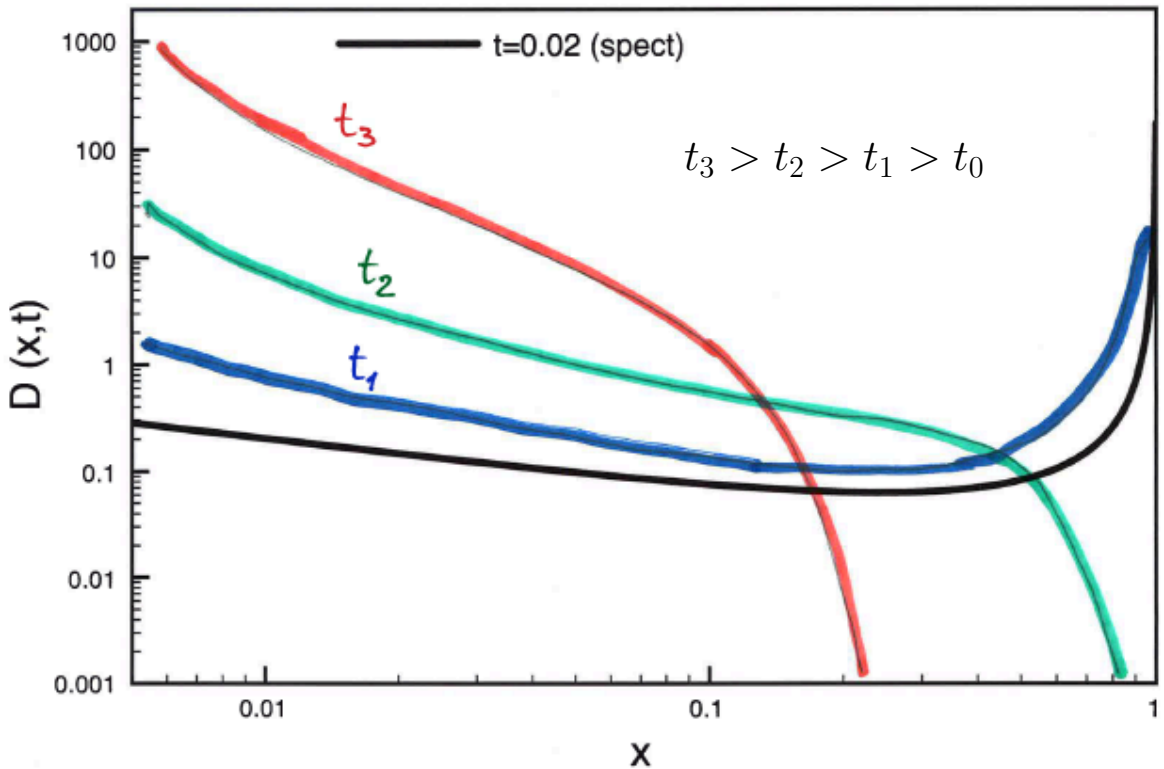

But this is not what happens !

One finds (exact result) $$D(x,t) \simeq \frac{t}{\sqrt{x}}\, \mathrm{e}^{-\pi t^2} \qquad \text{for } x \ll 1$$

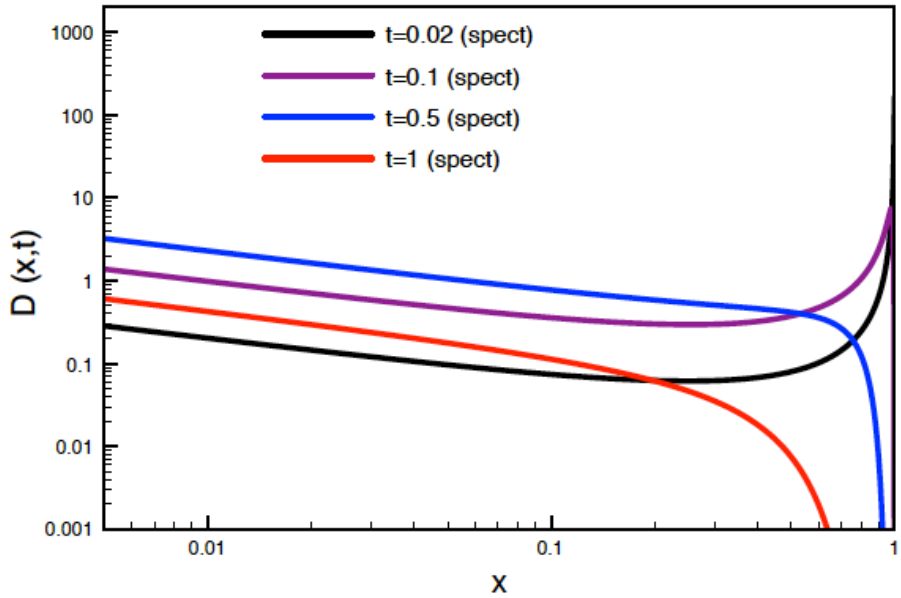

Fine (local) cancellations between gain and loss terms

BDMPS spectrum emerges as a fixed point, scaling, spectrum

Characteristic features of wave turbulence (Kolmogoroz, Zakharov)

The source problem

At this (fixed) point ALL the energy flows through the whole system

Energy is injected at x=1, at a constant rate

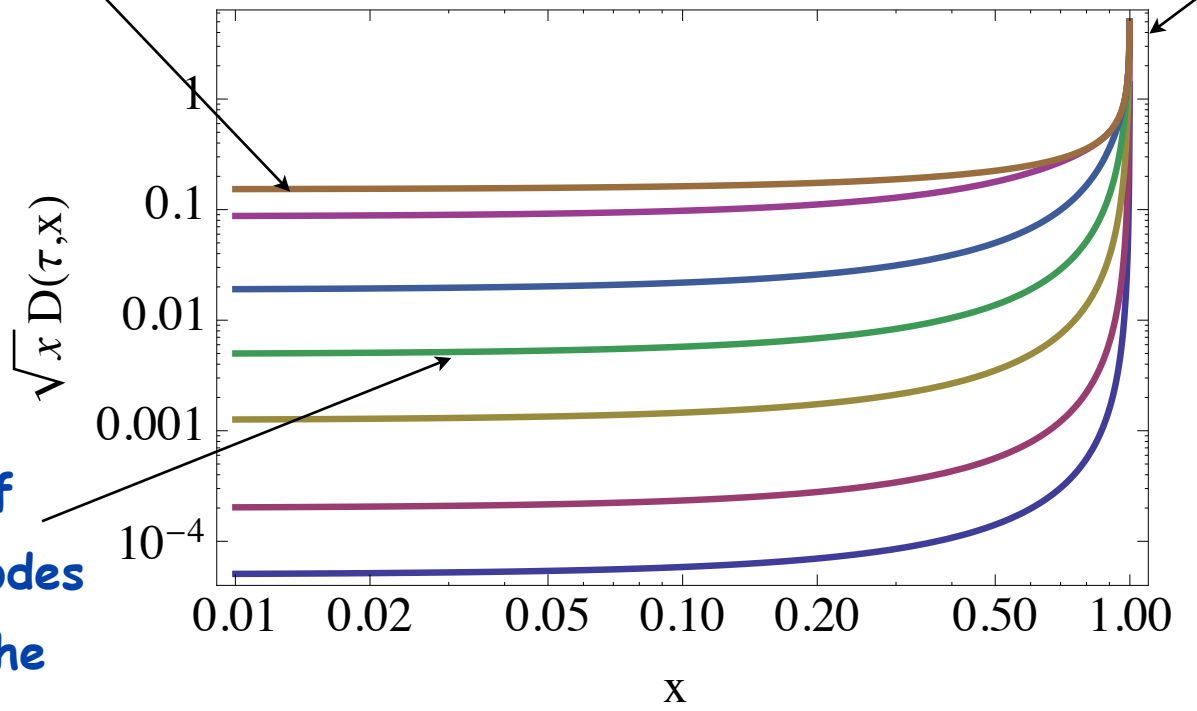

The population of the various x-modes grows, keeping the shape of the spectrum at small x

Relevance to di-jet asymmetry

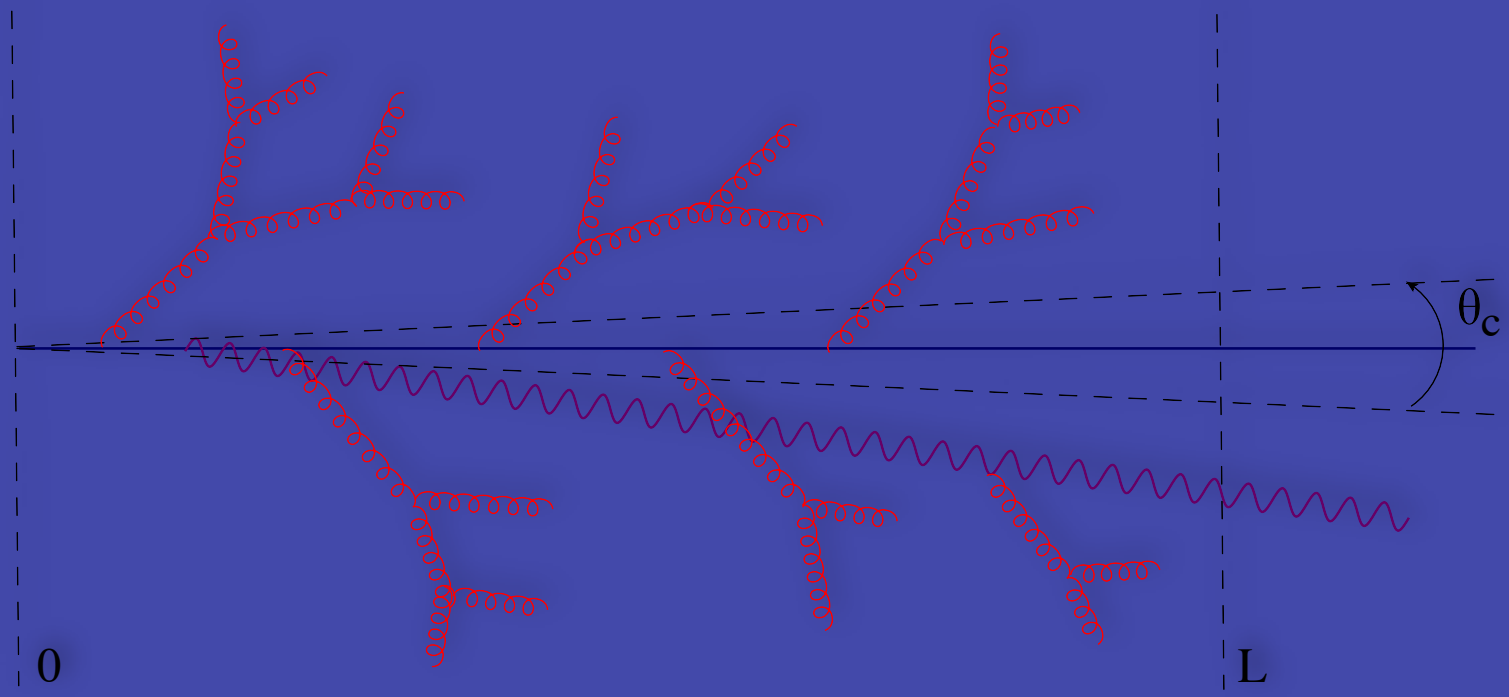

Evolution of the inclusive spectrum

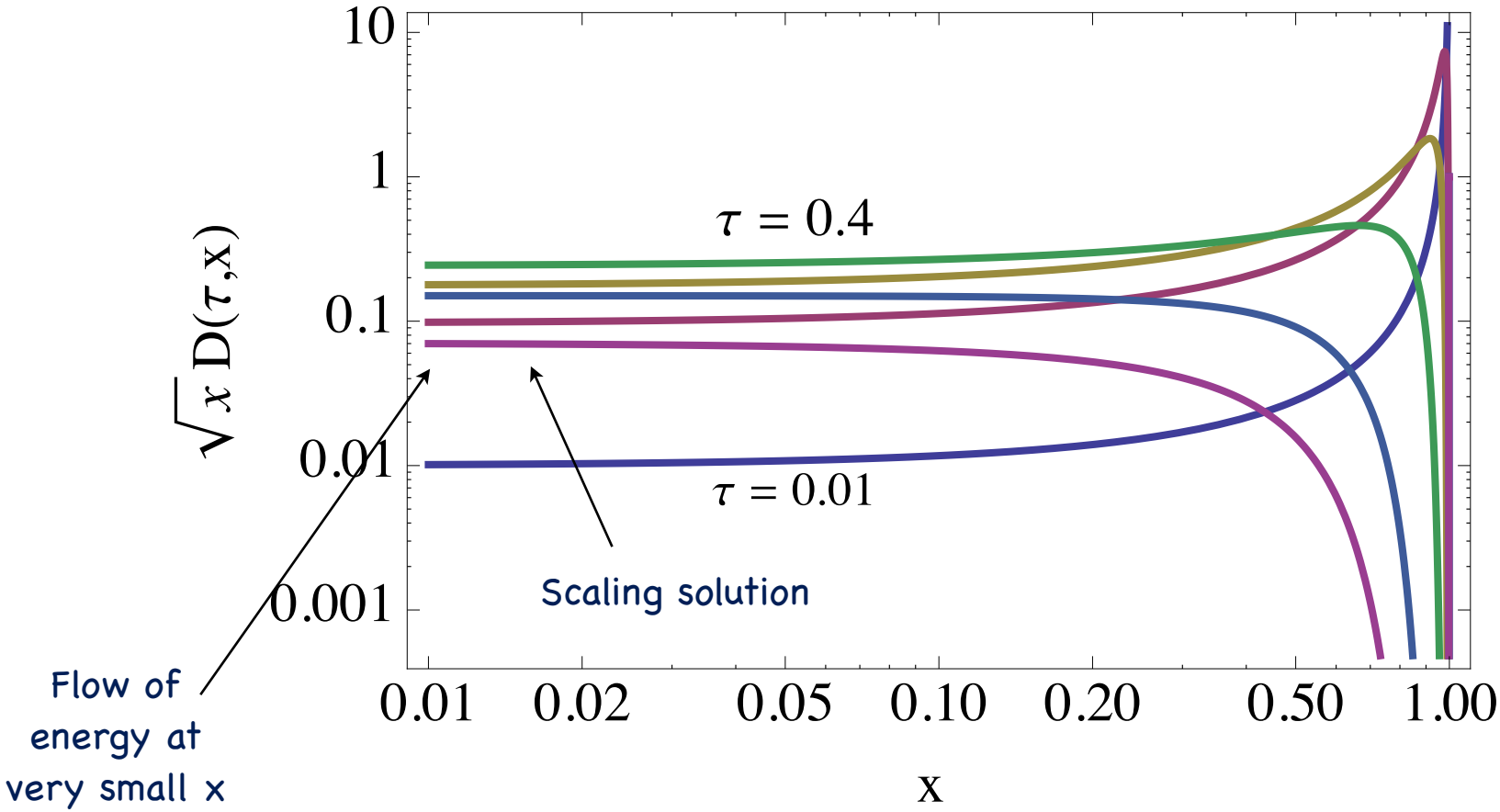

$$\mathcal{E}_{\rm flow} = E\frac{\upsilon\tau^2}{2} = \frac{\upsilon}{2}\,\bar{\alpha}^2\omega_c \qquad \omega_c \equiv \frac{\hat{q}L^2}{2} \qquad \upsilon \simeq 5$$

Estimate $\hat{q} = 1\,\mathrm{GeV}^2/\mathrm{fm}$ $\quad \omega_c \simeq 40$ Gev $\quad \bar{\alpha}^2 \simeq 0.1 \quad \mathcal{E}_{\rm flow} \simeq 15$ GeV

$L = 4$ fm

J.-P. B., E. Iancu, Y. Mehtar-Tani, arXiv: 1301.6102

Energy flow at large angle

$E_{\rm in}$ energy in the jet with x>xo

$E_{\rm out}$ energy in the spectrum with x<xo

$E_{\rm out} + E_{\rm flow}$ energy out of the jet cone

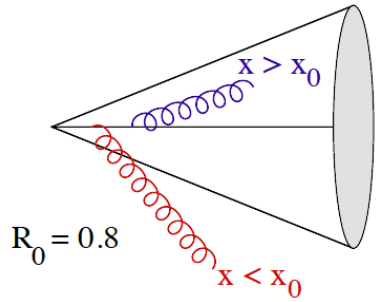

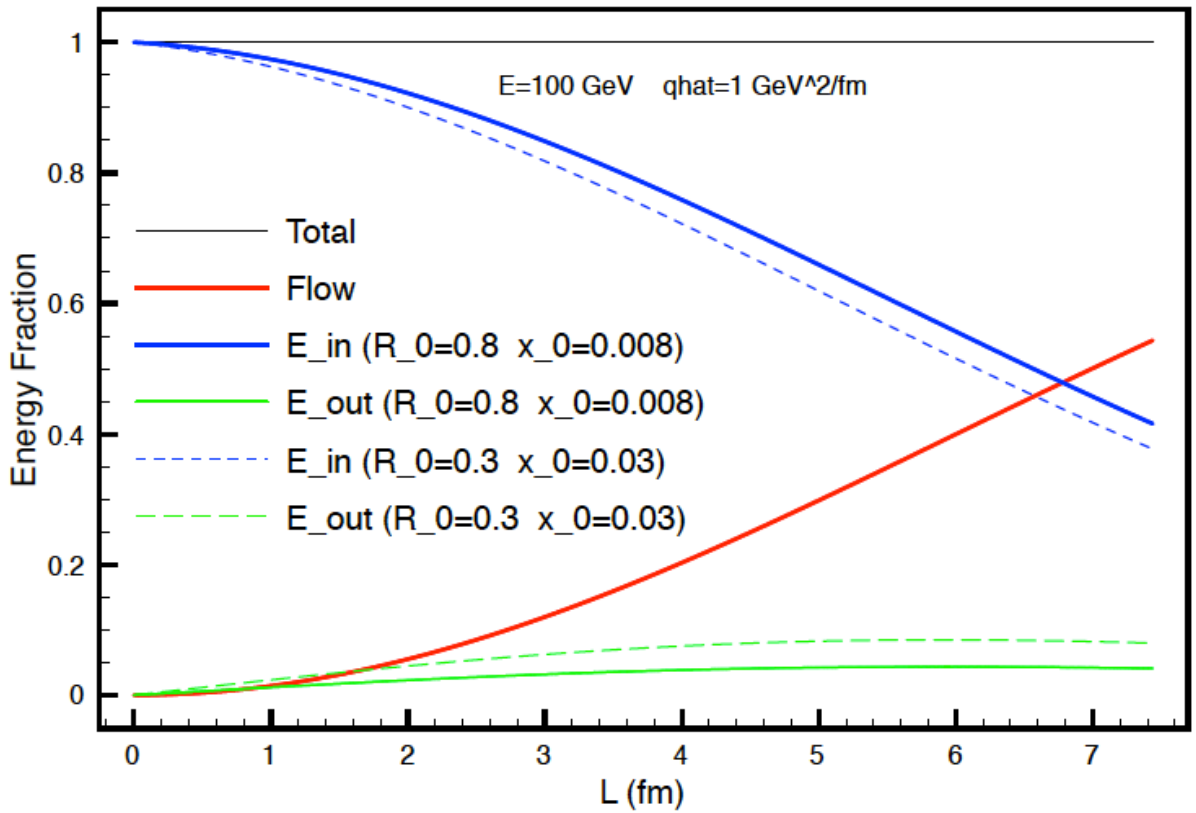

Conclusions

In-medium cascade is very different from the in-vacum cascade (no angular ordering, turbulent flow)

Provides a simple and natural mechanism for transfer of jet energy towards very small angles

Ridge correlations in pp/pPb: hydro perspective

Piotr Bożek

PB Phys. Rev. C85 (2012) 014911
PB, W. Broniowski Phys. Lett. B718 (2013) 1557
PB, W. Broniowski Phys. Lett. B720 (2013) 250
PB, W. Broniowski arXiv:1304.3044

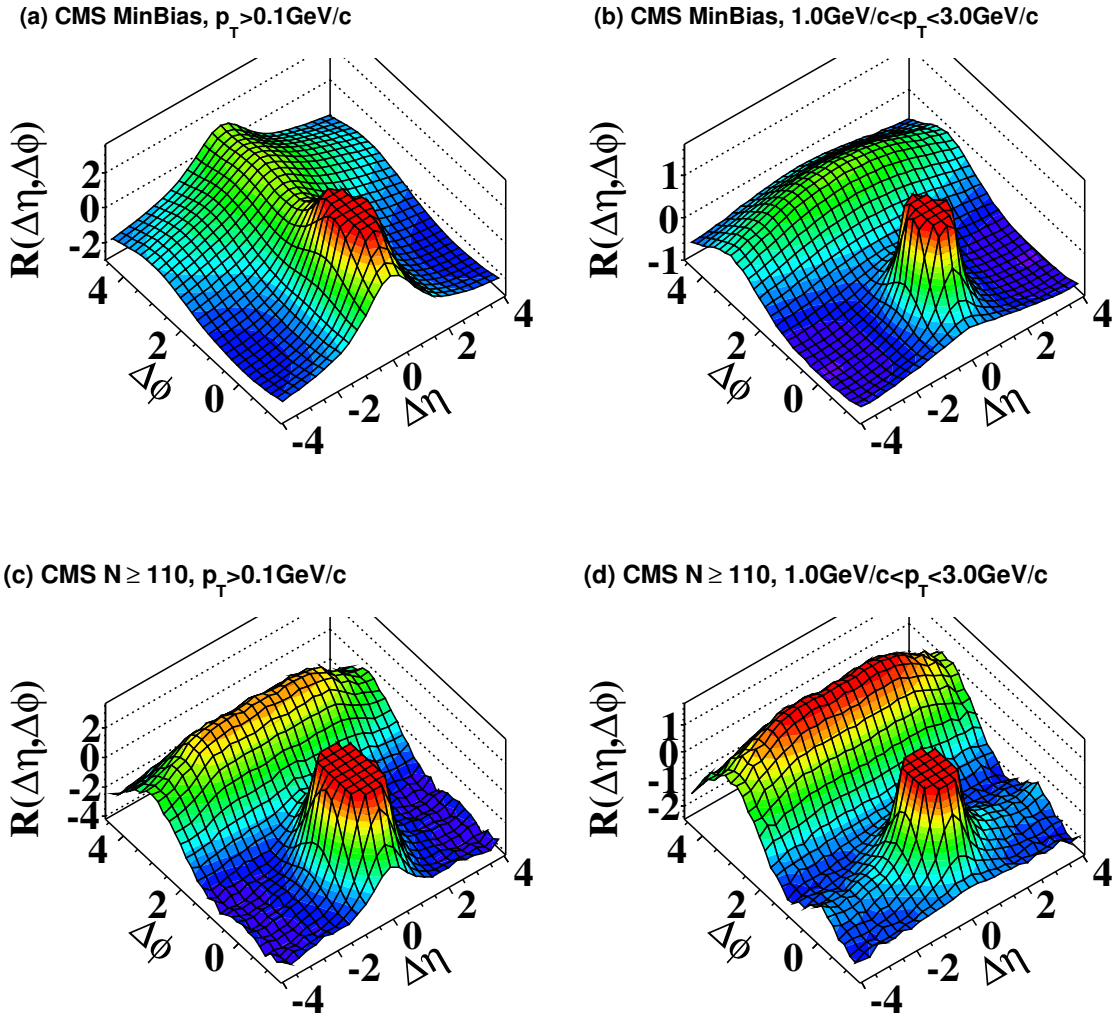

intriguing ridge seen in p-p

Flow in A-A

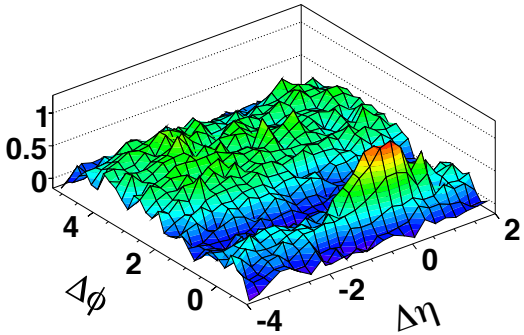

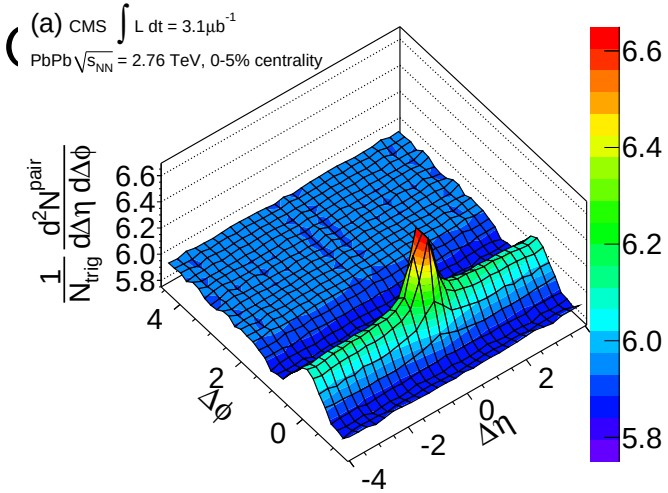

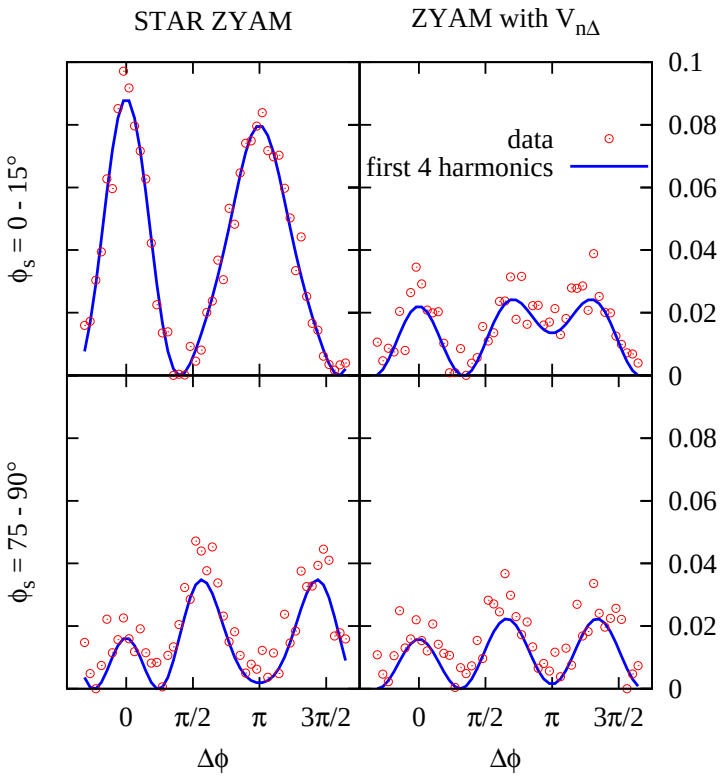

Luzum arXiv: 1011.5773 - flow harmonics

Collective elliptic flow in p-Pb?

- Large enough density? yes
- Large enough eccentricity? yes?
- Large enough size? (?) but should and can be tested in pA
- Small enough gradients? no - beyond viscous hydro

p-Pb, d-Pb @ LHC

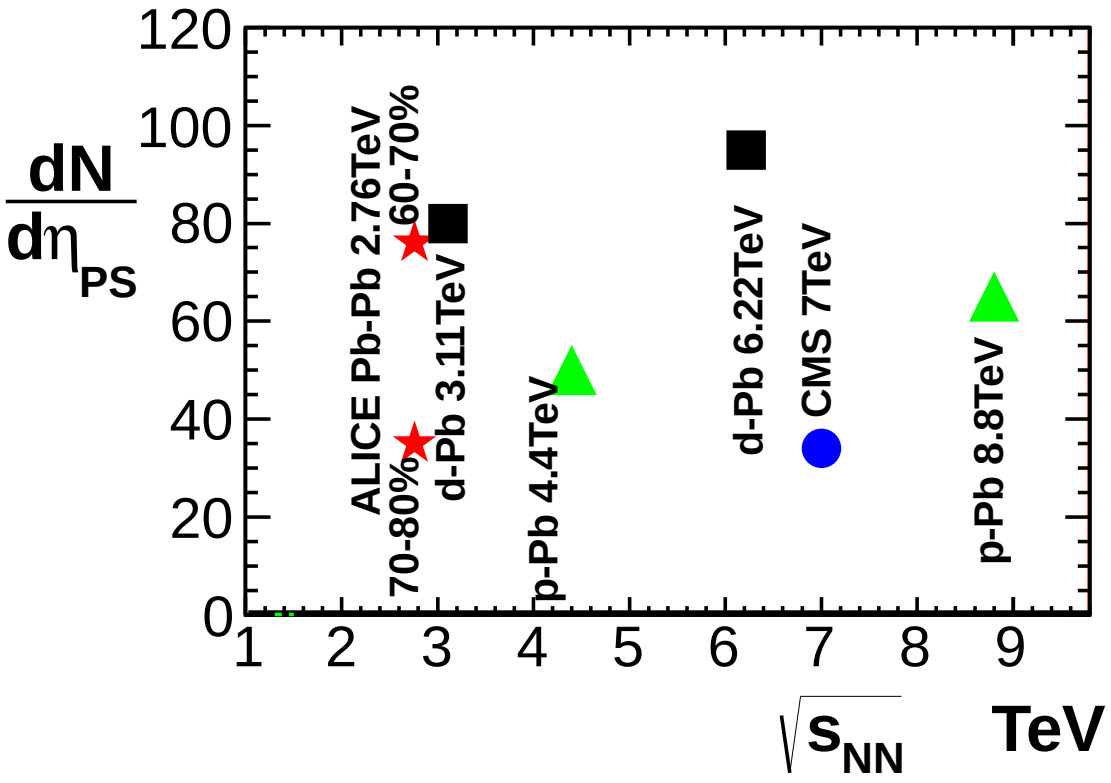

large multiplicity - large fireball - collective expansion?

Fireball in p-Pb

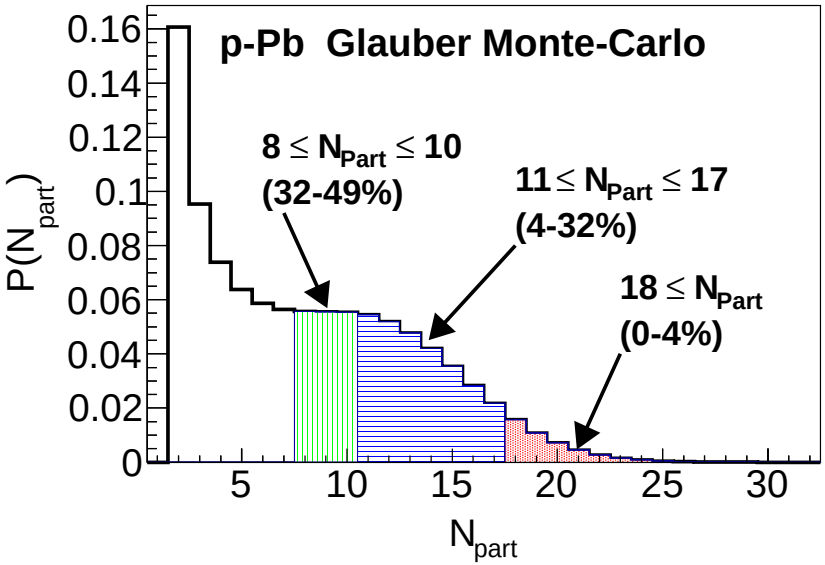

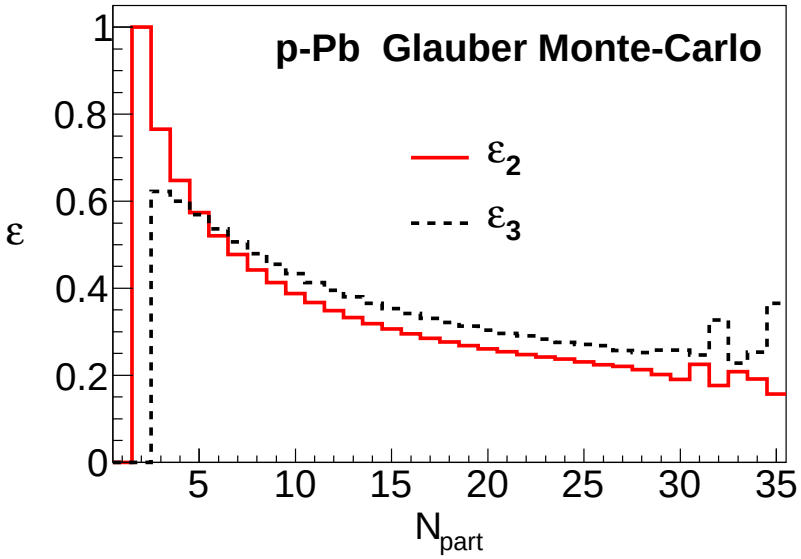

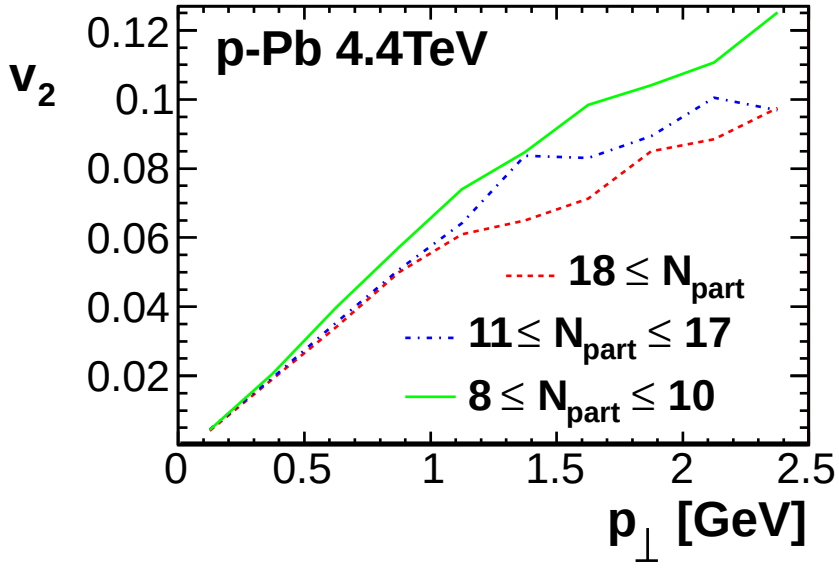

elliptic flow in p-Pb

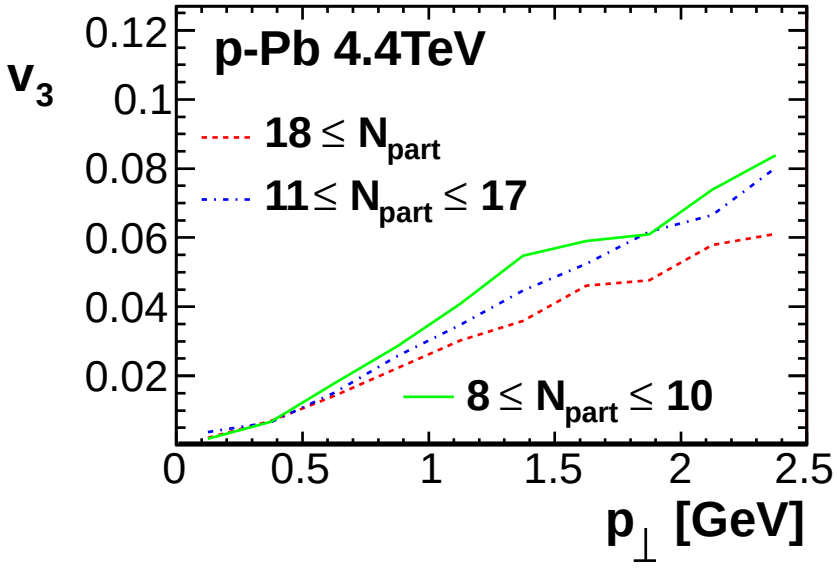

triangular flow

d-Pb

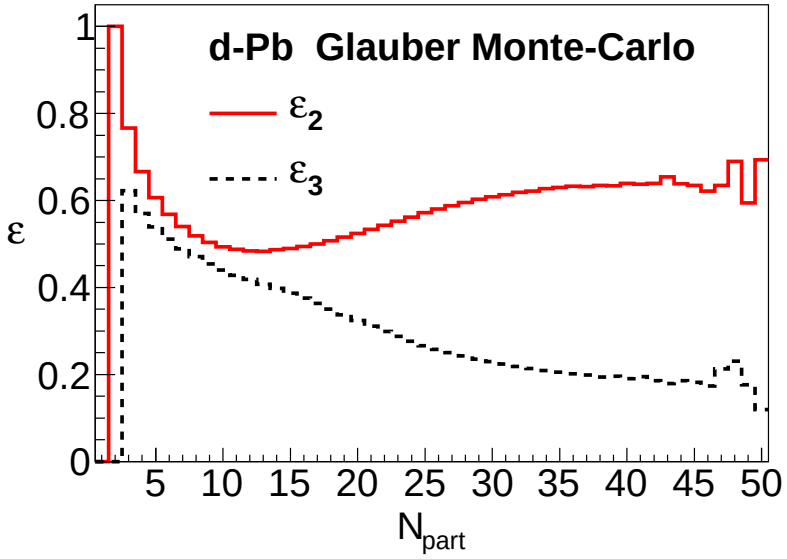

large elliptic flow

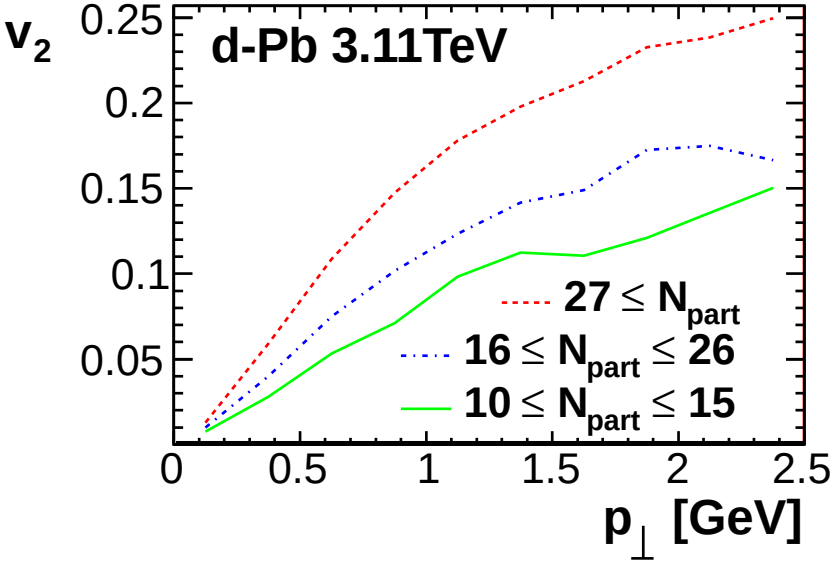

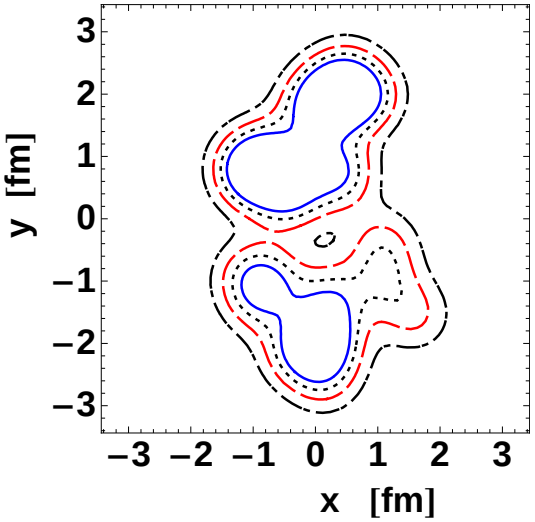

prediction 11.2011

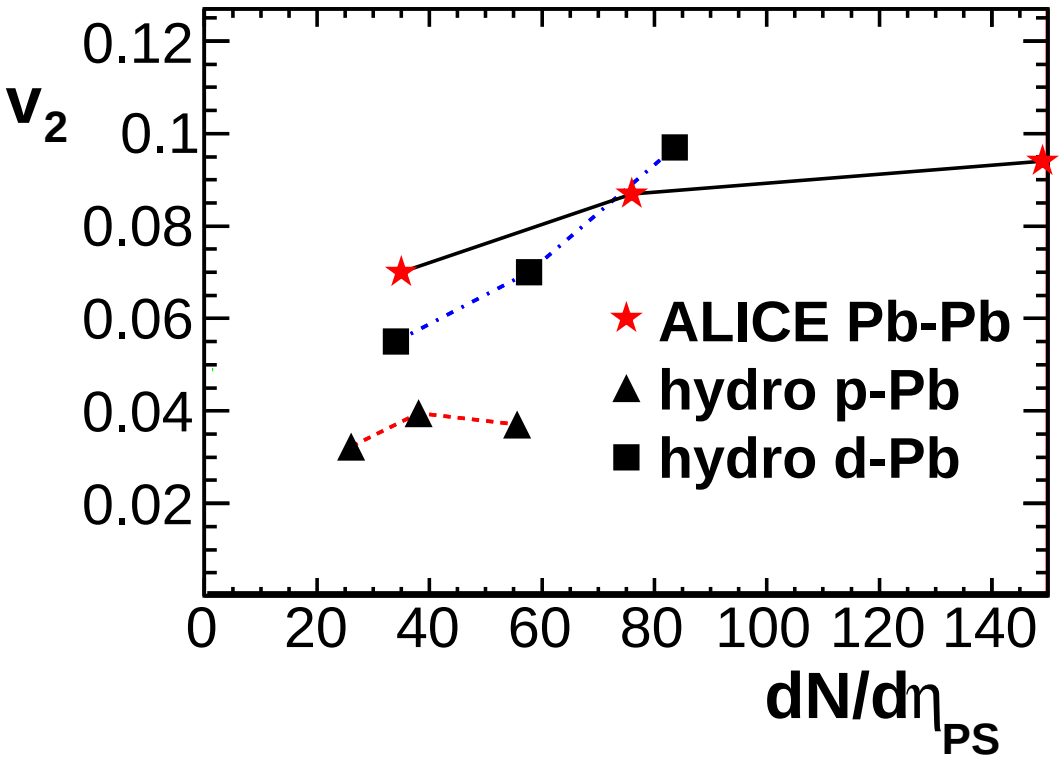

- collective flow effects $\simeq$ peripheral Pb-Pb
- can be observed
- p-Pb (d-Pb) is not p-p superposition
- only p-p as baseline

First results on pPb@5.02TeV - ALICE, CMS, ATLAS

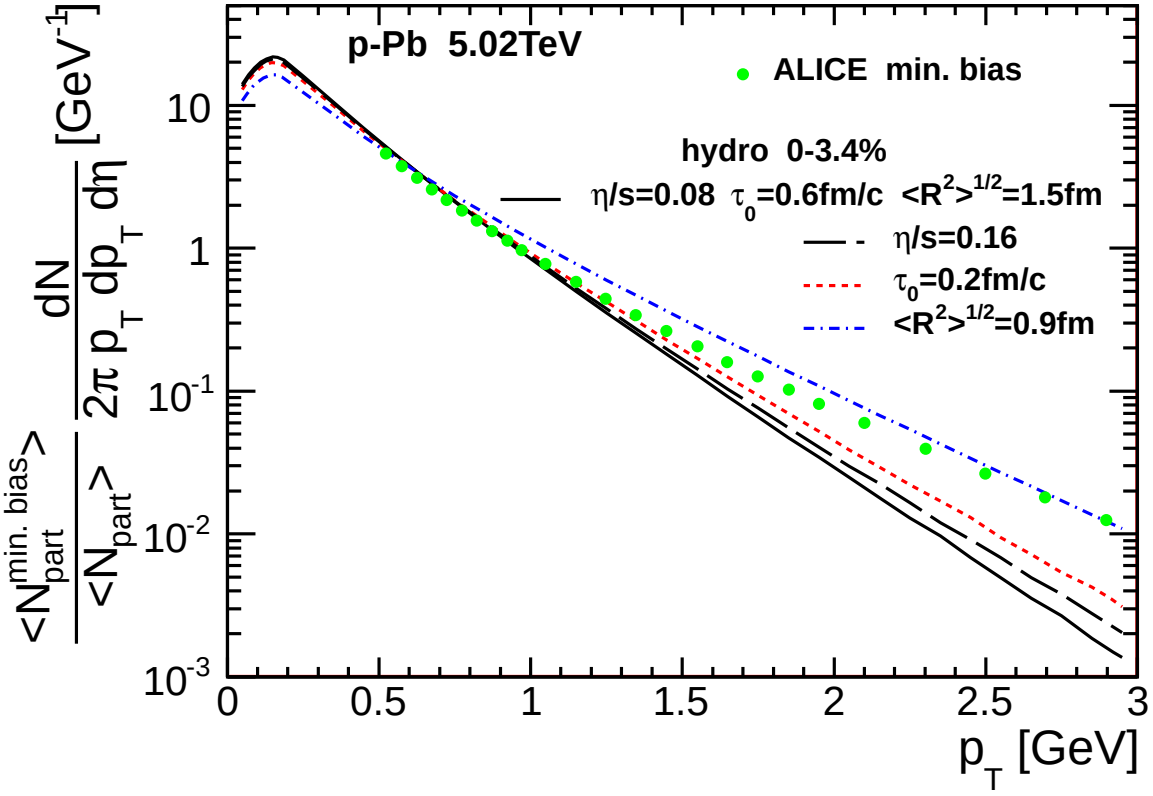

- statistical for $p_\perp < 1.5$-2Gev
- early flow, viscosity, density profile?

Ridge in p-Pb

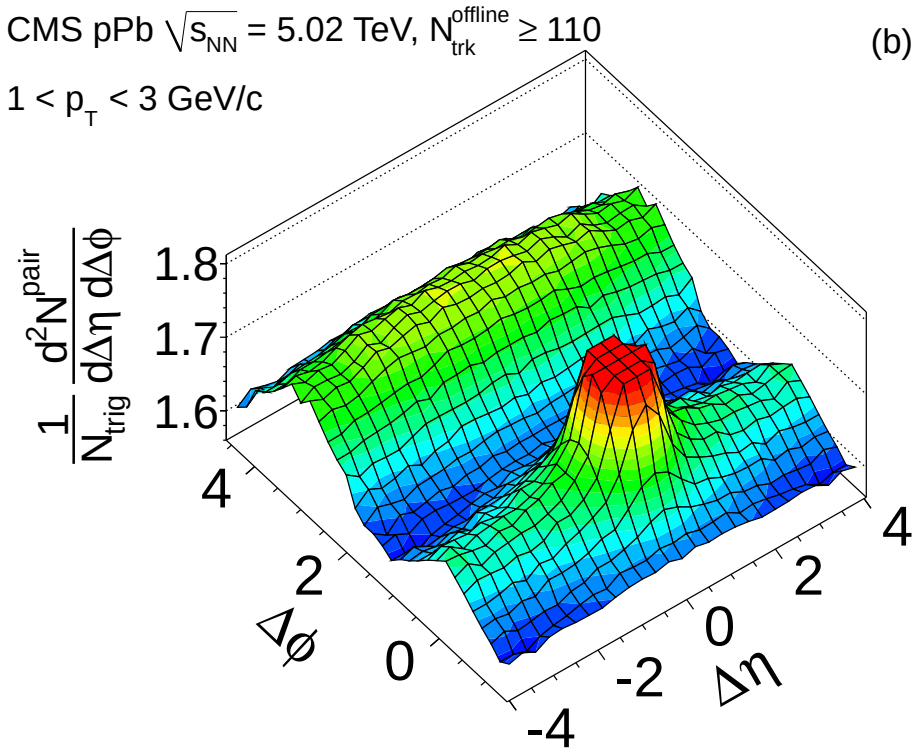
CMS pPb $\sqrt{s_{NN}}$ = 5.02 TeV, $N_{trk}^{offline} \geq 110$
$1 < p_T < 3$ GeV/c
$\frac{1}{N_{trig}} \frac{d^2N^{pair}}{d\Delta\eta\, d\Delta\phi}$
1.8
1.7
1.6
4
2
0
-4
-2
0
2
4
$\Delta\phi$
$\Delta\eta$

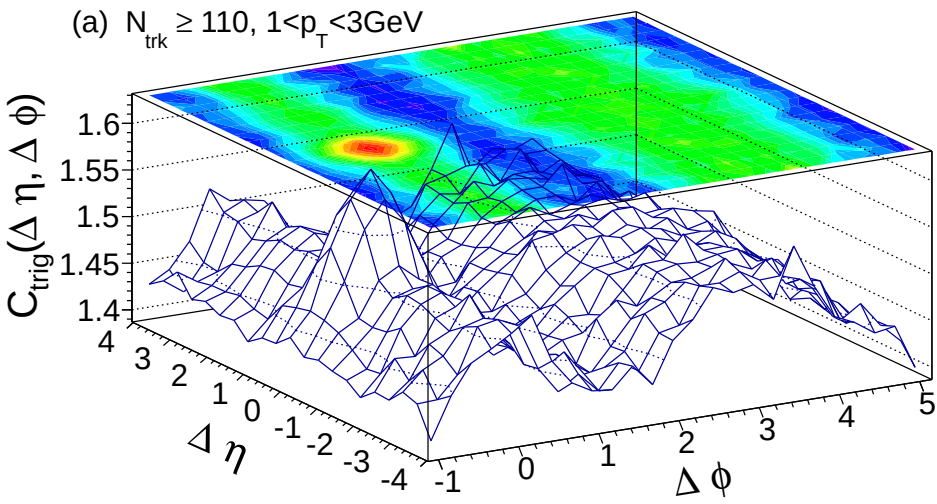
(a) $N_{trk} \geq 110$, $1<p_T<3$GeV
(b)
$C_{trig}(\Delta\eta, \Delta\phi)$
1.6
1.55
1.5
1.45
1.4
4
3
2
1
0
-1
-2
-3
-4
$\Delta\eta$
-1
0
1
2
3
4
5
$\Delta\phi$

Charge balancing

local charge conservation

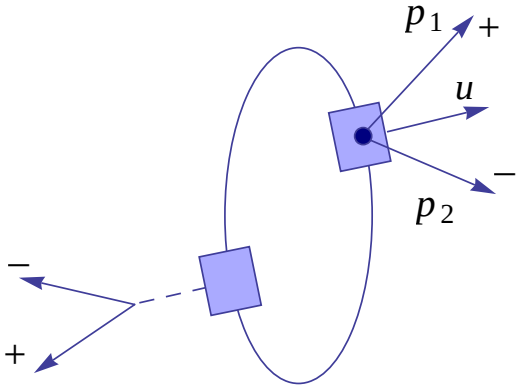

charge balance function

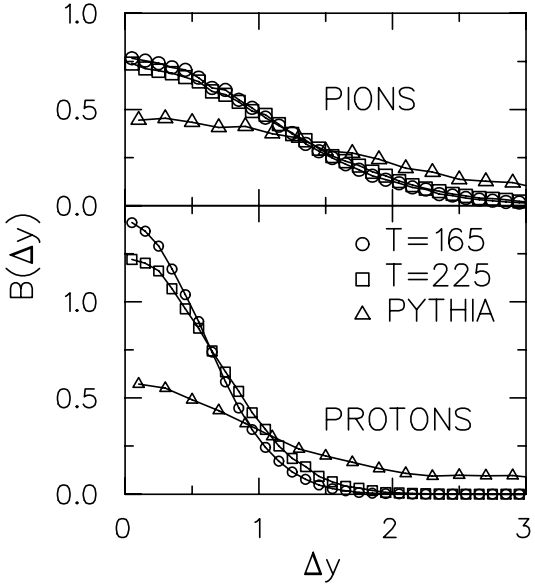

Bass et al. (2000)

Correlation function per pair

ATLAS

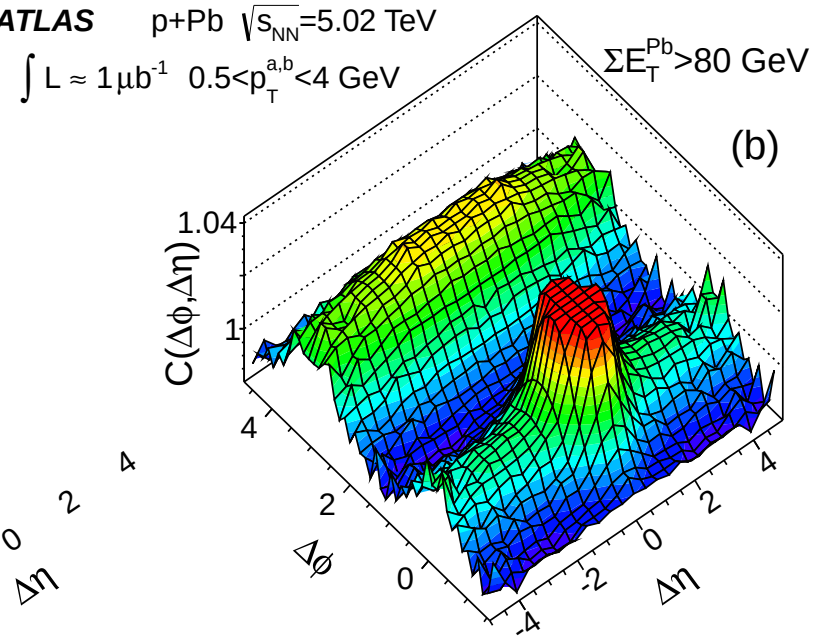

hydro

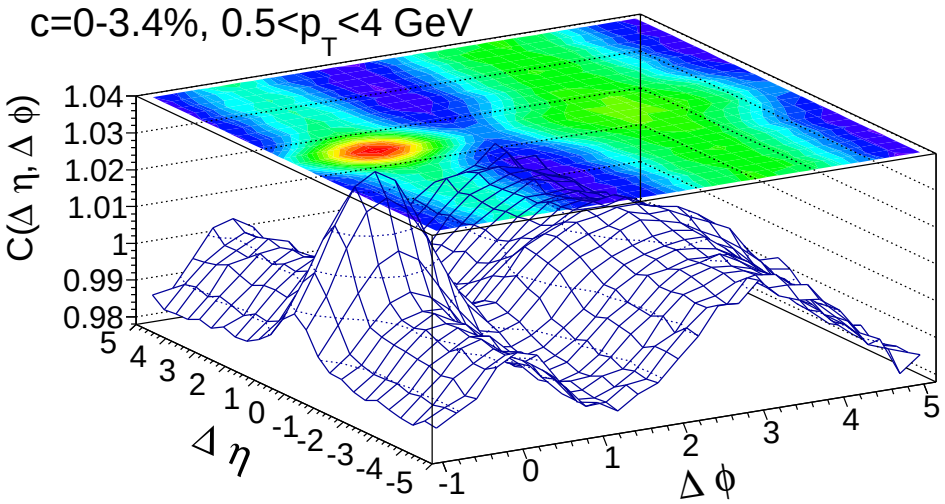

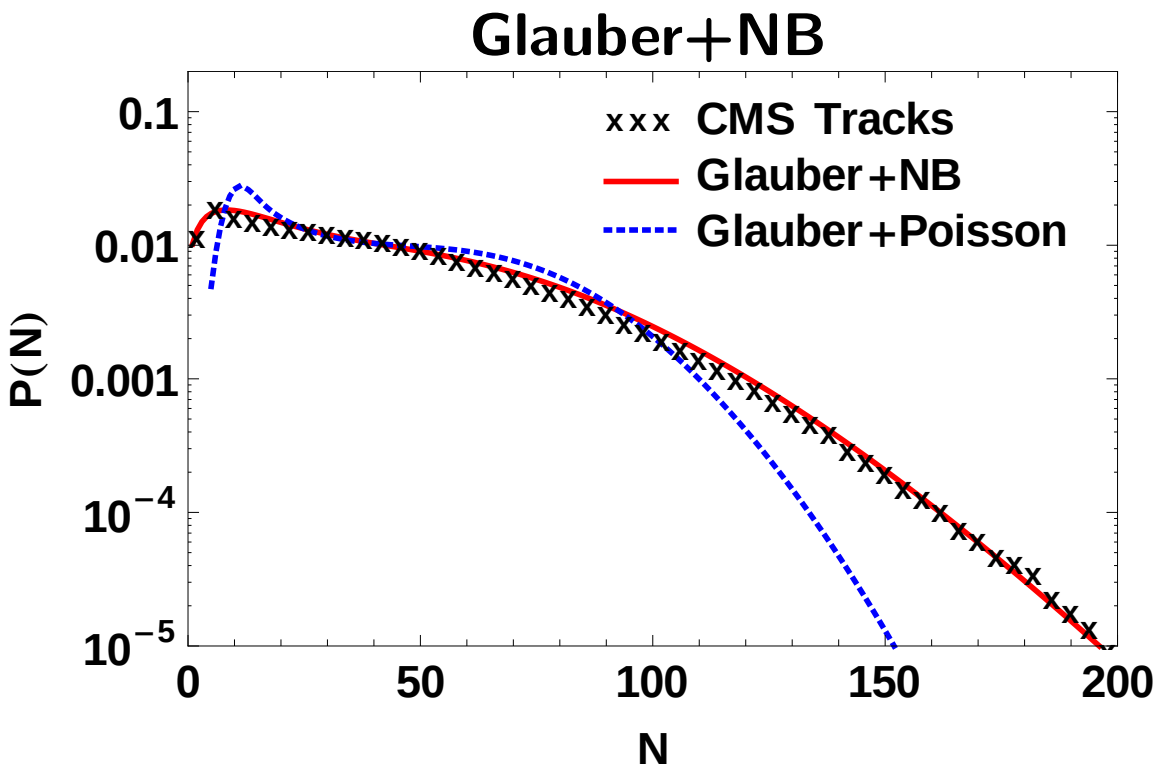

$P(n) = \sum_i P_{part}(i) N_{p\lambda i, \kappa i}(n)$

Additional fluctuations of density (compared to Glauber)

Very different fireball size

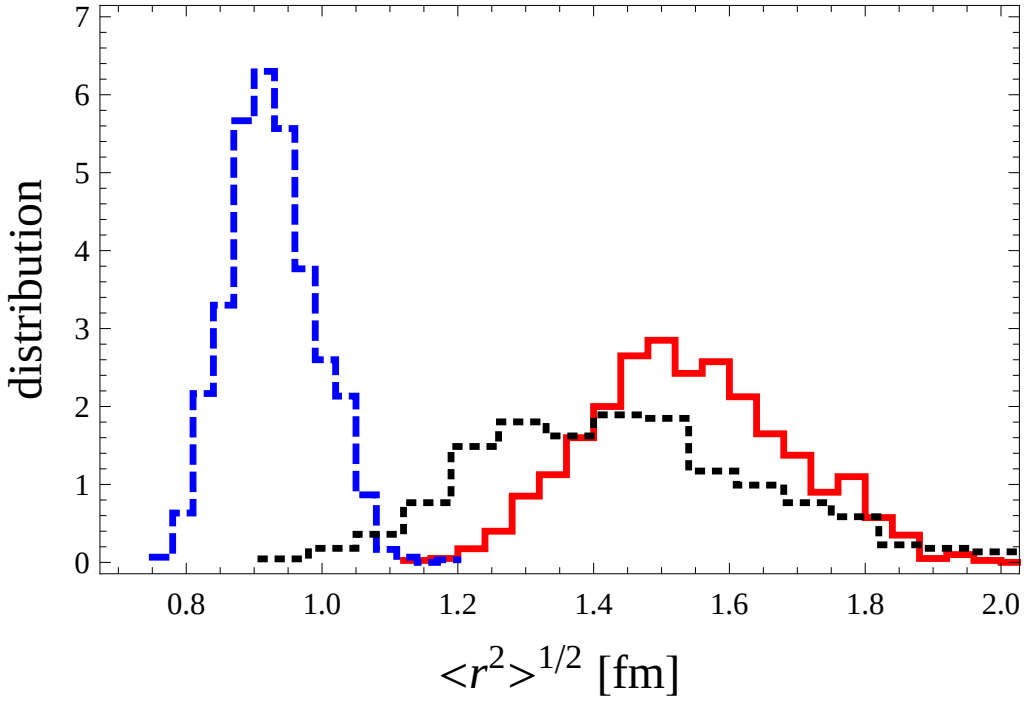

Compact (0.9fm), Glauber+NB (1.4fm), Standard (1.5fm)

Expansion of the fireball

Compact source

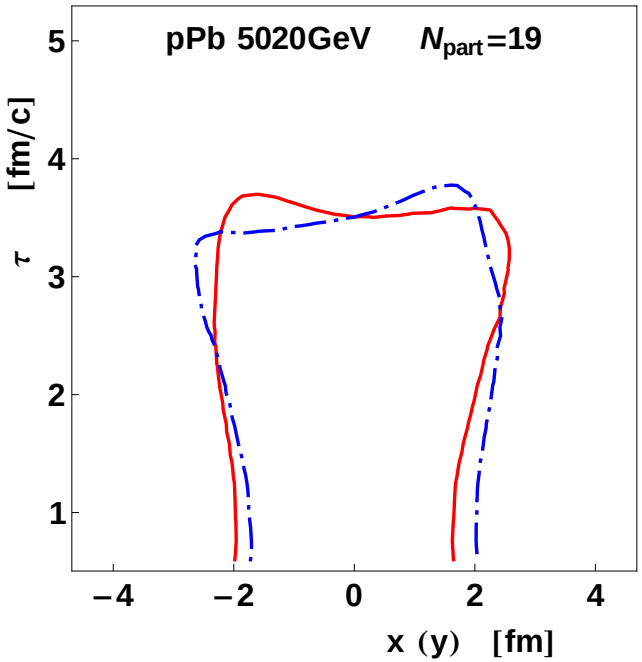

Standard (large) source

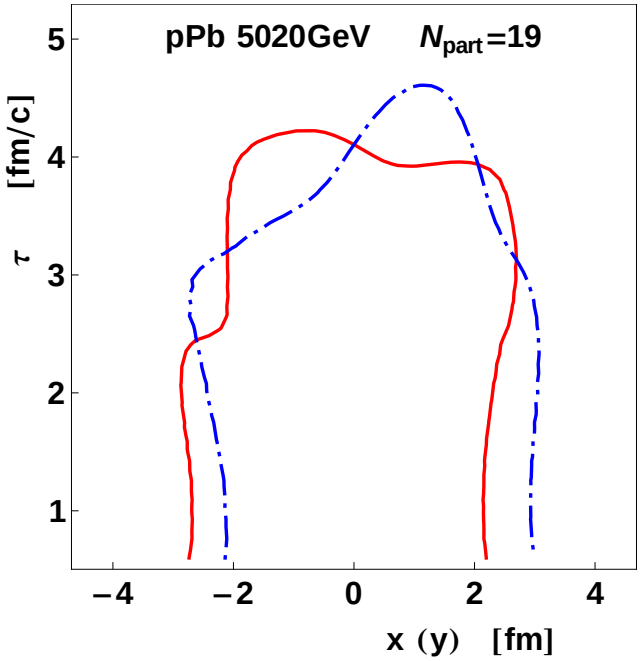

Azimuthal correlations

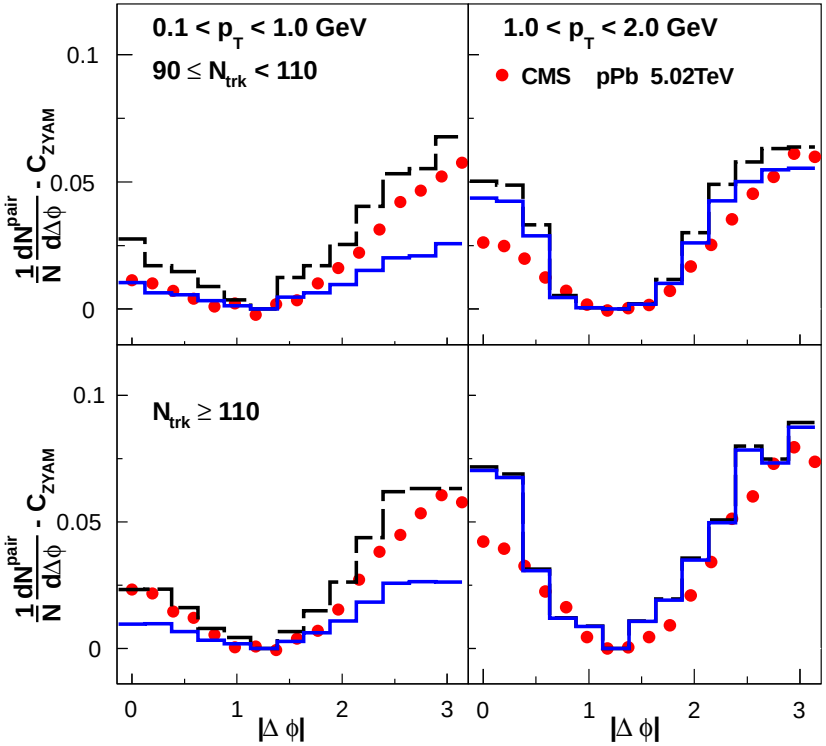

- collective flow

Azimuthal correlations ATLAS

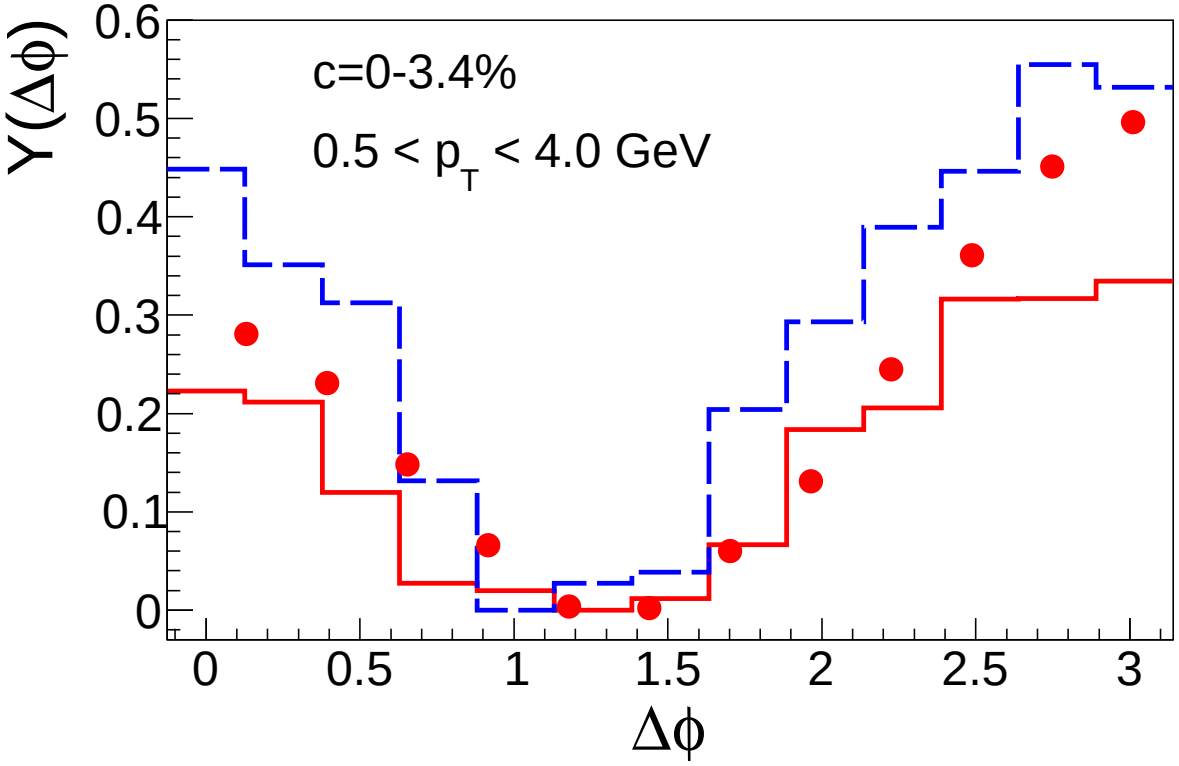

HBT systematics

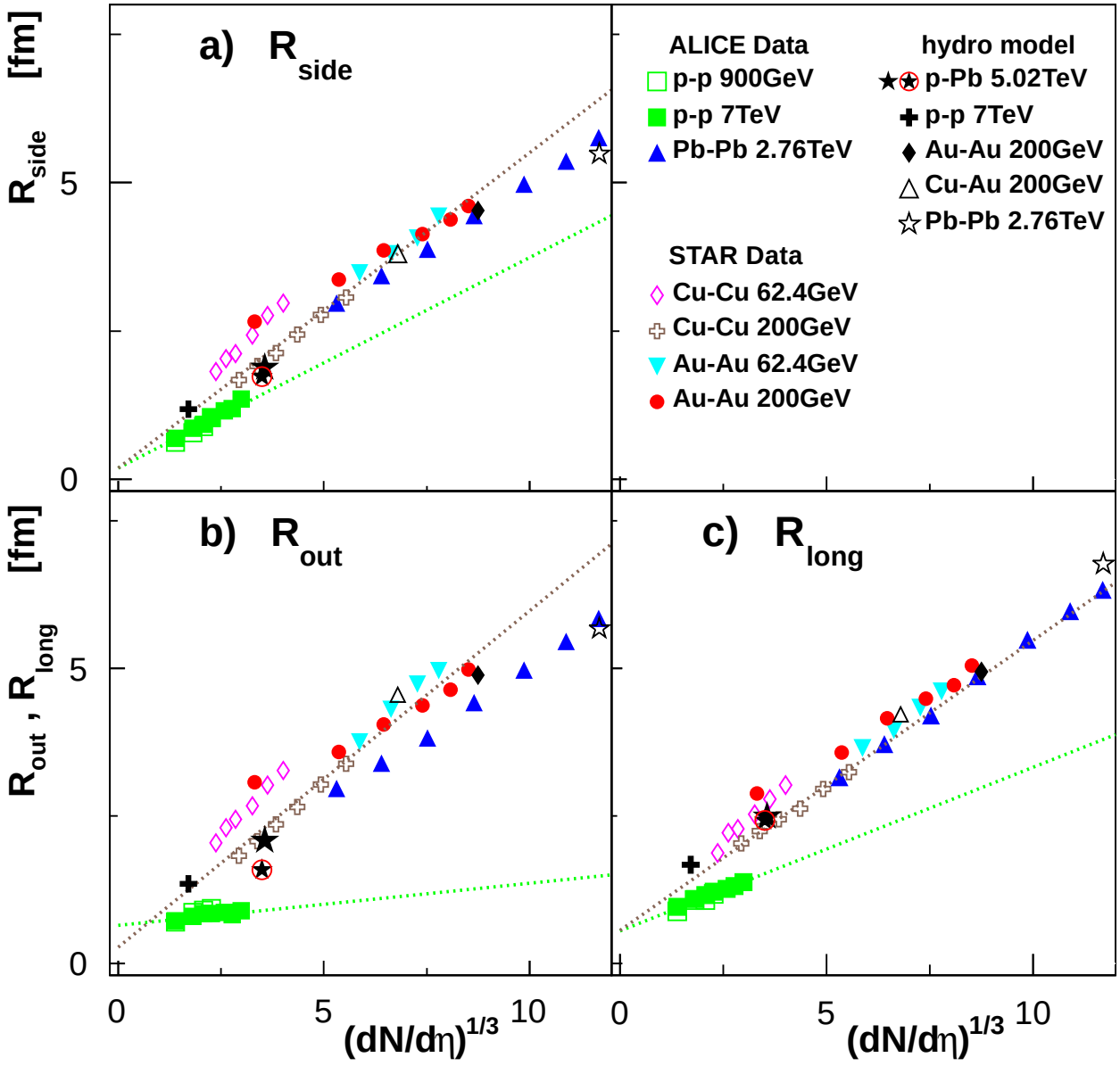

d-Au 200GeV

- large eccentricity
- large v_2
- small v_3

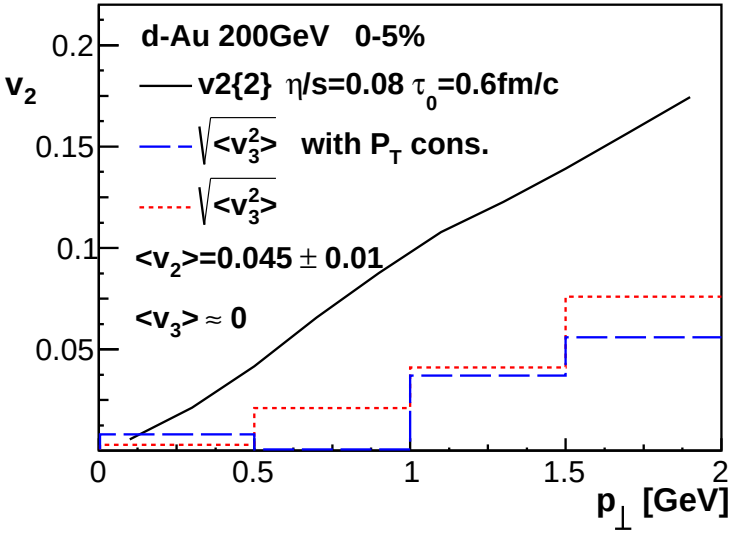

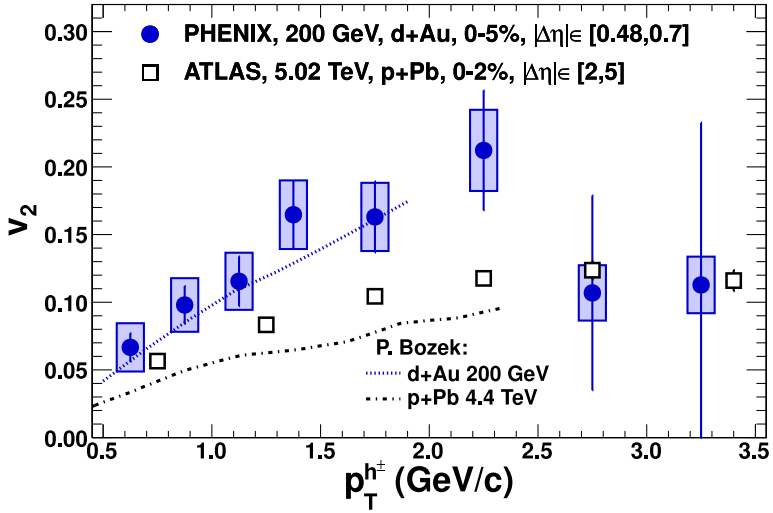

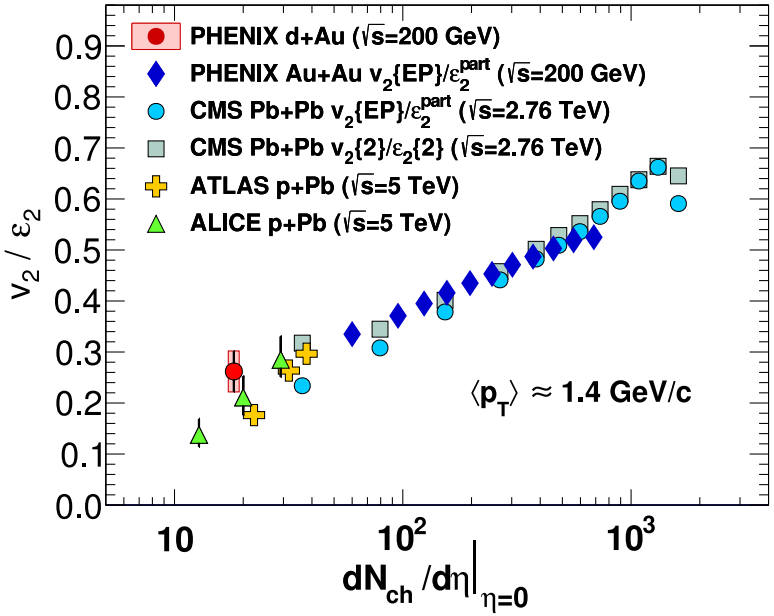

Hydro in pA, dA compares well with data

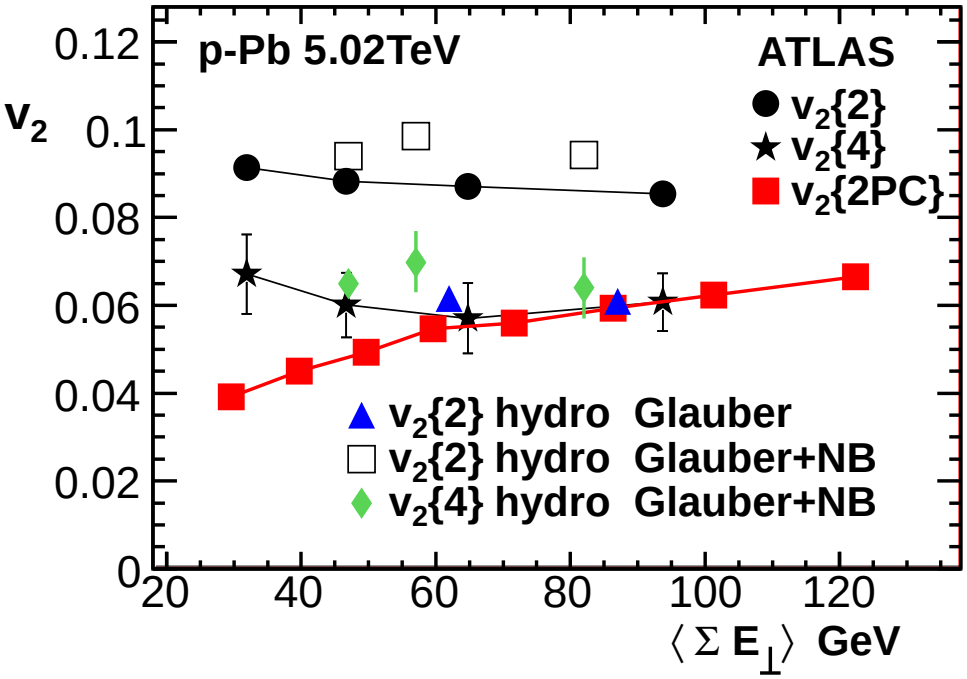

Initial conditions matter a lot!

Hydrodynamic flow in p-p?

- Romatschke, Luzum - arXiv: 0901.4588 (overlap)
- Bozek - arXiv: 0911.2392 (flux-tubes)
- Chaudhuri - arXiv: 0912.2578 (hot-spots)
- Werner, Karpenko, Pierog - arXiv: 1011.0375 (EPOS)
- Bzdak, Schenke, Tribedy, Venugopalan - arXiv: 1304.3403 (IP-Glasma)

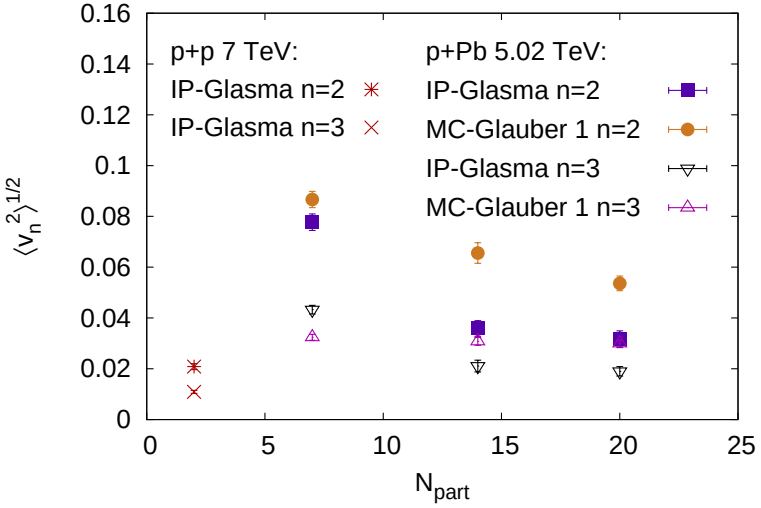

- Is hydrodynamics valid?
- What is the initial eccentricity ?

Fireball shape in pp

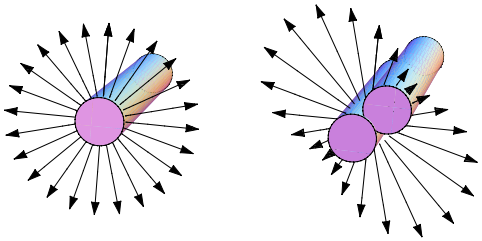

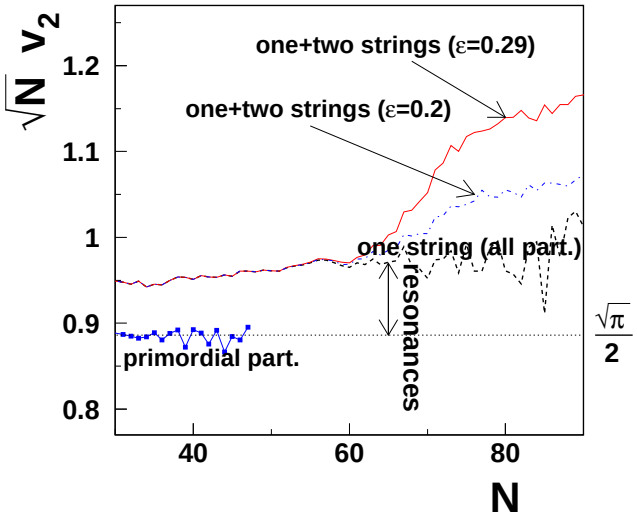

PB, 0911.2397

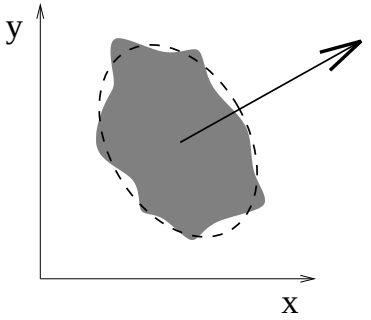

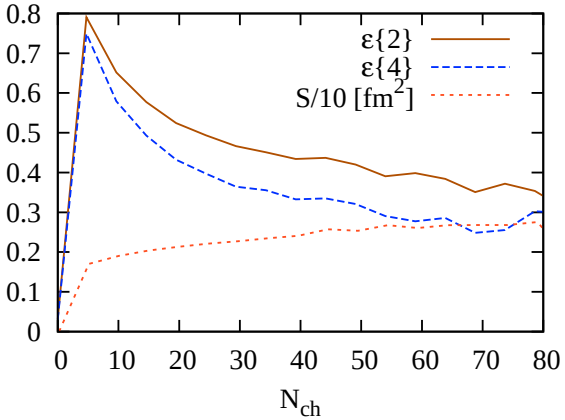

E.Asar et al., 1009.5643

EbE v_2 deconvolution? (ATLAS, Jia, Mohapatra)

Hydro ridge in p-p

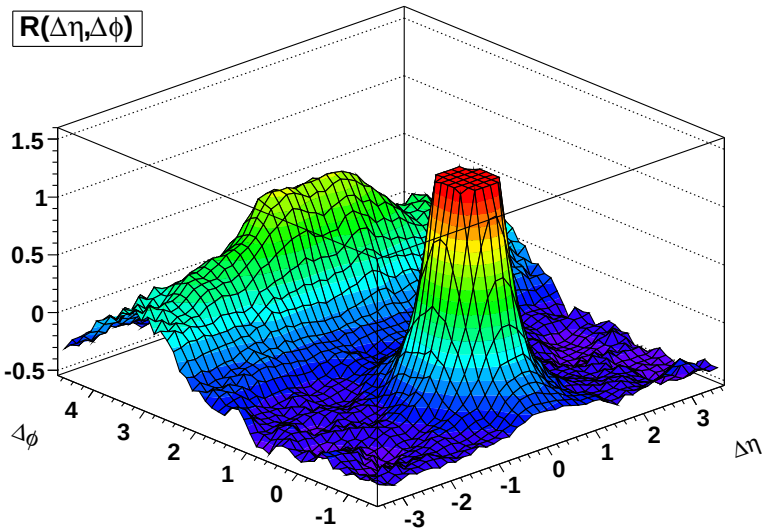

No collectivity

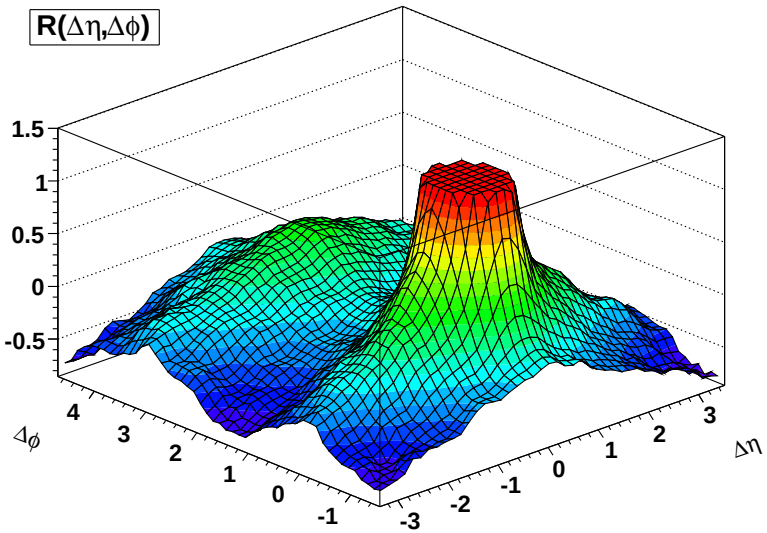

EPOS+hydro

Werner, Karpenko, Pierog arXiv: 1011.0375

Can we reduce the uncertainties

go back to very peripheral A-A

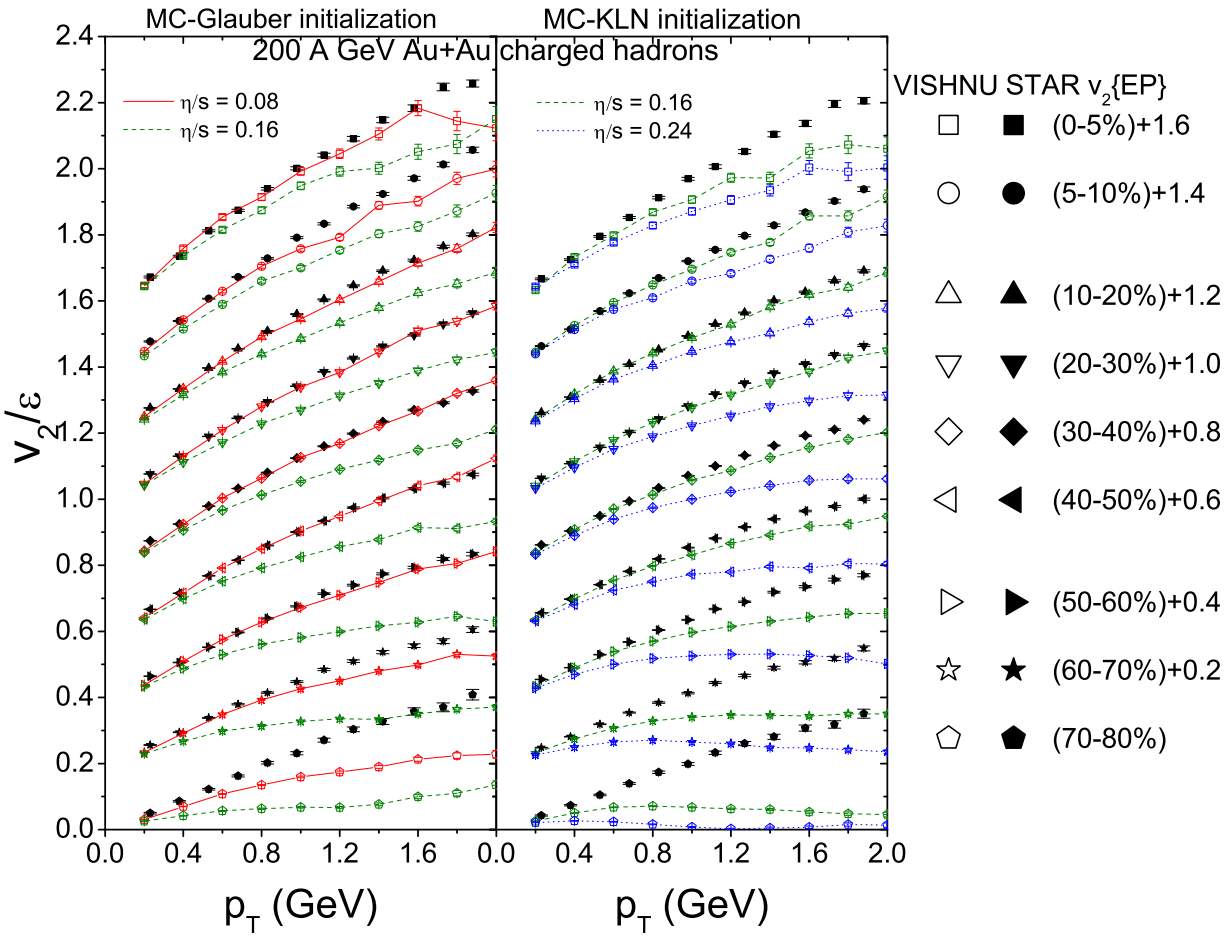

Song, Bass, Heinz, Hirano, Shen arXiv: 1101.4638

Summary

- Ev-by-ev hydro for pA, dA
- Collectivity (FSI) in pPb@LHC , explains observed ridge and v_2
- d-Au data consistent with collective picture
- HBT radii in p-Pb ?
- Is it collective flow ? - In manys ascpects consistent
- Other sources of correlations !
- Limits of hydro!

- Why hydrodynamics would work?

- Prospects: **Experiment**

... and initial state, peripheral A-A, p-p??, core-corona, disantengling: collectivity, CGC, jets ...

Pressure anisotropy

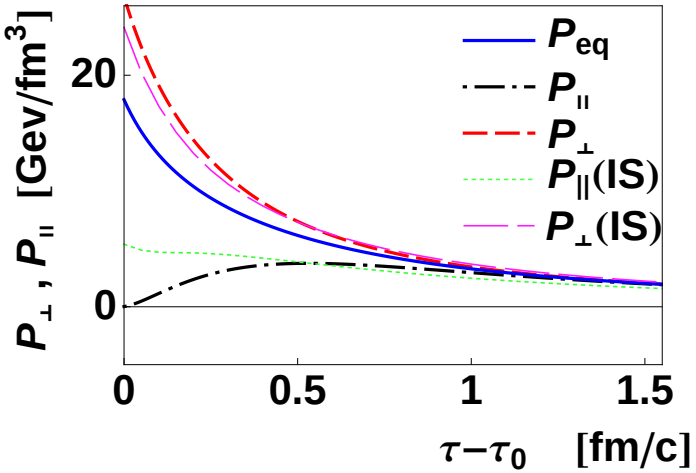

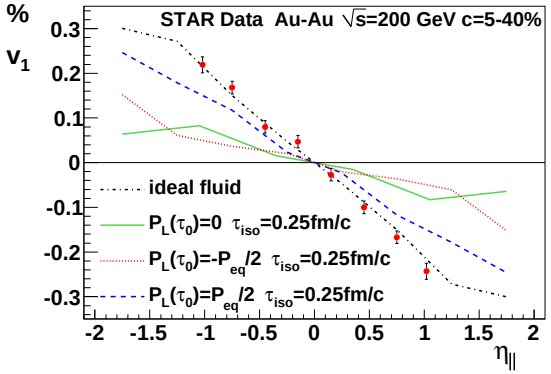

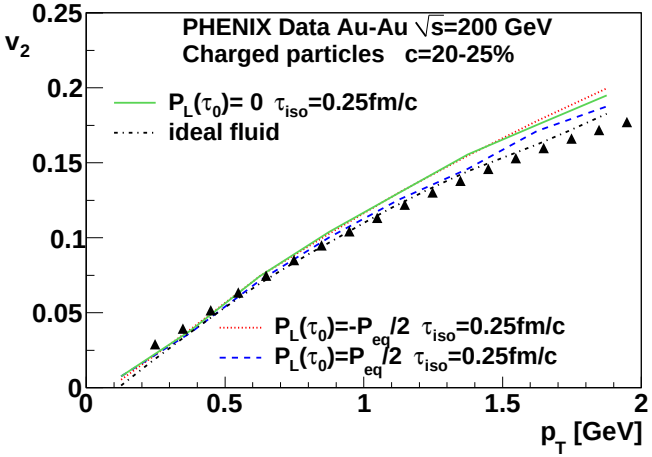

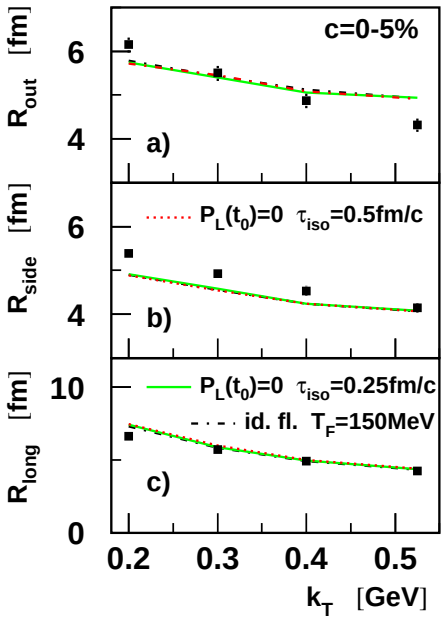

PB, I.Wyskiel, 2010

early pressure anisotropy irrelevant - Vredevoogd, Pratt, 2009

other higher gradients could be important ?

Fireball anisotropy - flow asymmetry

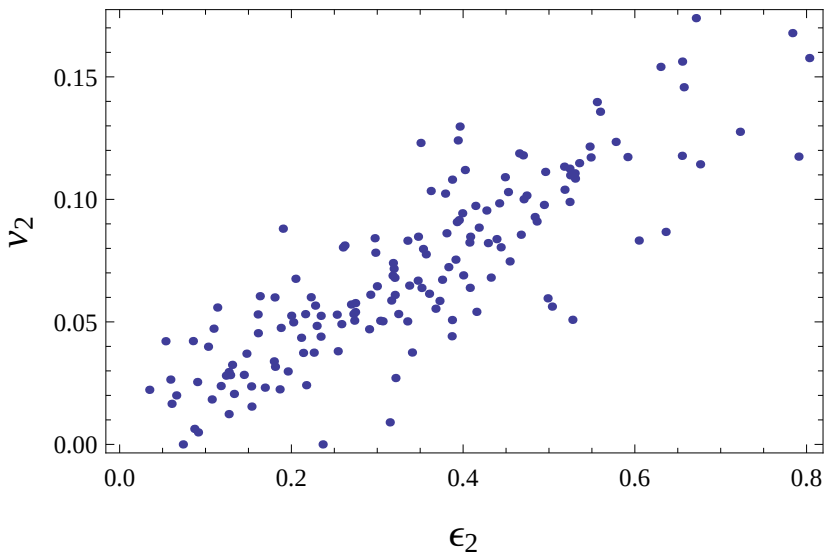

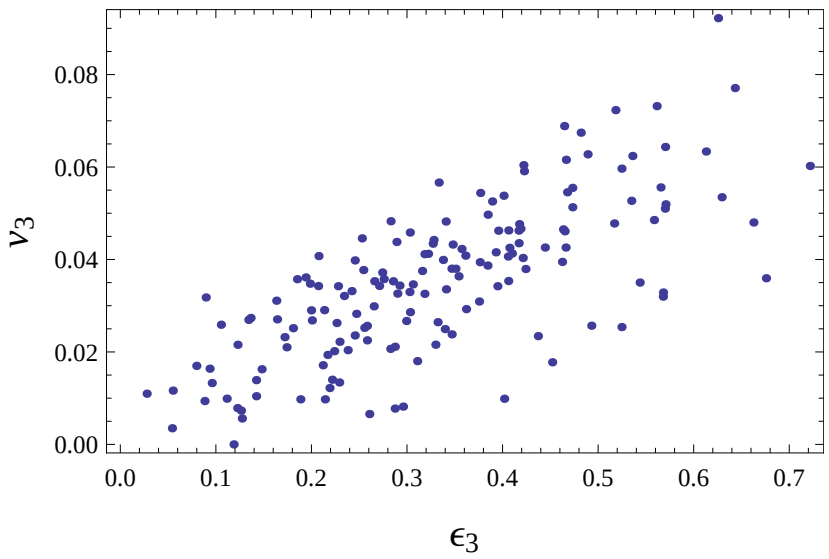

- Ev-by-Ev hydro response to geometry valid
- response strength depends on details

Eccentricity fluctuations, central collisions

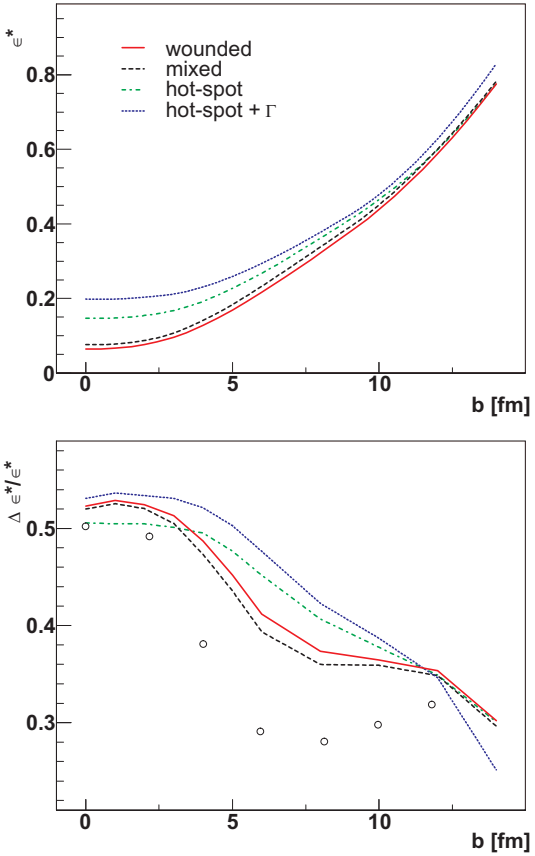

$$\frac{\Delta\epsilon}{\epsilon} = \sqrt{\frac{4}{\pi} - 1}$$

Broniowski, Bozek, Rybczynski arXiv: 0706.4266

central A-A, Gaussian limit $\longrightarrow$ $v_2\{4\} \simeq 0$

central p-A (Glauber+NB) $\frac{\Delta\epsilon}{\epsilon} < \sqrt{\frac{4}{\pi} - 1}$ and $v_2\{4\} > 0$

pA studies 1972-2013

reminiscences

The pA play
as seen through the eyes of one of the actors

Act 1 before the early 1970's	The "A" of "pA" is more of a nuisance than a help!
Act 2 The 1970's	Is there too much or too little cascading?
Act 3 late 1970's, early 1980's	Is there too much or too little quenching in the forward direction?
Act 4 Late 1980's, 1990's & 2000's	Who cares about the details of "pA" ? After all, it's only a reference!
Act 5 To-day	Who is helping whom? pp & pA the understanding of AA or AA the understanding of pp & pA?

Cosmic ray interactions in nuclear emulsions ≈ 1950

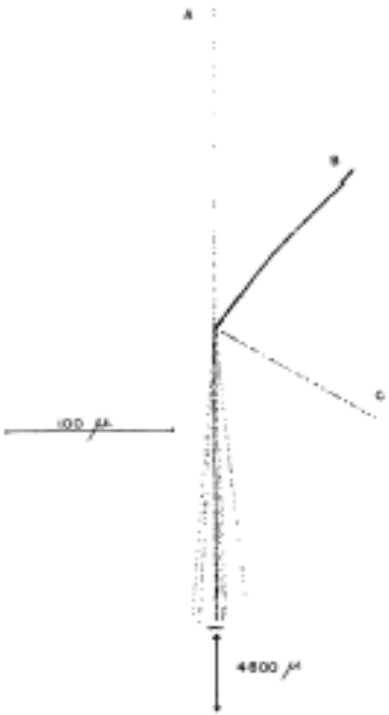

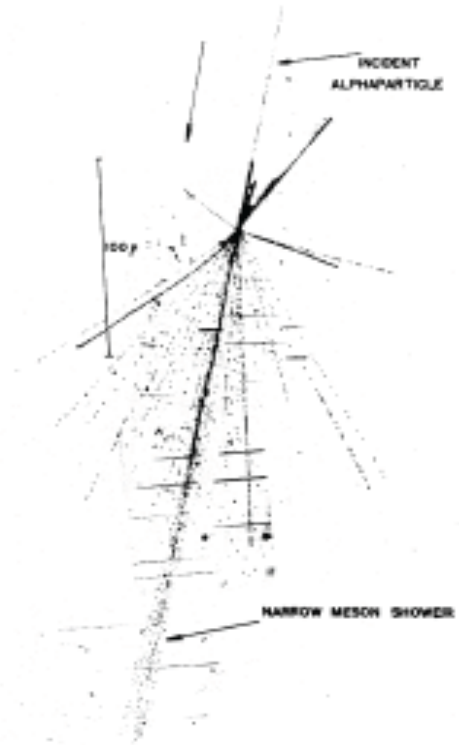

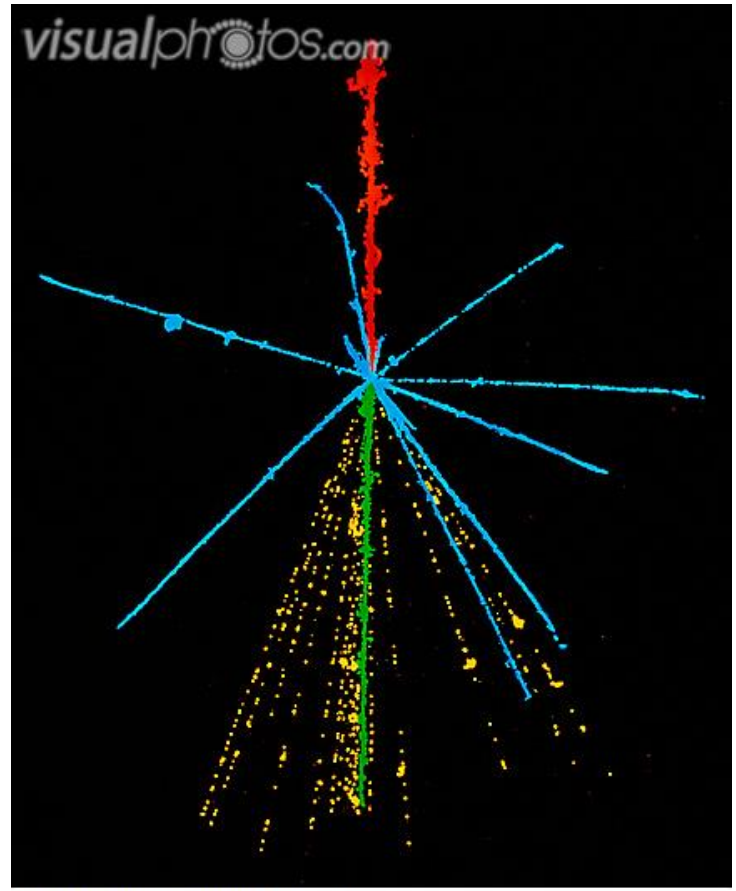

a134005 [RM] © www.visualphotos.com

p-p collision

α-emulsion collision

Composition of nuclear emulsion by weight: 83% (Ag+Br+I), 16% (C+N+O), 1% H

Echo Lake Calorimeter-Spark Chamber

(L.Jones et al. Preprint UM HE 74-23)

$$\sqrt{s_{NN}} = 13 - 31 GeV$$

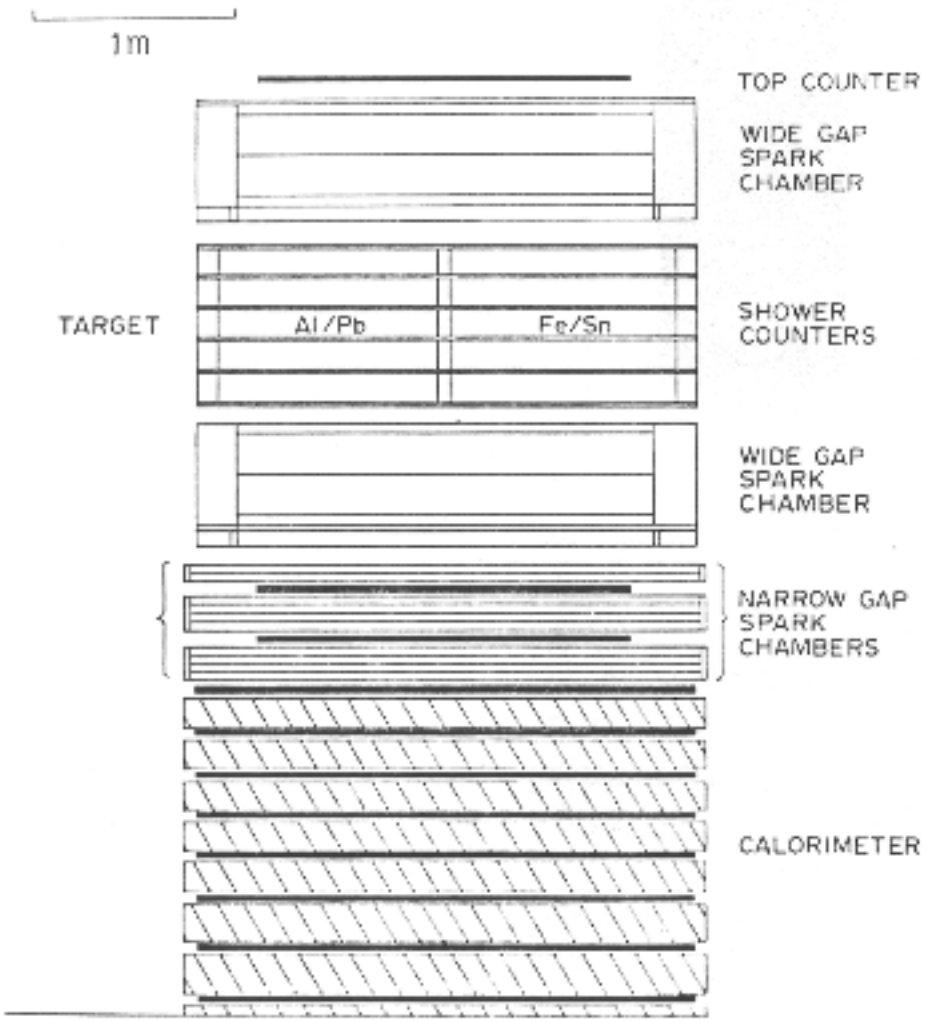

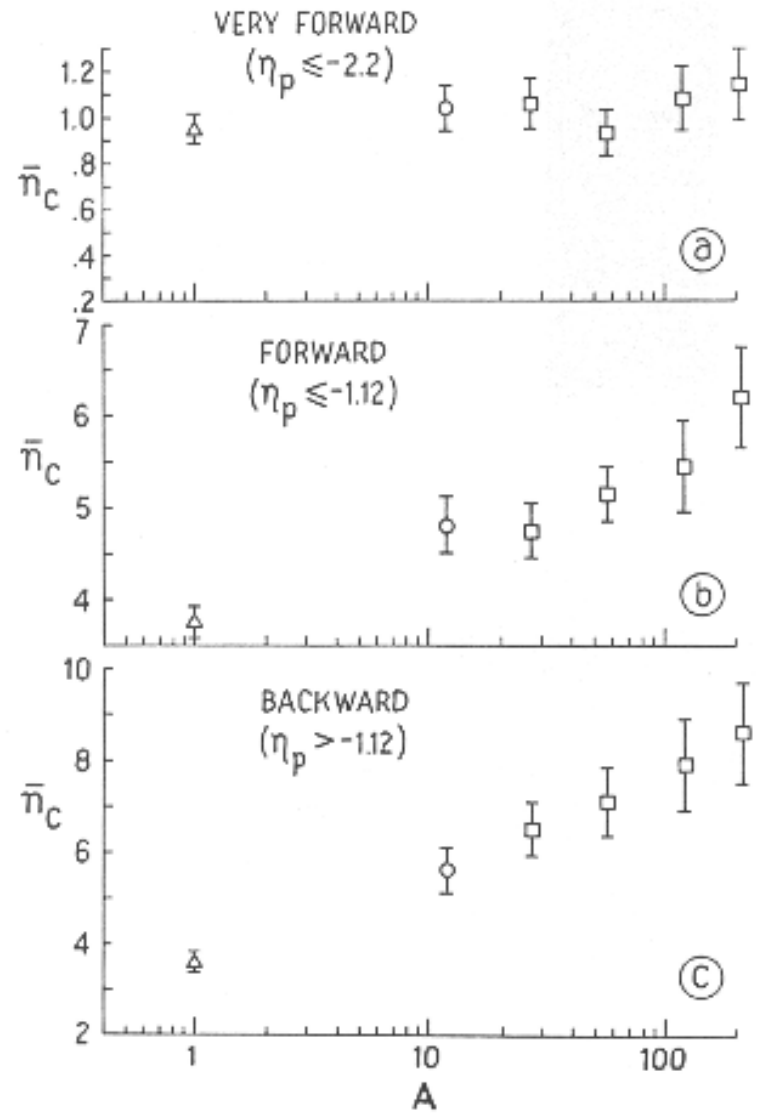

The pA play
as seen through the eyes of one of the actors

Act 1 before the early 1970's	The "A" of "pA" is more of a nuisance than a help!
Act 2 The 1970's	Is there too much or too little cascading?
Act 3 late 1970's, early 1980's	Is there too much or too little quenching in the forward direction?
Act 4 Late 1980's, 1990's & 2000's	Who cares about the details of "pA" ? After all, it's only a reference!
Act 5 To-day	Who is helping whom? pp & pA the understanding of AA or AA the understanding of pp & pA?

Questions from the early 1970's

- Mechanism of particle production in pp collisions?
- Space-Time evolution of the production process?

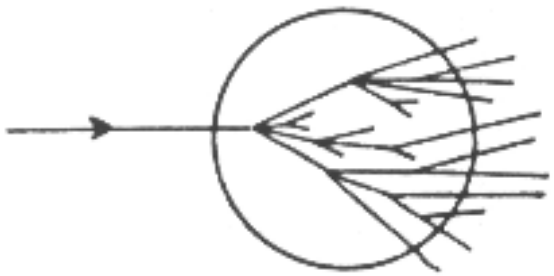

$\langle n \rangle_A \sim \langle n \rangle_p A^{1/3}$

or

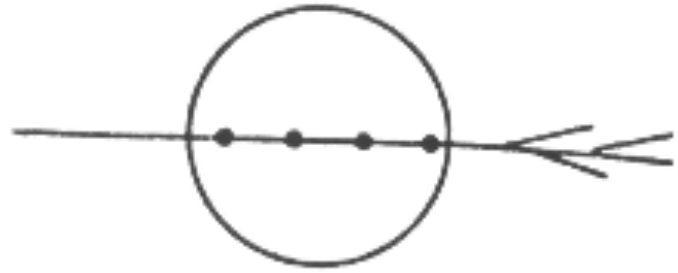

$\langle n \rangle_A \sim \langle n \rangle_p$ or

$\langle n(A,s) \rangle \sim \langle n(p,\bar{\nu}s) \rangle$

From Fermilab E178 proposal

Fashions in theory in 1970's

Godfried's energy cascade model

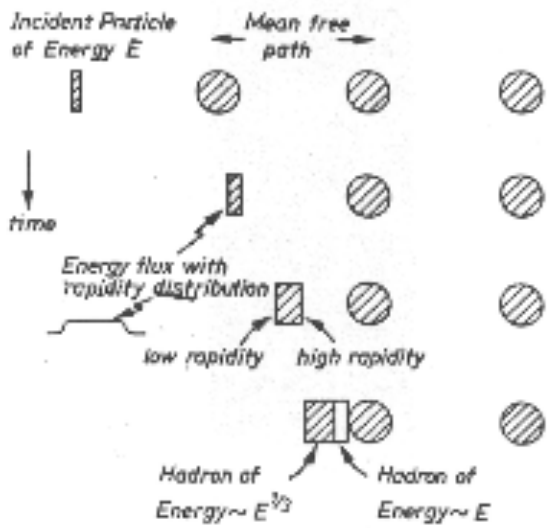

Parton and single chain multiperipheral type models

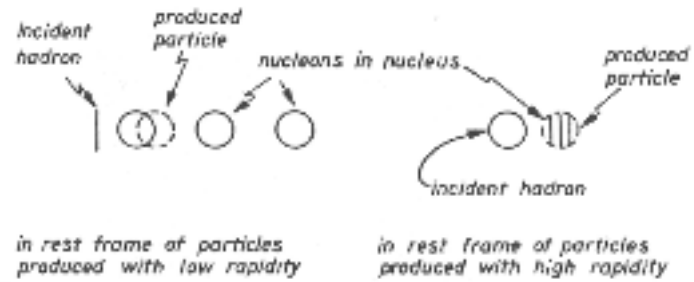

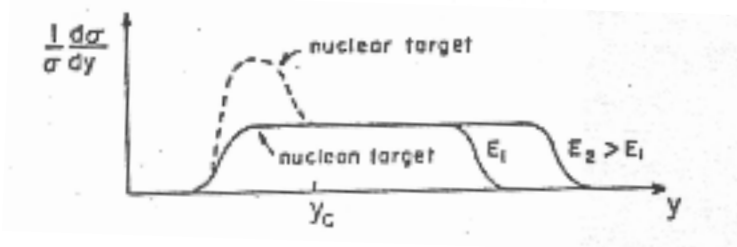

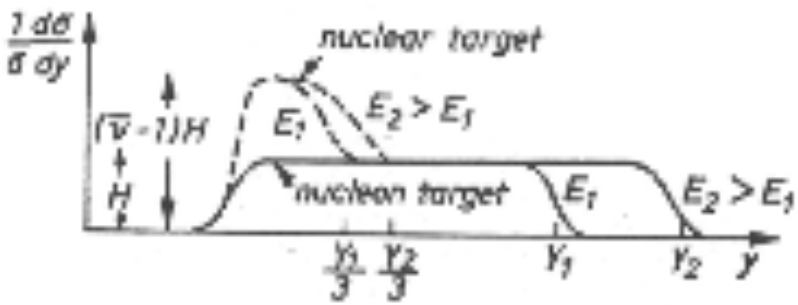

pA = pp at higher energy

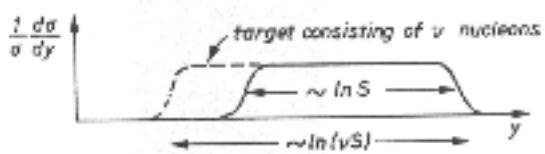

$$R_A \sim \frac{\ln(\nu S)}{\ln S} \sim 1 + \frac{\ln \nu}{\ln S} \to 1 \text{ as } E \to \infty.$$

None of these lead to the observed rapidity distributions, long range correlations, N_{part} -scaling or extended longitudinal scaling

From WB review,
Acta Phys. Pol. B8(1977)

1972 Fermilab E178 (PHOBOS - 1)

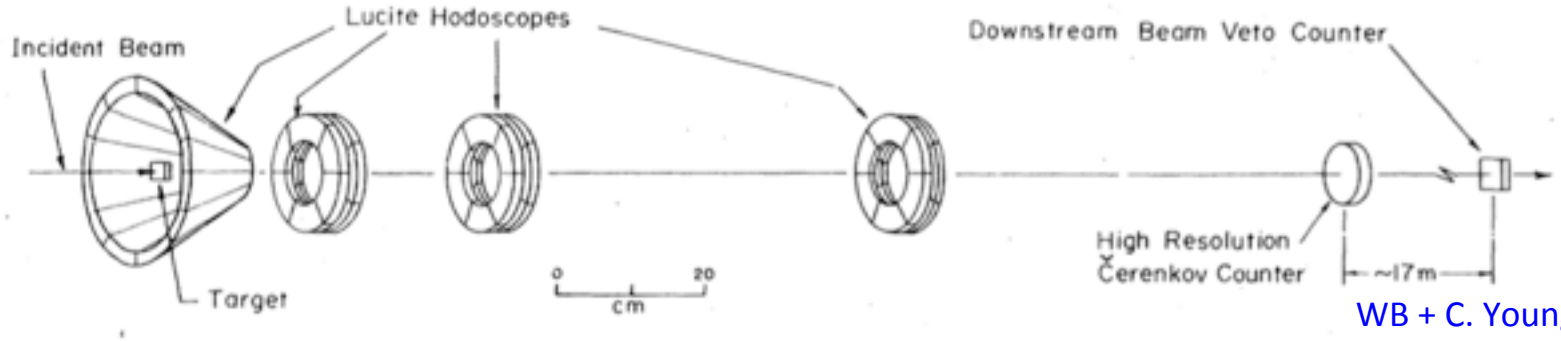

WB + C. Young

1991 PHOBOS

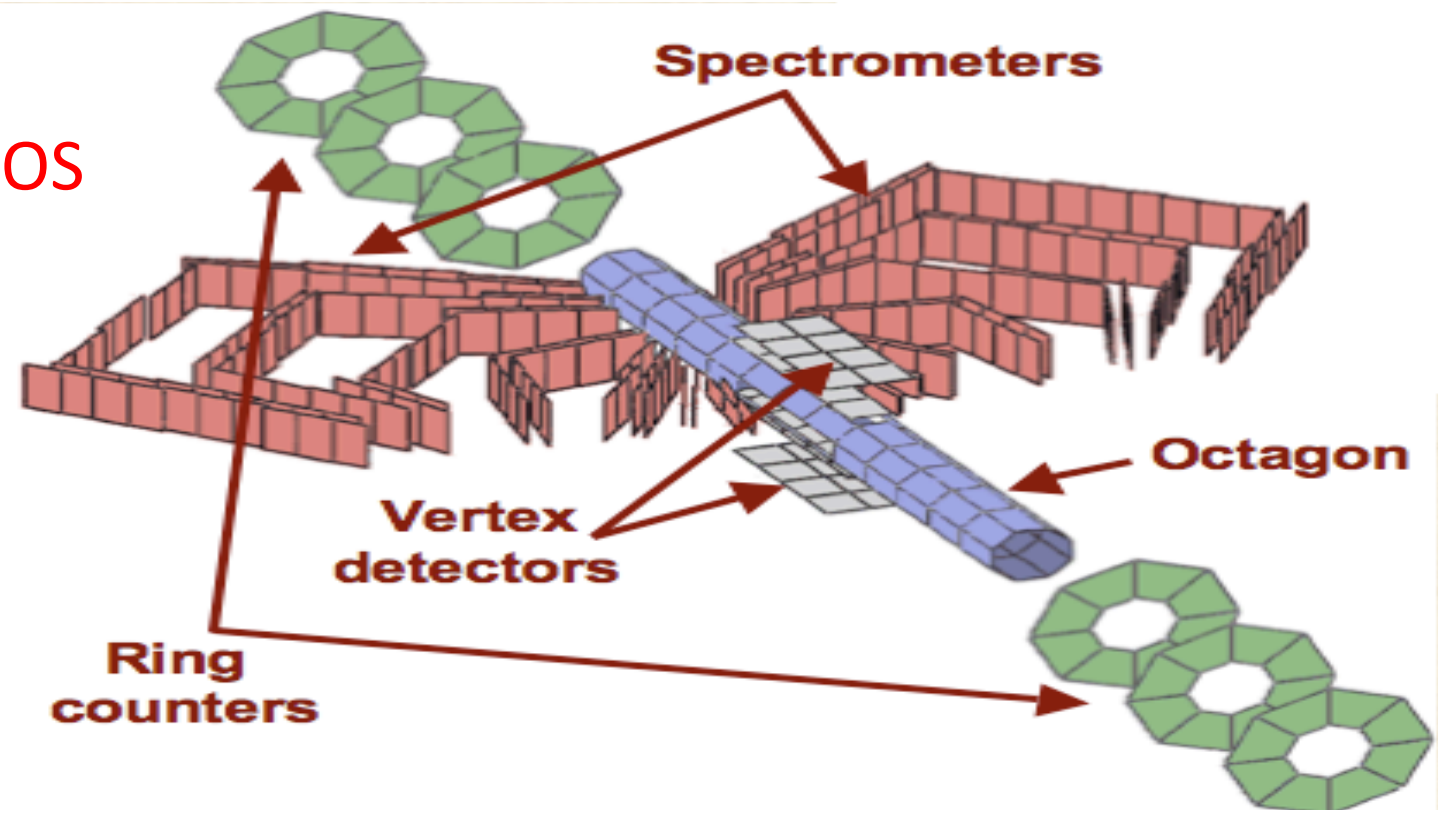

Surprise: participant scaling

$R_A = N_{pA} / N_{pp} = ½ + ½ \bar{\nu} = ½ + ½ N_{coll} = ½$ wounded nucleons $= ½ N_{part}$

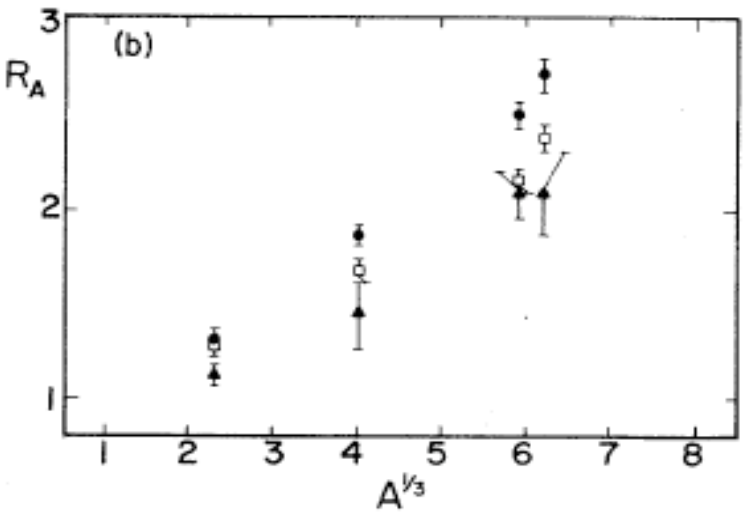

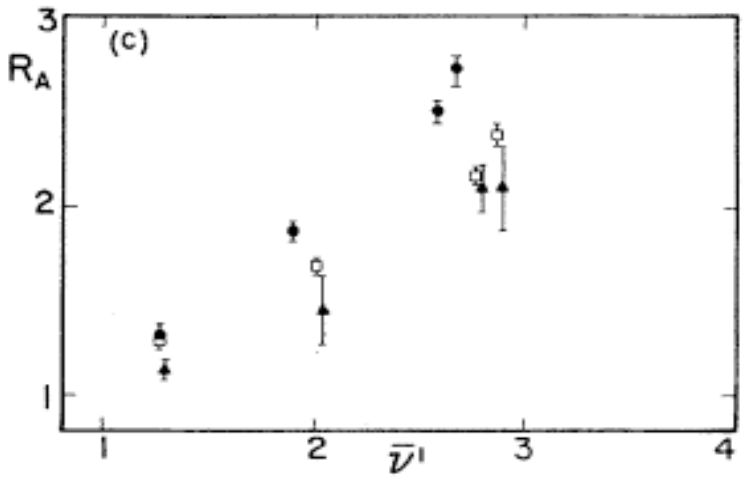

Different cross-section after the first collision

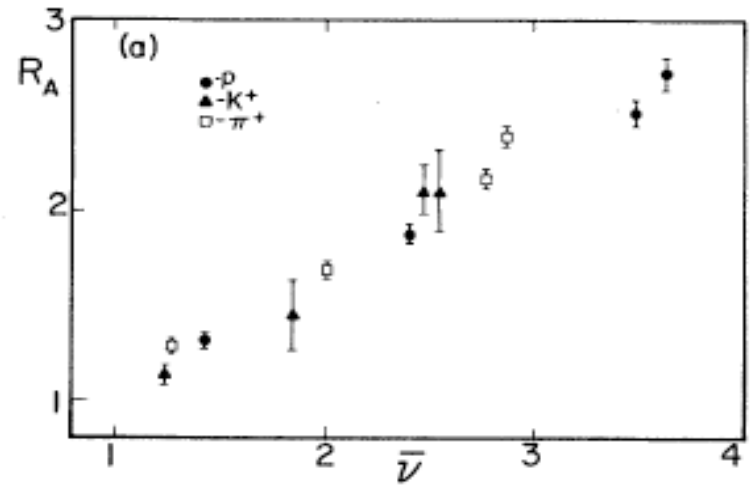

$\bar{\nu} = N_{coll} = N_{part} - 1 = A\sigma_{pp} / \sigma_{pA}$

π, *k*, *p* Data $\sqrt{S_{NN}}$ 10 to 20 GeV

W.Busza et al. (E178) PRL34 (1975) 836

J. E. Elias et al., (E178) PRL 41 (1978) 285

AA collisions consistent with N_{part} - Scaling

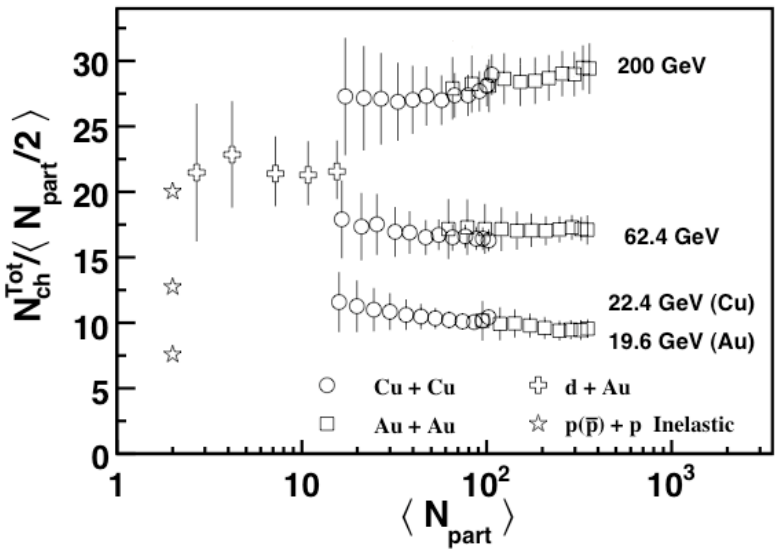

PHOBOS, arXiv:0709.4008 [nucl-ex]

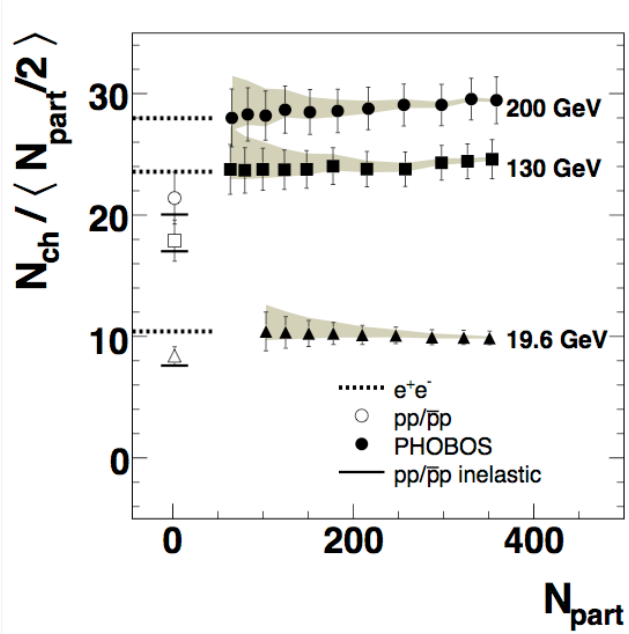

PHOBOS, Phys. Rev. C74 021902 (R) 2006

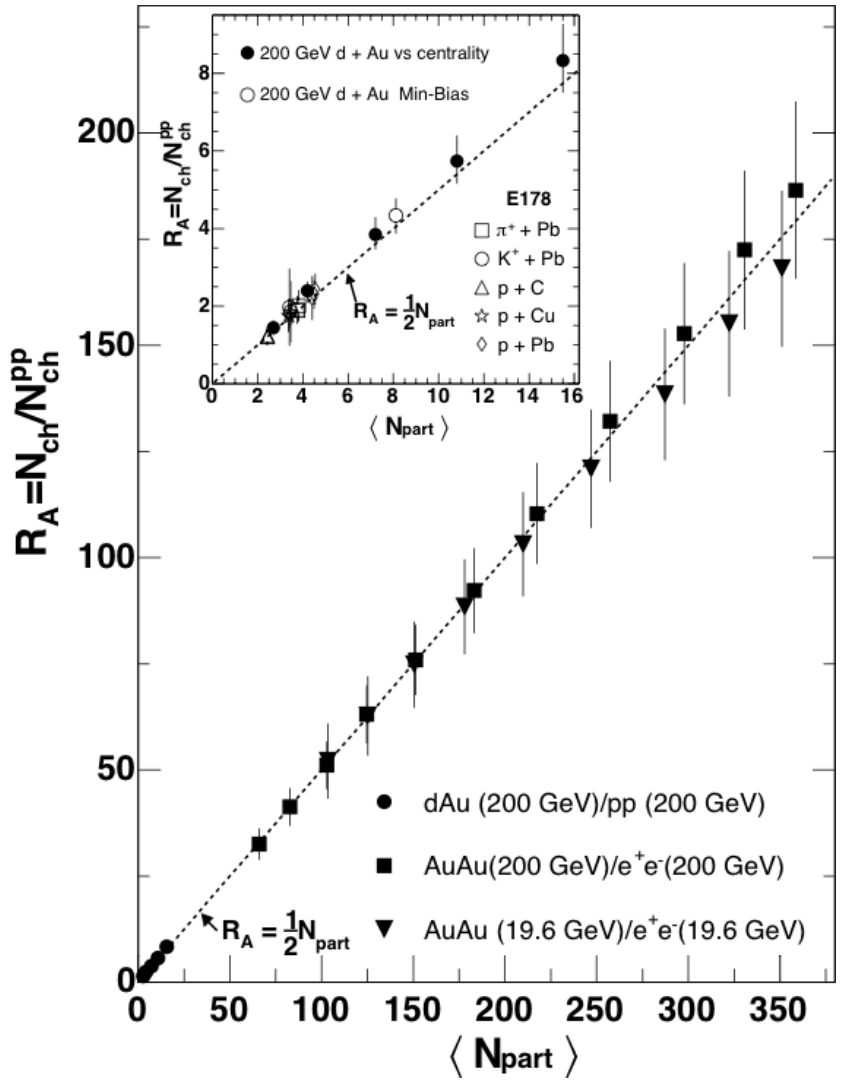

WB, Acta Phys. Pol. B35 (2004)2873

W.Busza et al. (E178) PRL34 (1975) 836

Extended Longitudinal Scaling in E178 Data for $\sqrt{s_{NN}}$ 10 - 20 GeV

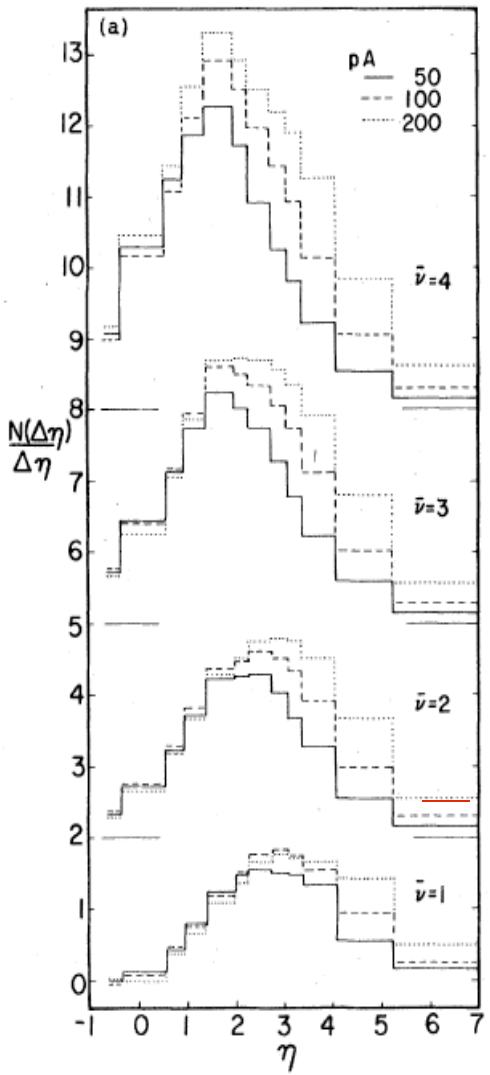

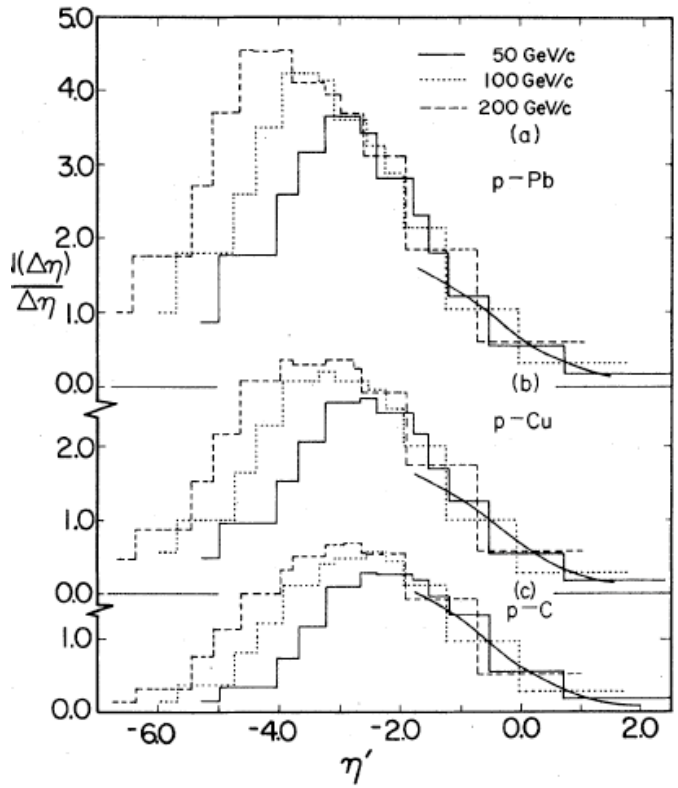

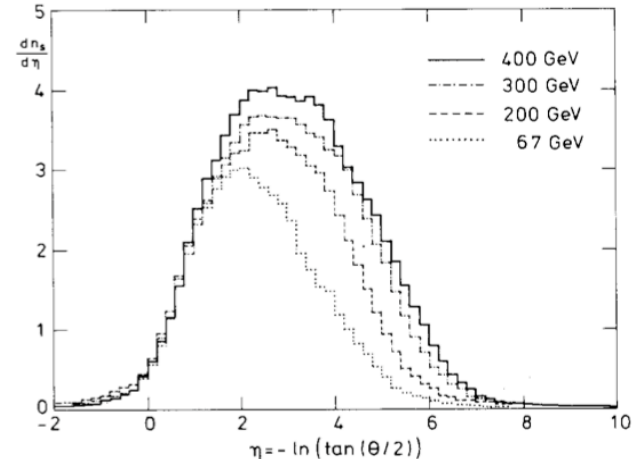

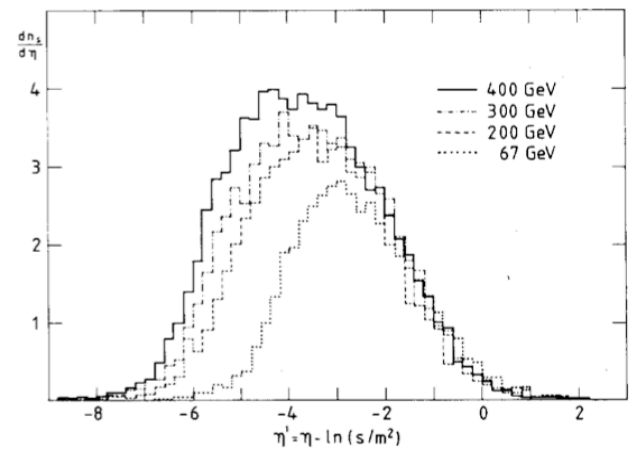

Nucleus rest frame

Projectile rest frame

pEmulsion data (Otterlund et al., compilation NP B142 (1978) 445

J. Elias et al., (E178) PR D22 (1980)13

Universality of extended longitudinal scaling

p,d-A

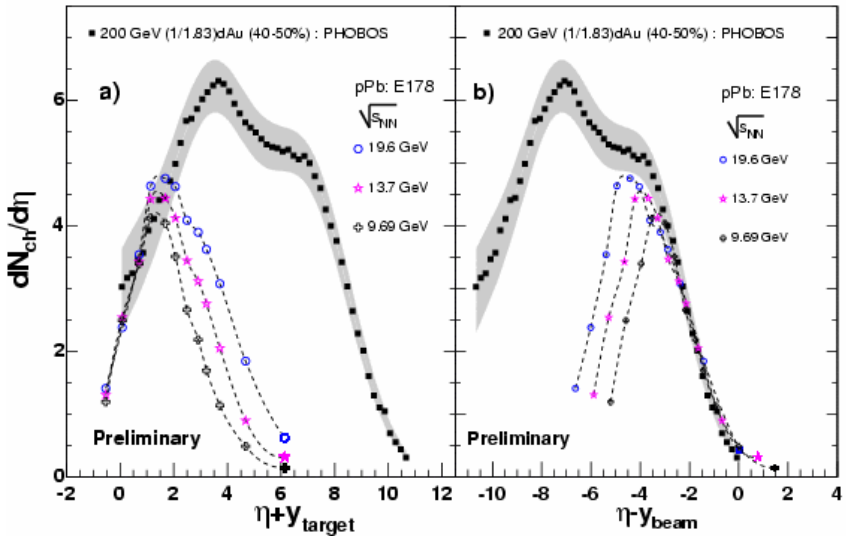

PHOBOS, Nucl. Phys. A 757 (2005) 28.
E178: PRD 22 (1980) 13

pp

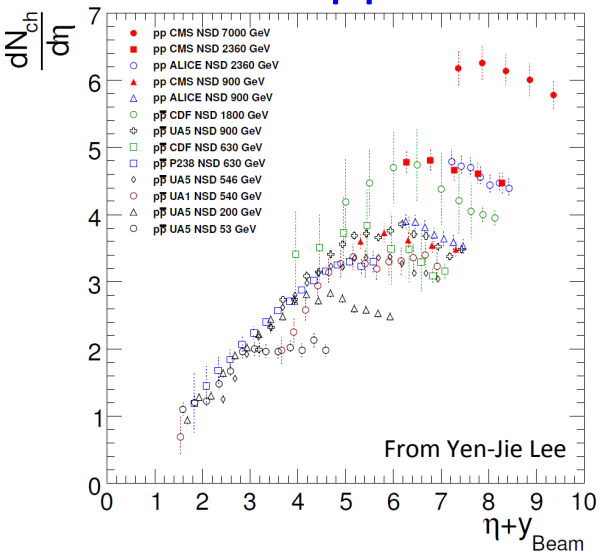

AA

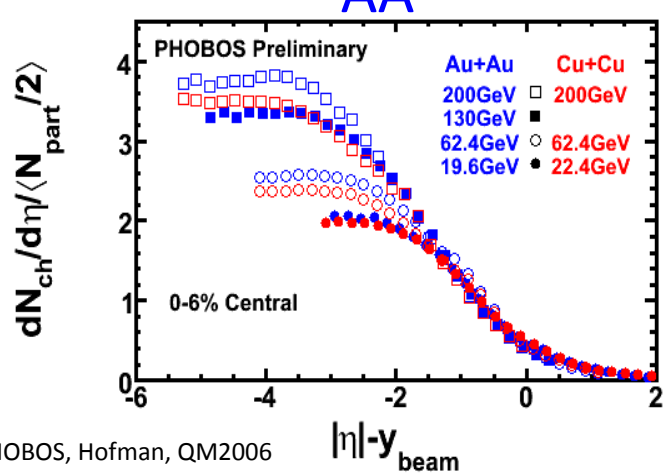

PHOBOS, Hofman, QM2006

AA

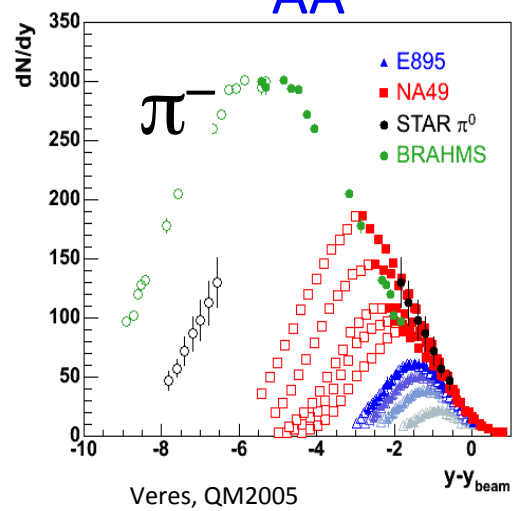

Veres, QM2005

First Reference to RHIC

PUGH: I wonder if you would like to say a few words about an additional dimension which seems to be on the verge of experimental feasibility. That is the study of collisions between nuclei at relativistic speeds. I am referring to the present feasibility or near-feasibility of accelerating particles up to carbon or so in the intersecting storage rings at CERN and of conceivably designing new facilities like Isabelle to include such possibilities.

MUZSA: If the interpretation that a few nucleons in a row behave like a single particle is so--and I don't personally believe that--then I think it would have tremendous consequences. If you had two U nuclei colliding with each other they would provide a source of energy much higher than accelerators normally give, but I find it difficult to understand how a few nucleons in a row can behave as a single object.

FESHBACH: Just wanted to ask a foolish question. It occurred to me while you were speaking: Why isn't the explanation of multiplicity trivial? The produced forward particles are peripheral and only interact with the edge of the nucleus and, therefore, just see a few particles while those which come off at larger angles go through the middle of the nucleus, see many nucleons, and, therefore, have increased multiplicity.

A. GOLDHABER: Forward particles are not produced only peripherally, since as $A^{2/3}$ even for them. I also have three comments: 1) Other-

Questions and Answers at “HE Physics and Nuclear Structure - 1975”, page 237 @ Santa Fe & Los Alamos

The “Cronin effect”: that’s another play!

The pA play
as seen through the eyes of one of the actors

Act 1 before the early 1970's	The "A" of "pA" is more of a nuisance than a help!
Act 2 The 1970's	Is there too much or too little cascading in pA?
Act 3 late 1970's, early 1980's	Is there too much or too little quenching in the forward direction?
Act 4 Late 1980's, 1990's & 2000's	Who cares about the details of "pA" ? After all, it's only a reference!
Act 5 To-day	Who is helping whom? pp & pA the understanding of AA or AA the understanding of pp & pA?

Forward production of particles in pA collsions (πA results are similar)

Various final states: ϕ, π^+, π^-,p ,p,n,Λ,K^0,Ξ,K^+,K^-
Various beam energies: 24, 100, 300, 400 GeV

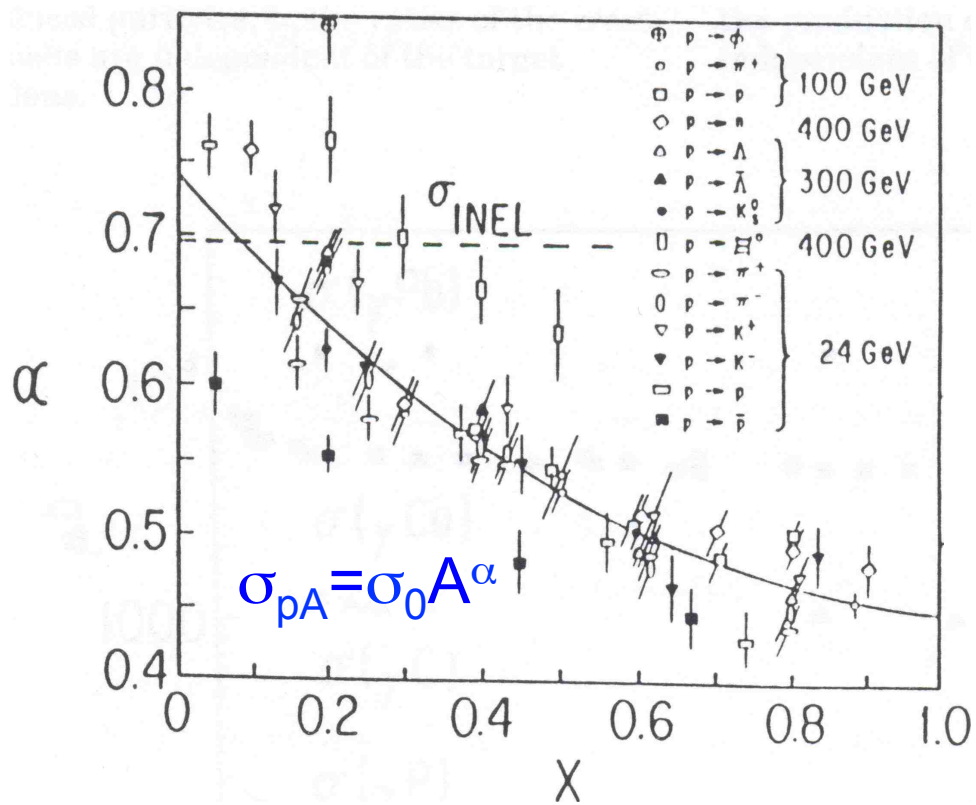

D.Barton et al. (E451) PRD27 (1983) 2580
WB, Nucl. Phys. A544:49 (1992)

800 GeV p-A (FNAL) $\sigma_A = \sigma_p * A^{\alpha}$
PRL 84, 3256 (2000); PRL 72, 2542 (1994)

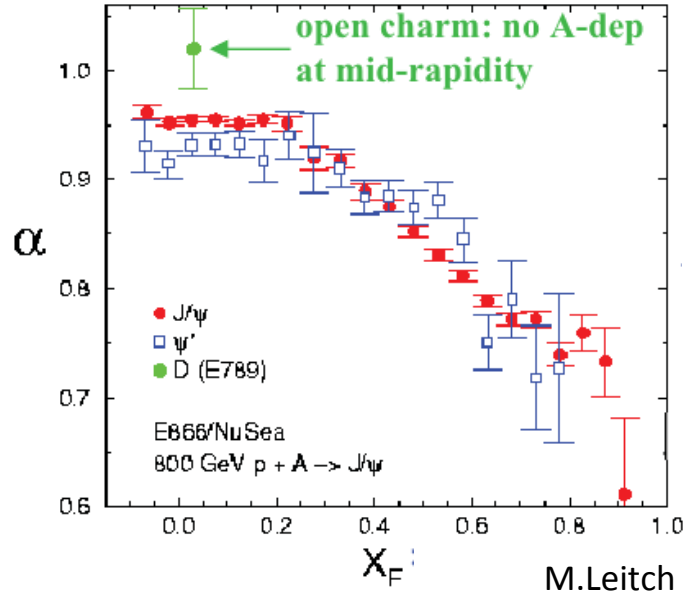

M.Leitch

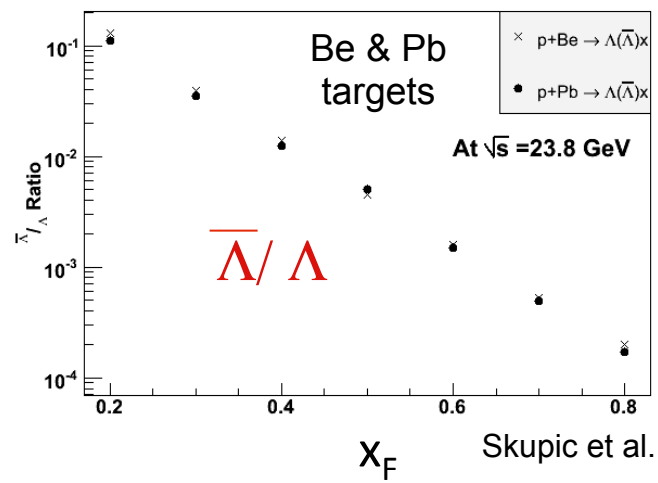

Skupic et al.

By-product of forward quenching studies:

estimate that, on average at RHIC, baryon will lose 85% of its energy as it goes through the center of the Au nucleus

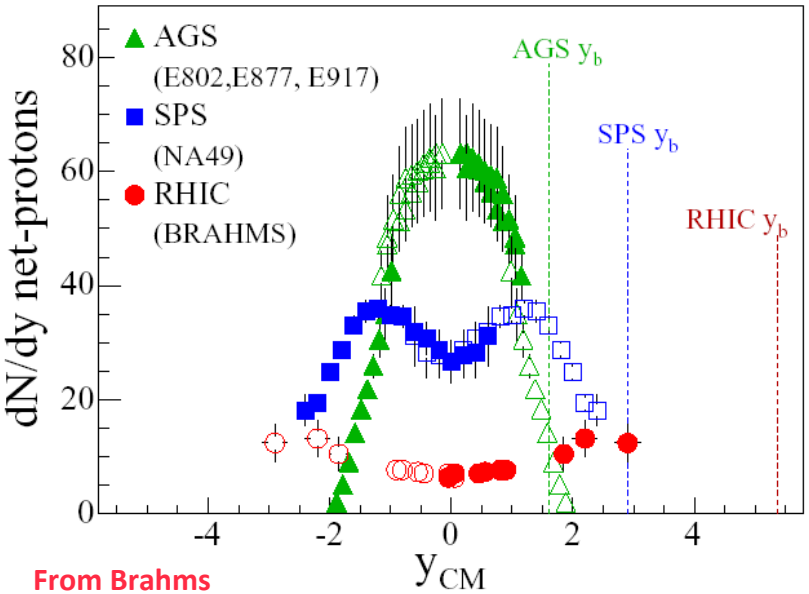

From Brahms

Baryon Rapidity Loss in pA Collisions

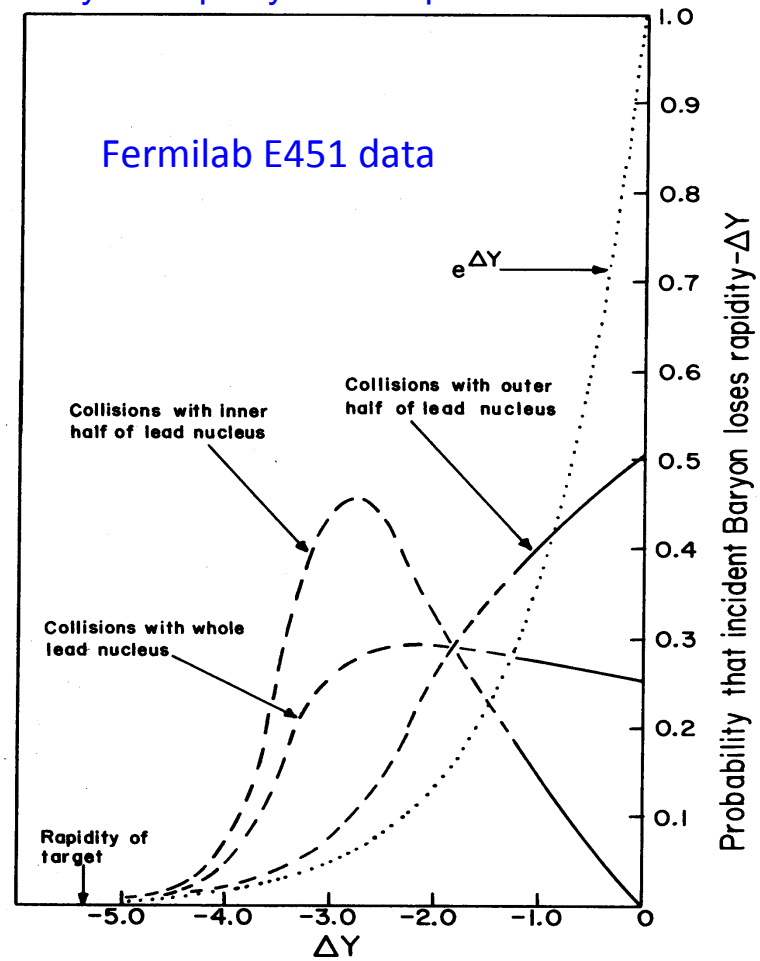

From WB and A.S. Goldhaber

The pA play
as seen through the eyes of one of the actors

Act 1 before the early 1970's	The "A" of "pA" is more of a nuisance than a help!
Act 2 The 1970's	Is there too much or too little cascading in pA?
Act 3 late 1970's, early 1980's	Is there too much or too little quenching in the forward direction?
Act 4 Late 1980's, 1990's & 2000's	Who cares about the details of "pA" ? After all, it's only a reference!
Act 5 To-day	Who is helping whom? pp & pA the understanding of AA or AA the understanding of pp & pA?

91
PHYSICAL REVIEW LETTERS
Articles published week ending
15 AUGUST 2003
Volume 91, Number 7
PRL 91 (7), 070401–079702, 15 AUGUST 2003 (256 total pages)
PHENIX
charged hadrons
neutral pions
p_T (GeV/c)
PHOBOS
70-100%
40-70%
20-40%
0-20%
R_{dAu}
p_T(GeV/c)
BRAHMS
d+Au (MB)
Au+Au (0-10%)
η=0
Nuclear Modification Factor
p_T [GeV/c]
STAR
$h^+ + h^-$
Au + Au Central
d + Au Central
p + p Minimum Bias
$(1/N_{Trigger})dN/d(\Delta\phi)$
Δφ (degrees)
7
APS Published by The American Physical Society

The pA play
as seen through the eyes of one of the actors

Act 1 before the early 1970's	The "A" of "pA" is more of a nuisance than a help!
Act 2 The 1970's	Is there too much or too little cascading in pA?
Act 3 late 1970's, early 1980's	Is there too much or too little quenching in the forward direction?
Act 4 Late 1980's, 1990's & 2000's	Who cares about the details of "pA" ? After all, it's only a reference!
Act 5 To-day	Who is helping whom? pp & pA the understanding of AA or AA the understanding of pp & pA?

Remarkable similarity of mass dependence of average P_t in AA and pp

CMS, pp, 0.9, 2.76 and 7 TeV

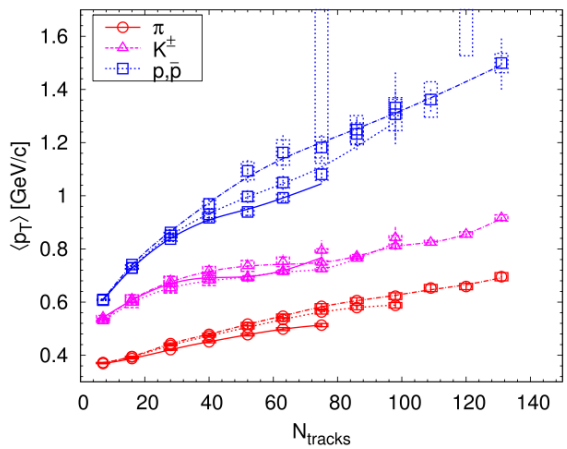

ALICE, UA5, STAR/PHENIX

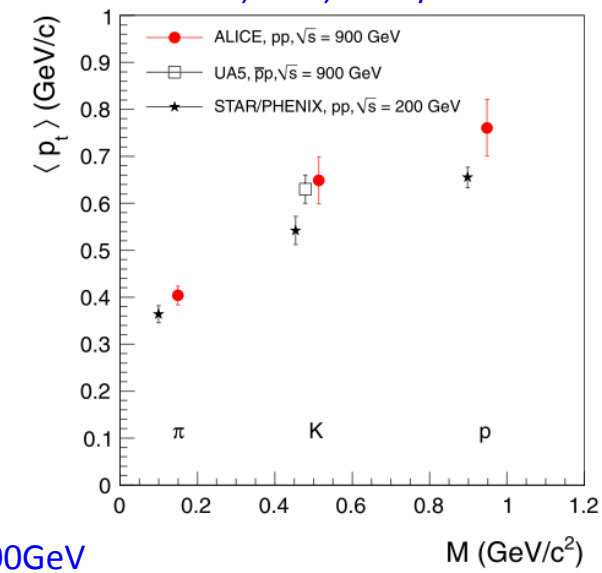

PHENIX, AuAu, 200GeV

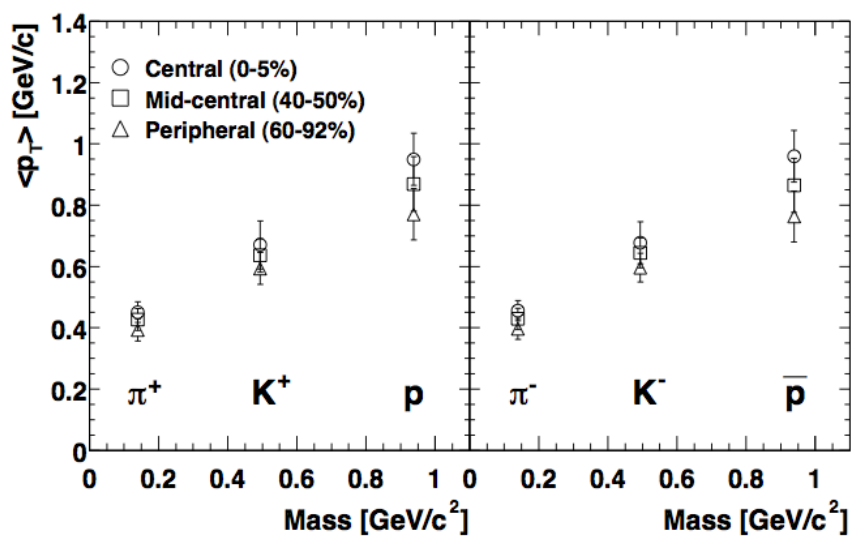

The ridge phenomenon

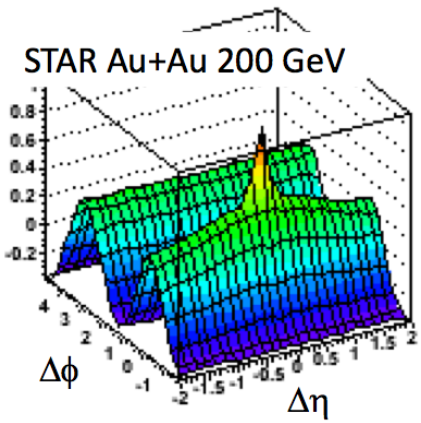

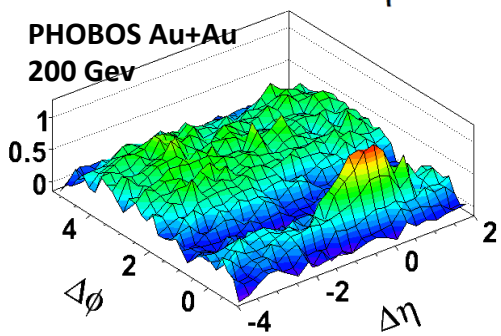

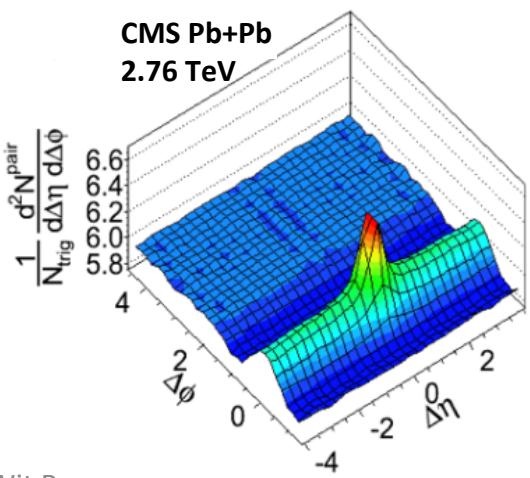

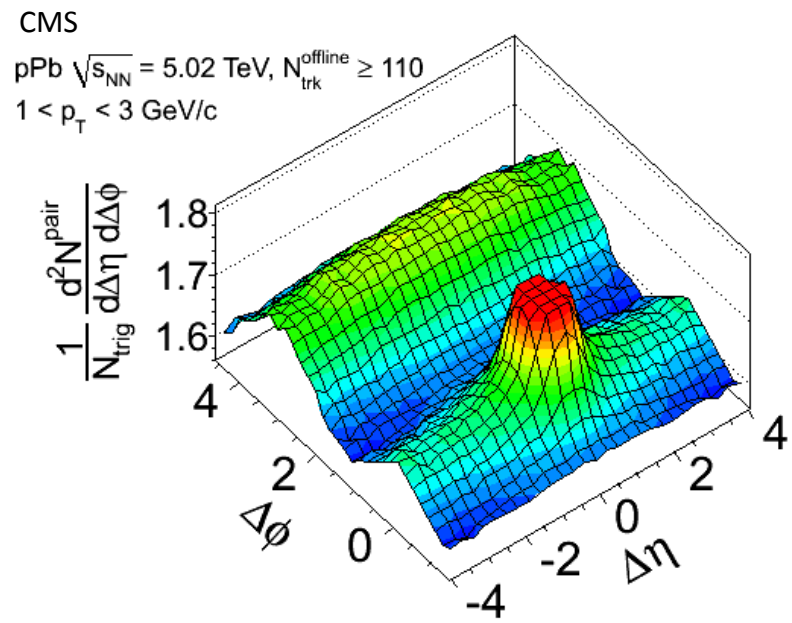

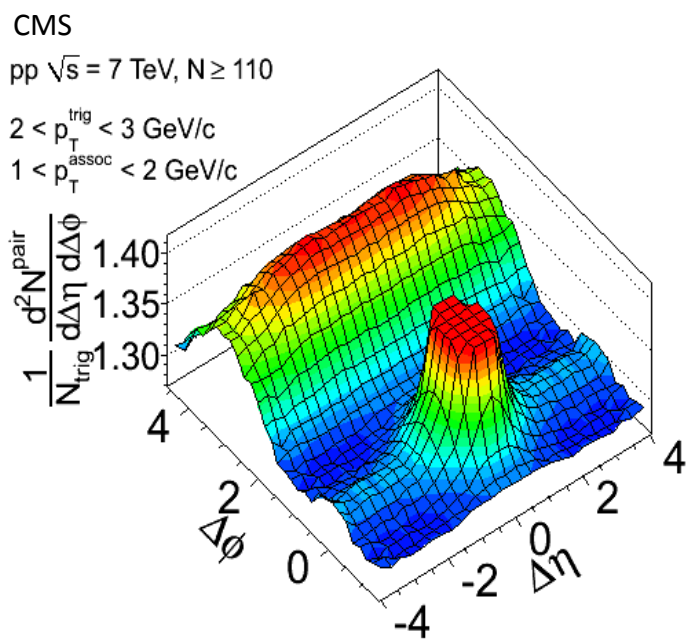

The pA play
as seen through the eyes of one of the actors

Act 1 before the early 1970's	The "A" of "pA" is more of a nuisance than a help!
Act 2 The 1970's	Is there too much or too little cascading in pA?
Act 3 late 1970's, early 1980's	Is there too much or too little quenching in the forward direction?
Act 4 Late 1980's, 1990's & 2000's	Who cares about the details of "pA" ? After all, it's only a reference!
Act 5 To-day	Who is helping whom? pp & pA the understanding of AA or AA the understanding of pp & pA?

Concluding remarks

pA data has, and continues to surprise us

- lack of cascading in the 1950' and 1960's
- long range correlations and simplicity of participant scaling in the 1970's
- "Cronin effect" in the the 1970's
- strong quenching of forward particles in the 1970's and 1980's
- "flow-like" behavior in the 2010's

pA is like a litmus test. Until we understand pA from our understanding of pp and AA, we cannot claim to have a deep understanding of pp and AA.

I take this opportunity to thank Andrzej Białas, Bj, Kurt Godfried, Freddie Goldhaber, Larry Jones, Miklos Gyulassy and Al Mueller, for helping make pA so much fun for me !

Flavor Tomography

Alessandro Buzzatti

Miklos Gyulassy

Outline

- Introduction
  - Jet tomography and jet quenching
- CUJET
  - Analysis of the model
  - Geometry, path integral, partonic spectra
- Jet tomography at RHIC and LHC
  - Heavy quark puzzle (RHIC)
  - Surprising transparency (LHC)
- Future developments
  - Elliptic flow
- Conclusions

Quark Gluon Plasma

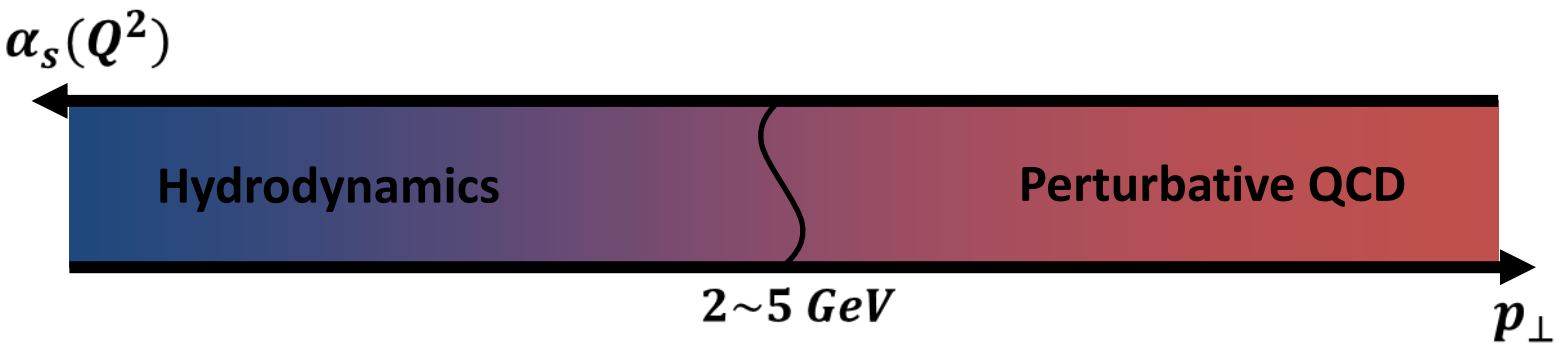

- Medium is strongly coupled
- Local thermal equilibrium is maintained
- Hydrodynamic expansion and collective flow
- Measurement of 'bulk' properties of QGP

- High-$p_\perp$ probes are weakly coupled with medium
- Perturbative QCD methods are applicable
- Indication of jet-medium coupling mechanism
- Indirect but `cleaner' measurements of QGP properties

Jet Tomography

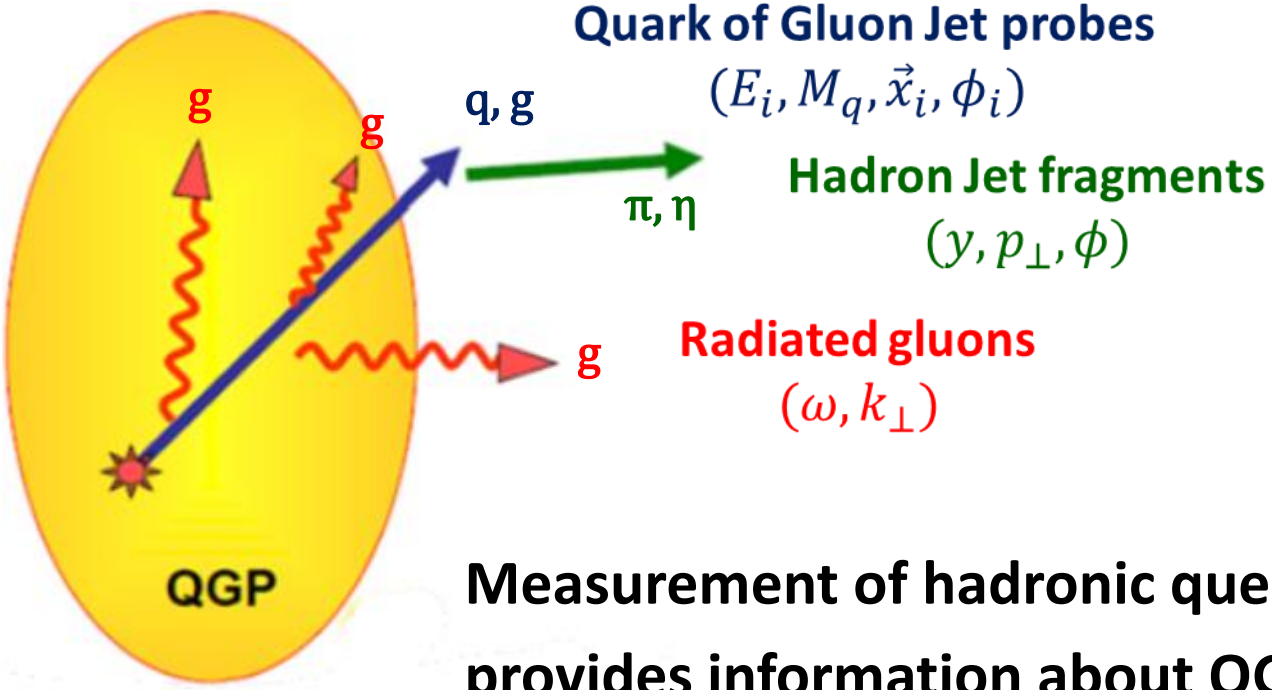

Measurement of hadronic quenching pattern provides information about QGP density

- Requires detailed knowledge of **jet-medium interaction mechanism** and **jet transverse diffusion**
- Knowledge of **initial conditions**, **`cold' nuclear matter effects** and **hadronization** process

R_{AA} measurements

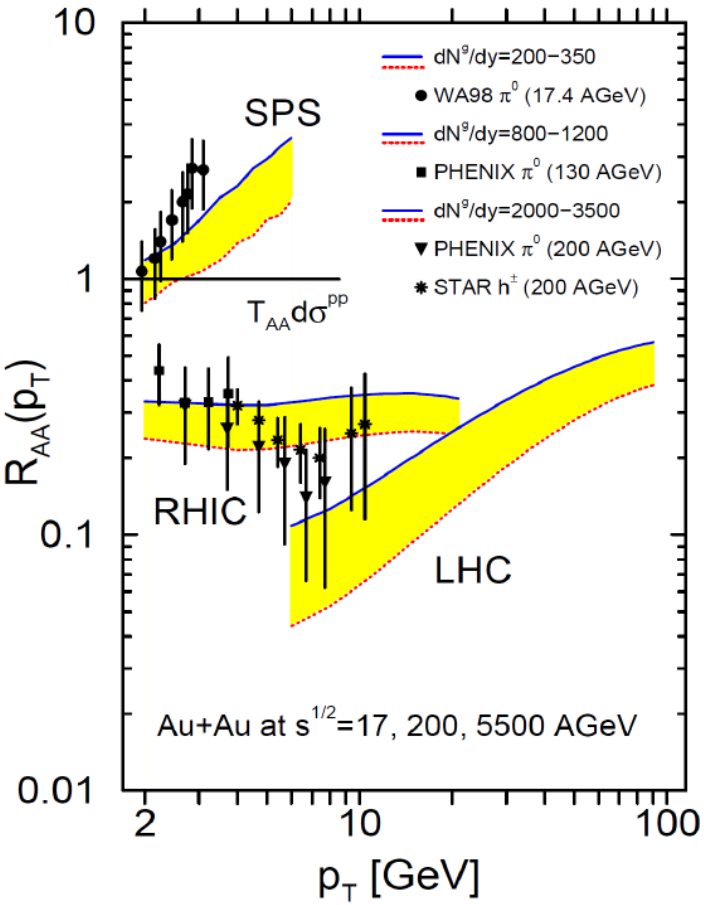

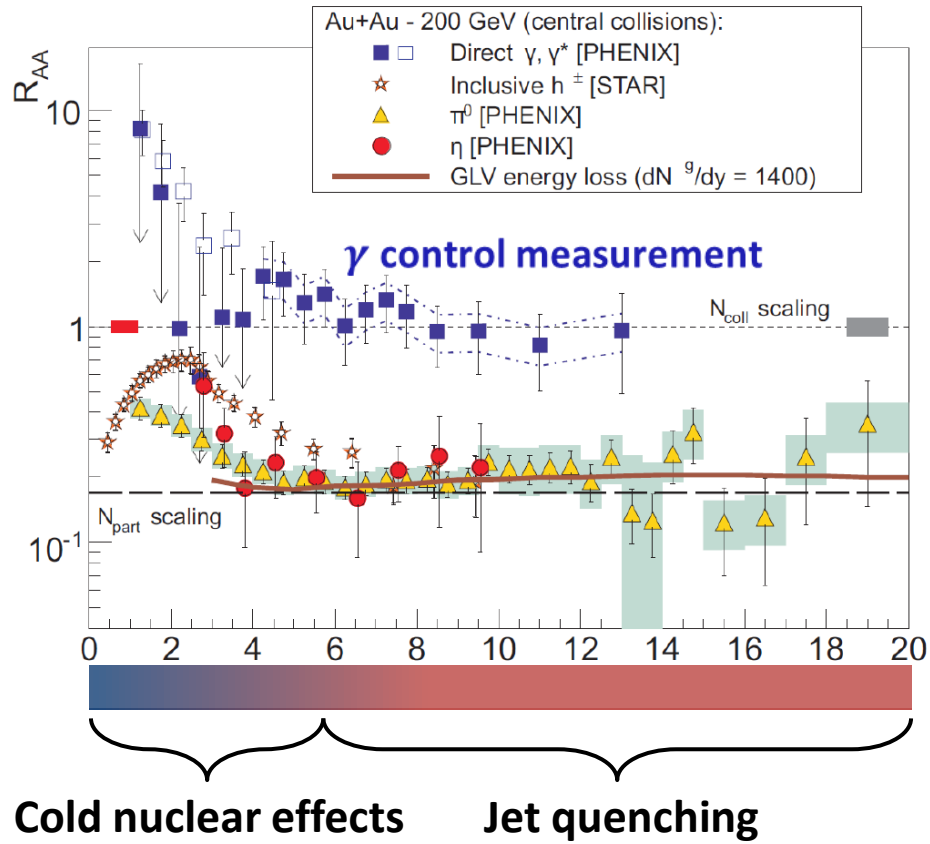

Relevance of 'cold' nuclear matter effects depends on $\sqrt{s}$ and $p_\perp$

- Use p+A collisions as control experiments

Jet quenching

- **Radiative** $\Delta E^{raditive} \propto \alpha_s^3 \int d\tau\, \tau\, \rho_{QGP}(\tau, \vec{r}(\tau)) \log\left(\frac{E_{jet}}{\mu_D}\right)$

(Soft eikonal approximation, incoherent multiple gluon emission)

  - Opacity expansion
    - Thin plasma approximation
    - Includes the hard tails of the transferred momentum distribution
    - Medium described by density ρ_{QGP} and Debye screening mass $\mu_D = gT$
  - Multiple soft scattering (MSS)
    - Thick plasma approximation
    - Gaussian transverse diffusion
    - Medium described by transport coefficient $\hat{q}$

- **Elastic** $\Delta E^{elastic} \propto \alpha_s^2 \int d\tau\, \rho_{QGP}^{2/3}(\tau, \vec{r}(\tau)) \log\left(\frac{E_{jet}}{T}\right)$
  - Bjorken collisional model

Model comparison

Characterize the medium by $\hat{q}$:

- **mean of the squared transverse momentum exchanged per unit path length**
- In the opacity expansion, $\hat{q} \sim \frac{\mu_D^2}{\lambda}$

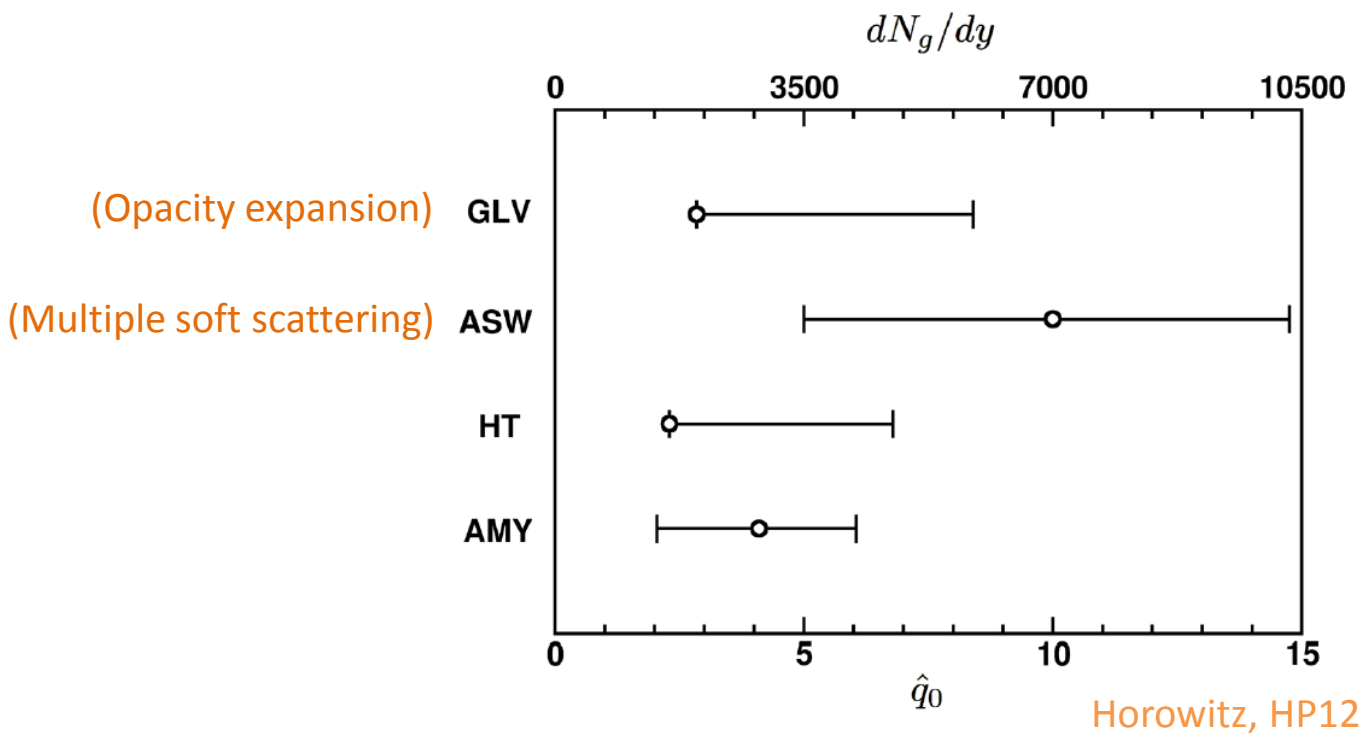

- **Need to reduce systematic uncertainties!**

Outline

- Introduction
  - Jet tomography and jet quenching
- CUJET
  - Analysis of the model
  - Geometry, path integral, partonic spectra
- Jet tomography at RHIC and LHC
  - Heavy quark puzzle (RHIC)
  - Surprising transparency (LHC)
- Future developments
  - Elliptic flow
- Conclusions

History

- Genealogy of Jet tomography at Columbia University: **Vitev**, **Molnar**, **Djordjevic**, **Adil**, **Wicks**, **Horowitz**, **Ficnar**.
- Past efforts culminated with the construction of the **WHDG** model
  - Radiative (static potential) + Elastic energy loss
  - Static medium (approximated at half the time of the expansion)
  - Static jet-medium coupling parameters
  - Simplified convolution over partonic spectra (spectral index approximation)
- Applications of WHDG to RHIC and LHC phenomenology got mixed response
  - Correct predictions of flat pion R_{AA} behavior at RHIC
  - Under-quenching of non-photonic electrons at RHIC
  - Over-quenching of pion R_{AA} at LHC

CUJET

- **Geometry**
  - **Glauber model**
  - **Bjorken longitudinal expansion**
- **Energy loss**
  - **Full jet path length integration**

$$\frac{dN_g}{dx}(x_\perp,\phi) = \frac{C_R}{\pi}\int d\tau\, \alpha_s(\tau)\frac{d^2k}{\pi}\frac{d^2q}{\pi}\frac{1}{x}\frac{\frac{9}{2}\pi\alpha_s^2(\tau)}{q^2\left(q^2+\mu^2(\tau)\right)}\times$$
$$\times\frac{2(k+q)}{(k+q)^2+\chi(\tau)}\left(\frac{(k+q)}{(k+q)^2+\chi(\tau)}-\frac{k}{k^2+\chi(\tau)}\right)\times$$
$$\times\left(1-cos\left[\frac{(k+q)^2+\chi(\tau)}{2xE}\tau\right]\right)\rho_{QGP}(x_\perp+\hat{\phi}\tau,\tau)$$

$$\mu(\tau) = gT(x_\perp+\hat{\phi}\tau,\tau)$$

$$\chi(\tau) = M^2x^2 + m_g{}^2(\tau)(1-x)$$

  - **Collisional energy losses**
  - **Gluon emission fluctuation effects**
- **Detailed convolution over initial production spectra**
- **In vacuum Fragmentation Functions**

Bjorken expansion

- The local thermal equilibrium is established at τ_0

$$s(\tau) = s_0 \frac{\tau_0}{\tau}$$ **(entropy density)**

$$s_0 \approx 3.6\, \rho_0 = 3.6\, \frac{1}{\pi R^2 \tau_0} \frac{dN}{dy}$$ *($\frac{dN}{dy}$ is the observed rapidity density)*

MONOTONIC density dependence

$$\rho_{QGP}(x_\perp, \tau) = \frac{1}{\tau_0} \frac{\rho_{part}(x_\perp)}{N_{part}} \frac{dN}{dy} f\left(\frac{\tau}{\tau_0}\right)$$

- Before equilibrium

Temporal envelopes: linear, divergent, free streaming

$$f\left(\frac{\tau}{\tau_0}\right) = \begin{cases} \frac{\tau}{\tau_0}, \frac{\tau_0}{\tau}, 0 & (\tau < \tau_0) \\ \frac{\tau_0}{\tau} & (\tau > \tau_0) \end{cases}$$

CUJET

- Geometry
  - Glauber model
  - Bjorken longitudinal expansion
- Energy loss
  - Full jet path length integration

Possibility to evaluate systematic theoretical uncertainties such as sensitivity to formation and decoupling phases of the QGP evolution, local running coupling and screening scale variations, and other effects out of reach with analytic approximations.

  - Collisional energy losses
  - Gluon emission fluctuation effects
- Detailed convolution over initial production spectra
- In vacuum Fragmentation Functions

Strong running coupling

- Introduce one-loop alpha running

$$\alpha_s \rightarrow \alpha_s(Q^2)\begin{cases} \alpha_0 & if\ Q \le Q_0 \\ \dfrac{2\pi}{9\log(Q/\Lambda)} & if\ Q > Q_0 \end{cases}$$

B. G. Zakharov, JETP Lett. 88 (2008) 781-786

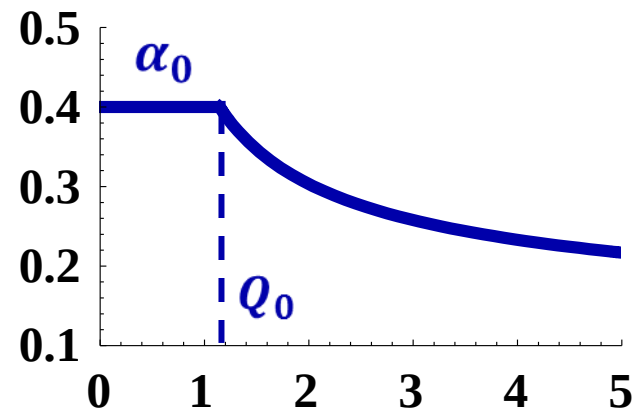

- $$Radiative = \begin{cases} \alpha(q^2)^2 \\ \alpha\left(\dfrac{k_\perp^2}{x(1-x)}\right) \\ \mu = g\big(\alpha(2T^2)\big)T \end{cases}$$

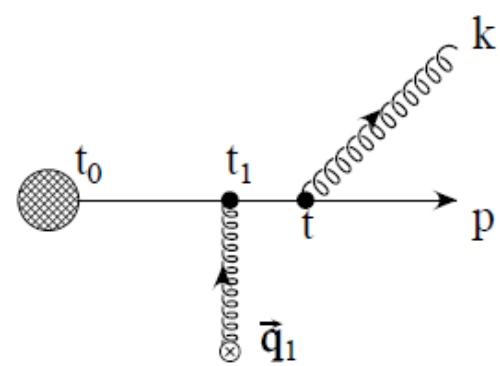

- $$Elastic = \begin{cases} \alpha(ET) \\ \alpha(\mu^2) \end{cases}$$

S. Peigne and A. Peshier, Phys.Rev. D77 (2008) 114017

CUJET

- Geometry
  - Glauber model
  - Bjorken longitudinal expansion
- Energy loss
  - Full jet path length integration

Possibility to evaluate systematic theoretical uncertainties such as sensitivity to formation and decoupling phases of the QGP evolution, local running coupling and screening scale variations, and other effects out of reach with analytic approximations.

  - Collisional energy losses
  - Gluon emission fluctuation effects
- Detailed convolution over initial production spectra
- In vacuum Fragmentation Functions

Production spectra

- Convolute over $\sqrt{s}$ and flavor dependent pQCD invariant jet spectra

$$\frac{d\sigma^{AA}}{dp_f} = \int \frac{d\phi}{2\pi} dx_\perp \bar{\rho}_{Jet}(x_\perp) \int dp_i \, P(p_f, p_i; x_\perp, \varphi;) \frac{d\sigma^{pp}}{dp_i}$$

RHIC

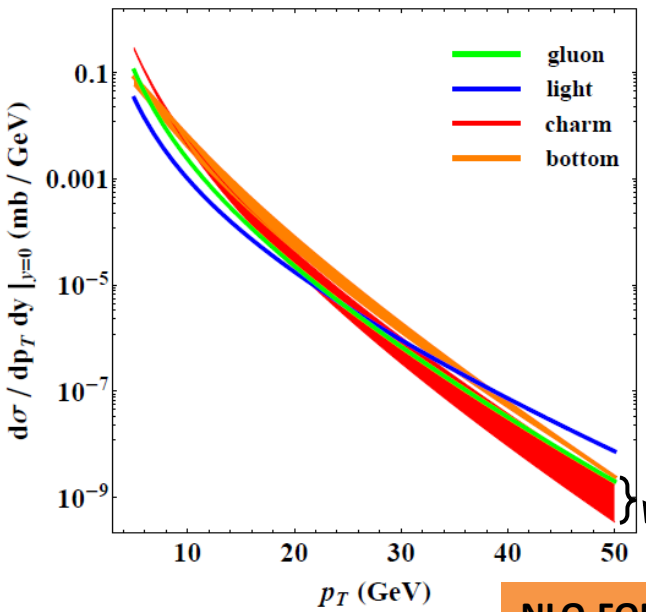

LHC

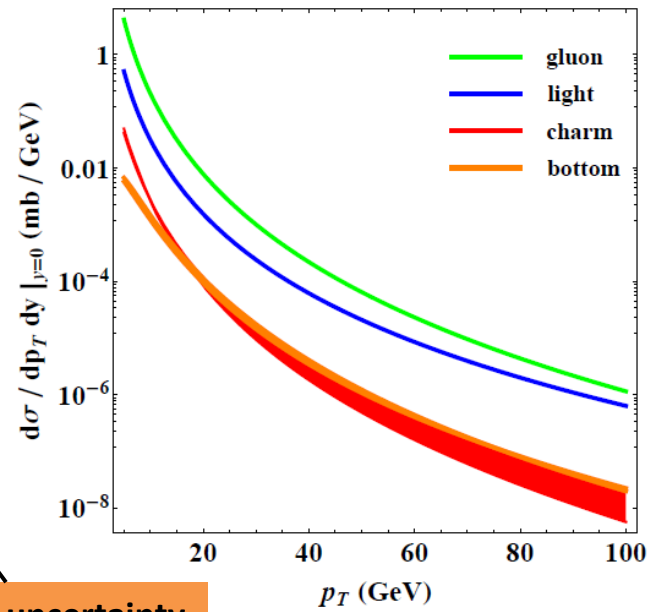

NLO-FONLL uncertainty

Vogt, Xin-Nian

CUJET

- Geometry
  - Glauber model
  - Bjorken longitudinal expansion
- Energy loss
  - Full jet path length integration

Possibility to evaluate systematic theoretical uncertainties such as sensitivity to formation and decoupling phases of the QGP evolution, local running coupling and screening scale variations, and other effects out of reach with analytic approximations.

  - Collisional energy losses
  - Gluon emission fluctuation effects
- Detailed convolution over initial production spectra
- In vacuum Fragmentation Functions

Systematic errors

- Initial conditions and plasma evolution
  - Thermalization phase, plasma density profile and fluctuations, plasma constituents, hydrodynamic expansion, freeze-out temperature
- pp reference spectra
- Jet-medium coupling
  - Interaction potential, order of opacity expansion, running coupling scales, multiple gluon emission, large angle radiation

1. One free parameter in the model: α_s (if fixed) or α_0 (if running)
2. Constraint α_s or α_0 to one $R_{AA}^h(p_\perp, \sqrt{s}, y, \mathcal{C})$ reference point
3. Extrapolations to different $(h; p_\perp, \sqrt{s}, y, \mathcal{C})$ are parameter free

Running coupling

- a-b-c model

  Gyulassy, Horowitz

$$\frac{dP}{d\tau} = -\kappa P^a \tau^b T^{2-a+b}$$

GLV → $a = \frac{1}{3} \sim \frac{1}{4}$ $\quad (\Delta E \propto \log(E/T)\, L^2 T^3)$

➢ **Contribution from hard $k_\perp$ tails**

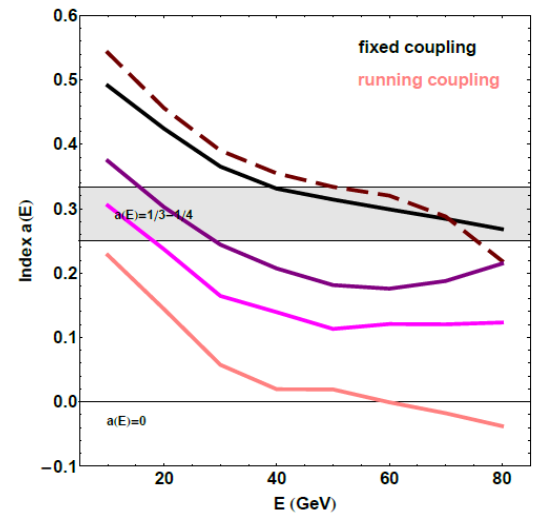

Running scales

fixed

only T

only $q_\perp$

only $k_\perp$

all

LHC

Solid: $\alpha_s(Q)$ with $\alpha_0 = 0.4$
Red Dotted: $\alpha_s(1.25 \times Q)$ with $\alpha_0 = 0.6$
Red Dashed: $\alpha_s(0.5 \times Q)$ with $\alpha_0 = 0.3$
Opaque: Fixed $\alpha_s = 0.3$

➢ Increase in the slope of R_{AA} over a broad range of momenta

Initial pQCD spectra

Initial quark production spectra

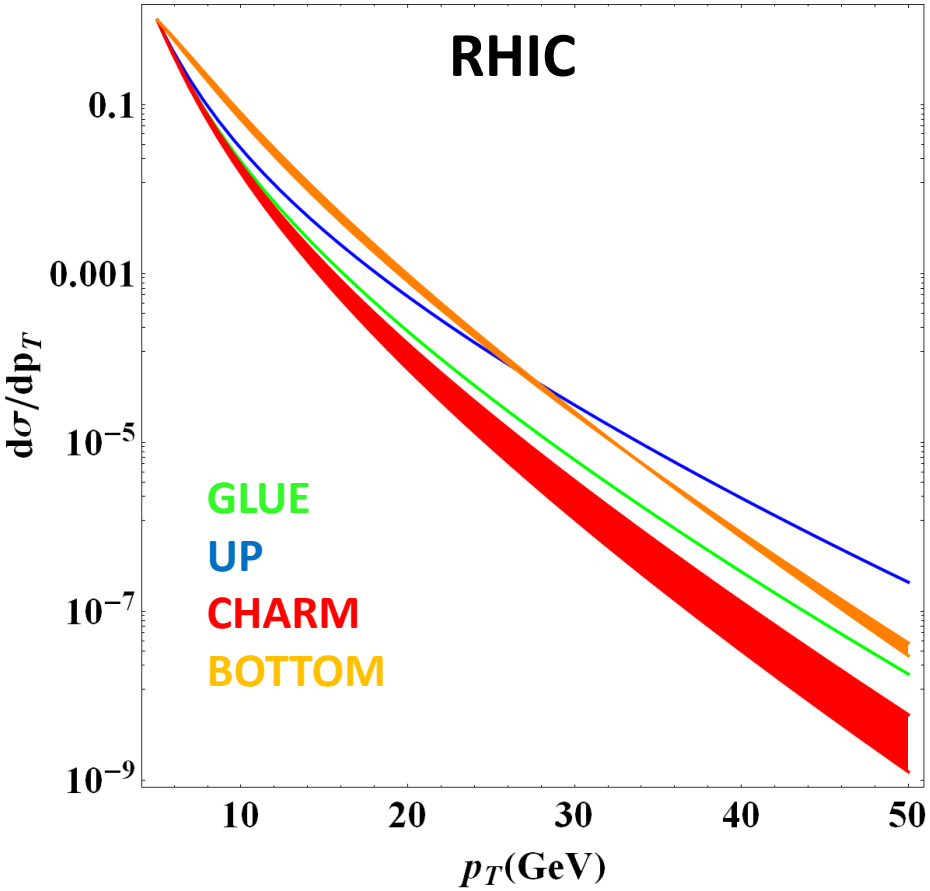

Competing effects between increased density and harder production spectra

- **RHIC density and spectra**
- LHC density, RHIC spectra
- LHC density and spectra

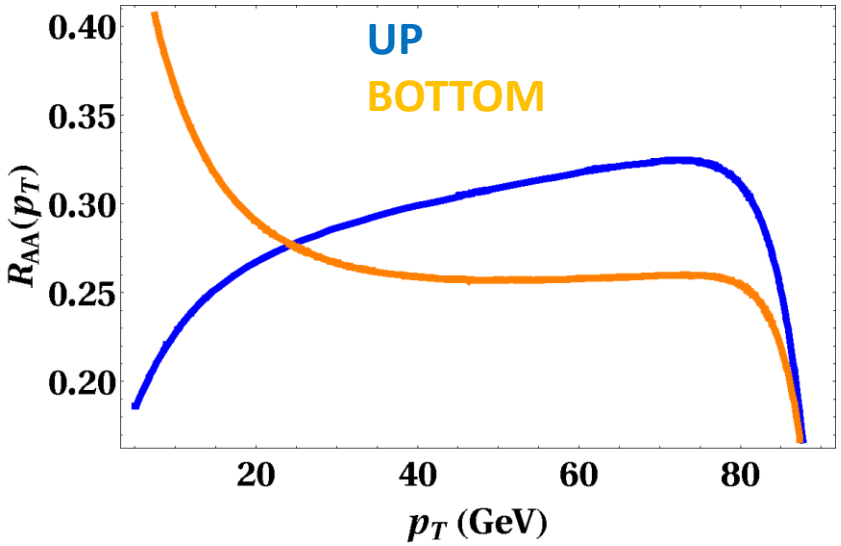

Initial pQCD spectra

Initial quark production spectra

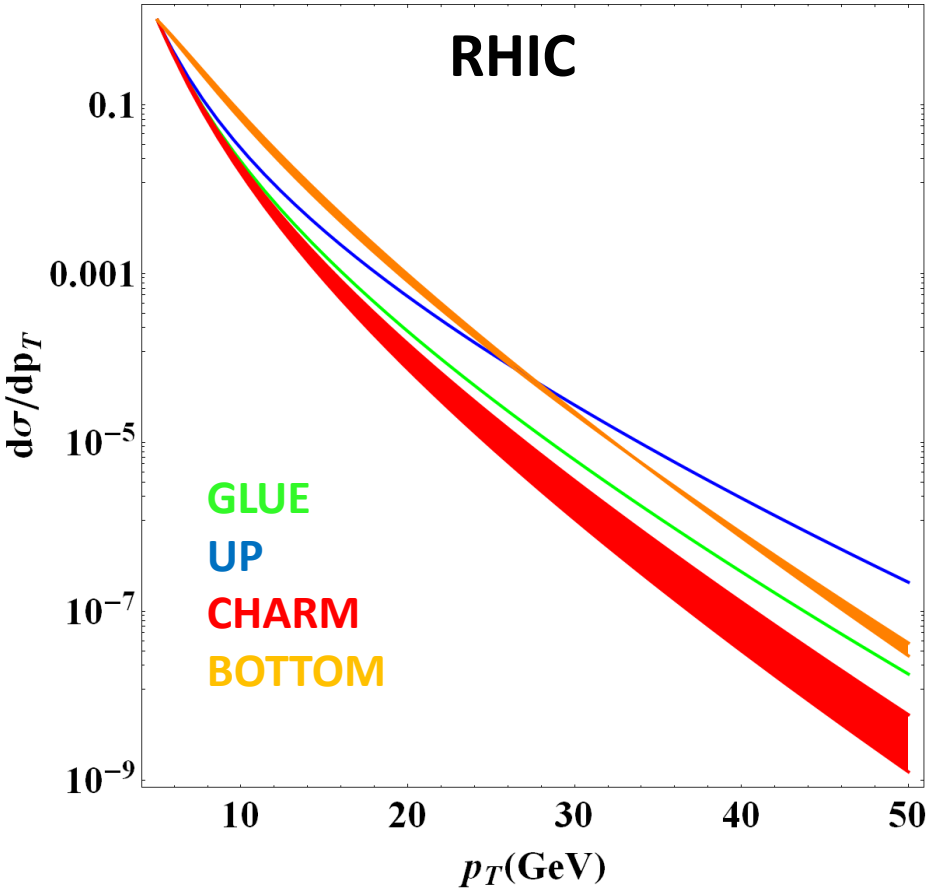

Competing effects between increased density and harder production spectra

- RHIC density and spectra
- **LHC density, RHIC spectra**
- LHC density and spectra

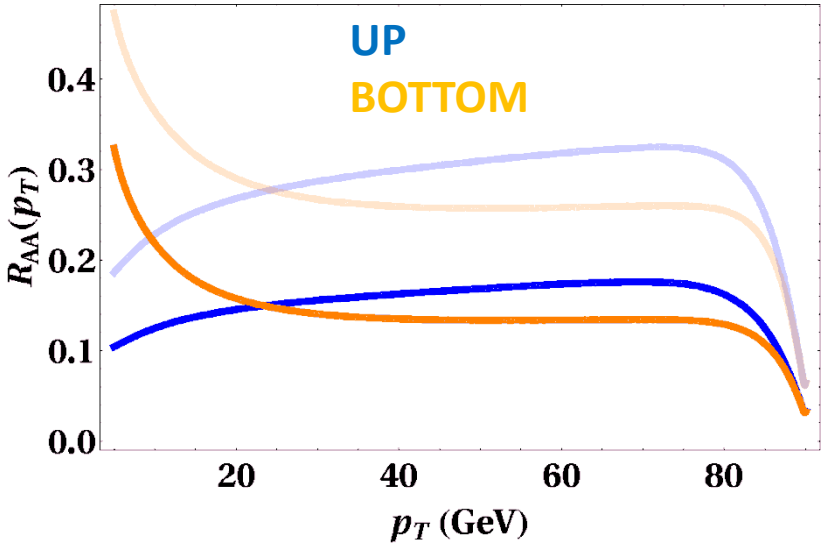

Initial pQCD spectra

Initial quark production spectra

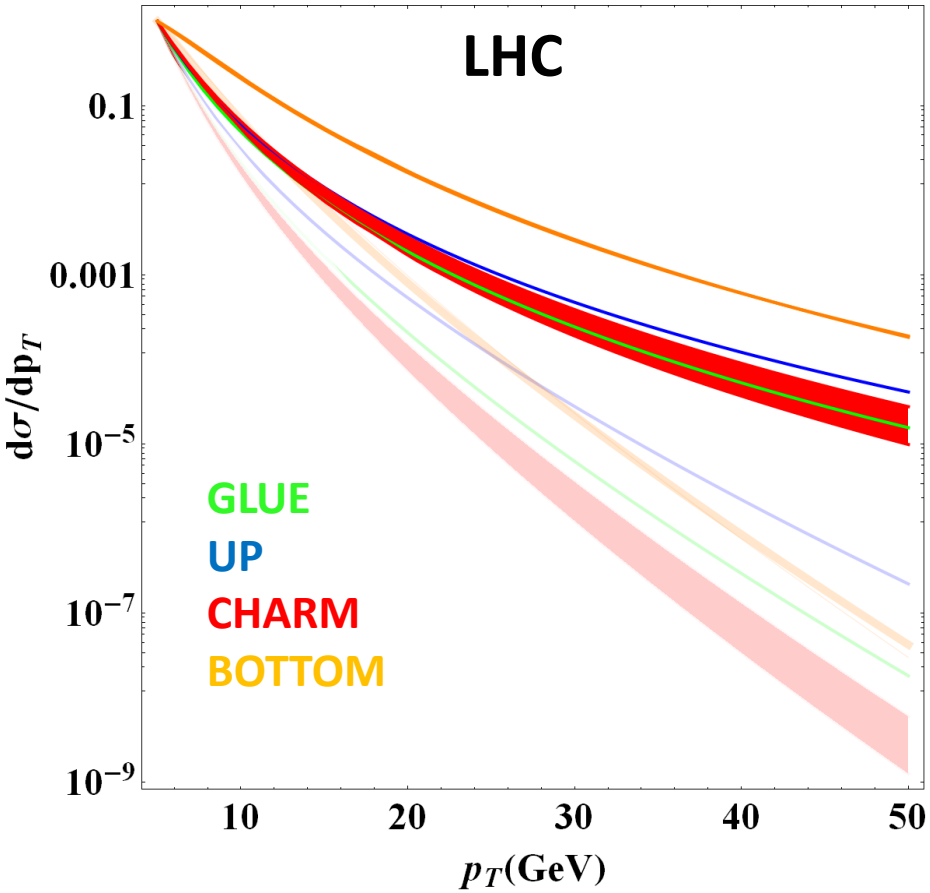

Competing effects between increased density and harder production spectra

- RHIC density and spectra
- LHC density, RHIC spectra
- **LHC density and spectra**

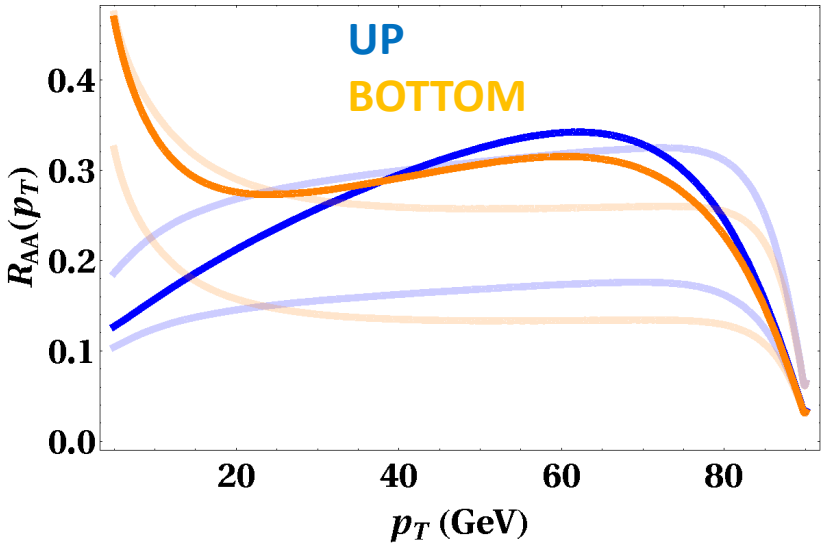

Outline

- Introduction
  - Jet tomography and jet quenching
- CUJET
  - Analysis of the model
  - Geometry, path integral, partonic spectra
- Jet tomography at RHIC and LHC
  - Heavy quark puzzle (RHIC)
  - Surprising transparency (LHC)
- Future developments
  - Elliptic flow
- Conclusions

Explained issues

Heavy quark puzzle (RHIC)

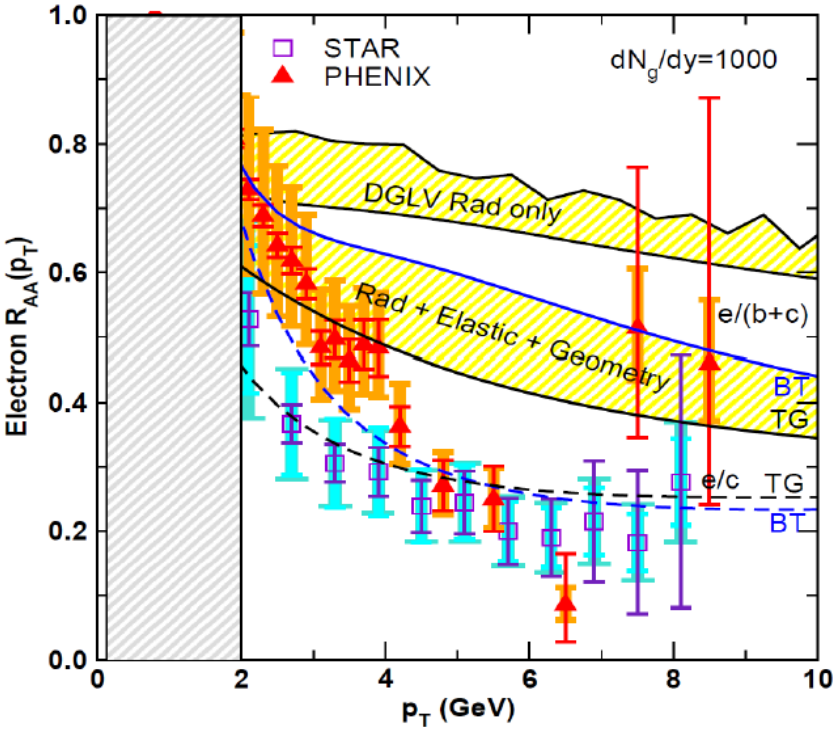

Surprising transparency (LHC)

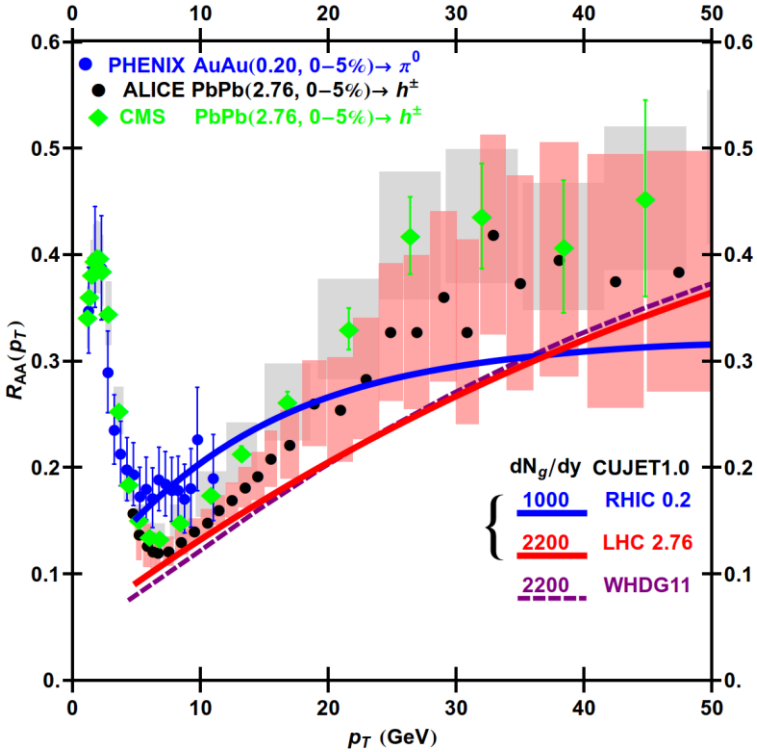

Level crossing at RHIC

RHIC fit
Glauber+Bjorken, dynamical, rad+col
central collision
dN/dy=1000
fixed coupling, α_s=0.3
τ_0=1 fm/c

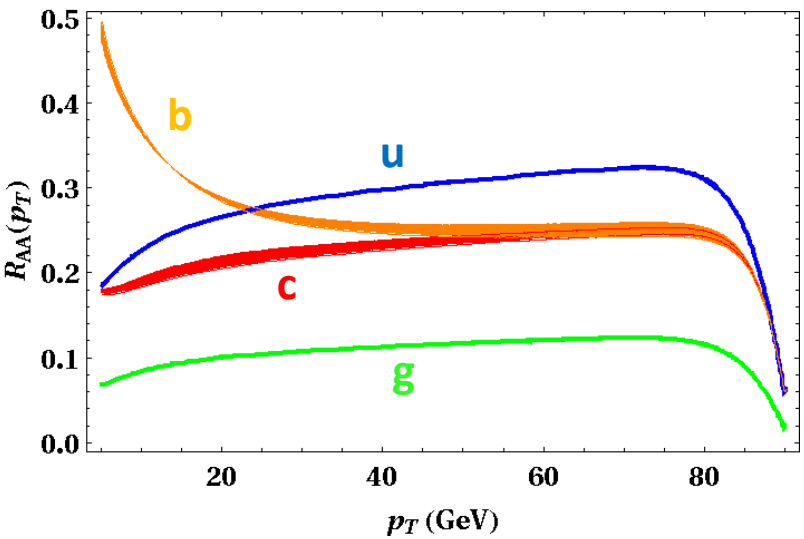

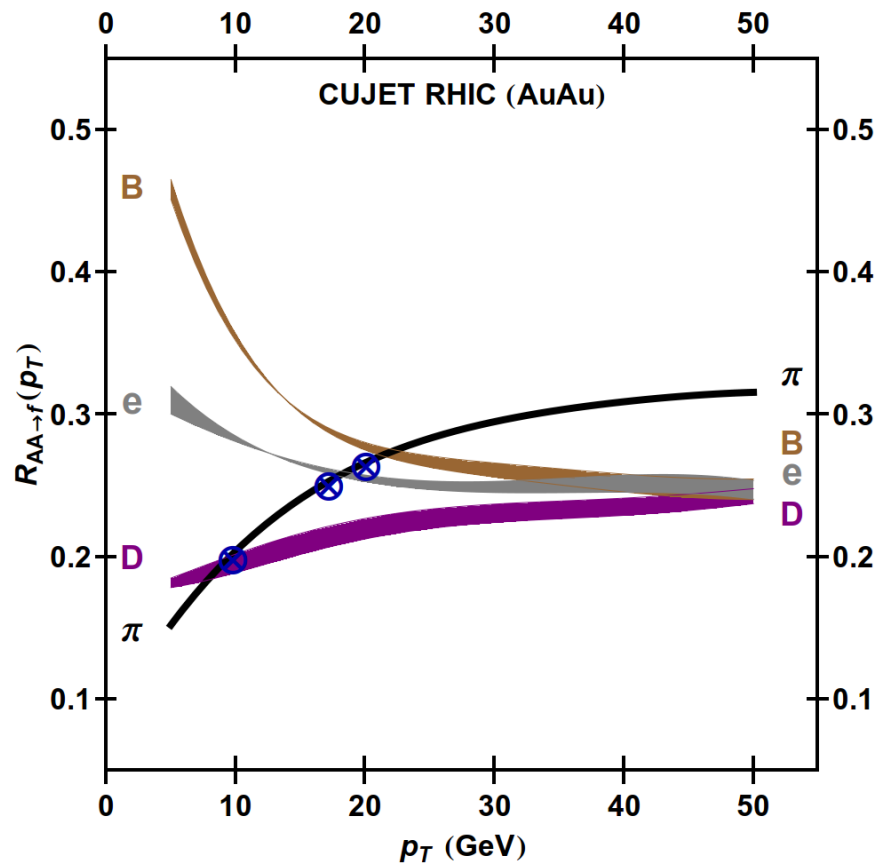

- Inversion of the expected hierarchy order $\pi < D < e < B$ at sufficiently high $p_\perp$
- Interplay between energy loss, initial partonic spectra and fragmentation functions

RHIC data

RHIC fit
Glauber+Bjorken, dynamical, rad+col
central collision
dN/dy=1000
fixed coupling, α_s=0.3

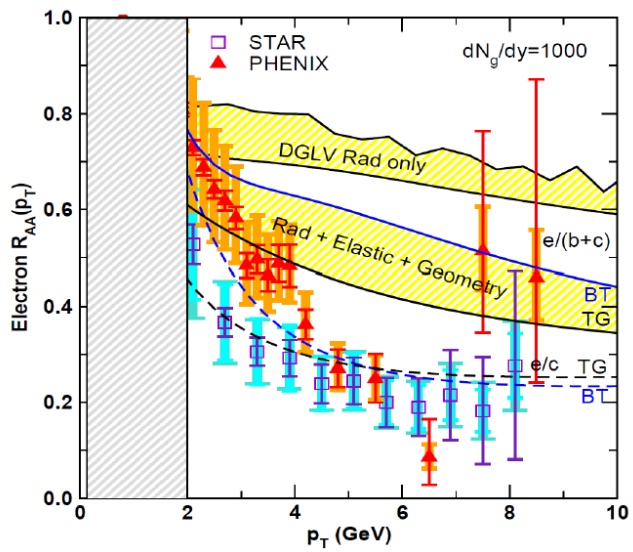

CUJET @ RHIC

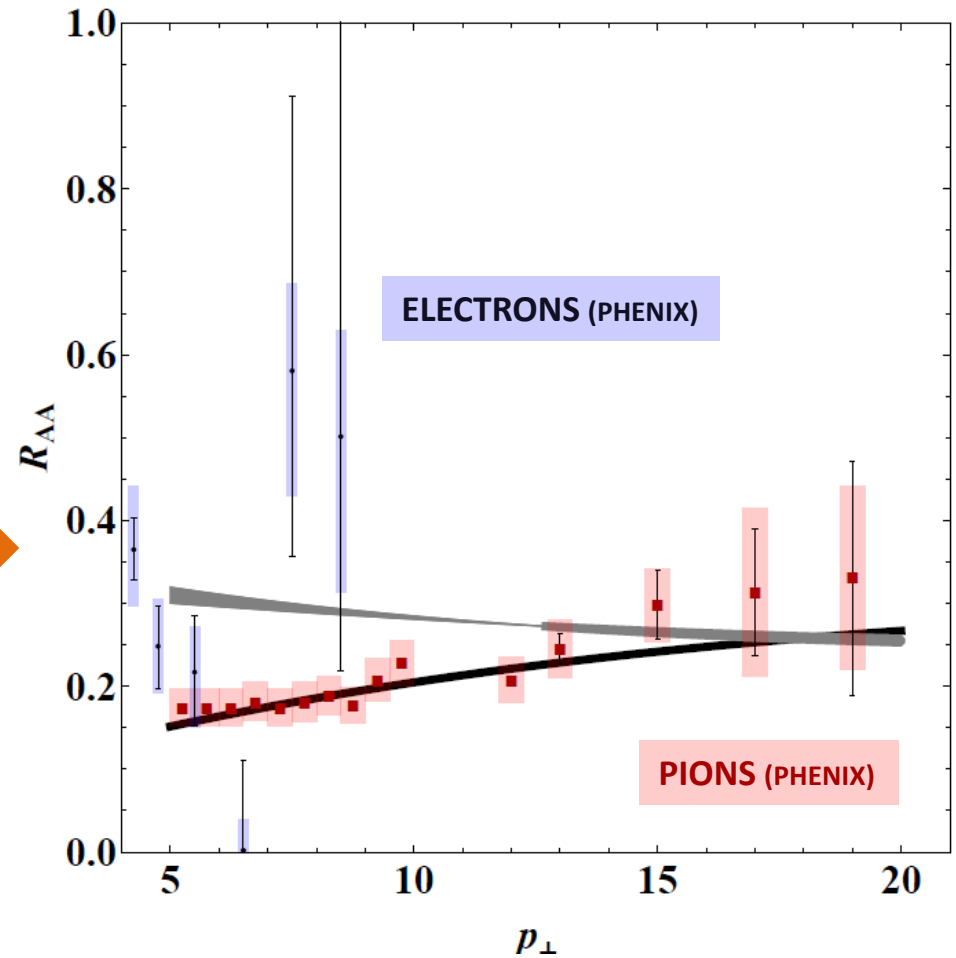

- **Reduced discrepancy between pions and non-photonic electrons**

Level crossing at LHC

LHC extrapolation parameter-free
dN/dy=2200
LHC production spectra

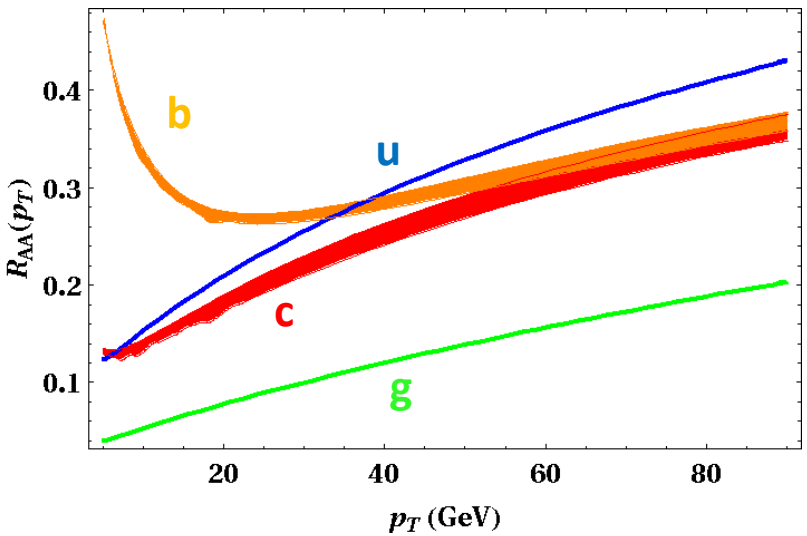

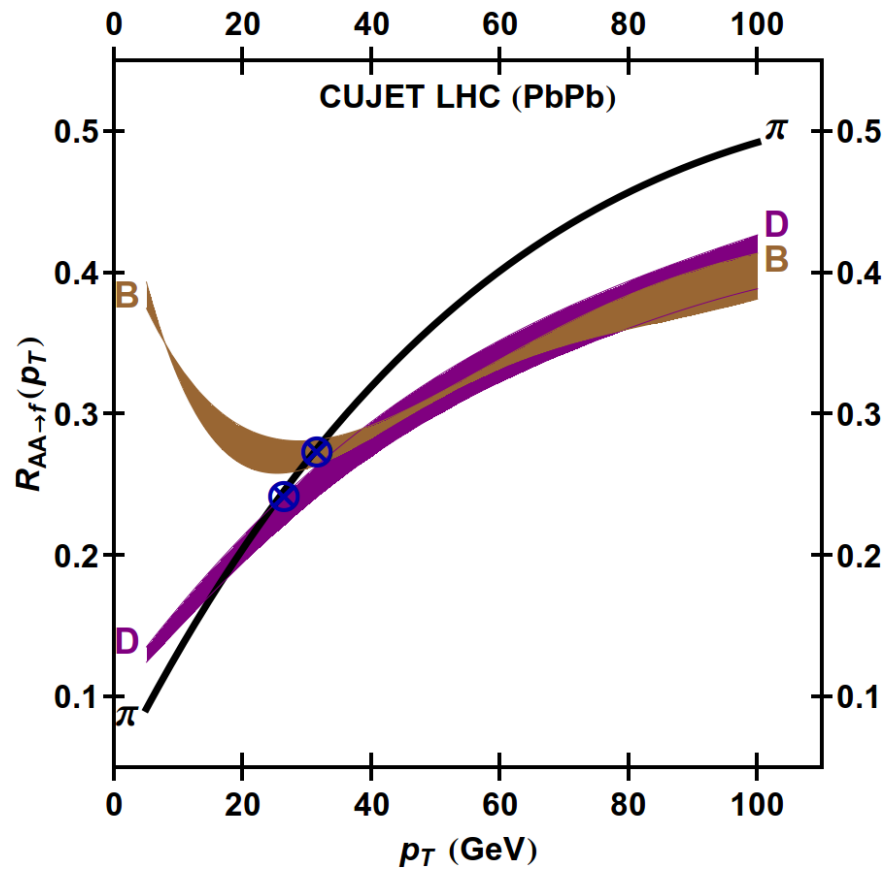

- Inversion of the expected hierarchy order $\pi < D < B$ at energies accessible experimentally
- Steep rise of R_{AA} with $p_\perp$

LHC data

LHC extrapolation parameter-free
(fixed coupling, α_s=0.3)
dN/dy=2200
LHC production spectra

- **Predictions are over-quenched: the QGP at LHC is surprisingly transparent to hard probes**
- **Possibility of reduced coupling?**

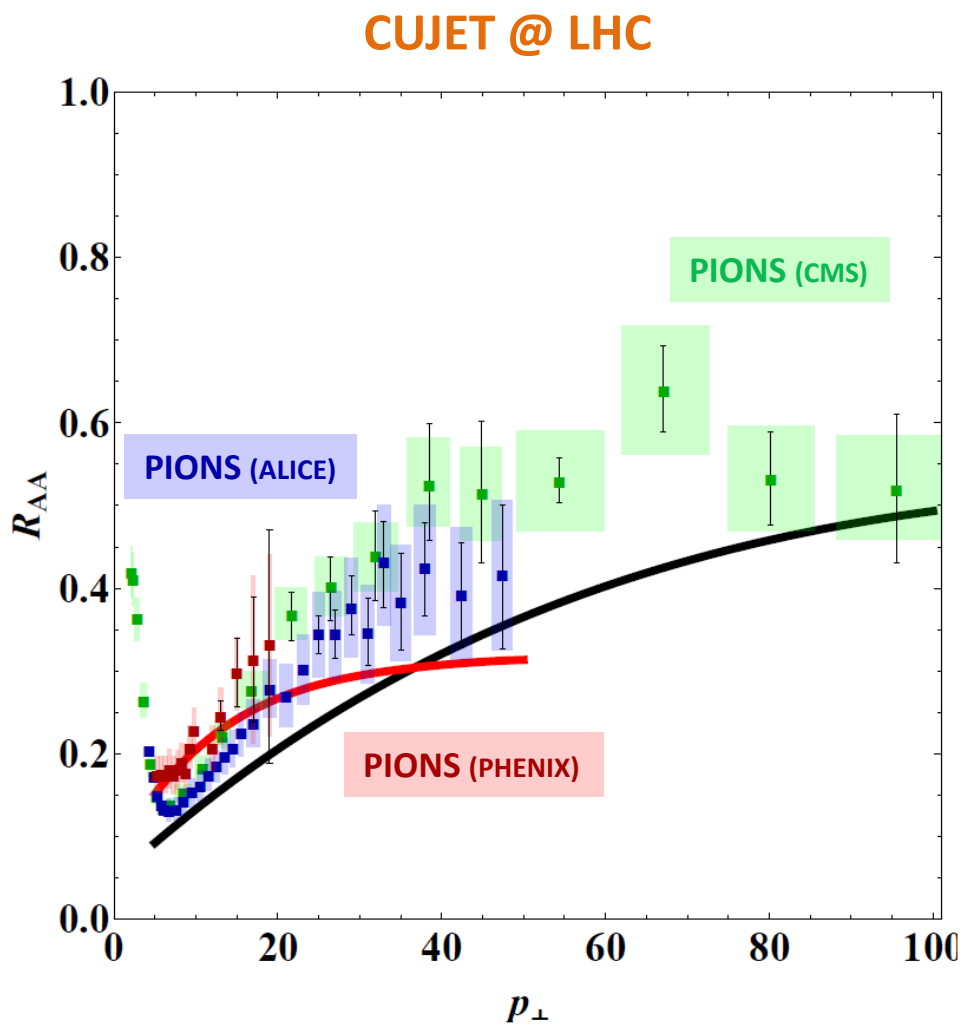

LHC data with running coupling

LHC fit, RHIC extrapolation parameter-free
Glauber+Bjorken, dynamical, rad+col
central collision
dN/dy=2200
running coupling, α_0=0.4

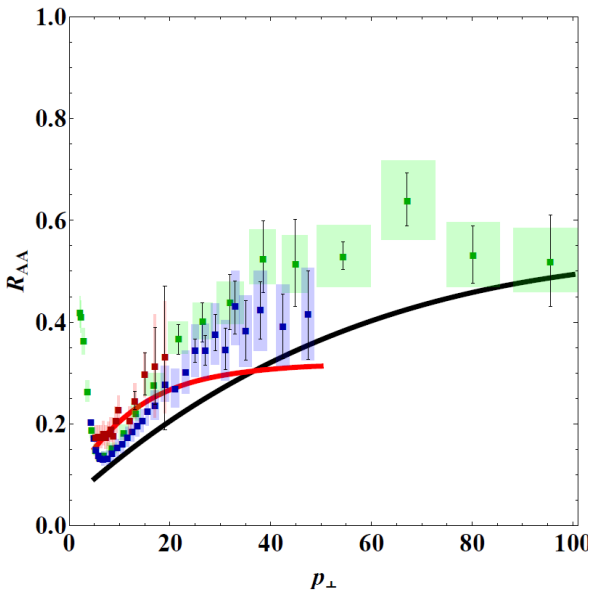

CUJET @ LHC

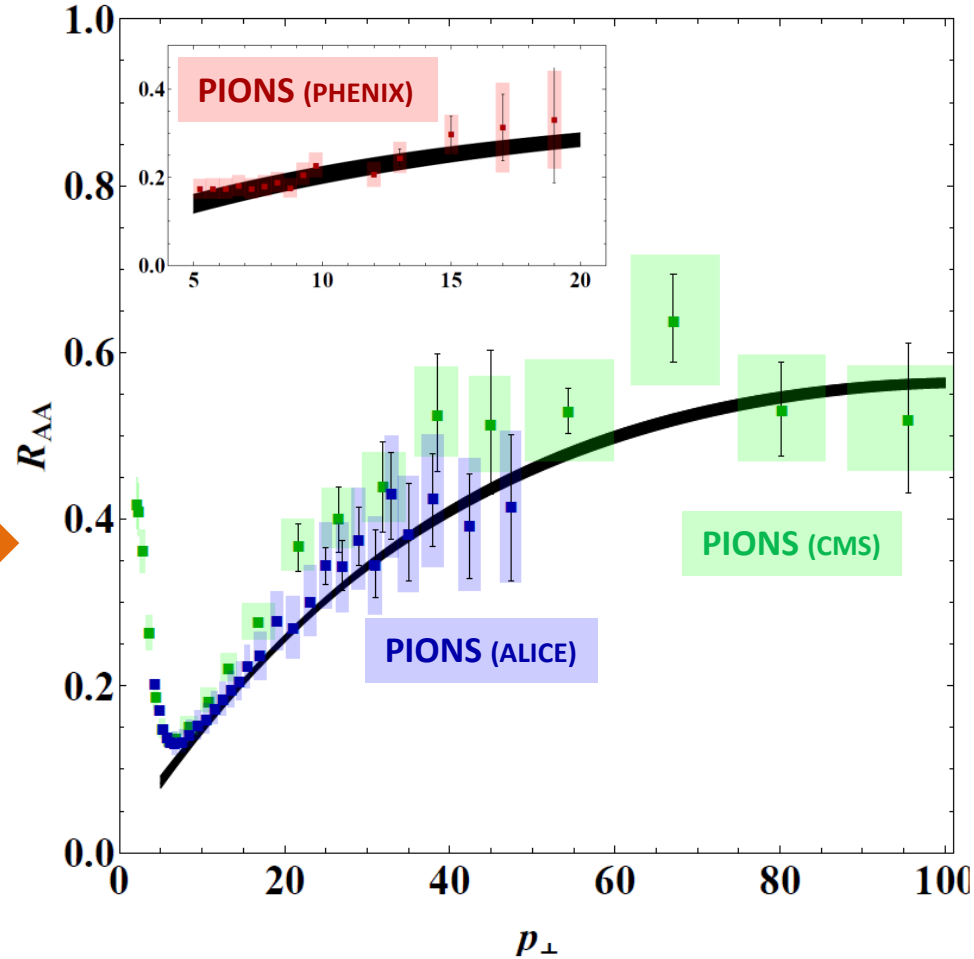

- **Surprising agreement with data**
- **Consistent with backward extrapolated RHIC predictions**

Open heavy flavor data

CUJET @ LHC

LHC fit, RHIC extrapolation parameter-free

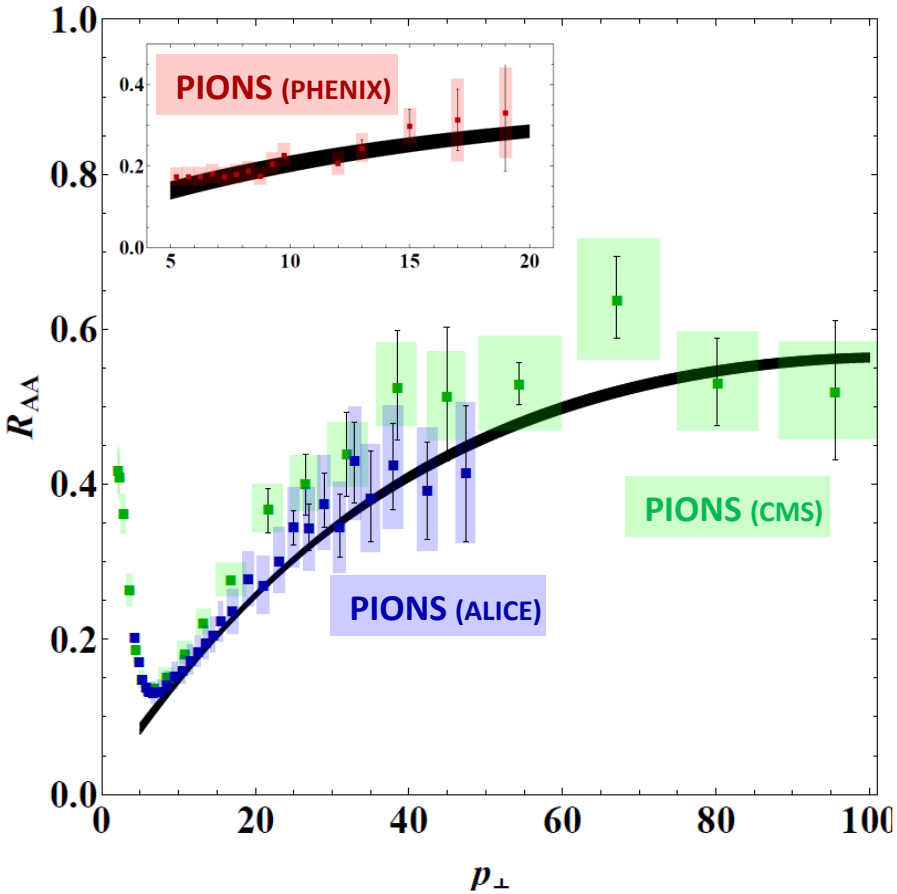

Constrained by LHC pion fit

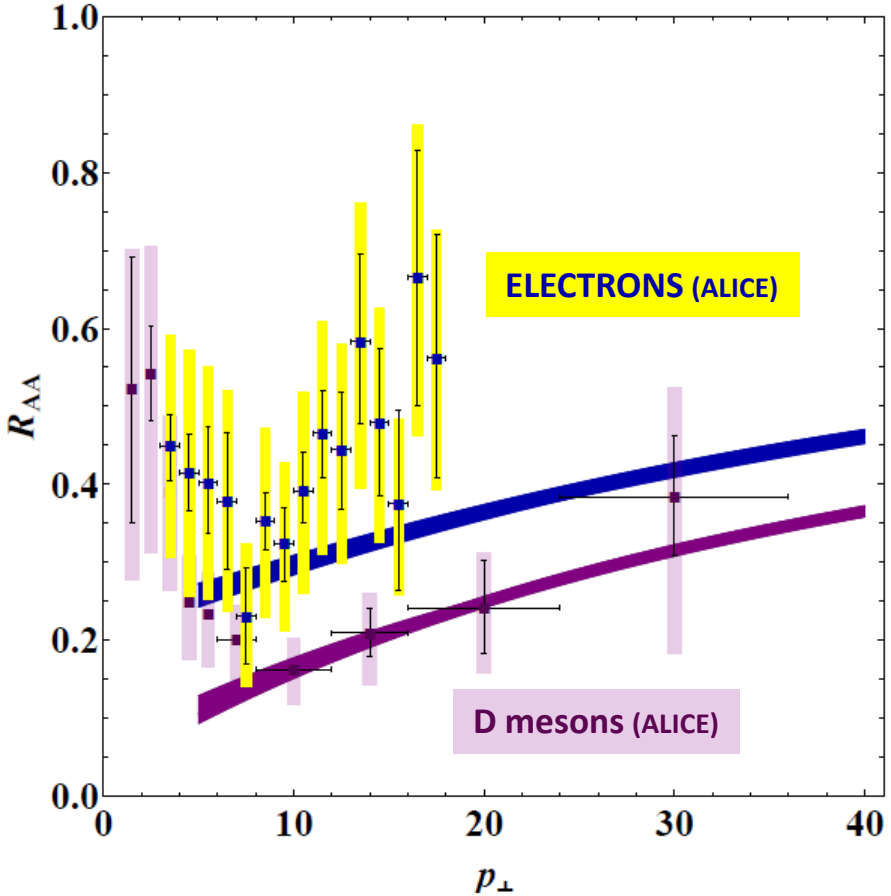

Open heavy flavor data

CUJET @ LHC

LHC fit, RHIC extrapolation parameter-free

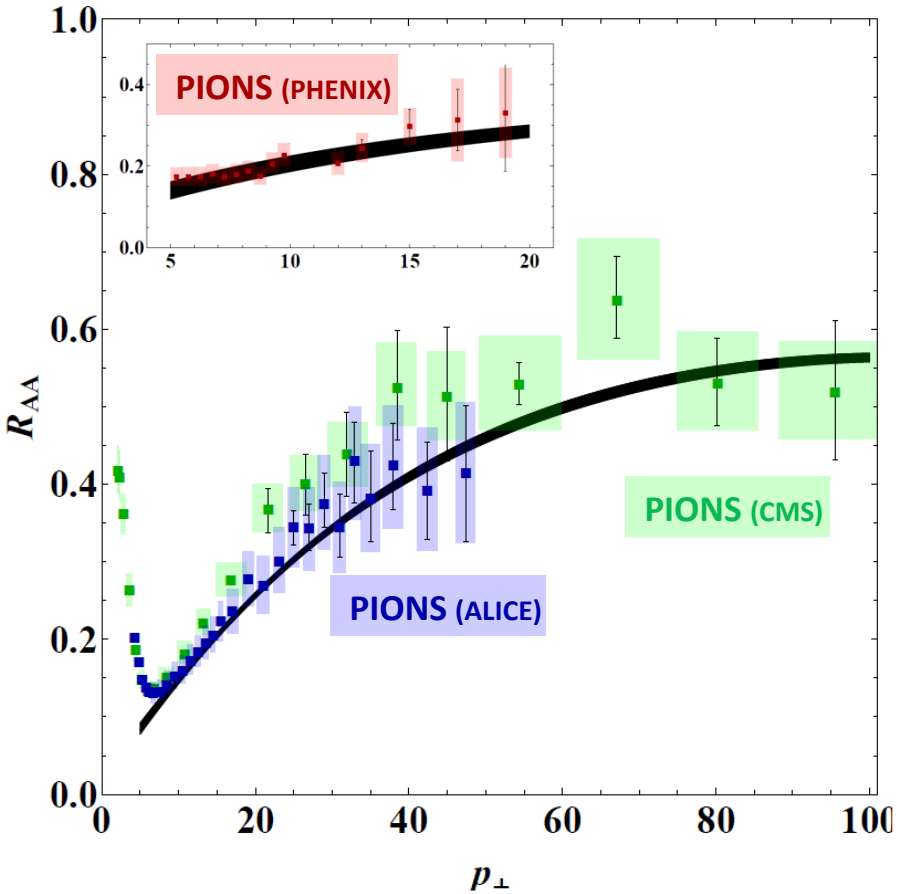

Constrained by LHC pion fit

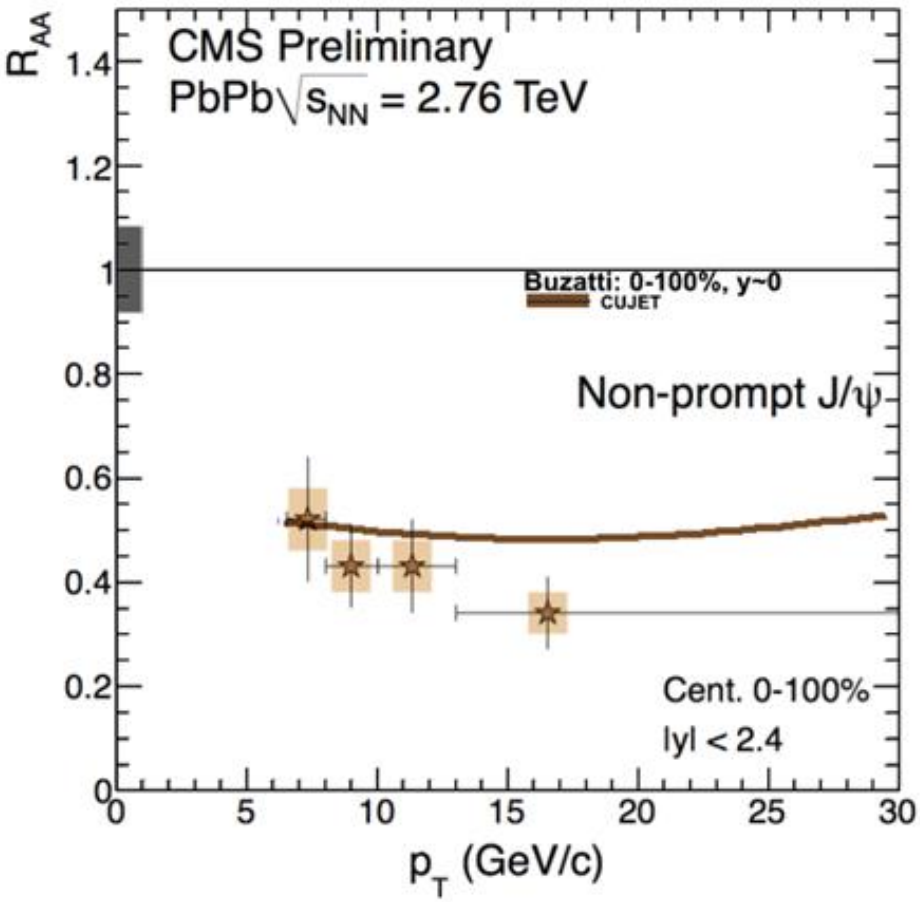

Outline

- Introduction
  - Jet tomography and jet quenching
- CUJET
  - Analysis of the model
  - Geometry, path integral, partonic spectra
- Jet tomography at RHIC and LHC
  - Heavy quark puzzle (RHIC)
  - Surprising transparency (LHC)
- Future developments
  - Elliptic flow
- Conclusions

Elliptic flow

Recent presliminary PHENIX/RHIC 2012 azimuthal tomography

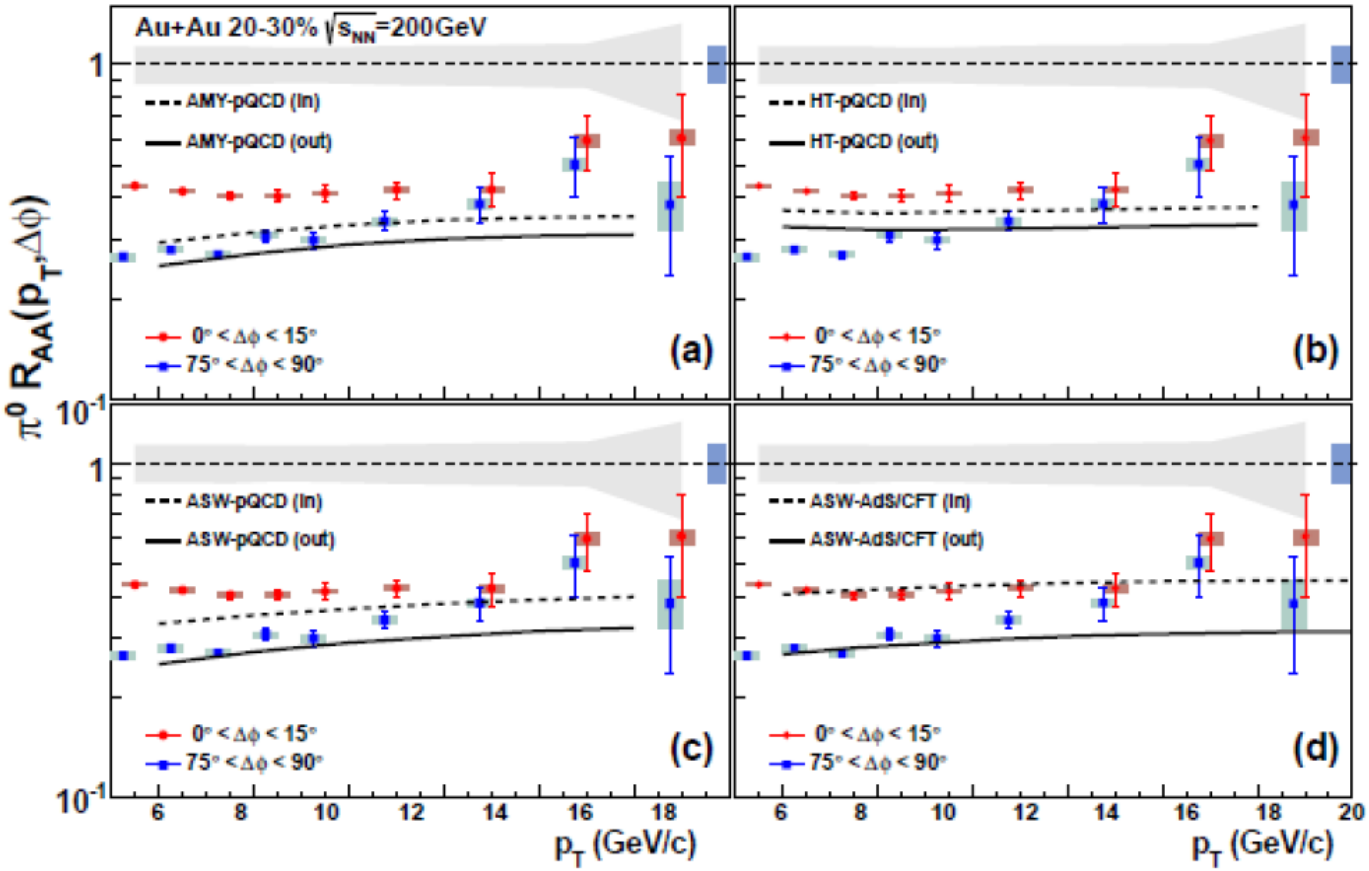

FIG. 22: (Color online) The data points are $R_{AA}(\Delta\phi)$ in 20–30% centrality as a function of p_T for in-plane (red, upper points) and out-of-plane π^0 (blue, lower points), compared to four model calculations (see text for description and references). (a) pQCD-based AMY [9, 42], (b) HT [10], (c) pQCD-based ASW [11], (d) ASW using AdS/CFT correspondence [12]. The curves on panels (a)-(c) are taken from [36]. The dotted and solid lines are the in-plane and out-of-plane predictions, respectively. The definition of the gray bands and blue boxes is same as in Fig. 20.

Elliptic flow

At LHC *Deep* UV Band pT>10 GeV seems to agree finally with pQCD tomography
An intermediate IM Band 2 < pT <10 interpolates between IR and UV bands

WAHorowitz, MG, JPG G38 (2011) QM11

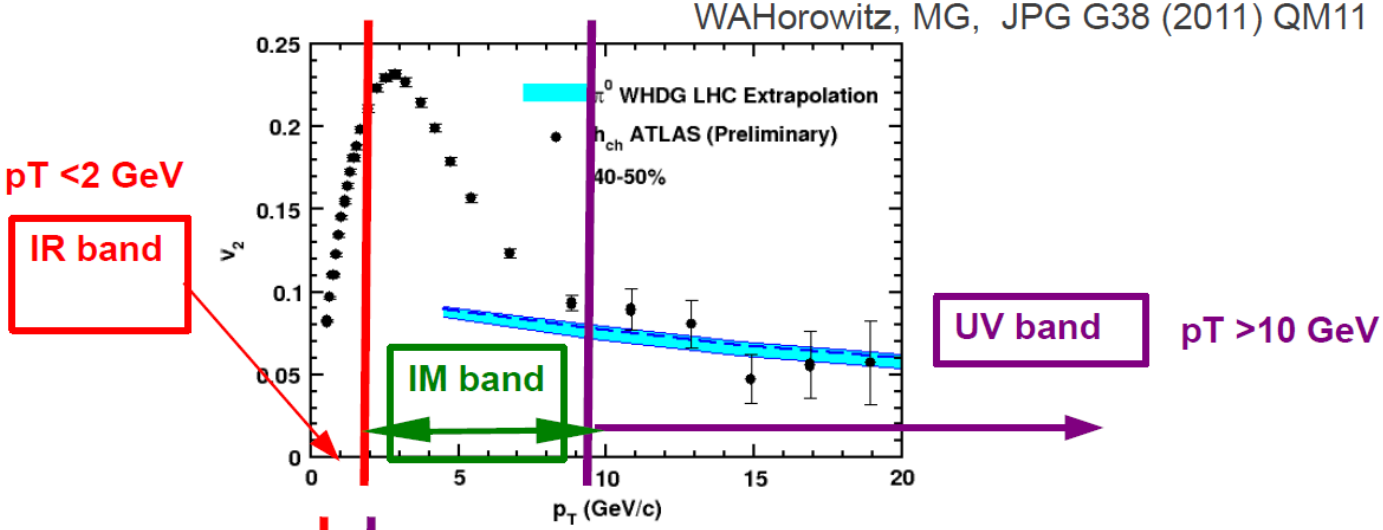

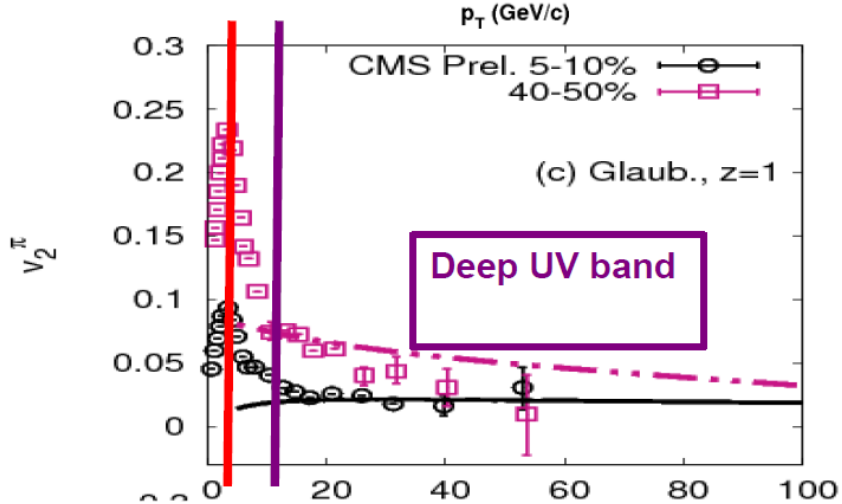

Latest CMS 2012
v2 data probe
very deep into UV ~ 60 GeV !

M Gyul 1

B.Betz, MG PRCC86 (2012) 024903

Hydro expansion

Denes Molnar, Deke Sun, QM12 used MPC bulk evolution to evaluate GLV En Loss

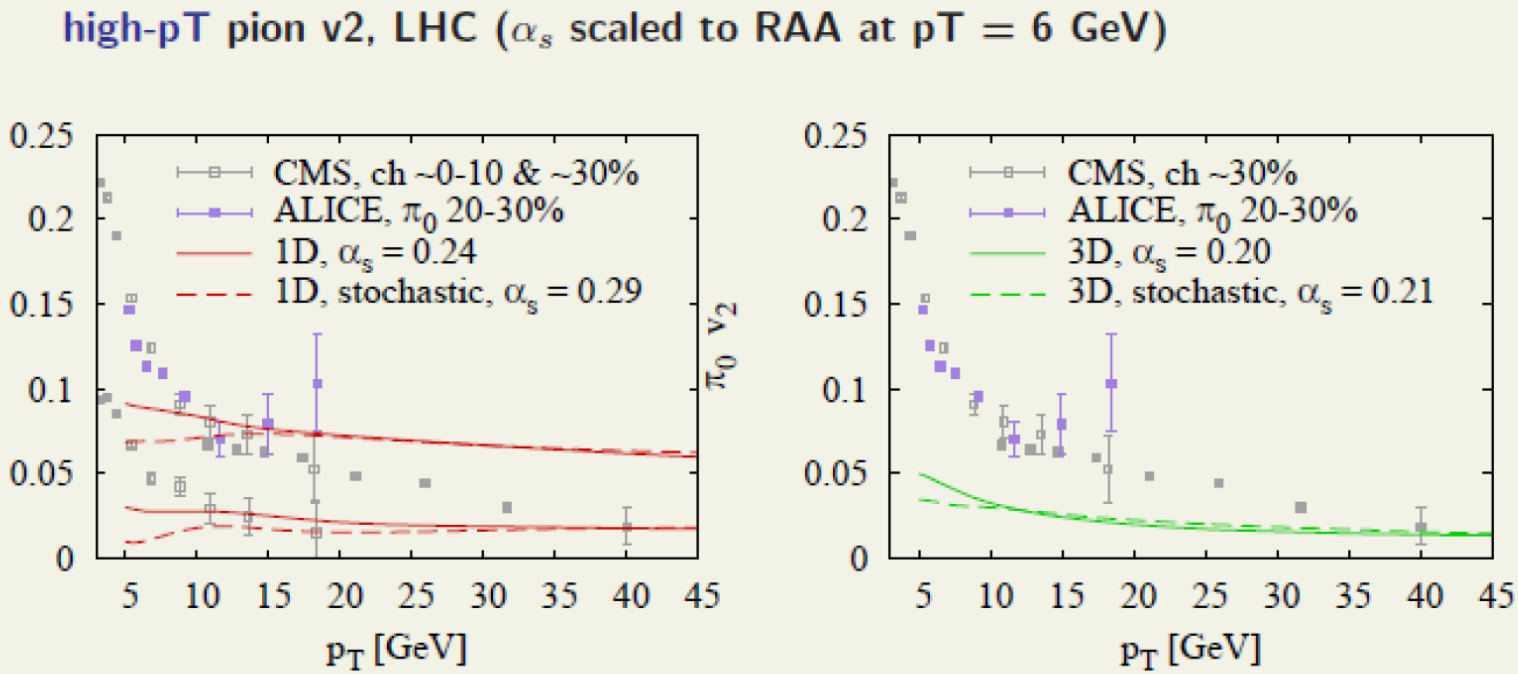

They concluded that transverse expansion reduced pQCD v2(pT) by factor ~ 2 below data

More on hydro expansion

Prelim
BBetz, MG
03/21/13 @
FNP13 Conf

pQCD plus
Romatschke
Visc.hydro
QGP

Consistent with
Recent
PHENIX v2(pT)

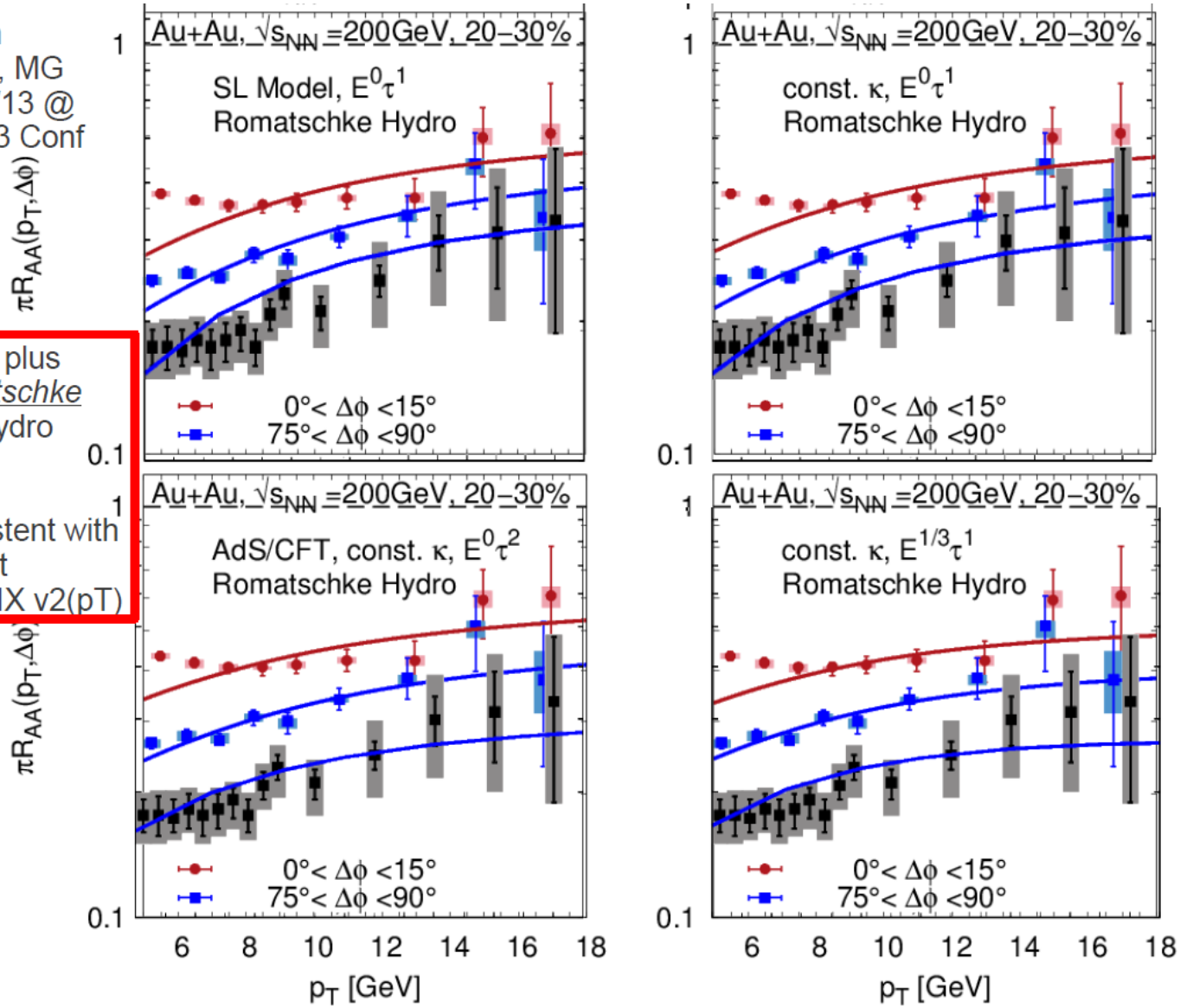

Conclusions

- Quark Gluon Plasma
  - Low- hydro vs. high- pQCD
  - QGP properties can be studied measuring high- Jets
  - Jet tomography requires knowledge of: (1) initial conditions (2) plasma evolution (3) energy loss (4) jet fragmentation
- CUJET
  - Quantitative predictions insensitive to many of the systematic theoretical uncertainties
  - Evolution over WHDG
    - » Geometry, Jet path integration, Partonic spectra, Dynamical potential
  - Predicted level crossing pattern, reduced light-bottom quark jets discrepancy, steep rise of R_{AA} at LHC
- Future
  - Address azimuthal asymmetry puzzle
    - » Include viscous hydrodynamics
  - Full jet measurements

WHDG

- Elliptic flow $$\frac{dN}{dp_\perp d\phi} = \frac{dN}{dp_\perp}\frac{1}{2\pi}(1 + 2v_1\cos\phi + 2v_2\cos 2\phi + \cdots)$$

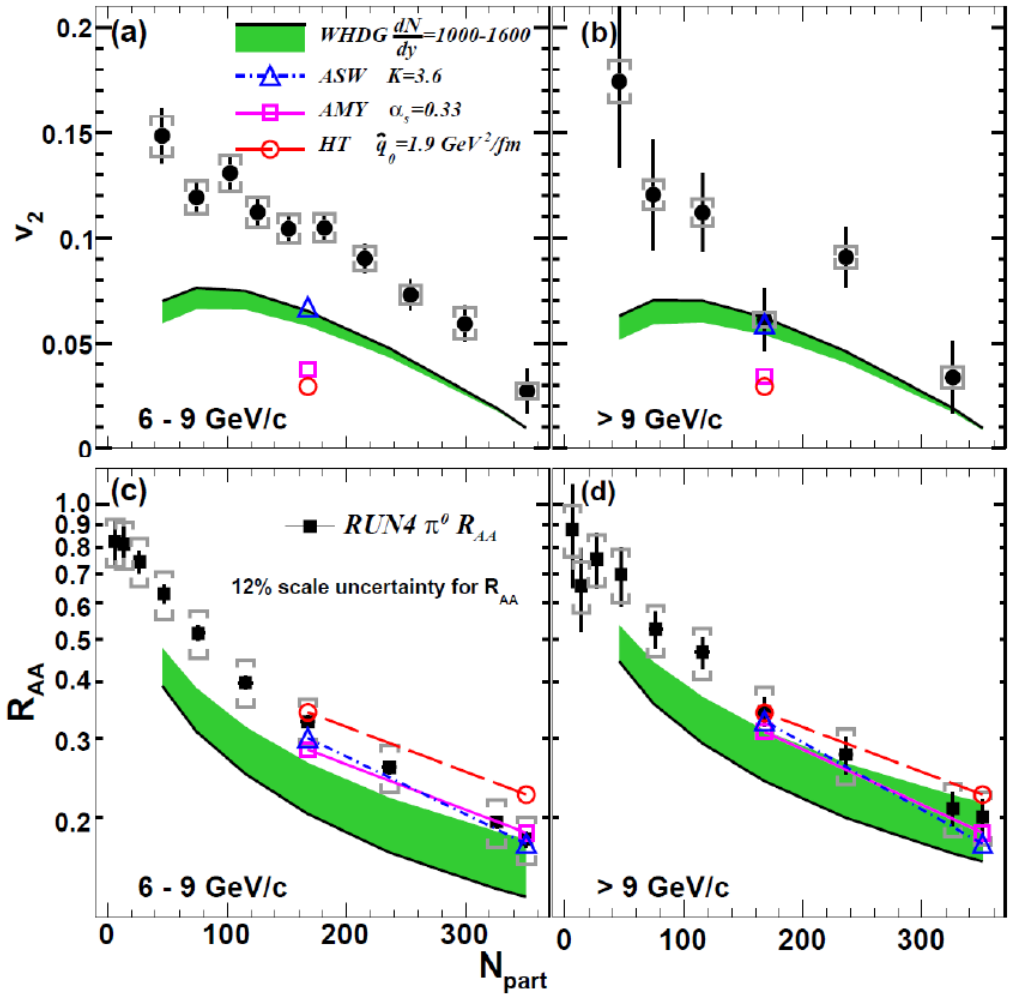

- Need stronger coupling between jet and medium, but R_{AA} will be over-quenched
- The agreement between data and theoretical curves worsen for higher centralities and lower transverse momenta.

Elliptic flow

BBMG 032112 FNP13

Azimuthal Tomography over full range RHIC pT=0-20 GeV , RAAin out

Sensistive to both dEdX as well as detailed spacetime QGP expansion
Results below couple pQCD with RL (Romatsch.Luzum) min visc hydro QGP

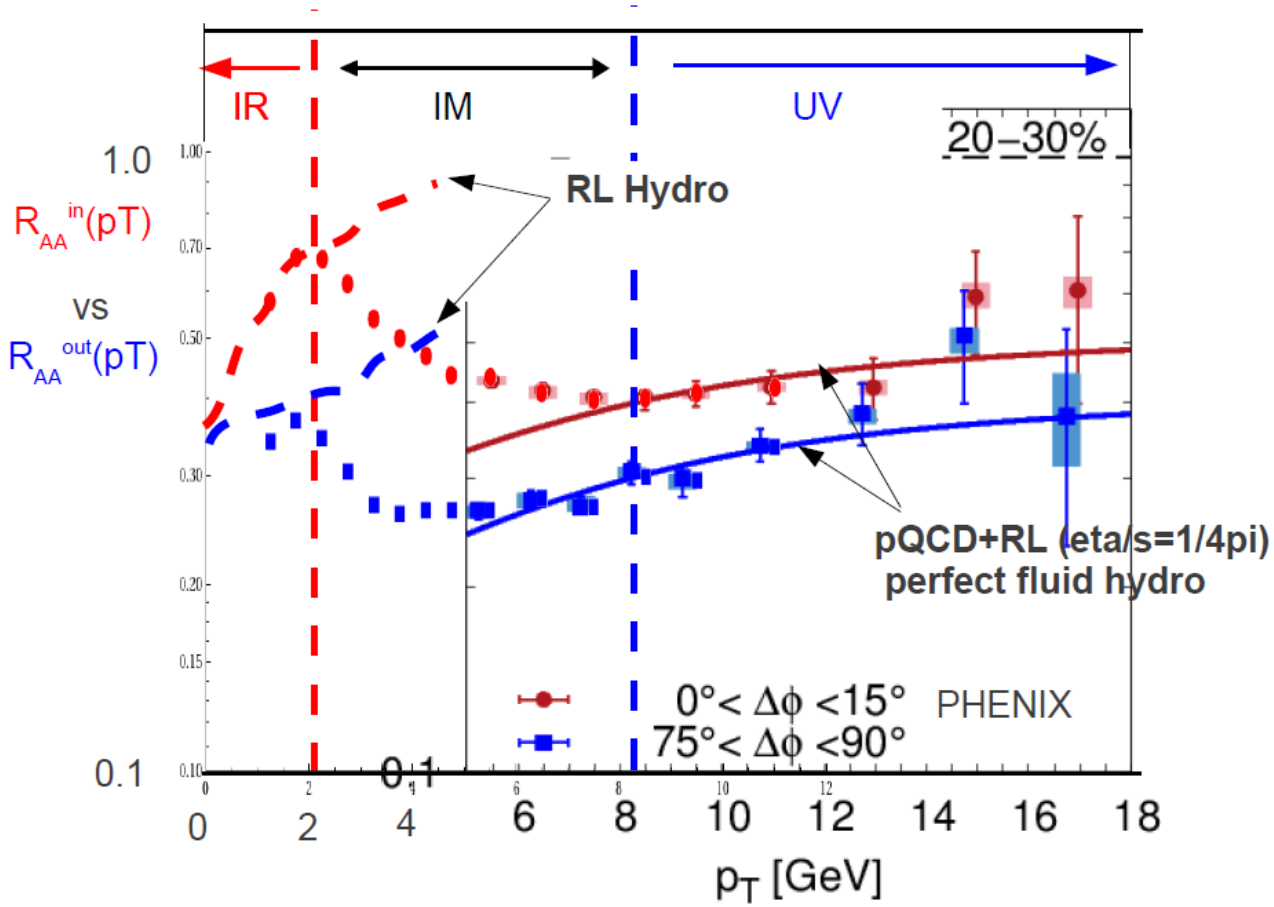

Radiative energy loss

Incoherent limit: Gunion-Bertsch

- $$\frac{dN}{dx dk_\perp} = \frac{1}{x}\frac{\alpha_s C_A}{\pi^2}\frac{q_\perp^2}{k_\perp^2 (q_\perp - k_\perp)^2}$$
  - Non-abelian equivalent of Bethe-Heitler limit
  - Flat distribution at mid-rapidity
  - Multiple scattering amplitudes are summed incoherently
  - Incoming quark is on-shell and massless

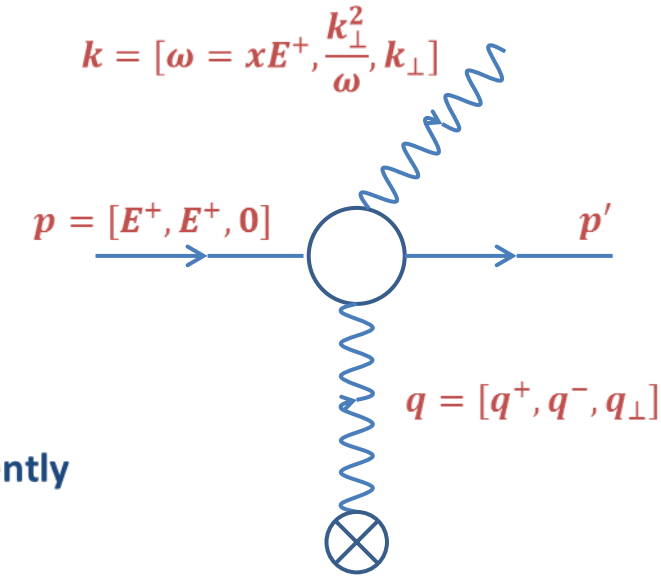

Formation time physics

- 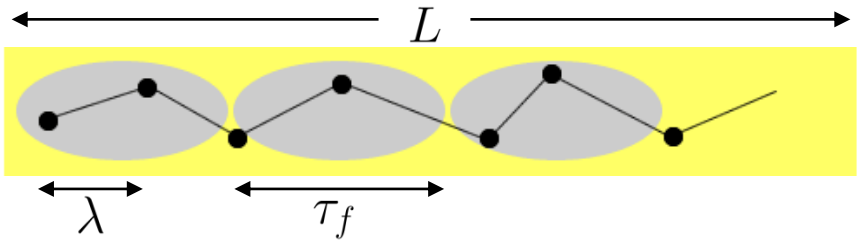

$$\tau_f \sim \frac{2\omega}{k_\perp^2}$$

  - $\tau_f < \lambda < L$ Incoherent multiple collisions
  - $\lambda < \tau_f < L$ LPM effect (radiation suppressed by multiple scatterings within one coherence length)
  - $\lambda < L < \tau_f$ Factorization limit (acts as one single scatterer)

GLV interference effects

- **Energy loss LPM interference effects with hard production vertex (jet created at finite time)**

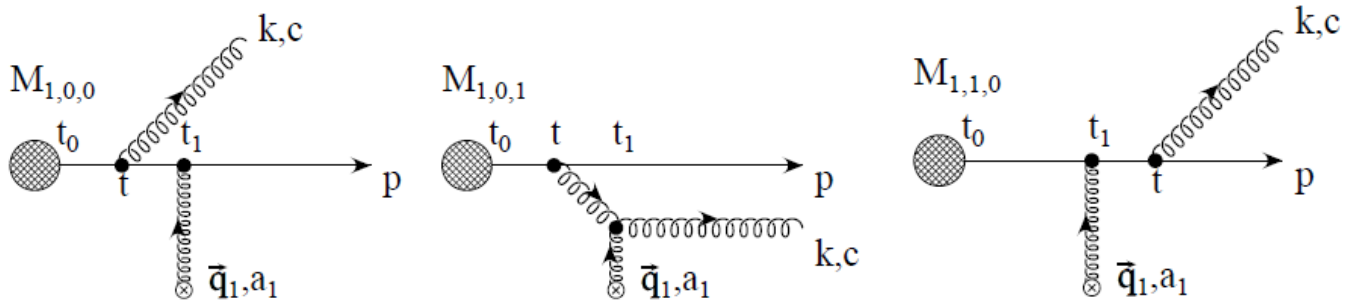

- **Transverse diffusion LPM interference effects with successive scatterings (gluon cascading)**

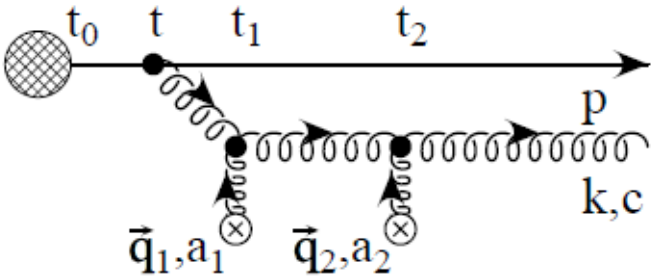

DGLV mass effects

$$x\frac{dN^{(n)}}{dx\,d^2\mathbf{k}} = \frac{C_R\alpha_s}{\pi^2}\frac{1}{n!}\int\prod_{i=1}^{n}\left(d^2\mathbf{q}_i\,\frac{L}{\lambda_g(i)}\left[\bar{v}_i^2(\mathbf{q}_i)-\delta^2(\mathbf{q}_i)\right]\right)\times$$

$$\times\left(-2\,\tilde{\mathbf{C}}_{(1,\cdots,n)}\cdot\sum_{m=1}^{n}\tilde{\mathbf{B}}_{(m+1,\cdots,n)(m,\cdots,n)}\left[\cos\left(\sum_{k=2}^{m}\Omega_{(k,\cdots,n)}\Delta z_k\right)-\cos\left(\sum_{k=1}^{m}\Omega_{(k,\cdots,n)}\Delta z_k\right)\right]\right)$$

Soft Radiation ($E \gg \omega$, $x \ll 1$)
Soft Scattering ($E \gg q$, $\omega \gg k_T$)

Opacity series expansion $\longrightarrow$ $\left(\frac{L}{\lambda}\right)^n$

Radiation antenna $\longrightarrow$ *Cascade terms*

$$\tilde{\mathbf{C}}_{(i_1 i_2\cdots i_m)} = \frac{(\mathbf{k}-\mathbf{q}_{i_1}-\mathbf{q}_{i_2}-\cdots-\mathbf{q}_{i_m})}{(\mathbf{k}-\mathbf{q}_{i_1}-\mathbf{q}_{i_2}-\cdots-\mathbf{q}_{i_m})^2+m_g^2+M^2x^2}\,,$$

$$\tilde{\mathbf{B}}_{(i_1 i_2\cdots i_m)(j_1 j_2\cdots i_n)} = \tilde{\mathbf{C}}_{(i_1 i_2\cdots j_m)} - \tilde{\mathbf{C}}_{(j_1 j_2\cdots j_n)}\,.$$

Gunion – Bertsch

$$\tilde{\mathbf{B}}_i = \tilde{\mathbf{H}} - \tilde{\mathbf{C}}_i\,,$$

Hard

$$\tilde{\mathbf{H}} = \frac{\mathbf{k}}{\mathbf{k}^2+m_g^2+M^2x^2}\,,$$

LPM effect $\longrightarrow$

$$\Omega_{(m,\cdots,n)} = \underbrace{\frac{(\mathbf{k}-\mathbf{q}_m-\cdots-\mathbf{q}_n)^2}{2xE}}_{\textit{Inverse formation time}} + \underbrace{\frac{m_g^2+M^2x^2}{2xE}}_{\textit{Mass effects}}$$

Scattering center distribution $\longrightarrow$ $\Delta z_k = z_k - z_{k-1} \sim L/(n+1)$

Effective Potential

Static potential (DGLV)

$$|\bar{v}_i(q_i)|^2 = \frac{1}{\pi}\frac{\mu(z_i)^2}{(q^2+\mu(z_i)^2)^2}$$

- Static scattering centers
- Color-electric screened Yukawa potential (Debye mass)
- Full opacity series

Dynamical potential (MD)

$$|\bar{v}_i(q_i)|^2 = \frac{1}{\pi}\frac{\mu(z_i)^2}{q^2(q^2+\mu(z_i)^2)}$$

- Dynamical scattering centers
- Includes screened color-magnetic effects (HTL gluon propagators)
- Only first order in opacity

Interpolating potential (CUJET)

$$|\bar{v}_i(q_i)|^2 = \frac{\mathcal{N}(\mu_m)}{\pi}\frac{\mu_e(z_i)^2}{(q^2+\mu_e(z_i)^2)(q^2+\mu_m(z_i)^2)}$$

- Introduces effective Debye magnetic mass
- Interpolates between the static and dynamical limits
- Magnetic screening allows full opacity series

Outline

- Introduction
  - QCD phase diagrams and equation of state
  - Heavy ion collisions and formation of Quark Gluon Plasma
  - Jet tomography and jet quenching
  - Energy loss models
- Opacity expansion series
  - Convergence of the series
  - Radiated gluon transverse momentum distribution
- CUJET
  - Analysis of the model
  - Geometry, path integral, partonic spectra
- Jet tomography at RHIC and LHC
  - Heavy quark puzzle (RHIC)
  - Surprising transparency (LHC)
- Conclusions

Convergence of the series

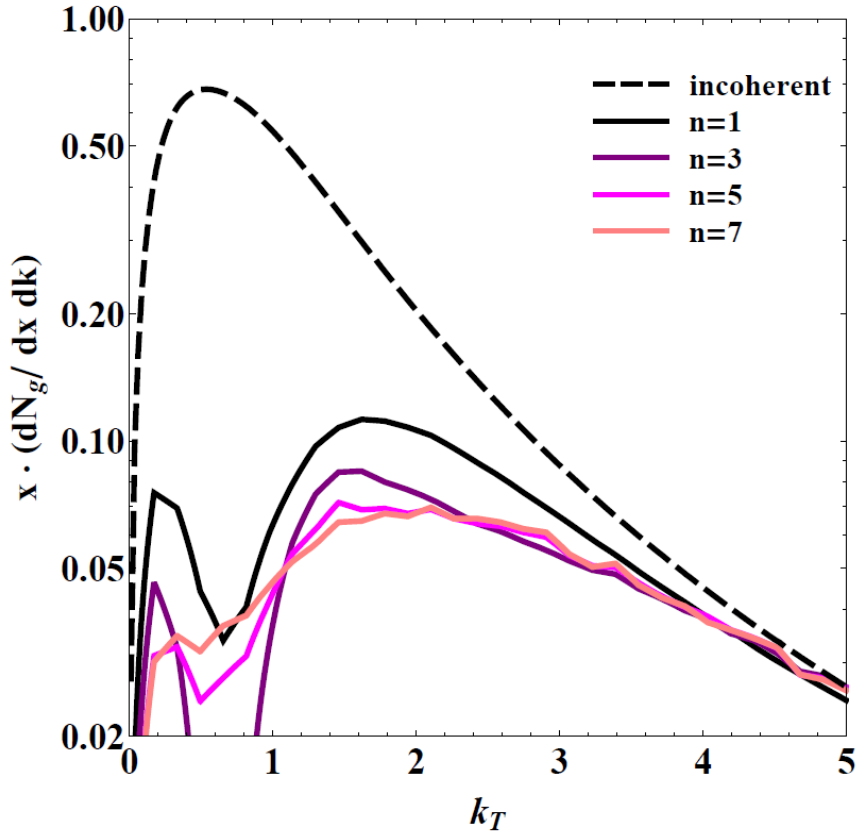

Static brick
E=50 GeV
ω=5 GeV (x=0.1)
L=5 fm
T=250 MeV

- **Interfering effects dominated by n=1 order in opacity**
- **Convergence already at n=5**

Light-charm quark similarity

Light (dashed) and **charm** (solid)

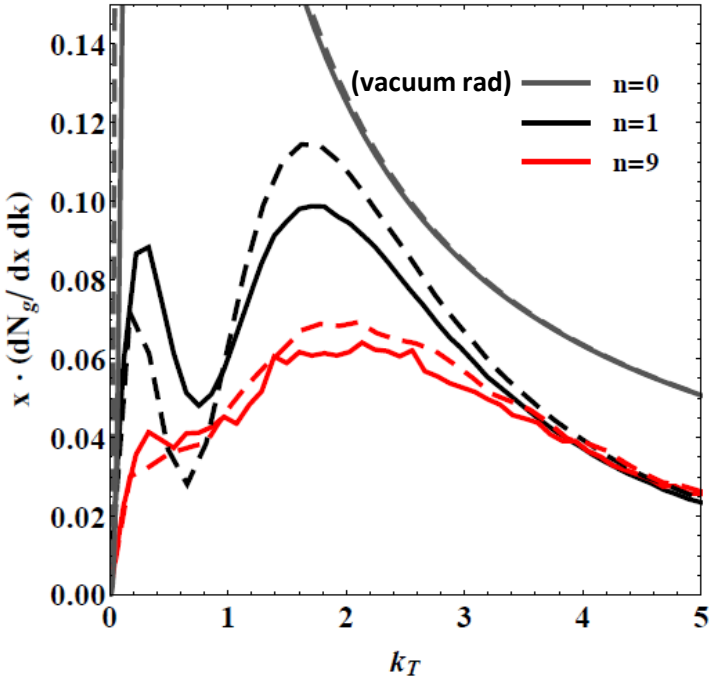

Bottom

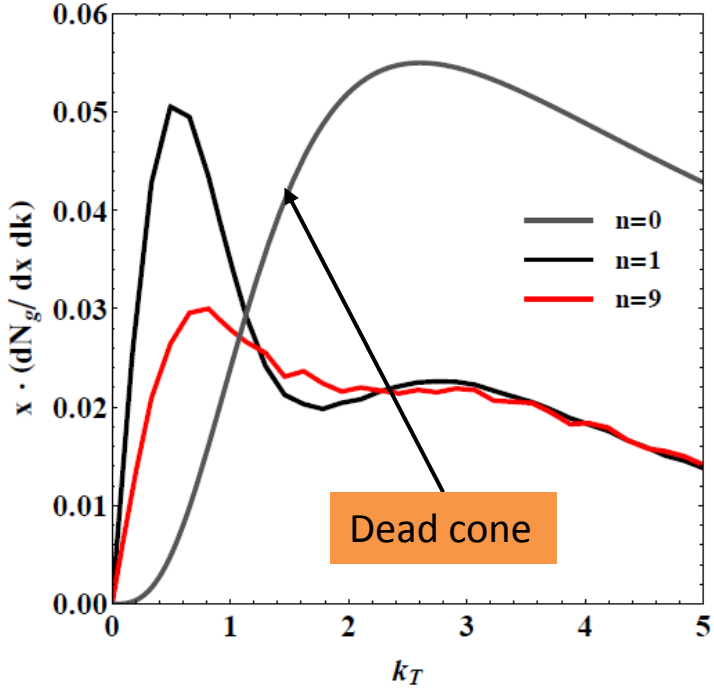

Static brick
E=20 GeV
ω=5 GeV (x=0.25)
M_l=0.2 GeV
M_c=1.2 GeV
M_b=4.75 GeV
L=5 fm
T=250 MeV

- **Charm and light quark transverse momentum spectra are almost identical**
- **Bottom quark radiation is suppressed by heavy mass**
- **Dead cone filled by induced radiation**

‘Thin’-‘thick’ plasma approximation

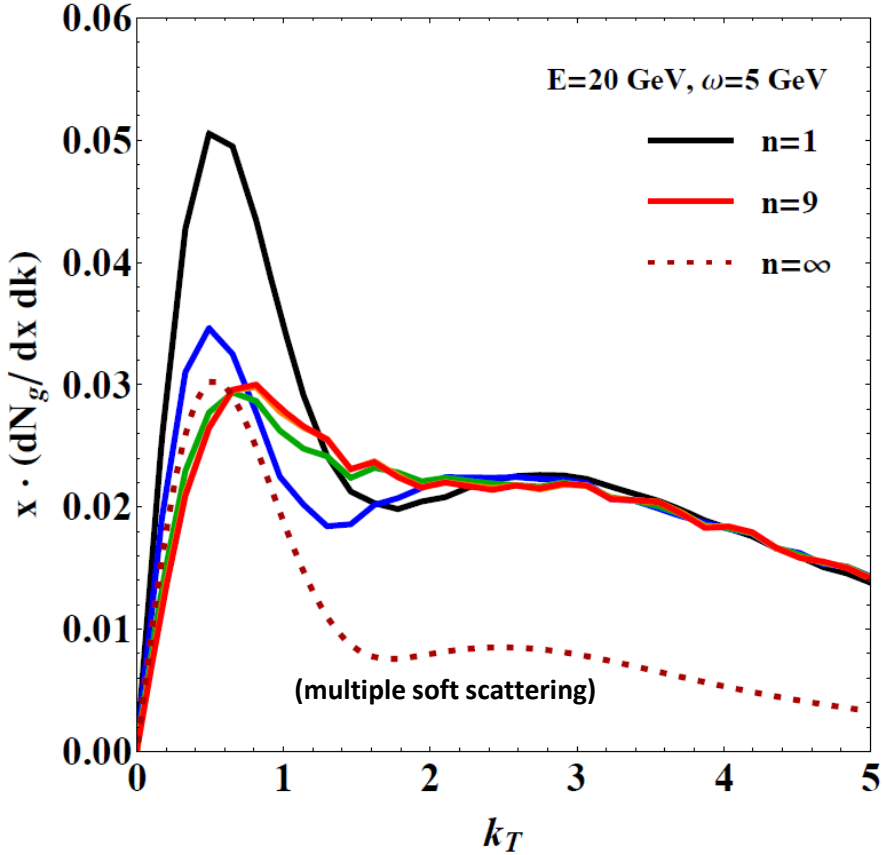

Static brick
E=20 GeV
ω=5 GeV (x=0.25)
L=5 fm
T=250 MeV

- At small emission angles, the opacity series converges to the m.s.s. limit
- At large $k_\perp$, the hard power-law tail of the distribution dominates

n=1 approximation

Light to heavy quark energy loss ratio

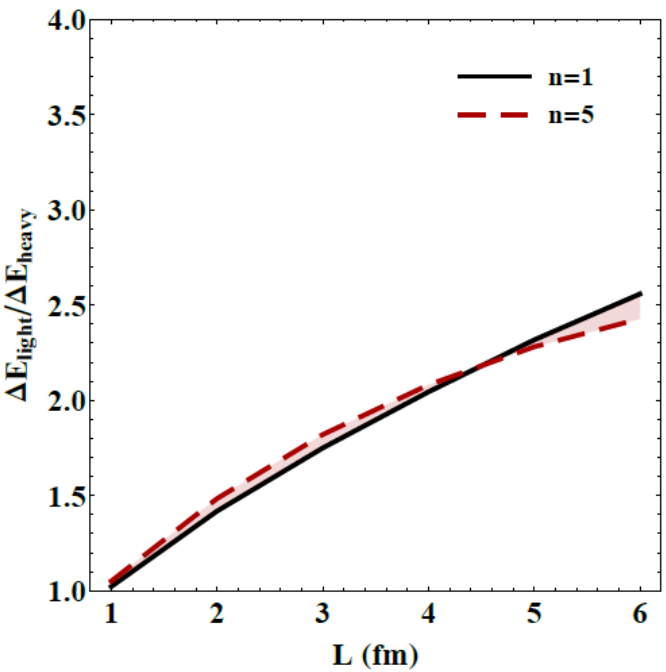

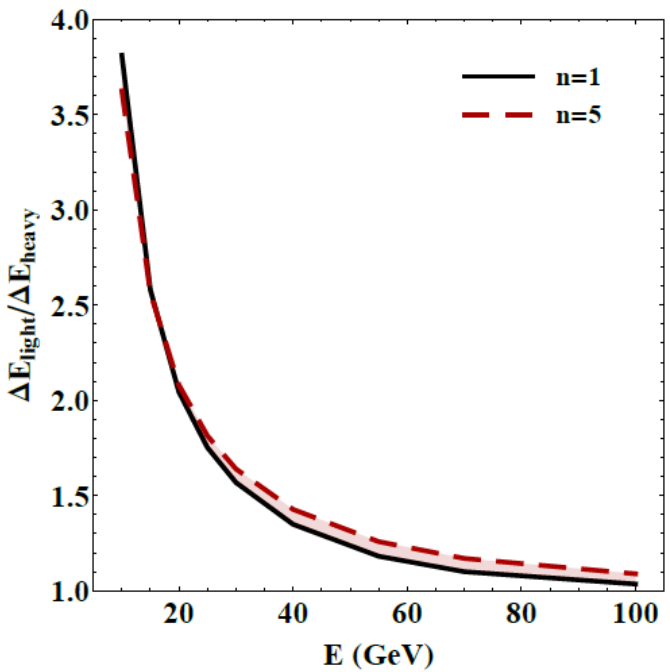

Static brick
E=20 GeV
ω=[integrated]
M_l=0.2 GeV
M_h=4.75 GeV
L=5 fm
T=250 MeV

- **The energy loss ratio between light and heavy quark jets is insensitive to higher order in opacity corrections**
- **Flavor tomography can be studied at n=1**
- **Jet measurements require full transverse radiative spectrum at high orders**

Interpolating potential

static → dynamical

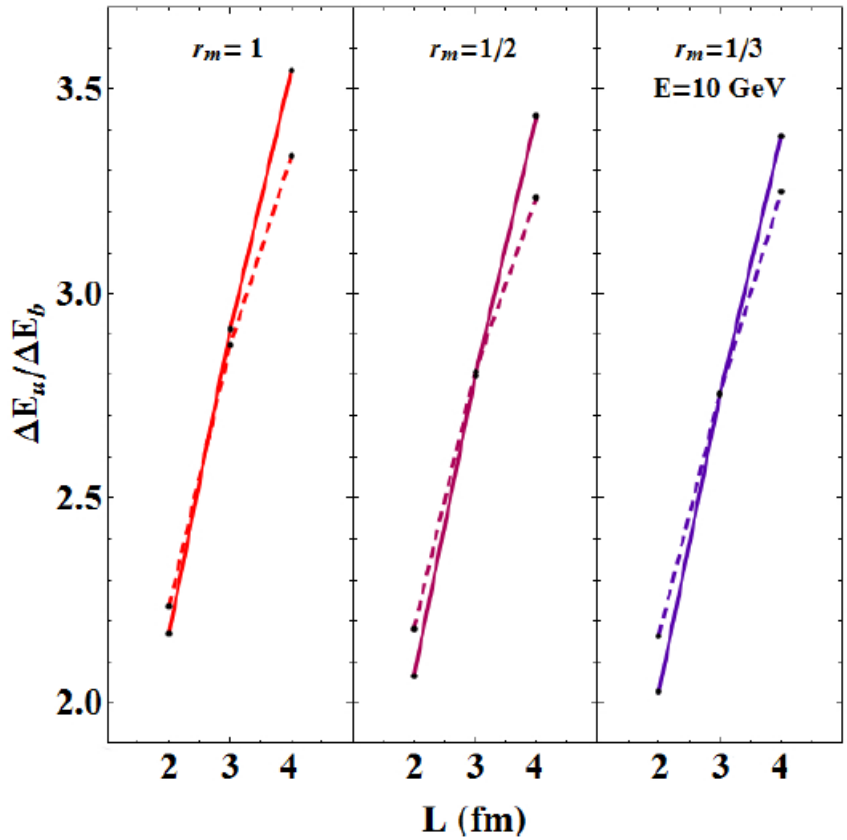

Static brick
E=10 GeV
ω=[integrated]
T=250 MeV

- **Strong indication of similar convergence for static and dynamical potentials**

Static and dynamical limits

Static (dashed) and **dynamical** (solid) **energy loss ΔE/E**

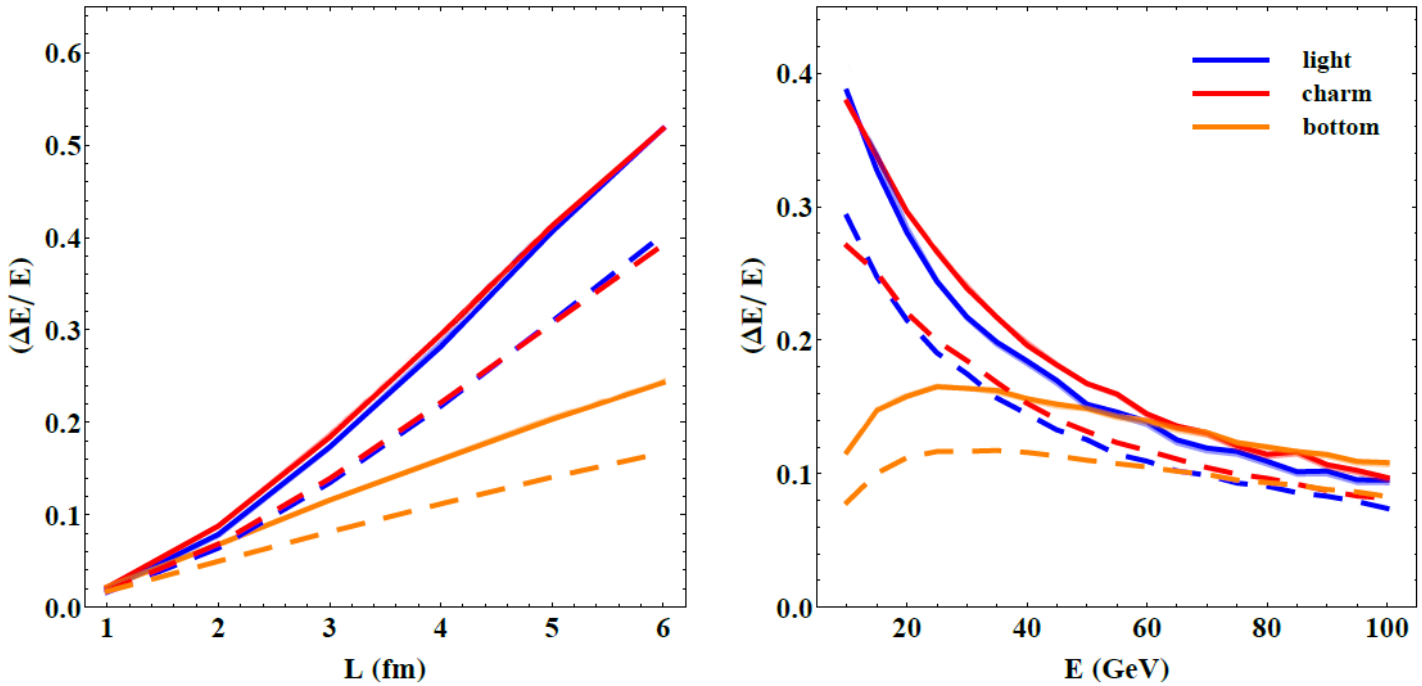

Static brick
E=20 GeV
M_l=0.2 GeV
M_c=1.2 GeV
M_b=4.75 GeV
L=5 fm
T=250 MeV

- **The dynamical potential increases the energy loss**
- **Quadratic L-dependence for light and charm (LPM effect) vs. linear for bottom**
- **Remarkably different dependence on E for bottom**

Thermalization

RHIC

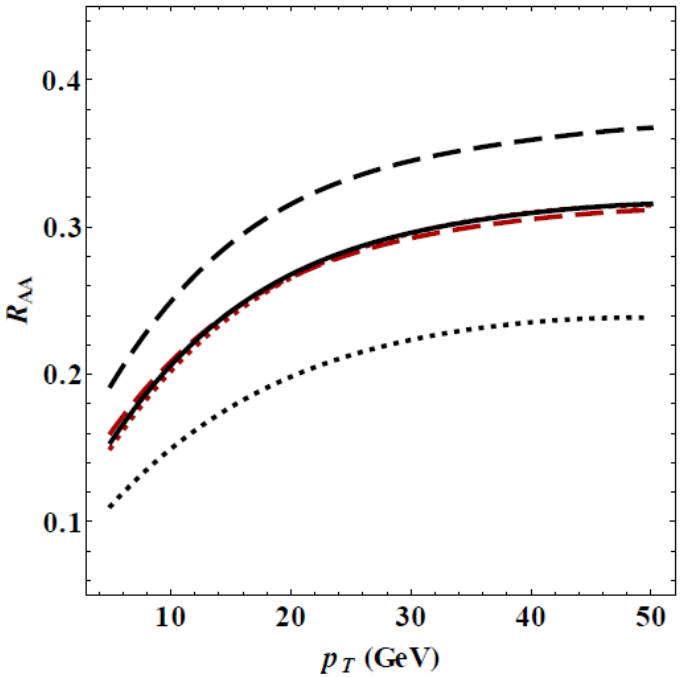

LHC

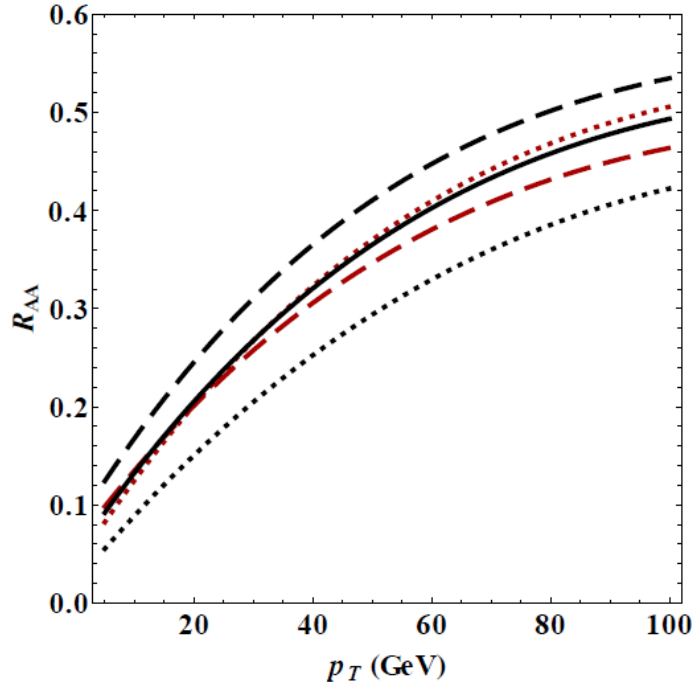

Glauber+Bjorken
dN/dy=1000 (RHIC)
2200 (LHC)
τ_0=1 fm/c
dynamical potential
fixed coupling
radiative+collisional

Solid: Linear with $\alpha_s = 0.3$
Dotted/Dashed: Divergent or *Free streaming* with $\alpha_s = 0.3$
Red: Divergent with $\alpha_s = 0.27$ or *Free streaming* with $\alpha_s = 0.325$

- **Large sensitivity to pre-thermalization phase, canceled by a small** (±10%) **rescaling of the coupling constant**

BDMPS

Baier, Dokshitzer, Mueller, Peigne, Schiff, Nucl.Phys.B483:291,1997

- **Multiple soft scattering approximation (N ~ ∞)**
  - **The quark performs a Brownian motion in transverse momentum**

START FROM PATH INTEGRAL FORMULATION

$$\omega \frac{dI}{d\omega} = \frac{\alpha_s C_R}{(2\pi)^2 \omega^2} 2\mathrm{Re} \int_{\xi_0}^{\infty} dy_l \int_{y_l}^{\infty} d\bar{y}_l \int d\mathbf{u} \int_0^{\chi\omega} d\mathbf{k}_\perp \, e^{-i\mathbf{k}_\perp \cdot \mathbf{u}} \, e^{-\frac{1}{2}\int_{\bar{y}_l}^{\infty} d\xi \, n(\xi)\, \sigma(\mathbf{u})}$$
$$\times \frac{\partial}{\partial \mathbf{y}} \cdot \frac{\partial}{\partial \mathbf{u}} \int_{\mathbf{y}=0}^{\mathbf{u}=\mathbf{r}(\bar{y}_l)} \mathcal{D}\mathbf{r} \exp\left[i \int_{y_l}^{\bar{y}_l} d\xi \frac{\omega}{2} \left(\dot{\mathbf{r}}^2 - \underbrace{\frac{n(\xi)\sigma(\mathbf{r})}{i\,\omega}}_{} \right) \right]$$

HARMONIC OSCILLATOR APPROXIMATION

$$n(\xi)\,\sigma(\mathbf{r}) \simeq \frac{1}{2}\,\hat{q}(\xi)\,\mathbf{r}^2$$

- $\hat{q} = \frac{\langle q_\perp^2 \rangle_{\mathrm{med}}}{\lambda}$ **is the transport coefficient that characterize the transverse momentum squared per unit path length transferred to the parton**

ASW

- **Without fixing kinematic limits**

  Peter Arnold, arXiv:0808.2767v2

$$\omega \frac{d}{d\omega}(I - I_{\rm vac}) = \frac{\alpha}{\pi}\, x\, P_{s\to g}(x)\, \ln|\cos(\omega_0 L)|$$

$$P_{q\to g}(x) = C_F \frac{[1+(1-x)^2]}{x}$$

$$\omega_0^2 = -i\,\frac{[C_F - x(1-x)C_A]\,\hat{\bar{q}}}{2x(1-x)E}$$

  - Scaling with z: $z \equiv |\omega_0^2| L^2$
  - Taylor expansion in z ~ O(L/ λ)[1]:

$$\ln\left[\cos(e^{i\pi/4} z^{1/2})\cos(e^{-i\pi/4} z^{1/2})\right] = \frac{1}{6}z^2 - \frac{17}{1260}z^4 + \frac{691}{467775}z^6 - \cdots$$

➢ Z scaling cannot hold at intermediate opacity, i.e. qhat alone is insufficient to describe radiative processes at intermediate opacity

- **Consider kinematic limits on k_T**

  Armesto, Salgado, Wiedemann, arXiv:hep-ph/0312106v1

$$\omega\frac{dI}{d\omega\, d\kappa^2} = \omega\frac{dI_4}{d\omega\, d\kappa^2} + \omega\frac{dI_5}{d\omega\, d\kappa^2} + \omega\frac{dI_6}{d\omega\, d\kappa^2}$$

OUR dN(0) ORIGIN OF DEAD CONE

  - I_5 and I_6 terms fill the dead cone
  - They depend on qhat, which is adjusted to obtain quenching

Dynamical potential

A.1.9 Recovering Djordjevic's 'dynamical medium'

We have just seen that the leading contribution to the collisional energy loss comes from the first term odd in ω in the $(\omega, q)/T$ expansion. But the leading contribution to the q_{perp} distribution for small momentum and energy exchange comes from the first term in the series. Taking the leading term in the q_{perp} integral, evaluating the $d\phi$ integral

$$\Gamma(E) = 4\pi C_J \alpha^2 T^3 (1 + \frac{n_f}{6}) \int \frac{d^2 q_\perp}{2\pi} \int \frac{d\omega}{q} \left(1 - \frac{\omega^2}{q^2}\right)^2 \times \left(|\Delta_L|^2 + \frac{1}{2} \left(\frac{v^2 - \frac{\omega^2}{q^2}}{1 - \frac{\omega^2}{q^2}} \right) |\Delta_T|^2 \right) \quad \text{(A.148)}$$

with $q_z \approx \frac{q^0}{v}$ and $q = \sqrt{q_\perp^2 + q_z^2} \approx \sqrt{q_\perp^2 + \omega^2/v^2}$. Note that the coefficient of the magnetic term has an explicit v dependence (not seen in Djordjevic). Also, if we had kept a mass for the medium particles, there would be a v_k dependence as well. Using the properties

$$\mathrm{Im}\,\Delta_L(Q) = \frac{\omega \pi \mu^2}{2q} \left(1 - \frac{\omega^2}{q^2}\right) |\Delta_L|^2 \quad \text{(A.149)}$$

$$\mathrm{Im}\,\Delta_T(Q) = -\frac{1}{2} \frac{\omega \pi \mu^2}{2q} \left(1 - \frac{\omega^2}{q^2}\right) |\Delta_T|^2 \quad \text{(A.150)}$$

and the change of variables

$$x = \frac{\omega}{q}, \quad \frac{dx}{x} = \frac{d\omega}{\omega} \left(1 - \frac{\omega^2}{q^2}\right) \quad \text{(A.151)}$$

produces, for $v = 1$,

$$\Gamma(E) = 4\pi C_J \alpha^2 T^3 (1 + \frac{n_f}{6}) \int \frac{d^2 q_\perp}{2\pi} \frac{2}{\pi \mu^2} \int \frac{dx}{x} \times \left(\frac{\mathrm{Im}\,\Delta_L}{(q_\perp^2 + \mathrm{Re}\,\Delta_L)^2 + (\mathrm{Im}\,\Delta_L)^2} - \frac{\mathrm{Im}\,\Delta_T}{(q_\perp^2 + \mathrm{Re}\,\Delta_T)^2 + (\mathrm{Im}\,\Delta_T)^2} \right) \quad \text{(A.152)}$$

Using the sum rule,

Aurenche, Gelis, et al, 2002

$$\int_{-1}^{1} \frac{dx}{x} \frac{1}{2\pi} \frac{2\,\mathrm{Im}\,\Delta_{L,T}}{(q_\perp^2 + \mathrm{Re}\,\Delta_{L,T})^2 + (\mathrm{Im}\,\Delta_{L,T})^2} = \frac{1}{q_\perp^2 + \mathrm{Re}\,\Pi_{L,T}(x = \infty)} - \frac{1}{q_\perp^2 + \mathrm{Re}\,\Pi_{L,T}(x = 0)} \quad \text{(A.153)}$$

This is an integral in the $\omega - q$ plane, with $q_\perp$ at a fixed value. This traces out a hyperbola. The asymptotic Πs satisfy:

Pisarski, 1980

$$\mathrm{Re}\,\Pi_L(x = \infty) = \frac{\mu^2}{3} \quad , \quad \mathrm{Re}\,\Pi_T(x = \infty) = \frac{\mu^2}{3} + \mu_{mag}^2 \quad \text{(A.154)}$$

$$\mathrm{Re}\,\Pi_L(x = 0) = \mu^2 \quad , \quad \mathrm{Re}\,\Pi_T(x = 0) = \mu_{mag}^2 \quad \text{(A.155)}$$

Hence,

Djordjevic, Heinz, 2007

$$\Gamma(E) = 4\pi C_J \alpha^2 T^3 (1 + \frac{n_f}{6}) \int \frac{d^2 q_\perp}{2\pi} \frac{2}{\mu^2} \left(\frac{1}{q_\perp^2 + \frac{\mu^2}{3}} - \frac{1}{q_\perp^2 + \mu^2} - \frac{1}{q_\perp^2 + \frac{\mu^2}{3} + \mu_{mag}^2} + \frac{1}{q_\perp^2 + \mu_{mag}^2} \right) \quad \text{(A.156)}$$

For the case of vanishing magnetic screening mass, this becomes

$$\Gamma(E) = 4\pi C_J \alpha^2 T^3 (1 + \frac{n_f}{6}) \int \frac{d^2 q_\perp}{2\pi} \frac{2}{\mu^2} \left(\frac{1}{q_\perp^2} - \frac{1}{q_\perp^2 + \mu^2} \right) \quad \text{(A.157)}$$

$$= 8\pi C_j \alpha^2 T^3 (1 + \frac{n_f}{6}) \int \frac{d^2 q_\perp}{2\pi} \frac{1}{q_\perp^2 (q_\perp^2 + \mu^2)} \quad \text{(A.158)}$$

Gunion-Bertsch

situation. The multiplicity distribution is then given by the differential of this expression, i.e.,

$$\frac{dn_g}{dx\, d^2q_\perp} = \frac{C_F\alpha_s}{\pi^2}\frac{1}{x{q_\perp}^2} \ . \tag{5}$$

This distribution is uniform in rapidity,

$$\frac{dn_g}{d\eta\, d^2q_\perp} = \frac{C_F\alpha_s}{\pi^2}\frac{1}{{q_\perp}^2} \ . \tag{6}$$

To relate this gluon distribution to an observable quantity, assume that $f_{\rm ch}$ charged particles are produced in the final state for each perturbative gluon. We also integrate over $q_\perp$, with a lower limit $q_\perp \sim \Lambda$ determined by confinement, and an upper limit ${q_\perp}^2 \sim s$ determined by kinematics. The charged-particle distribution is then

$$\frac{dn_{\rm ch}}{d\eta} \sim \frac{C_F f_{\rm ch}\alpha_s}{\pi}\ln(s/\Lambda^2) \ . \tag{7}$$

Elastic energy loss and Fluctuations

Bjorken elastic collisions

$$\frac{dE}{dx} = -C_R \pi \alpha^2 T^2 \log[B]$$

- Soft scattering
- Thoma-Gyulassy model $\longrightarrow$ $B_{TG} = \frac{4pT}{E-p+4T}/\mu$

Energy loss fluctuations

- **The probability of losing a fractional energy $\varepsilon = \frac{\Delta E}{E}$ is the convolution of Radiative and Elastic contributions**

$$P(\varepsilon) = \int dx\, P_{rad}(\varepsilon)\, P_{el}(x-\varepsilon)$$

- Radiative: $P_{rad}(\varepsilon) = P_0 \delta(\varepsilon) + \widetilde{P}(\varepsilon)|_0^1 + P_{stop}\delta(1-\varepsilon)$
- Elastic: $P_{el}(\varepsilon) = e^{-<N_c>}\delta(\varepsilon) + N e^{-\frac{(\varepsilon-\bar{\varepsilon})}{4T\bar{\varepsilon}}}$

Poisson expansion of the number of INCOHERENTLY emitted gluons

Gaussian fluctuations

Geometry of the collision

Glauber model is used to compute number of binary collisions and participant nucleons

- Start from Wood-Saxon nuclear density profile…
  - $\rho_A(r) \propto [1 + Exp[(r - R)/a]]^{-1}$
  - $T_A(x) = \int dz\, \rho_A(z, x)$
- …to obtain:
  - $\rho_{binary}(x, b)$
  - $\rho_{participants}(x, b)$

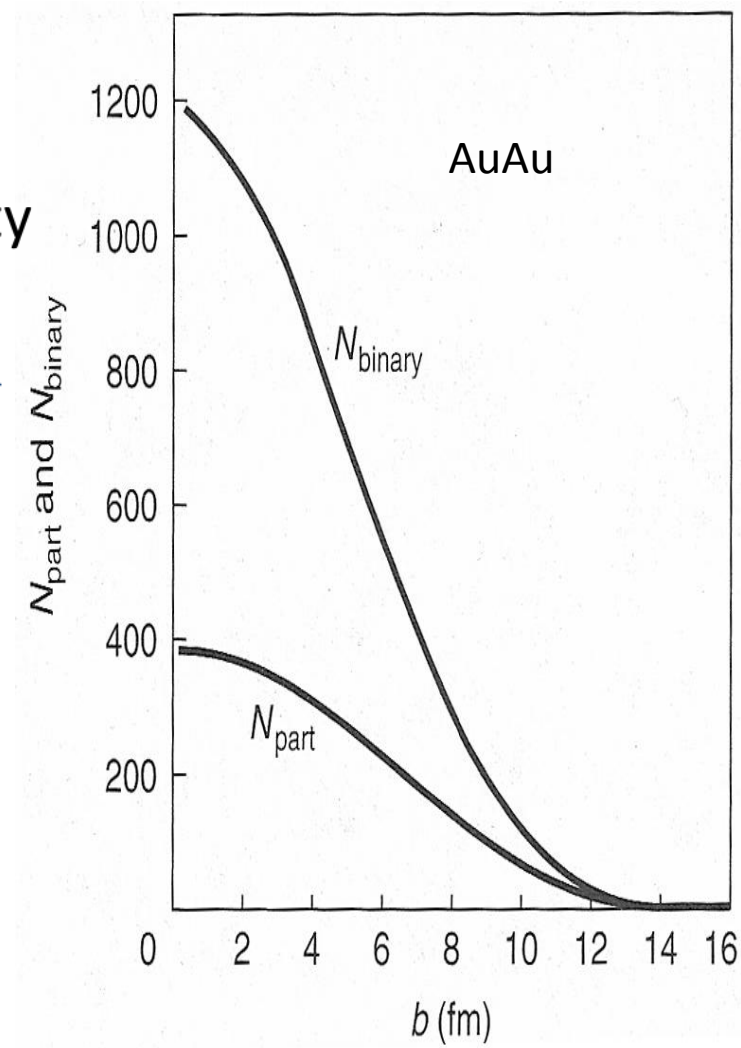

k_T sensitivity

- Collinear approximation: $x_E = x_+\left(1 + O\left(\frac{k_T}{x_+E^+}\right)^2\right)$
  - DGLV formula has the same functional form for x_E or x_+

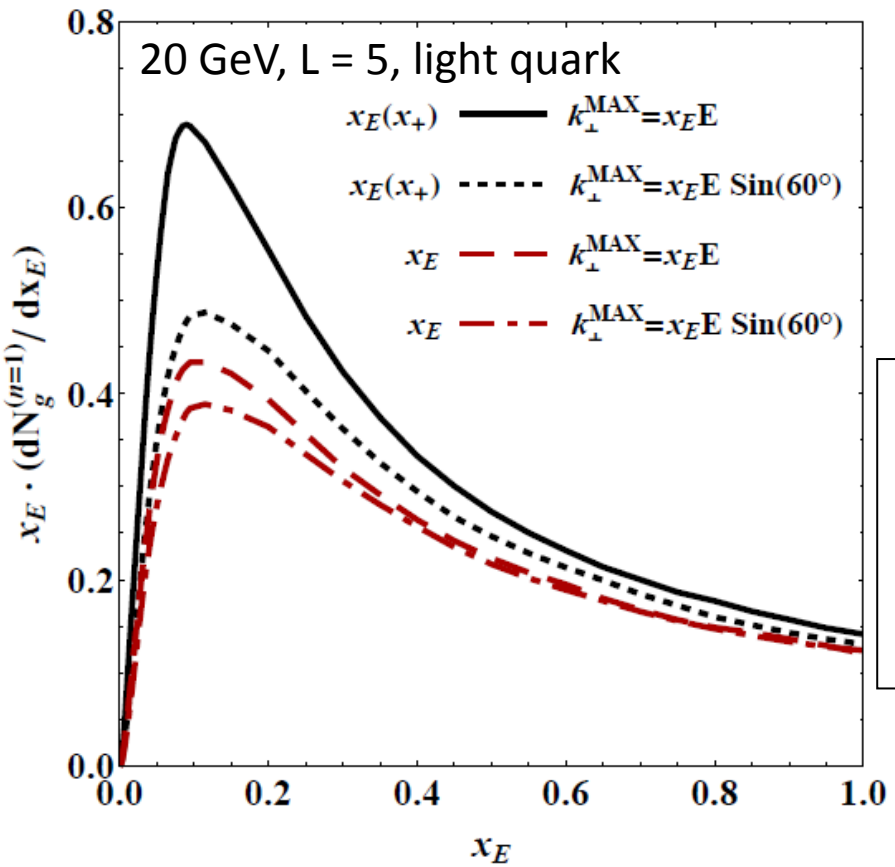

$$x_+ = \frac{1}{2}x_E\left(1 + \sqrt{1 - \left(\frac{k_T}{x_E E}\right)^2}\right)$$

$$\frac{dN_g^J}{dx_E}(x_E) \equiv \int^{x_E E \sin(\theta_{\max})} dk_T \frac{dx_+}{dx_E}\frac{dN_g}{dx_+ dk_T}(x_+(x_E)),$$

$$\frac{dx_+}{dx_E} = \frac{1}{2}\left[1 + \left(1 - \left(\frac{k_T}{x_E E}\right)^2\right)^{-1}\right].$$

Holographic models

- **AdS/CFT correspondence**: strong coupling between jet and medium
- The energy loss of a parton quenched in a thermal plasma is described by the dynamics of its dual classical string moving in a five-dimensional AdS space with a black hole

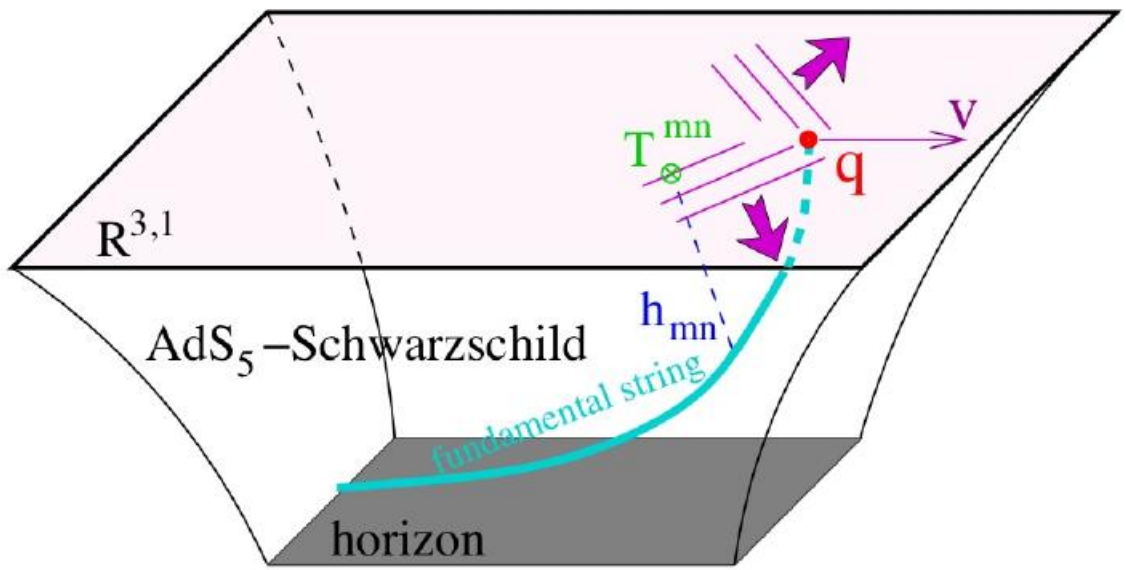

Jet Quenching and Initial Geometry/Conditions from the RHIC BES

Helen Caines - Yale University

BNL - April 2013

RHIC data available

Au-Au
200, 130, 62.4, 39, 27, 19.6,
11.5(STAR only), 7.7, 5(test run)

Cu-Cu
200, 62.4, 22.5

U-U
193

C-Au
200

p-p
200, 500

d-Au
200

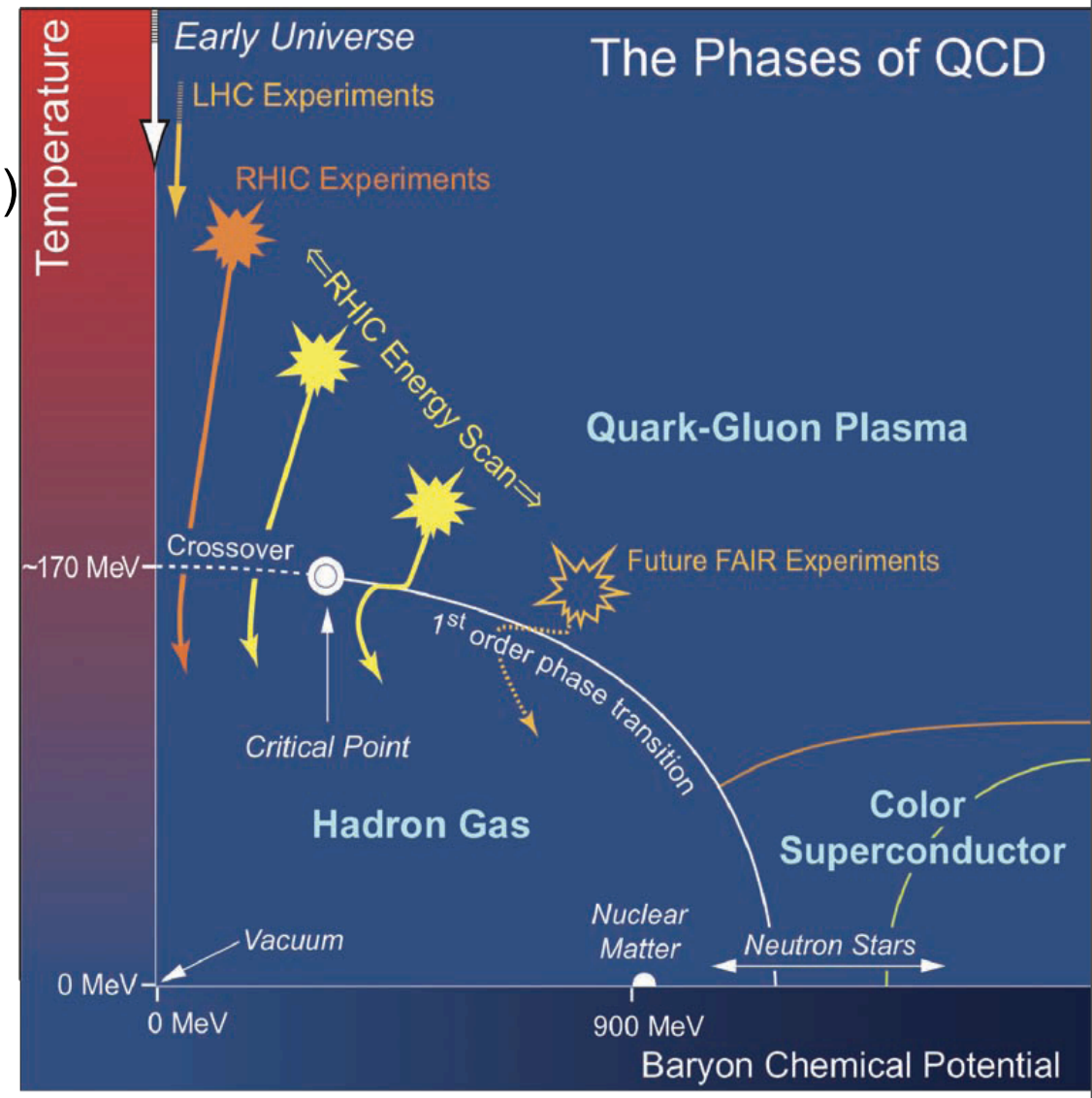

Generic features of A-A collisions - I

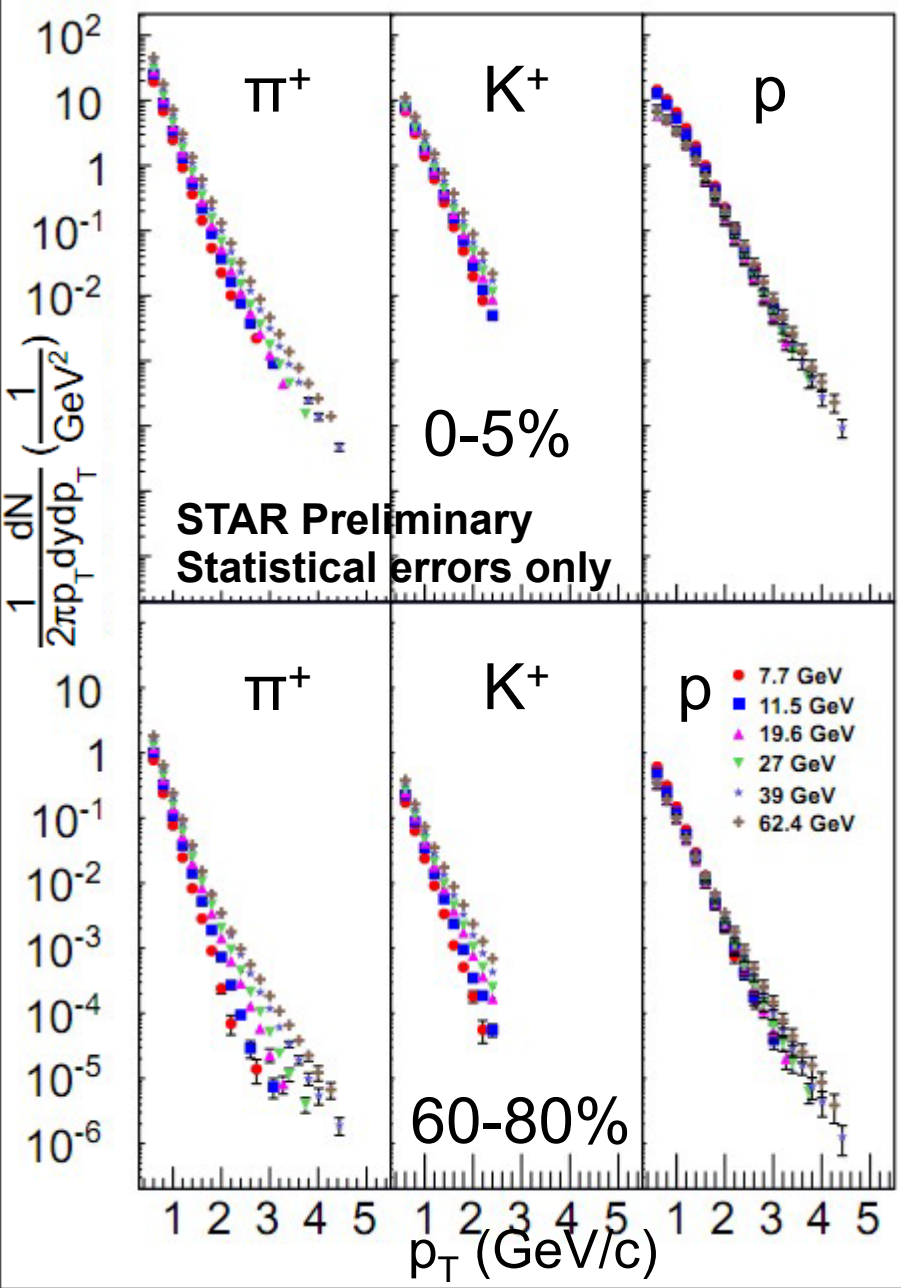

Pion spectra:

Significant change in slope for peripheral data with collision energy

Proton spectra:

Little change with collision energy

Strong species dependence in spectra change

Horvat CPOD

Generic features of A-A collisions - II

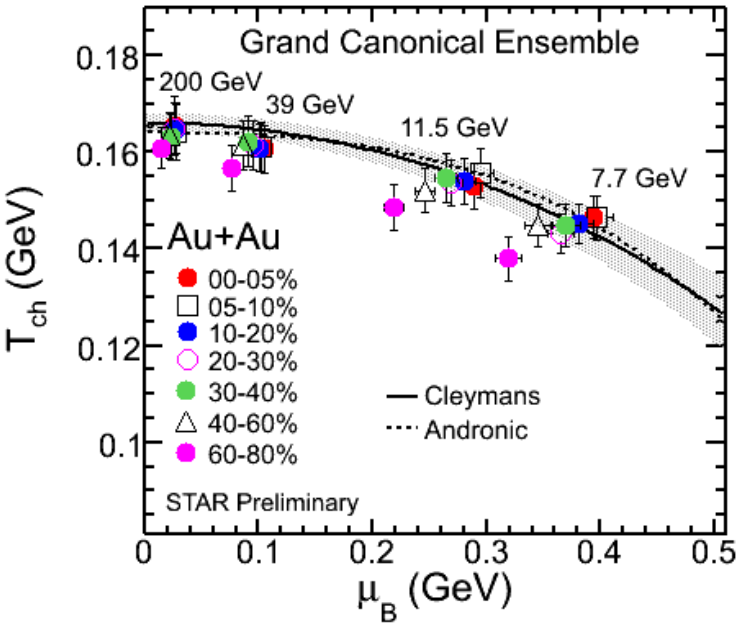

Particles used:
π, K, p, Λ, K^0_s, Ξ

THERMUS Model:
T_{ch} and μ_B

Chemical

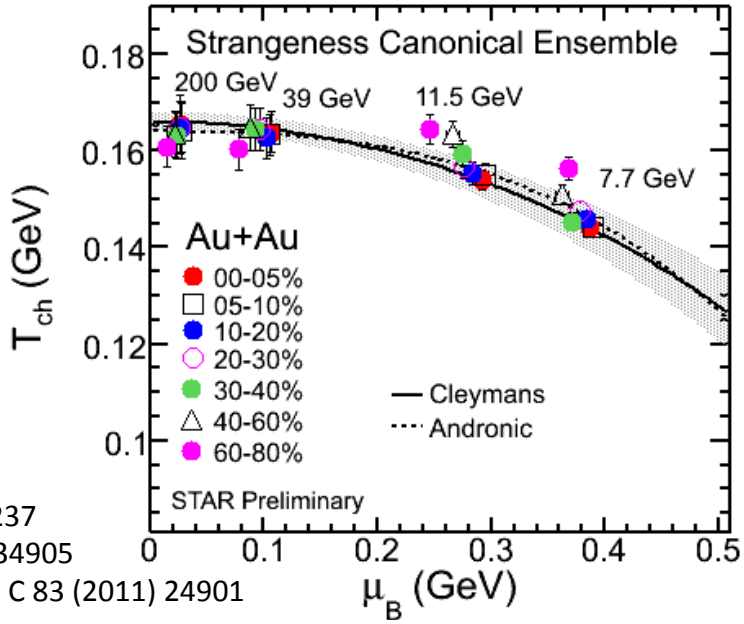

Andronic: NPA 834 (2010) 237
Cleymans: PRC 73 (2006) 034905
Au+Au 200 GeV : Phys. Rev. C 83 (2011) 24901

Opposite trends in centrality seen at lower energies for different ensembles

S. Das QM2012

Generic features of A-A collisions - II

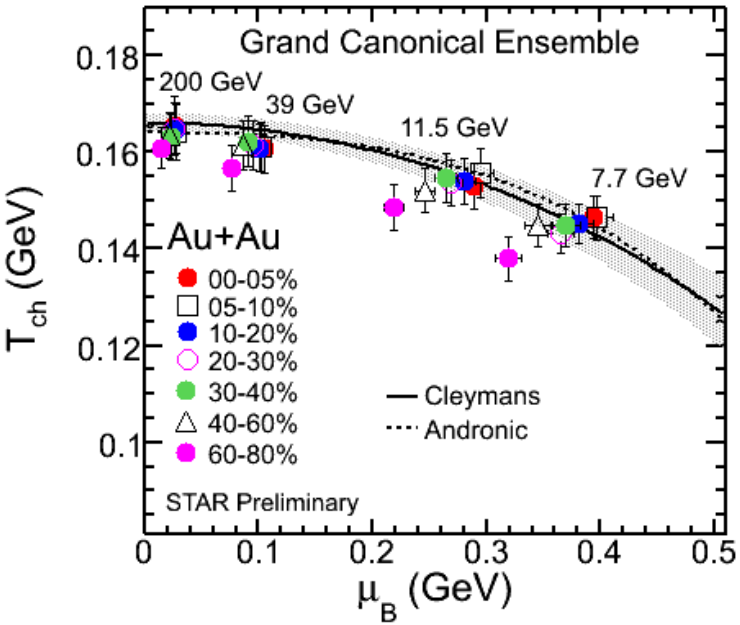

Particles used:
π, K, p, Λ, K^0_s, Ξ

THERMUS Model:
T_{ch} and μ_B

Chemical

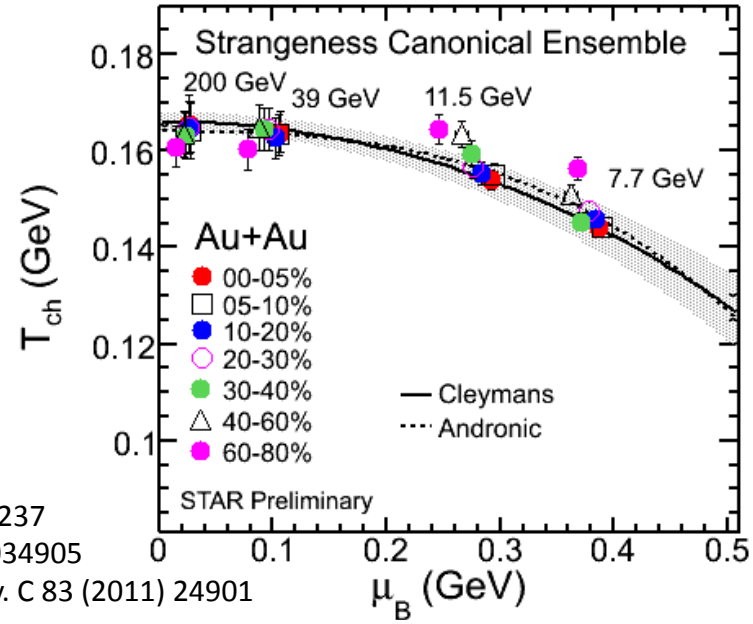

Andronic: NPA 834 (2010) 237
Cleymans: PRC 73 (2006) 034905
Au+Au 200 GeV : Phys. Rev. C 83 (2011) 24901

Opposite trends in centrality seen at lower energies for different ensembles

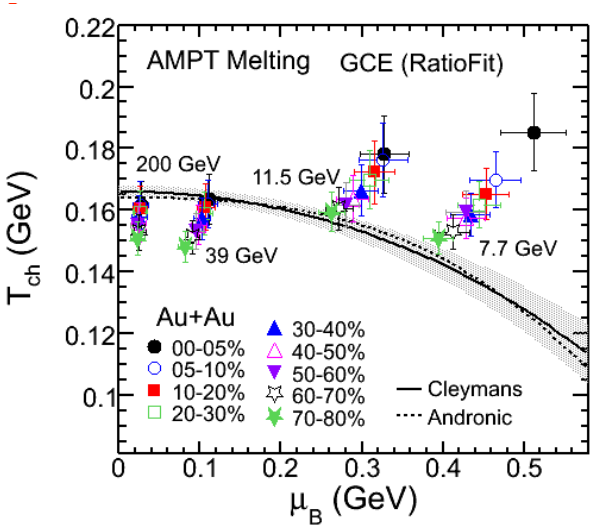

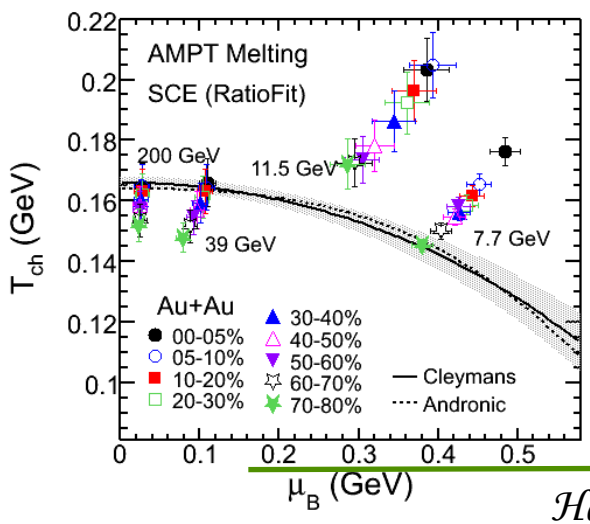

Not seen in simulations via AMPT

S. Das QM2012

Generic features of A-A collisions - III

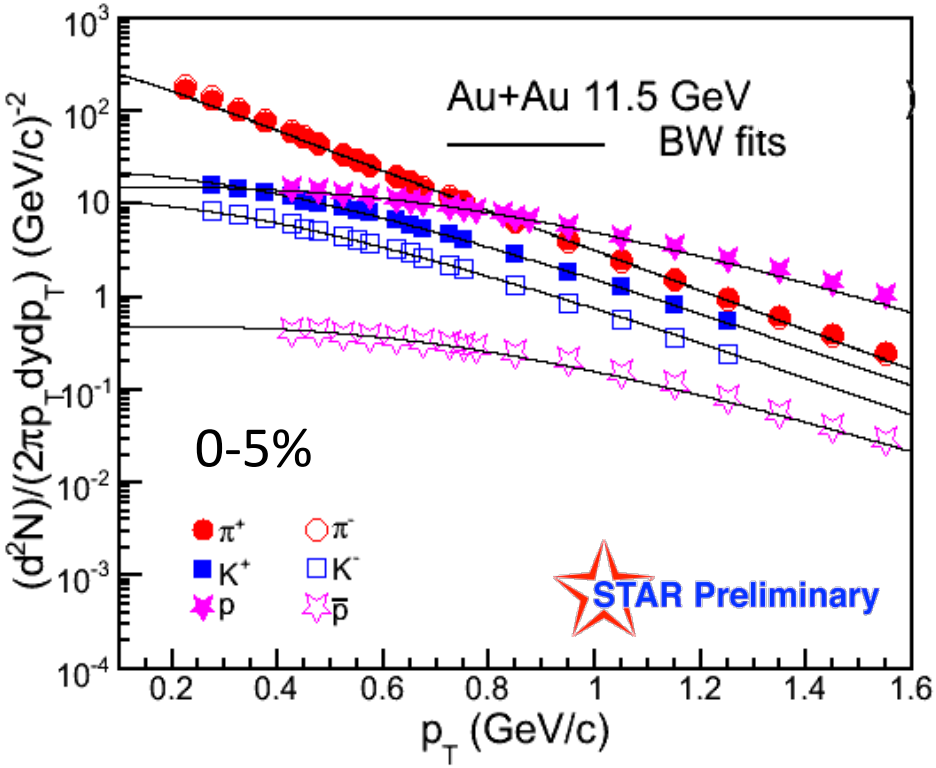

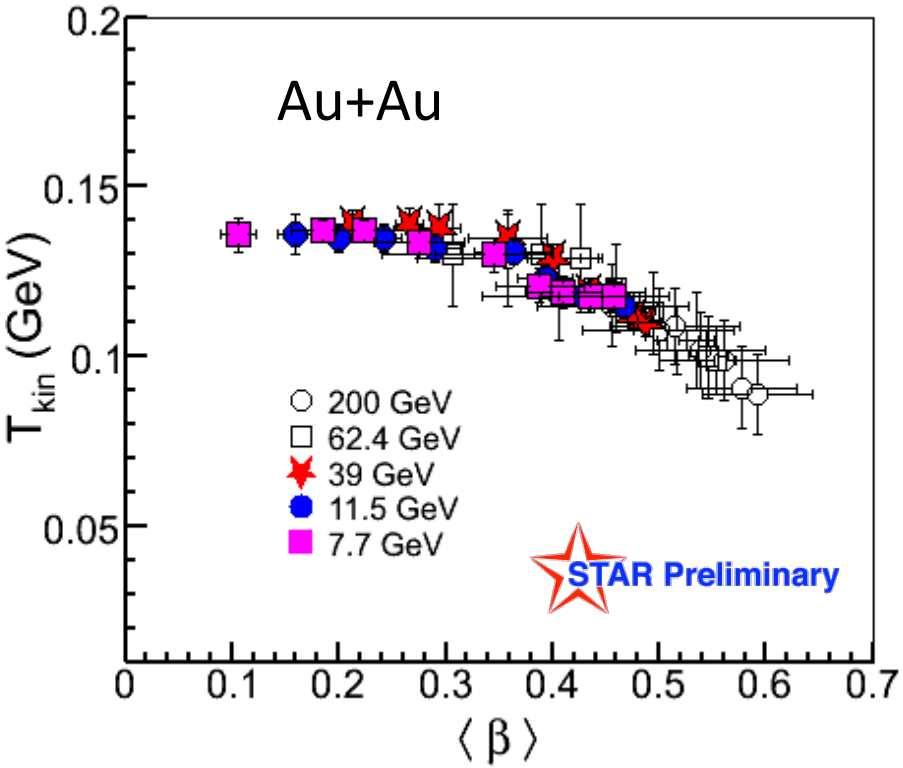

π, K, p used in fits

Blastwave fits seem OK even at lowest collision energies

Expansion gets less violent and kinetic freeze-out occurs "earlier" (or at least higher T)

Generic features of A-A collisions - III

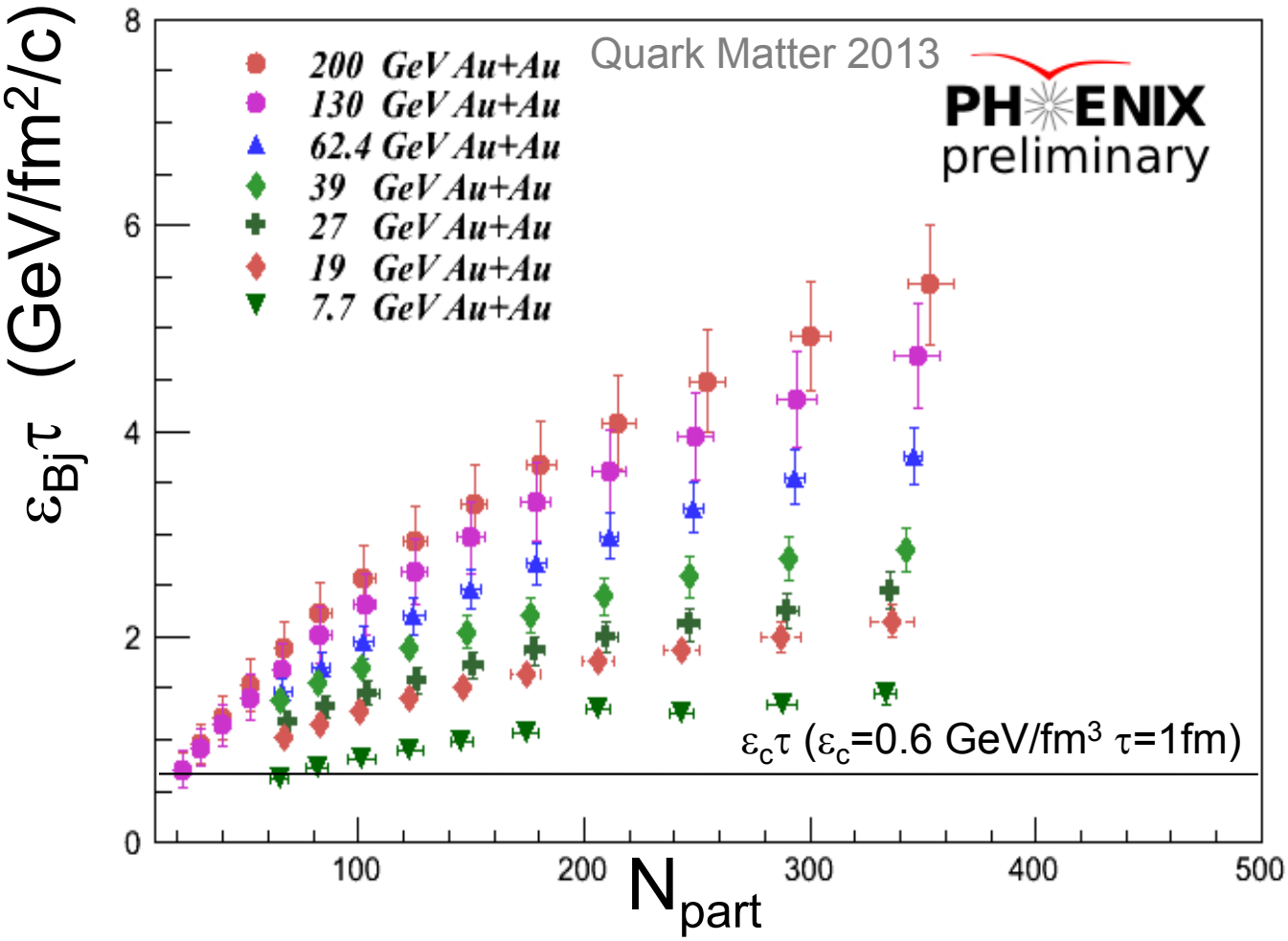

Lattice:
ε_c ~ 0.6 GeV/fm^3

Above critical density for all collision energies and centralities

QGP at all energies?

Charged hadron R_{CP}

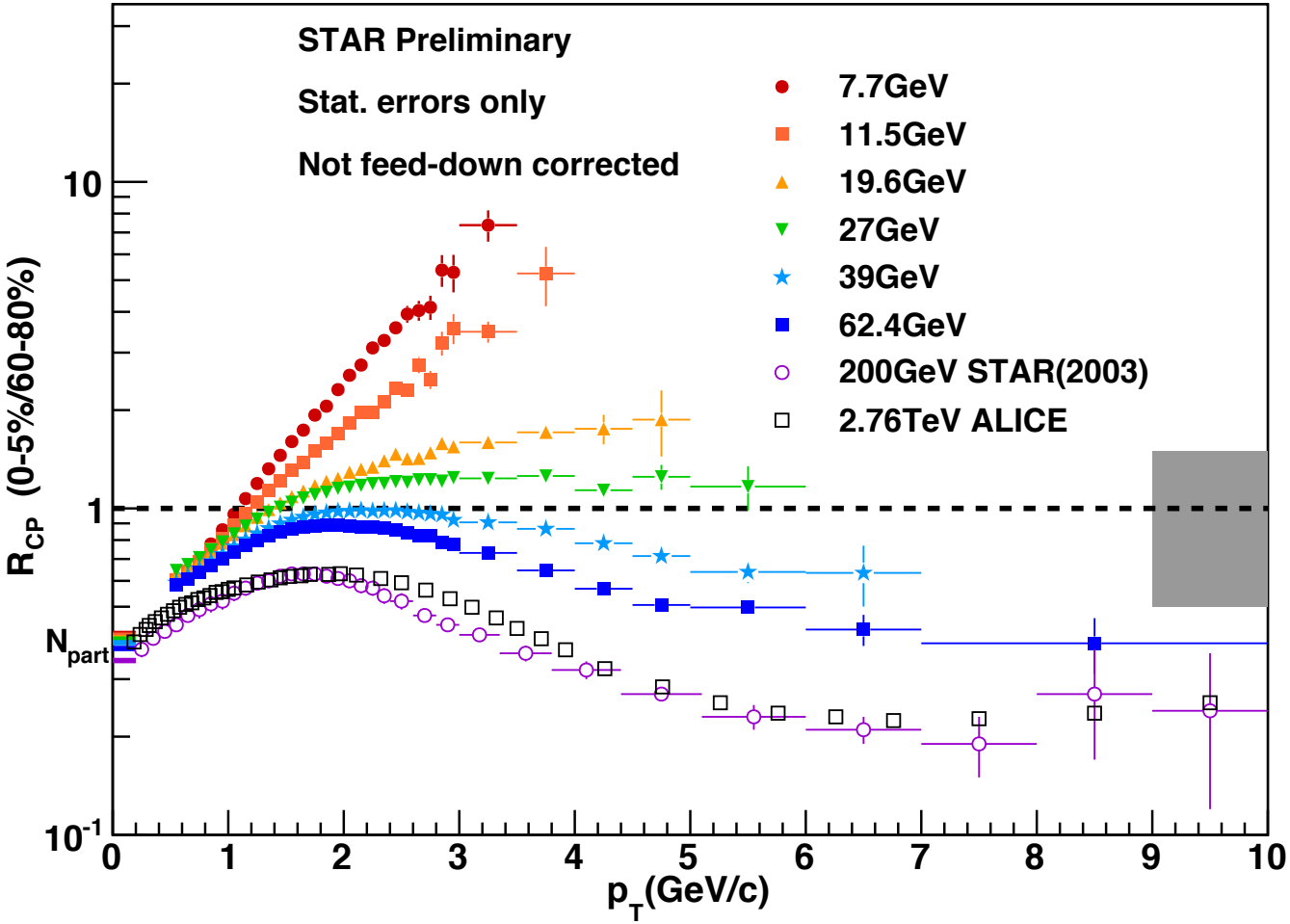

Lower energies strongly enhanced - Cronin effect?

Drops below unity for $\sqrt{s_{NN}} \geq 39$ GeV

Need to disentangle Cronin and jet quenching effects

Au-Au vs Cu-Cu

Mitchel CPOD

π^0

Cu-Cu

$R_{AA}^{22.4} > R_{AA}^{62} \sim R_{AA}^{200}$

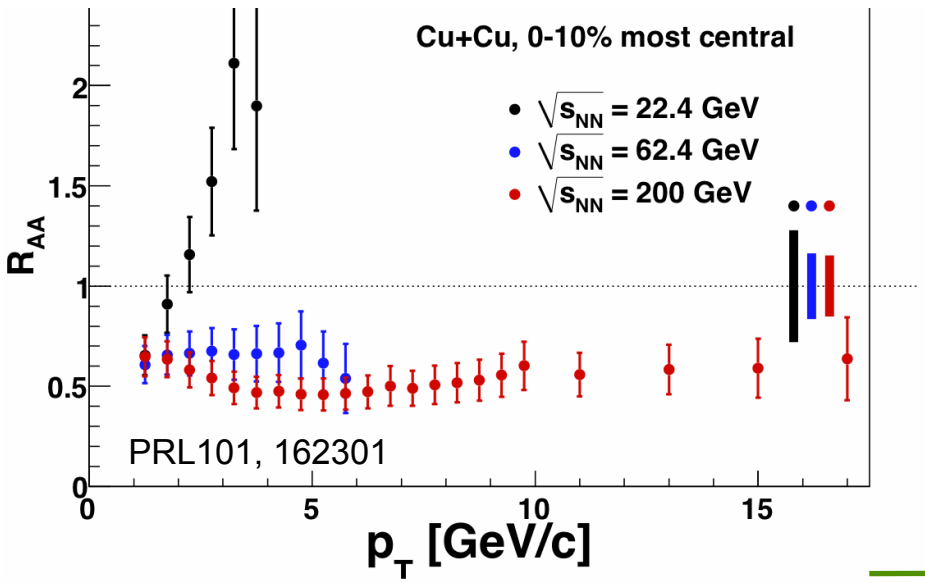

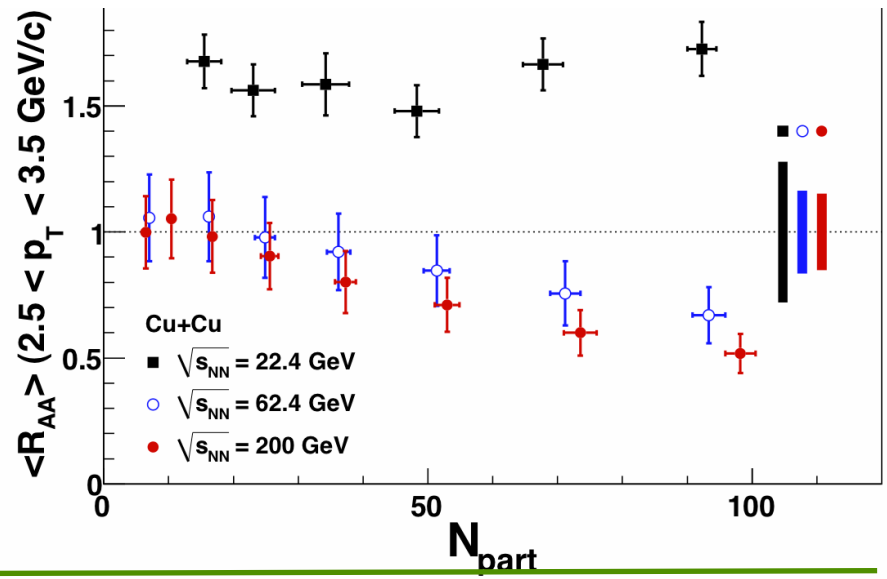

Au-Au vs Cu-Cu

Mitchel CPOD

π^0

Au-Au

$R_{AA}^{39} > R_{AA}^{62} \sim R_{AA}^{200}$

Cu-Cu

$R_{AA}^{22.4} > R_{AA}^{62} \sim R_{AA}^{200}$

Cu-Cu & Au-Au show similar trends

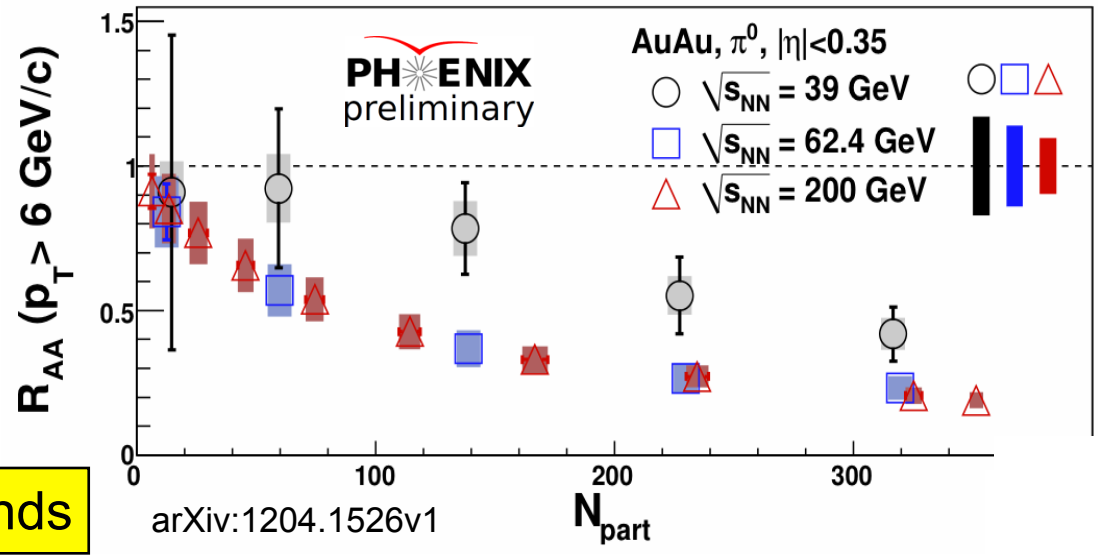

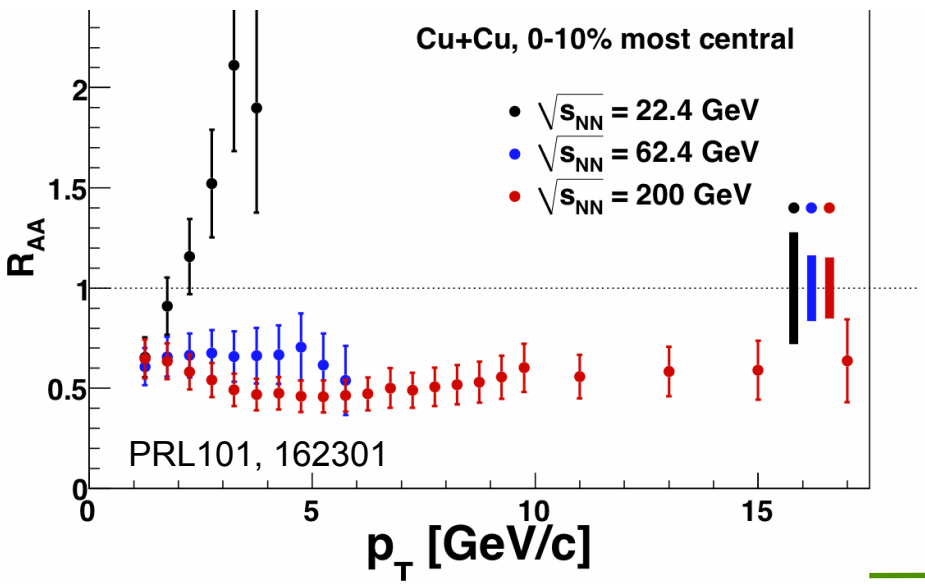

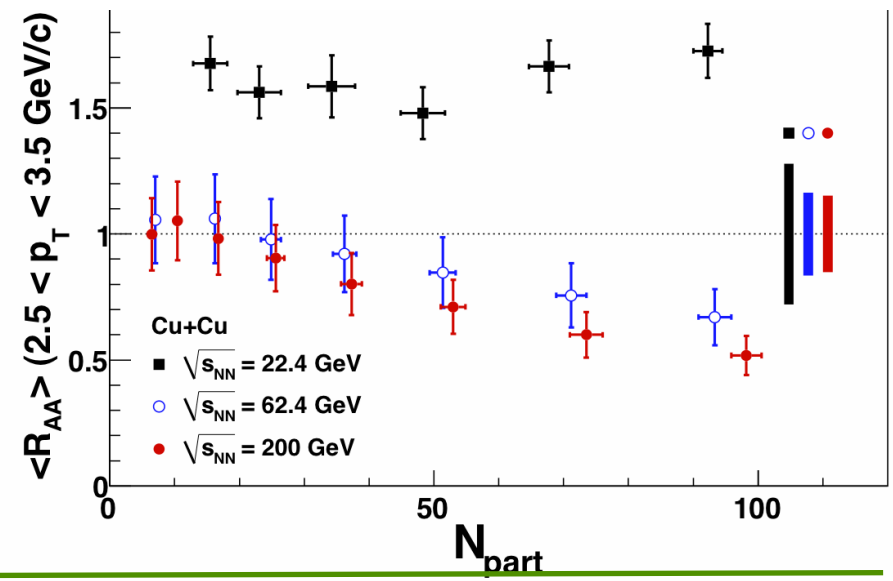

PID R_{CP}

Horvat CPOD

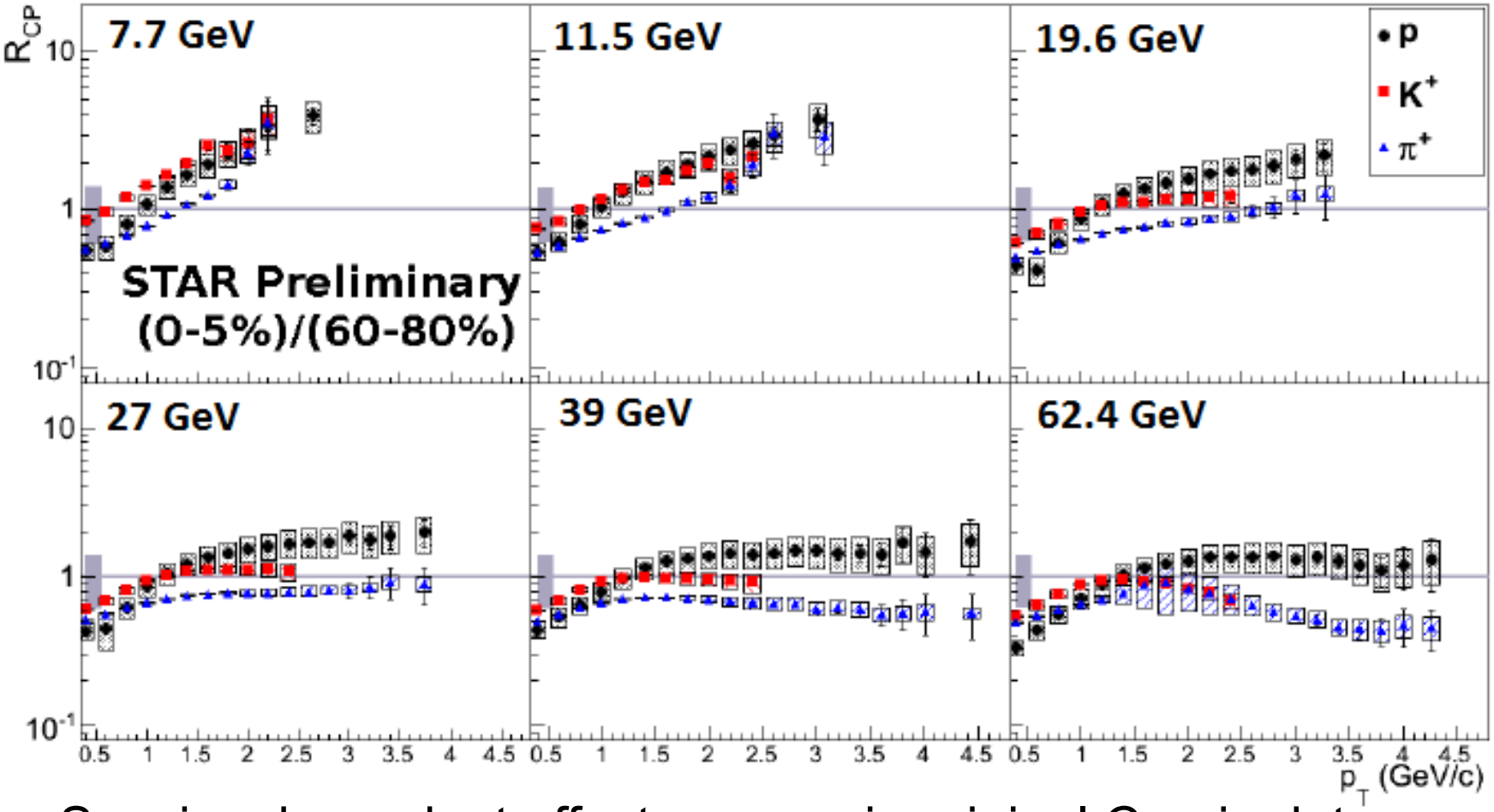

Species dependent effect seen as in original Cronin data

$R_{cp}^{p} > R_{cp}^{K} > R_{cp}^{\pi}$

Particle ratios changing as function of $\sqrt{s_{NN}}$

Similar features seen for anti-particles

Strangeness R_{CP}

Nasim CPOD

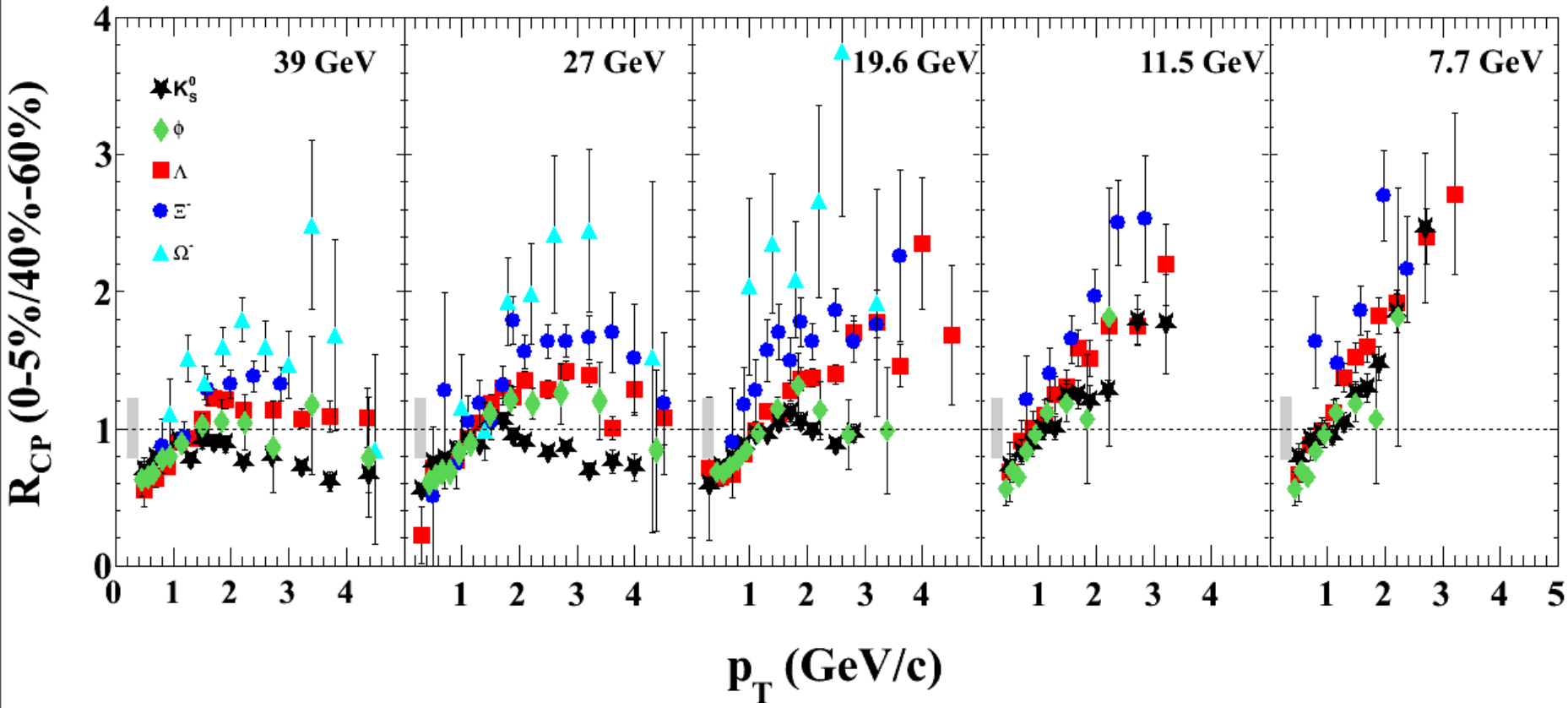

Cronin effect seems to be a mass effect - although errors large

Parton recombination ending

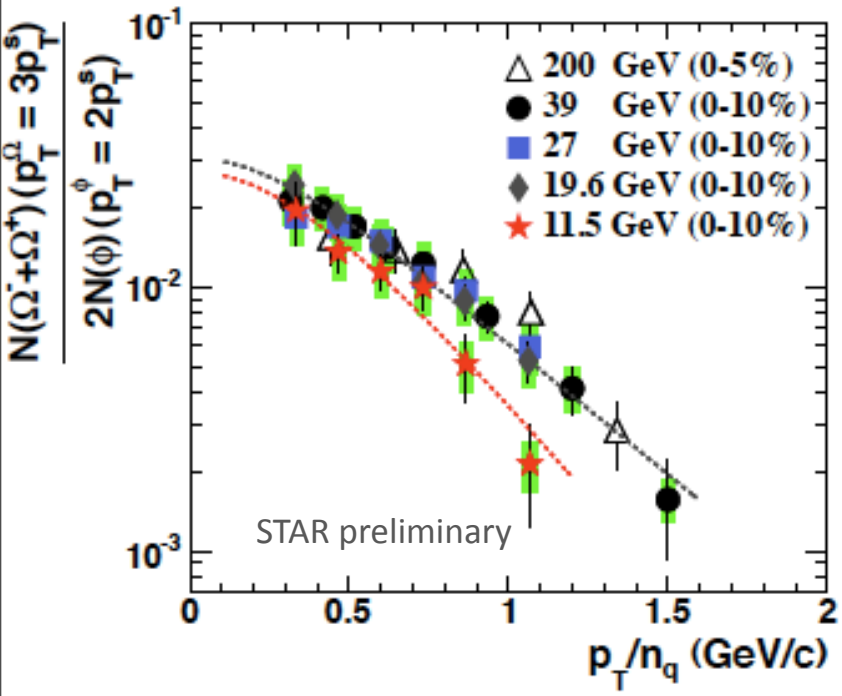

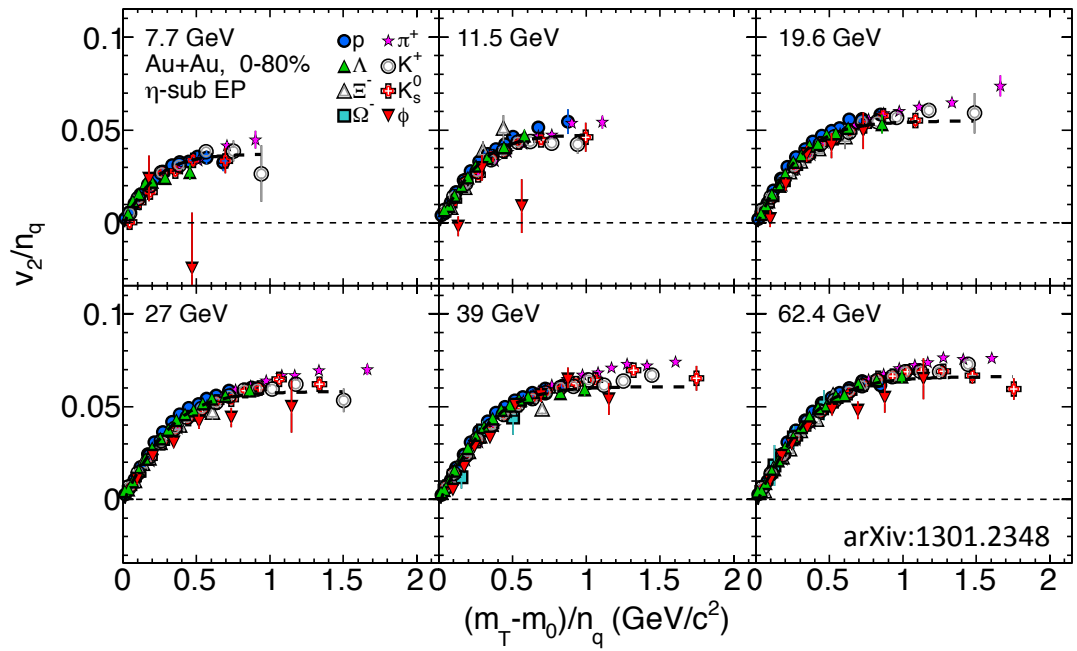

Between 19.6 and 11 GeV:

Derived s quark p_T distribution changes

Change in dominant particle production mechanisms?

ϕ v_2 no longer follows meson distribution
- low ϕ v_2 could imply hadronic dominance

(Better statistics would be nice)

R_{AA} vs R_{CP}

Peripheral

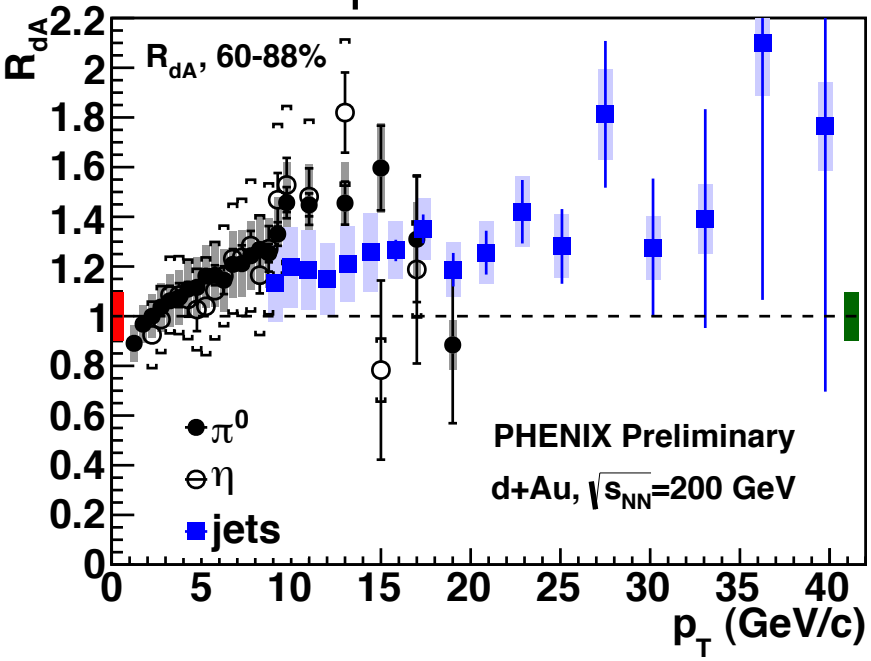

Central

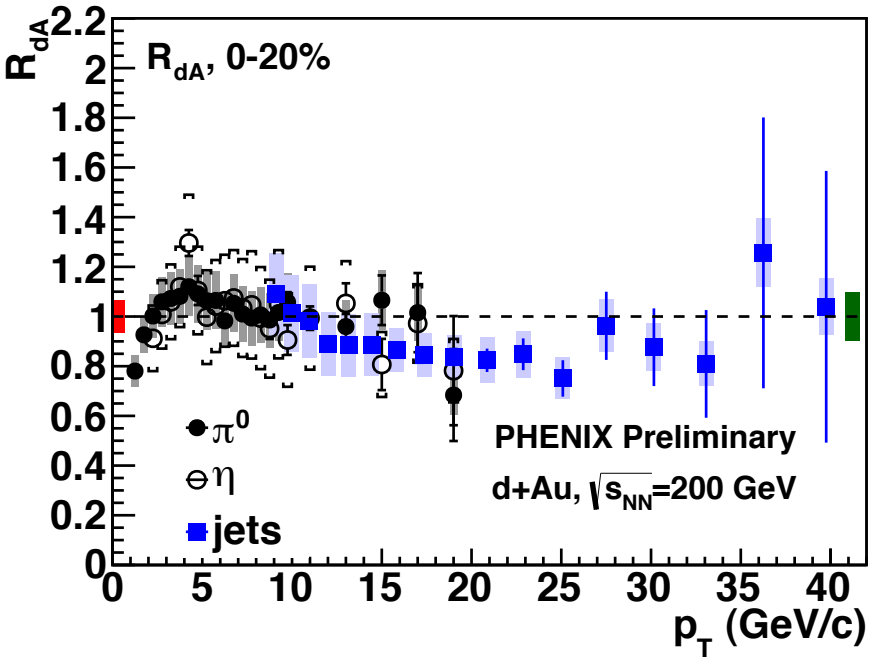

Centrality dependence to the Cronin Effect?

Au-Au 200

d-Au: enhancement larger in peripheral collisions

- were expected to be more “p-p” like

R_{AA} vs R_{CP}

Peripheral

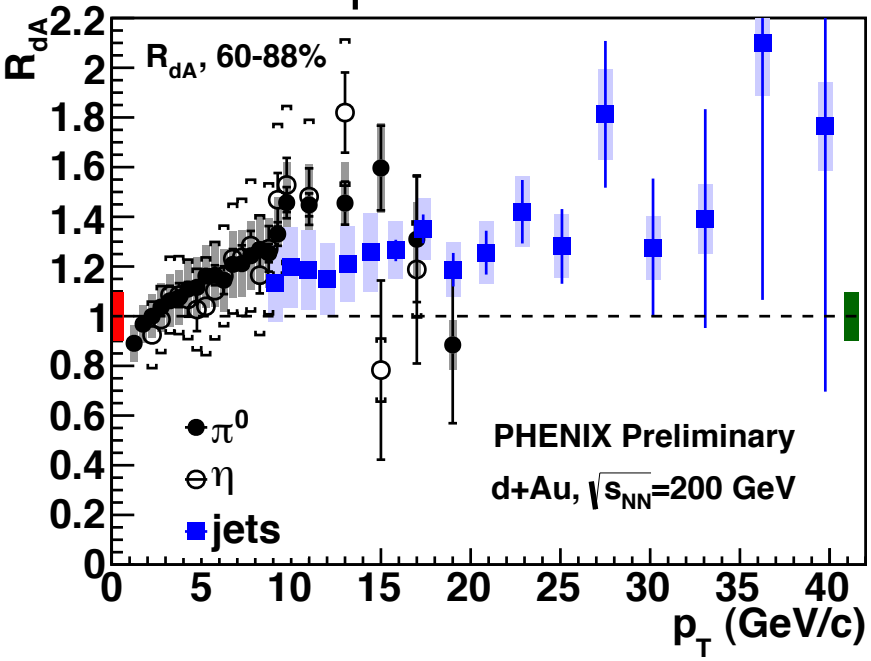

Central

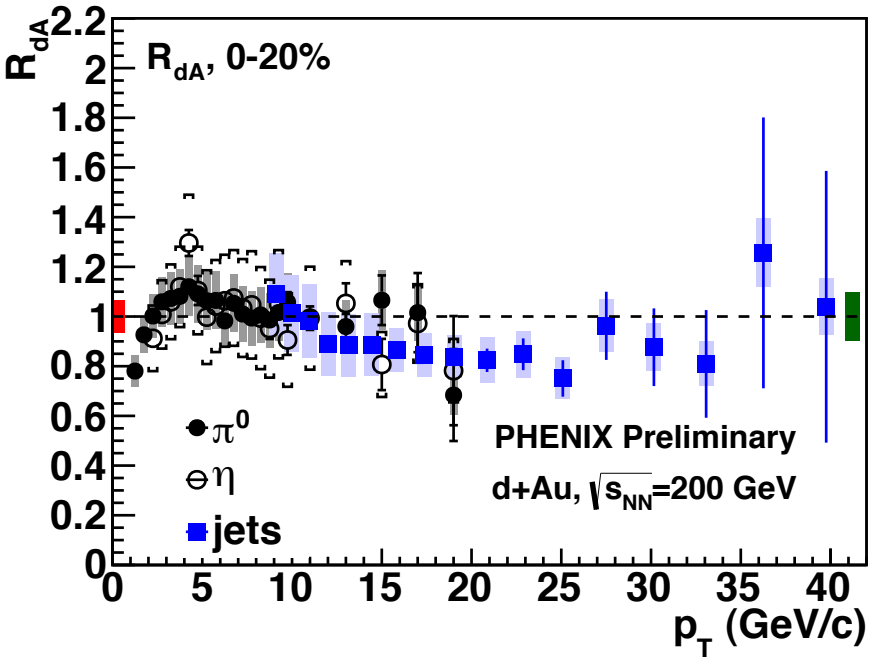

Centrality dependence to the Cronin Effect?

d-Au: enhancement larger in peripheral collisions
- were expected to be more “p-p” like

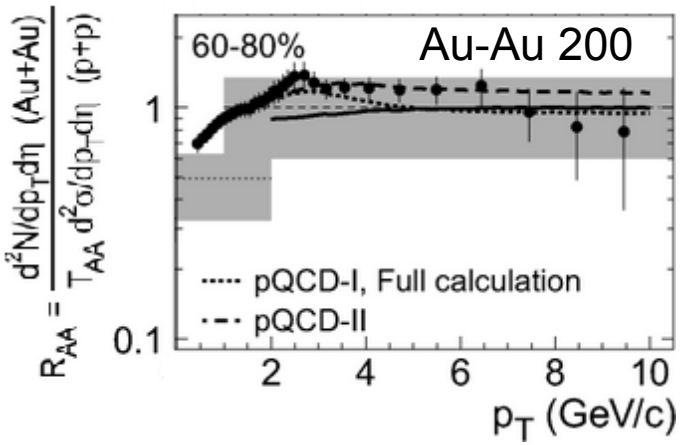

R_{AA} vs R_{CP}

Peripheral

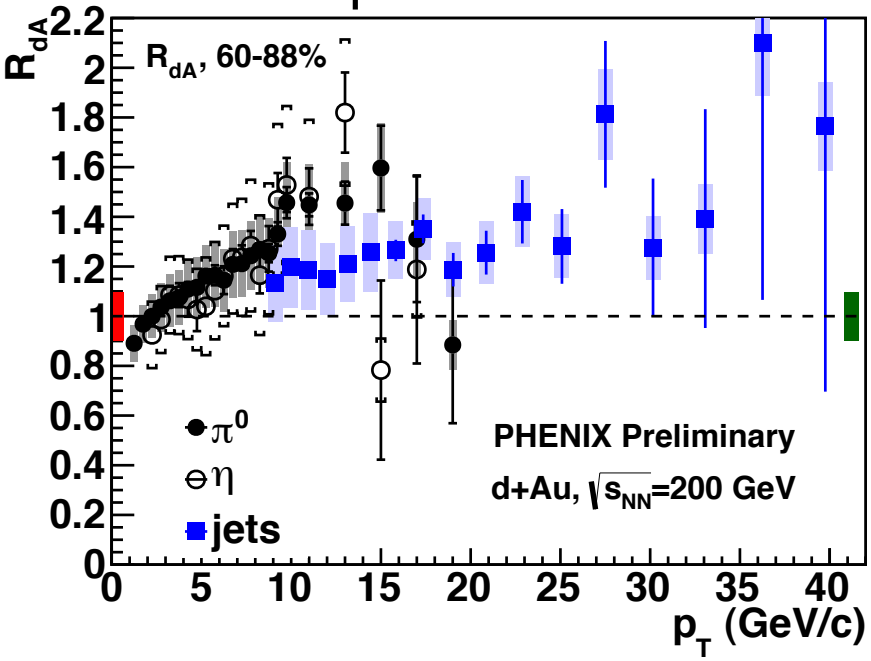

Central

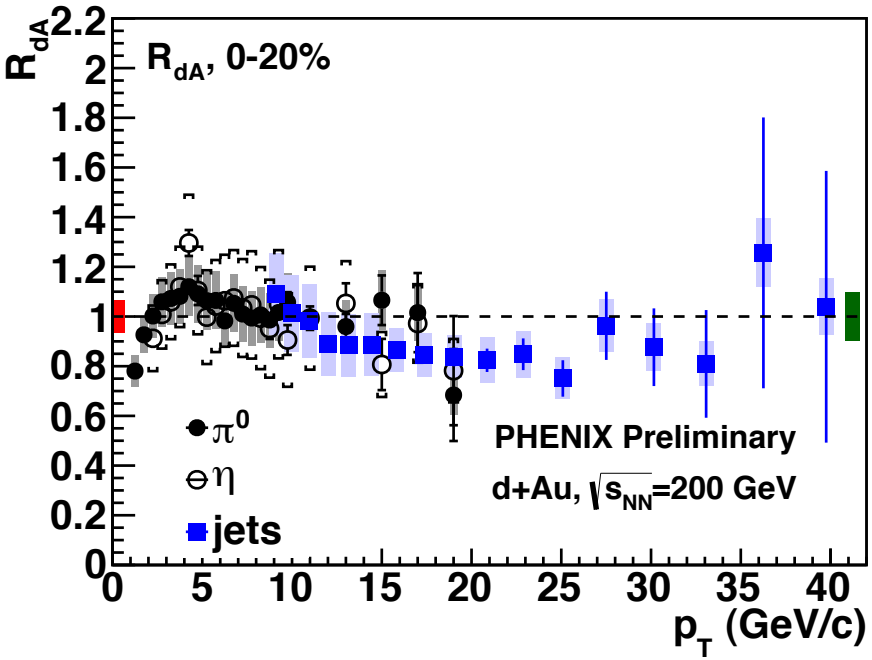

Centrality dependence to the Cronin Effect?

d-Au: enhancement larger in peripheral collisions
- were expected to be more "p-p" like

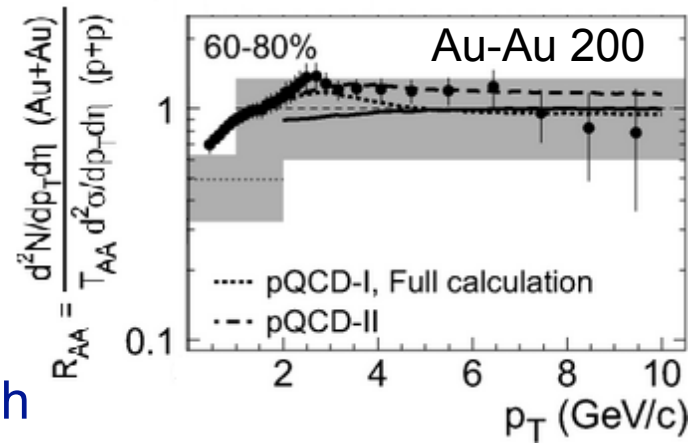

R_{CP} cancels some of the Cronin - maybe too much

Is x_T better variable than p_T?

Physics Letters B 637 (2006) 161–169

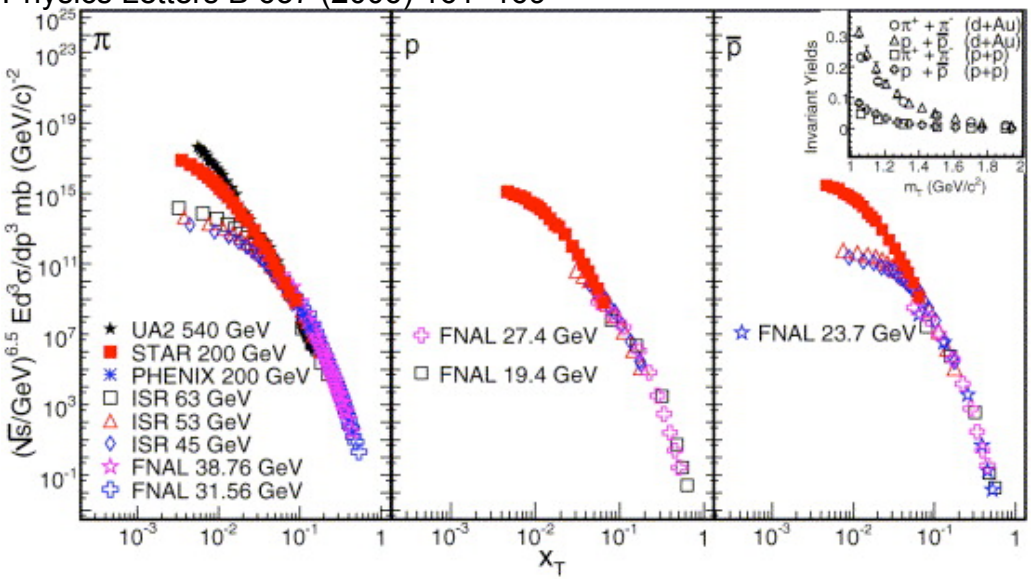

$$x_T = \frac{2p_T}{\sqrt{s}}$$

p-p spectra converge at large x_T over large range in $\sqrt{s_{NN}}$ when yield scaled by $(\sqrt{s}/GeV)^{6.5\pm0.8}$

Does this scaling persist in A-A collisions?

Is x_T better variable than p_T?

Physics Letters B 637 (2006) 161–169

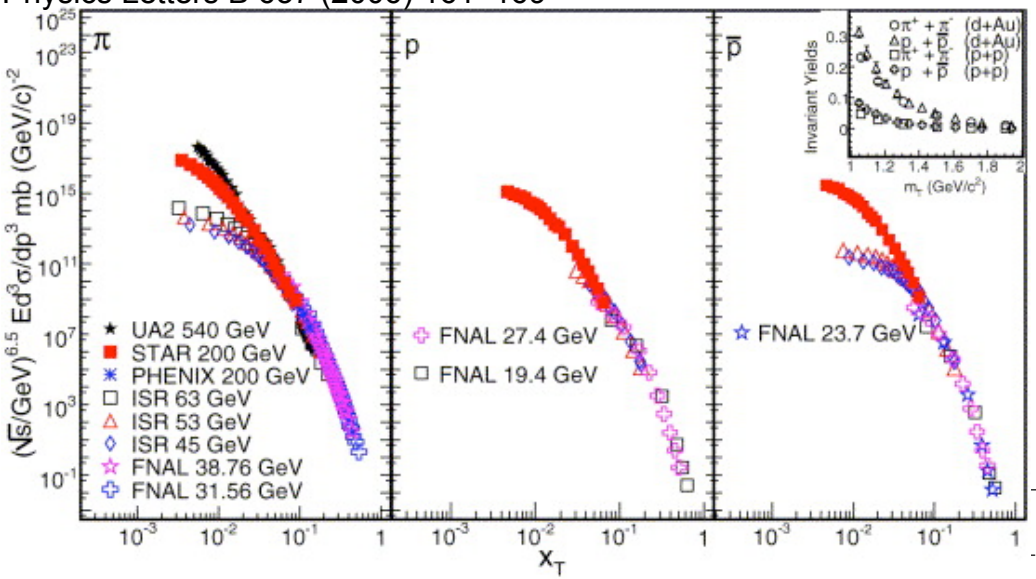

p-p spectra converge at large x_T over large range in $\sqrt{s_{NN}}$ when yield scaled by $(\sqrt{s}/GeV)^{6.5\pm0.8}$

Does this scaling persist in A-A collisions?

$$x_T = \frac{2p_T}{\sqrt{s}}$$

R_{CP}: $\sqrt{s_{NN}}$ dependence remains

x_T not the appropriate scaling and/or centrality dependence to exponent (6.5±0.8)

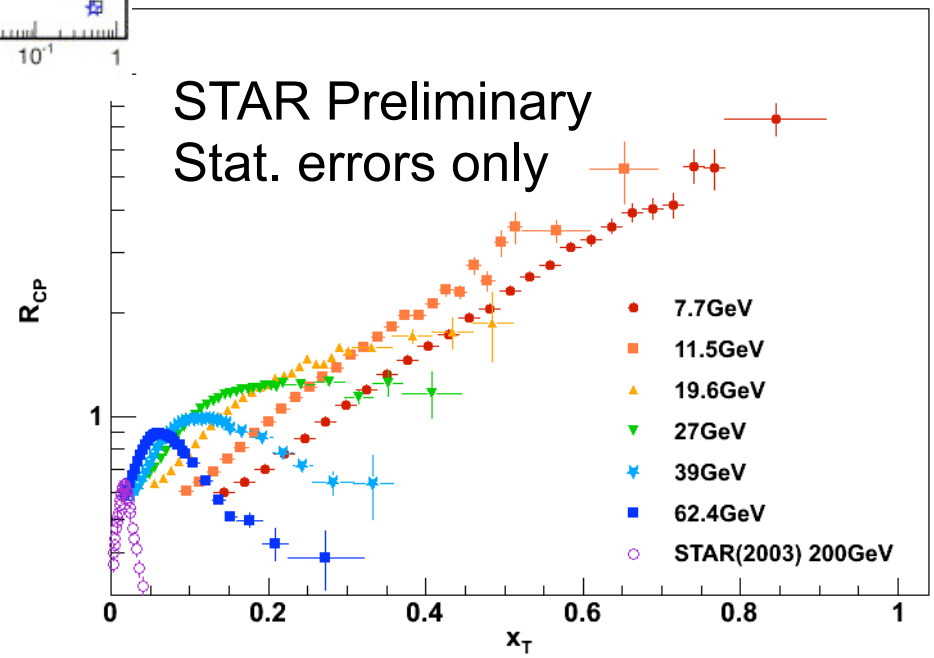

Can we extract Cronin from models

- HIJING 1.383
  - jet quenching on or off
  - modeled as -dE/dx within the medium
  - default Lund splitting parameters a=0.5,b=0.9

- AMPT v1.21/v2.21(uses HIJING 1.383)
  - string melting (SM) off uses Lund string fragmentation for hadronization (v1.21)
  - SM on uses quark coalescence for hadronization (v2.21)
  - default Lund splitting parameters a=2.2, b=0.5

Lund fragmentation formula: $f(z) \propto \frac{(1-z)^a}{z} e^{-bm_\perp^2/z}$

HIJING quenching on

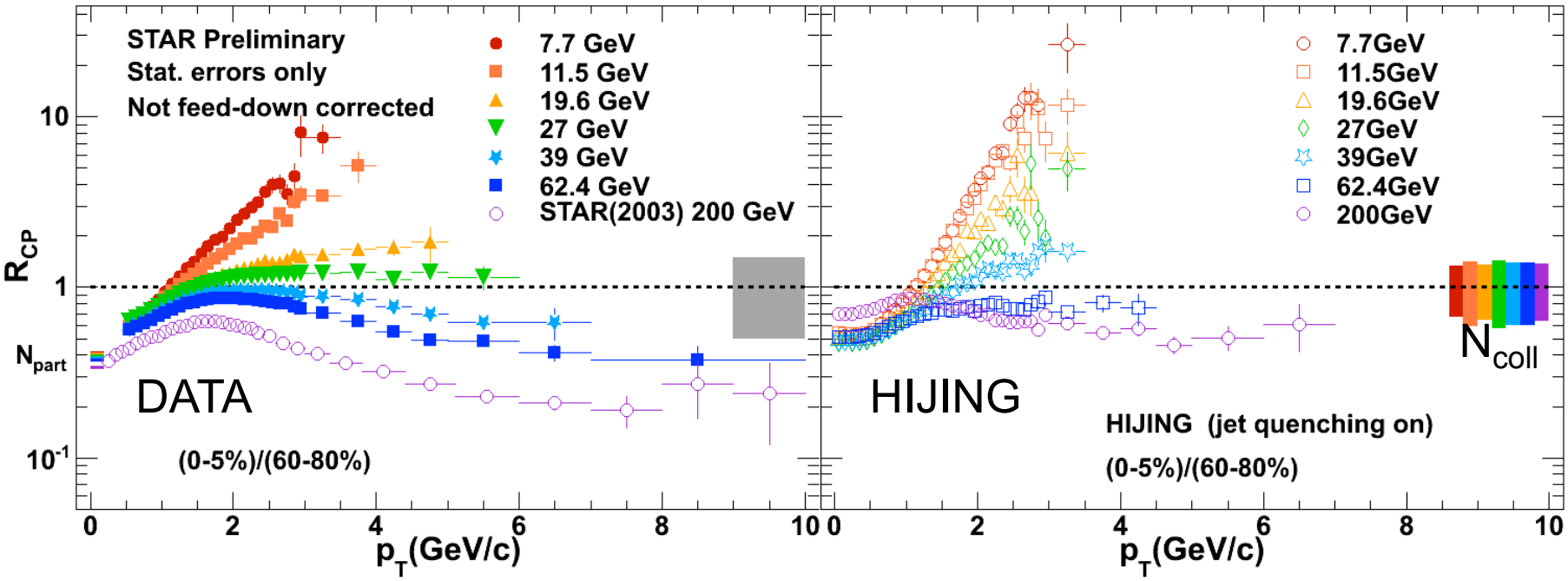

- Similar behavior to data
- 200 GeV has odd low p_T behavior
- Generally overestimates R_{CP}

HIJING quenching off

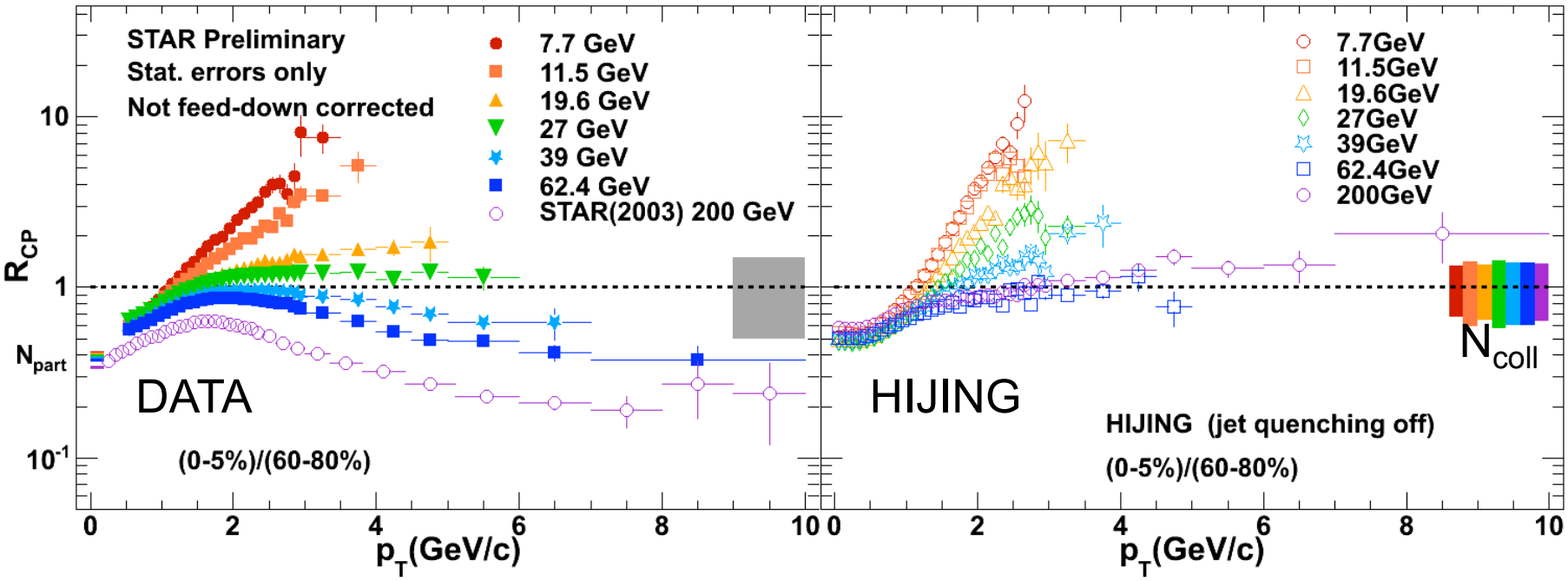

- 200 GeV better behaved at low p_T
- 7.7 GeV barely changed from quenching on

AMPT SM off

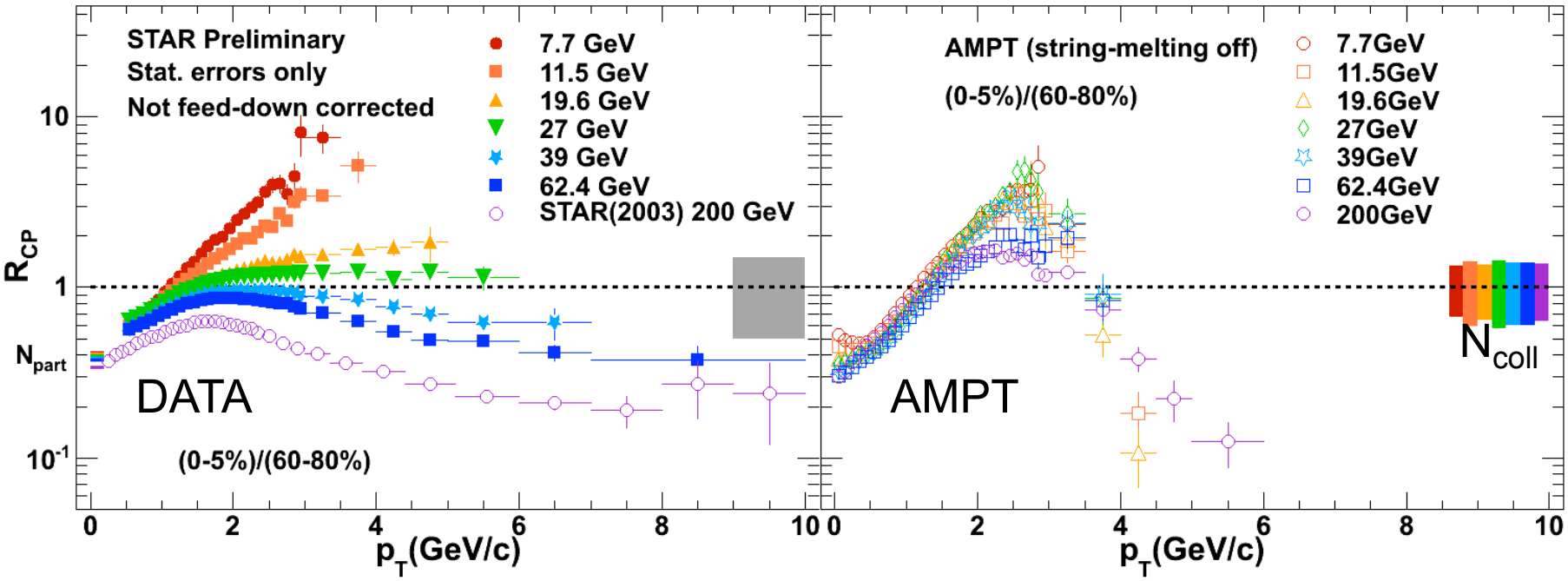

- Minimal beam energy dependence
- Sharp turn over near 2.5 GeV/c

AMPT SM on

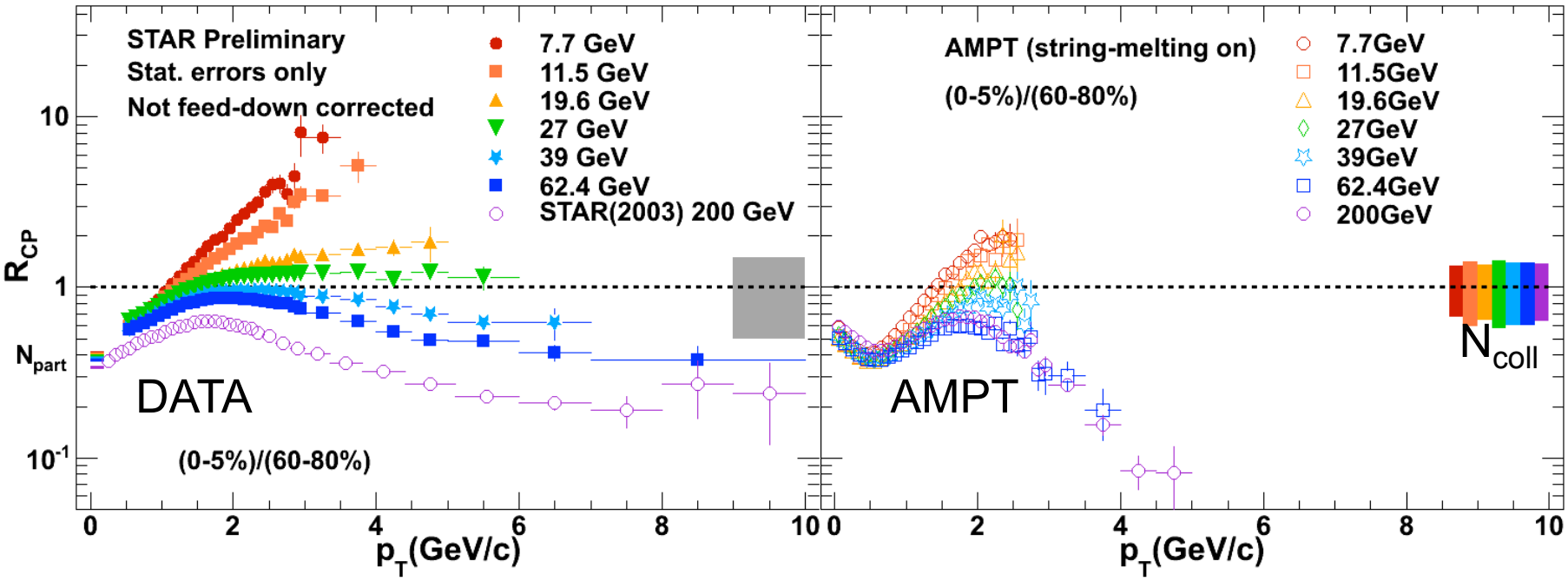

- recovers beam energy dependence
- limited p_T reach
  - same number of events for SM on/off

HIJING default/AMPT settings

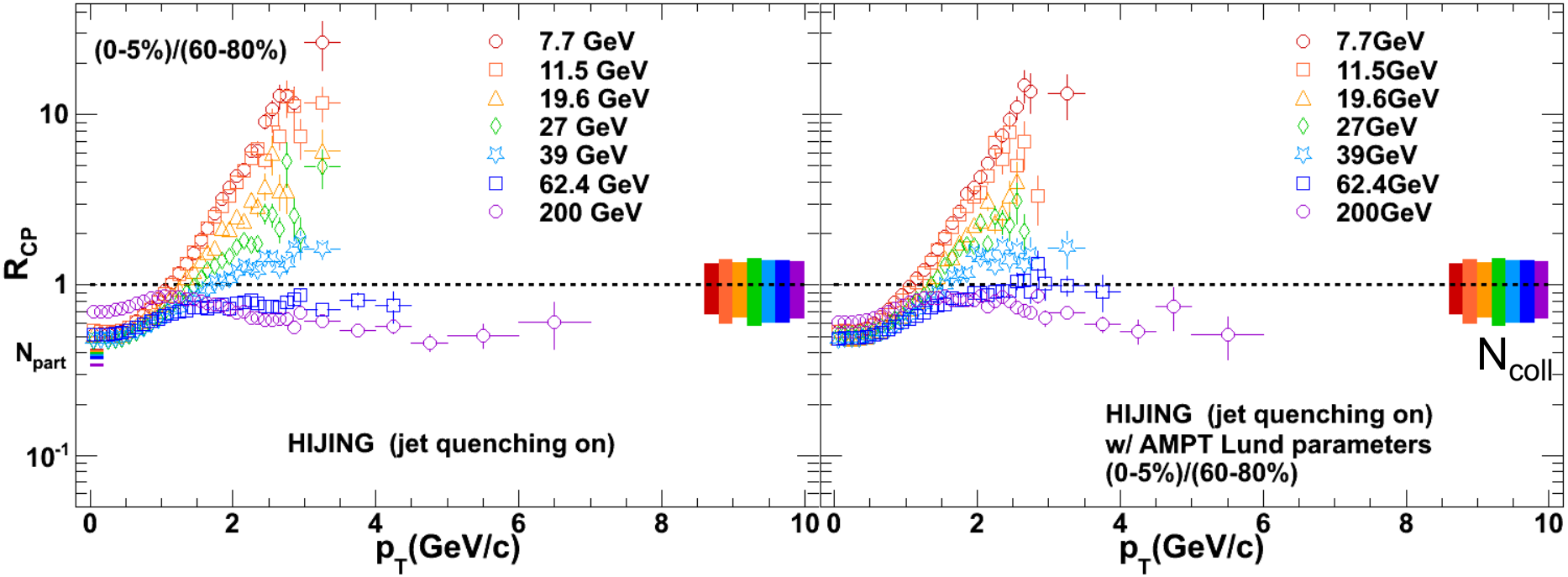

HIJING with default or AMPT's Lund splitting parameters

- small effect on R_{CP}

HIJING with differing Lund parameters

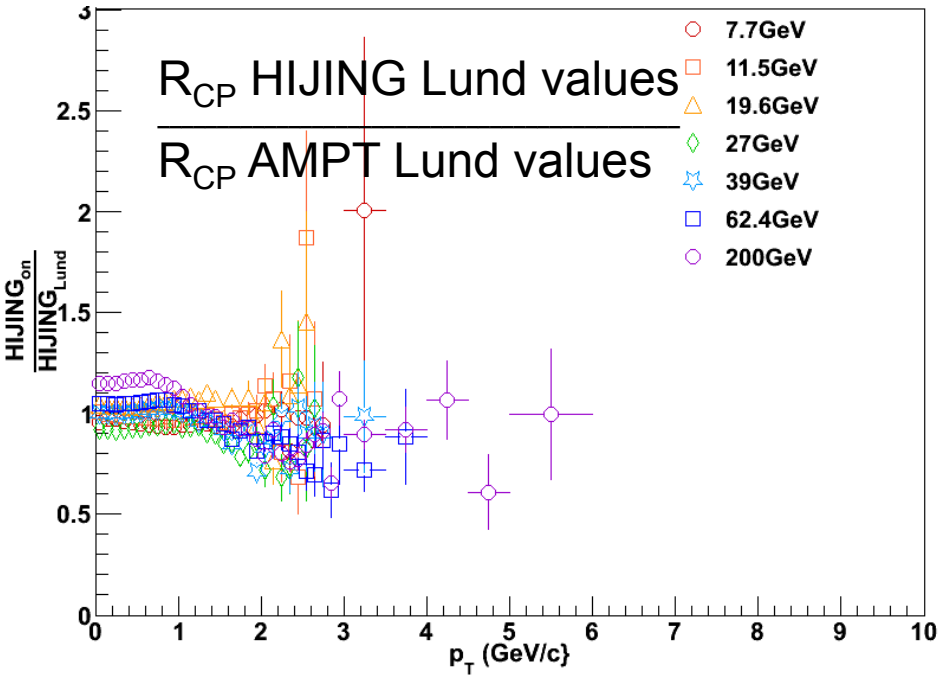

R_{CP} essentially unchanged

HIJING with differing Lund parameters

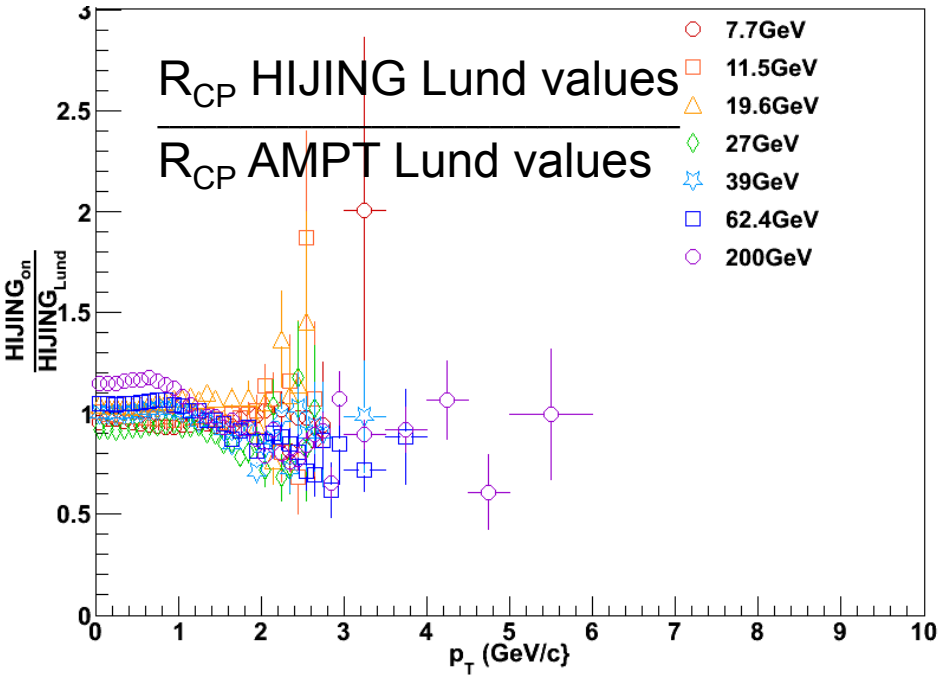

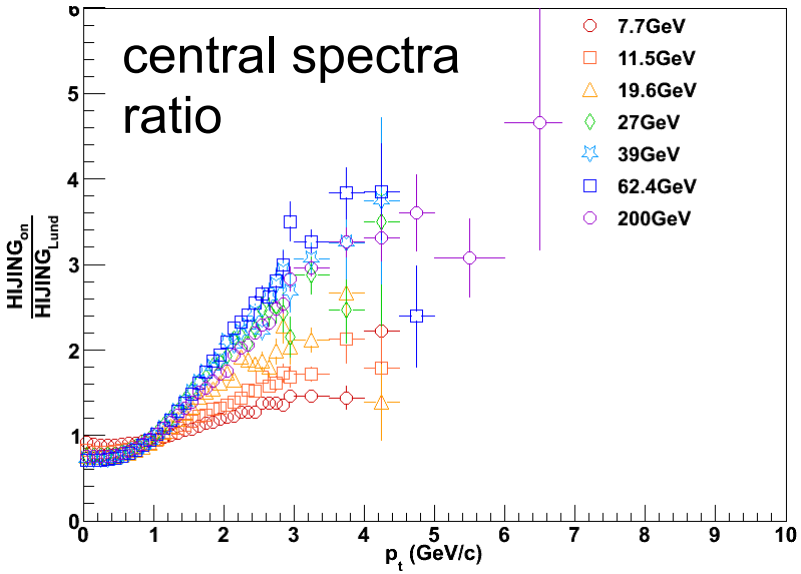

R_{CP} essentially unchanged

Peripheral and central spectra vary in same manner

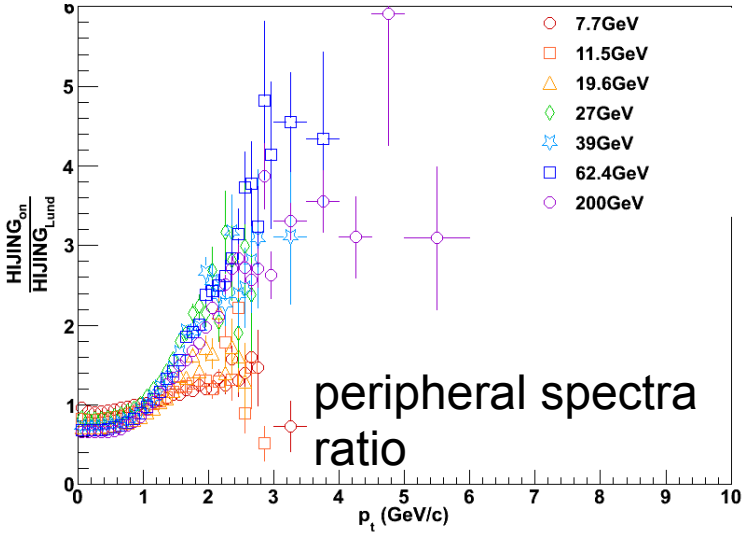

Conclusions on quenching

- Results taken at face value suggest QGP down to lowest beam energy
- Disentangling initial from final state close to impossible without control data
- (some) Models get trends OK but none get details
- Need to compare to numerous measurements to gain understanding
- BES data confusing, and more interesting than folks thought

Initial Conditions

Importance of initial conditions

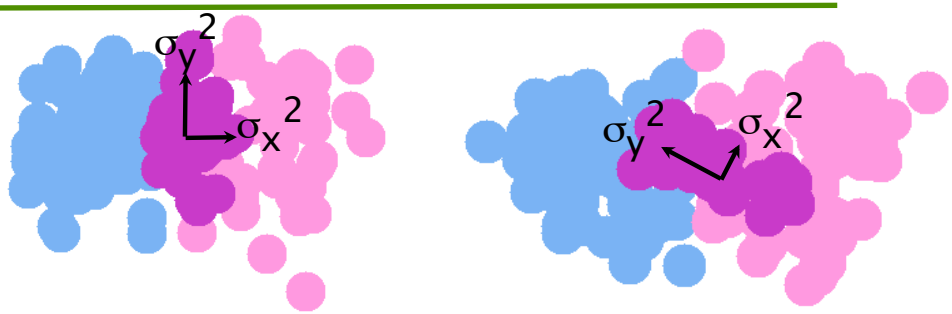

Phys. Rev. Lett. 98, 242302 (2007)

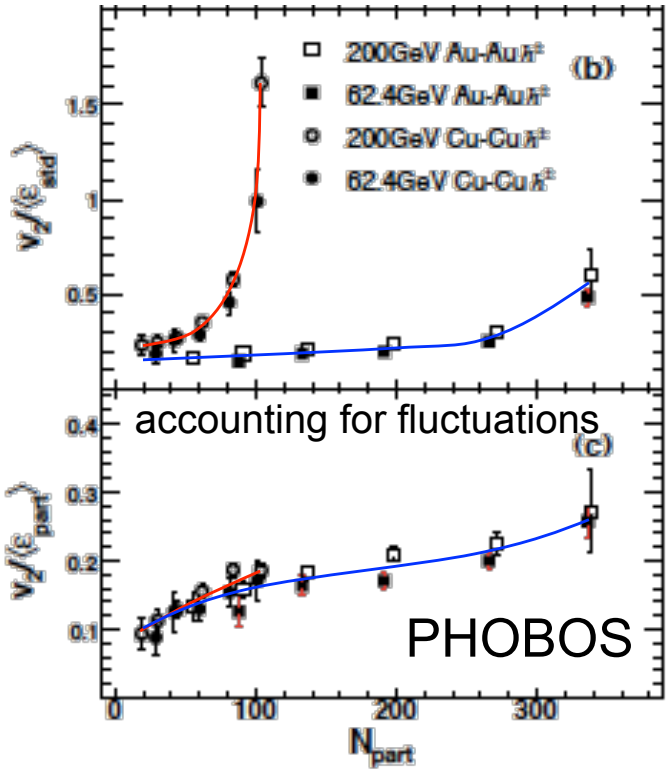

PHOBOS - Cu-Cu importance of principle axis

Alver and Roland - v_3 exists and plays key role

Importance of initial conditions

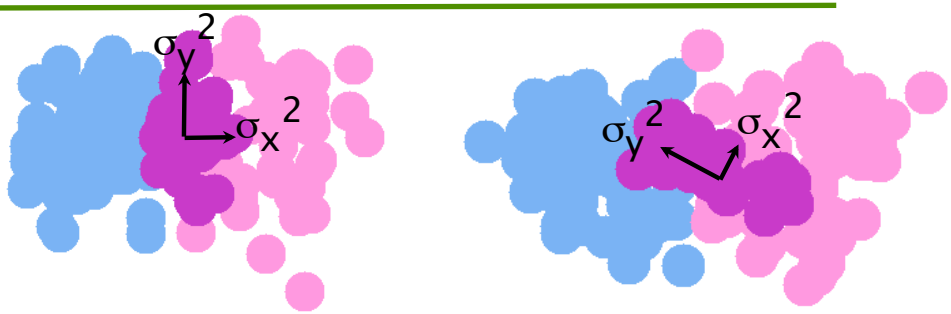

Phys. Rev. Lett. 98, 242302 (2007)

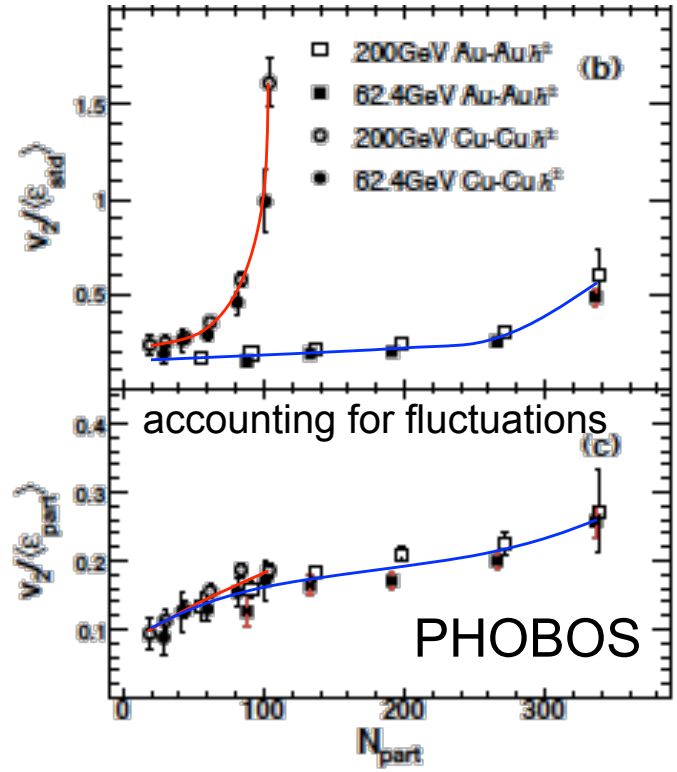

PHOBOS - Cu-Cu importance of principle axis

Alver and Roland - v_3 exists and plays key role

STAR Phys. Rev. C **85 (2012) 14903**

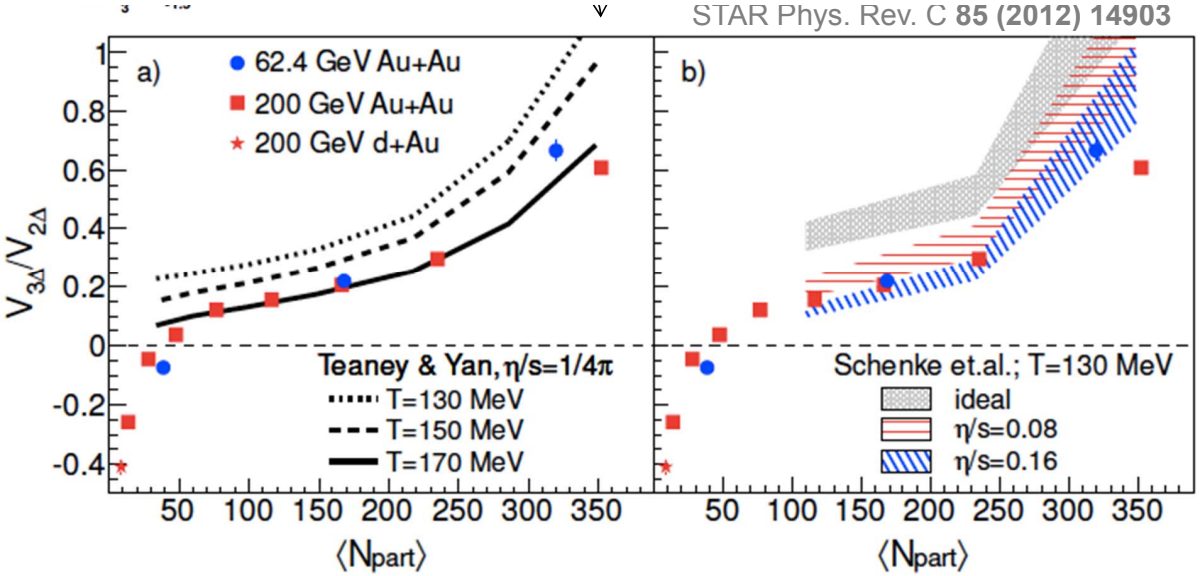

Viscosity or T can be tuned to match $V_{3\Delta}/V_{2\Delta}$

Need variety of data to pin down initial conditions

Importance of initial conditions - II

Song et al. PRL 106 192301 (2011)

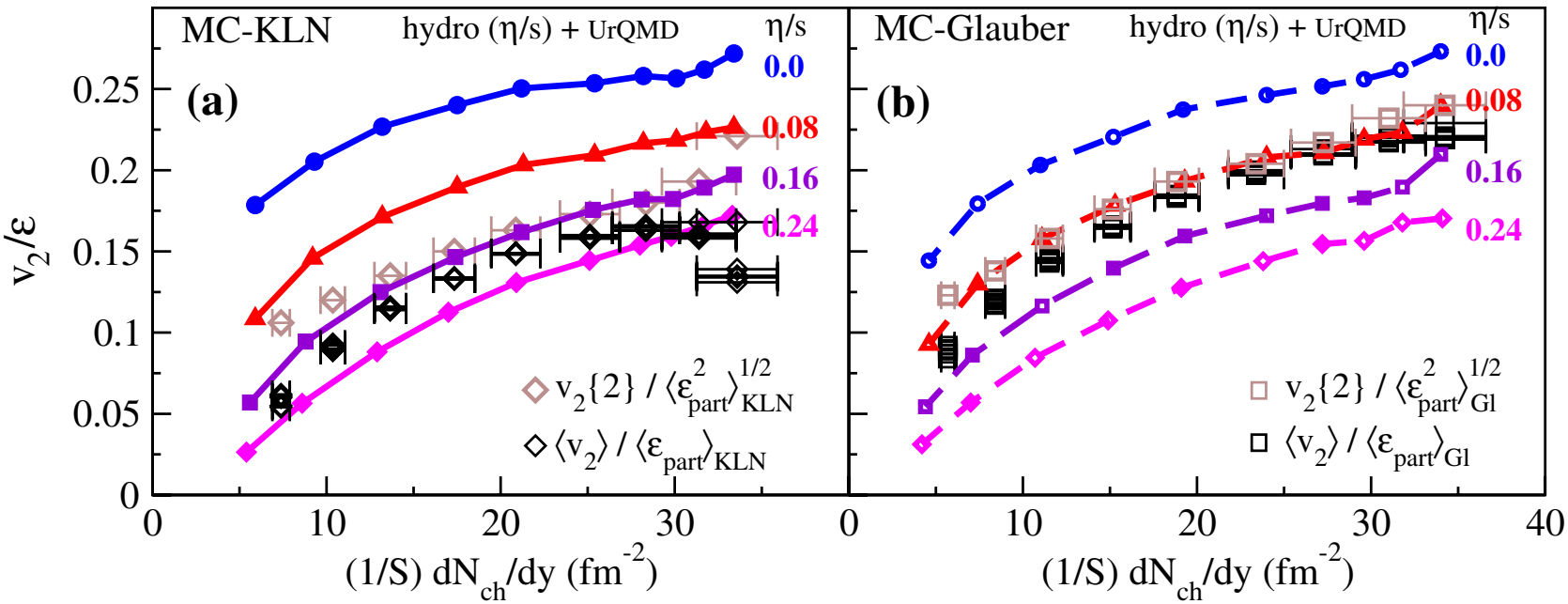

$$\frac{\eta}{s} = 0.08 \rightarrow 0.2$$

Details of initial configuration are large source of uncertainty

Importance of Initial conditions - III

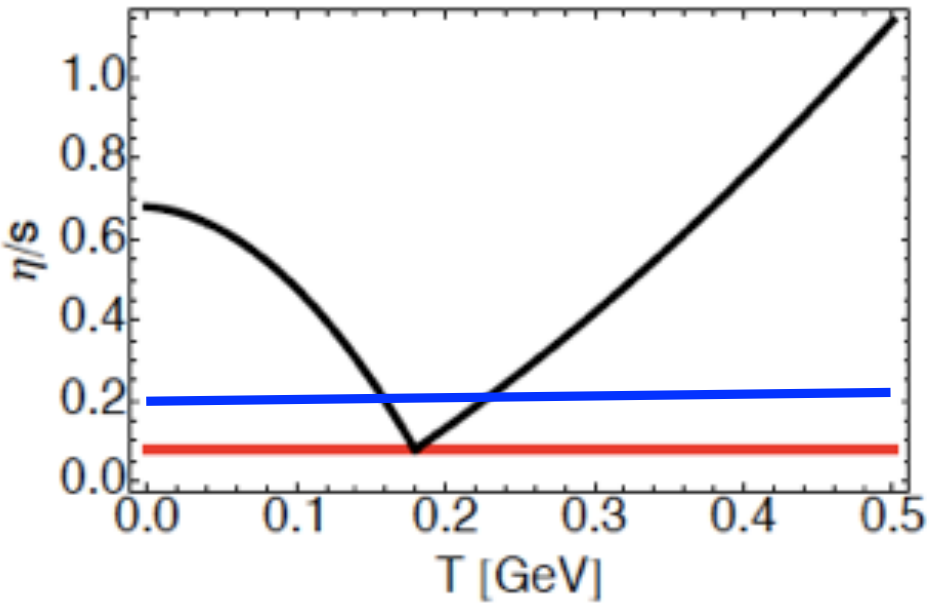

Gale, Jeon, Schenke, Tribedy, Venugopalan

Different functional forms for η/s(T) can result in similar mean η/s values

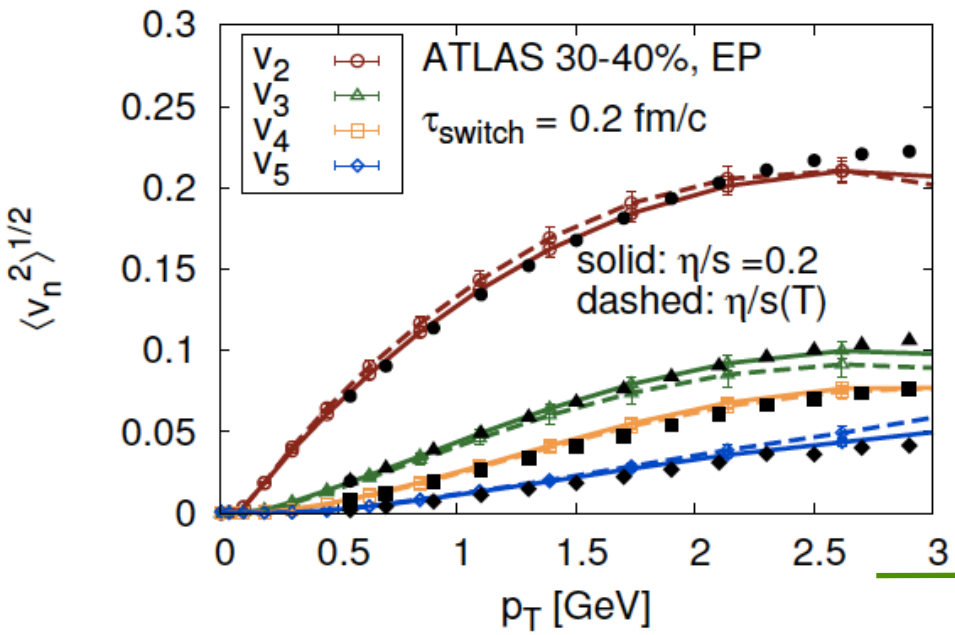

Can't distinguish with models between constant η/s or temperature dependent η/s with minimum at T_c with only one collision energy

Variety of collision energies needed to disentangle

η/s as a function of collision energy

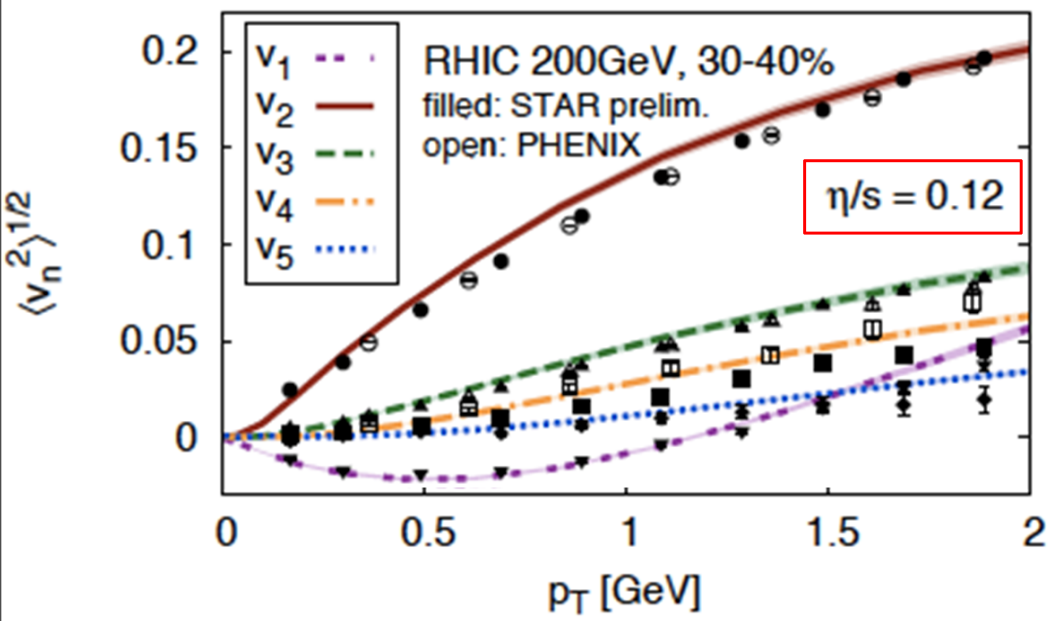

Mean η/s 40% smaller at top RHIC energies than at the LHC

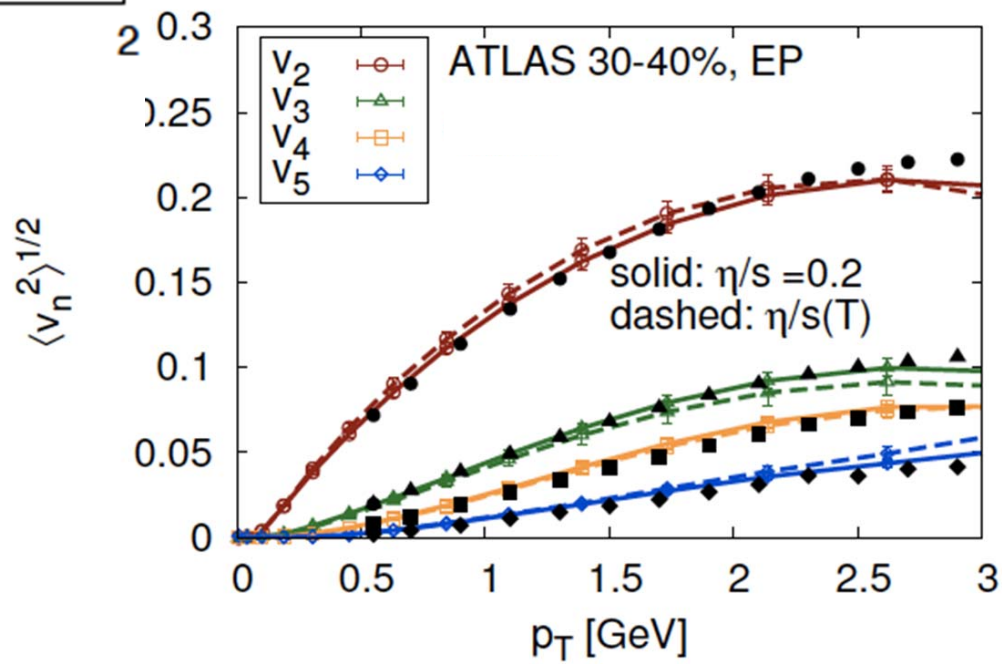

Does this keep dropping with beam energy?

V_n at top beam energies

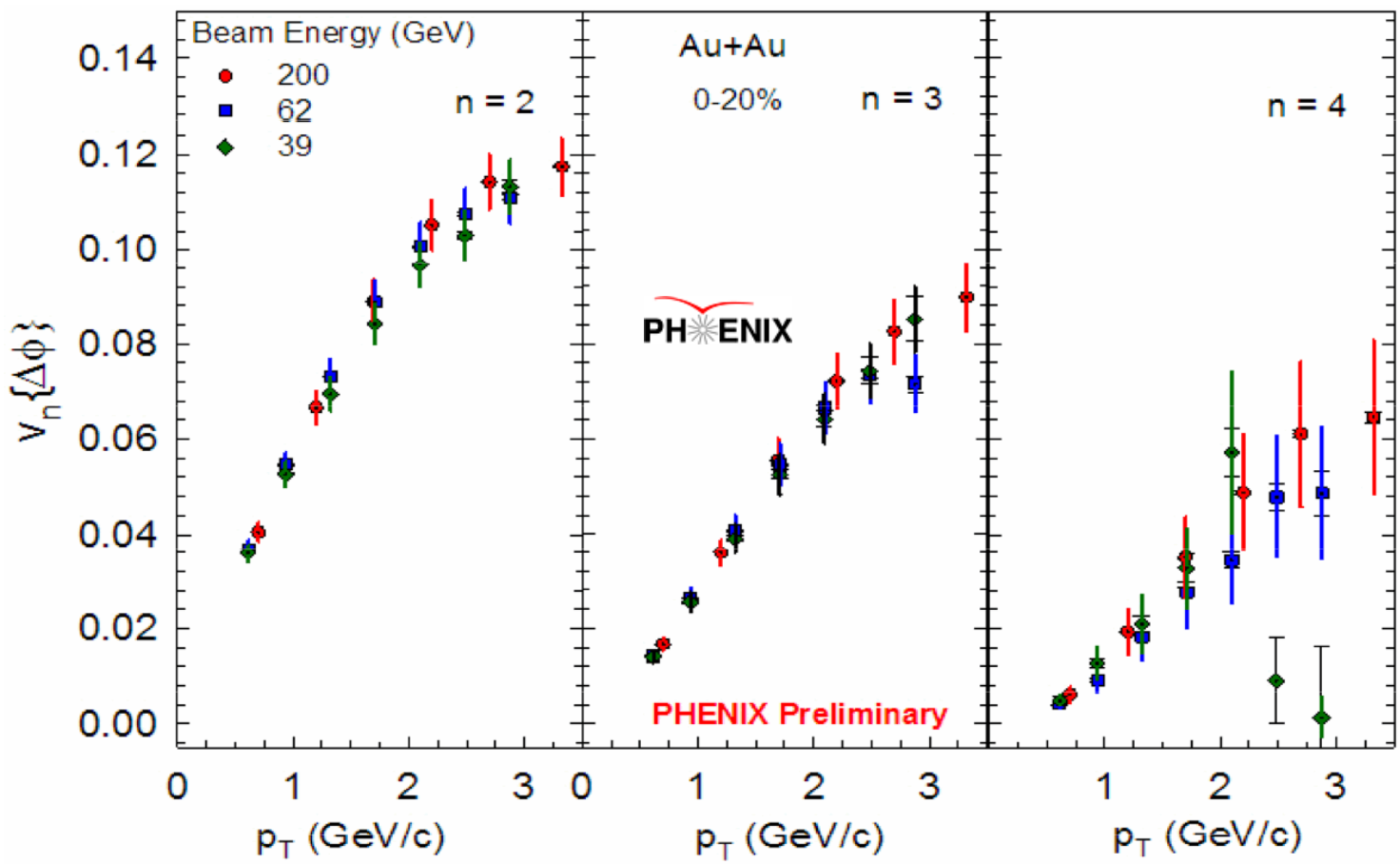

Similar p_T distributions for all v_n for $\sqrt{s_{NN}}$ = 39-200 GeV

Likely numerous things changing that happen to cancel out

v_3 and sensitivity to EoS

Y. Pandit, STAR, Quark Matter 2013

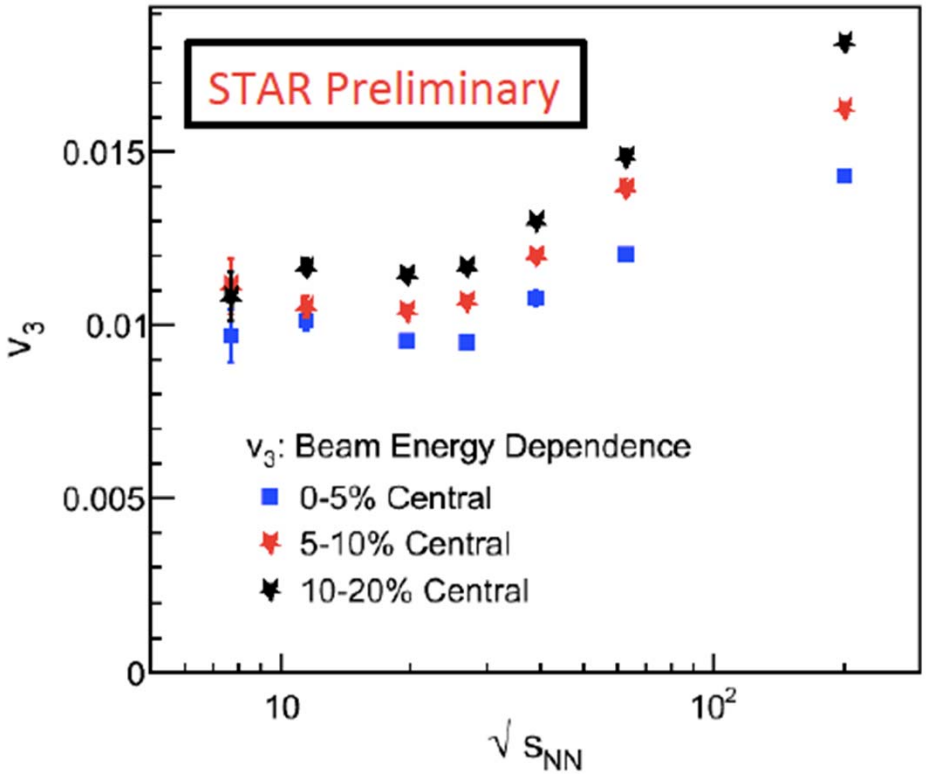

v_3 sizable even at 7.7 GeV
- jet contribution essentially zero

v_3 and sensitivity to EoS

Y. Pandit, STAR, Quark Matter 2013

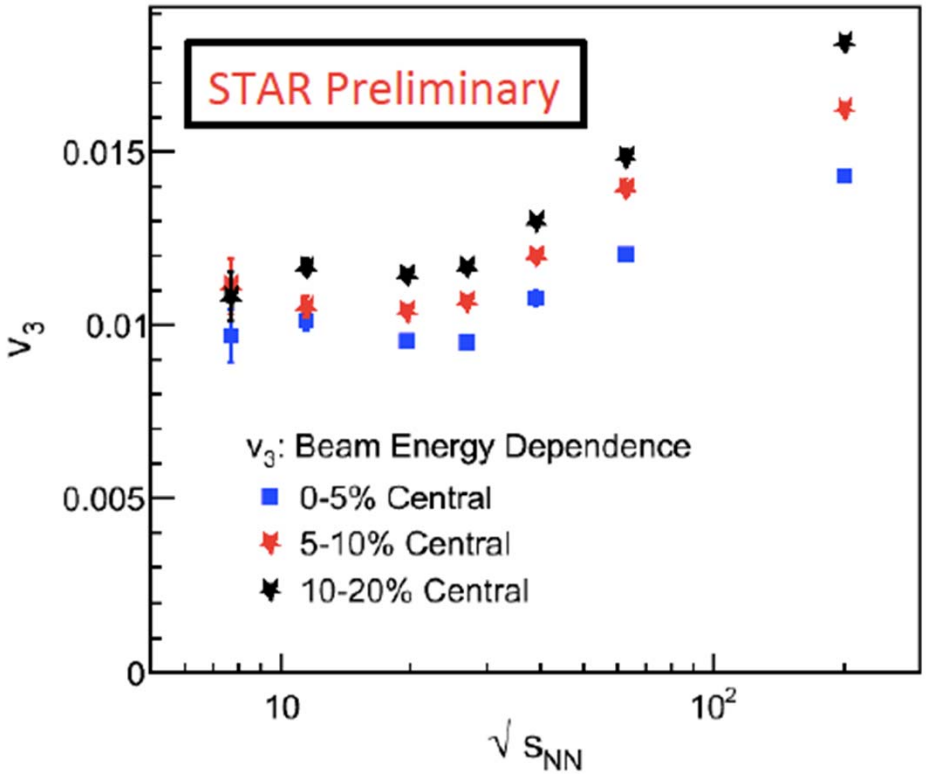

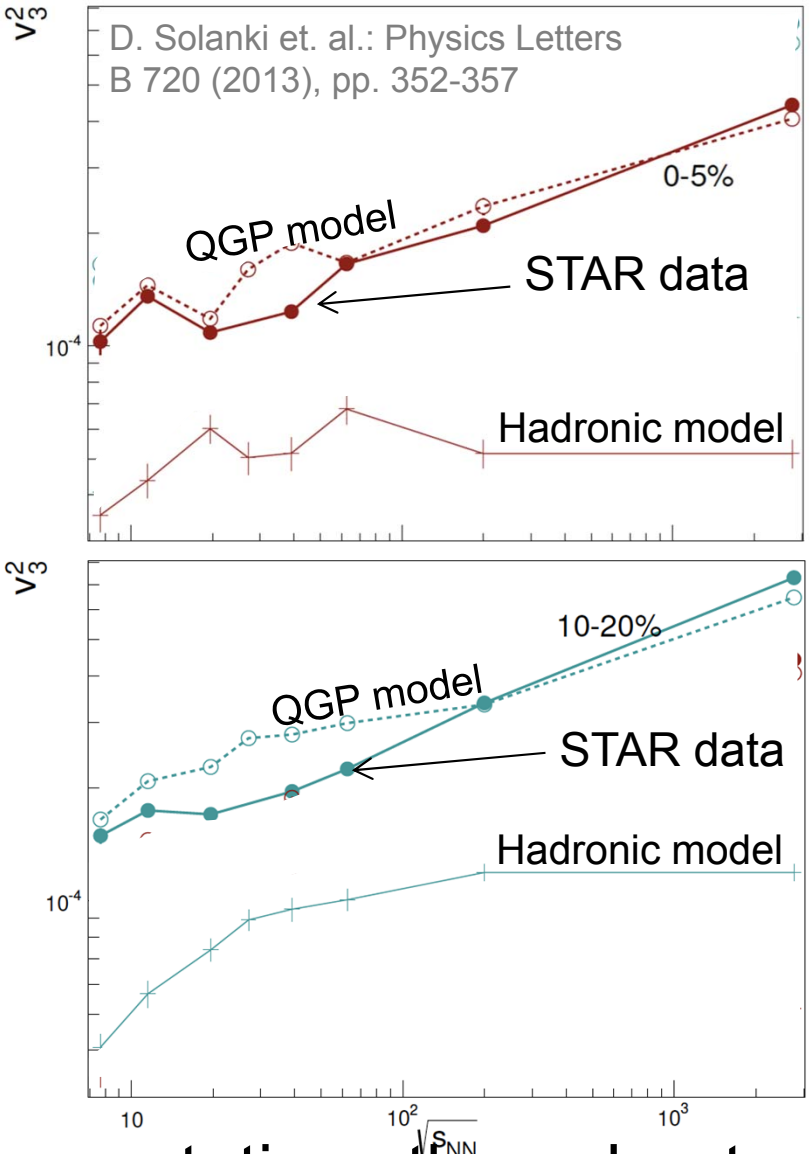

v_3 sizable even at 7.7 GeV
- jet contribution essentially zero

STAR data in reasonable agreement with QGP version of AMPT for all $\sqrt{s_{NN}}$

Pre BES - Azimuthally sensitive HBT

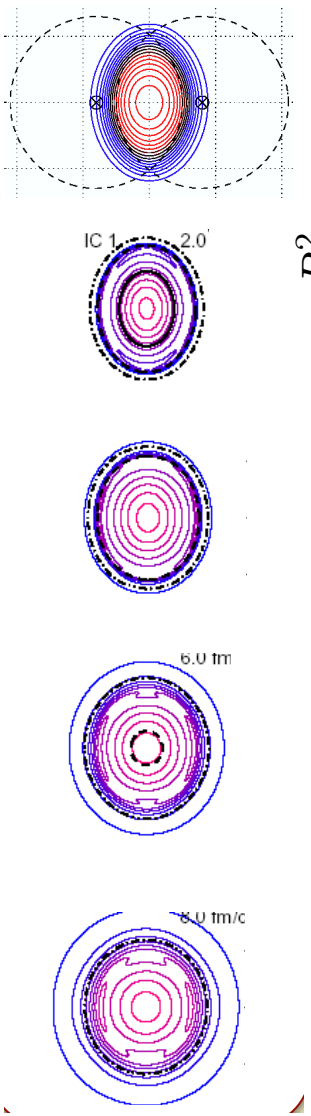

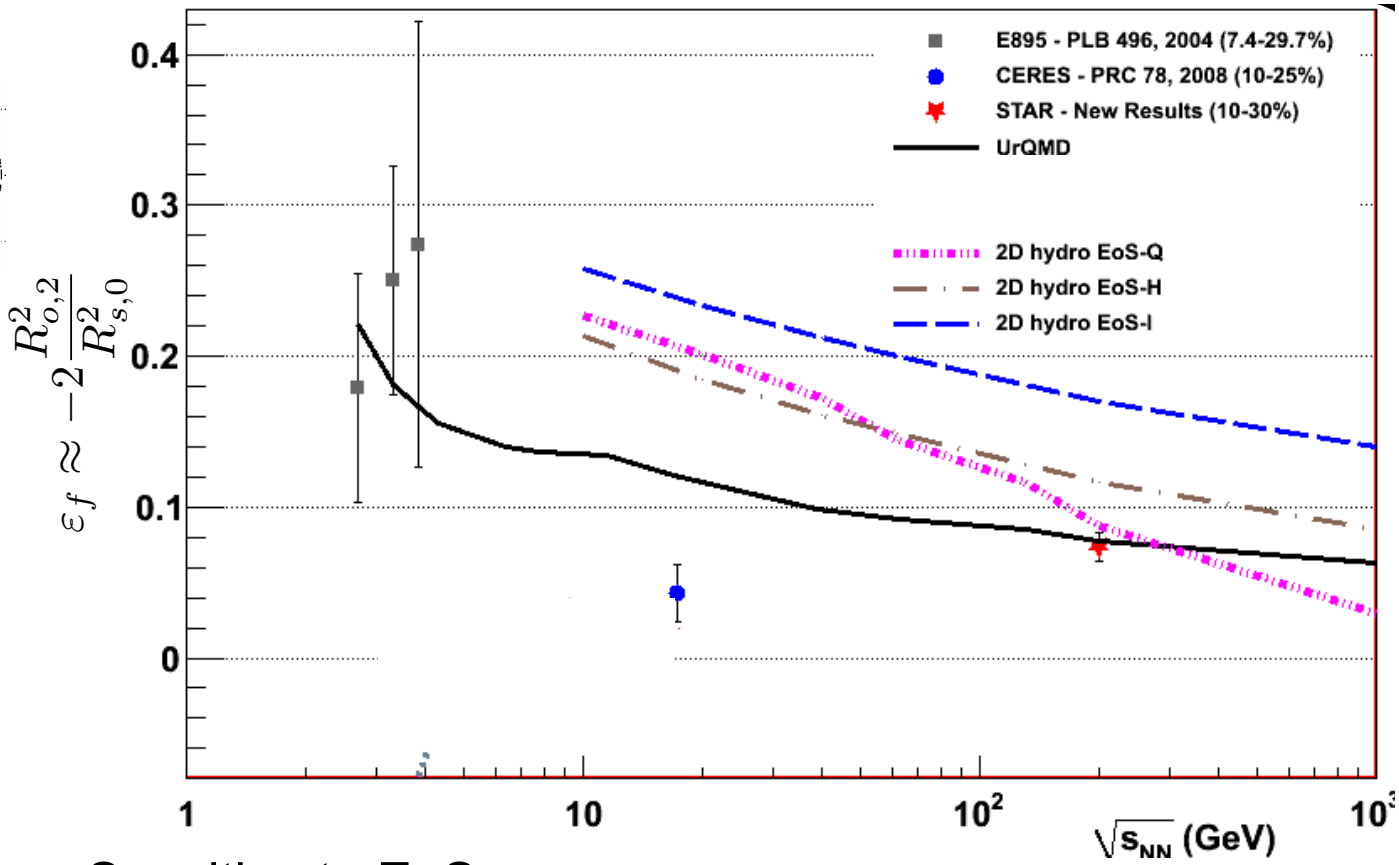

Sensitive to EoS

Naively:

higher $\sqrt{s_{NN}}$ → higher pressure → evolve to smaller ε_f

higher $\sqrt{s_{NN}}$ → longer lifetime → evolve to smaller ε_f

CERES data hint at something interesting

Azimuthal HBT

M.Lisa CPOD

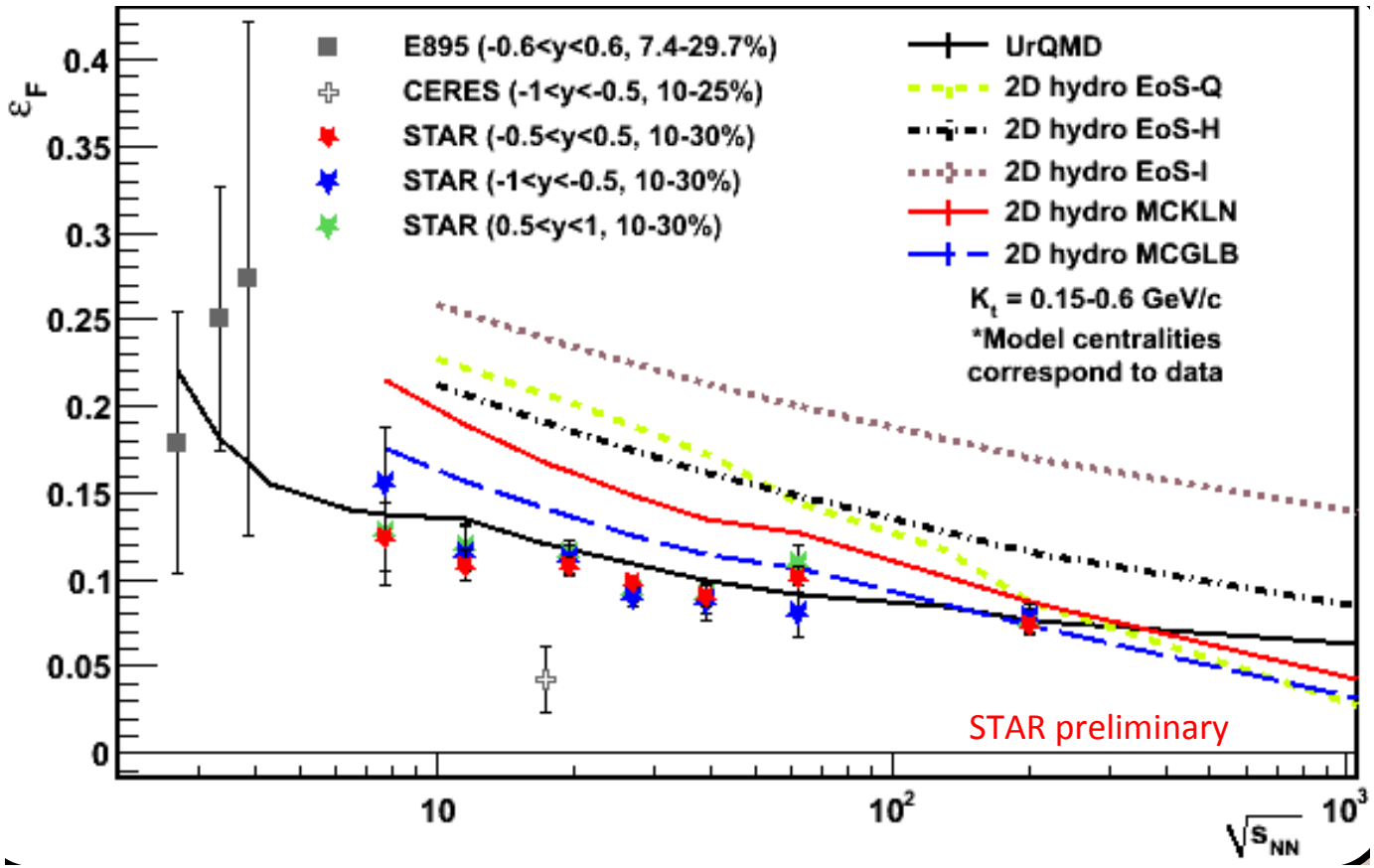

Shallow monotonic decrease for STAR data - even for CERES acceptance

Sensitivity to initial-state/viscosity

Azimuthal HBT

M.Lisa CPOD

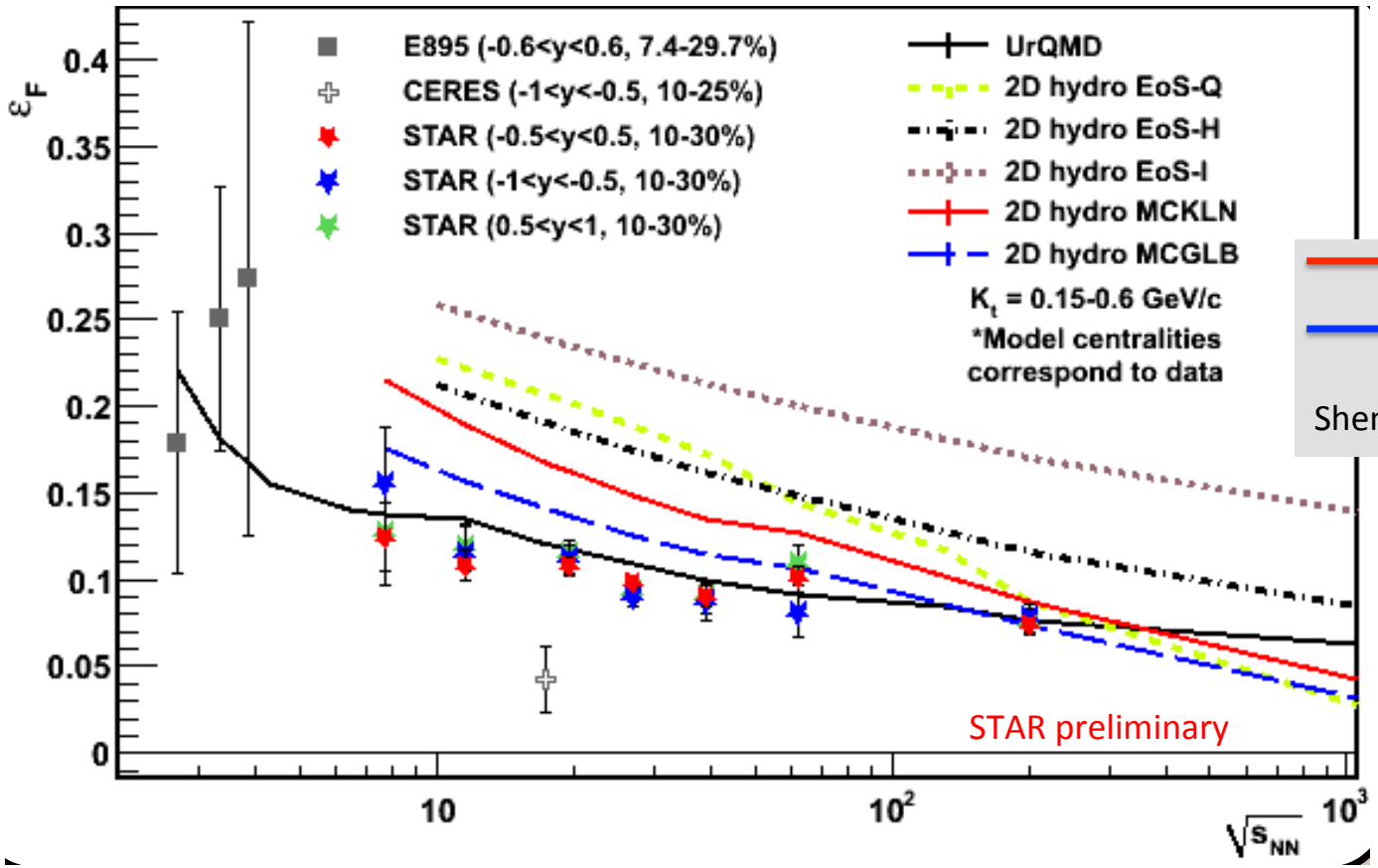

MC-KLN η/s = 0.2

MC-Glauber η/s = 0.08

Shen and Heinz (PRC85 054902 (2012)

Shallow monotonic decrease for STAR data - even for CERES acceptance

Sensitivity to initial-state/viscosity

Azimuthal Coordinate space measurement breaks degeneracy from azimuthal momentum space

Future prospects - BES-II and fixed target

$\sqrt{s_{NN}}$ (GeV)	μ_B (MeV)	BES-I	BES-II	Physics Motivation	Weeks**
200	24		**0.5-2** (B)	Heavy flavor hadron v_2 & R_{AA}	
39	112	130 (M)			
27	156	70 (M)			
19.6	206	36 (M)	**400** (M)	LMR di-electron*, net-p κ>5σ	**2**
15	250		**100** (M)	Ω yield, ϕ-meson v_2 (≤ 3GeV/c)	**2**
11.5	316	12 (M)	**120** (M)	net-p κ	**3.5**
7.7	420	5 (M)	**80** (M)	net-p κ	**10**

* Di-electron measurements below 19.6 GeV are not planned
** Estimates are based on electron cooling upgrade currently under development and are approximate without electron cooling, the program would require ~150 weeks

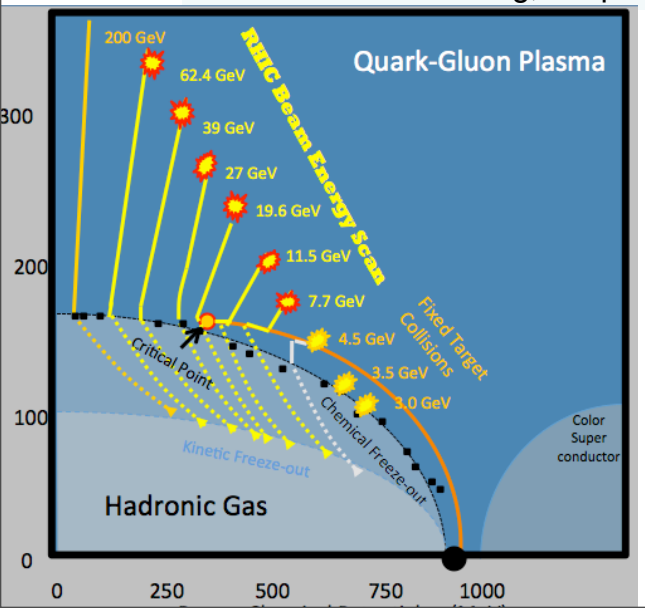

Fixed target experiment at STAR will push down to even lower μ_B

Collider mode $\sqrt{s_{NN}}$ (GeV)	Fixed-target mode $\sqrt{s_{NN}}$ (GeV)	Fixed-target mode μ_B (MeV)
19.6	4.5	585
15	4.0	625
11.5	3.5	670
7.7	3.0	720
5	2.5	775

Conclusions

- I'm in the minority but I think pA BES would be very interesting

- Hopeful can disentangle contributions to initial state via variety of measurements - HBT making a comeback?!?!!

- Lots of puzzles from the BES
  - even if hints for Critical Point and 1st order transitions are not leaping out

The End

Jet quenching II:
or
What do we know, and how well do we know it?

Brian. A Cole

April 16, 2013

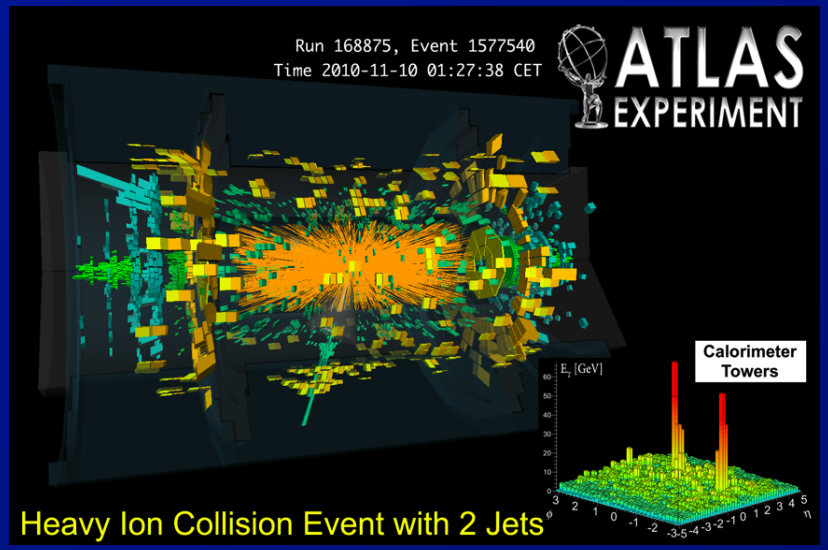

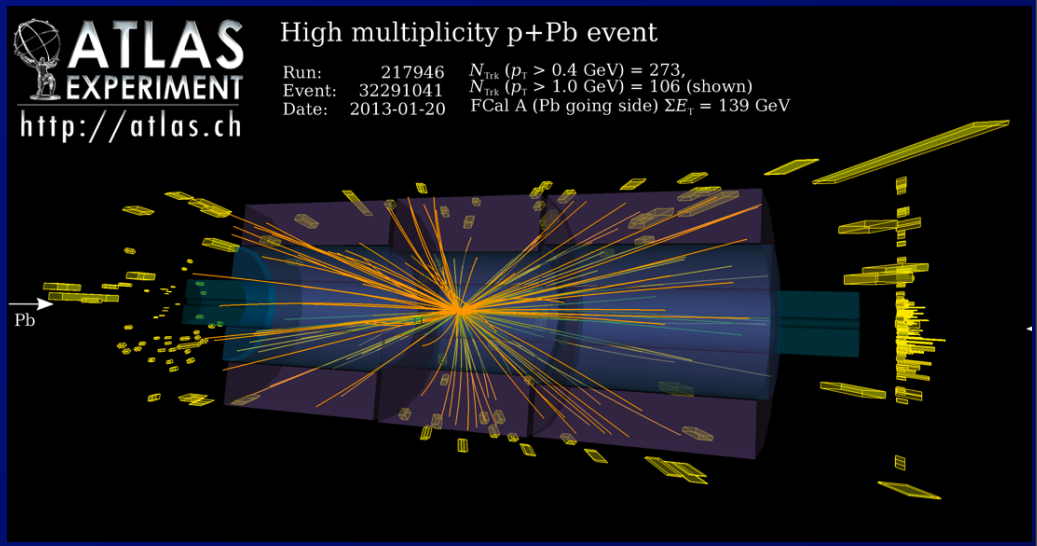

Overview

- From workshop web page:
  - Specific topics we plan to address include:
    - To what extent do we achieve control over initial state effects in light of the new dAu and pPb data?
    - How do the medium properties change from RHIC to LHC?
    - Can we achieve precision by combining the vast amount of data from RHIC and LHC?
    - How does the jet quenching response to fluctuating initial geometry (jet tomography) evolve from RHIC to LHC?
- Discuss:
  - Theory, p+Pb, Pb+Pb constraints on nuclear modifications on hard scattering rates at high p_T.
    - ⇒Single hadron, jet and heavy flavor suppression
  - Jet quenching probes insensitive to PDFs/rates
  - Tomographic measurements

Constraints on initial-state effects

Initial-state effects (not saturation)

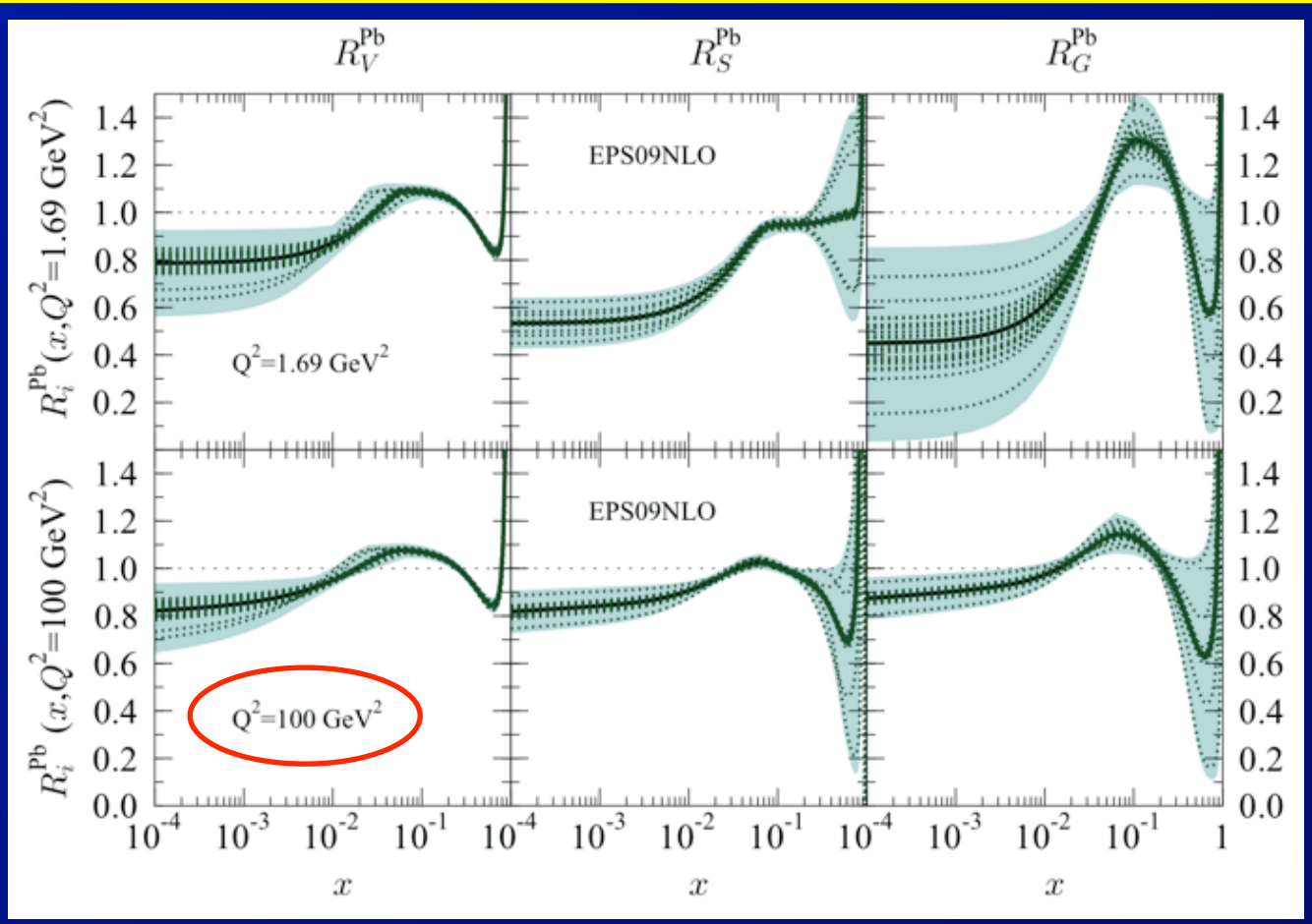

- For $Q^2 = 100\ GeV^2 \Rightarrow$ jet $p_T \sim 10$ GeV
  - Expect modest low x effects (b dependence?) for high-p_T processes

    $\Rightarrow$ p+Pb measurements will provide stringent test

p+Pb inclusive spectra

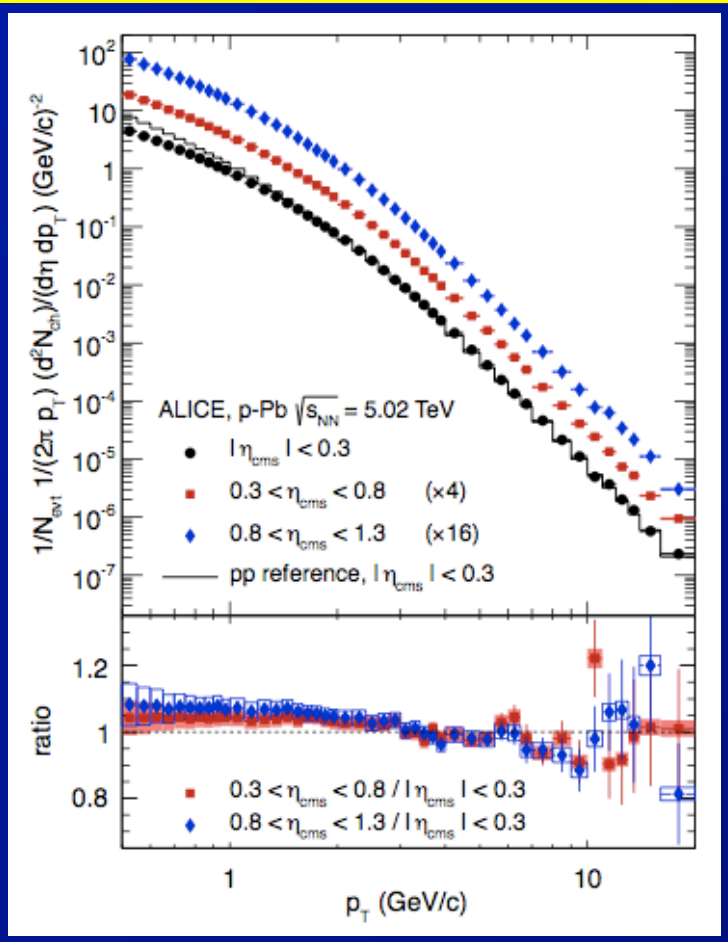

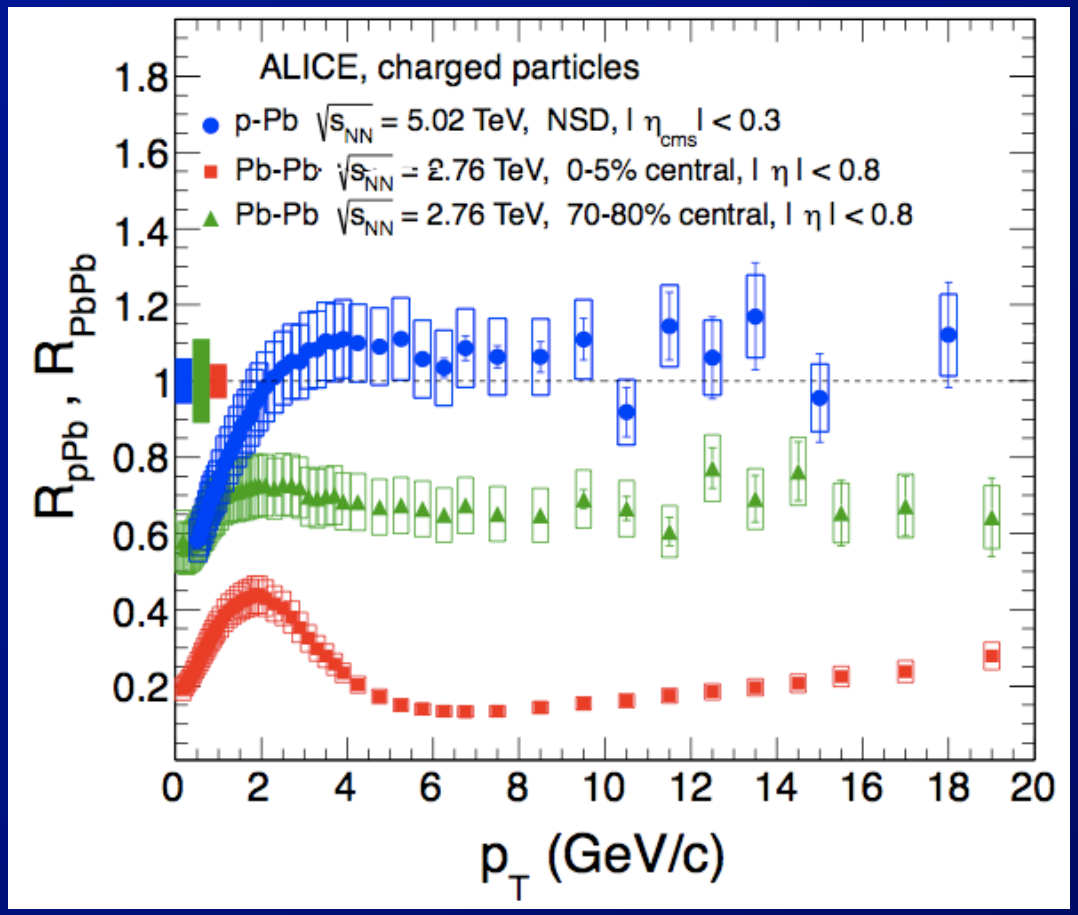

- 1st look at charged particle spectra
  - arXiv:1210.4520, ALICE inclusive, NSD
    - ⇒ R_{pPb} consistent with 1, no suppression at mid-rapidity, also little or no "Cronin"

Pb+Pb: Prompt photon production

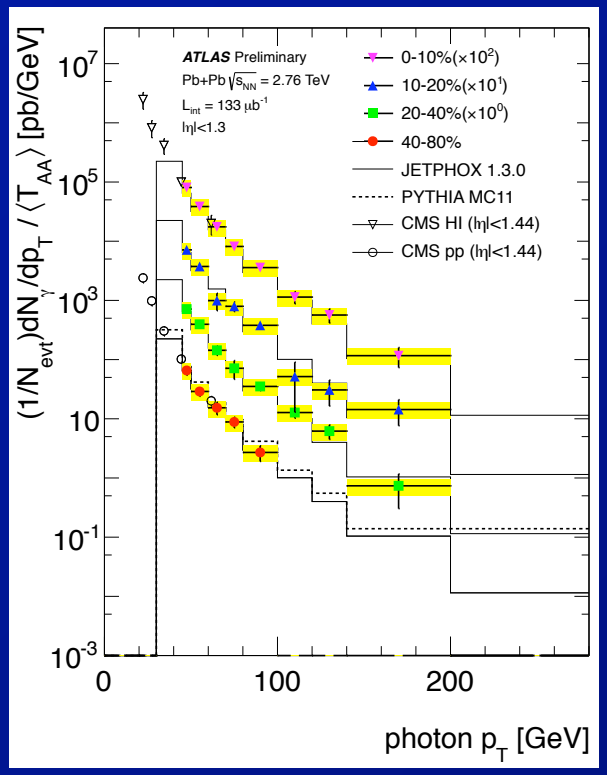

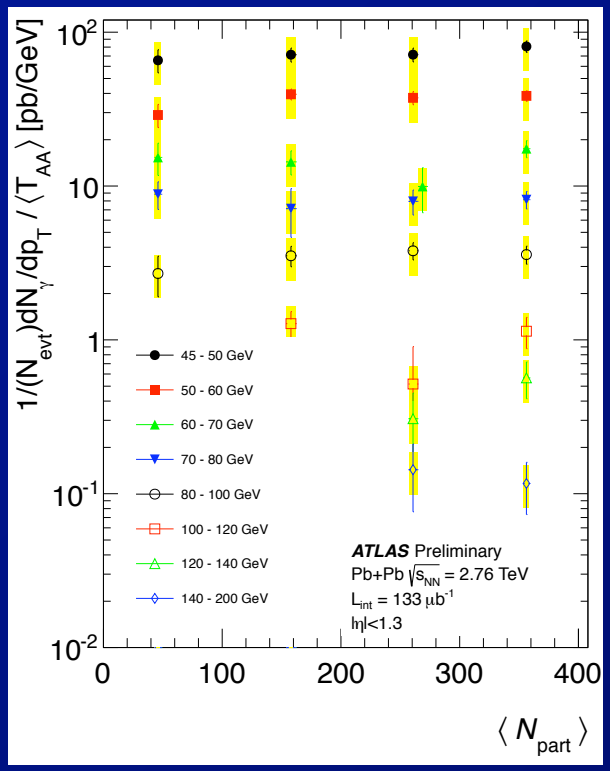

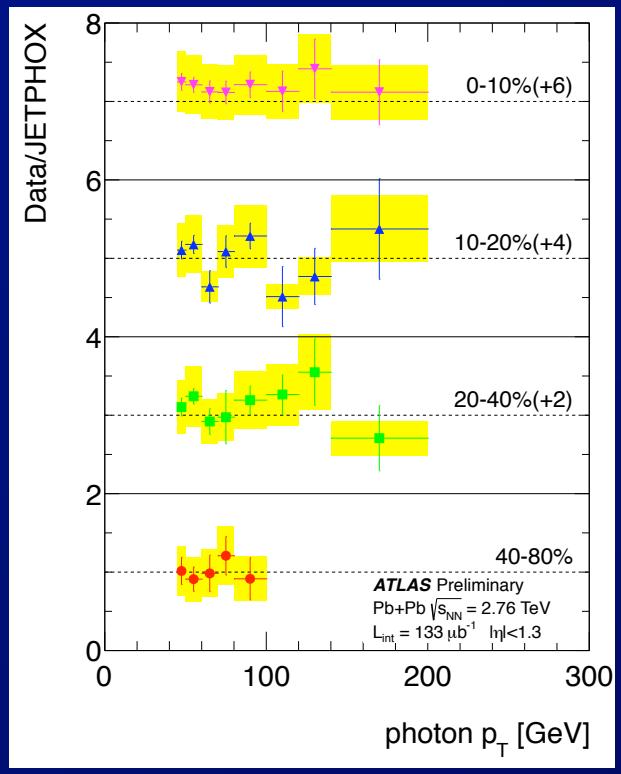

- **Photon spectra over 40 < p_T < 200 GeV**
  - well described by JETPHOX multiplied by T_{AA}
  - Yield / T_{AA} ~ independent of centrality

⇒ Hard QCD photon production varies with Pb+Pb centrality as expected

Pb+Pb: Z production

$Z \to e^+e^-$ event display

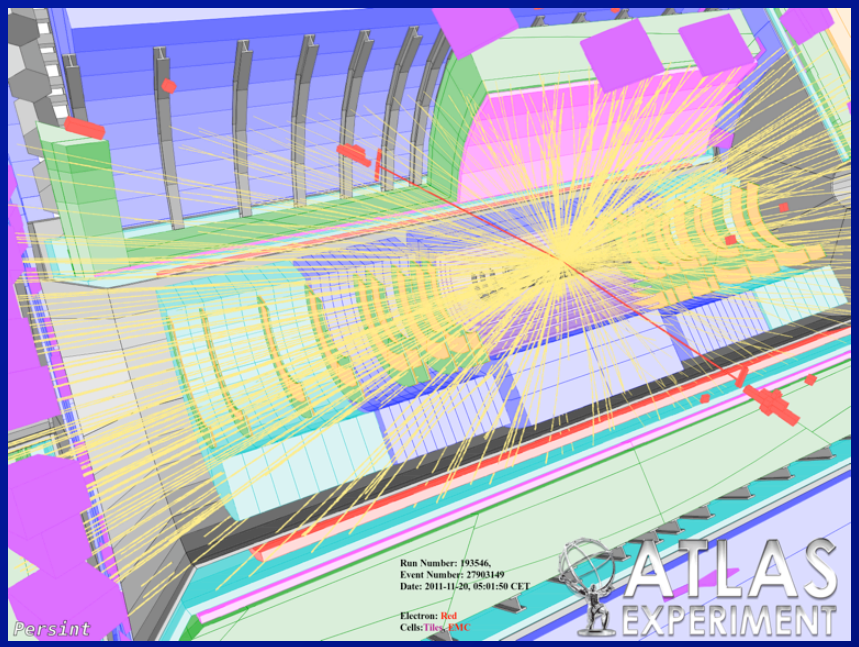

$Z \to \mu^+\mu^-$ event display

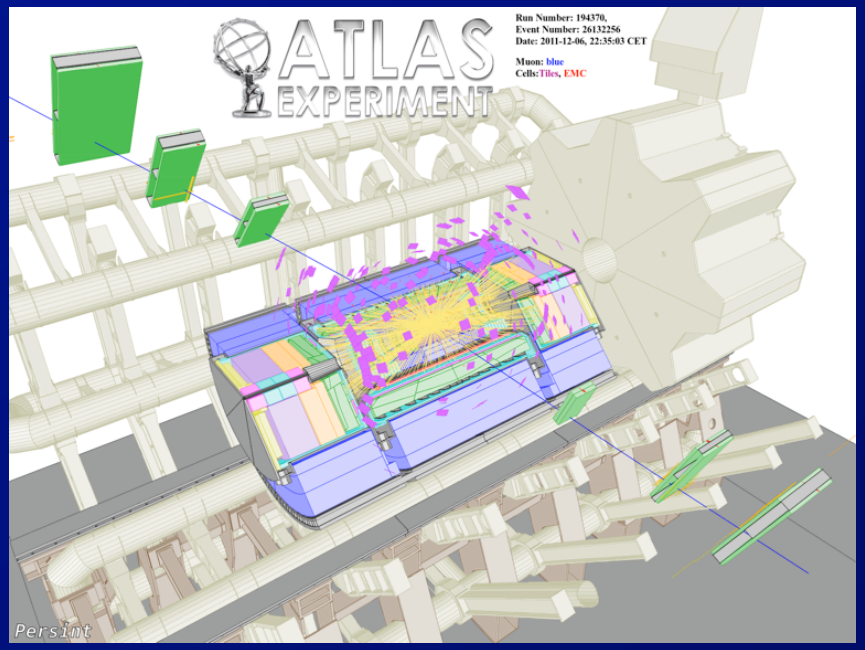

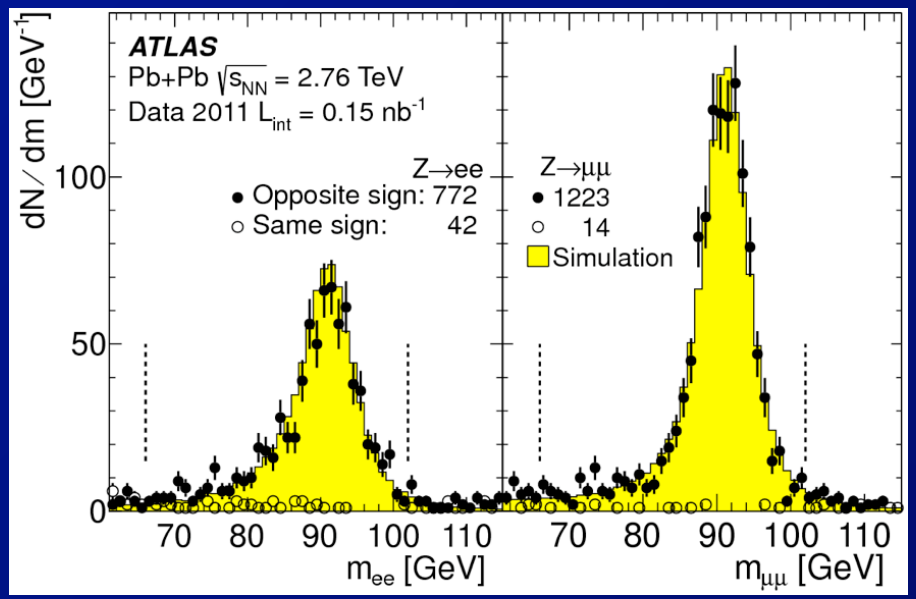

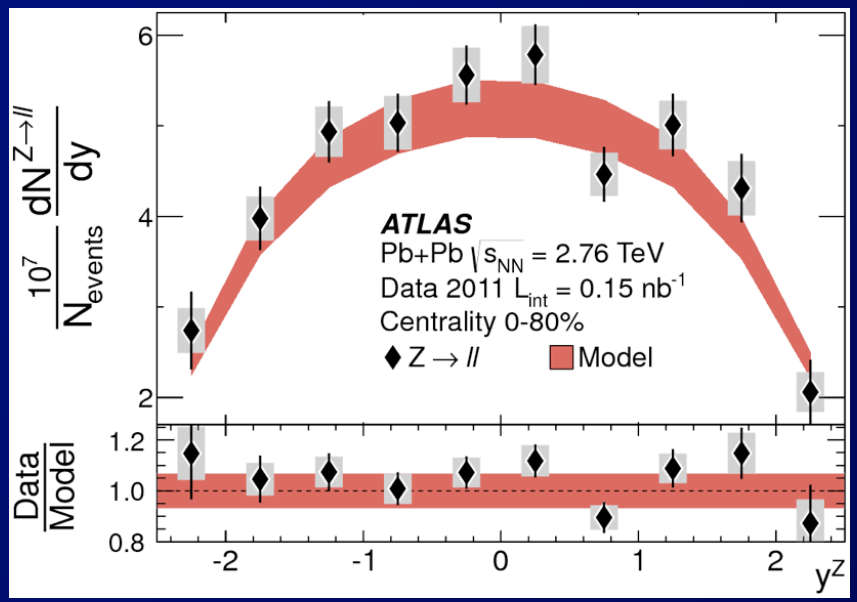

Pb+Pb: Z production (2)

Phys. Rev. Lett. 110, 022301 (2013)

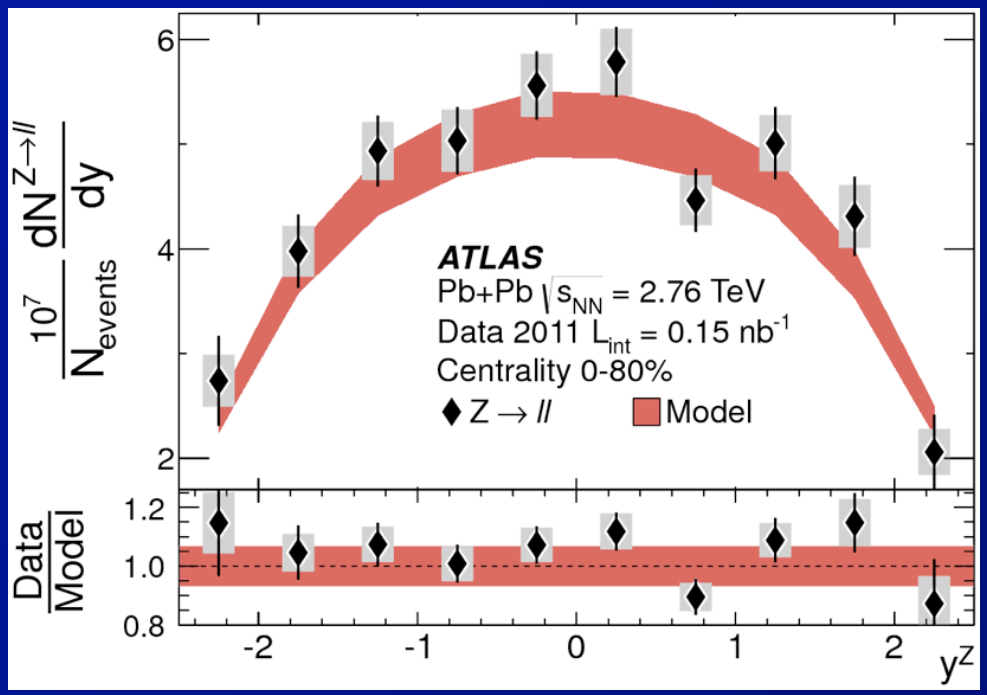

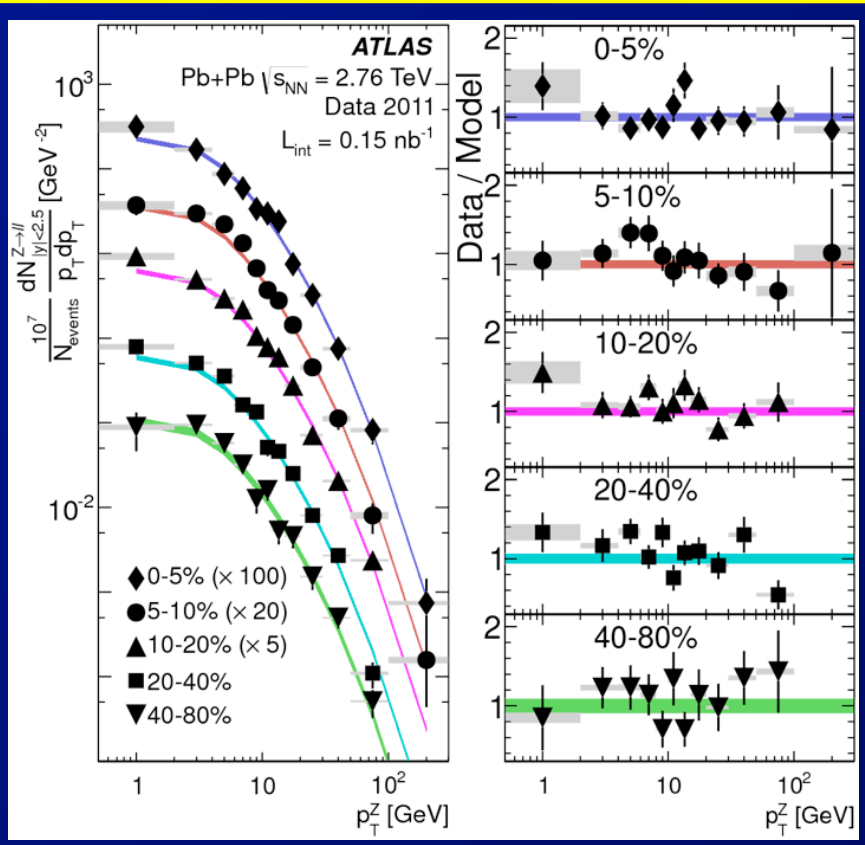

- Compare Pb+Pb Z rapidity distributions (minimum-bias) and pT spectra to PYTHIA scaled to NNLO calculations
  - No nuclear PDFs
    - ⇒ Nuclear PDF effects <~ 20%

Pb+Pb: Z production (3)

Phys. Rev. Lett. 110, 022301 (2013)

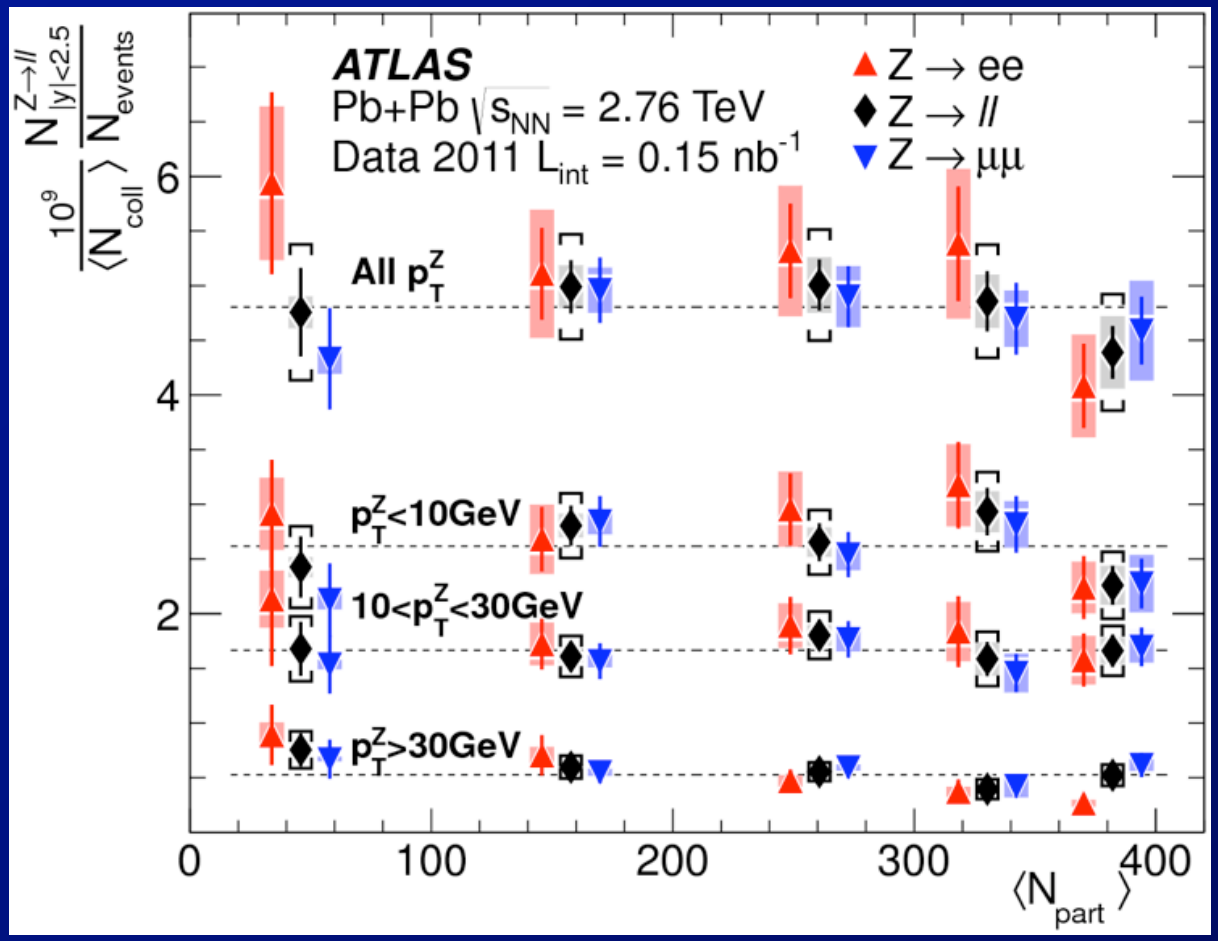

- Check Ncoll scaling of Z yield in different p_T intervals
  - Slight drop in central yield/Ncoll for p_T < 10 GeV
    - ⇒But not significant given errors. Expected?

Pb+Pb: Z production (4)

Guzey et al, Eur. Phys. J. A49 (2013) 35

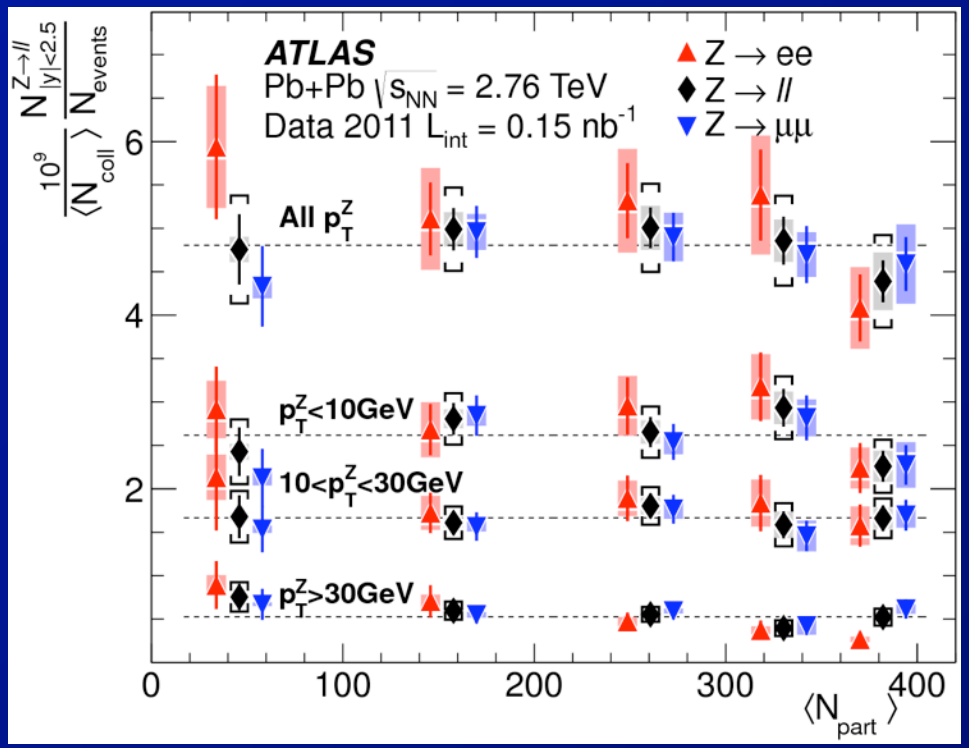

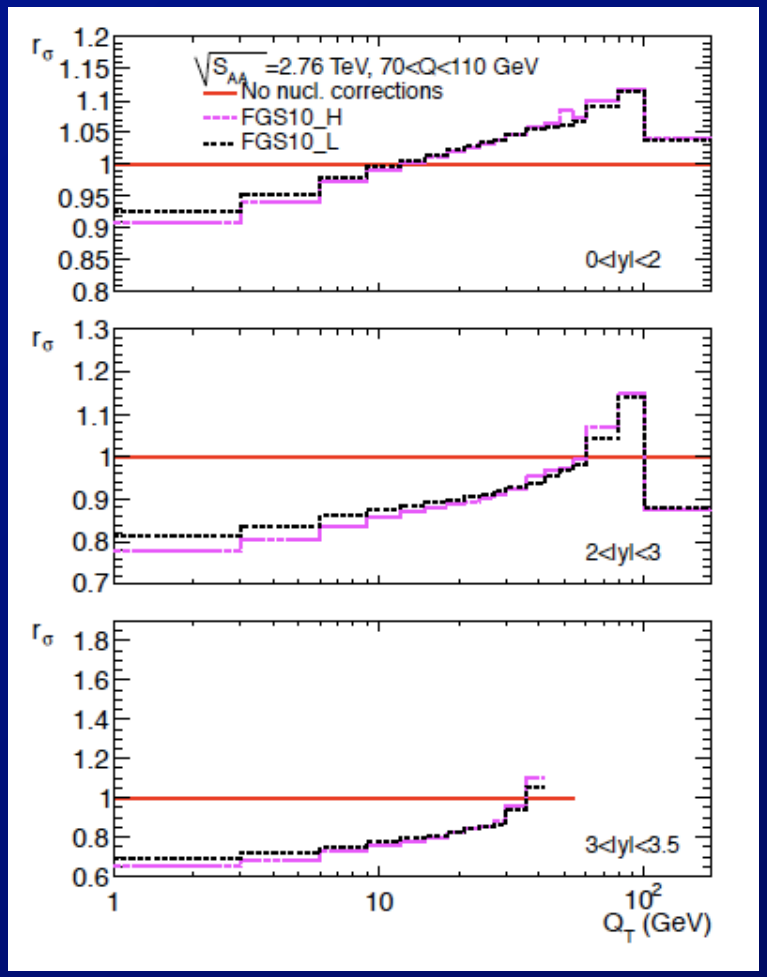

- Predictions of ~ 10% nuclear modifications in Pb+Pb at both low Q_T and high Q_T
  - ⇒Measurements not precise enough to test yet
  - ⇒But maybe with 2013 2.76 TeV p-p data

Single hadron, heavy flavor (muon), jet suppression

Charged particle R_{cp}

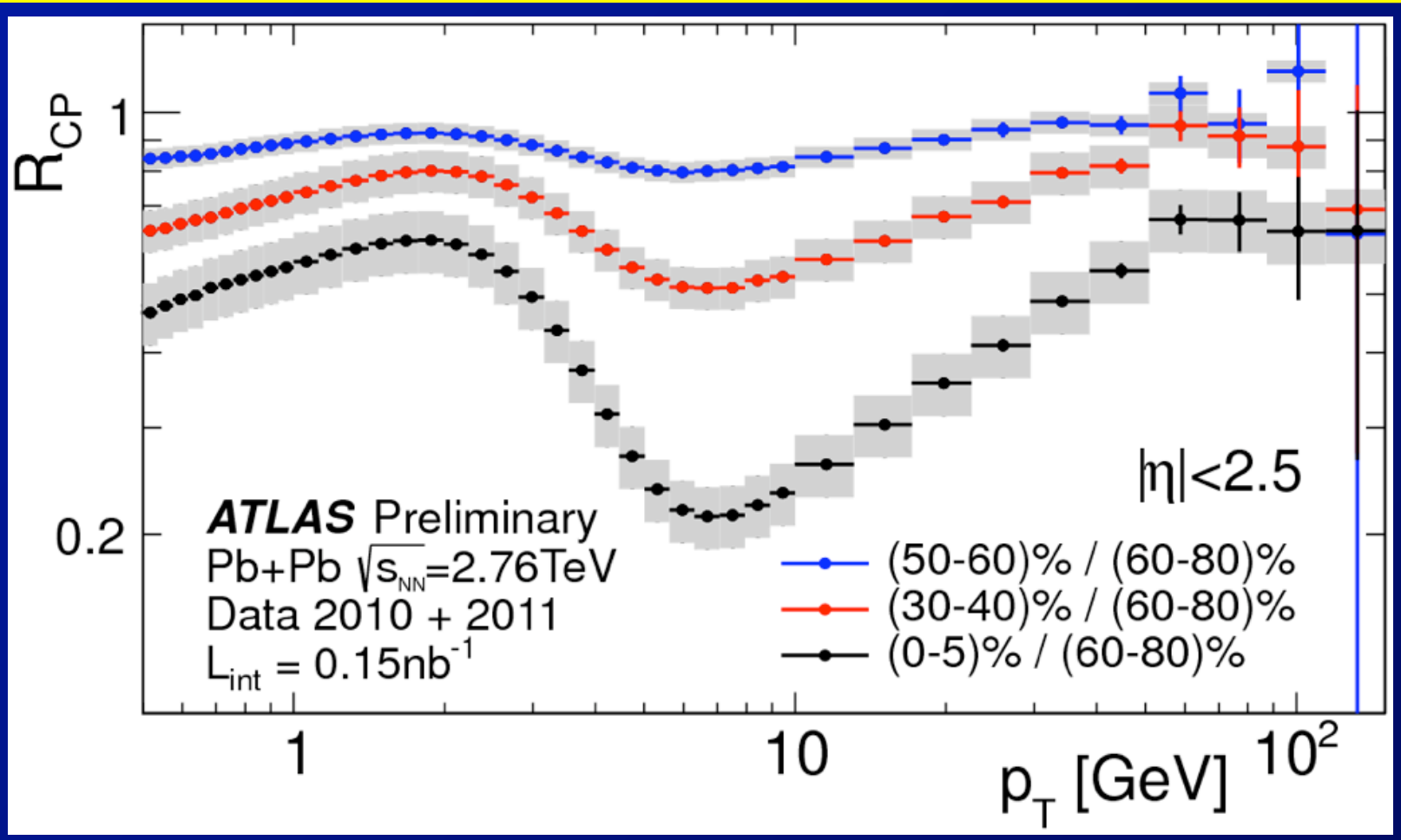

- **Similar to ALICE, CMS results**
  - **R_{cp} ~ 0.6 for p_T > 60 GeV**

    ⇒ (change in) slope for pT > 50 GeV important

Single muons from heavy quark decays

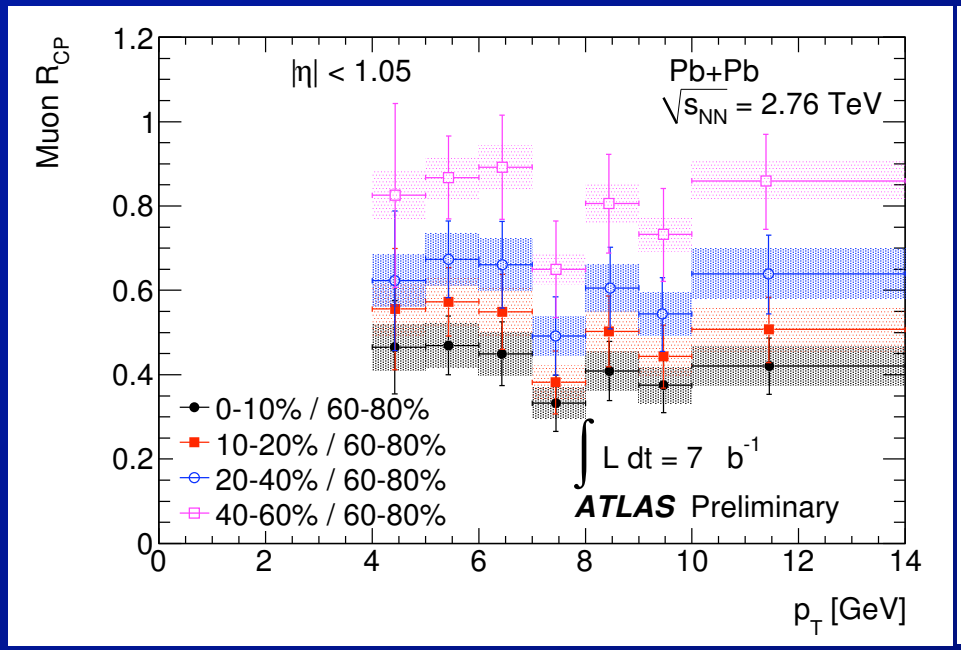

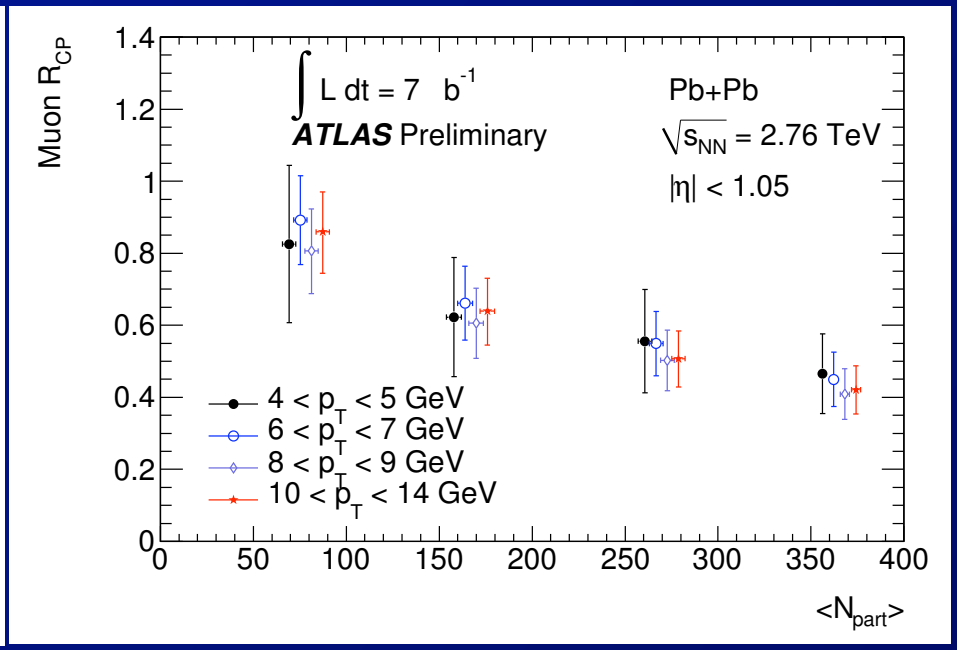

- In measured p_T range, muons primarily from charm and bottom decays.
  - J/ψ contribution ~ 1%
- Evaluate R_{cp} using 60-80% peripheral reference
  - ⇒ Factor of 2.5 suppression in 0-10% relative to 60-80%
  - ⇒ Independent of muon p_T within errors
  - ⇒ Evolution with N_{part} consistent between p_T bins

Single muons, charged comparison

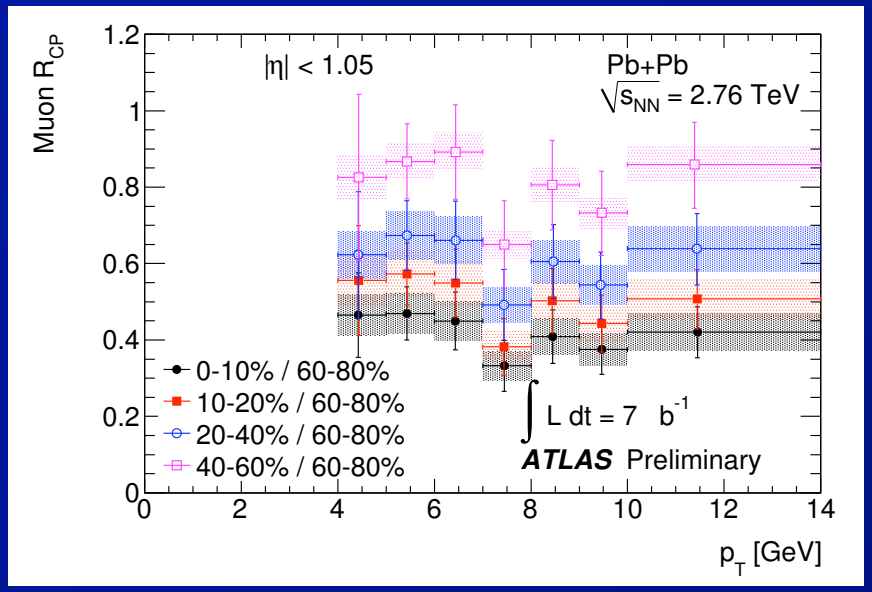

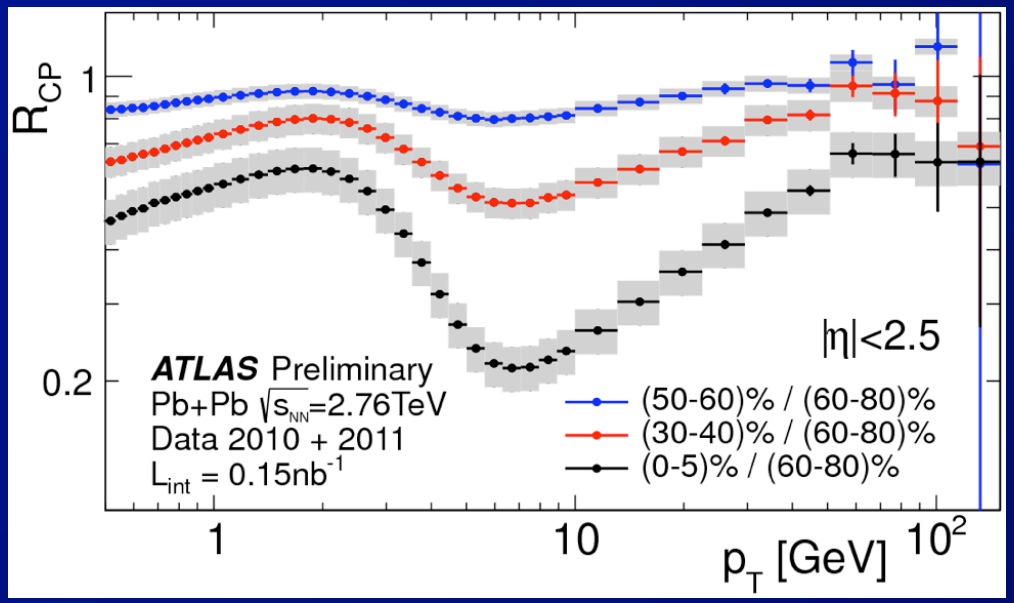

- See less suppression of heavy flavor decay muons than single hadrons @ lower p_T
  - But, both muon and hadron p_T poorly correlated with jet momentum.
    - ⇒ Single jets (below)
    - ⇒ b-tagged jets, especially at lower p_T (to come)

Pb+Pb Jet Spectra

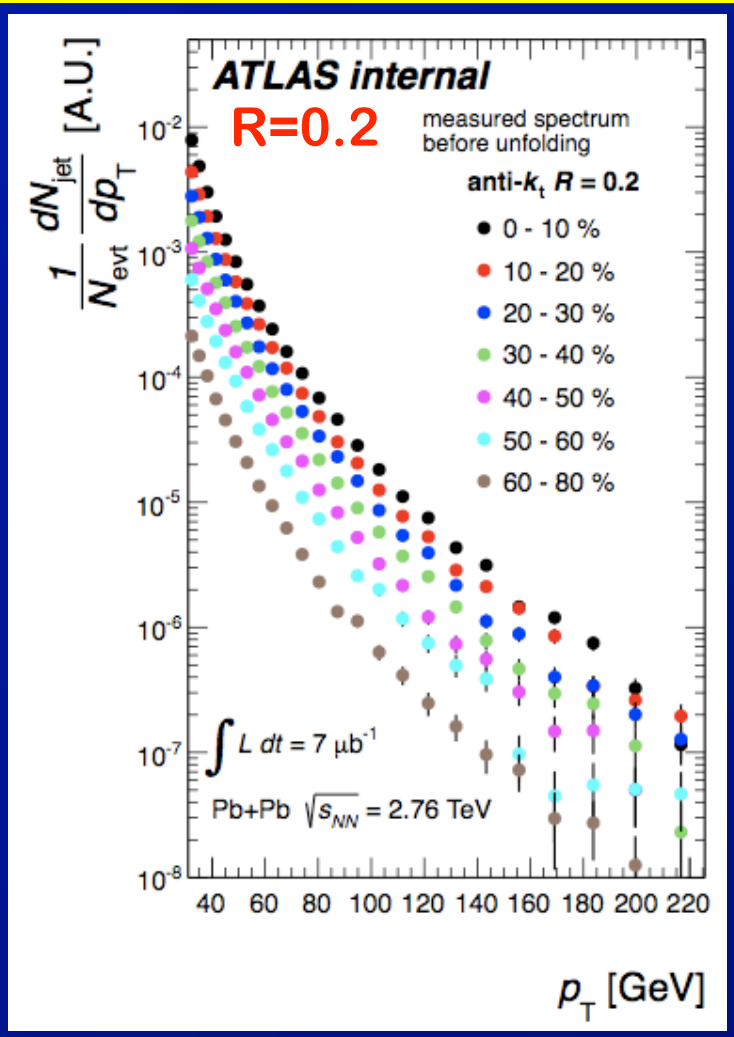

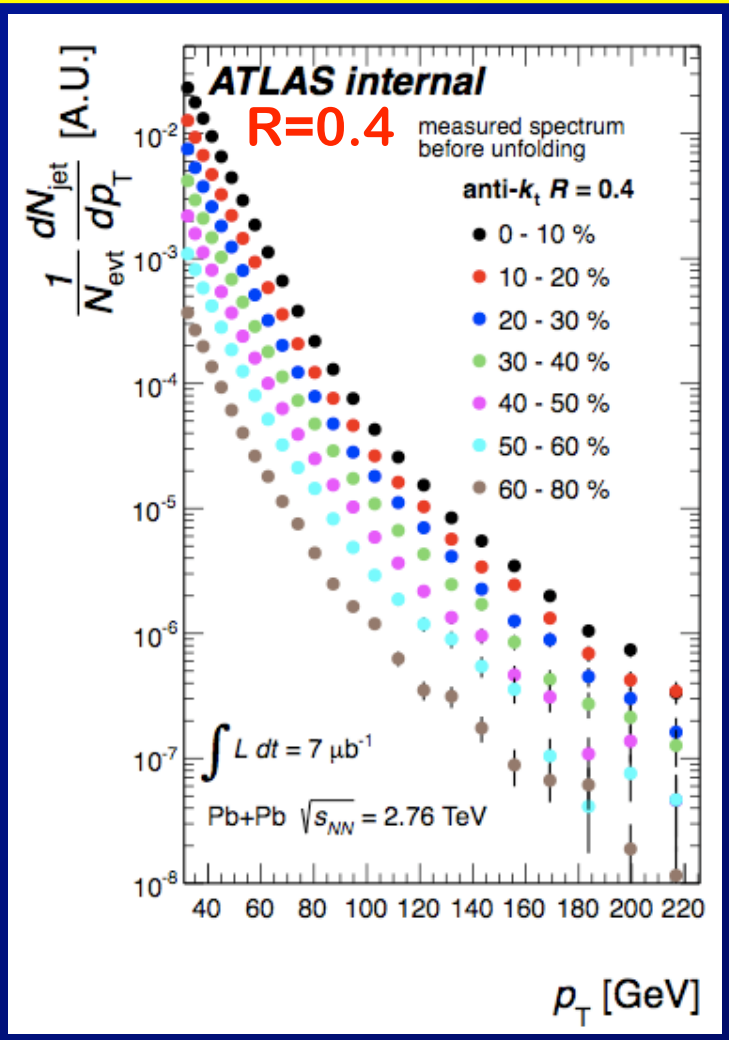

Unfolded (SVD) and efficiency corrected

- For these results, no absolute normalization
  - awaiting absolute jet energy scale uncertainty

⇒RSN

R = 0.4 Jet R_{cp}

Phys. Lett. B 719 (2013) 220-241

- Systematic errors
  - Black band: fully correlated systematics
    - ➡ all points move up/down together
    - ➡ JES, JER, efficiency, x_{ini}, R_{coll}
  - Red boxes: partially correlated systematics
    - ➡ unfolding
- Error bars: square root of diagonal elements of covariance matrix
- No significance to horizontal width of error bars

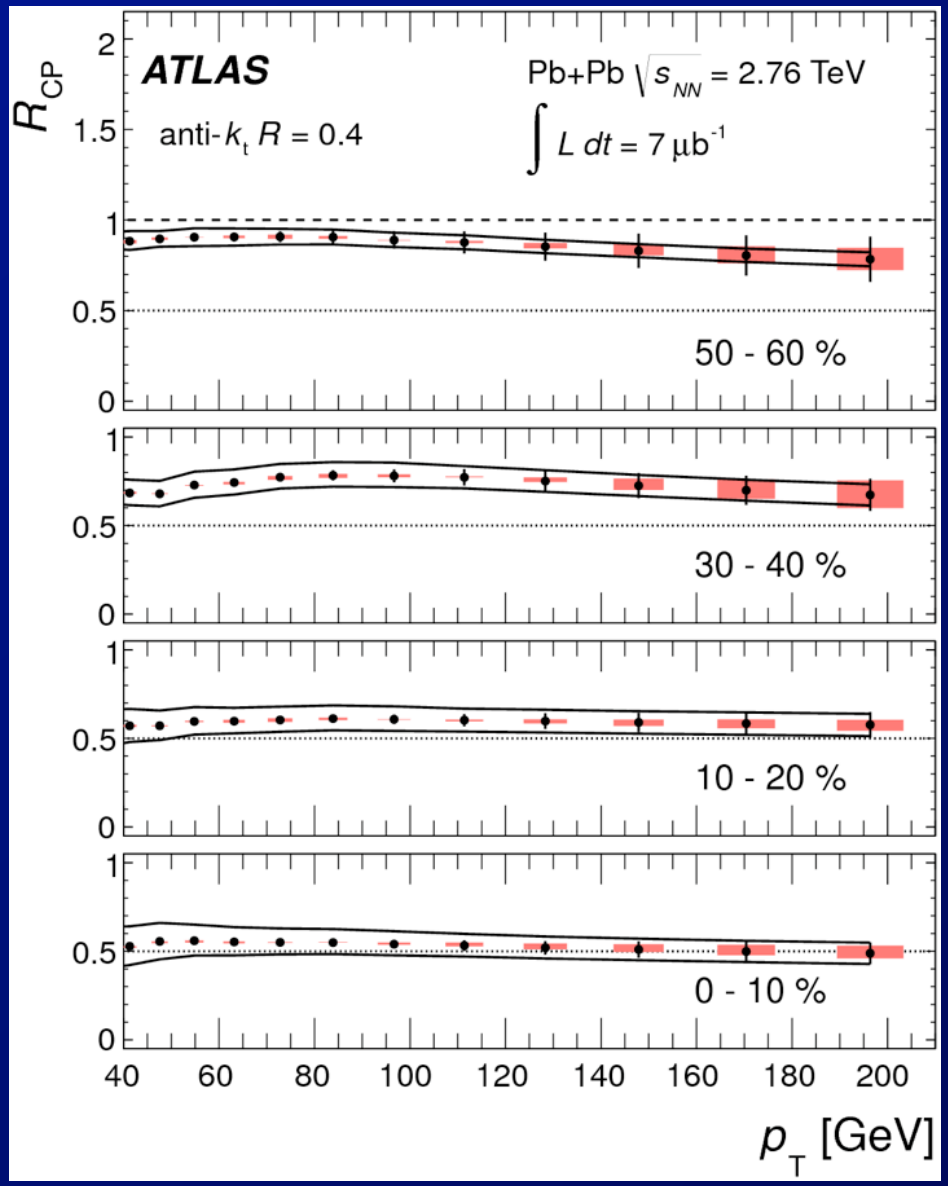

R = 0.4 Jet R_{cp} Uncertainties

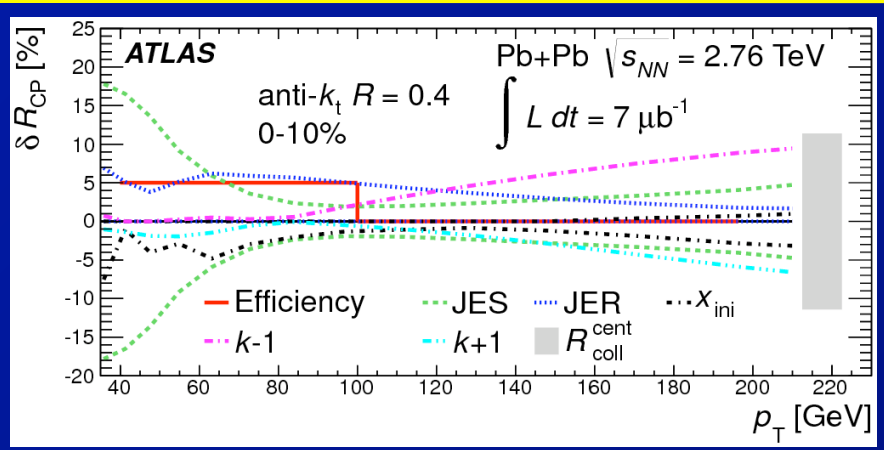

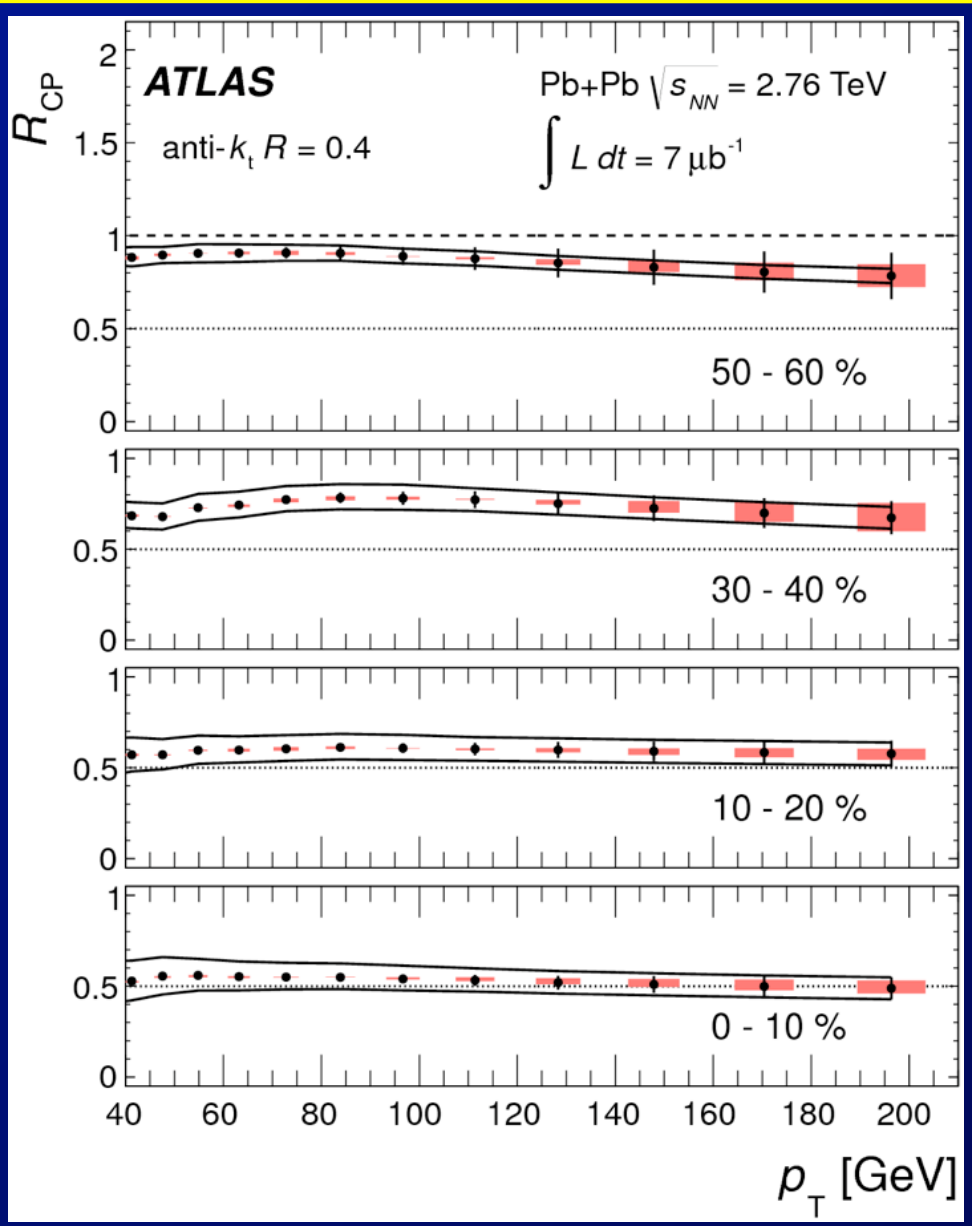

- All systematic uncertainties decrease w/ high-statistics 2011 data
  - Better control of unfolding
  - Better constraint on jet energy resolution, jet energy scale
    - ⇒MC, cross-checks

Jet yields: centrality dependence

Phys. Lett. B 719 (2013) 220-241

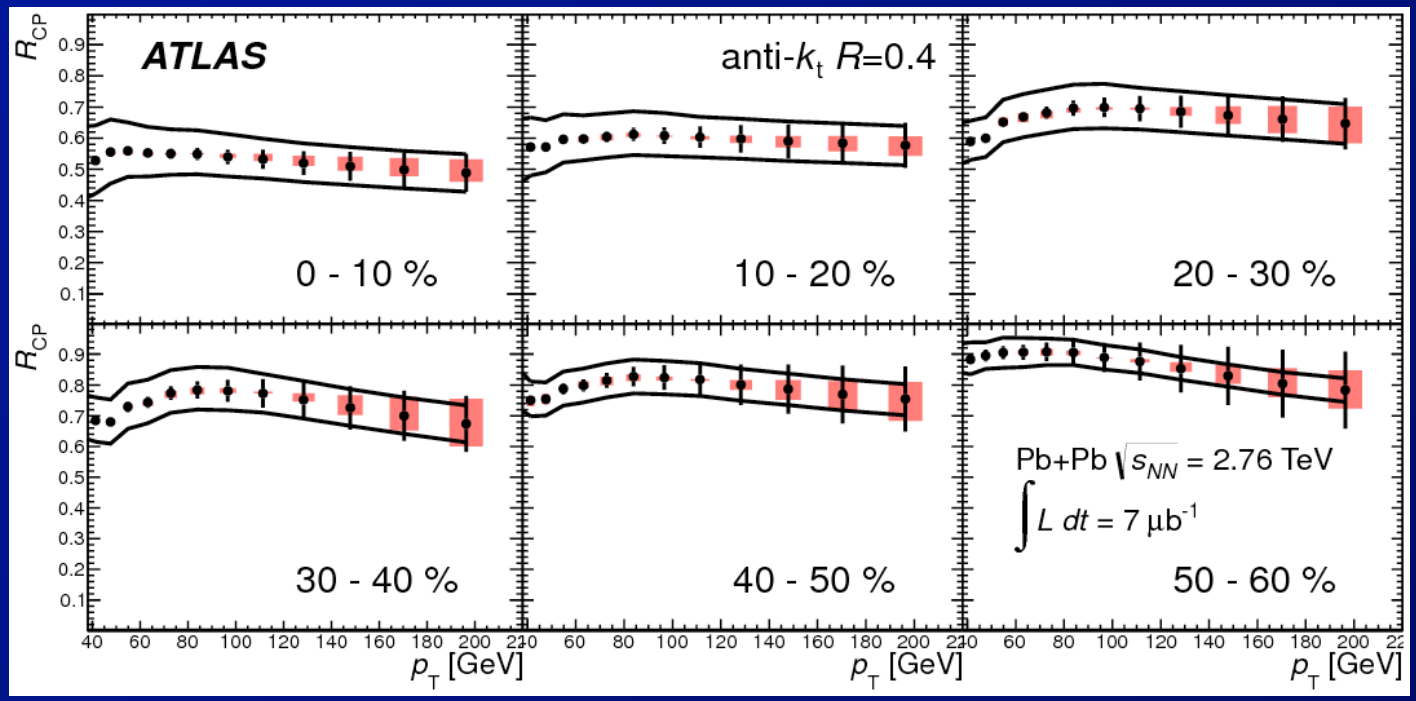

- **Consider systematics:**
  - Based on previous slides, γ, Z measurements constrain initial conditions to <~ 20%
    - ⇒ Will be reduced by p-Pb measurements
  - ~ 15% systematic uncertainties in R_{cp}
    - ⇒ Reduced in 2011 data, in R_{AA}

Jet radius dependence of R_{cp}

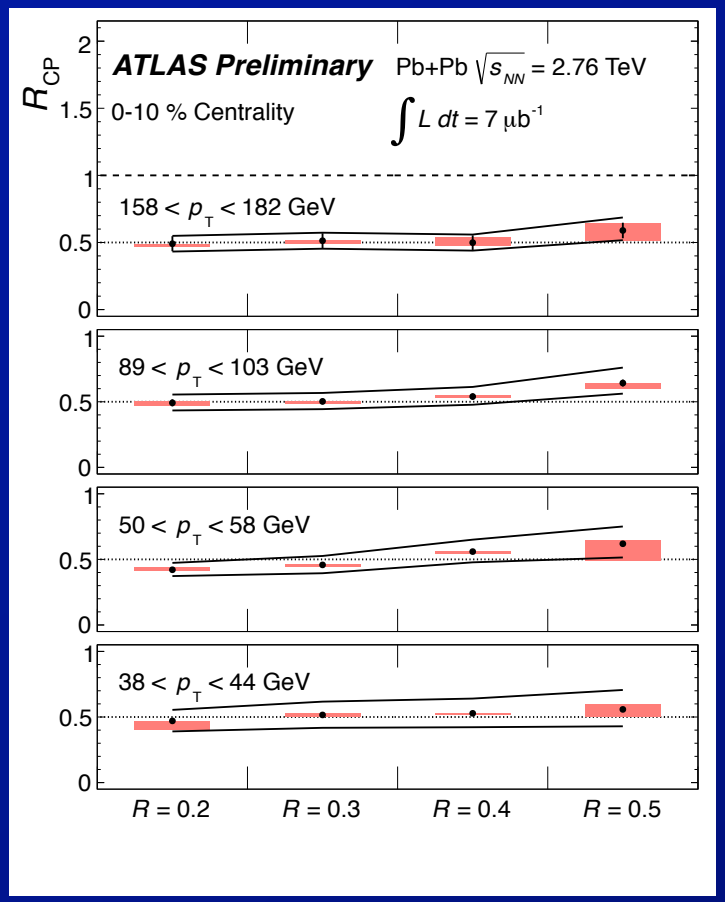

Significant cancellation of correlated errors

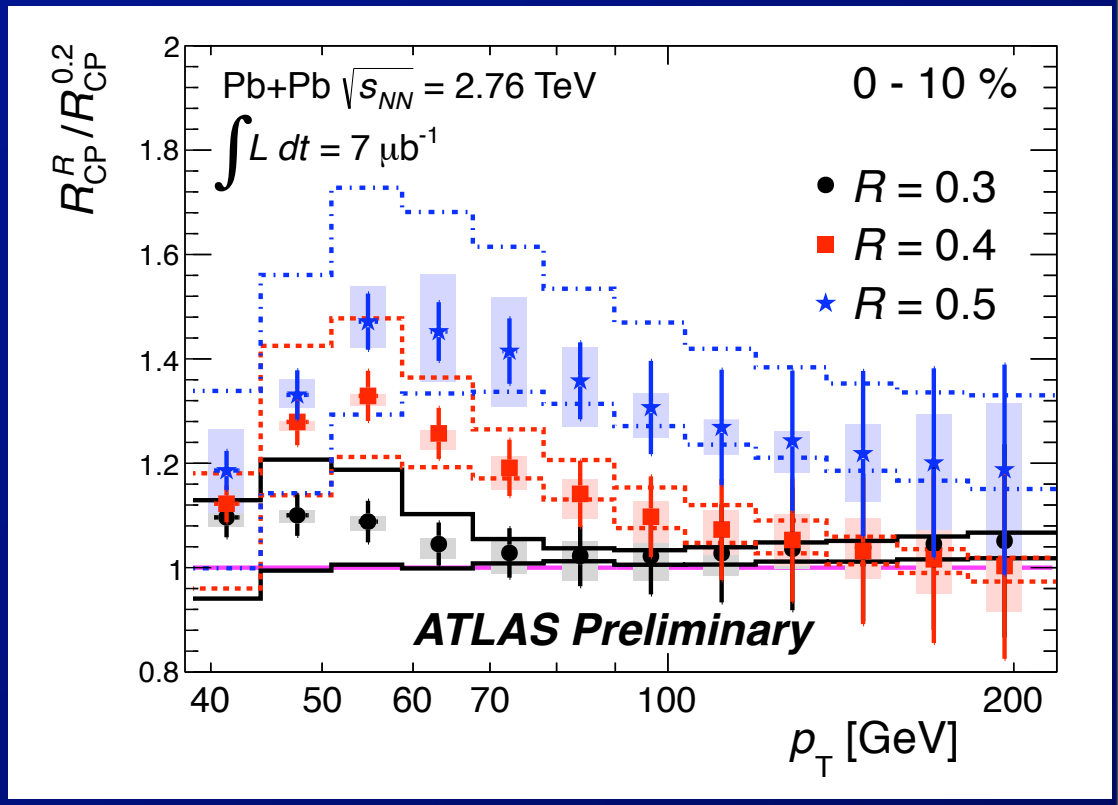

- Evaluate jet radius dependence of R_{cp}
  - Modest but significant variation of R_{cp}
  - Less suppression for larger R
    - ⇒An indication of jet broadening?

Probes insensitive to nuclear PDFs, hard-scattering rates

Inclusive jet fragmentation

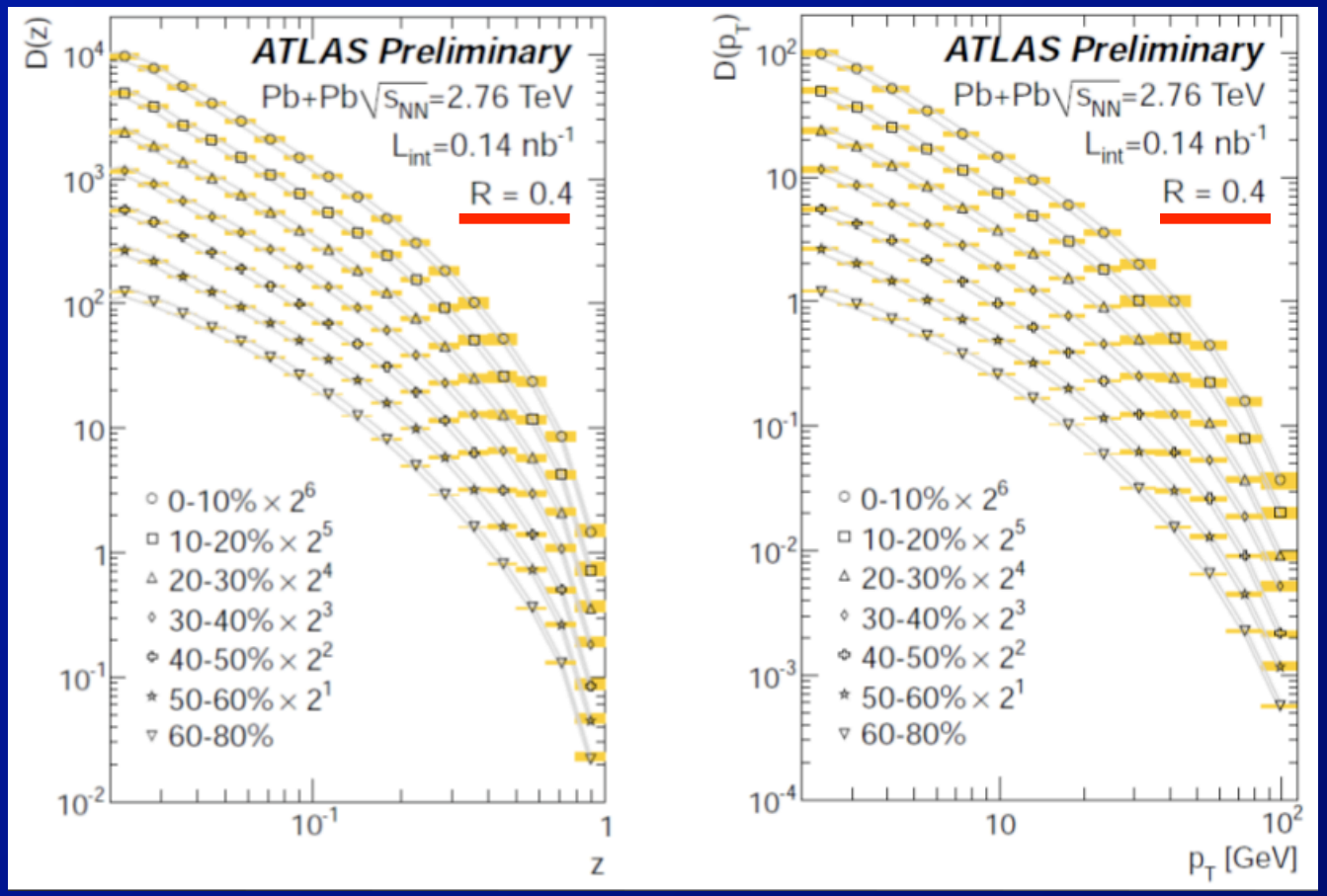

Unfolded for jet and charged particle resolution

$$D(z) = \frac{1}{N_{jet}} \frac{dN_{chg}}{dz}, z = \vec{p}_{chg} \cdot \vec{p}_{jet} / |\vec{p}_{jet}|$$

$$D(p_T) = \frac{1}{N_{jet}} \frac{dN_{chg}}{dp_T}$$

Inclusive jet fragmentation (2)

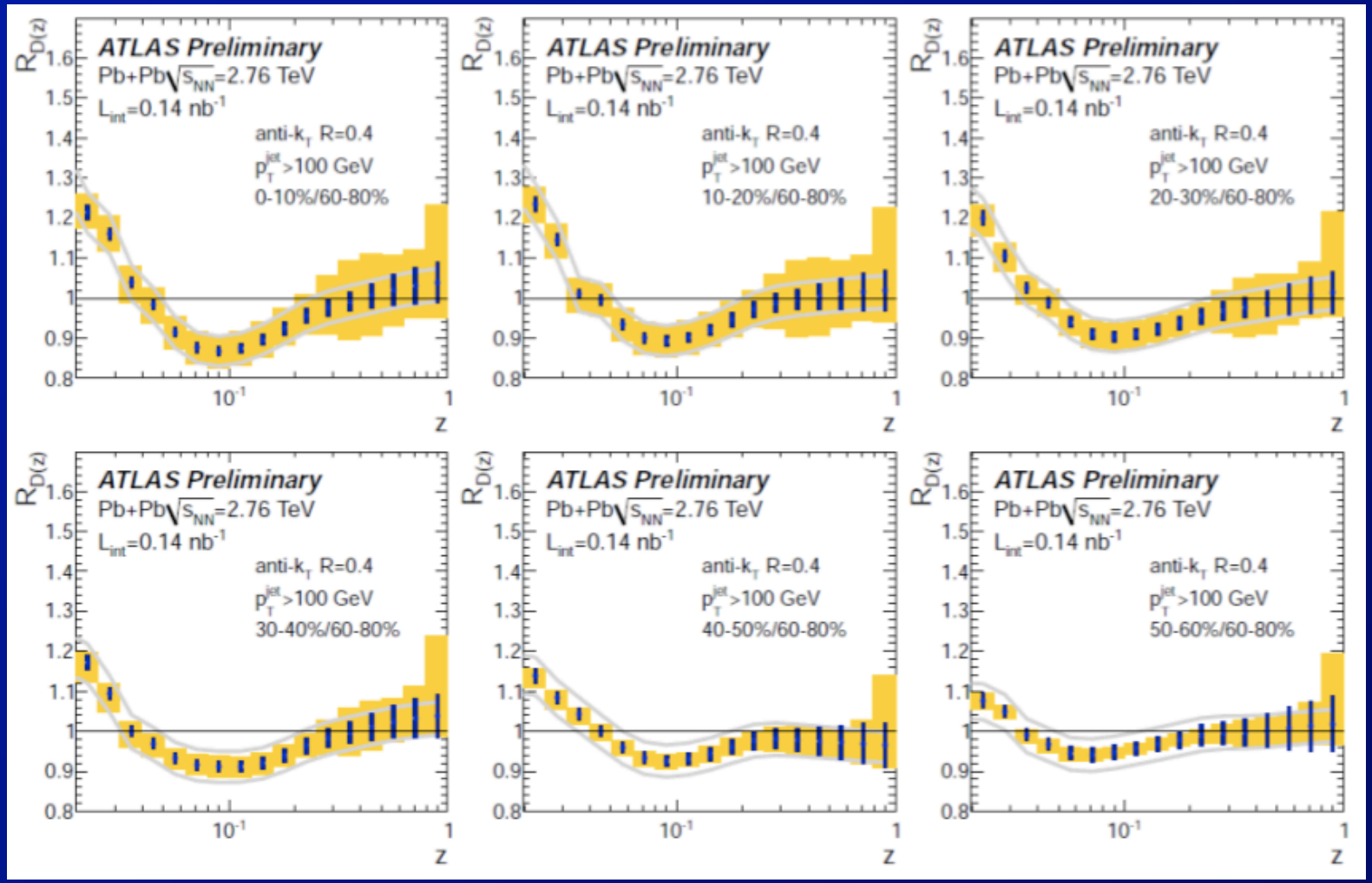

R = 0.4

- First observation of modified parton shower in inclusive jets

  ⇒Not only seeing "left over" unquenched jets.

Inclusive jet fragmentation (3)

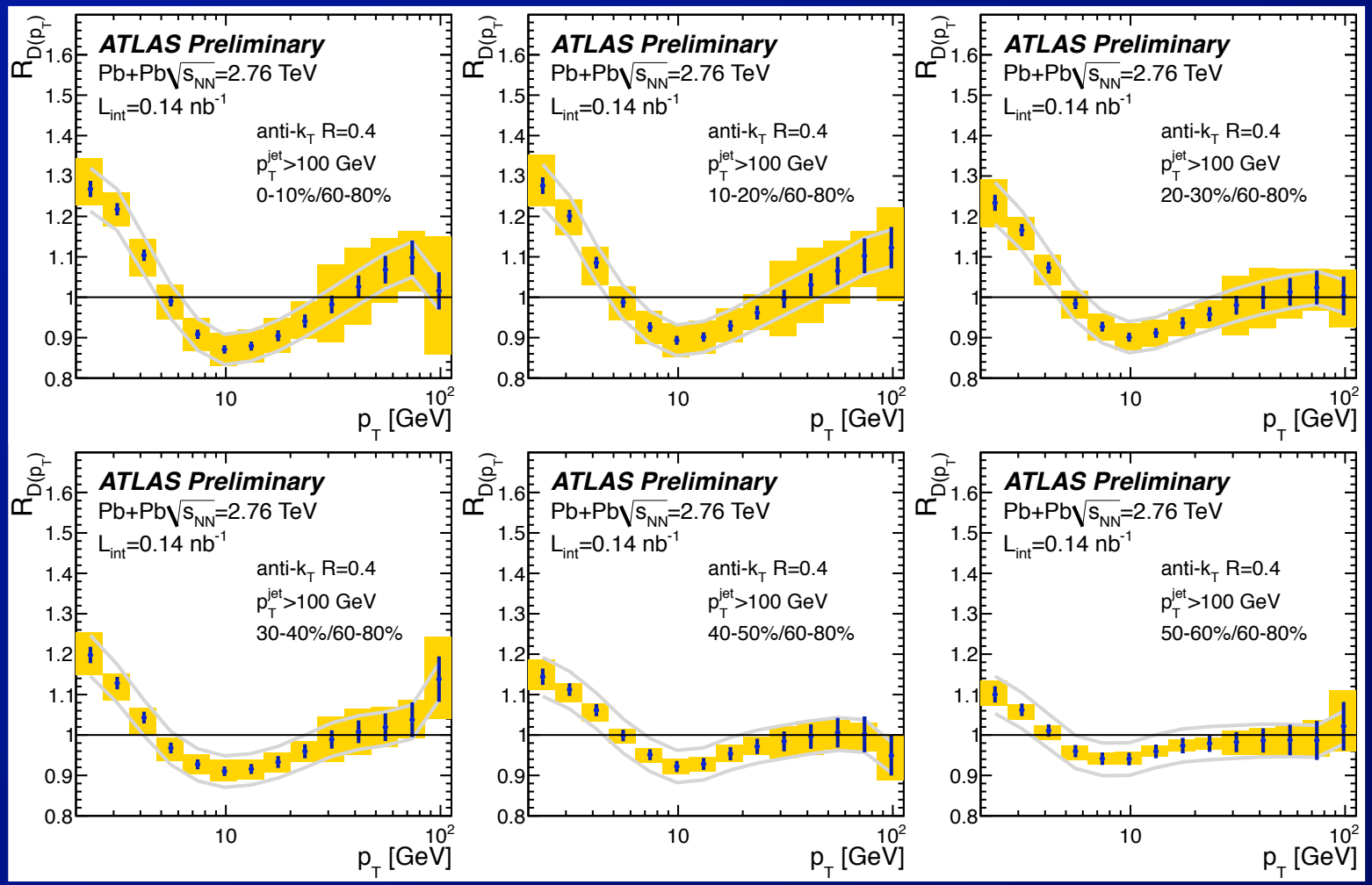

- Check that the modification is not due to the measurement of jet $p_T \Rightarrow D(p_T)$

  $\Rightarrow D(p_T)$ shows similar modifications

Jet fragmentation: R dependence

- Check that the modification is not due to underlying event fluctuations
  - Use different jet sizes: R = 0.2, 0.3
- Obtain the same results as R = 0.4

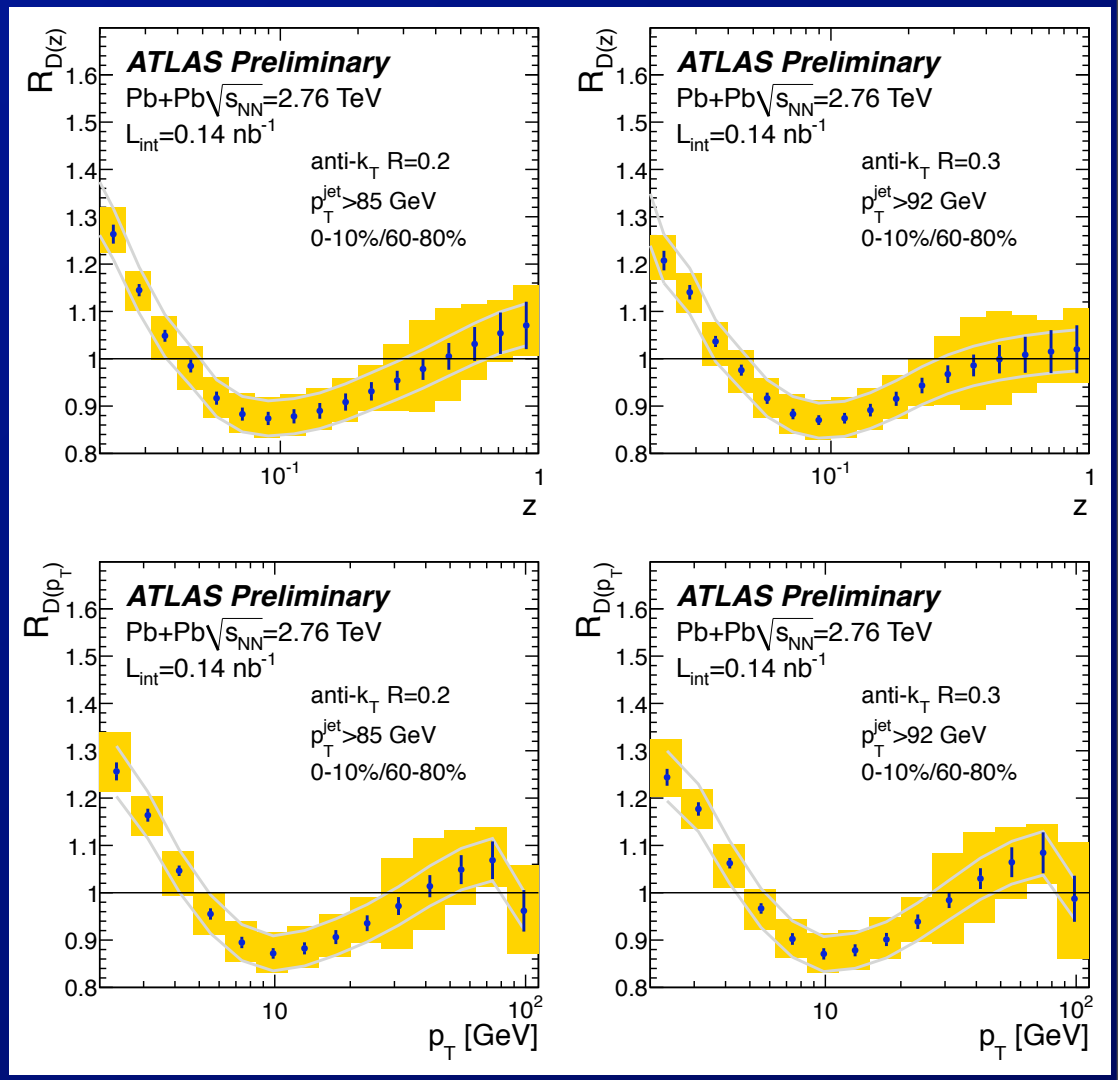

⇒Observed modifications are robust

Di-jet asymmetry & acoplanarity

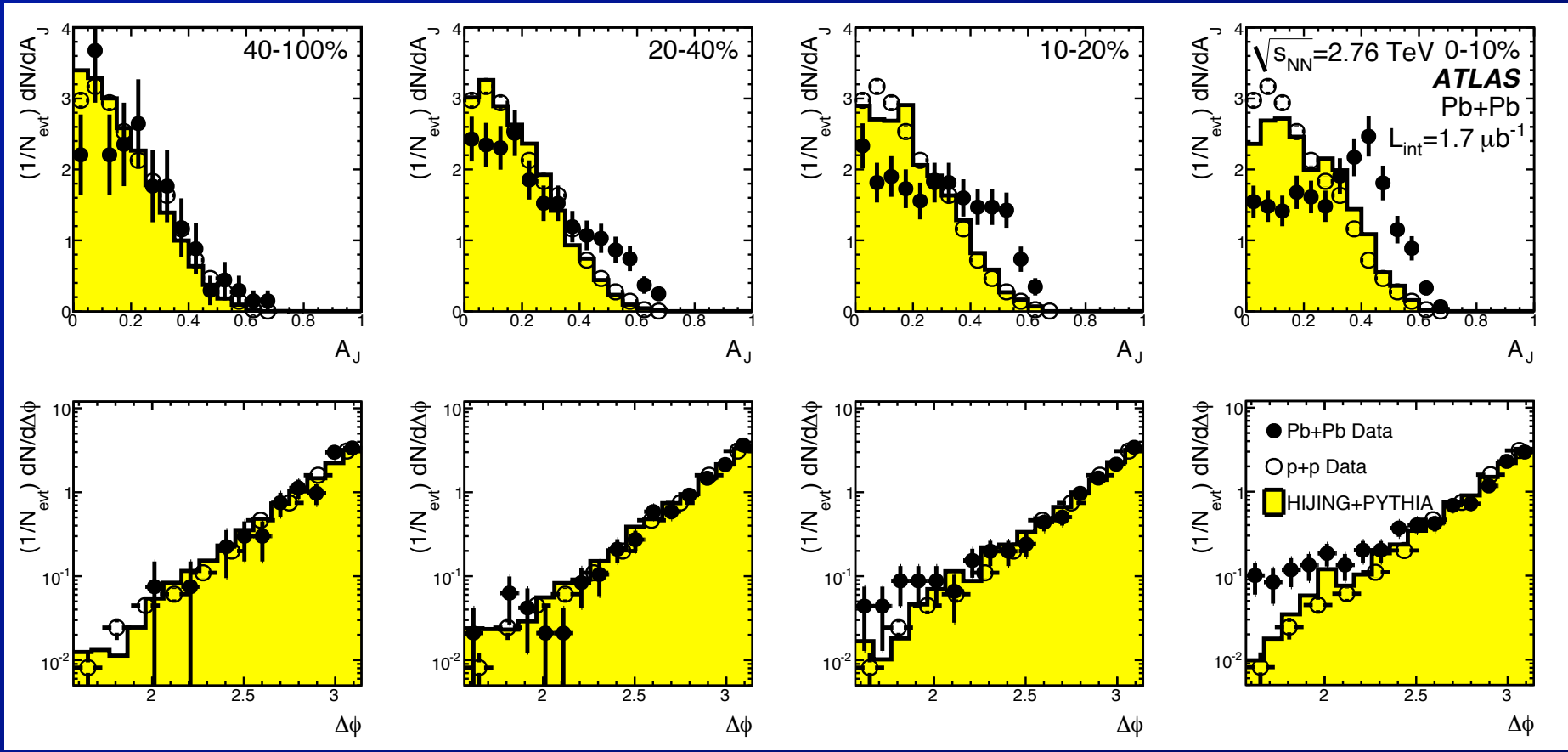

- For more central collisions, see:
  - Change in distribution of dijet asymmetry
  - While no change in the distribution of Δφ
    - ⇒Except for combinatoric pairs in central

Dijet acoplanarity, R = 0.2

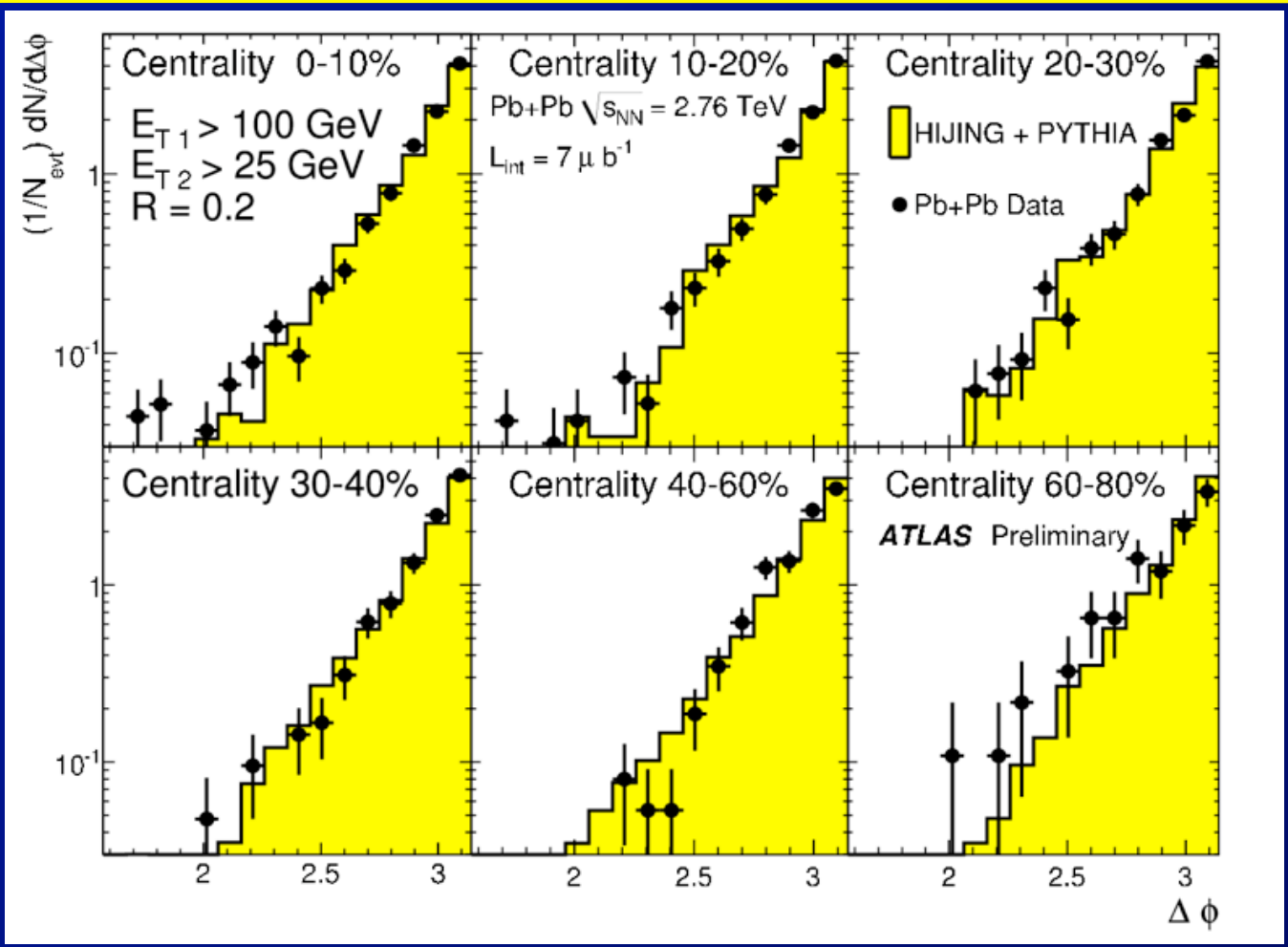

- Look at dijet acoplanarity w/ R = 0.2 jets
  - ⇒ small UE effects
  - ⇒ <NO> broadening

γ-jet angular distribution

Peripheral → central

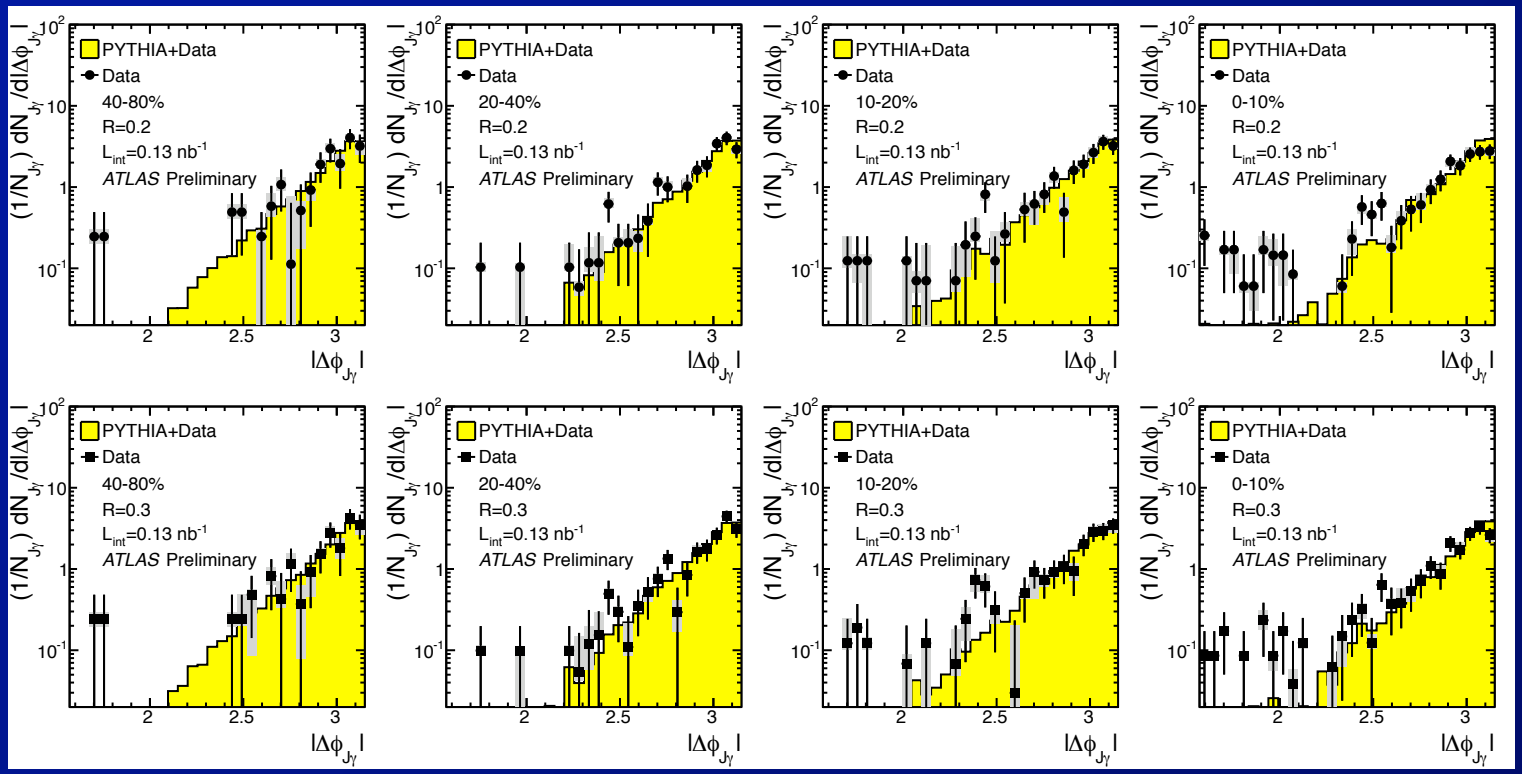

R = 0.2

R = 0.3

- Take leading jet in hemisphere opposite photons with 60 < p_T < 90 GeV
  - Jets with p_T > 25 GeV, R = 0.2 and 0.3
    - ⇒Distribution of Δϕ peaked at π
    - ⇒For following, apply cut $|\Delta\phi - \pi| < 7\pi/8$

γ-jet momentum balance

Peripheral → central

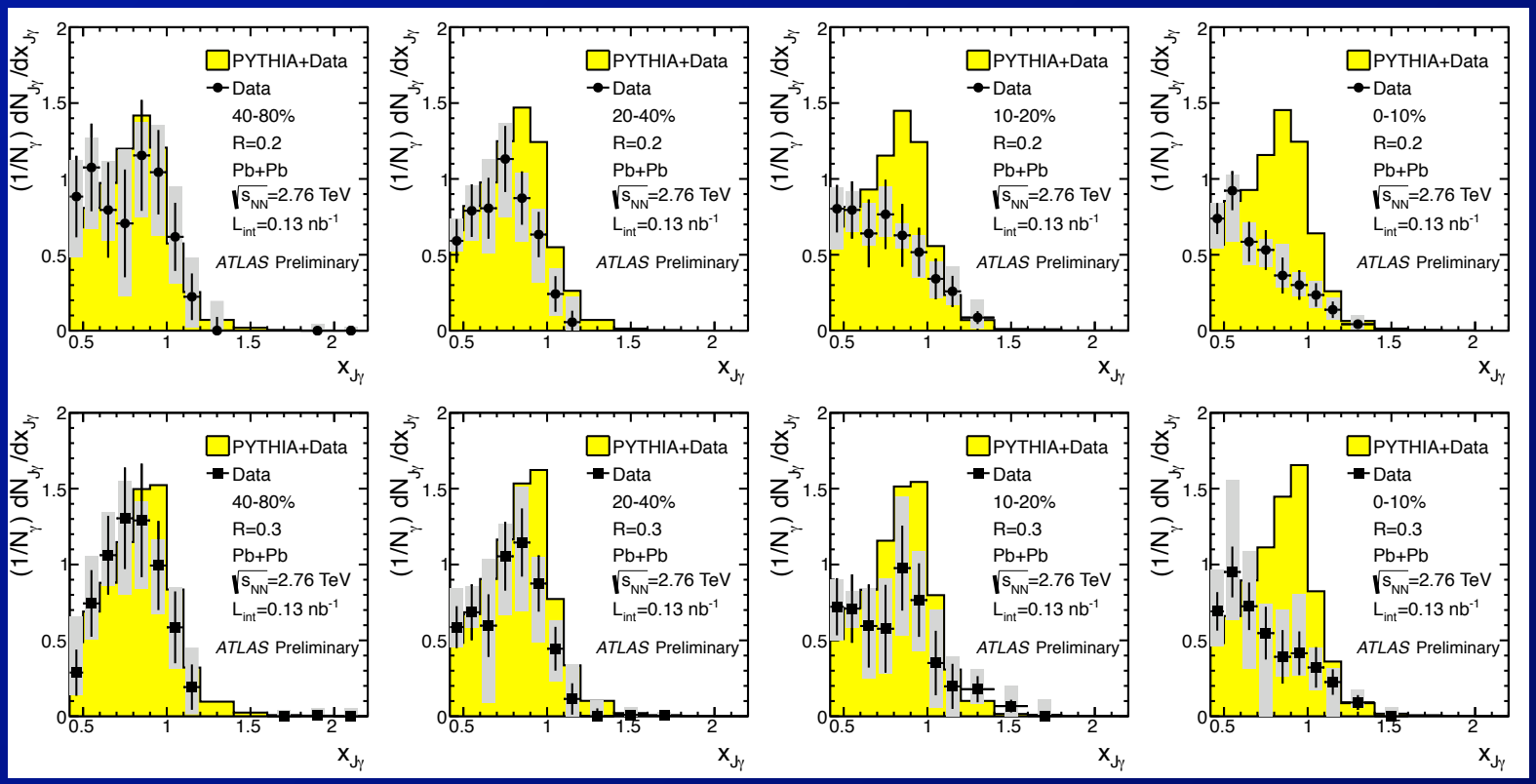

R = 0.2

R = 0.3

- Plot distribution of $x_J = p_T^{\mathrm{jet}} / p_T^{\gamma}$
  - photon background pairs subtracted
  - unfolded for jet energy resolution

    ⇒Substantial change in γ-jet balance

Pb+Pb Z-jet measurement

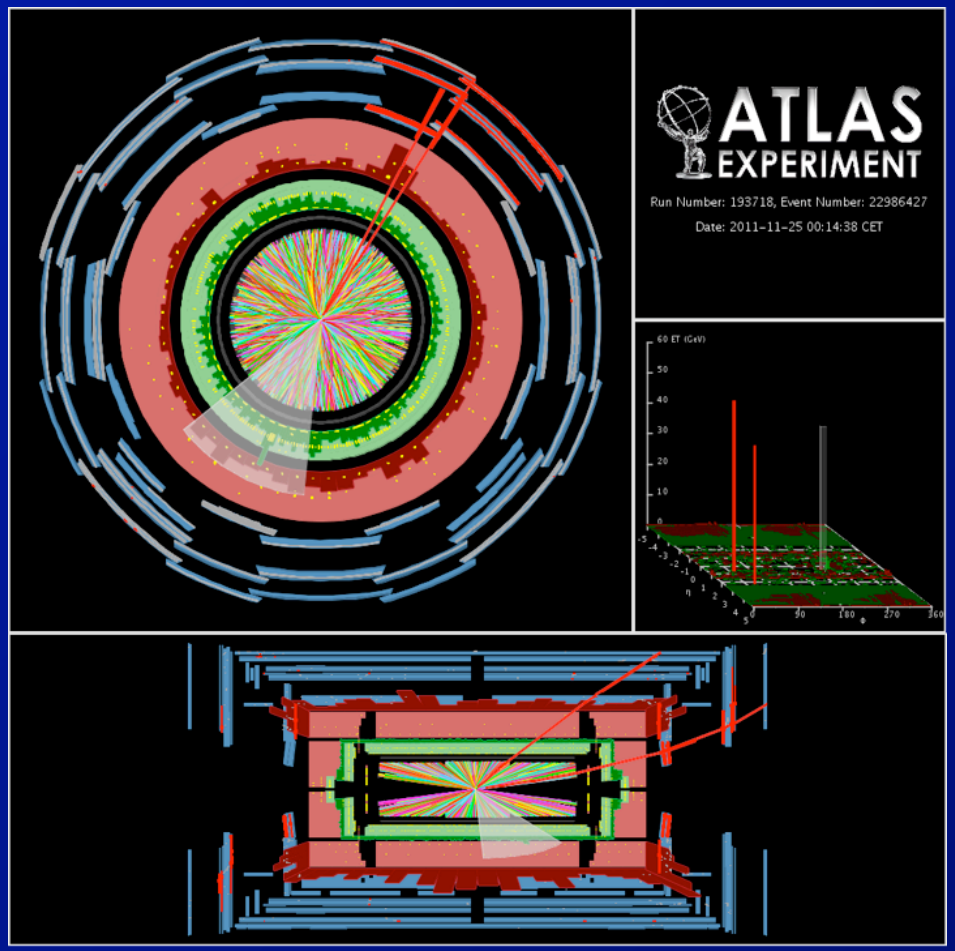

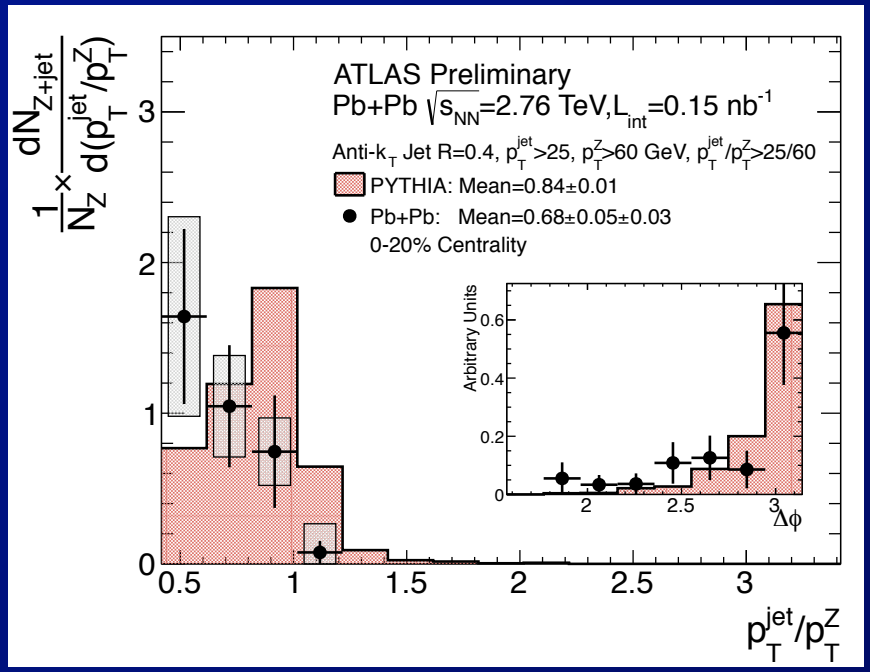

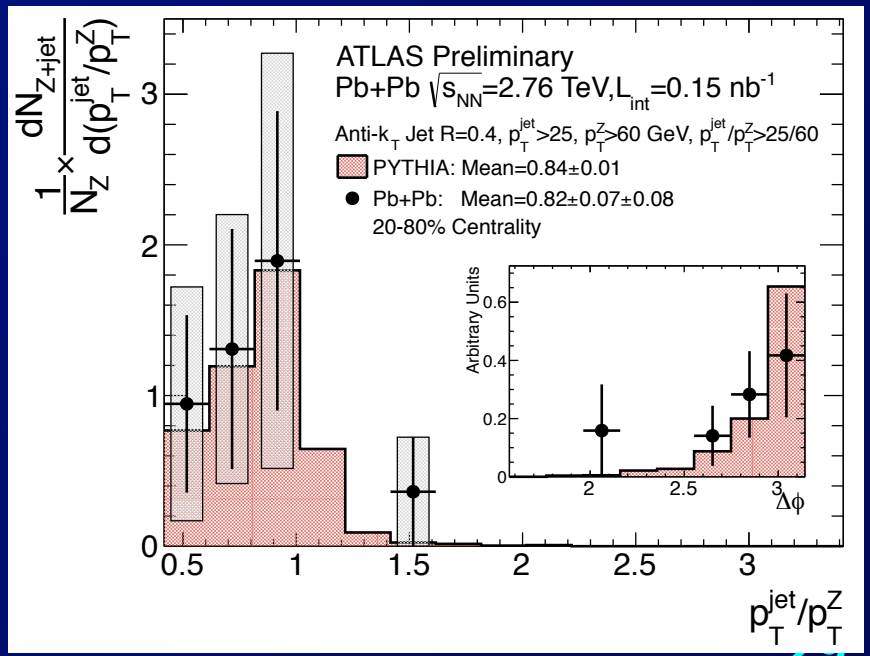

- Z-jet measurements have less background than γ-jet, but smaller rate

  ⇒1st results

Dijet (and gamma-jet) acoplanarity

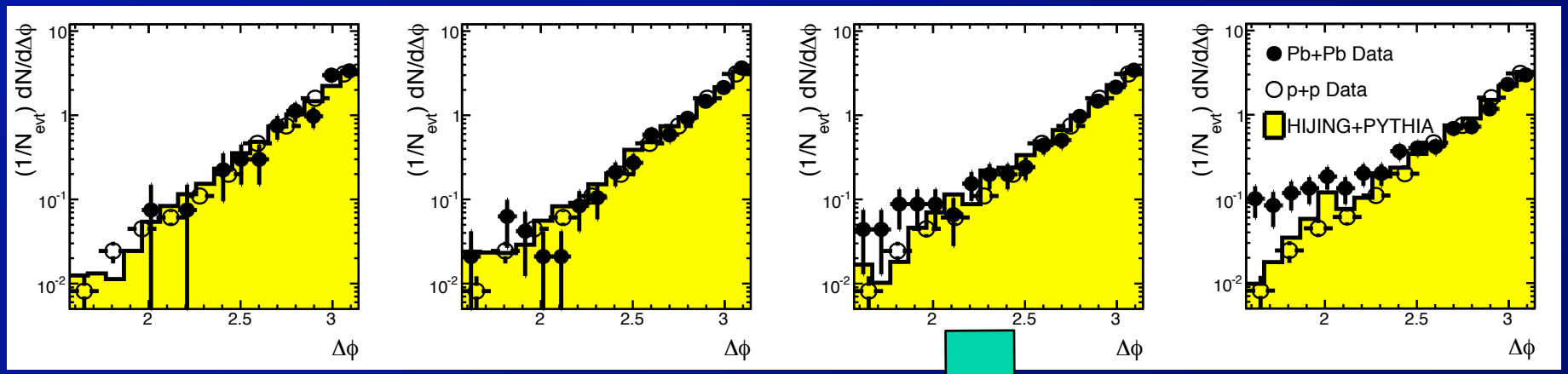

Virtuality matters

Virtuality Q^2 of the parton in the medium controls physics of radiative energy loss:

$$Q^2(L) \approx \max\left(\hat{q}L, \frac{E}{L}\right)$$

medium vacuum

Weak coupling scenario

RHIC: 20 GeV parton, $L = 3$ fm

$\hat{q}L \approx 4.5\,\mathrm{GeV}^2 \gg \frac{E}{L} \approx 1.5\,\mathrm{GeV}^2$

Virtuality of primary parton is medium dominated and small enough to "experience" the strongly coupled medium

LHC: 200 GeV parton, $L = 3$ fm

$\hat{q}L \approx 9\,\mathrm{GeV}^2 < \frac{E}{L} \approx 13\,\mathrm{GeV}^2$

Virtuality of primary parton is vacuum dominated and only its gluon cloud "experiences" the strongly coupled medium

Is the lack of k_T broadening in the presence of significant quenching a death knell for "leading parton" models of energy loss?

Tomography

ATLAS: Charged particle $v_2(p_T)$

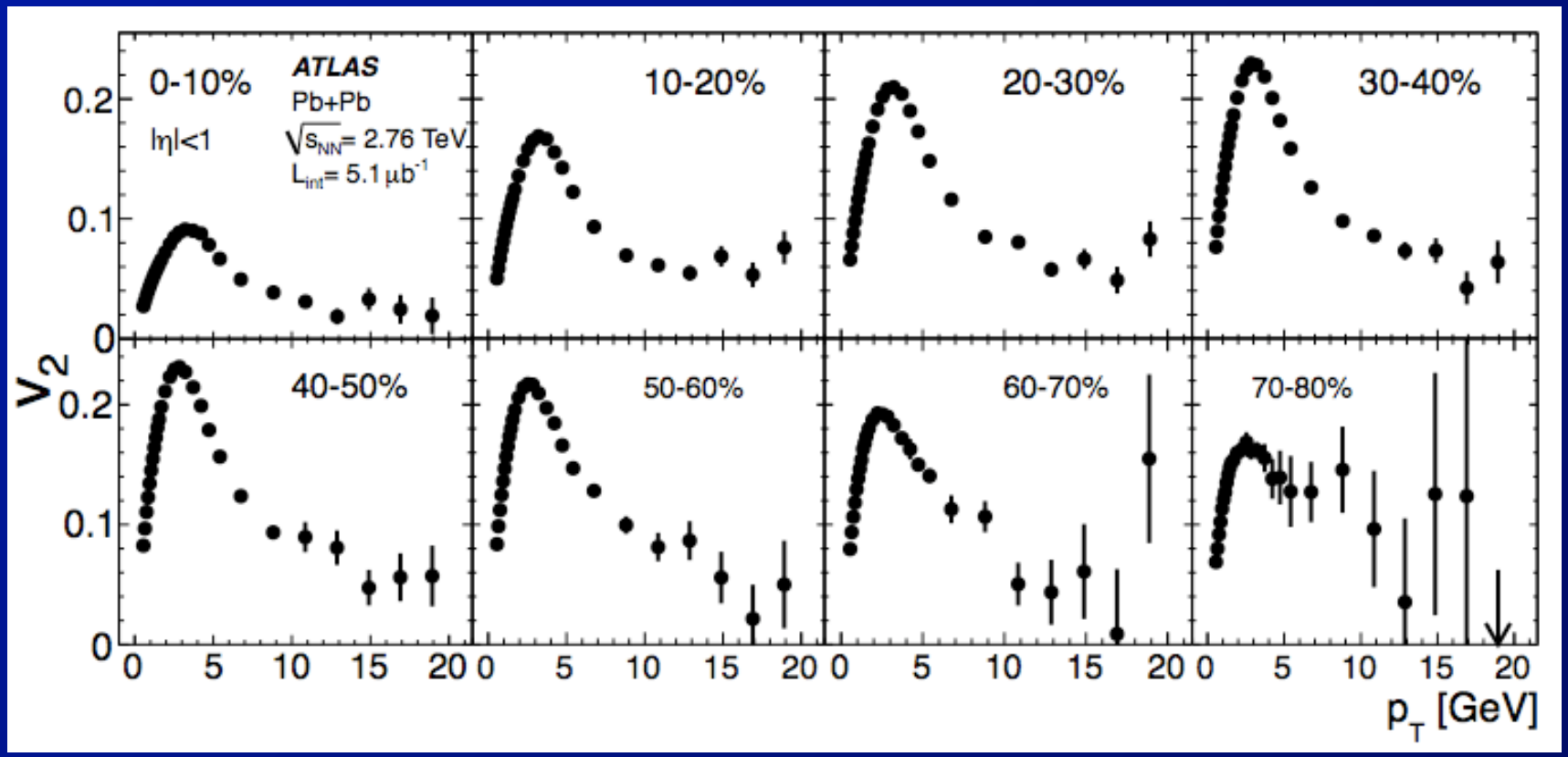

- **Single hadron $v_2(p_T)$:**
  - Evolution from flow (p_T < 6-7 GeV)
  - to quenching (p_T >~ 10 GeV)
    - ⇒Consistent with conclusions from similar analyses in PHENIX

ATLAS: Charged particle $v_2(p_T)$

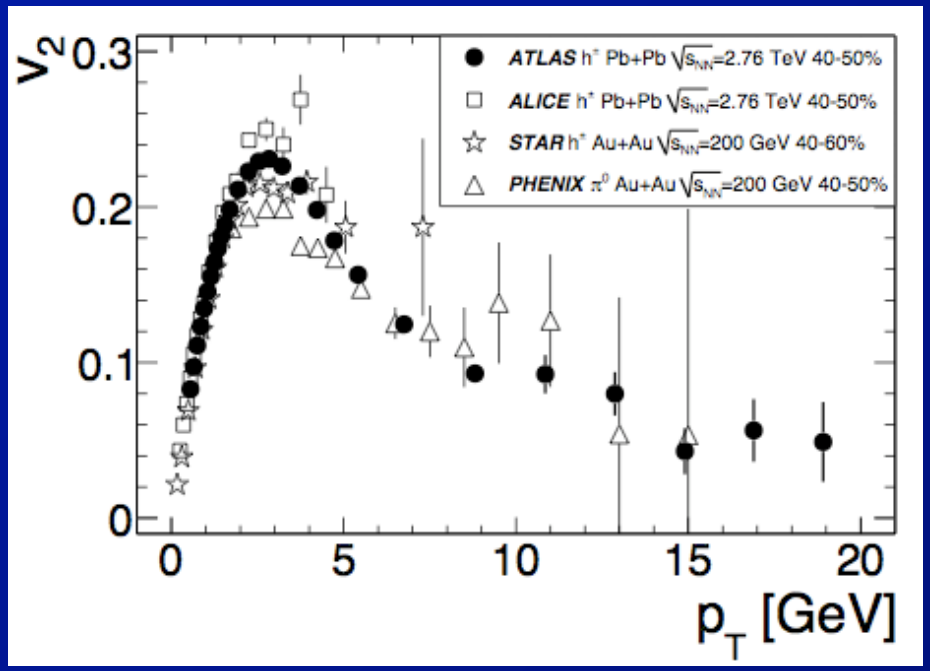

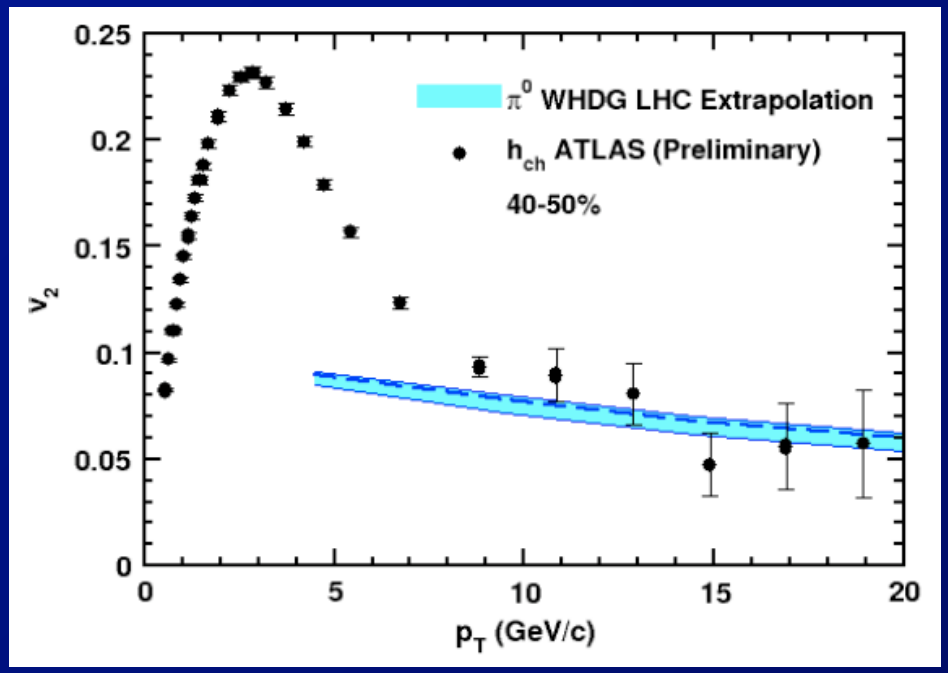

- Surprising agreement between RHIC and LHC $v_2(p_T)$, but beware "apples and oranges"
  - Charged (ATLAS, STAR), π^0 (PHENIX)
- WHDG energy loss describes $v_2(p_T)$ for $p_T > 10$

  ⇒ Flow dominates for p_T <~ 8 GeV

Differential jet suppression

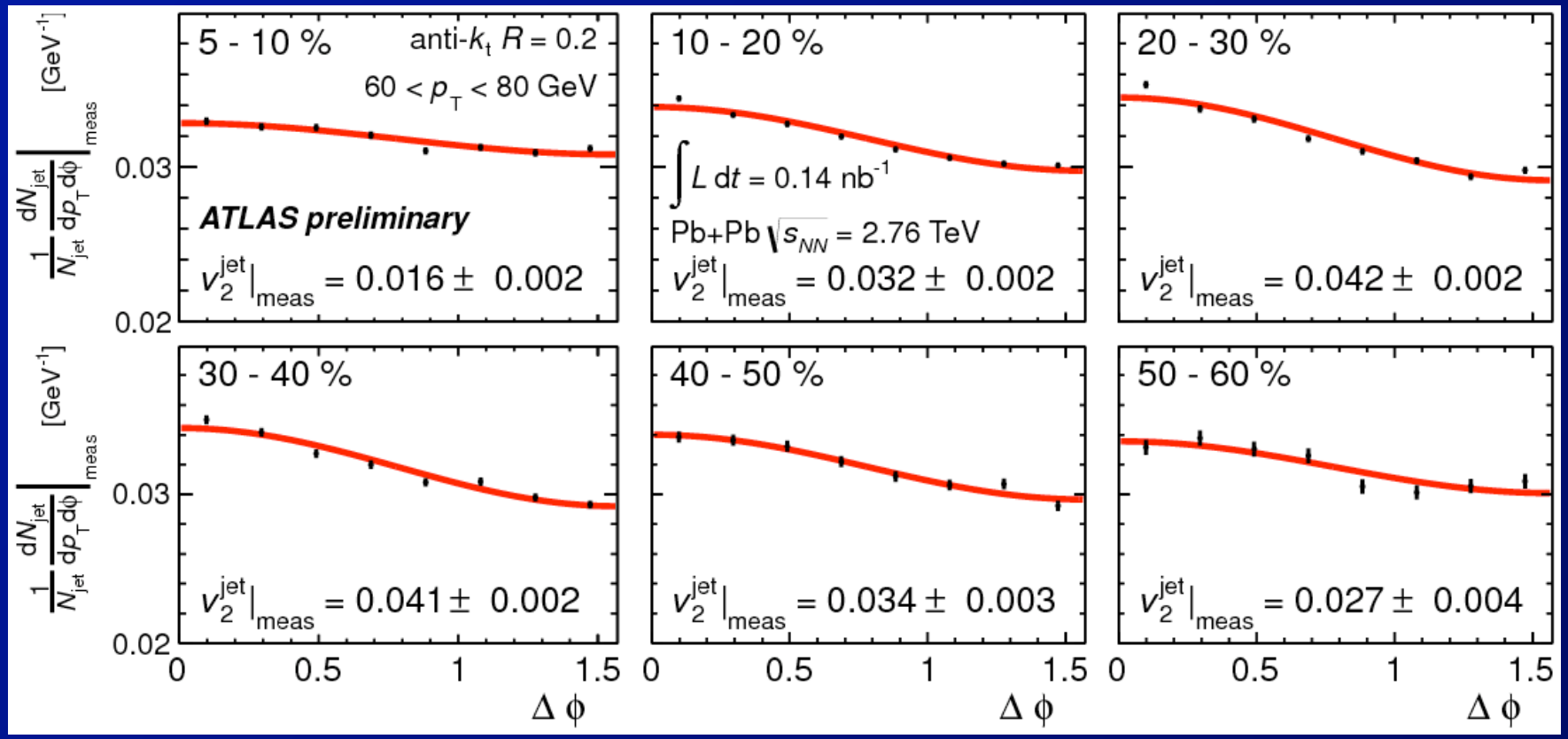

- Measure jet yields in 8 bins of $\Delta\phi$ with respect to the elliptic event plane
  - Here for R = 0.2 jets, $60 < p_T < 80$ GeV
    - ⇒UE subtraction corrected for elliptic flow modulation in calorimeter

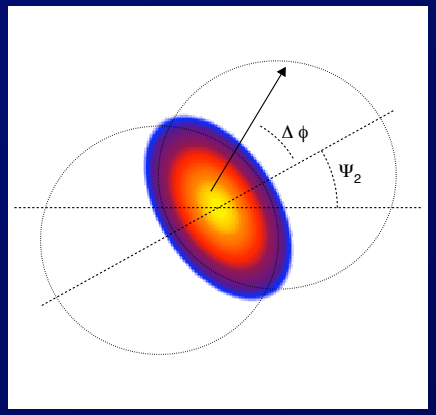

Differential jet suppression

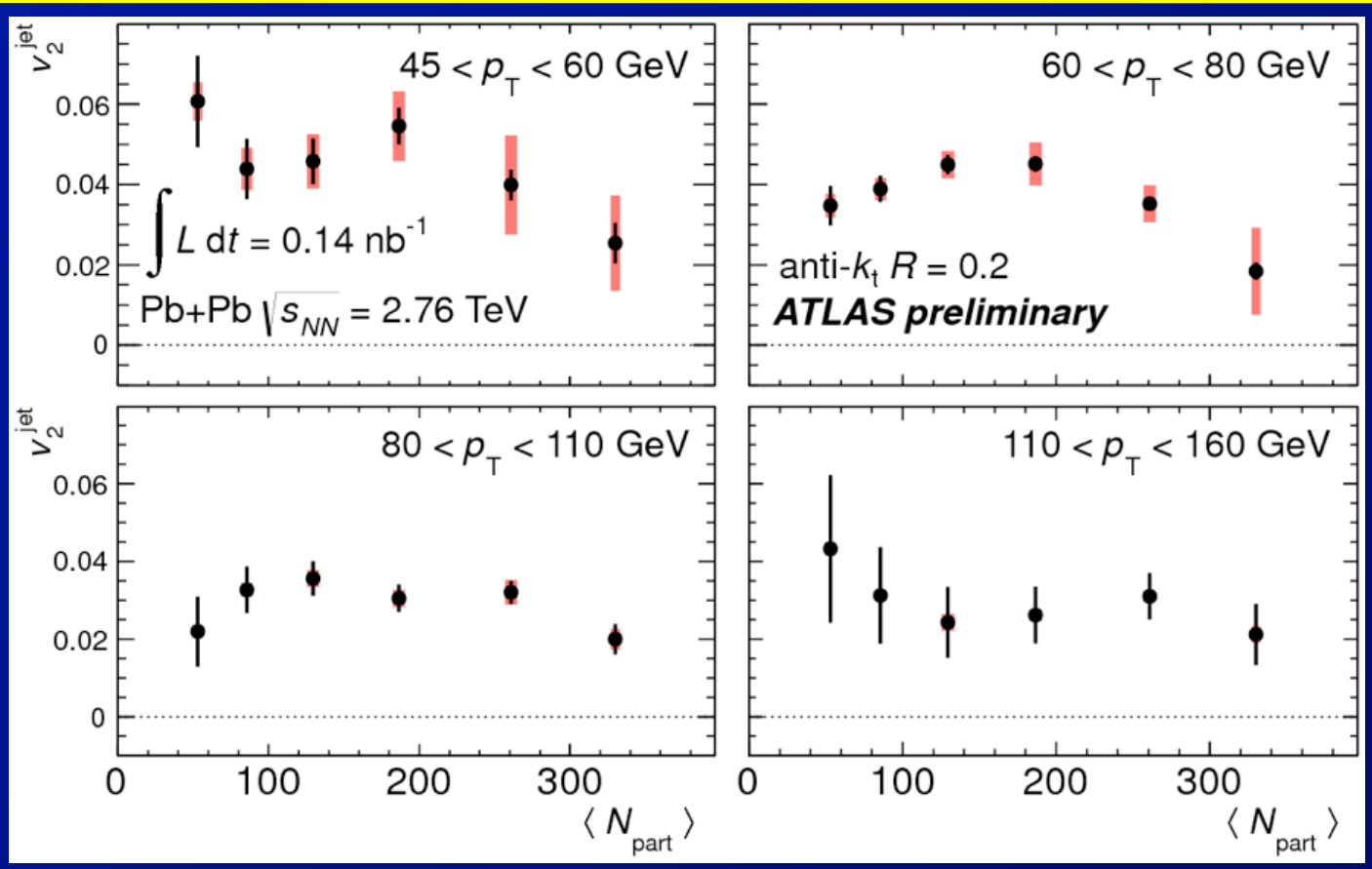

- Observe non-zero jet v_2 for (R = 0.2) p_T values > 100 GeV

  ⇒jet quenching clearly sensitive to initial geometry out to very high p_T

Jet $v_2(p_T)$

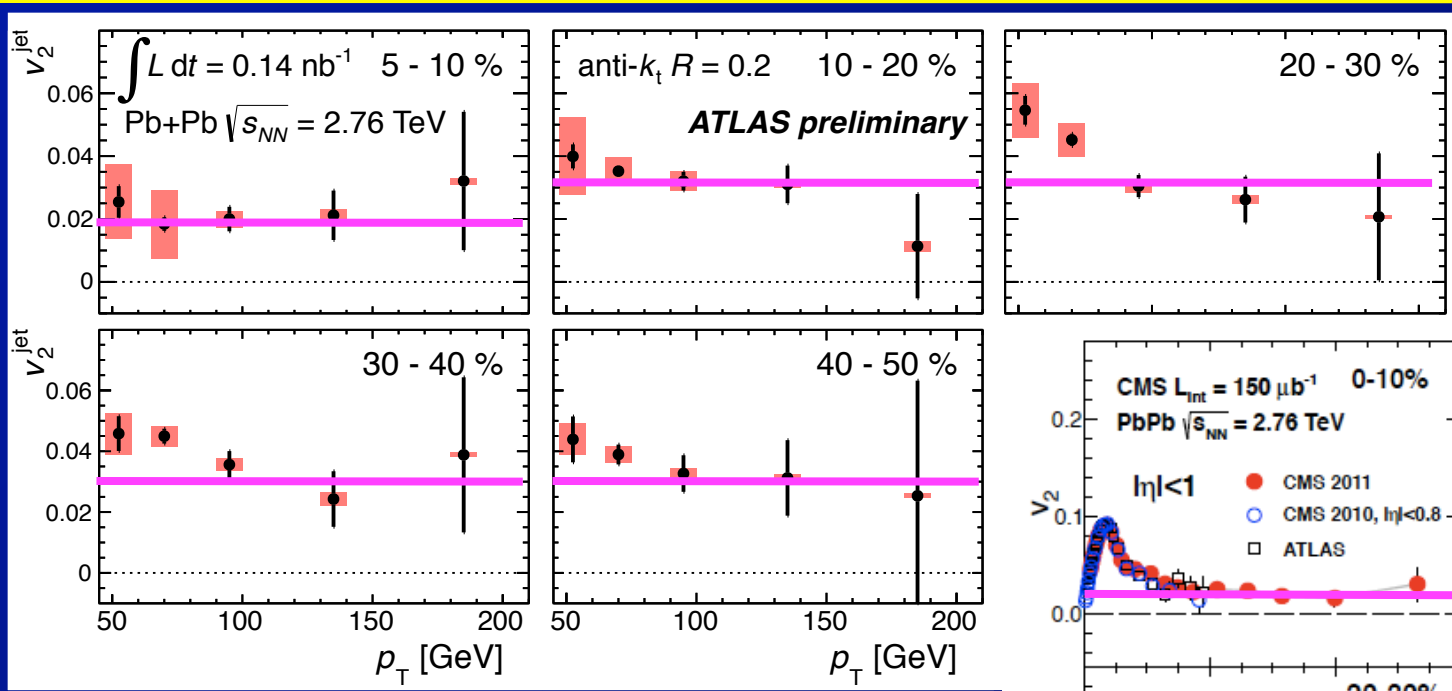

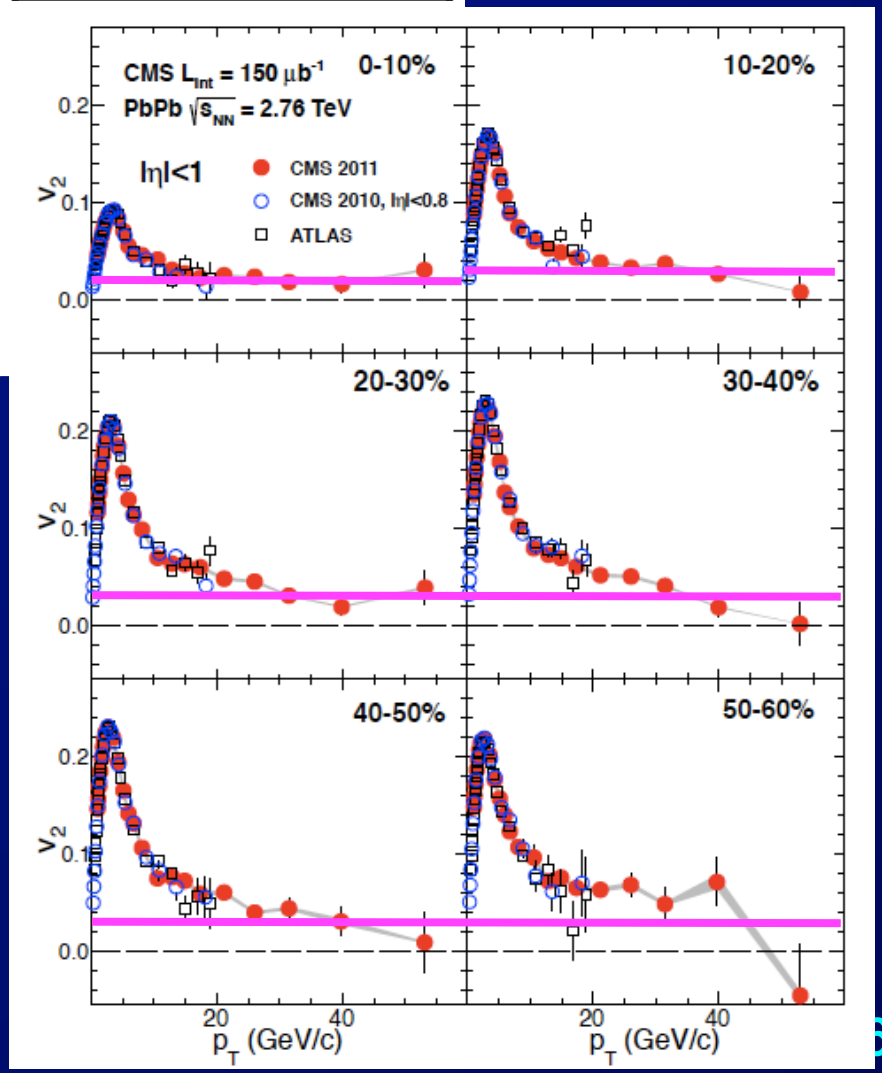

- Do rough comparison of jet, charged v2 at high p_T
  - plot 0.02 for 0/5-10%
  - plot 0.03 for > 10%

    ⇒As good as could be expected

Differential jet suppression

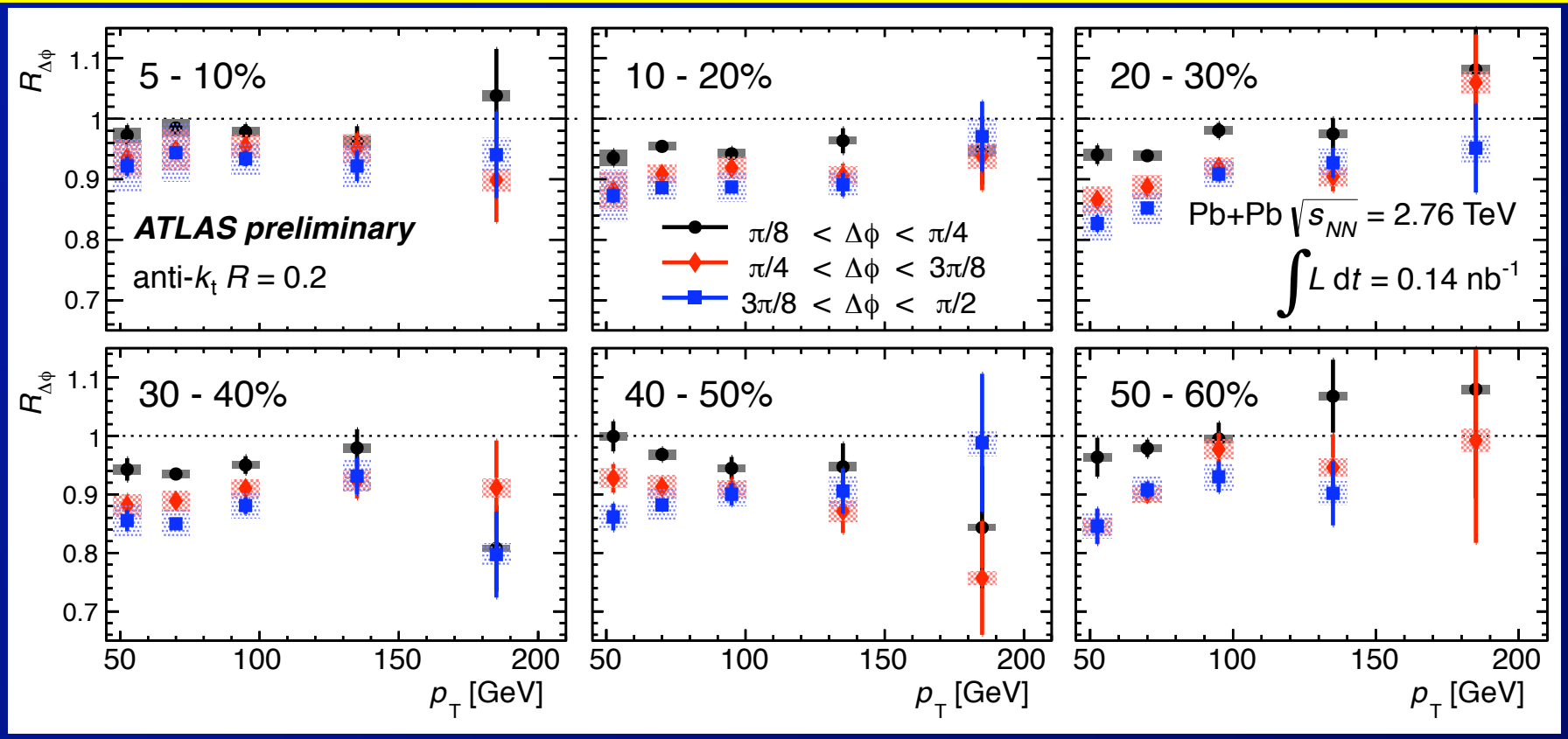

- Evaluate ratio of jet yields in different Δφ bins to the yield in 0 < Δφ < π/8.
  - $R_{AA}(\Delta\phi)/R_{AA}(0\text{-}\pi/8)$
    - ⇒ ~15% change in single jet suppression between in-plane, out-of-plane @ high p_T

n > 2 collective flow @ high(er) p_T

Phys. Rev. C86 (2012) 014907

- Full set of event plane $v_n(p_T)$ results
- Observe non-zero v_n for p_T > 10 GeV in central collisions

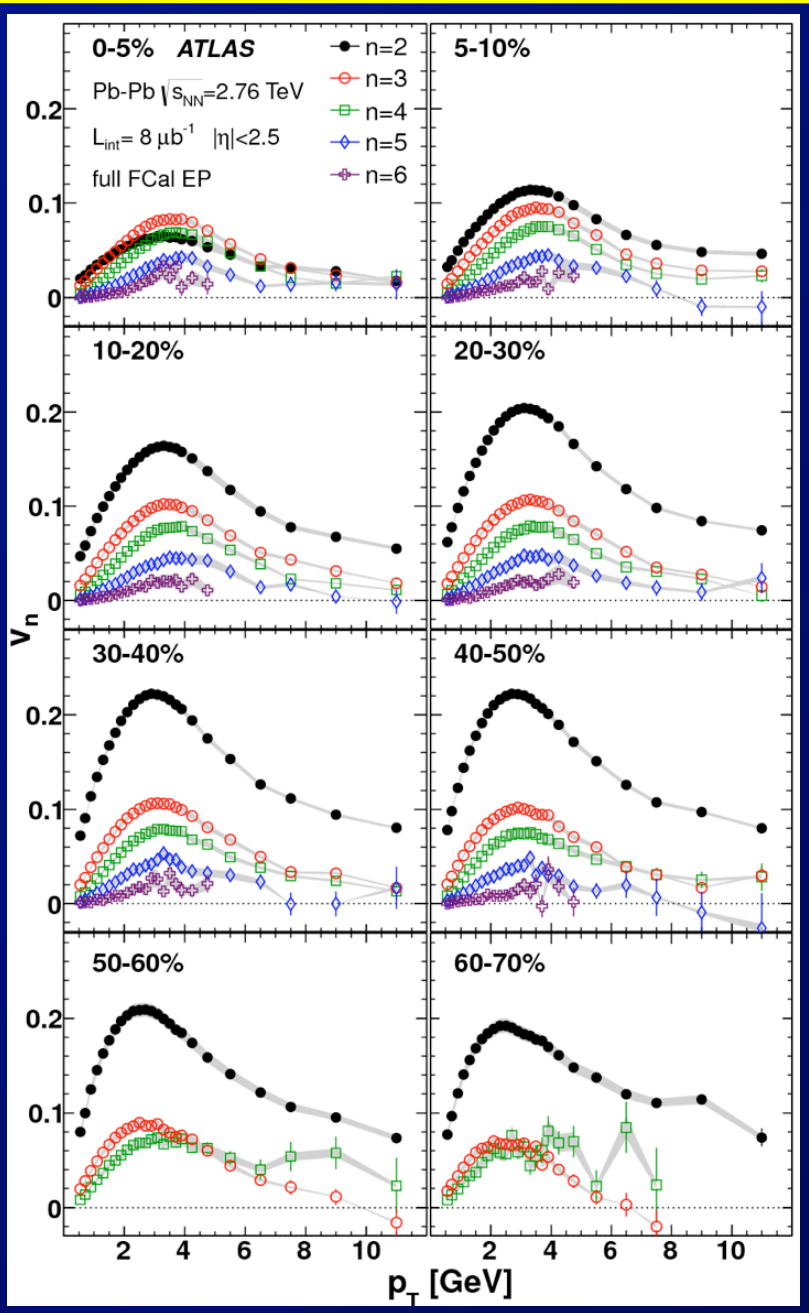

n > 2 collective flow @ high(er) p_T

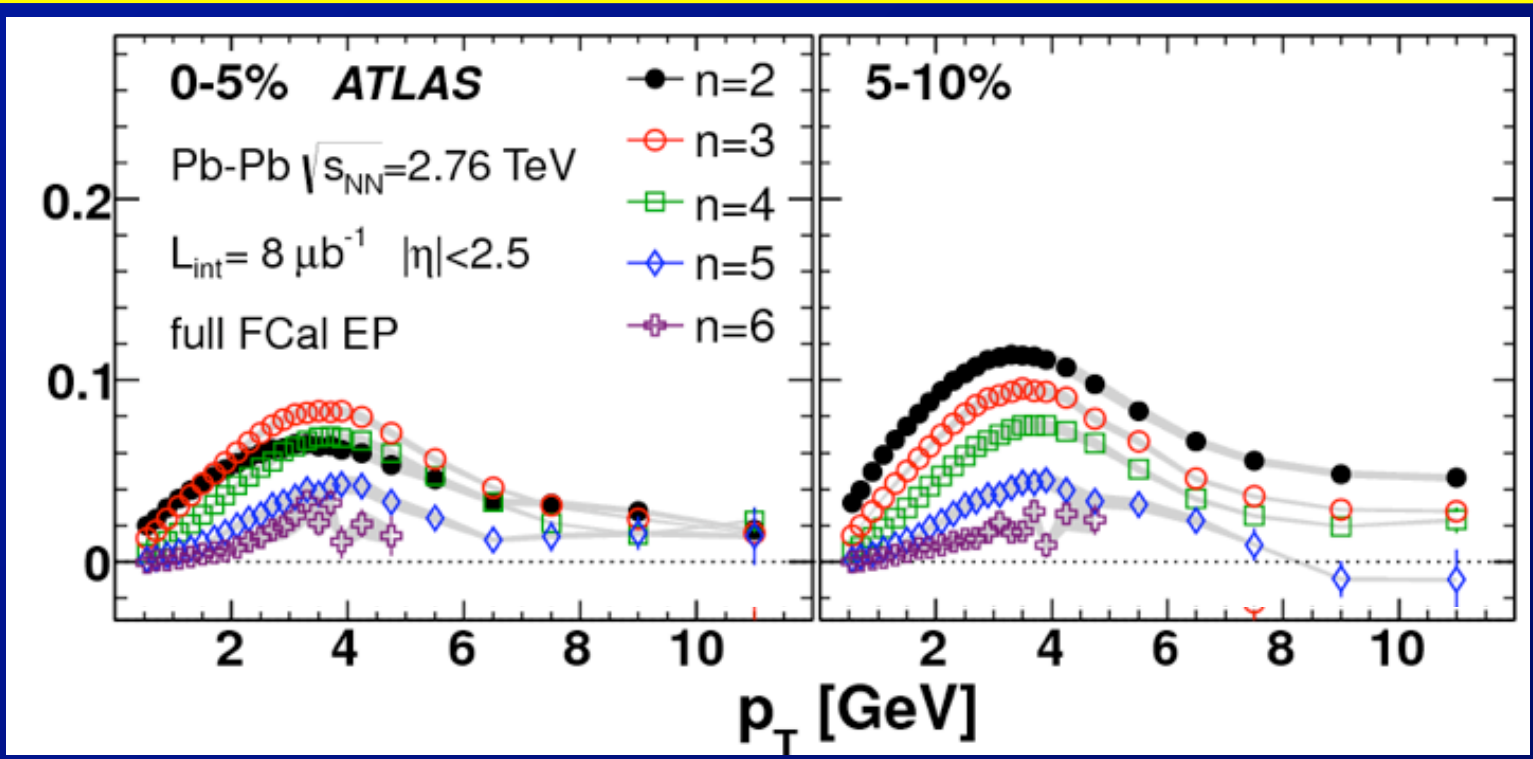

- For 0-5%, 5-10%
  - get non-zero, ~ flat v_n's in region where v_2 is due to quenching?
    - ⇒Suggestive, but not conclusive.

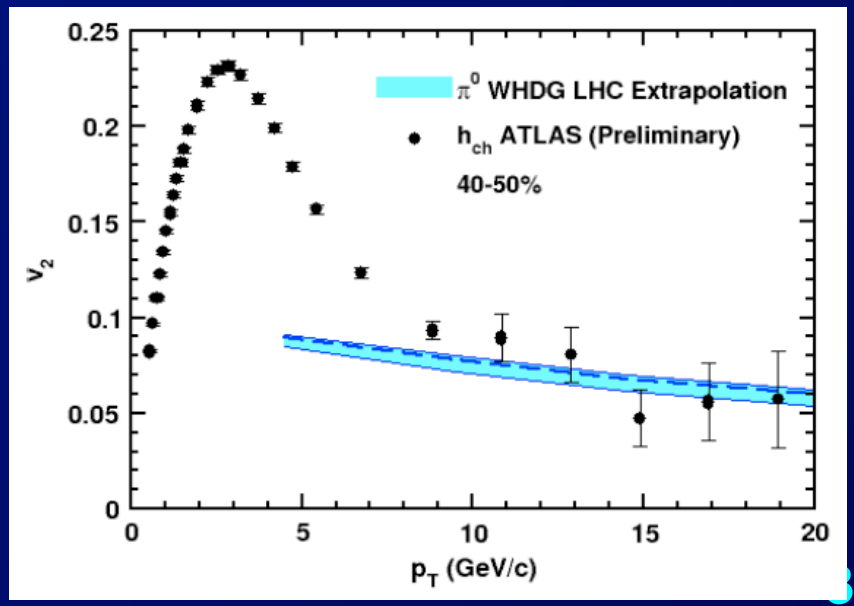

Summary, ruminations

Jet probes of the quark gluon plasma

Jet - QGP interactions schematically

From Quark Matter 2011 talk by Muller, Qiu

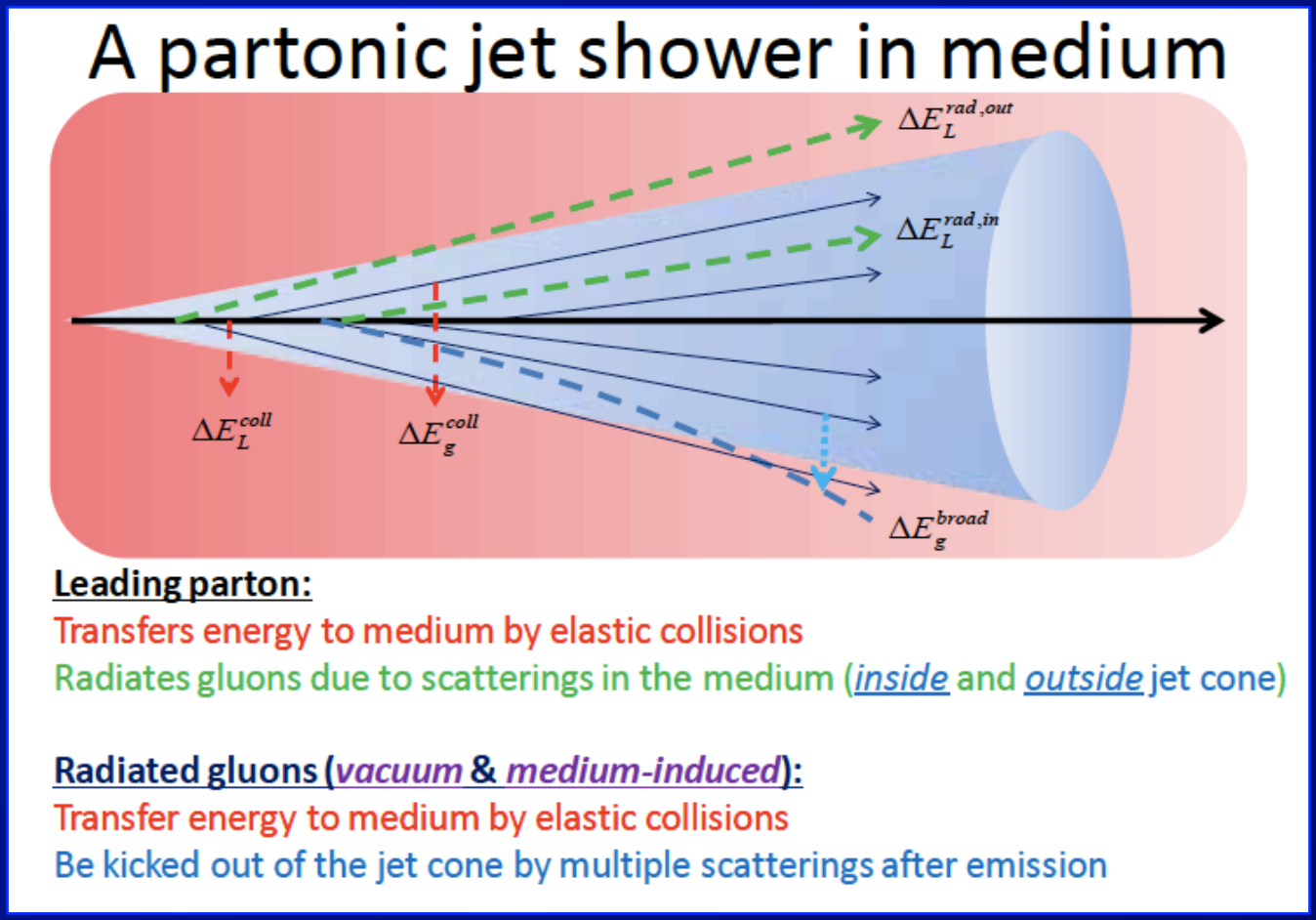

- Complicated theoretical problem
- Addressing complicated measurements
  - Need to be patient (but not too patient), but:
    - ⇒Are we asking, answering right questions?

Jet probes of the quark gluon plasma

A partonic jet shower in medium

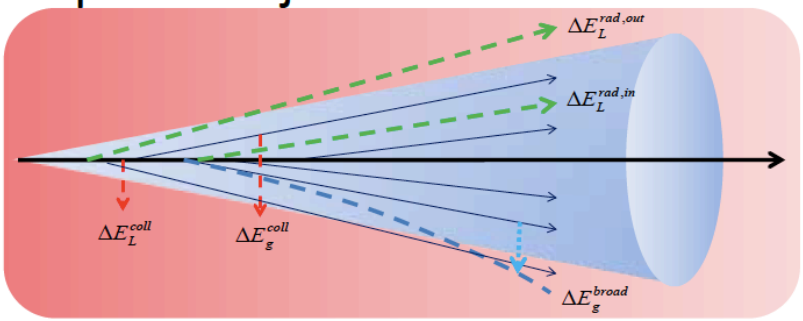

Leading parton:

Transfers energy to medium by elastic collisions

Radiates gluons due to scatterings in the medium (*inside* and *outside* jet cone)

Radiated gluons (*vacuum* & *medium-induced*):

Transfer energy to medium by elastic collisions

Be kicked out of the jet cone by multiple scatterings after emission

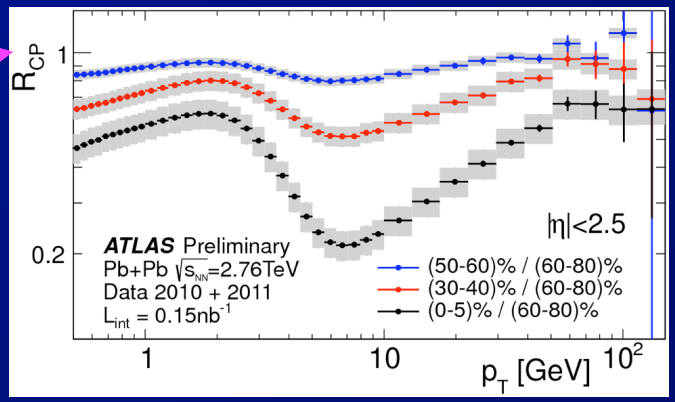

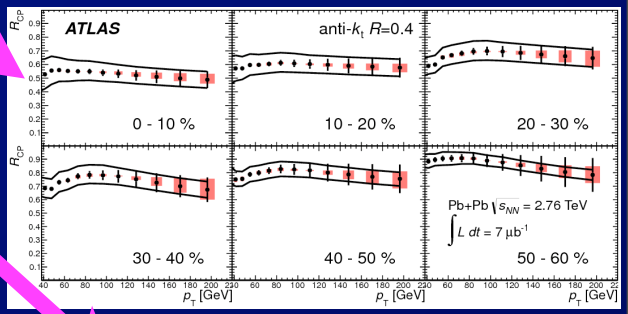

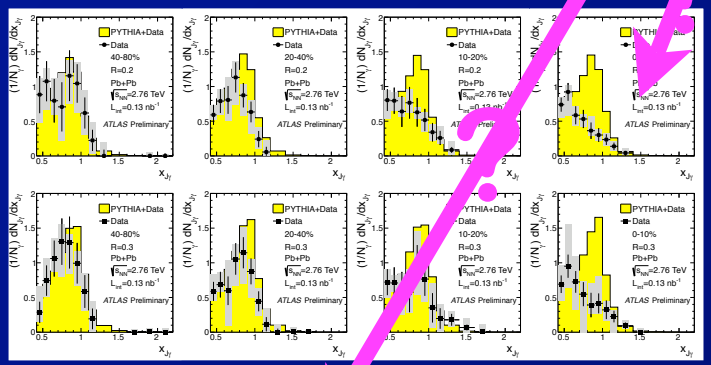

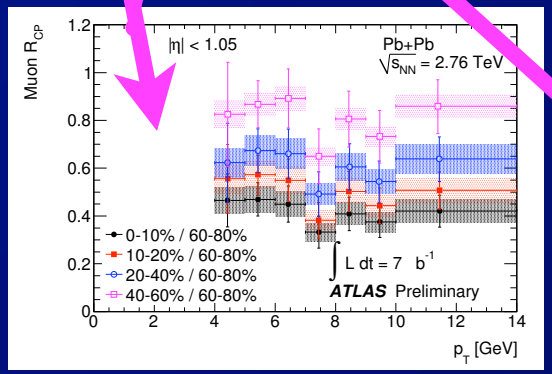

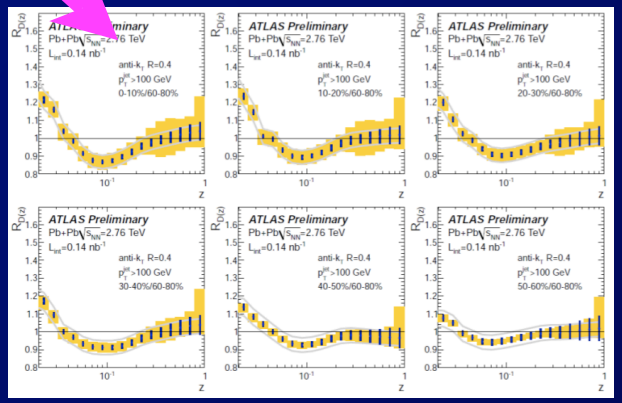

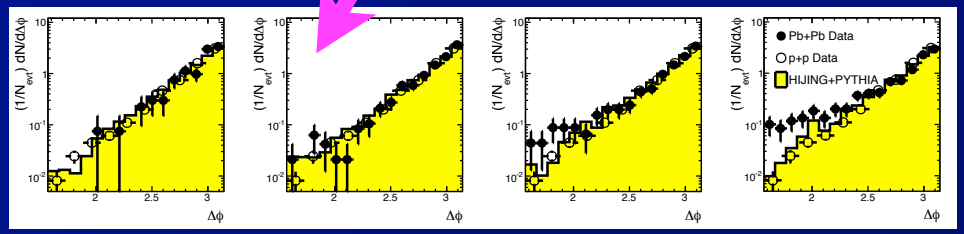

p+Pb ridges, who ordered that?

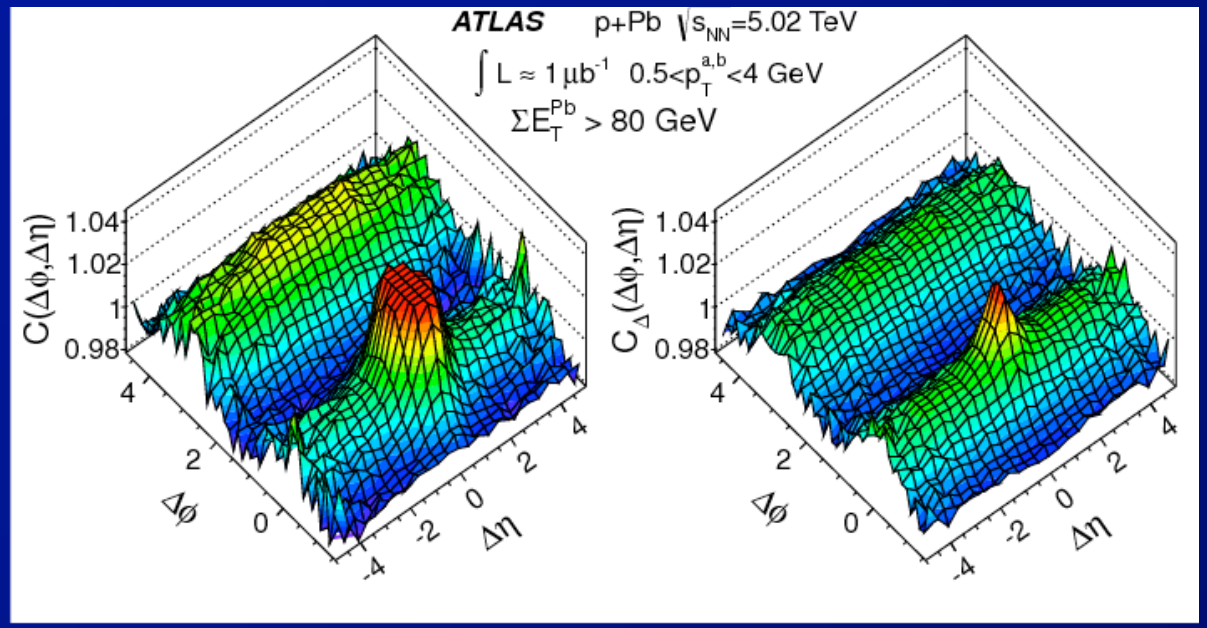

- **What are the implications of ridge(s) for understanding jet quenching in Pb+Pb?**
  - Improved understanding of initial conditions?
  - Yet more evidence of strong coupling?
  - Potential pre-equilibrium effects that we don't know (yet) know how to control?

  ⇒ Need to understand connection between ridges & hard scattering (if any) in p+Pb.

Wither the Glauber model …

Frankfurt, Strikman, Weiss, Phys. Rev. D83:054012,2011

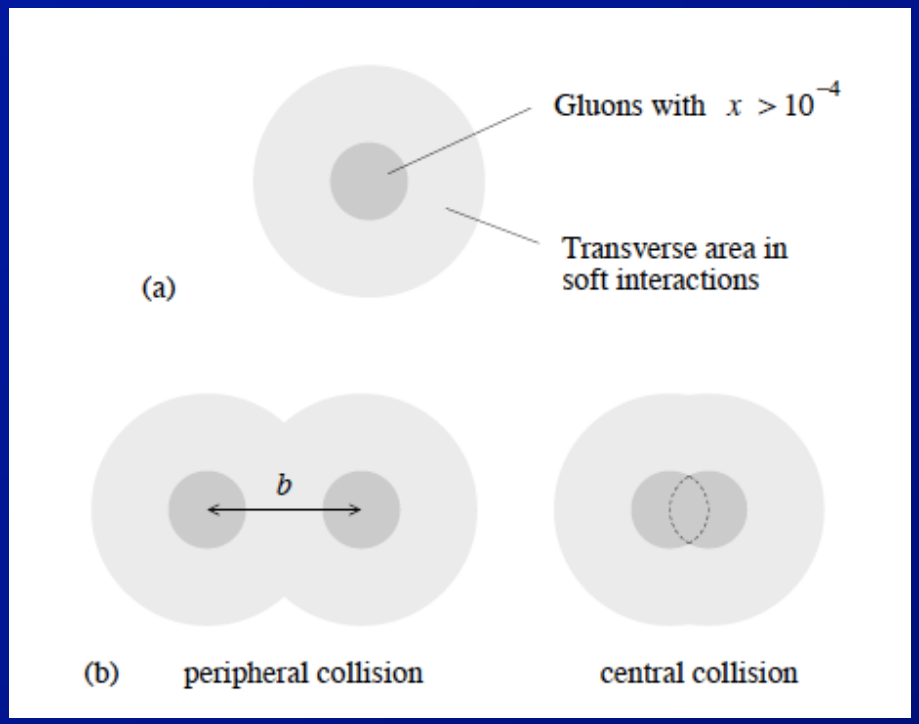

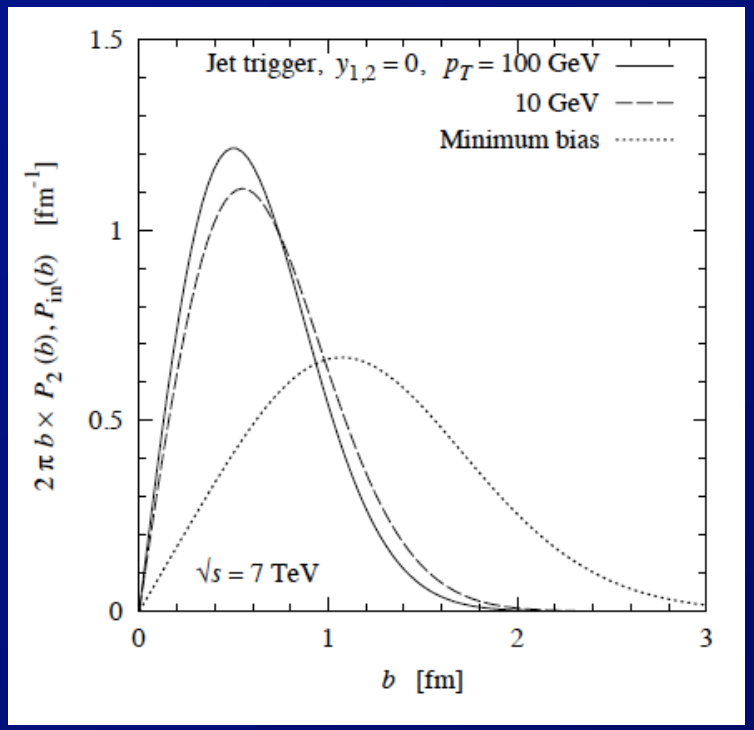

- Impact parameter dependence to physics in p-p collisions?
  - ⇒ Implications for d+A, p+A

Wither the Glauber model … (2)

M. Alvioli, M. Strikman, arXiv:1301.0728

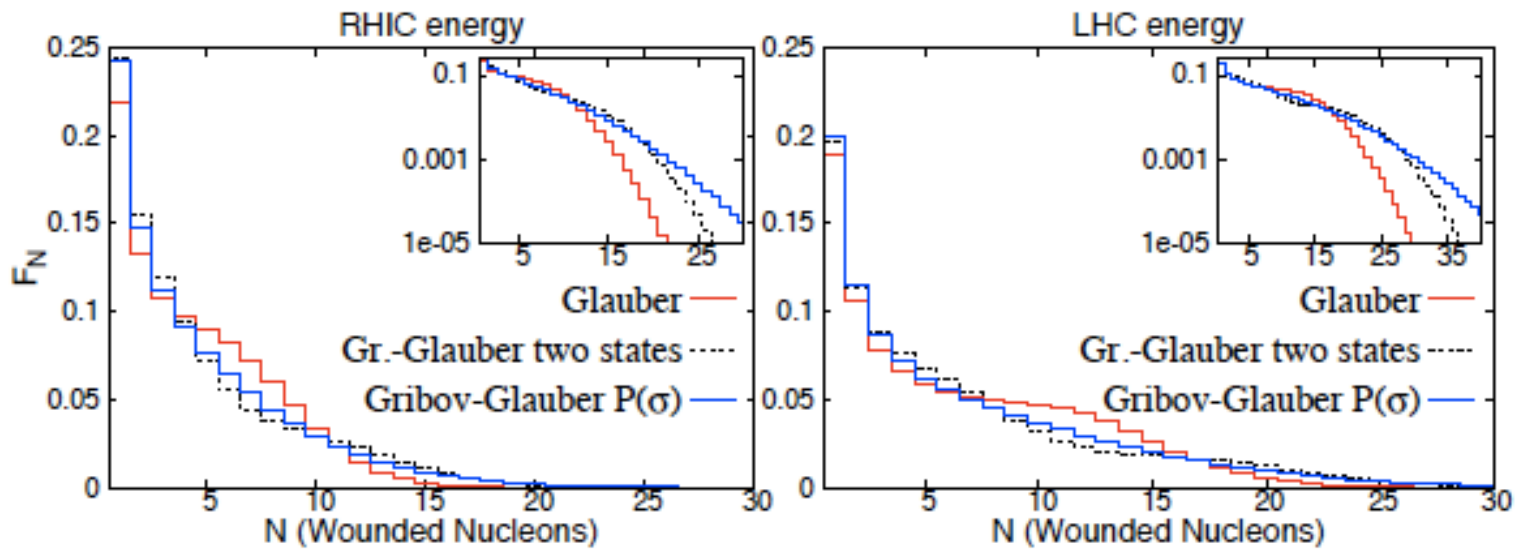

Figure 3: Effect of the event-by-event fluctuating values of σ_{tot}, for RHIC (left panel) and LHC energies (right panel) on the number of wounded nucleons, calculated as $F_N = \int db\, P_N(b)/\sigma_{in}^{hA}$. Red curves show the results obtained with the usual Glauber calculation with fixed cross section, black curves correspond to calculations with the two-component σ_{tot} model and blue curves correspond to calculations with fluctuating cross section with $P_h(\sigma_{tot})$ distribution. The insets show the same quantities in logarithmic scale.

- **The Glauber model works well … until it doesn't**

  ⇒ d/p-A may force us to go beyond Glauber.

Backup

20.1th century view of jet quenching

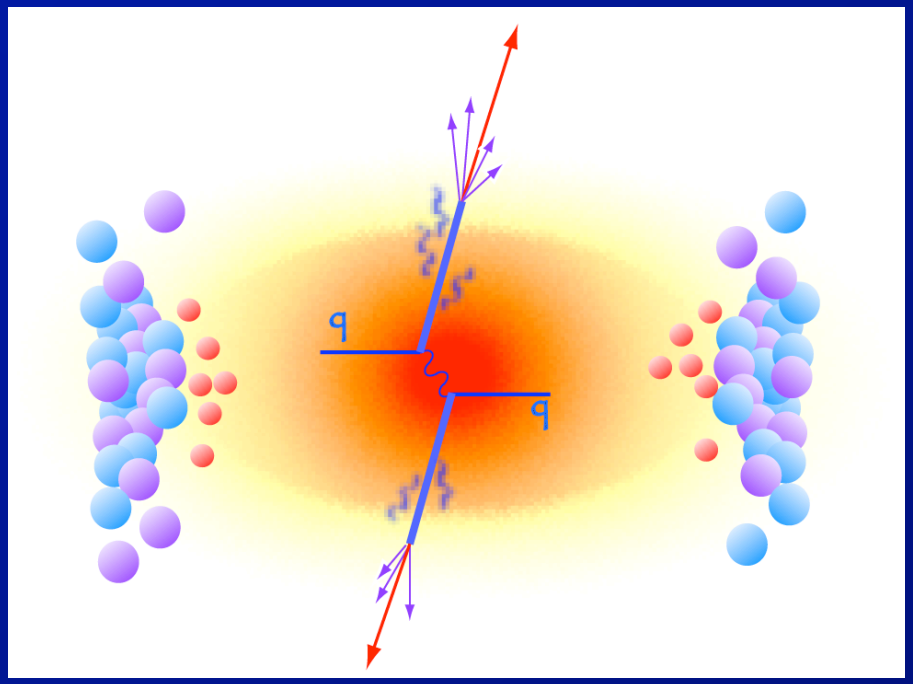

e.g. opacity expansion
a la GLV

- High-p_T quarks or gluons propagate through and scatter in the QGP
  - with collisional and radiative energy loss
  - interference between vacuum and medium-induced radiation + LPM interference of multiple emissions
  - Fragmentation in vacuum

20.1th century view of jet quenching

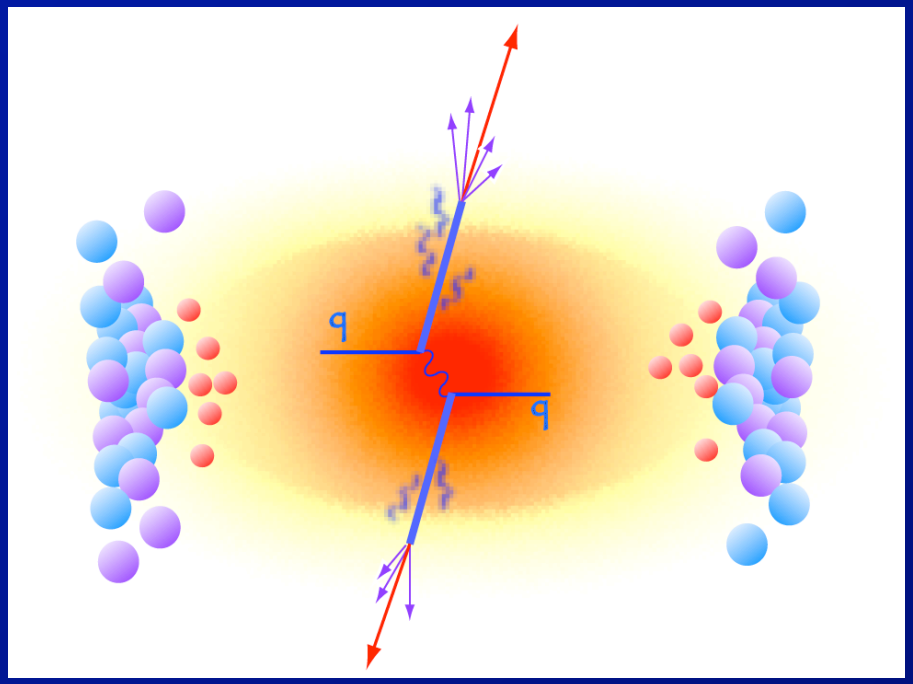

e.g. opacity expansion
a la GLV

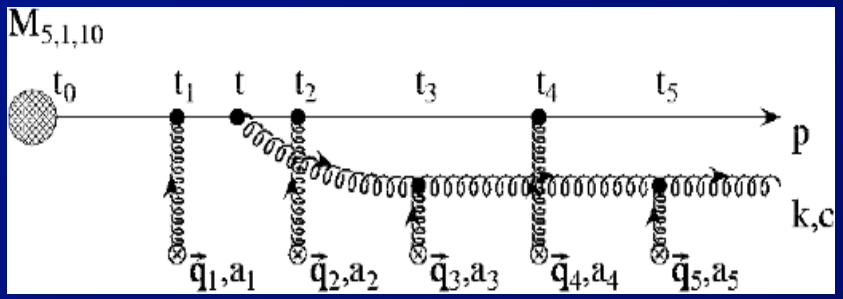

- High-p_T quarks or gluons propagate through and scatter in the QGP
  - with collisional and radiative energy loss
  - interference between vacuum and medium-induced radiation + LPM interference of multiple emissions
  - Fragmentation in vacuum

ATLAS: Pb+Pb centrality

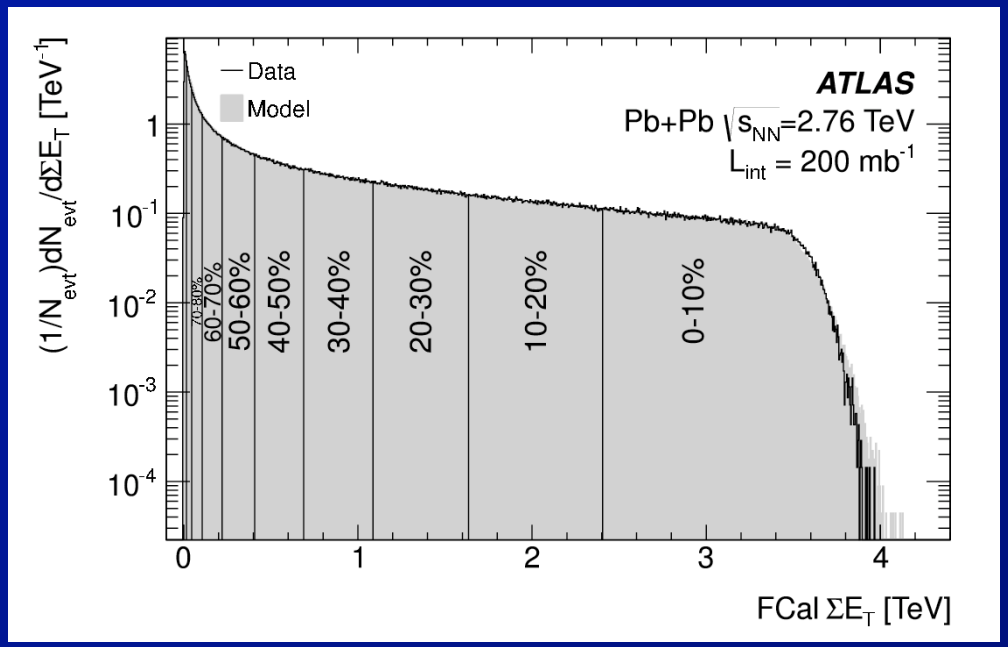

Centrality	$\langle N_{\rm part}\rangle$	$\langle N_{\rm coll}\rangle$
$0-10\%$	356 ± 2	1500 ± 115
$10-20\%$	261 ± 4	923 ± 68
$20-30\%$	186 ± 4	559 ± 41
$30-40\%$	129 ± 4	322 ± 24
$40-50\%$	86 ± 4	173 ± 14
$50-60\%$	53 ± 3	85 ± 8
$60-80\%$	23 ± 2	27 ± 4

- **Pb+Pb collision centrality characterized by ΣE_T in forward calorimeters ($3.2 < |\eta| < 4.9$).**
  - Also quantified using number of participants (N_{part})
  - Pb+Pb partonic luminosity expressed in terms of "number of nucleon-nucleon collisions" (N_{coll}) or T_{AA}

⇒Calculated using standard Glauber Monte Carlo.

Centrality dependence of jet R_{cp}

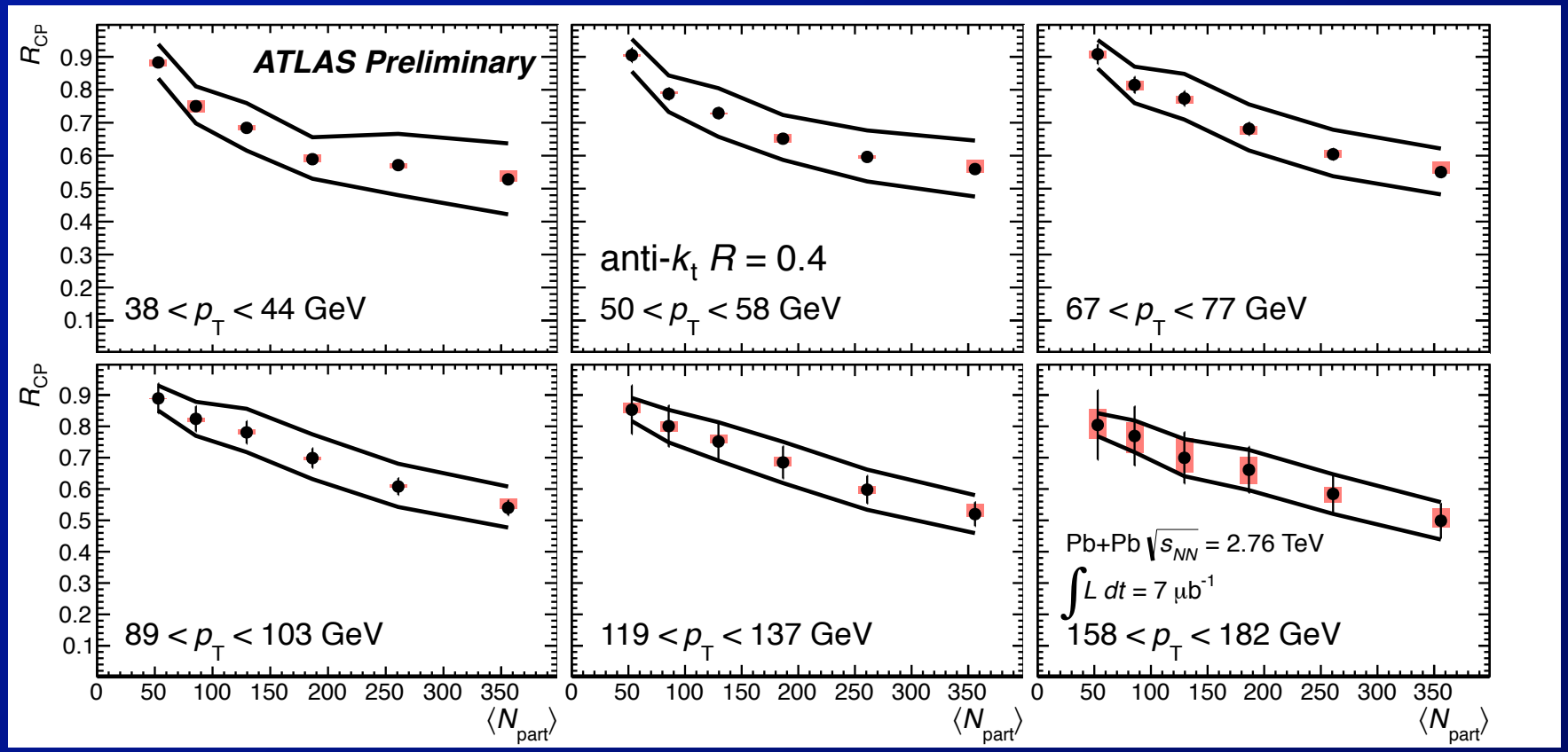

- Study centrality evolution for fixed jet p_T
  - R_{cp} vs N_{part}
    - ⇒Smooth turn on of jet suppression between peripheral and central collisions.

Jet Quenching at RHIC
vs LHC in Light of Recent dAu vs pPb Controls
RIKEN BNL Research Center Workshop
April 15-17, 2013 at Brookhaven National Laboratory

Experimental status of flavour tomography

Andrea Dainese
(INFN Padova, Italy)

Outline of the Talk

- Introduction: HF probes of the medium (→ see A.Buzzatti)
- Calibrating HF probes: pp results
- HF production in nucleus-nucleus:
  - Semi-leptonic decays
  - D mesons
  - B and b-jets
- Proton-nucleus control data
- HF azimuthal anisotropy
- Outlook: detector upgrades at RHIC and LHC

RHIC	PHENIX, STAR
	STAR

LHC	ALICE, ATLAS
	ALICE
	CMS

Outline of the Talk

- Introduction: HF probes of the medium
- Calibrating HF probes: pp results
- HF production in nucleus-nucleus:
  - Semi-leptonic decays
  - D mesons
  - B and b-jets
- Proton-nucleus control data
- HF azimuthal anisotropy
- Outlook: detector upgrades at RHIC and LHC

Heavy flavour production in pp

- State-of-the-art pQCD calculation: Fixed Order Next-to-Leading Log

$$\frac{d\sigma}{dp_T} = A(m)\,\alpha_s^2 + B(m)\,\alpha_s^3 + G(m,p_T)\left[\alpha_s^2 \sum_{i=2}^{\infty} a_i\,[\alpha_s \log(\mu/m)]^i + \alpha_s^3 \sum_{i=1}^{\infty} b_i\,[\alpha_s \log(\mu/m)]^i\right]$$

$\mu \approx p_T$

FONLL: Cacciari, Frixione, Mangano, Nason and Ridolfi, JHEP0407 (2004) 033

[coincides with NLO for low p_T (total cross section); more accurate at high p_T]

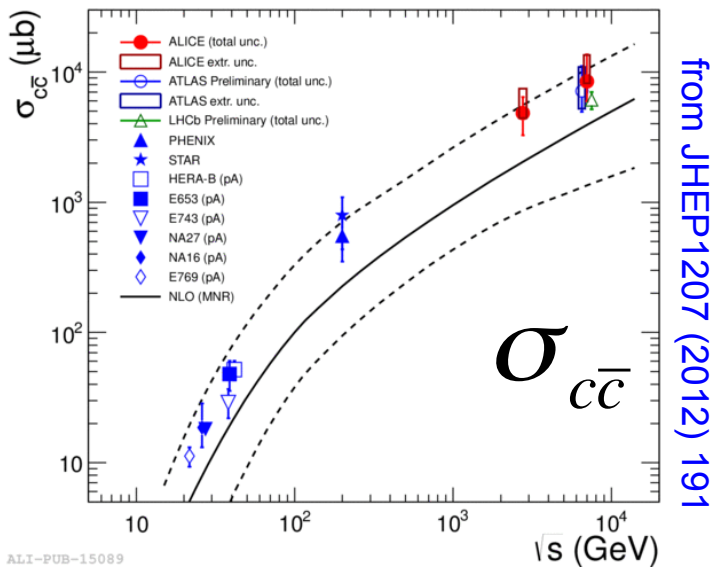

from JHEP1207 (2012) 191

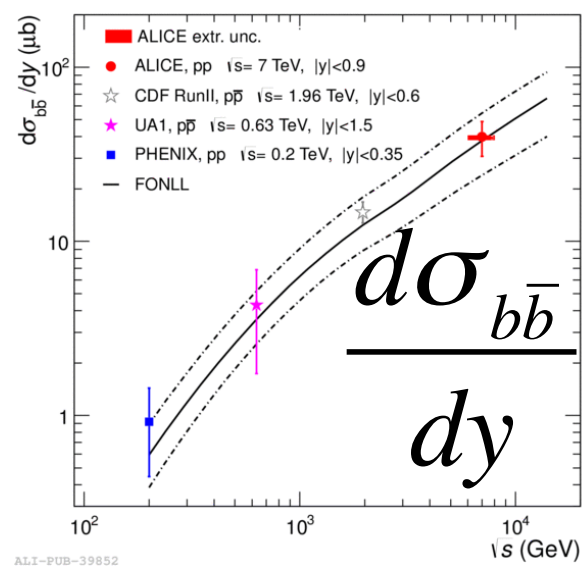

from JHEP1211 (2012) 065

- Describes consistently energy dependence of total cross sections
- Charm (beauty) x10 (100) from 0.2 to 2.76 TeV

pp: pQCD calculations vs data

Charm p_T-differential cross section

200, 500 GeV

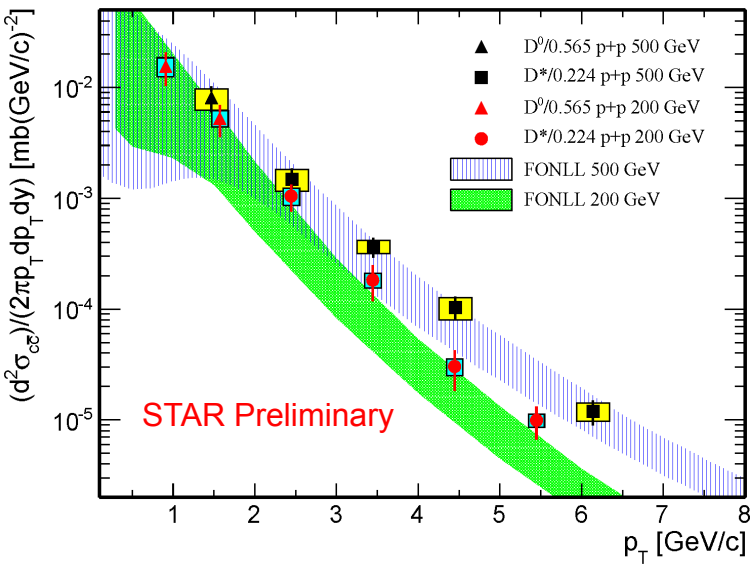

1.96 TeV

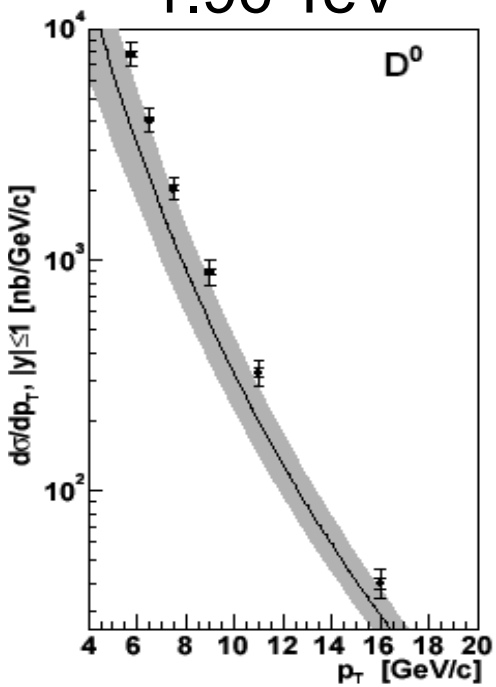

7 TeV

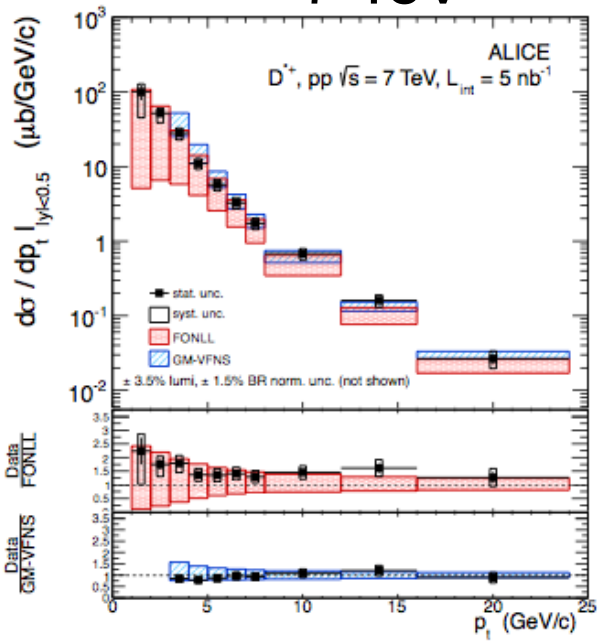

STAR, PRD 86 (2012) 72013 (200 GeV)
J. Bielcik (Moriond2013)

CDF, PRL91 (2003) 241804

ALICE, JHEP01 (2012) 128

- Charm production described within uncertainties
- Consistently at upper limit of theoretical band from 0.2 to 7 TeV

pp: pQCD calculations vs data

Beauty p_T-differential cross section

1.96 TeV

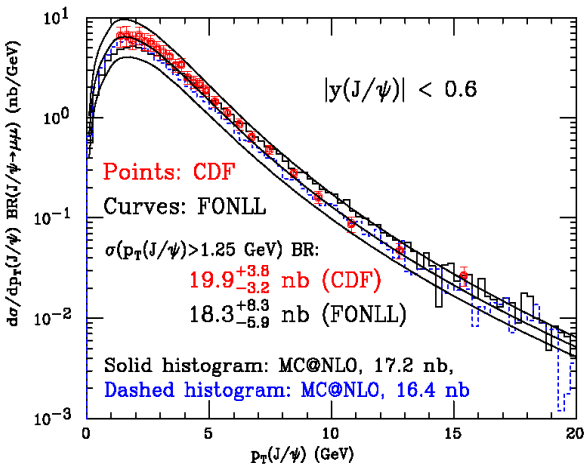

CDF, PRD71 (2005) 032001

7 TeV

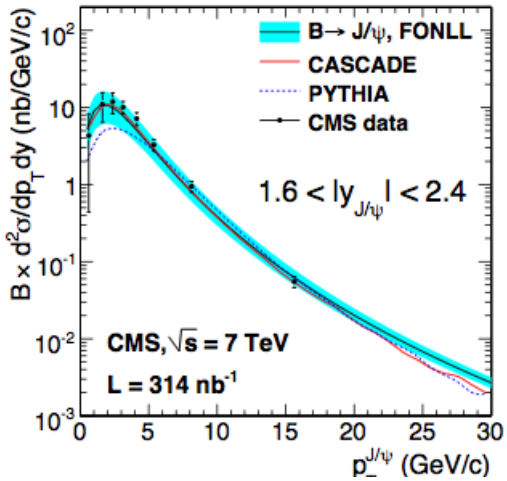

CMS, EPJC71 (2011) 1575

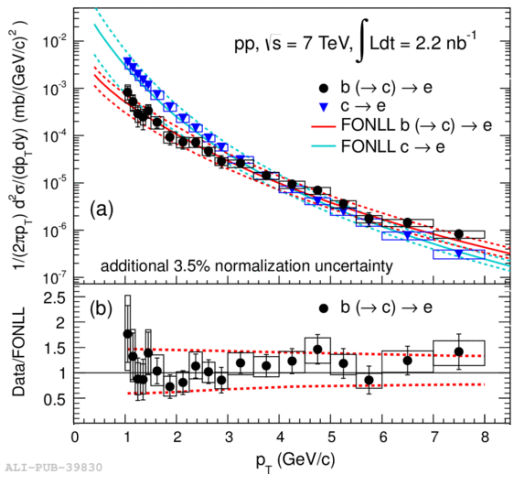

ALICE, PLB721 (2013) 13

- Beauty production described very well by central value of calculation

pp: pQCD calculations vs data

HF-lepton p_T-differential cross section

200 GeV

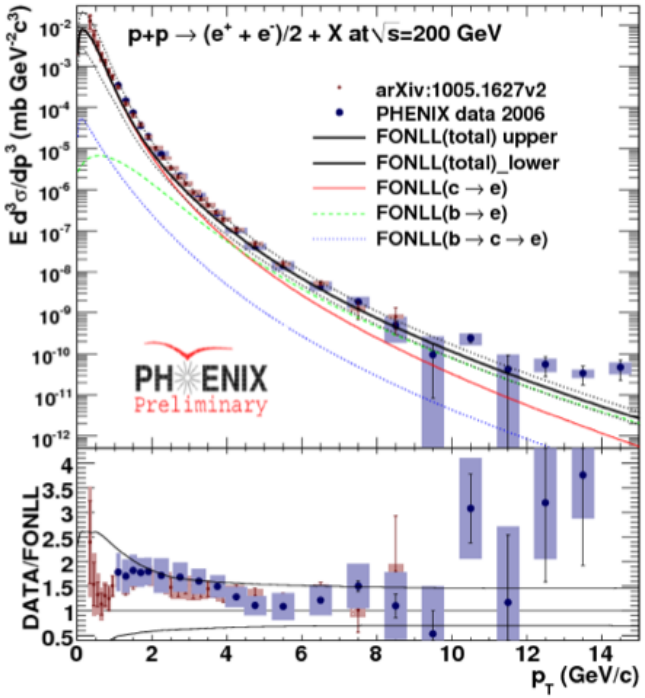

PHENIX, PRC84 (2011) 044905
N.Apadula (WWND2013)

2.76 TeV

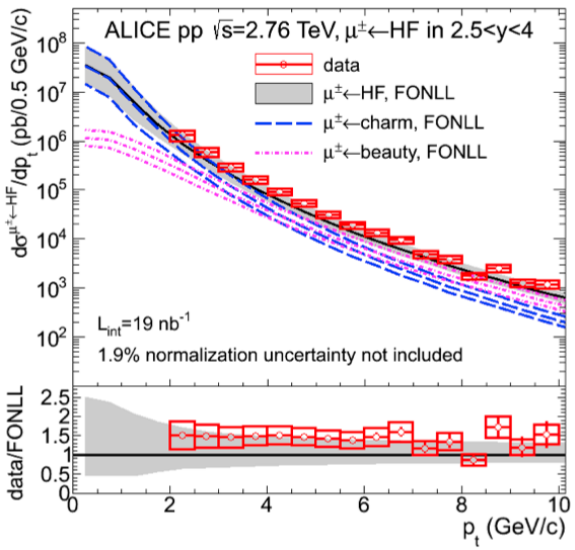

ALICE, PRL 109 (2012) 112301

7 TeV

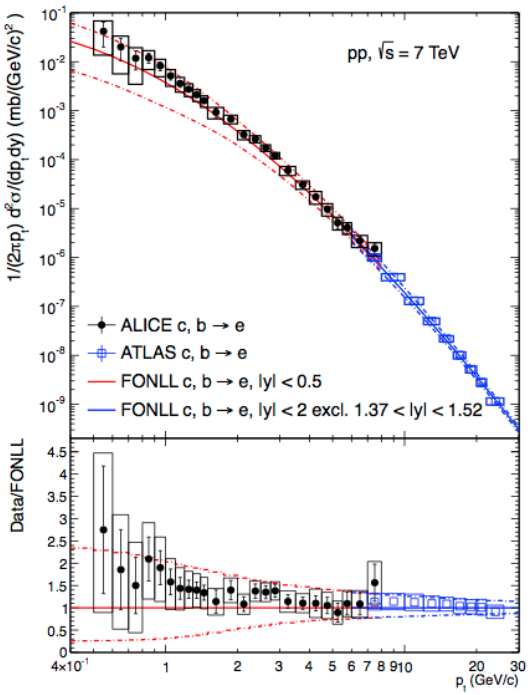

ALICE, PRD86 (2012) 112007
ATLAS, PLB707 (2012) 438

- HF-decay electrons and muons at central and forward y
- FONLL: “b > c” for p_T > 4 (5) GeV/c at RHIC (LHC)

Outline of the Talk

- Introduction: HF probes of the medium
- Calibrating HF probes: pp results
- HF production in nucleus-nucleus:
  - Semi-leptonic decays
  - D mesons
  - B and b-jets
- Proton-nucleus control data
- HF azimuthal anisotropy
- Outlook: detector upgrades at RHIC and LHC

RHIC	PHENIX, STAR	
	STAR	
LHC	ALICE, ATLAS	
	ALICE	
	CMS	

HF-decay electrons at RHIC (Au-Au)

- Inclusive measurement (c+b) using non-photonic electrons

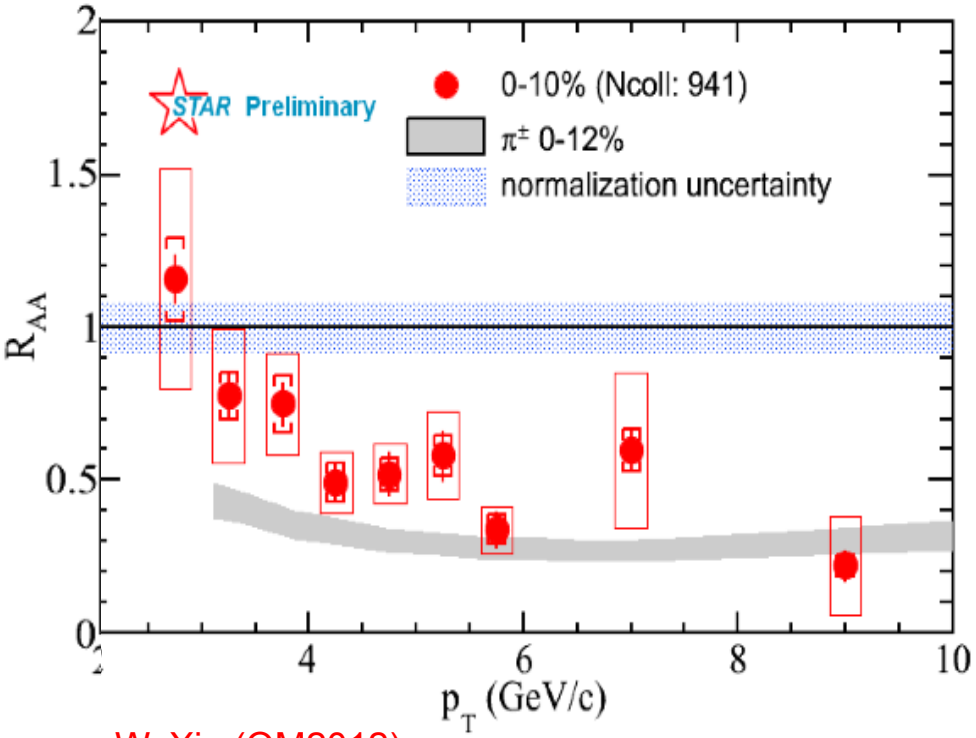

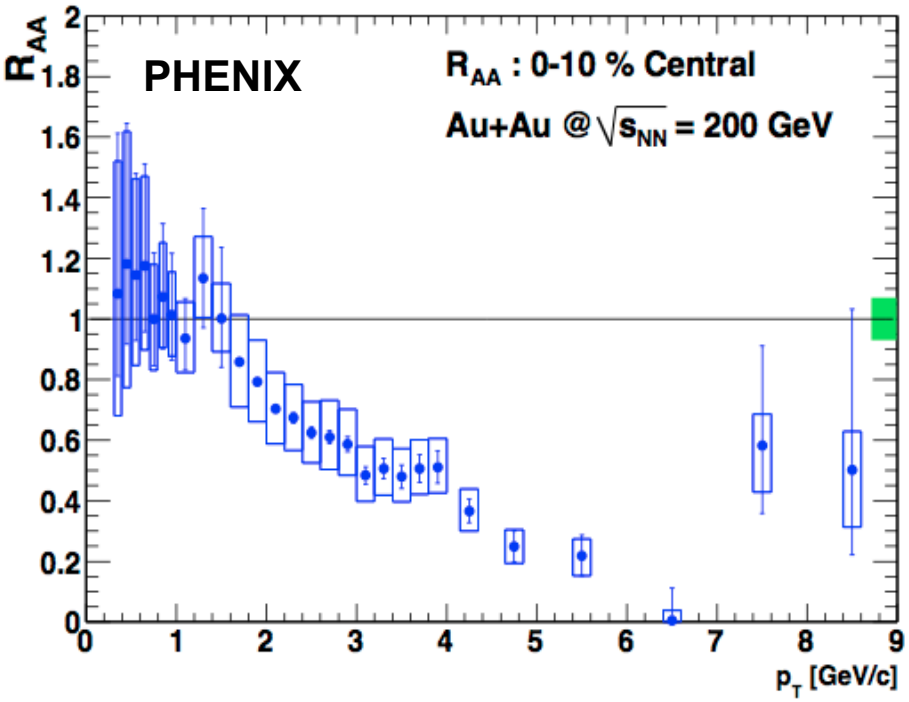

W. Xie (QM2012)
see also Phys. Rev. Lett. 98, 192301 (2007)

Phys. Rev. C 84, 044905 (2011)

- Same suppression as for light-flavour hadrons above 5 GeV/*c*
  - Mass already irrelevant?
- Smaller suppression at 2-3 GeV/c: is this the dead cone??

HF-decay e at RHIC (Cu-Cu vs. Au-Au)

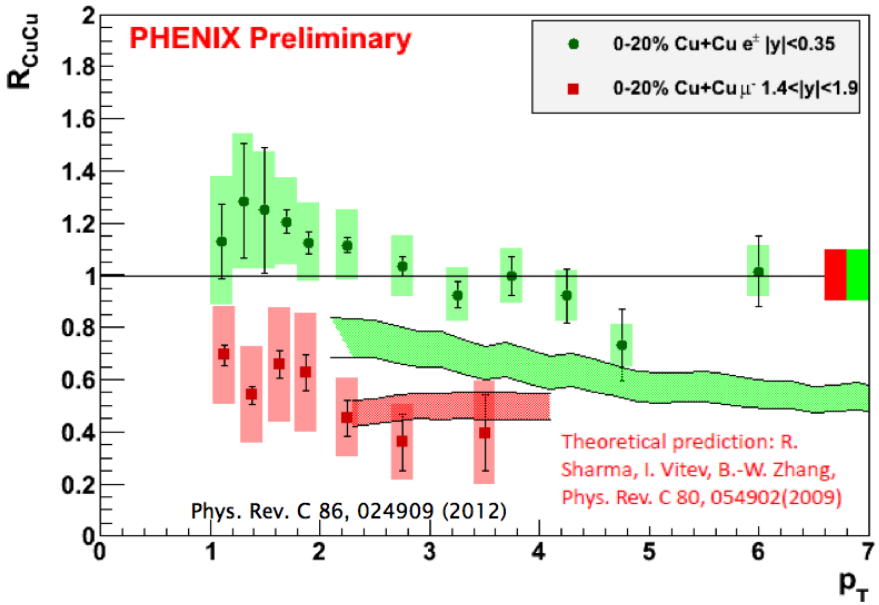

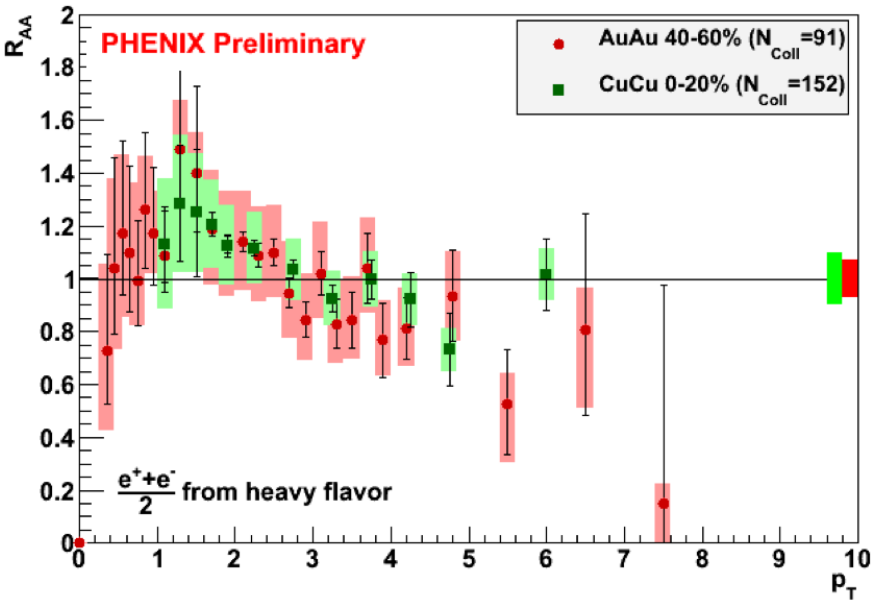

- Cu-Cu:
  - low p_T enhancement in central collisions?
  - no suppression even at 6 GeV/c: not expected in models!?
- Similar R_{AA} as in Au-Au for similar N_{coll} values

N.Apadula (WWND2013)

HF-decay e and μ at RHIC (Cu-Cu)

- Mid-rapidity (e): R_{AA}~1 → enhancement (from centr. to periph.)
- Forward rapidity (μ): suppression → R_{AA}~1

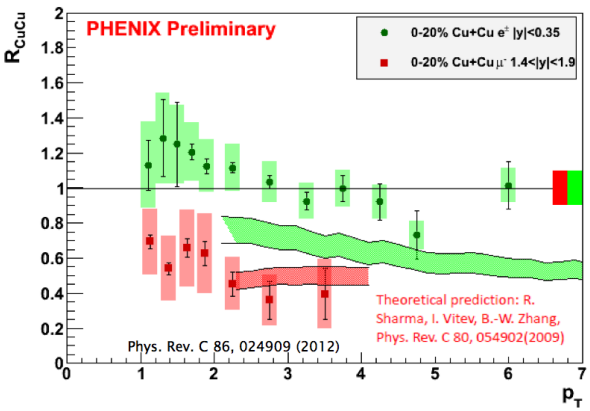

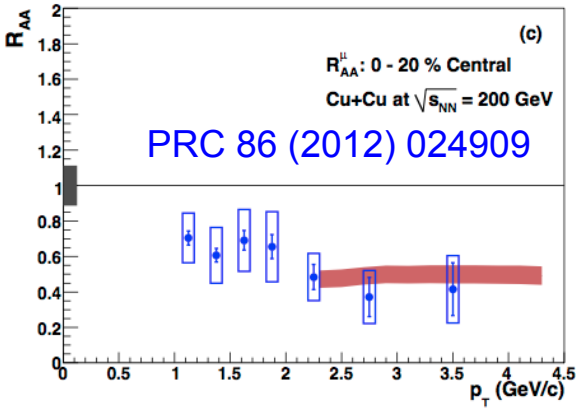

Theoretical prediction: R. Sharma, I. Vitev, B.-W. Zhang, Phys. Rev. C 80, 054902(2009)

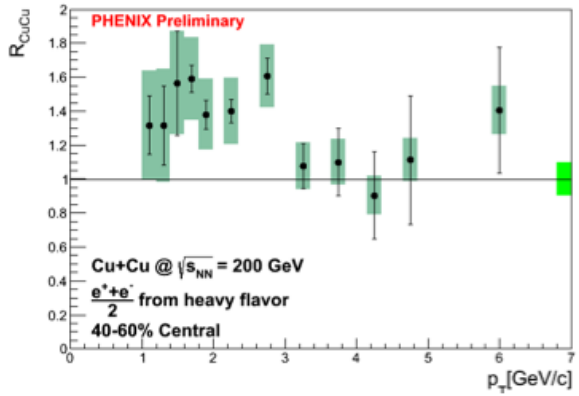

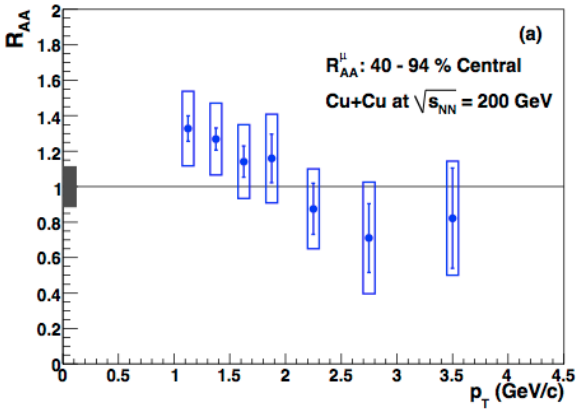

N.Apadula (WWND2013)

HF-decay e and μ at LHC: R_{AA} vs p_T

- Electrons and muons from D+B → e,μ decays

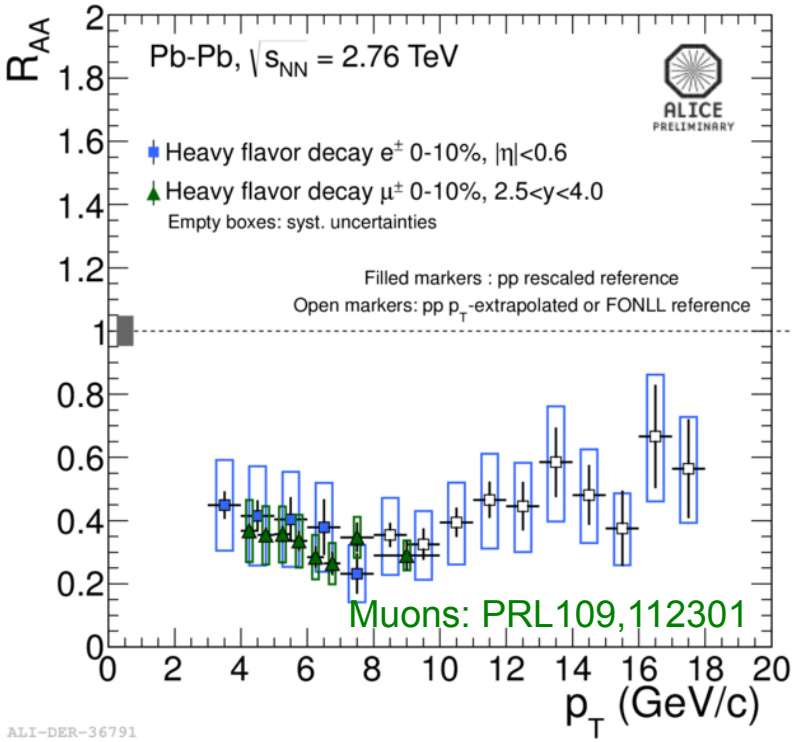

- Comparable suppression at central (|y|<0.6) and forward (2.5<y<4) rapidity

- Suppression by a factor about 2 up to 18 GeV/c
  - Dominated by beauty at such high p_T

Z.Conesa (QM2012)

HF-decay μ at LHC vs. centrality

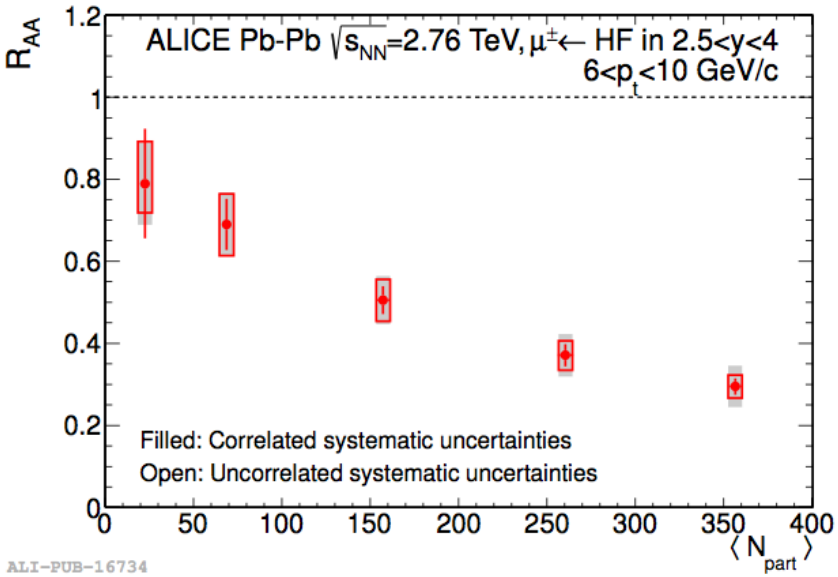

PRL 109 (2012) 112301

ATLAS-CONF-2012-081

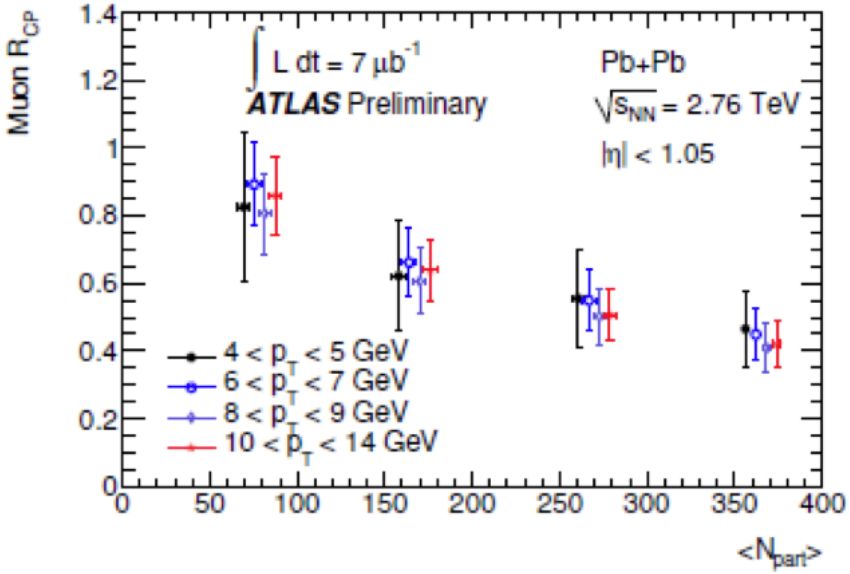

- Clear and consistent centrality dependence for
  - R_{AA} of muons at forward rapidity (ALICE)
  - R_{CP} of muons at central rapidity (ATLAS)
- No sign of p_T dependence from 4 to 12 GeV/c

Outline of the Talk

- Introduction: HF probes of the medium
- Calibrating HF probes: pp results
- HF production in nucleus-nucleus:
  - Semi-leptonic decays
  - D mesons
  - B and b-jets
- Proton-nucleus control data
- HF azimuthal anisotropy
- Outlook: detector upgrades at RHIC and LHC

RHIC	PHENIX, STAR	
	STAR	
LHC	ALICE, ATLAS	
	ALICE	
	CMS	

Charm: D mesons at RHIC

- STAR: first D R_{AA} in central Au-Au at RHIC

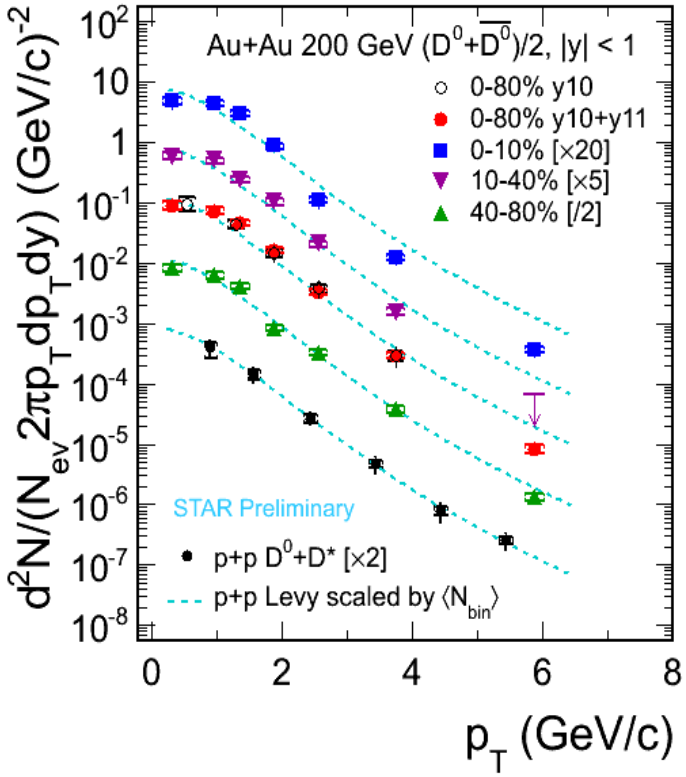

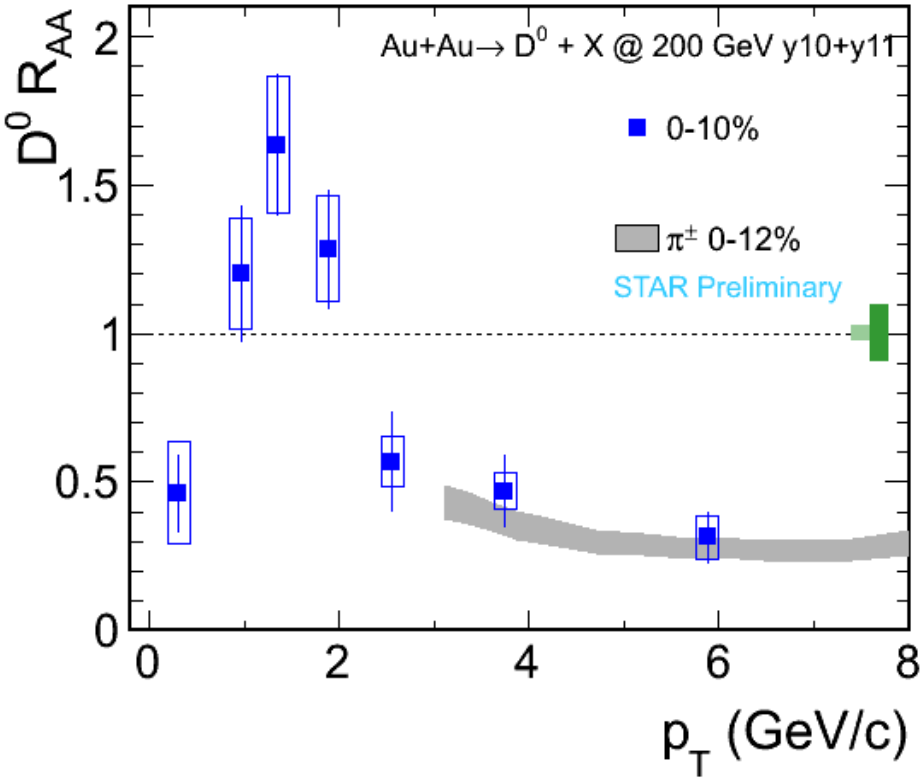

- Suppressed as much as pions at high p_T: no mass effect?
- Large enhancement at 1.5 GeV/c: radial flow + coalescence?

W.Xie (QM2012)

Charm: D mesons at LHC

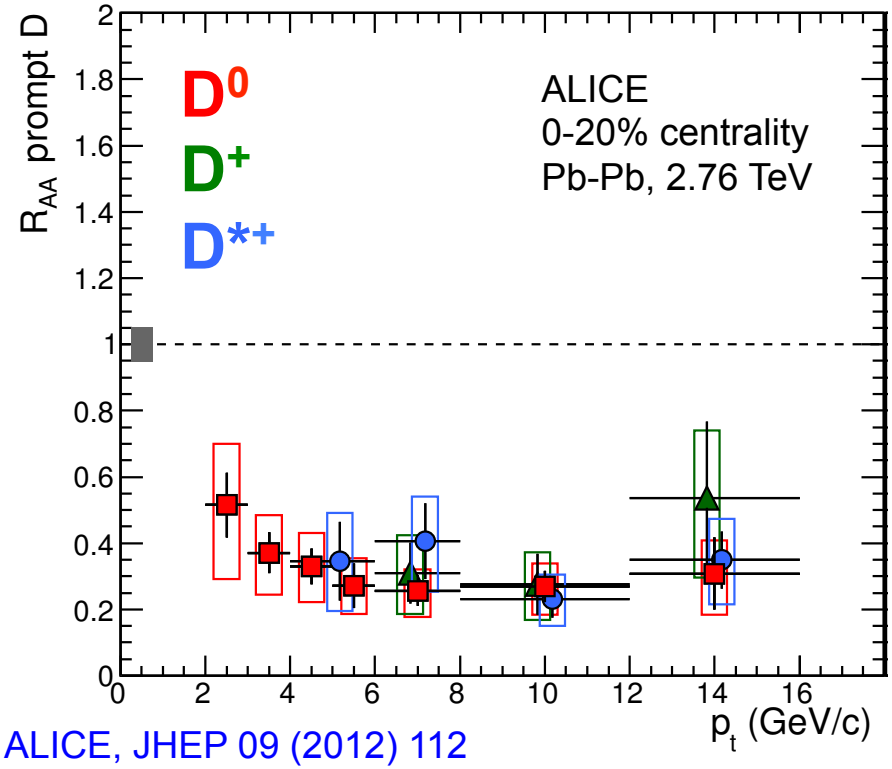

ALICE, JHEP 09 (2012) 112

Secondary vertex reconstruction (ALICE)

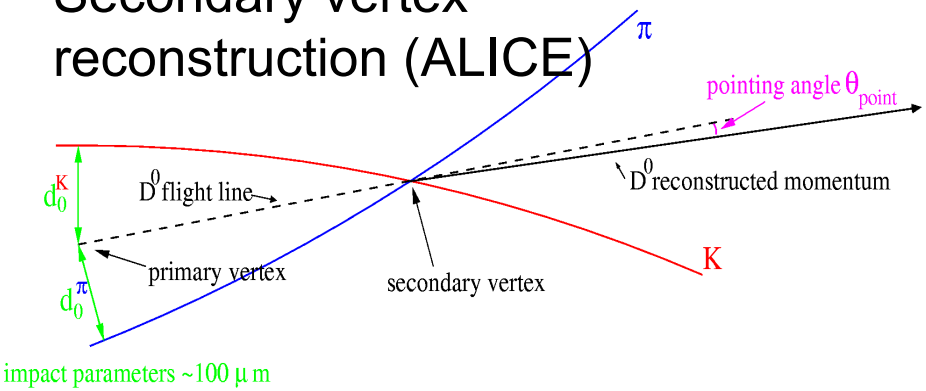

- First D R_{AA} measurement in heavy-ion collisions, presented by ALICE at QM2011 (LHC run 2010)
  - Strong suppression observed

Charm: D mesons at LHC

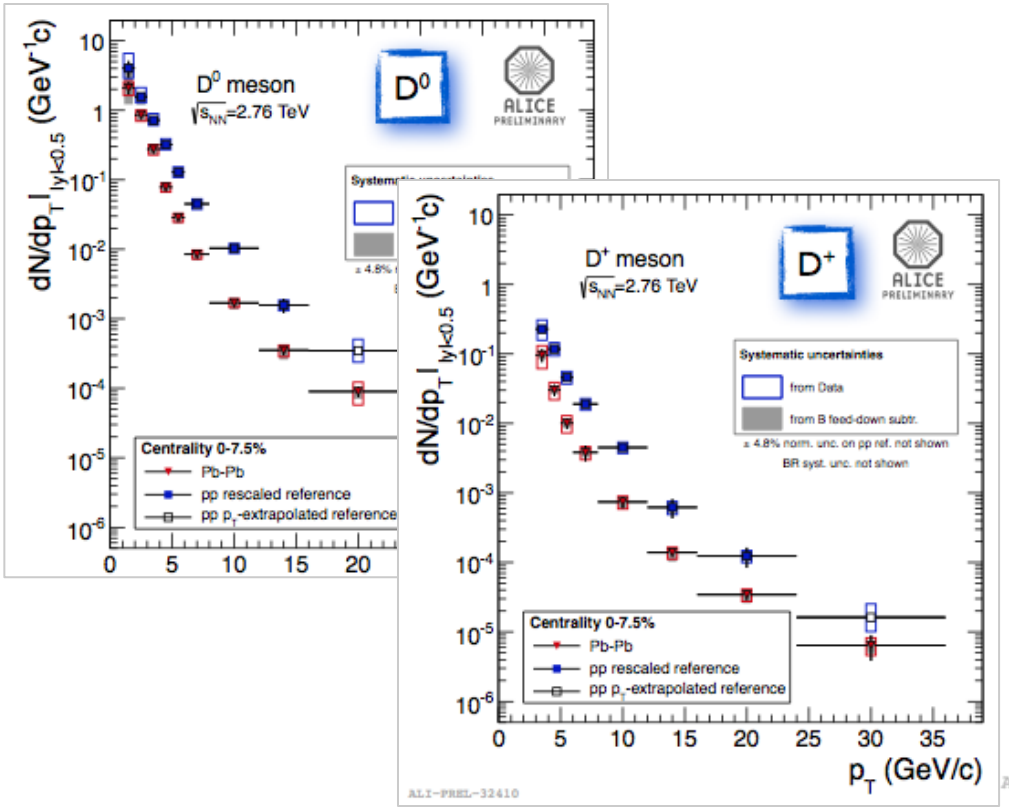

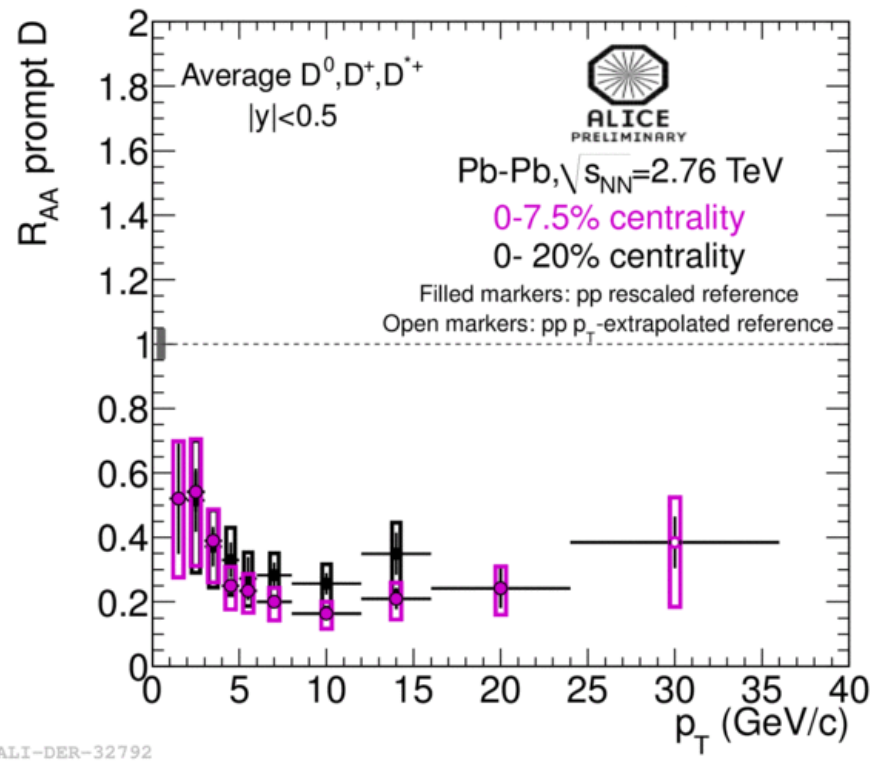

- First D R_{AA} measurement in heavy-ion collisions, presented by ALICE at QM2011 (LHC run 2010)
  - Strong suppression observed
- Measurement extended with LHC run 2011, from 1 to 30 GeV/c

Z.Conesa (QM2012)

Charm: D mesons vs. pions at RHIC and LHC

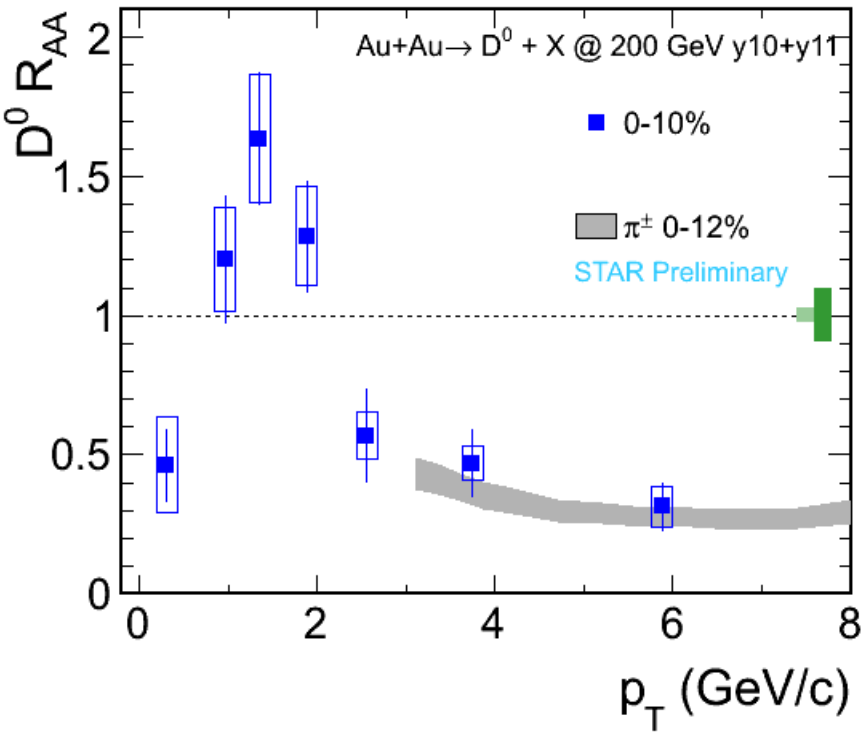

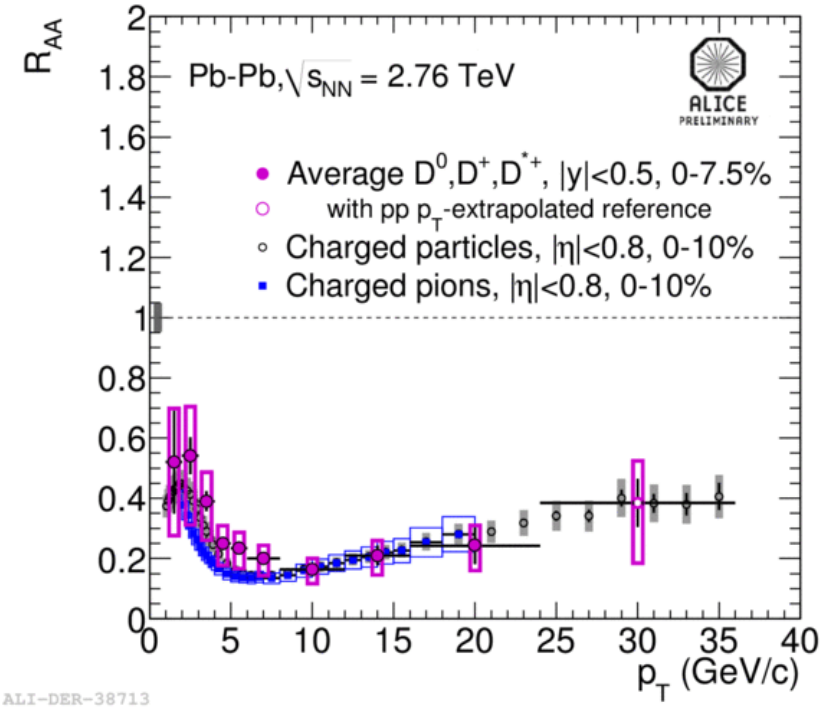

- D consistent with pions at both energies
  - Hint for D > π in 3-6 GeV/c at LHC?
- D meson R_{AA} similar at RHIC and LHC at 6 GeV/c
- Strikingly different at 1-2 GeV/c: stronger effect from coalescence at RHIC due to steeper spectra?

D_s meson R_{AA} at LHC

- First measurement of D_s in heavy ions
  - Large D_s enhancement expected, if *c* quarks recombine in the QGP

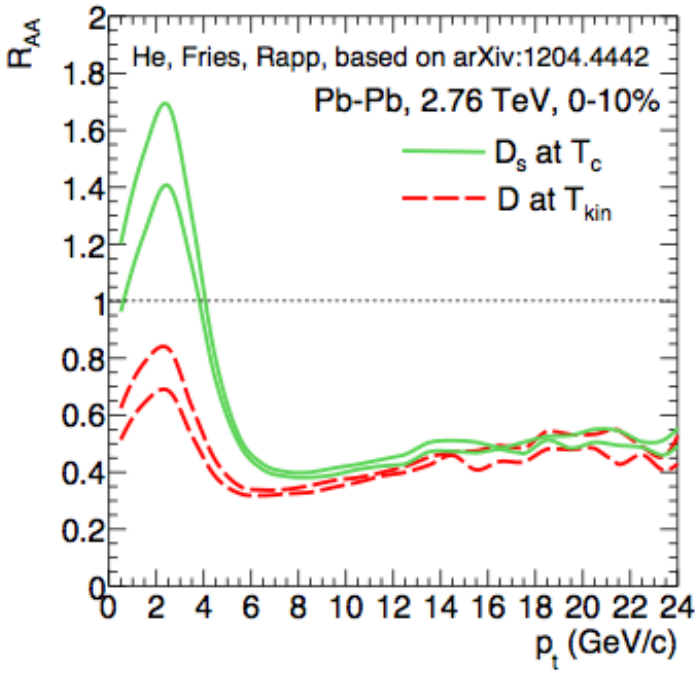

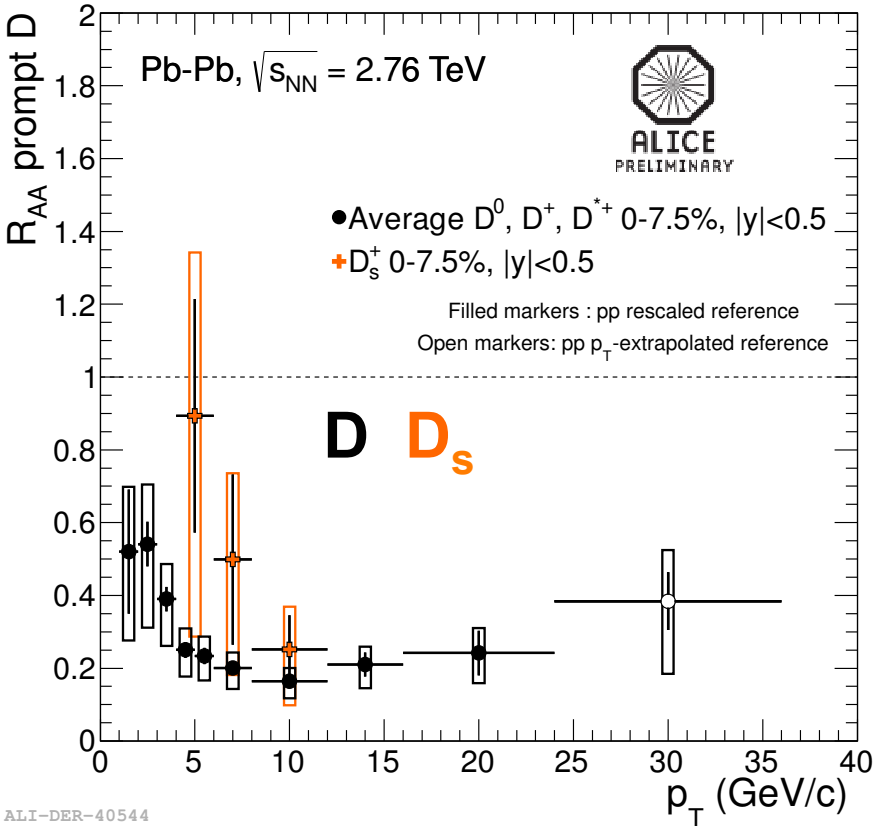

  - Data very intriguing, but not conclusive (→next LHC run, upgrades)

Z.Conesa (QM2012)

Outline of the Talk

- Introduction: HF probes of the medium
- Calibrating HF probes: pp results
- HF production in nucleus-nucleus:
  - Semi-leptonic decays
  - D mesons
  - B and b-jets
- Proton-nucleus control data
- HF azimuthal anisotropy
- Outlook: detector upgrades at RHIC and LHC

RHIC	PHENIX, STAR	
	STAR	
LHC	ALICE, ATLAS	
	ALICE	
	CMS	

Beauty suppression at LHC

- First measurement of beauty R_{AA} by CMS (CMS-PAS-HIN-12-014)

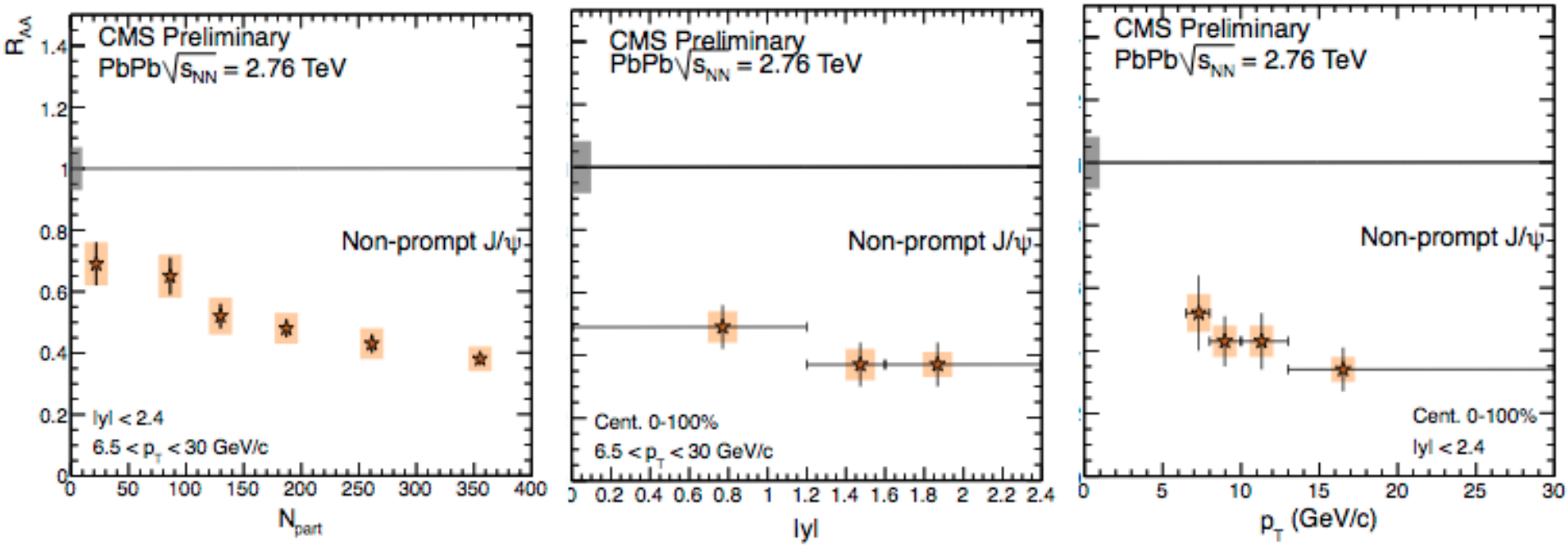

- Centrality dependence of B→J/ψ R_{AA}
  - 50-100%: factor ~1.4 → 0-5%: factor ~2.5
- Hint of less suppression at mid-rapidity
- Hint of larger suppression at higher p_T

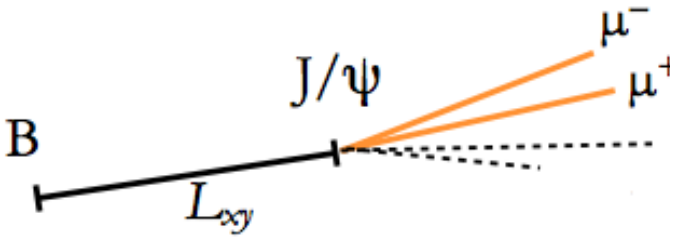

Is this the dead cone?

- Comparison of charmed mesons (ALICE) with J/ψ from beauty decays (CMS)

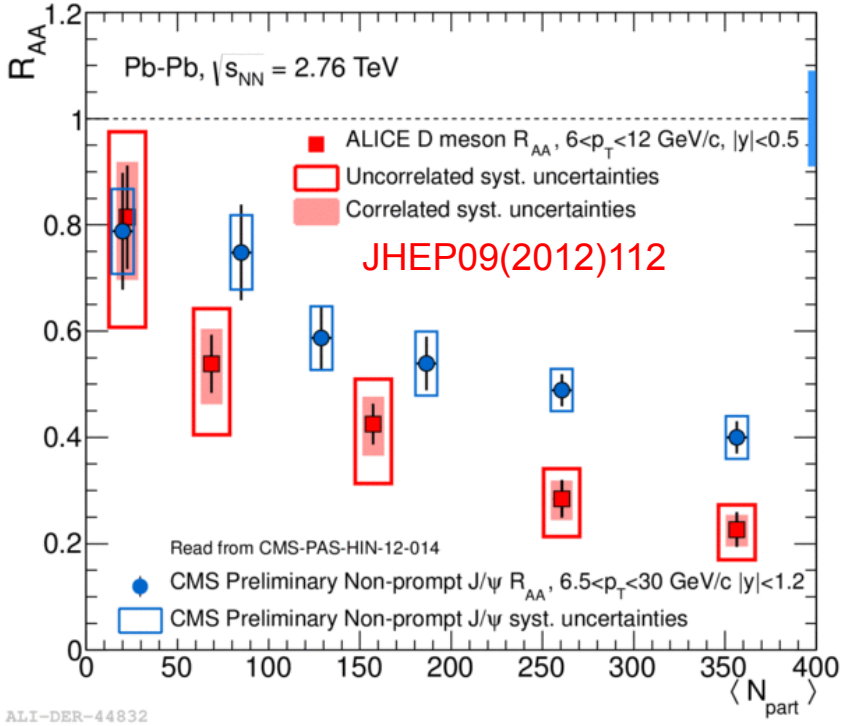

- First indication of a dependence on heavy quark mass:

$$R_{AA}^{B} > R_{AA}^{D}$$

  - However, kinematical ranges are not exactly the same

Large b-jet suppression at LHC

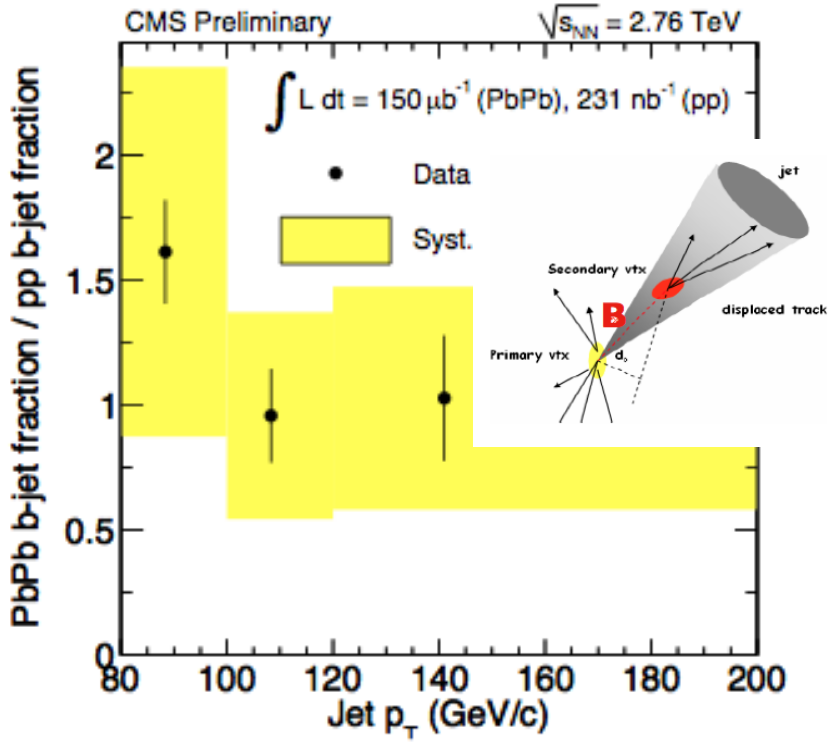

b-jet double_ratio =
b-fraction in PbPb / b-fraction in pp

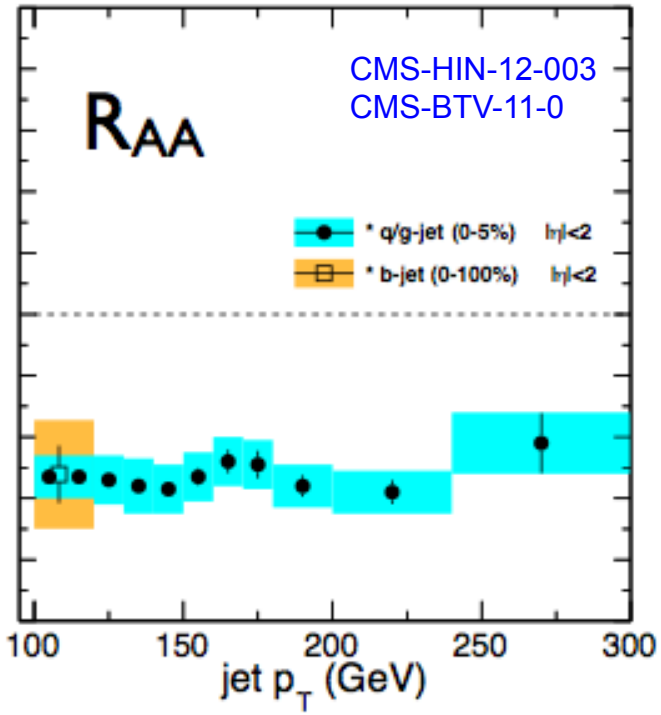

b-jet R_{AA} =
inclusive-jet R_{AA} * b-jet double_ratio

- CMS finds the same R_{AA} for b-jets as for q/g-jets, as expected at this p_T

Outline of the Talk

- Introduction: HF probes of the medium
- Calibrating HF probes: pp results
- HF production in nucleus-nucleus:
  - Semi-leptonic decays
  - D mesons
  - B and b-jets
- Proton-nucleus control data
- HF azimuthal anisotropy
- Outlook: detector upgrades at RHIC and LHC

Initial state effects on heavy quarks

- Charm production at low p_T: **Q^2 ($4m_c^2 \sim$ 5-10 GeV^2)**

Machine	SPS	RHIC	LHC	LHC
System	Pb–Pb	Au–Au	Pb–Pb	pp
$\sqrt{s_{NN}}$	17 GeV	200 GeV	5.5 TeV	14 TeV
$c\bar{c}$	$x \simeq 10^{-1}$	$x \simeq 10^{-2}$	$x \simeq 4 \times 10^{-4}$	$x \simeq 2 \times 10^{-4}$
$b\bar{b}$	–	–	$x \simeq 2 \times 10^{-3}$	$x \simeq 6 \times 10^{-4}$

→ interpretation of HF (charm) measurements in AA requires pA reference

→ charm in pA: access to small-*x* gluons with perturbative probes

Nuclear modification of PDFs

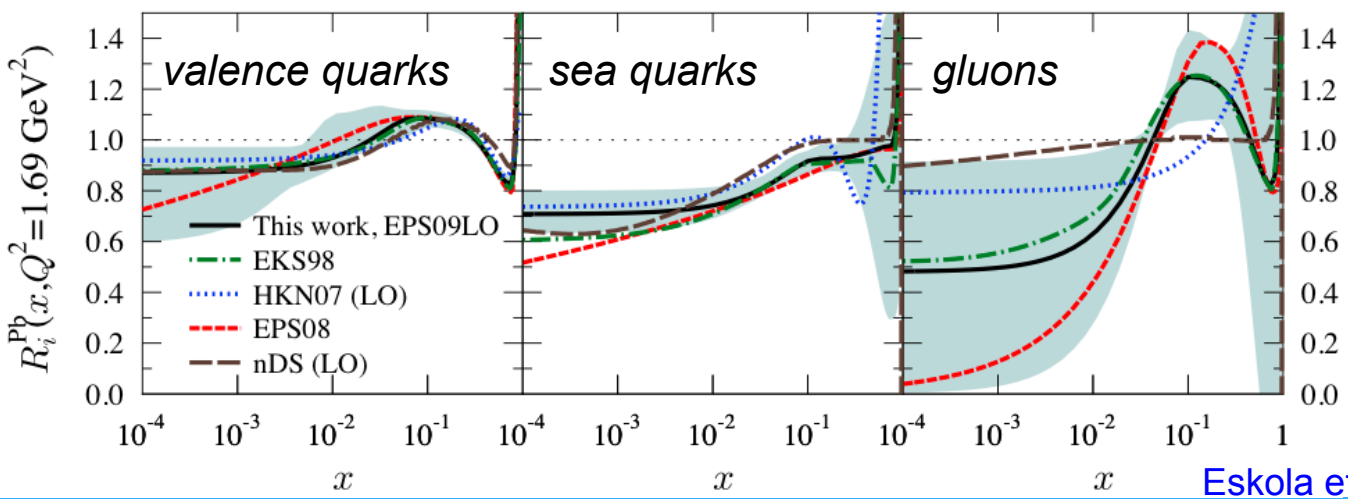

Eskola et al. JHEP0904(2009)065

Only a QCD medium effect? RHIC

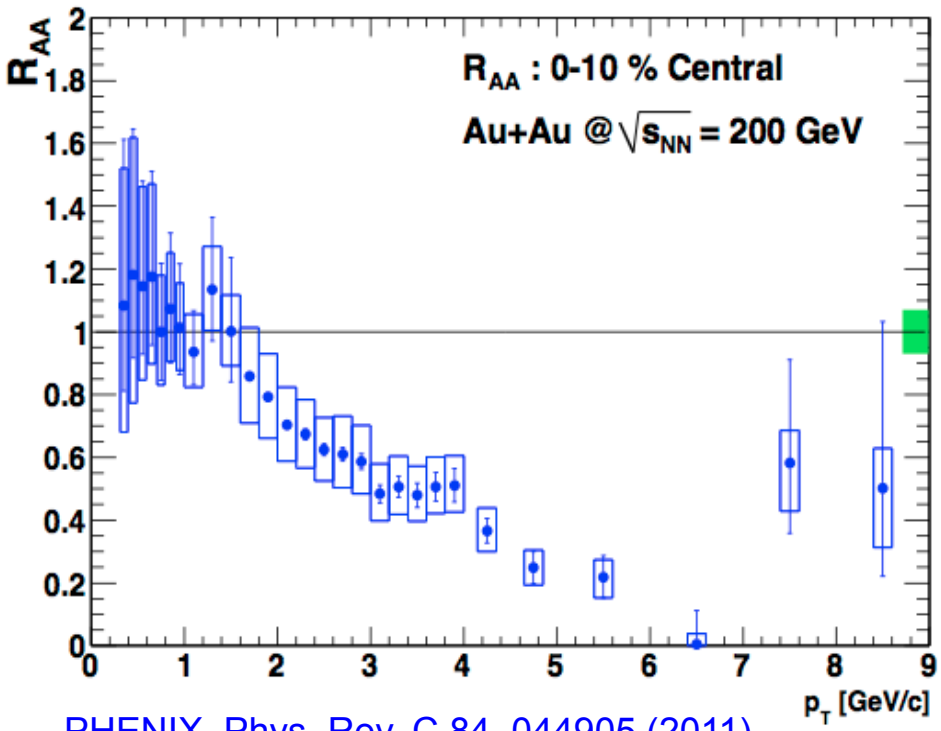

PHENIX, Phys. Rev. C 84, 044905 (2011)

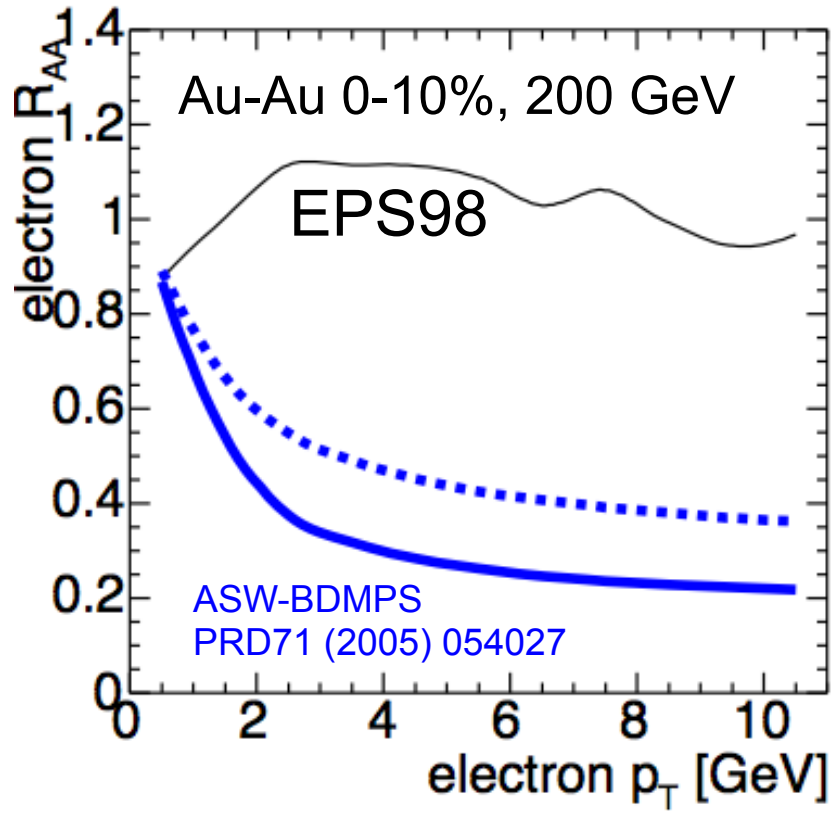

- Small effect expected from PDFs shadowing (<10%)
- Mostly a hot medium effect?
- <u>p/d-A control crucial to quantify initial-state effects</u>

Only a QCD medium effect? LHC

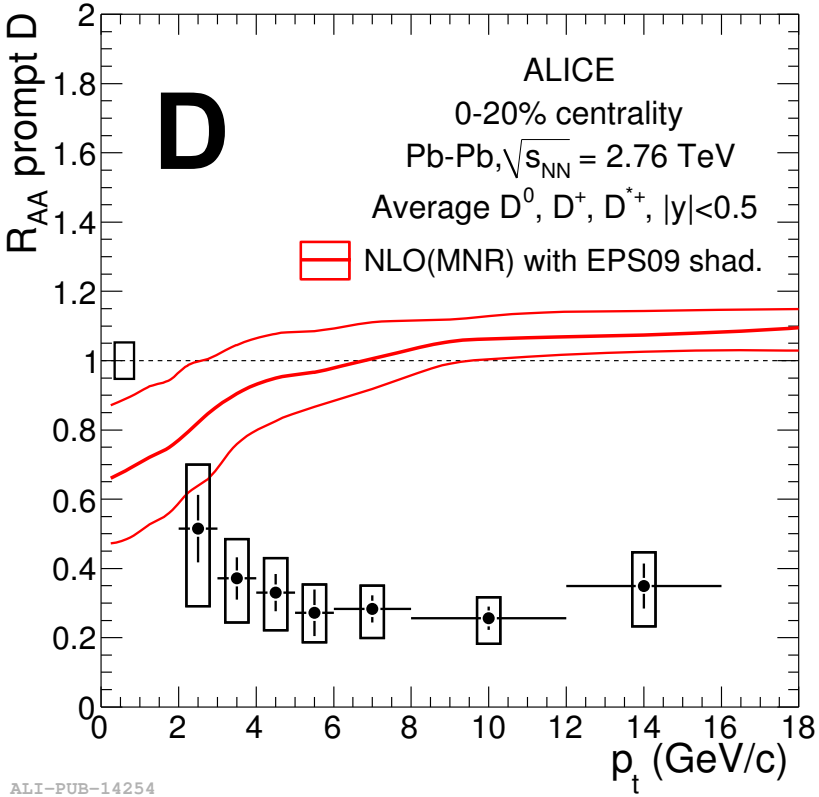

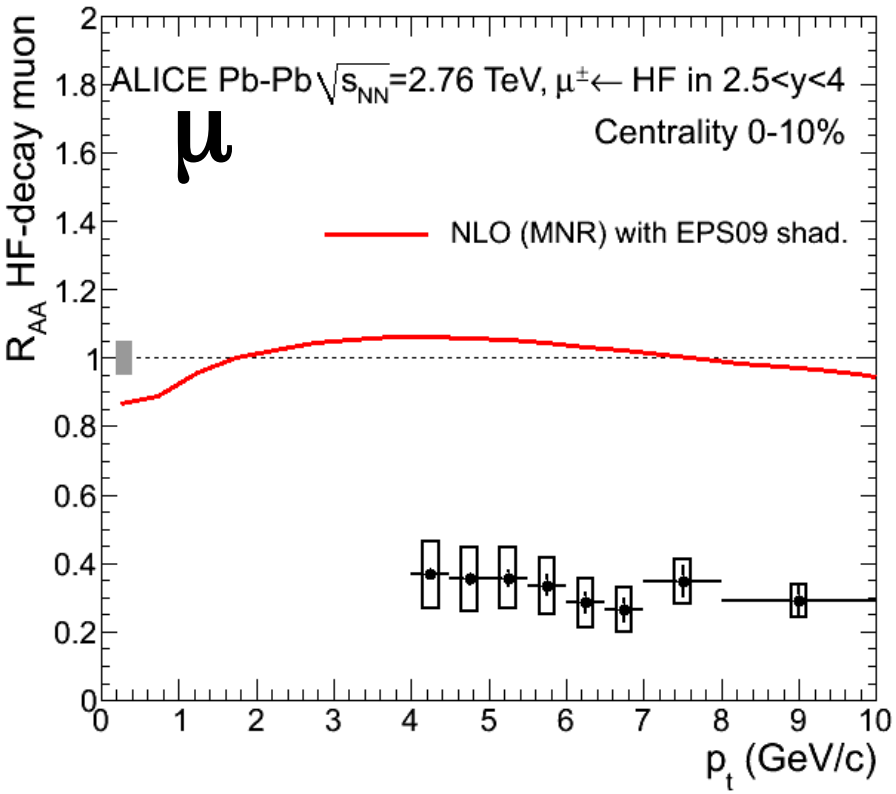

JHEP 09 (2012) 112
PRL 109 (2012) 112301

- Small effect expected from PDFs shadowing above 5 GeV/c
- Mostly a hot medium effect above 5 GeV/c?
- <u>p/d-A control crucial to quantify initial-state effects</u>

EPS09: Eskola et al. JHEP0904(2009)065

HF e in d-Au: RHIC results

Phys. Rev. Lett. 109, 242301 (2012)

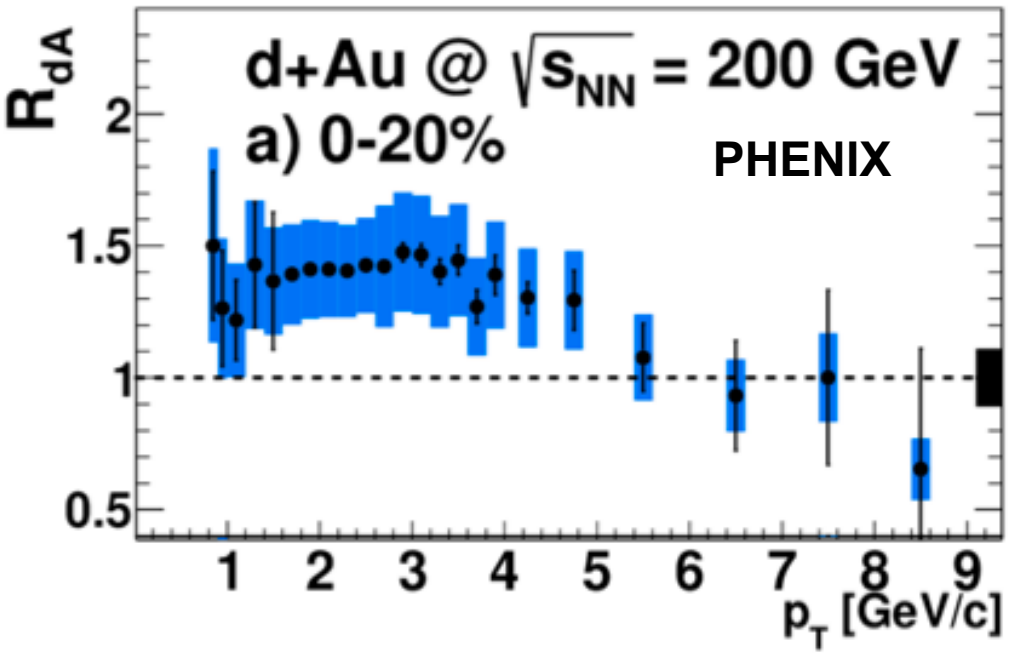

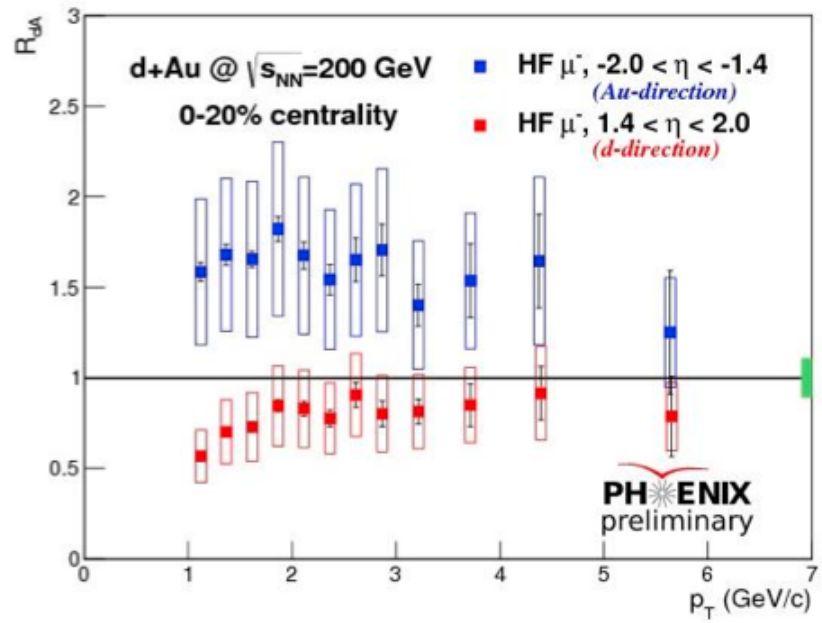

- Low-p_T electrons (mid-y) and muons (forward y) largely enhanced
- More than expected from anti-shadowing?

N.Apadula (WWND2013)

HF e in d-Au: RHIC results

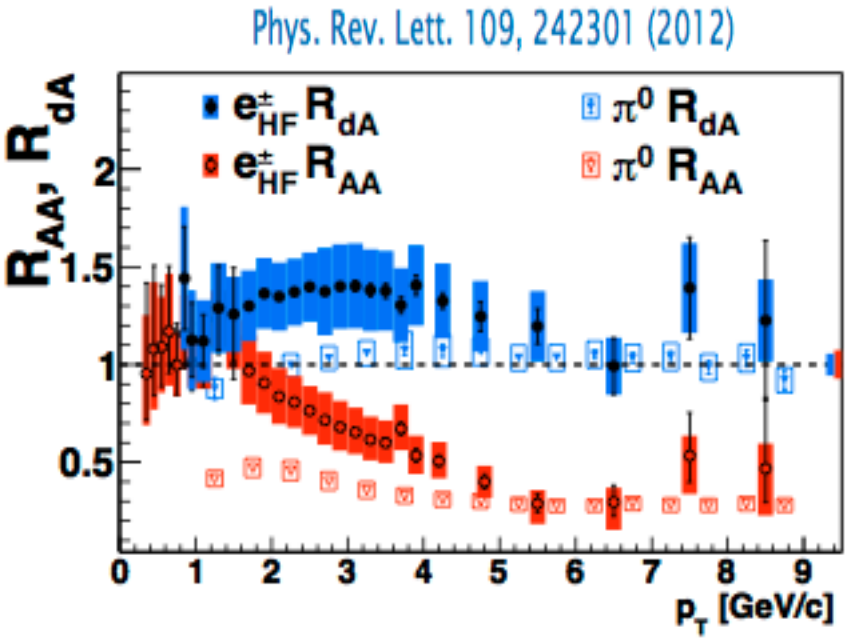

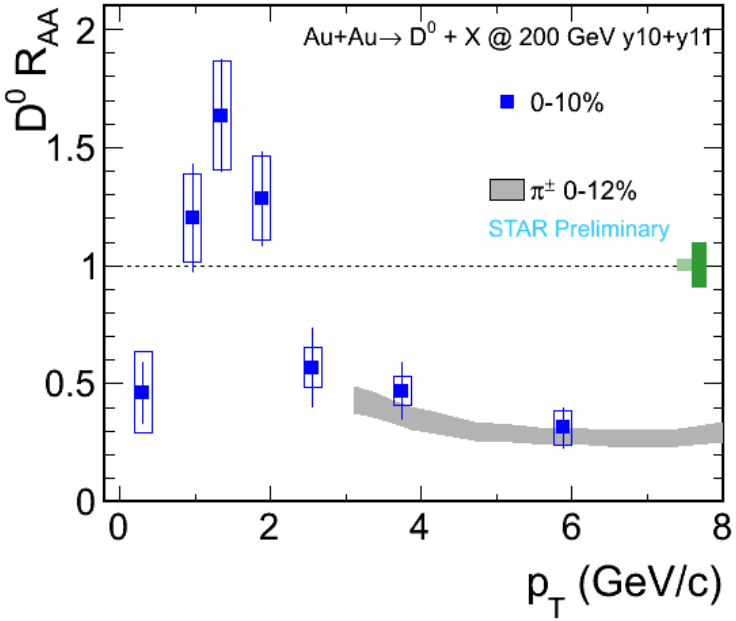

- Low-p_T electrons (mid-y) and muons (forward y) largely enhanced
- More than expected from anti-shadowing?
- Significant role of (mass-dependent?) k_T broadening / initial-state partonic scattering?
- Or is there some final-state "activity"? → need D mesons!!!

HF in p-Pb at LHC: analyses ongoing …

- Large integrated lumi of the p-Pb run (~30/nb) will allow the experiments (including LHCb!) to measure, with precision ~PbPb2011:
  - HF-decay electrons and muons
  - D mesons, including D_s
  - B→J/ψ, b-jets
- Example: D meson signals in ALICE

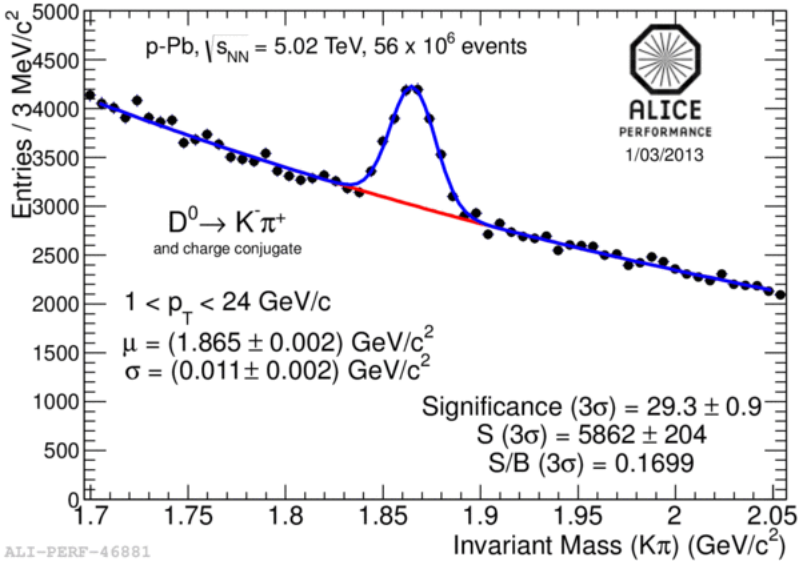

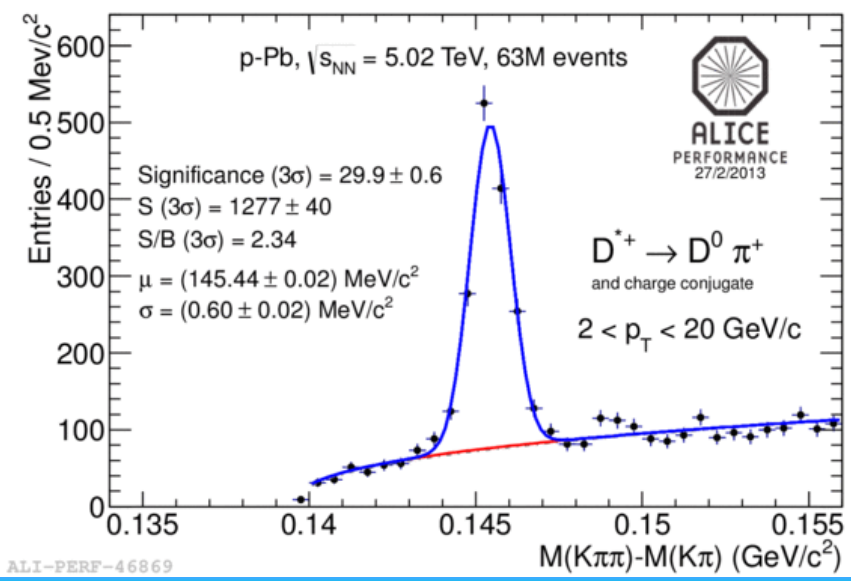

Outline of the Talk

- Introduction: HF probes of the medium
- Calibrating HF probes: pp results
- HF production in nucleus-nucleus:
  - Semi-leptonic decays
  - D mesons
  - B and b-jets
- Proton-nucleus control data
- HF azimuthal anisotropy
- Outlook: detector upgrades at RHIC and LHC

Heavy flavour v_2: a two-fold observable

- Low p_T: do heavy quarks take part in the "collectivity"?
  - Due to their large mass, c and b quarks should "feel" less the collective expansion
    - → need frequent interactions with large coupling to build v_2
    - → $v_2^b < v_2^c$
- High p_T: probe path length dependence of HQ energy loss

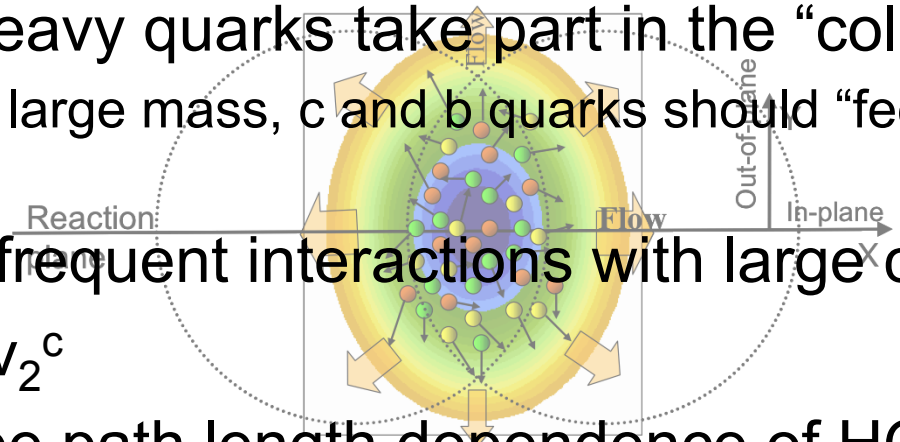

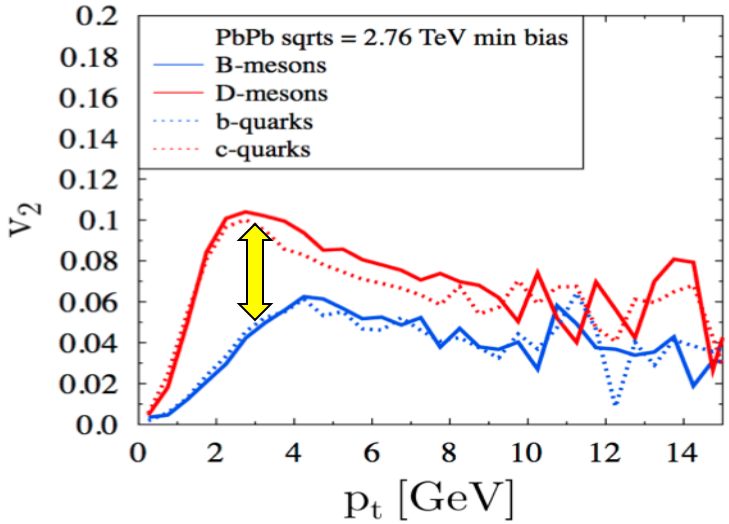

J. Aichelin et al. in arXiv:1201.4192

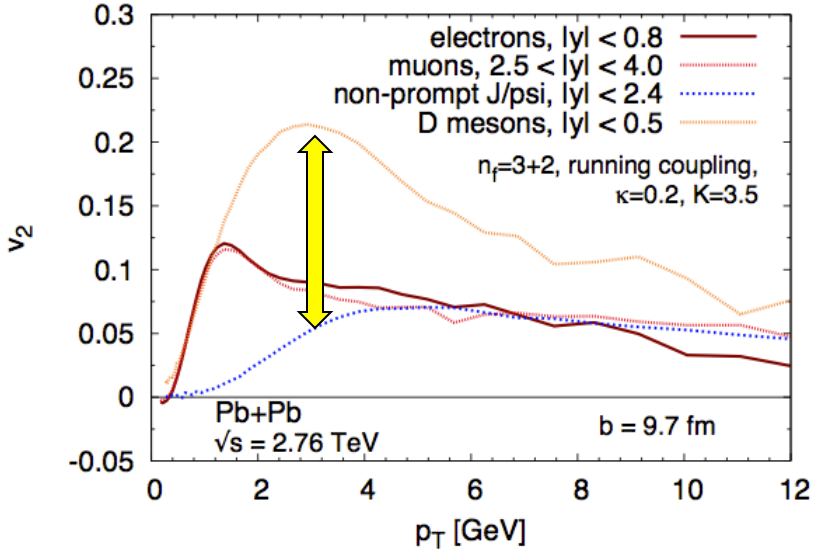

J. Uphoff et al. in arXiv:1205.4945

Heavy-flavour azimuthal anisotropy, from RHIC to LHC

- Electrons from HF show a v_2 of up to 0.15 at RHIC (PHENIX, STAR)
  - Charm does flow!
  - v_2 significantly smaller than for pions above 2 GeV/c (might be decay kinematics, rather than a difference heavy vs. light)
- First measurements at the LHC (ALICE): electron v_2 comparable to RHIC

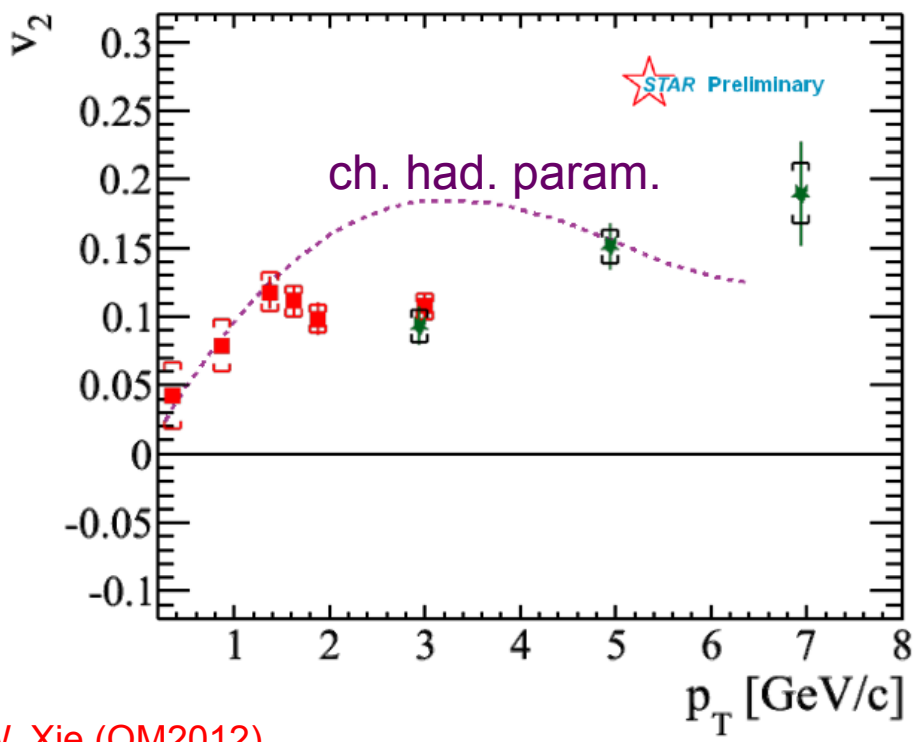

W. Xie (QM2012)

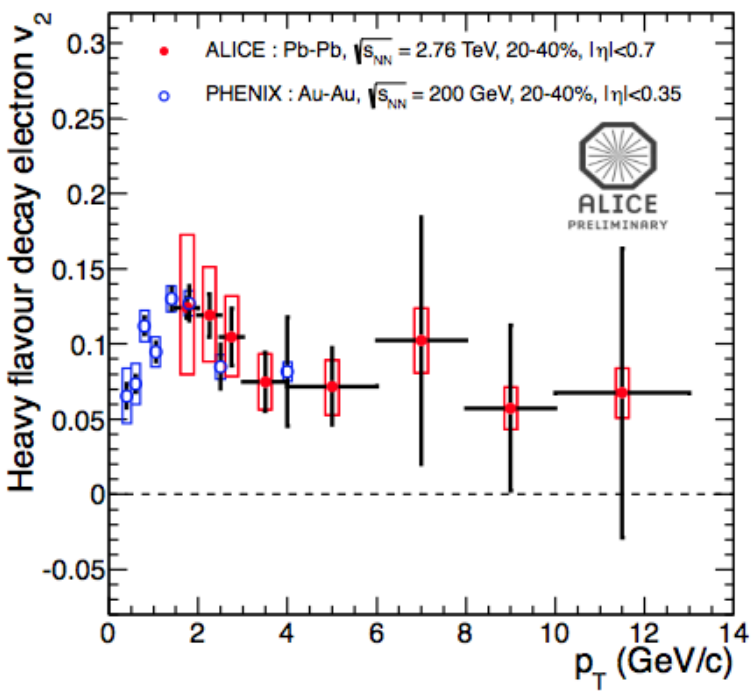

PHENIX, PRC84 (2011) 044905

Z. Conesa (QM2012)

Heavy-flavour azimuthal anisotropy, from RHIC to LHC

- First D measurements at the LHC (ALICE): D meson v_2>0 in 30-50% class
  - D meson v_2>0 in 30-50% class & Comparable to v_2 of charged hadrons
  - Suggests flow at low p_T and path-length dependent suppression at high p_T
- First D v_2 measurement at RHIC presented at QM by STAR (not shown)

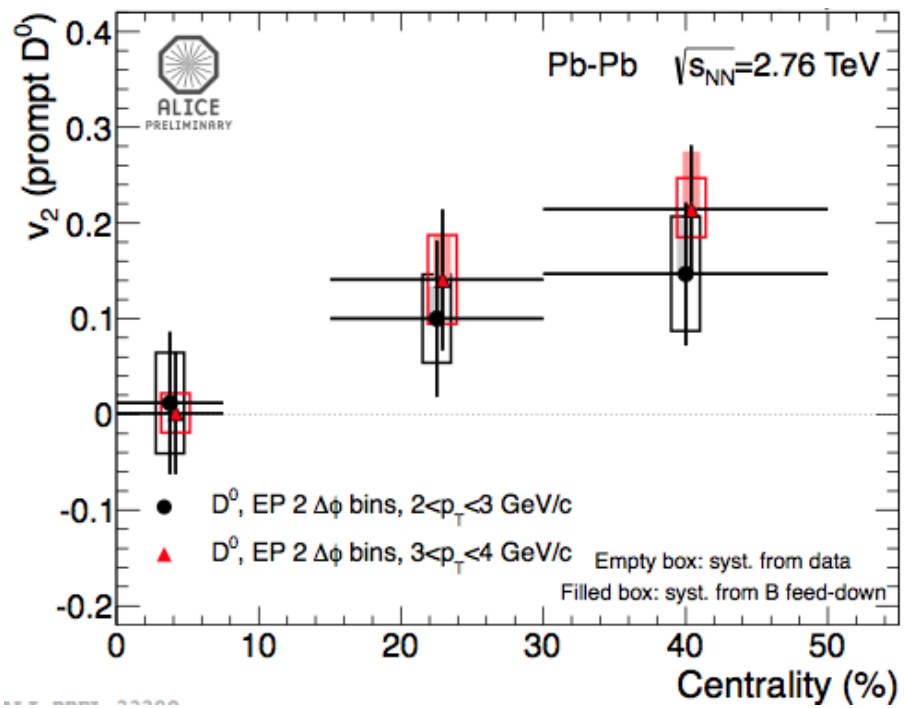

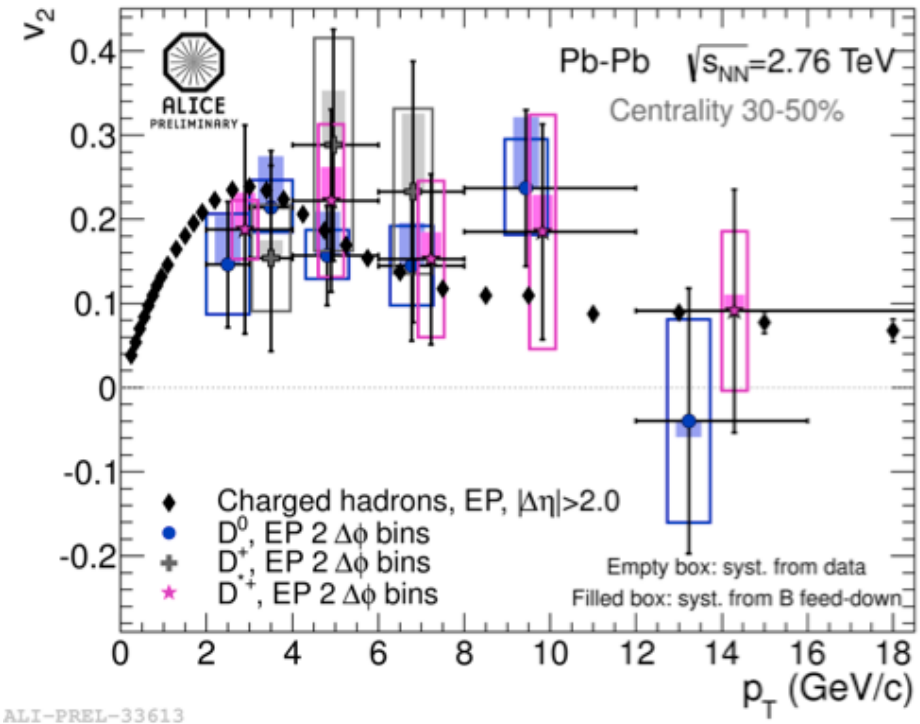

Z. Conesa (QM2012)

LHC: comparison with models (R_{AA})

- Several models based on E-loss and heavy-quark transport describe qualitatively the measured light, charm, and beauty R_{AA}

charm **"light"** **beauty**

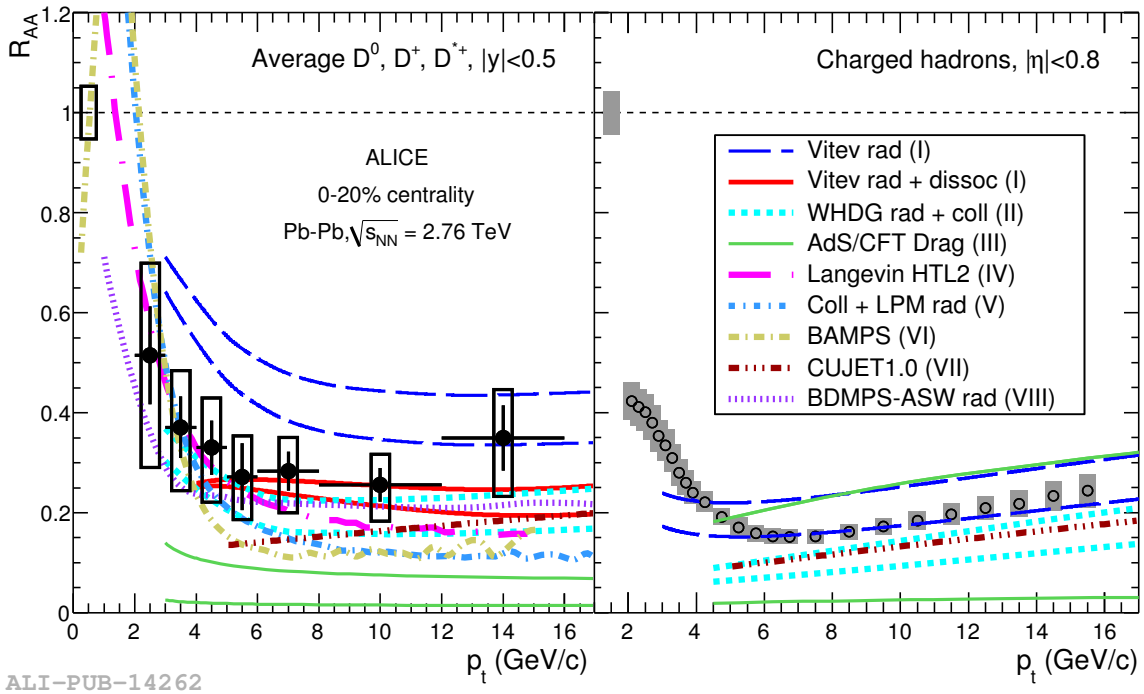

ALICE, JHEP 09 (2012) 112

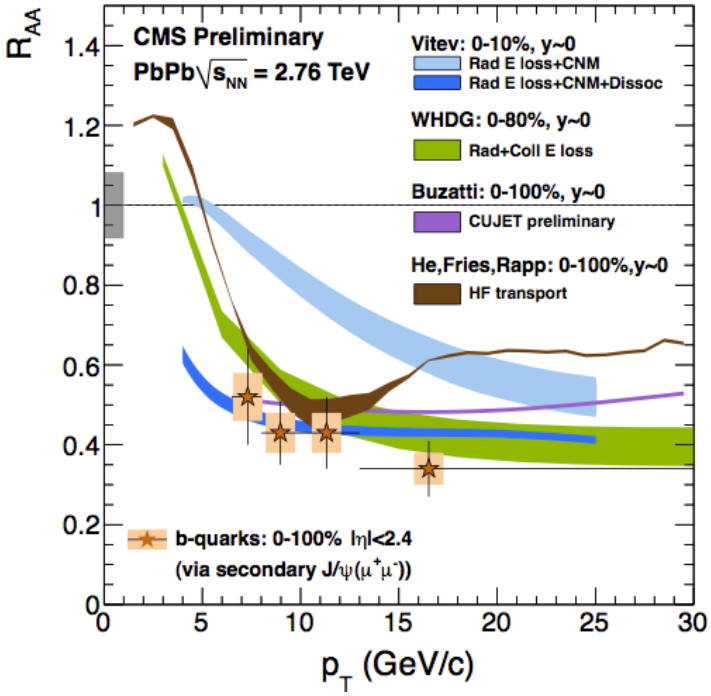

CMS-PAS-HIN-12-014

LHC: comparison with models (R_{AA} and v_2)

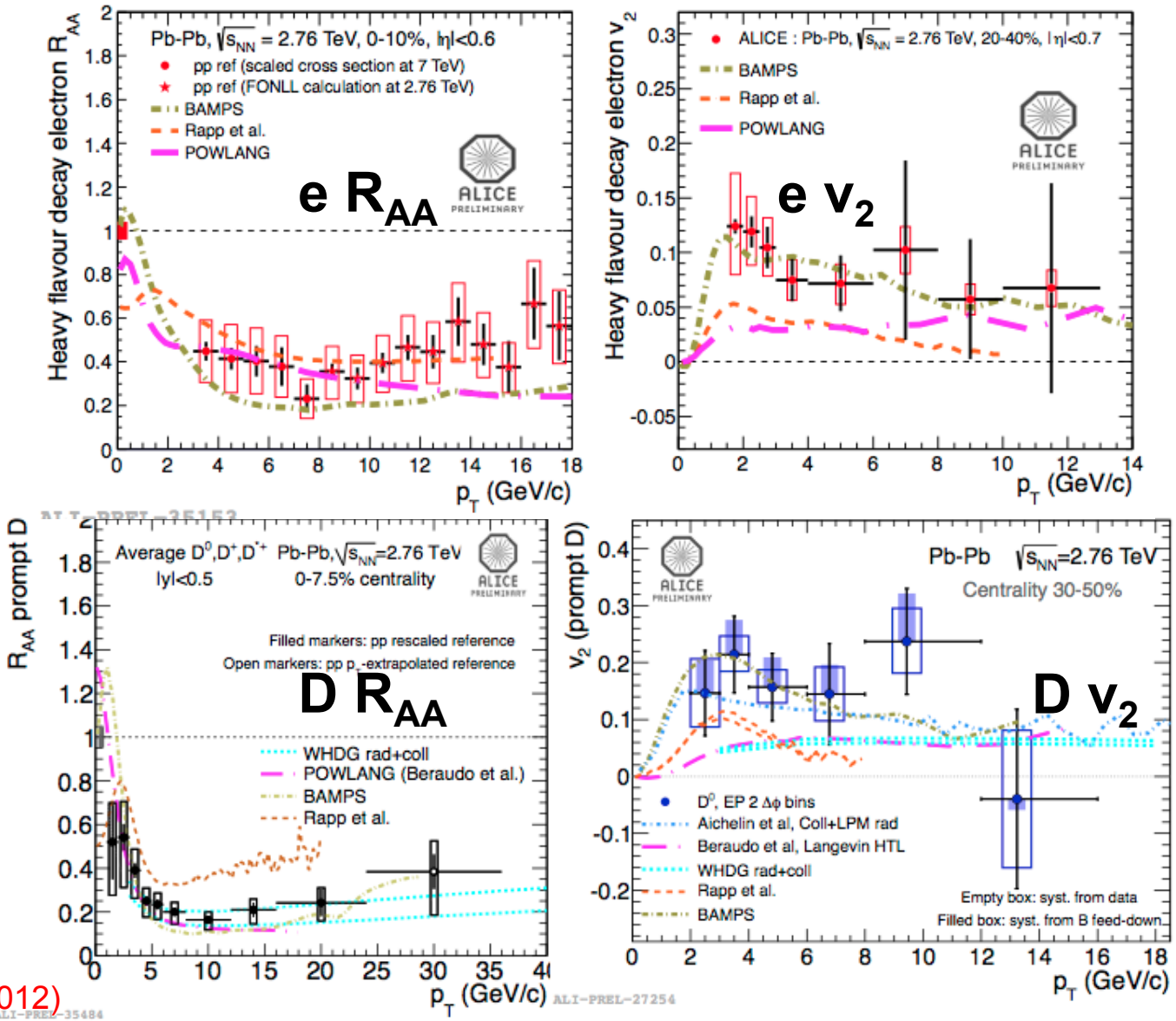

Z. Conesa (QM2012)

LHC: comparison with models (R_{AA} and v_2)

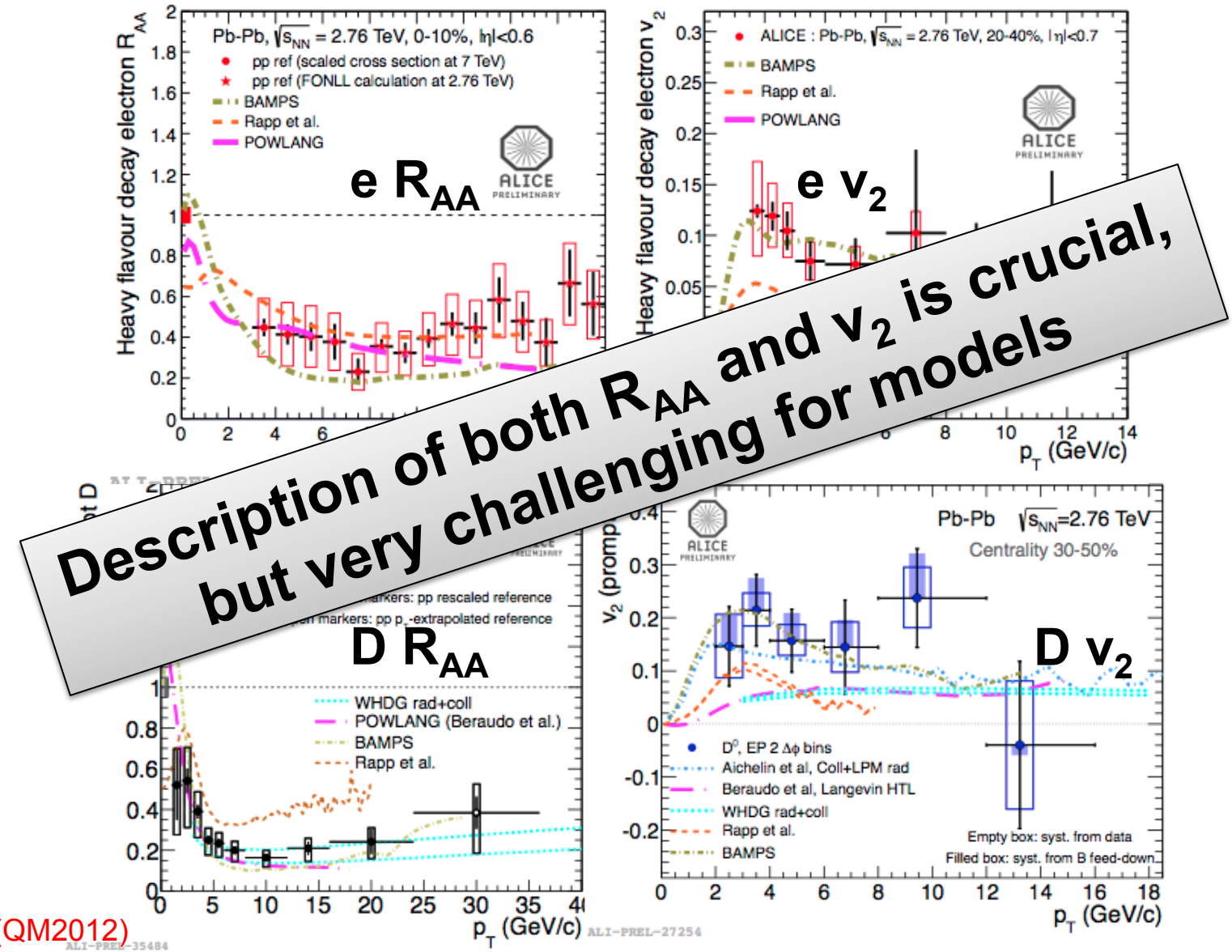

Z. Conesa (QM2012)

Towards HF tomography

- D suppression in different azimuthal directions

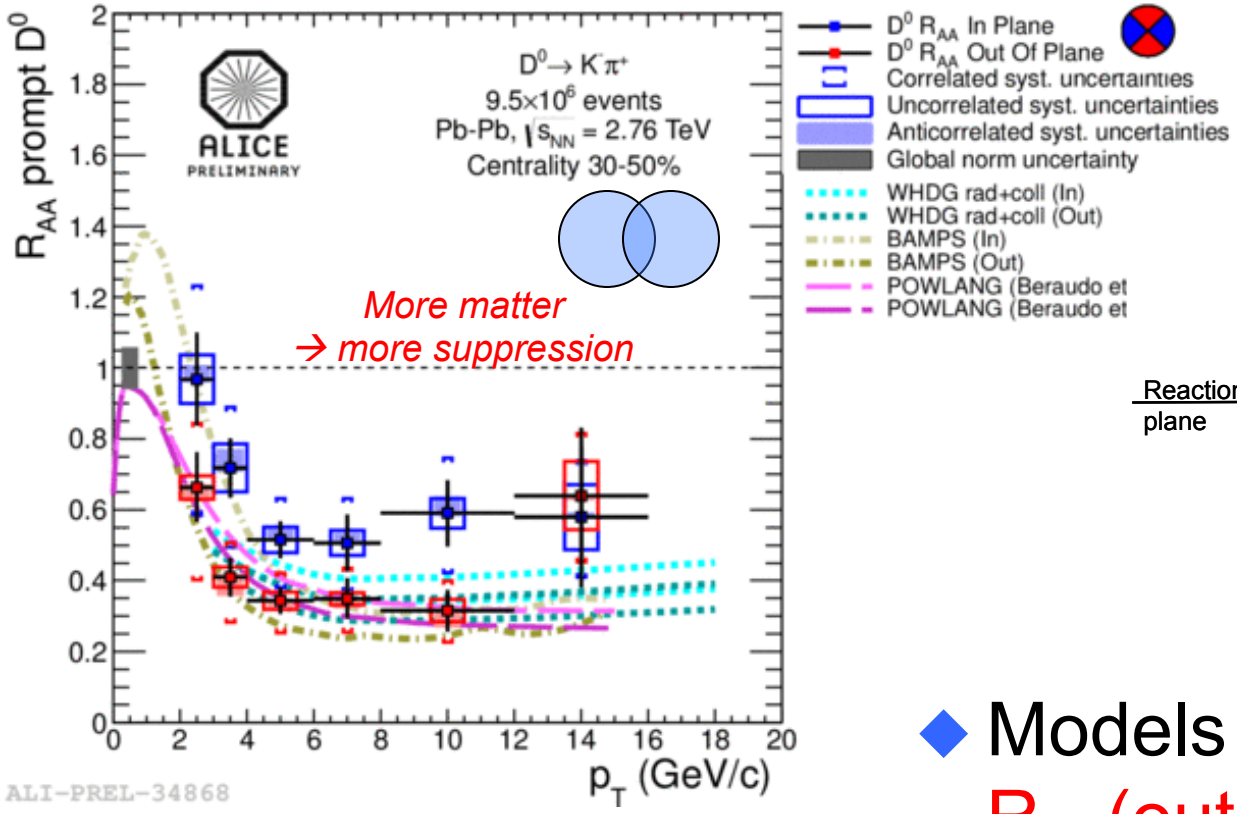

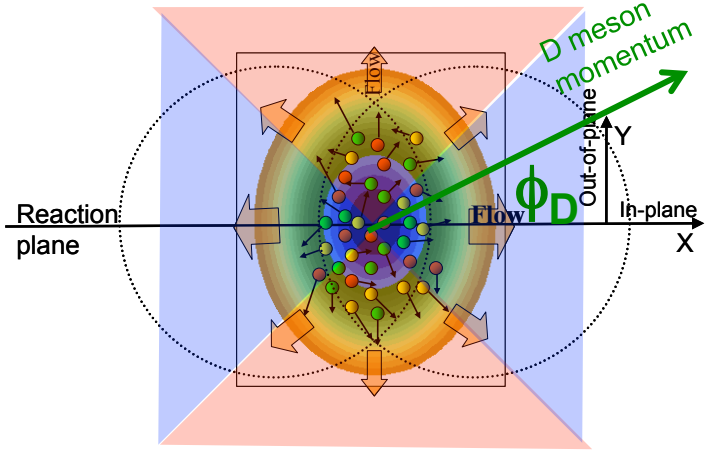

much more of this with next LHC run, then upgrades

- Models tend to describe R_{AA}(out-of-plane) better than R_{AA}(in-plane)

Z.Conesa (QM2012)

Outline of the Talk

- Introduction: HF probes of the medium
- Calibrating HF probes: pp results
- HF production in nucleus-nucleus:
  - Semi-leptonic decays
  - D mesons
  - B and b-jets
- Proton-nucleus control data
- HF azimuthal anisotropy
- Outlook: detector upgrades at RHIC and LHC
  - Heavy flavour: a central topic for upgrades of all the HI experiments!

PHENIX: Vertex Tracker (VTX)

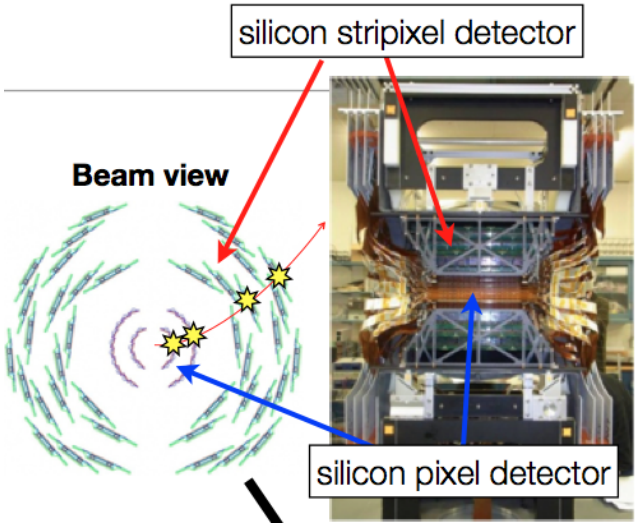

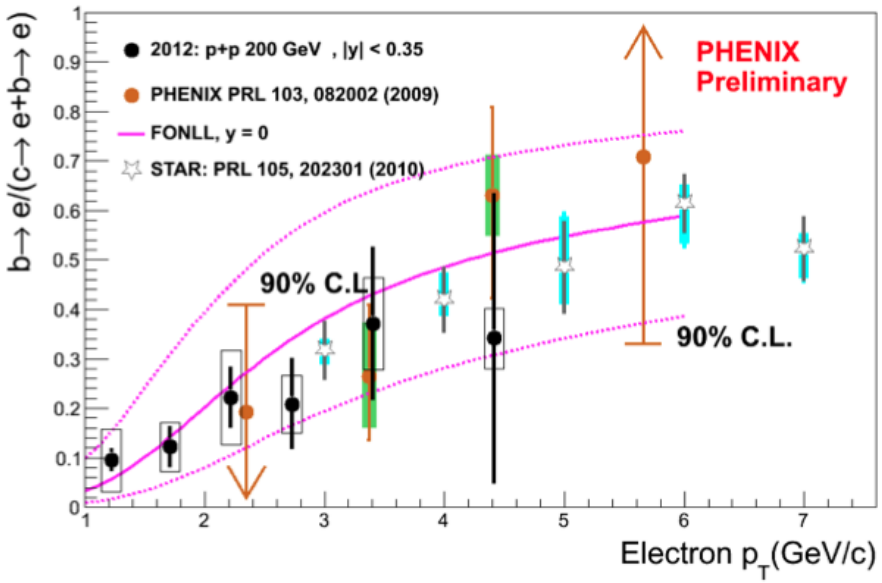

Projections 5B evts

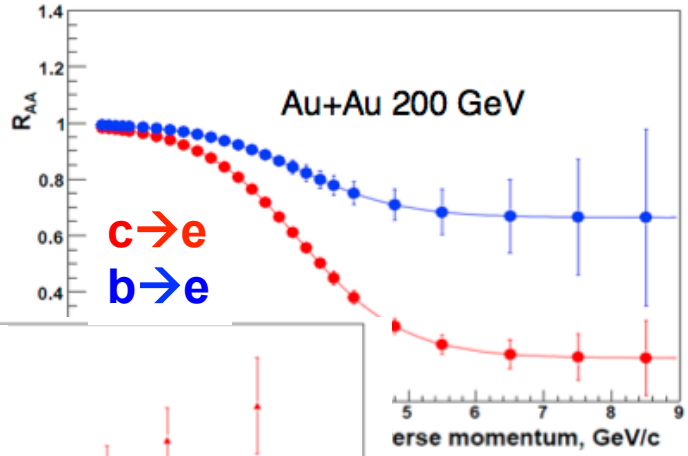

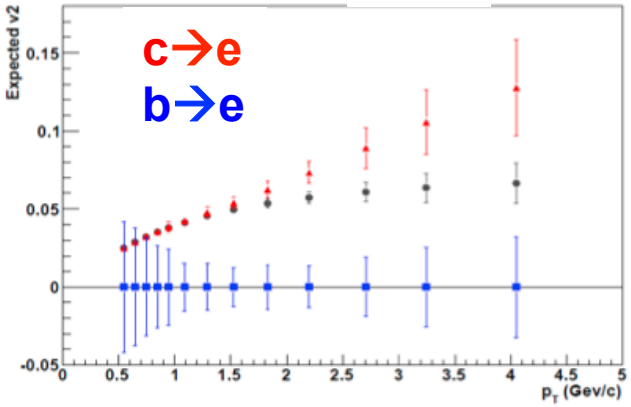

Electron b-fraction in pp

- Ongoing in Au-Au

M. Rosati, QM2012

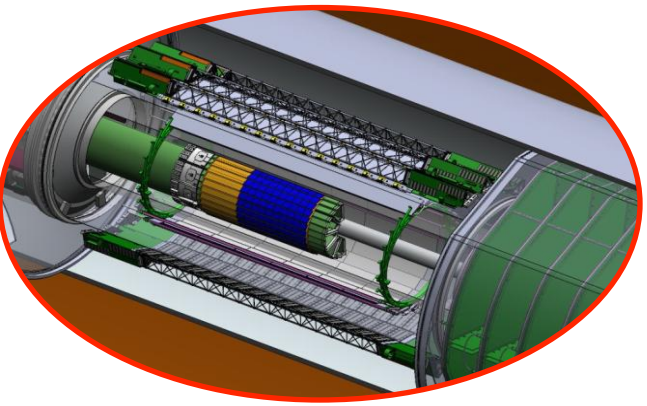

STAR: Heavy Flavour Tracker

Projections 500M evts

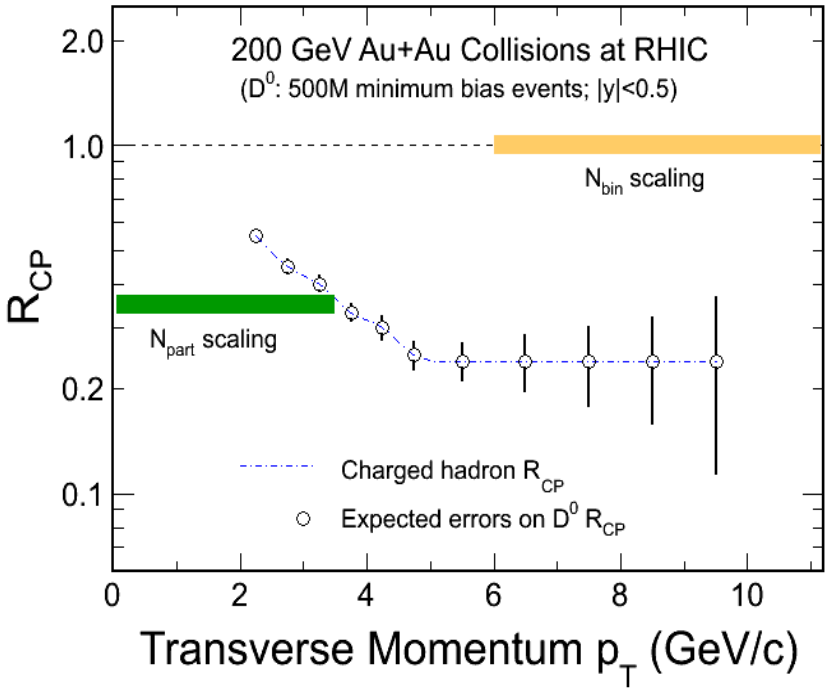

D meson R_{CP}

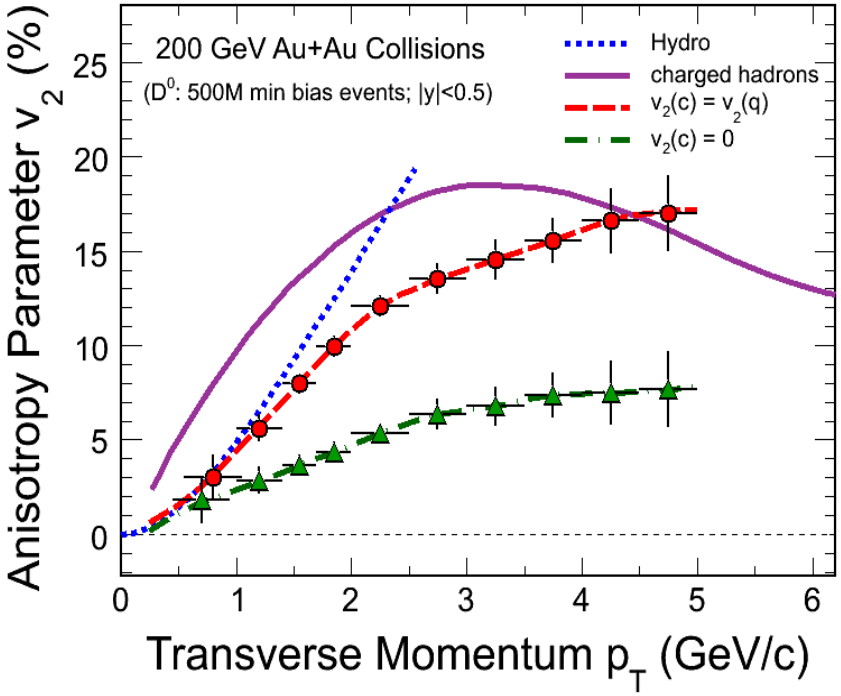

D meson v_2

J. Bielcik, Moriond2013

ALICE: new Inner Tracking System

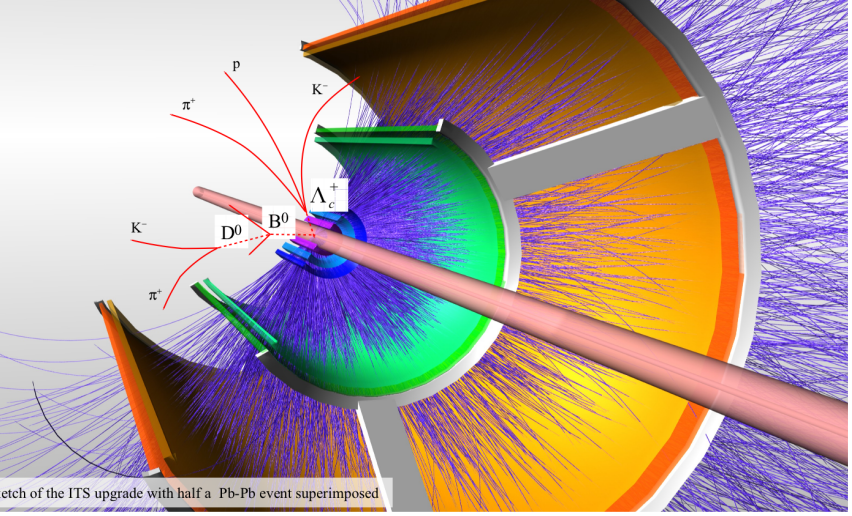

Projections LHC Run3 (10/nb)

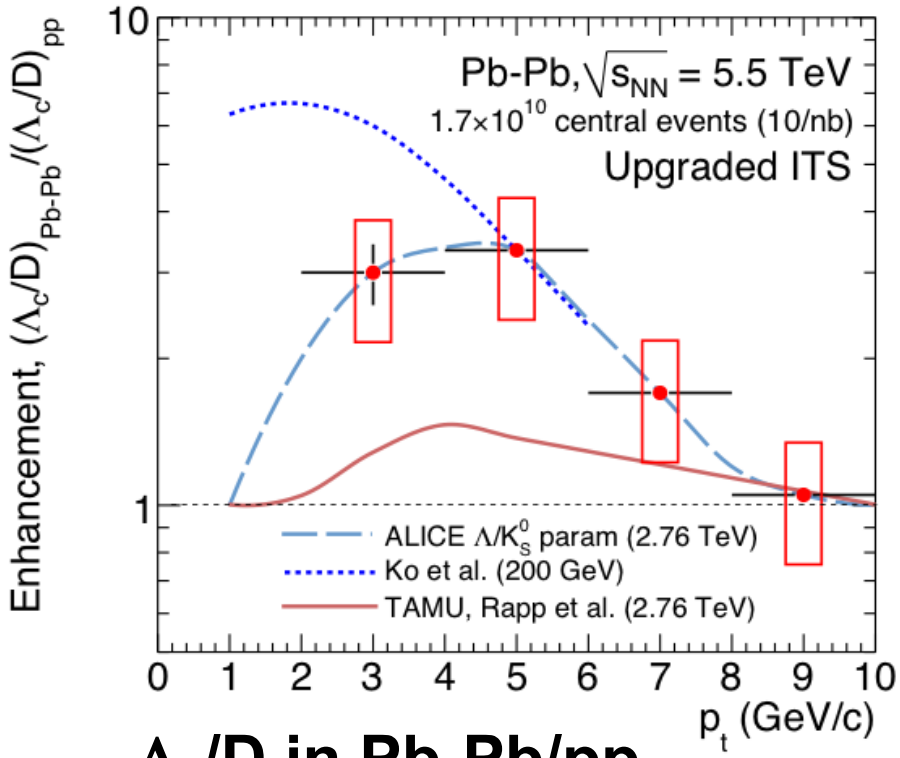

Λ_c/D in Pb-Pb/pp

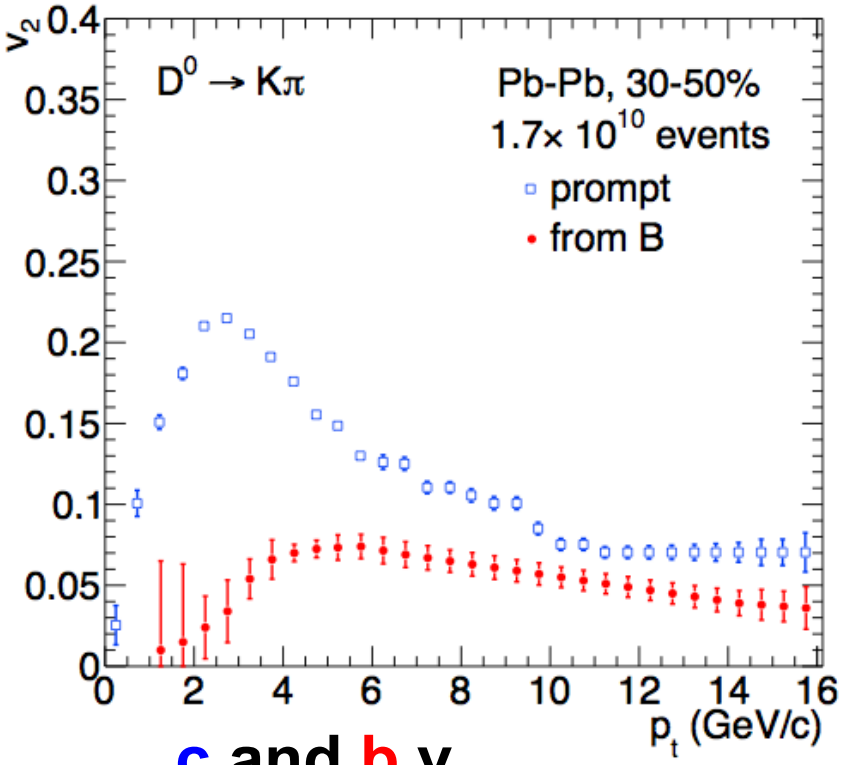

c and b v_2

CERN-LHCC-2012-013

Conclusions

- From the experimental point of view, we have just entered the "golden age" for heavy-flavour observables in HI collisions
  - Thanks to the LHC detectors and RHIC upgrades

Whom and What (in AA, as of today)

	PHENIX	STAR	ALICE	ATLAS	CMS
HF electrons	✔	✔	✔		
HF muons	✔		✔	✔	
D^0, D^+, D^{*+}		✔	✔		
D_s^+			✔		
$B \rightarrow J/\psi$					✔
B jets					✔

Conclusions

- From the experimental point of view, we have just entered the “golden age” for heavy-flavour observables in HI collisions
  - Thanks to the LHC detectors and RHIC upgrades

Whom and What (in AA, as of today)

	PHENIX	STAR	ALI	ATLAS	CMS
HF electrons					
HF muo					
D^0, D^+, D					
D_s^+					
$B \to J/\psi$					
B jets					

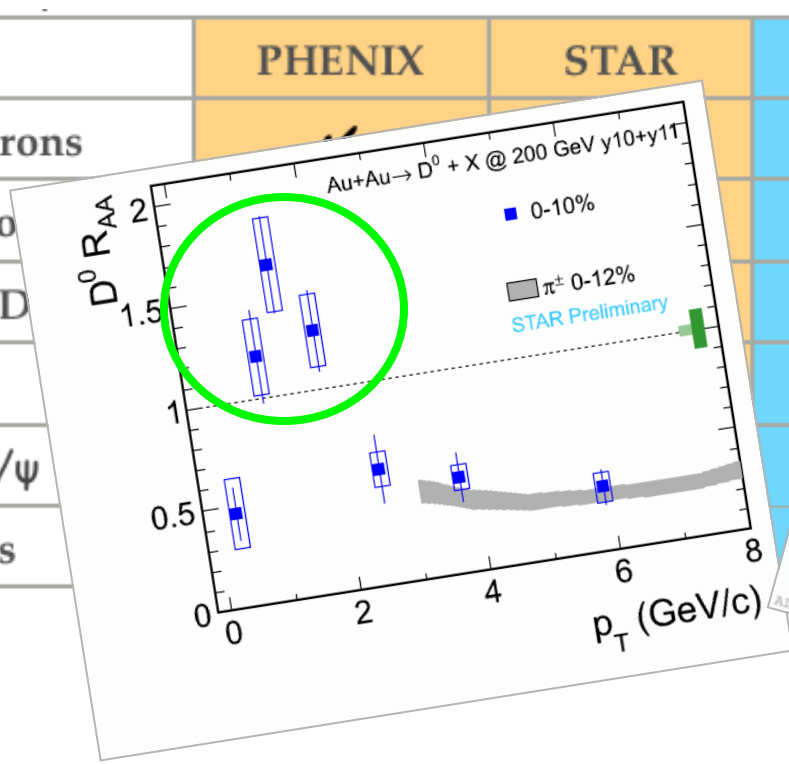

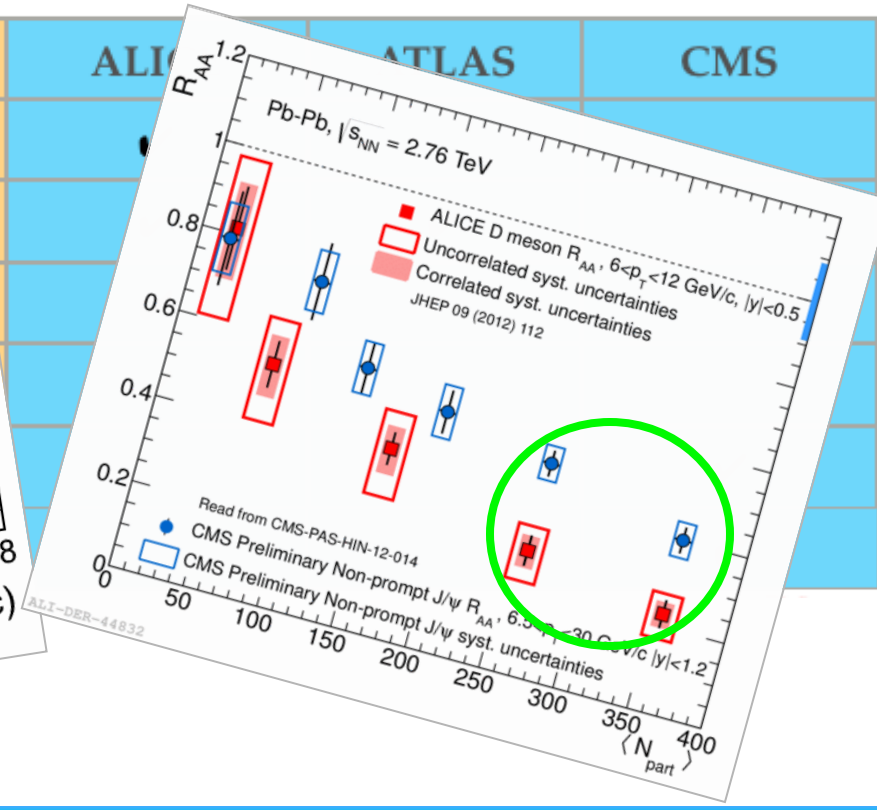

Conclusions

- From the experimental point of view, we have just entered the "golden age" for heavy-flavour observables in HI collisions
  - Thanks to the LHC detectors and RHIC upgrades

Whom and What (in dA, as of today)

	PHENIX	STAR	ALICE	ATLAS	CMS	LHCb
HF electrons	✔					
HF muons	✔					
D^0, D^+, D^*		✔				
D_s^+						
$B \to J/$						
B je						

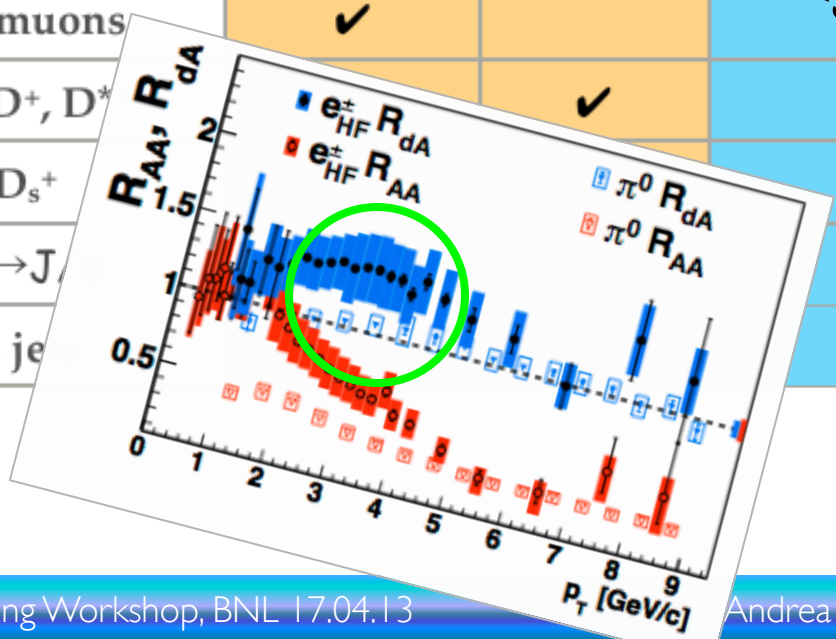

Eagerly waiting for LHC results!

EXTRA SLIDES

What's special about heavy quarks: probes through the full system history

- Large mass (m_c~1.5 GeV, m_b~5 GeV) → produced in large virtuality Q^2 processes at the initial stage of the collision with short formation time $\Delta t > 1/2m \sim 0.1$ fm << $\tau_{QGP} \sim 5\text{-}10$ fm
- Characteristic flavour, conserved in strong interactions
  - Production in the QGP is subdominant
  - Interactions with QGP don't change flavour identity
- Uniqueness of heavy quarks: cannot be "destroyed/created" in the medium → transported through the full system evolution

  → "Brownian motion markers of the medium" (*)

(*) Ralf Rapp

What's special about heavy quarks: probes through the full system history

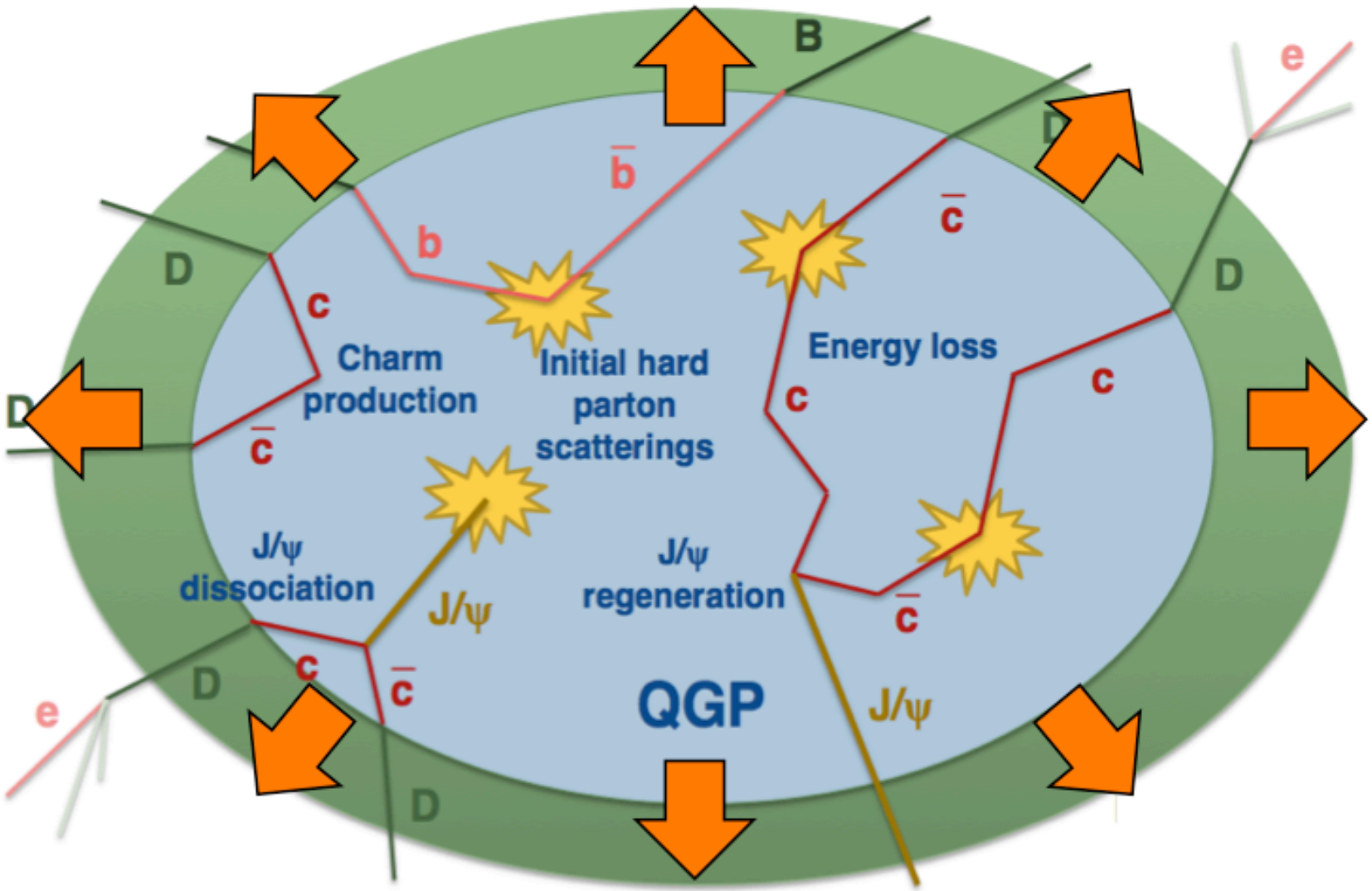

graphics courtesy J. Uphoff

What's special about heavy quarks: probing the properties of QCD E-loss

q: colour triplet
u,d,s: m~0, C_R=4/3

g: colour octet
g: m=0, C_R=3

Q: colour triplet
c: m~1.5 GeV, C_R=4/3
b: m~5 GeV, C_R=4/3

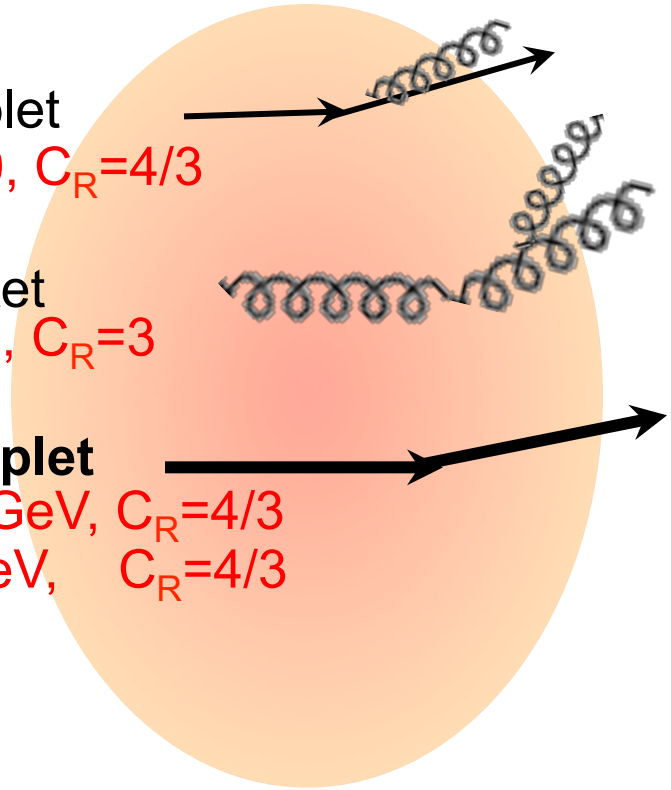

'QCD medium'

Parton Energy Loss by
- medium-induced gluon radiation
- collisions with medium gluons

$$\Delta E(\varepsilon_{medium}; C_R, m, L)$$

C_R: colour charge dep.
m: mass dep. (dead cone, …)

$$\rightarrow \quad \Delta E_g > \Delta E_{c\approx q} > \Delta E_b$$

pred: $$R_{AA}^{\pi} < R_{AA}^{D} < R_{AA}^{B}$$

Much more on this in the talk of A. Buzzatti

See e.g.:
Dokshitzer and Kharzeev, PLB 519 (2001) 199. Armesto, Salgado, Wiedemann, PRD 69 (2004) 114003.
Djordjevic, Gyulassy, Horowitz, Wicks, NPA 783 (2007) 493.

HF in heavy ion collisions: Who and What

	PHENIX	STAR	ALICE	ATLAS	CMS
HF electrons	✔	✔	✔		
HF muons	✔		✔	✔	
D^0, D^+, D^{*+}		✔	✔		
D_s^+			✔		
$B \to J/\psi$					✔
B jets					✔

Less gluon radiation for heavy quarks ?

- In vacuum, gluon radiation suppressed at $\theta < m_Q/E_Q$

  → "dead cone" effect

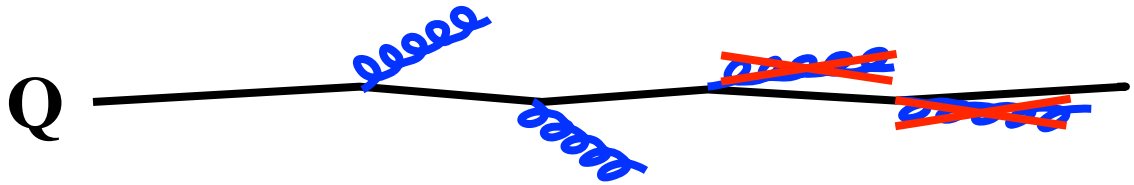

Gluonsstrahlung probability

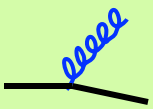

$$\propto \frac{1}{[\theta^2 + (m_Q / E_Q)^2]^2}$$

- *Dead cone implies lower energy loss* (Dokshitzer-Kharzeev, 2001):
  - energy distribution $\omega dI/d\omega$ of radiated gluons suppressed by angle-dependent factor
  - suppresses high-ω tail

$$\omega \frac{\mathrm{d}I}{\mathrm{d}\omega}\bigg|_{HEAVY} = \omega \frac{\mathrm{d}I}{\mathrm{d}\omega}\bigg|_{LIGHT} \times \left(1 + \left(\frac{m_Q}{E_Q}\right)^2 \frac{1}{\theta^2}\right)^{-2}$$

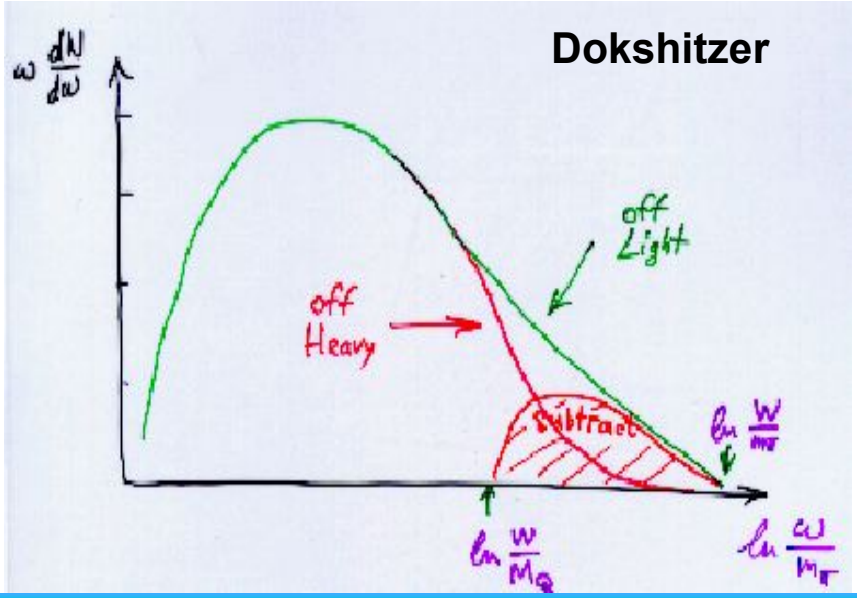

Dokshitzer, Khoze, Troyan, JPG 17 (1991) 1602.
Dokshitzer and Kharzeev, PLB 519 (2001) 199.

HQs E loss: some expectations …

- Energy loss based predictions: factor 3-5 suppression for D mesons
- Significantly smaller suppression for B

$$R_{AA}^{D}(p_T) \text{ and } R_{AA}^{B}(p_T)$$

Radiative E loss

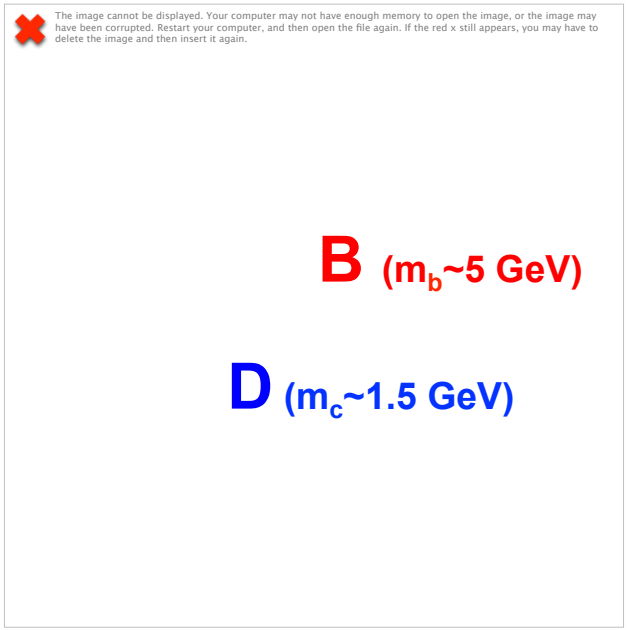

Radiative E loss + dissociation

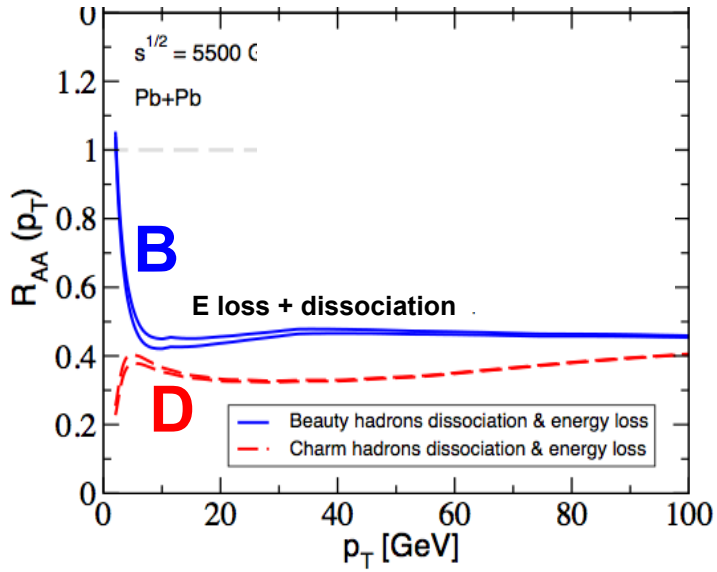

- Shorter formation time of heavy hadrons → additional R_{AA} suppression due to in-medium dissociation?

$$\tau_{form}(p_T = 10\ GeV)$$

π	D	B
25 fm	1.6 fm	0.4 fm

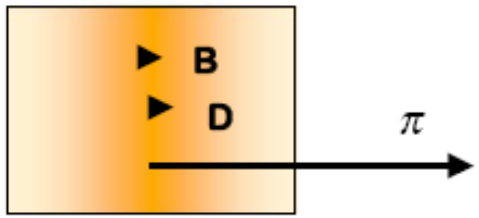

Wicks, Gyulassy, "Last Call for LHC Predictions" workshop, 2007

Vitev, et al, PRC80 (2009)

HQs E loss: the AdS/CFT way…?

- Maldacena conjecture: correspondence between super-gravity (Super Yang Mills) and QCD
- → calculate strongly-coupled QCD in SUGRA
- Model energy loss by embedding a string in AdS space
- One distinctive prediction:
  - Very strong suppression for charm
  - Small suppression for beauty up to very large p_T

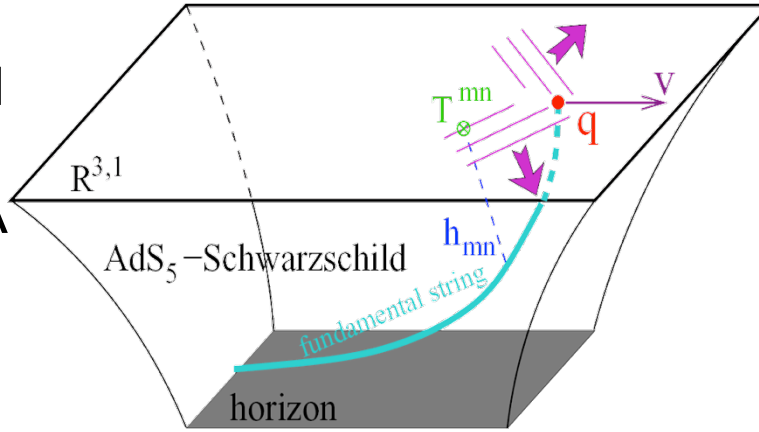

Friess, Phys Rev D75 (2007)

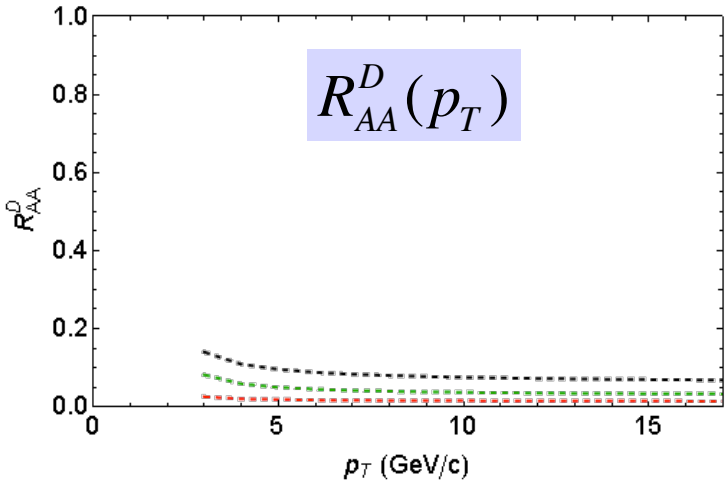

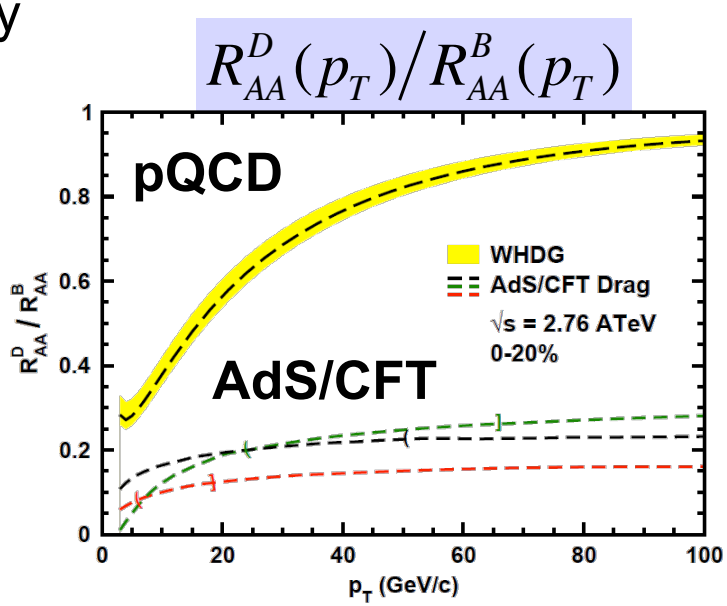

Horowitz, Gyulassy, PLB666 (2008), Horowitz, arXiv:1108.5876

pp reference at 2.76 TeV via √s-scaling (ALICE D mesons and electrons)

- Scale the 7 TeV cross sections by the 2.76/7 factor from FONLL, with full theoretical uncertainty
  - relative scaling uncertainty: 30% → 5% in the p_t range 2 → 16 GeV/*c*
- Validated by comparing to measured cross section at 2.76 TeV (fewer p_t bins)

$$R_{AA}(p_t) = \frac{1}{\langle T_{AA} \rangle} \frac{dN_{AA}/dp_t}{d\sigma_{pp}/dp_t}$$

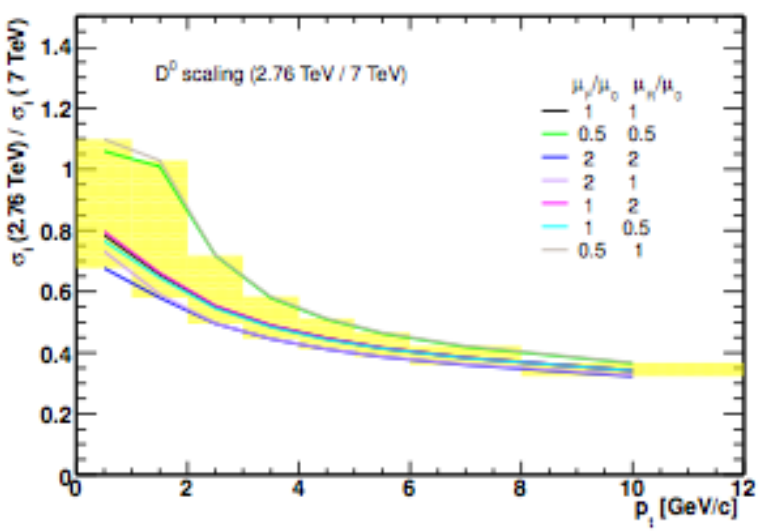

Averbeck et al., arXiv:1107.3243

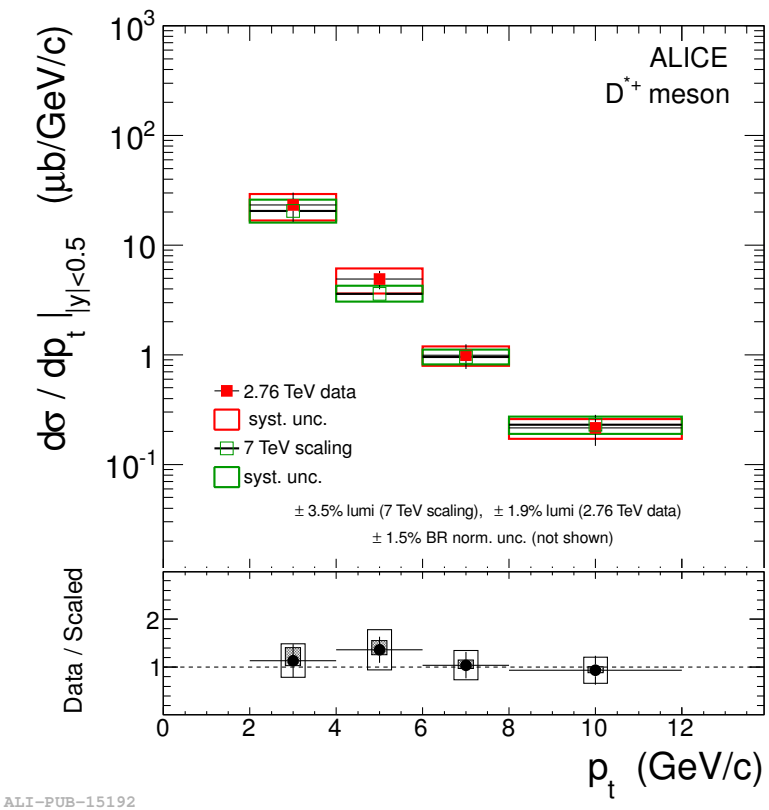

JHEP1207 (2012) 191

HF e in d-Au: RHIC results

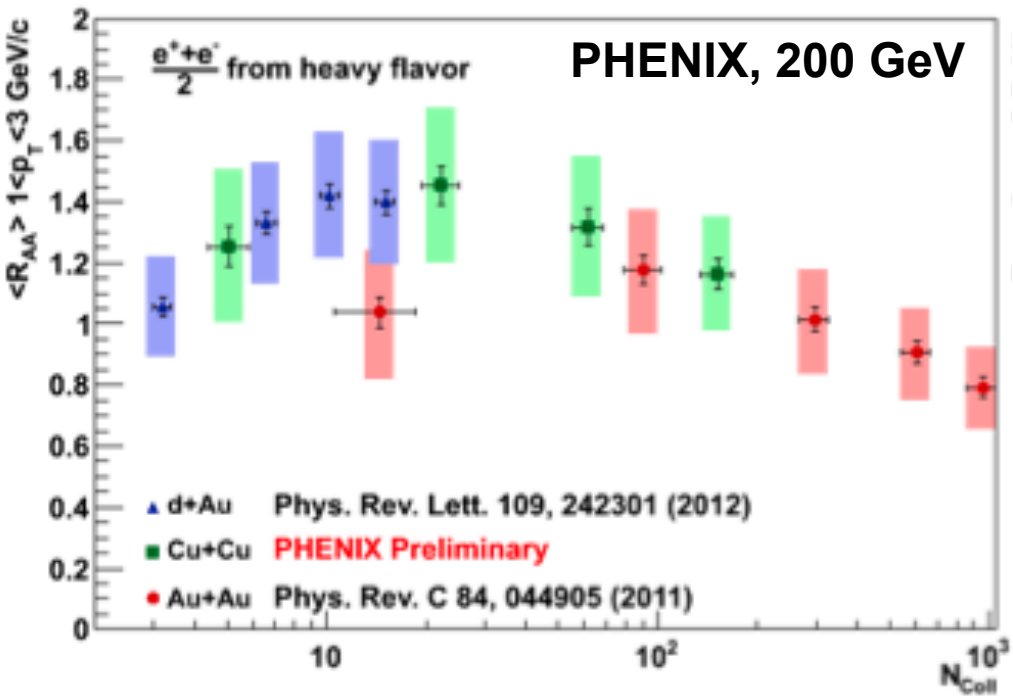

- Consistent N_{coll}-dependence in d-Au, Cu-Cu, Au-Au
- Move from initial-state effects in d-Au/peripheral Cu-Cu to where the hot medium takes over as system size increases in Cu-Cu and Au-Au

N.Apadula (WWND2013)

Updates/puzzles of dAu at RHIC

G. David, BNL

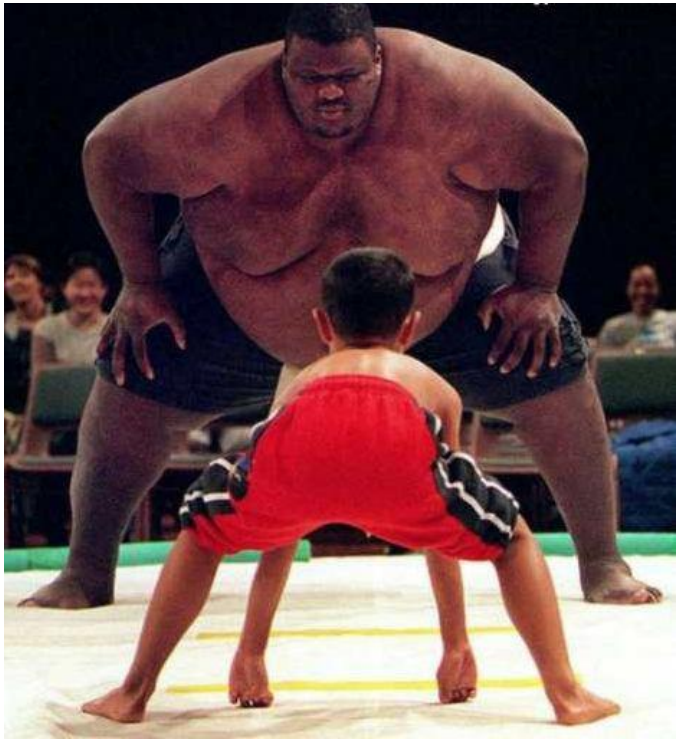

(Picture shamelessly stolen from Kwangbok Lee)

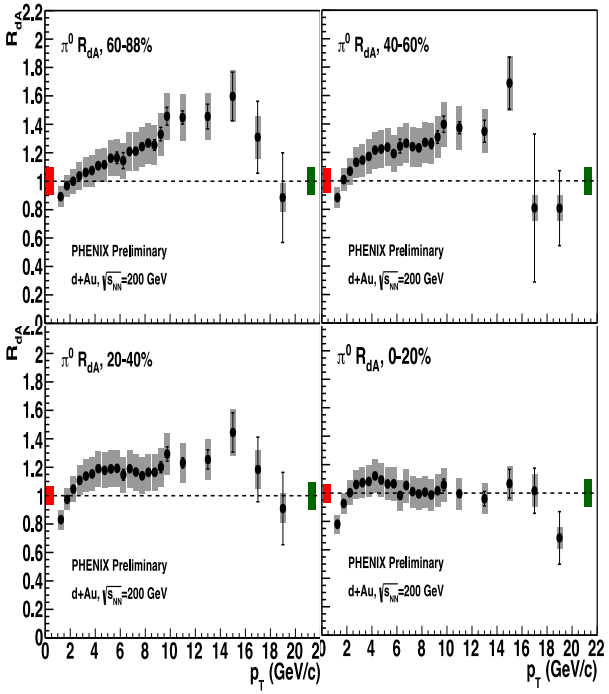

?

(Will focus on results at $\eta \sim 0$ and higher p_T)

In the beginning…

STAR, PRL 91 (2003) 072304

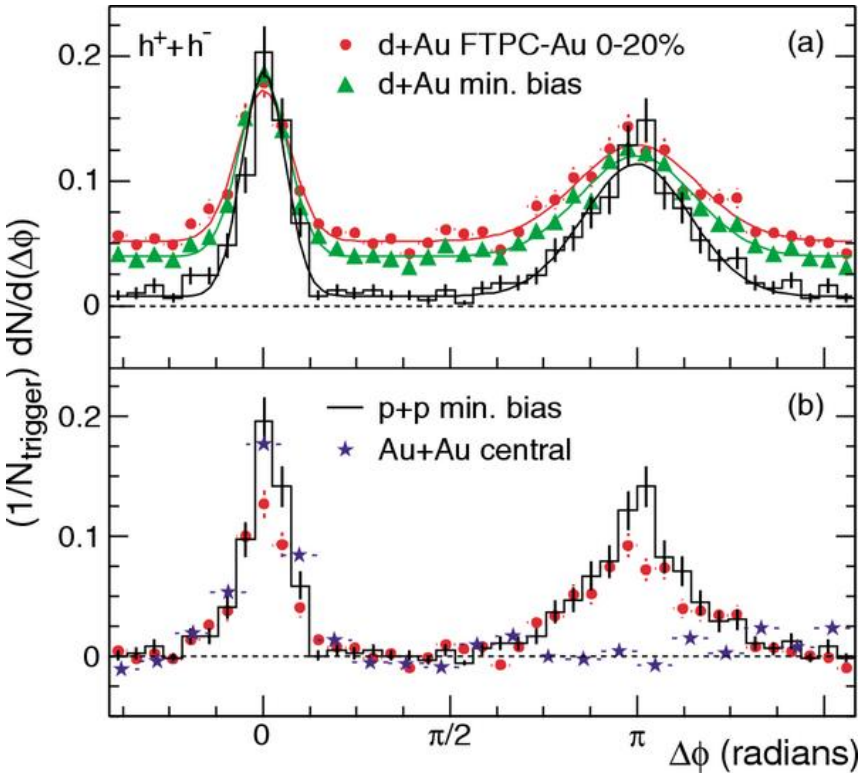

PHENIX, PRL 91 (2003) 072303

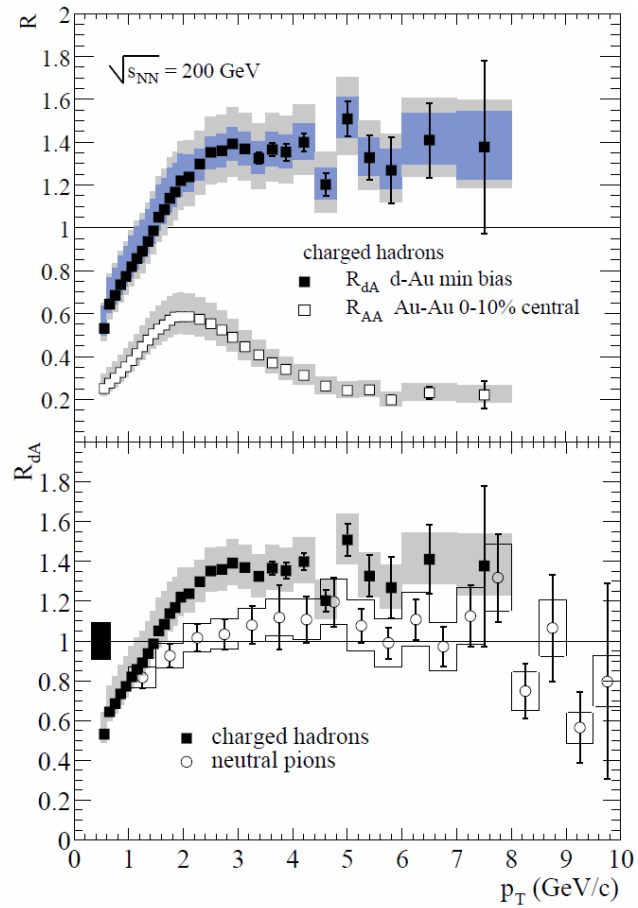

STAR: back-to-back jets reappear in d+Au
PHENIX: large suppression in Au+Au,
no suppression in d+Au
→ ***final state effect (as of 2003)***

What the photons tell

STAR, d+Au, PRC 81 (2010) 064904

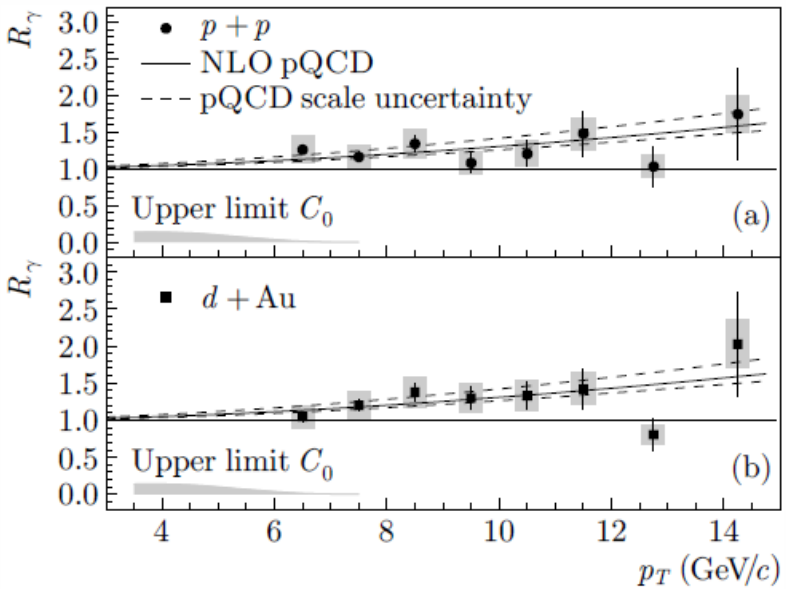

First published direct photons in d+Au at high p_T (shown here as R_γ)

No hint of medium formation so far

PHENIX, arXiv:1208.1234

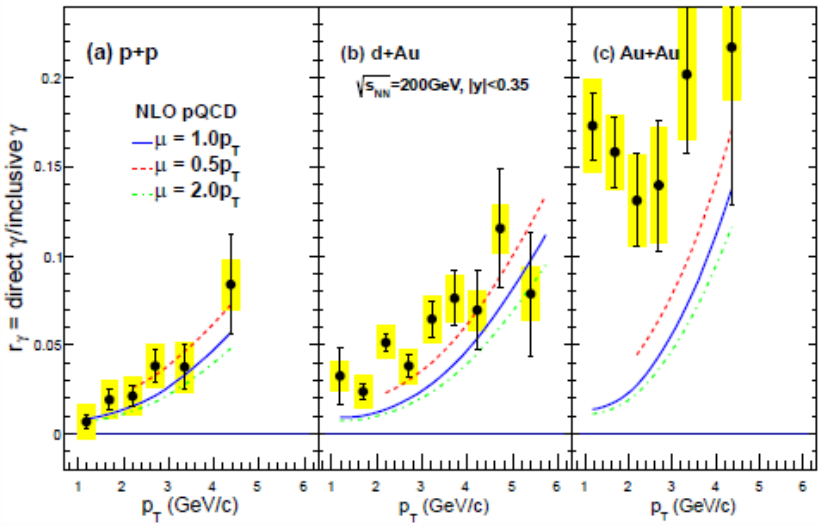

No (thermal) radiation at low p_T

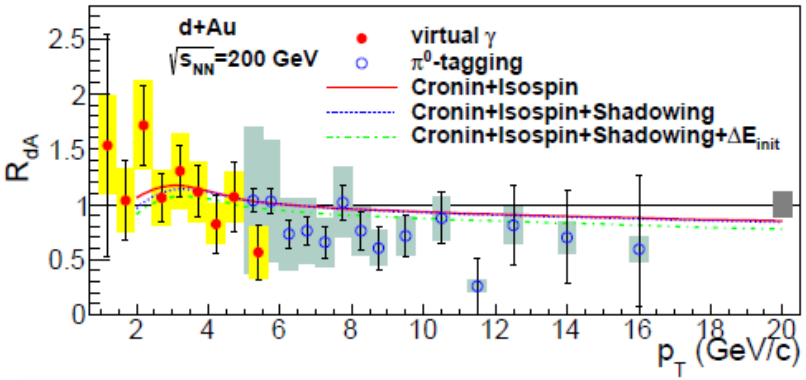

No nuclear modification (modulo isospin effect)

Low to medium p_T – Cronin-effect

ALICE, arXiv:1210.4520

For unidentified charged particles R_{AA} enhanced at RHIC, but consistent with one at LHC

The Cronin-effect appears to fade away at higher energies (why would it?) → but maybe it is because of some E_{loss}?

More pieces to the puzzle on the next slides

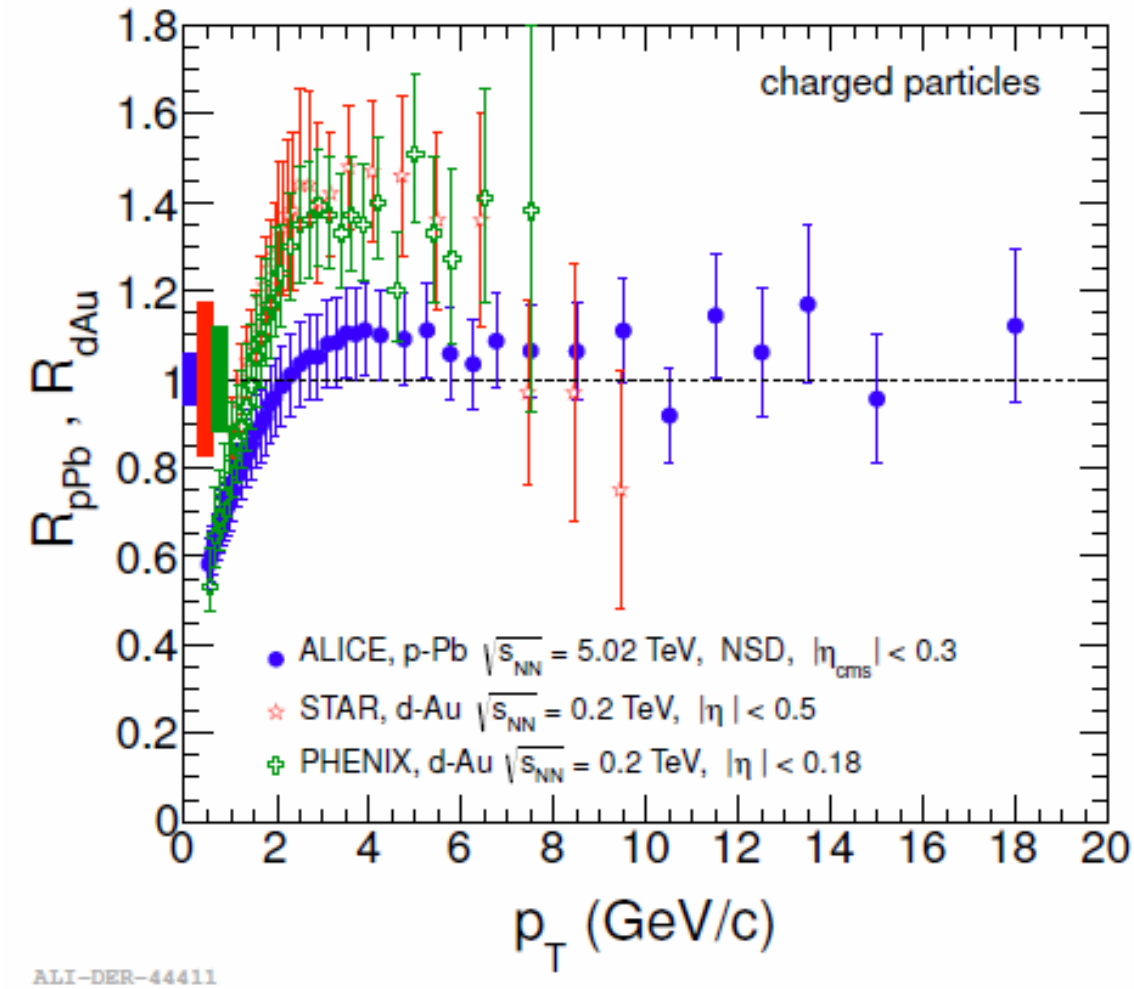

Identified hadron R_{AA} in Au+Au (medium p_T)

PHENIX, arXiv:1304.3410

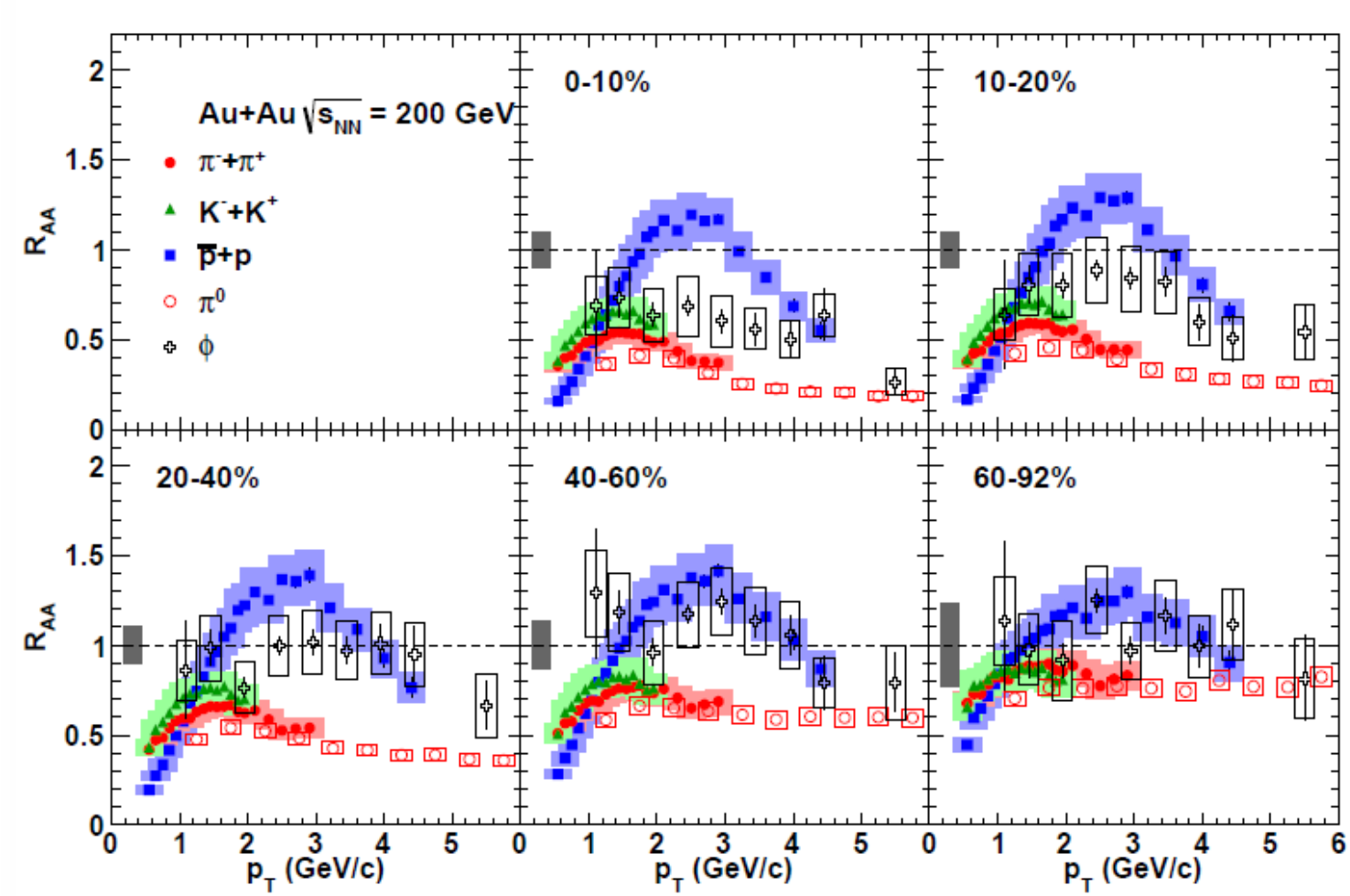

Proton: small variation with centrality.

K, π very similar (although kaons slightly higher): large variation with centrality

Φ: intermediate

Baryon vs meson; radial flow would order by mass

Identified hadron R_{dA} in d+Au (medium p_T)

PHENIX, arXiv:1304.3410

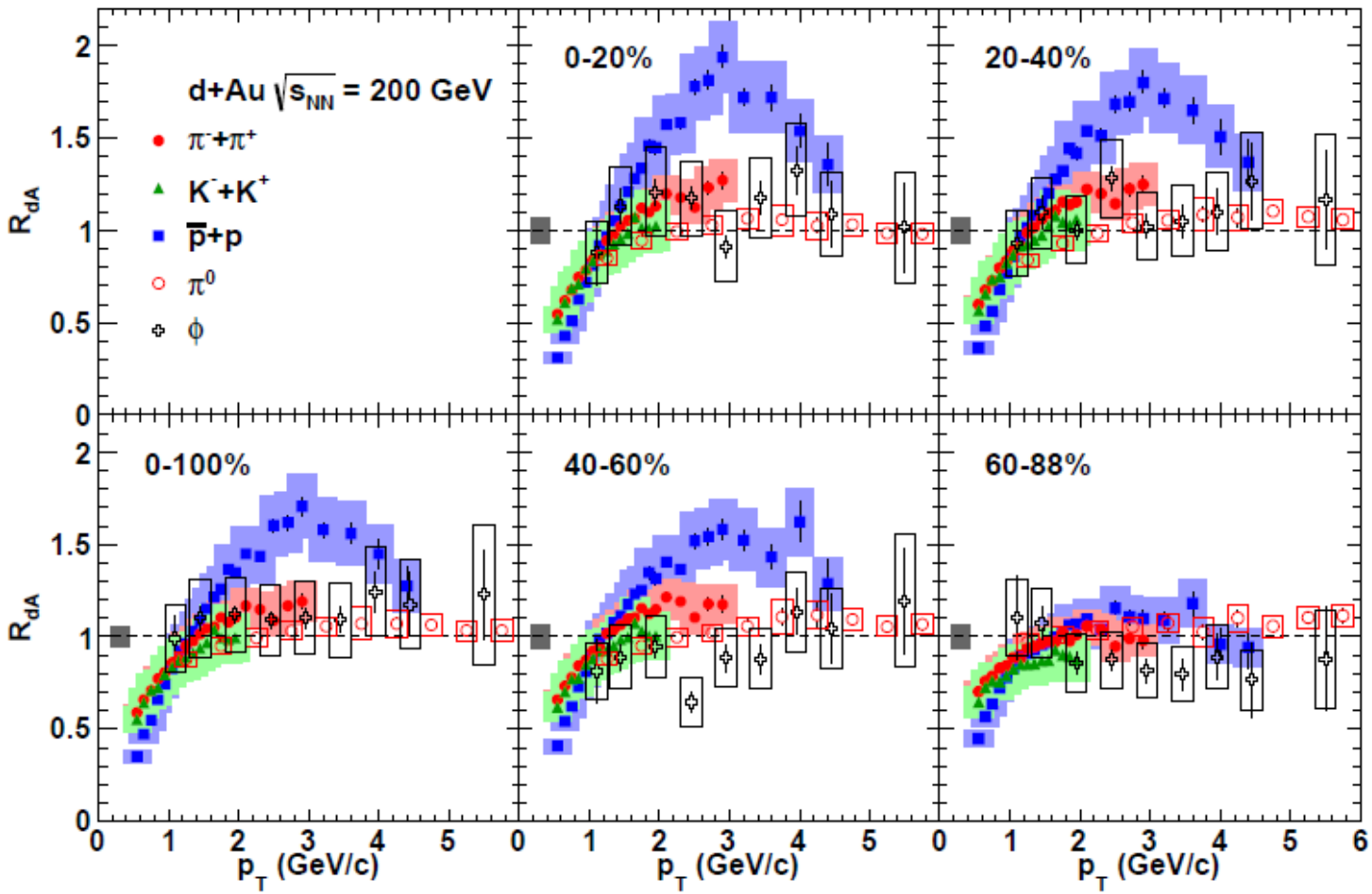

Proton: large variation → Cronin larger for baryons, and strongly depends on centrality

Φ, K, π very similar: little if any change with centrality

Mass irrelevant, valence quarks count – recombination?

Corollary: particle ratios

PHENIX, arXiv:1304.3410

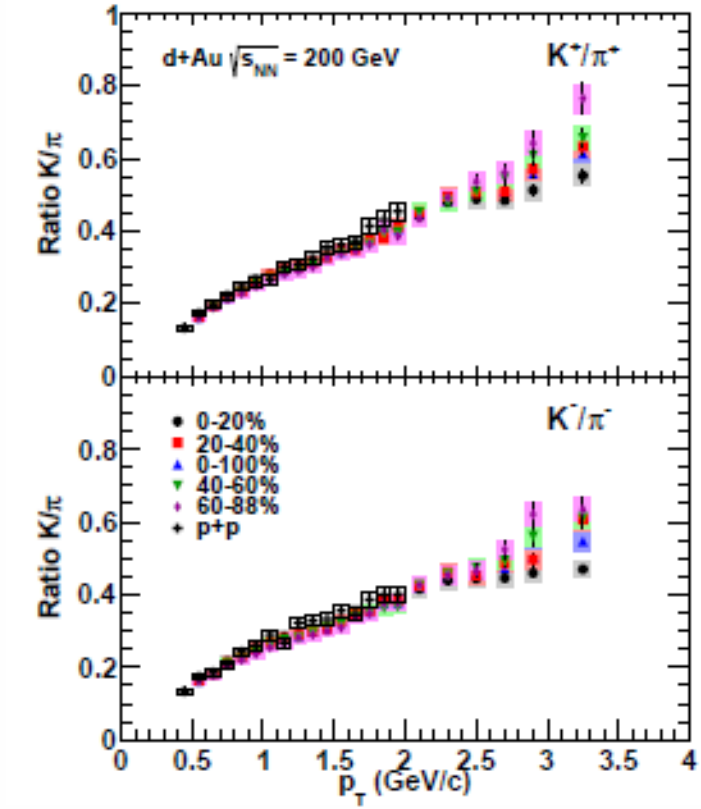

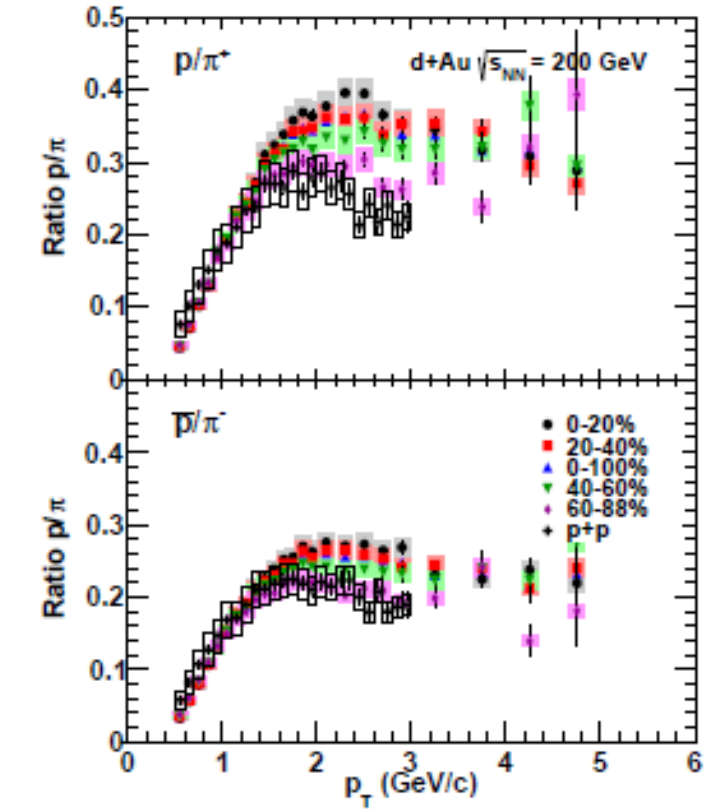

All very similar: strangeness production is the same for all centrality classes and consistent with p+p

Enhanced with centrality (similar trend as in Au+Au): recombination? (Which would favor protons.)

Peripheral Au+Au – central d+Au
Why are they similar?

PHENIX, arXiv:1304.3410

Au+Au 60-92% and d+Au 0-20% have similar N_{part}, N_{coll}.

The ratio of all ID'd hadron spectra are on the same curve, and go to a constant ~ 0.65

Common production mechanism?

Baryon enhancement the same?

If all CNM scales with N_{part}, does this ratio (non-unity) mean E_{loss} in the medium in peripheral Au+Au (even for protons?)

Rapidity shift in d+Au causing low p_T increase?

nPDF's modified?

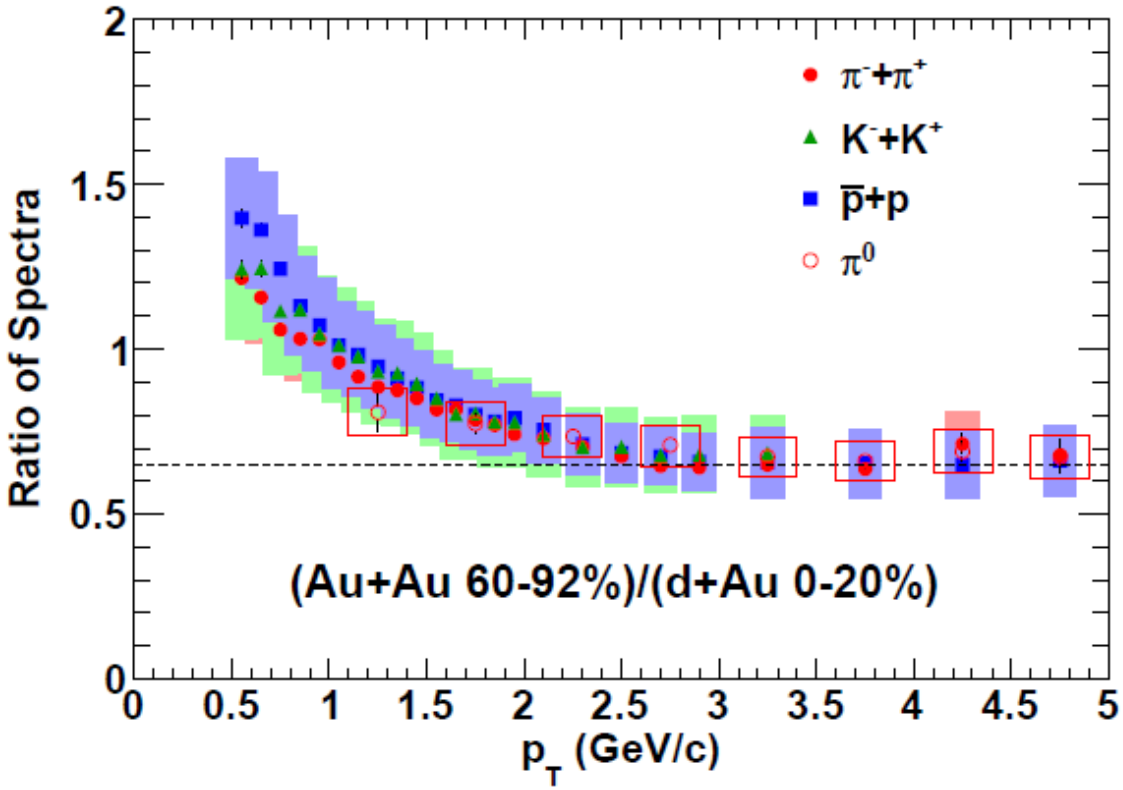

Now some results to lose sleep over

PHENIX preliminary, QM'12

2008 (high) statistics d+Au data, nuclear modification factors vs centrality

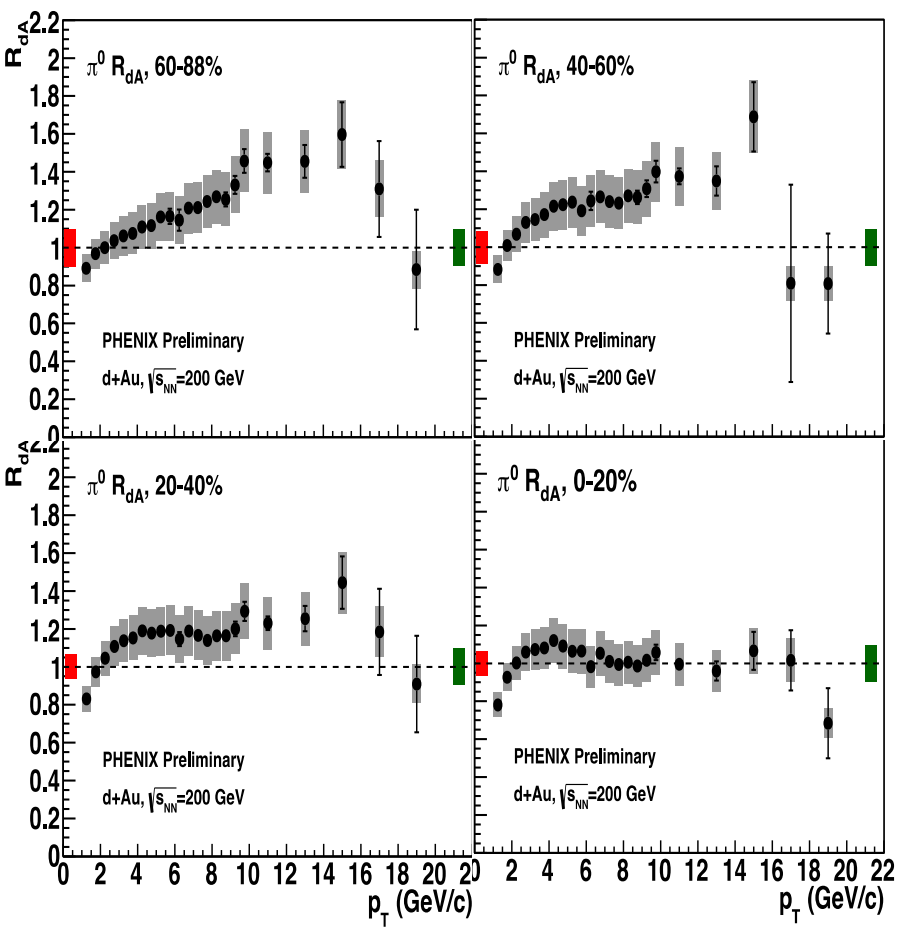

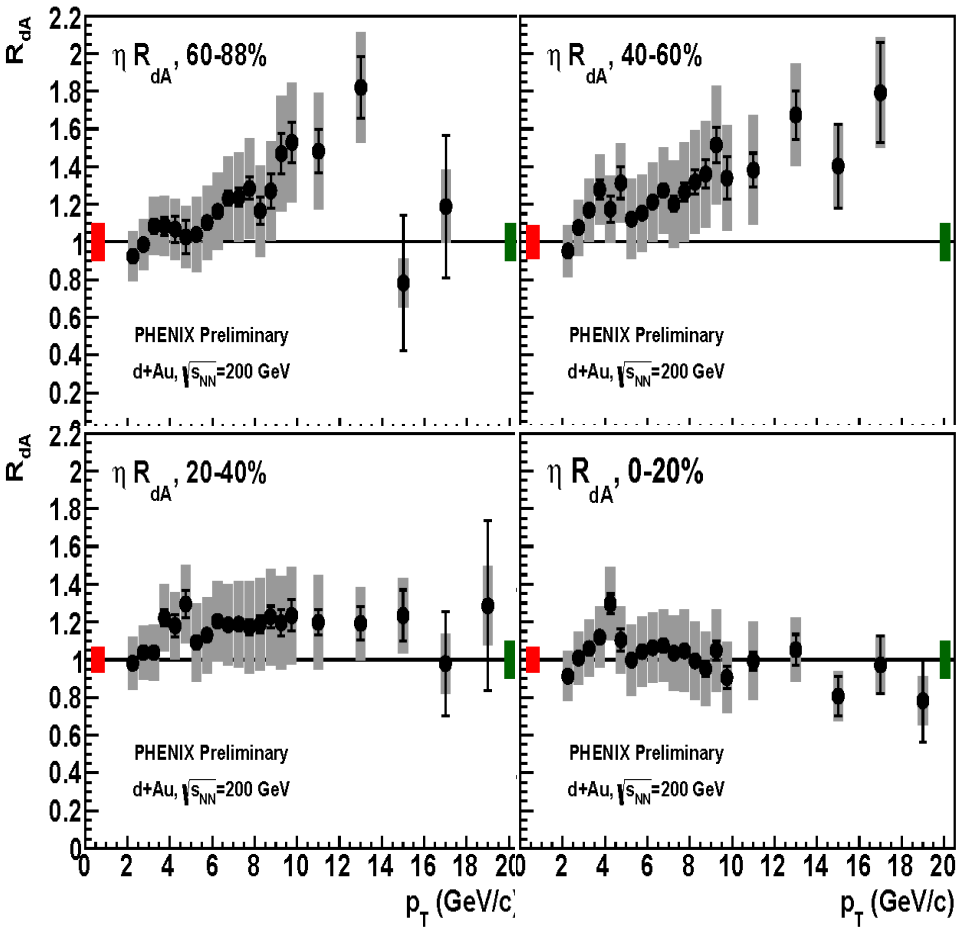

Is it possible that π_0, η production at high p_T in peripherals is enhanced???

Reminder: N_{coll} scaling works!

Remember: direct photons yields in Au+Au (presumed to be blind to any medium formed) should be proportional to the ("N_{coll}" times) ***increased, but still very-very small probability*** of photon production in p+p. And this is exactly what is seen here.

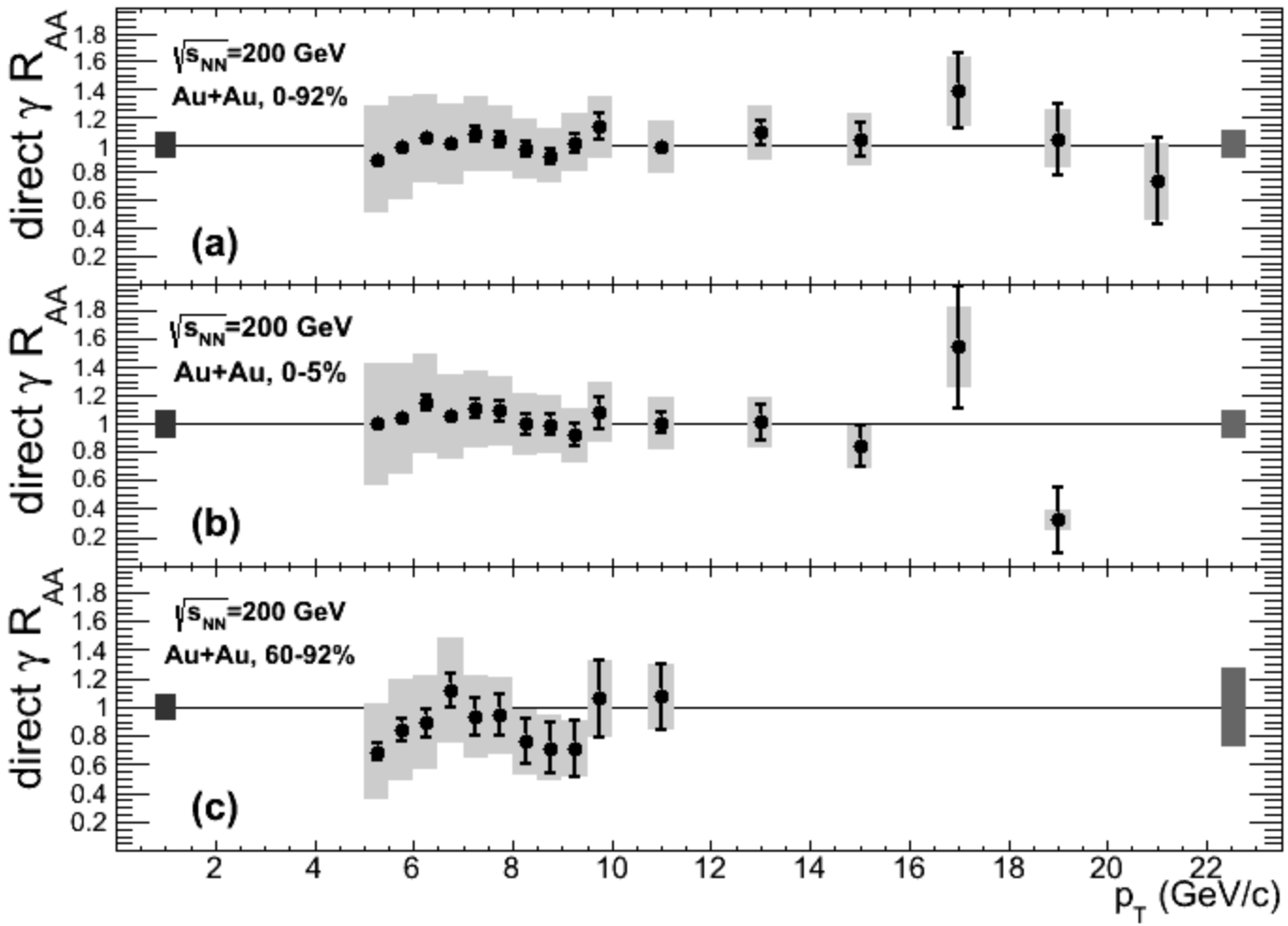

PHENIX, PRL 109, 152302 (2012)

Minimum bias R_{dA} is unity as expected everywhere

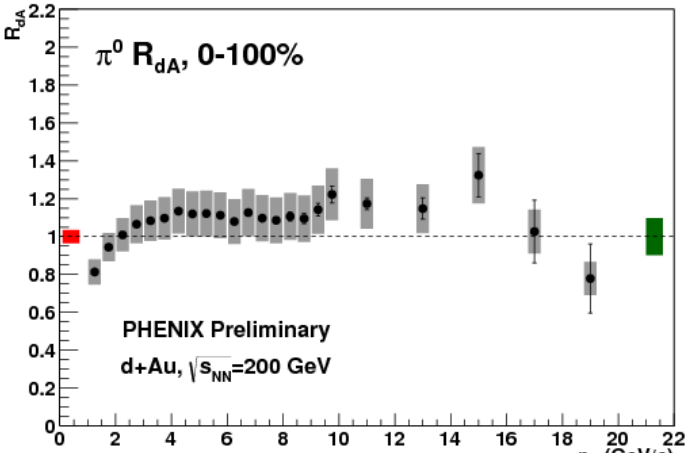

STAR, PRC 81 064904 (2010)

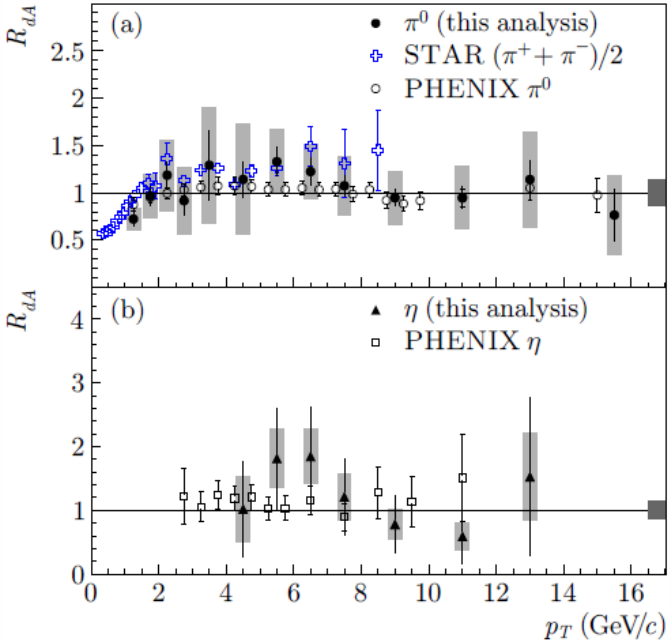

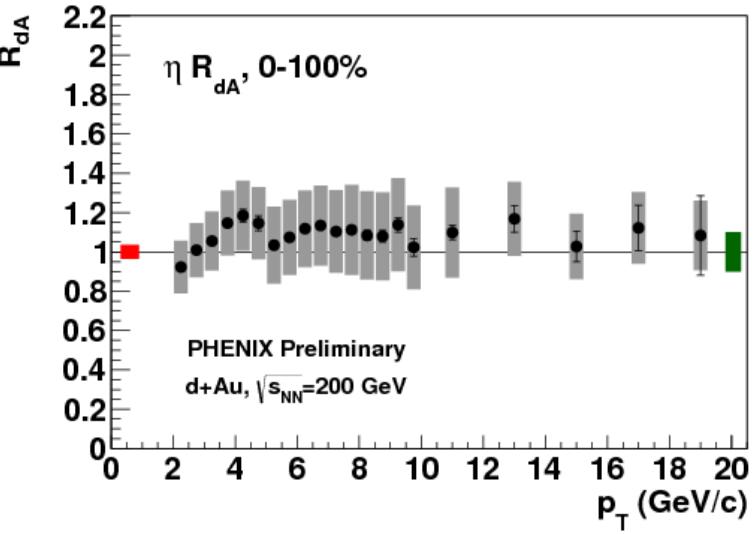

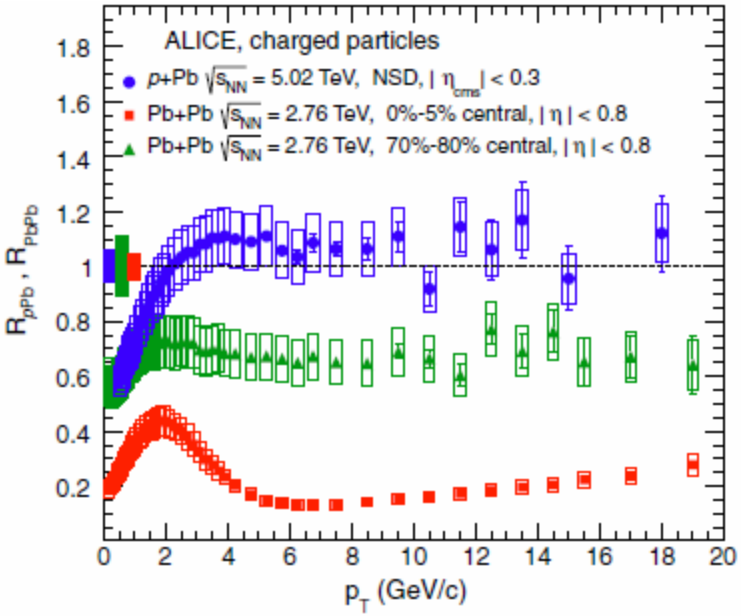

ALICE, PRL 110 082302 (2013)

Jets – a very different kind of analysis

Inclusive (leading) particle
vs jet reconstruction
(related, yet quite different
observable, analyzed differently)

Gaussian filter method

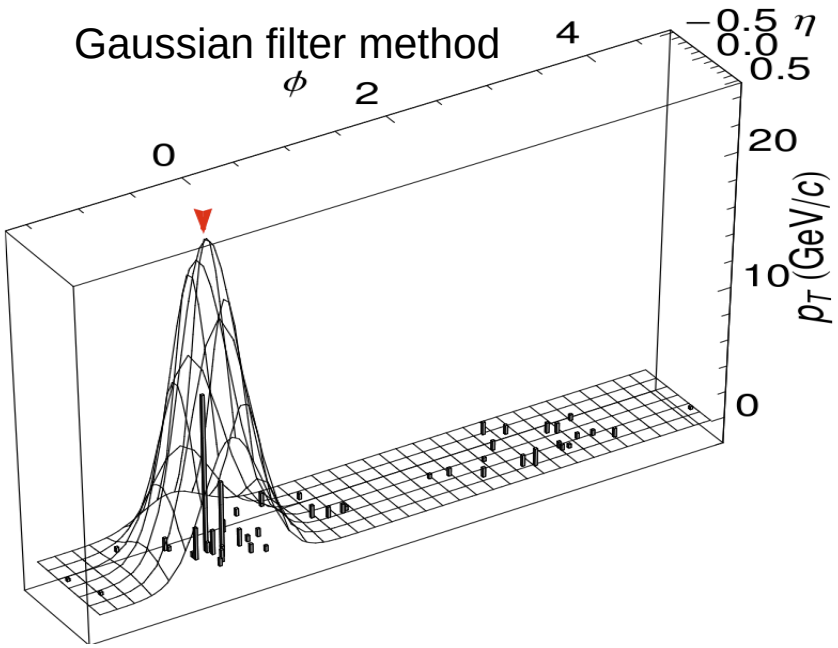

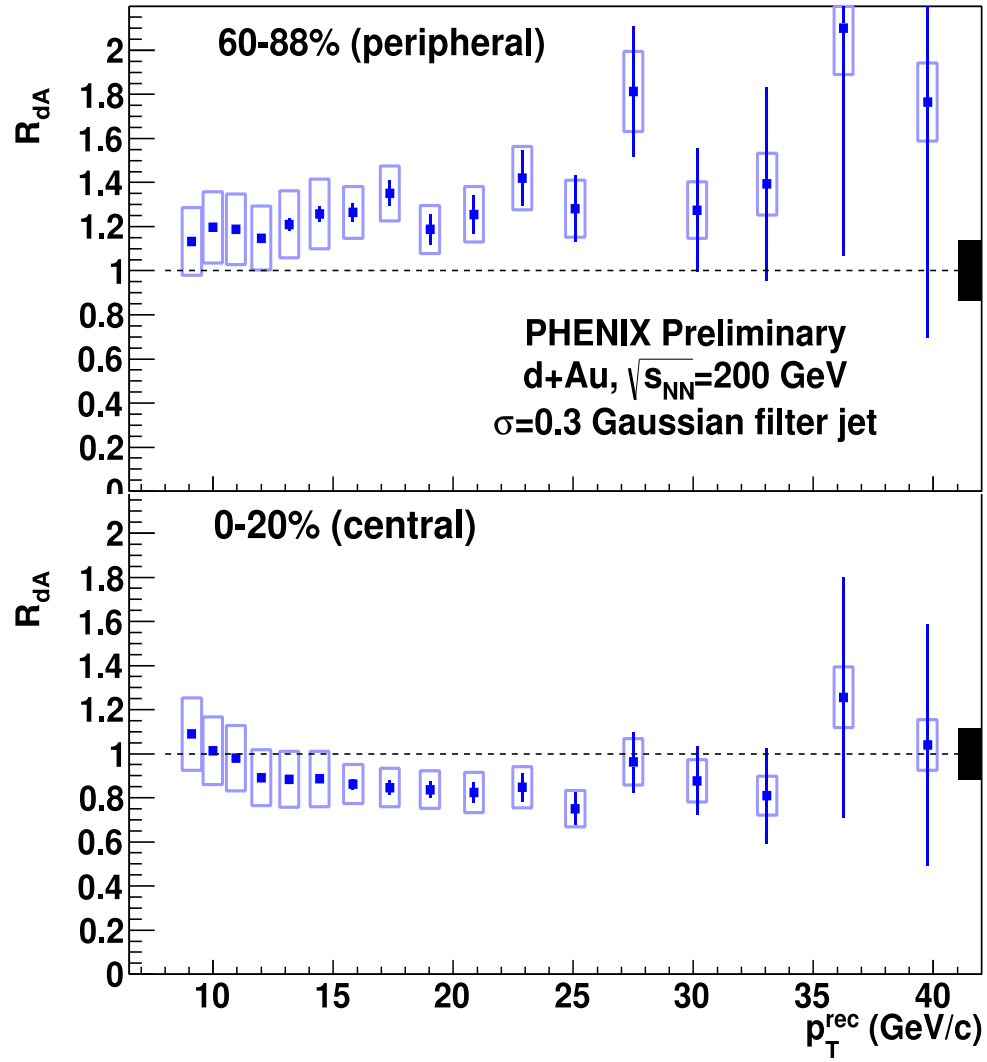

The energy scale is different,
but shows the same overall trend

Jets, π^0, η – central to peripheral

For π^0, η this is true p_T, for jets it is total jet energy.

There is no unambiguous transformation, but 1./0.7 is a reasonable compromise, and would put the points almost on top of each other.

Important: R_{CP} is *independent of any p+p reference*!

The only "external" quantity here is the N_{coll} value attributed to the individual centrality classes

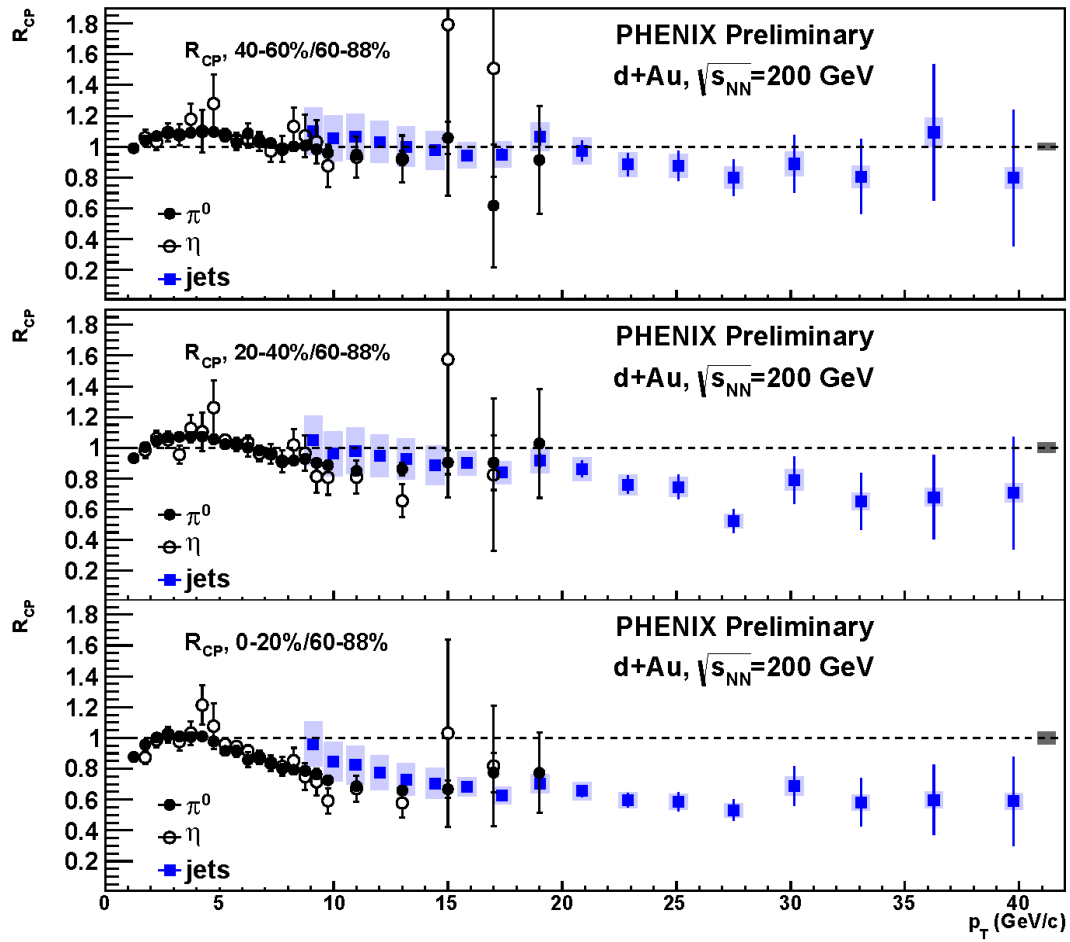

Note that R_{CP} drops sharply, indicating major shape change from peripheral to central

Something to be made VERY clear

I am **not** speaking for PHENIX this time – only and exclusively for myself

Of course I'm aware that there is very intense work going on in PHENIX to verify this result (there's a reason why it is called ***preliminary***!) The result, if it survives scrutiny, is extraordinary – extraordinary care is warranted.

However, even if I knew the answer, **I will not comment** on this specific work, checks, discussion in PHENIX related to this issue. Progress will be reported by the experiment in due time.

What I will do is to grab the opportunity to give a close look how ***centrality***, a crucial quantity in heavy ion collisions, is interpreted and connected between experiment and theory, deliberately avoiding (almost always) any numbers, since ***nothing here is specific to PHENIX***.

"Anybody thinking otherwise is itching for a fight" ☺

Centrality: thinking out loud

The theorist tends to think in terms of impact parameter (b), or N_{part}, N_{coll}, T_{AB}, ε, …
none of which is directly accessible in the experiment

The experimenter is concerned whether a/ the event is taken at all (*trigger* bias/efficiency)
b/ there are some *global* observables that can be tied to the theorists' quantities and while they are correlated to those quantities, they are as *uncorrelated* as possible to the *specific features* of the event (like presence of jets, flow, etc.)

Assuming such observable(s) exist, a model is agreed upon that makes the translation between experimental observables and theoretical quantities

Since you want to avoid introducing biases as much as possible, the model is *tuned with* a large number of (more or less) *average events*, in regions preferably "far" from the regions with the "specific features" studied (like a large η gap)

The correlation between the global observable and the theoretical quantity is typically wide: events on the average will be properly classified – but not necessarily individually.

Connecting theoretical and experimental quantitites

Ann.Rev.Nucl.Part.Sci.57:205-243,2007
(arXiv:nucl-ex/0701025)

3.1 Methodology

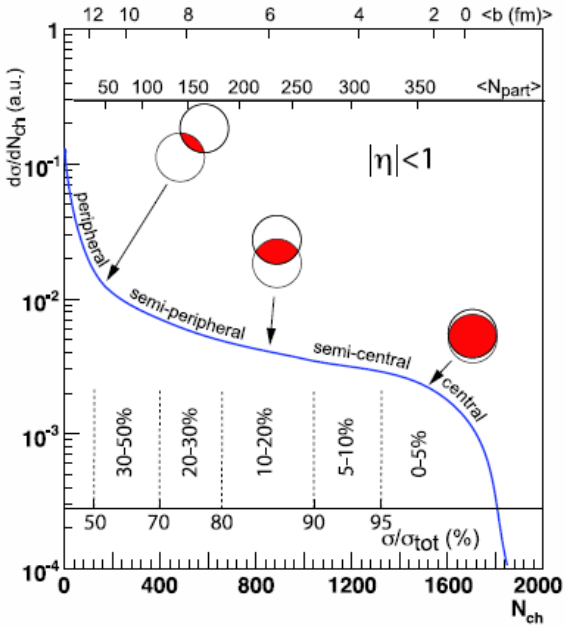

Figure 8: A cartoon example of the correlation of the final state observable N_{ch} with Glauber calculated quantities (b, N_{part}). The plotted distribution and various values are illustrative and not actual measurements (T. Ullrich, private communication).

Glauber Modeling in Nuclear Collisions 16

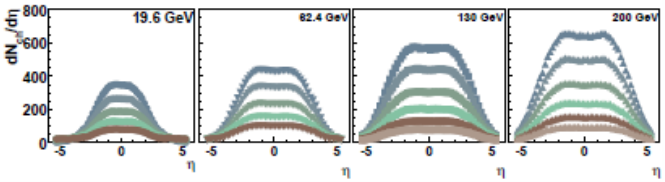

Figure 10: Charged particle multiplicity (PHOBOS) in Au+Au collisions at various center-of-mass energies for $|\eta| < 5$ (57,58). The different colors represent different centrality selections.

tion (41). However, the multiplicity is also known to scale with the hardness (q^2) of the collision – the multiplicity for hard jet events is significantly higher than that of MB collisions. In heavy ion collisions, we manipulate the fact that the majority of the initial state nucleon-nucleon collisions will be analogous to minimum bias p+p collisions, with a small perturbation from much rarer hard interactions. The final integrated multiplicity of heavy ion events is then roughly described as a superposition of many negative binomial distributions, which quickly approaches the Gaussian limit.

"In heavy ion collisions, we manipulate the fact that the majority of the initial state nucleon-nucleon collisions will be analogous to minimum bias p+p collisions…"

The verifiable case: p+p

Triggering and event characterization:
looking for activity (e.g. charged particle production N_{ch}, transverse energy E_T)
preferably **close to the beam and far from the region of interest** (mid-rapidity)

Now study those distributions as a function of the activity observed at η~0
"Activity" here is the **highest p_T for any particle seen around η~0**; could be jet energy, etc.
Can be done both in simulation and in data!

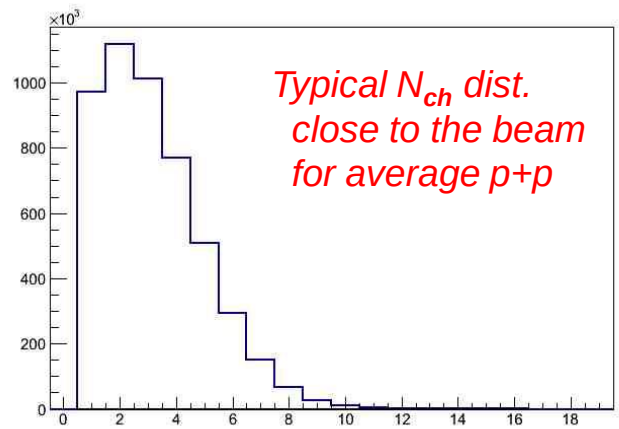

Note the characteristic rise initially (well-known: higher activity when hard scattering occurs)

However, at higher pT they start to drop slowly.
They have to, at least asymptotically, for simple kinematic reasons.

Mean and RMS of the N_{ch} dist. vs max p_T in the center

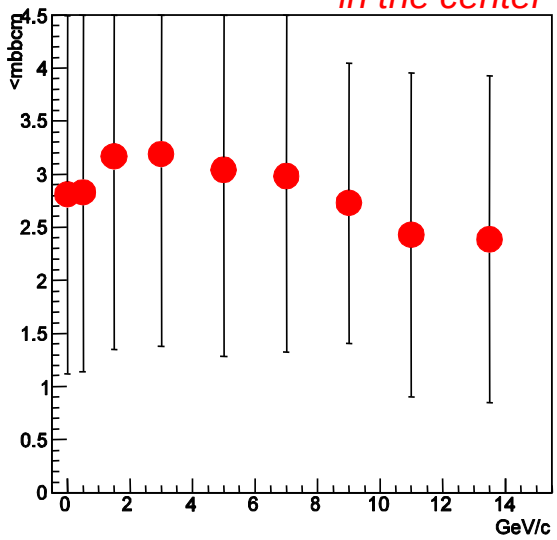

Trigger efficiency vs max p_T in the center

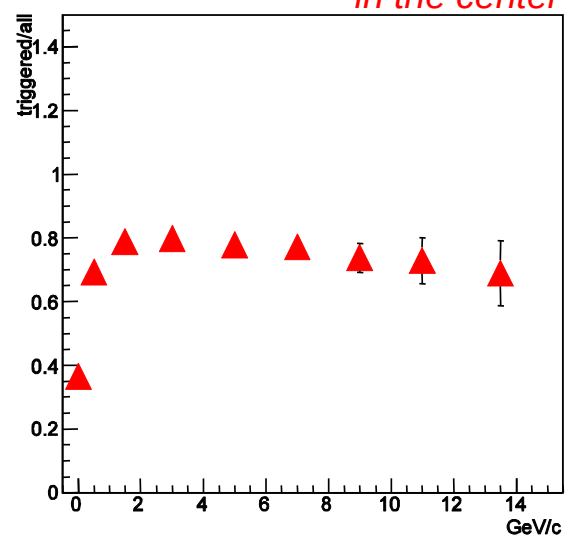

Of course *other mechanisms can deplete* forward activity way before kinematics does!

Glauber-model and centrality in p+A, d+A, …

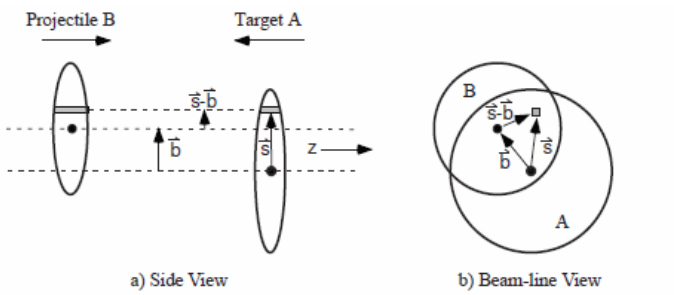

Straight path, independent collisions with the same probability (cross section) → N_{coll}, N_{part}

Folding with the *average response* observed in p+p can tie N_{coll}, N_{part} to observed N_{ch} *statistically*

Weather or not fluctuations are taken into account is irrelevant here

For instance:

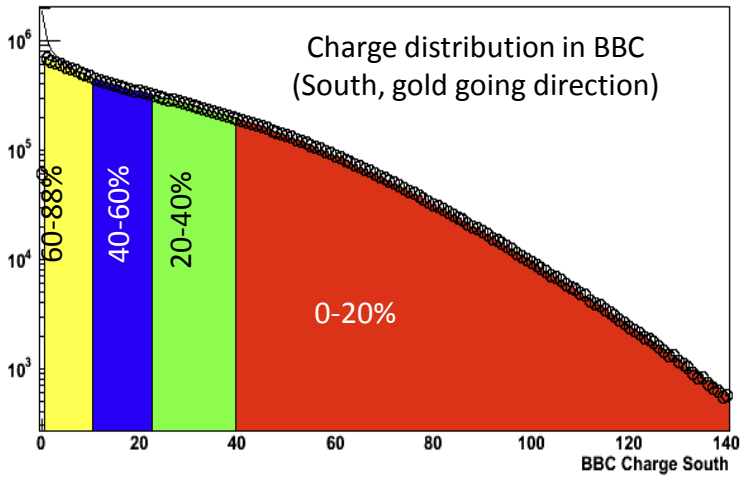

Experimentally defined centrality classes

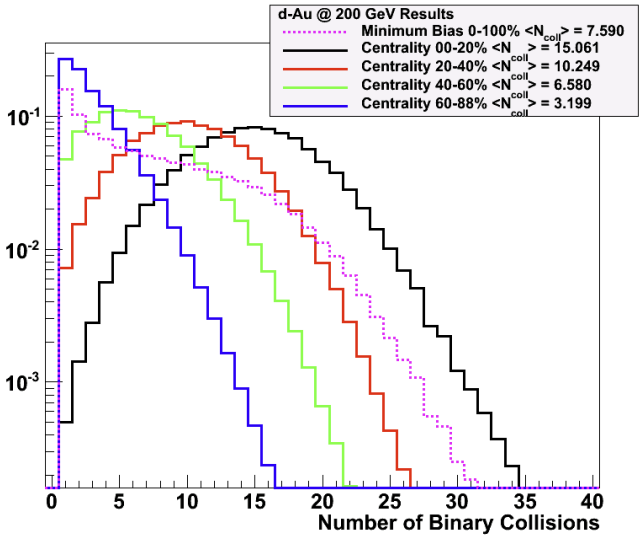

N_{coll} distribution for each class from the model

Based on average responses, does not take into account possible special features of rare events (like high p_T particle or jet in the central region)

Will this always work without further corrections?

Not necessarily.

For instance, as we have seen for p+p, the *trigger efficiency* decreases with increasing energy in the center. Since the trigger requires coincidence on both sides and in pA, dA on one side there are at most two nucleons, a similar drop in efficiency is expected. *This is well known and usually taken into account*.

Centrality is usually defined in the direction where the large ion goes. Assume the projectile makes **N** collisions, one of them with very high p_T. Then the expected multiplicity forward is only (**N**-1) times the average plus one reduced response
→ the multiplicity observed by the experimenter (forward) is smaller than it would be for an event that is identical except that no high p_T is present

If centrality is defined with fixed multiplicity thresholds based on the *average* events but applied to the *rare, special* ones, those rare events may be (mistakenly) classified as lower centrality (lower average N_{coll}) than they really are.

At higher p_T this effect typically shifts to lower multiplicity (i.e. lower centrality) classes events that N_{coll}-wise – i.e. from the point of view of how probable a rare, hard collision is – would belong in a higher centrality class.

Illustration: shift between multiplicity classes / 1

Here is your average, higher centrality event

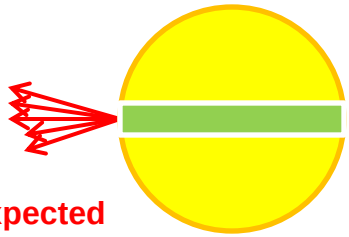

But now a very hard scattering happened (one in a million!), with reduced fwd. response, therefore…

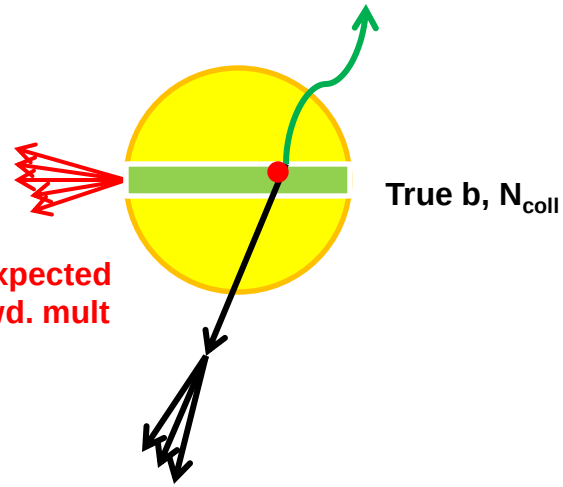

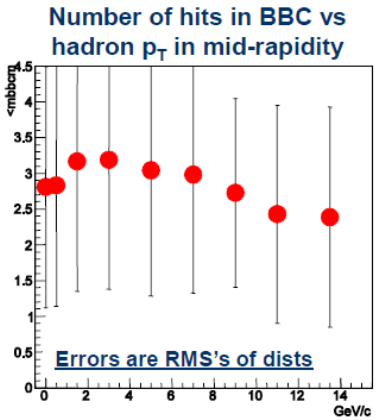

…this is how you classify the event…

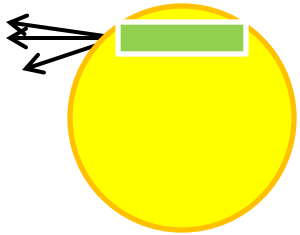

…and when you calculate R_{AA}, the denumerator ($N_{coll} * \sigma_{pp}$) will be smaller than it should be → R_{AA} increases

(There can be other, even more serious effects, as we'll theorize later)

Illustration: shift between multiplicity classes / 2

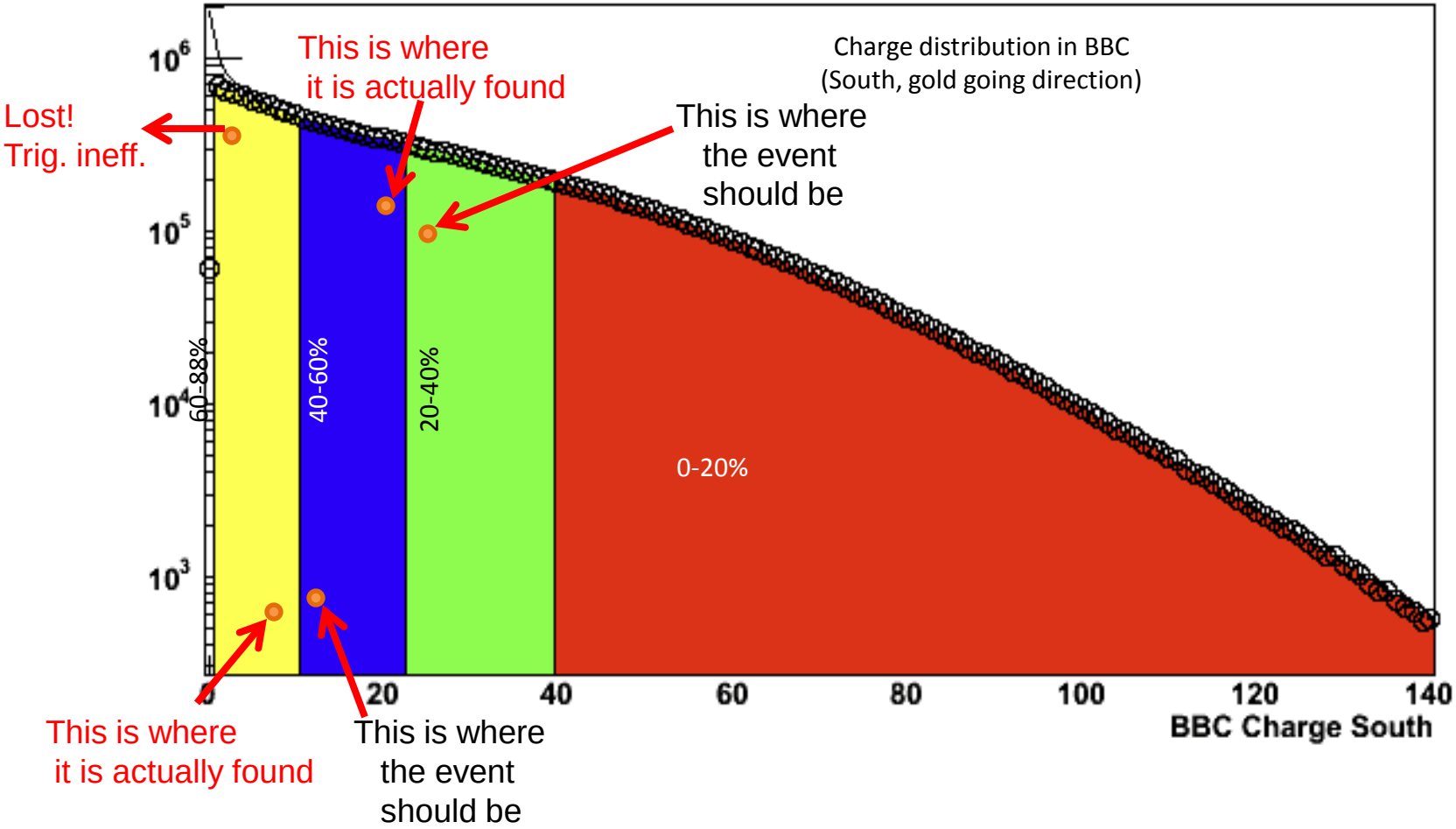

If (experimental) centrality is determined with fixed (forward) multiplicity thresholds, irrespective of what happened at η~0, events may end up in the wrong centrality class – and attributed an incorrect $\langle N_{coll} \rangle$

More exotic possibilities

Confusion from the dual use of N_{coll} (???)

We use it both to estimate the average soft response by folding the p+p distribution (which assumes that the likes of N_{coll} average p+p collisions in fact do happen in the event)

but then we also use N_{coll} to estimate how much an extremely rare p+p process (hard scattering) is enhanced in p/d+A,

where it is still very-very rare (<<1/event)

But in those very rare instances when hard scattering did in fact happen,

will the d/p nucleon for the rest of its path interact with the remaining A nucleons and original, intact nucleon (i.e. with the same σ_{pp} a la Glauber?)

If not, what will happen?

Will it keep interacting, but with reduced cross-section (like $\sigma_{\pi p}$)?

Will it be completely out of the pool (no more soft production whatsoever?)

Something in between? If so, what?

Can this be tested?

Reduced/vanishing cross-section in a different context:

Papp, Levai, Barnafoldi, Zhang, Fai -- nucl-th/0203075

A possible candidate for the reduction of the cross section in large systems is the proton dissociation mentioned in the introduction. Our pA collision study showed that each pp inelastic collision adds ~ 400 MeV transverse momentum to the partons inside the proton (on the average). After a few such collisions the partons gain high enough transverse momenta to become free of the proton and during this transition process they do not interact (dead time). We assume that such a proton is "lost" for the reaction and does not participate in particle production anymore. We note that such a picture corresponds to a modification of the original Glauber model. It re-

High p_T biases

Renk, arXiv:1212.0646

However, it has to be realized that almost all current high P_T observables measure conditional probabilities of events, not probabilities. Thus, the correct starting point for their theoretical understanding is Bayes' formula, and the biases introduced by the conditioning are crucial to understanding the outcome. Once this is introduced properly into the modelling process, the counter-intuitive results are seen to find a natural explanation in terms of various biases and the puzzles largely disappear.

Would comparison to LHC help?

If (with similar centrality determination) LHC would see no effect in our p_T range, but similar effect at higher p_T, the "kinematic" effect (depletion of available energy forward) could be the culprit (or dominant)

If LHC would see a similar effect already in our p_T range, the "dynamic" effect (reduced or vanishing cross section) could be the dominant contributor

Summary

In d+Au thermal radiation is not there, but identified hadrons up to 6 GeV/c show features consistent with some medium formation

Specifically, all hadron (baryon and meson) spectra are similar in peripheral Au+Au and central d+Au

Preliminary π^0, η and jet nuclear modification factors show a very unexpected rise in peripheral collisions, while for minimum bias $R_{AA} \sim 1$

Very large drop in R_{CP}, too – i.e. the reference p+p can not be the source of such effect

Different observables, different groups, codes, systematic uncertainties – unlikely that the spectra have a substantial problem

Is it some new physics – or can there be some problem with the way centrality is inferred for these very rare events?

One thing is certain: just redefining centrality such that $R_{AA} = 1$ is not a good idea ☺

Alfonso the Xth ("Alfonse the Wise")

1221-1284
Monarch of Castilia
One of the best scientists of his age
(and big time supporter of science)

"Alfonsine tables" used even by
Copernicus, superseded only
by Kepler in 1627

So he knew what he was talking about,
when sighed (and we all should agree…):

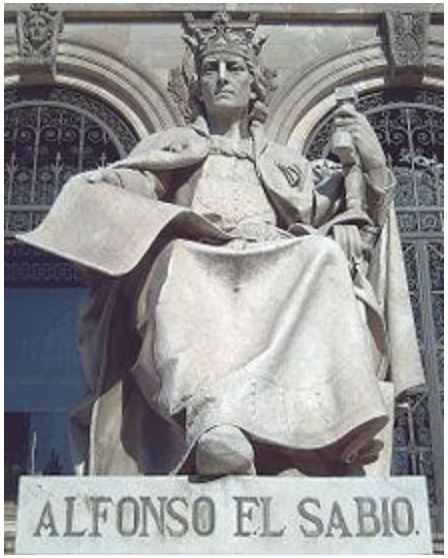

If the Lord Almighty had consulted me before embarking upon creation,

I should have recommended something simpler.

…or on a more serene note

Even if all these speculations turn out to be wrong, the measurement that prompted them is very tantalizing and certainly consequential – in one way or another. No matter what the outcome, the process itself has been fun. Or to quote…

Albert Szent-Györgyi

In later years, - he worked in his newly organized Muscle Research Laboratory at the Marine Biological Laboratory in Woods Hole, Mass., USA, – when asked why, he passionately used such a big hook for his beloved fishing, he used to say,
"I think it is more exciting not to catch a big fish, than not to catch a small one."
He really made some big catches in his lifetime: the Nobel-Prize for discovering the vitamin-C and the biochemical steps of catalysis of the fumaric acid in the tricarboxylic acid cycle.

Small-x physics and pA control measurements

Adrian Dumitru
RIKEN BNL and Baruch College, CUNY

Jet Quenching 2013
RBRC workshop 03/2013

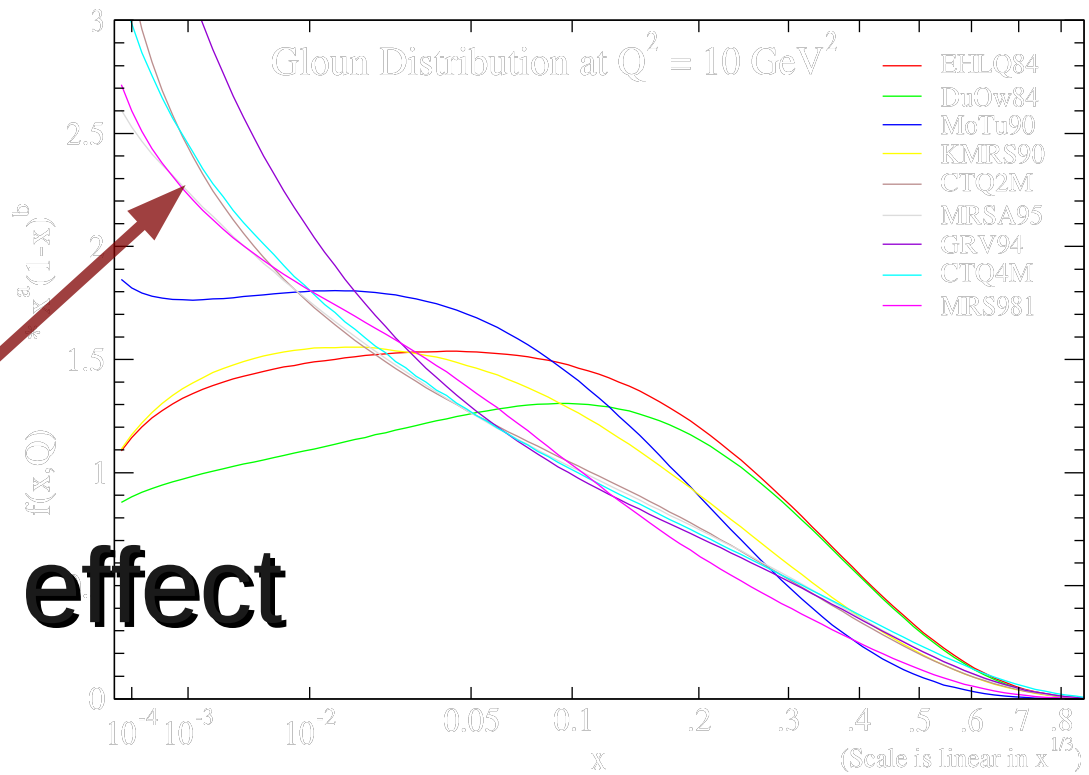

HERA effect

rcBK evolution:

basic “degrees of freedom”: dipole scattering amplitude in fund. rep. **(2-point fct)**

$$\mathcal{N}_F(r, Y; b, A) \equiv \frac{1}{N_c}\,\mathrm{tr}\,\langle 1 - V^\dagger(y)V(z)\rangle_Y$$

$$\mathbf{r} = \mathbf{y} - \mathbf{z}$$

BK equation (incl. non-linear terms → saturation of scattering amplitude!)

$$\frac{\partial \mathcal{N}(r,Y)}{\partial Y} = \int d^2 r_1\, K(r, r_1, r_2)\,[\mathcal{N}(r_1,Y) + \mathcal{N}(r_2,Y) - \mathcal{N}(r,Y) - \mathcal{N}(r_1,Y)\,\mathcal{N}(r_2,Y)]$$

$$\mathbf{r} = \mathbf{r}_1 - \mathbf{r_2}$$

running-coupling kernel (Balitsky prescription)

$$K(\mathbf{r}, \mathbf{r_1}, \mathbf{r_2}) = \frac{N_c\,\alpha_s(r^2)}{2\pi^2}\left[\frac{1}{r_1^2}\left(\frac{\alpha_s(r_1^2)}{\alpha_s(r_2^2)} - 1\right) + \frac{r^2}{r_1^2\,r_2^2} + \frac{1}{r_2^2}\left(\frac{\alpha_s(r_2^2)}{\alpha_s(r_1^2)} - 1\right)\right]$$

$$\alpha_s(r^2) = \frac{4\pi}{\beta \log\left(4\frac{C^2}{r^2\Lambda^2} + \mu\right)}$$

dipole scattering amplitude in adj. rep. $\mathcal{N}_A = 2\,\mathcal{N}_F - \mathcal{N}_F^2$

uGD at x = 3×10^{-4} (e.g. pt=2GeV, y=0, √s=7TeV)

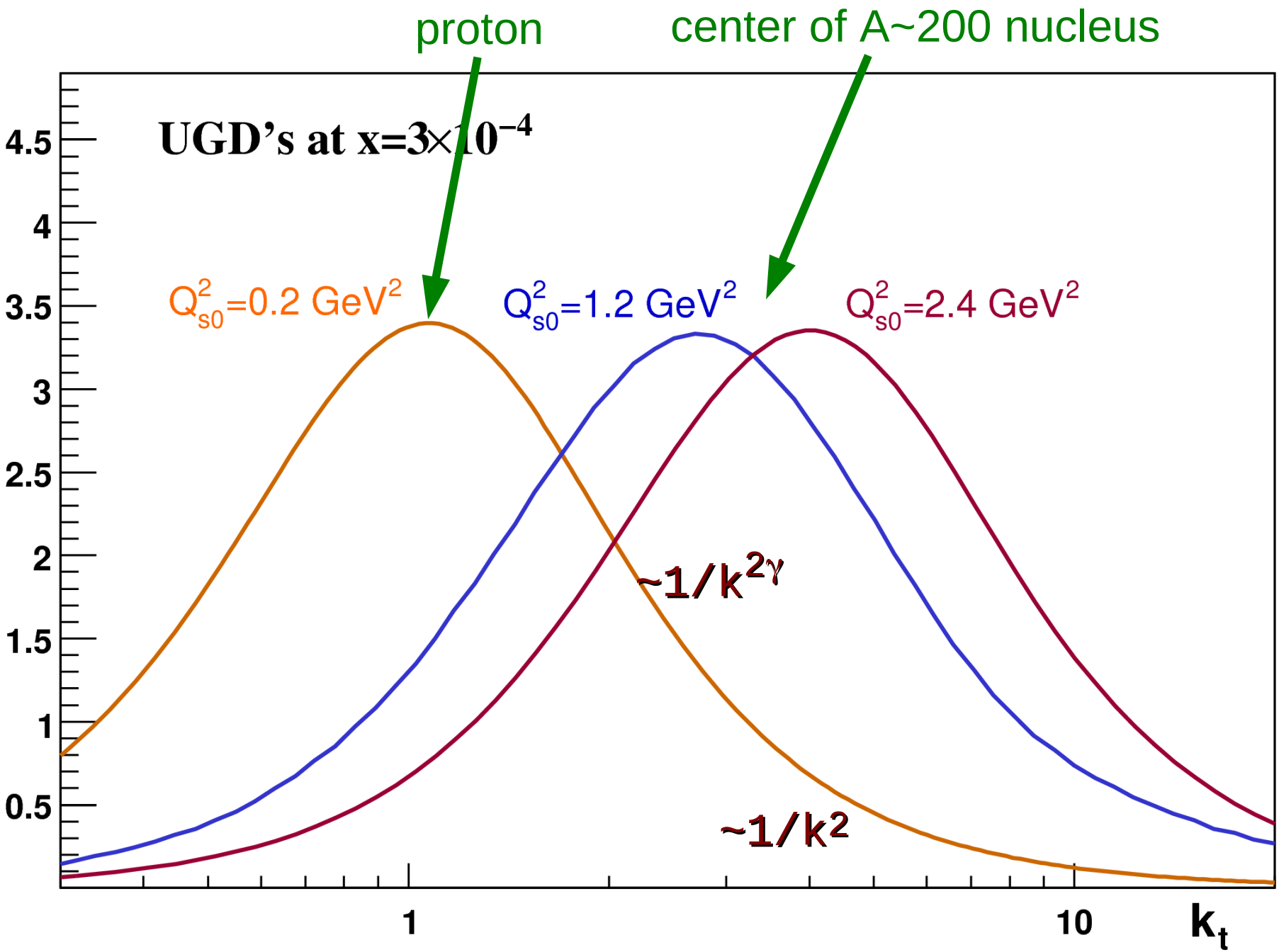

what is the initial condition for rcBK evolution ?

- don't really know, small-x doesn't tell
- needs to be set at “sufficiently” small x_0 so that rcBK can take it from there; in practice, x_0=0.01 ?
- for large A, MV model may provide a decent ini. cond. :

$$\mathcal{N}_F(r, Y=0; b) = 1 - \exp\left[-\frac{r^2\, Q_{s0}^2(b)}{4}\, \ln\left(\frac{1}{\Lambda\, r} + e\right)\right]$$

- alternative I.C. (AAMQS 2011), also denoted by MV^γ or Set 2 (γ>1 !):

$$\mathcal{N}_F(r, Y=0; b) = 1 - \exp\left[-\frac{\left[r^2\, Q_{s0}^2(b)\right]^\gamma}{4}\, \ln\left(\frac{1}{\Lambda\, r} + e\right)\right]$$

$\gamma^* p$

Fit with only light quarks

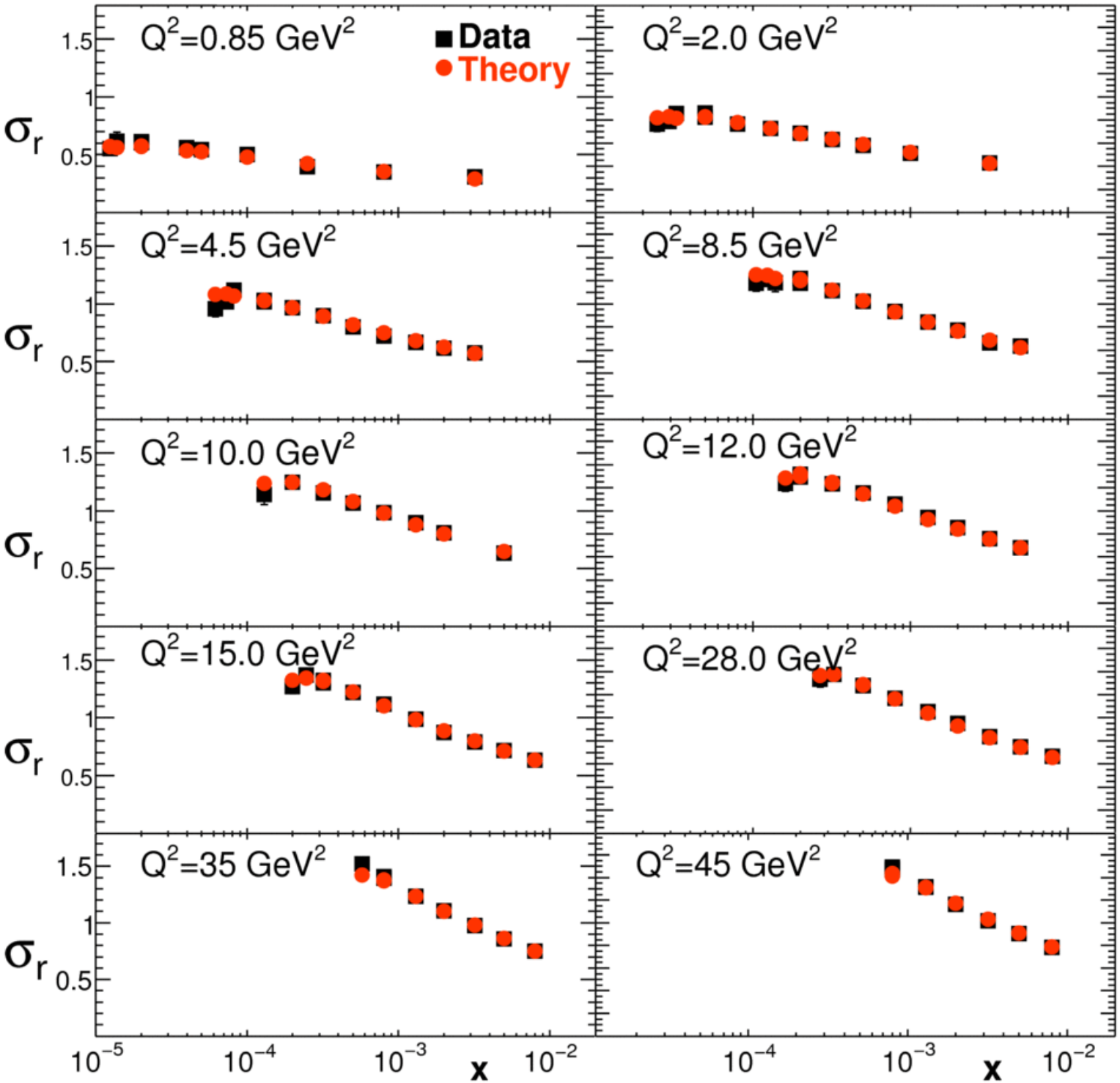

AAMQS:
EPJ C71 (2011)

J. Albacete et al (“AAMQS”): arXiv:1012.4408

	fit	$\frac{\chi^2}{d.o.f}$	Q^2_{s0}	σ_0	γ	C	m_l^2
	GBW						
a	$\alpha_{fr} = 0.7$	1.226	0.241	32.357	0.971	2.46	fixed
a’	$\alpha_{fr} = 0.7$ (Λ_{m_τ})	1.235	0.240	32.569	0.959	2.507	fixed
b	$\alpha_{fr} = 0.7$	1.264	0.2633	30.325	0.968	2.246	1.74E-2
c	$\alpha_{fr} = 1$	1.279	0.254	31.906	0.981	2.378	fixed
c’	$\alpha_{fr} = 1$ (Λ_{m_τ})	1.244	0.2329	33.608	0.9612	2.451	fixed
d	$\alpha_{fr} = 1$	1.248	0.239	33.761	0.980	2.656	2.212E-2
	MV						
e	$\alpha_{fr} = 0.7$	1.171	0.165	32.895	1.135	2.52	fixed
f	$\alpha_{fr} = 0.7$	1.161	0.164	32.324	1.123	2.48	1.823E-2
g	$\alpha_{fr} = 1$	1.140	0.1557	33.696	1.113	2.56	fixed
h	$\alpha_{fr} = 1$	1.117	0.1597	33.105	1.118	2.47	1.845E-2
h’	$\alpha_{fr} = 1$ (Λ_{m_τ})	1.104	0.168	30.265	1.119	1.715	1.463E-2

Table 1: Parameters from fits with only light quarks to data with $x \leq 10^{-2}$ and for all available values of $Q^2 \leq 50$ GeV^2 for different initial conditions, fixed values of the coupling in the infrared $\alpha_{fr} = 0.7$ and 1 and light quark masses either taken fixed $m_l = 0.14$ GeV or left as a free parameter. Fits a’, c’ and h’ correspond to taking the τ mass as reference scale for the running of the coupling. Units: Q^2_{s0} and m_l^2 are in GeV^2 and σ_0 in mb.

- in what follows, this I.C. is used even for a nucleon, with

MV: $Q^2_{s0,N} = 0.2\ \mathrm{GeV}^2$ MV^γ: $Q^2_{s0,N} = 0.168\ \mathrm{GeV}^2$

- for nucleus, at transv. position b:

$Q^2_{s0}(b)$ = (# nucleons at b) X $Q^2_{s0,N}$

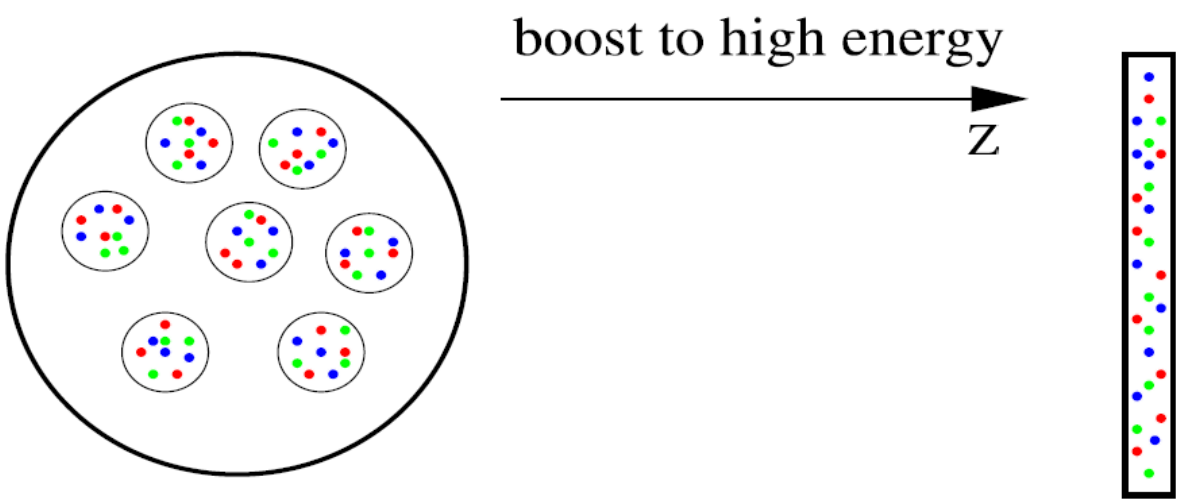

side view

McLerran & Venugopalan

fluctuations of valence partons in ⊥ plane

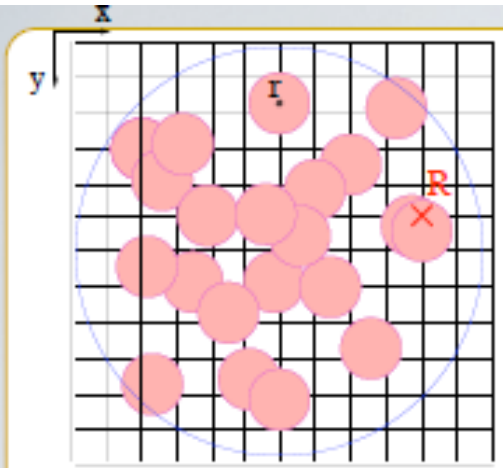

1. Initial conditions for the evolution (x=0.01)

$$N(\mathbf{R}) = \sum_{i=1}^{A} \Theta\left(\sqrt{\frac{\sigma_0}{\pi}} - |\mathbf{R} - \mathbf{r_i}|\right) \longrightarrow Q^2_{s0}(\mathbf{R}) = N(\mathbf{R})\, Q^2_{s0,\,\mathrm{nucl}}$$

$$\downarrow$$

$$\varphi(x_0 = 0.01, k_t, R)$$

2. Solve local running coupling BK evolution at each transverse point

rcBK equation or KLN model

$$\downarrow$$

$$\varphi(x, k_t, R)$$

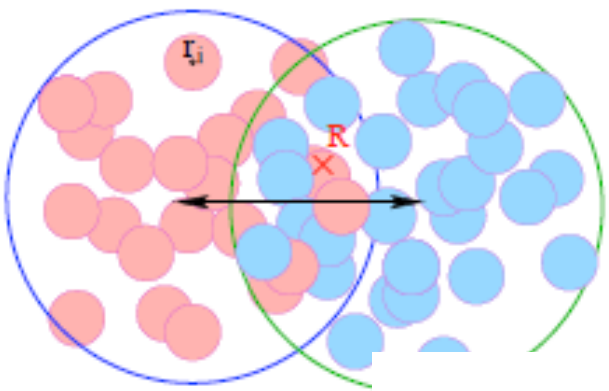

3 Calculate gluon production at each transverse point according to kt-factorization

INPUT: $\varphi(\mathbf{x} = \mathbf{0.01}, \mathbf{k_t})$ FOR A SINGLE NUCLEON:

$$N_{\mathrm{part,A}}(\vec{b}) = \sum_{i=1\cdots A} \Theta\left(P(\vec{b} - \vec{r}_i) - \nu_i\right) \quad .$$

$$P(b) = 1 - \exp[-\sigma_g T_{pp}(b)], \qquad T_{pp}(b) = \int d^2s\, T_p(s)\, T_p(s-b)$$

$$T_p(r) = \frac{1}{2\pi B} \exp[-r^2/(2B)] \qquad \sigma_{NN}(\sqrt{s}) = \int d^2b\, (1 - \exp[-\sigma_g T_{pp}(b)])$$

thickness fluctuations:

(average of 1 / 9 nucleon target compared to 5-nucl. target)

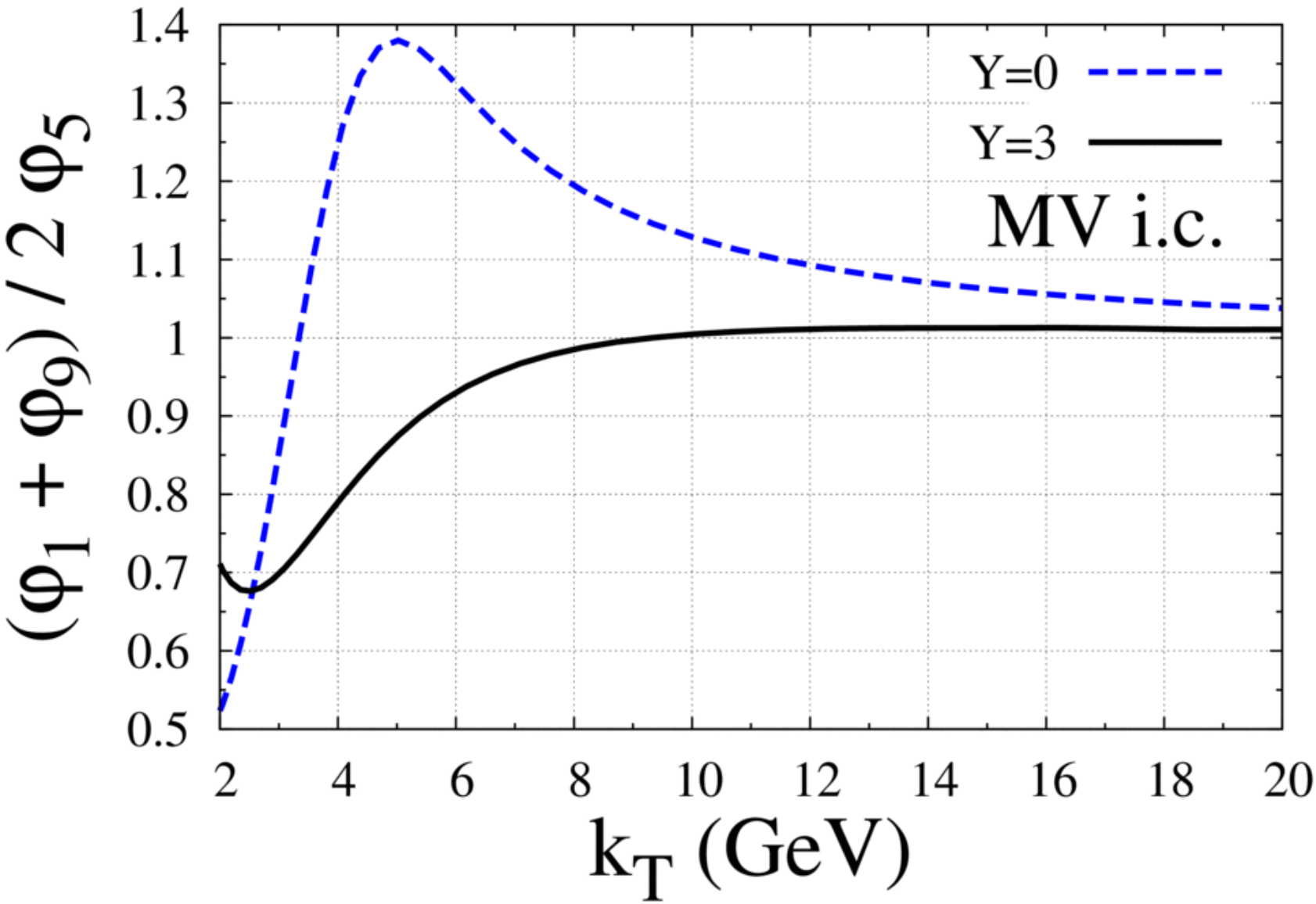

$k_\perp$-factorization, multiplicity in A+B --> g+X

unintegrated gluon distribution:

$$\varphi(k, Y; b, A) = \frac{C_F\, k^2}{\alpha_s(k)} \int \frac{d^2\mathbf{r}}{(2\pi)^3}\, e^{-i\mathbf{k}\cdot\mathbf{r}} \mathcal{N}_A(r, Y; b, A)$$

multiplicity:

$$\frac{dN^{A+B\to g}}{dy\, d^2p_t\, d^2b} = K\, \frac{2}{C_F} \frac{1}{p_t^2} \int^{p_t} \frac{d^2k_t}{4}\, \alpha_s(Q)\, \varphi\left(\frac{|p_t + k_t|}{2}, x_1\right) \varphi\left(\frac{|p_t - k_t|}{2}, x_2\right)$$

Notes:

- finite as $p_t \to 0$ if UGD does not blow up
- $x_{1,2} = (p_t/\sqrt{s}) \exp(\pm y)$; $Y_{1,2} = \log(x_0/x_{1,2})$ ←
  where x_0=0.01 is assumed onset of rcBK evol.
- K = 1.5 – 2, appears reasonable

high-pt hadron production in pp @ LHC requires steeper I.C.

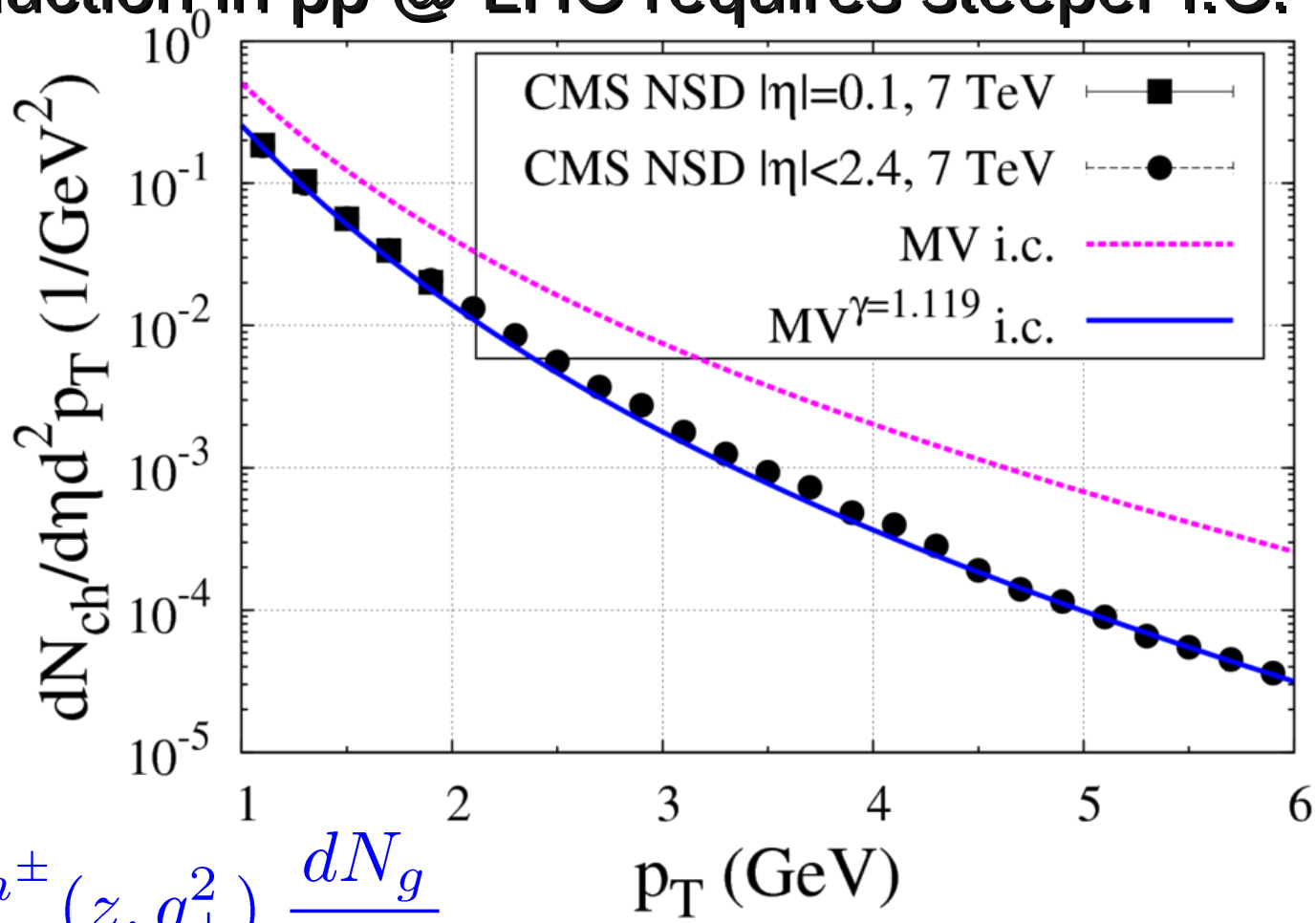

$$\frac{dN_{h^\pm}}{d^2p_\perp} = \int \frac{dz}{z^2} D_g^{h^\pm}(z, q_\perp^2) \, \frac{dN_g}{d^2q_\perp}$$

- no g $\longrightarrow$ h multiplication factor κ here!
  (normalization set by Fragm. Func.)
- rcBK in dilute regime
- LHC constrains initial condition

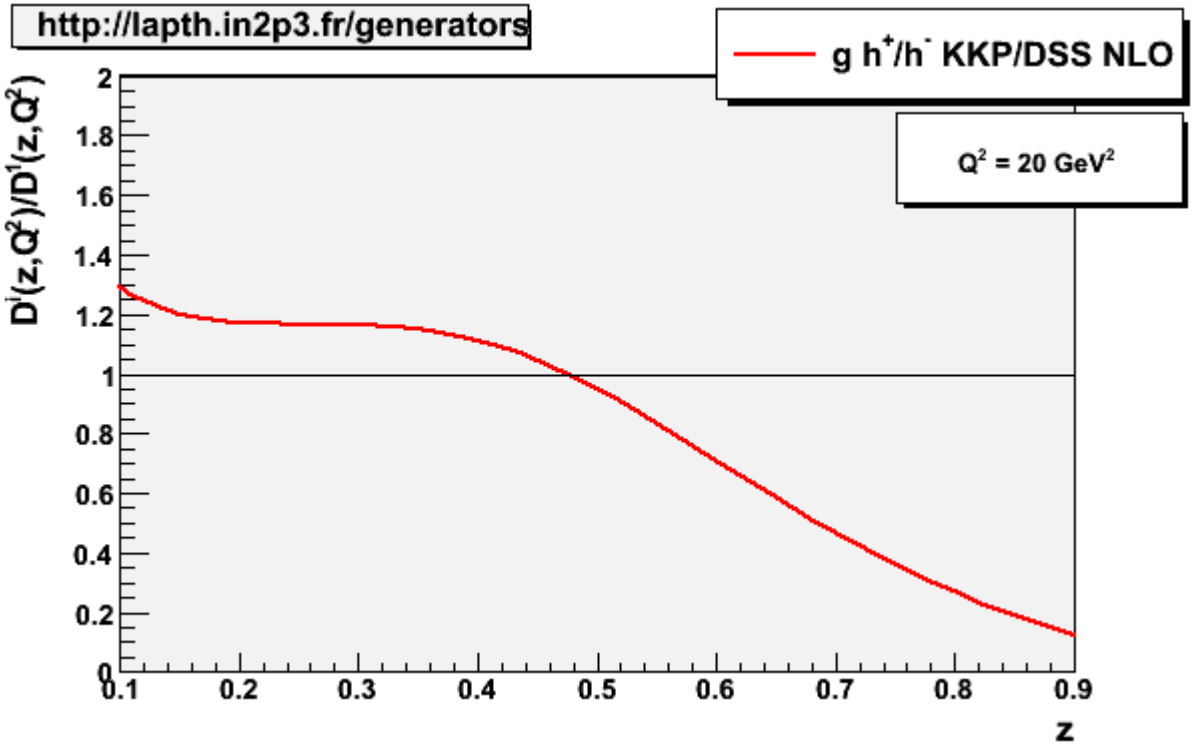
http://lapth.in2p3.fr/generators
g h+/h- KKP/DSS NLO
Q2 = 20 GeV2
Di(z,Q2)/D1(z,Q2)
z

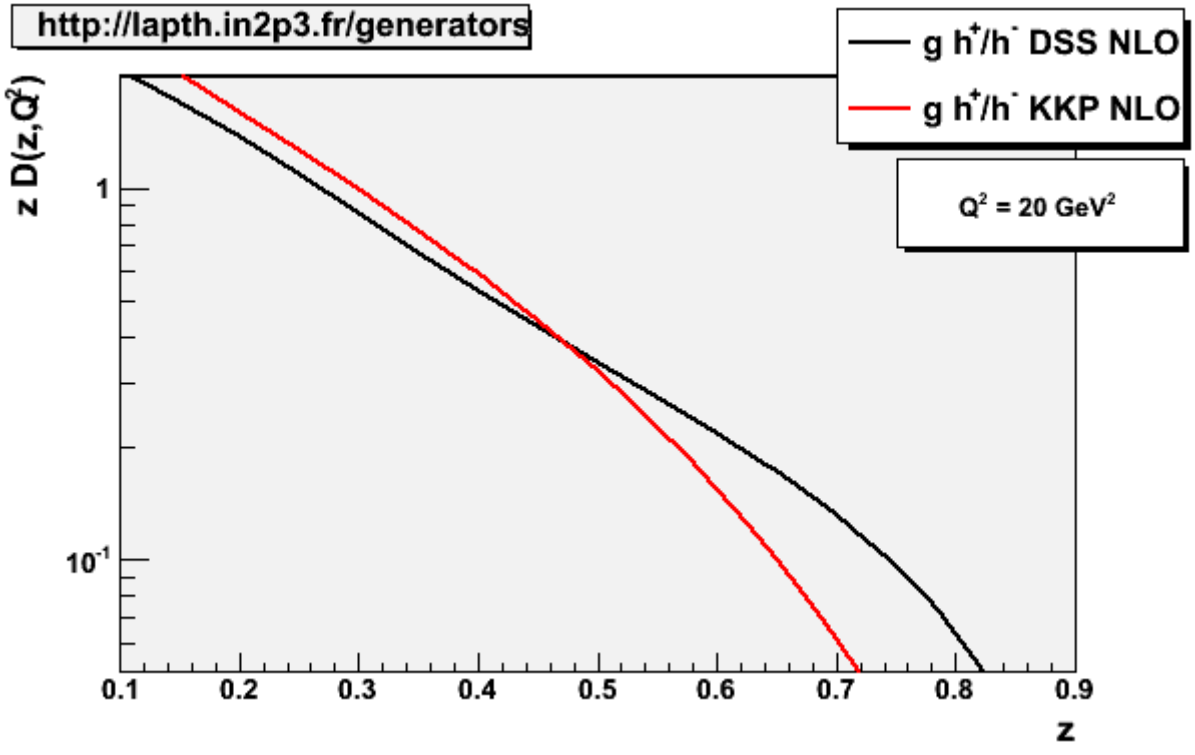
http://lapth.in2p3.fr/generators
g h+/h- DSS NLO
g h+/h- KKP NLO
Q2 = 20 GeV2
z D(z,Q2)
z

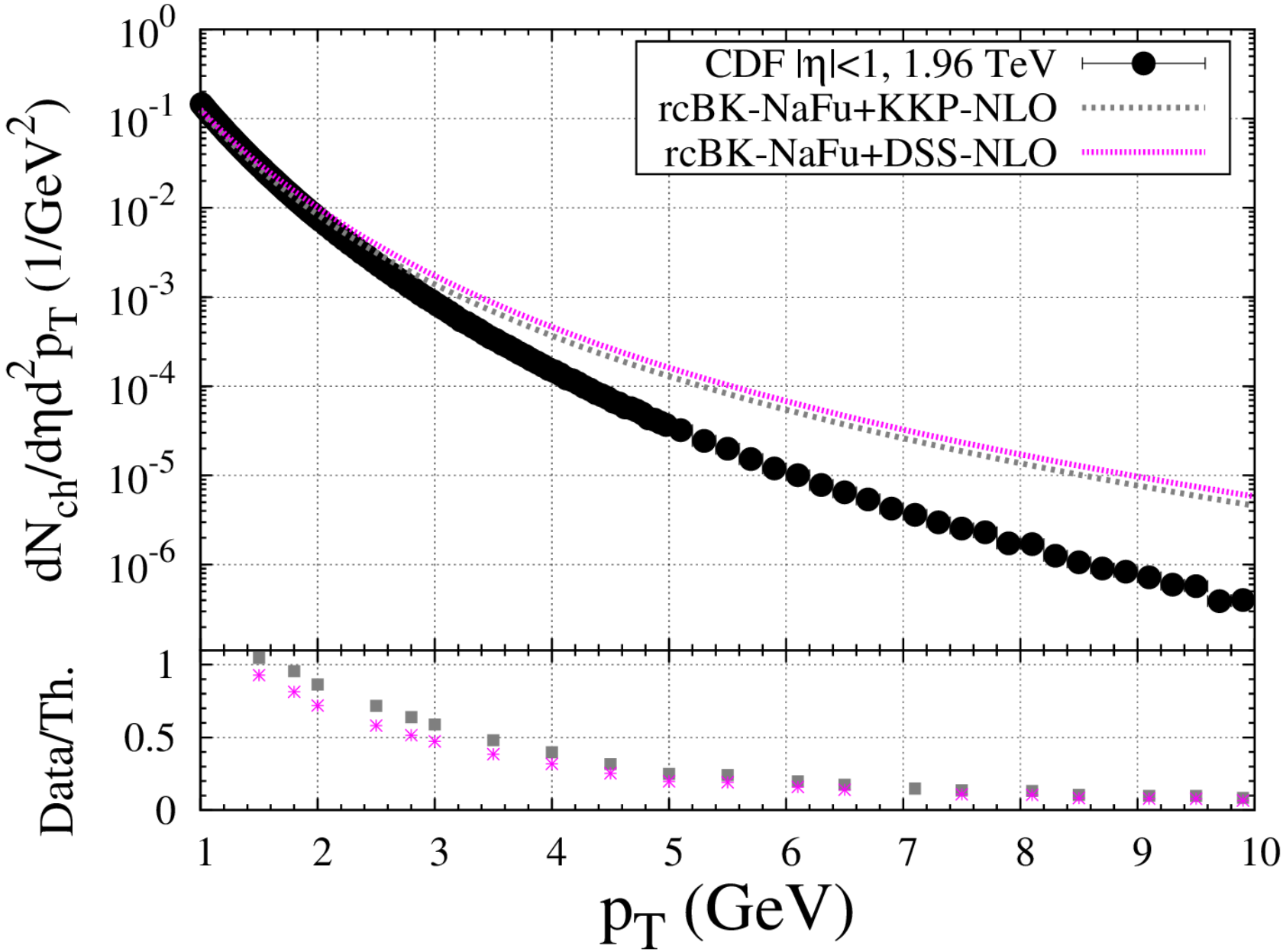
CDF |η|<1, 1.96 TeV
rcBK-NaFu+KKP-NLO
rcBK-NaFu+DSS-NLO
$dN_{ch}/d\eta d^2p_T$ (1/GeV^2)
Data/Th.
p_T (GeV)
10^0
10^{-1}
10^{-2}
10^{-3}
10^{-4}
10^{-5}
10^{-6}
1
0.5
0
1
2
3
4
5
6
7
8
9
10

pt distributions in pp → ch at TEVATRON / LHC energies

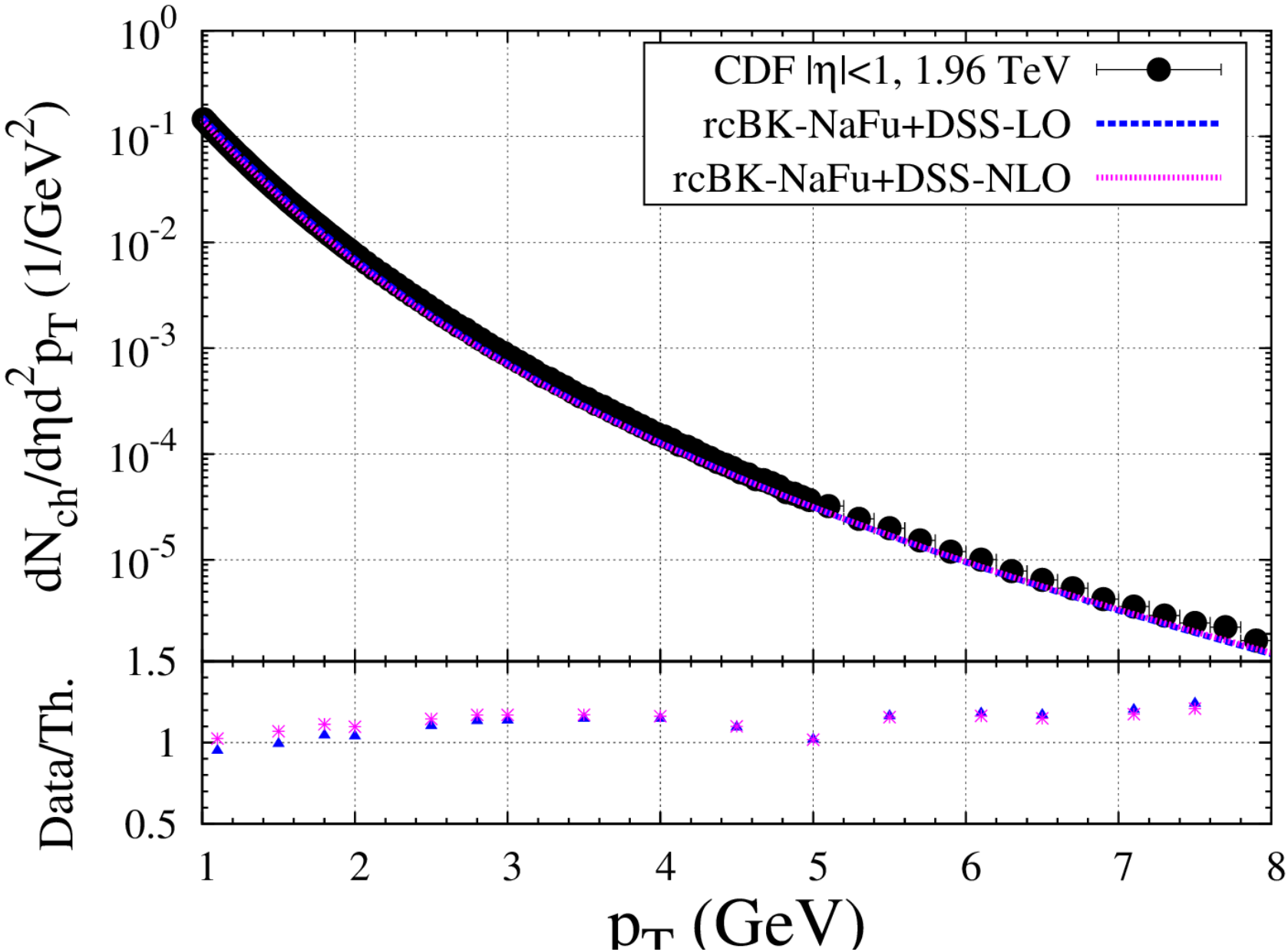

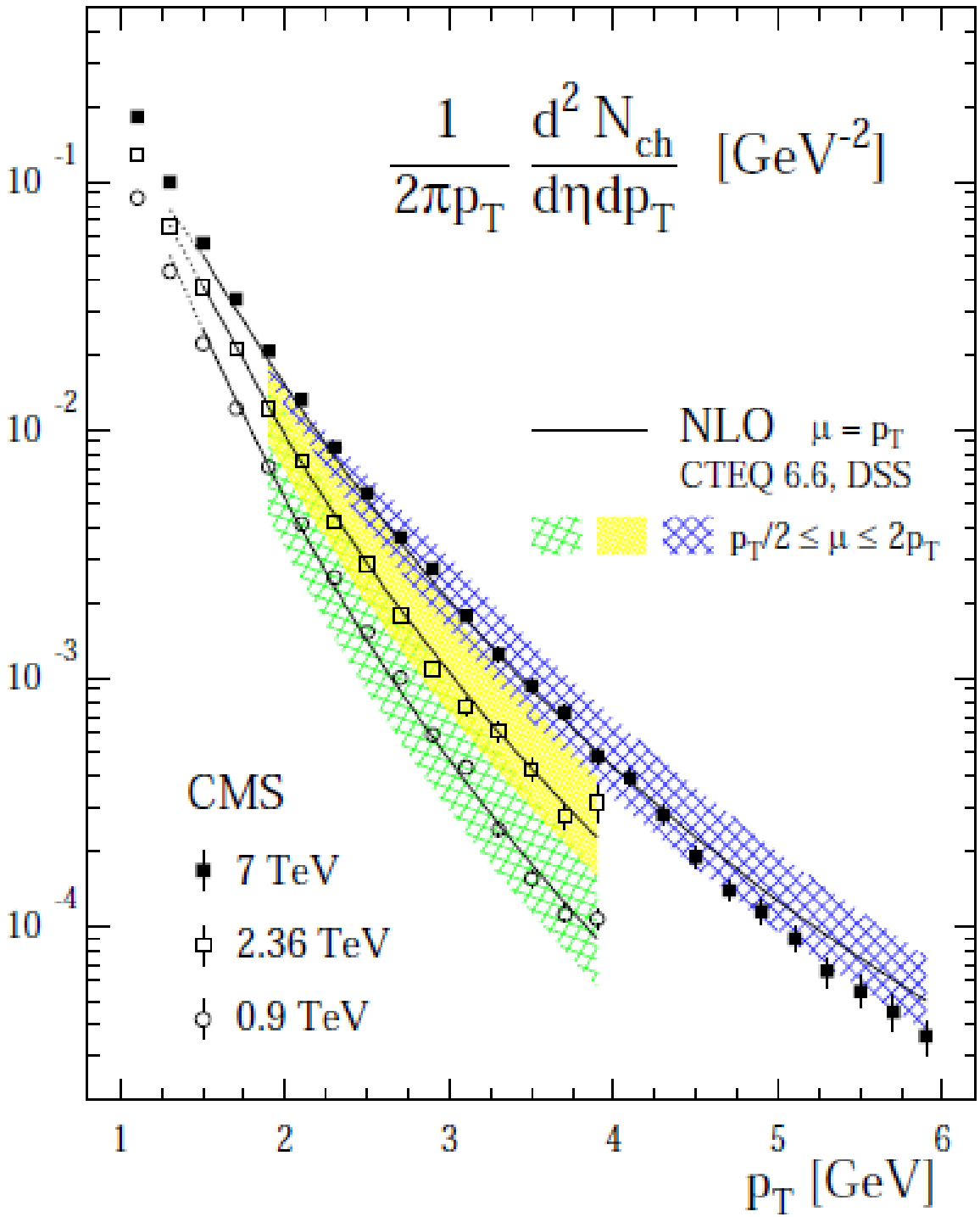

Collinear pQCD fact.

Sassot, Zurita, Stratmann
PRD 82 (2010)

$$\mathcal{N}_F(r, Y = 0; b) = 1 - \exp\left[-\frac{\left[r^2\, Q_{s0}^2(b)\right]^\gamma}{4}\, \ln\left(\frac{1}{\Lambda\, r} + e\right)\right]$$

for nuclei:

- do we use same γ as for a proton ?
- do we assume $Q_{s0}^2 \sim T_A$ or $Q_{s0}^2 \sim T_A^{1/\gamma}$

→ w/o a better idea of where the AAMQS parameter comes from, we need to factor this into uncertainties...

$A^{1/3}$ dependence of initial conditions for BK/JIMWLK beyond MV action

$$S = \int d^2x_\perp \left\{ \frac{1}{2\mu^2}\rho^a\rho^a - \frac{1}{\kappa_3} d^{abc}\rho^a\rho^b\rho^c + \left[\frac{1}{\kappa_4}\left(\delta^{ab}\delta^{cd} + \delta^{ac}\delta^{bd} + \delta^{ad}\delta^{bc}\right) + \frac{1}{\kappa_4'}\left(d^{abe}d^{cde} + d^{ace}d^{bde} + d^{ade}d^{bce}\right)\right]\rho^a\rho^b\rho^c\rho^d \right\}$$

+ soft YM fields + coupling of soft $\leftrightarrow$ hard

- $\mu^2 \sim g^2 A^{1/3}$; $\kappa_3 \sim g^3 A^{2/3}$; $\kappa_4 \sim g^4 A$

Elena Petreska et al:
PRD 2011

E. Petreska + A.D., NPA 2012

$$1-\mathcal{N}(r,x_0)=\frac{1}{4}r^2Q_{s0}^2\log\frac{1}{r\Lambda}-\frac{1}{6\pi^3}\frac{g^8}{\kappa_4}\left(\int dx^-\mu^4(x^-)\right)^2 r^2\log^3\frac{1}{r\Lambda}$$

(in log (1/rΛ) » 1 limit)

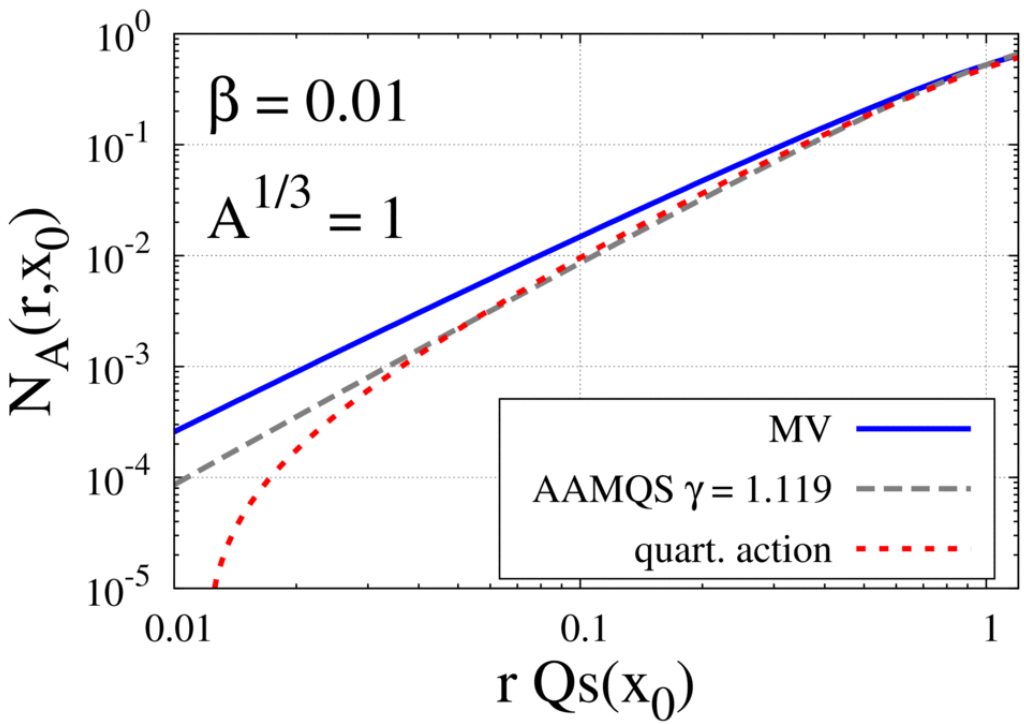

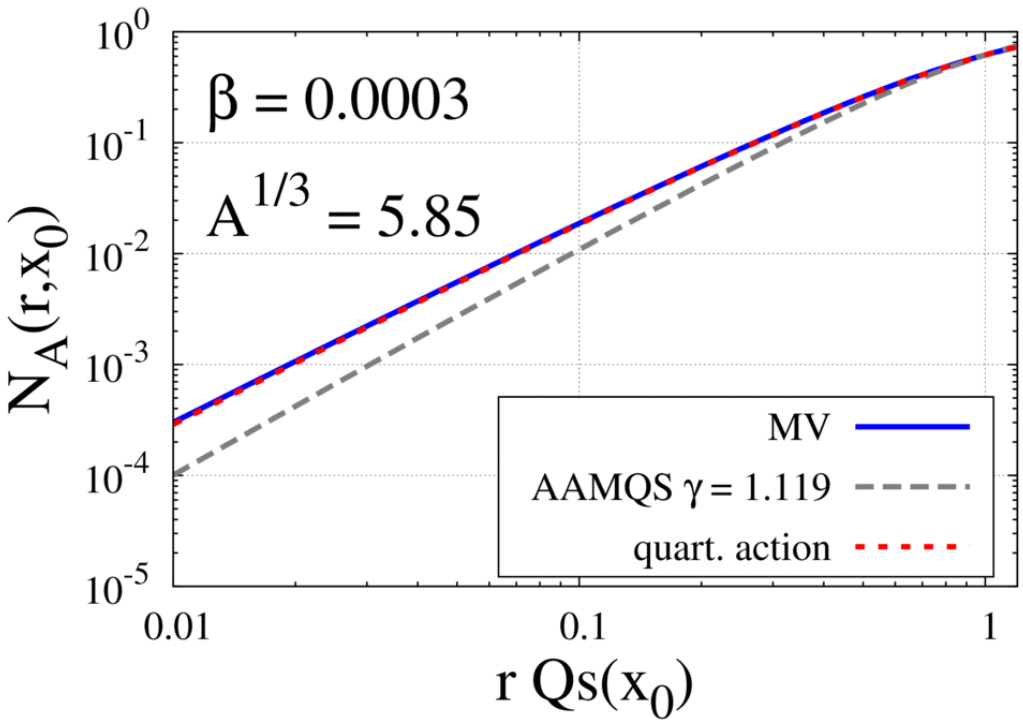

Let's start with AA : centrality and energy dependence of multiplicities; (confirms KLN idea)

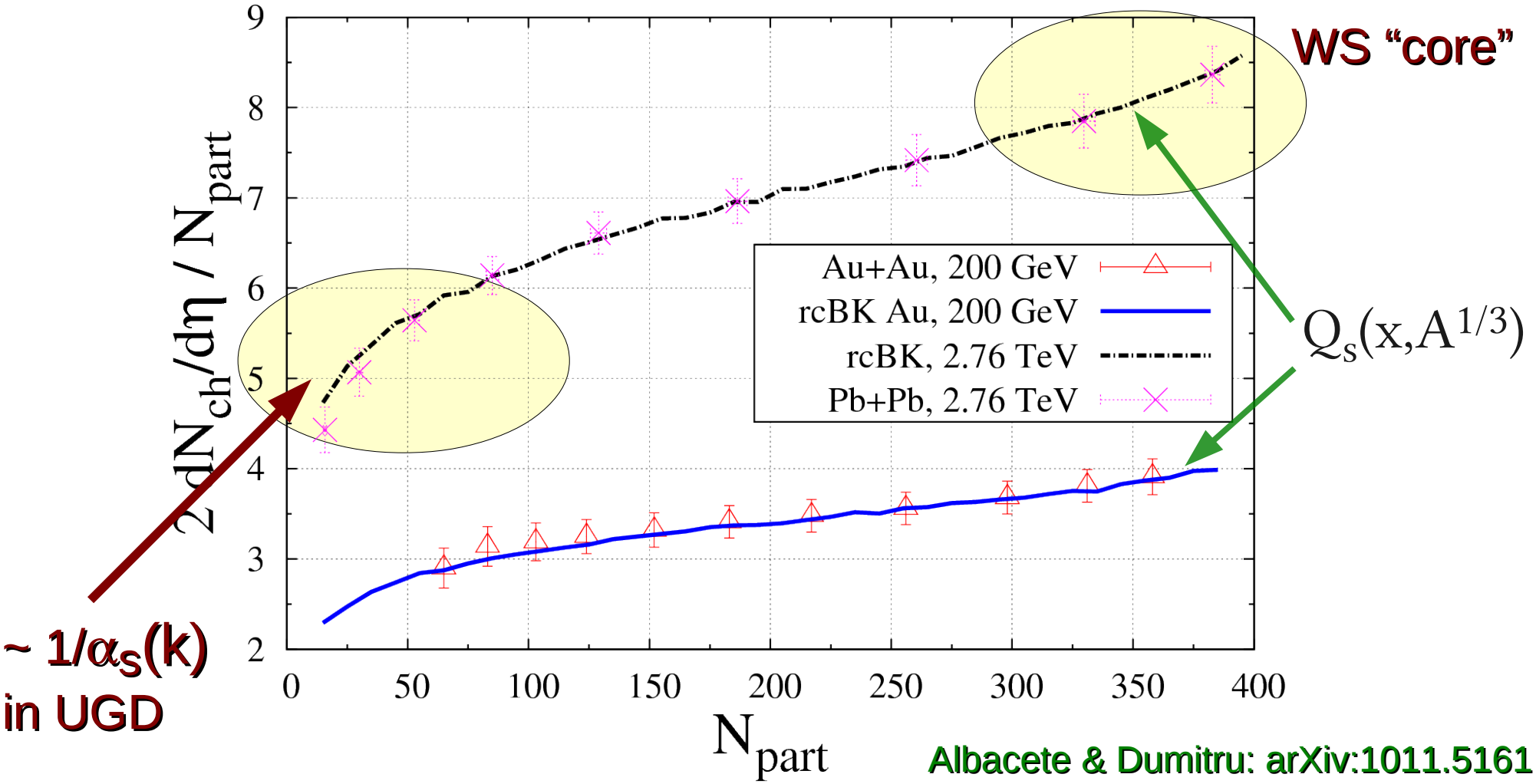

Albacete & Dumitru: arXiv:1011.5161

- assumes $N_{hadr} = \kappa \cdot N_{glue}$ with $\kappa \cong 5$

Back to AA : centrality and energy dependence of $E_\perp$

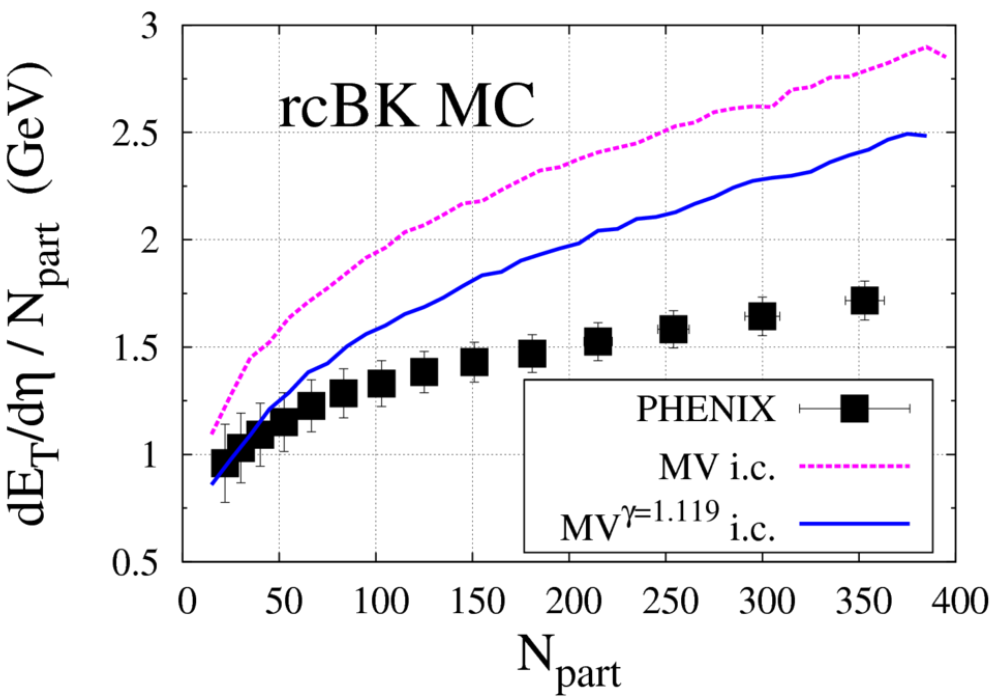

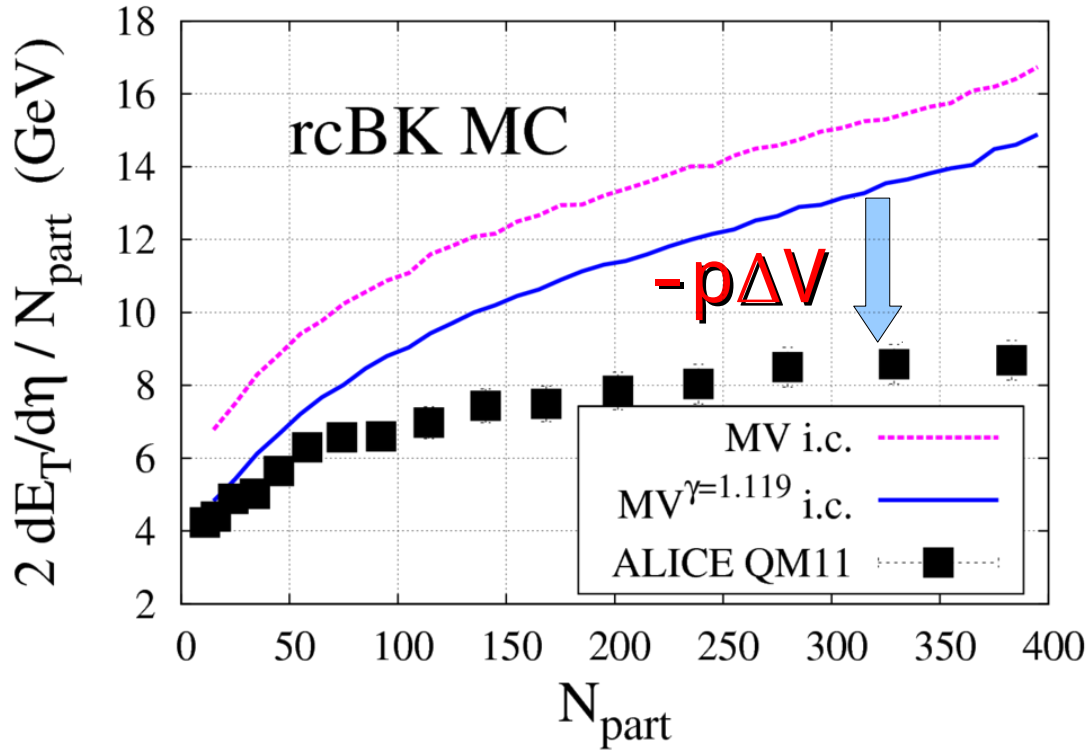

- (again, no g $\longrightarrow$ h multiplication factor κ here)
- 1d ideal hydro: $E_\perp^f / E_\perp^i \approx T_f / T_i \approx 1/2$
- interesting: $(dE_\perp/d\eta)$ / $(A\sqrt{s}) \approx 0.5\%$ at LHC_{2760}, centrl Pb+Pb !

R_{pA} for p+Pb at 5 TeV :

$$R_{pA}(p_T) = \frac{dN_{\rm ch}^{pA}/d^2p_T d\eta}{N_{\rm coll}\, dN_{\rm ch}^{pp}/d^2p_T d\eta}$$

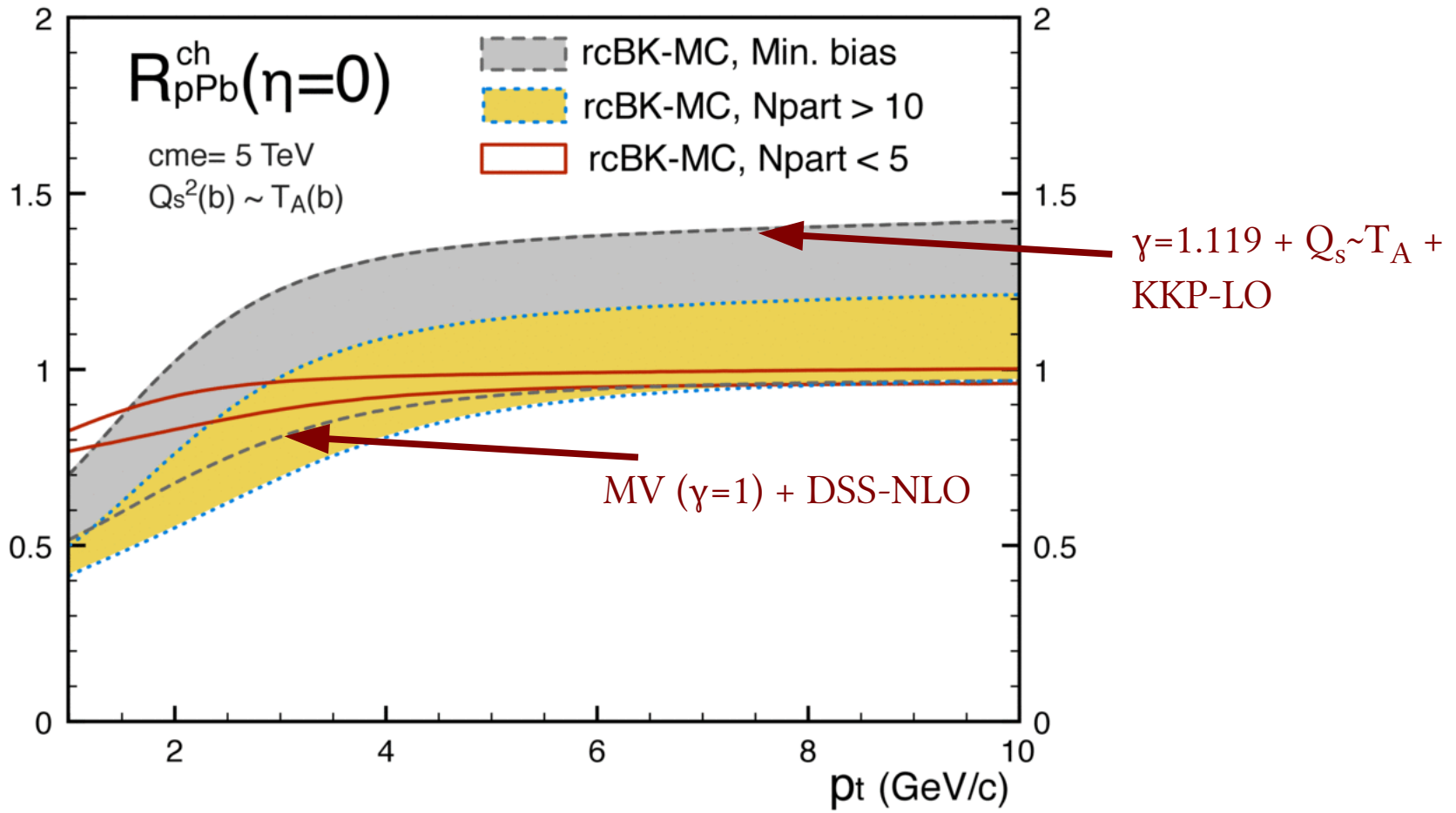

- $R_{pA} < 1$ at $p_{T(\rm hadron)} \sim$ 1-2 GeV
- R_{pA} decreases (slightly) with rapidity
- generically R_{pA}(central) < R_{pA}(mb)
- Cronin peak washed out by evolution

R_{p+Pb} at 5 TeV

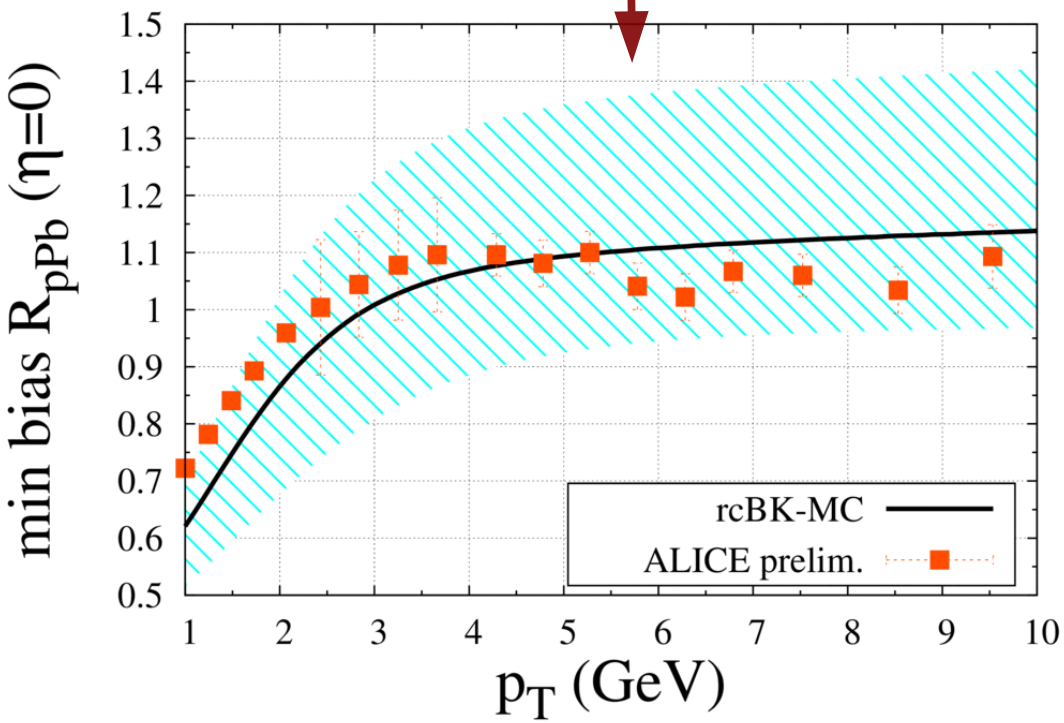

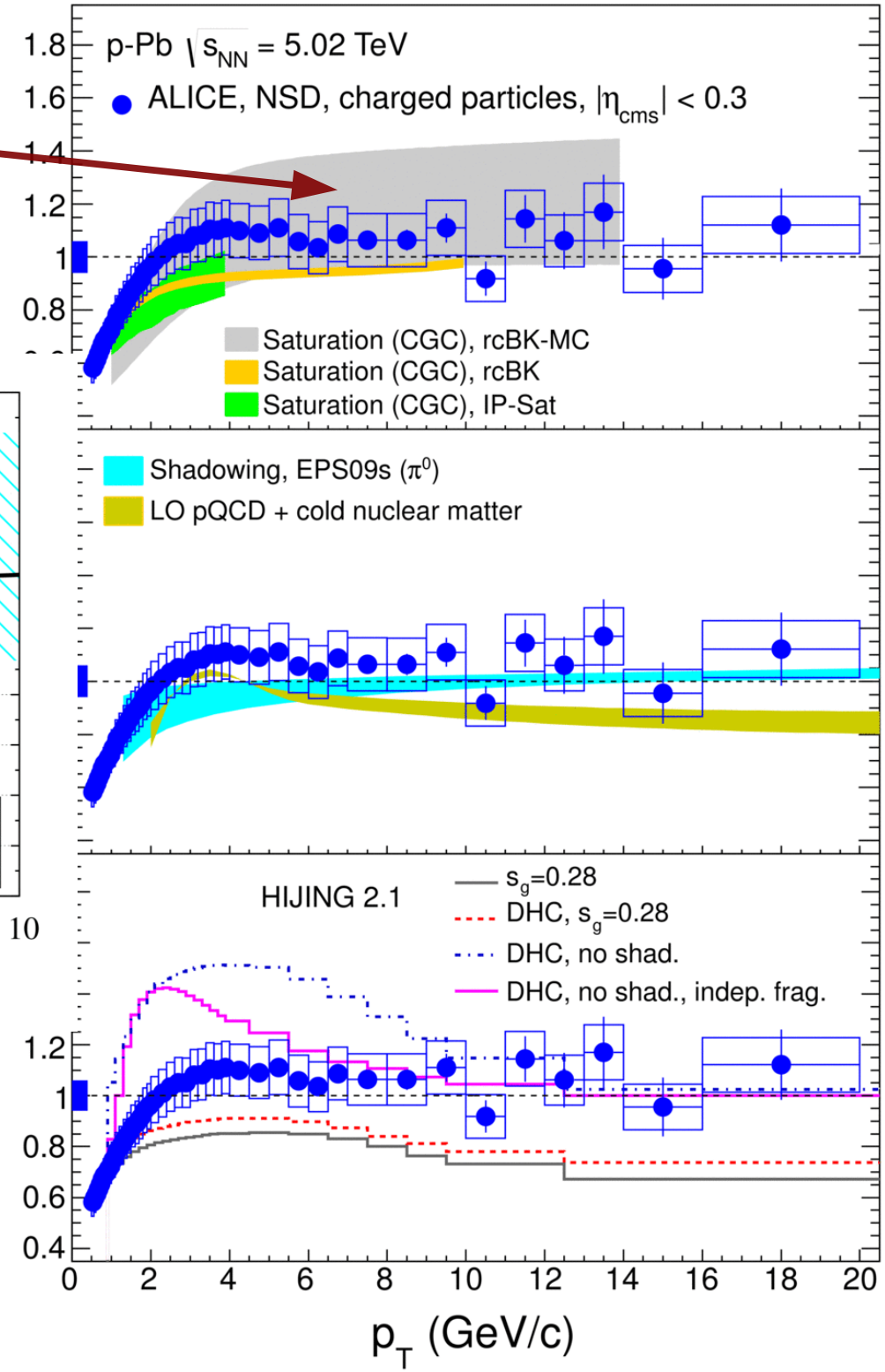

- clearly, no "initial state quenching" above ~ 3 GeV

forward rapidity :

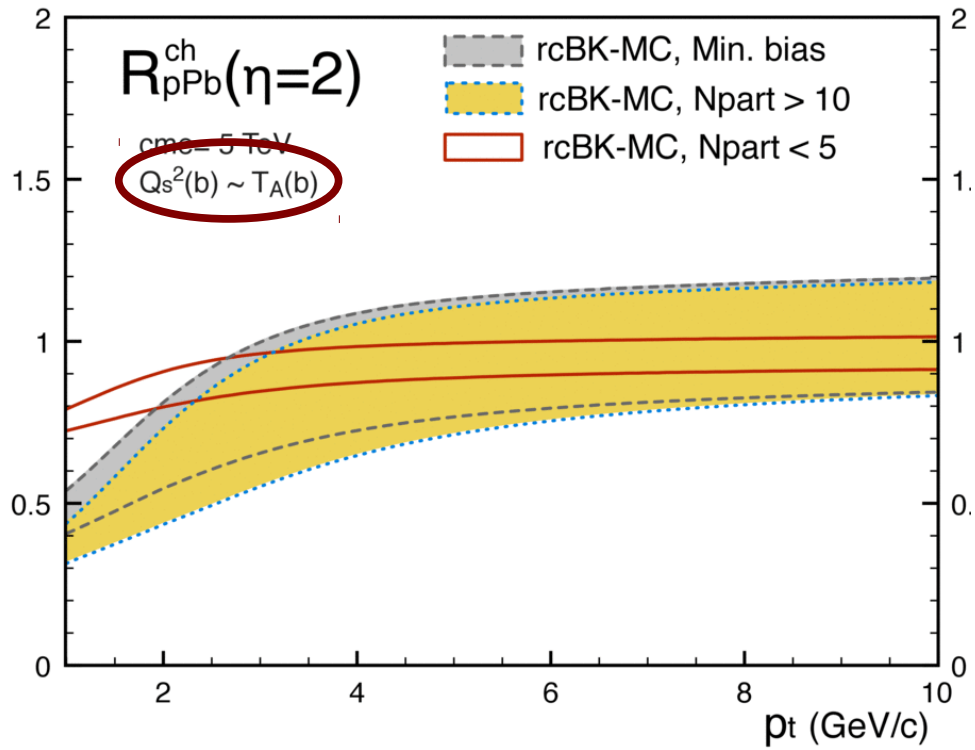

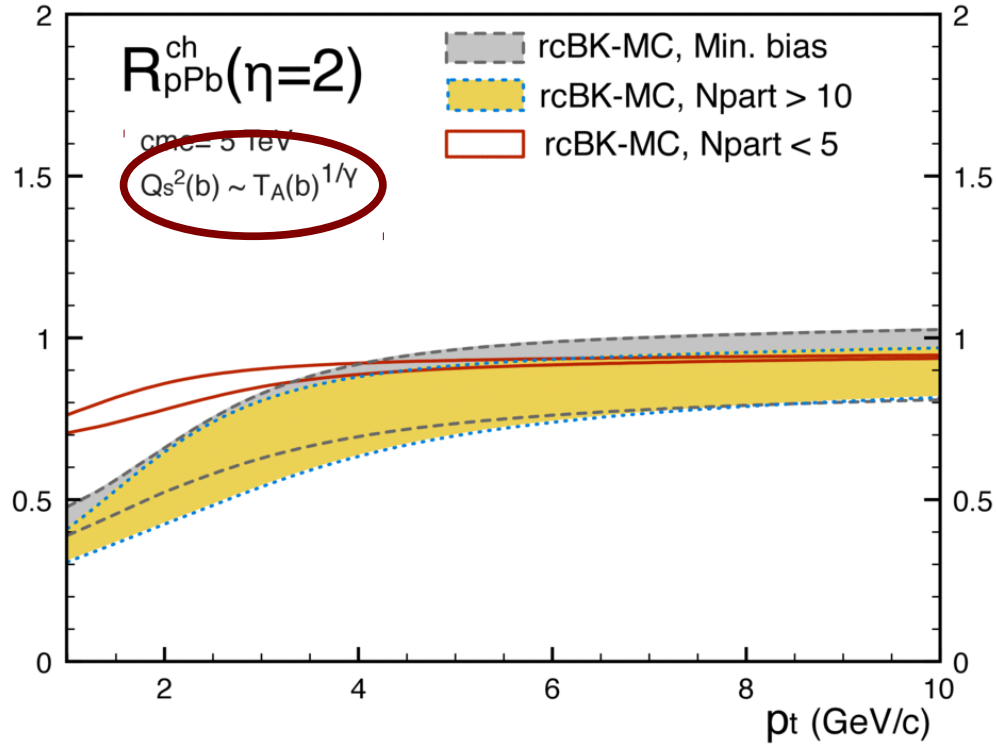

- more suppression due to small-x evolution
- R_{pA} goes down by some 0.1 – 0.2

More detailed view of the "medium" in AA ?

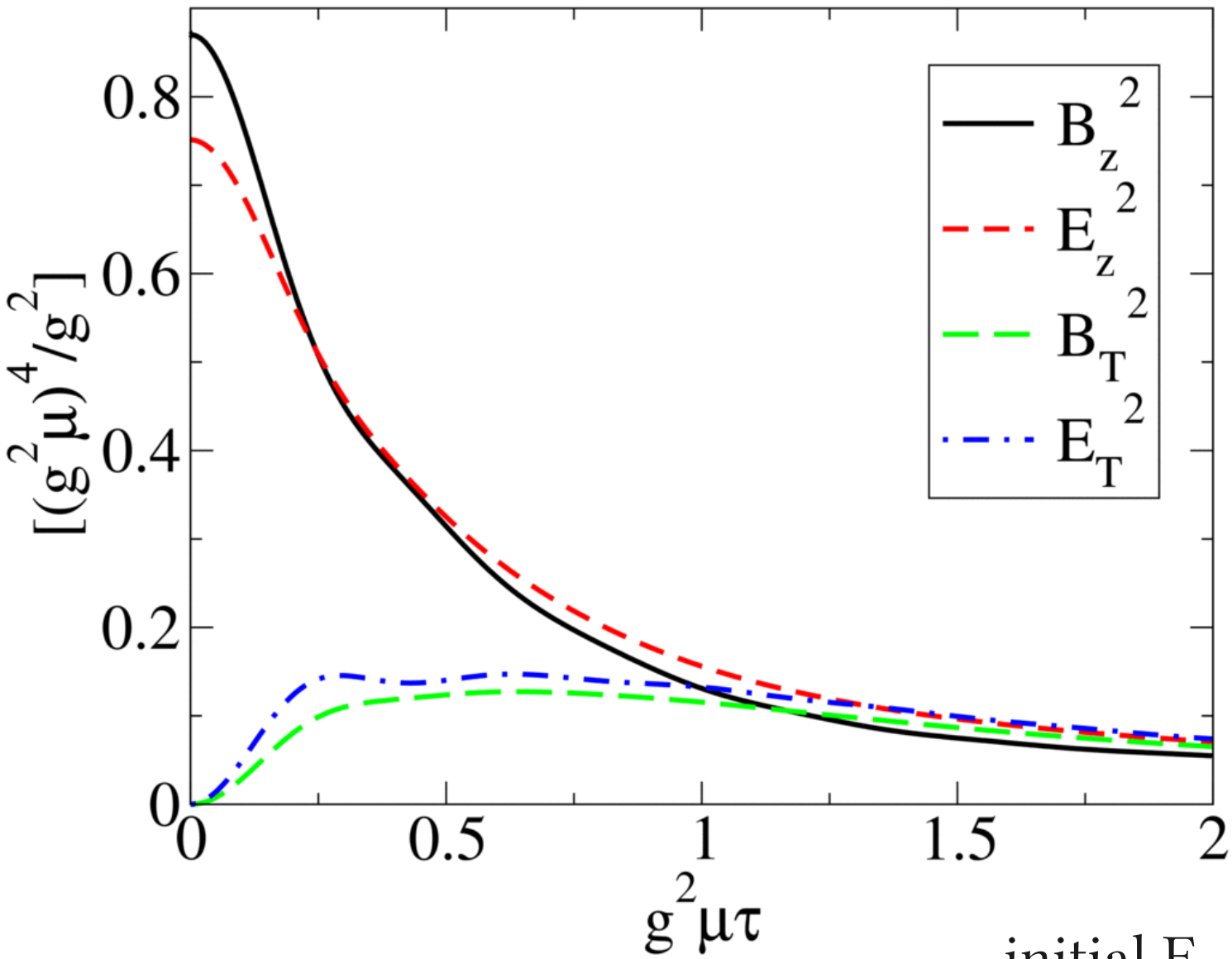

initial E_z, B_z fields

(Fries, Kapusta, Li;
Lappi, McLerran 2006)

Analyze classical field configurations at midrapidity: η=0, 2D

what is structure of B_z field ?

magnetic flux loop in x-y plane:

$$M(R) = \mathcal{P}\exp\left(ig\oint dx^i A^i\right)$$

$$W_M(R) = \frac{1}{N_c}\langle \mathrm{tr}\ M(R)\rangle$$

$$W_M^{Z(2)}(R) = \langle \mathrm{sgn\ tr}\ M(R)\rangle$$

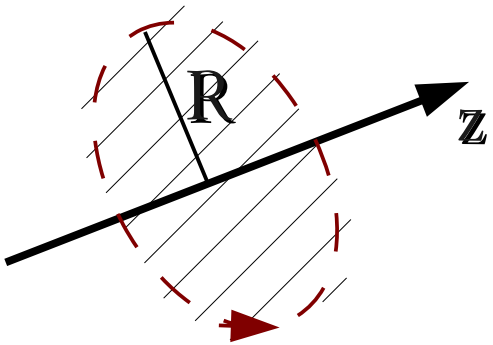

Magnetic field domains (B_z^3 at τ=0)

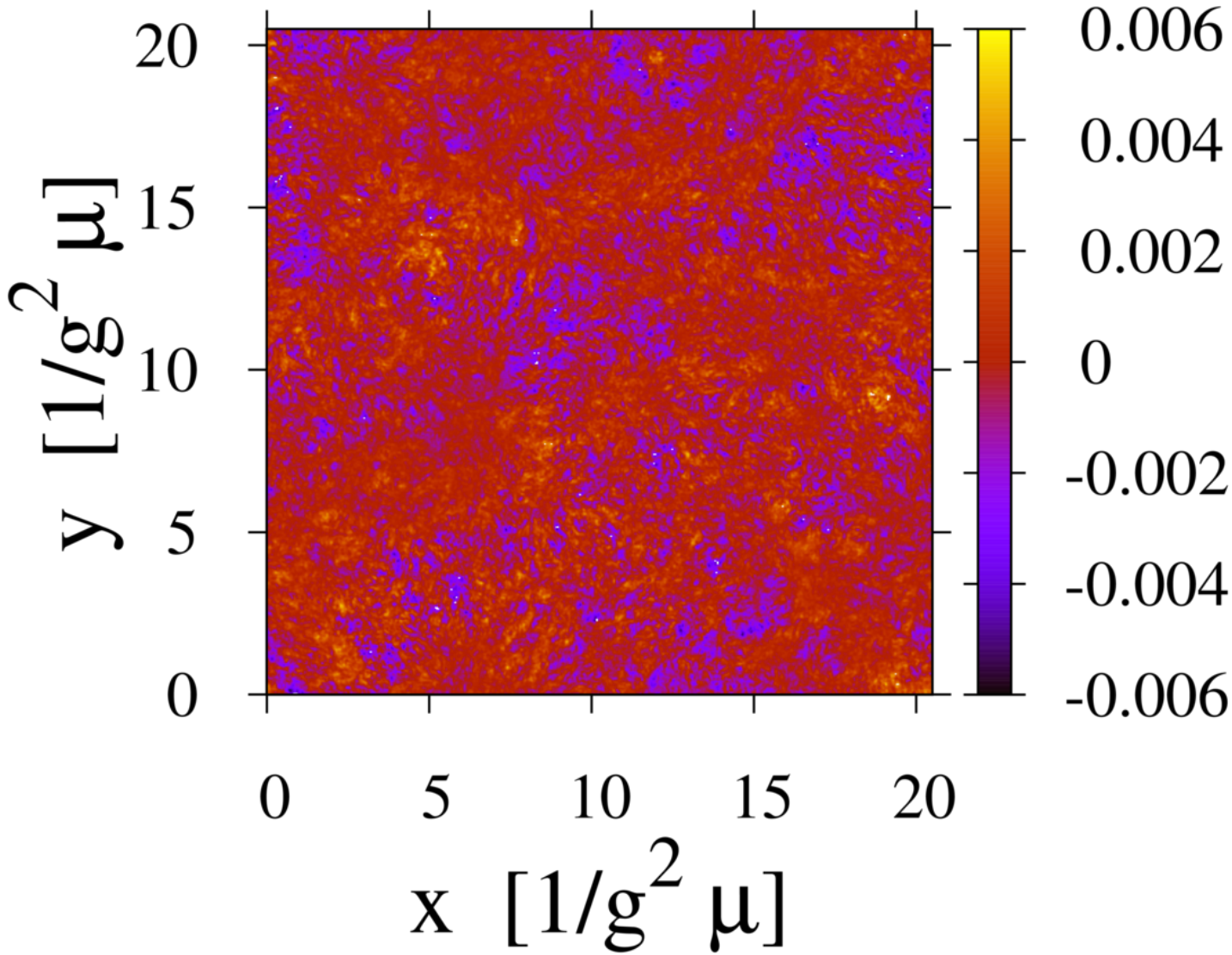

SU(2) solution :

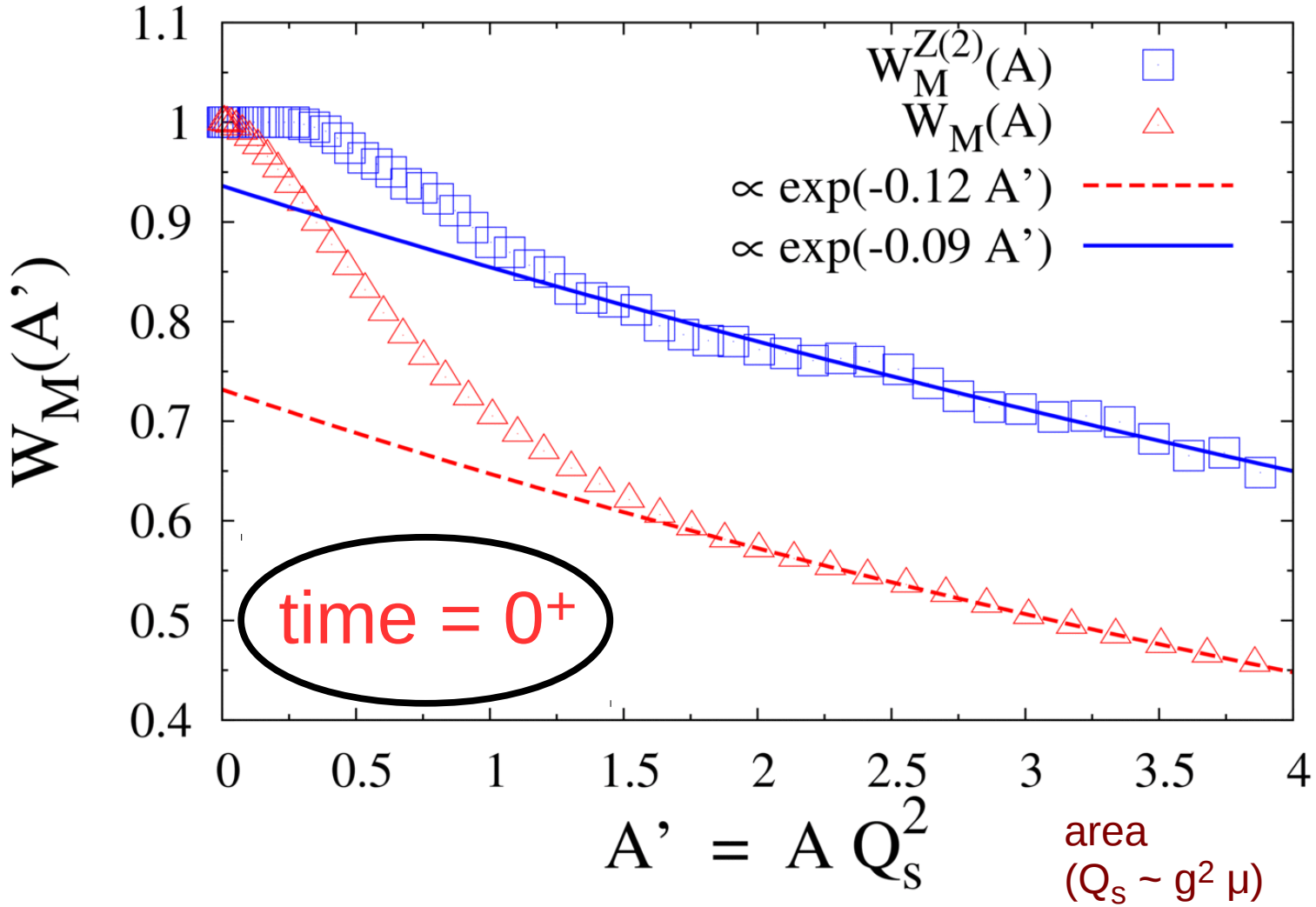

- area law for loops with area $A \geq 1.5 - 2$
- $\sigma_M \sim 0.12\ Q_s^2$; thermal SU(N): $\sigma_M \sim g_{3D}^2 \sim (g^2 T)^2$
- small loops $\notin Z(2)$ but roughly ok for large ones!
- structure of B_z ~ uncorrelated vortices ?!
- $R_{vtx} \sim 1/Q_s$ from onset of area law

A.D., Y. Nara, E. Petreska: arXiv:1302.2064

Propagation of hard particles in background of magnetic Z(N) vortices

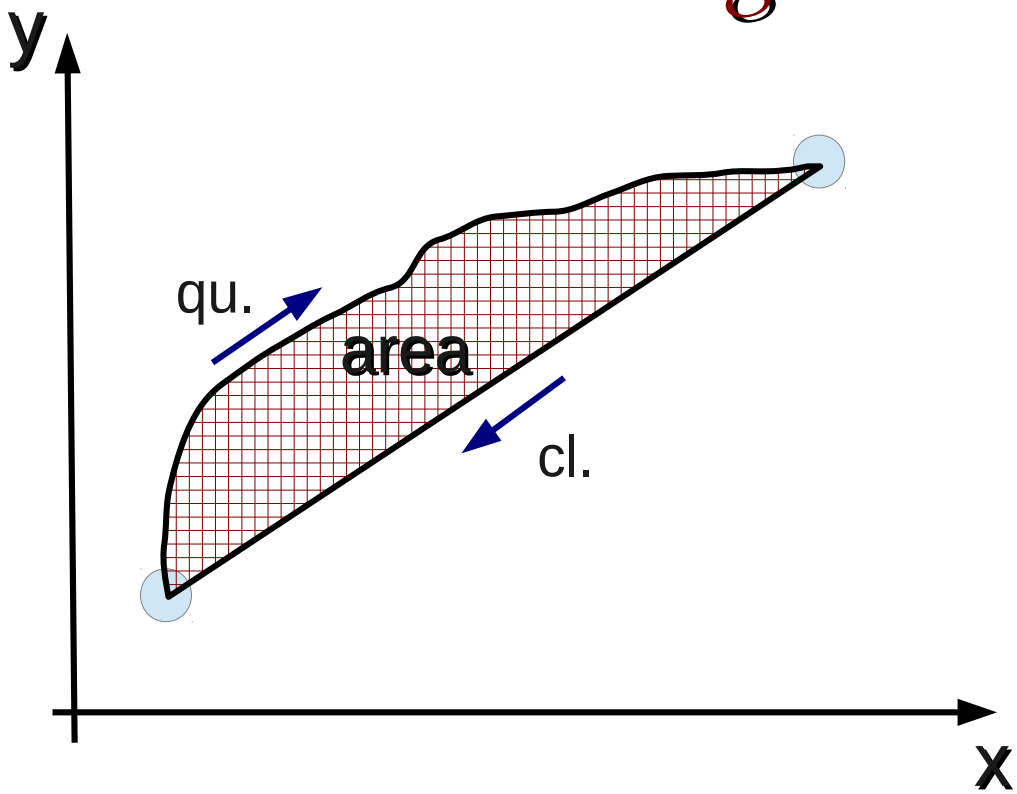

classical trajectory ?

- only if paths within one de Broglie length ($1/p_T$) have *same Aharonov-Bohm phase*
- destructive interference leads to Anderson localization

$$\int_0^\infty ds \int \mathcal{D}x^\mu \left\langle \exp i \int_0^s d\tau \left(m\dot{x}^2 + gA_\mu \dot{x}^\mu \right) \right\rangle \sim$$

$$\int_0^\infty ds \int \mathcal{D}x^\mu \exp \left(i \int_0^s d\tau \, m\dot{x}^2 \right) \exp(-\sigma_M A) = \frac{i}{p^2 + i\sigma_M \frac{m}{p_T}}$$

Summary

- p+Pb @ LHC control shows no “initial state jet quench”; (wasn't expected by more recent/realistic CGC predictions) suppression *was predicted and seen* at semi-hard pt ~ a few GeV
- forward rapidity data from LHC very important
- the “medium” appears much more interesting than featureless homogenous soup: density fluctuations, long. fields, vortices, ...

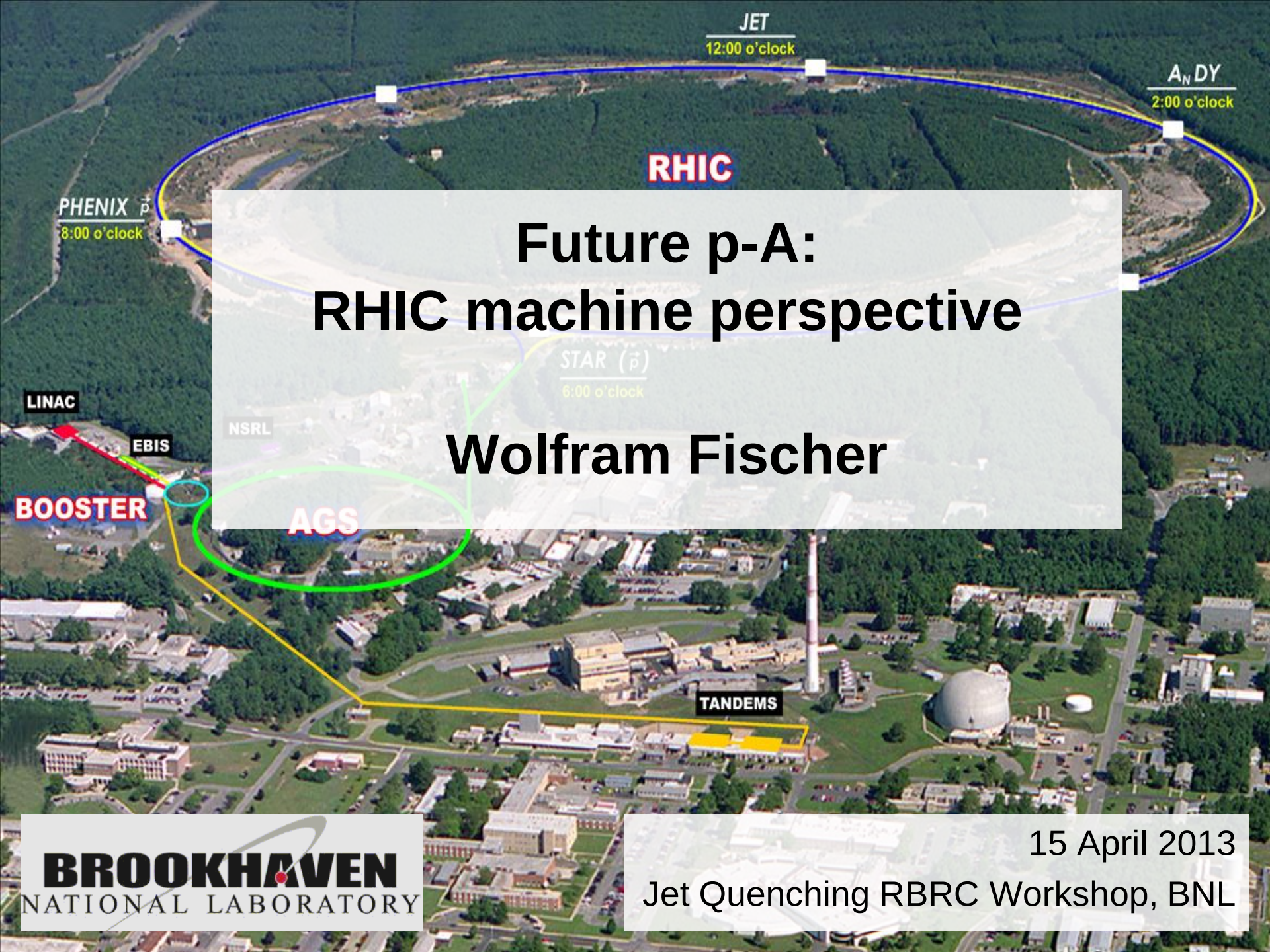

Future p-A: RHIC machine perspective

Wolfram Fischer

BROOKHAVEN NATIONAL LABORATORY

15 April 2013

Jet Quenching RBRC Workshop, BNL

Relativistic Heavy Ion Collider

1 of 2 ion colliders (other is LHC), only polarized p-p collider

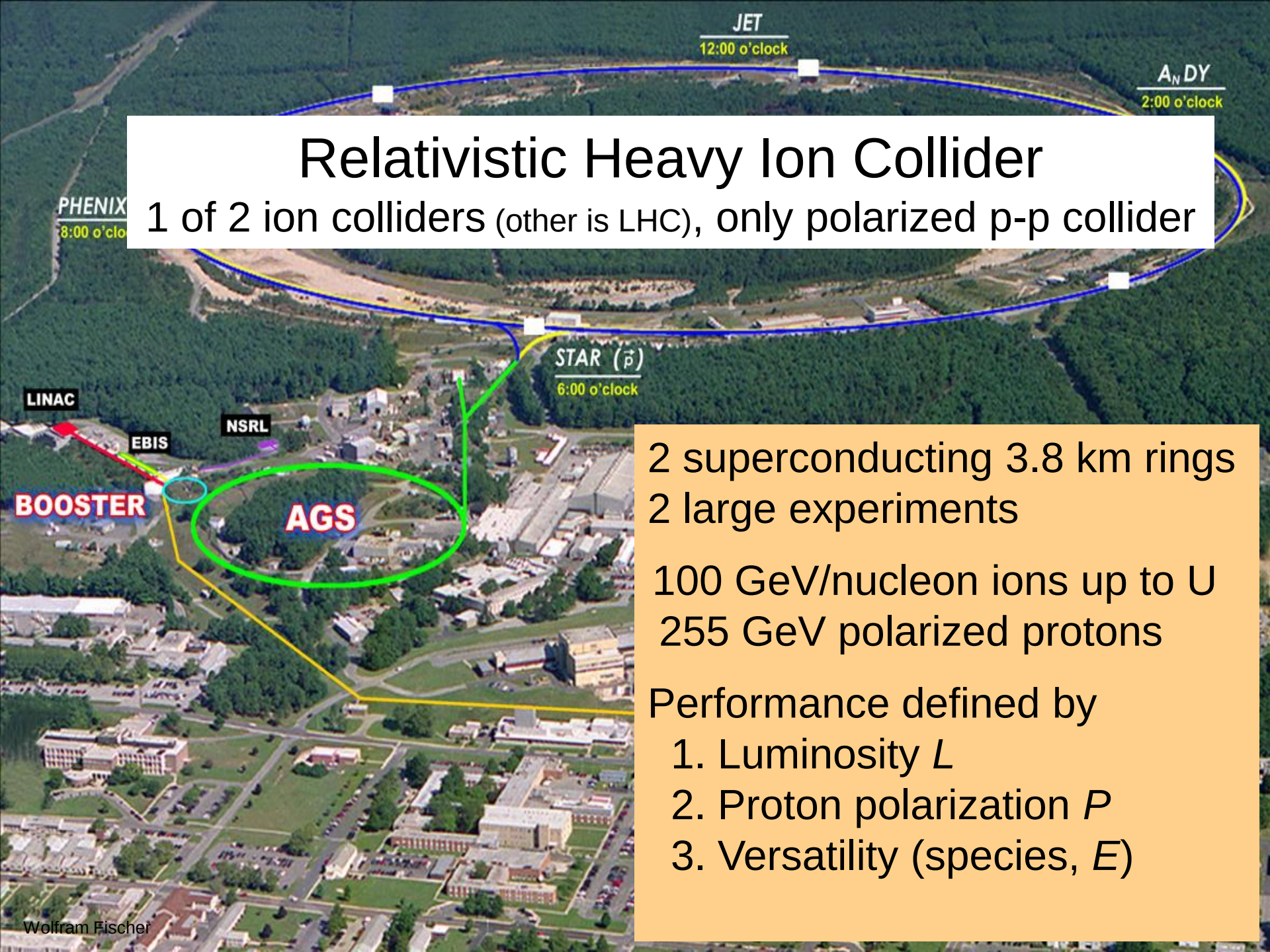

2 superconducting 3.8 km rings
2 large experiments

100 GeV/nucleon ions up to U
255 GeV polarized protons

Performance defined by

1. Luminosity *L*
2. Proton polarization *P*
3. Versatility (species, *E*)

Content

- What do we have for p+Au collisions?
- What do we still need for p+Au collisions?
- Luminosity projection

Delivered Integrated Luminosity and Polarization

--- RHIC-II performance is here ---

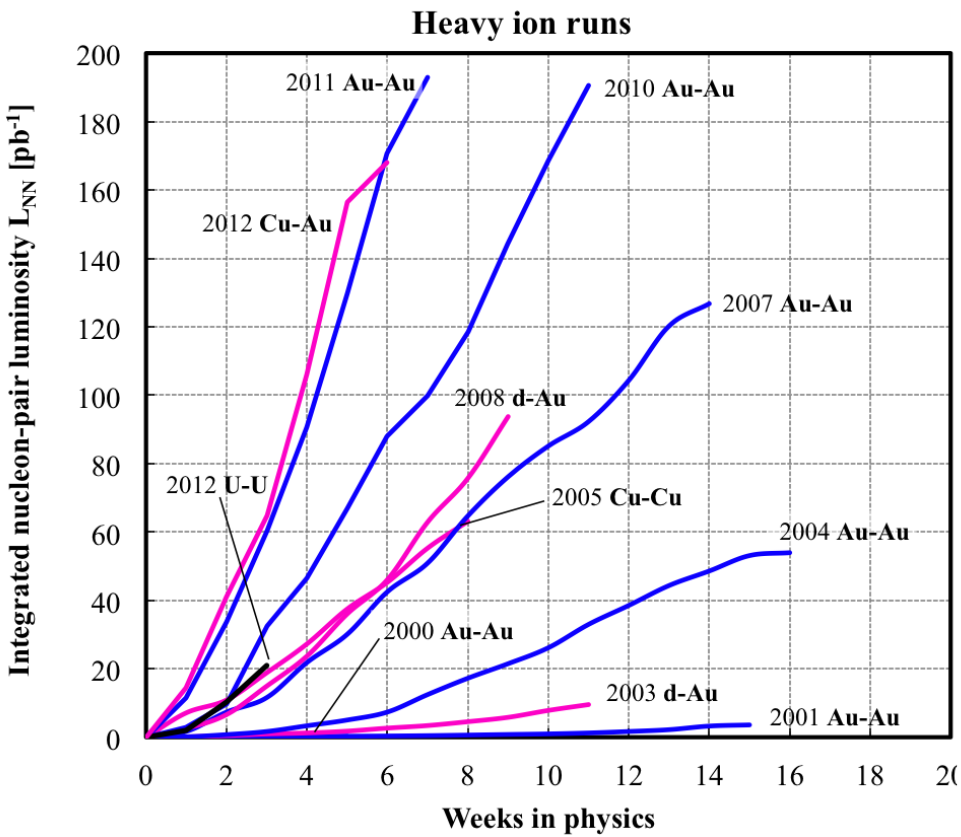

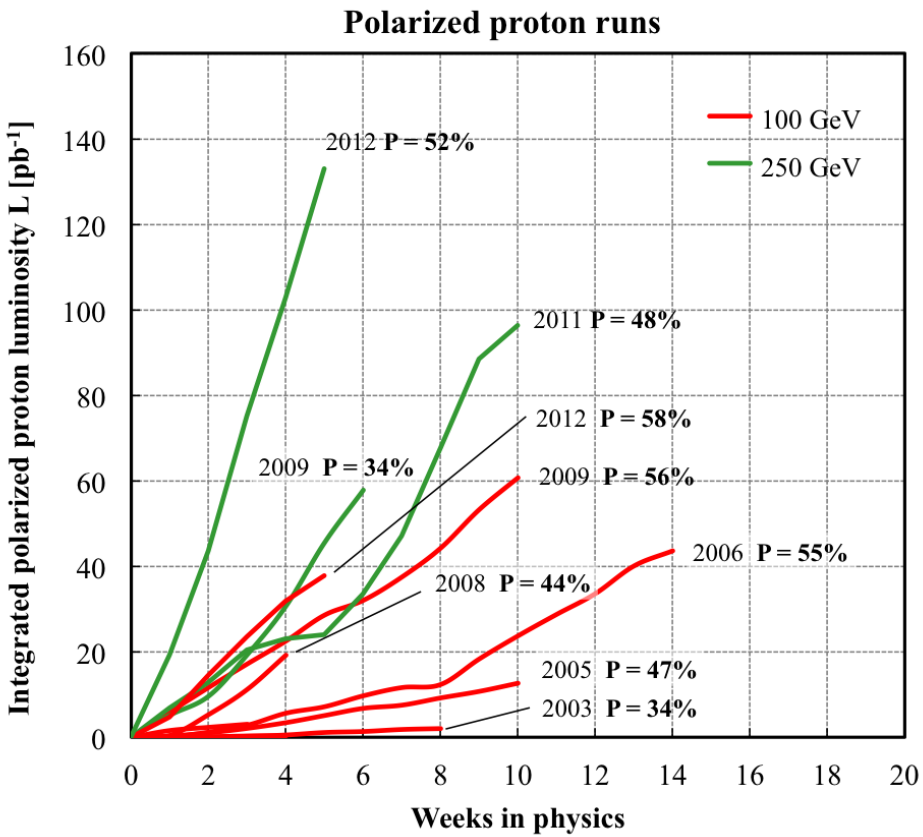

<u>Nucleon-pair luminosity</u>: luminosity calculated with nucleons of nuclei treated independently; allows comparison of luminosities of different species; appropriate quantity for comparison runs.

BROOKHAVEN NATIONAL LABORATORY

RHIC luminosity and polarization goals

parameter	unit	achieved		goals			
Au-Au operation		**2011**		**≥ 2014** 3D stochastic cooling + 56 MHz SRF			
energy	GeV/nucleon	100		100			
no colliding bunches	…	111		111			
bunch intensity	10^9	1.3		1.3			
avg. luminosity	$10^{26}\,cm^{-2}s^{-1}$	**30**		**40**			
p↑-p↑ operation		**2012**		**≥ 2013** source		**≥ 2014** source + e-lenses	
energy	GeV	100	255	100	250	100	250
no colliding bunches	…	– 107 –		– 107 –		– 107 –	
bunch intensity	10^{11}	1.6	1.7	1.6	2.0	1.8	2.5
avg. luminosity	$10^{30}\,cm^{-2}s^{-1}$	**33**	**105**	**30**	**150**	**60**	**300**
avg. polarization*	%	**59**	**52**	**– 60 –**		**– 65 –**	

*Intensity and time-averaged polarization as measured by the H-jet. Luminosity-averaged polarizations, relevant in single-spin colliding beam experiments, are higher. For example, for intensity-averaged P = 48% and $R_x = R_y$ = 0.2 (250 GeV, 2011), the luminosity-averaged polarization is P = 52%.

BROOKHAVEN NATIONAL LABORATORY

Asymmetric ion species under consideration in RHIC (to date)

proton-gold (p-Au)

- not yet done, part of the design
- requires moving IR6 and IR8 DX magnets horizontally by ~1 cm

deuteron-gold (d-Au)

- operated in 2003 and 2008

copper-gold (Cu-Au)

- operated in 2012

Polarized proton-polarized ^{3}He (p⇝-^{3}He⇝)

- likely request when ^{3}He⇝ is available
- RBRC Workshop on ^{3}He⇝ at BNL, 28-30 September 2011

What do we have for p+Au collisions?

- RHIC was designed for p+Au collisions
  - Independent rings except DX magnets
  - DX magnets movable (~1 shift)
- With stochastic cooling initial Au beam size is at its maximum
  - Allows for DX move in IR6 and IR8 only (~1 shift)
- Solutions for lattice, injection and acceleration
  - Lattice takes advantage of stochastic cooling
- Machine with fast setup (beam-based feedbacks)
- Experience with asymmetric collisions (d+Au, Cu+Au)

- Proton beam with $N_b = 2\text{x}10^{11}$, $P = 55\%$
  - with upgrades (OPPIS): $N_b = 3\text{x}10^{11}$, $P = 65\%$
- Au beam with $N_b = 1.3\text{x}10^{9}$
  - with upgrades (EBIS/Booster/AGS/RHIC): $2.0\text{x}10^{9}$ (emittance?)

Run-11: L_{avg} = 30 10^{26}cm^{-2}s^{-1}

Luminosity. The collider is designed for a Au-Au luminosity of about 2×10^{26} cm^{-2} sec^{-1} at top energy, while maintaining the potential for future upgrades by an order of magnitude. Operation with the heaviest ions imposes the most demanding requirements on the collider design, and gold-on-gold is taken as the prototypical example. The luminosity is energy dependent and decreases in first approximation propor **Run-12: L_{avg} = 10.5 10^{31}cm^{-2}s^{-1} (with P_{avg} = 53%)** will be higher, with ~1×10^{31} cm^{-2} sec^{-1} for pp collisions.

Range of ion masses. The expectations for interesting physics phenomena require a broad range of nuclei from the heaviest to the lightest, including protons. Asymmetric operation with heavy ions colliding on protons is considered to be crucial for the experimental program. The collider will allow collisions of beams of equal ion species from Au-Au all the way down to p-p. It will also allow operation of unequal species such as protons on gold ions.

Uranium is a viable species and can be considered as a future upgrade. However, at the present, an adequate source for uranium does not exist at Brookhaven and further R&D will be needed to achieve this goal.

Intersection Regions. The existing tunnel and the magnet lattice configuration provides for six experimental areas where the circulating beams cross. Three of the experimental areas presently

RHIC Design Manual (July 1998)

IR design with beam splitting DX dipoles first

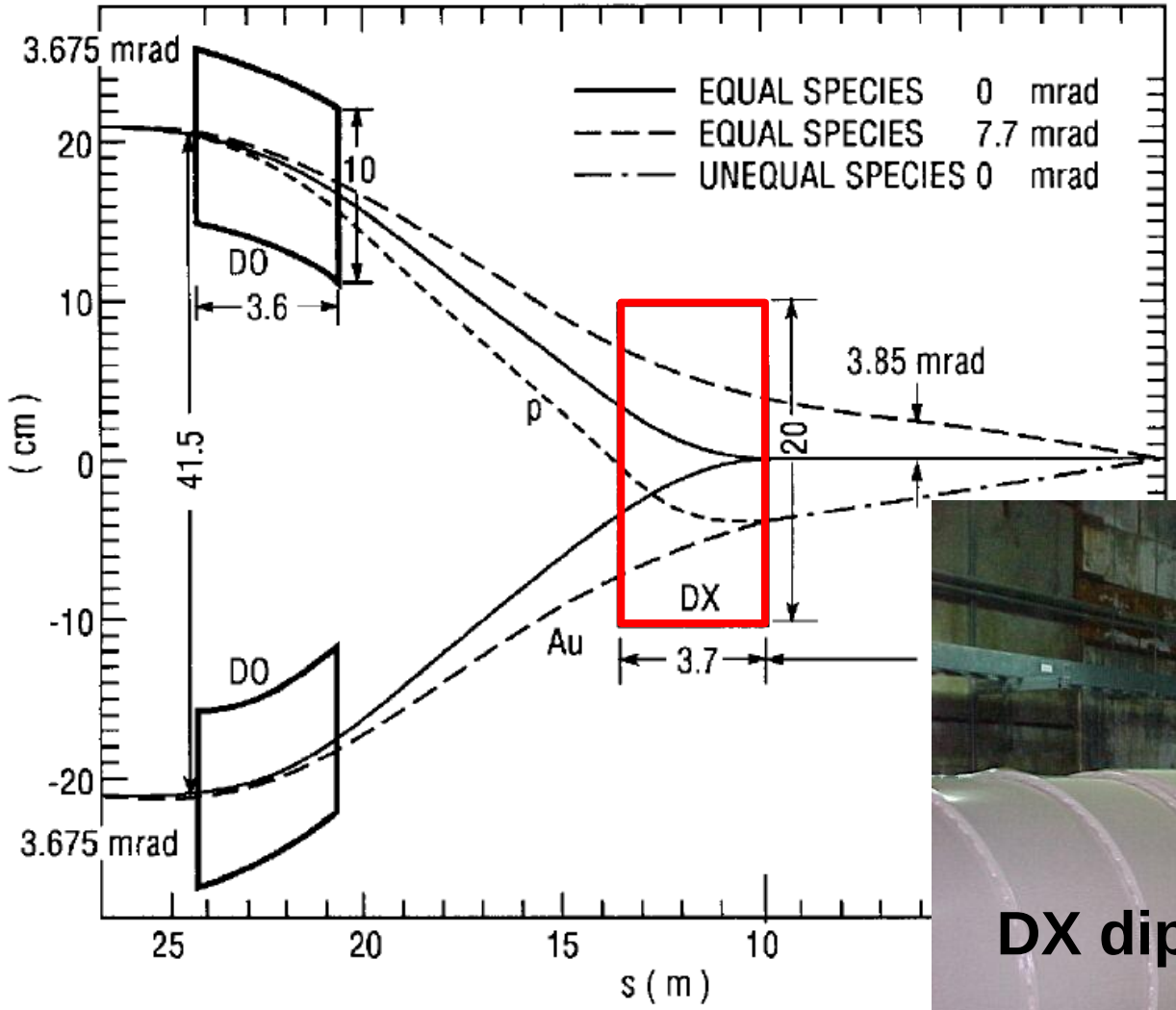

DX dipoles

- L_{mag} = 3.7 m, B_{max} = 4.3 T
- large aperture
  (18 cm coil ID)
- only magnets that need training
  (~5 for IR6/8 only)

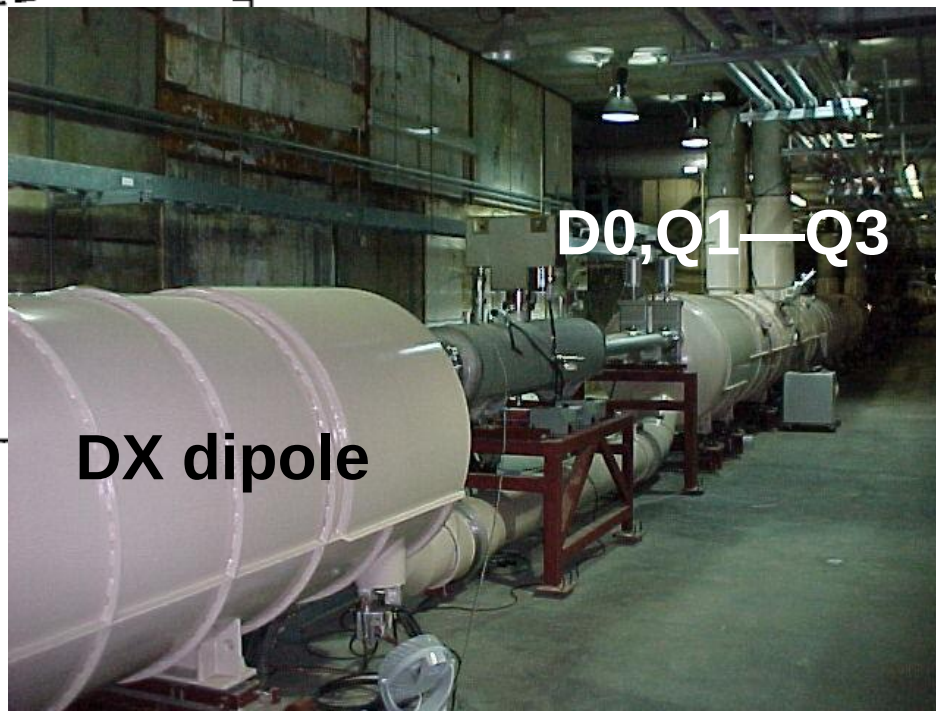

Now have full 3D stochastic cooling for heavy ions

longitudinal pickup

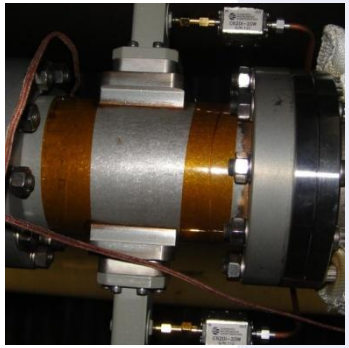

longitudinal kicker (closed)

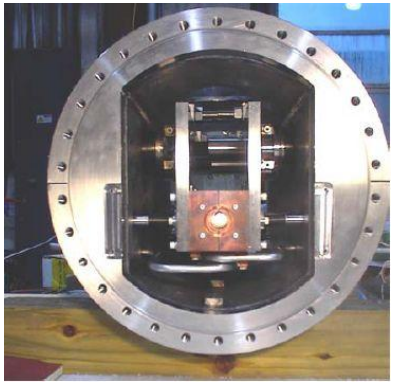

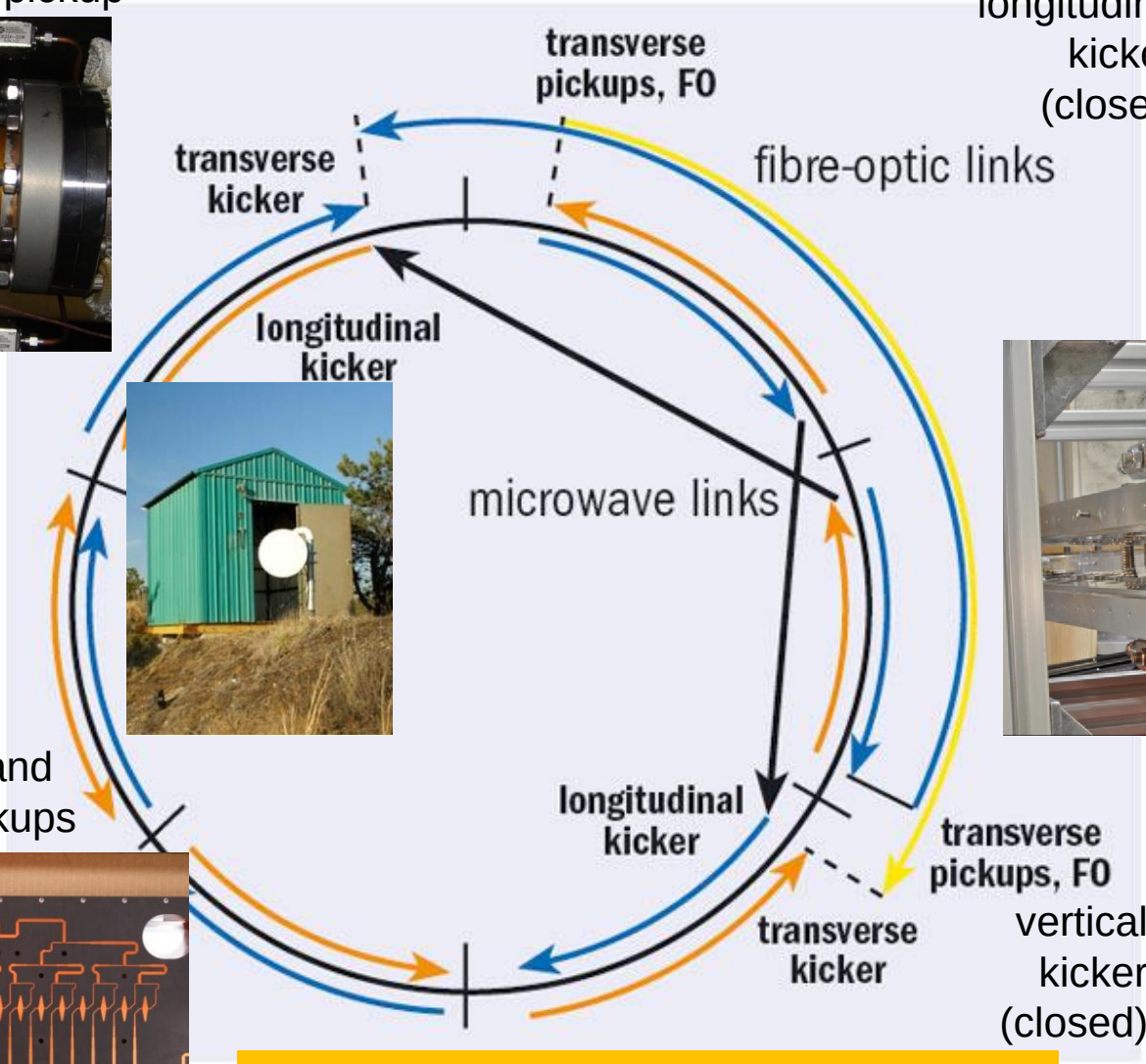

horizontal kicker (open)

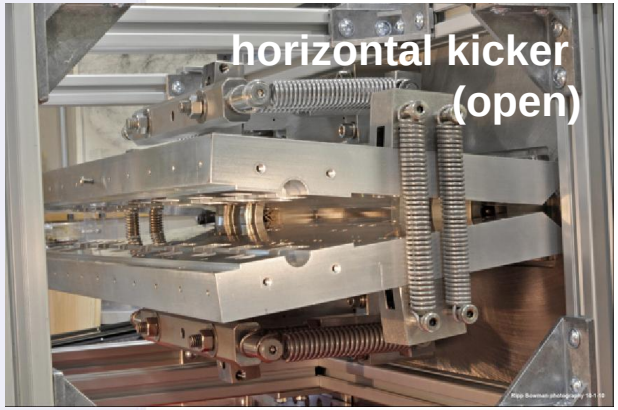

horizontal and vertical pickups

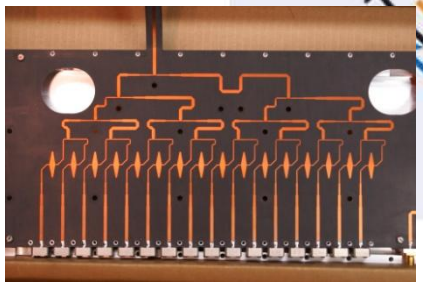

vertical kicker (closed)

5-9 GHz, cooling times ~1 h

M. Brennan, M. Blaskiewicz, F. Severino, PRL **100** 174803 (2008); PRSTAB, PAC, EPAC

Stochastic cooling in U—U operation

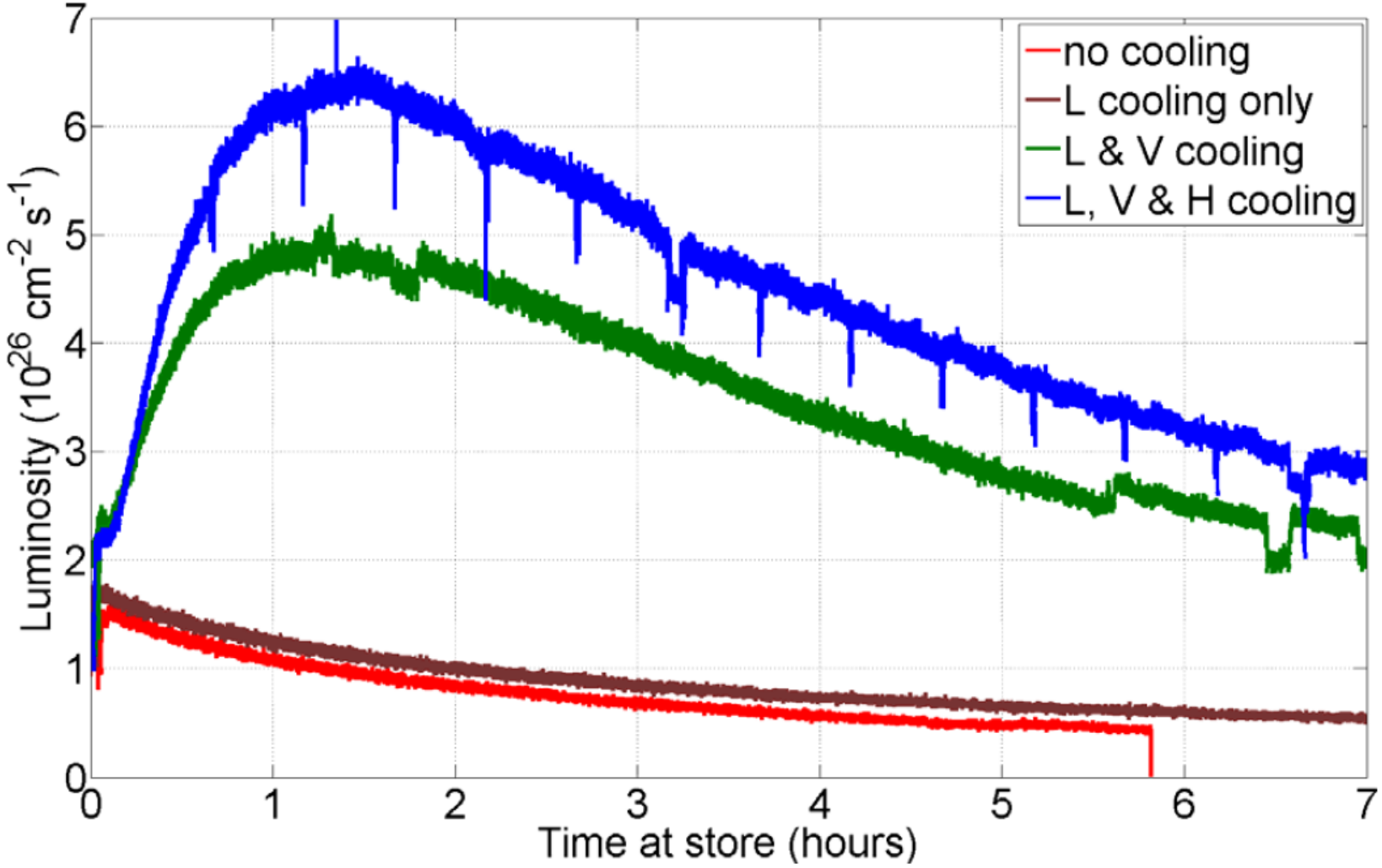

BROOKHAVEN NATIONAL LABORATORY

Cu-Au store – new mode in 2012

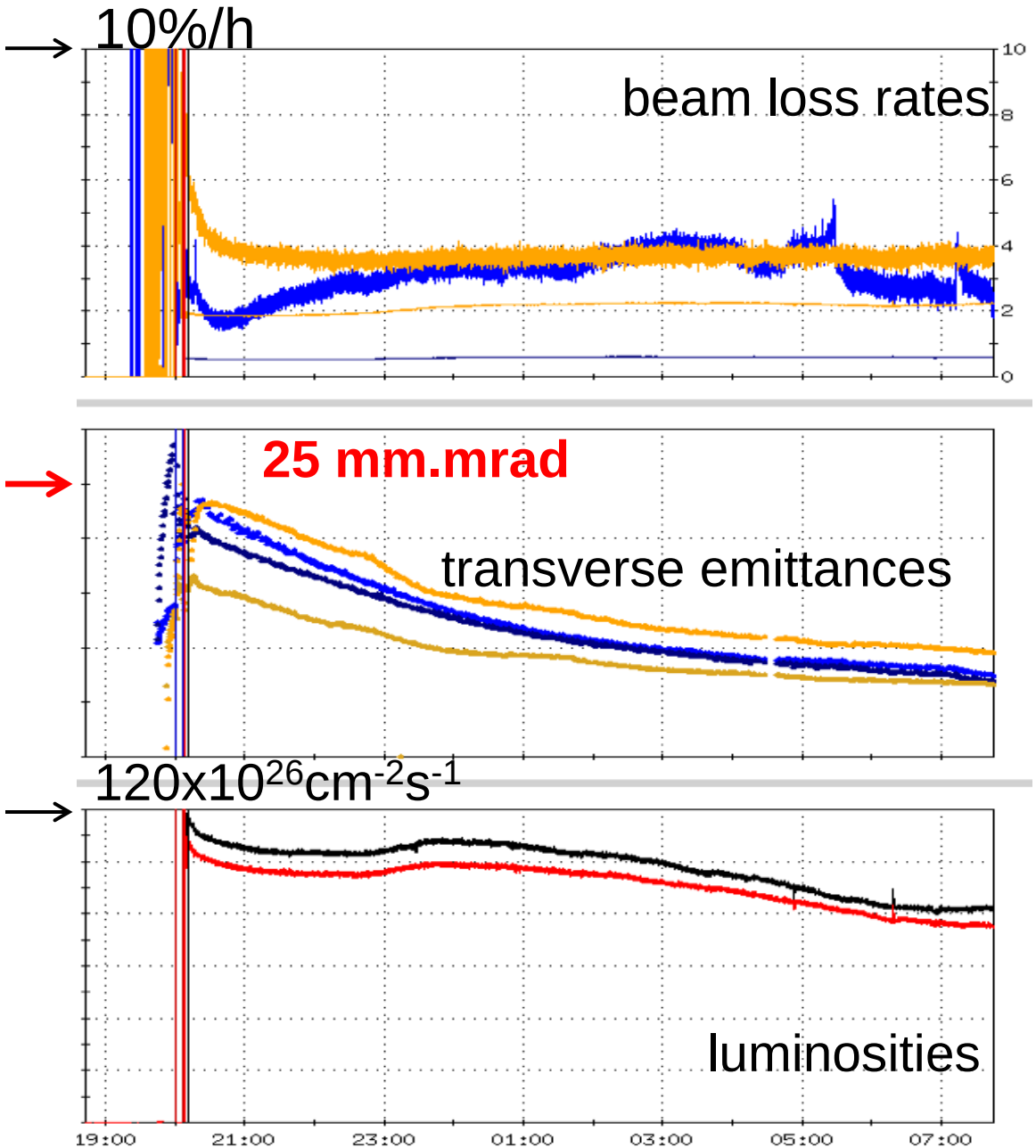

Cu and Au have different

- intrabeam scattering growth rates ($\sim Z^4 N_b/A^2$) $r_{IBS,Au} \approx 2x\ r_{IBS,Cu}$
- cooling rates ($\sim 1/N_b$) $r_{SC,Au} \approx 3x\ r_{SC,Cu}$

Stores start with large ε after undergoing instability at transition

Possible with stochastic cooling

Increase bunch intensity until loss at transition

p+Au easier with stochastic cooling

- only need to accommodate initial Au emittances
- sufficient to move IR6 and IR8 DX magnets

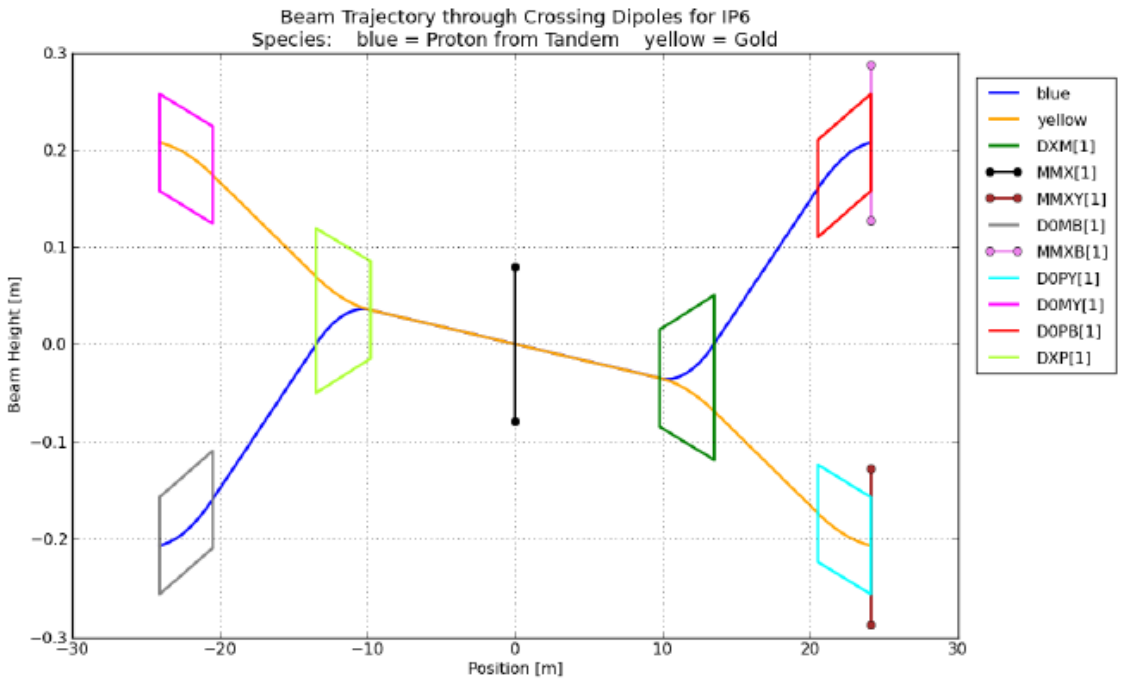

colliding IR
move DX by 1cm

Figure 1. The beam trajectory through the crossing dipoles D0 and DX. The Au beam is 69.4mm from the central line in the DX magnet in the worst case. Additional room for beam size must also be taken into account.

S. Tepikian, D. Trbojevic, C-A/AP/447 (Jan. 2012)

p+Au easier with stochastic cooling

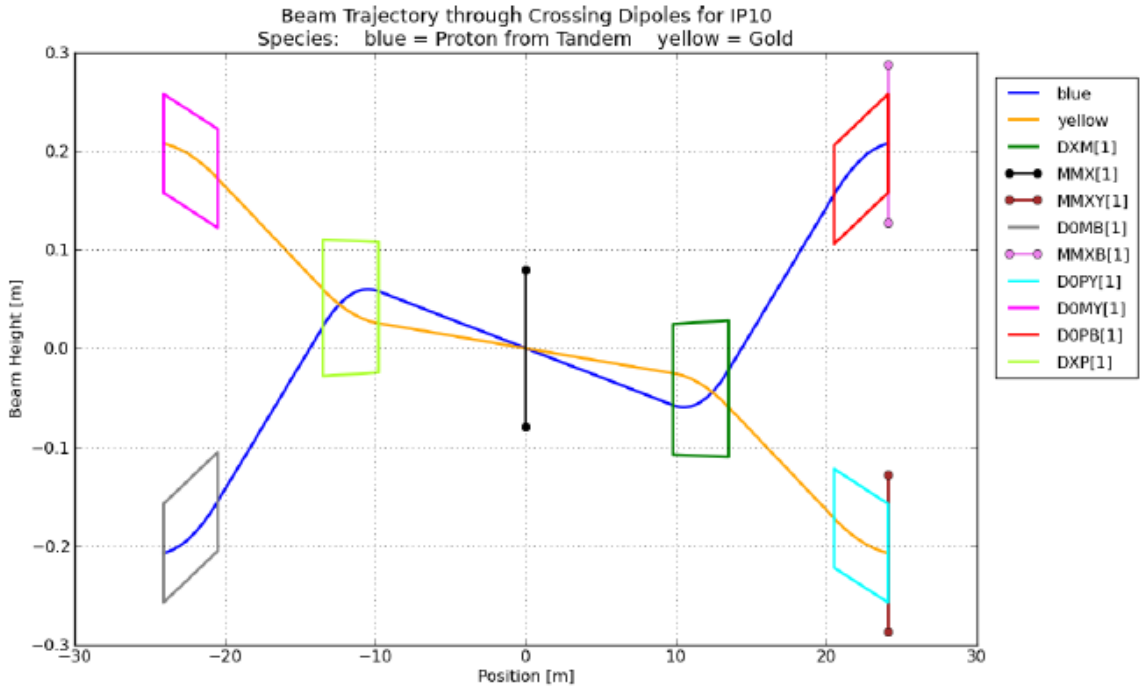

Figure 2. A non-colliding insertion. The crossing angle is -0.3305mrad. The beam trajectory is 59.8mm from the central axises for both beams in the DX magnet. The Blue beam reaches its peak at 10.5m from the IP, while the Yellow beam reaches its peak at 13.5m from the IP.

non-colliding IR
no DX move

S. Tepikian, D. Trbojevic, C-A/AP/447 (Jan. 2012)

Beam control improvement – feedbacks on ramp

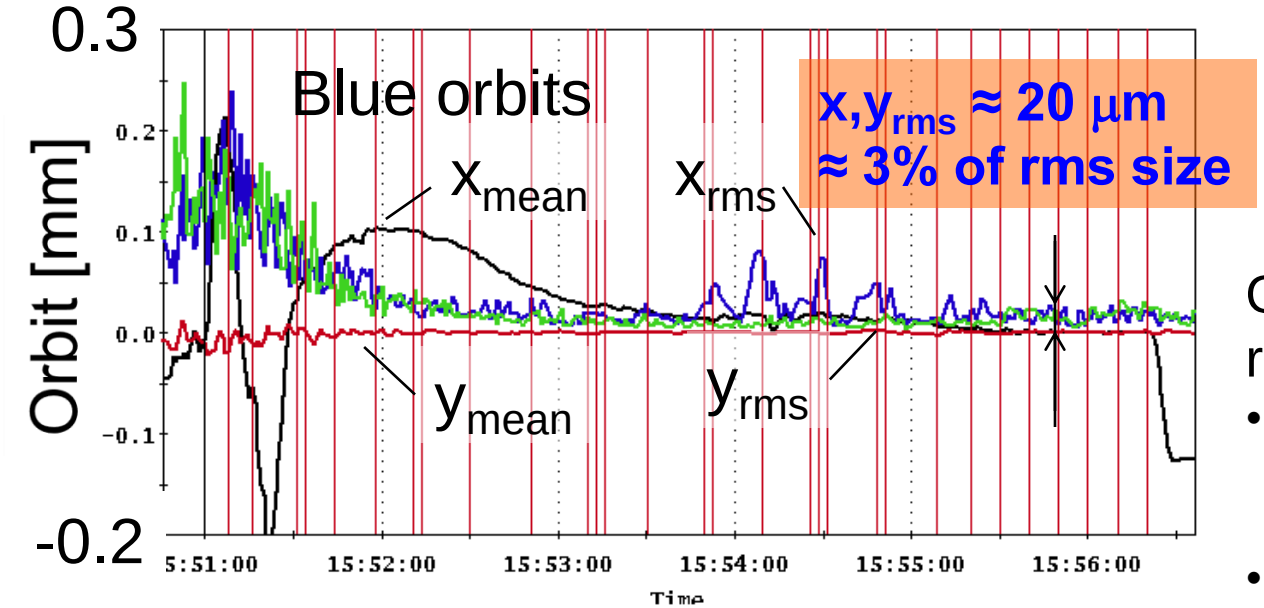

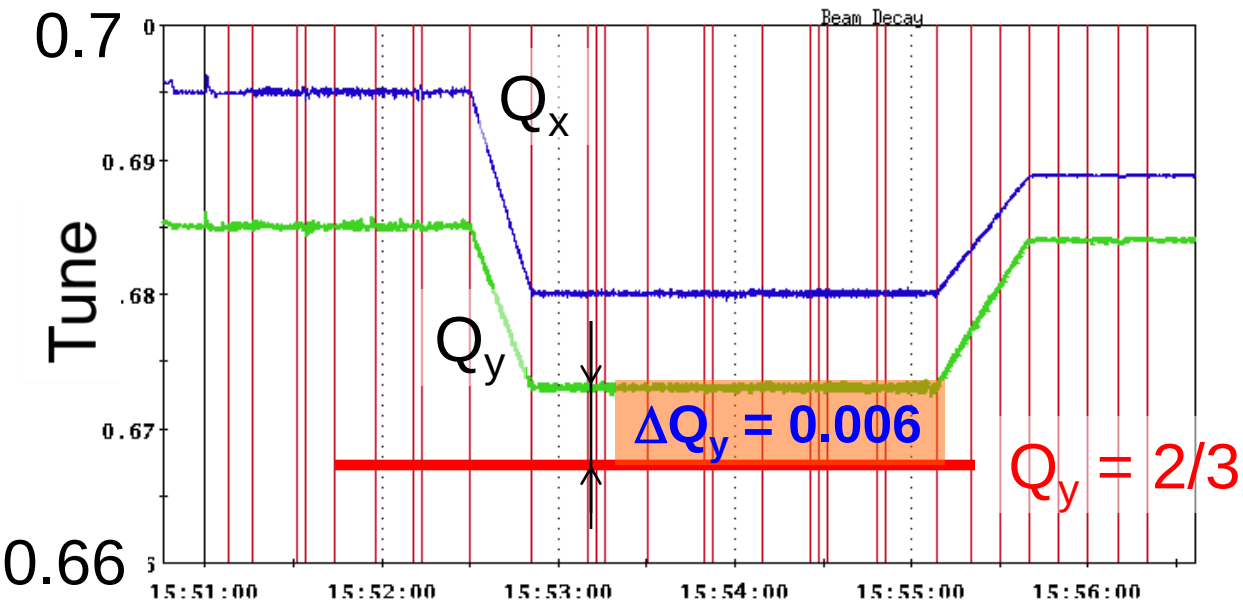

M. Minty,
A. Marusic et al.

Orbit feedback on every ramp allows for

- Smaller y_{rms} (smaller imperfection resonance strength)
- Ramp reproducibility (have 24 h orbit variation)

Tune/coupling feedback on every ramp allows for

- Acceleration near $Q_y = 2/3$ (better P transmission compared to higher tune)

Time-in-store as fraction of calendar time

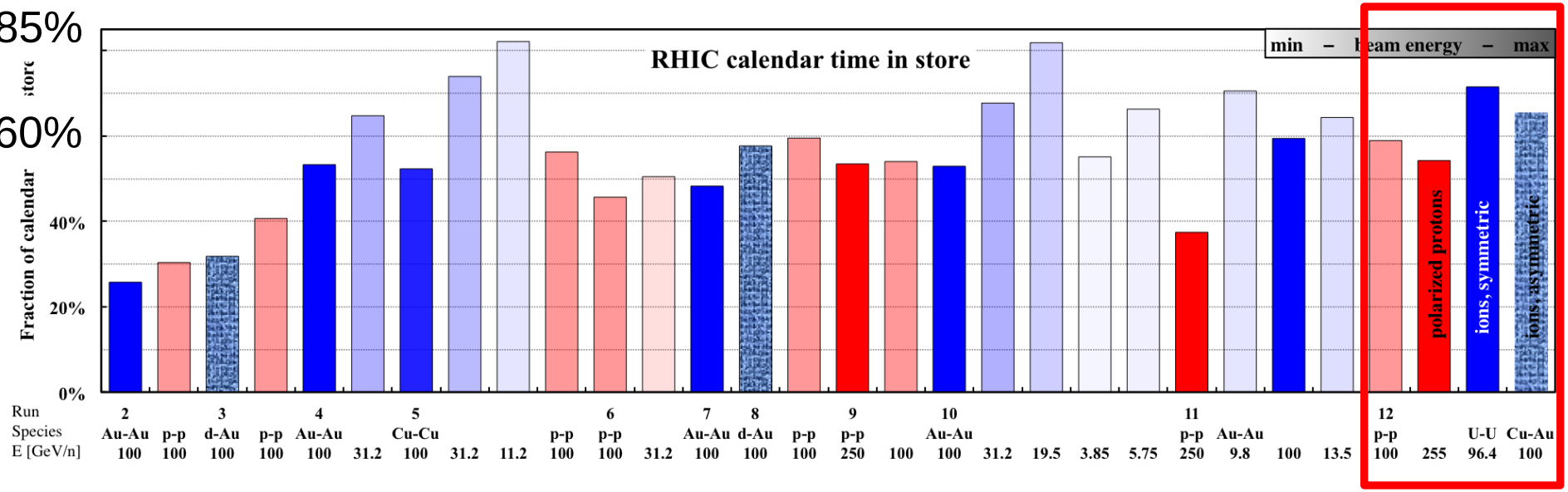

- Run-12 with low failure rates in all systems
- Highest time-in-store ratios to date
  even with increased APEX time during 255 GeV protons, and few weeks per species
- Have higher failure rates in Run-13 so far

What do we still need for p+Au?

- Demonstrate DX move by 1 cm
  - Can be done at end of Run-13
  - Move for p beam in Yellow, Au beam in Blue (different from d-Au)

- If p beam in Blue is needed (and Au beam in Yellow)
  - Modify vacuum pump stands in IR6 and IR8
  - Modify shielding IR6 and IR8

- Operate with new injection and acceleration scheme
  - Inject and accelerate Au to intermediate level above transition
  - Then inject p and accelerate both beams

- Ensure that luminosity can be measured
- Study DX aperture and possible experimental background

Moving IR6 and IR8 DX magnets by 1cm

- Bellows allow for 1 cm movement
- Installed shielding creates tight spaces but acceptable
  "6:00 the bellows and ion pump stand were swapped to make space for the shielding, … cannot be moved because of the ion pump stand" (M. Mapes)
- Easier to have p in Yellow, Au in Blue (different from d-Au!)

=> Clear preference for Au beam in Yellow ring.

(Workshop on Physics of p+A Collisioins in RHIC, 7-9 Jan 2013)

Can be done in ~ 1 shifts (i.e. during a run) when properly prepared in previous shut-down

p+Au injection and acceleration

maintains same f_{rev} for both beams

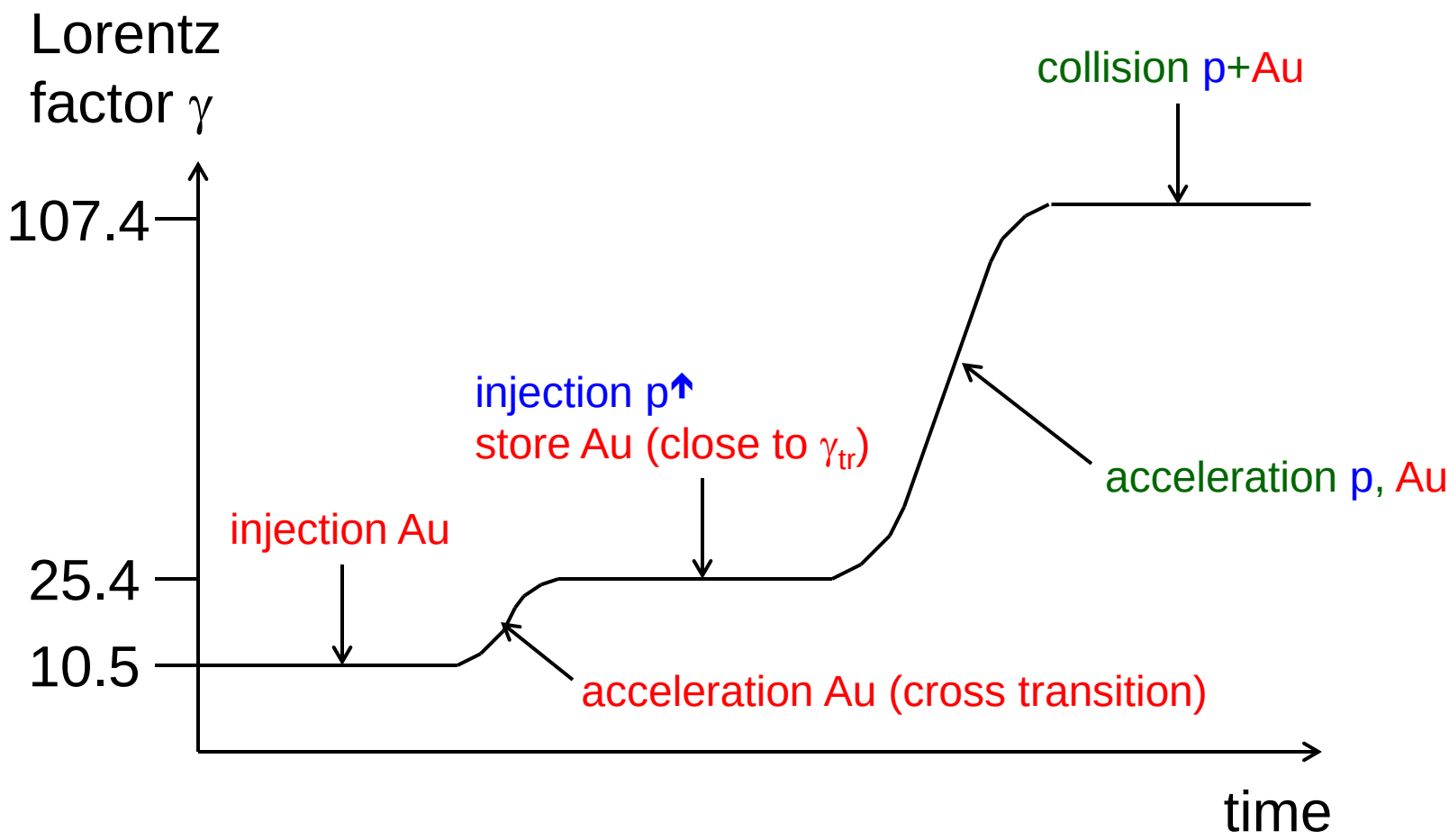

Note: now tolerate ion beam instabilities at transition to obtain higher intensity (can be cooled down again), not possible with p+Au since have smaller aperture available

ZDC Lumi Monitor Acceptance (M. Bai)

The 3.58 mrad common angle through IP for head-on collisions can blind the ZDC detector right behind DX magnet

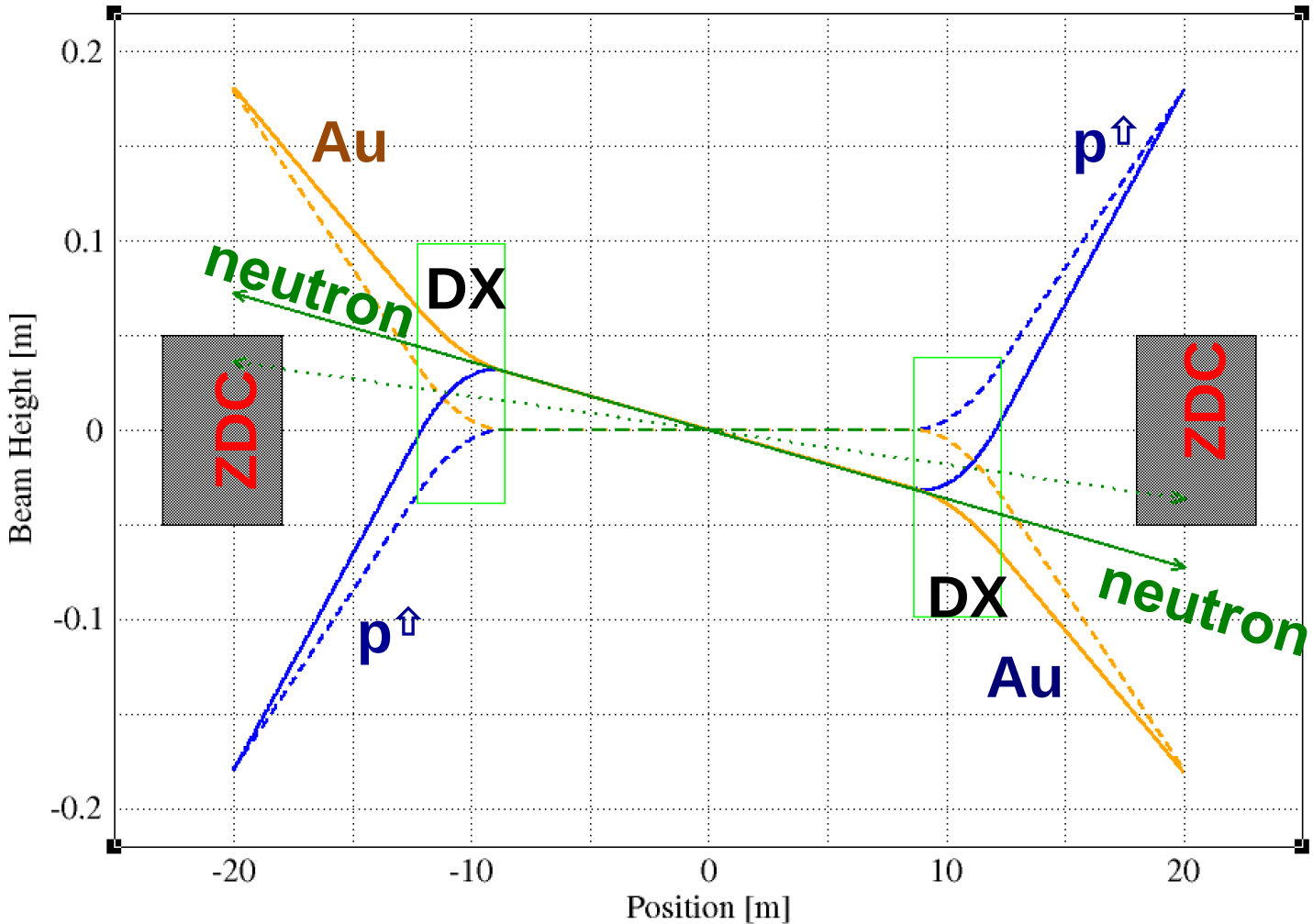

ZDC Lumi Monitor Acceptance (M. Bai)

Layout between DX and D0

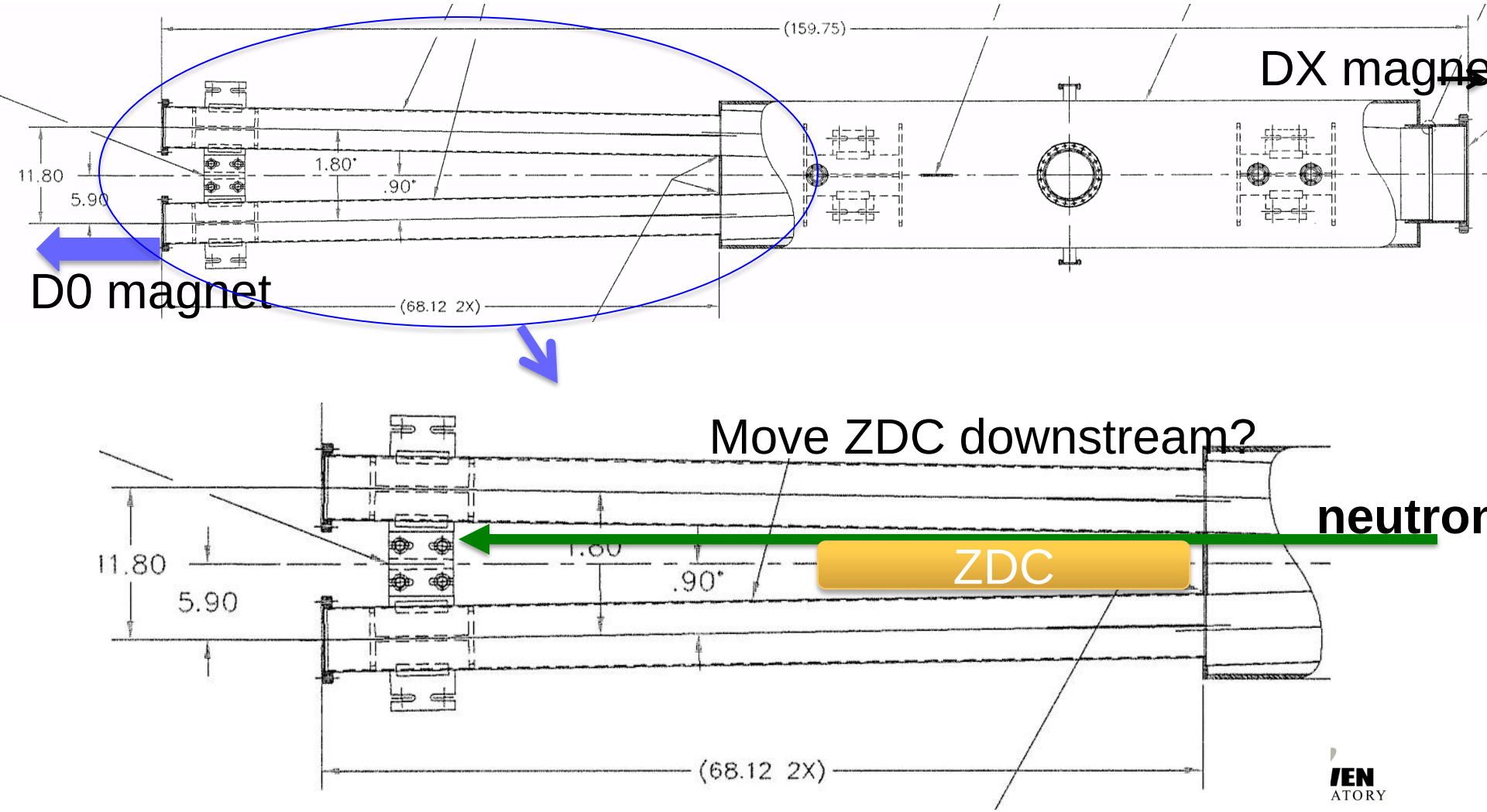

ZDC Lumi Monitor Acceptance (M. Bai)

If not enough room to move ZDC downstream, need to find a way to reposition ZDC

- move not only DX magnet but also the beam pipe between DX and D0
- Difficult but could be explored

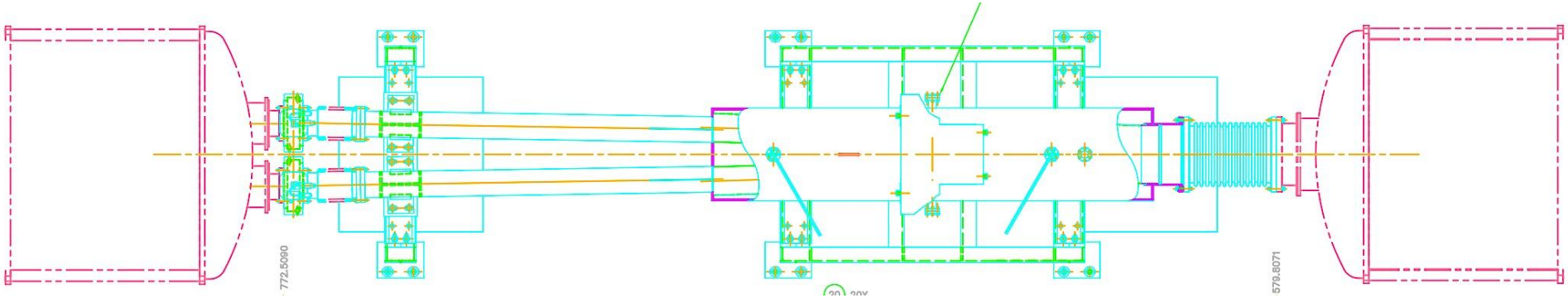

BROOKHAVEN NATIONAL LABORATORY

pA Collisions Beam Sizes

$$\sigma = \sqrt{\frac{\left(\frac{\epsilon_N}{\pi}\right)\left(\beta^* + \frac{s^2}{\beta^*}\right)}{6(\beta\gamma)}}$$

Store conditions:
Gold at Bρ = 831.763 *Tm* or (βY) = 107.391
Proton at Bρ = 358.647 *Tm* or (βY) = 114.593

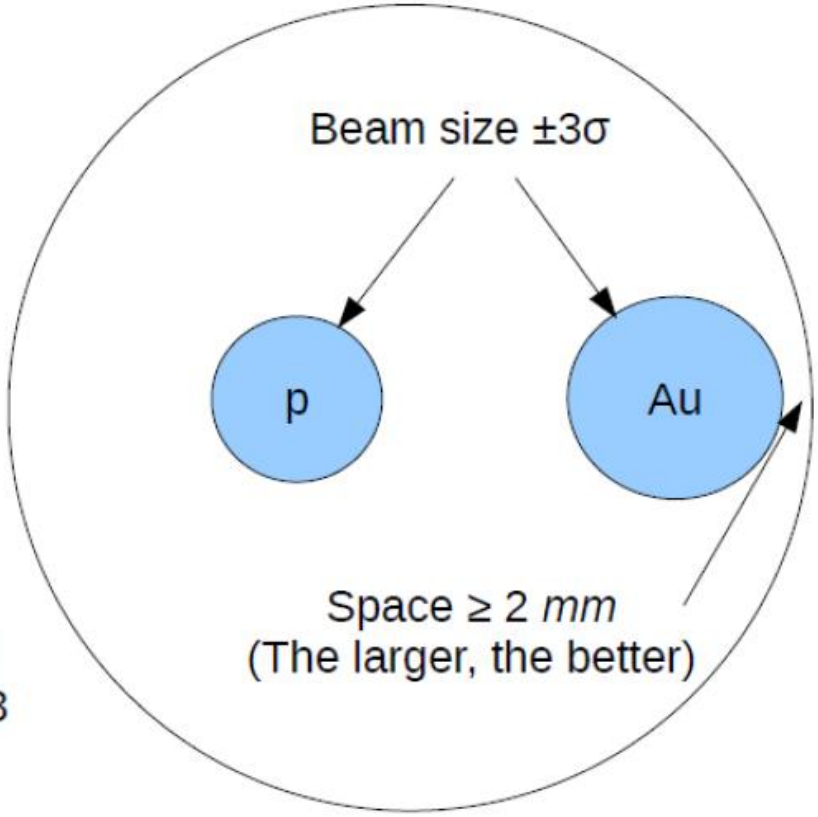

DX magnet (radius = 68.326 *mm*)

DX aperture measurement with beam, Y. Luo, A. Marusic, S. Tepikian

RUN 12 LATTICES:

04/10/13

Analysis pending.

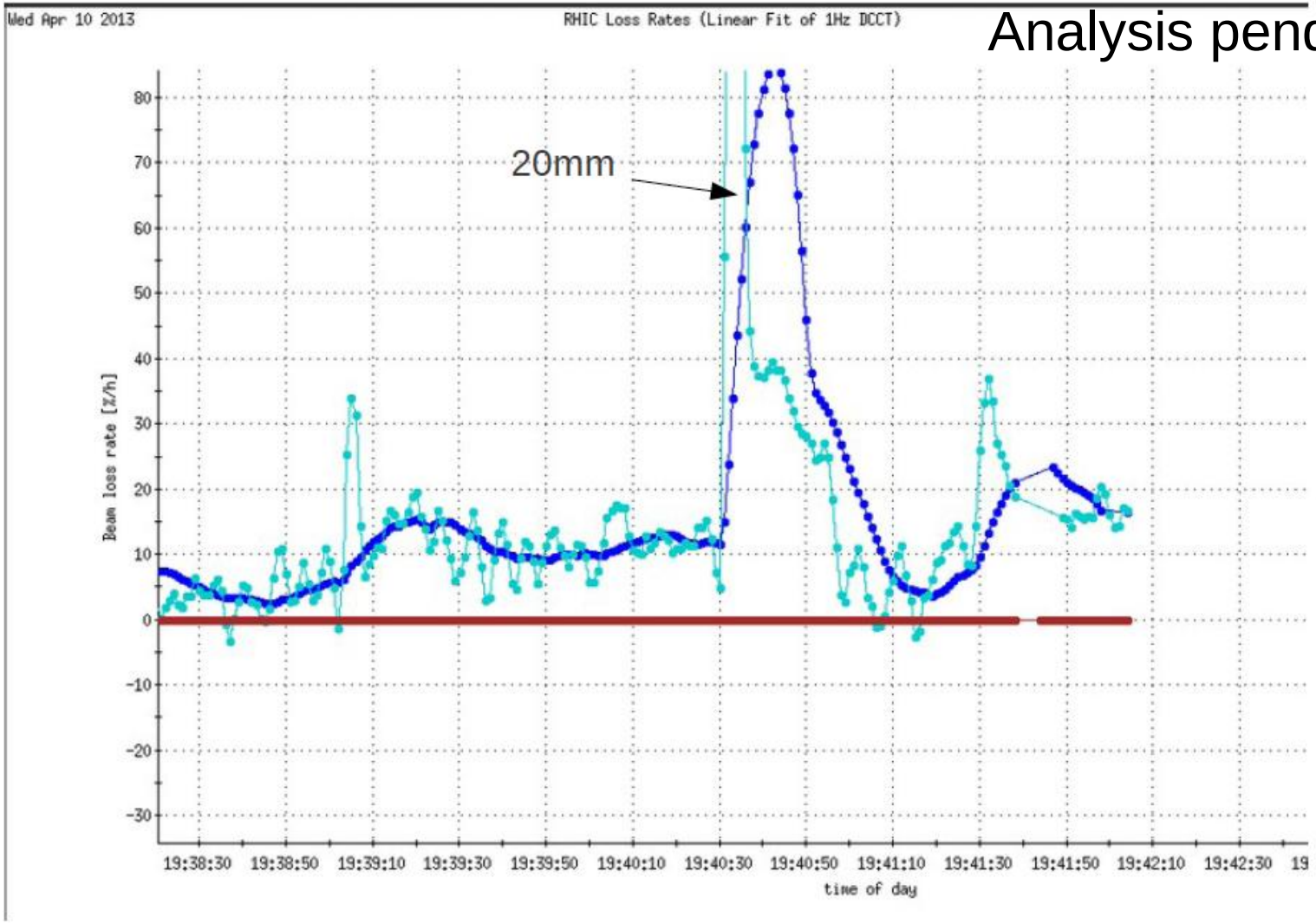

IR 12 Horizontal bump size 20mm
Zero crossing angle at IR2 (33mm offset at DX exit)
Vertical bump at IR2 removed during this measurement

Asymmetric collisions (p+Au)

- p+Au energies:

  100.8 GeV p on 100.0 GeV/nucleon Au ($\gamma_p = \gamma_{Au} = 107.4$)

- For energy scan need to match Lorentz factor γ of both beams

Au-Au history and projections for PHENIX Parameter	unit	p 2013E	Au	p 2013E	Au
no of colliding bunches	…	111	111	111	111
ions/bunch, initial	10^9	140	1.0	180	1.4
charges per bunch	10^9e	140	79	180	107
average beam current/ring I_{avg}	mA	194	110	250	148
stored energy per beam	MJ	0.25	0.35	0.32	0.47
transverse rms emittance ε_{xy}	mm.mrad	2.9	2.9	2.8	2.8
rms bunch length σ_s	m	0.5	0.3	0.5	0.3
envelope function at IP β^*	m	0.9	0.9	0.7	0.7
beam-beam parameter ξ/IP	10^{-3}	4.3	2.4	5.9	3.1
initial luminosity L/IP	**10^{26} cm^{-2}s^{-1}**	**39**		**82**	
events per bunch-bunch crossing	…				
average / initial luminosity	%	60		70	
average store luminosity L_{avg}	**10^{26} cm^{-2}s^{-1}**	**24**		**57**	
time in store	%	55		55	
max luminosity/week	μb^{-1}			190	
min luminosity/week	μb^{-1}	78			
L_{NN}/week, min/max	pb^{-1}	15		37	

Summary

- p+Au is possible
  max energy 100 GeV/nucleon for both beams
- Stochastic cooling for ion beams helps:
  DX move only in IR6 & IR8, no Au beam growth
- DX move in ~1 shifts
  possible upgrade for pp2pp in IR6 requires change of DX bellows
  will reduce flexibility, cannot move DX magnets during run
- New injection/acceleration scheme
  store Au beam above transition for ~15 min

- Luminosity estimate based on p↑ beam available (anticipated), and Au beam available (anticipated)

  L_{NN} = 15 pb/week min (now)
  L_{NN} = 37 pb/week max (few years)

Fluctuations, flow and viscosity in the Little Bang*

Ulrich Heinz (The Ohio State University)

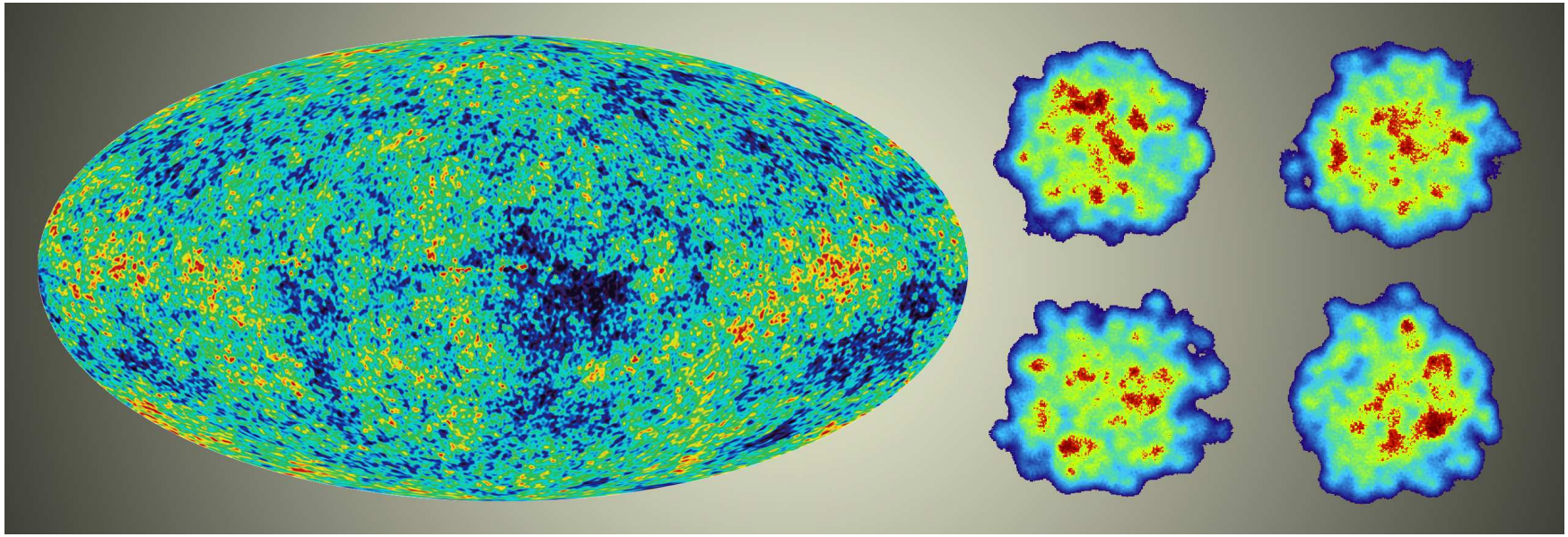

presented at:
Jet quenching at RHIC vs. LHC in Light of Recent dAu vs. pPb Controls
Brookhaven National Laboratory, 15-17 April 2013

THE OHIO STATE UNIVERSITY DEPARTMENT OF PHYSICS

*Supported by the U.S. Department of Energy

JET Collaboration

References: Heinz, Qiu, Shen, PRC 87 (2013) 034913
Qiu, Heinz, PLB 717 (2012) 261

Big Bang vs. Little Bang: The fluctuation power spectrum

Planck 2013 CMB temperature power spectrum

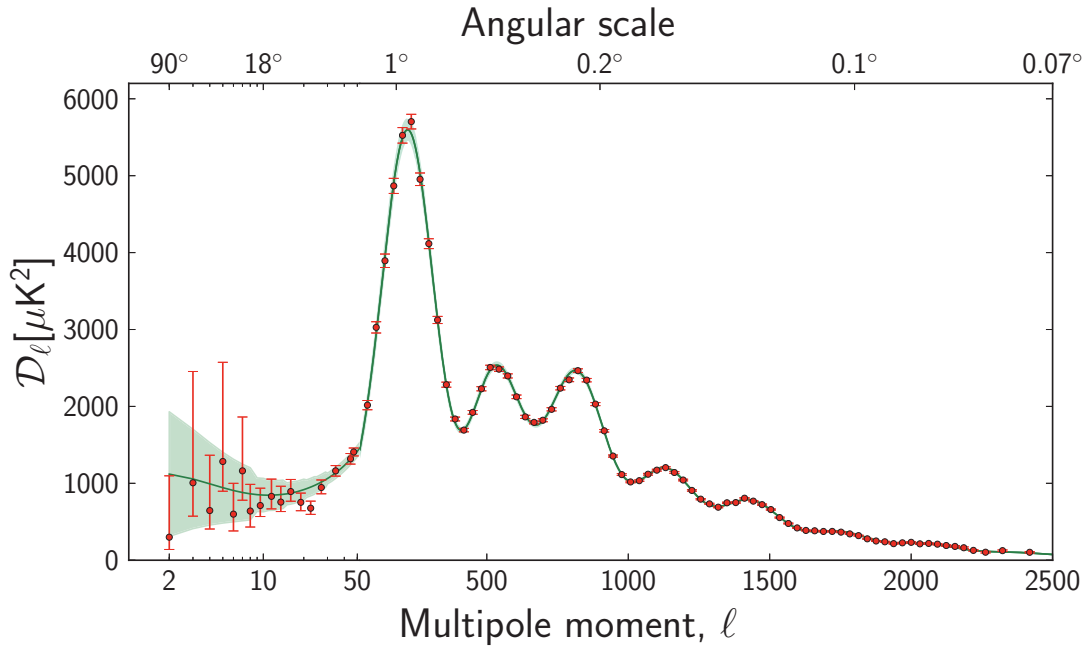

Little Bang density power spectra 2013

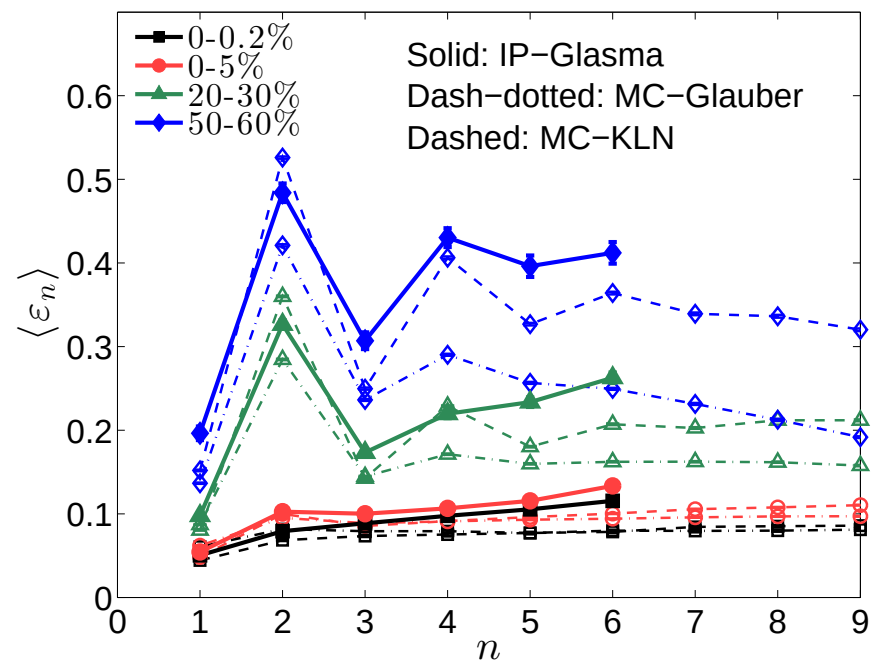

Initial eccentricities ε_n and associated participant-plane angles Φ_n of the Little Bang:

$$\varepsilon_1 e^{i\Phi_1} \equiv -\frac{\int r\,dr\,d\varphi\,r^3 e^{i\varphi}\,e(r,\varphi)}{\int r\,dr\,d\varphi\,r^3 e(r,\varphi)}, \qquad \varepsilon_n e^{in\Phi_n} \equiv -\frac{\int r\,dr\,d\varphi\,r^n e^{in\varphi}\,e(r,\varphi)}{\int r\,dr\,d\varphi\,r^n e(r,\varphi)} \quad (n>1)$$

A detailed study of fluctuations is a powerful discriminator between models!

The fluctuation power spectrum: initial vs. final

Little Bang density power spectra

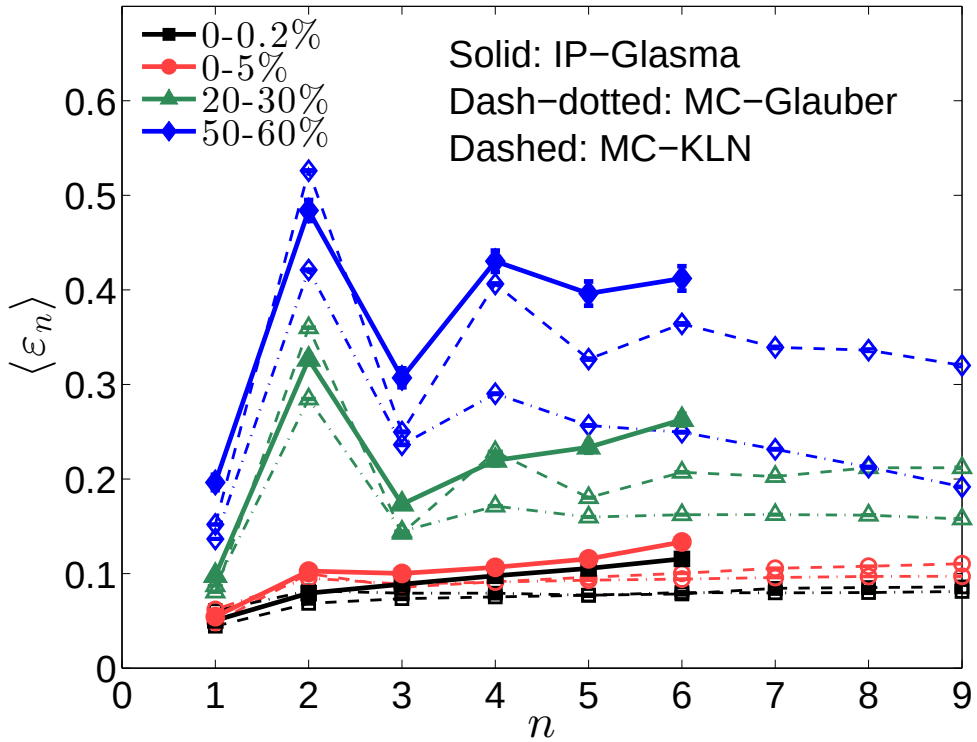

Flow power spectrum for ultracentral pPb Little Bangs

(CMS, Quark Matter 2012)

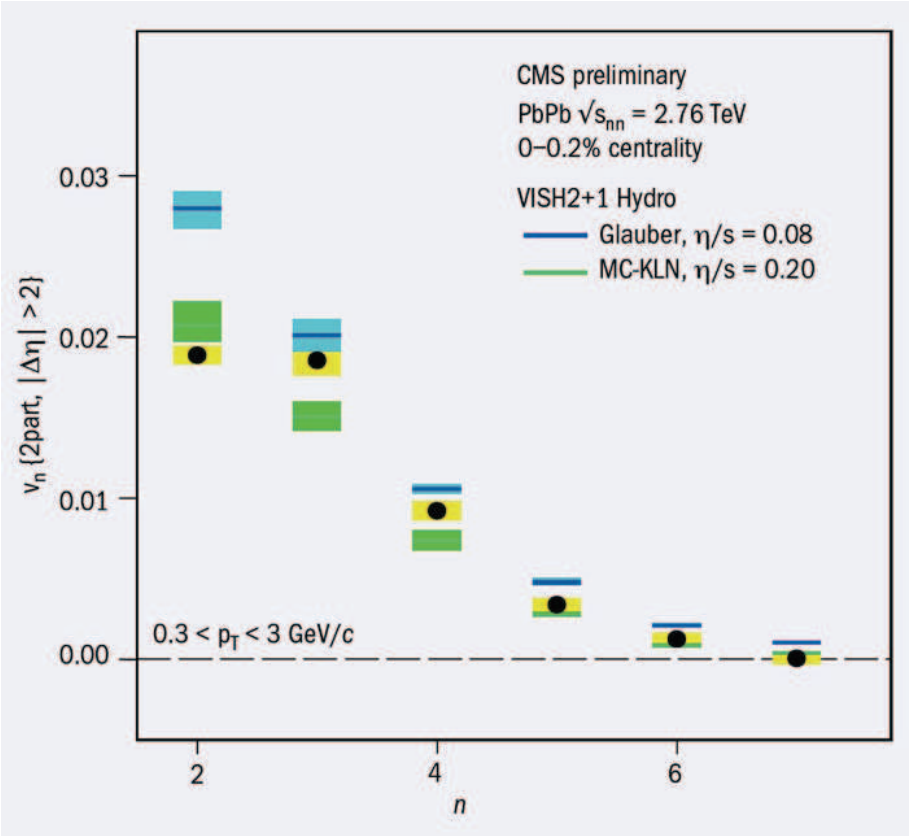

Higher flow harmonics get suppressed by shear viscosity

A detailed study of fluctuations is a powerful discriminator between models!

Each Little Bang evolves differently!

Density evolution of a single $b = 8$ fm Au+Au collision at RHIC, with IP-Glasma initial conditions, Glasma evolution to $\tau = 0.2\,\mathrm{fm}/c$ followed by (3+1)-d viscous hydrodynamic evolution with `MUSIC` using $\eta/s = 0.12 = 1.5/(4\pi)$

Schenke, Tribedy, Venugopalan, PRL 108 (2012) 252301:

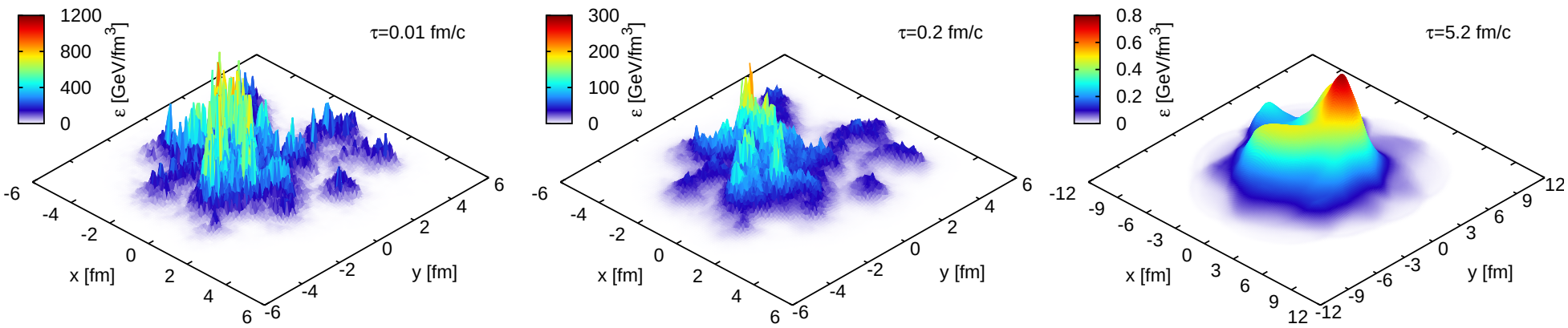

Single event anisotropic flow coefficients

In a single event, the specific initial density profile results in a set of complex, y- and p_T-dependent flow coefficients (we'll suppress the y-dependence):

$$V_n = v_n e^{in\Psi_n} := \frac{\int p_T dp_T d\phi \, e^{in\phi} \frac{dN}{dy p_T dp_T d\phi}}{\int p_T dp_T d\phi \, \frac{dN}{dy p_T dp_T d\phi}} \equiv \{e^{in\phi}\},$$

$$V_n(p_T) = v_n(p_T) e^{in\Psi_n(p_T)} := \frac{\int d\phi \, e^{in\phi} \frac{dN}{dy p_T dp_T d\phi}}{\int d\phi \, \frac{dN}{dy p_T dp_T d\phi}} \equiv \{e^{in\phi}\}_{p_T}.$$

Together with the azimuthally averaged spectrum, these completely characterize the measurable single-particle information for that event:

$$\frac{dN}{dy\, d\phi} = \frac{1}{2\pi} \frac{dN}{dy} \left(1 + 2 \sum_{n=1}^{\infty} v_n \, \cos[n(\phi - \Psi_n)] \right),$$

$$\frac{dN}{dy\, p_T\, dp_T\, d\phi} = \frac{1}{2\pi} \frac{dN}{dy\, p_T\, dp_T} \left(1 + 2 \sum_{n=1}^{\infty} v_n(p_T) \, \cos[n(\phi - \Psi_n(p_T))] \right).$$

- Both the magnitude v_n and the direction Ψ_n ("flow angle") depend on p_T.
- v_n, Ψ_n, $v_n(p_T)$, $\Psi_n(p_T)$ **all fluctuate from event to event.**
- $\Psi_n(p_T) - \Psi_n$ fluctuates from event to event.

Initial participant plane correlations in PbPb@LHC

Zhi Qiu, UH, PLB 717 (2012) 261

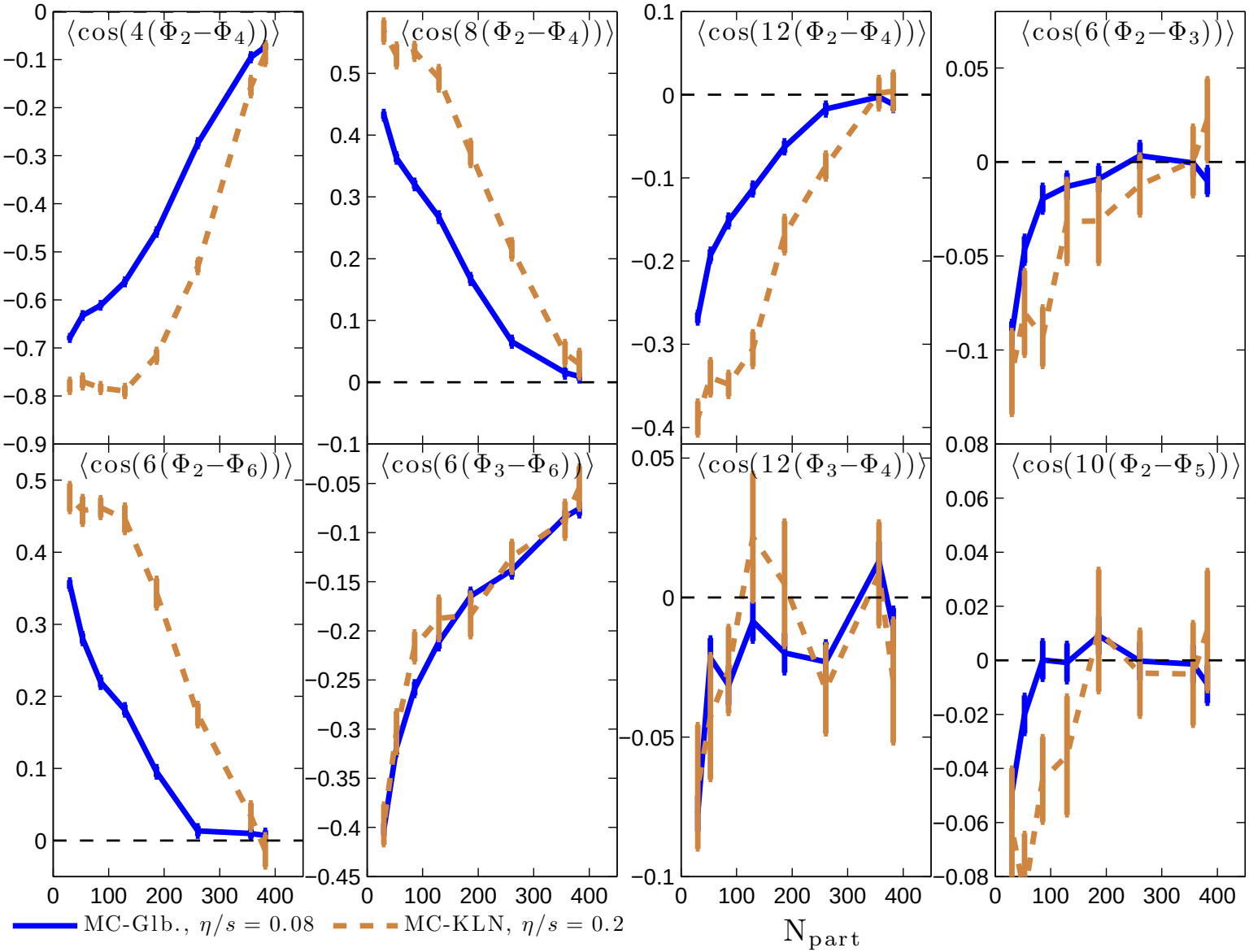

Qualitatively similar, but quantitative differences between models

Final flow angle correlations in PbPb@LHC

Data: ATLAS Coll., J. Jia et al., Hard Probes 2012

Event-by-event hydrodynamics: Zhi Qiu, UH, PLB 717 (2012) 261 (VISH2+1)

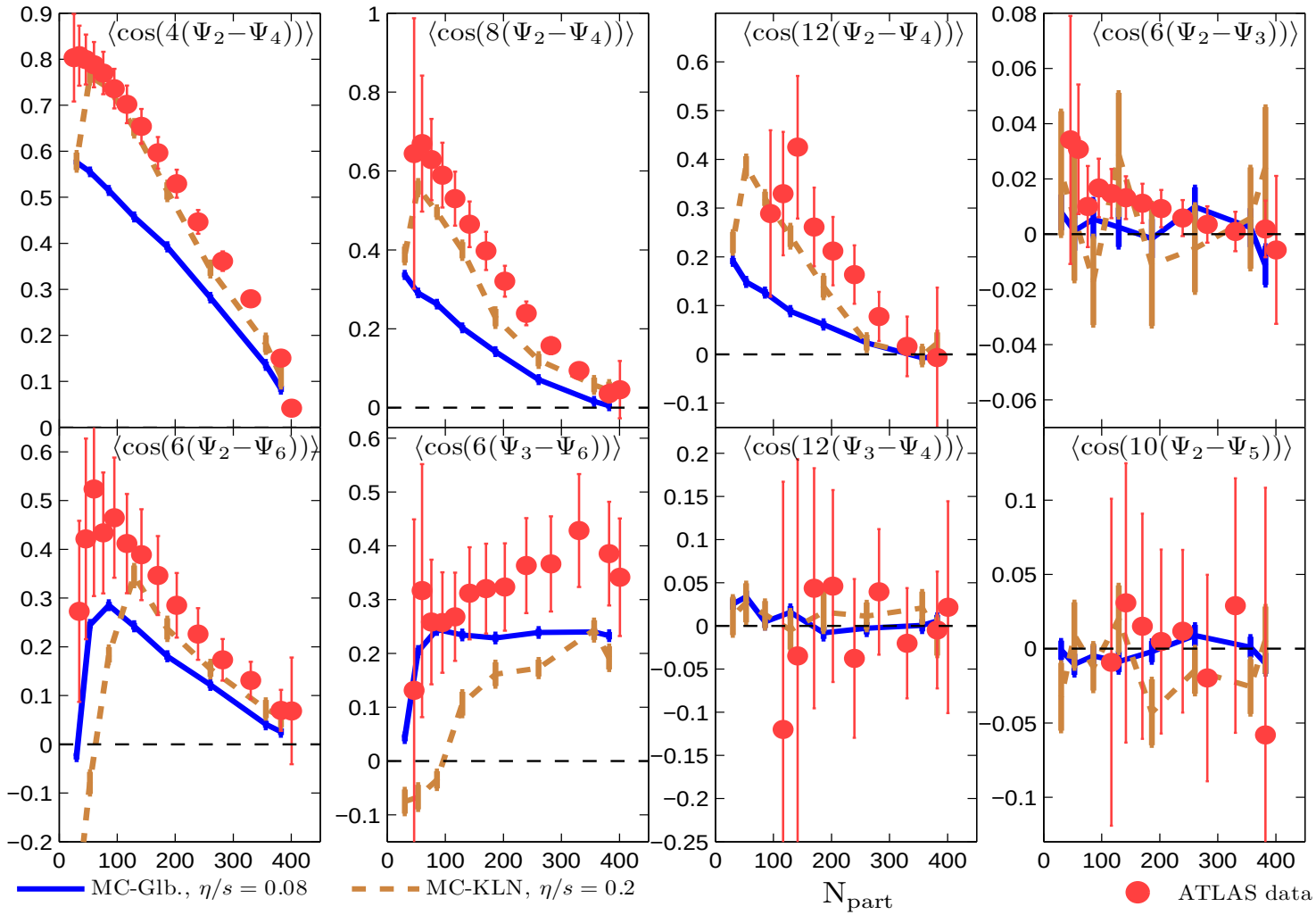

VISH2+1 reproduces qualitatively the centrality dependence of all measured event-plane correlations

Initial part.-plane correlations disagree qualitatively with the measured final-state flow-plane correlations

$\Longrightarrow$ Nonlinear mode coupling through hydrodynamic evolution essential to describe the data!

Larger viscosity appears to yield stronger flow-angle correlations

Initial three-plane correlations in PbPb@LHC

Zhi Qiu, UH, PLB 717 (2012) 261

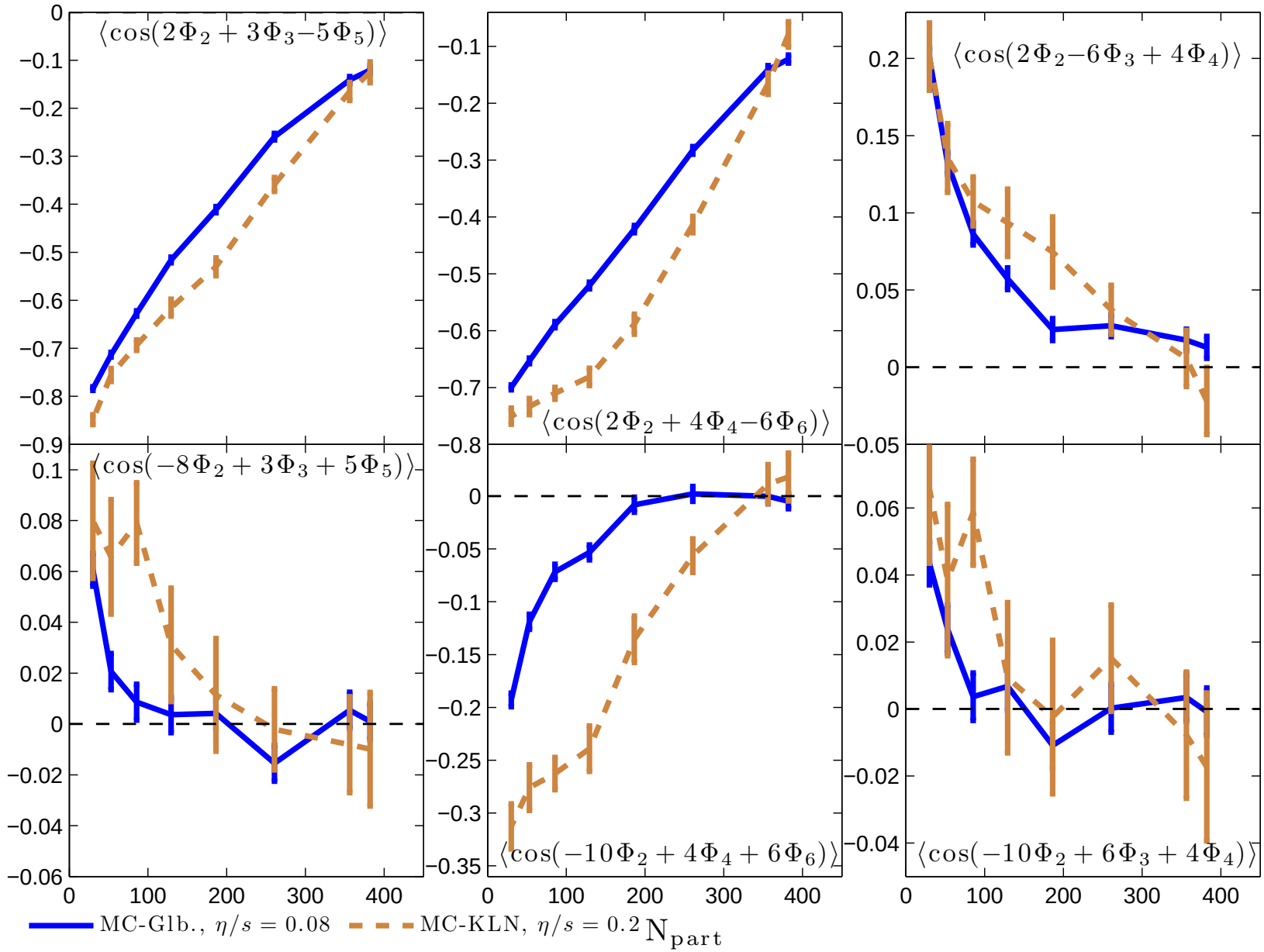

Final three-plane flow correlations in PbPb@LHC

Data: ATLAS Coll., J. Jia et al., Hard Probes 2012

Event-by-event hydrodynamics: Zhi Qiu, UH, PLB 717 (2012) 261 (VISH2+1)

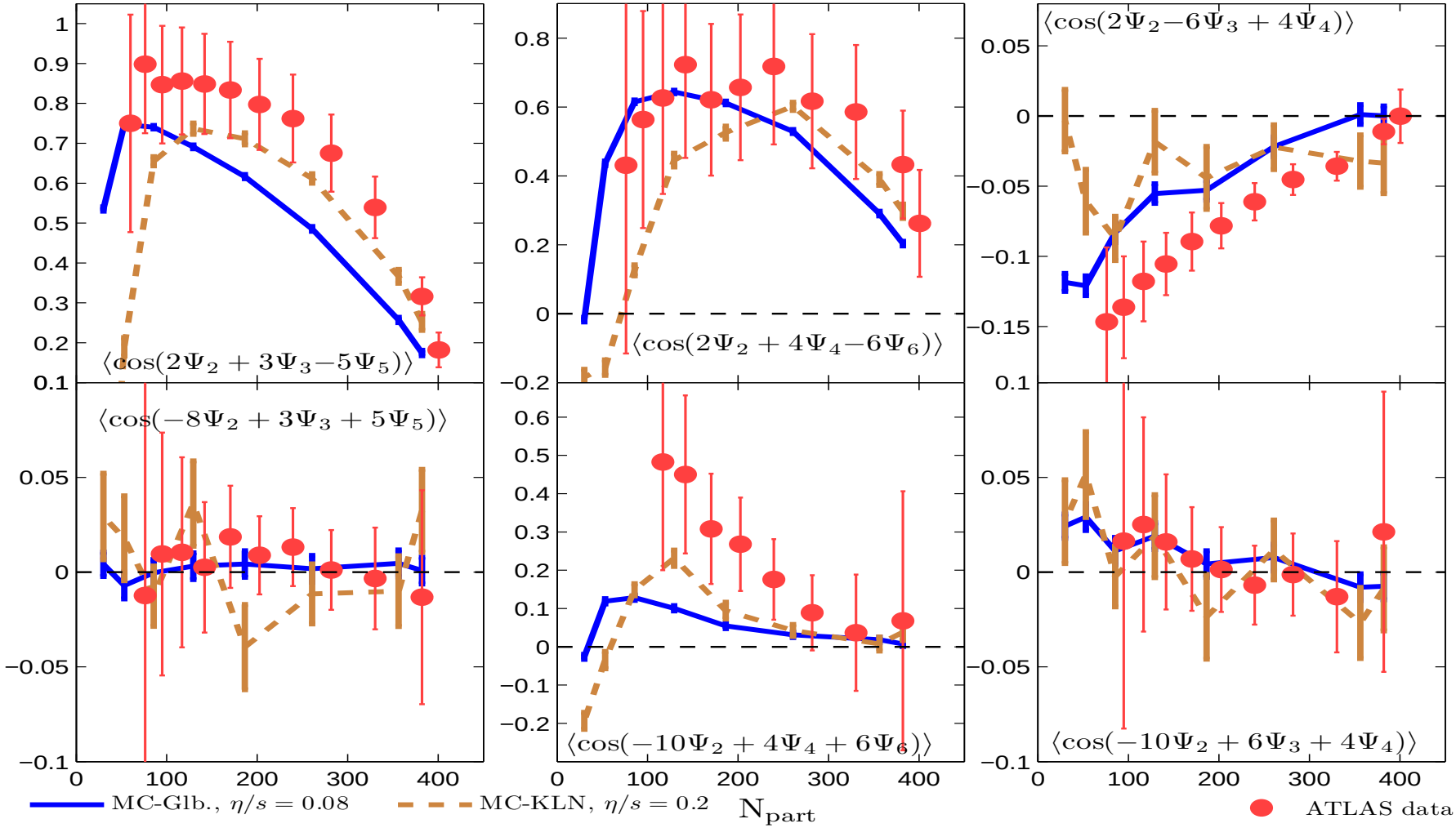

Nonlinear mode coupling through hydrodynamic evolution essential to describe the data!

Single event anisotropic flow coefficients

In a single event, the specific initial density profile results in a set of complex, y- and p_T-dependent flow coefficients (we'll suppress the y-dependence):

$$V_n = v_n e^{in\Psi_n} := \frac{\int p_T dp_T d\phi \, e^{in\phi} \frac{dN}{dy p_T dp_T d\phi}}{\int p_T dp_T d\phi \, \frac{dN}{dy p_T dp_T d\phi}} \equiv \{e^{in\phi}\},$$

$$V_n(p_T) = v_n(p_T) e^{in\Psi_n(p_T)} := \frac{\int d\phi \, e^{in\phi} \frac{dN}{dy p_T dp_T d\phi}}{\int d\phi \, \frac{dN}{dy p_T dp_T d\phi}} \equiv \{e^{in\phi}\}_{p_T}.$$

Together with the azimuthally averaged spectrum, these completely characterize the measurable single-particle information for that event:

$$\frac{dN}{dy\, d\phi} = \frac{1}{2\pi} \frac{dN}{dy} \left(1 + 2 \sum_{n=1}^{\infty} v_n \, \cos[n(\phi - \Psi_n)] \right),$$

$$\frac{dN}{dy\, p_T\, dp_T\, d\phi} = \frac{1}{2\pi} \frac{dN}{dy\, p_T\, dp_T} \left(1 + 2 \sum_{n=1}^{\infty} v_n(p_T) \, \cos[n(\phi - \Psi_n(p_T))] \right).$$

- Both the magnitude v_n and the direction Ψ_n ("flow angle") depend on p_T.
- v_n, Ψ_n, $v_n(p_T)$, $\Psi_n(p_T)$ **all fluctuate from event to event.**
- $\Psi_n(p_T) - \Psi_n$ fluctuates from event to event.

p_T-dependent flow angles and their fluctuations

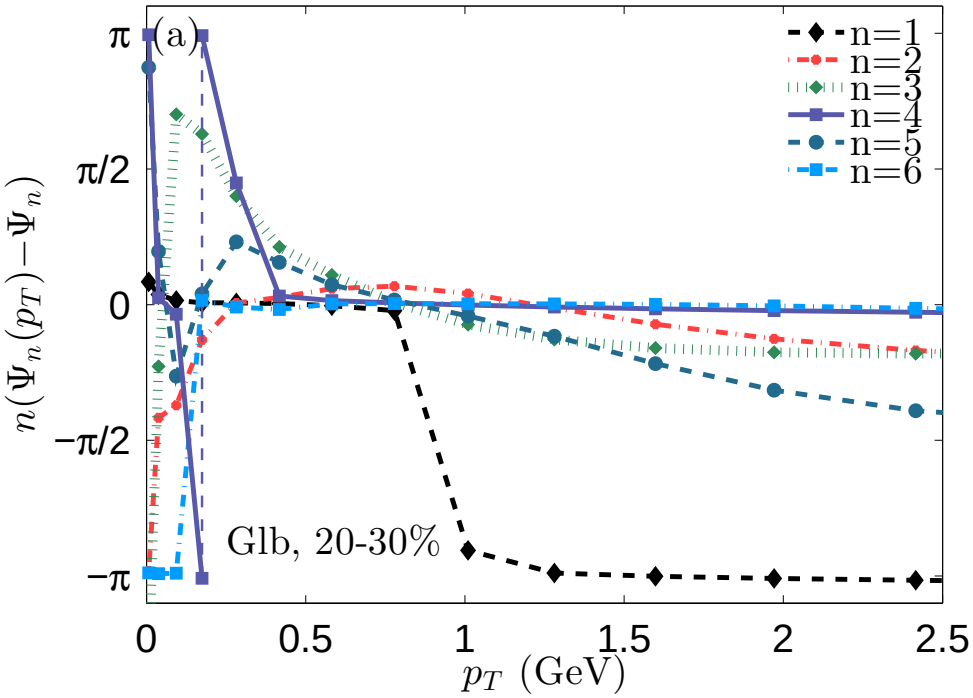

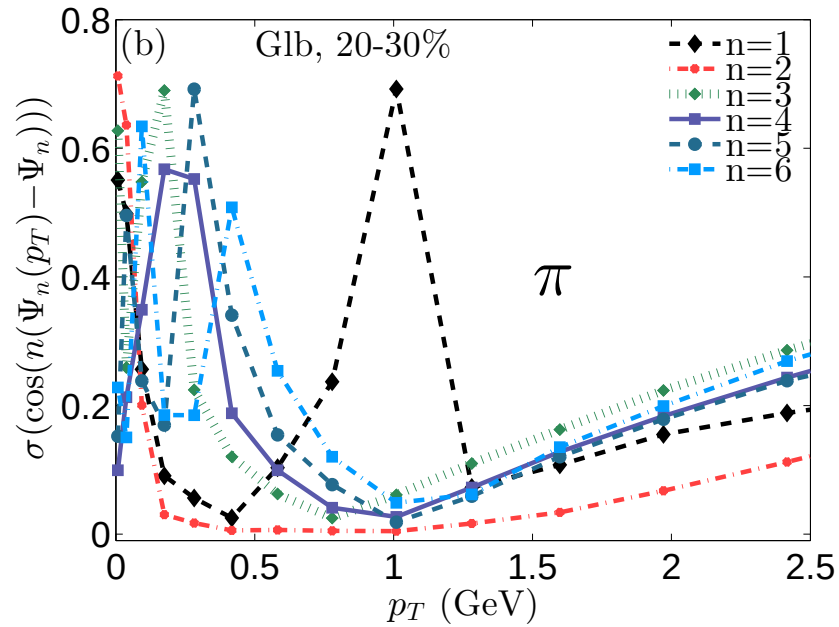

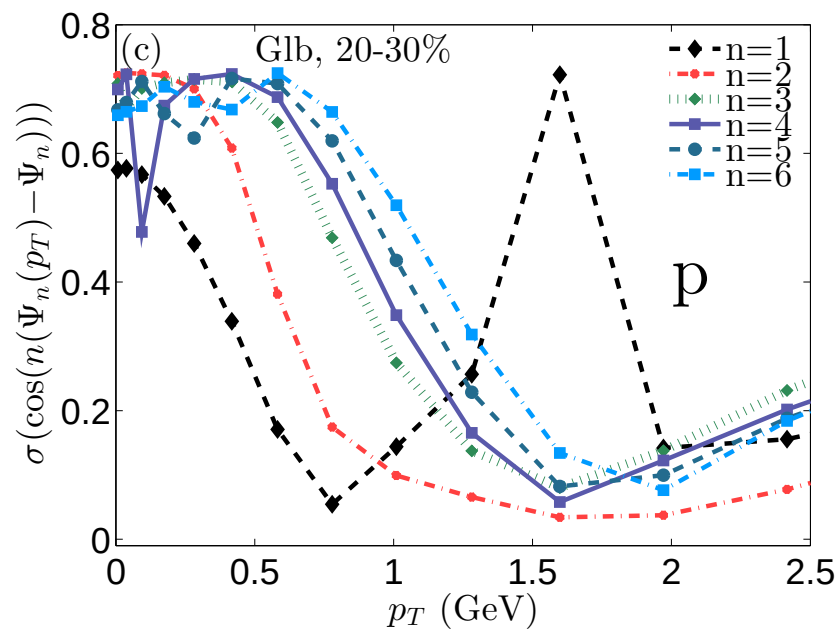

- Except for directed flow (n=1), $\Psi_n(p_T)-\Psi_n$ fluctuates most strongly at low p_T
- Directed flow angle $\Psi_1(p_T)$ flips by $180°$ at $p_T \sim 1$ GeV for charged hadrons (pions) and at $p_T \sim 1.5$ GeV for protons (momentum conservation)

Flow measures from two-particle correlations $\langle\{e^{in(\phi_1-\phi_2)}\}\rangle$

"rms flow":

$$v_n^2[2] := \langle\{e^{in\phi_1}\}\{e^{-in\phi_2}\}\rangle = \langle v_n^2\rangle \equiv v_n\{2\};$$
$$v_n^2[2](p_T) := \langle\{e^{in\phi_1}\}_{p_T}\{e^{-in\phi_2}\}_{p_T}\rangle = \langle v_n^2(p_T)\rangle \qquad (\neq v_n^2\{2\}(p_T)!).$$

"differential 2-particle cumulant flow":

$$v_n\{2\}(p_T) := \langle\{e^{in\phi_1}\}_{p_T}\{e^{-in\phi_2}\}\rangle / v_n\{2\} = \Big\langle v_n(p_T) v_n \cos[n(\Psi_n(p_T)-\Psi_n)]\Big\rangle \Big/ v_n[2]\ .$$

"event plane flow":

$$v_n\{\mathrm{EP}\}(p_T) := \Big\langle \{e^{in\phi}\}_{p_T} e^{-in\Psi_n}\Big\rangle = \Big\langle v_n(p_T)\cos[n(\Psi_n(p_T)-\Psi_n)]\Big\rangle.$$

"mean flow":

$$\langle v_n(p_T)\rangle := \Big\langle \Big|\{e^{in\phi}\}_{p_T} e^{-in\Psi_n}\Big|\Big\rangle = \Big\langle \sqrt{\{\cos(n\phi)\}_{p_T}^2 + \{\sin(n\phi)\}_{p_T}^2}\Big\rangle\ .$$

"two-particle flows":

$$\tilde{V}_{n\Delta}(p_{T1},p_{T2}) := \Big\langle \{e^{in(\phi_1-\phi_2)}\}_{p_{T1}p_{T2}}\Big\rangle = \Big\langle v_n(p_{T1})v_n(p_{T2})\cos[n(\Psi_n(p_{T1})-\Psi_n(p_{T2}))]\Big\rangle;$$
$$\Big\langle v_n(p_{T1})v_n(p_{T2})\Big\rangle := \Big\langle \sqrt{\{\cos(n\Delta\phi)\}_{p_{T1},p_{T2}}^2 + \{\sin(n\Delta\phi)\}_{p_{T1},p_{T2}}^2}\Big\rangle\ .$$

Here: both particles taken from same species (but this is not necessary).

Fluctation effects related to finite number of particles in the observed final state are ignored.

Elliptic and triangular flow comparison (I)

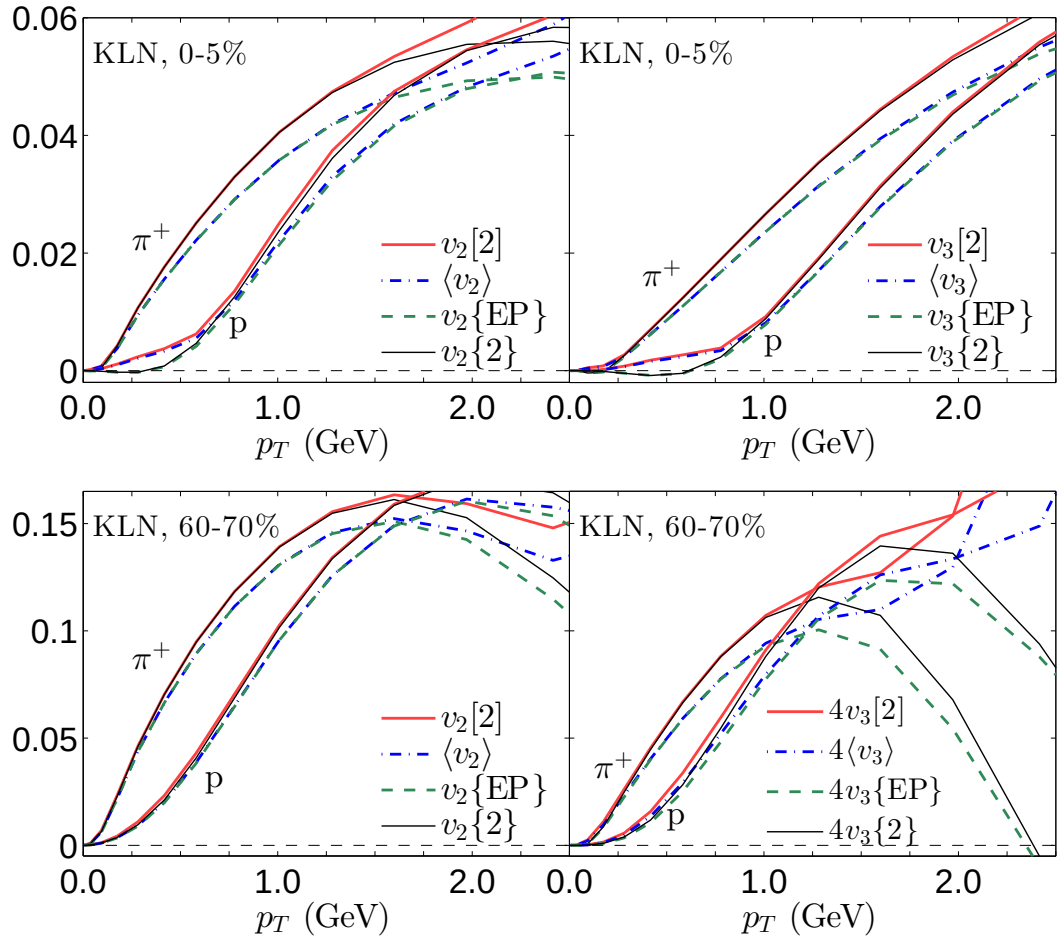

In central collisions, angular fluctuations suppress $v_n\{\mathrm{EP}\}(p_T)$ and $v_n\{2\}(p_T)$ below the mean and rms flows at low p_T (clearly visible for protons)

This effect disappears in peripheral collisions, but a similar effect then takes over at higher p_T, for both pions and protons.

Elliptic and triangular flow comparison (II): v_n ratios

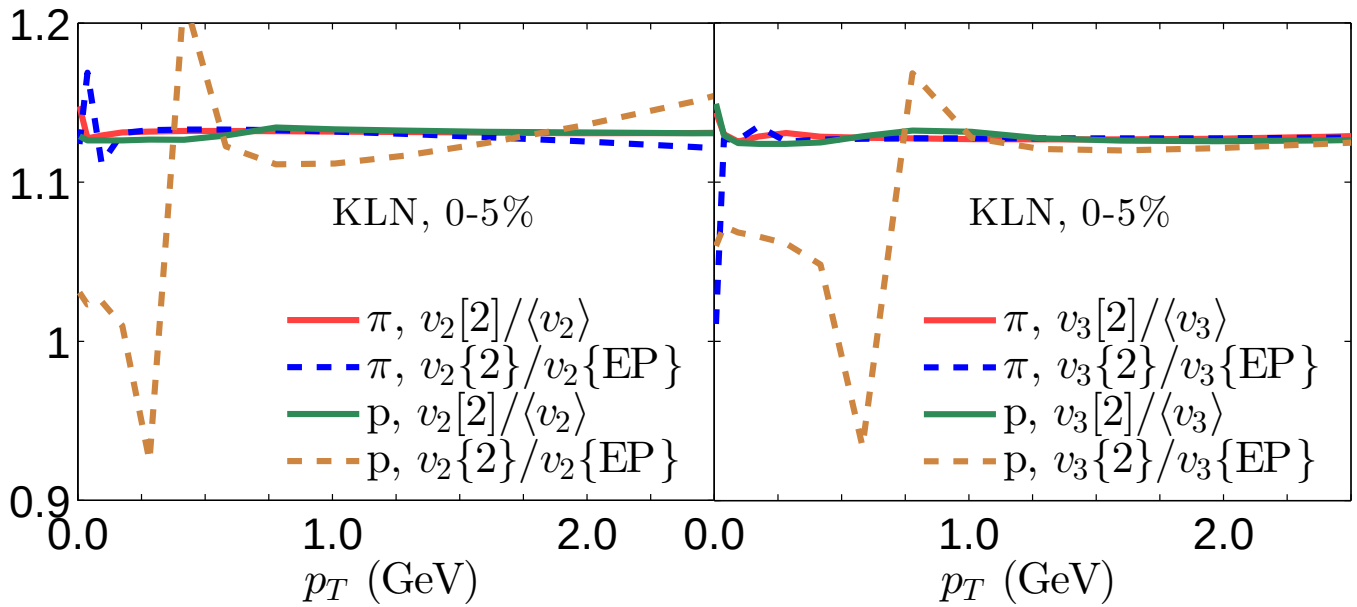

Except for where the numerator or denominator goes through zero, for central collisions these ratios are equal to $2/\sqrt{\pi} \approx 1.13$, independent of p_T. Expected if flow angles are randomly oriented (Bessel-Gaussian distribution for v_n, see Voloshin et al., PLB 659, 537 (2008)).

Not true in peripheral collisions, especially not for v_2 (Gardim et al., 1209.2323)

That this works even for $v_n\{2\}/v_n\{\mathrm{EP}\}$ suggests an approximate factorization of angular fluctuation effects!

Elliptic and triangular flow comparison (III): v_n ratios

Central collisions:

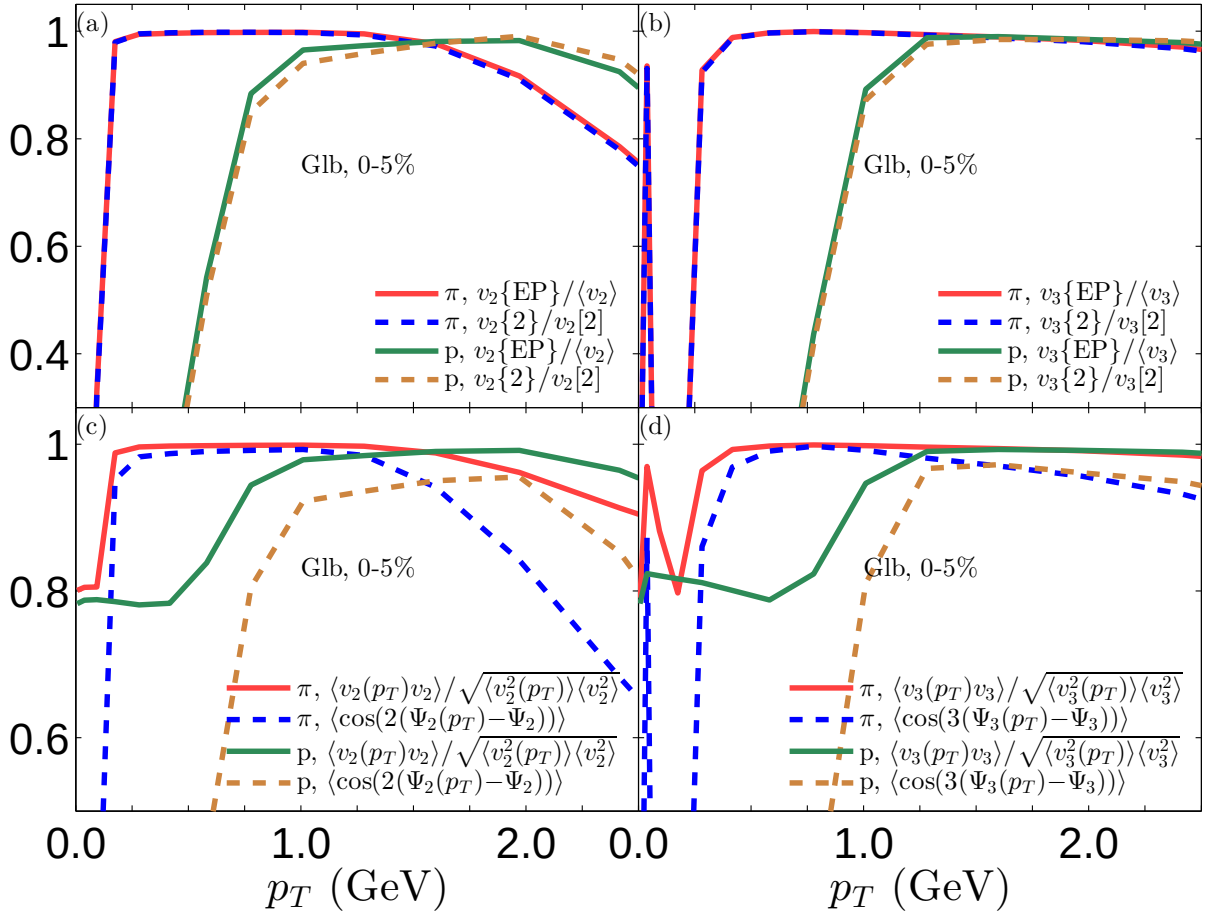

– The angular fluctuation factor $\langle\cos[n(\Psi_n(p_T)-\Psi_n)]\rangle$ completely dominates the p_T-dependence of these ratios!

– Angular fluctuations have similar effect as poor event-plane resolution: they reduce v_n.

– Angular fluctuations are effective both at low and high p_T, but not at intermediate p_T.

– The window for seeing flow angle fluctuation effects at low p_T is smaller for pions than for protons.

Elliptic and triangular flow comparison (IV): v_n ratios

Peripheral collisions:

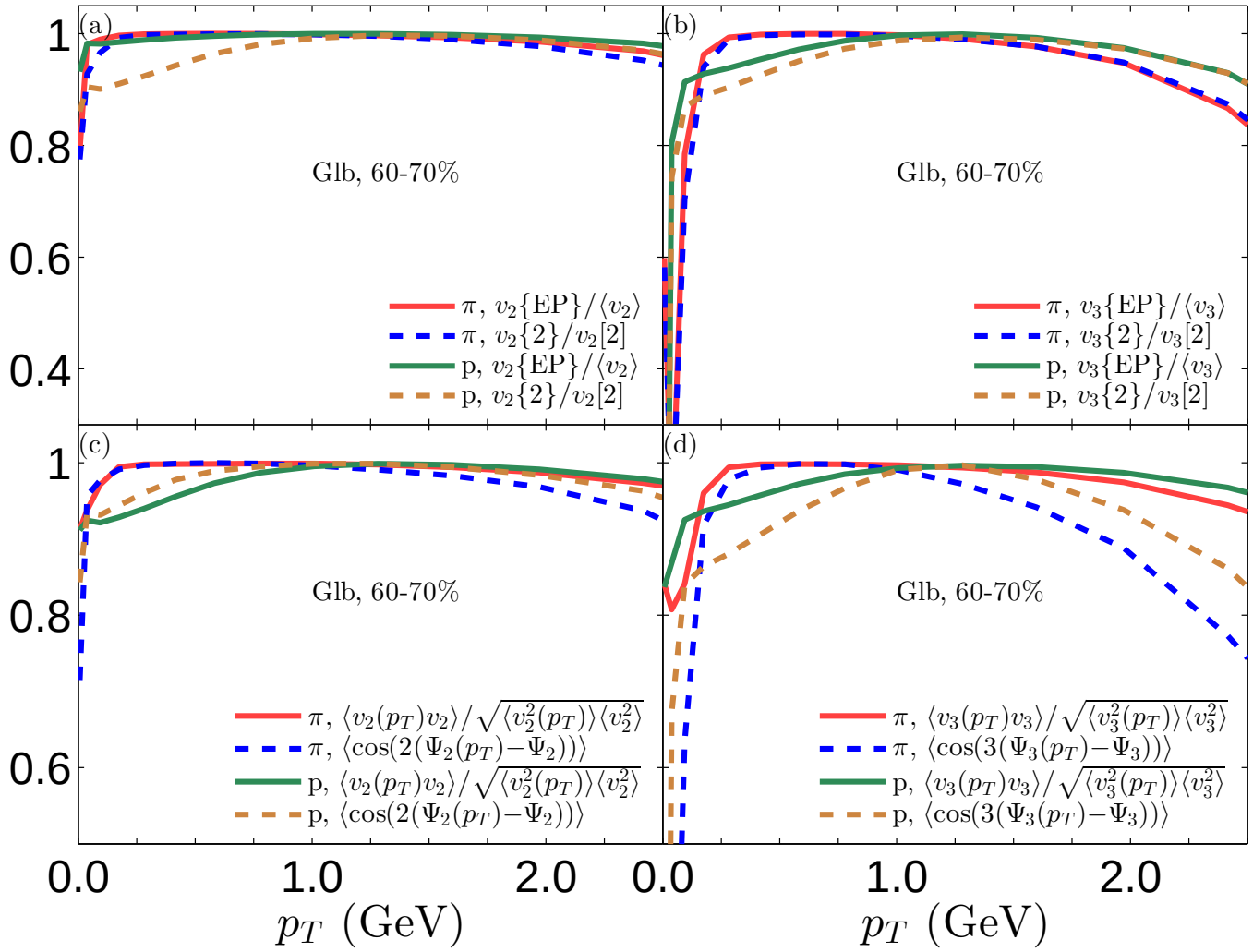

The window for seeing flow angle fluctuation effects at low p_T closes in peripheral collisions.

Flow angle fluctuation effects for higher order $v_n(p_T)$

Central collisions; solid: $\langle v_n(p_T)\rangle$; dashed: $v_n\{\mathrm{EP}\}(p_T)$:

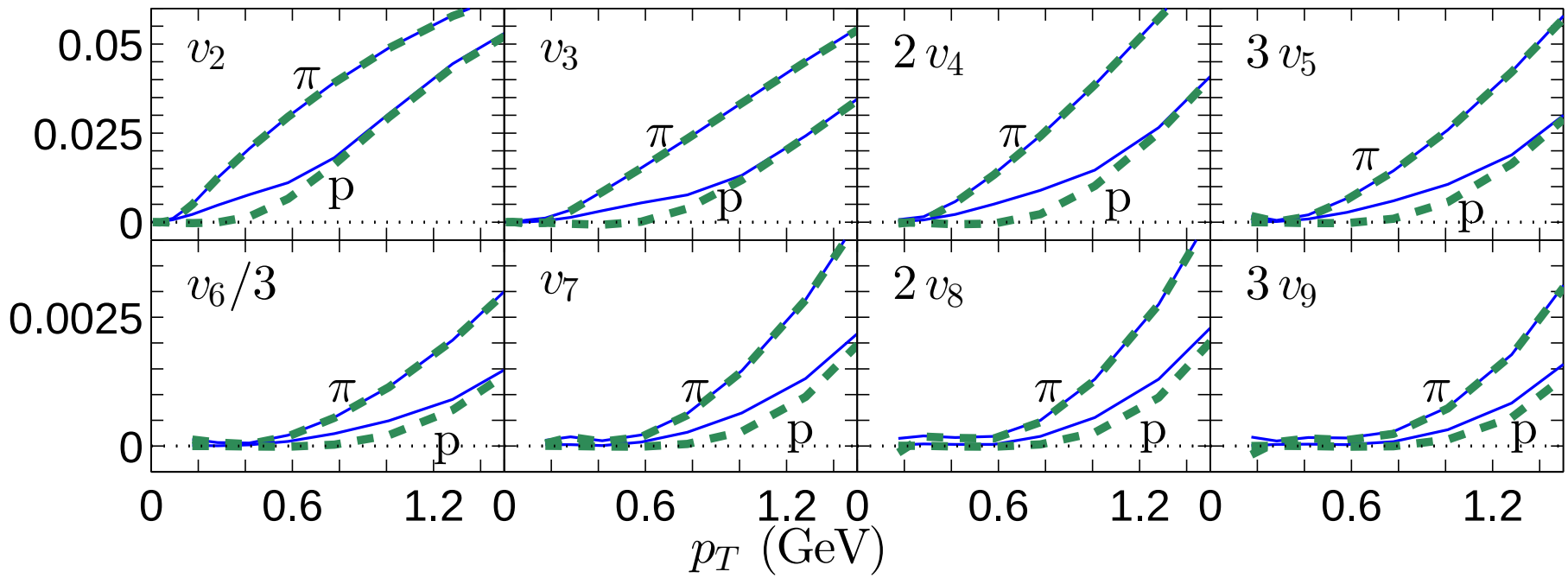

As harmonic order n increases, suppression of $v_n\{\mathrm{EP}\}(p_T)$ (or $v_n\{2\}(p_T)$) from flow angle fluctuations for protons gets somewhat weaker but persists to larger p_T.

Test of factorization of two-particle spectra

Factorization $V_{n\Delta}(p_{T1}, p_{T2}) := \left\langle \{\cos[n(\phi_1 - \phi_2)]\}_{p_{T1}p_{T2}} \right\rangle \approx$ "$v_n(p_{T1}) \times v_n(p_{T2})$" was checked experimentally as a test of hydrodynamic behavior, and found to hold to good approximation.

Gardim et al. (1211.0989) pointed out that event-by-event fluctuations break this factorization even if 2-particle correlations are exclusively due to flow.

They proposed to study the following ratio:

$$r_n(p_{T1}, p_{T2}) := \frac{V_{n\Delta}(p_{T1}, p_{T2})}{\sqrt{V_{n\Delta}(p_{T1}, p_{T1}) V_{n\Delta}(p_{T2}, p_{T2})}} = \frac{\langle v_n(p_{T1}) v_n(p_{T2}) \cos[n(\Psi_n(p_{T1}) - \Psi_n(p_{T2}))] \rangle}{v_n[2](p_{T1}) v_n[2](p_{T2})}.$$

Even in the absence of flow angle fluctuations, this ratio is < 1 due to v_n fluctuations (Schwarz inequality), except for $p_{T1} = p_{T2}$.

But it additionally depends on flow angle fluctuations.

To assess what share of the deviation from 1 is due to flow angle fluctuations, we can compare with

$$\tilde{r}_n(p_{T1}, p_{T2}) := \frac{\langle v_n(p_{T1}) v_n(p_{T2}) \cos[n(\Psi_n(p_{T1}) - \Psi_n(p_{T2}))] \rangle}{\langle v_n(p_{T1}) v_n(p_{T2}) \rangle}$$

which deviates from 1 **only** due to flow angle fluctuations. Again, this ratio approaches 1 for $p_{T1} = p_{T2}$.

Gardim et al. studied r_n for ideal hydro; we have studied r_n and $\tilde{r}_n$ for viscous hydro.

Breaking of factorization by e-by-e fluctuations (I)

Monte Carlo Glauber initial conditions, $\eta/s = 0.08 = 1/(4\pi)$:

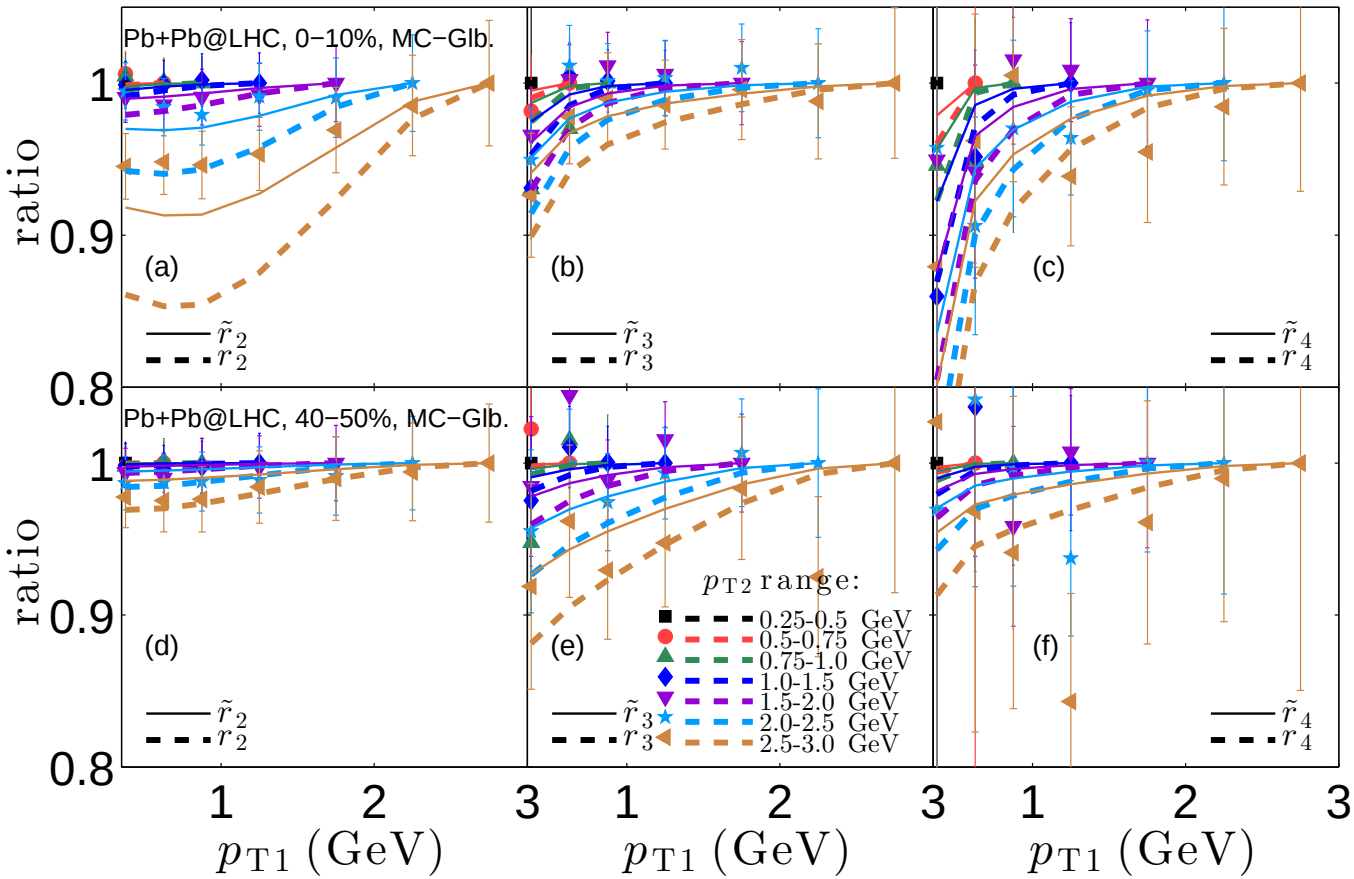

More than half of the factorization breaking effects are due to flow angle fluctuations.

In central collisions, $\eta/s = 0.08$ appears to overpredict the breaking of factorization (consistent with Gardim et al. who saw still larger effects for ideal hydro).

Factorization breaking effects appear to be larger for fluctuation-dominated flow harmonics.

Breaking of factorization by e-by-e fluctuations (II)

Monte Carlo KLN initial conditions, $\eta/s = 0.2 = 2.5/(4\pi)$:

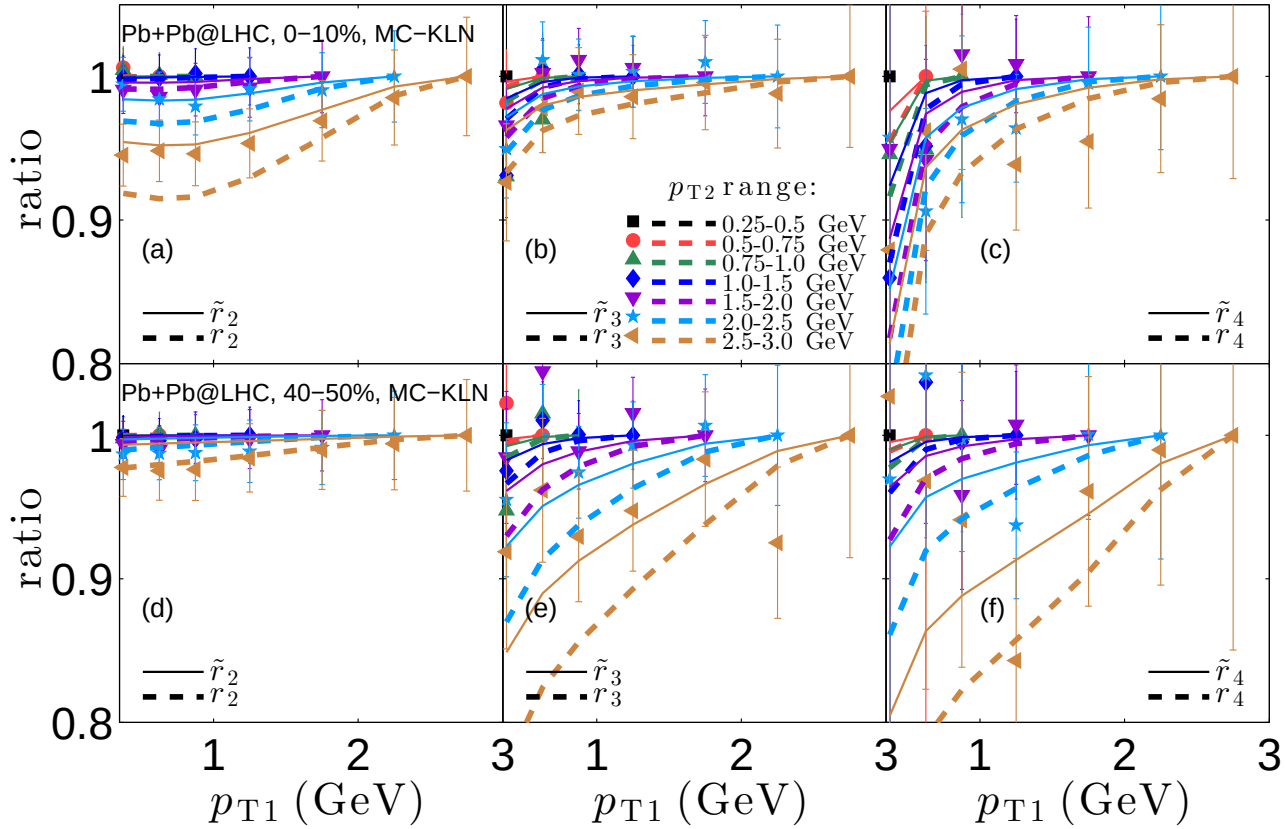

In central collisions, factorization-breaking effects decrease with increasing η/s.

In peripheral collisions, larger η/s appears to cause a larger breaking of factorization, mostly due to flow angle fluctuations.

Data may indicate slight preference for larger η/s value, but more experimental precision and more detailed theoretical studies are needed to settle this. Analysis of ATLAS data in progress.

Conclusions

- Both the magnitudes v_n and the flow angles Ψ_n depend on p_T and fluctuate from event to event.

- In each event, the "p_T-averaged" (total-event) flow angles Ψ_n are identical for all particle species, but their p_T distribution differs from species to species.

- The mean v_n values and their p_T-dependence at RHIC and LHC have already been shown to put useful constraints on the QGP shear viscosity and its temperature dependence (see next talk by B. Schenke)

- **The effects of v_n and Ψ_n fluctuations can be separated experimentally by studying different V_n measures based on two-particle correlations.**

- Flow angle correlations are a powerful test of the hydrodynamic paradigm and will help to further constrain the spectrum of initial-state fluctuations and QGP transport coefficients.

- Studying event-by-event fluctuations of the anisotropic flows v_n and their flow angles Ψ_n as functions of p_T, as well as the correlations between different harmonic flows (both their magnitudes and angles), provides a rich data base for identifying the **"Standard Model of the Little Bang"**, by pinning down its initial fluctuation spectrum and its transport coefficients.

Nuclear effects in pA

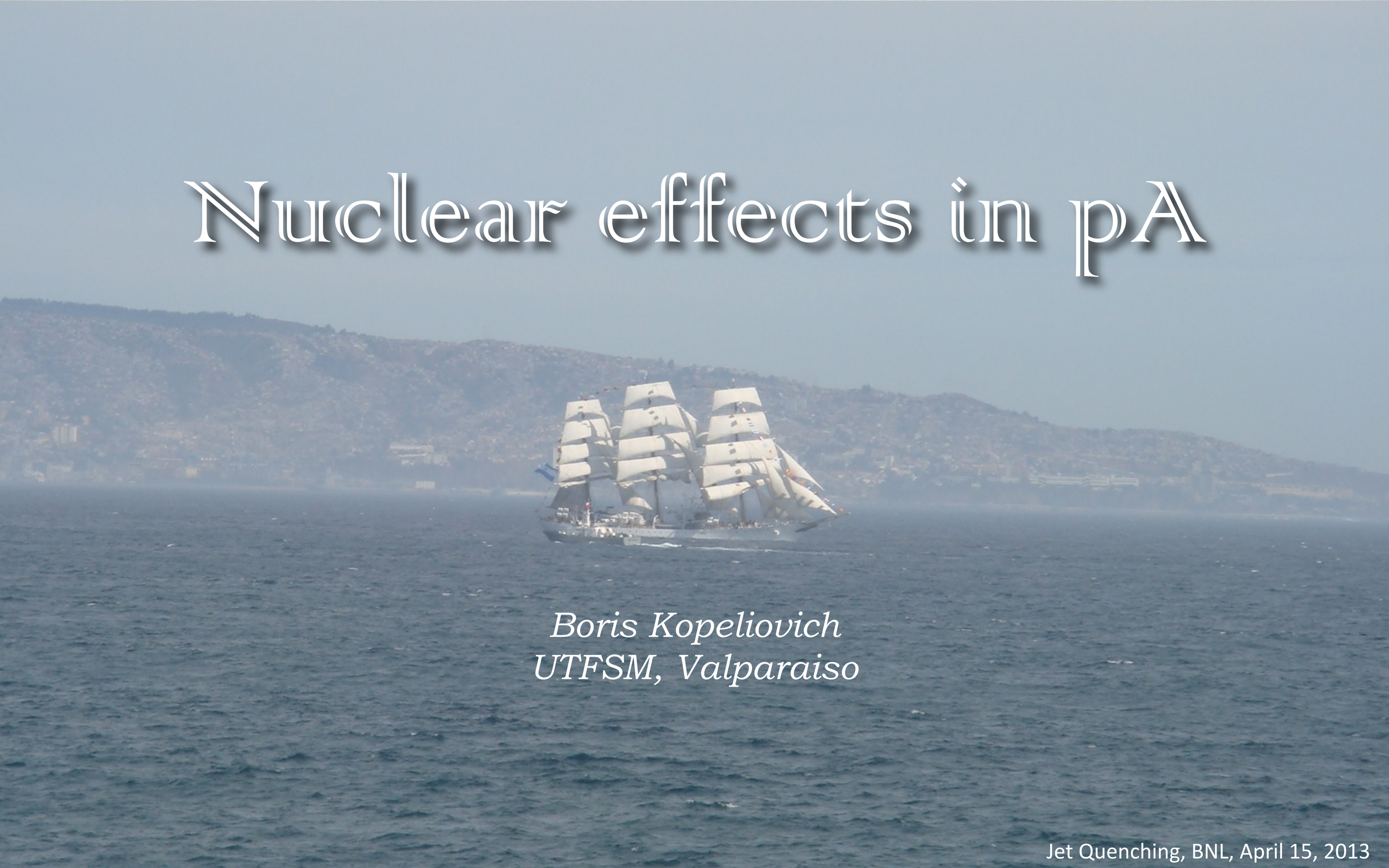

Boris Kopeliovich
UTFSM, Valparaiso

Jet Quenching, BNL, April 15, 2013

In collaboration with

Jan Nemchik
Irina Potashnikova
Ivan Schmidt

Cronin effect

High-pT hadrons can be produced coherently from multiple interactions in nuclei at very high energies (LHC), but not at low energies of fixed target experiments. Correspondingly, the mechanisms for the Cronin enhancement are different.

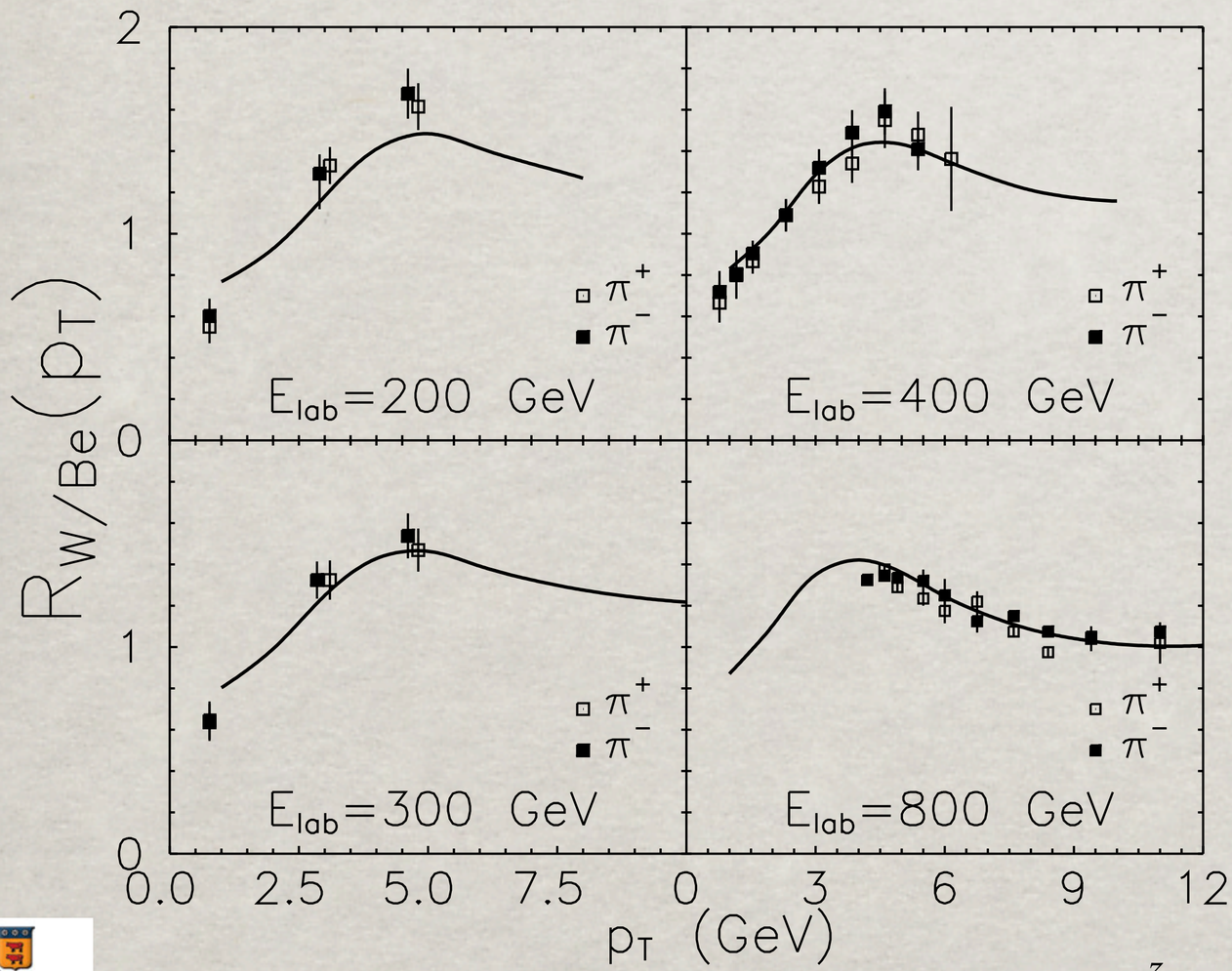

B.K., J.Nemchik, A.Schafer, A.Tarasov, PRL 88(2002)232303

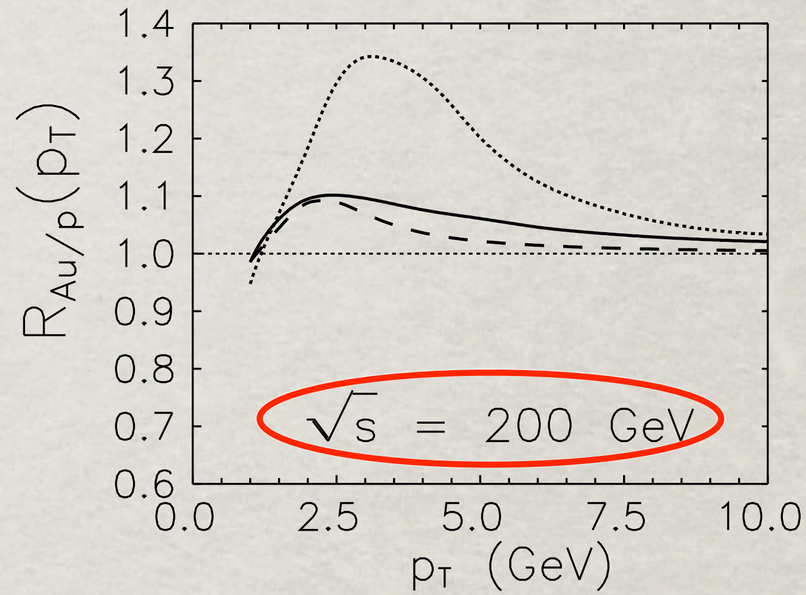

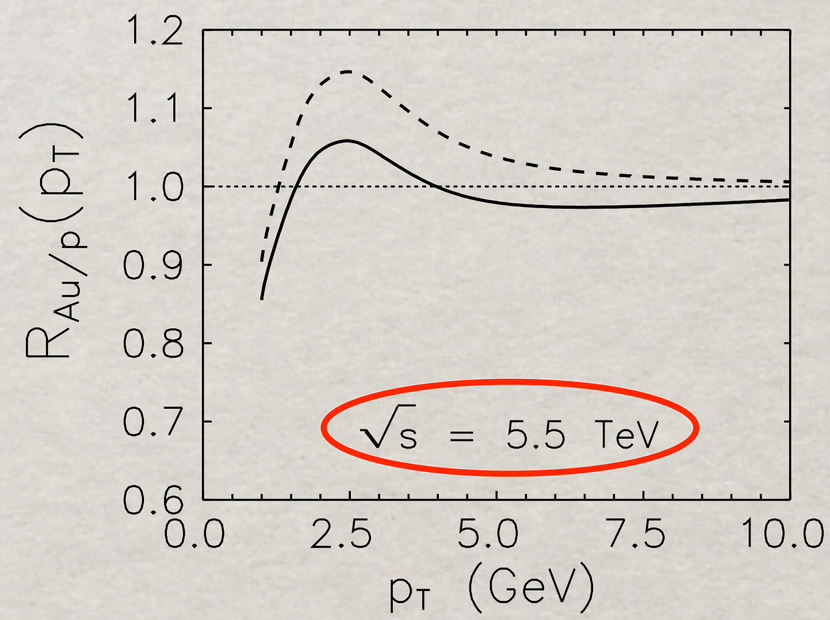

Cronin effect at RHIC: predicted and observed

The predicted magnitude was OK, but the shape was not. The employed unintegrated gluon density of K.J.Golec-Biernat & M.Wustoff, 1999 (GBW) peakes at too small pT.

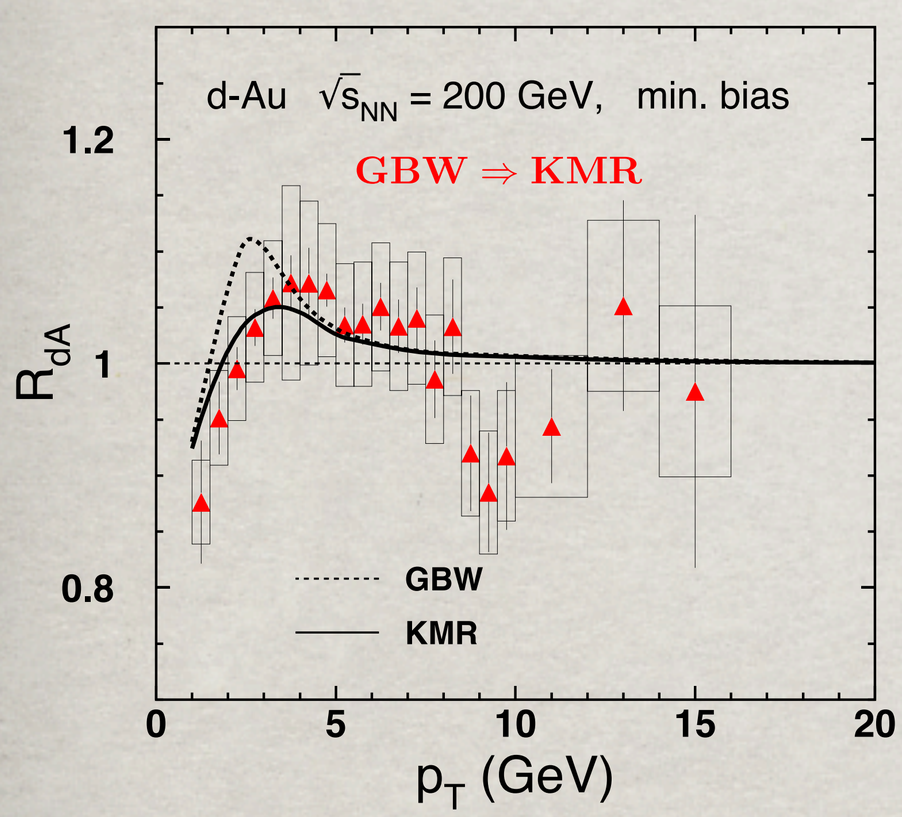

More realistic parametrization for the unintegrated gluon distribution proposed later,

M.Kimber, A.Martin & M.Ryskin, 2001 (KMR)

A.Martin, M.Ryskin & G.Watt, 2010

improves the shape (with no other modifications in the computing code).

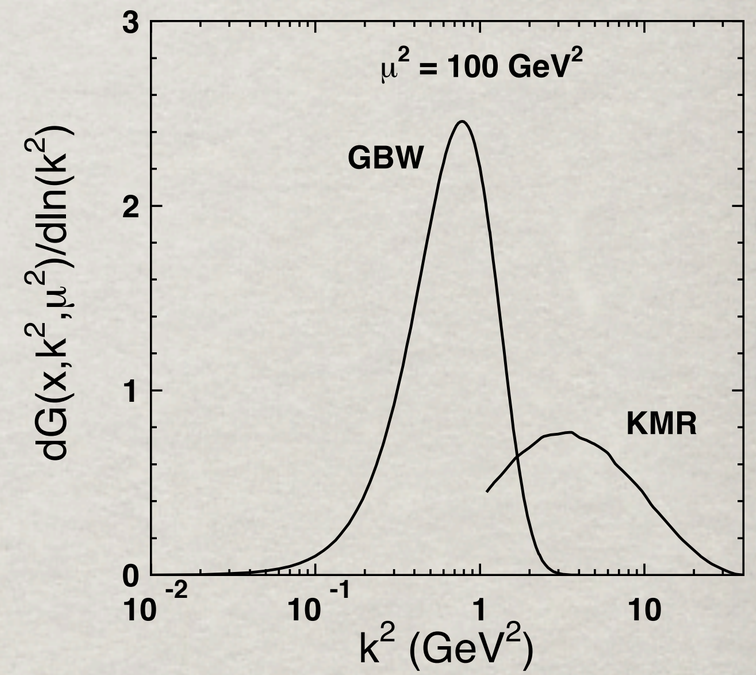

D.Kharzeev, E.Levin,L.McLerran, PL B561(2003)93:

Color Glass Condensate models exaggerated the magnitude of the coherence effects predicting a sizable suppression $\mathbf{R_{dA} = 0.75}$

Cronin effect at LHC: predicted and observed

R.Vogt et al, arXiv: 1301.3395

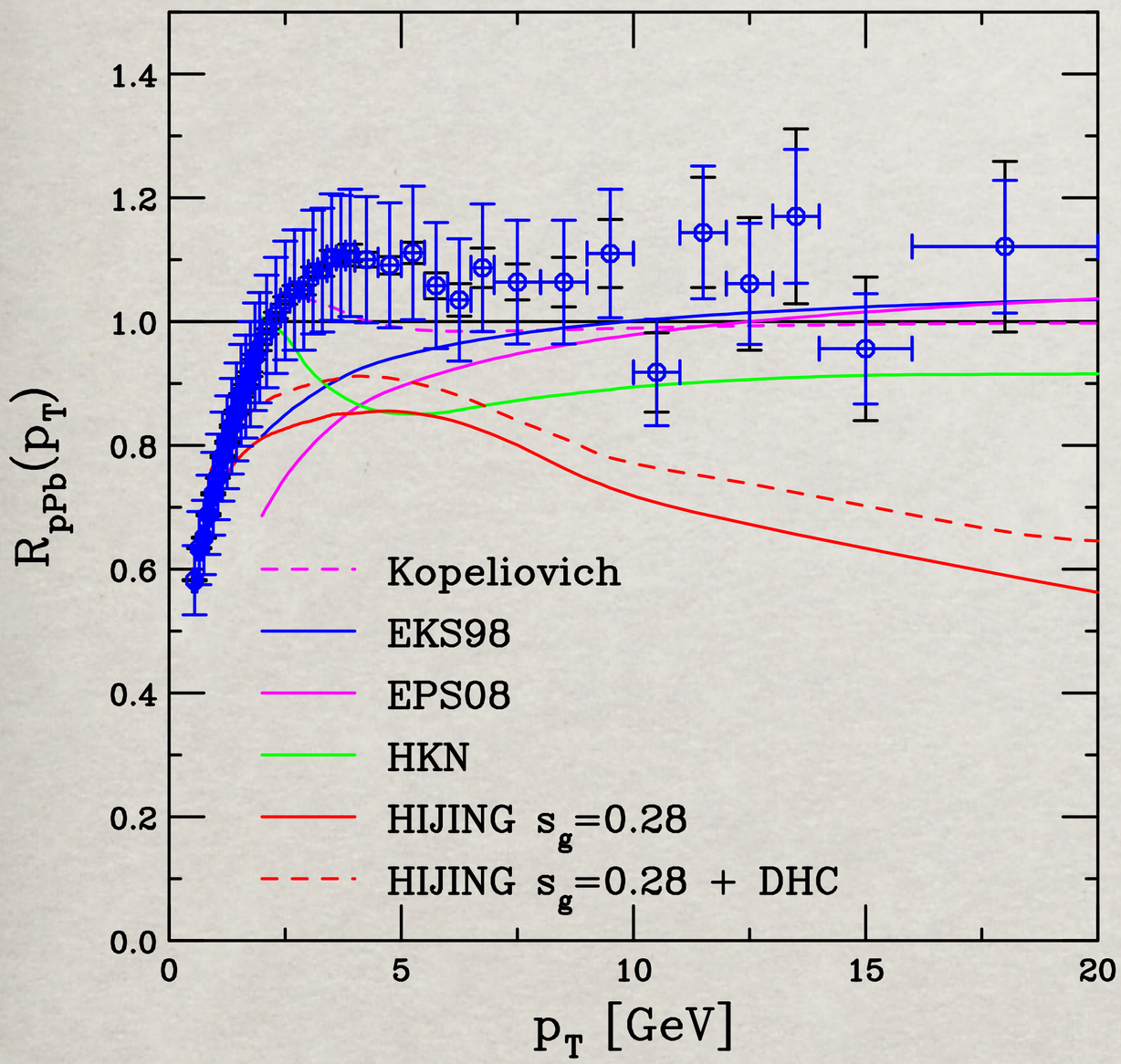

The first successful prediction

B.K., J.Nemchik, A.Schafer, A.Tarasov (2002)

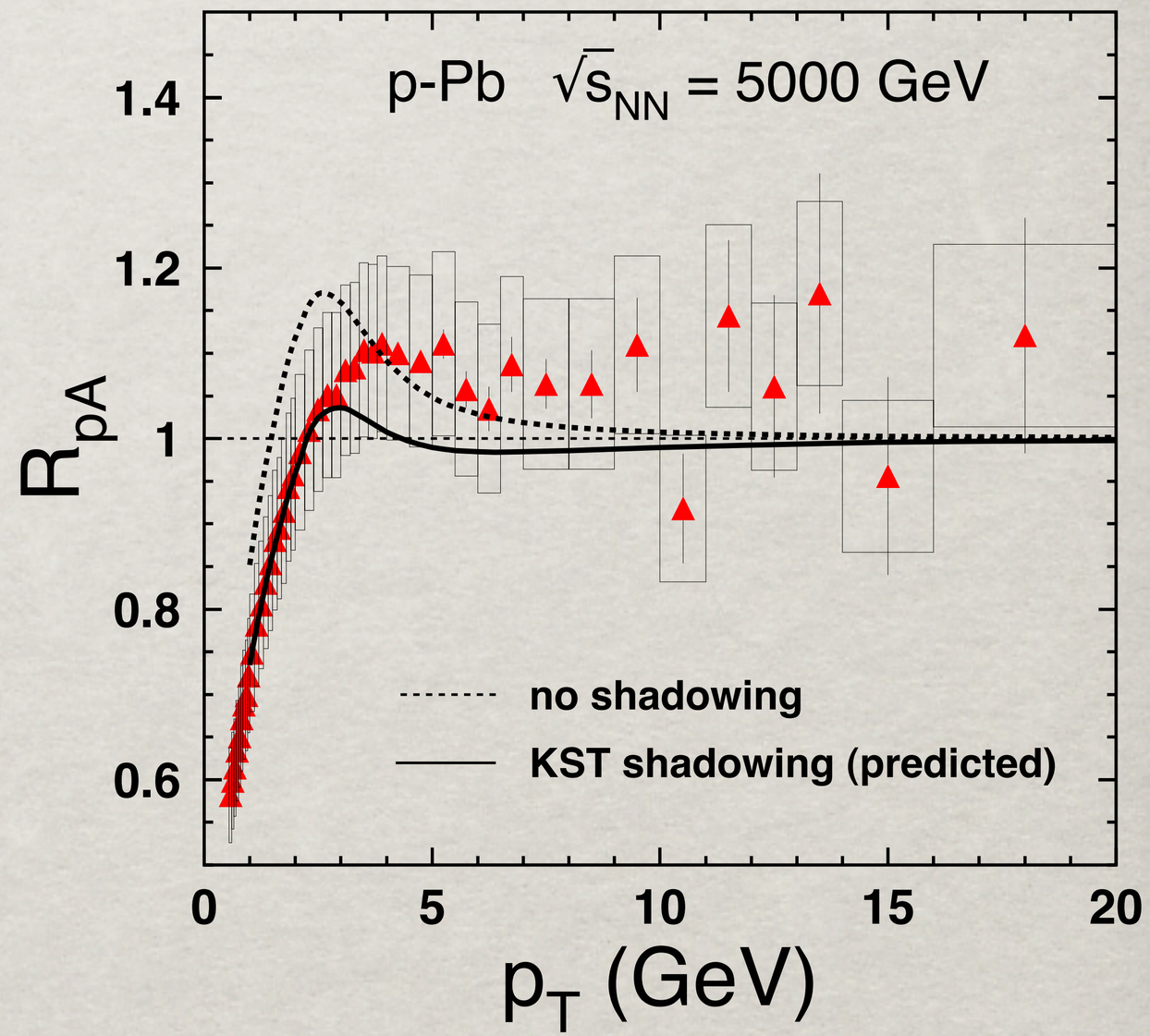

Predicted vs measured

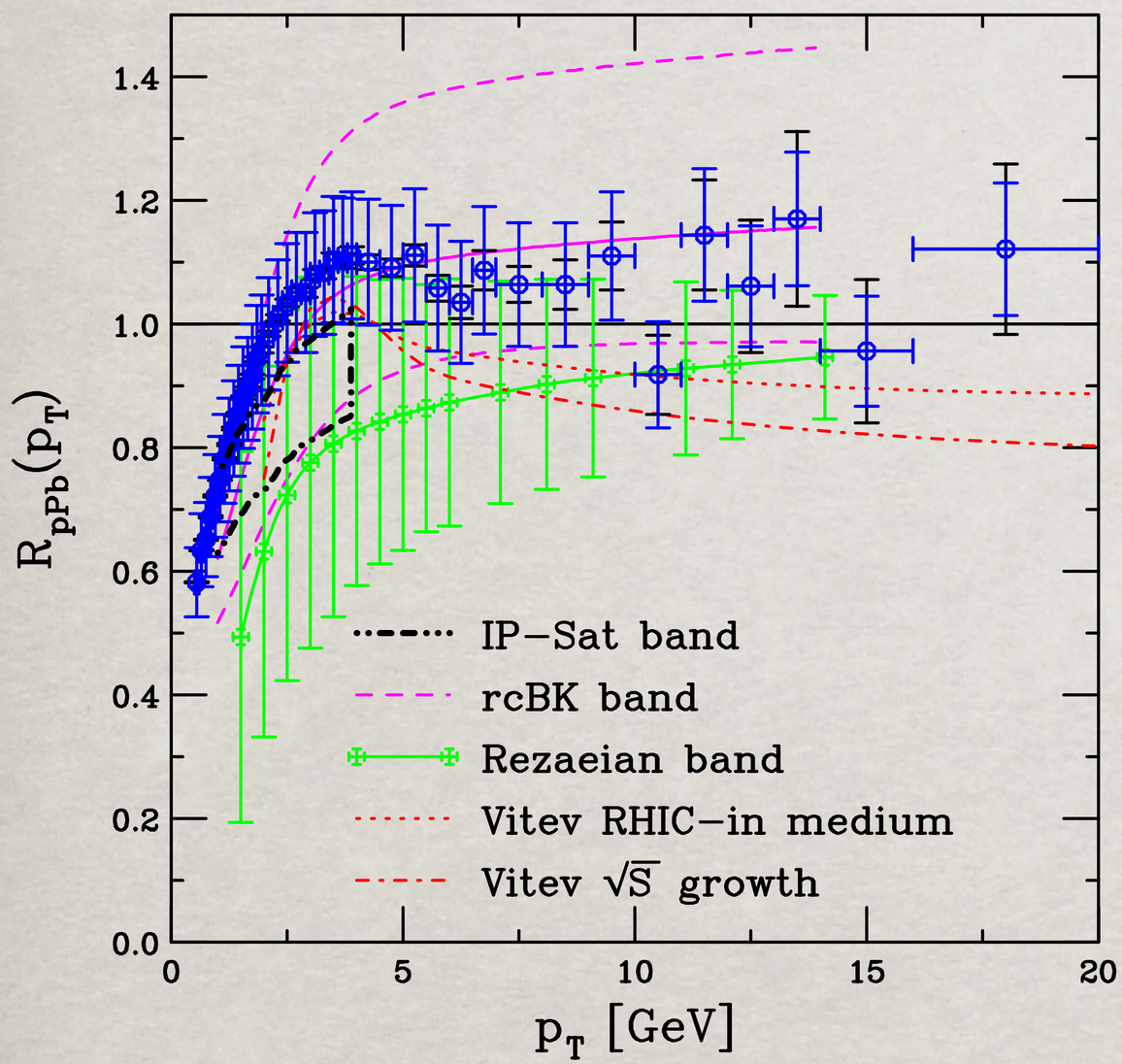

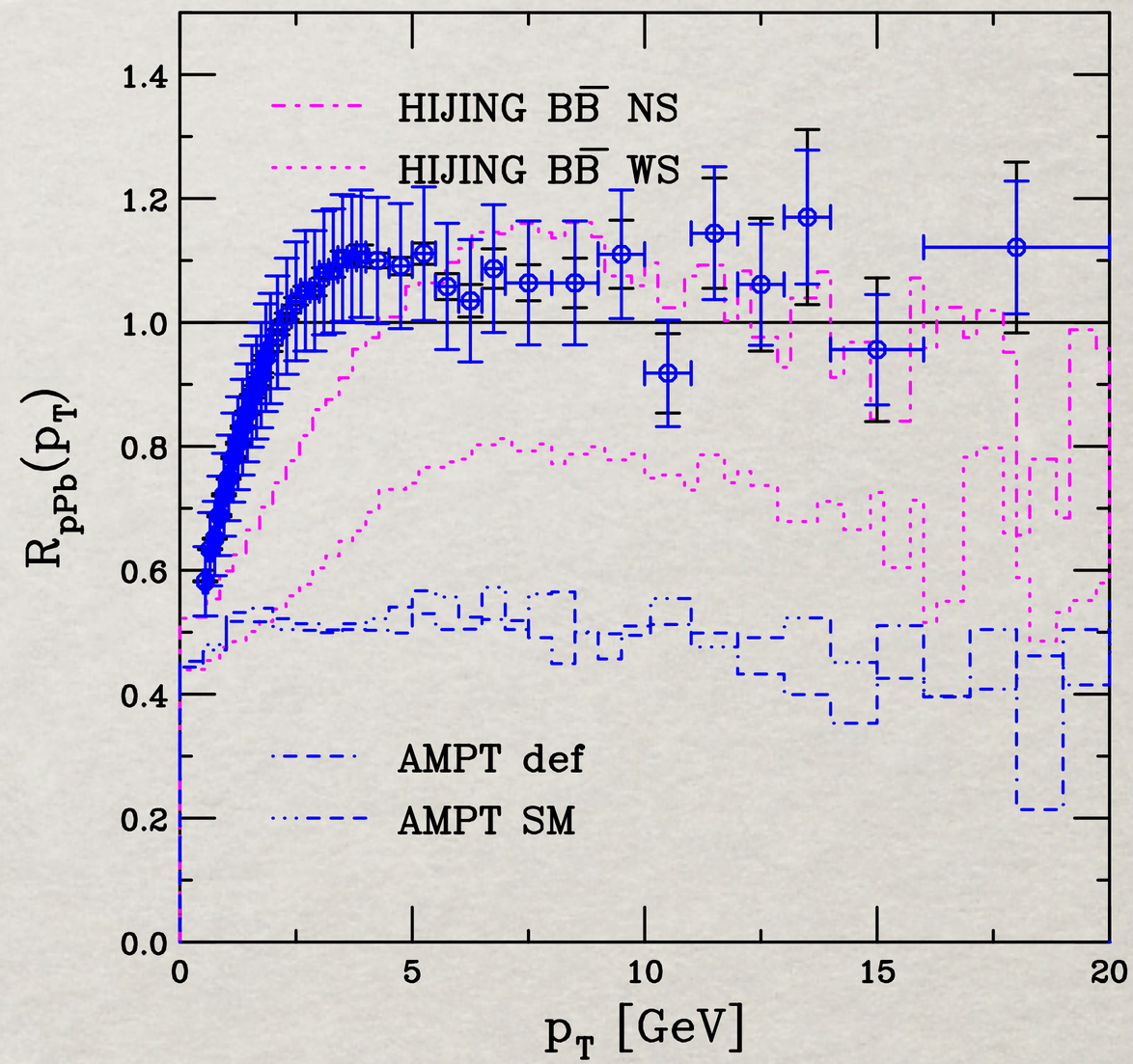

Not successful either

Details

parton model

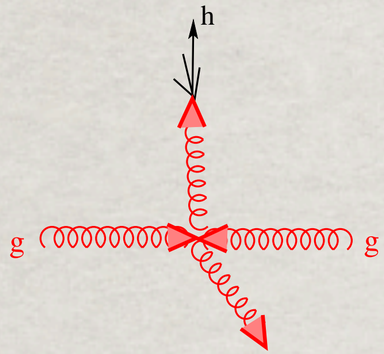

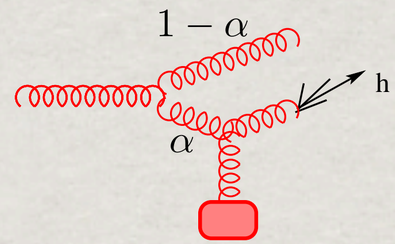

dipole description

$$\frac{\mathbf{d}\sigma^{\mathbf{N(A)}}_{\mathbf{g\to 2g}}(\alpha,\mathbf{x_2})}{\mathbf{d^2k_T\,dy}} = \int \mathbf{d^2r d^2r'\, e^{ik_T(r-r')}} \left\langle \mathbf{\Psi^\dagger_{gg}(r,\alpha)\Psi_{gg}(r',\alpha)} \right\rangle \mathbf{\Sigma^{N(A)}_{3g}(r,r',\alpha,x_2)}$$

$$\Sigma^{N(A)}_{3g}(\vec{r},\vec{r}\,',\alpha,x_2) = \begin{cases} \sigma^N_{3g}(r,\alpha)+\sigma^N_{3g}(r',\alpha)-\sigma^N_{3g}(\vec{r}-\vec{r}\,',\alpha); & \textbf{(pp)} \\ 2\int d^2b\left[1-e^{-\frac{1}{2}\sigma^N_{3g}(r,\alpha)T_A(b)}e^{-\frac{1}{2}\sigma^N_{3g}(r',\alpha)T_A(b)}+e^{-\frac{1}{2}\sigma^N_{3g}(\vec{r}-\vec{r}\,',\alpha)T_A(b)}\right] & \textbf{(pA)} \end{cases}$$

$$\sigma^N_{3g}(r,\alpha) = \frac{9}{8}\Big\{\sigma_{\bar{q}q}(r)+\sigma_{\bar{q}q}(\alpha r)+\sigma_{\bar{q}q}[(1-\alpha)r]\Big\}$$

$$\Psi_{gg}(\vec{r},\alpha) = \frac{\sqrt{8\alpha_s}}{\pi\, r^2}\exp\left[-\frac{r^2}{2\,r_0^2}\right]\left[\alpha(\vec{e}^{\,*}_1\cdot\vec{e})(\vec{e}^{\,*}_2\cdot\vec{r})(1-\alpha)(\vec{e}^{\,*}_2\cdot\vec{e})(\vec{e}^{\,*}_1\cdot\vec{r})-\alpha(1-\alpha)(\vec{e}^{\,*}_1\cdot\vec{e}^{\,*}_2)(\vec{e}\cdot\vec{r})\right]$$

$\mathbf{r_0 \approx 0.3fm}$

$$\left\langle \Psi^\dagger_{gg}(\vec{r})\Psi_{gg}(\vec{r}\,') \right\rangle = \frac{4\alpha_s}{\pi^2}\,\frac{\vec{r}\cdot\vec{r}\,'}{r^2\,r'^2}\exp\left[-\frac{r^2+r'^2}{2\,r_0^2}\right]\left[1+\alpha^4+(1-\alpha)^4\right]$$

$$\frac{d^2\sigma(pN(A)\to hX)}{d^2p_T\,dy} = \int_{z_{min}}^{1} \frac{dz}{z^2} D_{h/g}(z,k_T^2) \int_{x_{min}}^{1} dx_1\, g(x_1,k_T^2) \frac{d^2\sigma^{N(A)}_{g\to 2g}(\alpha,x_2)}{d^2k_T\,dy}$$

$$k_T = p_T/z$$

$$z_{min} = \frac{p_T}{\sqrt{s}} e^y\,; \qquad x_{min} = z_{min}/z\,;$$

$$\alpha = \frac{p_T\, e^y}{x_1 z \sqrt{s}}$$

$$x_2 = \frac{p_T^2}{x_1 z^2\, \alpha(1-\alpha) s}$$

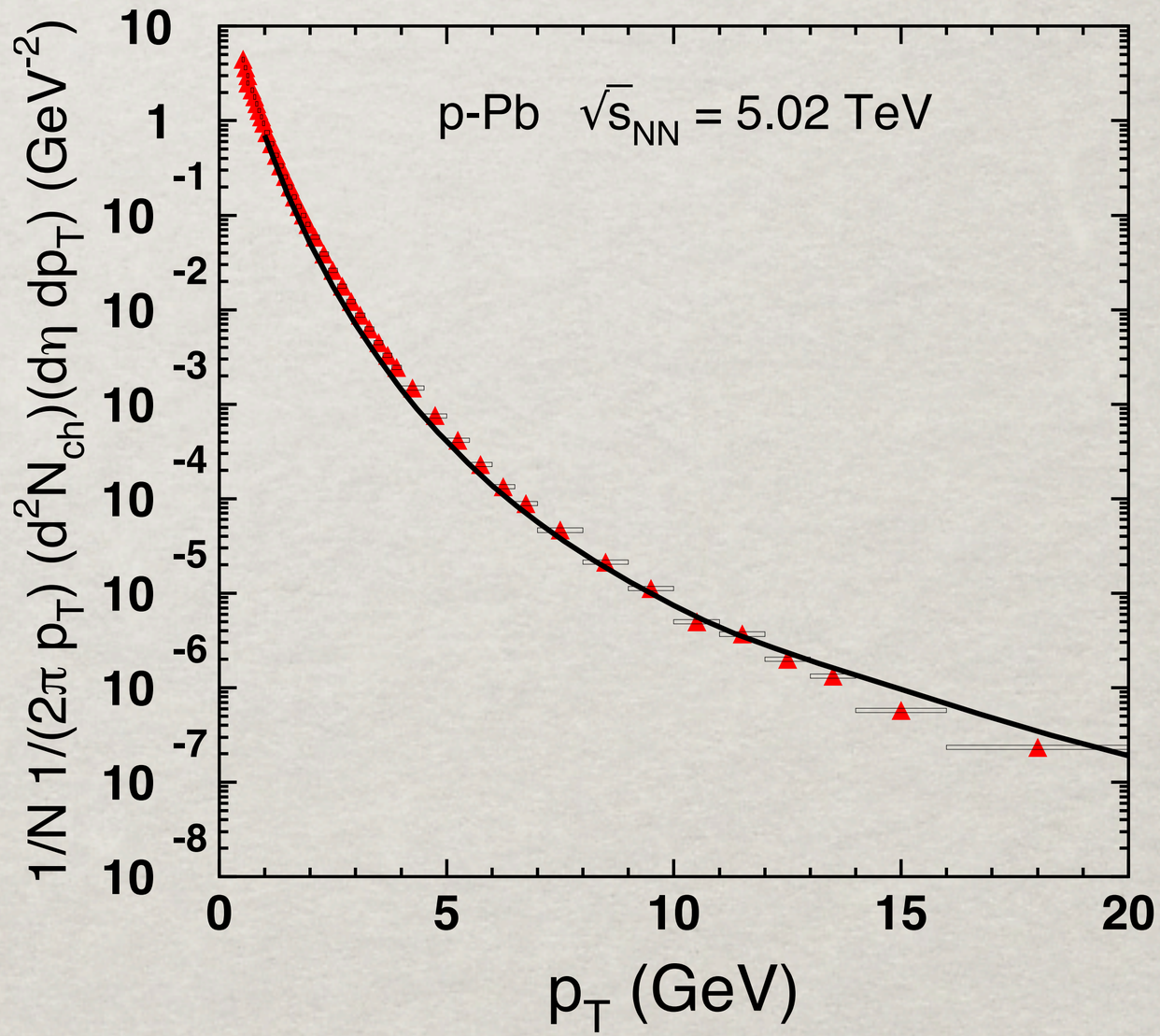

Weakness of gluon shadowing

Gluon shadowing is a part of the Gribov inelastic corrections related to the triple-Pomeron term in diffraction.

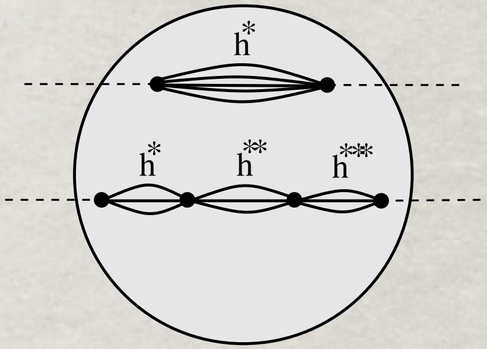

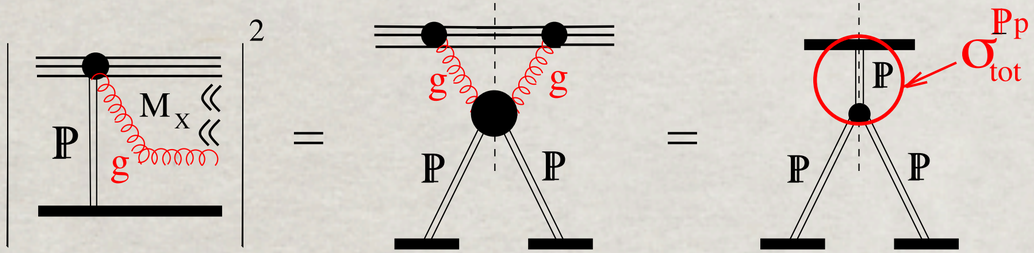

expected: $\sigma_{\mathbf{tot}}^{\mathbf{Pp}} \sim 50\,\mathrm{mb}$

measured: $\sigma_{\mathbf{tot}}^{\mathbf{Pp}} \lesssim 2\,\mathrm{mb}\,!!!$

Smallness of the diffractive cross section means weakness of gluon shadowing.

In terms of pQCD this shows a suppression of diffractive gluon radiation, which can only be related to smallness of gluonic dipoles.

Gluon shadowing from DIS

Gluon shadowing in DIS correspond to inclusion of the higher Fock components of the photon, $\gamma^* \to \bar{q}q + g$, B.K., A.Schaefer, A.Tarasov,1999 .

Gluon PDFs in DIS are probed via the DGLAP evolution from the Q^2 dependence of $F_2(x, Q^2)$
So far only the NMC experiment managed to detect a variation of the nuclear PDF with Q^2

B.K., A.Schaefer, A.Tarasov,1999 (KST)

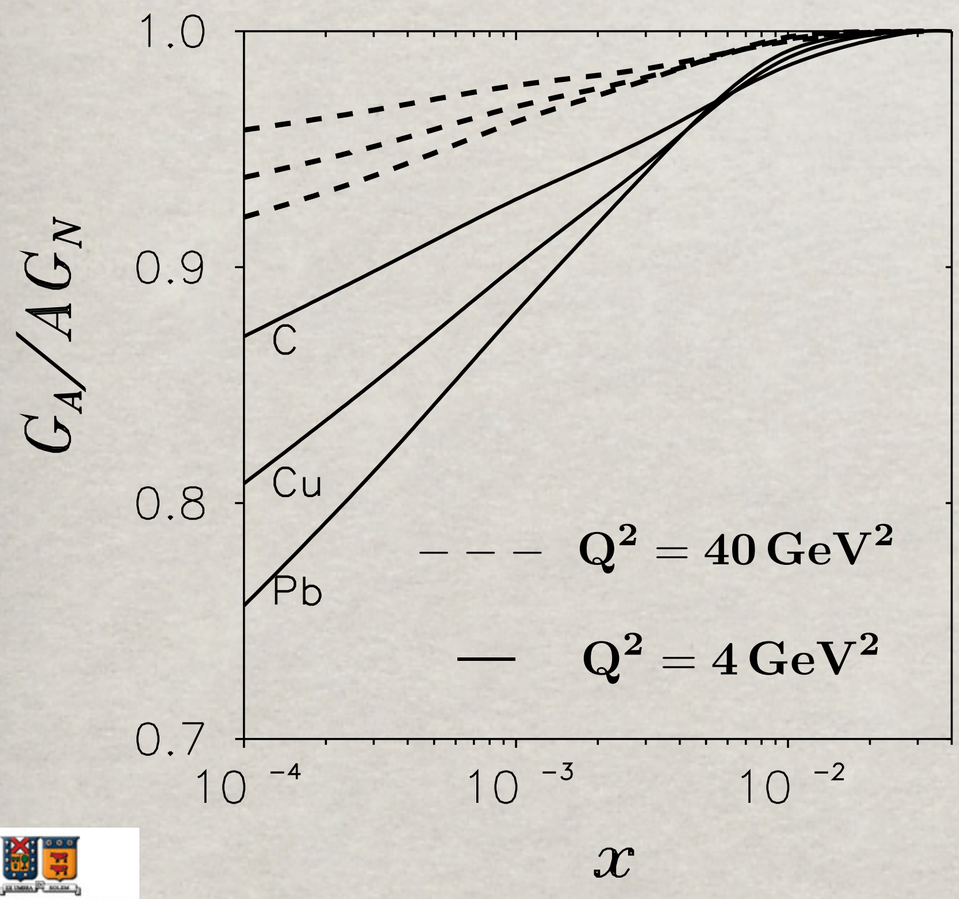

D.de Florian, R.Sassot, 2004 (DS)

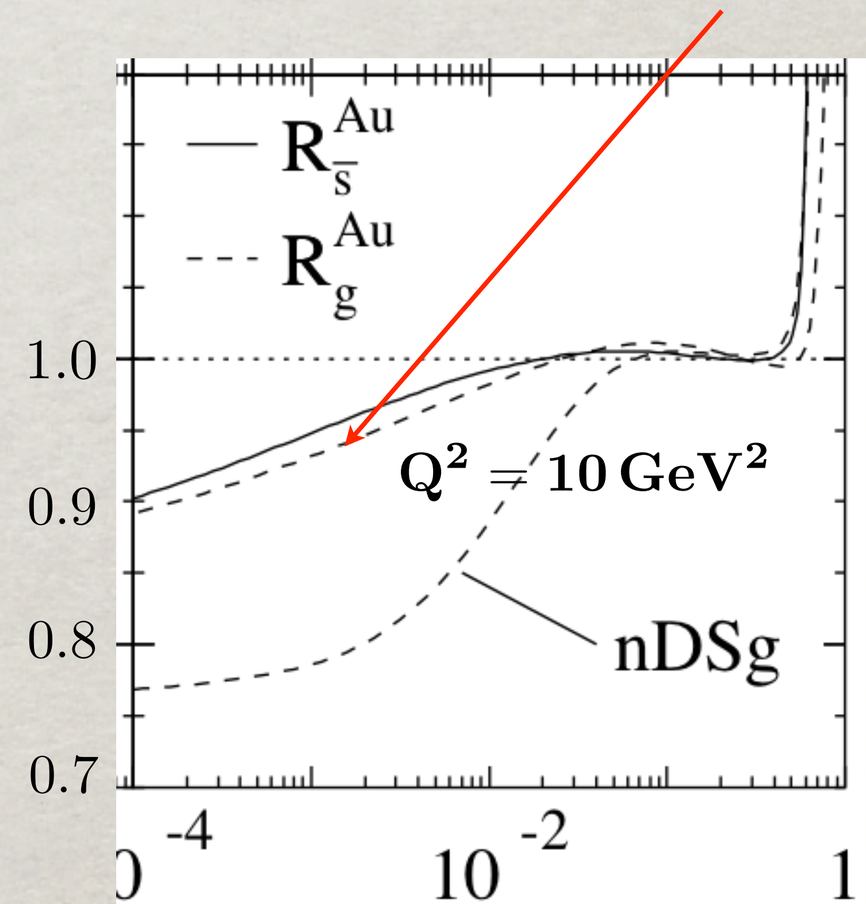

Two-scale hadronic structure

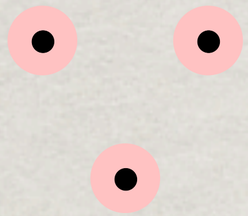

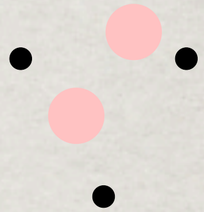

B.K., A.Schafer, A.Tarasov(1999):
the valence quarks carry small size gluon clouds, $r_0 \approx 0.3\mathrm{fm}$

Shuryak & Zakhed (2004):
gluonic spots of small size, $r_0 \approx 0.3\mathrm{fm}$ are floating in the proton.

Small gluonic spots ==> weak gluon shadowing:

$$\left.\frac{G_A(x)}{AG_N(x)}\right|_{x\ll 1} = \frac{2}{\langle\sigma_{GG}(r)\rangle}\int d^2b\left[1-\left\langle e^{-\frac{1}{2}\sigma_{GG}(r)T_A(b)}\right\rangle\right] = 1-\frac{3C}{8}\,r_0^2\,\rho_A R_A + \ldots \approx 0.8$$

Even if small-x gluons overlap in the longitudinal direction, they can miss each other in transverse plane, if they are located within small spots. Indeed, for a heavy nucleus (lead) the mean number of gluonic spots overlapping with a given one is,

$$\langle n\rangle = \frac{3\pi}{4}\,r_0^2\,\langle T_A\rangle = \pi\,r_0^2\,\rho_A\,R_A = 0.3$$

Evidences for two-scales

As far as gluon radiation is suppressed, hadronic cross sections should rise slowly with energy. Indeed, the observed energy dependence of the total **pp** cross section is well described [B.K., I.Potashnikova, E.Predazzi, B.Povh, PRL 85(2000)507]

$$\sigma_{tot} = \sigma_0 + \sigma_1 \left(\frac{s}{s_0}\right)^{\Delta}$$

$$\Delta = \frac{4\alpha_s}{3\pi} = 0.17$$

$$\sigma_1 = \frac{27}{4} C\, r_0^2$$

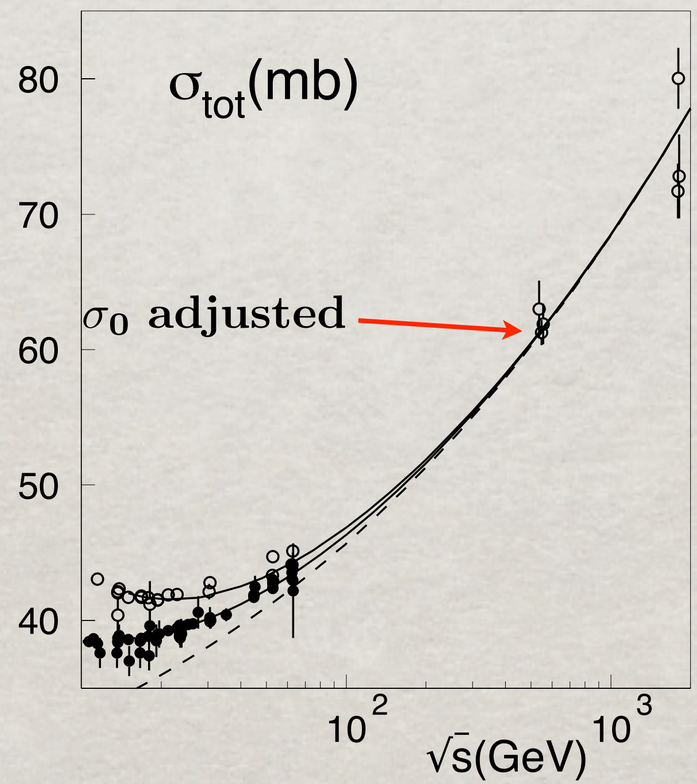

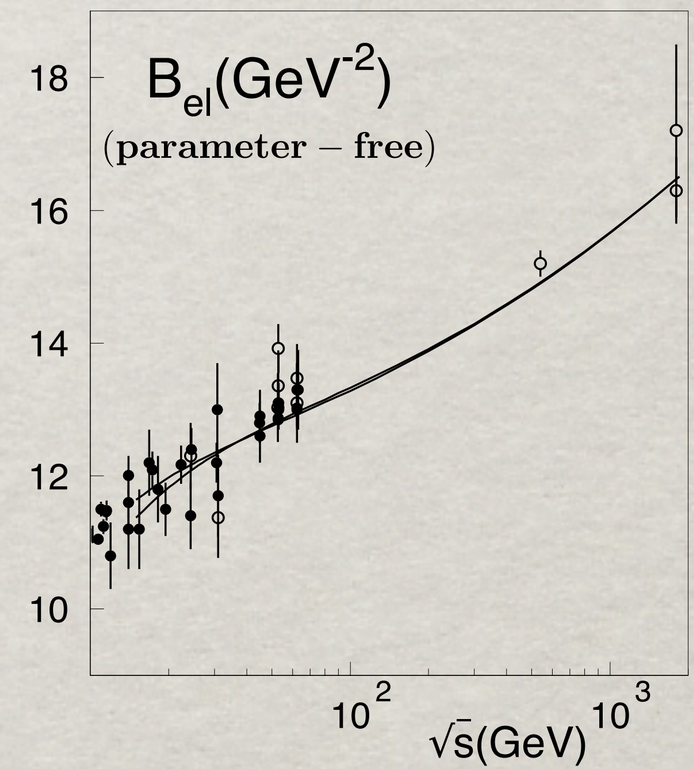

Evidences for two-scales

B.K., I.Potashnikova, B.Povh, E.Predazzi (2000)

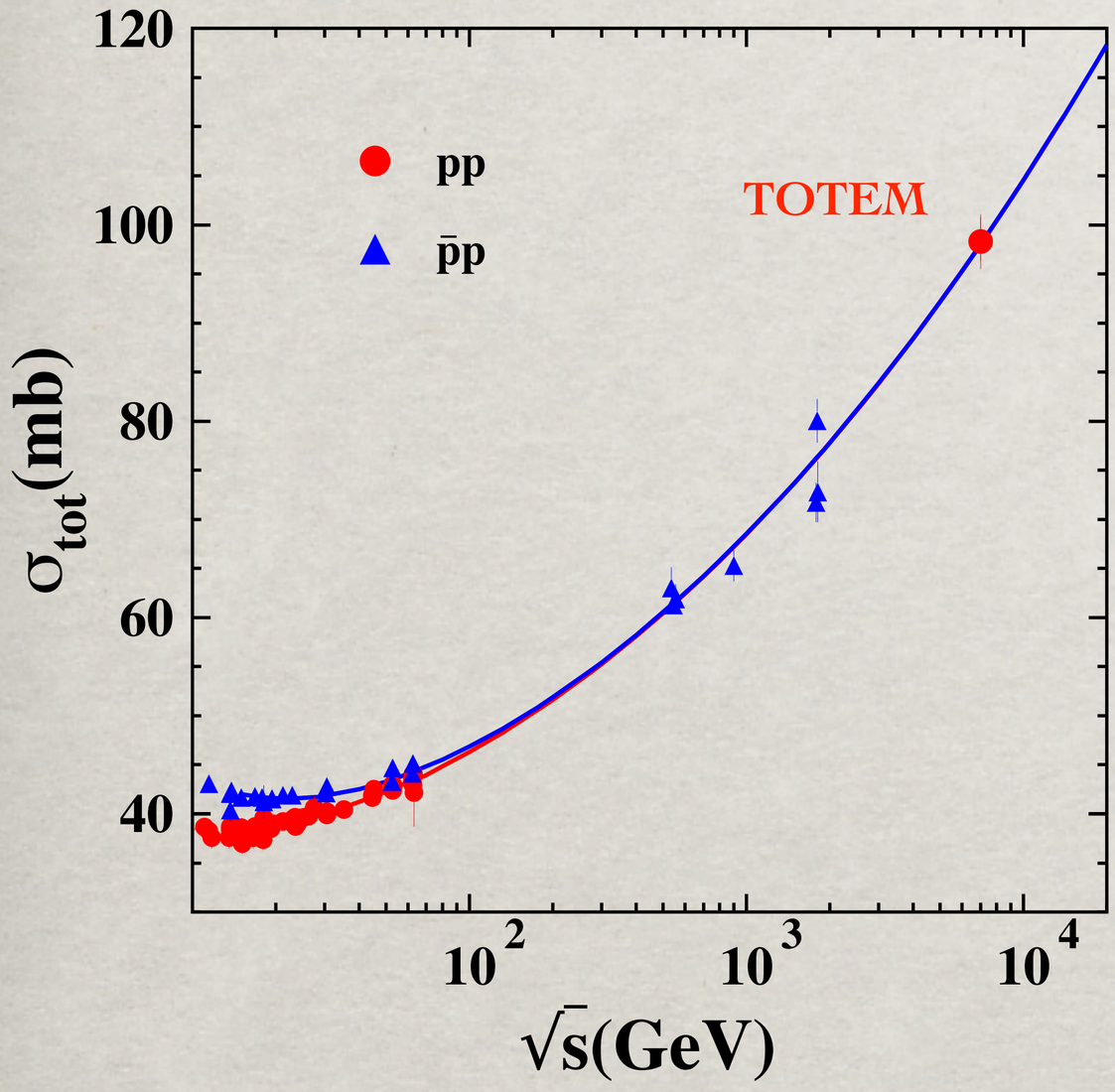

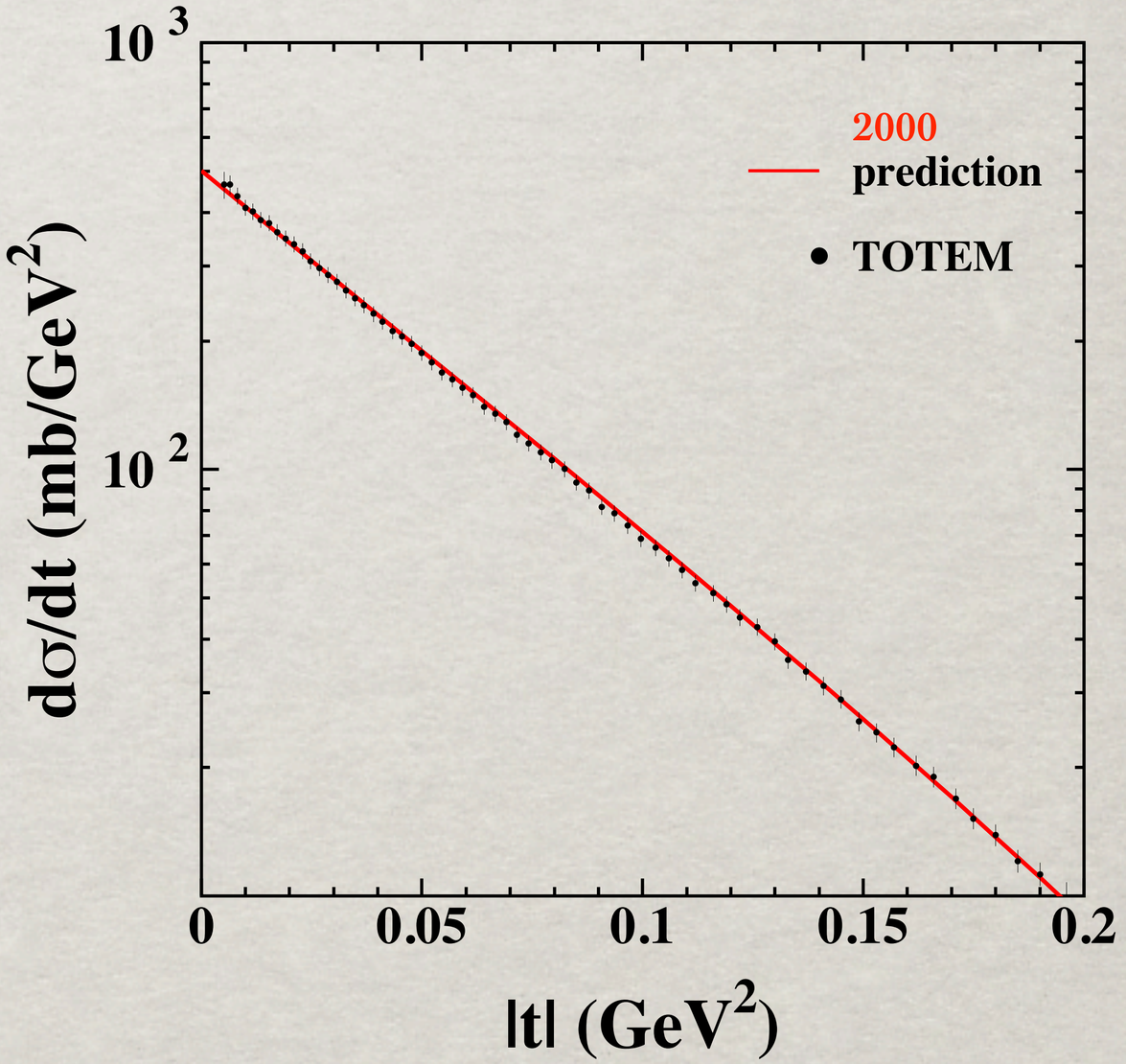

B.K., I.Potashnikova, B.Povh (2012)

Improved predictions

With the same 2002 computer code, but using a contemporary versions of the unintegrated gluon distribution (KMR) one can improve the shape of pT-dependence.

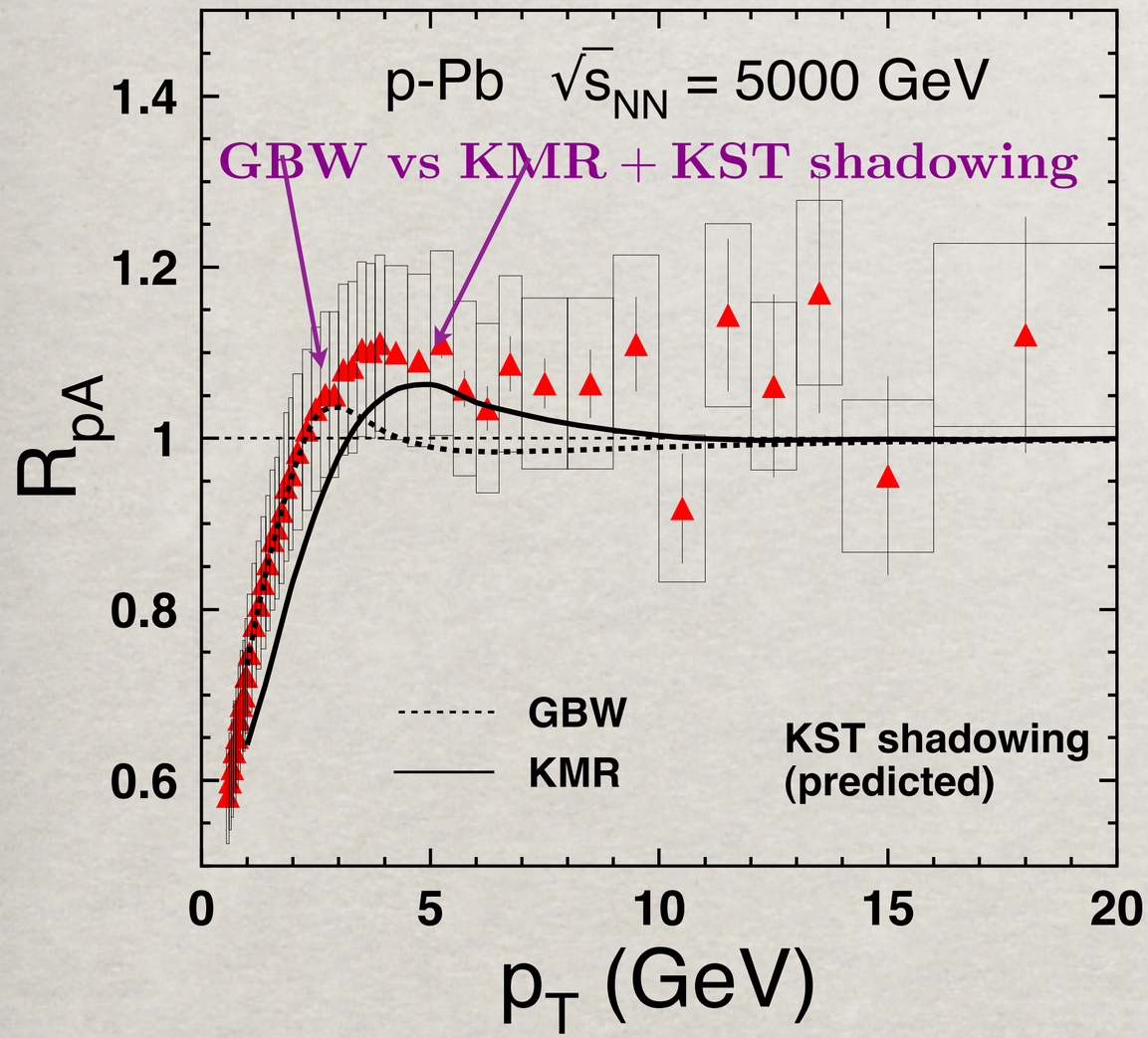

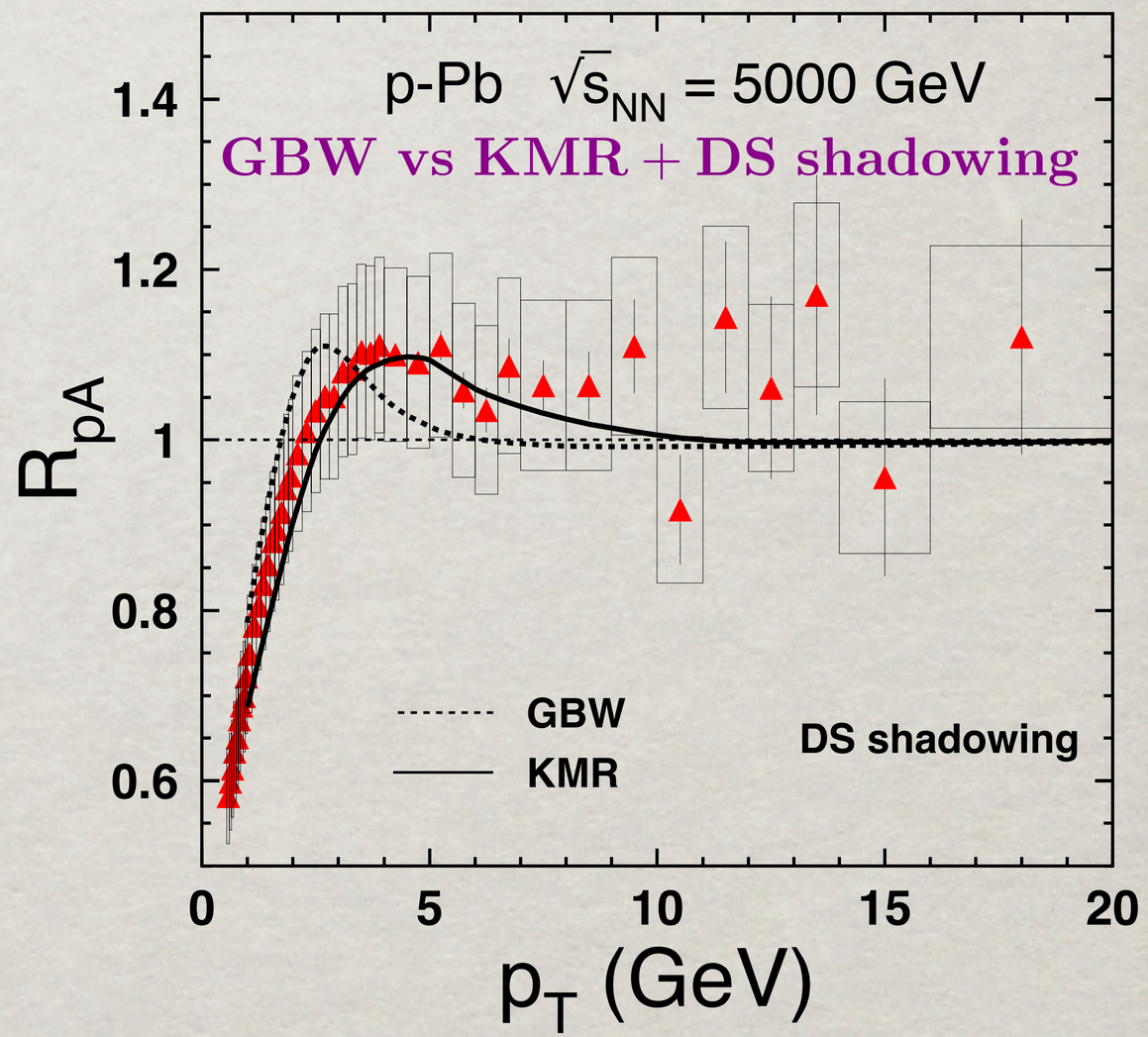

POSTDICTIONS: Further improvements

- A better choice of the scale for gluon shadowung.

$$Q^2 = \frac{4}{xg(x, k_T^2)} \int dq^2 \, \mathcal{F}_g(x, q, k_T^2)$$

- Alternative parametrizations for the dipole cross section:

J.Bartels, K.J.Golec-Biernat & H.Kowalsky, 2002 (BGBK)

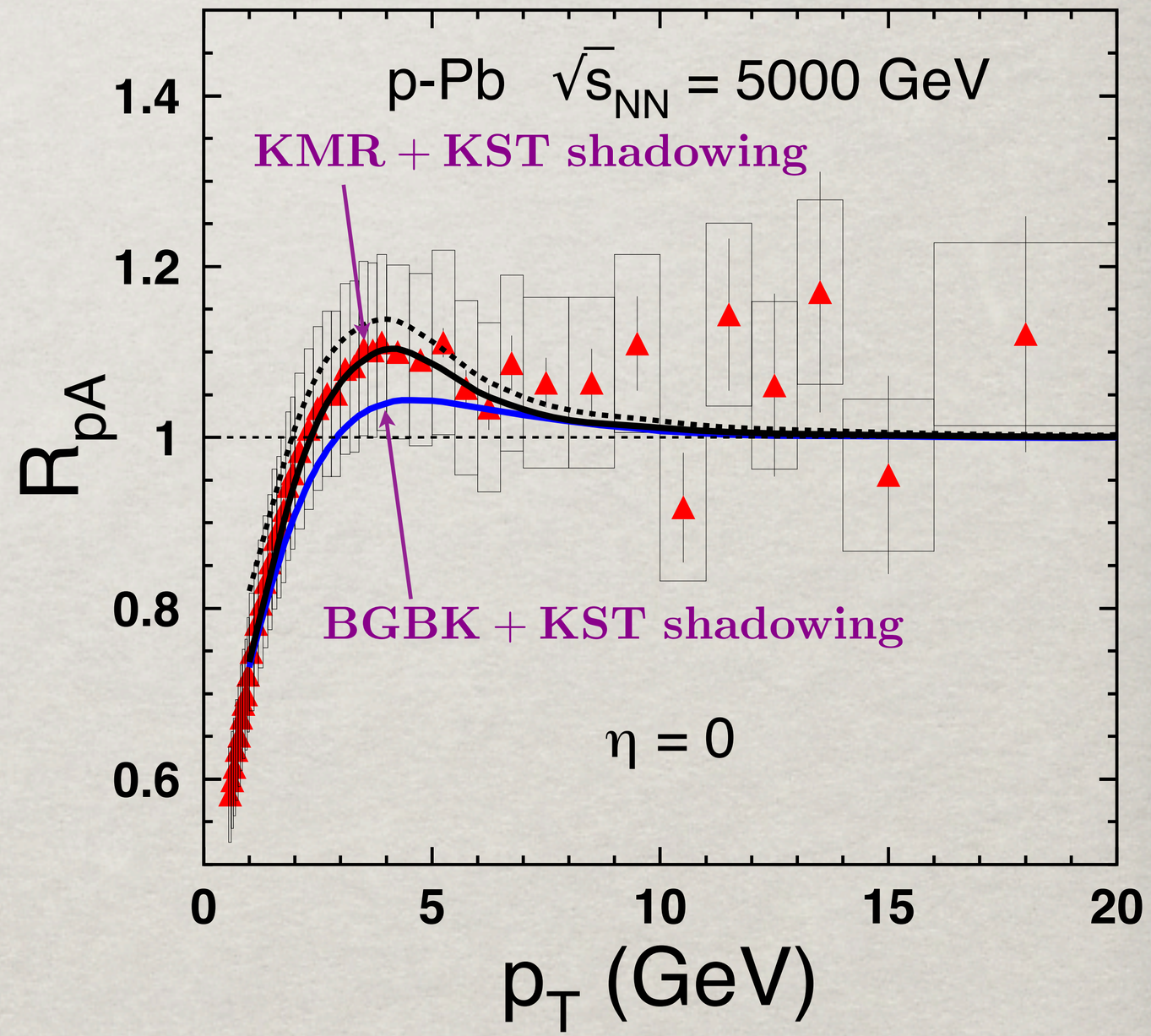

UNIVERSIDAD TECNICA FEDERICO SANTA MARIA

Toward the kinematic bound

Smallest x2 are reached at forward rapidities. This is why it was tempting to interpret the suppression observed at forward rapidities by BRAHMS and STAR, as a result of coherence, CGC [D.Kharzeev, Yu.Kovchegov, K.Tuchin (2003)]

Initial-state energy loss suppresses particle production toward the kinematic limit x1->1 [B.K., J.Nemchik, I.Potashnikova, I.Schmidt (2005)]

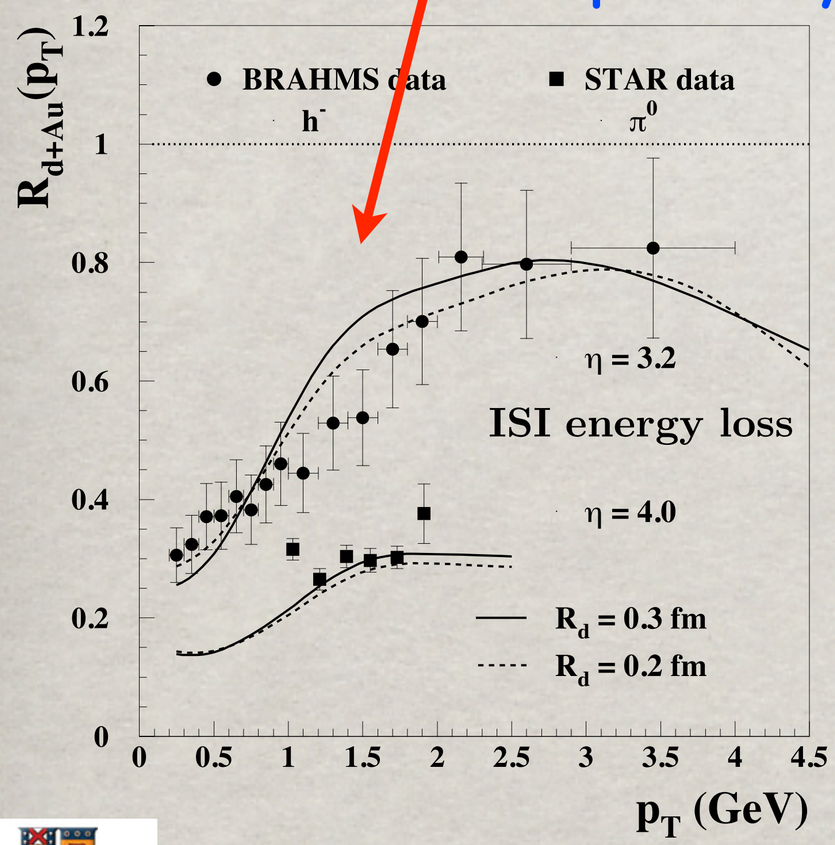

A possibility to settle this controversy would be to go to higher energies and check with the nuclear effects at the same x2, but further away from the kinematic limit (see LHC data below).

One also approaches the kinematic limit at the mid rapidity, but high pT.

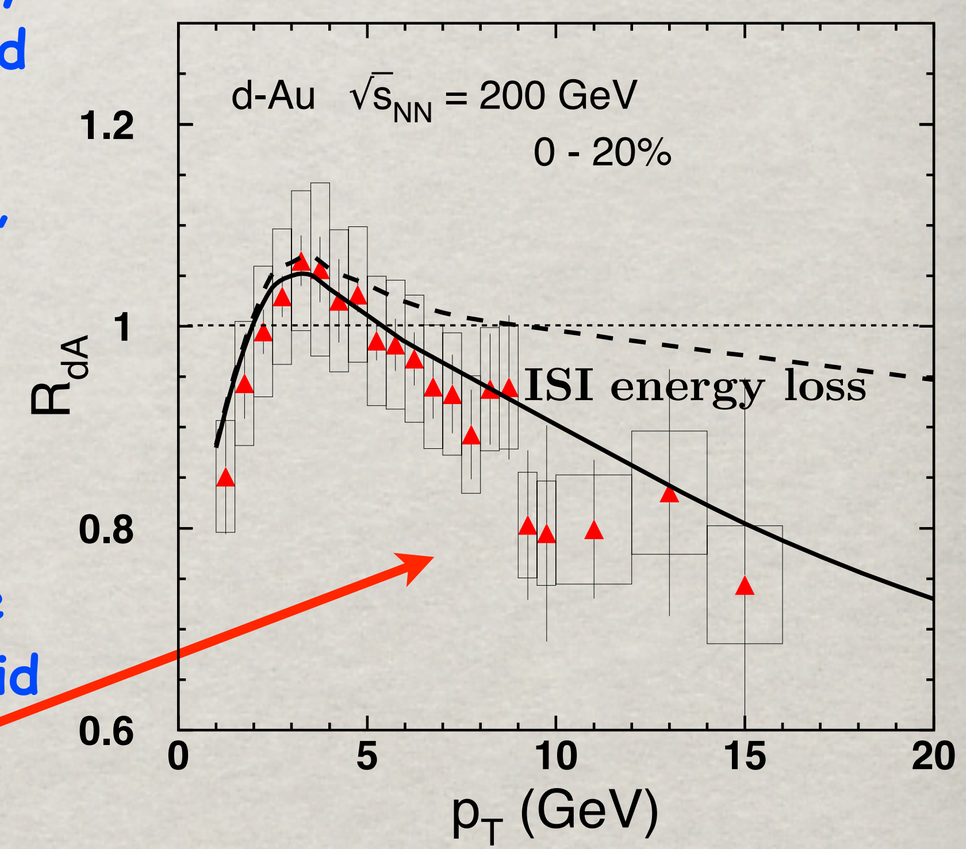

Lower energies - larger xT

Suppression of high-pT hadrons by ISI E-loss in AA collisions at RHIC

B.K., J.Nemchik, I.Potashnikova, I.Schmidt, PRC86(20012)054904

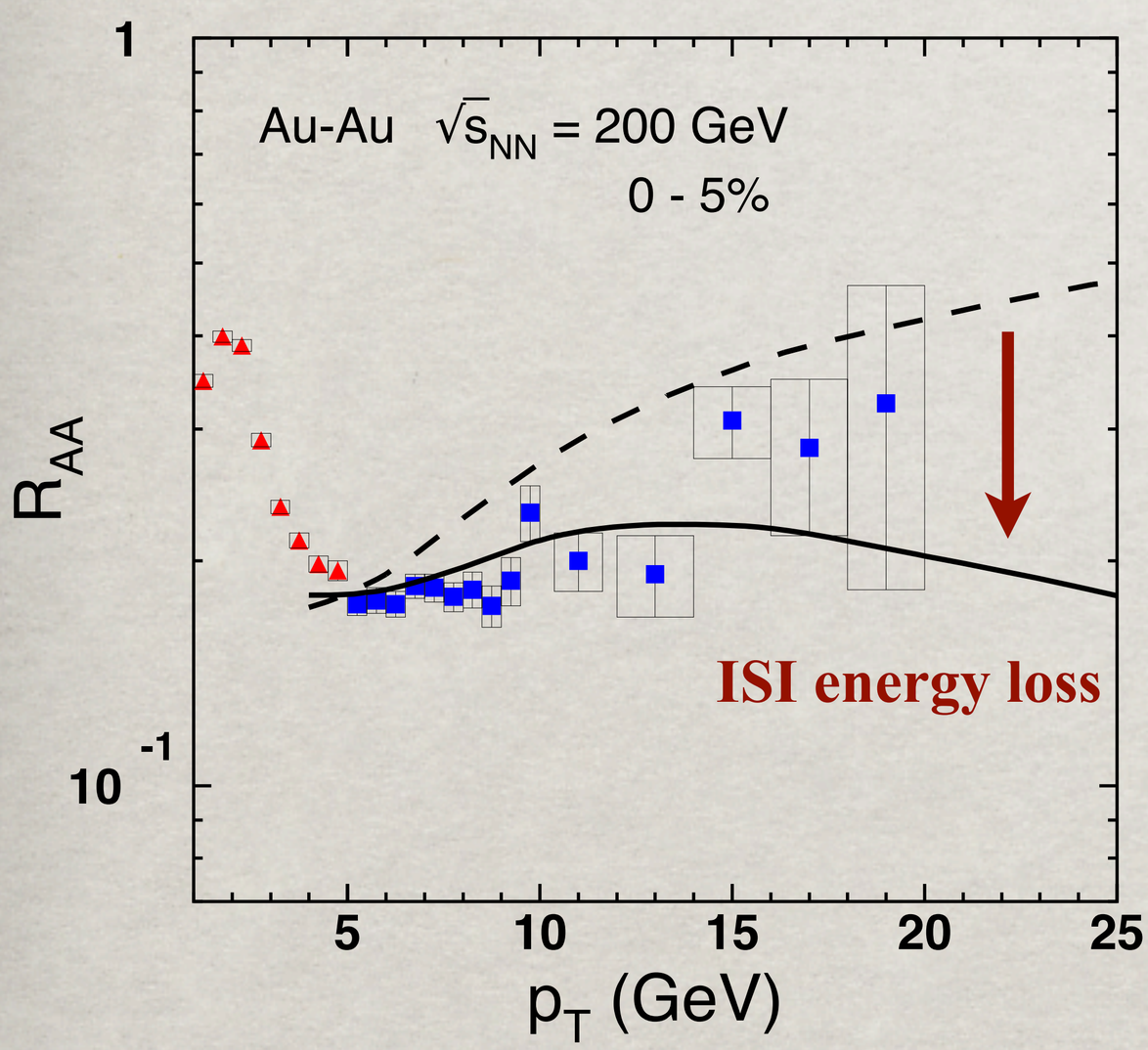

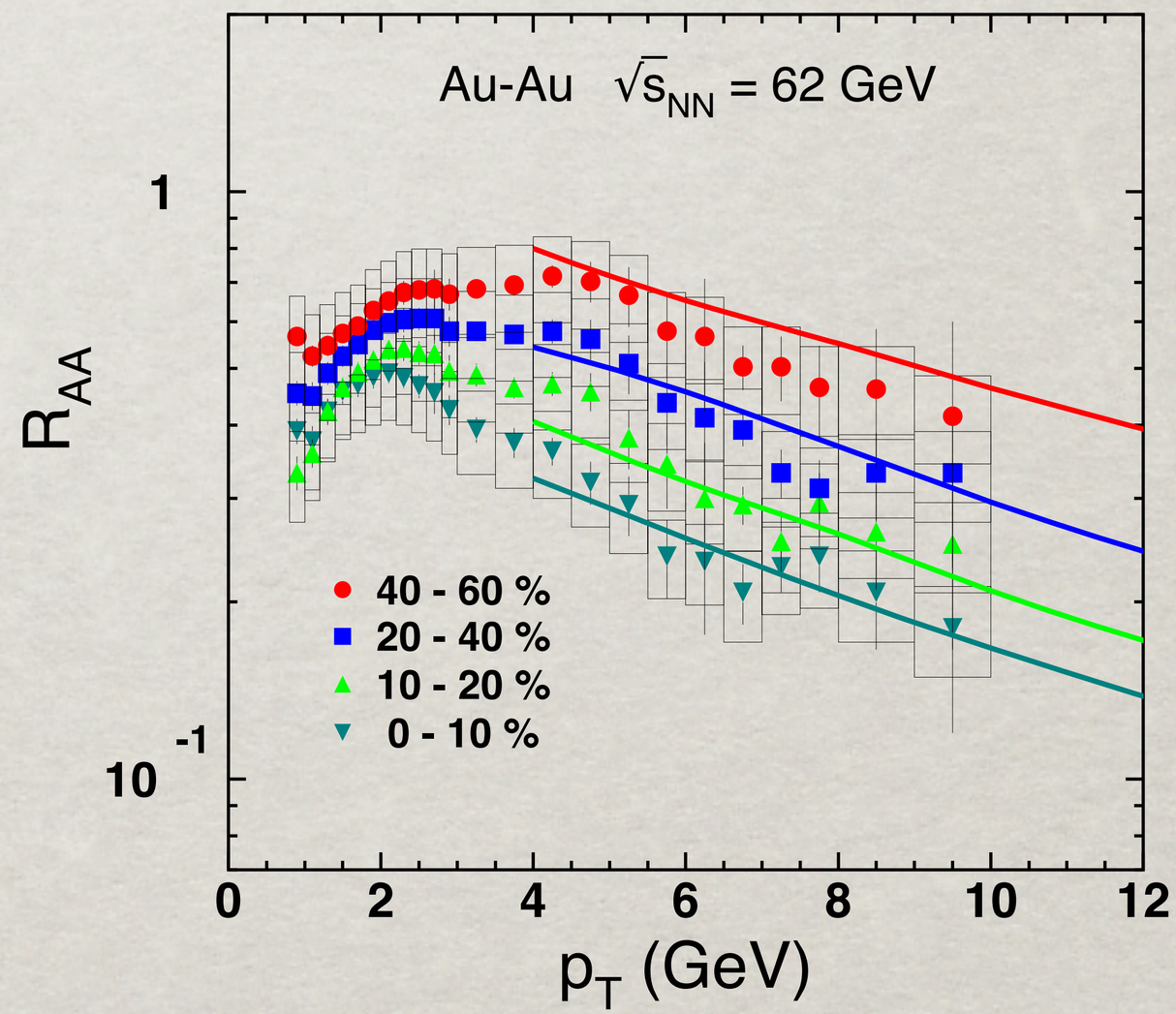

UNIVERSIDAD TECNICA FEDERICO SANTA MARIA

Cronin effect at forward rapidities

One can enhance the role of ISI energy loss either moving to forward rapidities, or higher pT, or both

····· no shadowing

----- KST shadowing

——— ISI E-loss added

KMR unintegrated gluon density

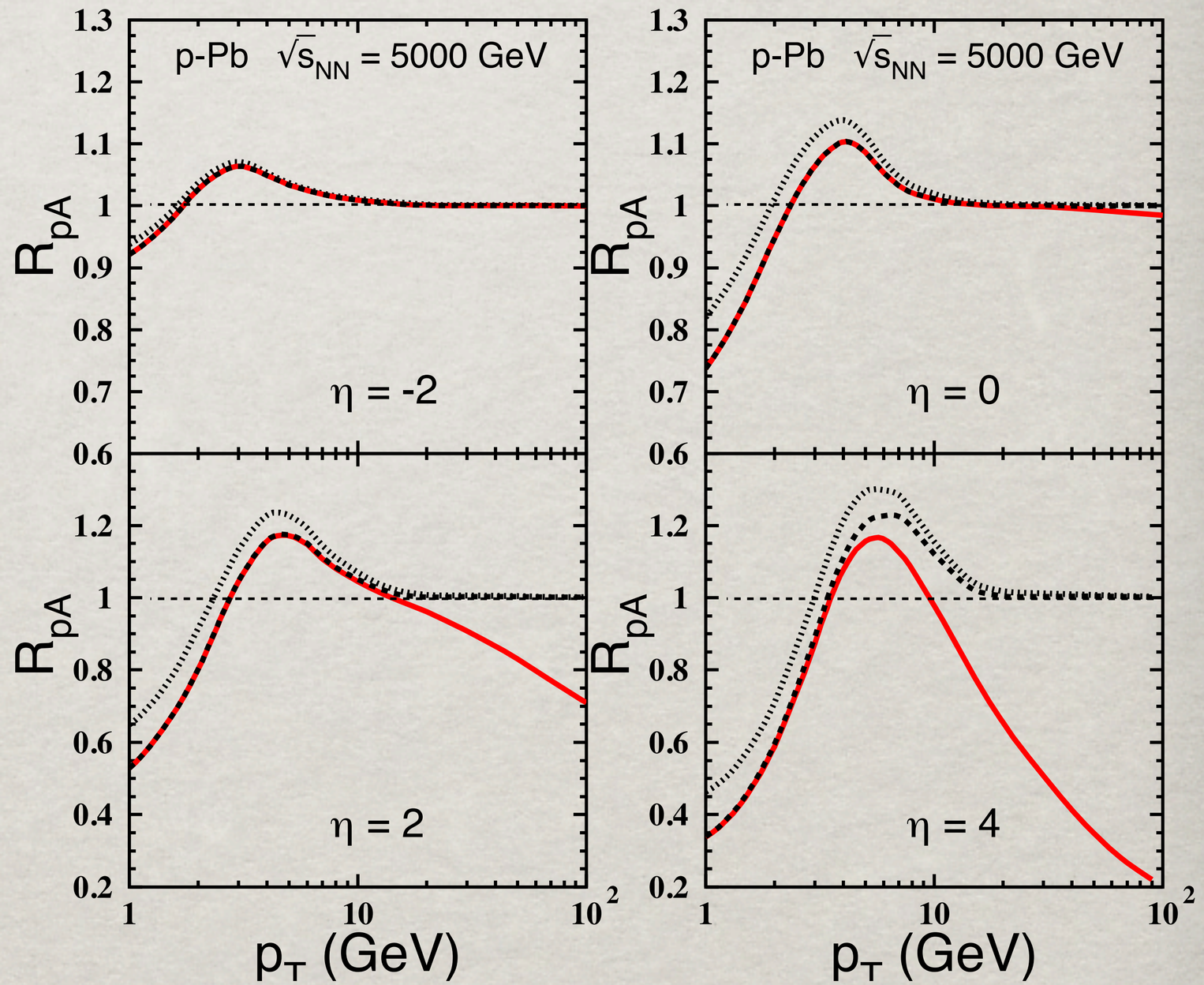

UNIVERSIDAD TECNICA FEDERICO SANTA MARIA

Summarizing,

For the first time high-pT hadrons can be produced in pA coherently. Data for the Cronin effect at LHC provide a strong support for the two-scale hadronic structure and weak gluon shadowing. Many popular models are "ruled out".

The magnitude of the Cronin enhancement predicted in 2002 was correct, while the shape of the pT dependence can be improved applying more realistic up-to-date phenomenology.

Initial state energy loss is expected to suppress significantly inclusive hadron production at large pT and/or at forward rapidities in pA, as well as in AA collisions.

BACKUPS

In order to study the sensitivity of different observables on the amount of shadowing in the nuclear gluon distribution, we have performed an alternative extraction of nPDF from the same data set but constraining the gluon density in heavy nuclei to show a stronger shadowing effect at small x_N. We provide the result in set called nDSg, constrained to satisfy $R_g^{Au} = 0.75$ at $x_N = 0.001$ and $Q^2 = 5$. The χ^2 value of this analysis is around 550, considerably larger than the *unconstrained* fit, and should be considered only as a mean to study variations on, mainly, the gluon nuclear distribution. An example

Long-Range Rapidity Correlations in Heavy-Light Ion Collisions

Yuri V. Kovchegov
The Ohio State University

based on arXiv:1212.1195 [hep-ph]
with Douglas Wertepny

Outline

- Long-range rapidity correlations in hadronic and nuclear collisions: general discussion
- Two-gluon production in heavy-light ion collisions:
  - Geometric correlations
  - Long-range rapidity correlations
  - Perturbative HBT correlations
- Conclusions

Introduction to saturation physics

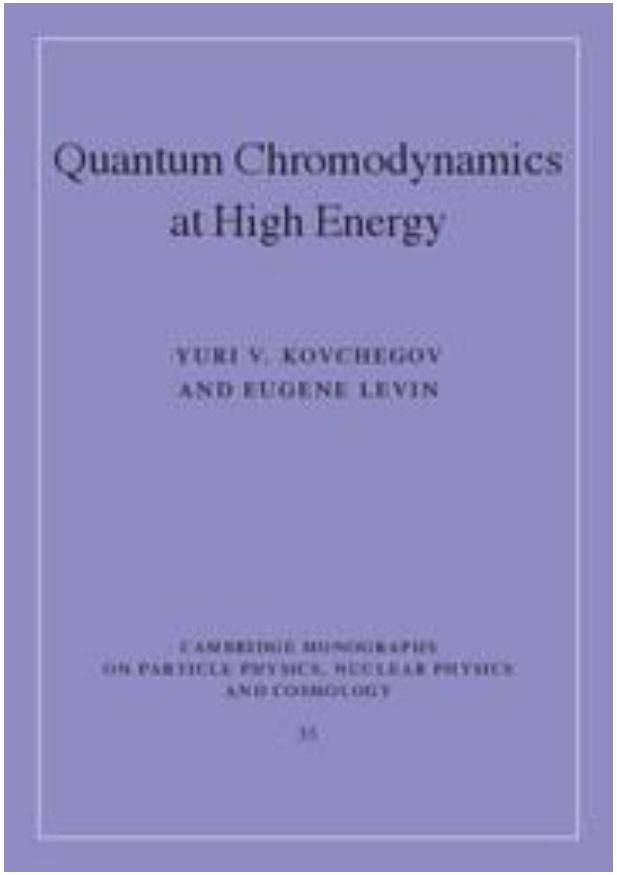

Published in September 2012
by Cambridge U Press

Long-range rapidity correlations

Ridge in heavy ion collisions

- Heavy ion collisions, along with high-multiplicity p+p and p+A collisions, are known to have long-range rapidity correlations, known as ‘the ridge’:

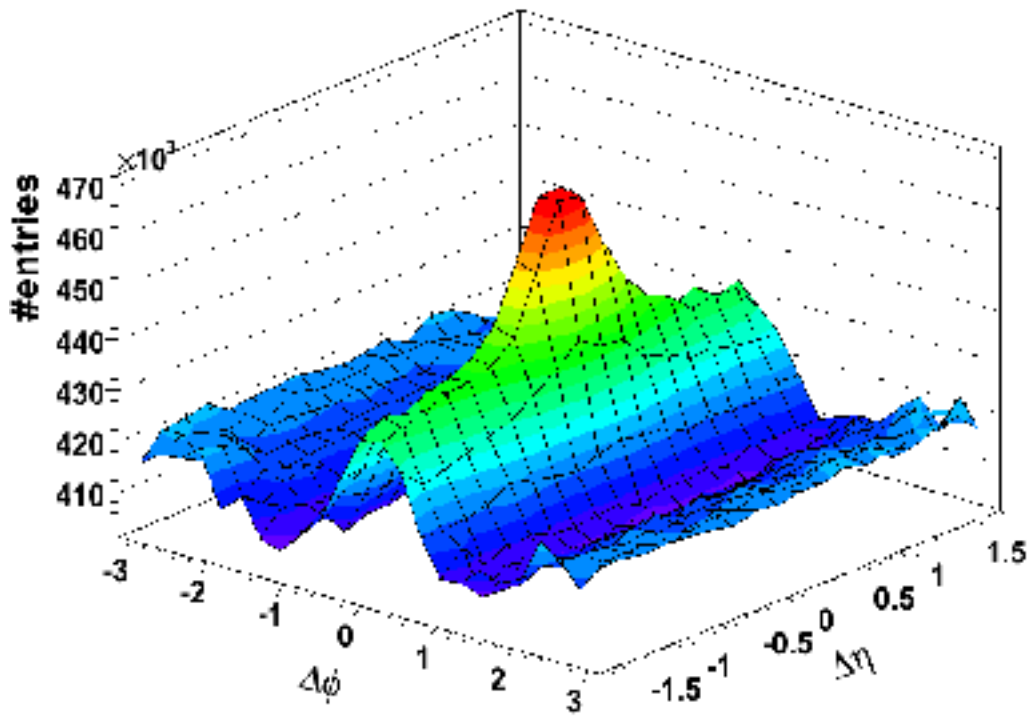

Origin of rapidity correlations

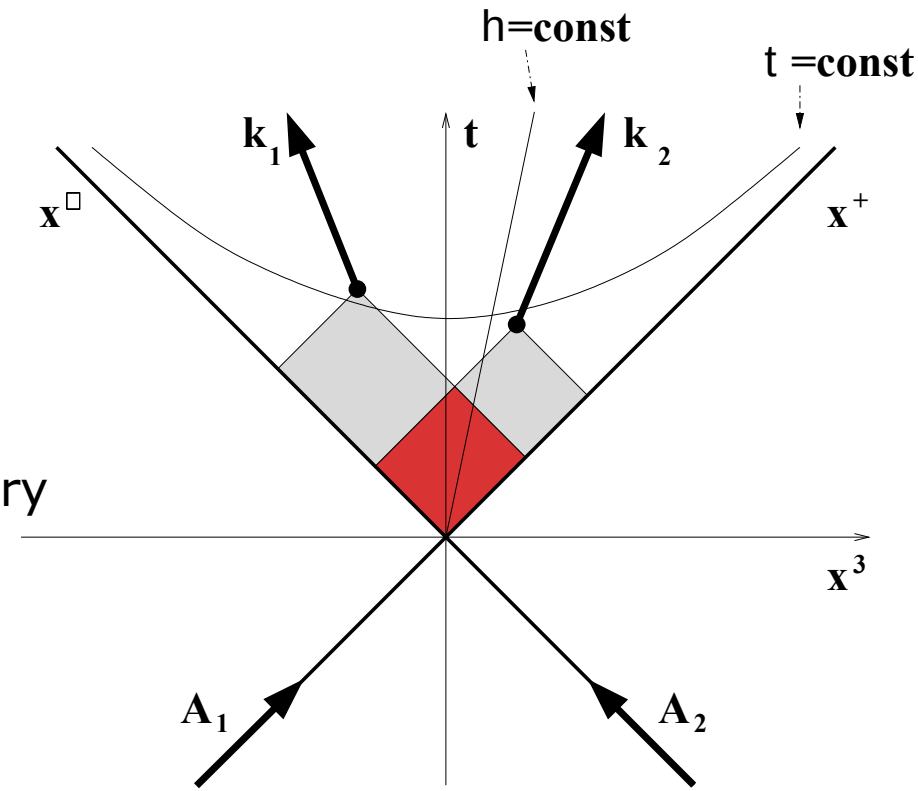

Causality demands that long-range rapidity correlations originate at very early times (cf. explanation of the CMB homogeneity in the Universe)

Gavin, McLerran, Moschelli '08;
Dumitru, Gelis, McLerran, Venugopalan '08.

Correlations in AdS shock wave collisions

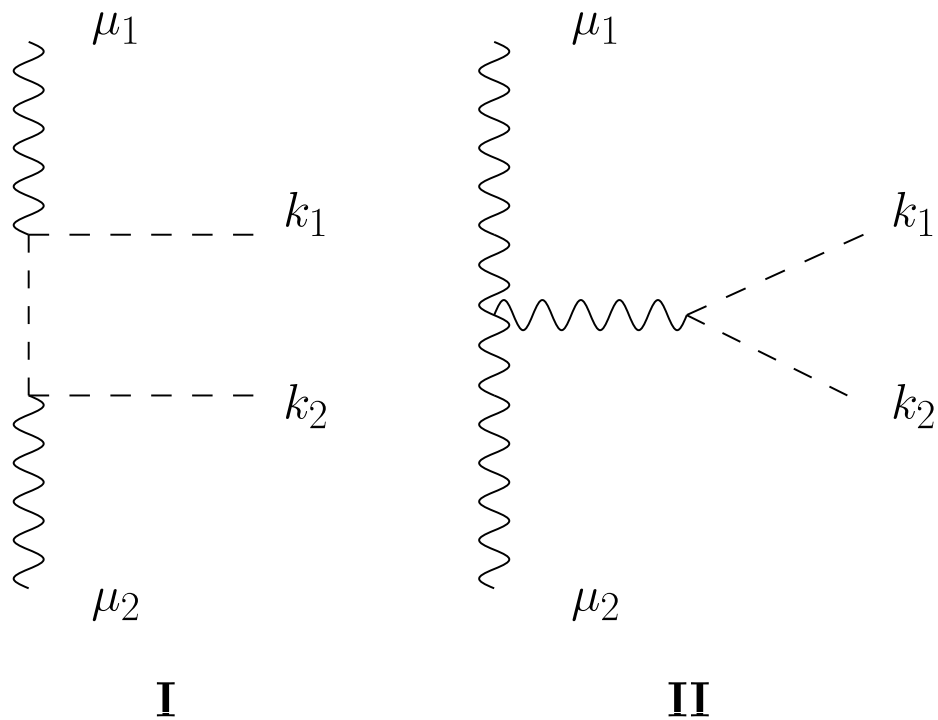

$$C(k_1, k_2) \sim \cosh(4\,\Delta y)$$

H. Grigoryan, Yu.K. ‘10

Correlations in AdS shock wave collisions

$$C(k_1, k_2) \sim \cosh(4\,\Delta y)$$

- Correlations grow with rapidity interval???
- It is possible that higher-order corrections in shock wave strengths will modify this result, making it closer to real life.
- However, such corrections are important at later times, and are less likely to affect the long-range rapidity correlation…
- This could be another argument in favor of weakly-coupled dynamics in the early stages of heavy ion collisions.

Ridge in CGC

- There are two explanations of the ridge in CGC:
  - Long-range rapidity-independent fields are created at early times, with correlations generated soon after and with azimuthal collimation produced by radial hydro flow. (Gavin, McLerran, Moschelli ’08)
  - Both long-range rapidity correlations and the azimuthal correlations are created in the collision due to a particular class of diagrams referred to as the “Glasma graphs”.

Glasma graphs

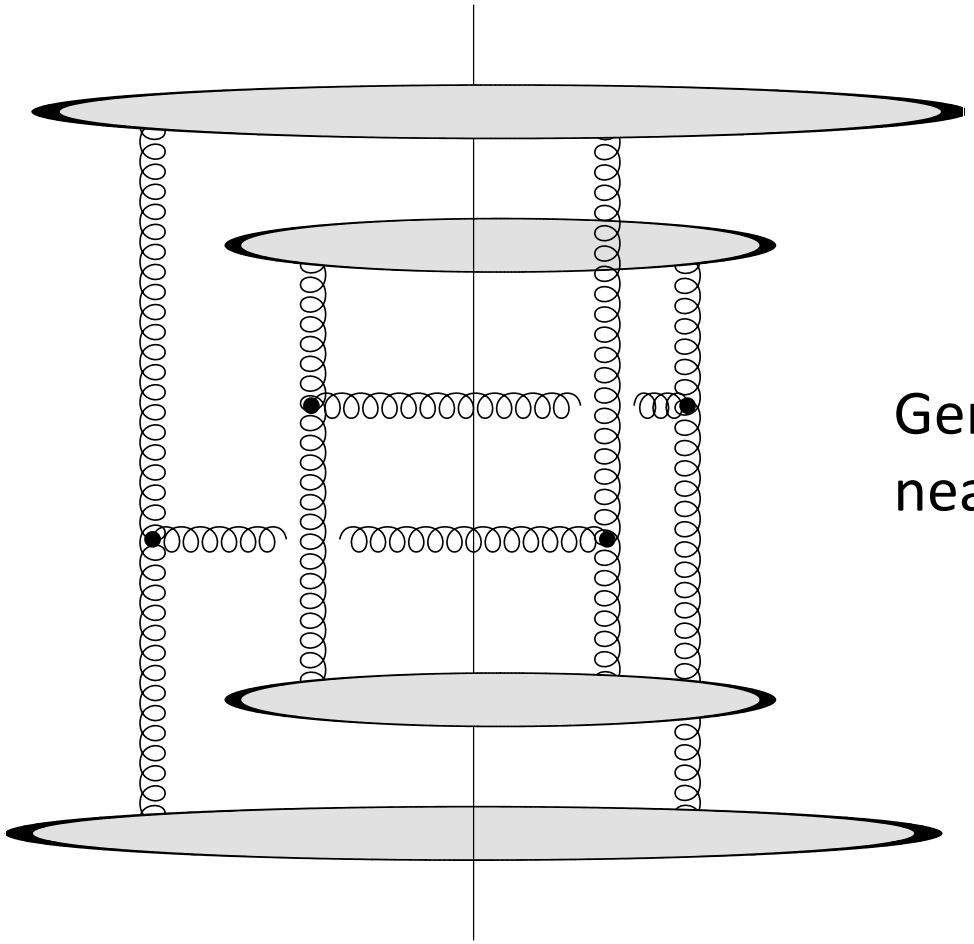

Generate back-to-back and near-side azimuthal correlations.

Dumitru, Gelis, McLerran, Venugopalan ‘08.

Glasma graphs in LC gauge

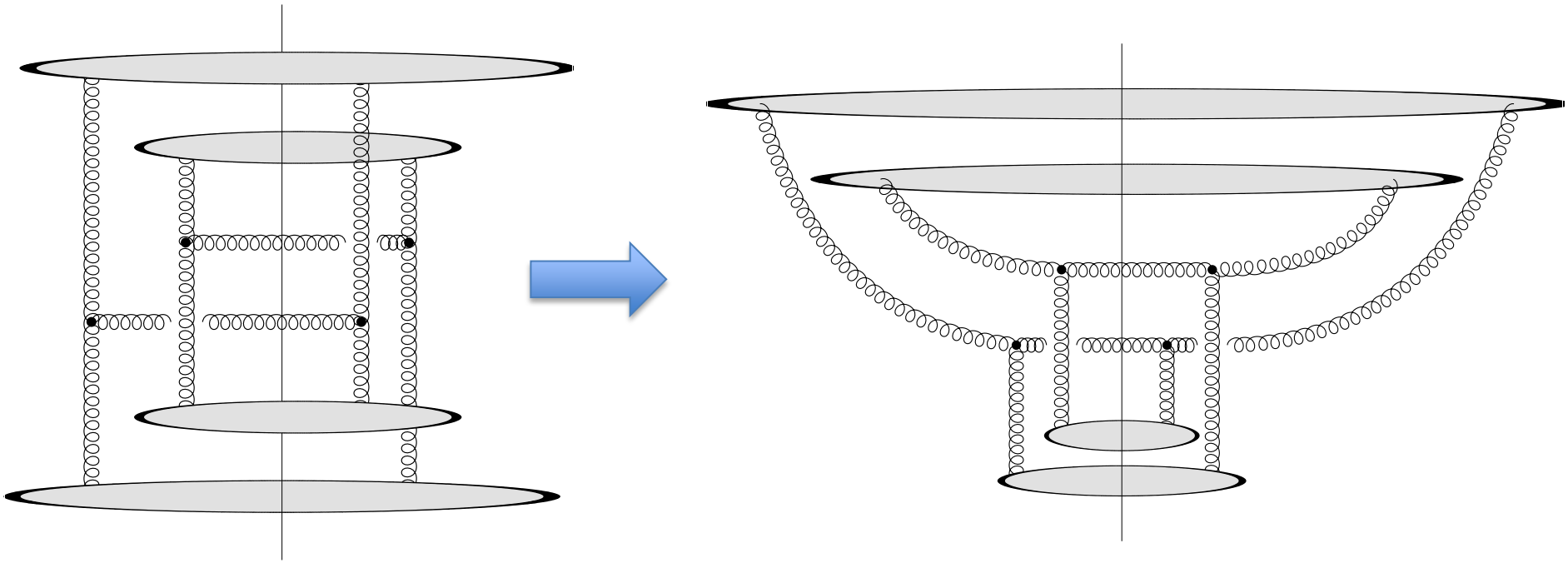

Glasma graphs are one of the many rescattering diagrams when two nucleons with a gluon each scatter on a nuclear target.

What to calculate?

- To systematically include Glasma graphs in the CGC formalism it would be great to solve the two-gluon inclusive production problem in the MV model, that is, including multiple rescatterings in both nuclei to all orders (the two produced gluons only talk to each other through sources):

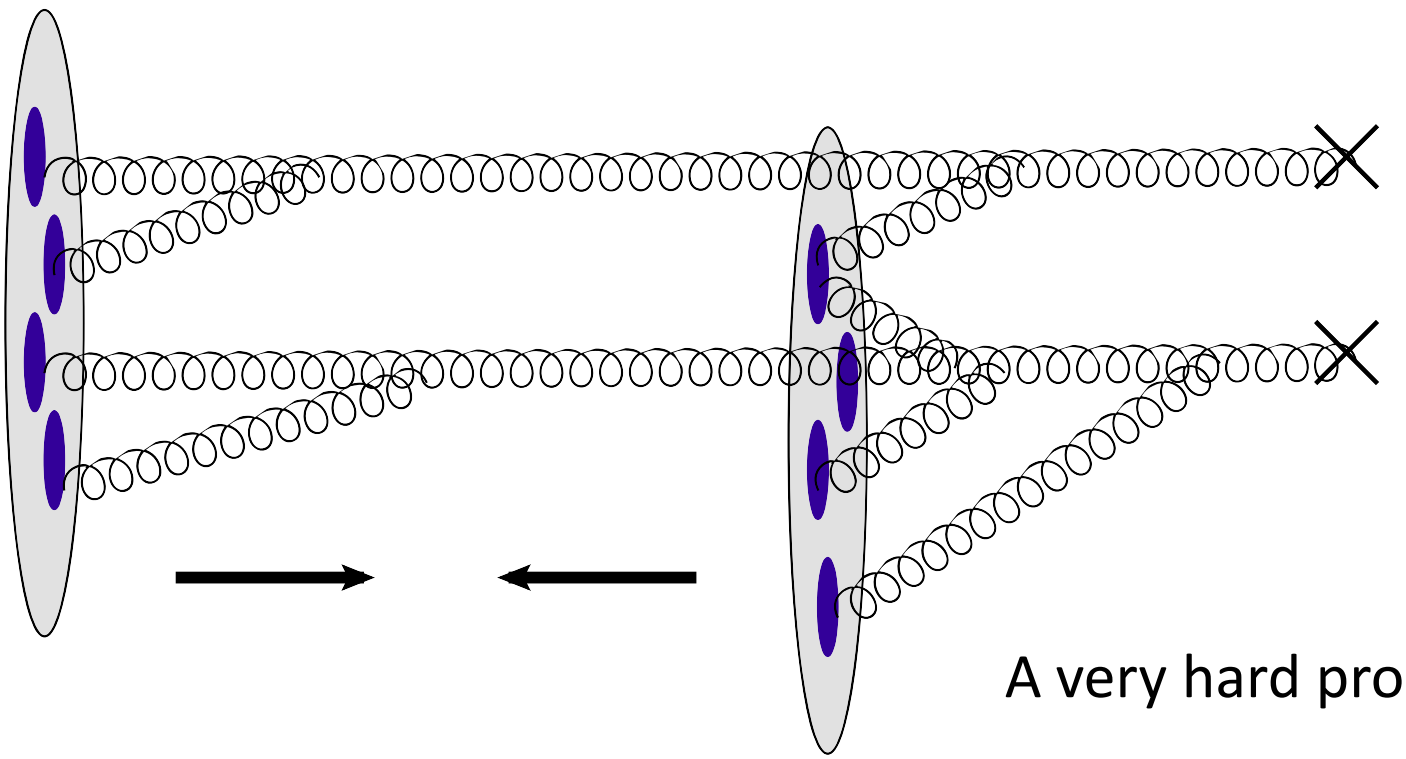

A very hard problem!

Heavy-Light Ion Collisions

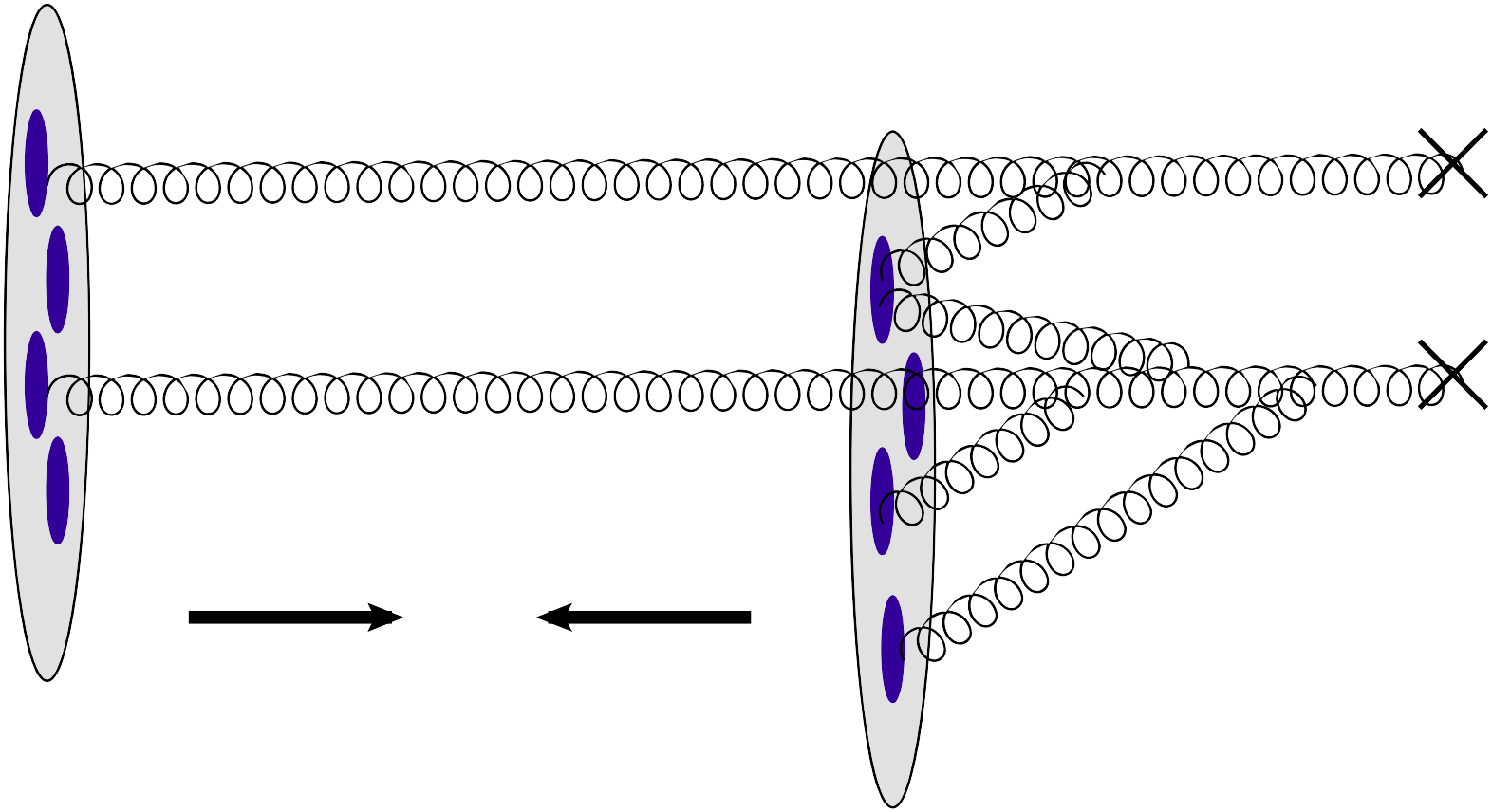

Little steps for the little feet: consider multiple rescatterings only in one of the two nuclei.

Double gluon production in heavy-light ion collisions

A. Setting up the problem: geometric correlations

Two-gluon production

- We want to calculate two gluon production in A_1+A_2 collisions with 1 << A_1 << A_2 resumming all powers of

$$\alpha_s^2 \, A_2^{1/3} \sim 1$$

(multiple rescatterings in the target nucleus)

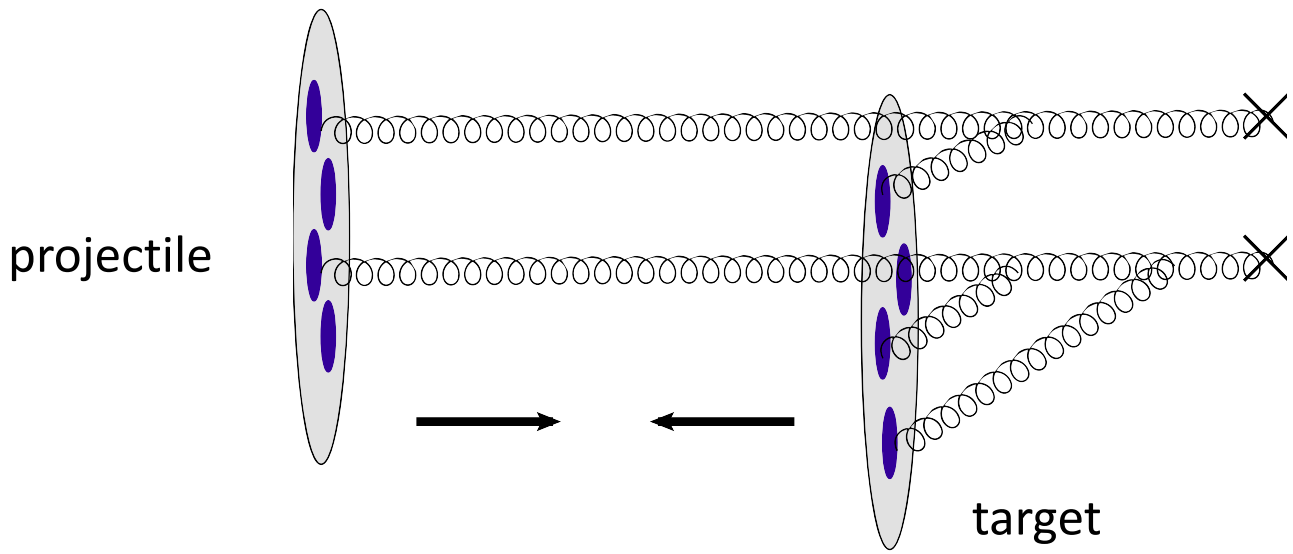

- The gluons come from different nucleons in the projectile nucleus as A_1>>1 and this is enhanced compared to emission from the same nucleon.

Applicability region

- The saturation scales of the two nuclei are very different:

$$\Lambda_{QCD} \ll Q_{s1} \ll Q_{s2}$$

- We are working above the saturation scale of the smaller nucleus:

$$k_T \gg Q_{s1}$$

- We thus sum all multiple rescatterings in the larger nucleus, $Q_{s2}/k_T \sim 1$, staying at the lowest non-trivial order in $Q_{s1}/k_T \ll 1$.

- Multiple interactions with the same nucleon in either nucleus are suppressed by $\Lambda_{QCD}/k_T \lll 1$.

Production cross-section

- The single- and double-inclusive cross sections can be written as

$$\frac{d\sigma}{d^2k\,dy} = \int d^2B\,d^2b\,|\Psi_I(\mathbf{B}-\mathbf{b})|^2 \left\langle \frac{d\sigma^{pA_2}}{d^2k\,dy\,d^2b} \right\rangle$$

$$\frac{d\sigma}{d^2k_1dy_1\,d^2k_2dy_2} = \int d^2B\,d^2b_1\,d^2b_2\,|\Psi_{II}(\mathbf{B}-\mathbf{b}_1,\mathbf{B}-\mathbf{b}_2)|^2 \left\langle \frac{d\sigma^{pA_2}}{d^2k_1dy_1d^2b_1}\,\frac{d\sigma^{pA_2}}{d^2k_2dy_2d^2b_2} \right\rangle$$

- Assume a large nucleus with uncorrelated nucleons (MV/Glauber model). Then the single- and double-nucleon wave functions are (with T_1 the nuclear profile function)

$$|\Psi_I(\mathbf{b})|^2 = T_1(\mathbf{b})$$

$$|\Psi_{II}(\mathbf{b}_1,\mathbf{b}_2)|^2 = T_1(\mathbf{b}_1)\,T_1(\mathbf{b}_2)$$

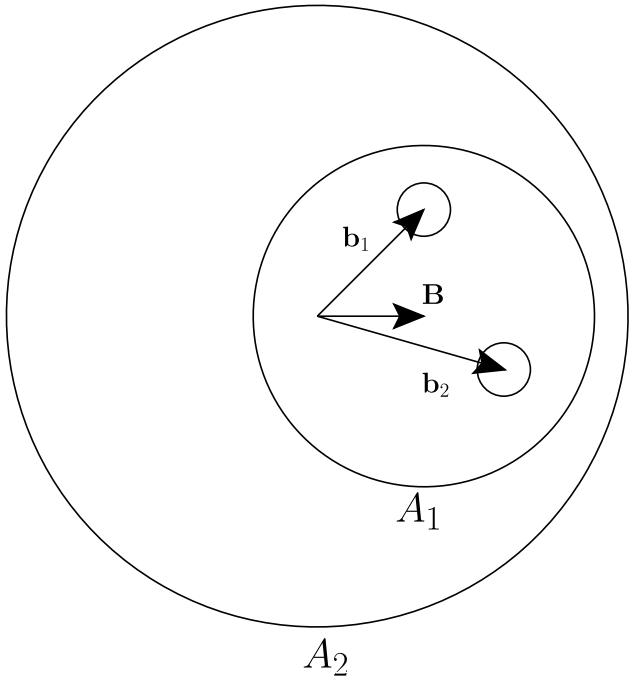

Geometric Correlations

- Assume uncorrelated interaction with the target:

$$\left\langle \frac{d\sigma^{pA_2}}{d^2k_1 dy_1 d^2b_1} \frac{d\sigma^{pA_2}}{d^2k_2 dy_2 d^2b_2} \right\rangle \approx \left\langle \frac{d\sigma^{pA_2}}{d^2k_1 dy_1 d^2b_1} \right\rangle \left\langle \frac{d\sigma^{pA_2}}{d^2k_2 dy_2 d^2b_2} \right\rangle$$

- For cross sections we have

$$\frac{d\sigma}{d^2k\, dy} = \int d^2B\, d^2b\, T_1(\mathbf{B}-\mathbf{b}) \left\langle \frac{d\sigma^{pA_2}}{d^2k\, dy\, d^2b} \right\rangle$$

$$\frac{d\sigma}{d^2k_1 dy_1\, d^2k_2 dy_2} = \int d^2B\, d^2b_1\, d^2b_2\, T_1(\mathbf{B}-\mathbf{b_1})\, T_1(\mathbf{B}-\mathbf{b_2}) \left\langle \frac{d\sigma^{pA_2}}{d^2k_1 dy_1 d^2b_1} \right\rangle \left\langle \frac{d\sigma^{pA_2}}{d^2k_2 dy_2 d^2b_2} \right\rangle$$

- Clearly

$$\frac{d\sigma}{d^2k_1\, dy_1\, d^2k_2\, dy_2} \nsim \frac{d\sigma}{d^2k_1\, dy_1} \frac{d\sigma}{d^2k_2\, dy_2}$$

- Correlations due to the integration over the impact parameter B
  -> Geometric correlations!

Geometric correlations: physical meaning

- In the same even the two nucleons are always within the smaller nucleus radius from each other (in transverse plane). In different events they can be anywhere in the larger nucleus.

$$C \propto \frac{\dfrac{d\sigma}{d^2k_1\, dy_1\, d^2k_2\, dy_2}}{\dfrac{d\sigma}{d^2k_1\, dy_1}\,\dfrac{d\sigma}{d^2k_2\, dy_2}}$$

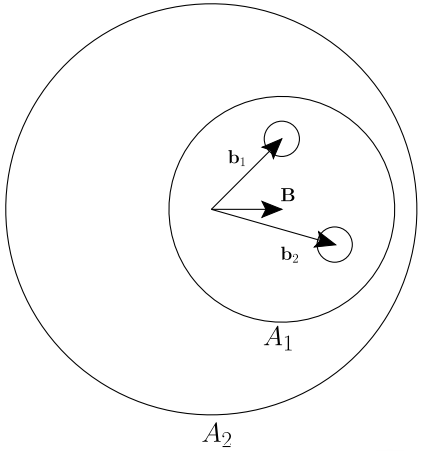

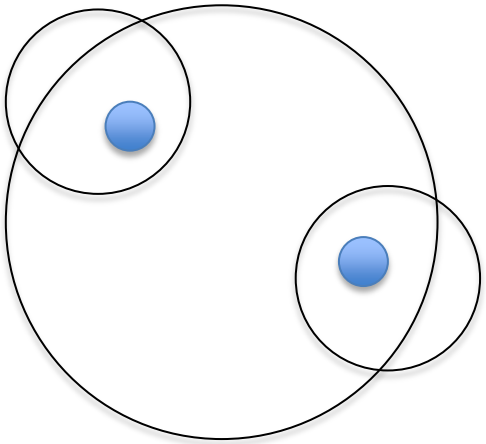

Geometric correlations at fixed B

- are zero as

$$\frac{d\sigma}{d^2k_1\,dy_1\,d^2k_2\,dy_2\,d^2B} = \frac{d\sigma}{d^2k_1\,dy_1\,d^2B}\,\frac{d\sigma}{d^2k_2\,dy_2\,d^2B}$$

which is clear from

$$\frac{d\sigma}{d^2k\,dy} = \int d^2B\,d^2b\,T_1(\mathbf{B}-\mathbf{b})\left\langle\frac{d\sigma^{pA_2}}{d^2k\,dy\,d^2b}\right\rangle$$

$$\frac{d\sigma}{d^2k_1dy_1\,d^2k_2dy_2} = \int d^2B\,d^2b_1\,d^2b_2\,T_1(\mathbf{B}-\mathbf{b_1})\,T_1(\mathbf{B}-\mathbf{b_2})\left\langle\frac{d\sigma^{pA_2}}{d^2k_1dy_1d^2b_1}\right\rangle\left\langle\frac{d\sigma^{pA_2}}{d^2k_2dy_2d^2b_2}\right\rangle$$

- Note that direction of B has to be fixed (to remove the geometric correlations), in other words the *vector* B should be fixed with respect to *vectors* k_1 and k_2. Maybe hard to do, but perhaps possible.

B. Two-gluon production

(i) Single gluon production in pA

Single gluon production in pA

Model the proton by a single quark (can be easily improved upon).
The diagrams are shown below (Yu.K., A. Mueller '97):

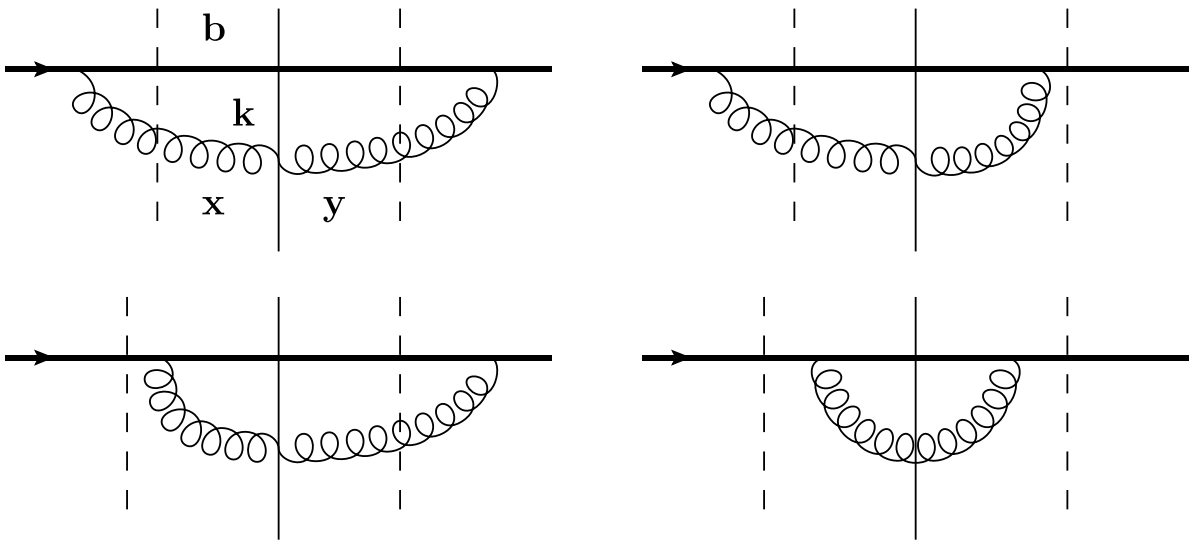

Multiple rescatterings are denoted by a single dashed line:

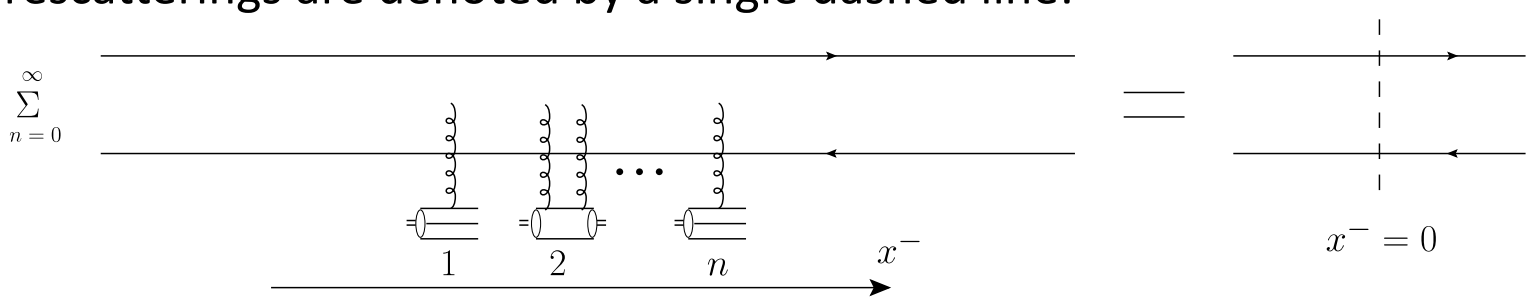

Single gluon production in pA

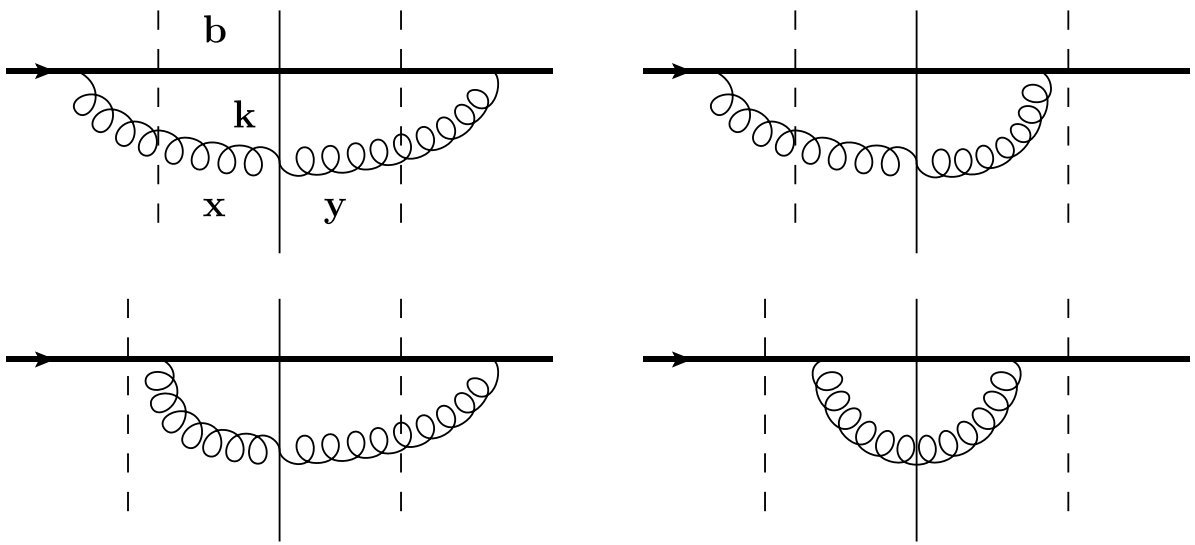

The gluon production cross section can be readily written as (U = Wilson line in adjoint representation, represents gluon interactions)

$$\left\langle \frac{d\sigma^{pA_2}}{d^2k\,dy\,d^2b} \right\rangle = \frac{\alpha_s\,C_F}{4\,\pi^4} \int d^2x\,d^2y\;e^{-i\,\mathbf{k}\cdot(\mathbf{x}-\mathbf{y})}\;\frac{\mathbf{x}-\mathbf{b}}{|\mathbf{x}-\mathbf{b}|^2}\cdot\frac{\mathbf{y}-\mathbf{b}}{|\mathbf{y}-\mathbf{b}|^2}$$

$$\times\left\langle \frac{1}{N_c^2-1}\,Tr[U_{\mathbf{x}}U_{\mathbf{y}}^\dagger] \;-\; \frac{1}{N_c^2-1}\,Tr[U_{\mathbf{x}}U_{\mathbf{b}}^\dagger] \;-\; \frac{1}{N_c^2-1}\,Tr[U_{\mathbf{b}}U_{\mathbf{y}}^\dagger] \;+\; 1 \right\rangle$$

Forward dipole amplitude

- The eikonal quark propagator is given by the Wilson line

$$V(\underline{x}) = \mathrm{P}\exp\left[i\,g\int_{-\infty}^{\infty} dx^+\,A^-(x^+, x^- = 0, \underline{x})\right]$$

with the light cone coordinates $$x^{\pm} = \frac{t \pm z}{\sqrt{2}}$$

- The quark dipole scattering amplitude is

$$N(\underline{x}_1, \underline{x}_2) = 1 - \frac{1}{N_c}\left\langle \mathrm{tr}\left[V(\underline{x}_1)\,V^\dagger(\underline{x}_2)\right]\right\rangle$$

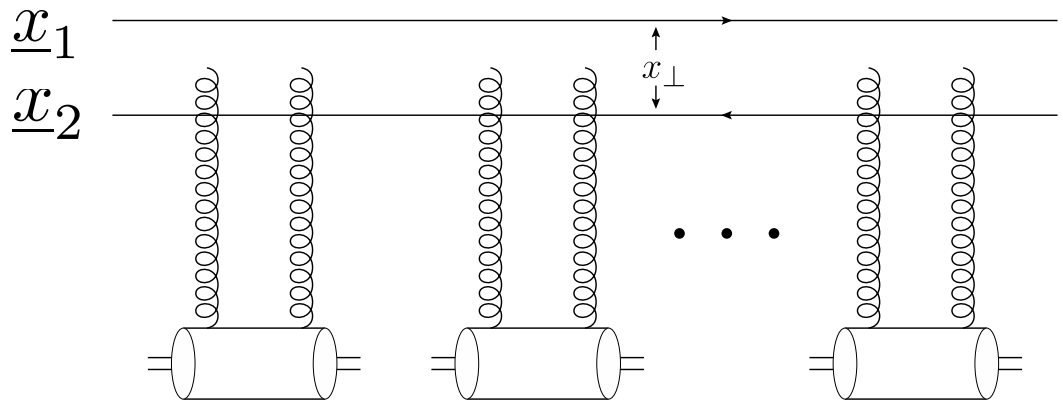

(ii) Two-gluon production in heavy-light ion collisions

The process

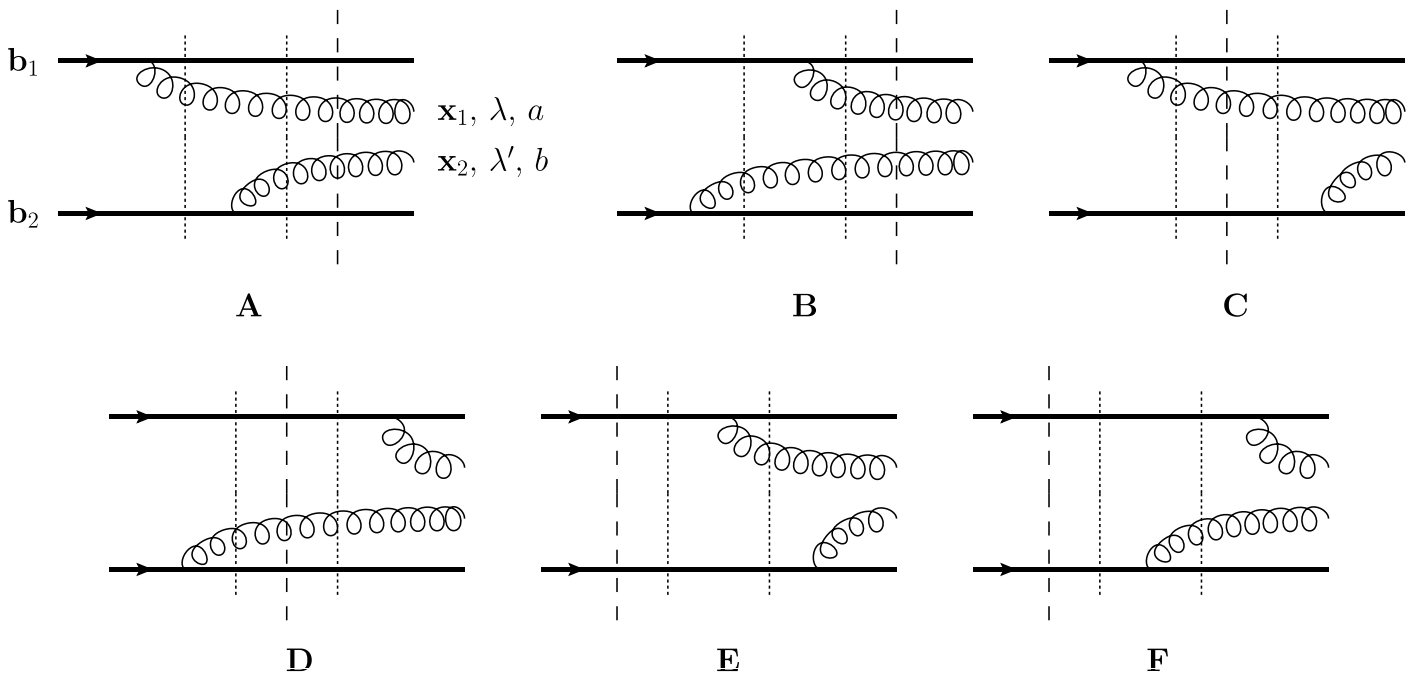

Solid horizontal lines = quarks in the incoming nucleons.
Dashed vertical line = interaction with the target.
Dotted vertical lines = energy denominators.

Amplitude squared

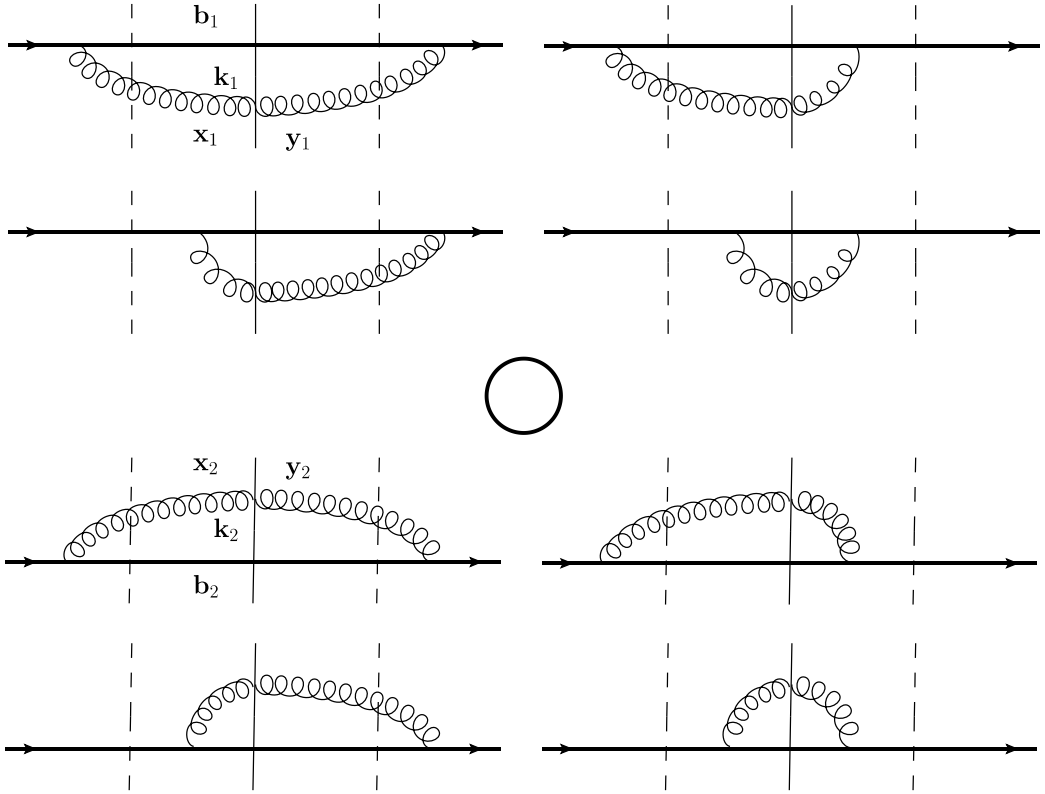

This contribution to two-gluon production looks like one-gluon production squared, with the target averaging applied to both.

Amplitude squared

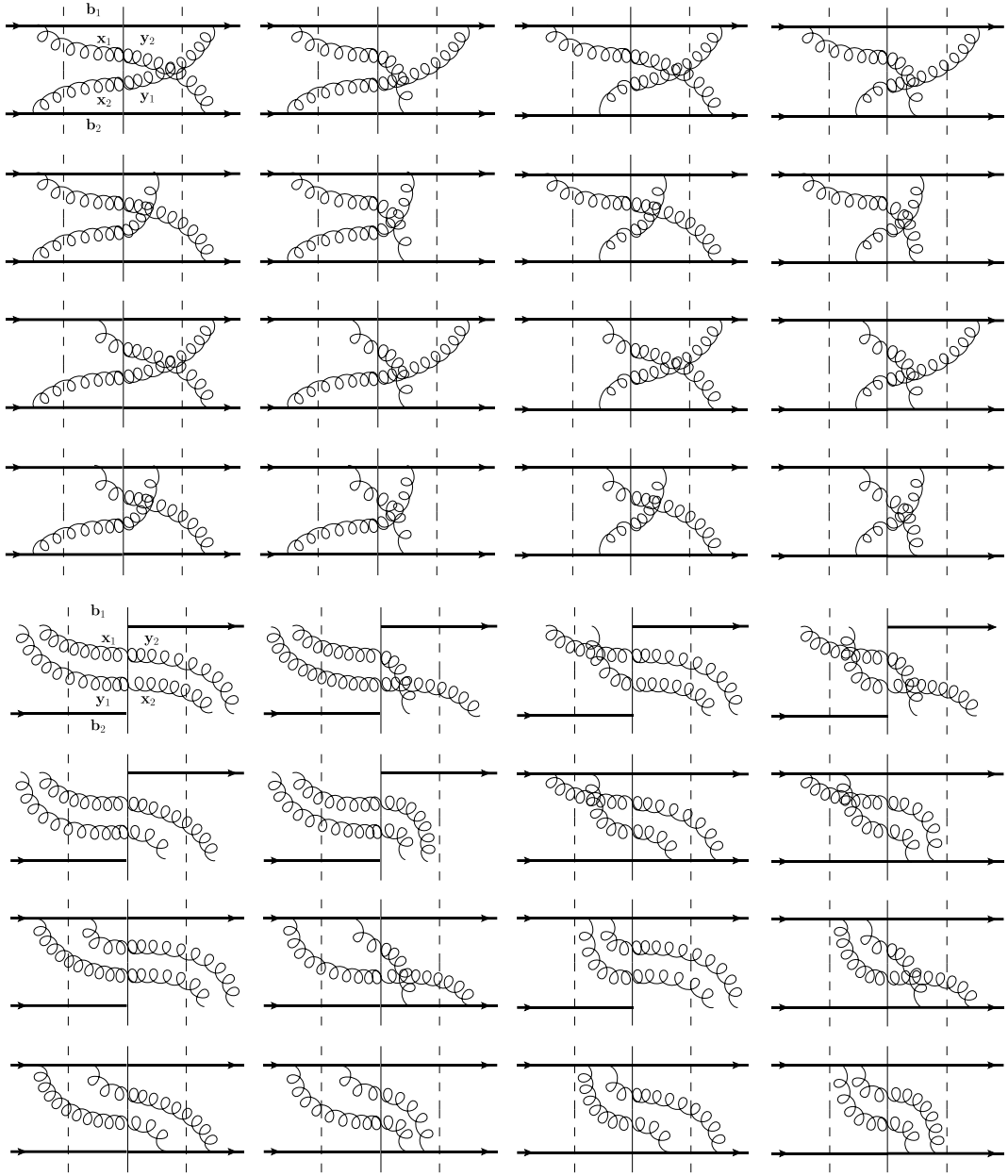

These contributions to two-gluon production contain cross-talk between the emissions from different nucleons.

Two-gluon production cross section

- "Squaring" the single gluon production cross section yields

$$\frac{d\sigma}{d^2k_1 dy_1 d^2k_2 dy_2} = \frac{\alpha_s^2\, C_F^2}{16\,\pi^8} \int d^2B\, d^2b_1\, d^2b_2\, T_1(\mathbf{B}-\mathbf{b}_1)\, T_1(\mathbf{B}-\mathbf{b}_2)\, d^2x_1\, d^2y_1\, d^2x_2\, d^2y_2\, e^{-i\,\mathbf{k}_1\cdot(\mathbf{x}_1-\mathbf{y}_1)-i\,\mathbf{k}_2\cdot(\mathbf{x}_2-\mathbf{y}_2)}$$
$$\times\ \frac{\mathbf{x}_1-\mathbf{b}_1}{|\mathbf{x}_1-\mathbf{b}_1|^2}\cdot\frac{\mathbf{y}_1-\mathbf{b}_1}{|\mathbf{y}_1-\mathbf{b}_1|^2}\ \frac{\mathbf{x}_2-\mathbf{b}_2}{|\mathbf{x}_2-\mathbf{b}_2|^2}\cdot\frac{\mathbf{y}_2-\mathbf{b}_2}{|\mathbf{y}_2-\mathbf{b}_2|^2}$$
$$\times\ \left\langle\left(\frac{1}{N_c^2-1}\,Tr[U_{\mathbf{x}_1}U^\dagger_{\mathbf{y}_1}]\ -\ \frac{1}{N_c^2-1}\,Tr[U_{\mathbf{x}_1}U^\dagger_{\mathbf{b}_1}]\ -\ \frac{1}{N_c^2-1}\,Tr[U_{\mathbf{b}_1}U^\dagger_{\mathbf{y}_1}]\ +\ 1\right)\right.$$
$$\left.\times\ \left(\frac{1}{N_c^2-1}\,Tr[U_{\mathbf{x}_2}U^\dagger_{\mathbf{y}_2}]\ -\ \frac{1}{N_c^2-1}\,Tr[U_{\mathbf{x}_2}U^\dagger_{\mathbf{b}_2}]\ -\ \frac{1}{N_c^2-1}\,Tr[U_{\mathbf{b}_2}U^\dagger_{\mathbf{y}_2}]\ +\ 1\right)\right\rangle$$

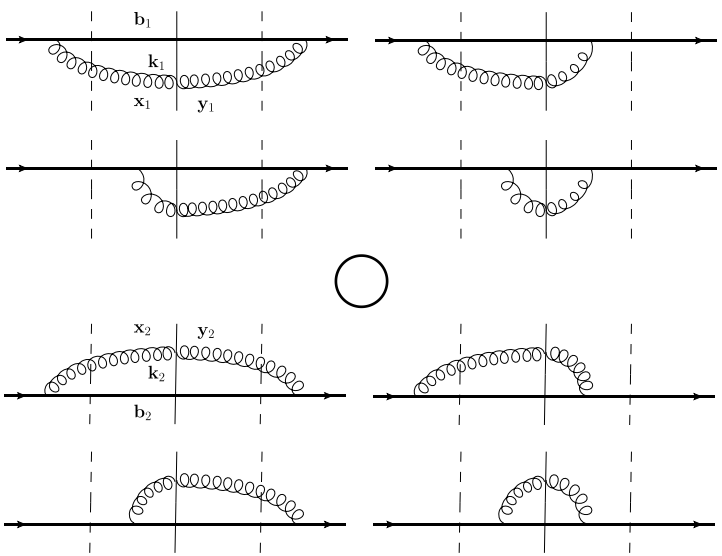

(cf. Kovner & Lublinsky, '12)

Two-gluon production cross section

- The "crossed" diagrams give

$$\frac{d\sigma_{crossed}}{d^2k_1 dy_1 d^2k_2 dy_2} = \frac{1}{[2(2\pi)^3]^2} \int d^2B\, d^2b_1\, d^2b_2\, T_1(\mathbf{B}-\mathbf{b}_1)\, T_1(\mathbf{B}-\mathbf{b}_2)\, d^2x_1\, d^2y_1\, d^2x_2\, d^2y_2$$

$$\times \left[e^{-i\,\mathbf{k}_1\cdot(\mathbf{x}_1-\mathbf{y}_2)-i\,\mathbf{k}_2\cdot(\mathbf{x}_2-\mathbf{y}_1)} + e^{-i\,\mathbf{k}_1\cdot(\mathbf{x}_1-\mathbf{y}_2)+i\,\mathbf{k}_2\cdot(\mathbf{x}_2-\mathbf{y}_1)} \right]$$

$$\times \frac{16\,\alpha_s^2}{\pi^2} \frac{C_F}{2N_c} \frac{\mathbf{x}_1-\mathbf{b}_1}{|\mathbf{x}_1-\mathbf{b}_1|^2} \cdot \frac{\mathbf{y}_2-\mathbf{b}_2}{|\mathbf{y}_2-\mathbf{b}_2|^2} \frac{\mathbf{x}_2-\mathbf{b}_2}{|\mathbf{x}_2-\mathbf{b}_2|^2} \cdot \frac{\mathbf{y}_1-\mathbf{b}_1}{|\mathbf{y}_1-\mathbf{b}_1|^2}$$

$$\times \Big[Q(\mathbf{x}_1,\mathbf{y}_1,\mathbf{x}_2,\mathbf{y}_2) - Q(\mathbf{x}_1,\mathbf{y}_1,\mathbf{x}_2,\mathbf{b}_2) - Q(\mathbf{x}_1,\mathbf{y}_1,\mathbf{b}_2,\mathbf{y}_2) + S_G(\mathbf{x}_1,\mathbf{y}_1) - Q(\mathbf{x}_1,\mathbf{b}_1,\mathbf{x}_2,\mathbf{y}_2)$$

$$+ Q(\mathbf{x}_1,\mathbf{b}_1,\mathbf{x}_2,\mathbf{b}_2) + Q(\mathbf{x}_1,\mathbf{b}_1,\mathbf{b}_2,\mathbf{y}_2) - S_G(\mathbf{x}_1,\mathbf{b}_1) - Q(\mathbf{b}_1,\mathbf{y}_1,\mathbf{x}_2,\mathbf{y}_2) + Q(\mathbf{b}_1,\mathbf{y}_1,\mathbf{x}_2,\mathbf{b}_2)$$

$$+ Q(\mathbf{b}_1,\mathbf{y}_1,\mathbf{b}_2,\mathbf{y}_2) - S_G(\mathbf{b}_1,\mathbf{y}_1) + S_G(\mathbf{x}_2,\mathbf{y}_2) - S_G(\mathbf{x}_2,\mathbf{b}_2) - S_G(\mathbf{b}_2,\mathbf{y}_2) + 1 \Big]$$

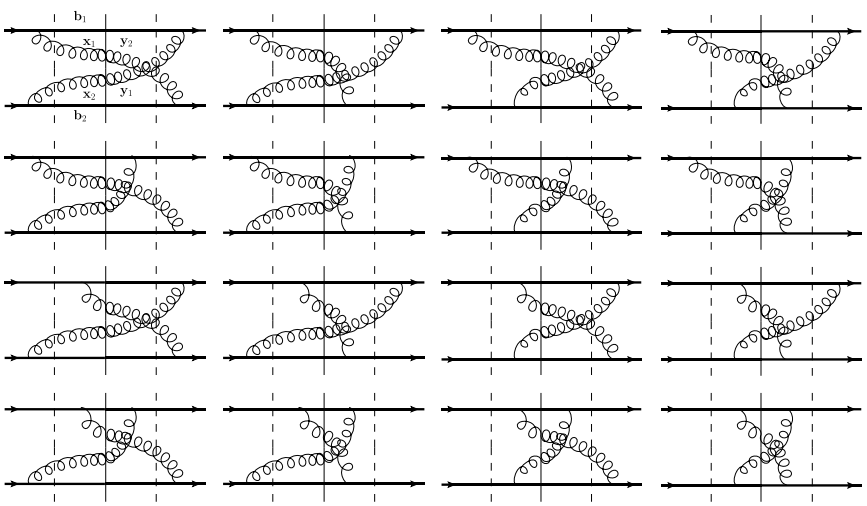

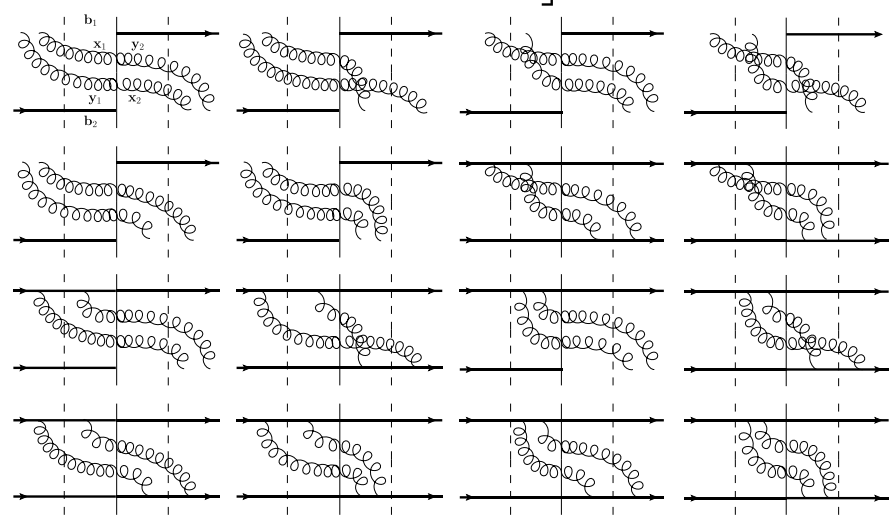

Two-gluon production cross section

- The "crossed" diagrams give

$$\frac{d\sigma_{crossed}}{d^2k_1 dy_1 d^2k_2 dy_2} = \frac{1}{[2(2\pi)^3]^2} \int d^2B\, d^2b_1\, d^2b_2\, T_1(\mathbf{B}-\mathbf{b}_1)\, T_1(\mathbf{B}-\mathbf{b}_2)\, d^2x_1\, d^2y_1\, d^2x_2\, d^2y_2$$
$$\times \left[e^{-i\,\mathbf{k}_1\cdot(\mathbf{x}_1-\mathbf{y}_2)-i\,\mathbf{k}_2\cdot(\mathbf{x}_2-\mathbf{y}_1)} + e^{-i\,\mathbf{k}_1\cdot(\mathbf{x}_1-\mathbf{y}_2)+i\,\mathbf{k}_2\cdot(\mathbf{x}_2-\mathbf{y}_1)} \right]$$
$$\times \frac{16\,\alpha_s^2}{\pi^2} \frac{C_F}{2N_c} \frac{\mathbf{x}_1-\mathbf{b}_1}{|\mathbf{x}_1-\mathbf{b}_1|^2} \cdot \frac{\mathbf{y}_2-\mathbf{b}_2}{|\mathbf{y}_2-\mathbf{b}_2|^2} \frac{\mathbf{x}_2-\mathbf{b}_2}{|\mathbf{x}_2-\mathbf{b}_2|^2} \cdot \frac{\mathbf{y}_1-\mathbf{b}_1}{|\mathbf{y}_1-\mathbf{b}_1|^2}$$
$$\times \Big[Q(\mathbf{x}_1,\mathbf{y}_1,\mathbf{x}_2,\mathbf{y}_2) - Q(\mathbf{x}_1,\mathbf{y}_1,\mathbf{x}_2,\mathbf{b}_2) - Q(\mathbf{x}_1,\mathbf{y}_1,\mathbf{b}_2,\mathbf{y}_2) + S_G(\mathbf{x}_1,\mathbf{y}_1) - Q(\mathbf{x}_1,\mathbf{b}_1,\mathbf{x}_2,\mathbf{y}_2)$$
$$+ Q(\mathbf{x}_1,\mathbf{b}_1,\mathbf{x}_2,\mathbf{b}_2) + Q(\mathbf{x}_1,\mathbf{b}_1,\mathbf{b}_2,\mathbf{y}_2) - S_G(\mathbf{x}_1,\mathbf{b}_1) - Q(\mathbf{b}_1,\mathbf{y}_1,\mathbf{x}_2,\mathbf{y}_2) + Q(\mathbf{b}_1,\mathbf{y}_1,\mathbf{x}_2,\mathbf{b}_2)$$
$$+ Q(\mathbf{b}_1,\mathbf{y}_1,\mathbf{b}_2,\mathbf{y}_2) - S_G(\mathbf{b}_1,\mathbf{y}_1) + S_G(\mathbf{x}_2,\mathbf{y}_2) - S_G(\mathbf{x}_2,\mathbf{b}_2) - S_G(\mathbf{b}_2,\mathbf{y}_2) + 1 \Big]$$

- We introduced the adjoint color-dipole and color quadrupole amplitudes:

$$S_G(\mathbf{x}_1,\mathbf{x}_2,y) \equiv \frac{1}{N_c^2-1} \left\langle Tr[U_{\mathbf{x}_1} U^\dagger_{\mathbf{x}_2}] \right\rangle$$

$$Q(\mathbf{x}_1,\mathbf{x}_2,\mathbf{x}_3,\mathbf{x}_4) \equiv \frac{1}{N_c^2-1} \left\langle Tr[U_{\mathbf{x}_1} U^\dagger_{\mathbf{x}_2} U_{\mathbf{x}_3} U^\dagger_{\mathbf{x}_4}] \right\rangle$$

Two-gluon production: properties

$$\frac{d\sigma}{d^2k_1 dy_1 d^2k_2 dy_2} = \frac{\alpha_s^2 C_F^2}{16\,\pi^8} \int d^2B\, d^2b_1\, d^2b_2\, T_1(\mathbf{B}-\mathbf{b}_1)\, T_1(\mathbf{B}-\mathbf{b}_2)\, d^2x_1\, d^2y_1\, d^2x_2\, d^2y_2\, e^{-i\,\mathbf{k}_1\cdot(\mathbf{x}_1-\mathbf{y}_1)-i\,\mathbf{k}_2\cdot(\mathbf{x}_2-\mathbf{y}_2)}$$
$$\times\ \frac{\mathbf{x}_1-\mathbf{b}_1}{|\mathbf{x}_1-\mathbf{b}_1|^2}\cdot\frac{\mathbf{y}_1-\mathbf{b}_1}{|\mathbf{y}_1-\mathbf{b}_1|^2}\ \frac{\mathbf{x}_2-\mathbf{b}_2}{|\mathbf{x}_2-\mathbf{b}_2|^2}\cdot\frac{\mathbf{y}_2-\mathbf{b}_2}{|\mathbf{y}_2-\mathbf{b}_2|^2}$$
$$\times\ \left\langle\left(\frac{1}{N_c^2-1}\,Tr[U_{\mathbf{x}_1}U^\dagger_{\mathbf{y}_1}]\ -\ \frac{1}{N_c^2-1}\,Tr[U_{\mathbf{x}_1}U^\dagger_{\mathbf{b}_1}]\ -\ \frac{1}{N_c^2-1}\,Tr[U_{\mathbf{b}_1}U^\dagger_{\mathbf{y}_1}]\ +\ 1\right)\right.$$
$$\left.\times\ \left(\frac{1}{N_c^2-1}\,Tr[U_{\mathbf{x}_2}U^\dagger_{\mathbf{y}_2}]\ -\ \frac{1}{N_c^2-1}\,Tr[U_{\mathbf{x}_2}U^\dagger_{\mathbf{b}_2}]\ -\ \frac{1}{N_c^2-1}\,Tr[U_{\mathbf{b}_2}U^\dagger_{\mathbf{y}_2}]\ +\ 1\right)\right\rangle$$

- Note that if the interaction with the target factorizes,

$$\left\langle Tr[U_{\mathbf{x}_1}U^\dagger_{\mathbf{y}_1}]\ Tr[U_{\mathbf{x}_2}U^\dagger_{\mathbf{y}_2}]\right\rangle\Big|_{\mathrm{large}-N_c,\,\mathrm{large}-A_2} \approx \left\langle Tr[U_{\mathbf{x}_1}U^\dagger_{\mathbf{y}_1}]\right\rangle\ \left\langle Tr[U_{\mathbf{x}_2}U^\dagger_{\mathbf{y}_2}]\right\rangle$$

  we still have **<u>the geometric correlations</u>**.

- The geometric correlations lead to non-zero cumulants! (Like everything that depends on geometry.)

Two-gluon production: properties

$$\frac{d\sigma}{d^2k_1 dy_1 d^2k_2 dy_2} = \frac{\alpha_s^2 C_F^2}{16\,\pi^8} \int d^2B\, d^2b_1\, d^2b_2\, T_1(\mathbf{B}-\mathbf{b}_1)\, T_1(\mathbf{B}-\mathbf{b}_2)\, d^2x_1\, d^2y_1\, d^2x_2\, d^2y_2\, e^{-i\,\mathbf{k}_1\cdot(\mathbf{x}_1-\mathbf{y}_1)-i\,\mathbf{k}_2\cdot(\mathbf{x}_2-\mathbf{y}_2)}$$
$$\times \frac{\mathbf{x}_1-\mathbf{b}_1}{|\mathbf{x}_1-\mathbf{b}_1|^2}\cdot\frac{\mathbf{y}_1-\mathbf{b}_1}{|\mathbf{y}_1-\mathbf{b}_1|^2}\,\frac{\mathbf{x}_2-\mathbf{b}_2}{|\mathbf{x}_2-\mathbf{b}_2|^2}\cdot\frac{\mathbf{y}_2-\mathbf{b}_2}{|\mathbf{y}_2-\mathbf{b}_2|^2}$$
$$\times \left\langle \left(\frac{1}{N_c^2-1}\,Tr[U_{\mathbf{x}_1}U^\dagger_{\mathbf{y}_1}] - \frac{1}{N_c^2-1}\,Tr[U_{\mathbf{x}_1}U^\dagger_{\mathbf{b}_1}] - \frac{1}{N_c^2-1}\,Tr[U_{\mathbf{b}_1}U^\dagger_{\mathbf{y}_1}] + 1\right)\right.$$
$$\left.\times \left(\frac{1}{N_c^2-1}\,Tr[U_{\mathbf{x}_2}U^\dagger_{\mathbf{y}_2}] - \frac{1}{N_c^2-1}\,Tr[U_{\mathbf{x}_2}U^\dagger_{\mathbf{b}_2}] - \frac{1}{N_c^2-1}\,Tr[U_{\mathbf{b}_2}U^\dagger_{\mathbf{y}_2}] + 1\right)\right\rangle$$

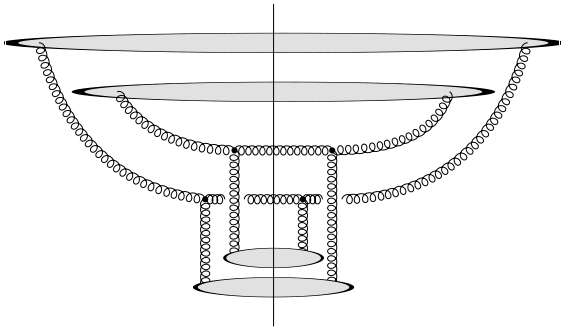

- If we expand the interaction with the target to the lowest non-trivial order, one reproduced the contribution of the 'glasma' graphs:

$$\left.\frac{d\sigma_{corr}}{d^2k_1 dy_1 d^2k_2 dy_2}\right|_{LO} = \frac{\alpha_s^2}{4\,\pi^4}\int d^2B\, d^2b\,[T_1(\mathbf{B}-\mathbf{b})]^2\,\frac{Q_{s0}^4(\mathbf{b})}{\mathbf{k}_1^2\,\mathbf{k}_2^2}\int_\Lambda \frac{d^2l}{(\mathbf{l}^2)^2}\left[\frac{1}{(\mathbf{k}_1-\mathbf{l})^2\,(\mathbf{k}_2+\mathbf{l})^2}+\frac{1}{(\mathbf{k}_1-\mathbf{l})^2\,(\mathbf{k}_2-\mathbf{l})^2}\right]$$

away-side correlations

$$\sim \frac{1}{(\mathbf{k}_1+\mathbf{k}_2)^2}$$

near-side correlations

$$\sim \frac{1}{(\mathbf{k}_1-\mathbf{k}_2)^2}$$

(cf. Dumitru, Gelis, McLerran, Venugopalan '08)

Two-gluon production: properties

- Crossed diagrams at lowest nontrivial order

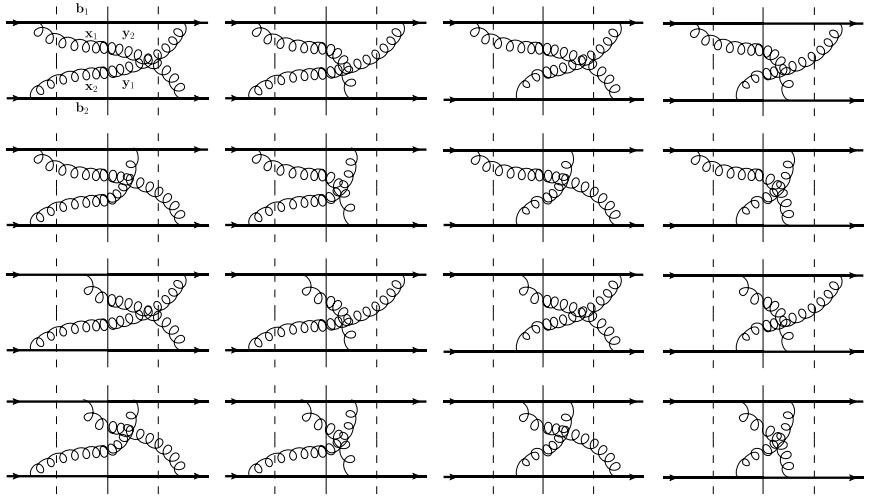

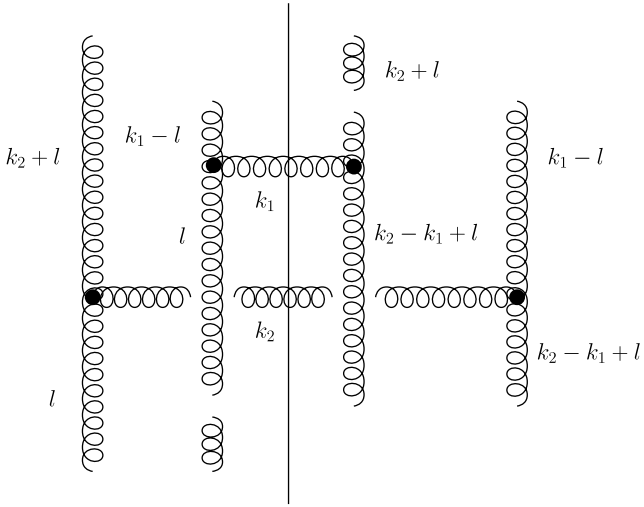

$$\sim \cos 2\Delta\phi \left[\frac{1}{(\mathbf{k}_1 - \mathbf{k}_2)^2} + \frac{1}{(\mathbf{k}_1 + \mathbf{k}_2)^2} \right]$$

Stronger correlations!

Two-gluon production: properties

$$\frac{d\sigma}{d^2k_1 dy_1 d^2k_2 dy_2} = \frac{\alpha_s^2 C_F^2}{16\,\pi^8} \int d^2B\, d^2b_1\, d^2b_2\, T_1(\mathbf{B}-\mathbf{b}_1)\, T_1(\mathbf{B}-\mathbf{b}_2)\, d^2x_1\, d^2y_1\, d^2x_2\, d^2y_2\, e^{-i\,\mathbf{k}_1\cdot(\mathbf{x}_1-\mathbf{y}_1)-i\,\mathbf{k}_2\cdot(\mathbf{x}_2-\mathbf{y}_2)}$$
$$\times\ \frac{\mathbf{x}_1-\mathbf{b}_1}{|\mathbf{x}_1-\mathbf{b}_1|^2}\cdot\frac{\mathbf{y}_1-\mathbf{b}_1}{|\mathbf{y}_1-\mathbf{b}_1|^2}\ \frac{\mathbf{x}_2-\mathbf{b}_2}{|\mathbf{x}_2-\mathbf{b}_2|^2}\cdot\frac{\mathbf{y}_2-\mathbf{b}_2}{|\mathbf{y}_2-\mathbf{b}_2|^2}$$
$$\times\ \left\langle\left(\frac{1}{N_c^2-1}\,Tr[U_{\mathbf{x}_1}U^\dagger_{\mathbf{y}_1}]\ -\ \frac{1}{N_c^2-1}\,Tr[U_{\mathbf{x}_1}U^\dagger_{\mathbf{b}_1}]\ -\ \frac{1}{N_c^2-1}\,Tr[U_{\mathbf{b}_1}U^\dagger_{\mathbf{y}_1}]\ +\ 1\right)\right.$$
$$\left.\times\ \left(\frac{1}{N_c^2-1}\,Tr[U_{\mathbf{x}_2}U^\dagger_{\mathbf{y}_2}]\ -\ \frac{1}{N_c^2-1}\,Tr[U_{\mathbf{x}_2}U^\dagger_{\mathbf{b}_2}]\ -\ \frac{1}{N_c^2-1}\,Tr[U_{\mathbf{b}_2}U^\dagger_{\mathbf{y}_2}]\ +\ 1\right)\right\rangle$$

- The cross section is symmetric under (ditto for the “crossed” term)

$$\mathbf{k}_1 \leftrightarrow \mathbf{k}_2$$ (just coordinate relabeling)

$$\mathbf{k}_2 \to -\mathbf{k}_2$$ as $$Tr\left[U_{\mathbf{x}}\,U^\dagger_{\mathbf{y}}\right] = Tr\left[U_{\mathbf{y}}\,U^\dagger_{\mathbf{x}}\right]$$

- Hence the correlations generate only even azimuthal harmonics

$$\sim \cos 2\,n\,(\phi_1-\phi_2)$$

Correlation function

May look like this (a toy model; two particles far separated in rapidity, jets subtracted, pA and AA):

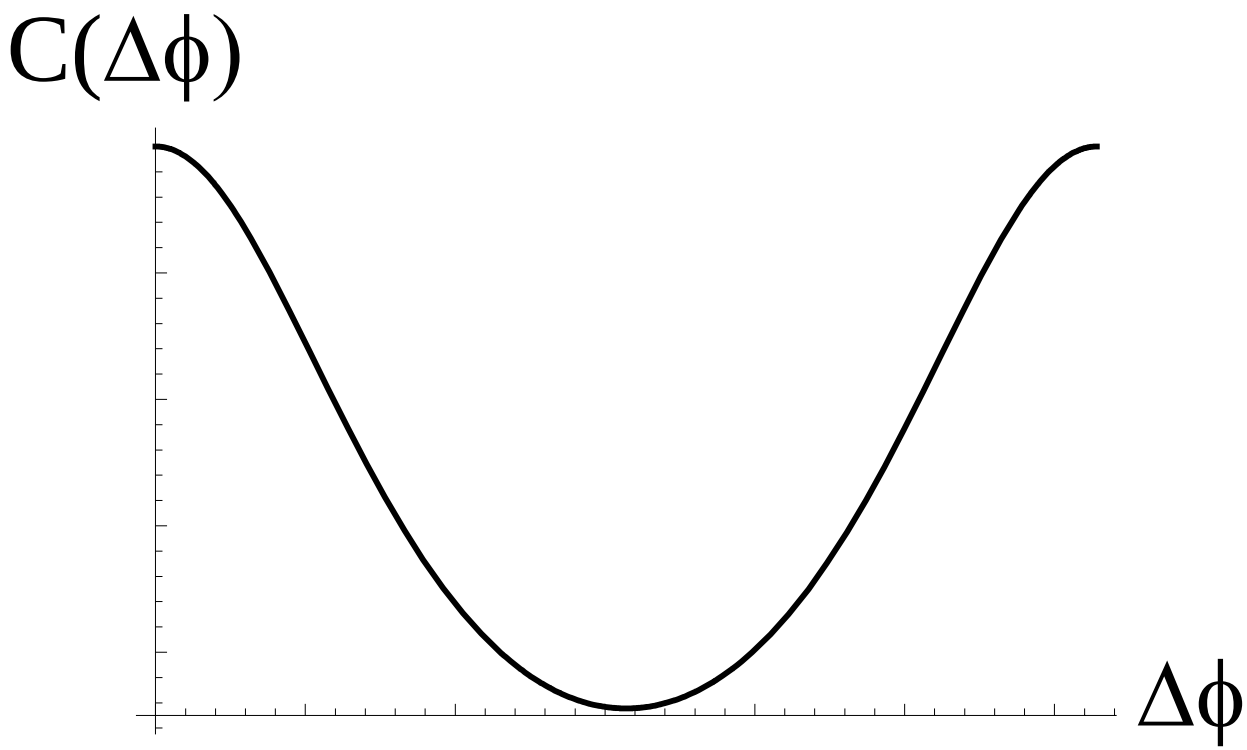

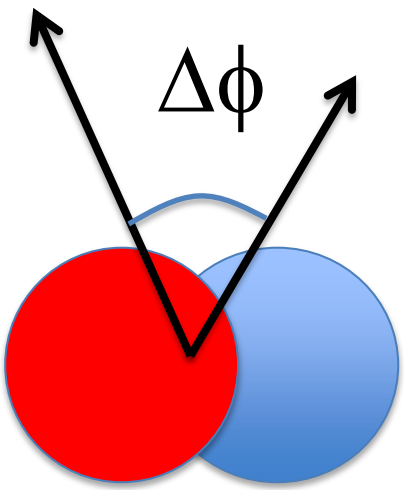

Dumitru, Gelis, McLerran, Venugopalan ’08; Yu.K., D. Wertepny ‘12; Lappi, Srednyak, and Venugopalan ‘09

This conclusion is consistent with the data

Long-Range Rapidity Correlations in Heavy-Light Ion Collisions

Yuri V. Kovchegov, Douglas E. Wertepny

(Submitted on 5 Dec 2012)

We study two-particle long-range rapidity correlations arising in the early stages of heavy ion collisions in the saturation/Color Glass Condensate framework, assuming for simplicity that one colliding nucleus is much larger than the other. We calculate the two-gluon production cross section while including all-order saturation effects in the heavy nucleus with the lowest-order rescattering in the lighter nucleus. We find four types of correlations in the two-gluon production cross section: (i) geometric correlations, (ii) HBT correlations, (iii) back-to-back correlations, and (iv) near-side azimuthal correlations which are long-range in rapidity. The geometric correlations (i) are due to the fact that nucleons are correlated by simply being confined within the same nucleus and may lead to long-range rapidity correlations for the produced particles without strong azimuthal angle dependence. Somewhat surprisingly, long-range rapidity correlations (iii) and (iv) have exactly the same amplitudes along with azimuthal and rapidity shapes: one centered around \Delta \phi = \pi\ with the other one centered around \Delta \phi = 0 (here \Delta \phi\ is the azimuthal angle between the two produced gluons). We thus observe that the early-time CGC dynamics in nucleus-nucleus collisions generates azimuthal non-flow correlations which are qualitatively different from jet correlations by being long-range in rapidity. If strong enough, they have the potential of mimicking the elliptic (and higher-order even-harmonic) flow in the di-hadron correlators: one may need to take them into account in the experimental determination of the flow observables.

This conclusion is consistent with the data

Long-range angular correlations on the near and away side in p-Pb collisions at sqrt(sNN) = 5.02 TeV

ALICE Collaboration

(Submitted on 10 Dec 2012)

Angular correlations between charged trigger and associated particles are measured by the ALICE detector in p-Pb collisions at a nucleon-nucleon centre-of-mass energy of 5.02 TeV for transverse momentum ranges within 0.5 < pT,assoc < pT,trig < 4 GeV/c. The correlations are measured over two units of pseudorapidity and full azimuthal angle in different intervals of event multiplicity, and expressed as associated yield per trigger particle. Two long-range ridge-like structures, one on the near side and one on the away side, are observed when the per-trigger yield obtained in low-multiplicity events is subtracted from the one in high-multiplicity events. The excess on the near-side is qualitatively similar to that recently reported by the CMS collaboration, while the excess on the away-side is reported for the first time. The two-ridge structure projected onto azimuthal angle is quantified with the second and third Fourier coefficients as well as by near-side and away-side yields and widths. The yields on the near side and on the away side are equal within the uncertainties for all studied event multiplicity and pT bins, and the widths show no significant evolution with event multiplicity or pT. These findings suggest that the near-side ridge is accompanied by an essentially identical away-side ridge.

LHC p+Pb data from ALICE

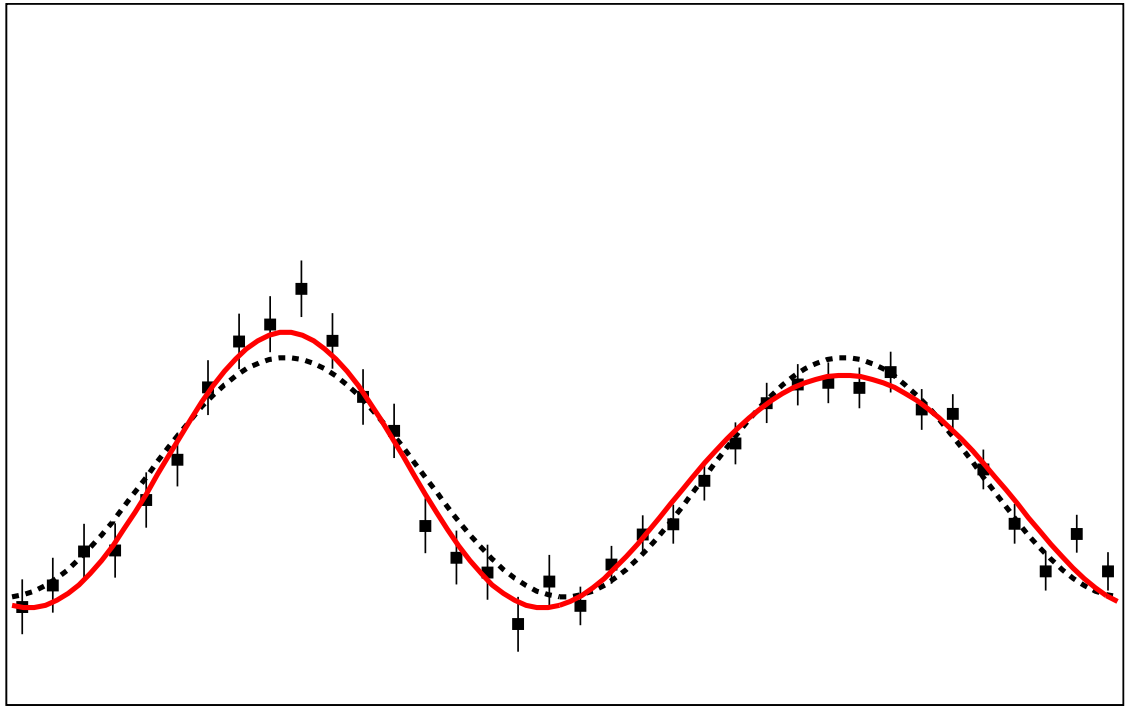

- These are high-multiplicity collisions: it is possible that quark-gluon plasma is created in those, with the hydrodynamics contributing to these correlations.

- Saturation approach is lacking the odd harmonics, like cos (3 $\Delta\phi$) , etc. Can they be generated in a pure CGC approach EBE?

C. HBT correlations

HBT diagrams

- There is another contribution coming from the “crossed” diagrams

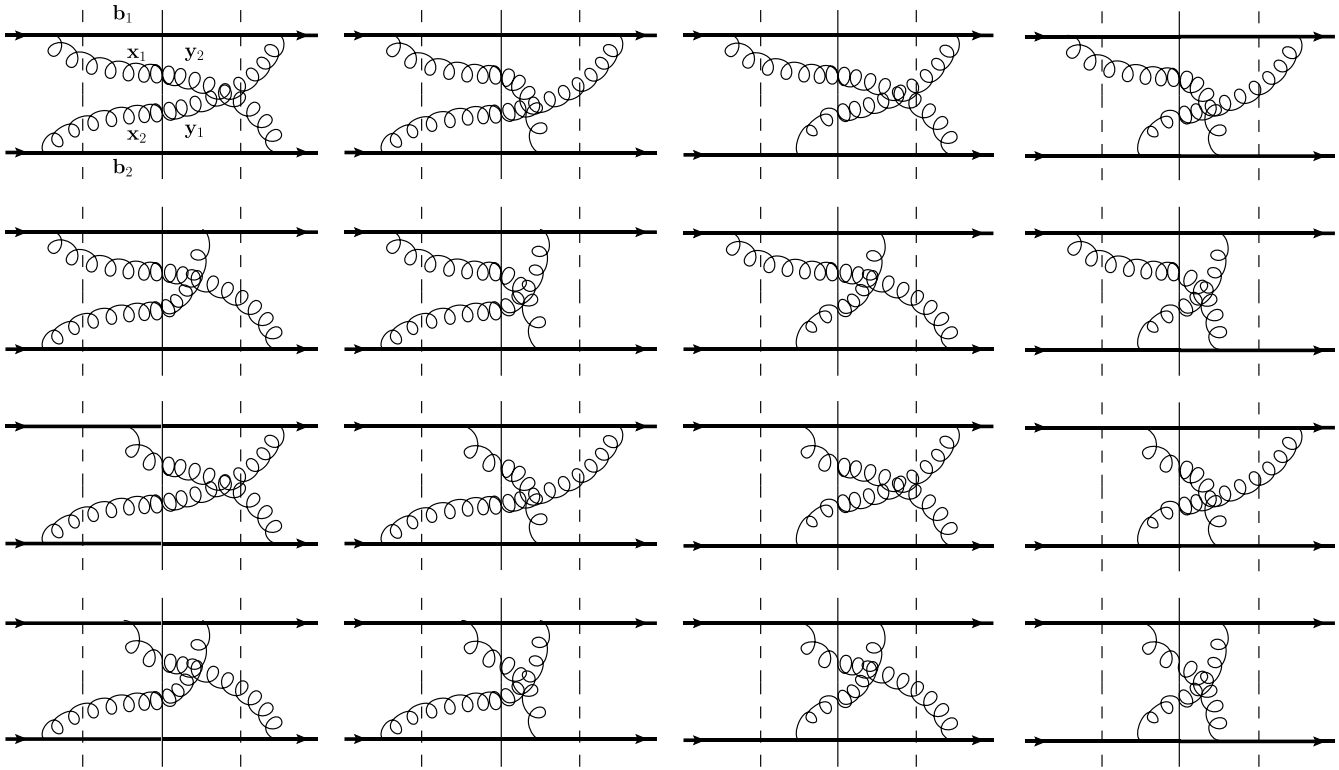

HBT diagrams

- They give HBT correlations (with R_{long} =0 due to Lorentz contraction)

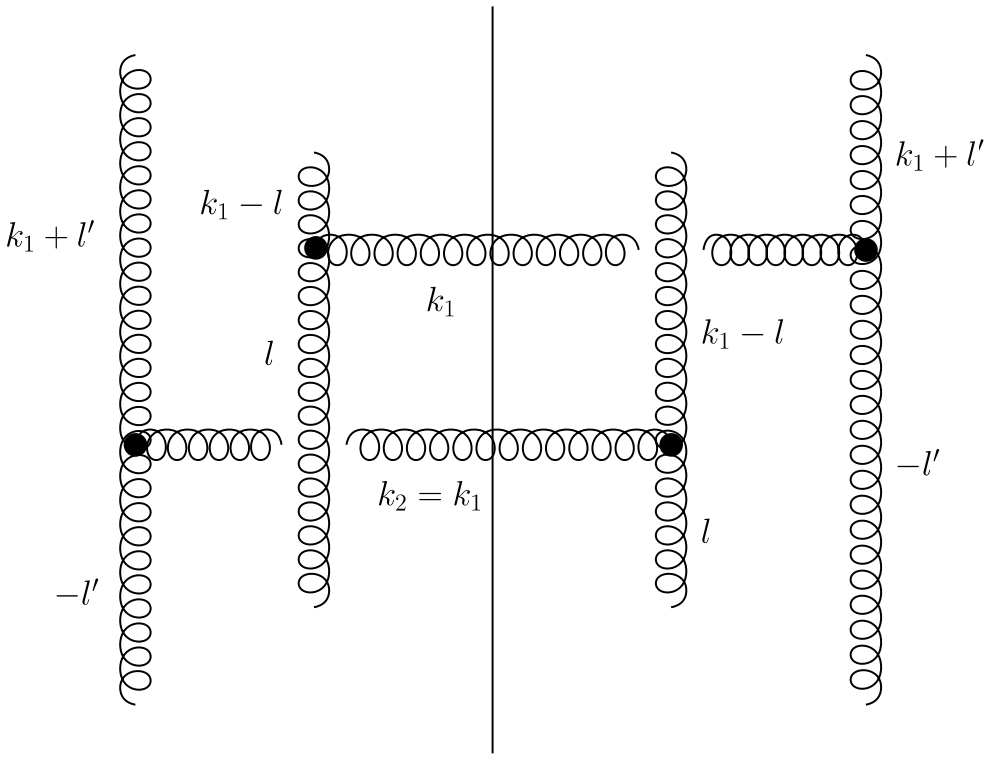

$$\sim \delta^2(\mathbf{k}_1 - \mathbf{k}_2)$$

- Just like the standard HBT correlations

$$|\Psi_1(\mathbf{k}_1)\,\Psi_2(\mathbf{k}_2) + \Psi_1(\mathbf{k}_2)\,\Psi_2(\mathbf{k}_1)|^2 \to \Psi_1(\mathbf{k}_1)\,\Psi_2(\mathbf{k}_2)\,\Psi_1^*(\mathbf{k}_2)\,\Psi_2^*(\mathbf{k}_1) + c.c. + \ldots$$

- Possibly fragmentation would break phase coherence making these perturbative HBT correlations not observable.

Back-to-back HBT?

- Note that all our formulas are symmetric under

$$\mathbf{k}_2 \to -\mathbf{k}_2$$

- Therefore, the HBT correlation is accompanied by the identical back-to-back HBT correlation

$$\sim \delta^2(\mathbf{k}_1 + \mathbf{k}_2)$$

- Note again that this correlation may be destroyed in hadronization.

Conclusions

- In this talk I have shown a calculation of the two-gluon production cross section in nuclear collisions including saturation effects in one nucleus to all orders (heavy-light ion collisions).

- Correlations we see:
  - Geometric correlations ✓
  - HBT correlations (along with b2b HBT ones)
  - Away-side correlations ✓
  - Near-side long-range rapidity correlations ✓
    (✓ = long-range in rapidity)

- Near- and away-side correlations are identical to all orders in saturation effects: this is mainly consistent with the recent p+Pb data from LHC.

- Seems like geometric correlations are hard to remove by cumulants!

Backup Slides

Ridge in heavy ion collisions

- Heavy ion collisions, along with high-multiplicity pp collisions, are known to have long-range rapidity correlations, known as ‘the ridge’:

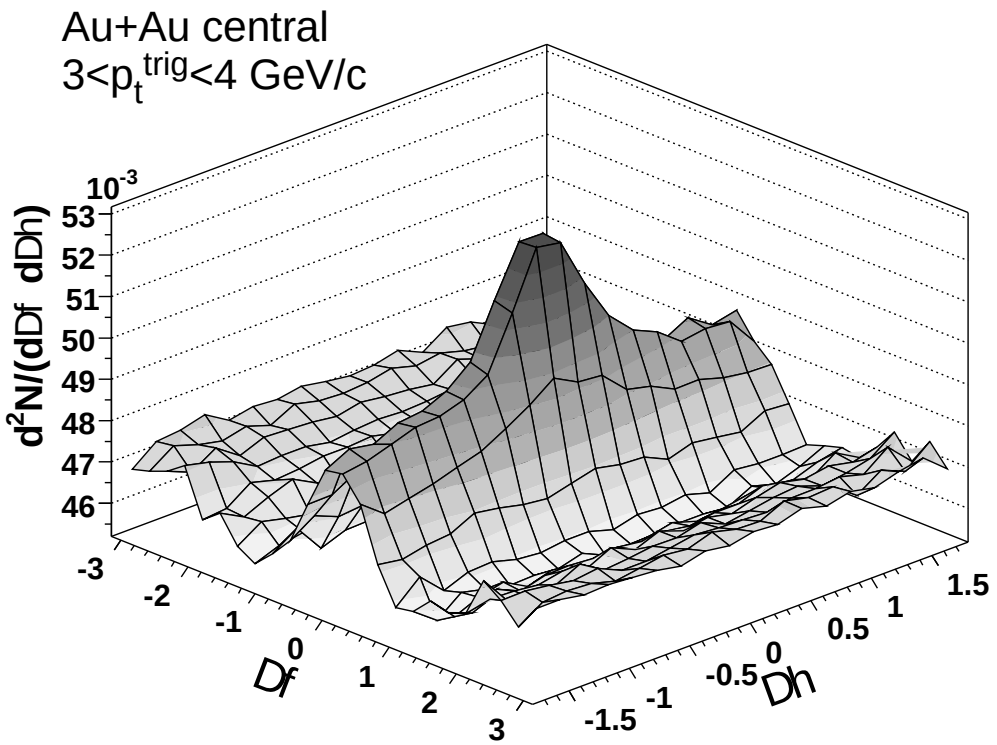

What to calculate?

- To systematically include glasma graphs in the CGC formalism it would be great to solve the two-gluon inclusive production problem in the MV model, that is, including multiple rescatterings in both nuclei to all orders:

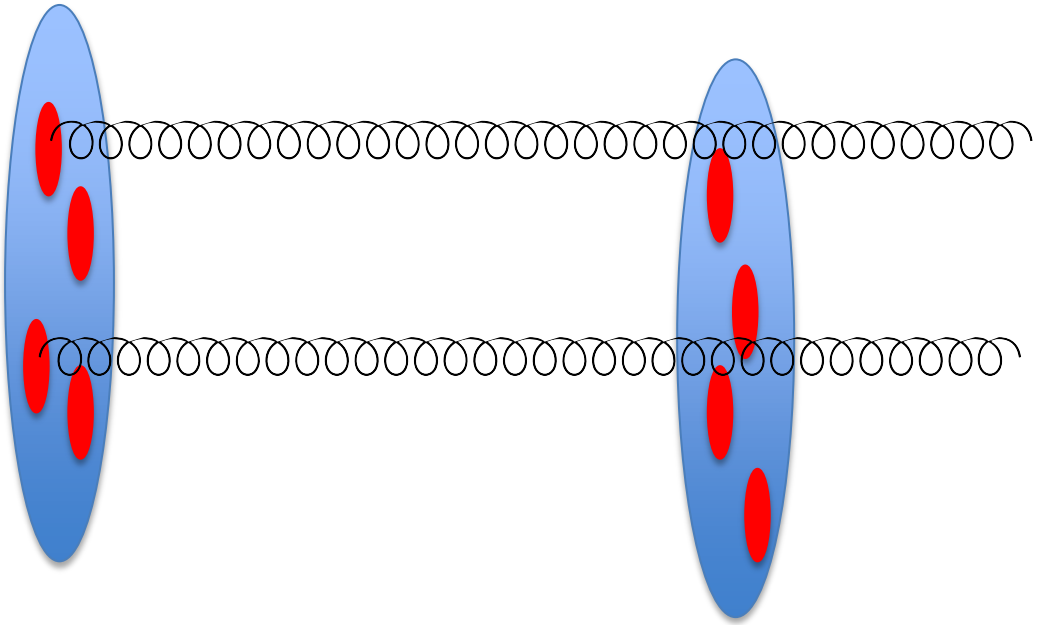

Forward dipole amplitude

$$N(\underline{x}_1, \underline{x}_2) = 1 - \frac{1}{N_c} \langle \mathrm{tr} \left[V(\underline{x}_1)\, V^\dagger(\underline{x}_2) \right] \rangle$$

- Valid both in the quasi-classical Glauber-Mueller/McLerran-Venugopalan multiple-rescattering approximation and for the LLA small-x evolution (BFKL/BK/JIMWLK).

Two-gluon production

- The approximation can also be formulated as resumming all powers of target color charge density ρ_2 while staying at the order- ρ_1^2 in the projectile charge density.

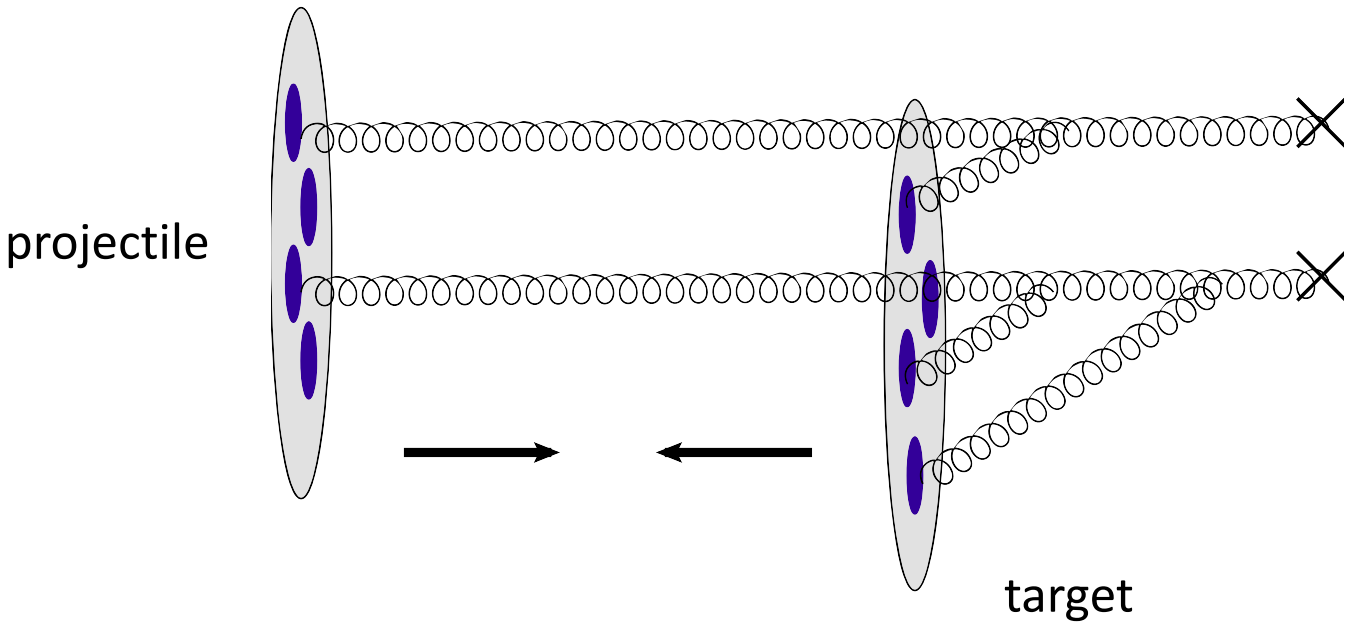

Origin of correlations

- It appears that the correlation is in the connected part Δ of the double-trace correlator

$$\frac{1}{(N_c^2-1)^2}\langle Tr[U_{\mathbf{x}_1}U^\dagger_{\mathbf{x}_2}]\,Tr[U_{\mathbf{x}_3}U^\dagger_{\mathbf{x}_4}]\rangle = \frac{1}{(N_c^2-1)^2}\langle Tr[U_{\mathbf{x}_1}U^\dagger_{\mathbf{x}_2}]\rangle\langle Tr[U_{\mathbf{x}_3}U^\dagger_{\mathbf{x}_4}]\rangle + \Delta(\mathbf{x}_1,\mathbf{x}_2,\mathbf{x}_3,\mathbf{x}_4)$$

- We evaluated the correlator in the Gaussian (MV) approximation in the large-N_c limit.

- Its evolution is not straightforwards: JIMWLK gives a pretty hard to work with expression.

Correlations in AdS shock wave collisions

$$C(k_1, k_2) \sim \cosh(4\,\Delta y)$$

- Correlations grow with rapidity interval???
- It is possible that higher-order corrections in shock wave strengths will modify this result, making it closer to real life.
- However, such corrections are important at later times, and are less likely to affect the long-range rapidity correlation…
- This could be another argument in favor of weakly-coupled dynamics in the early stages of heavy ion collisions.

CGC 2013 - A PERSPECTIVE.

Alex Kovner

University of Connecticut

p-A COLLISIONS A NATURAL HABITAT FOR SATURATION.

SO IS IT THERE? IS IT NOT THERE? CAN WE EVEN TELL IF IT IS THERE?

A WONDERFUL AND SIMPLE IDEA

IN A DENSE SYSTEM (HADRON OR NUCLEUS) THE AVERAGE DENSITY OF PARTONS (OR FIELDS OR WHAT NOT...) DEFINES A TRANSVERSE SCALE $Q_S^2 \propto \rho$.

AT DISTANCE SCALES $\Delta x^2 < Q_S^{-2}$ THE SYSTEM IS DILUTE PARTONIC: GLUON DENSITY AT HIGH MOMENTUM $\Phi(k) \propto 1/k^2$ (up to logarithmic corrections)

AT LOW RESOLUTION SCALES $\Delta x^2 > Q_S^{-2}$ THE SYSTEM IS SATURATED. THERE ARE MUCH LESS GLUONS THAN PERTURBATIVE EXPECTATION: AT $k < Q_S$, $\Phi(k) \propto const$, OR MAYBE EVEN $\Phi(k) \propto k^2$.

Q_S IS ALWAYS THERE - EVEN FOR A PROTON AT REST, BUT $Q_s^2 \sim 0.04 Gev^2$ - NONPERTURBATIVELY SMALL AND SATURATED REGIME IS INTRACTABLE.

BUT IT GROWS WITH ATOMIC NUMBER AND WITH ENERGY $Q_S^2 \propto A^{1/3} s^{\#\alpha_s}$

SO NATURALLY THE BEST WAY TO GET INTO "'PERTURBATIVE SATURATION REGIME"' (CGC ?) IS TO PROBE HEAVY NUCLEUS AT HIGH ENERGY.

TO MINIMIZE STRONG FINAL STATE EFFECTS THE PROBE BETTER BE SMALL, SO IN THE ABSENCE OF e-A MACHINE, THE BEST REACTION IS p-A.

WHAT DO WE EXPECT FORM CGC?

WITH WHAT LEVEL OF ACCURACY CAN WE CALCULATE INTERESTING OBSERVABLES?

MULTIPLICITES

k_T SPECTRUM AND R_{pA}

TWO PARTICLE CORRELATIONS - "THE RIDGE"

MULTIPLICITIES

THE SIMPLEST OBSERVABLE. ROUGHLY SPEAKING PROPORTIONAL TO THE SATURATION MOMENTUM

$$\frac{dN}{dy} \propto \frac{1}{\alpha_S(Q_S^2)} S Q_S^2 \times ln \frac{Q_S^2(1)}{Q_S^2(2)}$$

ASSUMES $\phi(k) \sim const; \quad k < Q_S$ AND k_T FACTORISED GLUON PRODUCTION, AND LOCAL GLUON-HADRON DUALITY - KLN MODEL

Q_S DEPENDS ON ENERGY, RAPIDITY AND CENTRALITY

$$Q_S^2 = Q_0^2 N_{part} \left[x_0 \frac{W}{Q_0} e^{\pm y} \right]^{\lambda}; \qquad Q_0 = 0.6\ Gev; \quad x_0 = 0.01; \quad \lambda = 0.205$$

THIS SIMPLE INPUT PLUS SOME MODELLING AT $x \to 1$ PLUS GLAUBER MONTE CARLO FOR FLUCTUATIONS OF N_{part} AND THEREFORE Q_S OF Pb PRODUCES VERY COMPELLING RESULTS.

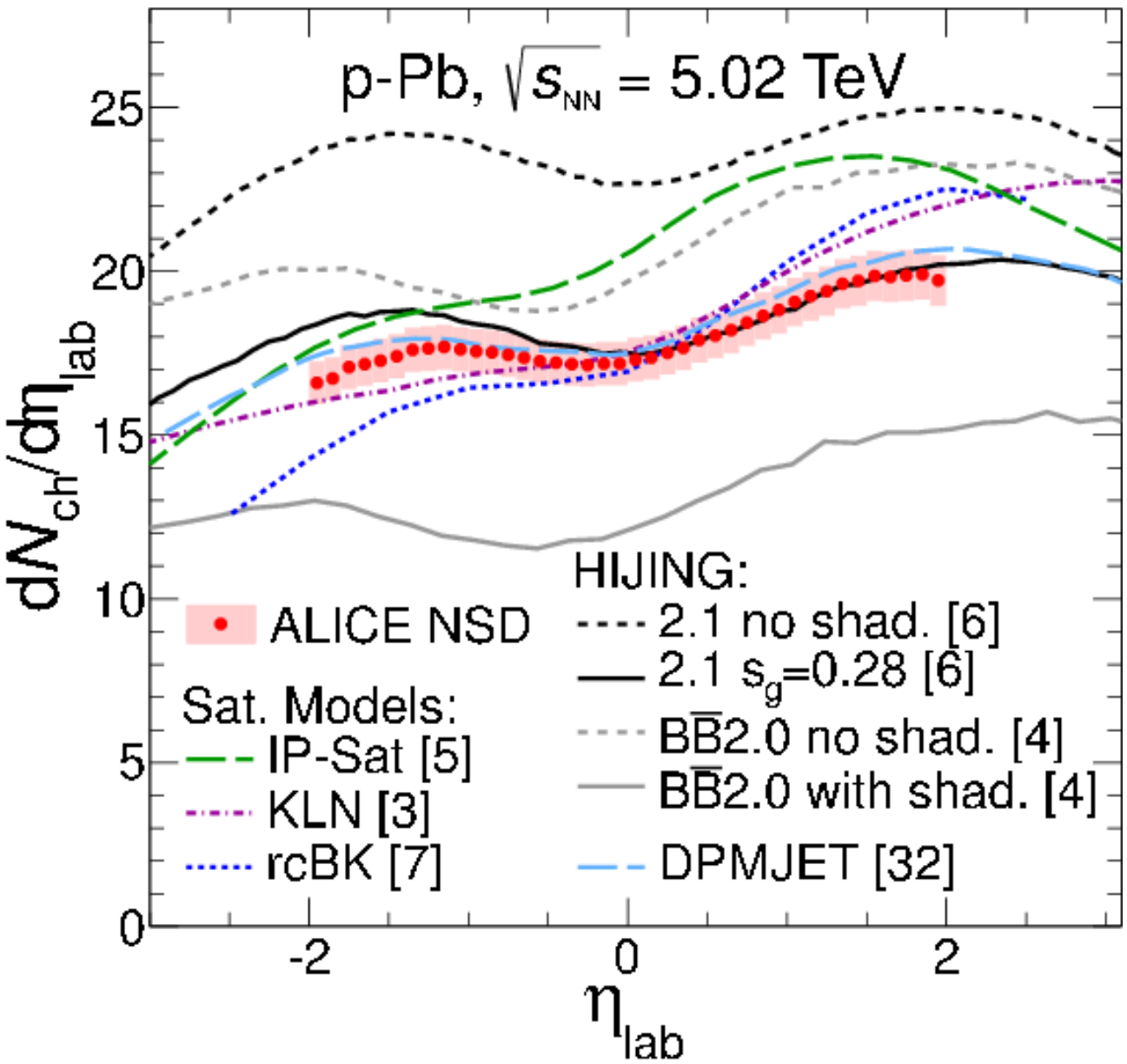
p-Pb, $\sqrt{s_{NN}}$ = 5.02 TeV
$dN_{ch}/d\eta_{lab}$
η_{lab}
ALICE NSD
Sat. Models:
IP-Sat [5]
KLN [3]
rcBK [7]
HIJING:
2.1 no shad. [6]
2.1 s_g=0.28 [6]
B$\bar{B}$2.0 no shad. [4]
B$\bar{B}$2.0 with shad. [4]
DPMJET [32]

rc BK AND FRIENDS

BUT ONE WANTS TO DO MORE AND TO DO IT BETTER.

IN PRINCIPLE WE DO NOT HAVE TO MODEL THE DEPENDENCE OF Q_S ON W AND y. THIS DEPENDENCE SHOULD FOLLLOW FROM THE QCD EVOLUTION: BK/JIMWLK EQUATION.

LAST SEVERAL YEARS "rcBK" APPROACH HAS BEEN DEVELOPED AND VIGOROUSLY APPLIED.
ONE CHOOSES A "REASONABLE" INITIAL CONDITION FOR $\Phi(k)$ AT INITIAL x_0 AND EVOLVES IT IN RAPIDITY WITH THE BALITSKY-KOVCHEGOV EQUATION, WHERE THE COUPLING CONSTANT RUNS AT THE SCALE CHOSEN TO MINIMIZE SOME NEXT TO LEADING ORDER CONTRIBUTIONS.

NEED TO CHOOSE INITIAL CONDITIONS.

$$N(r,x_0) = 1 - \exp\Big[- \frac{(r^2 Q^2_{0S,\ proton})^\gamma}{4} \ln(\frac{1}{\Lambda r})\Big]; \qquad \Phi(k) \propto \frac{1}{\alpha_s(k)} k^2 N(k)$$

PARAMETERS Q_{0s} AND γ ARE CONSTRAINED TO A DEGREE BY FITS TO **DIS HERA** DATA (ANOTHER ADJUSTABLE PARAMETER OR TWO IN α_S)

NEED TO MODEL THE Q_S OF NUCLEUS.

TWO BASIC APPROACHES:

1. THE SIMPLEST IS FIX ONE $Q_{0S,\ nucleus}$ AND SOLVE BK EQUATION WITH THIS INITIAL CONDITION (REZAEIAN also TRIBEDY-VENUGOPALAN).

2. MORE ELABORATE: GLAUBER MONTE CARLO FOR DISTRIBUTION OF NUCLEONS IN THE NUCLEUS YIELDS TRANSVERSE POSITION DEPENDENT Q_S. CALCULATE PARTICLE PRODUCTION LOCALLY IN b AND INTEGRATE OVER b IN THE END (ALBACETE, DUMITRU, FUJII, NARA)

FINALLY: HOW DO WE CALCULATE HADRON PRODUCTION?

1. k_T FACTORIZATION:

$$\frac{dN}{dyd^2p_Td^2R} \propto \frac{1}{p_T^2}\int d^2k_T \int d^2b\alpha_S(Q)\Phi_P(k_T,x_1,b)\Phi_T(p_T-k_T,x_2,R-b)$$

R-NUCLEAR IMPACT PARAMTER, b TRANSVERSE COORDINATE IN THE PROTON. AT HIGH P_T CONVOLUTED WITH GLUON FRAGMENTATION FUNCTION. THIS IS DERIVED FOR PRODUCTION OF SOFT GLUONS - FAR IN RAPIDITY FROM VALENCE PARTONS.

2. FOR MORE FORWARD RAPIDITIES - HYBRID FORMALIZM:

$$\frac{dN}{d\eta d^2k} = \left[\frac{dN}{d\eta d^2k}\right]_{elastic} + \left[\frac{dN}{d\eta d^2k}\right]_{inelastic}$$

$$\left[\frac{dN}{d\eta d^2k}\right]_{elastic} \propto \Sigma_{q,g}x_1 f_{q,g/p}(x_1)N_{q,g}(x_2,k_T)$$

$$\left[\frac{dN}{d\eta d^2k}\right]_{inelastic} \propto \alpha_S(Q)\frac{1}{k^4}\int d^2pp^2N(x_2,p)\int\frac{d\zeta}{\zeta}\omega_j(\zeta)f_j(\frac{x_1}{\zeta},Q^2)$$

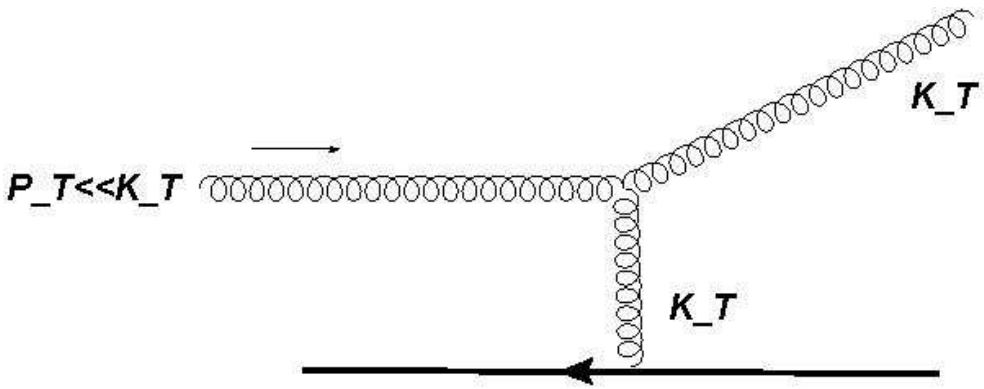

Figure 1: Elastic contribution to particle production.

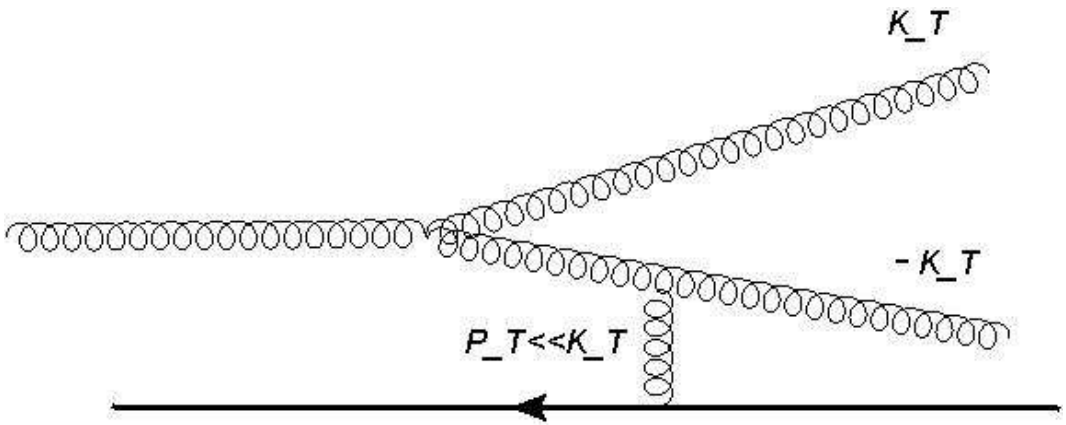

Figure 2: Inelastic contribution to particle production.

INELASTIC CONTRIBUTION FORMALLY A PERTURBATIVE CORRECTION, BUT IS OF THE SAME ORDER AS DGLAP EVOLUTION OF PARTONIC DISTRIBUTIONS IN THE ELASTIC PART.

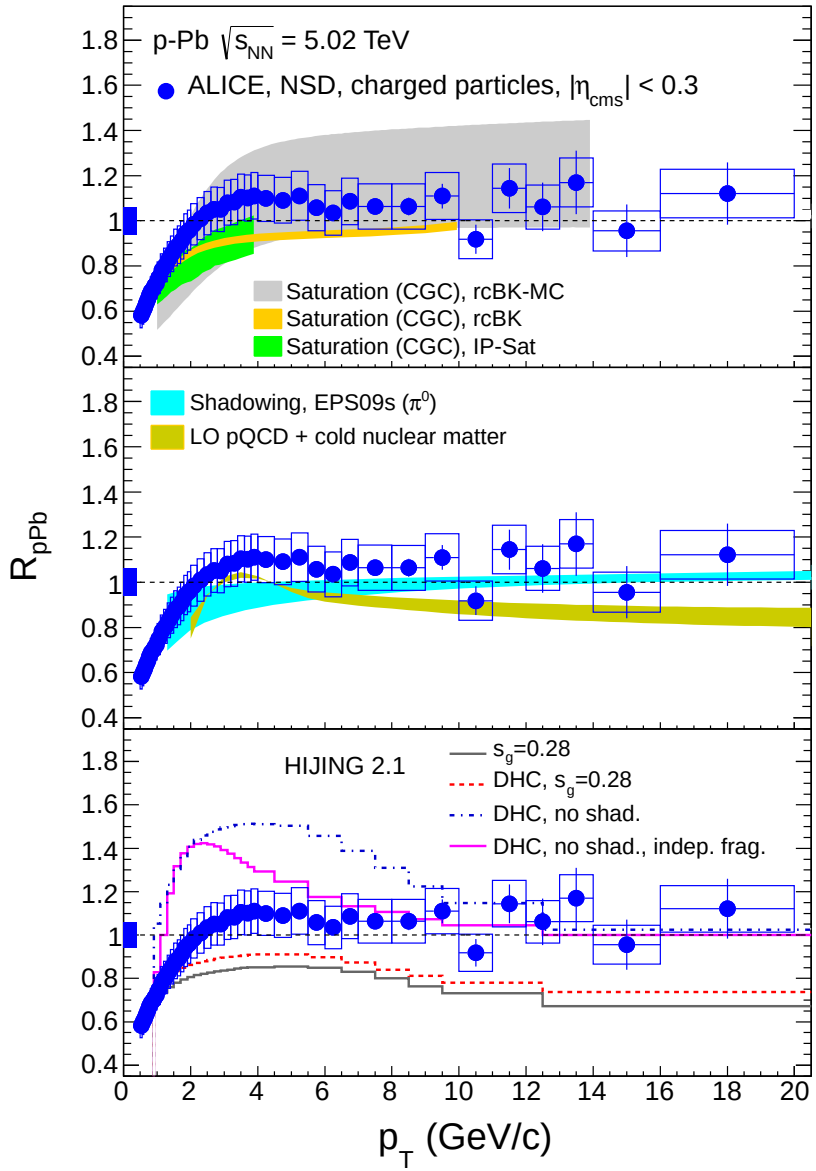

Figure 3: ALICE data: NO CRONIN PEAK (check), SUPPRESSION UP TO 2 Gev (check), VERY FLAT $R_{pA} \sim 1$ ABOVE 2-3 Gev (kh-m, check)

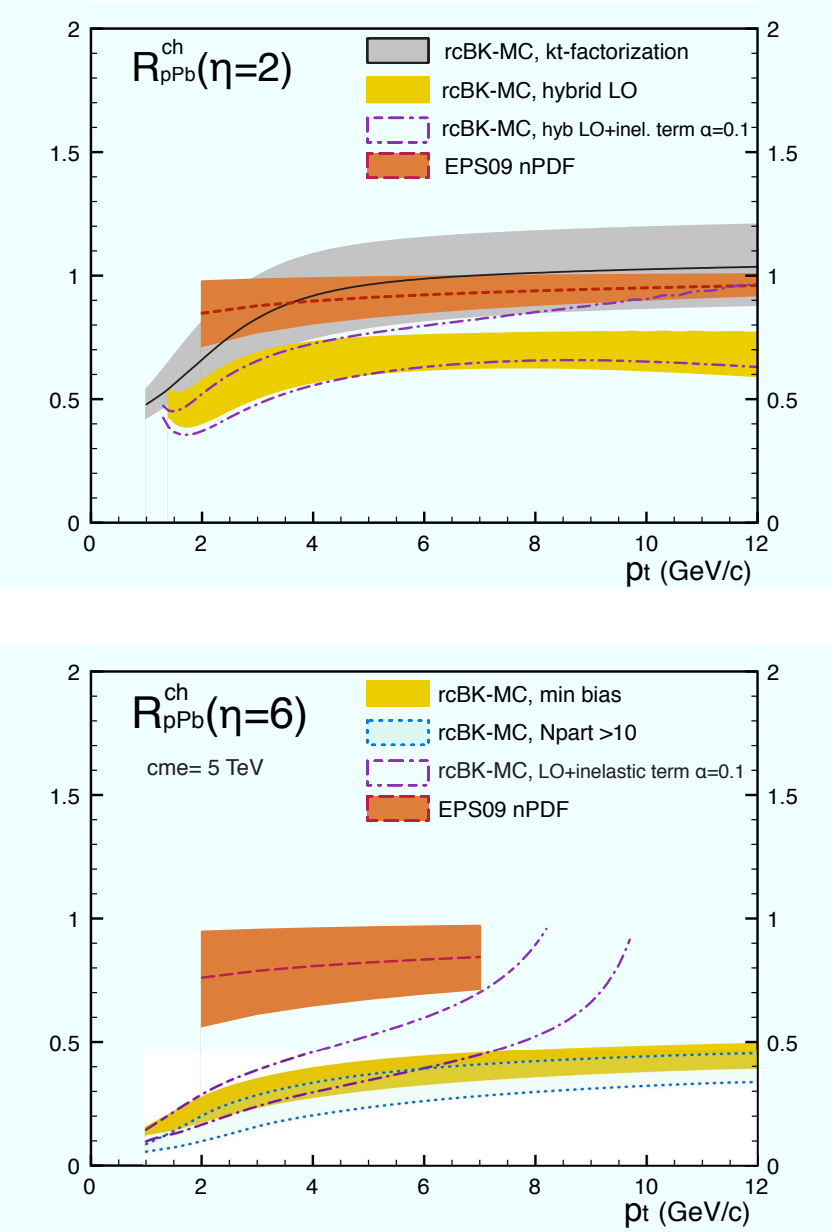

Figure 4: Albacete et.al. - predictions for p-Pb at 5 Tev

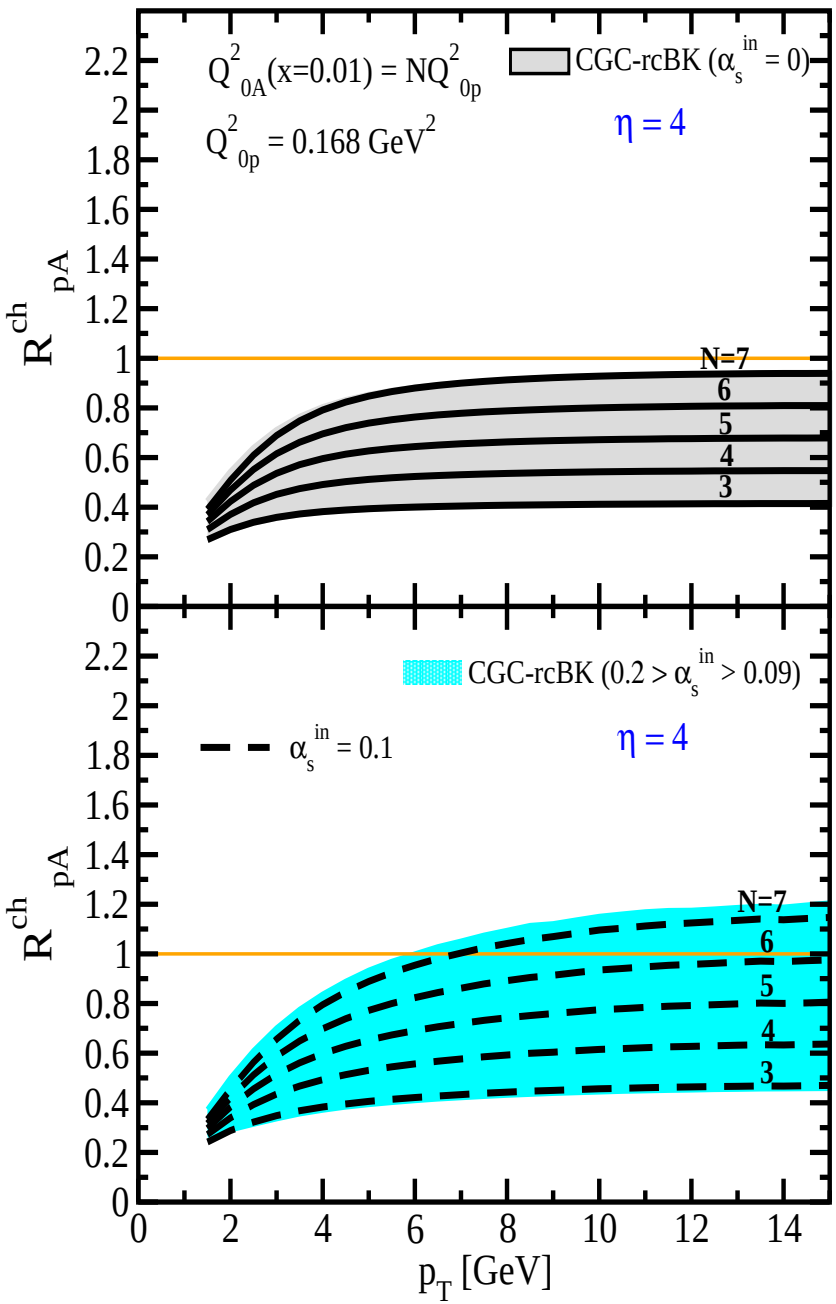

Figure 5: Rezaeian - predictions for p-Pb at 5 Tev

CLEARLY THE PREDICTION BAND IS VERY WIDE

CLEARLY THE EFFECT OF THE PERTURBATIVE CORRECTION - THE INELASTIC TERM IS VERY LARGE.

SO WE NEED TO UNDERSTAND THINGS BETTER.

IS PERTURBATION THEORY UNSTABLE? POSSIBLY. THEN WE ARE IN TROUBLE.

MORE LIKELY, I THINK, THE INELASTIC CORRECTION IS NOT AS BIG AS IT LOOKS. AT FORWARD RAPIDITIES AND LARGE TRANSVERSE MOMENTA THE PARTON PAIR ONLY EXIST FOR A SHORT TIME AND SHOULD NOT BE ABLE TO SCATTER COHERENTLY OFF THE TARGET. COHERENT SCATTERING APPROXIMATION MAY WELL BE AT FAULT.

MORE COMPLETE PERTURBATIVE CORRECTION EXISTS: CHIRILLI, XIAO, YUAN - BUT THE SCATTERING IS STILL TREATED THERE AS COHERENT.

rcBK ALSO PRODUCES PARTICLE MULTIPLICITIES. SO DO OTHER PHENOMENOLOGICAL SATURATION ANSATZE FOR THE GLUON DENSITY (IP-SAT, b-CGC)

IRONICALLY THE "OF THE SHELF" KLN MODEL STILL DOES THE BEST JOB.

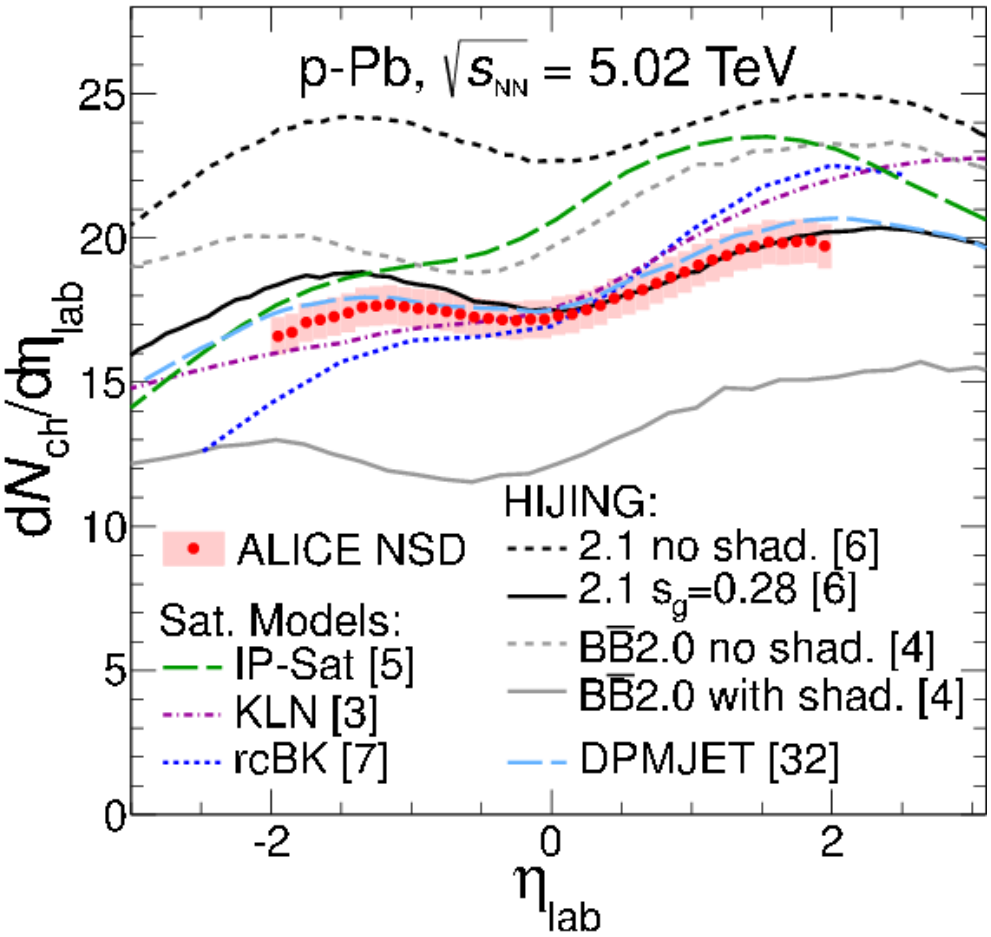

THE RIDGE

CMS OBSERVATION OF RIDGE IN p-p FOLLOWED BY ALICE AND ATLAS OBSERVATION IN p-Pb

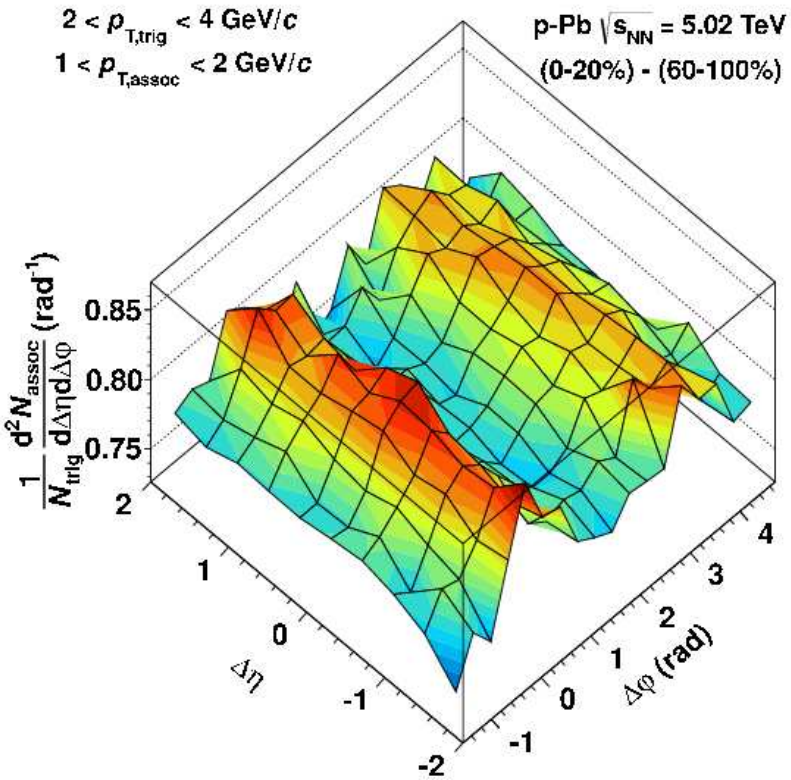

Figure 6: ALICE RIDGE

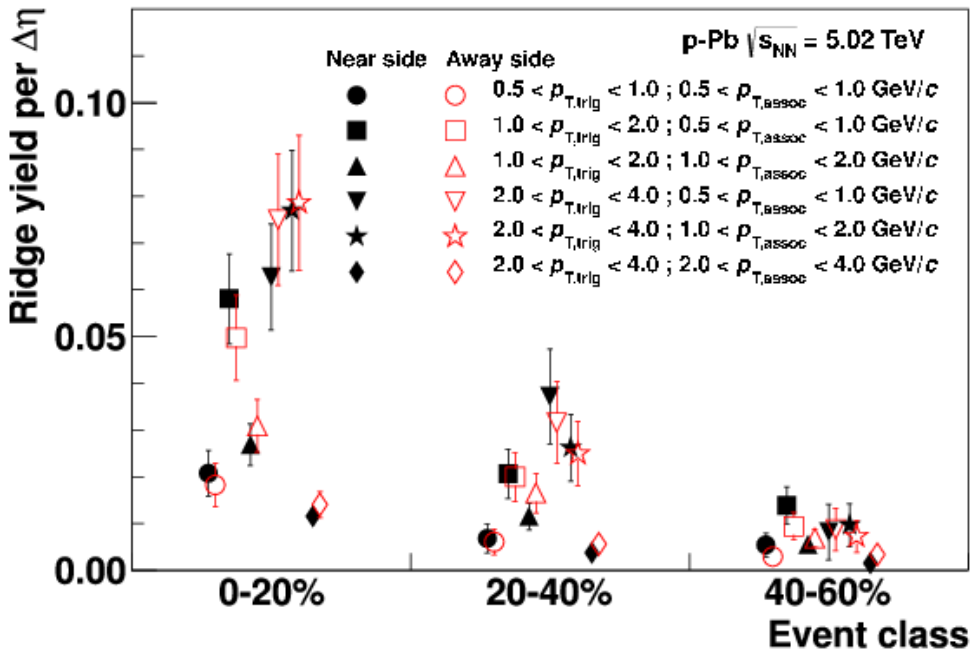

Figure 7: ALICE ridge at different p_T

QUALITATIVELY SIMILAR STRUCTURE: TWO PARTICLE CORRELATIONS LONG RANGE IN RAPIDITY (> 4 UNITS); AND COLLIMATED IN AZYMUTHAL ANGLE.
p-Pb SIGNAL IS STRONGER (ABOUT A FACTOR OF 2.5-3 FOR CORRELATED YIELD).
THE PLOTS ARE FOR ASSOCIATED YIED $R(\Delta\eta) \sim \frac{N_{correlated\ pairs}}{N_{trigger\ particles}}$

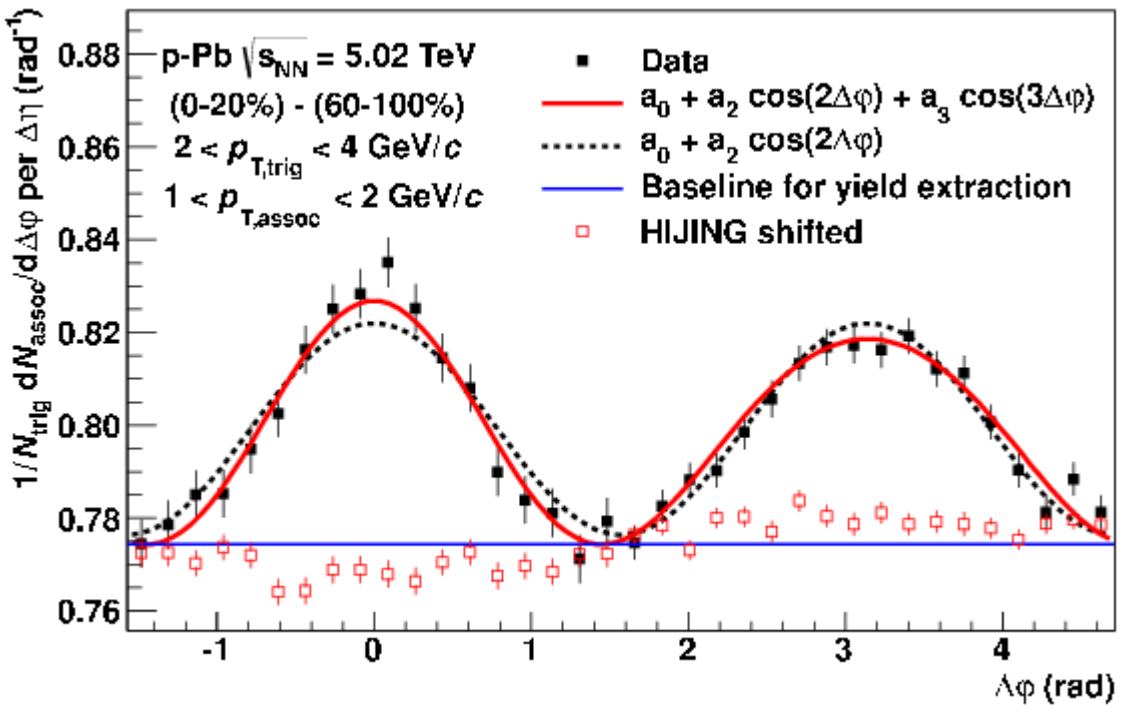

Figure 8: ALICE RIDGE IS SYMMETRIC

ALSO THE p-Pb SIGNAL IS SYMMETRIC IN $\Delta\phi \to \Delta\phi + \pi$.

VIGOROUS ACTIVITY TO DESCRIBE THE RIDGE WITHIN CGC APPROACH - **DUSLING AND VENUGOPALAN**

IT IS CERTAINLY CGC INSPIRED.
INVOLVES QUITE A BIT OF MODELING. E.G. REQUIRES A CHOICE OF Q_S FOR EVERY MULTIPICITY CLASS (NOT UNREASONABLE).
MOST IMPORTANT LIMITATION IN MY VIEW IS THAT IT TAKES AN ANSATZ FOR TWO PARTICLE PRODUCTION PROBABILITY FROM DILUTE LIMIT (HIGH p_T), AND APPLIES IT TO ALL MOMENTA.
THE VALIDITY IS NOT UNDER THEORETICAL CONTROL.
SOME IMPORTANT LEADING IN N_C EFFECTS ARE NOT INCLUDED. THE RESULTS OF DV ARE BASED ON A SUBLEADING IN N_C CONTRIBUTION.

A SHORT RUNDOWN OF EFFECTS THAT LEAD TO COLLIMATION.

1. DIRECTED COLOR FIELDS IN THE TARGET (KOVNER, LUBLINSKY). COLOR FIELDS IN THE TARGET HAVE FINITE CORRELATION LENGTH GIVEN BY $Q_{S,TARGET}$. WHEN TWO GLUONS FROM THE PROJECTILE SCATTER OFF THE SAME FIELD, THEY PICK UP THE SAME MOMENTUM TRANSFER. THIS LEADS TO POSITIVE ANGULAR CORRELATIONS. THIS IS LEADING N_C EFFECT. AT PRESENT WE DO NOT UNDERSTAND ITS ENERGY DEPENDENCE.
THIS EFFCT IS NOT INCLUDED IN DV

2. VARIATION OF COLOR FILED DENSITY IN THE TARGET (LEVIN AND REZAEIAN). IF THE SIZE OF THE INCOMING TWO GLUON STATE IS COMPARABLE TO THE SIZE OF THE REGION OVER WHICH Q_S VARIES, THERE IS A PREFERRED DIRECTION FOR SCATTERING - ALONG THE GRADIENT OF Q_S. THIS IS ALSO A LEADING N_C EFFECT AND HAS LEADING BEHAVIOR AT HIGH ENERGY. THE RELEVANT MOMENTUM RANGE HOWEVER IS NOT Q_S, BUT "THE CORRELATION LENGTH OF Q_S". STILL, GIVEN THAT Q_S FLUCTUATES IN IMPACT PARAMETER, IT MAY BE QUITE IMPORTANT.
THIS EFFCT IS NOT INCLUDED IN DV

3. BOSE CORRELATIONS BETWEEN THE GLUONS OF PROJECTILE. (DUMITRU, DUSLING, GELIS, JALILIAN MARIAN, LAPPI, MCLERRAN, VENUGOPALAN) DENSITY OF PROJECTILE GLUONS WITH THE SAME QUANTUM NUMBERS (TRANSVERSE MOMENTUM AND COLOR) IS ENHANCED DUE TO BOSE CORRELATIONS. THE GLUONS IN THIS CORRELATED CONFIGURATION PREFER TO SCATTER IN THE SAME DIRECTION. SINCE THE INCOMING GLUONS HAVE TO BE IN THE SAME COLOR STATE, THIS IS A SUBLEADING IN N_C CONTRIBUTION RELATIVE TO GENERIC SITUATION WHERE THE COLOR OF INCOMING GLUONS IS INDEPENDENT.
THIS EFFCT IS INCLUDED IN DV AND GIVES ALL THE CORRELATED CONTRIBUTION.

ALL THE ABOVE MECHANISMS LEAD TO SYMMETRIC CONTRIBUTIONS AT ϕ AND $\phi + \pi$.

DV CALCULATION IS AN INTERESTING MODEL, BUT IT IS HARD TO SEE HOW IT CAN BE THE LAST WORD. TANTALIZING THAT IT GIVES SUCH GOOD QUANTITIVE AGREEMENT WITH THE DATA. COULD BE AN ACCIDENT, OR COULD BE THAT THE OTHER EFFECTS ARE FOR SOME REASON SUPPRESSED.

IT IS IMPORTANT THAT THIS CALCULATION IS OUT THERE AS A BASELINE FOR FUTURE, HOPEFULLY MORE COMPLETE ONES

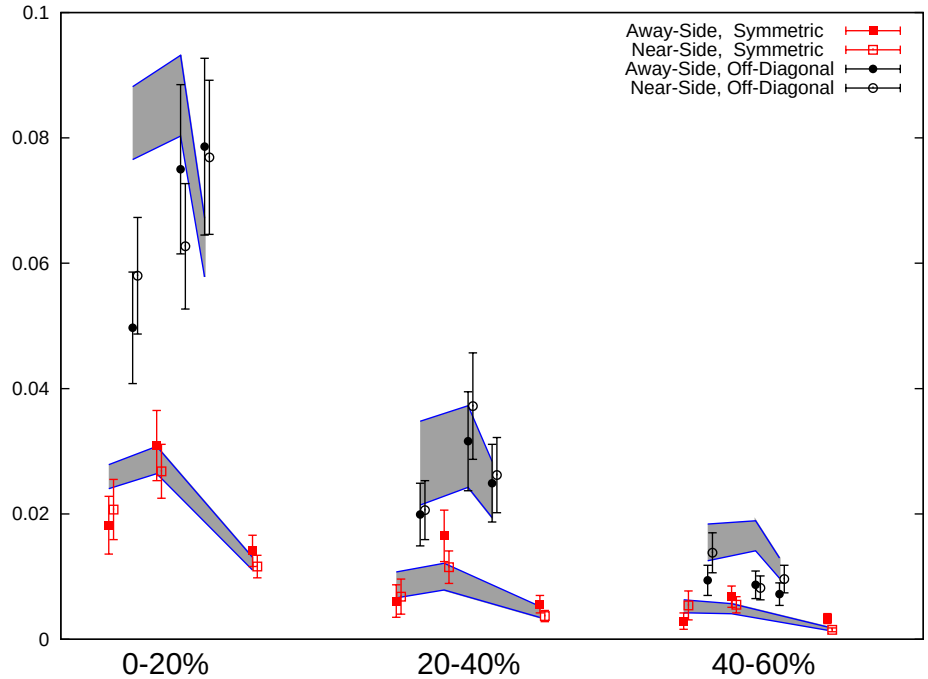

Figure 9: DUSLING-VENUGOPALAN FIT TO ALICE (LARGE FLUCTUATIONS IN Q_S?)

CONCLUSIONS

A MIXED BAG: QUALITATIVELY THINGS WORK QUITE WELL - A LOT OF FEATURES OF THE DATA ARE REPRODUCED.

IS IT A **THEORY** AS OPPOSED TO **MODEL**? NOT YET. STILL MANY AD HOC APPROXIMATIONS WITH NO OBVIOUS CONTROL ON THEIR VALIDITY PLUS A LOT OF FREEDOM IN FITTING (CHANGING) PARAMETERS.

THE USUAL ANNOYING THING. HERE IS A GOOD, SIMPLE IDEA. YOU MAKE THE SIMPLEST POSSIBLE ESTIMATE INSPIRED BY IT, AND IT WORKS BETTER THAN IT HAS THE RIGHT TO WORK. YOU IMPROVE IT BY MAKING REAL CALCULATION (INCLUDING PERTURBATIVE CORRECTIONS AND SUCH) AND THINGS GET ONLY WORSE. USUALLY ONE HAS TO WORK REALLY HARD TO GET BACK THE ACCURACY OF THE ORIGINAL BACK-OF-THE ENVELOPE ESTIMATE FROM THE REAL CONTROLLABLE CALCULATION.

TYPICAL TEENAGER: SHOOTS UP A FOOT IN HIGHT IN A YEAR, BUT DOES NOT QUITE KNOW WHAT TO DO WITH HIS LONG ARMS, PLUS HAS TONS OF PIMPLES. IT WILL TAKE TIME AND EFFORT TO GROW HIM INTO A PROFESSIONAL ATHLETE WITH SMOOTH SKIN (OR ALTERNATIVELY INTO A RESPECTED UNIVERSITY PROFESSOR). BUT IN THE END IT MAY HAPPEN.

SO I HOPE THAT WE ARE AT THIS STAGE IN THE CHAIN - MOVING FROM BACK OF THE ENVELOPE STUFF TO REAL CALCULATIONS, ALTHOUGH NOT QUITE THERE YET.

Combined analysis of RHIC to LHC suppression & Geometry

Roy A. Lacey
Chemistry Dept.,
Stony Brook University

Primary focus:

Scaling properties of flow & Jet quenching

Flow & Jet quenching are important probes of the QGP!

3-4 < pT < 8-10 GeV/c

Transition Region

pT < 3 - 4 GeV/c **Flow**

pT > 8 - 10 GeV/c **Jet suppression**

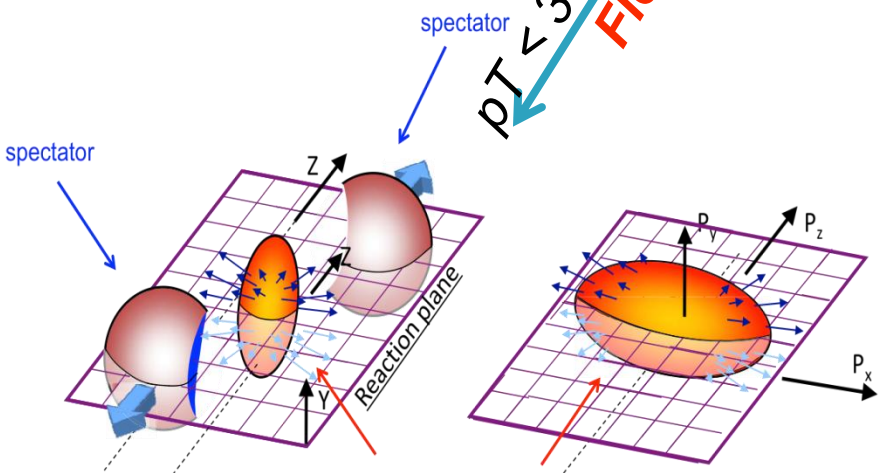

Eccentricity driven & acoustic

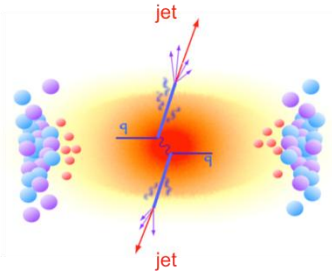

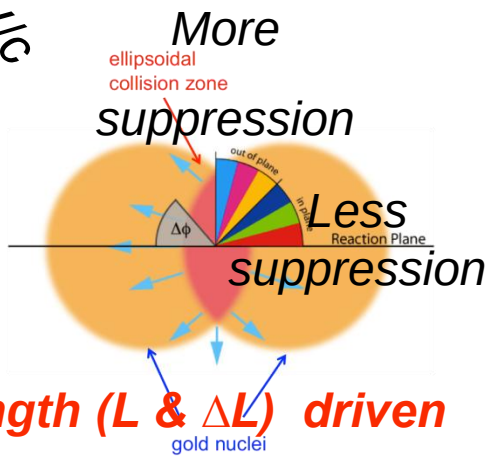

Path length (L & ΔL) driven

Flow and Jet suppression are linked to Geometry & the interactions in the QGP

- **This implies very specific scaling properties for flow and jet suppression (respectively), which can be tested experimentally**

✓ ***Scaling validation provide important insights, as well as straightforward probes of transport coefficients***

Geometric Quantities for scaling

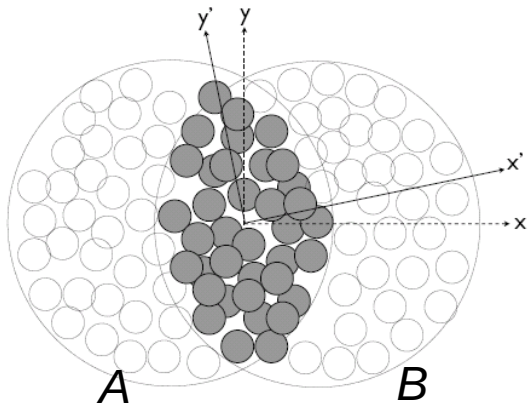

Phys. Rev. C 81, 061901(R) (2010)

$$S_{nx} \equiv S_n \cos(n\Psi_n^*) = \int d\mathbf{r}_\perp \rho_s(\mathbf{r}_\perp)\omega(\mathbf{r}_\perp)\cos(n\phi)$$

$$S_{ny} \equiv S_n \sin(n\Psi_n^*) = \int d\mathbf{r}_\perp \rho_s(\mathbf{r}_\perp)\omega(\mathbf{r}_\perp)\sin(n\phi),$$

$$\Psi_n^* = \frac{1}{n}\tan^{-1}\left(\frac{S_{ny}}{S_{nx}}\right)$$

$$\varepsilon_n = \left\langle \cos n\left(\phi - \psi_n^*\right)\right\rangle$$

$$\frac{1}{\bar{R}} = \sqrt{\left(\frac{1}{\sigma_x^2} + \frac{1}{\sigma_y^2}\right)}$$

$\omega(r_\perp) = r^n$

$L = \bar{R}$

$\Delta L \sim \varepsilon \bar{R}$

arXiv:1203.3605

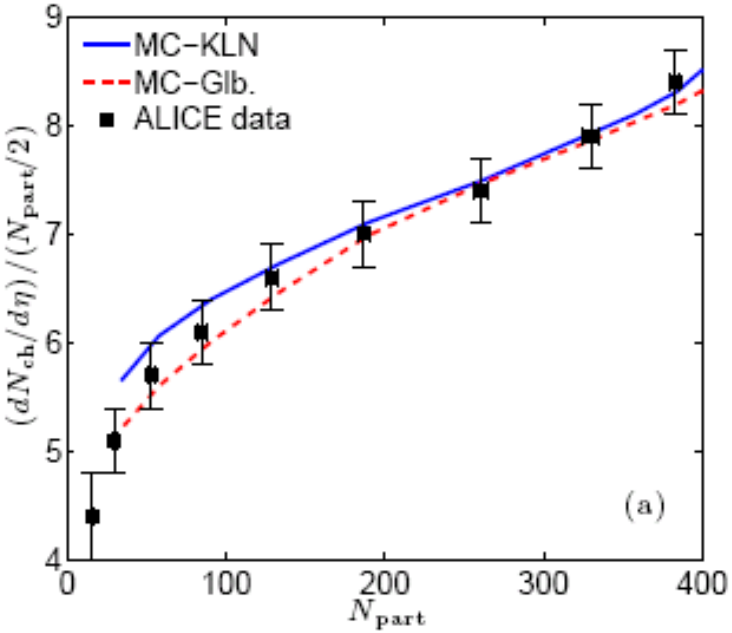

σ_x & σ_y → *RMS widths of density distribution*

- ***Geometric fluctuations included***
- ***Geometric quantities constrained by multiplicity density.***

The Flow Probe

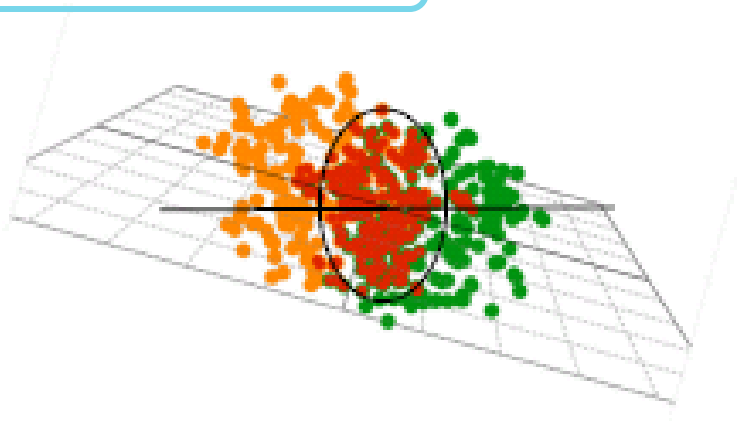

Initial Geometry characterized by many shape harmonics (ε_n) → drive v_n

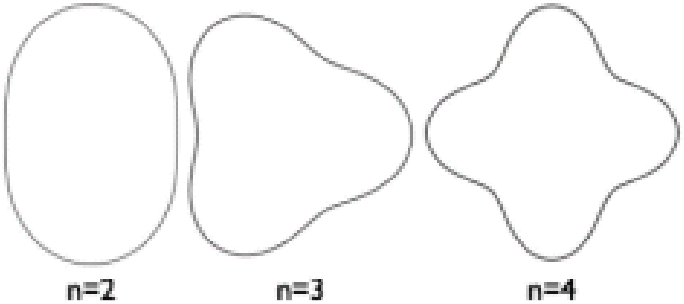

$$\frac{dN}{d\phi} \propto \left(1 + 2\sum_{n=1} v_n(p_T)\cos n(\phi - \psi_n)\right)$$

Acoustic viscous modulation of v_n

$$\delta T_{\mu\nu}(t,k) = \exp\left(-\frac{2}{3}\frac{\eta}{s}k^2\frac{t}{T}\right)\delta T_{\mu\nu}(0)$$

Staig & Shuryak **arXiv:1008.3139**

$$k = n / \bar{R}$$

$$\delta T_{\mu\nu}(n,t) = \exp\left(-\beta n^2\right)\delta T_{\mu\nu}(0), \quad \beta = \frac{2}{3}\frac{\eta}{s}\frac{1}{\bar{R}^2}\frac{t}{T}$$

Particle Distribution

$$f = f_0 + \delta f(\tilde{p}_T), \quad \tilde{p}_T = \frac{p_T}{T}$$

Scaling expectations

$$\frac{v_n(p_T)}{\varepsilon_n} \propto \exp\left(-\beta' n^2\right)$$

$$\frac{v_n(p_T)}{v_2(p_T)} = \frac{\varepsilon_n}{\varepsilon_2}\cdot\exp\left(-\beta'(n^2-4)\right)$$

Note that v_n is related to v_2

$$\ln\left(\frac{v_n}{\varepsilon_n}\right) \propto \frac{-\beta''}{\bar{R}}$$

$$\beta''(\tilde{p}_T) \propto p_T^{\alpha'}$$

$v_n(\psi_n)$ Measurements - ATLAS

ATLAS data - Phys. Rev. C86, 014907 (2012) & ATLAS-CONF-2011-074

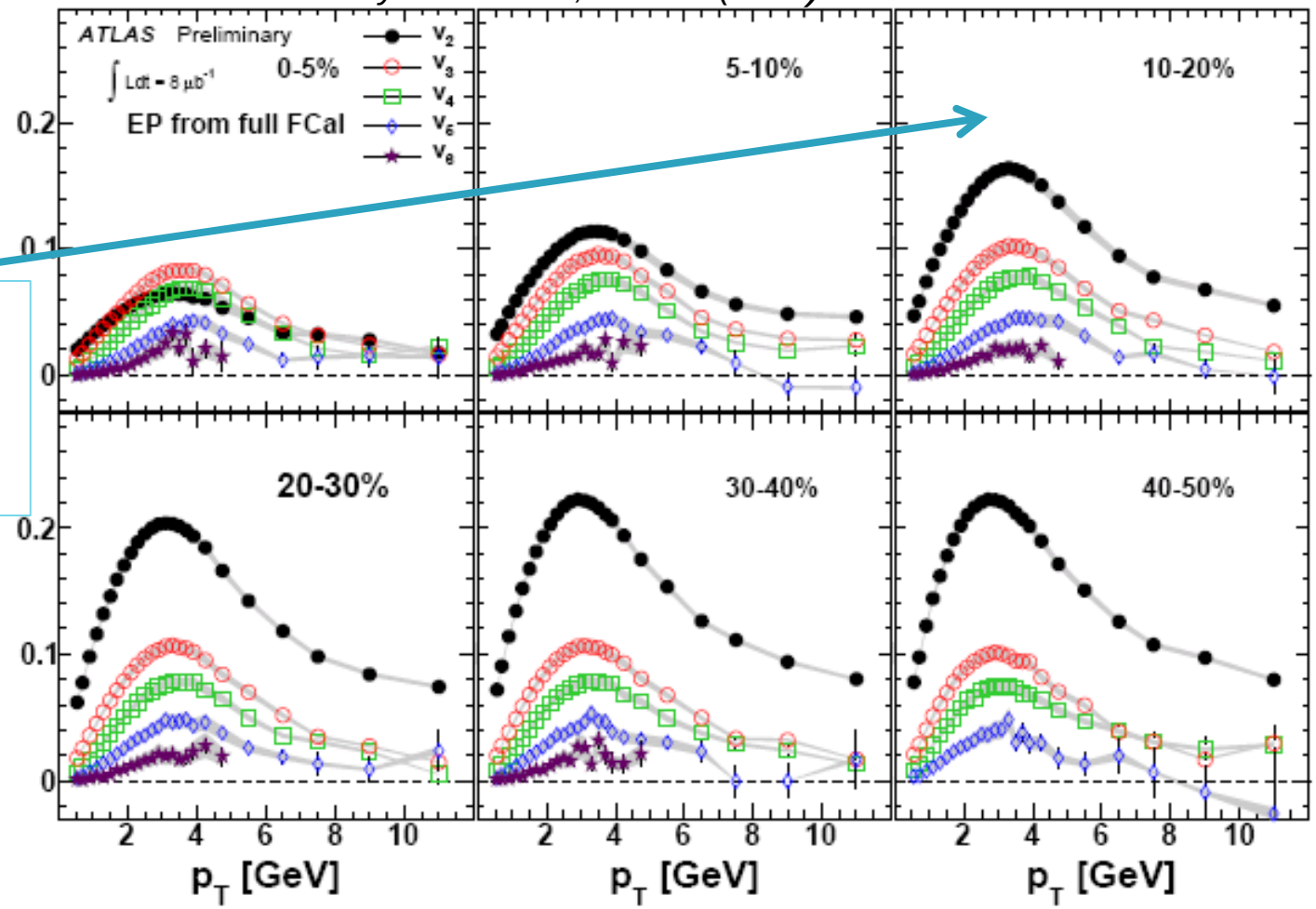

Note v_n increase from central to peripheral collisions

High precision double differential Measurements for Pb+Pb are pervasive → Do they scale?

$v_n(\psi_n)$ Measurements - LHC

Recent p+Pb measurements

ATLAS Data - arXiv:1212.5198.

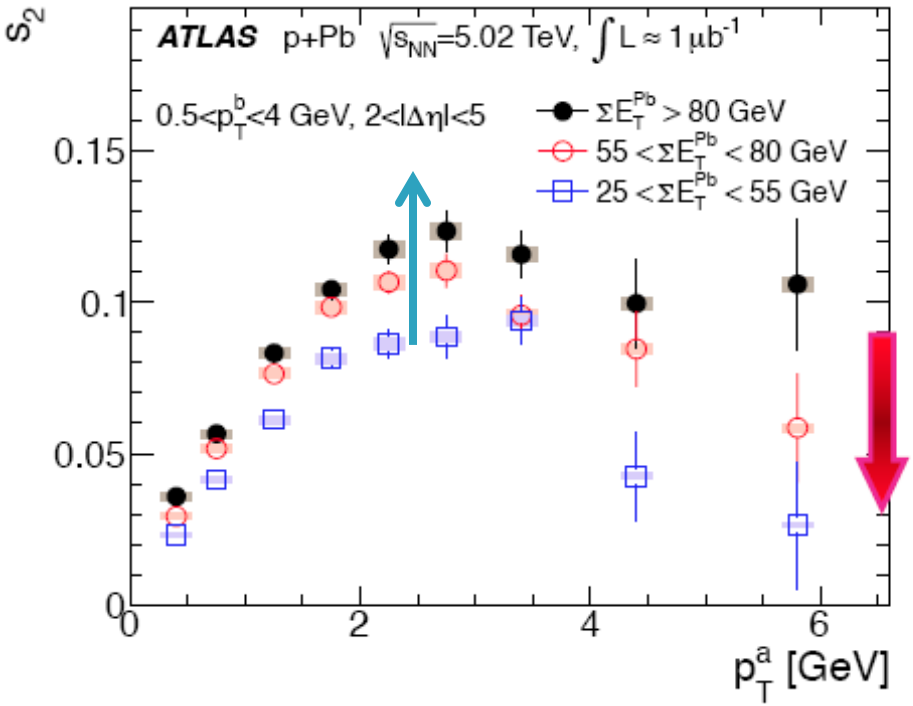

ALICE Data - arXiv:1212.2001

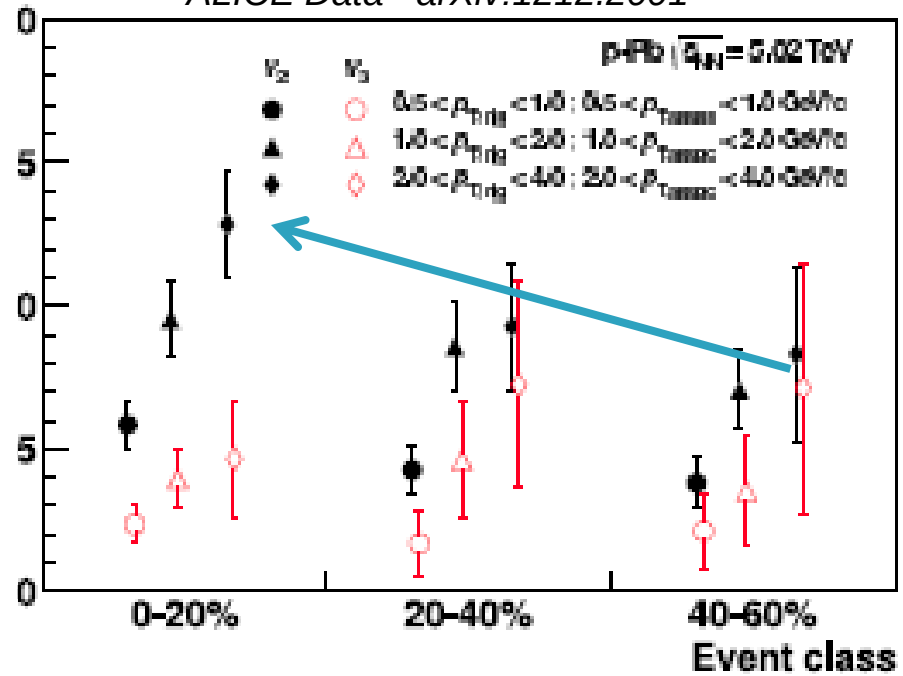

✓ **Note increase of v_2 (or s_2) from peripheral to central collisions**

Double differential Measurements for p+Pb are pervasive → Do they scale?

Acoustic Scaling – n^2

$$\frac{v_n(p_T)}{\varepsilon_n} \propto \cdot \exp\left(-\beta' n^2\right)$$

ATLAS data - Phys. Rev. C86, 014907 (2012)

arXiv:1301.0165

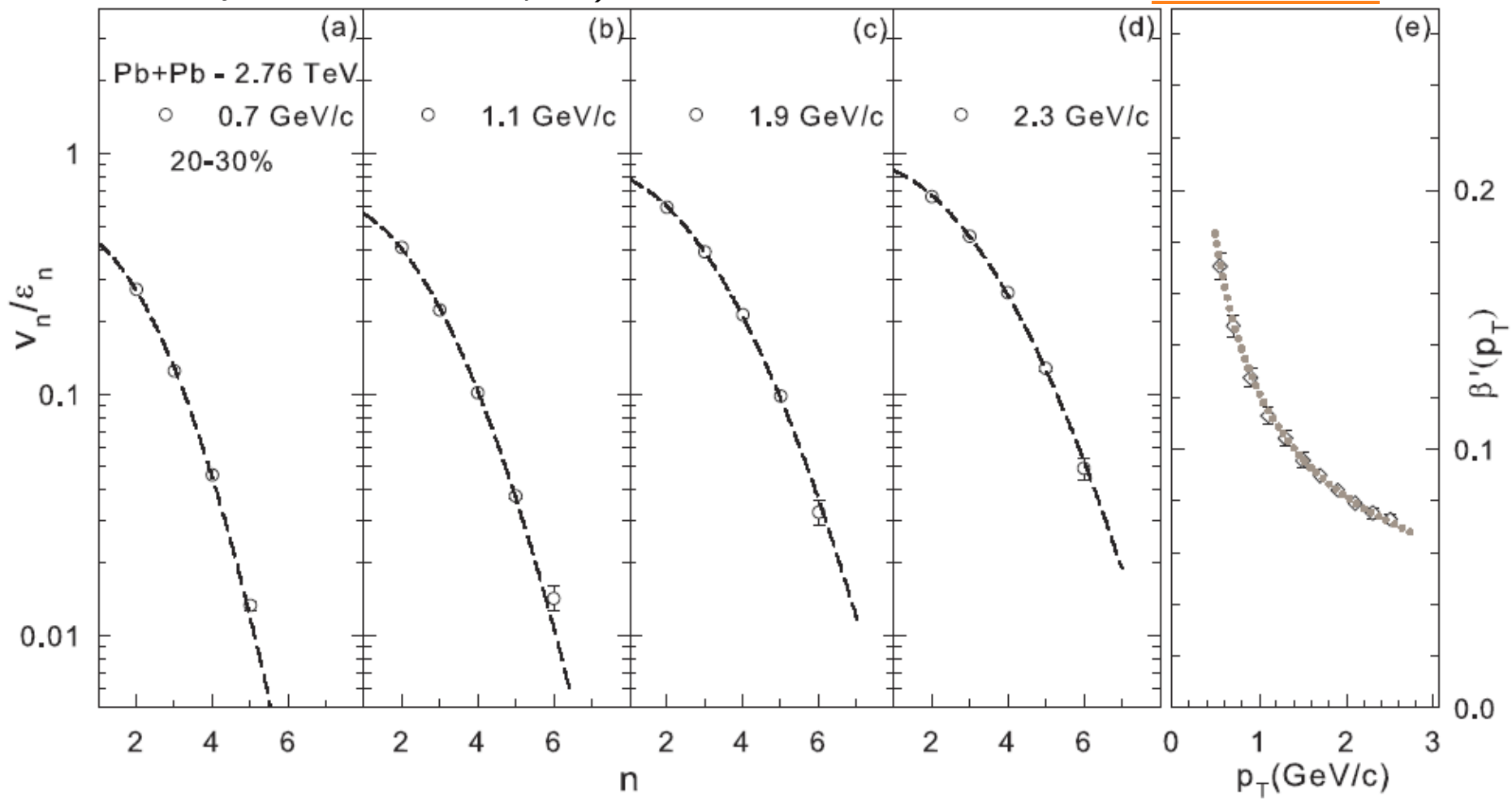

- ✓ **Characteristic n^2 viscous damping validated**
- ✓ **Characteristic *$1/(p_T)^\alpha$ dependence of extracted β values validated***

Constraint for η/s and δf

Acoustic Scaling - Ratios

$$\frac{v_n(p_T)}{v_2(p_T)} = \frac{\varepsilon_n}{\varepsilon_2} \exp\left(-\beta'(n^2-4)\right)$$

arXiv:1301.0165

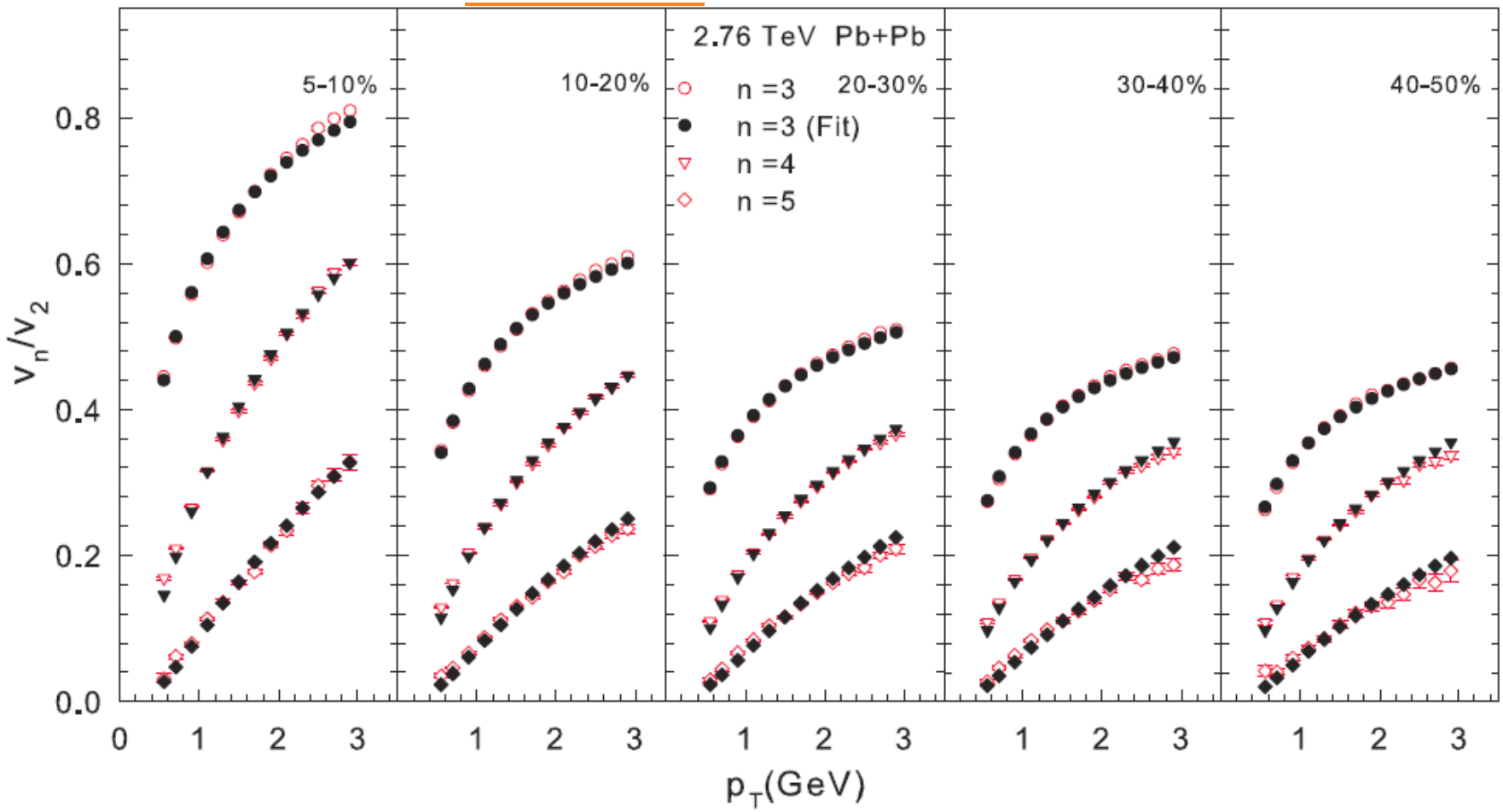

- ✓ **Characteristic (n^2 – 4) viscous damping validated**
- ✓ **Characteristic *$1/(p_T)^\alpha$ dependence of β validated***

Constraint for η/s

Acoustic Scaling - Ratios

$$\frac{v_n(p_T)}{v_2(p_T)} = \frac{\varepsilon_n}{\varepsilon_2} \exp\left(-\beta'(n^2-4)\right)$$

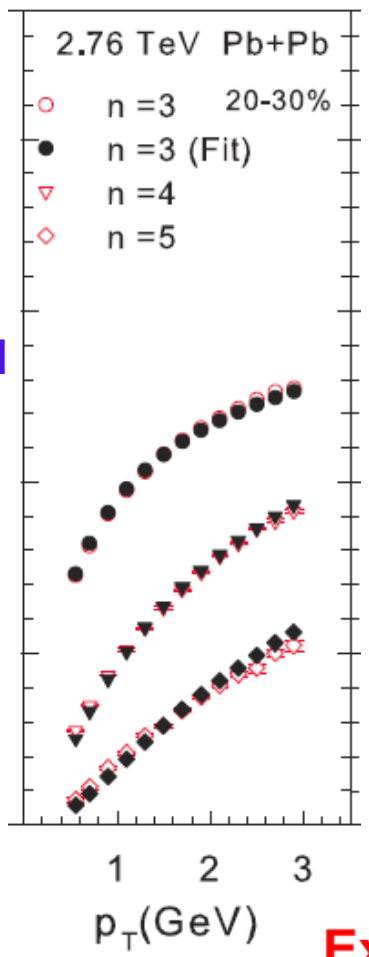

Fits performed for each centrality

arXiv:1301.0165

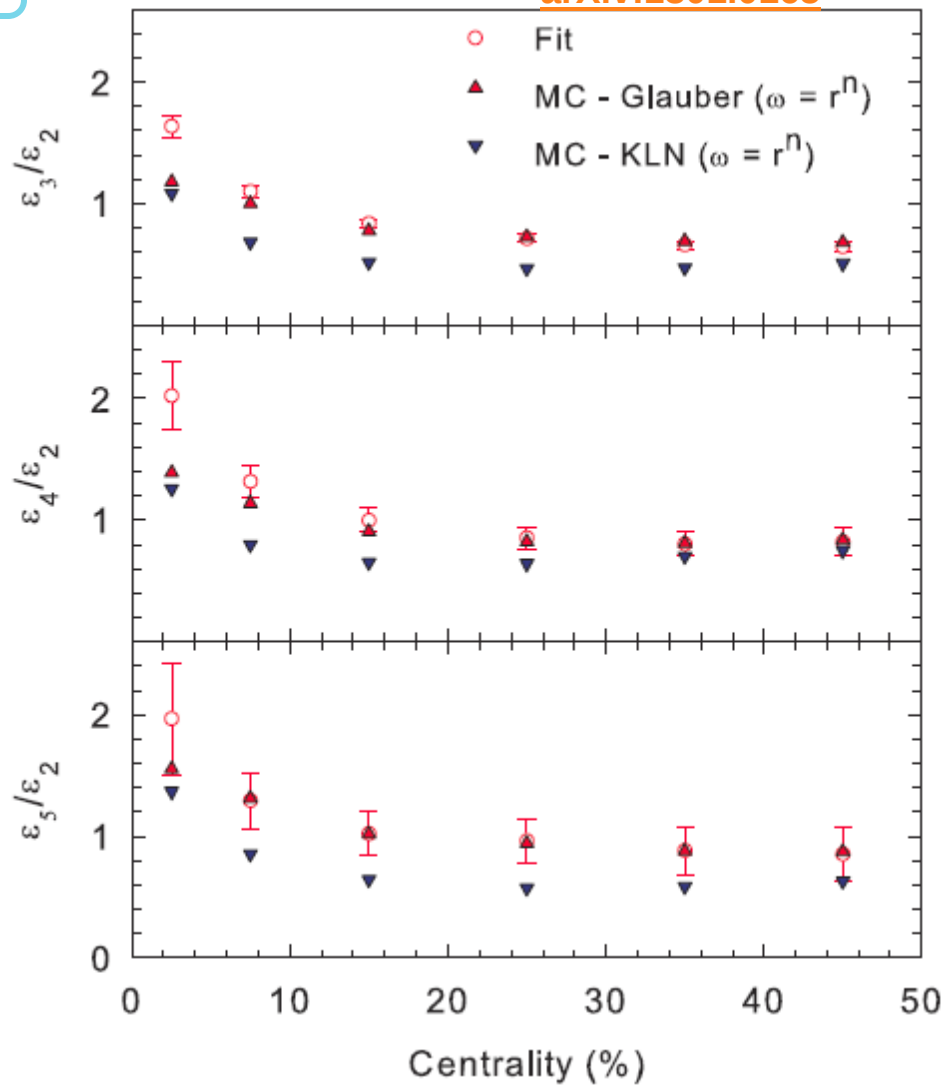

Extracted ratios for $\frac{\varepsilon_n}{\varepsilon_2}$ provide straightforward constraints for eccentricity models

Acoustic Scaling - Ratios

arXiv:1105.3782

$$\frac{v_n(p_T)}{v_2(p_T)} = \frac{\varepsilon_n}{\varepsilon_2} \exp\left(-\beta'(n^2-4)\right)$$

$$v_n(p_T) \propto (v_2)^{n/2}$$

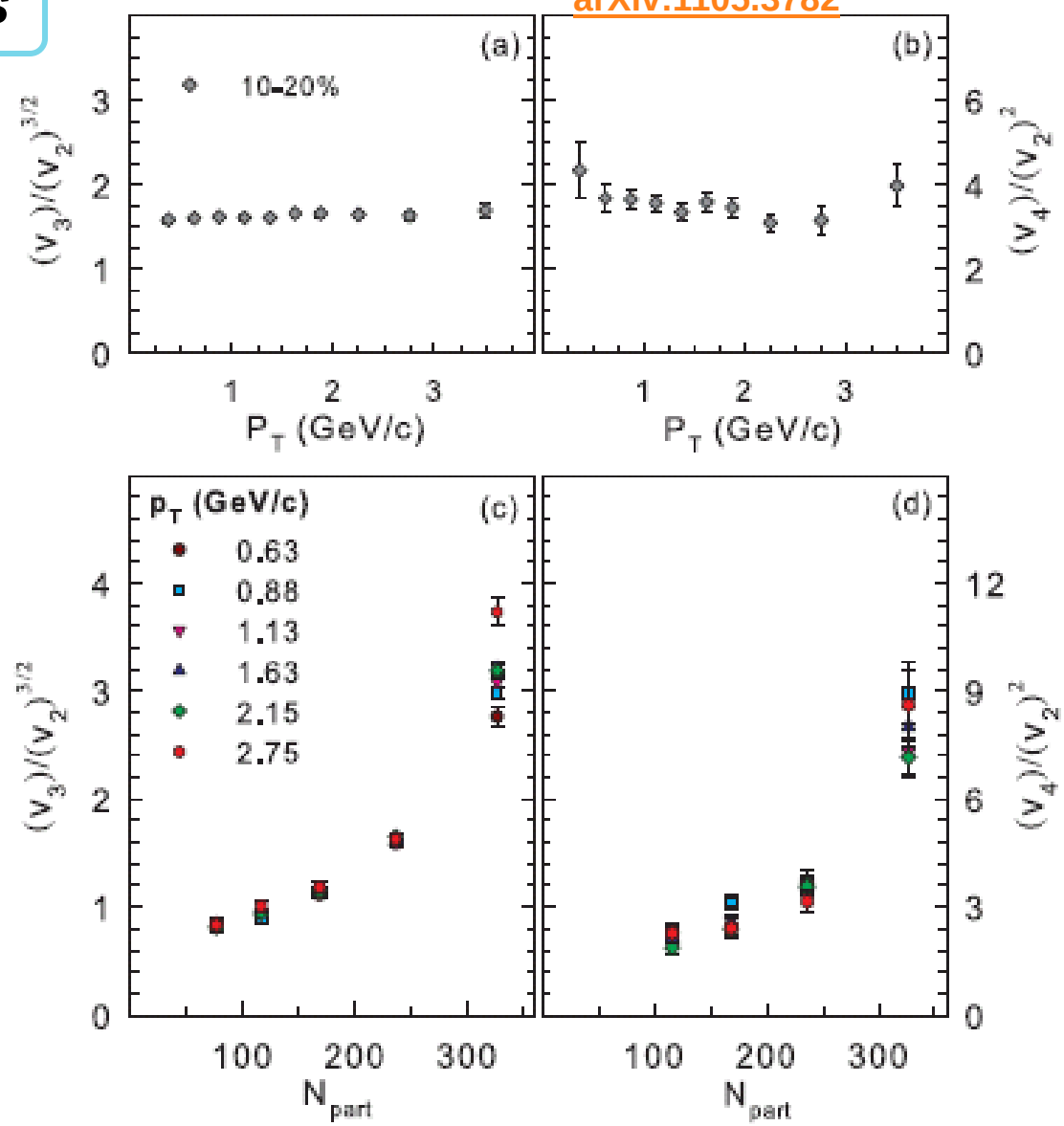

The expected relation between v_n and v_2 is validated

Flow is partonic & Acoustic?

arXiv:1211.4009

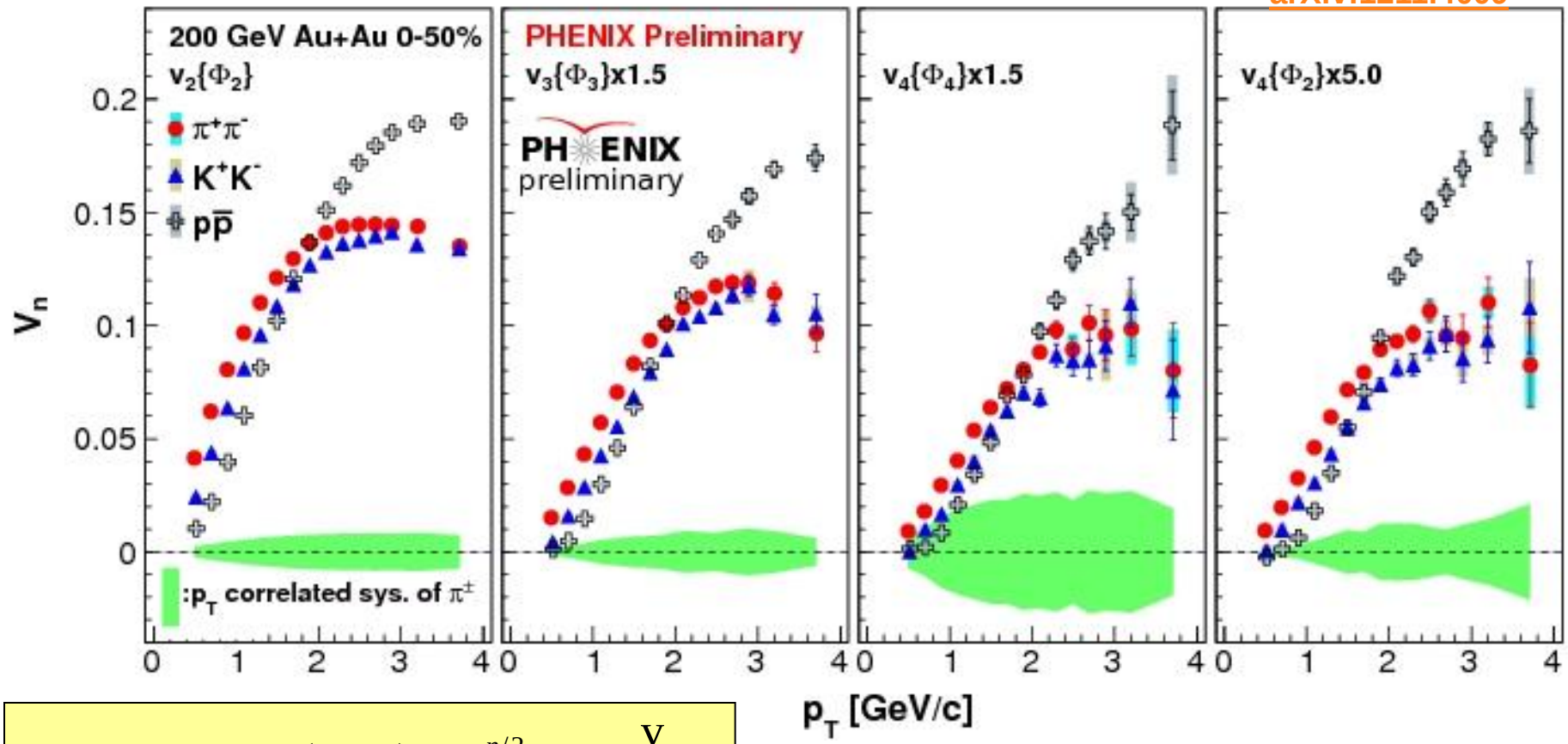

$$\text{Expectation: } v_n(KE_T) \sim v_2^{n/2} \text{ or } \frac{v_n}{(n_q)^{n/2}}$$

Note species dependence for all v_n

For partonic flow, quark number scaling expected
→ single curve for identified particle species v_n

Flow is partonic & acoustic

J.Phys. G38 (2011) 124048 arXiv:1211.4009

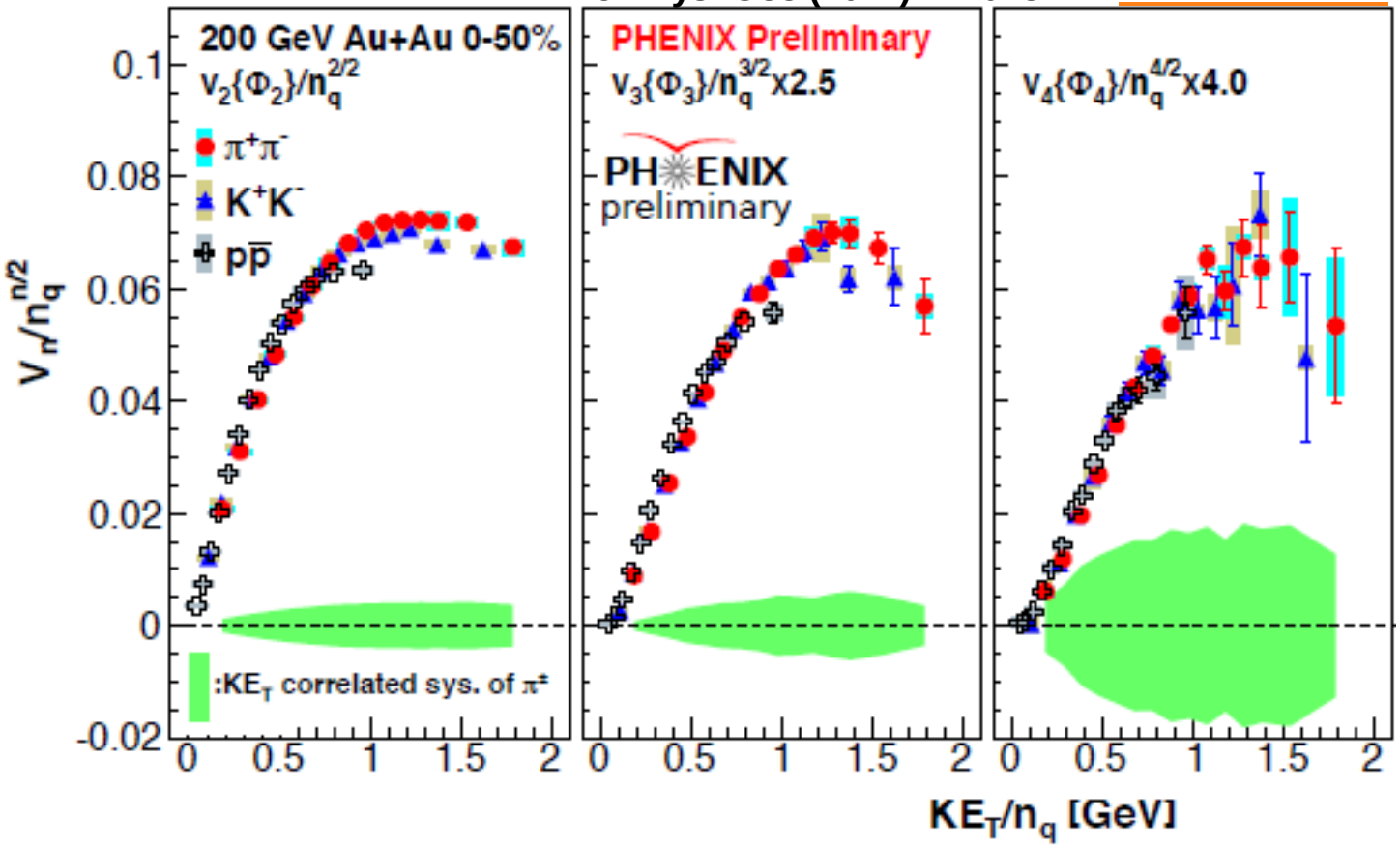

KE_T & $(n_q)^{n/2}$ scaling validated for v_n
→ Partonic flow

Acoustic Scaling – 1/R

ATLAS data - Phys. Rev. C86, 014907 (2012)

Specific dependence dictated by sound attenuation

$$\ln\left(\frac{v_n}{\varepsilon_n}\right) \propto \frac{-\beta''}{\bar{R}}$$

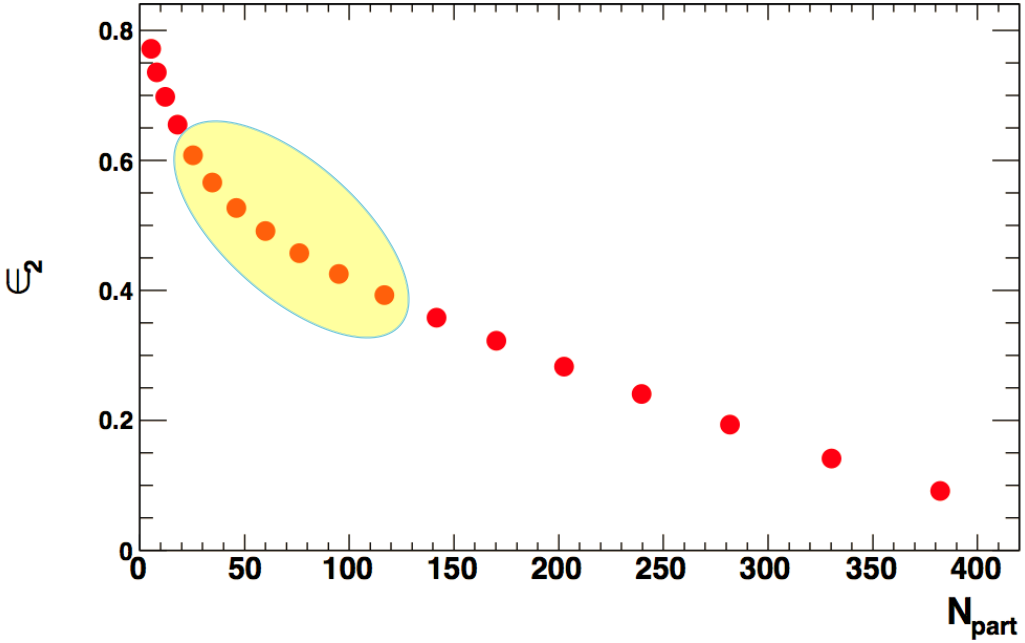

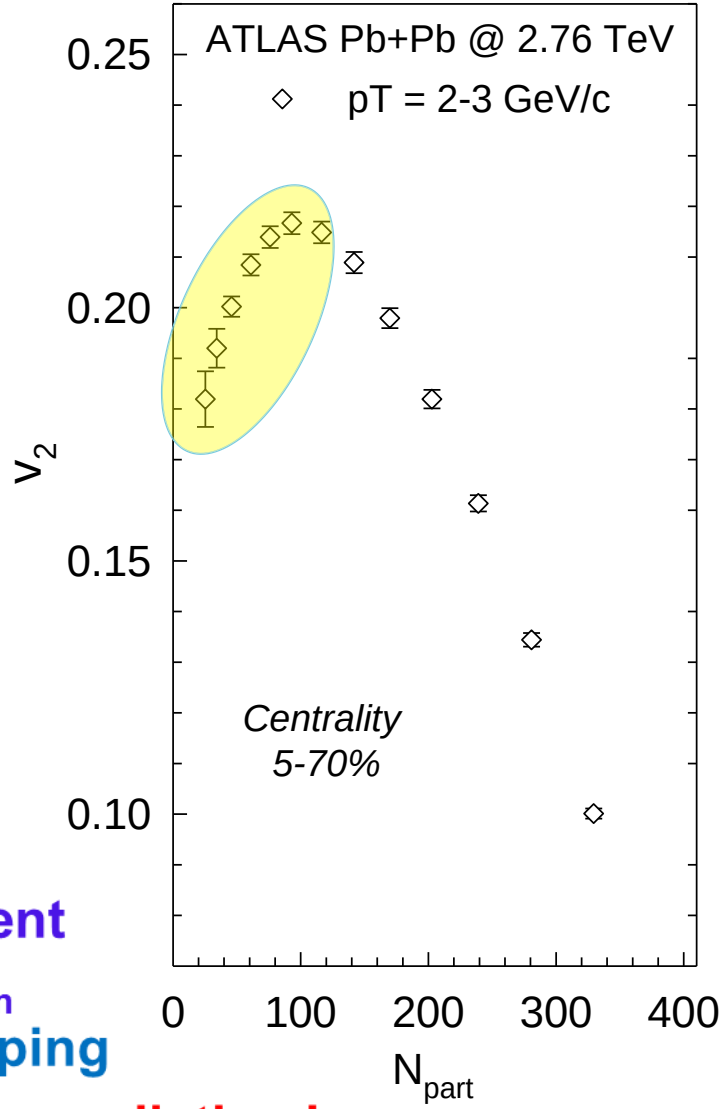

- **Eccentricity change <u>alone</u> is not sufficient To account for the N_{part} dependence of v_n**

Transverse size ($\bar{R}$) influences viscous damping

✓ **Characteristic $1/\bar{R}$ scaling prediction is non-trivial**

Acoustic Scaling – 1/R

$$\ln\left(\frac{v_n}{\varepsilon_n}\right) \propto \frac{-\beta''}{\bar{R}}$$

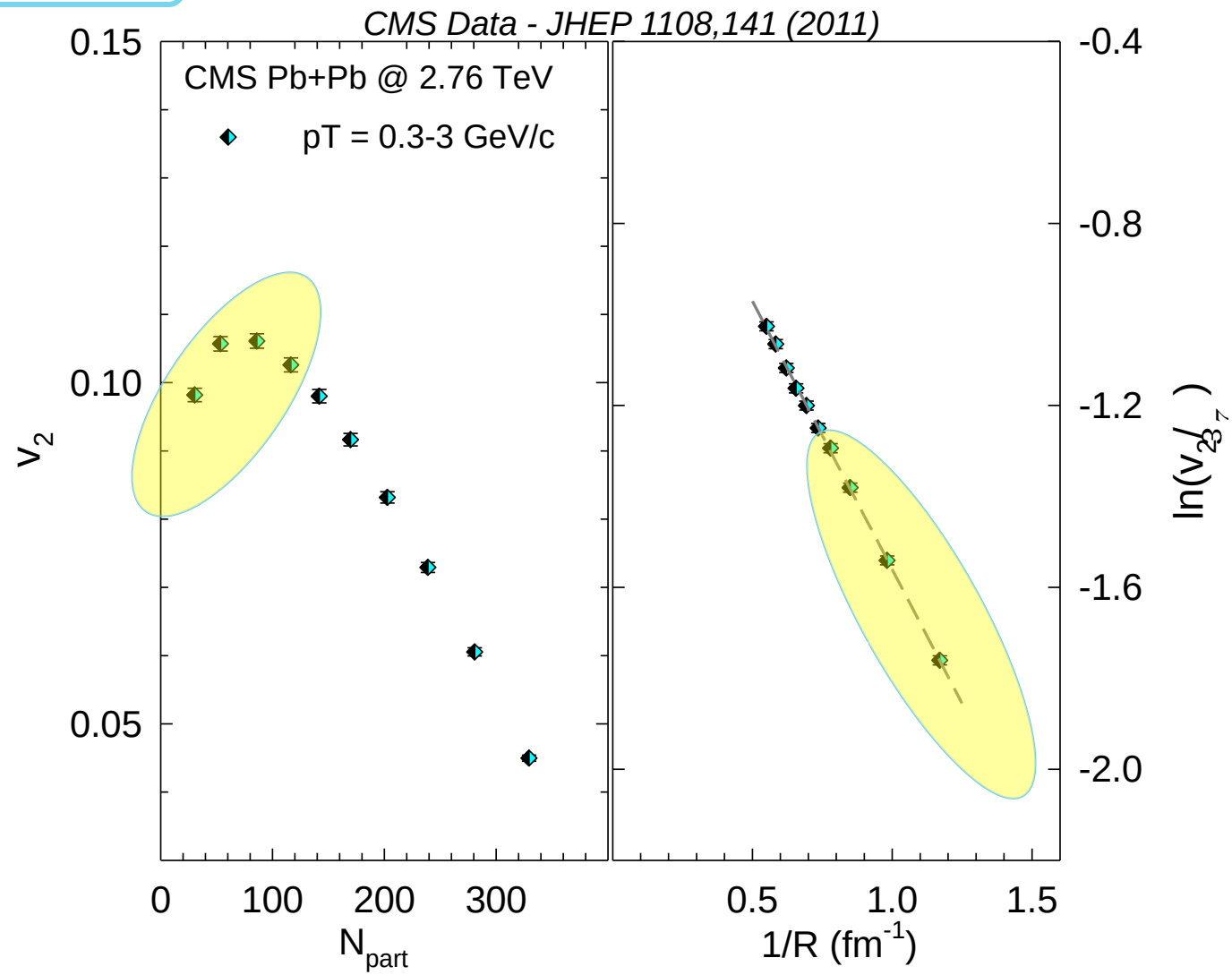

✓ **Characteristic $1/\bar{R}$ viscous damping validated**

✓ ***A further constraint for η/s δf***

Acoustic Scaling – 1/R

$$\ln\left(\frac{v_n}{\varepsilon_n}\right) \propto \frac{-\beta''}{\bar{R}}$$

STAR Data - PhysRevC.81.044902

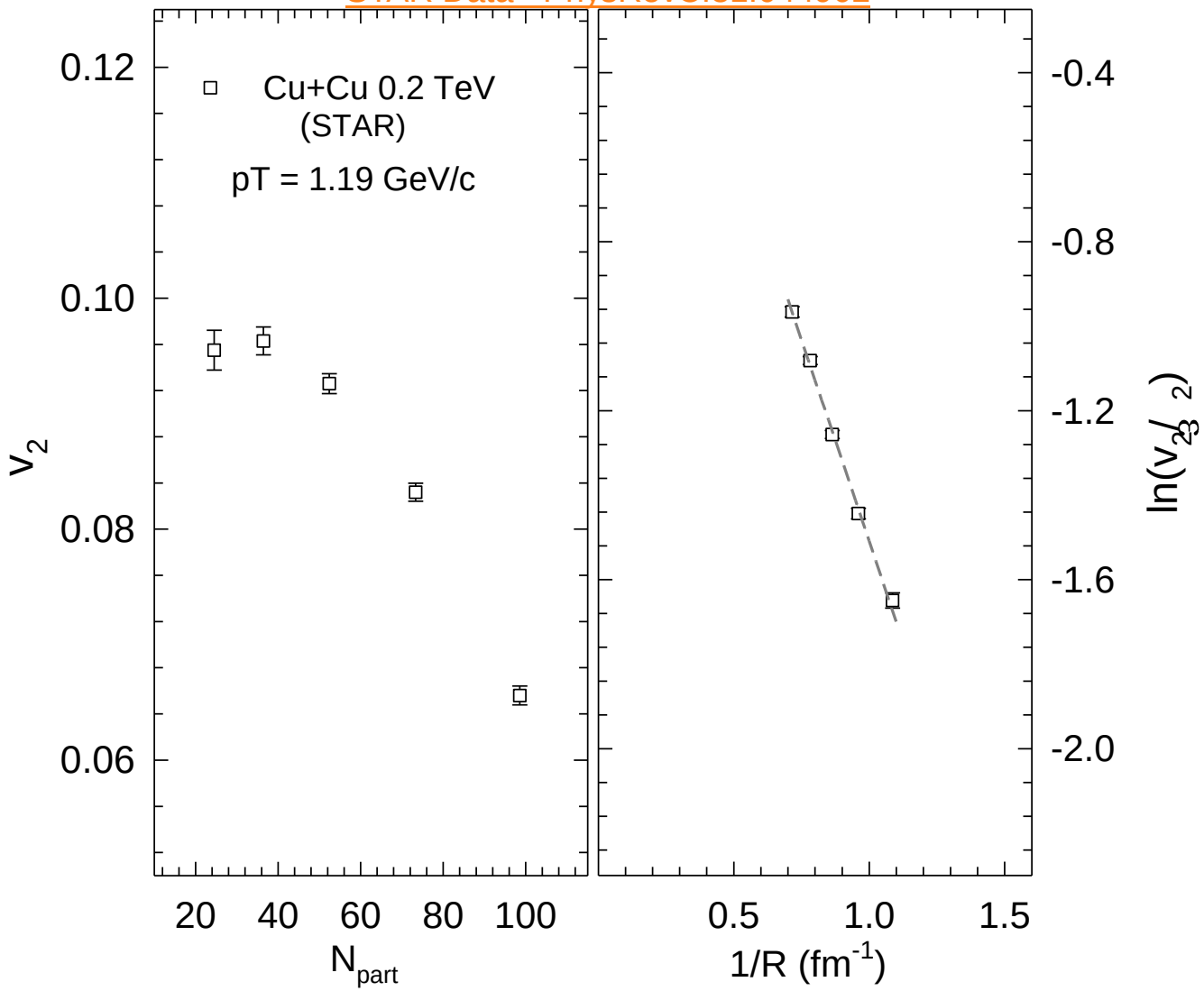

slope → β constraint

✓ **Characteristic $1/\bar{R}$ viscous damping validated for light system**

✓ ***A further constraint for η/s***

Acoustic Scaling – 1/R

$$\ln\left(\frac{v_n}{\varepsilon_n}\right) \propto \frac{-\beta''}{\bar{R}}$$

ATLAS data - Phys. Rev. C86, 014907 (2012)

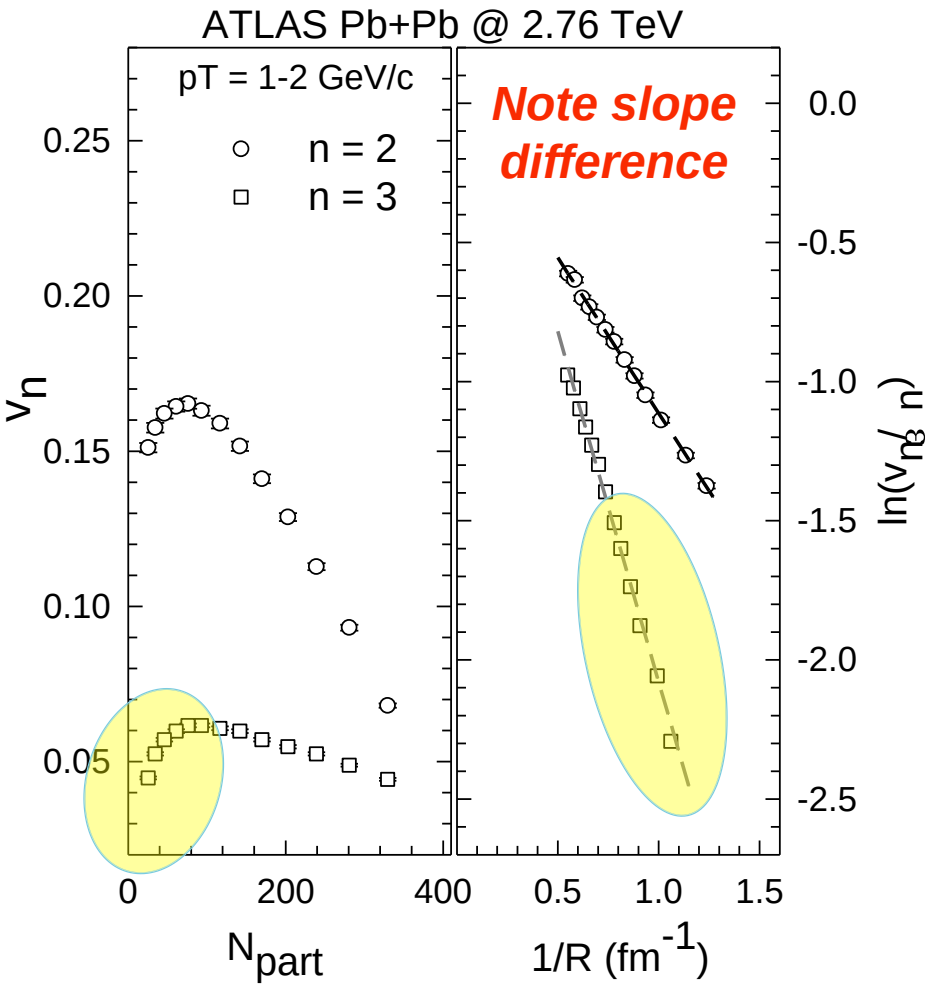

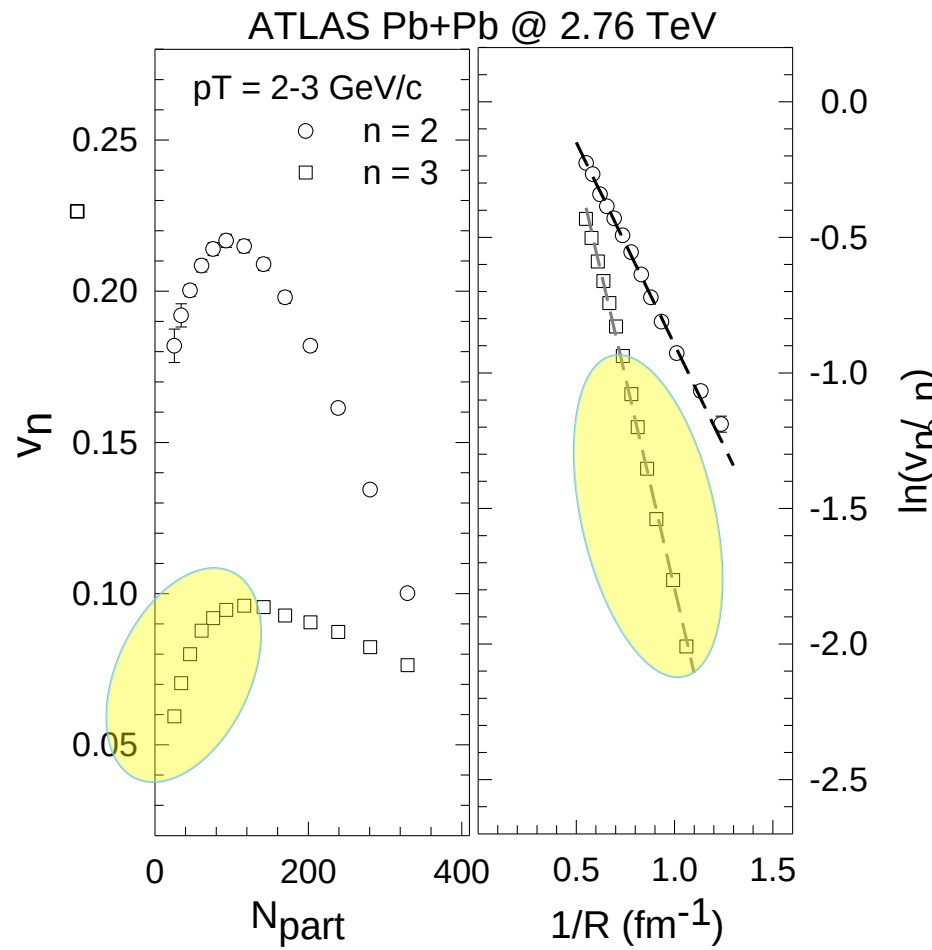

✓ **Characteristic $1/\bar{R}$ viscous damping validated**

✓ ***A further constraint for η/s and δf***

Acoustic Scaling – 1/R

$$\ln\left(\frac{v_n}{\varepsilon_n}\right) \propto \frac{-\beta''}{\bar{R}}$$

ATLAS Data - arXiv:1212.5198.

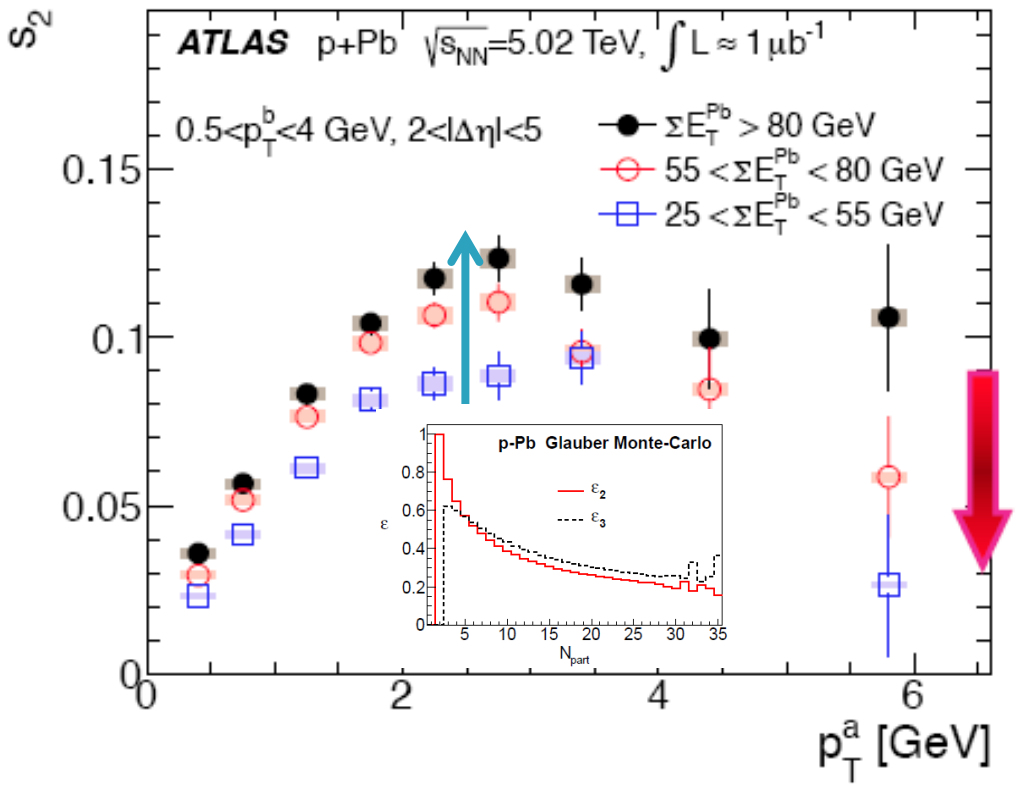

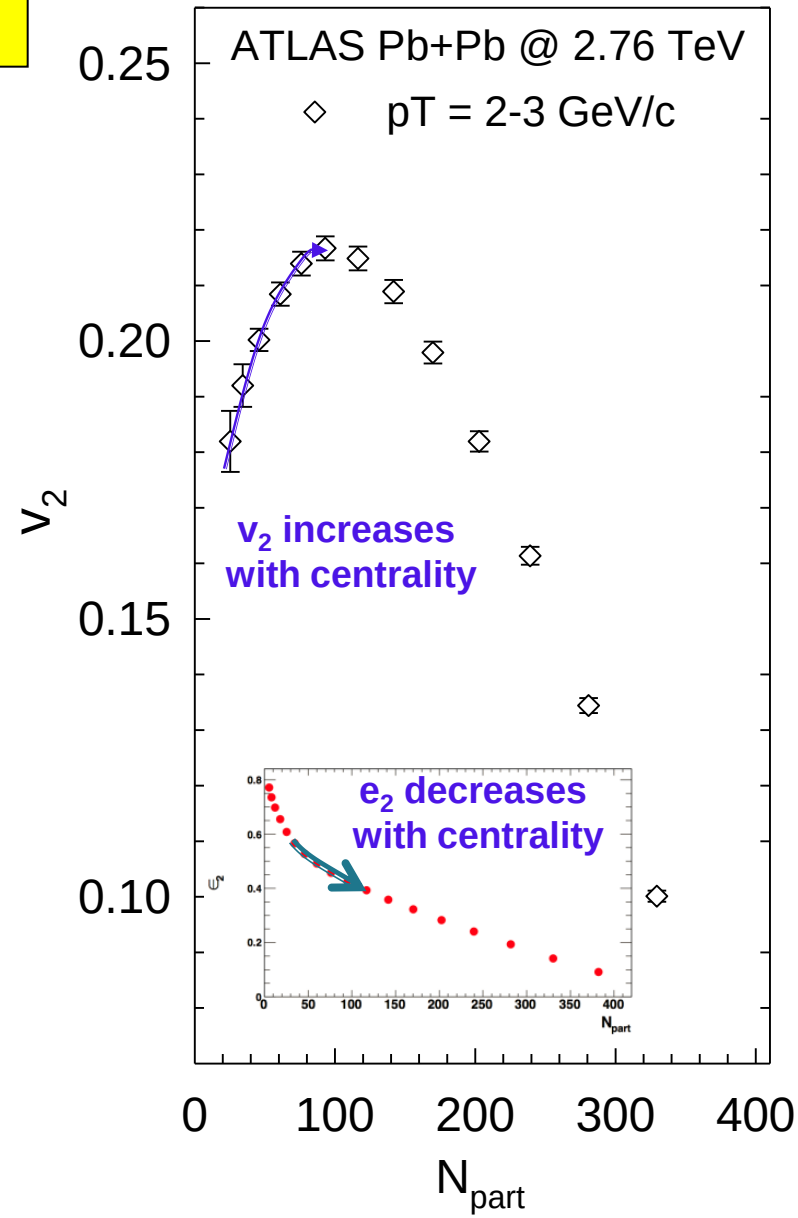

✓ **Increase of s_2 (v_2) with centrality for p+Pb collisions is to be expected**

If the mechanism is similar!

→ Effects of system size (R) dominates

Acoustic Scaling – 1/R

$$\ln\left(\frac{v_n}{\varepsilon_n}\right) \propto \frac{-\beta''}{\bar{R}}$$

Compare system size @ RHIC

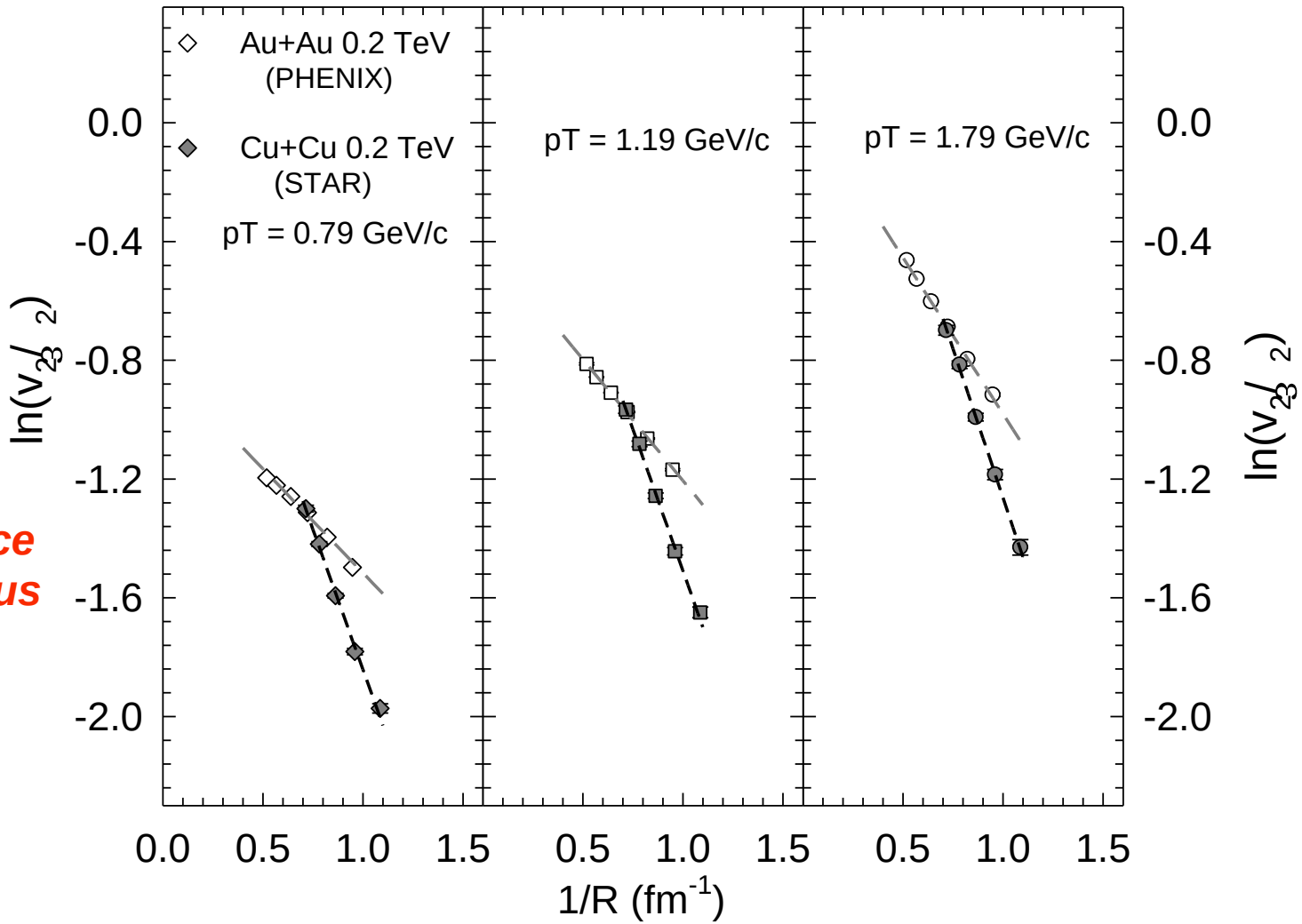

Slope difference encodes viscous coefficient difference

✓ **Viscous coefficient larger for more dilute system**

Acoustic Scaling – 1/R

$$\ln\left(\frac{v_n}{\varepsilon_n}\right) \propto \frac{-\beta''}{\bar{R}}$$

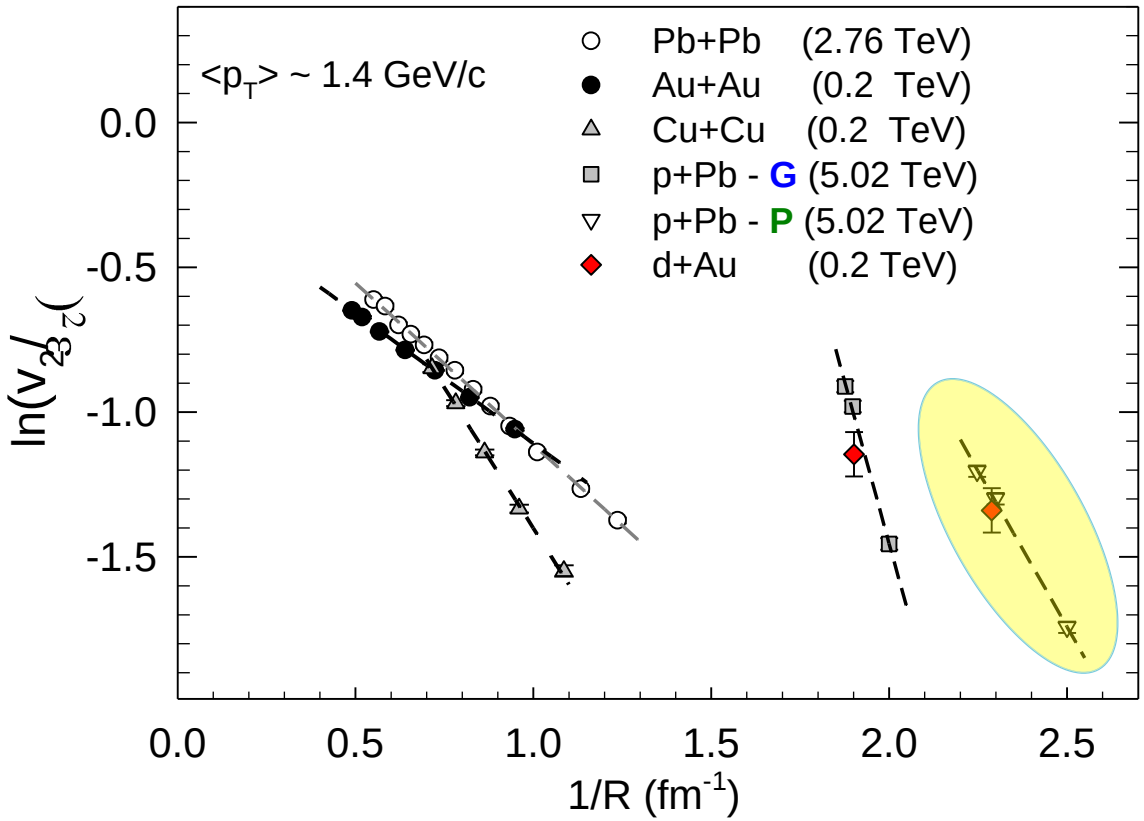

- ✓ **Characteristic $1/\bar{R}$ viscous damping validated across systems**
  → Similar mechanism
- ✓ ***Clear system size dependence of β → signature of dilute fluid?***
  This is very important

Jet suppression Probe

Modified jet

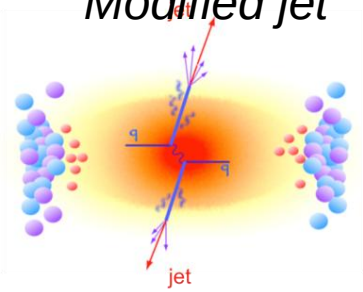

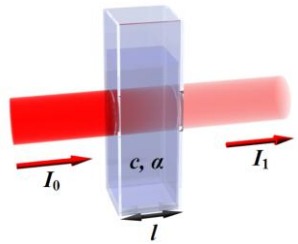

$$T = \frac{I}{I_0} = e^{-\varepsilon L c}$$

Fixed Geometry

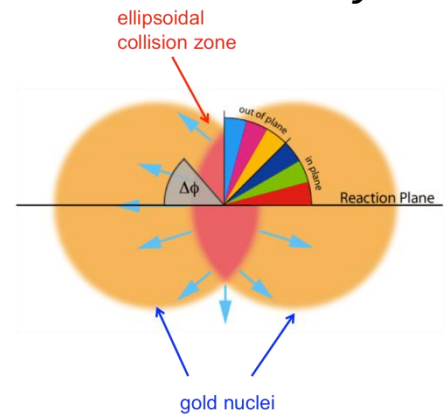

More suppression

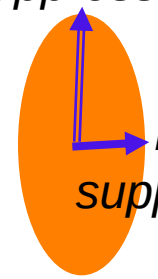

Less suppression

$$Yield(\Delta\phi, p_T) \propto [1 + 2v_2(p_T)\cos(2\Delta\phi)]$$

Suppression (L)

$$R_{AA}(p_T, L) = \frac{Yield_{AA}}{\langle N_{binary}\rangle_{AA}\, Yield_{pp}}$$

Path length (related to collision centrality)

Suppression (ΔL) – pp yield unnecessary

$$R_2(p_T, \Delta L) = \frac{R_{AA}(90^o, p_T)}{R_{AA}(0^0, p_T)} = \frac{1 - 2v_2(p_T)}{1 + 2v_2(p_T)}$$

For Radiative Energy loss:

Dokshitzer and D. E. Kharzeev , Phys.Lett.B519:199-206,2001

$$R_{AA}(p_T, L) \simeq \exp\left[-\frac{2\alpha_s C_F}{\sqrt{\pi}} L\sqrt{\hat{q}\frac{\mathcal{L}}{p_\perp}} + \frac{16\alpha_s C_F}{9\sqrt{3}} L\left(\frac{\hat{q}\ M^2}{M^2 + p_\perp^2}\right)^{1/3}\right]$$

$$\mathcal{L} \equiv \frac{d}{d\ln p_\perp}\ln\left[\frac{d\sigma^{vac}}{dp_\perp^2}(p_\perp)\right]$$

***Jet suppression drives R_{AA} & azimuthal anisotropy* with specific scaling properties**

R_{AA} Measurements - CMS

Eur. Phys. J. C (2012) 72:1945
arXiv:1202.2554

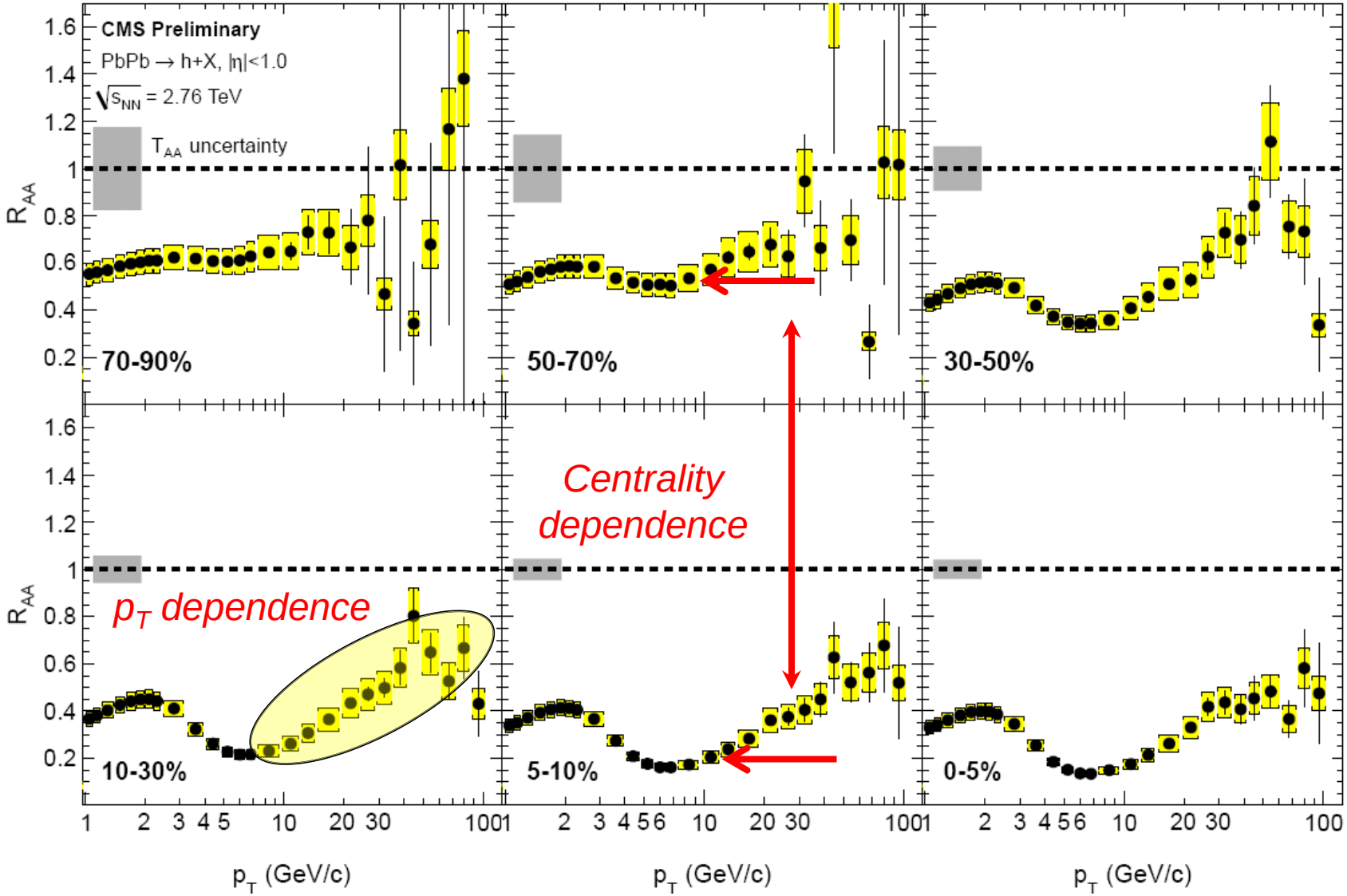

Specific p_T and centrality dependencies – Do they scale?

L scaling of Jet Quenching - LHC

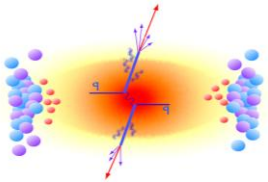

Dokshitzer and D. E. Kharzeev, Phys.Lett.B519:199-206,2001

$$R^{l}_{\mathrm{AA}}(p_T, L) \simeq \exp\left[-\frac{2\alpha_s C_F}{\sqrt{\pi}} L \sqrt{\hat{q}\frac{\mathcal{L}_l}{p_T}}\right]$$

arXiv:1202.5537

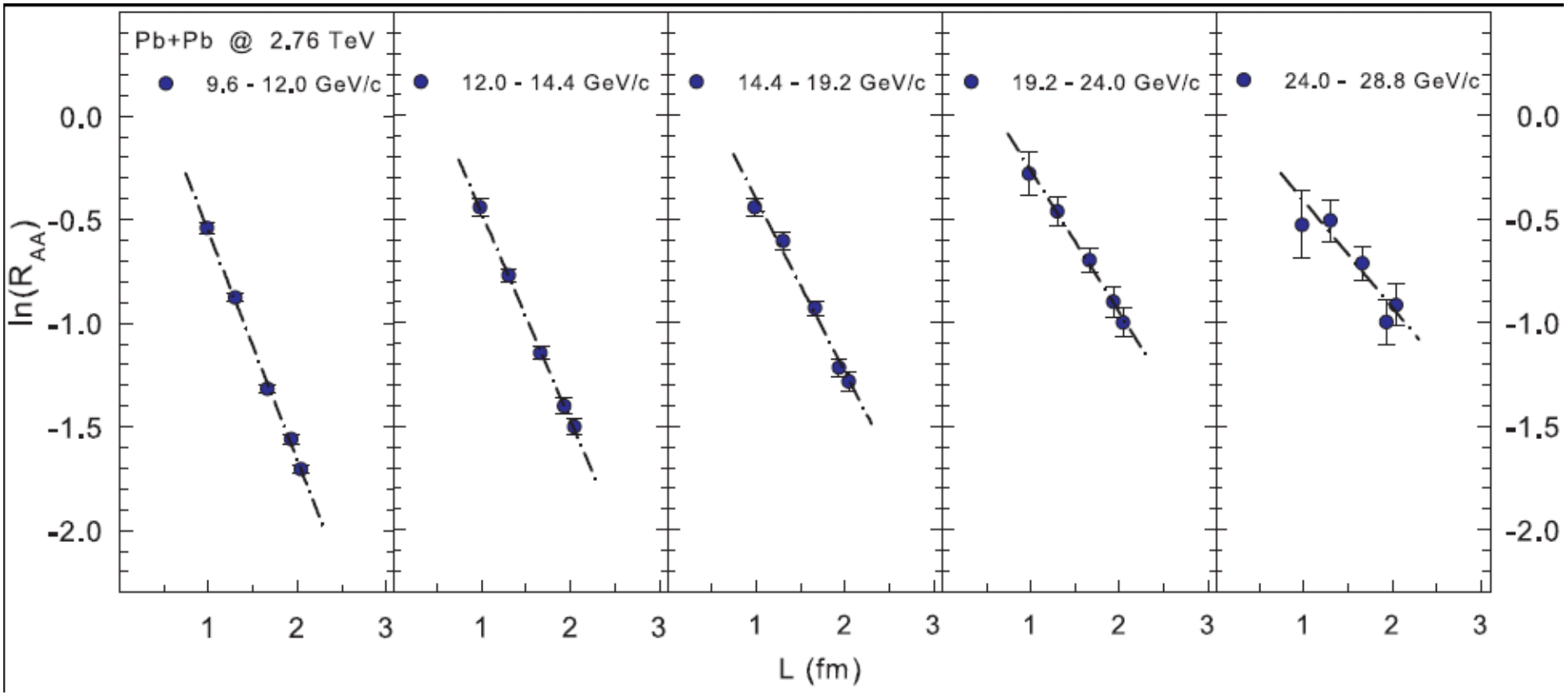

R_{AA} scales with L, slopes (S_L) encodes info on α_s and $\hat{q}$

✓Compatible with the dominance of radiative energy loss

L scaling of Jet Quenching - RHIC

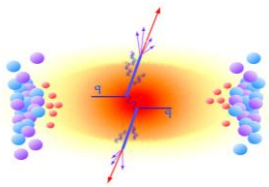

$$R^{l}_{AA}(p_T, L) \simeq \exp\left[-\frac{2\alpha_s C_F}{\sqrt{\pi}}\, L\sqrt{\hat{q}\frac{\mathcal{L}_l}{p_T}}\right]$$

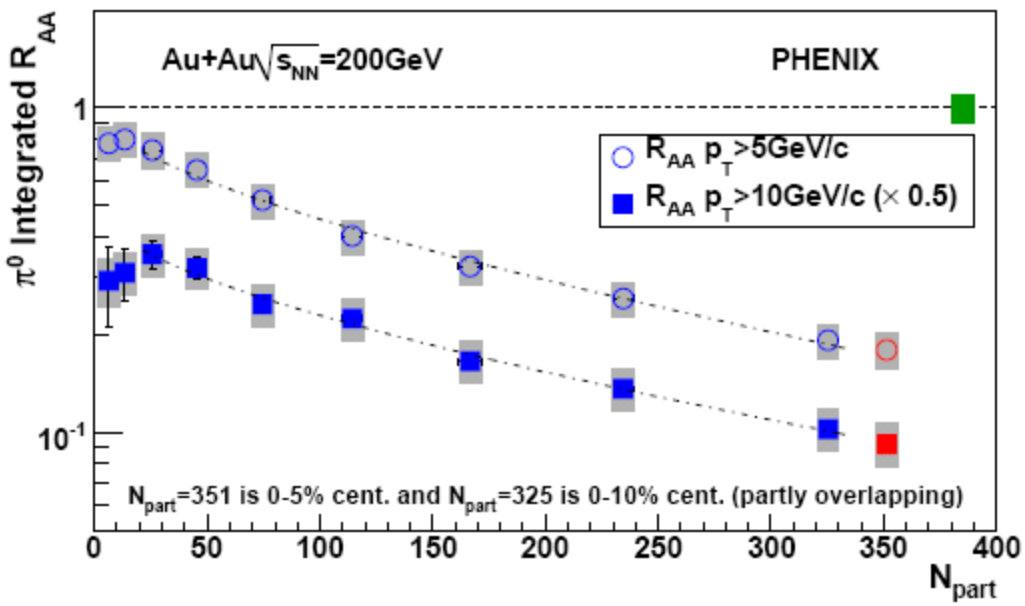

Phys.Rev.C80:051901,2009

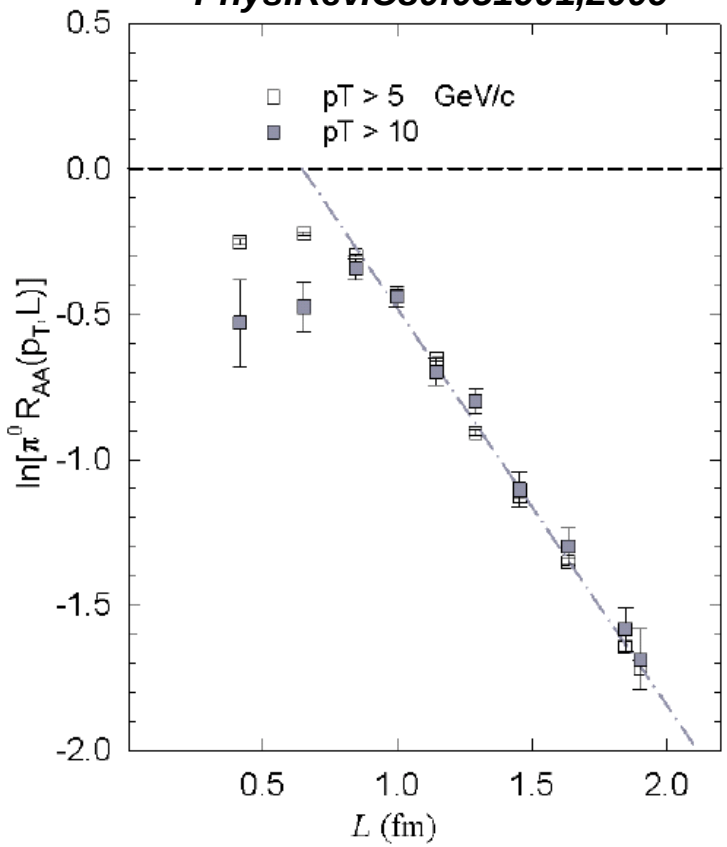

R_{AA} scales with L, slopes (S_L) encodes info on α_s and $\hat{q}$

✓Compatible with the dominance of radiative energy loss

p_T scaling of Jet Quenching

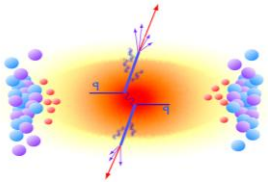

Dokshitzer and D. E. Kharzeev, Phys.Lett.B519:199-206,2001

$$R^l_{AA}(p_T, L) \simeq \exp\left[-\frac{2\alpha_s C_F}{\sqrt{\pi}} L \sqrt{\hat{q}\frac{\mathcal{L}_l}{p_T}}\right]$$

arXiv:1202.5537

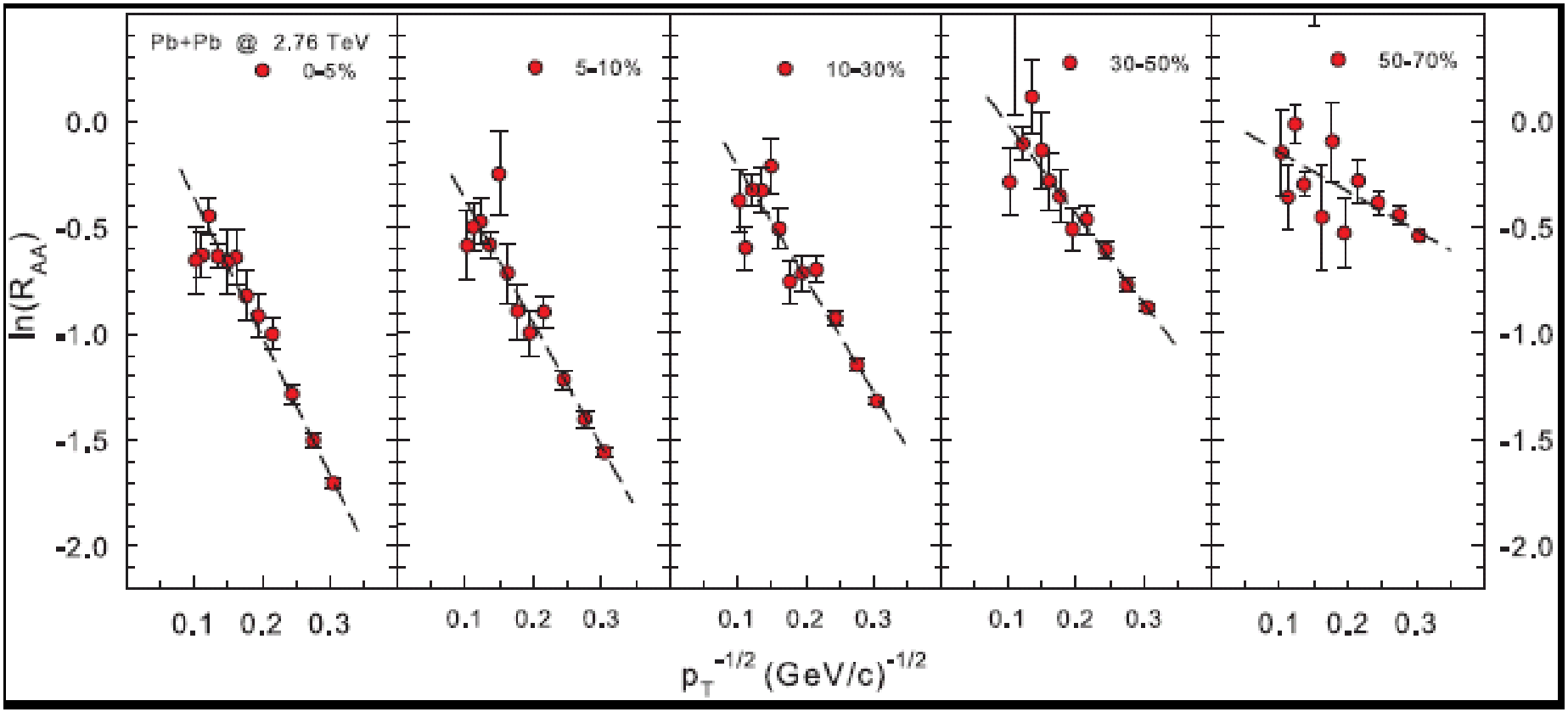

R_{AA} scales as $1/\sqrt{p_T}$; slopes (S_{pT}) encode info on α_s and $\hat{q}$

- ✓ ***L and $1/\sqrt{p_T}$ scaling → single universal curve***
- ✓ ***Compatible with the dominance of radiative energy loss***

Heavy quark suppression

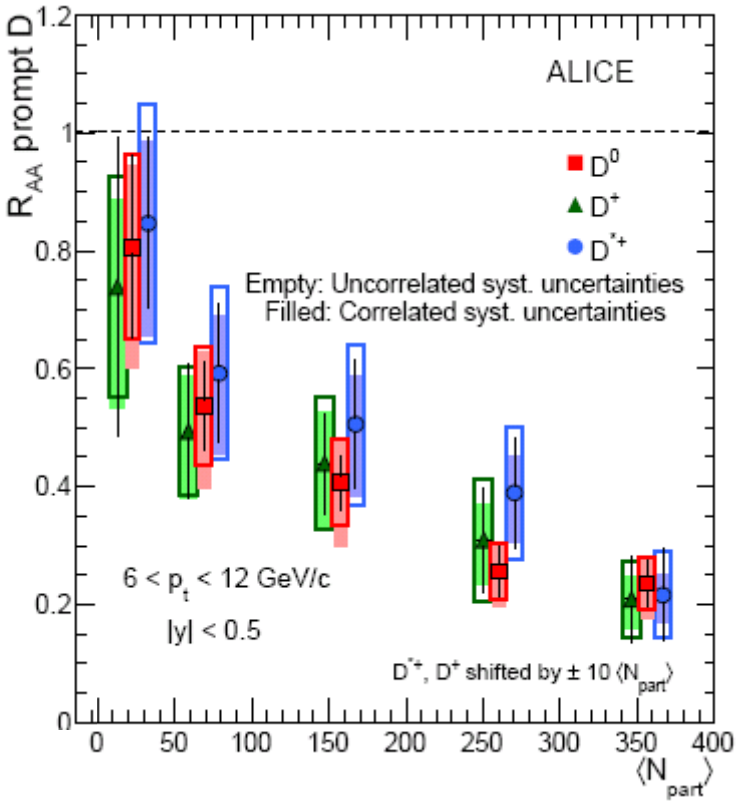

$$R_{AA}(p_T, L) \simeq \exp\left[-\frac{2\alpha_s C_F}{\sqrt{\pi}} L \sqrt{\hat{q}\frac{\mathcal{L}}{p_\perp}} + \frac{16\alpha_s C_F}{9\sqrt{3}} L \left(\frac{\hat{q}\ M^2}{M^2 + p_\perp^2}\right)^{1/3}\right]$$

$$\mathcal{L} \equiv \frac{d}{d\ln p_\perp} \ln\left[\frac{d\sigma^{vac}}{dp_\perp^2}(p_\perp)\right]$$

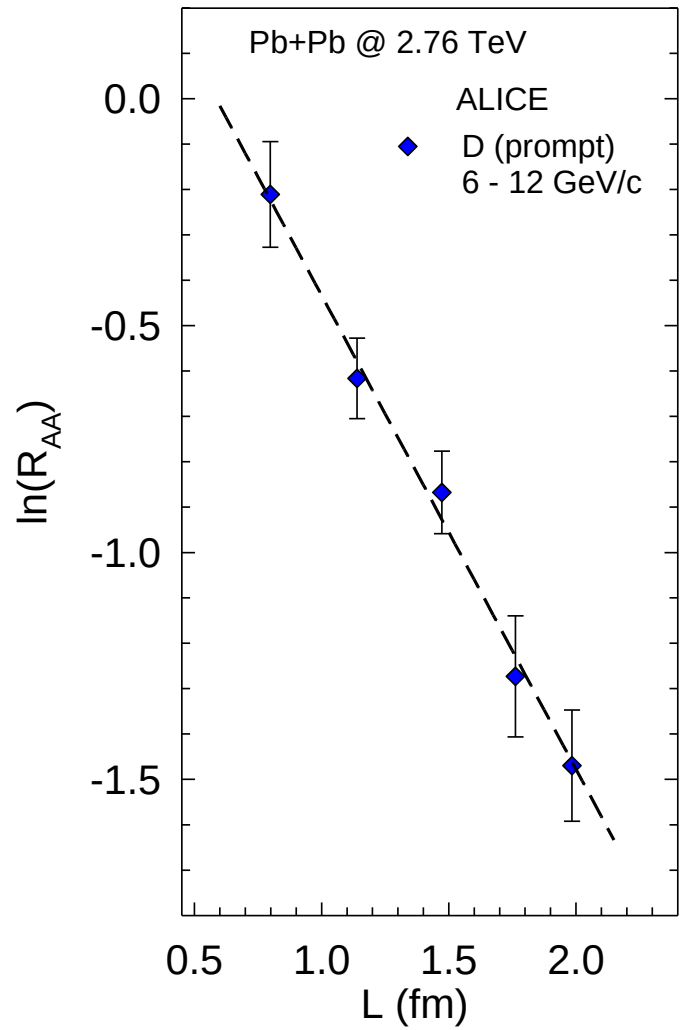

Consistent $\hat{q}_{LHC}$ obtained

High-pT v_2 measurements - PHENIX

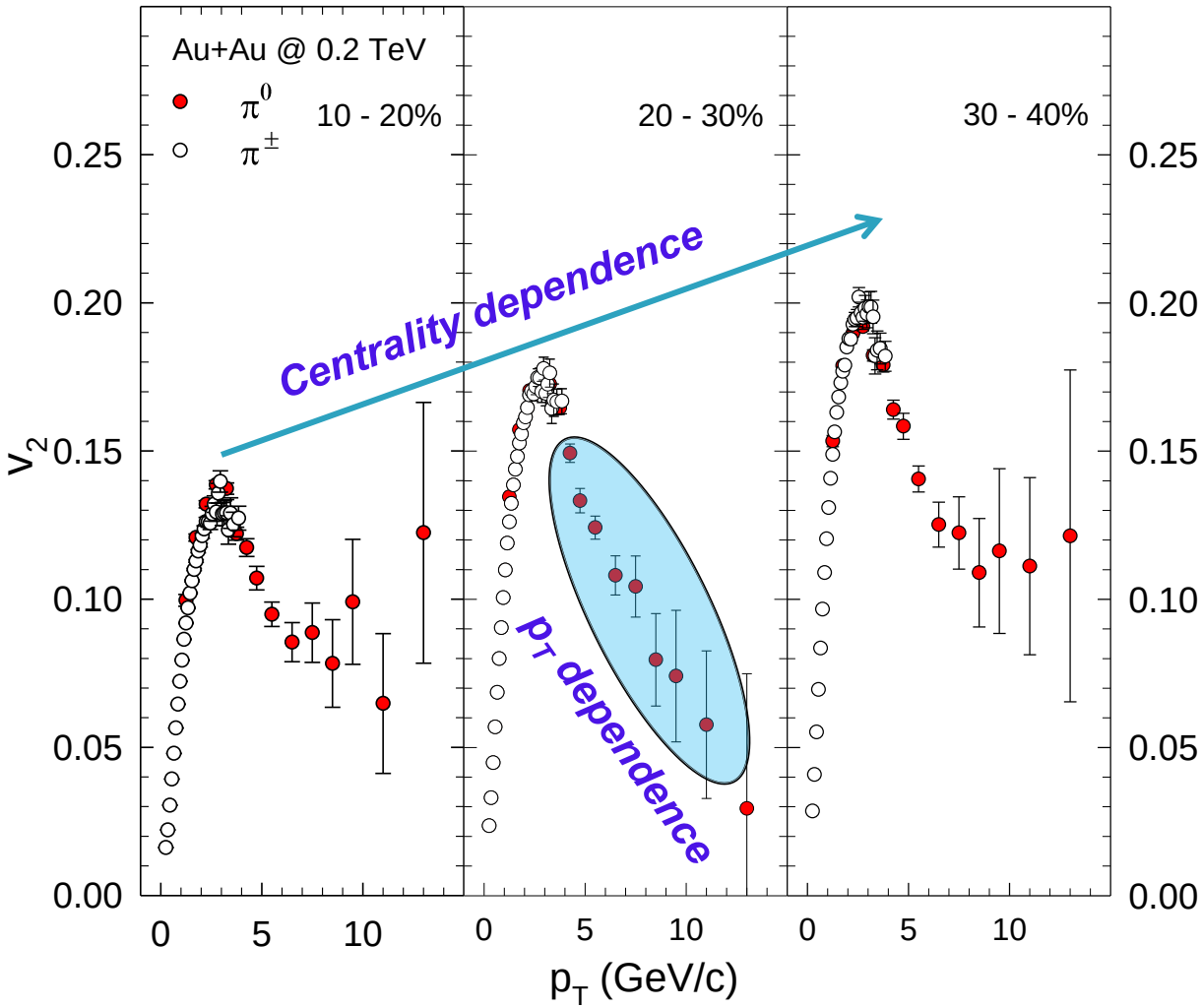

Specific p_T and centrality dependencies – Do they scale?

High-pT v_2 measurements - CMS

arXiv:1204.1850

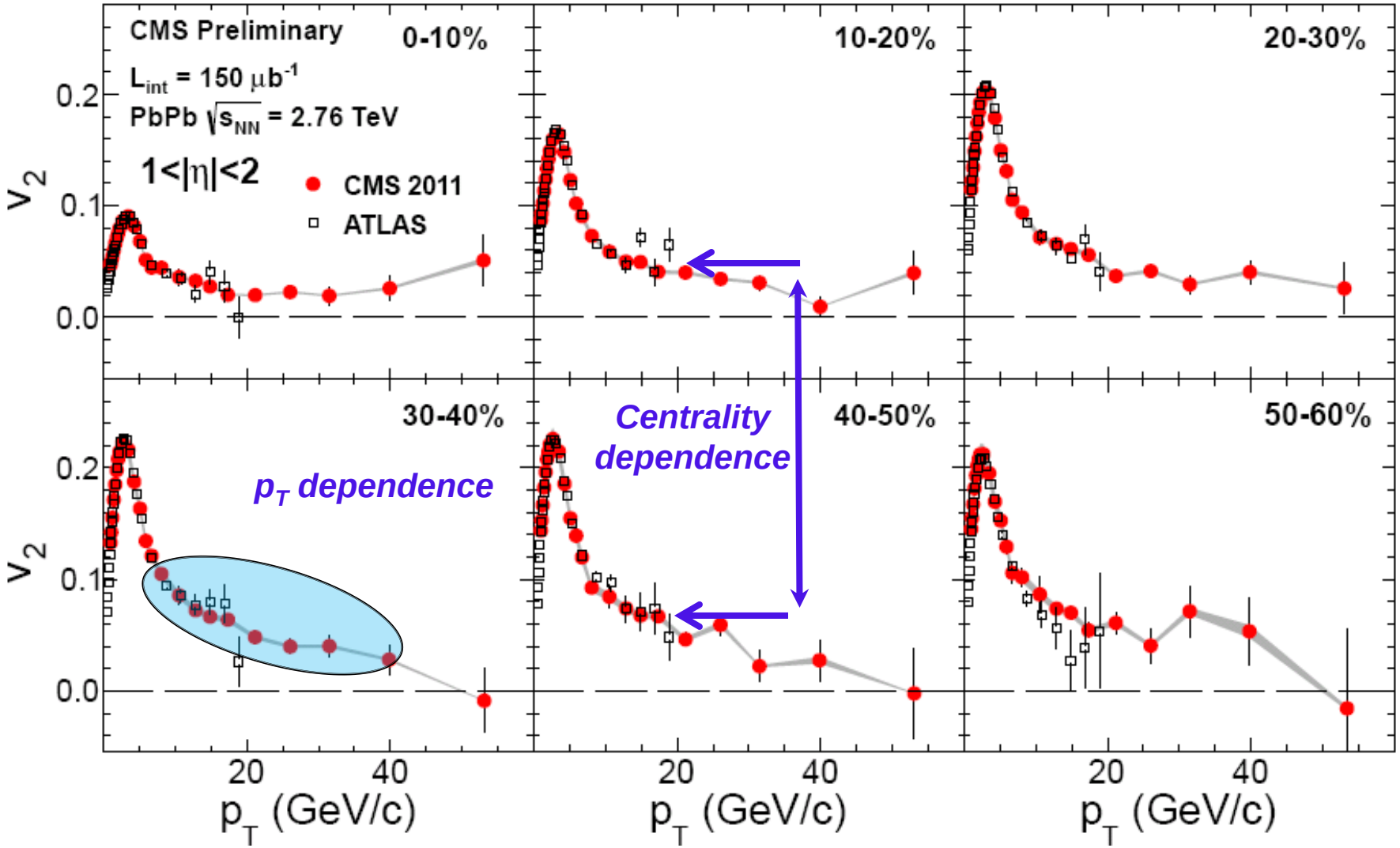

Specific p_T and centrality dependencies – Do they scale?

High-pT v_2 scaling - LHC

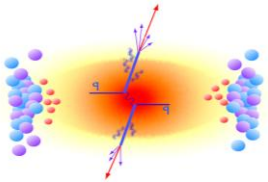

$$R^l_{AA}(p_T, L) \simeq \exp\left[-\frac{2\alpha_s C_F}{\sqrt{\pi}}\, L \sqrt{\hat{q}\frac{\mathcal{L}_l}{p_T}}\right]$$

arXiv:1203.3605

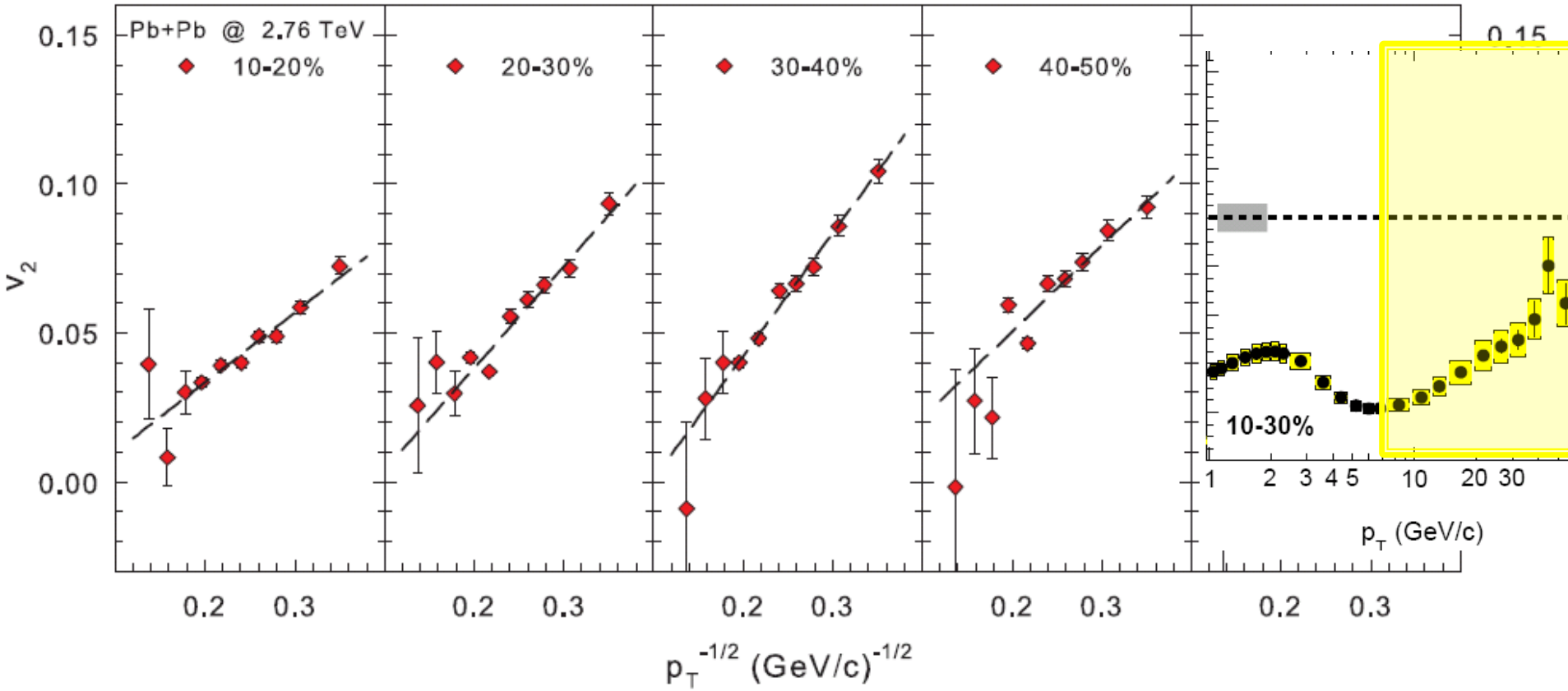

v_2 follows the p_T dependence observed for jet quenching

Note the expected inversion of the $1/\sqrt{p_T}$ dependence

ΔL Scaling of high-pT v_2 – LHC & RHIC

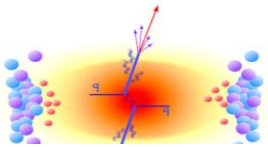

$$R^{l}_{AA}(p_T, L) \simeq \exp\left[-\frac{2\alpha_s C_F}{\sqrt{\pi}} L \sqrt{\hat{q}\frac{\mathcal{L}_l}{p_T}}\right]$$

arXiv:1203.3605

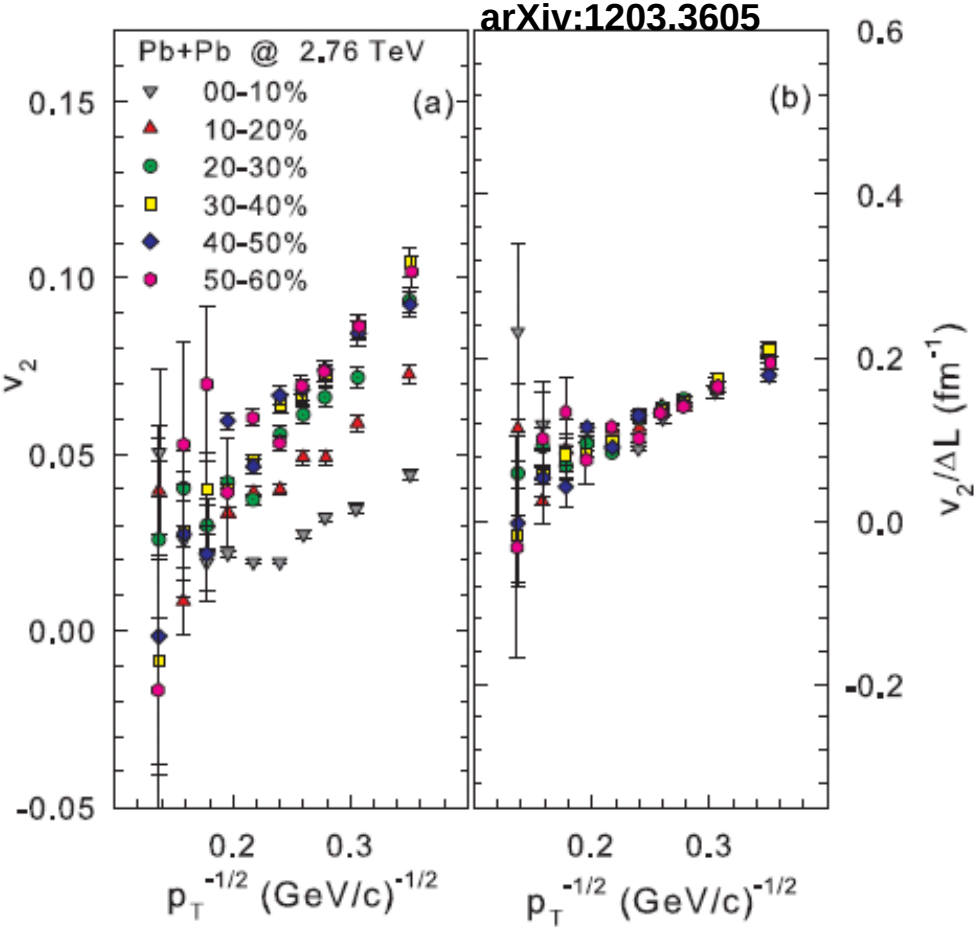

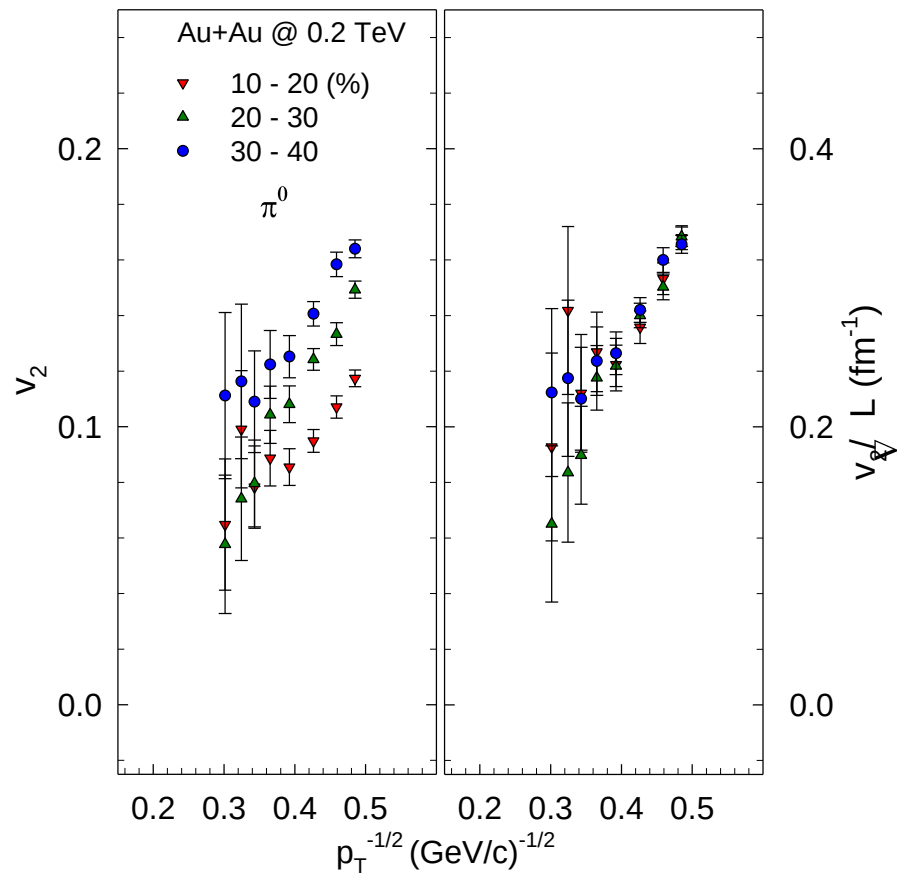

Combined ΔL and $1/\sqrt{p_T}$ scaling → single universal curve for v_2

ΔL Scaling of high-pT v_2 - RHIC

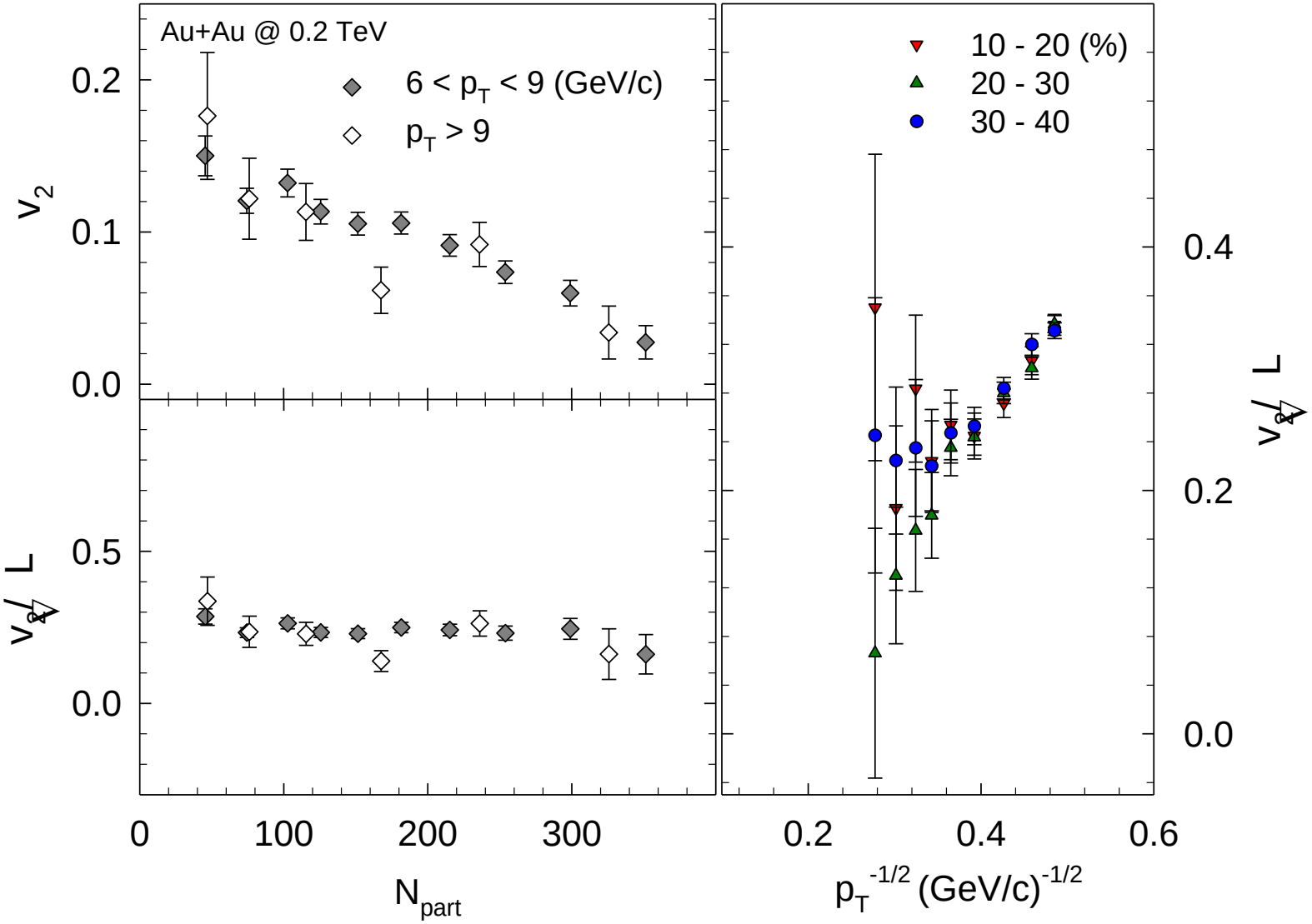

Combined ΔL and $1/\sqrt{p_T}$ scaling → single universal curve for v_2

→ Constraint for ε_n

Jet v_2 scaling - LHC

$$R^l_{AA}(p_T, L) \simeq \exp\left[-\frac{2\alpha_s C_F}{\sqrt{\pi}}\, L \sqrt{\hat{q}\frac{\mathcal{L}_l}{p_T}}\right]$$

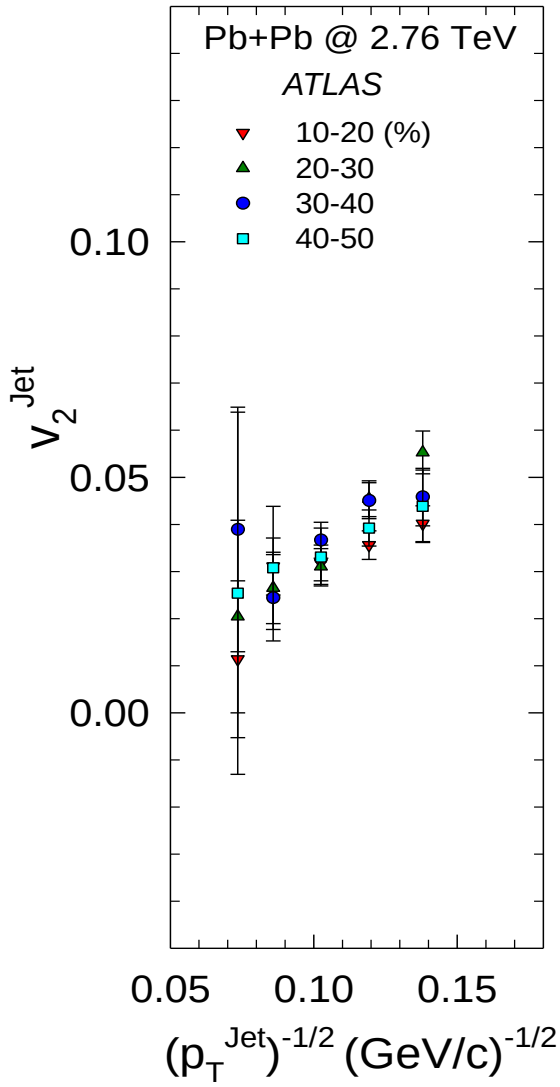

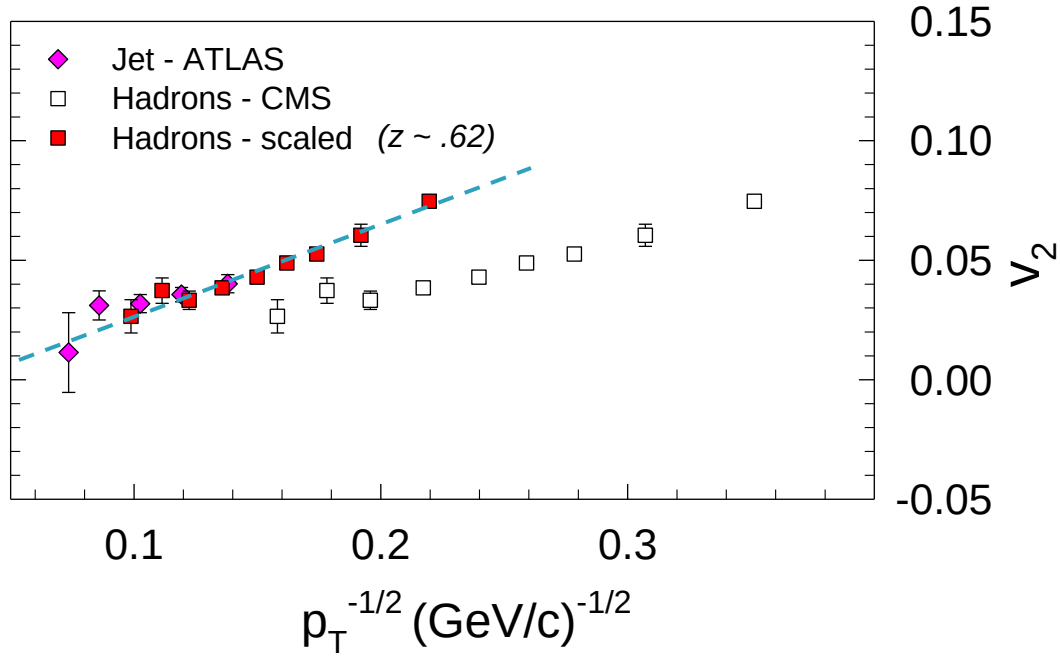

v_2 for reconstructed Jets follows the p_T dependence for jet quenching

Similar magnitude and trend for Jet and hadron v_2 after scaling

Jet suppression from high-pT v_2

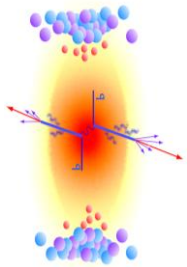

$$R^{l}_{AA}(p_T, L) \simeq \exp\left[-\frac{2\alpha_s C_F}{\sqrt{\pi}}\, L \sqrt{\hat{q}\frac{\mathcal{L}_l}{p_T}}\right]$$

$$N(\Delta\phi, p_T) \propto [1 + 2v_2(p_T)\cos(2\Delta\phi)]$$

$$R_{v_2}(p_T, \Delta L) = \frac{R_{AA}(90^o, p_T)}{R_{AA}(0^0, p_T)} = \frac{1 - 2v_2(p_T)}{1 + 2v_2(p_T)}$$

arXiv:1203.3605

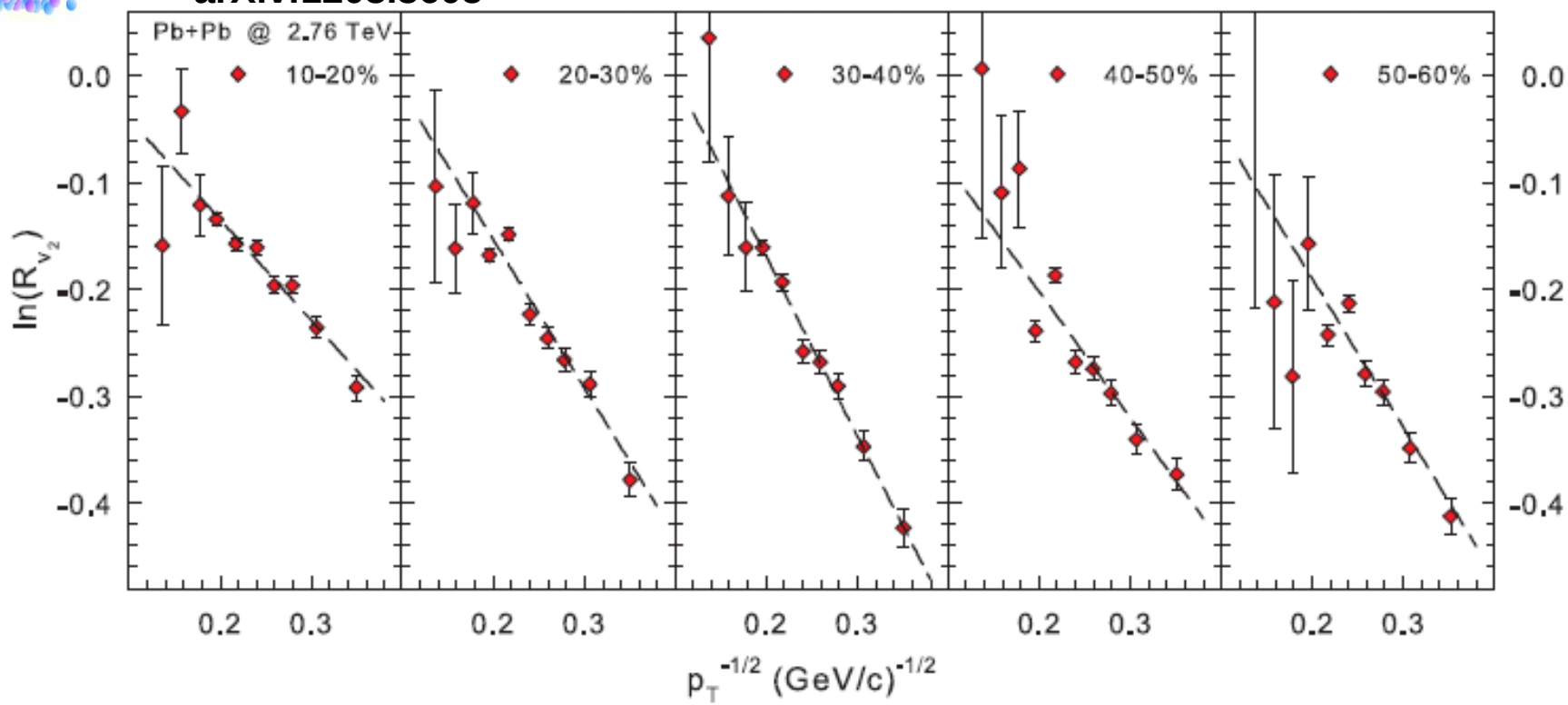

Jet suppression obtained directly from pT dependence of v_2

R_{v2} scales as $1/\sqrt{p_T}$, slopes encodes info on α_s and $\hat{q}$

Extracted stopping power

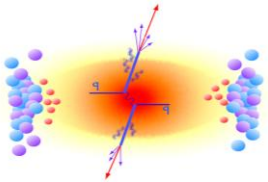

$$R^{l}_{AA}(p_T, L) \simeq \exp\left[-\frac{2\alpha_s C_F}{\sqrt{\pi}}\, L \sqrt{\hat{q}\frac{\mathcal{L}_l}{p_T}}\right]$$

arXiv:1202.5537 **arXiv:1203.3605**

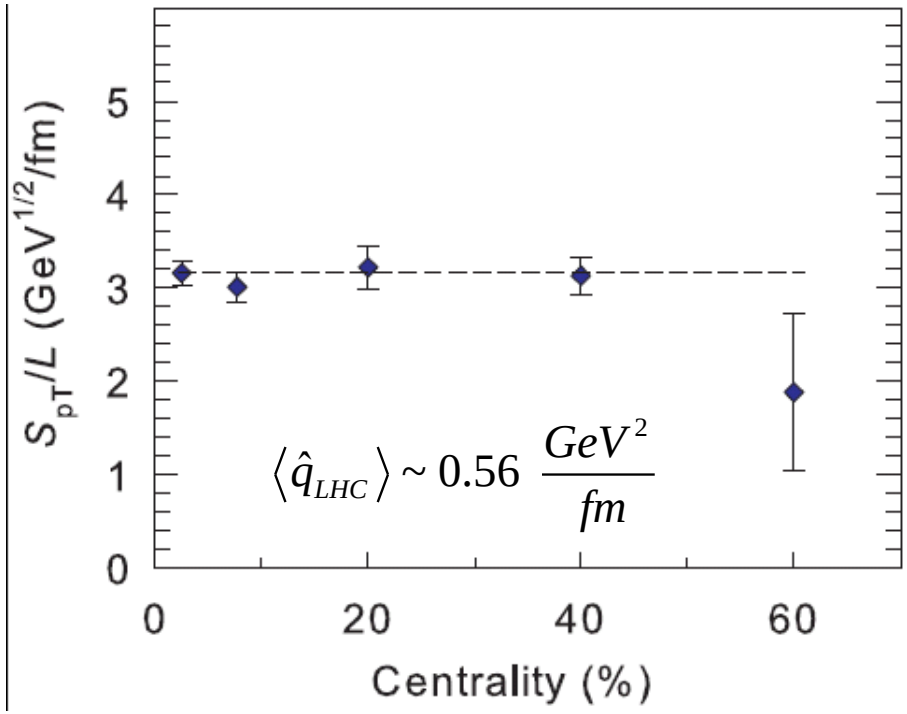

Phys.Rev.C80:051901,2009

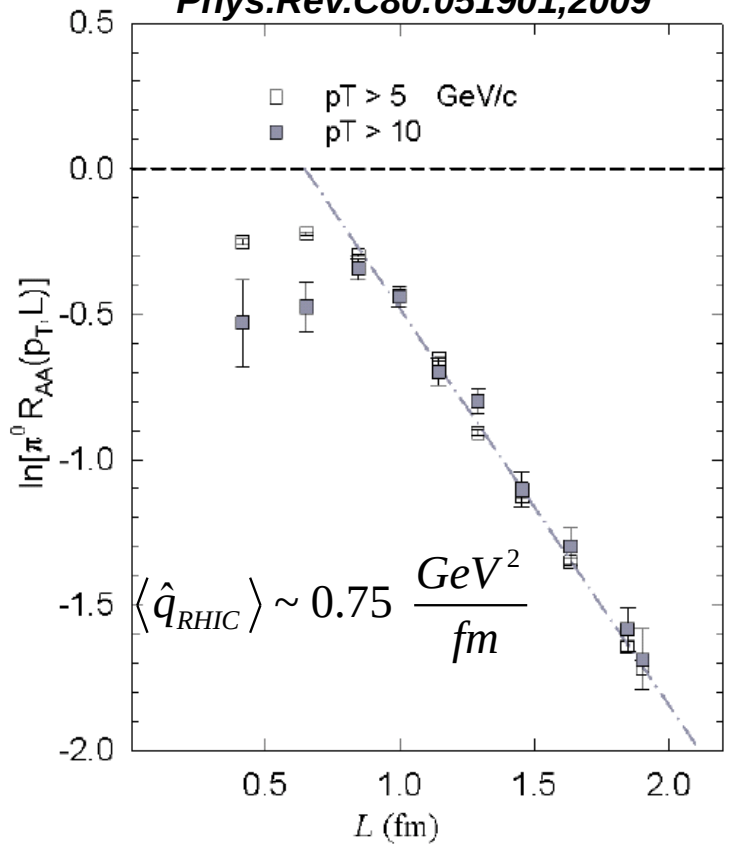

- ***$\hat{q}_{LHC}$ obtained from high-pT v_2 and R_{AA} [same α_s] → similar***
- ***$\hat{q}_{RHIC} > q_{LHC}$ - medium produced in LHC collisions less opaque!***

Conclusion similar to those of Liao, Betz, Horowitz,
→ Stronger coupling near T_c?

Summary

Robust scaling observed for both Flow and Jet Quenching

They lend profound mechanistic insights, as well as New constraints for estimates of the transport and thermodynamic coefficients!

What do we learn?

- **R_{AA} and high-pT azimuthal anisotropy stem from the same energy loss mechanism**
- **Energy loss is dominantly radiative**
- **R_{AA} and anisotropy measurements give consistent estimates for <ˆq >**
- **R_{AA} for D's give consistent estimates for <ˆq >**
- **The QGP created in LHC collisions is less opaque than that produced at RHIC – Note density increase from RHIC to LHC**

- ***Flow is acoustic***
  - ✓ ***Flow is pressure driven***
  - ✓ ***Obeys the dispersion relation for sound propagation***
  - ✓ ***clear system size dependence***
- ***Flow is partonic***
  - ✓ ***exhibits scaling***

$$v_{n,q}(KE_T) \sim v_{2,q}^{n/2} \text{ or } \frac{v_n}{(n_q)^{n/2}}$$

- ***Constraints for:***
  - ✓ ***ε, β, and δf***
  - ✓ ***η/s @ RHIC (~ 1/4π)***
  - ✓ ***η/s @ LHC a bit larger than at RHIC***

End

Acoustic Scaling – 1/R

$$\ln\left(\frac{v_n}{\varepsilon_n}\right) \propto \frac{-\beta''}{\bar{R}}$$

Centrality – 5-70%

ATLAS data - Phys. Rev. C86, 014907 (2012)

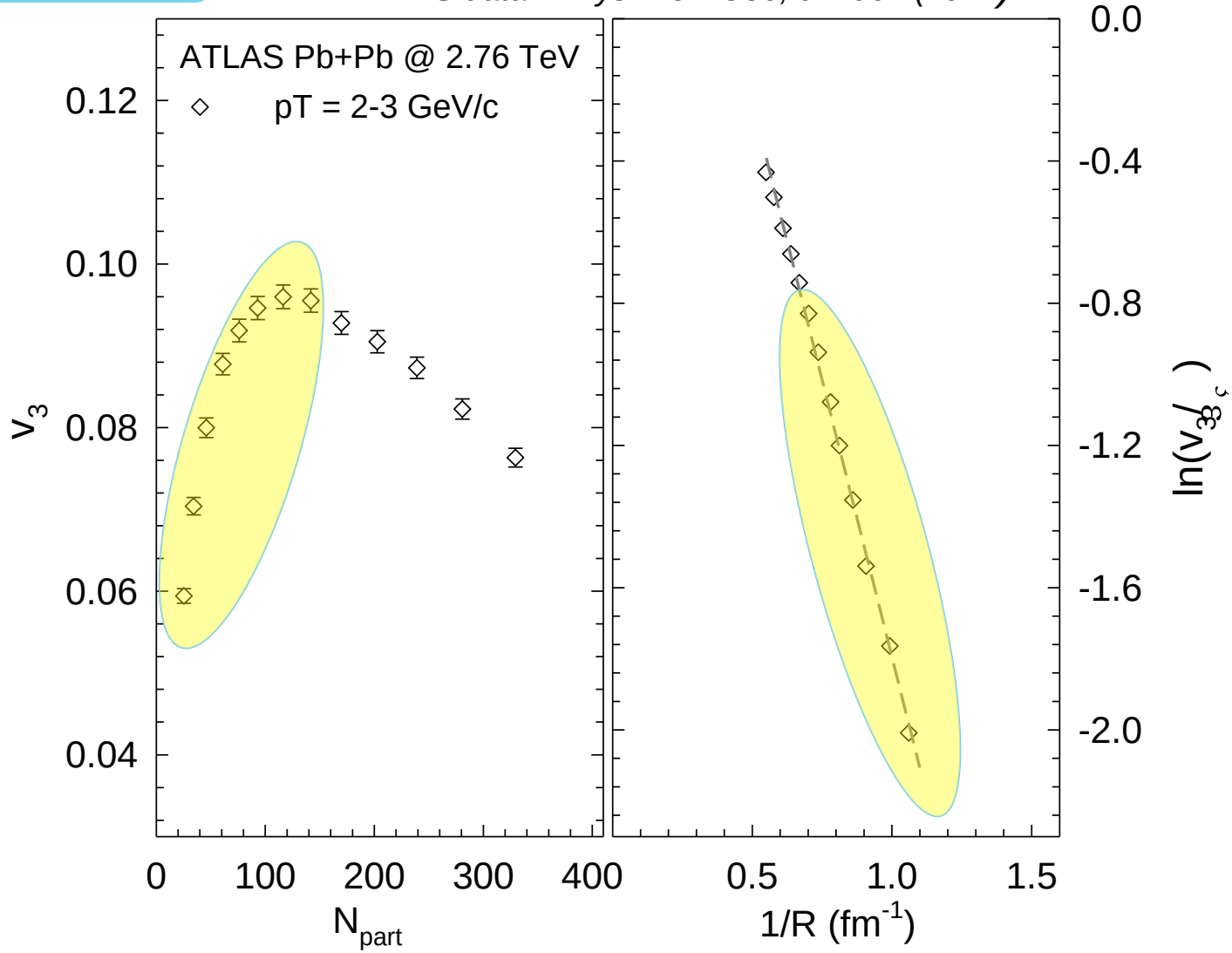

✓ **Characteristic $1/\bar{R}$ viscous damping validated**

✓ ***A further constraint for η/s and δf***

Acoustic Scaling – 1/R

$$\ln\left(\frac{v_n}{\varepsilon_n}\right) \propto \frac{-\beta''}{\bar{R}}$$

STAR Data - PhysRevC.81.044902

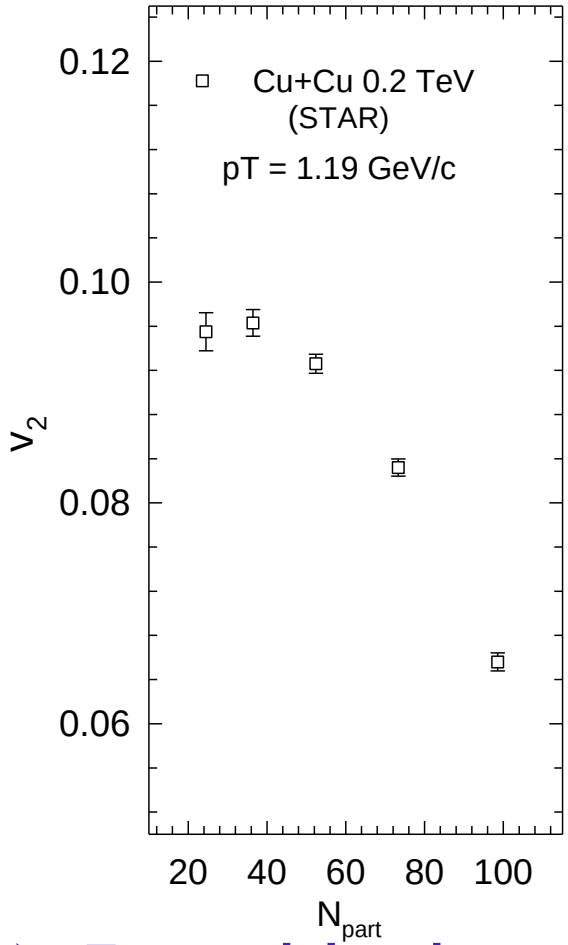

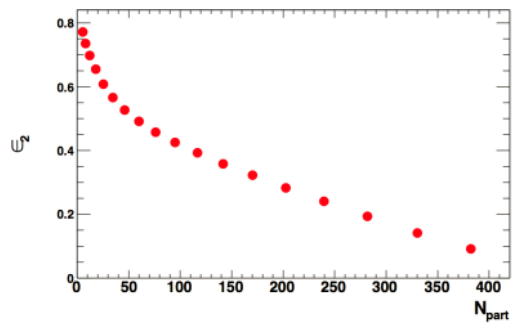

ATLAS data - Phys. Rev. C86, 014907 (2012)

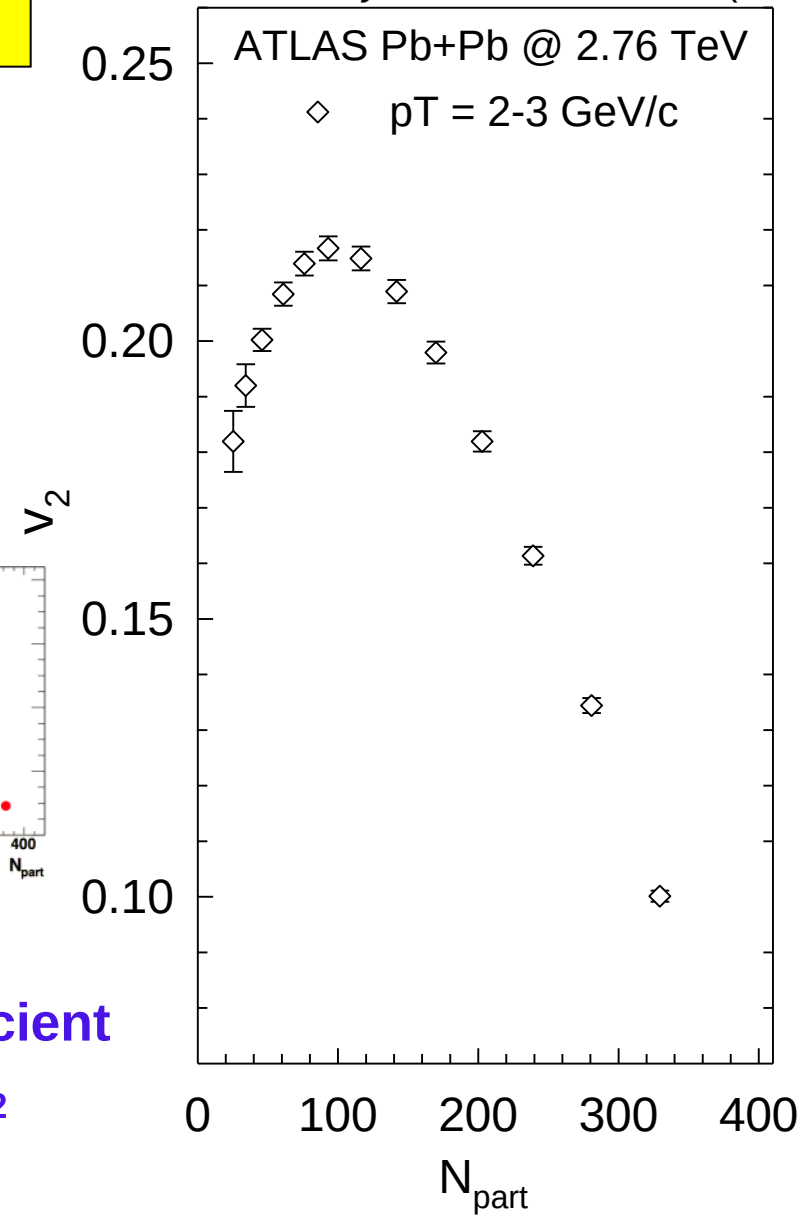

- **Eccentricity change <u>alone</u> is not sufficient To account for N_{part} dependence of v_2 In light & heavy systems**

Acoustic Scaling – 1/R

Compare RHIC & LHC

$$\ln\left(\frac{v_n}{\varepsilon_n}\right) \propto \frac{-\beta''}{\bar{R}}$$

p_T dependence of slope → δf constraint

Larger Slope for LHC → Viscosity larger @ LHC than @ RHIC

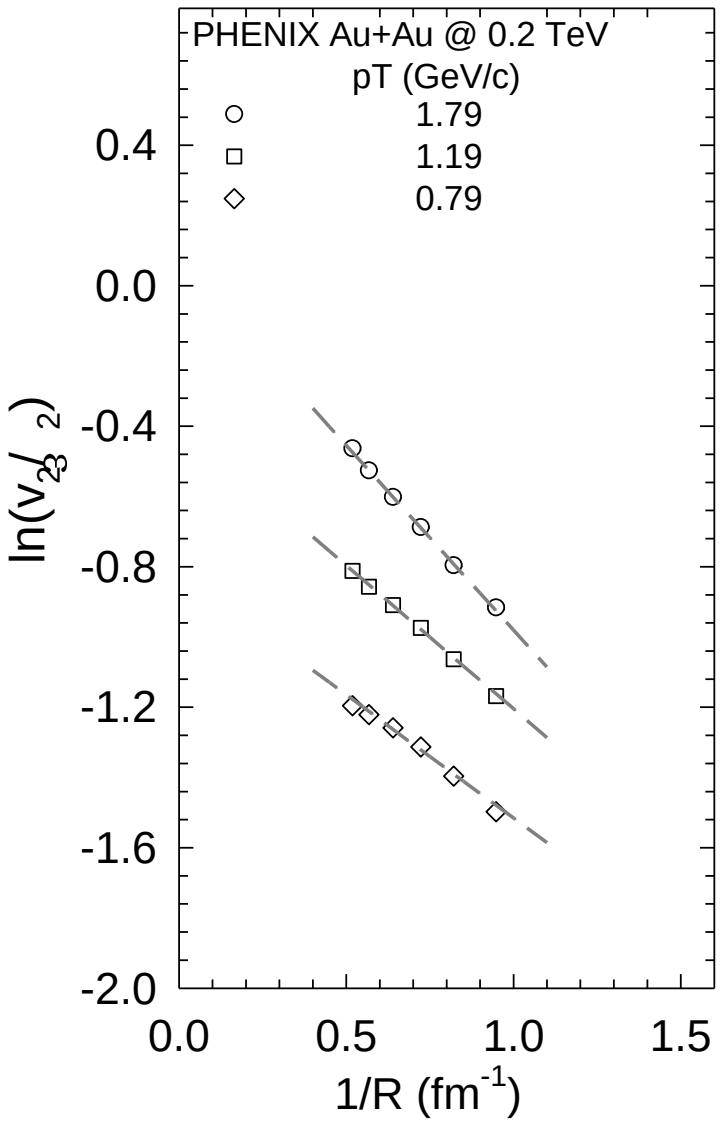

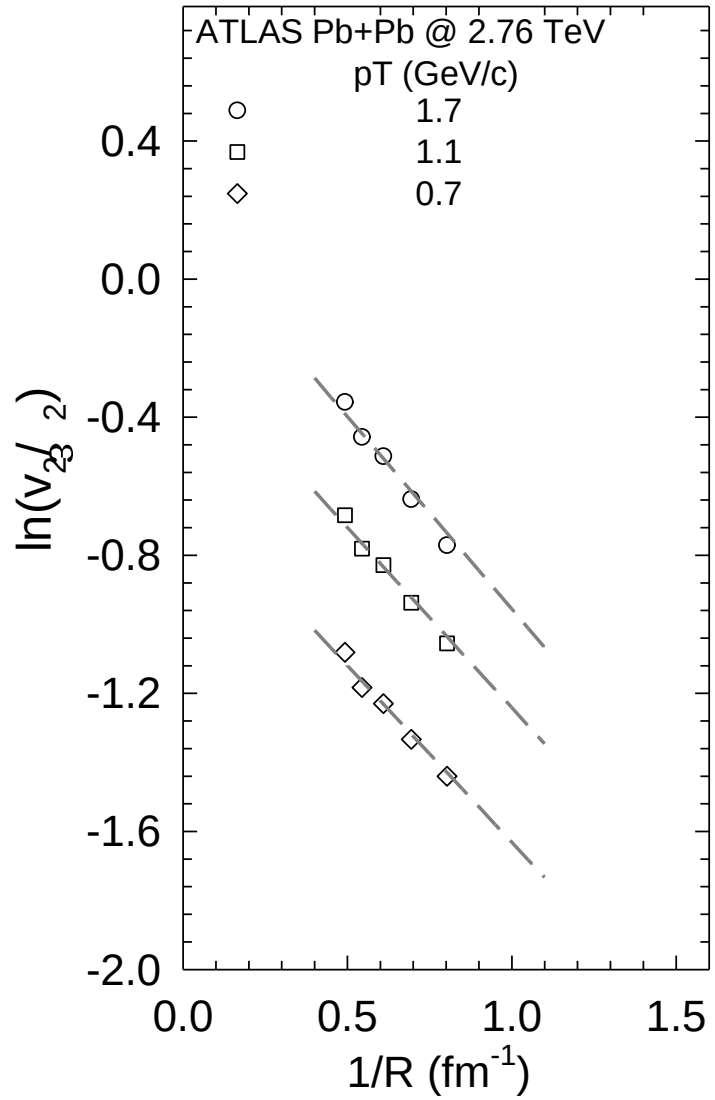

✓ **Characteristic $1/\bar{R}$ viscous damping validated**

✓ ***A further constraint for η/s***

Opaqueness Evolution from Color Liberation

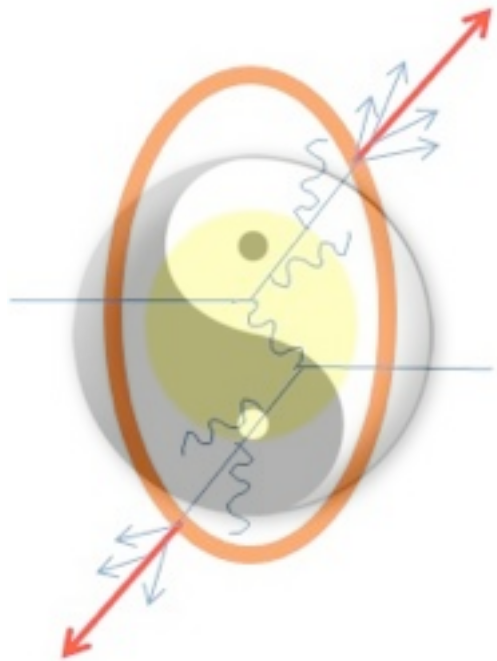

Jinfeng Liao
Indiana University, Physics Dept. & CEEM
RIKEN BNL Research Center

Outline

- Introduction: An Opaque QCD Plasma
- What We Learn From Geometry of Jet Quenching
- Opaqueness Evolution from RHIC to LHC
- Discussions & Summary

X. Zhang, JL, arXiv:1208.6361; 1210.1245;
JL, arXiv:1109.0271;
J.Jia, W.Horowitz, JL, Phys.Rev. C84 (2011) 034904
JL, Shuryak, Phys.Rev.Lett. 102 (2009) 202302

40 Years of Asymptotic Freedom

Nuclear Physics

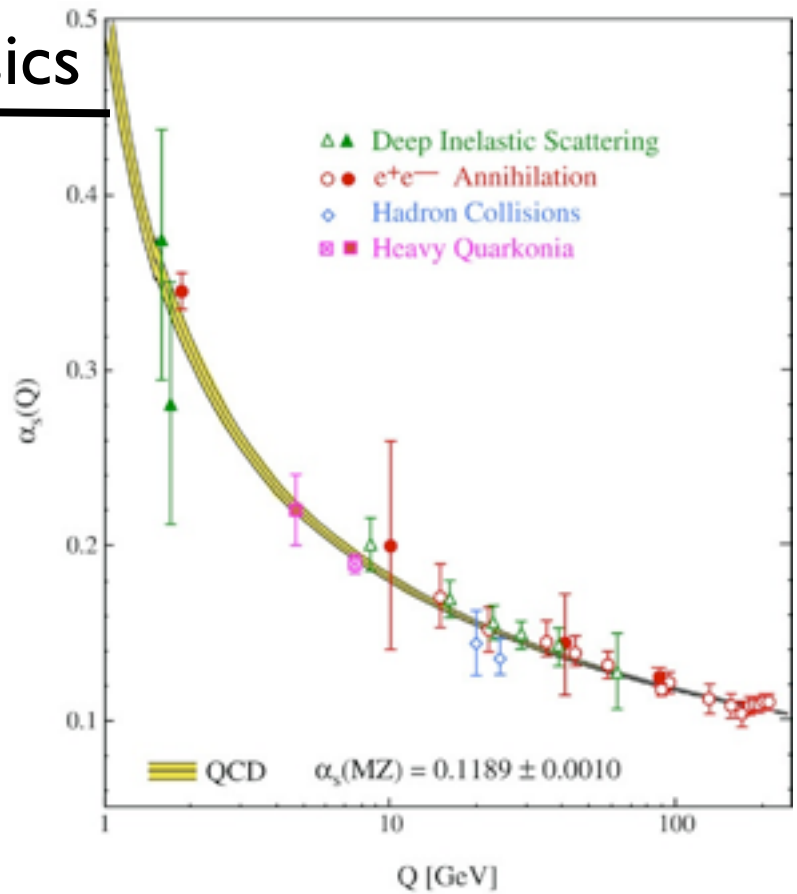

Asymptotically Free Matter

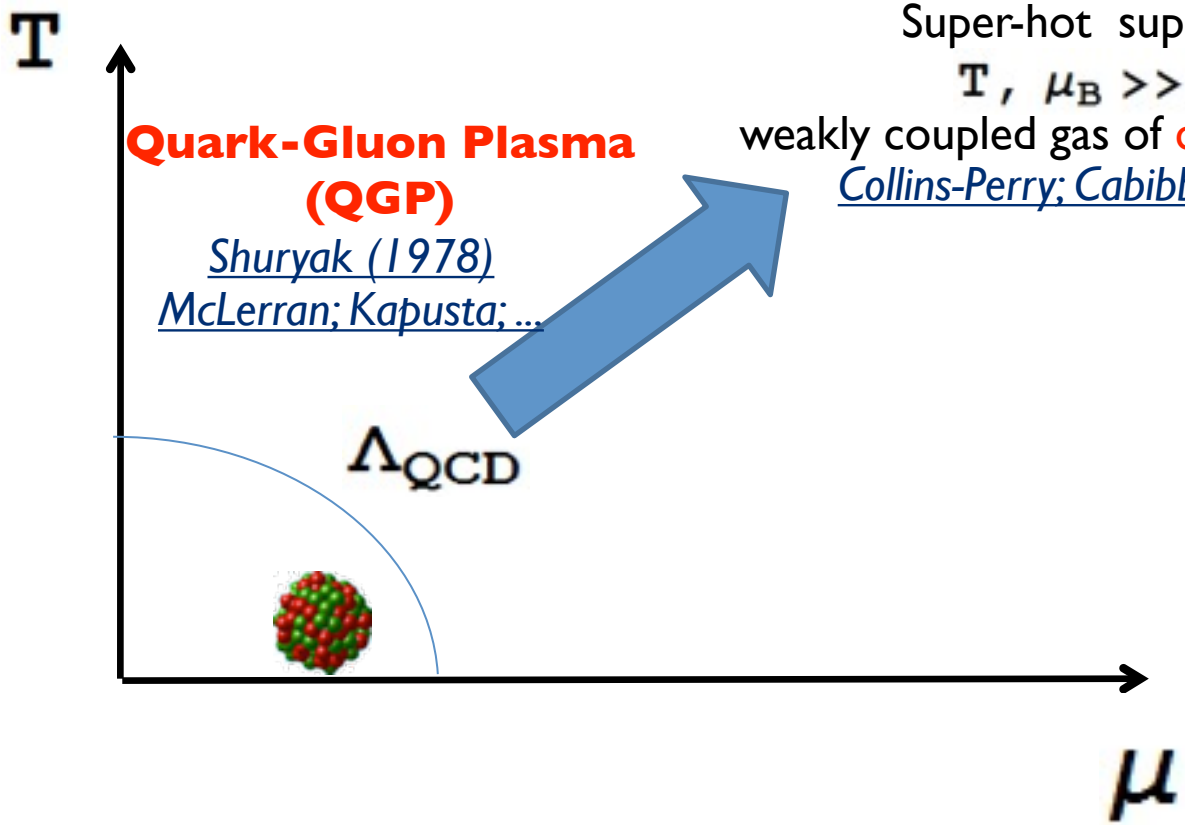

Super-hot super-dense:

$T,\ \mu_B >> \Lambda_{QCD}$

weakly coupled gas of quarks and gluons

Collins-Perry; Cabibbo-Parisi (1975)

color confined world --> color (fully) liberated world

Hot off the Lattice: **Crossover**, but **Rapid**

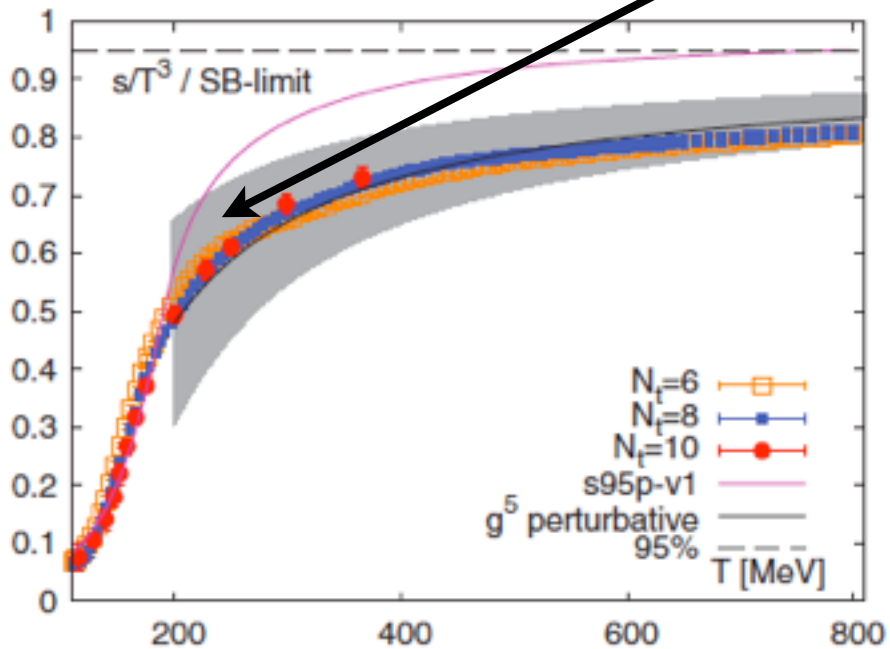

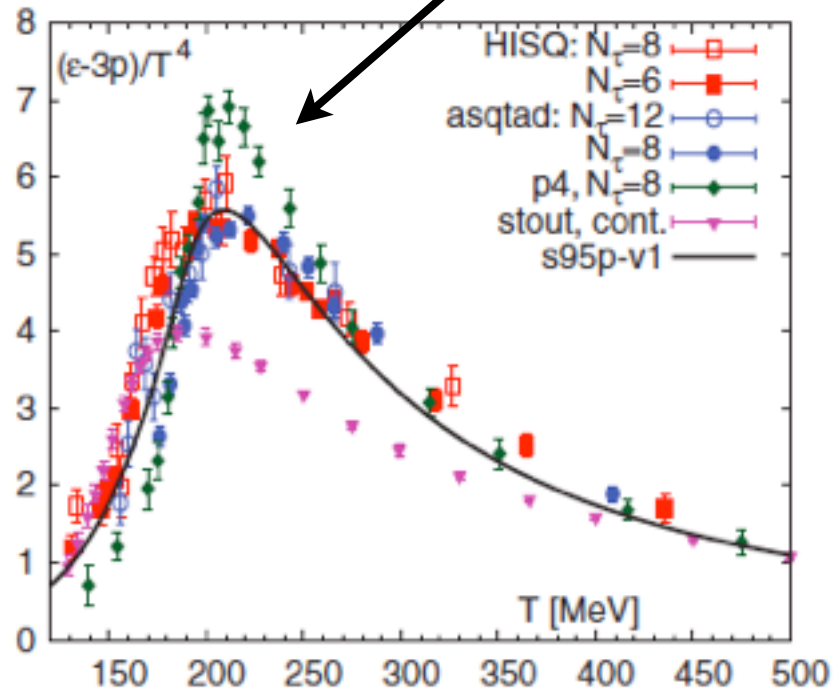

"Rapid Up" or "Rapid Down":
pressure/energy density/entropy density/
2-nd q-susceptibilities/
chiral condensate/Q-bar-Q free energy/...

"Peak" or "Dip":
trace anomaly/chiral susceptibility/
4-th q-susceptibilities/
Q-bar-Q internal energy/
speed of sound//...

Liberation of Color?

Degrees of freedom

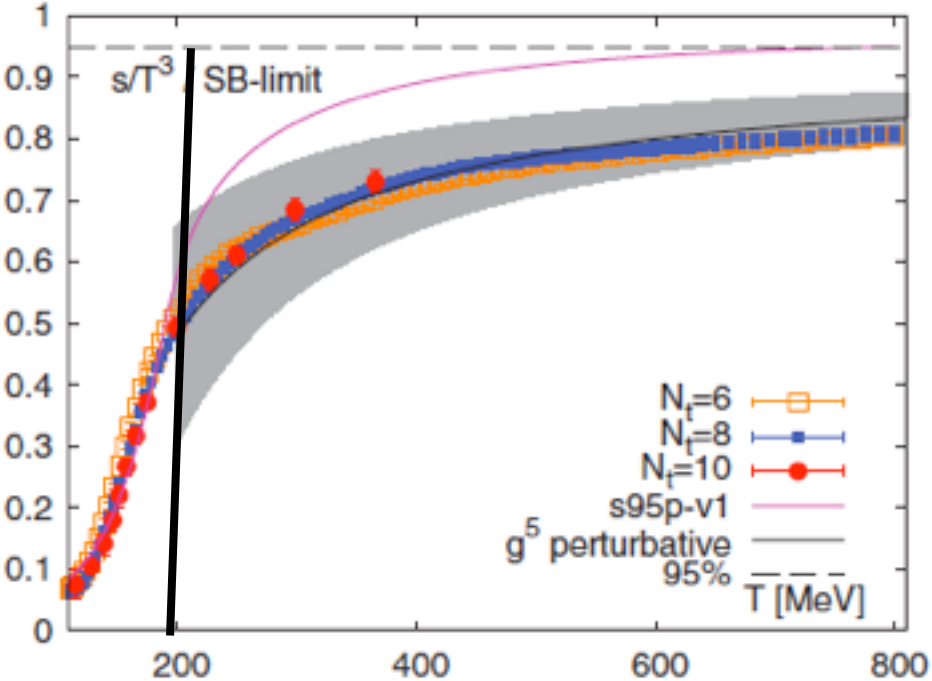

Degree of color liberation

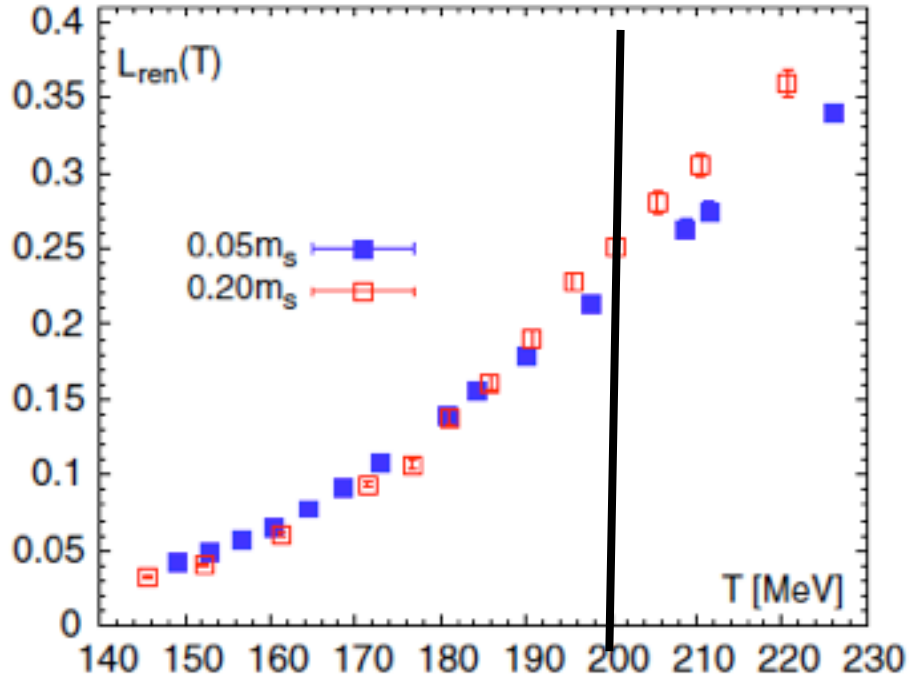

A region around Tc with liberated degrees of freedom

but only partially liberated color-electric objects.

(Pisarski & collaborators: semi-QGP --- see Skokov's talk)

Then what are the "extra" dominant DoF here???

Let's come to this later, for the moment: sth. special Near Tc, not yet the AFM

QGP from the "Little Bangs"

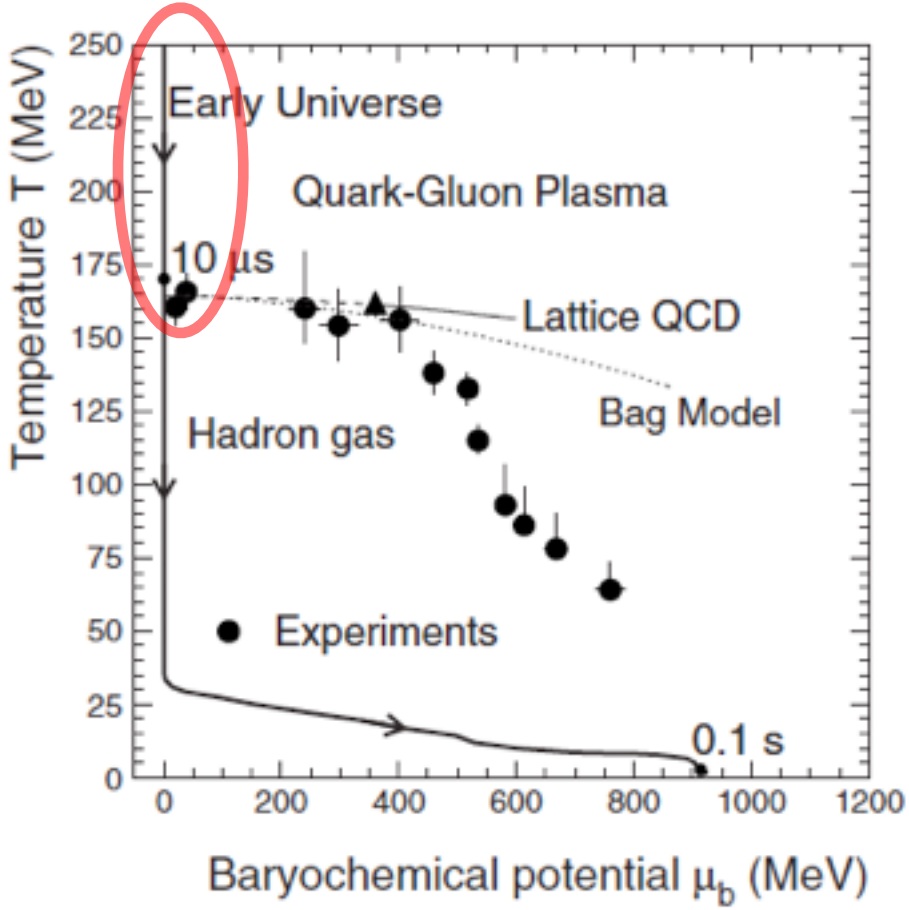

Surprising QGP: nearly perfect fluid; color opaque; .....

It is not the Asymptotically Free Matter yet!

(not unrelated to the partial liberation of color)

A Color-Opaque Plasma

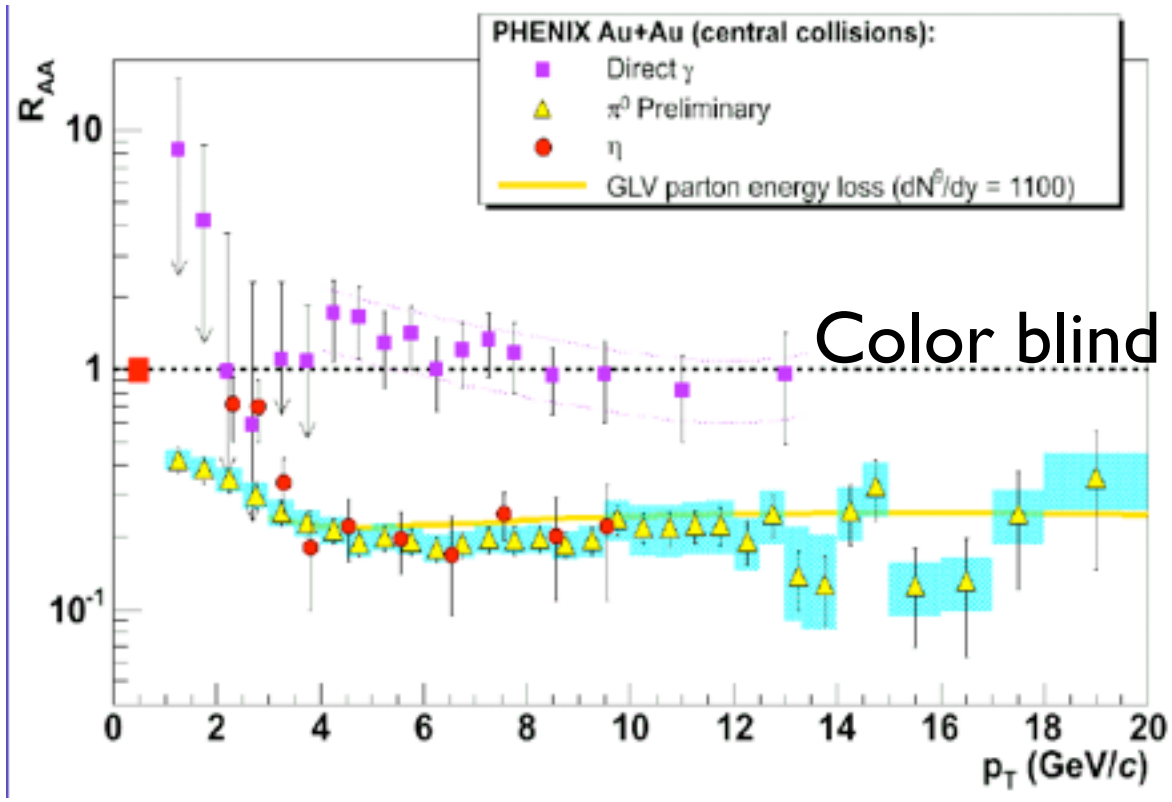

Color blind probe

Colorful probe

A qualitatively different medium

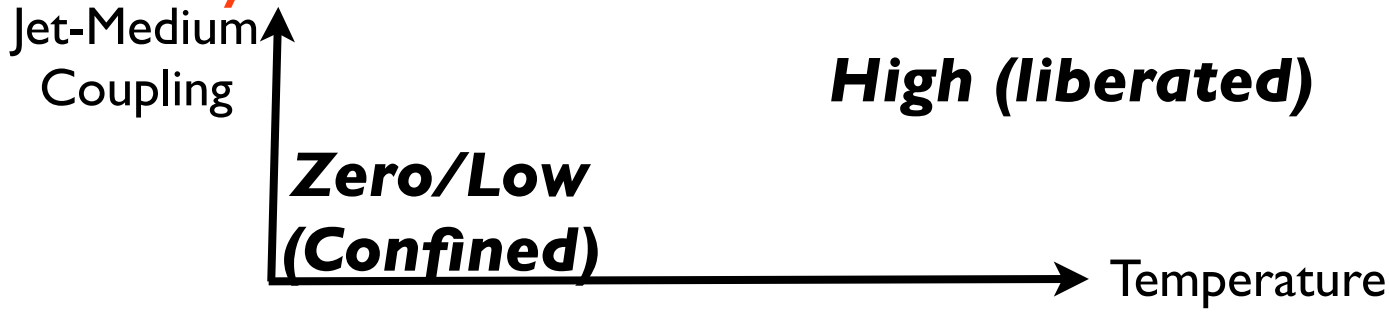

From Transparency to Opaqueness

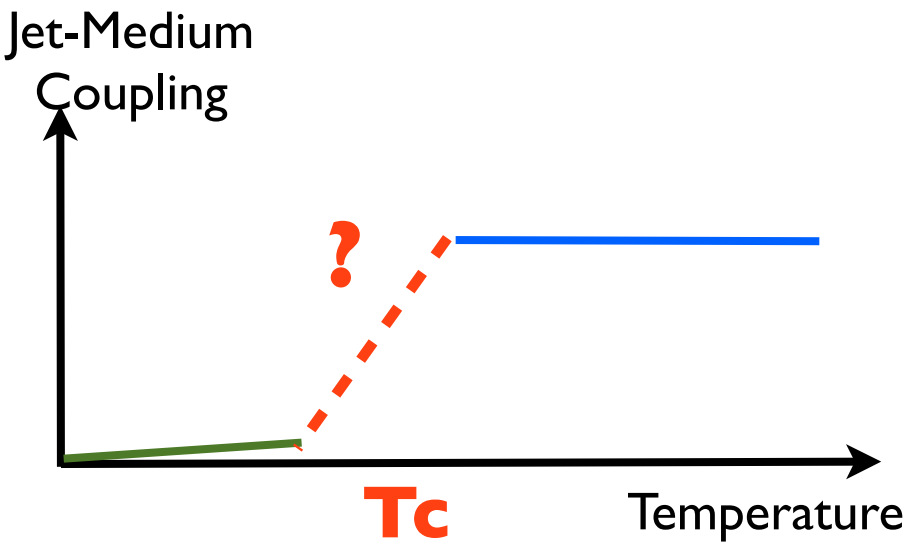

"Waterfall" scenario

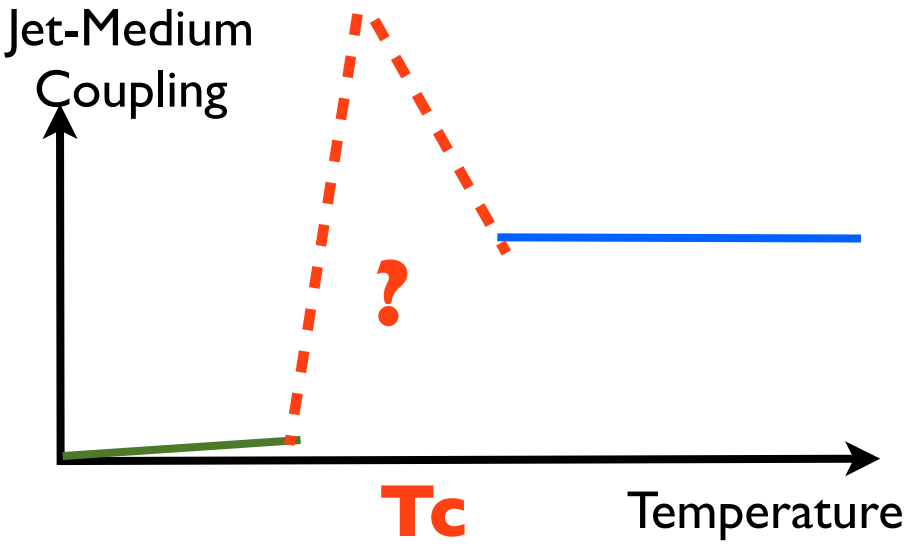

"Volcano" scenario

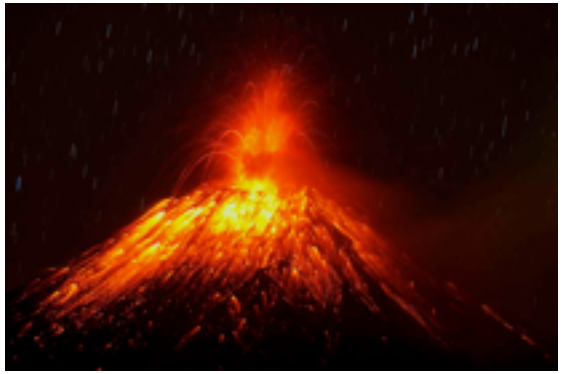

To me, this is a question of fundamental interest, and one we must answer for understanding of jet-quenching & of the medium itself.

V.S.

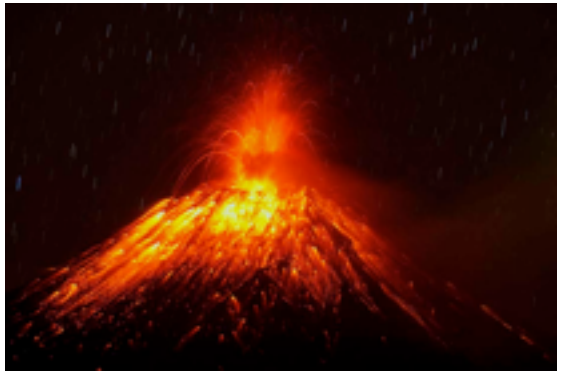

How can we get the answer?

Do we even have a chance
to find out the answer?

Luckily, we seem to be able to:
Geometry ; evolution RHIC --> LHC

Geometric Anisotropy of Jet Quenching

Geometric tomography(~2001): Gyulassy,Vitev,Wang,...
Geometric limit of high-pt v2: Shuryak; Drees,Feng,Jia;...
Till ~2008: clear discrepancy between data / any model

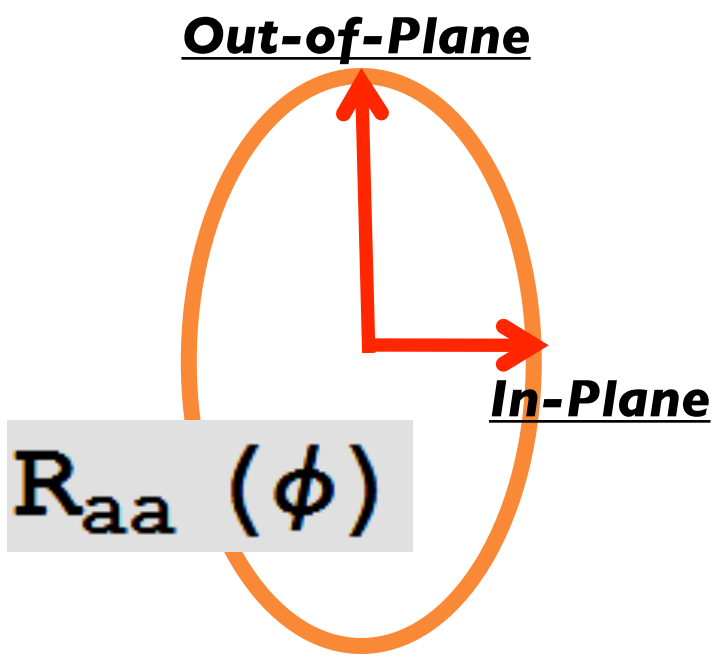

$I_{in} < I_{out} \Rightarrow (R_{aa})_{in} > (R_{aa})_{out}$

Positive v2 for high Pt hadrons

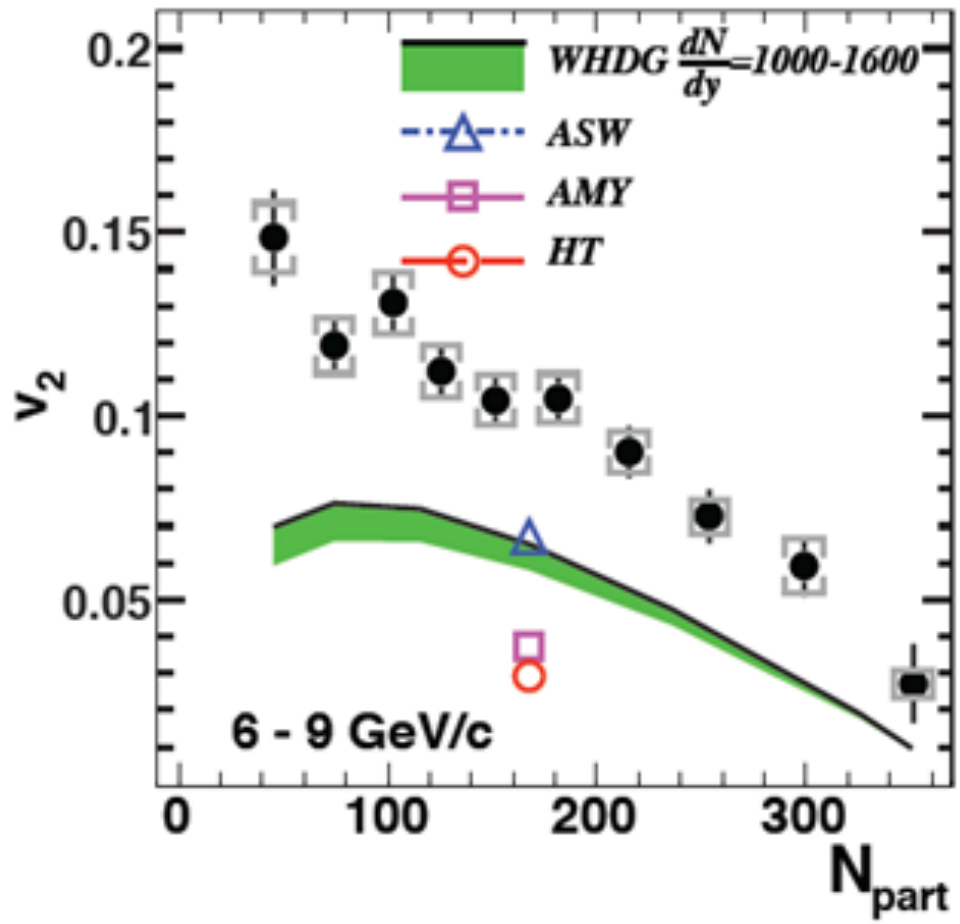

Where Are Jets Quenched (More Strongly)?

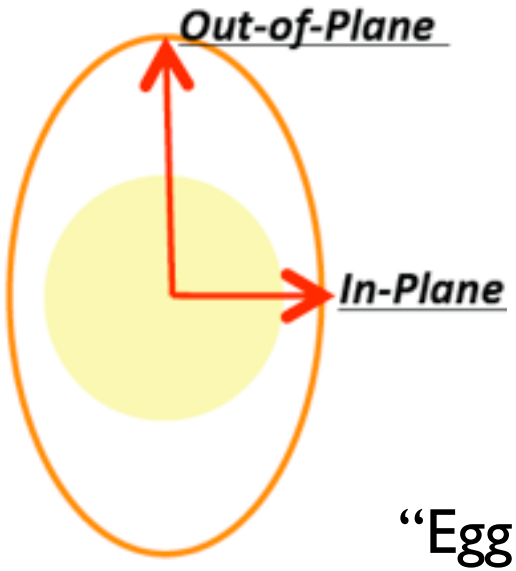

Taken for granted in all previous models: "waterfall" scenario.

We realized the puzzle may concern more radical questions:

Where are jets quenched (more strongly)?

Geometry is a sensitive feature:
"Egg yolk" has one geometry, "Egg white" has another.

PRL 102, 202302 (2009) PHYSICAL REVIEW LETTERS week ending 22 MAY 2009

Angular Dependence of Jet Quenching Indicates Its Strong Enhancement near the QCD Phase Transition

Jinfeng Liao[1,2,*] and Edward Shuryak[1,†]
[1]*Department of Physics and Astronomy, State University of New York, Stony Brook, New York 11794, USA*
[2]*Nuclear Science Division, Lawrence Berkeley National Laboratory, Berkeley, California 94720, USA*
(Received 22 October 2008; revised manuscript received 19 February 2009; published 22 May 2009)

Layer-wise Jet Quenching

$$f_P = exp\left\{-\int_P \kappa[s(l)]\, s(l)\, l^m dl\right\}$$

$$R_{AA}(\phi) = < (f_P)^{n-2} >_{P(\phi)}$$

scan the jet quenching geometry layer by layer in density

$$\kappa[s] = \kappa_c * \theta[s - s_a] * \theta[s_b - s]$$

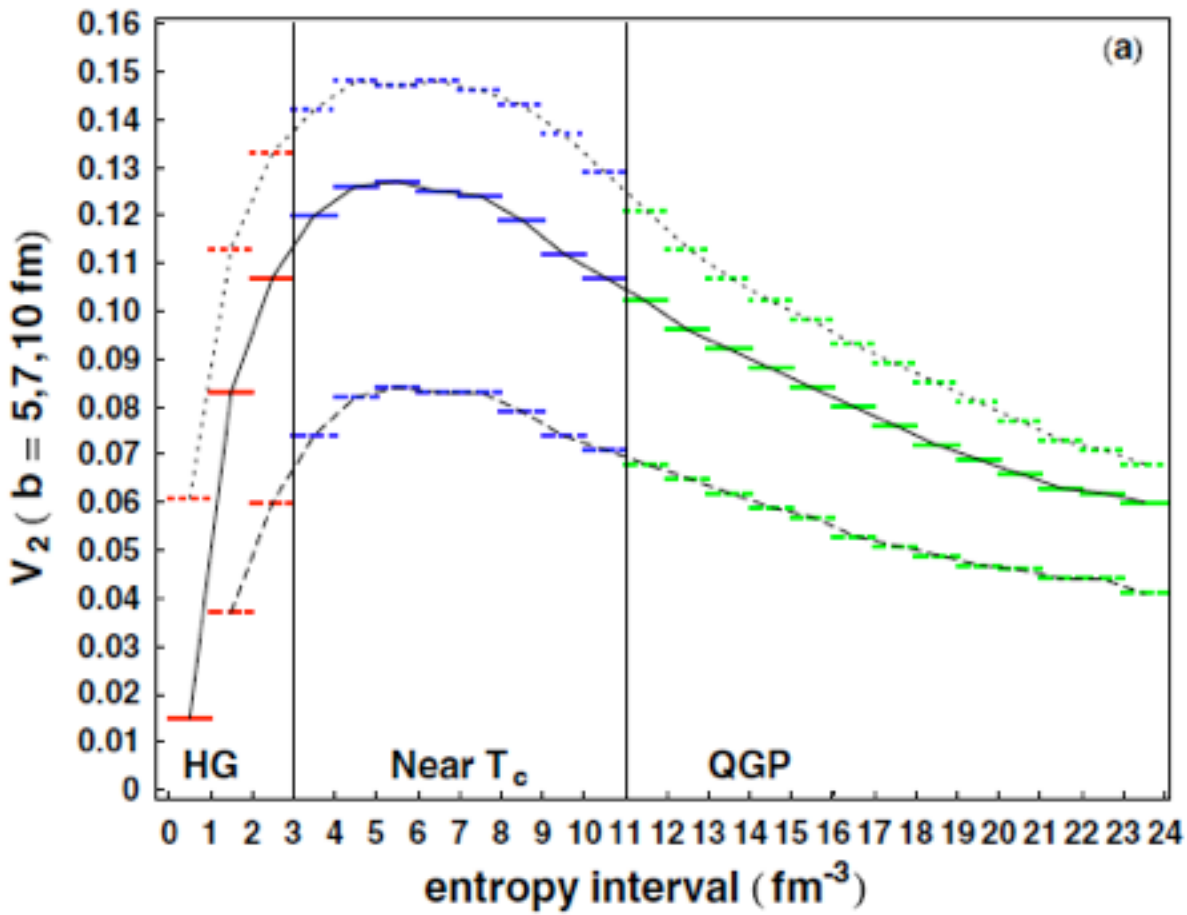

Assume jet quenching occurs only in a specific density interval with constraint from overall Raa

-->

look at v2 from that layer:

Near-Tc layers give the strongest anisotropy!

Near-Tc Enhancement (NTcE)

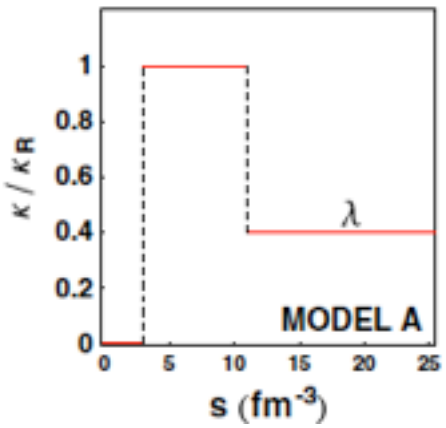

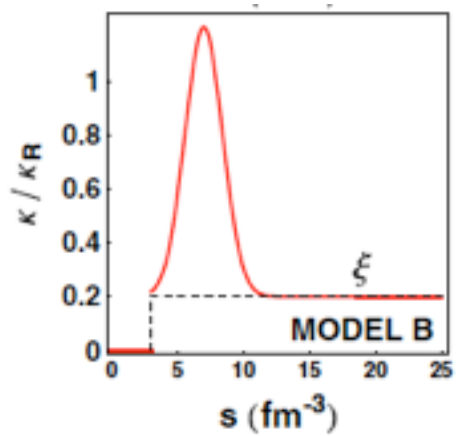

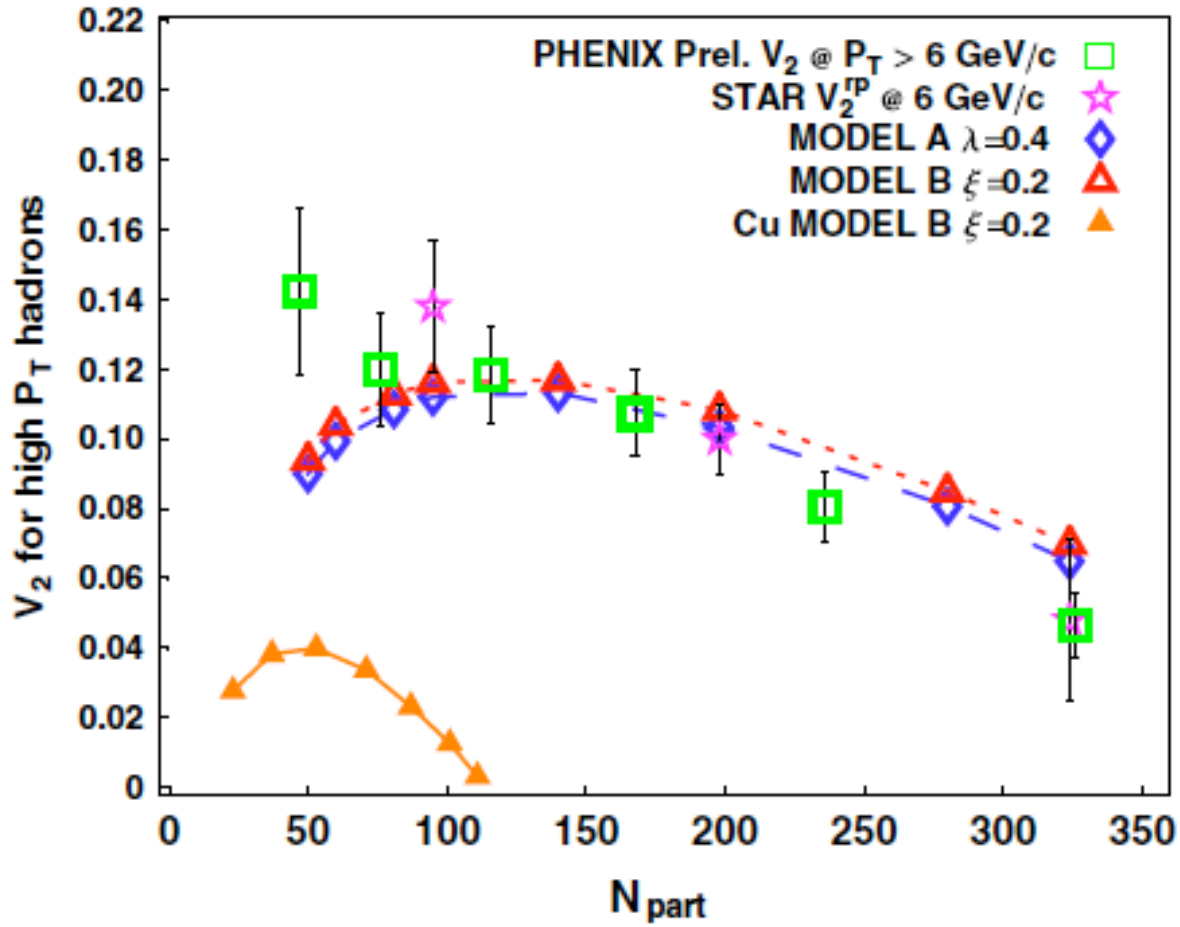

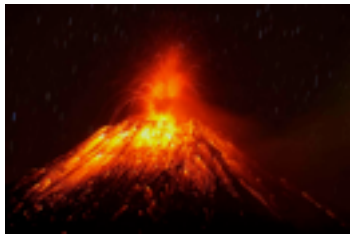

Models based on "volcano" scenario gave the first simultaneous description of high Pt Raa and V2 at RHIC!

NTcE as a Generic Mechanism

Near Tc Enhancement (the "volcano") generically increases the contribution to jet quenching from later stage and outer layer of the fireball, and "picks" up more anisotropy.

* relatively insensitive to detailed shape of "volcano"

* works in jet quenching modelings with varied implementations (e.g. geometric models, or GLV/WHDG/CUJET, or ASW, with/without fluctuations/transverse expansions)

Francesco-Di Toro-Greco

Renk-Holopainen-Heinz-Shen

Gyulassy,Buzzatti,Bezt

Fries & students

Marquet & Renk

Jia & Wei

The RHIC+LHC Era

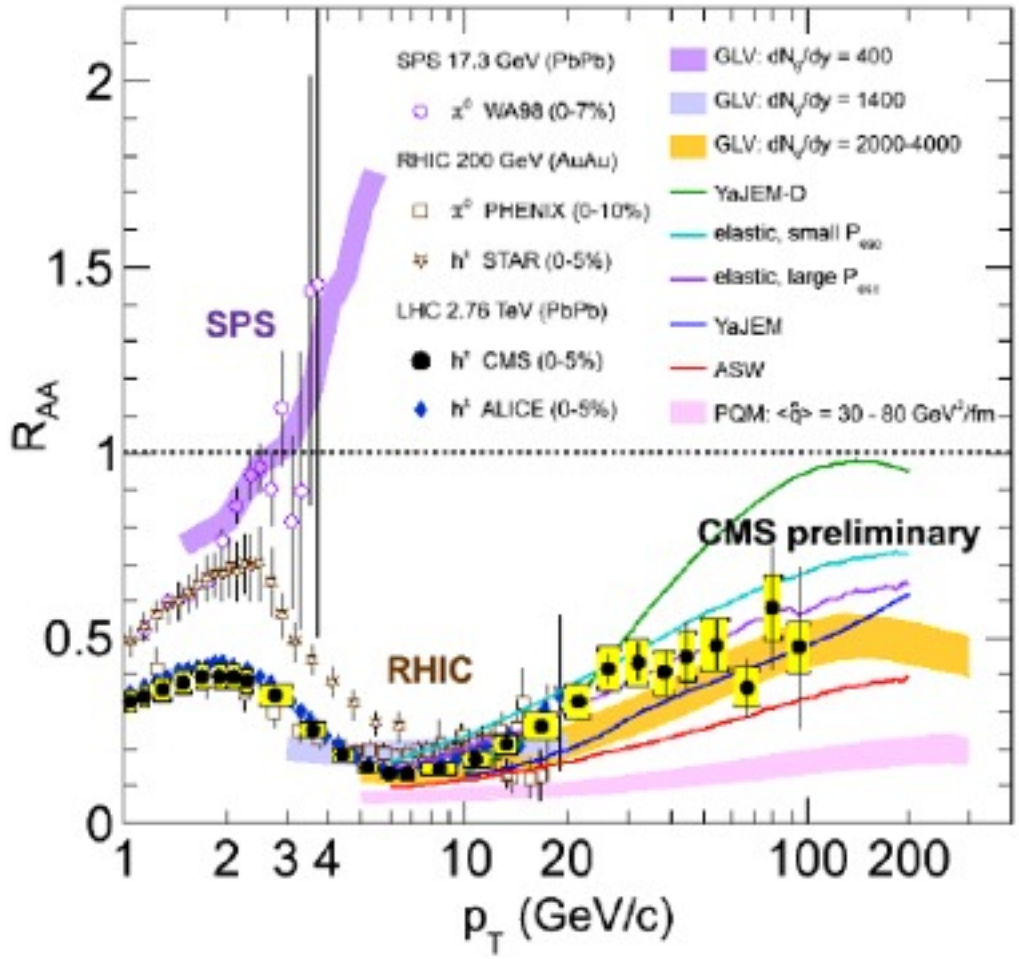

Beautiful jet quenching measurements from ALICE,ATLAS,CMS

NTcE: Shift to Less Opaque Medium at LHC

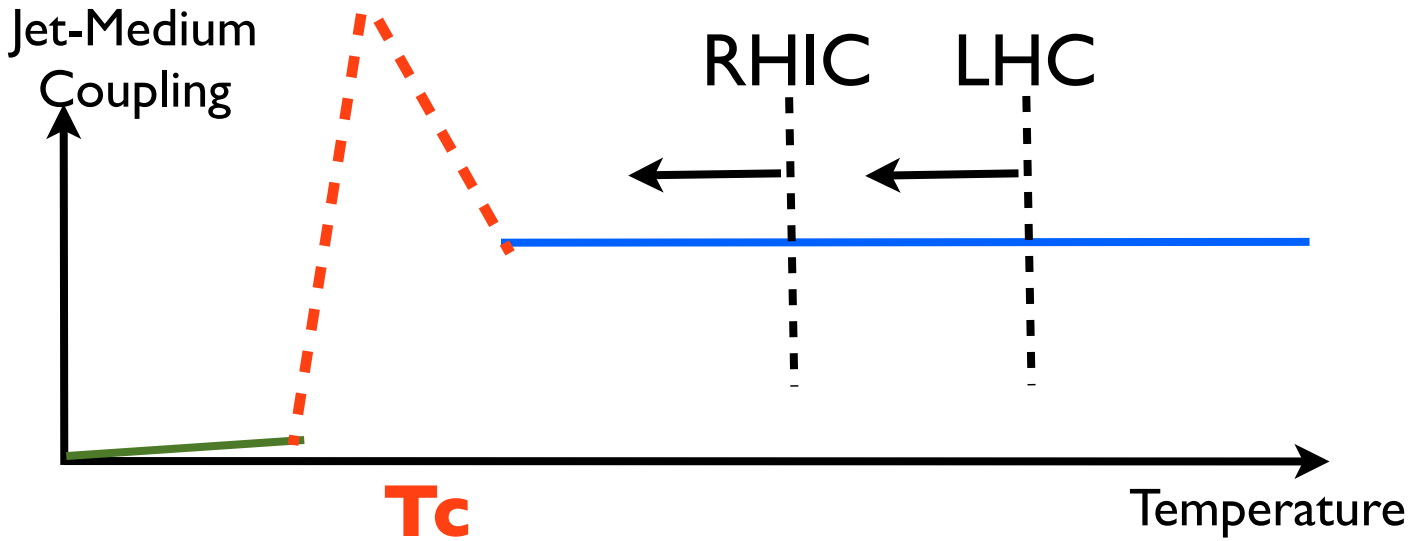

LHC compared with RHIC:

* high T QGP occupies more space-time evolution
* the near-Tc will weigh less, with "volcano" effect reduced

-->

* Naturally predicts a less opaque (on average) medium seen by jets (note however density doubles)
* Anisotropy from the "volcano" and "waterfall" scenarios will become closer

Raa from RHIC to LHC

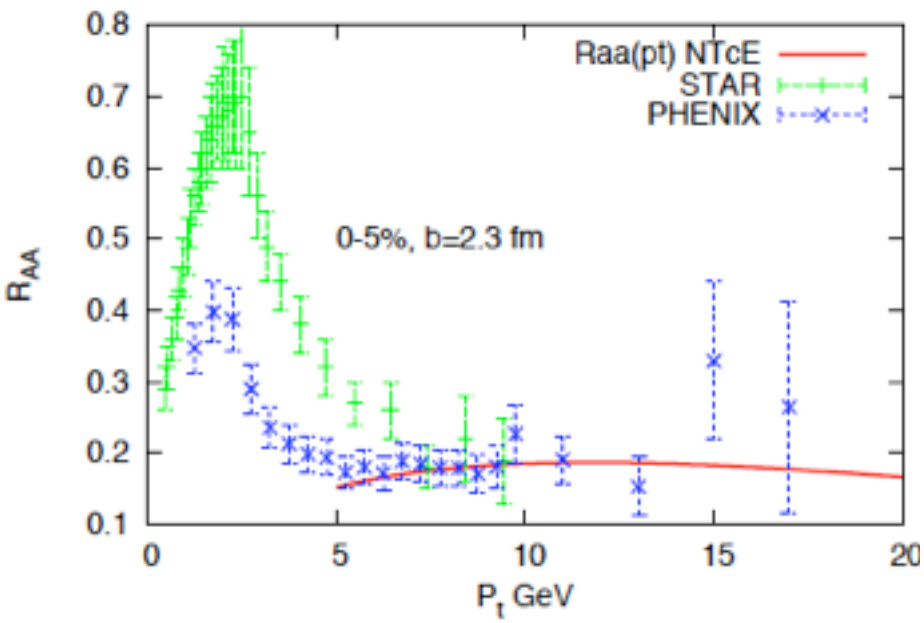

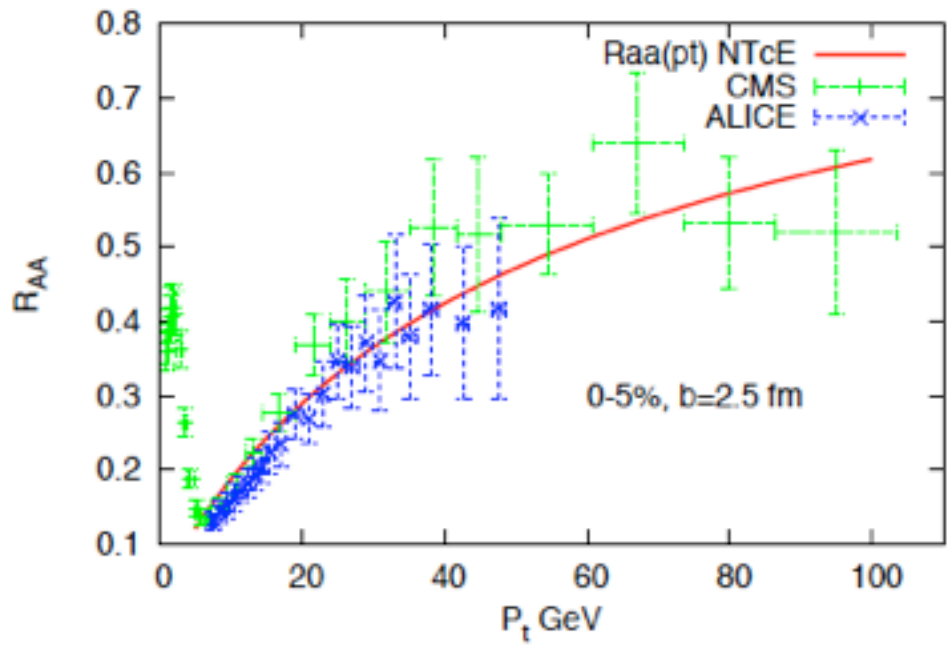

Average jet-medium coupling from RHIC to LHC: reduced by ~30%

$$< \kappa[s(l)] >_P = \frac{\int_P \kappa[s(l)]\, s(l)\, l\, dl}{\int_P s(l)\, l\, dl}$$

$$< \kappa >_{\mathrm{RHIC}} : < \kappa >_{\mathrm{LHC}} \approx 1 : 0.72$$

V2 from RHIC to LHC

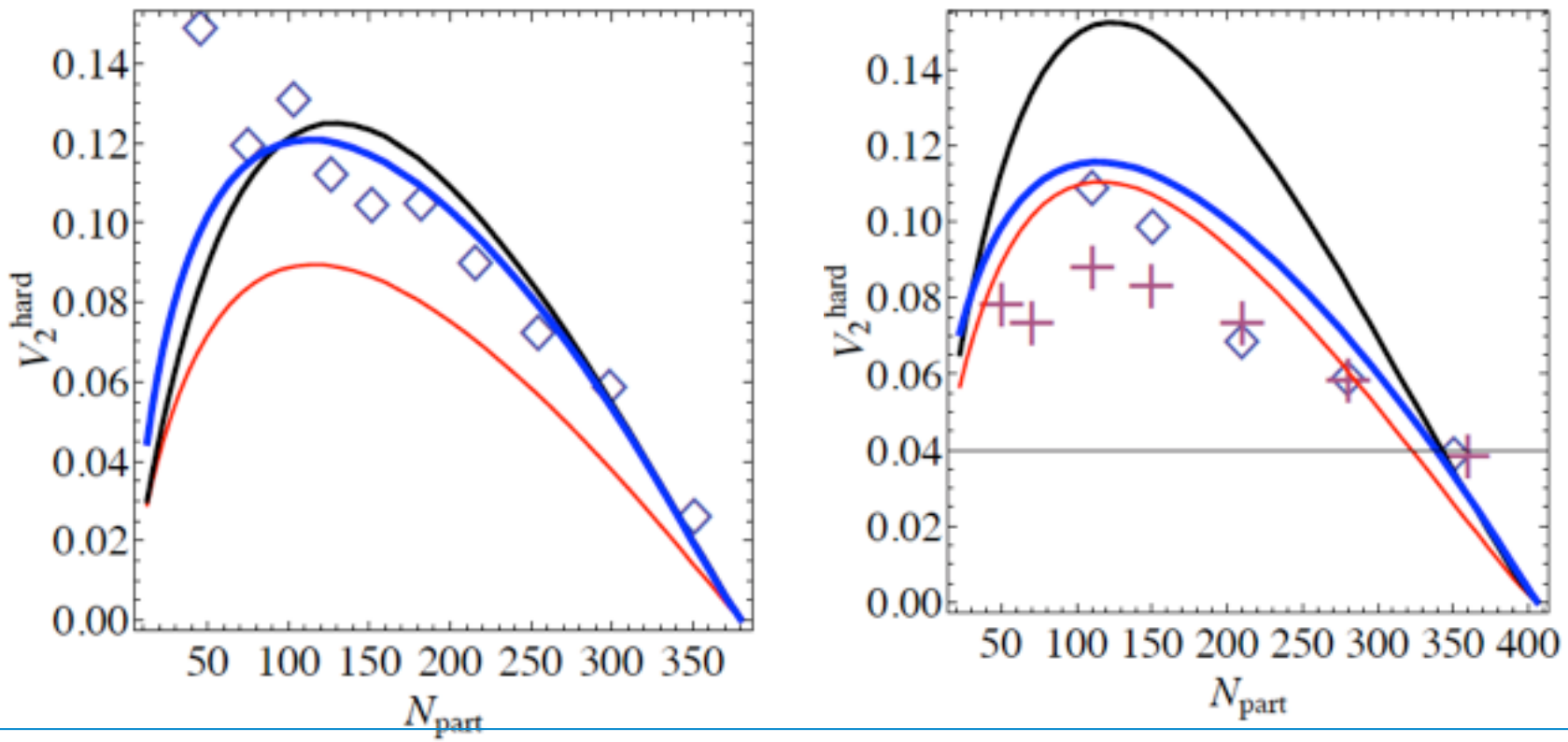

RED: L^2 model+waterfall **BLUE: L^2+volcano** **BLACK: L^3+waterfall**

* We do see big difference between waterfall/volcano at RHIC, and this difference becomes much smaller at LHC
* RHIC + LHC data are in favor of the L^2 + Volcano scenario
(See Xilin Zhang talk tomorrow for newest results with initial fluctuations and higher harmonics)

"Volcano" Seen from "Different Angles"

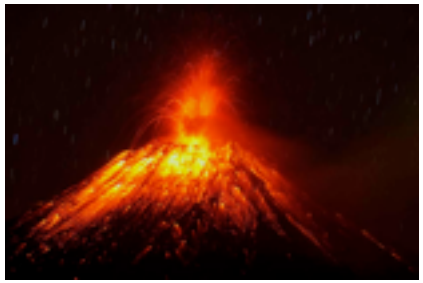

* Horowitz & Gyulassy:
  "surprising transparency" when
  simply extrapolating RHIC to LHC
* Betz & Gyulassy:
  10~30% reduction in "polytrope" model
* Buzzatti & Gyulassy:
  Strong running coupling at T --> Tc
  (also in Zakharov calculation)

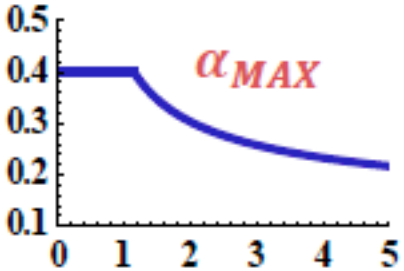

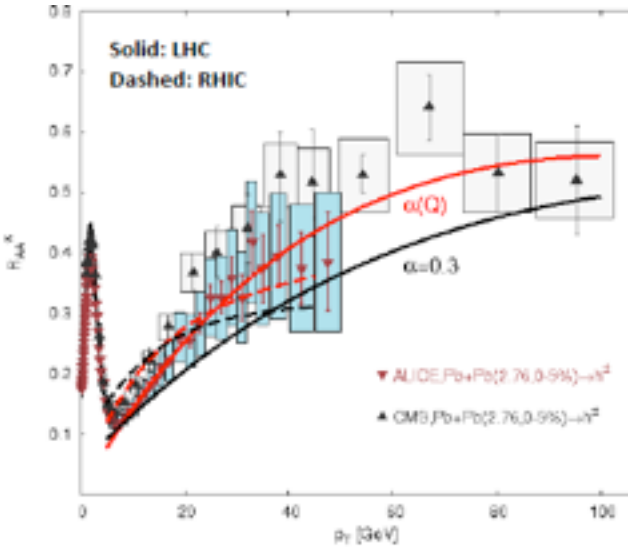

* Lacey et al, scaling analysis: q-hat(LHC) ~ q-hat(RHIC) despite twice the density
* Lattice QCD: Q-bar-Q internal energy shows strong peak at Tc
* Muller-Majumder-Wang, Dusling-Moore-Teaney:
  peak in q-hat/density related with dip in \eta/s ?
* Majumder: lattice attempt -->q-hat/density showing peak?

What are Underlying the "Volcano"?

T<< Lambda_QCD | T ~ Lambda_QCD | T>> Lambda_QCD

Vacuum: confined | **Tc** | sQGP | ***wQGP: screening*** → **T**

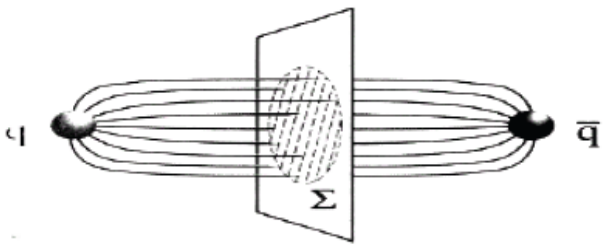

Emergent plasma with E & M charges:
chromo-magnetic monopoles are the "missing DoF"

Plasma of E-charges
E-screening: g T
M-screening: g^2 T

Electric Flux Tube:
Magnetic Condensate

$$\alpha_E * \alpha_M = 1.$$

$$\kappa \sim \frac{\alpha_E(T)\alpha_M(T)n_m(T)}{s(T)} = \frac{n_m/T^3}{s/T^3}$$

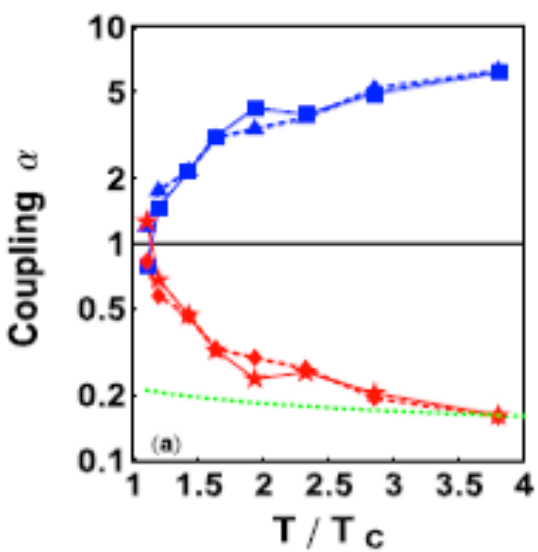

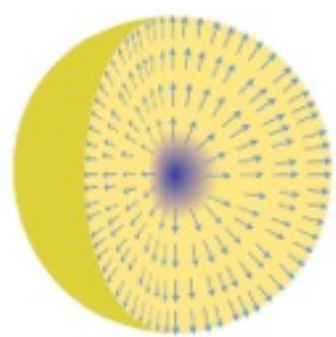

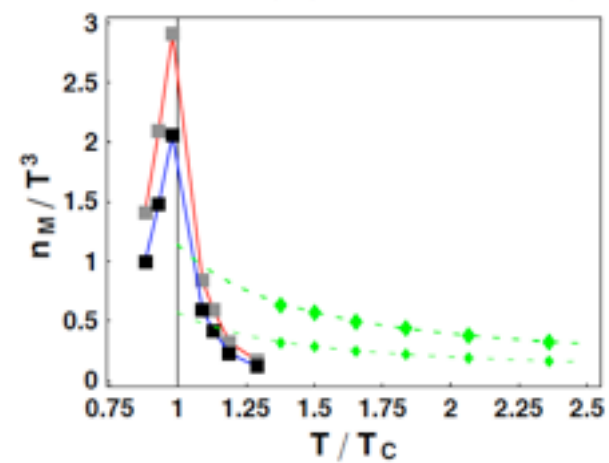

JL & Shuryak:
Phys.Rev.C75:054907,2007; Phys.Rev.Lett.101:162302,2008; Phys.Rev.C77:064905,2008; Phys.Rev.D82:094007,2010; Phys.Rev.Lett.109:152001,2012.

Summary

* An exciting problem: determine and understand the temperature dependence of jet-medium coupling

* Geometry + Evolution from RHIC to LHC: strong evidences for Near-Nc Enhancement

* RHIC + LHC together provide unique opportunities for mapping out the detailed shape of the "volcano" and for probing the fascinating midland between the confined world and the asymptotically free matter.

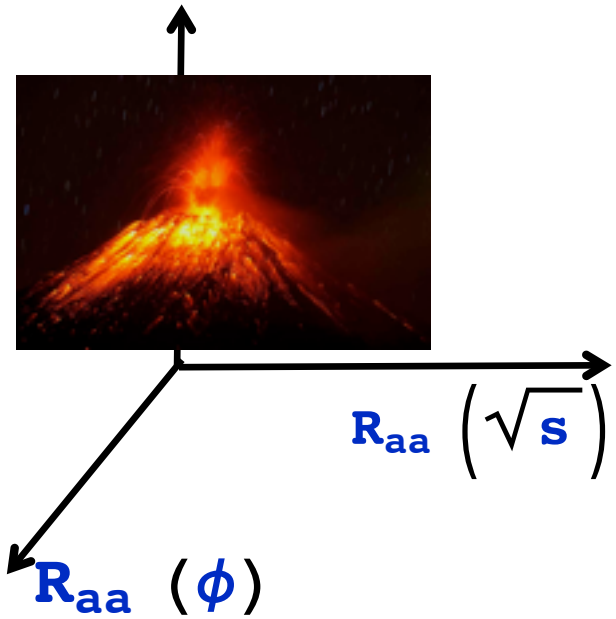

BACKUP SLIDES

Near-Tc Matter: Thermodynamics

Near Tc: <u>a wide window</u> in terms of entropy density !

What is the nature of confinement transition?

Can H.I.C. help us understand the matter just about to confine?

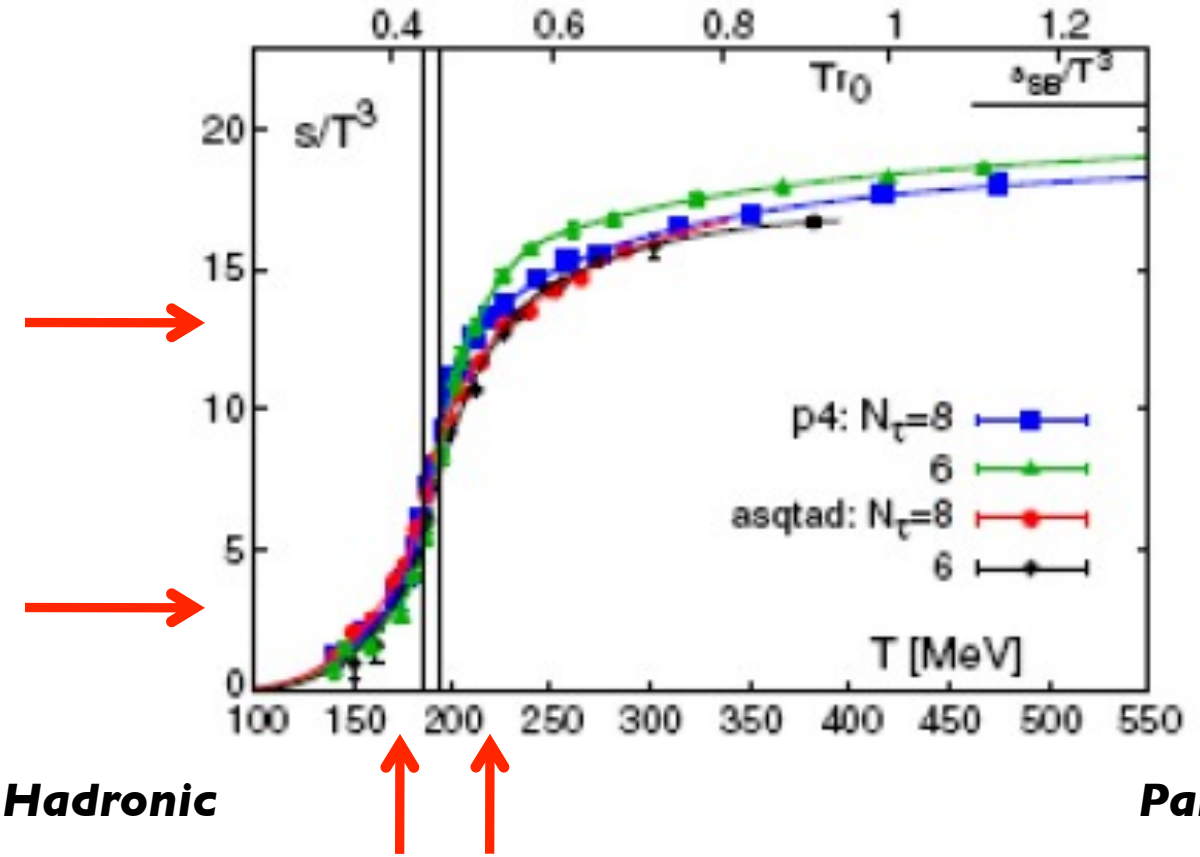

Hadronic ***Partonic***

The world is much richer than just a HRG and a Stefan-Boltzmann QGP!

Near-Tc Matter: Hydrodynamics

Near Tc Matter (between HRG and QGP) occupies
large space time volume (~1/3) during the fireball evolution.

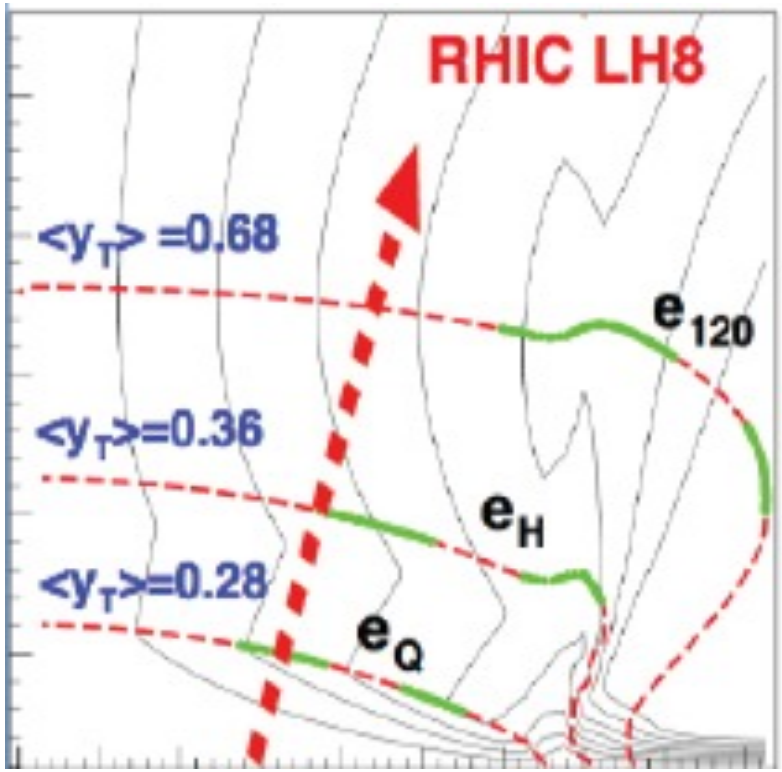

Teaney & Shuryak

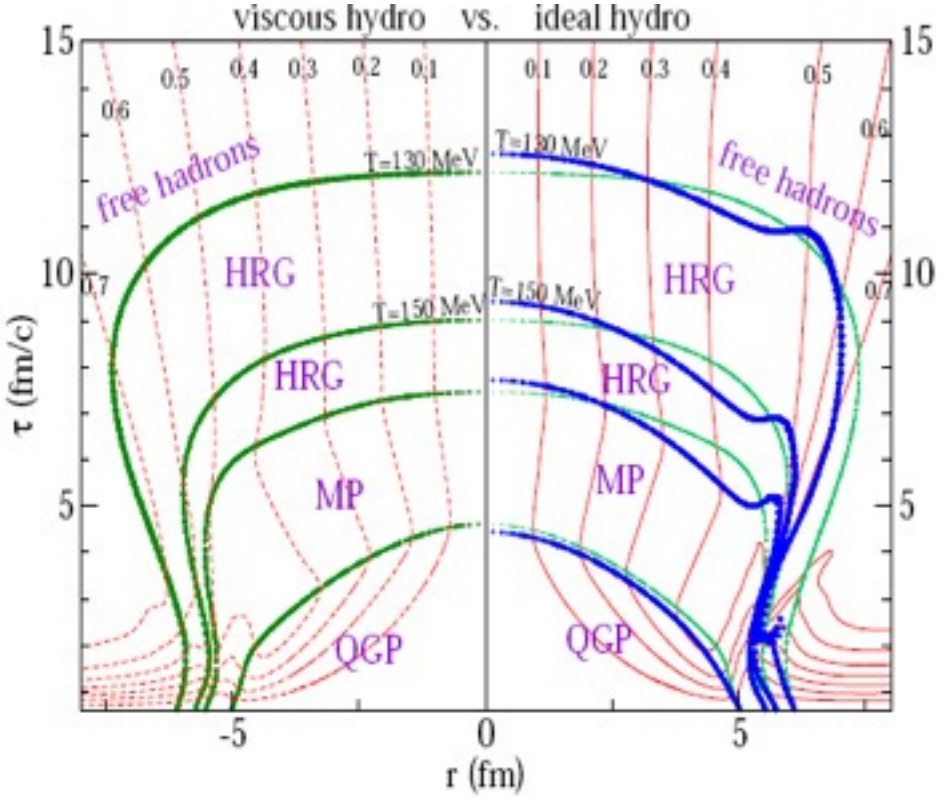

Heinz & Song

Sensitivity to T-dependence of Energy Loss

Francesco-Di Toro-Greco (arXiv:1009.1261)

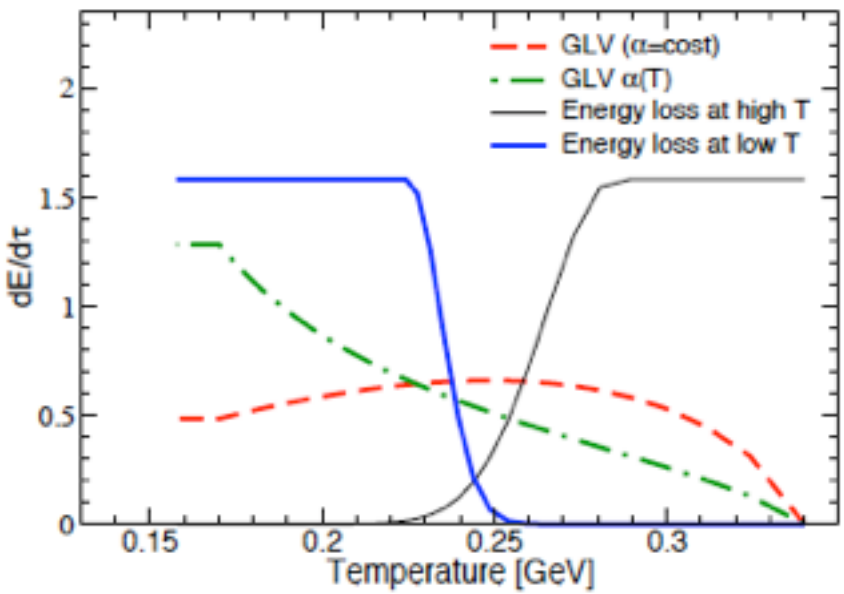

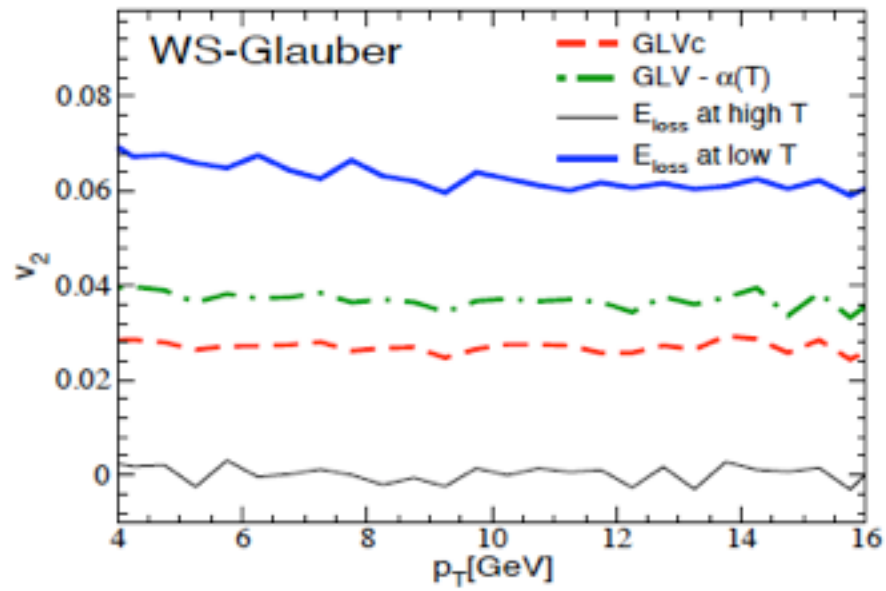

Magnetic Monopoles & E-M Duality

't Hooft-Polyakov (1974):
monopoles naturally arise as topological solutions to classical EoM in non-Abelian gauge theories;
<u>Dirac Quantization obeyed, mass & size ~ 1/g</u>

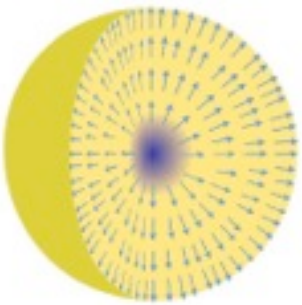

$$\boxed{\text{Dirac}: e^* g = 1}$$

What happens if the gauge theory with monopoles is in strongly coupled regime?

E-M Duality: (Motonen, Olive, 1977)

strong coupling → change of D.o.F. toward emergent ones ;

Dirac condition → E and M couplings inversely related

E weakly coupled → theory in terms of E language

E strongly coupled → theory better described by Magnetic.

Recent results from pPb collisions at the LHC

Constantin Loizides
(LBNL/EMMI)

15.04.2013

RBRC Workshop on “Jet quenching at RHIC vs LHC in light of recent dAu vs pPb controls”

LHC p+Pb runs at 5.02 TeV

- LHC operated with
  - 4 TeV proton beam and 1.57 TeV / nucleon Pb beam
    - Center of mass energy 5.02 per nucleon pair
    - Center of mass rapidity shift dY = -0.465 in direction of proton
- 2012 pilot run (4 hours of data taking)
  - About 1/μb per experiment with very low pileup
- 2013 long run (3 weeks of data taking)
  - Delivered about 30/nb to ATLAS, CMS and ALICE
    - ALICE required about 50/μb with μ<0.003 (for the rest μ<0.05)
    - Few 1/nb for LHCb (new to heavy-ion operation)
  - Beam reversal (relevant for ALICE and LHCb) for about half of statistics
  - Van der Meer scans in both beam configuations
- No pp run at 5.02 TeV until 2015
  - Instead a run at 2.76 TeV with 0.1/pb for ALICE and 5/pb for the rest

Acceptance of LHC experiments

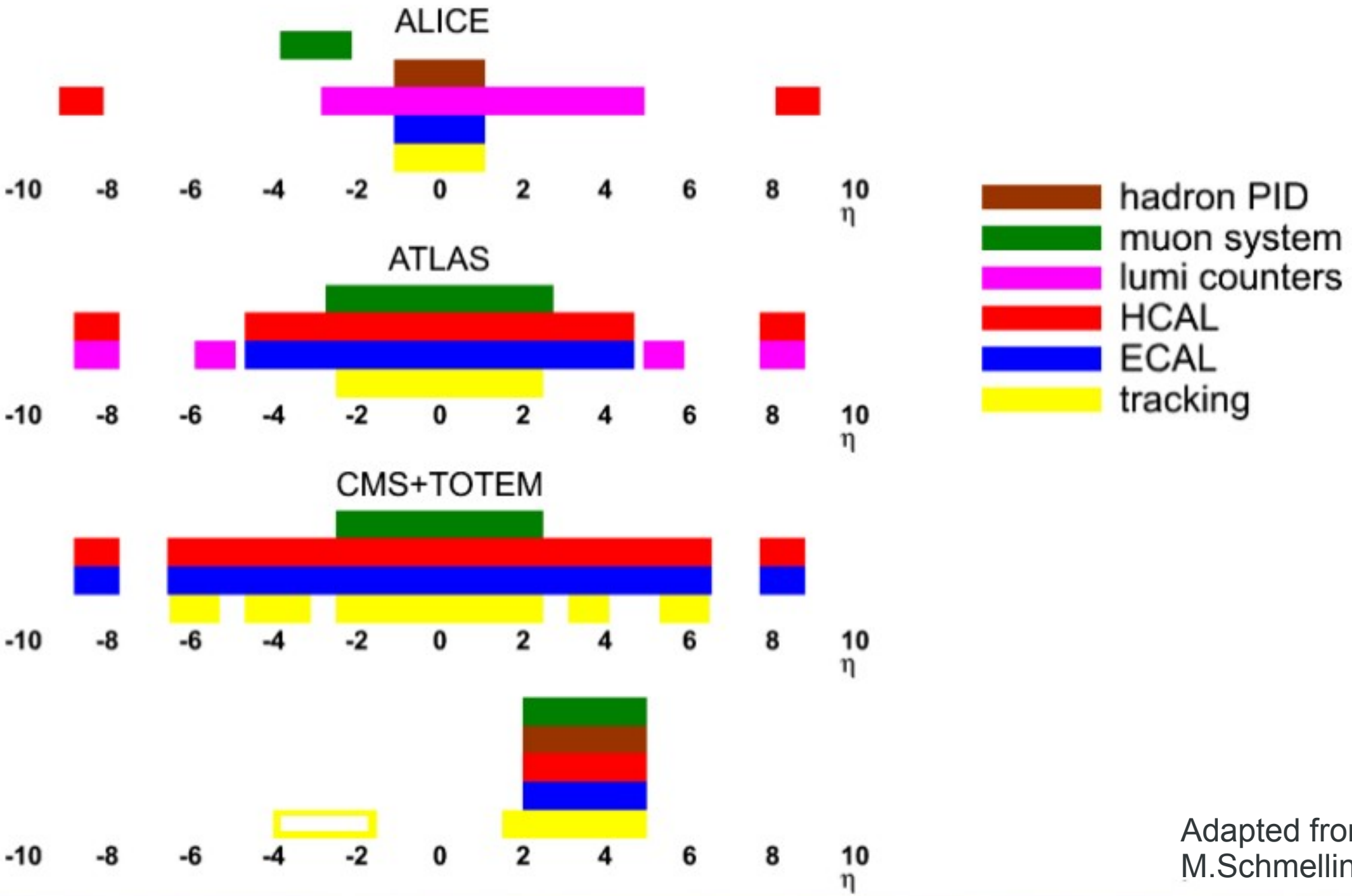

Adapted from M.Schmelling

Physics results from pilot run

ALICE, PRL 110 (2013) 032301

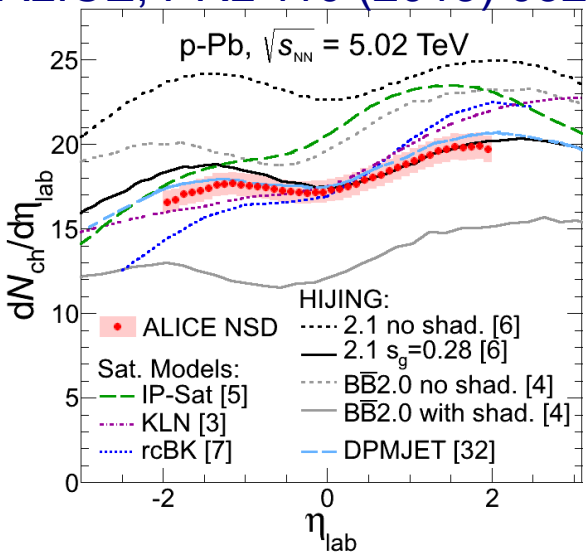

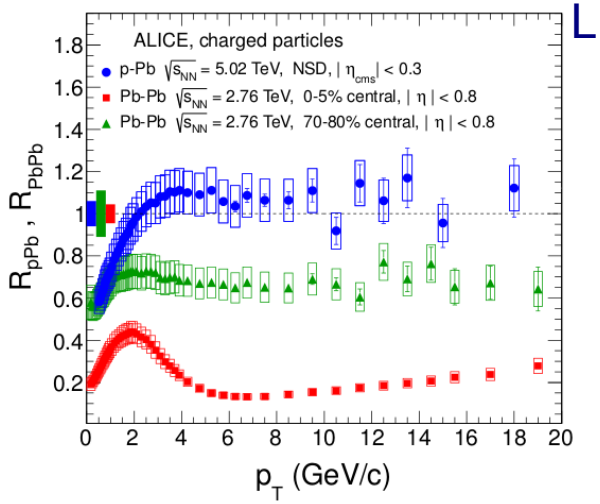

LHCb, CERN-LHCb-CONF-2012-034

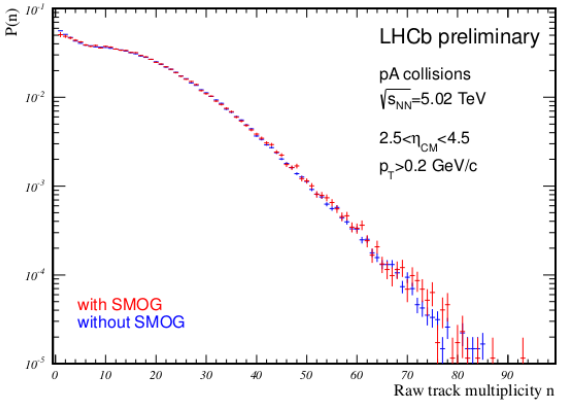

ALICE, PRL 110 (2013) 082302

ATLAS, arXiv:1212.5198

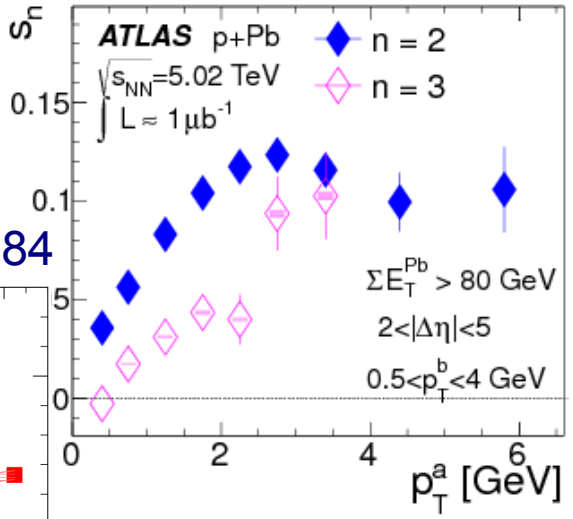

CMS, PLB 718 (2012) 795

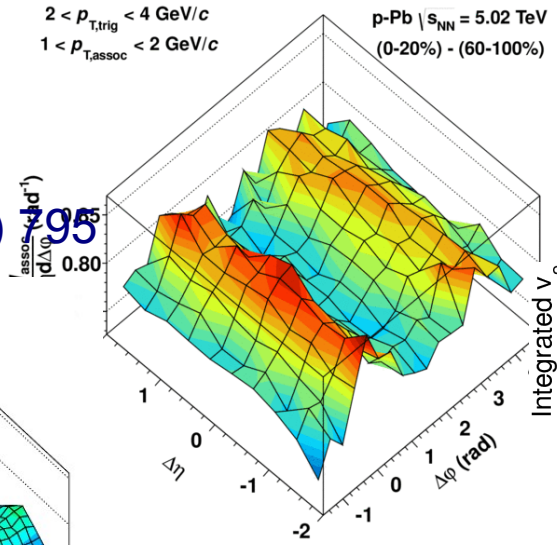

ATLAS, arXiv:1303.2084

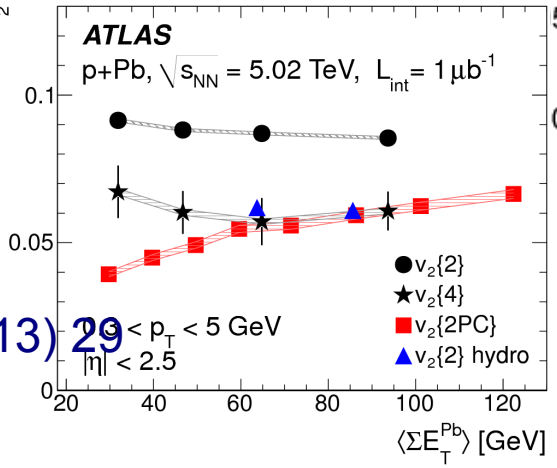

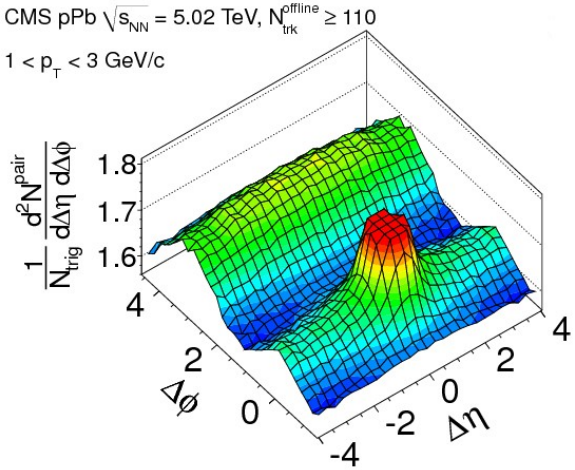

ALICE, PLB 719 (2013) 29

LHCb: Normal and SMOG running

LHCb, CERN-LHCb-CONF-2012-034

- Two running scenarios:
  - Normal background conditions
  - Running with “SMOG” (System for Measuring Overlap with Gas)
    - Ne injection to measure beam-profile + luminosity (JINST 7 P01010)
    - Increase beam-gas factor by ~100
    - Obtain 0.569/μb (SMOG) and 0.361/μb (normal) with 5.2% systematic uncertainty
- Need to perform beam-gas subtraction
  - Measure observables with BX1 (beam1), BX2 (beam2) and BX3 (coll.beams)
  - Calculate BX3 – a_1 BX1 – a_2 BX2
  - Determine a_1 and a_2 from primary vertex distribution for |z|>300 mm
    - Common for w and w/o SMOG
    - Same weights apply for other observables

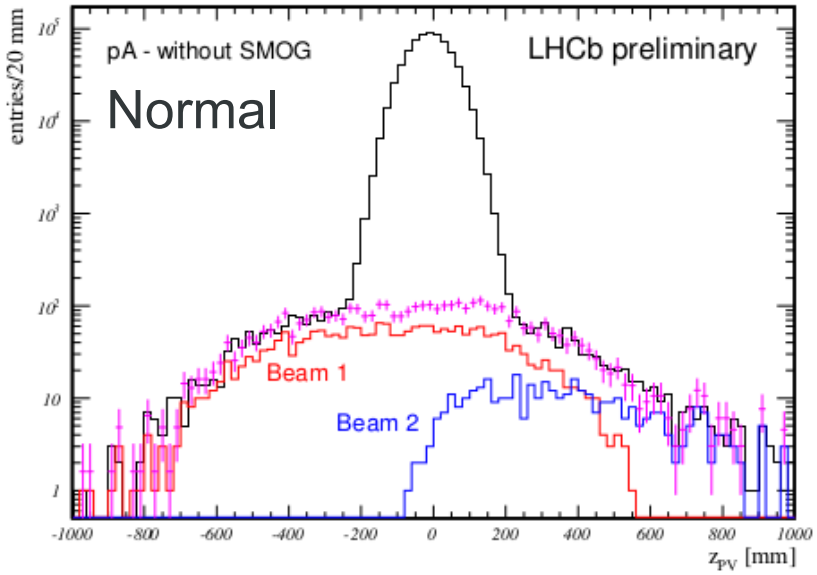

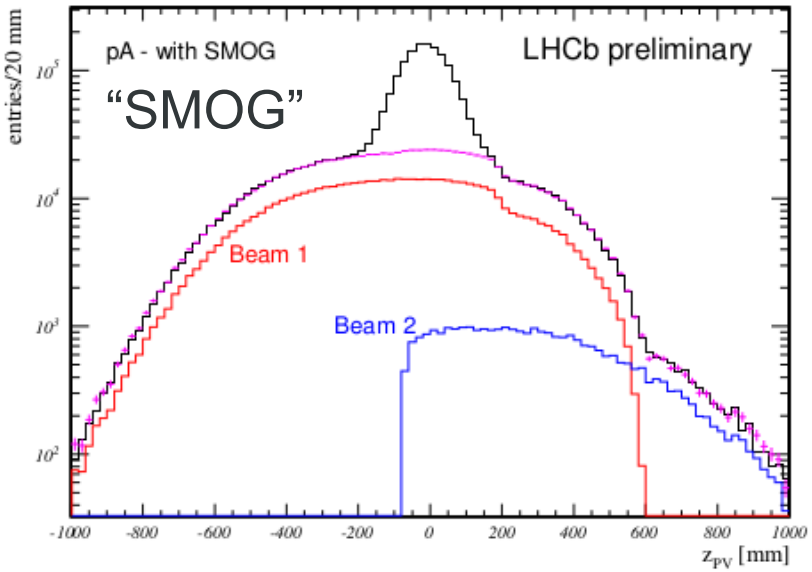

LHCb: Beam gas subtraction

LHCb, CERN-LHCb-CONF-2012-034

z-vertex positions of primary vertices in pPb and pp

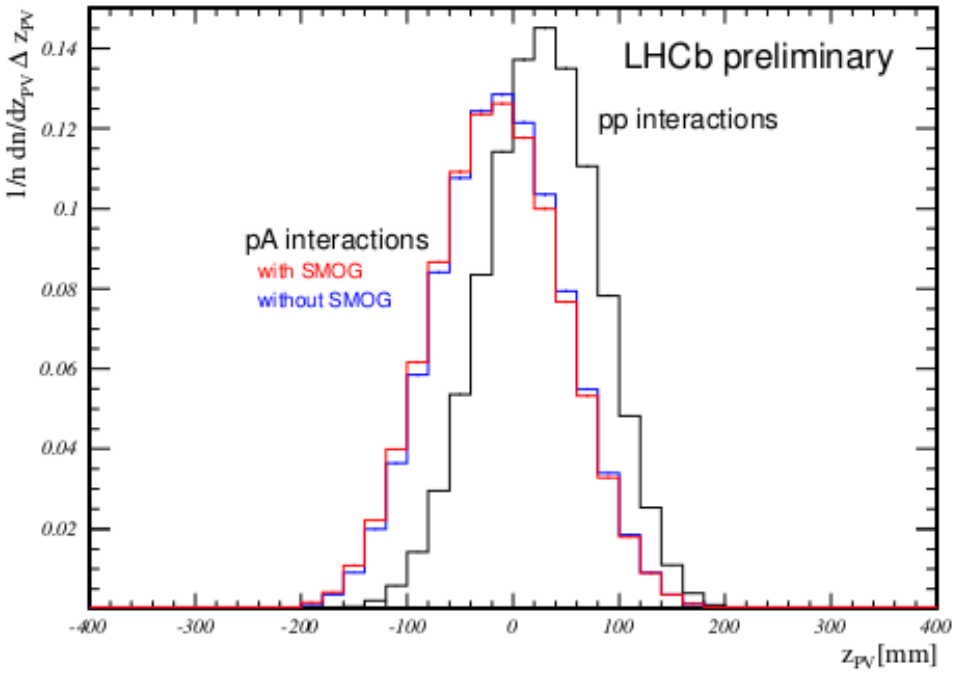

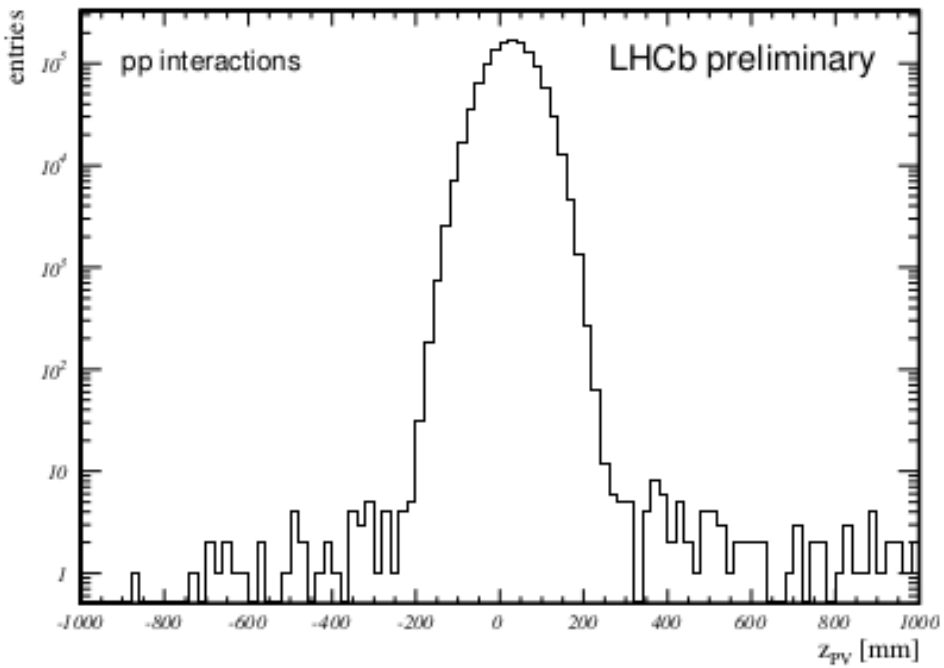

- After beam-gas subtraction vertex distributions in pPb are very similar for collisions taken with and without SMOG
- Differences in luminous region between pPb and pp
- Luminous region in $|z_{PV}|<200$mm for pPb and pp

Inelastic pPb cross section

LHCb, CERN-LHCb-CONF-2012-034

- Count collisions which produce at least one track in 2.5<η<4.5 (proton side) with p_T>0.2 GeV/c
  - In HIJING/DPMJET only 1-2% events without a charged particle
- Analysis steps
  - Beam gas subtraction
  - Pileup below permille level ignored
  - Trigger efficiency 100% ±1%
  - Correction for finite single track finding efficiency: 98% ± 2%
  - Convert using integrated luminosity measured with SMOG
  - Systematic uncertainty dominated by 5.2% error on luminosity

Raw distribution after beam-gas subtraction

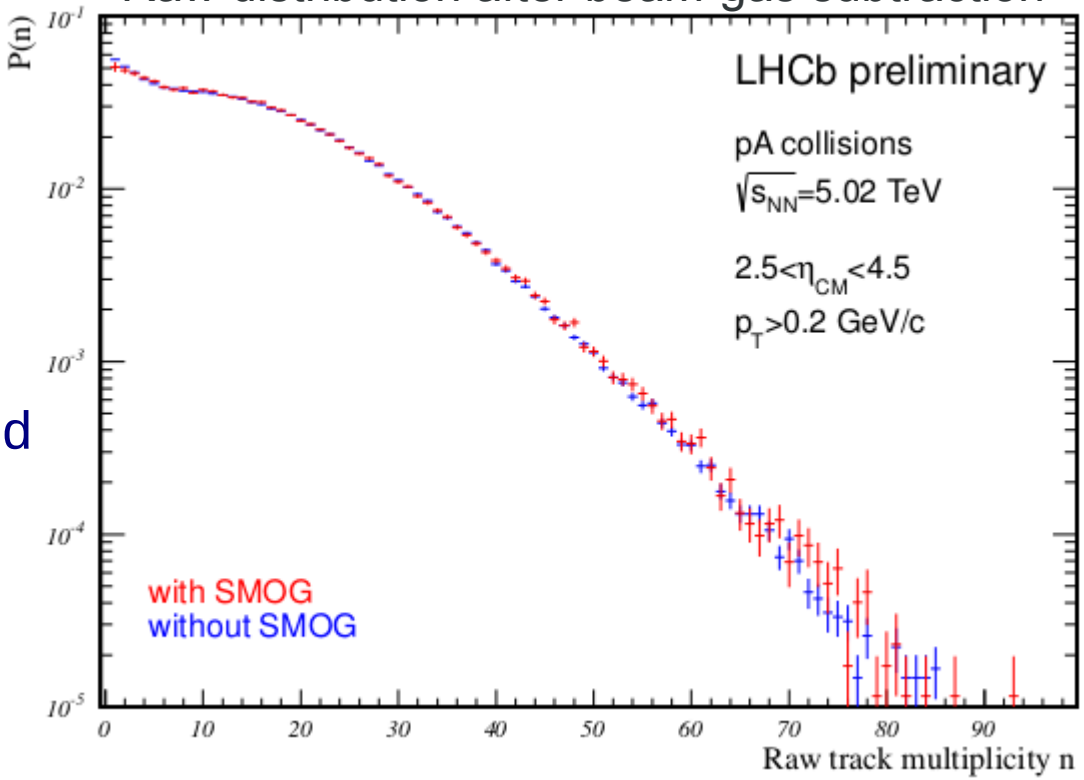

$$\sigma_{inel}(2.5 < \eta_{cm} < 4.5,\ p_T > 0.2\,\mathrm{GeV}/c) = 2.09 \pm 0.12\,\mathrm{b}$$

(consistent with HIJING, DPMJET and Glauber with σ_{NN}=70mb)

NSD pPb normalization

ALICE, PRL 110 (2013) 032301

- Event selection
  - VZERO-A (2.8<η<5.1) and VZERO-C (-3.7<η<-1.7) incl. time cuts
  - Systematic variation using ZDC on nucleus side (ZNA)
- Resulting event sample
  - Non single-diffractive (NSD)
    - At least one binary N+N interaction is NSD (Glauber picture)
    - Inspired from DPMJET, which includes incoherent SD of the projectile with target nucleons that are mainly concentrated on the surface of the nucleus
    - SD about 4% from HIJING, DPMJET or standalone Glauber
  - Negligible contamination from SD and EM processes
- Validated with a cocktail of generators
  - DPMJET for NSD (2b)
  - PHOJET + Glauber for incoherent SD part (0.1b)
    - SD/INEL = 0.2 in pp at 7 TeV (arXiv:1208.4968)
  - EM with STARLIGHT (0.1-0.2b)

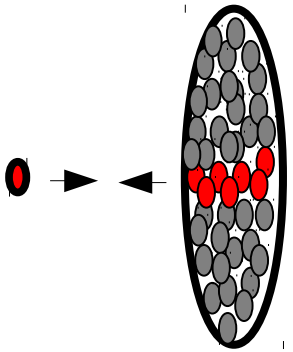

Pseudorapidity density

ALICE, PRL 110 (2013) 032301

- Tracklet analysis using SPD hits
  - Dominant systematic uncertainty from NSD normalization of 3.1%
- Reach of SPD extended to $|\eta|<2$ by extending the z-vertex range
- Results in ALICE laboratory system
  - $y_{cms} = -0.465$
- Comparison
  - Most models within 20%
  - Saturation models have to steep rise between p and Pb region

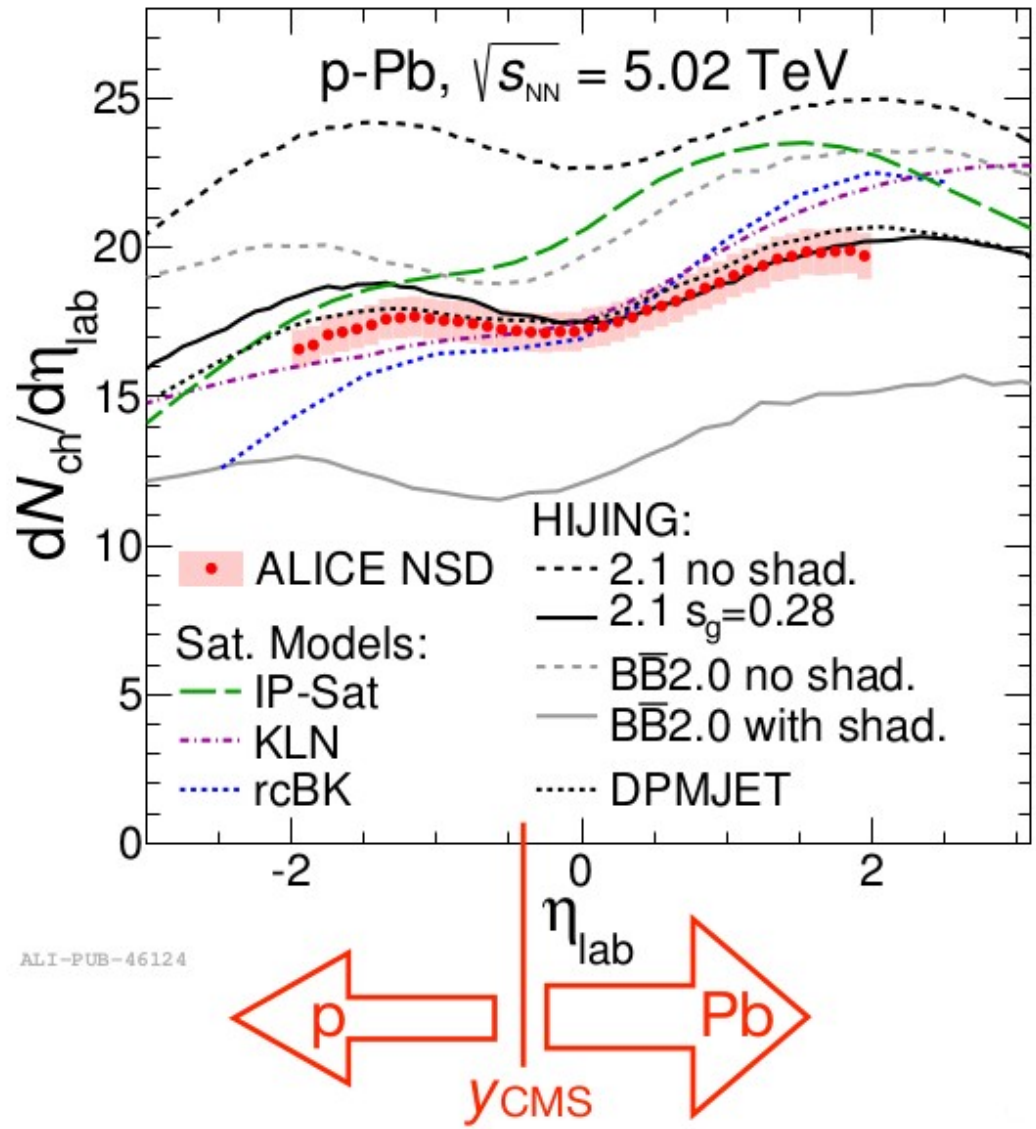

NB: HJING calculations for NSD expected to increase by ~4%

Pseudorapidity density at midrapidity

ALICE, PRL 110 (2013) 032301

- Measurement (tracklet based)
  - dN/dη = 16.81 ± 0.71 (syst)
  - Converted into centre-of-mass system using HIJING
  - Dominant uncertainty from NSD normalization of 3.1%
- Glauber model for pPb
  - With σ_{INEL}= 70 ± 5 mb
  - <Npart> = 7.9 ± 0.6 (syst)
- Participant scaled value
  - (dN/dη)/<Npart> = 2.14 ± 0.17 (syst)
  - About 15% below NSD pp
  - Similar to pp INEL
- Inelastic pPb would be 4% lower (estimate from models)

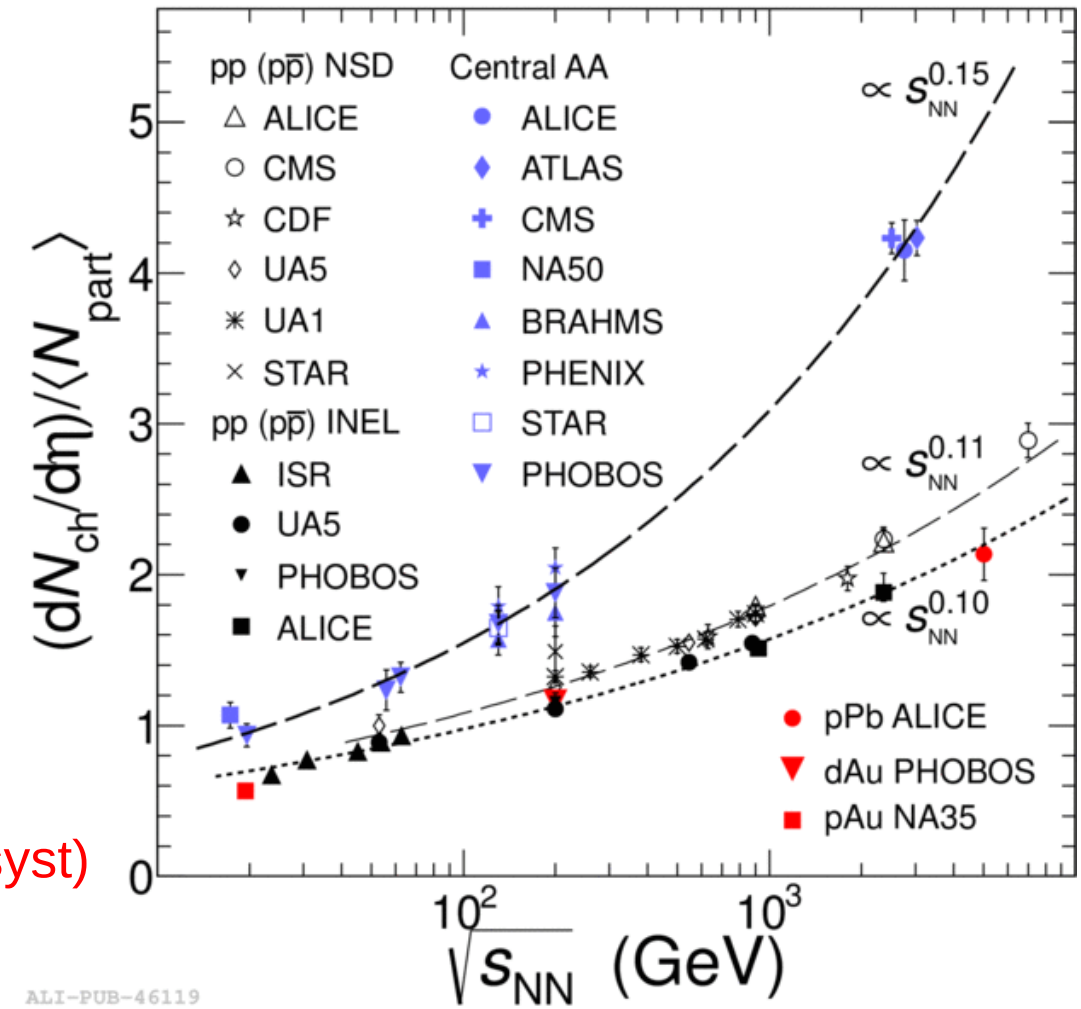

Charged particle spectrum

- Primary charged tracks (3 η bins)
  - Reconstructed in ITS+TPC (|η|<0.8)
  - Assume $\eta_{cms} = \eta_{lab} - y_{cms}$, then correct
  - Systematic uncertainty: 5.2-7.1%
  - NSD normalization: 3.1 %
- Hint for slightly softer spectrum at higher η (Pb side)?
- Reference constructed from pp (INEL) data at 2.76 and 7 TeV
  - Interpolation below 5 GeV/c, and above scaled by factor obtained from NLO calculation
    - Systematic uncertainty: 8%
    - Normalization uncertainty: 3.6%
  - $\langle T_{pPb} \rangle = 0.0983 \pm 0.0035\ mb^{-1}$ from Glauber model

ALICE, PRL 110 (2013) 082302

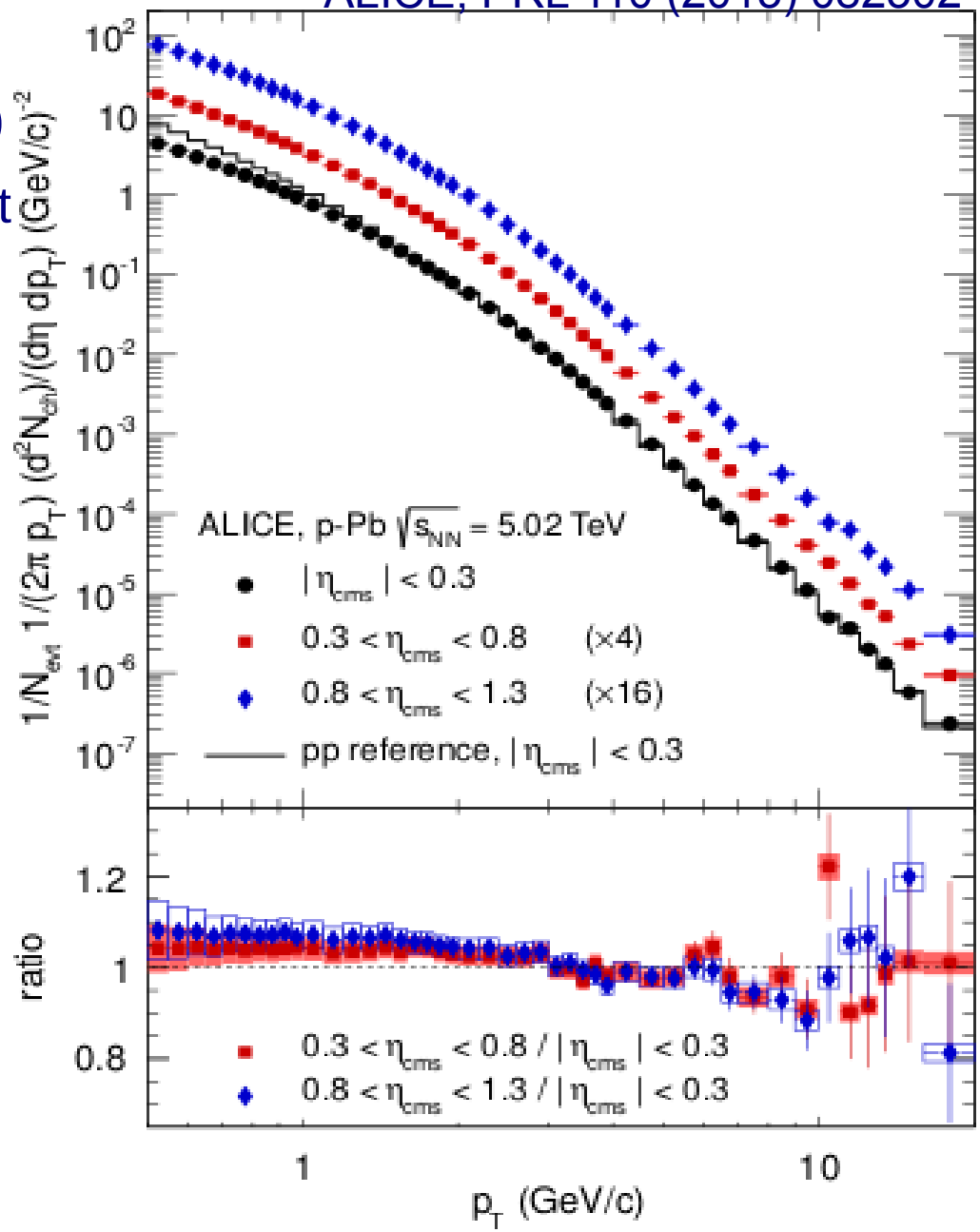

Nuclear modification factor

ALICE, PRL 110 (2013) 082302

$$R_{AB} = \frac{\mathrm{d}N_{AB}/\mathrm{d}p_{\mathrm{T}}}{\langle N_{\mathrm{coll}}\rangle \mathrm{d}N_{\mathrm{pp}}/\mathrm{d}p_{\mathrm{T}}}$$

- R_{pPb} (at mid-rapidity) consistent with unity for p_T > 2 GeV/c
- High-p_T charged particles exhibit binary scaling
- Unlike in PbPb, no suppression is observed
- Suppression in PbPb is not an initial state effect

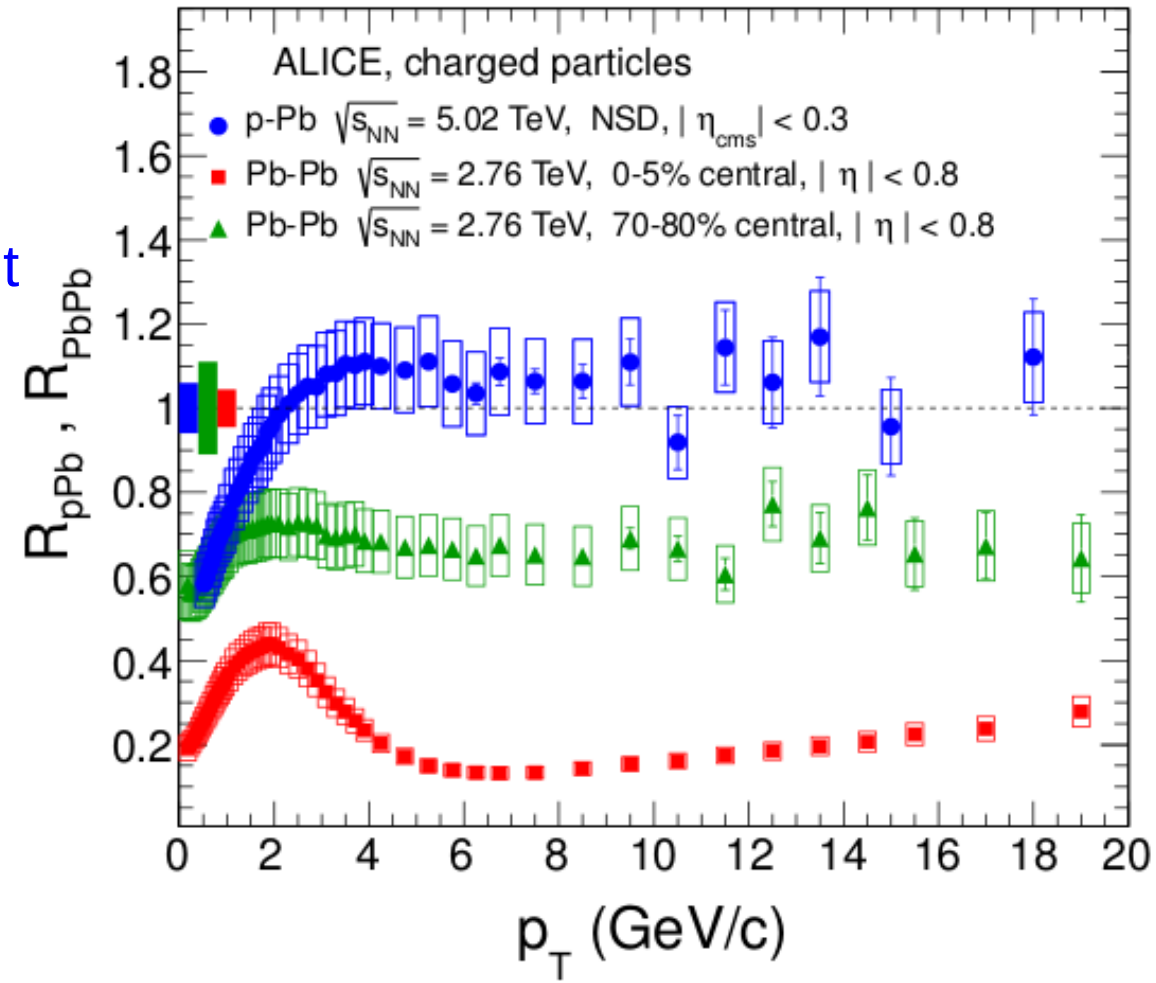

Cronin effect at RHIC and LHC

ALICE, PRL 110 (2013) 082302
STAR, PRL 91 (2003) 072304
PHENIX, PRL 91 (2003) 072030

$$R_{AB} = \frac{\mathrm{d}N_{AB}/\mathrm{d}p_{\mathrm{T}}}{\langle N_{\mathrm{coll}}\rangle \mathrm{d}N_{\mathrm{pp}}/\mathrm{d}p_{\mathrm{T}}}$$

- $R_{AB} > 1$ at intermediate p_T observed in dAu collisions at RHIC typically attributed to Cronin effect
- No enhancement seen in pPb at the LHC
- No Cronin effect?

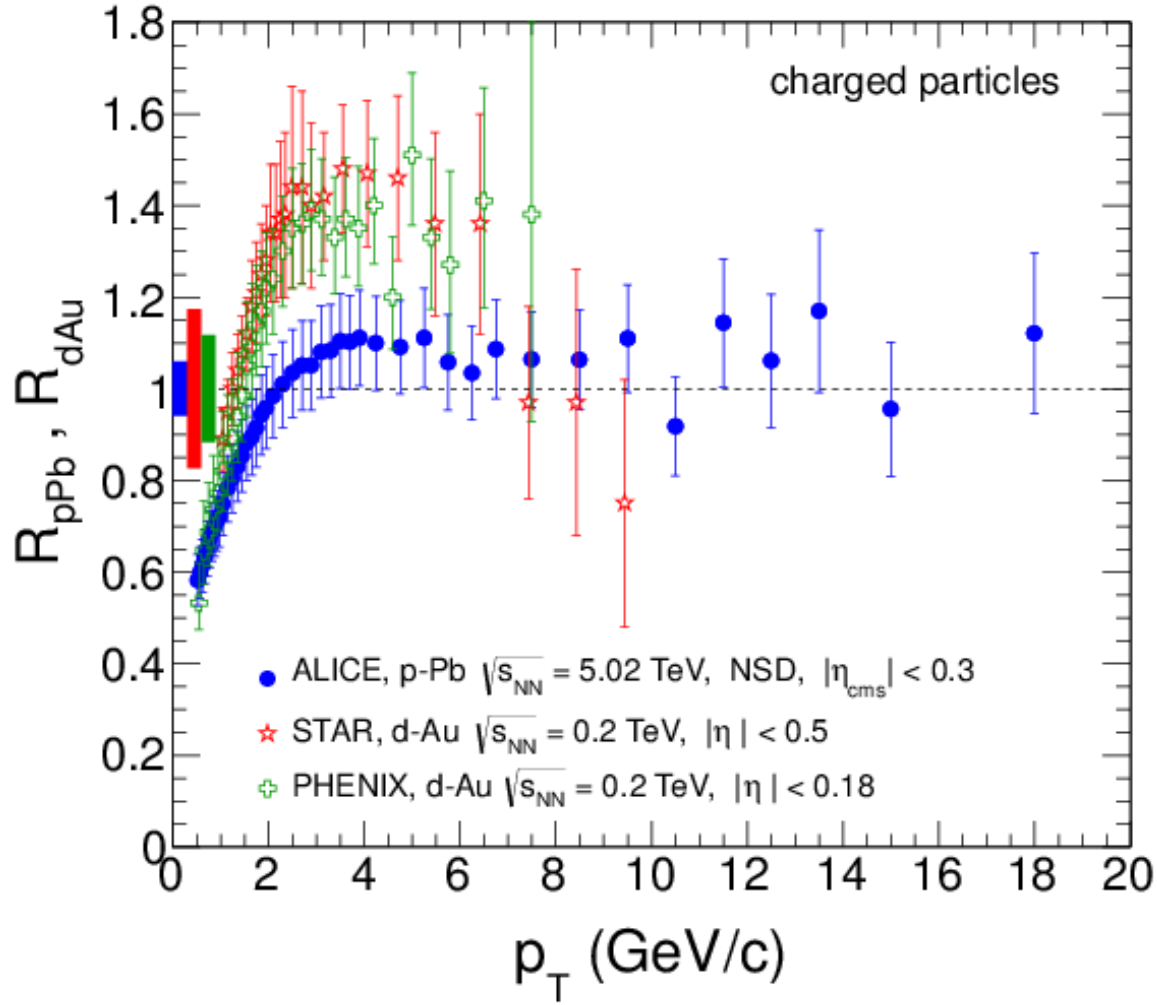

Cronin effect at SPS

- Reminder from SPS energies: RAB ≈ 1 does not necessarily imply absence of effects

NA49, NPA 783 (2007) 65
WA98, PRL 89 (2002) 252301

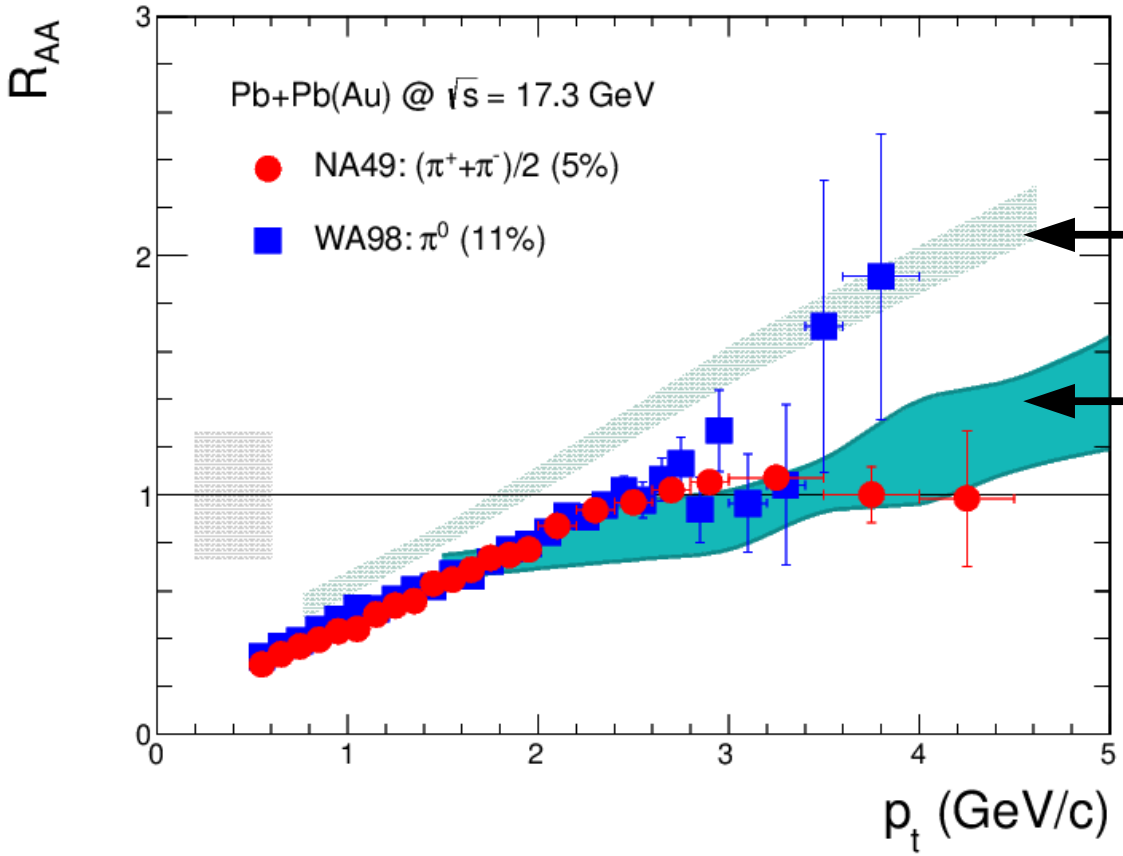

Calculation taking into account:

Cronin effect + shadowing

Cronin effect, shadowing plus partonic energy loss

- Model comparisons are required to understand R_{pPb} at the LHC

Nuclear modification factor vs models

- Saturation (CGC) models:
  - Consistent with the data
  - Large uncertainties
- pQCD models with shadowing
  - Consistent at low p_T
  - Discrepancies at high p_T
- HIJING
  - With shadowing describes η and low p_T better
  - No shadowing better at high p_T
- Spectrum on its own interesting
  - Neither HIJING nor DPMJET do describe the p-Pb p_T spectra

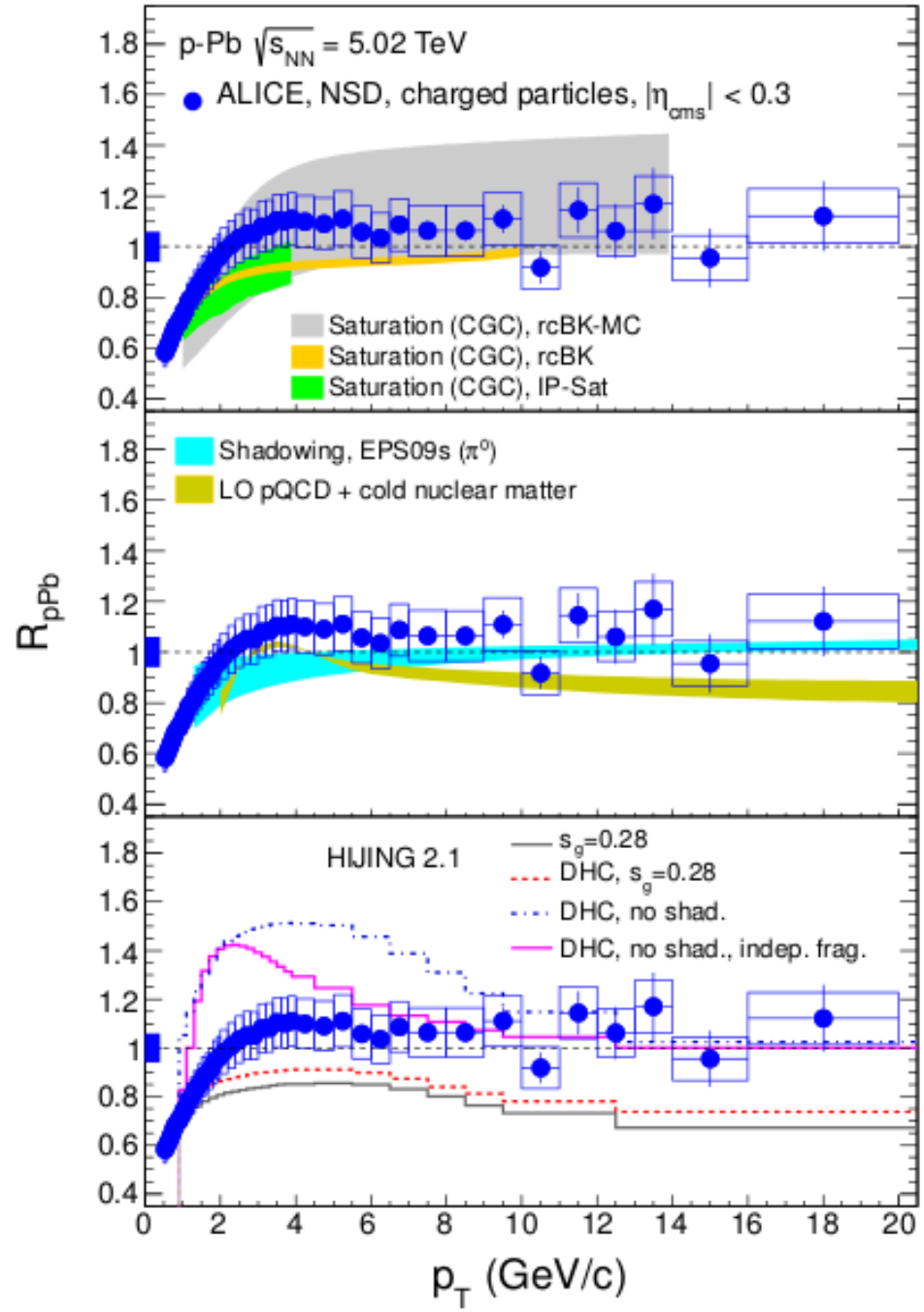

NB: HJING calculations for NSD expected to increase by ~4%

Di-Hadron Correlations (DHC)

- CMS: pp, pPb at LHC
  - Long-range near-side correlations (ridge) appear at high-multiplicity
    - Collective effects in pp and pPb?
    - CGC initial state effects?

CMS, JHEP 1009 (2010) 91

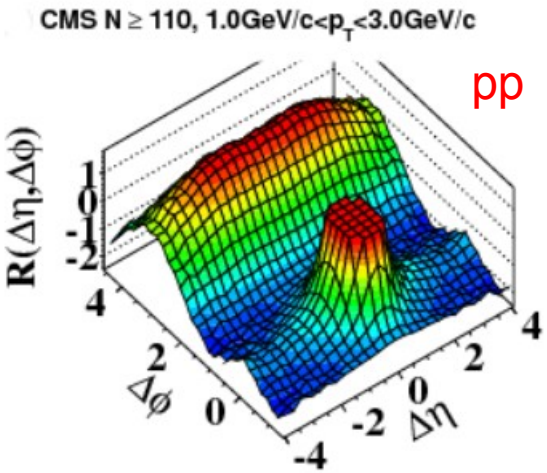

CMS, PLB 718 (2012) 795

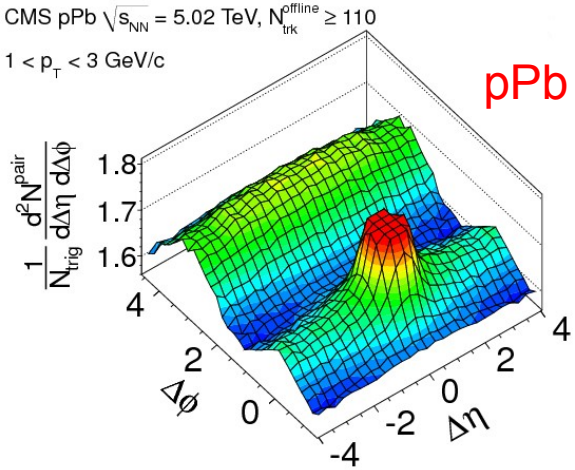

- STAR: dAu at RHIC
  - Back-to-back (jet-like) correlations in forward π^0 correlations disappear in high-multiplicity events
    - Compatible with CGC predictions
- LHC mid- and RHIC forward-η probe a similar x regime

STAR, arXiv:1005.2378

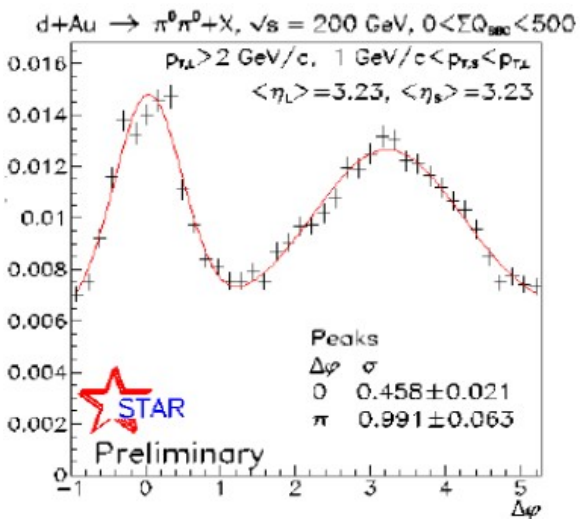

Peripheral

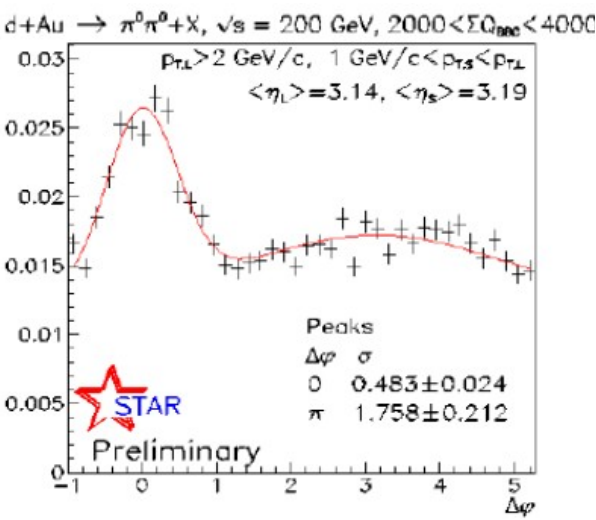

Central

DHC: Multiplicity classes

ALICE, PLB 719 (2013) 29

- Correlation between geometry and multiplicity in pA is not as strong as in AA
  - System also shows features of biased pp (NN) collisions in the low and high multiplicity tails
- Define multiplicity classes
  - Use charge in VZERO to avoid correlation with tracks in barrel
  - V0M: sum of amplitudes from
    - VZERO-A (2.8<η<5.1)
    - VZERO-C (-3.7<η<-1.7)
- Systematic checks using
  - SPD (|η|<1.4)
  - ZNA (beam neutron on Pb side)

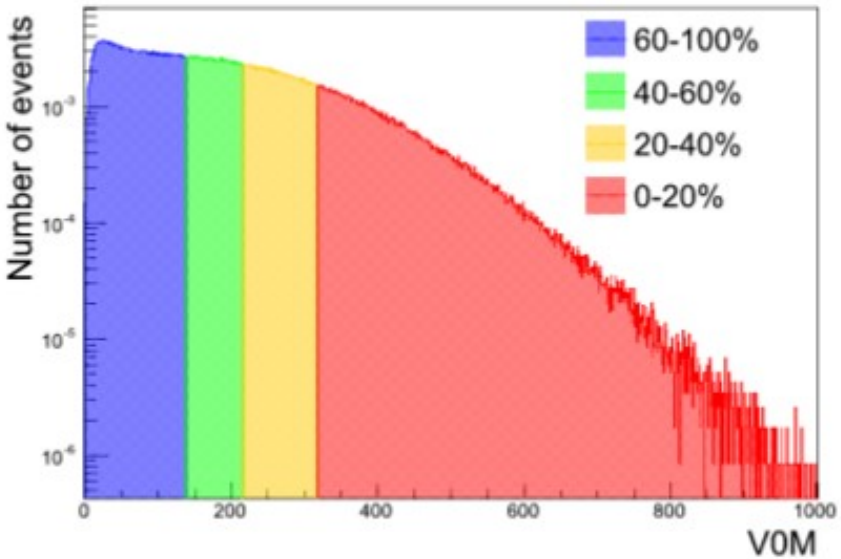

Event class	V0M range (a.u.)	$\langle dN_{ch}/d\eta \rangle \|_{\|\eta\|<0.5}$ $p_T > 0$ GeV/c	$\langle N_{trk} \rangle \|_{\|\eta\|<1.2}$ $p_T > 0.5$ GeV/c
60–100%	< 138	6.6 ± 0.2	6.4 ± 0.2
40–60%	138–216	16.2 ± 0.4	16.9 ± 0.6
20–40%	216–318	23.7 ± 0.5	26.1 ± 0.9
0–20%	> 318	34.9 ± 0.5	42.5 ± 1.5

DHC: Correlation measure

ALICE, PLB 719 (2013) 29

- Associated yield per trigger particle (with $p_T^{trig} > p_T^{assoc}$)

$$\frac{1}{N_{\mathrm{trig}}} \frac{\mathrm{d}^2 N_{\mathrm{assoc}}}{\mathrm{d}\Delta\eta\, \mathrm{d}\Delta\varphi} = \frac{S(\Delta\eta, \Delta\varphi)}{B(\Delta\eta, \Delta\varphi)}$$

- Signal (same event) pair yield

$$S(\Delta\eta, \Delta\varphi) = \frac{1}{N_{\mathrm{trig}}} \frac{\mathrm{d}^2 N_{\mathrm{same}}}{\mathrm{d}\Delta\eta\, \mathrm{d}\Delta\varphi}$$

  - Definition as ratio of sums is multiplicity independent

$$\begin{aligned} \frac{N_{pair}}{N_{trig}} &= \frac{\sum_{i=1}^{N_{evt}} \sum_{j=1}^{N^i_{source}} \frac{1}{2} n_{ij}(n_{ij}-1)}{\sum_{i=1}^{N_{evt}} \sum_{j=1}^{N^i_{source}} n_{ij}} \\ &= \frac{N_{evt}\langle N_{source}\rangle \frac{1}{2}\langle n(n-1)\rangle}{N_{evt}\langle N_{source}\rangle \langle n\rangle} \\ &= \frac{1}{2}\frac{\langle n(n-1)\rangle}{\langle n\rangle} \end{aligned}$$

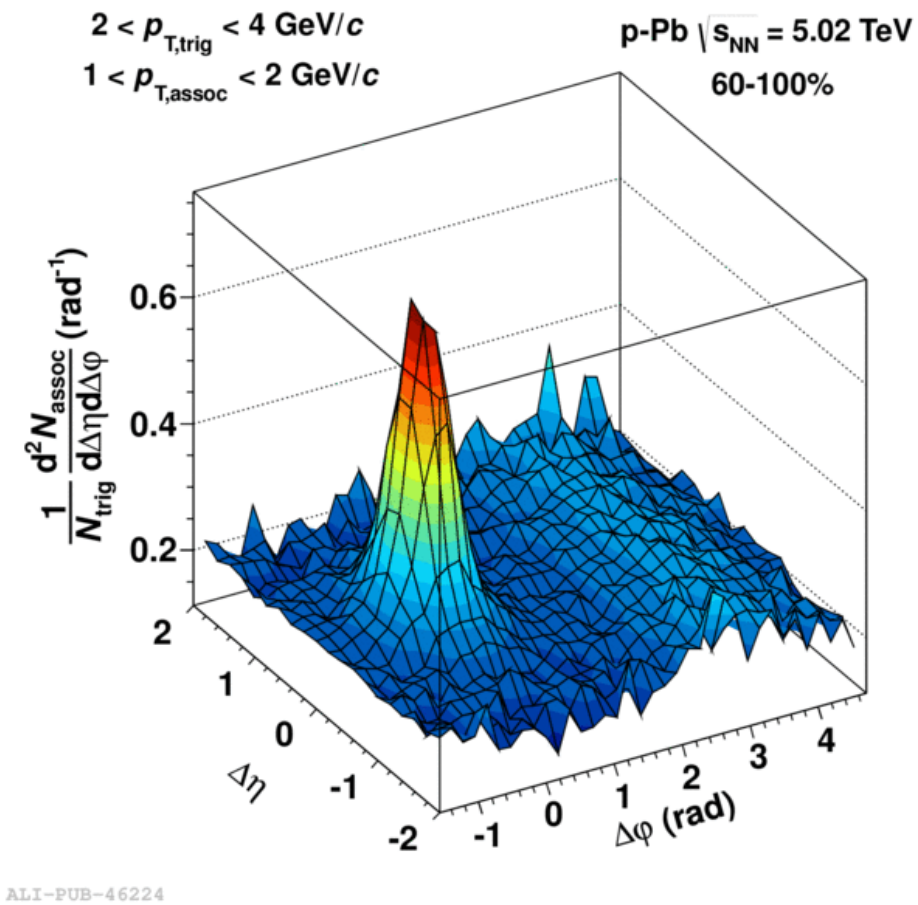

- Background (mixed event) pair yield

$$B(\Delta\eta, \Delta\varphi) = \frac{1}{B(0,0)} \frac{\mathrm{d}^2 N_{\mathrm{mixed}}}{\mathrm{d}\Delta\eta\, \mathrm{d}\Delta\varphi}$$

DHC: Multiplicity dependence

ALICE, PLB 719 (2013) 29

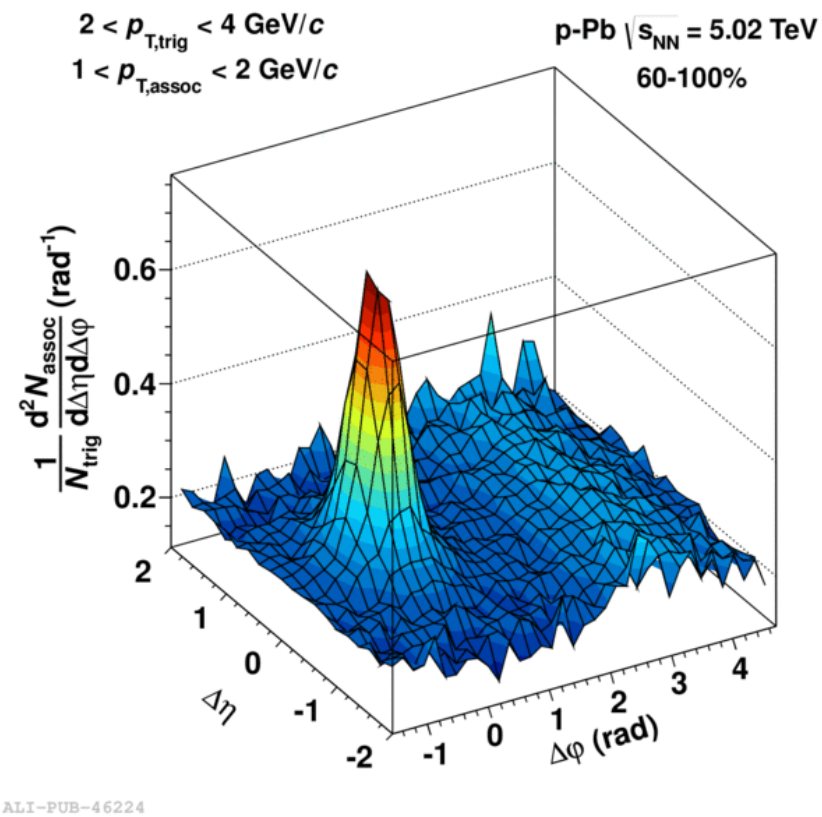

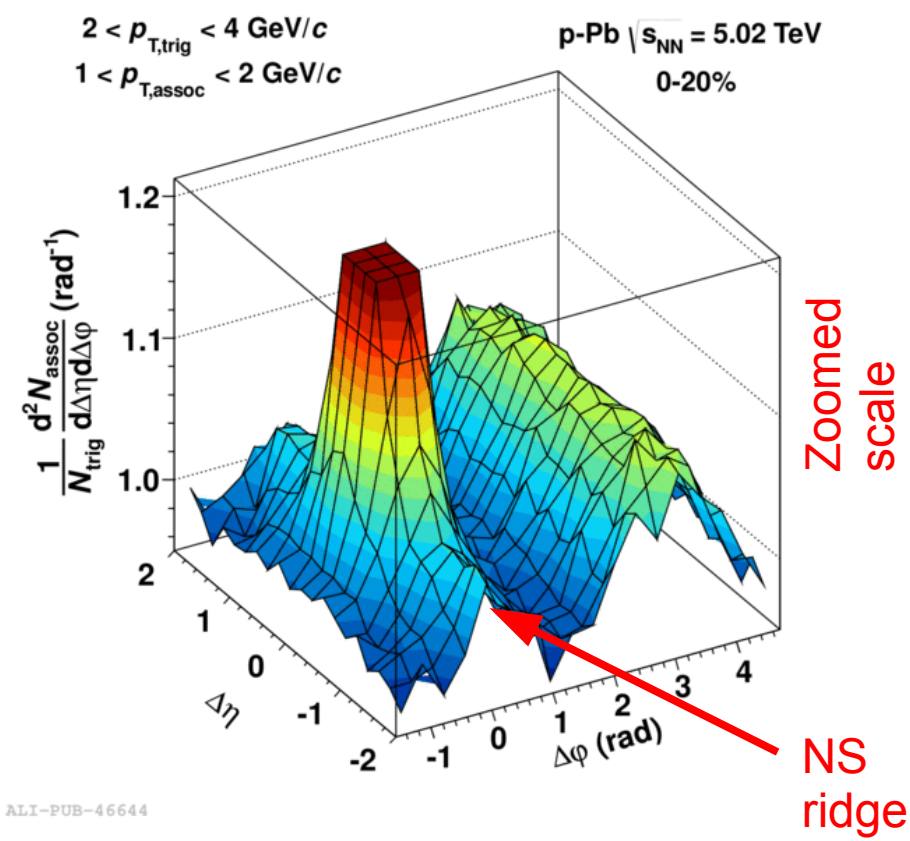

- Low-multiplicity p-Pb (60-100%)
  - pp-like (jet-like) correlation structures

- High-multiplicity p-Pb (0-20%)
  - Near-side ridge appears (first seen in CMS)
  - Higher yields on near- and away-side

DHC: Multiplicity dependence

ALICE, PLB 719 (2013) 29

- Compare associated yield in pPb multiplicity classes and pp
  - Project to Δφ over |Δη|<1.8
  - Subtract baseline at Δφ~1.3
- Low multiplicity pPb is similar to pp (at 7 TeV)
- Yield rises on near and away side with increasing multiplicity
- In contrast with away-side suppression observed in dAu at RHIC at forward η (similar x)

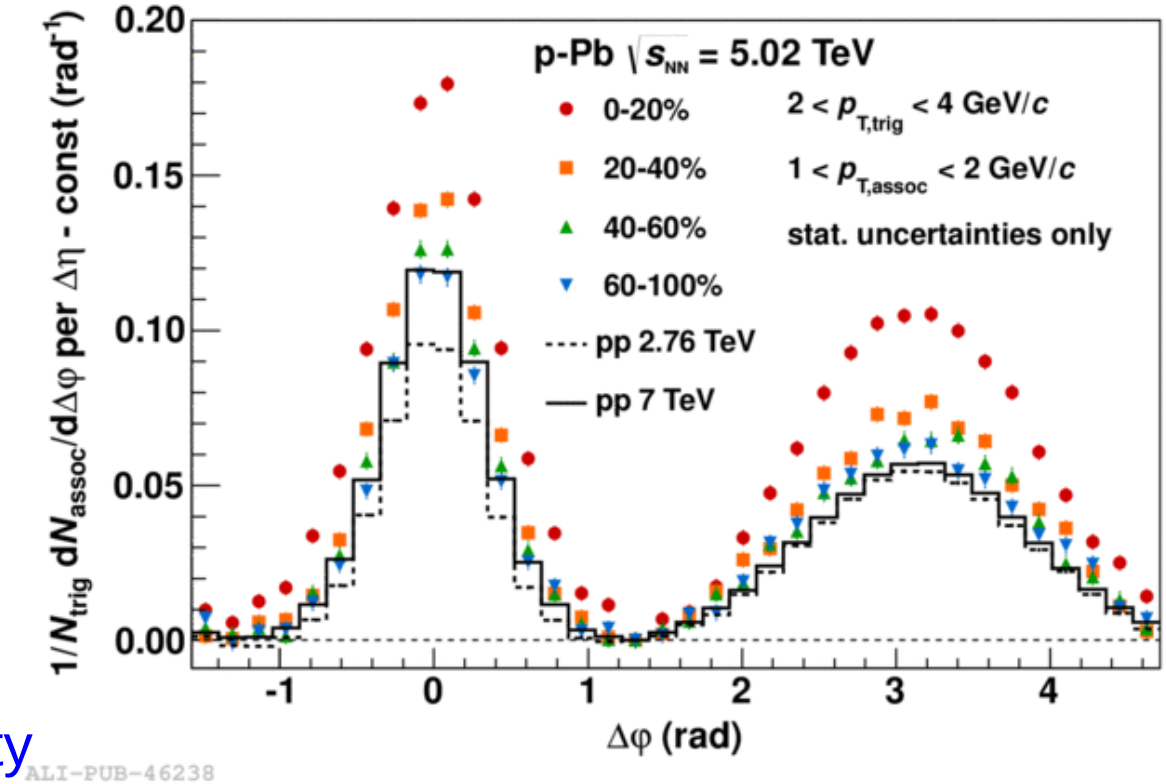

DHC: Two ridges

ALICE, PLB 719 (2013) 29

- Quantify the excess in high-multiplicity pPb by subtracting the jet-like correlations:

0-20% minus 60-100% =

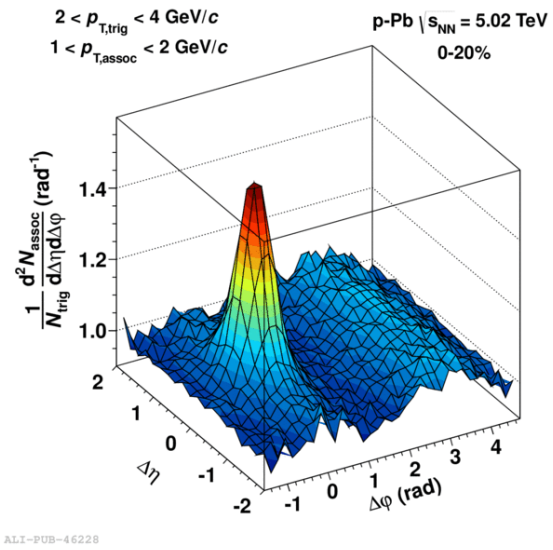

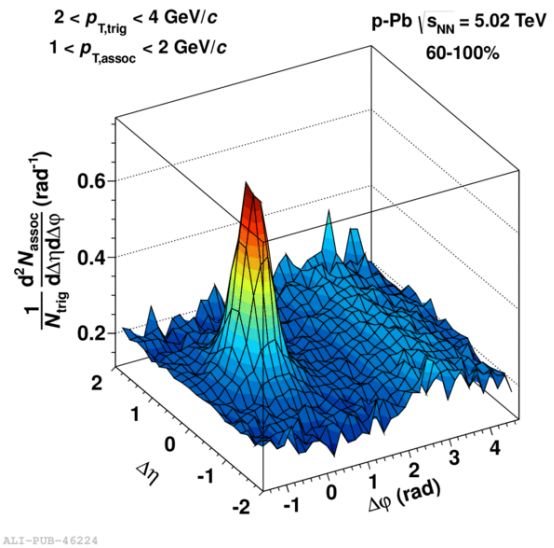

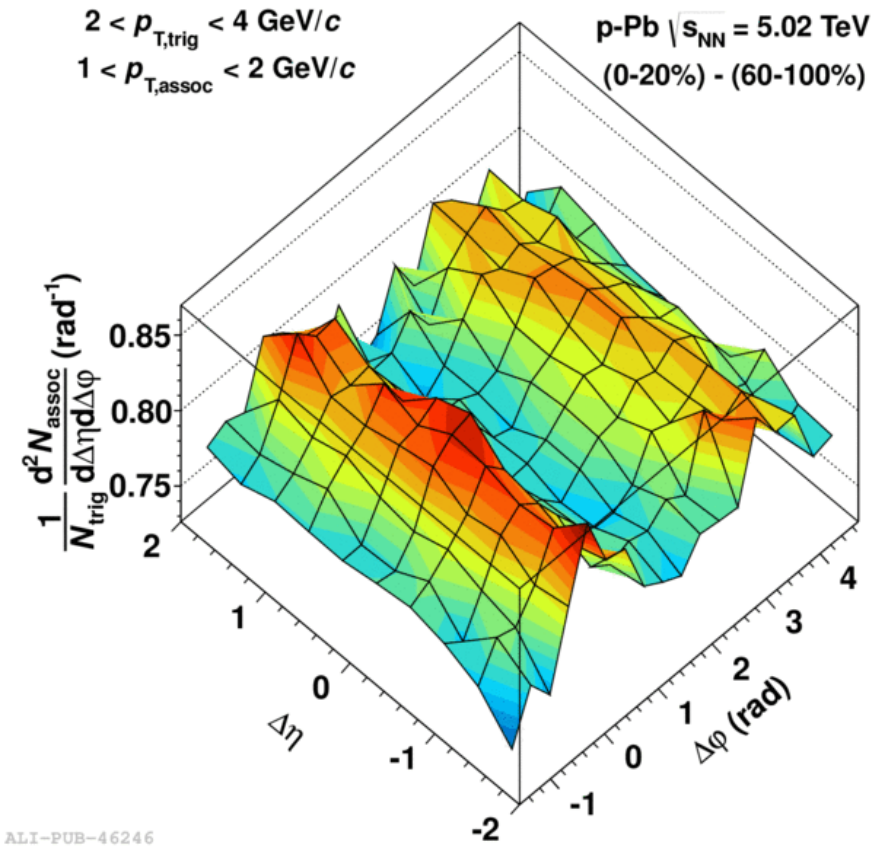

- The near-side is accompanied by an almost identical ridge structure on the away-side

DHC: Two ridges

ALICE, PLB 719 (2013) 29

- A residual jet peak at (0,0) remains even after subtraction of 60-100% from the 0-20% multiplicity class
- Compare effects using different event class definition

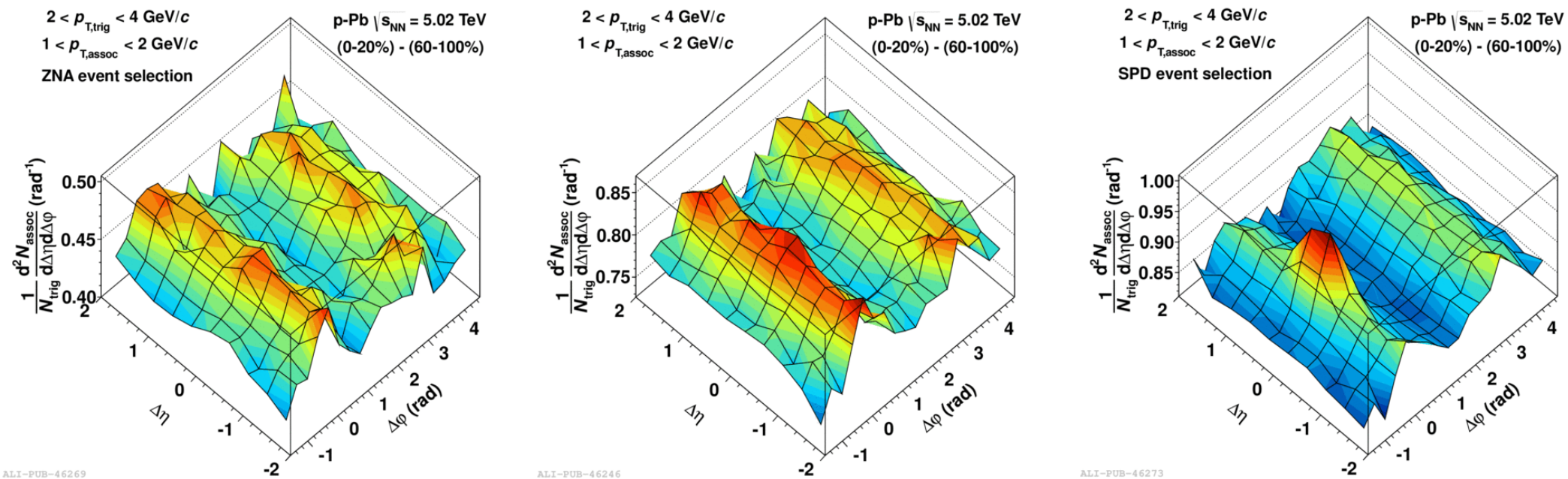

ZNA VZERO SPD

auto-correlation →

← η separation

DHC: Selection bias on fragmentation (pp) 30

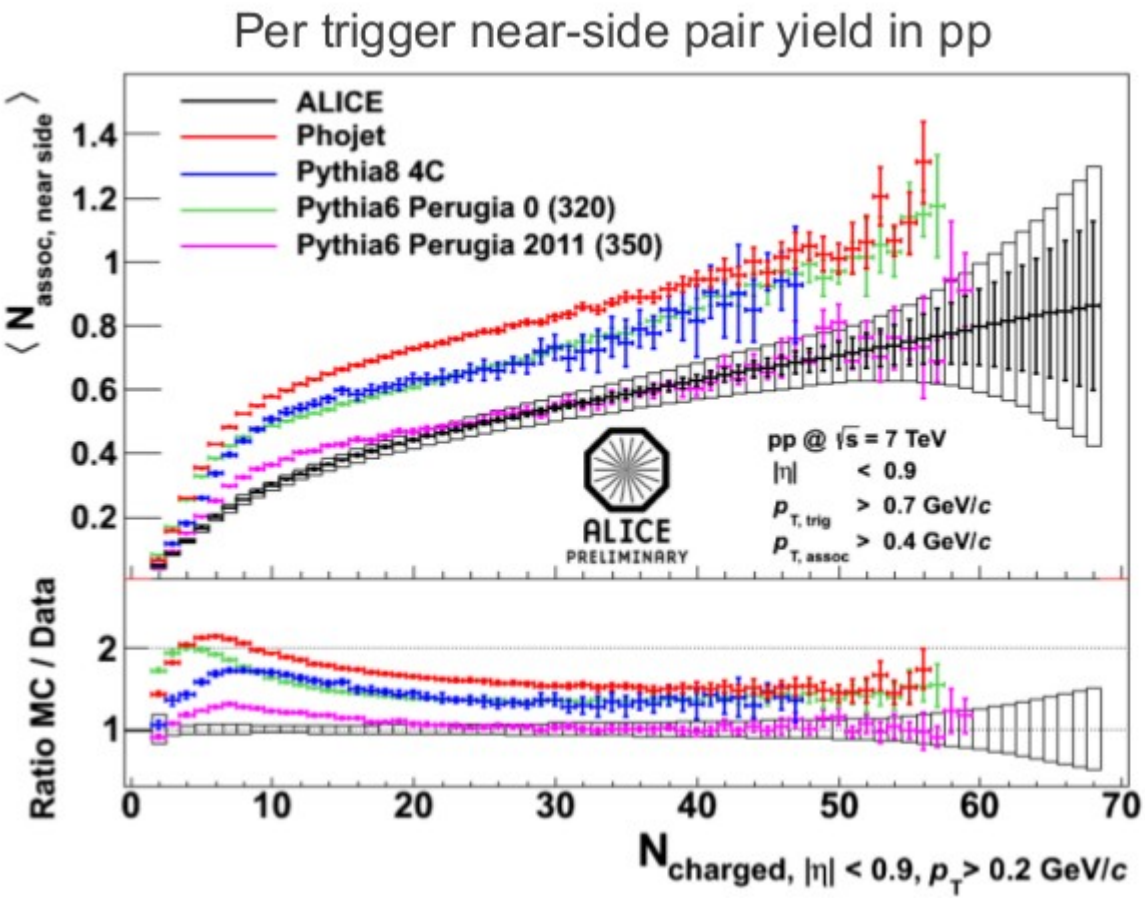

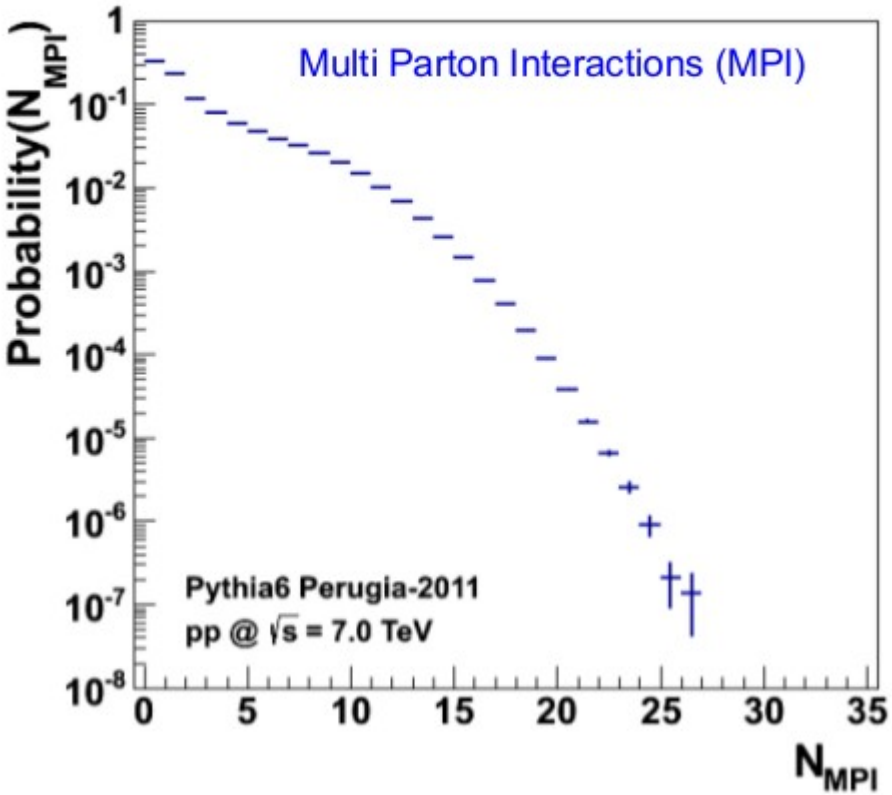

- By selecting on multiplicity, jet fragmentation is biased towards higher number of fragmenting products
- Competition between higher number of MPI and fragmentation

DHC: Two ridges (ATLAS)

ATLAS, arXiv:1212.5198

- Similar two ridge structures also observed by ATLAS
  - Event multiplicity classes defined by sum of transverse energy (3.1<η<4.9) on the Pb nucleus side
  - Also here, the jet peak at (0,0) remains even after subtraction of 50-100% from the 0-2% multiplicity class

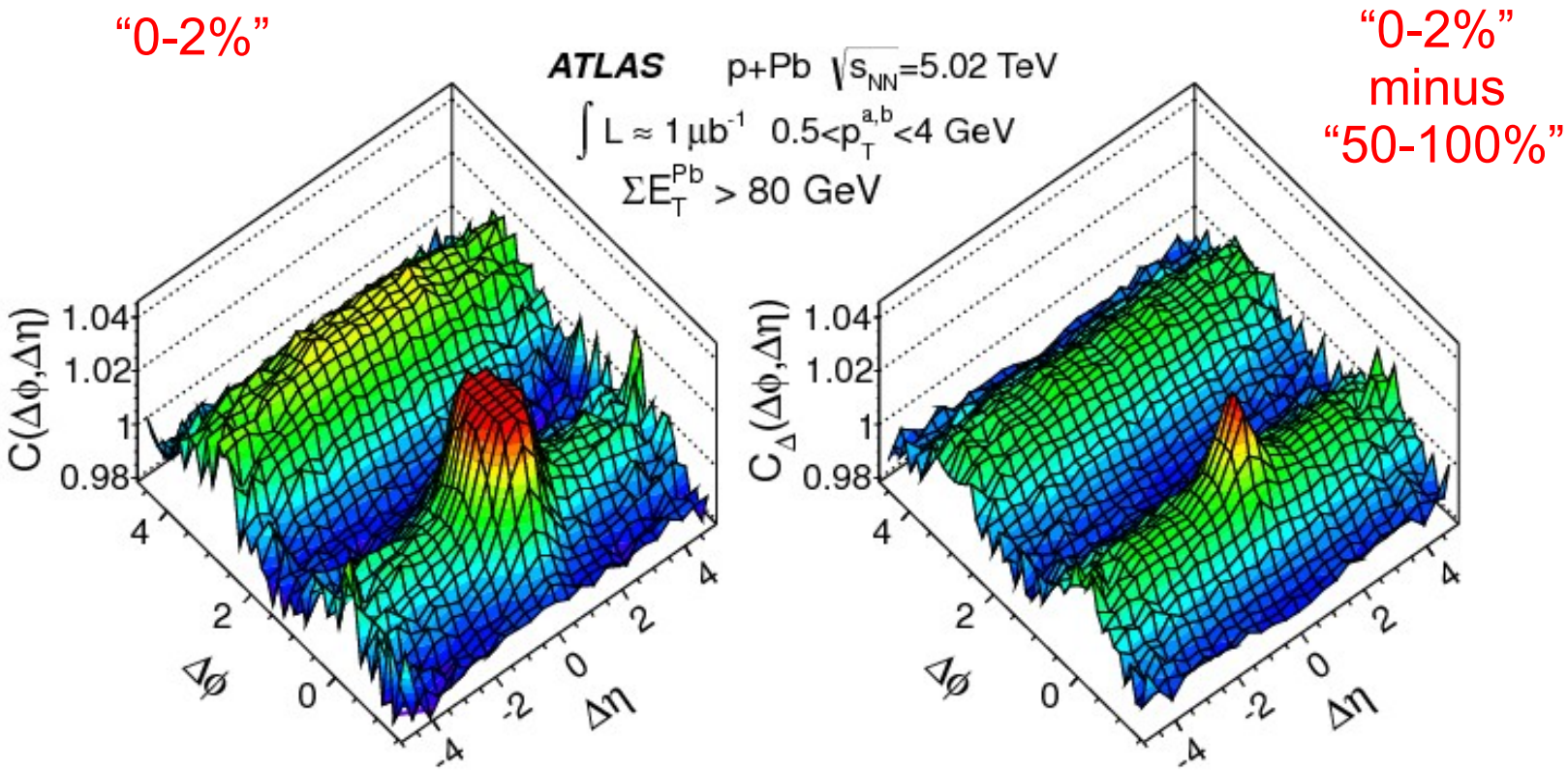

DHC: Two ridges

- A closer look at the two ridges: the near- and away-side ridges
  - Are essentially flat in Δη
    - Slight excess on near side due to small residual jet peak
  - Have the same magnitude
- Projection to Δφ
  - Exclude residual peak (|Δη<0.8| on near-side) exhibits a modulation
  - In HIJING, the correlation shows no qualitative changes with multiplicity
  - Quantify the ridges
    - Ridge yields
    - Fourier coefficients

ALICE, PLB 719 (2013) 29

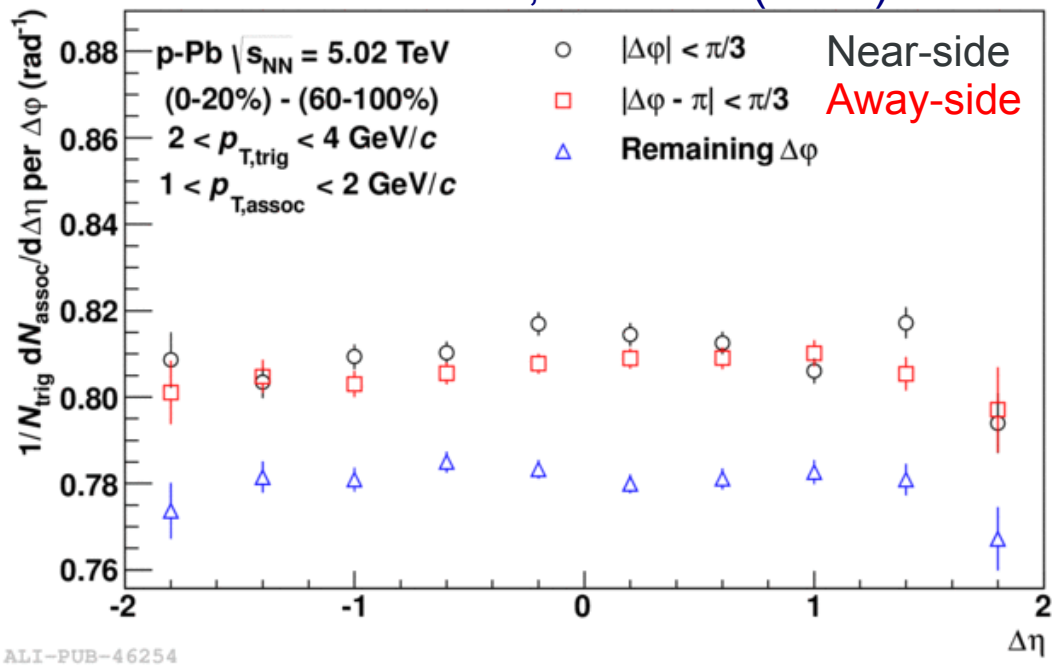

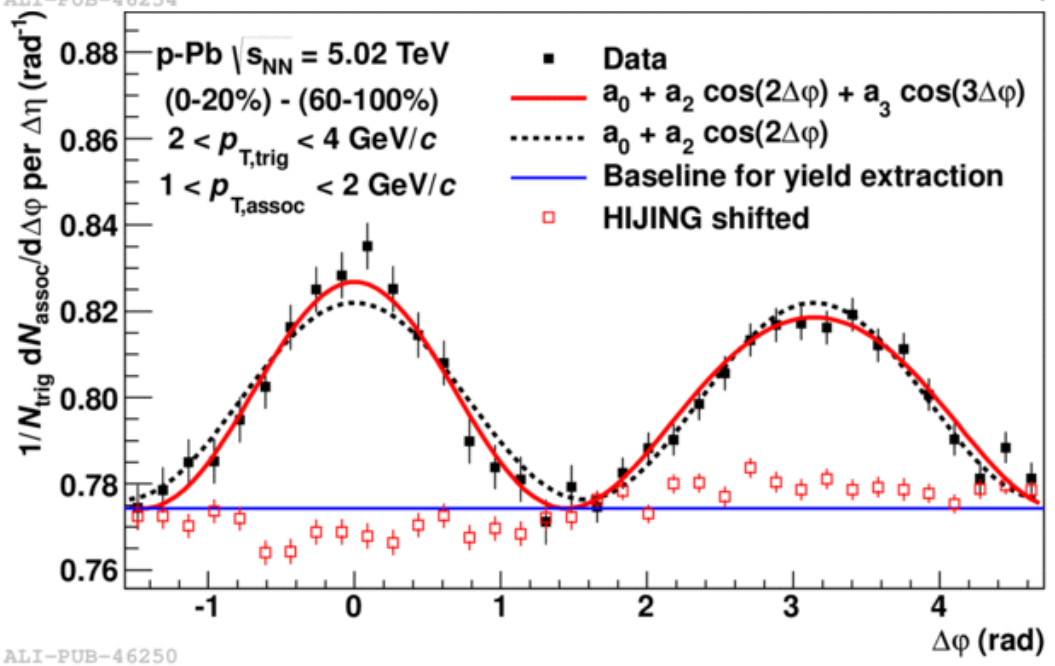

DHC: Ridge yields

- Integrate two ridges above baseline on the
  - Near side ($|\Delta|<\pi/2$)
  - Away side ($\pi/2<|\Delta|<3\pi/2$)
- Near and away-side ridge yields
  - Change significantly
  - Agree for all p_T and multiplicity ranges
  - Increase with trigger p_T and multiplicity
  - Widths are approximately the same (not shown)
- The correlation between near- and away-side yields suggests a common underlying origin

ALICE, PLB 719 (2013) 29

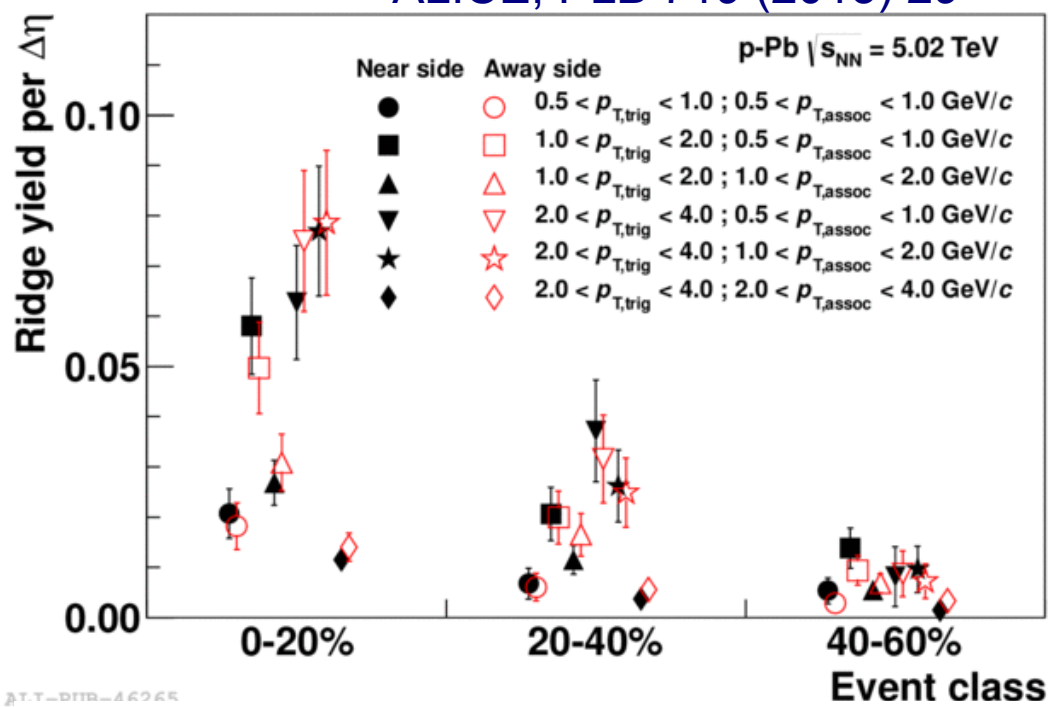

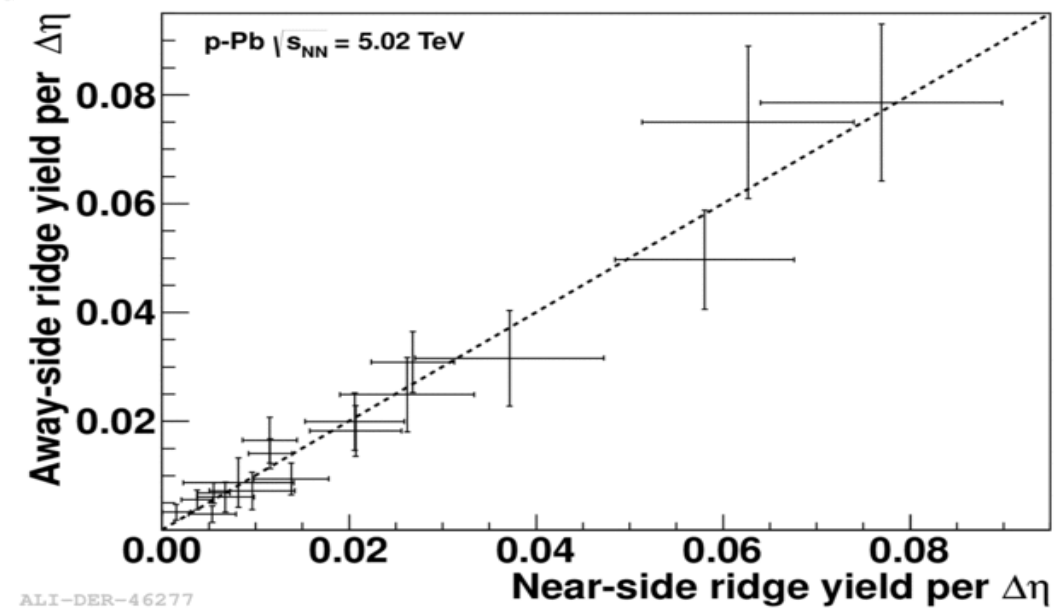

DHC: Ridge modulation

ALICE, PLB 719 (2013) 29

- Obtain $v_n = \sqrt{(a_n/b)}$ from $a_0+2a_2\cos(2\Delta\varphi)+2a_3\cos(3\Delta\varphi)$ fit where b is baseline in higher multiplicity class
  - v_2 increases strongly with p_T and mildly with multiplicity
  - v_3 increases with p_T within large uncertainties
  - These trends are in qualitative agreement with expectations from viscous hydrodynamical predictions

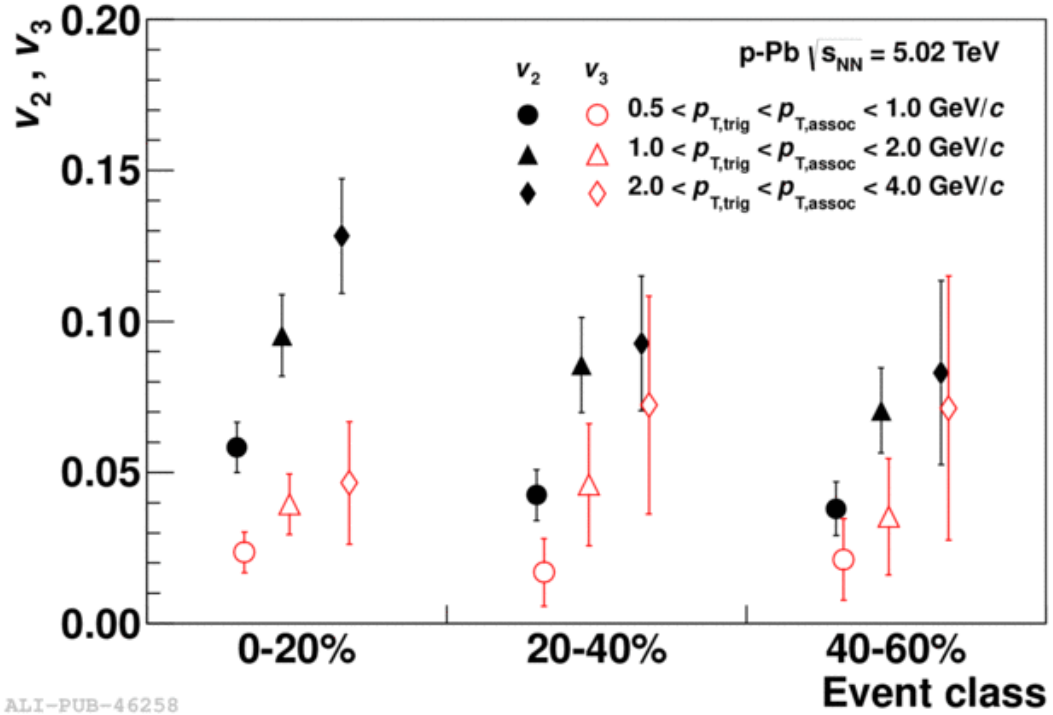

Bozek, PRC 85 (2012) 014911

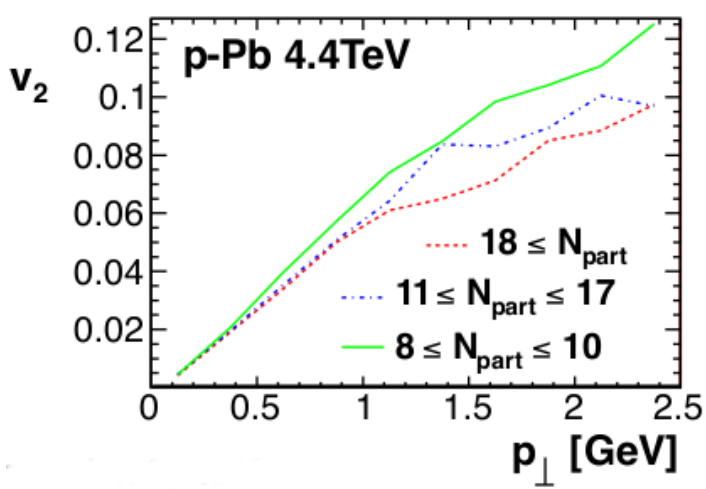

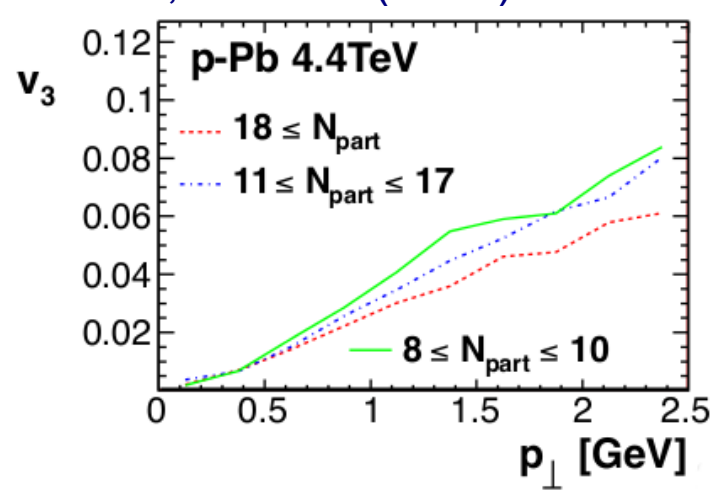

DHC: Ridge modulation

- Two ridges are also predicted by CGC

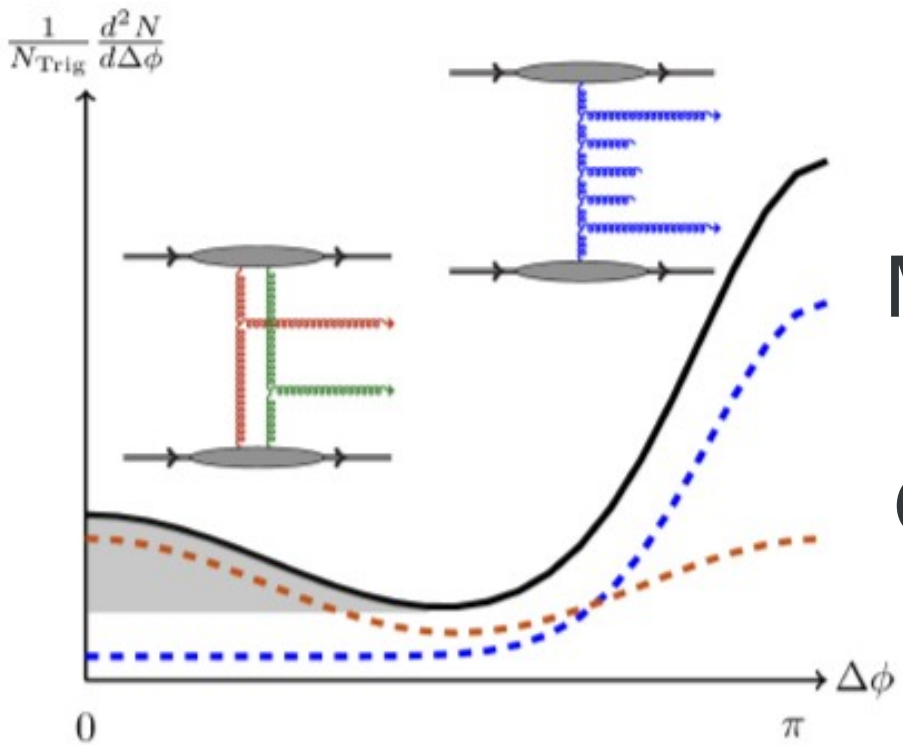

Dusling and Venugopalan, arXiv:1302.7018

Minijets

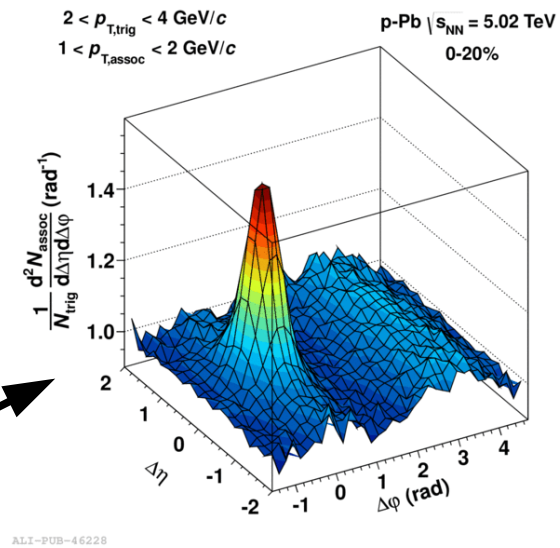

Glasma

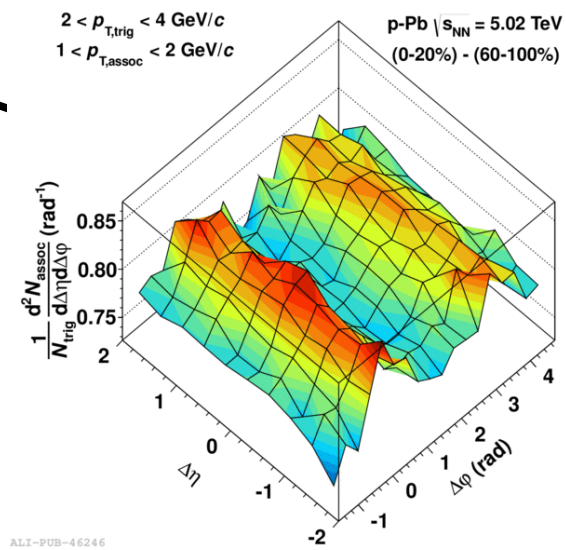

DHC: Symmetric ridge

ALICE, PLB 719 (2013) 29

- What would the assumption of a symmetric ridge give?
  - Determine the near-side ridge in 1.2 < |Δη| < 1.8
  - Mirror to away-side and subtract

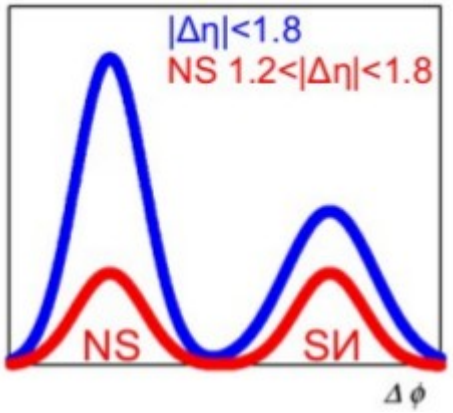

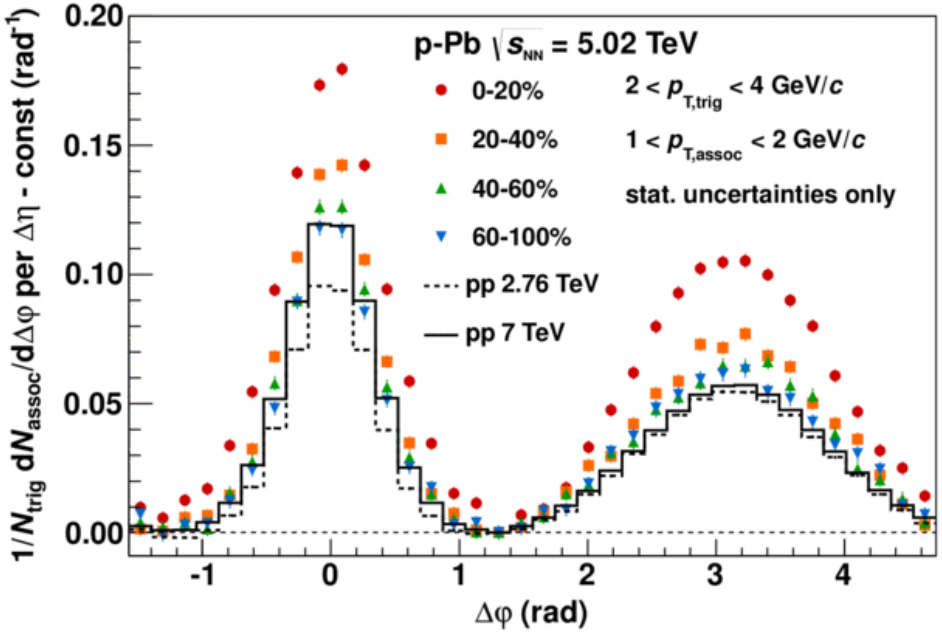

Subtract →

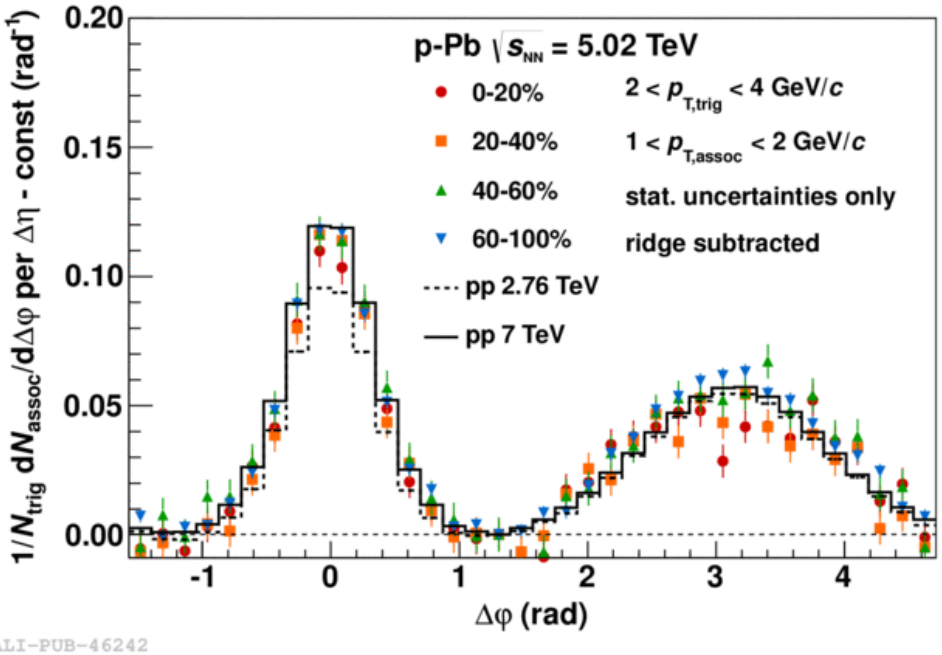

- No significant other multiplicity dependent structures left over

DHC: CMS and ATLAS

- CMS
  - Reported near-side ridge
- ATLAS
  - Confirms two-ridge structure
    - Larger acceptance
    - More p_T and multiplicity bins

CMS, PLB 718 (2012) 795

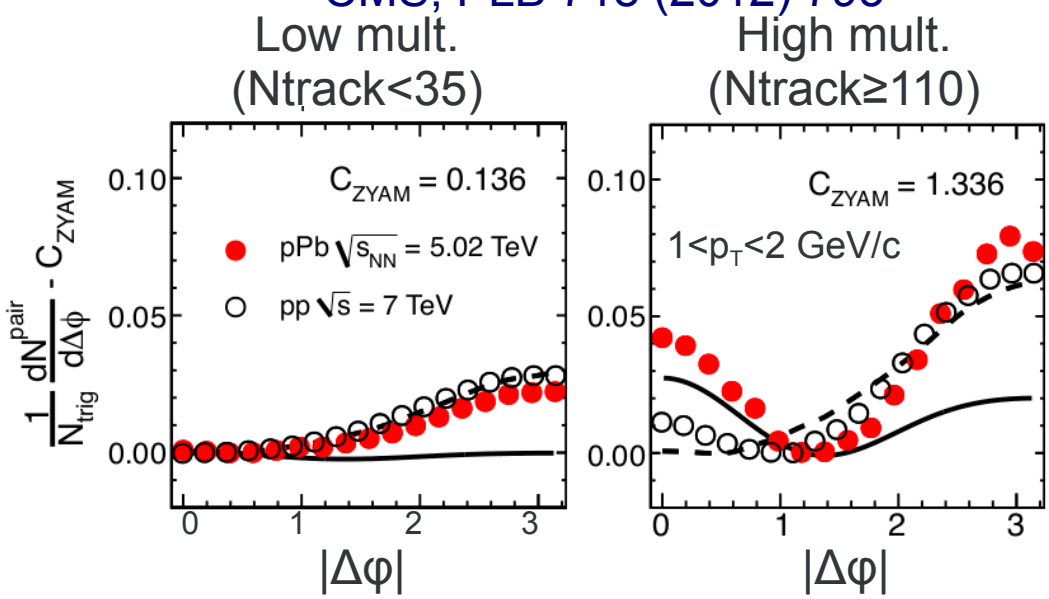

- Results by the 3 collaborations are qualitatively similar
  - Differences in event selection, normalization, acceptance and p_T ranges, as well as in the per-trigger yield definition make direct comparisons difficult
  - A few cases were checked "together" and found to be consistent
  - See appendix: arXiv:1302.7018

ATLAS, arXiv:1212.5198

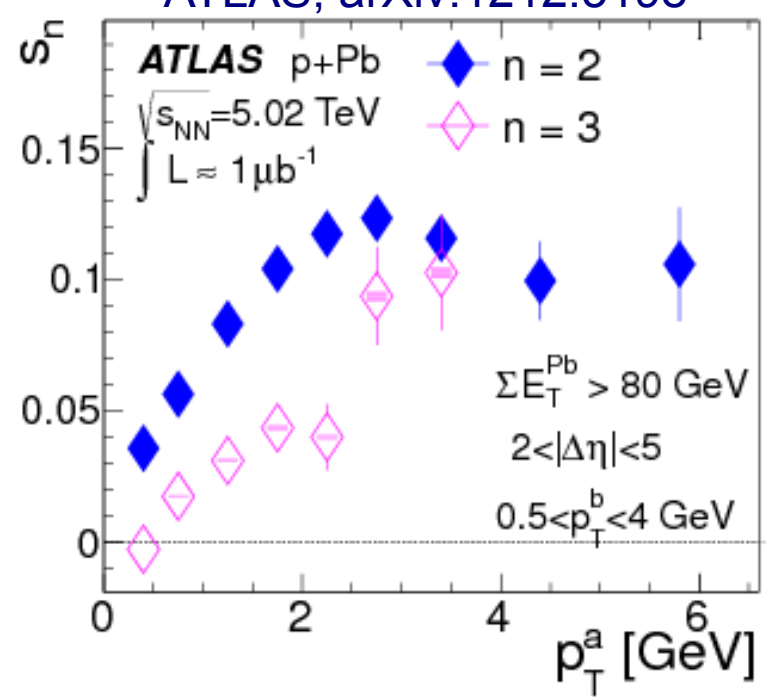

Multi-particle correlations in PbPb

- Cumulants to extract genuine k-particle correlations excluding those from k-1 particles
- Higher order cumulant nicely work out in PbPb, where multiplicity is large
- Definitions
  - $v_2\{2\}^2 = \langle v_2 \rangle^2 + \sigma_{v_2}^2 + \delta$
    $v_2 \gg 1/\sqrt{M}$
  - $v_2\{4\}^2 = \langle v_2 \rangle^2 - \sigma_{v_2}^2$
    $v_2 \gg 1/M^{3/4}$
    - eg. M=100, v_2>>0.03
  - Care is needed when averaging over M, as cumulants are also sensitive to multiplicity fluctuations

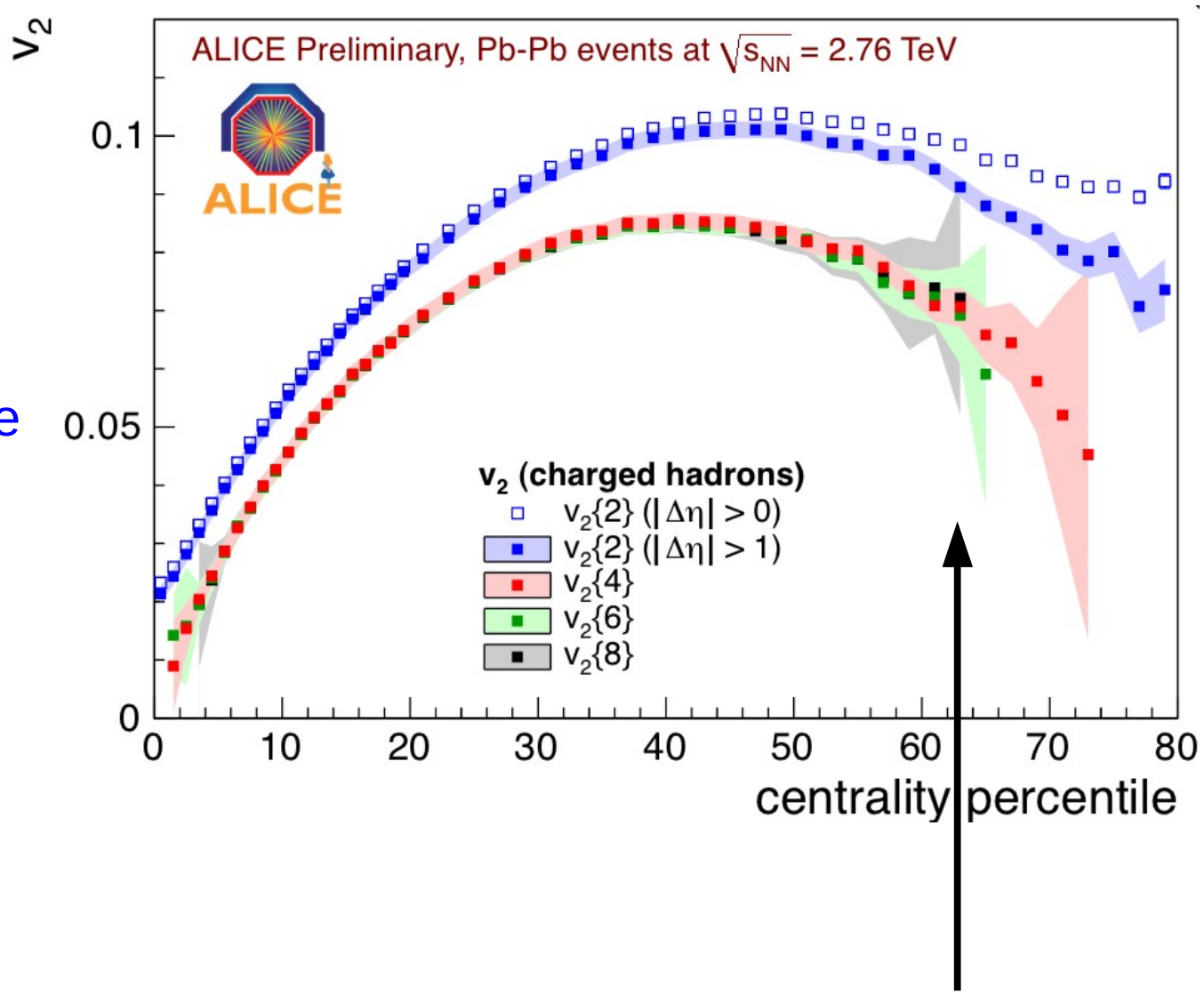

$\langle N_{ch} \rangle \approx 100$

Multi-particle correlations in pPb

ATLAS, arXiv:1303.2084

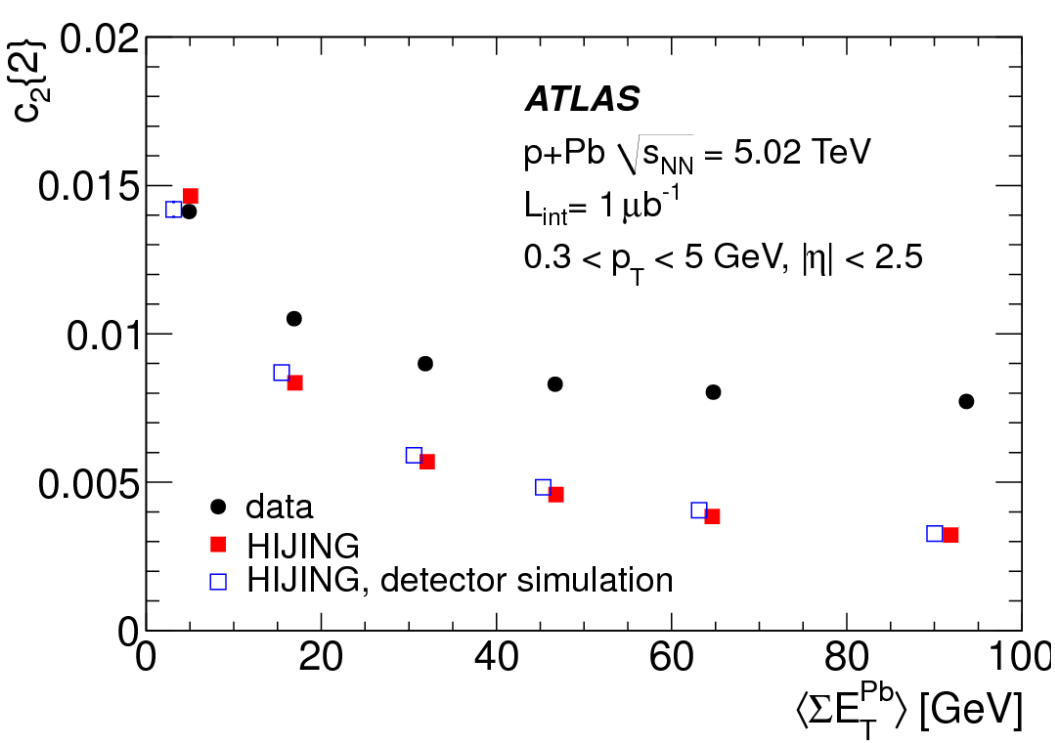

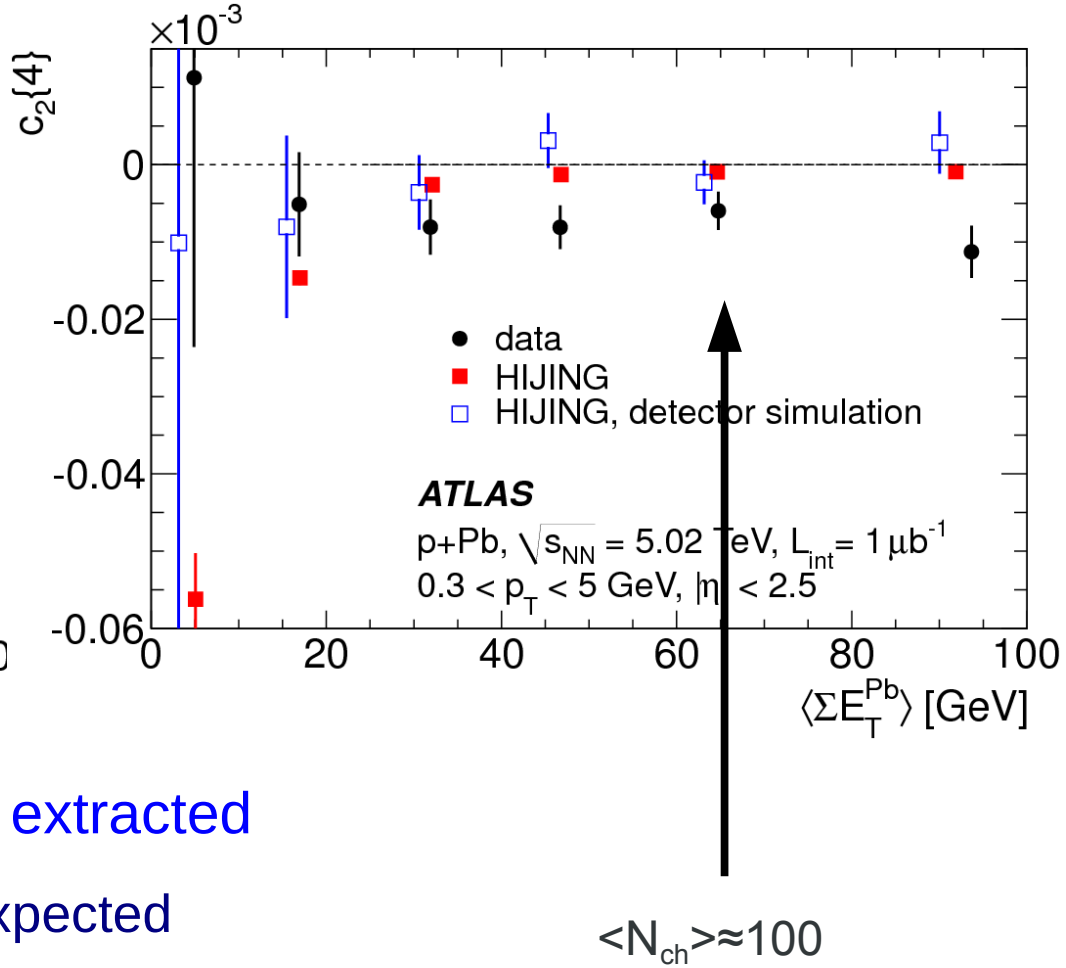

$\langle N_{ch} \rangle \approx 100$

- Second and fourth order cumulant extracted
  - Second order above HIJING as expected if additional correlations present
  - Fourth order has different trend than HIJING
    - In high-multiplicity region there are four or higher particle correlations not present in HIJING

Integrated v_2 for pPb

ATLAS, arXiv:1303.2084

In PbPb one would expect

$$v_2\{2\}^2 = \langle v_2 \rangle^2 + \sigma_{v_2}^2 + \delta$$

$$v_2\{4\}^2 = \langle v_2 \rangle^2 - \sigma_{v_2}^2$$

$$v_2\{2PC\}^2 = \langle v_2 \rangle^2 + \sigma_{v_2}^2$$

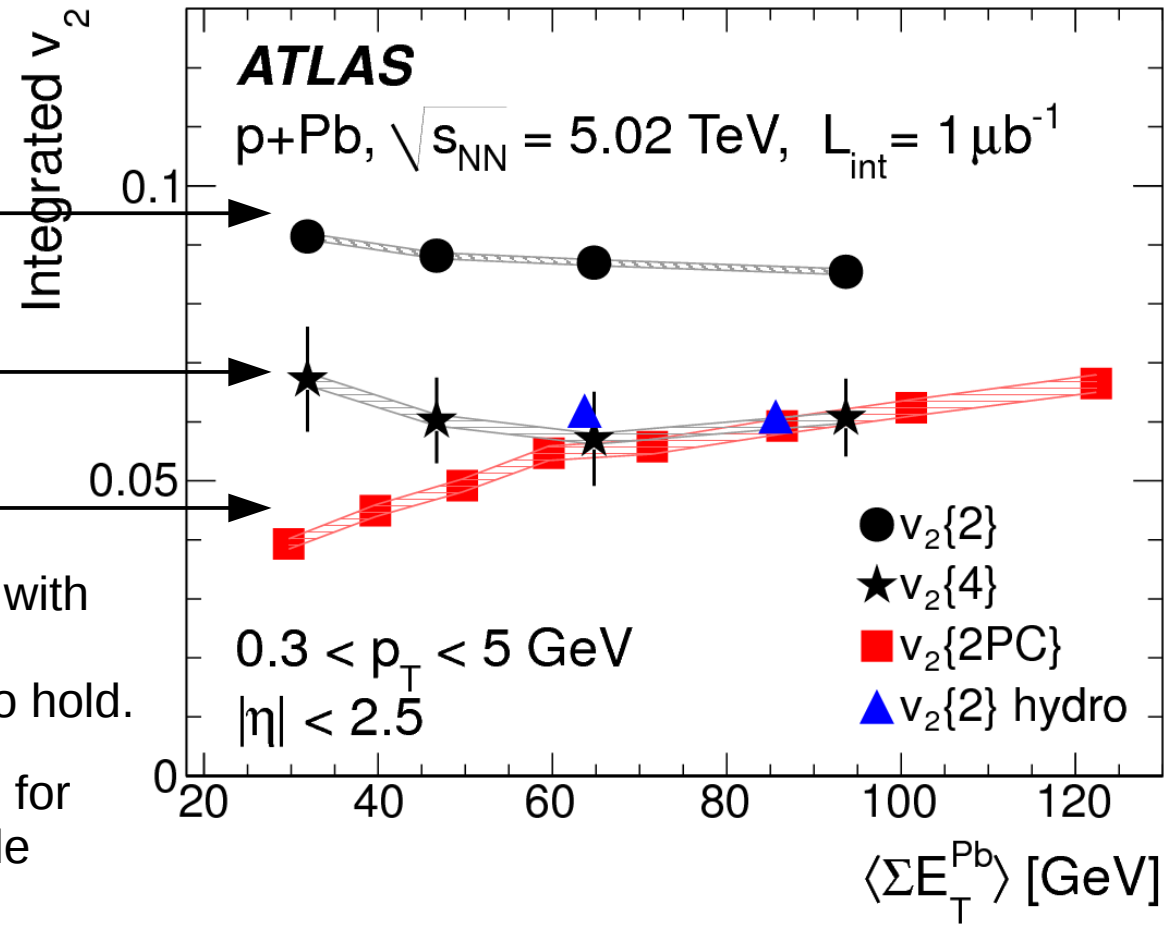

- Equations derived for heavy-ions with guidance from Bessel-Gauss and eccentricity studies do not need to hold.
- Nevertheless taken at face value, for high multiplicity events, compatible solution can exist within errors.

$v_2\{4\}$ compatible with $v_2\{PC\}$ supports the importance of final state effects, even in pPb. Or else, are there other Glasma contributions (or different theory) which predict four azimuthally correlated particles?

Summary

ALICE, PRL 110 (2013) 032301

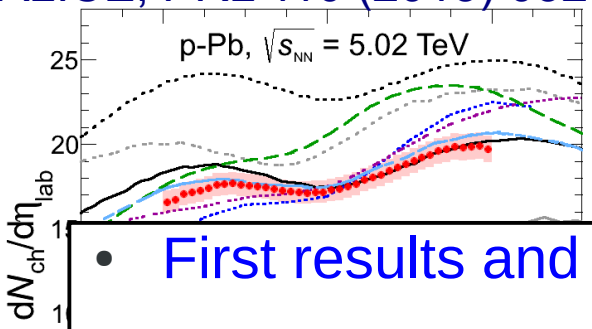

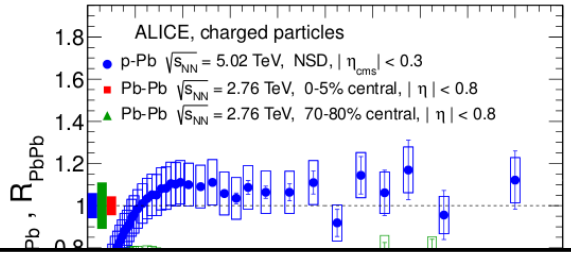

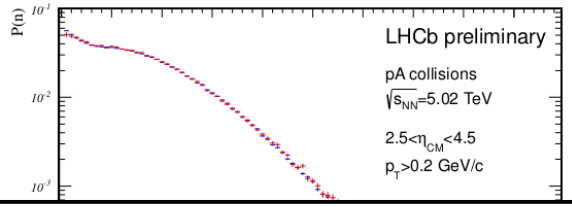

- First results and surprises already from the pilot run in 2012
  - First measurements (pPb cross section, dN/dη and dN/dp_T spectra)
  - More fundamental work needed (diffraction, fluctuations and centrality)
  - Ridge and higher cumulant results lead to interesting debate of the role of initial and final state effects in pPb
- Thanks to successful LHC operations in 2013, there are soon many more results to come

198

CMS

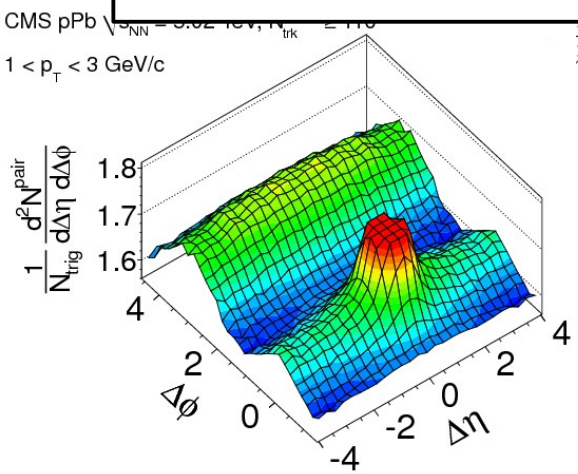

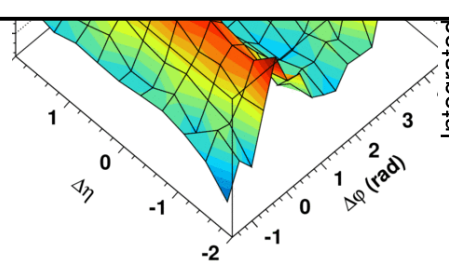

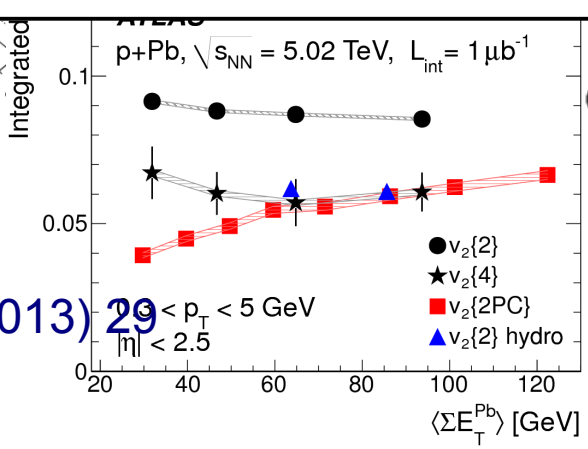

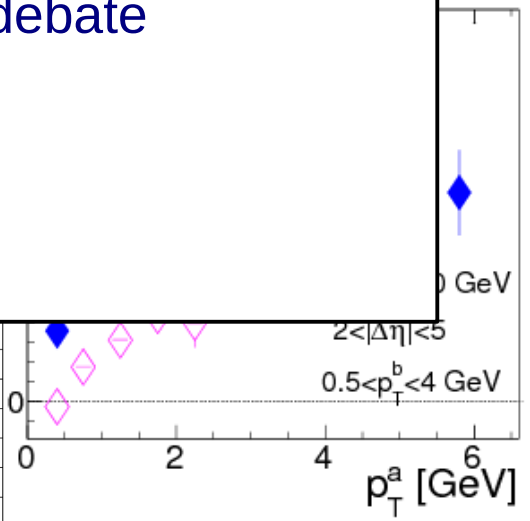

ALICE, PLB 719 (2013) 29

Extra

ALICE configuration (pilot run)

Illustration (HIJING at 4.4 TeV)

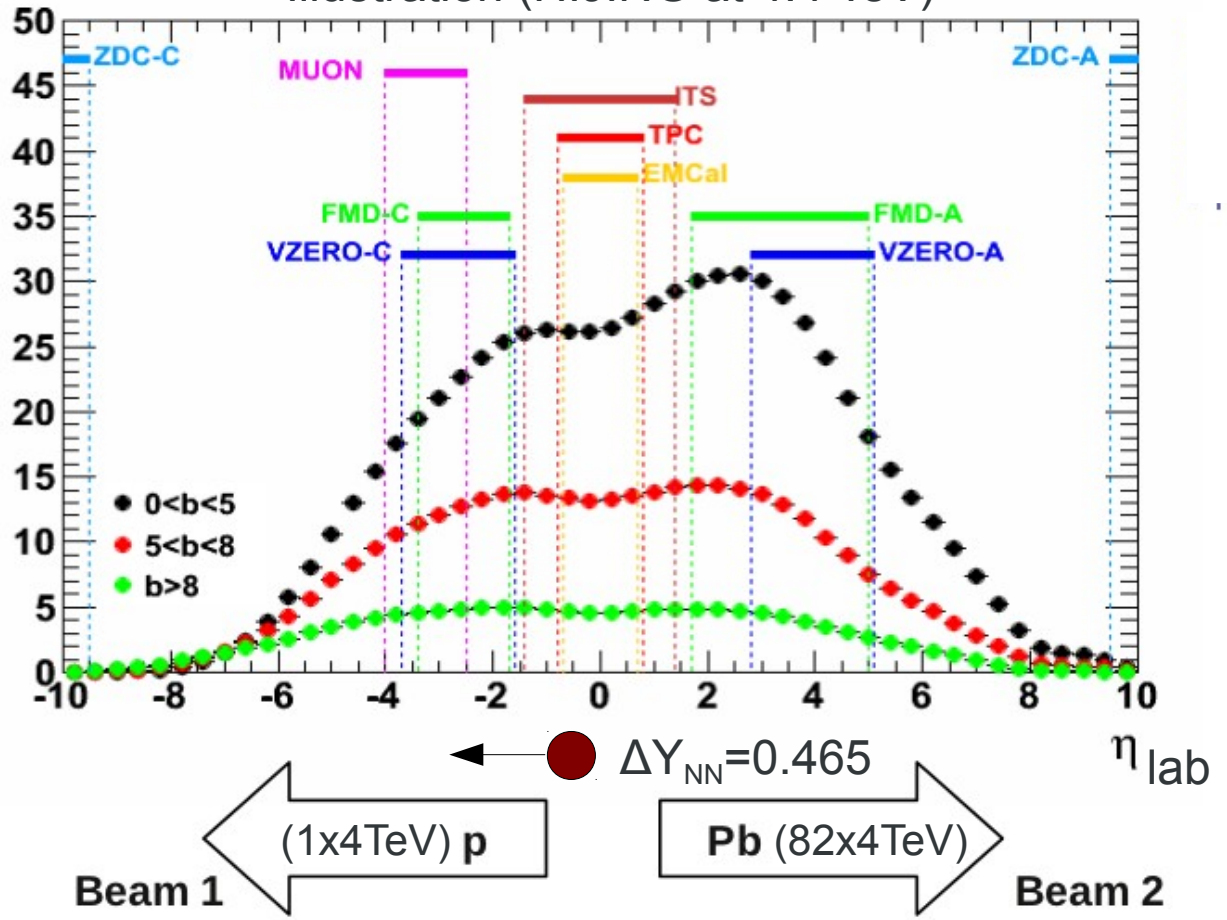

- Trigger
  - VZERO-A or C
  - ZDC-A or ZDC-C
- Dataset
  - One fill (a few millions triggers)
  - A part with displaced vertex to have ITS coverage over 6 units in η

Nuclear modification factor

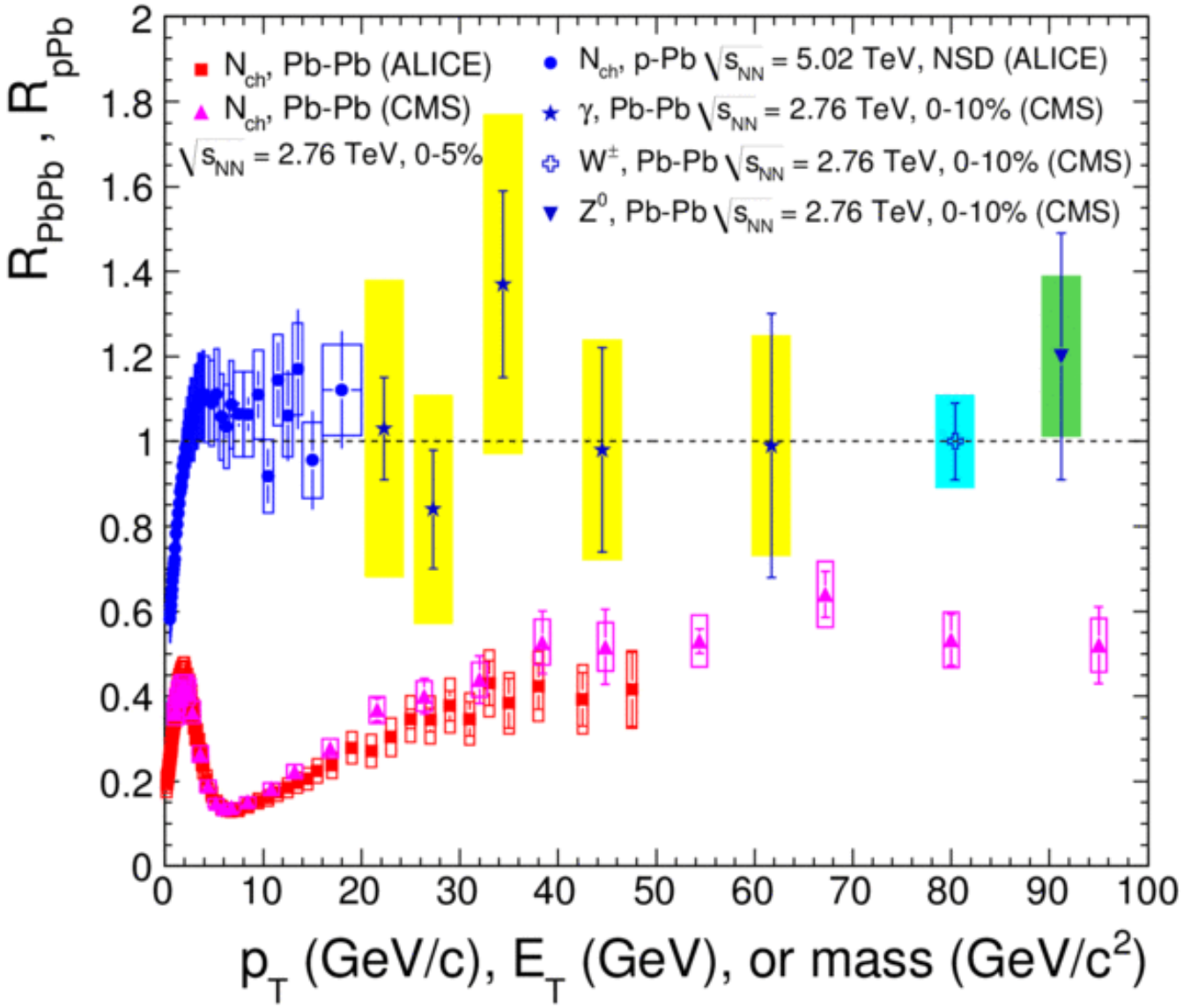

Jet quenching and fragmentation from an exactly soluble model

Frashër Loshaj

Department of Physics & Astronomy
Stony Brook University

16 April 2013

based on *F.L. and D. E. Kharzeev, Int.J.Mod.Phys. E21 (2012) 1250088, arXiv:1111.0493 [hep-ph]*; *D. E. Kharzeev and F.L., to appear in Phys. Rev. D, arXiv:1212.5857 [hep-ph]*

Outline

1. Introduction and motivation
2. Overview of the model
3. Jet fragmentation in vacuum
4. In-medium fragmentation
5. Summary and Outlook

Jet quenching - General introduction

- It is observed at RHIC and LHC that large p_T hadron yields are suppressed in heavy ion collisions.
- This suppression is attributed to jet quenching.
- Traditional approaches to jet quenching are:
  - Perturbative QCD ($pQCD$)

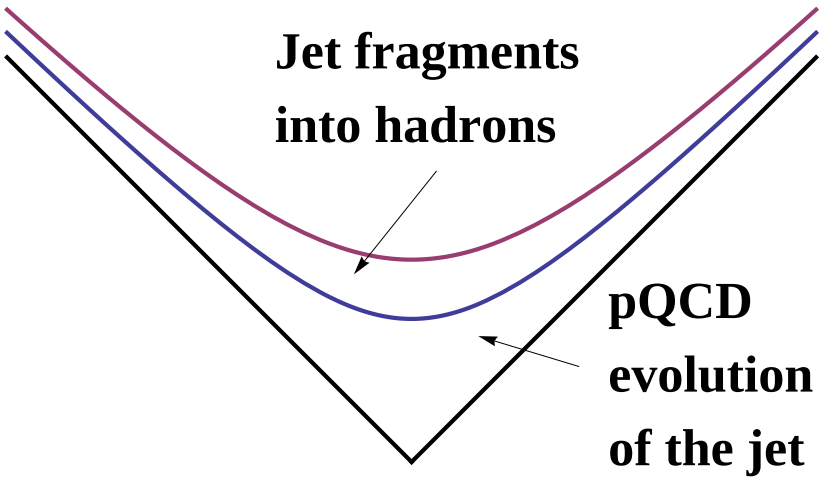

- At some scale $Q_0^2 \sim 1 - 3$ GeV^2, $pQCD$ is not valid anymore.
- Fragmentation functions are used to describe hadronization phenomenologically.

  - Gauge/Gravity duality

General properties of the model

We want to study nonperturbative effects on jet fragmentation. Properties we would like to have:

- Confinement in the presence of light quarks - screening of color charge.
- Chiral symmetry breaking, topology, anomalies.

Other assumptions

- We study very energetic jets, therefore we assume effective dimensional reduction - namely a $1+1$ dimensional theory, where the spatial direction is along jet axis.
- The picture of confinement we adopt is one based on the Abelian projection - we project the non Abelian theory to N_c (number of colors) Abelian sectors (e.g. condensation of magnetic monopoles).

The Model

In the large N_c approximation we can neglect interference between individual Abelian sectors. We then have N_c independent Abelian sectors in the theory. We assume that the dynamics in these sectors is described by the Schwinger model or QED in $1+1$ dimensions.

$$\mathcal{L} = -\frac{1}{4}F_{\mu\nu}F^{\mu\nu} + \bar{\psi}(i\gamma^\mu\partial_\mu - g\gamma^\mu A_\mu - m_q)\psi$$

It is very well known that this theory is exactly soluble when $m_q = 0$.
Dimensional analysis:

$$[A] = 0, \quad [\psi] = 1/2 \Rightarrow \boxed{[g] = 1}$$

Vector current

$$J_V^\mu(x) = \bar{\psi}(x)\gamma^\mu\psi(x)$$

Is conserved. For the massless case, $m_q = 0$, the axial current

$$J_A^\mu(x) = \bar{\psi}(x)\gamma^\mu\gamma^5\psi(x)$$

is conserved classically. Quantum corrections give rise to axial anomaly.
We will illustrate some of the properties in the following slides.

The theta angle [*Coleman, 1975*]

- In $1+1$ dimensions, in the $A_1 = 0$ gauge, we can write

$$F_{01} = g\partial_1^{-1} j_0 + F$$

- the constant electric field is allowed in $1+1$ dimensions

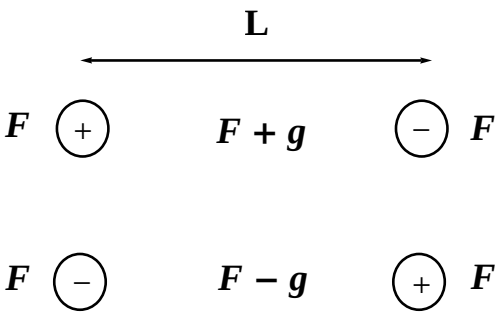

- Energy difference

$$\Delta E = \frac{1}{2}\int dx[F_{01}^2 - F^2] = \frac{1}{2}L[(F \pm g)^2 - F^2]$$

- Pair creation favorable for $|F| > \frac{1}{2}g$, until $|F| \leq \frac{1}{2}g$

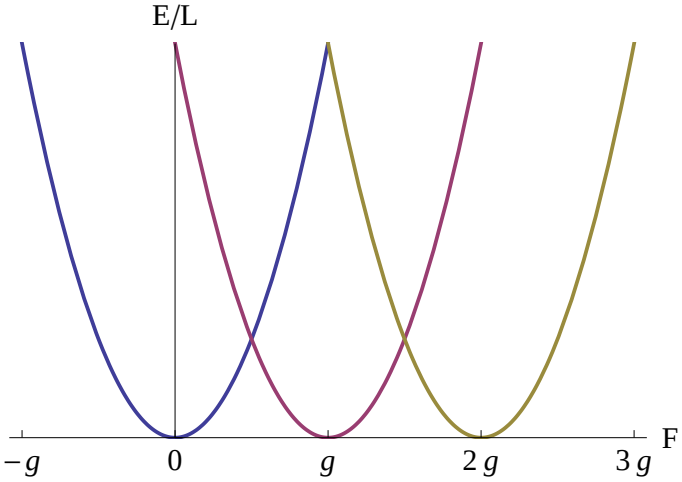

Ground state energy per unit length.

Physics is periodic with period g.

$$\theta = \frac{2\pi F}{g}$$

Confinement and chiral symmetry breaking

Let's consider two infinitely heavy quarks with charges $\pm g$, separated by $2L$

$$J^0_{ext}(x) = \delta(z+L) - \delta(z-L)$$

The potential can be computed to be

$$\begin{aligned} V(L) &= 2\pi^2 M^2 2L + \frac{g\sqrt{\pi}}{2}\left(1 - e^{-\frac{g}{\sqrt{\pi}}2L}\right) \\ M^2 &\propto m_q g \end{aligned}$$

$m_q = 0$ - Charge screening.
$m_q \neq 0$ - Linear confinement.

Axial anomaly in $1+1$ dimensions has the form

$$\partial_\mu J^\mu_A = \frac{g}{2\pi}\epsilon^{\mu\nu}F_{\mu\nu} = \frac{g}{\pi}F_{01}$$

Using Gauss' theorem

$$\int dzdt\partial_\mu\, J^\mu_A = Q_A(t=\infty) - Q_A(t=-\infty) = N_R - N_L = \frac{g}{2\pi}\int dzdt\, \epsilon^{\mu\nu}F_{\mu\nu}$$

If we have a nonzero background electric field F

$$\boxed{N_R - N_L = \frac{g}{\pi}\int dzdt\, F}$$

Chiral symmetry is not spontaneously broken, but explicitly through anomaly

Abelian bosonization

In $1+1$ dimensions we can use bosonization

$$J_V^\mu(x) = \bar{\psi}(x)\gamma^\mu\psi(x) = -\frac{1}{\sqrt{\pi}}\epsilon^{\mu\nu}\partial_\nu\phi(x)$$

where ϕ is a real scalar field. Using the identity $\gamma^\mu\gamma^5 = -\epsilon^{\mu\nu}\gamma_\nu$, we have

$$J_A^\mu(x) = \bar{\psi}(x)\gamma^\mu\gamma^5\psi(x) = \frac{1}{\sqrt{\pi}}\partial^\mu\phi(x)$$

Bosonized Lagrangian can be written as ($m_q = 0$)

$$\begin{aligned}
\mathcal{L} &= -\frac{1}{4}F_{\mu\nu}F^{\mu\nu} + \frac{1}{2}\partial_\mu\phi\partial^\mu\phi + \frac{g}{\sqrt{\pi}}\epsilon^{\mu\nu}\partial_\nu\phi A_\mu \\
&= \frac{1}{2}F_{01}^2 + \frac{1}{2}\partial_\mu\phi\partial^\mu\phi - \frac{g}{\sqrt{\pi}}\epsilon^{\mu\nu}\partial_\nu A_\mu \\
&= \frac{1}{2}F_{01}^2 + \frac{1}{2}\partial_\mu\phi\partial^\mu\phi + \frac{g}{\sqrt{\pi}}\phi\, F_{01}
\end{aligned}$$

We can integrate F_{01} (e.g. choose the gauge $A_0 = 0$, Jacobian of $\int \mathcal{D}A_1 \to \int \mathcal{D}F_{01}$ doesn't depend on F_{01}) to get

$$\boxed{\mathcal{L}_{eff} = \frac{1}{2}\partial_\mu\phi\partial^\mu\phi - \frac{1}{2}\frac{g^2}{\pi}\phi^2}$$

This is just a free massive scalar field, with mass $m = \frac{g}{\sqrt{\pi}}$.

Anomaly equation

From Maxwell's equations

$$\partial_1 F^{10} = -\frac{g}{\sqrt{\pi}}\partial_1\phi \Rightarrow F_{01} = \frac{-g}{\sqrt{\pi}}\phi$$

We have assumed that fields vanish at infinity.
Equation of motion for ϕ is just the Klein-Gordon equation

$$(\Box + \frac{g^2}{\pi})\phi = 0$$

Using bosonization relations

$$\partial_\mu J_A^\mu = \partial_\mu \left(\frac{1}{\sqrt{\pi}}\partial^\mu\phi\right) = \frac{1}{\sqrt{\pi}}\Box\phi$$

Using EOM for ϕ and relation between F_{01} and ϕ, we get

$$\partial_\mu J_A^\mu = \frac{g}{\pi}F_{01} = \frac{g}{2\pi}\epsilon^{\mu\nu}F_{\mu\nu}$$

This is the same expression we saw before for the axial anomaly for QED in $1+1$ dimensions.

Adding an external source

Consider a general external source $J^{\mu}_{ext}(x) = j^{\mu}_{ext}(z,t)$. We use the parametrization

$$J^{\mu}_{ext}(x) = -\frac{1}{\sqrt{\pi}}\epsilon^{\mu\nu}\partial_{\nu}\phi_{ext}(x)$$

In the same way as before, we get the effective Lagrangian

$$\mathcal{L}_{eff} = \frac{1}{2}(\partial_{\mu}\phi)^2 - \frac{1}{2}\frac{g^2}{\pi}(\phi + \phi_{ext})^2$$

Which gives

$$\boxed{(\Box + m^2)\phi(x) = -m^2\phi_{ext}(x)}$$

- Corresponds to a massive scalar field, coupled to a classical source.
- Coherent particle creation.

Jet fragmentation by quark-antiquark pair production

We consider the source (*Casher, Kogut and Susskind,1974*)

$$J^0_{ext}(x) = \delta(z-t)\theta(z) - \delta(z+t)\theta(-z)$$

Quark anti quark pair, moving back to back.

Using bosonization relations we have

$$\phi_{ext}(x) = -\theta(t-z)\theta(t+z)$$

We therefore have to solve

$$(\Box + m^2)\phi = m^2\theta(t-z)\theta(t+z)$$

The solution to the equation of motion is (*F.L. and D. E. Kharzeev, arXiv:1111.0493 [hep-ph]*)

$$\phi(x) = \theta(t+z)\theta(t-z)(1 - J_0(m\sqrt{x^2}))$$

where $x^2 = t^2 - z^2$.

Jet fragmentation (cont'd)

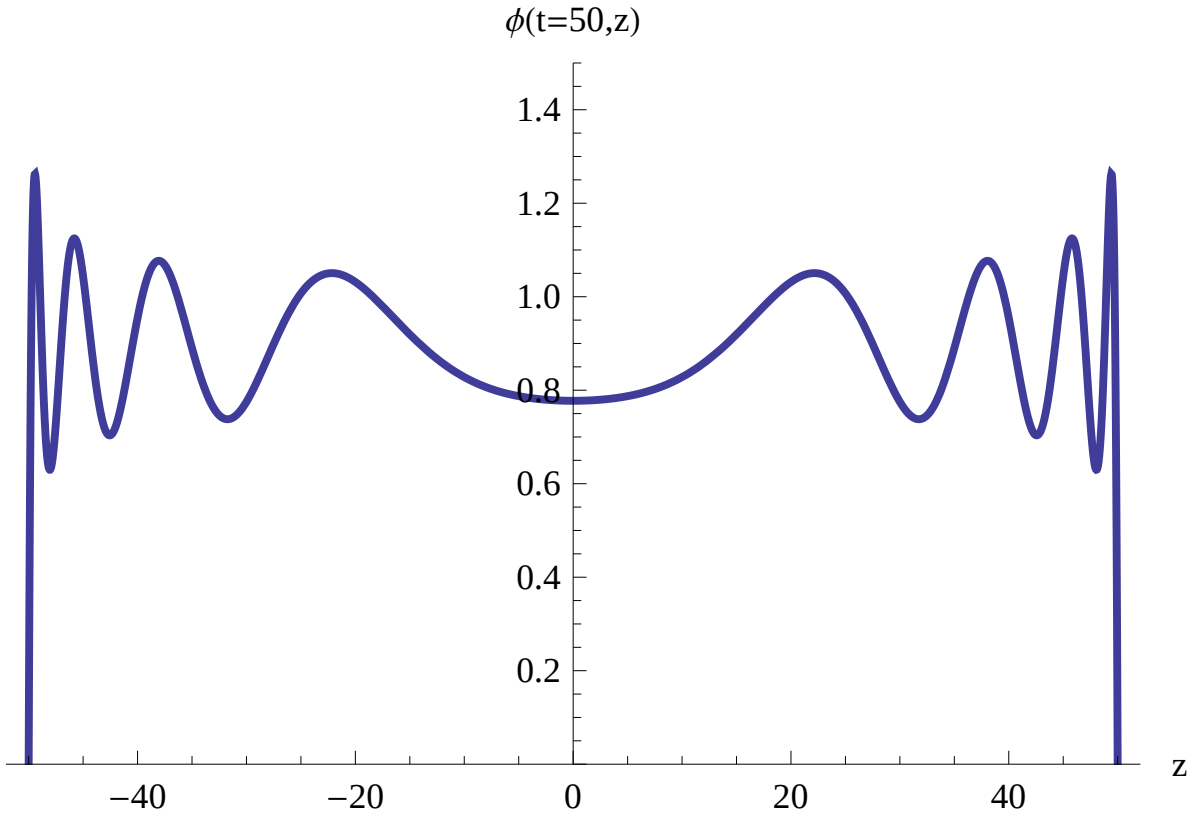

Quark anti quark pair, moving back to back.

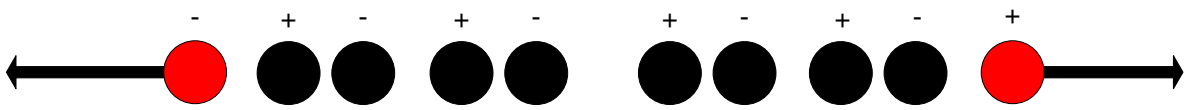

Quark anti quark pair, moving back to back.

[*D. E. Kharzeev and F.L., arXiv:1212.5857 [hep-ph]*]

(Anti-)Kinks correpond to (anti-)fermions. Quark fragmentation in the θ-vacuum.

Particle creation by a general source

Let's consider

$$(\Box + m^2)\phi(x) = f(x)$$

It is known that

$$\begin{aligned} \frac{dN}{dp} &= \frac{|\tilde{f}(p)|^2}{2E_p}, \\ \tilde{f}(p) &= \int d^2x\, e^{ip\cdot x} f(x), \quad E_p = \sqrt{p^2 + m^2} \end{aligned}$$

For jets with finite energy - quarks move with velocity v

$$j^0_{ext}(x) = \delta(z - vt)\theta(z) - \delta(z + vt)\theta(-z)$$

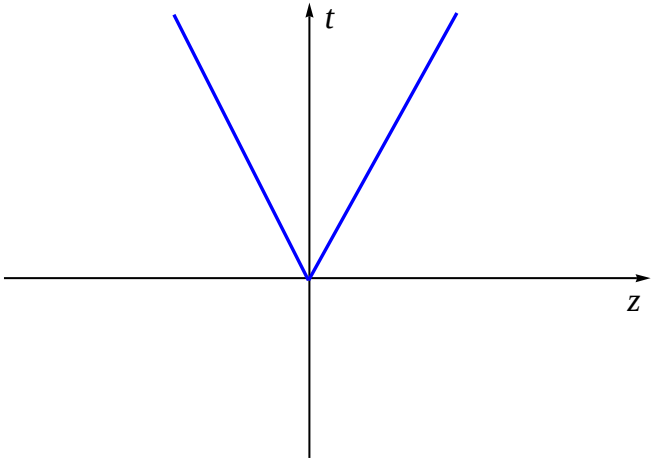

Velocity is calculated from

$$v = \frac{p_q}{E_q} = \frac{p_{jet}}{\sqrt{p_{jet}^2 + Q_0^2}}$$

$$\frac{dN}{dp} = 2\pi \frac{v^2 m^4}{E_p (E_p^2 - v^2 p^2)^2}$$

We fix Q_0 by comparing our result to experimental data.

Rapidity distribution

We now change variables to $y = \frac{1}{2} \ln \frac{E_p + p}{E_p - p}$

$$\frac{dN}{dy} = 2\pi \frac{v^2}{(\cosh^2 y - v^2 \sinh^2 y)^2}$$

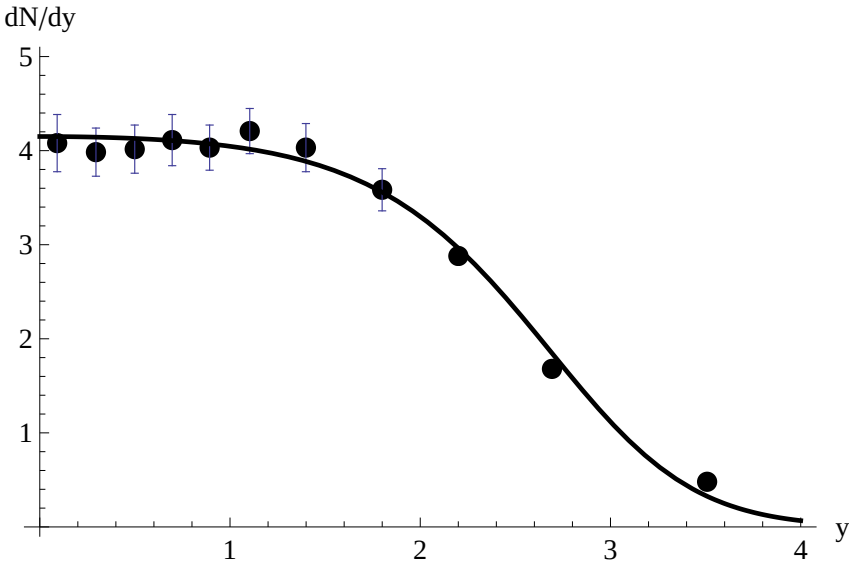

Comparison to experimental data [*Aiphara (TPC/Two Gamma Collaboration), 1988*], for $\sqrt{s} = 29$ GeV

- Q_0 is fixed by above fit. We get $Q_0 \approx 1.8$ GeV.
- Since $\sqrt{s}$ is small, the effect of jet evolution is small and our model fits the data well.

Fragmentation functions

Fragmentation function for e^+e^- annihilation

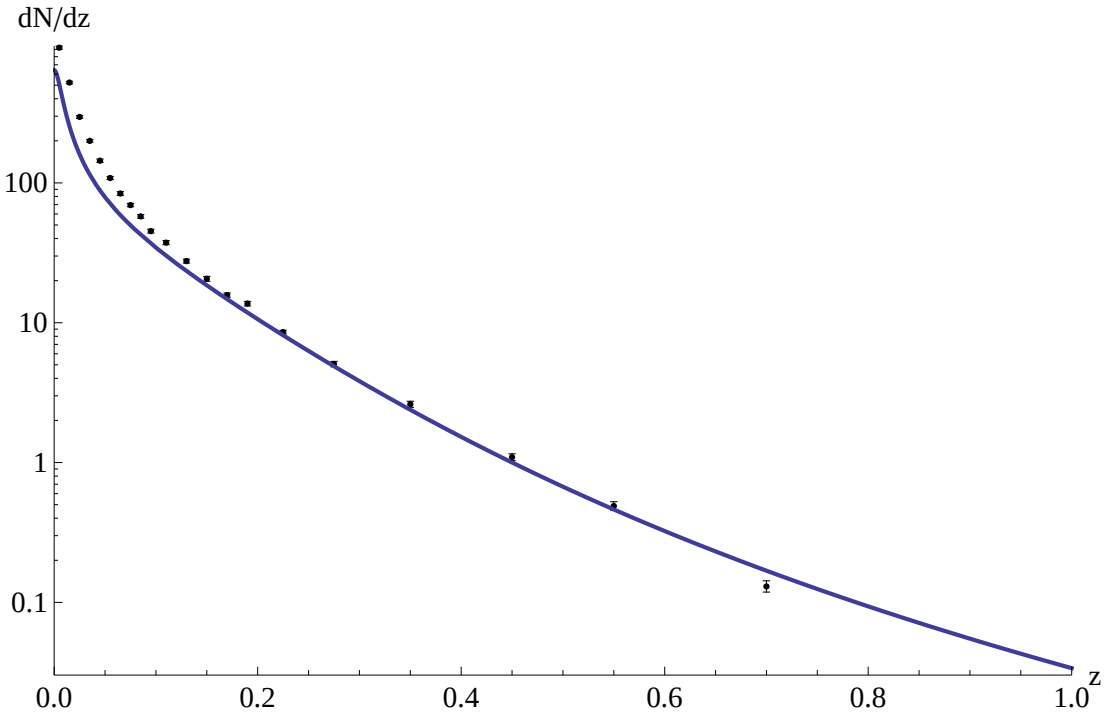

Charged particle distribution for $\sqrt{s} = 201.7$ GeV, [*Abbiendi (OPAL Collaboration), 2003*].

- Reasonable agreement with the data for $\frac{p}{p_{jet}} = z > 0.1$.
- By fitting to data at different center of mass energies $m \simeq 0.6$ GeV.
- Enhancement at small z and suppression at large z are attributed to $pQCD$ evolution of the jet, which is not included in our model.

Medium modified fragmentation functions [*CMS Collaboration, 2012*], [*PHENIX Collaboration, 2012*]

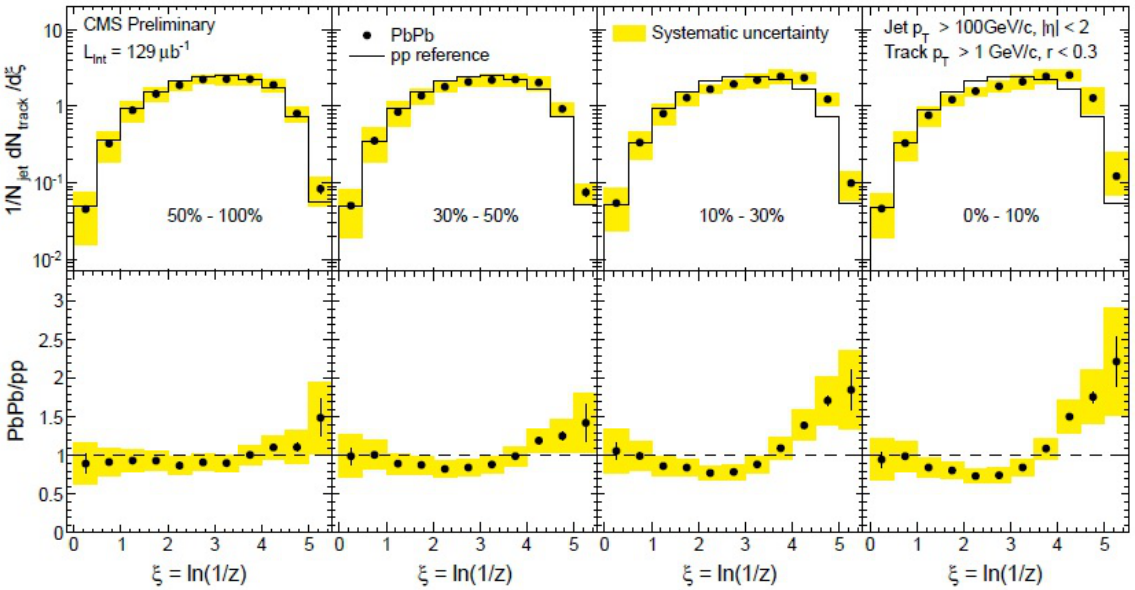

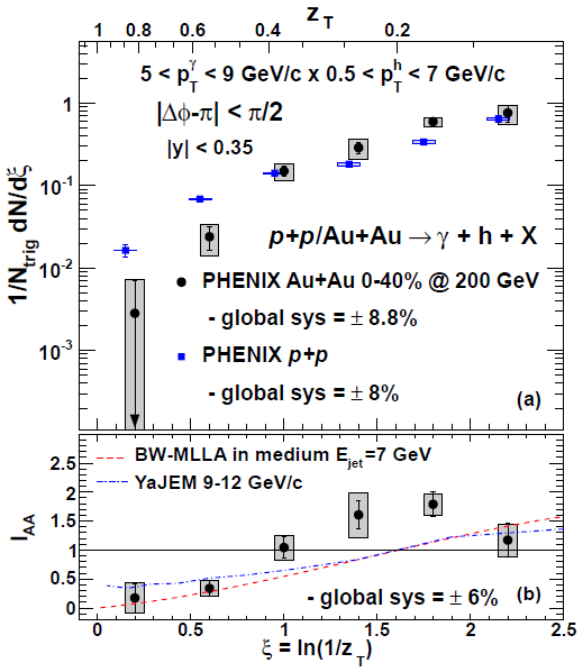

$$z = \frac{p^h}{p^{jet}}, \quad \xi = \ln\frac{1}{z}$$

- There is enhancement of soft particles for central collisions.
- For the most central collisions, we also see a depletion of particles for intermediate ξ.

In-medium scattering

We consider a very simple model: static scatterers, no expansion of the medium. [*D. E. Kharzeev and F.L., arXiv:1212.5857 [hep-ph]*]

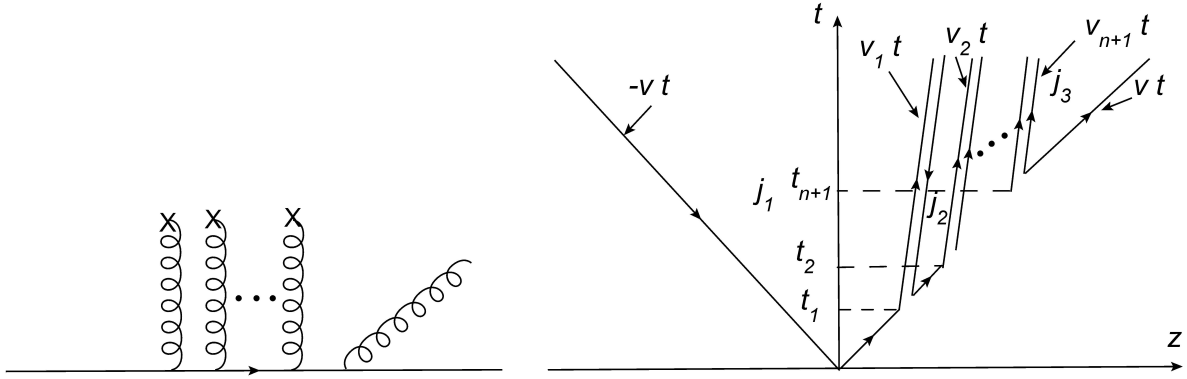

We have three types of currents and their Fourier transform is

$$
\begin{aligned}
\tilde{j}_1^0(p) &= \frac{ip}{E_p - vp}\left[\frac{2v}{E_p + vp} - \frac{v - v_1}{E_p - v_1 p} e^{i(E_p - vp)t_1}\right] \\
\tilde{j}_2^0(p) &= \frac{-ip}{E_p - vp}\left[\frac{v - v_2}{E_p - v_2 p} e^{i(E_p - vp)t_2} - \frac{v - v_1}{E_p - v_1 p} e^{i(E_p - vp)t_1}\right] \\
\tilde{j}_3^0(p) &= \frac{ip}{E_p - vp}\frac{v - v_{n+1}}{E_p - v_{n+1} p} e^{i(E_p - vp)t_{n+1}}
\end{aligned}
$$

Nonperturbative LPM effect

Total momentum distribution is given by

$$\frac{dN^{med}}{dp} = \frac{1}{2E_p}|\tilde{f}(p)|^2 = \frac{1}{2E_p}\left(|\tilde{f}_1(p)|^2 + \sum_{i=1}^{N-1}|\tilde{f}_2(p)|^2 + |\tilde{f}_3(p)|^2\right)$$

where as before we construct f_i's from j_i^0's.
$\tilde{j}_2^0(p)$ responsible for soft radiation. We can define the formation time

$$t_f = \frac{1}{E_p - vp} \simeq \frac{2p}{m^2}$$

Similar to the perturbative result $t_f = \frac{2\omega}{k_\perp^2}$. Radiation is suppressed when mean free path $\lambda = t_2 - t_1 << t_f$ - LPM effect.

Medium fragmentation functions - results

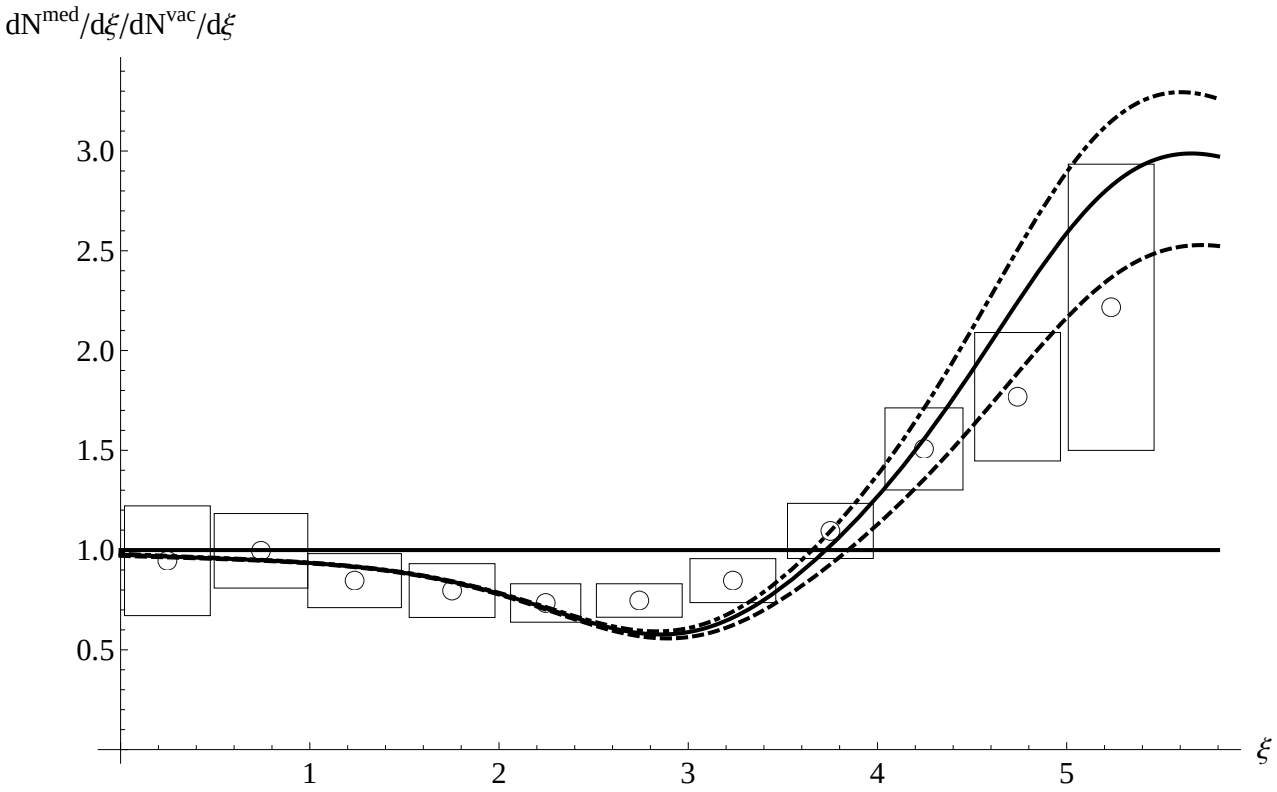

The ratio of in-medium and vacuum fragmentation functions for $p_{jet} = 120$ GeV. The first scattering occurs at $t_1 \simeq 1$ fm, which is the assumed thermalization time. The length of the medium is $L = 5$ fm. The curves correspond to mean free paths of $\lambda = 0.57$, 0.4 and 0.2 fm from top to bottom respectively.

- Scaling for small ξ - Nonperturbative LPM effect.
- Suppression at intermediate ξ is a result of the partial screening of the color charge of the jet by a comoving medium-induced gluon.

Transverse-momentum difference - D_{AA} (Talk by J. Putschke)

We study jet modification using another observable proposed in [*STAR Collaboration, arXiv:1302.6184 [nucl-ex]*]

$$D_{AA}(p) = Y_{Au-Au}(p)\,\langle p\rangle_{Au-Au} - Y_{p-p}(p)\,\langle p\rangle_{p-p}$$

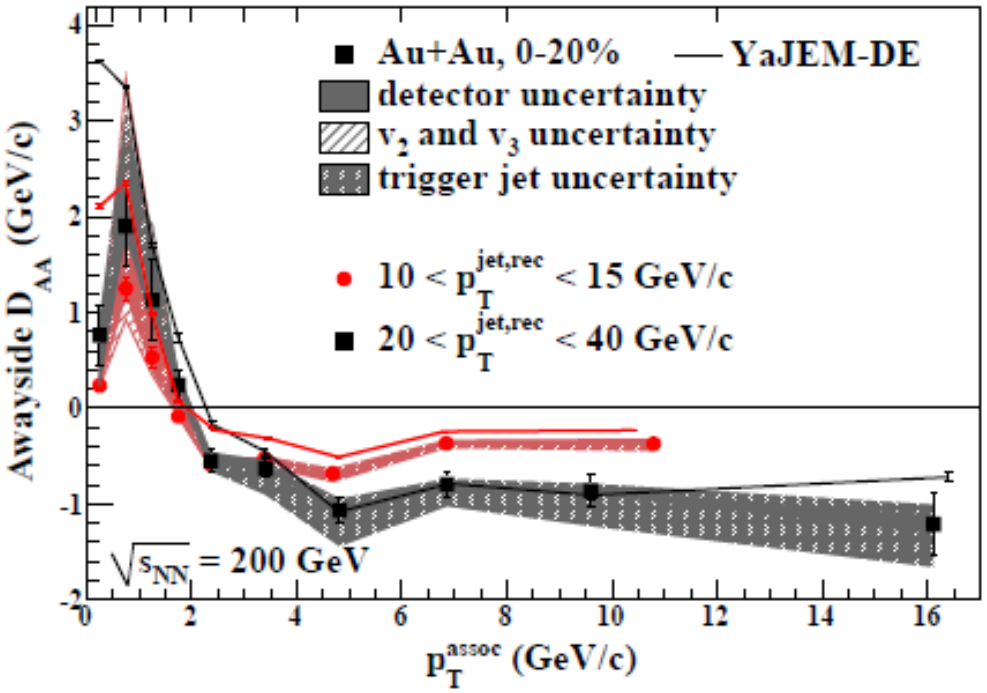

Y are yields in $Au-Au$ and $p-p$ and $\langle p\rangle$ is the average momentum inside a bin.

In our case

$$D_{AA}(p) = \langle p\rangle \int_{\text{bin with average}\,\langle p\rangle} dp'\,\frac{dN^{\text{med}}}{dp'} - \langle p\rangle \int_{\text{bin with average}\,\langle p\rangle} dp'\,\frac{dN^{\text{vac}}}{dp'}$$

Transverse-momentum difference - D_{AA} - Results

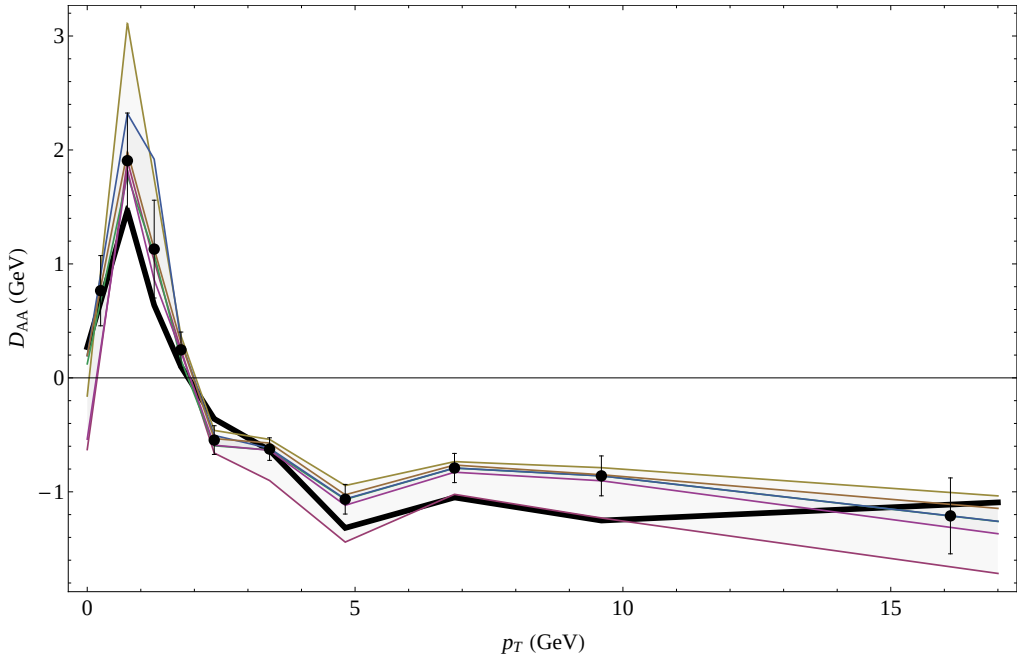

Circles show the data for the awayside momentum difference for 20<$p_T^{jet,rec} < 40$ GeV and shaded areas show jet energy scale, v2/v3 and detector uncertainties (taken from [*STAR Collaboration, arXiv:1302.6184 [nucl-ex]*]). Calculations are done using $\lambda = 0.4$ fm (solid black line).

Transverse-momentum difference - D_{AA} - Results

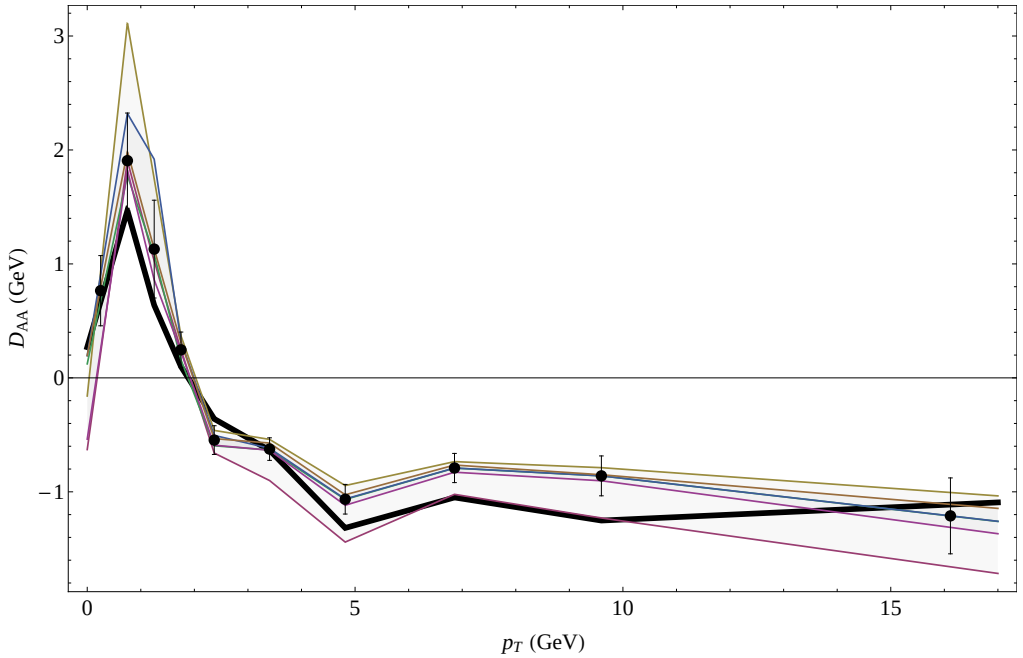

Circles show the data for the awayside momentum difference for 20<$p_T^{jet,rec} < 40$ GeV and shaded areas show jet energy scale, v2/v3 and detector uncertainties (taken from [*STAR Collaboration, arXiv:1302.6184 [nucl-ex]*]). Calculations are done using $\lambda = 0.4$ fm (solid black line).

D_{AA} was also addressed in [*T. Renk, Phys.Rev. C87 (2013) 024905*]
In this approach jet broadening contributes to jet modification and energy loss.
In our $1+1$ model we only have energy redistribution in the longitudinal (along jet axis) direction.
Two models could be distinguished experimentally by looking for the modification of the jet cone.

Summary and Outlook

- We considered an effective theory of jet fragmentation based on an exactly soluble model
- This model incorporated confinement in the presence of light quarks, topology and chiral symmetry breaking.
- Topology was shown to be responsible for particle production.

- Would be interesting to investigate further the effects of topology in high energy processes.
- A systematic derivation of the dimensionally reduced theory for high energy processes is needed.

Jet modification in A-A, p-A and D-A at RHIC and LHC

(within HT scheme)

Abhijit Majumder
Wayne State University

RIKEN BNL workshop on Jet Quenching at RHIC and LHC ... , BNL, April 15-17

Outline

- The present status of HT jet modification
- Some background on HT E-loss + MC routines
- Observables that are easily understood
- Observables less easily understood
- Really difficult observables!
- What else are we doing...

What goes into HT-E-loss

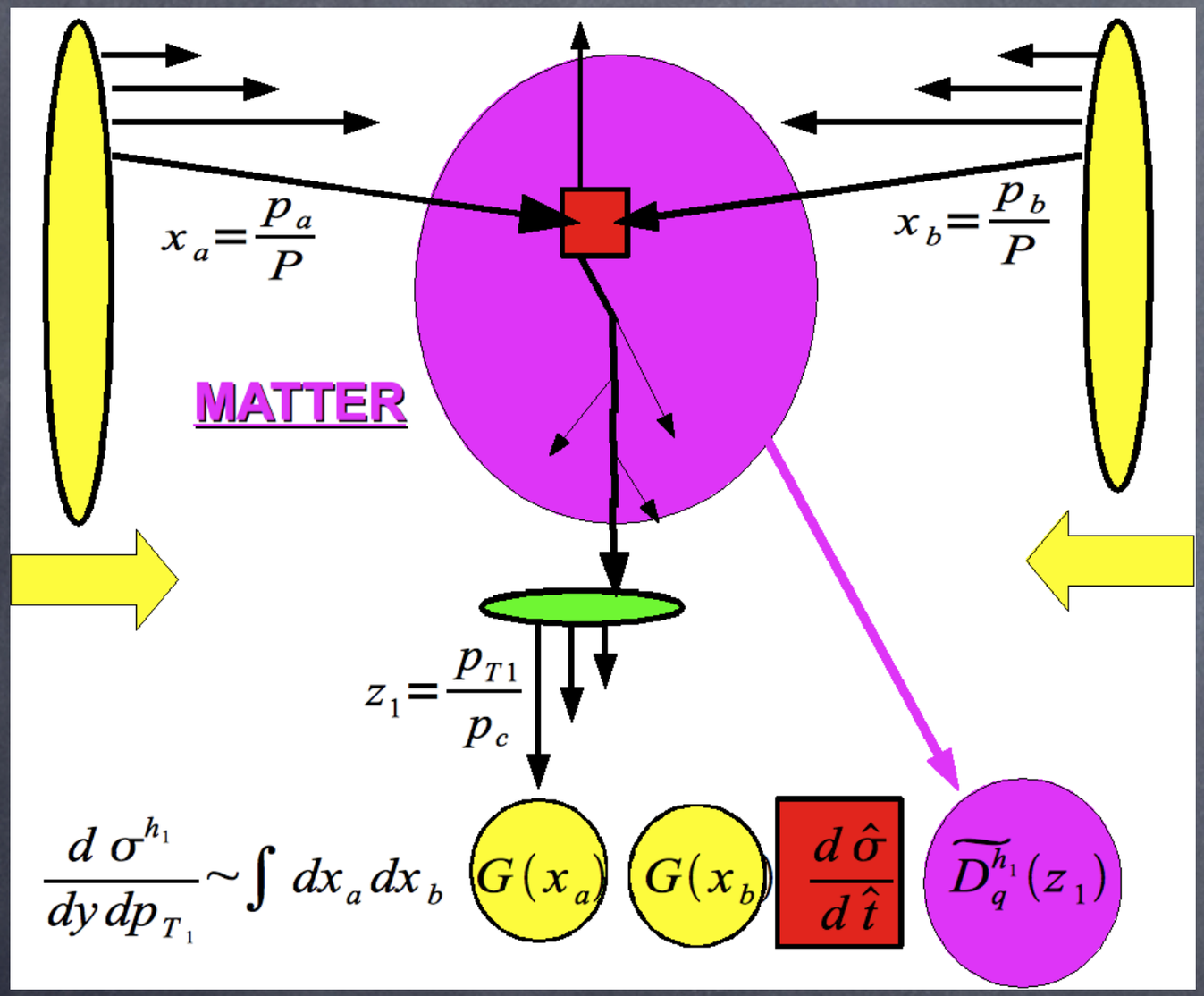

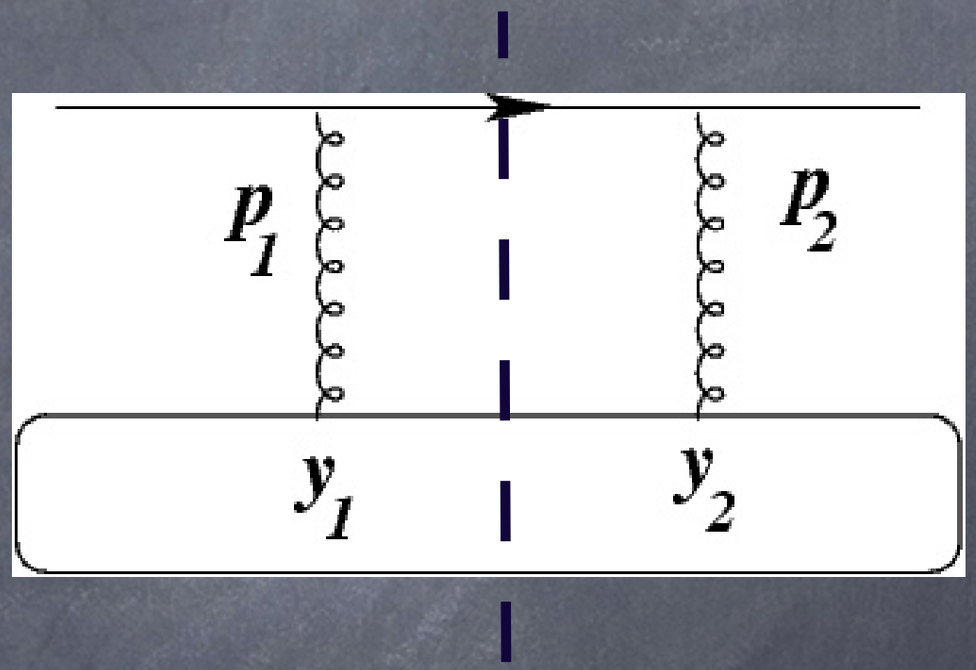

Double factorized perturbative approach

What goes into this calculation

Modification derived in A-DIS and applied to HIC
(implied factorization of hard scattering)

Jet scale assumed much harder than medium scale
(factorization of jet from soft matrix element)

Multiple scatterings resummed in single gluon emission

Expansion in powers of Λ^2/Q^2

DGLAP k_T^2 systematics assumed for multiple emissions

Fluid dynamical simulation of medium and trans. coeffs.

How the medium affects the parton.

A parton in a jet shower, has momentum components

$q = (q^-, q^+, q_T) = (1, \lambda^2, \lambda)Q$, Q: Hard scale, $\lambda \ll 1$, $\lambda Q \gg \Lambda_{QCD}$

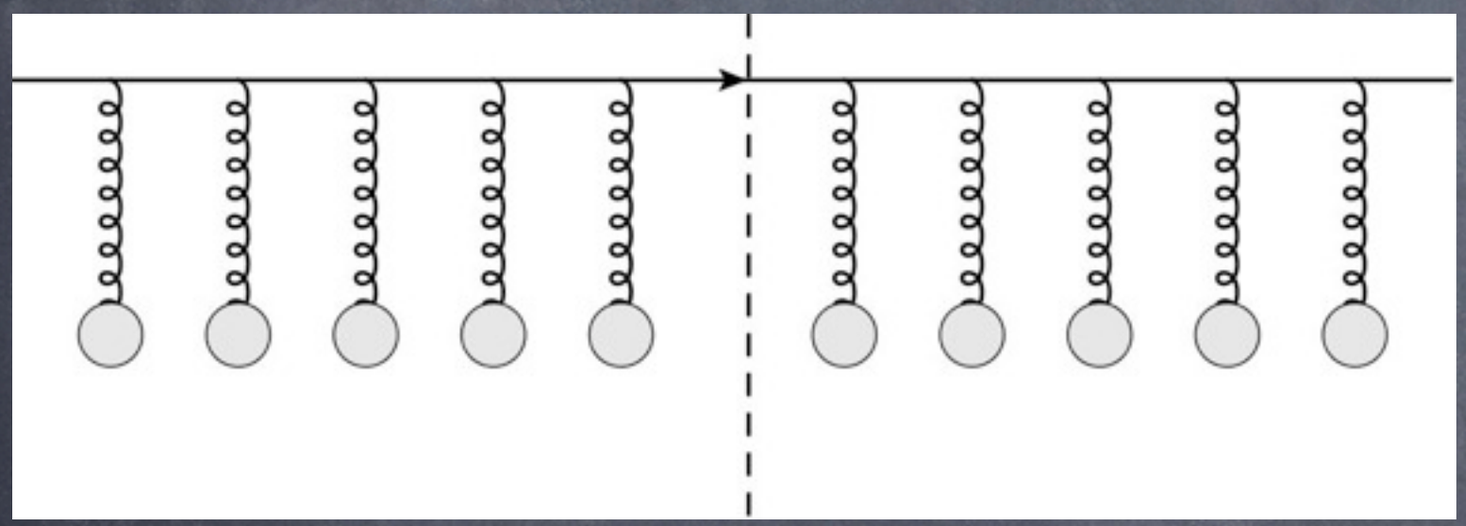

$$p^+ = \frac{p^0 + p_z}{\sqrt{2}}$$

$$p^- = \frac{p^0 - p_z}{\sqrt{2}}$$

hence, gluons have

$$k_\perp \sim \lambda Q, \qquad k^+ \sim \lambda^2 Q$$

could also have $k^- \sim \lambda Q$

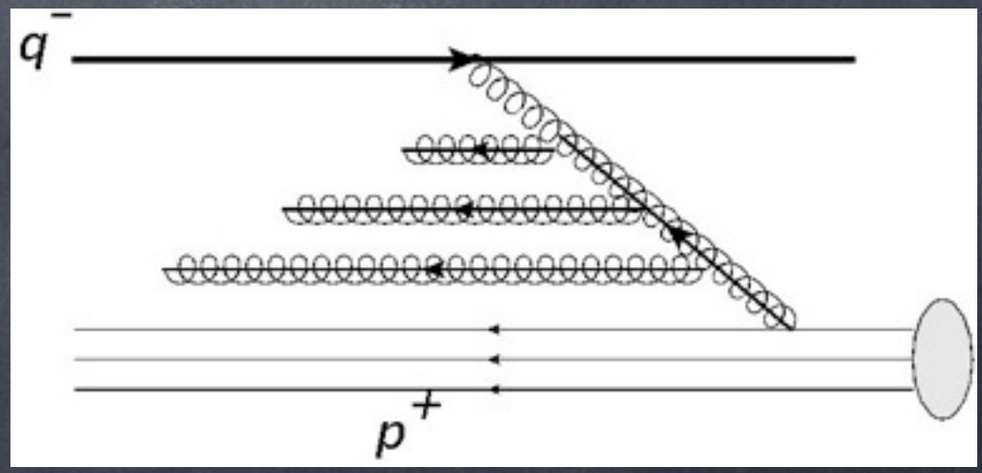

Idlilbi, Majumder PRD 80 054022 2008

So what do we get from resumming ?

transverse broadening

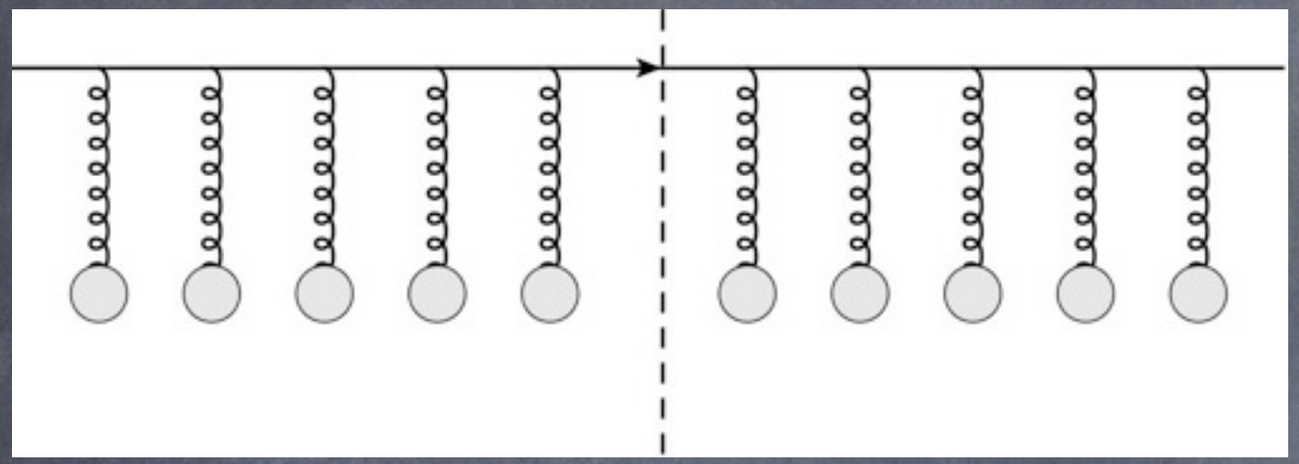

$$q^- \to \infty$$

Assuming independent scattering of nucleons gives a diff. equation

These cannot be soft, they must have transverse momentum, Glauber gluons.

$$\frac{\partial f(p_\perp, t)}{\partial t} = \nabla_{p_\perp} \cdot D \cdot \nabla_{p_\perp} f(p_\perp, t)$$

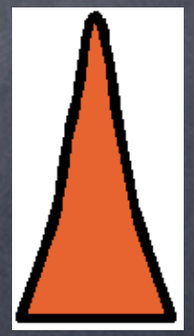

$$\langle p_\perp^2 \rangle = 4Dt$$

$$\hat{q} = \frac{p_\perp^2}{t} = \frac{2\pi^2 \alpha_s C_R}{N_c^2 - 1} \int d\tilde{t} \left\langle F^{\mu\alpha}(\tilde{t}) v_\alpha F^\beta_\mu(0) v_\beta \right\rangle$$

There are a bunch of medium properties which modify the parton and frag. func.

$\hat{q}$, $\hat{e}$ = dE/dL and f = dN/dL

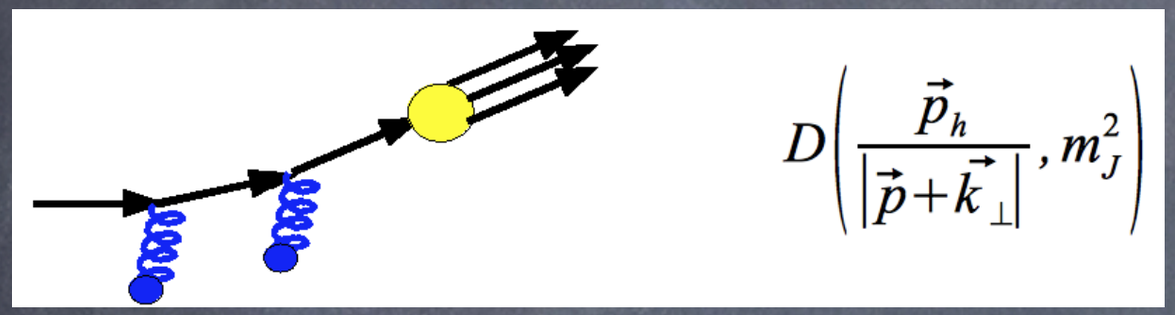

$$\hat{q} = \frac{\langle p_T^2 \rangle_L}{L}$$

Transverse momemtum diffusion rate

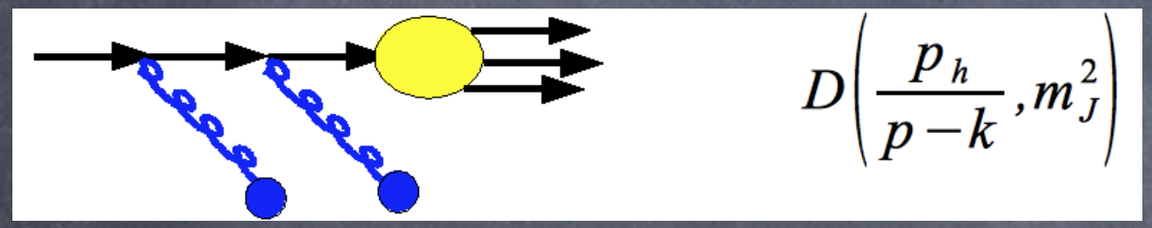

$$\hat{e} = \frac{\langle \Delta E \rangle_L}{L}$$

Elastic energy loss rate also diffusion rate e_2

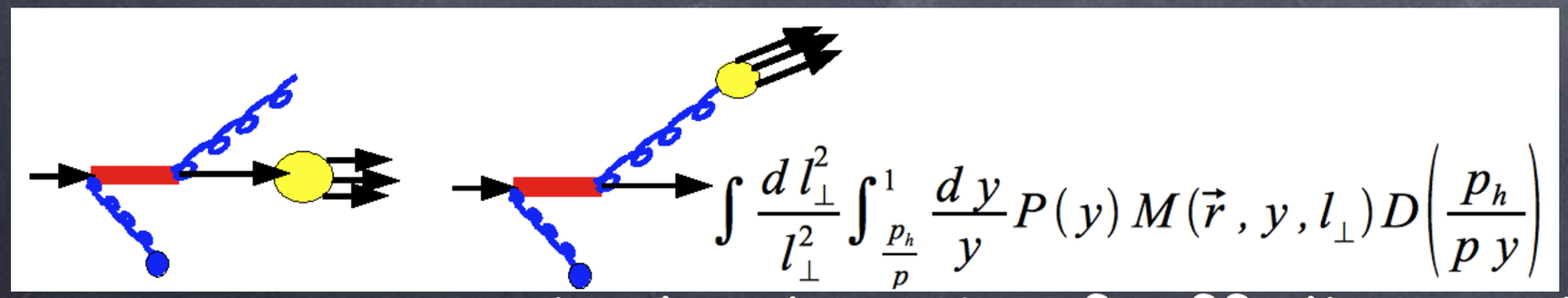

Gluon radiation is sensitive to all these transport coefficients

And a bunch of off diagonal and higher order transport coefficients

Need to repeat the kernel

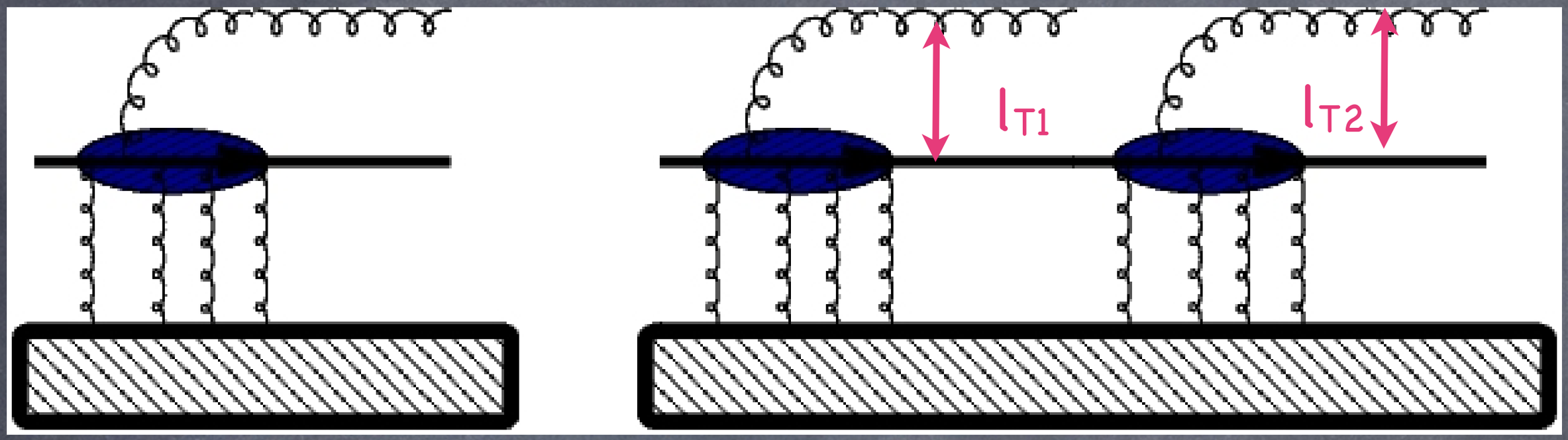

What is the relation between subsequent radiations ?

In the large Q^2 we can argue that there should be ordering of l_T.

$$if \;\; \hat{q}L \;\; < \;\; Q^2$$

$$\text{then} \qquad \frac{dQ^2}{Q^2}\left[1 + c_1 \frac{\hat{q}L}{Q^2}\right] \leq \frac{dQ^2}{Q^2}[1 + c_1]$$

A DGLAP formalism requires an upper scale
and a lower scale

Upper scale is p_T^2 , same as in vacuum
What is the lower scale?
what is the virtuality of a parton on exit ?

Natural choice
$Q^2_{min} = E/L$

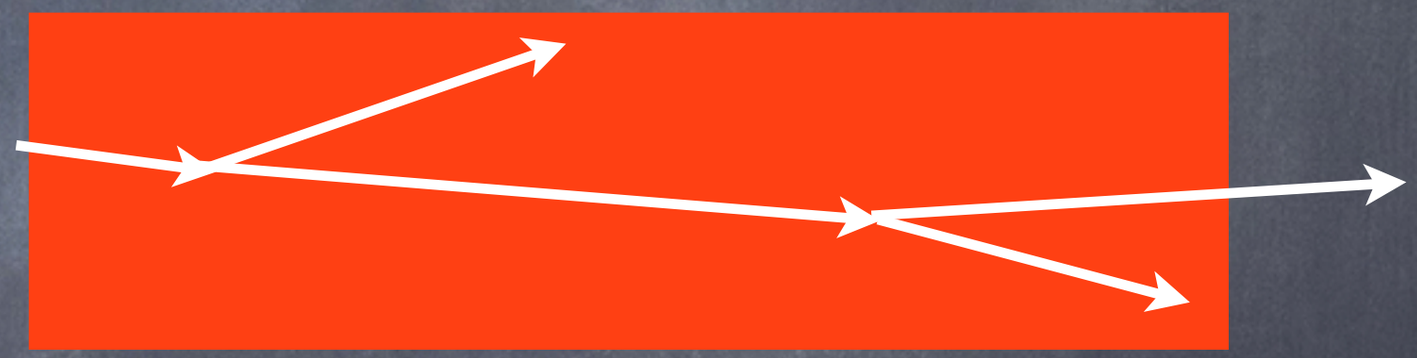

Realistically, this should be done for each path
In reality we average kernel over many paths
and calculate a mean distance based on the maximum length
that the jet can travel in the representative brick

Gaussian distribution/temperature dependence/fit parameter !!!

Multiple scattering off any distribution samples a Gaussian

$$\hat{q} \sim T^3, s, \epsilon^{3/4}$$

is basically a model

$$\frac{d\sigma}{dk_\perp^2}$$

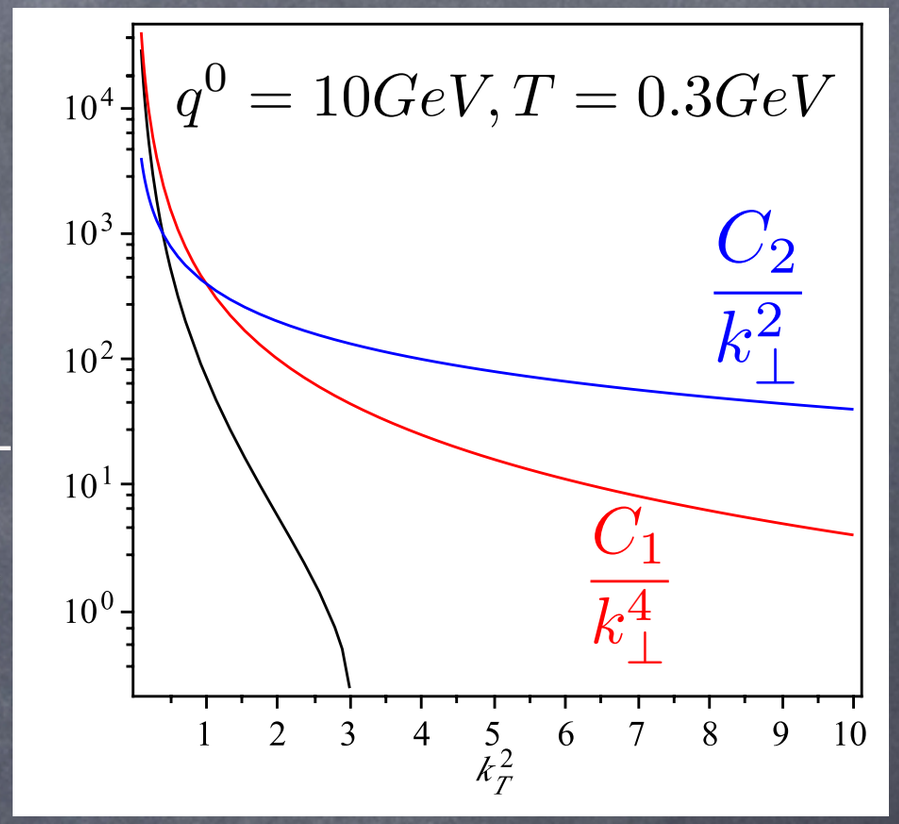

Ultimately you have to fit the normalization to 1 data point at one centrality, one value of p_T , one HIC energy

Bulk medium described by viscous fluid dynamics

Medium evolves hydro-dynamically as the jet moves through it

Fit the q for the initial T in the hydro in central coll.

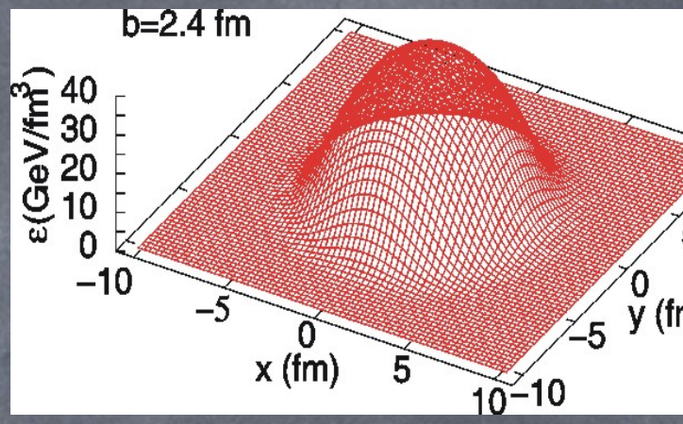

$$\hat{q}_0 \sim (10-20)\hat{q}_{Nucleus}$$

$$\hat{q}(\vec{r},t) = \hat{q}_0 \frac{s(\vec{r},t)}{s_0}$$

$$s_0 = s(T_0)$$

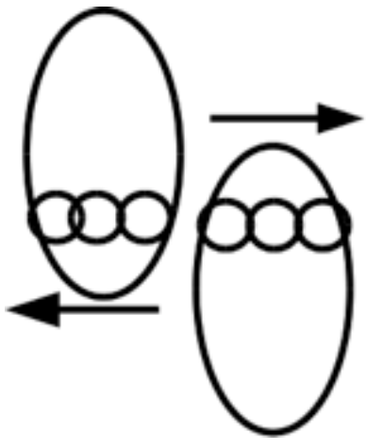

$$R_{AA} \sim \frac{\frac{dN_{AA}}{dp_T dy}}{N_{bin}\frac{dN_{pp}}{dp_T dy}}$$

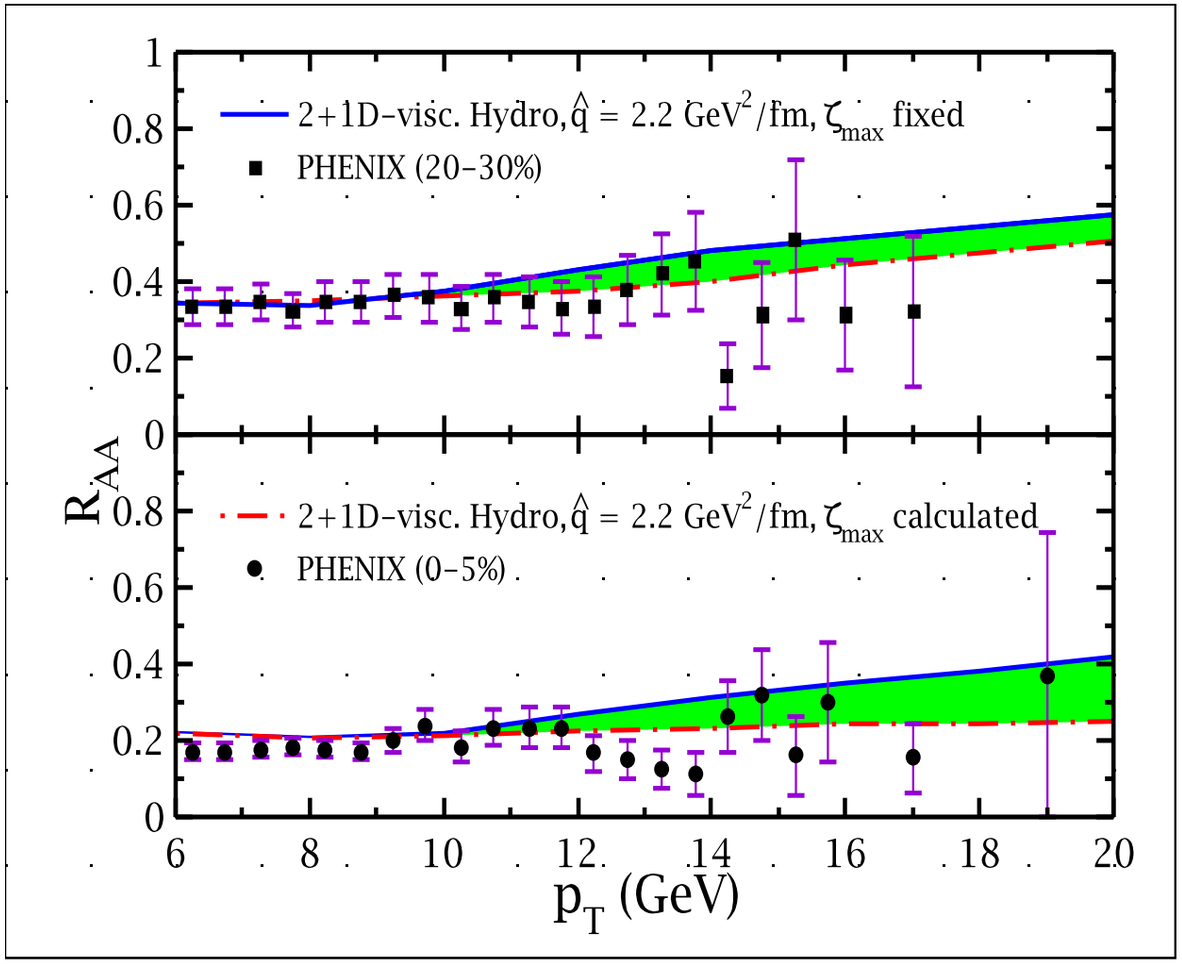

Note: no refitting between RHIC and LHC.

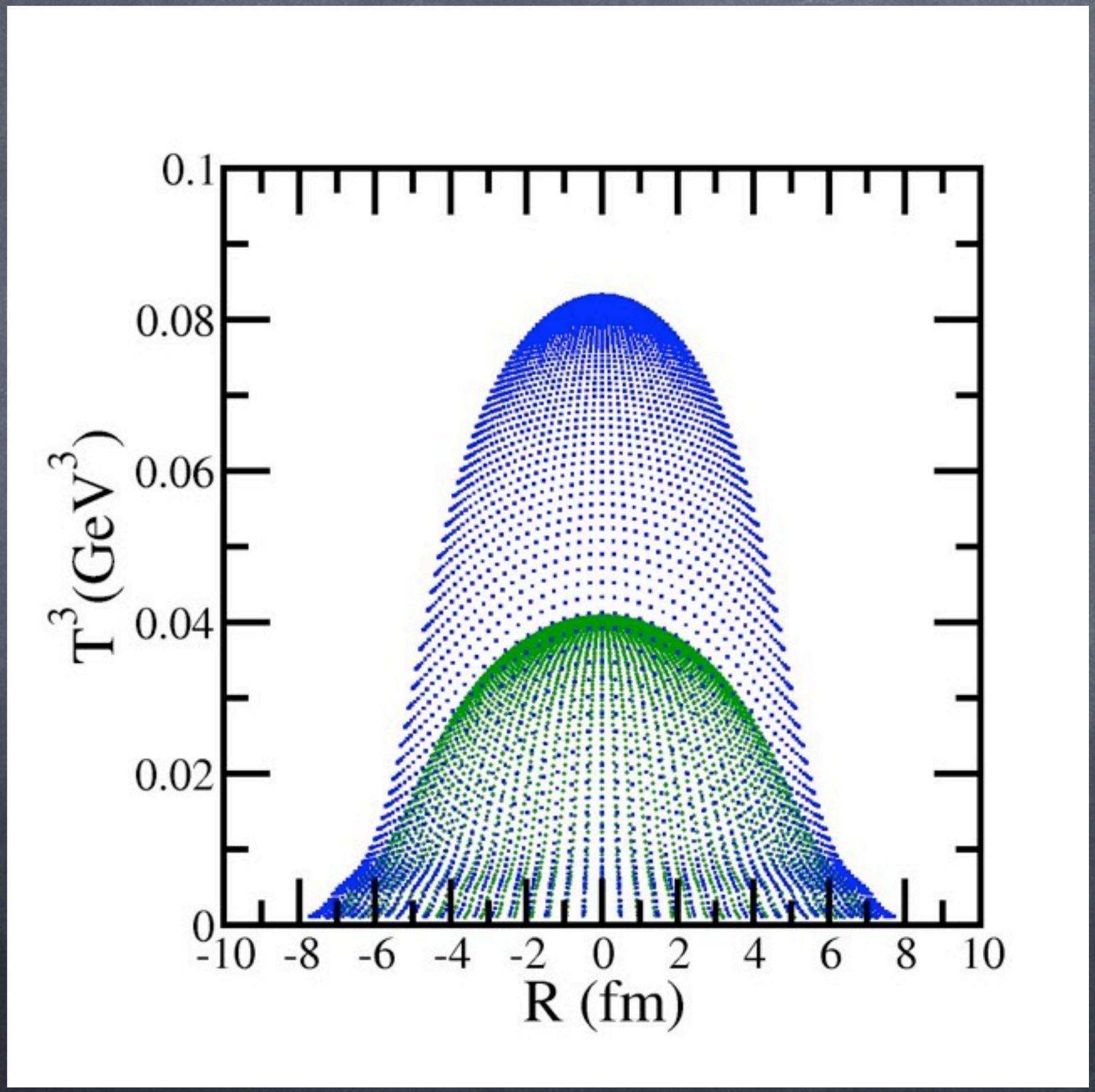

Versus reaction plane, versus energy

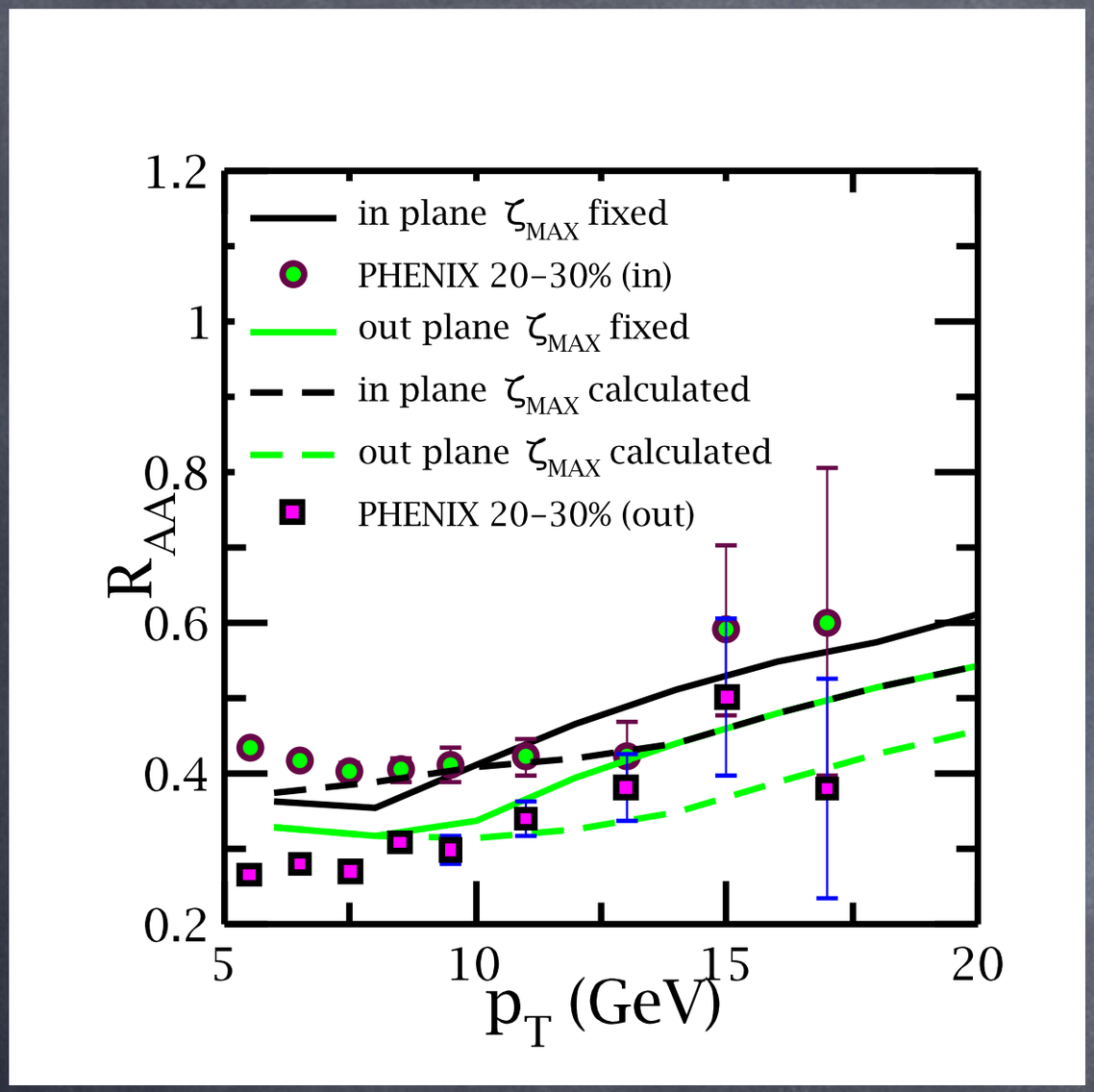

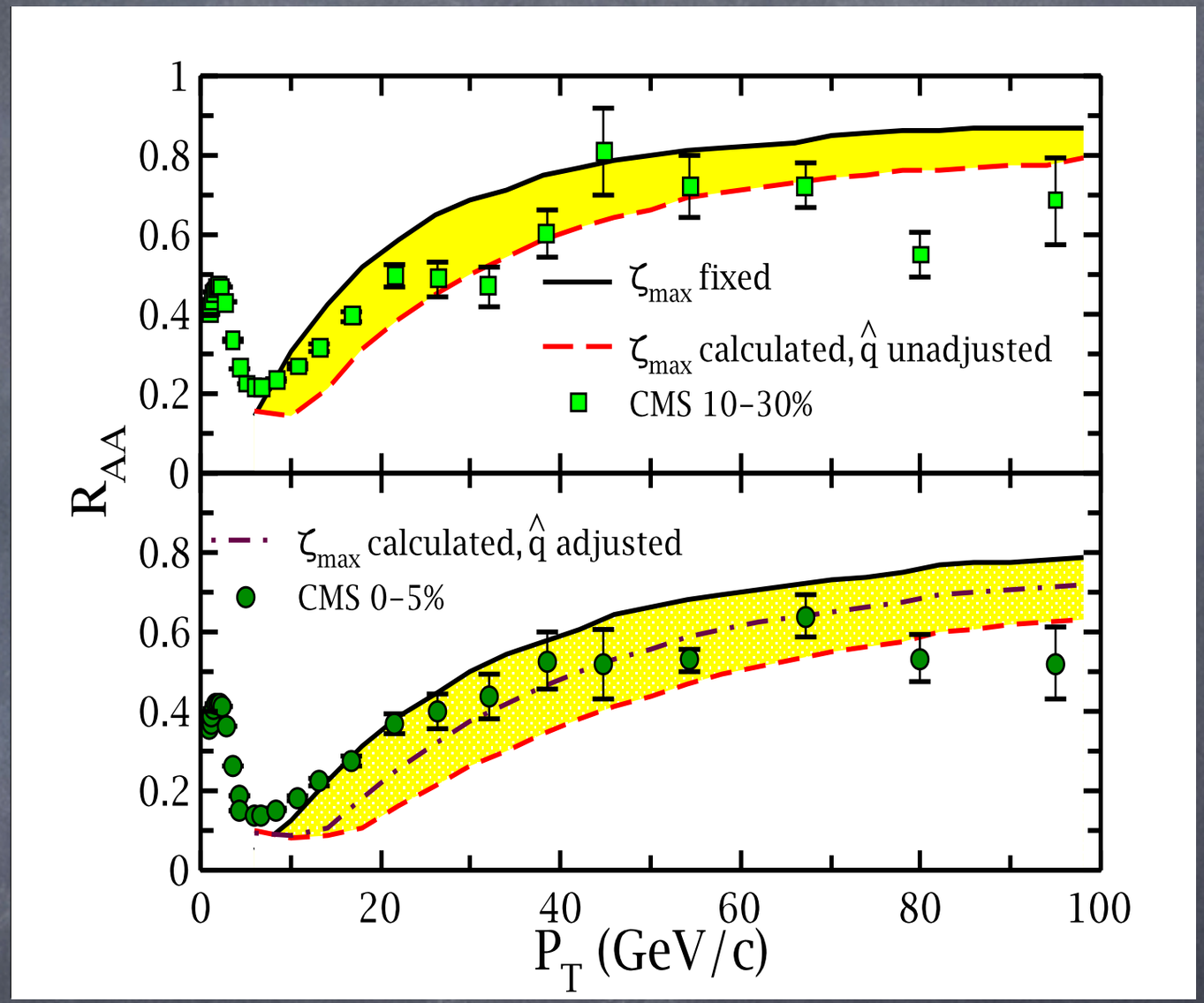

AM, C. Shen, PRL 109 202301 2012

Reasonable agreement with data

The band is from the uncertainty in Q_{min}

Predictions for p-Pb R_{AA} at mid-rapidity

No surprises here!

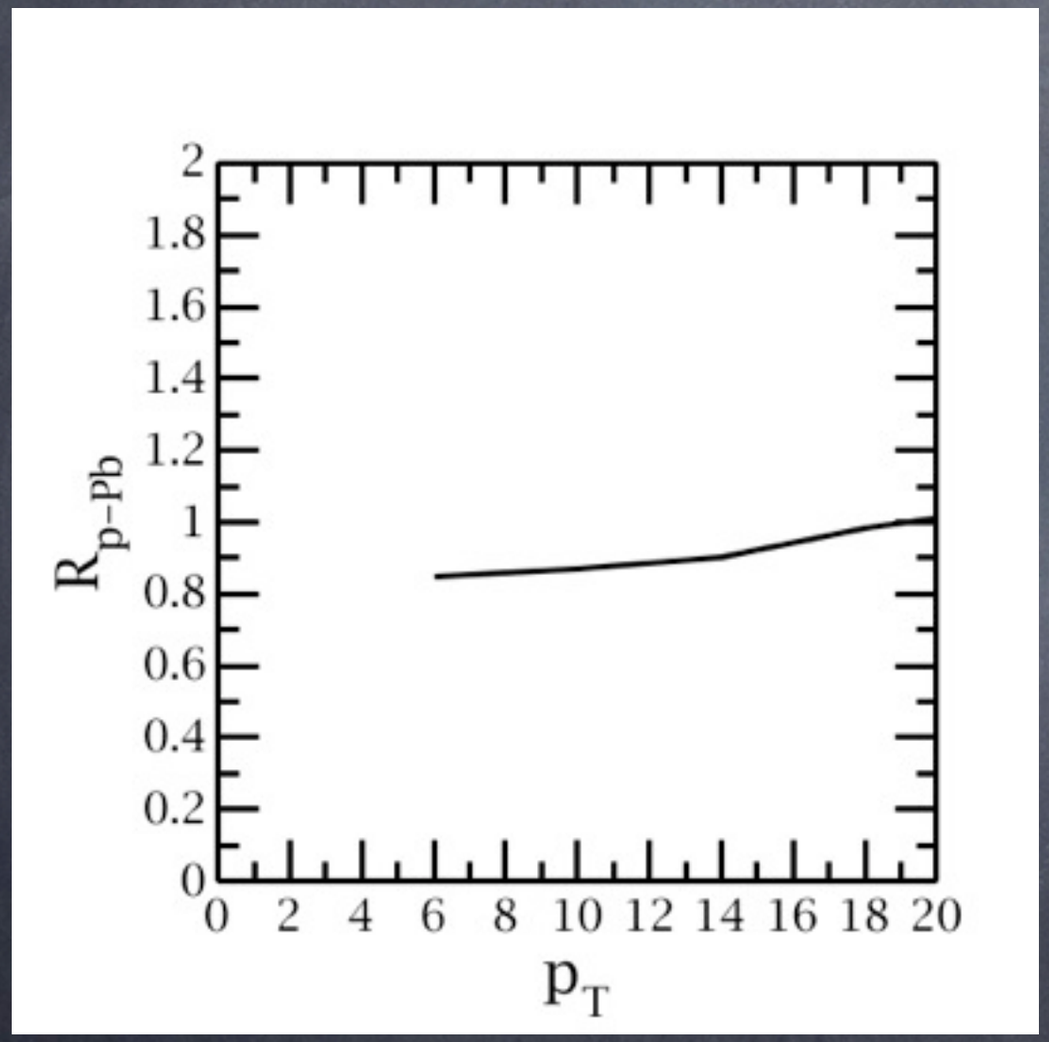

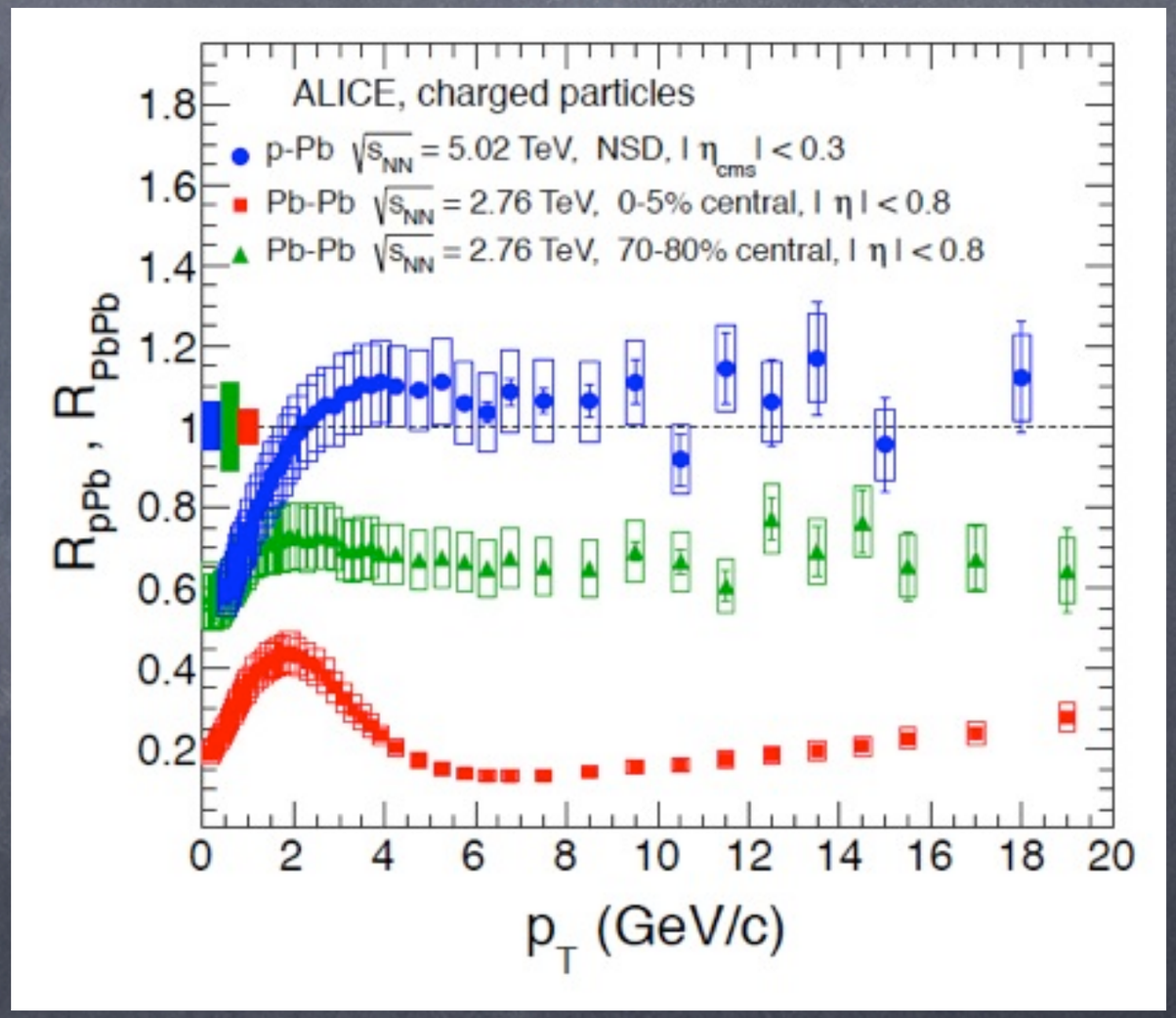

This means that our baseline is in control
We can do more detailed analysis

Predictions for p-Pb R_{AA} at mid-rapidity

No surprises here!

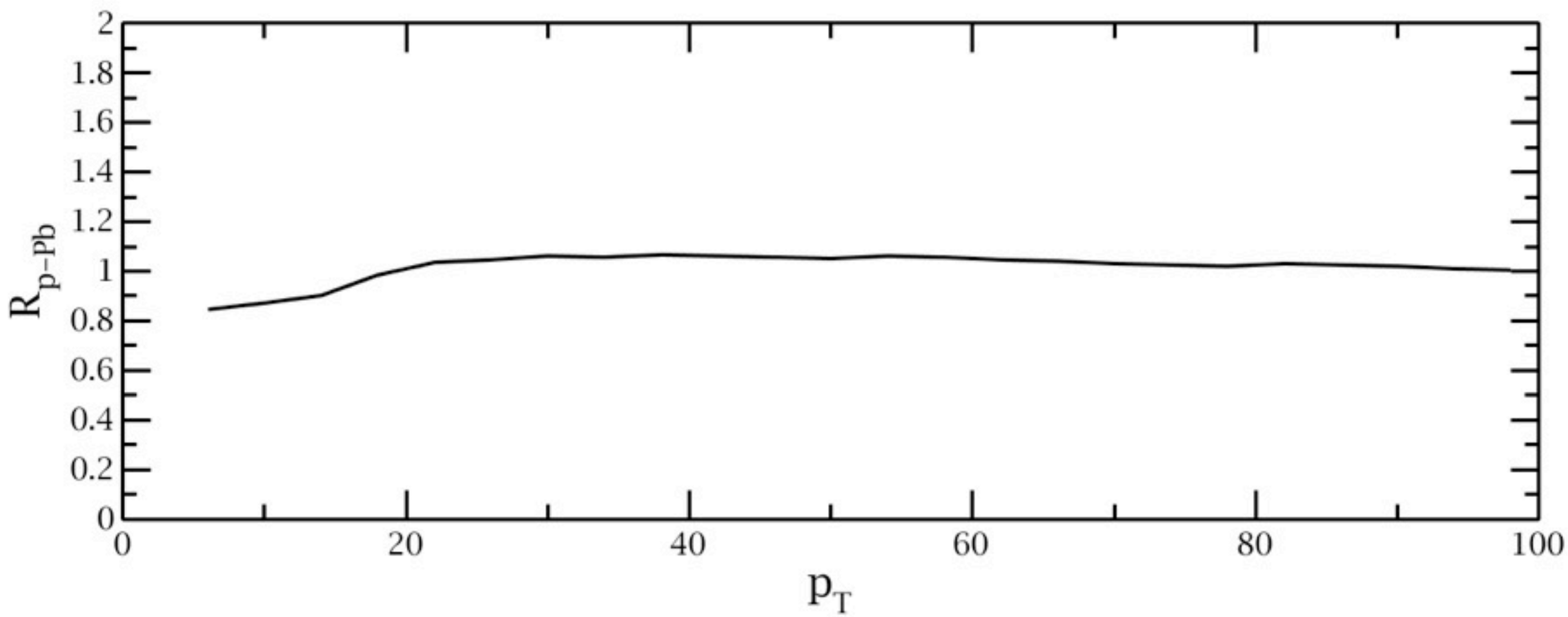

This means that our baseline is in control
We can do more detailed analysis

Four ways to go from here

Four ways to go from here

Move from a few particles to full jets... Need MC

Four ways to go from here

Move from a few particles to full jets... Need MC

Progress towards a first principles calculation... Lattice QCD

Four ways to go from here

Move from a few particles to full jets... Need MC

Progress towards a first principles calculation... Lattice QCD

Improve the error in current calculations... NLO

Four ways to go from here

Move from a few particles to full jets... Need MC

Progress towards a first principles calculation... Lattice QCD

Improve the error in current calculations... NLO

Study flavor/mass dependence... more transport coefficients

MATTER++ a HT based MC event generator

Main problem: Introducing distance into a DGLAP shower

No space-time in the usual Monte-Carlo showers

$$\bar{z} = \frac{z + z'}{2}$$

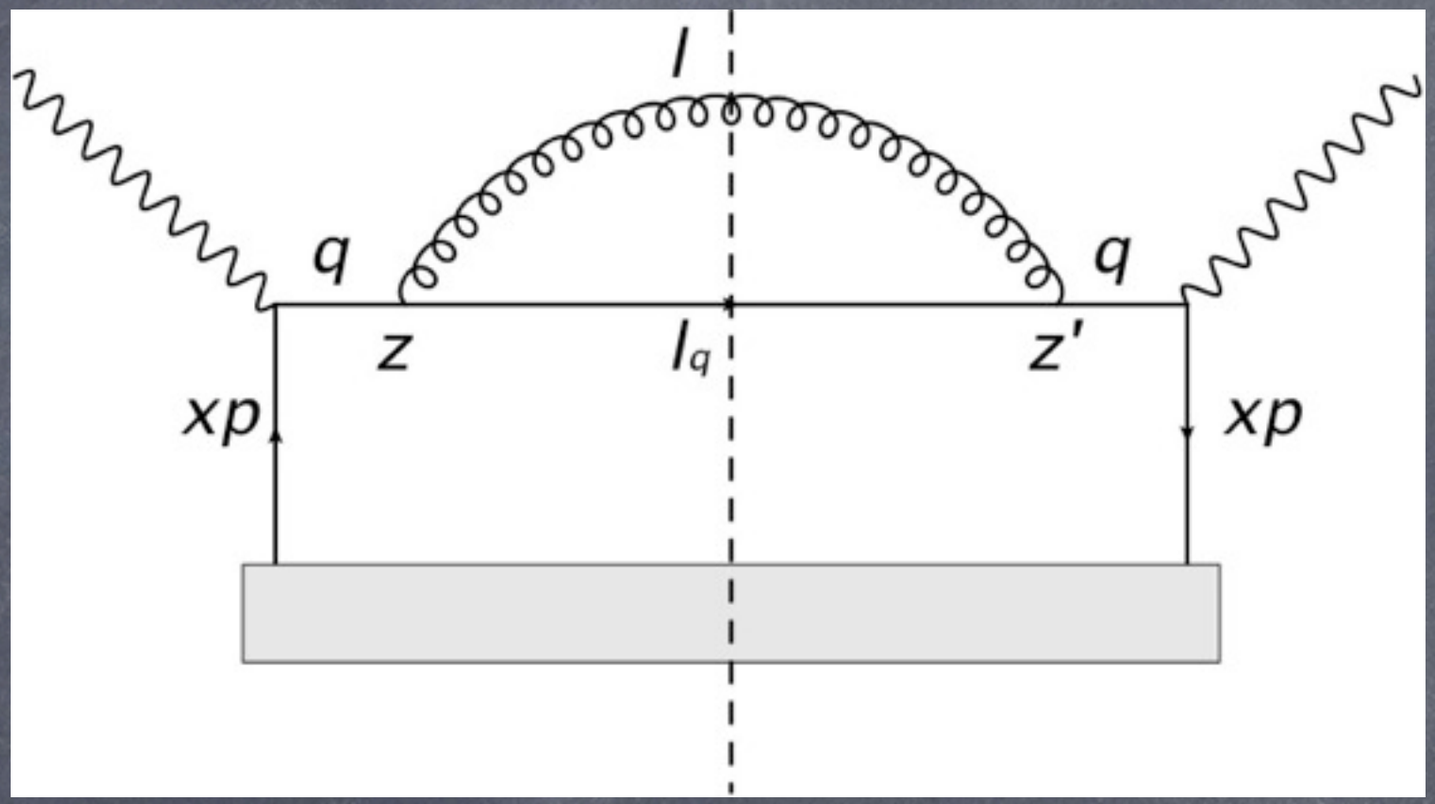

$$\delta z = z - z'$$

what is the role of z and z' ?

$$\int_0^\infty d^4\bar{z} \exp\left[i(\delta q)\bar{z}\right]$$

$$\int d^4\delta z \exp\left[i\delta z(l + l_q - q)\right]$$

δq is the uncertainty in q,

How much uncertainty can there be ?

To be sensible: $\delta q \ll q$

we assume a Gaussian distribution around q^+

And try different functional forms of the width

We set the form by insisting $\langle \tau \rangle = 2q^-/(Q^2)$

to obtain the z^- distribution only need to assume a δq^+ distribution

$$\rho(\delta q^+) = \frac{e^{-\frac{(\delta q^+)^2}{2[2(q^+)^2/\pi]}}}{\sqrt{2\pi[2(q^+)^2/\pi]}}$$

A normalized Gaussian with a variance $2q^+/\pi$

FT gives the following distribution in distance

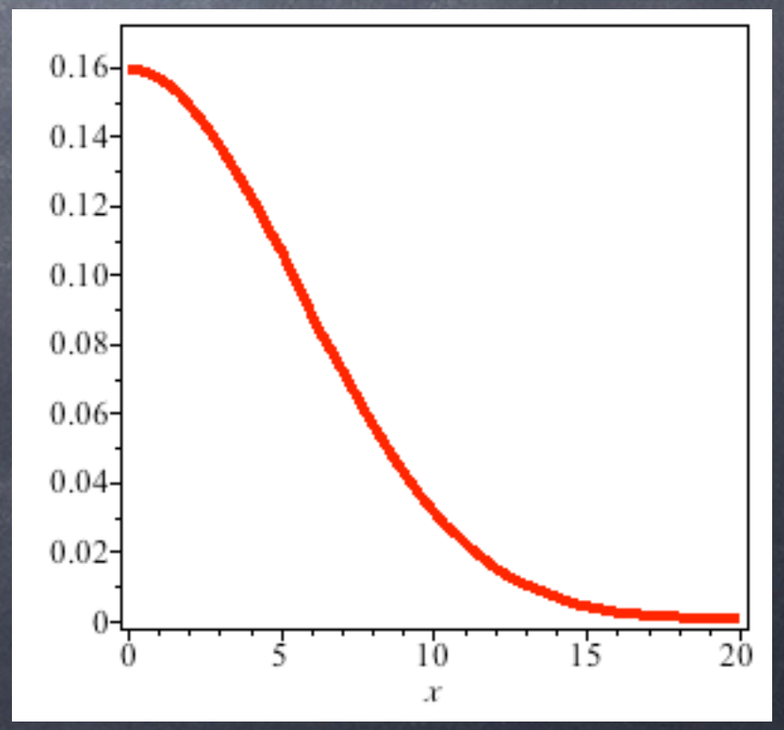

Consider a jet moving through a QGP Brick

We now construct a Sudakov with the constraint

$$\frac{Q_0^2}{Q^2} < z < 1 - \frac{Q_0^2}{Q^2}$$

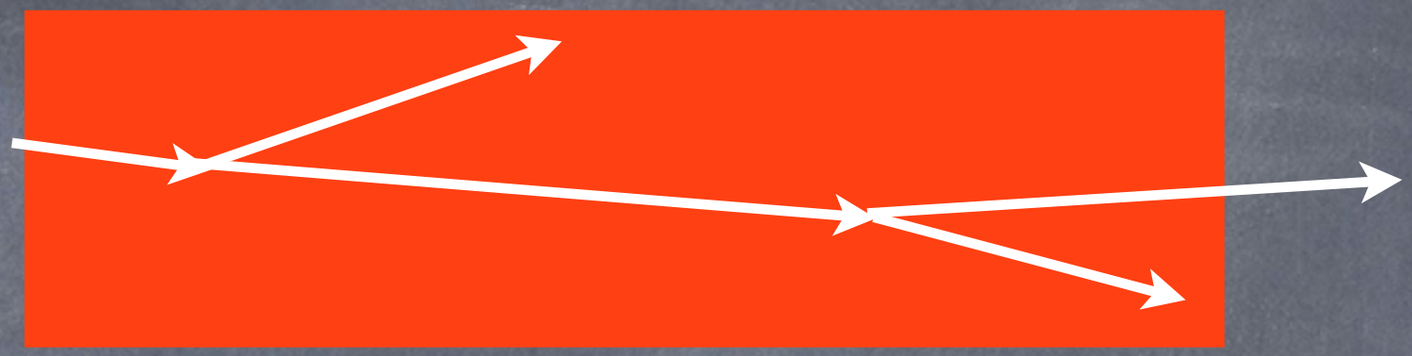

Have a distribution of locations of splittings

length dependent transverse broadening

Partons whose virtuality drops below 1 GeV are removed form cascade

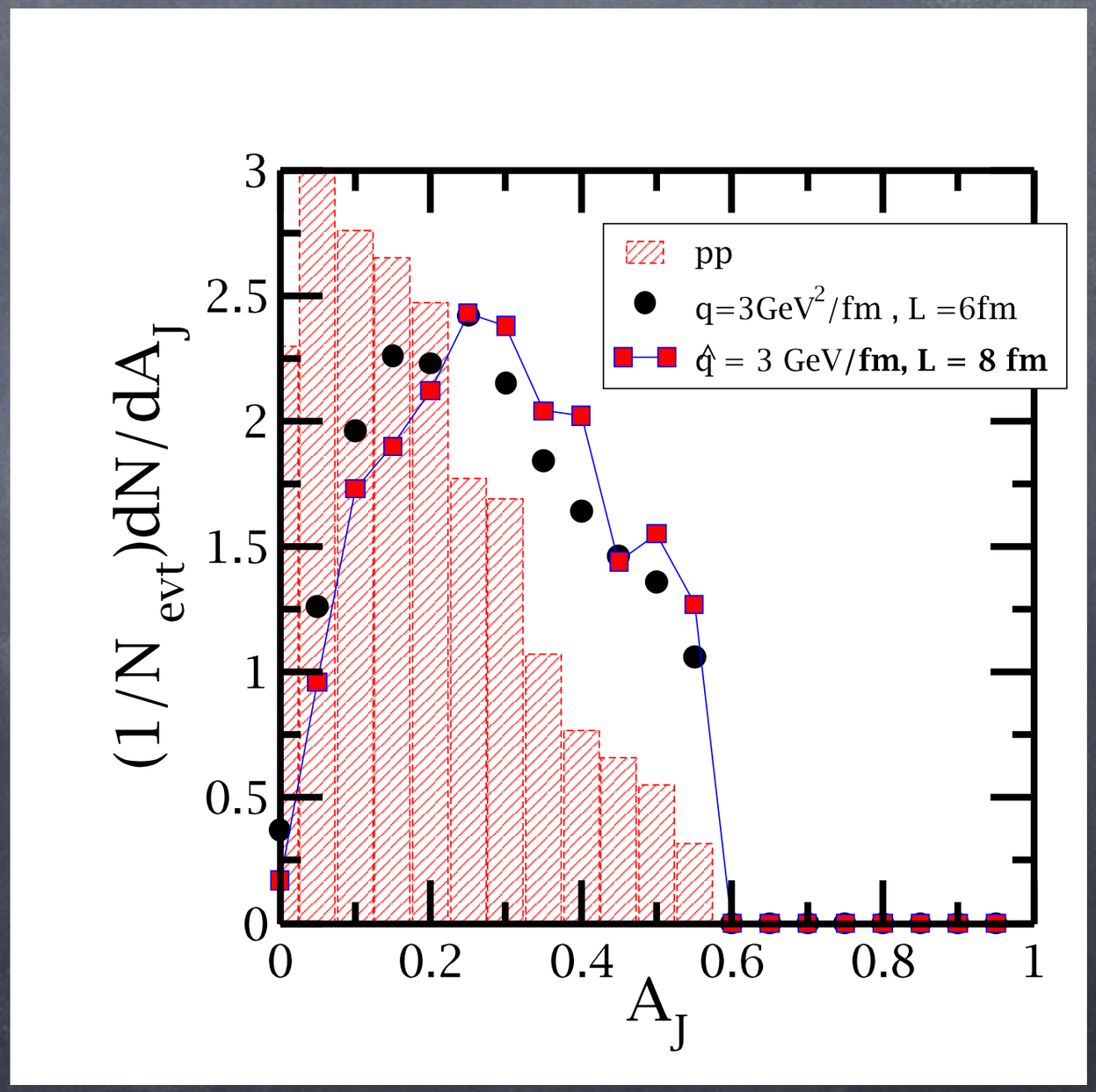

Getting around to the CMS/ATLAS Fragmentation function

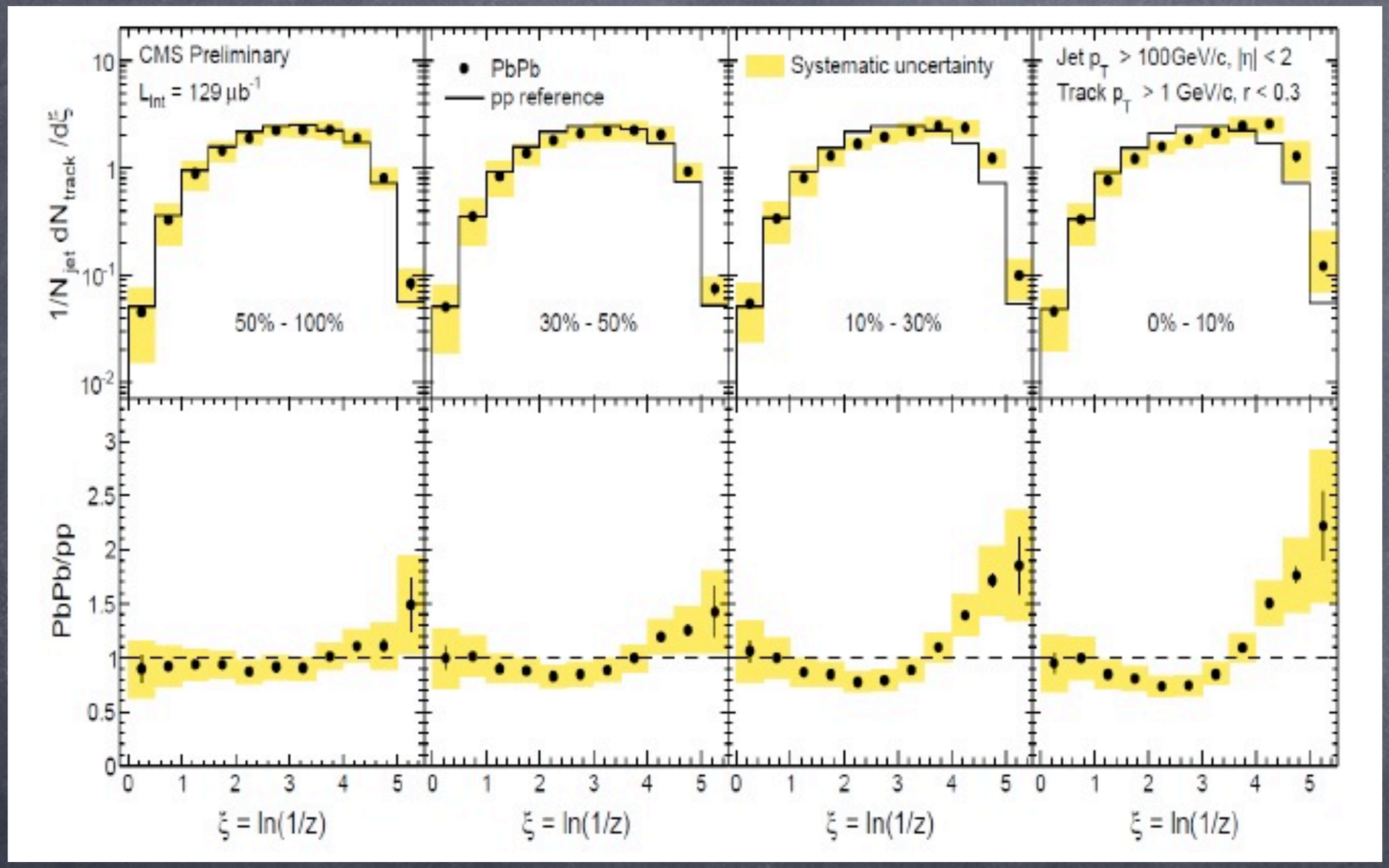

AM, arXiv:1301.5323 [nucl-th]

Brick MC, need E-by-E hydro and realistic hadronization

Getting around to the CMS/ATLAS Fragmentation function

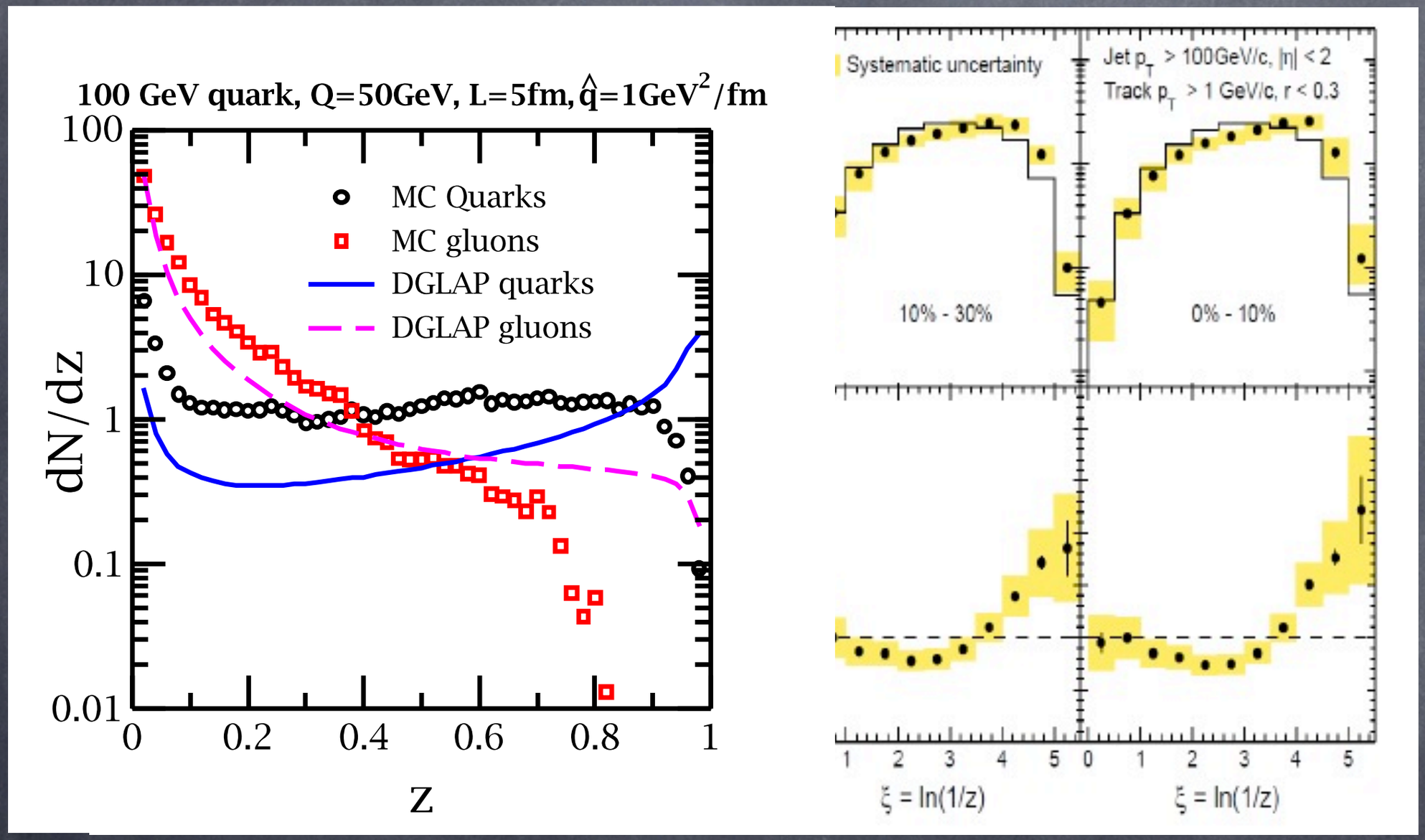

AM, arXiv:1301.5323 [nucl-th]

Brick MC, need E-by-E hydro and realistic hadronization

Getting around to the CMS/ATLAS Fragmentation function

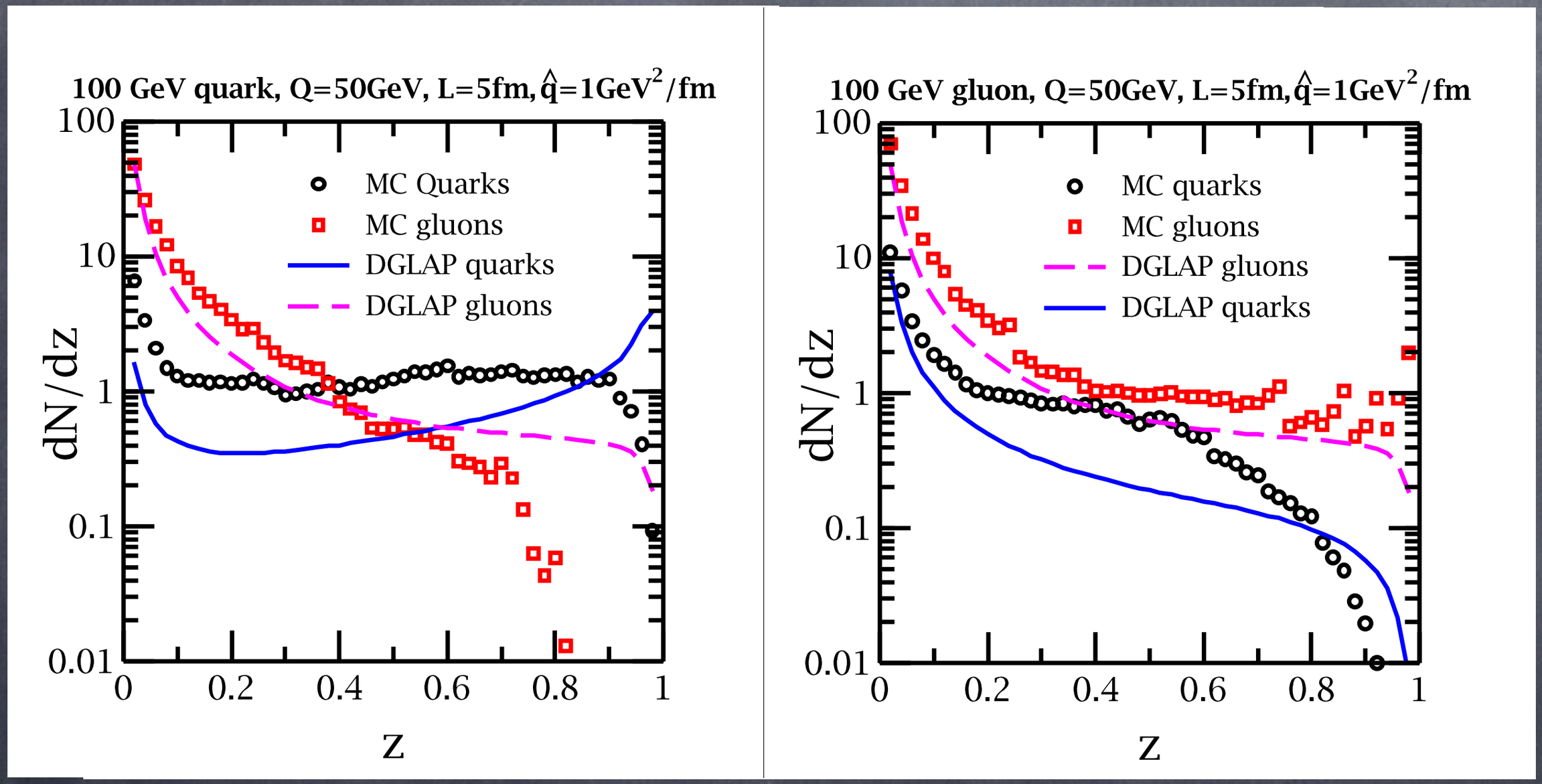

AM, arXiv:1301.5323 [nucl-th]

Brick MC, need E-by-E hydro and realistic hadronization

Getting around to the CMS/ATLAS Fragmentation function

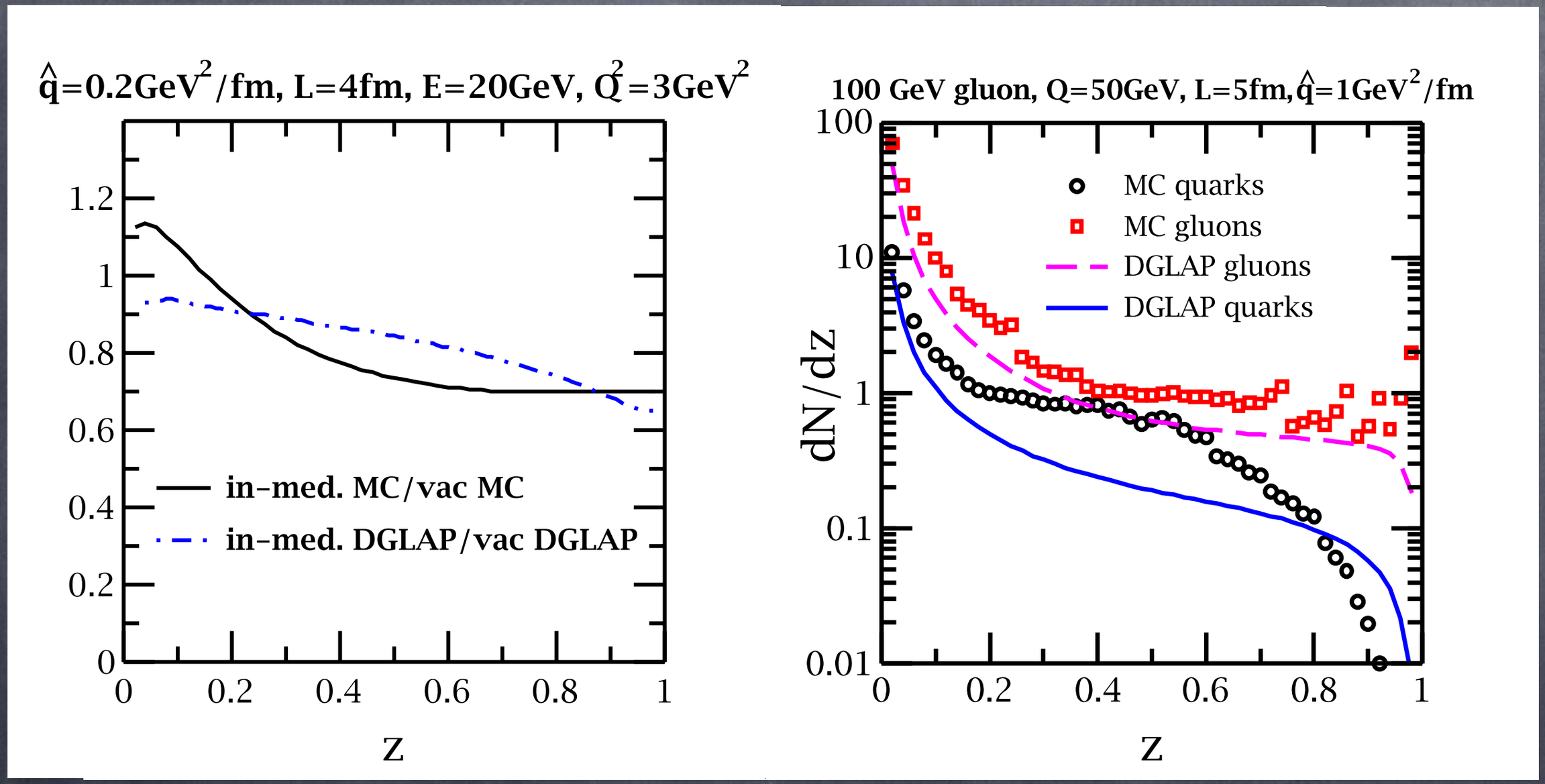

AM, arXiv:1301.5323 [nucl-th]

Brick MC, need E-by-E hydro and realistic hadronization

Getting around to the CMS/ATLAS Fragmentation function

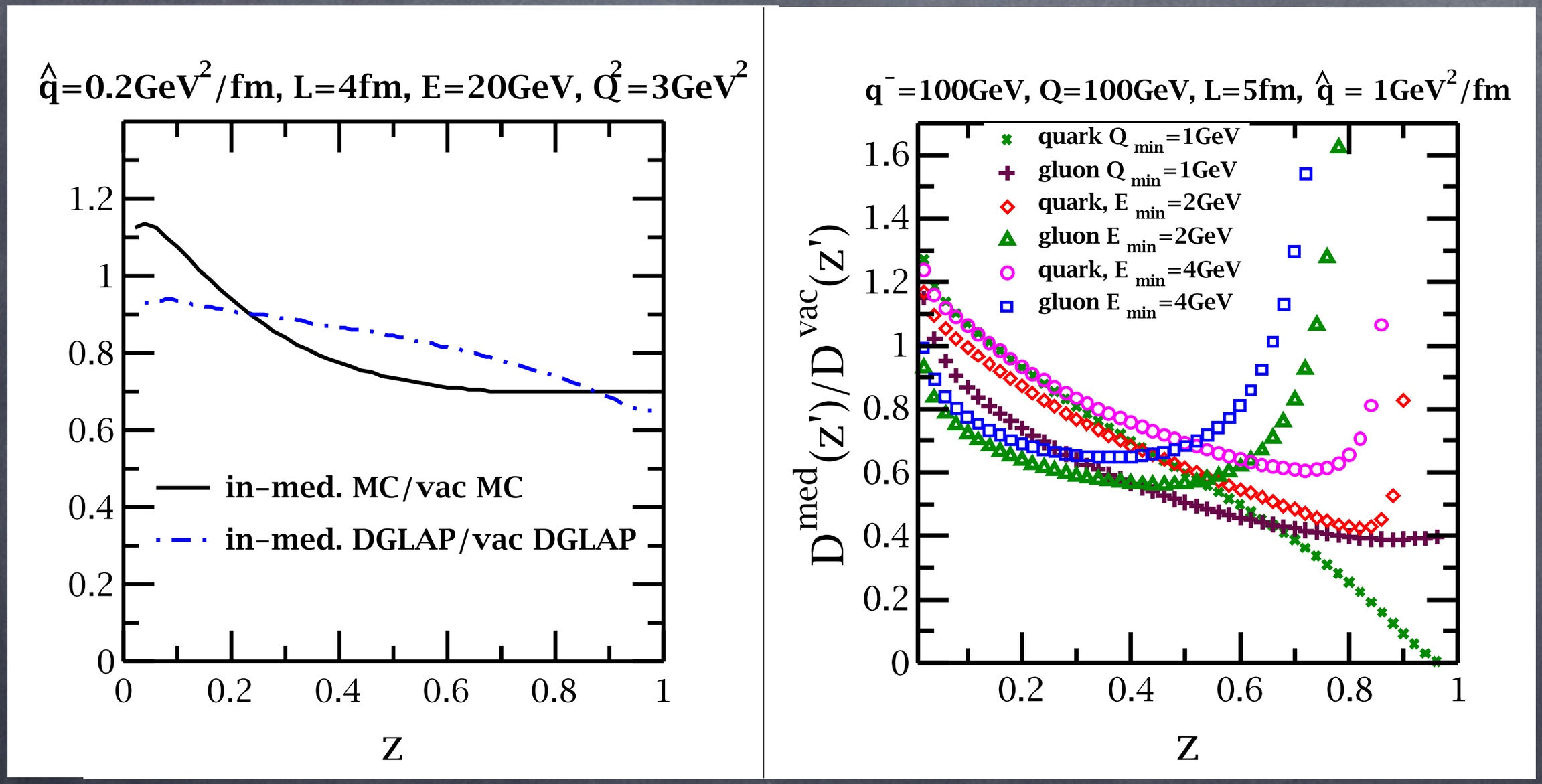

AM, arXiv:1301.5323 [nucl-th]

Brick MC, need E-by-E hydro and realistic hadronization

Energy in and out of cone!

answering this question is not trivial!

From the surviving hard partons, very little energy ~ 5% is outside R=1 cone

A lot of the energy is lost as particles become less energetic or less virtual than 1 GeV, thus strongly interacting with the medium

So far cannot estimate in MC,
no Sudakov, which readjusts formation time
by removing deposited energy from shower

No single gluon emission with coherent drag calculation

G.Y. Qin, AM to appear

However, can be analytically estimated

At lower momentum need some no-pert. input

A single parton deposits energy and transverse momentum in medium. This just q and e

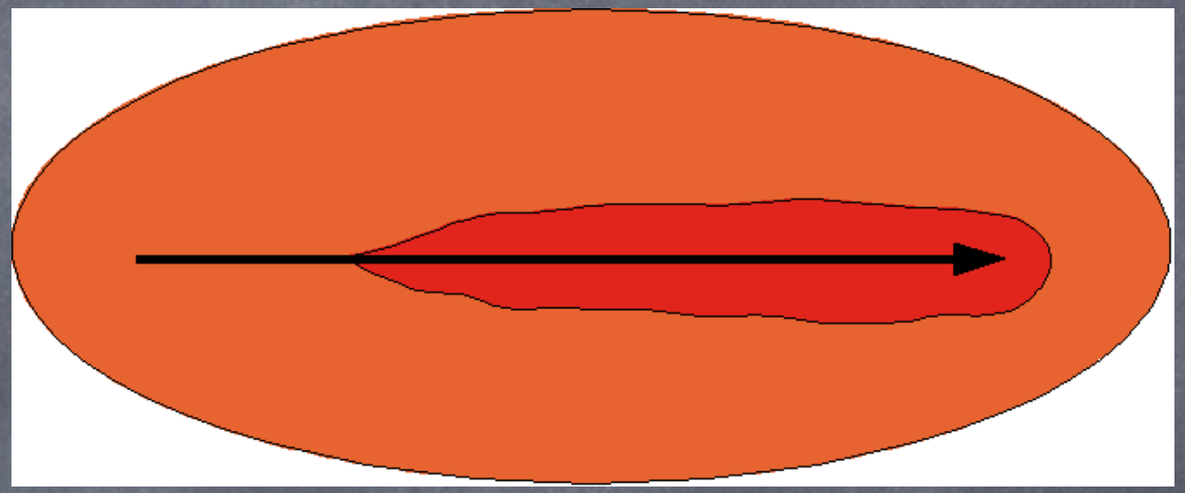

multiple radiation increases the sources of mom. dep. We know how much radiation as we already calculated it for energy loss

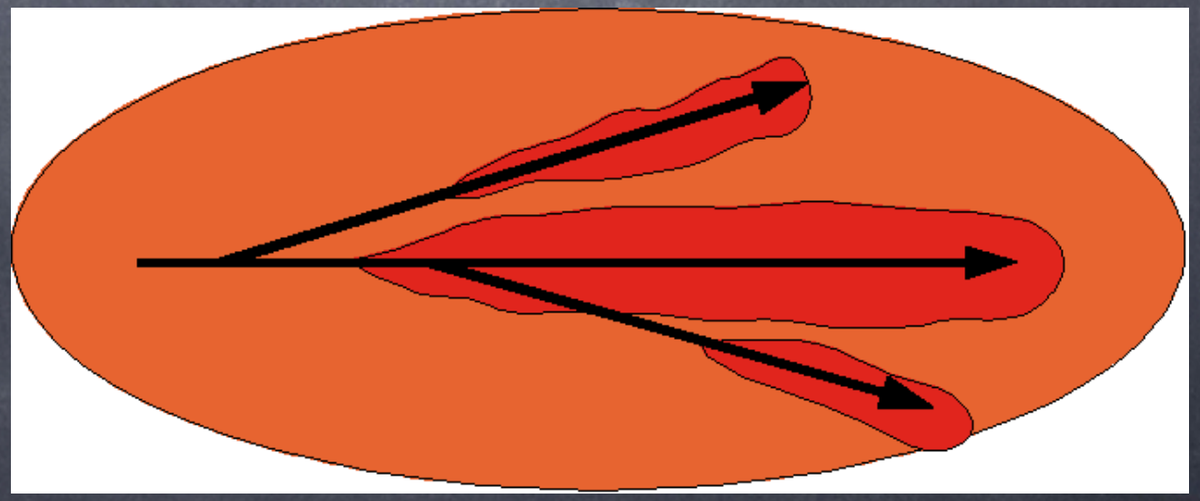

Radiative loss enhances the deposited energy

Do a DGLAP with $\Delta E = \hat{e}\, L$ as input

partons with E= 4T and Q<1GeV are added to medium

Energy

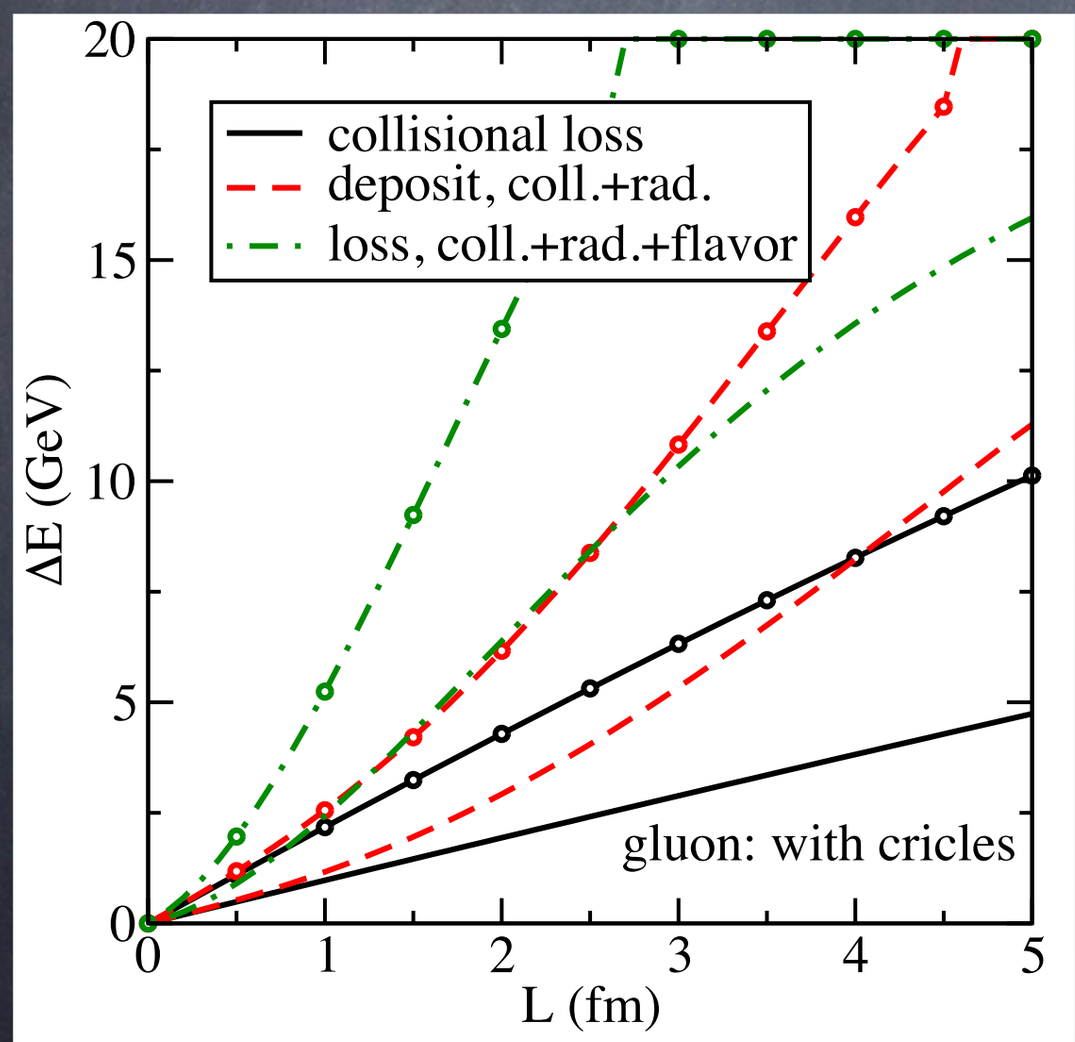

Deposited energy will thermalize and spread out

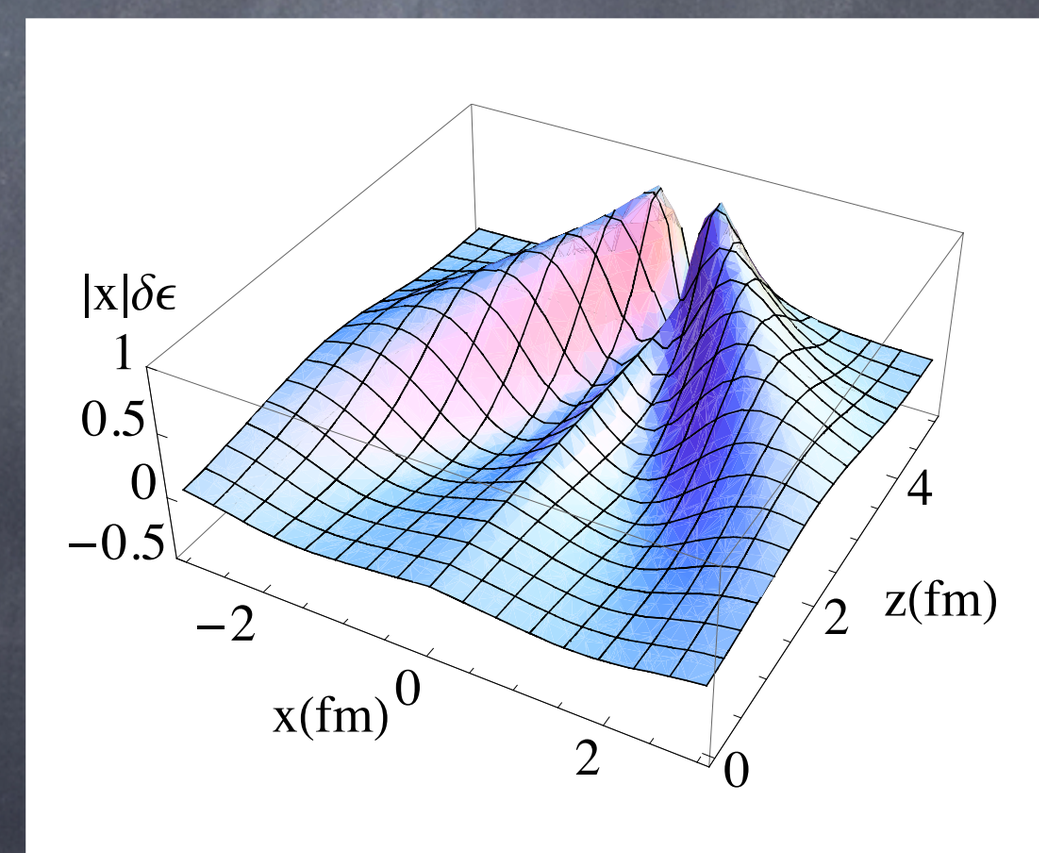

G.Y. Qin, AM, H. Song, U. Heinz, PRL **103 (2009) 152303**

A simple picture

Assign E deposited before L/2 as early deposition.

L=4fm (RHIC) and L= 6fm (LHC)

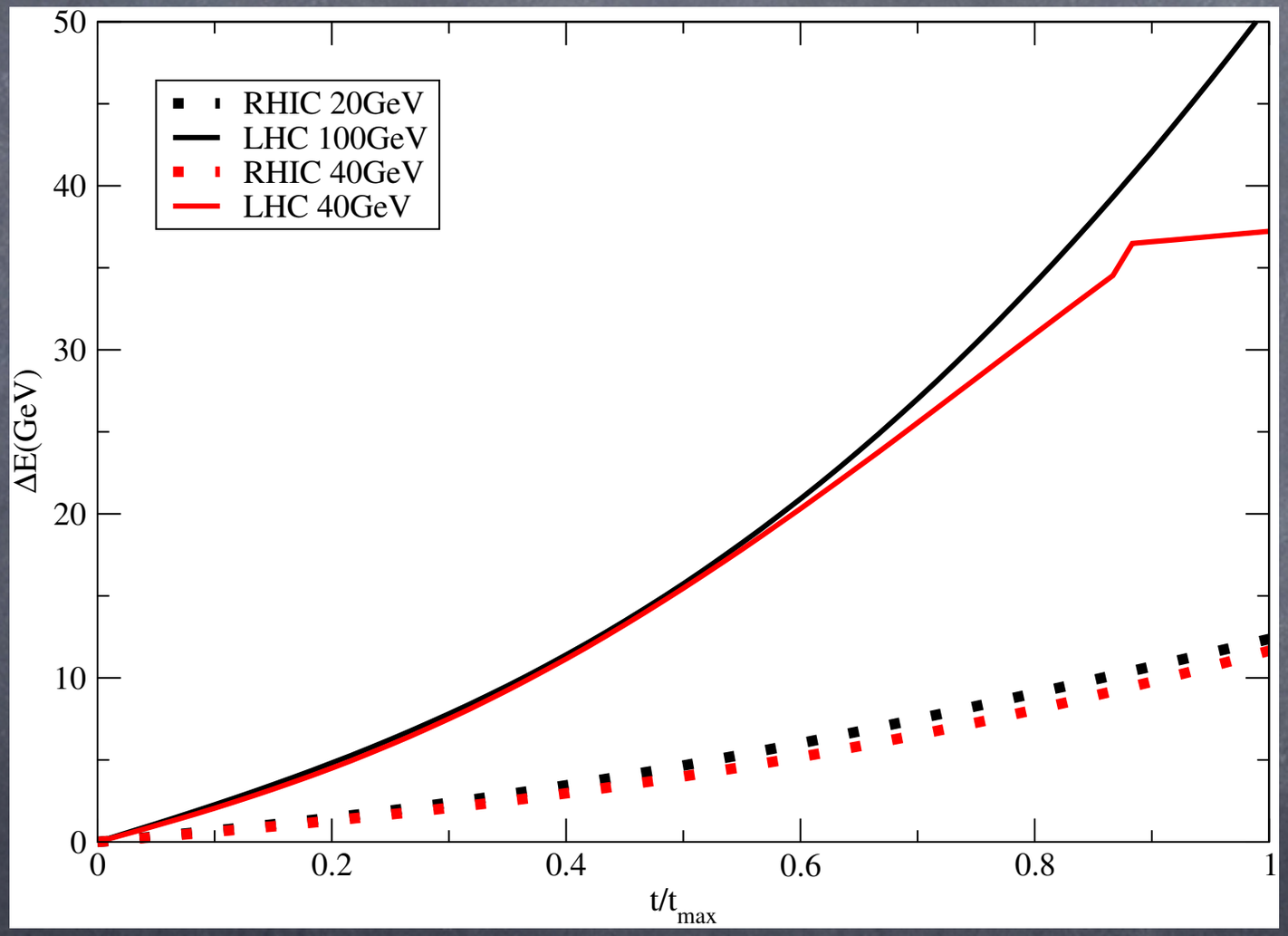

G.Y. Qin, AM, J. Putschke

A complete understanding requires a MC and a new soft-hard transport coefficient

A simple picture

Assign E deposited before L/2 as early deposition.

L=4fm (RHIC) and L= 6fm (LHC)

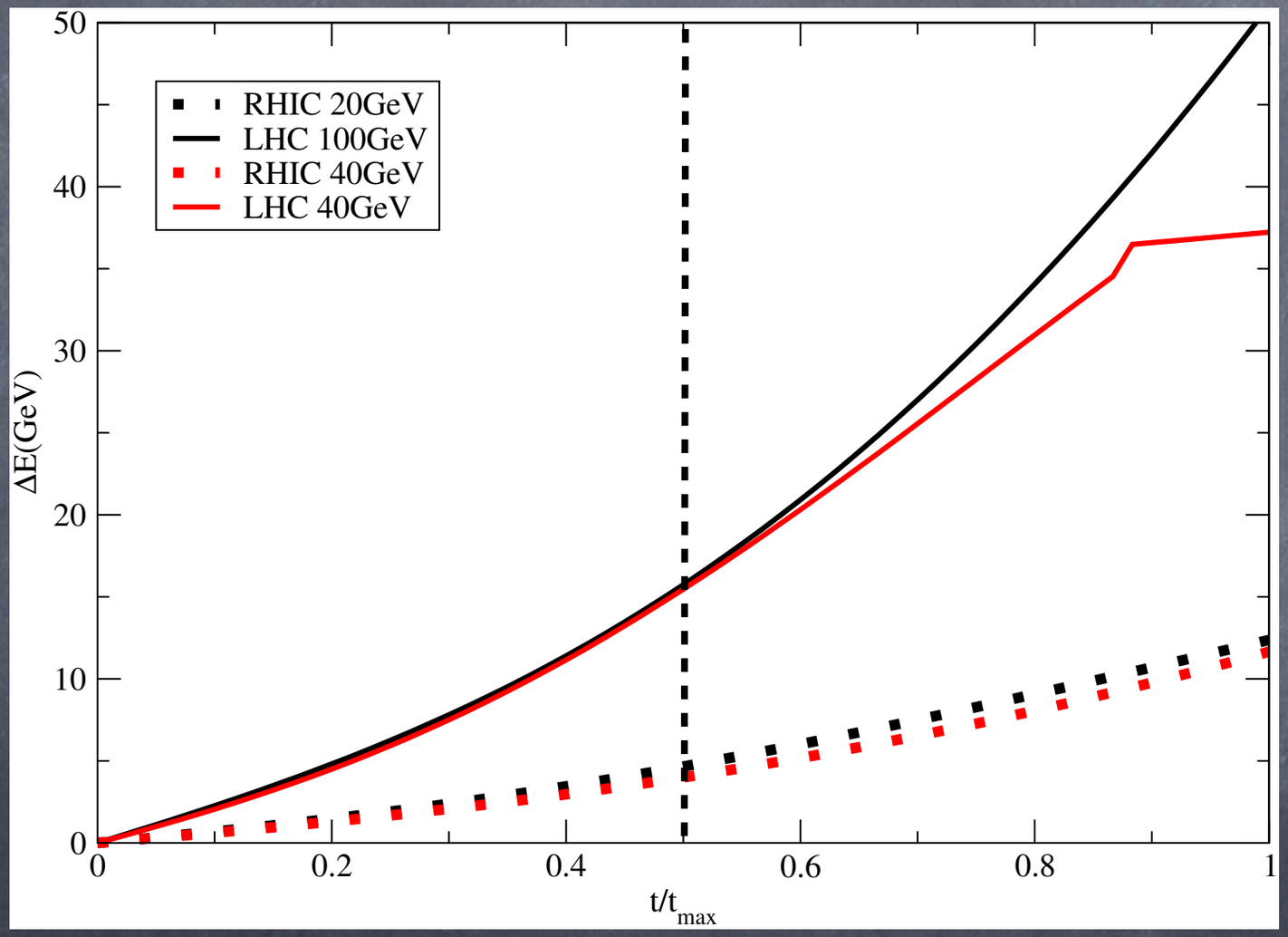

G.Y. Qin, AM, J. Putschke

A complete understanding requires a MC and a new soft-hard transport coefficient

Even with the best MC energy loss routine on the best E-by-E hydro

The exchange momentum distribution of $\hat{q}$,$\hat{e}$ and their normalization are assumptions!

A first principles method to calculate $\hat{q}$

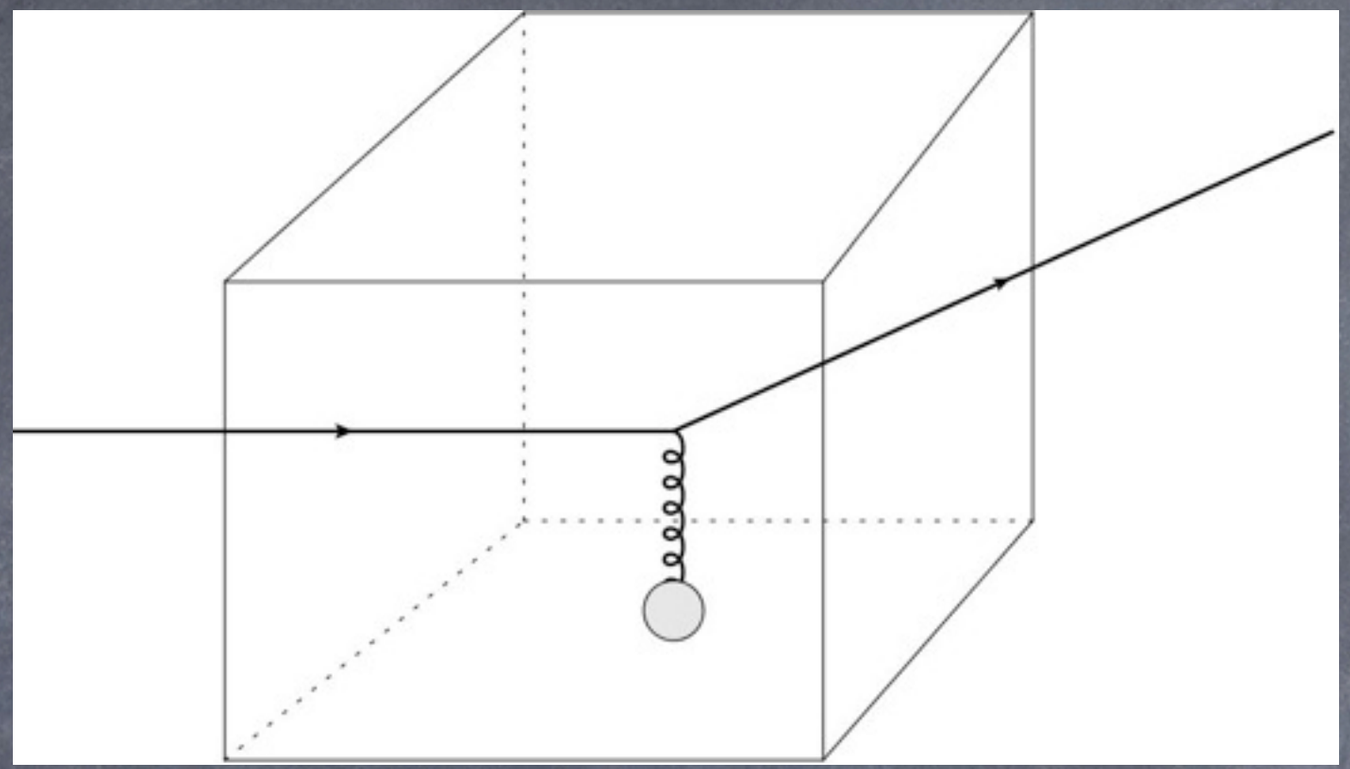

$$
\begin{aligned}
W(k) &= \frac{g^2}{2N_c}\langle q^-; M| \int d^4x d^4y \bar{\psi}(y) \not{A}(y)\psi(y) \\
&\times \quad |q^- + k_\perp; X\rangle\langle q^- + k_\perp; X| \\
&\times \quad \bar{\psi}(x) \not{A}(x)\psi(x)|q^-; M\rangle
\end{aligned}
$$

in terms of W, we get

$$\hat{q} = \sum_k k_\perp^2 \frac{W(k)}{t},$$

Final state is ``on-shell''

$$\delta[(q+k)^2] \simeq \frac{1}{2q^-}\delta\left(k^+ - \frac{k_\perp^2}{2q^-}\right).$$

Also we are calculating in a finite temperature heat bath

$$\hat{q} = \frac{4\pi^2\alpha_s}{N_c}\int \frac{dy^- d^2y_\perp}{(2\pi)^3} d^2k_\perp e^{-i\frac{k_\perp^2}{2q^-}\cdot y^- + i\vec{k}_\perp\cdot\vec{y_\perp}}$$

$$\langle n|\frac{e^{-\beta E_n}}{Z}F^{+,}{}_\perp(y^-)F_\perp^+(0)|n\rangle$$

physical $\hat{q}(q^-, q^+)$ where $q^+ \sim \lambda^2 Q$

Consider a more general object

$$\hat{Q} = \frac{4\pi^2\alpha_s}{N_c}\int \frac{d^4y d^4k}{(2\pi)^4} e^{ik\cdot y} \frac{2(q^-)^2}{\sqrt{2}q^-} \frac{\langle M|F^{+\perp}(0)F^+_{\perp,}(y)|M\rangle}{(q+k)^2+i\epsilon}.$$

Consider q^- large (~Q) and fixed

Consider q^+ to be a variable

$\frac{d^2\hat{Q}}{dk_\perp^2}$ has a pole at $q^+ = \frac{k_\perp^2}{2q^-}$

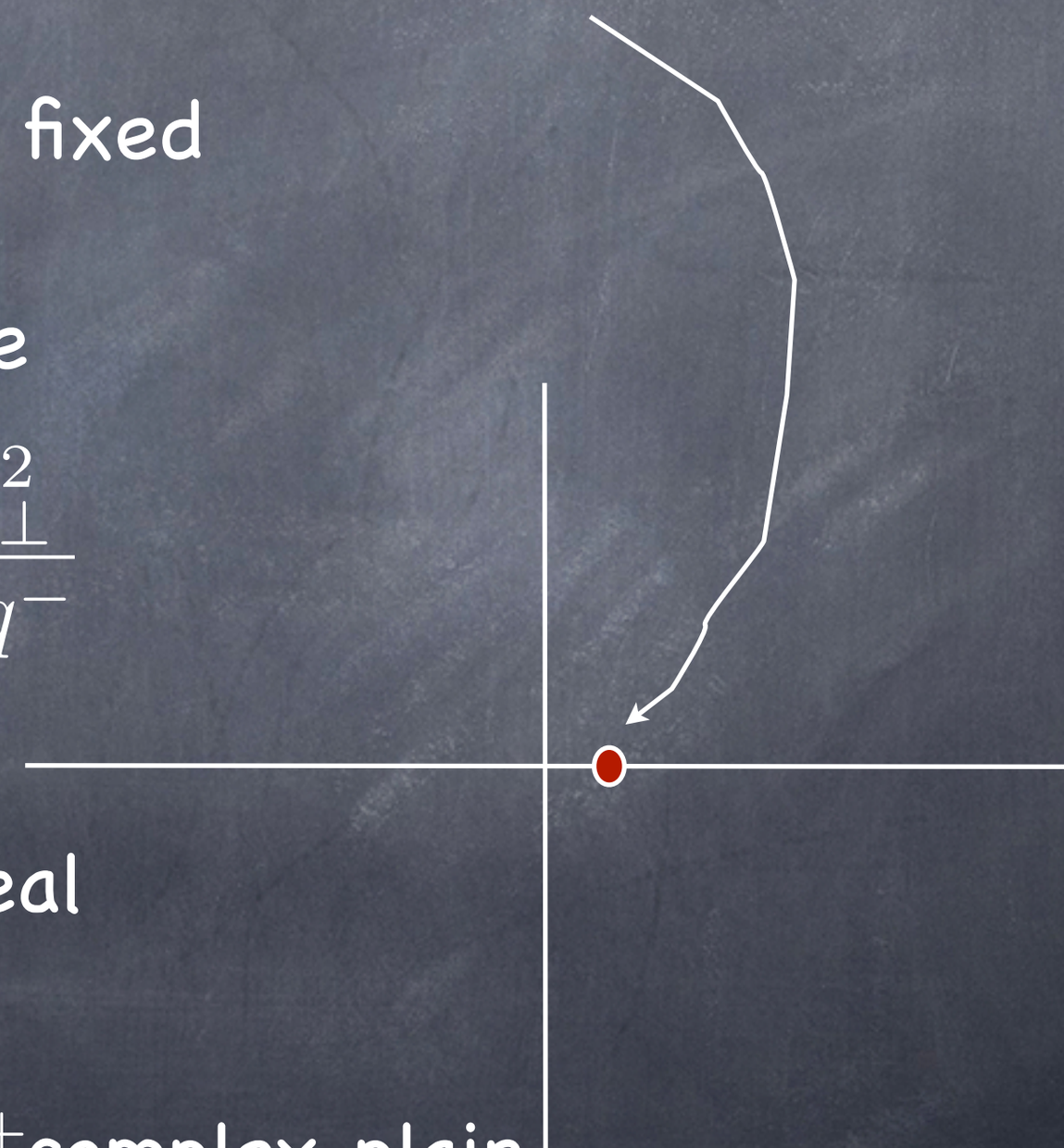

$\hat{Q}$ has a branch cut on the real axis at $q^+ \sim \lambda^2 Q$

$\hat{q} = Im(\hat{Q})$

q^+complex plain

Consider a more general object

$$\hat{Q} = \frac{4\pi^2\alpha_s}{N_c}\int \frac{d^4y d^4k}{(2\pi)^4} e^{ik\cdot y} \frac{2(q^-)^2}{\sqrt{2}q^-} \frac{\langle M|F^{+\perp}(0)F^+_{\perp,}(y)|M\rangle}{(q+k)^2+i\epsilon}.$$

Consider q^- large (~Q) and fixed

Consider q^+ to be a variable

$\frac{d^2\hat{Q}}{dk_\perp^2}$ has a pole at $q^+ = \frac{k_\perp^2}{2q^-}$

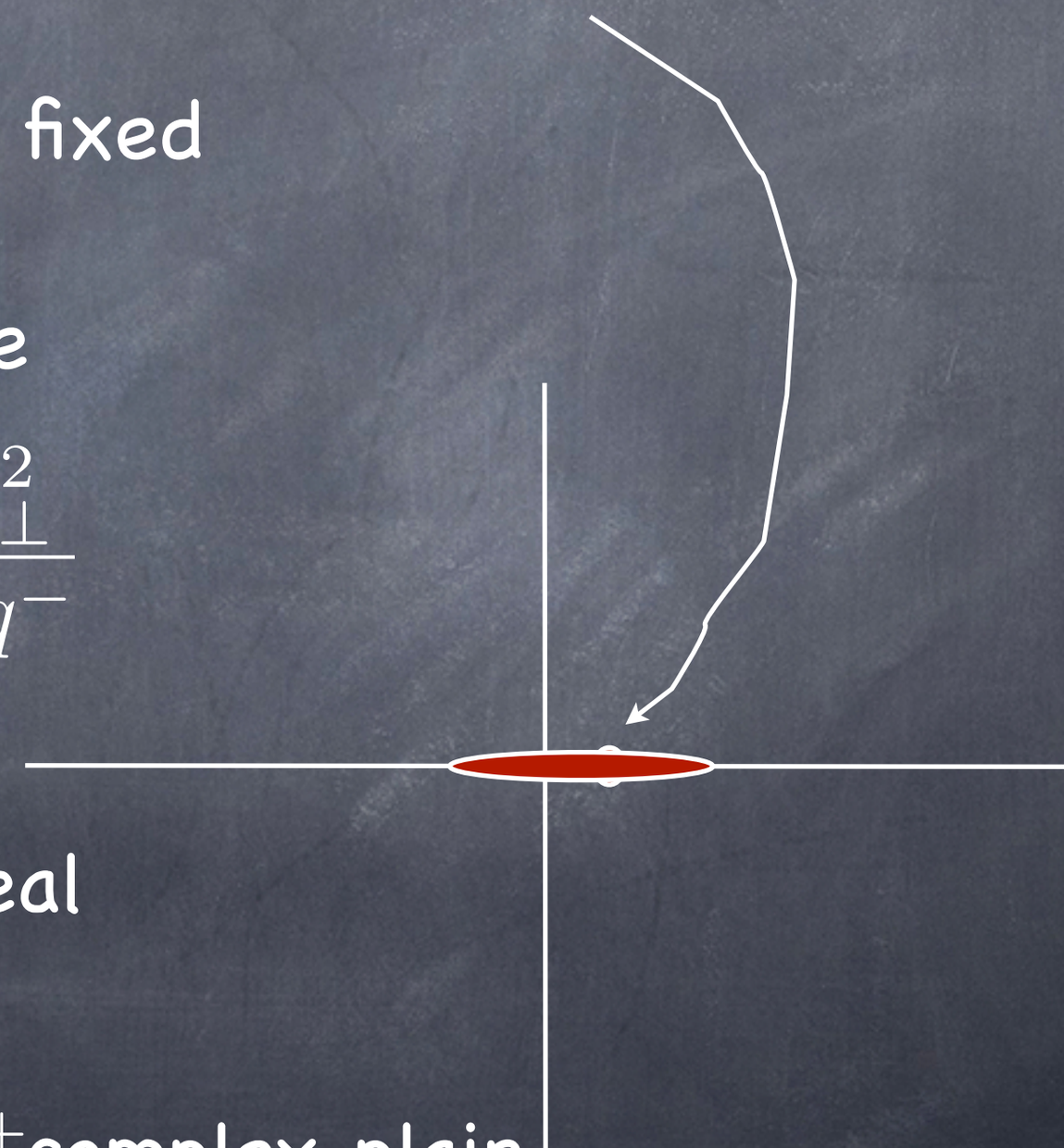

$\hat{Q}$ has a branch cut on the real axis at $q^+ \sim \lambda^2 Q$

$\hat{q} = Im(\hat{Q})$

q^+complex plain

Consider the following integral

$$I_1 = \oint \frac{dq^+}{2\pi i} \frac{\hat{Q}(q^+)}{(q^+ + Q_0)}$$

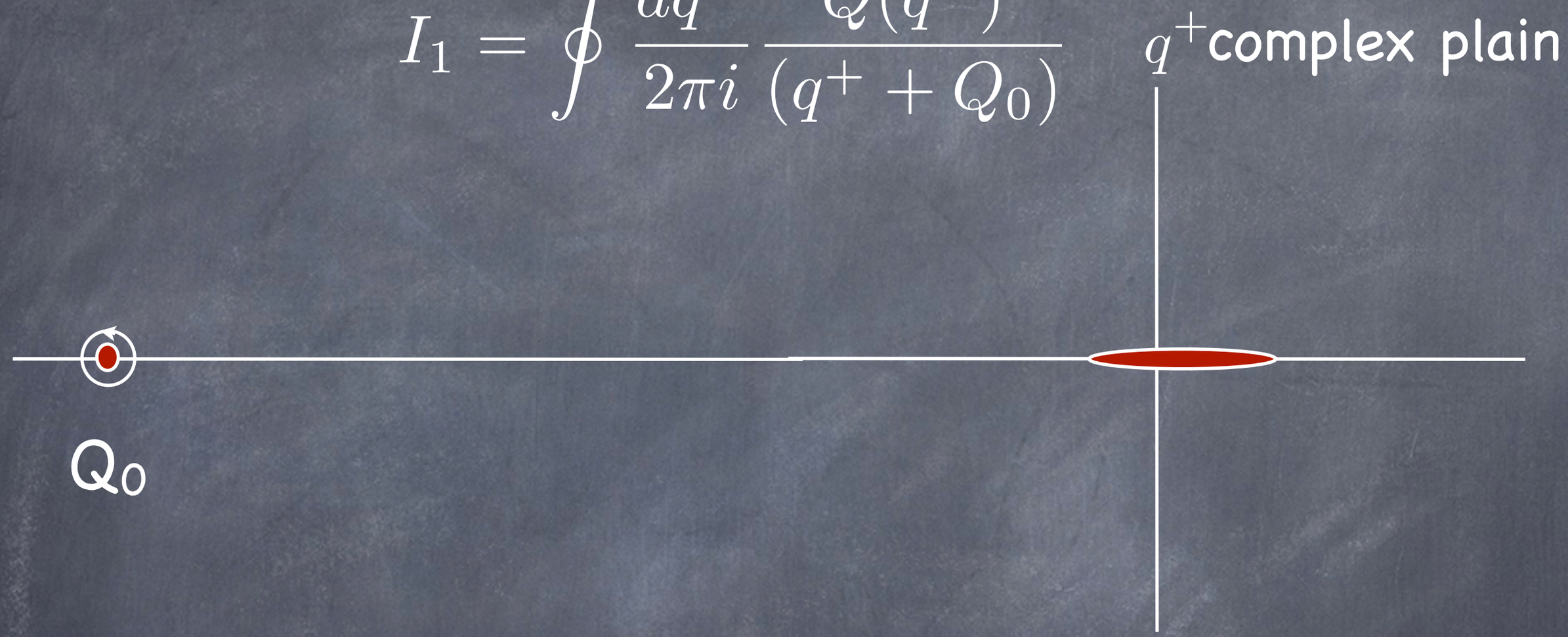

For Q_0 ~ -Q, can Taylor expand $\hat{Q}$ in terms of local operators

$$I_1 = \frac{4\sqrt{2}\pi^2\alpha_s \langle M|F_\perp^{+\mu} \sum_{n=0}^{\infty} \left(\frac{-q\cdot i\mathcal{D} - \mathcal{D}_\perp^2}{2q^- Q_0}\right)^n F_{\perp,\mu}^+ |M}{N_c 2Q_0}$$

Consider the following integral

$$I_1 = \oint \frac{dq^+}{2\pi i} \frac{\hat{Q}(q^+)}{(q^+ + Q_0)}$$

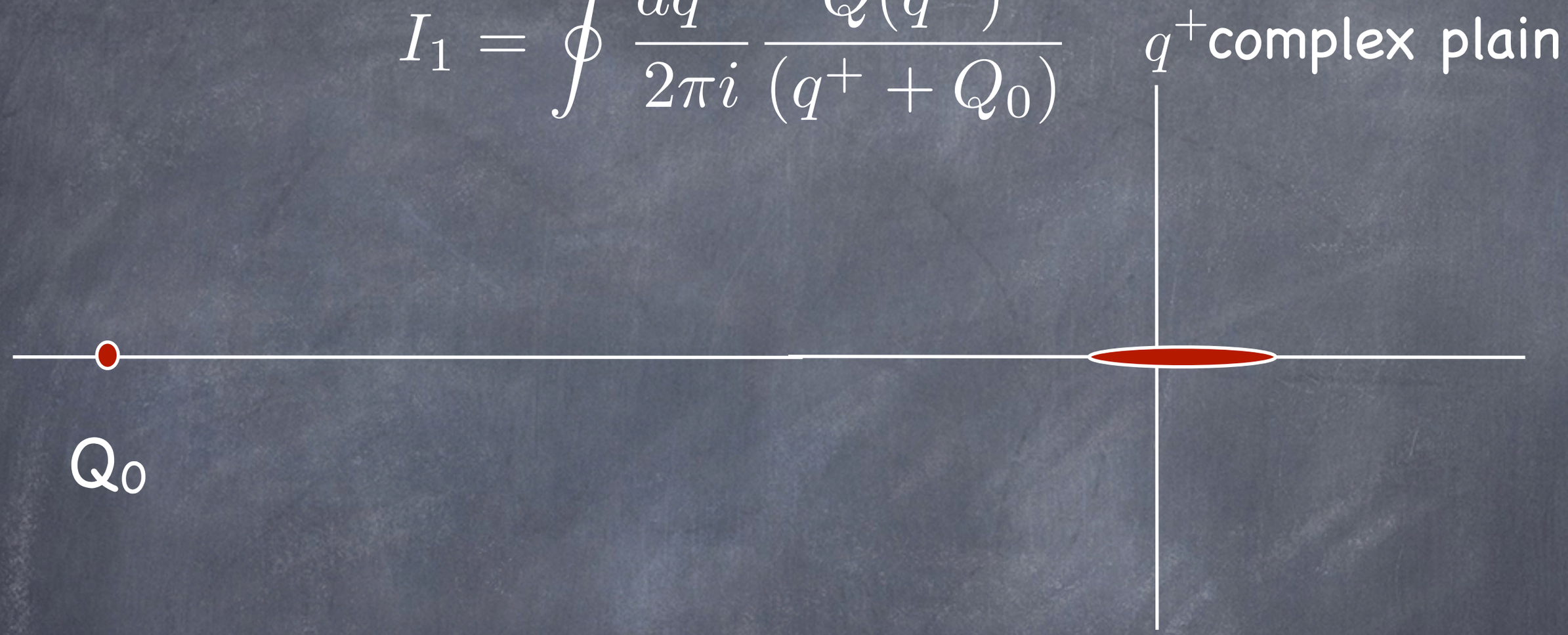

For Q_0 ~ -Q, can Taylor expand $\hat{Q}$ in terms of local operators

$$I_1 = \frac{4\sqrt{2}\pi^2\alpha_s \langle M|F_\perp^{+\mu} \sum_{n=0}^{\infty} \left(\frac{-q\cdot i\mathcal{D} - \mathcal{D}_\perp^2}{2q^- Q_0}\right)^n F_{\perp,\mu}^+ |M}{N_c 2Q_0}$$

Consider the following integral

$$I_1 = \oint \frac{dq^+}{2\pi i} \frac{\hat{Q}(q^+)}{(q^+ + Q_0)}$$

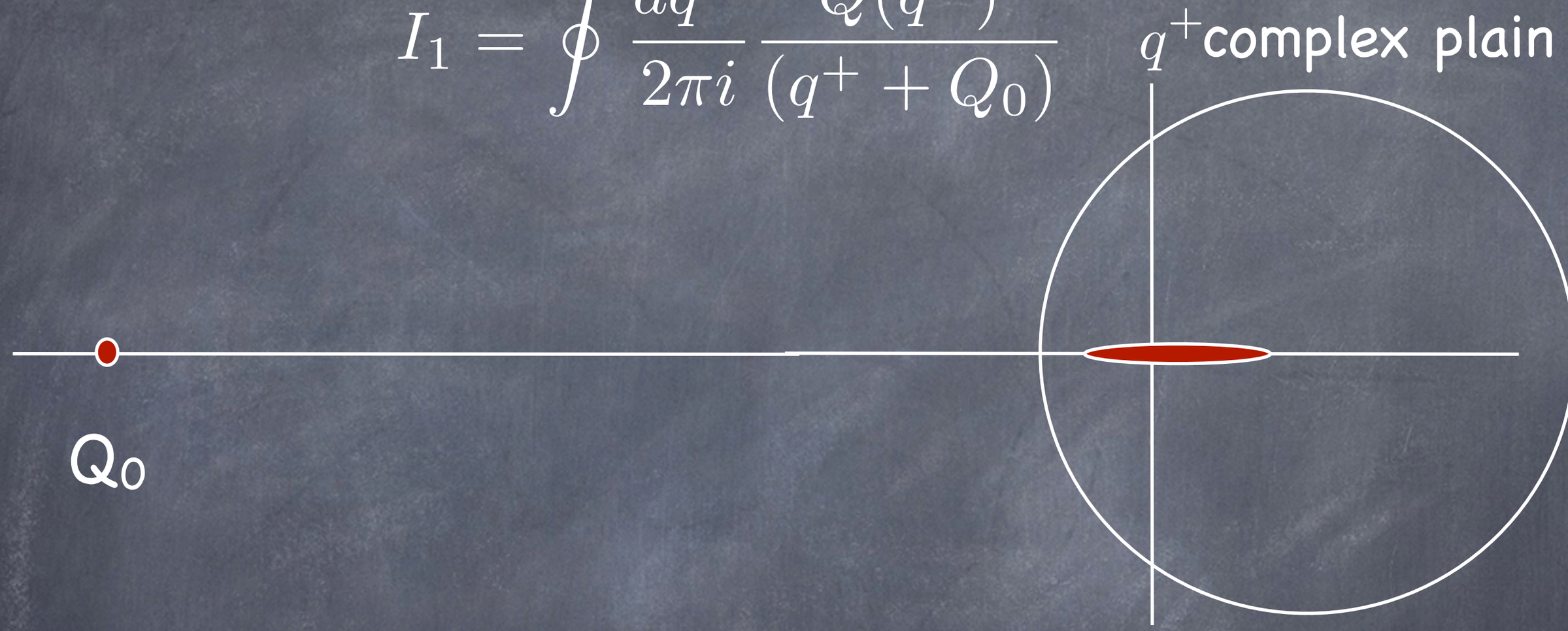

For Q_0 ~ -Q, can Taylor expand $\hat{Q}$ in terms of local operators

$$I_1 = \frac{4\sqrt{2}\pi^2\alpha_s \langle M|F_\perp^{+\mu} \sum_{n=0}^{\infty} \left(\frac{-q\cdot i\mathcal{D} - \mathcal{D}_\perp^2}{2q^- Q_0}\right)^n F_{\perp,\mu}^+ |M}{N_c 2Q_0}$$

Consider the following integral

$$I_1 = \oint \frac{dq^+}{2\pi i} \frac{\hat{Q}(q^+)}{(q^+ + Q_0)}$$

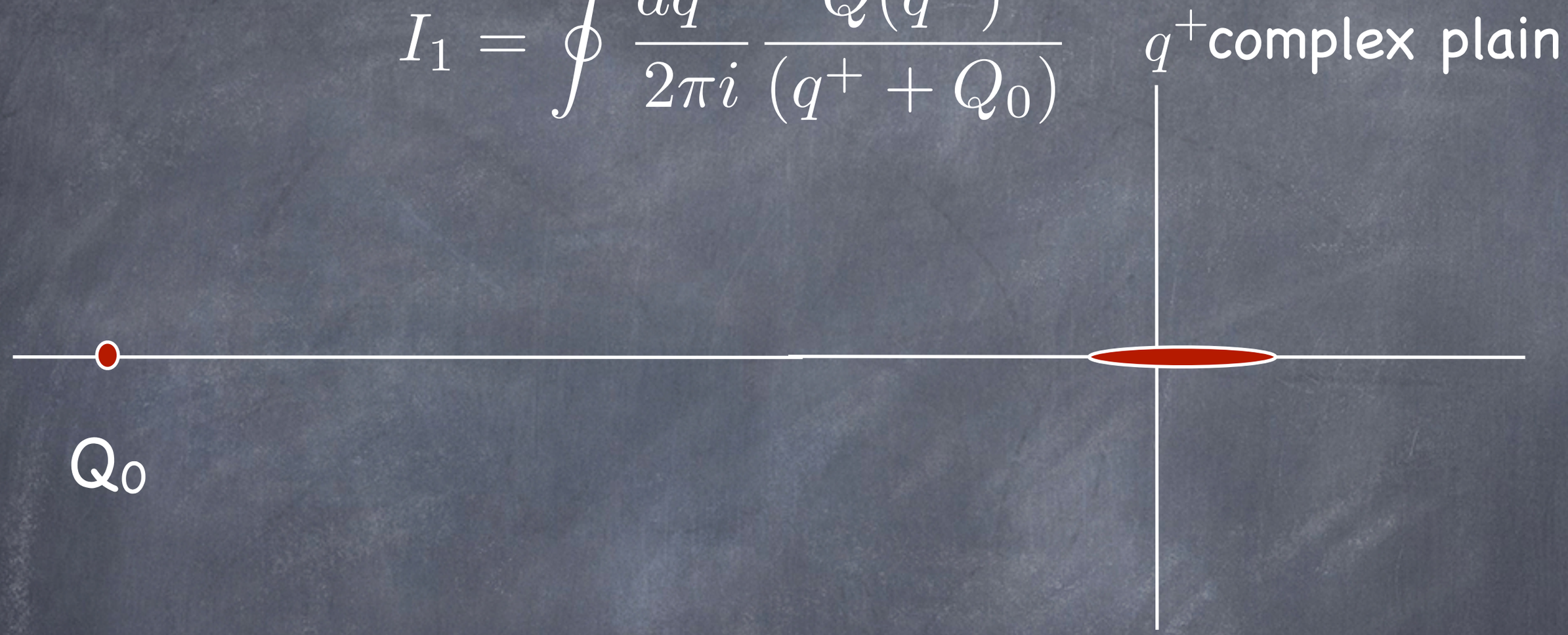

For Q_0 ~ -Q, can Taylor expand $\hat{Q}$ in terms of local operators

$$I_1 = \frac{4\sqrt{2}\pi^2\alpha_s \langle M|F_\perp^{+\mu} \sum_{n=0}^{\infty} \left(\frac{-q\cdot i\mathcal{D} - \mathcal{D}_\perp^2}{2q^- Q_0}\right)^n F_{\perp,\mu}^+ |M}{N_c 2Q_0}$$

Consider the following integral

$$I_1 = \oint \frac{dq^+}{2\pi i} \frac{\hat{Q}(q^+)}{(q^+ + Q_0)}$$

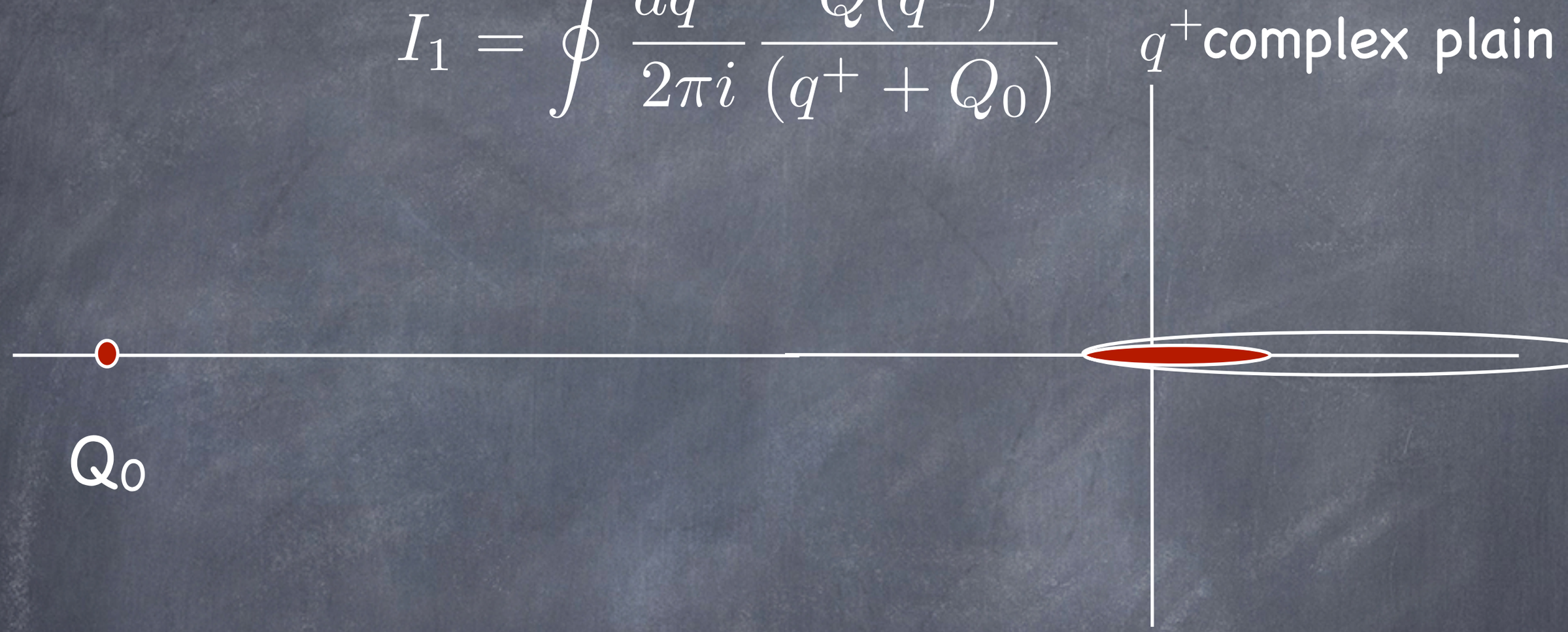

For Q_0 ~ -Q, can Taylor expand $\hat{Q}$ in terms of local operators

$$I_1 = \frac{4\sqrt{2}\pi^2\alpha_s \langle M|F_\perp^{+\mu} \sum_{n=0}^{\infty} \left(\frac{-q\cdot i\mathcal{D} - \mathcal{D}_\perp^2}{2q^- Q_0}\right)^n F_{\perp,\mu}^+ |M}{N_c 2Q_0}$$

Rotating everything to Euclidean space and calculating

$$x^0 \to -ix^4 \text{ and } A^0 \to iA^4$$

$$\to F^{0i} \to iF^{4i}$$

Calculate in quark less SU(2) gauge theory

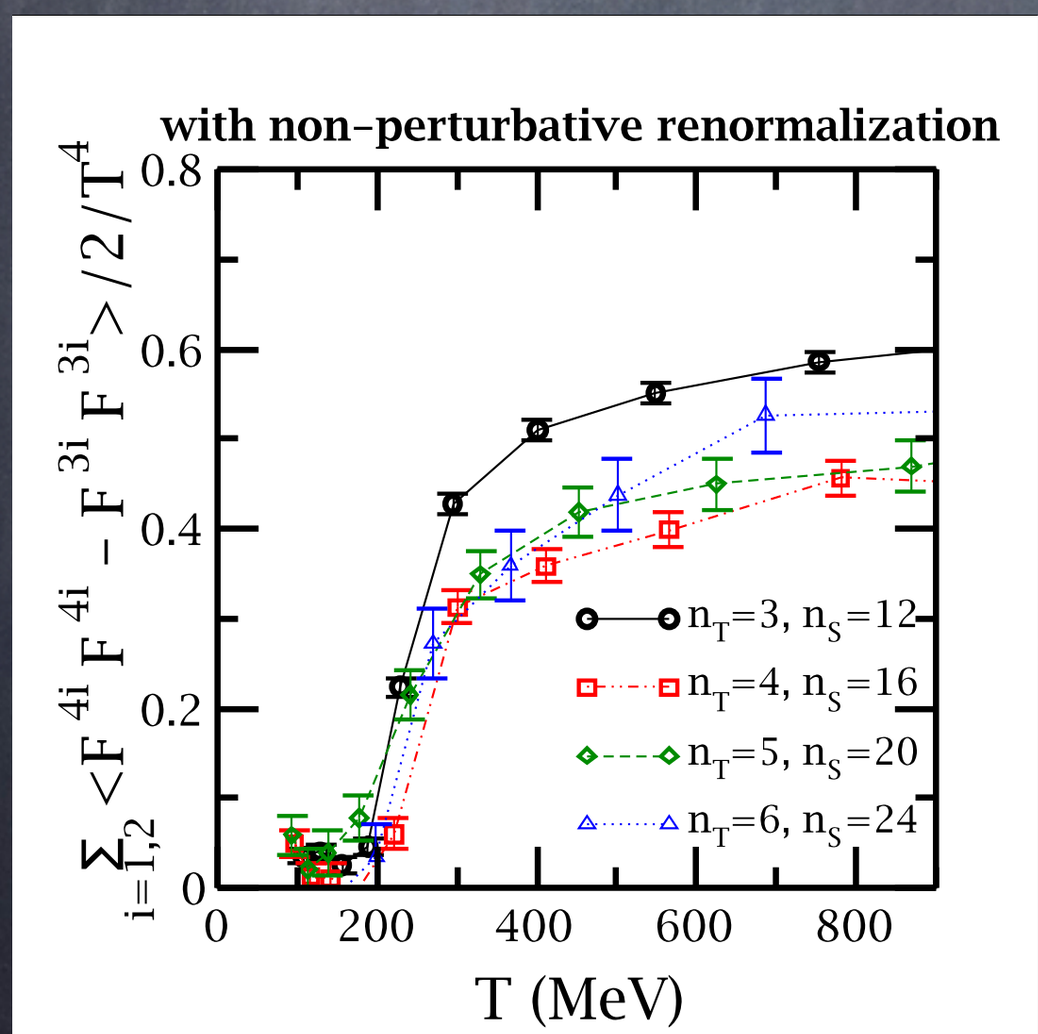

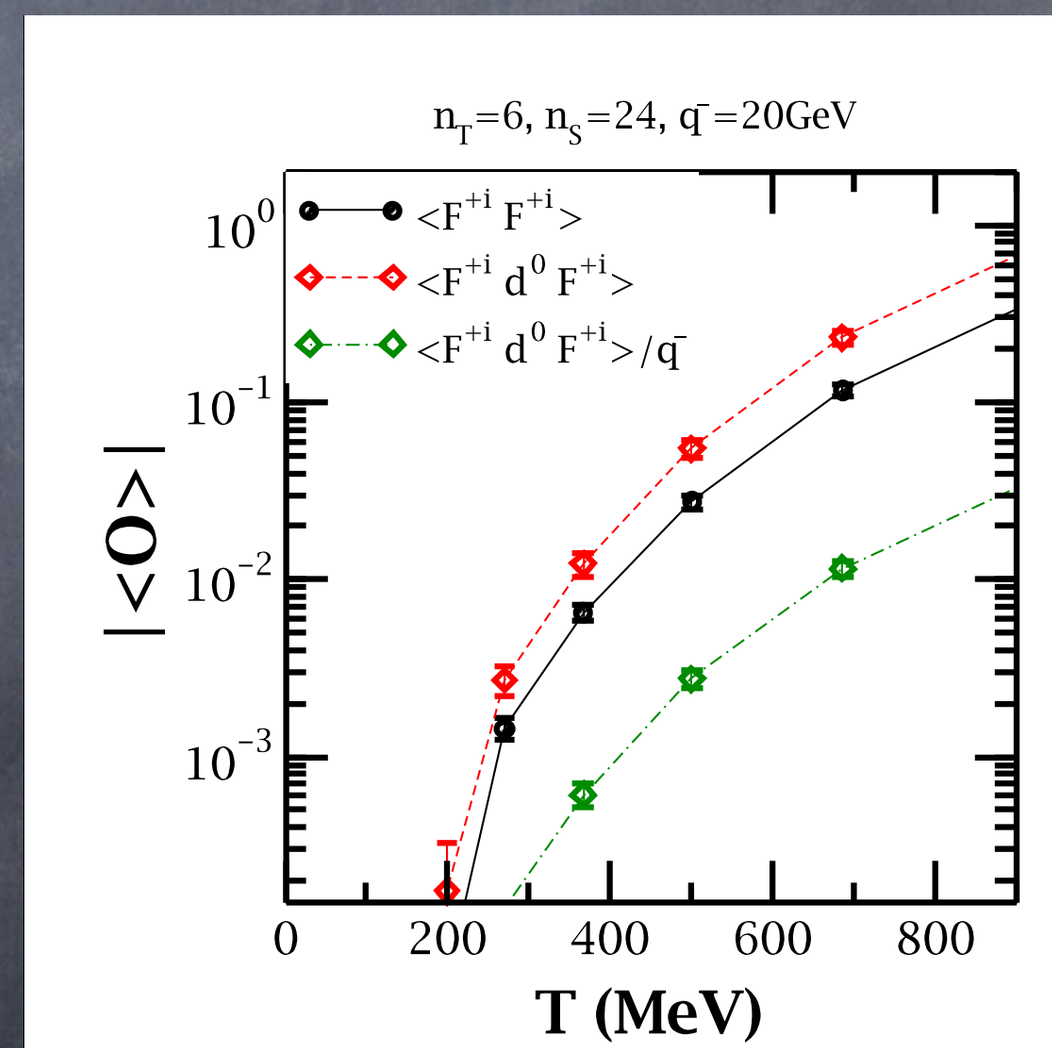

AM, PRC 87 034905

Concluding and Extrapolating !

Need to calculate in SU(3)
Better renormalization prescription
More complicated processes on the lattice
Need to do a higher order perturbative calculation
But lets estimate anyways

at T=400, FF = 0.01 GeV^4
Lattice size ~ 2fm, E = 20 GeV, μ^2 = 1.3 GeV^2

Gluon $\hat{q}$ is C_A/C_F of quark $\hat{q}$

SU(2) has 3 gluons, SU(3) has 8,
and 6 quarks + antiquarks

$$\hat{q}(T = 400\mathrm{MeV}) = 1\mathrm{GeV}^2/\mathrm{fm} - 2\mathrm{GeV}^2/\mathrm{fm}$$

A lingering problem with D-Au

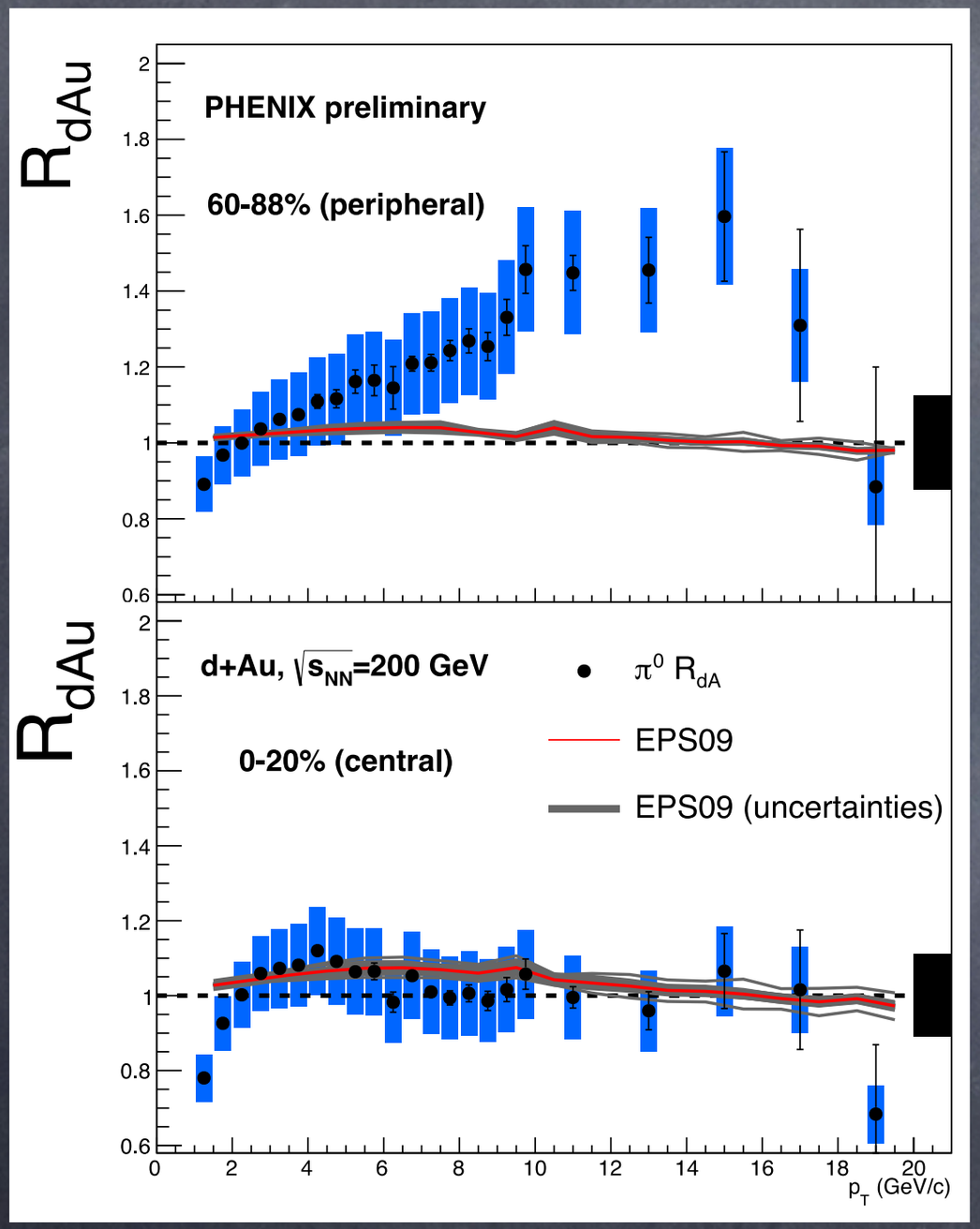

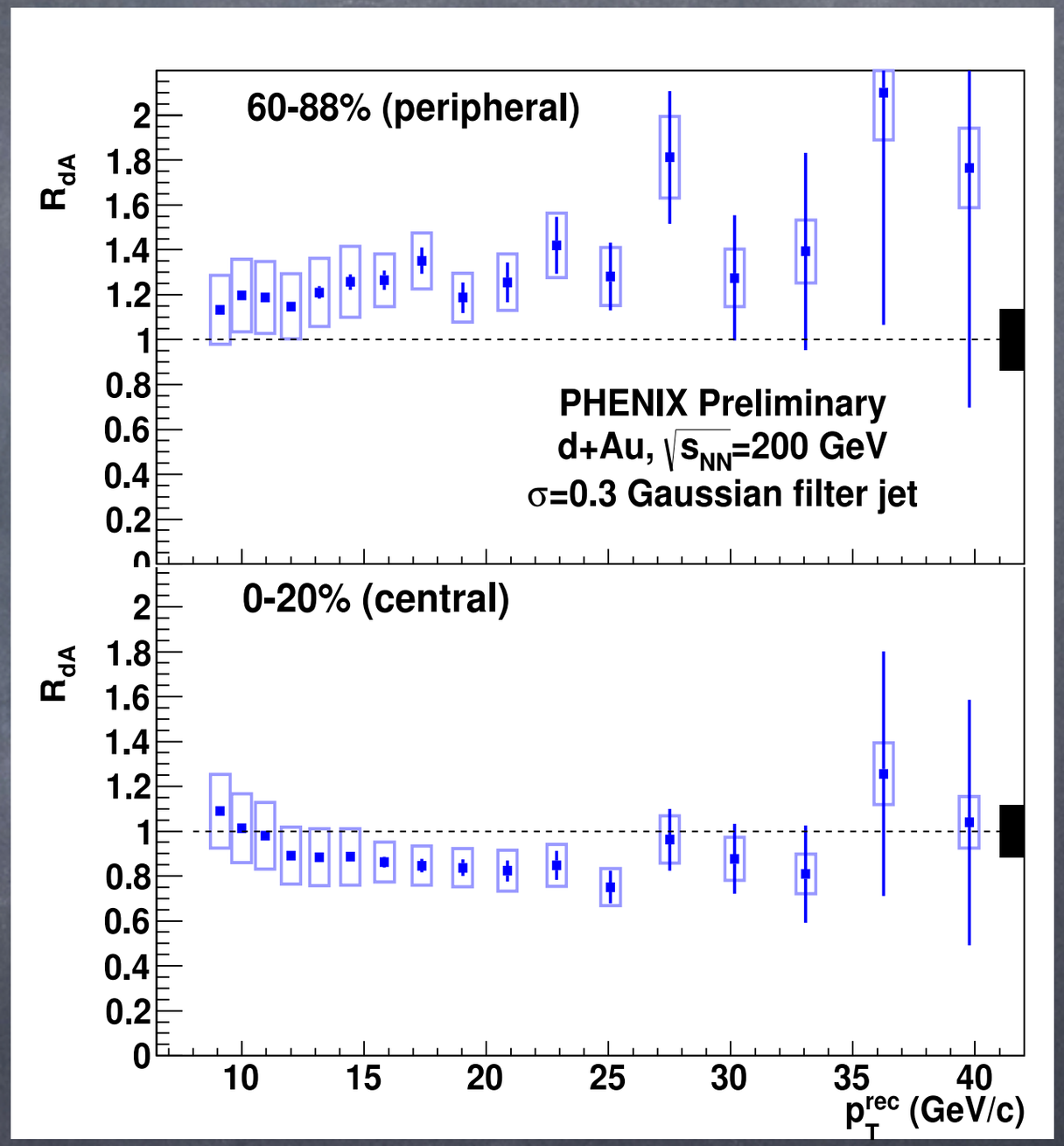

Why does this happen ?

Are there more scatterings per nucleon in peripheral vs. central D-Au

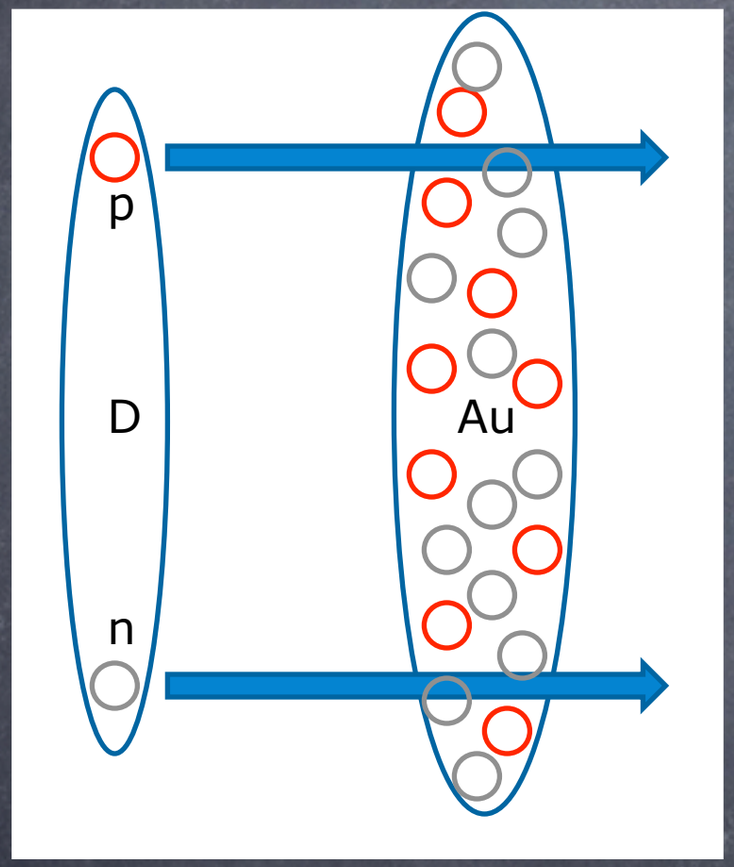

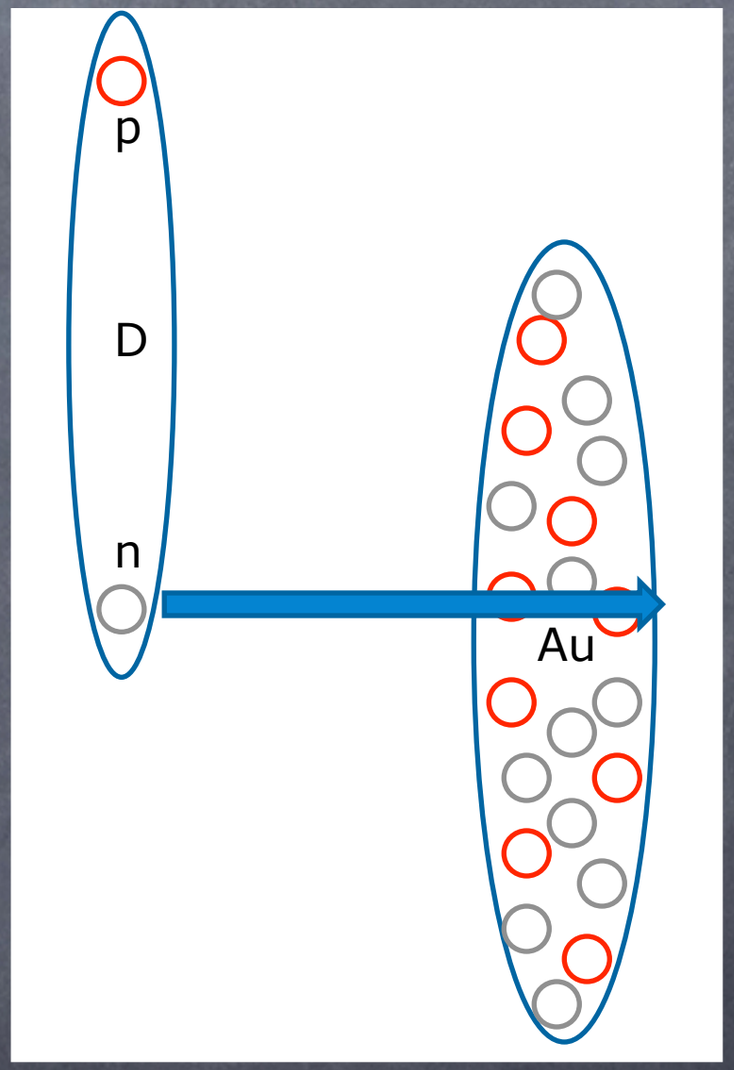

No, but the numbers are very close.
Testing to see if correlated initial state and final state scattering can explain the data.

M. Kordell, AM and S. Gavin

Done more carefully than you would think!

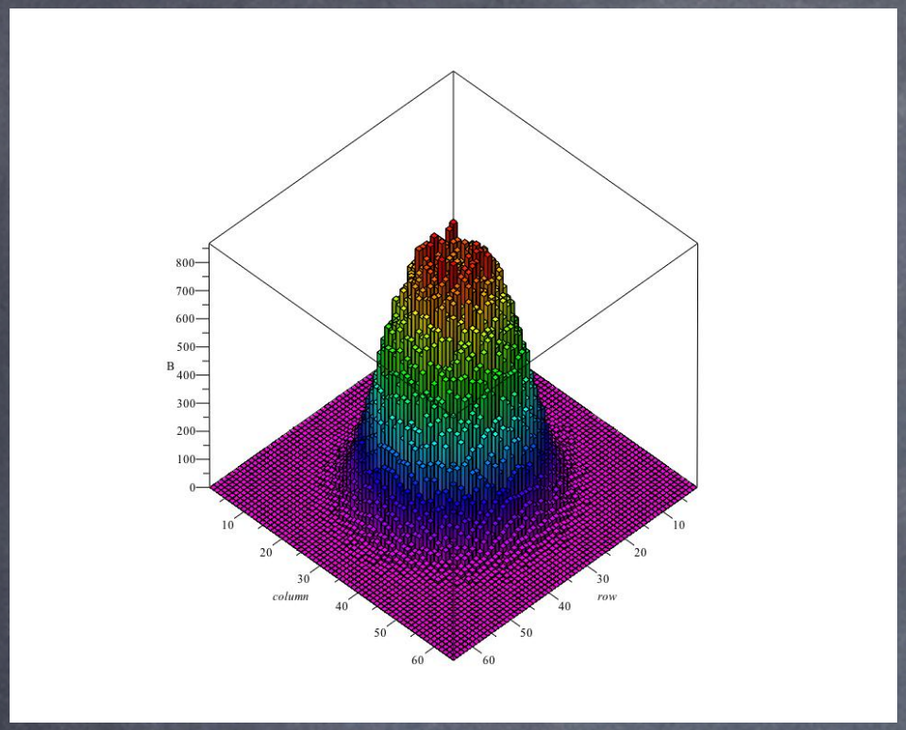

Hulthen for D
Woods-Saxon for A
Shell model for A

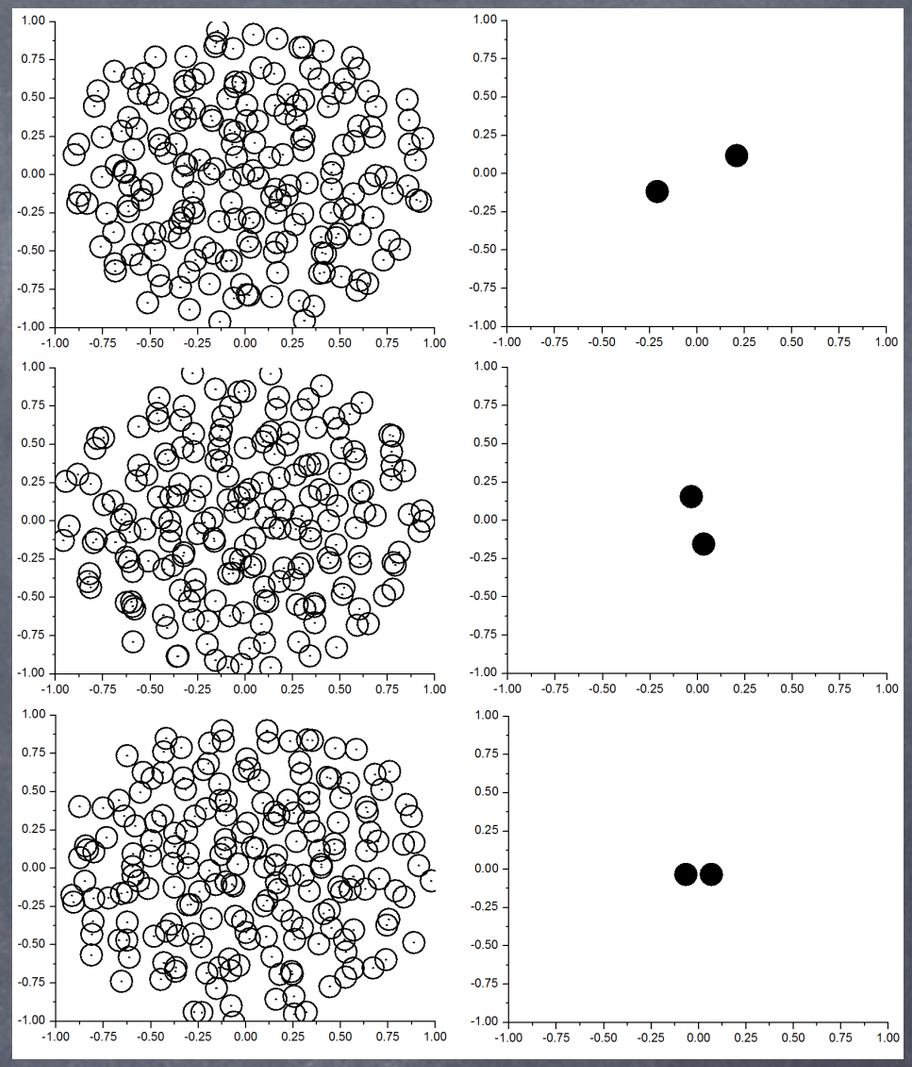

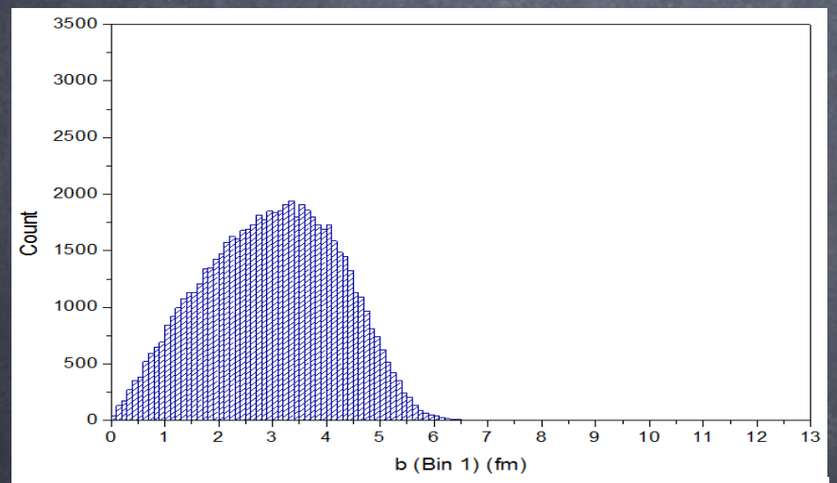

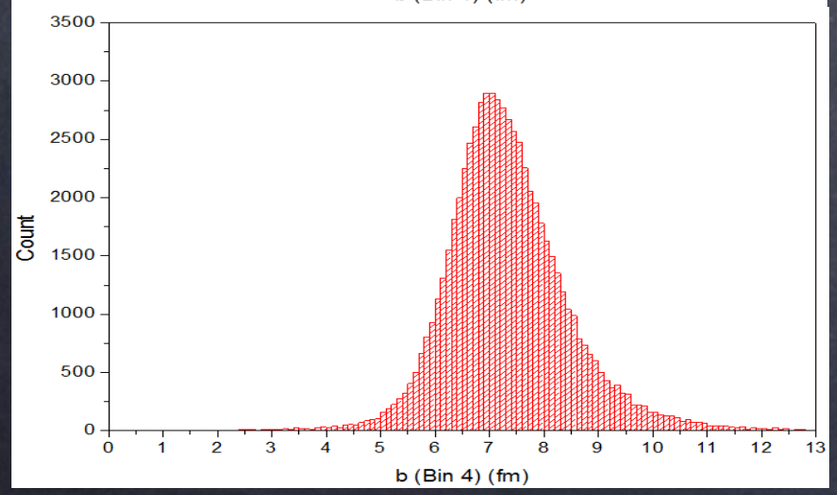

Sum of 1M events
Distribution of b for each N_{bin}

A new e-by-e shadowing

Summary

After R_{AA} test HT energy loss scheme on the expansion

Full Jet MC being incorporated with E-by-E hydro

Energy deposition calculations being developed

Lattice QCD calculations of transport parameters

Detailed phenomenology for D-A and AA being set up

Interesting issues with heavy-quarks and NLO

Jets at Detroit, part II

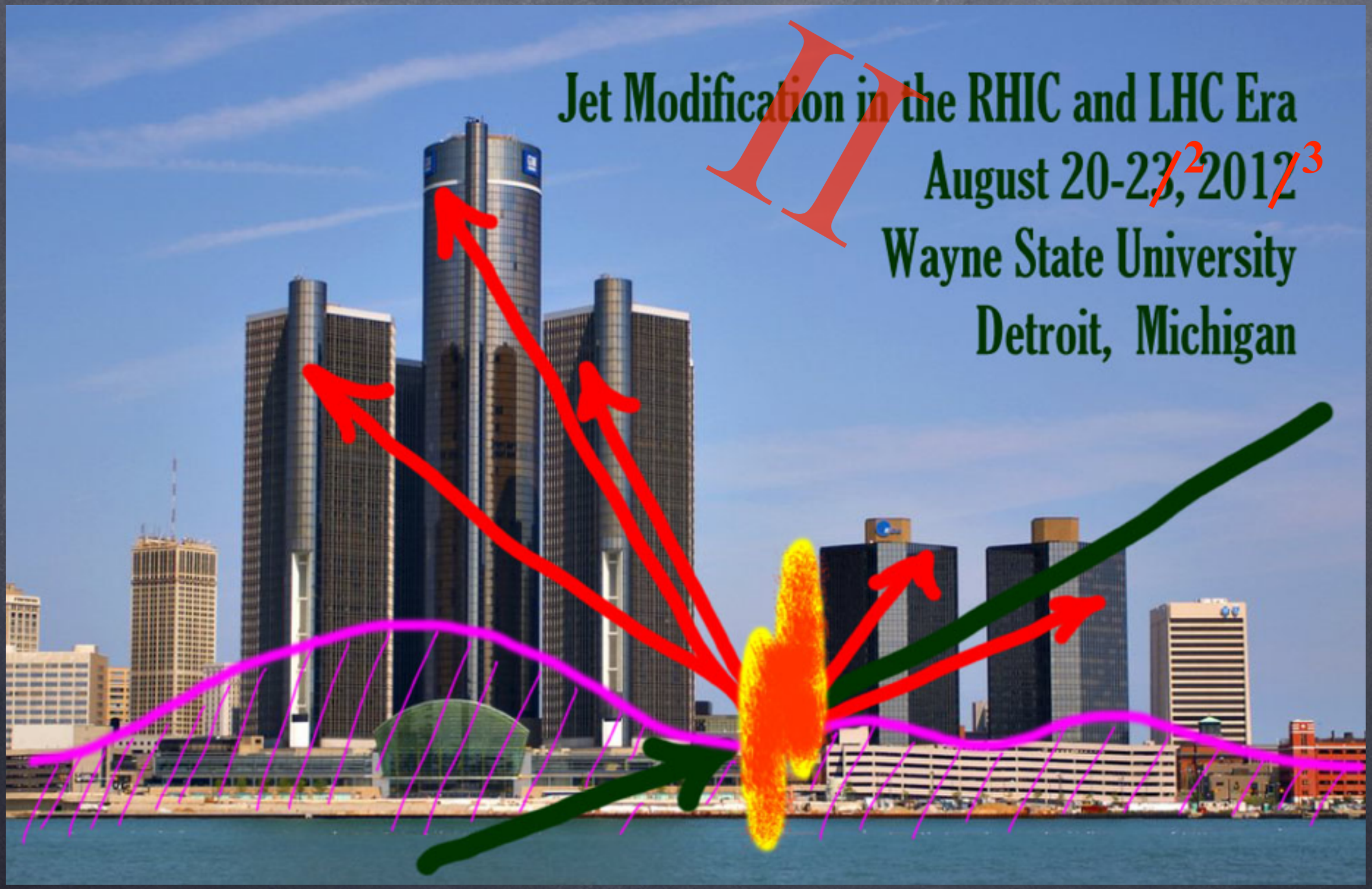

Event-by-event flow and initial geometry from LHC

Soumya Mohapatra

Stony Brook University

Jet Quenching Workshop, BNL
16th April 2013

Importance of fluctuations

- Initial spatial fluctuations of nucleons lead to higher moments of deformations in the fireball, each with its own orientation.

Alver, Roland (arXiv:1003.0194)

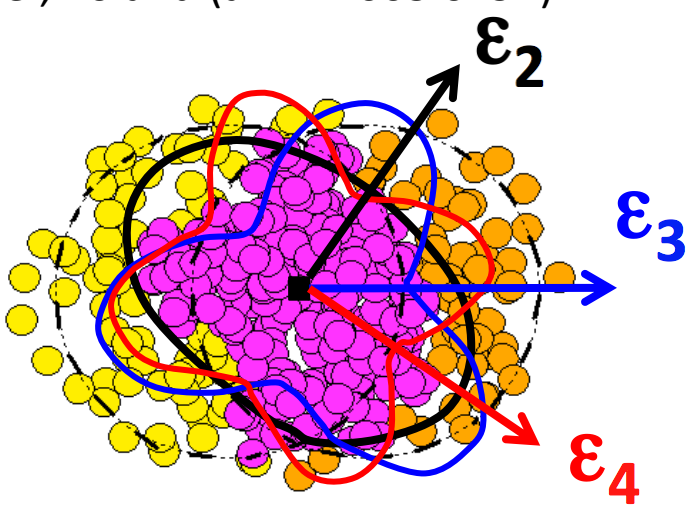

1. Odd harmonics present
2. v_n is a distribution, can be characterized by mean and width
3. Each harmonic has a separate phase (phases may be correlated)

$$\varepsilon_n = \sqrt{\frac{\langle r^n \cos(n\phi)\rangle + \langle r^n \sin(n\phi)\rangle}{r^n}} \qquad \tan(n\Phi_n^*) = \frac{\langle r^n \sin(nf)\rangle}{\langle r^n \cos(nf)\rangle}$$

Large acceptance of the LHC experiments coupled with the increased multiplicity has allowed for great precision is studying the nature of these fluctuations

Understanding the initial geometry is critical for understanding jet-suppression

OUTLINE

- Multi-particle correlation measurements
  - Cumulants, 2PC, LYZ
- Event by Event v_n measurements
- Event-plane correlations

Emphasis on

- Removing non-flow
- Comparison between experiments and methods
- Theory interpretation

Gaussian model of flow fluctuations

$$\vec{e}_n = (e_x, e_y)$$

$$p(\vec{e}_n) \mu \exp\left(\frac{-(\vec{e}_n - \vec{e}_n^{RP})^2}{2\delta_n^2}\right)$$

$$\vec{e}_n^{RP} \rightarrow Mean\,Geometry$$

$$\delta_n \rightarrow Fluctuations$$

arXiv: 0708.0800

arXiv:0809.2949

$$p(\vec{v}_n) \mu \exp\left(\frac{-(\vec{v}_n - \vec{v}_n^{RP})^2}{2\delta_n^2}\right)$$

$$p(v_n) \mu\, v_n \exp\left(\frac{-(v_n^2 + (v_n^{RP})^2}{2\delta_n^2}\right) I_0\left(\frac{v_n v_n^{RP}}{\delta_n^2}\right)$$

For pure fluctuations $v_n^{RP}=0$

$$p(v_n) \propto v_n \exp\left(\frac{-(v_n^2)}{2\delta_n^2}\right)$$

Multi-particle correlations

$$v_n\{2\} = \sqrt{\left(v_n^{RP}\right)^2 + 2\delta_n^2}$$

Sensitive to mean geometry and fluctuations

arXiv: 0708.0800
0809.2949

$$v_n\{4\} = v_n\{6\} = v_n\{8\} = v_n^{RP}$$

Mean geometry only

$$\frac{\sigma_n}{\langle v_n \rangle} \gg \sqrt{\frac{v_n\{2\} - v_n\{4\}}{v_n\{2\} + v_n\{4\}}}$$

Limit when $v_n^{RP} >> \delta_n$ (i.e. Average geometry dominates over fluctuations)
Expected for v_2 in mid-central events

$$\frac{\sigma_n}{\langle v_n \rangle} \gg \sqrt{\frac{4}{\pi} - 1}$$

Limit when $v_n^{RP} \to 0$ (Pure fluctuations)
Expected to hold for v_2 in central events and for higher order harmonics in all centralities

Lee-Yang Zeros : Multi-particle correlations involving all particles in the event. suppresses non-flow

Two particle correlations: similar to $v_n\{2\}$, but often done with dh gap to suppress non-flow. Measures $\langle v_n^2 \rangle$

Event Plane (EP) Method : Returns a value in between $\langle v_n \rangle$ and $\langle v_n^2 \rangle$

v_2 from multi-particle correlations

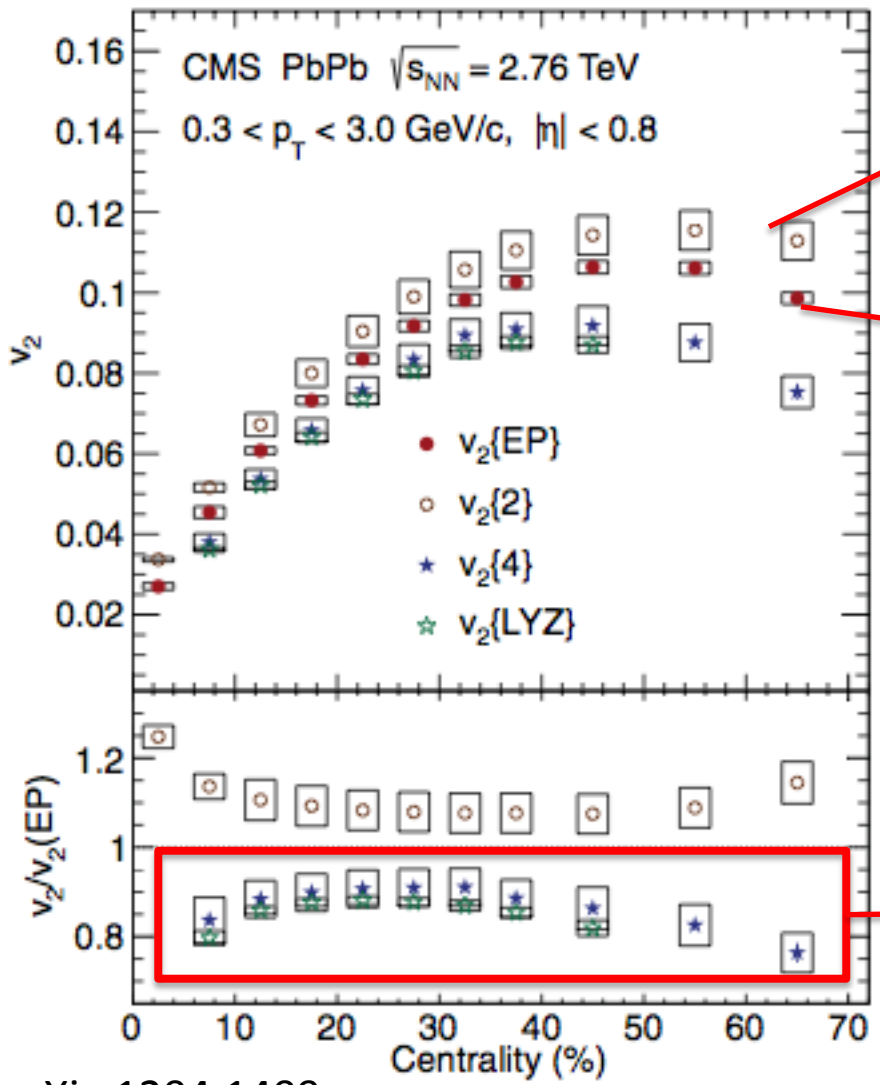

$v_2\{2\}$ probably over-estimates $\langle v_2^2 \rangle$
Due to non-flow

$v_2\{EP\}$ probably under-estimates $\langle v_2^2 \rangle$

Good consistency between LYZ and 4-particle cumulants :
Reliable handle on average geometry!

arXiv:1204.1409

Comparison across experiments

ATLAS-CONF-2012-118

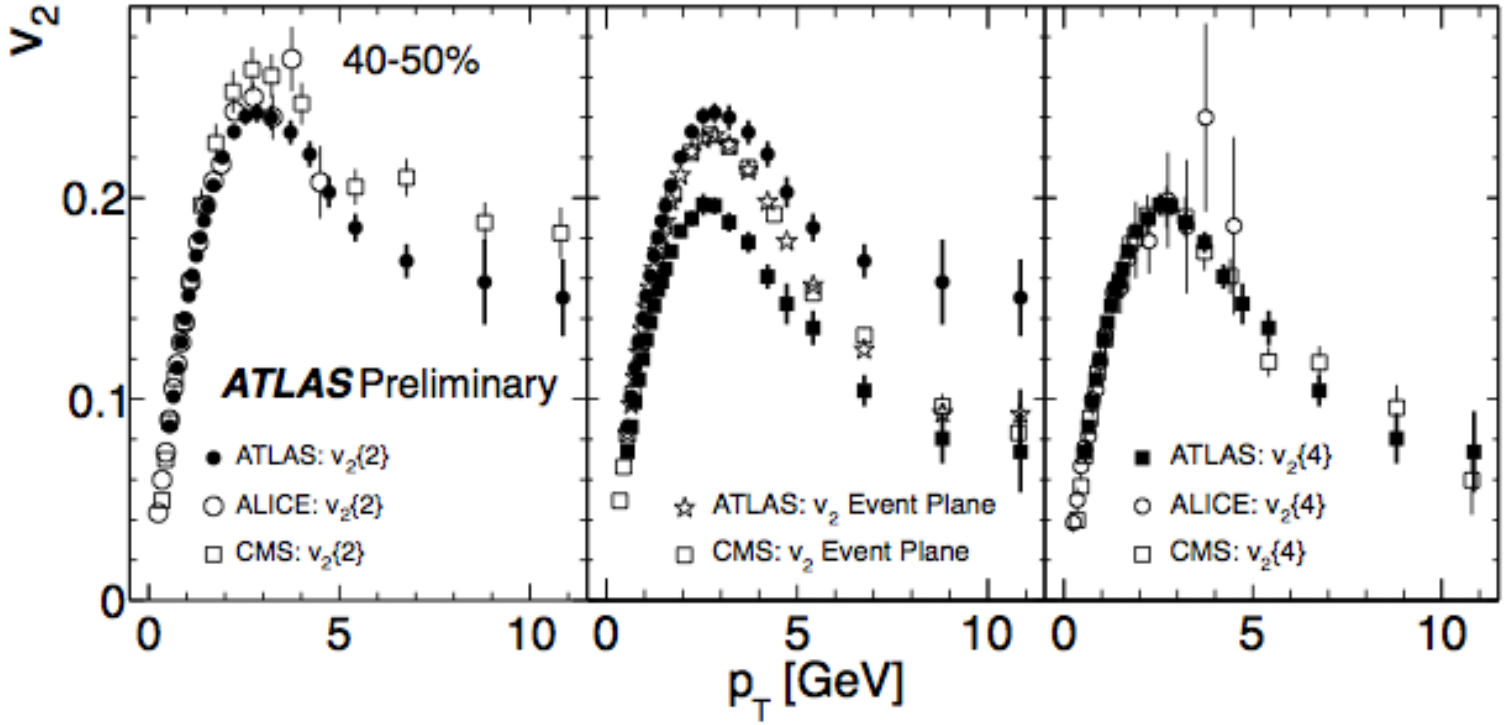

Good agreement among experiments for cumulants and even $v_2\{EP\}$

pT dependence of EbE fluctuations

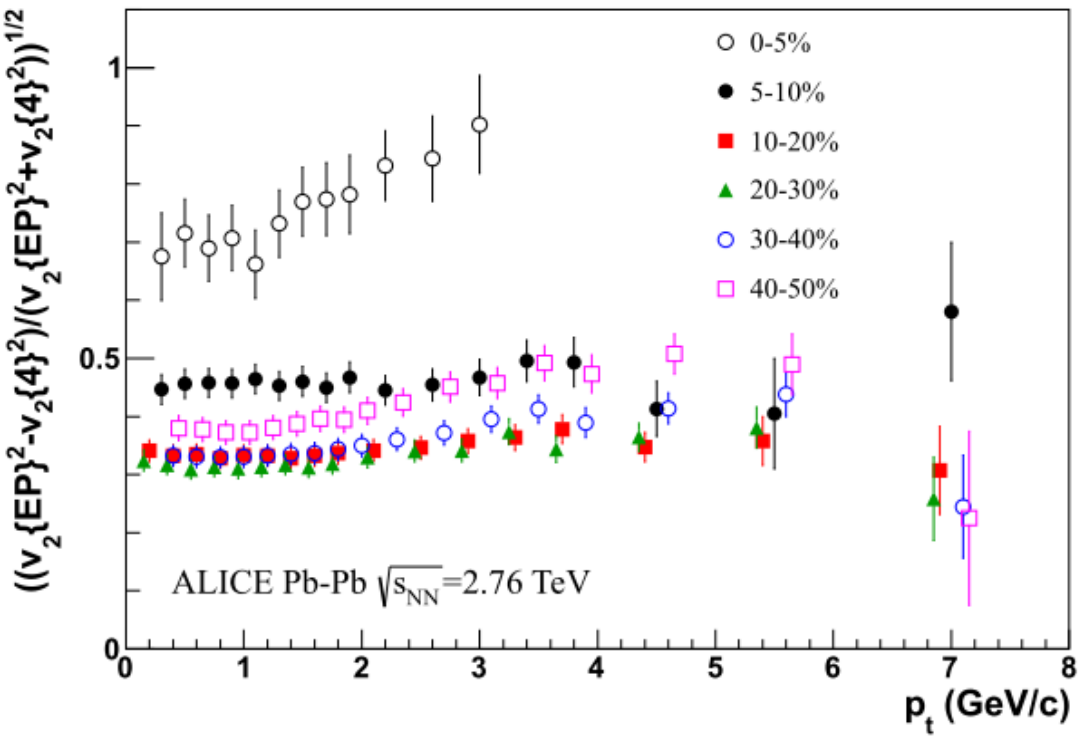

arXiv:1205.5761

$$\frac{s_2}{\langle v_2 \rangle} \approx \sqrt{\frac{v_2\{EP\} - v_2\{4\}}{v_2\{EP\} + v_2\{4\}}}$$

Ratio of fluctuations in v_2 to mean v_2 is relatively independent of p_T

Note that $v_2\{EP\}$ changes by an order of magnitude over this p_T range but ratio is remarkably stable

Hydro response factorizes of function of p_T and initial geometry!

Higher order cumulants for v_2

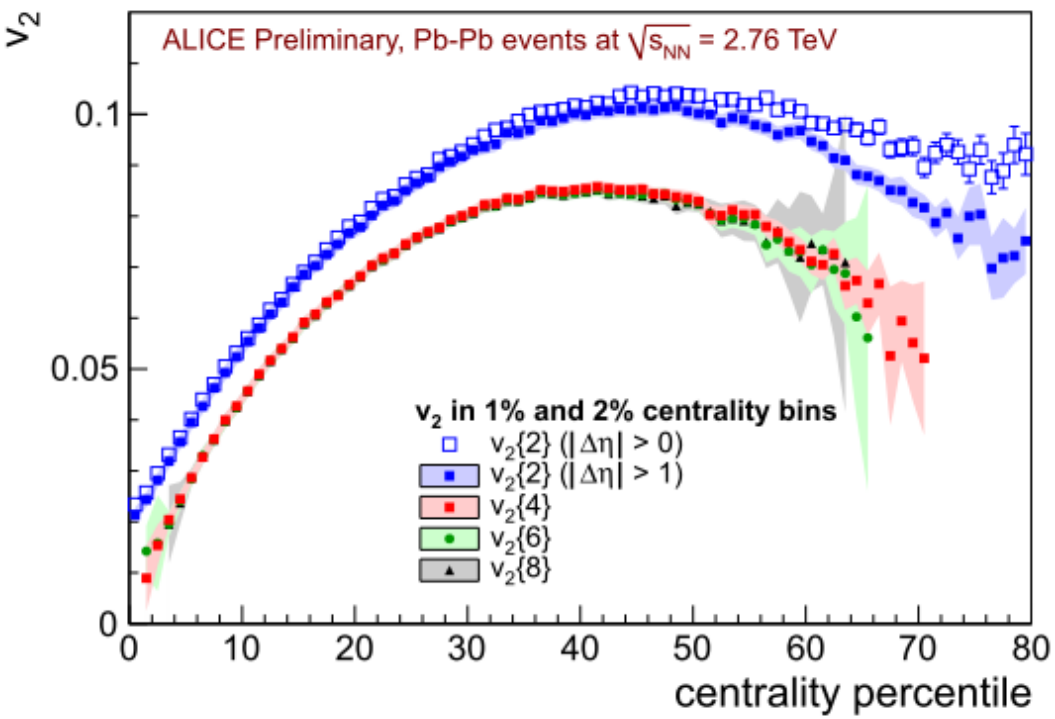

- Higher order cumulants such as $v_n\{6\}$,$v_n\{8\}$ all measure v_n^{RP}
- v_n^{RP} is less susceptible to non-flow and so are $v_n\{4\}$, $v_n\{6\}$,$v_n\{8\}$.
- ALICE results show consistency among them
- Note these measurements are done in 1% bins (Good!)

Cumulant results v3

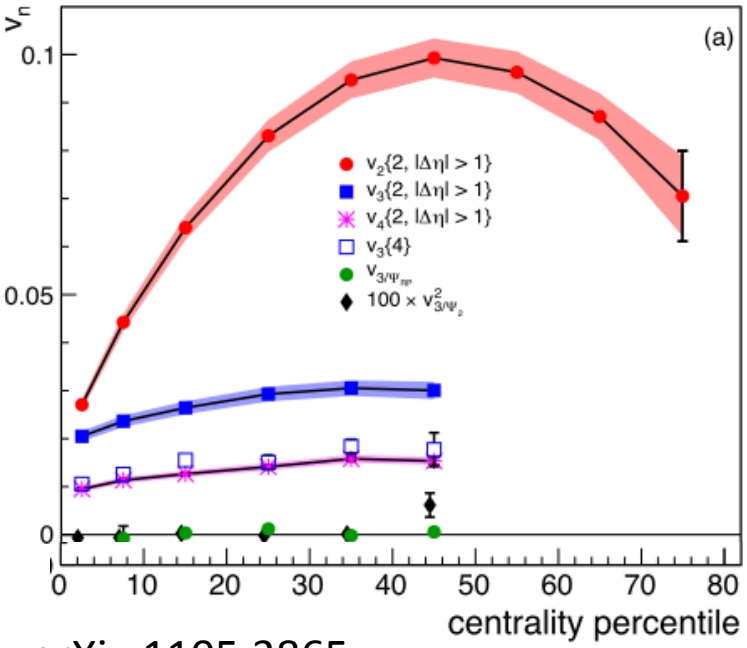

arXiv:1105.3865

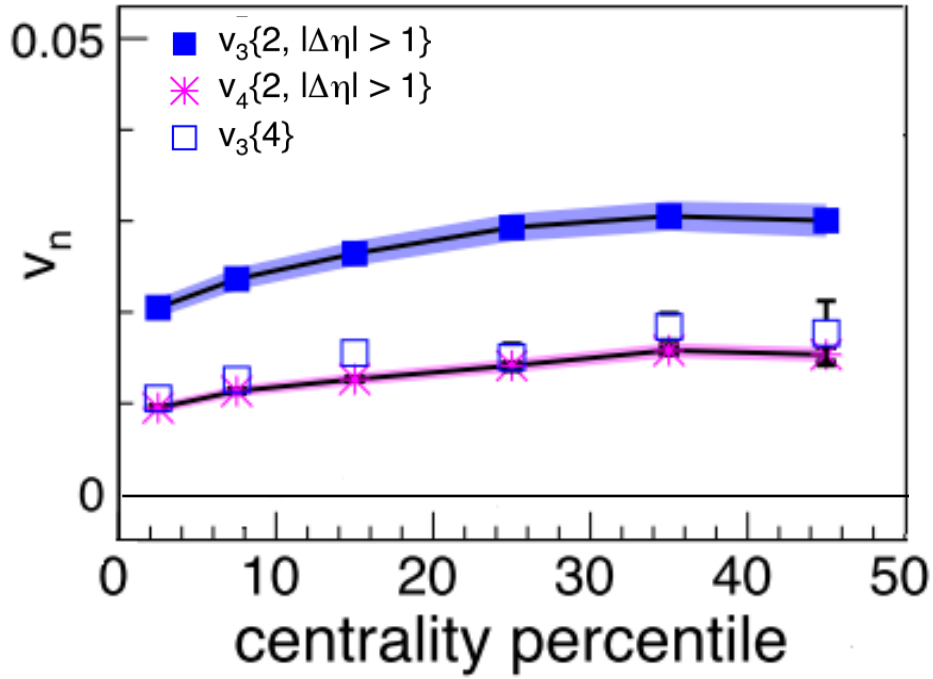

- Relatively weak centrality dependence as compared to v_2
- Sizable $v_3\{4\}$ is seen ~50% of $v_3\{2\}$
  - Implies mean geometry effects for v_3 !
- $v_3\{4\} / v_3\{2\} = 0.5 \Rightarrow v_3^{RP}/\delta_3 = 0.8$

$v_3\{4\}$ and average geometry

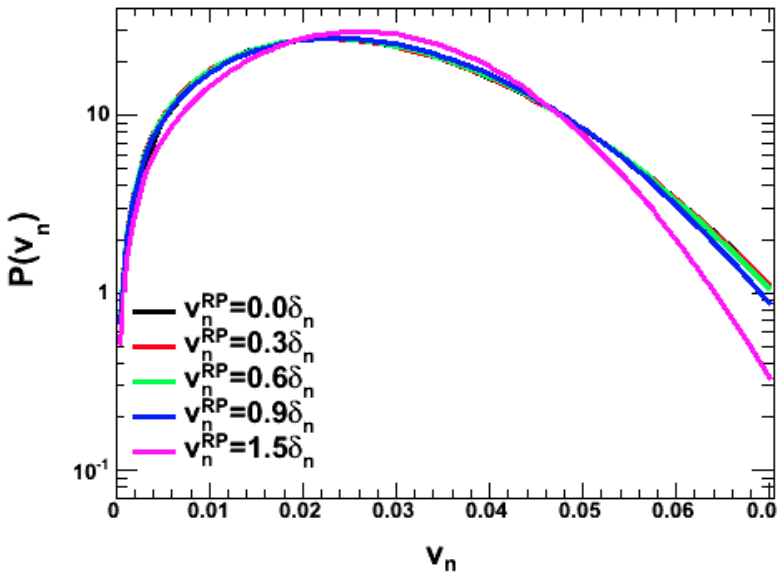

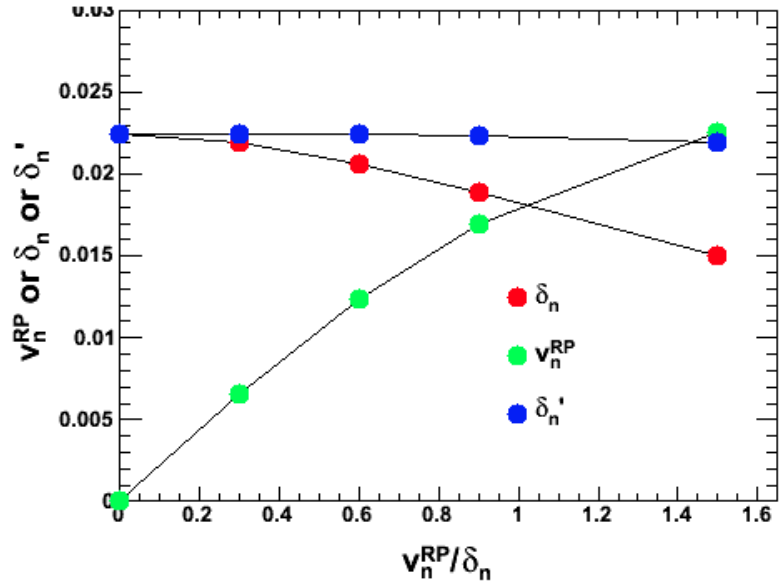

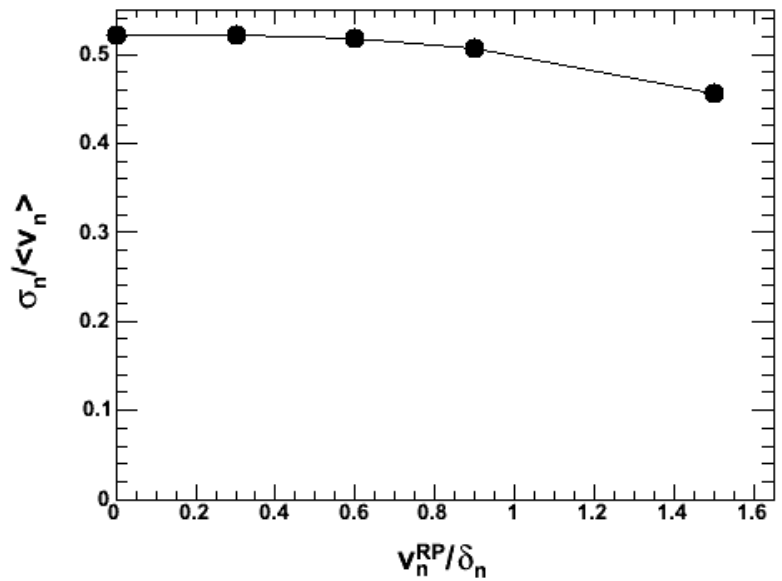

$$\begin{pmatrix} d_n \\ v_n^{RP} \end{pmatrix} \rightarrow \begin{pmatrix} d_n' = \sqrt{d_n^2 + \left(v_n^{RP}\right)^2/2} \\ v_n^{RP}{}' = 0 \end{pmatrix}$$

$$Valid\ till\ \frac{v_n^{RP} v_n}{d_n^2} \gg 2$$

Event by Event flow measurements

Track distribution in three central events

Corresponding two-particle correlations

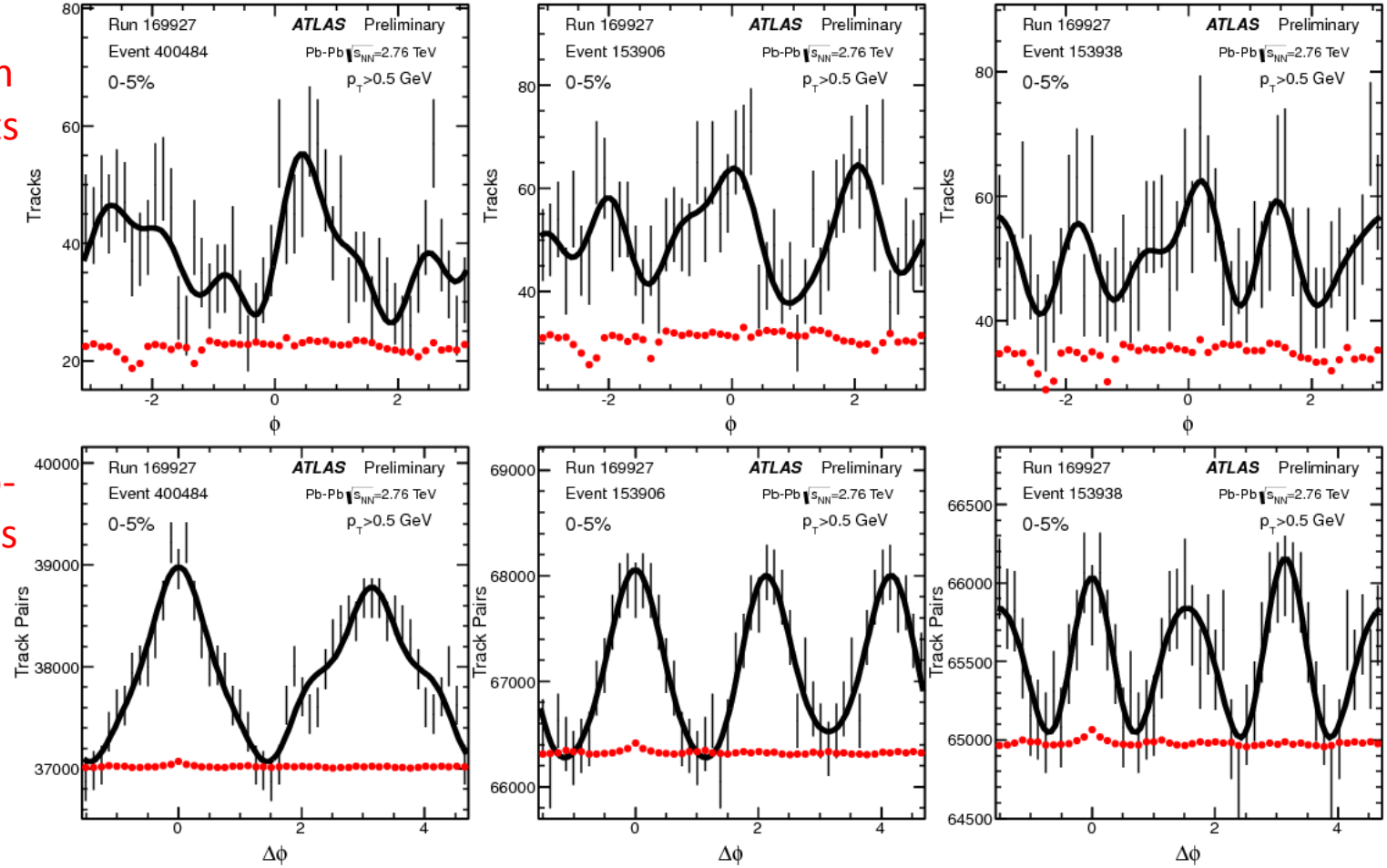

The large acceptance of the ATLAS/ALICE detectors and large multiplicity at LHC makes EbE v_n measurements possible for the first time.

v_2-v_3 probability distributions

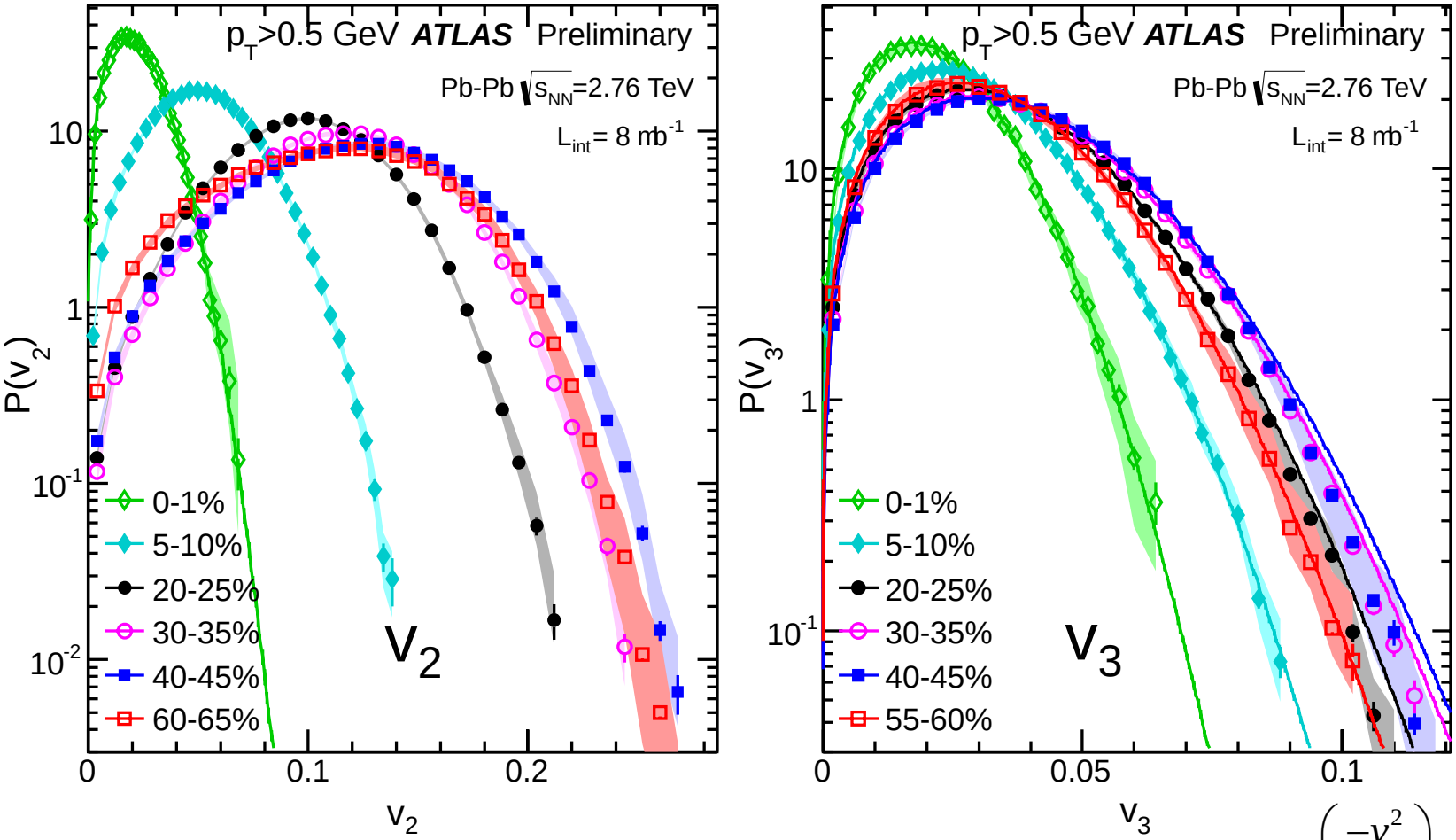

v_3 distributions are consistent with pure Gaussian fluctuations $p(v_n) \propto v_n \exp\left(\frac{-v_n^2}{2\delta_n^2}\right)$

deviations in the tail (increases central->midcentral), Also see caveat in slide 11

For v_2 pure Gaussian fits only work for most central (2%) events

v_2 probability distributions via 2PC

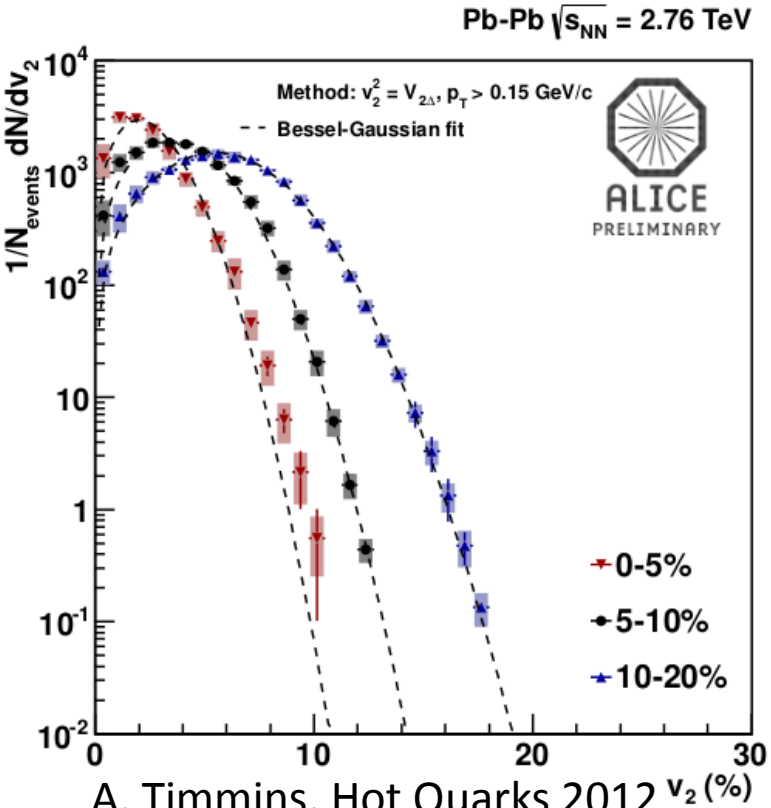

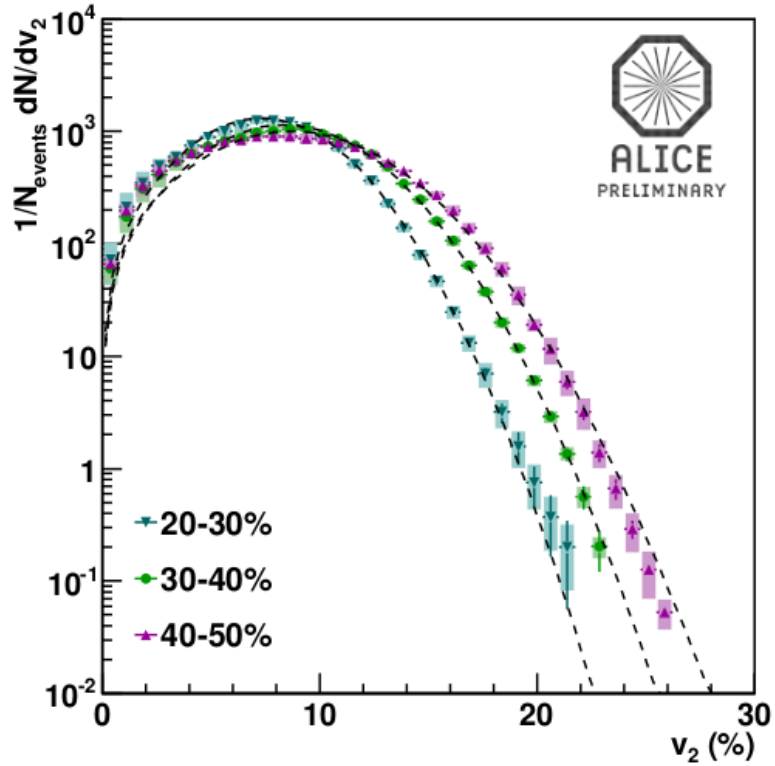

A. Timmins, Hot Quarks 2012

ALICE EbE v_2 measurements obtained via 2PC followed by unfolding.

v_2 described by Bessel-Gaussian distribution: Contribution from mean geometry+fluctuations.

$$p(v_n) \propto v_n \exp\left(-\frac{(v_n^2 + (v_n^{RP})^2)}{2\sigma_n^2}\right) I_0\left(\frac{v_n v_n^{RP}}{\sigma_n^2}\right)$$

Relative fluctuations of v_2

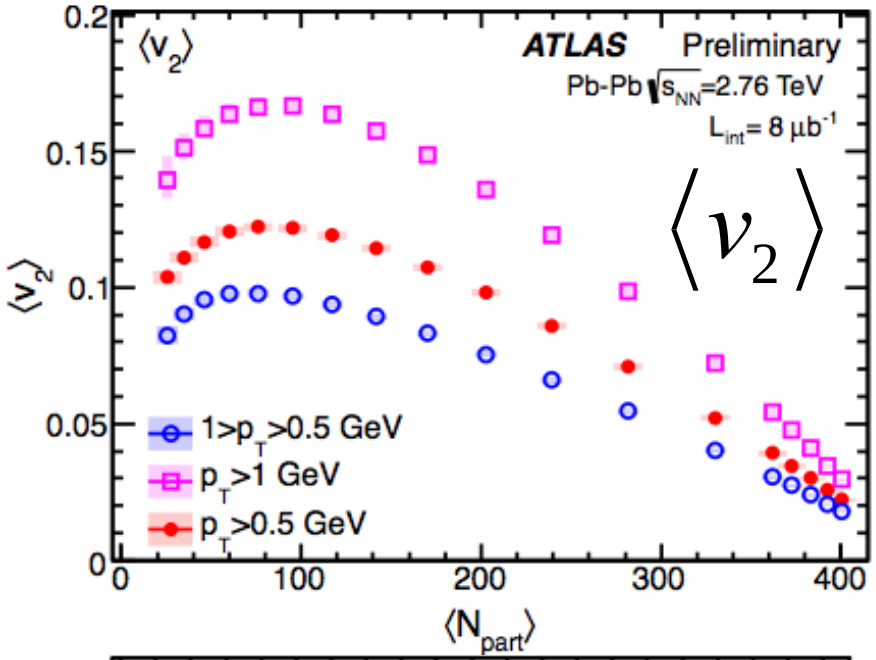

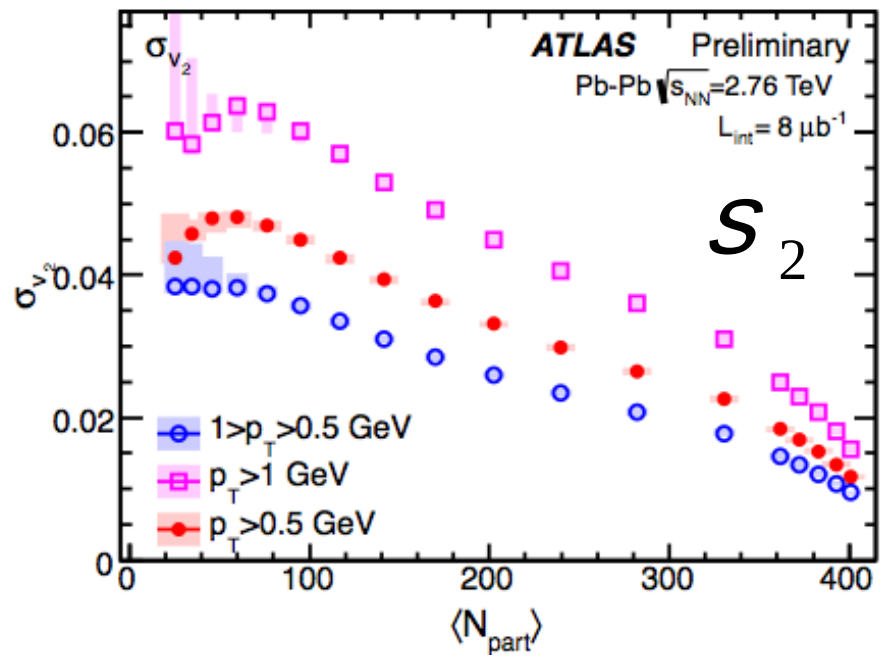

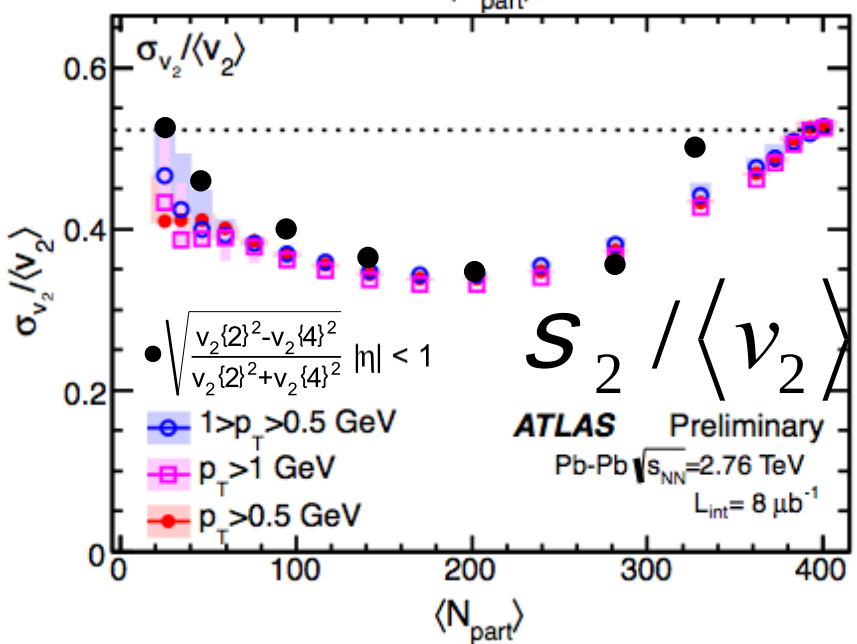

Can obtain mean, σ from EbE distributions
And calculate σ/mean

for gaussian fluctuations : $s_n / \langle v_n \rangle \approx 0.523$

Black points are fluctuations estimated from cumulant method :

$$\bullet \sqrt{\frac{v_2\{2\}^2 - v_2\{4\}^2}{v_2\{2\}^2 + v_2\{4\}^2}}$$

Relative fluctuations of v_3

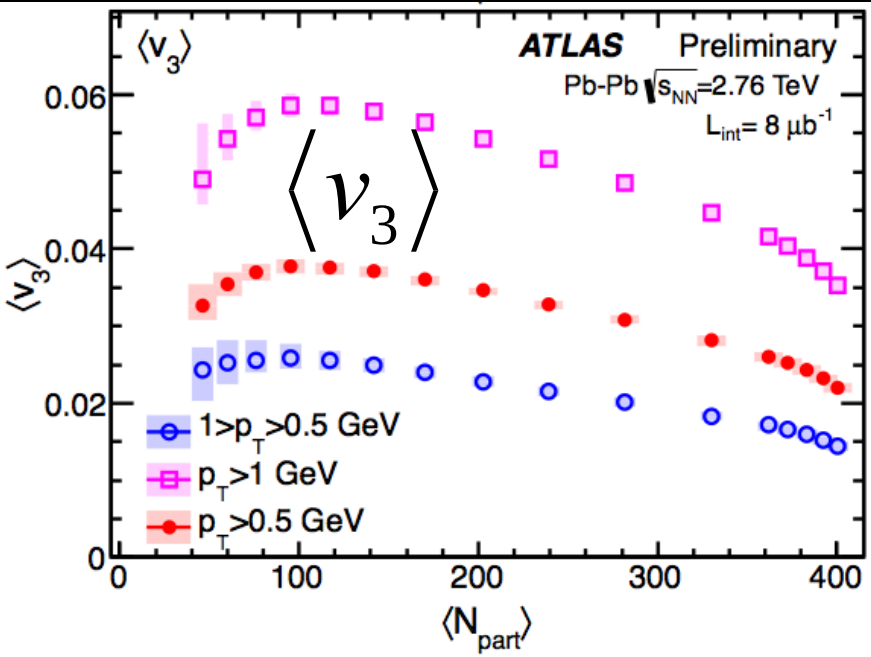

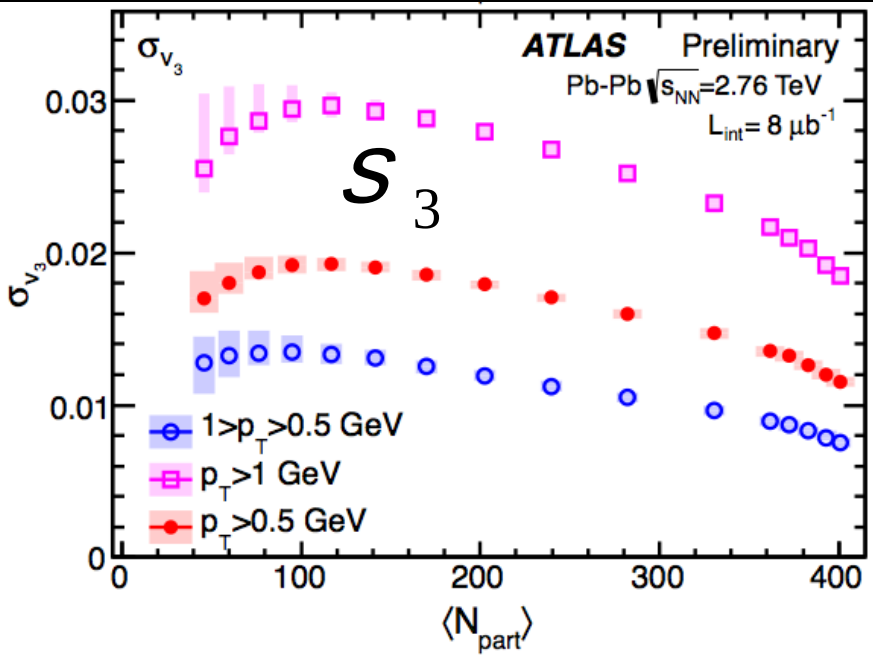

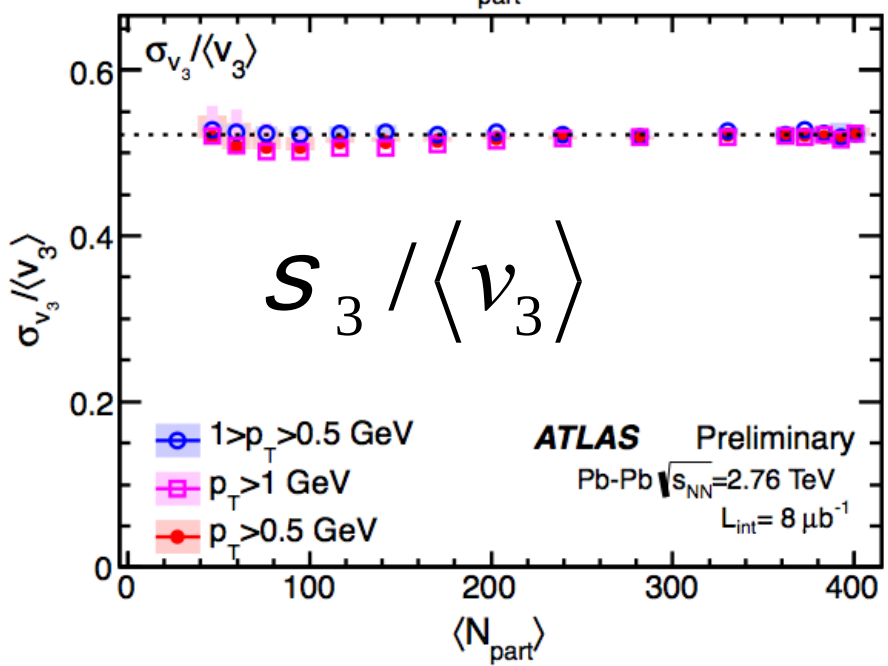

for gaussian fluctuations : $s_n / \langle v_n \rangle \approx 0.523$

Comparison to cumulant results

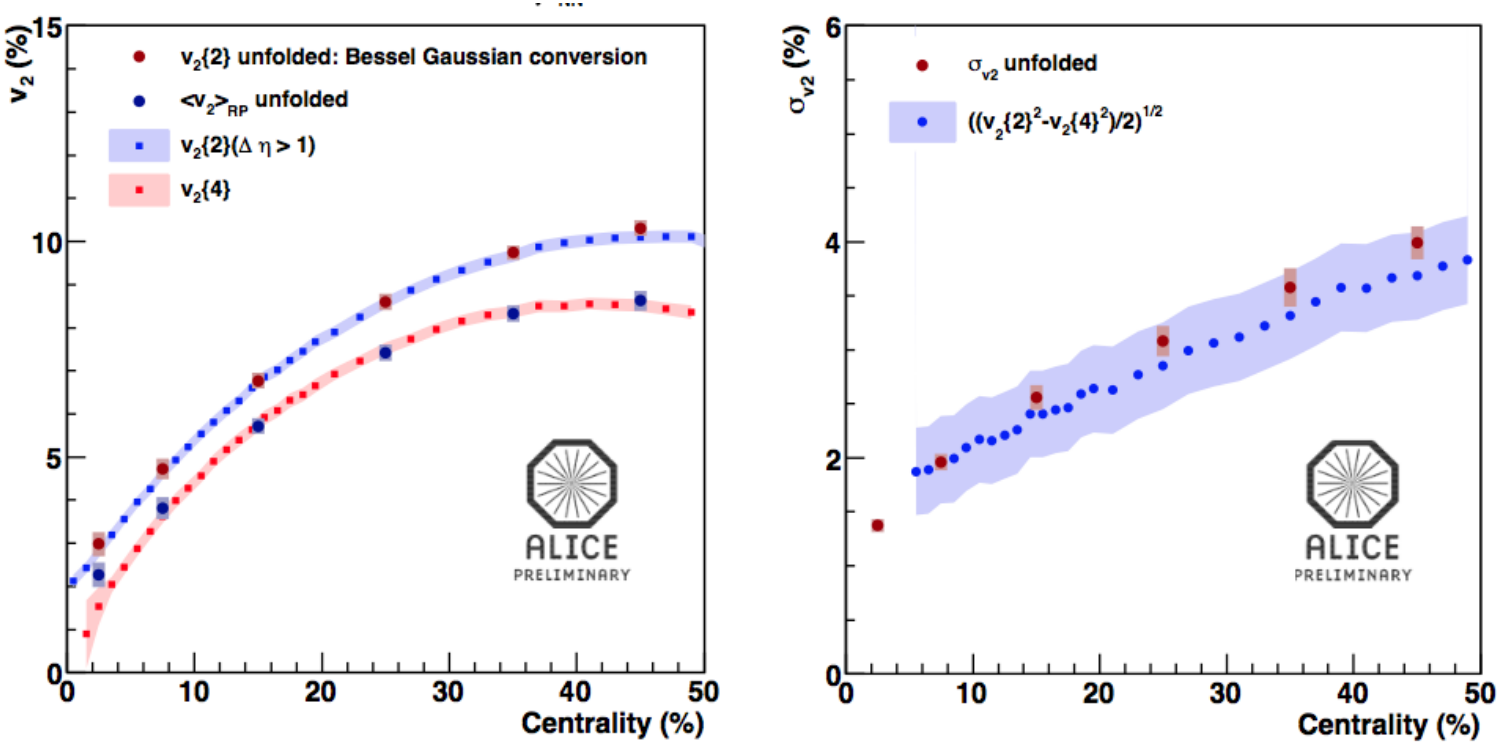

A. Timmins
Hot Quarks 2012

Extracted $v_2\{2\}$, $v_2\{4\}$ and sigma from EbE distributions are consistent with cumulant measurements

Non-flow bias on fluctuation measurements

- Non-flow effects can bias the cumulant and EbE results

- For cumulant the main effect is to enhance $v_n\{2\}$
  - Can use $v_n\{2\}$ with $\Delta\eta$ gap as substitute
- $v_n\{4\}$ and higher cumulants relatively unaffected by non-flow

- Can estimate non-flow from MC (ALICE EbE Measurements)
  - Not data driven
- For EbE v_n measurement the unfolding procedure can be used to remove non-flow (ATLAS Measurements)
  - Data driven procedure

Non-flow effects : ATLAS EbE

- Non-flow effects are mostly uncorrelated between sub-events
  - They are removed during unfolding
- HIJING+Flow afterburner test demonstrates this
  - Get response function by dividing tracks with η>0 and η<0 into sub-events
  - Get response function by randomly dividing tracks into sub-events
  - Do unfolding with both response functions and compare to input vn distribution

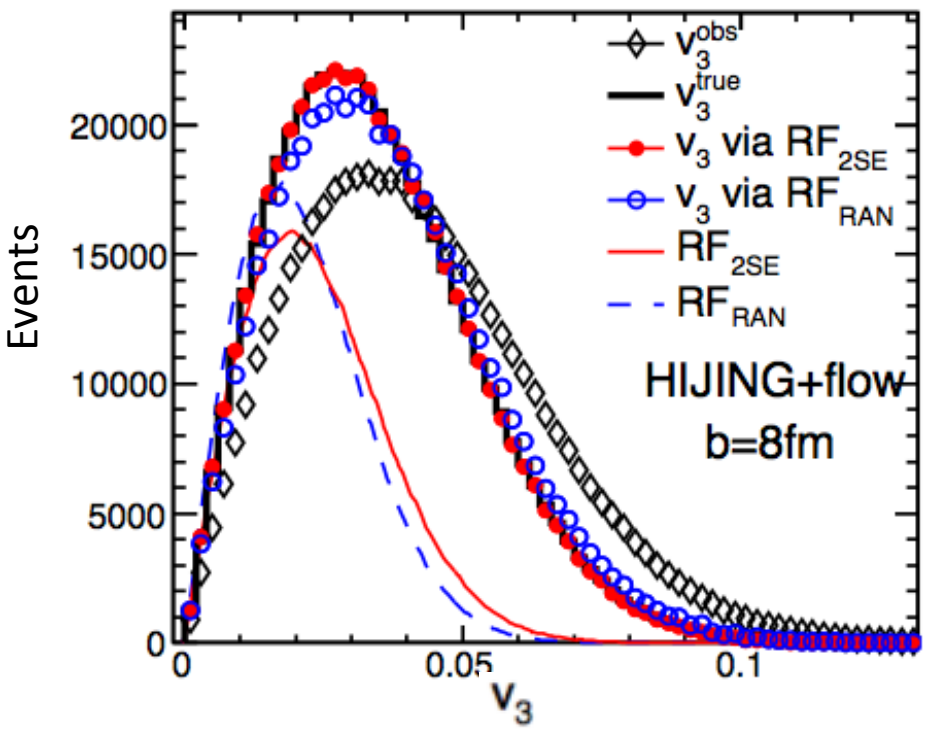

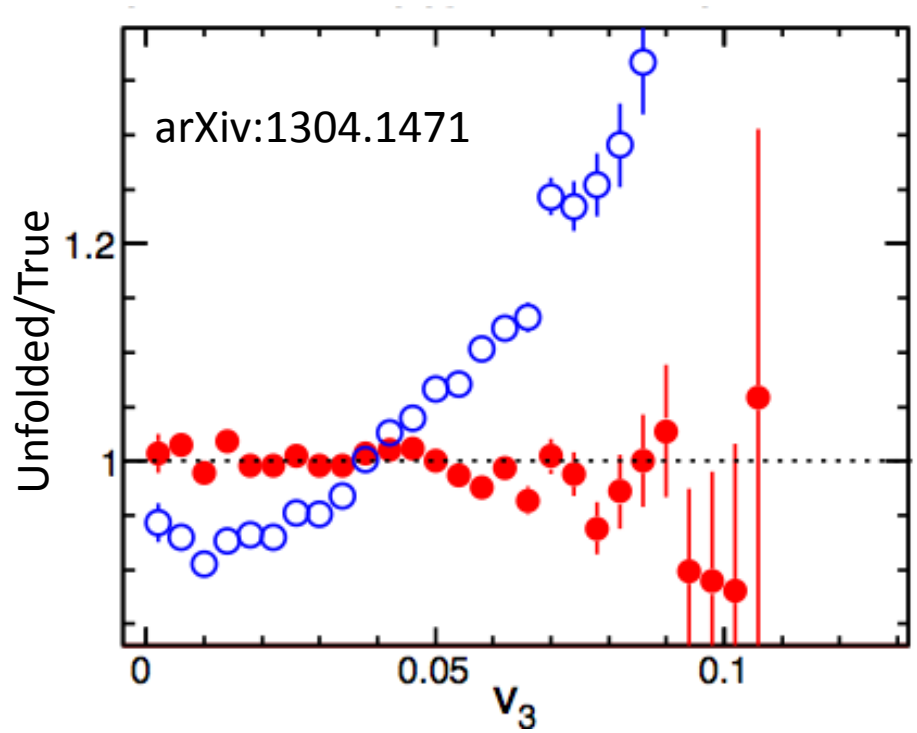

Comparison to initial geometry: v_2

$$v_n \propto \epsilon_n = \frac{\sqrt{\langle r^n \cos n\phi \rangle^2 + \langle r^n \sin n\phi \rangle^2}}{\langle r^n \rangle}$$

For Glauber and CGC mckln

Rescale ε_n distribution to the mean of data

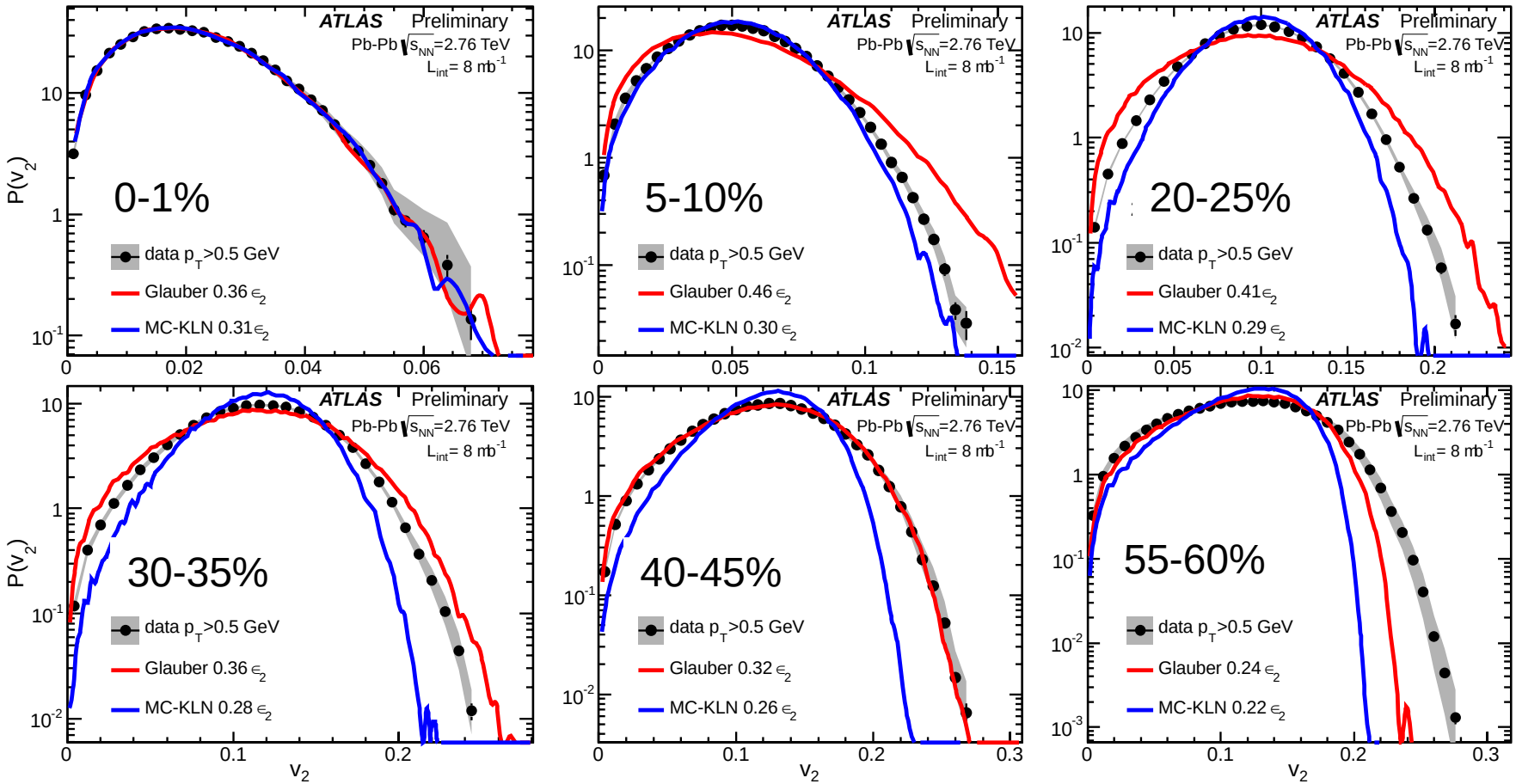

Both models fail describing $p(v_2)$ across the full centrality range

Comparison to IP-Glasma model

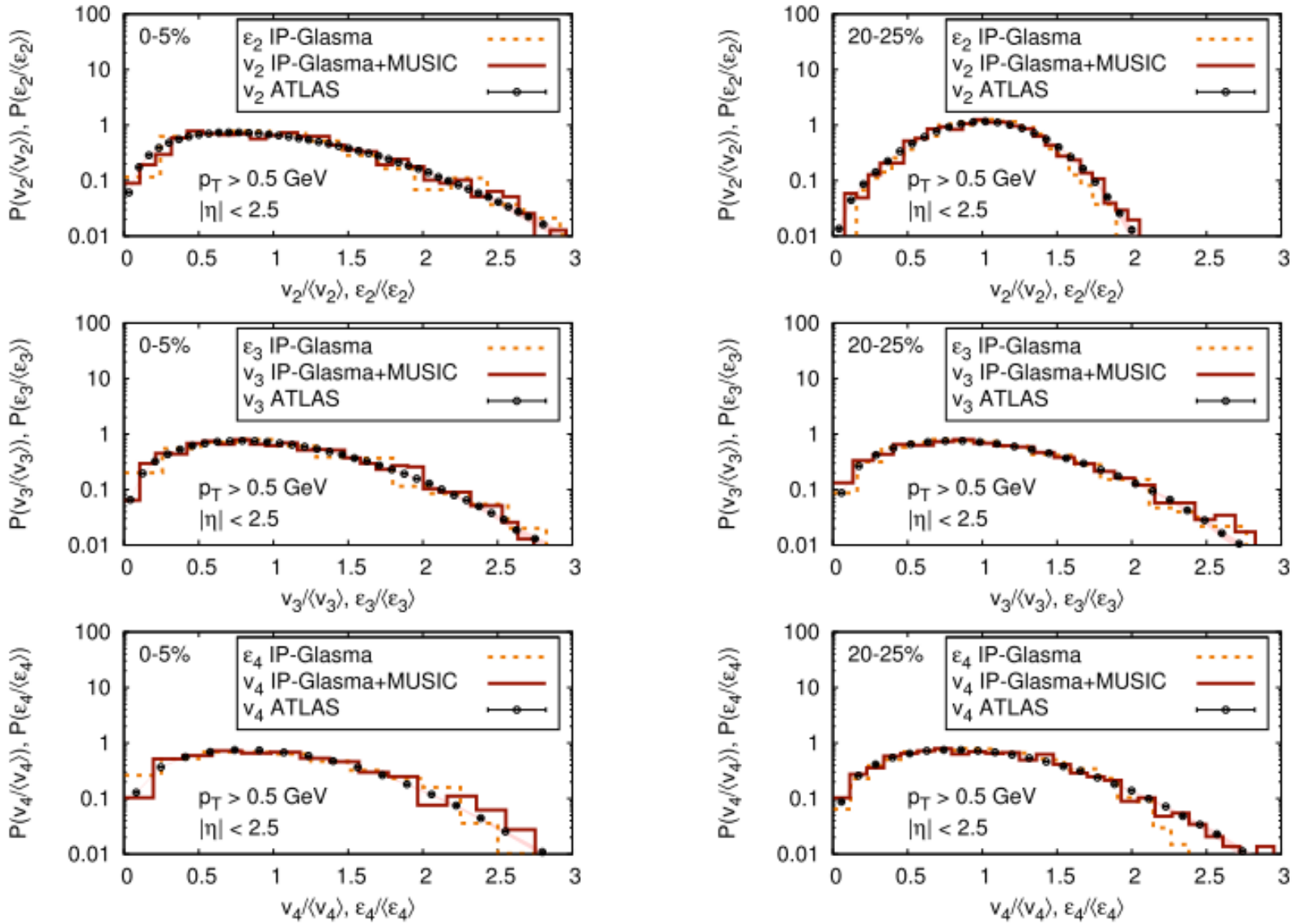

arXiv:1301.5893

1209.6330 (Gale, Jeon, Schenke, Tribedi, Venugopalan)

Talk tomorrow by Bjorn Schenke

Correlation between phases of harmonic flow

- Complementary observables to v_n
- Correlation can exist in the initial geometry and also generated during hydro evolution
- The correlation can be quantified via a set of correlators

$$\frac{dN_{events}}{d(k(\Phi_n - \Phi_m))} = 1 + 2\sum_{j=1}^{\infty} V_{n,m}^{j} \cos(jk(\Phi_n - \Phi_m))$$

arXiv:1205.3585

$$V_{n,m}^{j} = \left\langle \cos(jk(\Phi_n - \Phi_m)) \right\rangle$$

arXiv:1203.5095

- This can be generalized into multi-plane correlations

$$\left\langle \cos(c_1\Phi_1 + 2c_2\Phi_2 \ldots lc_l\Phi_l) \right\rangle \quad c_1 + 2c_2 + \ldots lc_l = 0$$

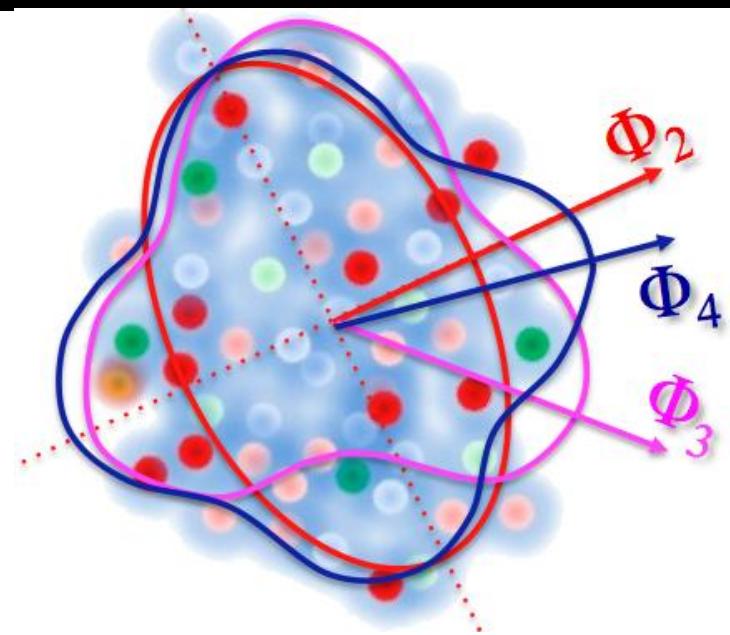

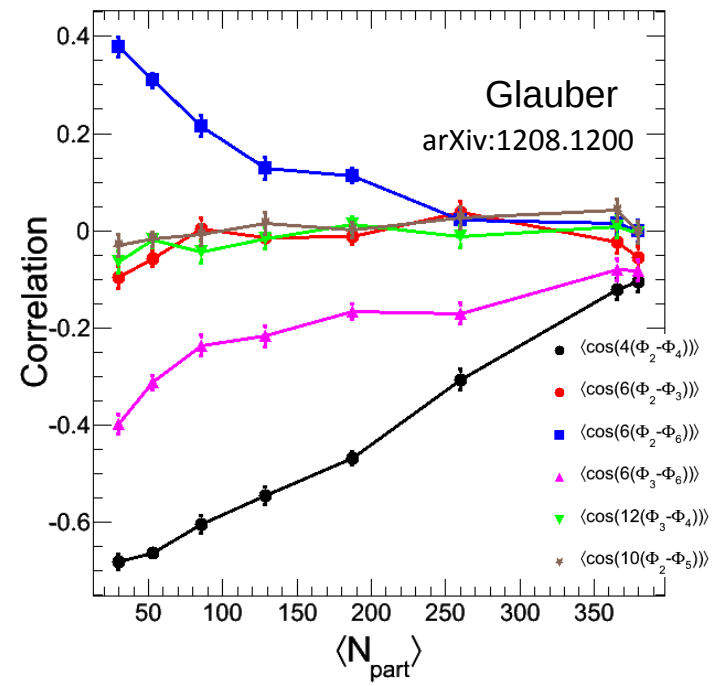

Event plane correlations

Initial geometry
+ hydrodynamic

ATLAS data

MC-Glb., $\eta/s = 0.08$

MC-KLN, $\eta/s = 0.2$

ATLAS-CONF-2012-049

arXiv:1208.1200
Heinz & Qui

geometry only

MC-Glb.

MC-KLN

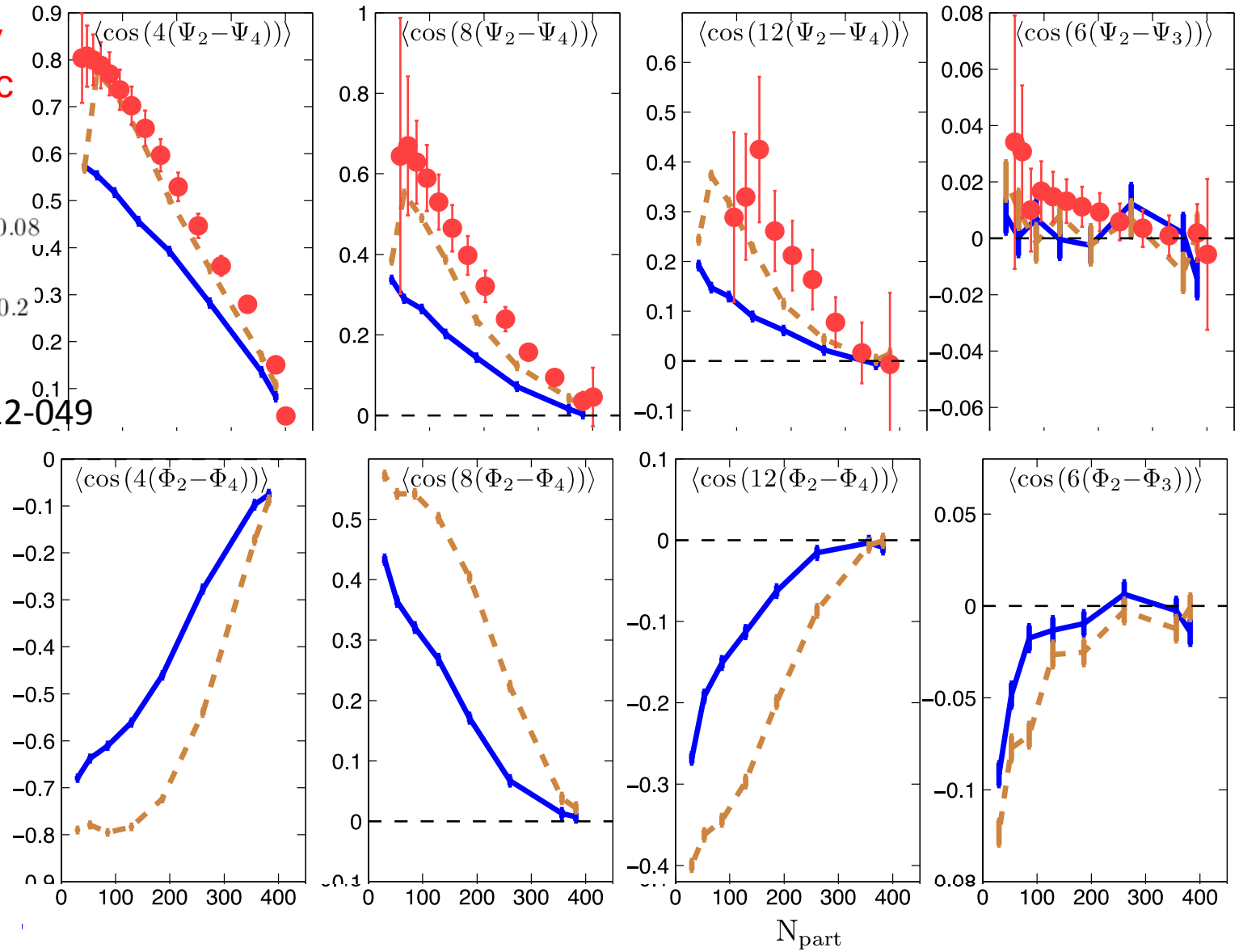

EbE hydro qualitatively reproduces features in the data

Compare with EbE hydro calculation: 3-plane

Initial geometry
+ hydrodynamic

ATLAS data

MC-Glb., $\eta/s = 0.08$

MC-KLN, $\eta/s = 0.2$

ATLAS-CONF-2012-049

arXiv:1208.1200
Heinz & Qui

geometry only

MC-Glb.

MC-KLN

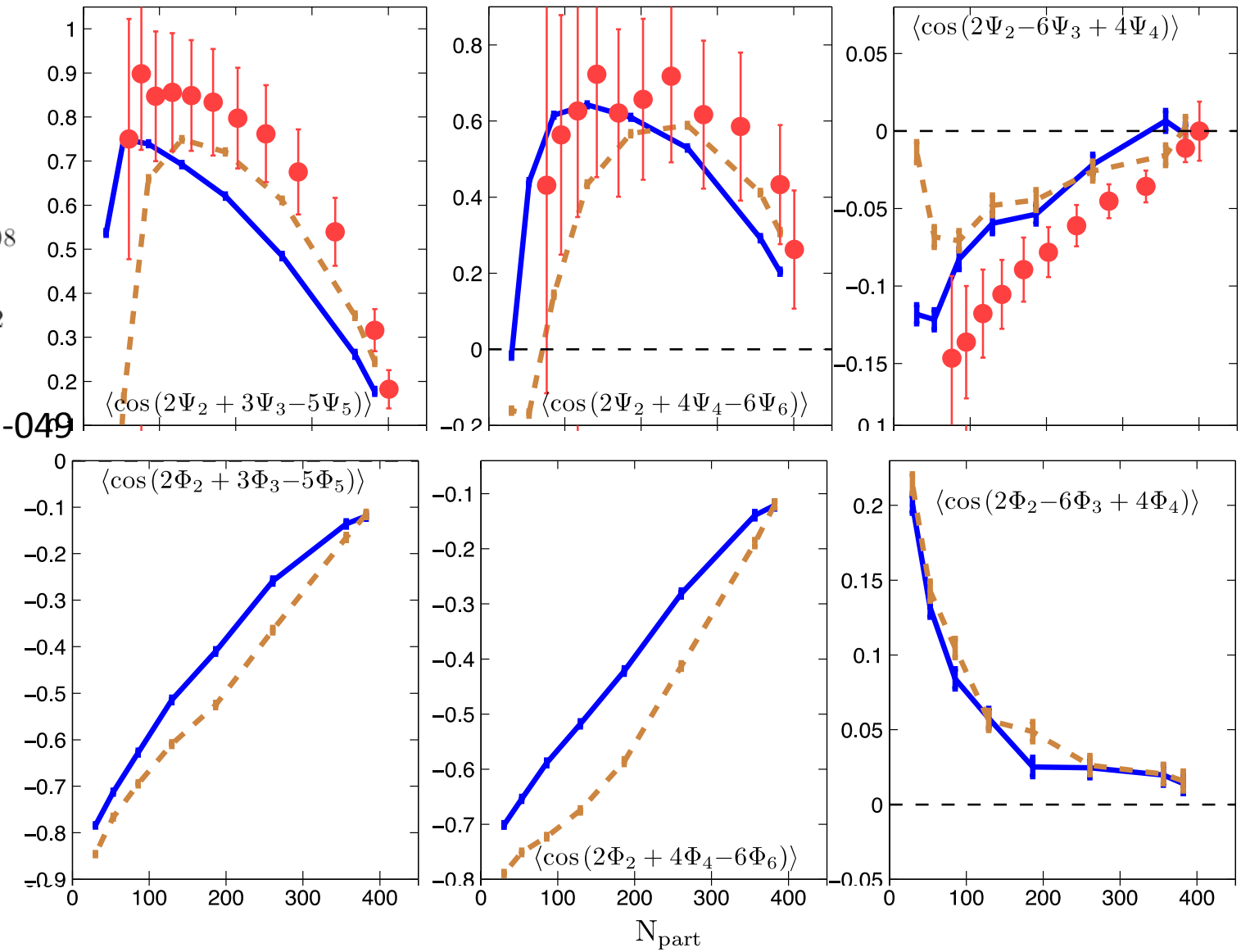

EbE hydro qualitatively reproduces features in the data

Summary

- Cumulants provide overview into nature of fluctuations
  - $v_2\{2\}$ used to probe average geometry+fluctuations.
  - $v_2\{4\}=v_2\{6\}=v_2\{8\}=v_2^{RP}$ and LYZ probe average geometry.
  - Dependence of v_n on p_T and initial geometry factorizes.
- EBE measurements of v_2, v_3 and v_4 distributions done by ATLAS and ALICE(v_2).
  - EbE measurement handles non-flow.
  - Does not assume a particular form of the EbE distributions.
  - Distributions look Bessel-Gaussian like (deviations in the tail).
  - Distributions for v_2, v_3 and v_4 well reproduced by IP-Glasma+MUSIC, but not by Glauber.
- EP Corrs give further insight into initial geometry as well as hydro-evolution
  - Can differentiate hydro-effects from initial geometry effects.
  - Also gives information on initial geometry.

Hard and soft responses from parton transport

Denes Molnar, Purdue University

Workshop on Jet Quenching at RHIC vs LHC

in Light of Recent dAu vs pPb controls

Apr 15-17, 2013, Brookhaven National Laboratory, Upton, NY

in collaboration with Deke Sun

(parton) transport can give you:

- **bulk medium evolution**
- **nonequilibrium effects**
- **fluctuations**

Covariant transport

(on-shell) phase-space density $f(x,\vec{p}) \equiv \frac{dN(\vec{x},\vec{p},t)}{d^3x d^3p}$

transport equation:

$$p^\mu \partial_\mu f_i(x,p) = C^i_{2\to 2}[\{f_j\}](x,p) + C^i_{2\leftrightarrow 3}[\{f_j\}](x,p) + \cdots$$

with, e.g.,

$$C^i_{2\to 2} = \frac{1}{2}\sum_{jkl}\int_{234} (f^k_3 f^l_4 - f^i_1 f^j_2) W^{ij\to kl}_{12\to 34} \qquad \left(\int_j \equiv \int \frac{d^3p_j}{2E_j}\,, \quad f^k_a \equiv f^k(x,p_a) \right)$$

fully causal and stable, can handle large gradients

near hydrodynamic limit, transport coefficients and relaxation times:

$$\eta \approx 1.2T/\sigma_{tr}, \qquad \tau_\pi \approx 1.2\lambda_{tr}$$

Freezeout

Cooper-Frye: <u>assumed</u> sudden transition to a gas on a 3D hypersurface

$$E\,dN = p^\mu d\sigma_\mu(x)\,d^3p\,f_{gas}(x,\vec{p})$$

Huovinen & Holopainen (QM2012): $T_{FO} = const$ **vs** $\tau_{scatt}/\tau_{exp} = const$ **?!**

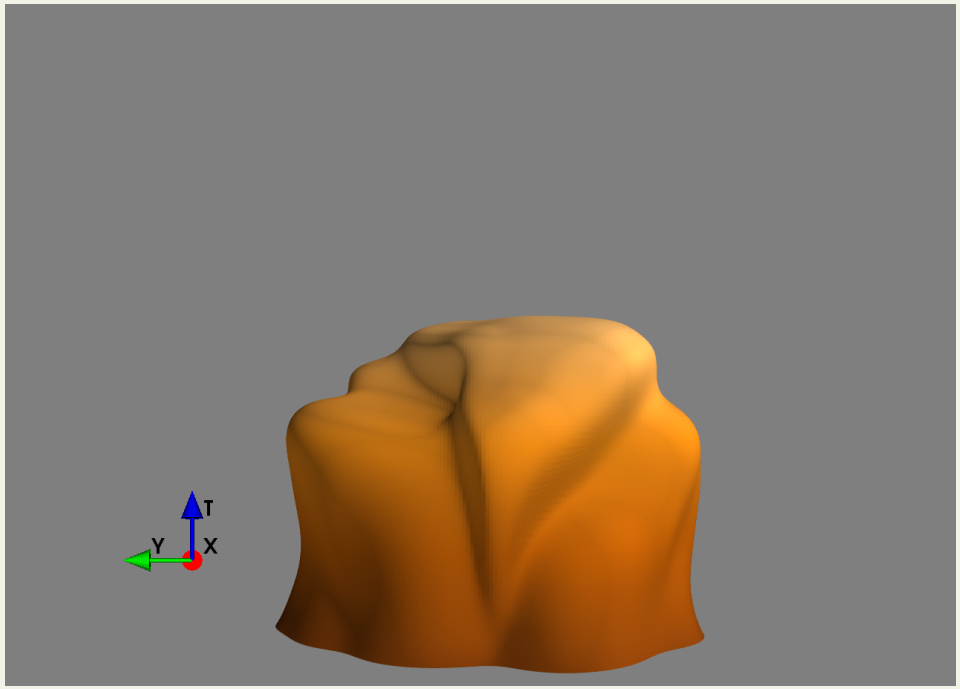

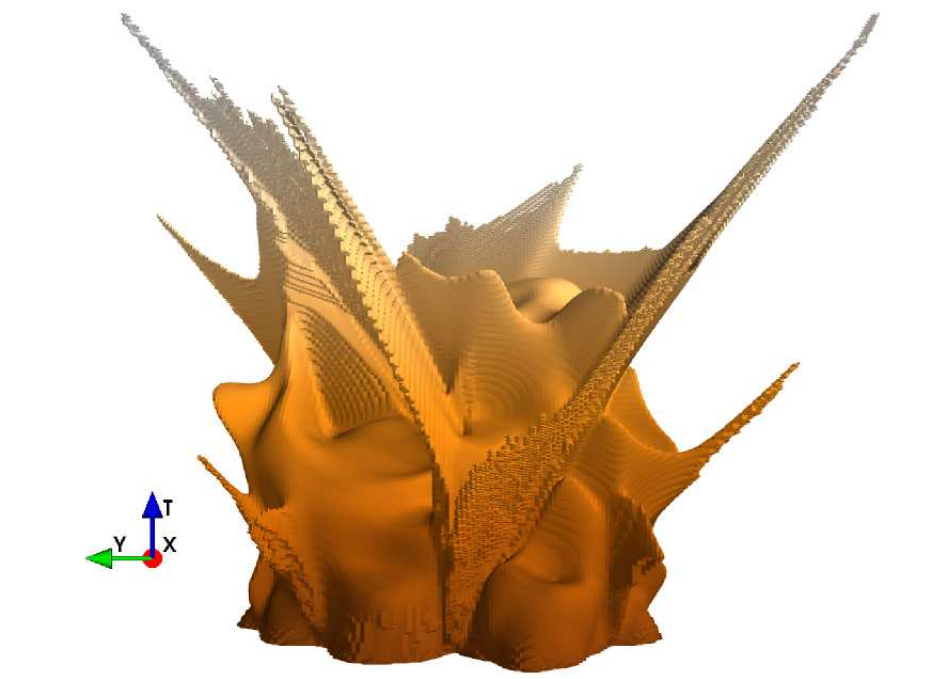

also need viscous corrections $f_{gas} = f_{equil} + \delta f$ **(e.g.,** Wolff & Molnar @ QM2012**)**

Collectivity with suitable rates

Zhang, Gyulassy & Ko ('99):

$2 \to 2$ **transport ZPC**

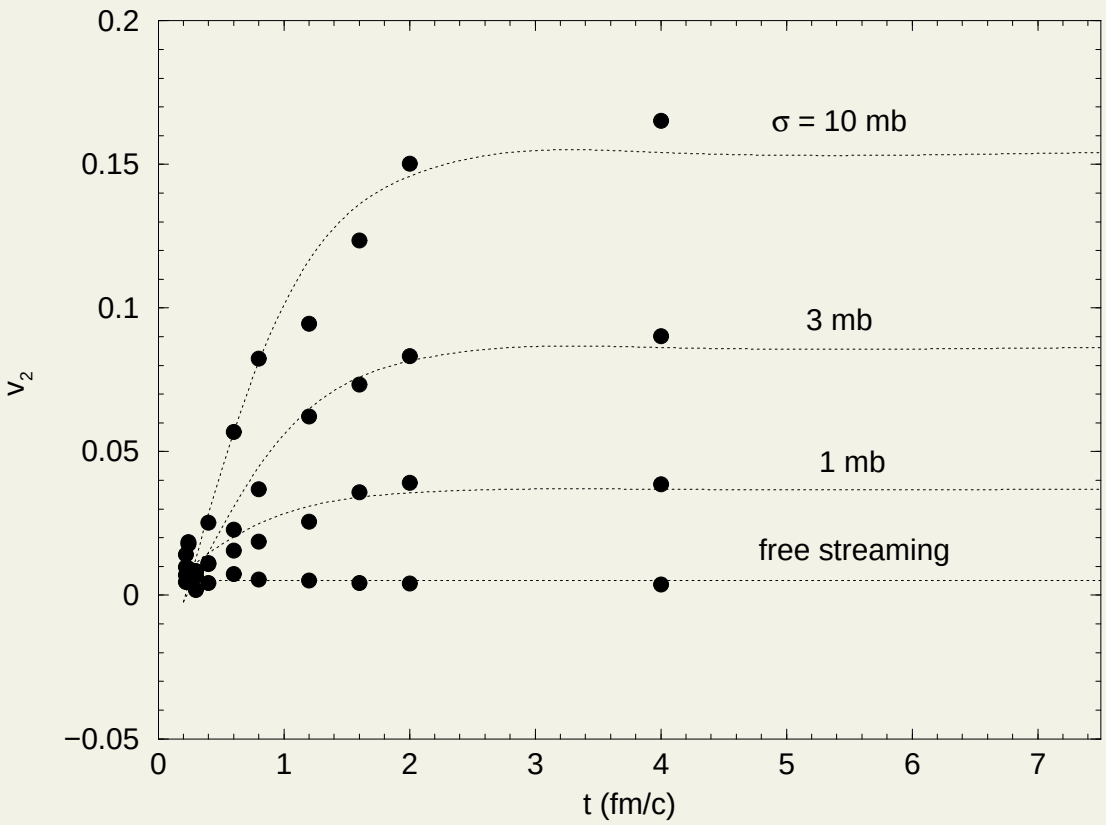

DM & Gyulassy, NPA 697 ('02):

$2 \to 2$ **transport MPC**

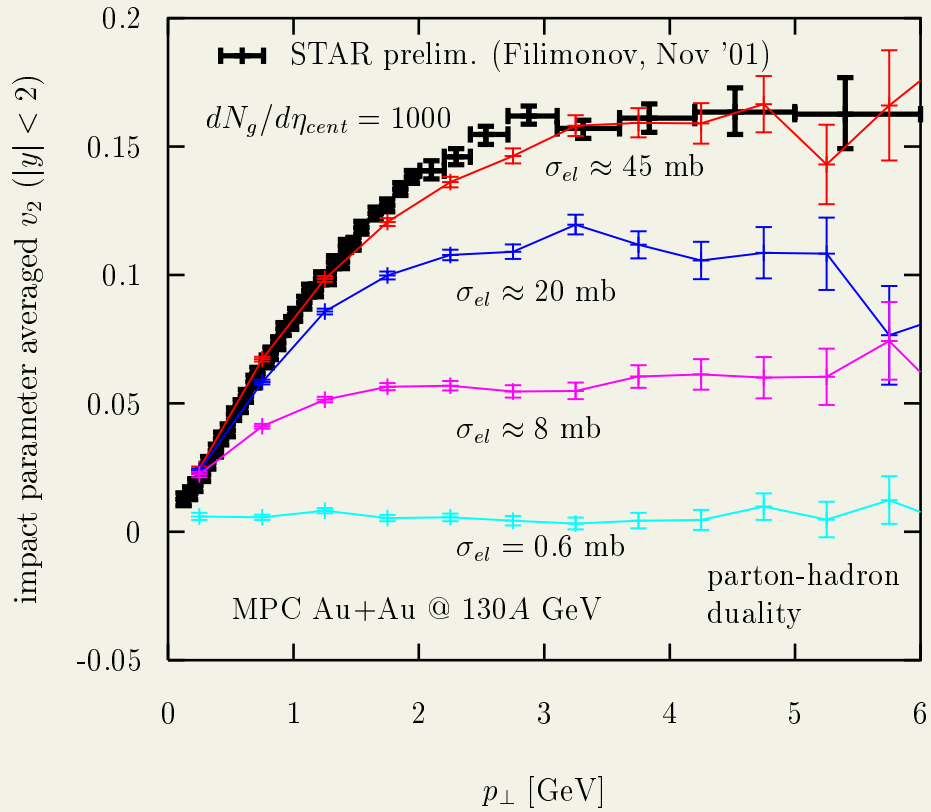

Xu & Greiner, ('08) **BAMPS claim: perturbative $3 \leftrightarrow 2$ rates thermalize**

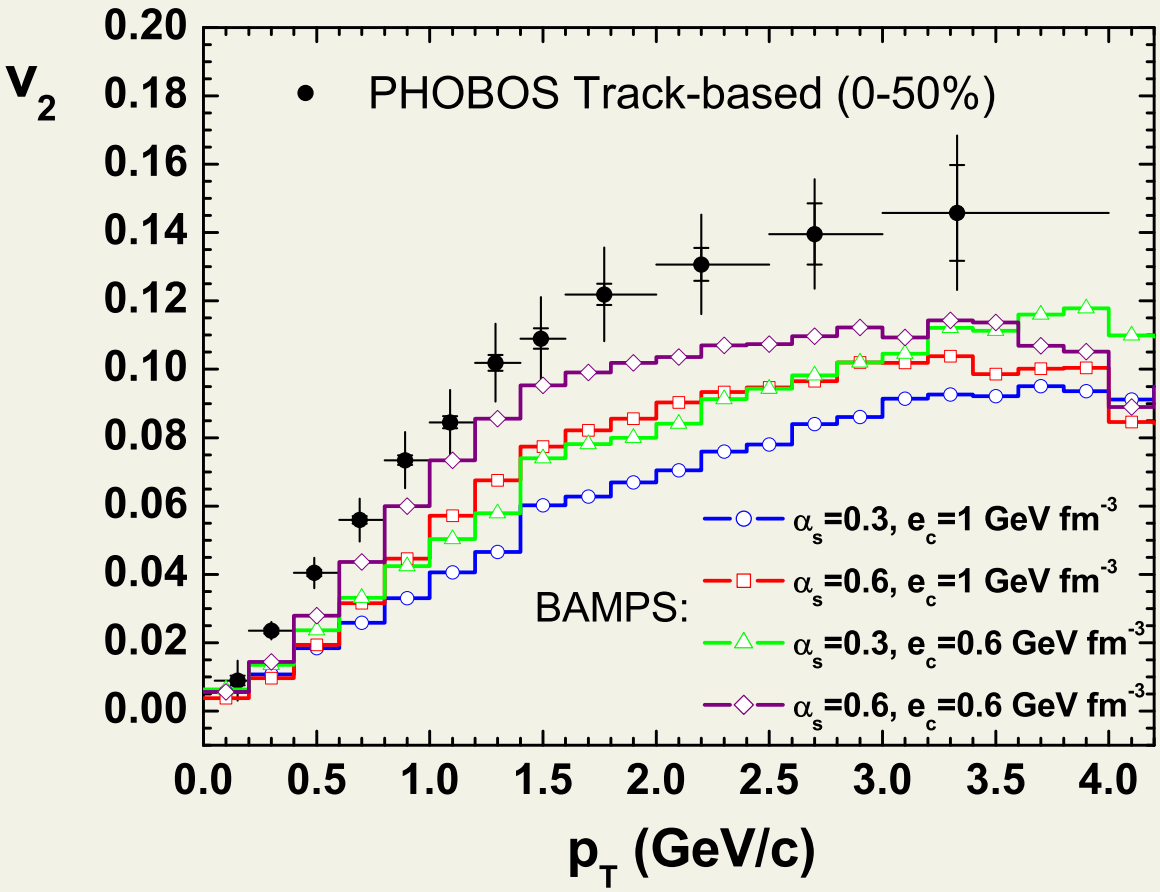

Still to be confirmed... **matrix elements?**

Application: bulk medium for jet quenching

E.g., line integrals

$$\Delta E^{(1)}_{GLV} \approx \frac{9\pi C_R \alpha_s^3}{4} \int d\tau\, \tau\, \rho(z_0 + v\tau, \tau) \ln \frac{2E}{\mu^2 \tau}$$

Gyulassy, Vitev, et al...

$$\frac{dE}{dL} = \kappa[s(L)]s(L)L$$

Shuryak & Liao

$$\frac{dE}{dL} = const \times E^{\alpha} L^{\beta} T^{2-\alpha+\beta}(L)$$

Betz et al

or stochastic E-loss

ΔE **depends on the medium. E.g, GLV needs scattering center information**

$\rightarrow$ **natural to combine (D)GLV with a parton transport model (MPC)**

GLV - opacity expansion

Gyulassy, Levai, Vitev NPB594 ('00)

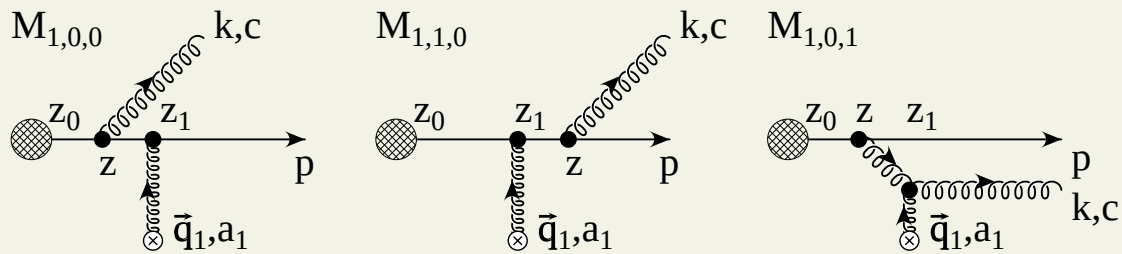

$$x\frac{dN^{(n)}}{dx\,d^2\mathbf{k}} = \frac{C_R\alpha_s}{\pi^2}\frac{\chi^n}{n!}\int\prod_{i=1}^{n}\left\{d\mathbf{q}_i\left(\frac{dz_i\rho_i\sigma_i}{\chi}\right)(\bar{v}_i^2(\mathbf{q}_i)-\delta^2(\mathbf{q}_i))\right\}$$

$$\times\left[-2\,\mathbf{C}_{(1,\cdots,n)}\cdot\sum_{m=1}^{n}\mathbf{B}_{(m+1,\cdots,n)(m,\cdots,n)}\left(\cos\left(\sum_{k=2}^{m}\omega_{(k,\cdots,n)}\Delta z_k\right)-\cos\left(\sum_{k=1}^{m}\omega_{(k,\cdots,n)}\Delta z_k\right)\right)\right]$$

formation time $\omega_{n\cdots m}=\frac{2xE}{(\mathbf{k}-\mathbf{q}_n-\cdots\mathbf{q}_m)^2}$

key assumptions: static Yukawa scatterers, soft emission, $\lambda_{MFP}\gg 1/\mu_D$

as usual, in the end interpret $\rho_i(\vec{x})\to\rho_i(\vec{x},t)$ **along jet trajectory**

Setup:

- **Bulk dynamics evolution computed from covariant transport (MPC code)**

DM & Gyulassy, PRC62 ('00)

- **Here: only use the density $\rho(x_\perp, \tau)$**
  - **in principle, we could use spacetime location of scatterers for external jets embedded in transport (no jet recoil, forward scattering)**
- **Keep energy loss stochastic (no averaging over scattering location)**
- **Radiated glue considered "lost" and feedback on medium ignored - focus on high p_T**

After E-loss, fragment as in vacuum (LO pQCD) to get some hadronic observables: R_{AA} and v_2

Medium evolution from kinetic theory (MPC transport code):

- $2 \to 2$ **with massless gluons**
- **opacity set to generate sufficient** $v_2(p_T) \sim 0.2$ **at RHIC / LHC**
- $\eta/s \approx 0.1$ **dynamics via** $\sigma_{gg} \sim 1/T^2 \sim \tau^{2/3}$ DM, arXiv:0806.0026
- **boost-invariant initial conditions in** $|\eta| < 5$ **window**

- **LO pQCD jet production & fragmentation (CTEQ5L, BKK95,** $K_{NLO} \approx 2.5$**)**
- **jet and bulk transverse profiles** $\propto \rho^{binary}(x_\perp)$**, with** $dN^{bulk}/dy \propto N_{part}$
- T **set by** $\rho(T)$ **for massless gluon gas,** $\mu_D = gT$
- $\tau_0 = 0.6$ **fm formation, and LINEAR density buildup** $\rho(\tau) \propto \tau$ **for** $\tau < \tau_0$

Two centralities: $0 - 10$**% (**$b \approx 3$ **fm) and** $25 - 35$**% (**$b \approx 8$ **fm)**

4 scenarios:

1D = longitudinal Bjorken expansion, $\langle \Delta E \rangle$

1D, stochastic = longitudinal Bjorken expansion, $\Delta E(z)$

3D = Bjorken AND transverse expansion, $\langle \Delta E \rangle$

3D, stochastic = Bjorken AND transverse expansion, $\Delta E(z)$

not the most sophisticated E-loss treatment

but we <u>did</u> include transverse expansion (unlike Buzzatti et al, Horowitz et al, Betz et al**)**

Finite energy & kinematics crucial:

$$|k| \; < \sim xE$$
$$|q| \; < \sim \sqrt{s} \; \sim \; \sqrt{6ET}$$
$$xE \; > \sim \mu \qquad \textbf{(plasma)}$$

$$\Delta E^{(1)}_{GLV}(z) = \frac{C_R \alpha_s}{\pi^2} \chi \int dx\, d\mathbf{k}\, d\mathbf{q}\, \frac{\mu^2}{\pi(\mathbf{q}^2+\mu^2)^2} \frac{2\mathbf{k}\cdot\mathbf{q}}{\mathbf{k}^2(\mathbf{k}-\mathbf{q})^2}(1-\cos\omega\Delta z)$$
$$\equiv \frac{2C_R\alpha_s}{\pi} E\,\chi\, I(\Delta z/\tau(z), E/\mu(z)) \qquad , \qquad \omega \equiv (\mathbf{k}-\mathbf{q})^2/(2Ex)$$

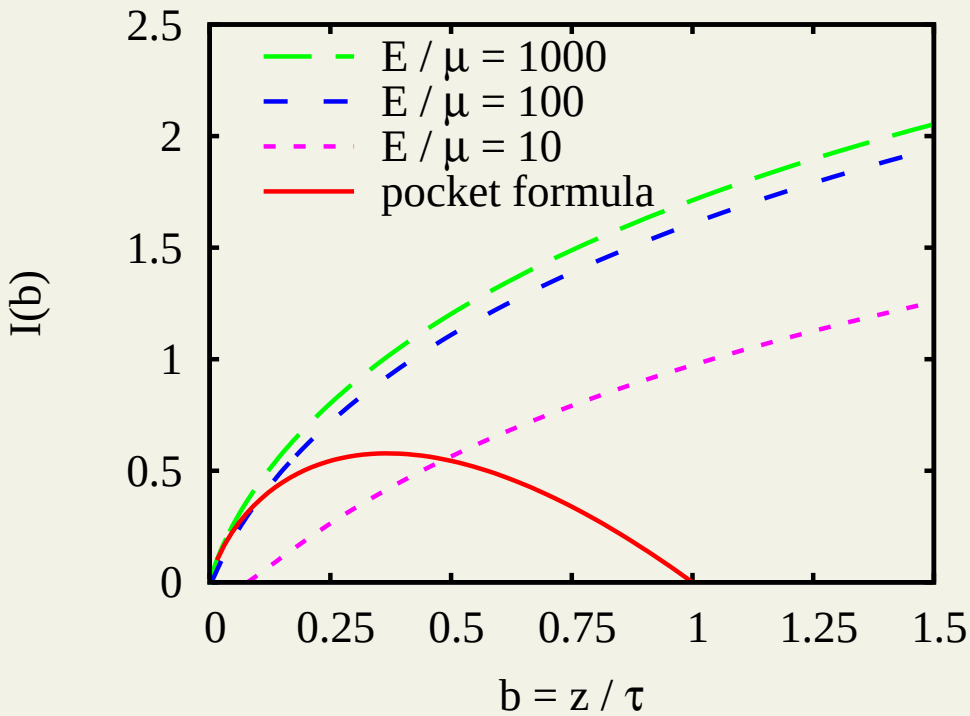

$$\tau(z) \equiv \frac{2E}{\mu^2(z)}$$

"pocket formula"

$$\langle \Delta E^{(1)}_{GLV} \rangle \sim \int \rho(z_0 + v\tau, \tau) \ln \frac{2E}{\mu^2 \tau}$$

not reliable

pion RAA, RHIC

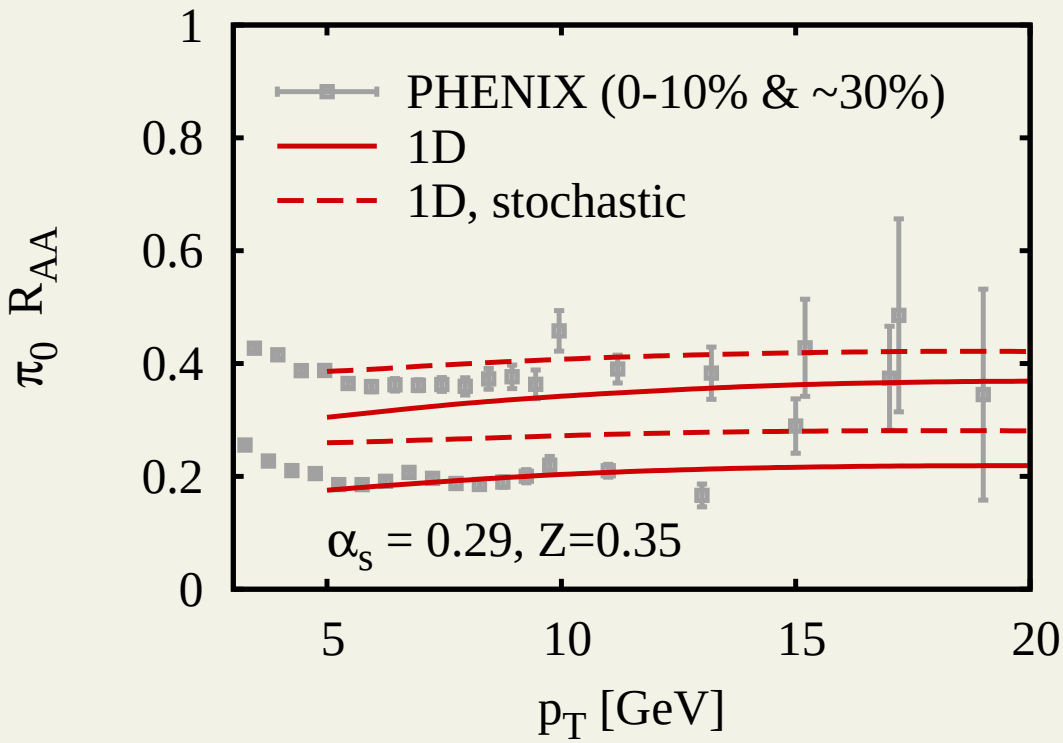

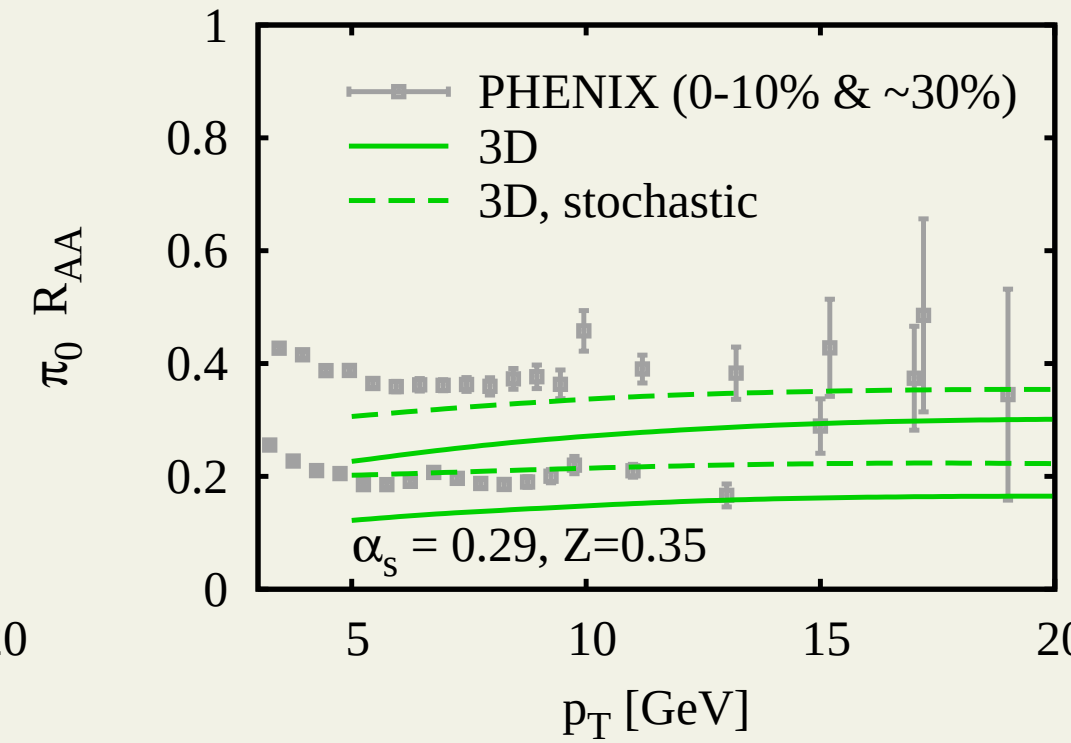

fluctuations and transverse expansion matter

more energy loss with transverse expansion because GLV favors large $\Delta z/\tau_f$

pion RAA, RHIC - α_s scaled to RAA for central

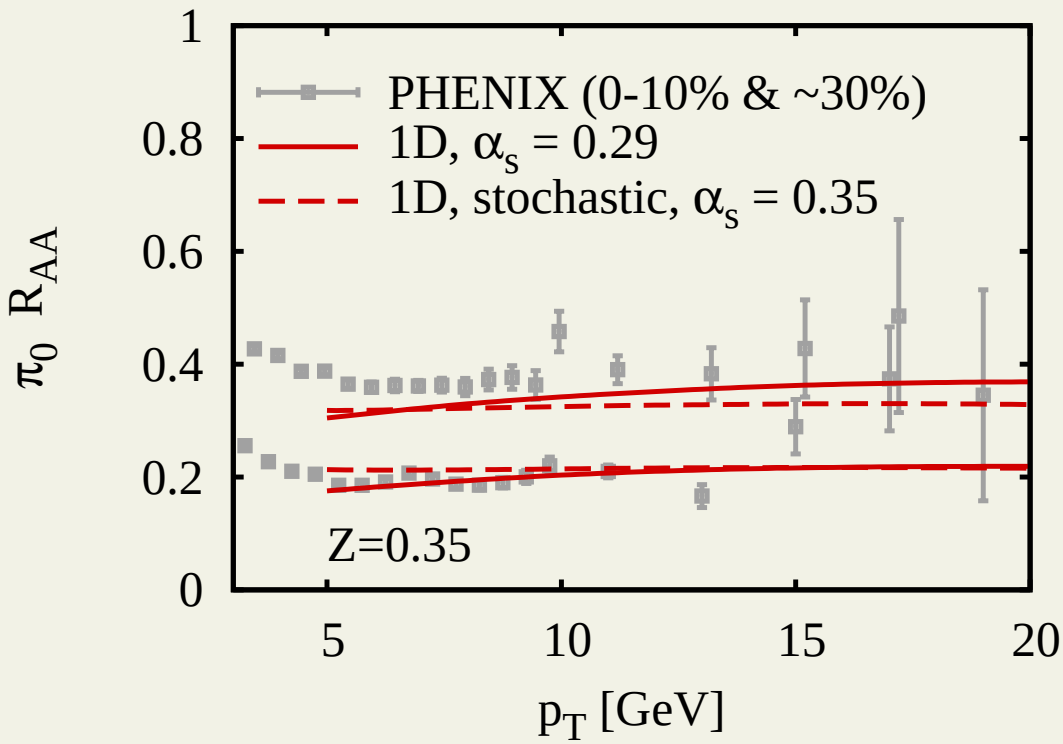

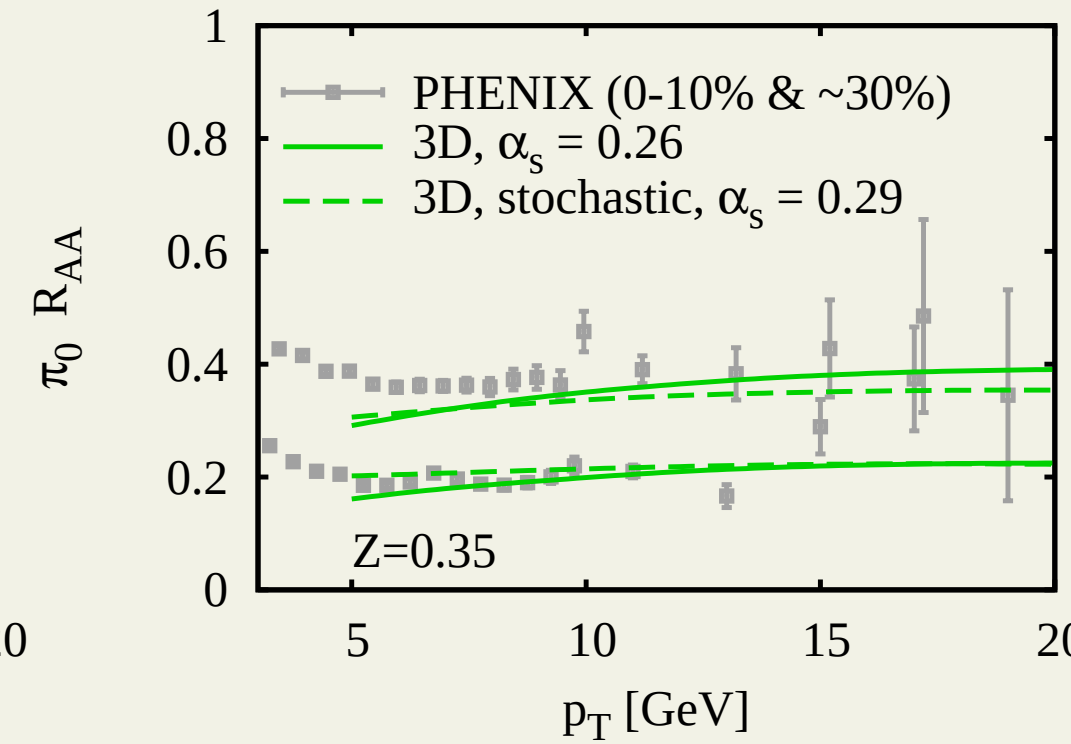

only small 10-15% differences after tuning parameters to central data

pion v2, RHIC

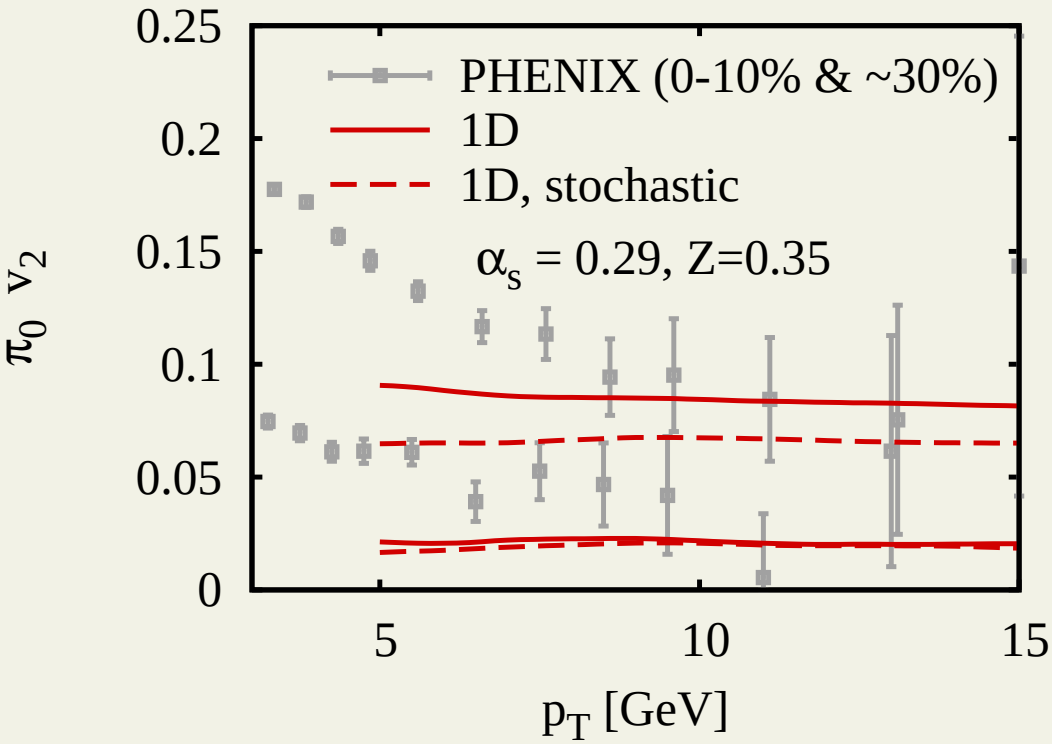
PHENIX (0-10% & ~30%)
1D
1D, stochastic
α_s = 0.29, Z=0.35
π_0 v_2
p_T [GeV]
0.25
0.2
0.15
0.1
0.05
0
5
10
15

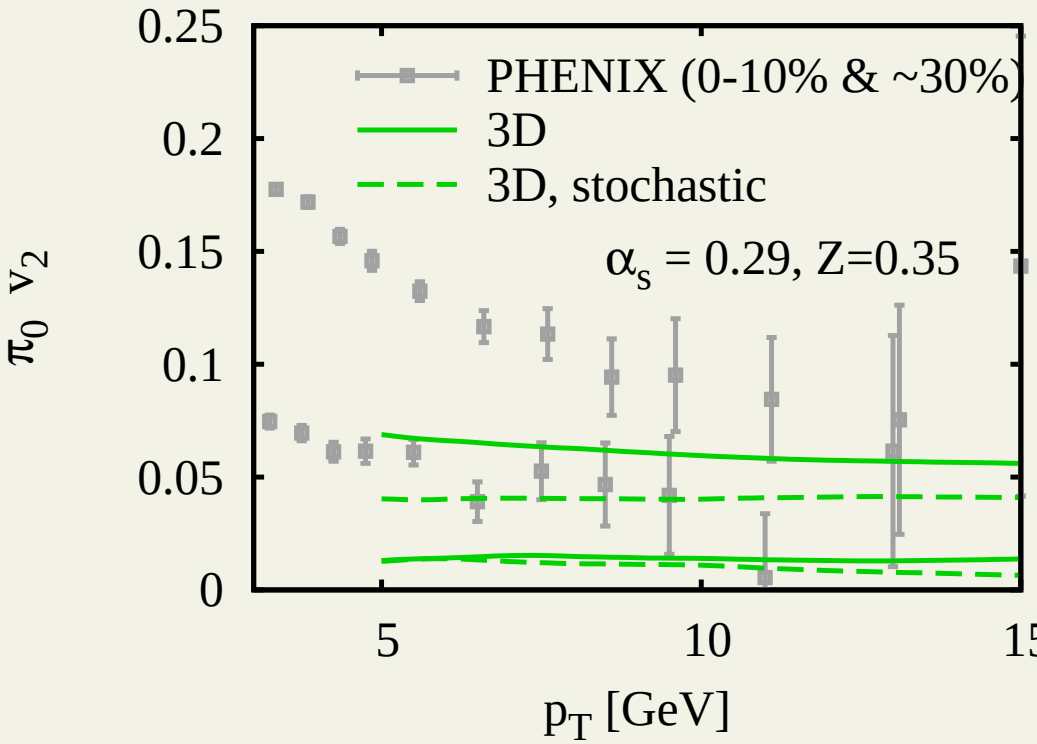
PHENIX (0-10% & ~30%)
3D
3D, stochastic
α_s = 0.29, Z=0.35
π_0 v_2
p_T [GeV]
0.25
0.2
0.15
0.1
0.05
0
5
10

pion v2, RHIC - α_s scaled to RAA for central

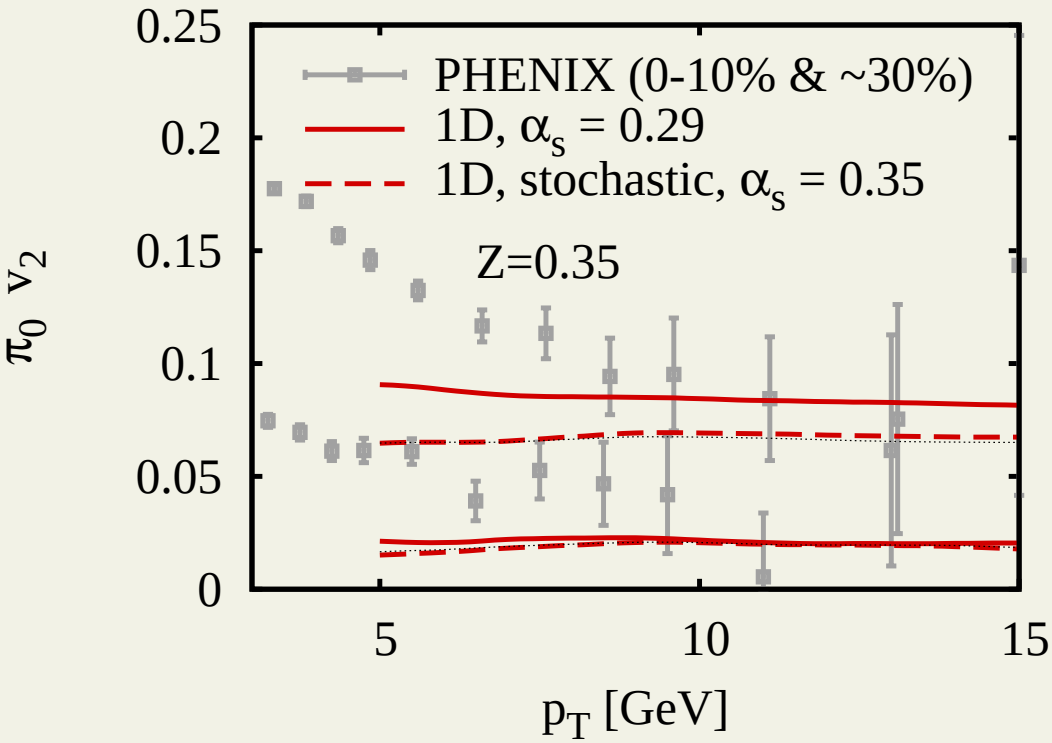

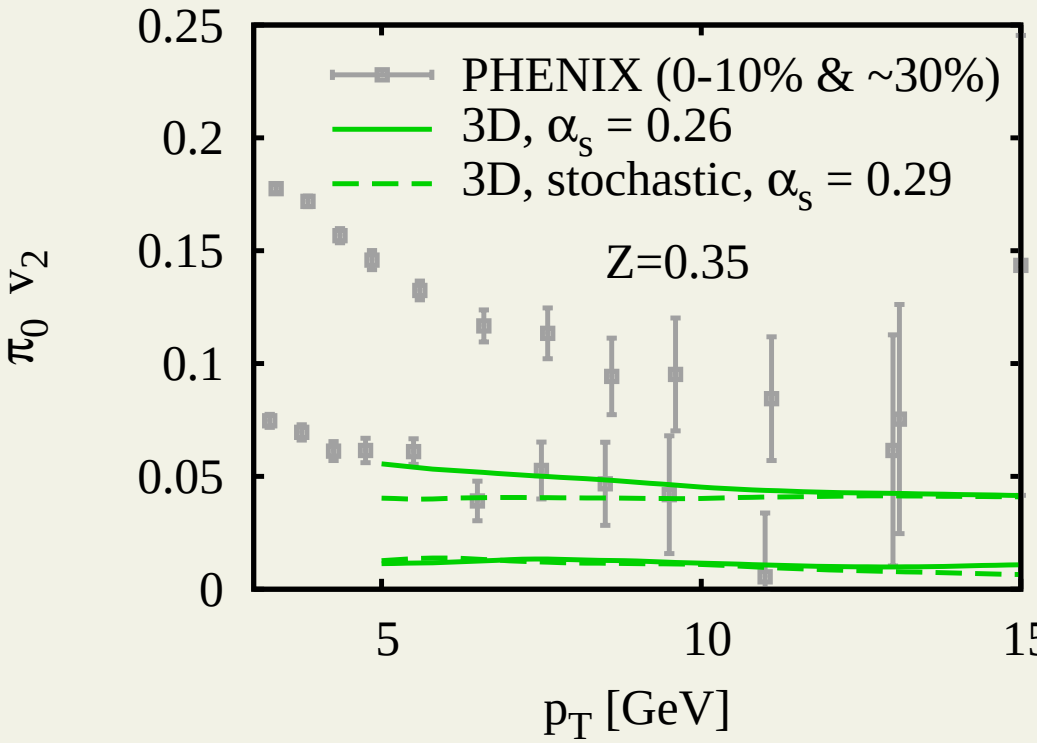

challenging to get enough $v_2 > 4 - 5\%$ with expanding medium

smaller v_2 with transverse expansion - GLV favors later times (large $\Delta z/\tau_f$)

Now move to LHC energies. Simple assumption:

- **higher** $dN/d\eta = 2400$ **in central collisions (**$b = 0$**)**
- **all other ingredients stay same**

at present we only have mid-peripheral results in the 3D case

pion RAA, LHC

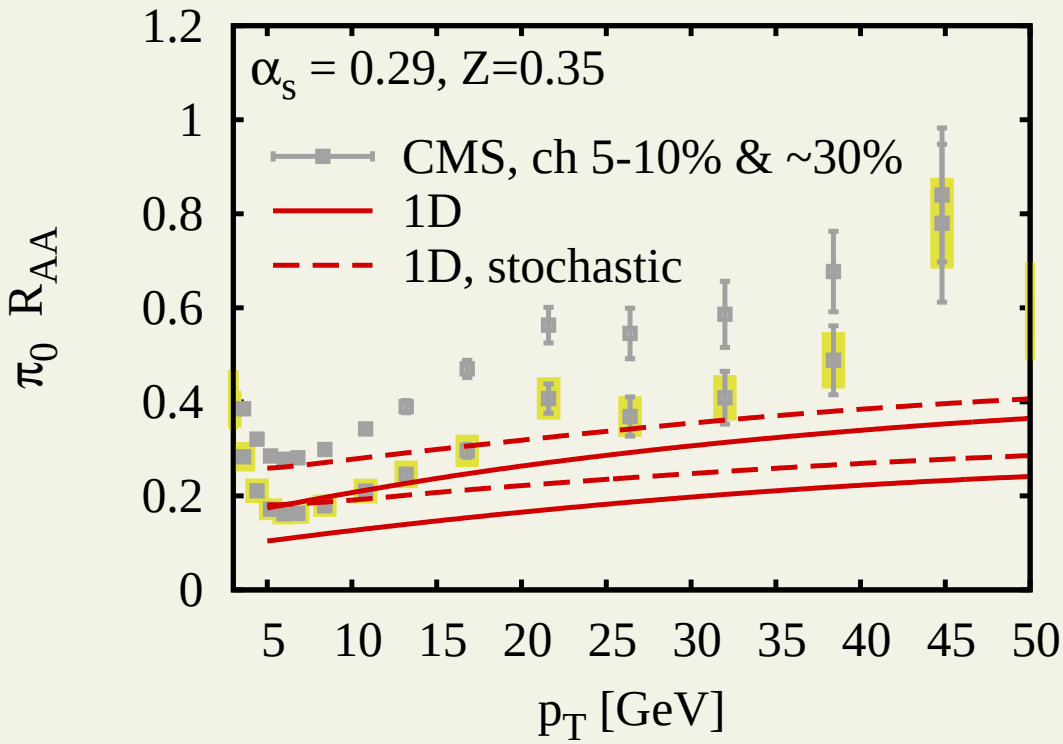
α_s = 0.29, Z=0.35
CMS, ch 5-10% & ~30%
1D
1D, stochastic
π_0 R_{AA}
p_T [GeV]
0
0.2
0.4
0.6
0.8
1
1.2
5
10
15
20
25
30
35
40
45
50

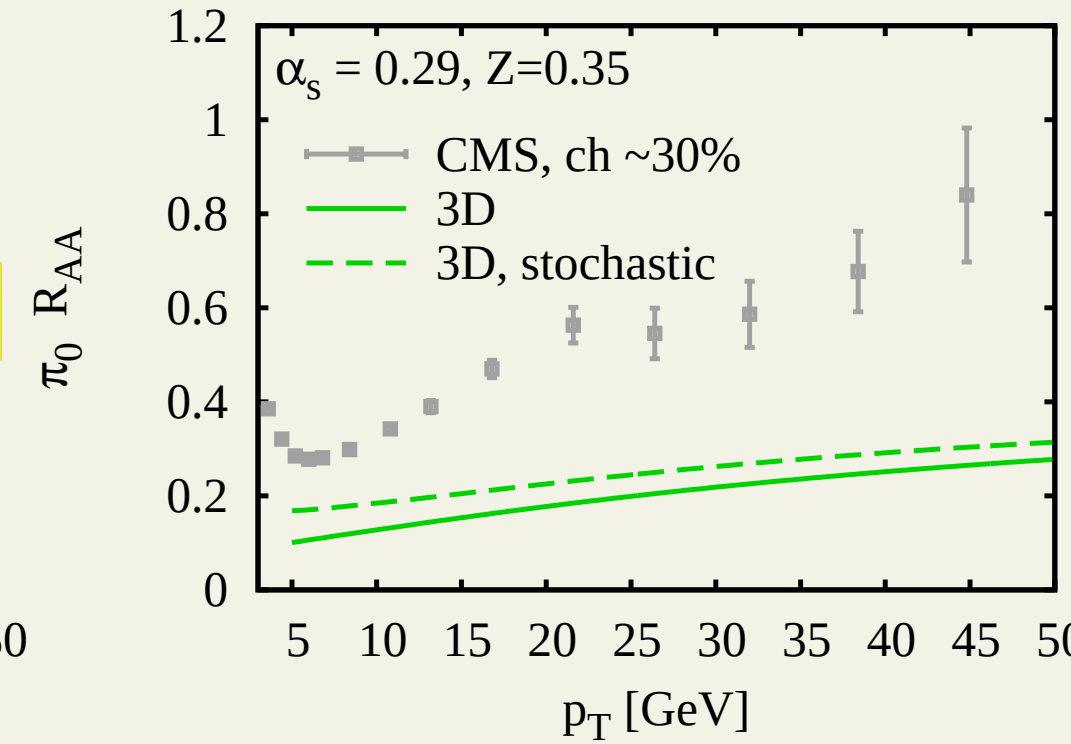
α_s = 0.29, Z=0.35
CMS, ch ~30%
3D
3D, stochastic
π_0 R_{AA}
p_T [GeV]
0
0.2
0.4
0.6
0.8
1
1.2
5
10
15
20
25
30
35
40
45
50

pion RAA, LHC - α_s scaled to RAA for central at pT = 6 GeV

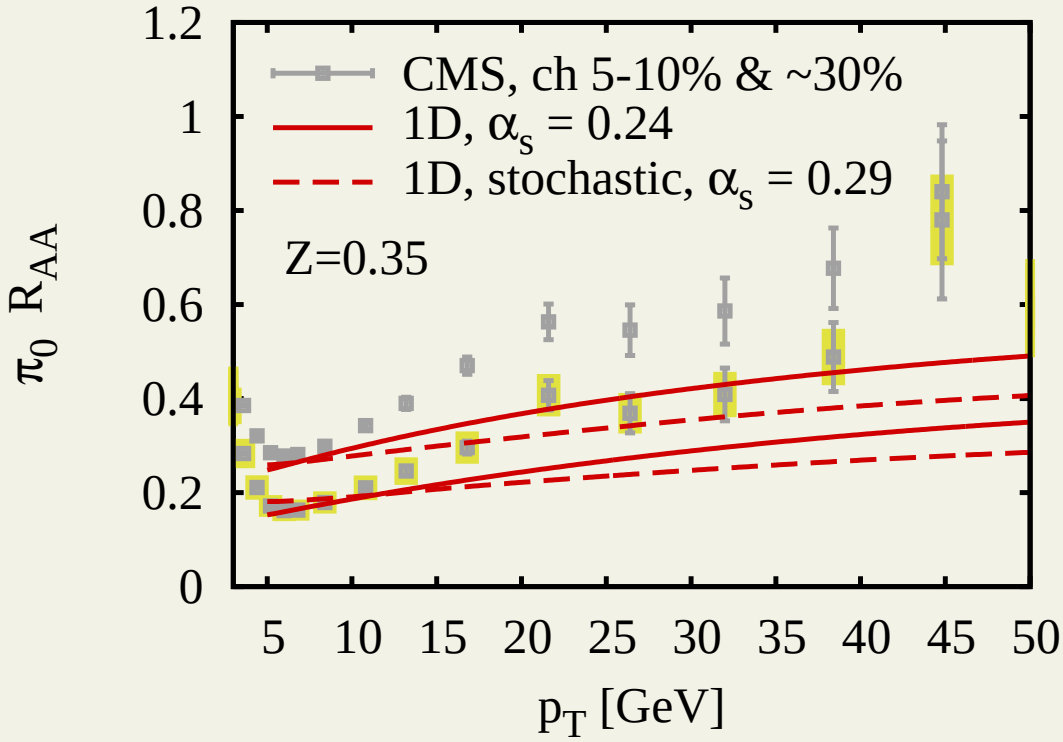

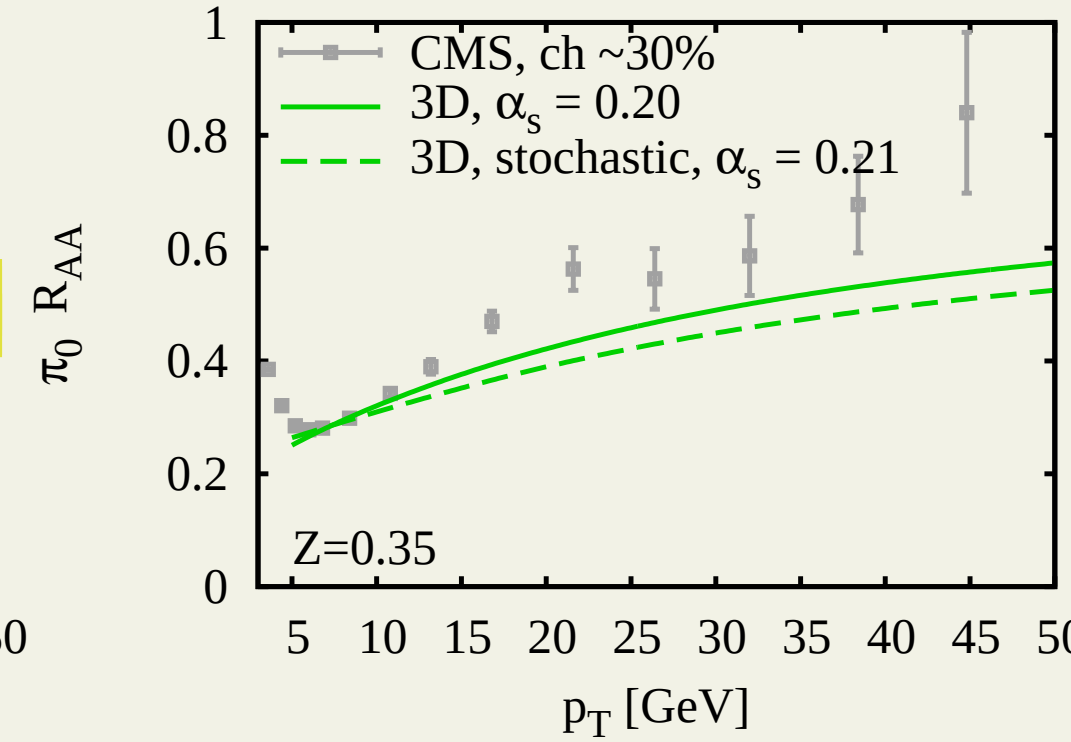

GLV implementation here is simplified, also $\alpha_s = const$ (no running)

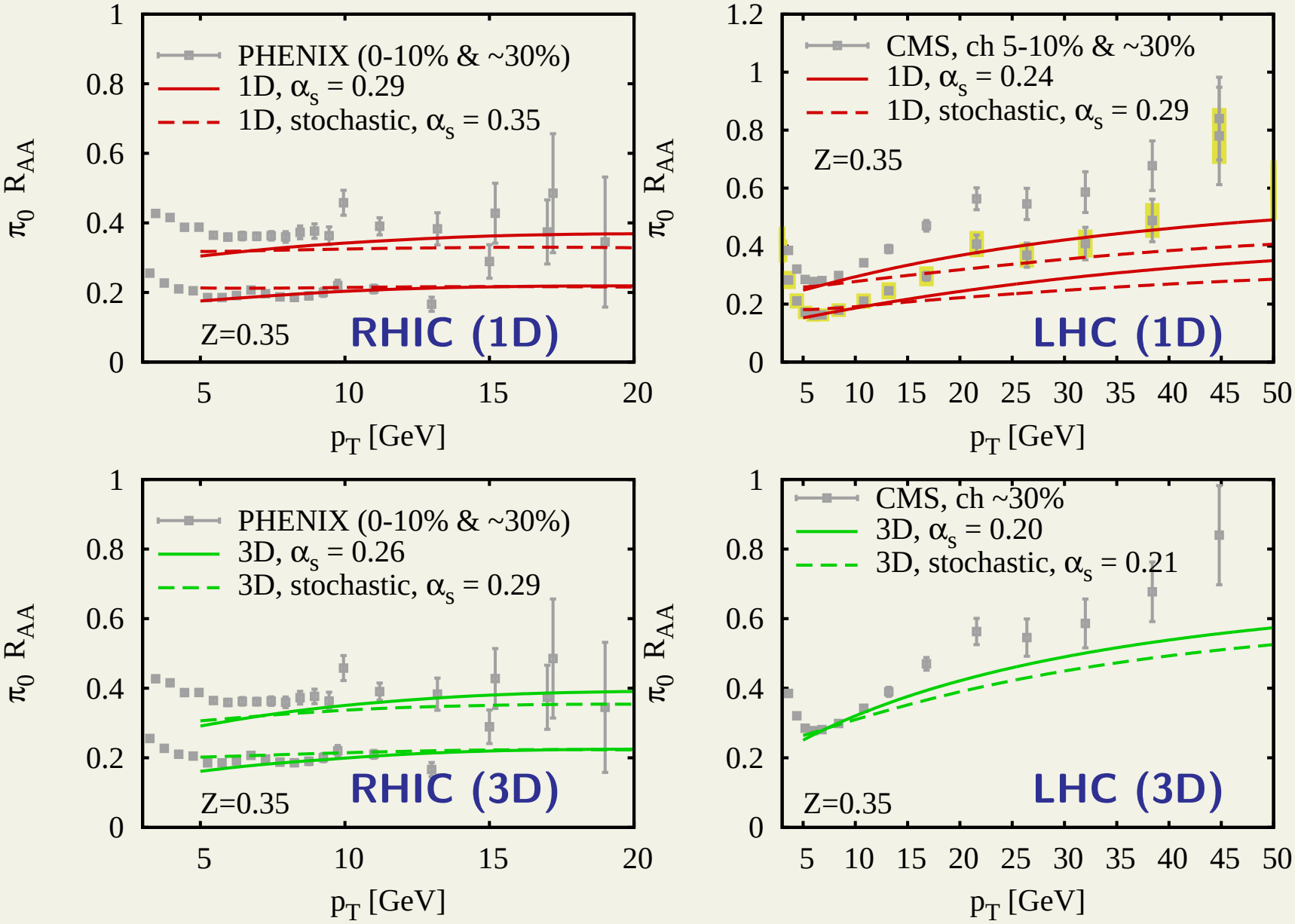

need $20-25$% smaller α_s at LHC than at RHIC - similar to Betz et al, 1201.0281

pion v2, LHC

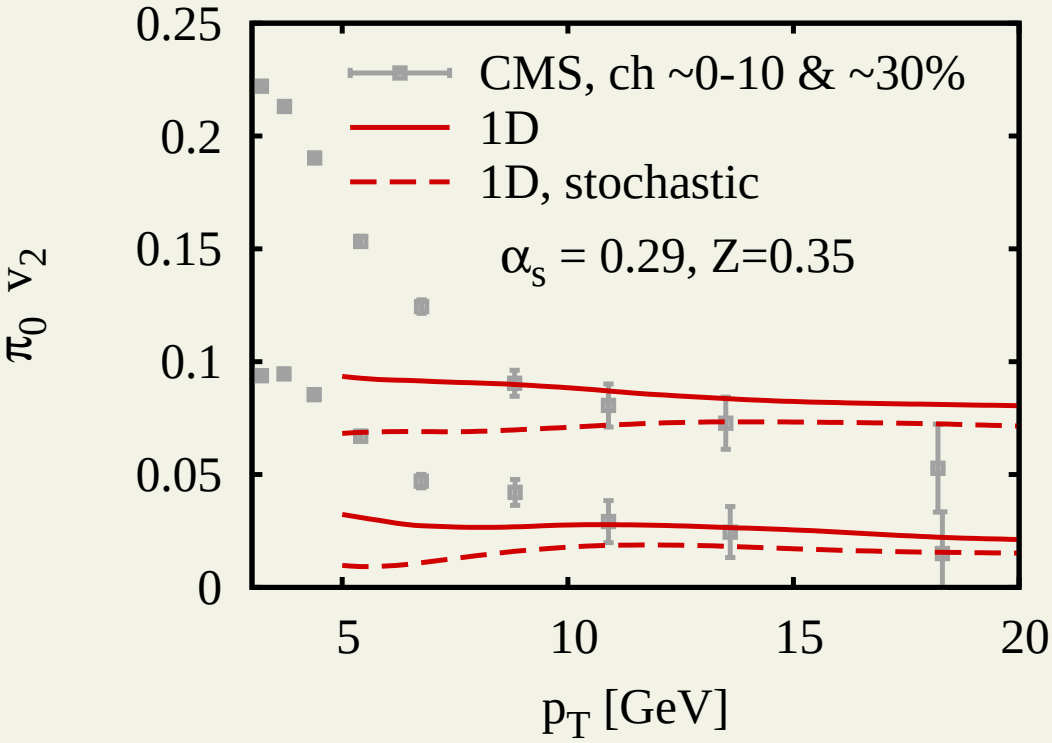
0.25
0.2
0.15
0.1
0.05
0
5
10
15
20
π_0 v_2
p_T [GeV]
CMS, ch ~0-10 & ~30%
1D
1D, stochastic
α_s = 0.29, Z=0.35

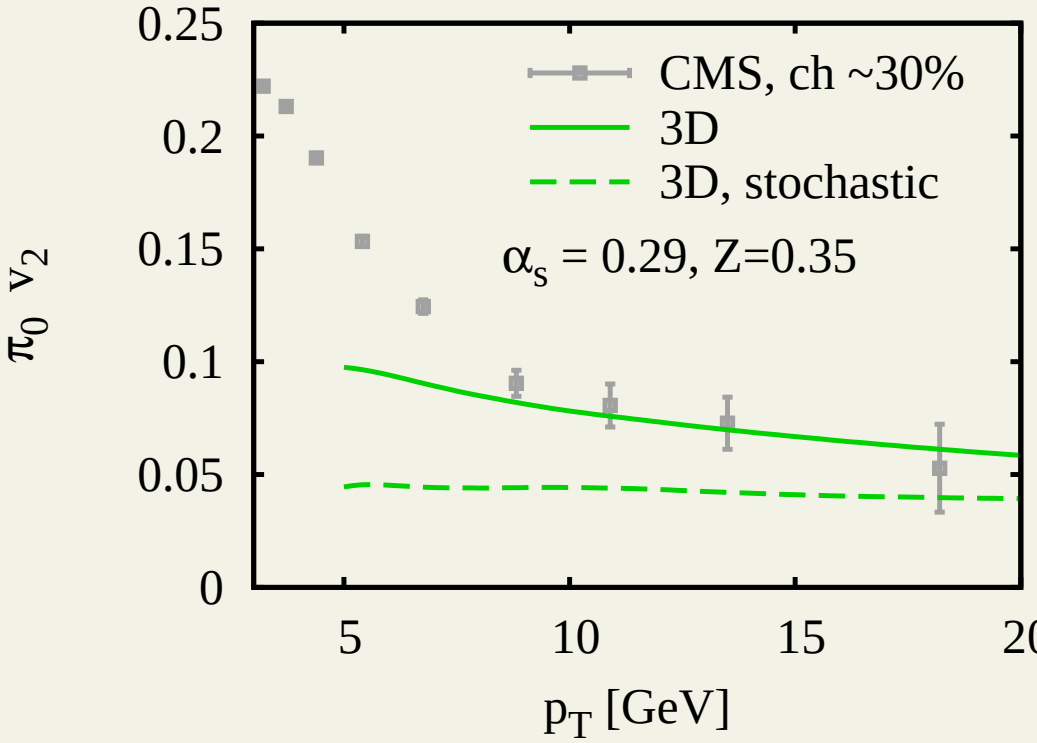
0.25
0.2
0.15
0.1
0.05
0
5
10
15
20
π_0 v_2
p_T [GeV]
CMS, ch ~30%
3D
3D, stochastic
α_s = 0.29, Z=0.35

pion v2, LHC - α_s scaled to RAA at pT = 6 GeV

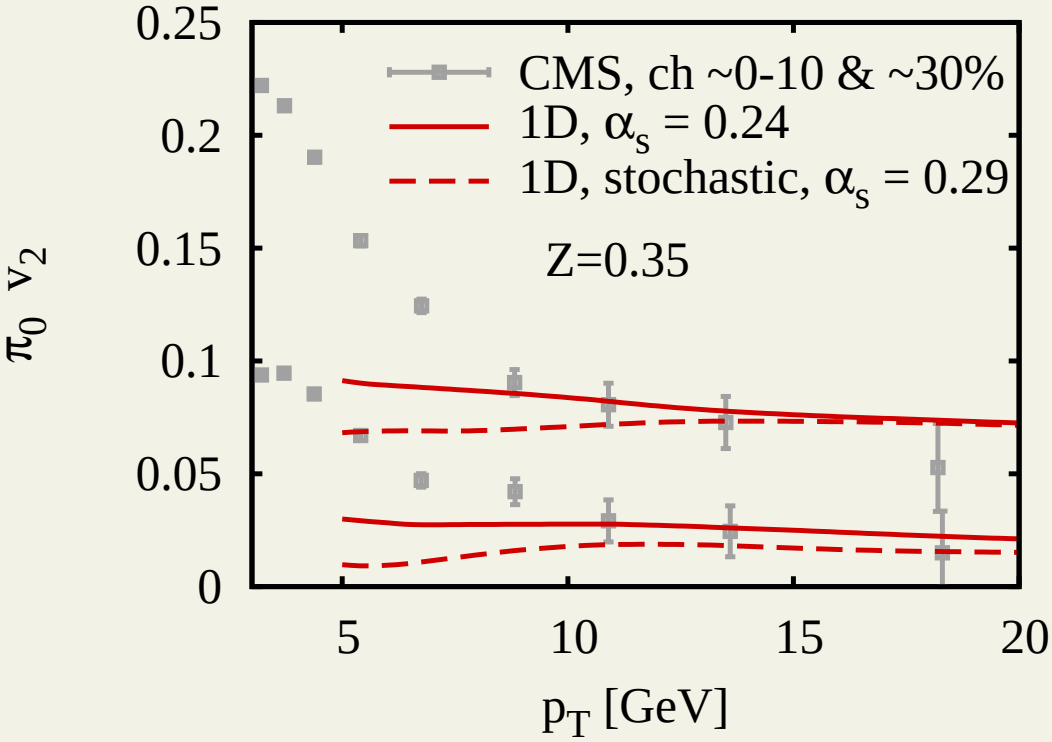

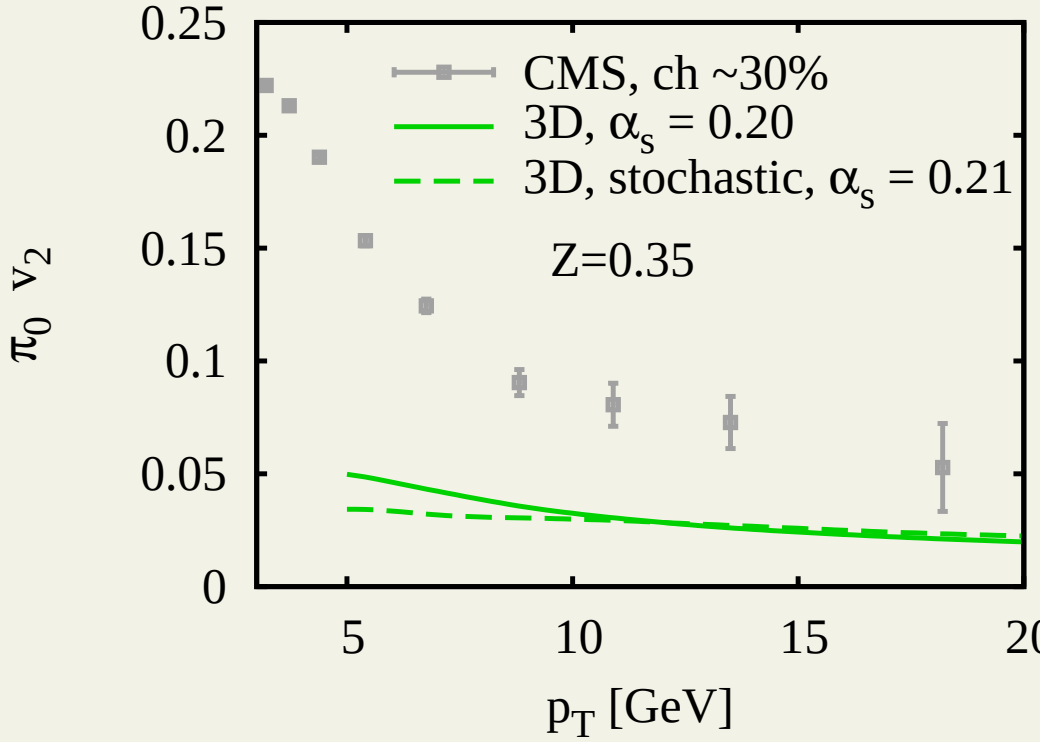

similar reduction in 3D case as at RHIC energies

high-pT pion v2, LHC (α_s scaled to RAA at pT = 6 GeV)

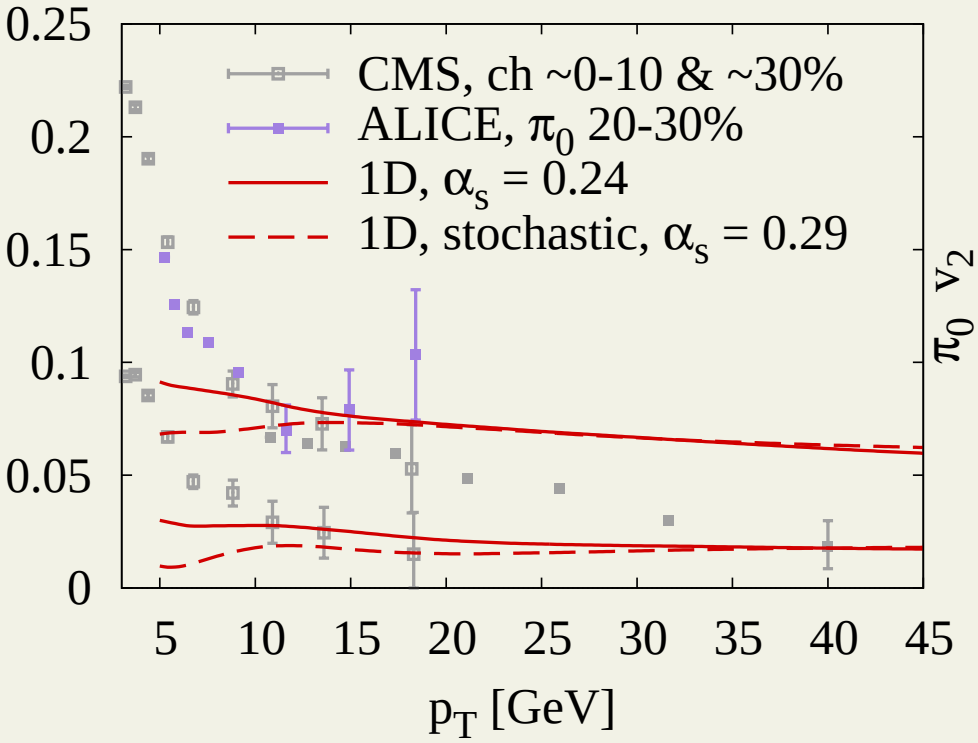

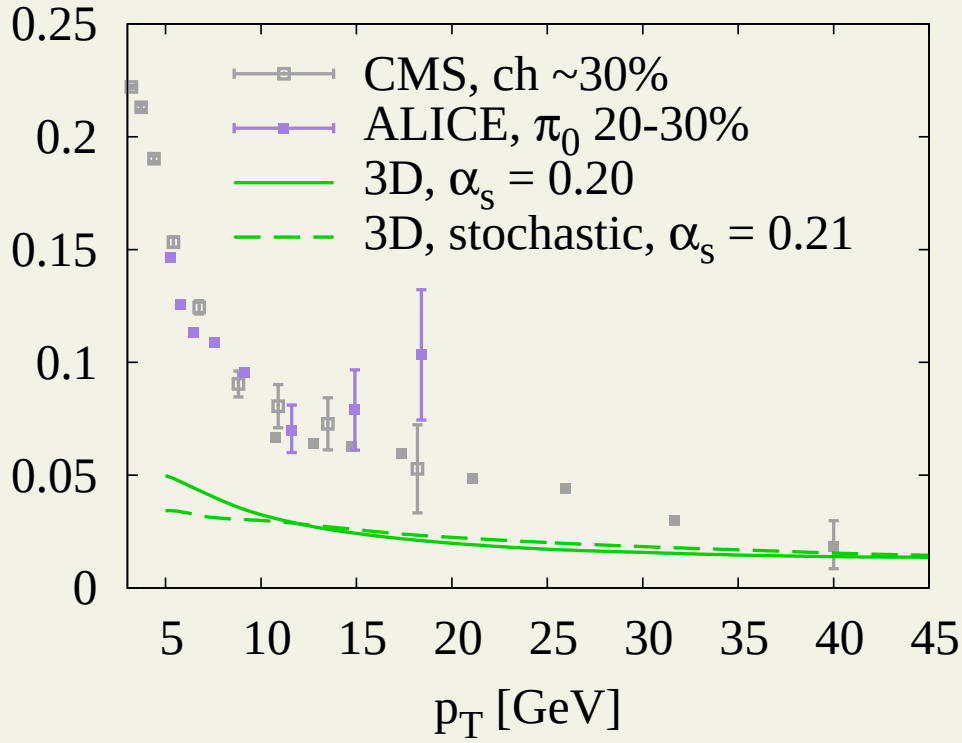

<u>In short:</u> for transversely expanding medium, both R_{AA} and v_2 are smaller with GLV energy loss. LPM interference favors late scattering.

$$\Delta E^{(1)}_{GLV}(z) \quad \propto \quad \int dx\, d\mathbf{k}\, d\mathbf{q}\, \frac{\mu^2}{\pi(\mathbf{q}^2+\mu^2)^2}\frac{2\mathbf{k}\cdot\mathbf{q}}{\mathbf{k}^2(\mathbf{k}-\mathbf{q})^2}(1-\cos\omega\Delta z) \;\propto\; I(\Delta z/\tau(z), E/\mu(z))$$

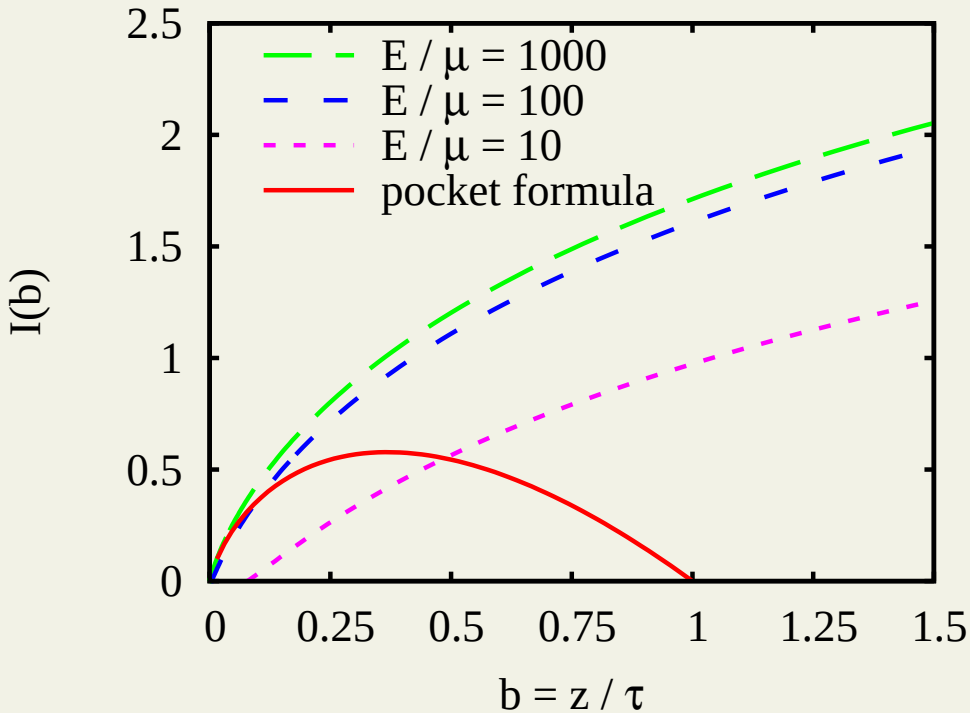

$$\tau(z) \equiv \frac{2E}{\mu^2(z)}$$

Could fluctuations help?

- **MC Glauber initconds (binary)**
- **RHIC Au+Au at $b = 8$ fm, 200A GeV**
- **same $2 \to 2$ transport (MPC)**

average Au+Au, b=8 fm

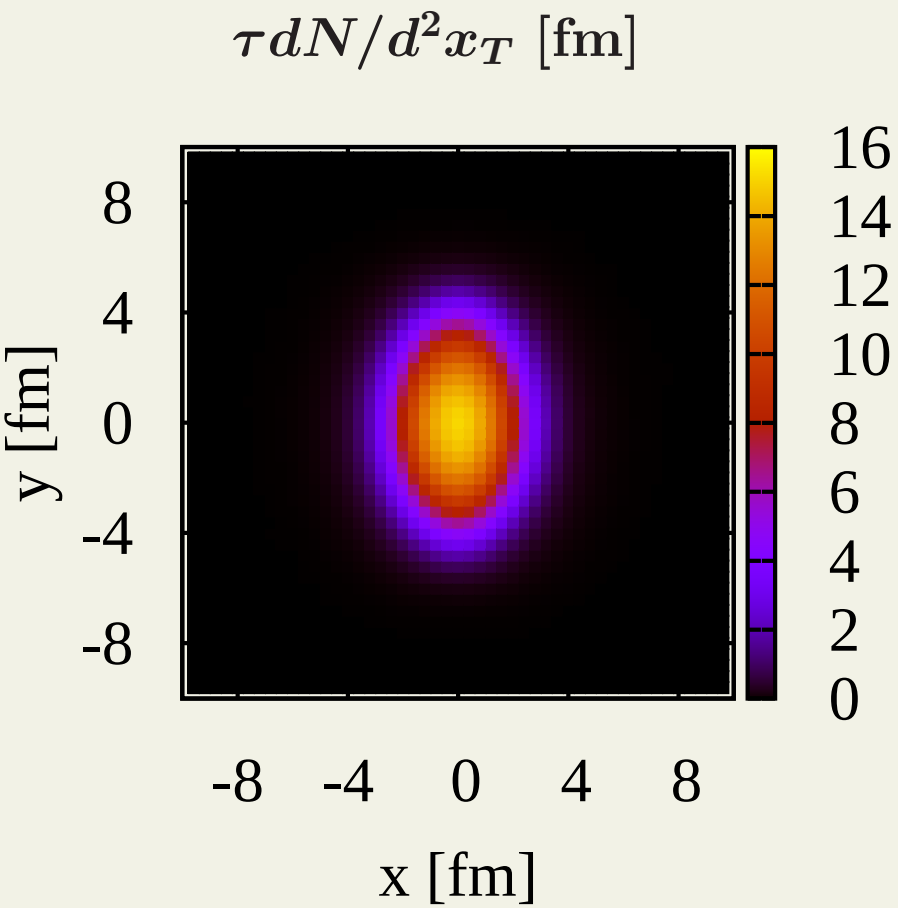

single MC Glauber

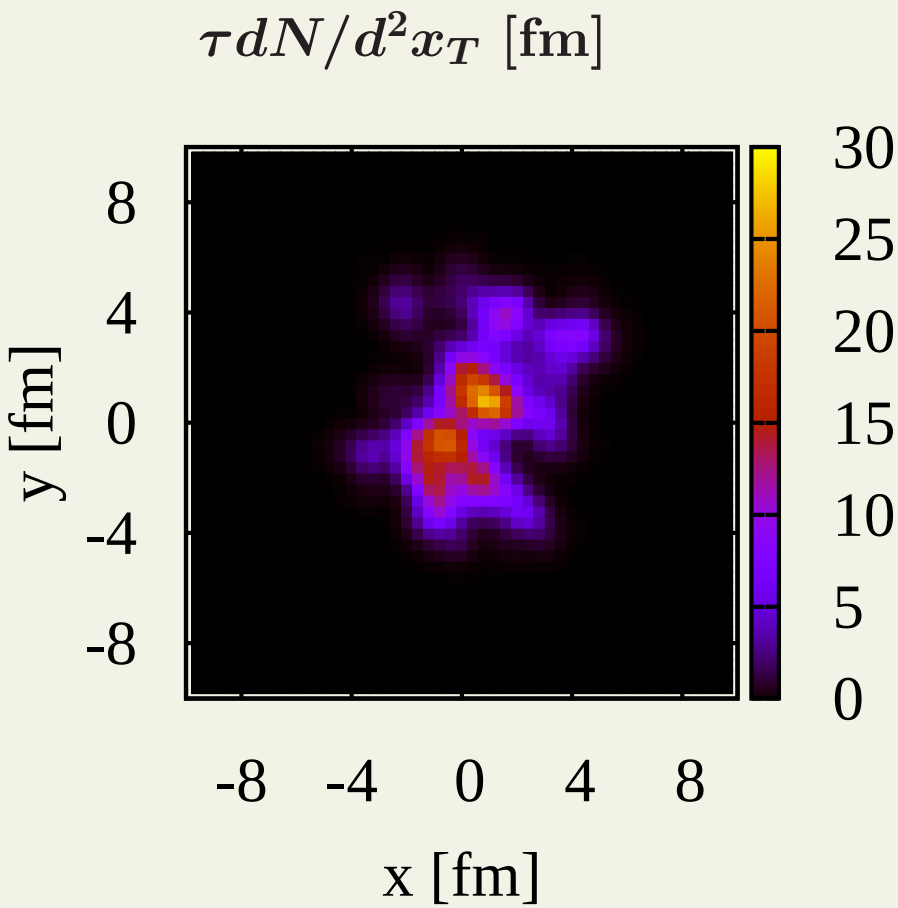

$\tau = 0.6$ fm

average Au+Au, b=8 fm

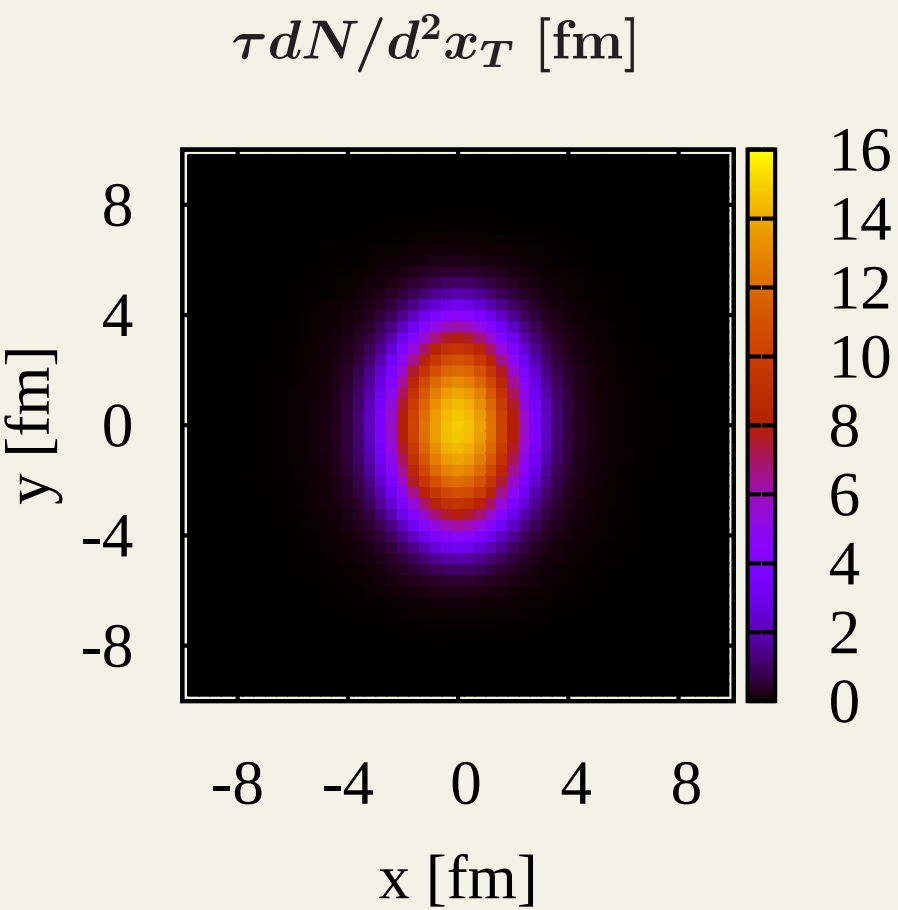

single MC Glauber

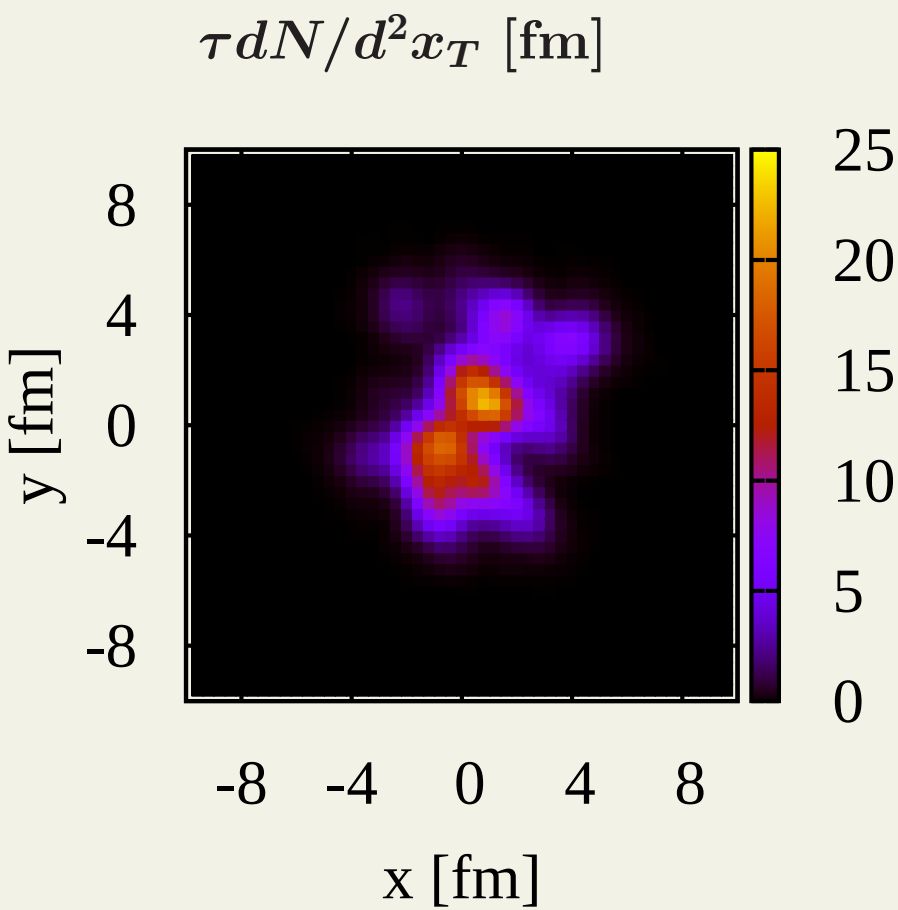

$\tau = 1.2$ fm

average Au+Au, b=8 fm

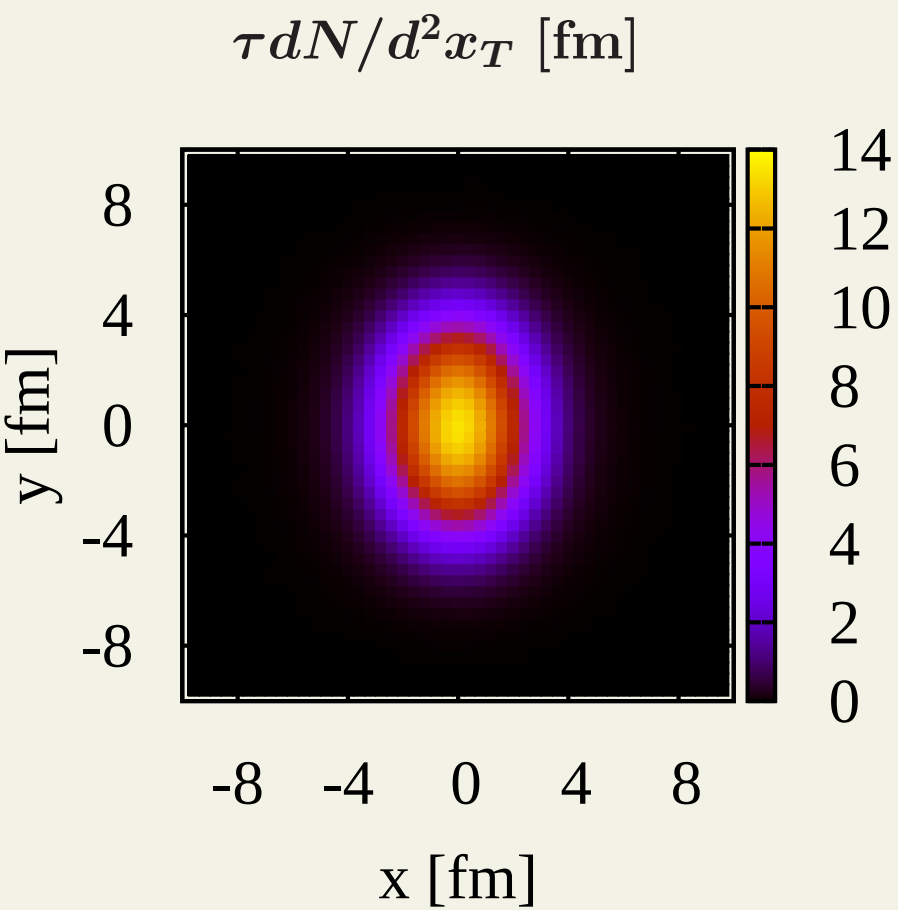

single MC Glauber

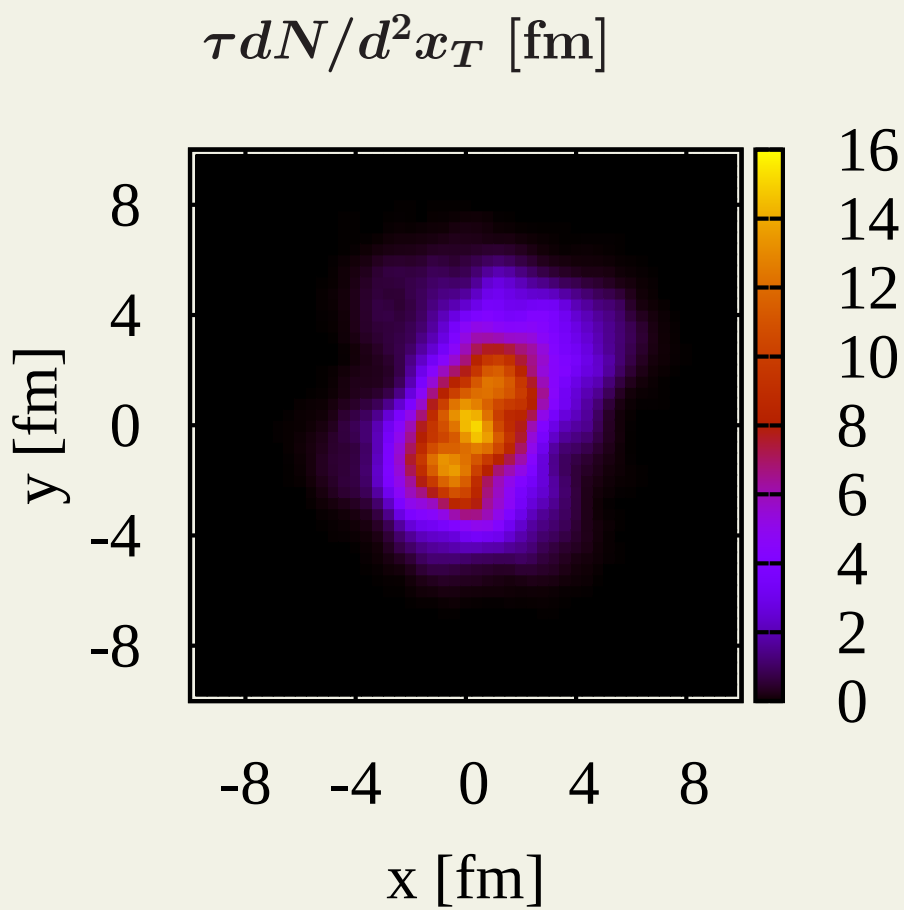

$\tau = 2.1$ fm

average Au+Au, b=8 fm

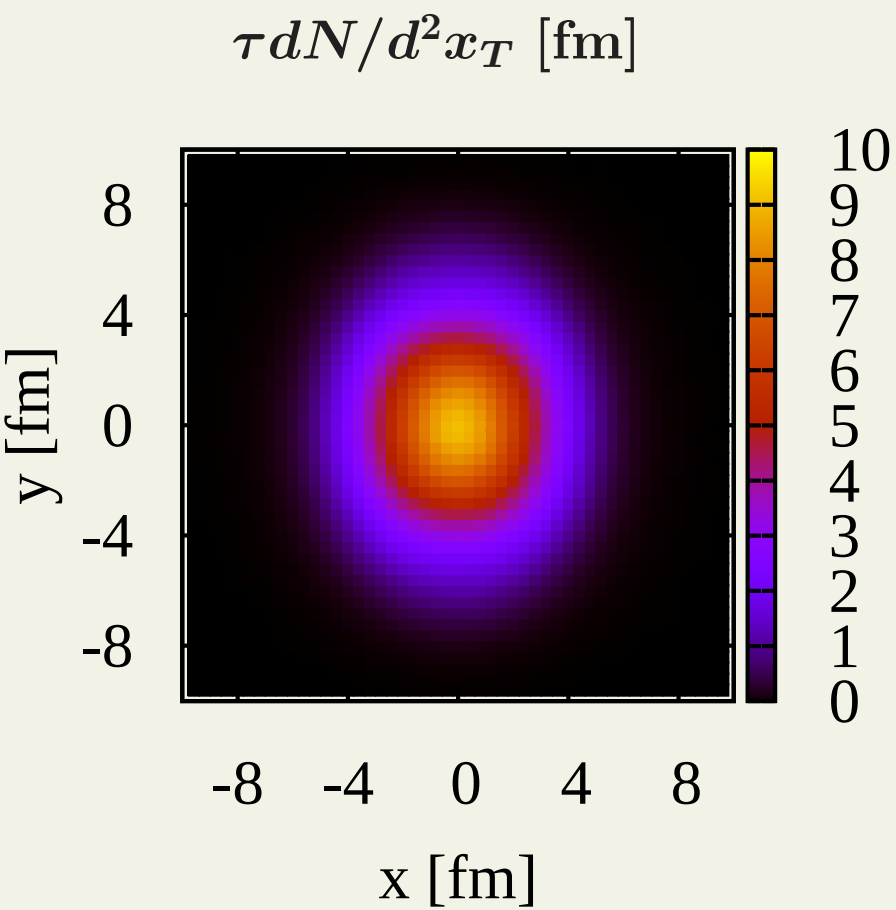

single MC Glauber

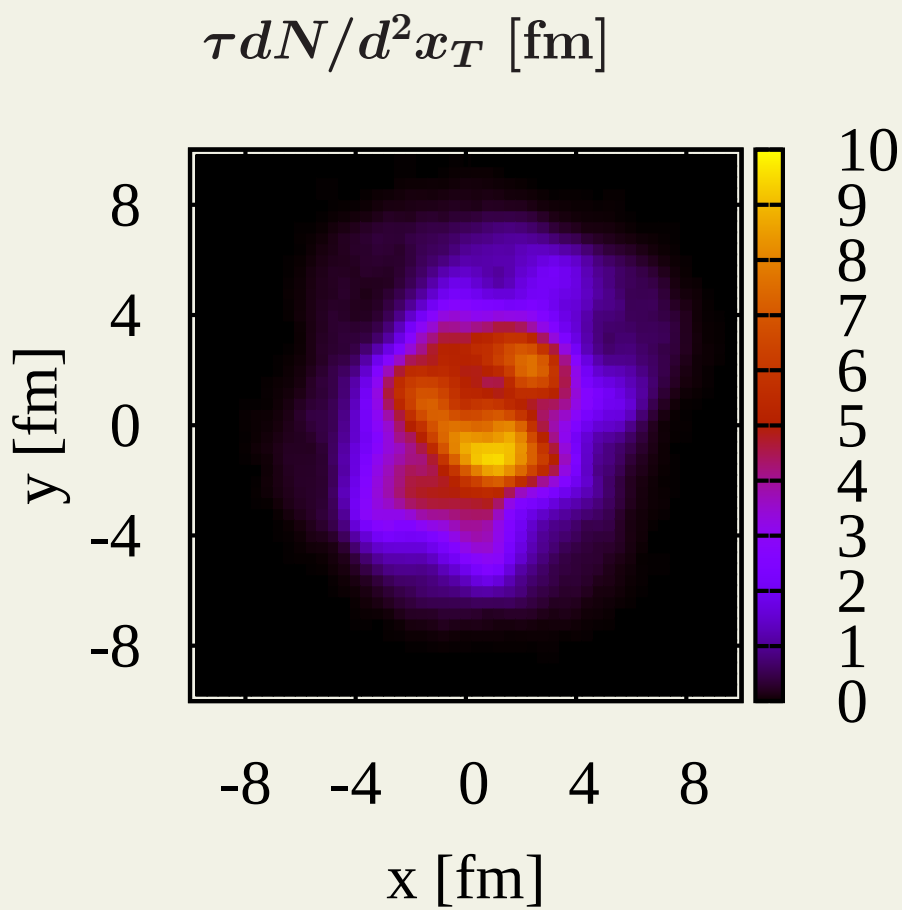

$\tau = 3.6$ fm

average Au+Au, b=8 fm

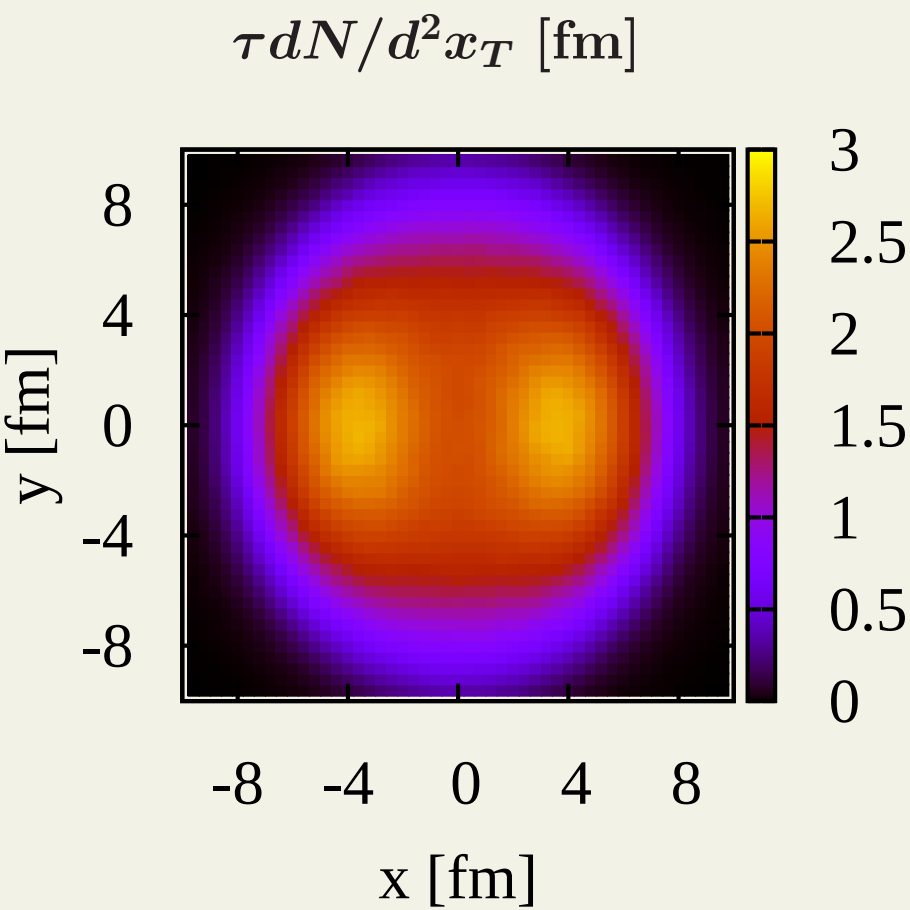

single MC Glauber

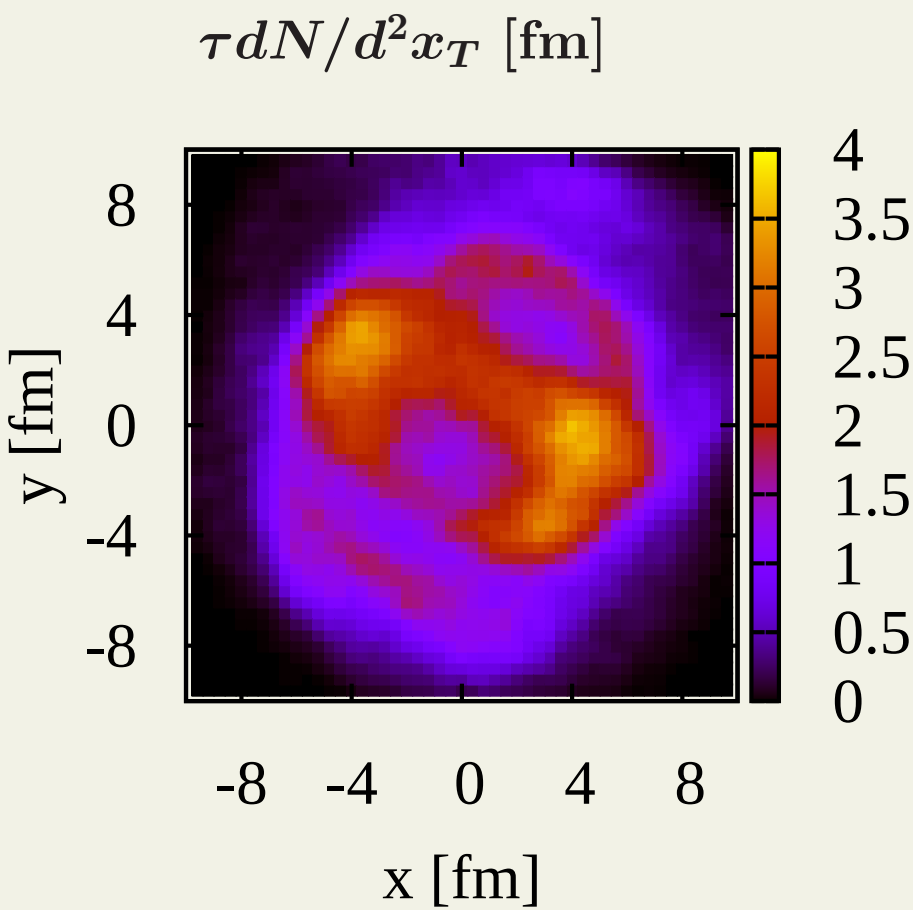

$\tau = 6.6$ fm

average Au+Au, b=8 fm

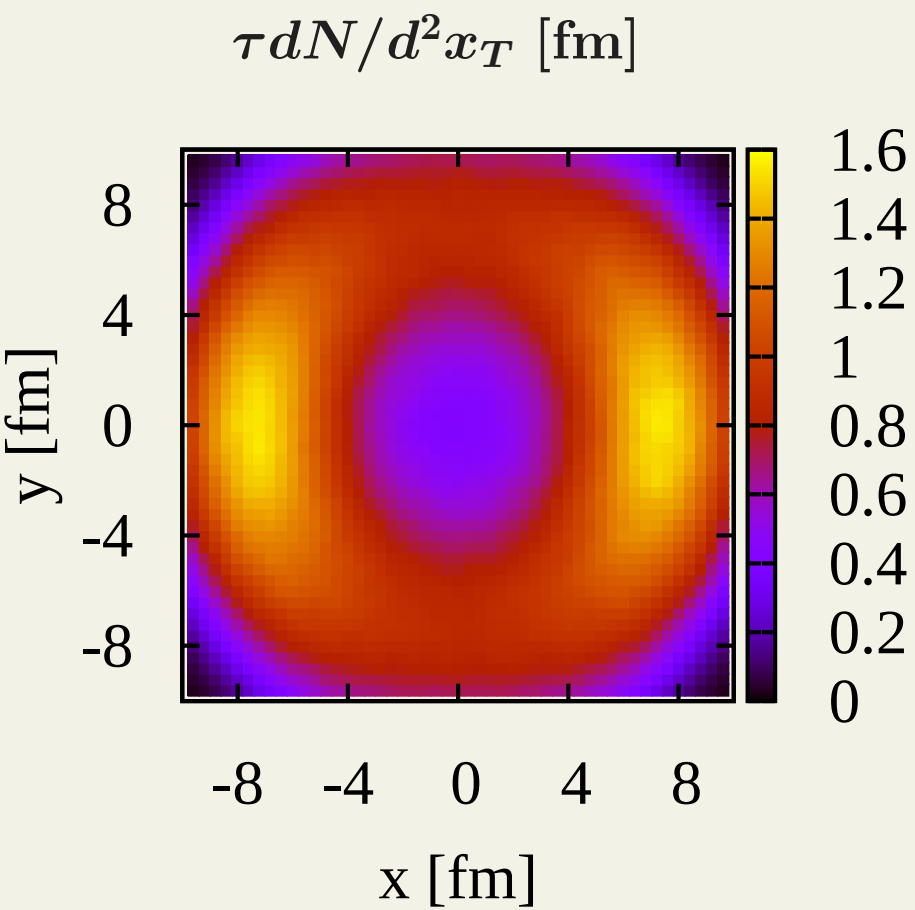

single MC Glauber

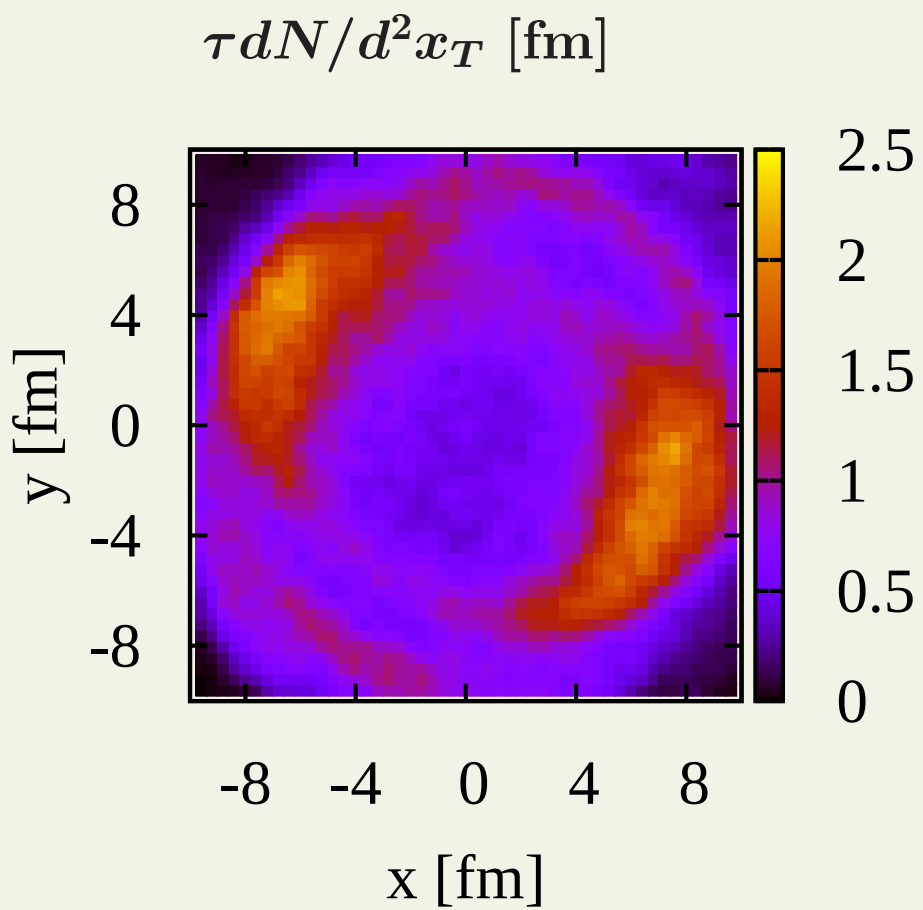

$\tau = 9.6$ fm

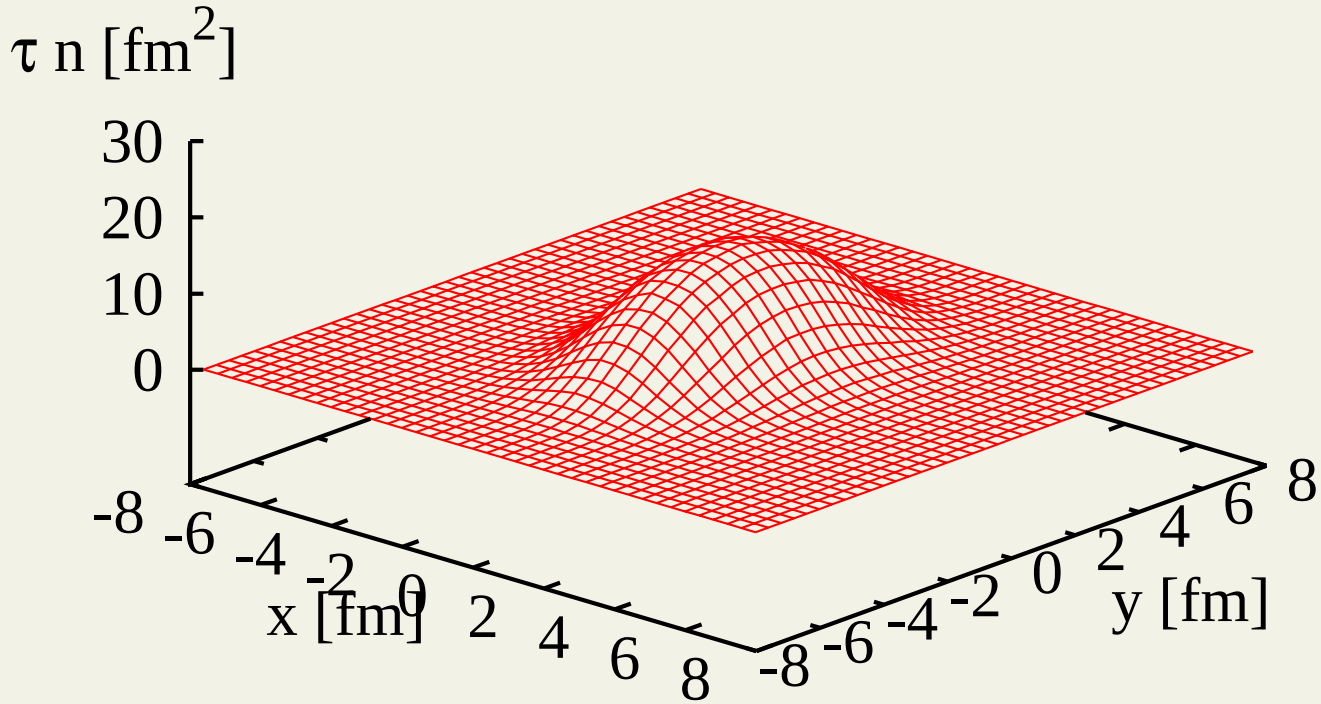
τ n [fm2]
30
20
10
0
-8
-6
-4
-2
0
2
4
6
8
x [fm]
-8
-6
-4
-2
0
2
4
6
8
y [fm]

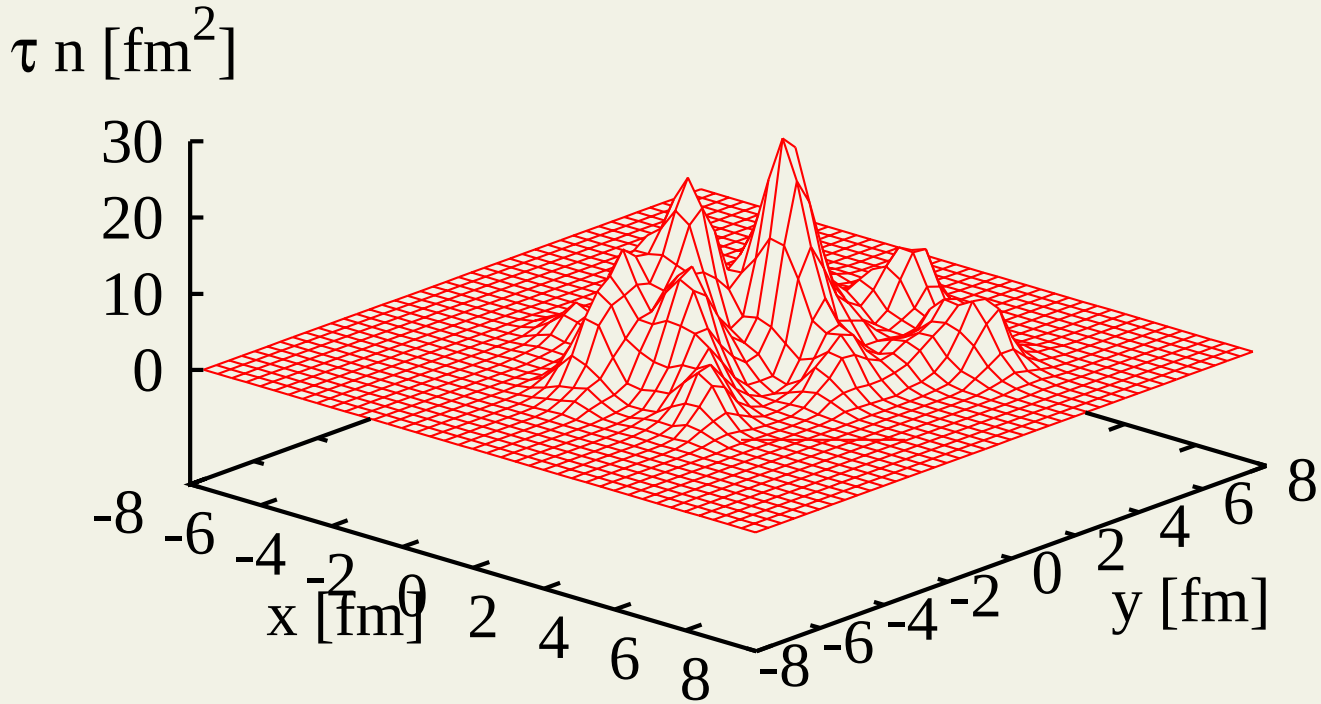
τ n [fm2]
30
20
10
0
-8
-6
-4
-2
0
2
4
6
8
x [fm]
-8
-6
-4
-2
0
2
4
6
8
y [fm]

"./flu

Analyze MEDIUM and JET response using eccentricity coefficients

$$\begin{aligned}\vec{\epsilon}_{n,k} &\equiv \frac{1}{\langle r^k \rangle}\left(\langle r^k \cos(n\phi_x)\rangle, \langle r^k \sin(n\phi_x)\rangle\right) \\ &= \epsilon^*_{n,k}\left(\cos\Phi_{n,k}, \sin\Phi_{n,k}\right)\end{aligned}$$

and similar decomposition for transverse momenta (v_n, Φ_n)

$$\frac{dN}{d\varphi} \propto 1 + \sum_{n=1}^{\infty} 2v_n \cos n(\varphi - \Phi_n)$$

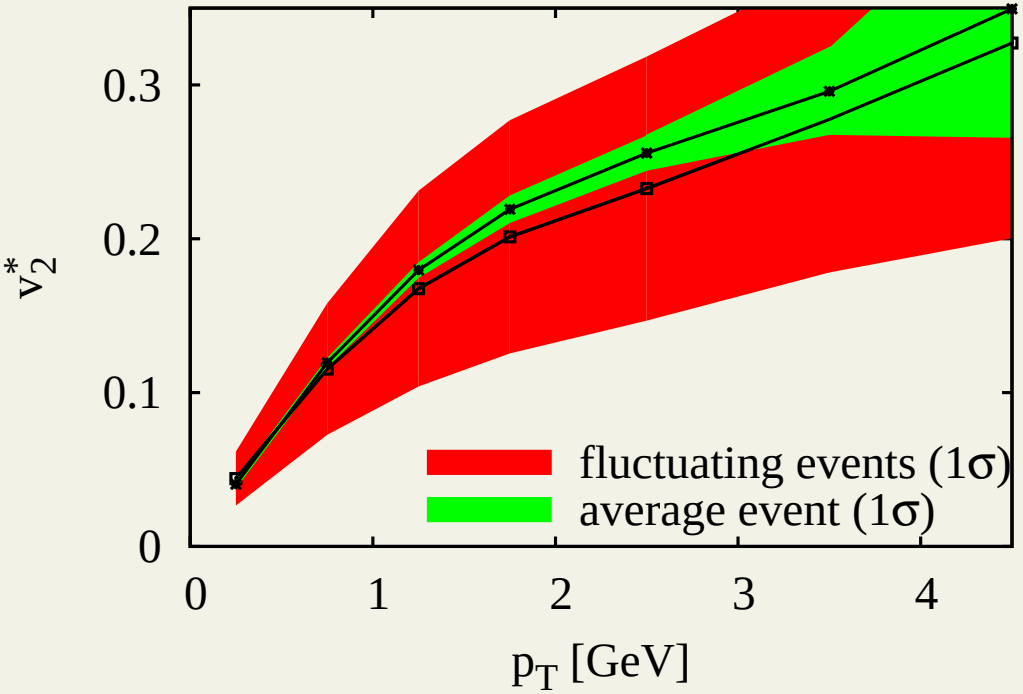

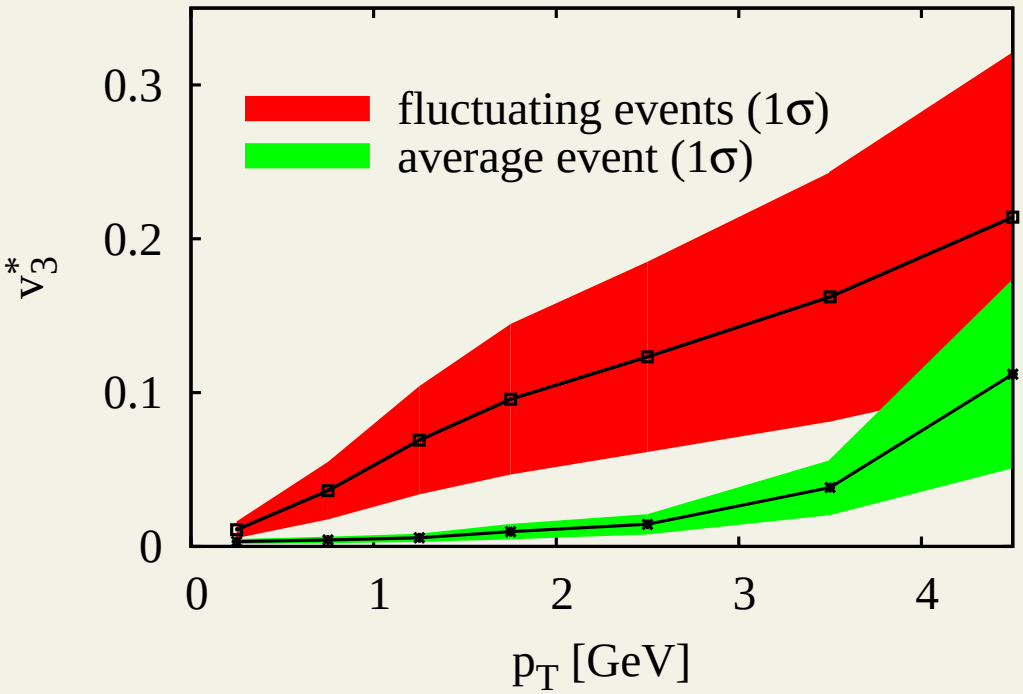

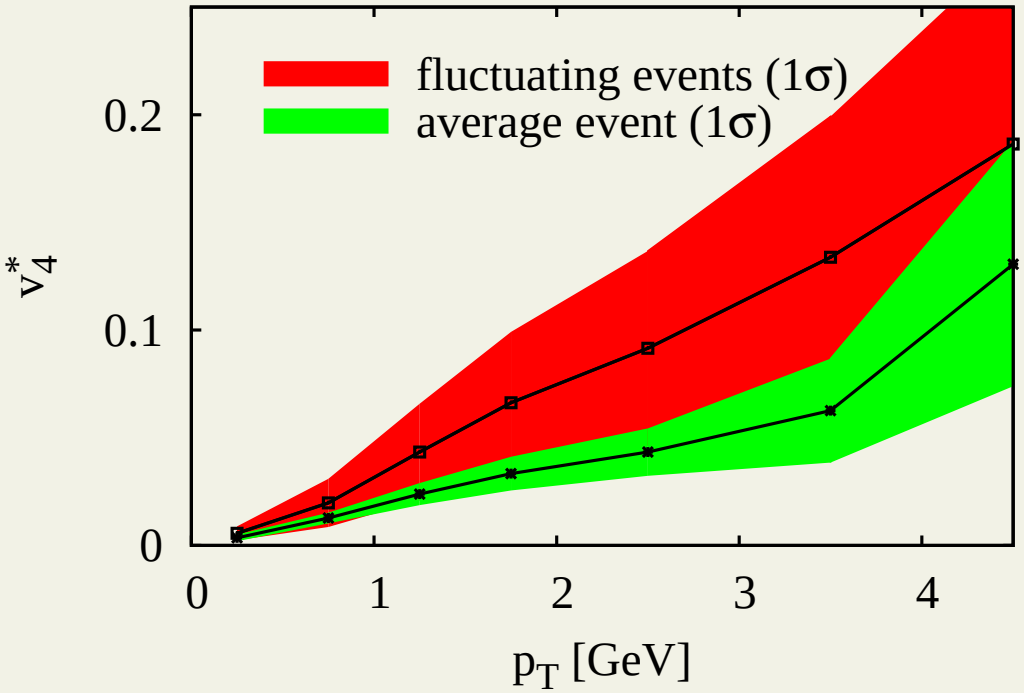

average v_2 essentially same as from averaged initcond

v_n increase with p_T

(shades represent $\sqrt{\langle \delta v_n^2 \rangle}$)

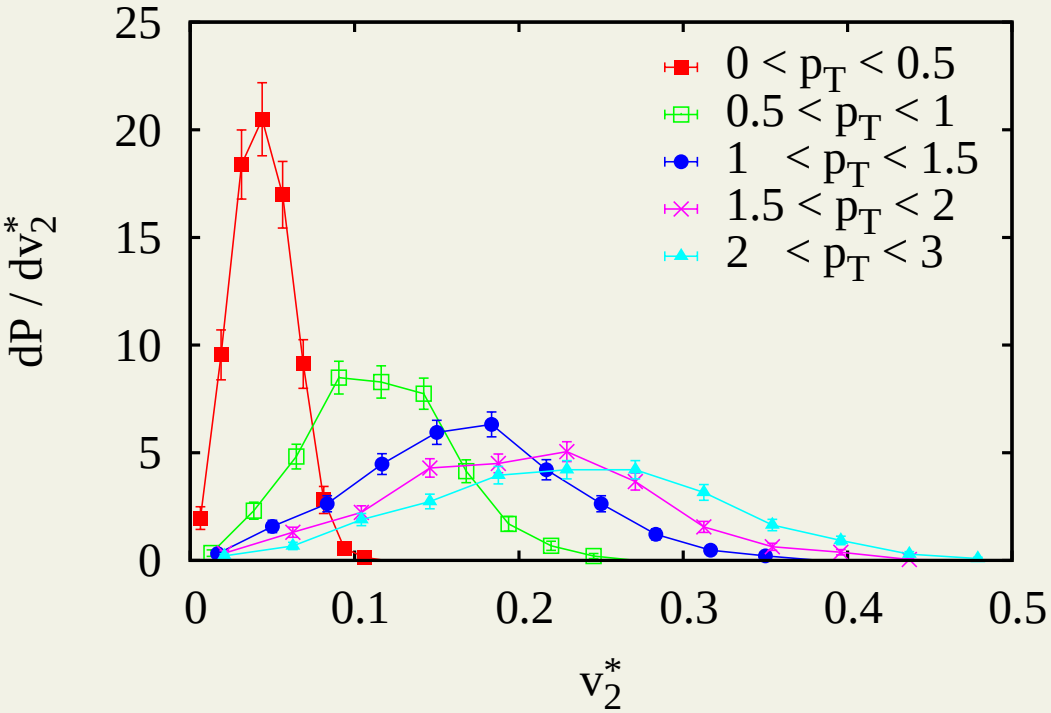

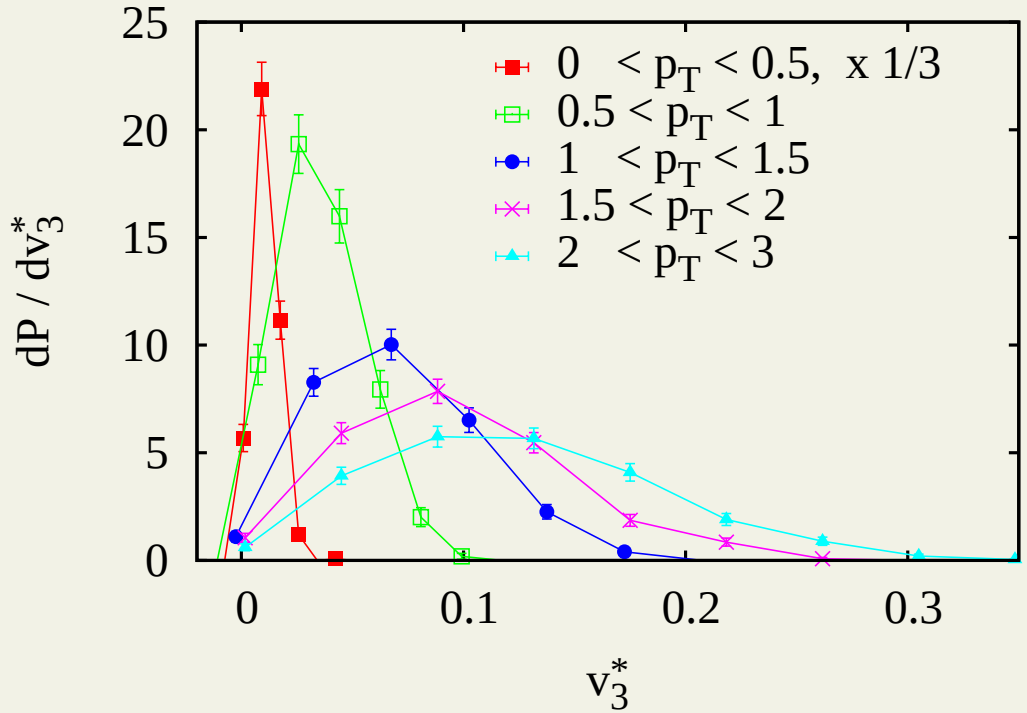

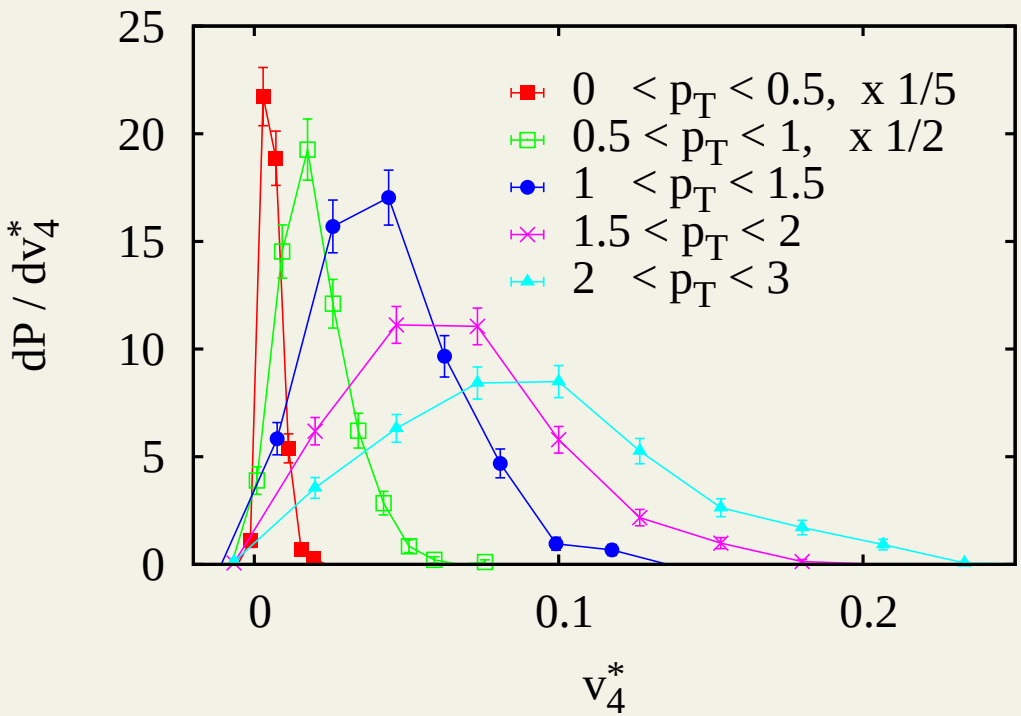

MC Glauber initial conditions induce large v_2, v_3, v_4 fluctuations in bulk transport medium

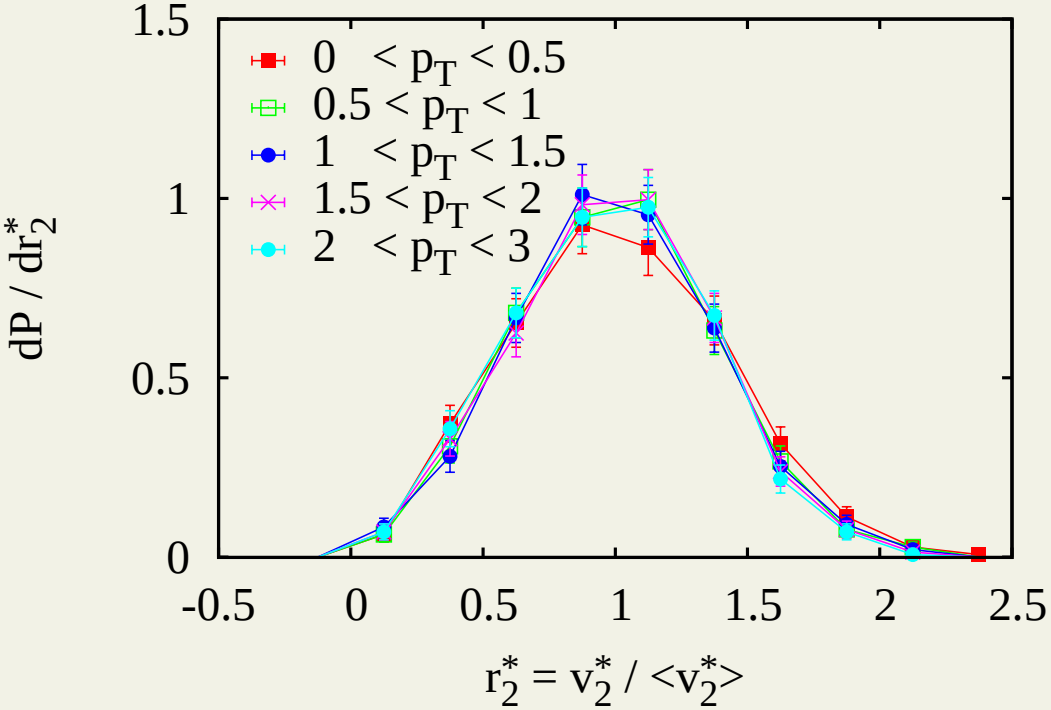

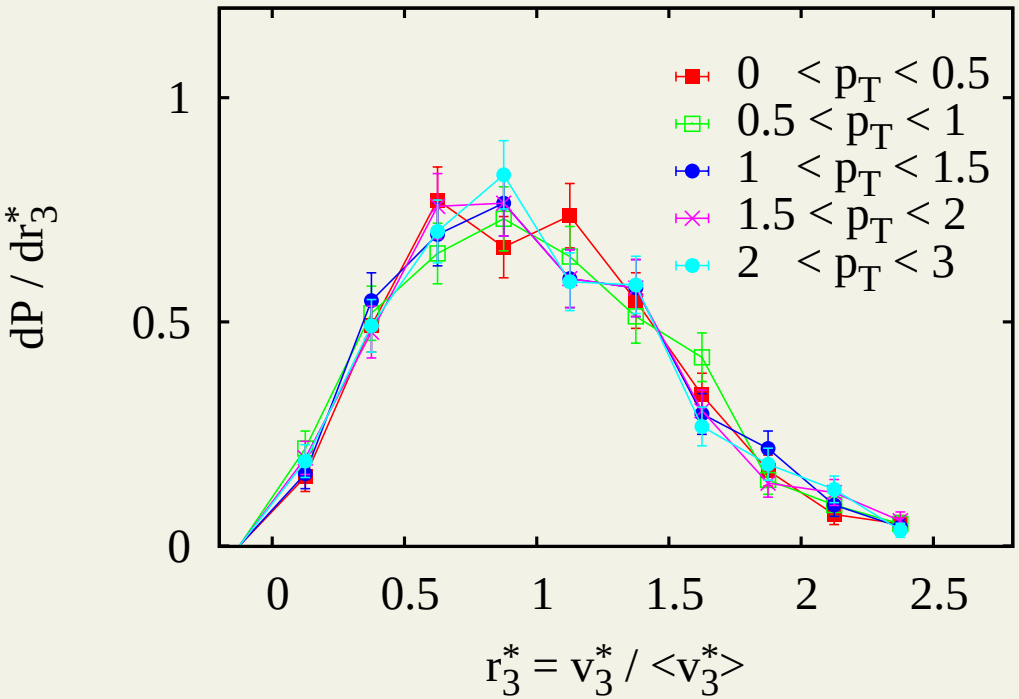

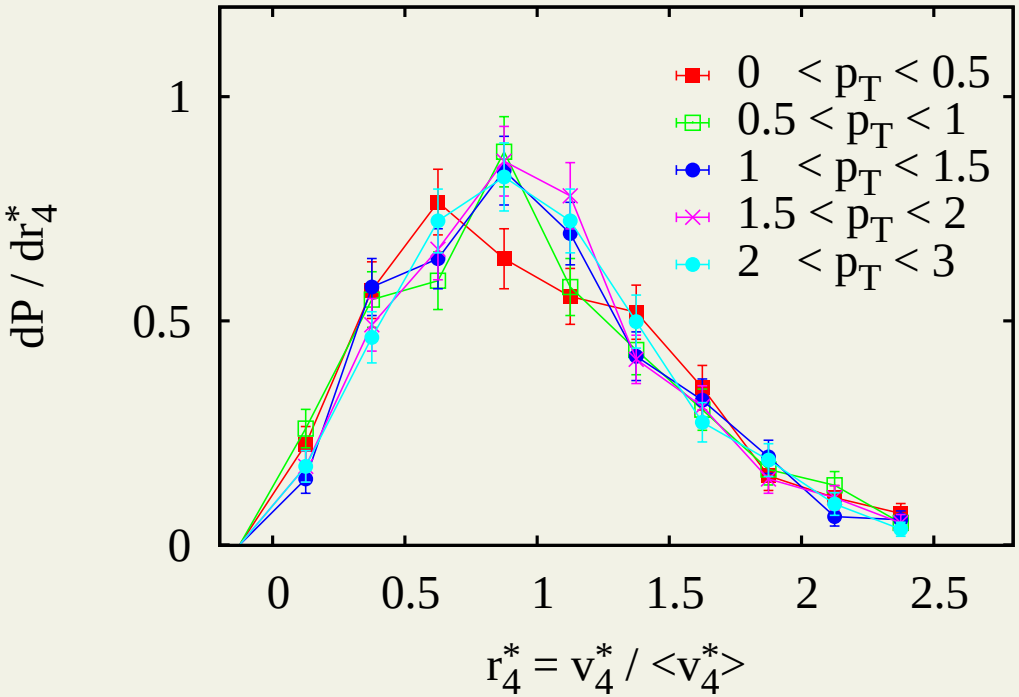

$v_n/\langle v_n\rangle$ **nearly universal independent of** p_T

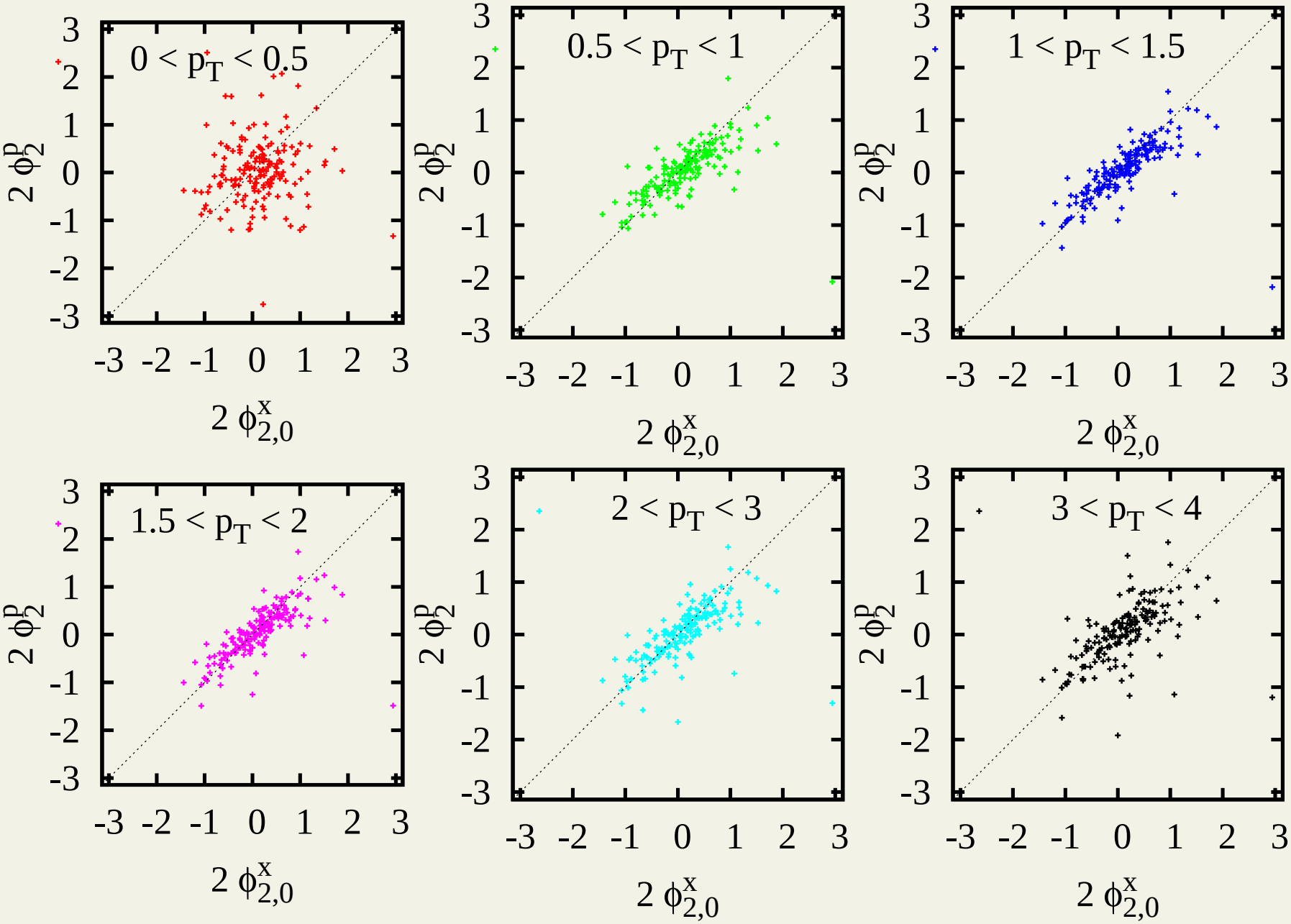
0 < p_T < 0.5
0.5 < p_T < 1
1 < p_T < 1.5
1.5 < p_T < 2
2 < p_T < 3
3 < p_T < 4
2 φ^P_2
2 φ^x_{2,0}
-3 -2 -1 0 1 2 3

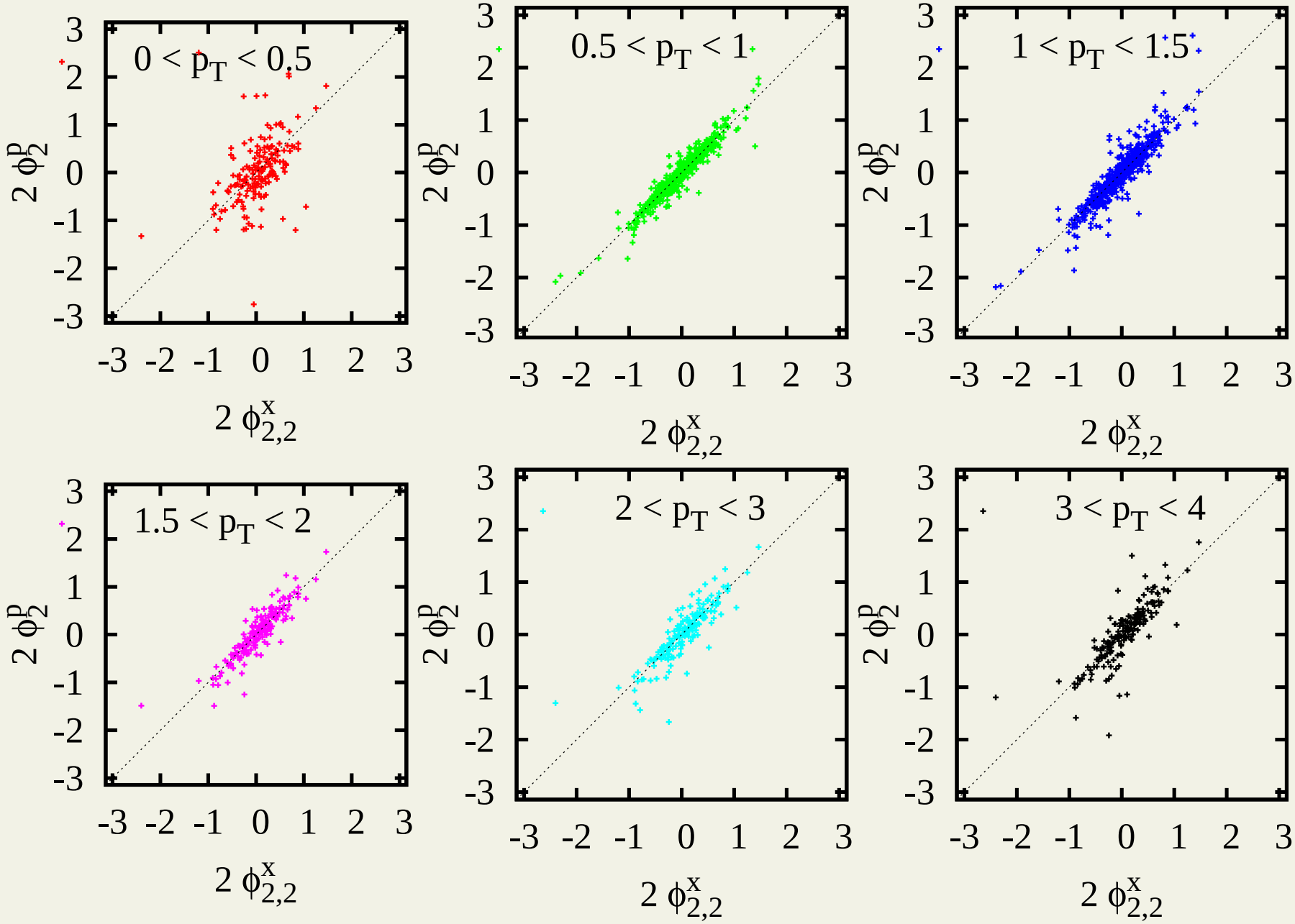

$\epsilon_{2,2}$ orientation correlates best with v_2 orientation

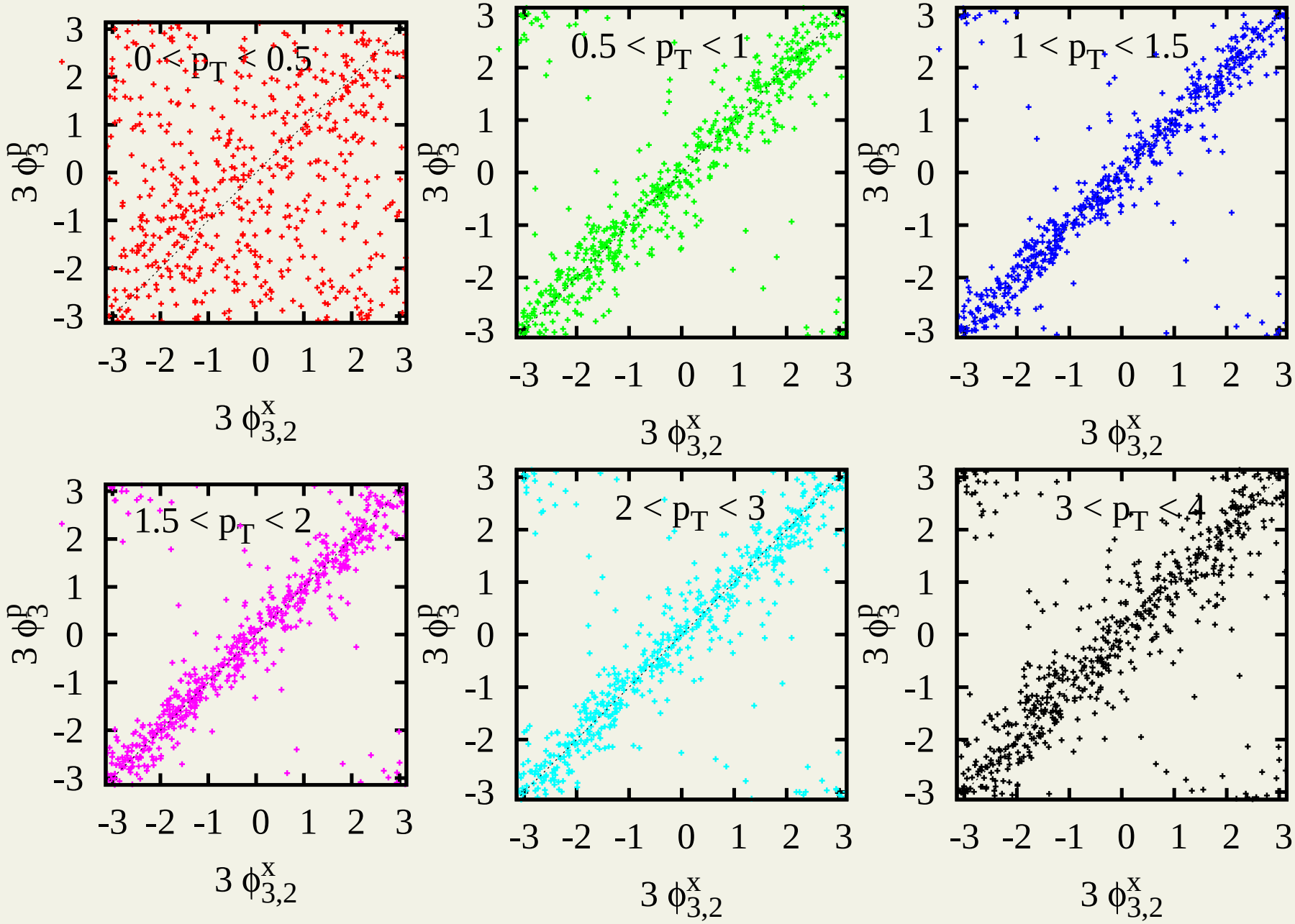

$\epsilon_{3,2}$ **correlates strongly with** v_3 **orientation**

Bulk medium response qualitatively similar to hydrodynamics.

What about the jets?

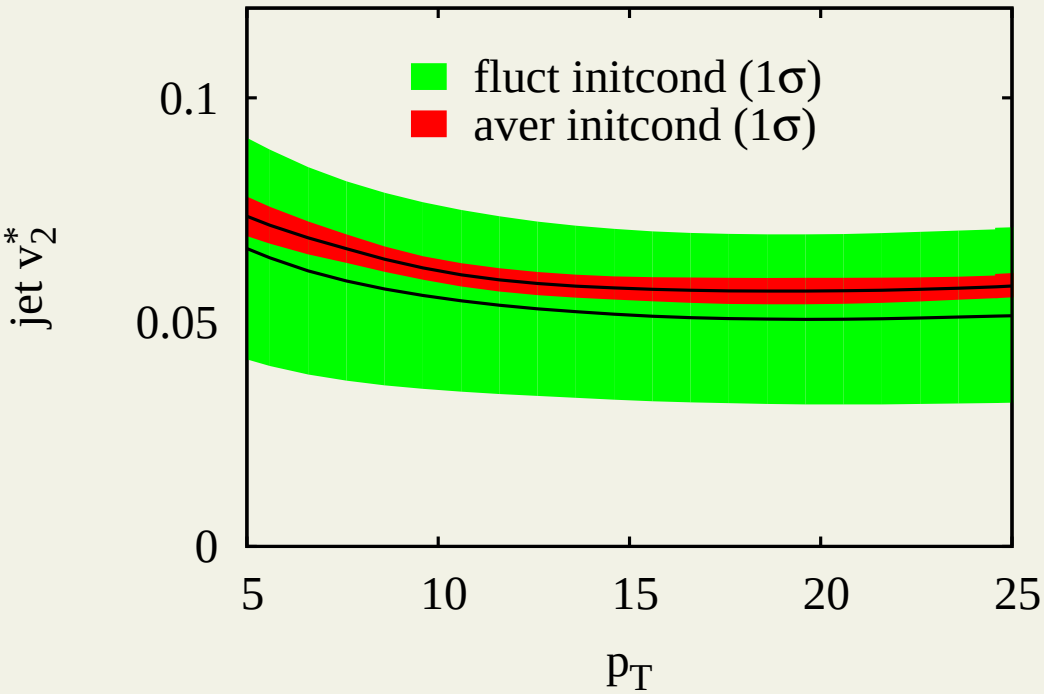

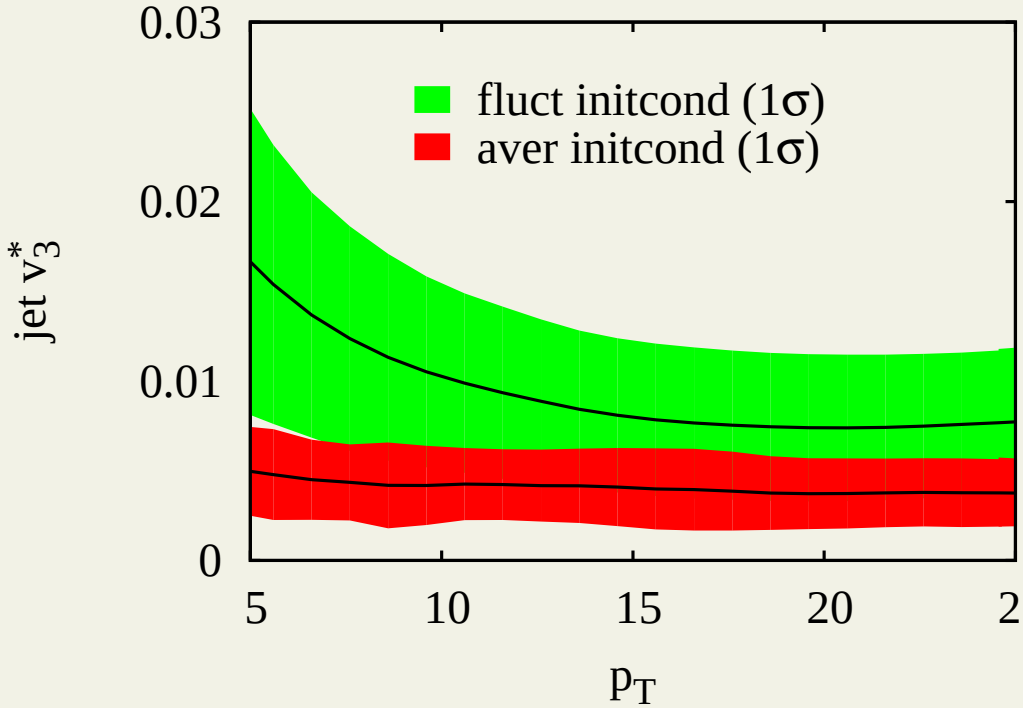

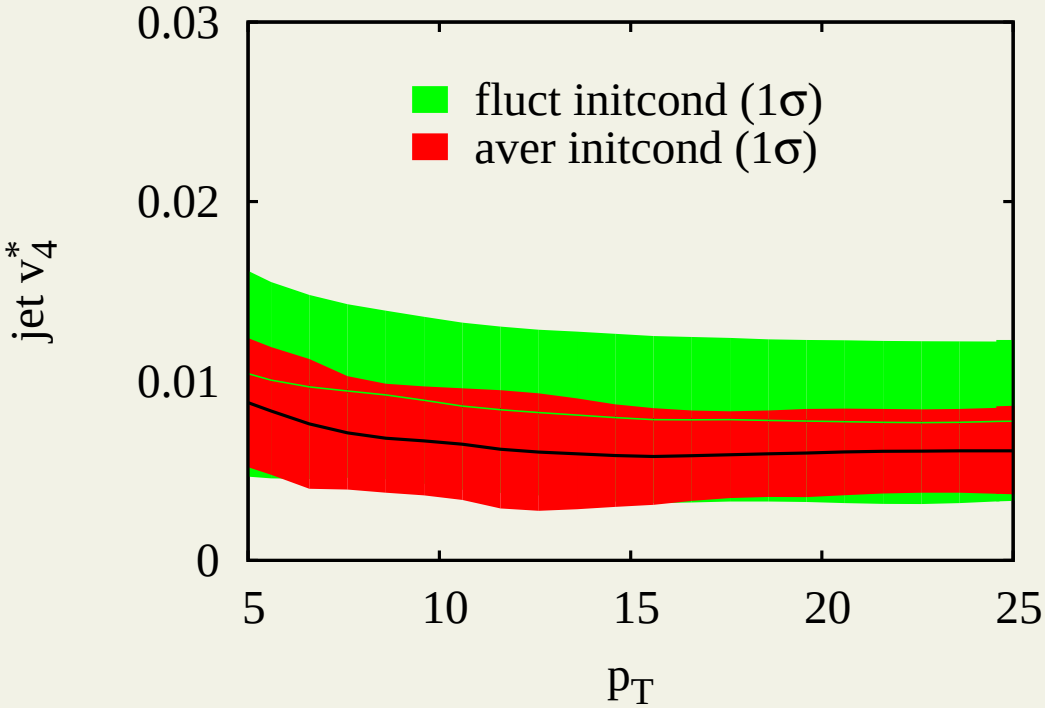

noticeable fluctuations in jet v_n

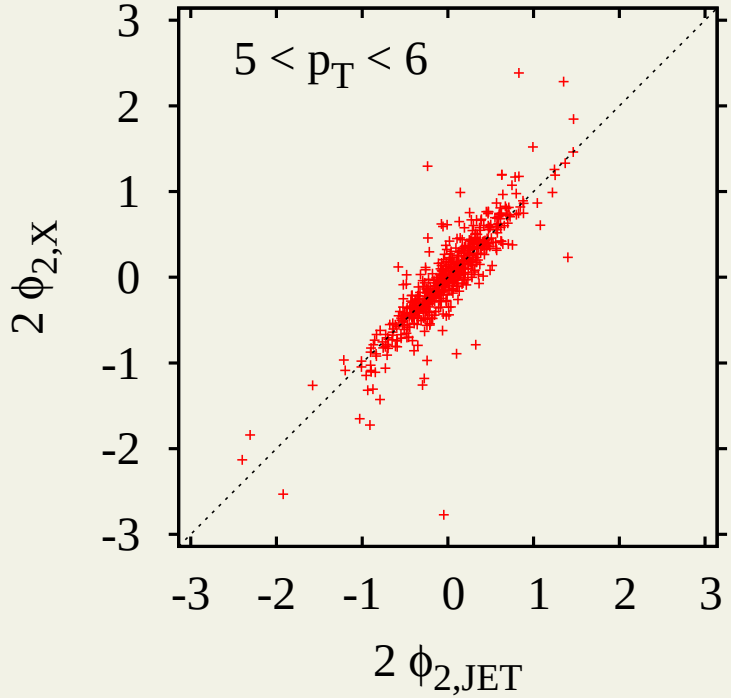

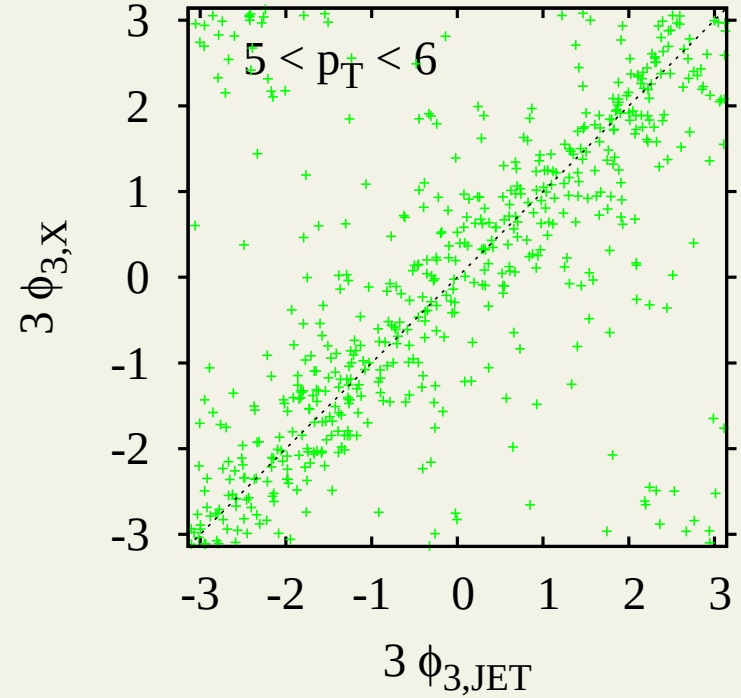

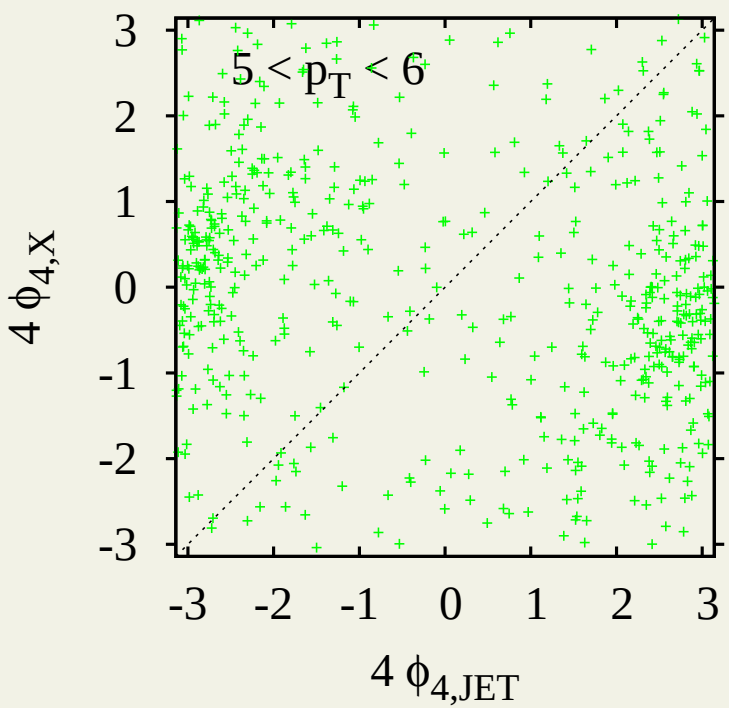

JET v_2 and v_3 correlate with orientation of $\epsilon_{2,3}$

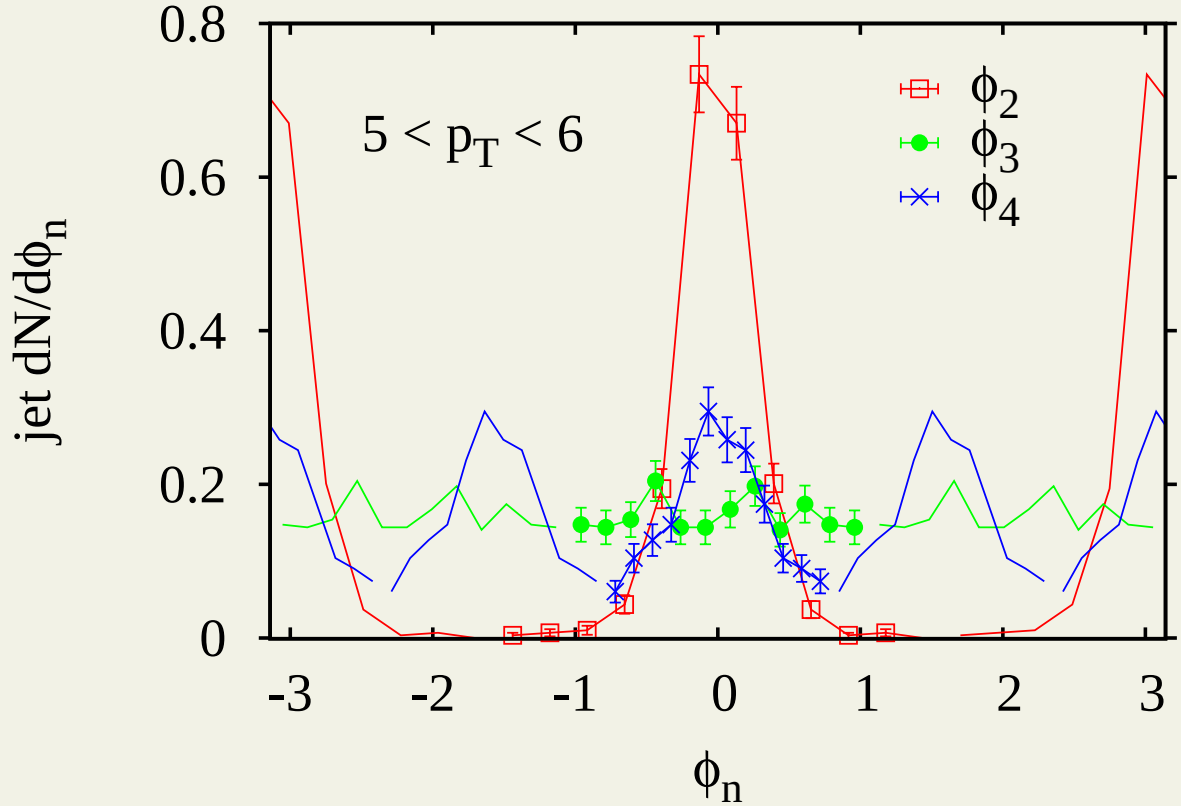

angles relative to theorist's reaction plane $\rightarrow$ positive v_4

Summary

Parton transport can serve as bulk medium model. It responds to fluctuating initial conditions similarly to hydrodynamics.

Though initial fluctuations NOT small perturbations, jet and medium $v_{2,3,4}$ correlate well with initial $\vec{\epsilon}_{2,3,4}$. For basic observables averaging even appears to nearly commute with evolution. (Where is the nonlinearity??)

We also find that, with GLV energy loss, transverse expansion reduces both R_{AA} and v_2 at high p_T.

Some interesting avenues to investigate:

- **dynamical fluctuations in transport**
- **migration in p_T ("plasma push"** DM nucl-th/0503051**)**
- **corona**

DM ('05):

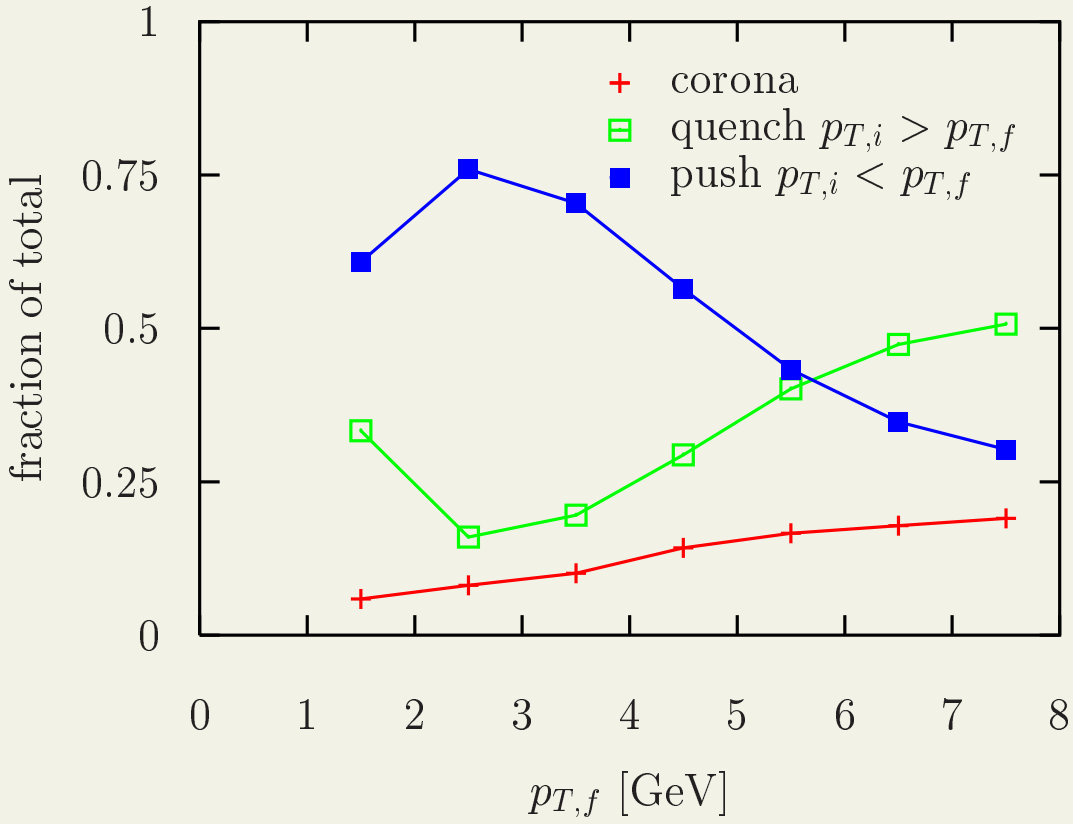
fraction of total
$p_{T,f}$ [GeV]
corona
quench $p_{T,i} > p_{T,f}$
push $p_{T,i} < p_{T,f}$

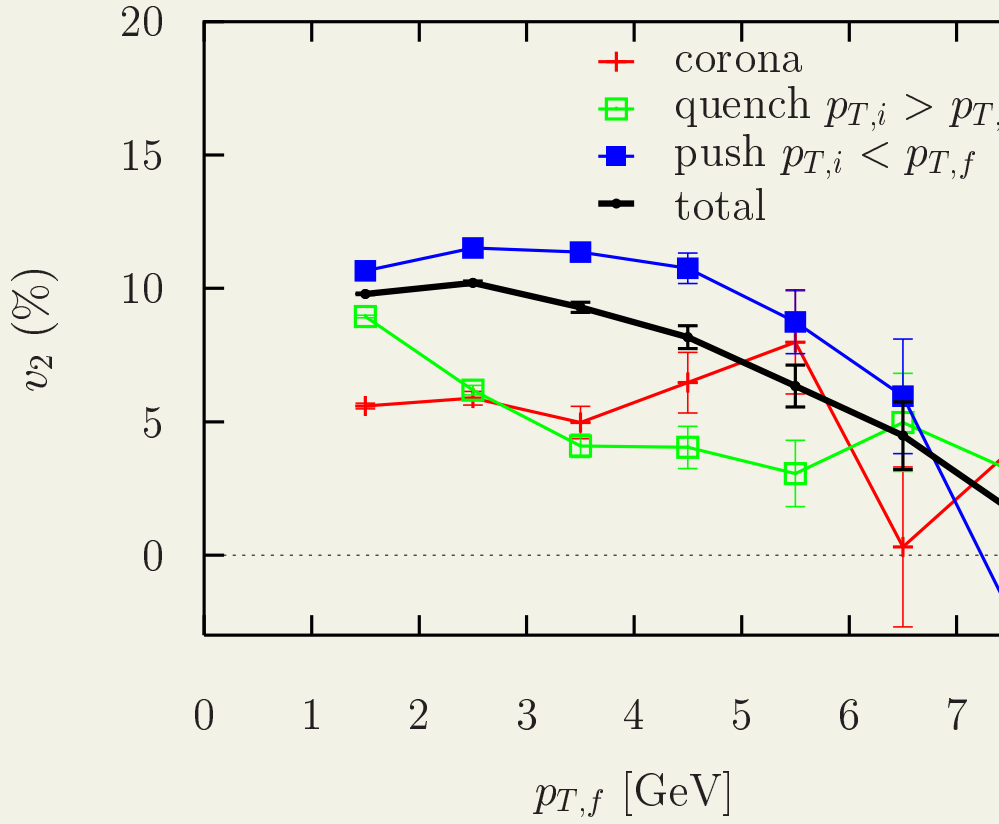
v_2 (%)
$p_{T,f}$ [GeV]
corona
quench $p_{T,i} > p_{T,}$
push $p_{T,i} < p_{T,f}$
total

average Au+Au, b=8 fm **600 averaged MC Glauber runs**

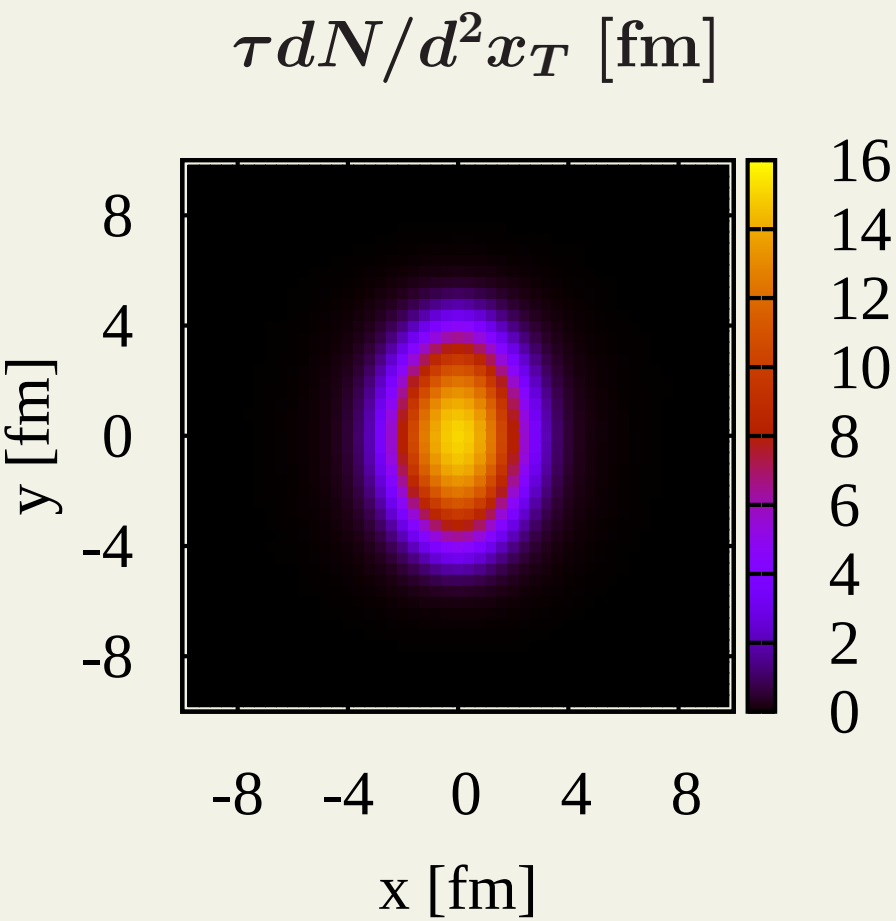

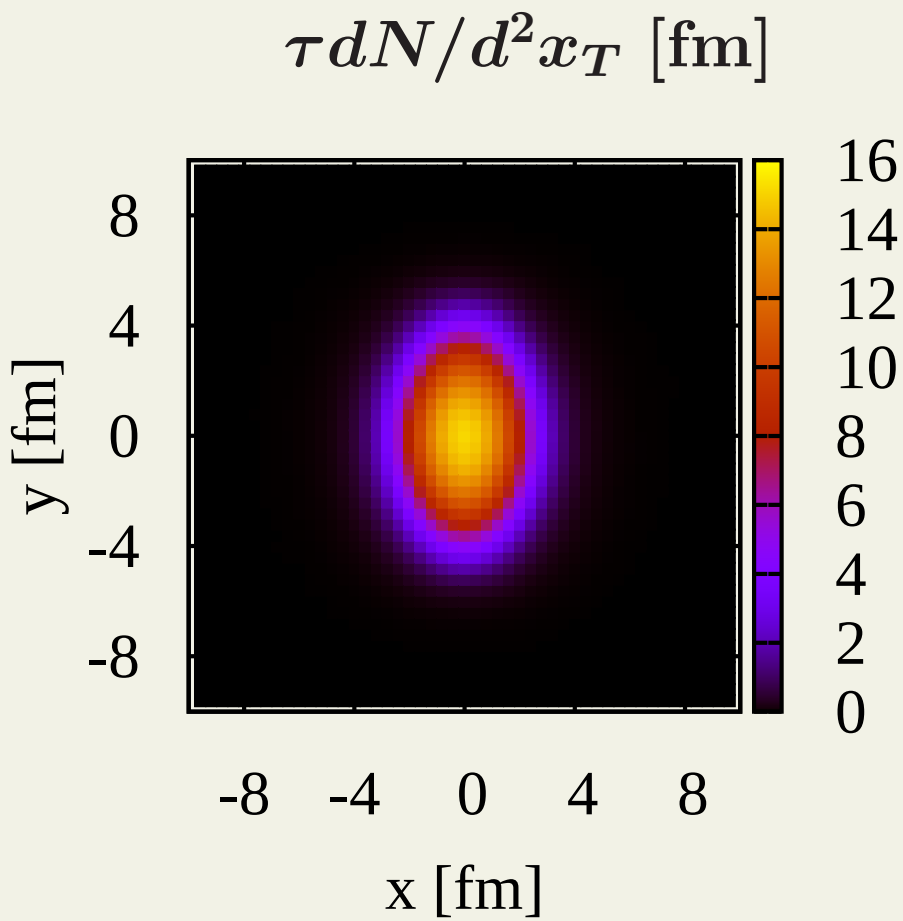

$\tau = 0.6$ fm

average Au+Au, b=8 fm **600 averaged MC Glauber**

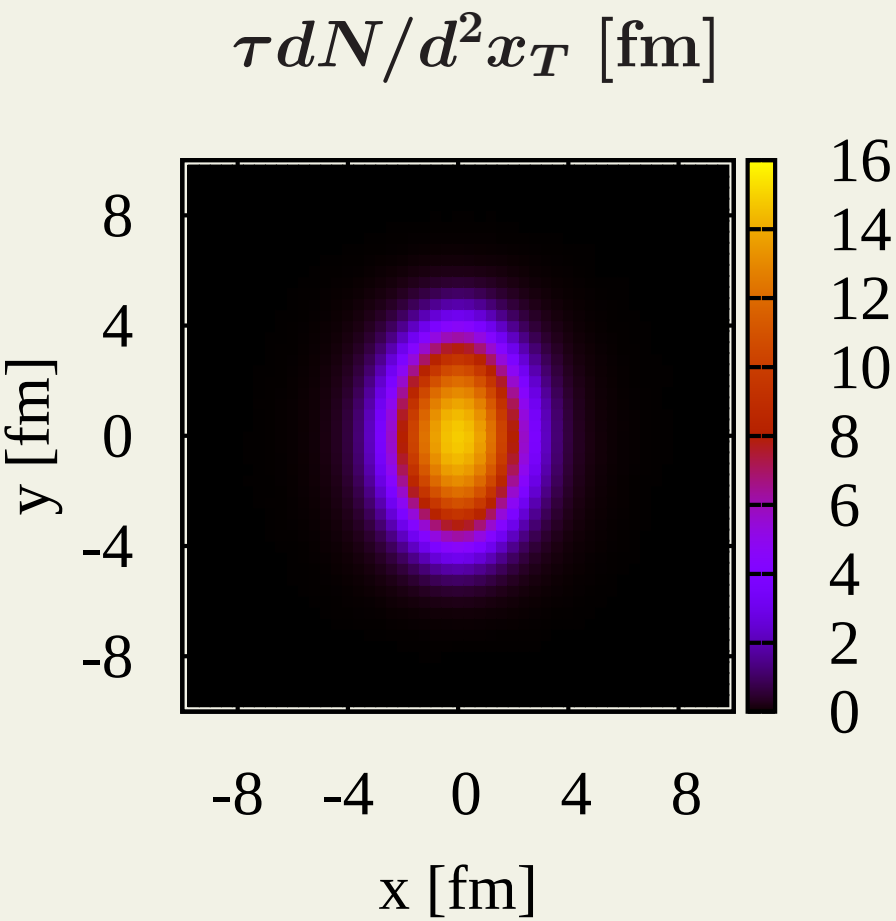

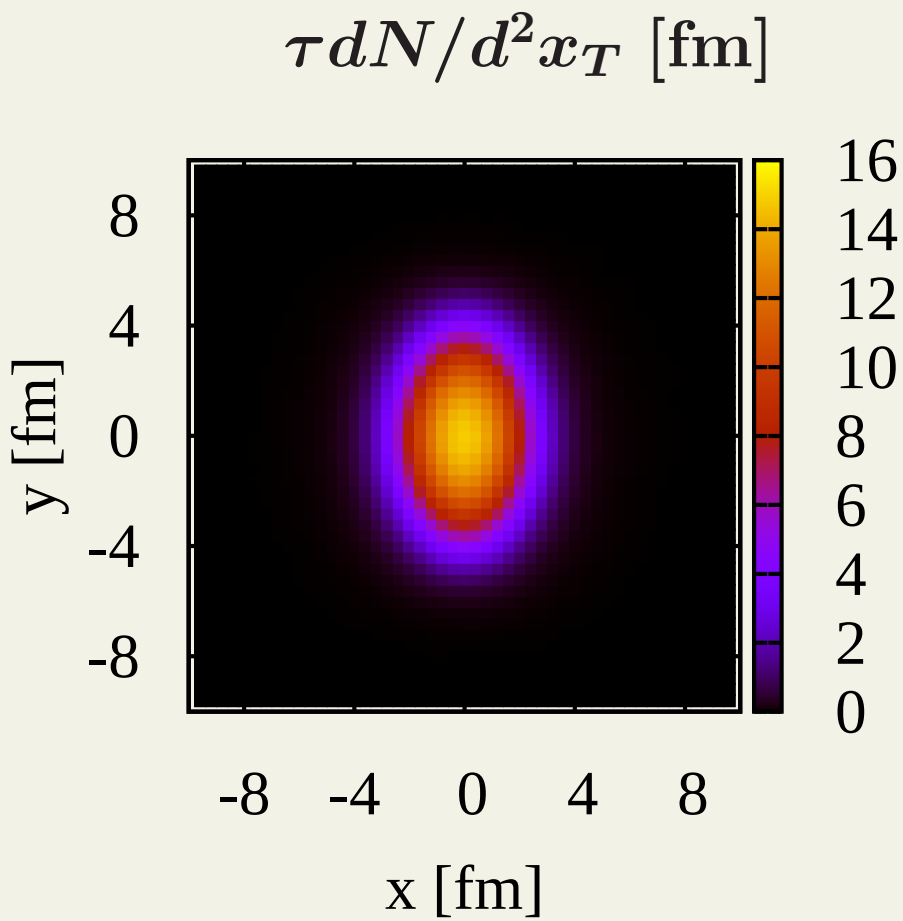

$\tau = 1.2$ fm

average Au+Au, b=8 fm **600 averaged MC Glauber**

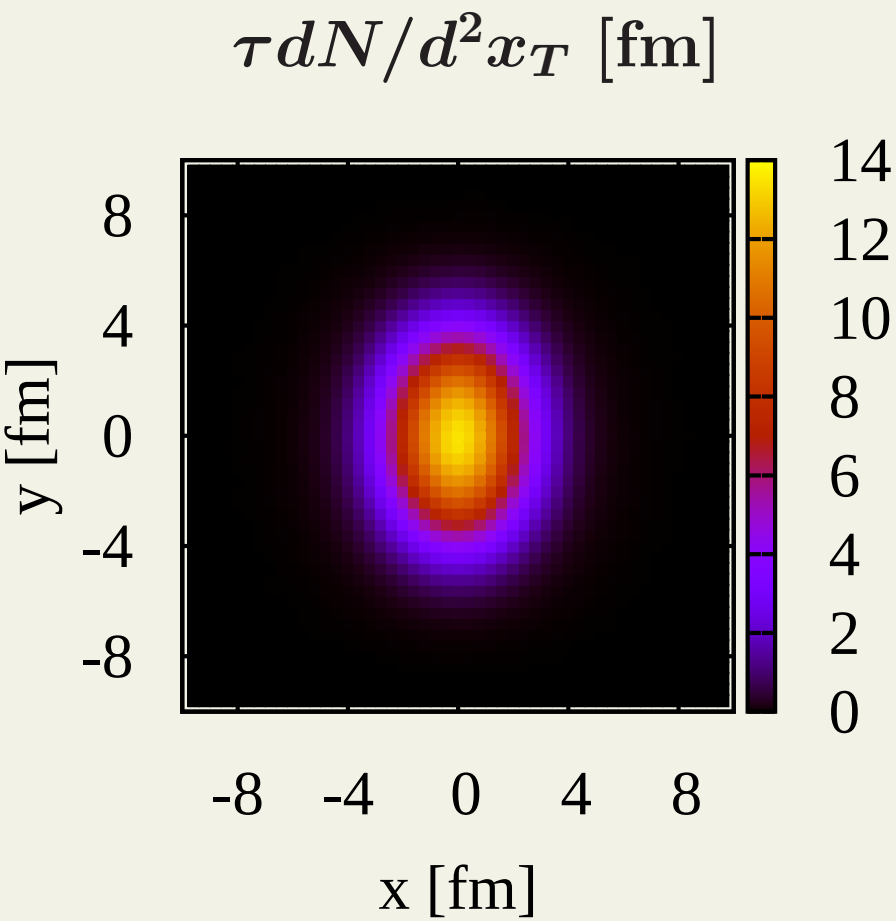

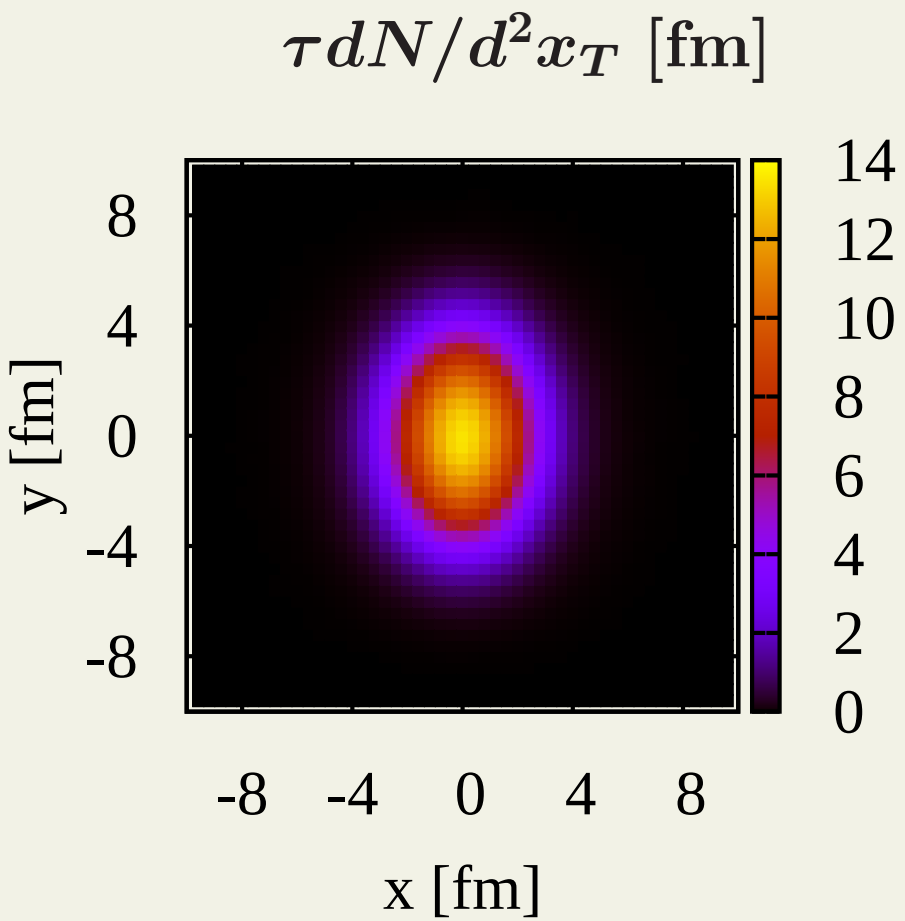

$\tau = 2.1$ fm

average Au+Au, b=8 fm

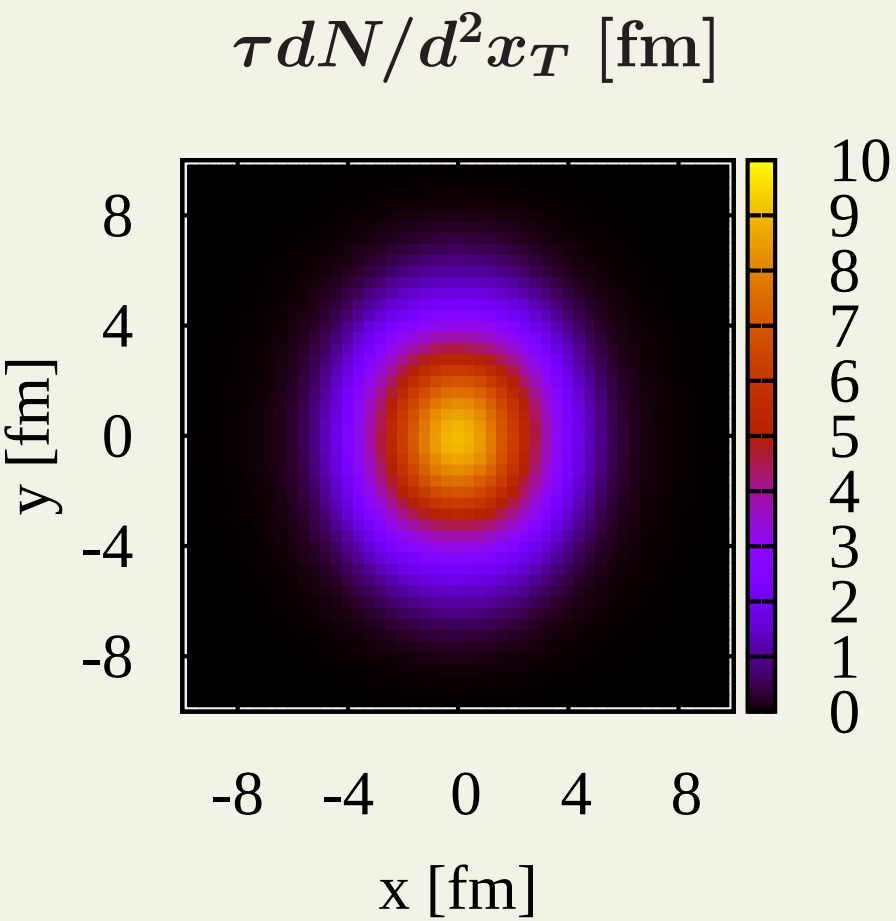

600 averaged MC Glauber

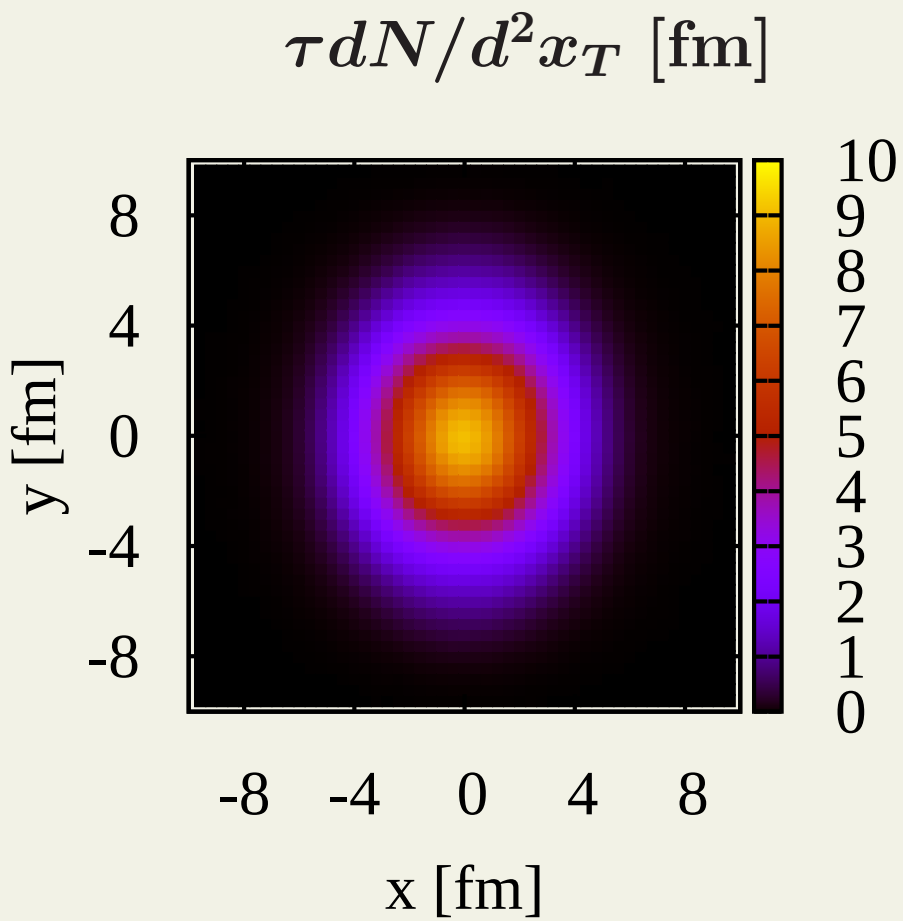

$\tau = 3.6$ fm

average Au+Au, b=8 fm **600 averaged MC Glauber**

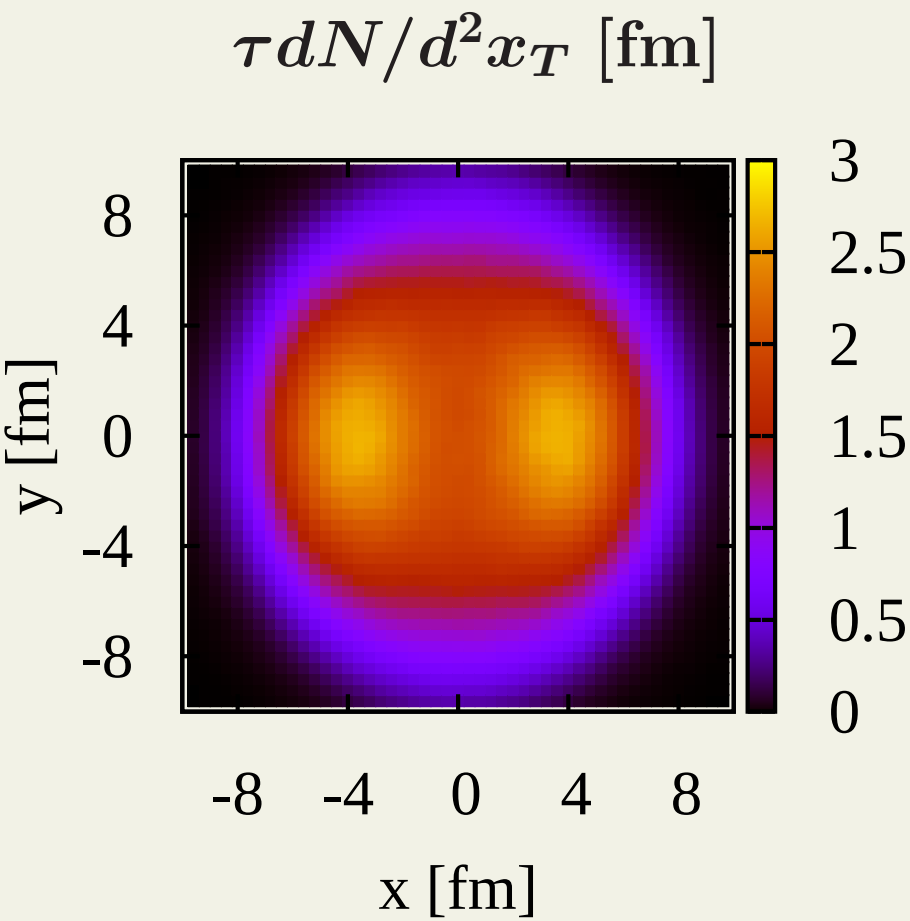

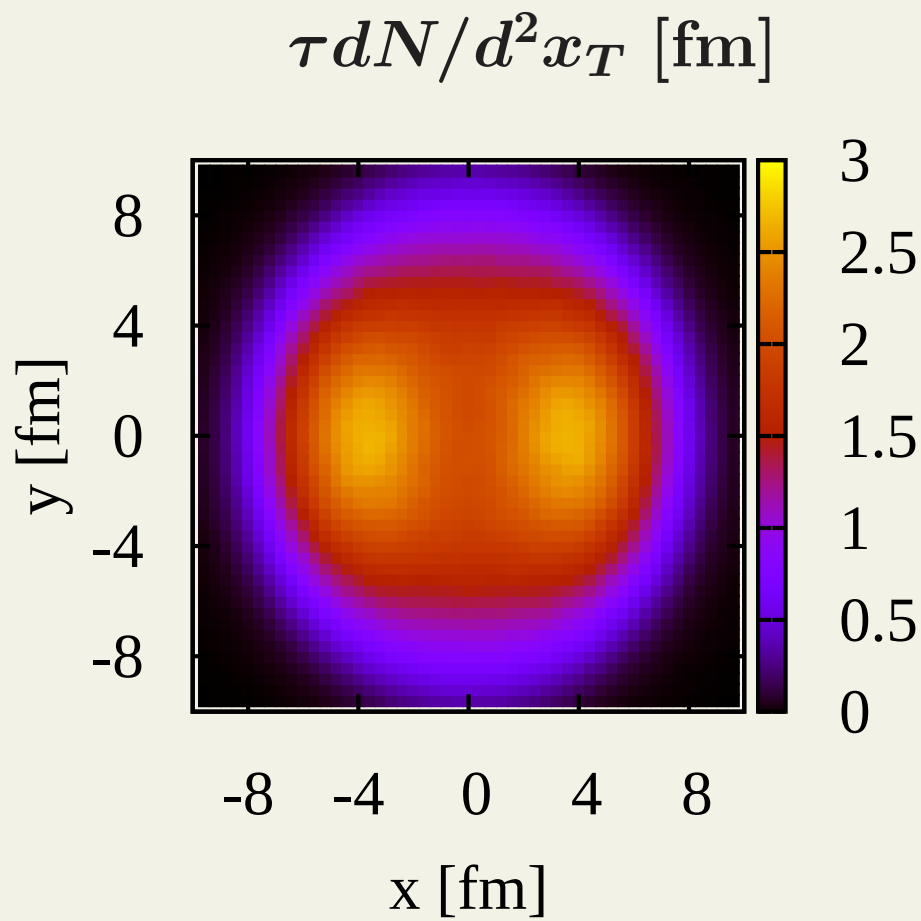

$\tau = 6.6$ fm

average Au+Au, b=8 fm **600 averaged MC Glauber**

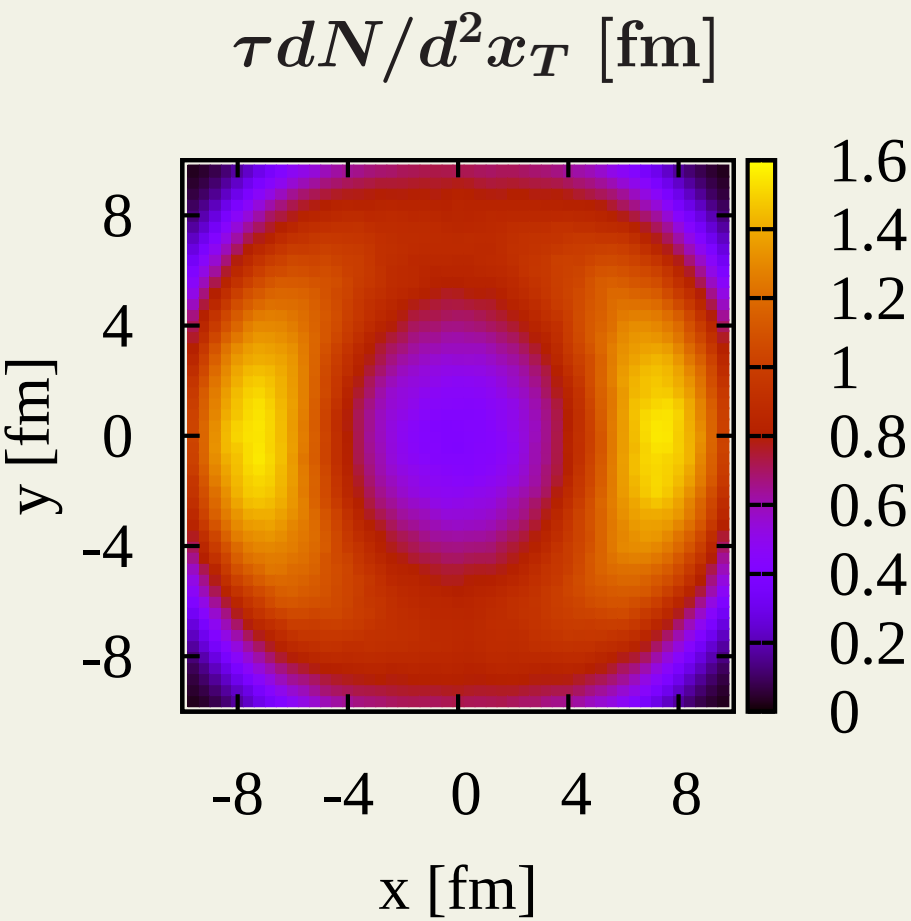

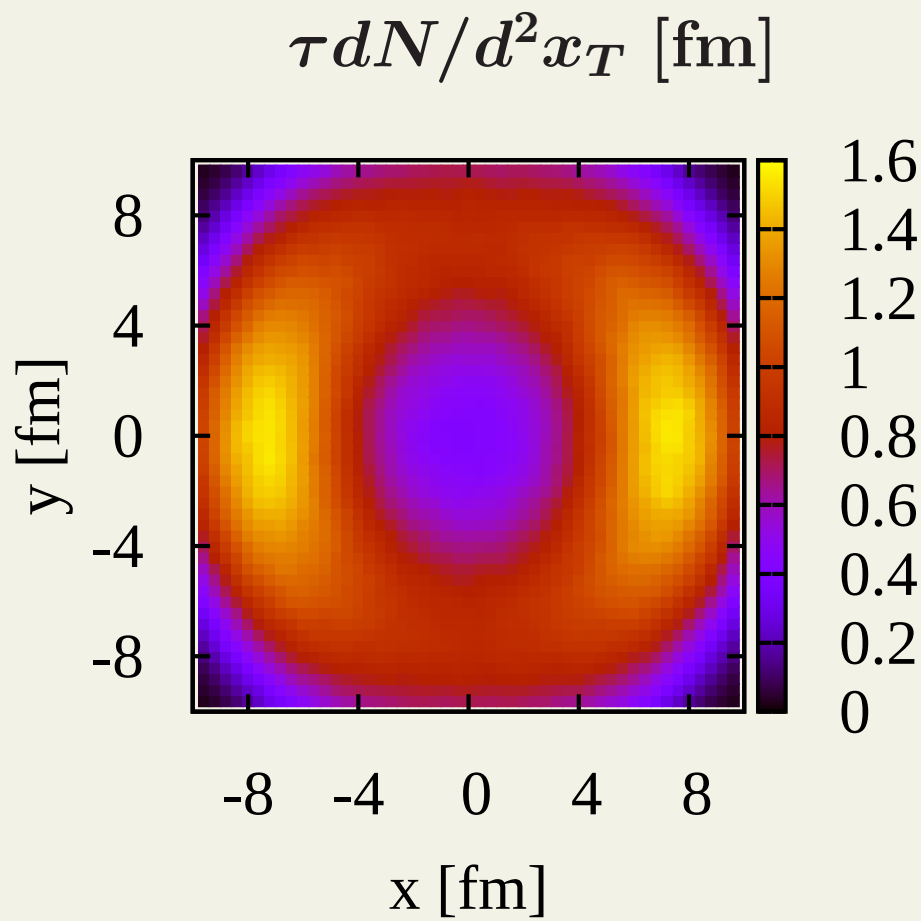

$\tau = 9.6$ fm

Backup slides

CUJET 1.0 Buzzatti et al ('11)

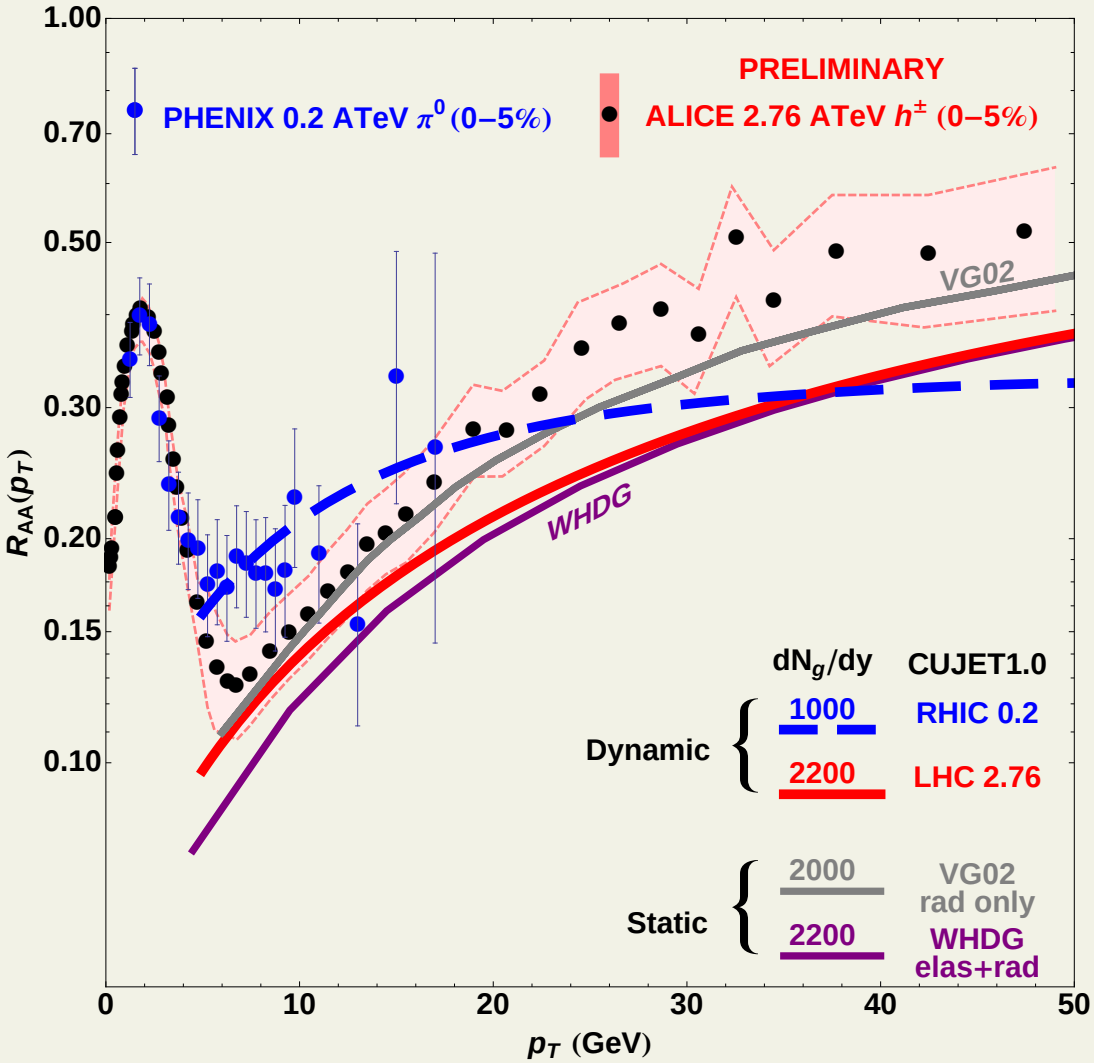

Betz & Gyulassy, arXiv:1201.0281

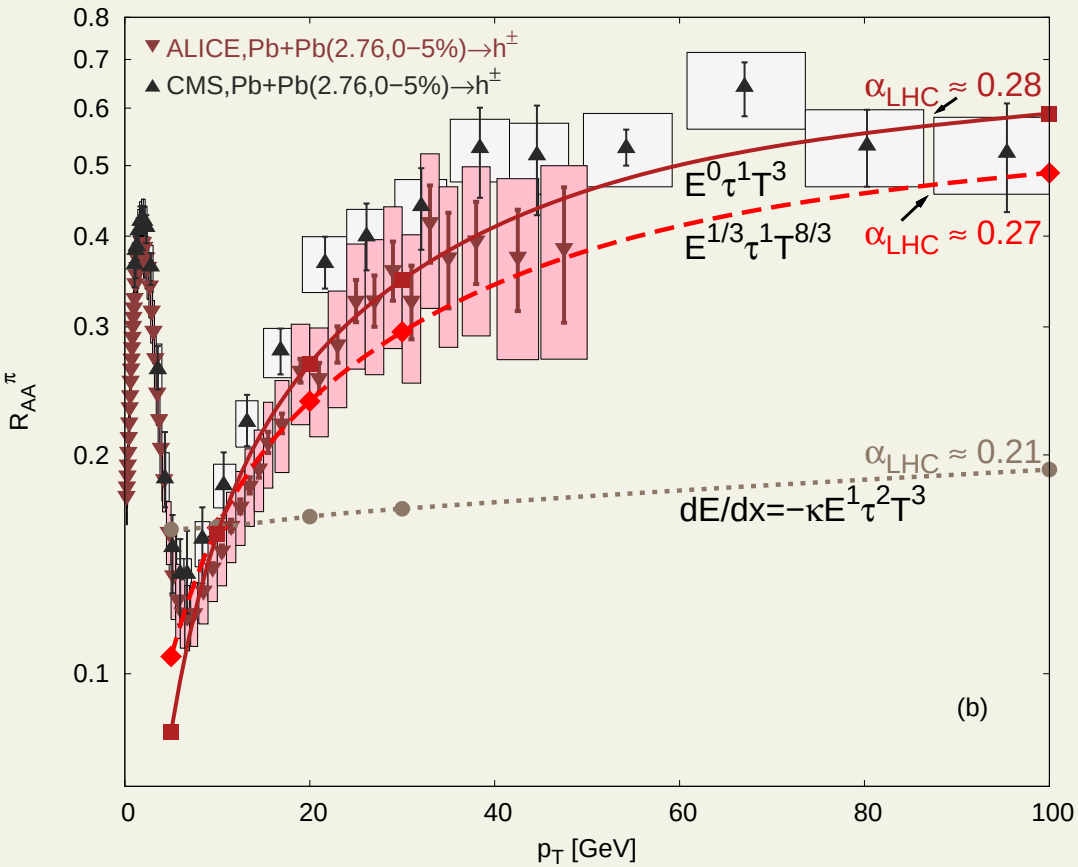

$$\alpha_s^{RHIC} = 0.3$$

ALICE v2,v3,v4 arXiv:1205.5761v2

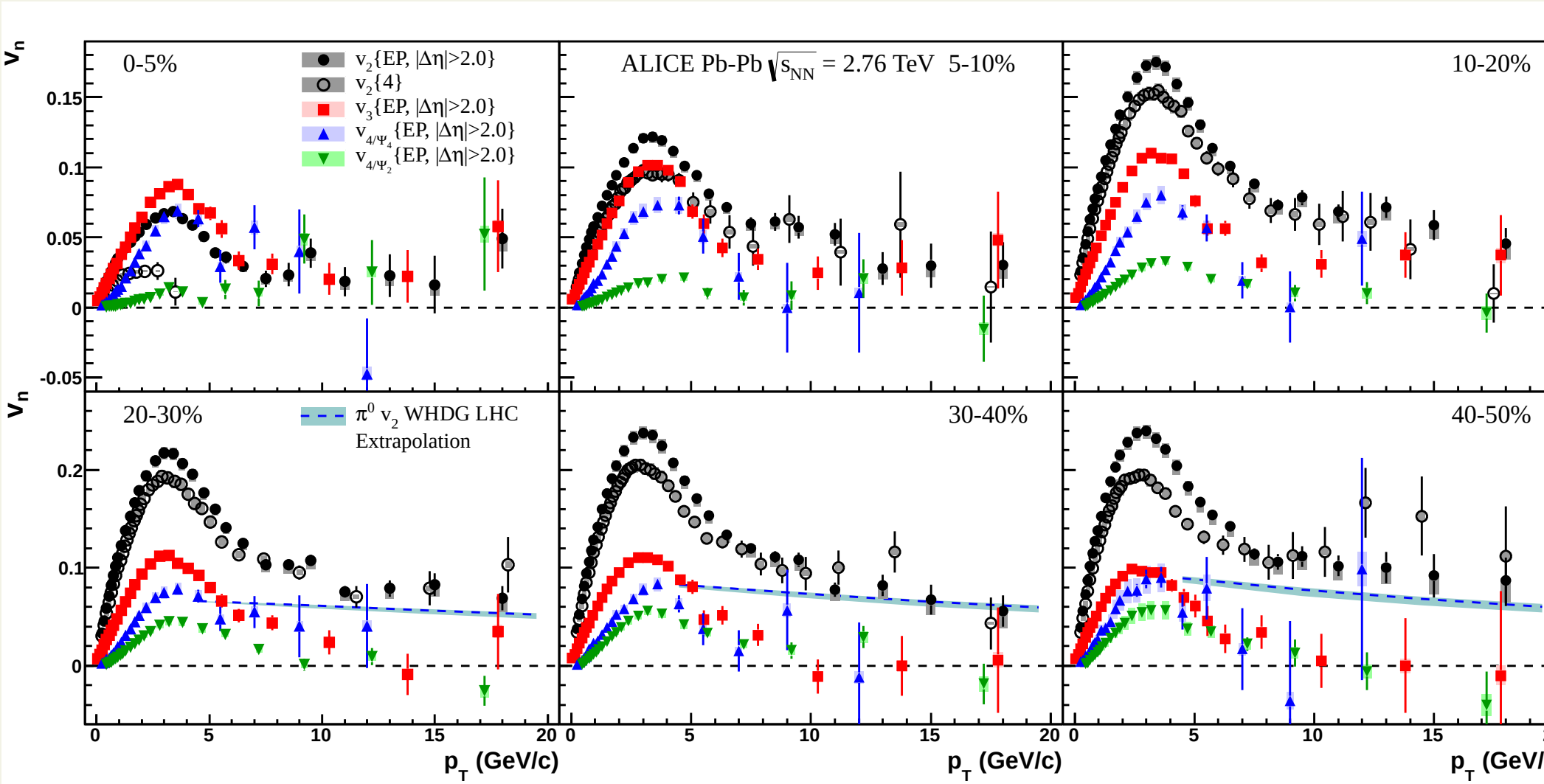

CYM eccentricity Venugopalan & Lappi, PRC74 ('06):

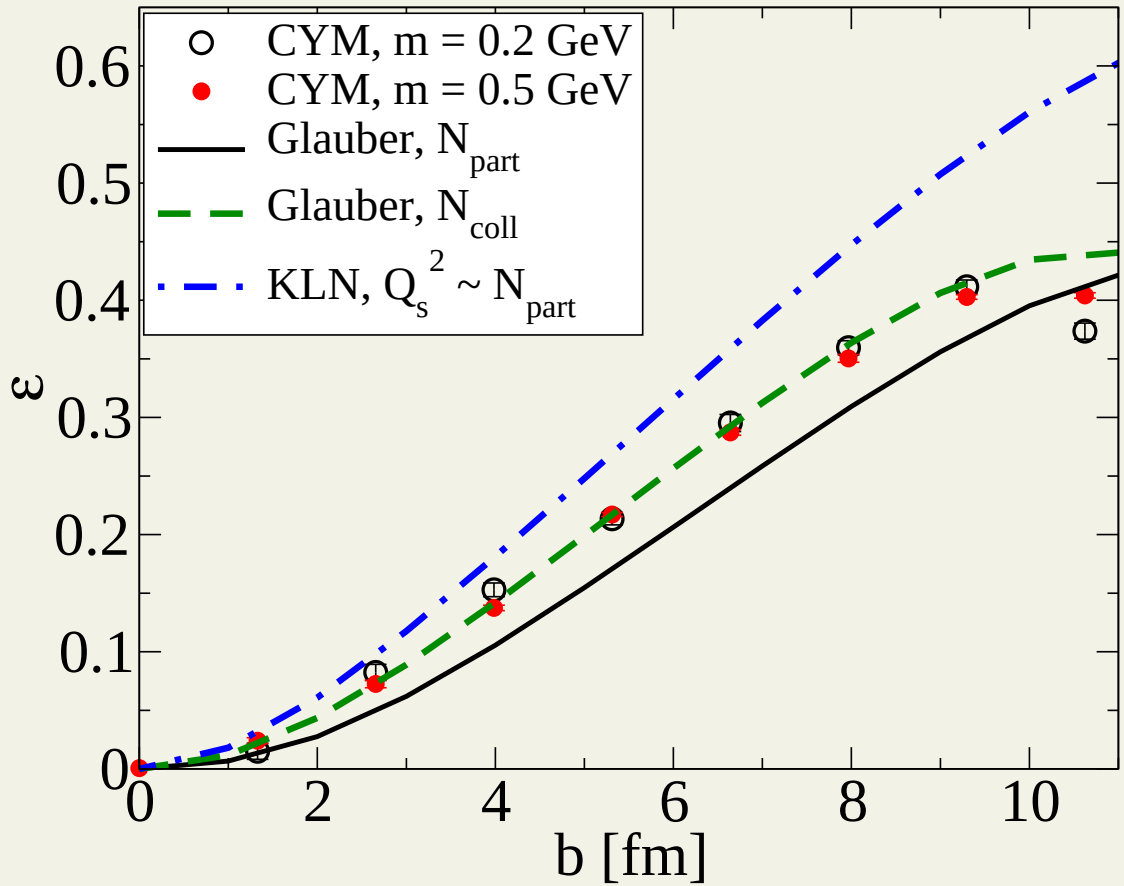

MARTINI $R_{AA}(\phi)$ Schenke et al, PRC80 ('09):

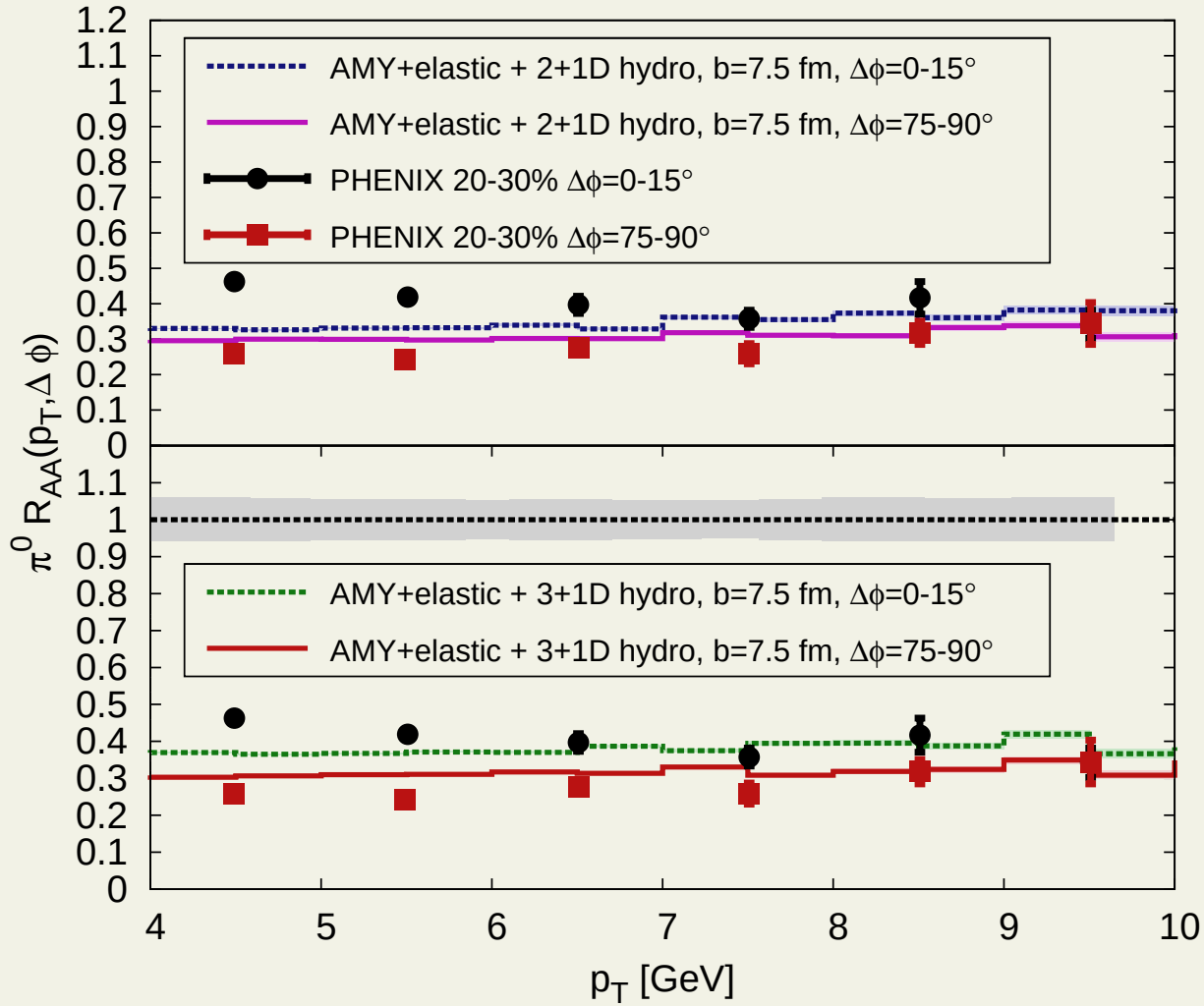

Parton subdivision

Naive $2 \to 2$ cascade nonlocal - action at distance $d < \sqrt{\frac{\sigma}{\pi}}$

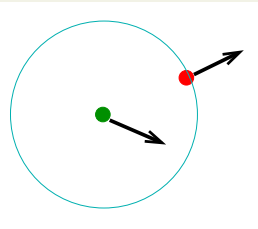

subdivision: **rescale** $f \to f \cdot \ell$, $\sigma \to \sigma/\ell$ $\Rightarrow$ $d \propto \ell^{-1/2}$ **local as** $\ell \to \infty$

DM & Gyulassy ('02): $v_2(p_T)$

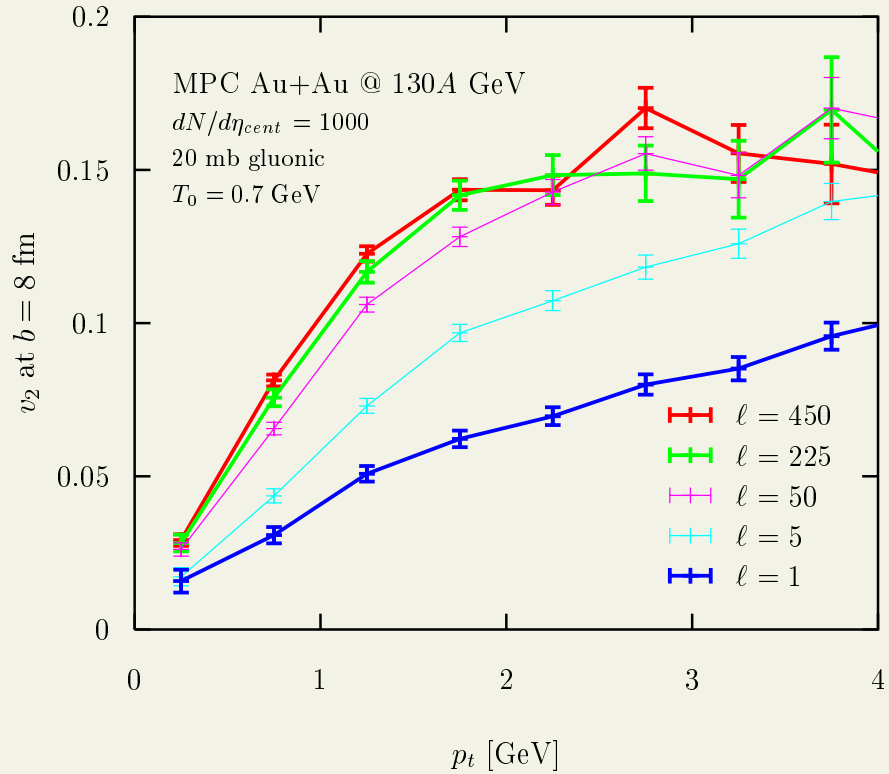

spectra

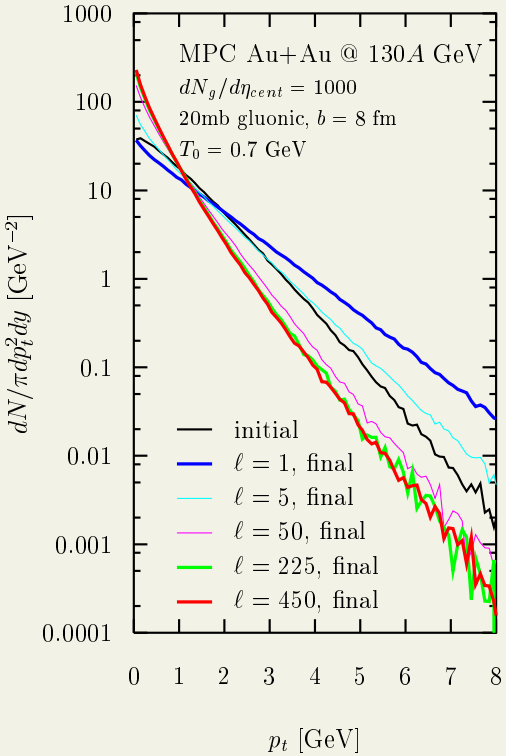

at RHIC: need subdivision $\ell \sim 200$ **to eliminate large artifacts**

$\to$ **computational challenge** - **CPU time scales as** $\ell^{\sim 3/2}$ **per run** $\to$ **barely fits on PC**

RHIC/LHC Complementarity

Jörn Putschke

(Wayne State University)

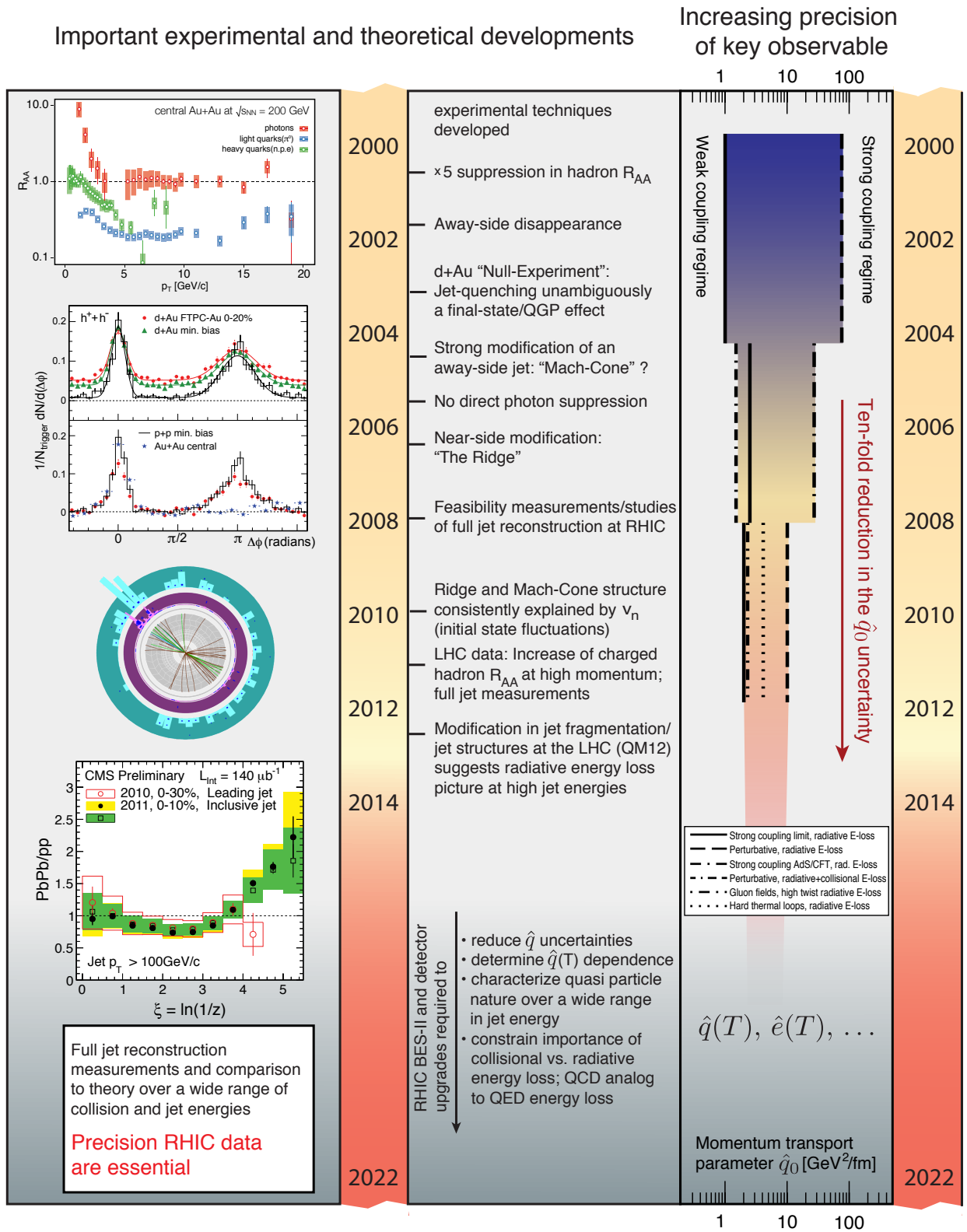

Used as a guideline ...

RHIC White Paper: "Hot and Dense QCD Matter"

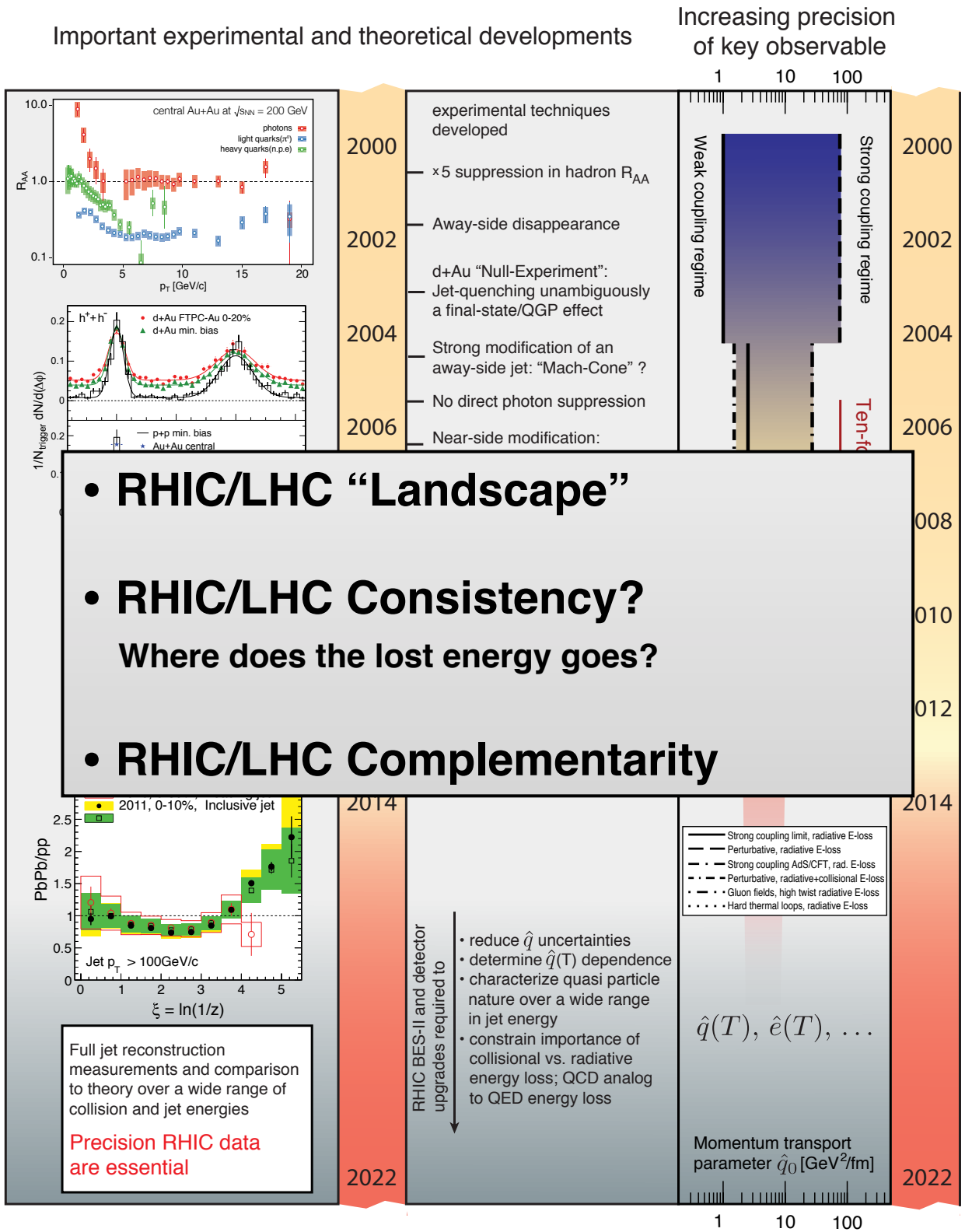

Used as a guideline ...

RHIC White Paper: "Hot and Dense QCD Matter"

RHIC and LHC "Landscape"

The QGP at the LHC:

- fireball hotter (~20%) and denser (~x2) and longer lifetime wrt RHIC

- bulk dynamics, $v_n(p_T)$, similar at RHIC and LHC, mainly driven by initial state "geometry"

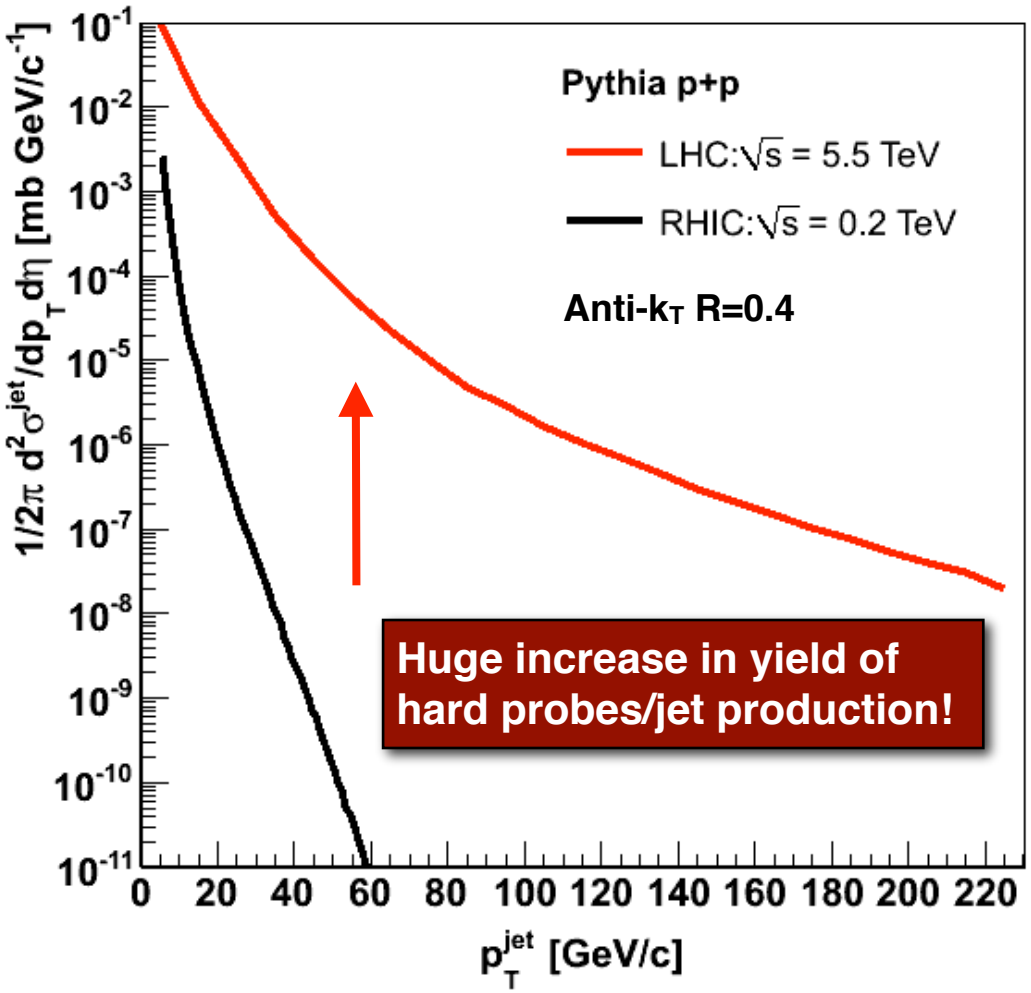

RHIC and LHC "Landscape"

The QGP at the LHC:

- fireball hotter (~20%) and denser (~x2) and longer lifetime wrt RHIC

- bulk dynamics, $v_n(p_T)$, similar at RHIC and LHC, mainly driven by initial state "geometry"

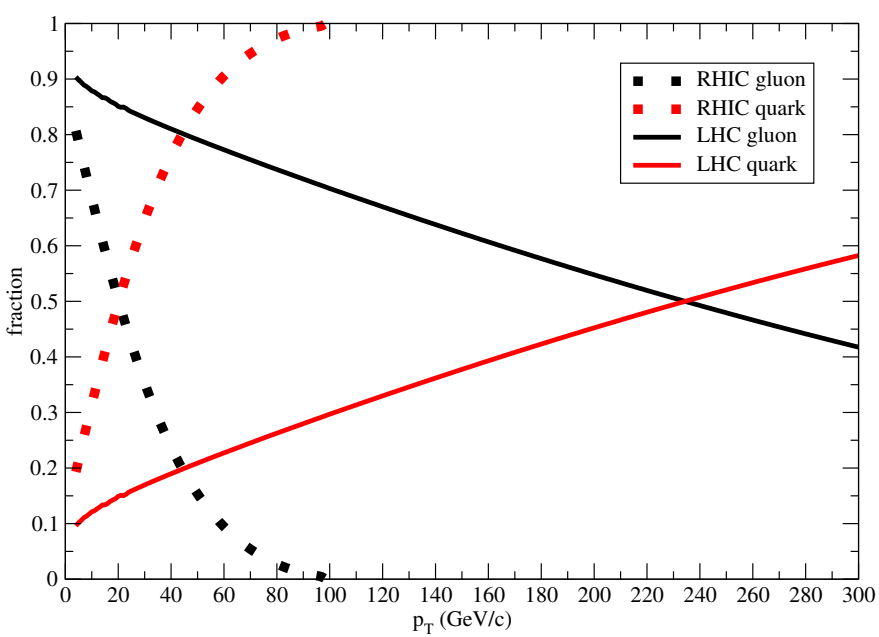

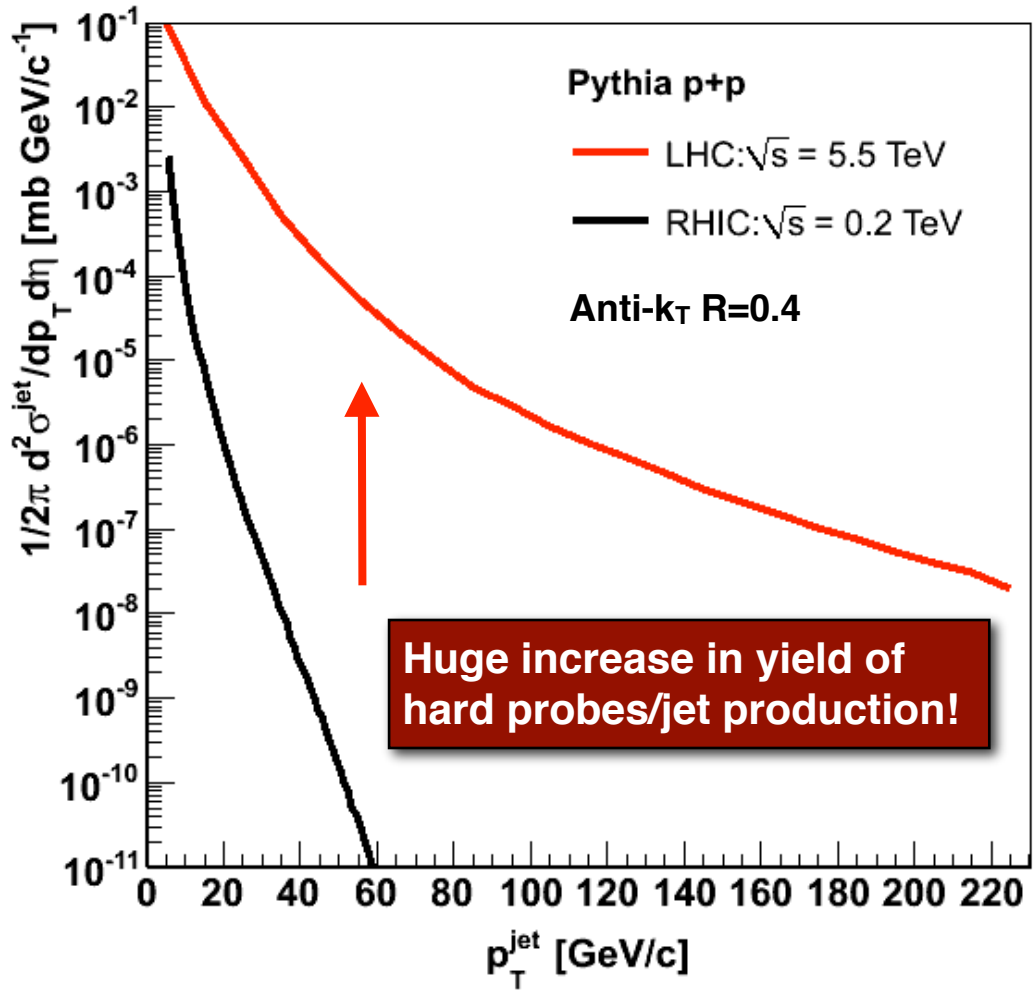

Huge increase in yield of hard probes/jet production!

Mainly gluon jets (p_T<200 GeV) at the LHC. Quark jets at RHIC p_T>40 GeV.

The issue: Background in HI collisions

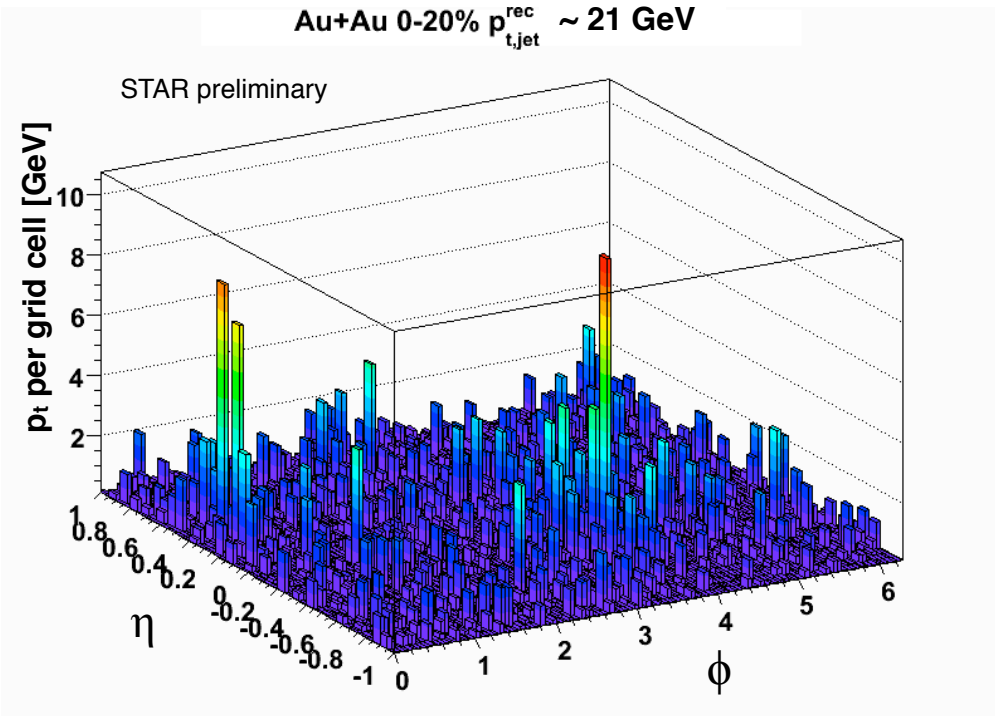

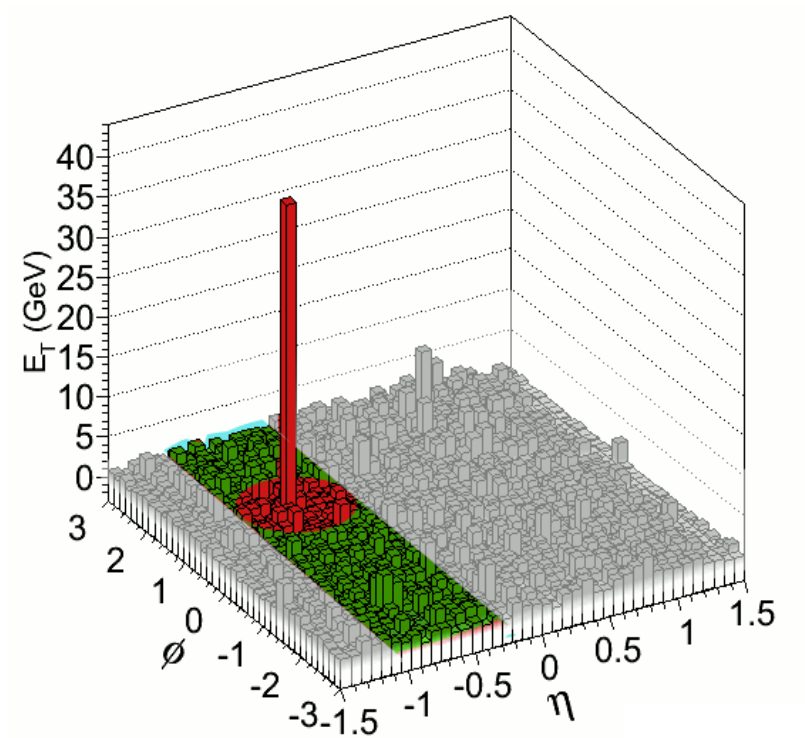

Full jet reconstruction in HI collisions is a challenge due to the underlying background

- Overall background pedestal
- Region-to-region background fluctuations and v_n contributions
- Multiple independent hard scattering in HI collisions

Different contributions depending on coincidence vs. inclusive measurements!

Remark: I will not talk about this in detail, a comprehensive summary concerning the different approaches currently used can be found in a talk by G. Roland: https://indico.cern.ch/getFile.py/access?contribId=3&sessionId=0&resId=0&materialId=slides&confId=198761

LHC and RHIC R_{AA}

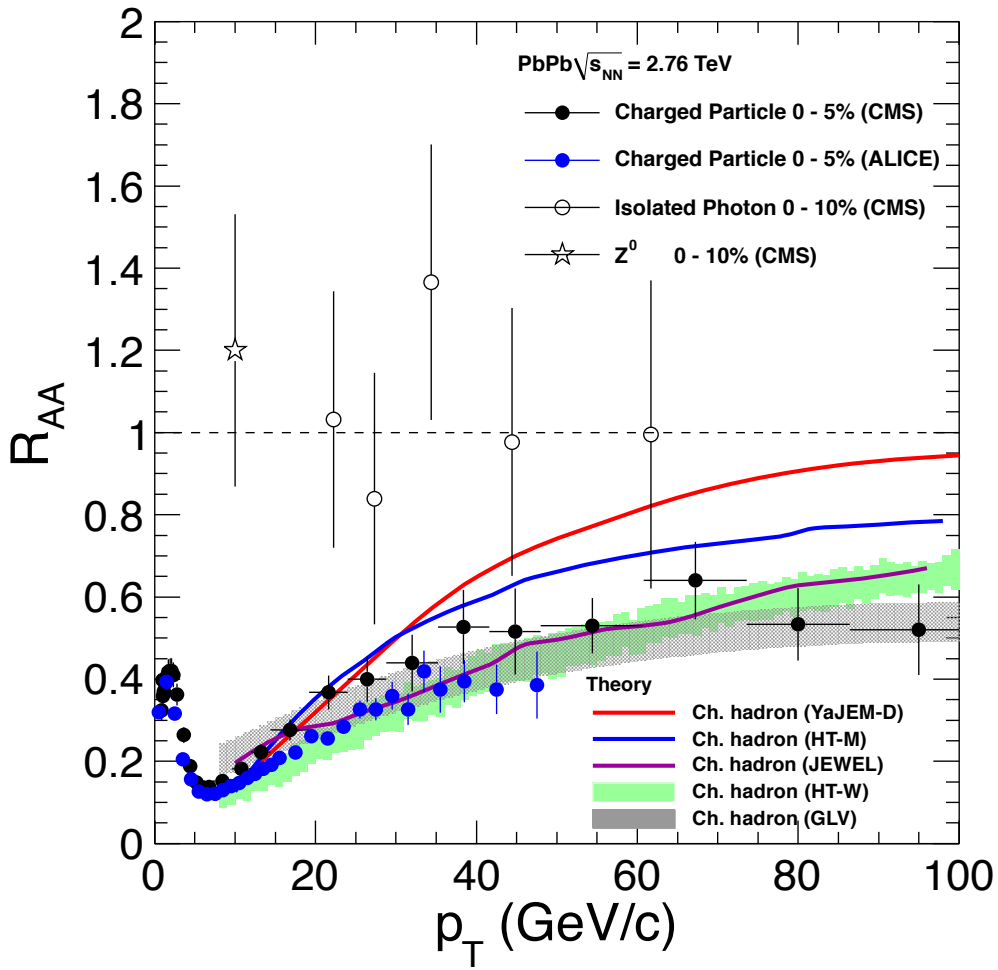

R_{AA} rising as function of p_T; constant for p_T>50 GeV?

LHC and RHIC R_{AA}

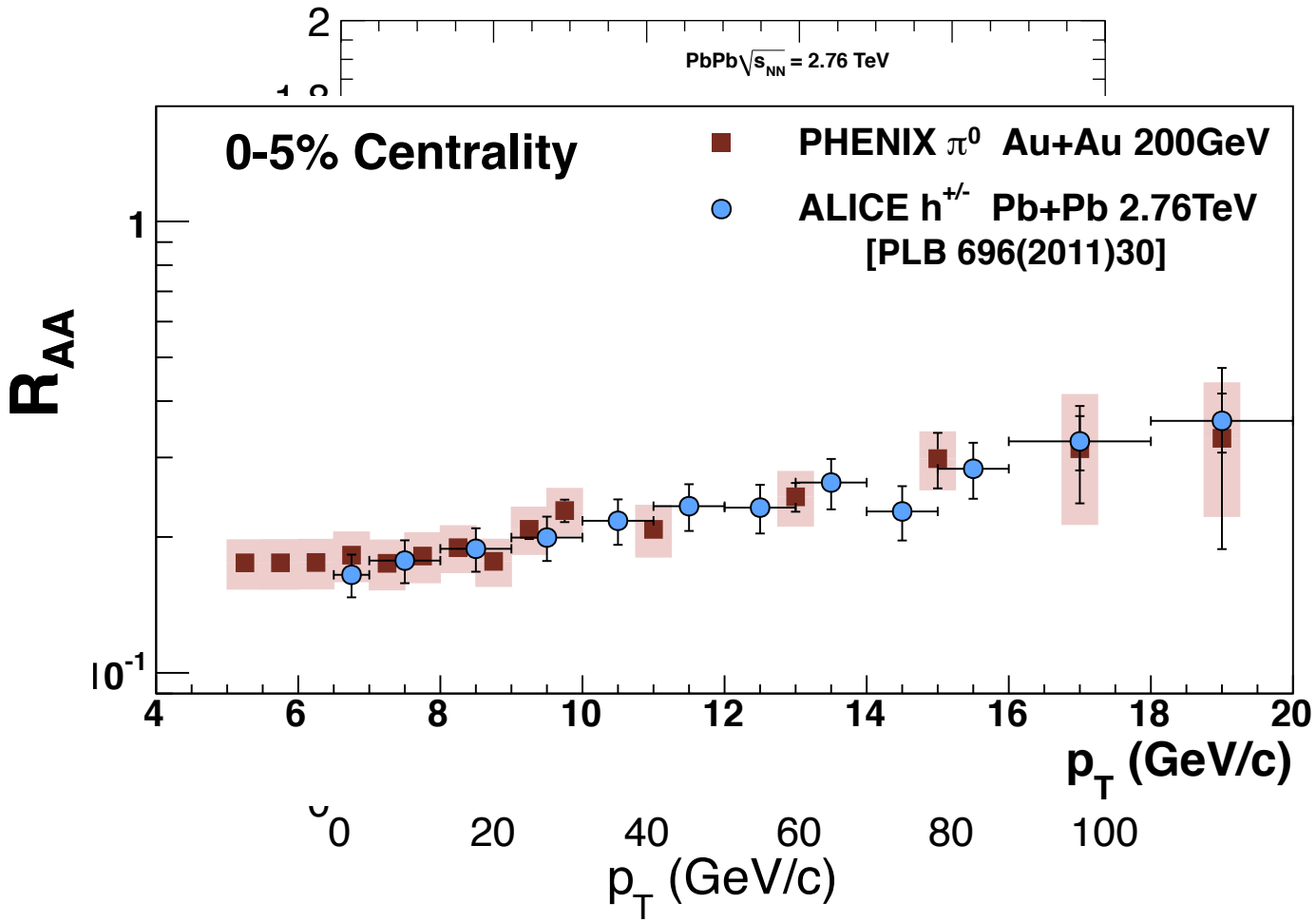

R_{AA} rising as function of p_T; constant for p_T>50 GeV?

RHIC R_{AA} ~ LHC R_{AA} up to p_T~20 GeV

Jet R_{AA}/R_{CP} at the LHC

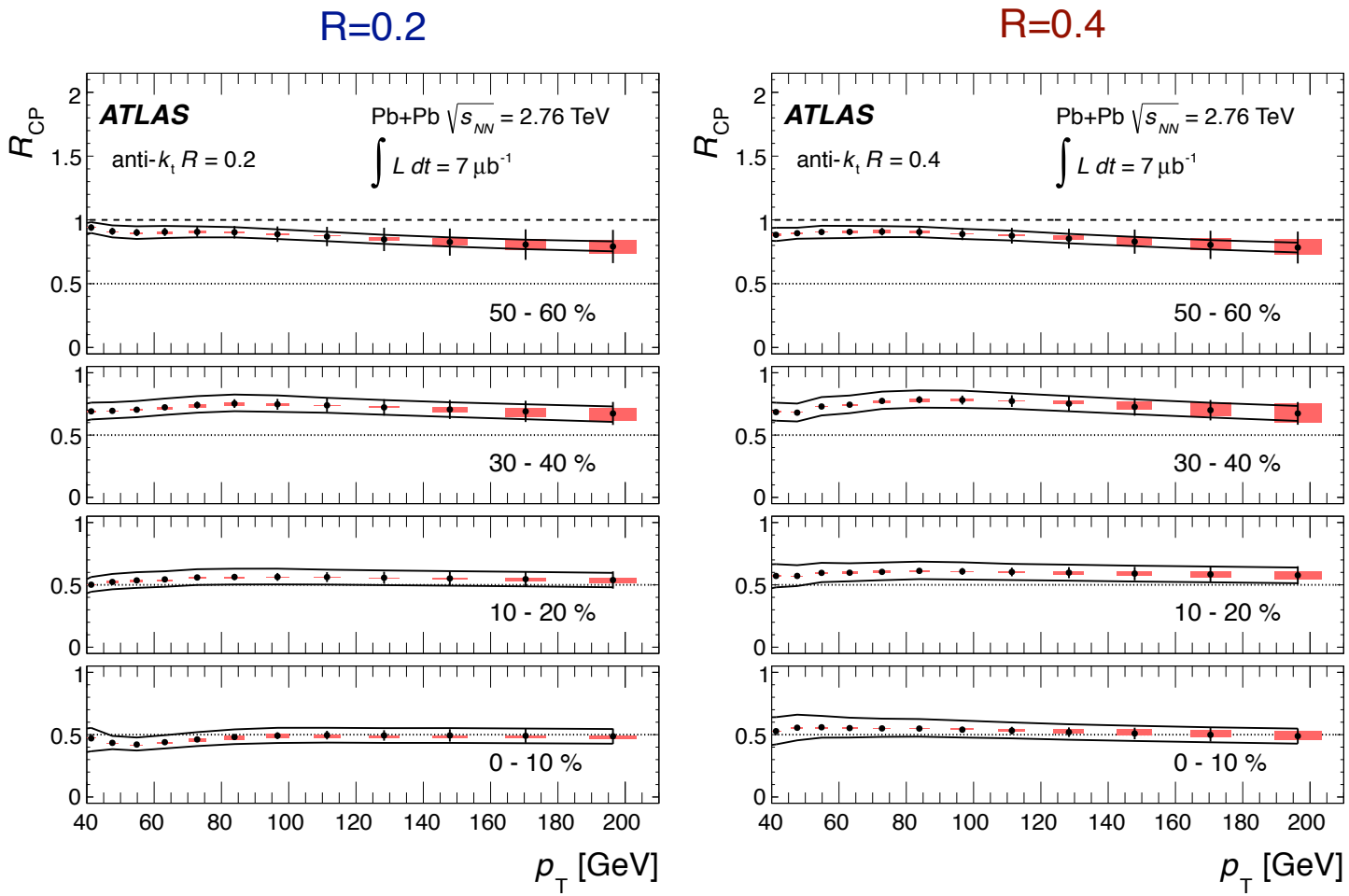

R_{CP}^{Jet}~ R_{AA} ~ 0.5 (>50 GeV)

No significant p_T and R dependence of R_{CP} for p_T>100 GeV

Jet R_{AA}/R_{CP} at the LHC

R=0.2

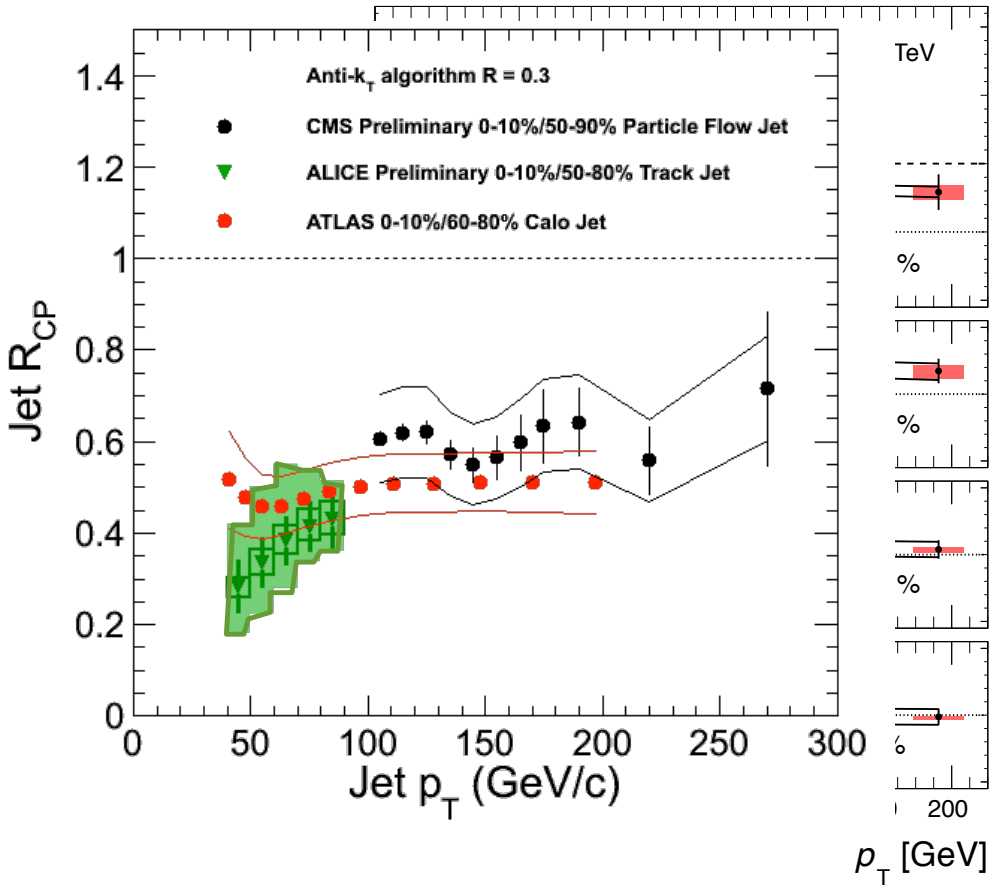

R=0.4

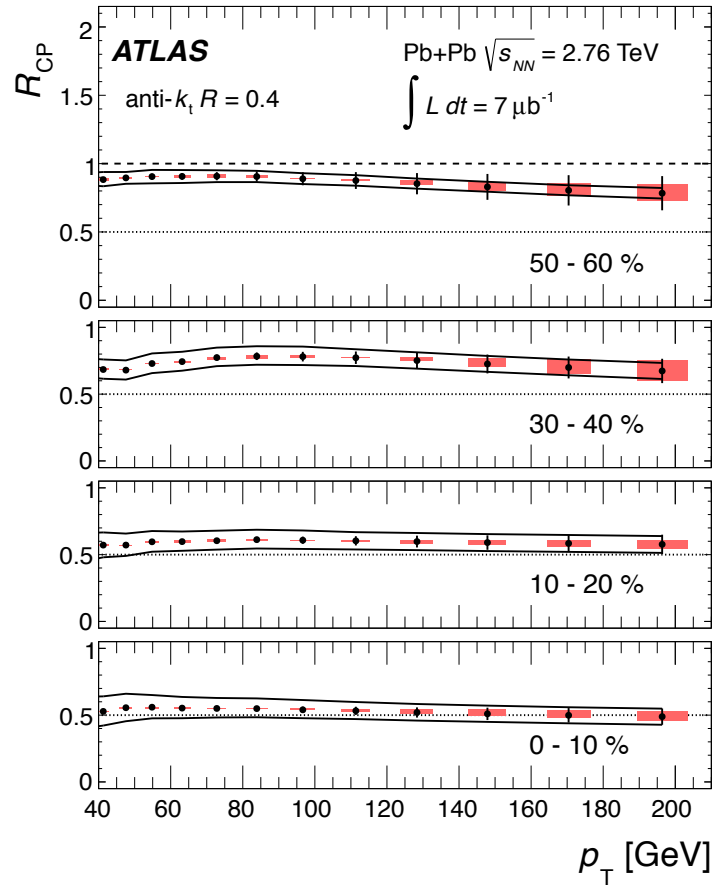

R_{CP}^{Jet}~ R_{AA} ~ 0.5 (>50 GeV)

No significant p_T and R dependence of R_{CP} for p_T>100 GeV

Jet R_{AA}/R_{CP} at the LHC

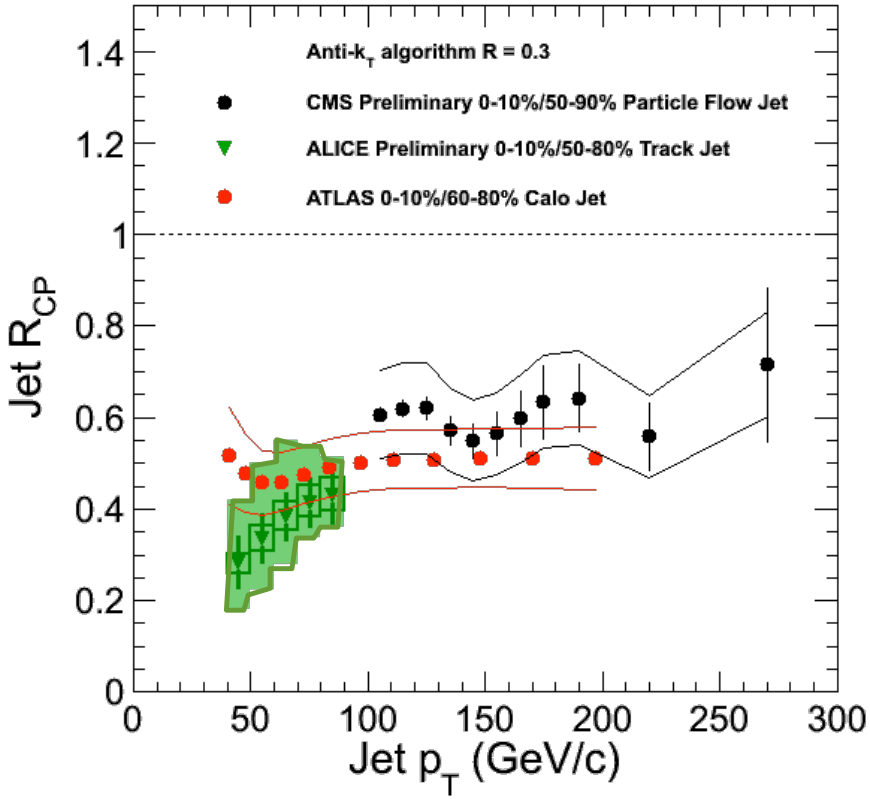

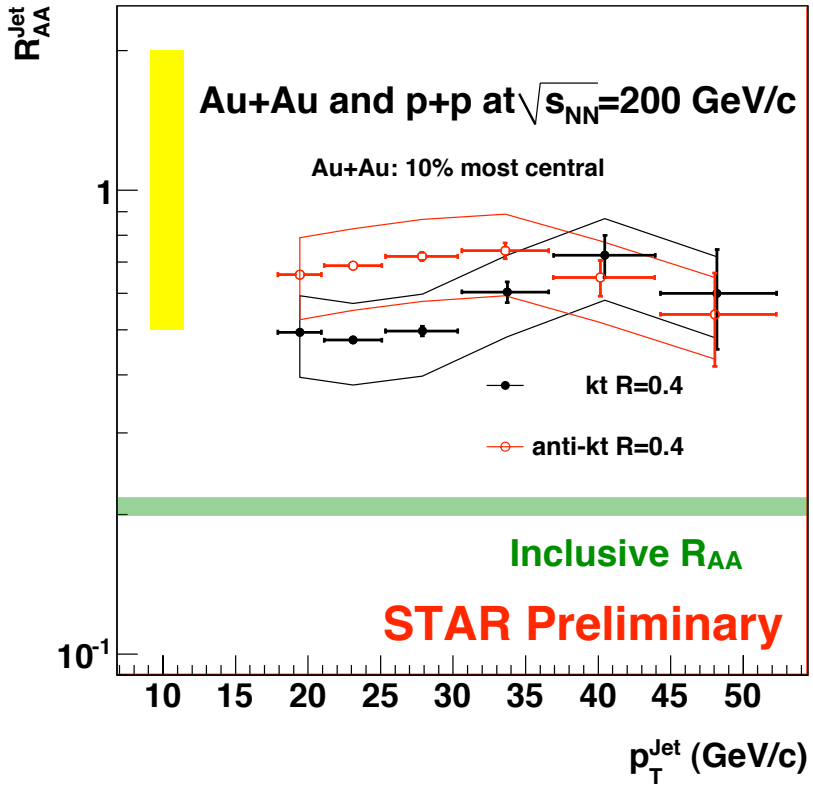

R_{CP}^{Jet}~ R_{AA} ~ 0.5 (>50 GeV)

No significant p_T and R dependence of R_{CP} for p_T>100 GeV

***RHIC:* Jet R_{AA} less suppressed than hadrons!**

Caveat: Large systematic uncertainties

Di-jet asymmetry/imbalance as function of leading jet p_T

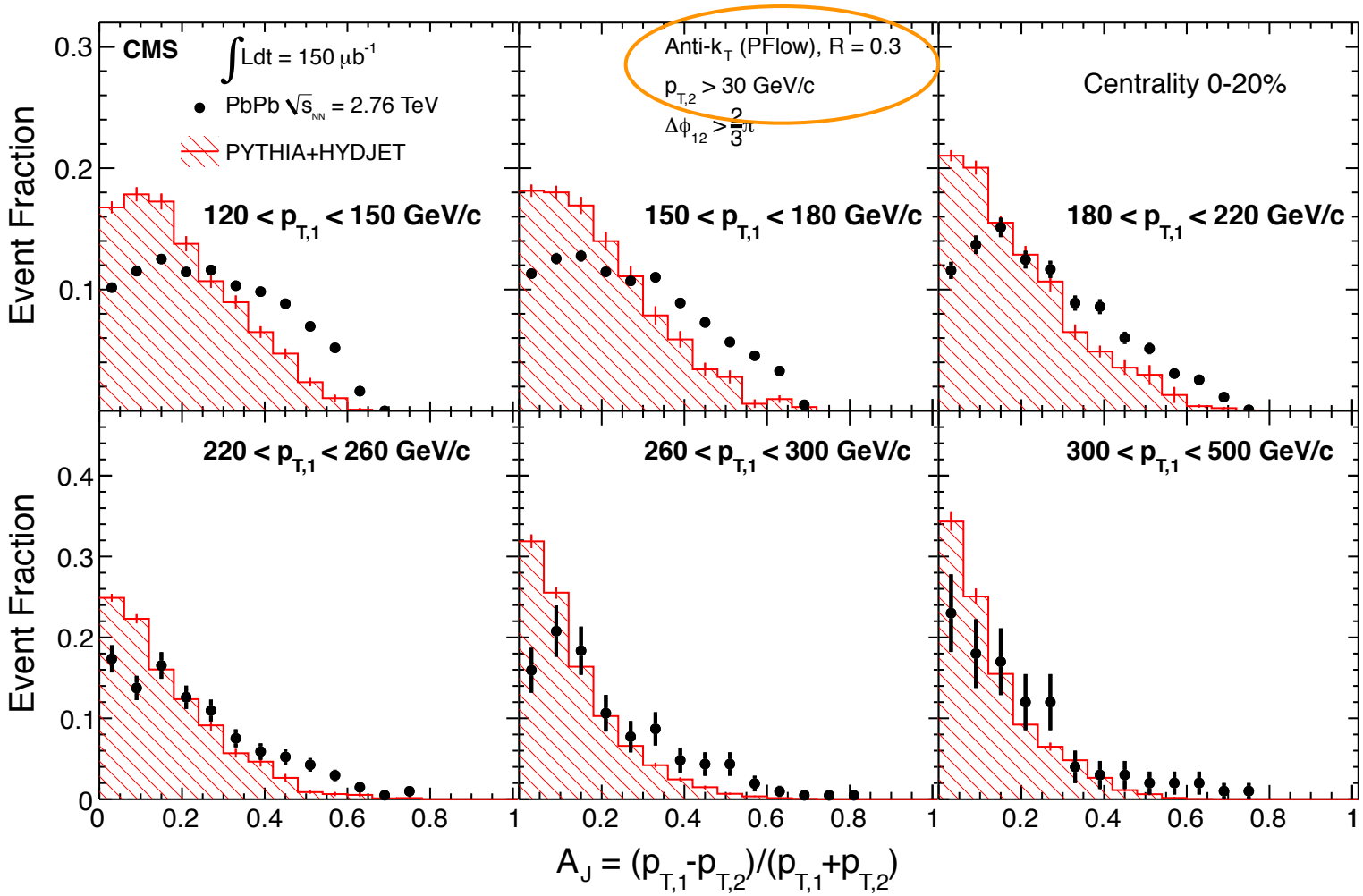

Di-jet asymmetry/imbalance as function of leading jet p_T

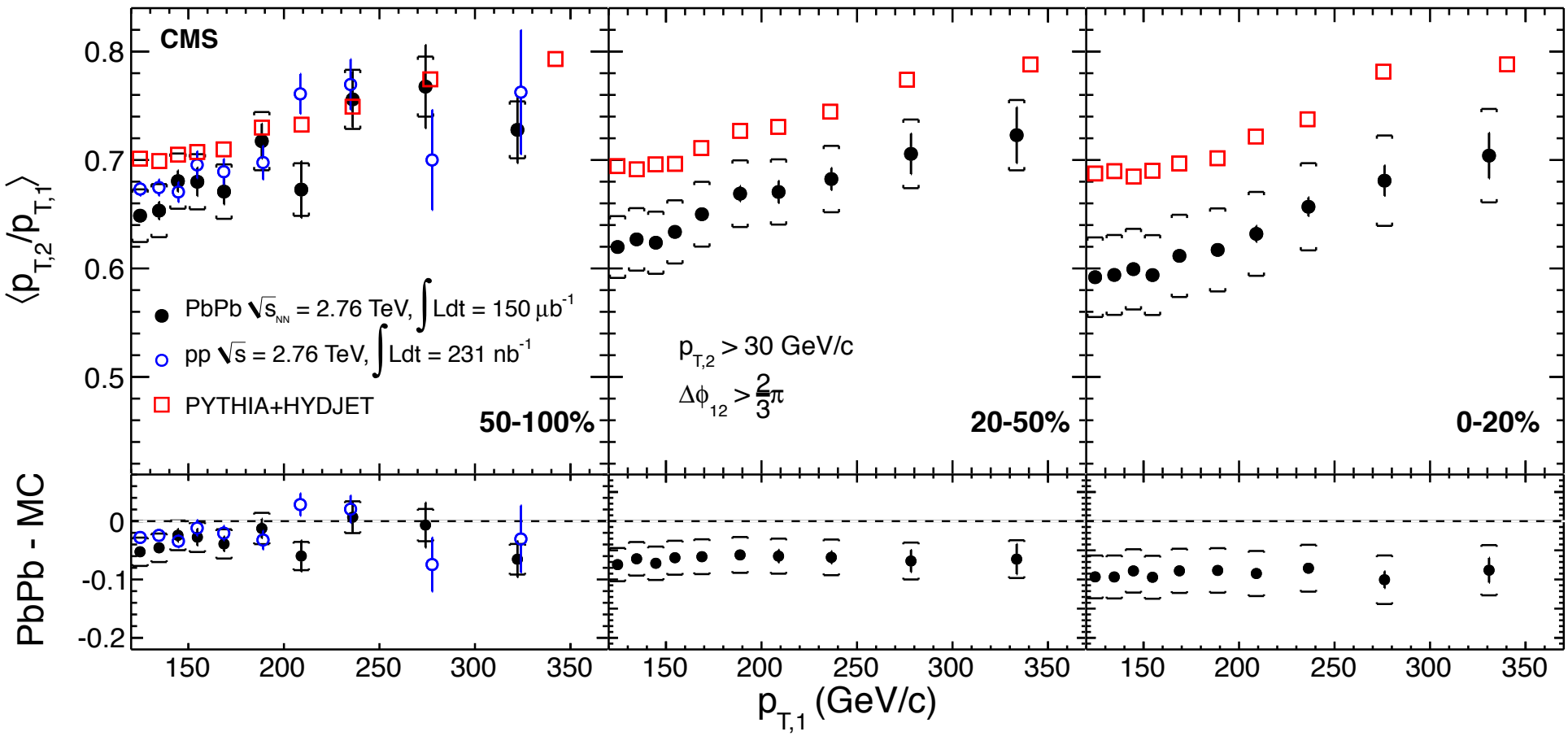

Di-Jet imbalance decreasing with increasing jet energy!

"Can be explained in terms of essentially known physics, i.e. the increased collimation of jets due to kinematics and a transition to a less gluon- dominated regime." : T.Renk, arXiv:1204.5572

Direct Photon-Jet Measurements

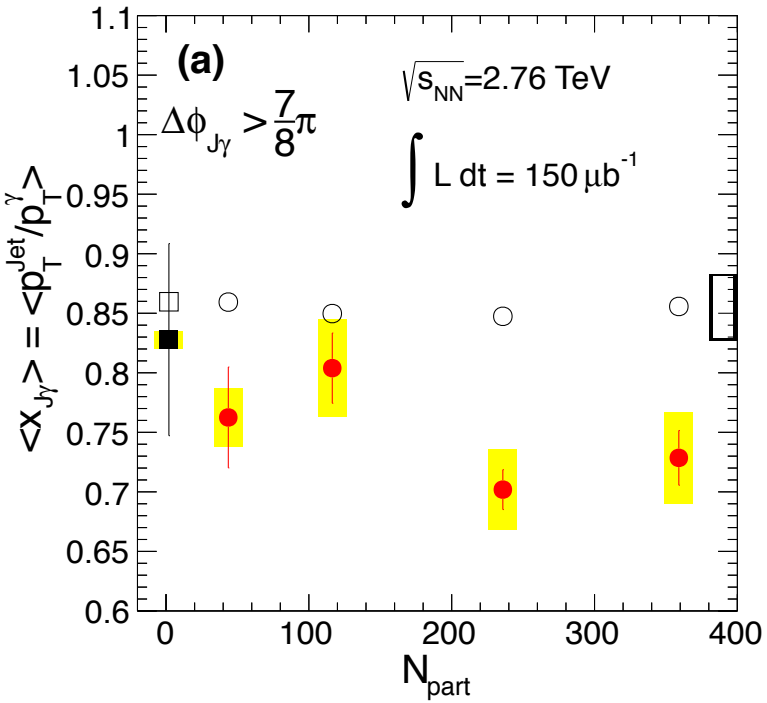

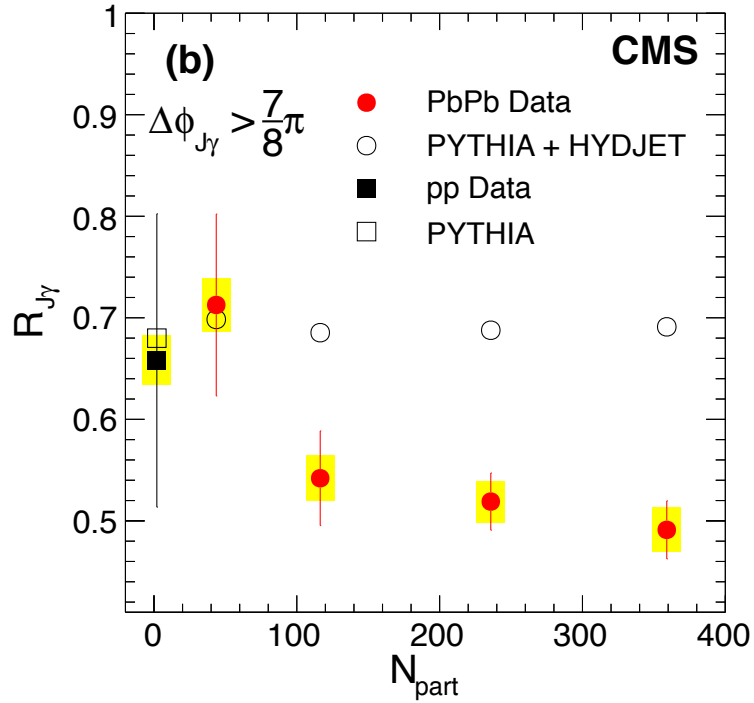

p_T^{γ}>60 GeV
p_T^{Jet}>30 GeV

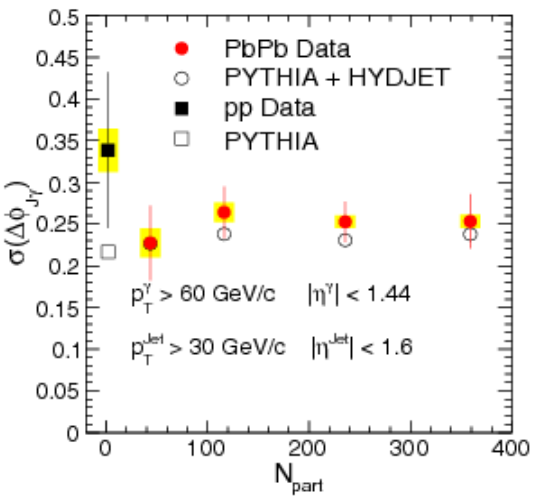

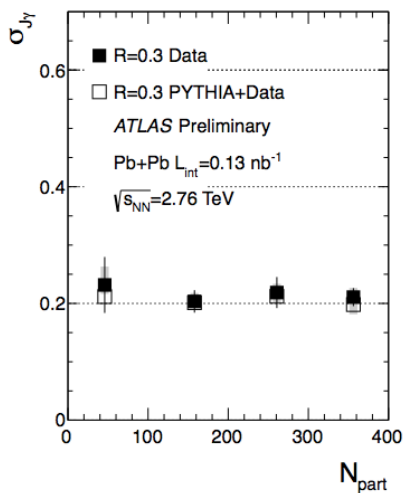

Large quenching effects seen in direct photon measurements

(Consistent with jets measurements? Quark vs. gluon energy loss?)

No angular de-correlation

(also seen in di-jets @RHIC)

Fragmentation Functions in Pb+Pb at the LHC

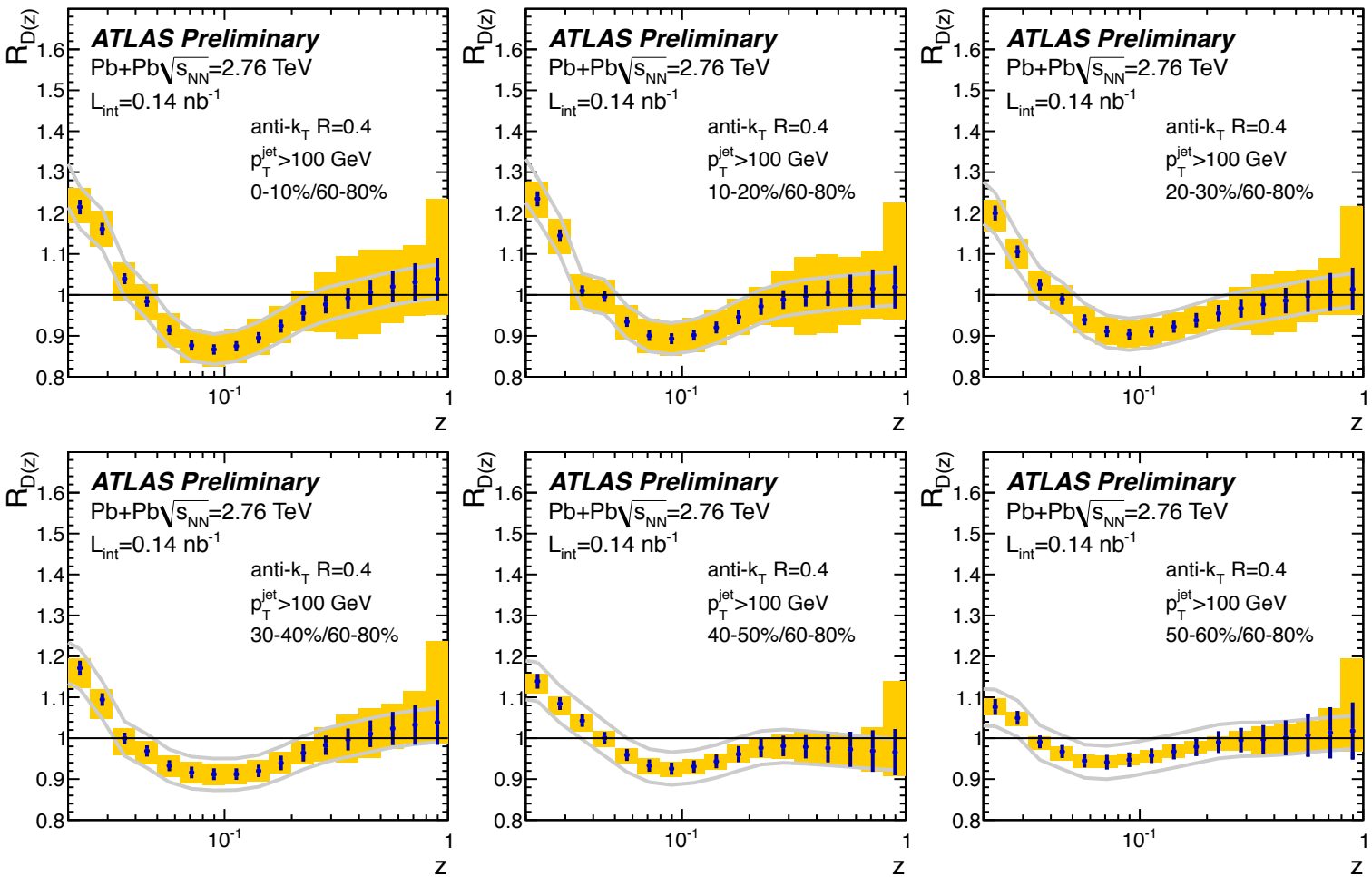

Enhancement at low z

Suppression at intermediate z

No suppression at high z

Fragmentation Functions in Pb+Pb at the LHC

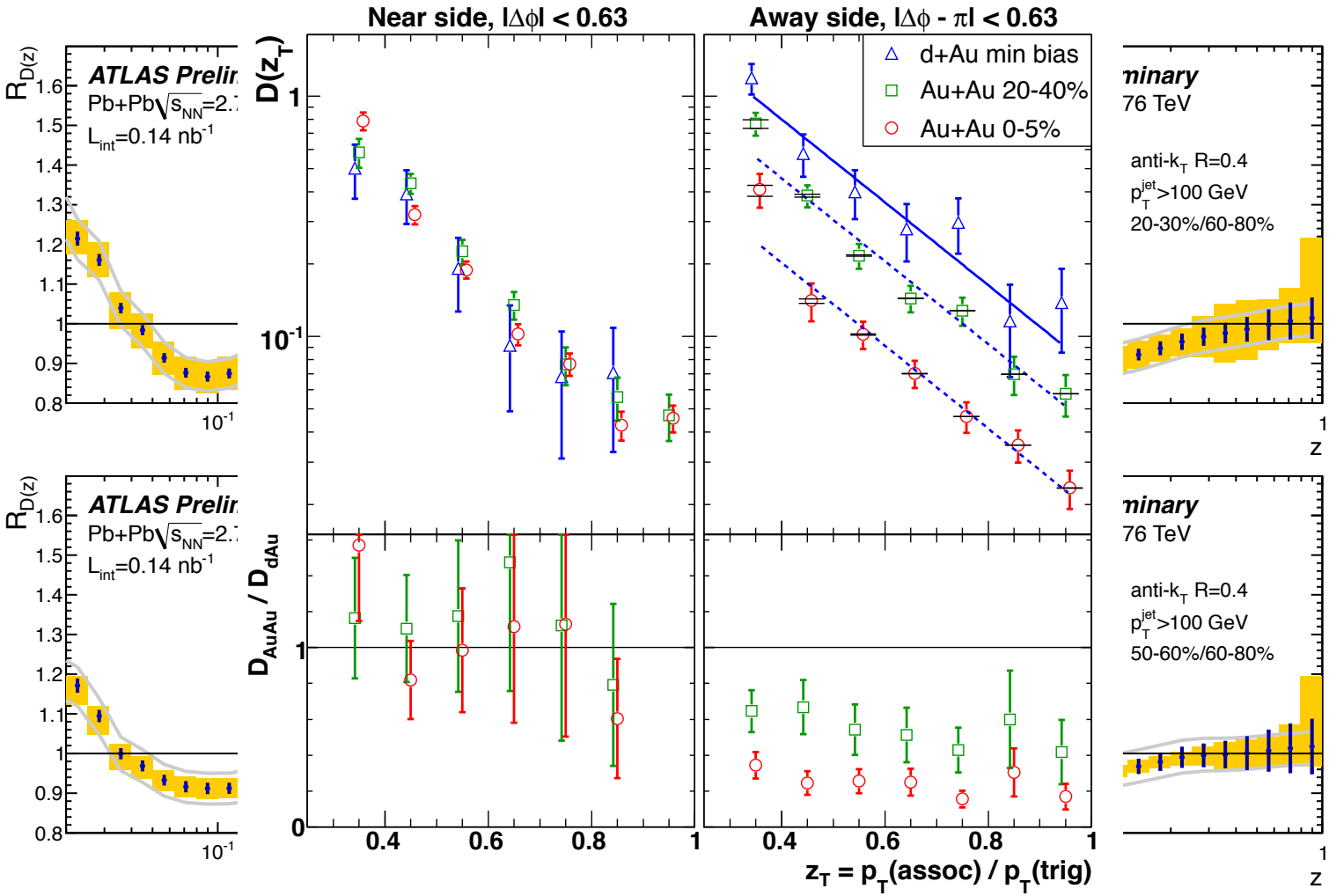

Enhancement at low z

Suppression at intermediate z

No suppression at high z

***RHIC:* Suppression at high di-hadron z_T**

Caveat: Not apple to apple comparison!

Jet Shape Observables

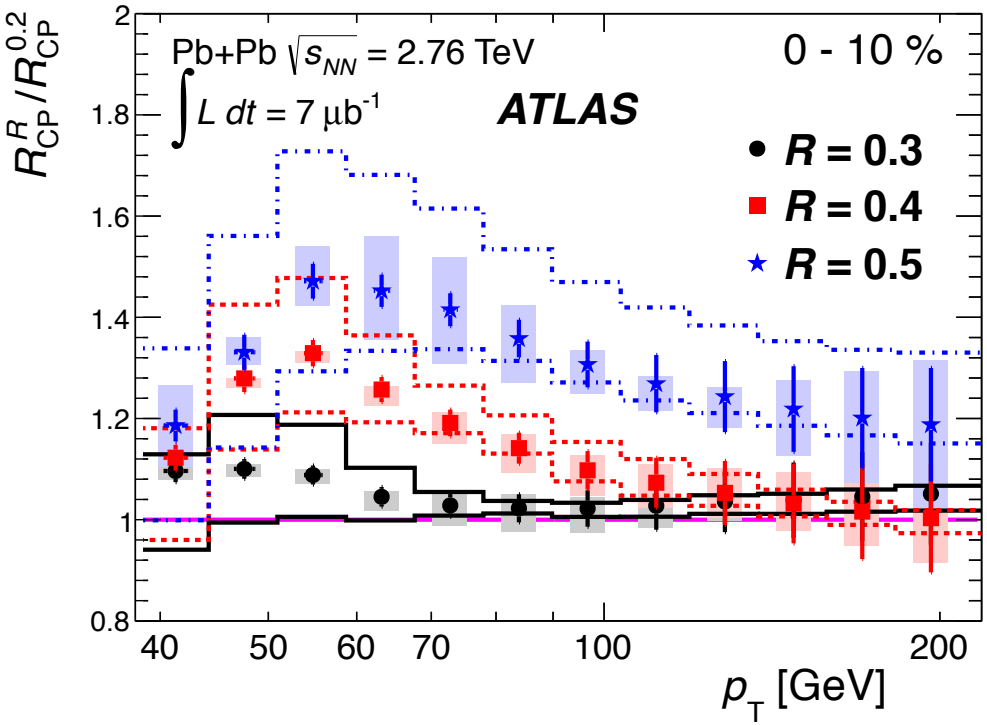

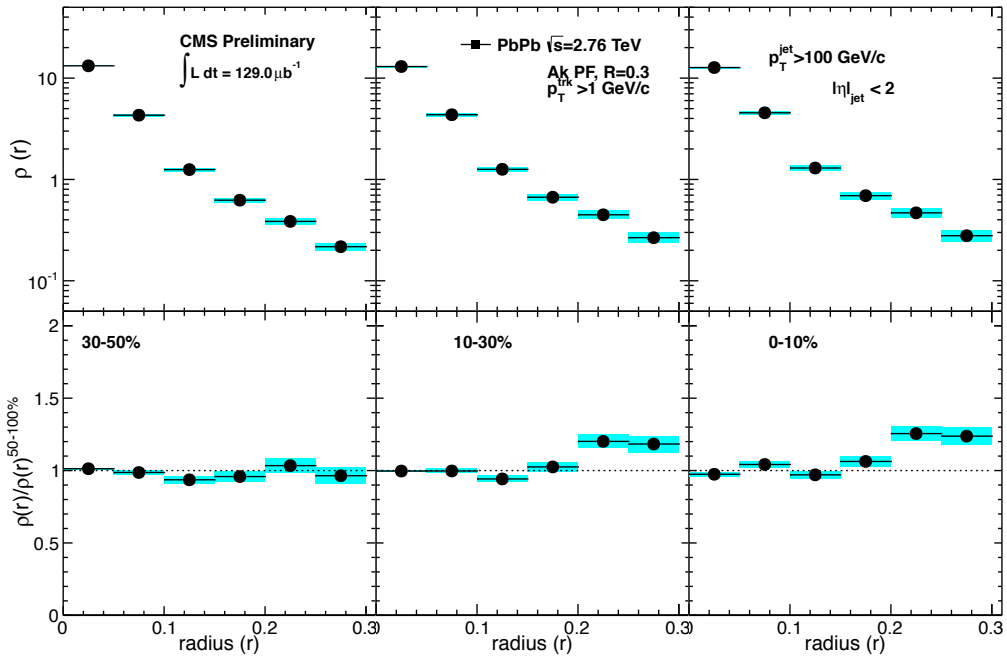

Jet broadening at the LHC:
Seen in differential jet shape and R dependence of jet R_{CP}
(especially at lower jet p_T)

Jet Shape Observables

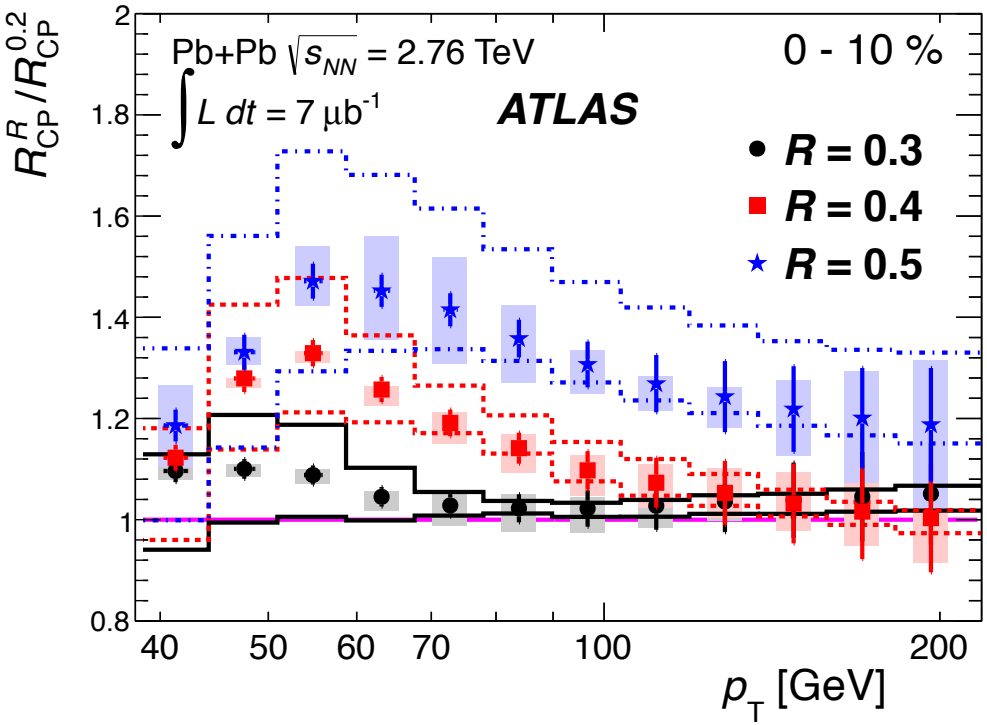

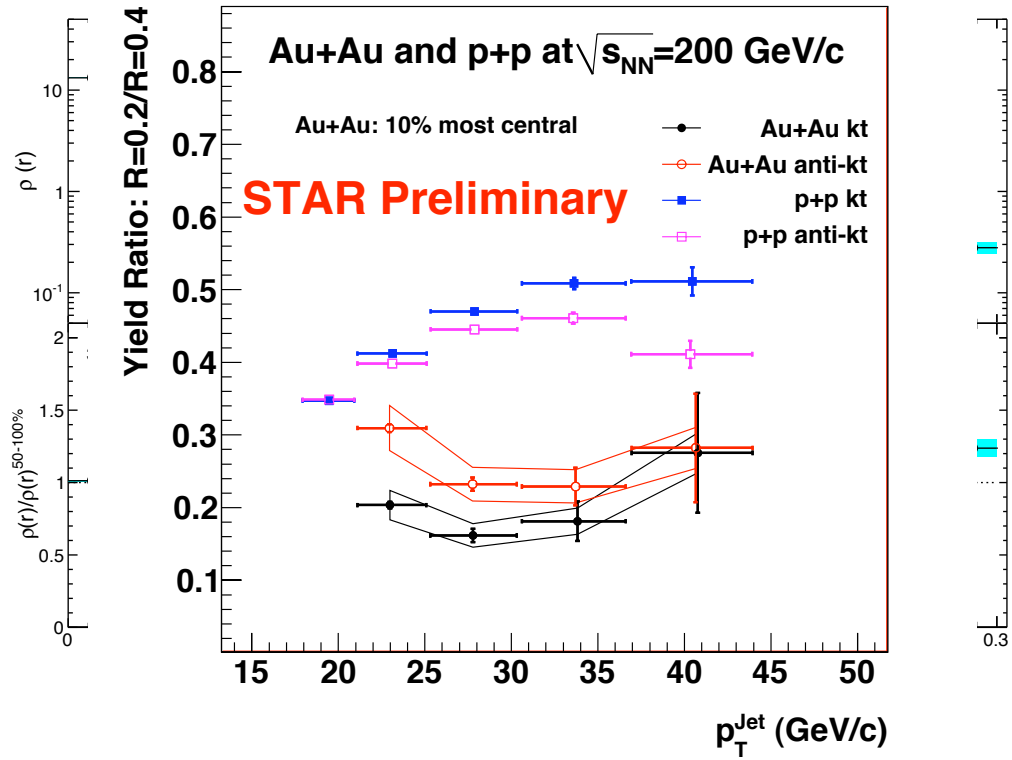

Jet broadening at the LHC:
Seen in differential jet shape and R dependence of jet R_{CP}
(especially at lower jet p_T)

***RHIC:* Stronger broadening observed**

Reminder: These measurements look at the jet shape in a cone of R=0.2-0.5!

Where does the lost energy go? Missing p_T^{ll}

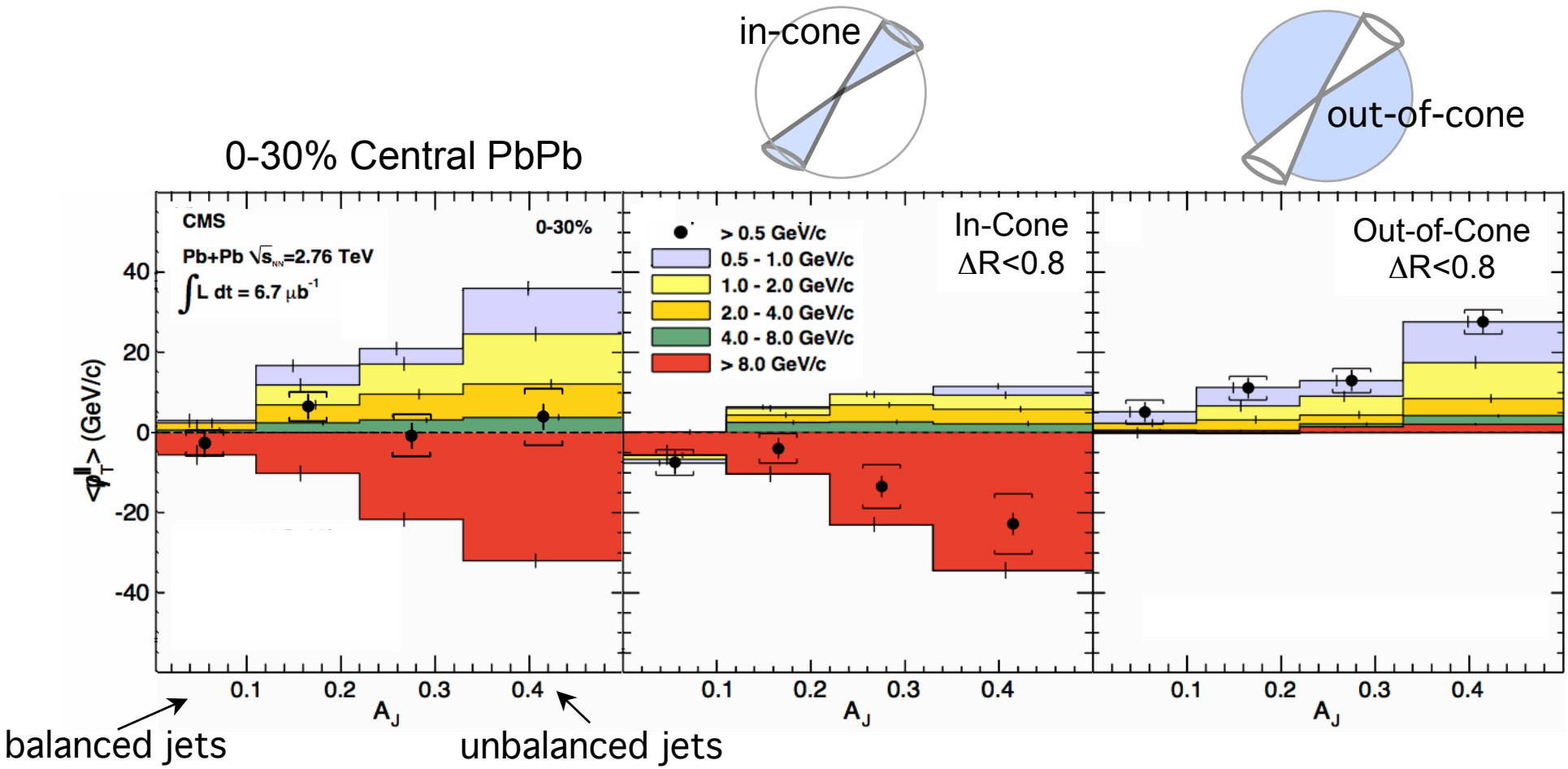

The momentum difference in the di-jet is balanced by low p_T particles at large angles relative to the away side jet axis

RHIC: Direct Photon - Hadron Correlations

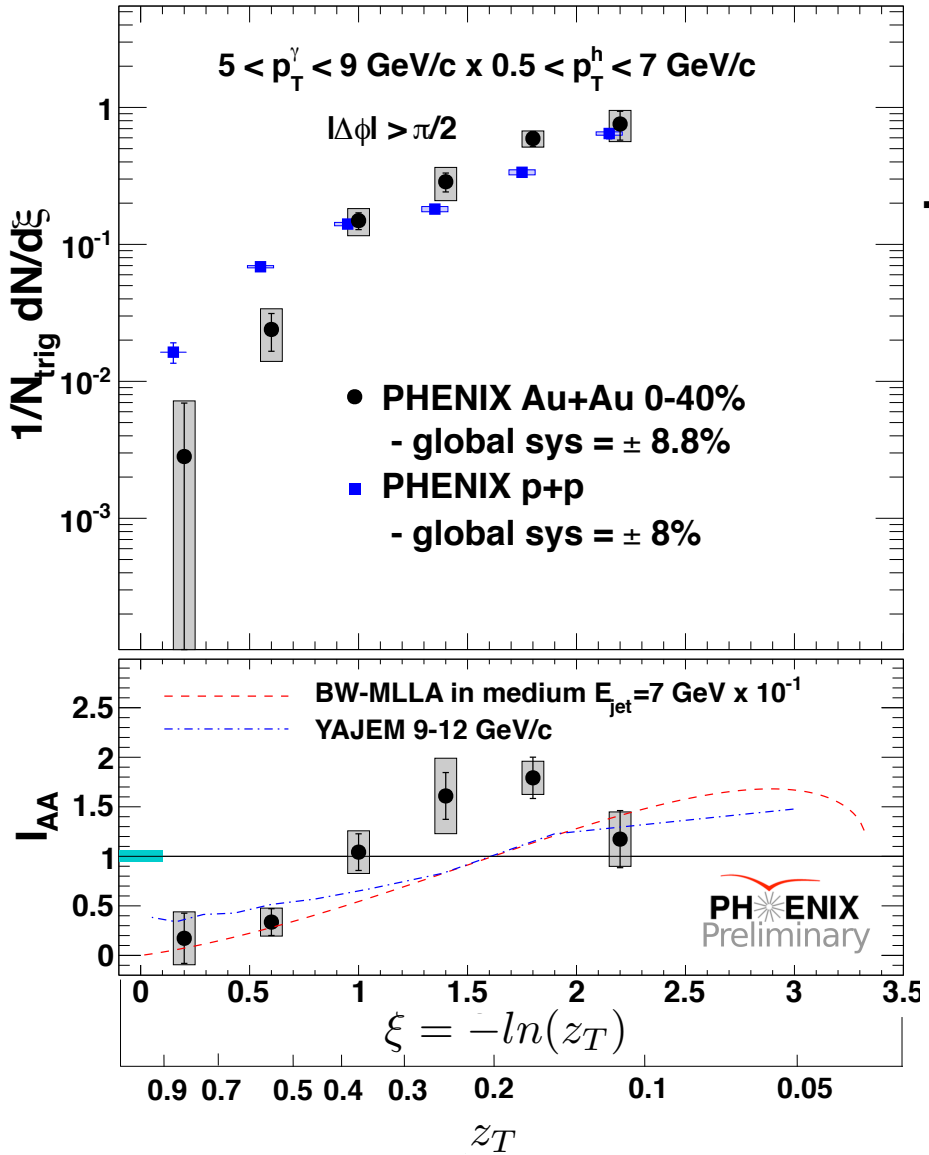

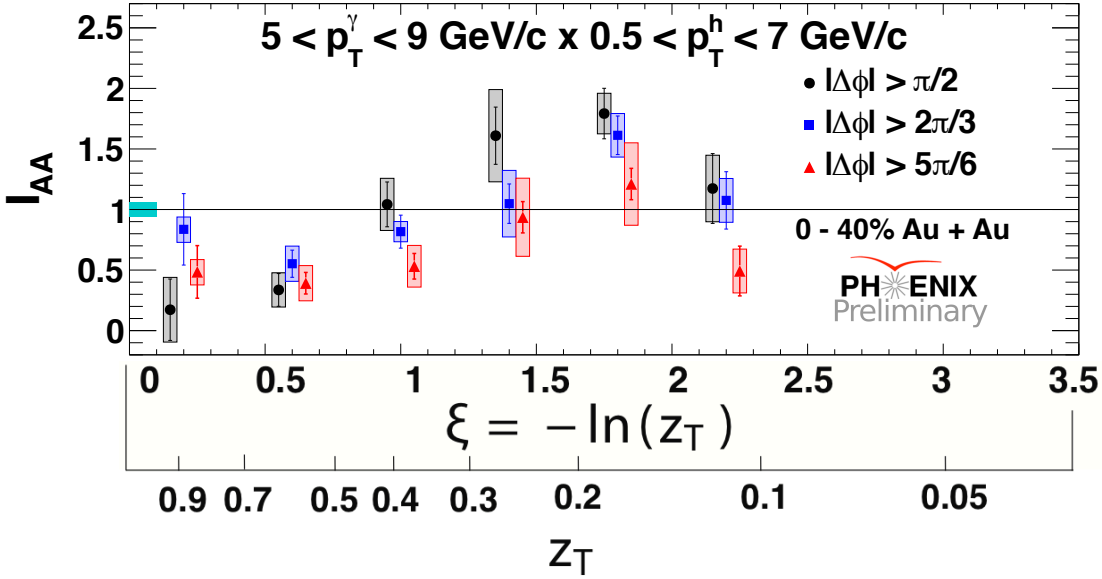

Enhancement at low z

Suppression at high z

Broadening at low z

RHIC: Jet-Hadron Correlations

Trigger Jet: R=0.4, $p_{T,cut}$=2 GeV/c and EMCal Tower>6 GeV

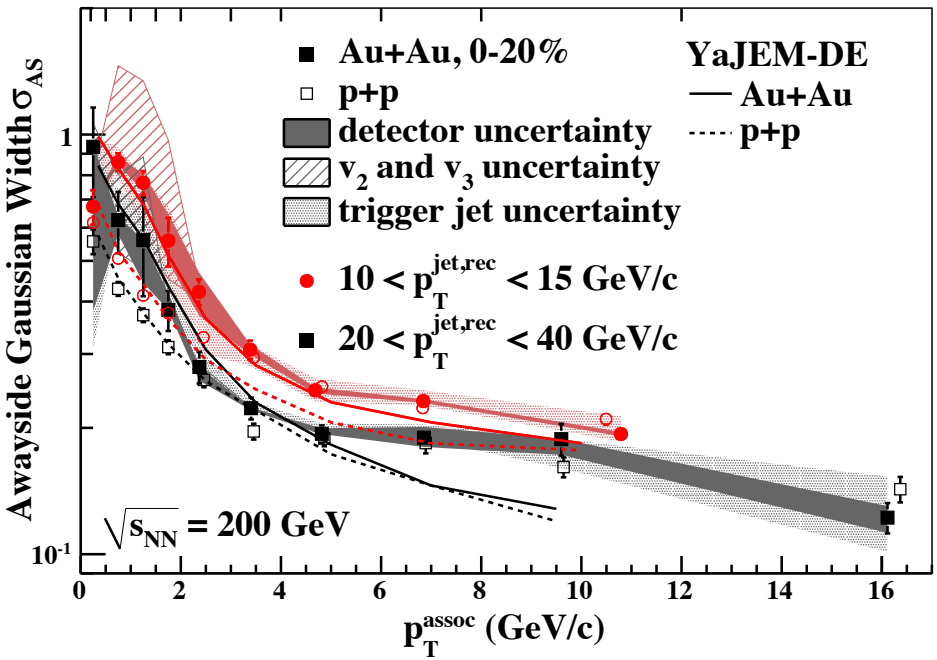

Energy difference: AuAu-pp

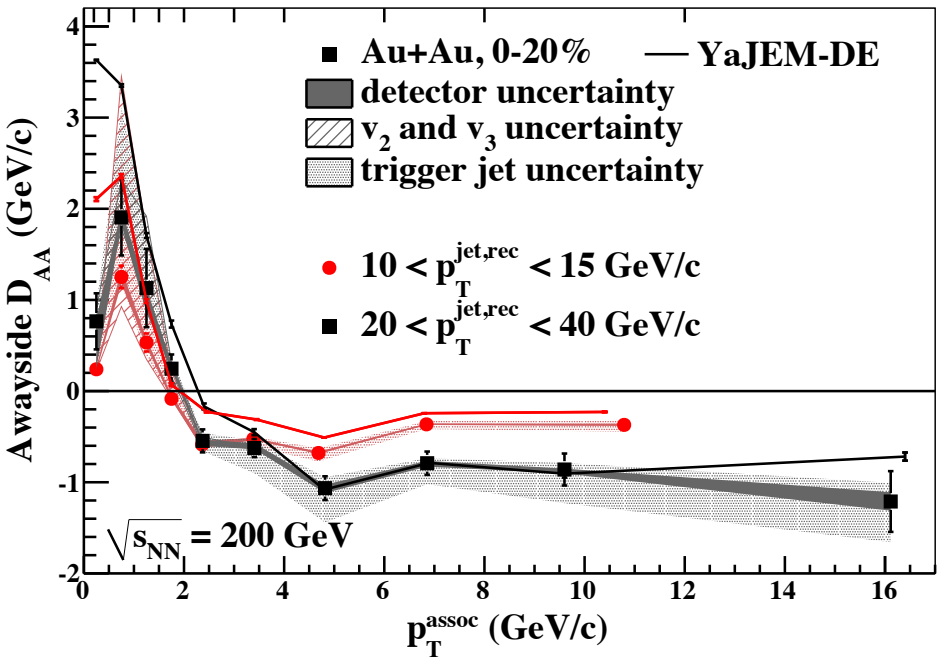

Hint of Jet Broadening at low p_T (large uncertainties due to potential jet v_2/v_3)

Quenched energy at high p_T balanced by low p_T enhancement
Consistent picture between γ^{direct}/jet-hadron correlations @ RHIC!

RHIC: Jet-Hadron Correlations

Trigger Jet: R=0.4, $p_{T,cut}$=2 GeV/c and EMCal Tower>6 GeV

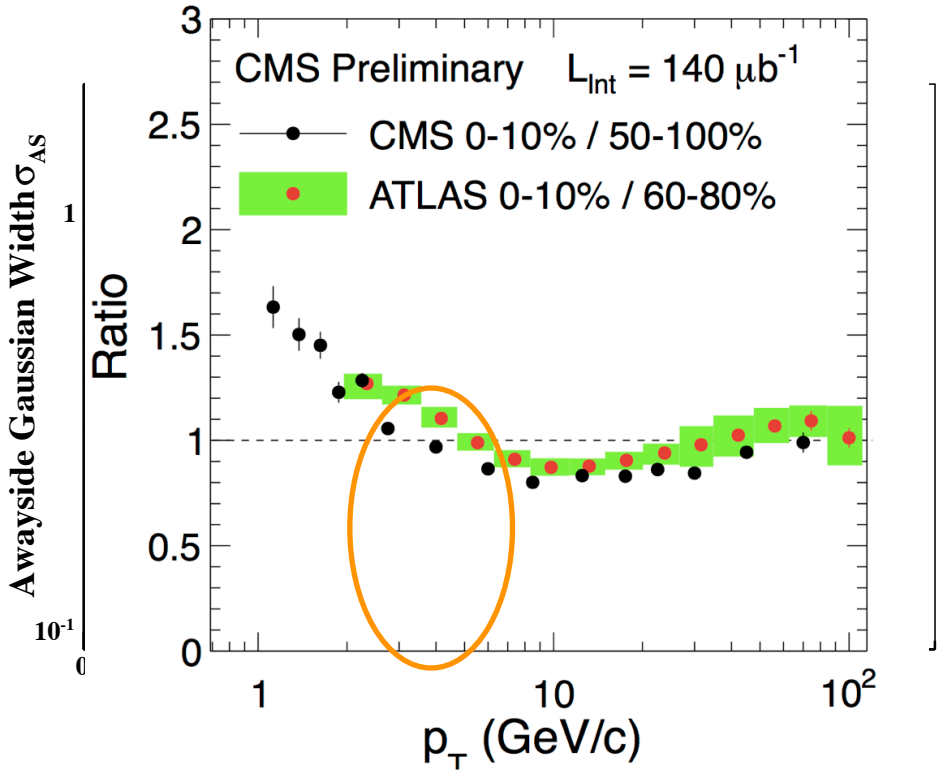

Energy difference: AuAu-pp

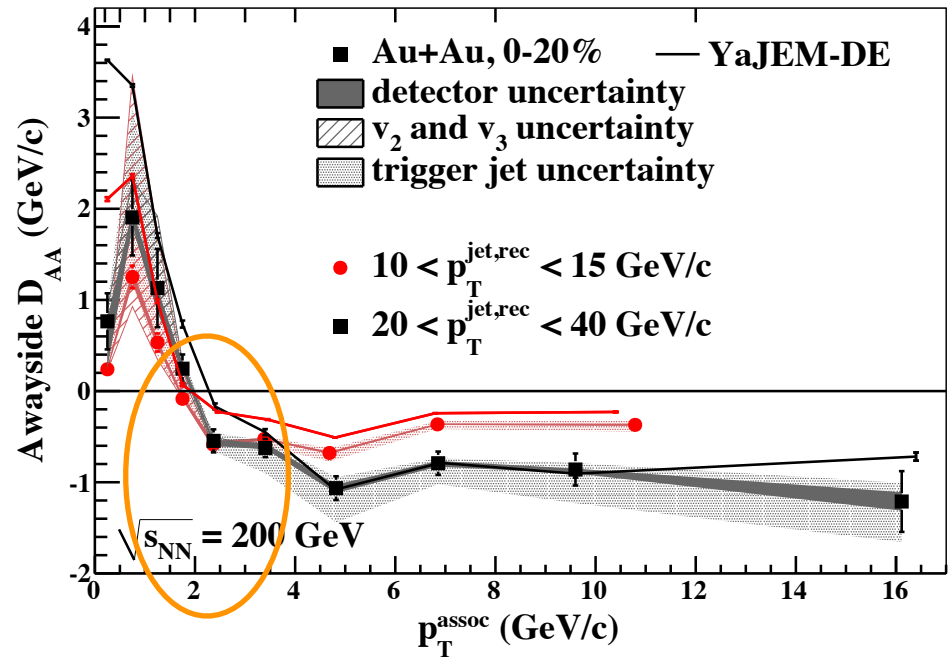

Hint of Jet Broadening at low p_T (large uncertainties due to potential jet v_2/v_3)

Quenched energy at high p_T balanced by low p_T enhancement
Consistent picture between γ^{direct}/jet-hadron correlations @ RHIC!

p_T scale of low p_T enhancement: ~2 GeV RHIC, 3-4 GeV LHC

Caveat: RHIC measurement: Statistical. Need per jet quantities (A_j, FF) to allow one-to-one comparison to LHC.

Consistency or a way too simplistic explanation?

We heard about this in more detail in A Majumder's talk today.

Integrated energy loss (in a brick)

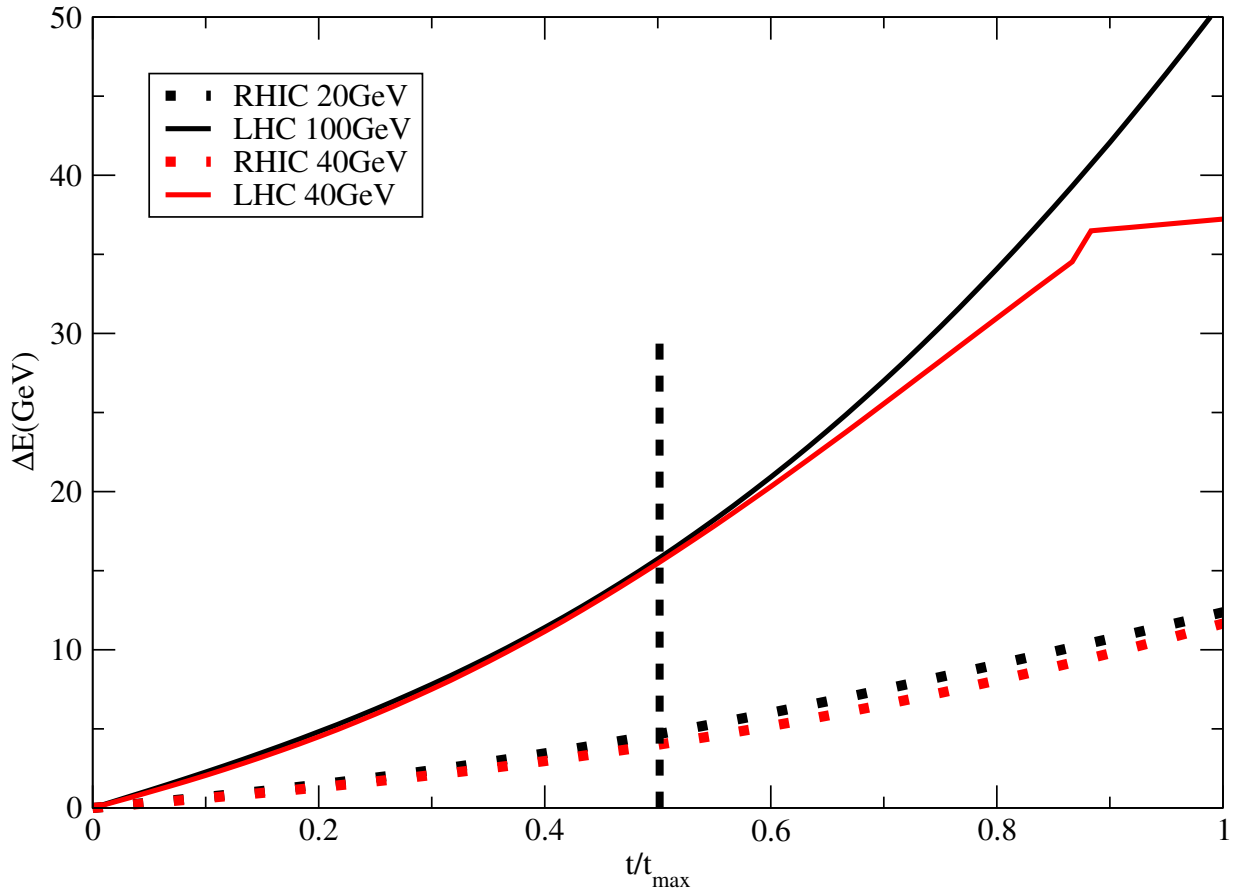

t_{max}(LHC)=6fm
t_{max}(RHIC)=4fm

LHC larger energy loss at early times → diffusion in medium → larger angles

RHIC smaller energy loss at early times→ less diffusion in the medium → closer to jet axis → can qualitatively explain the differences RHIC/LHC (!?)

Easier to study details of soft gluon radiation at RHIC!?

Caveat: Realistic calculation needed? Can current MC models explain RHIC and LHC at the same time?

Biases are not always bad ...

T. Renk, Phys.Rev. C87 (2013) 024905

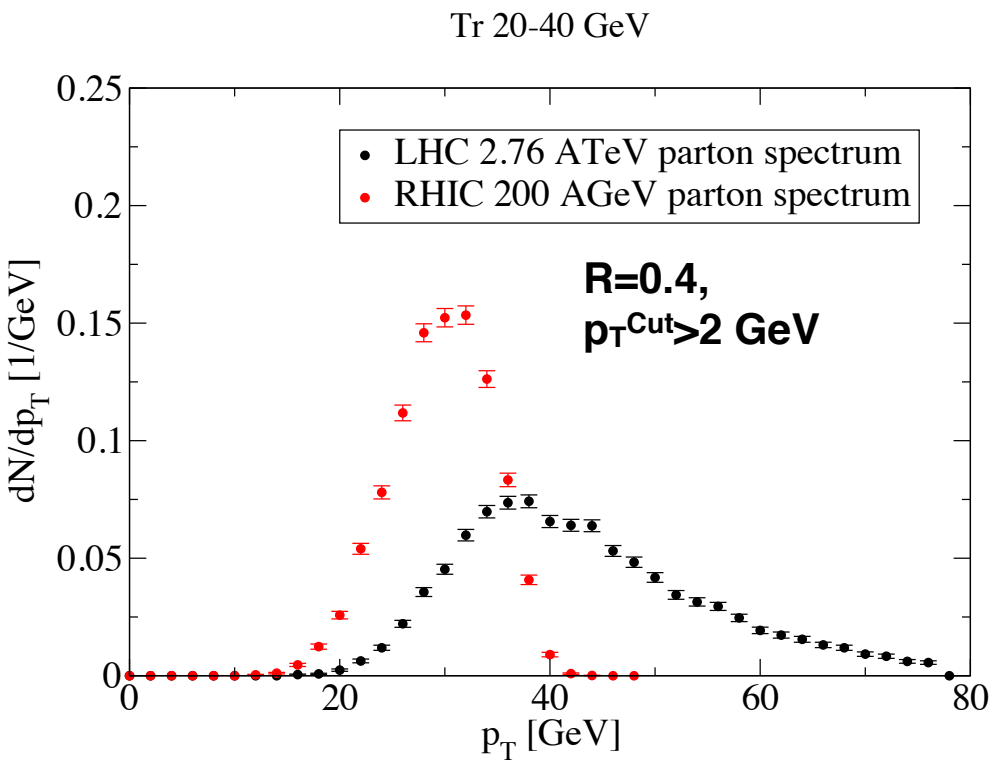

Due to the steeply falling spectrum at RHIC, even with imposing biases (p_T^{Cut}, ...), a good correlation to the initial parton energy is preserved

Biases are not always bad ...

T. Renk, Phys.Rev. C87 (2013) 024905

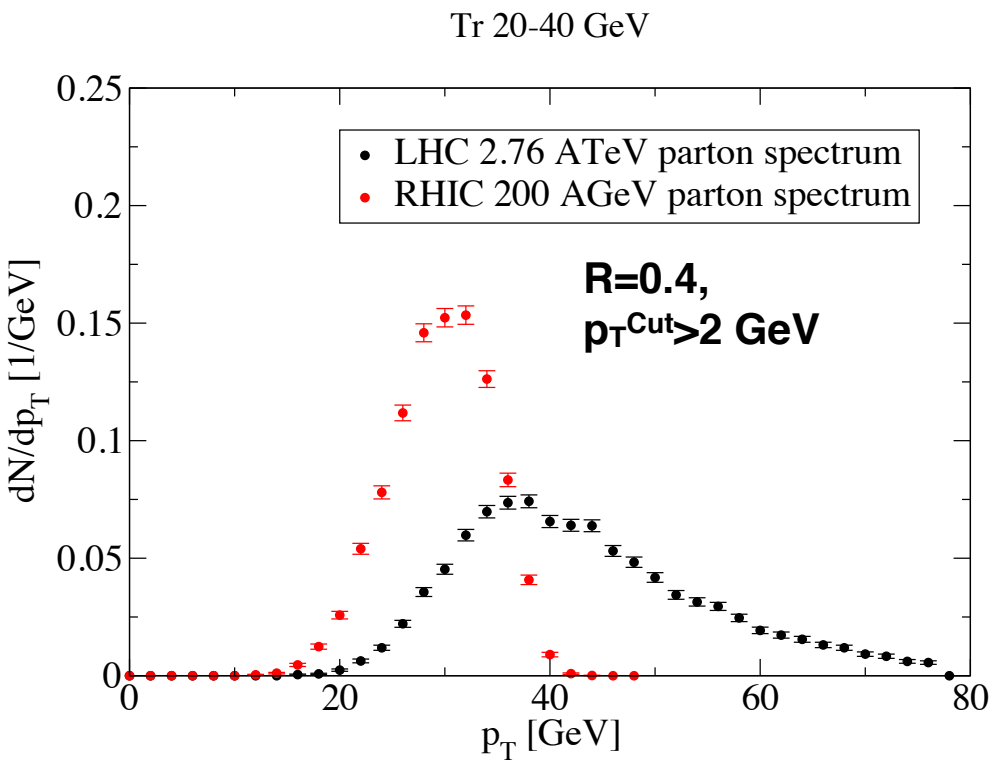

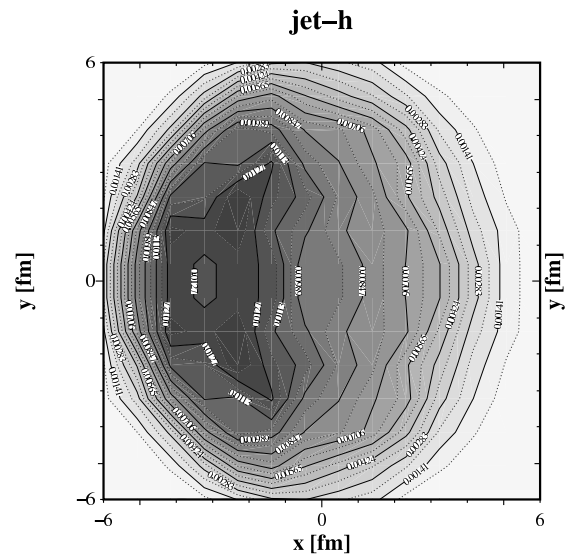

p_T^{Cut}>2 GeV

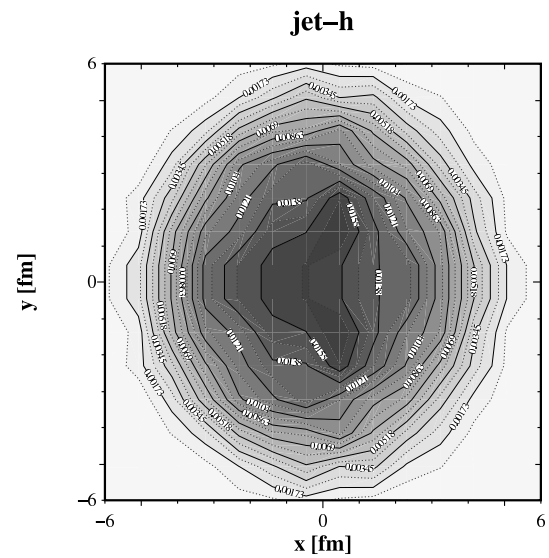

Ideal

Due to the steeply falling spectrum at RHIC, even with imposing biases (p_T^{Cut}, ...), a good correlation to the initial parton energy is preserved

Biases (p_T^{Cut}, ...) can be used to change systematically the pathlength of the recoil jet

Biases (p_T^{Cut}, ...) can be further utilized to favor gluon recoil jets

Caveat: Can only compare to MC models!

“Direct” Comparison of RHIC and LHC energy loss

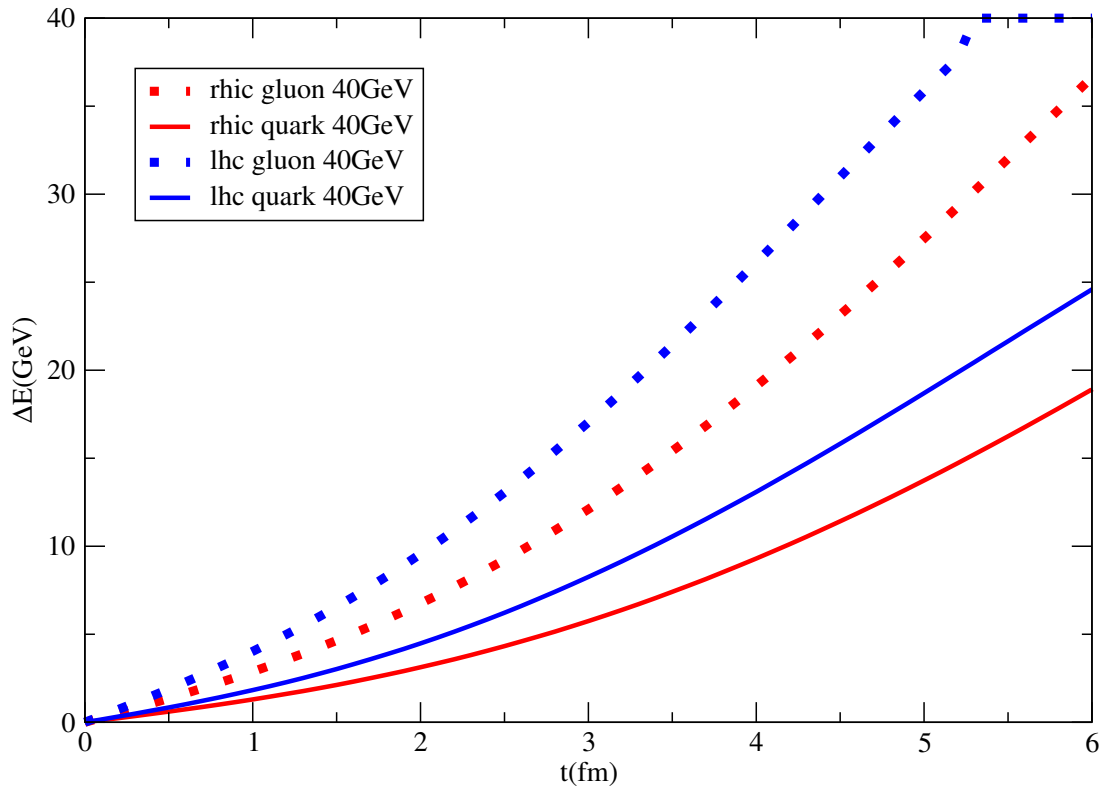

γ^{direct}-jet at the LHC (quark jet) compared to di-jets at RHIC (quark jets) @ 40-50 GeV

Caveat: To remove geometric biases one needs an unbiased jet measurement at RHIC!

Temperature dependence of energy loss

We had talks this morning discussing this in more detail!

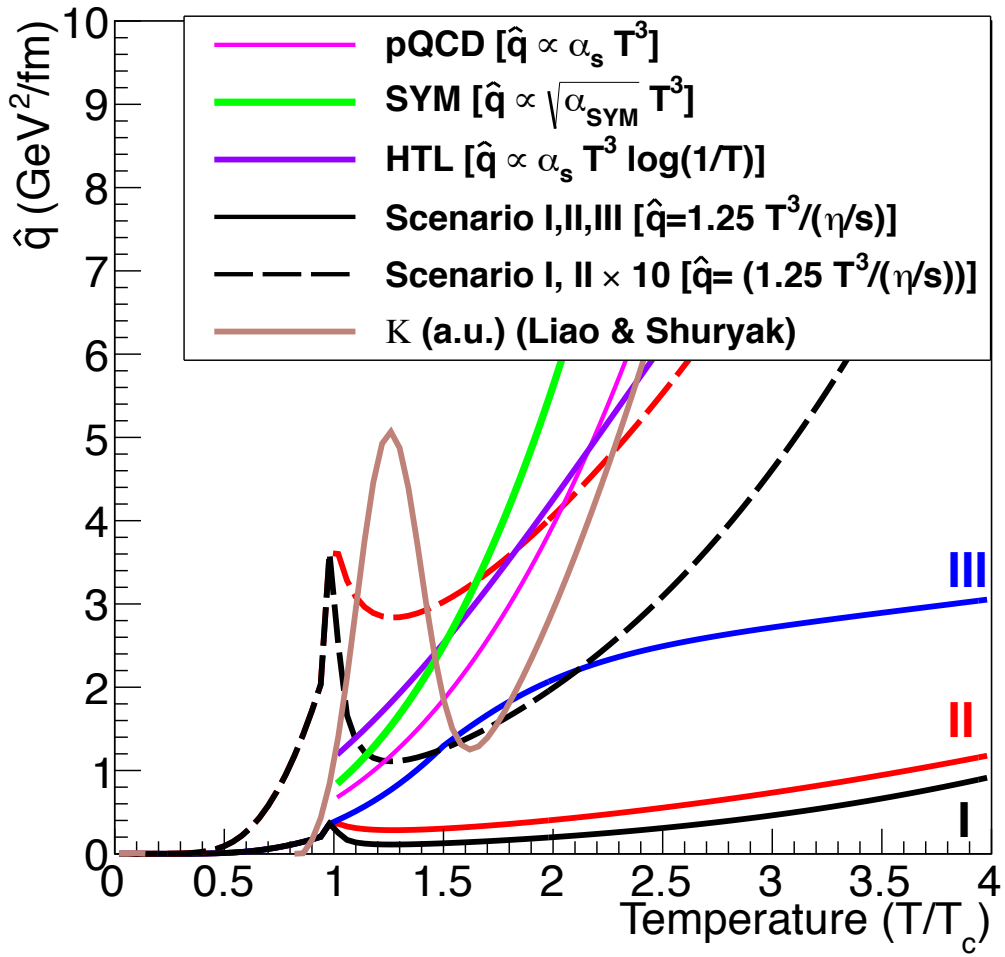

$$\eta / s = \text{const} \times T^3 / \hat{q}$$

for weak coupling (PRL 99, 192301, 2007)

Differential measurements of transport properties of the QGP: Temperature dependence of q (ê, η/s, ..)

Sensitivity of q to 1-2 T_C requires RHIC measurements for different colliding systems and smaller √s (LHC larger initial T)

Testing the quasi-particle nature of the QGP

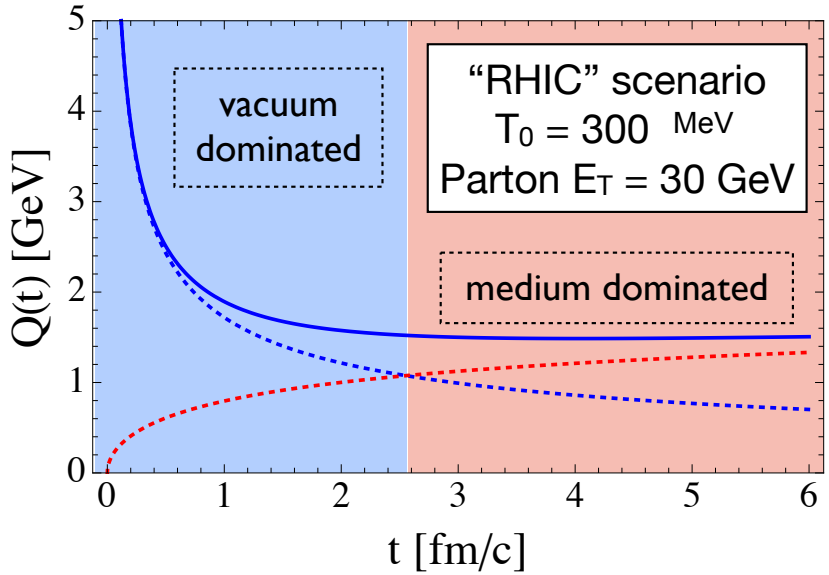

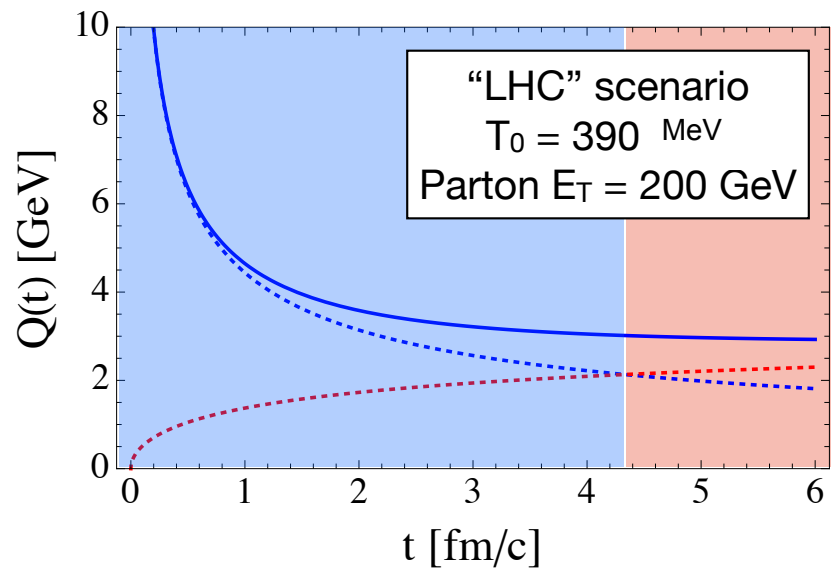

Jet Virtuality: Controls the Physics of Radiative Energy Loss

$$Q^2(L) \approx \max\left(\hat{q}\,L, \frac{E}{L}\right)$$

medium *vacuum*

RHIC: 20 GeV parton, L = 3 fm

$$\hat{q}\,L \approx 1.5\,\mathrm{GeV}^2 \quad \approx \quad \frac{E}{L} \approx 1.5\,\mathrm{GeV}^2$$

Virtuality of primary parton is medium influenced and small enough to "experience" the strongly coupled medium

LHC: 200 GeV parton, L = 3 fm

$$\hat{q}\,L \approx 3.5\,\mathrm{GeV}^2 \quad < \quad \frac{E}{L} \approx 13\,\mathrm{GeV}^2$$

Virtuality of primary parton is vacuum dominated and only its gluon cloud "experiences" the strongly coupled medium

RHIC can explore the region between the weak and strong coupling limits!

"QCD Analog of Bethe-Bloch"

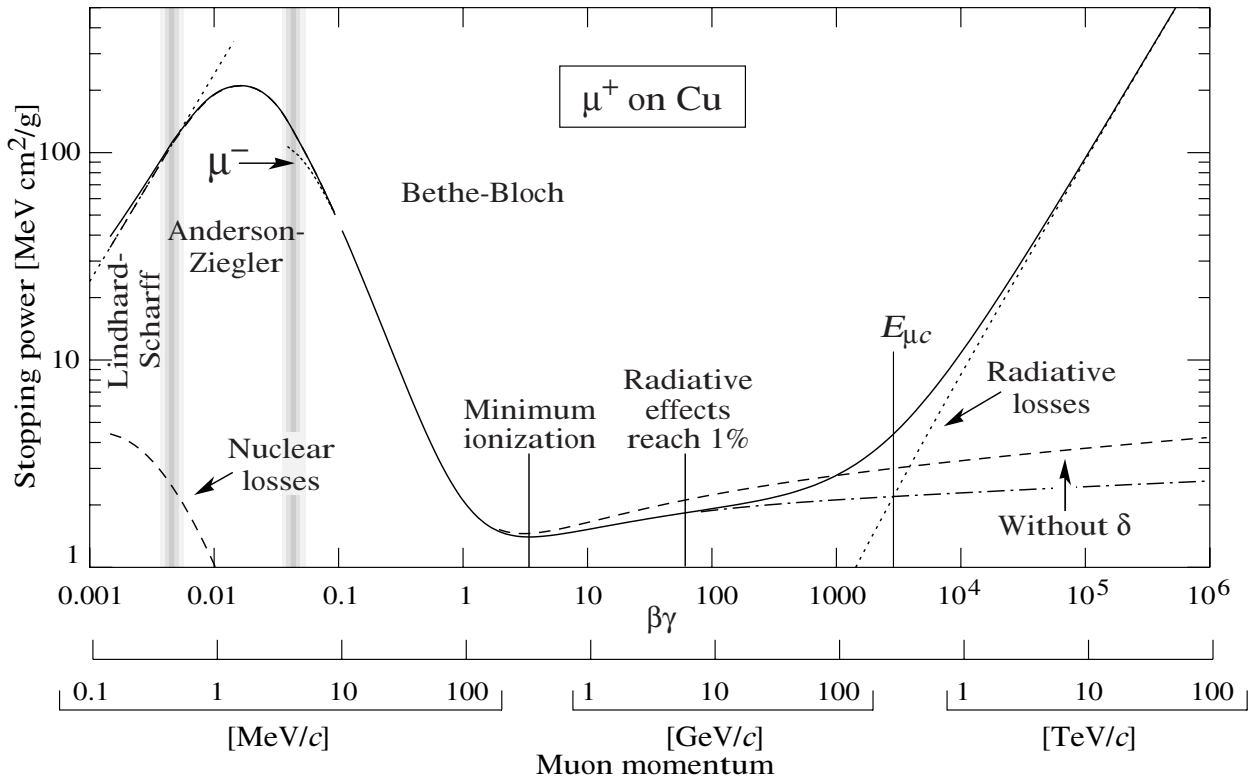

At the LHC/at large jet energies, jet modification dominated by radiative energy loss

At lower jet energies balance/interplay between radiative energy and collisional energy loss

RHIC and LHC combined will map out the stopping power –dE/dx of hot and dense QGP for colored patrons

RHIC is always good for surprises: d+Au R_{AA}

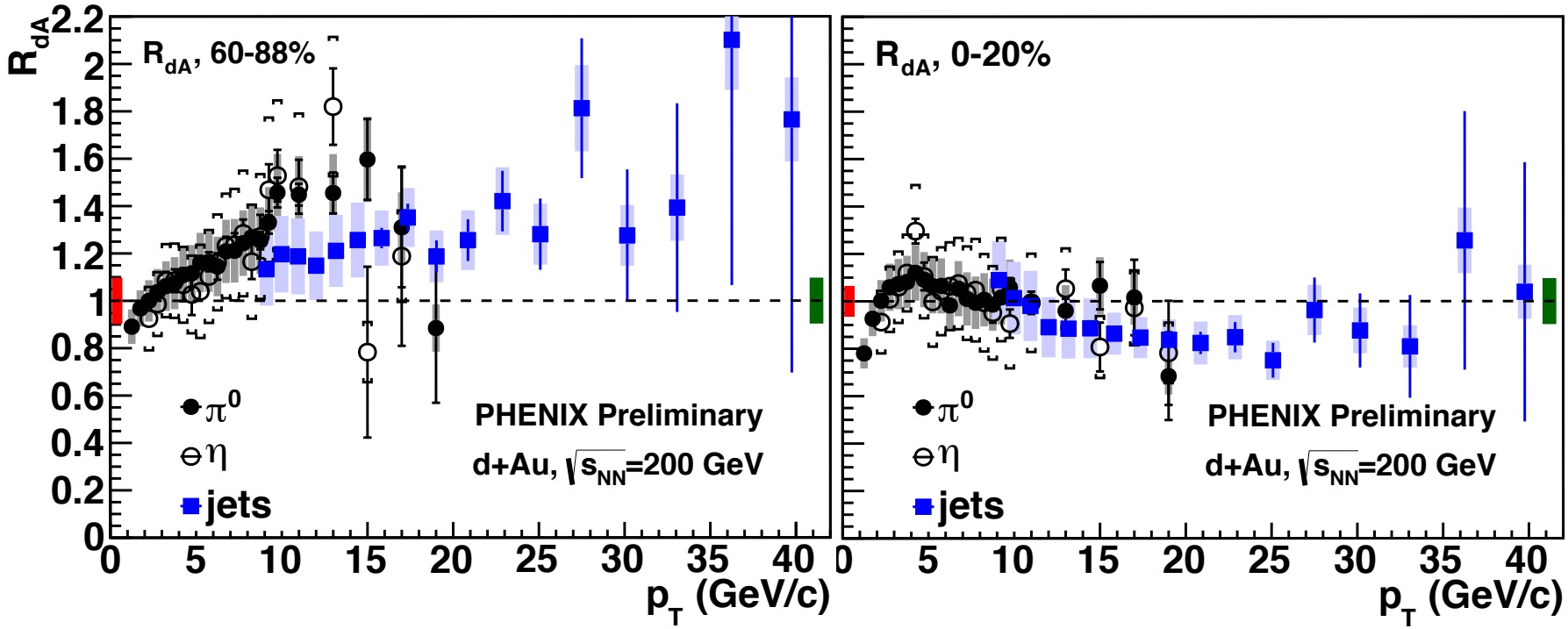

Enhancement of Jet R_{AA} in peripheral d+Au collision?

<u>Caveat:</u> We saw yesterday (G. David) that centrality determination in d+Au is not trivial ...

Future: Precision Jet Measurements @ RHIC / sPhenix

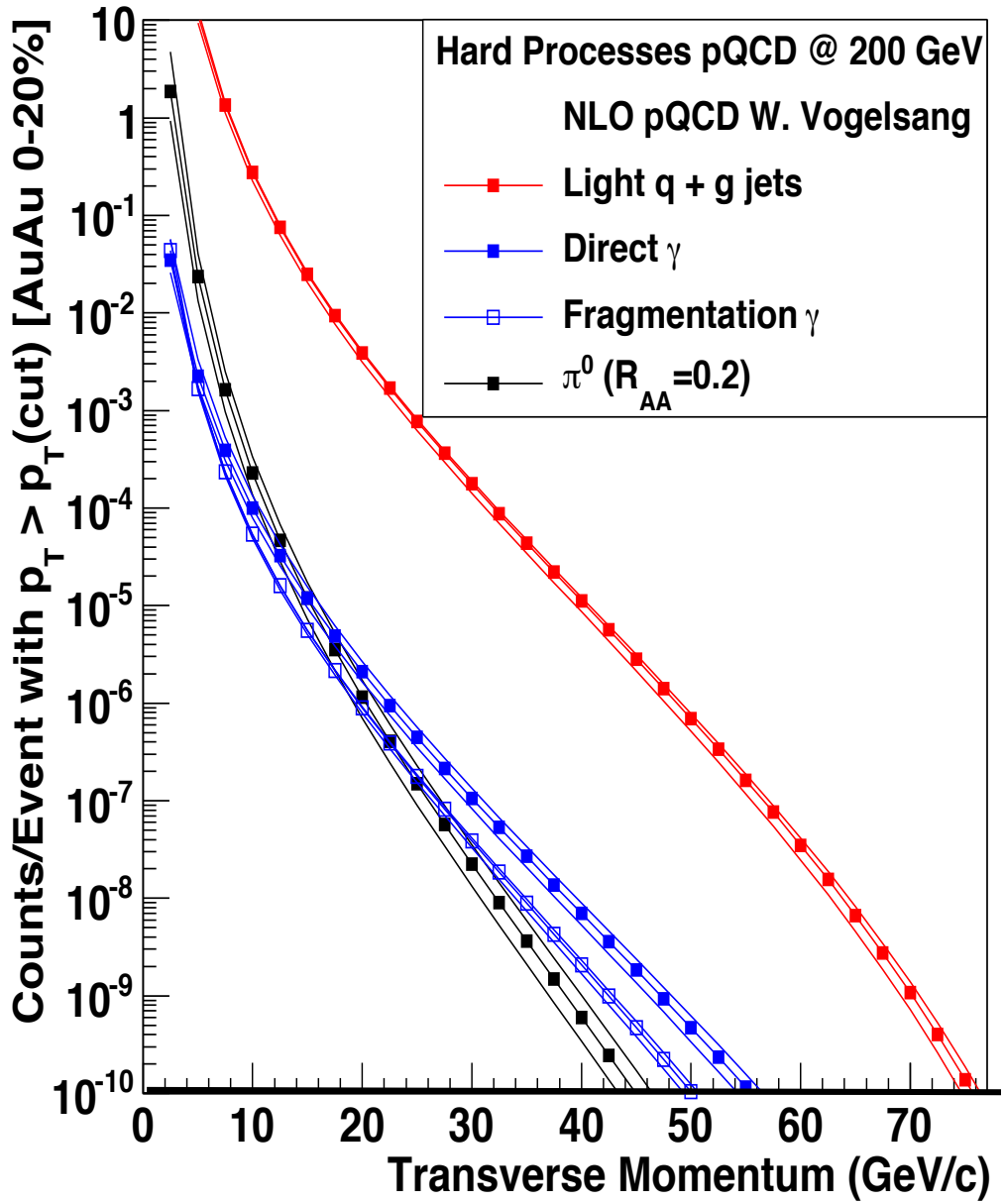

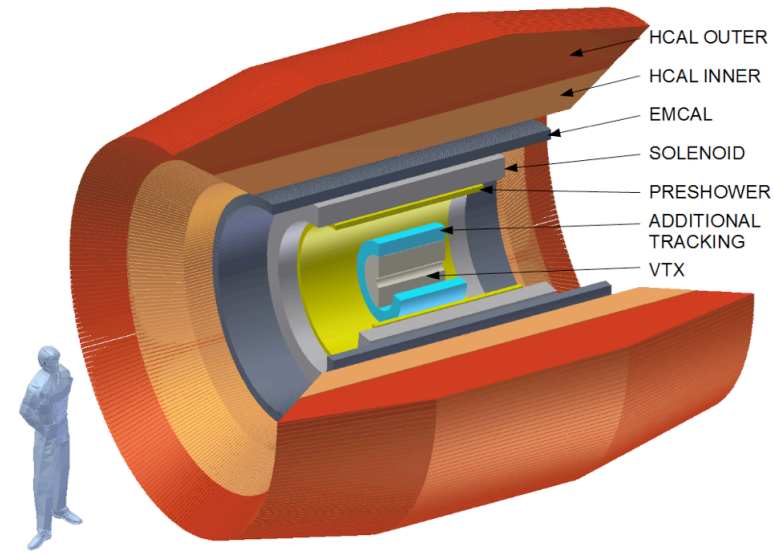

Full Calorimetry

Large kinematic reach
(can be used to reduce current biases)

Precision Jet measurements with the flexibility of RHIC concerning collision energy and system sizes

Can this be utilized to study pre-equilibrium effects?

Summary

Consistent (qualitative) jet quenching picture at RHIC emerging: suppression at high z, enhancement at low z. Jet broadening has to be quantified.

Can current LHC and RHIC quenching measurements be explained in a consistent picture?

In many respects RHIC and LHC a complementary and an active jet program at RHIC is essential to further and quantify our understanding of partonic energy loss in the future!

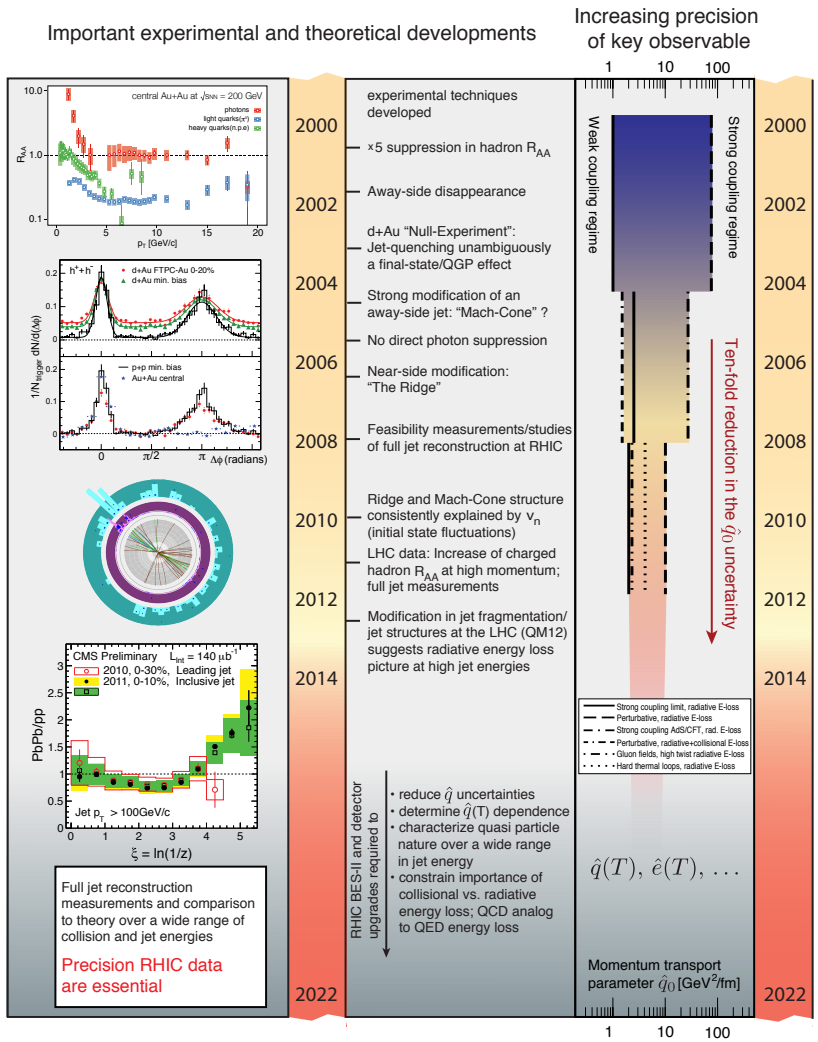

Near Future: RJE(T)T ?

RJE(T)T=RHIC **J**et **E**xperiments (& **T**heory) **T**askforce

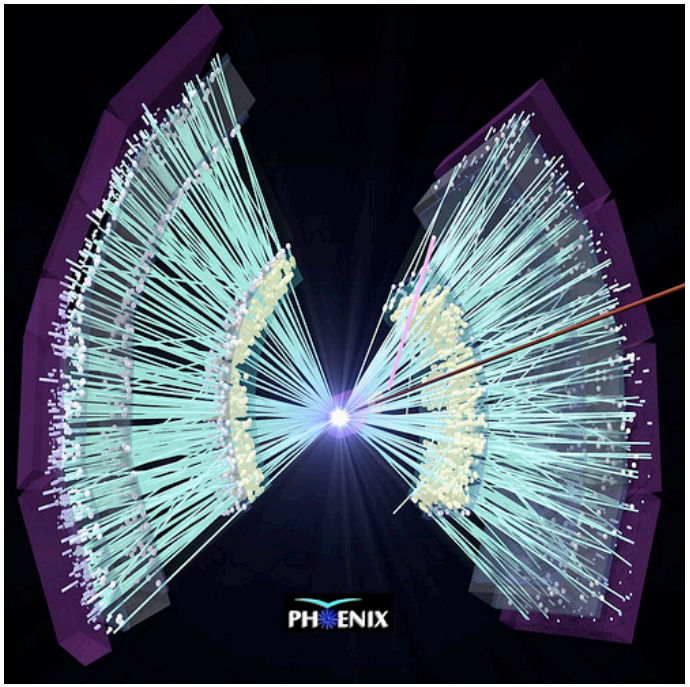

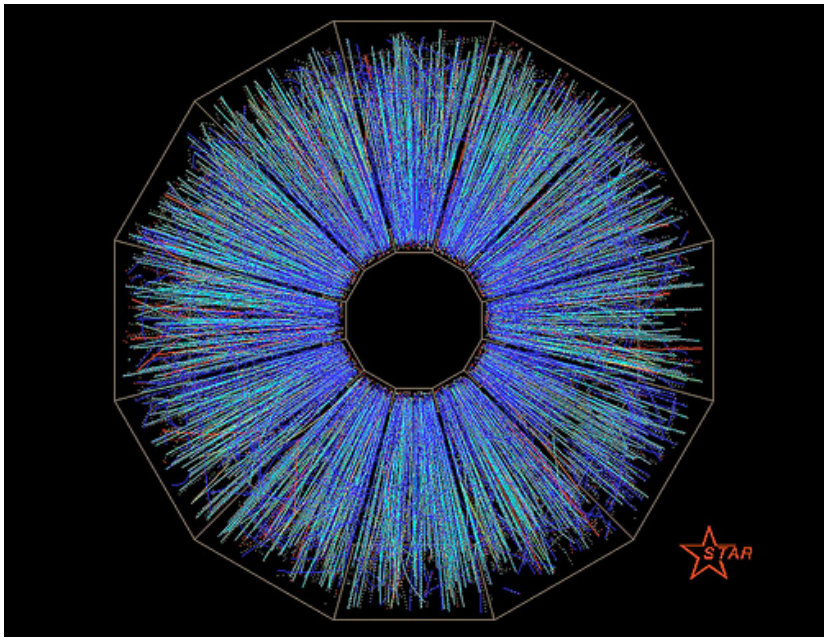

Can something like this be realized at RHIC?

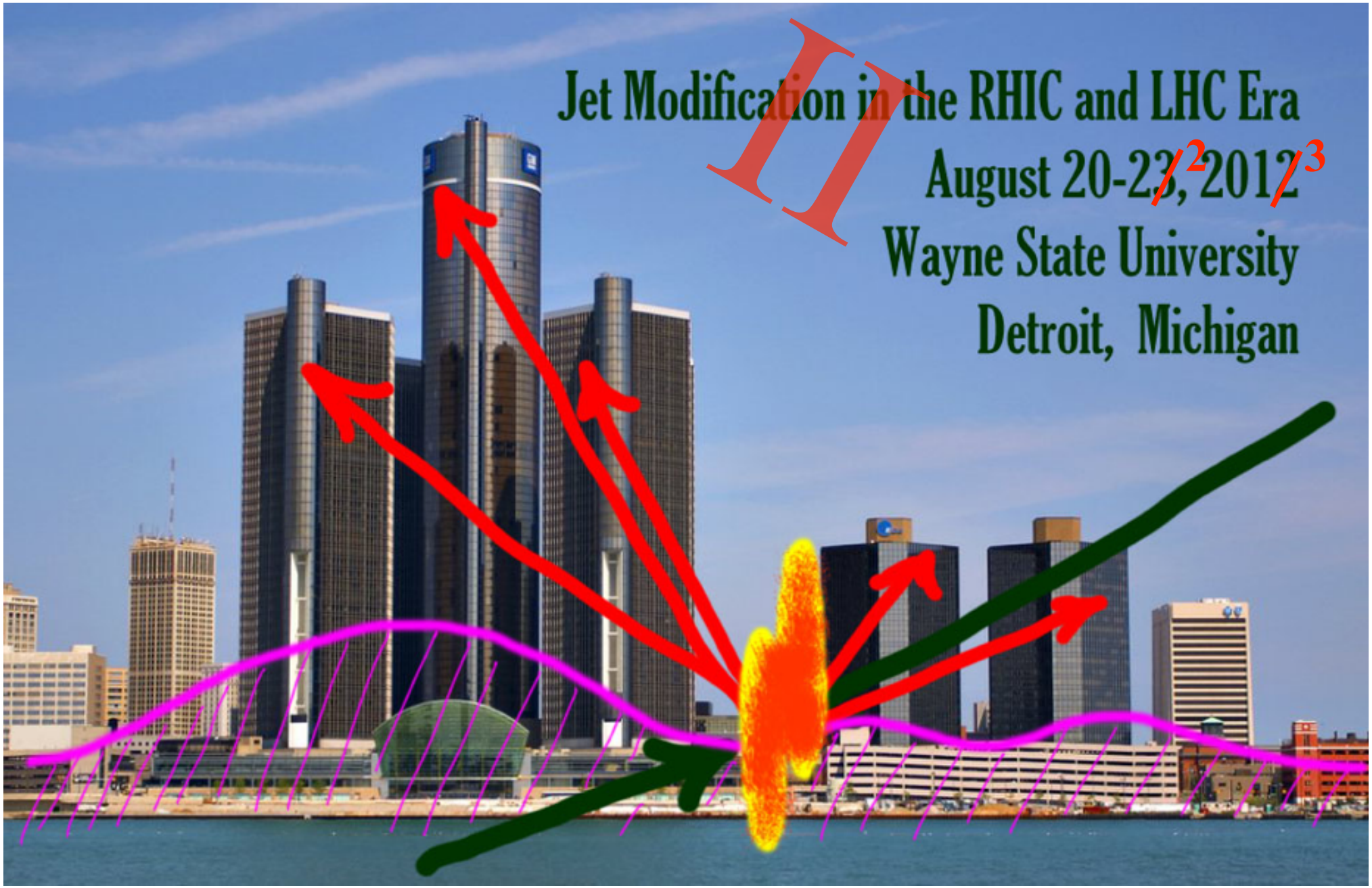
Jet Modification in the RHIC and LHC Era
August 20-23, 2012
Wayne State University
Detroit, Michigan

Backup

Temperature dependence of energy loss

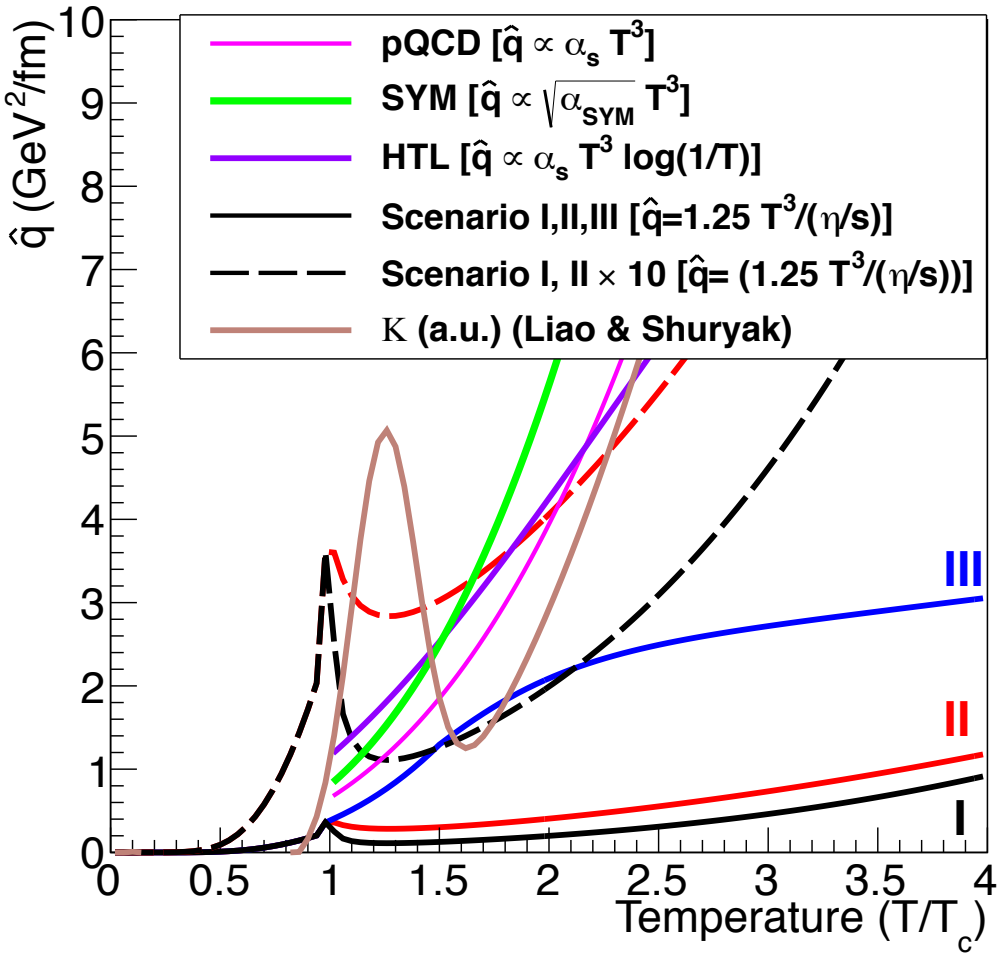

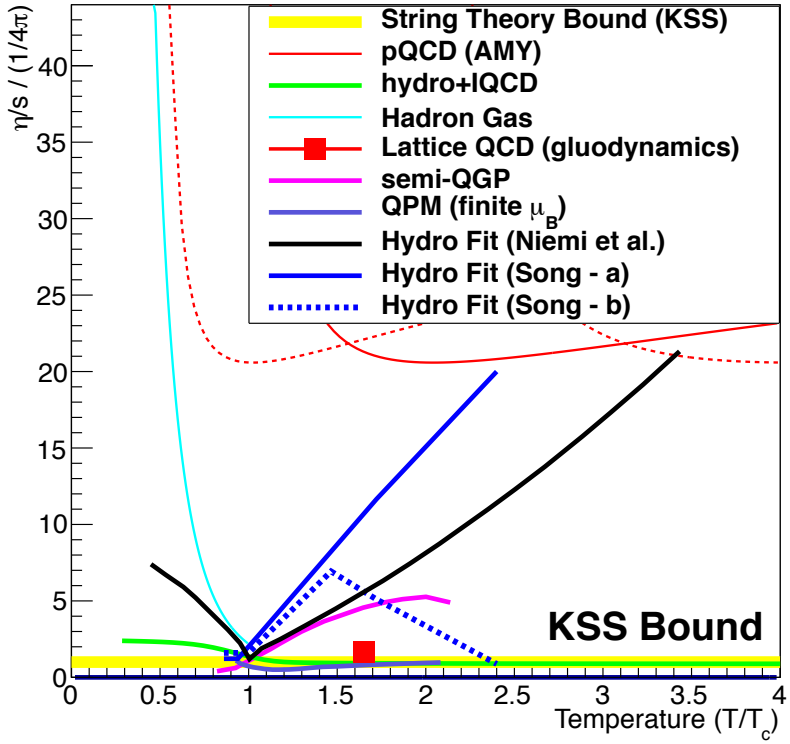

Majumder, BM, W
that η/s and q̂ are
weak coupling in
[PRL 99, 192301

$\eta / s = \text{const} \times$

$\eta / s = \text{const} \times \mathrm{T}^3 / \hat{q}$ for weak coupling (PRL 99, 192301, 2007)

η/s saturates in strong coupling, but energy loss increases w/o limit

At strong couplin
at 1/4π, but q̂ incr
limit. Unambiguou
weak vs. strong c

Where does the lost energy go? Missing $p_T^{||}$

Taken from C. Roland (CMS), QM11

Missing $p_T^{||}$: $$\not{p}_T^{||} = \sum_{\text{Tracks}} -p_T^{\text{Track}} \cos\left(\phi_{\text{Track}} - \phi_{\text{Leading Jet}}\right)$$ $|\eta| < 2.4$

Calculate projection of p_T on leading jet axis and average over selected tracks with

$p_T > 0.5$ GeV/c and

$|\eta| < 2.4$

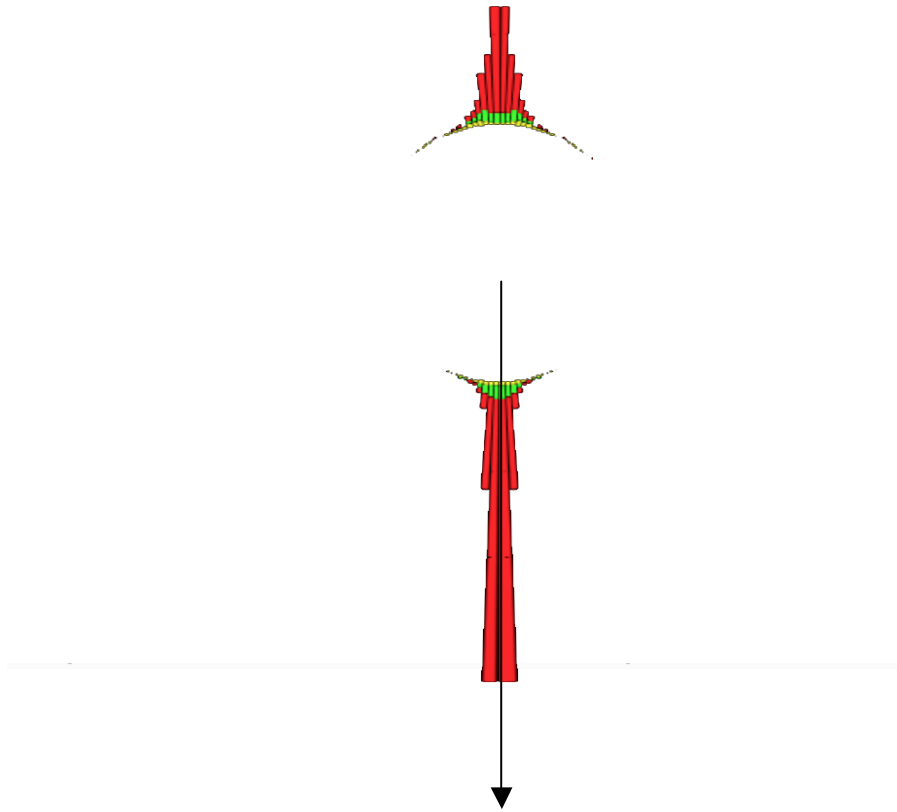

Leading Jet defines direction

Where does the lost energy go? Missing $p_T^{||}$

Taken from C. Roland (CMS), QM11

Missing $p_T^{||}$: $$\not{p}_T^{||} = \sum_{\text{Tracks}} -p_T^{\text{Track}} \cos\left(\phi_{\text{Track}} - \phi_{\text{Leading Jet}}\right)$$ $|\eta| < 2.4$

Calculate projection of p_T on leading jet axis and average over selected tracks with

$p_T > 0.5$ GeV/c and

$|\eta| < 2.4$

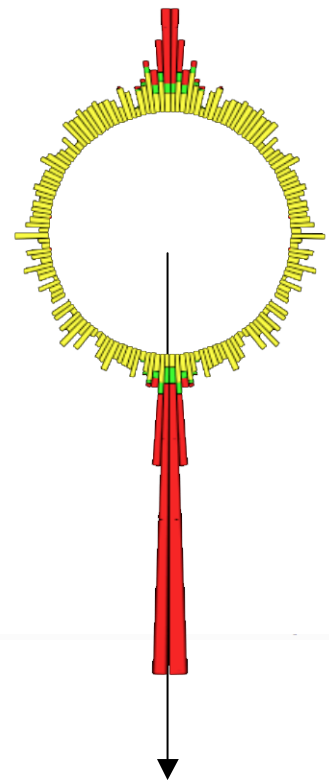

Sum all tracks in the event

Where does the lost energy go? Missing $p_T^{||}$

Taken from C. Roland (CMS), QM11

Missing $p_T^{||}$: $$\not{p}_T^{||} = \sum_{\text{Tracks}} -p_T^{\text{Track}} \cos\left(\phi_{\text{Track}} - \phi_{\text{Leading Jet}}\right)$$ $|\eta| < 2.4$

0-30% Central PbPb

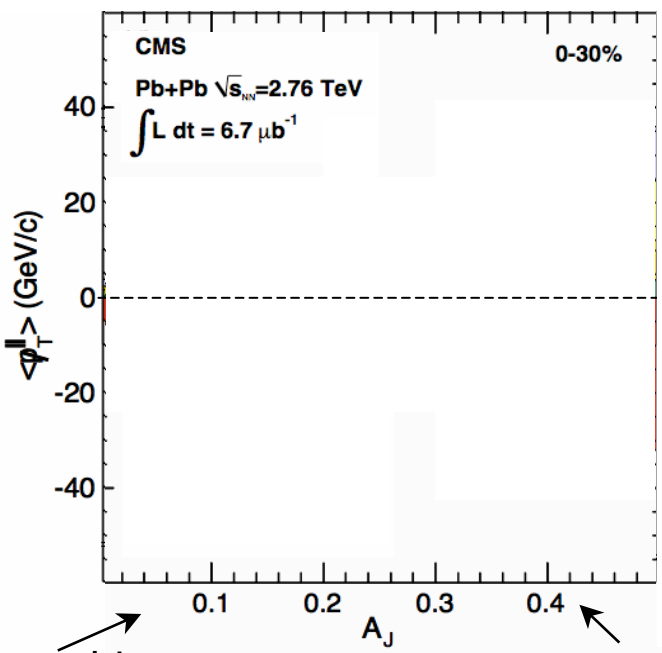

excess away from leading jet

excess towards leading jet

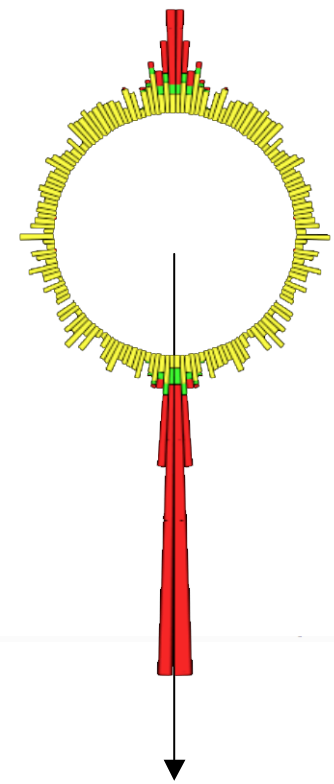

alanced jets

unbalanced jets

Where does the lost energy go? Missing $p_T^{||}$

Taken from C. Roland (CMS), QM11

Missing $p_T^{||}$: $$\not{p}_T^{||} = \sum_{\text{Tracks}} -p_T^{\text{Track}} \cos\left(\phi_{\text{Track}} - \phi_{\text{Leading Jet}}\right)$$ $|\eta| < 2.4$

0-30% Central PbPb

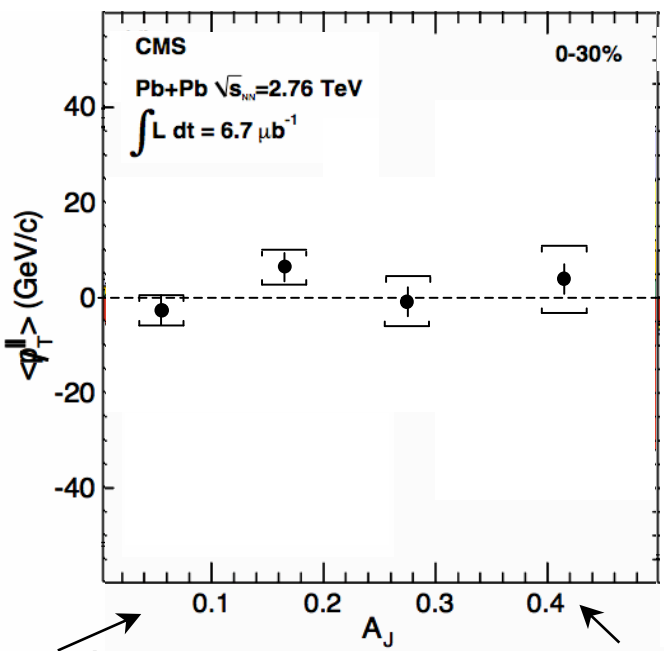

excess away from leading jet

excess towards leading jet

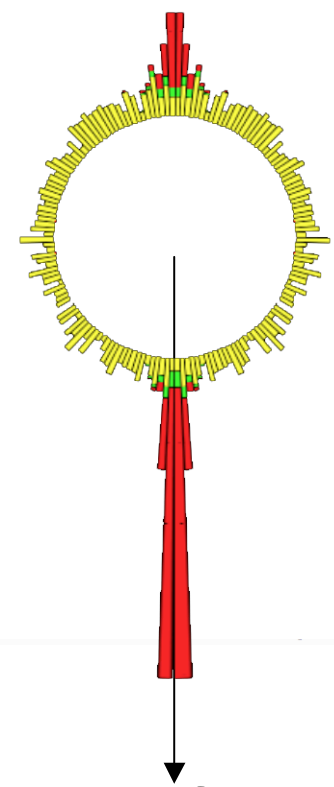

alanced jets

unbalanced jets

Integrating over the whole event final state the momentum balance is restored

Where does the lost energy go? Missing $p_T^{||}$

Taken from C. Roland (CMS), QM11

Missing $p_T^{||}$: $$\not{p}_T^{||} = \sum_{\text{Tracks}} -p_T^{\text{Track}} \cos\left(\phi_{\text{Track}} - \phi_{\text{Leading Jet}}\right)$$ $|\eta| < 2.4$

0-30% Central PbPb

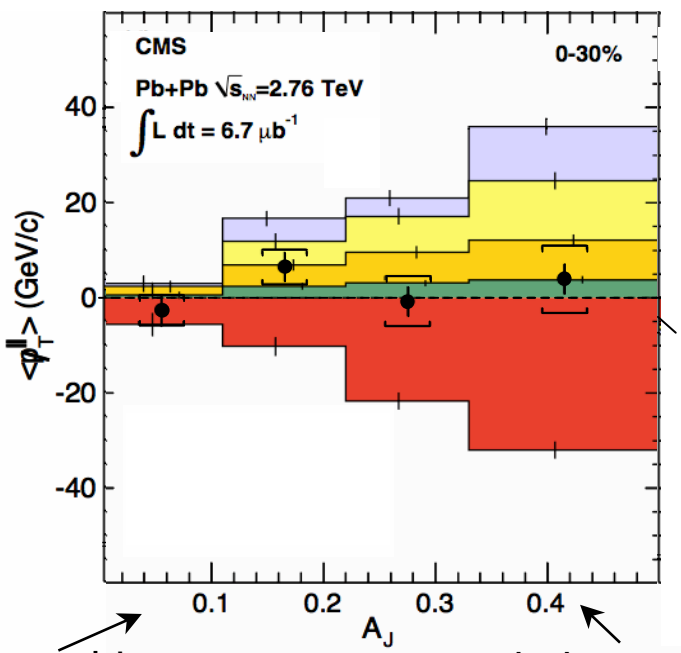

excess away from leading jet

excess towards leading jet

balanced jets

unbalanced jets

Calculate missing p_T in ranges of track p_T:

- > 0.5 GeV/c
- 0.5 - 1.0 GeV/c
- 1.0 - 2.0 GeV/c
- 2.0 - 4.0 GeV/c
- 4.0 - 8.0 GeV/c
- > 8.0 GeV/c

The momentum difference in the dijet is balanced by low p_T particles

Jet R_{AA} in central Au+Au and Cu+Cu

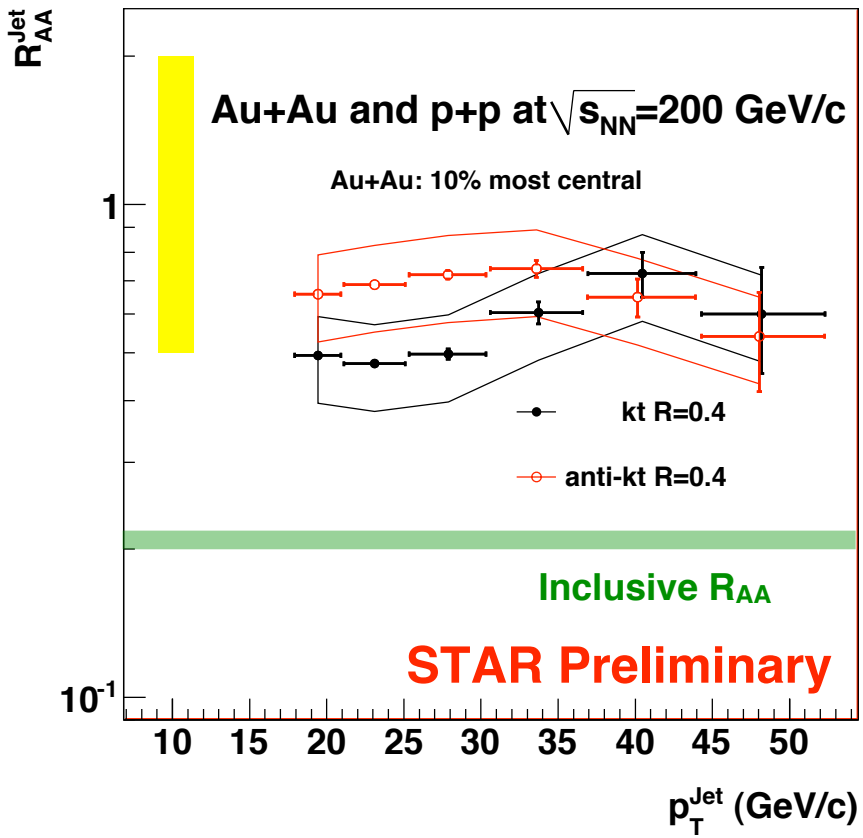

Y. Lai QM2009

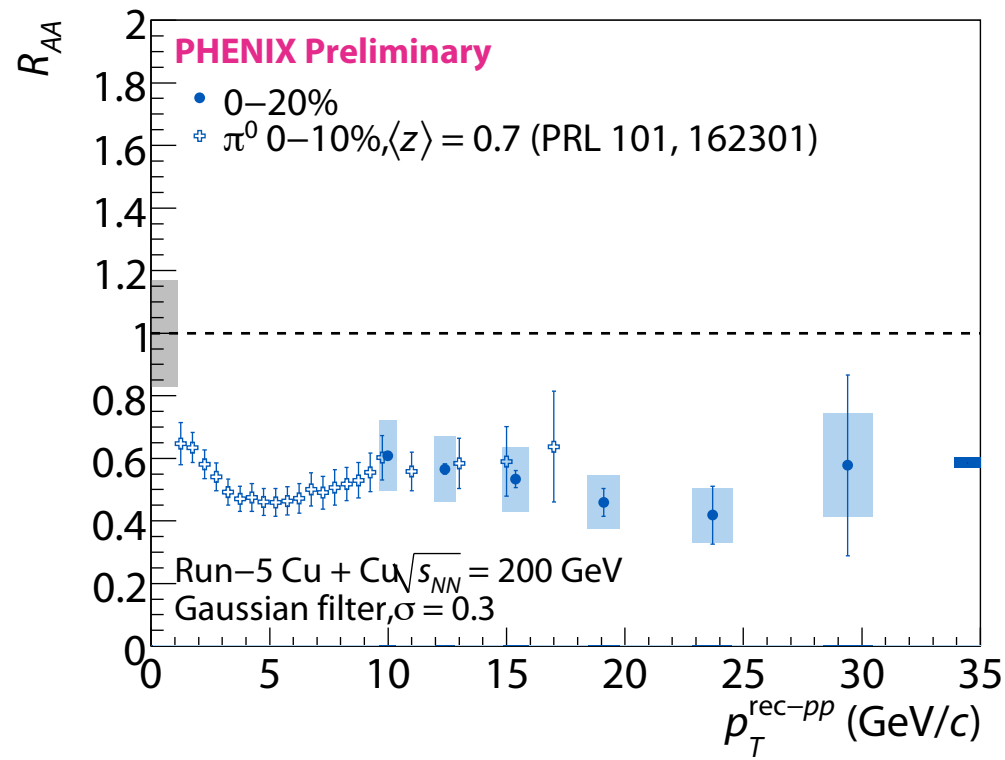

STAR sees a substantial fraction of jets in Au+Au
- in contrast to x5 suppression for light hadron R_{AA}

Strong suppression (similar to single particle)
in Cu+Cu measured by PHENIX

Recoil jet spectrum R_{AA}

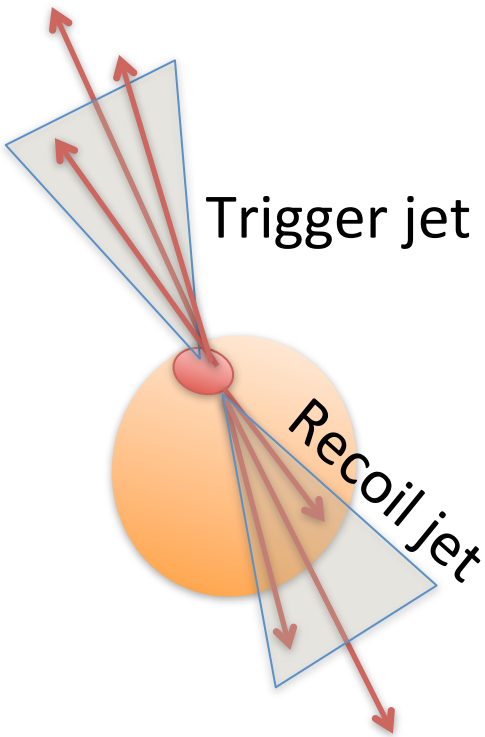

E. Bruna QM2009

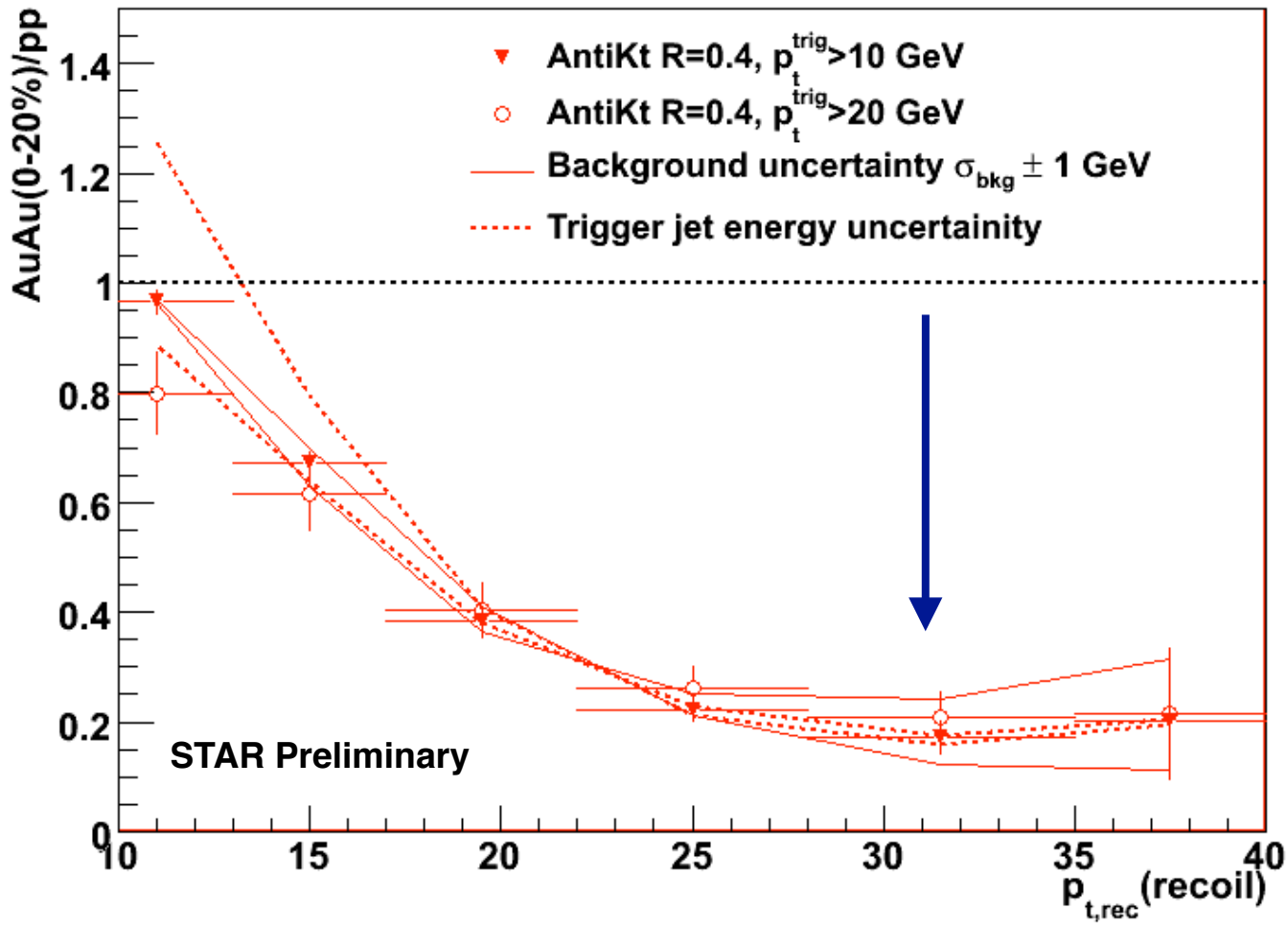

- **Selecting biased trigger jet maximizes pathlength for the back-to-back jets: *extreme selection of jet population***
- **Significant suppression in di-jet coincidence measurements!**

CMS results on jet quenching and pPb collisions

Gunther Roland
(MIT)
for the CMS Collaboration

RBRC Workshop
"Jet Quenching at RHIC vs LHC in Light of Recent dAu vs pPb Controls"
BNL Apr 15-17, 2013

CMS results on jet quenching and pPb collisions

Gunther Roland
(MIT)
for the CMS Collaboration

RBRC Workshop
"Jet Quenching at RHIC vs LHC in Light of Recent dAu vs pPb Controls"
BNL Apr 15-17, 2013

CMS Detector

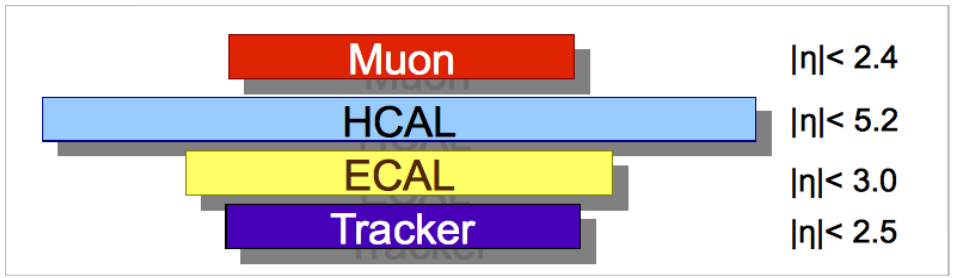

PbPb dijet phenomenology

Leading jet (p_T>120GeV/c)

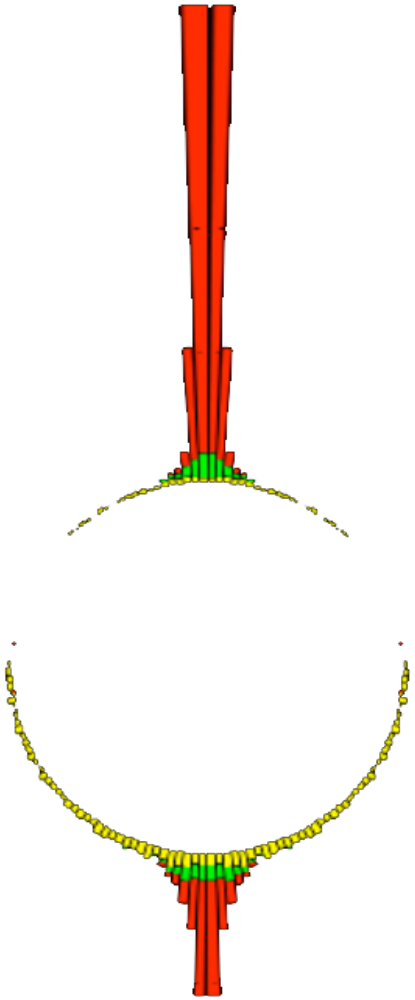

Subleading jet (p_T>30GeV/c)

PbPb dijet phenomenology

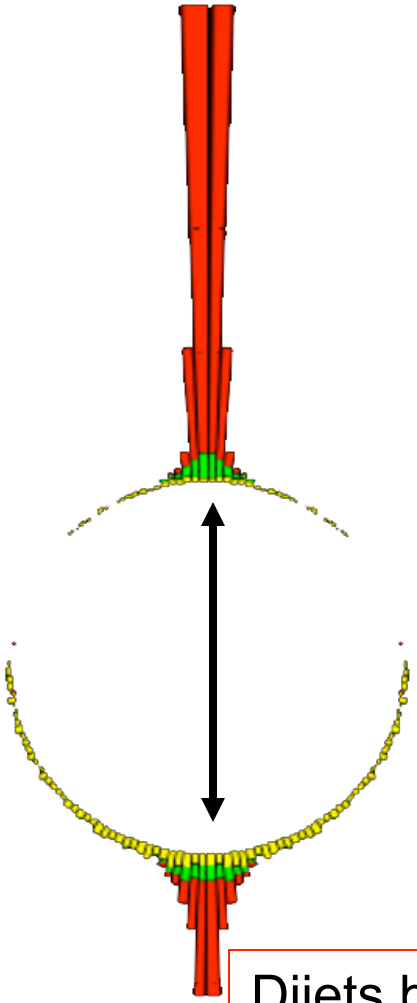

PRC 84 (2011) 024906

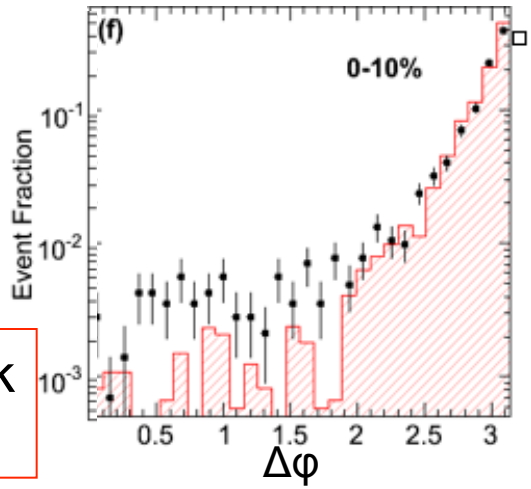

Dijets back-to-back in central PbPb

PbPb dijet phenomenology

PLB 712 (2012) 176

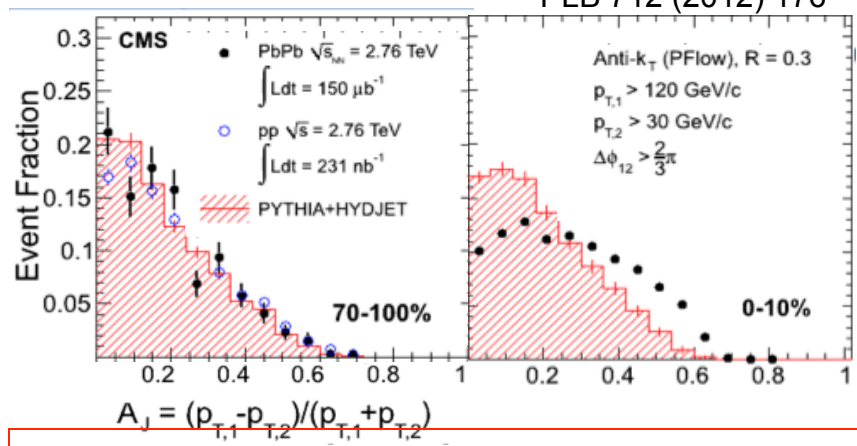

Large dijet momentum asymmetry in central PbPb

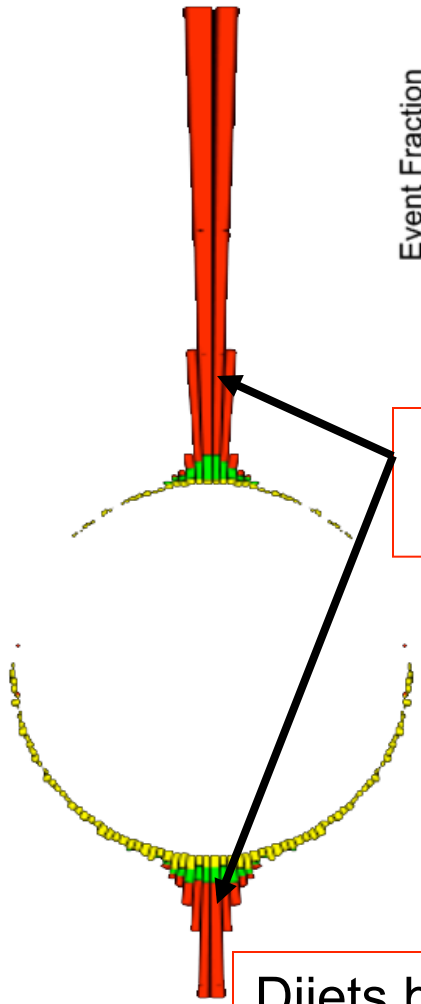

PRC 84 (2011) 024906

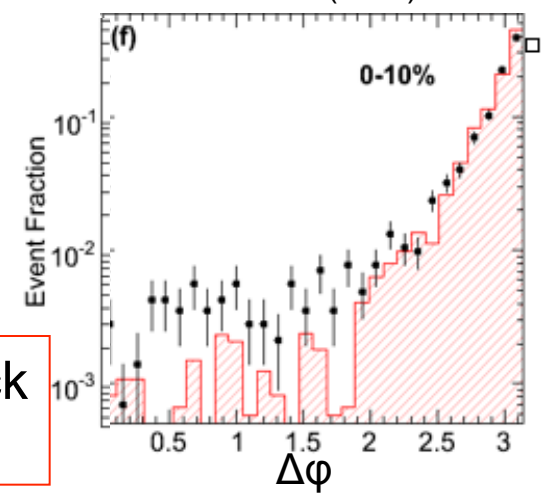

Dijets back-to-back in central PbPb

PbPb dijet phenomenology

$$\not{p}_T^{\parallel} = \sum_{\text{Tracks}} -p_T^{\text{Track}} \cos\left(\phi_{\text{Track}} - \phi_{\text{Leading Jet}}\right)$$

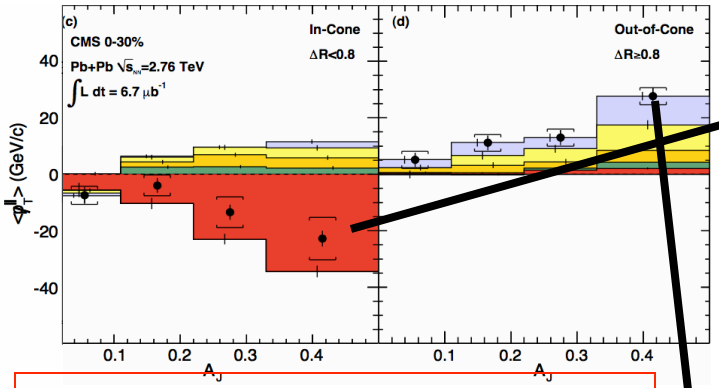

Jet asymmetry balanced by soft particles at large angles

PRC 84 (2011) 024906

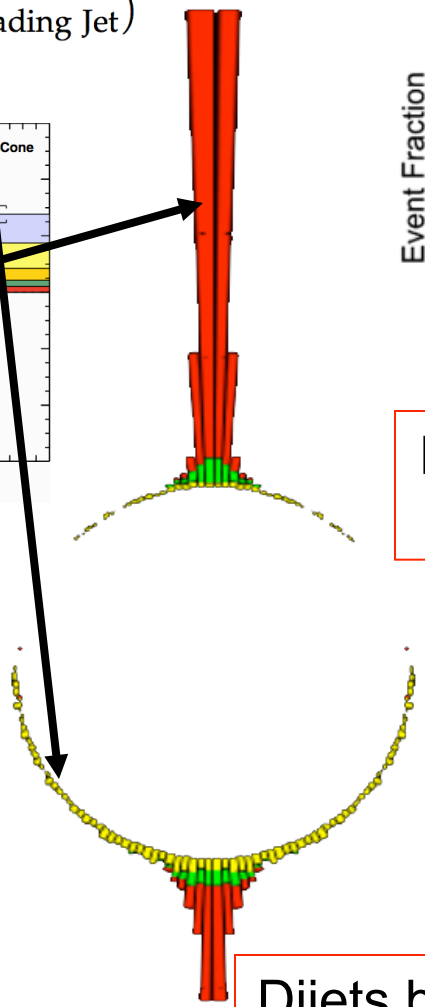

PLB 712 (2012) 176

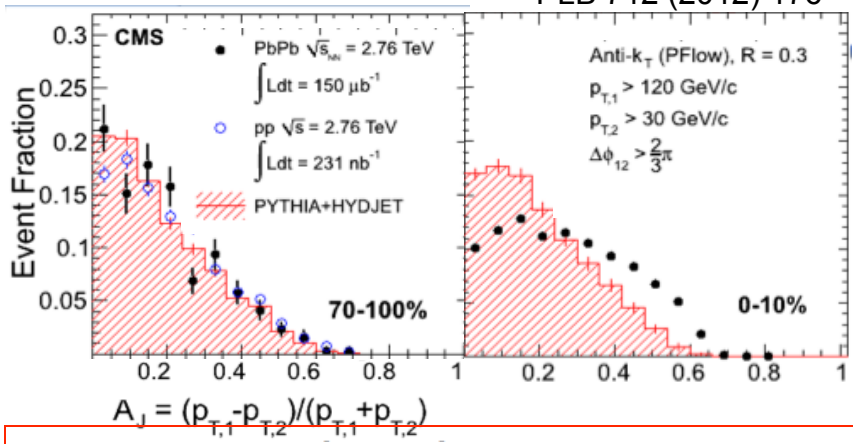

Large dijet momentum asymmetry in central PbPb

PRC 84 (2011) 024906

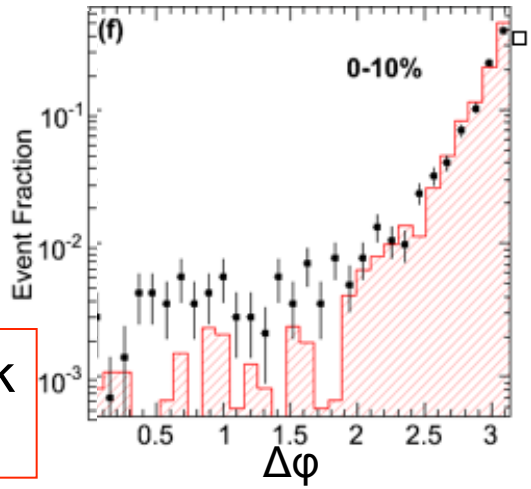

Dijets back-to-back in central PbPb

Jet anatomy

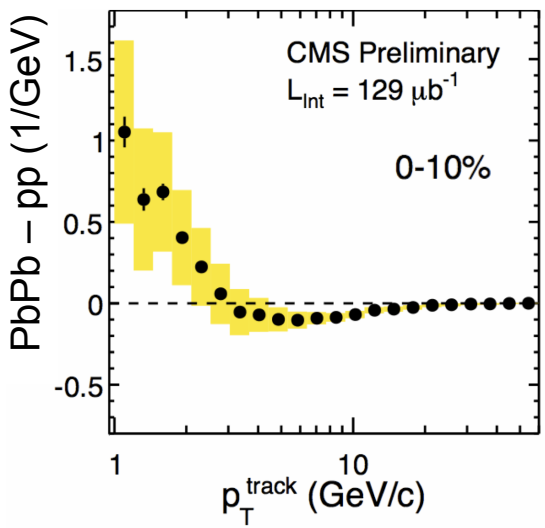

Fragmentation function difference (PbPb – pp):
Shows redistribution of particles in p_T

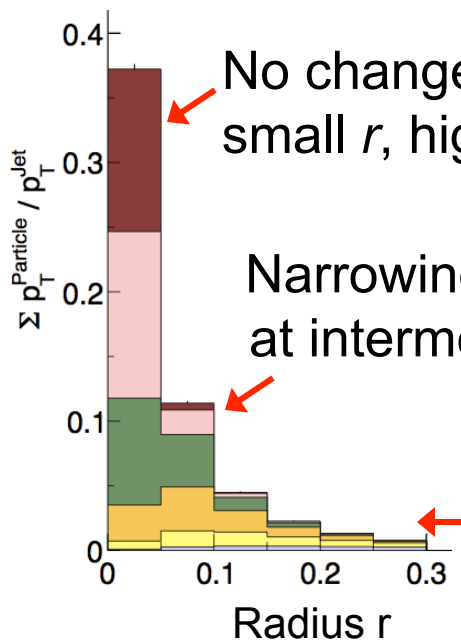

No change at small *r*, high p_T

Narrowing/depletion at intermediate *r*, p_T

Broadening/excess at large *r*, low p_T

(3-5% of jet energy)

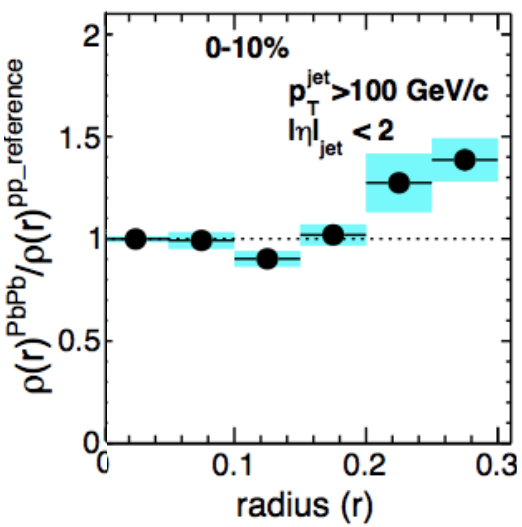

Jet shape ratio (PbPb/pp):
Shows redistribution of energy in *r* from jet axis

γ+jet: u,d quark energy loss

PLB 718 (2013) 773

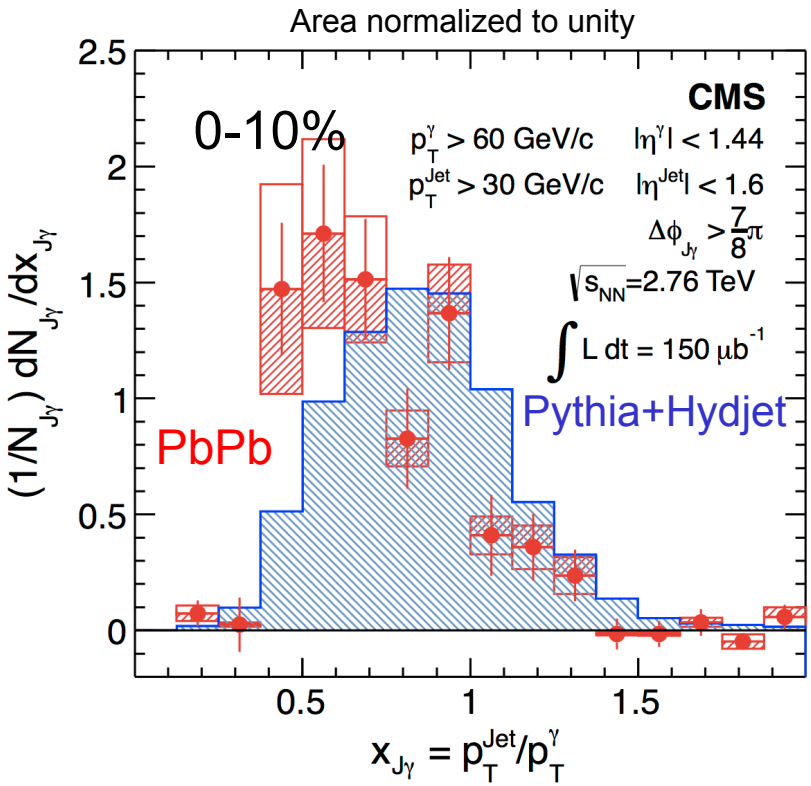

Photon-jet momentum balance

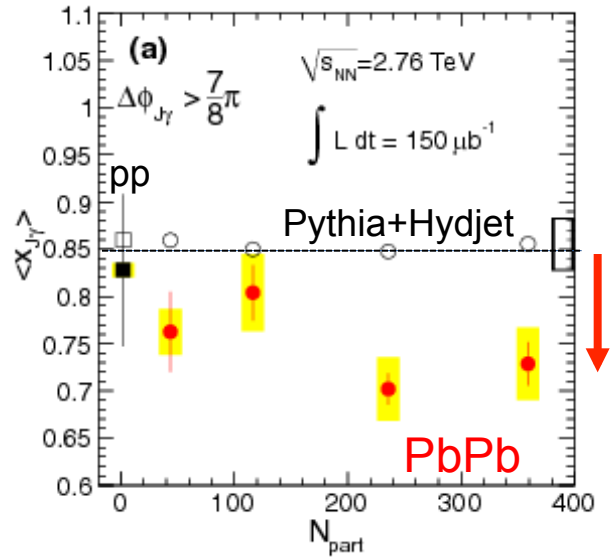

Jet-photon p_T balance drops by 14%

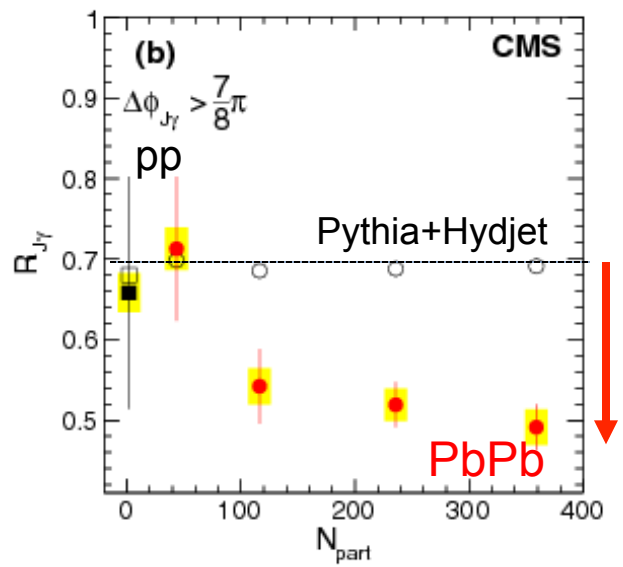

20% of photons lose jet partner

R_{AA} Zoo: Signal and Control

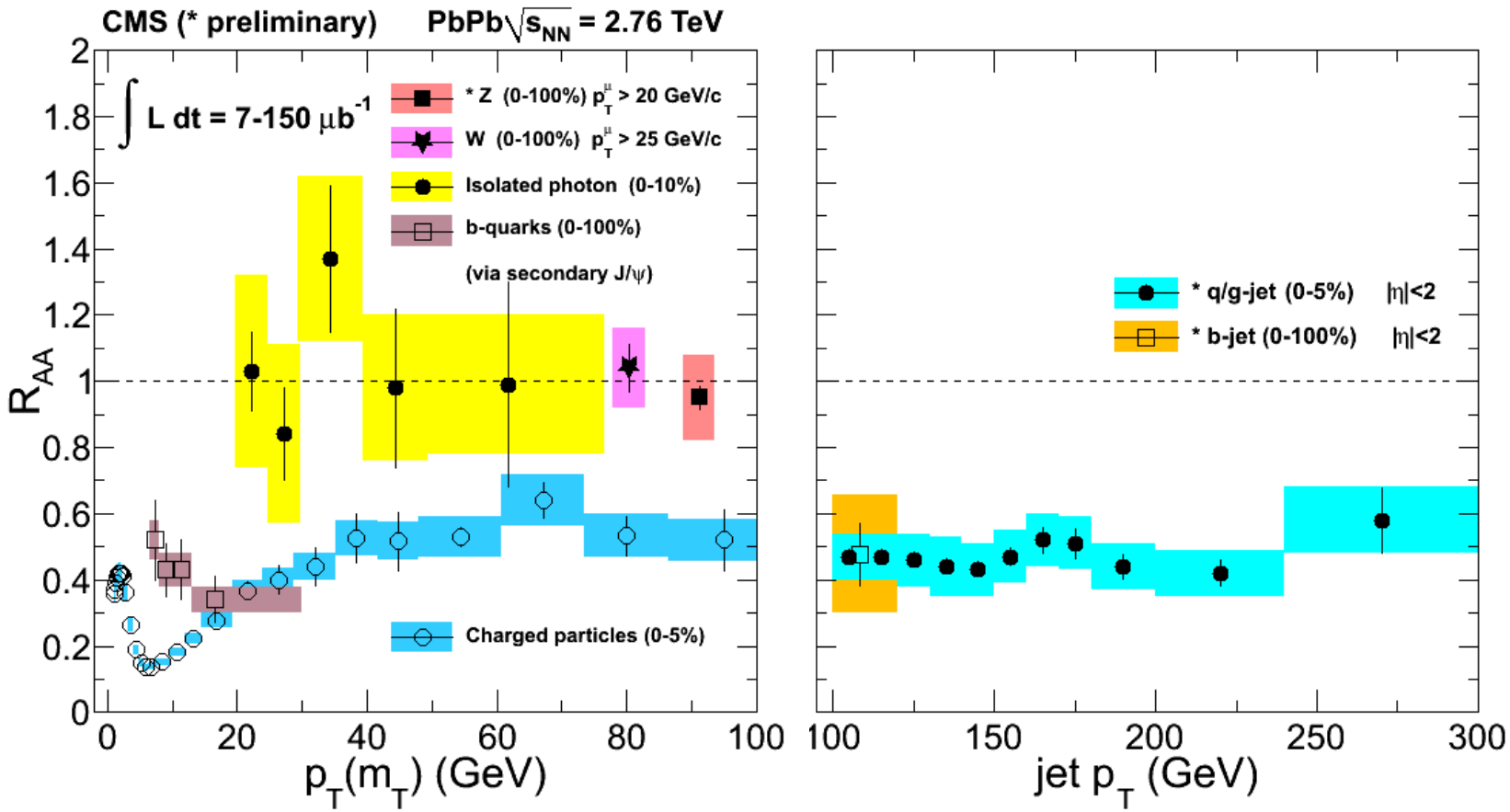

Vector-bosons show that hard scattering rates are under good control

Long-range correlations in pp and pPb

JHEP

PUBLISHED FOR SISSA BY SPRINGER

RECEIVED: *September 22, 2010*
ACCEPTED: *September 23, 2010*
PUBLISHED: *September 27, 2010*

Observation of long-range, near-side angular correlations in proton-proton collisions at the LHC

Physics Letters B 718 (2013) 795–814

Contents lists available at SciVerse ScienceDirect

Physics Letters B

www.elsevier.com/locate/physletb

ELSEVIER

Observation of long-range, near-side angular correlations in pPb collisions at the LHC ☆

CMS Collaboration *

CERN, Switzerland

Observed “flow-like” effects raise possibility of “final state” effects in pPb for many observables, incl. e.g. jets (but this is going to be subject of a talk at a different meeting…)

Correlations in 7TeV pp collisions

Results based on $1fb^{-1}$,
i.e. sampling 50billion pp events
with high multiplicity trigger

Intermediate p_T: 1-3 GeV/c

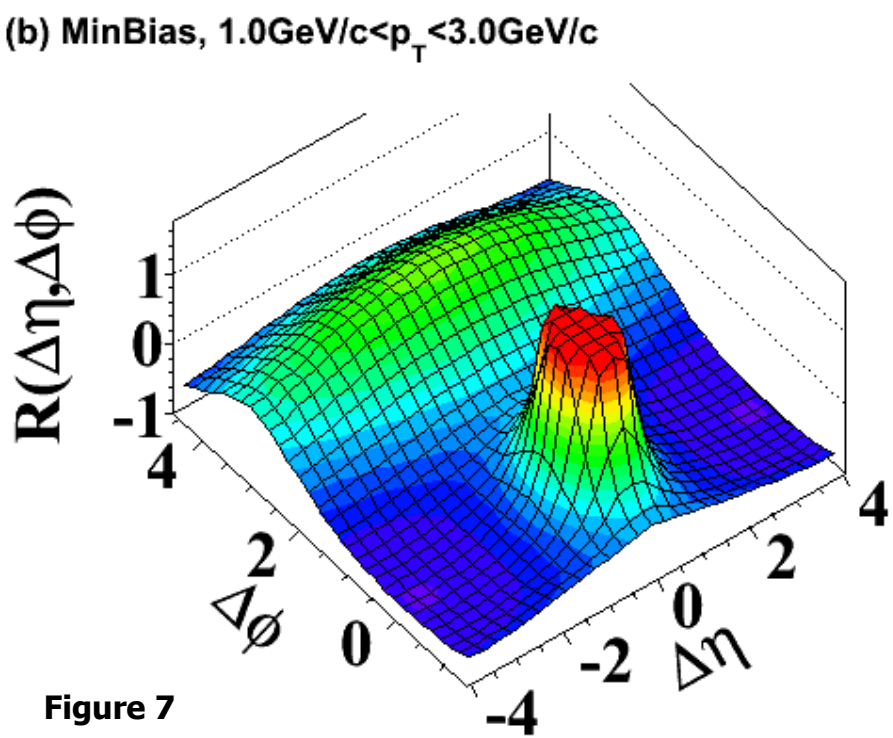

Figure 7

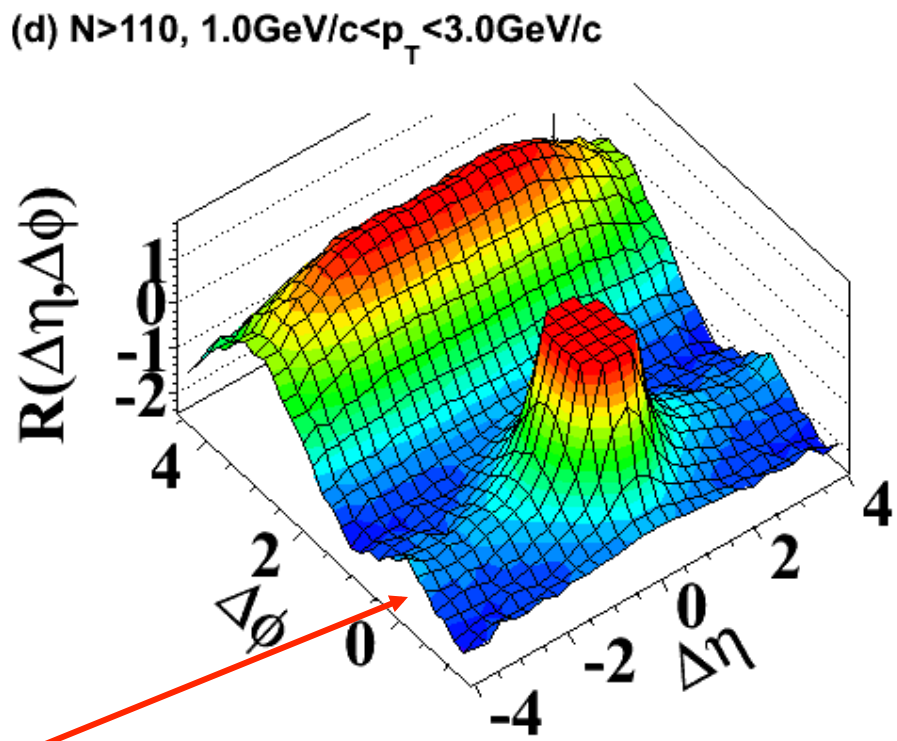

Pronounced structure at large $\delta\eta$ around $\delta\phi \sim 0$!

Multiplicity Evolution in pPb

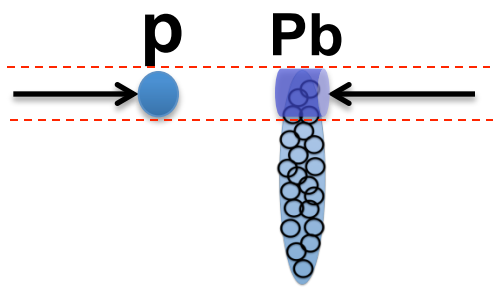

Low multiplicity

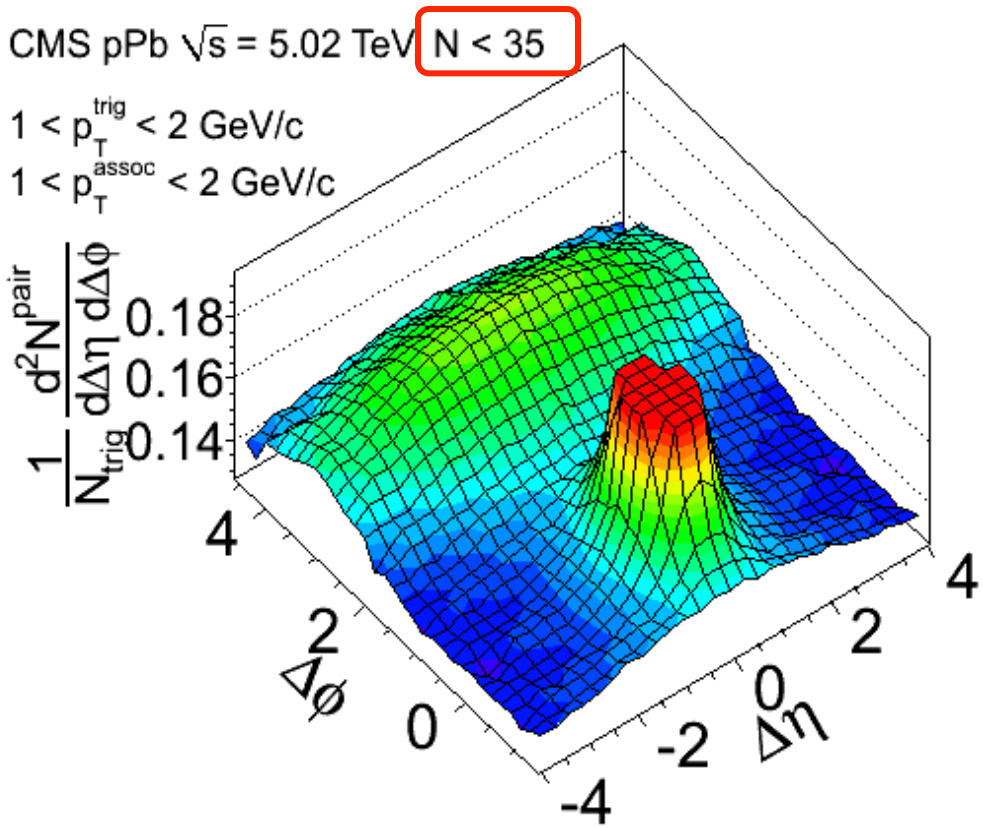

Divide into 4 multiplicity bins:

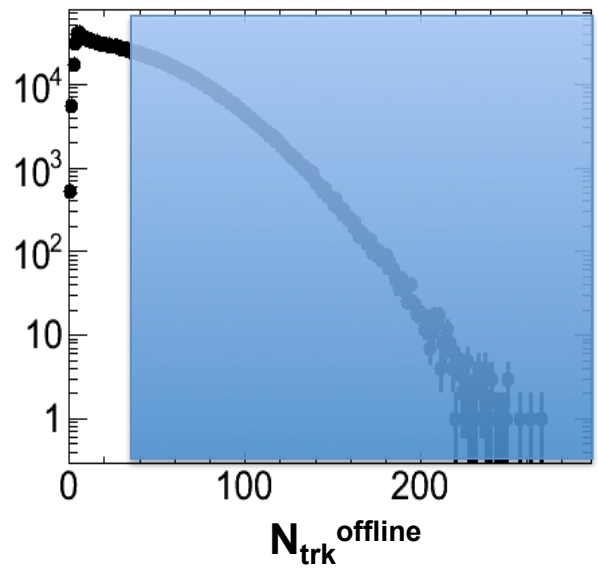

Multiplicity Evolution in pPb

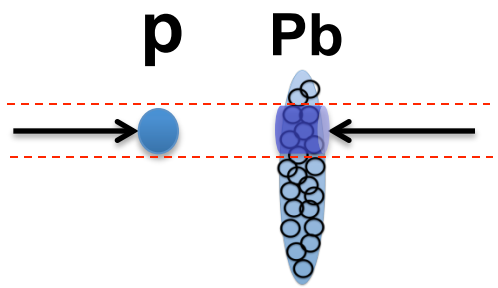

Increasing multiplicity

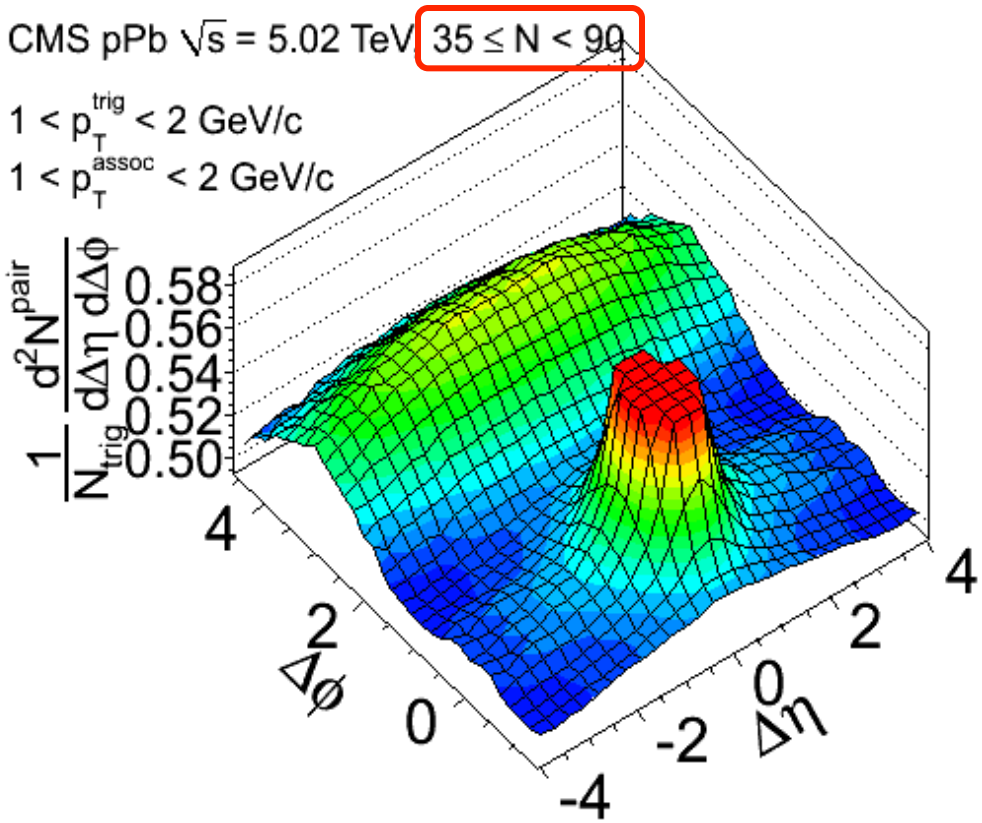

Divide into 4 multiplicity bins:

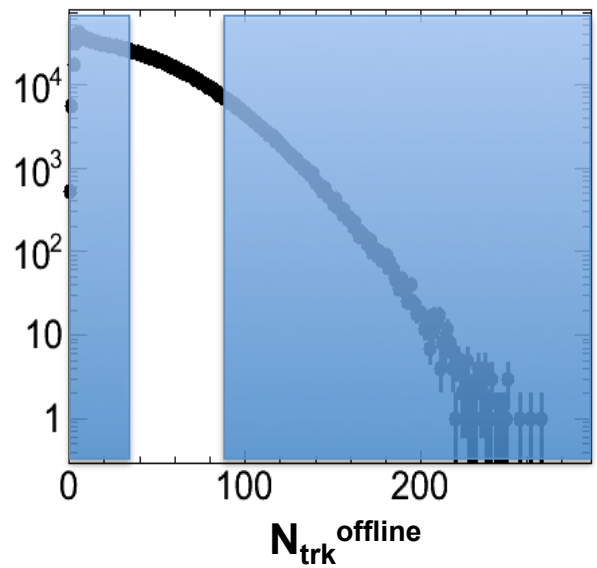

Multiplicity Evolution in pPb

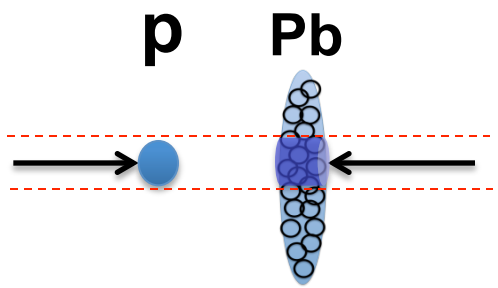

Increasing multiplicity

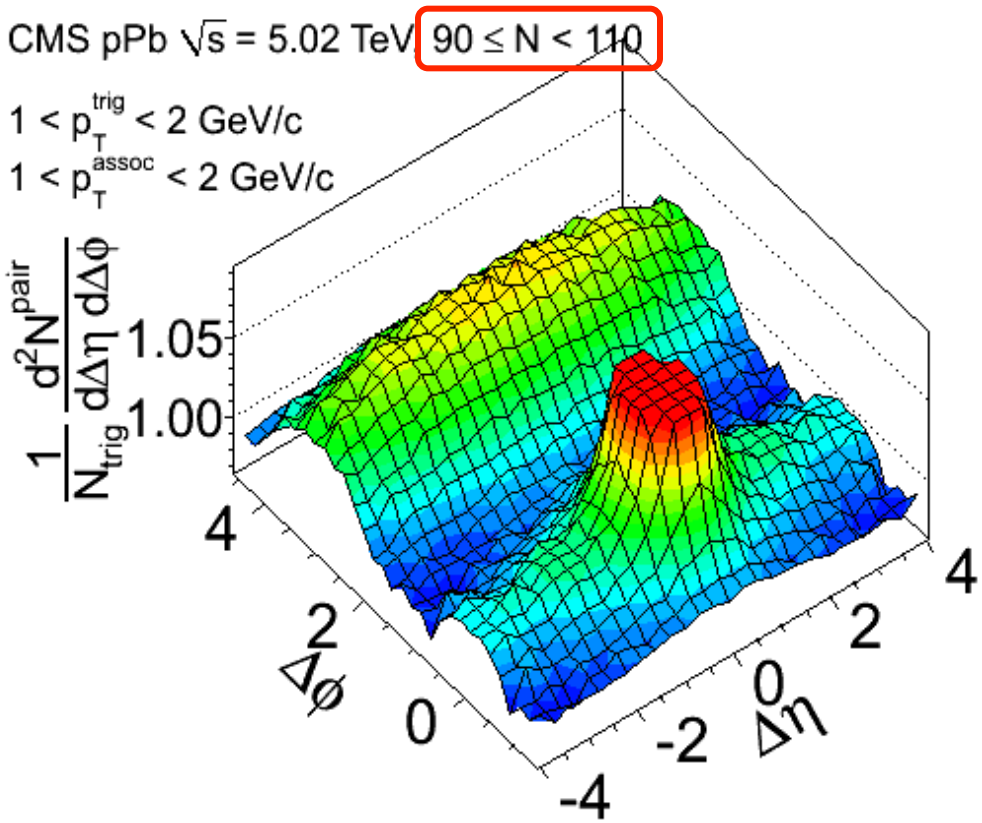

Divide into 4 multiplicity bins:

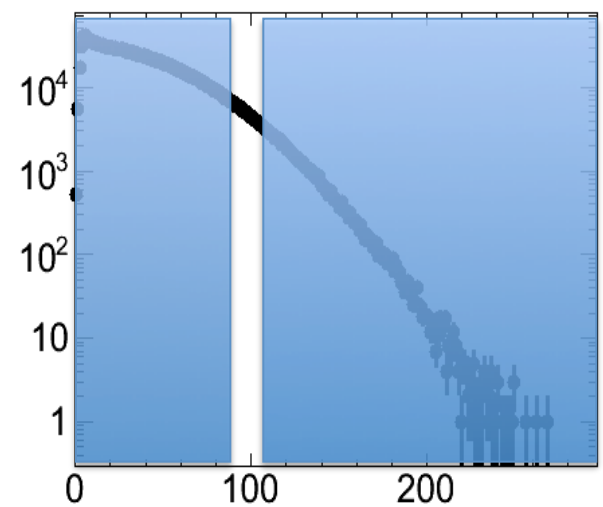

Multiplicity Evolution in pPb

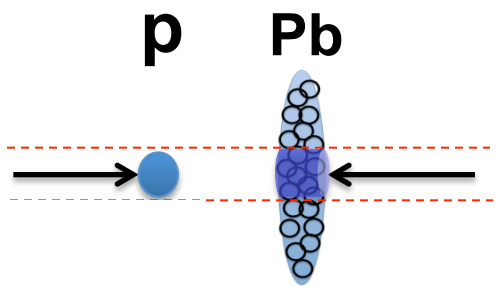

Increasing multiplicity

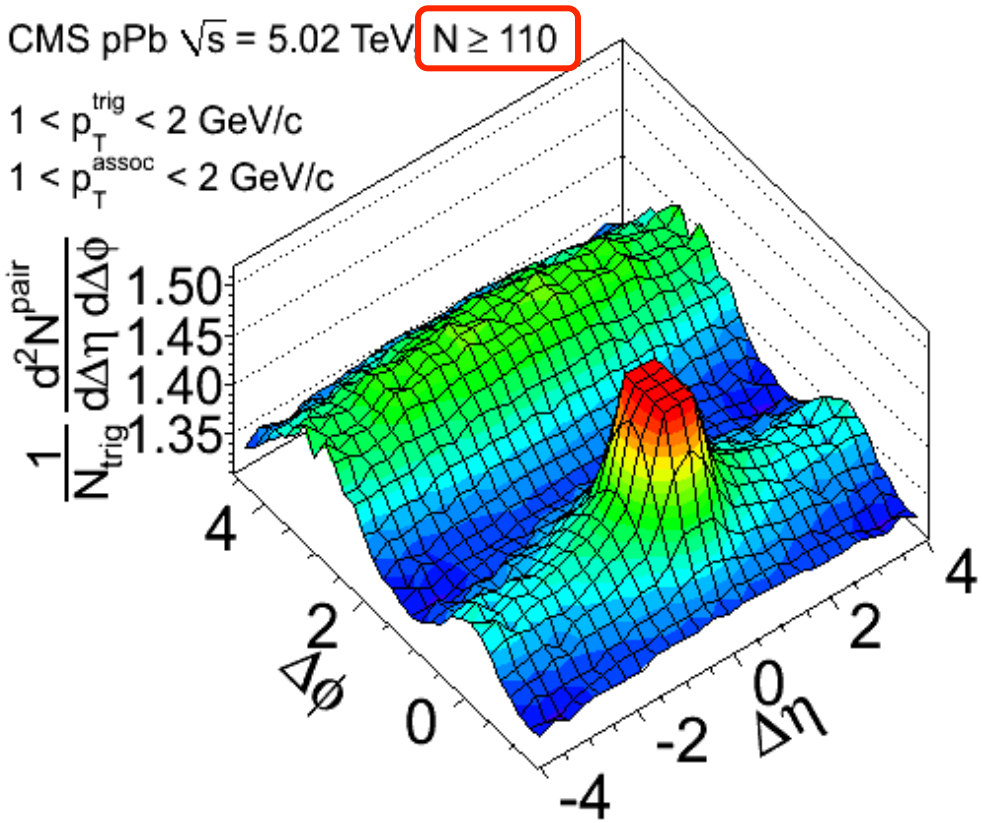

Divide into 4 multiplicity bins:

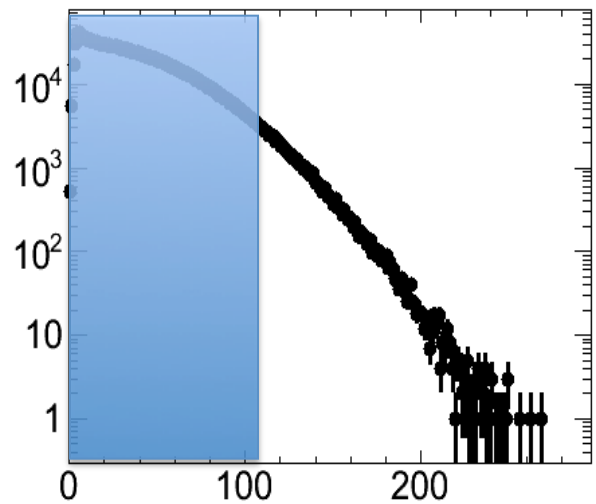

Ridge Associated Yield

ZYAM example

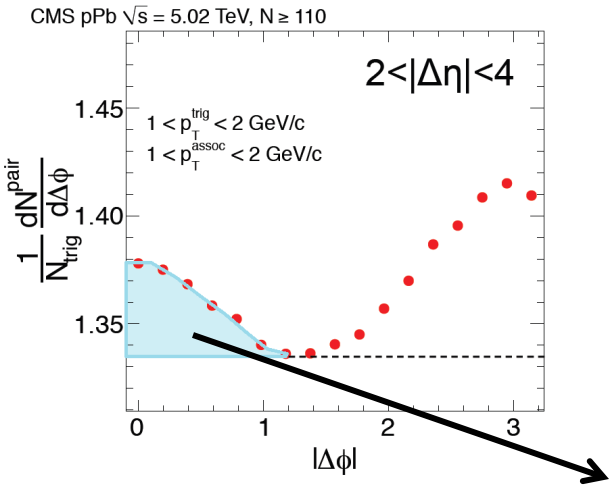

In the signal (N>110) region, the strength of the effect rises and falls with p_T

In the p_T range where the yield is the strongest, the ridge turns on at N≈40

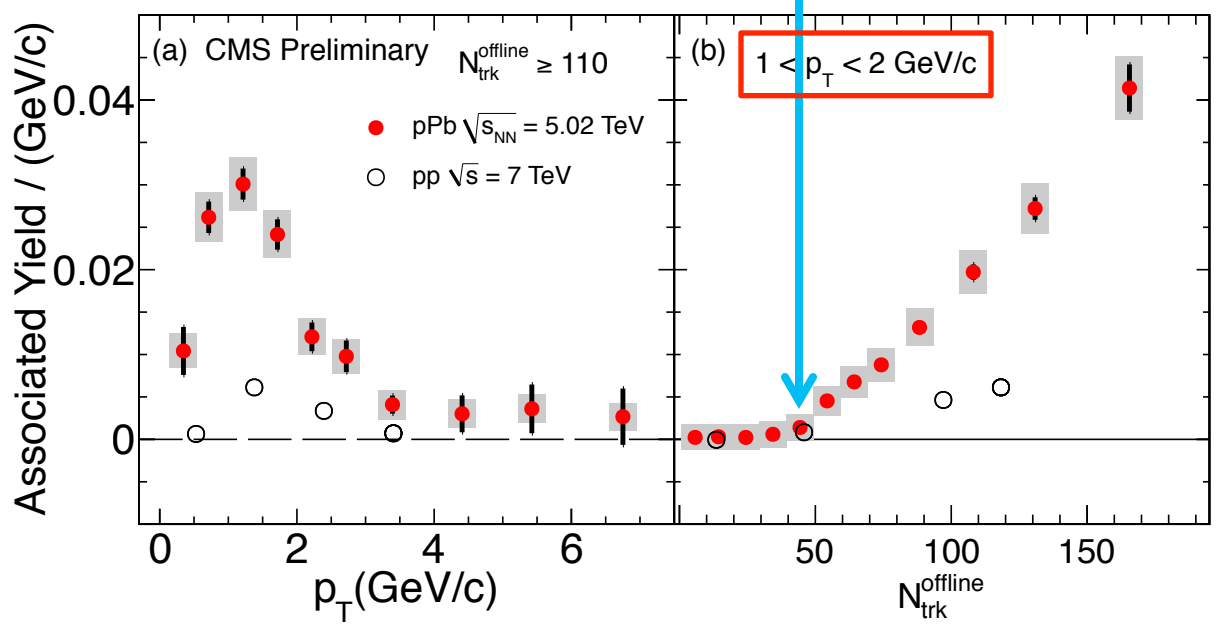

New results on pPb correlations

- Analysis of 2013 pPb data set
  - Including high multiplicity triggers sampling full luminosity of 31/nb (30000x pilot run stat's)
- Re-analysis of peripheral PbPb using identical reconstruction, event selection, analysis code,…
- Comprehensive set of observables
  - Associate yields (as in previous CMS pp and pPb analyses)
  - v_2 and v_3 from two particle correlations (w/ η gap)
  - "Peripheral subtraction" a la ALICE, ATLAS
  - $v_2\{4\}$ four-particle cumulants

“Centrality” (multiplicity density) binning

n.b., particles are counted for $p_T > 0.4$GeV/c, $|\eta| < 2.4$

	pPb data			PbPb data		
$N_{trk}^{offline}$ bin	Fraction	$\langle N_{trk}^{offline} \rangle$	$\langle N_{trk}^{corrected} \rangle$	<Centrality> ± RMS (%)	$\langle N_{trk}^{offline} \rangle$	$\langle N_{trk}^{corrected} \rangle$
$[0,\infty)$	1.00	40	50±2			
$[0,20)$	0.31	10	12±1	92±4	10	13±1
$[20,30)$	0.14	25	30±1	86±4	24	30±1
$[30,40)$	0.12	35	42±2	83±4	34	43±2
$[40,50)$	0.10	45	54±2	80±4	44	55±2
$[50,60)$	0.09	54	66±3	78±3	54	68±3
$[60,80)$	0.12	69	84±4	75±3	69	87±4
$[80,100)$	0.07	89	108±5	72±3	89	112±5
$[100,120)$	0.03	109	132±6	70±3	109	137±6
$[120,150)$	0.02	132	159±7	67±3	134	168±7
$[150,185)$	4×10^{-3}	162	195±9	64±3	167	210±9
$[185,220)$	5×10^{-4}	196	236±10	62±2	202	253±11
$[220,260)$	6×10^{-5}	232	280±12	59±2	239	299±13
$[260,300)$	3×10^{-6}	271	328±14	57±2	279	350±15
$[300,350)$	1×10^{-7}	311	374±16	55±2	324	405±18

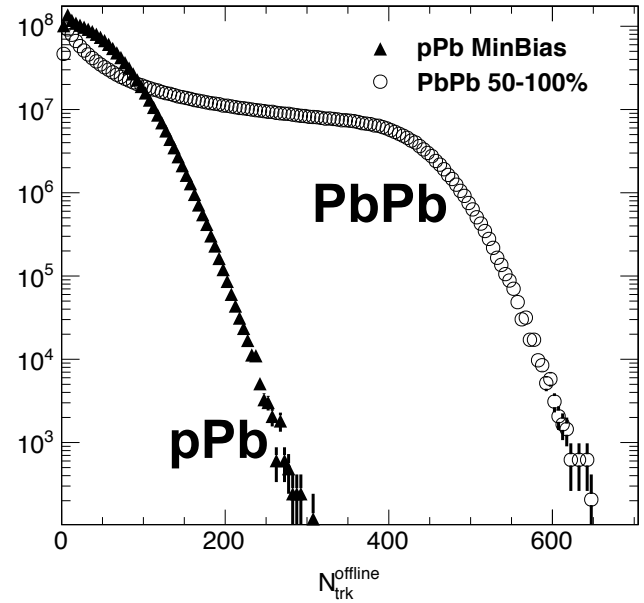

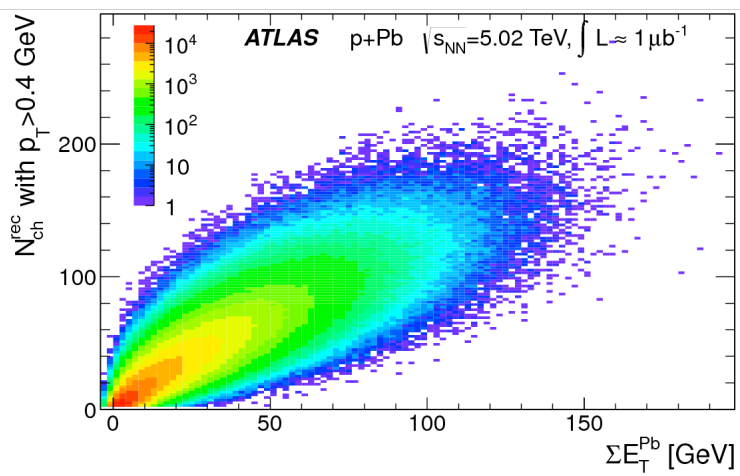

pPb vs PbPb

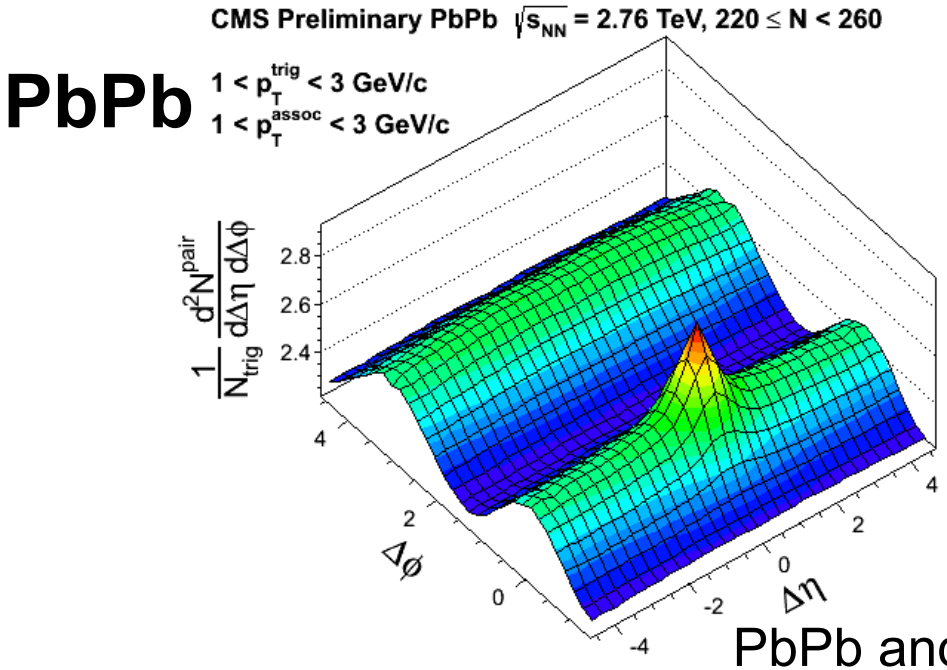

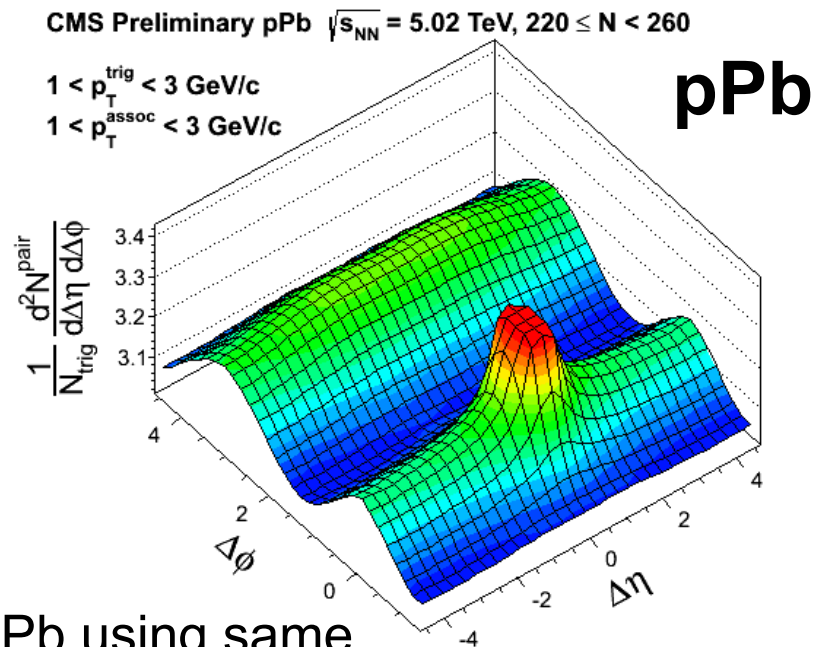

PbPb and pPb using same multiplicity selection, 220 < N < 260

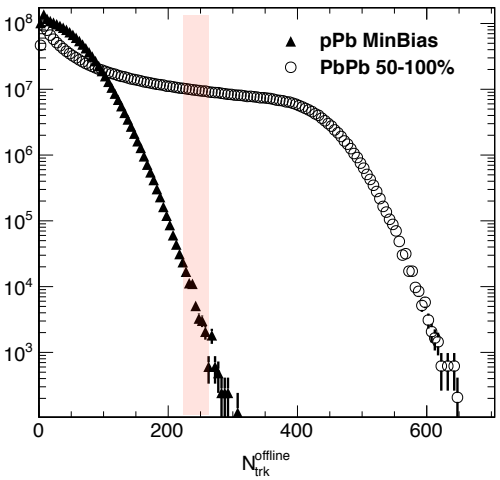

n.b., particles are counted for $p_T > 0.4$GeV/c, $|\eta| < 2.5$

pPb vs PbPb: p_T dependence

PbPb

$|\Delta\eta| > 2$

$|\Delta\eta| < 1$

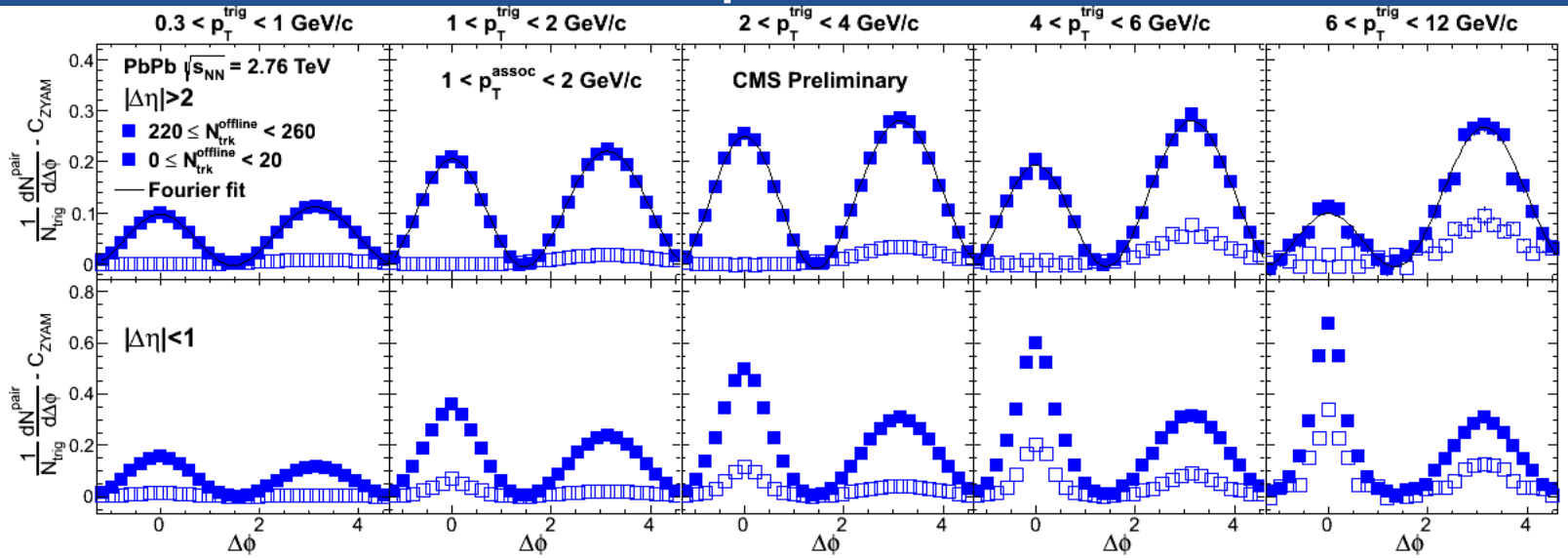

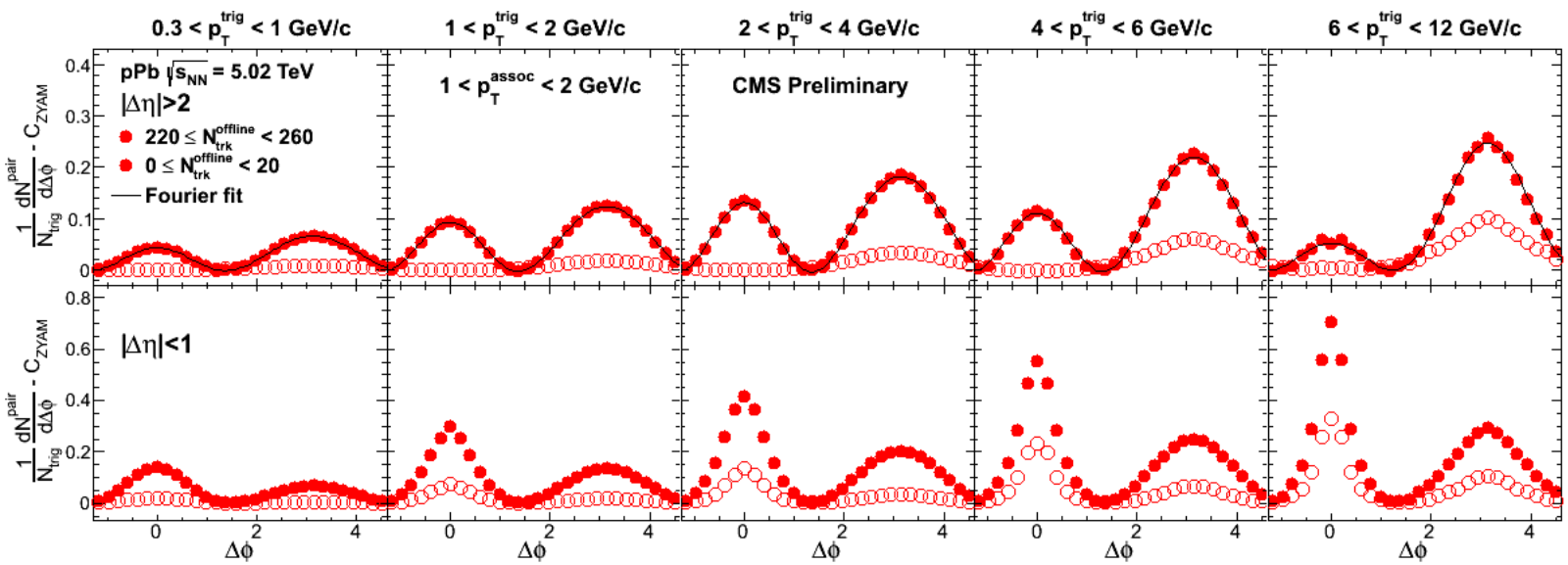

$|\Delta\eta| > 2$

$|\Delta\eta| < 1$

pPb

Multiplicity dependence

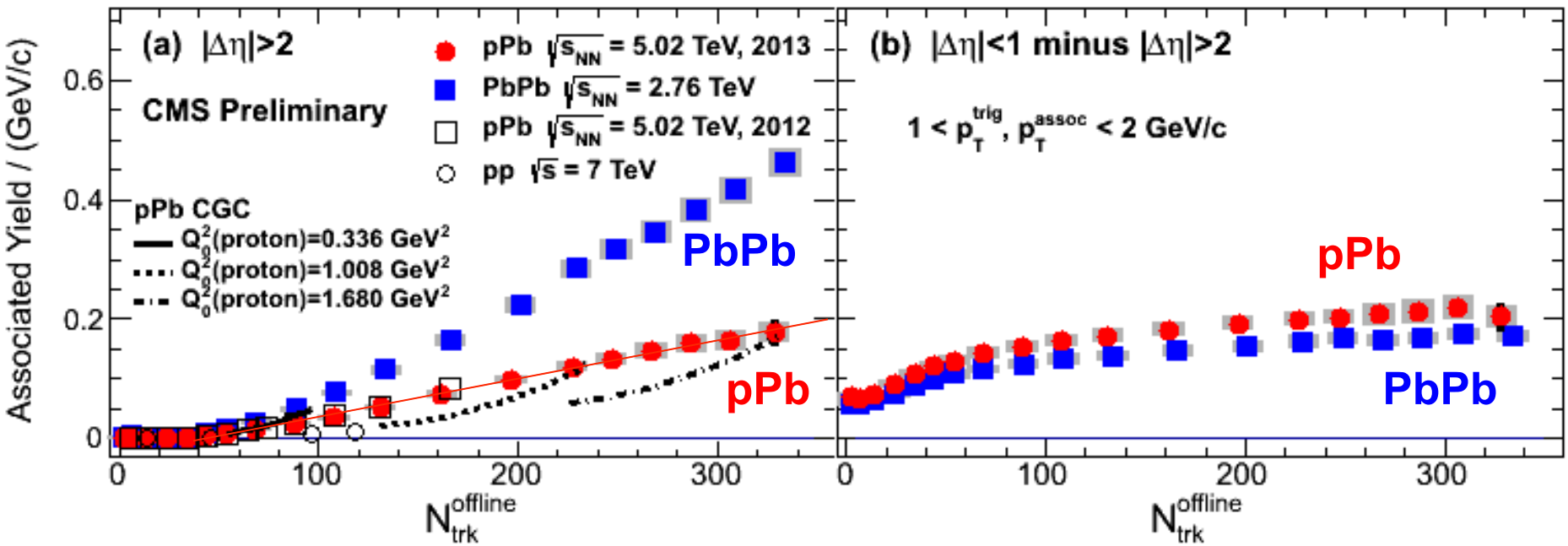

"Long-range" associated yield:
Similar multiplicity dependence for pPb and PbPb

"Jet" yield:
Nearly identical for pPb and PbPb

Difference in absolute yield

4th order cumulants in multiplicity bins

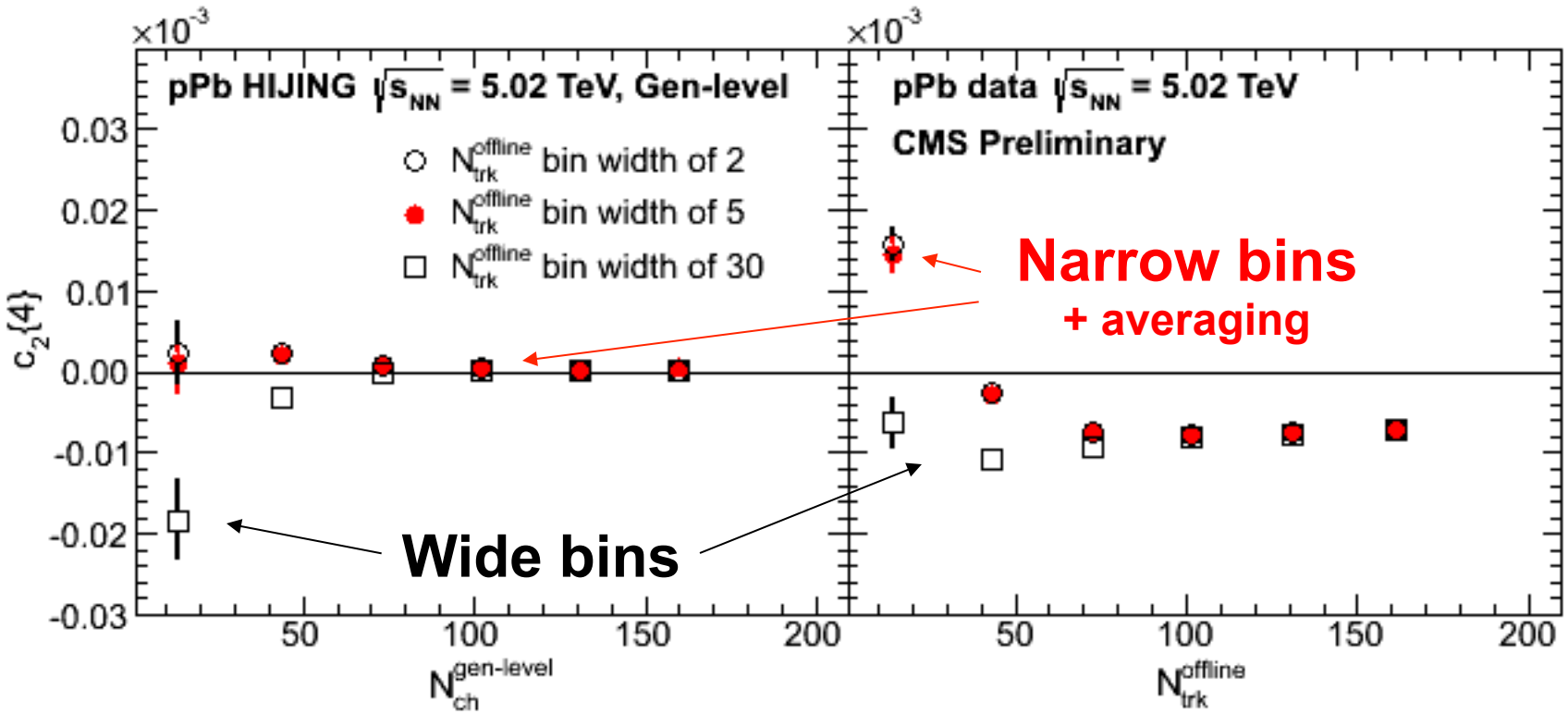

Cumulant analysis in bins of multiplicity
Need to consider bin widths carefully
CMS analysis: (narrow bins + averaging)

v_2 in pPb and PbPb

Dash-dot line: peripheral subtracted

multiplicity →

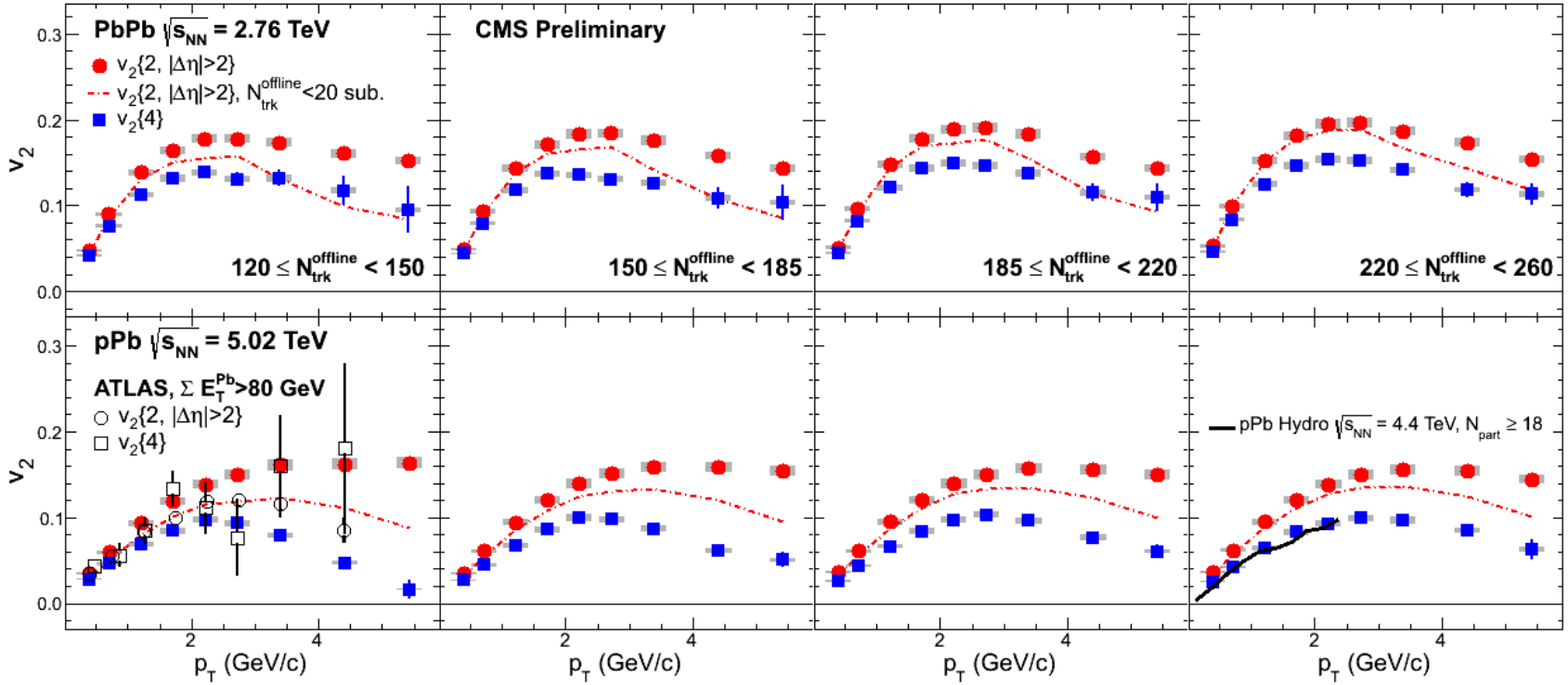

PbPb

pPb

v_2 shows similar shape in pPb and PbPb, but is smaller in pPb

$v_2\{4\}$ is only 20% smaller than $v_2\{2\}$ below 2 GeV/c

"Peripheral subtraction" has small effect at high multiplicity

v_2 in pPb and PbPb

PbPb

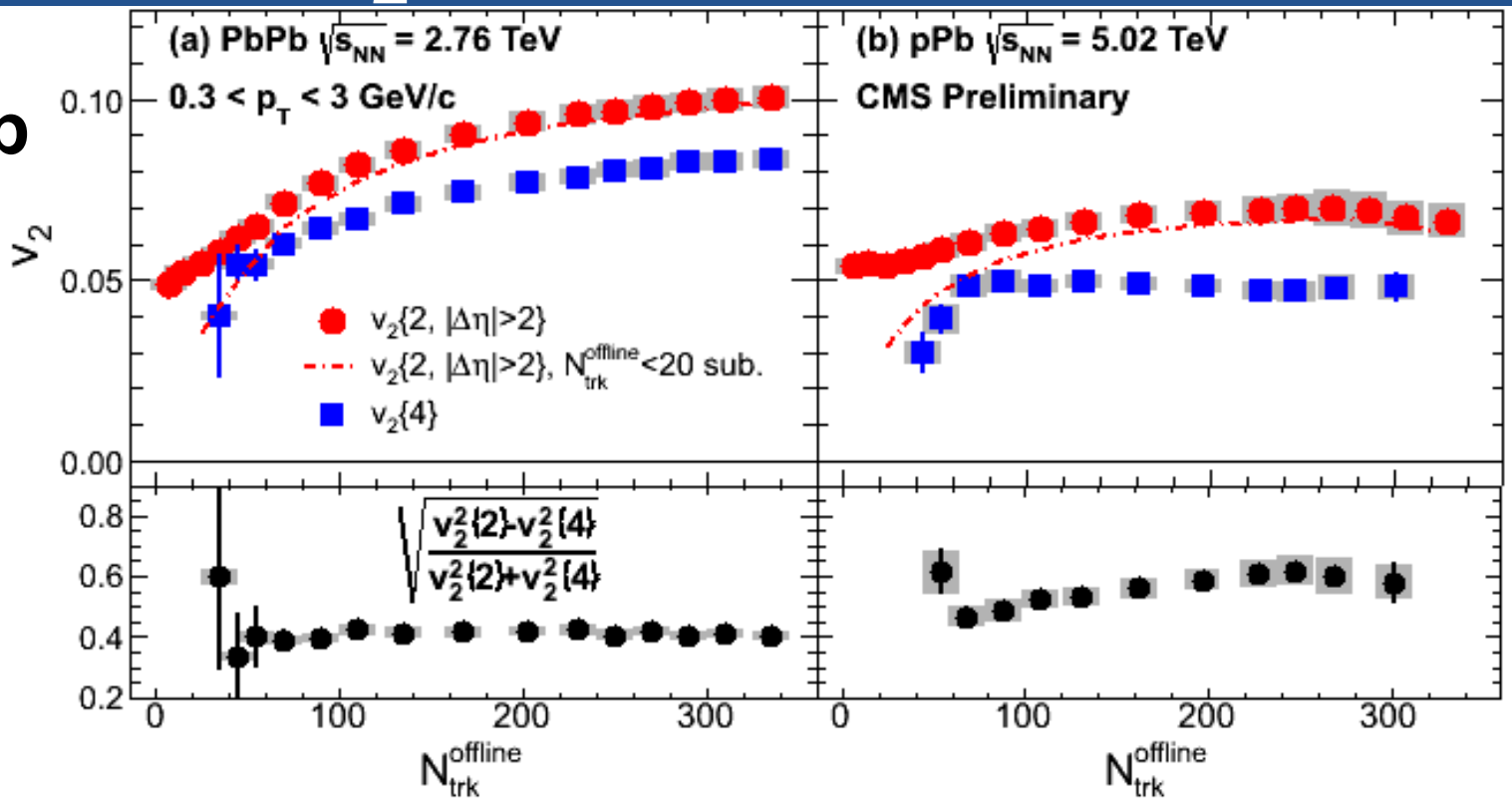

pPb

v_2 smaller in pPb than PbPb

$v_2\{4\}$ drops at low multiplicity

"Peripheral subtraction" has small effect at high multiplicity

v_2 in pPb and PbPb

PbPb

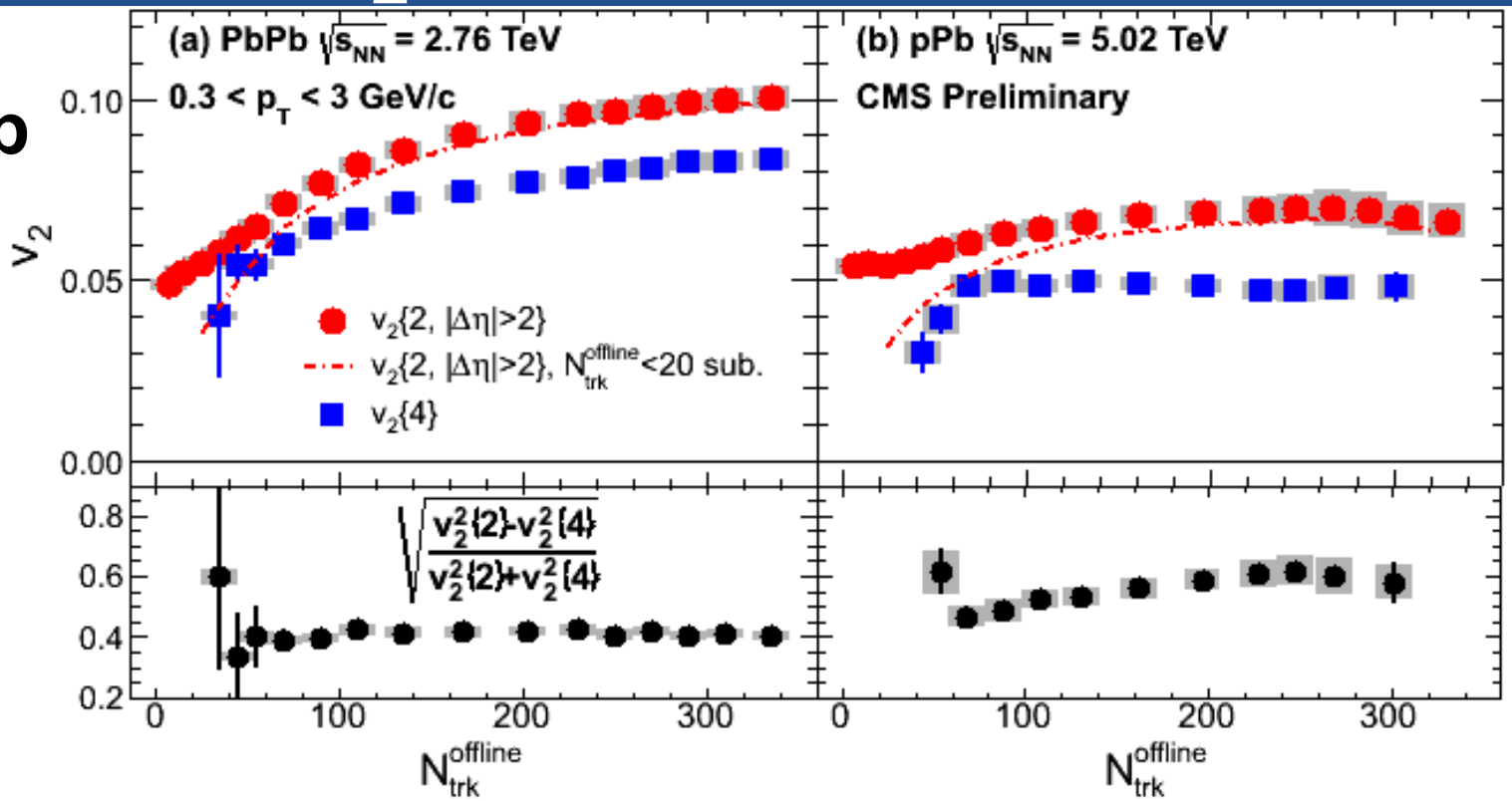

pPb

$$v_2\{2\} = \sqrt{< v_2 >^2 + \sigma_{v_2}^2}$$
$$v_2\{4\} = \sqrt{< v_2 >^2 - \sigma_{v_2}^2},$$

$$\frac{\sigma_{v_2}}{v_2} = \sqrt{\frac{v_2^2\{2\} - v_2^2\{4\}}{v_2^2\{2\} + v_2^2\{4\}}}.$$

"Fluctuations" larger in pPb, with moderate multiplicity dependence

v_3 in pPb and PbPb

Dash-dot line: peripheral subtracted

multiplicity →

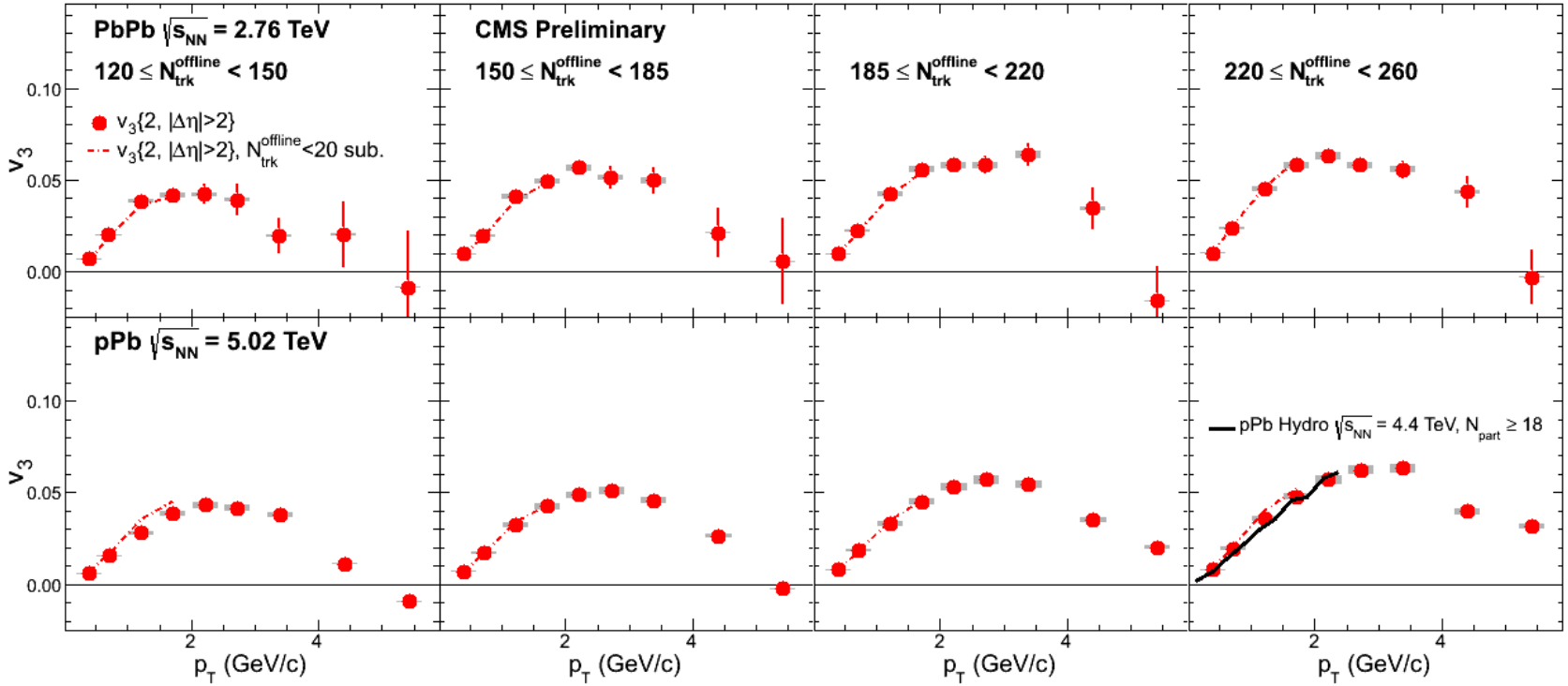

PbPb

pPb

v_3 has similar shape in pPb and PbPb; magnitude comparable

"Peripheral subtraction" makes essentially no difference

Hydro prediction: Bozek, $v_3\{PP\}$, not including fluctuations

v_3 in pPb and PbPb

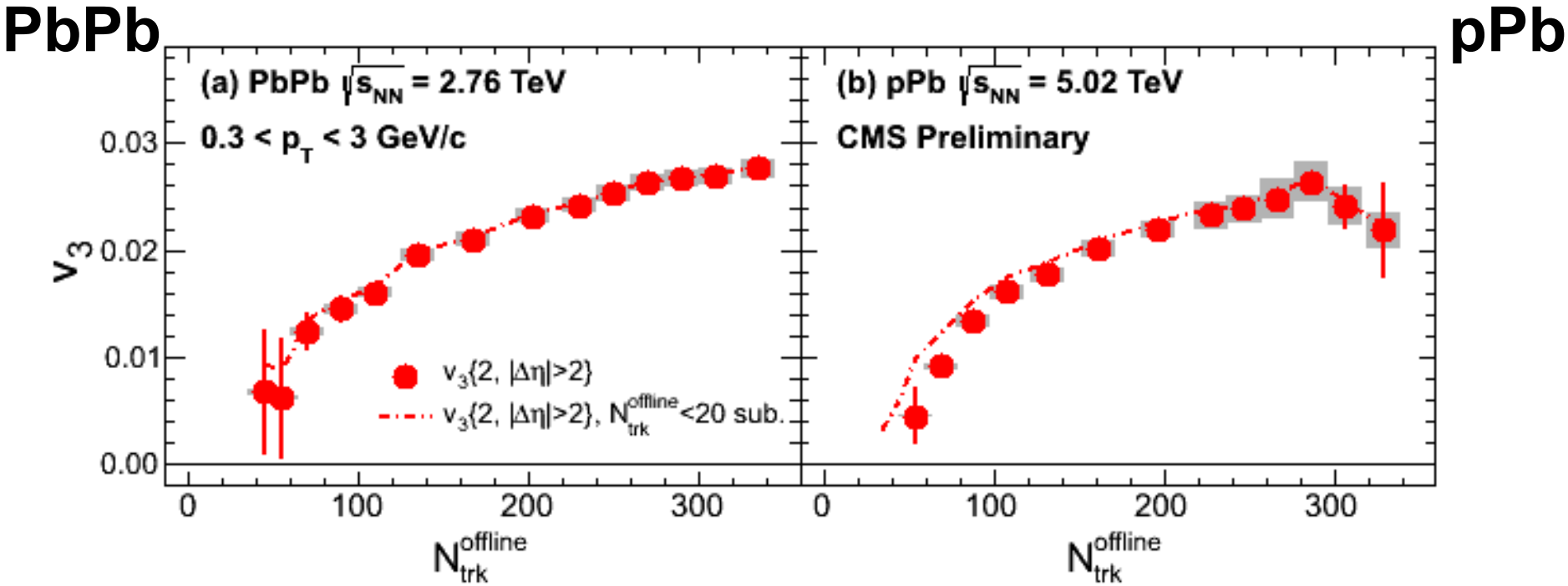

v_3 shows similar shape in pPb and PbPb; magnitude comparable

"Peripheral subtraction" makes essentially no difference

v_2 comparison with ATLAS in pPb

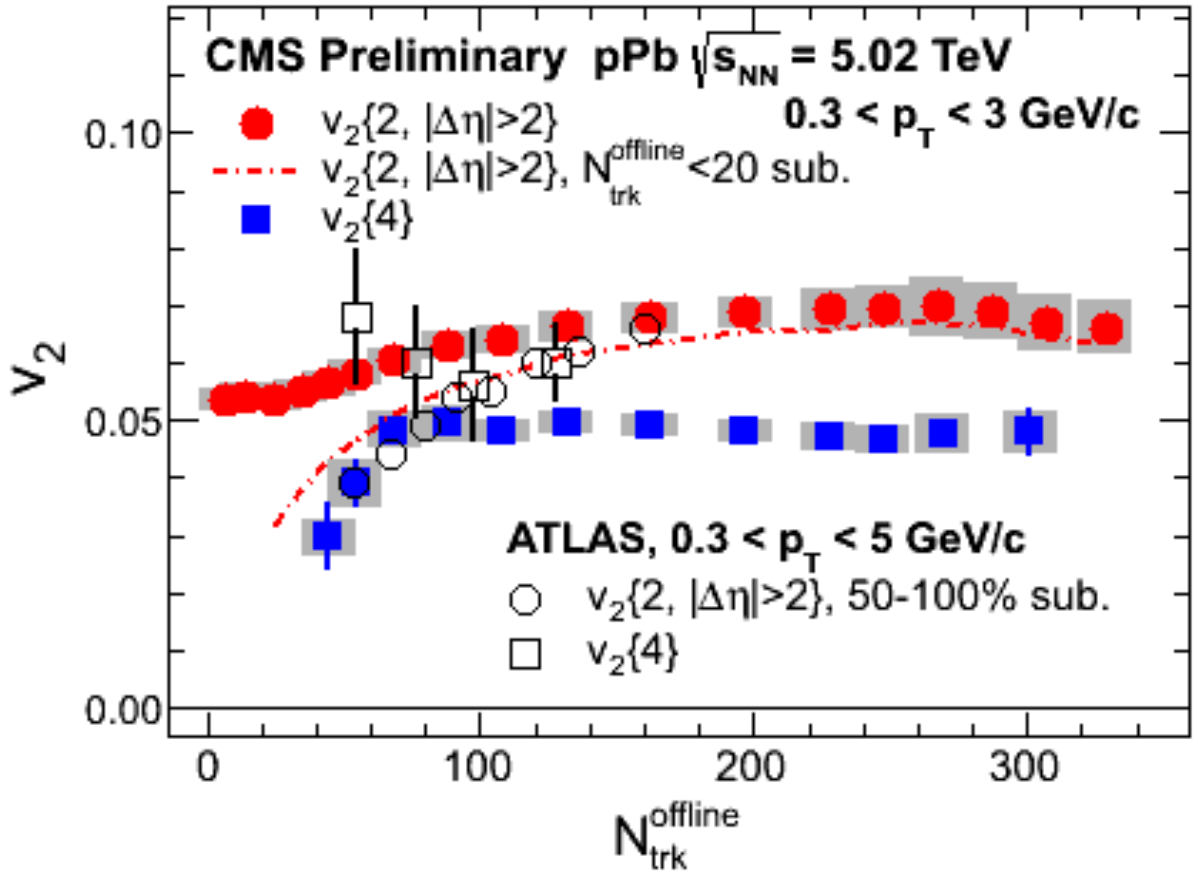

pPb

ATLAS: arXiv: 1303.2084

Subtract $N_{trk}^{offline}$<20 (70-100%) to avoid removing signal

- ATLAS subtract 50-100%; forward-calorimeter centrality

Some difference vs ATLAS in $v_2\{4\}$: multiplicity fluctuations?

Summary

- Direct comparison of high statistics, high multiplicity pPb and PbPb data
  - Studied v_2 multiplicity dependence in pPb and PbPb
  - Somewhat smaller magnitude of v_2 in pPb
  - Large $v_2\{4\}$ in pPb
  - Large $v_3\{2\}$ in pPb (comparable to PbPb)
- Ready to use full arsenal of jet studies in pPb

No ridge anywhere in pPb MC

Compare to AMPT and HIJING pPb

HIJING pPb, N>=120

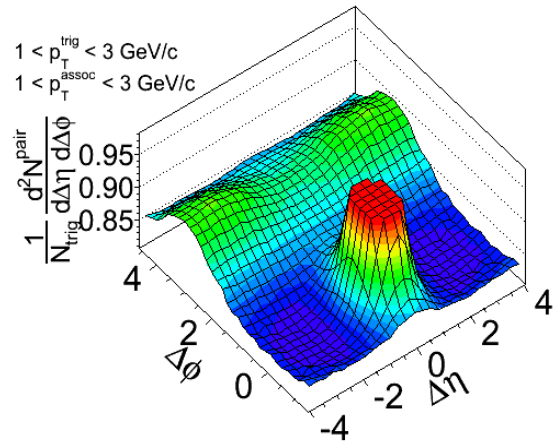

AMPT pPb, N>=100

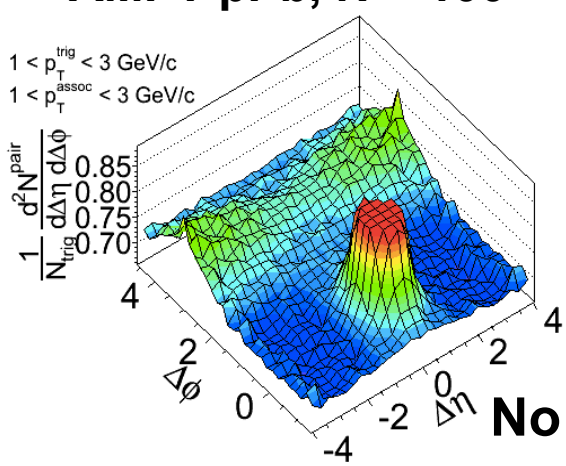

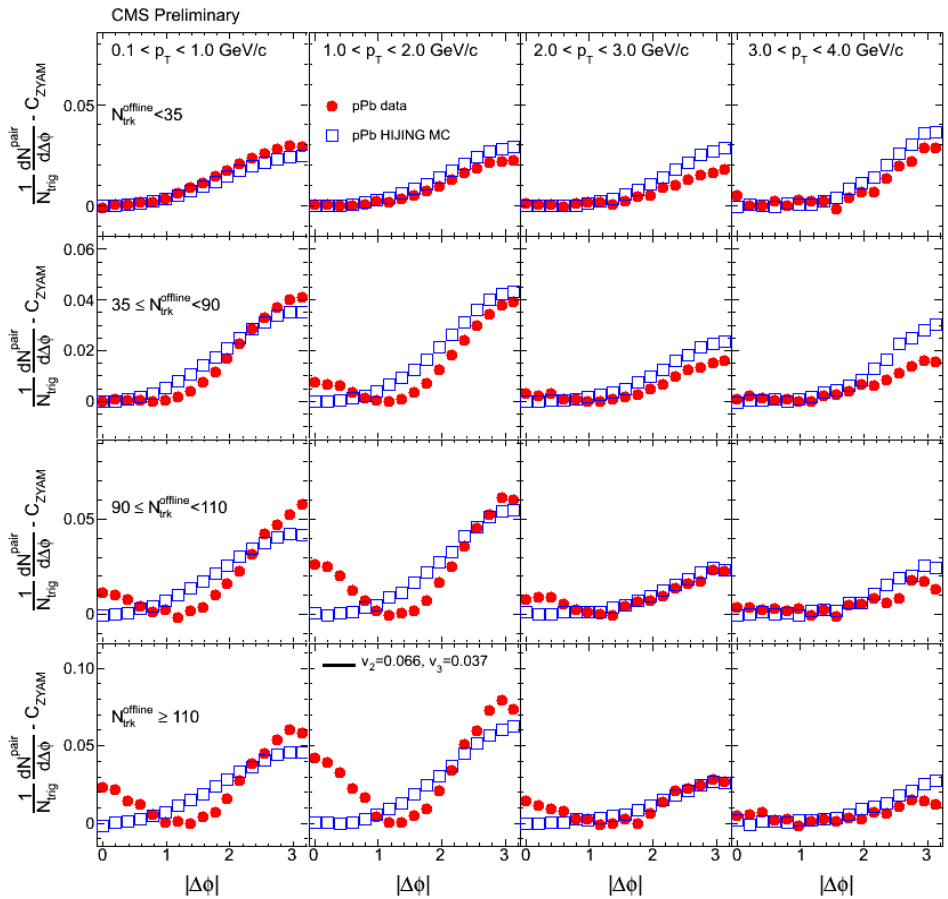

No ridge in these pPb MC!

Triggers and event selection

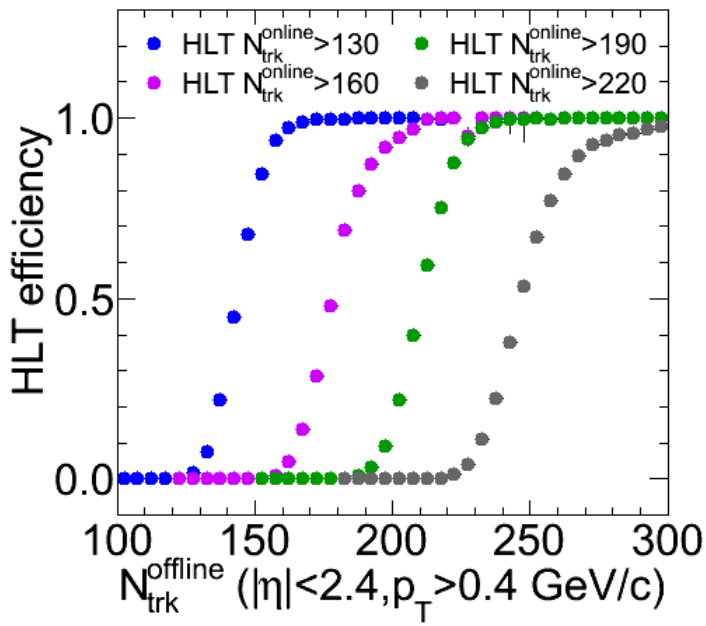

Event selection:

- HF coincidence of at least 1 tower above 3 GeV
- Vertex requirement: !isFake & $|v_z|$<15 cm & position.Rho<0.15 cm & nTracks>=2
- Fraction of highPurity tracks > 25% to remove beam scraping events

Initial conditions in A+A, p+A, d+A and p+p collisions

Björn Schenke
Physics Department, Brookhaven National Laboratory, Upton, NY, USA

April 17 2013

Jet Quenching at RHIC vs LHC in Light of Recent dAu and pPb Controls

BNL, Upton, NY

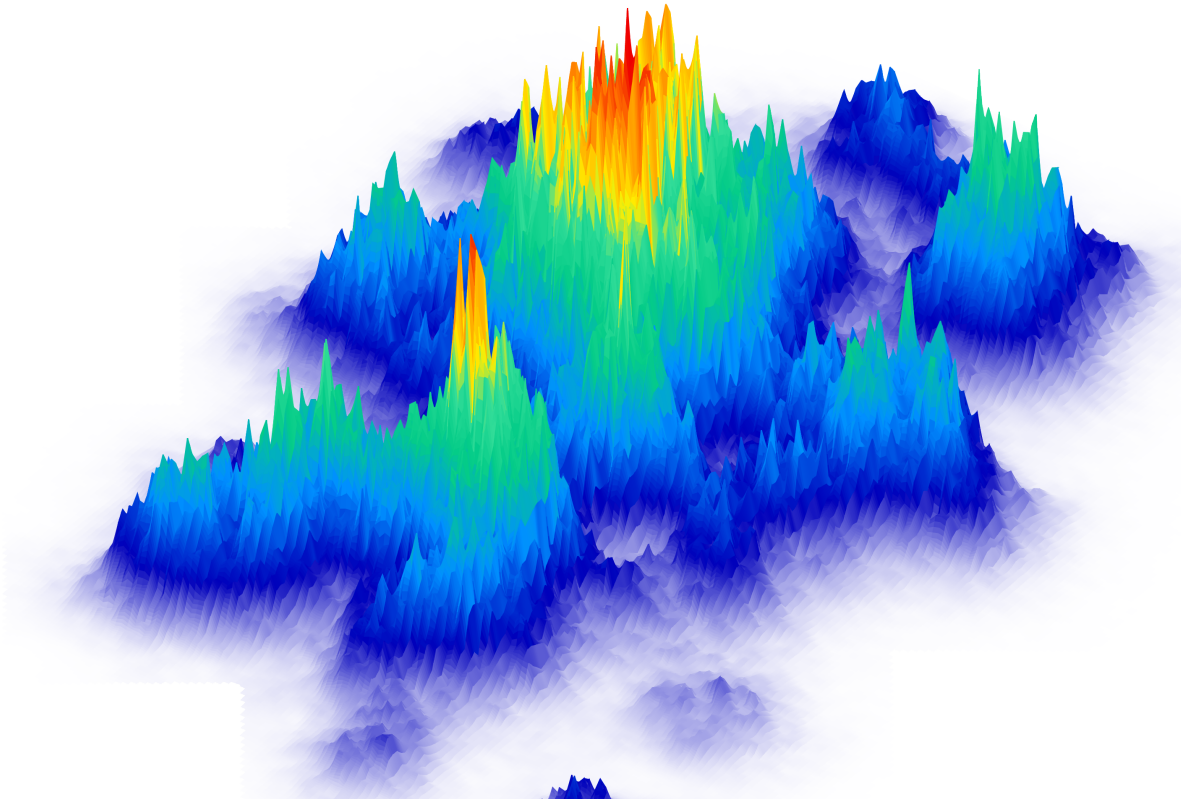

Introduction - Initial state fluctuations and flow

- Large elliptic flow has indicated fluid behavior of matter created at RHIC in early 2000's BNL announces "perfect liquid" in 2005 press release
- The importance of fluctuations in the initial state was realized later and analysis of odd flow harmonics began in 2010
- Measured anisotropic flow is largely due to the response to the initial fluctuating geometry
- Geometry of the medium is relevant for jet evolution
- I will
  - present different models for the initial state in A+A
  - show some results of harmonic flow from these models
  - apply the models to p+p, p+A and d+Au collisions

Modeling the initial state

Flow is driven by the initial geometry
Final result depends on what we start with

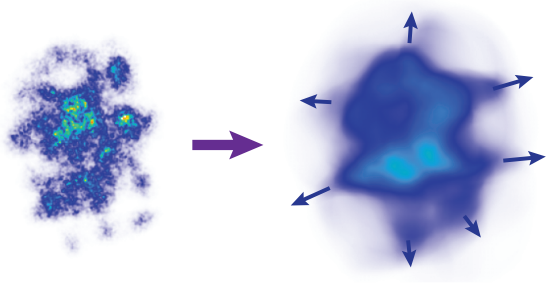

Hard partons are affected by the geometry of the background

We need a rigorous understanding
of the initial state and its fluctuations

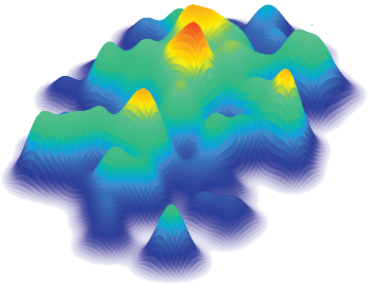

?

MC-Glauber

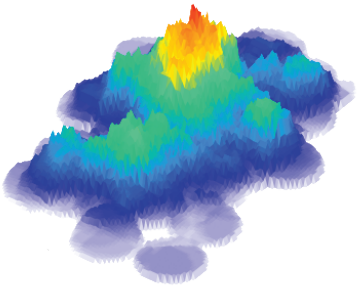

?

MC-KLN

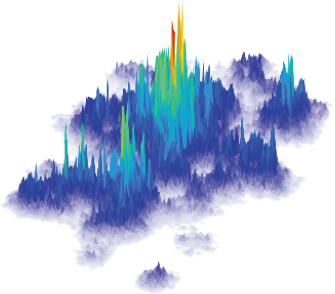

?

IP-Glasma

MC-Glauber

- Sample (un-)correlated nucleons in nucleus A and B, then overlap the two distributions with impact parameter b
- Interaction when the distance d between a nucleon from nucleus A and one from nucleus B fulfills (black disk):

$$d \leq \sqrt{\sigma_{\text{inel}}^{NN}/\pi}$$

(alternatively use a Gaussian overlap function)

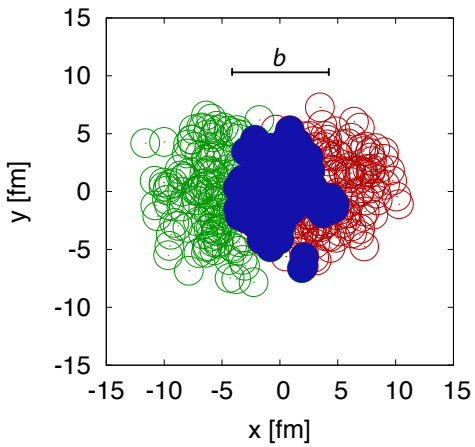

- Add Gaussian energy density with width σ_0 for every wounded nucleon, binary collision, or combination

$$\sigma_0 = 0.4\,\text{fm}$$

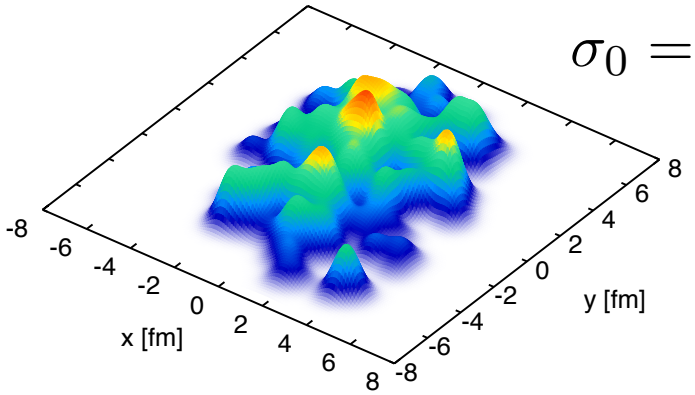

MC-KLN

- Sample nucleon positions from Woods-Saxon distribution
- Local nucleon density $T_{A,B}(\mathbf{x}_\perp)$ from counting nucleons in tube of transverse area $S = \sigma_{\text{inel}}^{NN}$
- Kharzeev-Levin-Nardi (KLN) model for uGDF ϕ:

$$\phi_{A,B}(x, k_\perp^2, \mathbf{r}_\perp) \sim \frac{1}{\alpha_s(Q_s^2)} \frac{Q_s^2}{\max(Q_s^2, k_\perp^2)}$$

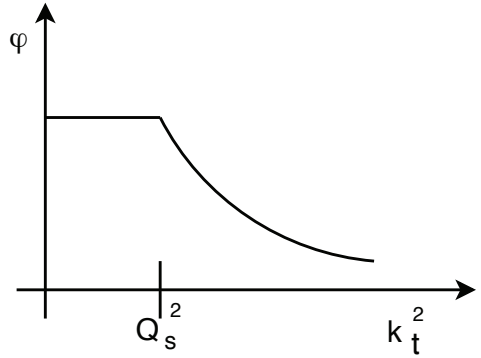

with $Q_{s,A}^2(x, \mathbf{r}_\perp) = 2\,\text{GeV}^2 \frac{T_A(\mathbf{x}_\perp)}{1.53\,\text{fm}^{-2}} \left(\frac{0.01}{x}\right)^\lambda, \lambda = 0.28$

- Determine gluon production using k_T-factorization:

cannot be derived for dense-dense systems
$\rightarrow$ assume it works

$$\frac{dN}{dr_\perp^2 dy} \sim \int \frac{d^2 p_\perp}{p_\perp^2} \int d^2 k_\perp \alpha_s \phi_A(x_1, k_\perp^2) \phi_B(x_2, (p_\perp - k_\perp)^2)$$

- Energy density analogously

Drescher, Nara, Phys.Rev. C75 (2007) 034905

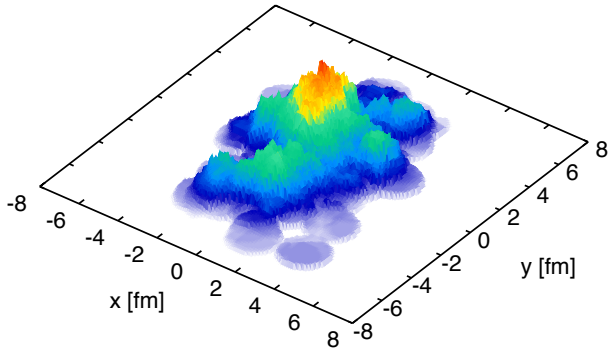

IP-Glasma: before the collision

- Energy and impact parameter b dependence of $Q_s(x, \mathbf{b})$ can be modeled in the IP-Sat model Kowalski, Teaney, Phys.Rev. D68 (2003) 114005
- Parametrize cross sections for DIS on protons and fit to HERA diffractive data
  A. Rezaeian, M. Siddikov, M. Van de Klundert, R. Venugopalan
  Phys.Rev. D87 (2013) 034002

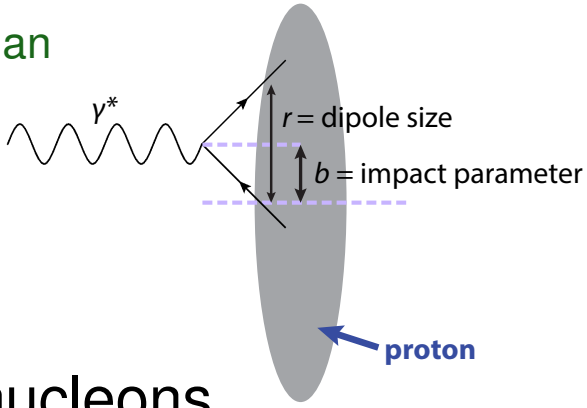

- Sample nucleon positions from Woods-Saxon distribution
- Sum Gaussian thickness functions T_p of A nucleons

$$\frac{\mathrm{d}\sigma^{\mathrm{p}}_{\mathrm{dip}}}{\mathrm{d}^2\mathbf{b}_\perp}(\mathbf{r}_\perp, x, \mathbf{b}_\perp) = 2\,\mathcal{N}(\mathbf{r}_\perp, x, \mathbf{b}_\perp) = 2\left[1 - \exp\left(-\frac{\pi^2}{2N_c}\mathbf{r}_\perp{}^2\alpha_s(Q^2)xg(x, Q^2)\sum_{i=1}^{A} T_p(\mathbf{b}_\perp - \mathbf{b}_T^i)\right)\right]$$

then determine local $Q_s(\mathbf{x}_\perp)$ $(\mathcal{N}(1/Q_s(x, \mathbf{x}_\perp), x, \mathbf{x}_\perp) = 1 - e^{-1/2})$

- Color charge density $g\mu(\mathbf{x}_\perp)$ is proportional to $Q_s(\mathbf{x}_\perp)$

IP-Glasma: before the collision

- Self-consistently solve $x = Q_s(\mathbf{x}_\perp, x)/\sqrt{s}$
- Run the coupling with $Q_s(\mathbf{x}_\perp)$
- Sample color charges ρ^a from local Gaussian

$$\langle \rho^a(\mathbf{x}_\perp)\rho^b(\mathbf{y}_\perp)\rangle = \delta^{ab}\delta^2(\mathbf{x}_\perp - \mathbf{y}_\perp)g^2\mu^2(\mathbf{x}_\perp)$$

- Color charges determine incoming color currents:

$$J_1^\nu = \delta^{\mu+}\rho_1(x^-, \mathbf{x}_\perp)$$
$$[D_\mu, F^{\mu\nu}] = J_1^\nu$$

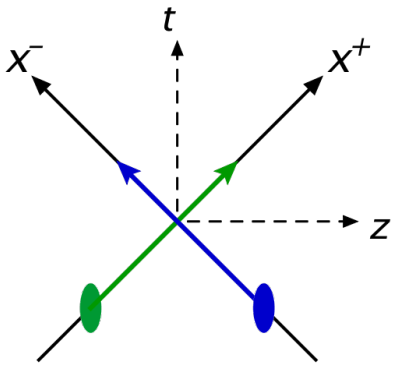

$$J_2^\nu = \delta^{\mu-}\rho_2(x^+, \mathbf{x}_\perp)$$
$$[D_\mu, F^{\mu\nu}] = J_2^\nu$$

- Solve Yang-Mills equations for the gauge fields
  $A^+(x^-, \mathbf{x}_\perp) = -\frac{g\rho(x^-, \mathbf{x}_\perp)}{\nabla_\perp^2 + m^2}$

IP-Glasma: after the collision

Initial condition on the lightcone:

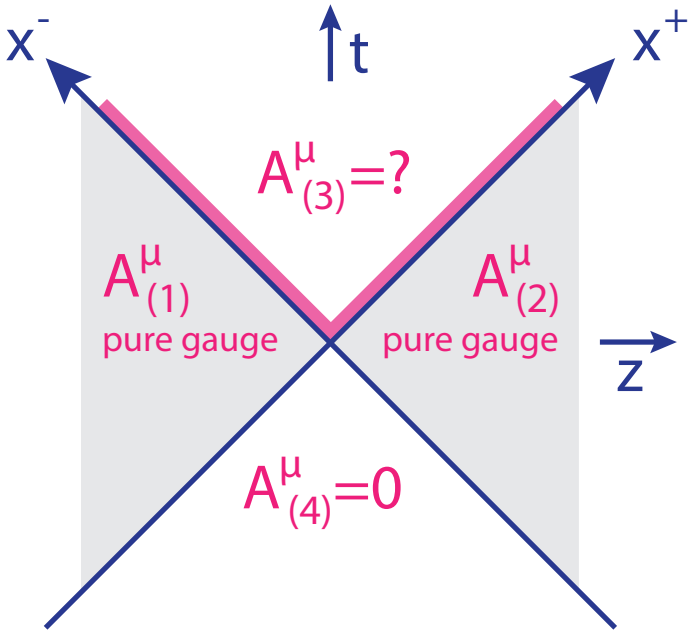

Configuration in Schwinger gauge $A^\tau = 0$

Solution:

Kovner, McLerran, Weigert, Phys. Rev. D52, 3809 (1995)

$$A^i_{(3)}|_{\tau=0} = A^i_{(1)} + A^i_{(2)}$$

$$A^\eta_{(3)}|_{\tau=0} = \frac{ig}{2}[A^i_{(1)}, A^i_{(2)}]$$

Numerical solution

Krasnitz, Venugopalan, Nucl.Phys. B557 (1999) 237

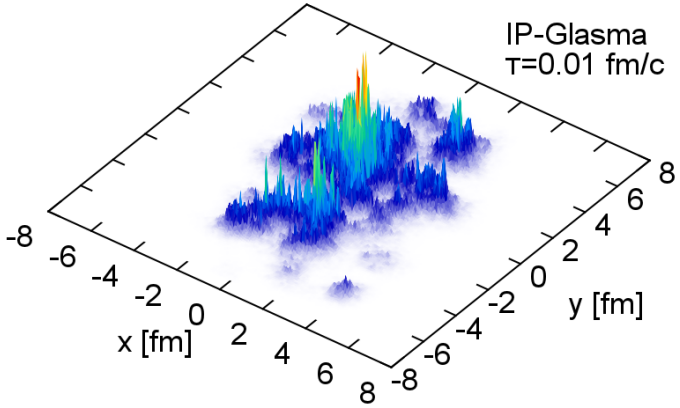

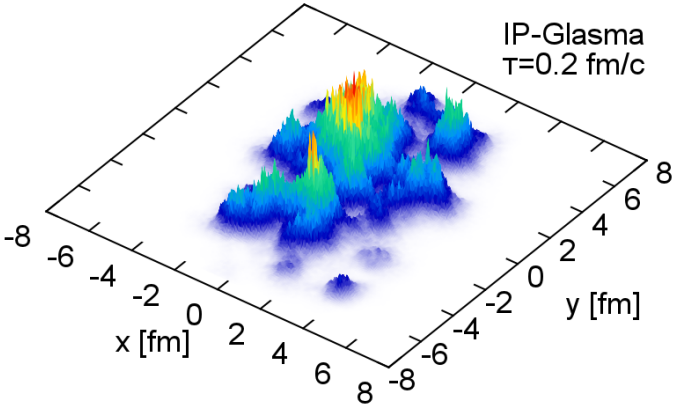

Eccentricities B.Schenke, P.Tribedy, R.Venugopalan, Phys.Rev.Lett. 108, 252301 (2012)

Characterize the initial distribution by its ellipticity, triangularity, etc...

$$\varepsilon_n = \sqrt{\langle r^n \cos(n\phi)\rangle^2 + \langle r^n \sin(n\phi)\rangle^2} / \langle r^n \rangle$$

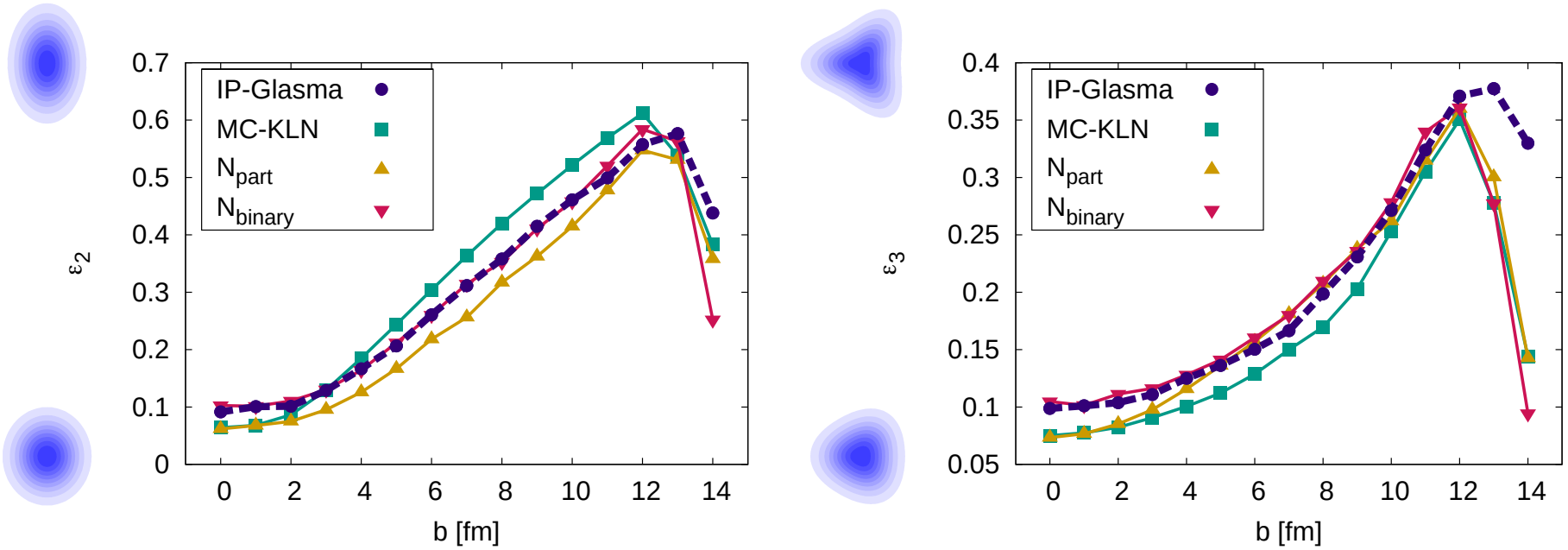

- ε_2 smaller in IP-Glasma than MC-KLN for (for $b > 3\,\mathrm{fm}$)
- ε_2 and ε_3 very similar between IP-Glasma and MC-Glauber with binary collision scaling

Multiplicity B.Schenke, P.Tribedy, R.Venugopalan, Phys. Rev. C86, 034908 (2012)

$P(dN_g/dy)$ at time $\tau = 0.4\,\mathrm{fm}$ with $P(b)$ from a Glauber model

Experimental data: STAR, Phys. Rev. C79, 034909 (2009)

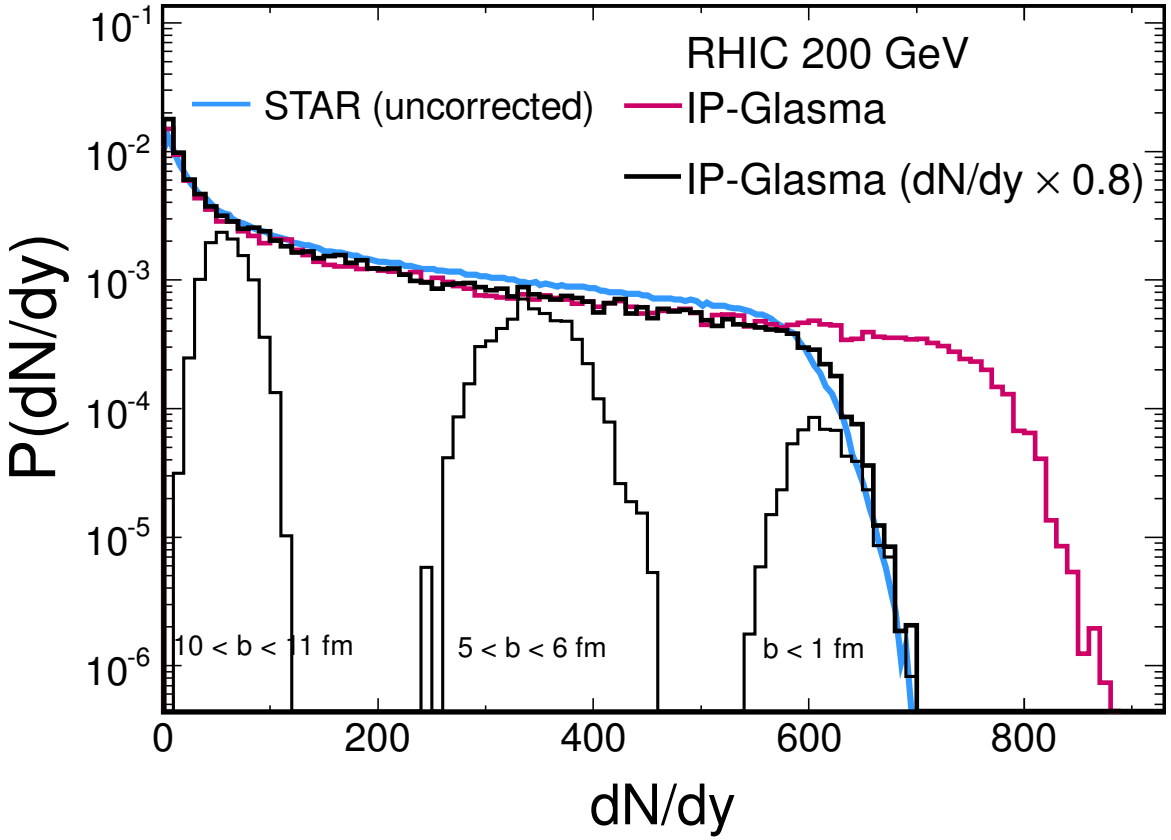

Glasma model gives a convolution of negative binomial distributions

No need to put them in by hand

Negative binomial fluctuations

B.Schenke, P.Tribedy, R.Venugopalan, Phys.Rev.Lett.108, 252301 (2012)

Fluctuations in the total energy per unit rapidity produce negative binomial distribution (NBD).

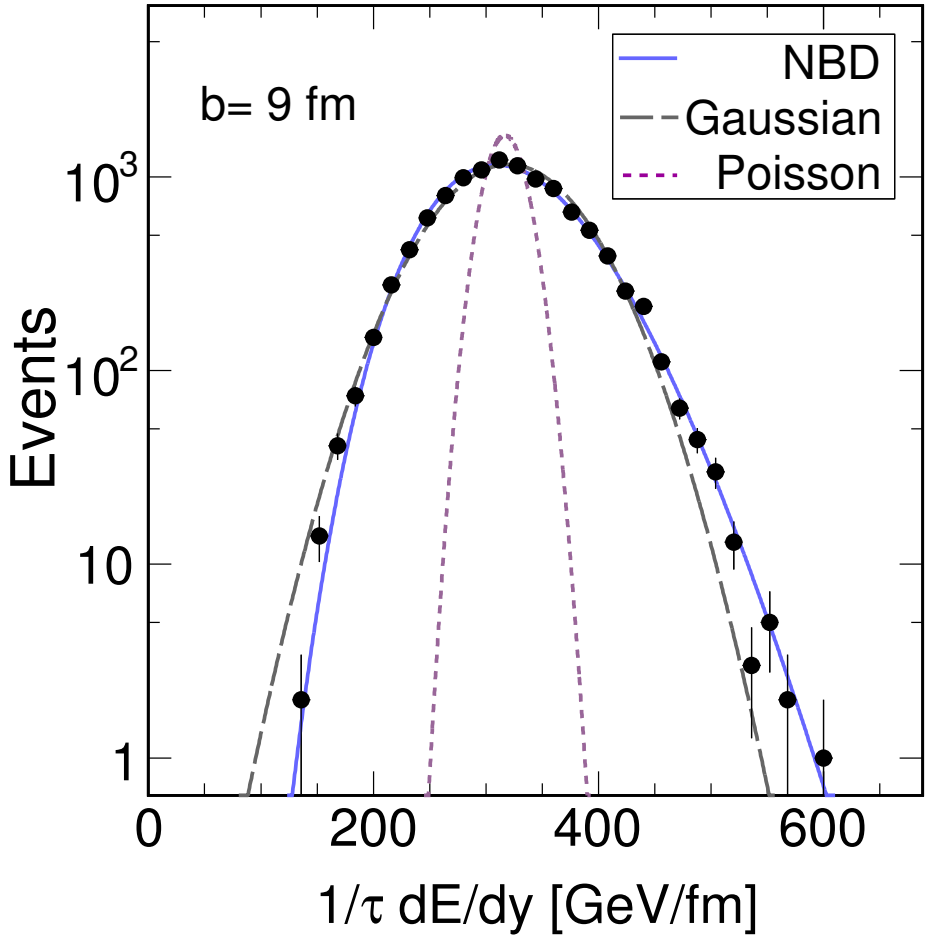

$$P(n) = \frac{\Gamma(k+n)}{\Gamma(k)\Gamma(n+1)} \frac{\bar{n}^n k^k}{(\bar{n}+k)^{n+k}}$$

Good, since multiplicity in pp collisions can be described well with NBD.

In AA, convolution of NBDs at all impact parameters describes data well too.

P. Tribedy and R. Venugopalan
Nucl.Phys. A850 (2011) 136-156

MC-KLN does not do that - these fluctuations need to be added by hand.
see Dumitru and Nara, Phys.Rev. C85 (2012) 034907

Viscous flow at RHIC and LHC

C. Gale, S. Jeon, B.Schenke, P.Tribedy, R.Venugopalan, PRL110, 012302 (2013)

RHIC $\eta/s = 0.12$

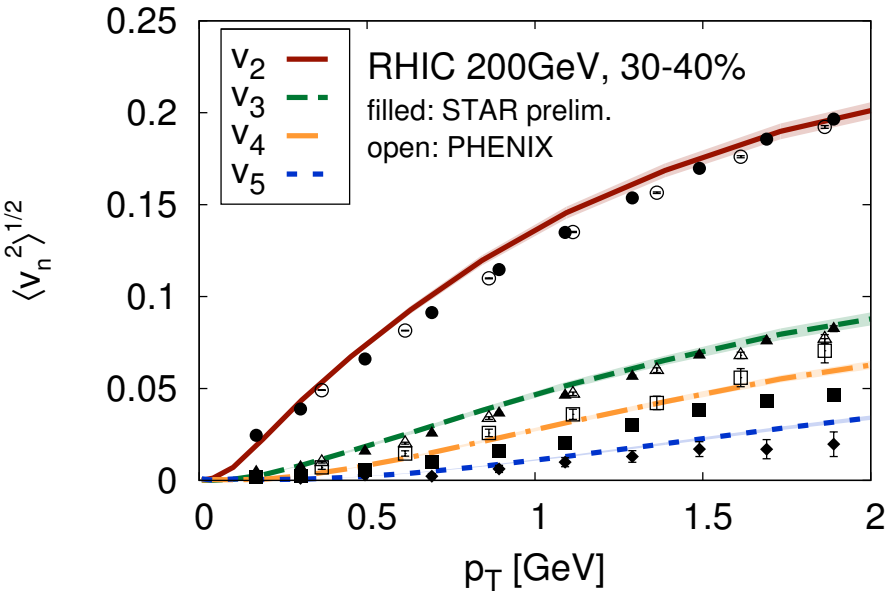

LHC $\eta/s = 0.2$

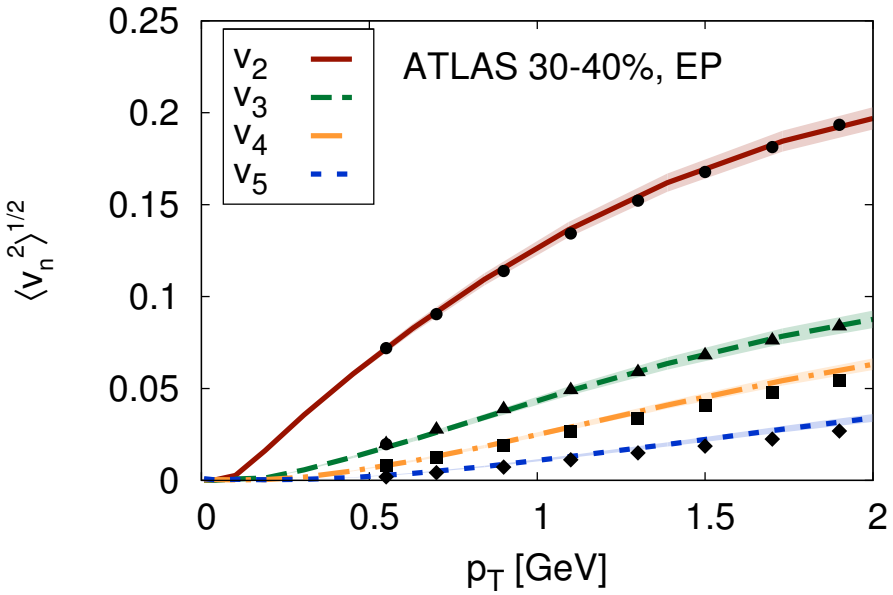

Initial state fluctuations + flow work to describe v_n in A+A

Lower effective η/s at RHIC than at LHC needed to describe data

Hints at increasing η/s with increasing temperature

Experimental data:

A. Adare et al. (PHENIX Collaboration), Phys.Rev.Lett. 107, 252301 (2011)

Y. Pandit (STAR Collaboration), Quark Matter 2012, (2012)

ATLAS collaboration, Phys. Rev. C 86, 014907 (2012)

Event-by-event distributions of v_n

Experimenatal data:
ATLAS collaboration https://atlas.web.cern.ch/Atlas/GROUPS/PHYSICS/CONFNOTES/ATLAS-CONF-2012-114/
J. Jia, S. Mohapatra, arXiv:1304.1471

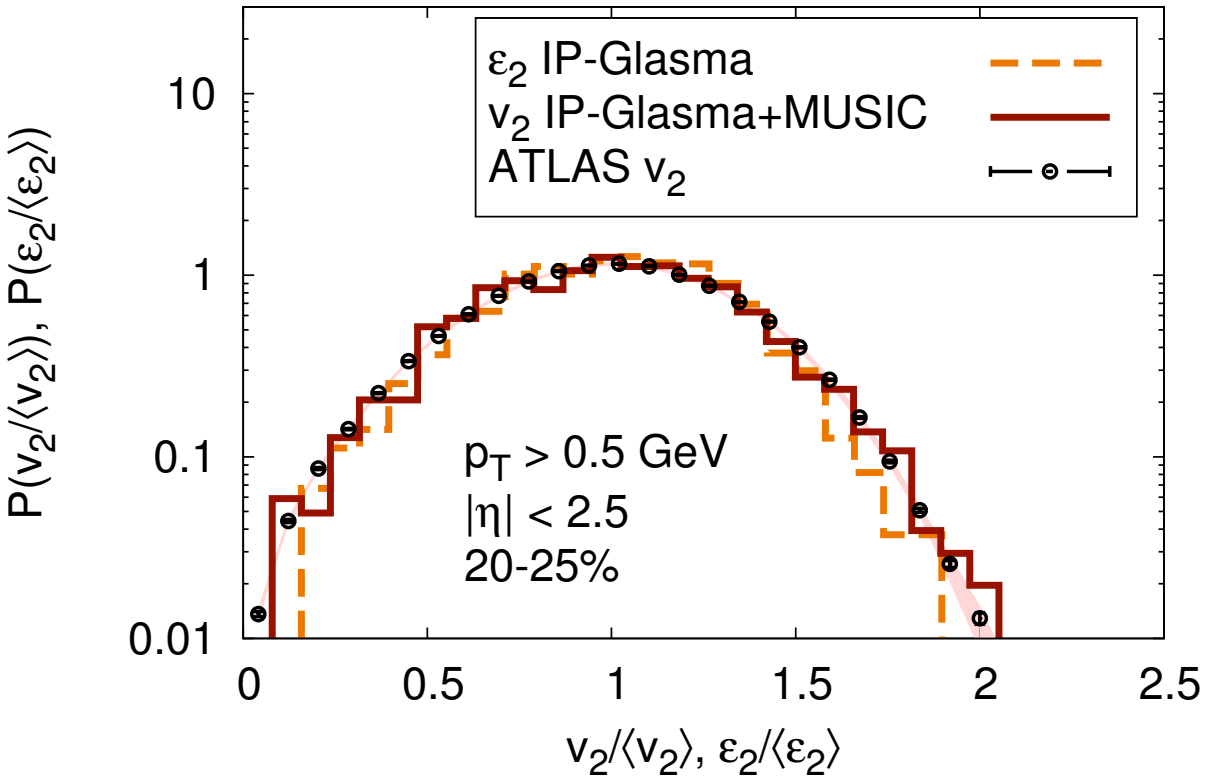

C. Gale, S. Jeon, B.Schenke, P.Tribedy, R.Venugopalan, PRL110, 012302 (2013)

Event-by-event distributions of v_n

Experimenatal data:
ATLAS collaboration https://atlas.web.cern.ch/Atlas/GROUPS/PHYSICS/CONFNOTES/ATLAS-CONF-2012-114/
J. Jia, S. Mohapatra, arXiv:1304.1471

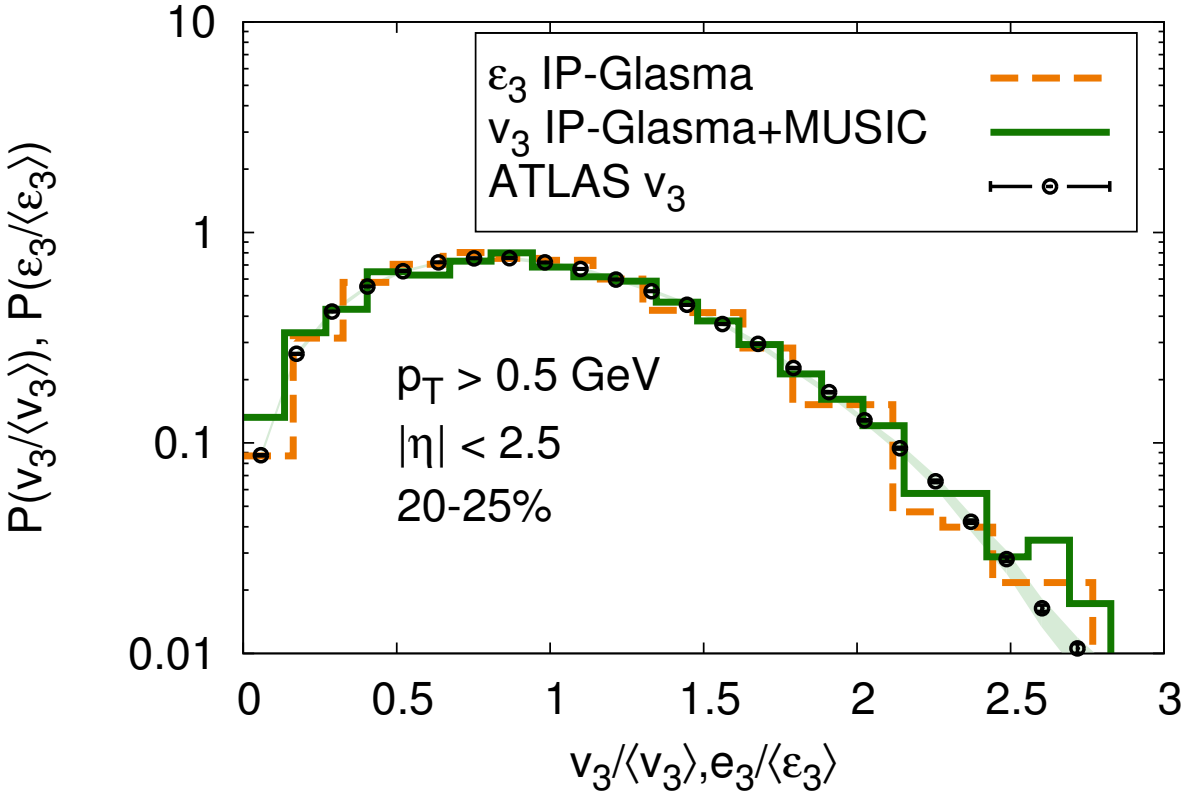

C. Gale, S. Jeon, B.Schenke, P.Tribedy, R.Venugopalan, PRL110, 012302 (2013)

Event-by-event distributions of v_n

Experimenatal data:
ATLAS collaboration https://atlas.web.cern.ch/Atlas/GROUPS/PHYSICS/CONFNOTES/ATLAS-CONF-2012-114/
J. Jia, S. Mohapatra, arXiv:1304.1471

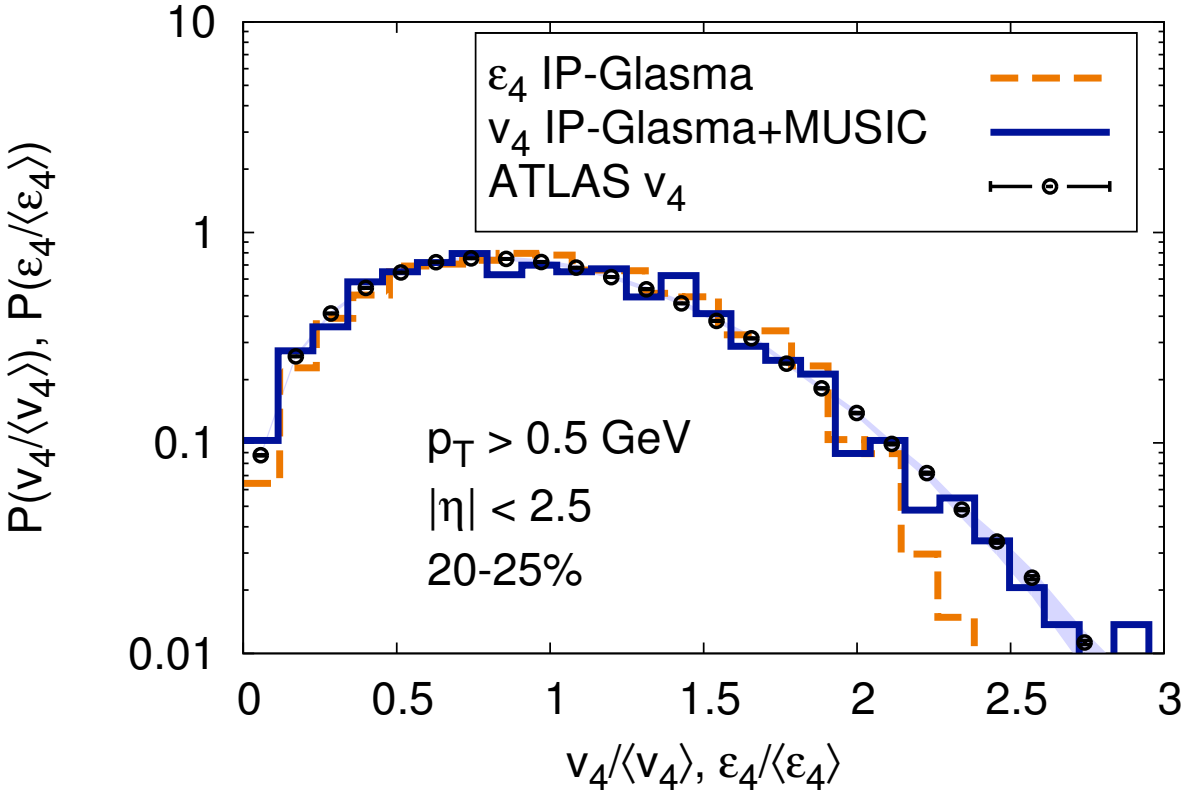

C. Gale, S. Jeon, B.Schenke, P.Tribedy, R.Venugopalan, PRL110, 012302 (2013)

Event-by-event distributions of v_n

Experimenatal data:
ATLAS collaboration https://atlas.web.cern.ch/Atlas/GROUPS/PHYSICS/CONFNOTES/ATLAS-CONF-2012-114/
J. Jia, S. Mohapatra, arXiv:1304.1471

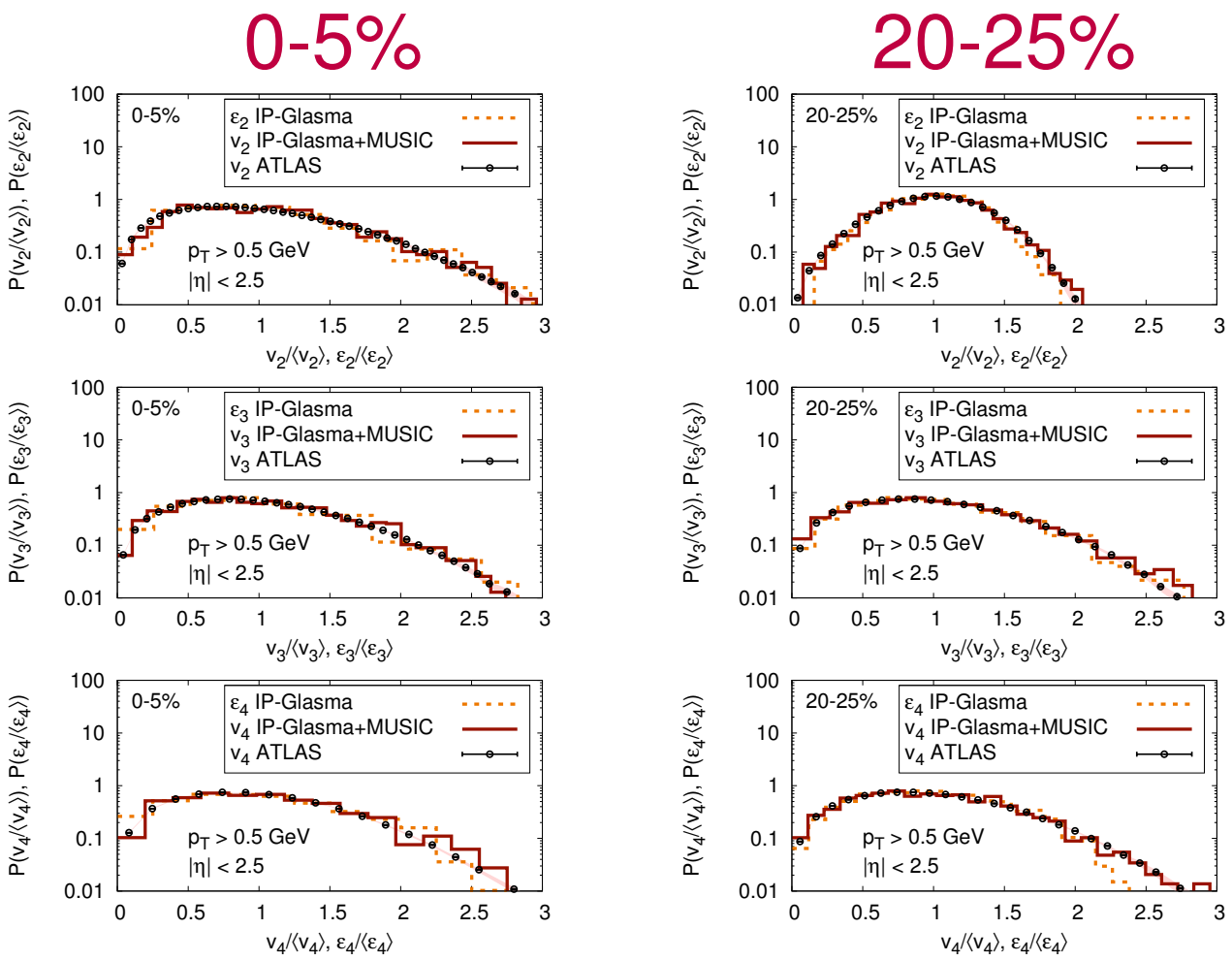

C. Gale, S. Jeon, B.Schenke, P.Tribedy, R.Venugopalan, PRL110, 012302 (2013)

Event-by-event distributions of v_n - other models

Showing eccentricity distributions (yellow on the right)

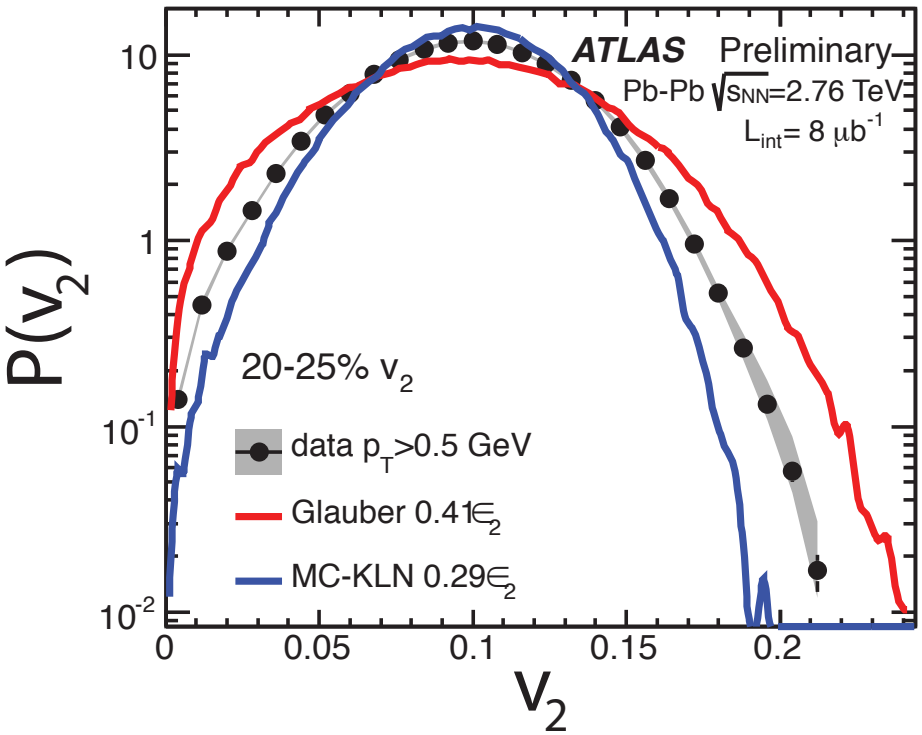

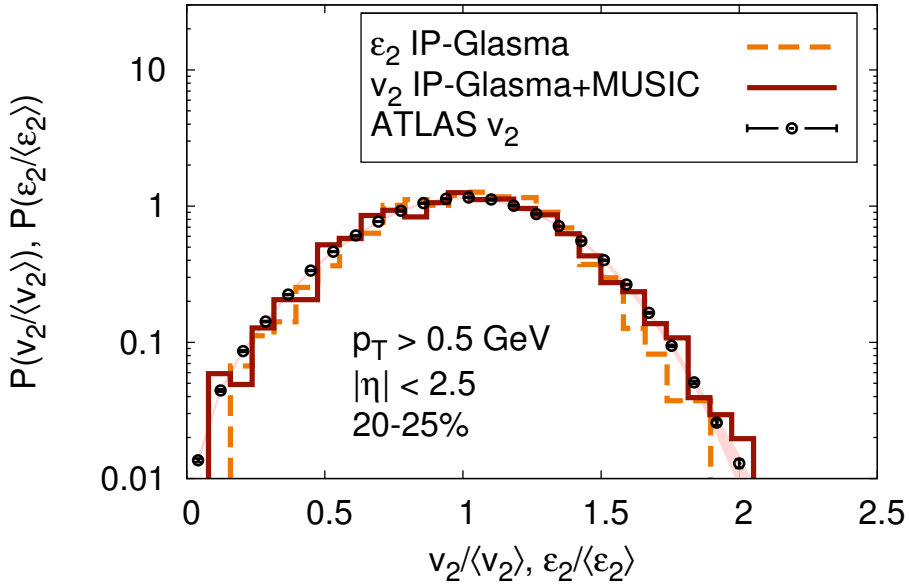

Event-by-event distributions can potentially distinguish between different initial state models

Experimental data: `https://atlas.web.cern.ch/Atlas/GROUPS/PHYSICS/CONFNOTES/ATLAS-CONF-2012-114/`

d+Au collisions A. Bzdak, B. Schenke, P. Tribedy, R. Venugopalan, arXiv:1304.3403

In small systems the different models lead to very different intial states

Energy density for the same nucleon positions:

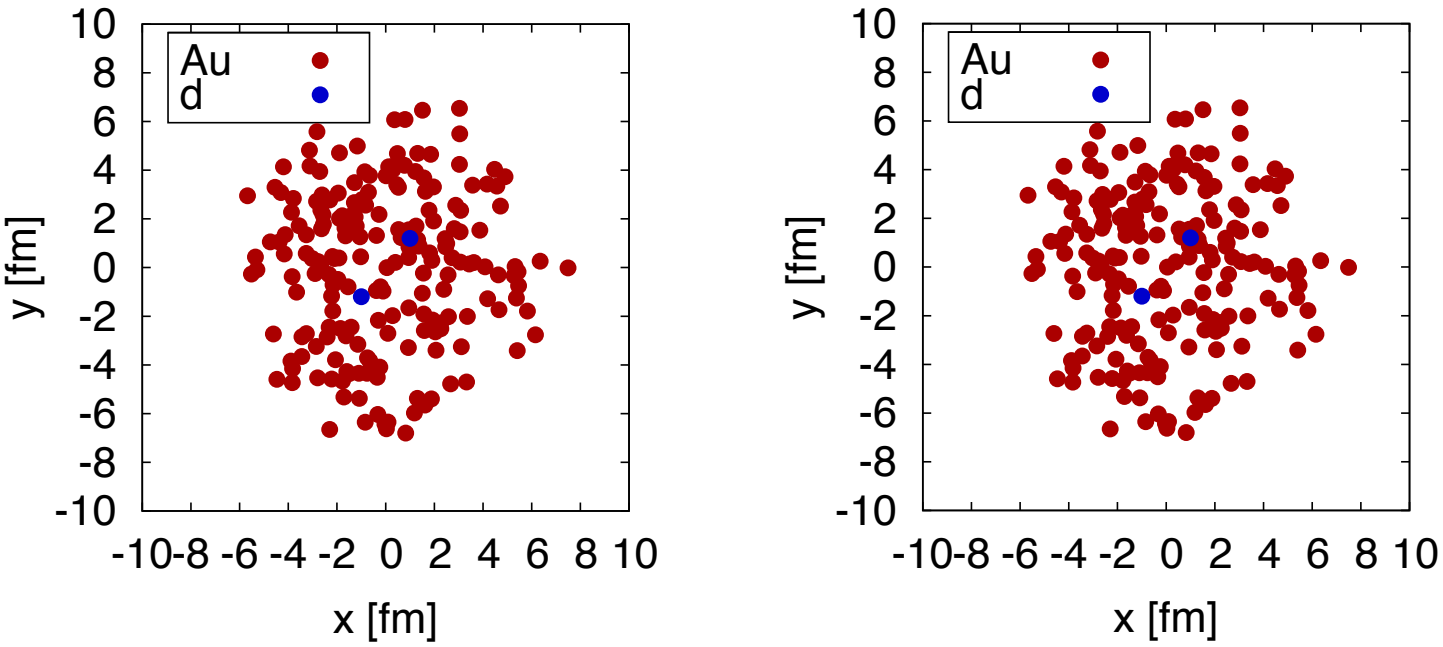

In MC-Glauber all nucleons that are barely 'touched' contribute fully to the energy density

an MC-Glauber implementation is used in e.g. P. Bozek, Phys.Rev. C85 (2012) 014911

d+Au collisions A. Bzdak, B. Schenke, P. Tribedy, R. Venugopalan, arXiv:1304.3403

In small systems the different models lead to very different intial states

Energy density for the same nucleon positions:

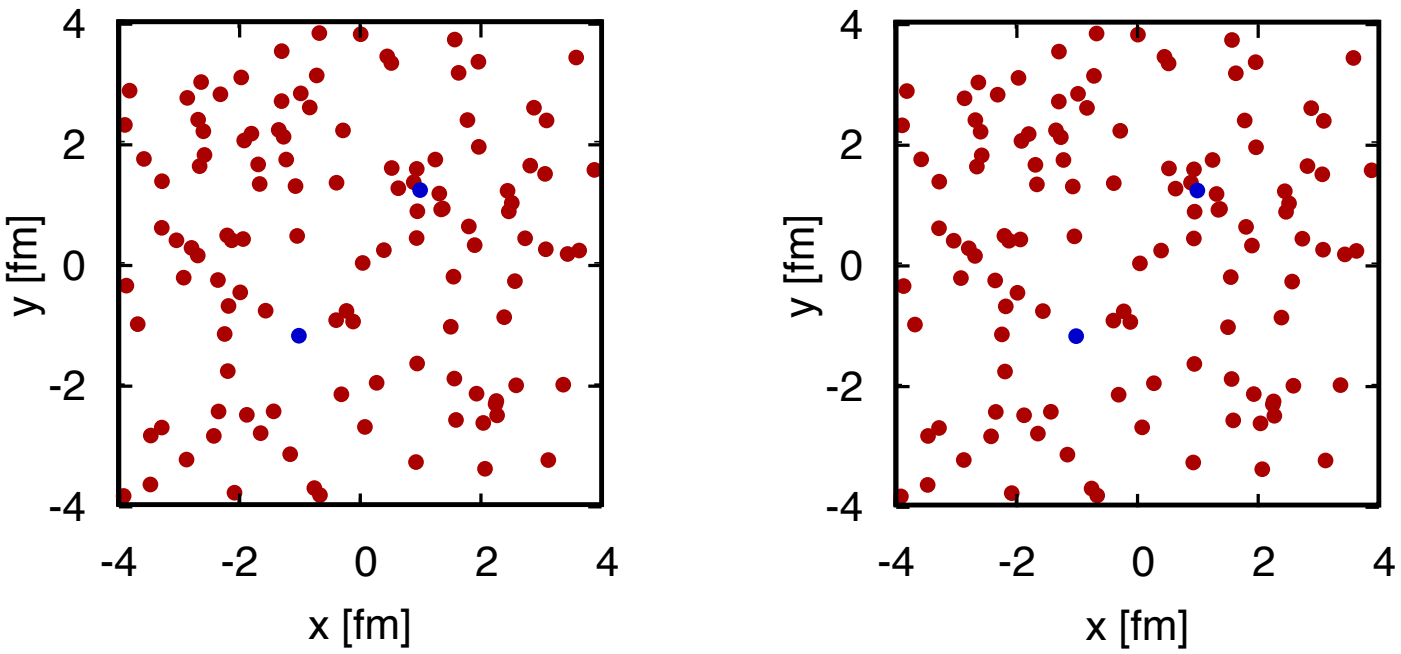

In MC-Glauber all nucleons that are barely 'touched' contribute fully to the energy density

an MC-Glauber implementation is used in e.g. P. Bozek, Phys.Rev. C85 (2012) 014911

d+Au collisions A. Bzdak, B. Schenke, P. Tribedy, R. Venugopalan, arXiv:1304.3403

In small systems the different models lead to very different intial states

Energy density for the same nucleon positions:

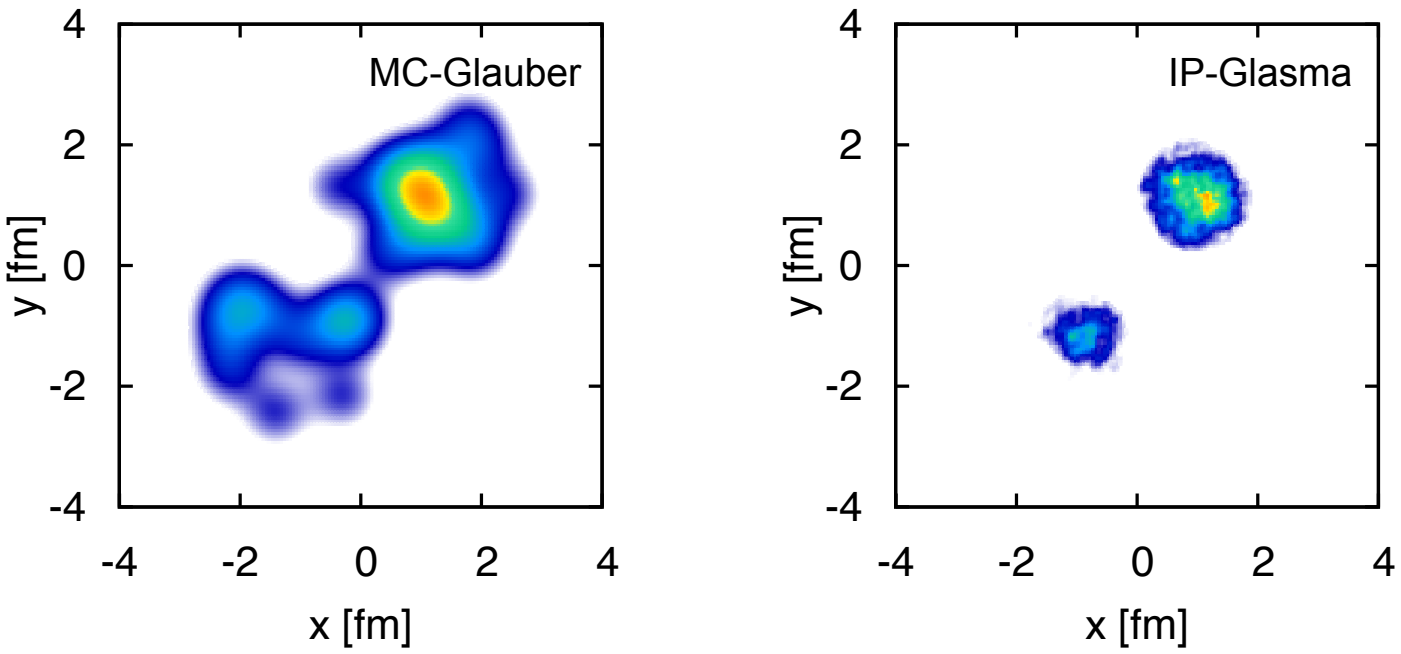

In MC-Glauber all nucleons that are barely 'touched' contribute fully to the energy density

an MC-Glauber implementation is used in e.g. P. Bozek, Phys.Rev. C85 (2012) 014911

d+Au collisions A. Bzdak, B. Schenke, P. Tribedy, R. Venugopalan, arXiv:1304.3403

In small systems the different models lead to very different intial states

Energy density for the same nucleon positions:

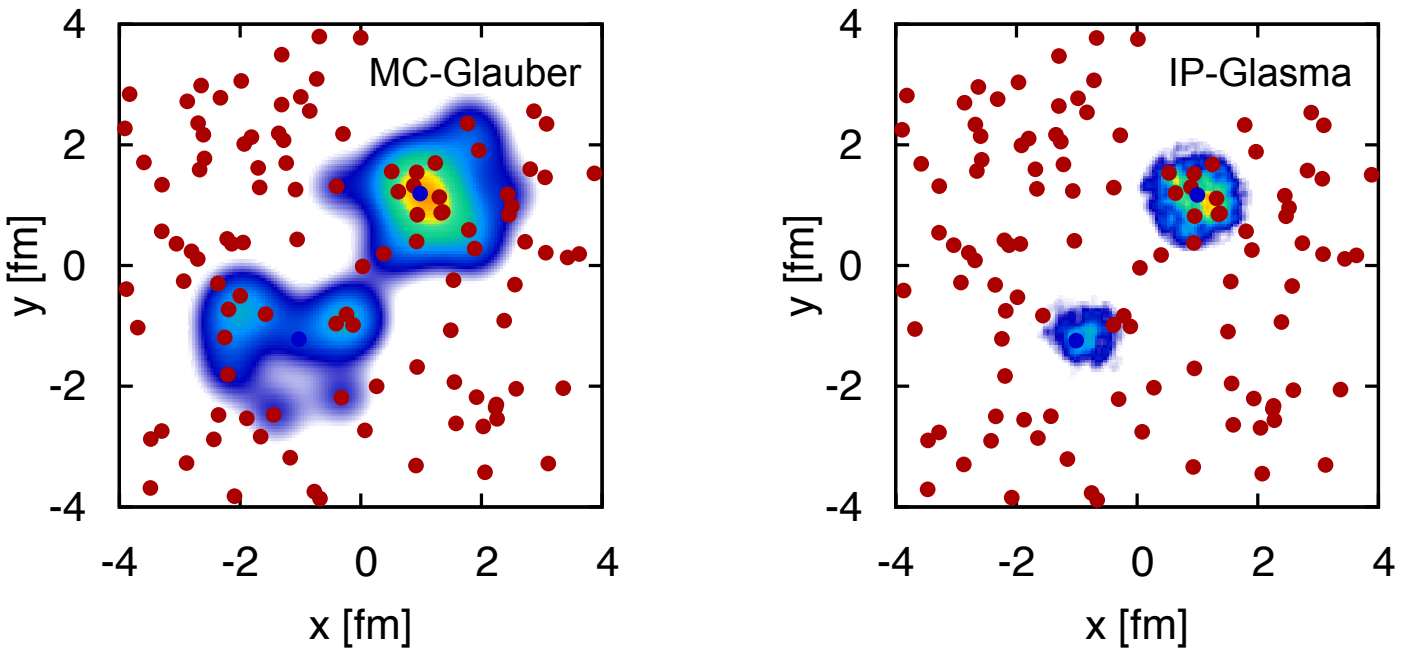

In MC-Glauber all nucleons that are barely 'touched' contribute fully to the energy density

an MC-Glauber implementation is used in e.g. P. Bozek, Phys.Rev. C85 (2012) 014911

Evolution in d+Au

Energy density and initial flow velocity from $u_\mu T^{\mu\nu} = \varepsilon u^\nu$ as input for hydrodynamic simulation

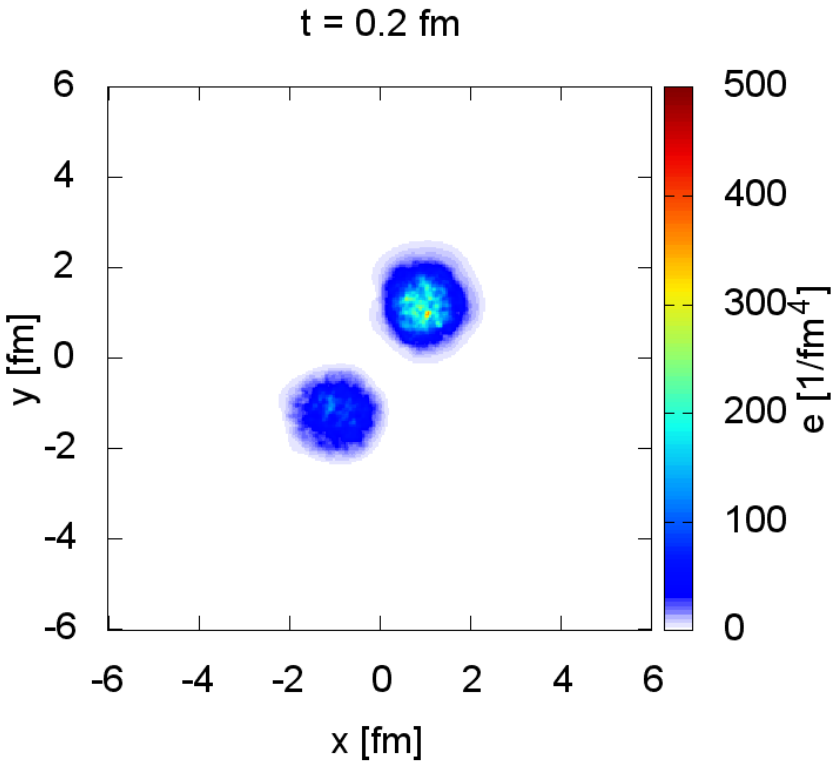

Evolution in d+Au

Energy density and initial flow velocity from $u_\mu T^{\mu\nu} = \varepsilon u^\nu$ as input for hydrodynamic simulation

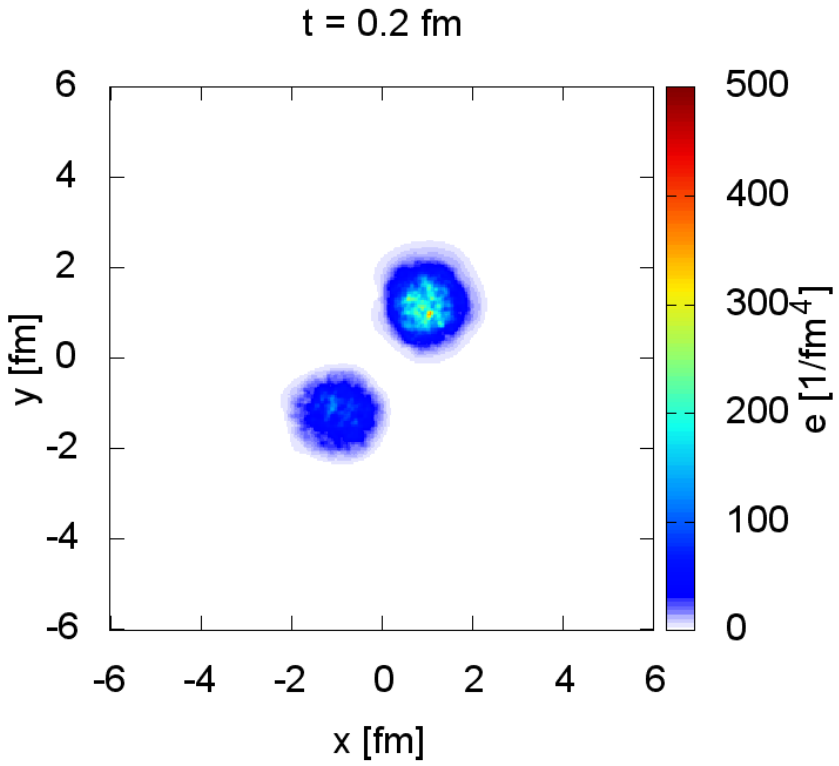

p+p and p+Pb collisions A. Bzdak, B. Schenke, P. Tribedy, R. Venugopalan, arXiv:1304.3403

Initial system size (vs dN/dy) in p+p and p+Pb collisions is very similar in the IP-Glasma model

$r_{\max}$ = maximal radius at which energy density is above $\sim \Lambda^4_{\mathrm{QCD}}$

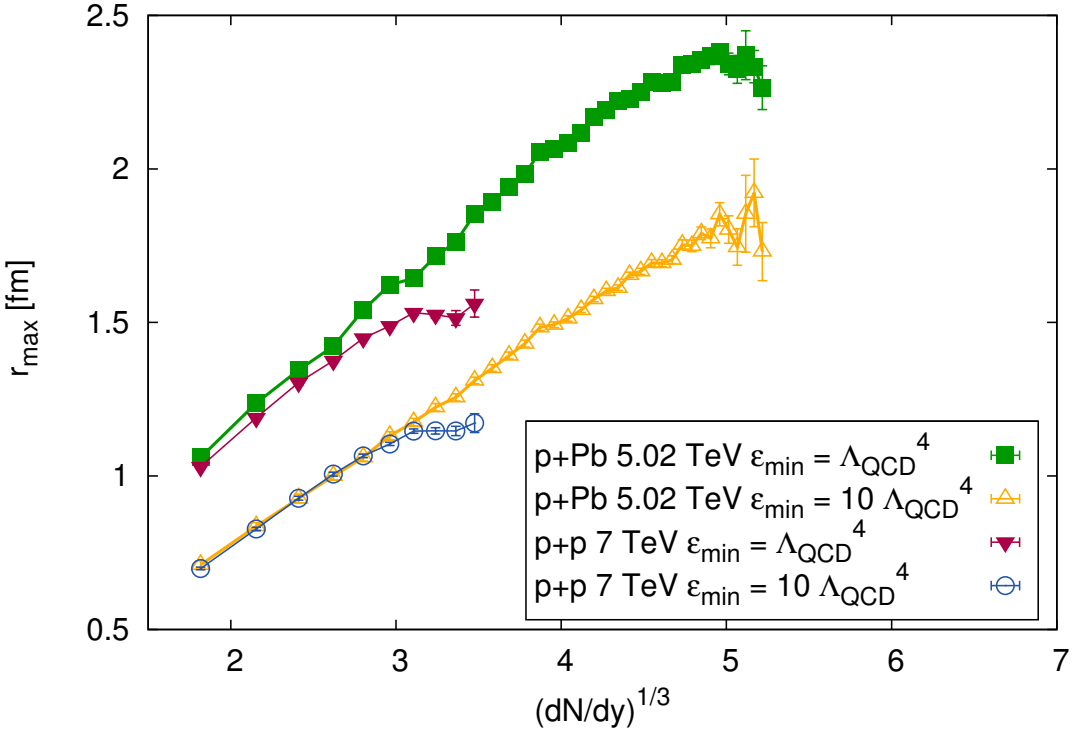

If there is no flow in either system, HBT radii will be similar

p+p and p+Pb collisions A. Bzdak, B. Schenke, P. Tribedy, R. Venugopalan, arXiv:1304.3403

Initial eccentricities (vs dN/dy) in p+p and p+Pb collisions are quite different in the IP-Glasma model

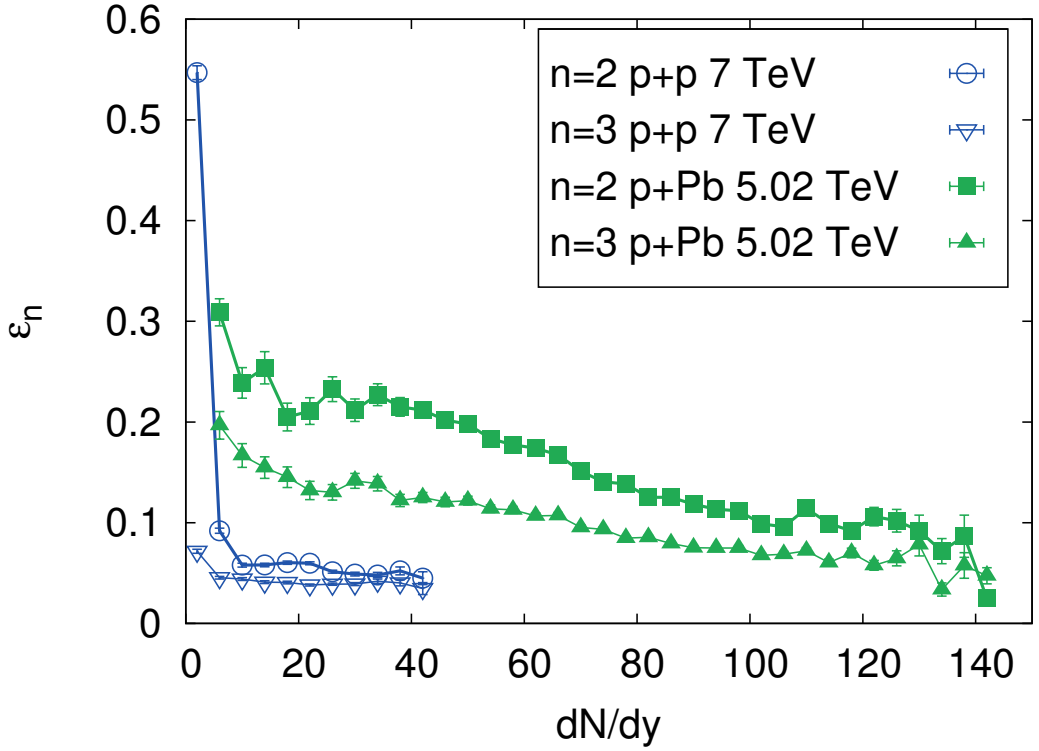

How well do eccentricities represent flow in p+p and p+Pb collisions?

p+Pb collisions A. Bzdak, B. Schenke, P. Tribedy, R. Venugopalan, arXiv:1304.3403

Eccentricities from different models can differ significantly

MC-Glauber 1 MC-Glauber 2

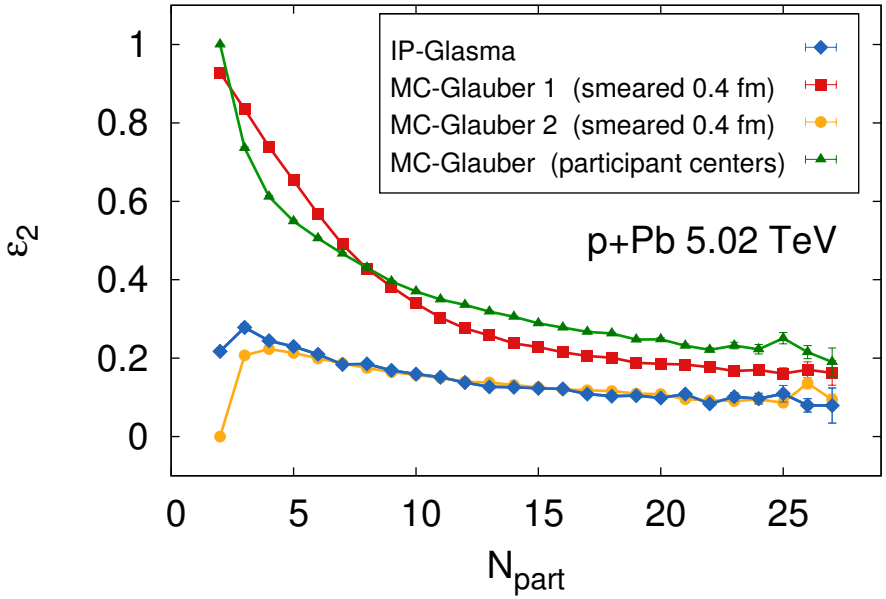

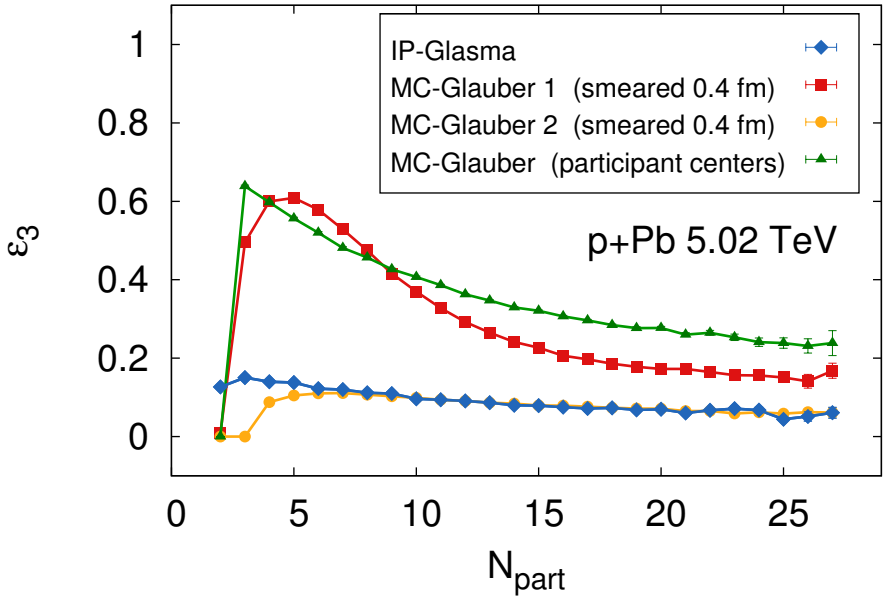

Lesson: Do not divide v_n by ε_n in small systems

Flow in p+p, p+Pb and d+Au collisions

Only qualitative scaling between flow and eccentricities

p+p (at $b = 0\,\mathrm{fm}$) and p+Pb

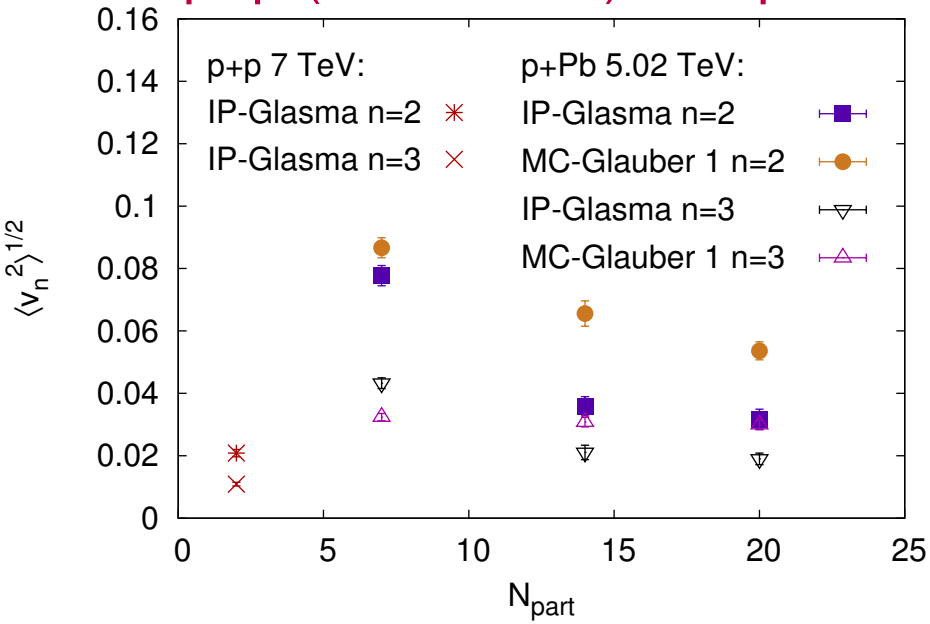

d+Au

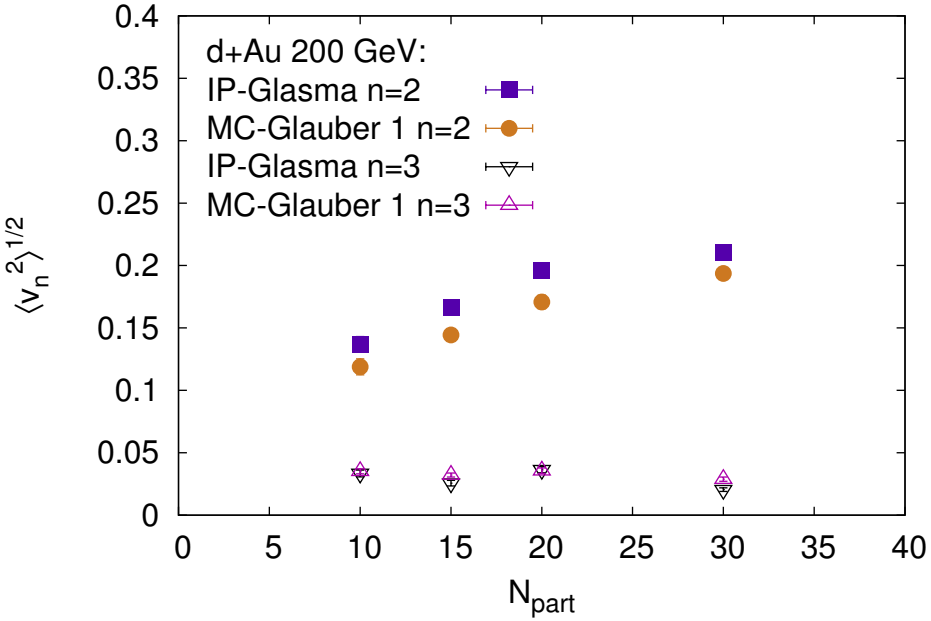

p+Pb: Ellipitc flow decreases with N_{part}
d+Au: Elliptic flow increases with N_{part}
p+p: Elliptic flow small, but not as small as expected from eccentricity
Need sophisticated centrality selection to compare with experiments

A. Bzdak, B. Schenke, P. Tribedy, R. Venugopalan, arXiv:1304.3403

p+A collisions - is viscous hydro valid?

How “crazy” is it to use hydrodynamics in p+A?

Initial $\pi_0^{\mu\nu} = 0$, $b = 0$ fm, IP-Glasma. Cells within f.o. surface that have $> 25\%$ viscous correction in p+Pb and Pb+Pb:

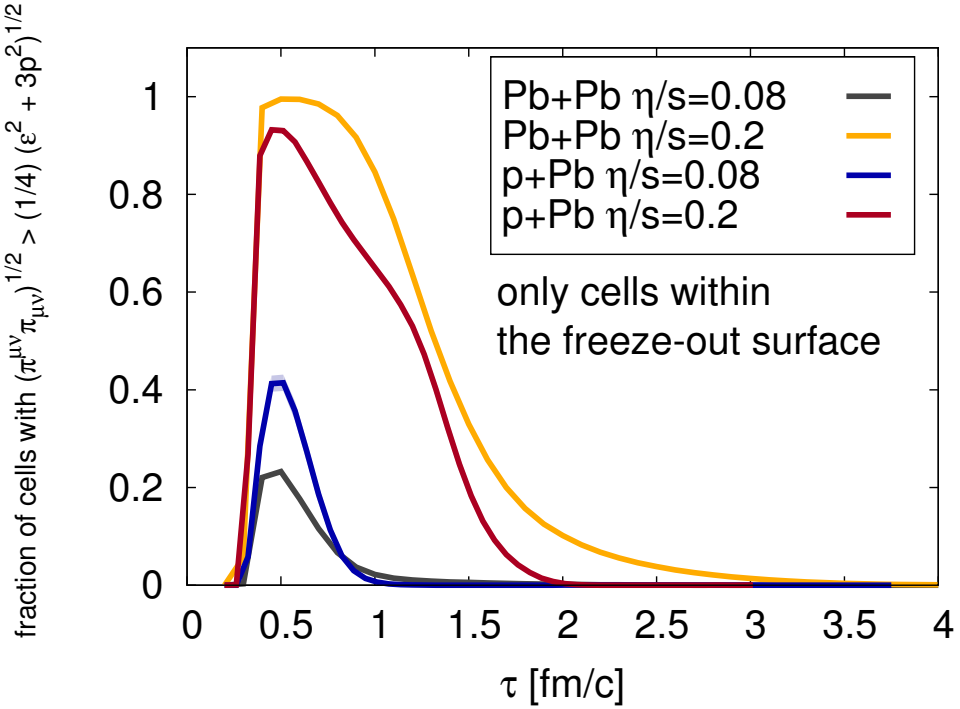

Important: Lifetime in Pb+Pb is about 6 times longer than in p+Pb

Also see Dumitru, Molnar, Nara, Phys.Rev. C76 (2007) 024910

p+A collisions - is viscous hydro valid?

same with Navier-Stokes $\pi_0^{\mu\nu}$, count cells within f.o. surface that have more than a 25% viscous correction in p+Pb and Pb+Pb:

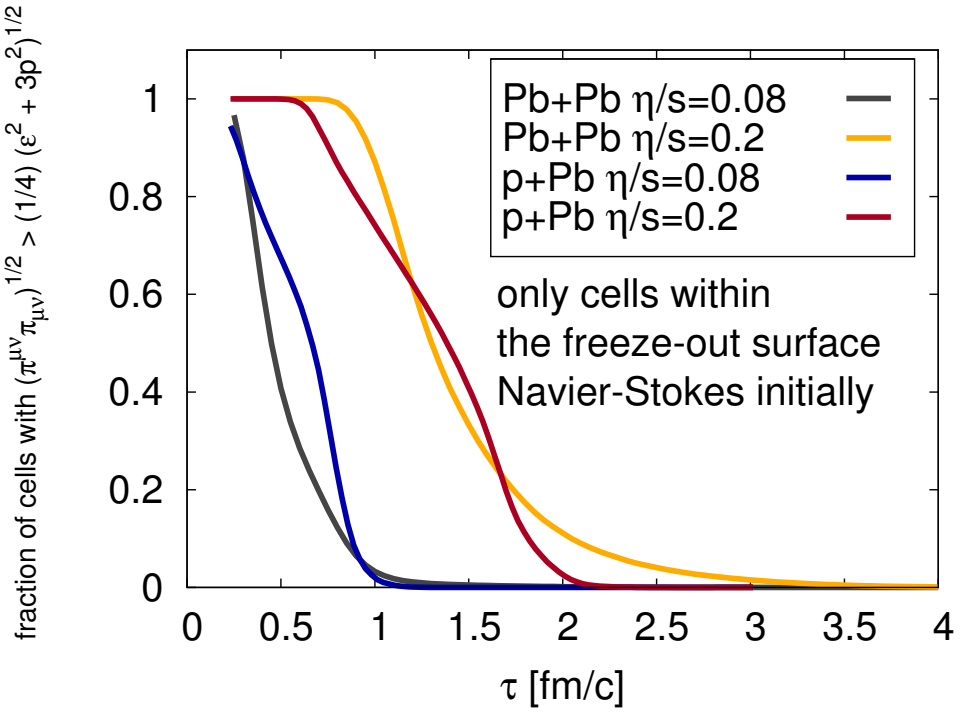

Important: Lifetime in Pb+Pb is about 6 times longer than in p+Pb

p+A collisions - is viscous hydro valid?

Initial Navier-Stokes $\pi_0^{\mu\nu}$, count cells within f.o. surface that have more than a 50% viscous correction in p+Pb and Pb+Pb:

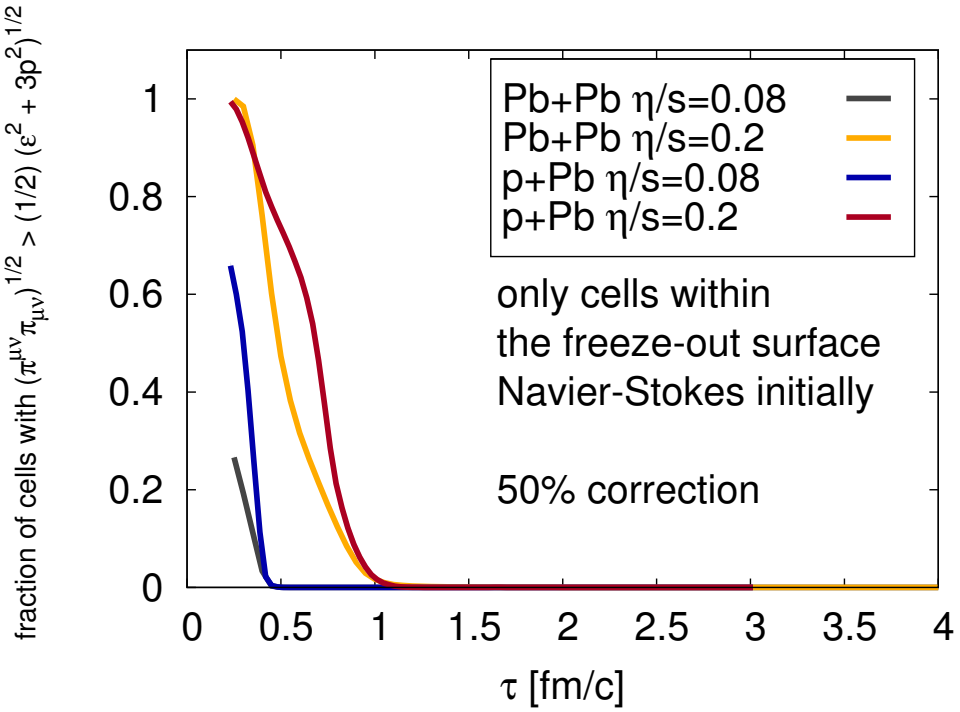

Important: Lifetime in Pb+Pb is about 6 times longer than in p+Pb

Summary and conclusions

- Different initial state models produce different geometries
- Differences are not very large in A+A, details still relevant for flow and jet energy loss studies (e.g. jet v_2)
- Differences are much larger in small systems (p+p, p+A, d+A)
- Eccentricites not the only relevant measure/predictor of flow
- Correct centrality selection in the model important
- Viscous corrections: Large at early times - affect larger fraction of total evolution time in p+A than A+A

BACKUP

Flow in p+Pb

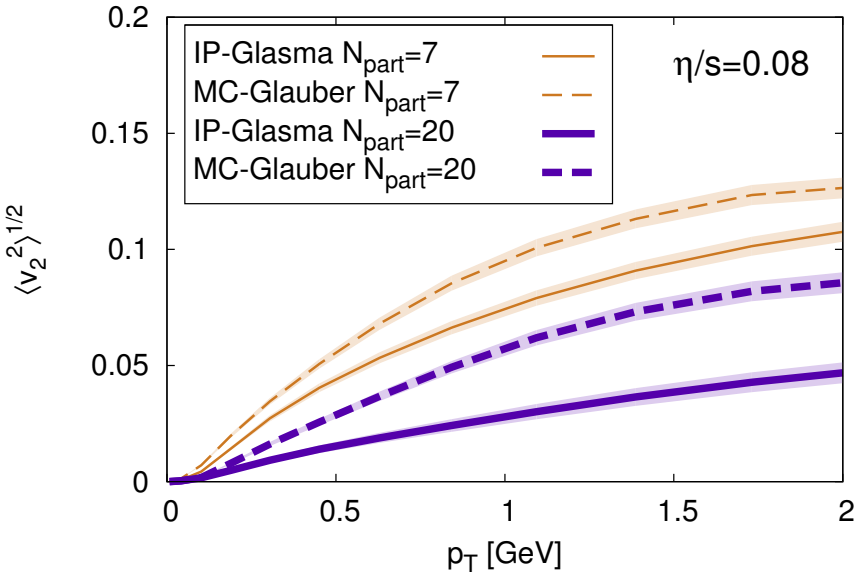

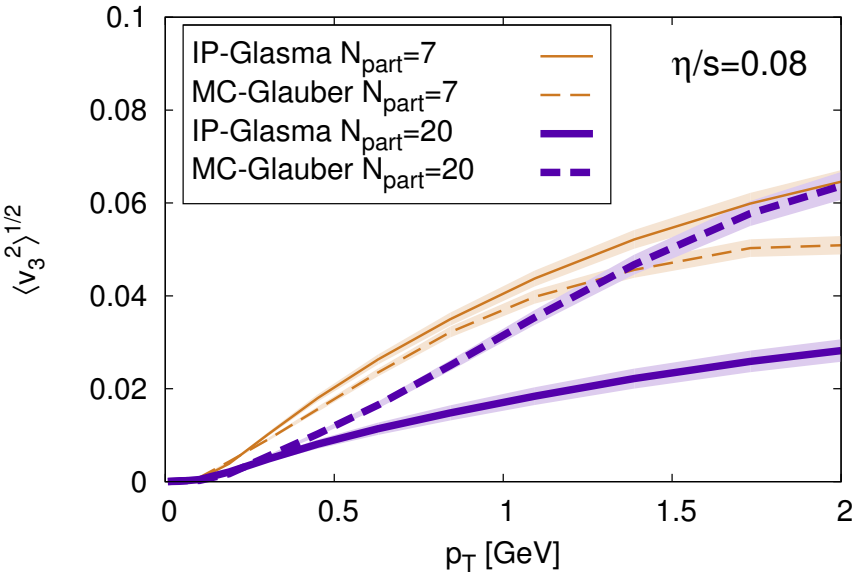

A. Bzdak, B. Schenke, P. Tribedy, R. Venugopalan, arXiv:1304.3403

Flow in d+Au

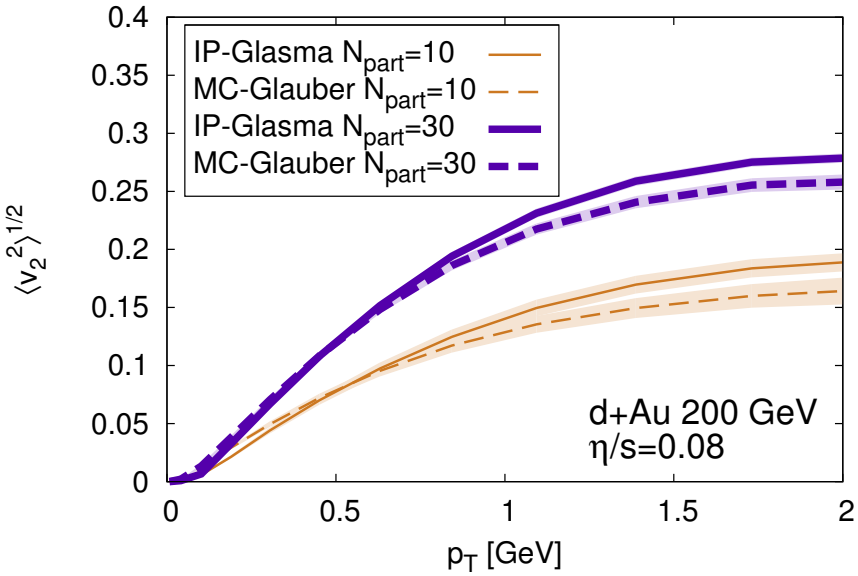

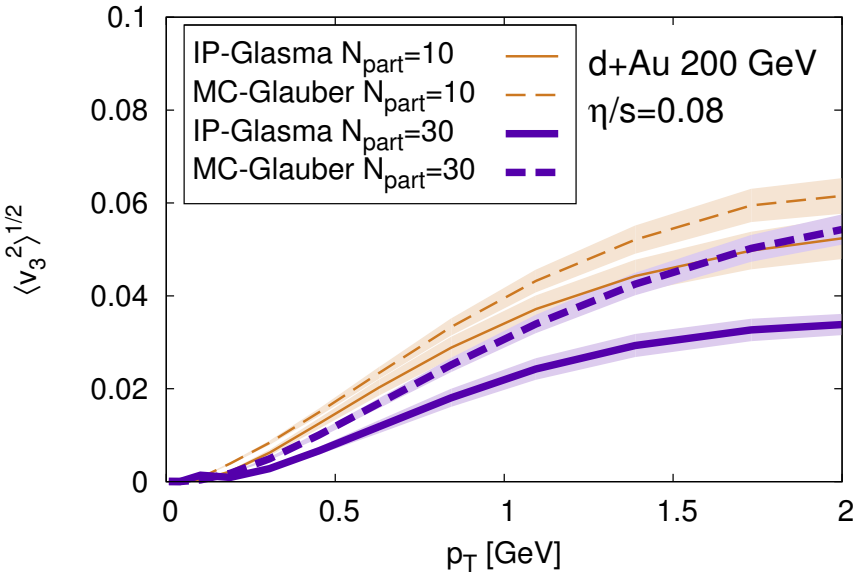

A. Bzdak, B. Schenke, P. Tribedy, R. Venugopalan, arXiv:1304.3403

Learning about QCD

Example: extraction of $(\eta/s)(T)$

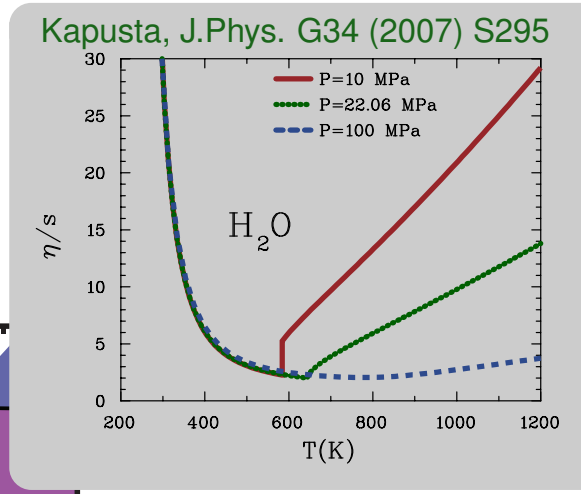

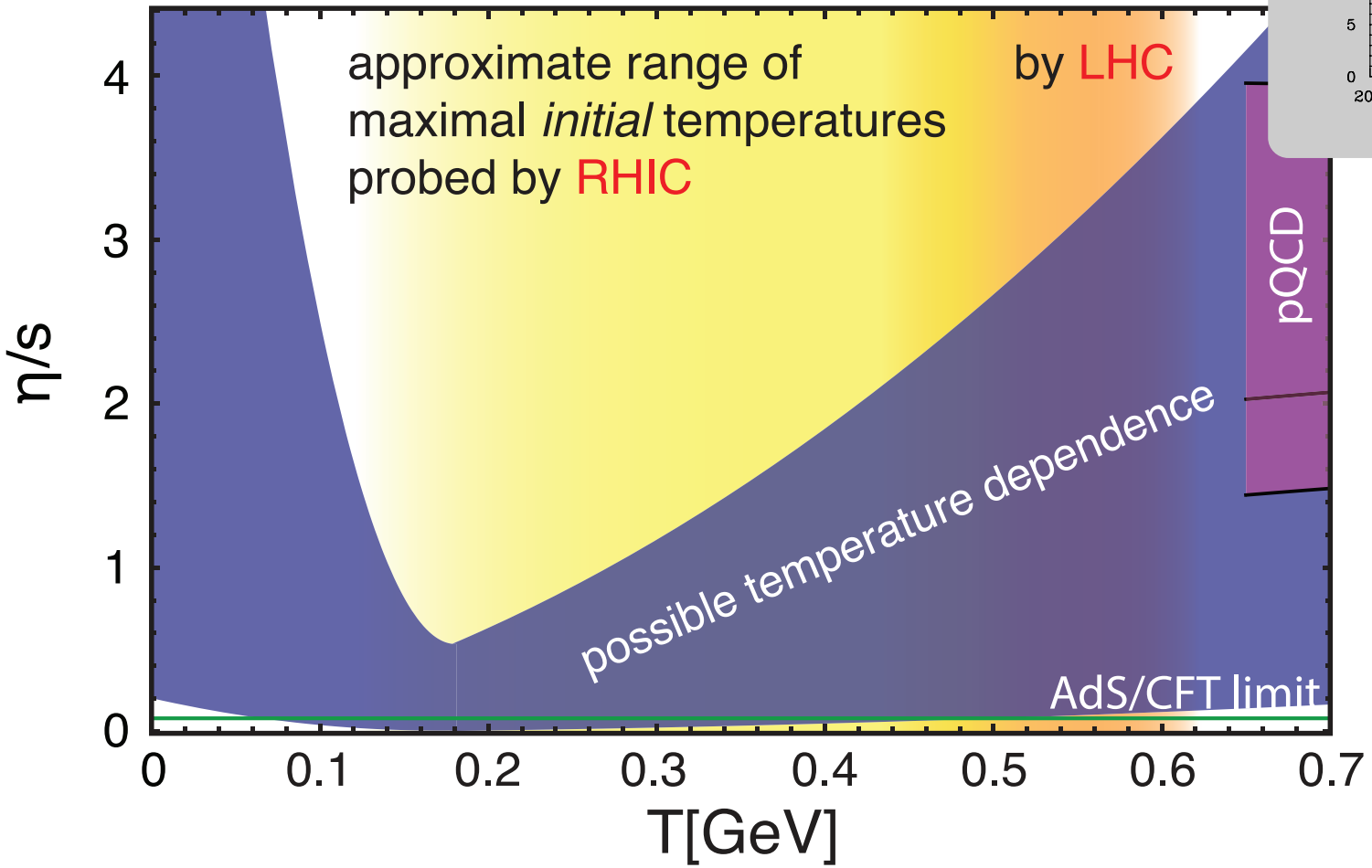

Temperature dependent η/s

C. Gale, S. Jeon, B.Schenke,
P.Tribedy, R.Venugopalan, PRL110, 012302 (2013)

Use $\eta/s(T)$ as in Niemi et al., Phys.Rev.Lett. 106 (2011) 212302

Experimental data: A. Adare et al. (PHENIX), Phys.Rev.Lett. 107, 252301 (2011)
Y. Pandit (STAR), Quark Matter 2012, (2012)
ATLAS collaboration, Phys. Rev. C 86, 014907 (2012)

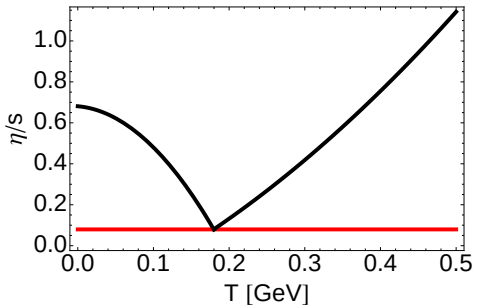

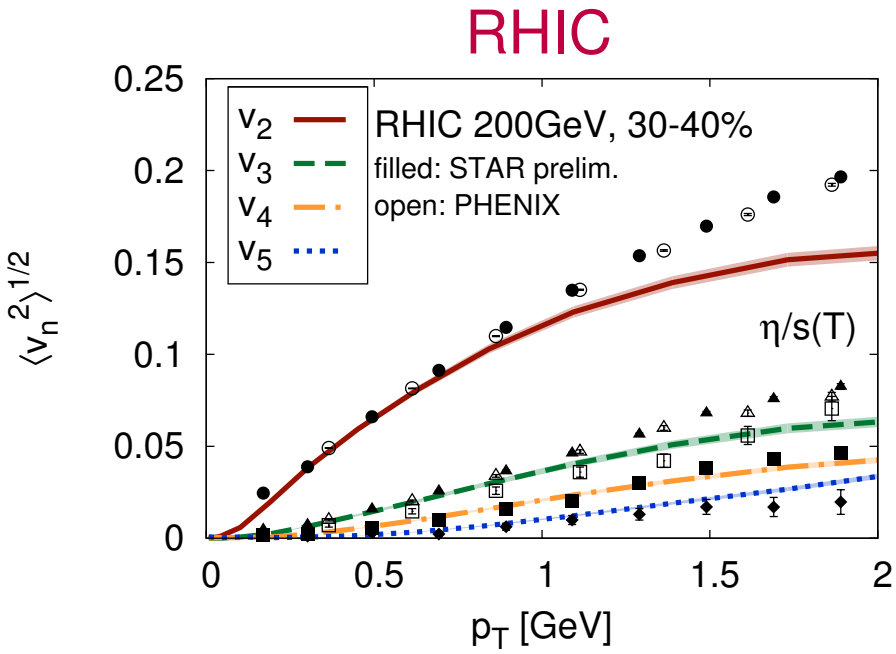

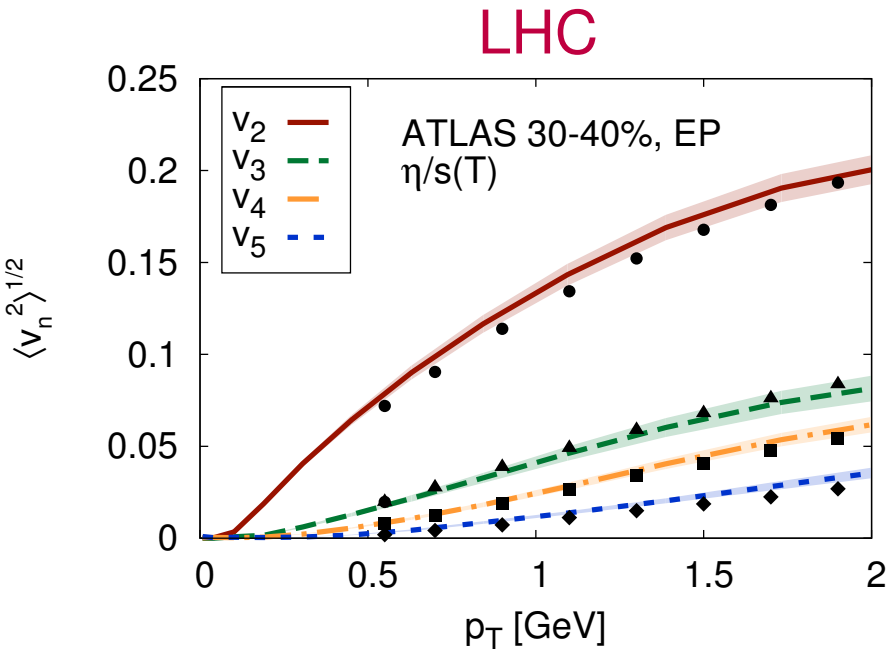

One $(\eta/s)(T)$ will be able to describe both RHIC and LHC data
Used parametrization not yet perfect: no surprise
More detailed study needed - include different RHIC energies and LHC

Eccentricities B.Schenke, P.Tribedy, R.Venugopalan, Phys.Rev.C86, 034908 (2012)

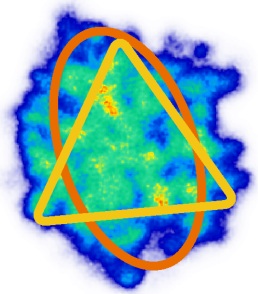

Characterize the initial distribution by its ellipticity, triangularity, etc...

$$\varepsilon_n = \sqrt{\langle r^n \cos(n\phi)\rangle^2 + \langle r^n \sin(n\phi)\rangle^2}/\langle r^n\rangle$$

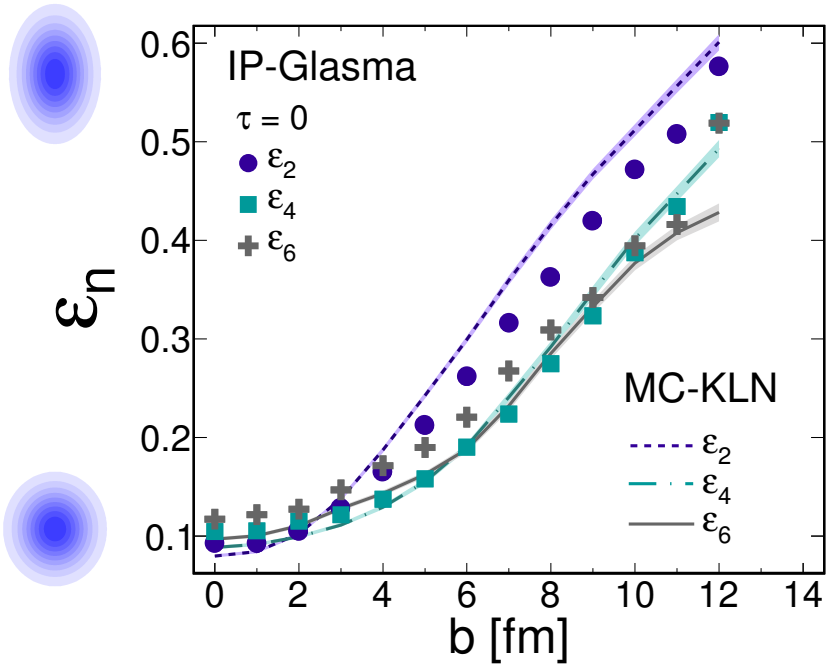

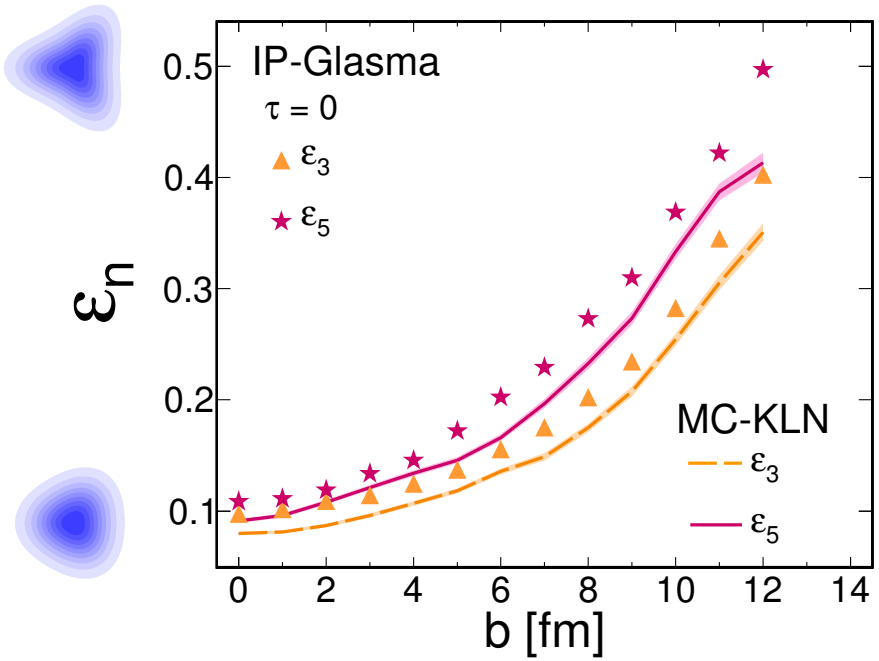

- ε_n larger in Glasma model for odd n
- ε_n smaller in Glasma model for $n = 2$ (for $b > 3\,\mathrm{fm}$) about equal for $n = 4$, larger for $n = 6$

Viscous flow at LHC

C. Gale, S. Jeon, B.Schenke, P.Tribedy, R.Venugopalan, PRL110, 012302 (2013)

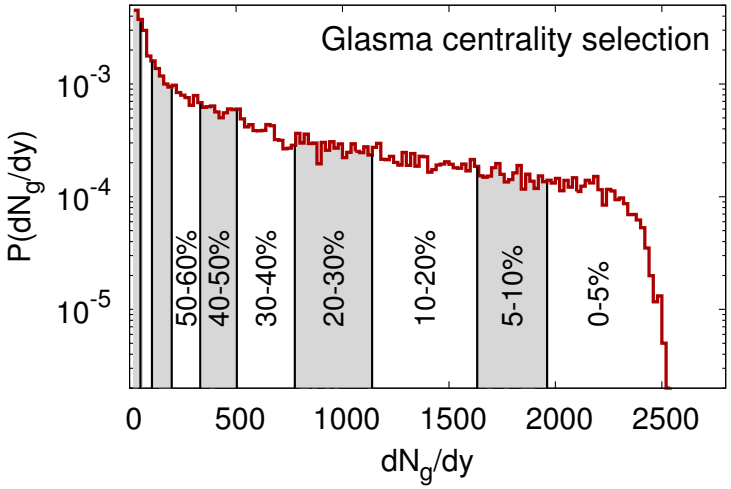

Viscous flow at LHC

C. Gale, S. Jeon, B.Schenke, P.Tribedy, R.Venugopalan, PRL110, 012302 (2013)

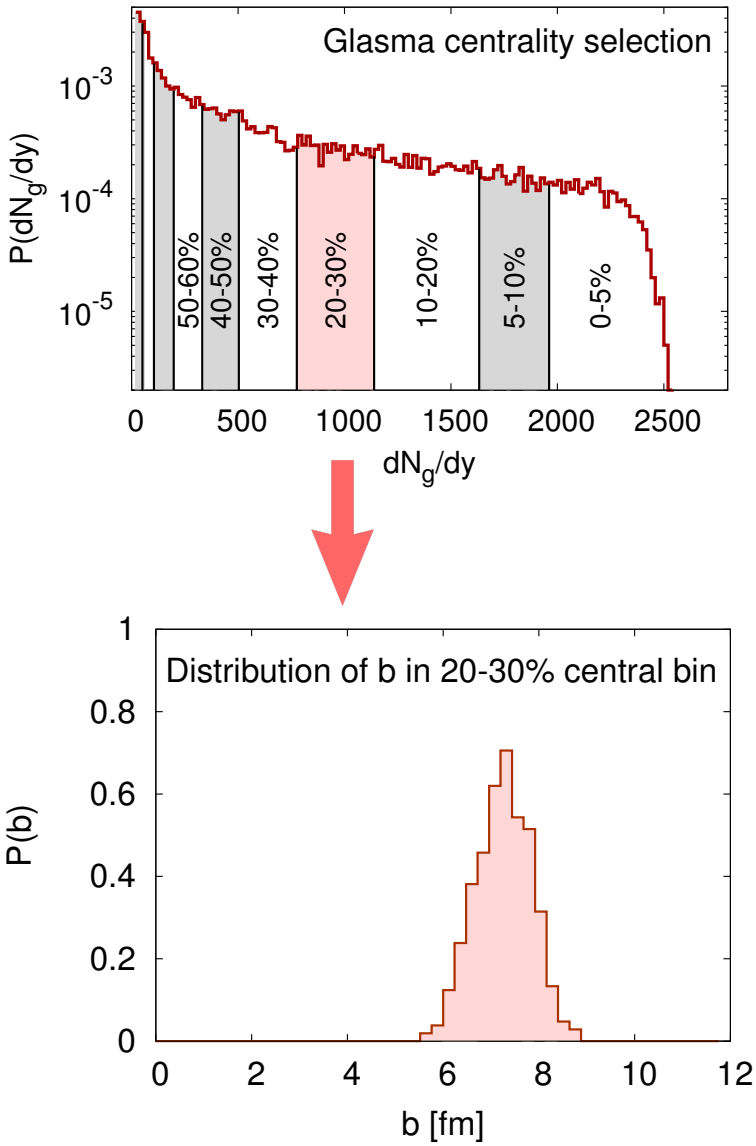

Viscous flow at LHC

C. Gale, S. Jeon, B.Schenke, P.Tribedy, R.Venugopalan, PRL110, 012302 (2013)

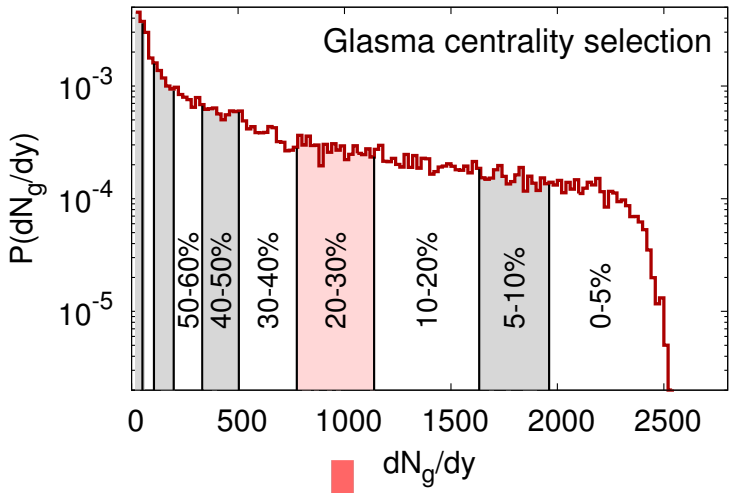

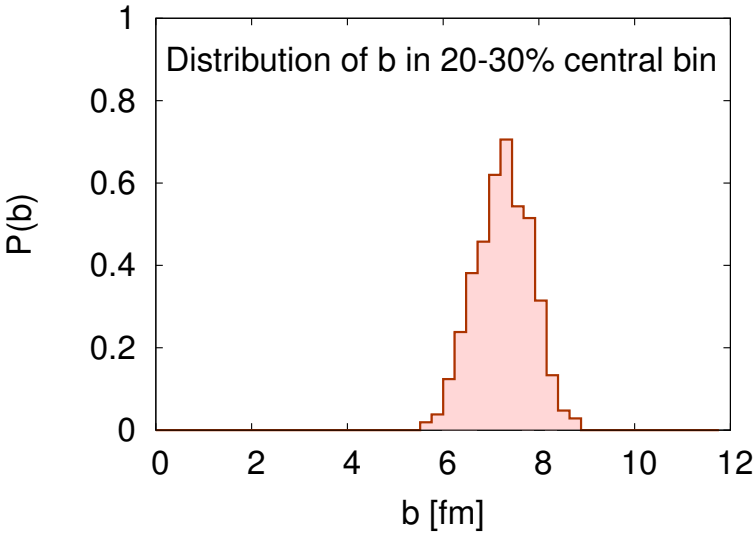

Hydro evolution

MUSIC

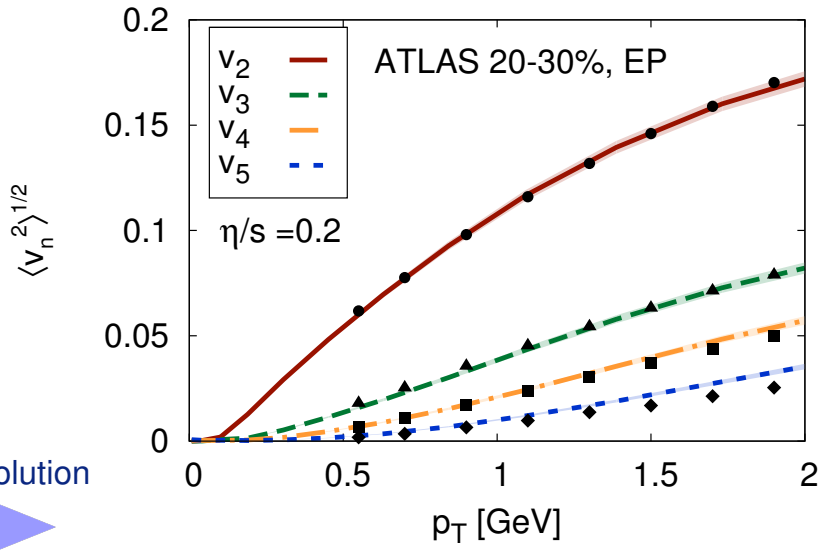

Viscous flow at LHC

C. Gale, S. Jeon, B.Schenke, P.Tribedy, R.Venugopalan, PRL110, 012302 (2013)

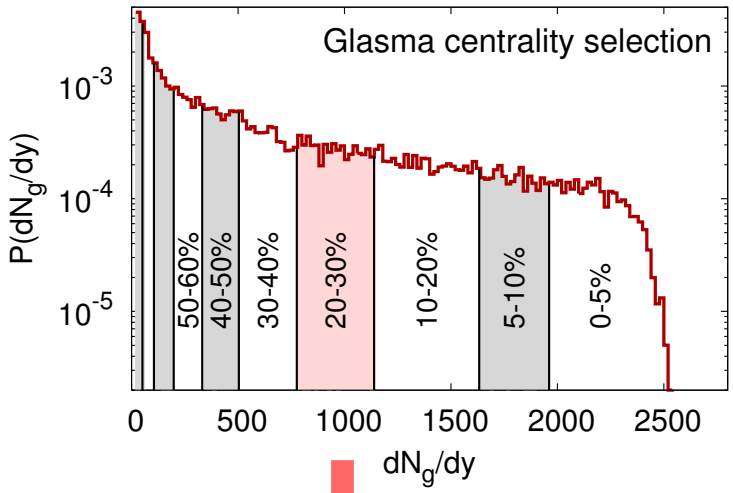

Hydro evolution

MUSIC

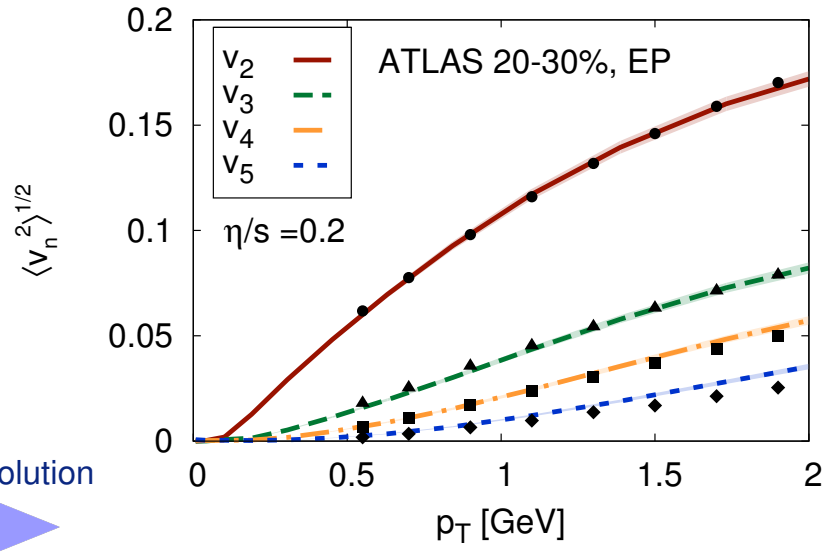

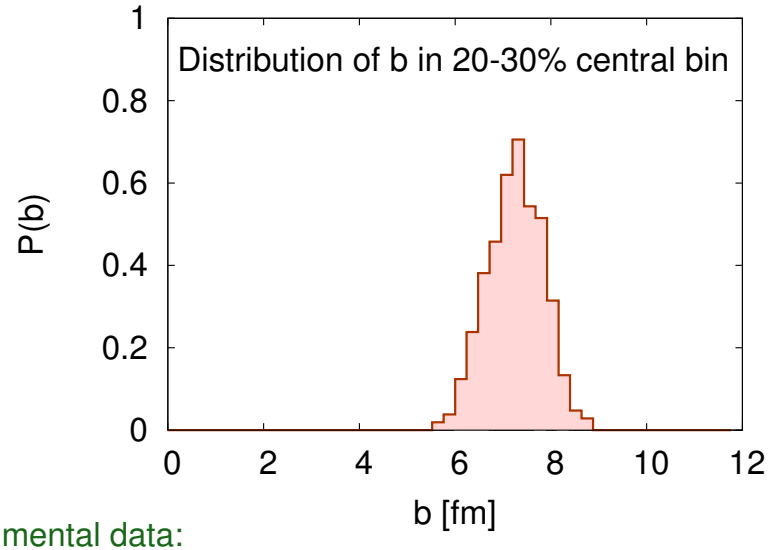

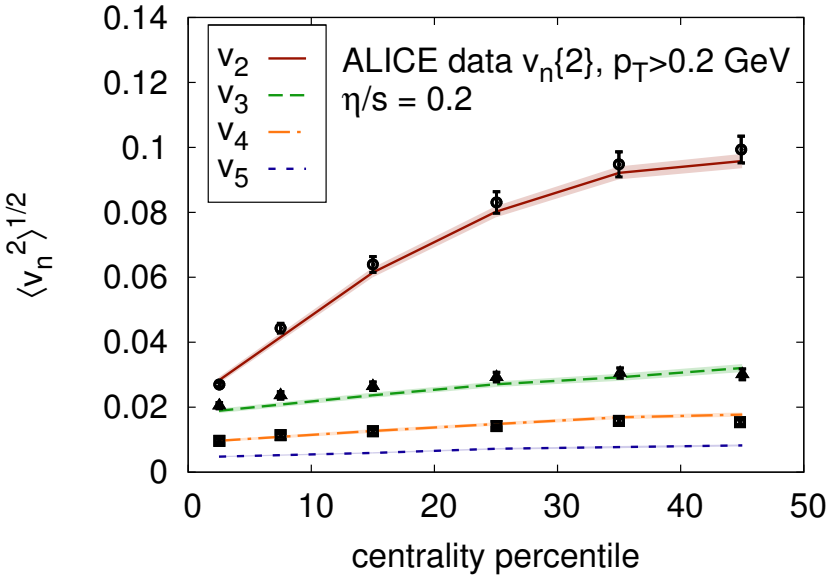

Experimental data:
ATLAS collaboration, Phys. Rev. C 86, 014907 (2012)
ALICE collaboration, Phys. Rev. Lett. 107, 032301 (2011)

Relativistic fluid-dynamics

Bulk of the matter produced in heavy-ion collisions
is well described by fluid-dynamics...

... and that is just energy and momentum conservation
in a system with small mean free path (compared to the system size)

$$\partial_\mu T^{\mu\nu} = 0$$

$$T^{\mu\nu} = (\epsilon + P)u^\mu u^\nu - P g^{\mu\nu} + \pi^{\mu\nu}$$

need additional equation to close the set:

Equation of state: $P = P(\epsilon)$

(comes e.g. from lattice QCD / hadron gas model)

$\pi^{\mu\nu}$ contains dissipative effects

Event-by-event fluctuations

- Fluctuations are important
  Affect all harmonics v_1, v_2, v_3, etc.

$$\frac{dN}{d\phi} = \frac{N}{2\pi}\left(1 + \sum_n 2v_n \cos(n(\phi - \psi_n))\right)$$

  In particular: odd harmonics are not zero
  Mishra et al., Phys.Rev. C77, 064902 (2008), Takahashi et al., Phys. Rev. Lett. 103, 242301 (2009)
  Alver and Roland, Phys. Rev. C81, 054905 (2010)

- Axes and eccentricities determined by fluctuating geometry

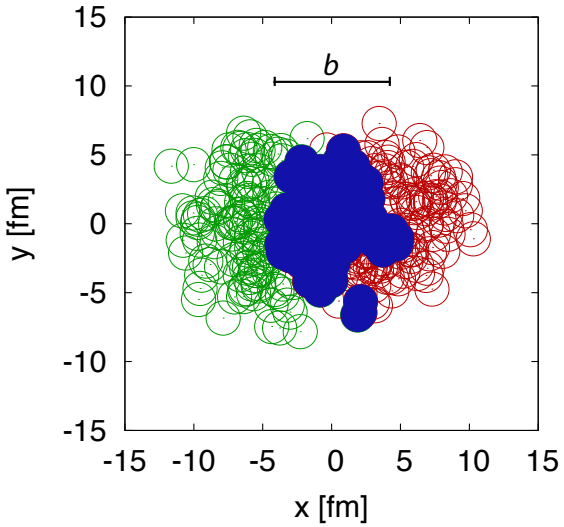

Event-by-event fluctuations

- Fluctuations are important
  Affect all harmonics v_1, v_2, v_3, etc.

$$\frac{dN}{d\phi} = \frac{N}{2\pi}\left(1 + \sum_n 2v_n \cos(n(\phi - \psi_n))\right)$$

  In particular: odd harmonics are not zero
  Mishra et al., Phys.Rev. C77, 064902 (2008), Takahashi et al., Phys. Rev. Lett. 103, 242301 (2009)
  Alver and Roland, Phys. Rev. C81, 054905 (2010)

- Axes and eccentricities determined by fluctuating geometry

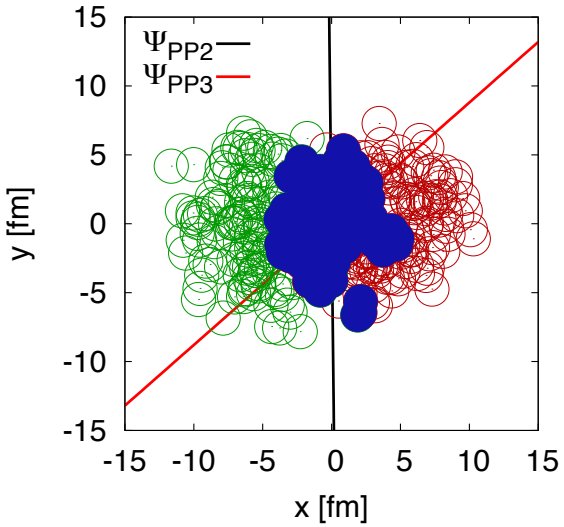

Participant plane angle (spatial):

$$\psi_{PPn} = \frac{1}{n}\arctan\frac{\langle r^n \sin(n\phi)\rangle}{\langle r^n \cos(n\phi)\rangle}$$

average over nucleon positions

Event plane angle (momentum):

$$\psi_{EPn} = \frac{1}{n}\arctan\frac{\langle p_T^\alpha \sin(n\psi)\rangle}{\langle p_T^\alpha \cos(n\psi)\rangle}$$

average over produced particles, $\alpha = 0, 1, ...$

Event-by-event fluctuations

- Fluctuations are important
  Affect all harmonics v_1, v_2, v_3, etc.

$$\frac{dN}{d\phi} = \frac{N}{2\pi}\left(1 + \sum_n 2v_n \cos(n(\phi - \psi_n))\right)$$

  In particular: odd harmonics are not zero
  Mishra et al., Phys.Rev. C77, 064902 (2008), Takahashi et al., Phys. Rev. Lett. 103, 242301 (2009)
  Alver and Roland, Phys. Rev. C81, 054905 (2010)

- Axes and eccentricities determined by fluctuating geometry

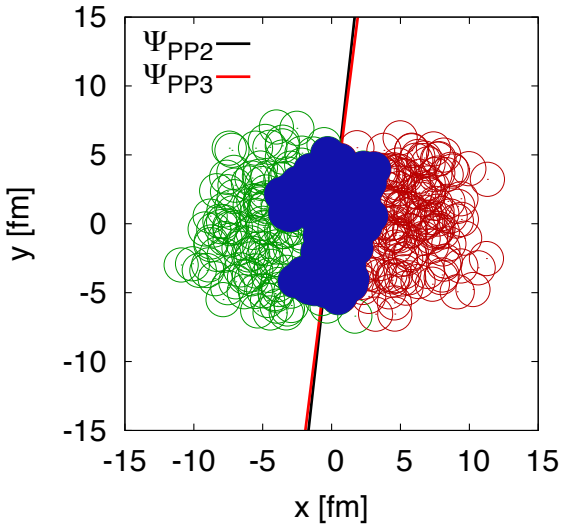

Participant plane angle (spatial):

$$\psi_{PPn} = \frac{1}{n}\arctan\frac{\langle r^n \sin(n\phi)\rangle}{\langle r^n \cos(n\phi)\rangle}$$

average over nucleon positions

Event plane angle (momentum):

$$\psi_{EPn} = \frac{1}{n}\arctan\frac{\langle p_T^\alpha \sin(n\psi)\rangle}{\langle p_T^\alpha \cos(n\psi)\rangle}$$

average over produced particles, $\alpha = 0, 1, ...$

Event-by-event fluctuations

- Fluctuations are important
  Affect all harmonics v_1, v_2, v_3, etc.

$$\frac{dN}{d\phi} = \frac{N}{2\pi}\left(1 + \sum_n 2v_n \cos(n(\phi - \psi_n))\right)$$

  In particular: odd harmonics are not zero
  Mishra et al., Phys.Rev. C77, 064902 (2008), Takahashi et al., Phys. Rev. Lett. 103, 242301 (2009)
  Alver and Roland, Phys. Rev. C81, 054905 (2010)

- Axes and eccentricities determined by fluctuating geometry

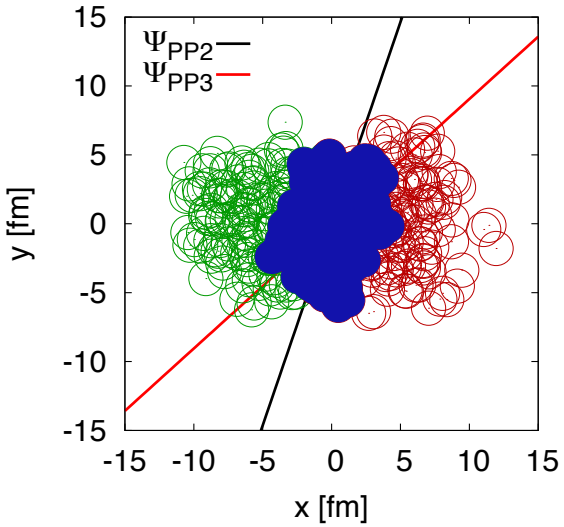

Participant plane angle (spatial):

$$\psi_{PPn} = \frac{1}{n}\arctan\frac{\langle r^n \sin(n\phi)\rangle}{\langle r^n \cos(n\phi)\rangle}$$

average over nucleon positions

Event plane angle (momentum):

$$\psi_{EPn} = \frac{1}{n}\arctan\frac{\langle p_T^\alpha \sin(n\psi)\rangle}{\langle p_T^\alpha \cos(n\psi)\rangle}$$

average over produced particles, $\alpha = 0, 1, ...$

Event-by-event fluctuations

- Fluctuations are important
  Affect all harmonics v_1, v_2, v_3, etc.

$$\frac{dN}{d\phi} = \frac{N}{2\pi}\left(1 + \sum_n 2v_n \cos(n(\phi - \psi_n))\right)$$

  In particular: odd harmonics are not zero
  Mishra et al., Phys.Rev. C77, 064902 (2008), Takahashi et al., Phys. Rev. Lett. 103, 242301 (2009)
  Alver and Roland, Phys. Rev. C81, 054905 (2010)

- Axes and eccentricities determined by fluctuating geometry

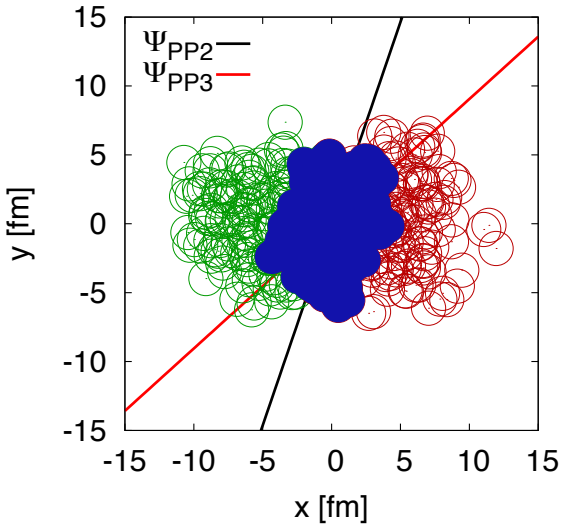

Eccentricities:

$$\varepsilon_n = \frac{\sqrt{\langle r^n \cos(n\phi)\rangle^2 + \langle r^n \sin(n\phi)\rangle^2}}{\langle r^n \rangle}$$

All $\varepsilon_n = 0 \rightarrow$ perfect circle
$\varepsilon_n \neq 0$: shape modulation in the nth harmonic

3+1D event-by-event viscous fluid-dynamics

The first relativistic hydrodynamic simulation to include viscosity, fluctuations and 3+1 dimensions:

MUSIC: MUScl for Ion Collisions

MUSCL = Monotonic Upstream Centered Scheme for Conservation Laws

B. Schenke, S. Jeon, and C. Gale, Phys.Rev.Lett.106, 042301 (2011)

- 3+1 dimensions
- Kurganov-Tadmor algorithm
  A. Kurganov, E. Tadmor, Journal of Computational Physics **160**, 241-282 (2000)
- expanding geometry
- viscous effects (2nd order Israel-Stewart formalism)
- fluctuating initial conditions
- equation of state from lattice QCD and hadron resonance gas

MUSIC: studying the effect of viscosity and fluctuations

energy density

- Setup:
  Wounded nucleons are assigned
  a Gaussian energy density distribution
  width σ_0 is a free parameter
- Evolution:
  Hydrodynamic evolution with shear viscous effects
  System expands, becomes dilute, freezes out
  Initial spatial anisotropy is transformed into momentum anisotropy
- Energy density $\rightarrow$ Particle spectra:
  Cooper-Frye formula:

$$E\frac{dN}{d^3p} = \int_\Sigma d\Sigma_\mu p^\mu f(T, p_\mu u^\mu, \pi^{\mu\nu})$$

followed by resonance decays

$\Sigma =$ freeze-out surface (surface of constant temperature)
$f =$ particle distribution

Cooper and Frye, Phys.Rev.D10, 186 (1974)

Sensitivity of v_n on viscosity and fluctuations

B. Schenke, S. Jeon, C. Gale, Phys.Rev.C85, 024901 (2012)

viscous to ideal results

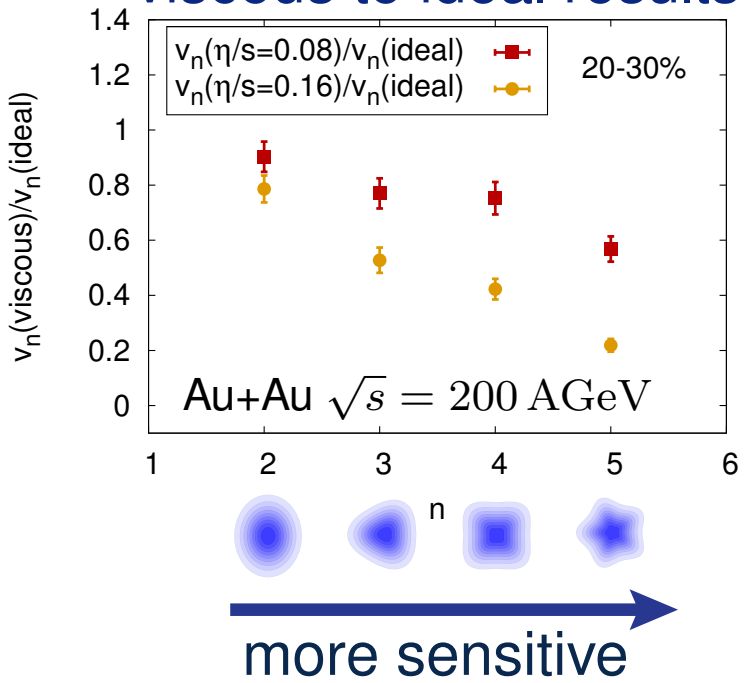

more sensitive

smoother to more granular results

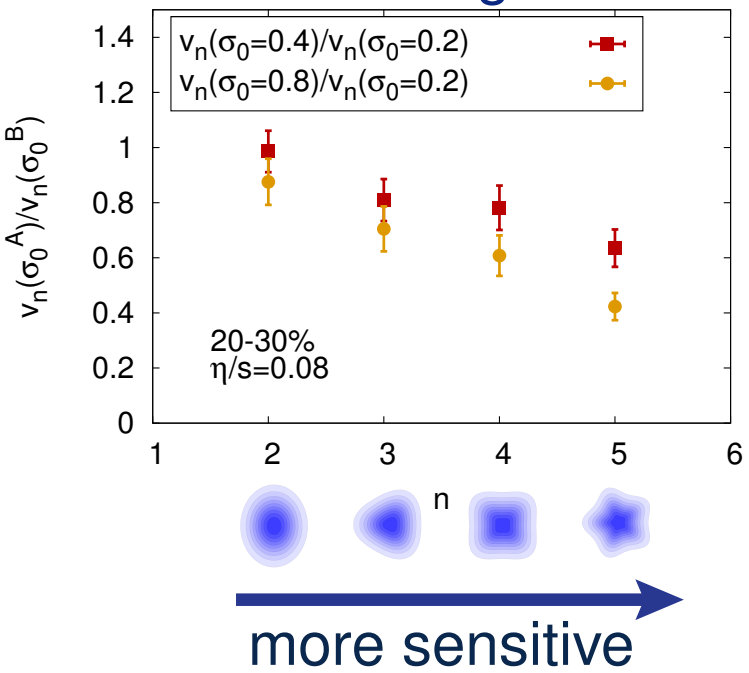

more sensitive

Viscosity decreases anisotropic flow (it's friction)
Smoother initial conditions decrease anisotropic flow

Sensitivity to viscosity and initial state structure increases with n

Nuclei at high energy: Gluon saturation

As we go to higher energy / smaller x, gluons split, number increases:

BFKL (Balitsky,Fadin,Kuraev,Lipatov) equation describes x-evolution but violates unitarity: cross-sections grow without bound

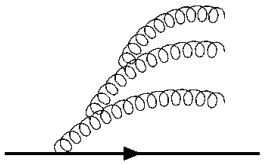

JIMWLK (Jalilian-Marian, Iancu, McLerran, Weigert, Leonidov, Kovner) and BK (Balitsky, Kovchegov) equations include non-linear evolution $\rightarrow$ saturation

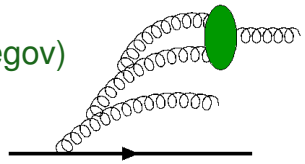

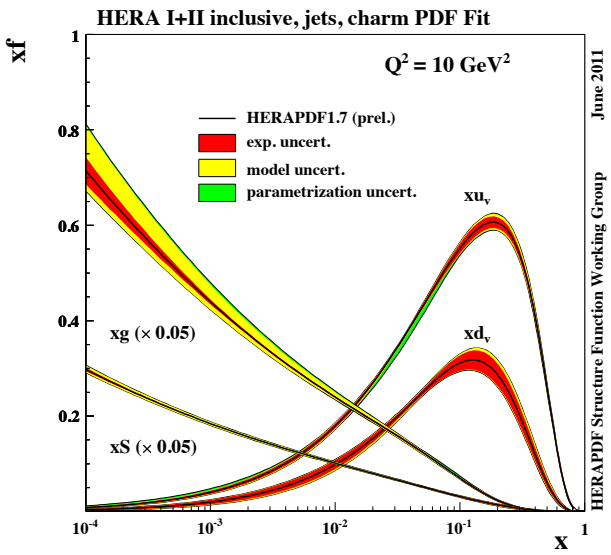

- Transverse gluon density:
  $\rho \sim \frac{xg_A(x,Q^2)}{S_\perp} \sim \frac{Axg(x,Q^2)}{A^{2/3}} \sim A^{1/3}xg(x,Q^2)$
- Recombination cross section:
  $\sigma_{gg\rightarrow g} \sim \frac{\alpha_s}{Q^2}$
- Saturation when
  $\rho\sigma_{gg\rightarrow g} \gtrsim 1$

$\Rightarrow$ Saturation at scale $Q_s^2 = \alpha_s A^{1/3} xg(x, Q_s^2)$

x = longitudinal momentum fraction of partons in a hadron or nucleus

Nuclei at high energy: Gluon saturation

As we go to higher energy / smaller x, gluons split, number increases:

BFKL (Balitsky,Fadin,Kuraev,Lipatov) equation describes x-evolution
but violates unitarity: cross-sections grow without bound

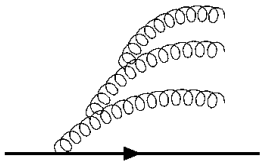

JIMWLK (Jalilian-Marian, Iancu, McLerran, Weigert, Leonidov, Kovner) and BK (Balitsky, Kovchegov)
equations include non-linear evolution $\rightarrow$ saturation

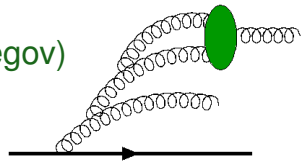

$\mathbf{p}_T \lesssim Q_s(x)$:

- strong saturated fields $A_\mu \sim 1/g$
- occupation numbers $\sim 1/\alpha_s$
- $\Rightarrow$ classical field approximation

McLerran and Venugopalan, Phys.Rev. D49 (1994) 2233-2241

Energy density B.Schenke, P.Tribedy, R.Venugopalan, Phys.Rev.Lett. 108, 252301 (2012)

Compute energy density in the fields at $\tau = 0$ and later times with CYM evolution

arbitrary units
same nucleon positions
in all events, b=4fm

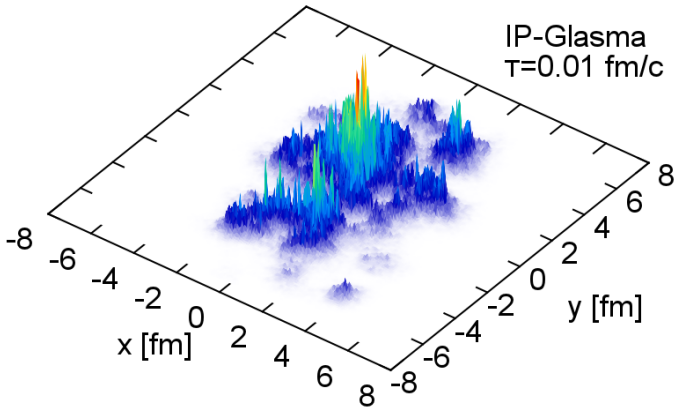

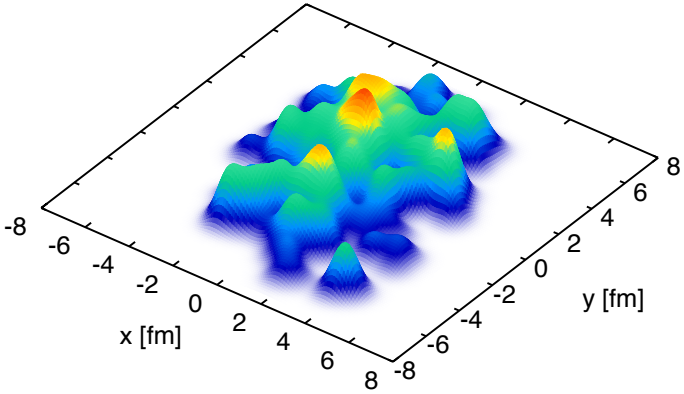

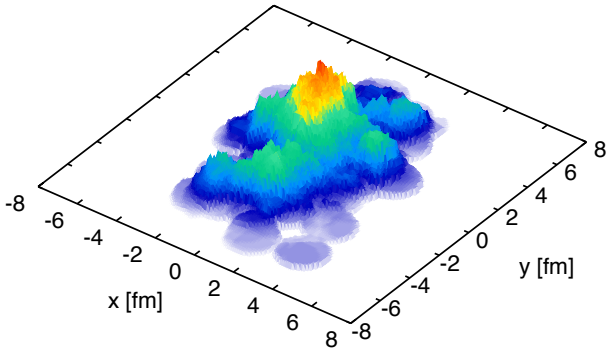

MC-KLN: Drescher, Nara, nucl-th/0611017
mckln-3.52 from `http://physics.baruch.cuny.edu/files/CGC/CGC_IC.html` with defaults, energy density scaling

Energy density B.Schenke, P.Tribedy, R.Venugopalan, Phys.Rev.Lett. 108, 252301 (2012)

Compute energy density in the fields at $\tau = 0$ and later times with CYM evolution

arbitrary units
same nucleon positions
in all events, b=4fm

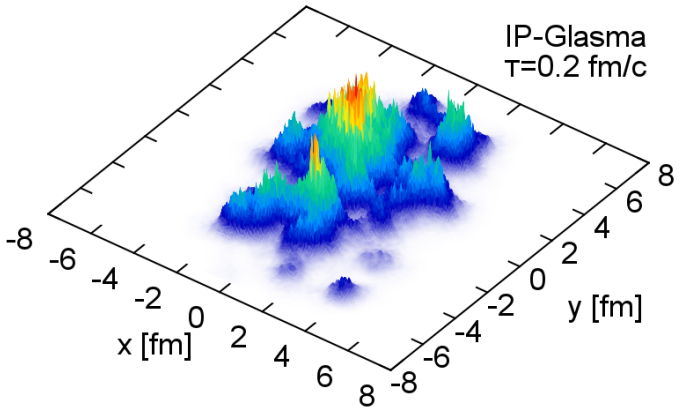

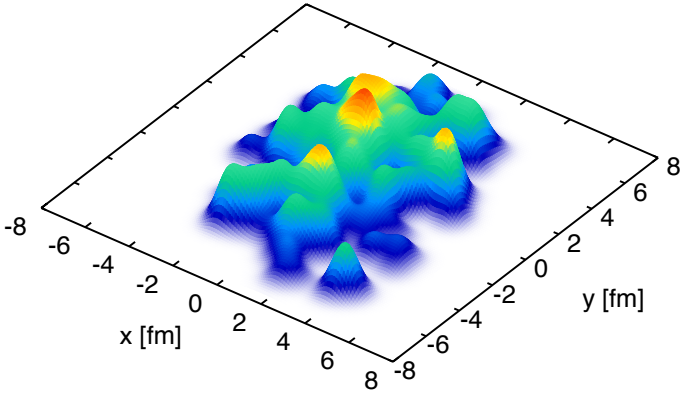

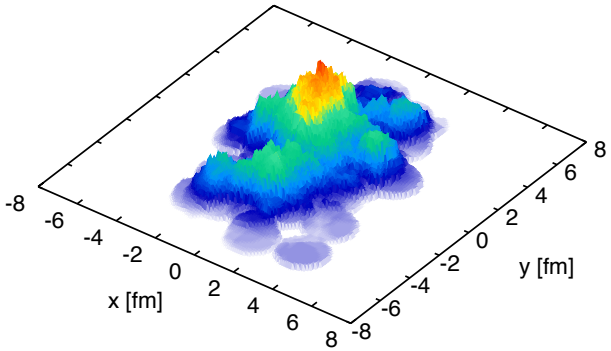

MC-KLN: Drescher, Nara, nucl-th/0611017
mckln-3.52 from `http://physics.baruch.cuny.edu/files/CGC/CGC_IC.html` with defaults, energy density scaling

Multiplicity B.Schenke, P.Tribedy, R.Venugopalan, Phys. Rev. C86, 034908 (2012)

dN_{g}/dy in transverse Coulomb gauge $\partial_i A^i = 0$
N_{part} from MC-Glauber with $\sigma_{NN} = 42\,\mathrm{mb}$ and $64\,\mathrm{mb}$ respectively

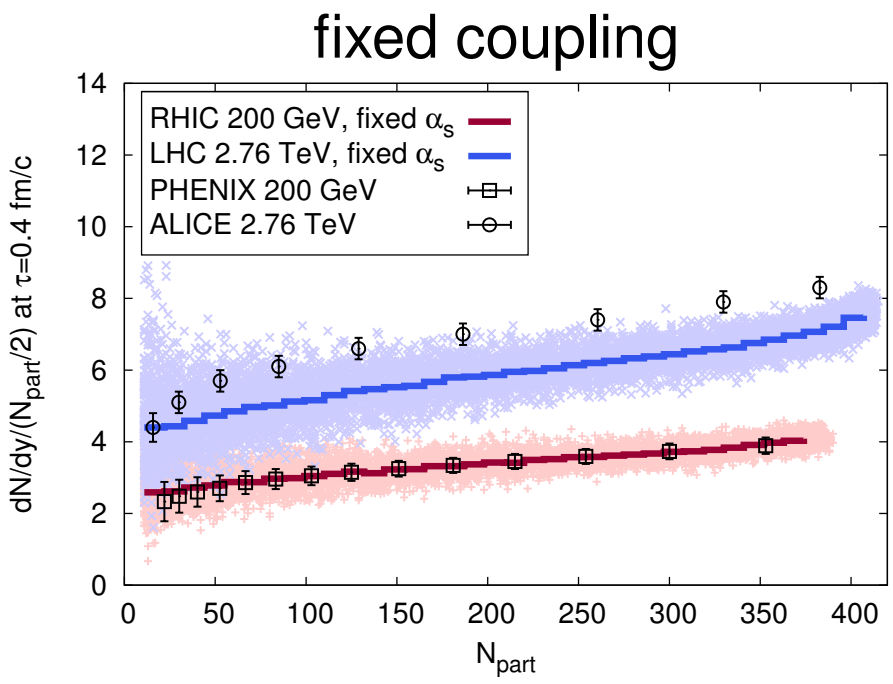

Experimental data: PHENIX, Phys.Rev.C71 034908 (2004) and ALICE, Phys.Rev.Lett. 106, 032301 (2011)

Scaled by $2/3$ to compare to charged particles.
Original version. Nuclear 'oomph' added by hand.

Multiplicity B.Schenke, P.Tribedy, R.Venugopalan, Phys. Rev. C86, 034908 (2012)

dN_{g}/dy in transverse Coulomb gauge $\partial_i A^i = 0$
N_{part} from MC-Glauber with $\sigma_{NN} = 42\,\mathrm{mb}$ and $64\,\mathrm{mb}$ respectively

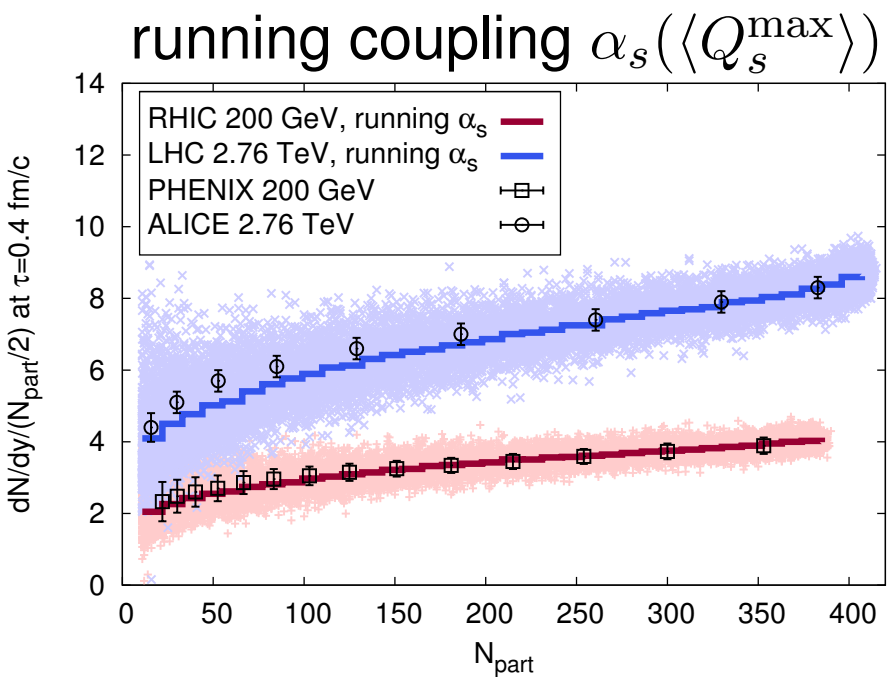

Experimental data: PHENIX, Phys.Rev.C71 034908 (2004) and ALICE, Phys.Rev.Lett. 106, 032301 (2011)

Scaled by $2/3$ to compare to charged particles.
Original version. Nuclear 'oomph' added by hand.

Multiplicity B.Schenke, P.Tribedy, R.Venugopalan, Phys. Rev. C86, 034908 (2012)

New version. Using IP-Sat for nuclei. No adjustments by hand anymore.

running coupling $\alpha_s(Q_s^{\max}(\mathbf{x}_\perp))$

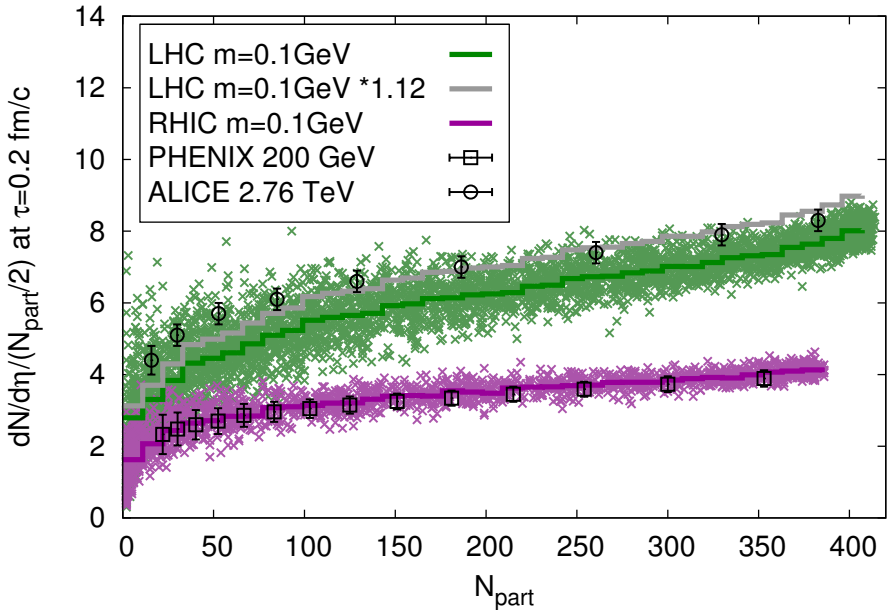

Experimental data: PHENIX, Phys.Rev.C71 034908 (2004) and ALICE, Phys.Rev.Lett. 106, 032301 (2011)

Expect more entropy production at LHC - need hydro results to check

Negative binomial fluctuations

B.Schenke, P.Tribedy, R.Venugopalan, Phys.Rev.C86, 034908 (2012)

Extract k and $\bar{n}$ using a fit with

$$P(n) = \frac{\Gamma(k+n)}{\Gamma(k)\Gamma(n+1)} \frac{\bar{n}^n k^k}{(\bar{n}+k)^{n+k}}$$

at fixed impact parameters

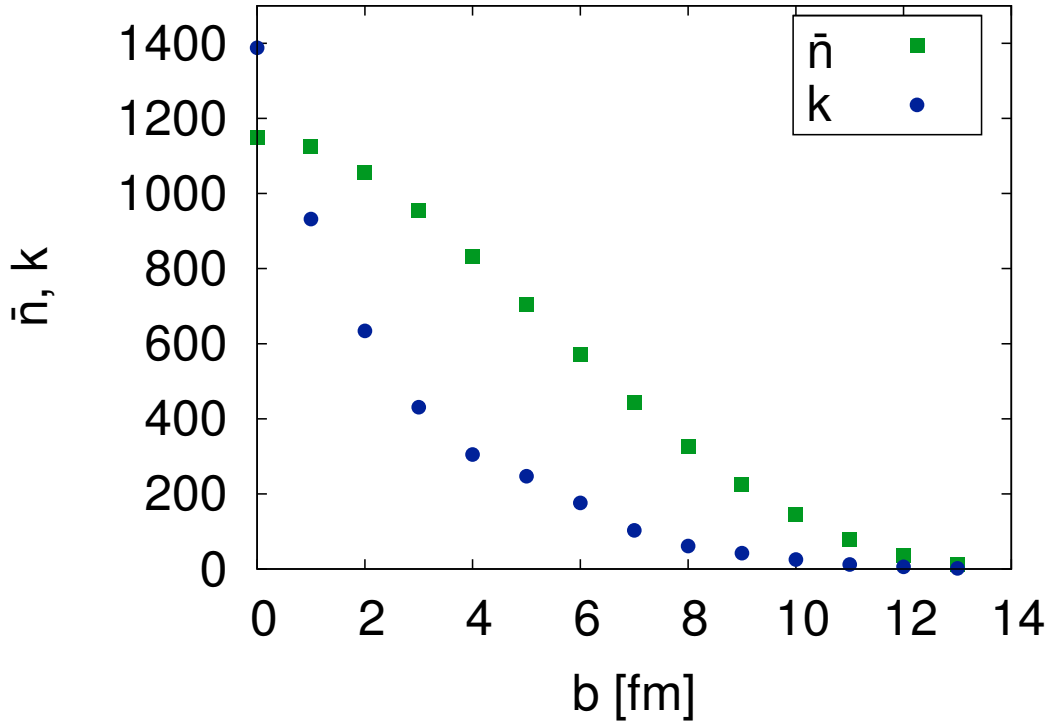

Ratio of $k/\bar{n}$ is > 1 for small b and becomes small ~ 0.14 for large b.
That is close to the value extracted for $p+p$ collisions: Dumitru and Nara arXiv:1201.6382

NBDs and Glasma flux tubes

B.Schenke, P.Tribedy, R.Venugopalan, Phys.Rev.C86, 034908 (2012)

Glasma flux tube picture:

$$k = \zeta \frac{N_c^2 - 1}{2\pi} Q_s^2 S_\perp$$

Gelis, Lappi, Mclerran, arXiv:0905.3234

Width of NBD is inversely proportional to the number of flux tubes $Q_s^2 S_\perp$.
$S_\perp =$ interaction area

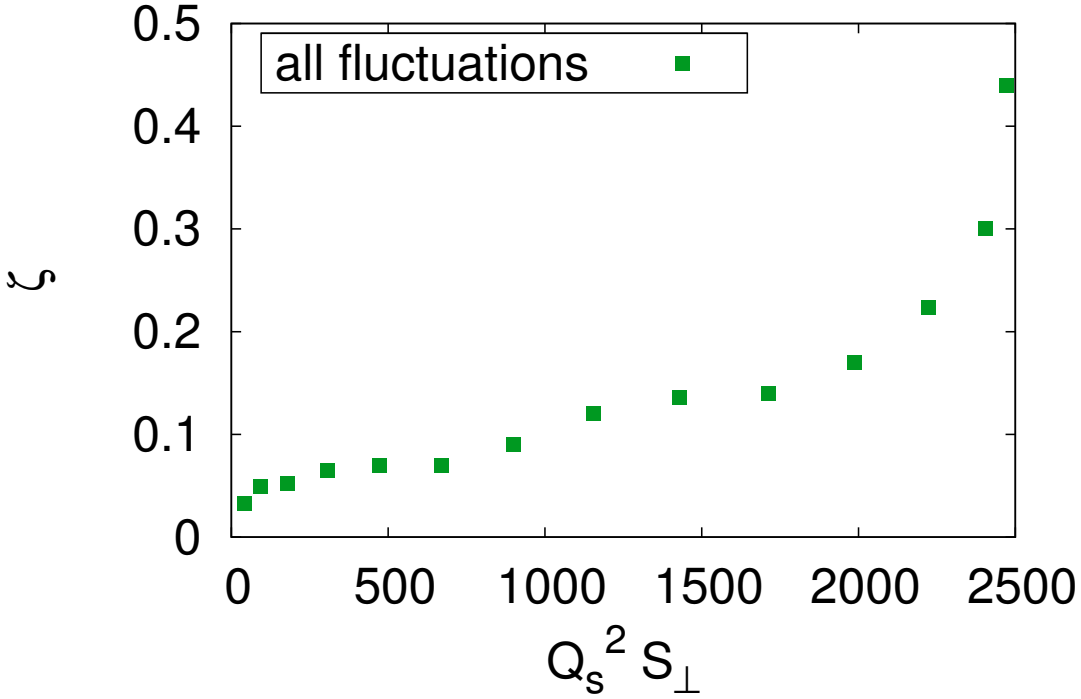

ζ should be close to constant in the flux tube picture

NBDs and Glasma flux tubes

B.Schenke, P.Tribedy, R.Venugopalan, Phys.Rev.C86, 034908 (2012)

ζ is not constant because geometric fluctuations are very important
Were not considered in the derivation of

$$k = \zeta \frac{N_c^2 - 1}{2\pi} Q_s^2 S_\perp$$

Eliminate by using smooth nucleon distributions:

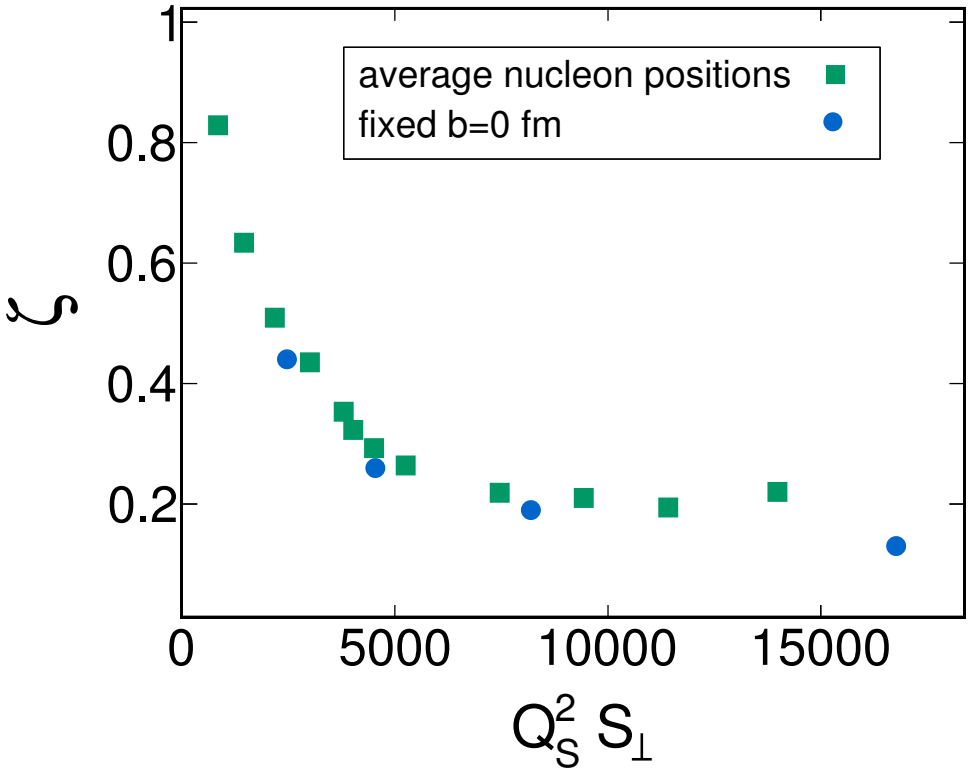

Color charge densities of incoming nuclei

- Sample positions of nucleons from Woods-Saxon distributions in nucleus A and B.
- IP-Sat provides $Q_s^2(x, \mathbf{b}_\perp)$ for each nucleon.
  The color charge density squared $g^2\mu^2$ is proportional to Q_s^2.
  (proportionality factor depends on details of calculation - see Lappi, arXiv:0711.3039)
- We add all $g^2\mu^2(\mathbf{x}_\perp)$ in each nucleus to obtain $g^2\mu_1^2(\mathbf{x}_\perp)$ and $g^2\mu_2^2(\mathbf{x}_\perp)$.

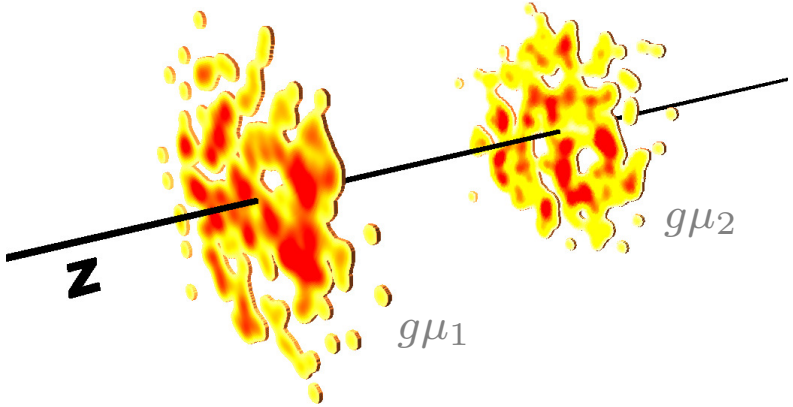

- Sample ρ^a from local Gaussian distribution for each nucleus

$$\langle \rho^a(\mathbf{x}_\perp)\rho^b(\mathbf{y}_\perp)\rangle = \delta^{ab}\delta^2(\mathbf{x}_\perp - \mathbf{y}_\perp)g^2\mu^2(\mathbf{x}_\perp)$$

Gauge fields before the collision

Color currents:

$$J_1^\nu = \delta^{\mu+}\rho_1(x^-, \mathbf{x}_\perp)$$
$$[D_\mu, F^{\mu\nu}] = J_1^\nu$$

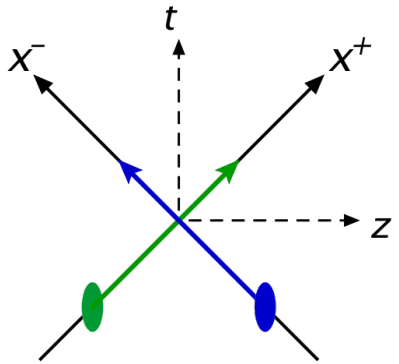

$$J_2^\nu = \delta^{\mu-}\rho_2(x^+, \mathbf{x}_\perp)$$
$$[D_\mu, F^{\mu\nu}] = J_2^\nu$$

Solution in covariant gauge:

$$A^+_{\mathrm{cov}(1,2)}(x^-, \mathbf{x}_\perp) = -\frac{g\rho_{(1,2)}(x^-, \mathbf{x}_\perp)}{\nabla_\perp^2 + m^2}$$

with infrared cutoff m of order Λ_{QCD}.

Solution in light cone gauge:

$$A^+_{(1,2)}(\mathbf{x}_\perp) = A^-_{(1,2)}(\mathbf{x}_\perp) = 0$$
$$A^i_{(1,2)}(\mathbf{x}_\perp) = \frac{i}{g} V_{(1,2)}(\mathbf{x}_\perp)\partial_i V^\dagger_{(1,2)}(\mathbf{x}_\perp)$$

V is the path-ordered exponential of $A^+_{\mathrm{cov}(1,2)}$

Gauge fields before the collision

The correlator of the Wilson lines (same one we looked at before)

$$C_{(1,2)}(\mathbf{x}_\perp) = \frac{1}{N_c}\mathrm{Re}[\mathrm{tr}(V(1,2)^\dagger(0,0)V(1,2)(x,y))]$$

with

$$V_{(1,2)}(\mathbf{x}_\perp) = P\exp\left(-ig\int dx^- \frac{\rho_{(1,2)}(x^-,\mathbf{x}_\perp)}{\nabla_\perp^2 + m^2}\right)$$

shows the degree of correlations and fluctuations in the gluon fields.

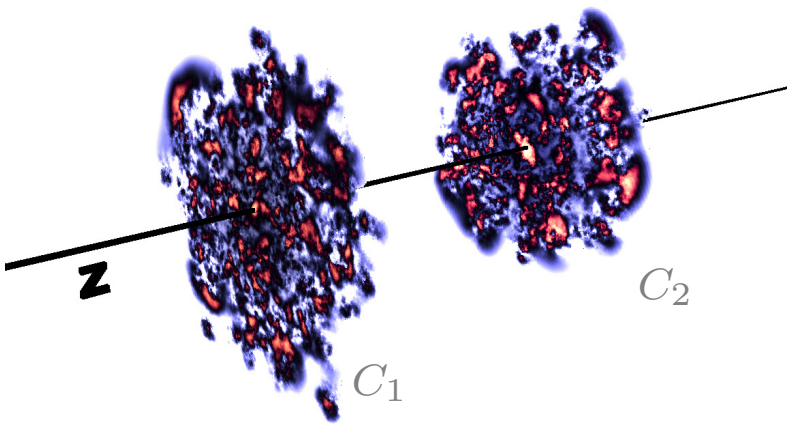

The length scale of fluctuations is $1/Q_s$. Not the nucleon size.

IP-Glasma: Gauge fields after the collision (Glasma)

Initial condition on the lightcone:

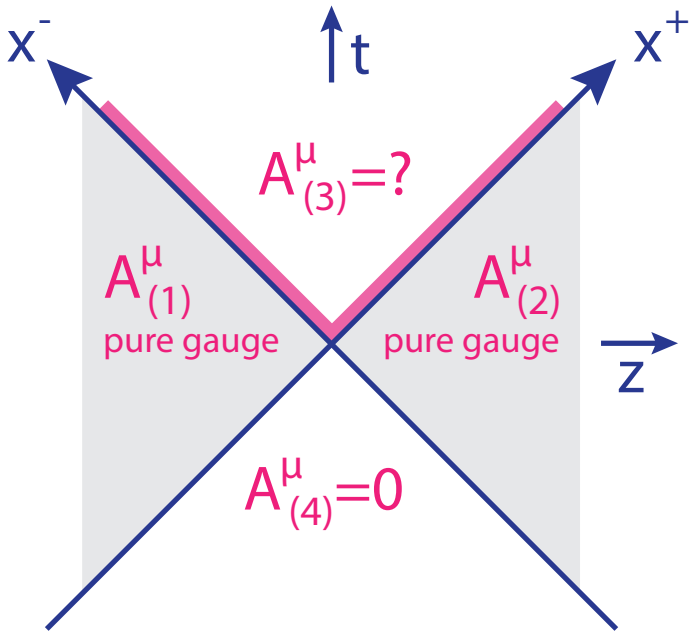

Configuration in Schwinger gauge $A^\tau = 0$

Solution:

$$A^i_{(3)}|_{\tau=0} = A^i_{(1)} + A^i_{(2)}$$

$$A^\eta_{(3)}|_{\tau=0} = \frac{ig}{2}[A^i_{(1)}, A^i_{(2)}]$$

We solve for the gauge fields numerically

Krasnitz, Venugopalan, Nucl.Phys. B557 (1999) 237

Time evolution follows Yang-Mills equations

Modeling x and b dependence: IP-Sat model

Want to determine color charge distribution in a nucleus. Proton first:
Use IP-Sat model to parametrize

- x-dependence
- Impact parameter dependence (IP)

  Kowalski, Teaney, Phys.Rev. D68 (2003) 114005

x-evolution can be computed using JIMWLK,
but parametrization is easier for now

Modeling x and b dependence: IP-Sat model

Want to determine color charge distribution in a nucleus. Proton first:
Use IP-Sat model to parametrize

- x-dependence
- Impact parameter dependence (IP)

  Kowalski, Teaney, Phys.Rev. D68 (2003) 114005

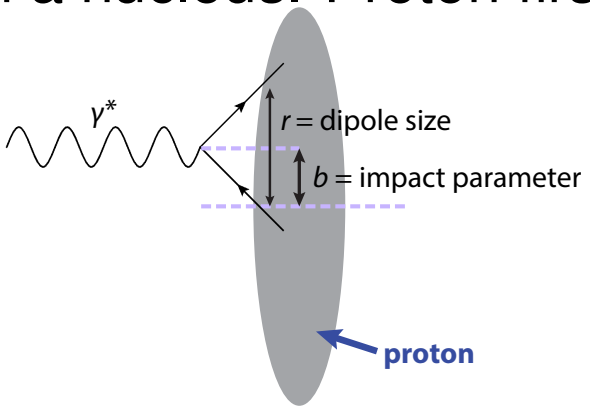

x-evolution can be computed using JIMWLK, but parametrization is easier for now

IP-Sat proton dipole cross section in deeply inealstic scattering (DIS):

$$\frac{\mathrm{d}\sigma^{\mathrm{p}}_{\mathrm{dip}}}{\mathrm{d}^2\mathbf{b}_\perp}(\mathbf{r}_\perp, x, \mathbf{b}_\perp) = 2\mathcal{N}(\mathbf{r}_\perp, x, \mathbf{b}_\perp) = 2\left[1 - \exp\left(-\frac{\pi^2}{2N_c}\mathbf{r}_\perp{}^2\alpha_s(Q^2)xg(x,Q^2)T_p(\mathbf{b}_\perp)\right)\right]$$

with Q^2 an energy scale related to the dipole size $\mathbf{r}_\perp$

gluon density

Gaussian shape

Parameters fit to HERA diffractive data

Q_s is defined by the scale r where $\mathcal{N}$ reaches the saturated regime

$\mathcal{N}(R_s, x, \mathbf{b}_\perp) = 1 - e^{-1/2}$, with $Q_s^2 = \frac{2}{R_s^2}$

Gauge fields after the collision (Glasma)

Initial condition on the lightcone: require that fields match smoothly on the lightcone.

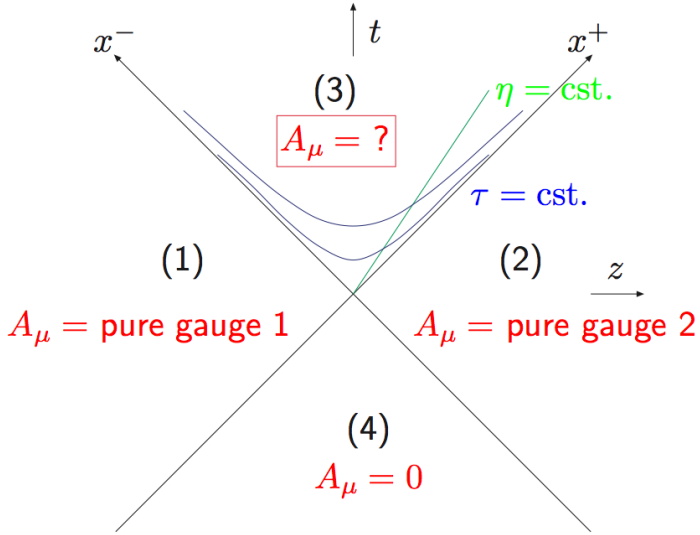

figure from Lappi, arXiv:1003.1852

Solution:

$$A^i_{(3)}|_{\tau=0} = A^i_{(1)} + A^i_{(2)}$$

$$A^\eta_{(3)}|_{\tau=0} = \frac{ig}{2}[A^i_{(1)}, A^i_{(2)}]$$

On the lattice the Wilson lines in the future lightcone are obtained from the condition:

$$\mathrm{tr}\left\{t^a\left[\left(U^i_{(1)} + U^i_{(2)}\right)\left(1 + U^{i\dagger}_{(3)}\right) - \left(1 + U^i_{(3)}\right)\left(U^{i\dagger}_{(1)} + U^{i\dagger}_{(2)}\right)\right]\right\} = 0$$

where t^a are the generators of $SU(N_c)$ in the fundamental representation. Solve iteratively.

Krasnitz, Venugopalan, Nucl.Phys. B557 (1999) 237

$$U^i_{(1,2),j} = V_{(1,2),j} V^\dagger_{(1,2),j+\hat{e}_i}$$ (gauge transform of $\mathbf{1}$: pure gauge)

E_η can be obtained from $U^i_{(1,2,3)}$

Modeling x and b dependence of Q_s: IP-Sat model

After fitting parameters to HERA DIS data the model provides a distribution of $Q_s^2(x, \mathbf{b}_\perp)$ of the proton, which will be our input

It is determined self consistently from the requirement that

$$\mathcal{N}(R_s, x, \mathbf{b}_\perp) = 1 - e^{-1/2}, \quad \text{with } Q_s^2 = \frac{2}{R_s^2}$$

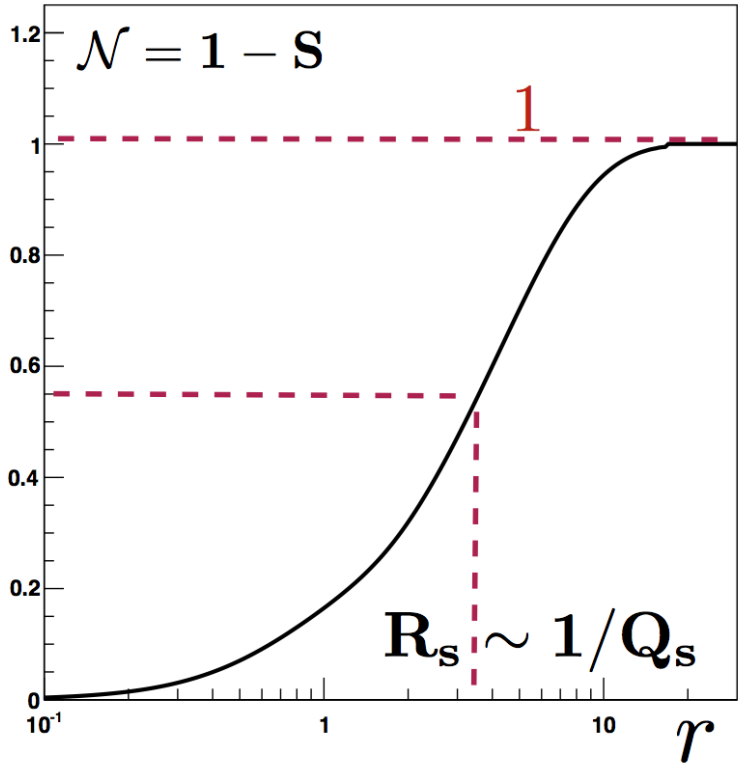

Multiplicity B.Schenke, P.Tribedy, R.Venugopalan, Phys. Rev. C86, 034908 (2012)

dN_{g}/dy in transverse Coulomb gauge $\partial_i A^i = 0$
N_{part} from MC-Glauber with $\sigma_{NN} = 42\,\mathrm{mb}$ and $64\,\mathrm{mb}$ respectively

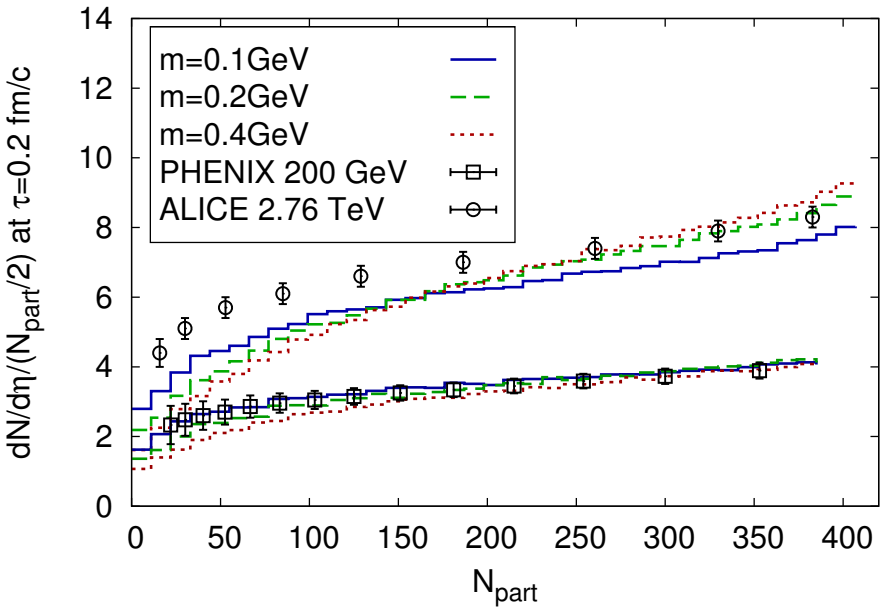

Experimental data: PHENIX, Phys.Rev.C71 034908 (2004) and ALICE, Phys.Rev.Lett. 106, 032301 (2011)

Scaled by $2/3$ to compare to charged particles.
New version. Using IP-Sat for nuclei. m-dependence.

Equations to be solved

Explicit version of $\partial_\mu T^{\mu\nu} = 0$ in an appropriate coordinate system that expands longitudinally

proper time $\tau = \sqrt{t^2 - z^2}$, space-time rapidity $\eta_s = \frac{1}{2} \ln \frac{t+z}{t-z}$

$$\partial_\tau(\tau T^{\tau\tau}) + \partial_v(\tau T^{v\tau}) + \partial_{\eta_s}(T^{\eta_s\tau}) + T^{\eta_s\eta_s}$$
$$+\partial_\tau(\tau\pi^{\tau\tau}) + \partial_v(\tau\pi^{v\tau}) + \partial_{\eta_s}(\pi^{\eta_s\tau}) + \pi^{\eta_s\eta_s} = 0$$

$$\partial_\tau(\tau T^{\tau\eta_s}) + \partial_v(\tau T^{v\eta_s}) + \partial_{\eta_s}(T^{\eta_s\eta_s}) + T^{\tau\eta_s}$$
$$+\partial_\tau(\tau\pi^{\tau\eta_s}) + \partial_v(\tau\pi^{v\eta_s}) + \partial_{\eta_s}(\pi^{\eta_s\eta_s}) + \pi^{\tau\eta_s} = 0$$

$$\partial_\tau(\tau T^{\tau v}) + \partial_w(\tau T^{wv}) + \partial_{\eta_s}(T^{\eta_s v})$$
$$+\partial_\tau(\tau\pi^{\tau v}) + \partial_w(\tau\pi^{wv}) + \partial_{\eta_s}(\pi^{\eta_s v}) = 0$$

spatial derivatives (computed using Kurganov-Tadmor method) treated as sources

Equations to be solved

In addition, we have to solve the equation for $\pi^{\mu\nu}$
(2nd order Israel-Stewart viscous fluid-dynamics)

$$\begin{aligned}\partial_c(u^c\pi^{ab}) = &-\frac{1}{2\tau}u^\tau\pi^{ab} + \frac{1}{\tau}\Delta^{a\eta}u^\eta\pi^{b\tau} - \frac{1}{\tau}\Delta^{a\tau}u^\eta\pi^{b\eta} \\ &- g_{cf}\pi^{cb}u^a Du^f - \frac{\pi^{ab}}{2\tau_\pi} - \frac{1}{6}\pi^{ab}\partial_c u^c \\ &+ \frac{\eta}{\tau_\pi}\left(-\frac{1}{\tau}\Delta^{a\eta}g^{b\eta}u^\tau + \frac{1}{\tau}\Delta^{a\eta}g^{b\tau}u^\tau \right. \\ &\qquad \left. + g^{ac}\partial_c u^b - u^a Du^b - \frac{1}{3}\Delta^{ab}\partial_c u^c\right) \\ &+ (a \leftrightarrow b)\,,\end{aligned}$$

relaxation time τ_π
$\Delta^{\mu\nu} = g^{\mu\nu} - u^\mu u^\nu$
$D = u^\mu\partial_\mu$
$\tau_\pi = 3\eta/(\varepsilon + P)$: shear relaxation time

Yang-Mills evolution

The equations of motion are formulated on the lattice in 2+1D ($\phi = A_\eta$)

$$\dot{U}_i = i\frac{g^2}{\tau}E^i U_i \text{ (no sum over } i)$$
$$\dot{\phi} = \tau E^\eta$$
$$\dot{E}^1 = \frac{i\tau}{2g^2}[U_{1,2} + U_{1,-2} - U^\dagger_{1,2} - U^\dagger_{1,-2} - T_1] + \frac{i}{\tau}[\tilde{\phi}_1, \phi]$$
$$\dot{E}^2 = \frac{i\tau}{2g^2}[U_{2,1} + U_{2,-1} - U^\dagger_{2,1} - U^\dagger_{2,-1} - T_2] + \frac{i}{\tau}[\tilde{\phi}_1, \phi]$$
$$\dot{E}^\eta = \frac{1}{\tau}\sum_i \left[\tilde{\phi}_i + \tilde{\phi}_{-i} - 2\phi\right]$$

where $T_1 = \frac{1}{N_c}\mathrm{tr}[U_{1,2} + U_{1,-2} - U^\dagger_{1,2} - U^\dagger_{1,-2}]\,\mathbf{1}$, and
$T_2 = \frac{1}{N_c}\mathrm{tr}[[U_{2,1} + U_{2,-1} - U^\dagger_{2,1} - U^\dagger_{2,-1}]\,\mathbf{1}$ with the $N_c \times N_c$ unit matrix $\mathbf{1}$
$\tilde{\phi}^j_i = U^i_j \phi_{j+\hat{e}_i} U^{i\dagger}_j$ and $U^j_{1,2} = U^1_j\, U^2_{j+\hat{e}_1}\, U^{1\dagger}_{j+\hat{e}_2}\, U^{2\dagger}_j$

Event plane

To get non-zero odd moments, we rotate the event plane in each event.
Event plane is defined by the angle:

$$\psi_n = \frac{1}{n} \arctan \frac{\langle w \sin(n\phi) \rangle}{\langle w \cos(n\phi) \rangle}$$

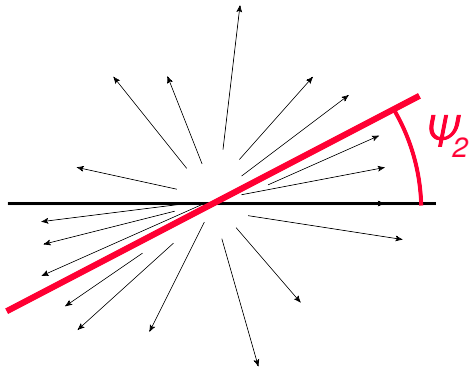

using particle momenta.
($w = p_T$ (first results) or 1 (later results))

A.Poskanzer and S.Voloshin, Phys.Rev.C58:1671-1678 (1998)

$$v_n = \langle \cos(n(\phi - \psi_n)) \rangle$$

... different angle for every flow coefficient.

In the simulation we know the true event-plane (no correction factor).

Effect of initial flow

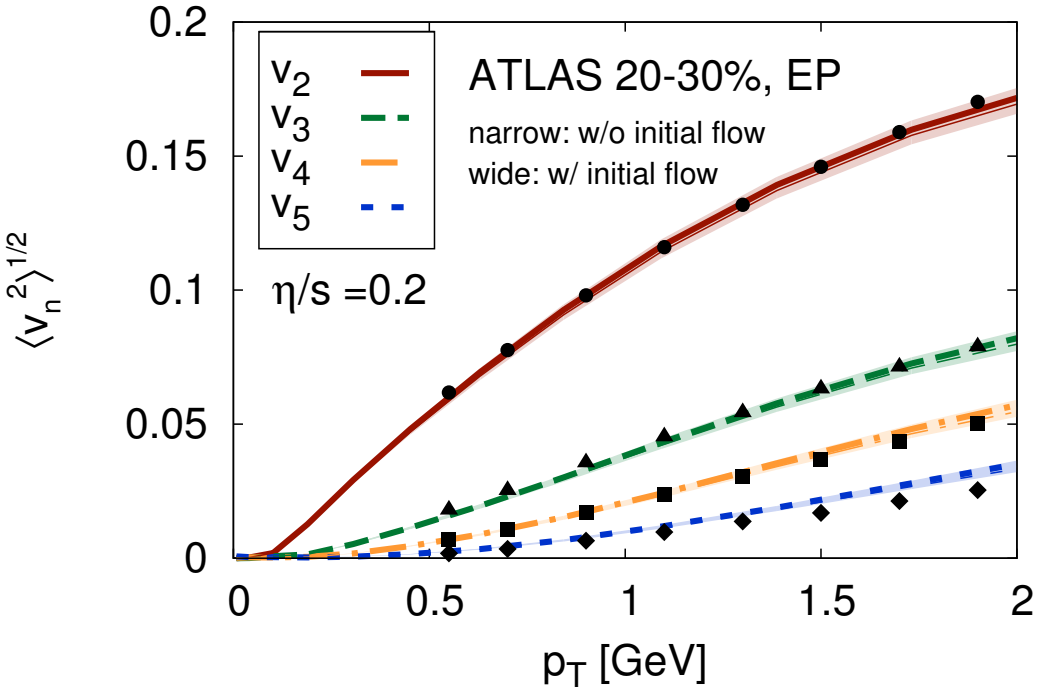

Weak effect of initial flow on hadron $v_n(p_T)$

Expect stronger effect for photon v_n:
Photons are mostly produced early at high temperatures

Effect of different switching time $0.4\,\mathrm{fm}/c$ is very weak

Experimental data:
ATLAS collaboration, Phys. Rev. C 86, 014907 (2012)

Directed flow v_1

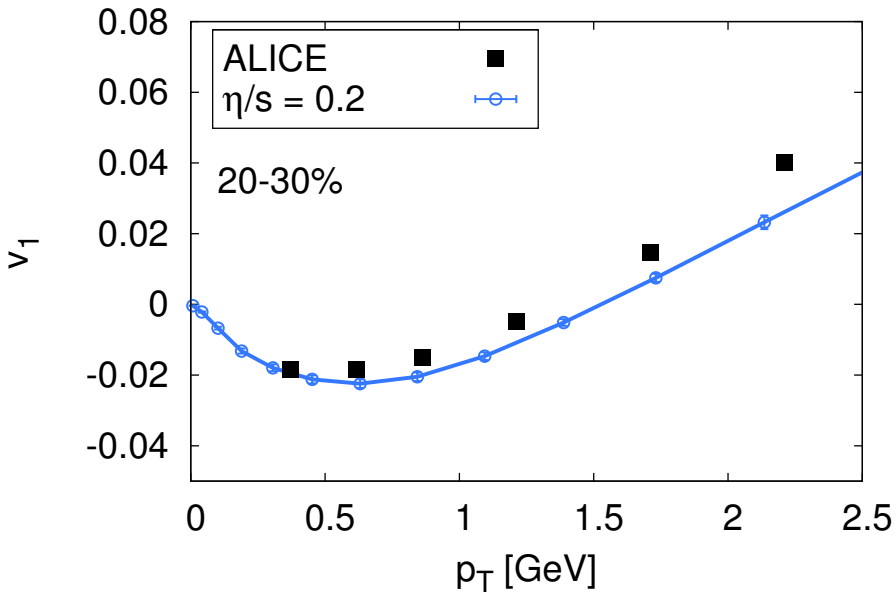

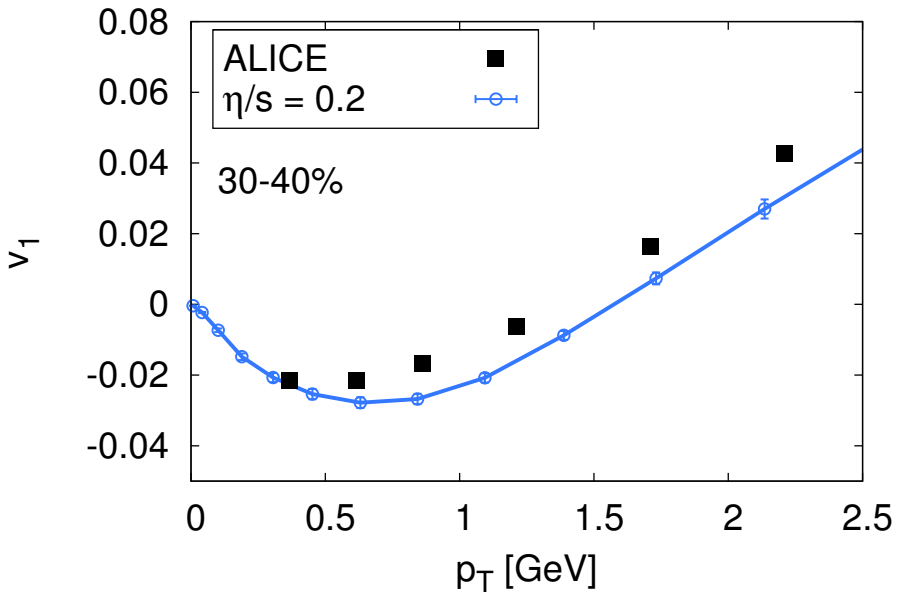

Experimental data:

extracted in Retinskaya et al., Phys.Rev.Lett. 108 (2012) 252302

from ALICE data in K. Aamodt et al., Phys. Lett. B 708, 249 (2012)

More centrality classes: IP-Glasma + MUSIC

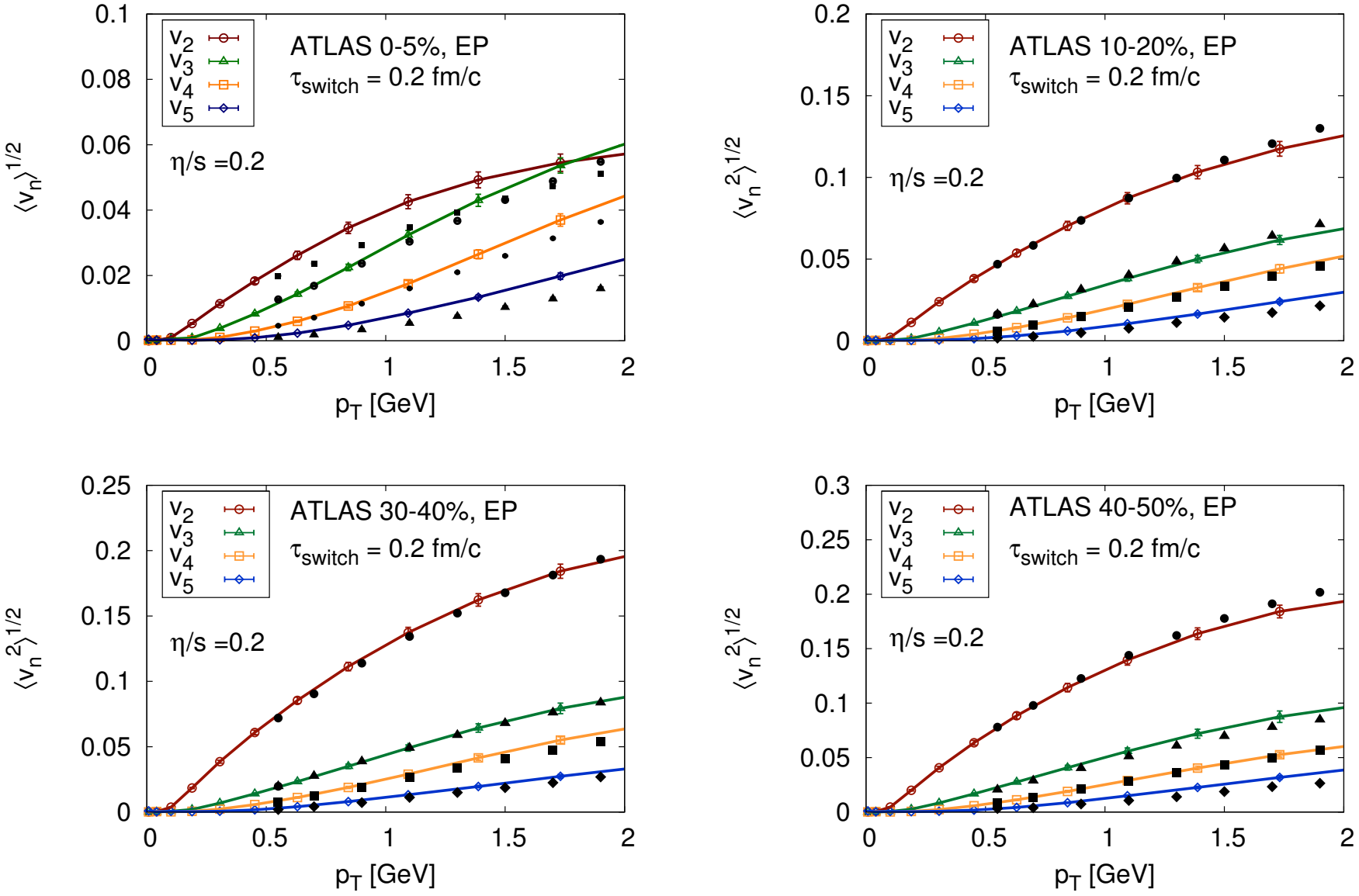

Smaller average η/s

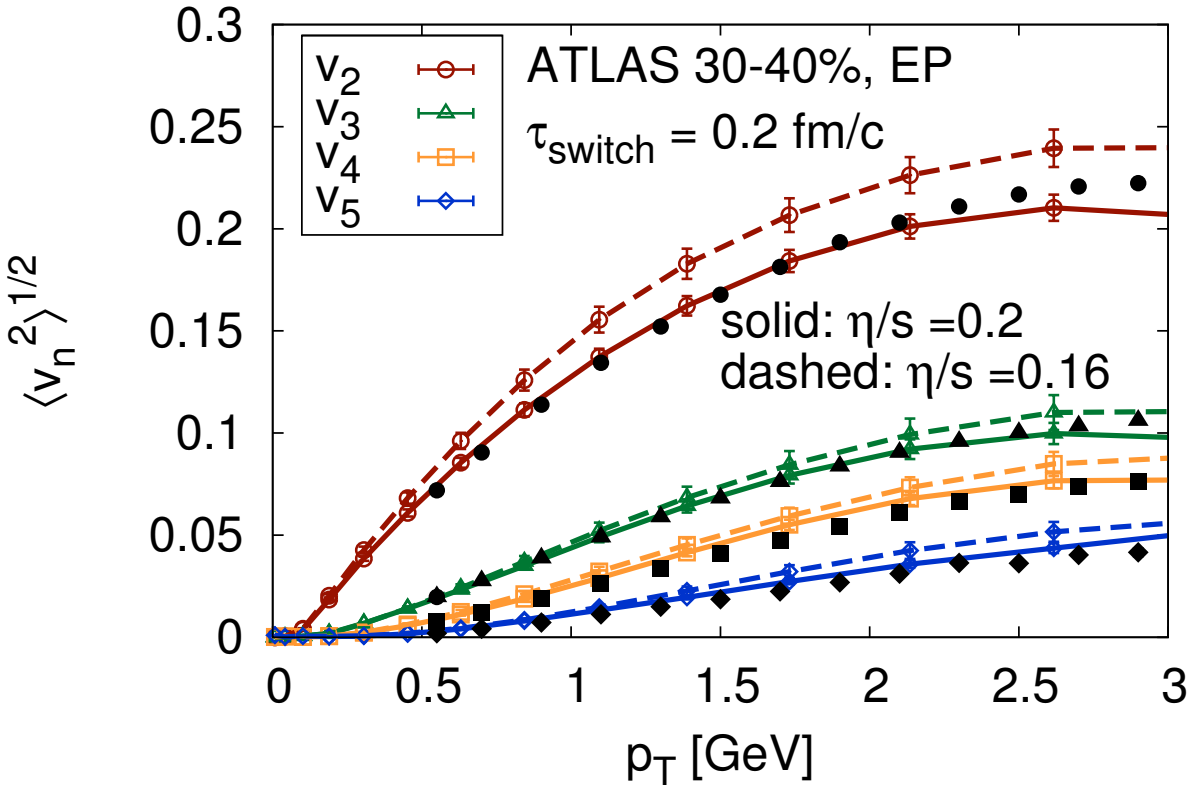

Using $\eta/s = 0.16$ overestimates all v_n

Experimental data:
ATLAS collaboration, Phys. Rev. C 86, 014907 (2012)

High Multiplicity pp and pA: explosive Stringy Pomeron and Hydrodynamics at its Edge

arXiv:1301.4470

Edward Shuryak and Ismail Zahed

Stony Brook

Talk at RBRC workshop, April 2013

2 parts:

micro=>macro

macro=>micro

micro-to-macro: excitation of stringy Pomeron

- stringy Pomeron: Stoffers-Zahed model
- T=>T(Hagedorn) in bulk and for one string
- transition to explosive regime
- black hole connection

stringy Pomeron

A. Stoffers and I. Zahed, arXiv:1211.3077 [nucl-th].
I. Zahed, arXiv:1211.6421 [hep-ph].

At very high energies the rapidity interval parameter is large

$$\chi = \ln(s/s_0) \gg 1 \tag{48}$$

and will play the role of the *effective time* in

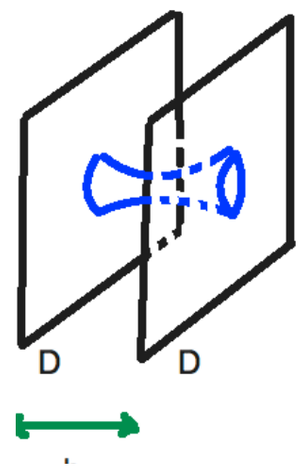

sion. Two longitudinal directions – time and the beam direction, also often used as light cone variables $x_\pm$ – are complemented by two transverse coordinates plus a *"scale coordinate" z*. Its initial value corresponds to a physical size of the colliding dipoles and diffusion means the production of small size closed strings. The z-coordinate is not flat. We will model its metric by an AdS_5 with a wall. The number of transverse coordinates, which will play an important role in the following, is thus

$$D_\perp = 3 \tag{49}$$

$$\frac{1}{-2is}\mathcal{T}(s,t;k) \approx g_s^2 \int d^2\mathbf{b}\, e^{iq\cdot\mathbf{b}}\, \mathbf{K}_T(\beta,\mathbf{b};k) \tag{50}$$

where $\mathbf{K}_T$ is the pomeron propagator for dipole sources of color N_c-ality k describing the string flux. k runs over all integers till $N_c/2$ for even N_c and $N_c/2+1/2$ for odd ones. In the real world with the SU(3) color group, $k=1$ is the usual string between fundamental charges (quarks) and the largest tension $k=2$ is the one between two baryon junctions. The first argu-

$$\mathcal{T}(s,t;k) \approx i g_s^2 \left(\frac{s}{s_0}\right)^{1+\frac{kD_\perp}{12}+\frac{\alpha'}{2k}t} \tag{59}$$

Thus the resulting pomeron is supercritical, with the intercept above 1

$$\alpha_{\mathbf{P},k}(0) = 1 + \frac{kD_\perp}{12} \to 1 + \frac{kD_\perp}{12} - \frac{(D_\perp-1)^2}{8\sqrt{\lambda}} \tag{60}$$

where the first term is due to Casimir-Luscher contribution and the $1/\sqrt{\lambda}$ correction follows from the tachyonic correction (58) as discussed in [1].

$D_k\chi$. A more precise bound follows from the inclusion of the $1/\lambda$ corrections in the tachyon mass (58) or

$$\beta > \sqrt{2(\alpha_{\mathbf{P}}-1)}\,\beta_H \tag{61}$$

This leads to the bound $\chi < 10$ for the corrected phenomenological value of the pomeron intercept $\alpha_{\mathbf{P}} - 1 = 0.08$ in (60), which roughly corresponds to energies below the LHC. This

now our paper

a stringy cylinder generates temperature, entropy and even viscosity (Kubo)

1/T is circle's sircumference,

so T is highest at the middle

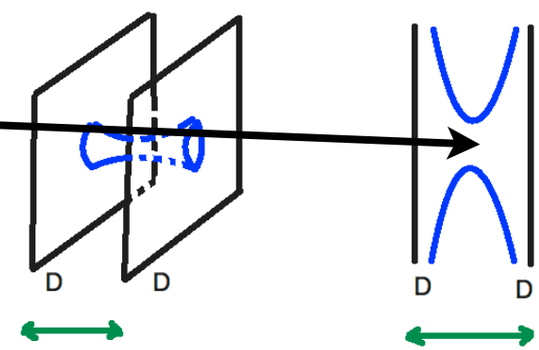

$$\mathbf{S} = -D_\perp \sum_{n=1}^{\infty} \left(\ln\left(1 - e^{-\beta_k n}\right) + \frac{\beta_k n}{e^{\beta_k n} - 1} \right) + D_\perp \left(\frac{\beta_k}{12} - \frac{1}{2}\left(1 + \ln\left(\frac{\beta_k}{2\pi}\right)\right)\right)$$

Pure glue thermodynamics

Near-Hagedorn regime: a string gets excited into a **string ball,** with growing **entropy,energy** but **not free energy (=p)!**

a b

Polyakov, Susskind 1978

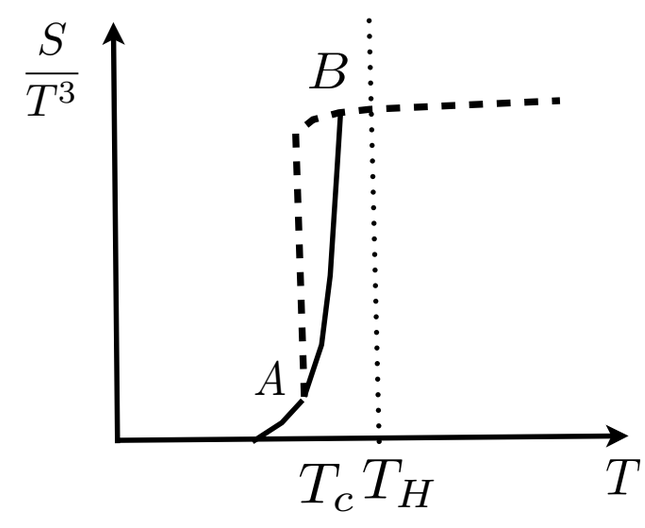

FIG. 2: Schematic temperature dependence of the entropy density. The dashed line represents equilibrium gluodynamics with a first order transition at $T = T_c$. The solid line between points A and B represents the expected behavior of a single string approaching its Hagedorn temperature T_H.

but when T is too close to T(Hagedorn), transition to QGP happens, pressure grows and the ball can explode!

$T \Rightarrow T_H$

Hagedorn regime
string makes a ball
small F,p
large E,S

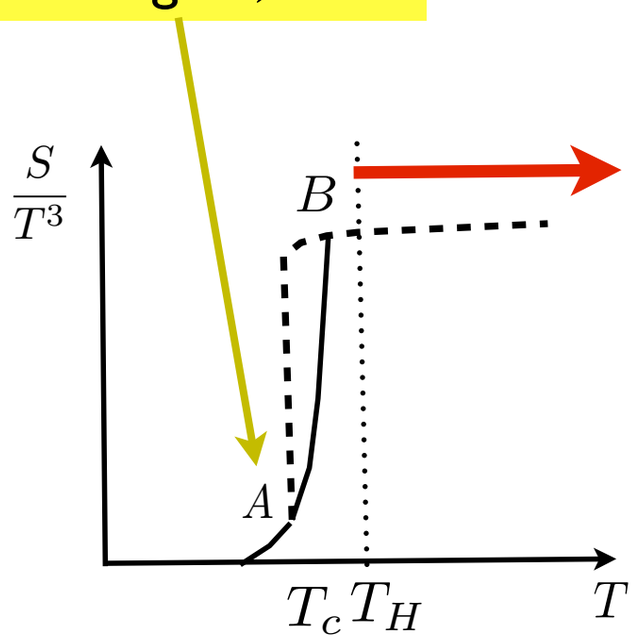

FIG. 2: Schematic temperature dependence of the entropy density. The dashed line represents equilibrium gluodynamics with a first order transition at $T = T_c$. The solid line between points A and B represents the expected behavior of a single string approaching its Hagedorn temperature T_H.

$$\frac{\Delta\beta}{\beta_H} = \frac{T_H}{T} - 1 = \mathcal{O}\left(\frac{1}{N_c}\right)$$

The ratio of the high multiplicity events to the minimum bias events can be estimated as

$$\frac{\sigma_{HM}}{\sigma_{MB}} \approx g_s^2 \frac{1}{\chi^{D_\perp/2}} \left(\frac{\Delta\beta}{\beta_H}\right) e^{-\chi\sqrt{\Delta\beta/2\beta_H}} \quad (72)$$

where we have dropped an overall number of order 1 and $D_\perp = 3$. For near critical strings we have (70) and $g_s \approx 1/N_c$. At LHC, $\chi \approx 10$ so that

$$\frac{\sigma_{HM}}{\sigma_{MB}} \approx 10^{-5} \quad (73)$$

This estimate is comparable to the probability of the high multiplicity trigger used by the CMS collaboration for events displaying the ridge in pp collisions at LHC.

a string ball is dual to a black hole

The correspondence is usually derived via the entropy

(=Hawking-Bekenstein)

But one can also calculate viscosity, which gives 1/4pi

although the calculation is stringy not BH. (And even if BH it is very different from that in AdS/CFT , not located in 5-th dimension, so were surprised)

Kubo

tensor. To assess the primordial viscosity, we follow [2] and write the needed expression on the streched horizon for the excited string

$$\eta_R = \lim_{\omega_R \to 0} \frac{A_R}{2\omega_R} \int_0^\infty d\tau e^{i\omega_R \tau} \mathbf{R}_{23,23}(\tau) \quad (87)$$

with A_R the area of the black-hole and τ a dimensionless Rindler time. The retarded commutator of the normal ordered transverse stress tensor for the Polyakov string on the Rindler horizon reads

$$\mathbf{R}_{23,23}(\tau) = \left\langle \left[T_\perp^{23}(\tau), T_\perp^{23}(0) \right] \right\rangle \quad (88)$$

with

$$T_\perp^{23}(\tau) = \frac{1}{2A_R} \sum_{n \neq 0} : a_n^2 a_n^3 : e^{-2in\tau} \quad (89)$$

and the canonical rules $\left[a_m^i, a_n^j\right] = m\delta_{m+n,0}\delta^{ij}$. The averaging in (88) is carried using the black-body spectrum as in (84). The result is

$$\eta_R = \lim_{\omega_R \to 0} \frac{A_R}{2\omega_R} \frac{\pi}{2A_R^2} \frac{(\omega_R/2)^2}{e^{\beta_R \omega_R/2} - 1} = \frac{1}{A_R} \frac{\pi}{8\beta_R} \quad (90)$$

We note the occurence of the Bekenstein-Hawking or Rindler temperature $\beta_{BH} = \beta_R$ in the thermal factor.

Combining (86) for the entropy to (90) yields the viscosity on the streched horizon

$$\frac{\eta_R}{\mathbf{S_R}/A_R} = \frac{1}{4\pi} \left(\frac{3}{D_\perp} \right) \equiv \frac{1}{4\pi} \quad (91)$$

summary
micro=>macro

- at very high energy the strings of the Pomeron gets longer and effectively hotter
- as its T approach Haderon temperature, a string ball regime appears => high S,E but not p
- as T grows too close to T(Hagedorn), string ball saturates the space and transition to sQGP happens. => p grows =>hydro explosion

Macro to micro: Outline

Macro to micro: Outline

- history before LHC

Macro to micro: Outline

- history before LHC
- 4 papers from LHC experiments

Macro to micro: Outline

- history before LHC
- 4 papers from LHC experiments
- two small parameters of hydro

Macro to micro: Outline

- history before LHC
- 4 papers from LHC experiments
- two small parameters of hydro
- the radial flow, gradients and viscosity

Macro to micro: Outline

- history before LHC
- 4 papers from LHC experiments
- two small parameters of hydro
- the radial flow, gradients and viscosity
- higher harmonics, sound damping

Macro to micro: Outline

- history before LHC
- 4 papers from LHC experiments
- two small parameters of hydro
- the radial flow, gradients and viscosity
- higher harmonics, sound damping
- higher harmonics for pp and pA

Macro to micro: Outline

- history before LHC
- 4 papers from LHC experiments
- two small parameters of hydro
- the radial flow, gradients and viscosity
- higher harmonics, sound damping
- higher harmonics for pp and pA
- higher gradients and LS resummation

prehistory:
Can there be hydro in pp?

prehistory:
Can there be hydro in pp?

- **the radial flow should affect pi,K,p differently** => but pp ISR data showed no effect (excellent Mt scaling)

  E. V. Shuryak and O. V. Zhirov, Phys. Lett. B 89, 253 (1979).

prehistory:
Can there be hydro in pp?

- **the radial flow should affect pi,K,p differently** => but pp ISR data showed no effect (excellent Mt scaling)
  E. V. Shuryak and O. V. Zhirov, Phys. Lett. B 89, 253 (1979).

- 20 years later Bjorken and co [MiniMax Collaboration], T. C. Brooks et al. Phys. Rev. D 61, 032003 (2000) [hep-ex/9906026] took data at TEVATRON: minor effect, inconclusive

prehistory:
Can there be hydro in pp?

- **the radial flow should affect pi,K,p differently** => but pp ISR data showed no effect (excellent Mt scaling)
  E. V. Shuryak and O. V. Zhirov, Phys. Lett. B 89, 253 (1979).

- 20 years later Bjorken and co [MiniMax Collaboration], T. C. Brooks et al. Phys. Rev. D 61, 032003 (2000) [hep-ex/9906026] took data at TEVATRON: minor effect, inconclusive

- the radial flow was seen in AA at AGS/SPS
  Good pre-RHIC hydro description C.Hung,E.Shuryak Phys.Rev. C57 (1998) 1891-1906

prehistory:
Can there be hydro in pp?

- **the radial flow should affect pi,K,p differently** => but pp ISR data showed no effect (excellent Mt scaling)
  E. V. Shuryak and O. V. Zhirov, Phys. Lett. B 89, 253 (1979).

- 20 years later Bjorken and co [MiniMax Collaboration], T. C. Brooks et al. Phys. Rev. D 61, 032003 (2000) [hep-ex/9906026] took data at TEVATRON: minor effect, inconclusive

- the radial flow was seen in AA at AGS/SPS
  Good pre-RHIC hydro description C.Hung,E.Shuryak Phys.Rev. C57 (1998) 1891-1906

- and everyone knows what happened at RHIC, v_n etc

LHC era begins

Observation of long-range, near-side angular correlations in pPb collisions at the LHC

arXiv:1210.5482v2 [nucl-ex] 22 Oct 2012

The CMS Collaboration*

high multiplicity trigger in pp reveals a ``ridge" which is also there in pPb

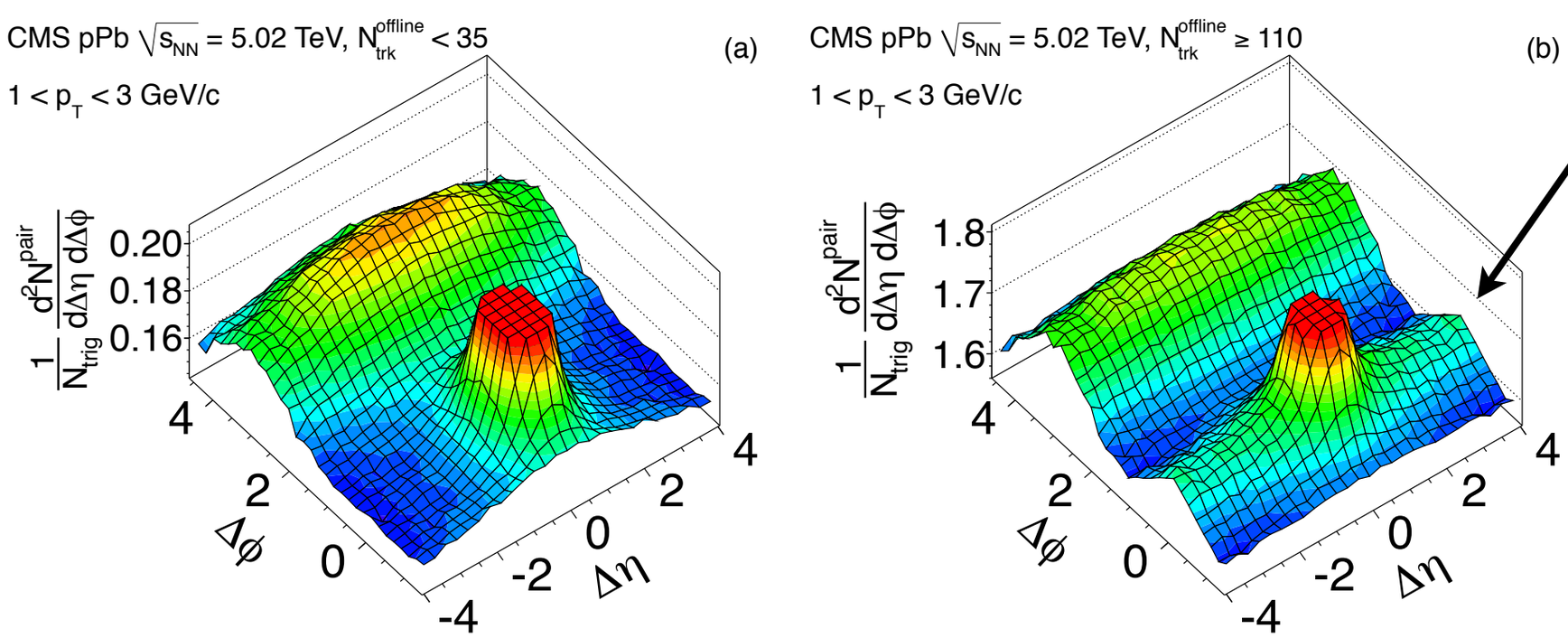

Figure 1: 2-D two-particle correlation functions for 5.02 TeV pPb collisions for pairs of charged particles with $1 < p_T < 3\,\mathrm{GeV}/c$. Results are shown (a) for low-multiplicity events ($N_{trk}^{offline} < 35$) and (b) for a high-multiplicity selection ($N_{trk}^{offline} \geq 110$). The sharp near-side peaks from jet correlations have been truncated to better illustrate the structure outside that region.

- all bins show back-to-back correlation well described by ``minijet'' models like HIJING
- Ridge is a peak at the same azimuth, seen at highest multiplicity only and at pr=1-2 GeV
- it is stronger in pA than at pp, yet the same multiplicity is needed

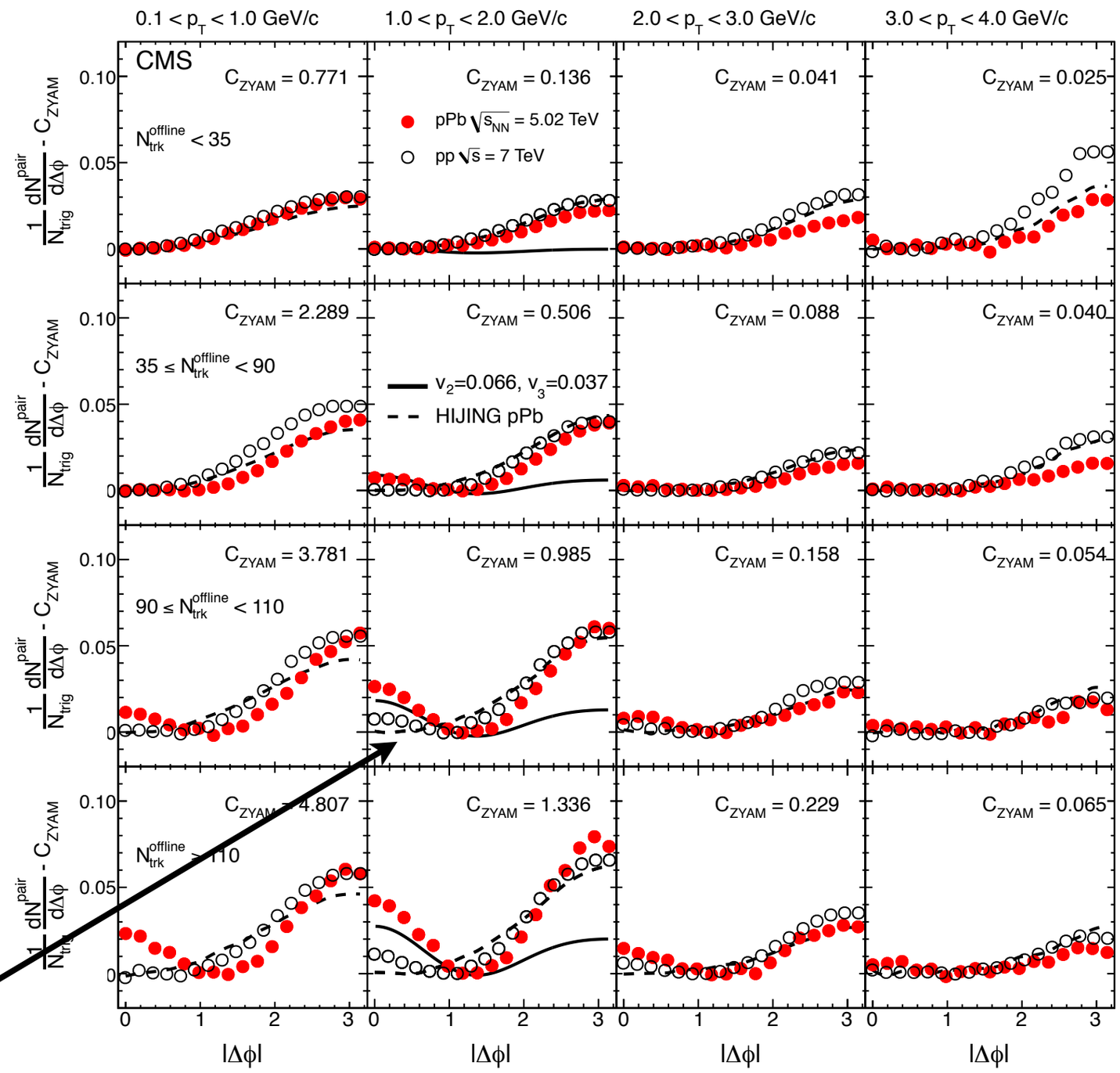

Figure 2: Correlated yield obtained from the ZYAM procedure as a function of $|\Delta\phi|$ averaged over $2 < |\Delta\eta| < 4$ in different p_T and multiplicity bins for 5.02 TeV pPb data (solid circles) and 7 TeV pp data (open circles). The p_T selection applies to both particles in each pair. Statistical uncertainties are smaller than the marker size. The subtracted ZYAM constant is listed in each panel. Also shown are pPb predictions for HIJING [24] (dashed curves) and a hydrodynamic model [25] (solid curves shown for $1 < p_T < 2$ GeV/c).

• a ``double ridge" in ALICE and ATLAS

Long-range angular correlations on the near and away side in p–Pb collisions at $\sqrt{s_{NN}}$= 5.02 TeV

arXiv:1212.2001v1 [nucl-ex] 10 Dec 2012

ALICE Collaboration*

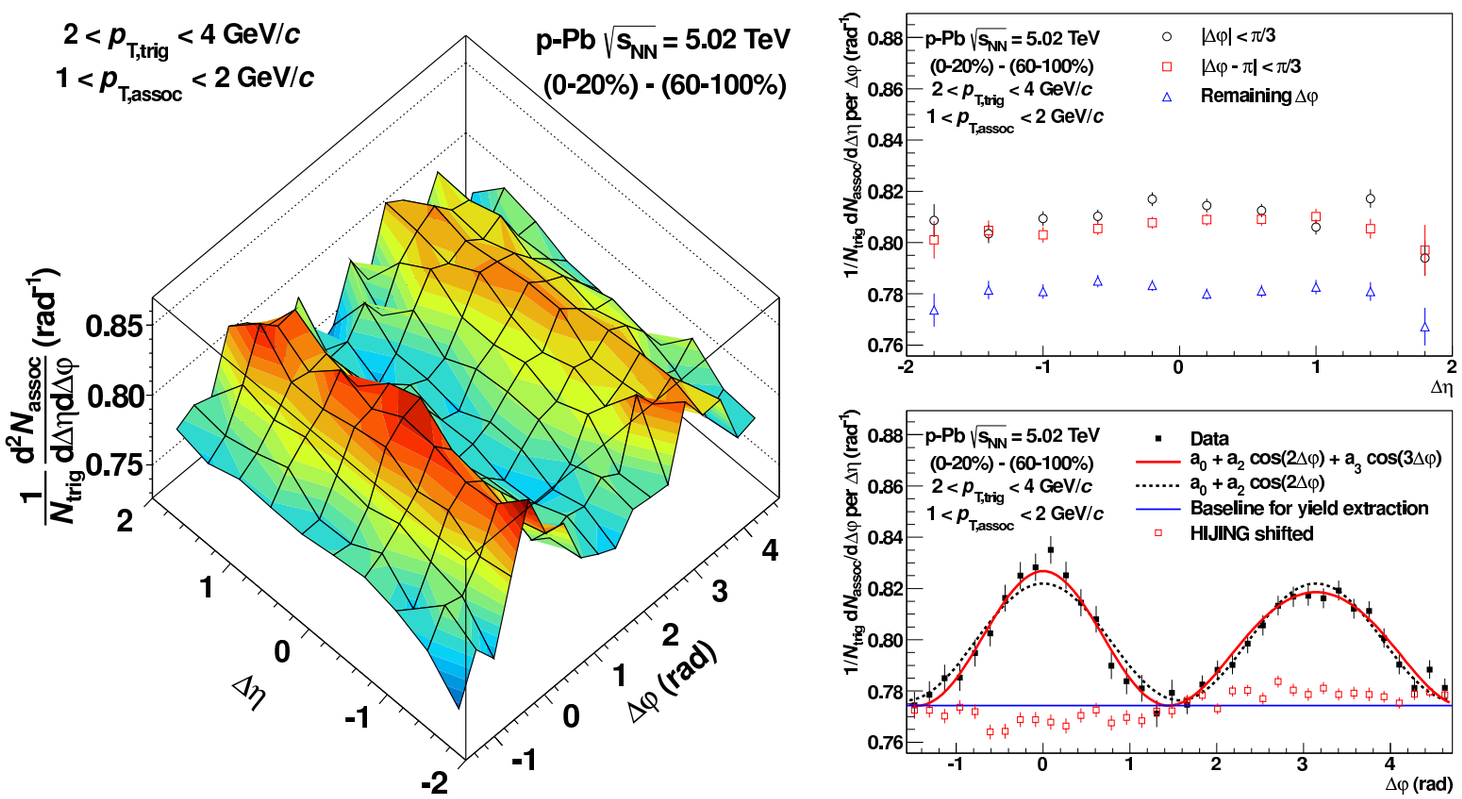

Fig. 3: Left: Associated yield per trigger particle in $\Delta\varphi$ and $\Delta\eta$ for pairs of charged particles with $2 < p_{T,trig} < 4$ GeV/c and $1 < p_{T,assoc} < 2$ GeV/c in p–Pb collisions at $\sqrt{s_{NN}} = 5.02$ TeV for the 0–20% multiplicity class, after subtraction of the associated yield obtained in the 60–100% event class. Top right: the associated per-trigger yield after subtraction (as shown on the left) projected onto $\Delta\eta$ averaged over $|\Delta\varphi| < \pi/3$ (black circles), $|\Delta\varphi - \pi| < \pi/3$ (red squares), and the remaining area (blue triangles, $\Delta\varphi < -\pi/3$, $\pi/3 < \Delta\varphi < 2\pi/3$ and $\Delta\varphi > 4\pi/3$). Bottom right: as above but projected onto $\Delta\varphi$ averaged over $0.8 < |\Delta\eta| < 1.8$ on the near side and $|\Delta\eta| < 1.8$ on the away side. Superimposed are fits containing a $\cos(2\Delta\varphi)$ shape alone (black dashed line) and a combination of $\cos(2\Delta\varphi)$ and $\cos(3\Delta\varphi)$ shapes (red solid line). The blue horizontal line shows the baseline obtained from the latter fit which is used for the yield calculation. Also shown for comparison is the subtracted associated yield when the same procedure is applied on HIJING shifted to the same baseline. The figure shows only statisti-

• a ``double ridge" in ALICE and ATLAS

arXiv:1212.2001v1 [nucl-ex] 10 Dec 2012

Long-range angular correlations on the near and away side in p–Pb collisions at $\sqrt{s_{NN}}$= 5.02 TeV

ALICE Collaboration*

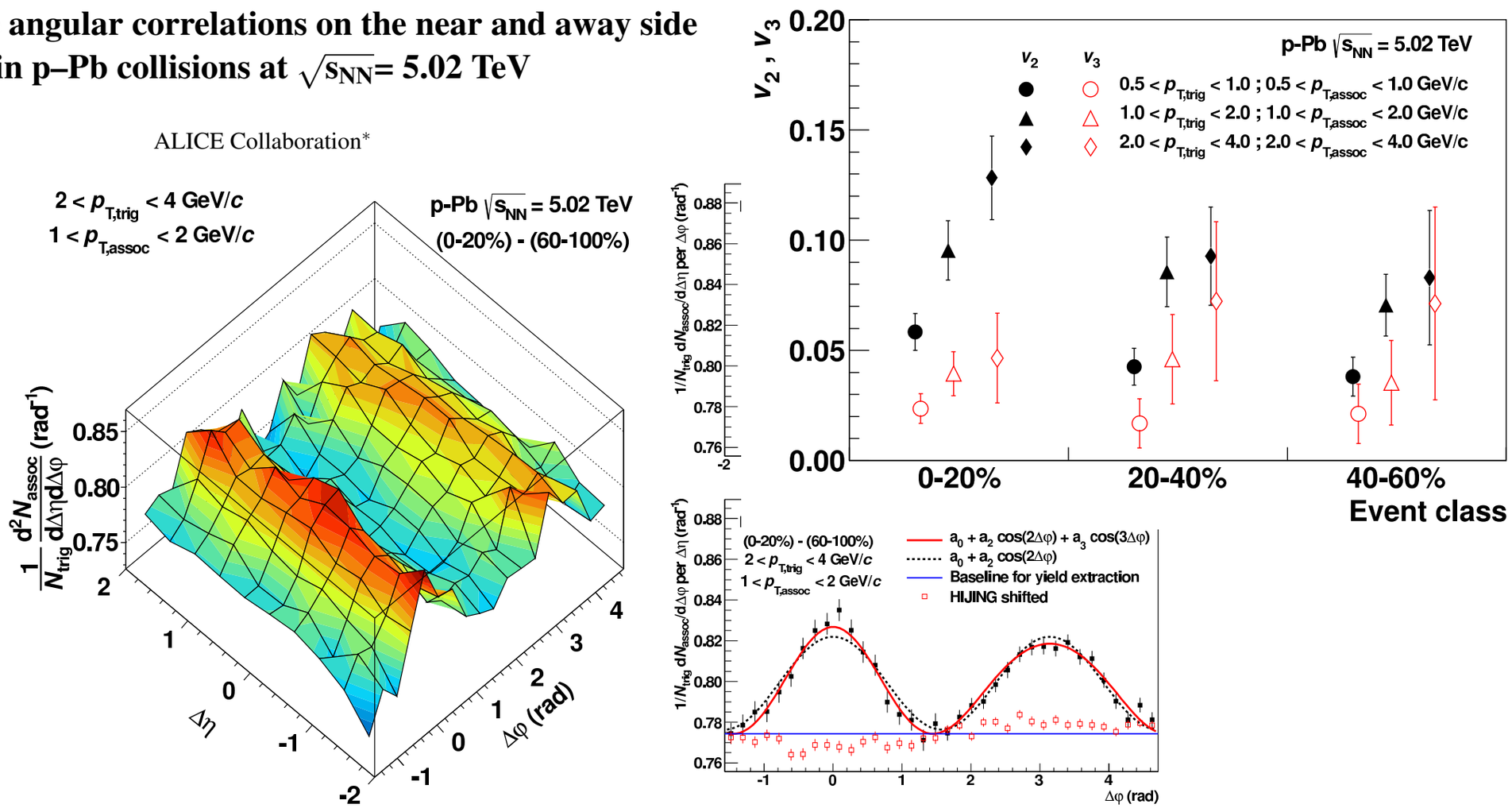

Fig. 3: Left: Associated yield per trigger particle in $\Delta\varphi$ and $\Delta\eta$ for pairs of charged particles with $2 < p_{T,trig} < 4$ GeV/c and $1 < p_{T,assoc} < 2$ GeV/c in p–Pb collisions at $\sqrt{s_{NN}} = 5.02$ TeV for the 0–20% multiplicity class, after subtraction of the associated yield obtained in the 60–100% event class. Top right: the associated per-trigger yield after subtraction (as shown on the left) projected onto $\Delta\eta$ averaged over $|\Delta\varphi| < \pi/3$ (black circles), $|\Delta\varphi - \pi| < \pi/3$ (red squares), and the remaining area (blue triangles, $\Delta\varphi < -\pi/3$, $\pi/3 < \Delta\varphi < 2\pi/3$ and $\Delta\varphi > 4\pi/3$). Bottom right: as above but projected onto $\Delta\varphi$ averaged over $0.8 < |\Delta\eta| < 1.8$ on the near side and $|\Delta\eta| < 1.8$ on the away side. Superimposed are fits containing a $\cos(2\Delta\varphi)$ shape alone (black dashed line) and a combination of $\cos(2\Delta\varphi)$ and $\cos(3\Delta\varphi)$ shapes (red solid line). The blue horizontal line shows the baseline obtained from the latter fit which is used for the yield calculation. Also shown for comparison is the subtracted associated yield when the same procedure is applied on HIJING shifted to the same baseline. The figure shows only statisti-

• a ``double ridge" in ALICE and ATLAS

arXiv:1212.2001v1 [nucl-ex] 10 Dec 2012

Long-range angular correlations on the near and away side in p–Pb collisions at $\sqrt{s_{NN}}$= 5.02 TeV

ALICE Collaboration*

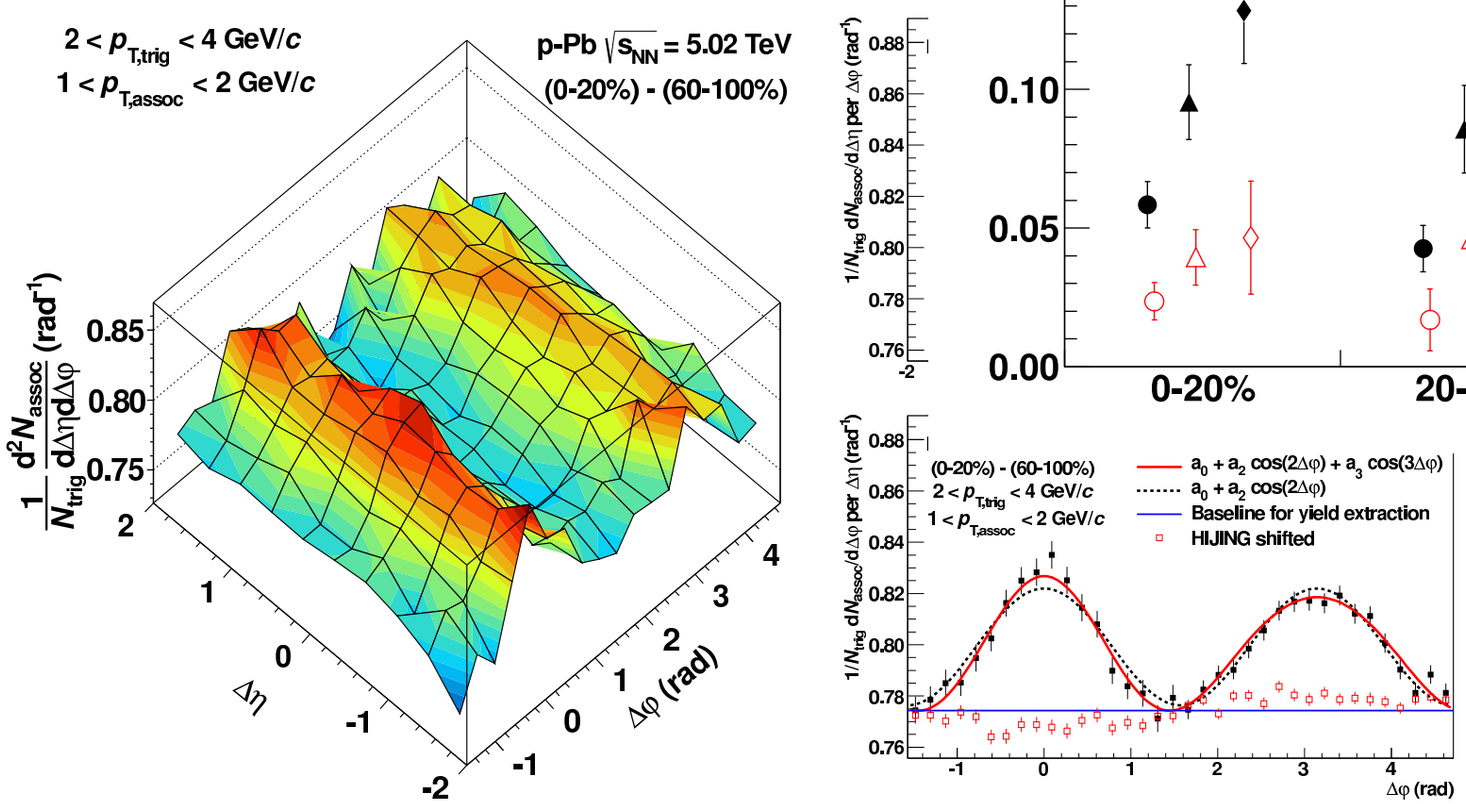

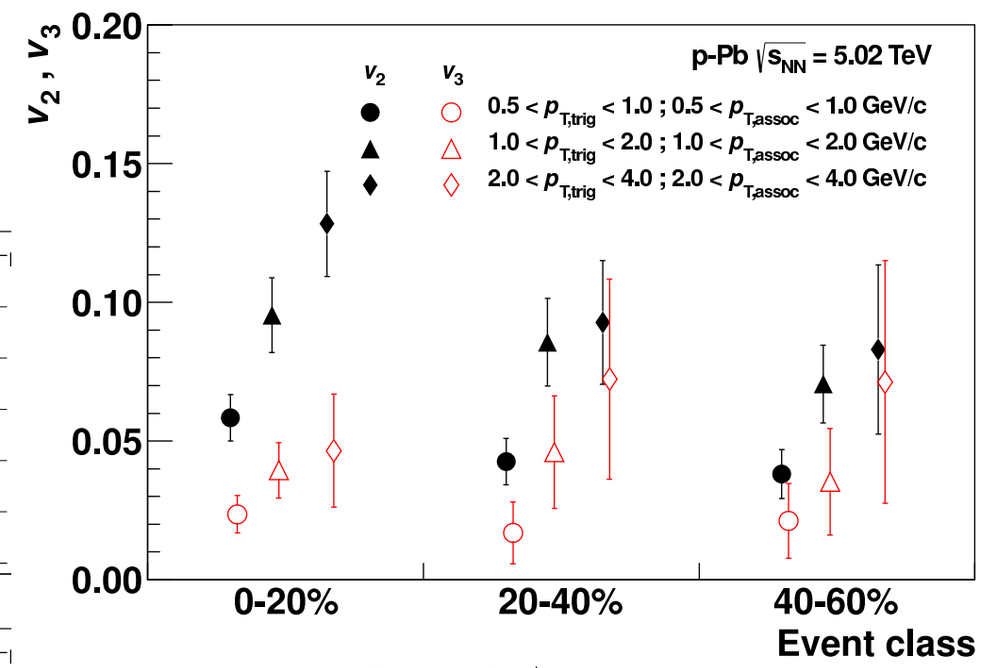

unlike AA, the v2 is dominant
v3/v2 = 1/3 or so

all moments grow with pt!

Fig. 3: Left: Associated yield per trigger particle in $\Delta\varphi$ and $\Delta\eta$ for pairs of charged particles with $2 < p_{T,trig} < 4$ GeV/c and $1 < p_{T,assoc} < 2$ GeV/c in p–Pb collisions at $\sqrt{s_{NN}} = 5.02$ TeV for the 0–20% multiplicity class, after subtraction of the associated yield obtained in the 60–100% event class. Top right: the associated per-trigger yield after subtraction (as shown on the left) projected onto $\Delta\eta$ averaged over $|\Delta\varphi| < \pi/3$ (black circles), $|\Delta\varphi - \pi| < \pi/3$ (red squares), and the remaining area (blue triangles, $\Delta\varphi < -\pi/3$, $\pi/3 < \Delta\varphi < 2\pi/3$ and $\Delta\varphi > 4\pi/3$). Bottom right: as above but projected onto $\Delta\varphi$ averaged over $0.8 < |\Delta\eta| < 1.8$ on the near side and $|\Delta\eta| < 1.8$ on the away side. Superimposed are fits containing a $\cos(2\Delta\varphi)$ shape alone (black dashed line) and a combination of $\cos(2\Delta\varphi)$ and $\cos(3\Delta\varphi)$ shapes (red solid line). The blue horizontal line shows the baseline obtained from the latter fit which is used for the yield calculation. Also shown for comparison is the subtracted associated yield when the same procedure is applied on HIJING shifted to the same baseline. The figure shows only statisti-

Observation of Associated Near-side and Away-side Long-range Correlations in $\sqrt{s_{\mathrm{NN}}} = 5.02\ \mathrm{TeV}$ Proton–lead Collisions with the ATLAS Detector

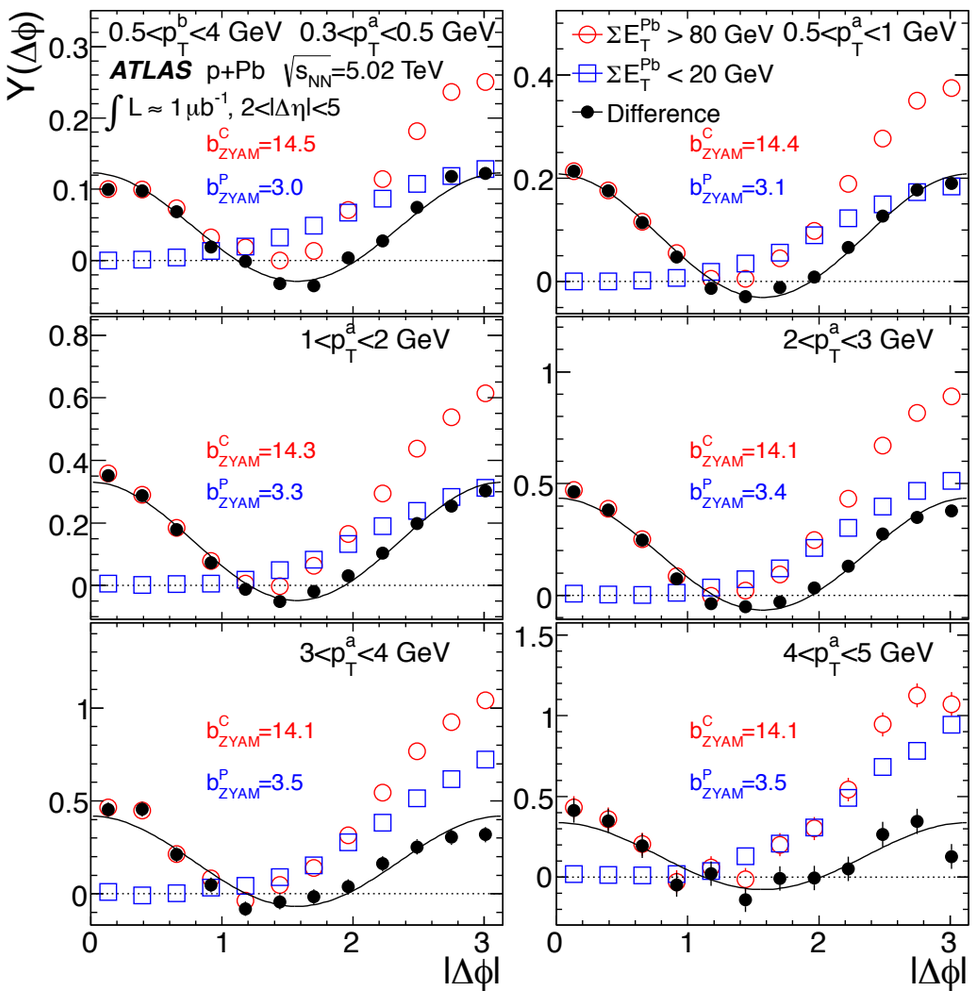

FIG. 3. Distributions of per-trigger yield in the peripheral and the central event activity classes and their differences (solid symbols), for different ranges of $p_{\mathrm{T}}^{\mathrm{a}}$ and $0.5 < p_{\mathrm{T}}^{\mathrm{b}} < 4$ GeV, together with functions $a_0 + 2a_2 \cos 2\Delta\phi$ obtained via a Fourier decomposition (see text). The values for the ZYAM-determined pedestal levels are indicated on each panel for peripheral ($b^{\mathrm{P}}_{\mathrm{ZYAM}}$) and central ($b^{\mathrm{C}}_{\mathrm{ZYAM}}$) $\Sigma E_{\mathrm{T}}^{\mathrm{Pb}}$ bins.

TLAS C

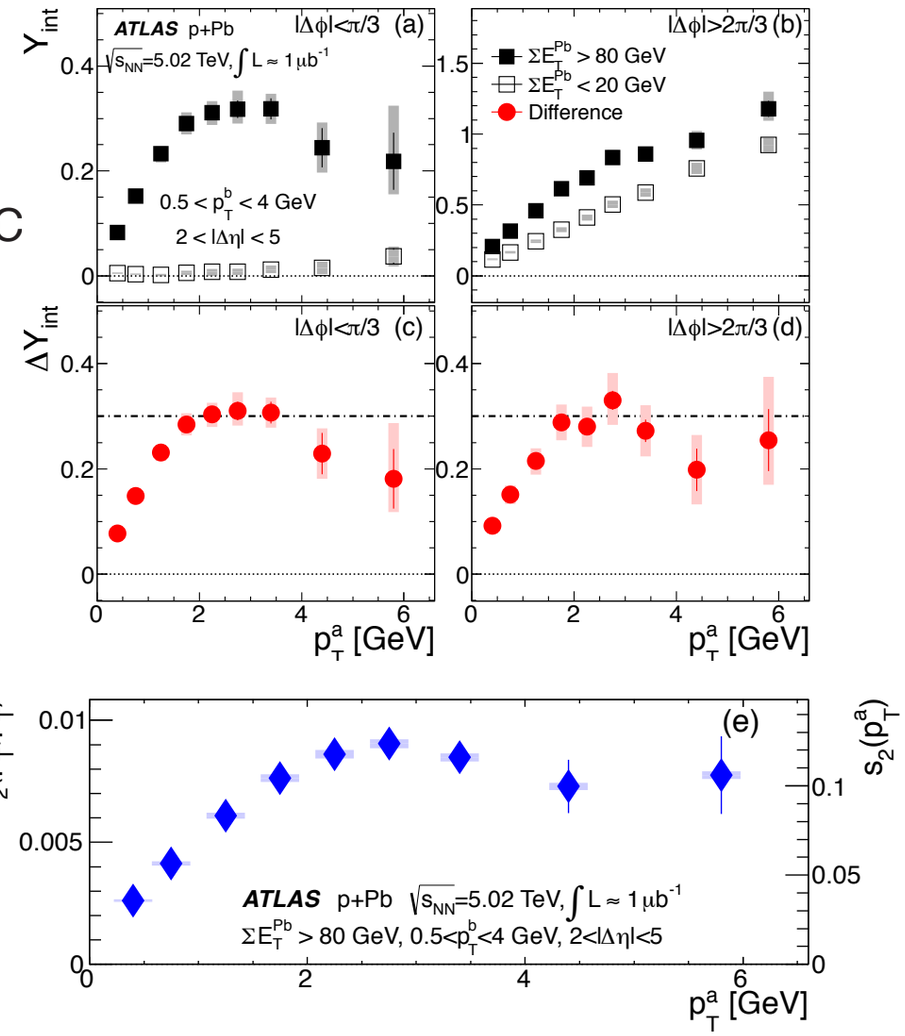

FIG. 4. Integrated per-trigger yields, Y_{int}, (see text) vs $p_{\mathrm{T}}^{\mathrm{a}}$ for $0.5 < p_{\mathrm{T}}^{\mathrm{b}} < 4$ GeV in peripheral and central events, on the (a) near-side and (b) away-side. The panels (c) and (d) show the difference, ΔY_{int}. Panel (e) shows the p_{T} dependence of c_2 (left axis) and s_2 (right axis). The right axis of (e) differs from the left only by a multiplicative factor $1/\sqrt{5.4 \times 10^{-3}}$ (see text). The error bars and shaded boxes represent the statistical and systematic uncertainties, respectively.

arXiv:1212.5198v1 [hep-ex] 20 Dec 2012

Observation of Associated Near-side and Away-side Long-range Correlations in $\sqrt{s_{\mathrm{NN}}} = 5.02\ \mathrm{TeV}$ Proton–lead Collisions with the ATLAS Detector

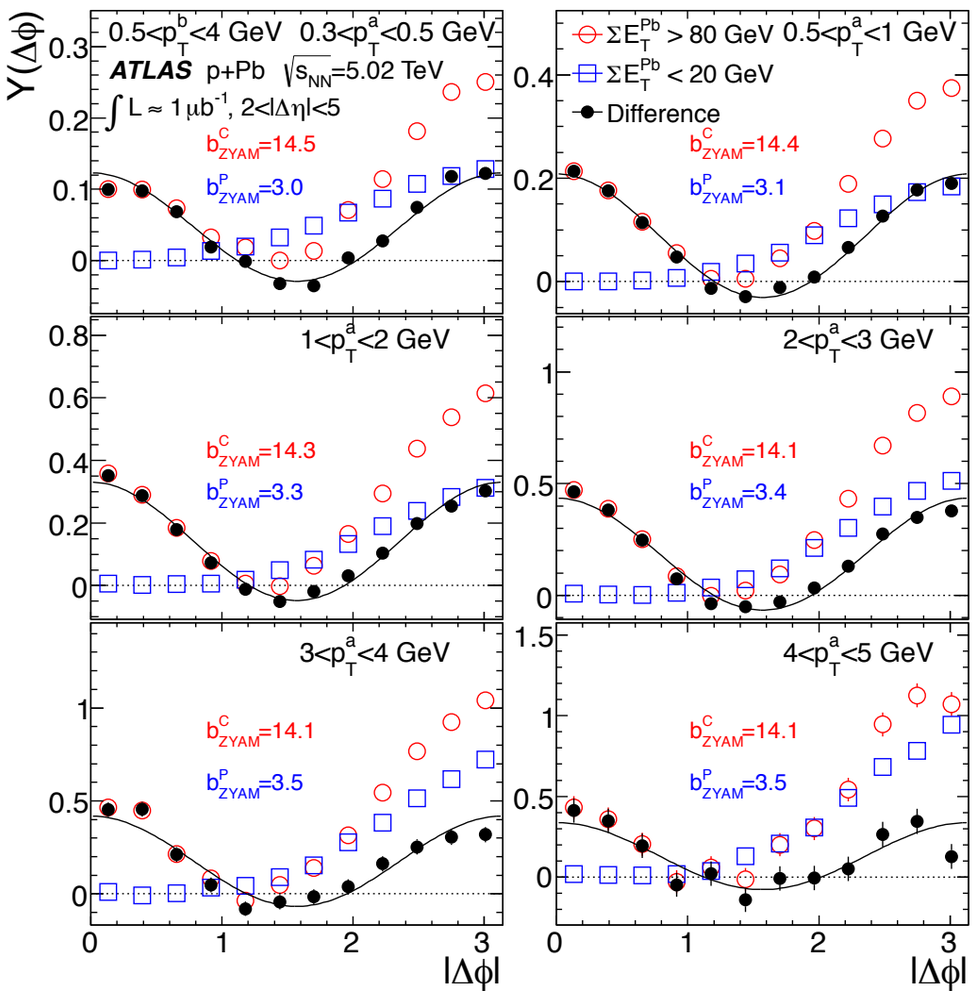

FIG. 3. Distributions of per-trigger yield in the peripheral and the central event activity classes and their differences (solid symbols), for different ranges of $p_{\mathrm{T}}^{\mathrm{a}}$ and $0.5 < p_{\mathrm{T}}^{\mathrm{b}} < 4$ GeV, together with functions $a_0 + 2a_2 \cos 2\Delta\phi$ obtained via a Fourier decomposition (see text). The values for the ZYAM-determined pedestal levels are indicated on each panel for peripheral ($b^{\mathrm{P}}_{\mathrm{ZYAM}}$) and central ($b^{\mathrm{C}}_{\mathrm{ZYAM}}$) $\Sigma E_{\mathrm{T}}^{\mathrm{Pb}}$ bins.

TLAS C

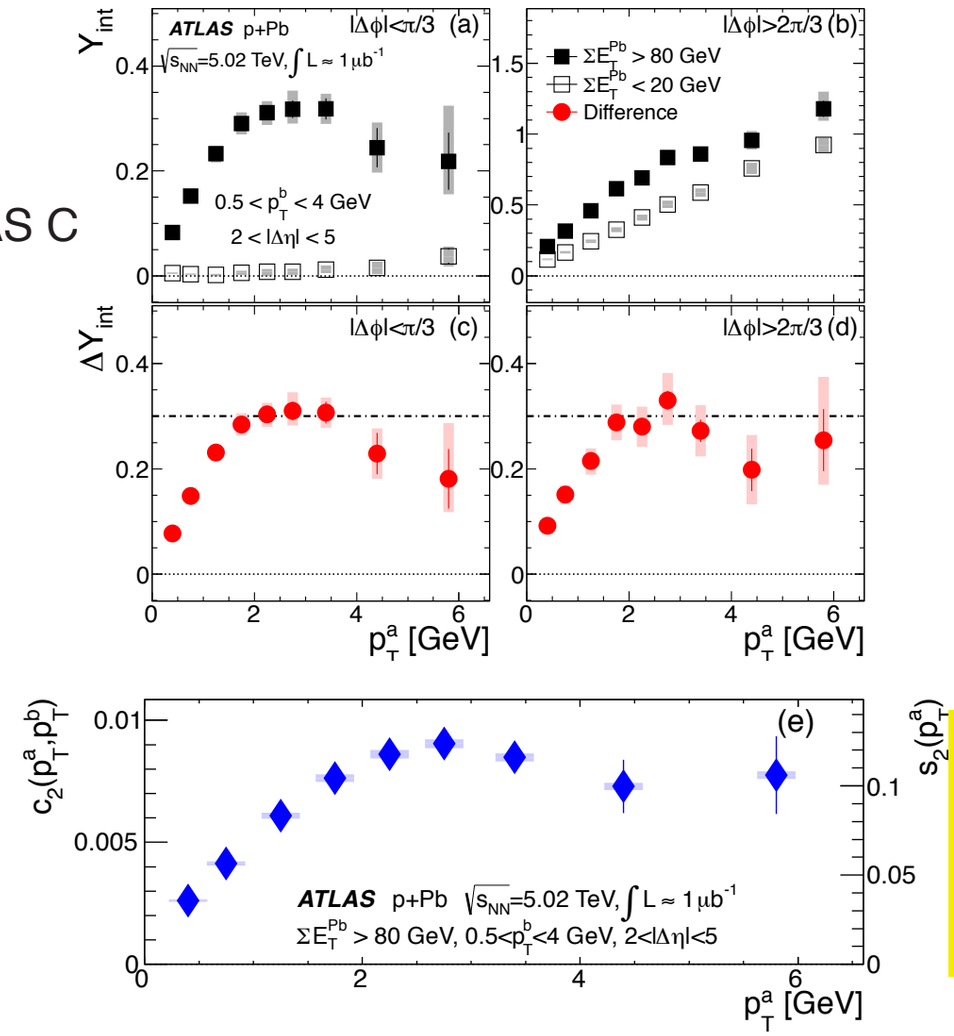

FIG. 4. Integrated per-trigger yields, Y_{int}, (see text) vs $p_{\mathrm{T}}^{\mathrm{a}}$ for $0.5 < p_{\mathrm{T}}^{\mathrm{b}} < 4$ GeV in peripheral and central events, on the (a) near-side and (b) away-side. The panels (c) and (d) show the difference, ΔY_{int}. Panel (e) shows the p_{T} dependence of c_2 (left axis) and s_2 (right axis). The right axis of (e) differs from the left only by a multiplicative factor $1/\sqrt{5.4 \times 10^{-3}}$ (see text). The error bars and shaded boxes represent the statistical and systematic uncertainties, respectively.

arXiv:1212 p-ex] 20 Dec 2012

persists to high pt

High Multiplicity pp and pA Collisions: Hydrodynamics at its Edge and Stringy Black Hole

Edward Shuryak and Ismail Zahed

- What is the smallest system size which still undergoes a hydrodynamical explosion?

- How do all hydrodynamical observables scale with the system size R and viscosity-to-entropy ratio η/s, for such systems? In particular, how large are the viscous corrections for radial and elliptic flows?

- How do amplitudes of higher angular harmonics v_n scale with n,R and η/s? In which p_t region do we expect hydrodynamics to work, and for each v_n?

- Do high multiplicity pp and pA collisions in which the (double) "ridge" has been recently observed at LHC [7–9] fit into such a hydrodynamical scaling?

two small parameters of hydro

$$\mathcal{O}(1) \approx \frac{1}{TR^{pp,high\,mutiplicity}} > \frac{1}{TR^{central\,pA}} > \frac{1}{TR^{central\,AA}} \approx \mathcal{O}(1/10) \tag{2}$$

Another important small parameter which we seem to have for strongly coupled Quark-Gluon Plasma (sQGP) is the *viscosity-to-entropy-density ratio*

$$\frac{\eta}{s} \approx \mathcal{O}(1/10) \ll 1 \tag{3}$$

Roughly speaking, it tells us that viscous effects – or the mean free path – is additionally suppressed compared to the micro scale $1/T$.

the radial (Gubser's) flow

$$v_\perp^{max}[AA, pA, pp] = [0.69, 0.83, 0.95]$$

Gubser's solution of ideal relativistic hydrodynamics, for the transverse velocity and the energy density reads

$$v_\perp(t,r) = \frac{2tr}{1+t^2+r^2} \qquad (10)$$

$$\frac{\epsilon}{q^4} = \frac{\hat{\epsilon}_0 2^{8/3}}{t^{4/3}\left[1+2(t^2+r^2)+(t^2-r^2)^2\right]^{4/3}}$$

$$t = q\bar{\tau}, \quad r = q\bar{r}$$

$$q_{AA}^{-1} = 4.3, \; q_{pA}^{-1} = 1, \; q_{pp}^{-1} = 0.5\,(fm)$$

my guesses of the
system's size
central PbPb 400
pA: 15-20 participants
pp 2

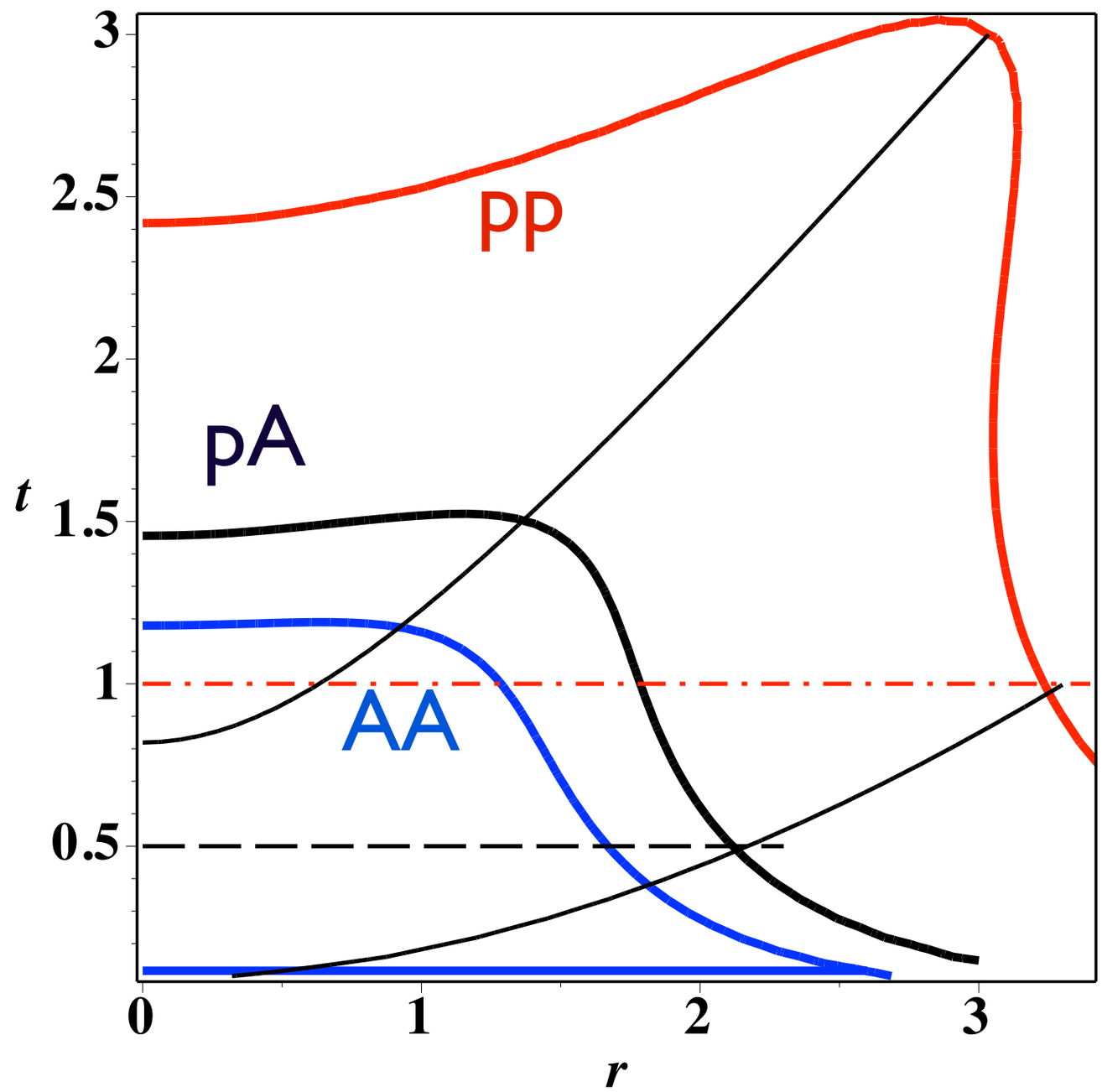

the role of viscosity

$$H_0 = \frac{\eta}{\epsilon^{3/4}} = \frac{\eta}{s}\frac{4}{3} f_*^{1/4} \qquad (20)$$

for $\eta/s = 0.134$ we will use as representative number $H_0 = 0.33$.

nonzero viscosity the solution is

$$\hat{T} = \frac{\hat{T}_0}{(\cosh\rho)^{2/3}} + \frac{H_0 \sinh^3\rho}{9(\cosh\rho)^{2/3}} \times {}_2F_1\left(\frac{3}{2}, \frac{7}{6}; \frac{5}{2}, -\sinh^2\rho\right) \qquad (27)$$

with $\hat{T} = \tau f_*^{1/4} T$ and $f_* = \epsilon/T^4 = 11$ as in [18].

In [19] Gubser and Yarom re-derived the radial solution by going into the co-moving frame via a coordinate transformation from the τ, r to a new set ρ, θ given by:

$$\sinh\rho = -\frac{1-\tau^2+r^2}{2\tau} \qquad (25)$$

$$\tan\theta = \frac{2r}{1+\tau^2-r^2} \qquad (26)$$

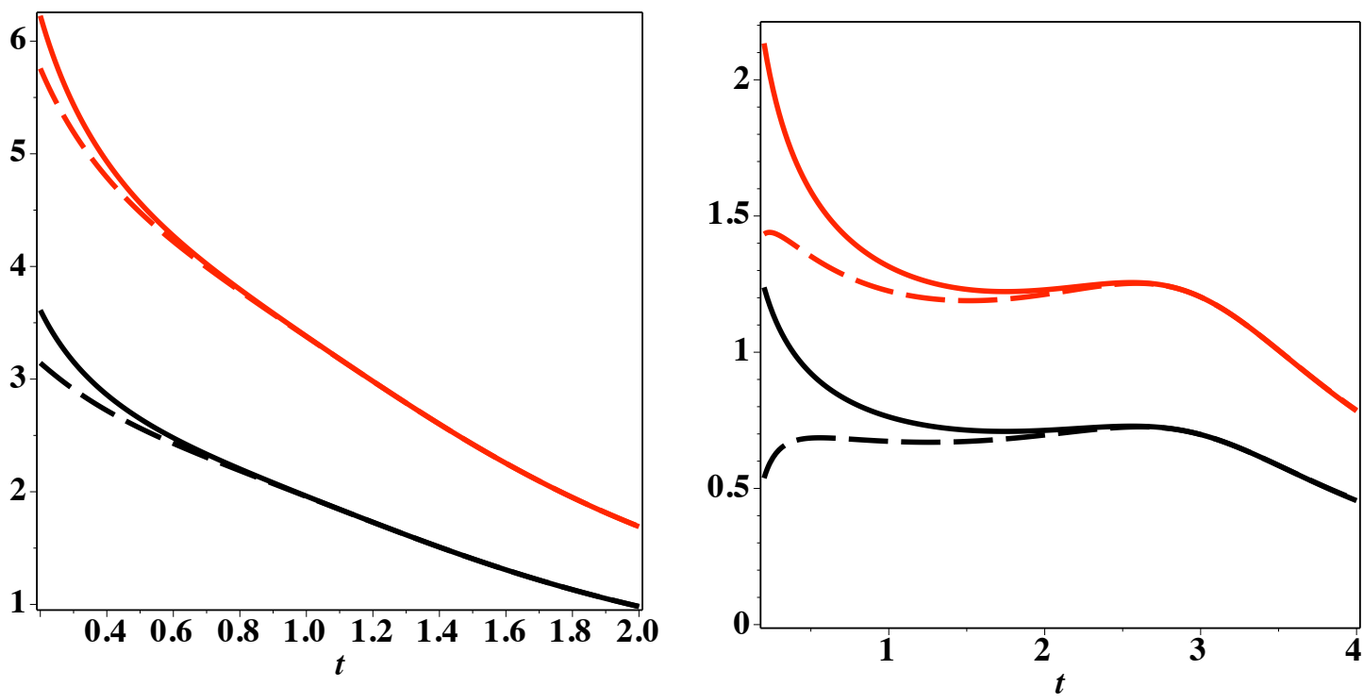

The radial flow in pA,pp has moderate corrections!

FIG. 3: (color online) The temperature versus dimensionless time t, for ideal hydrodynamics (solid) and viscous hydrodynamics with $\eta/s = 0.132$ (dashed) lines. The upper pair of (red) curves are for pp, the lower (black) ones for pA collisions. The upper plot is for $r = 1$, the lower plot for $r = 3$.

viscosity for higher harmonics

Staig+ES (2010) suggested to use ``acoustic'' damping expression

t=O(R)

$$P_m = \exp\left[-m^2 \frac{4}{3}\left(\frac{\eta}{s}\right)\left(\frac{1}{TR}\right)\right]$$

AA

pA

pp

viscosity for higher harmonics

Staig+ES (2010) suggested to use ``acoustic'' damping expression

t=O(R)

$$P_m = \exp\left[-m^2 \frac{4}{3}\left(\frac{\eta}{s}\right)\left(\frac{1}{TR}\right)\right]$$

In AA: (m/10)^2
in pA/pp (m/3)^2

AA

pA

pp

viscosity for higher harmonics

Staig+ES (2010) suggested to use ``acoustic'' damping expression

t=O(R)

$$P_m = \exp\left[-m^2 \frac{4}{3}\left(\frac{\eta}{s}\right)\left(\frac{1}{TR}\right)\right]$$

In AA: (m/10)^2
in pA/pp (m/3)^2

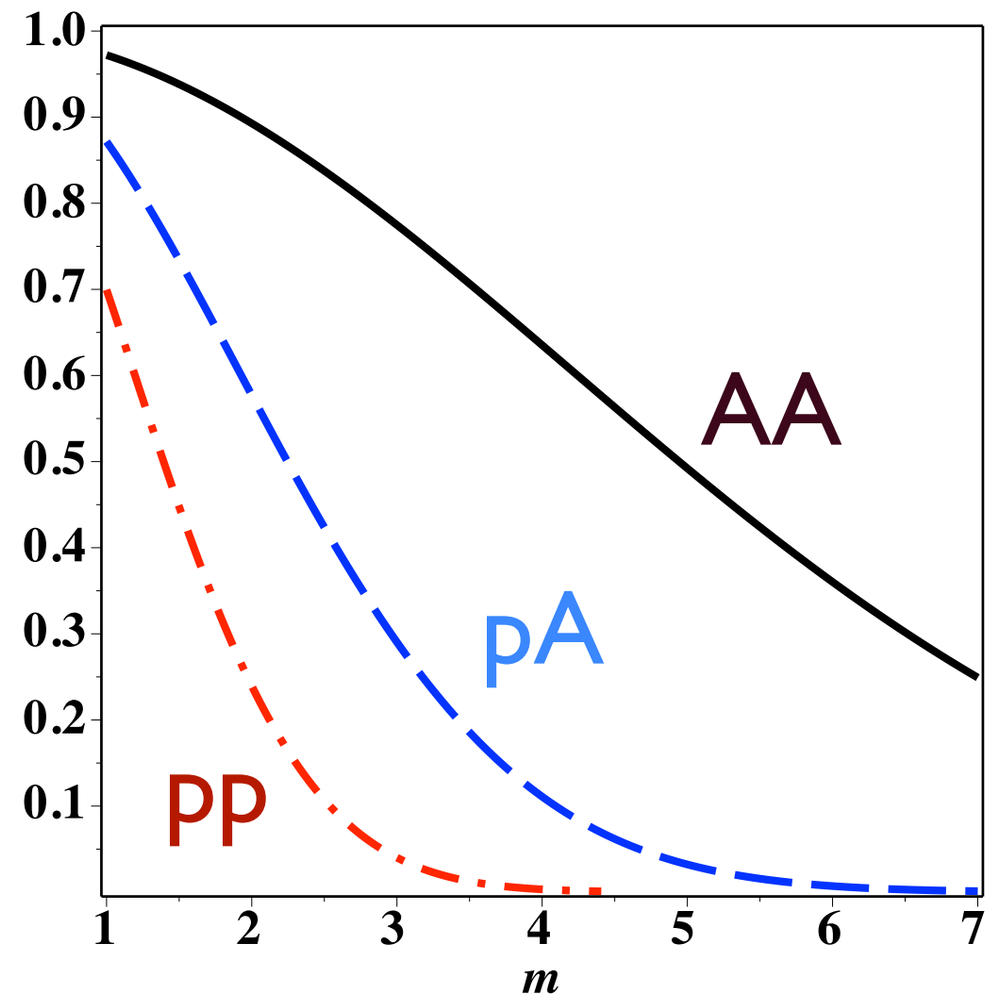

FIG. 4: (color online) Squared amplitude dissipation factor P_m^2 (as it appears in 2-particle correlators) for $\eta/s = .134$ as a function of the azimuthal harmonics m for AA (black) solid, pA (blue) dash and pp (red) dash-dot.

arXiv:1301.0165v1 [nucl-ex] 2 Jan 2013

Is anisotropic flow really acoustic?

Roy A. Lacey,[1,*] Yi Gu,[1] X. Gong,[1] D. Reynolds,[1] N. N. Ajitanand,[1] J. M. Alexander,[1] A. Mawi,[1] and A. Taranenko[1]

[1] *Department of Chemistry, Stony Brook University, Stony Brook, NY, 11794-3400, USA*

(Dated: January 3, 2013)

$$P_m = \exp\left[-m^2 \frac{4}{3}\left(\frac{\eta}{s}\right)\left(\frac{1}{TR}\right)\right]$$

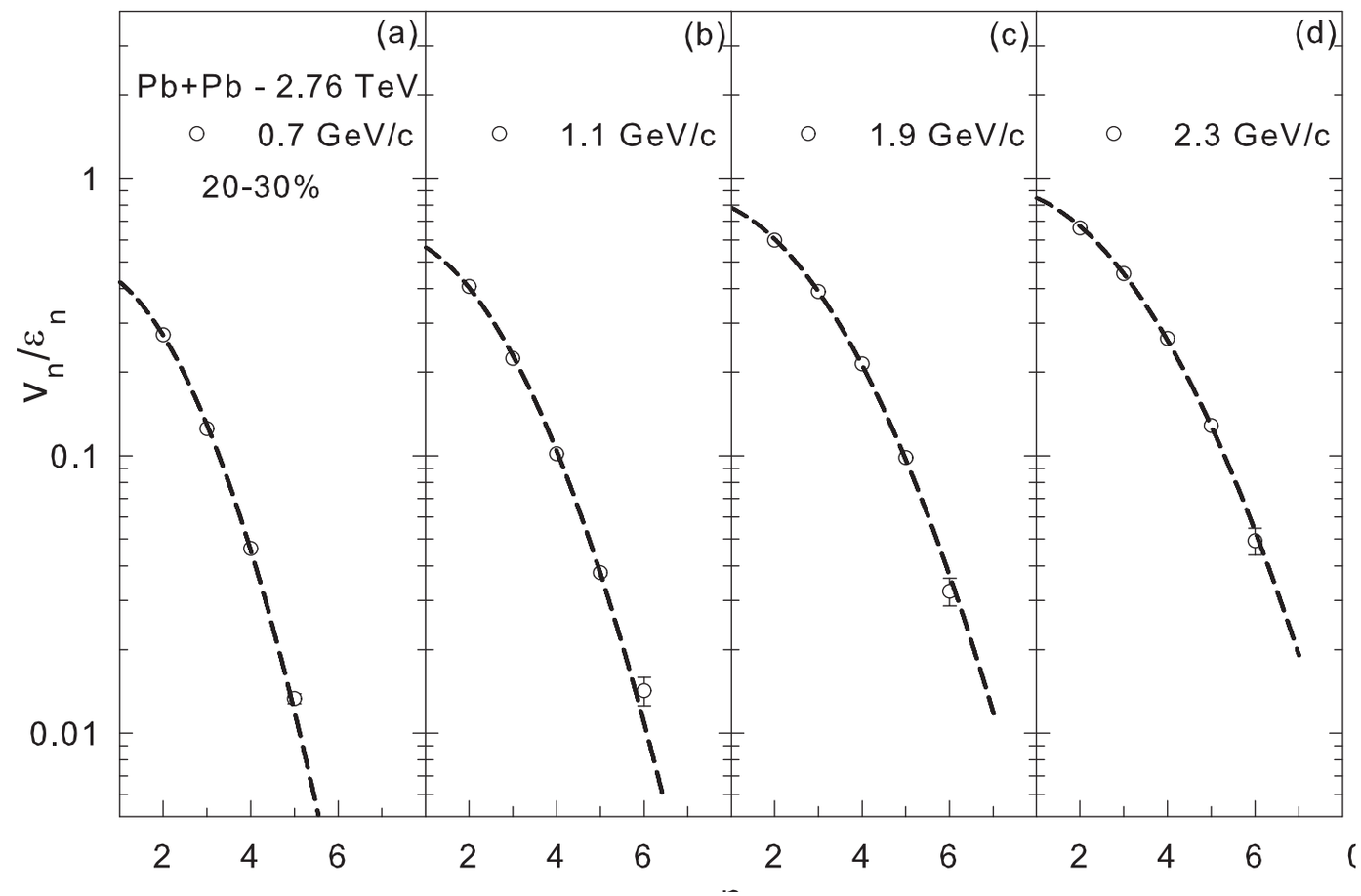

Harmonics 2,3,4 for AA,pA,pp

stronger damping in pA,pp

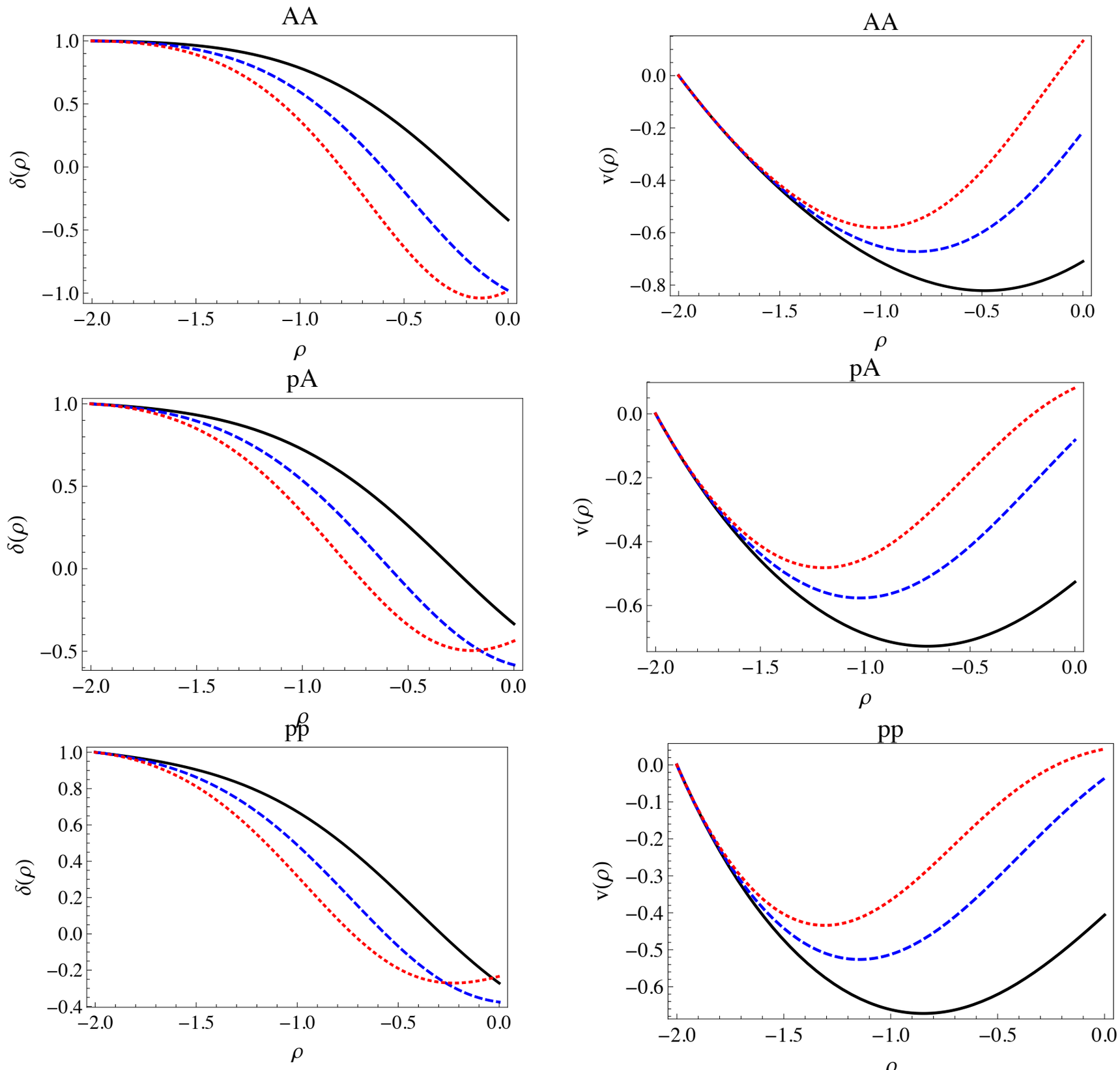

$$(v_2^{AA})^2 : (v_2^{pA})^2 : (v_2^{pp})^2$$
$$= 0.5(\epsilon_2^{AA})^2 : 0.3(\epsilon_2^{pA})^2 : 0.16(\epsilon_2^{pp})^2 \quad (36)$$

This is qualitatively consistent with the *squared* damping of the amplitude of the previous section, for $m = 2$.

A comparison to CMS data shows that the pp data show smaller v_2 as compared to pA data. Quantitatively, the ratio is about factor 1/4 (see Fig.3 of [7]) rather than 1/2 which the hydro solution provides. Perhaps it is because the pp collisions create a somewhat more spherical fireball, with $\epsilon_2^{pp} < \epsilon_2^{pA}$, in spite of being smaller in size. We will return to this issue at the end of the paper.

small v3/v2

ratio of the $m = 3$ to $m = 2$ harmonics

$$\left(\frac{v_3^{AA}}{v_2^{AA}}\right)^2 \approx 0.12 \left(\frac{\epsilon_3^{AA}}{\epsilon_2^{AA}}\right)^2 \quad (37)$$
$$\left(\frac{v_3^{pA}}{v_2^{pA}}\right)^2 \approx 0.09 \left(\frac{\epsilon_3^{pA}}{\epsilon_2^{pA}}\right)^2$$
$$\left(\frac{v_3^{pp}}{v_2^{pp}}\right)^2 \approx 0.02 \left(\frac{\epsilon_3^{pp}}{\epsilon_2^{pp}}\right)^2$$

Assuming $\epsilon_3/\epsilon_2 \sim 1$ one finds that in pA we predict $v_3/v_2 \approx 1/3$, which agrees nicely with the ALICE data [8]. For pp we have $v_3/v_2 \approx 1/7$ which is probably too small to be seen.

resummation of higher gradients a la Lublinsky-Shuryak

An approximate PADE-like re-summation of the higher order terms has been suggested by Lublinsky and Shuryak (LS) [20]. The main point is to notice the alternating signs of the series, which calls for an resummation a la geometrical series. Here we discuss only the single pole resummation model or LS2 in [20] in which the Navier-Stokes viscosity or NS is subtituted by an effective viscosity

$$\eta_{LS2}(\omega,k) = \frac{\eta_{NS}}{1-\eta_{2,0}k^2/(2\pi T)^2 - i\omega\eta_{0,1}/(2\pi T)} \tag{40}$$

Note that (40) involves only two dimensionless coefficients

$$\eta_{2,0} = -\frac{1}{2}\,\eta_{0,1} = 2-\ln 2 = 1.30 \tag{41}$$

Schematically the resummed hydro equations look as

$$(Euler) = \eta \mathbf{O}_{LS}(Navier-Stokes) \tag{44}$$

where $\mathbf{O}_{LS}$ is an integral operator. However, one can act with its inverse on the hydrodynamical equation as a whole, acting on the Euler part but canceling it in the viscous term

$$\mathbf{O}_{LS}^{-1}(Euler) = \eta(Navier-Stokes) \tag{45}$$

These are the equations of the LS hydrodynamics. Obviously they have two extra derivatives and thus need more initial conditions for solution

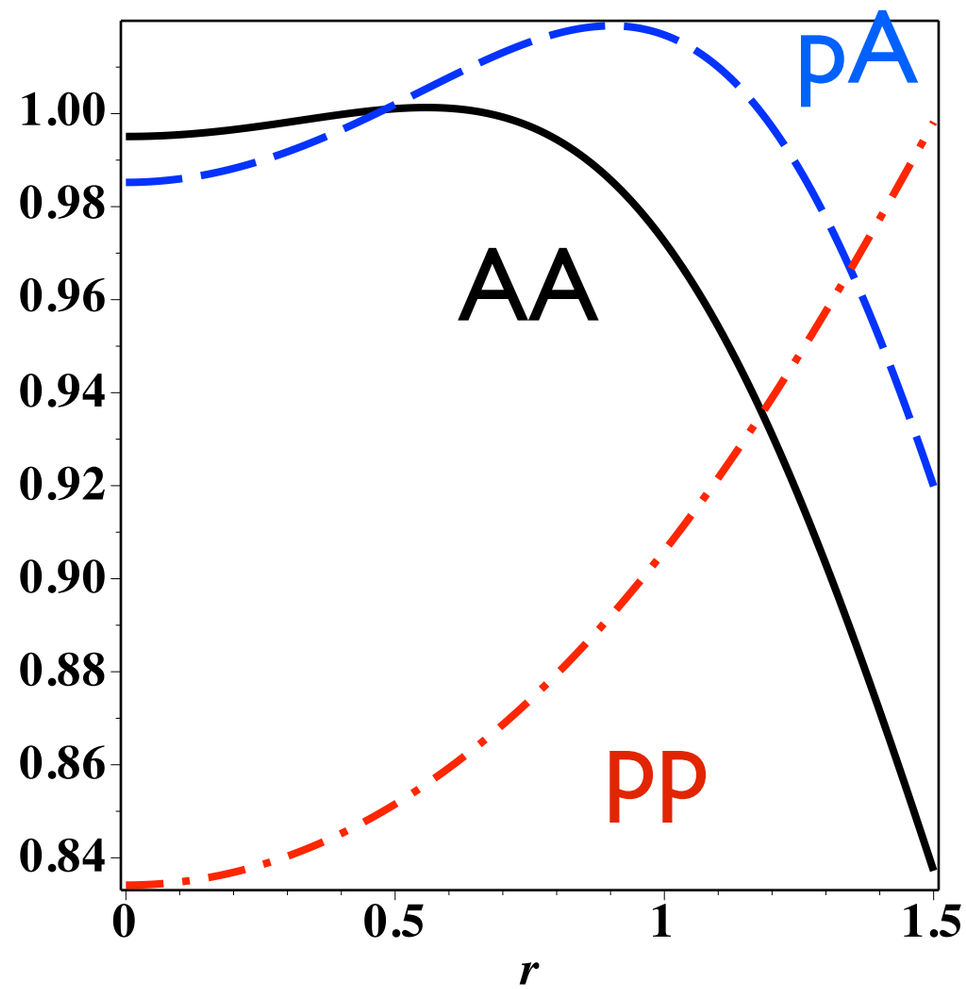

$$\mathbf{O}_{LS}^{-1}(f) = 1 + \frac{q^2}{2(2\pi T)^2}\left(\frac{\partial^2 f}{\partial r^2} + \frac{1}{r}\frac{\partial f}{\partial r}\right)\frac{1}{f} + (2-\ln 2)\,\frac{q}{2\pi T}\frac{\partial f}{\partial t}\frac{1}{f} \tag{43}$$

summary of the hydro

- the applicability of hydrodynamics rests on two small parameters:
  (i) **the micro-to- macro ratio 1/TR, (ii) the viscosity-to-entropy ratio η/s.**
  For central AA collisions, both are O(1/10). For high multiplicity pA and pp collisions, the first parameter is no longer small 1/TR = O(1), prompting us to ask which hydrodynamical predictions are preserved by the smallness of only the second parameter η/s.

- After solving the hydrodynamical equations we found that **the radial (axially symmetric) flow is little modified by viscosity and is in fact enhanced** by higher transverse gradients. Thus our main prediction is an enhanced radial flow => a change in the observed pt spectra on the particle mass, or growing proton-to-pion-ratio with pt. The magnitude of the effect should be even larger **(=> ALICE ?)**

- **Higher harmonics are penalized by larger viscous corrections**. We obtained explicit solution for Gubser flow for m = 2, 3, 4 as shown in Fig.5. We have found a small v3/v2 ≈ 1/3 ratio for pA in agreement with the reported ALICE data (in contrast to v3/v2 >1 in central AA). The value of v2 itself is also suppressed by viscosity, and the relative suppression we have found between the pp and pA collisions agree reasonably with the CMS data.

Staig+ES 2011
prediction vs ATLAS data

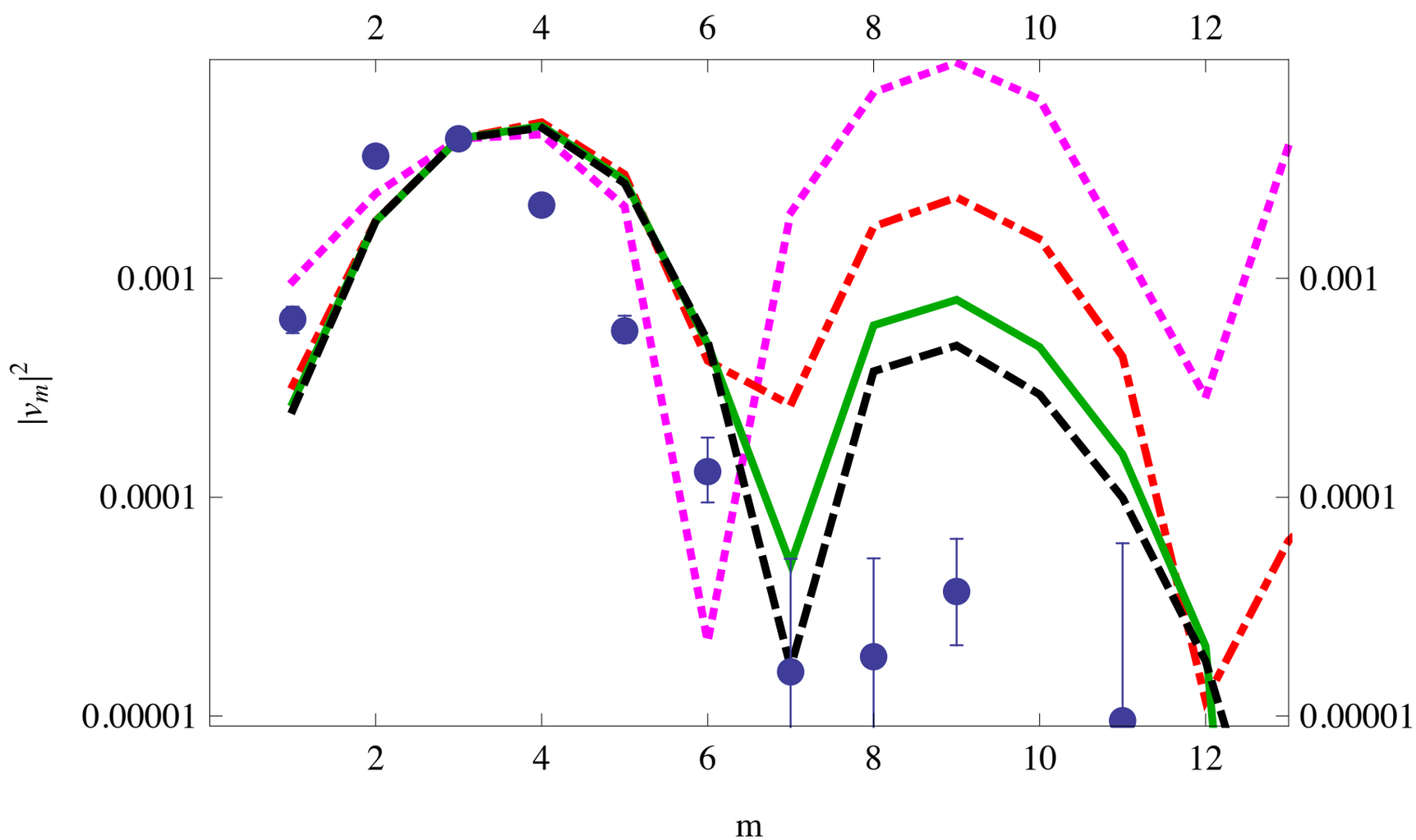

Jets Quenching at RHIC: Present and Future

Anne Sickles
Brookhaven National Lab

- LHC has brought the field fantastic new jet measurements
  - high jet rates, huge detectors, new system, large kinematic reach

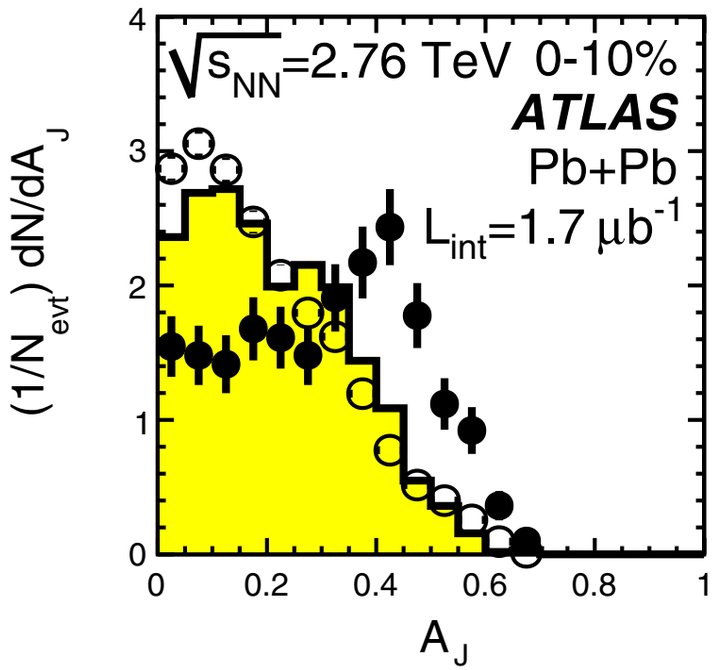

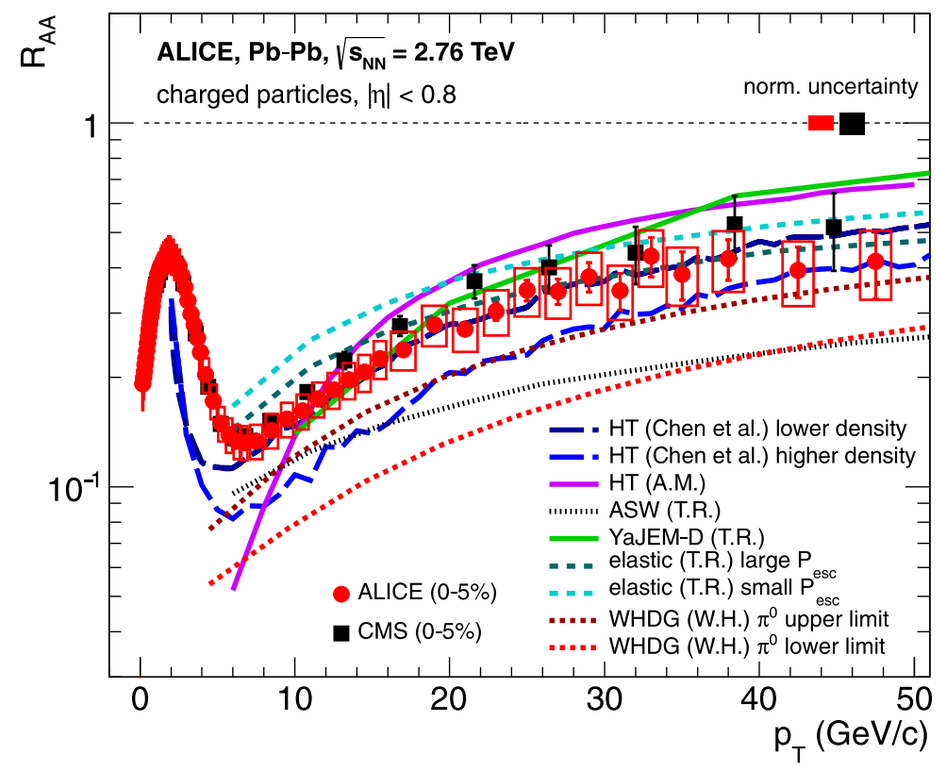

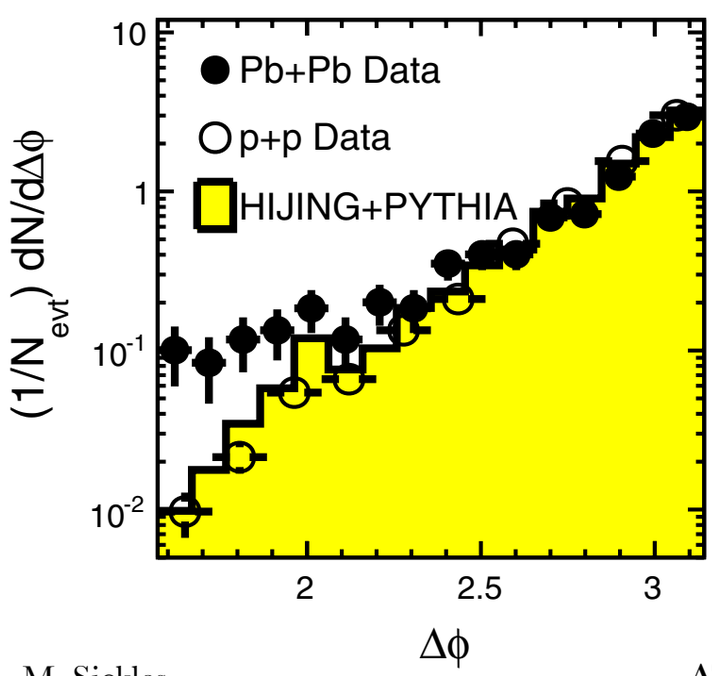

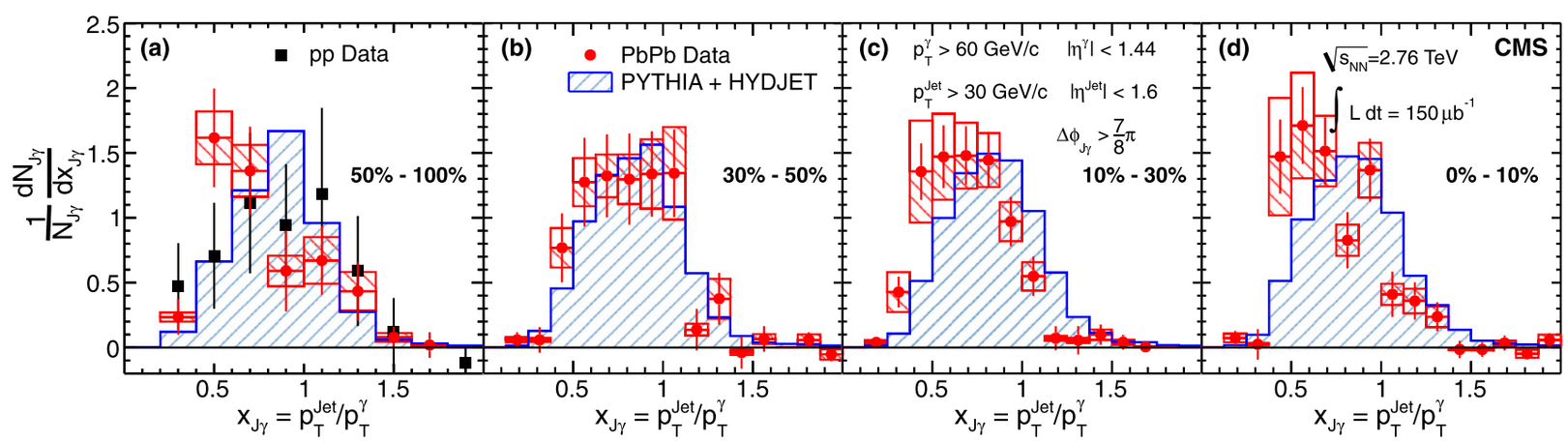

ATLAS PRL 105 252303, ALICE PLB 720 52, CMS PLB 718 773

what do we want from jets @ RHIC?

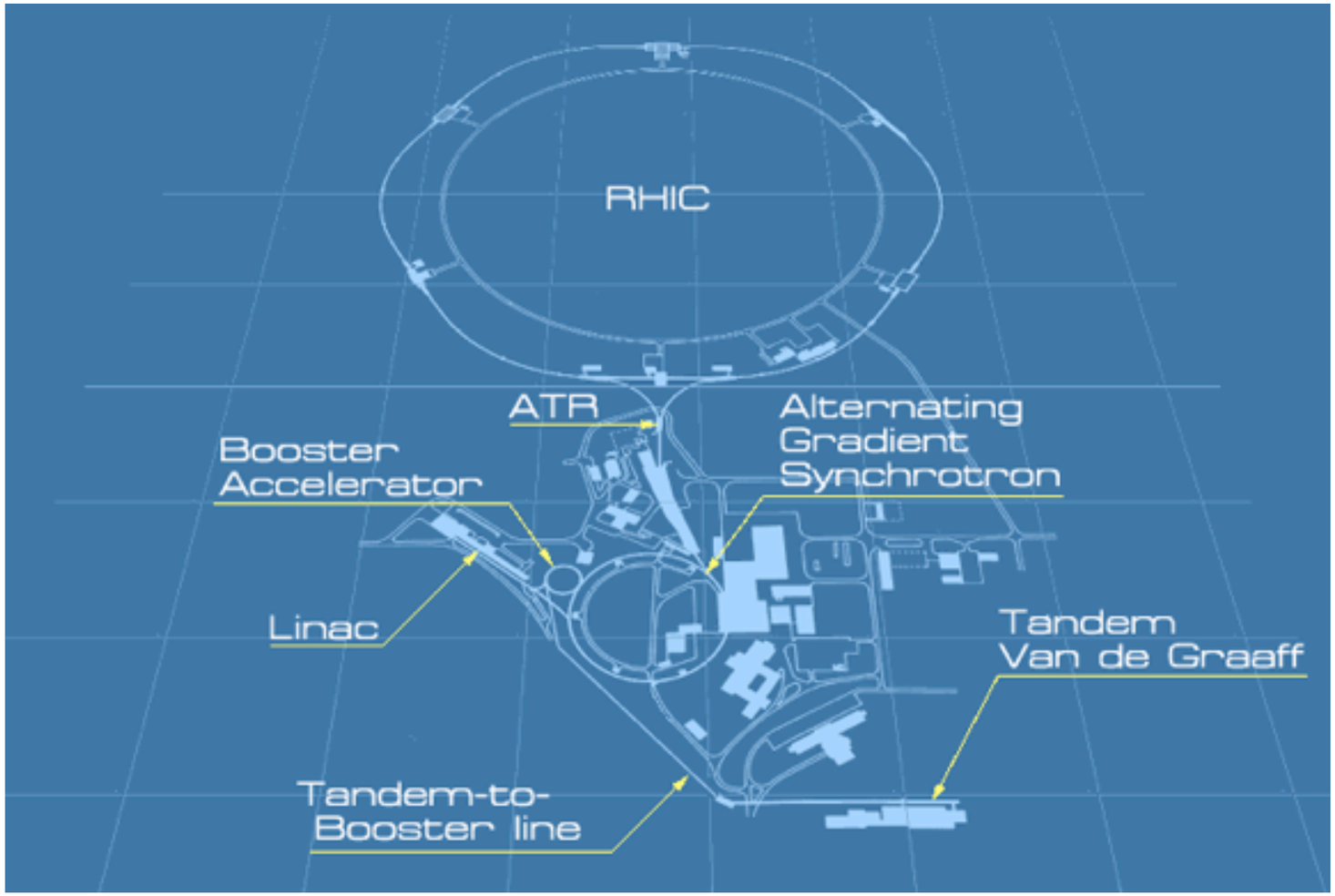

- probe the properties of jets near Tc
- exploit the large collision energy difference between RHIC and LHC to understand the physics of quenching
- exploit RHIC's flexibility to study different systems, small and large:
  - geometry, initial state effects...

quenching vs temperatue

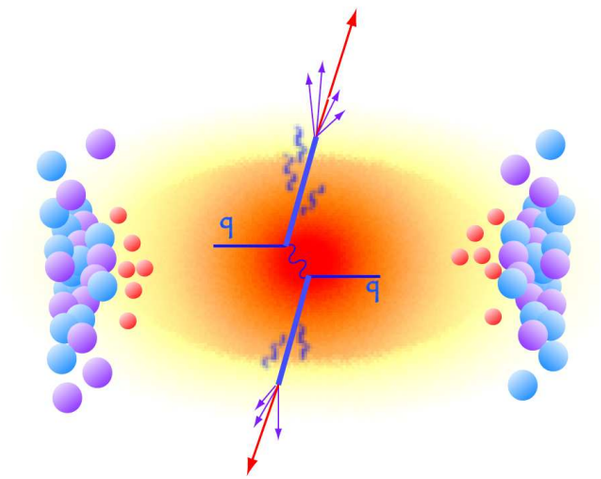

strongest quenching at the highest temperature in the collision

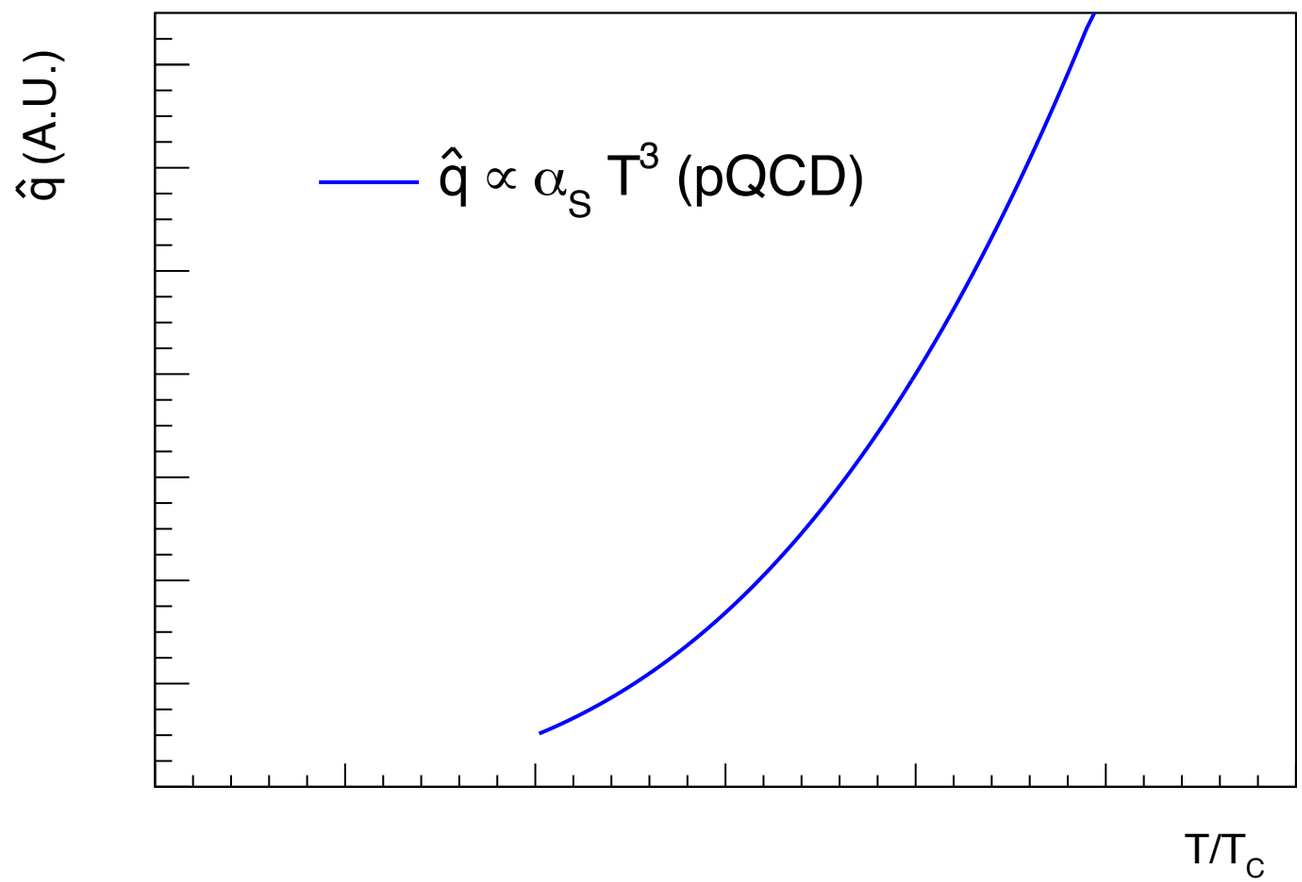

q(T) change the initial collision temperature by changing the collision energy

modified fragmentation patterns

CMS: balancing energy at low p_T and large angles

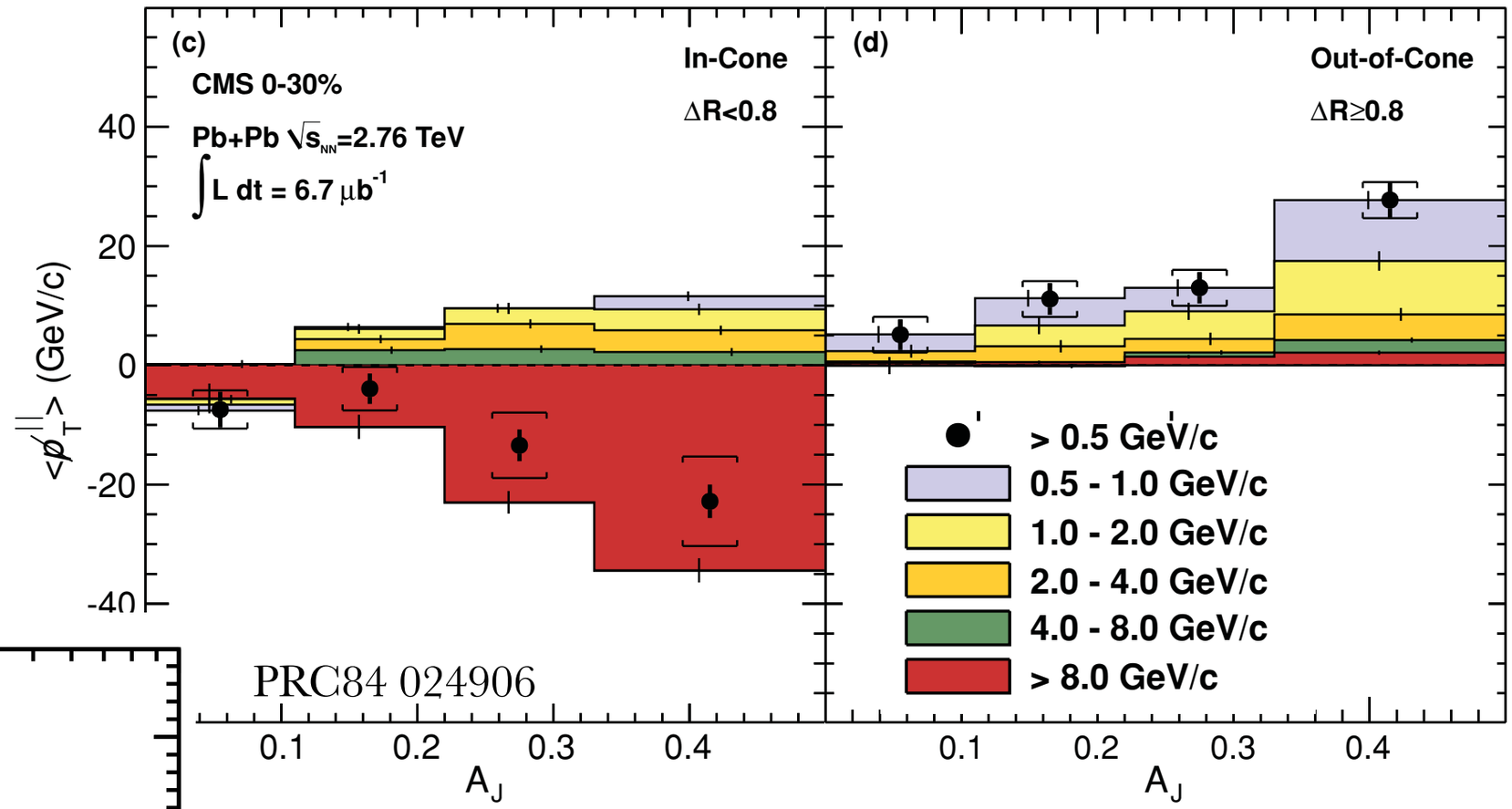

PRC84 024906

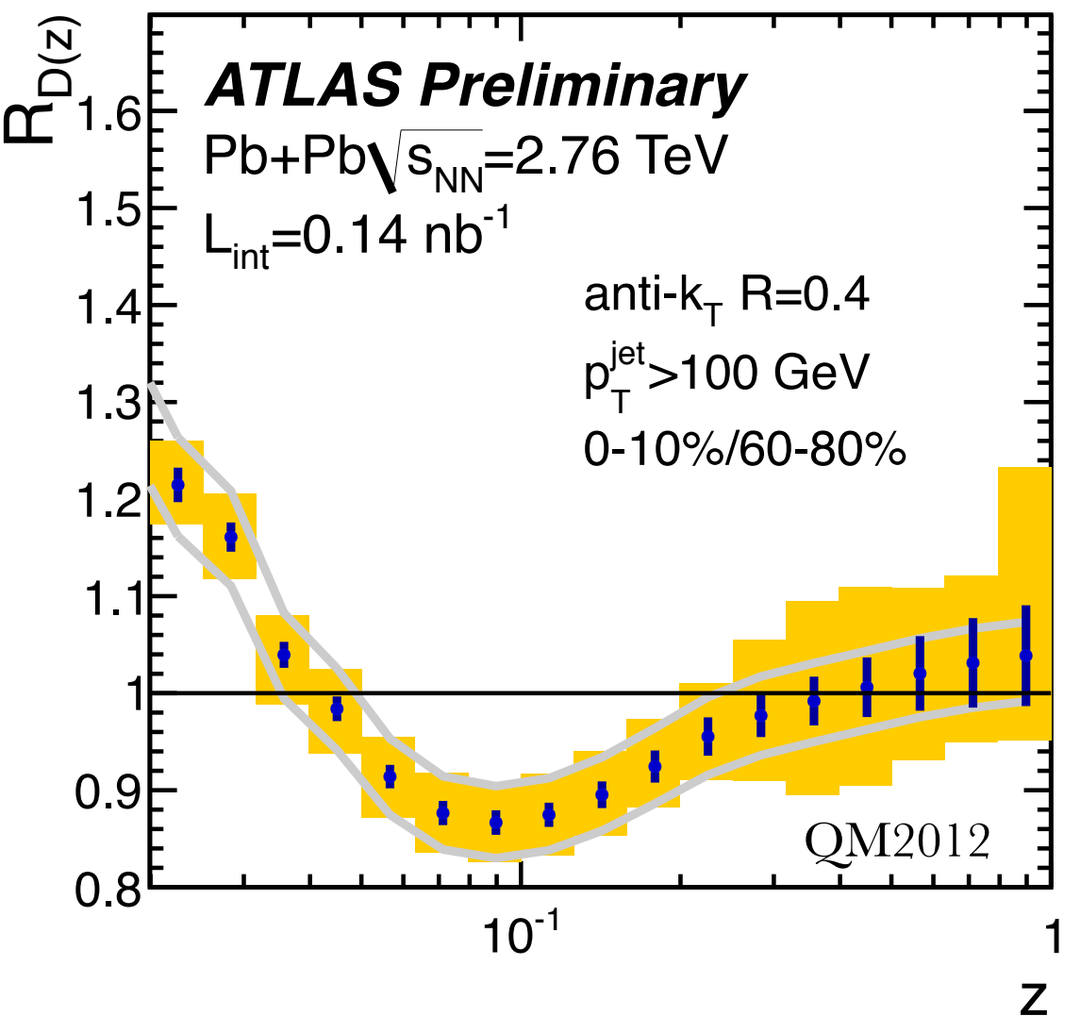

QM2012

ATLAS: softening of jet fragmentation functions

modifying fragmentation patterns

γ-hadron correlations

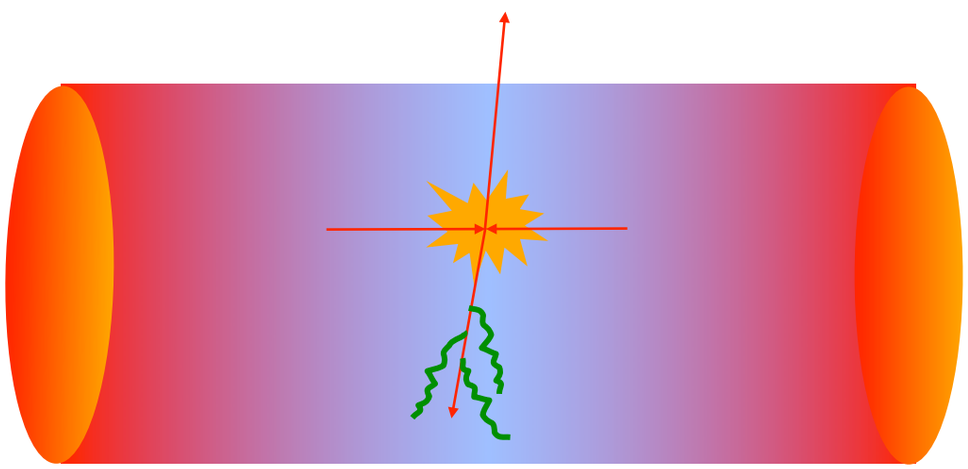

PHENIX: extra low p_T (<2GeV) hadrons in AuAu

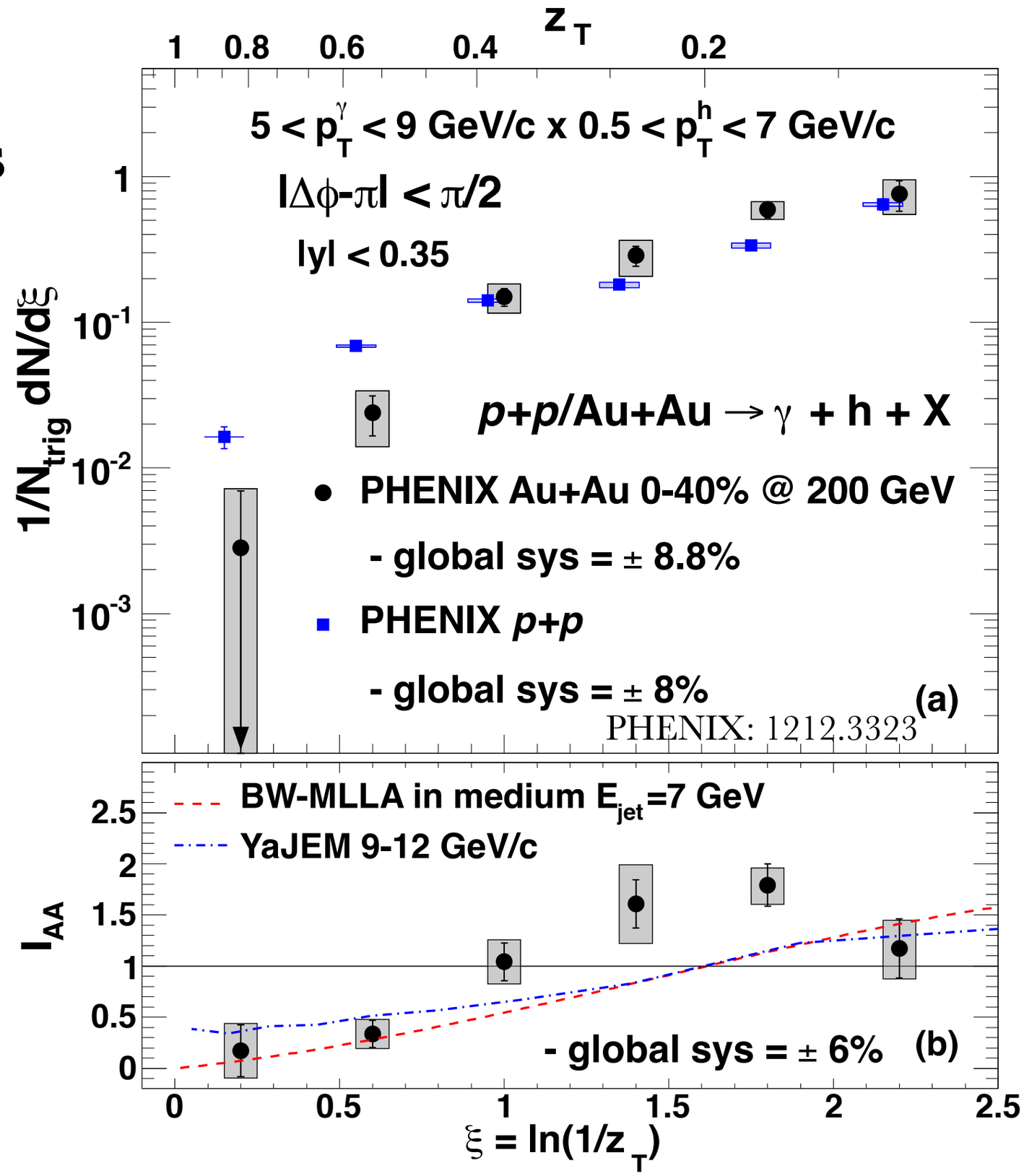

broadening of angular distribution

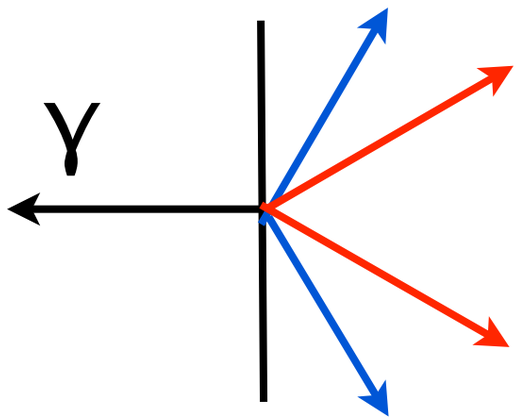

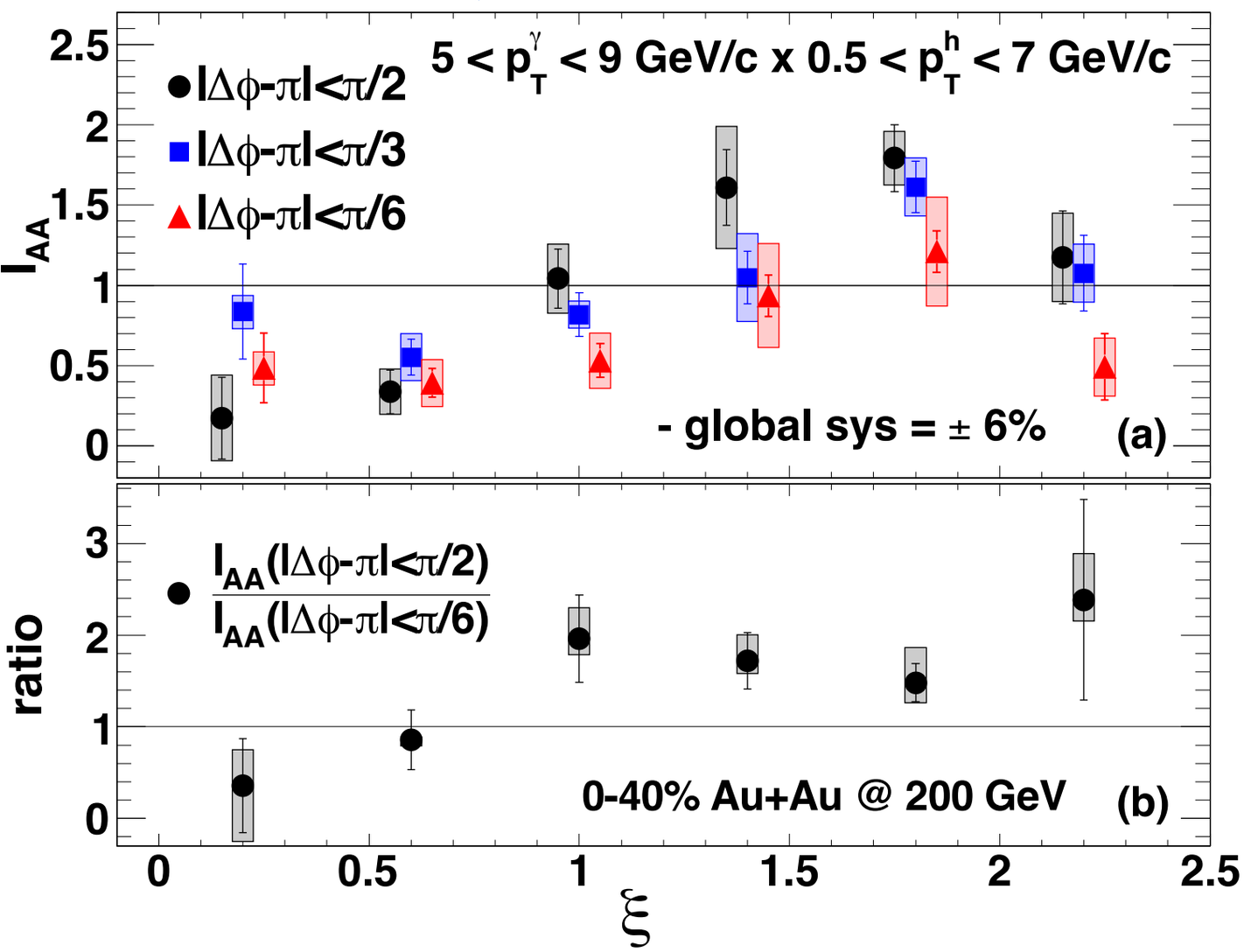

PHENIX: 1212.3323

broadening of angular distribution

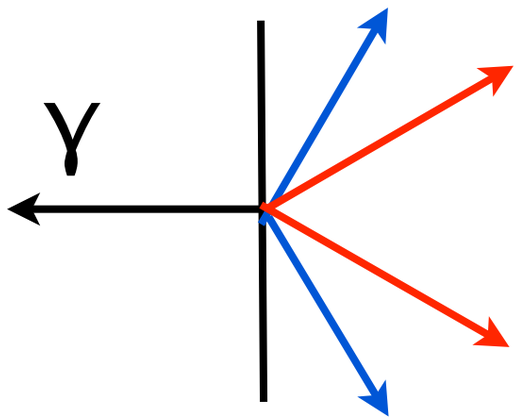

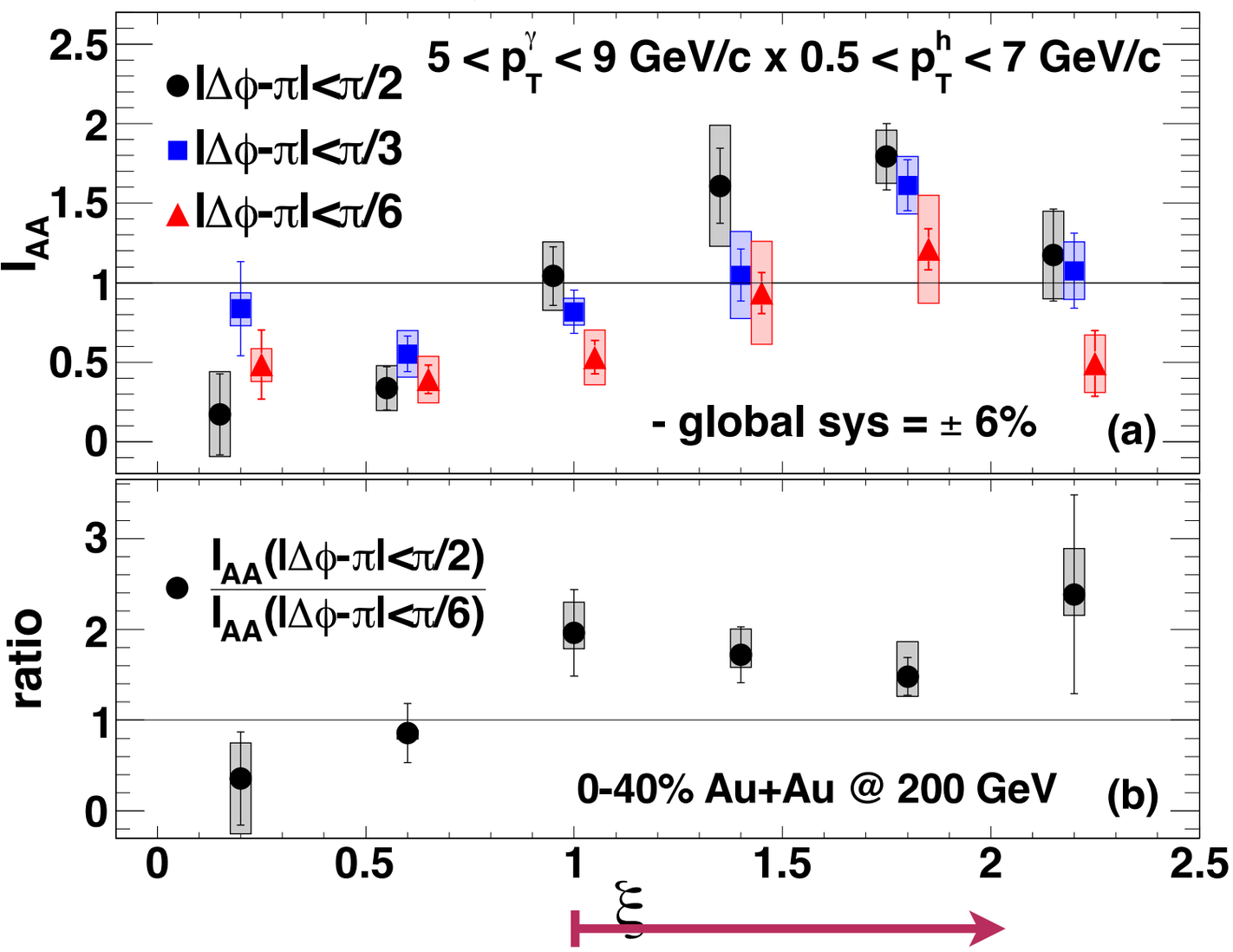

broadening of hadron distribution for pT < 2GeV/c

PHENIX: 1212.3323

broadening of angular distribution

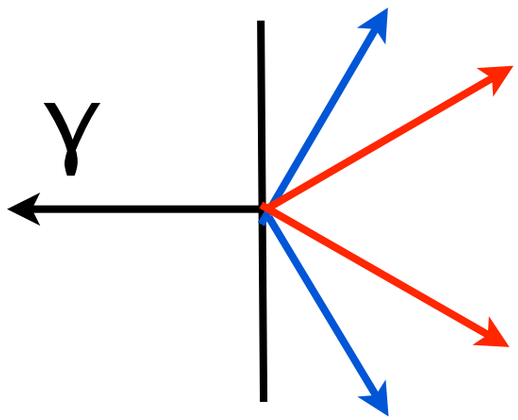

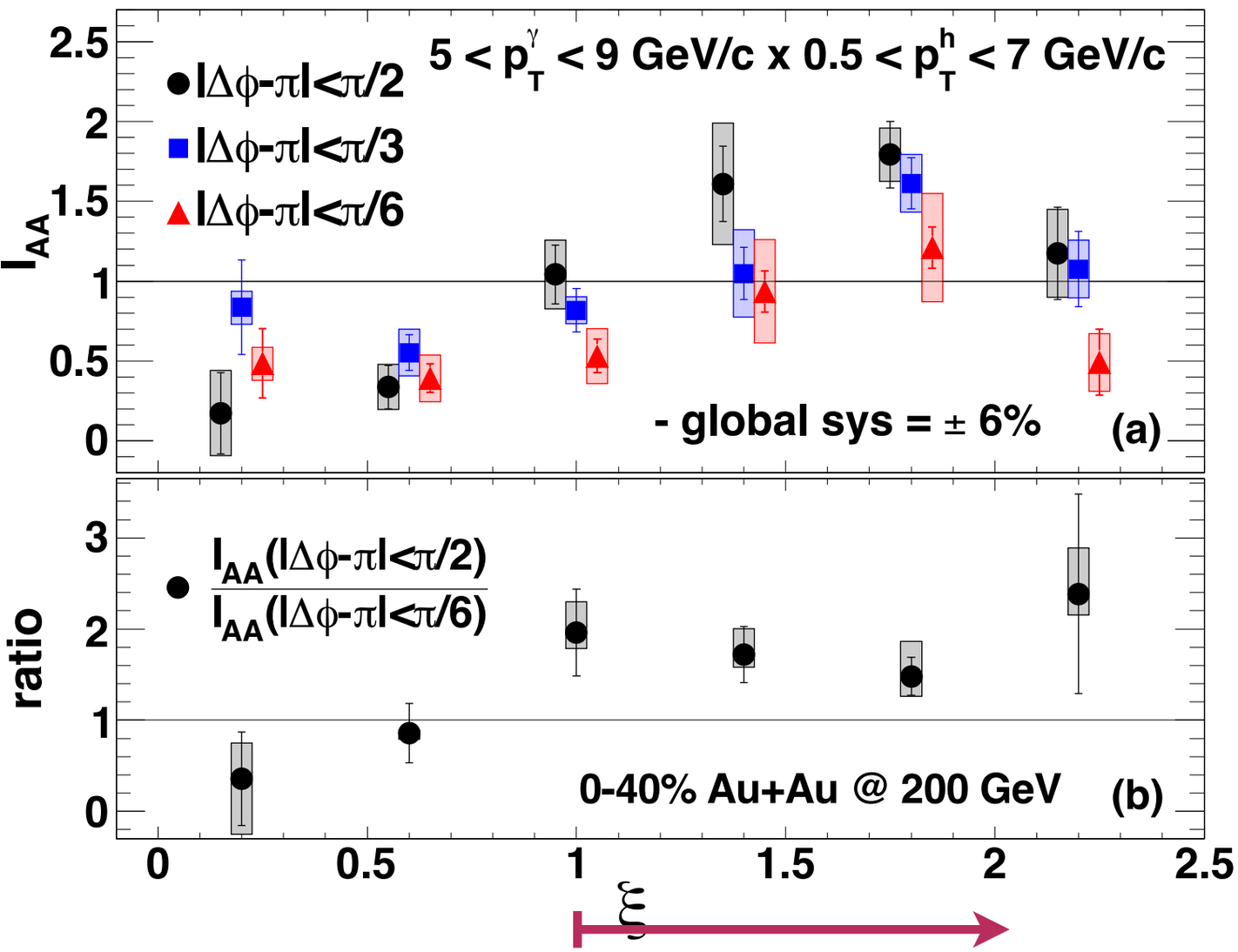

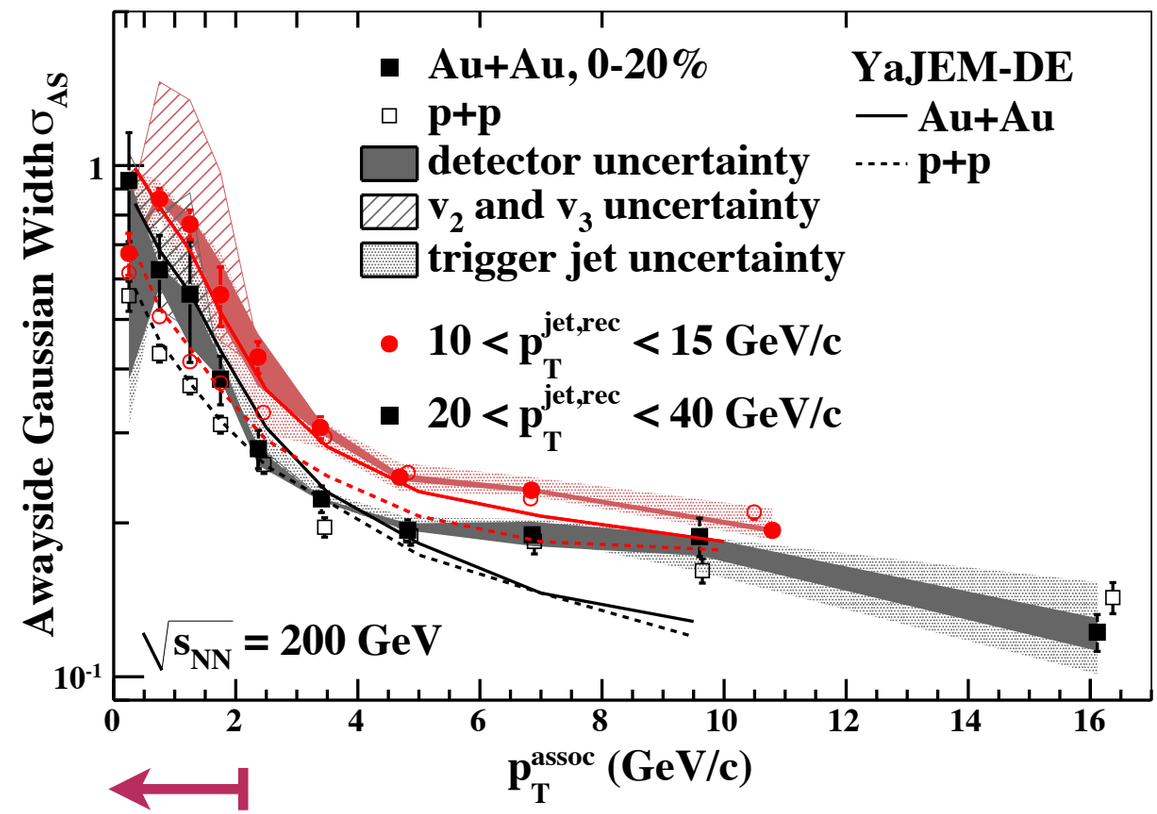

STAR: 1302.6184

broadening of hadron distribution for pT < 2GeV/c

PHENIX: 1212.3323

broadening of angular distribution

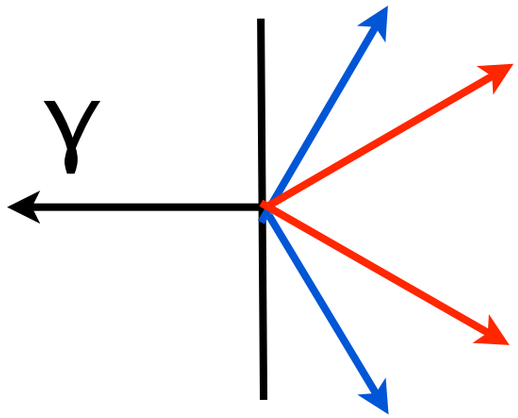

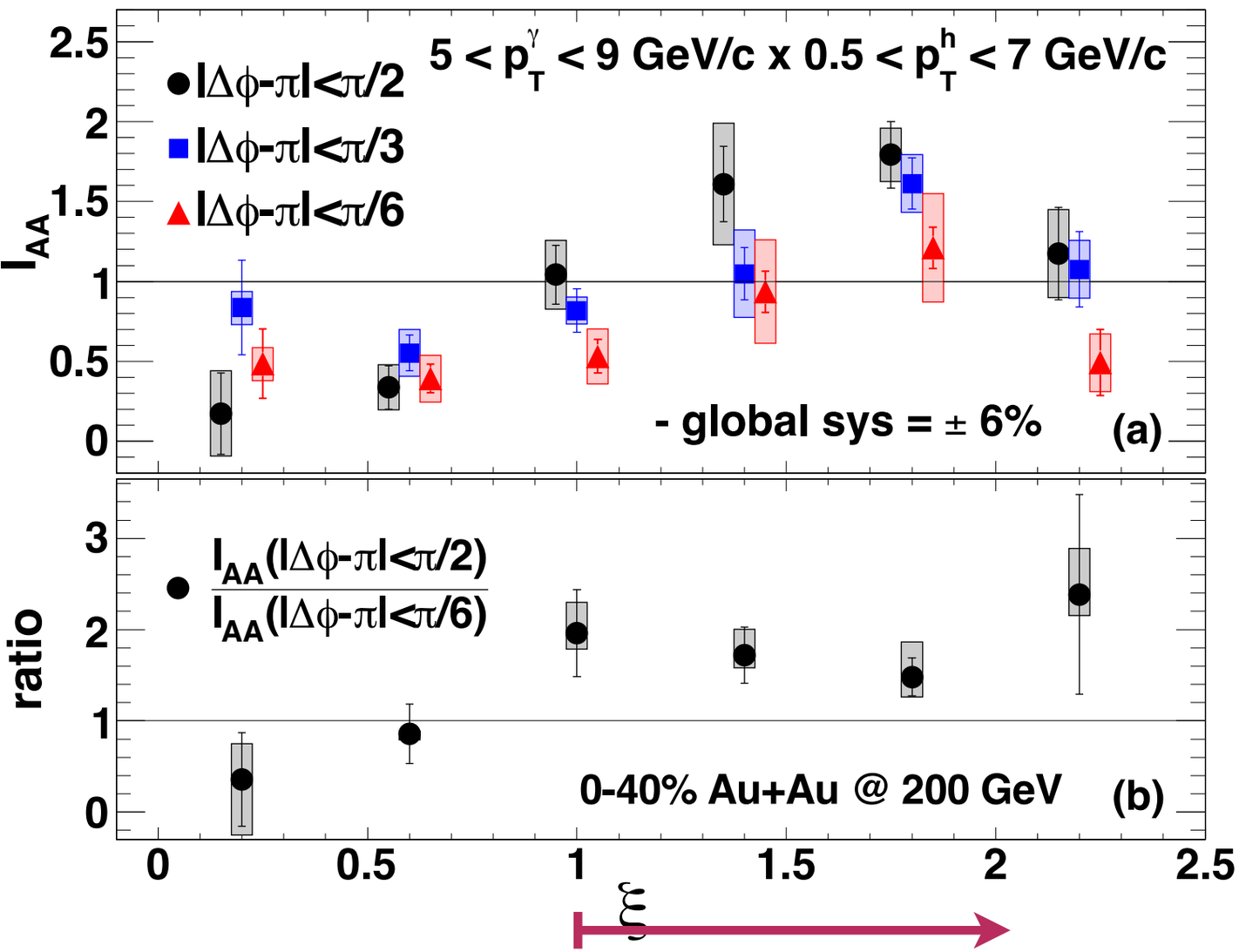

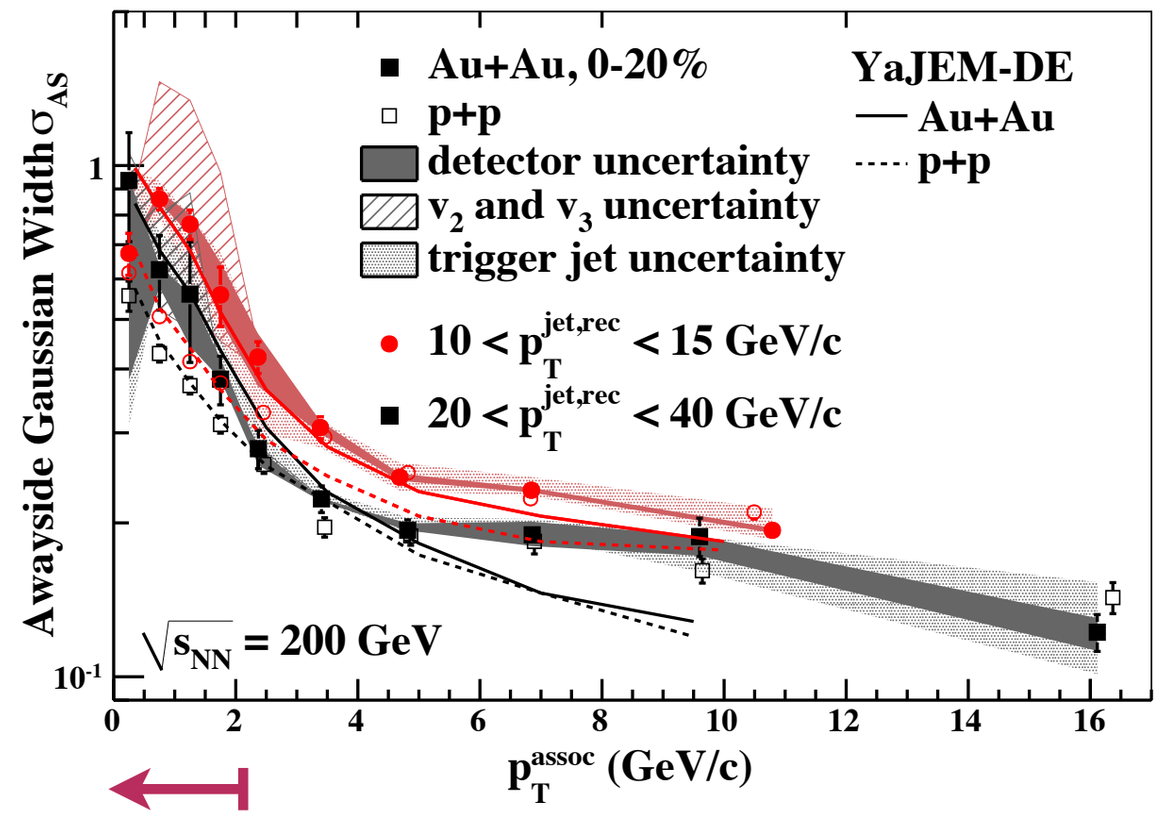

STAR: 1302.6184

evidence for low p_T broadening of hadrons opposite jets/photons

broadening of hadron distribution for pT < 2GeV/c

PHENIX: 1212.3323

quenching vs $\sqrt{s_{NN}}$

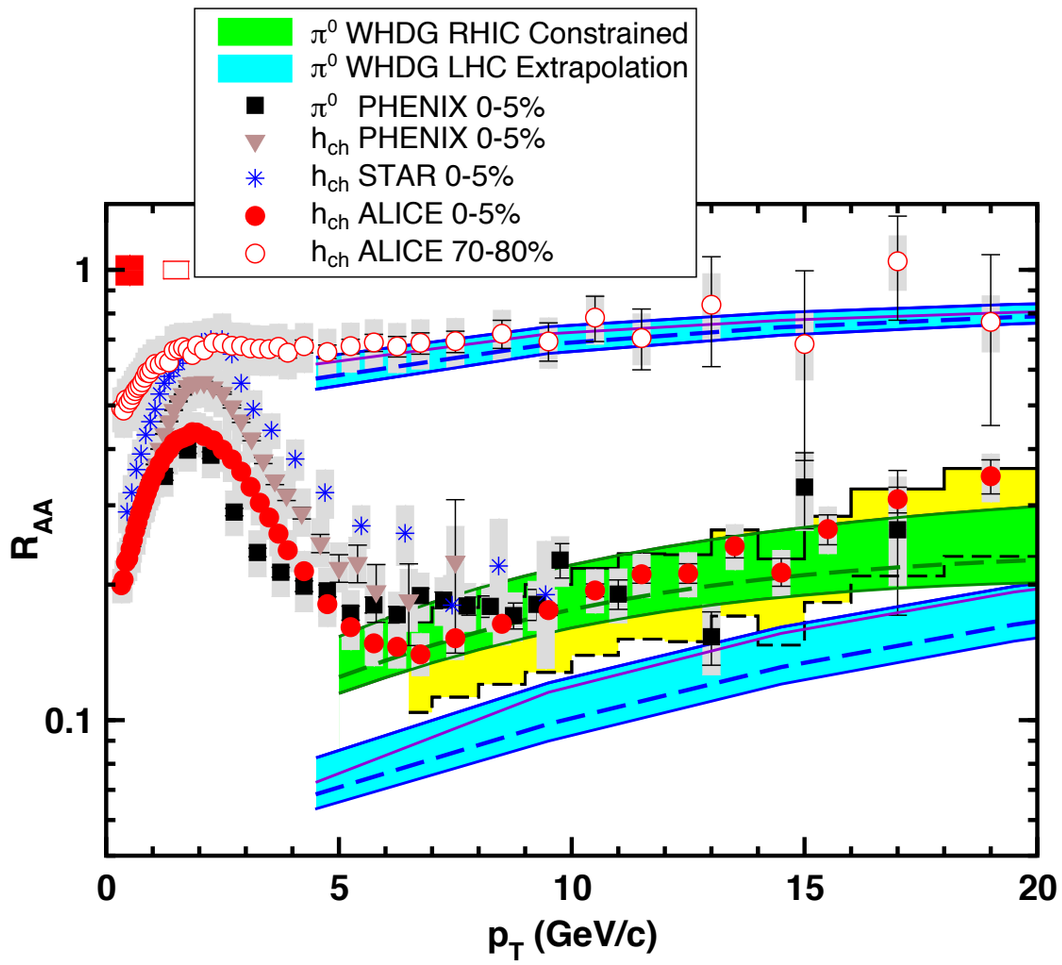

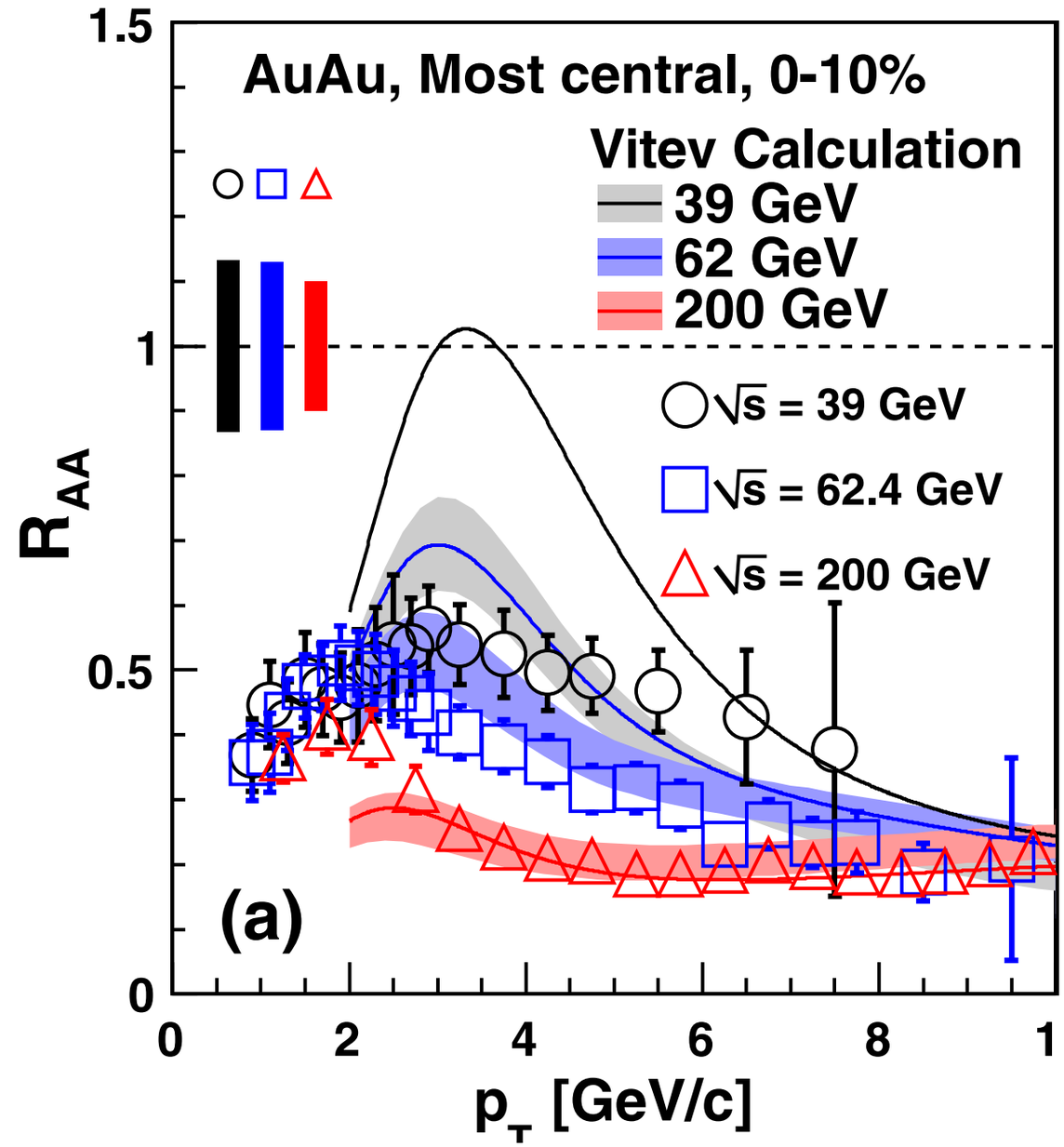

- $R_{AA} \sim 0.5$ at 39GeV
- p_T reach ~10GeV at 62.4GeV, R_{AA} consistent with 200GeV
- *pA measurements needed to understand initial state effect

Horowitz & Gyulassy NPA872 265, PHENIX PRL 109 152301

a peak into the future of hard probes...

using RHIC and LHC to constrain temperature dependence of η/s within hydro

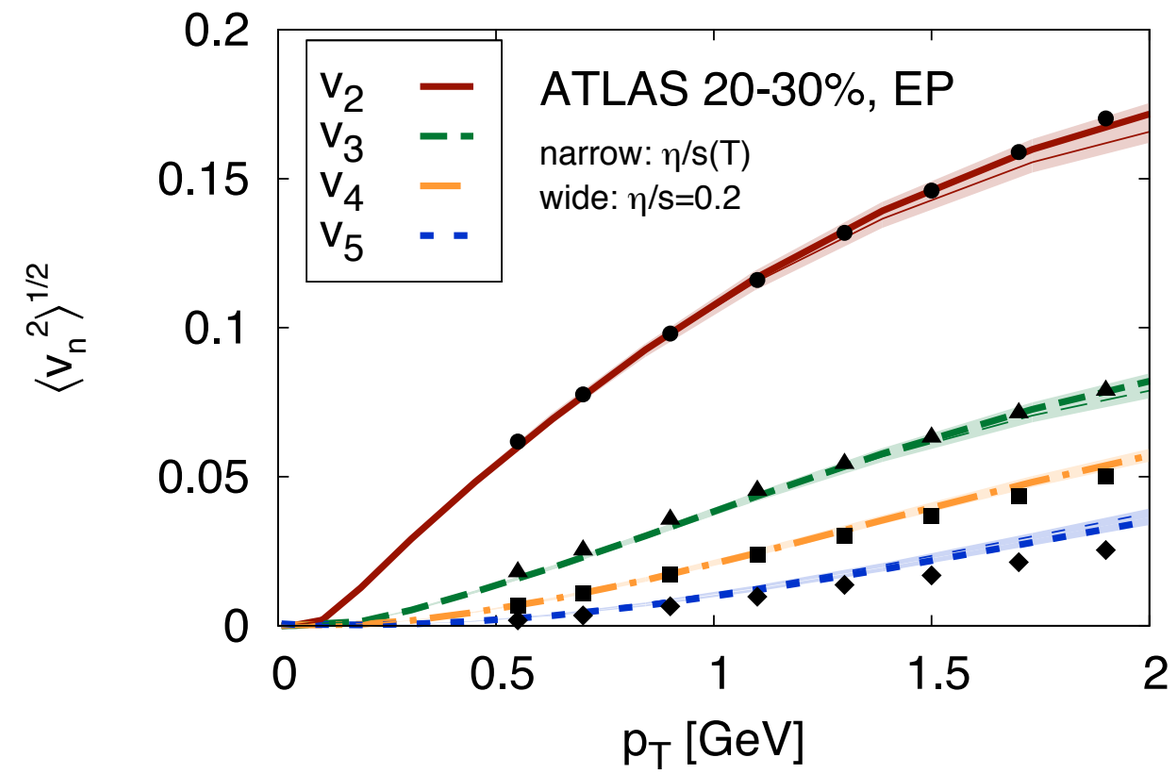

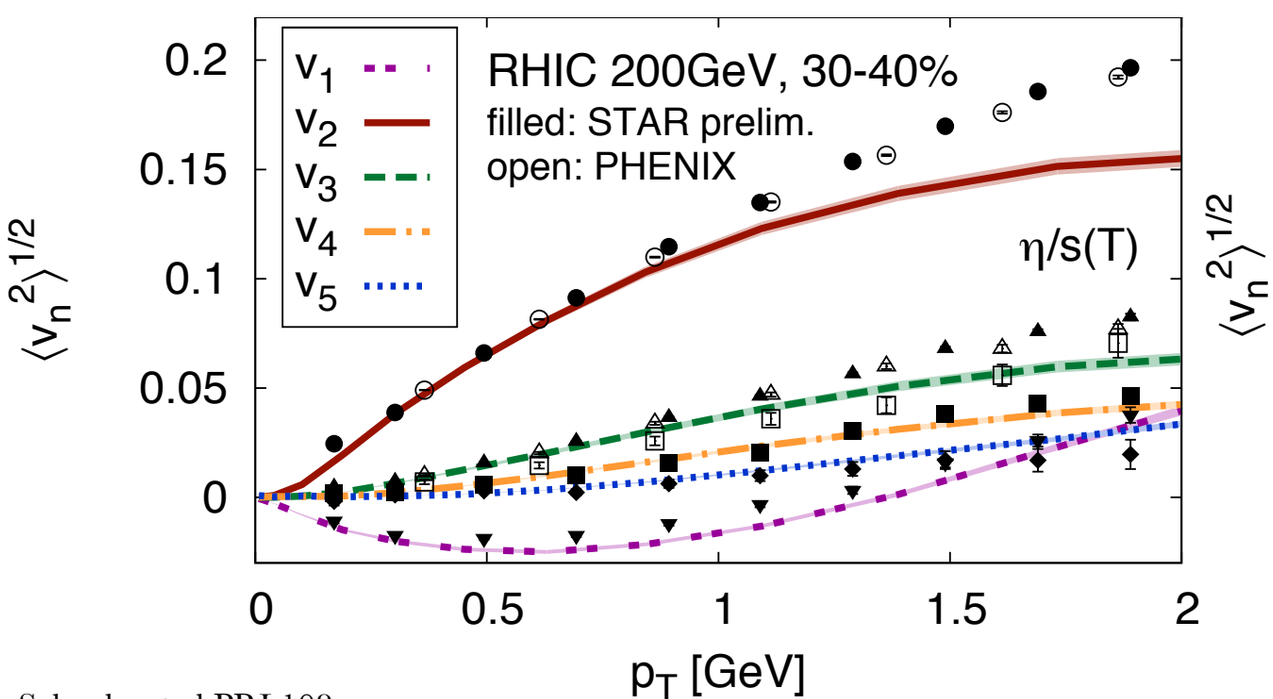

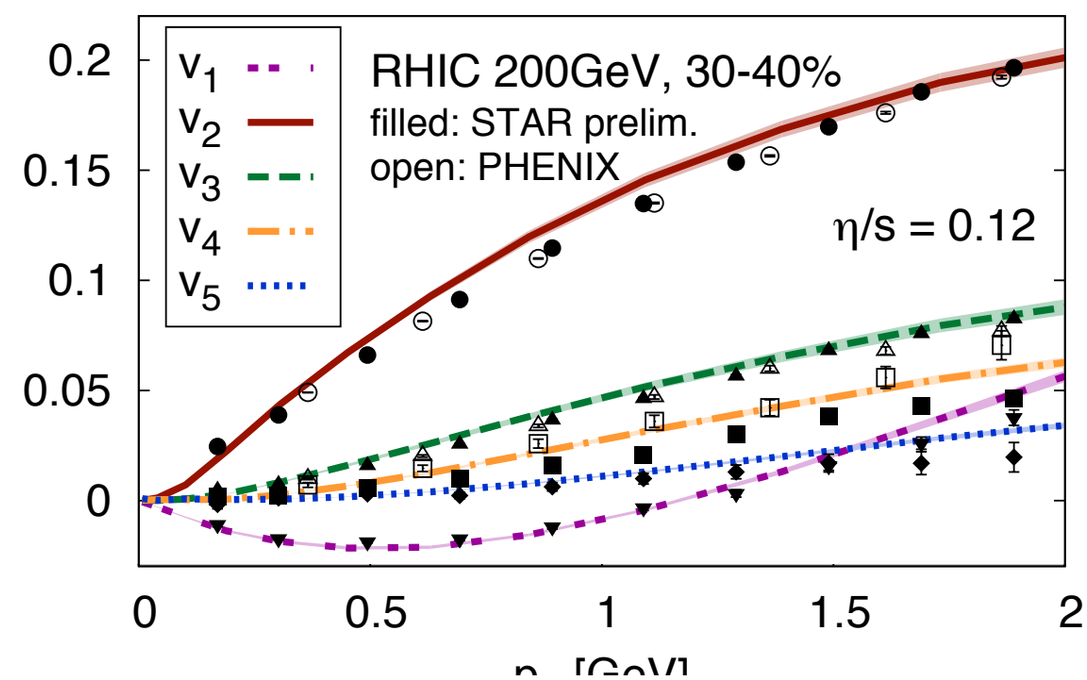

Schenke et al PRL108 252301
Gale et al 1209.6330

leveraging RHIC/LHC differences

initial entropy densitiy

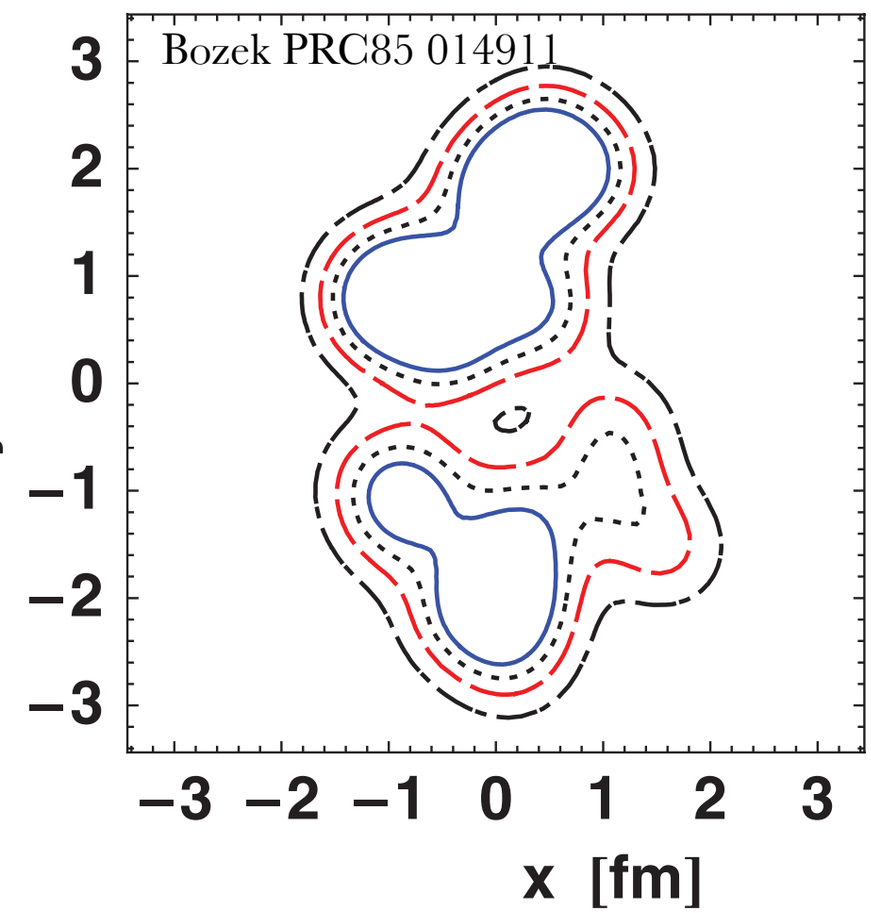

1303.1794

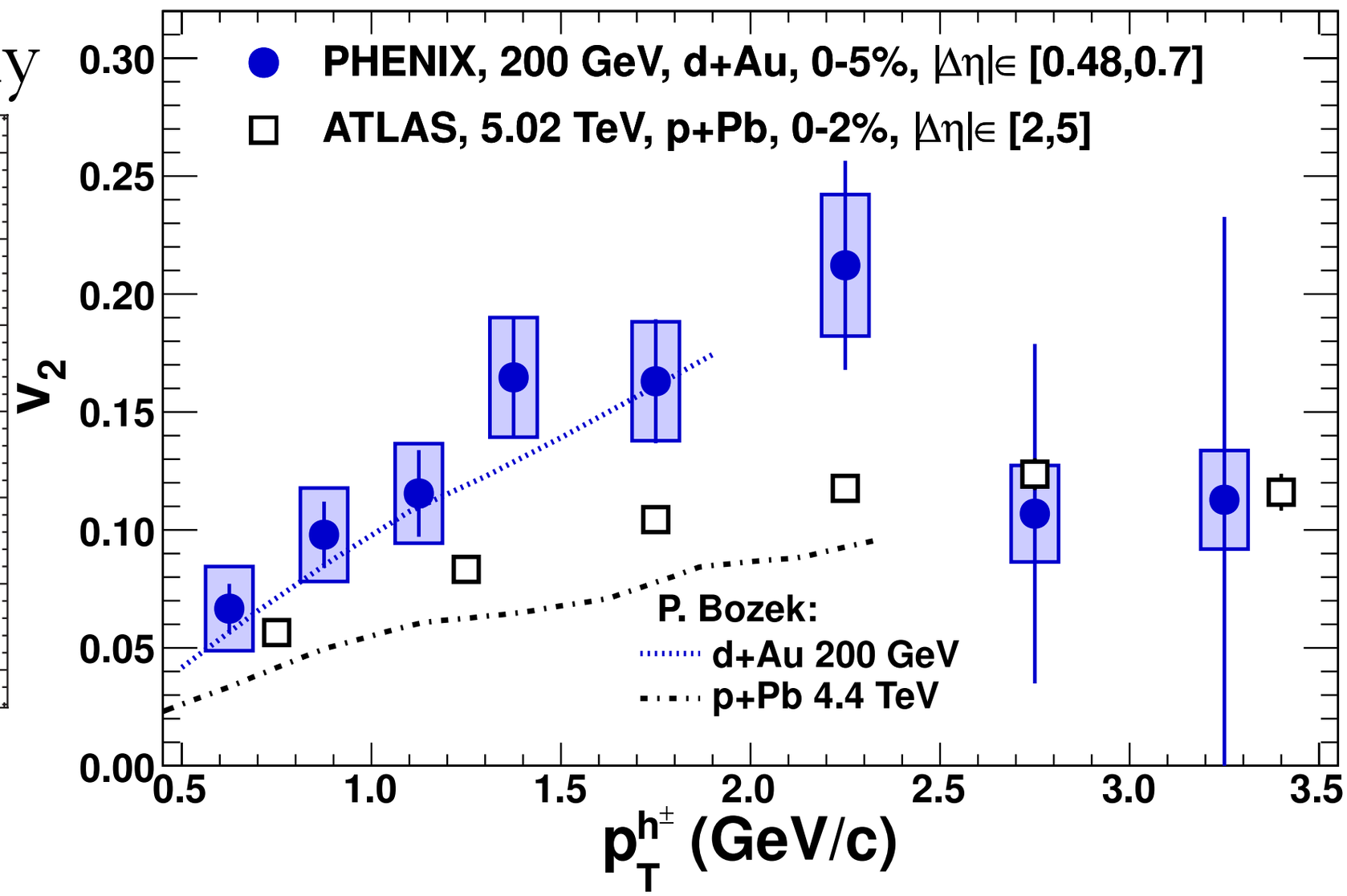

- changing both the collision energy and the shape of the initial system as compared to the ridge seen in pPb

sPHENIX

- upgrade optimized around jet/di-jet/photon measurements
- high rate, large uniform acceptance over $|\eta|<1$, hadronic calorimetry
- submitted last month to DOE for CD-0 review

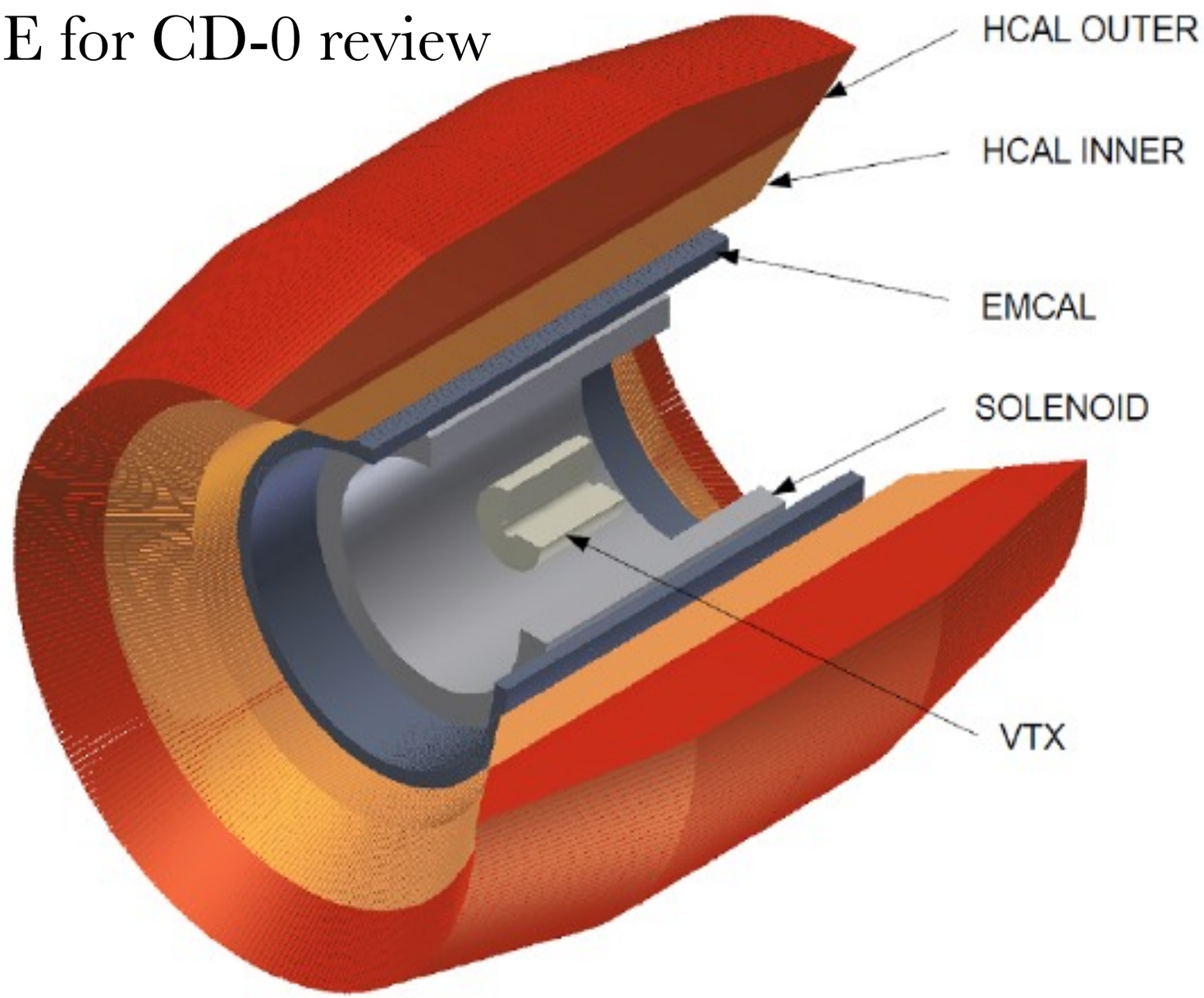

inside sPHENIX

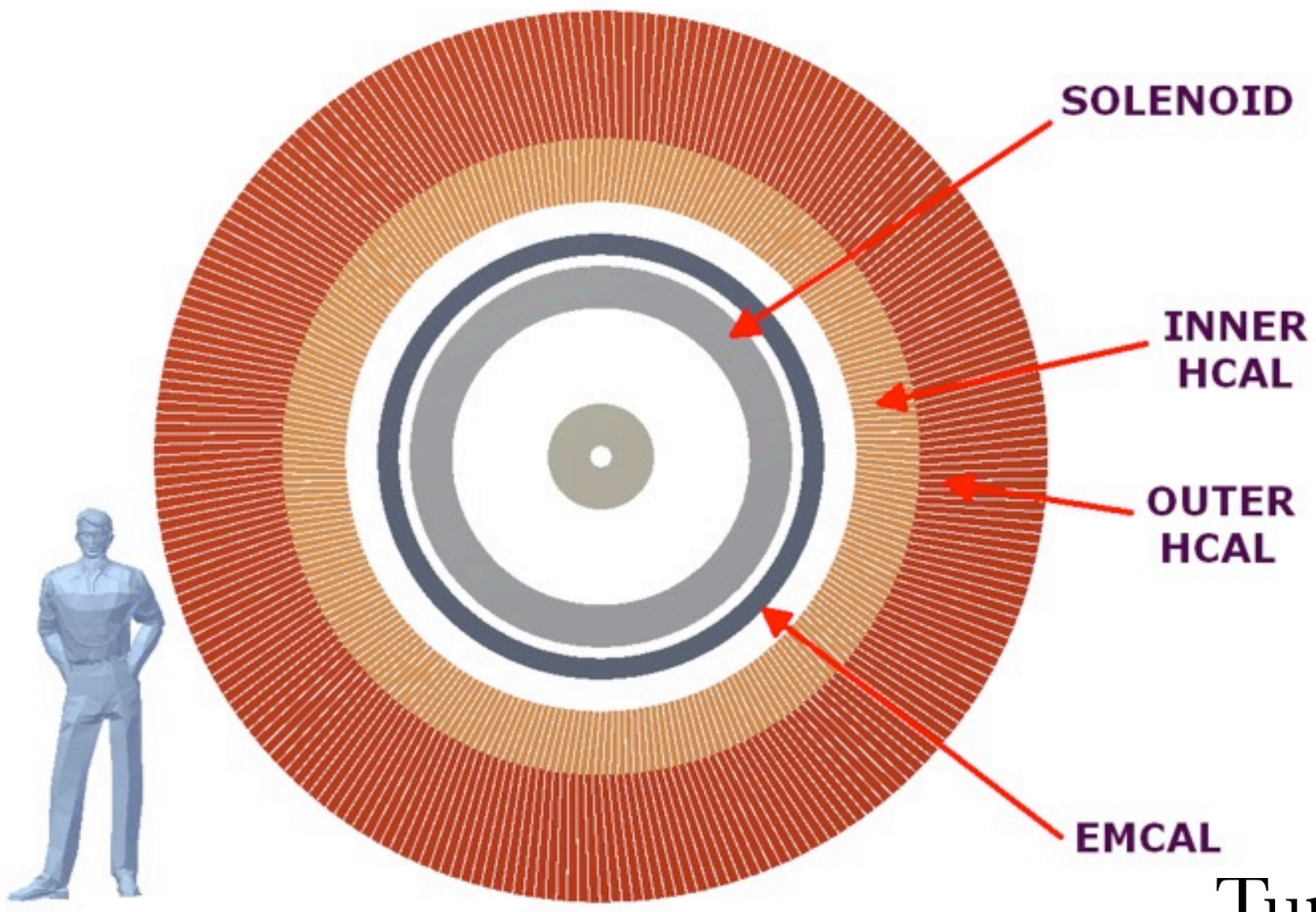

Rin = 70cm
2T, $1X_0$

Fe-Scintillator
HCal

Tungsten-scintillator
10cm thick

How Realistic Is this at RHIC?

RHIC Jet Rates

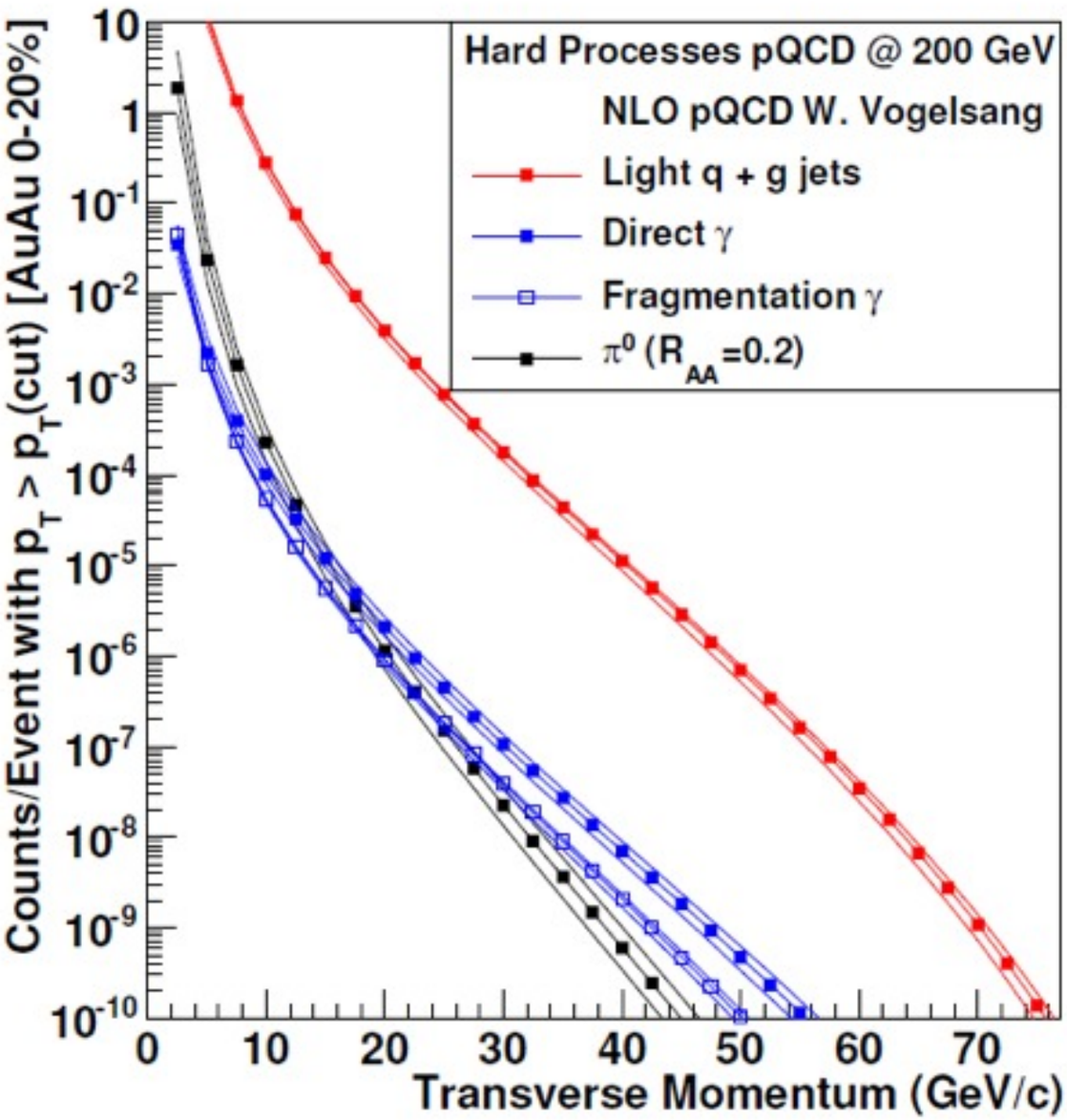

rates based on full stochastic cooling, but no additional accelerator upgrades

	Au+Au (central 20%)	p+p	d+Au
>20GeV	10^7 jets 10^4 photons	10^6 jets 10^3 photons	10^7 jets 10^4 photons
>30GeV	10^6 jets 10^3 photons	10^5 jets 10^2 photons	10^6 jets 10^3 photons
>40GeV	10^5 jets	10^4 jets	10^5 jets
>50GeV	10^4 jets	10^3 jets	10^4 jets

Huge rates allow differential measurements with geometry (v_2, v_3, A+B, U+U, ...) & precise control measurements (dAu & pp) over 80% as dijets!

jet reconstruction performance

- how well can we measure real jets?
  - jet energy scale, jet energy resolution
- how are the jet measurements impacted by background fluctuations masquerading as jets--fakes

- large HIJING study
  - embedding PYTHIA jets into HIJING events to evaluate jet reconstruction performance
  - 750M minimum bias HIJING events to study relative rates of fake and real jets in HI background
- iterative background subtraction as in ATLAS

detailed study in: Hanks, Sickles et al: PRC86 024908

reconstruction performance

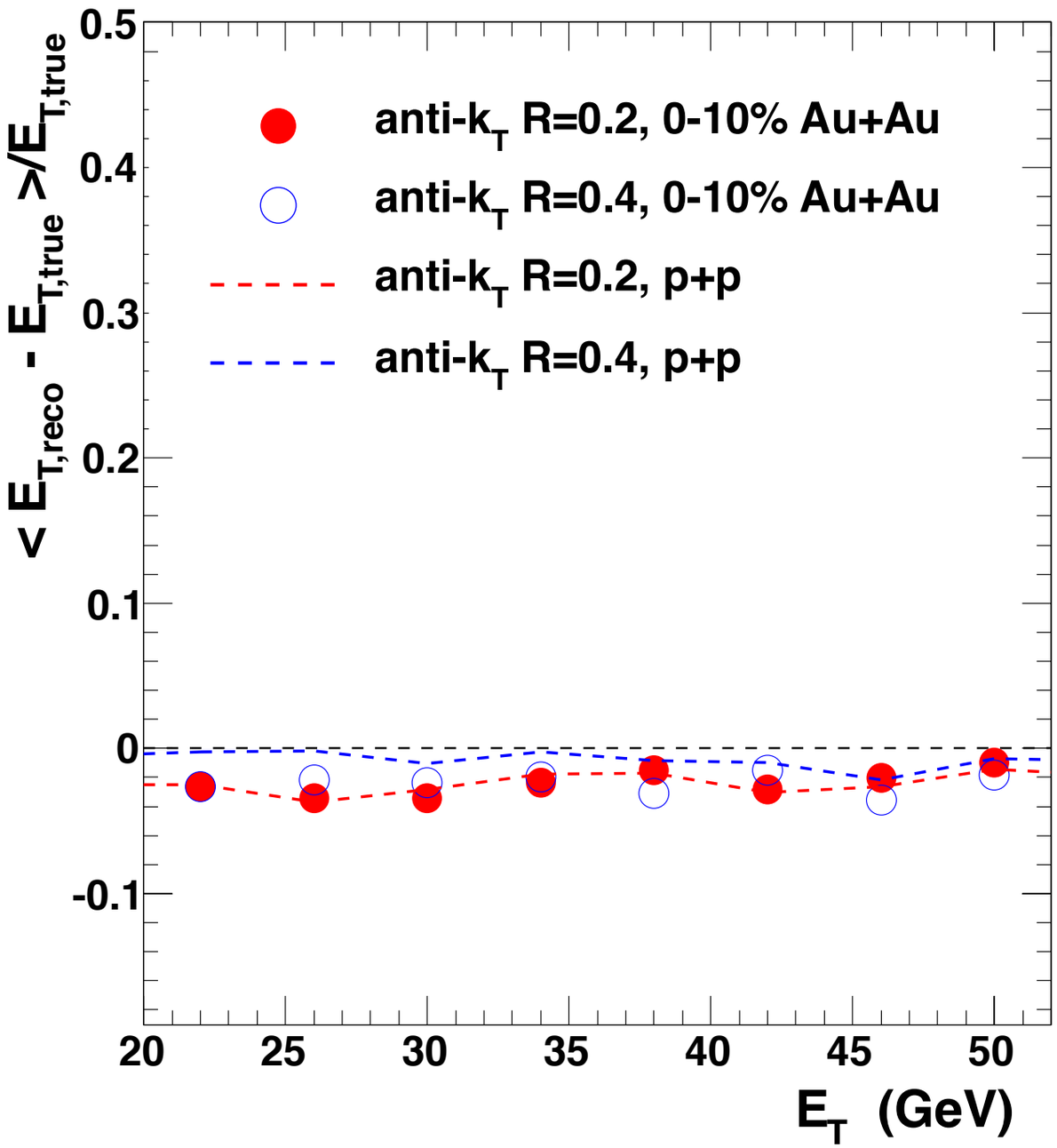

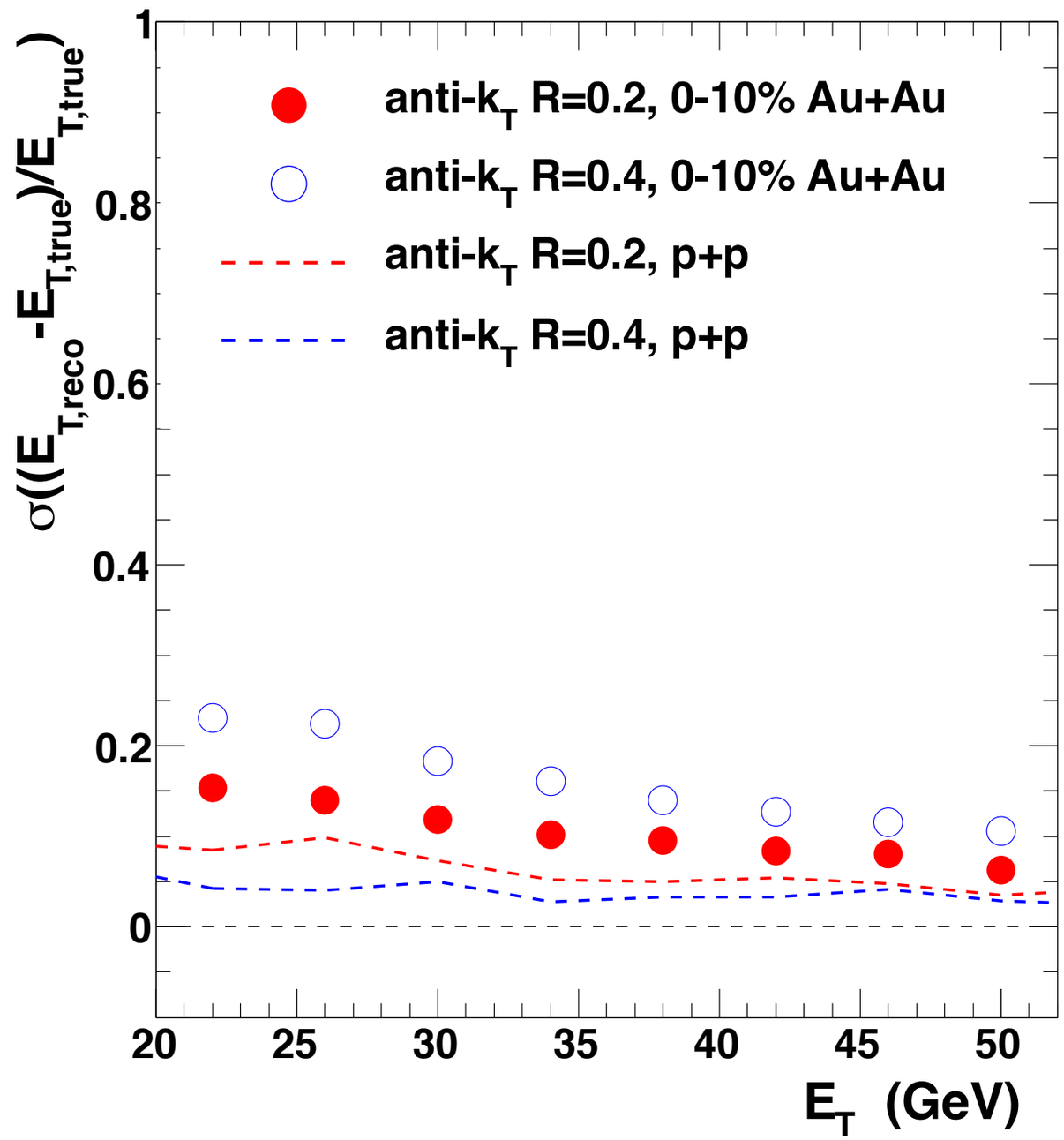

- good performance in heavy ion background
- resolution only from the underlying event, no detector resolution included

reconstructed jets

reconstructed jets

matched jets:
within ΔR< 0.25 of a HIJING truth jet (>5GeV)

not matched jets:
no nearby HIJING jets
"fakes"

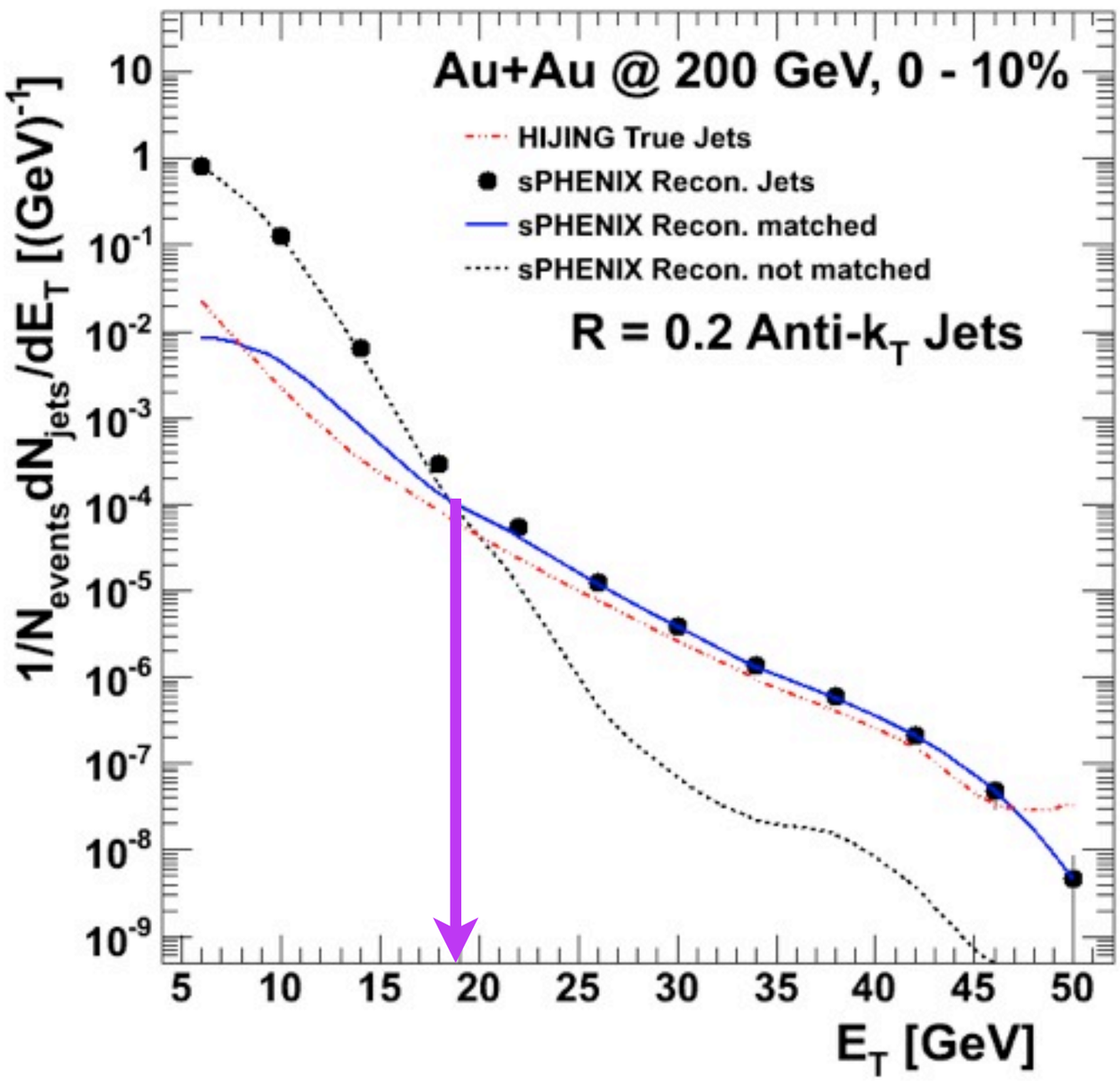

Fake Jets at RHIC (R=0.2)

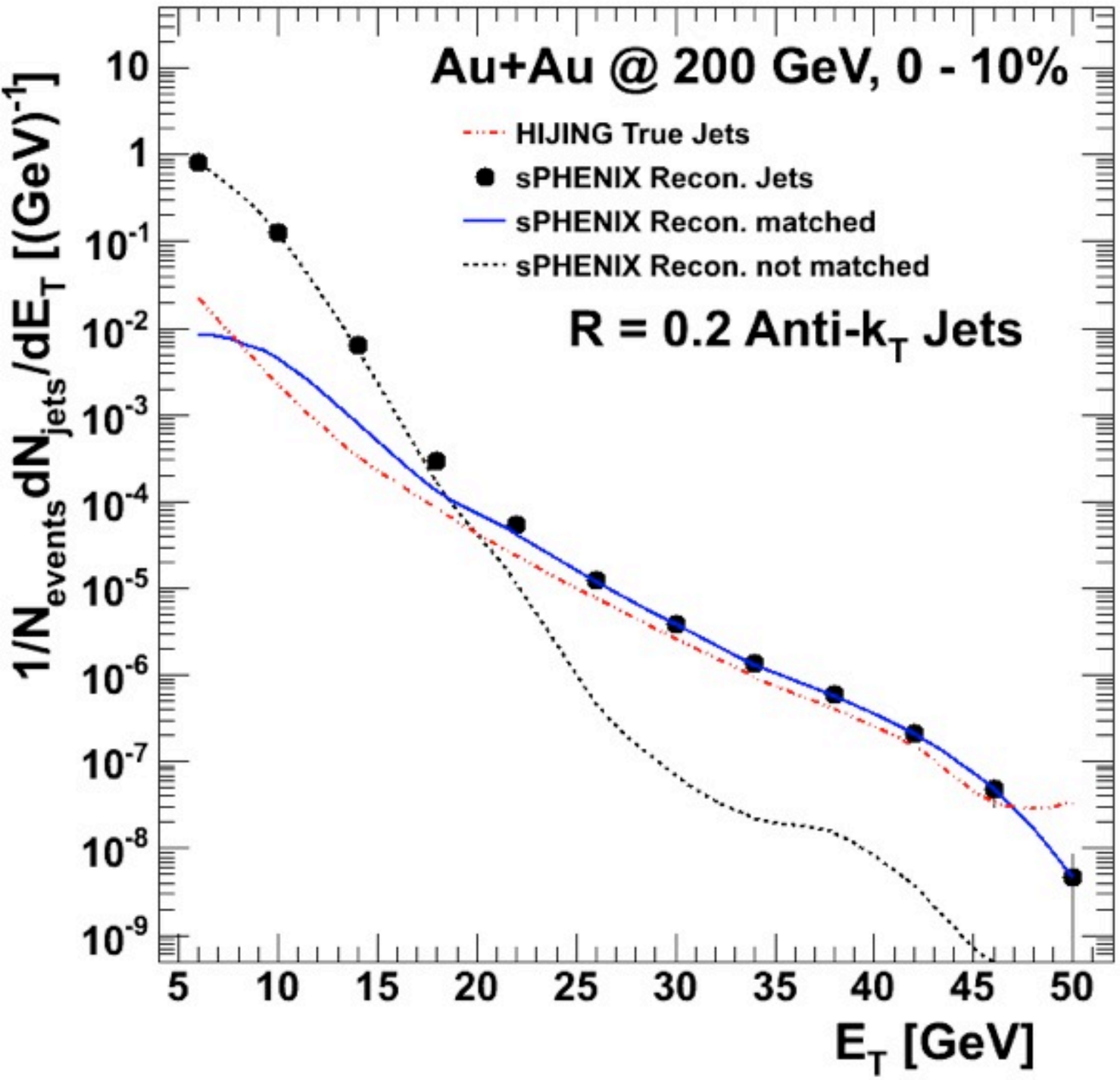

Fake Jets at RHIC (R=0.2)

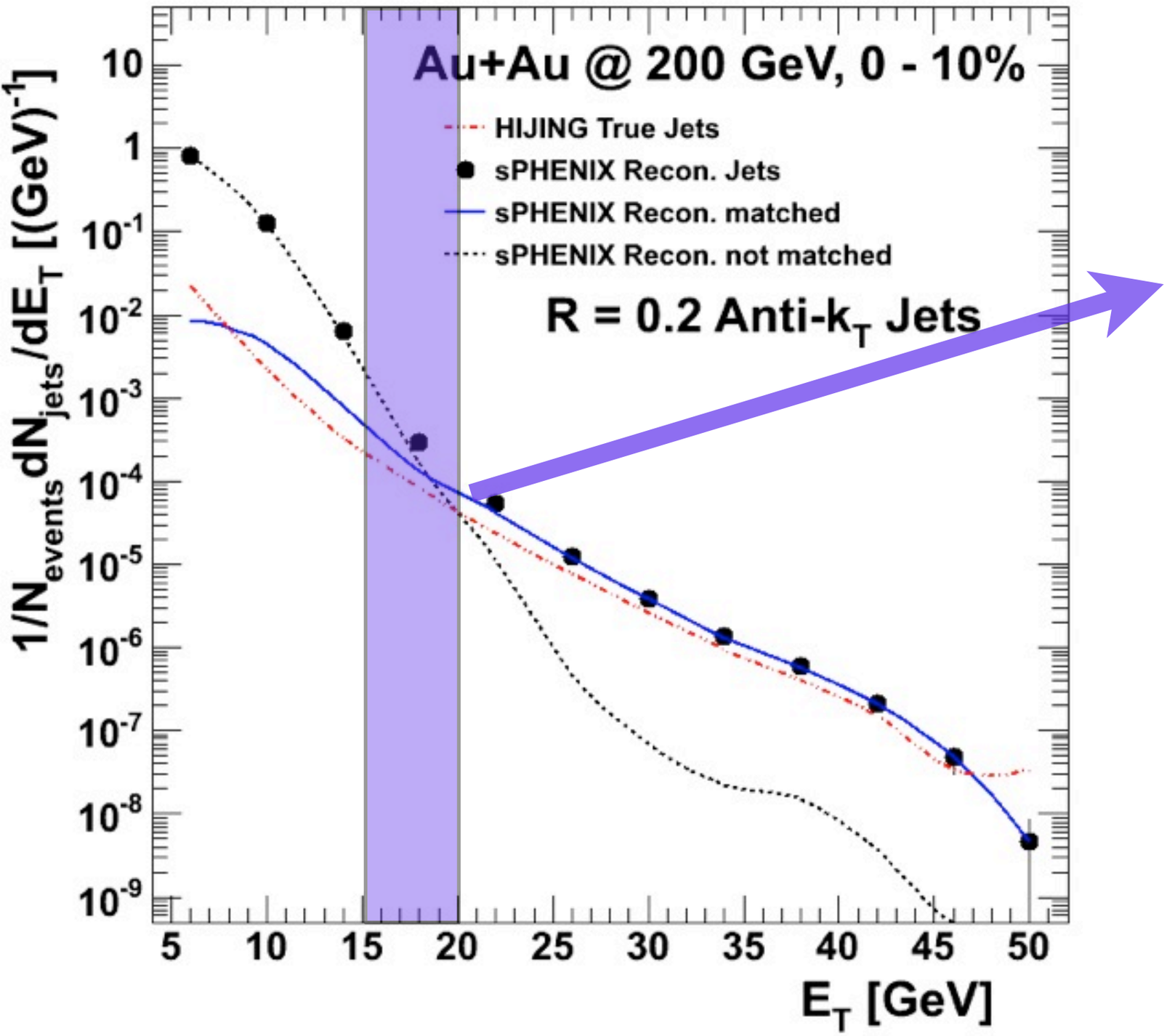

Fake Jets at RHIC (R=0.2)

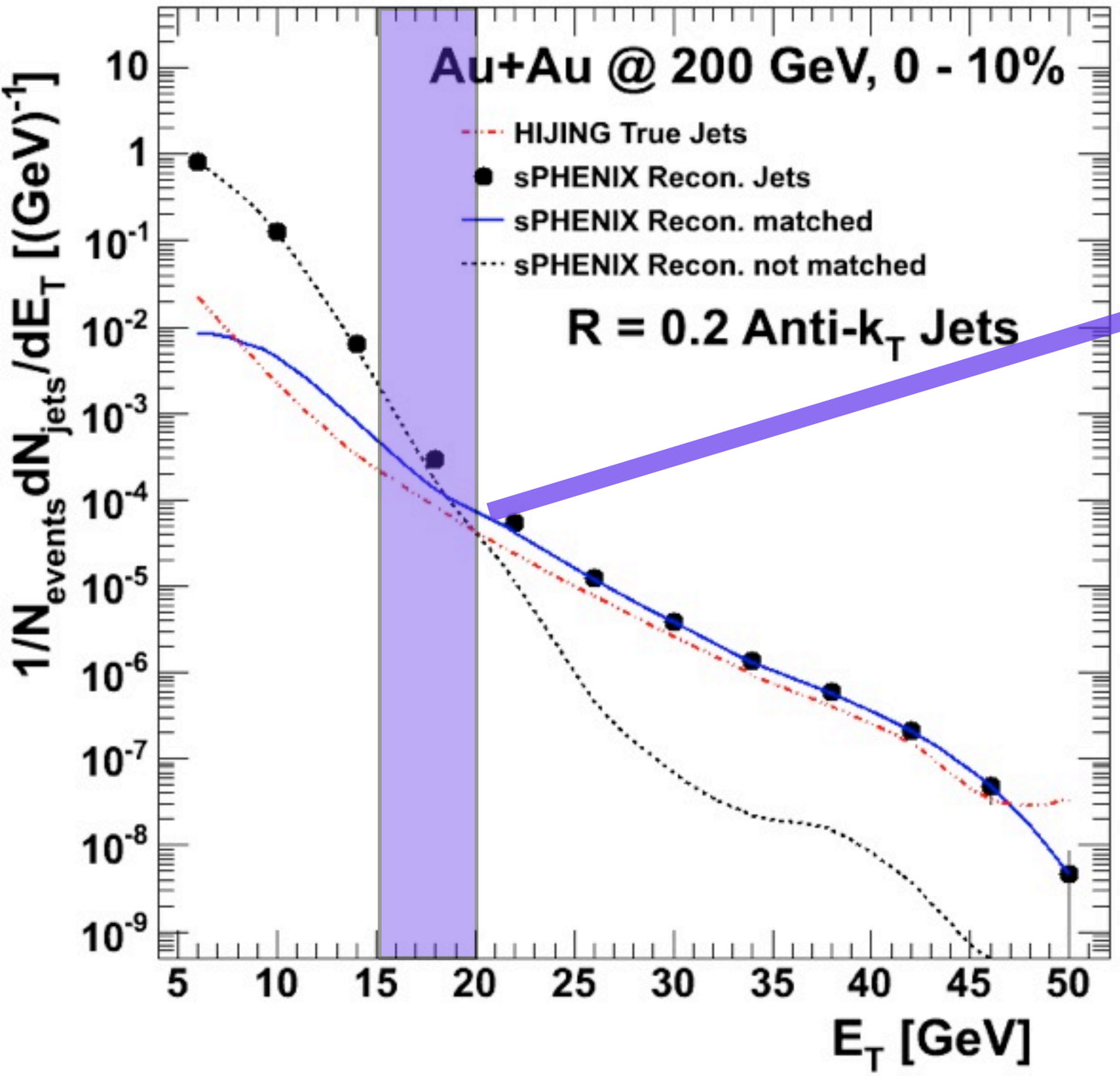

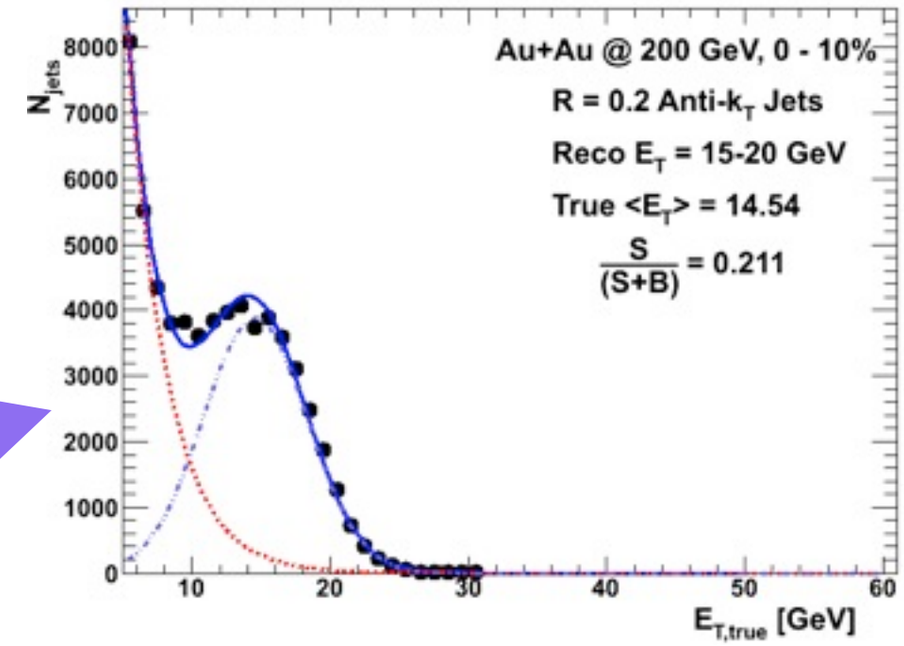

Fake Jets at RHIC (R=0.2)

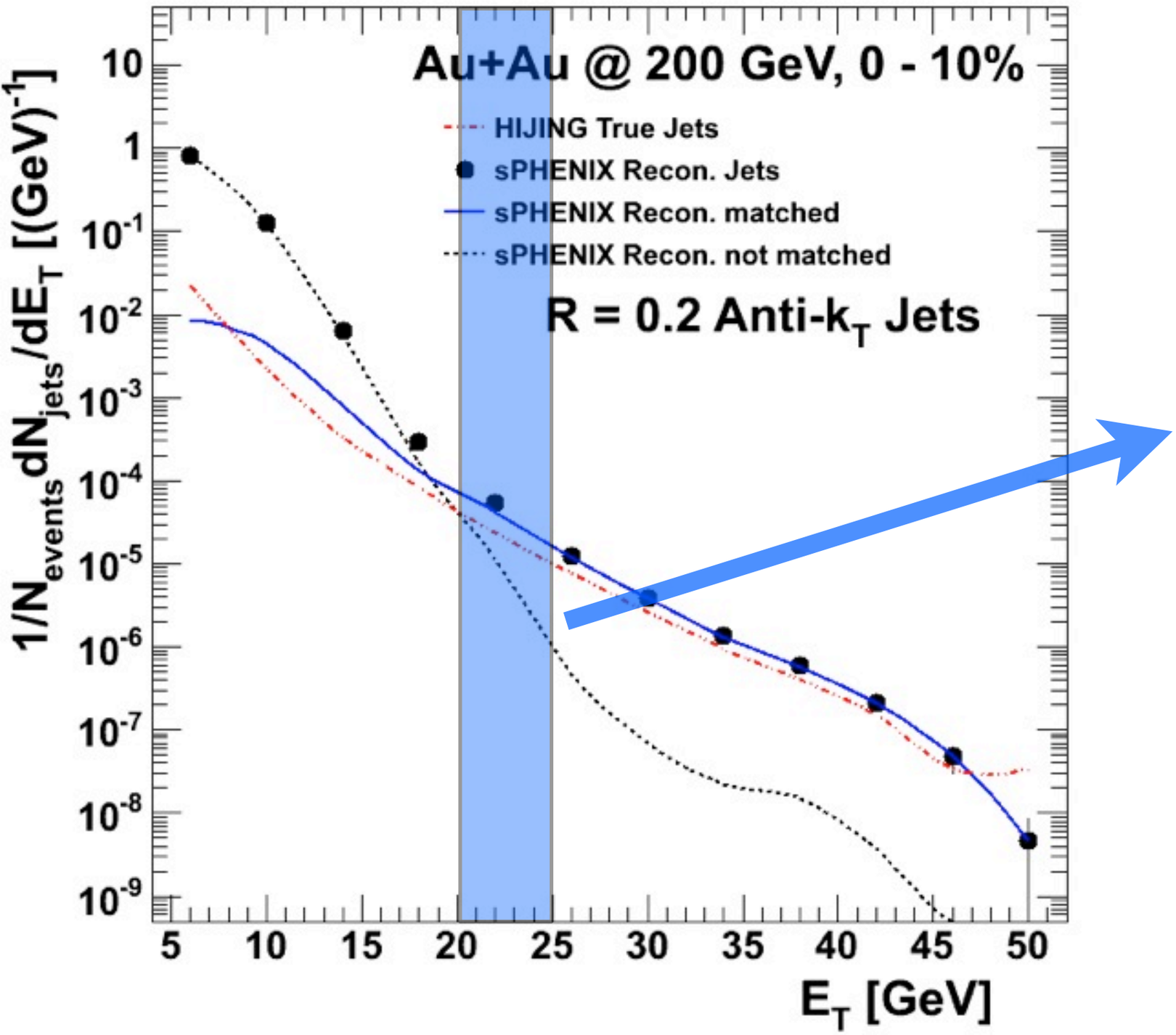

Fake Jets at RHIC (R=0.2)

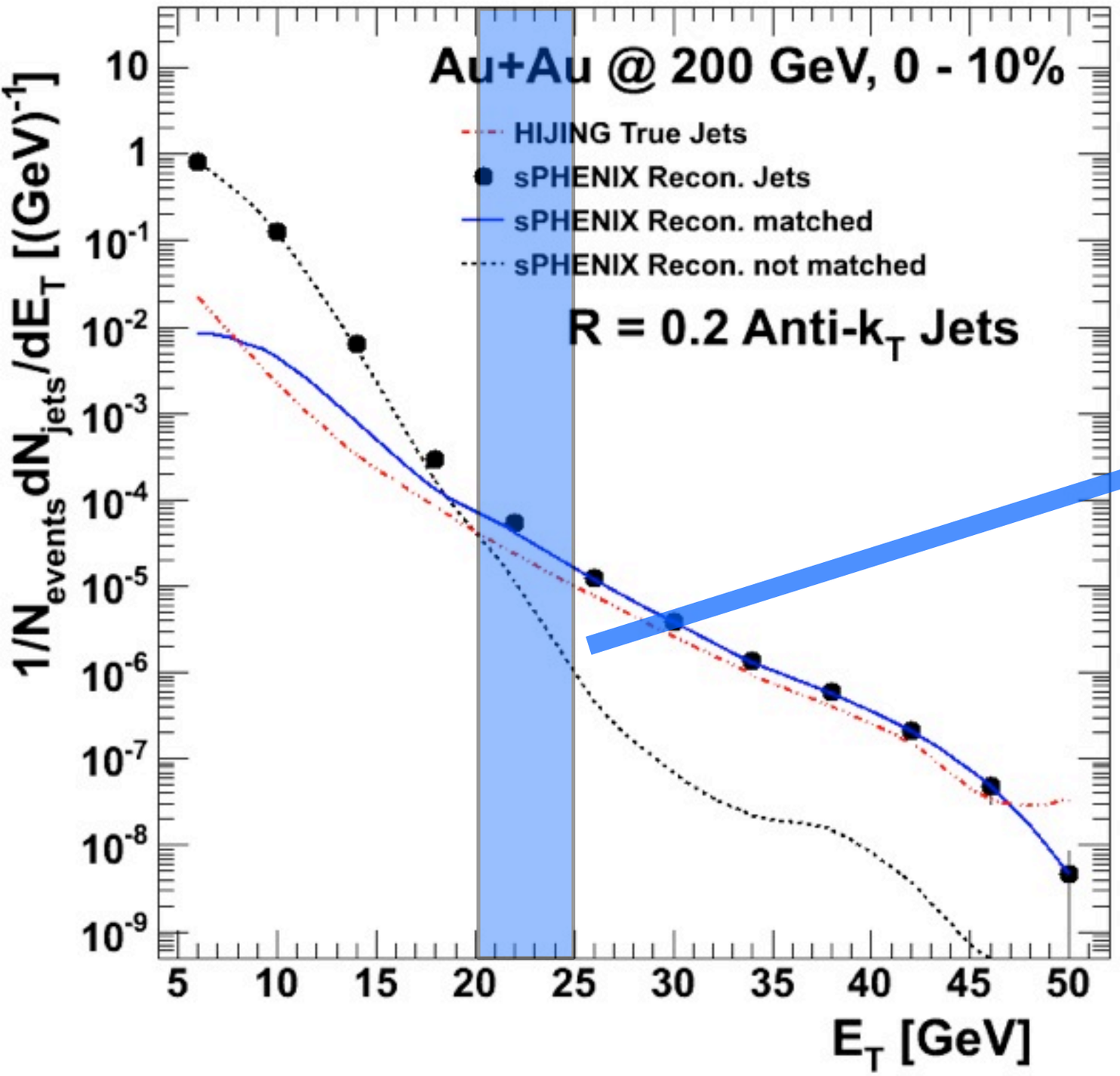

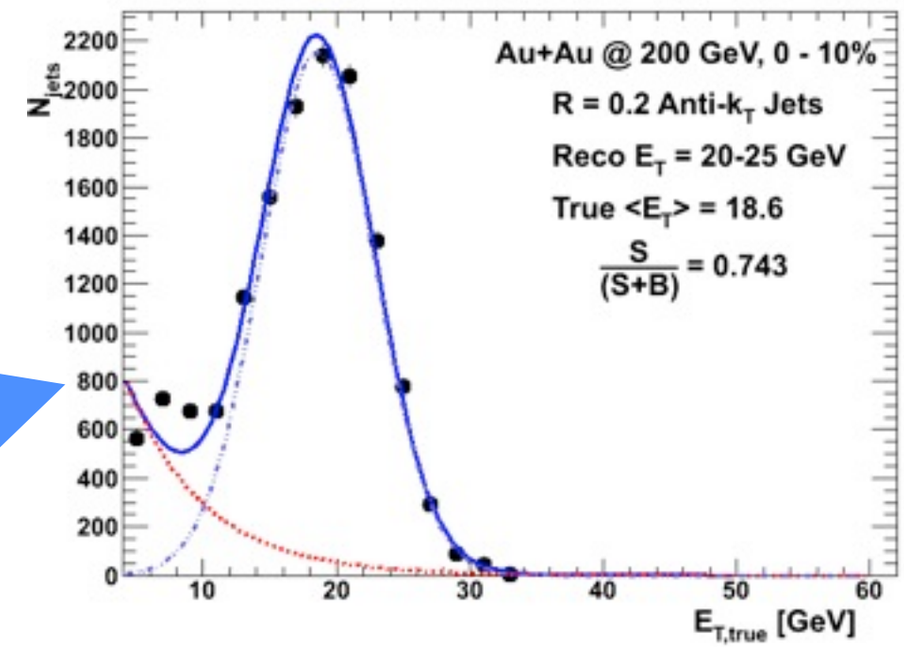

Fake Jets at RHIC (R=0.2)

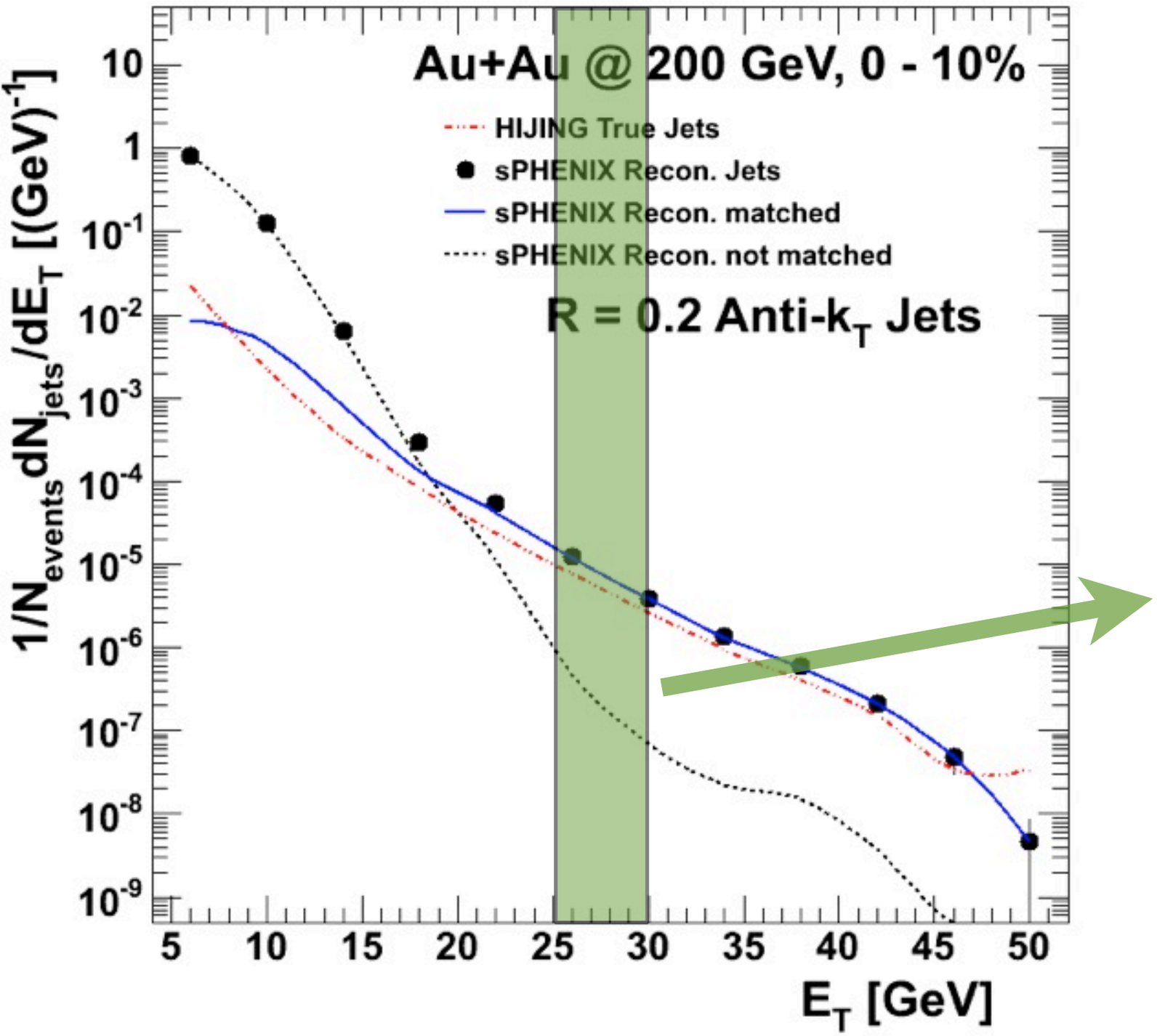

Fake Jets at RHIC (R=0.2)

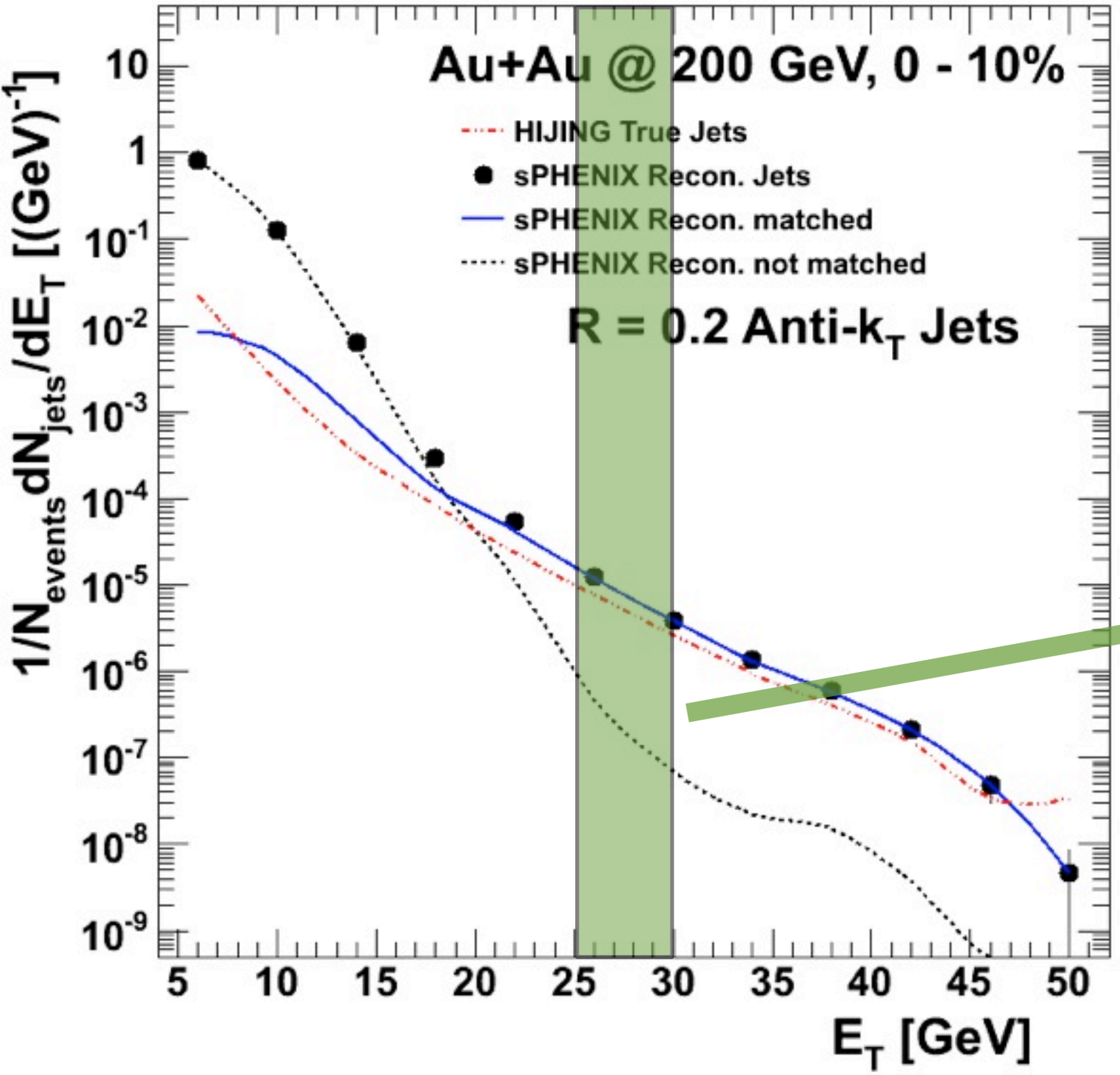

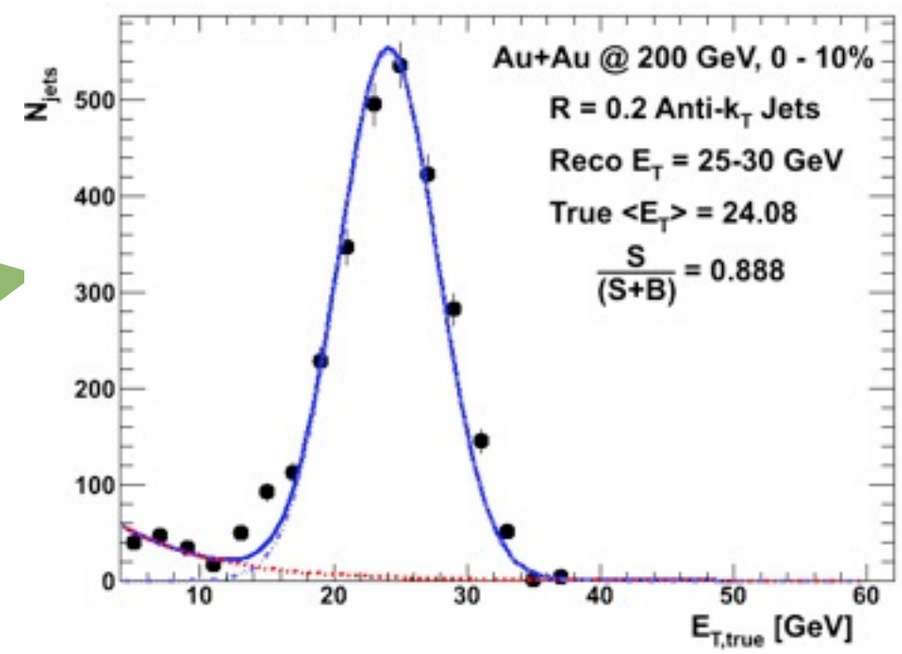

Fake Jets at RHIC (R=0.2)

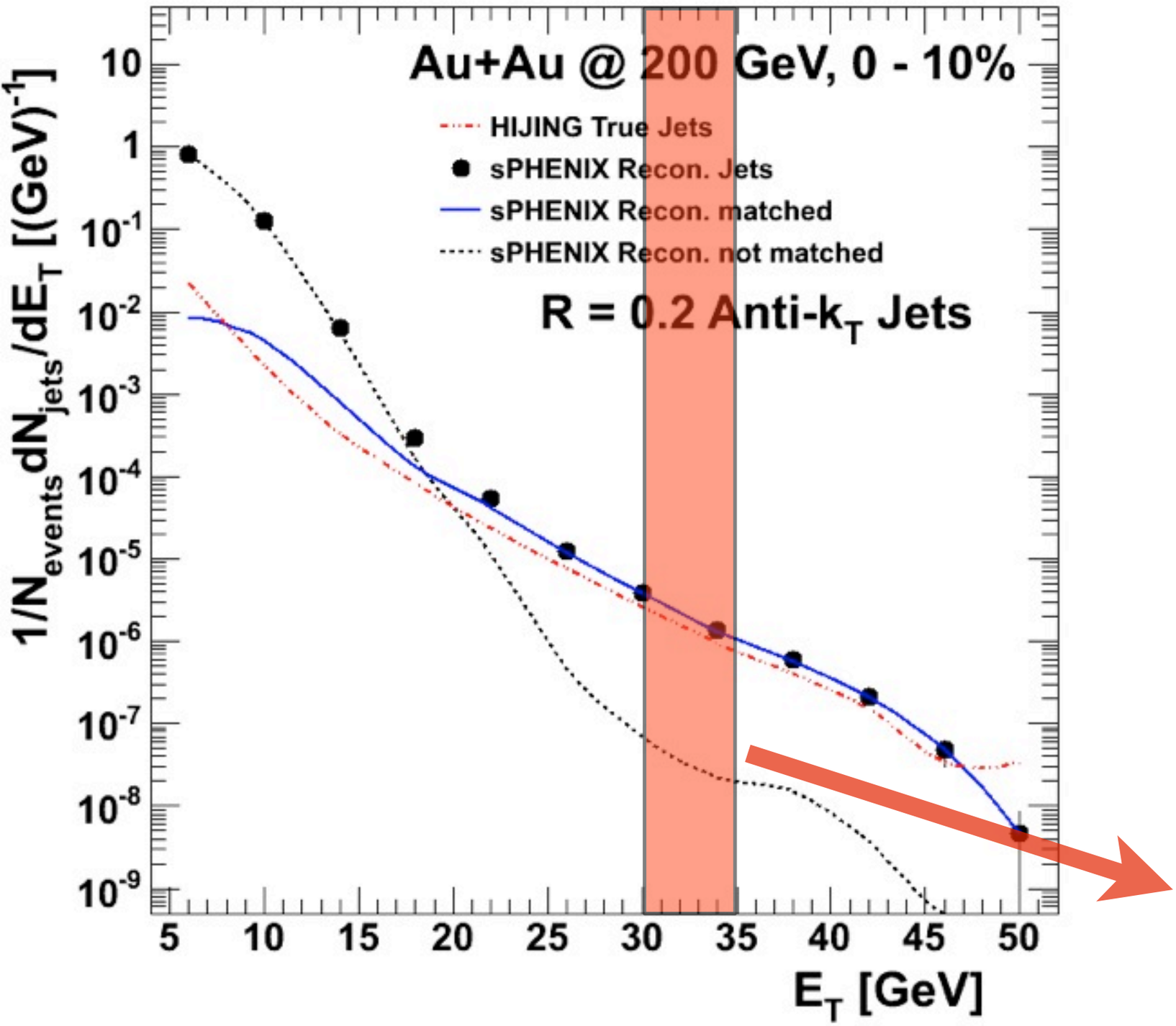

Fake Jets at RHIC (R=0.2)

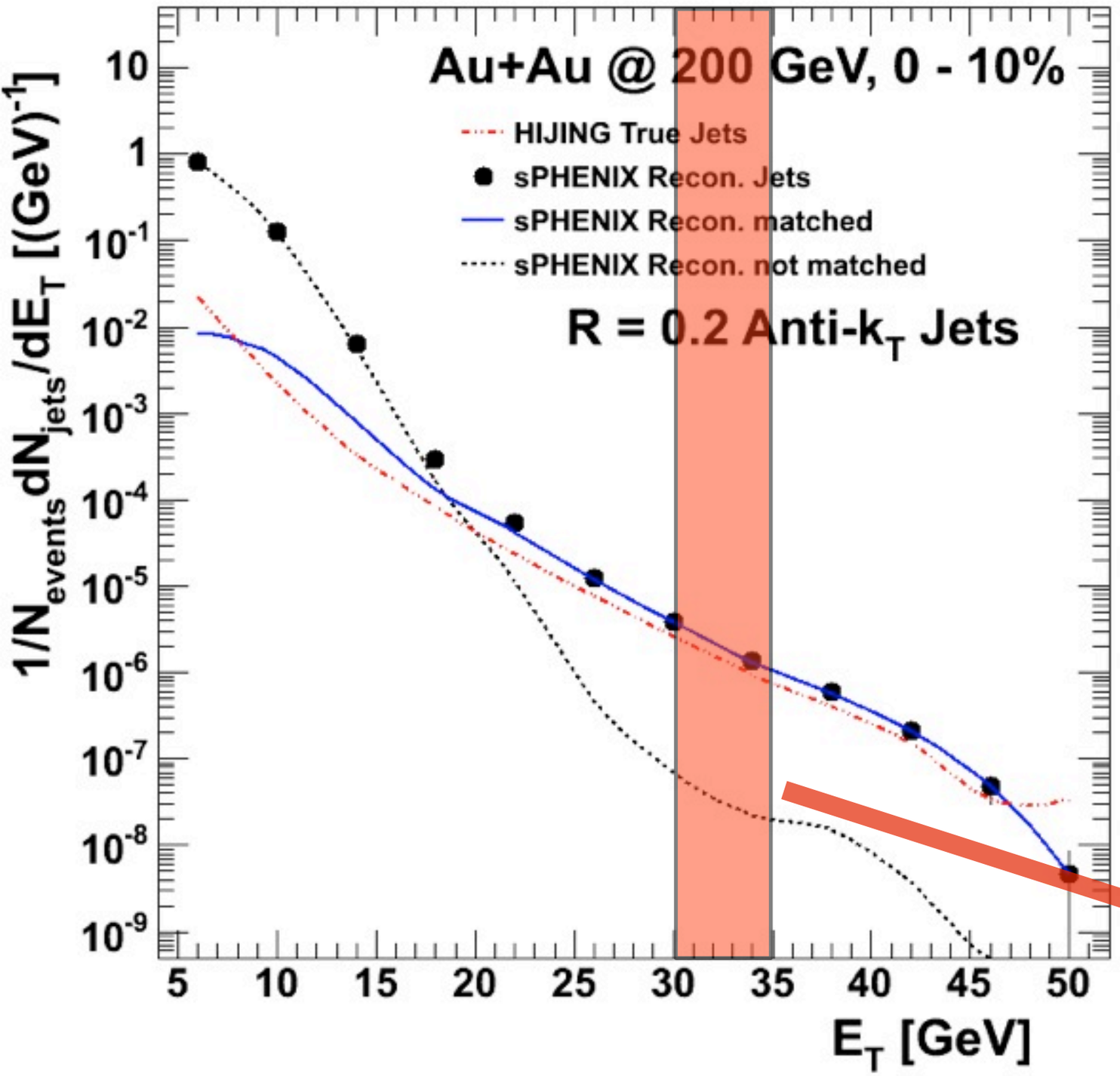

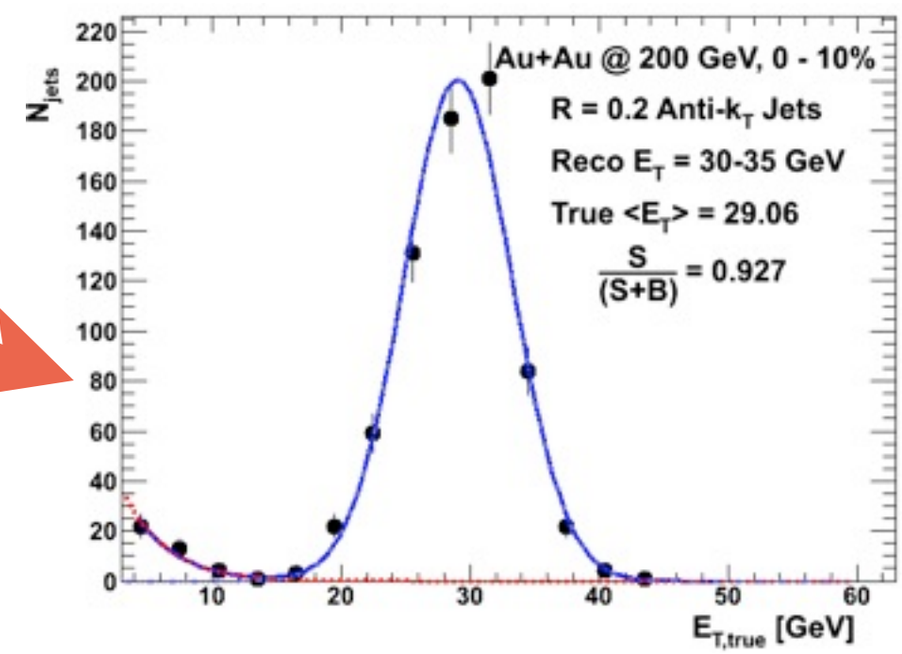

Fake Jets at RHIC (R=0.2)

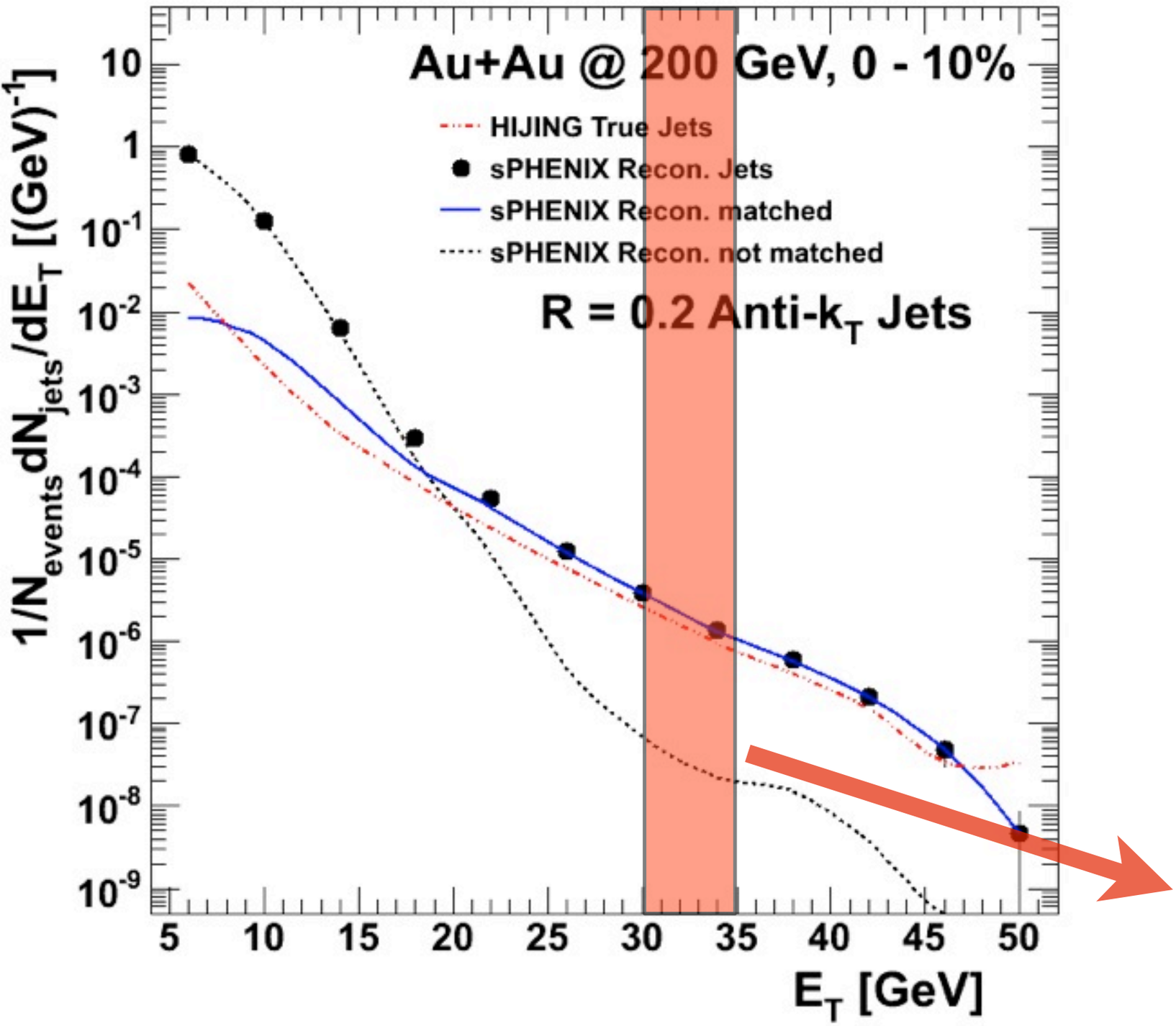

Fake Jets at RHIC (R=0.4)

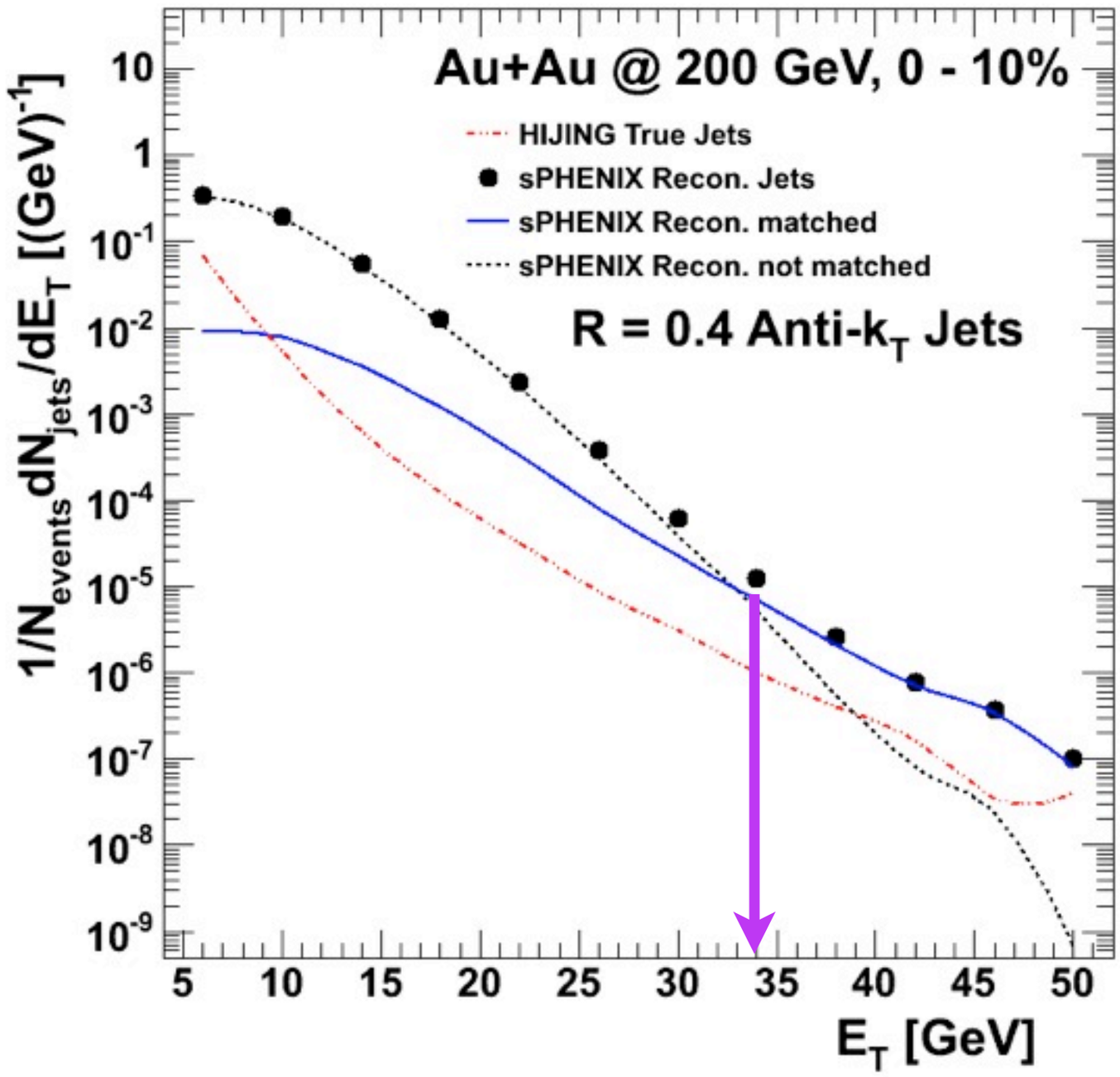

real jets outnumber fakes by ~35GeV

however, no fake jet rejection done yet

optimistic about lowering this crossover!

why are large jets so interesting?

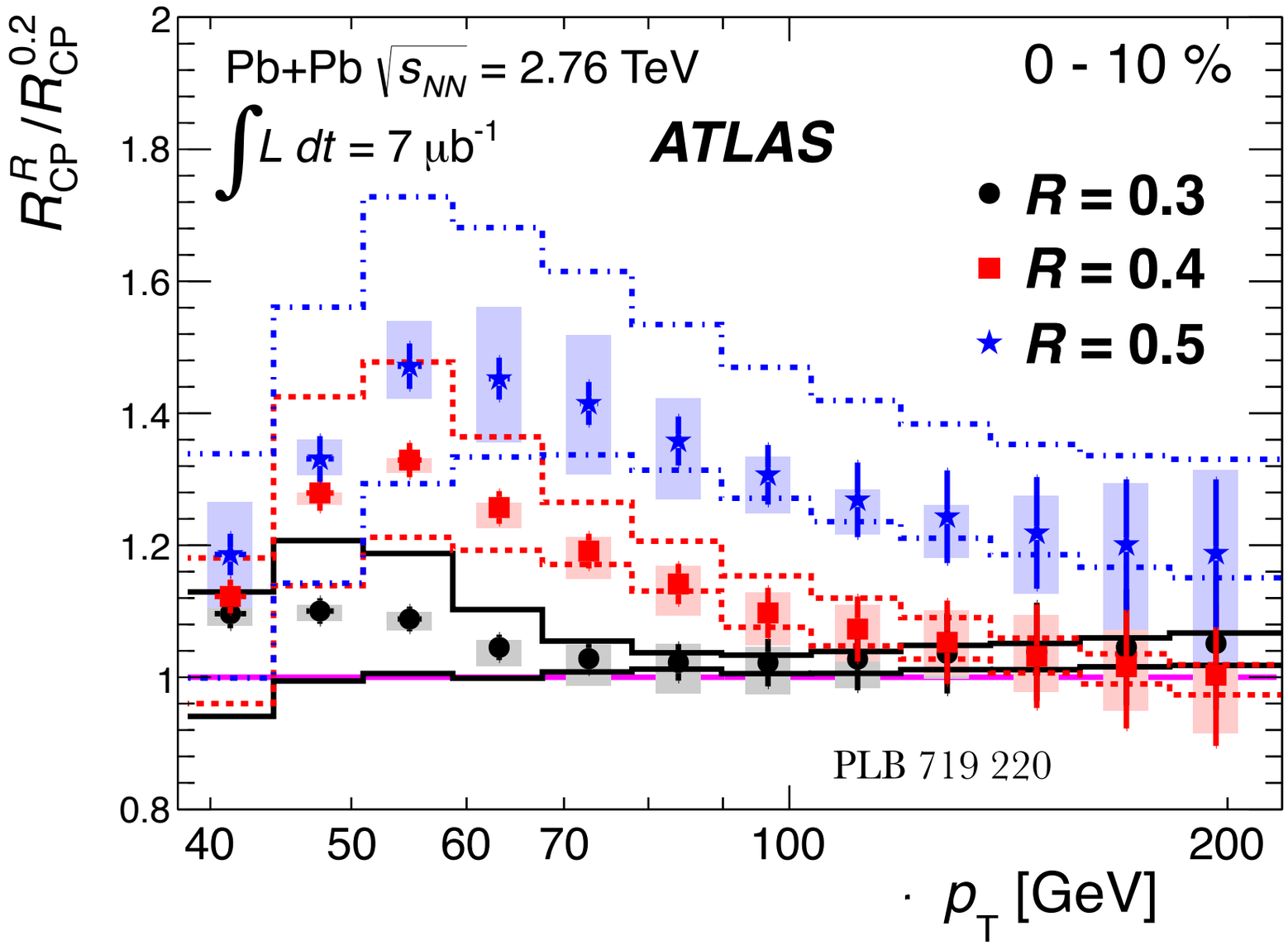

- evidence for large shape modifications in the region accessible at RHIC
- experimentally: require high statistics & good control of systematics

dijet measurements

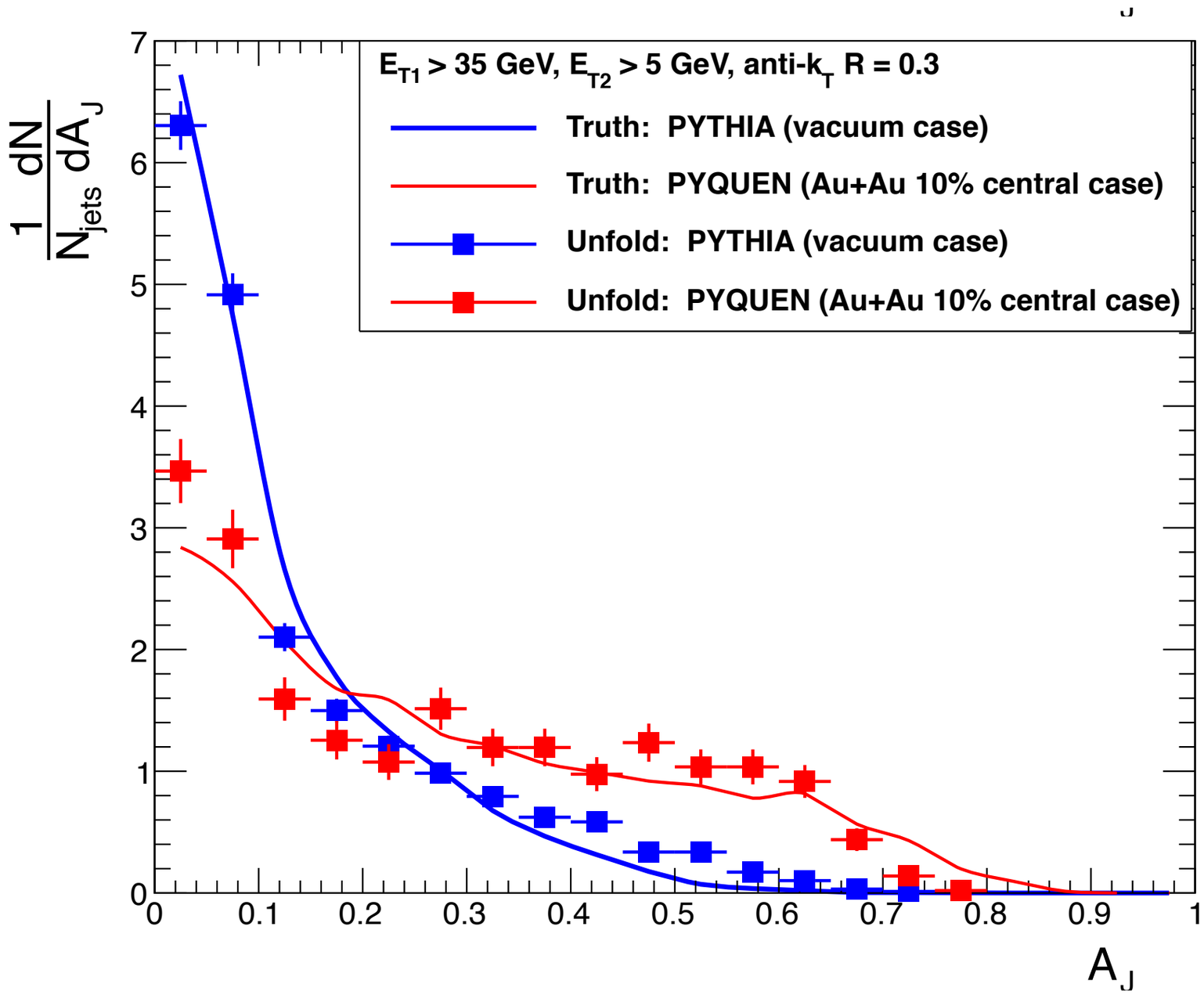

- full Geant 4 detector simulation of dijets embedded in 0-10% central HIJING
- unfolding recovers the truth distribution very well

γ-jet measurements

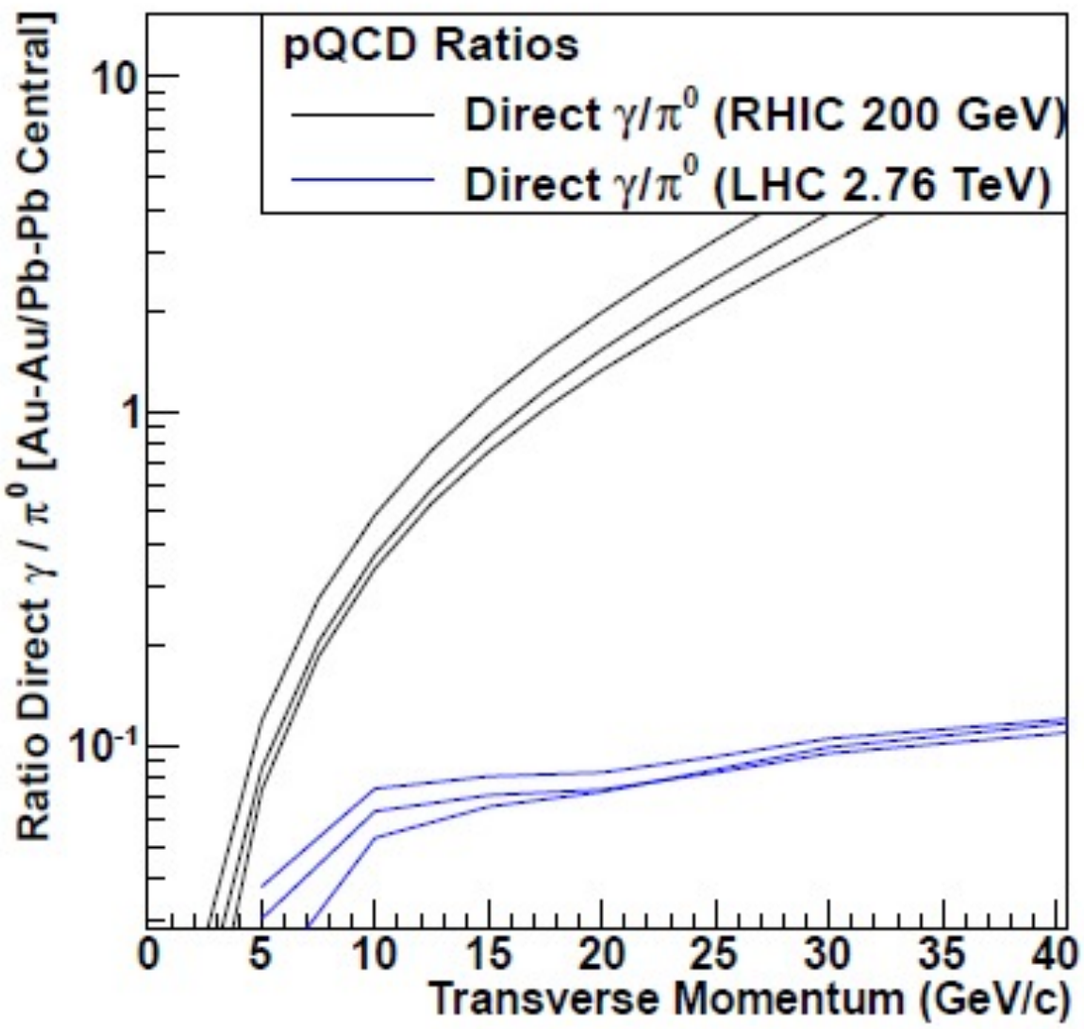

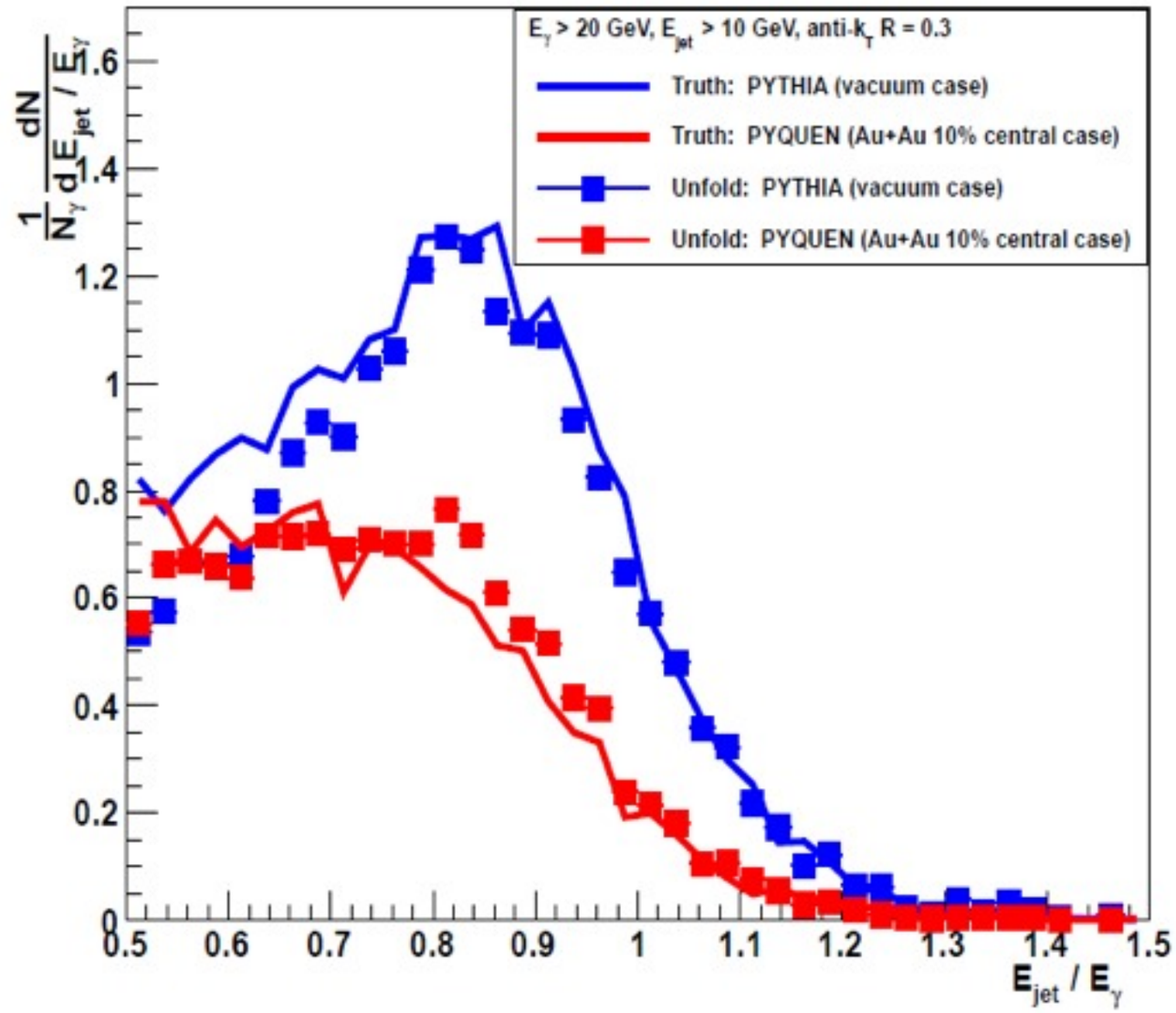

- γ/π0 very large at RHIC, large numbers out >30GeV
- unfolding the jet energy recovers the truth distributions from Geant4 simulation into central HIJING

heavy flavor at RHIC

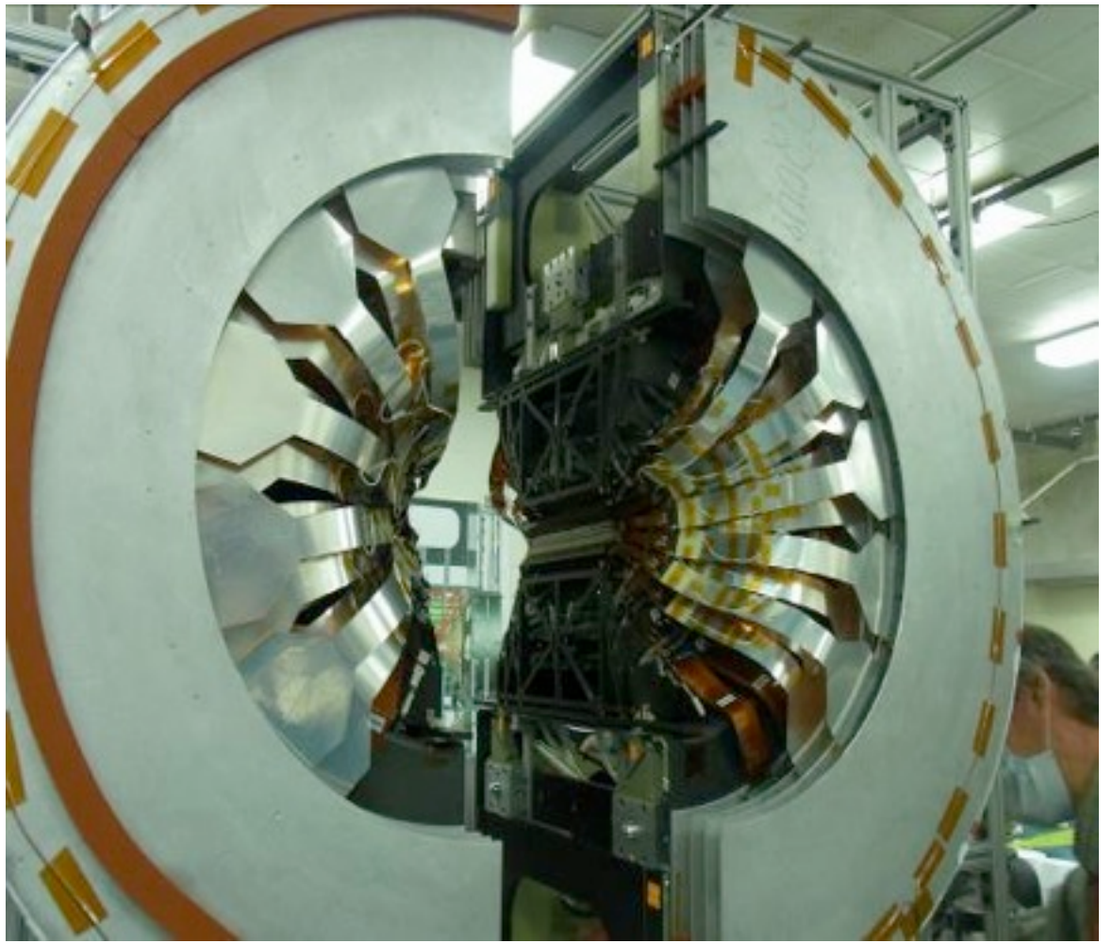

PHENIX (F)VTX

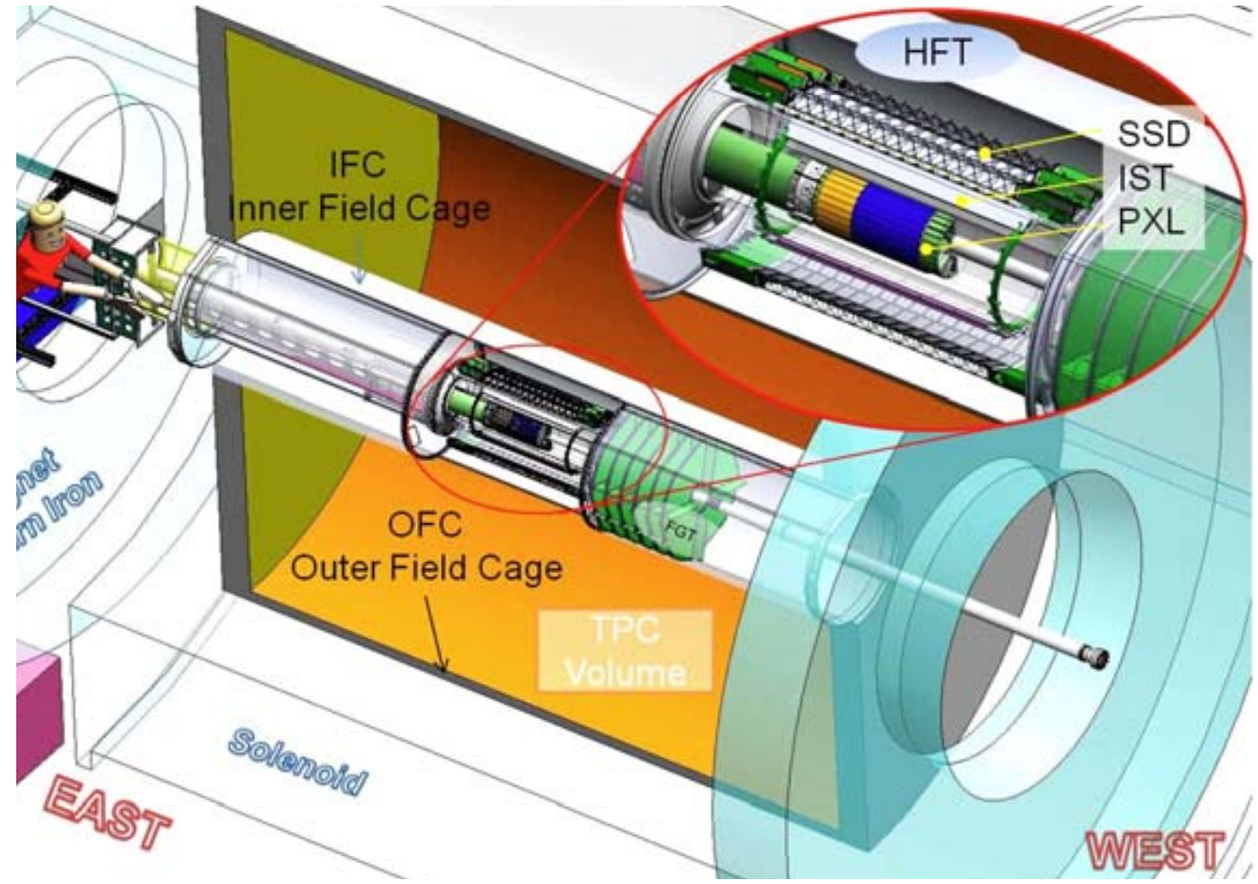

STAR HFT

- upgrades coming online to address charm and bottom separation at RHIC
- essential piece of the jet quenching puzzle

jet quenching at RHIC

- **current measurements show evidence for softening of fragmentation and broadening of angular correlations**
- **ATLAS measurements show R dependence of jet suppression at jet energies accessible at RHIC**
- **together with LHC constrain T dependence of jet quenching**
- **extremely interesting physics accessible at RHIC**
- **sPHENIX: full calorimeter coverage at mid-rapidity**
  - take advantage of full RHIC luminosity: large acceptance, high rate
  - becomes central to ePHENIX
  - proposal submitted to DOE for CD-0 review last month!
- **silicon detectors at STAR and PHENIX will provide handle on heavy flavor**
- **detector upgrades critical to the success of hard probes at RHIC**

backups

further exploration of T dependence

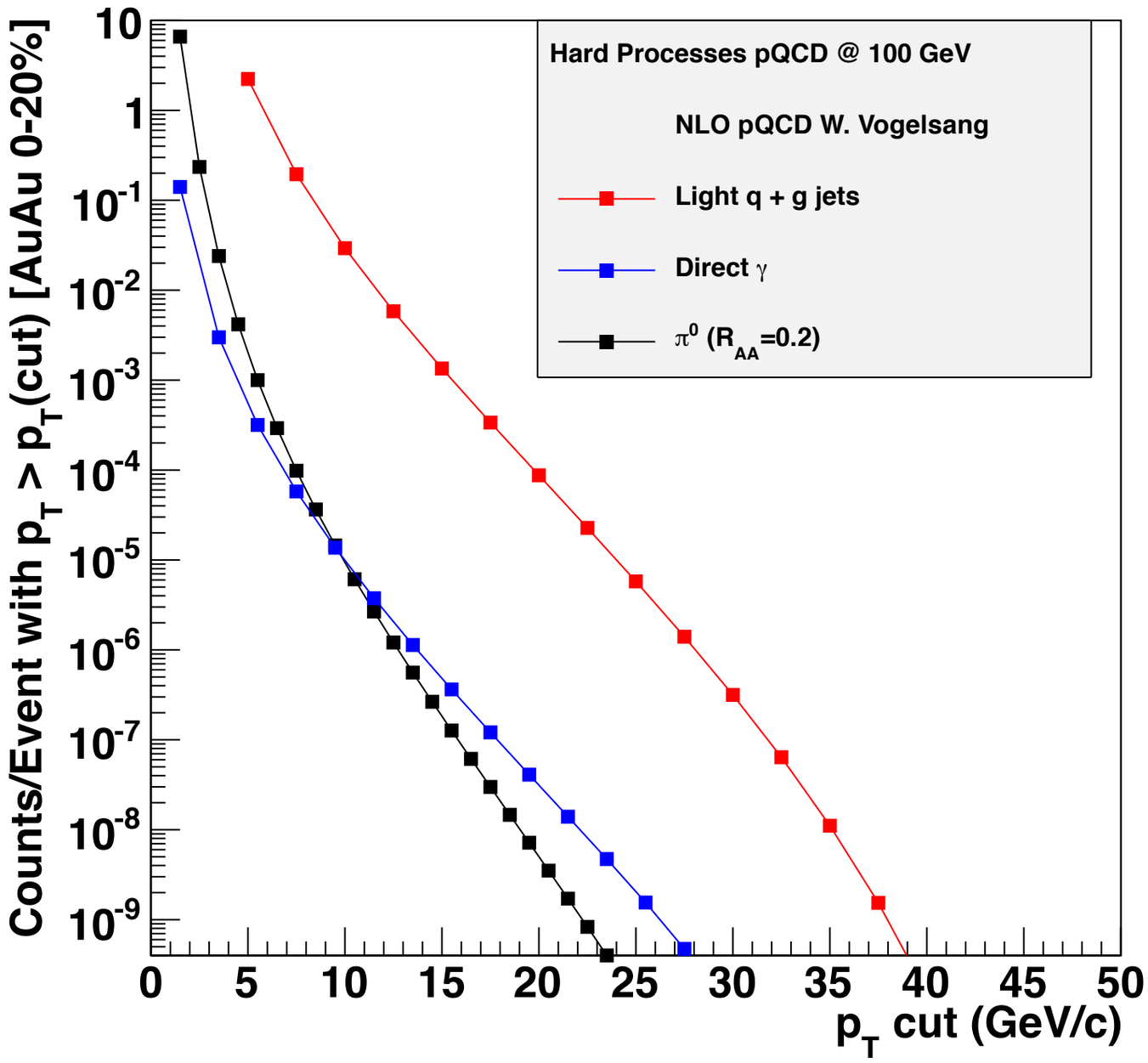

heavy quarks

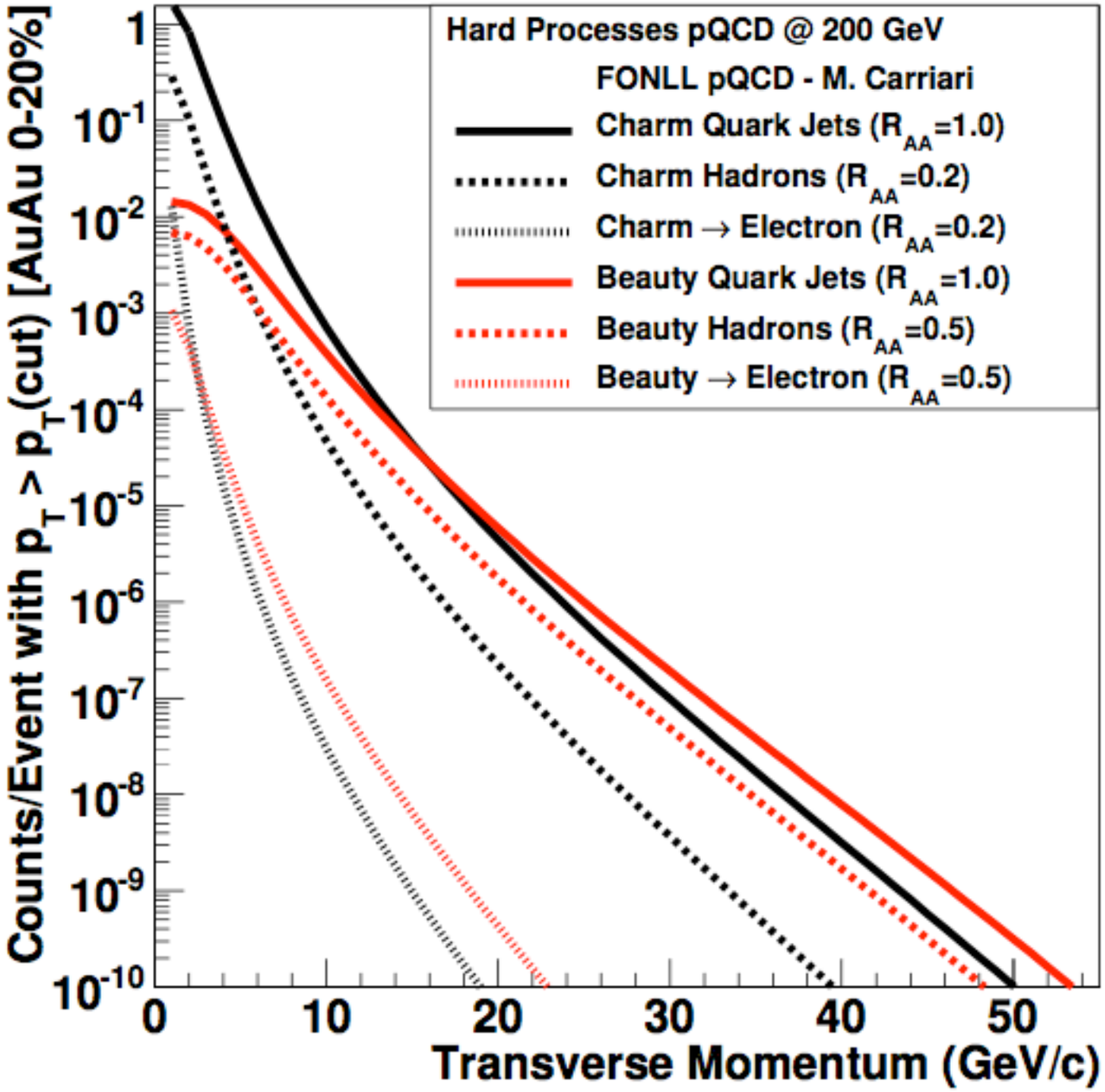

identifying truth jets

identifying truth jets

deep within the HIJING Event Generation...

identifying truth jets

deep within the HIJING Event Generation...

parton 1

identifying truth jets

deep within the HIJING Event Generation...

parton 1

↓

hadrons A

identifying truth jets

deep within the HIJING Event Generation...

parton 1

↓

hadrons A

↓

FastJet
anti-k_T

identifying truth jets

deep within the HIJING Event Generation...

parton 1

↓

hadrons A

↓

FastJet
anti-k_T

↓

jet A(R=0.2)
jet A(R=0.3)
jet A(R=0.4)

identifying truth jets

deep within the HIJING Event Generation...

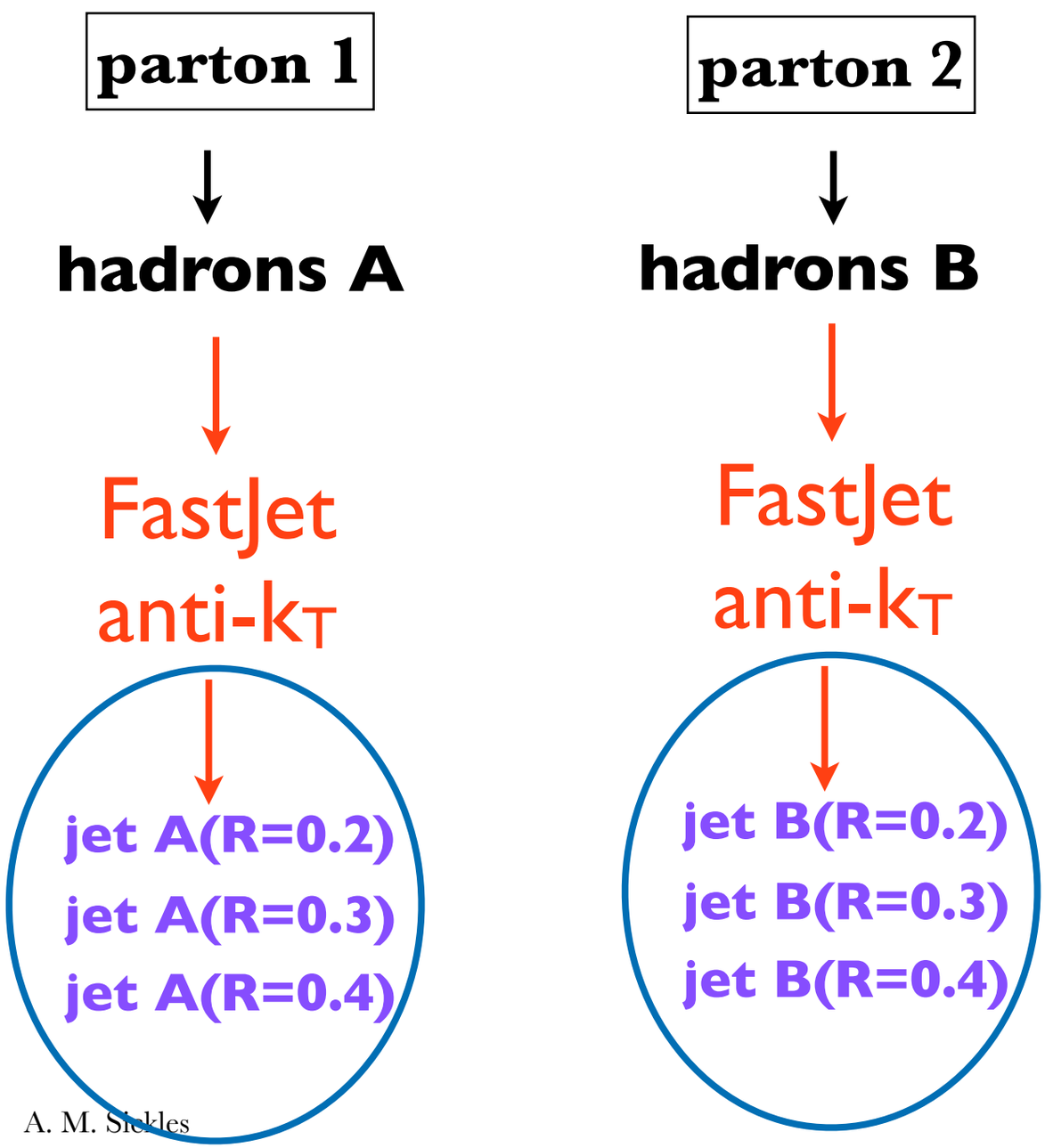

identifying truth jets

deep within the HIJING Event Generation...

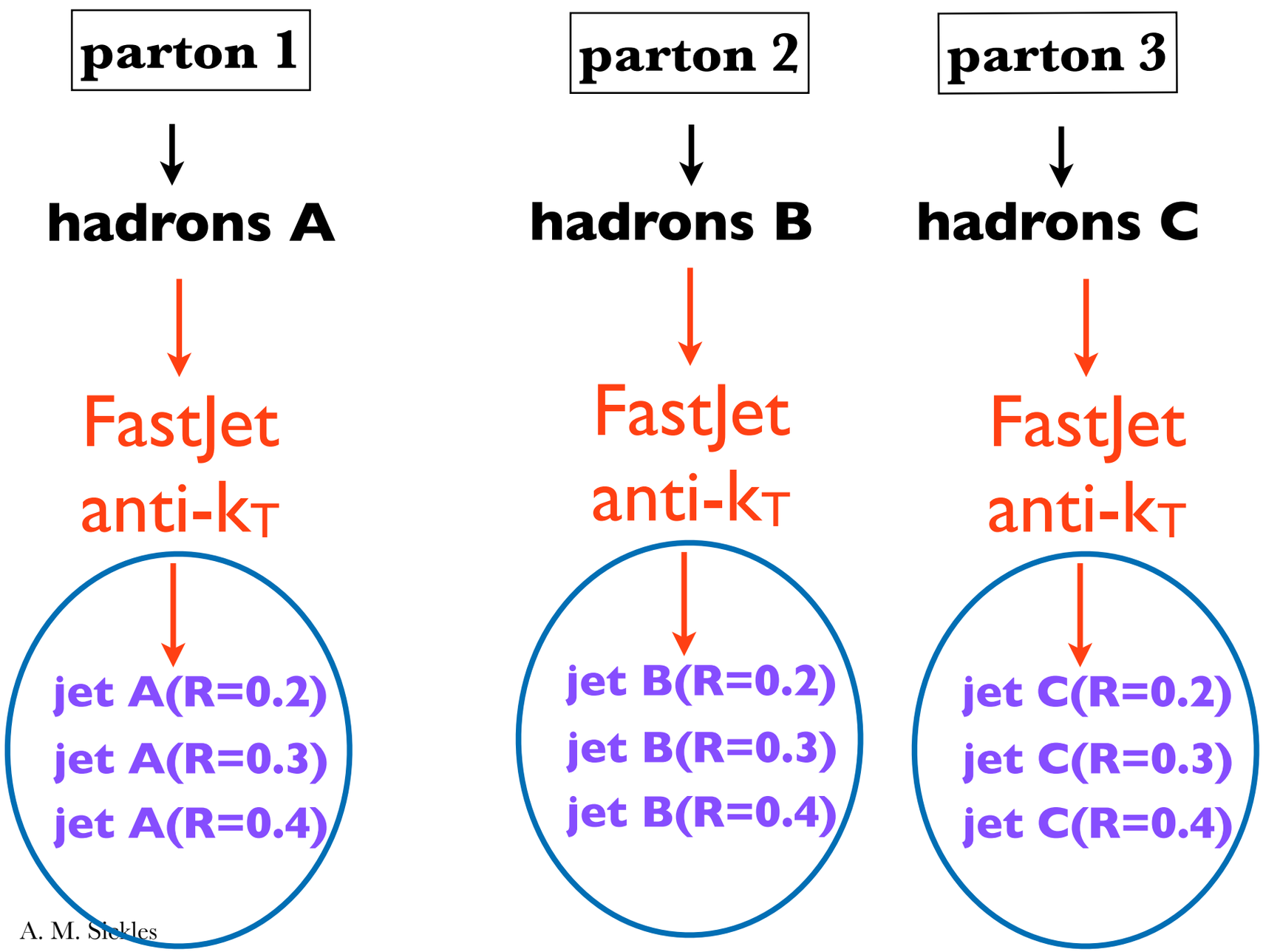

identifying truth jets

deep within the HIJING Event Generation...

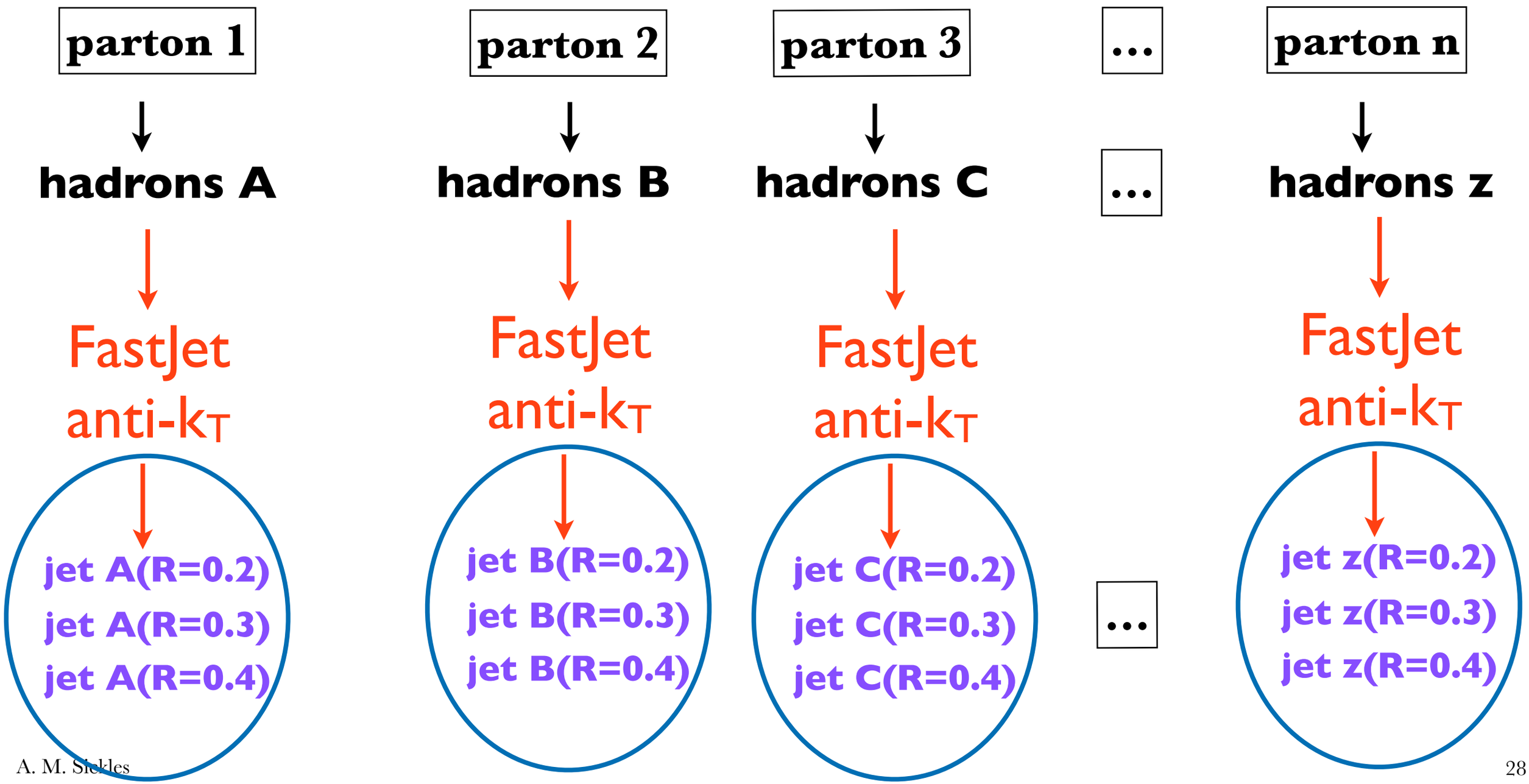

well reconstructed jets

- b = 1.8fm HIJING dijet event
- well reconstructed with anti-k_T R=0.2

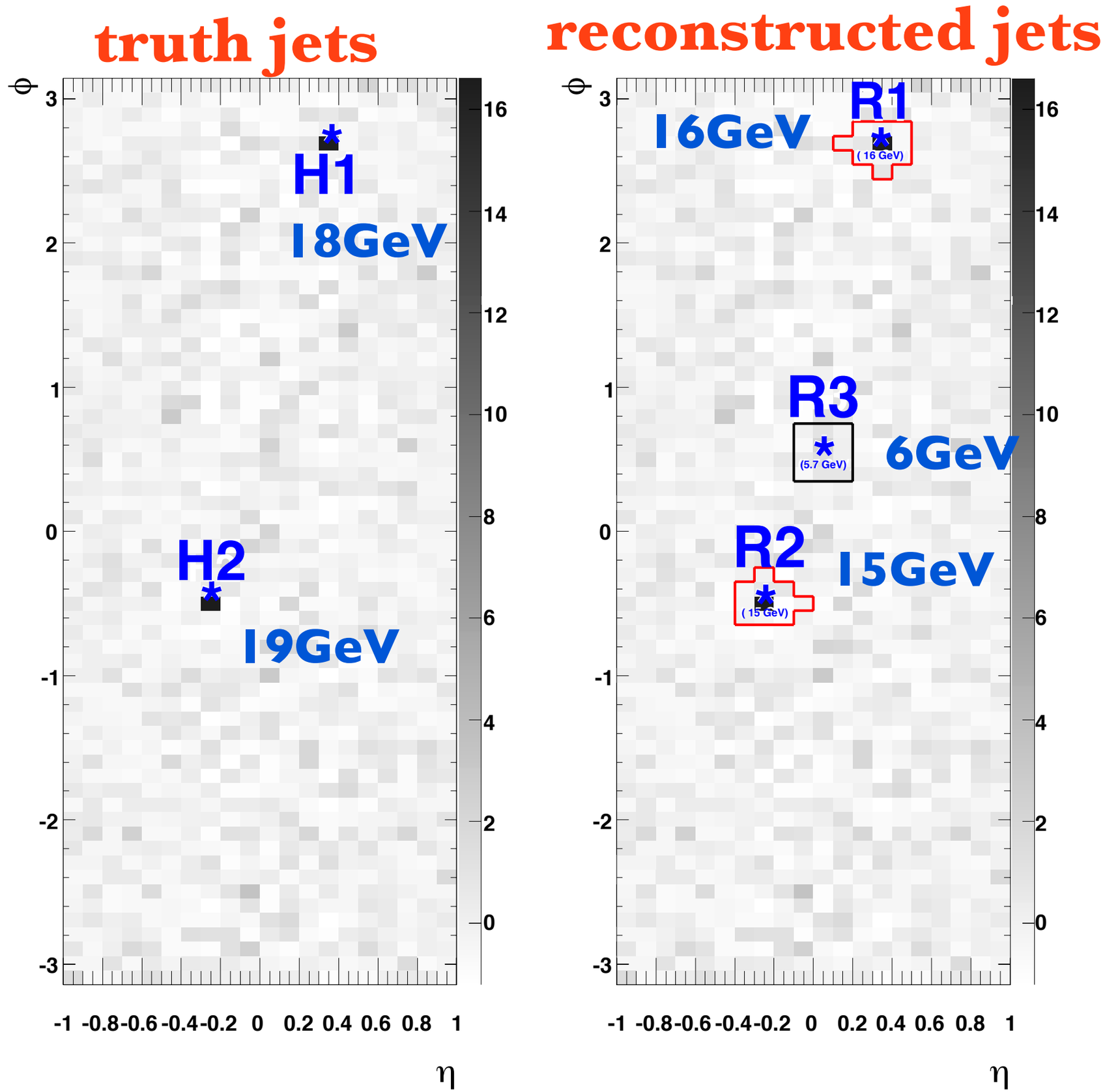

fake jets

truth jets

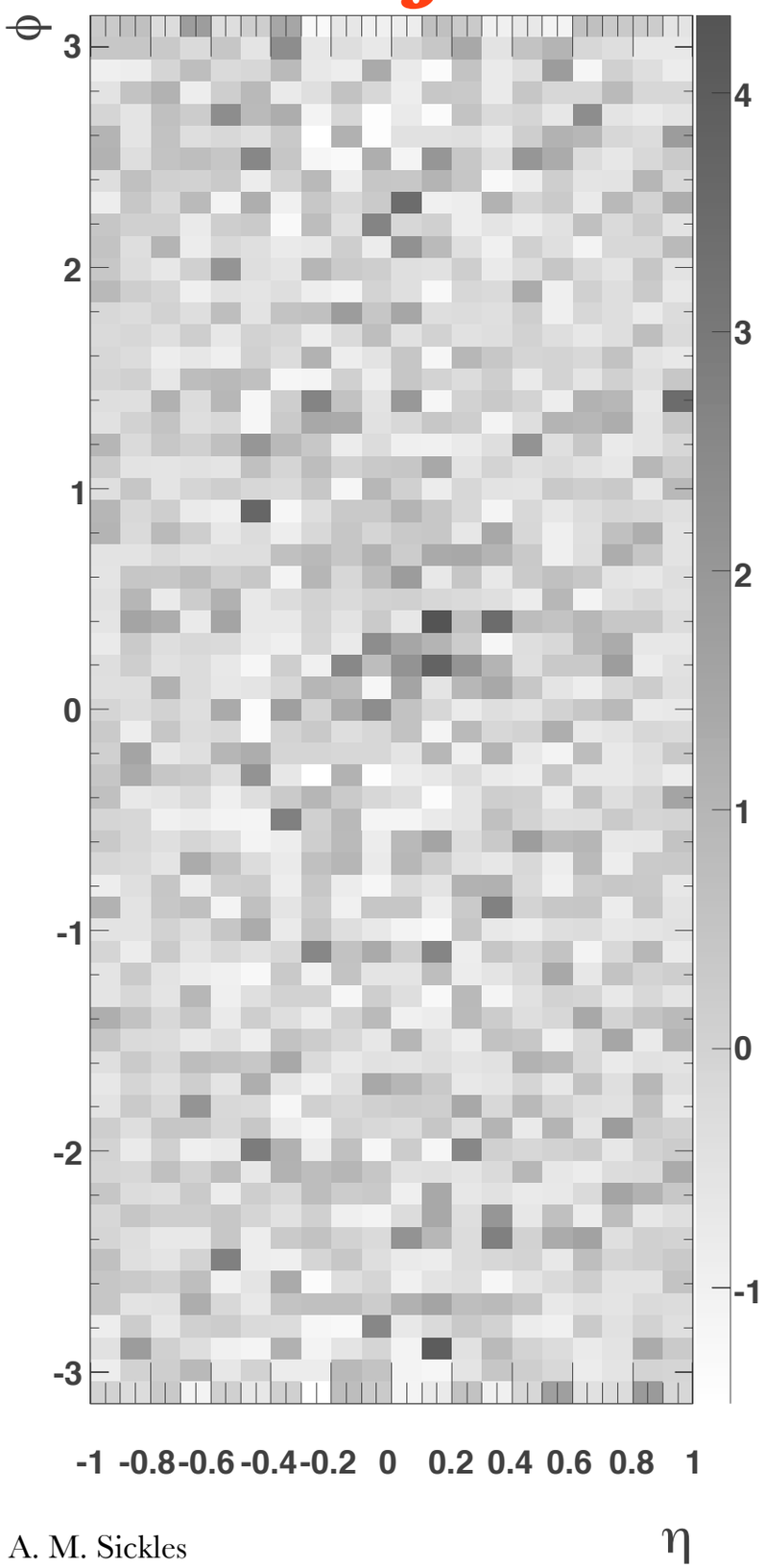

reconstructed jets

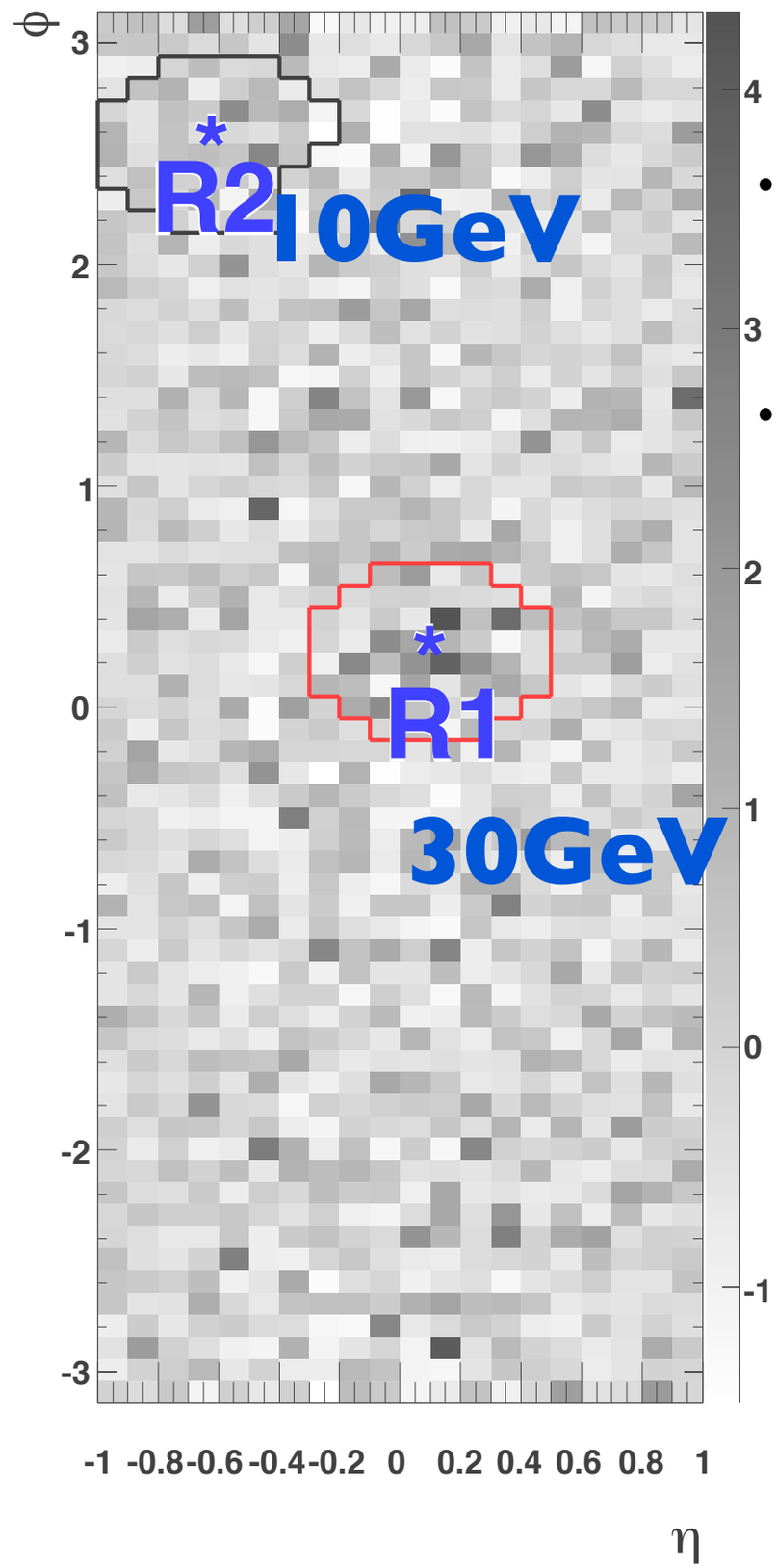

- b=2.4 HIJING event, no true jets
- 30 & 10GeV fake jets with anti-k_T R=0.4

however, we looked at 750M+ events! need quantitative rate assessment

iterative jet finding algorithm

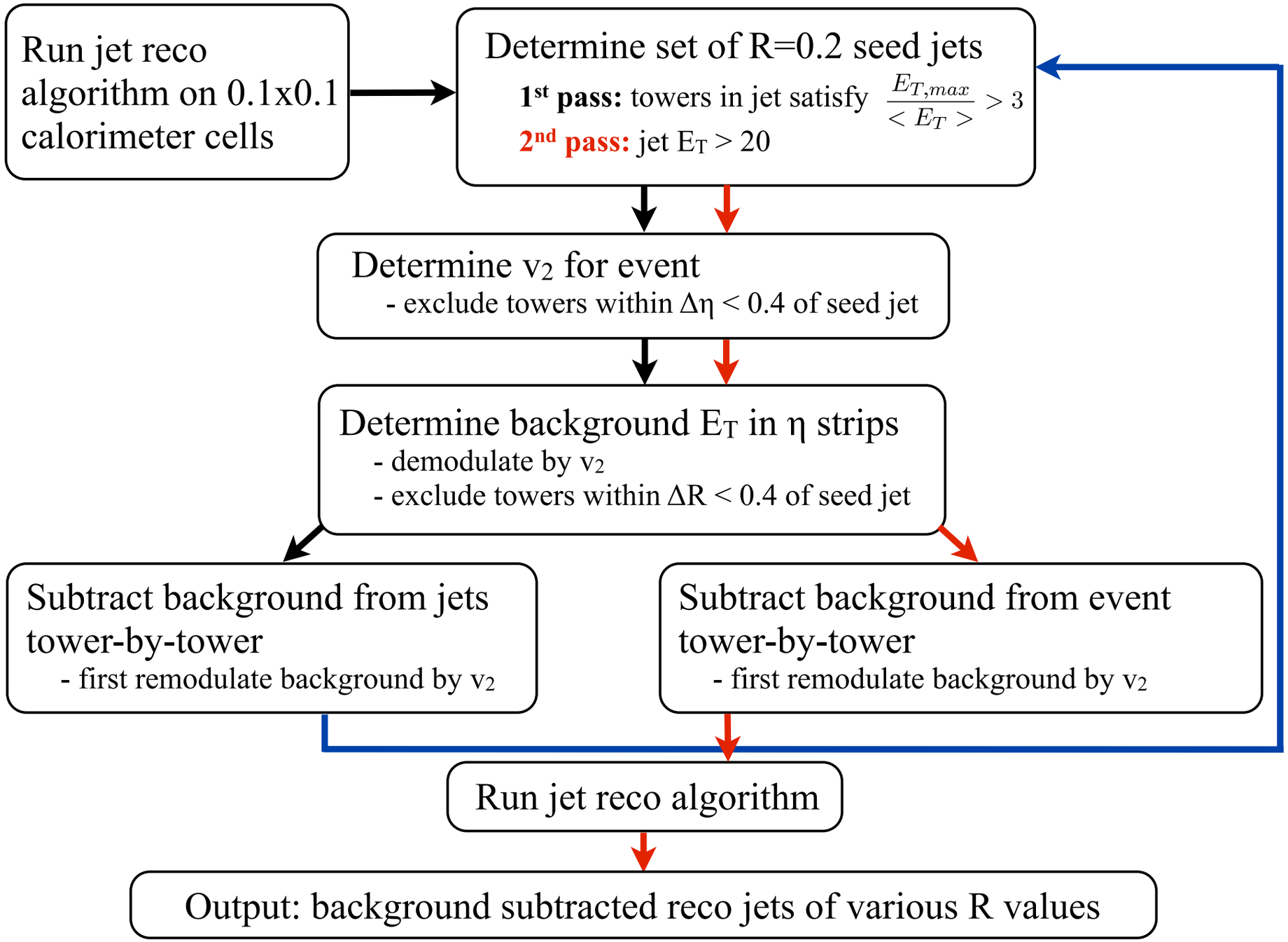

- uses anti-k_T algorithm
- inspired by ATLAS algorithm

Suppression of energy loss from partially ionized color

Vladimir Skokov
Y. Hidaka, S. Lin, R. Pisarski

pA workshop BNL 2013

Outline

- Introduction: ionization in QED/QCD plasmas

Outline

- Introduction: ionization in QED/QCD plasmas
- Collisional energy loss in partially ionized plasma

Outline

- Introduction: ionization in QED/QCD plasmas
- Collisional energy loss in partially ionized plasma
- Conclusions

Ionization in QED plasma

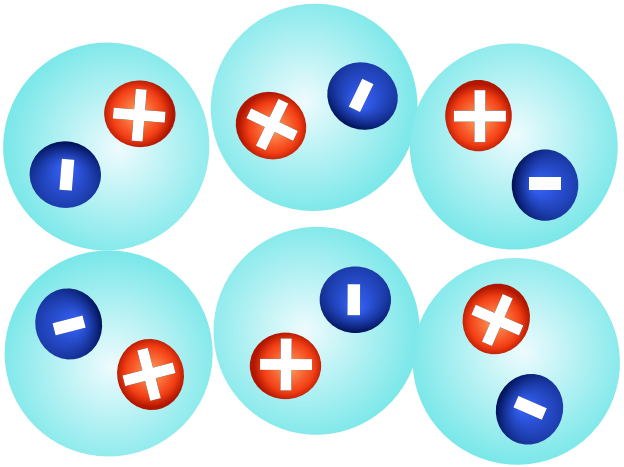

Neutral state $\rightsquigarrow$ atoms,
electric neutrality > atomic scales

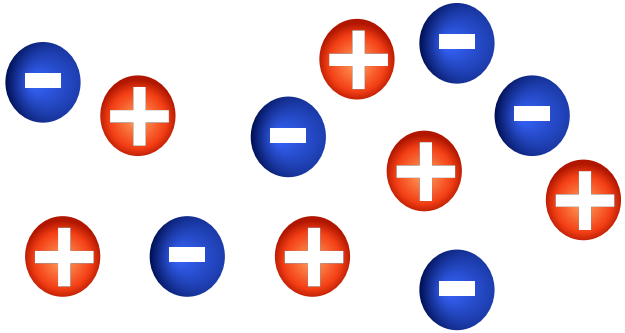

Completely ionized plasma $\rightsquigarrow$ plasma
with freely moving electric charges

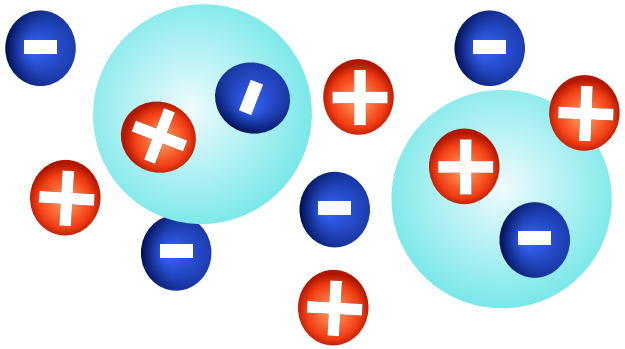

Partially ionized plasma $\rightsquigarrow$ *partially* ionized plasma with atoms and electric charges

Ionization in QCD plasma

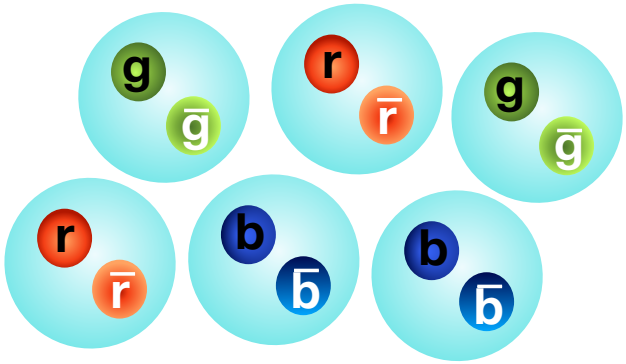

Neutral state ⇝ confined phase, color neutrality > hadronic scale

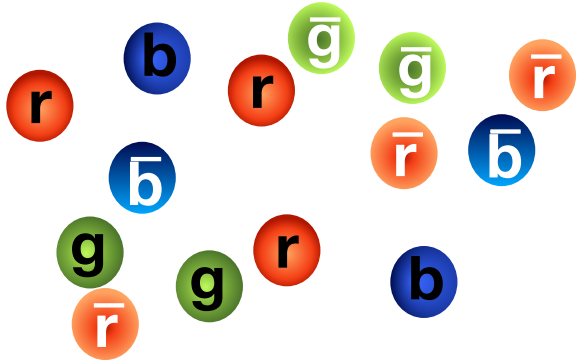

Completely ionized plasma ⇝ perturbative QGP with freely moving charges

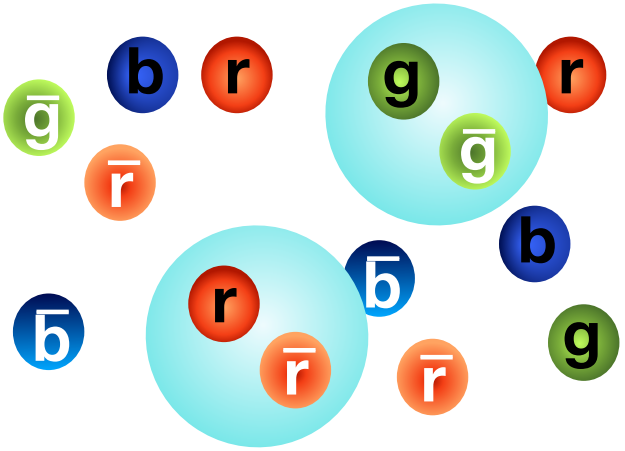

Partially ionized plasma ⇝ *partial* ionization of color: hadrons and color charges; semi-QGP, nontrivial holonomy

Polyakov loop as a measure of partial ionization: pure glue

Polyakov loop: $\langle L \rangle \sim e^{-F_{\text{test qk}}/T}$

Confined: $F_{\text{test qk}} \to \infty$, $\langle L \rangle \to 0$

Semi QGP: $0 < \langle L \rangle < 1$
$\langle L \rangle$ measures degree of ionization

Perturbative QGP:
$F_{\text{test qk}}/T \to 0$, $\langle L \rangle \to 1$

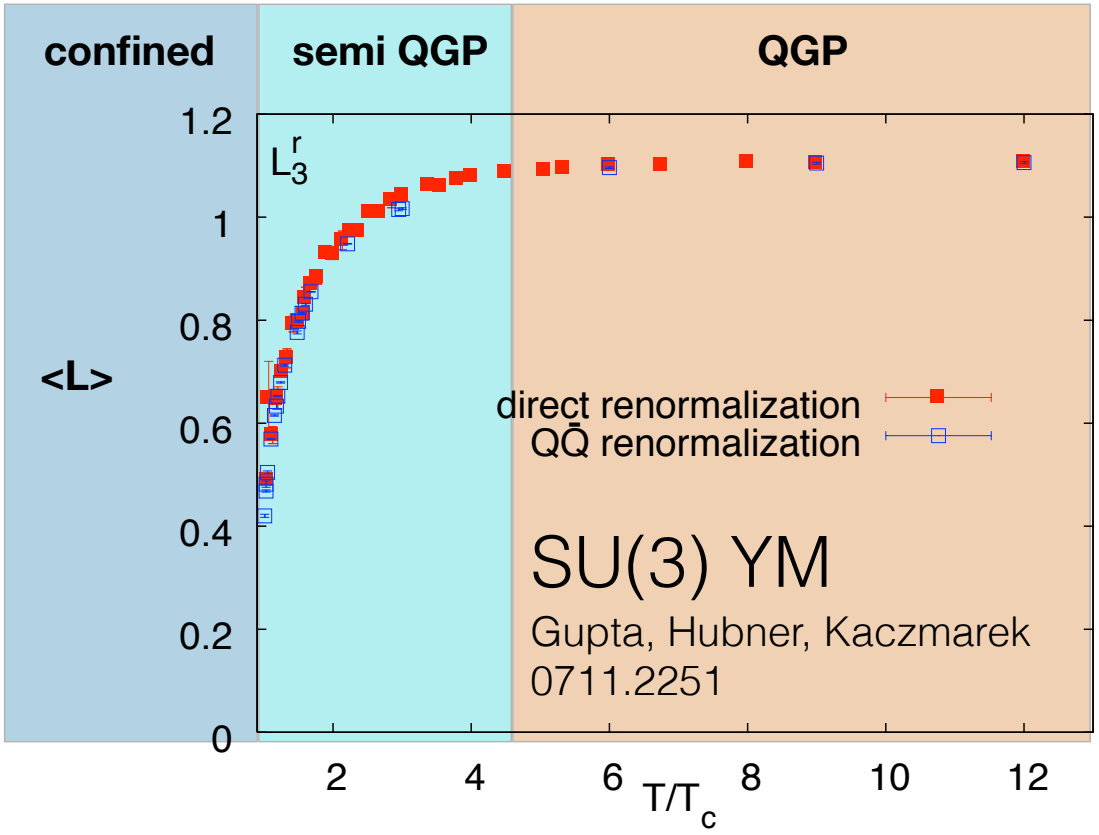

Polyakov loop as a measure of partial ionization: LQCD

Polyakov loop: $\langle L \rangle \sim e^{-F_{\text{test qk}}/T}$

Confined: $F_{\text{test qk}} \to \infty$, $\langle L \rangle \to 0$

Intermediate regime: $0 < \langle L \rangle < 1$
$\langle L \rangle$ measures degree of ionization

Deconfined: $F_{\text{test qk}}/T \to 0$, $\langle L \rangle \to 1$

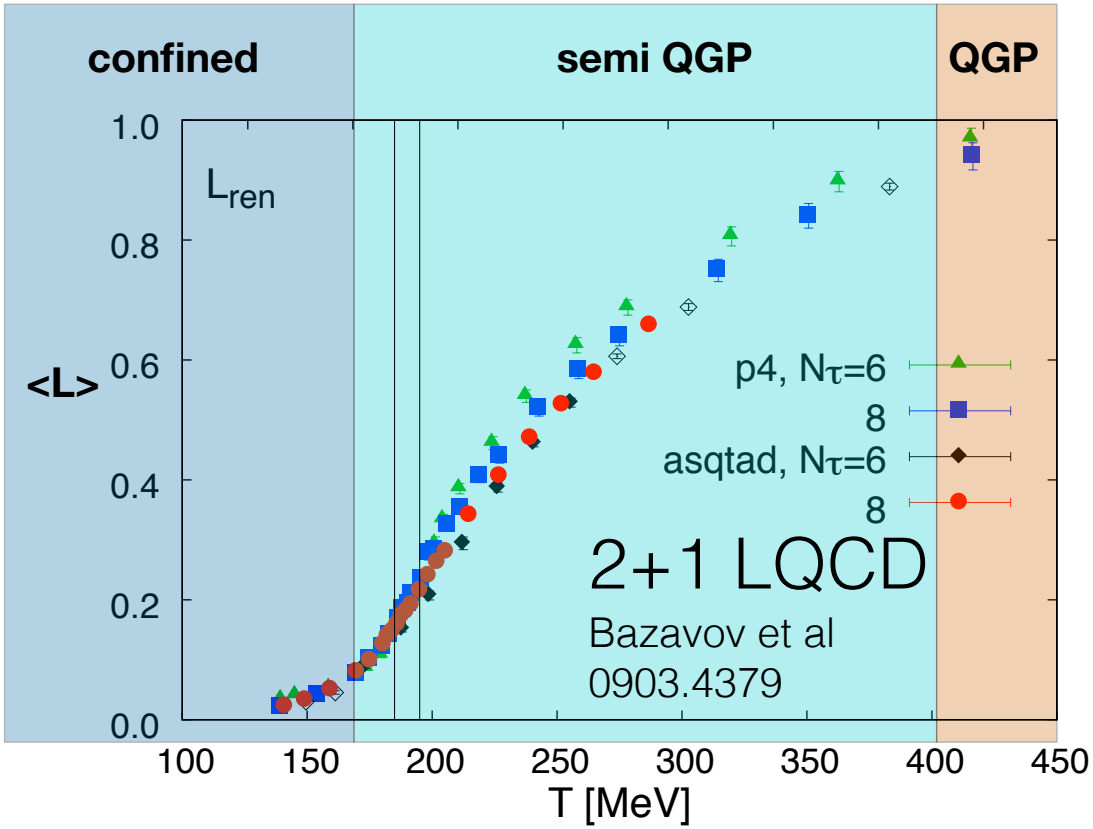

Polyakov loop: matrix model

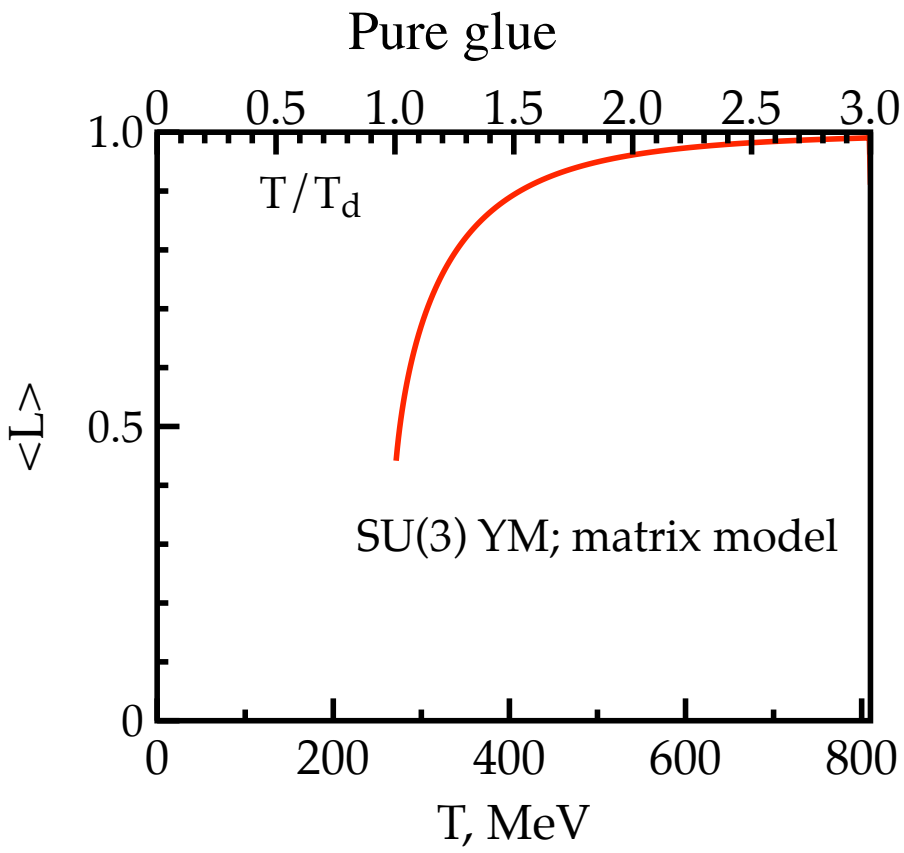

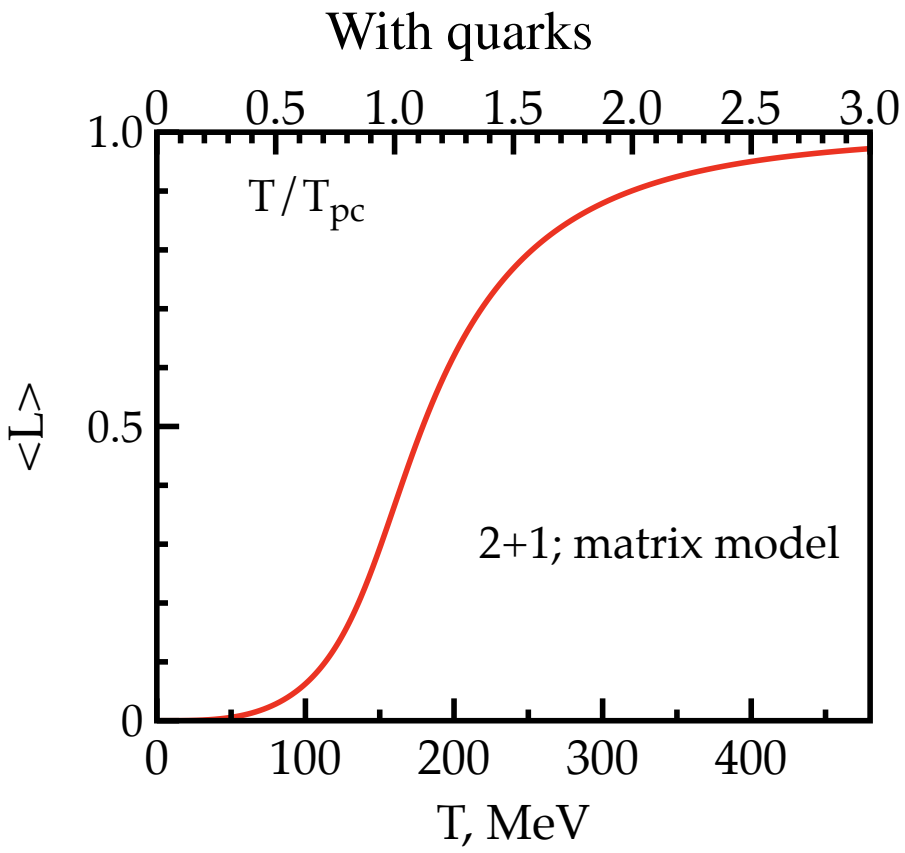

Punchline: transition region ("semi"-QGP): must exhibit partial ionization of color shear viscosity, energy loss…must depend upon the degree of ionization

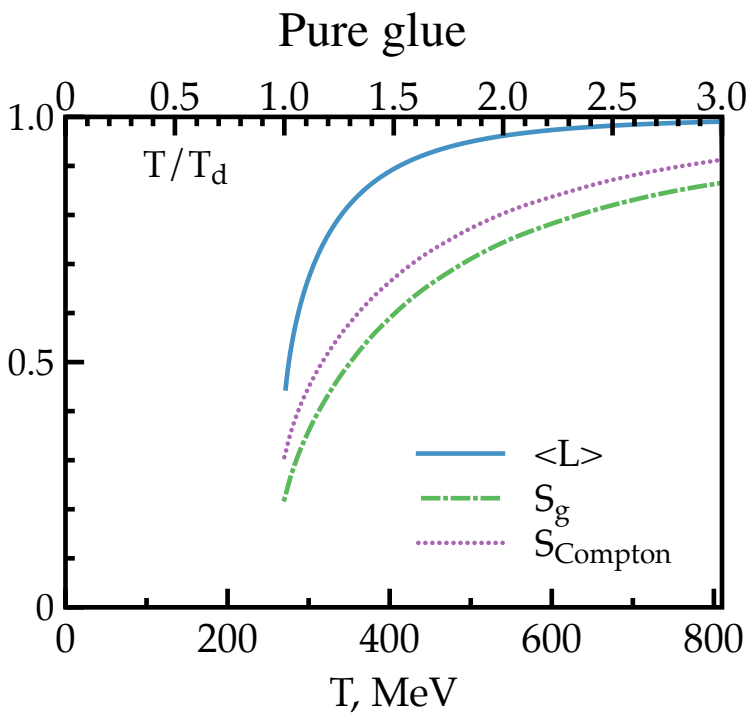

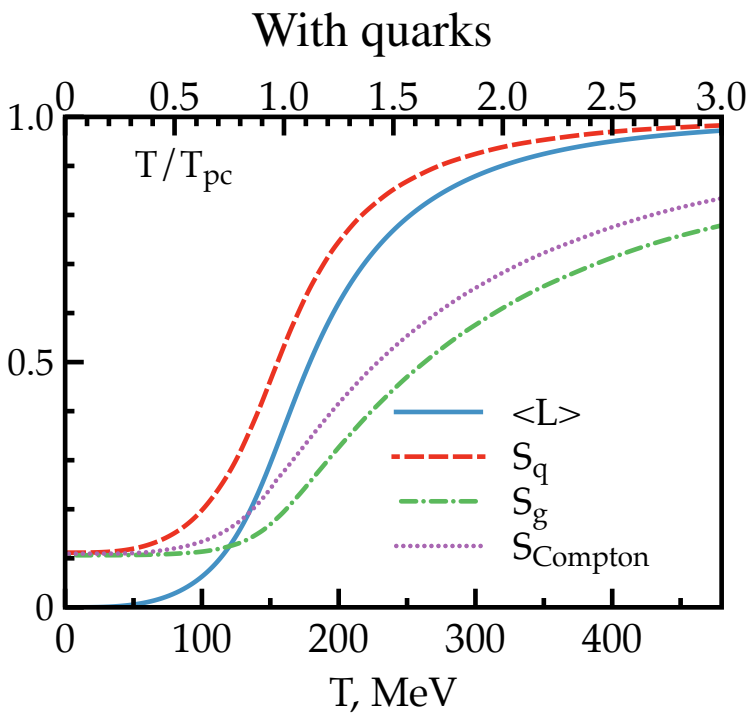

$$S_i = \frac{\text{energy loss in semi-QGP}}{\text{energy loss inperturbative QGP}}$$

S_i increases as color is ionized

- $i = q$ scattering on light quark (t channel)
- $i = g$ scattering on gluons (t channel)
- $i =$ Compton scattering on gluons, Compton scattering (u channel)

Perturbative vs semi-QGP

Usual argument of kinetic theory

Majumder, Muller and Wang, hep-ph/0703082

Liao and Shuryak, 0810.4116

Asakawa, Bass, and Muller, hep-ph/0603092, 1208.2426

- Viscosity $\eta \sim \rho^2/\sigma$
  - ρ - density of color charges $\rho \sim 1$
  - σ - crossection: $\sigma \sim g^4$, g - coupling
  - large $g \rightsquigarrow$ small η

- Energy loss $\frac{dE}{dx} \sim g^2\rho^2$
  - large $g \rightsquigarrow$ large $\frac{dE}{dx}$

Semi-QGP

Y. Hidaka, R, Pisarski 0912.0940

R. Pisarksi, V. Skokov proceedings of QM2013

- Viscosity $\eta \sim \rho^2/\sigma$
  - ρ - density of color charges, $\rho \sim \langle L \rangle^2$
  - σ - crossection: $\sigma \sim \langle L \rangle^2$
  - $\eta \sim \langle L \rangle^2$, small in semi-QGP

- Energy loss (large N_c)
  - $\frac{dE}{dx} \sim \langle L \rangle \cdot \frac{dE}{dx}$ on light quarks $+\langle L \rangle^2 \cdot \frac{dE}{dx}$ on gluons

Details

- Matrix model
- Collisional energy loss in large N_c limit
- Collisional energy loss due to scattering on light quark, $N_c = 3$
- Collisional energy loss due to scattering on gluons, $N_c = 3$
- Outlook: radiative?!

Non-zero Polyakov loop $\rightsquigarrow$ non-trivial holonomy

- Polyakov loop $L = \mathrm{Tr}\,\mathcal{P}\exp\left(ig\int_0^{1/T} A_0 d\tau\right)$
- Anzatz for $[A_0]_{ab} = \delta_{ab}\frac{Q^a}{g}$, for the sake of simplicity $Q^a = 2\pi T \cdot q^a$
- Tracelessness tr $A_0 = 0 \rightsquigarrow \sum_a Q^a = \sum_a q^a = 0$
- Classical approximation: zero action for A_0
- One loop about A_0: Gross, Pisraski, Yaffe '81:

$$U_{\text{pert}} = -2\pi^2 T^4 \left[\frac{N^2-1}{45} - \frac{1}{3}\sum_{a,b}(q_a - q_b)^2\,(1 - |q_a - q_b|)^2\right]$$

  Gives only trivial A_0
- Non-perturbative contribution are modeled by (R. Pisarski et al)

$$U_{\text{non-pert}} = T^2 T_d^2 \left[c_1 \sum_{a,b}^{N} |q_a - q_b|\,(1 - |q_a - q_b|) + c_2 \sum_{a,b}^{N}(q_a - q_b)^2\,(1 - |q_a - q_b|)^2 + c_3\right]$$

- c_i are fixed to get transition at $T = T_d$, and describe lattice data
- three colors: $q_1 = -q_2 = q$, $q_3 = 0$. Confining at $q = 1/3$ and perturbative $q = 0$.

Model vs lattice

Pressure for pure glue

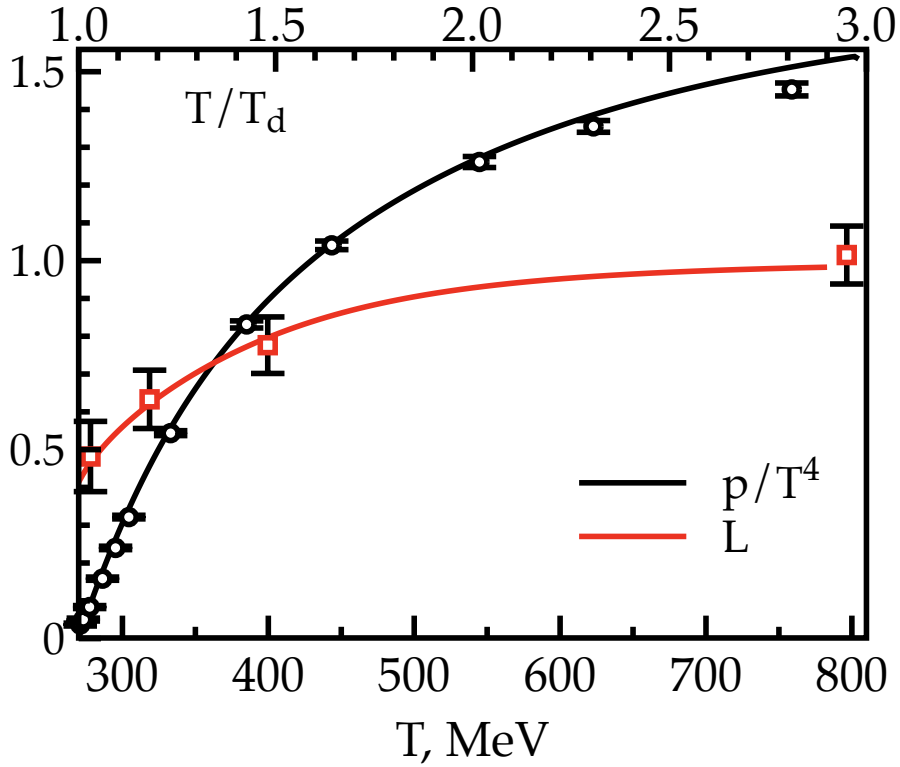

t'Hooft loop
(interface between different $Z(N)$ sectors)

Dumitru et al, 1011.3820

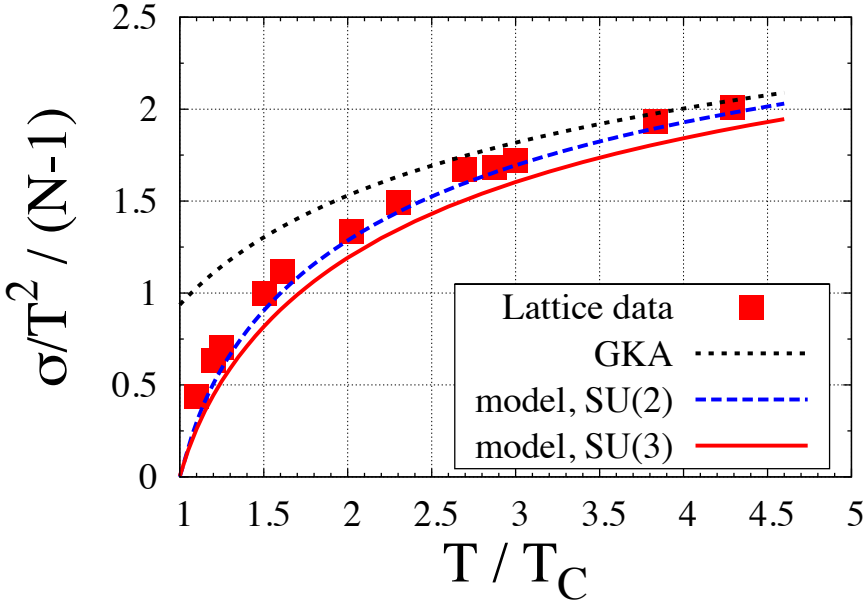

$$V \to V + \frac{1}{g^2} \sum_a^N \left(\frac{\partial Q_a}{\partial z} \right)^2$$

Quark and gluon propagator in a background A_0 field: Hidaka, Pisarski 0906.1751

- Distribution function for gluons

$$n^g_{a,b}(p,Q) = \left[\exp\left(\frac{E - i(Q_a - Q_b)}{T}\right) - 1\right]^{-1}$$

- Distribution function for quarks

$$n^q_a(p,Q) = \left[\exp\left(\frac{E - iQ_a}{T}\right) + 1\right]^{-1}$$

Limits:

- Trivial holonomy or perturbative QGP, $Q = 0$

$$n^g(p, Q = 0) = \left[\exp\left(\frac{E}{T}\right) - 1\right]^{-1}$$

$$n^q(p, Q = 0) = \left[\exp\left(\frac{E}{T}\right) + 1\right]^{-1}$$

- Confining limit, large N:

$$n^q = 0$$

$$n^g = 0$$

Large N limit for scattering off light quark: birdtracks

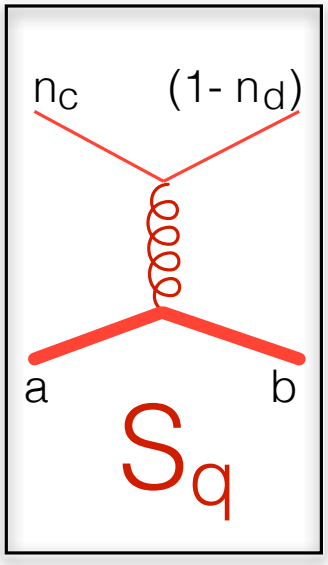

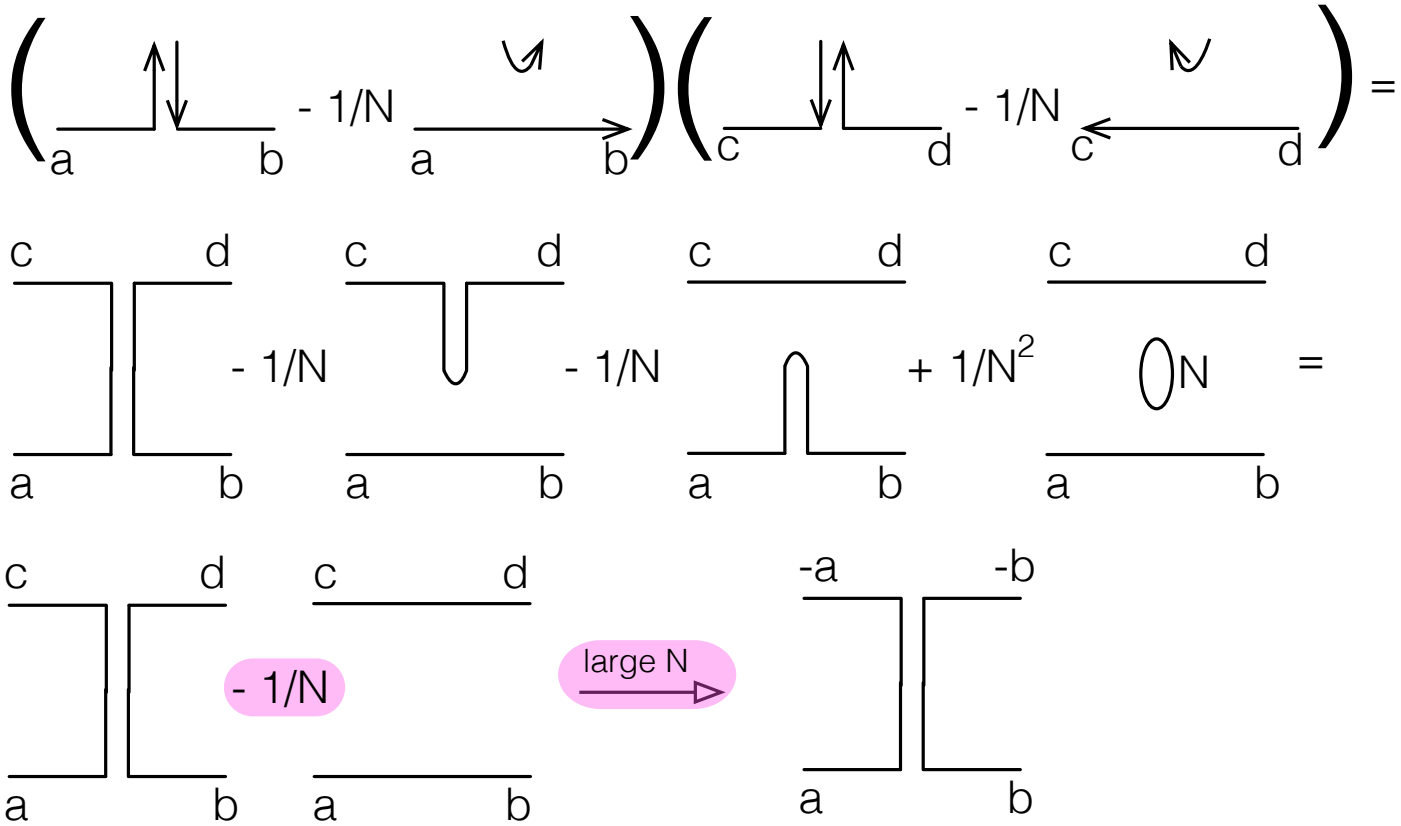

$$\sim \sum_{ab} n_a(1-n_b)$$

Large N limit

$$\frac{dE}{dx} \propto \sum_{a,b}^{N} \int [dk][dk'][dp'] f(p,k,k',p') n(E_k + iQ_a)\,[1 - n(E_{k'} + iQ_b)]$$

$$\sum_a n(E_k + iQ_a) = \sum_a [\exp(\beta E_k + i\beta Q_a) + 1]^{-1}$$

$$= \sum_{n=1}^{\infty} (-1)^n \exp(-\beta E_k) \sum_a \exp(in\beta Q_a) = \sum_{n=1}^{\infty} (-1)^n \exp(-\beta E_k)\, \mathrm{tr}\, L^a$$

for small tr L scattering off **light quarks**

$$\frac{dE}{dx} \propto \mathrm{tr} L \cdot \left(\frac{dE}{dx}\right)_{\text{pert.}}$$

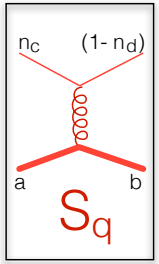

Similar argument for scattering off **gluons** gives

$$\frac{dE}{dx} \propto (\mathrm{tr}\, L)^2 \cdot \left(\frac{dE}{dx}\right)_{\text{pert.}}$$

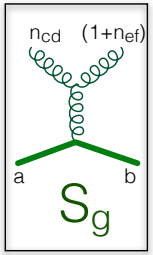

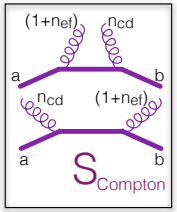

N=3

As in pQCD, but taking into account modification of distribution function in final/initial state.

N=3: Scattering off light quarks

$$S_i = \left(\frac{dE}{dx}\right)_i \Big/ \left(\frac{dE}{dx}\right)_{i,\text{pert.}}$$

- Scattering off light quark

$$S_q = \frac{12}{\pi^2(N^2-1)} \sum_{l=1}^{\infty} \sum_{m=0}^{l-1} (-1)^{l+1} \frac{l-2m}{l^3} \left(\text{tr}\, L^{l-m} \text{tr}\, L^m - \frac{1}{N} \text{tr}\, L^l \right)$$

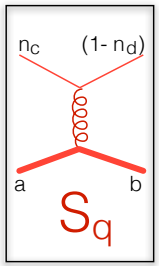

- Perturbative limit $Q \to 0$, so $\forall i \quad \text{tr}\, L^i \to 1$:

$$S_q(Q=0) = \frac{12}{\pi^2(N^2-1)} \sum_{l=1}^{\infty} \sum_{m=0}^{l-1} (-1)^{l+1} \frac{l-2m}{l^3} (N^2-1) = 1$$

- Confining limit $q \to 1/3$, so $\forall i = kN$, where k is integer, $\text{tr}\, L^i \to N$, otherwise $\text{tr}\, L^{j \neq kN} \to 0$:

$$S_q(q=1/3) = \frac{12}{\pi^2(N^2-1)} \sum_{k=1}^{\infty} \sum_{m=0}^{Nk-1} (-1)^{kN+1} \delta_m j N \frac{kN-2m}{k^3 N^3} (N^2-1)$$

$$= \frac{1}{N^2} \text{for odd } N, \ \frac{2}{N^2} \text{ otherwize}$$

N=3: Scattering off gluons

$$S_i = \left(\frac{dE}{dx}\right)_i \Big/ \left(\frac{dE}{dx}\right)_{i,\text{pert.}}$$

- Scattering off gluons (t channel)

$$S_g = \frac{6}{\pi^2(N^2-1)} \sum_{l=1}^{\infty} \sum_{m=0}^{l-1} \frac{l-2m}{l^3} \left(\text{tr}\, L^{l-m} \cdot \text{tr}\, L^{l} \cdot \text{tr}\, L^{m} - \text{tr}\, L^{2l}\right)$$

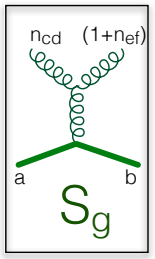

- Compton scattering off gluons (u channel), only Polyakov loop terms

$$S_{\text{Compton}} = \cdots \Big(\text{tr}\, L^{l} \text{tr}\, L^{l-m} \text{tr}\, L^{m}$$
$$- \frac{2}{N} \text{tr}\, L^{m} \text{tr}\, L^{2l-m} - \frac{2}{N} \text{tr}\, L^{l-m} \text{tr}\, L^{l+m} + \frac{4}{N} \text{tr}\, L^{2l}$$
$$+ \frac{1}{N^2} (\text{tr}\, L^{m})^2 \, \text{tr}\, L^{2(l-m)} + \frac{1}{N^2} \left(\text{tr}\, L^{l-m}\right)^2 \text{tr}\, L^{2m} - \frac{4}{N^2} \text{tr}\, L^{2(l-m)} \text{tr}\, L^{2m}$$
$$+ \frac{1}{N^3} \left(\text{tr}\, L^{2m}\right)^2 \text{tr}\, L^{2(l-m)} \Big)$$

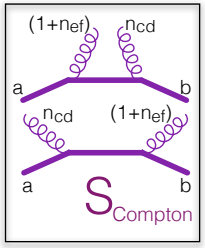

Numerical results

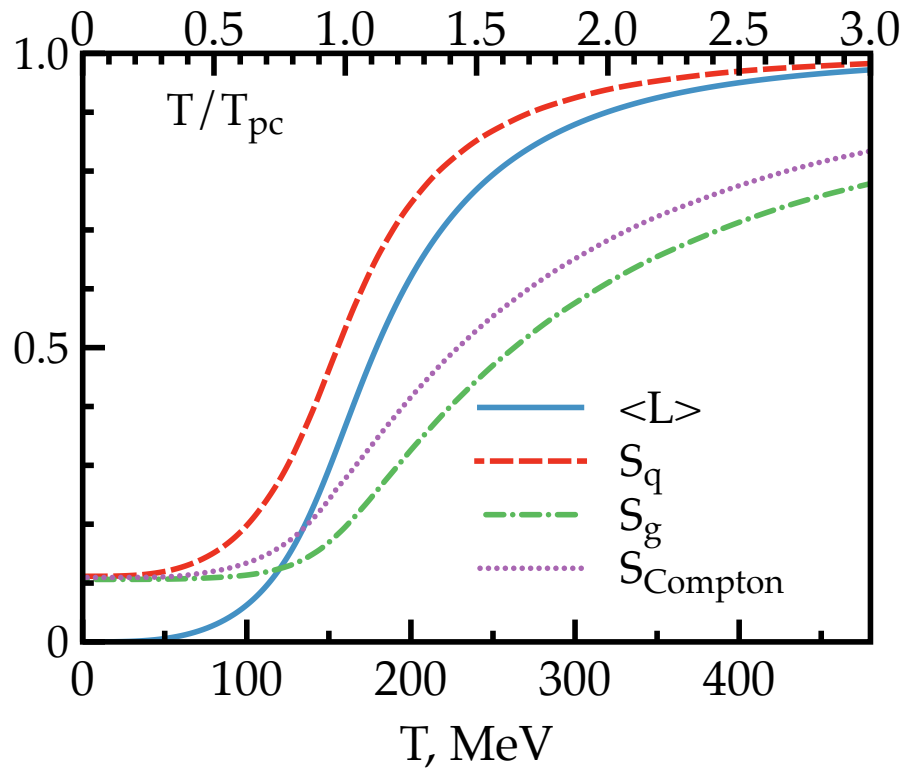

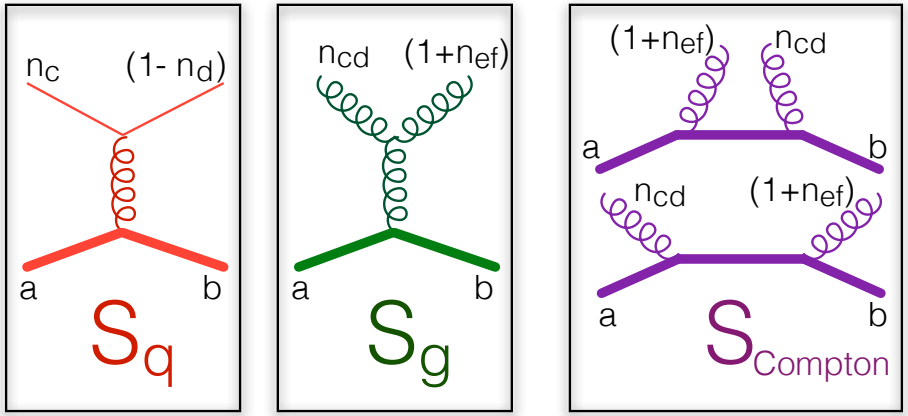

$$S_i = \left(\frac{dE}{dx}\right)_i \Big/ \left(\frac{dE}{dx}\right)_{i,\text{pert.}}$$

- Different processes are supressed dufferently
- Processes with gluons are supressed stronger then thouse with quarks
- $\forall i; S_i \to 1/N^2$ at low temperatures

Radiative energy loss: preliminary large N result

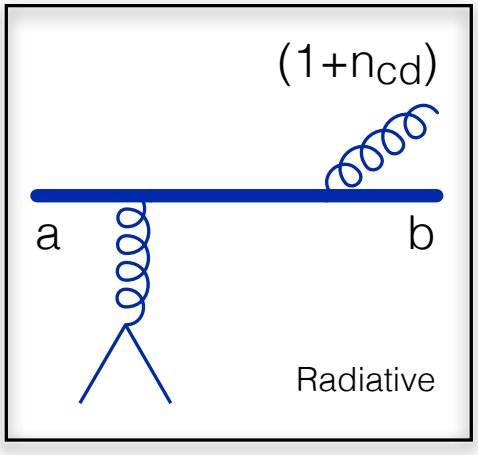

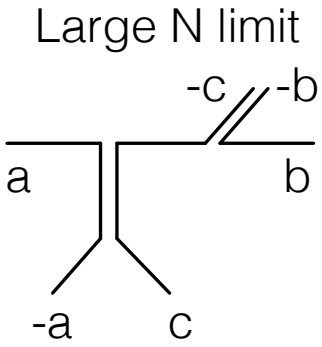

Suppressed by

$$n_{-a}(1-n_c)(1+n_{-c,-b}) \sim \mathrm{tr}\, L$$

Conclusions

- LQCD: shallow dependence of $\langle L \rangle$ on T
- This suggest that **semi-QGP** region (region with partial ionization of color) is broad and has to be taken into account when computing energy loss viscosity and etc
- Collisional energy loss is supressed in semi-QGP either linearly (for scattering off light quarks) or quadratically (for scattering off gluons) by Polyakov loop
- Radiative energy loss is harder to cumpute, but, at least, in large N limit it also gets supressed at least quadratically by Polyakov loop

Thank you!

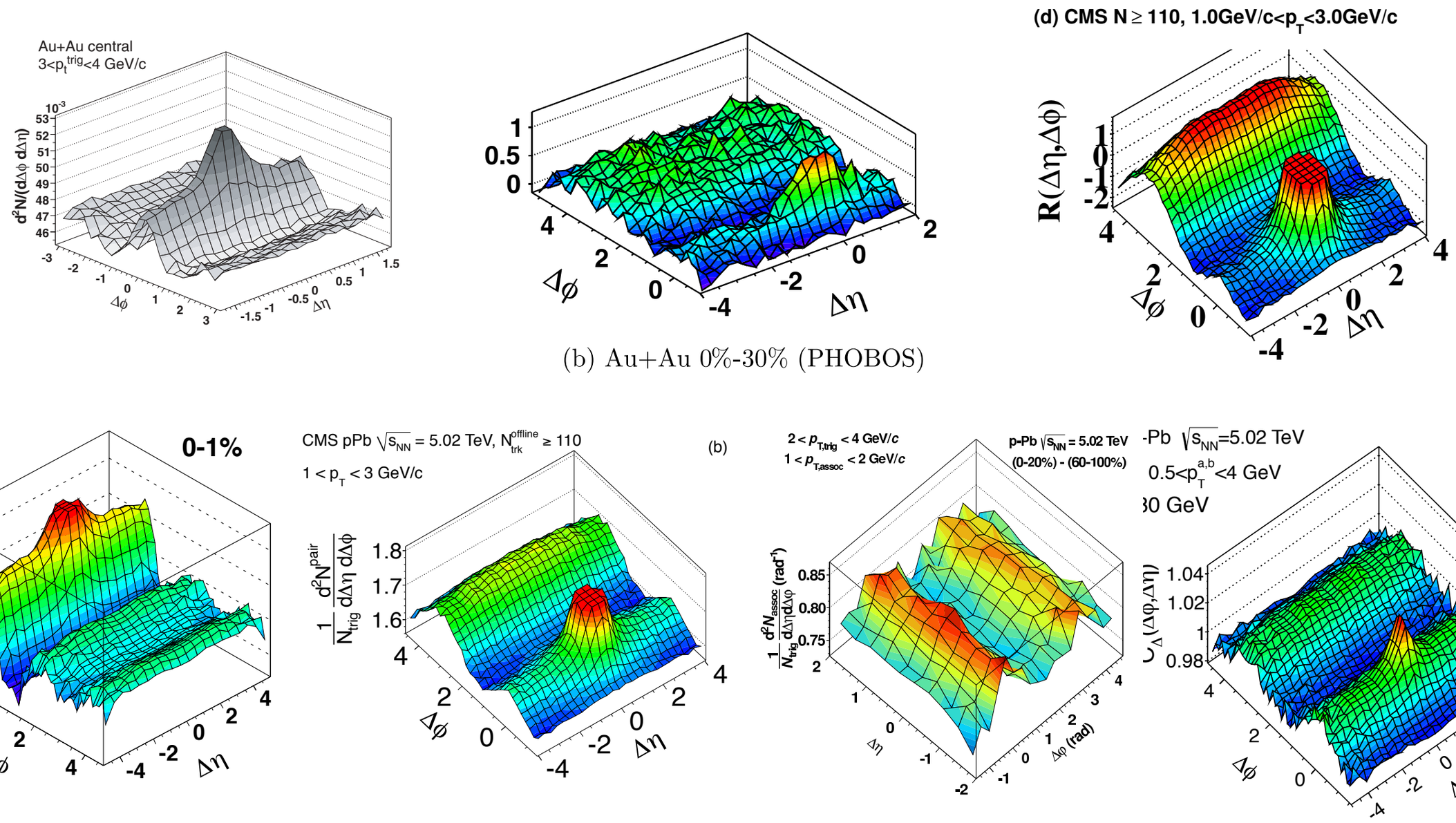

(b) Au+Au 0%-30% (PHOBOS)

PROJECT

THE RIDGE AT RHIC & THE LHC

PETER STEINBERG, BNL

DATE APRIL 15, 2013

CLIENT JQR2013 @ BNL

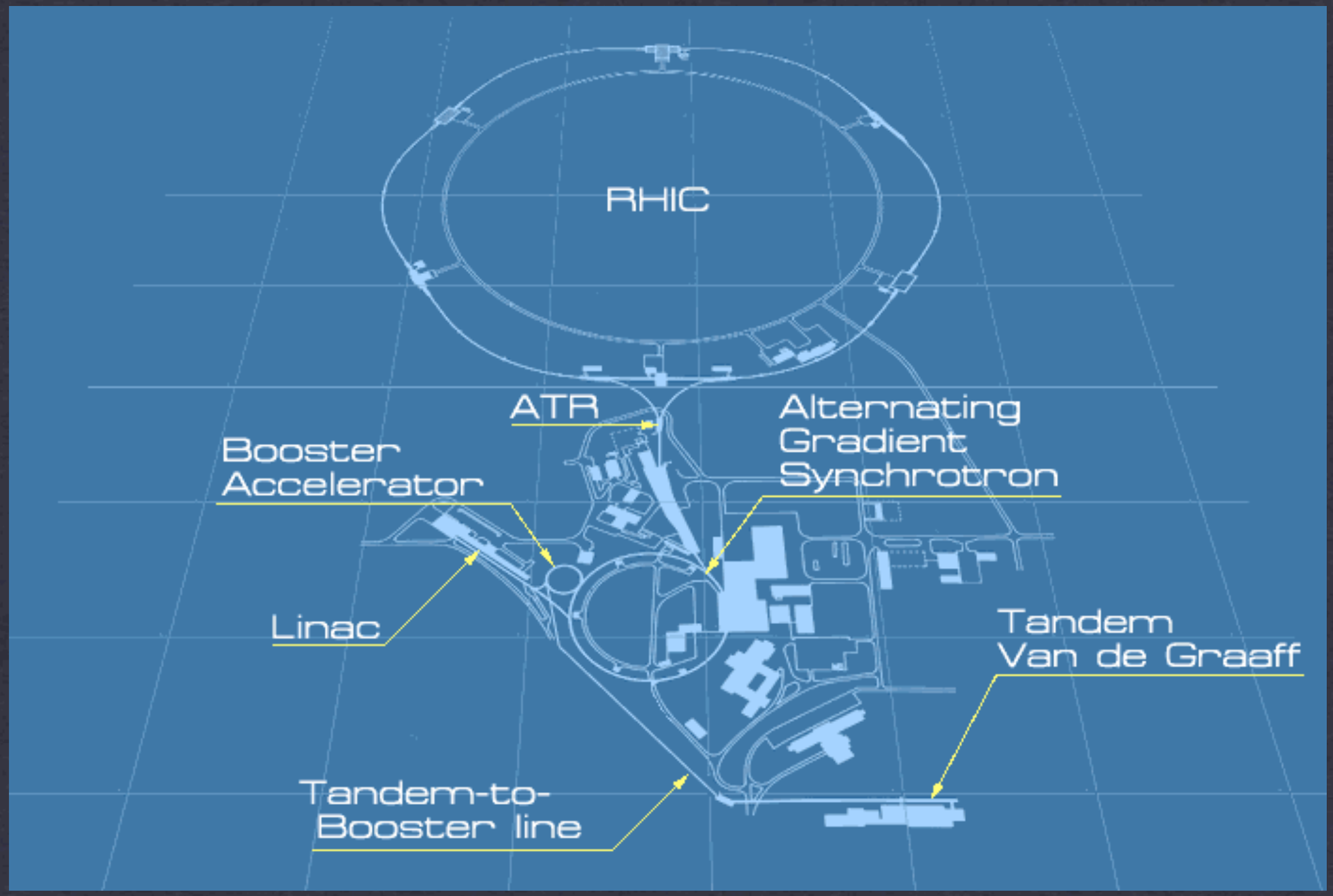

PROJECT

RELATIVISTIC HEAVY ION COLLIDER
BROOKHAVEN NATIONAL LABORATORY, USA

DATE JUNE 2000

CLIENT HEAVY ION & SPIN COMMUNITIES

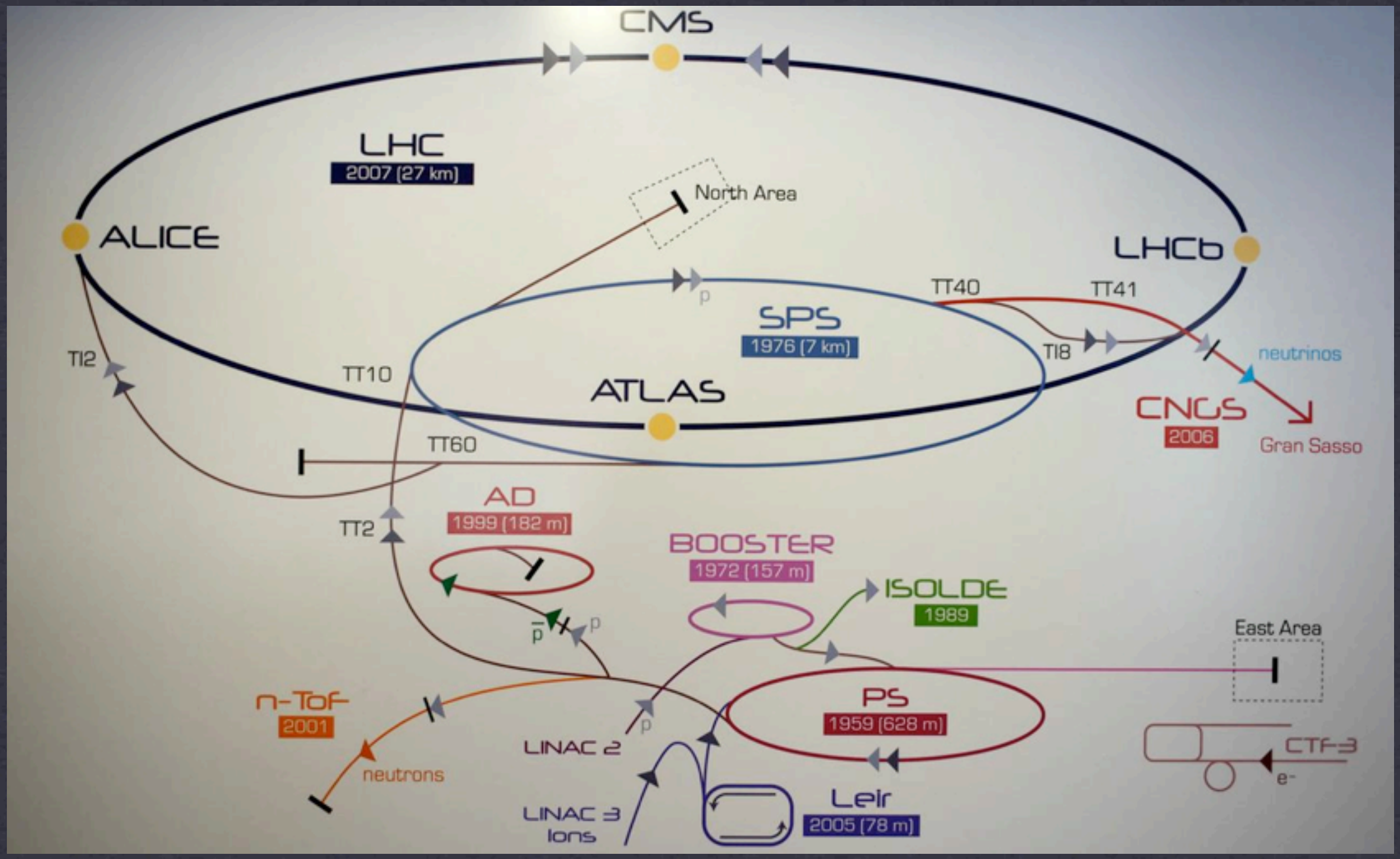

PROJECT

LARGE HADRON COLLIDER
CERN, SWITZERLAND

DATE	CLIENT
NOVEMBER 2009	HEP & HI COMMUNITIES

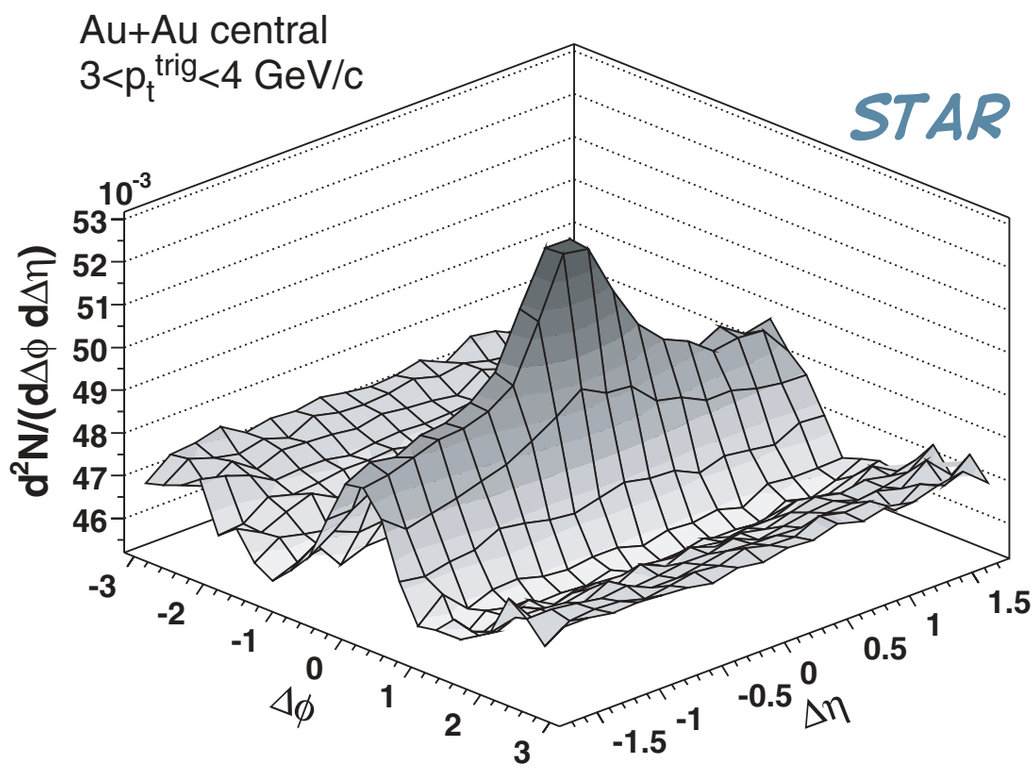

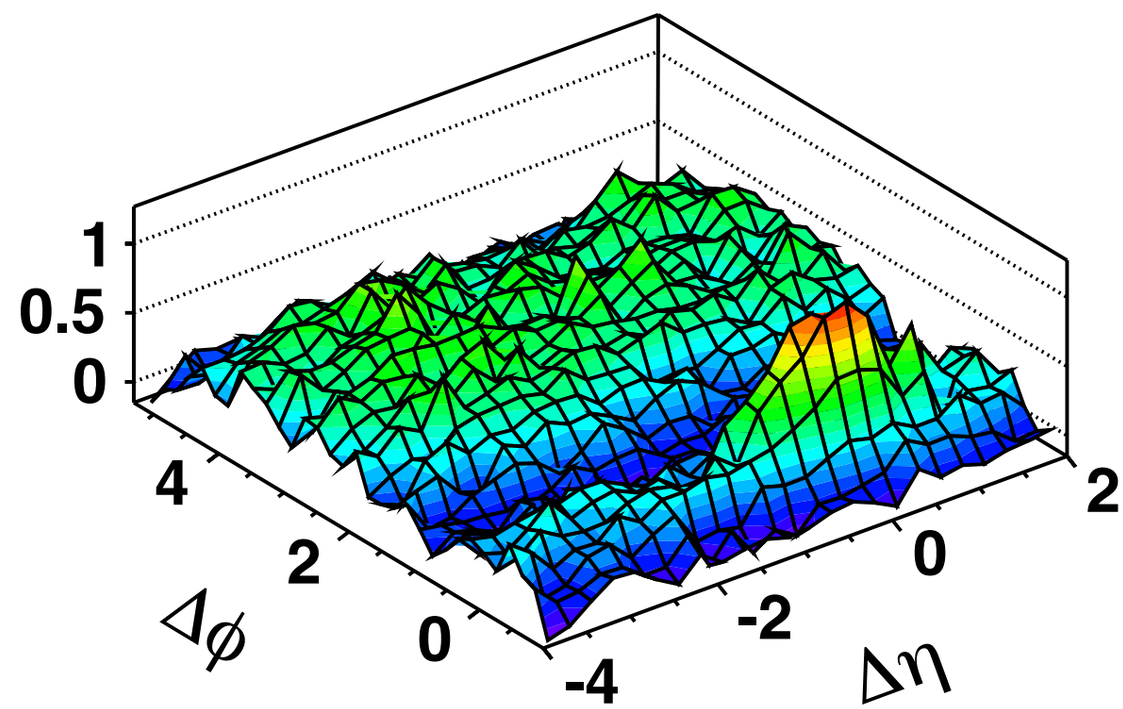

(b) Au+Au 0%-30% (PHOBOS)

• • •

PROJECT

THE RHIC RIDGE

PHENIX, PHOBOS, AND STAR

DATE 2004-2010

CLIENT HEAVY ION COMMUNITY

STAR AU+AU RIDGE

- RIDGE FIRST OBSERVED AT RHIC IN AU+AU
- BY-PRODUCT OF STUDY OF HIGH P_T CORRELATIONS
- CLEAR STRUCTURE EXTENDED IN ETA, BUT LOCALIZED IN PHI

CLEARLY SEEN IN AU+AU ...BUT NOT OBSERVED IN D+AU COLLISIONS!

STAR, PRC 80 064912 (2009)

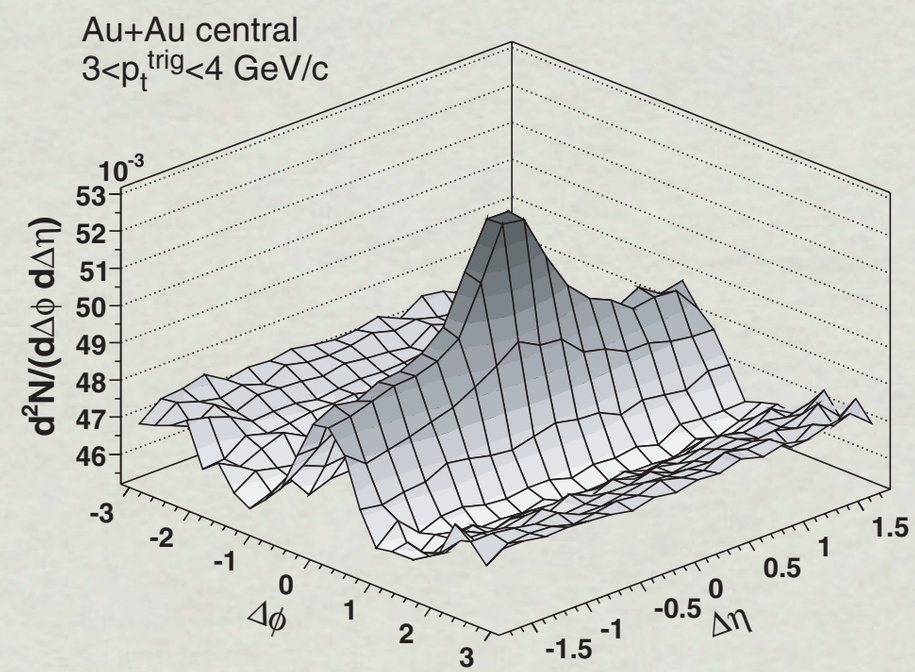

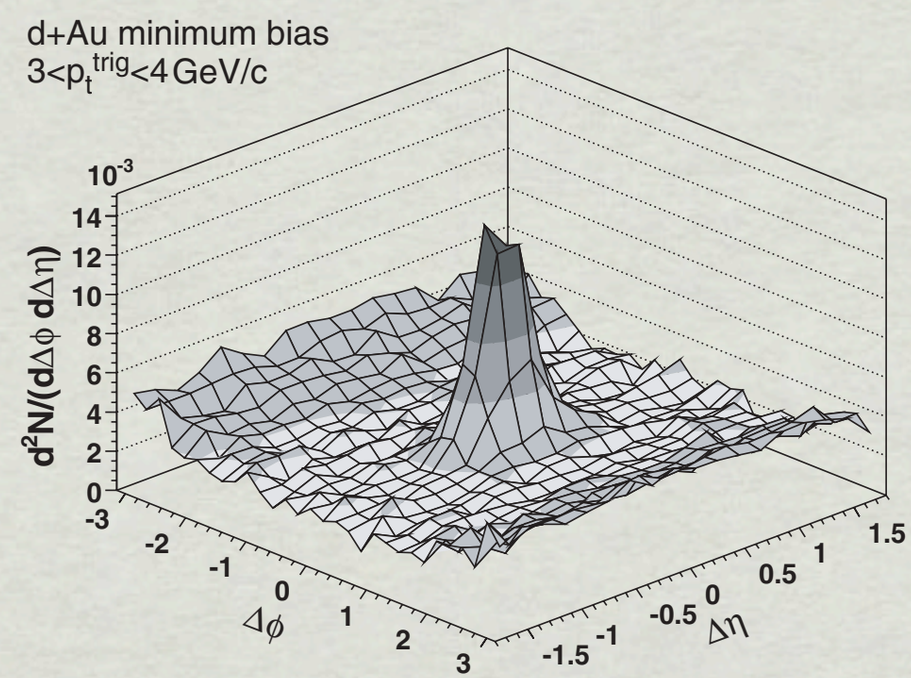

PHOBOS AU+AU RIDGE

PHOBOS, PRL 104 062301 (2010)

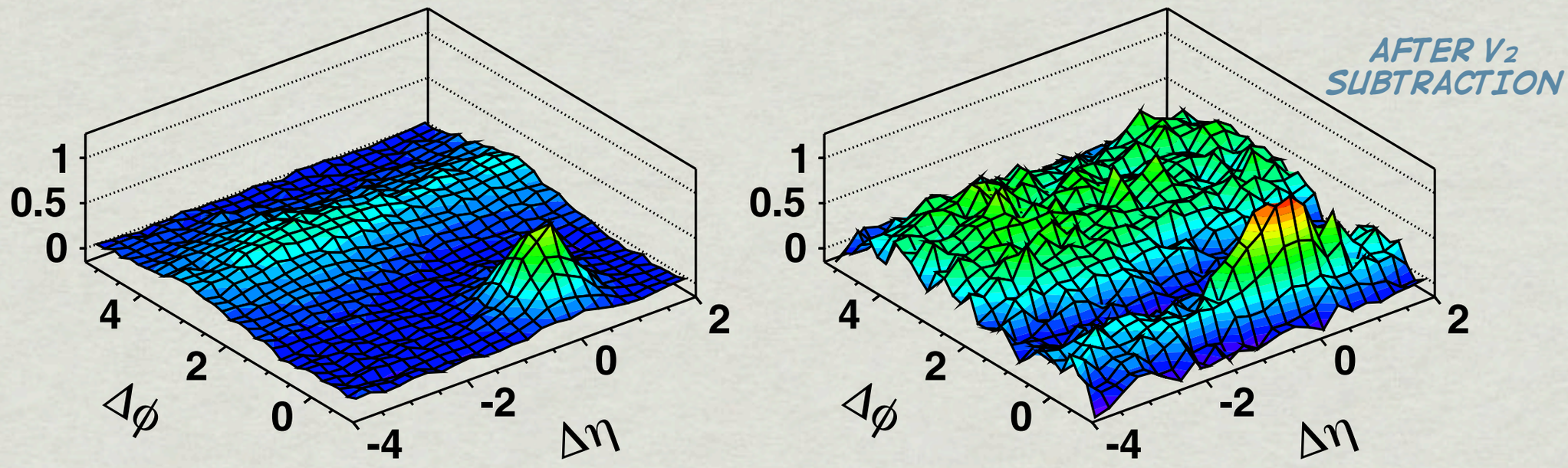

(a) p+p PYTHIA (version 6.325) (b) Au+Au 0%-30% (PHOBOS)

WHILE PHOBOS COULD NOT PROVIDE P_T DEPENDENCE, THE LARGE ETA COVERAGE GAVE FIRST LOOK AT THE RIDGE AT VERY LARGE ΔETA SEPARATIONS...

...AND THERE WAS NO END IN SIGHT!

MANY EXPLANATIONS...

...FROM A 2008 TALK BY ED WENGER (PHOBOS)

- **Coupling of induced radiation to longitudinal flow**
  Armesto et al., PRL 93, 242301
- **Recombination of shower + thermal partons**
  Hwa, arXiv:nucl-th/0609017v1
- **Anisotropic plasma**
  Romatschke, PRC 75, 014901
- **Turbulent color fields**
  Shuryak, arXiv:0706.3531v1
- **Bremsstrahlung + transverse flow + jet-quenching**
  Majumder, Muller, Bass, arXiv:hep-ph/0611135v2
- **Splashback from away-side shock**
  Pantuev, arXiv:0710.1882v1
- **Momentum kick imparted on medium partons**
  Wong, arXiv:0707.2385v2
- **Glasma Flux Tubes**
  Dumitru, Gelis, McLerran, Venugopalan, arXiv:0804.3858; Gavin, McLerran, Moscelli, arXiv:0806.4718

"RIDGE & CONE" KEPT US BUSY FOR 6 YEARS!

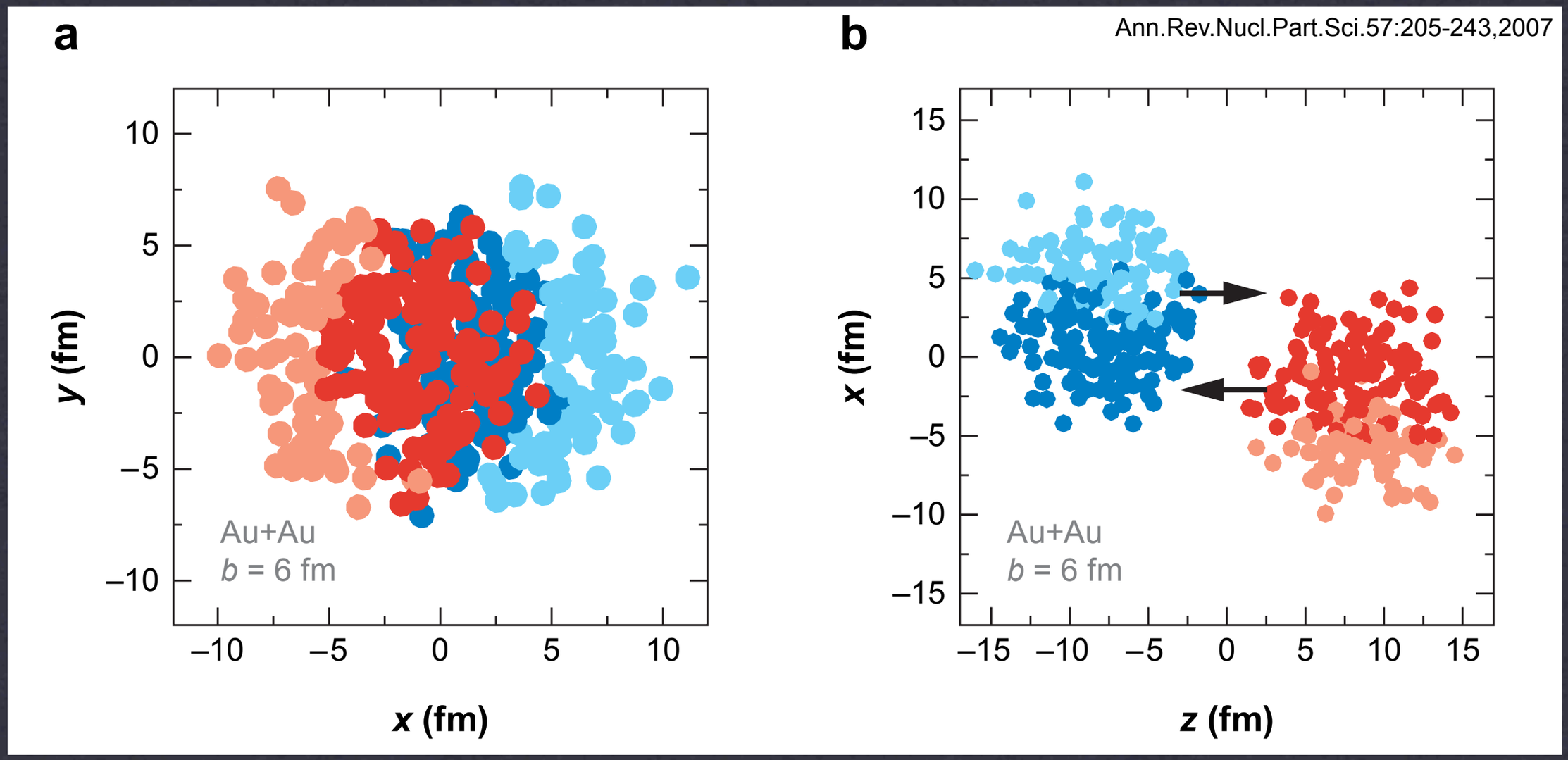

PROJECT

MONTE CARLO GLAUBER
PHOBOS (& ALVER & ROLAND)

DATE JUNE 2005–MARCH 2010

CLIENT HI COMMUNITY

INITIAL STATE MATTERS

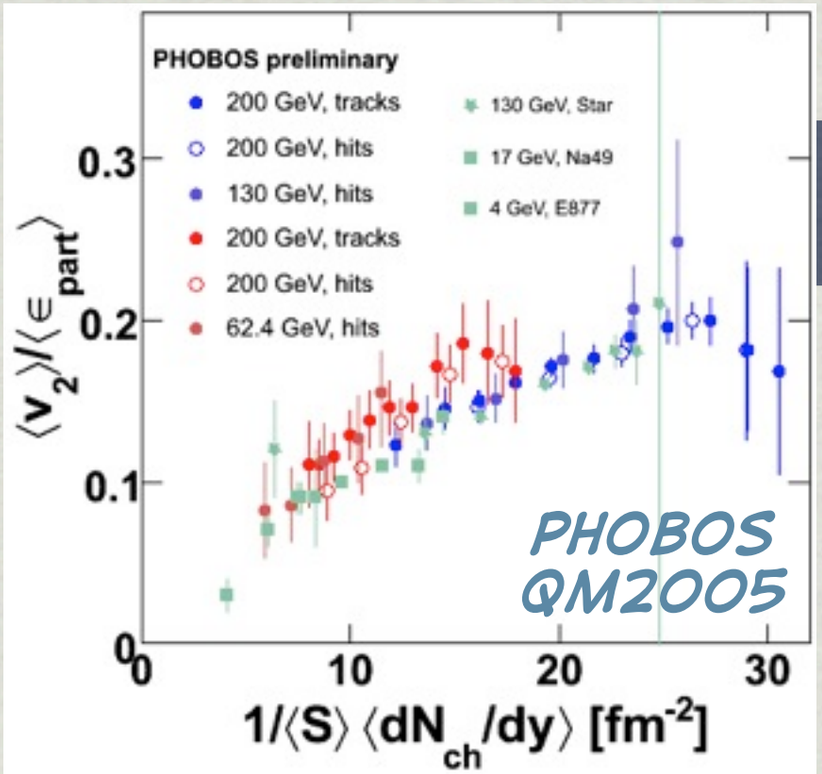

STAR, PRC 81 054905 (2010)

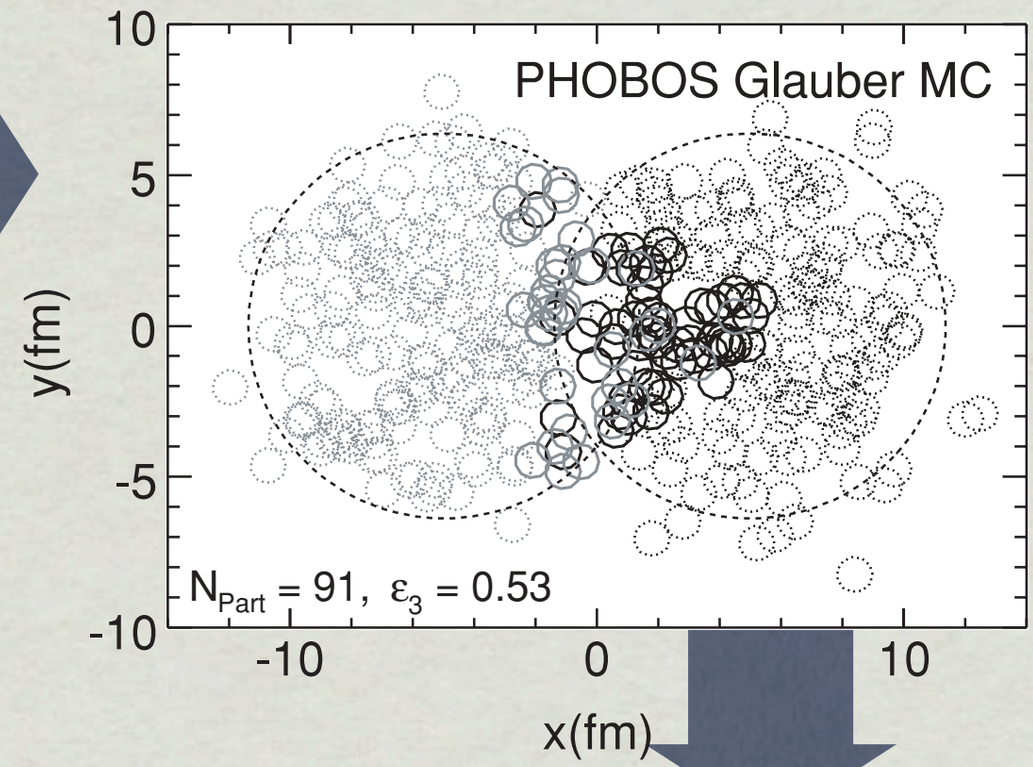

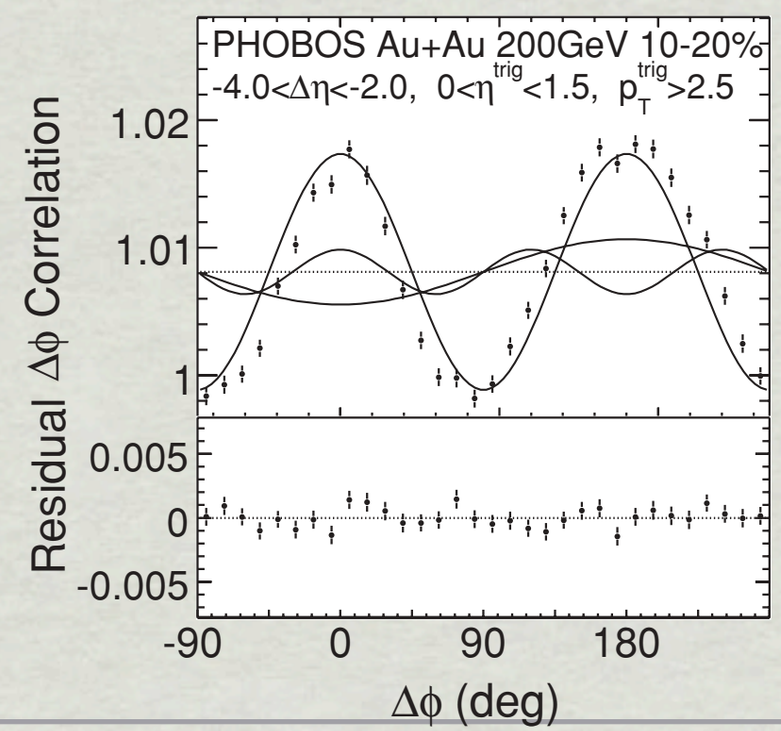

PARTICIPANT ECCENTRICITY BROUGHT AU+AU & CU+CU TOGETHER! **(PHOBOS 2005)**

ALVER & ROLAND WERE FIRST TO MAKE IT CLEAR THAT V_3 SHOULD EXIST AND, MORE IMPORTANTLY, **RIDGE AND CONE ARE "LEFT BEHIND" IF V_2 SUBTRACTED**

THE RIDGE, POST V_3

* ONCE SEEN, DIFFICULT TO FORGET
* FLUCTUATIONS IN THE INITIAL STATE PROVIDE SIMPLEST WAY TO HARMONIZE FLOW SYSTEMATICS
* THEY ARE ALSO THE SIMPLEST WAY TO UNDERSTAND THE RIDGE **AND** MACH CONE

...WAS THIS THE END OF THE RIDGE??

NOT SO FAST!...

JHEP

Published for SISSA by Springer

Received: September 22, 2010
Accepted: September 23, 2010
Published: September 27, 2010

Observation of long-range, near-side angular correlations in proton-proton collisions at the LHC

The CMS collaboration

Abstract: Results on two-particle angular correlations for charged particles emitted in proton-proton collisions at center-of-mass energies of 0.9, 2.36, and 7 TeV are presented, using data collected with the CMS detector over a broad range of pseudorapidity (η) and azimuthal angle (ϕ). Short-range correlations in $\Delta\eta$, which are studied in minimum bias

JHEP09(2010)

PROJECT

THE PP RIDGE

CMS COLLABORATION

DATE SEPT. 2010–MARCH 2011

CLIENT HEP (& HI?) COMMUNITY

SEPTEMBER SURPRISE

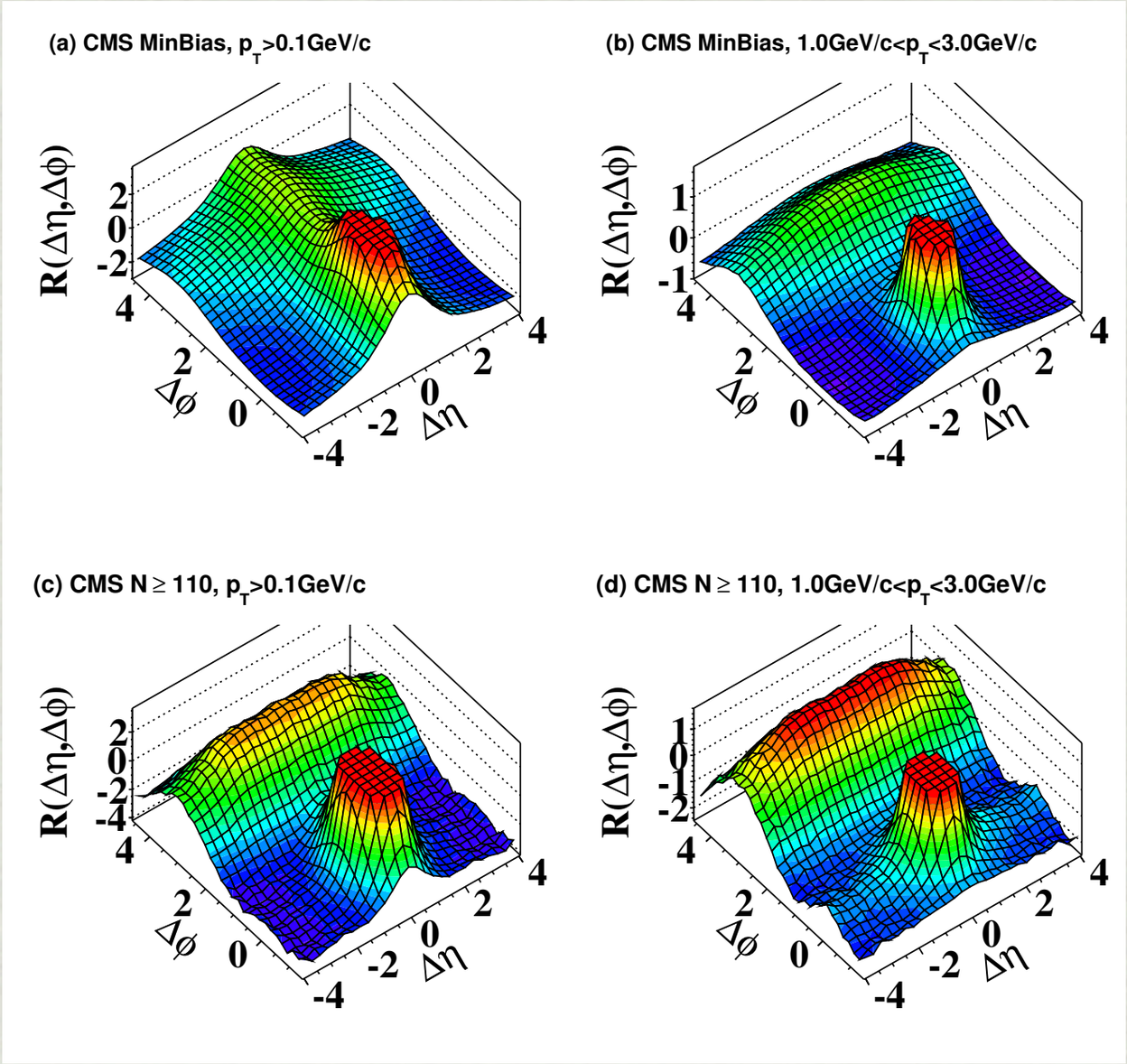

CMS, JHEP 1009 091 (2010)

$$R(\Delta\eta,\Delta\phi) = \left\langle (\langle N\rangle - 1)\left(\frac{S_N(\Delta\eta,\Delta\phi)}{B_N(\Delta\eta,\Delta\phi)} - 1\right)\right\rangle_{\text{bins}}$$

$$S_N(\Delta\eta,\Delta\phi) = \frac{1}{N(N-1)}\frac{d^2N^{\text{signal}}}{d\Delta\eta d\Delta\phi}$$

$$B_N(\Delta\eta,\Delta\phi) = \frac{1}{N^2}\frac{d^2N^{\text{mixed}}}{d\Delta\eta d\Delta\phi}$$

USING A **SPECIAL HIGH MULTIPLICITY TRIGGER**, A DATA SAMPLE UNAVAILABLE TO THE OTHER EXPERIMENTS REVEALED **A RIDGE IN PP!**

PHYSICS OF THE RIDGE

* I DEFER TO MY THEORIST COLLEAGUES, SPEAKING NEXT
* BUT THE **SAME DATA** LED TO A **WIDE VARIETY** OF EXPLANATIONS
  * PARTON SATURATION (VENUGOPALAN ET AL)
  * MULTIPARTON INTERACTIONS (STRIKMAN)
  * BREMSSTRAHLUNG IN STRONG FIELDS
  * "JET-MEDIUM" (HWA, WONG,...)
  * HYDRODYNAMICS (WERNER, AVSAR, ETC.)
* AS WITH THE RHIC RIDGE, MANY EXPLANATIONS BUT NO CLEAR WINNER
  * ABSENCE OF CRISP PREDICTIONS CONFRONTING NEW PP RIDGE DATA

PP RIDGE VS. P_T

CMS, PAS-HIN-2011-006 (Mar 2011)

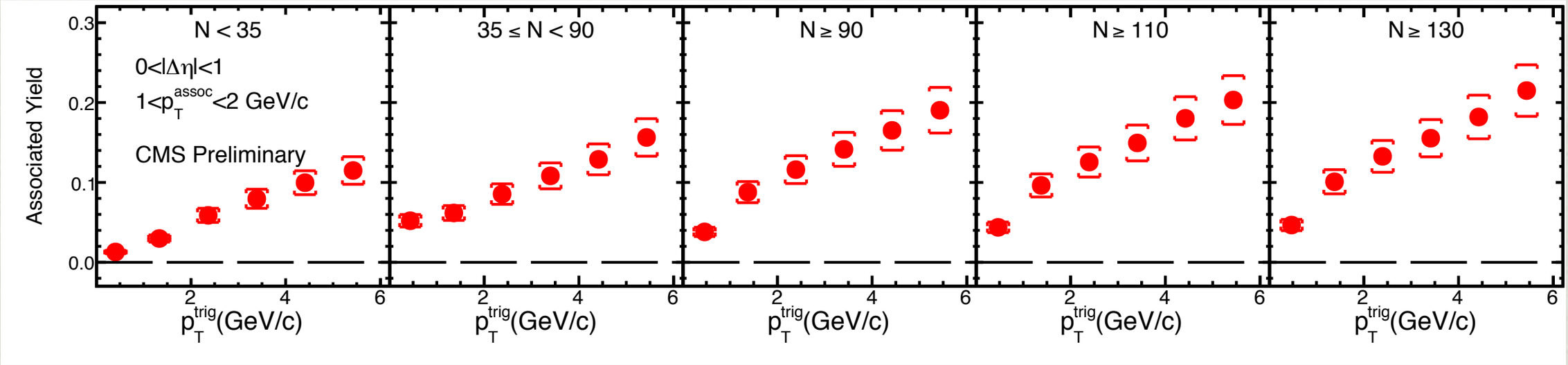

A SYSTEMATIC INCREASE IN JET REGION (ΔETA<1)

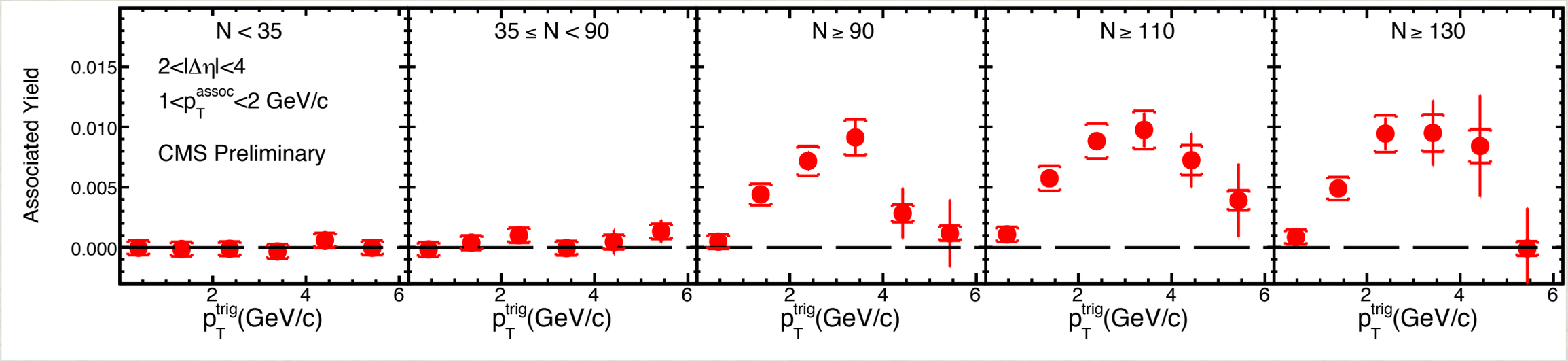

A CHARACTERISTIC PT DEPENDENCE IN "RIDGE" REGION: ONE WHICH LOOKED FAMILIAR FROM A+A

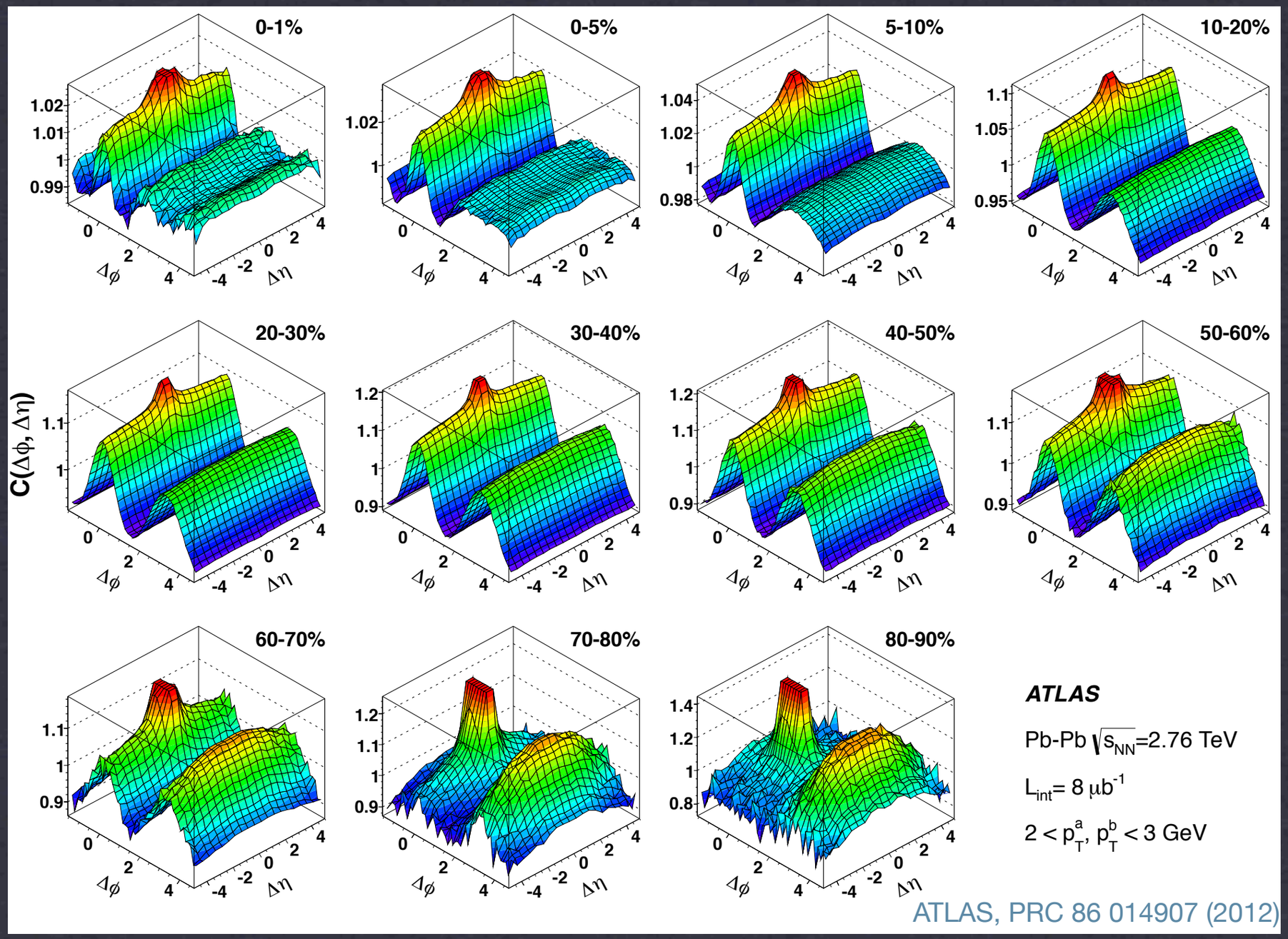

ATLAS, PRC 86 014907 (2012)

PROJECT

THE PB+PB RIDGE

ALICE, ATLAS, CMS

DATE SPRING 2011

CLIENT HEAVY ION COMMUNITY

FOURIER DECOMPOSITION

ATLAS, PRC 86 014907 (2012)

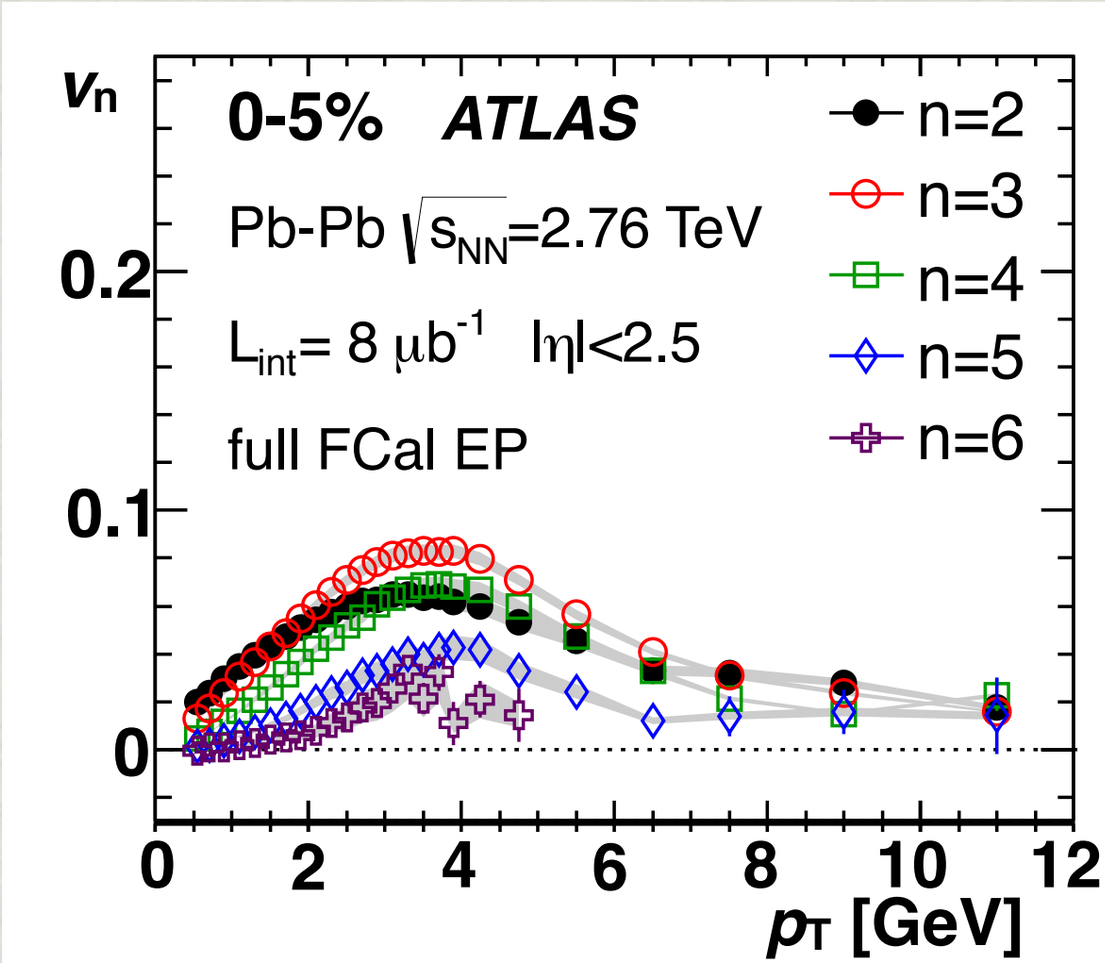

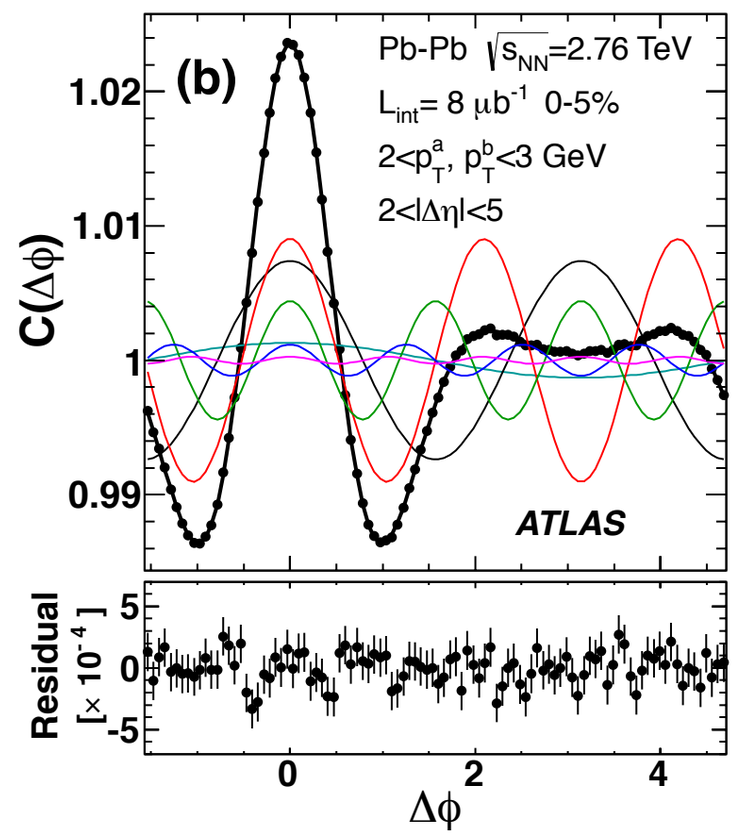

WHY STOP AT TRIANGULAR FLOW?

IN THIS VIEW, THE 2PC RIDGE IS SIMPLY ALL FOURIER COMPONENTS CONTRIBUTING AT ΔPHI=0!

AND NOTE VERY SIMILAR SHAPE OF P_T DEPENDENCE TO PP RIDGE!

v_N FROM FLOW

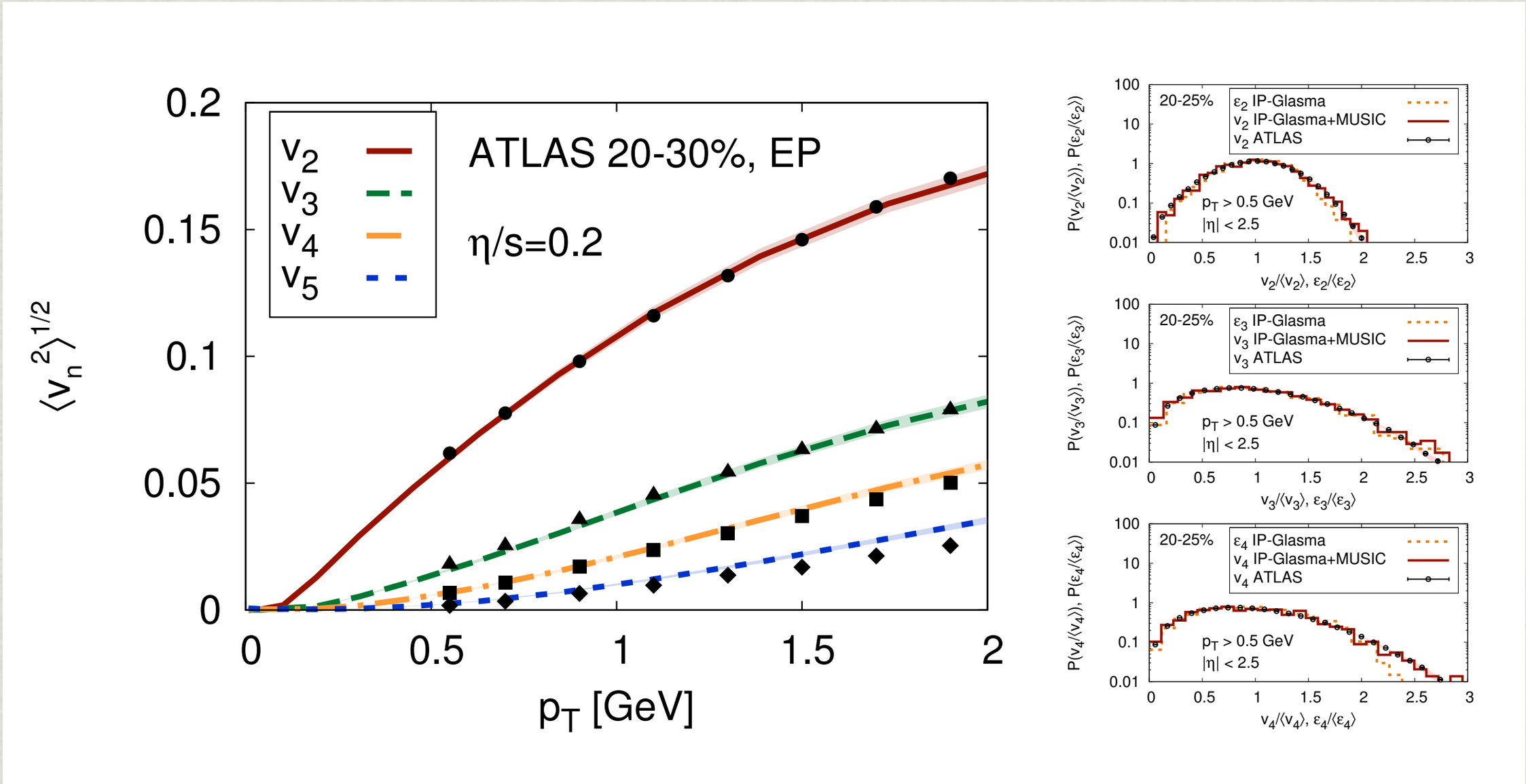

BOTH MEAN VALUES AND FLUCTUATIONS NICELY DESCRIBED BY **EVENTWISE VISCOUS HYDRO WITH IP GLASMA IC.** (& OTHERS)

(SCHENKE ET AL, HEINZ ET AL, LUZUM ET AL,...)

WITH THE HIGHER-ORDER HARMONICS...

HAD WE FINALLY BURIED THE RIDGE?...

...AT LEAST IN A+A, WHERE FLOW WAS ALREADY THE LEADING HYPOTHESIS

NOT SO FAST!...

EUROPEAN ORGANIZATION FOR NUCLEAR RESEARCH (CERN)

CERN-PH-EP/2012-320
2012/10/23

CMS-HIN-12-015

Observation of long-range, near-side angular correlations in pPb collisions at the LHC

The CMS Collaboration*

PROJECT

DISCOVERY OF A P+PB RIDGE

THE CMS COLLABORATION

DATE OCTOBER 23, 2013

CLIENT HEAVY ION COMMUNITY

EAT A MICROBARN OF LEAD, PROTONS!...

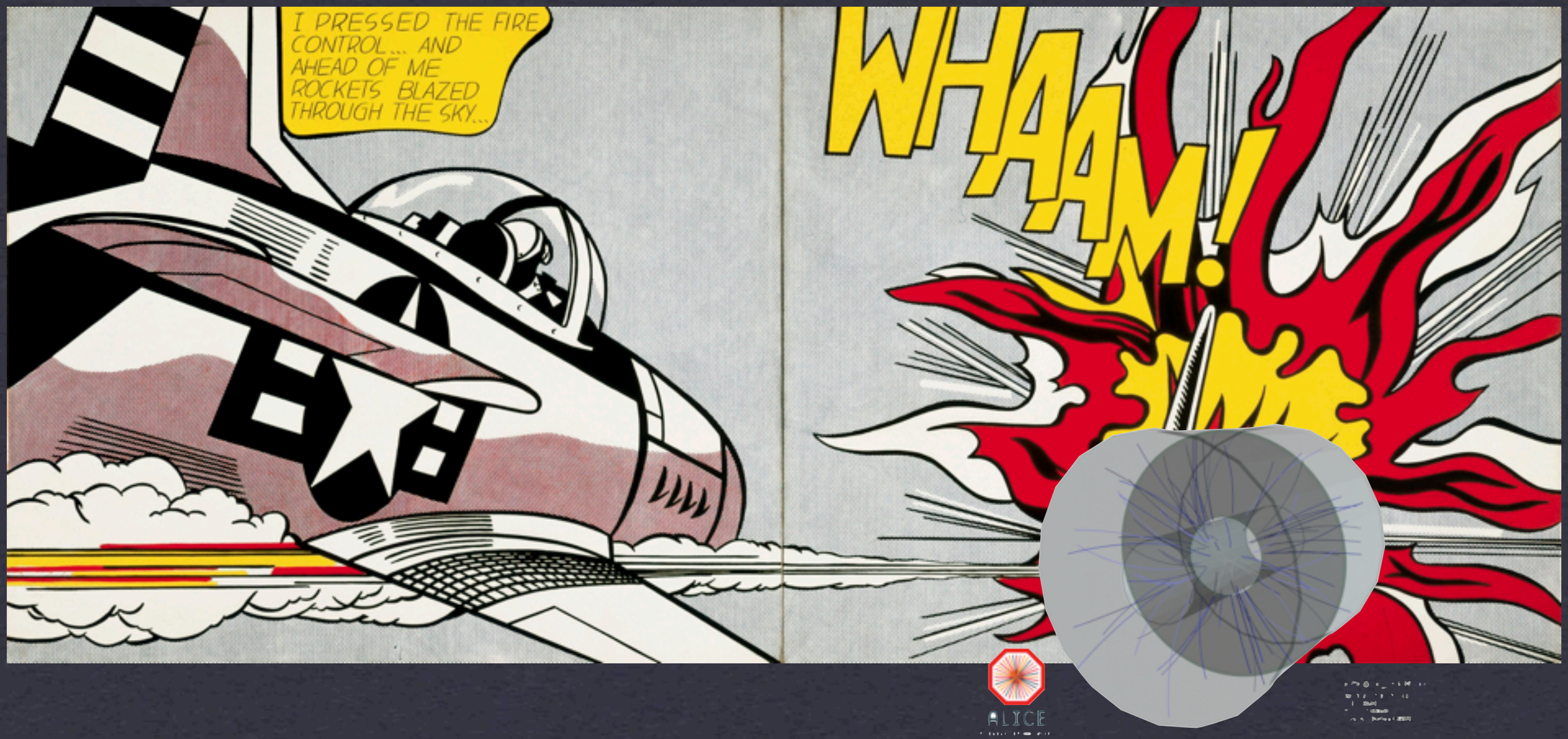

PROJECT

THE P+PB PILOT RUN

LARGE HADRON COLLIDER (J. JOWETT, ET AL)

DATE	CLIENT
SEPTEMBER 12, 2012	HI COMMUNITY & LHCB

RIDGE REDISCOVERED

CMS, PLB 718 795 (2013)

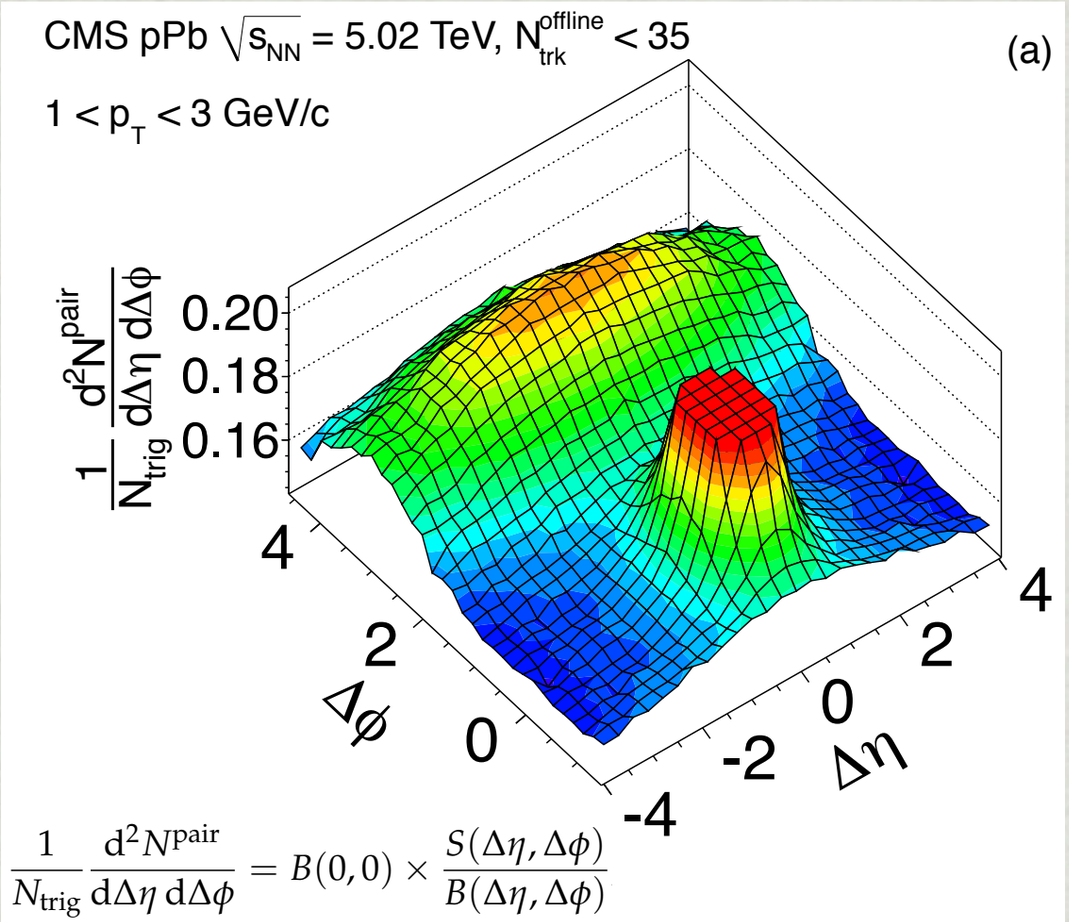

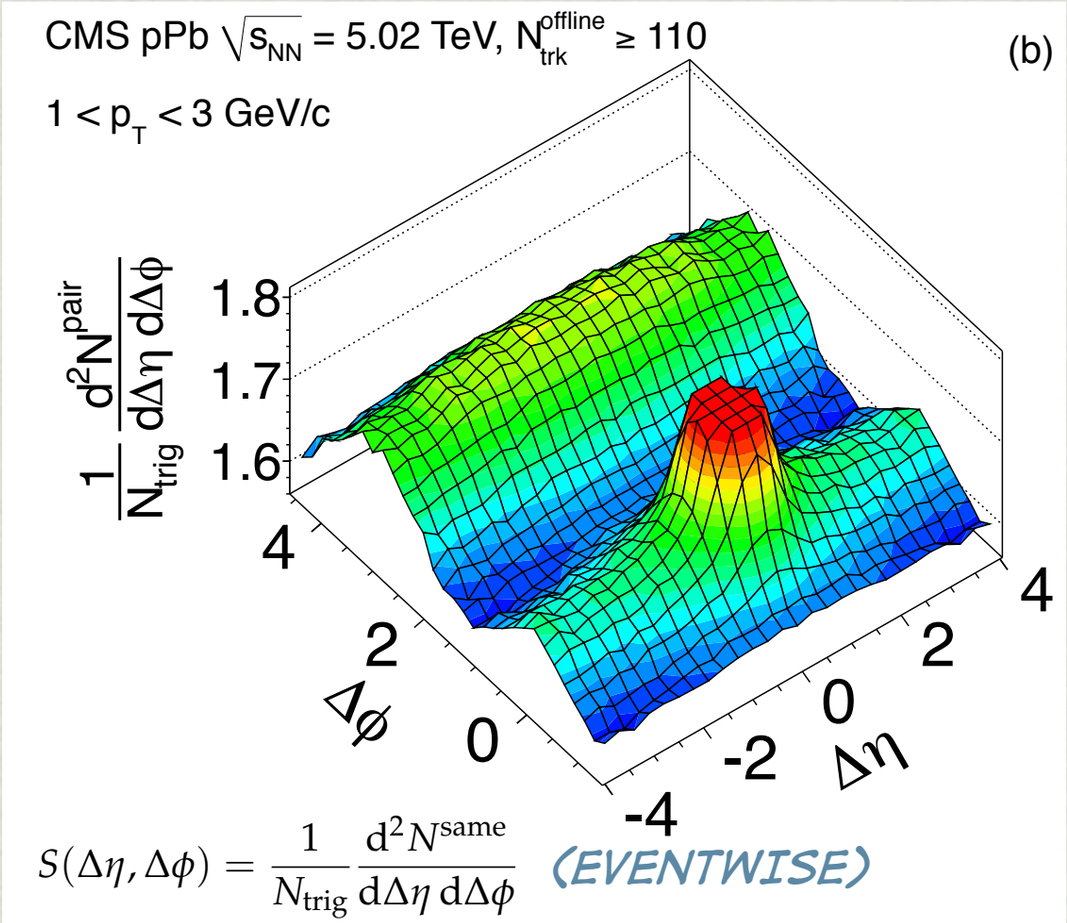

IN PP, RIDGE REQUIRED HIGHEST MULTIPLICITY COLLISIONS TO BE SEEN NEXT TO ENORMOUS NEAR-SIDE PEAK,

IN P+PB RIDGE WAS VISIBLE WITH RATHER MODEST MULTIPLICITIES (DUE TO MULTIPLE COLLISIONS)

CORRELATION FUNCTIONS

EQUAL MOMENTUM BINS

MULTIPLICITY BINS

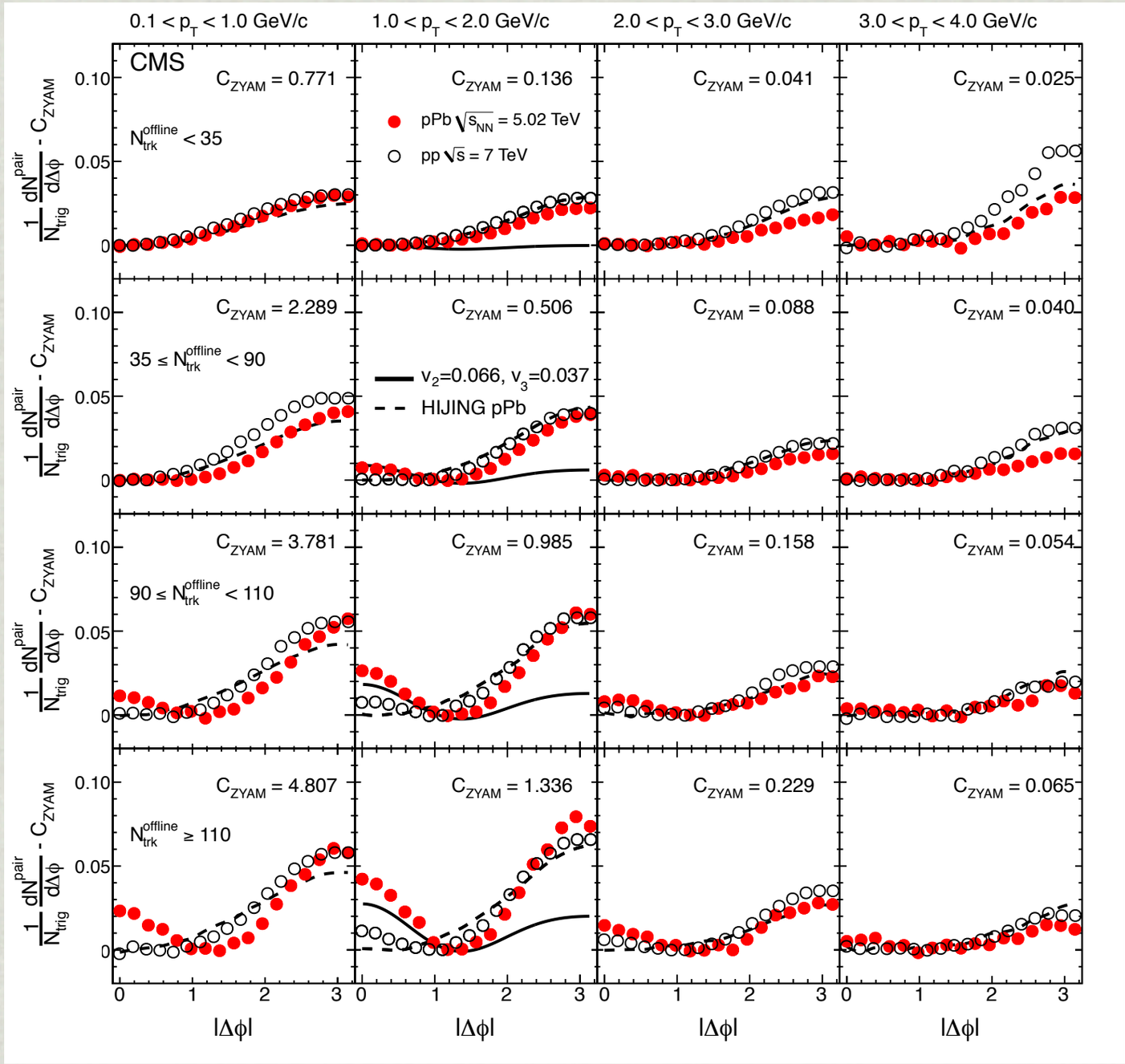

CMS, PLB 718 795 (2013)

COMPARISONS TO HIJING & HYDRO PREDICTIONS

CGC MODELING

Dusling & Venugopalan, prd 87 054014 (2013)

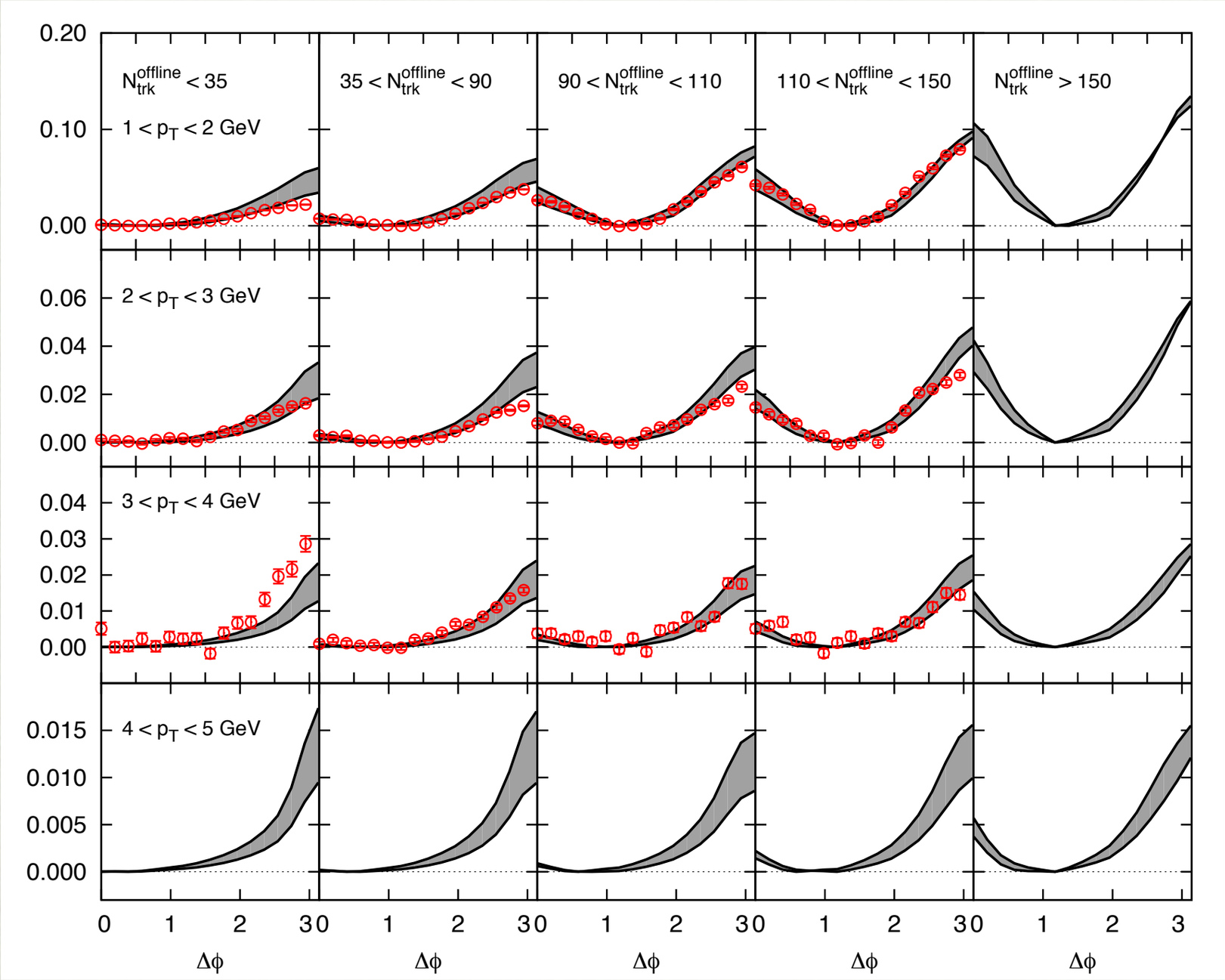

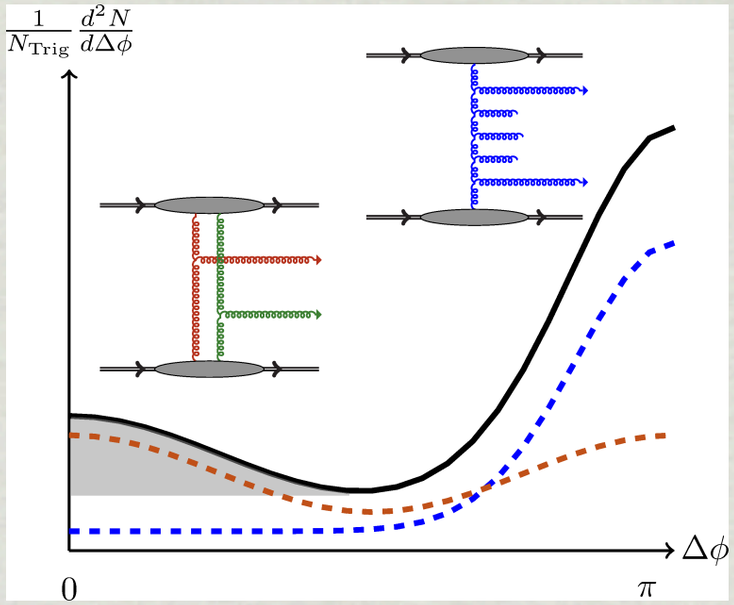

BASED ON PP EXPERIENCE, CGC GROUPS WERE **READY!**

THIS WORK AND COMPARISONS TO LATER DATA WILL BE COVERED IN RAJU'S TALK!...

ALSO WORK BY: KOVCHEGOV & WERPERTNY

MEANWHILE...

THE OTHER LHC EXPERIMENTS WERE BUSY AT WORK!...

...FINALIZING PAPERS SIMULTANEOUSLY (ALTHOUGH ALICE GOT THE JUMP ON ATLAS!)

EUROPEAN ORGANIZATION FOR NUCLEAR RESEARCH

CERN-PH-EP-2012-359
03 Dec 2012

Long-range angular correlations on the near and away side in p–Pb collisions at $\sqrt{s_{NN}}$= 5.02 TeV

ALICE Collaboration*

] 10 Dec 2012

Abstract

Angular correlations between charged trigger and associated particles are measured by the ALICE detector in p–Pb collisions at a nucleon–nucleon centre-of-mass energy of 5.02 TeV for transverse momentum ranges within $0.5 < p_{T,assoc} < p_{T,trig} < 4$ GeV/c. The correlations

PROJECT

THE P+PB RIDGE
ALICE COLLABORATION

DATE DECEMBER 10, 2012

CLIENT HEAVY ION COMMUNITY

EUROPEAN ORGANISATION FOR NUCLEAR RESEARCH (CERN)

CERN-PH-EP-2012-366

Submitted to: Phys. Rev. Lett.

Observation of Associated Near-side and Away-side Long-range Correlations in $\sqrt{s_{\mathrm{NN}}} = 5.02\ \mathrm{TeV}$ Proton–lead Collisions with the ATLAS Detector

The ATLAS Collaboration

PROJECT

THE P+PB RIDGE

ATLAS COLLABORATION

DATE DECEMBER 20, 2012

CLIENT HEAVY ION COMMUNITY

"EVENT ACTIVITY"

ATLAS, arXiv:1212.5198 (2013, accepted by PRL)

OVERALL ACTIVITY CHARACTERIZED BY ATLAS WITH E_T SUM IN $3.2<\eta<4.9$,

AND ALICE WITH VOM, MULTIPLICITY IN FORWARD DIRECTION

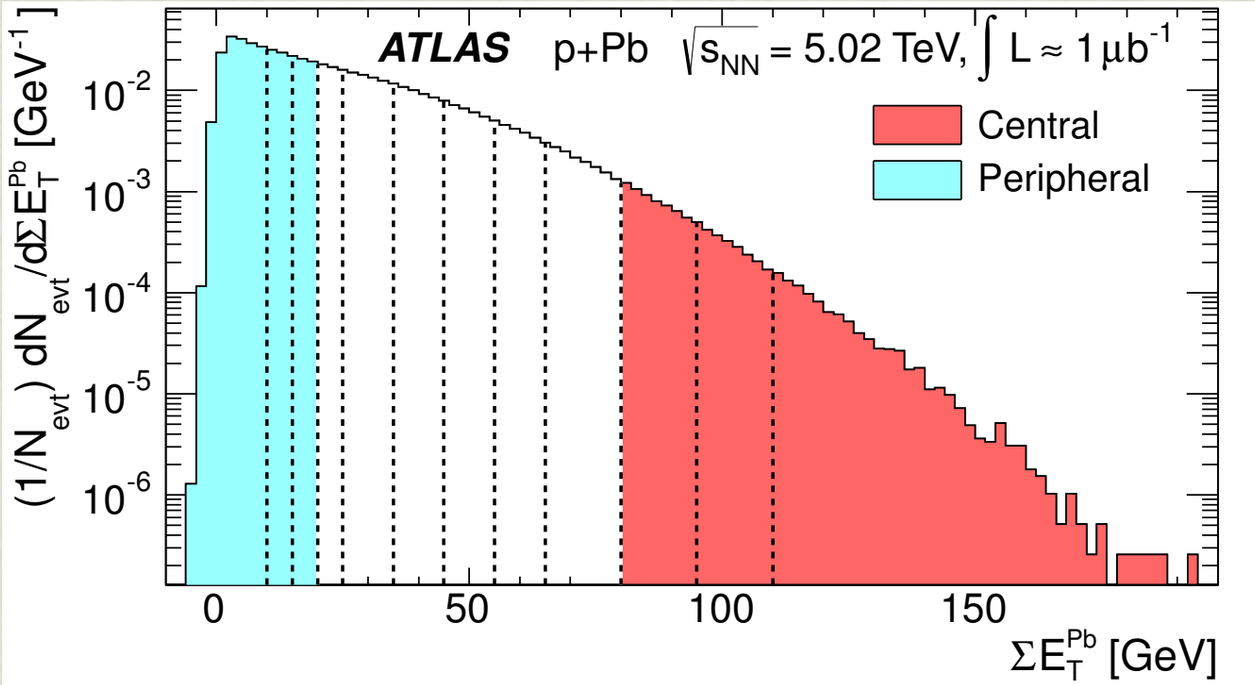

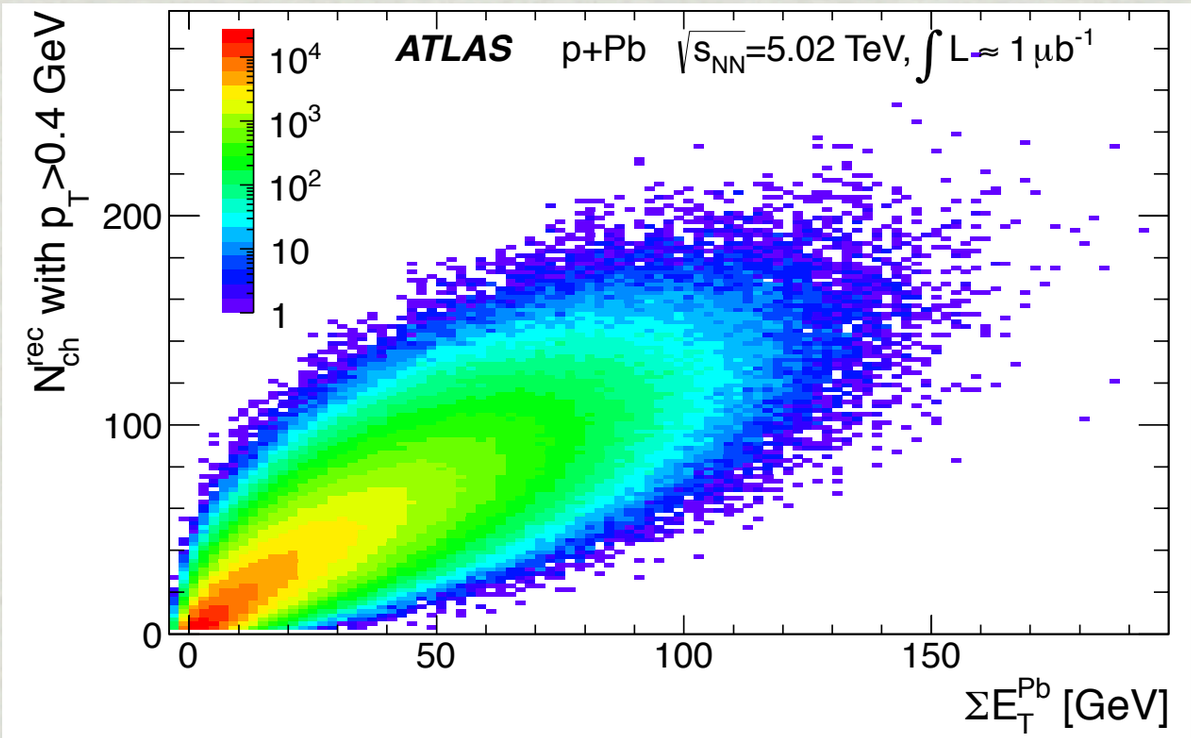

IMPORTANT TO AVOID CUTTING DIRECTLY INTO MULTIPLICITY DISTRIBUTION AT ETA~0

SECOND OBSERVATION!

ALICE, PLB 719 29 (2013)

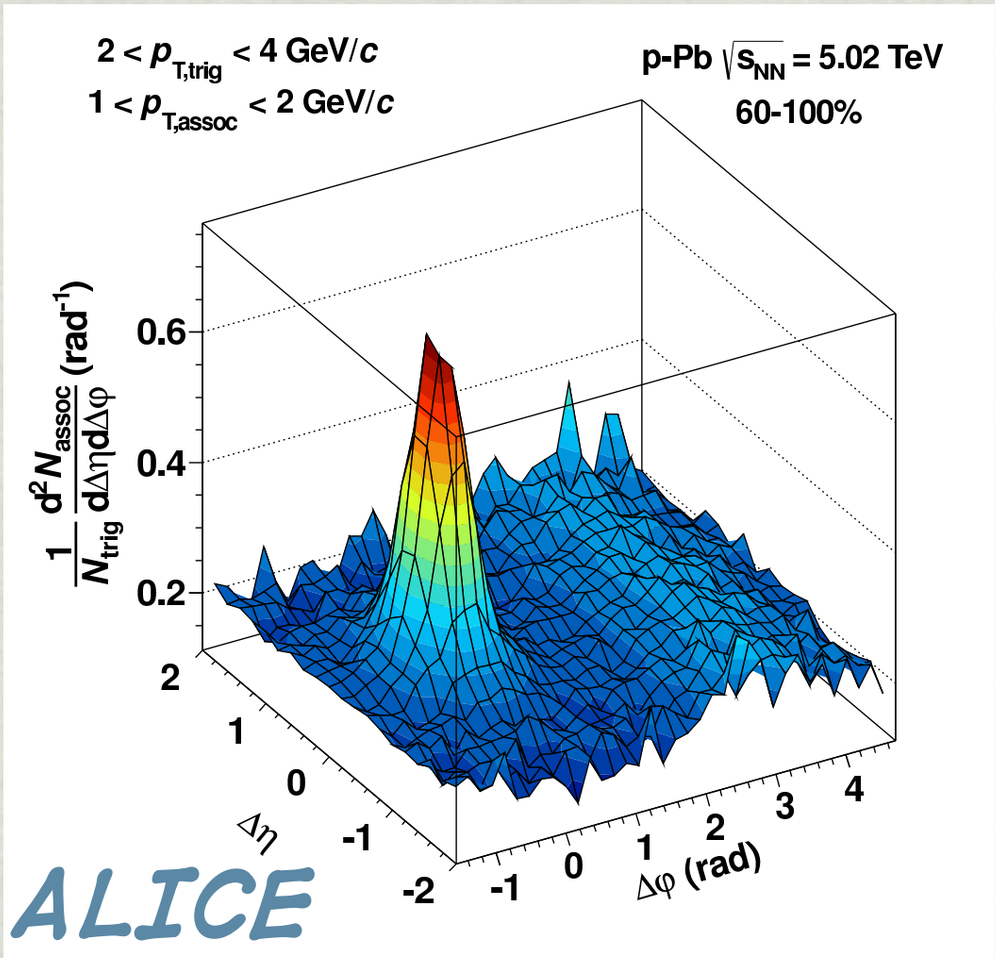

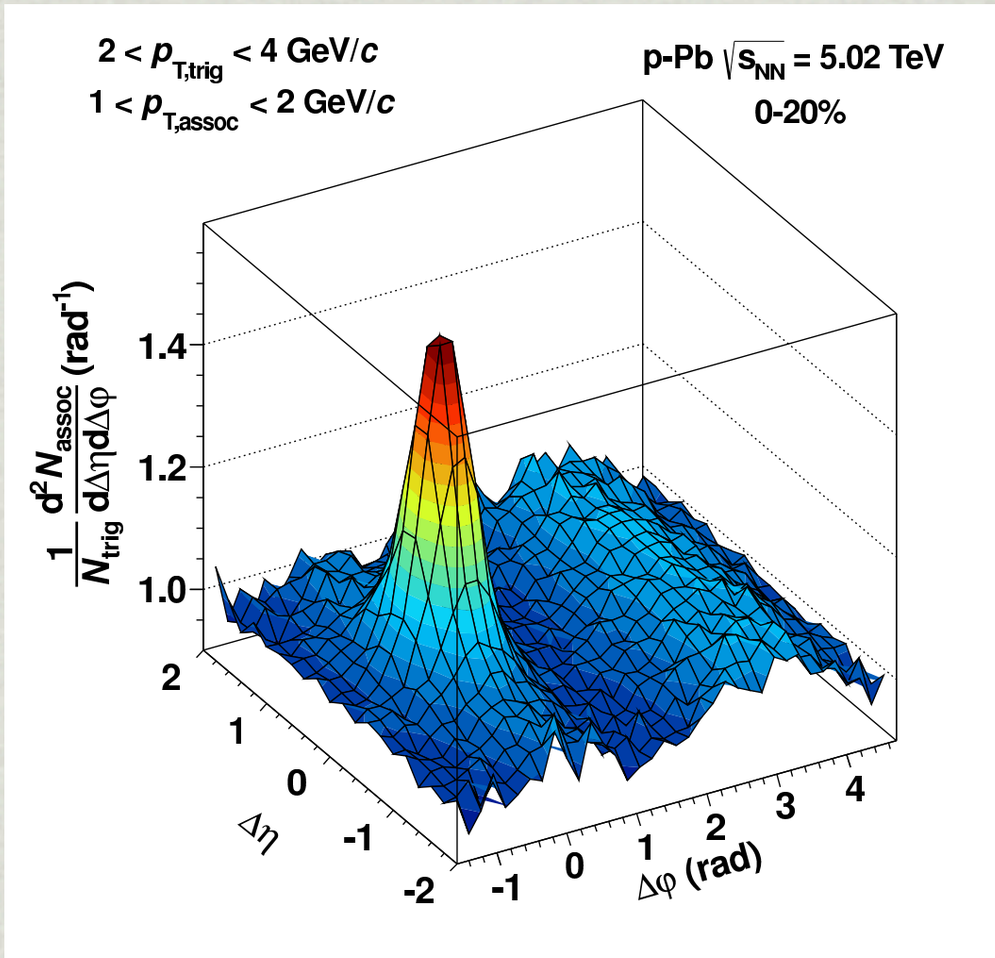

EVEN WITH A SMALLER ΔETA ACCEPTANCE,
THE RIDGE WAS OBSERVED BY ALICE
AT THE FOOT OF THE JET MOUNTAIN...

$$\frac{1}{N_{\rm trig}}\frac{{\rm d}^2N_{\rm assoc}}{{\rm d}\Delta\eta{\rm d}\Delta\varphi} = \frac{S(\Delta\eta,\Delta\varphi)}{B(\Delta\eta,\Delta\varphi)}$$

$$S(\Delta\eta,\Delta\varphi) = 1/N_{\rm trig}{\rm d}^2N_{\rm same}/{\rm d}\Delta\eta{\rm d}\Delta\varphi$$

(SUMMED OVER MULTIPLICITY CLASS)

ATLAS VS. CMS

CMS

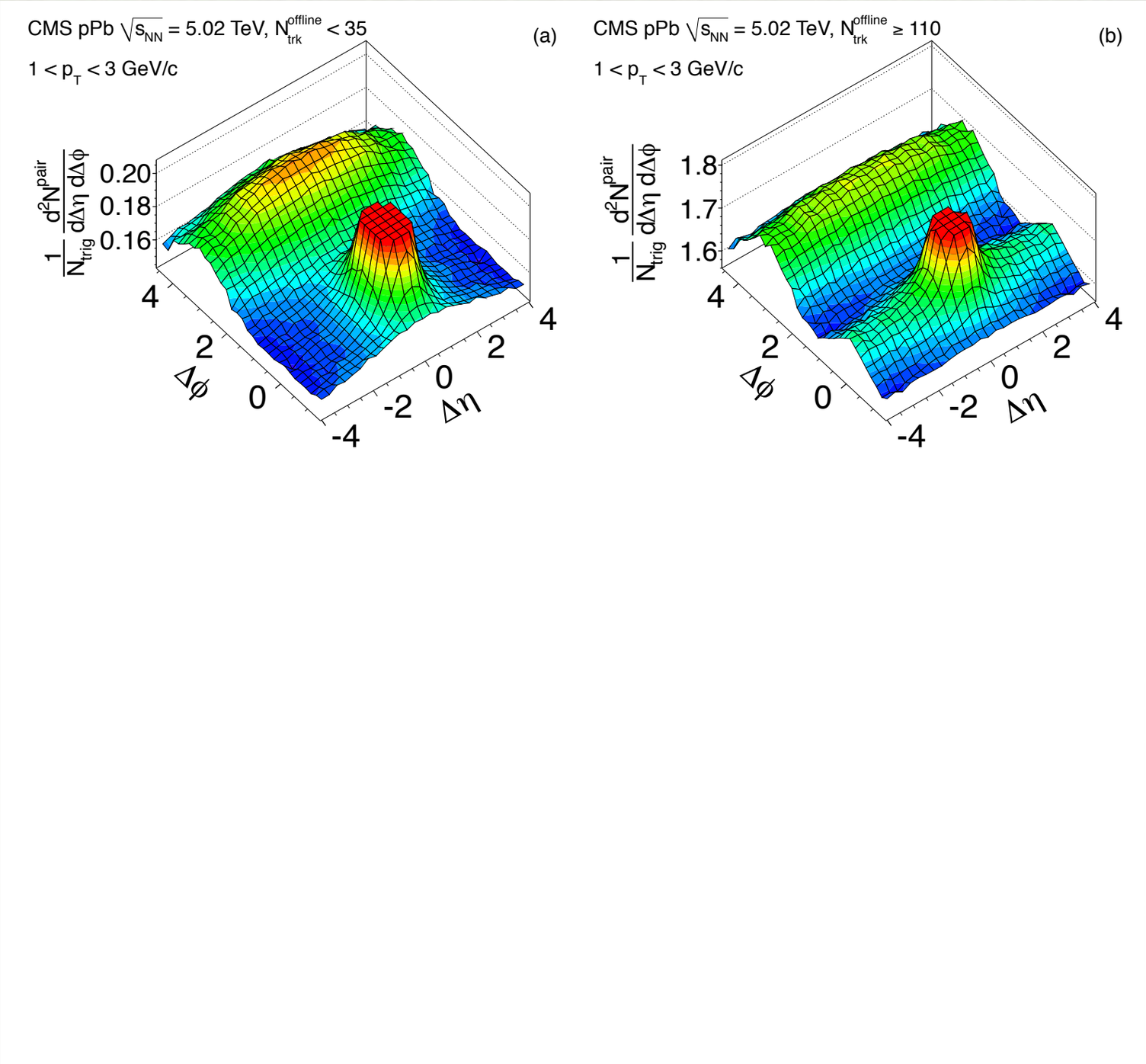

ATLAS

PERI. CENT.

ATLAS VS. CMS

CMS

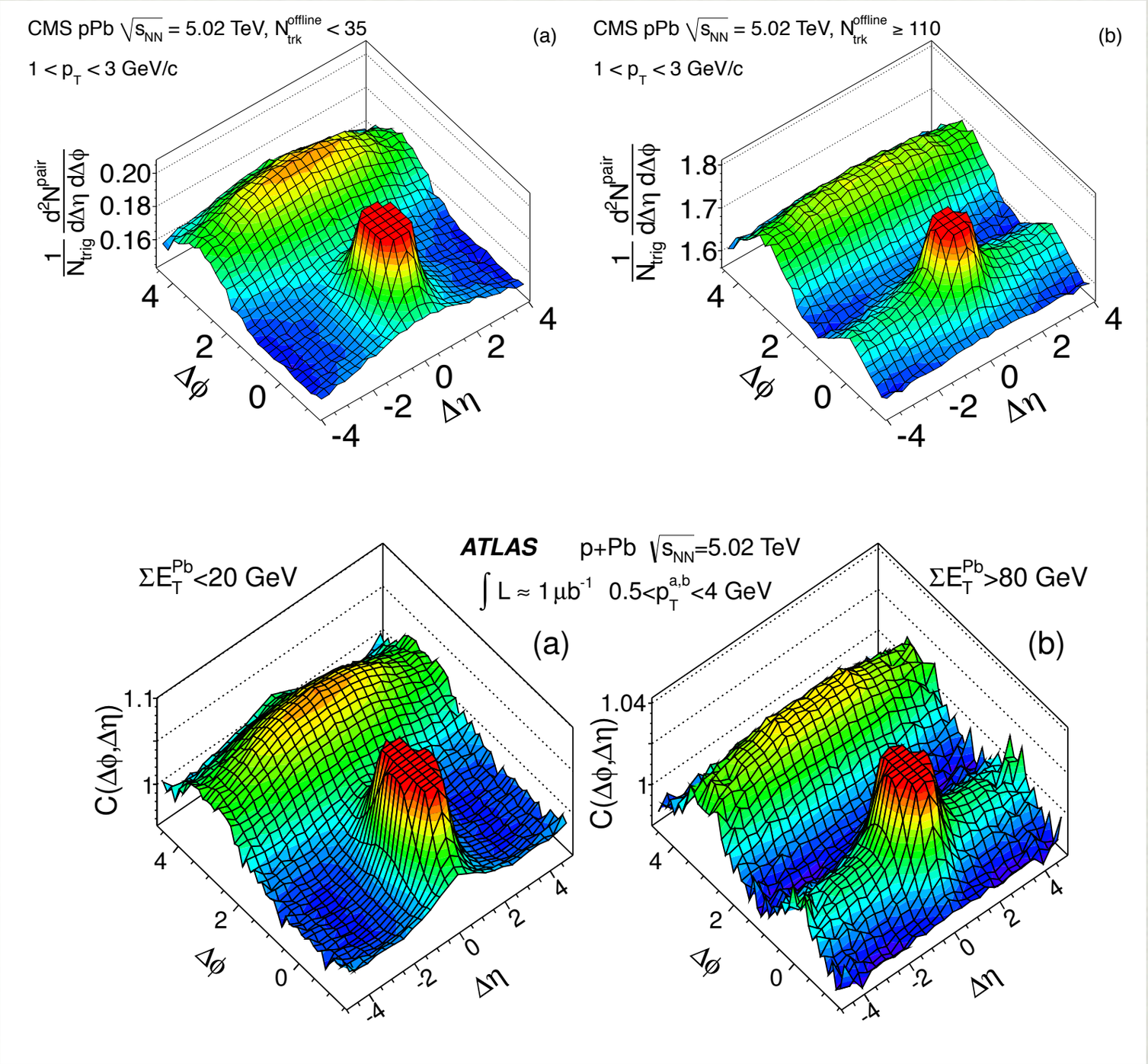

ATLAS

VERY SIMILAR OBSERVATION!

$$C(\Delta\phi, \Delta\eta) = \frac{S(\Delta\phi, \Delta\eta)}{B(\Delta\phi, \Delta\eta)}$$

(SUMMED OVER MULTIPLICITY CLASS)

PERI. CENT.

A TWIN?

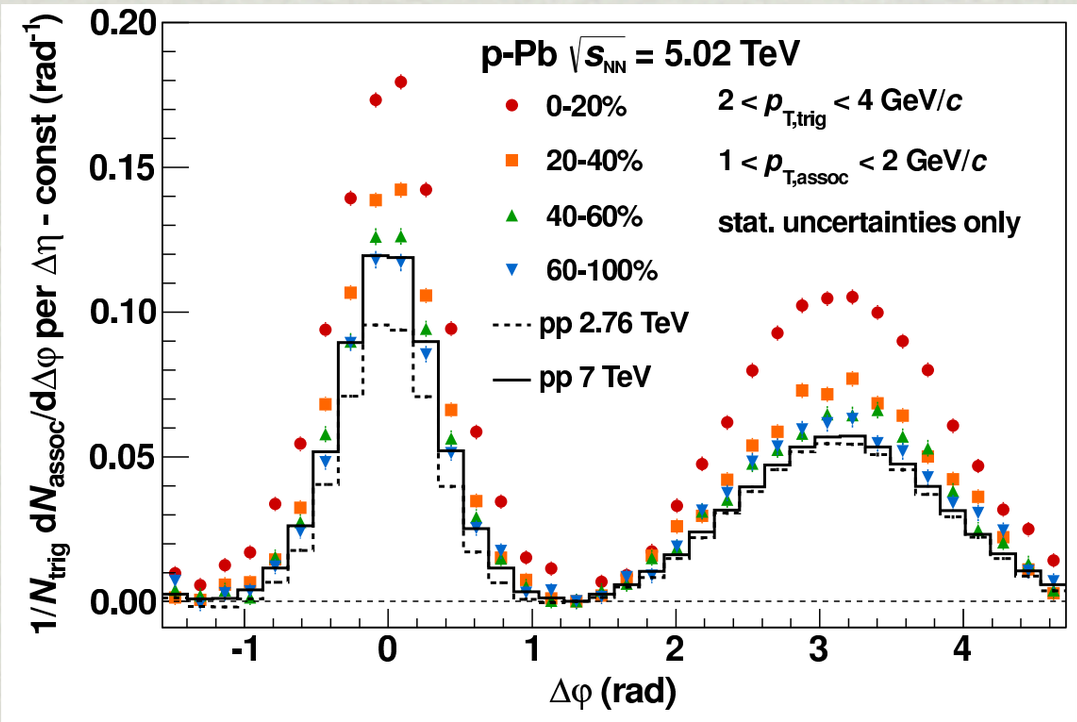

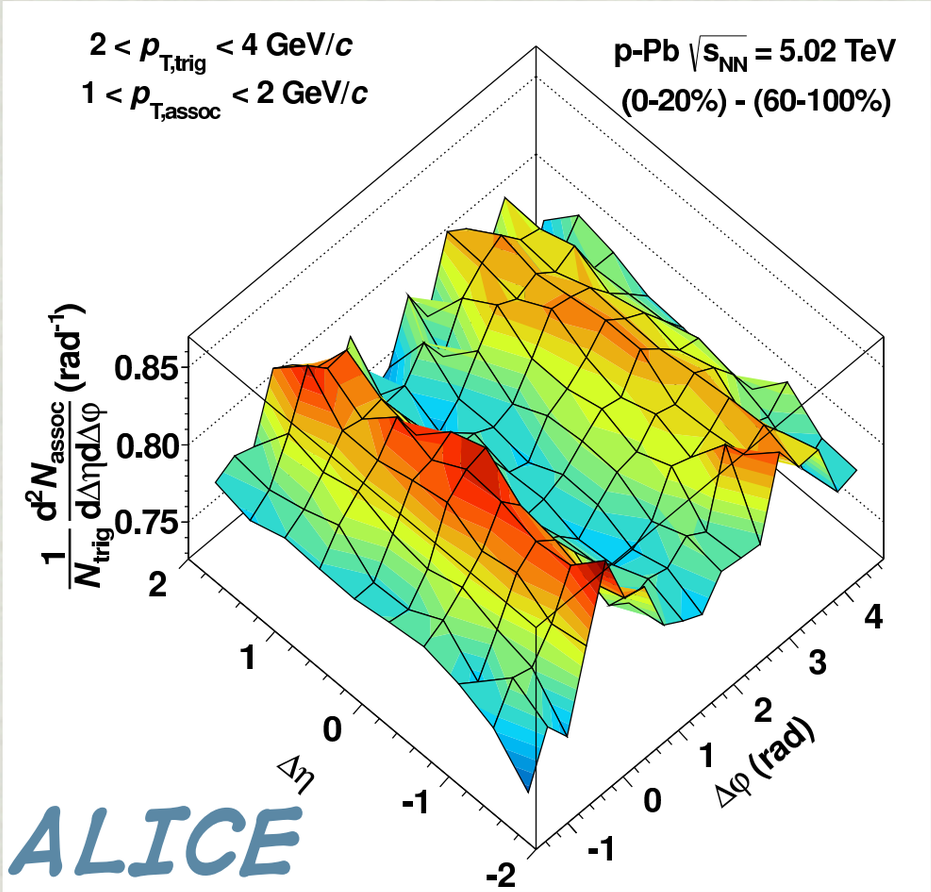

PERIPHERAL P+PB GAVE A SIMILAR YIELD AS SEEN IN PP AT SIMILAR ENERGIES...

USE PERIPHERAL AS A PROXY FOR PP

PERIPHERAL TURNED OUT TO SUBTRACT CLEANLY: LEAVING BEHIND **TWO RIDGES!**

ATLAS RECOIL REMOVAL

ATLAS, arXiv:1212.5198 (2013)

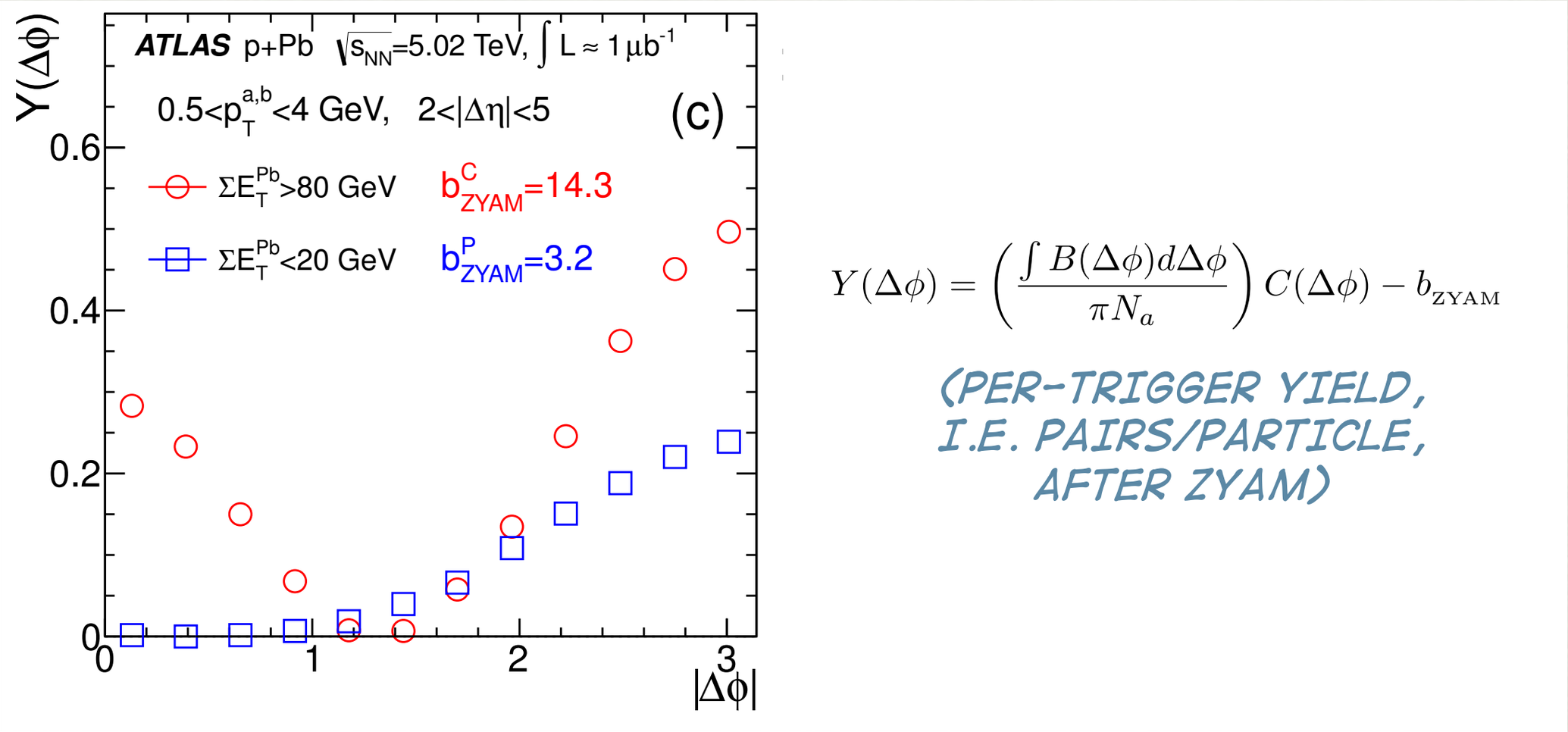

$$Y(\Delta\phi) = \left(\frac{\int B(\Delta\phi)d\Delta\phi}{\pi N_a}\right) C(\Delta\phi) - b_{\mathrm{ZYAM}}$$

(PER-TRIGGER YIELD, I.E. PAIRS/PARTICLE, AFTER ZYAM)

COMPARING Y(Δφ) IN CENTRAL TO PERIPHERAL:
OBSERVED THE DIFFERENCE IN YIELDS
TO BE ~**CONSTANT VS. CENTRALITY!**
STRAIGHTFORWARD INTERPRETATION AS "**RECOIL**"

ATLAS RECOIL REMOVAL

ATLAS, arXiv:1212.5198 (2013)

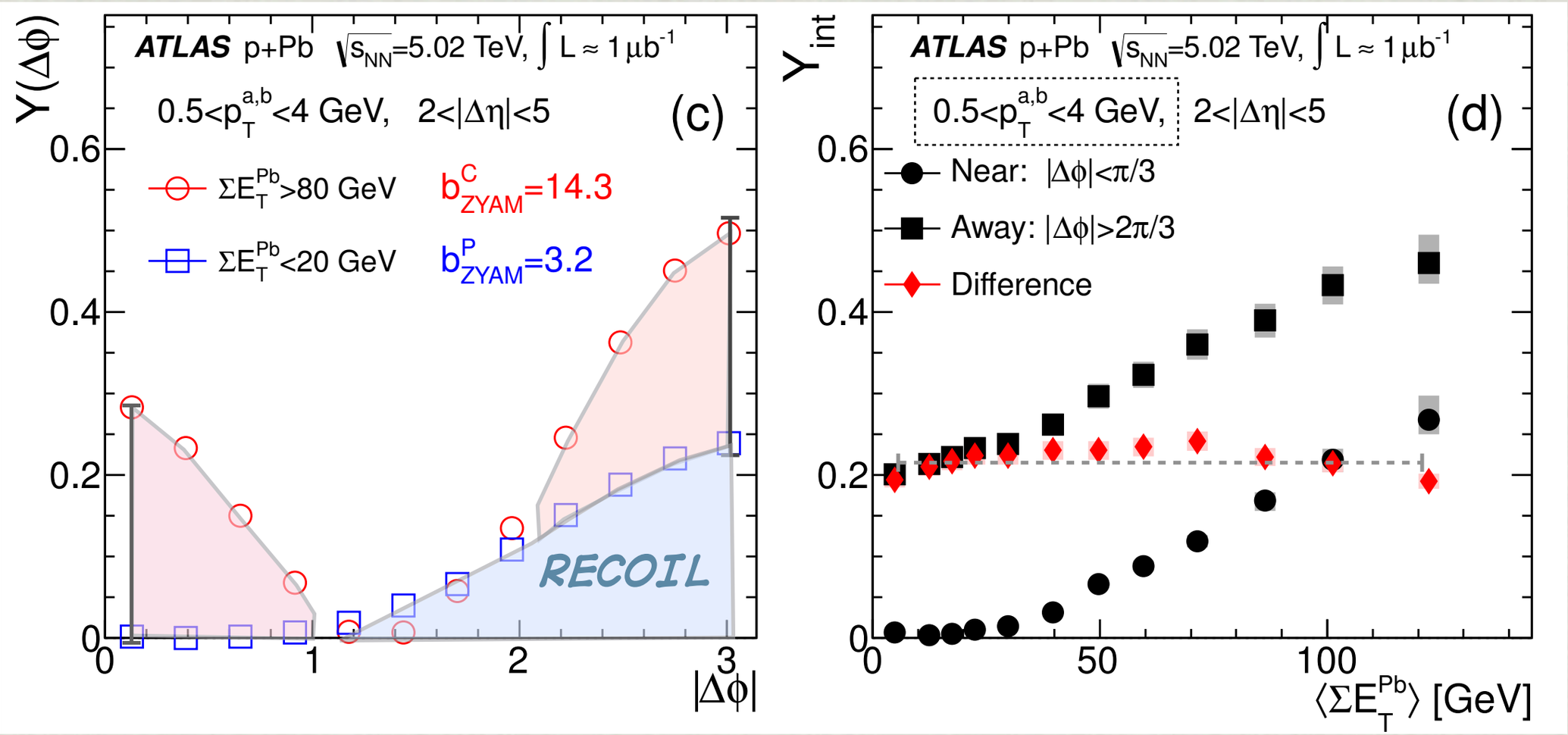

COMPARING Y(Δφ) IN CENTRAL TO PERIPHERAL:
OBSERVED THE DIFFERENCE IN YIELDS
TO BE ~**CONSTANT VS. CENTRALITY!**
STRAIGHTFORWARD INTERPRETATION AS "**RECOIL**"

AN IDENTICAL TWIN? (ALICE)

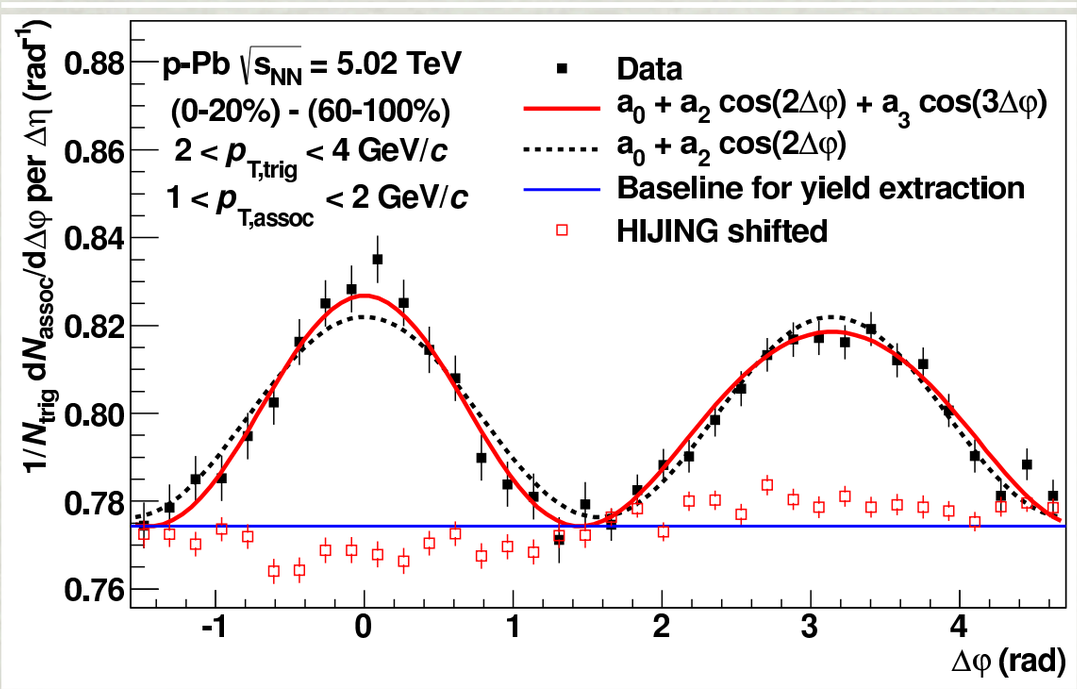

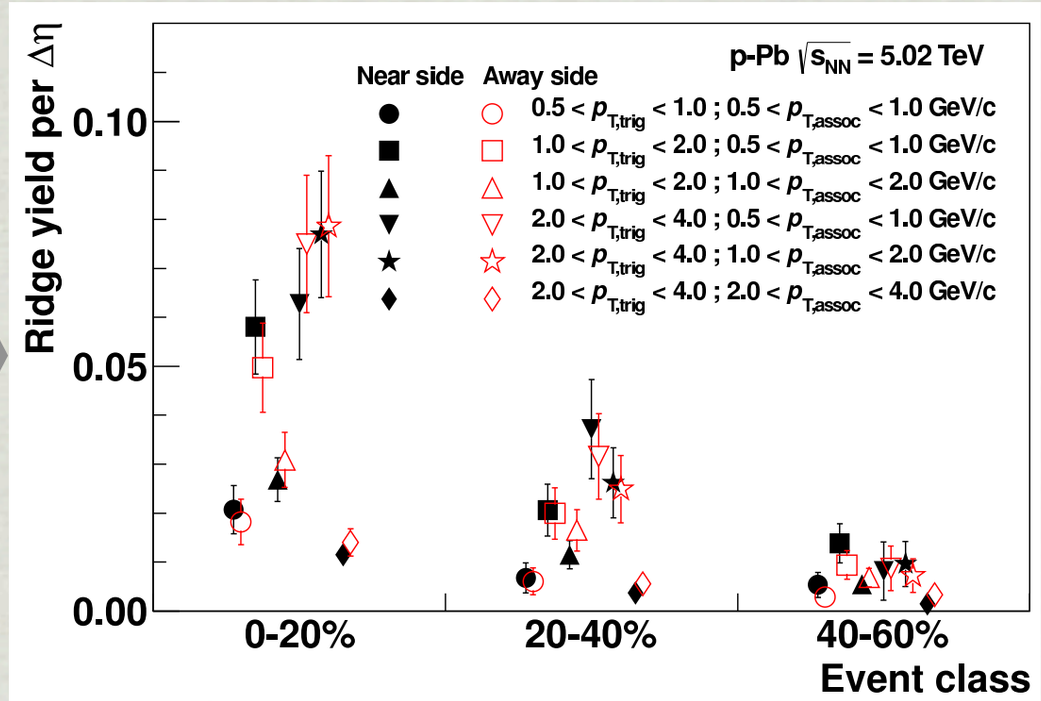

NEAR AND AWAY-SIDE RESPOND **IDENTICALLY** TO P_T SELECTIONS

AN IDENTICAL TWIN? (ATLAS)

NEAR AWAY

ATLAS, arXiv:1212.5198 (2013)

CENTRAL & PERIPH.

SUBTRACTED

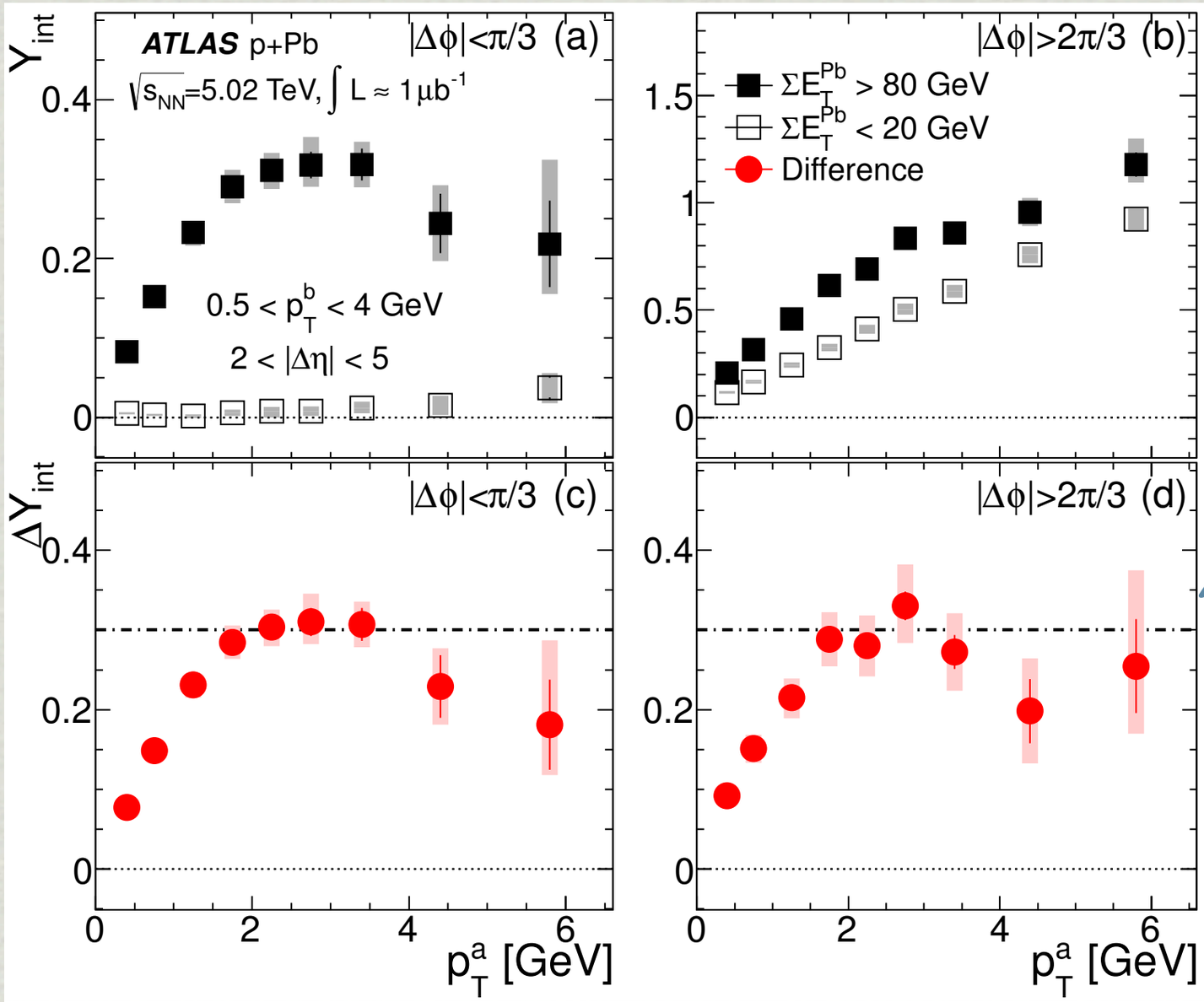

ATLAS RIDGE & ITS TWIN ARE **IDENTICAL!**

"THE RIDGE" ITS TWIN

FLOW IN P+PB? (ALICE)

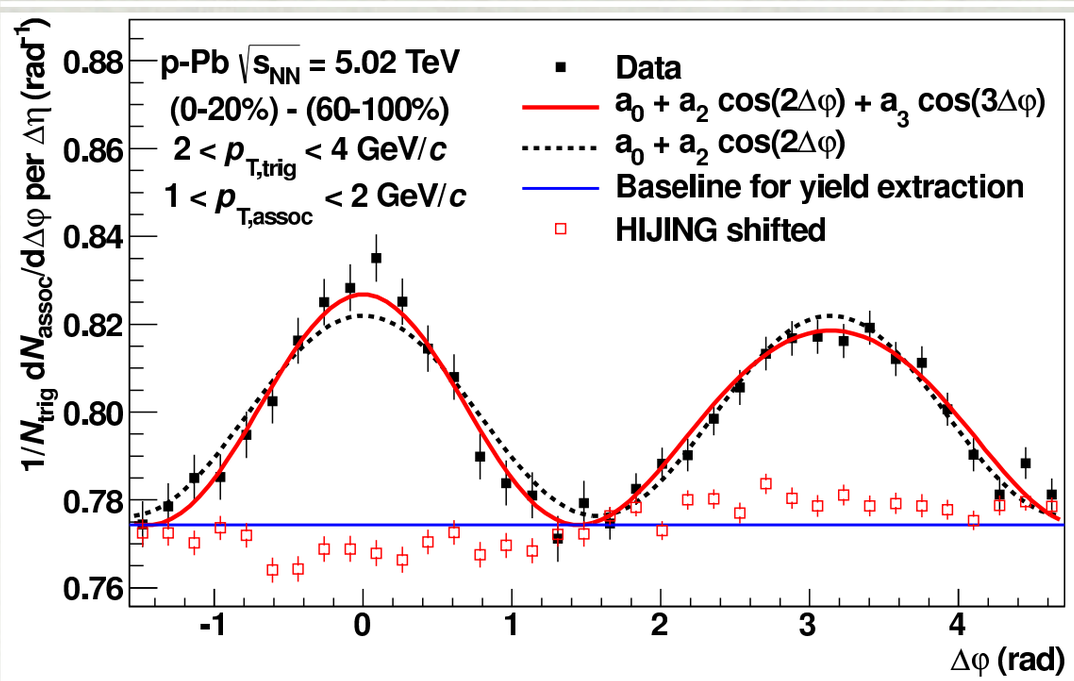

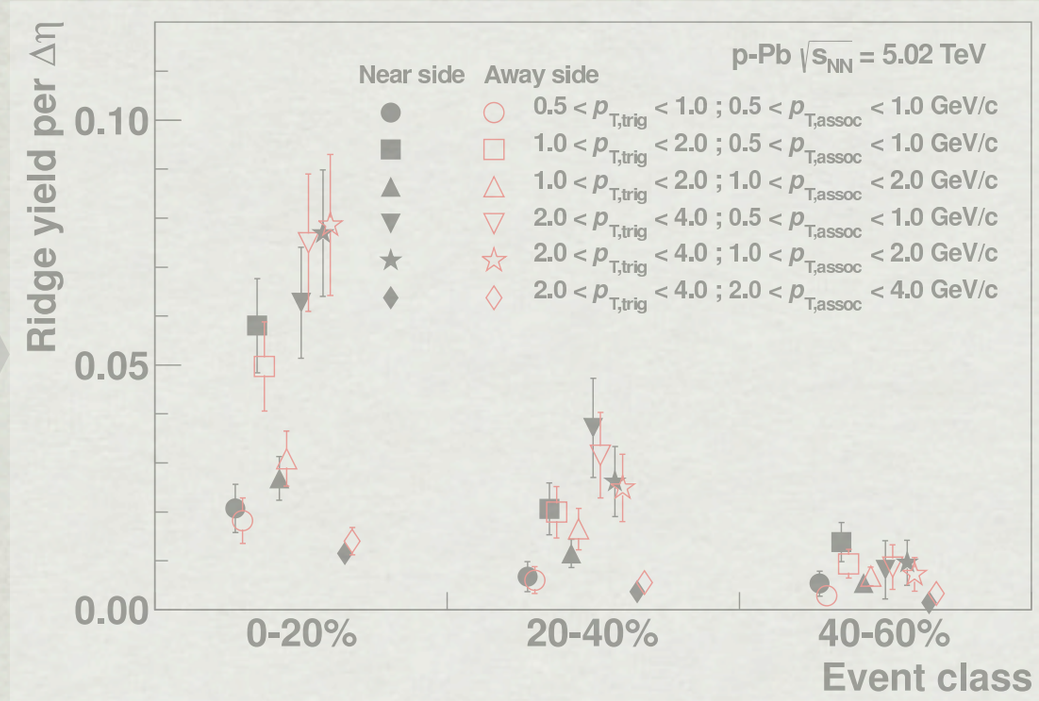

AFTER SUBTRACTION FOURIER COEFFS. DETERMINED BY FITS, IMPROVED BY A_3. V_2,V_3 EXTRACTED ASSUMING FACTORIZATION

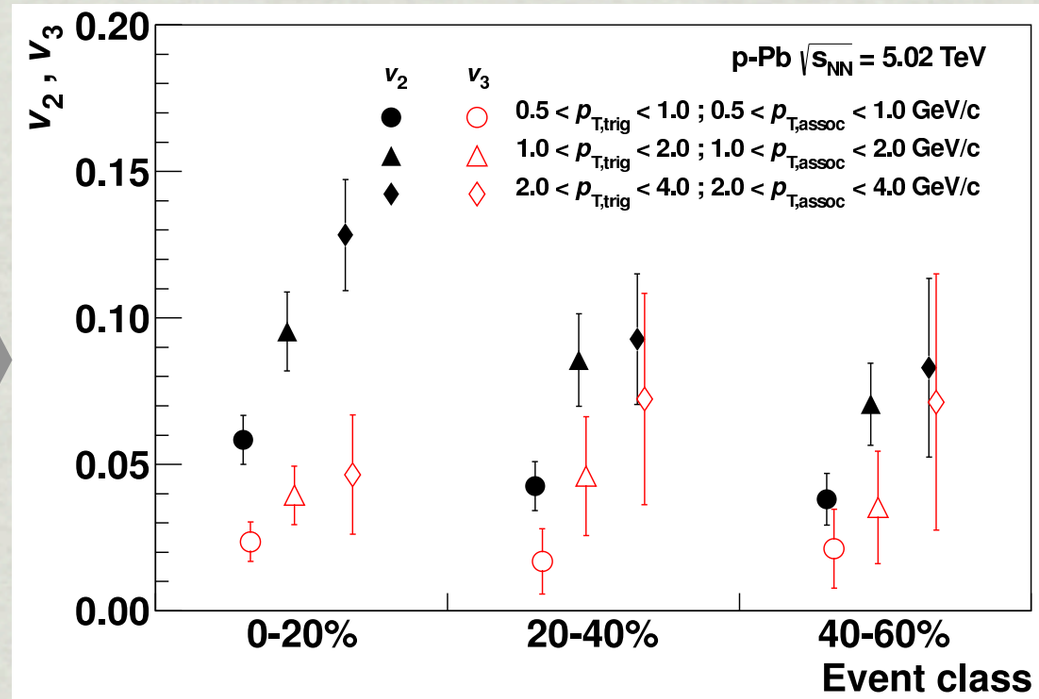

SIGNIFICANT V_2 AND V_3 CONTRIBUTIONS!

HOLY SNEAKY SINUSOIDS!

FOR NEAR-INCLUSIVE ASSOCIATED PARTICLES (0.5-4 GEV), **SINUSOID DOMINATES** AFTER RECOIL SUBTRACTION FOR ALL P_T INTERVALS

SHOWN ARE:

$$a_0 + 2a_2 \cos 2\Delta\phi$$ (SOLID)

$$a_0 + 2a_2 \cos 2\Delta\phi + 2a_3 \cos 3\Delta\phi$$ (DOTTED)

FOURIER COEFFS. CALCULATED USING DFT:

$$a_n = \langle \Delta Y(\Delta\phi) \cos n\Delta\phi \rangle$$

P_T(ASSOC) = 0.5-4 GEV

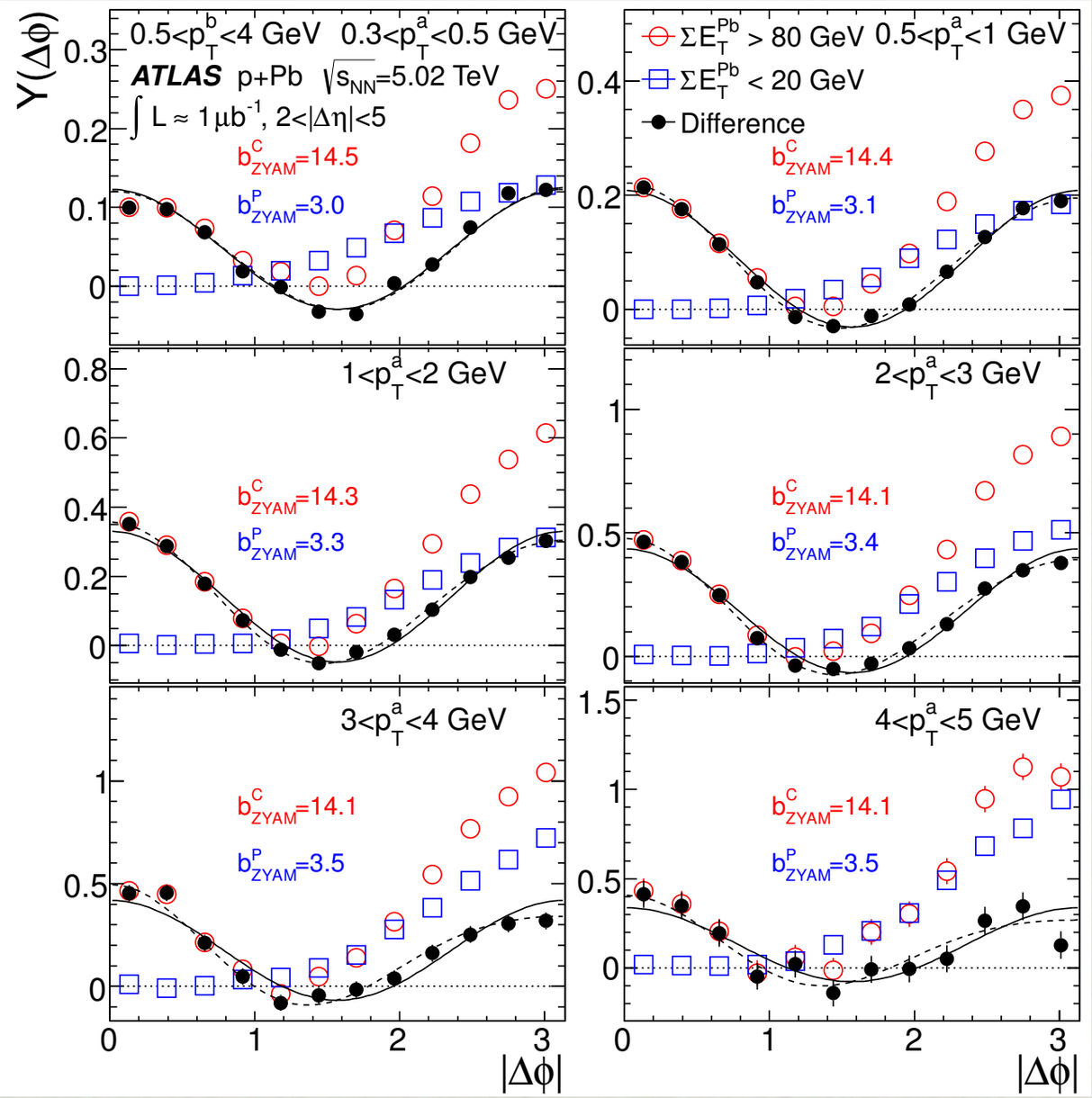

ATLAS, arXiv:1212.5198 (2013)

FLOW IN P+PB? (ATLAS)

ATLAS, arXiv:1212.5198 (2013), accepted to PRL with new data!

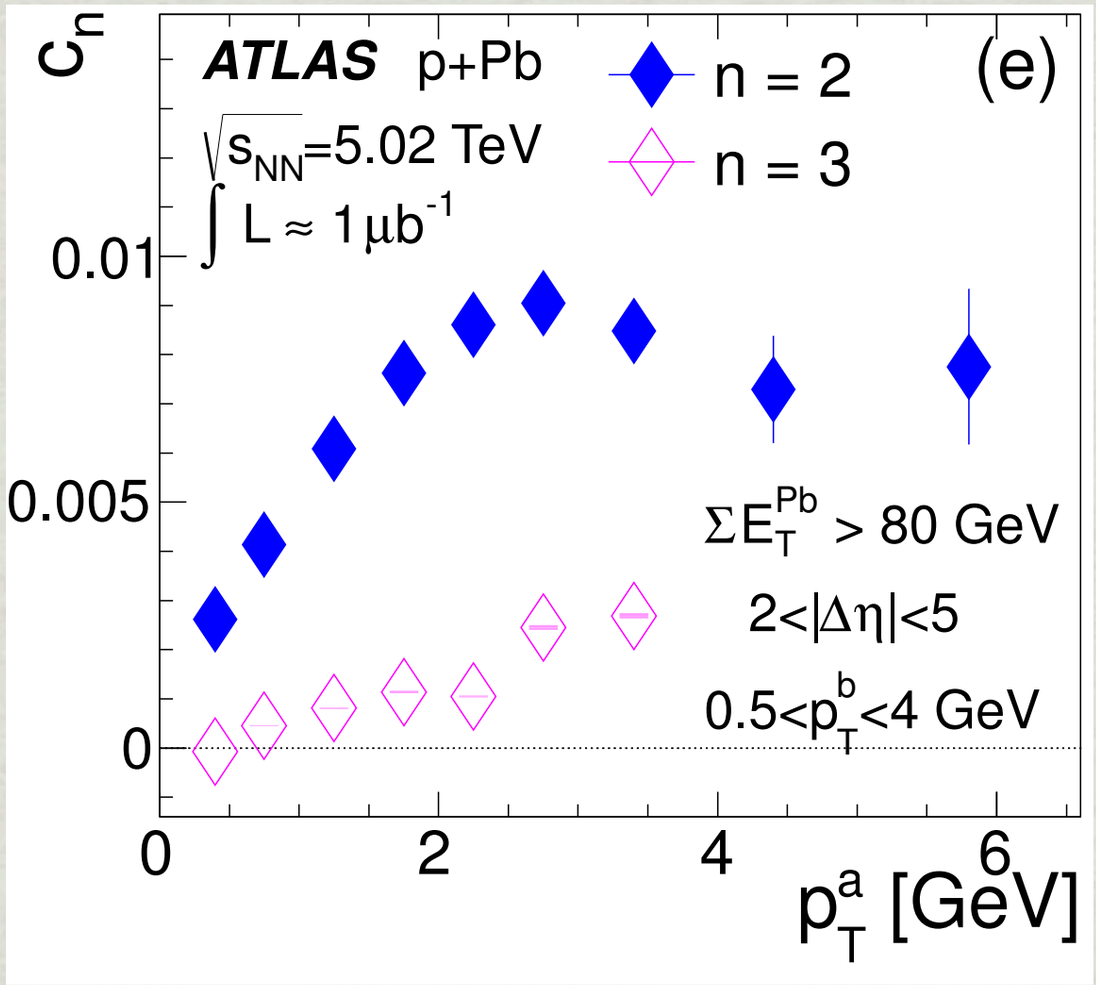

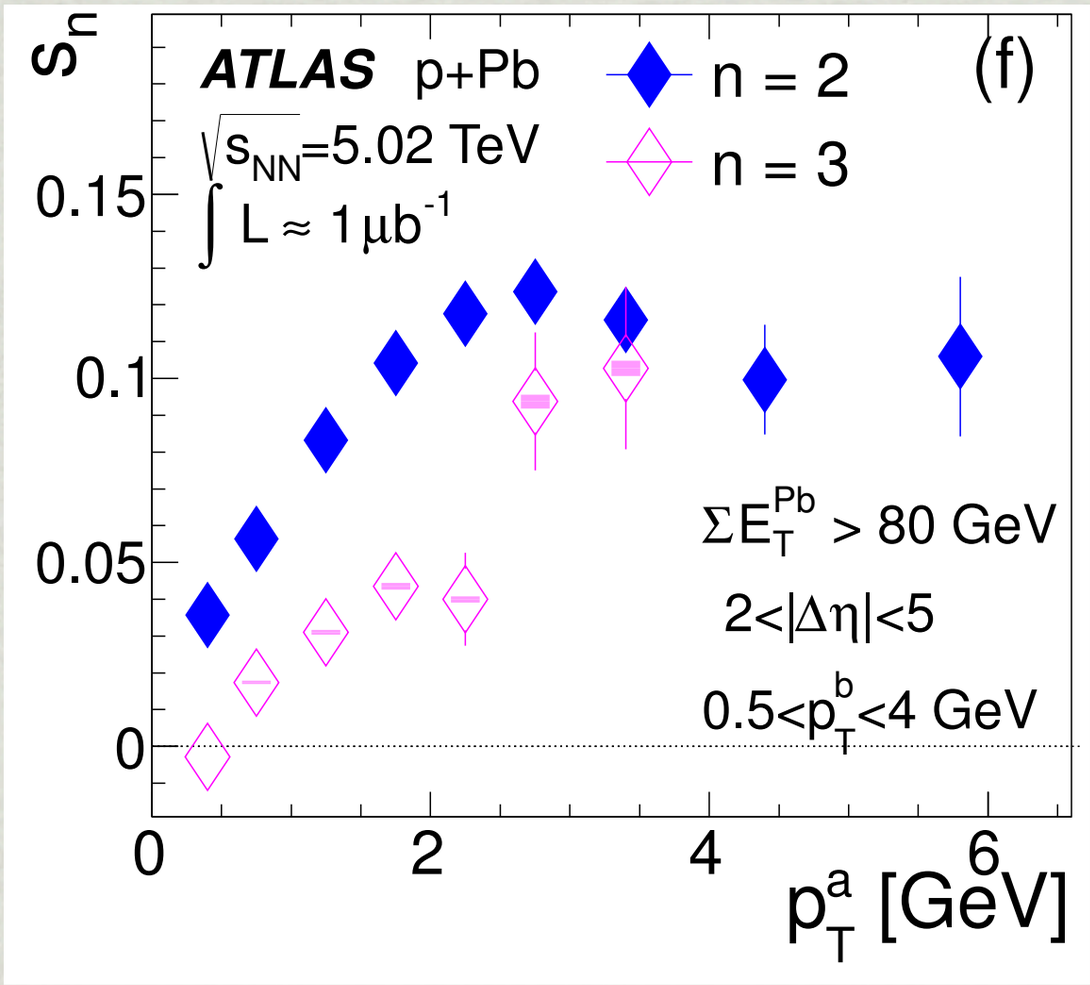

IF MODULATION OF 2PC **FACTORIZES** INTO CONVOLUTION OF **SINGLE-PARTICLE SINUSOIDS**, CAN EXPRESS MODULATION IN TERMS OF "S_N" (SAME PROCEDURE USED IN HI TO EXTRACT V_N): ...**ATLAS** EXTRACTS SIGNIFICANT S_2 **AND** S_3!

AT THE LHC, THE RIDGE IS NOT ALONE!

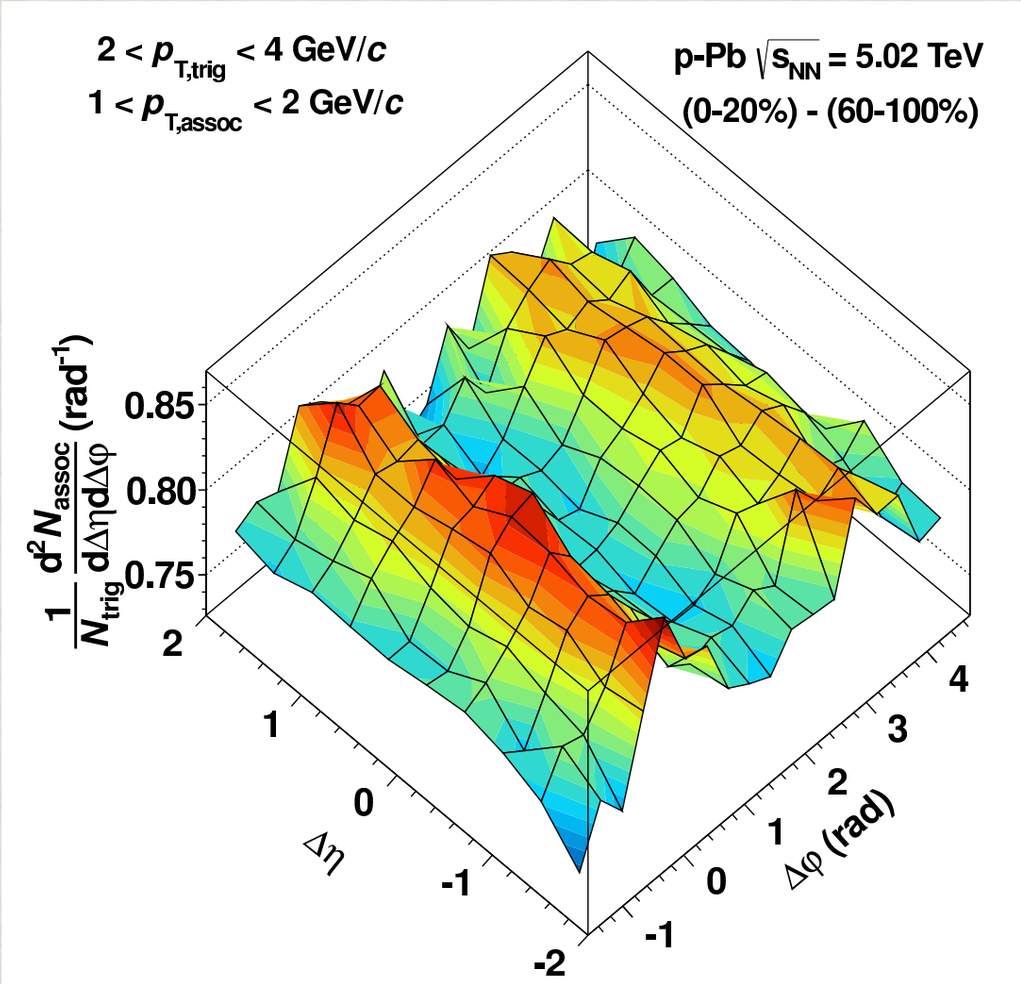

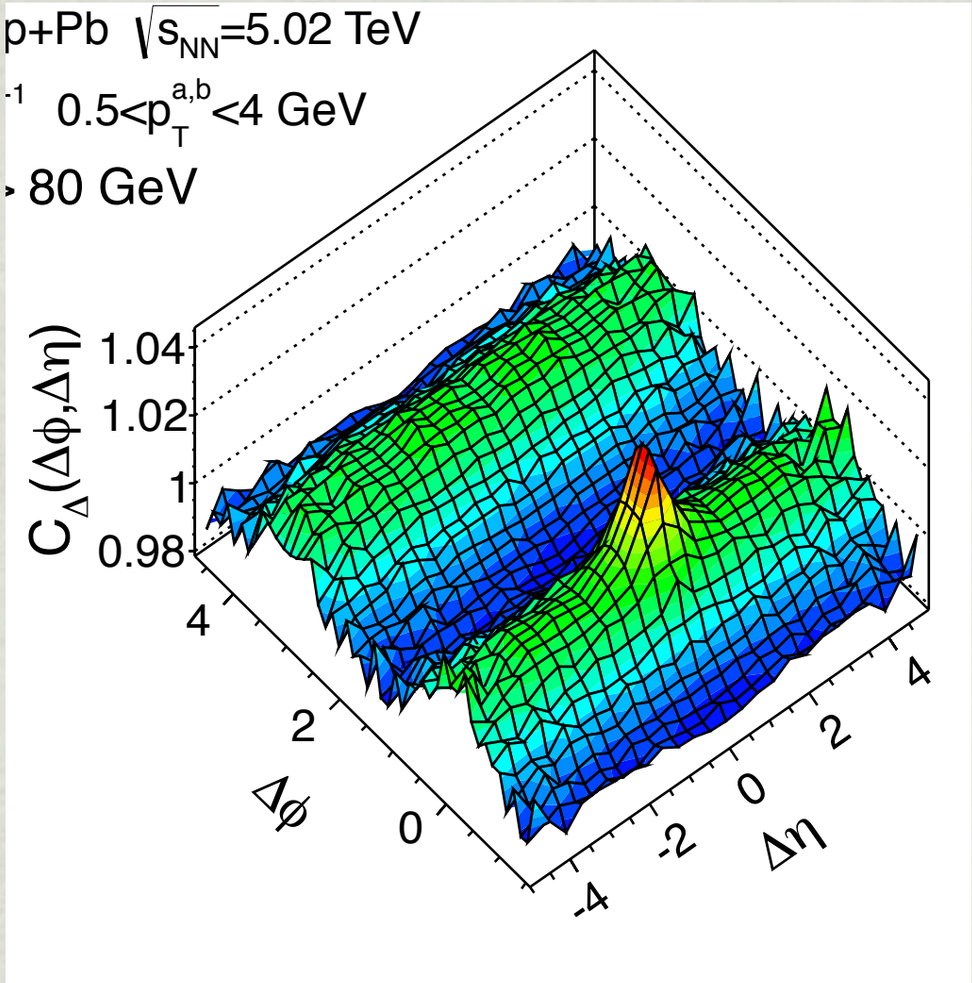

AND SOON AFTER, ACROSS THE ATLANTIC (& NEXT TO MY BNL OFFICE)...

AND SOON AFTER, ACROSS THE ATLANTIC (& NEXT TO MY BNL OFFICE)...

LO AND BEHOLD...

Quadrupole anisotropy in dihadron azimuthal correlations in central d+Au collisions at $\sqrt{s_{NN}}$=200 GeV

A. Adare,[13] C. Aidala,[41,42] N.N. Ajitanand,[58] Y. Akiba,[54,55] H. Al-Bataineh,[48] J. Alexander,[58] A. Angerami,[14] K. Aoki,[33,54] N. Apadula,[59] Y. Aramaki,[12,54] E.T. Atomssa,[34] R. Averbeck,[59] T.C. Awes,[50] B. Azmoun,[7] V. Babintsev,[23] M. Bai,[6] G. Baksay,[19] L. Baksay,[19] K.N. Barish,[8] B. Bassalleck,[47] A.T. Basye,[1] S. Bathe,[5,8,55] V. Baublis,[53] C. Baumann,[43] A. Bazilevsky,[7] S. Belikov,[7,*] R. Belmont,[63] R. Bennett,[59] J.H. Bhom,[67] D.S. Blau,[32] J.S. Bok,[67] K. Boyle,[59] M.L. Brooks,[37] H. Buesching,[7] V. Bumazhnov,[23] G. Bunce,[7,55] S. Butsyk,[37] S. Campbell,[59] A. Caringi,[44] C.-H. Chen,[59] C.Y. Chi,[14] M. Chiu,[7] I.J. Choi,[67] J.B. Choi,[10] R.K. Choudhury,[4] P. Christiansen,[39] T. Chujo,[62] P. Chung,[58] O. Chvala,[8] V. Cianciolo,[50] Z. Citron,[59] B.A. Cole,[14] Z. Conesa del Valle,[34] M. Connors,[59] M. Csanád,[17] T. Csörgő,[66] T. Dahms,[59] S. Dairaku,[33,54] I. Danchev,[63] K. Das,[20] A. Datta,[41] G. David,[7] M.K. Dayananda,[21] A. Denisov,[23] A. Deshpande,[55,59] E.J. Desmond,[7] K.V. Dharmawardane,[48] O. Dietzsch,[57] A. Dion,[27] M. Donadelli,[57] O. Drapier,[34] A. Drees,[59] K.A. Drees,[6] J.M. Durham,[59] A. Durum,[23] D. Dutta,[4] L. D'Orazio,[40] S. Edwards,[20] Y.V. Efremenko,[50] F. Ellinghaus,[13] T. Engelmore,[14] A. Enokizono,[50] H. En'yo,[54,55] S. Esumi,[62] B. Fadem,[44] D.E. Fields,[47] M. Finger,[9] M. Finger, Jr.,[9] F. Fleuret,[34] S.L. Fokin,[32] Z. Fraenkel,[65,*] J.E. Frantz,[49,59] A. Franz,[7] A.D. Frawley,[20] K. Fujiwara,[54] Y. Fukao,[54] T. Fusayasu,[46] I. Garishvili,[60] A. Glenn,[36] H. Gong,[59] M. Gonin,[34] Y. Goto,[54,55] R. Granier de Cassagnac,[34] N. Grau,[2,14] S.V. Greene,[63] G. Grim,[37] M. Grosse Perdekamp,[24] T. Gunji,[12] H.-Å. Gustafsson,[39,*] J.S. Haggerty,[7] K.I. Hahn,[18] H. Hamagaki,[12] J. Hamblen,[60] R. Han,[52] J. Hanks,[14] E. Haslum,[39] R. Hayano,[12] X. He,[21] M. Heffner,[36] T.K. Hemmick,[59] T. Hester,[8] J.C. Hill,[27] M. Hohlmann,[19] W. Holzmann,[14] K. Homma,[22] B. Hong,[31] T. Horaguchi,[22] D. Hornback,[60]

• • •

PROJECT

QUADRUPOLES IN D+AU

PHENIX COLLABORATION

DATE MARCH 7, 2013

CLIENT HEAVY ION COMMUNITY

PHENIX D+AU

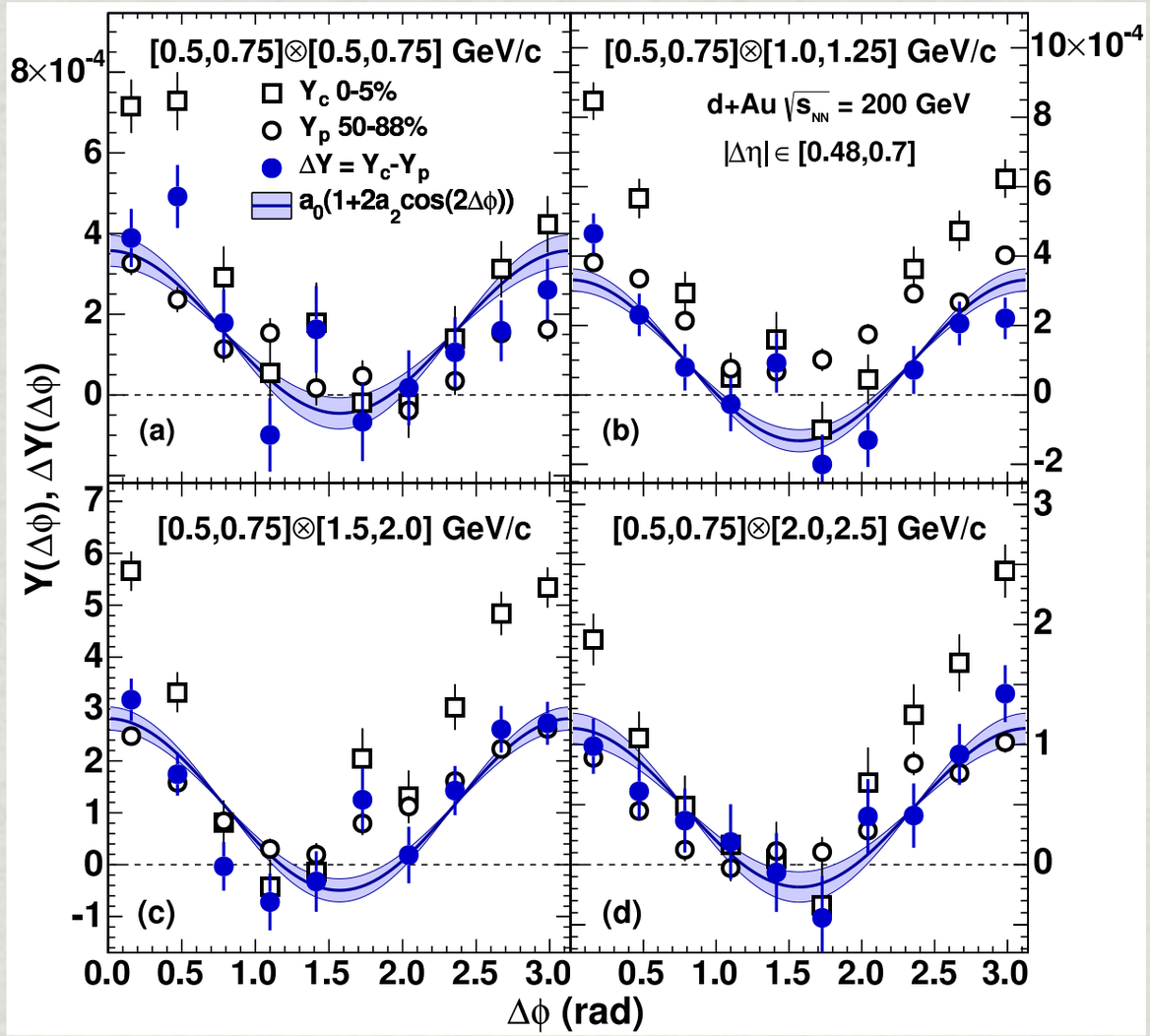

PHENIX, arXiv:1303.1794 (2013)

DESPITE SMALL ETA COVERAGE OF PHENIX,
MADE GOOD USE OF THEIR **1.6 BILLION** EVENTS:
CORRELATIONS WITH SOFT PARTICLES (0.5–0.75 GEV)
ALSO EVINCE **QUADRUPOLE MODULATION**

MODULATIONS @ RHIC

PHENIX, arXiv:1303.1794 (2013)

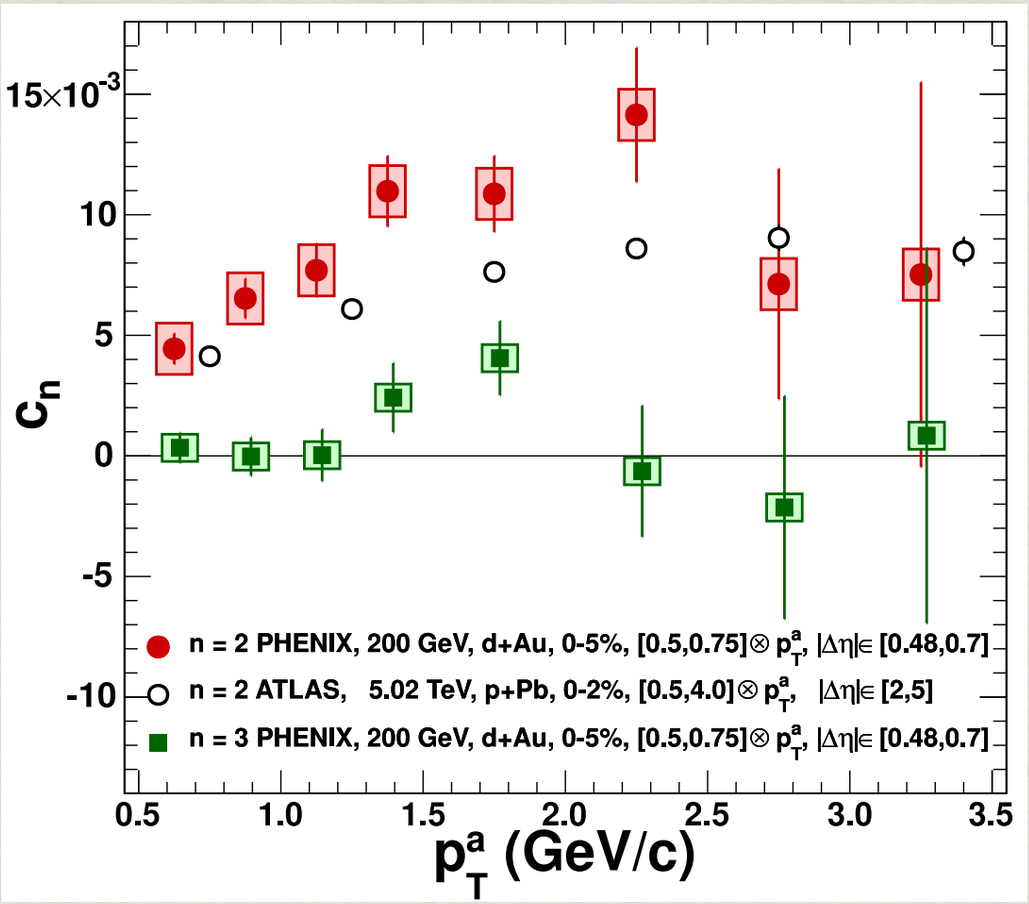

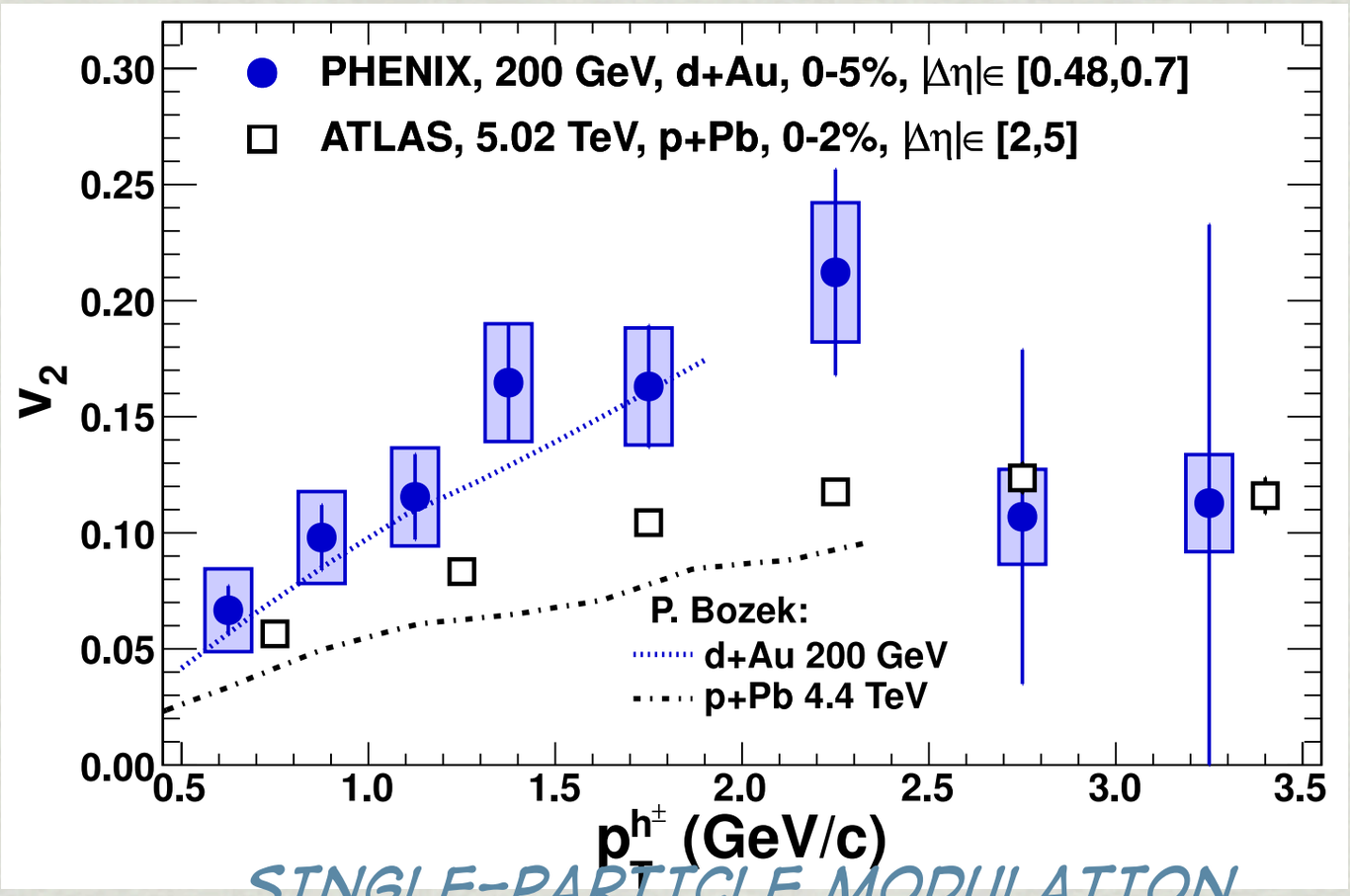

2PC MODULATIONS ARE OF **SIMILAR ORDER** TO THOSE SEEN @LHC

(QUANTITATIVE COMPARISON IS **NOT POSSIBLE** GIVEN DIFFERENT P_T AND ΔETA CUTS)

SINGLE-PARTICLE MODULATION CAN BE DIRECTLY COMPARED, AND **D+AU@RHIC** IS FOUND TO HAVE **LARGER V_2** THAN **P+PB@LHC!...**

REASONABLE AGREEMENT W/ HYDRO PREDICTIONS (N.B. LHC PREDICTIONS AT WRONG ENERGY!)

HYDRO SCALING OF P/D+A?

PHENIX, arXiv:1303.1794 (2013)

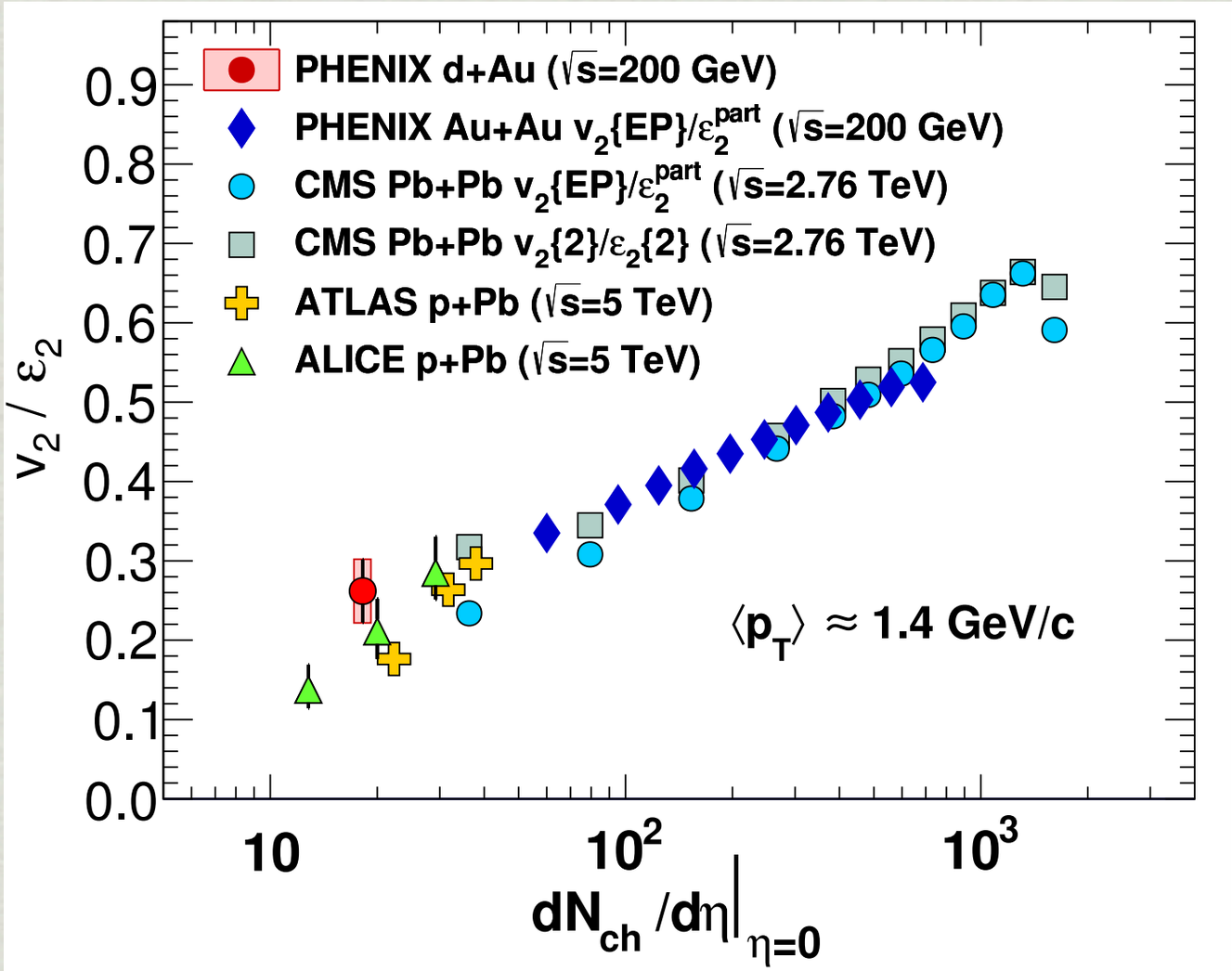

SIMILAR, BUT **NOT IDENTICAL** TO OLDER VERSION (LEAVES OUT TRANSVERSE AREA).
DESPITE USE OF HIJING MULTIPLICITIES AND ECCENTRICITIES NOT PROVIDED BY THE EXPERIMENTS, DO **P/D+A DATA SCALE** TO THE O(50%) LEVEL?

BUT WAIT,
THERE'S MORE!

FOR NO ADDITIONAL RUNNING, WE CAN ADD TWO MORE PARTICLES!

EUROPEAN ORGANISATION FOR NUCLEAR RESEARCH (CERN)

CERN-PH-EP-2013-029

Submitted to: Physics Letters B

[hep-ex] 8 Mar 2013

Measurement with the ATLAS detector of multi-particle azimuthal correlations in p+Pb collisions at $\sqrt{s_{\mathrm{NN}}} = 5.02$ TeV

The ATLAS Collaboration

PROJECT

4-PARTICLE CORRELATIONS

ATLAS COLLABORATION

DATE MARCH 8, 2013

CLIENT HEAVY ION COMMUNITY

CUMULANTS IN P+PB

IF THE EFFECT IS DUE TO FINAL-STATE DYNAMICS, SHOULD OBSERVE TRUE **MULTIPARTICLE** CORRELATIONS: **CUMULANTS** ARE THE NATURAL WAY TO CHECK

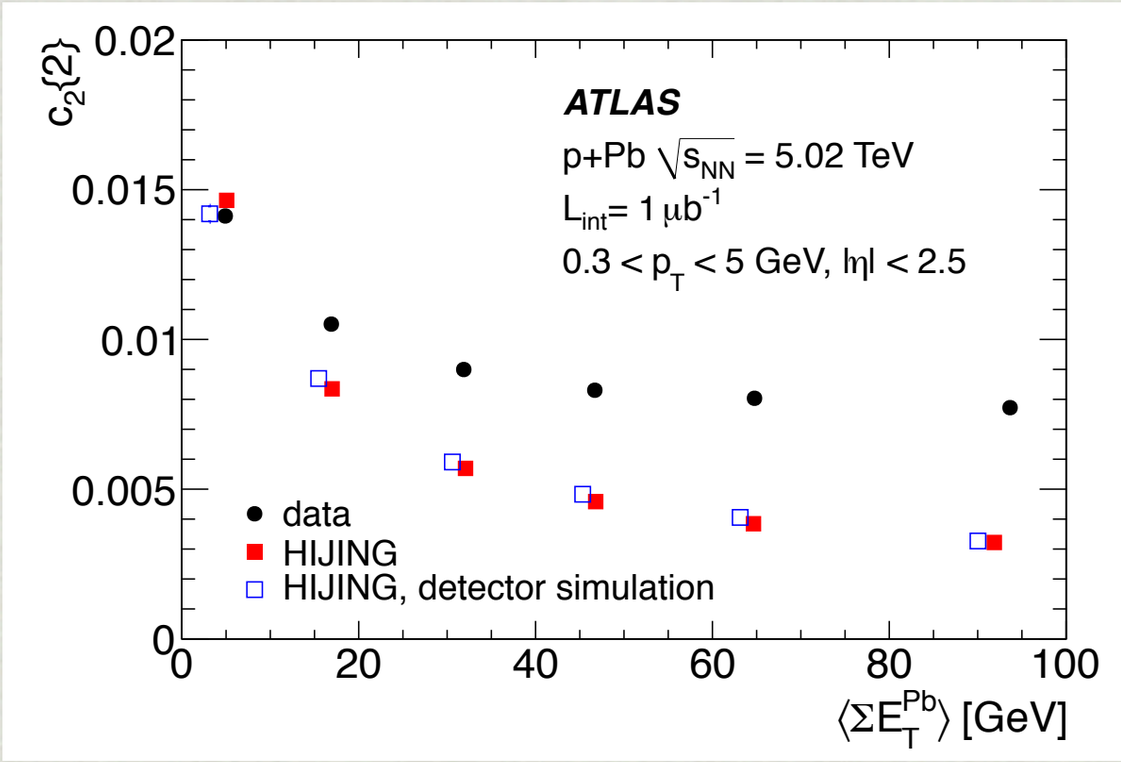

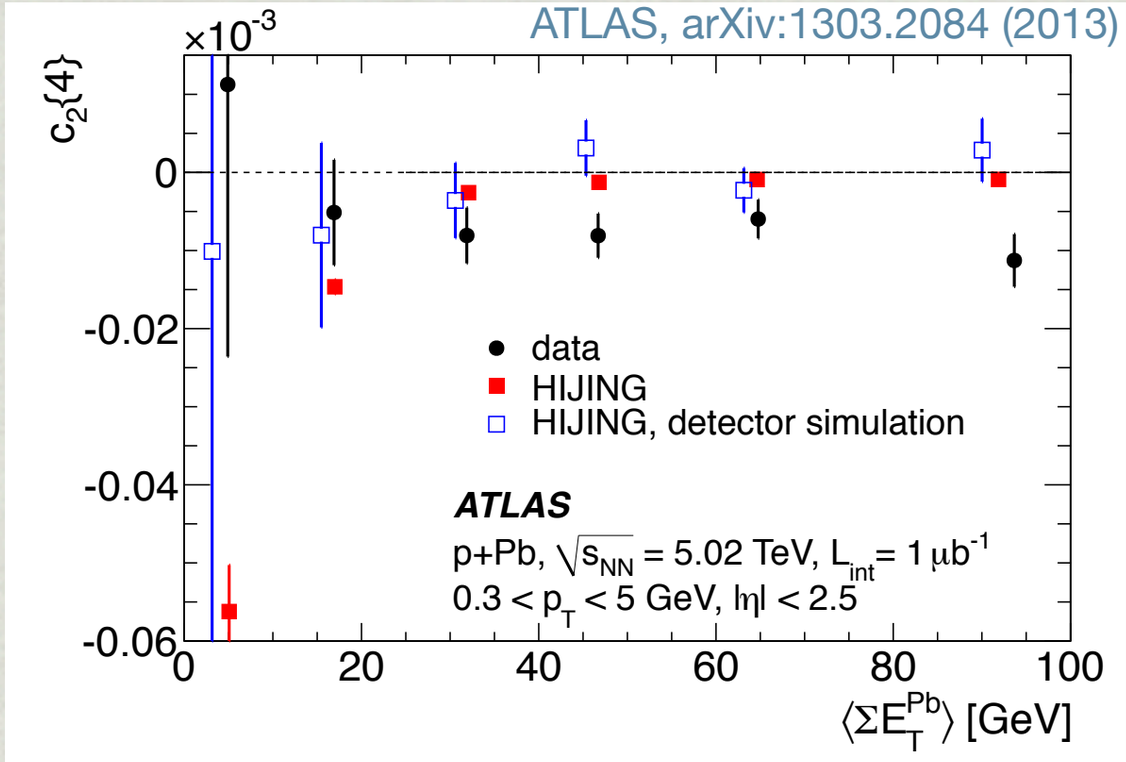

$$corr_n\{2\} = \langle e^{in(\phi_1-\phi_2)} \rangle$$

$$c_n\{2\} = \langle corr_n\{2\} \rangle$$

$$v_2^{\mathrm{ref}}\{2\} = \sqrt{c_2\{2\}}$$

$$corr_n\{4\} = \langle e^{in(\phi_1+\phi_2-\phi_3-\phi_4)} \rangle$$

$$c_n\{4\} = \langle corr_n\{4\} \rangle - 2 \cdot \langle corr_n\{2\} \rangle^2$$

$$v_2^{\mathrm{ref}}\{4\} = \sqrt[4]{-c_2\{4\}}$$

4 PARTICLE CUMULANT IS **NEGATIVE**
(BUT SO IS PERIPHERAL **HIJING**, UNLESS WE USE |ETA|<1)

P_T DEPENDENCE

ATLAS, arXiv:1303.2084 (2013)

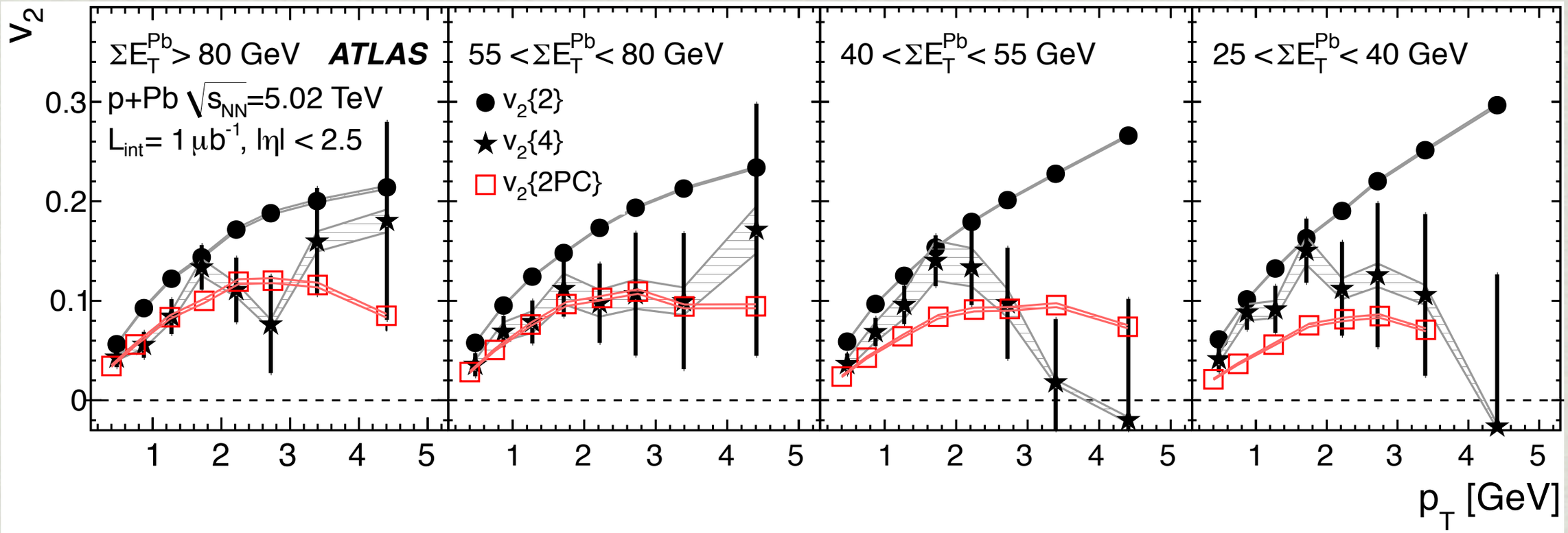

PT DEPENDENCE FROM CUMULANTS SHOWS:

1) CLEAR **DIJET CONTAMINATION** IN 2-PARTICLE

2) SIGNIFICANT 4-P, AND GOOD AGREEMENT OF 4-P WITH **2PC** IN CENTRAL EVENTS

3) SIMILAR PT SHAPE FOR 4-P AS FOUND IN **PB+PB** (EP METHOD)

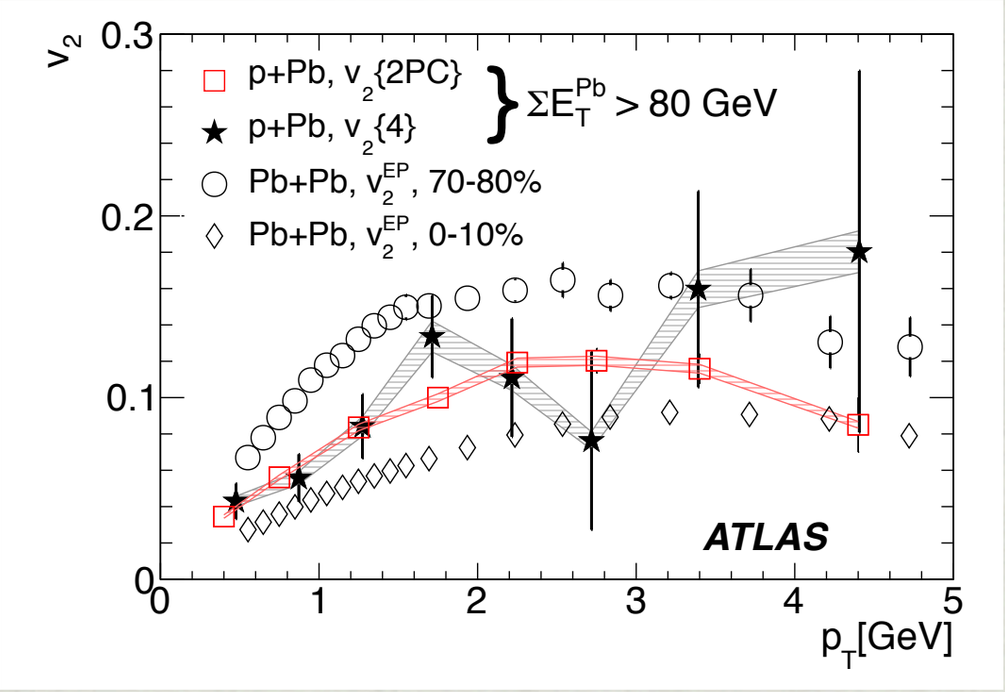

INTEGRATED V_2

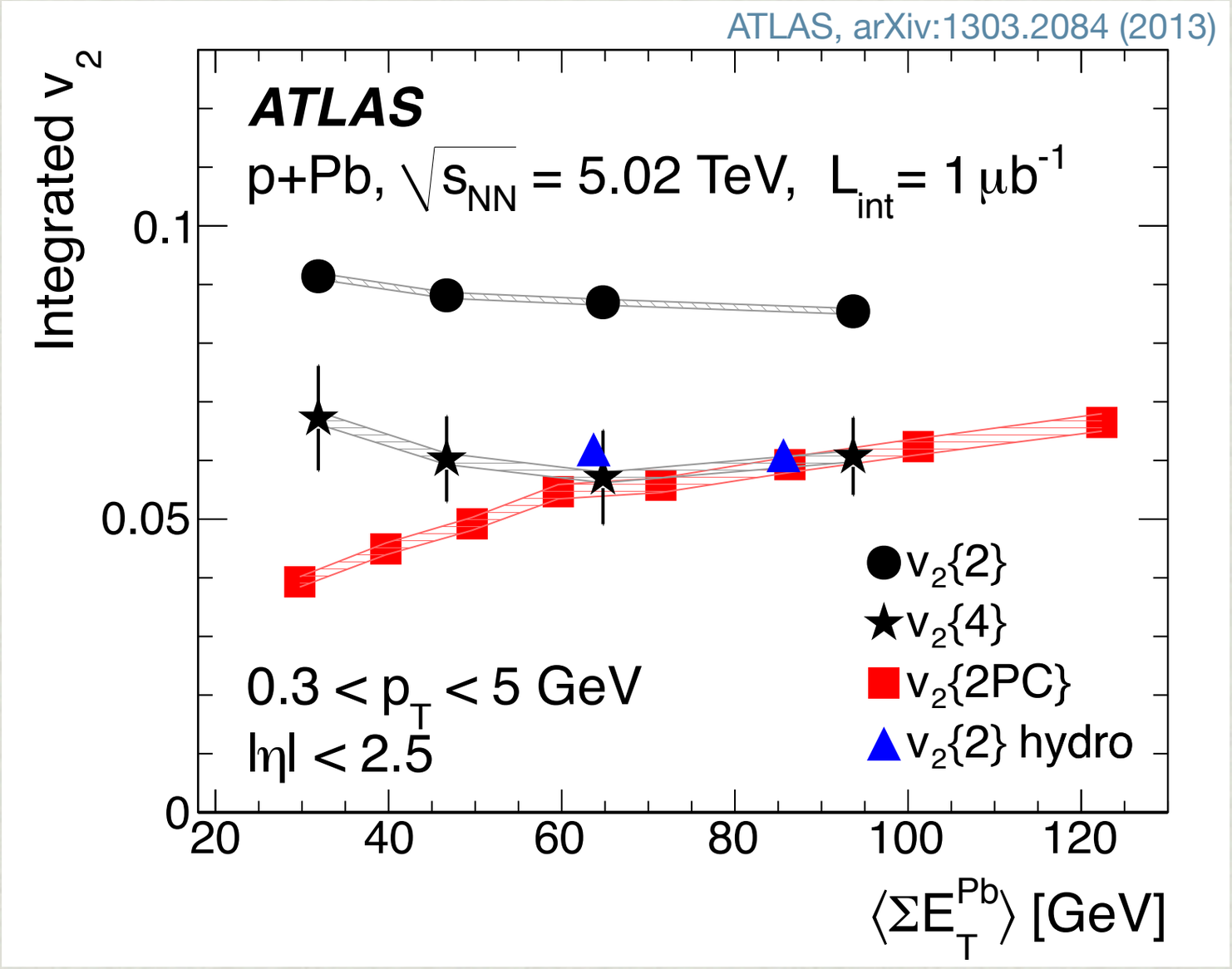

BOZEK ET AL, 5.02 TEV, PRIVATE COMM.

AGREEMENT WITH HYDRO IN MORE CENTRAL EVENTS:
SUPPORT FOR FINAL STATE INTERACTIONS?
SOME ISSUES: 1) HYDRO V2 DECREASES WITH CENTRALITY (DATA INCREASES) 2) SENSITIVITY OF CUMULANTS TO FLUCTUATIONS IN SMALL SYSTEMS

THE STORY SO FAR

* RIDGE DISCOVERED IN AU+AU @ RHIC
  * "EXPLAINED" BY TRIANGULAR FLOW, I.E. FLUCTUATIONS IN THE INITIAL STATE
  * STRONG SUPPORT FROM **LHC PB+PB**
* RIDGE REDISCOVERED IN PP
  * LET A MILLION EXPLANATIONS BLOOM, FROM CGC TO HYDRO
* NEAR-SIDE RIDGE DISCOVERED IN P+PB
  * IDENTICAL AWAY-SIDE RIDGE --> **ONE PHENOMENON!**
    * CGC INTERFERENCE GRAPHS?
    * HYDRODYNAMIC RESPONSE TO FLUCTUATIONS?
* D+AU DATA SHOW THE "DOUBLE RIDGE", I.E. QUADRUPOLE MODULATIONS
  * HYDRO PREDICTIONS, FLOW SCALING
* 4-PARTICLE CUMULANTS TILT TOWARDS HYDRO INTERPRETATION OF THE DATA...FOR NOW

STAY TUNED, FOR THE NEXT EPISODE!

IMPORTANT QUESTIONS!

* P+PB WAS SUPPOSED TO BE ABOUT INITIAL STATE (I.E. CGC) BUT WE HAVE A SURPRISING HINT OF FINAL STATE DYNAMICS (I.E. FLOW)
  * CGC & FLOW BOTH CLAIM TO HAVE **DESCRIPTIVE** AND **PREDICTIVE** POWER
* LIMITS OF HYDRODYNAMICS
  * CAN **THERMALIZATION** BE ACHIEVED FOR SUCH SMALL SPACE/TIME SCALES?
  * ARE **VISCOUS CORRECTIONS** TOO LARGE?
  * WHAT ABOUT **CUMULANTS**?
* SCOPE/PREDICTIVE POWER OF CGC APPROACH
  * IF MODEL IS COMPLETE, THEN **PREDICTIONS** ARE ESSENTIAL
  * WHAT ABOUT **MULTIPARTICLE EFFECTS**? v_3?
* WHAT ABOUT PP?
  * IN LIGHT OF P+PB, P+P RIDGE SUGGESTS THAT WE SHOULD BE THINKING MORE CAREFULLY ABOUT **PP INITIAL STATE**
  * HOW TO HANDLE **GEOMETRY/FLUCTUATIONS** IN **PP**?

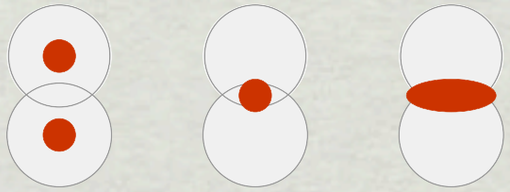

BZDAK, ET AL, STRIKMAN, ...

* EXPLANATION FOR LONG RANGE CORRELATIONS
  * CGC (FLUX TUBES) VS. HYDRO (BUILT IN, BUT 3+1D??)

AVENUES FOR PROGRESS

* EVEN MORE MULTIPARTICLE OBSERVABLES $V_2(6)$, AND HIGHER ORDER MODULATION
* EVEN LONGER RANGE CORRELATIONS
  * PREDICTIONS FOR ETA DEPENDENCE FROM CGC OR HYDRO?
* PARTICLE SPECIES DEPENDENCE (CQ SCALING?)
* A COMPREHENSIVE DESCRIPTION, FROM SMALL TO LARGE SYSTEMS, ESPECIALLY WHERE THEY OVERLAP IN SIZE/DENSITY
* **PREDICTIONS ARE CRUCIAL, SINCE VERY DIFFERENT APPROACHES ARE ABLE TO DESCRIBE THE SAME DATA!**

A PARTING (PERSONAL) QUESTION:
WOULD WE HAVE IMAGINED DISCUSSING 4-PARTICLE CUMULANTS IN P+PB @ LHC?

I DIDN'T, BUT IT'S A VERY EXCITING MOMENT!

"THE BEST LAID SCHEMES OF MICE AND MEN GANG AFT AGLEY..."

("THE BEST LAID PLANS OF MICE AND MEN OFTEN GO ASTRAY")

IT SEEMS THE SAME IS TRUE FOR
MICE (PROTONS), MAMMOTHS (IONS), AND THE RIDGE!

THANKS!!

(SPECIAL THANKS TO J. JIA FOR DISCUSSIONS)

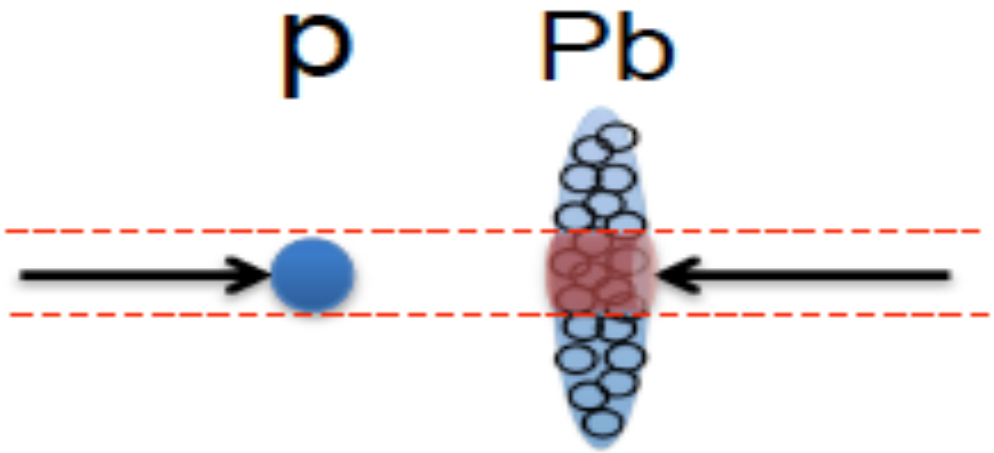

Large ridges in small systems: gluon entanglement in the Glasma

Raju Venugopalan

Brookhaven National Laboratory

RBRC jet quenching workshop, BNL, April 15, 2013

Talk outline

- Multi-particle dynamics in dense-dense systems:
  an ab initio CGC EFT approach

- The ridge in p+p collisions: Glasma + BFKL - QCD contributions

- The ridge in A+A collisions: the dominance of flow
  generated from the Glasma pedestal (IP-Glasma model)

- The ridge in p/d+A: like p+p or A+A ?
  Relative role of Glasma + flow contributions

High multiplicity events:

"dense-dense" hadron-hadron collisions

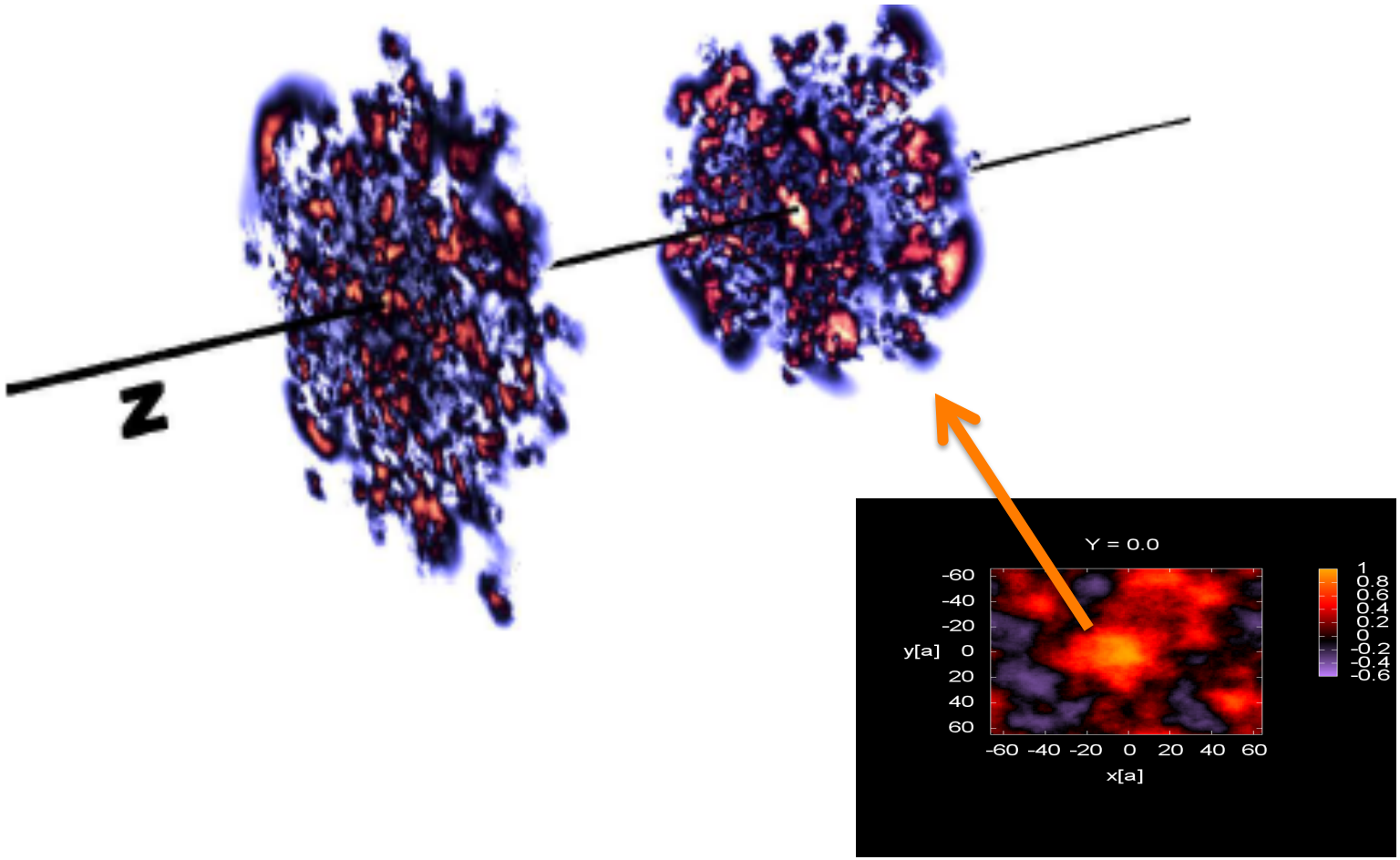

Incoming nuclei are Color Glass Condensates: Highly occupied gluon states with maximal occupancy allowed in QCD

High parton densities: multi-particle production

Counting powers of "effective" color charge density $\rho = g\, n_{occ}$

$k_T \leq Q_S$, $n_{occ} = 1/g^2 \Rightarrow \rho \approx 1/g$

$k_T \gg Q_S$, $n_{occ} = 1 \Rightarrow \rho \approx 1$

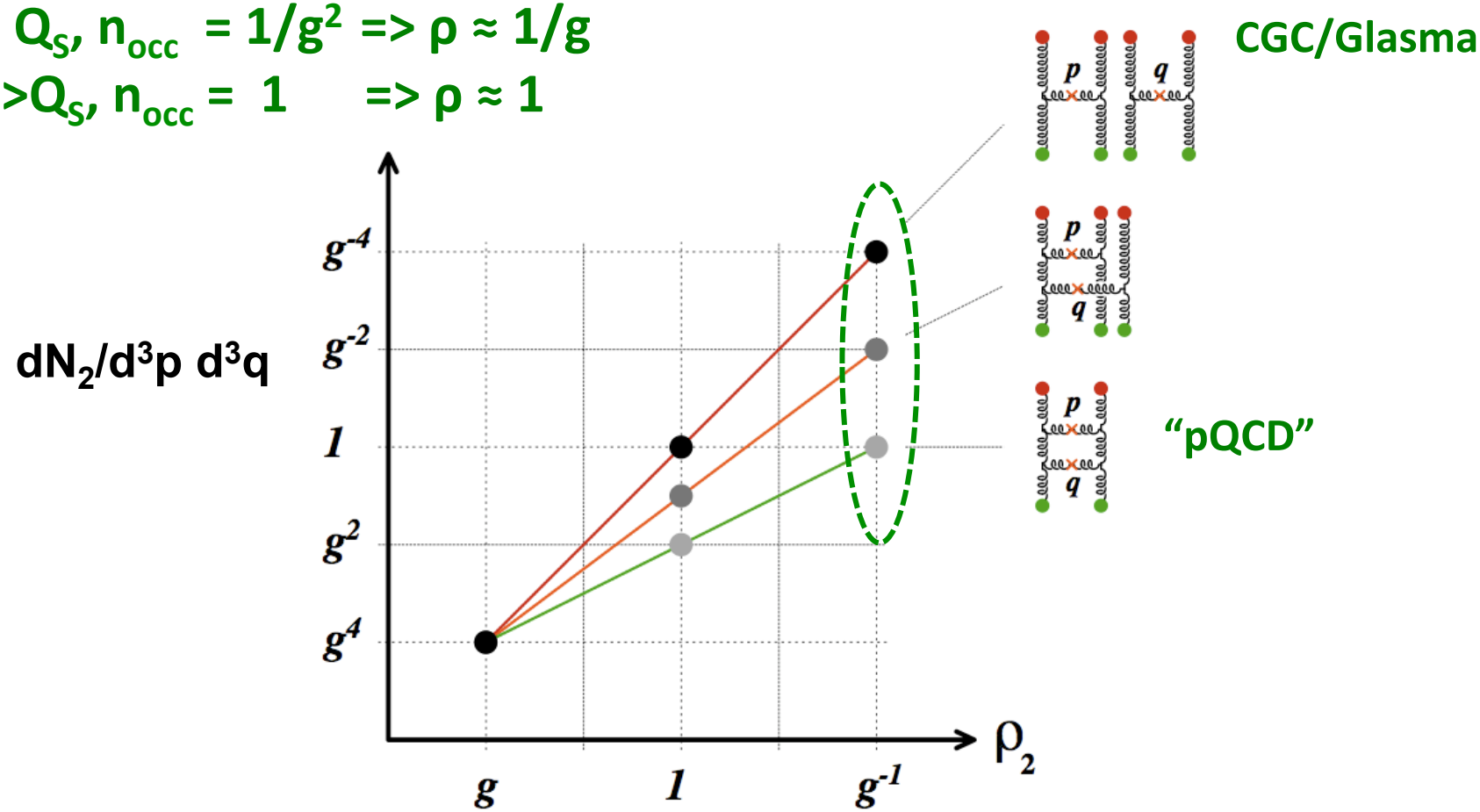

"Dense-dense" limit relevant for high multiplicity events: $\rho_1, \rho_2 \sim 1/g$

High multiplicity events: single inclusive production

Gelis,Lappi,RV
arXiv:0804.2630 [hep-ph];
arXiv:0807.1306 [hep-ph]
arXiv:0810.4829 [hep-ph]

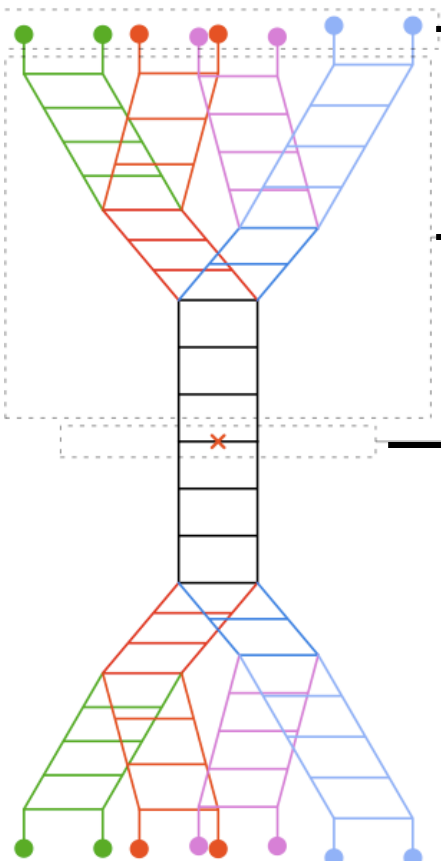

Initial configuration of sources for nucleus 1

BK/JIMWLK evolution for nucleus 1

$$\frac{dN_{\rm LO}}{d^3p}$$

Computed from Yang-Mills **Glasma** gluon fields

Krasnitz, Nara, RV; Lappi

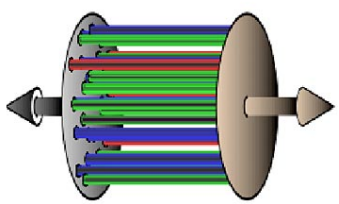

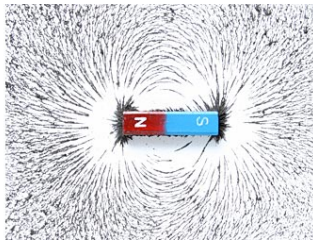

Identical evol. for nucleus 2

- Full JIMWLK+YM evolution feasible Lappi, PLB 703 (2011)209
- In practice: approximations of varying rigor

High multiplicity events: two particle correlations

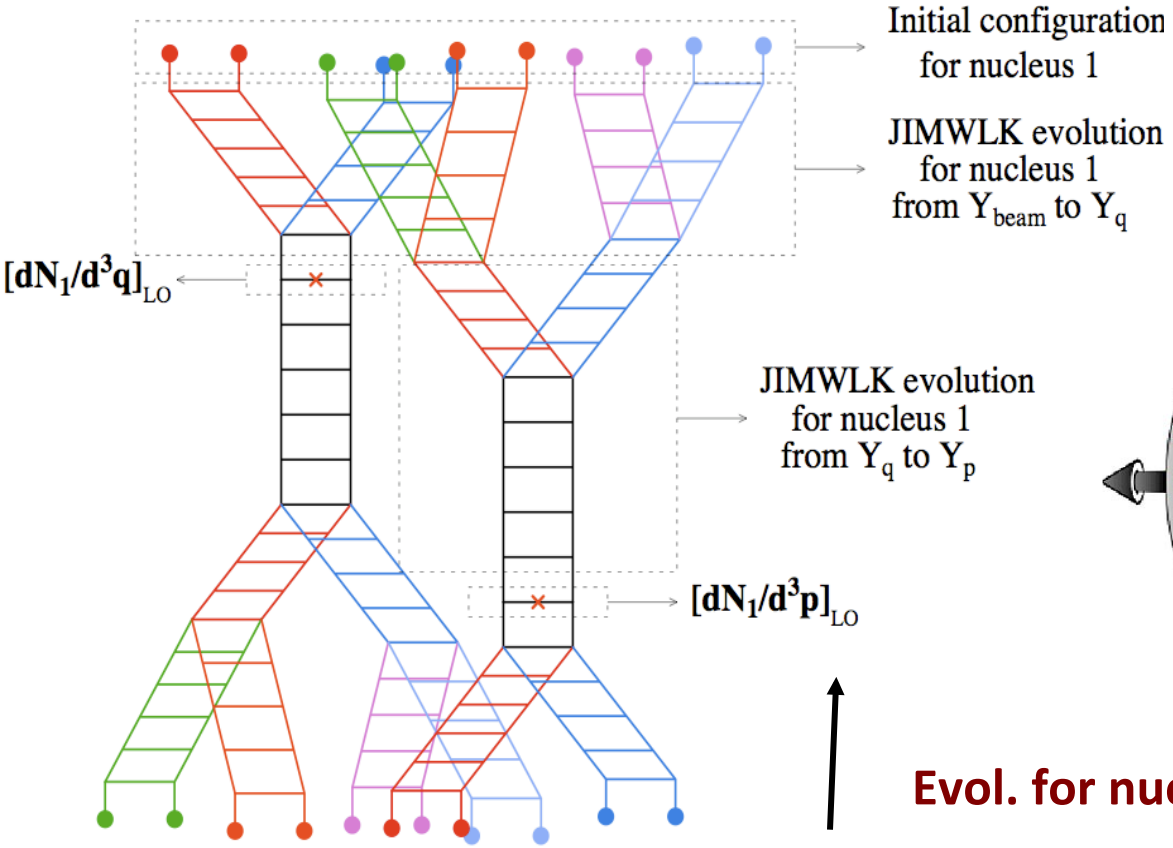

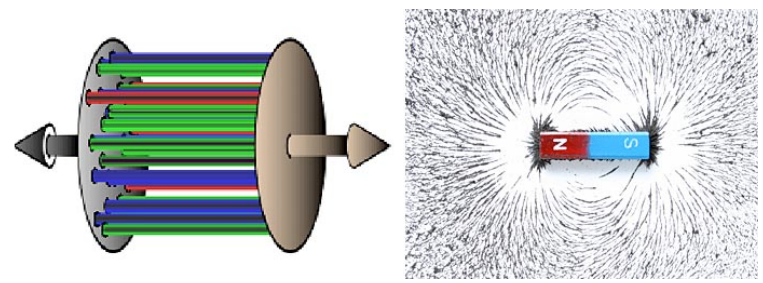

Evol. for nucl. 2

- **Full YM+JIMWLK evolution – not available yet** Lappi,Schenke,RV in progress
- **Approximations: BK Gaussian truncation approximation for $k_T \geq Q_S$; YM results for MV model available for all k_T**

Dusling,Gelis,Lappi,RV:0911.2720; Lappi,Srednyak,RV:0911.2068; Kovchegov,Wertepny: 1212.1195

The saturated hadron: Glasma graphs -I

RG evolution:

Dumitru,Gelis,McLerran,RV: 0804.3858
Gelis, Lappi, RV, arXiv: 0807.1306

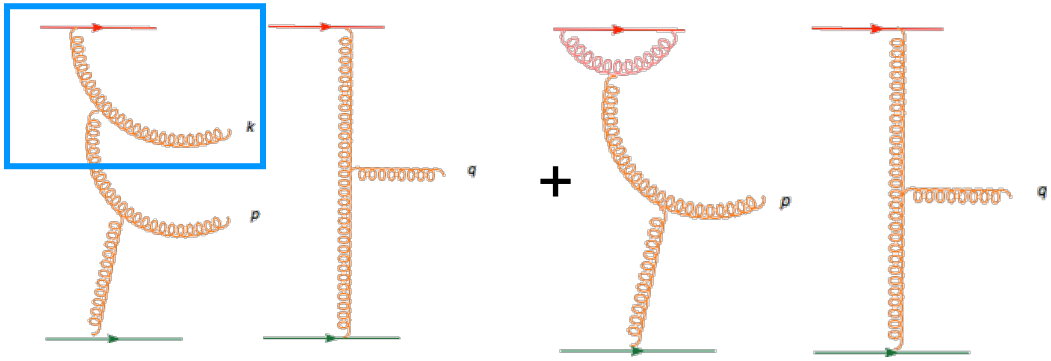

+ . . .

Keeping leading logs to all orders (NLO+NNLO+…)

= LO graph with evolved sources

avg. over sources in each event and over all events gives correlation

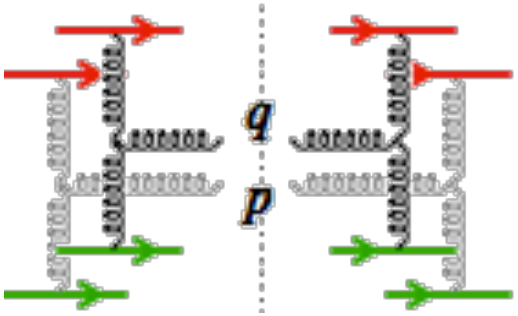

$$\langle \frac{dN_2}{d^3p\, d^3q} \rangle_{\rm LLogs} = \int [d\rho_1][d\rho_2] W_{Y_1}[\rho_1]\, W_{Y_2}[\rho_2]\, \frac{dN}{d^3p}|_{\rm LO}\, \frac{dN}{d^3q}|_{\rm LO}$$

From solns. of Yang-Mills eqns.with two light cone sources
Includes all mult. scat. contributions $(g\rho_1)^n$ and $(g\rho_2)^n$

The saturated hadron: Glasma graphs -II

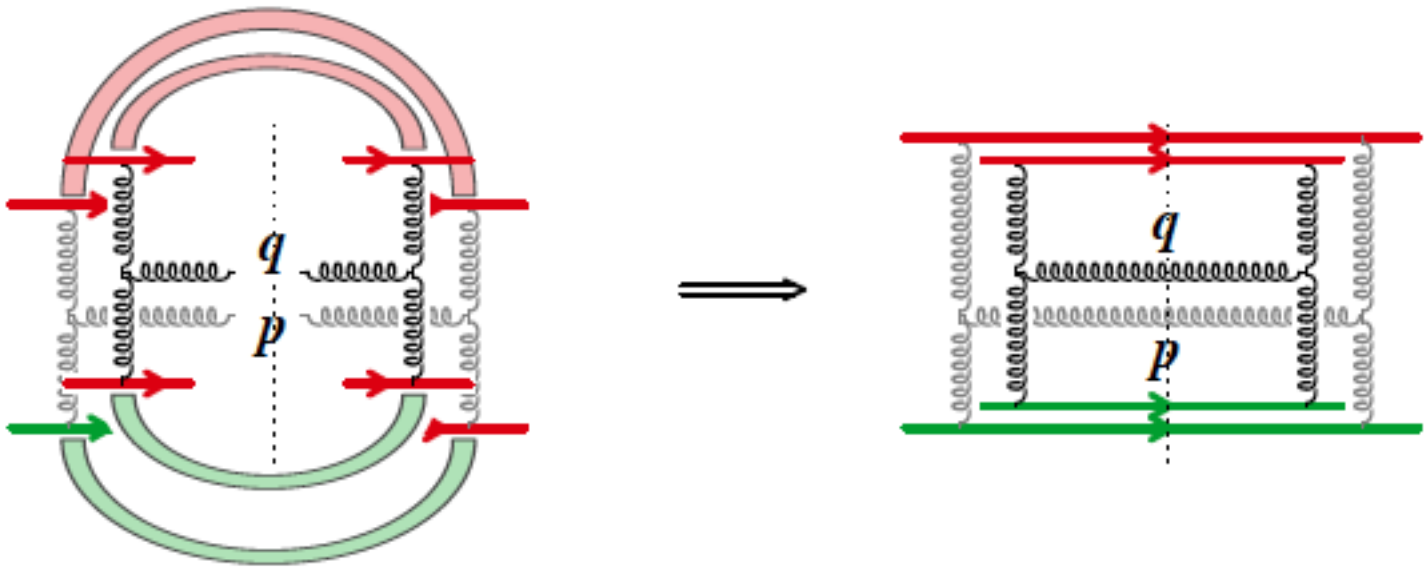

Disconnected graphs: $d^2N_{pedestal} \approx N_{incl.} \times N_{incl.}$

Dominant contribution to the "uncollimated" pedestal

Other sources in CGC EFT – 4 particle correlations

Kovner, Lublinsky, 1211:1298

The saturated hadron: Glasma graphs-III

Correlations are induced by color fluctuations that vary event to event – for Gaussian weight functionals in ρ, have color screening radius ~ $1/Q_S$

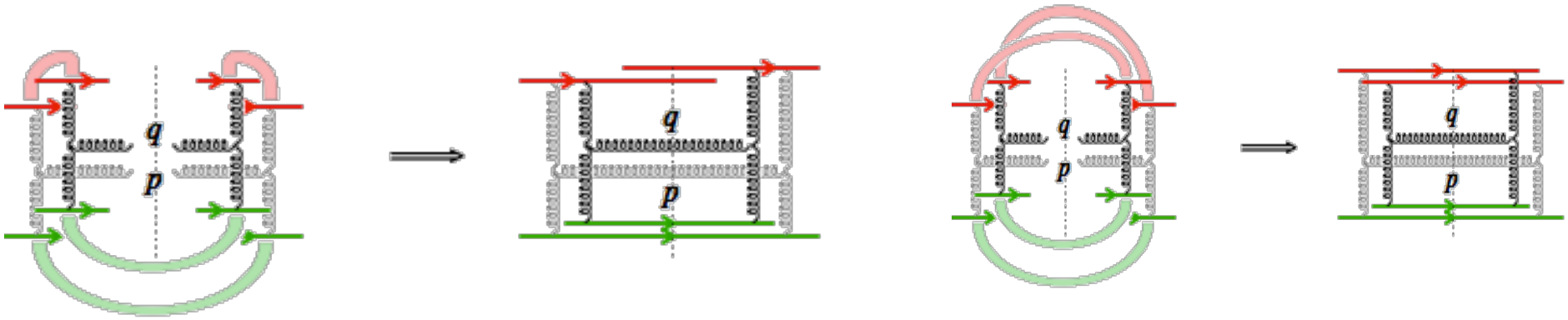

Glasma graphs generate long range rapidity correlations, are suppressed for $Q_S << p_T$ by powers of α_S AND N_C
(At high p_T, large x or large impact parameters)

However recall: coupling of sources to fields with $k_T \leq Q_S = 1/g$ not g for high occupancy fields
(central impact parameters, small x, low p_T, large nuclei)

The saturated hadron: Glasma graphs-III

Correlations are induced by color fluctuations that vary event to event – for Gaussian weight functionals in ρ, have color screening radius ~ $1/Q_S$

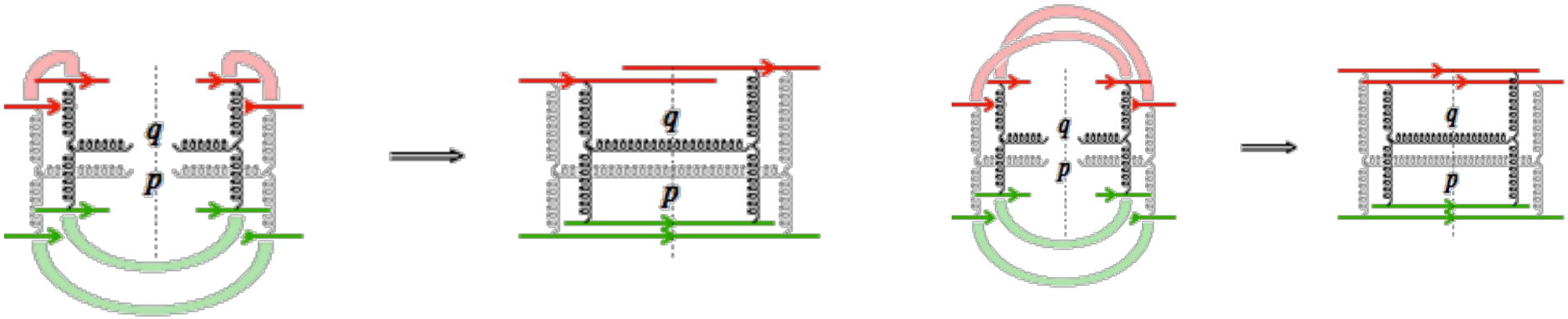

- **Glasma graphs enhanced for high multiplicity events by α_S^{-8} -- a factor of 10^5 !**

- **Collimated contributions competitive with pQCD back-to-back graphs for high multiplicity events**

2-particle → n-particle correlations

Dusling,Fernandez-Fraile, RV
Gelis,Lappi,McLerran

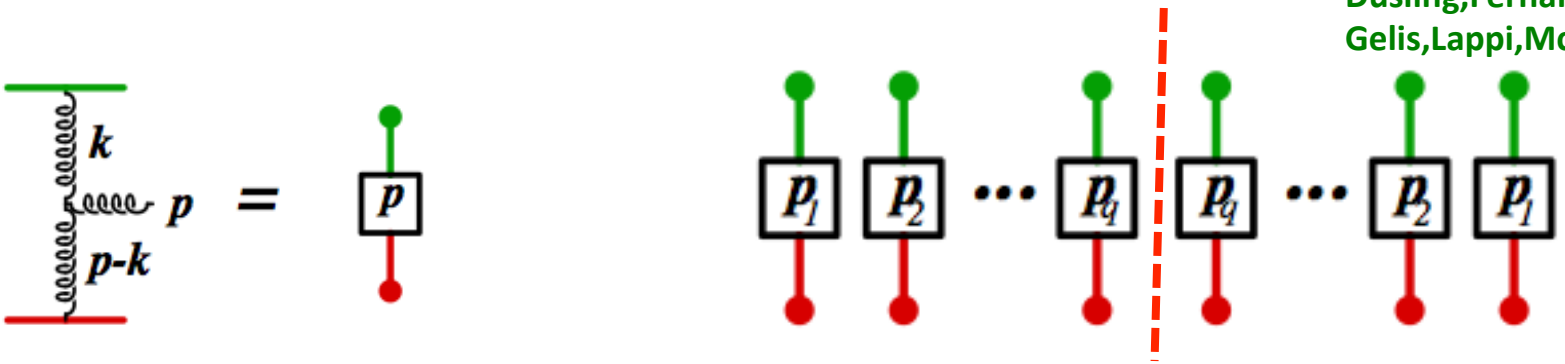

Multiplicity distribution: Leading combinatorics -> negative binomial dist.

$$P_n^{\mathrm{N.B.}}(\bar{n},k) = \frac{\Gamma(k+n)}{\Gamma(k)\Gamma(n+1)} \frac{\bar{n}^n k^k}{(\bar{n}+k)^{n+k}}$$

$$k = \zeta \frac{(N_c^2-1)Q_S^2 S_\perp}{2\pi}$$

k = 1 : Bose-Einstein
k = ∞ : Poisson

From Yang-Mills: ζ ~ 1/6

Lappi, Srednyak, RV, 0911.2068
Schenke, Tribedy, RV, 1206.6805

High Multiplicity pp collisions

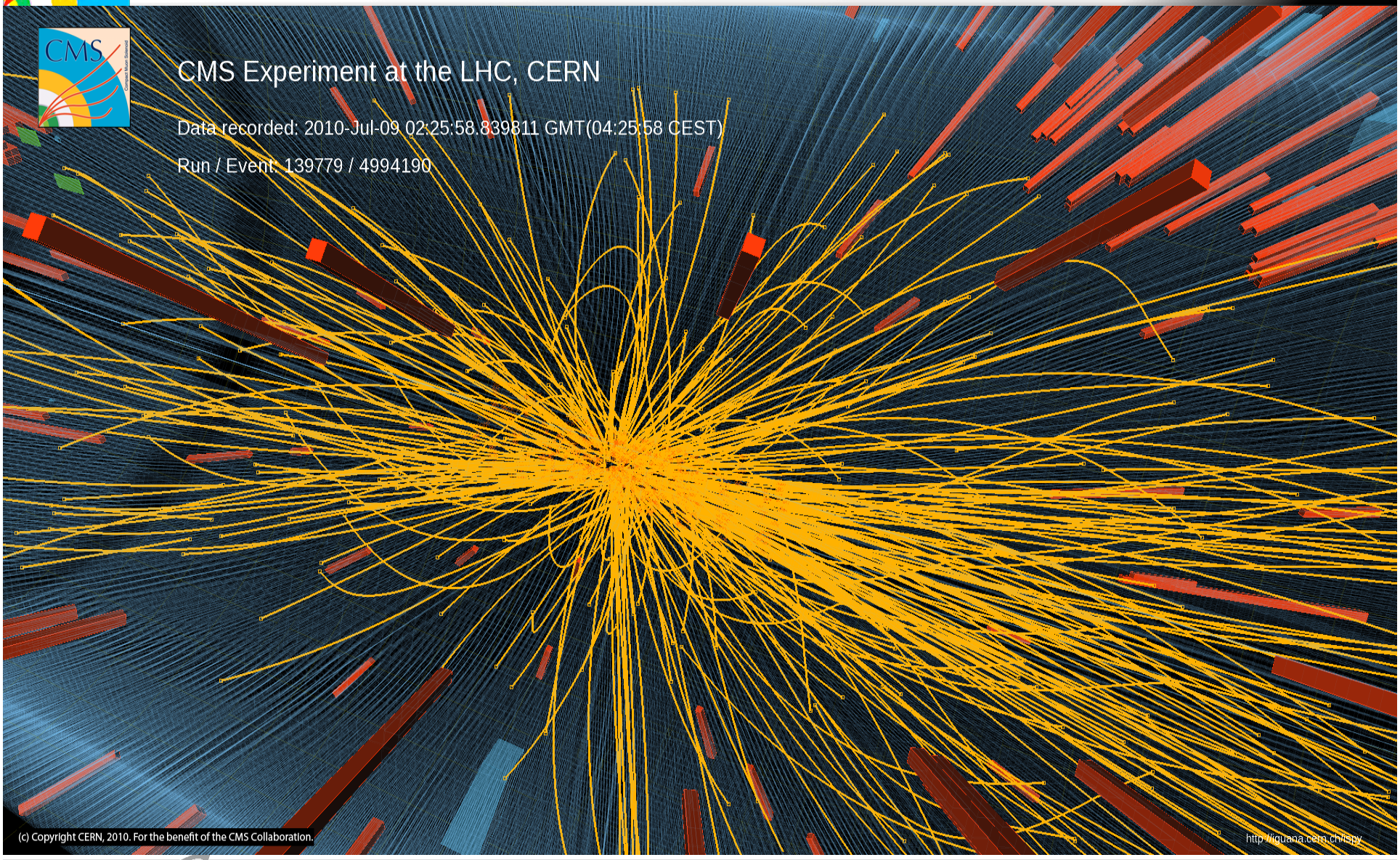

n-particle Glasma correlations describe p+p multiplicity dist.

Tribedy, RV
1112.2445

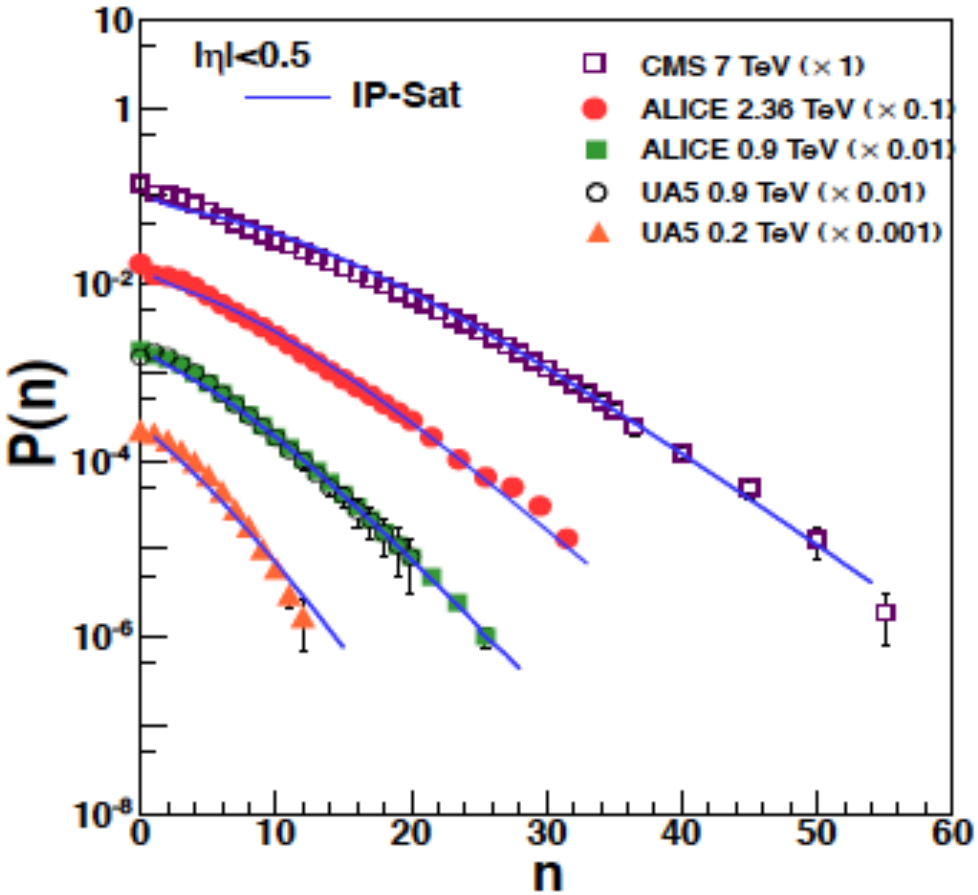

Approx: k_T factorization; more detailed YM treatment in progress

Schenke,Tribedy,RV

High multiplicity events in p+p

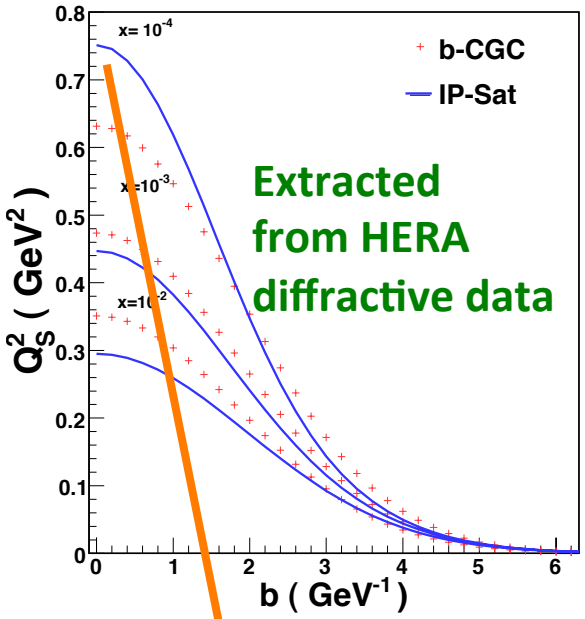

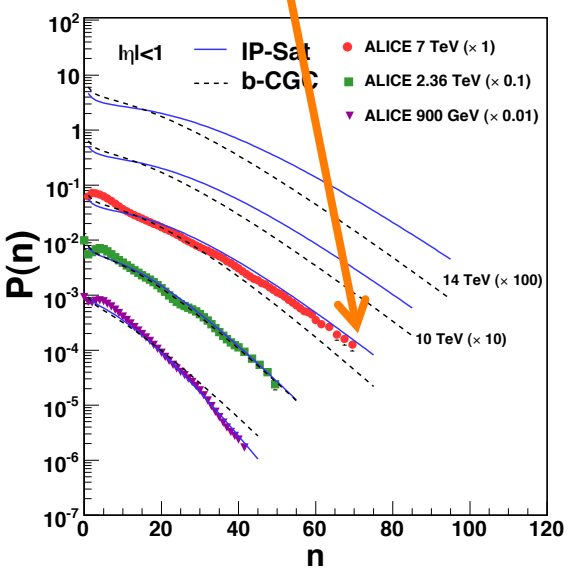

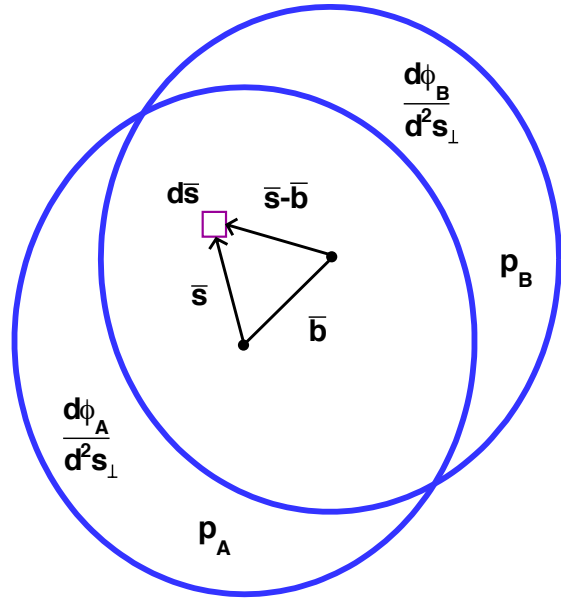

High multiplicity events likely correspond to high occupation numbers ($1/\alpha_S$) in the proton wave functions

-- use "dense-dense" EFT framework

The ridge in high mult. p+p collisions

CMS 1009.4122

"Discovery"

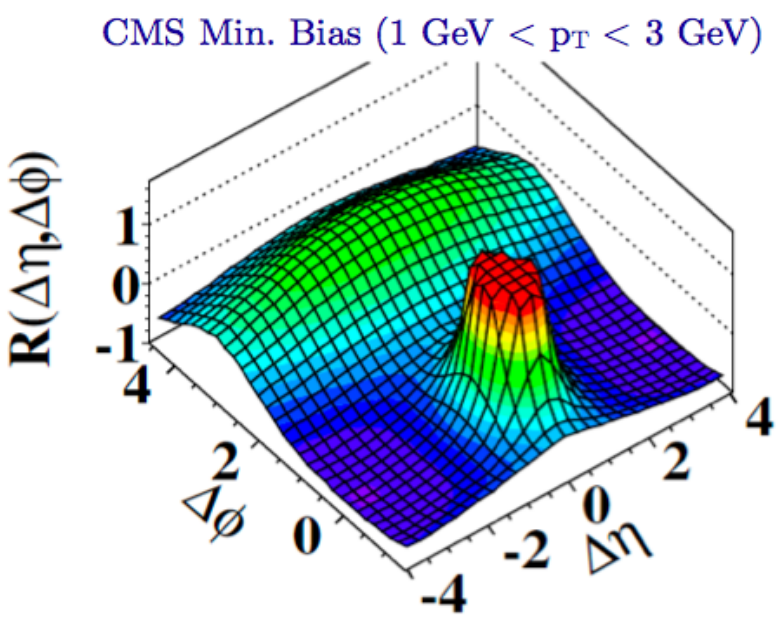

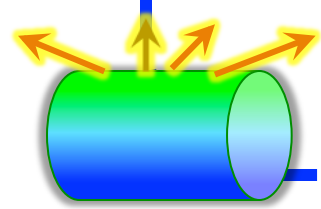

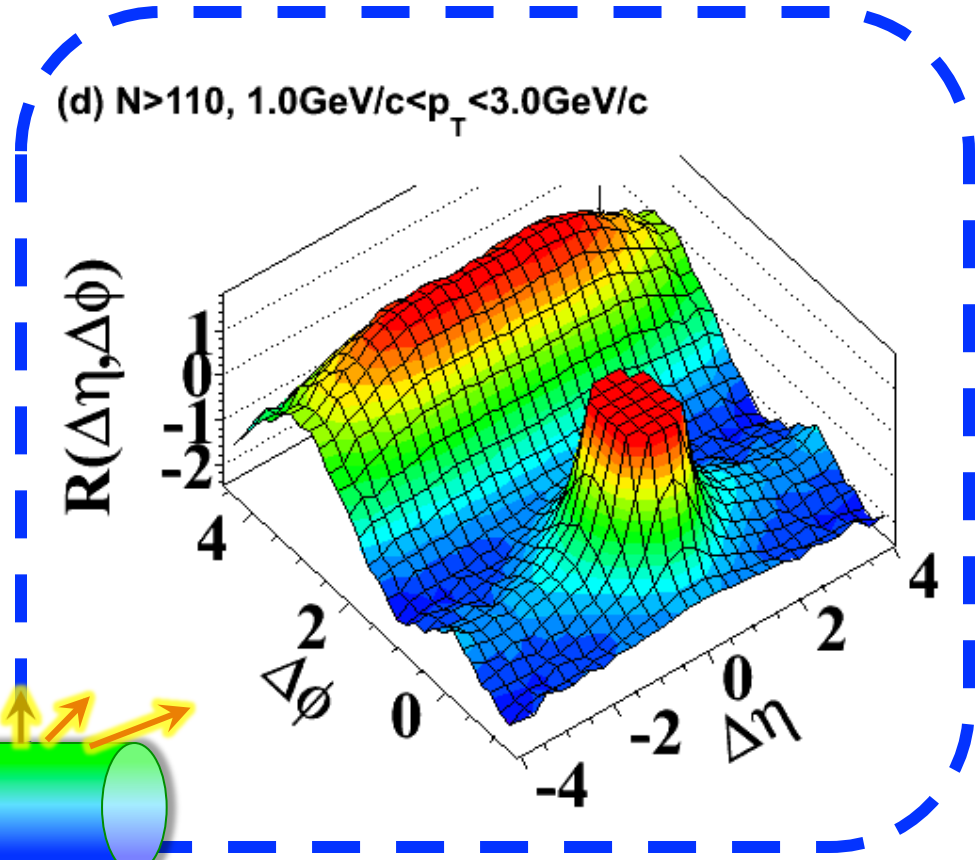

Anatomy of long range di-hadron collimation

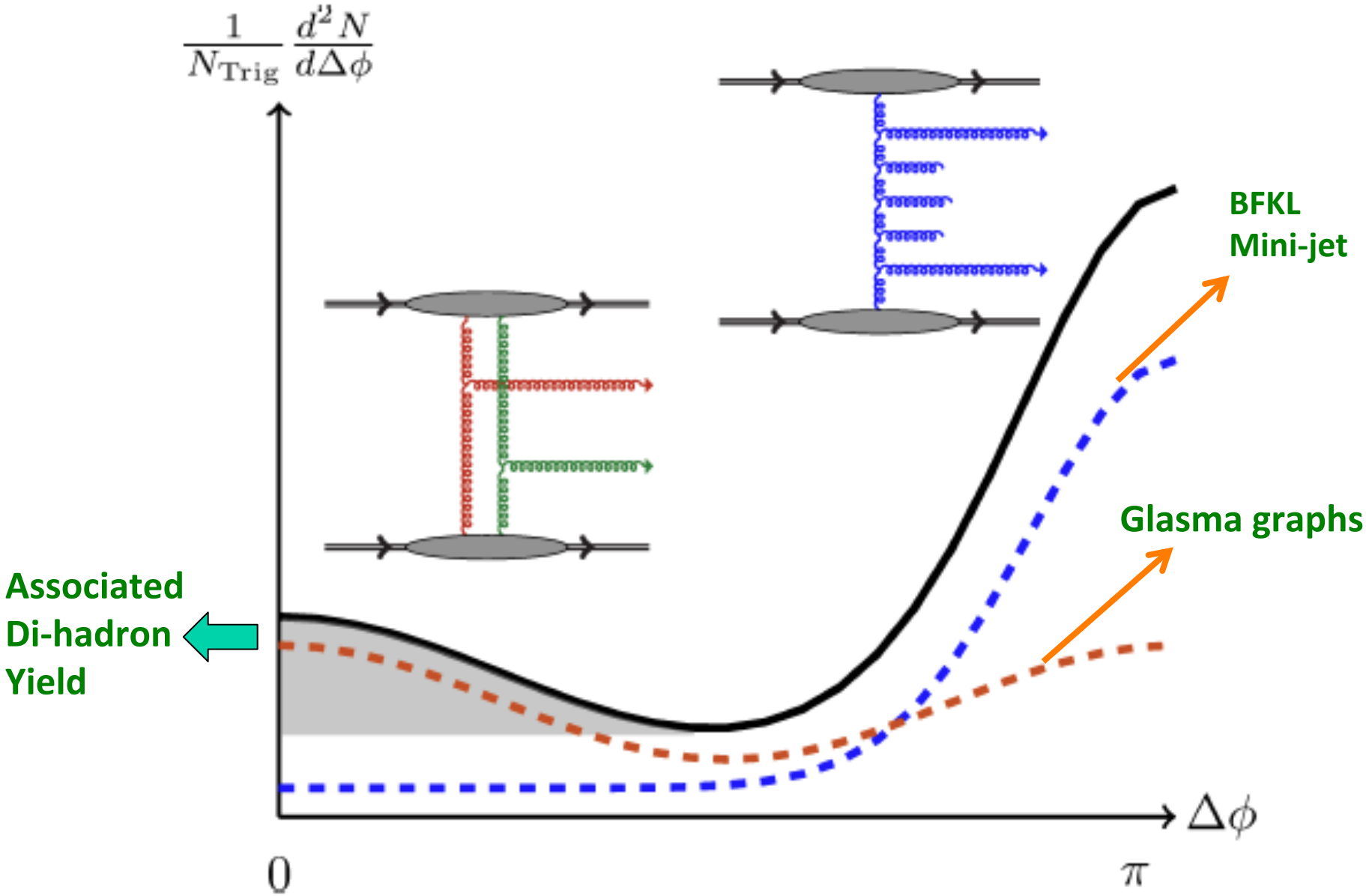

Long range di-hadron Glasma correlations

Dumitru,Dusling,Gelis,Jalilian-Marian,Lappi,RV, arXiv:1009.5295

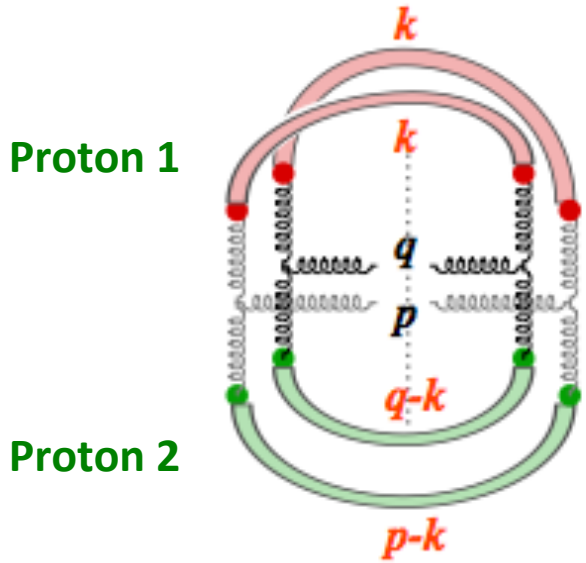

$$C(\mathbf{p},\mathbf{q}) \propto \frac{g^4}{\mathbf{p}_\perp^2 \mathbf{q}_\perp^2} \int \mathrm{d}^2\mathbf{k}_{1\perp}\, \Phi^2_{A_1}(y_p,\mathbf{k}_{1\perp})\Phi_{A_2}(y_p,\mathbf{p}_\perp-\mathbf{k}_{1\perp})\Phi_{A_2}(y_q,\mathbf{q}_\perp-\mathbf{k}_{1\perp}) + \text{permutations}$$

RG evolution of two particle correlations C(p,q) expressed in terms of "unintegrated gluon distributions" in the proton

Collimated Glasma yield

$$C(\mathbf{p},\mathbf{q}) \propto \frac{g^4}{\mathbf{p}_\perp^2 \mathbf{q}_\perp^2} \int \mathrm{d}^2\mathbf{k}_{1\perp}\, \Phi^2_{A_1}(y_p,\mathbf{k}_{1\perp})\Phi_{A_2}(y_p,\mathbf{p}_\perp-\mathbf{k}_{1\perp})\Phi_{A_2}(y_q,\mathbf{q}_\perp-\mathbf{k}_{1\perp}) + \text{permutations}$$

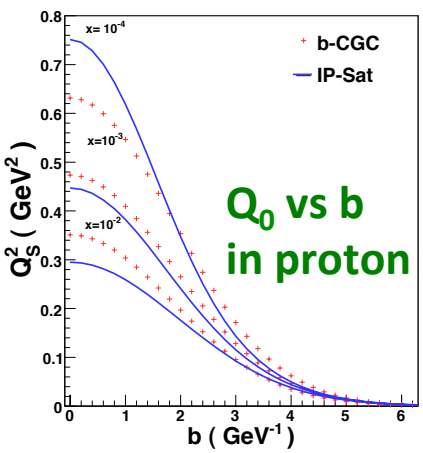

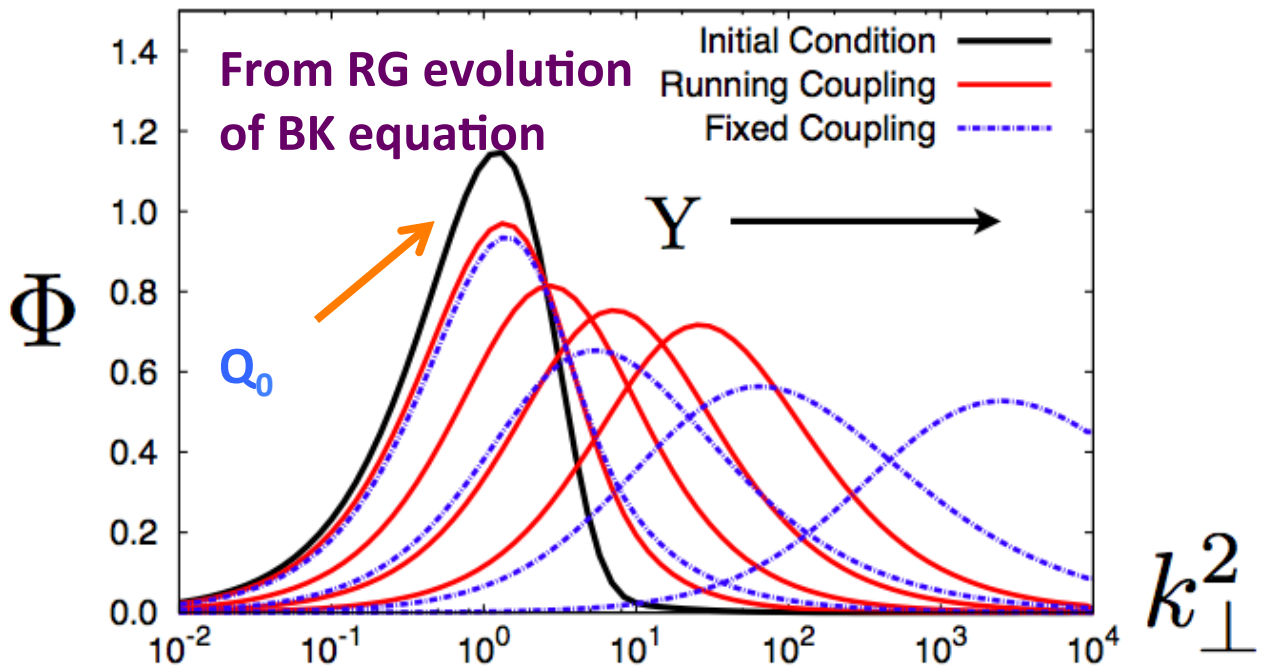

Dominant contribution from $|p_T - k_T| \sim |q_T - k_T| \sim |k_T| \sim Q_S$

This gives a collimation for $\Delta\Phi \approx 0$ and π

Angular structure from (mini-) jet radiation

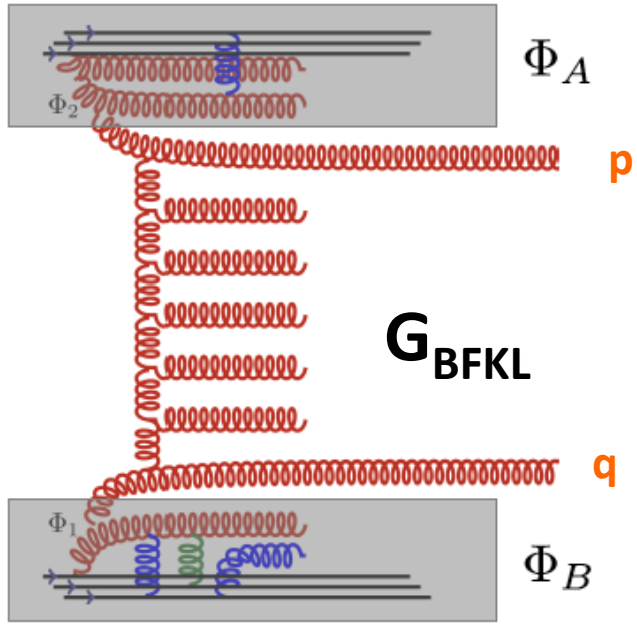

$$C_{\mathrm{BFKL}}(\mathbf{p},\mathbf{q}) \propto \Phi_A \otimes \Phi_B \otimes G_{\mathrm{BFKL}}$$

Mini-jets: O (1) in high multiplicity events
- give an angular collimation at $\Delta\Phi \cong \pi$

LHC results also test the structure of bremsstrahlung radiation between jets

Quantitative description of ridge

Dusling,RV:PRL108 (2012)262001

$$\frac{d^2N}{d\Delta\phi} = K \int_{-2.4}^{+2.4} d\eta_p\, d\eta_q\, \mathcal{A}(\eta_p, \eta_q)$$

$$\times \int_{p_T^{\min}}^{p_T^{\max}} \frac{dp_T^2}{2} \int_{q_T^{\min}}^{q_T^{\max}} \frac{dq_T^2}{2} \int d\phi_p \int d\phi_q\, \delta(\phi_p - \phi_q - \Delta\phi)$$

$$\times \int_0^1 dz_1 dz_2 \frac{D(z_1)}{z_1^2} \frac{D(z_2)}{z_2^2} \frac{d^2 N^{\text{corr.}}_{\text{Glasma}}}{d^2\mathbf{p}_T d^2\mathbf{q}_T d\eta_p d\eta_q} \left(\frac{p_T}{z_1}, \frac{q_T}{z_2}, \Delta\phi\right)$$

(6

$$\mathcal{A}(\eta_p, \eta_q) = \theta(|\eta_p - \eta_q| - \Delta\eta_{\min})\, \theta(\Delta\eta_{\max} - |\eta_p - \eta_q|)$$

$$N_{\text{trig}} = \int_{-2.4}^{+2.4} d\eta \int_{p_T^{\min}}^{p_T^{\max}} d^2\mathbf{p}_T \int_0^1 dz \frac{D(z)}{z^2} \frac{dN}{d\eta\, d^2\mathbf{p}_T} \left(\frac{p_T}{z}\right)$$

$$\text{Assoc. Yield} = \frac{1}{N_{\text{trig}}} \int_0^{\Delta\phi_{\min.}} d\Delta\phi \frac{d^2N}{d\Delta\phi} - \left.\frac{d^2N}{d\Delta\phi}\right|_{\Delta\phi_{\min.}}$$

Dependence on transverse area cancels in ratio…

Rarer and rarer gluon configurations probed In the proton

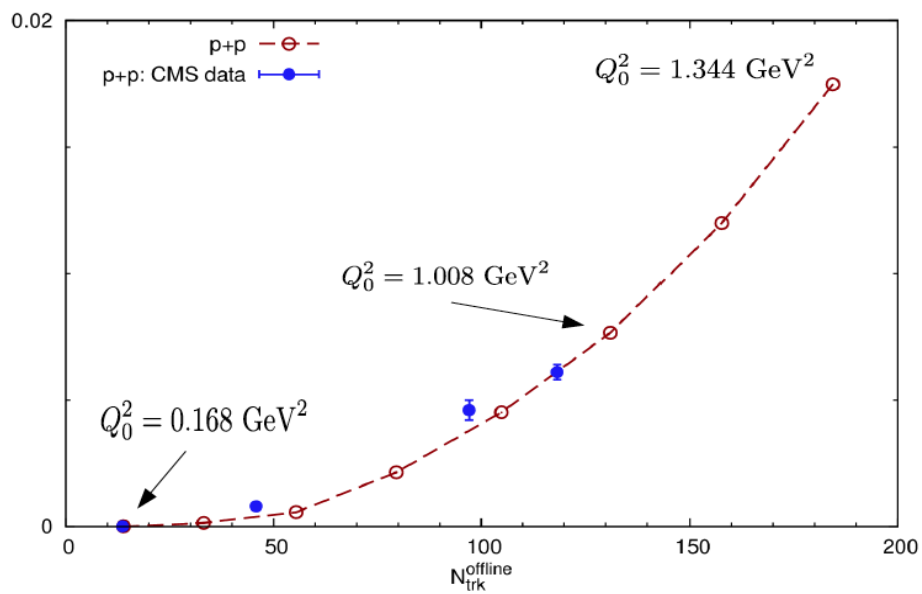

CMS data: JHEP 1009, 091 (2010); PLB 718, 795 (2013)

Assoc. yield per. trig.

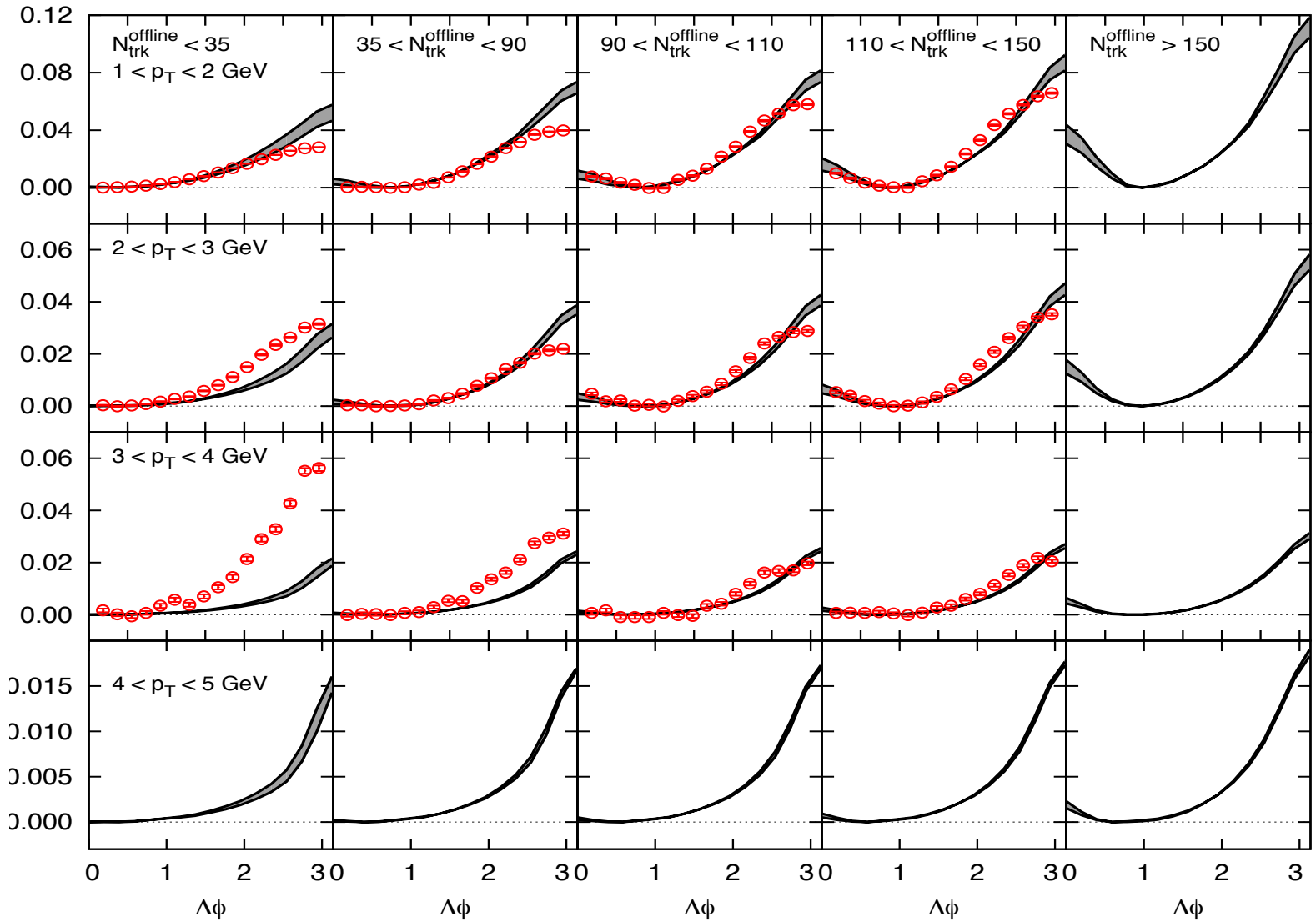

$K_{BFKL}=K_{Glasma}= 1$
KKP fragmentation

Dusling,RV, PRD 87, 051502 (R) (2013); arXiv:1302.7018

Dusling,RV, PRD 87, 051502 (R) (2013); arXiv:1302.7018

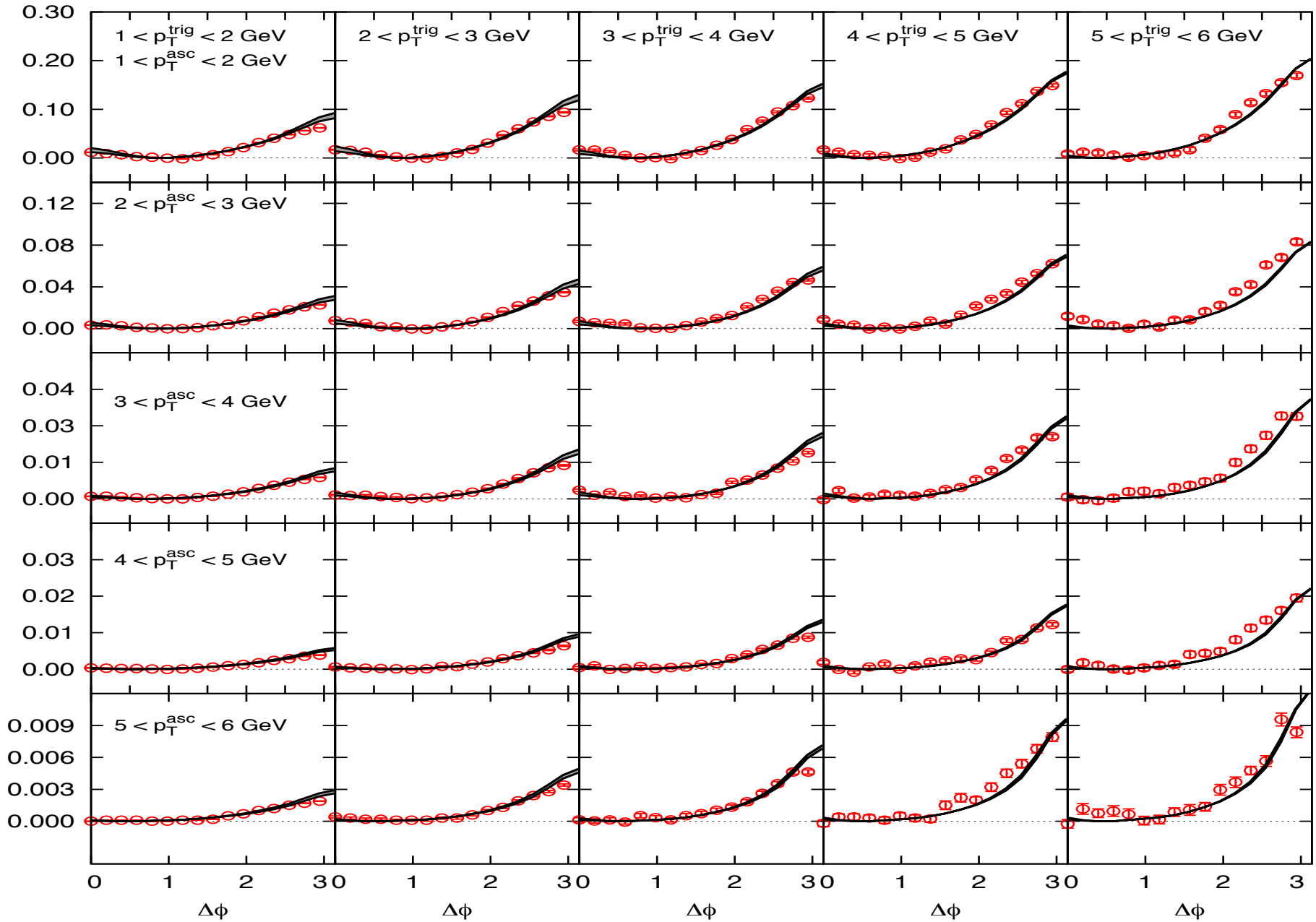

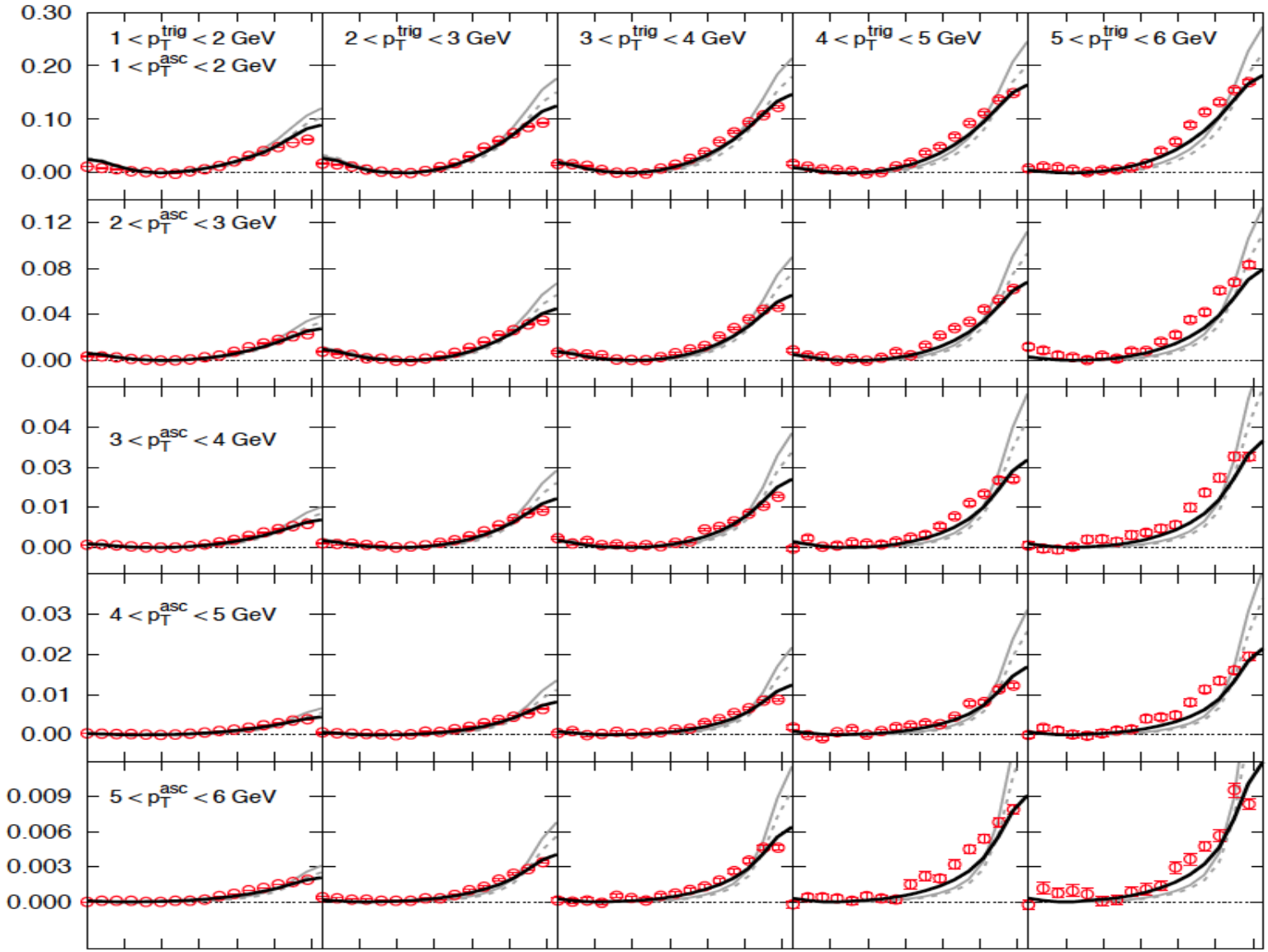

Grey curves: 2 -> 4 QCD (Multi-Regge) QCD results
– no emission in Δη between jets

p+p vs A+A

In p+p we are seeing the intrinsic collimation from a single flux tube

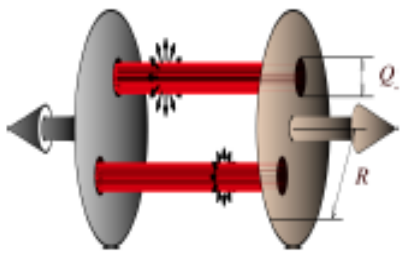

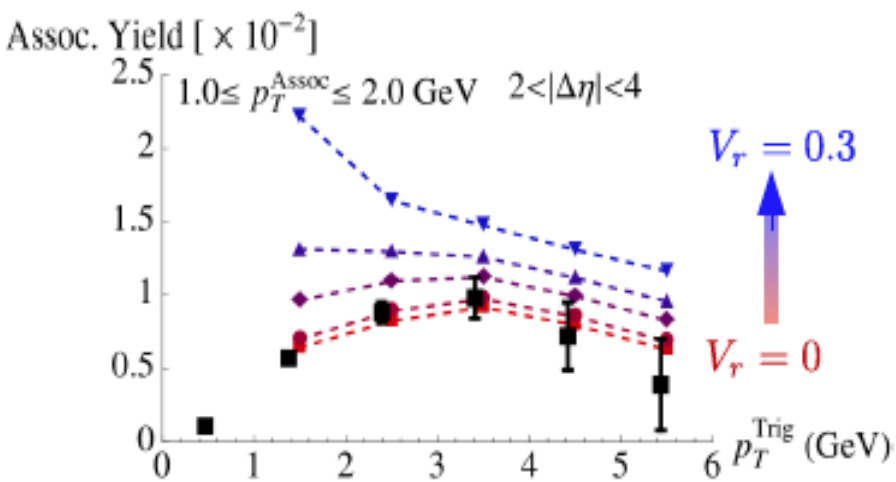

Increasing transverse flow in p+p creates a discrepancy with data.

In A+A there are many such tubes each with an intrinsic correlation enhanced by flow

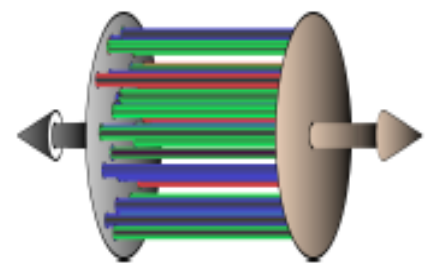

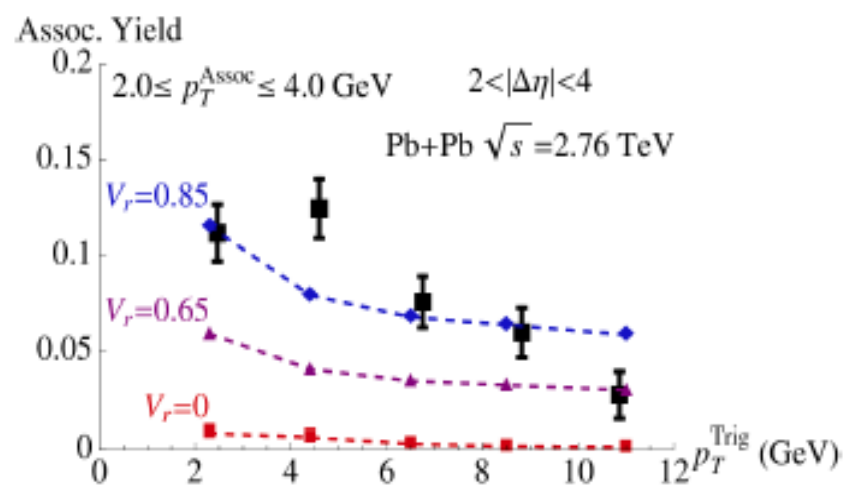

Yet, transverse flow is needed to explain identical measurements in Pb+Pb

Analysis of "pilot run" on proton lead collisions

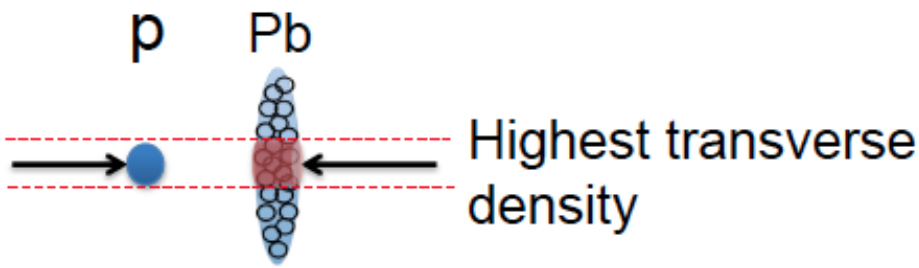

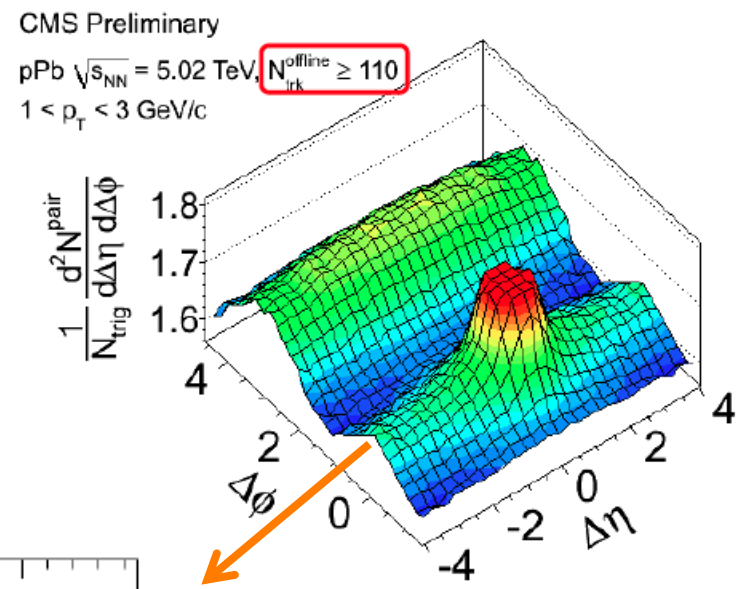

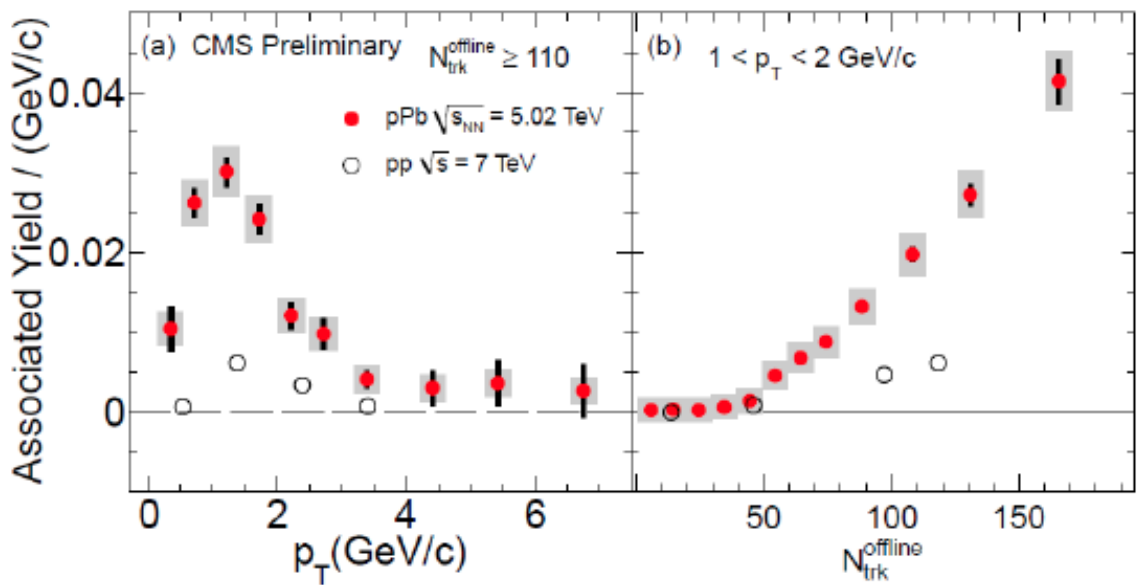

Ridge much bigger than p+p for the same multiplicity !

CMS p+Pb nearside per trigger yield-I

Dusling, RV: PRD87, 054014 (2013); arXiv:1302.7018

$Q_0^2(\text{lead}) = N_{Part}^{Pb} * Q_0^2(\text{proton})$

of "wounded" nucleons in Lead nucleus

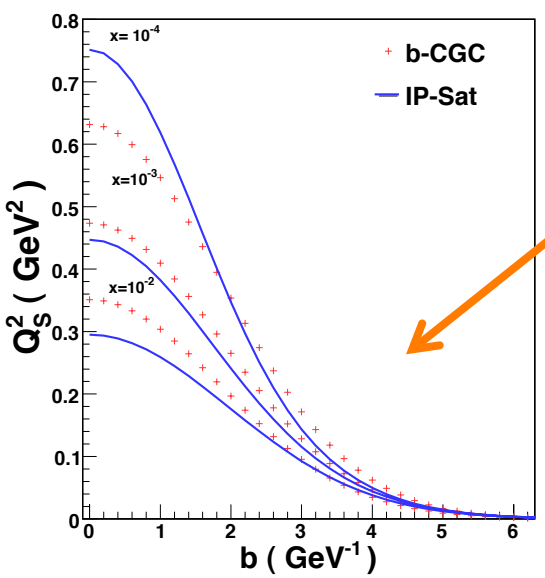

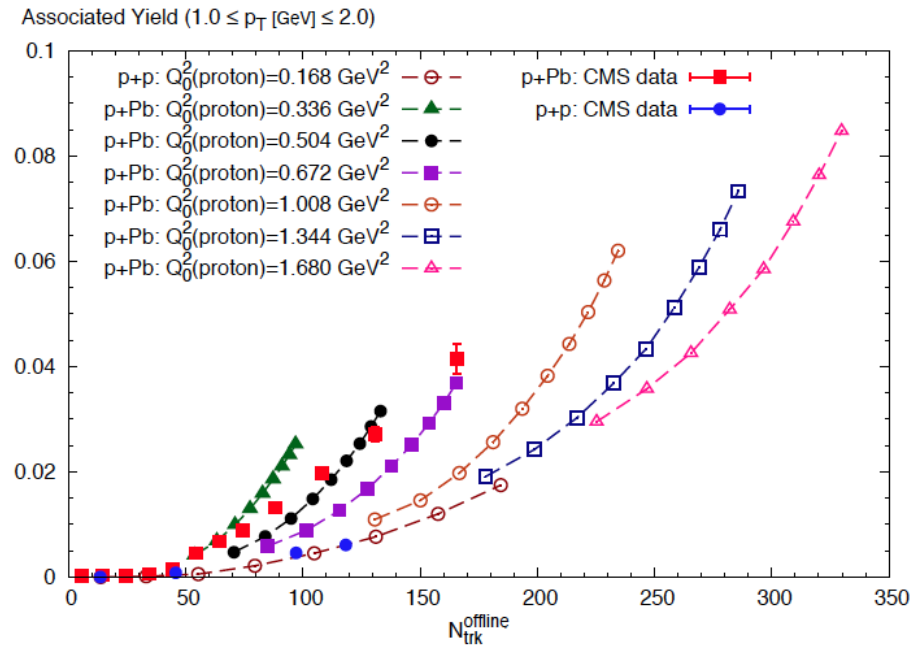

CMS p+Pb nearside yield per trigger-II

Dusling, RV: 1302.7018

$Q_0^2(\text{lead}) = N_{Part}^{Pb} * Q_0^2(\text{proton})$

of "wounded" nucleons in Lead nucleus

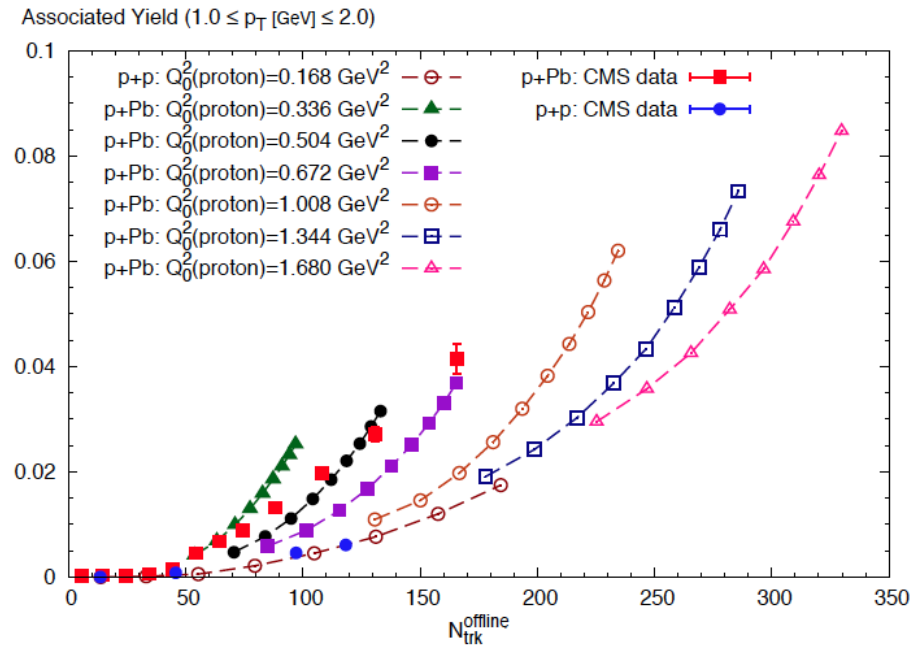

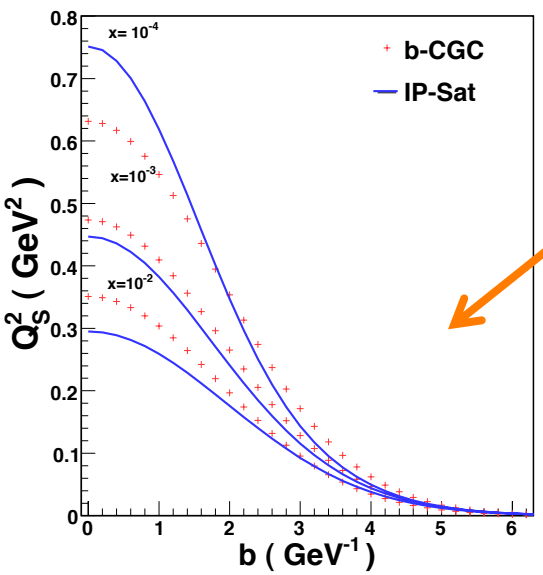

Large "ridge" seen by varying saturation scale in proton and # of wounded nucleons

--rarer and rarer Fock configurations probed in both proton and nucleus

CMS p+Pb nearside yield per trigger-III

Dusling, RV: 1211.3701
1302.7018

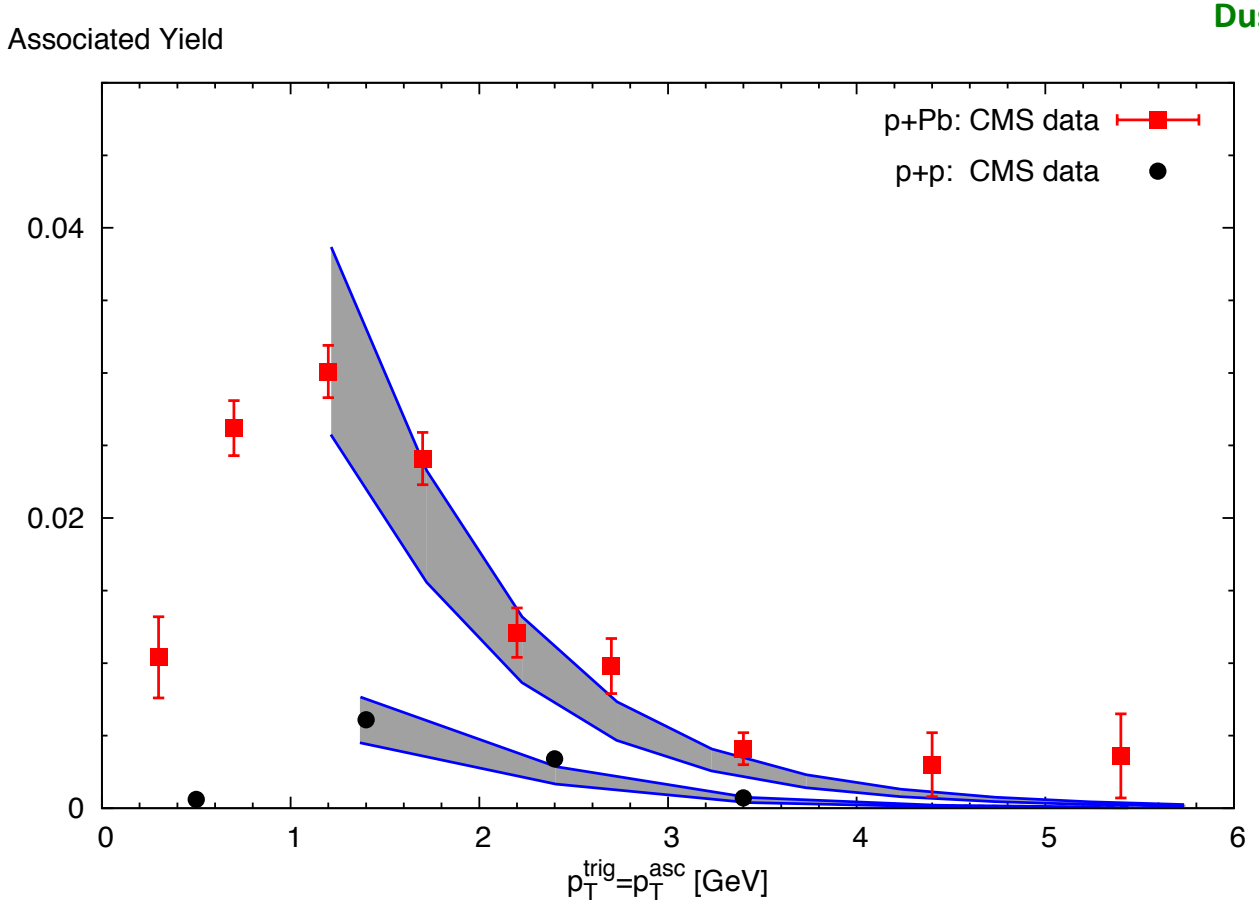

$N_{trk} > 110$

p+Pb Upper curve: $(Np^{Part}, N_A^{Part}) = (3,22)$

p+Pb Lower curve: $(Np^{Part}, N_A^{Part})=(4,14)$

p+p $N_{part} = 5,6$

CMS p+Pb yield compared to Glasma + BFKL

Dusling, RV: 1211.3701
1302.7018

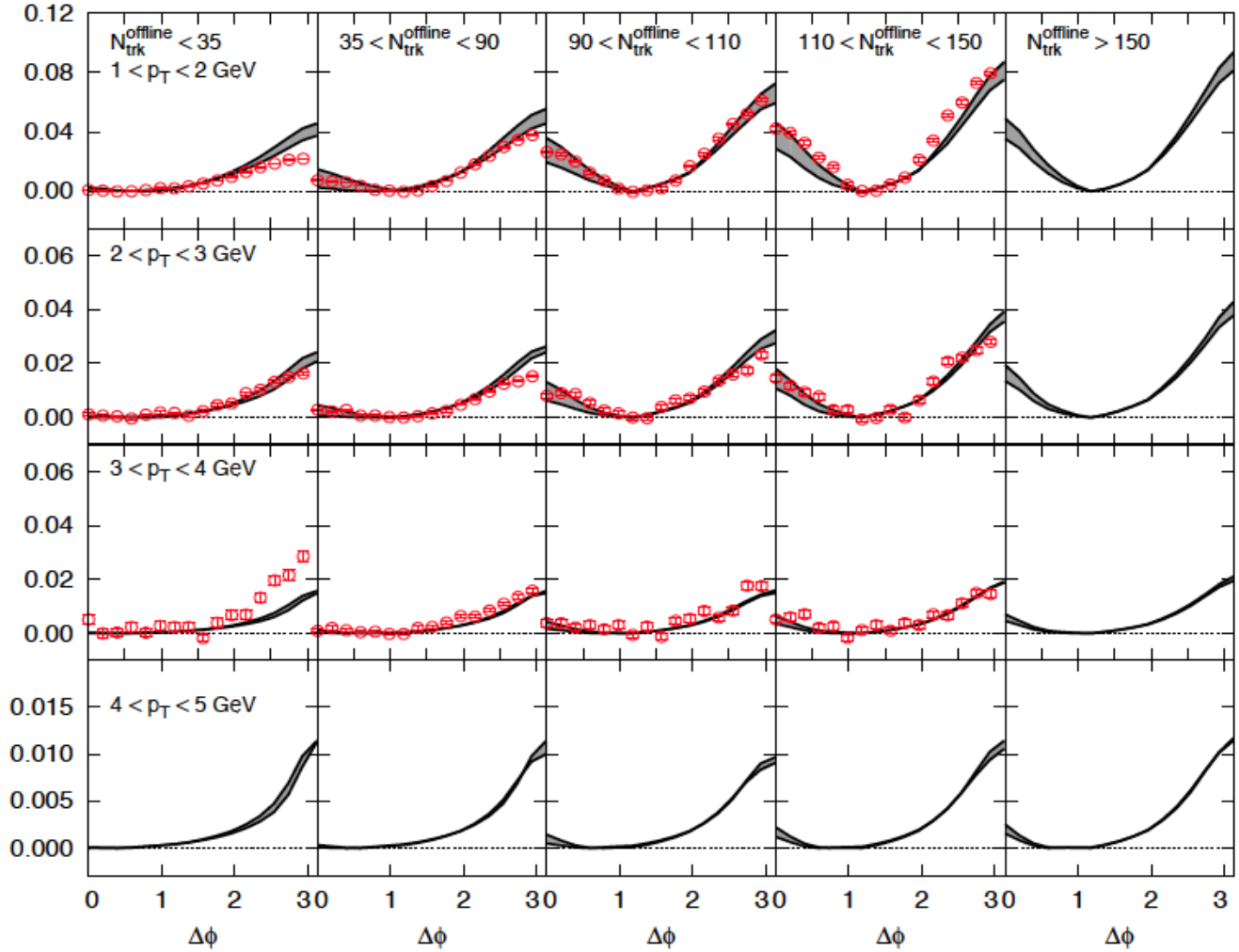

Smoking gun for gluon saturation and BFKL dynamics ?

ALICE data on the p+Pb ridge

ALICE coll. PLB 719, 29 (2013)

Different acceptance ($|\Delta\eta| < 1.8$) than CMS ($2 < |\eta| < 4$) and ATLAS ($2 < |\eta| < 5$).

ALICE subtracts away-side "jet" contribution at 40-60% centrality from most central events –can interpret as v_2

–this gives symmetric "dipole" shape of correlation – expected for Glasma contribution

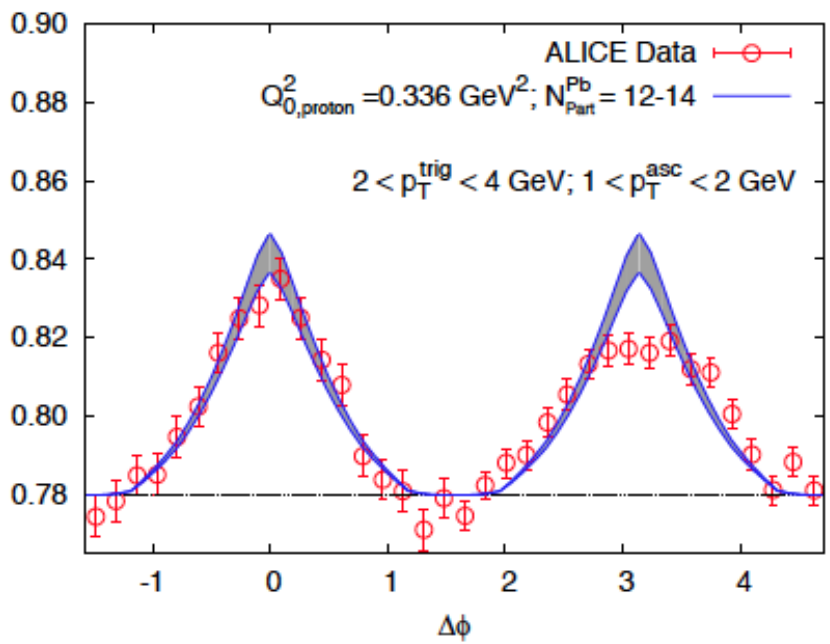

Dusling, RV: 1302.7018

Different analysis technique from CMS/ATLAS

-- same normalization as for CMS/ATLAS

Curves for $Q_{0,proton}^2$ =0.336 GeV^2 & N_{part}^{Pb} = 12 - 14

Comparison to ATLAS p+Pb ridge

ATLAS coll. arXiv: 1212.5198, PRL in press

p+A centralities
(N_{part}^{P},N_{part}^{A})

= (3,22) upper
= (4,14) lower

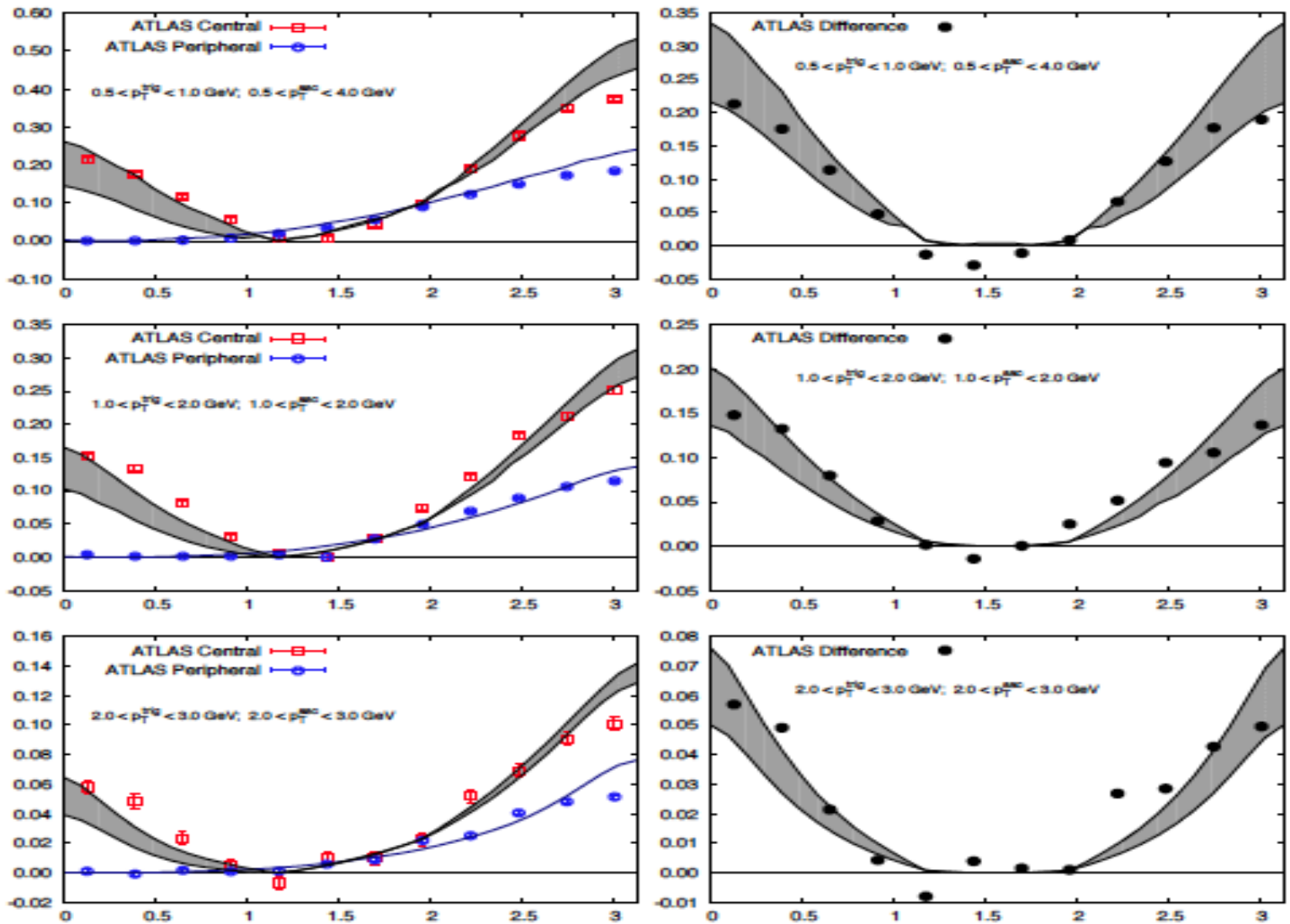

Comparison to ATLAS p+Pb ridge

ATLAS coll. arXiv: 1212.5198

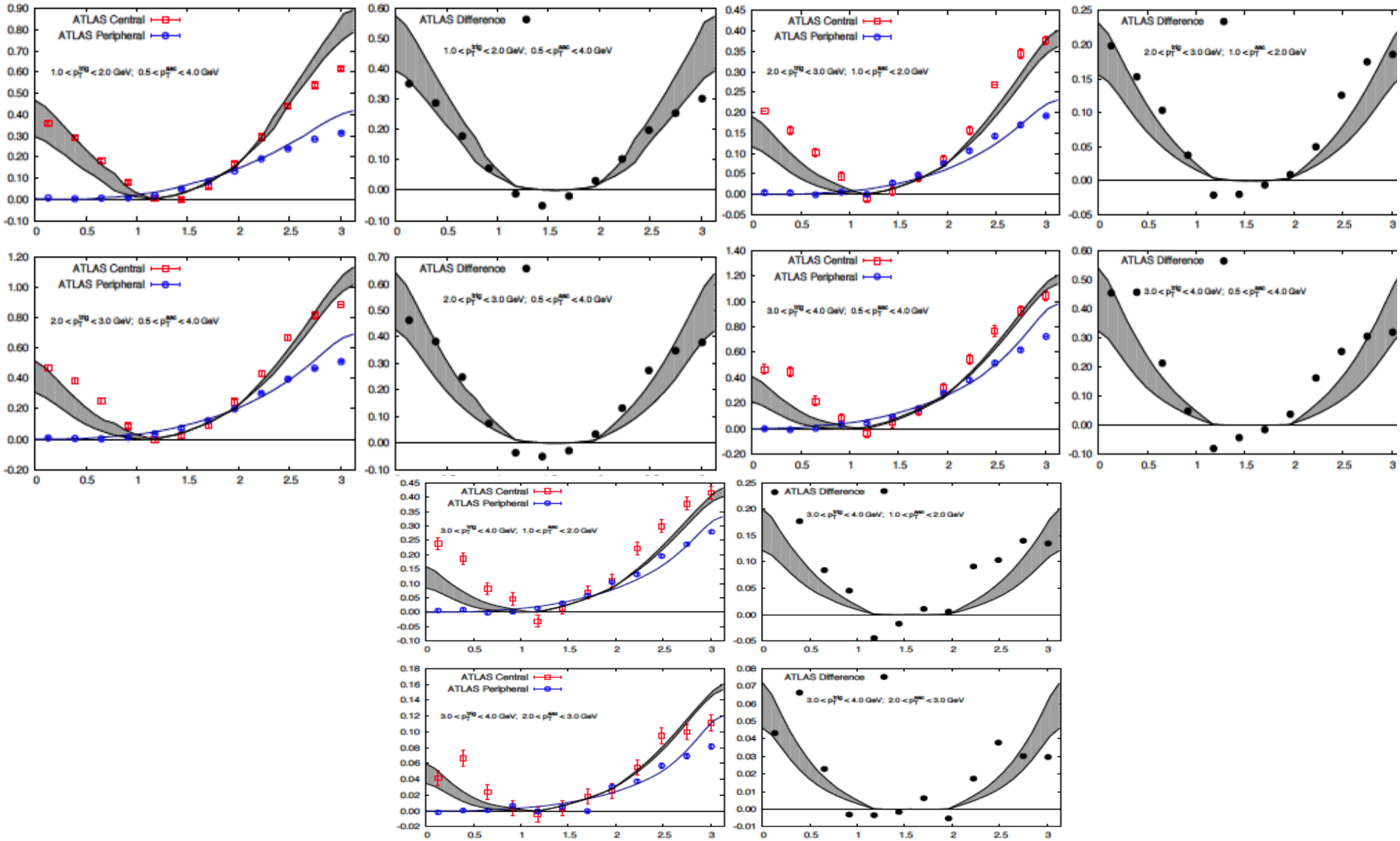

Physics underlying the ridge

Look at ratio of yield at $\Delta\phi_{pq} = 0$ to $\Delta\phi_{pq}=\pi$ for $|p_T|=|q_T|$

$$\mathrm{CY} \propto \frac{\int d^2k_T\ \Phi_A^2(k_T)\ \Phi_B^2(|p_T - k_T)}{\int d^2k_T\ \Phi_A^2(k_T)\ \Phi_B(|p_T - k_T|)\Phi_B(|p_T + k_T|)}$$

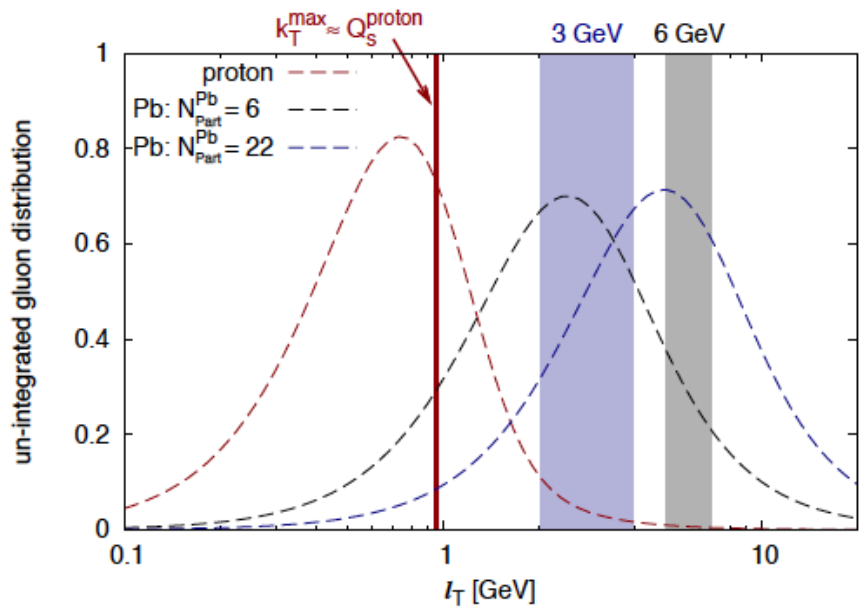

$$\mathrm{CY} \propto \frac{\Phi_B(Q_B)}{\Phi_B(\sqrt{2p_T^2 + 2Q_A^2 - Q_B^2})} \propto 1 + \frac{(Q_B - Q_A)^2}{Q_A^2} \sim N_{\mathrm{part}}$$

As seen in the LHC p+Pb data…

RHIC d+Au data

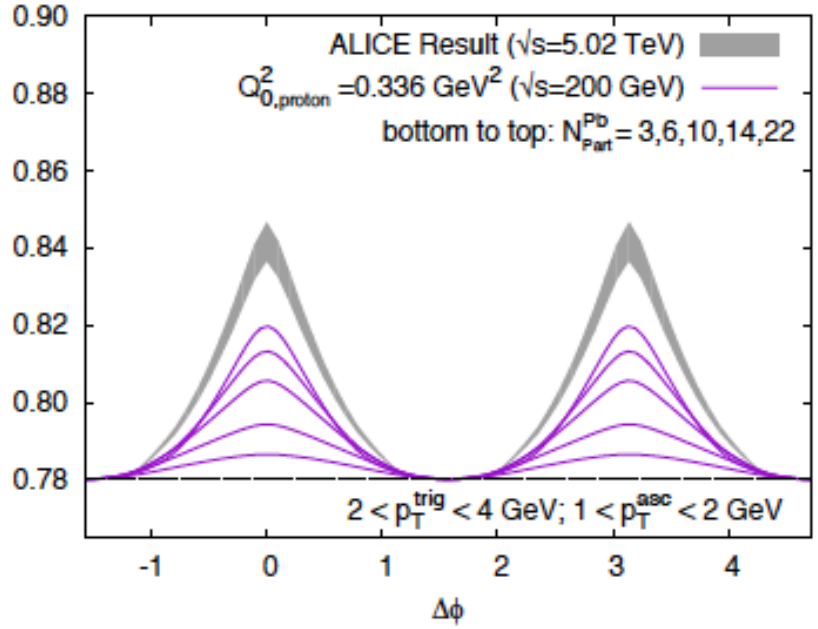

Dusling,RV: 1302.7018

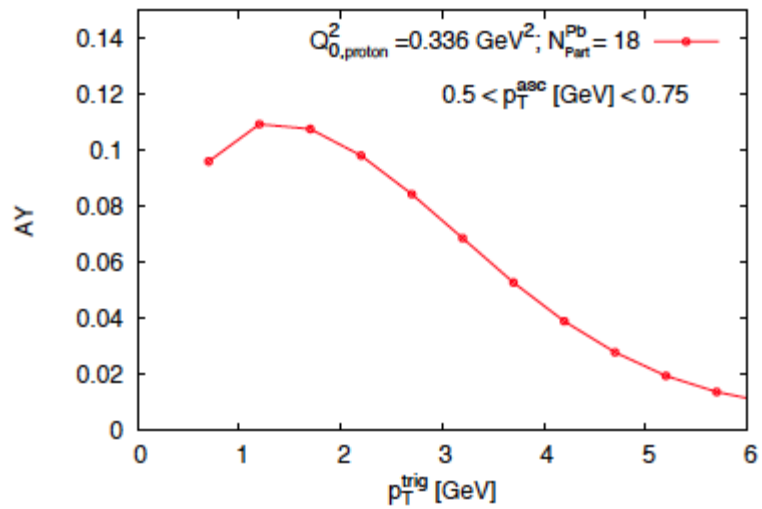

PHENIX has measured large v2 in 0-5% d+Au collisions: arXiv:1303.1794

We compute correlated yield

$$d^2N_{corr} \approx d^2N_{pedestal}\, v_2^2$$

Strong function of p_T^a, p_T^b – larger at LHC

Extraction of d^2N_{corr} would allow quantitative study in our framework

Are there signficant final state effects ?

Why is jet unmodified while Glasma graph (which generates the v_2) is ?

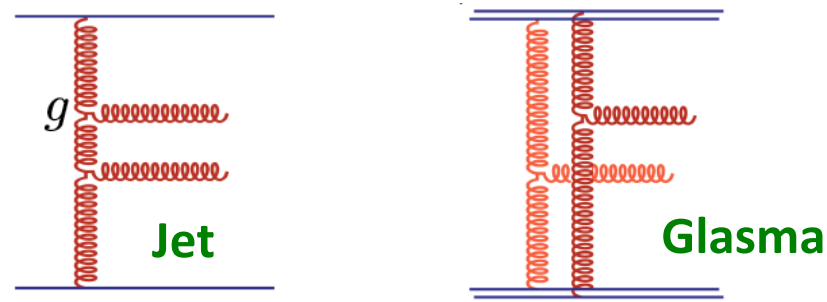

Appears quite different in p+p and p/A versus A+A

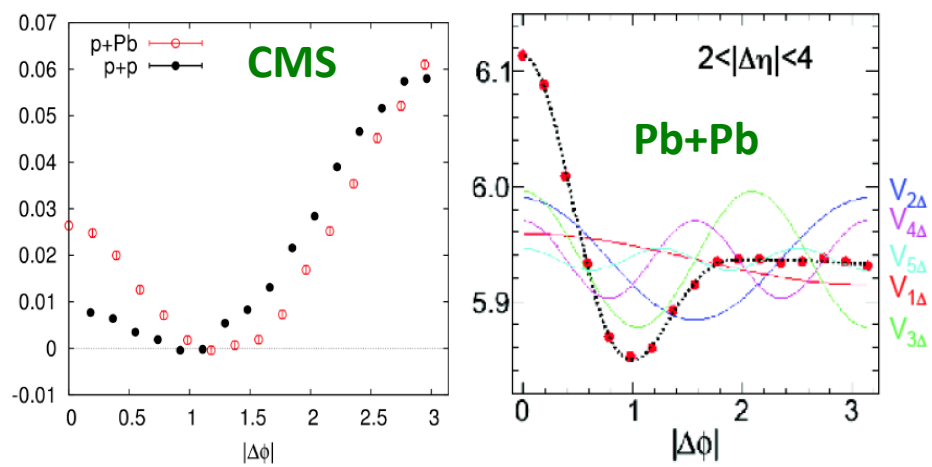

Are there signficant final state effects ?

Why is jet unmodified while Glasma graph (which generates the v_2) is ?

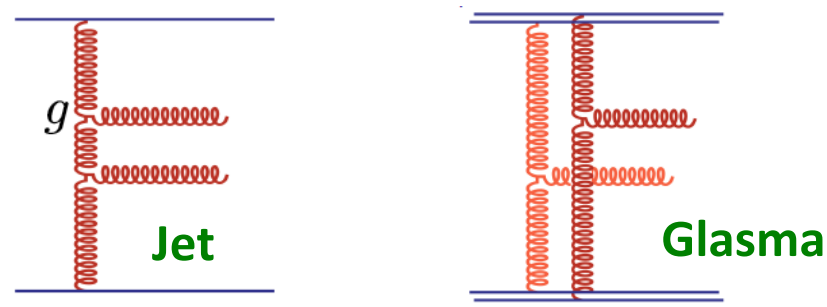

Appears quite different in p+p and p/A versus A+A

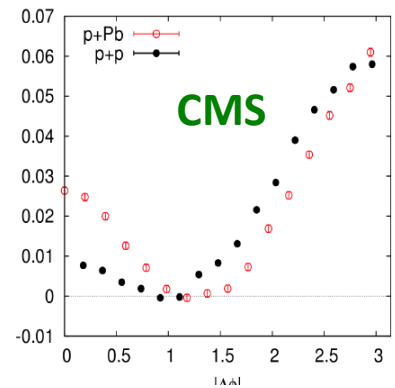

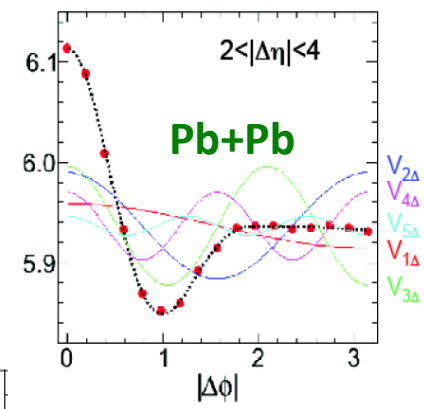

Sizes are the same in p+p and p+Pb whose ``v_2" is ~ 4 times larger

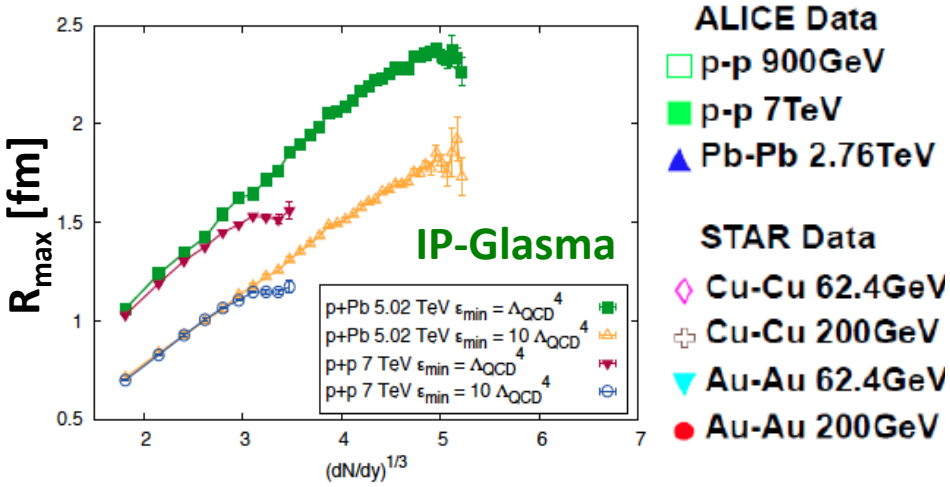

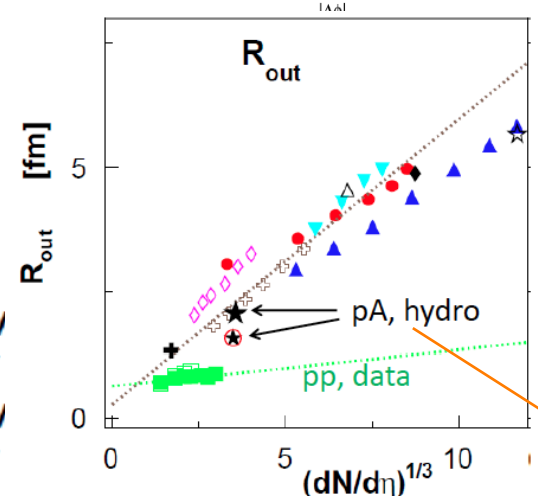

HBT radii in p+A will be very helpful !

Bozek,Broniowski, PLB 720 (2013) 250

Role of flow in p+p, p/d+A

- Is there room for flow in these systems ? See next talk by Piotr Bozek

- Our view: hydro results very sensitive to initial conditions

  -- significant differences seen between IP-Glasma and MC-Glauber models

  -- flow in p+p is small and at most 50% less than p+A even for "nearly ideal" flow simulations

  -- large viscous corrections in small size systems

  -- talk on Wednesday by Bjoern Schenke Bzdak,Schenke,Tribedy,RV, arXiv:1304.3403

Role of flow in p+p, p/d+A

- Is there room for flow in these systems ? See next talk by Piotr Bozek

- Our view: hydro results very sensitive to initial conditions
  - -- significant differences seen between IP-Glasma and MC-Glauber models
  - -- flow in p+p is small and at most 50% less than p+A even for "nearly ideal" flow simulations
  - -- large viscous corrections in small size systems
  - -- talk on Wednesday by Bjoern Schenke Bzdak,Schenke,Tribedy,RV, arXiv:1304.3403

- Trend/magnitude of flow different from p+Pb data – note Glasma η/s=0.08 !

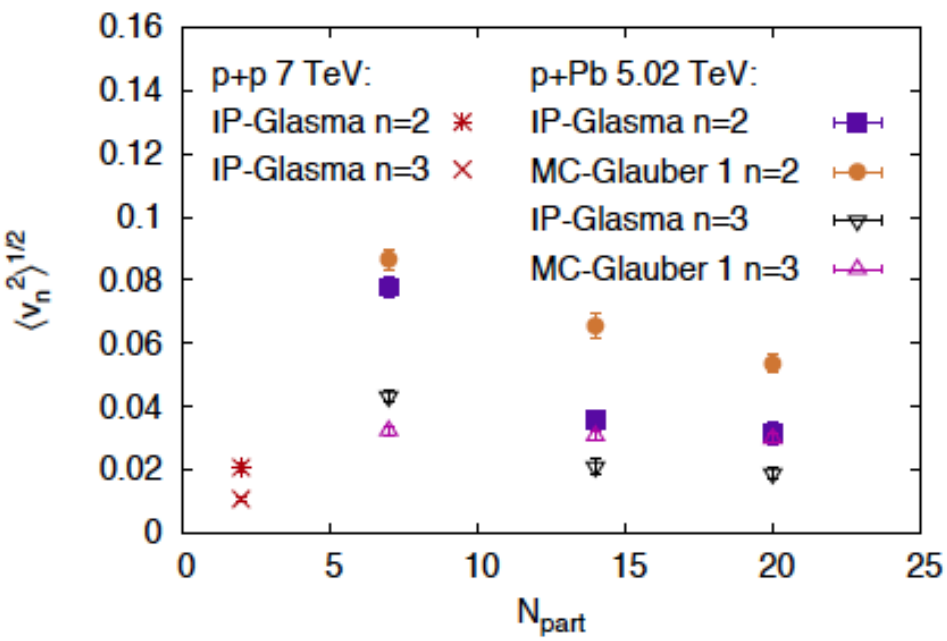

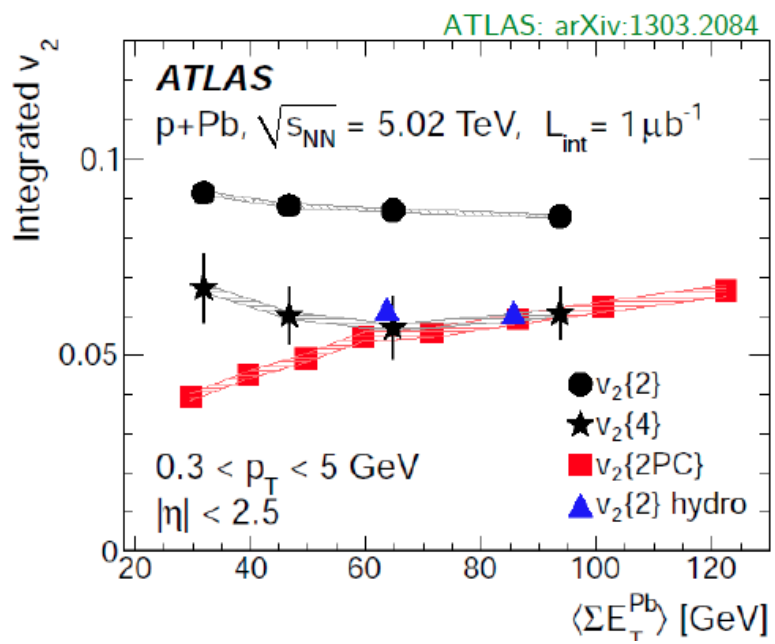

Conclusions

- The Glasma framework provides a systematic description of multi-particle production in p+p, p+A and A+A collisions
- The p+p ridge can be quantitatively understood from gluon saturation enhanced quantum interference Glasma graphs + BFKL graphs
- The A+A ridge and v_n moments are quantitatively described by IP-Glasma initial conditions + flow
- The p/d+A ridge situation is not completely clear yet
  - but will be clarified soon. 2-part corr. data presented thus far are quantitatively described by Glasma+BFKL dynamics

EXTRA SLIDES

The big picture: many-body universal gluodynamics

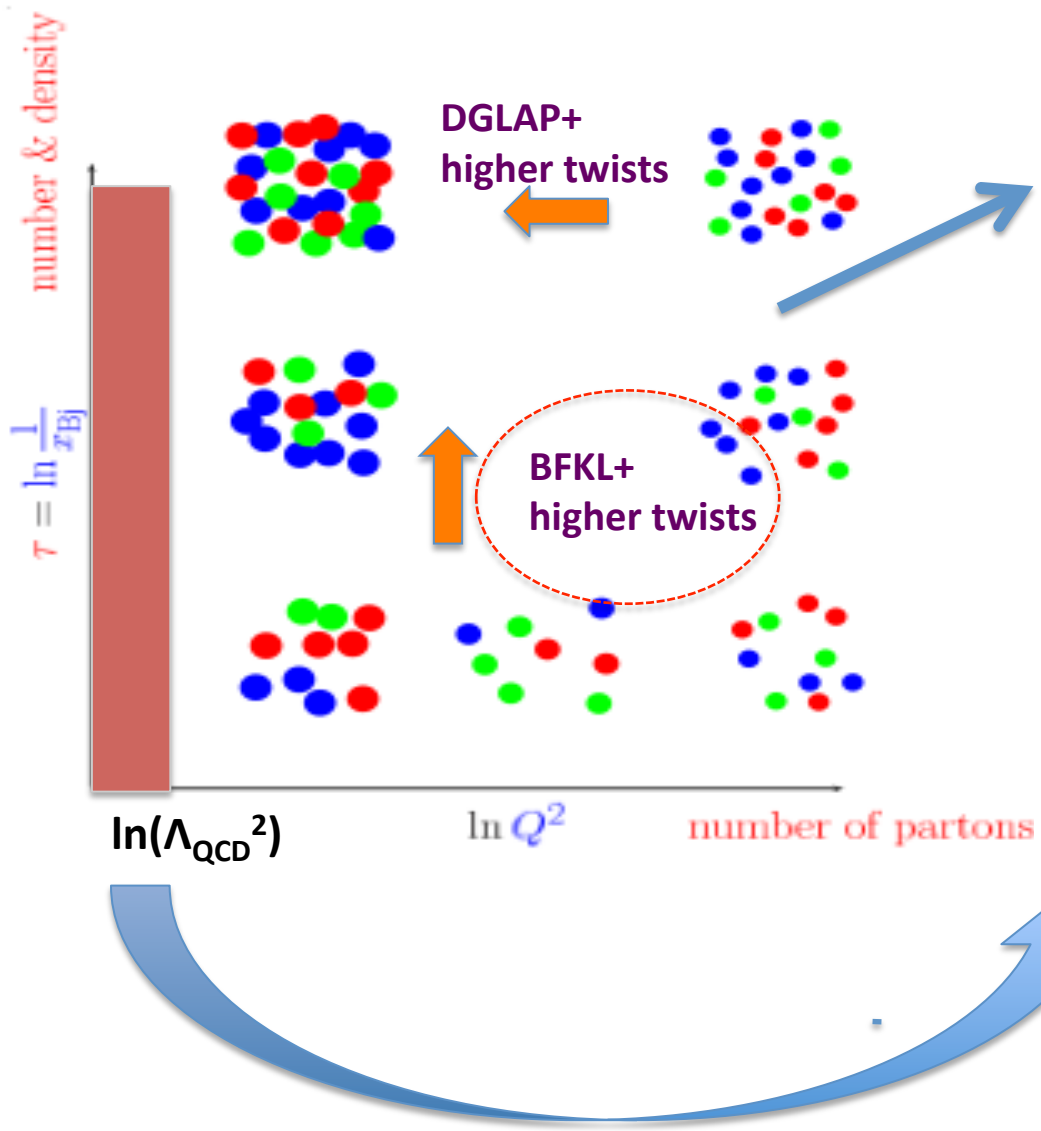

How does this happen ? What are the right degrees of freedom ?

How do correlation functions of these evolve ?

Is there a universal fixed point for the RG evolution of d.o.f

Does the coupling run with Q_s^2 ?

How does saturation transition to chiral symmetry breaking and confinement

Physics underlying systematics of the ridge

For Glasma graphs

$$d^2N \propto \int d^2k_T\ \Phi_A^2(k_T)\ \Phi_B(|p_T - k_T|)\ \Phi_B(|q_T - k_T|)$$

For $|p_T| = |q_T|$, from the Cauchy-Schwarz inequality:

$$\int d^2k_T\ \Phi_A^2(k_T)\ \Phi_B(|p_T - k_T|)\ \Phi_B(|q_T - k_T|) \leq \int d^2k_T\ \Phi_A^2(k_T)\Phi_B^2(|p_T - k_T|)$$

Equality implies no collimation; satisfied only iff $\Phi_B(|p_T - k_T|) \propto \Phi_B(|q_T - k_T|)$

True only if Φ is flat in k_T - for above fns. Else, there must be a collimation

Physics underlying the ridge

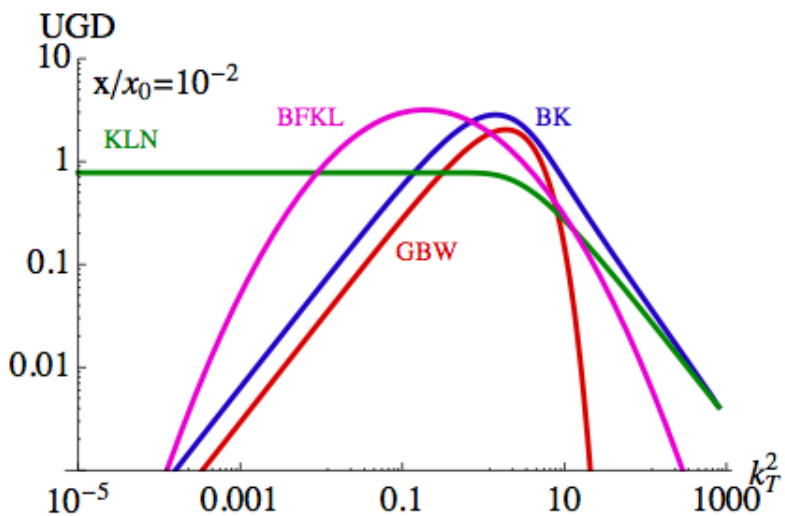

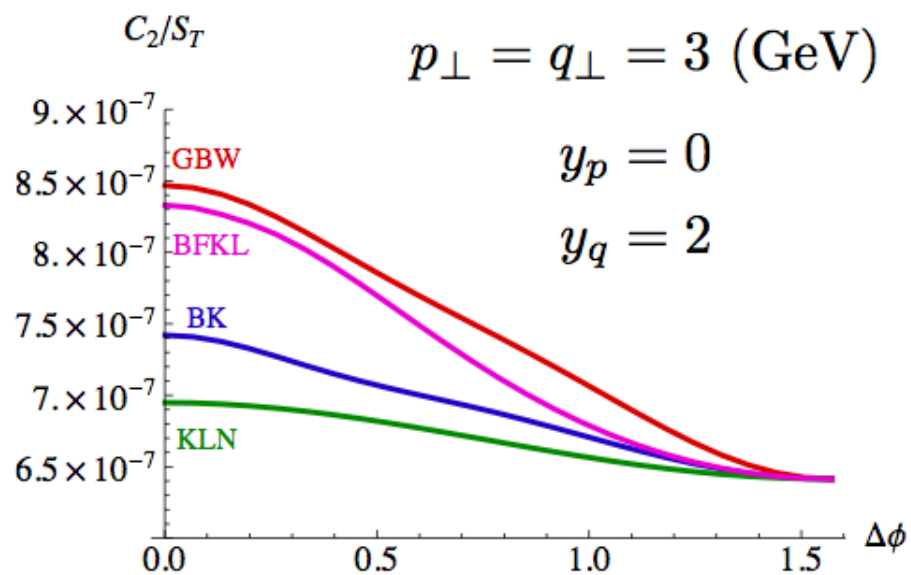

Physics underlying the ridge

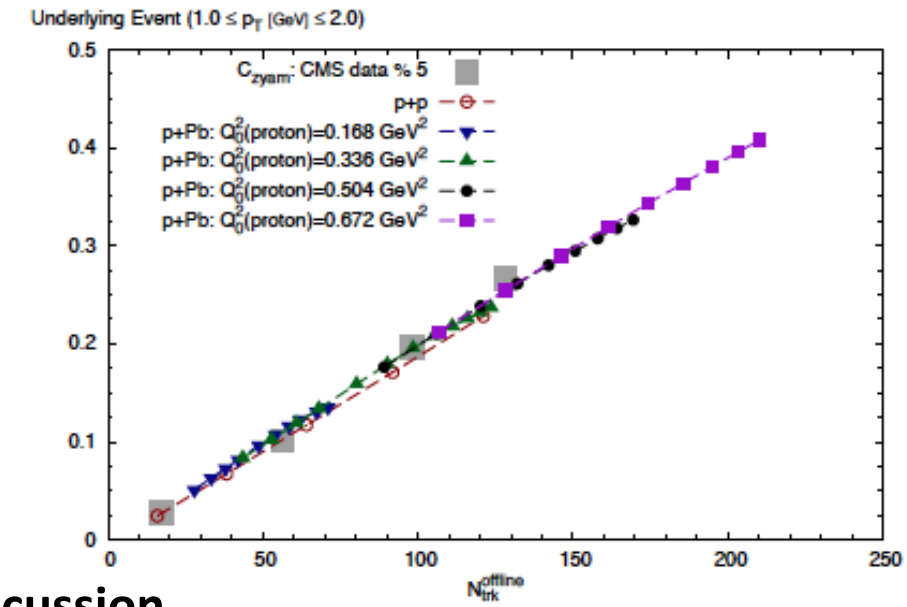

From previous discussion

$$\mathrm{UE} \propto \frac{\int d^2k_T\ \Phi_A^2(k_T)\ \Phi_B^2(|p_T - k_T)}{\int d^2k_T\ \Phi_A(k_T)\ \Phi_B(|p_T - k_T|)} \propto N_{\mathrm{track}}$$

rcBK vs IP-Sat evolution

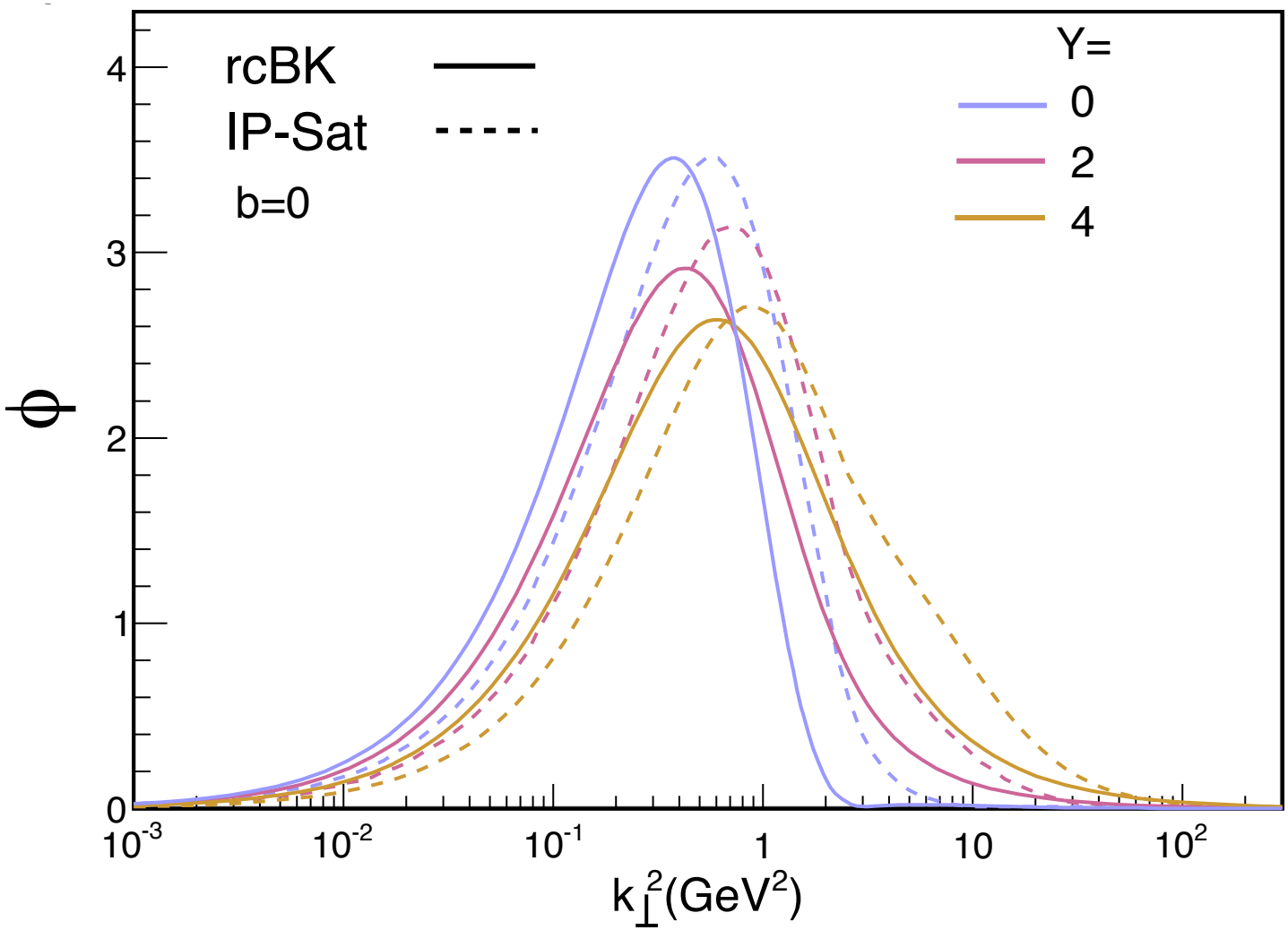

Jet Quenching at RHIC
vs LHC in Light of Recent dAu vs pPb Controls

RIKEN BNL Research Center Workshop
April 15-17, 2013 at Brookhaven National Laboratory

Particle Correlations at RHIC: Present & Future

Fuqiang Wang

Purdue University

U.S. DEPARTMENT OF ENERGY | Office of Science

PURDUE UNIVERSITY

BROOKHAVEN NATIONAL LABORATORY

Two types of correlations

FLOW

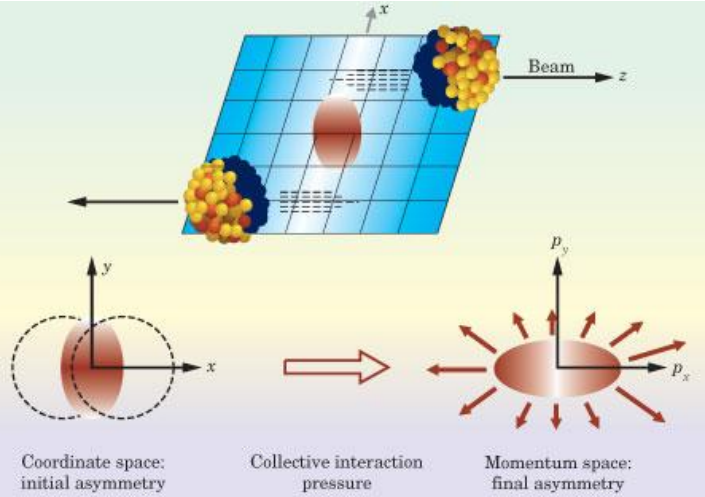

Initial-state anisotropy + fluctuations
Hydrodynamic evolution
Final-state event-wise correlations
Bulk medium properties

JET QUENCHING

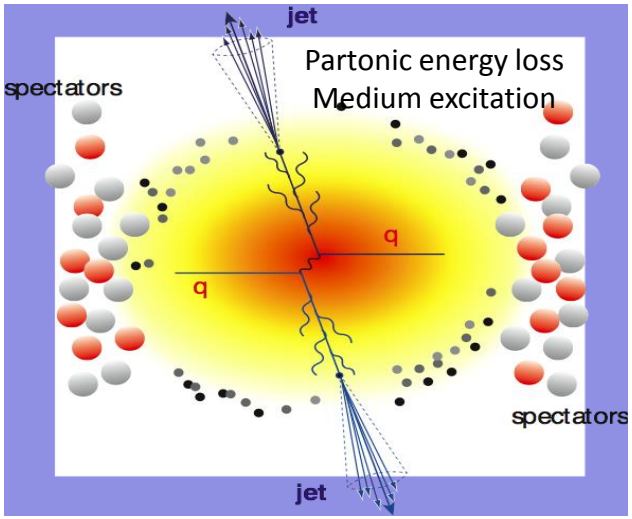

Initial-state hard processes
Jet-medium interactions
Final-state modified particle correlations
Probe ΔE mechanisms, medium properties

Flow and nonflow

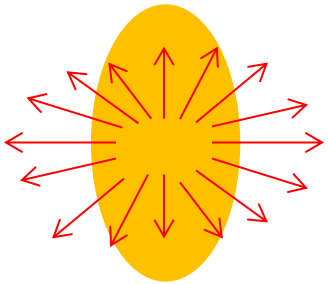

Flow due to hydrodynamic pressure

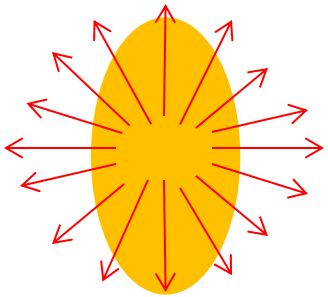

Anisotropy due to pathlength-dep. energy loss

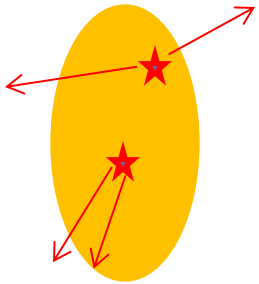

Nonflow correlations

High p_T suppression & re-emergence

STAR, PRL91 (2003)

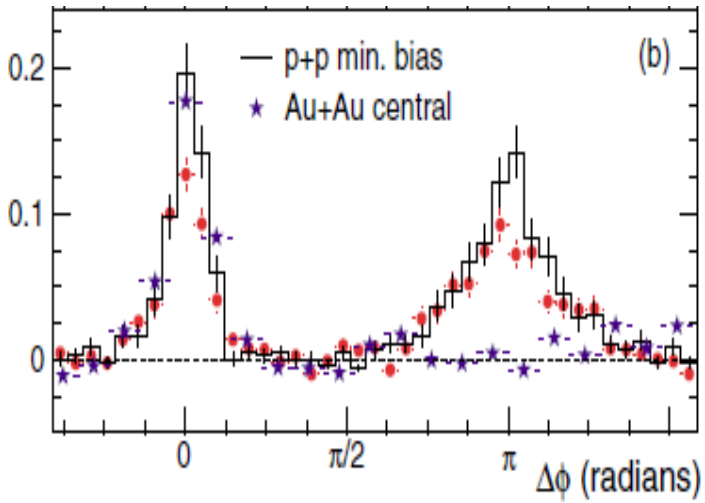

STAR, PRL97 (2006)

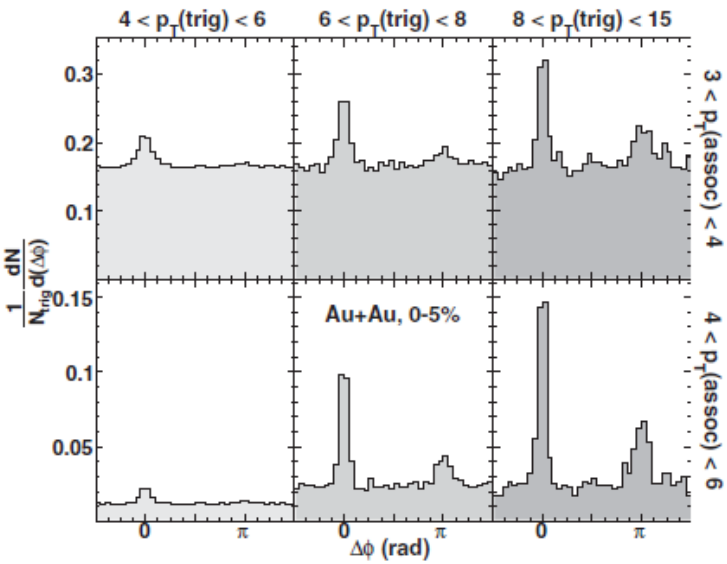

- Clear evidence of jet-quenching, and it's a final-state effect
- Finite probability of non-interacting jets at high p_T.

Low-intermediate p_T broadening

STAR, PRL 95 (2005); PRC82 (2010)

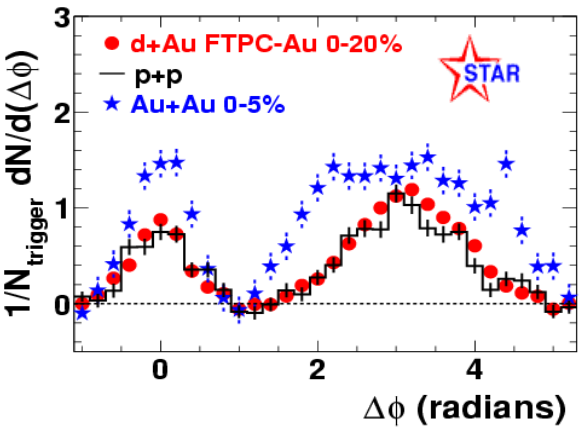

STAR, PRC80 (2009)

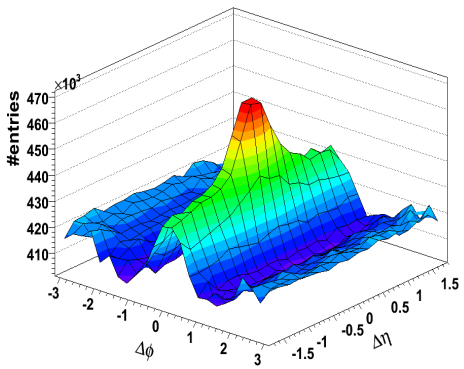

PHOBOS, PRL104 (2010)

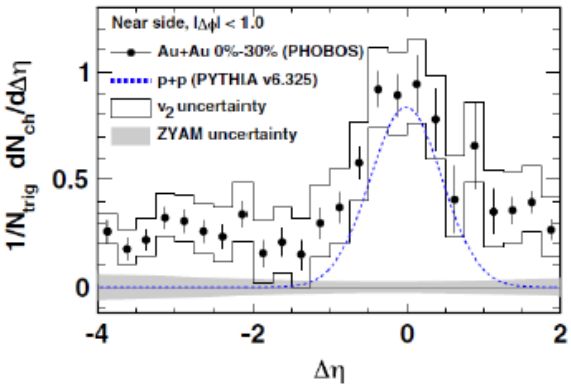

PHENIX,PRL97(2006);PRC78(2008)

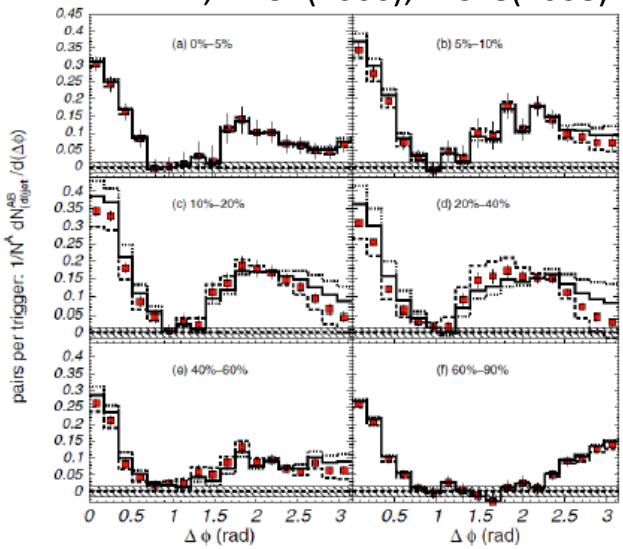

- Low p_T enhancement and broadening
- Large-$\Delta\eta$ small-$\Delta\phi$ ridge correlation
- Away-side double peak
- v_2 subtracted but not higher harmonics

All v_n's are possible

Mishra et al. PRC77 (2008)
Alver, Roland, PRC81 (2010)

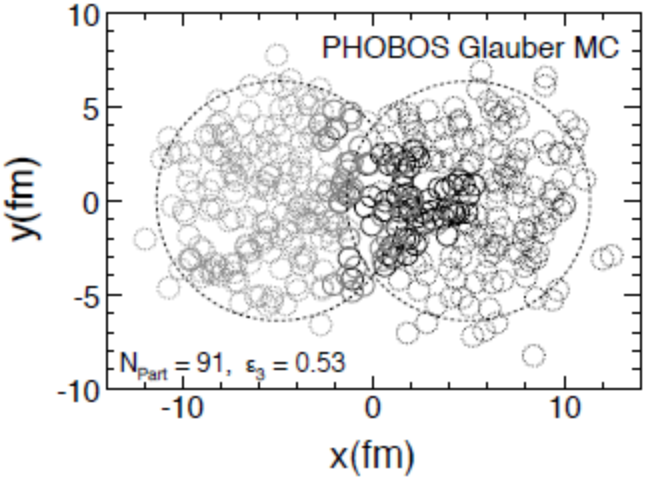

Schenke et al. PRL106 (2011)
Qiu, Heinz, PRC84 (2011)

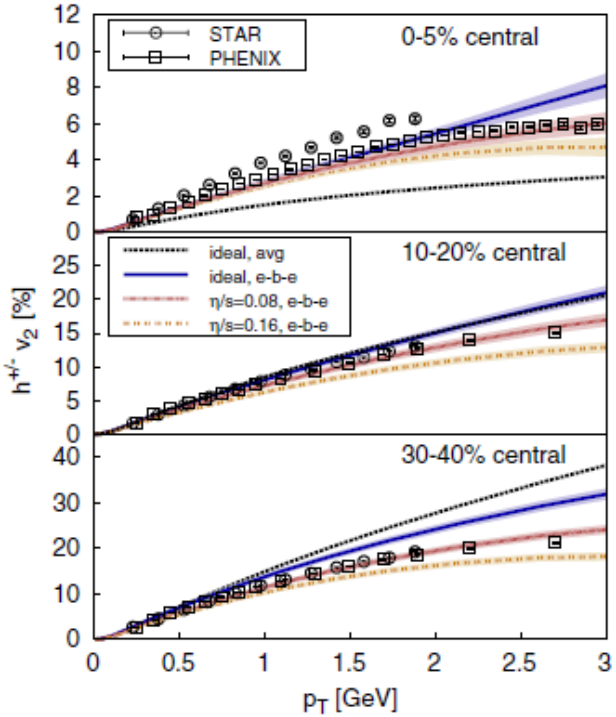

- Event-by-event fluctuations can generate initial-state triangular anisotropy
- Observable consequence in the final-state due to hydro evolution

v_3 measurements at RHIC

PHENIX, PRL107 (2011)

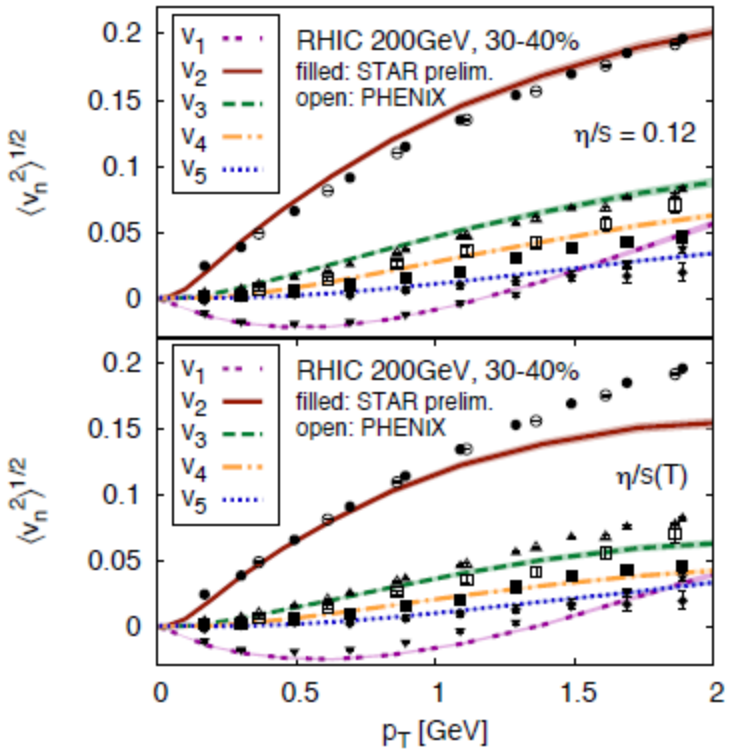

STAR, arXiv:1301.2187

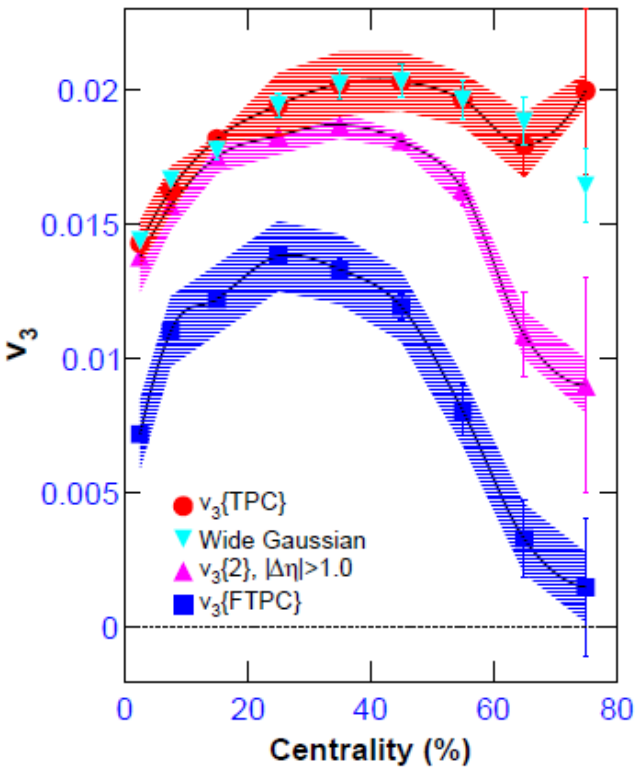

- There might be tension between STAR/PHENIX

v_3 decreases with $\Delta\eta$

STAR, arXiv:1301.2187

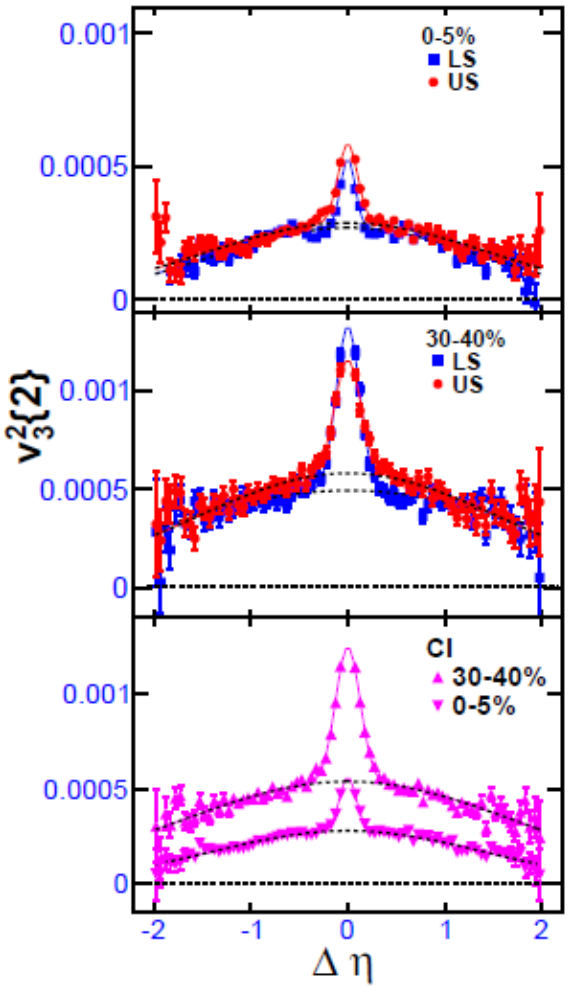

- v_3 decreases with $\Delta\eta$
- Consistent with untriggered correlations

STAR, PRC86 (2012)

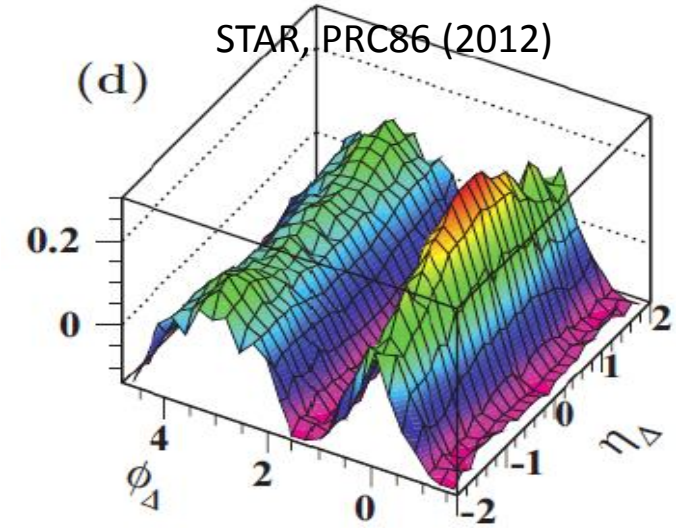

v_3 depends $\Delta\eta$

STAR, arXiv:1301.2187

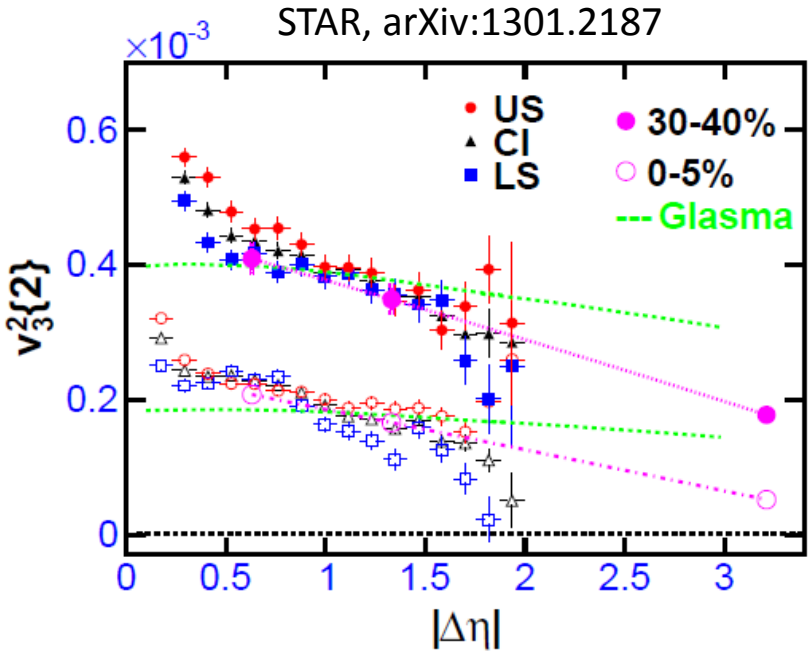

- Nonflow?

- $\Delta\eta$-dependent flow fluctuations? Harmonic planes may decorrelate over $\Delta\eta$

  Bozek et al. PRC83 (2011)
  Petersen et al. PRC84 (2011)
  Xiao et al. PRC87 (2013)

Petersen, QM 2012

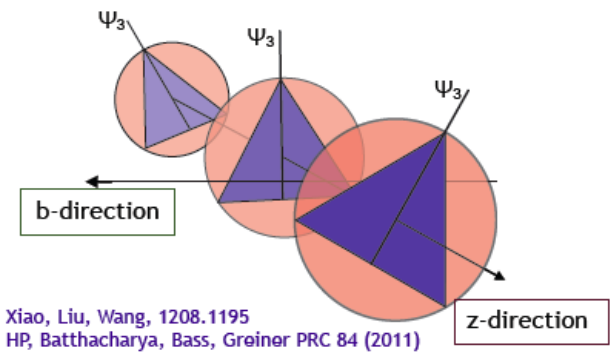

- $\Delta\eta$-gap method may not be suitable

Flow/nonflow vs. η

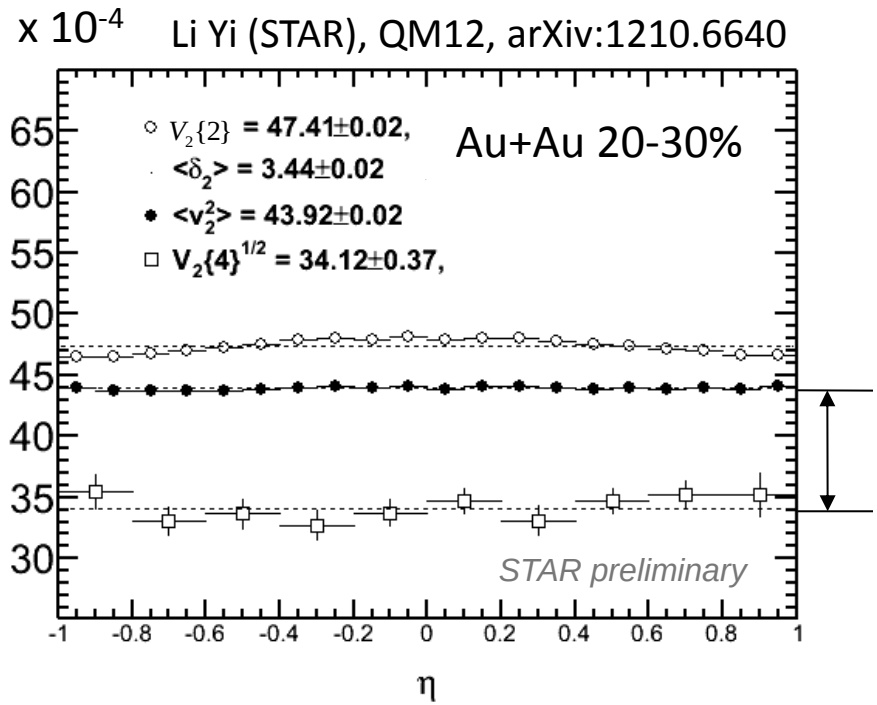

$$\frac{\sigma_2^{\ 2}}{\langle v_2 \rangle^2} \sim \frac{\langle v_2^2 \rangle - V_2\{4\}^{1/2}}{\langle v_2^2 \rangle - V_2\{4\}^{1/2}} \sim 13\%$$

- Method does not assume flow shape vs. η
- Flow seems independent of η.
- (Nonflow/flow)^2 ~ 4%, (Nonflow/flow) ~ 20%,
- (Fluctuation/flow)^2 ~ 13%, Fluctuation/flow ~ 36%

Why is `flow' factorization so good? Because it is bootstrapped!

$$V_n(p_T^a, p_T^b) \times V_n(p_T^{ref}, p_T^{ref}) \approx V_n(p_T^a, p_T^{ref}) \times V_n(p_T^b, p_T^{ref})$$

Kikola et al. PRC86 (2012) 014901

Independent jet fragmentation → Jet correlation may approximately factorize!

$$\langle \cos n(\phi_i - \phi_j) \rangle = \langle \cos n[(\phi_i - \psi_{jet}) - (\phi_j - \psi_{jet})] \rangle = \langle \cos n(\phi_i - \psi_{jet}) \rangle \langle \cos n(\phi_j - \psi_{jet}) \rangle$$

Anisotropic flow + non-flow: $V_{2\Delta}(p_T^a, p_T^b) = v_2(p_T^a) v_2(p_T^b) + \delta_2(p_T^a) \delta_2(p_T^b)$

$$\frac{V_{n\Delta}(p_T^b, p_T^a)}{v_n'(p_T^a) v_n'(p_T^b)} - 1$$

$$= \frac{v_n(p_T^b) v_n(p_T^c) + \delta_n(p_T^b) \delta_n(p_T^c)}{\frac{v_n(p_T^a) v_n(p_T^c) + \delta_n(p_T^a) \delta_n(p_T^c)}{\sqrt{v_n^2(p_T^c) + \delta_n^2(p_T^c)}} \frac{v_n(p_T^b) v_n(p_T^c) + \delta_n(p_T^b) \delta_n(p_T^c)}{\sqrt{v_n^2(p_T^c) + \delta_n^2(p_T^c)}}} - 1$$

$$\approx \left(\frac{\delta_n(p_T^a)}{v_n(p_T^a)} - \frac{\delta_n(p_T^c)}{v_n(p_T^c)} \right) \left(\frac{\delta_n(p_T^b)}{v_n(p_T^b)} - \frac{\delta_n(p_T^c)}{v_n(p_T^c)} \right) \quad (14)$$

- $\delta_n(p_T) / v_n(p_T) \sim 20\%$ → deviation ~ 10^{-2} - 10^{-3}
- $\delta_n(p_T) \propto v_n(p_T)$ → precise factorization

Is it important to remove nonflow?

Important because it affects extracted QGP medium property, such as η/s.

Hydro-data comparison (e.g. Uli Heinz): $v/\varepsilon \rightarrow \eta/s \sim (1\text{-}2) * 1/4\pi$
20% error on ε (Glauber vs CGC) → 100% uncertainty on η/s.

The question is how to reduce uncertainty in v_2/ε :
1. ε from theoretical part
2. v_2 from experimental part

Song, Bass, Heinz, etal. PRL 106, 192301 (2011)

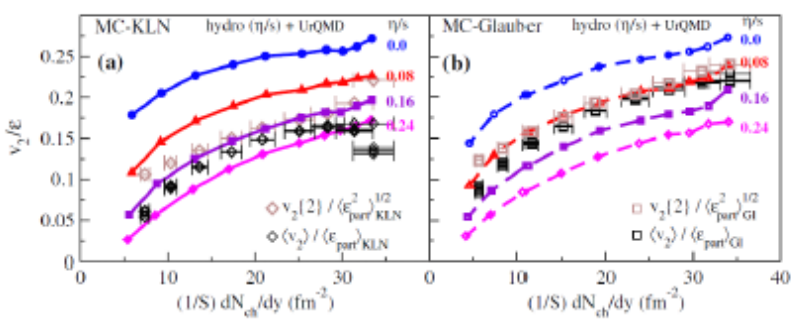

"The extraction of η/s from a comparison with hydrodynamics thus requires careful treatment of both fluctuation and nonflow effects"

v_n background subtraction

- It's absolutely important to remove all sizeable v_n's in jet-correlations
- What v_n to subtract? v_n with minimal jet (nonflow) contributions
- But v_n have to be measured by final-state particle correlations

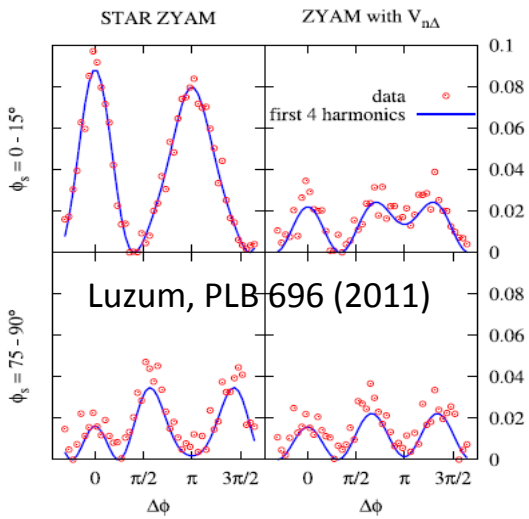

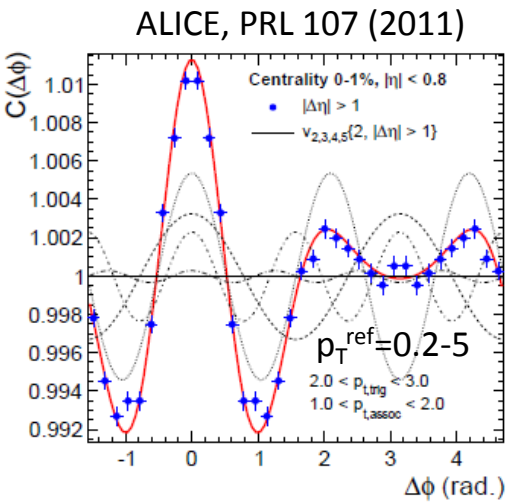

Word of caution: With non-vanishing odd harmonics, nothing really prevents people from fitting everything to v_n. Fine in itself, but dangerous if people subsequently take it as entirely hydro flow.
The real question is what's in v_n?

- Apply $\Delta\eta$-gap: may not work because of potential $\Delta\eta$-dep. flow fluctuations
- Viable way is to use as low p_T reference particles as possible. Disadvantage is flow is small at low p_T.

Dihadron correl. with vn subtractions

Todoroki (PHENIX), QM12, arXiv:1304.2852

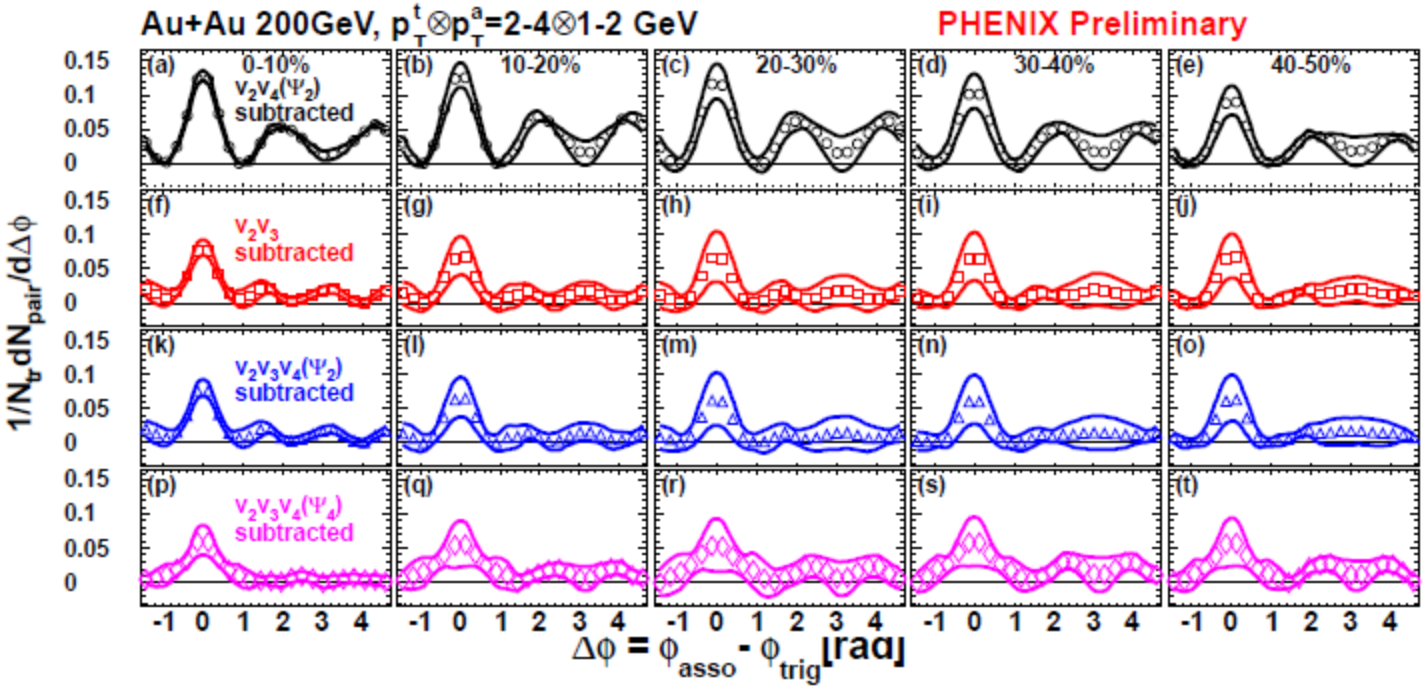

Relative to the Event Plane

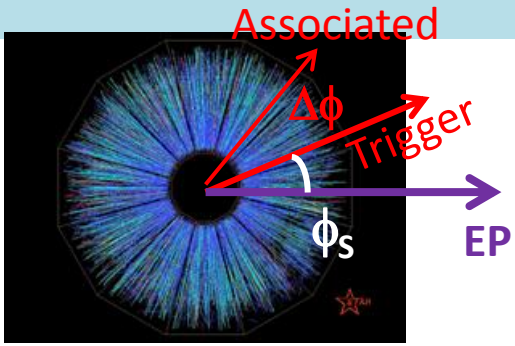

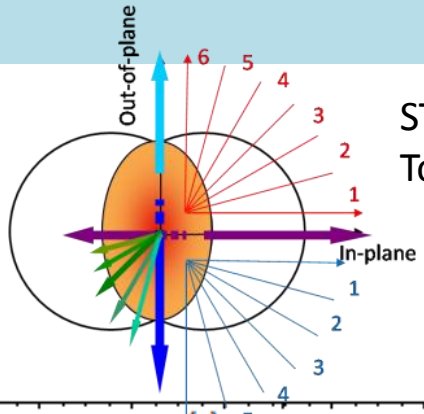

STAR, arXiv:1010.0690v1
Todoroki (PHENIX) 1304.2852

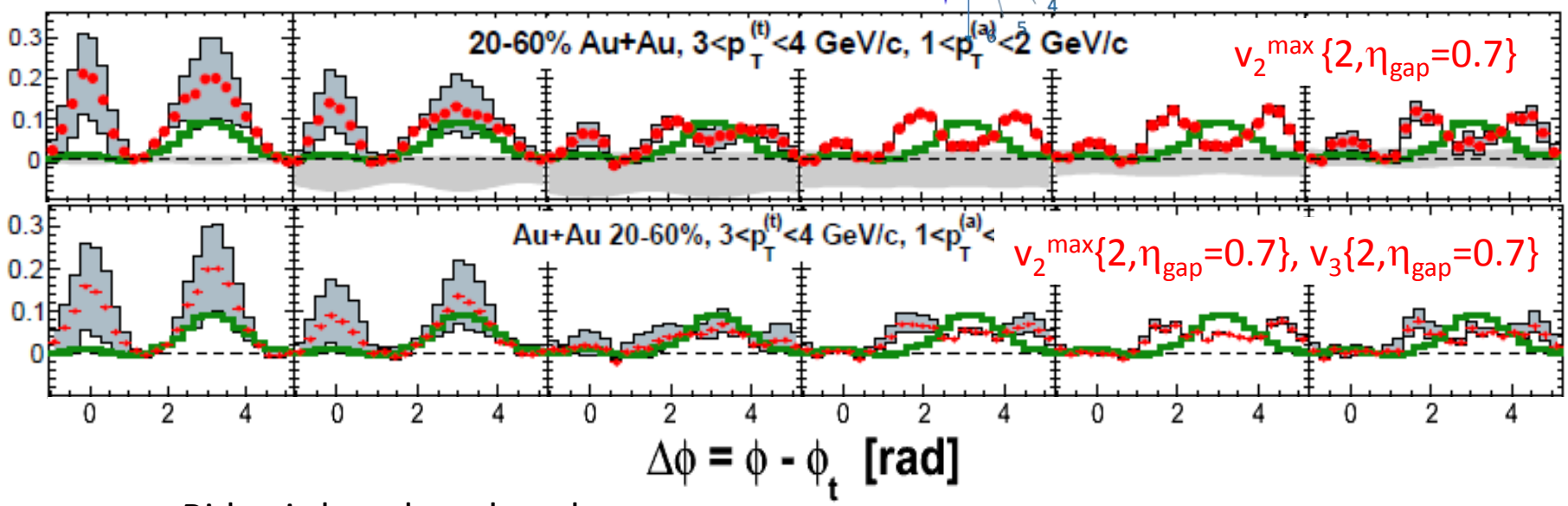

- Ridge is largely reduced.
- Evolution of structure seems to remain from in-plan to out-of-plane.
- Possible biases in EP reconstruction due to jet-correlations?

v_3 effect on 3-particle correl.

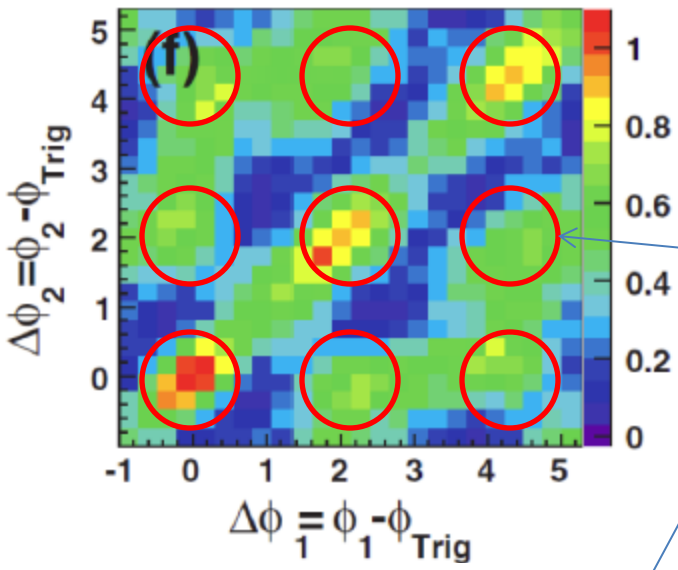

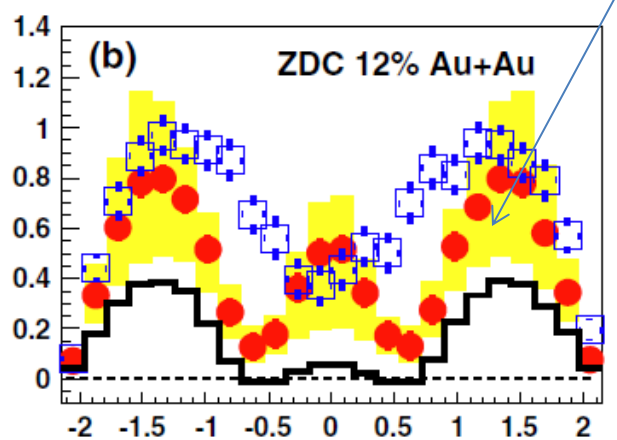

- v2 and v4 subtracted.
- Does v3 remove all of the off-diag. peak strength? Need further study.
- Deflected jets contributions (to diag. peaks) must be present.
- Need to be followed up.

pA and dA ridge

PHENIX, arXiv:1303.1794

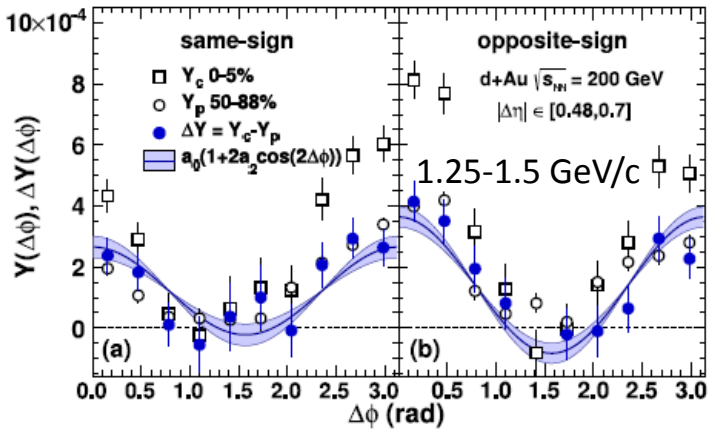

$0.15 < p_T^{trig} < 3$ GeV/c

$1 < p_T^{assoc} < 2$ GeV/c

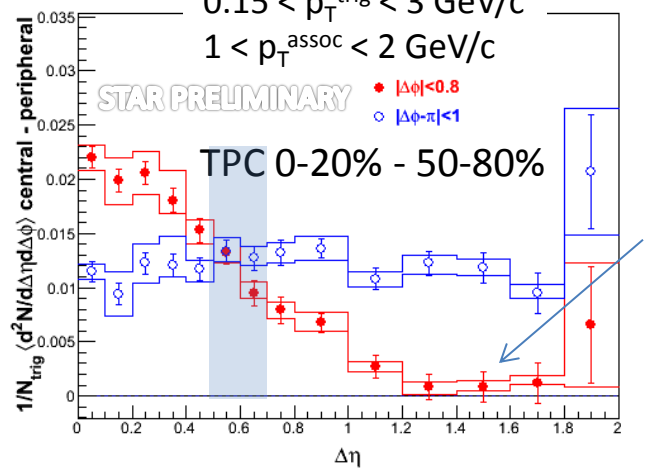

Minimal ridge

Bozek, PRC85 (2012)

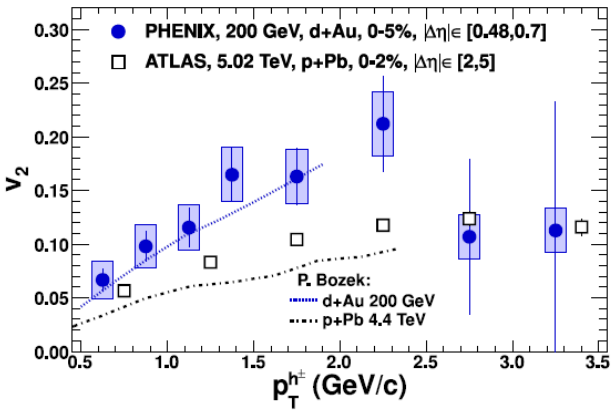

Dusling and Venugopalan, arXiv:1302.7018

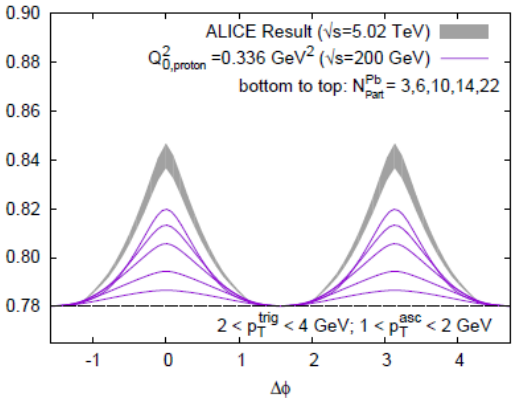

- LHC+RHIC more stringent test on theoretical models.

Where is hydro bkgd to triggers?

C. Shen et al. PRC82 (2010) 054904

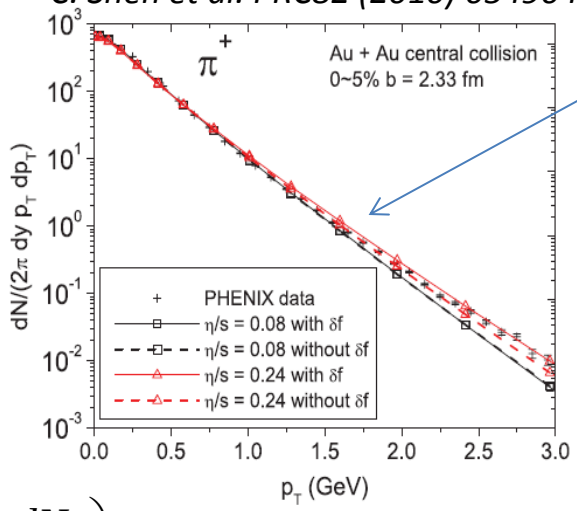

- Going to lower trigger p_T, expect large hydro contribution to particle production → Jet-like correlations should be reduced.

- Surprisingly similar Au+Au and d+Au near-side jet-like signal strength
- No evidence of trigger dilution from hydro background triggers

$$\frac{1}{N_{trig}}\left(\frac{dN}{d\Delta\phi}\right)$$

Konzer (STAR) QM 2012, STAR preliminary

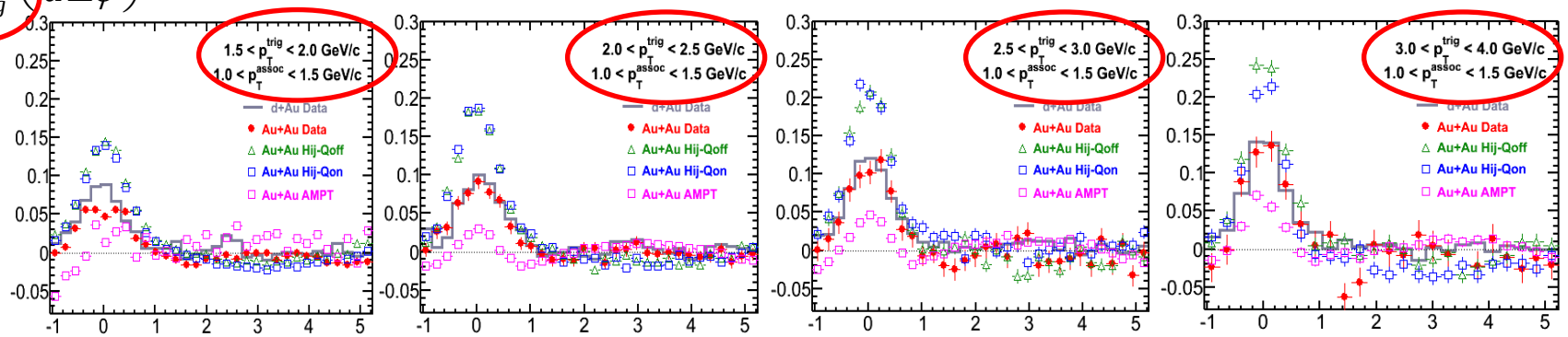

Prospective future measurements

- Hydro v_n explains majority of ridge and double-peak correlations in heavy-ions. Does hydro v_n explain all of the correlation signals?
- v_n measurements with minimal nonflow: go to low p_T reference particles, $\Delta\eta$-gap?
- Precision measurements of jet-correlations with v_n subtraction
- Dihadron correlations w.r.t. EP with EP far removed in η.
- More clever way to separate flow/nonflow?

- γ-jet with no flow background
- Heavy flavor induced correlations

- Can we learn something fundamental from small systems?
- How high dA multiplicity can we reach at RHIC?

Harmonic jet tomography at RHIC+LHC

Xilin Zhang (Ohio U)

Jet Quenching Workshop, RIKEN BNL, April 2013

X.Z. and Jinfeng Liao,
*PLB **713,** 35 (2012)*
*arXiv:**1208.6361**, **1210.1245**.*

Outline

- Jet tomography: geometry and fluctuations; different jet energy loss models
- High-pt Vn at different centralities from RHIC to LHC
- Hard-soft correlation
- P-Pb case
- Conclusion and outlook

Jet tomography: geometry

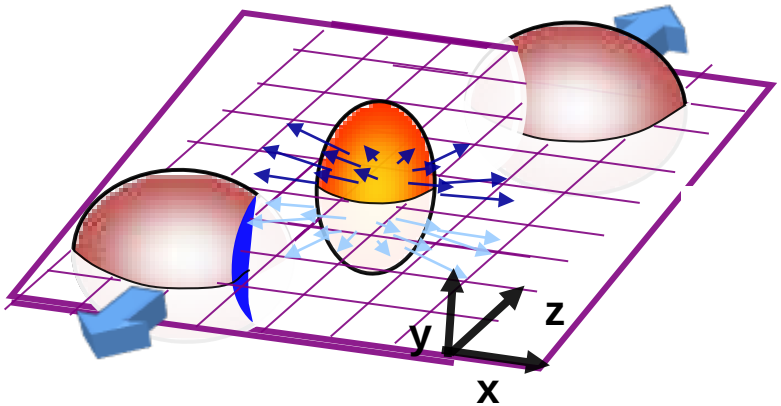

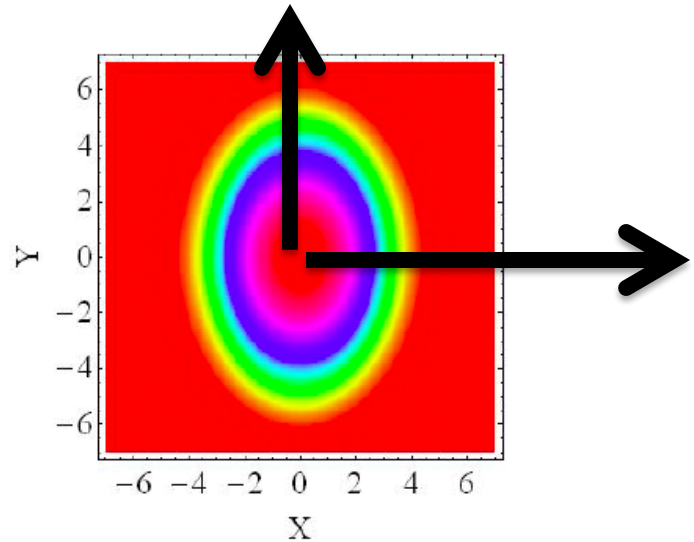

$$\frac{dN^h}{d\phi} \sim R_{AA}(\phi) \sim 1 + 2v_2 \cos[2(\phi - \Psi_R)]$$

Can V2 be understood in a consistent picture <u>from</u> RHIC <u>to</u> LHC?

Jet tomography: **High pt Vn!**

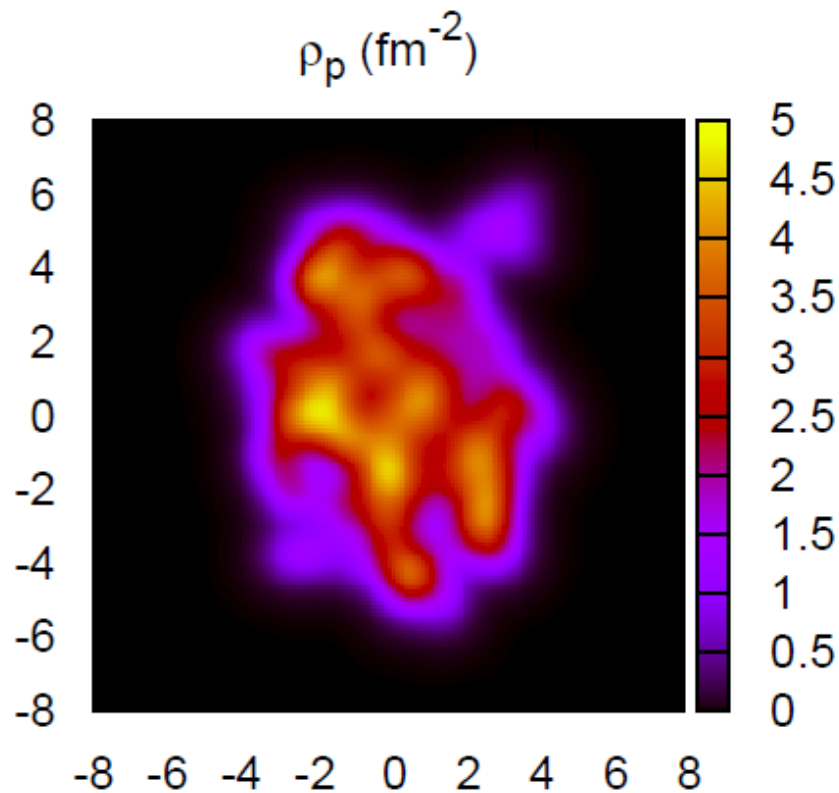

Initial state, and jet production fluctuations

Glauber model

$$R_{AA}(\phi) \sim 1 + 2\sum_n v_n \cos[n(\phi - \Psi_n^J)]$$

- **Consistent picture and more information!**
- **Hard-soft correlation.**

Jet energy loss

- Length dependence?
- Density dependence?

*J. Liao and E. Shuryak, PRL **102**, 202302 (2009)*

$$\Delta E = -E\,\kappa[s(l)] \times s(l) \times l^m \times \Delta l$$

- NTcE model: m=1.
  (Nontrivial matter near Tc)
- L^2 model: m=1, κ const.
  (pQCD)
- L^3 model: m=2, κ const.
  (AdS/QCD)

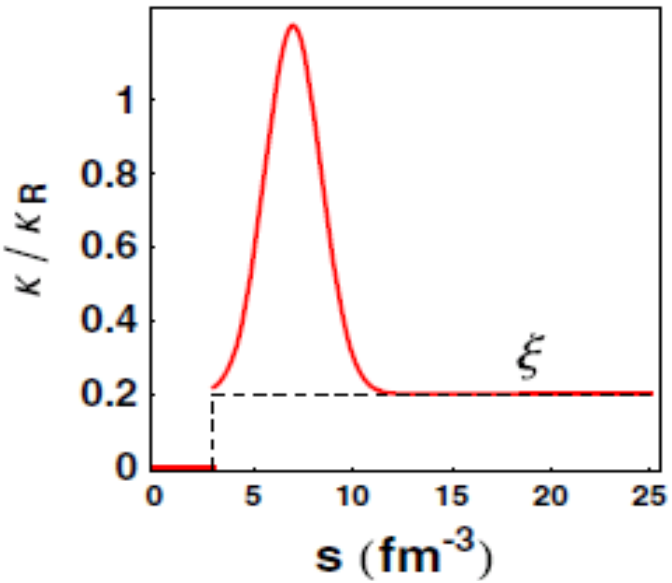

*Barbara Betz et.al., PRC **84**, 024913 (2011)*
*W.A. Horowitz and M. Gyulassy, NPA **872**, 265 (2011)*

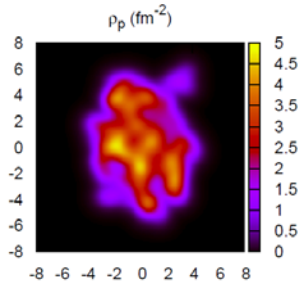

MC: one event

$$g_{pp}(p_t) \propto \frac{1}{p_t^n}$$

$$E_f = E_i \times f_{\vec{p}} \qquad R_{AA} = < (f_{\vec{p}})^{n-2} >_{\vec{p}}$$

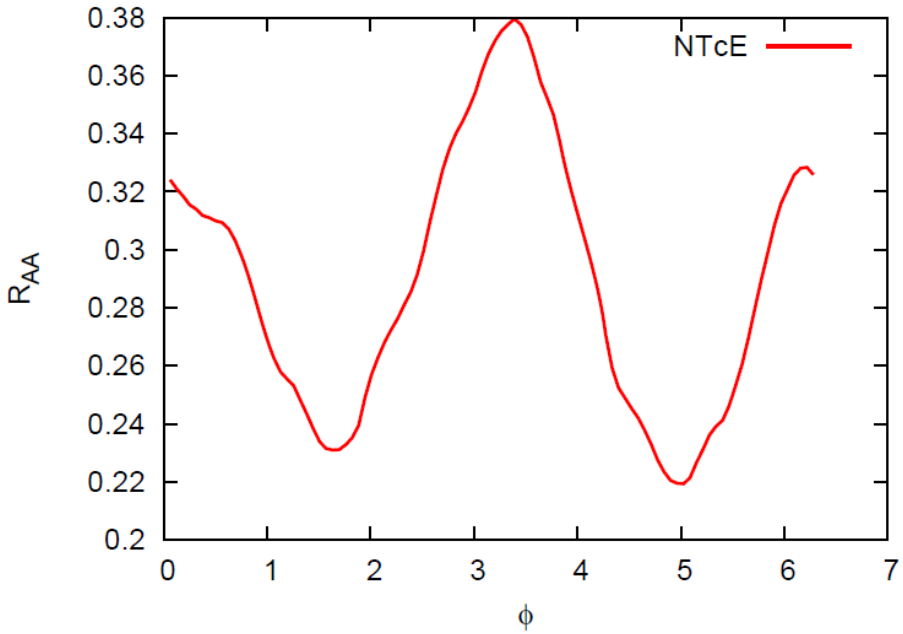

Sum over all the jet spots and jet paths

n= 8.1 (200 GeV), n=6.0 (2.76 TeV)

$$R_{AA}(\phi) \sim 1 + 2\sum_n v_n \cos[n(\phi - \Psi_n^J)]$$

Results: V2, RHIC 200 GeV

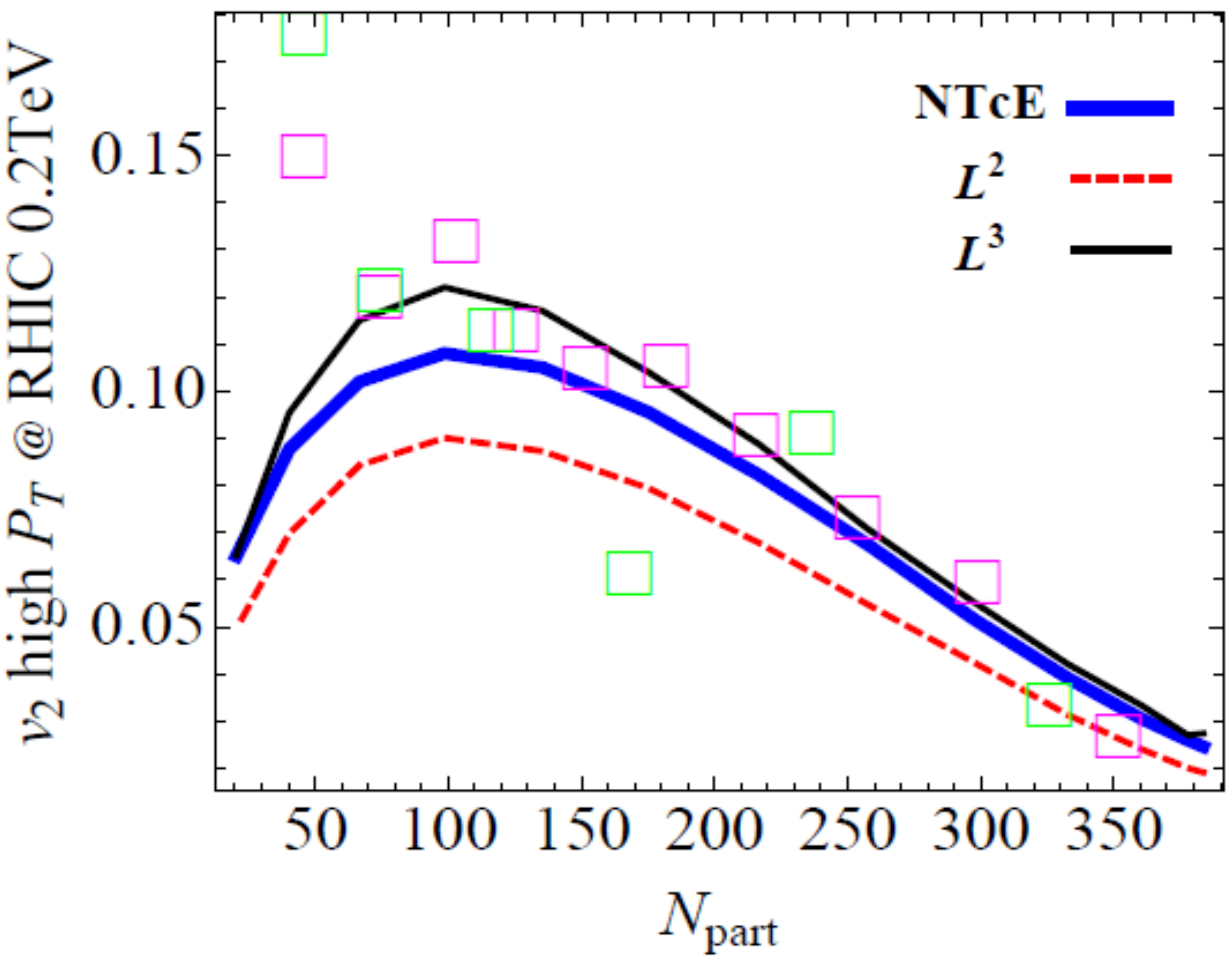

*PHENIX, Pt: 6--9 GeV and > 9 GeV, PRL **105**, 142301 (2010).*

Results: V2, LHC 2.76 TeV

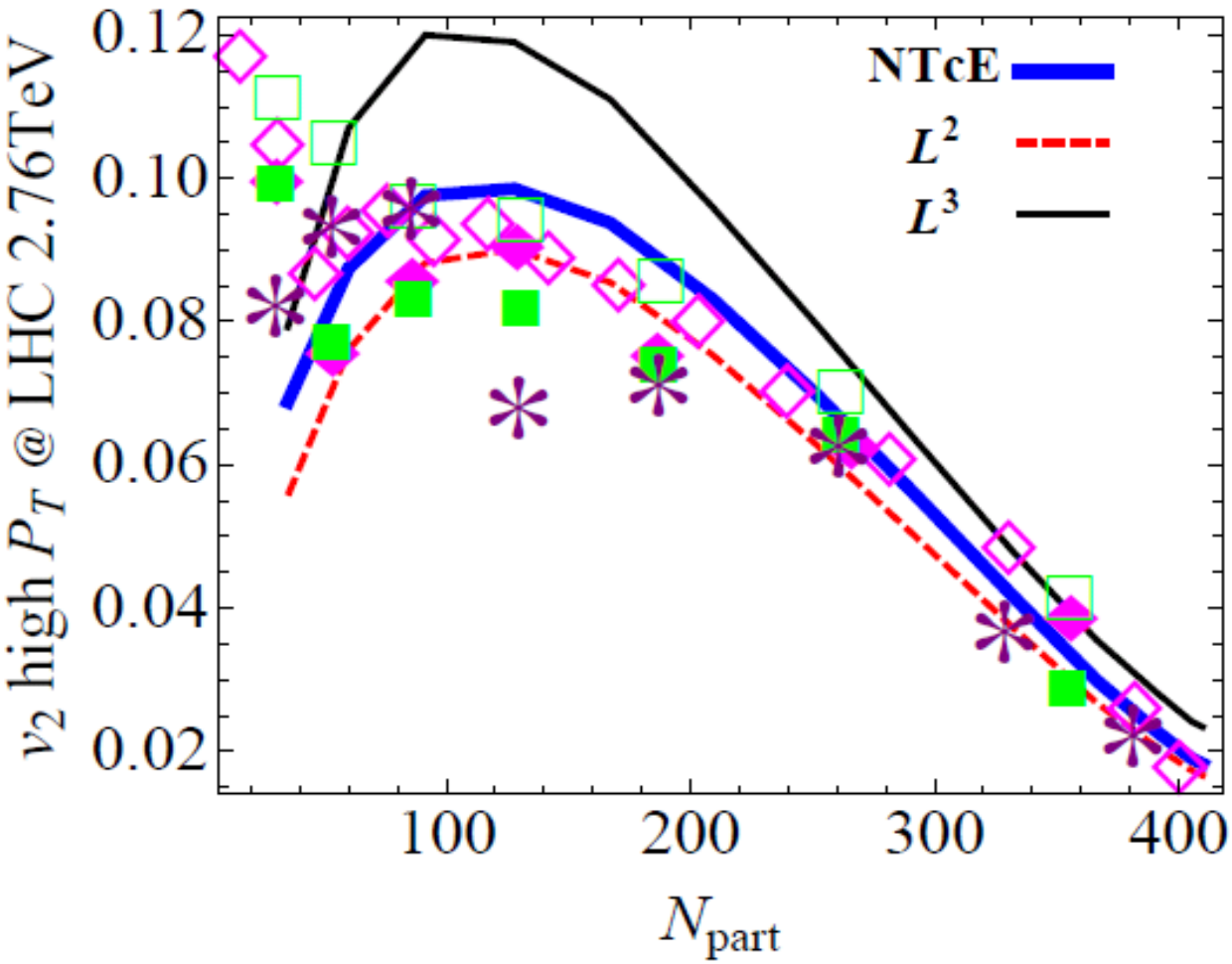

ATLAS, CMS, and ALICE, Pt: ~10--20 GeV,
*arXiv:1205.5761, 1204.1850, PLB **707**, 330 (2012)*

From RHIC to LHC

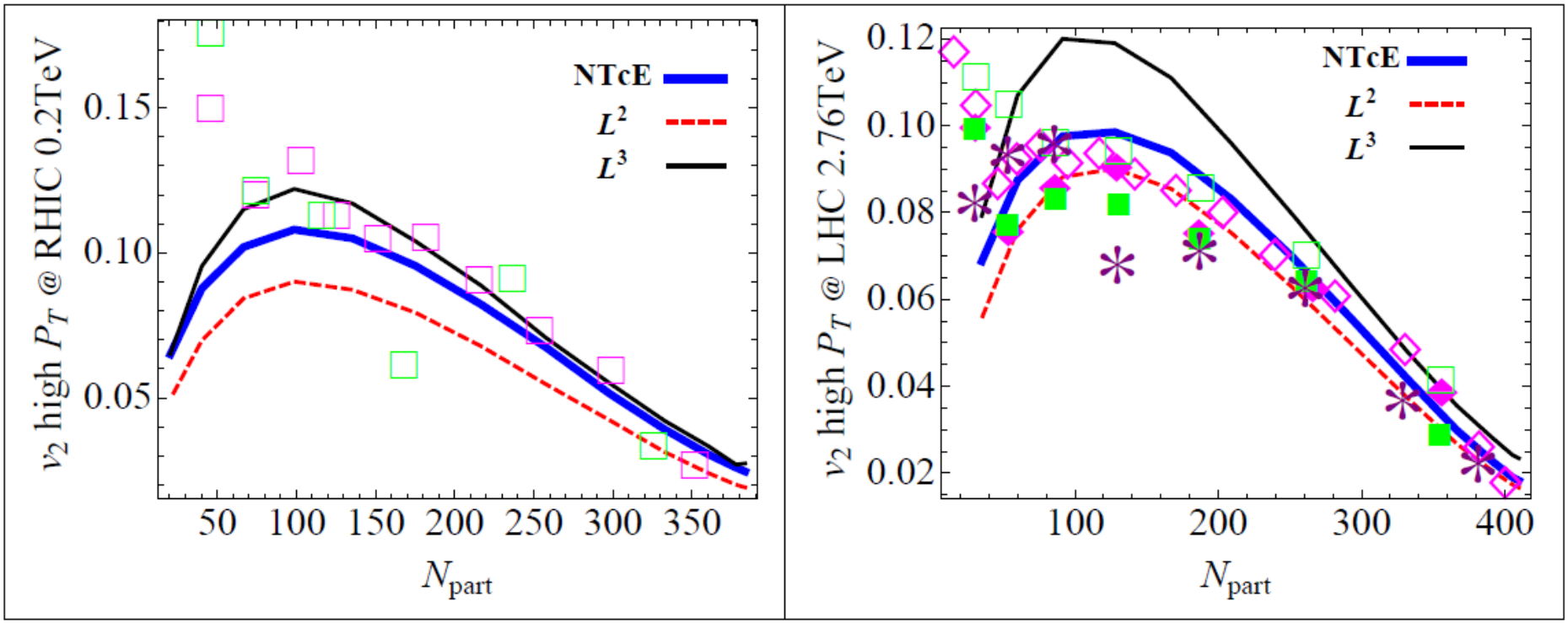

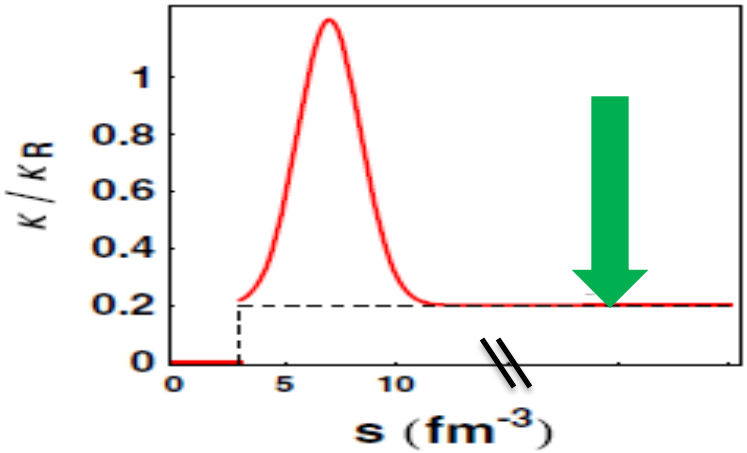

X.Z. and J. Liao, arXiv:1208.6361

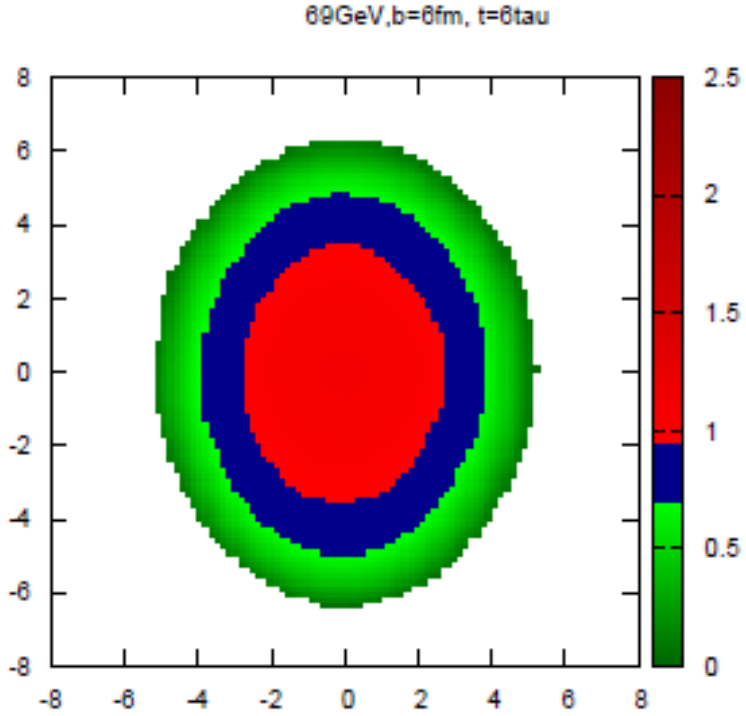

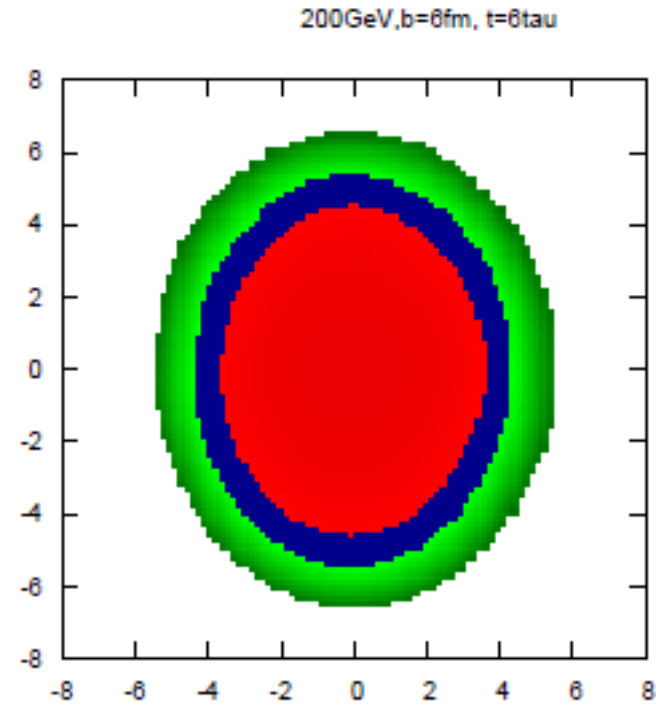

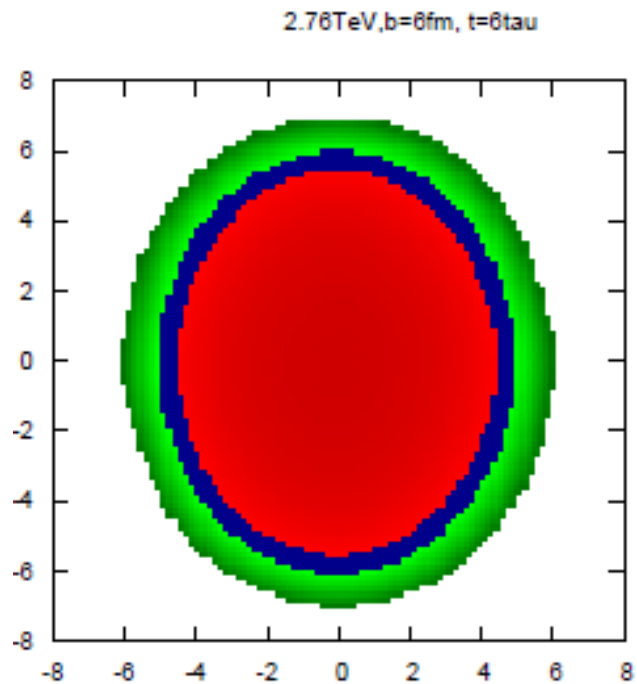

Entropy density

Results: Vn, LHC 2.76 TeV

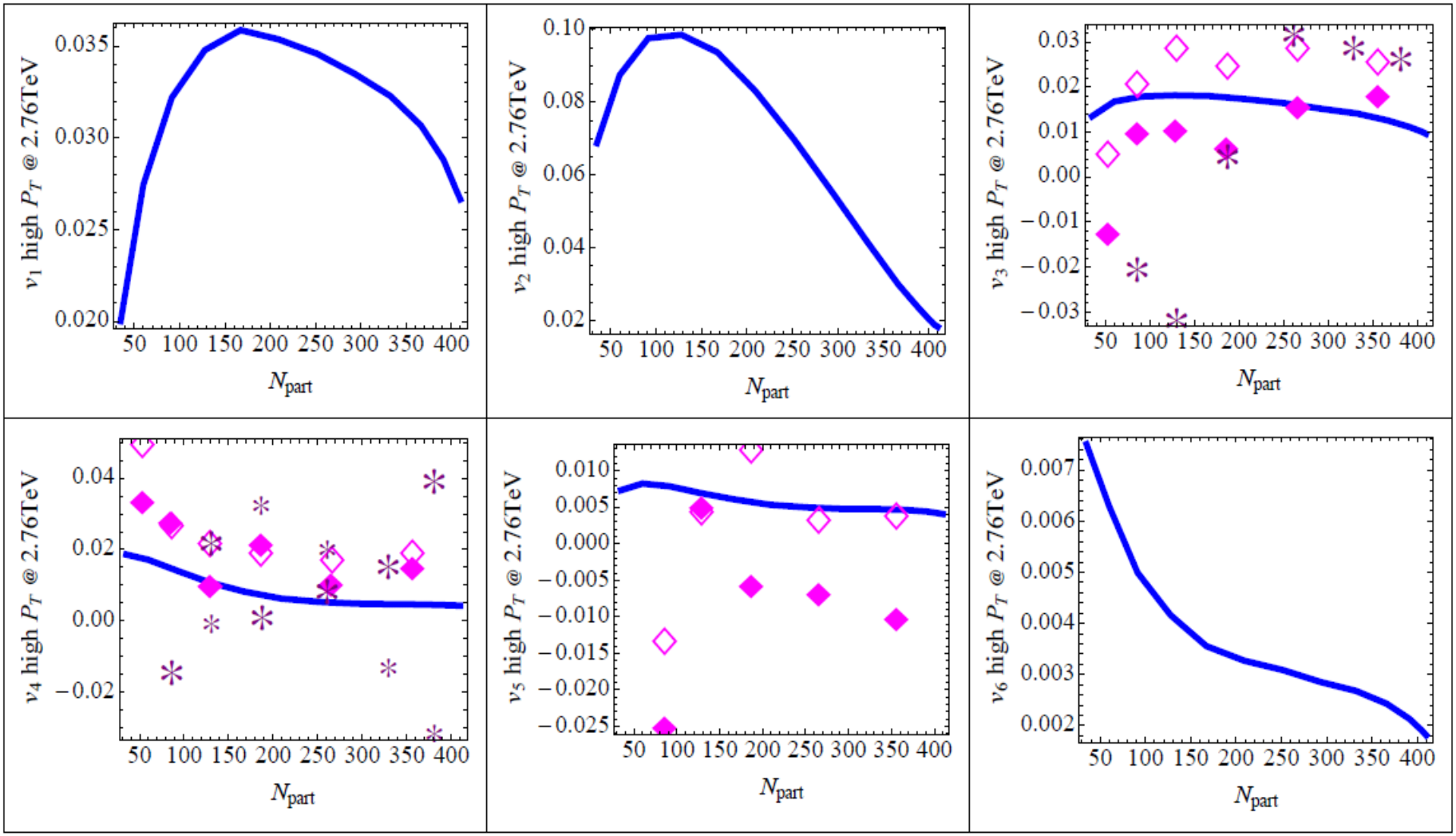

Based on NTcE model

Some details: Vn spectrum

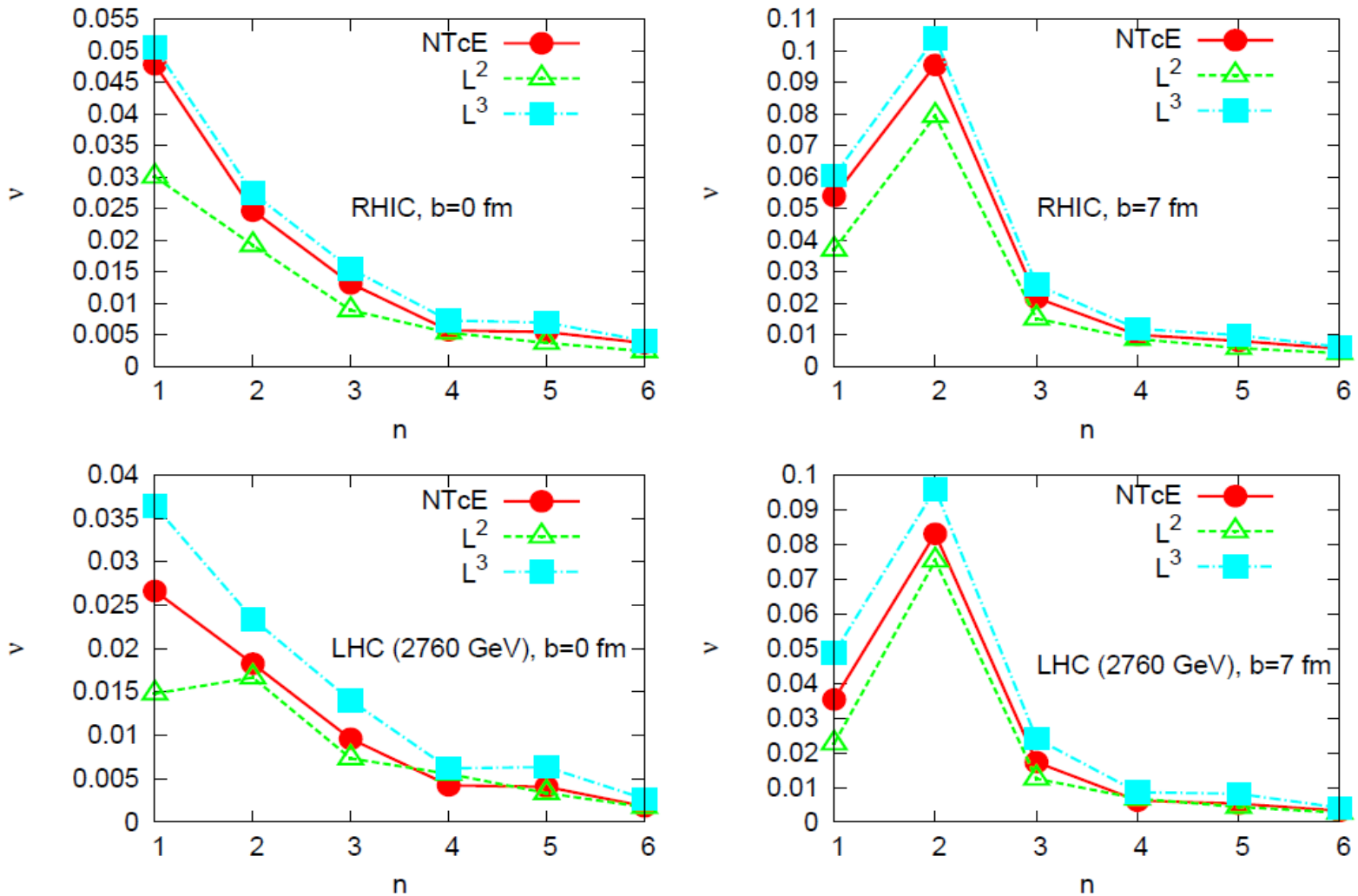

X.Z. and J. Liao, arXiv:1210.1245

Some details: angle dispersion

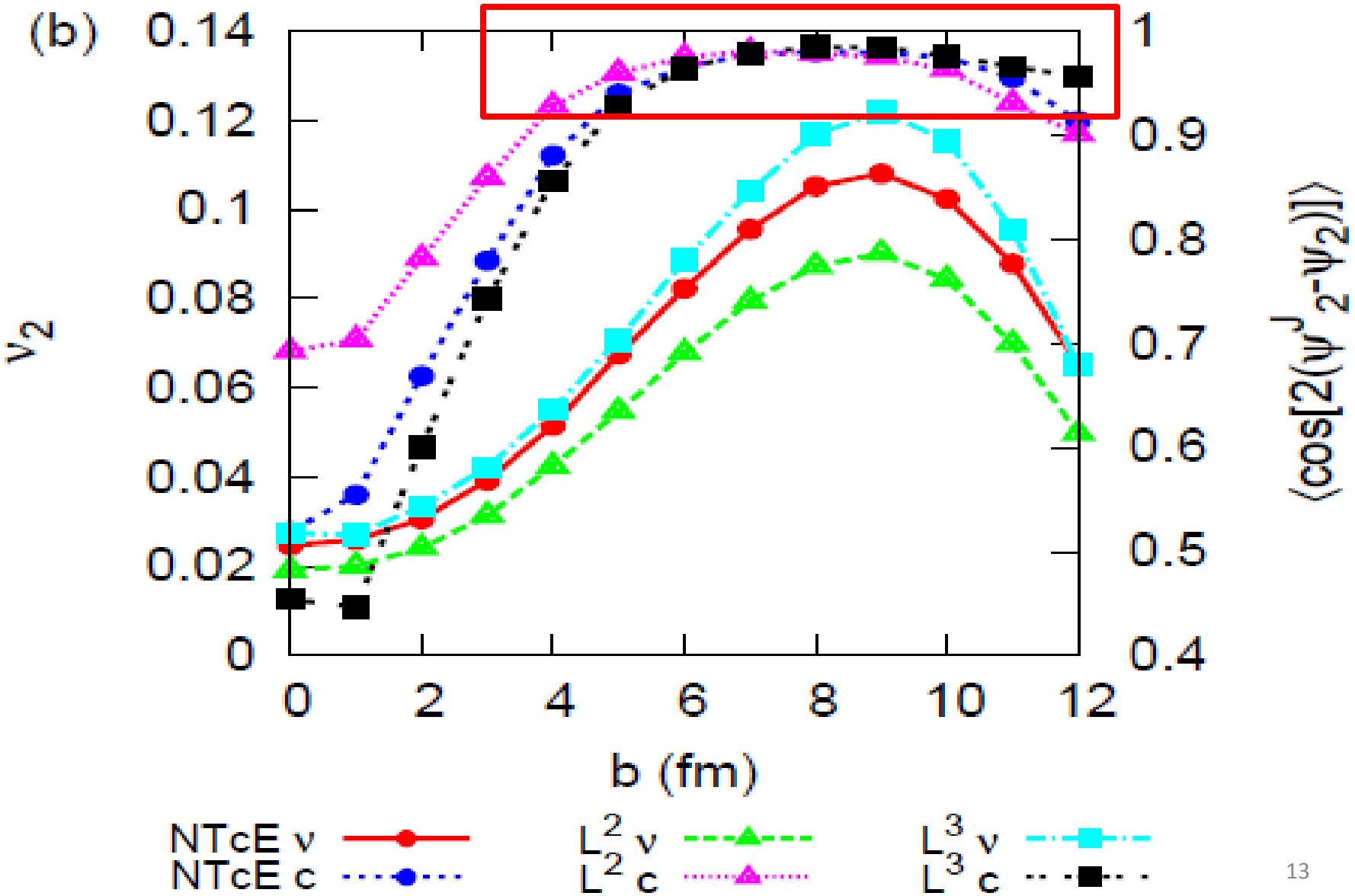

Some details: angle dispersion

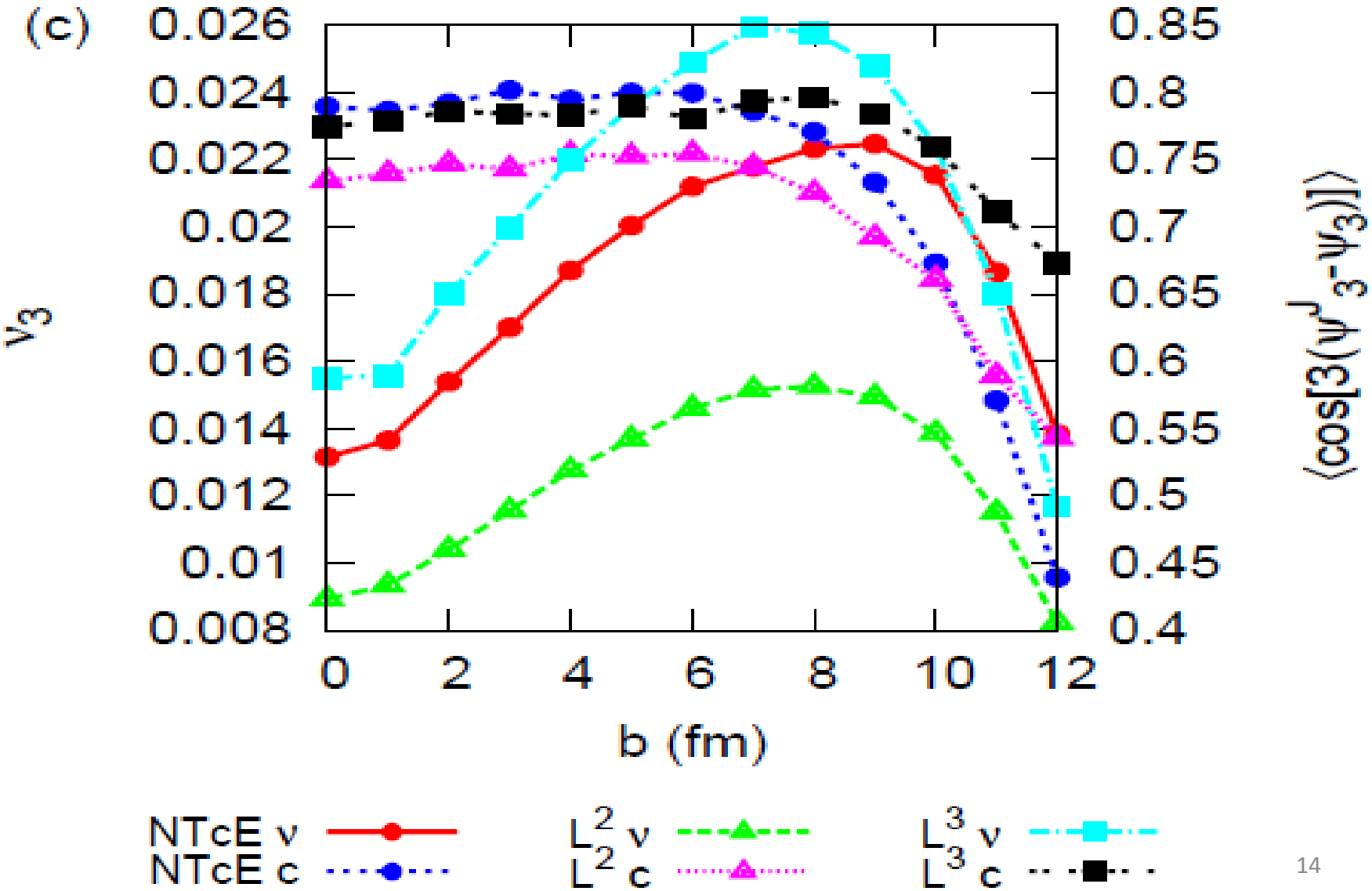

Hard-soft Correlation

p^t_T 4-6, p^a_T 2-4, 0-5% centrality, Pb-Pb (2.76 TeV)

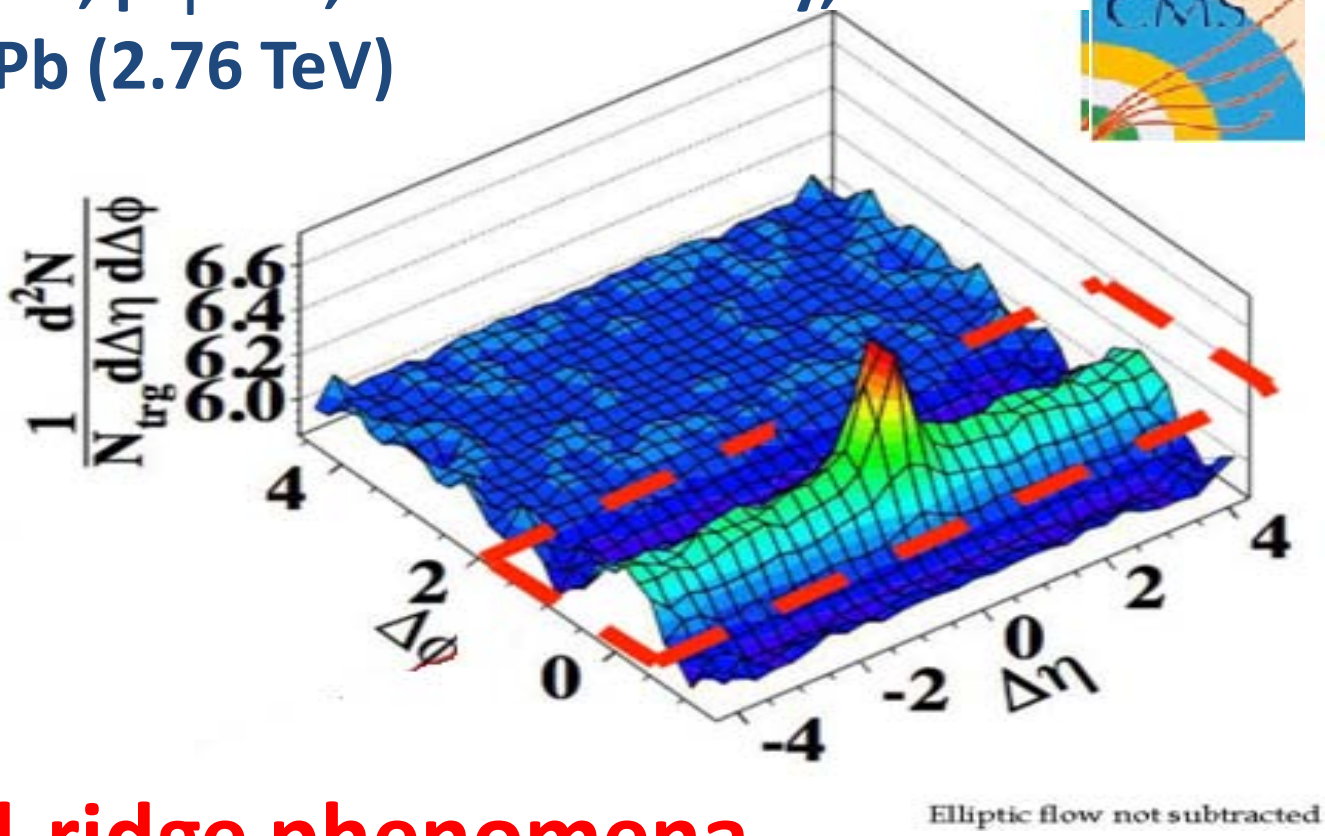

Hard-ridge phenomena

From Olga Evdokimov's talk at NNPSS2011

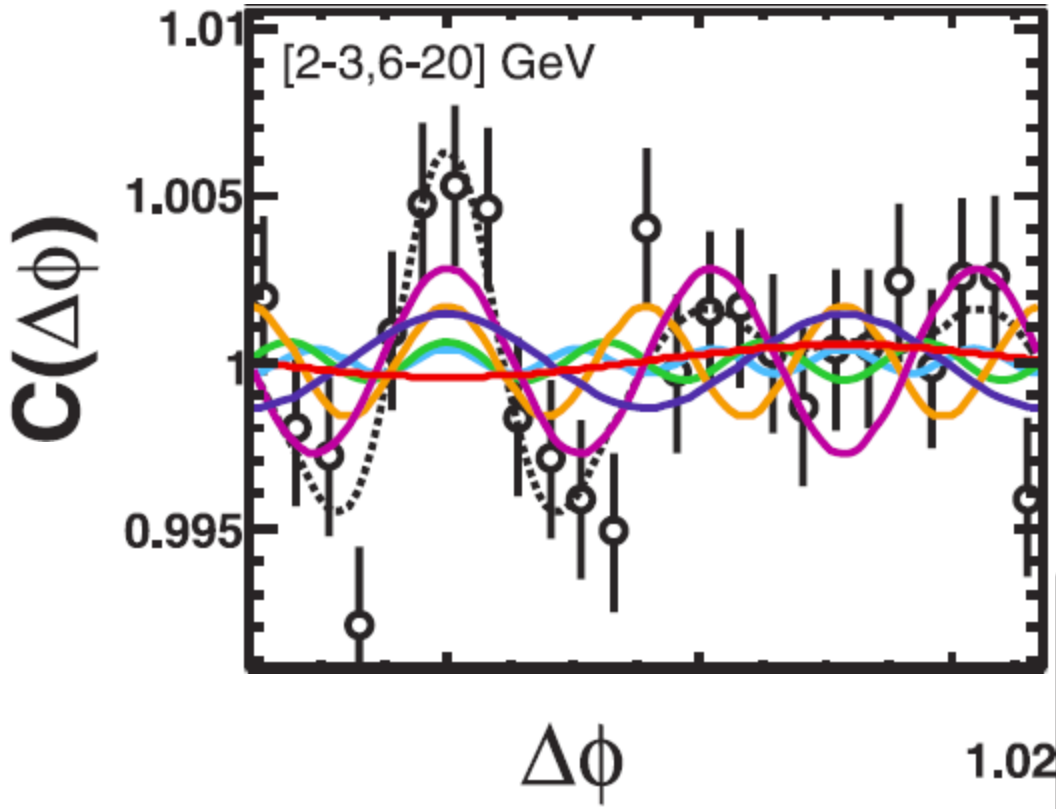

ATLAS,
*PRC **86**, 014907 (2012)*

0-1% centrality,

$2 < |\Delta\eta| < 5$

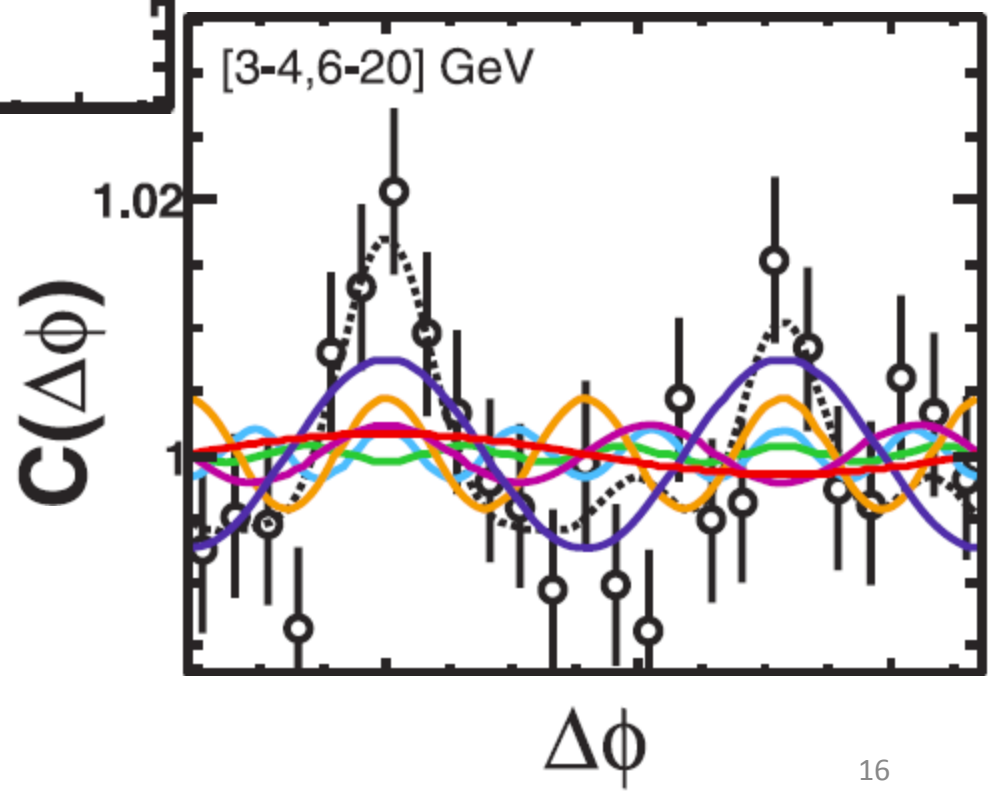

Hard-soft Correlation

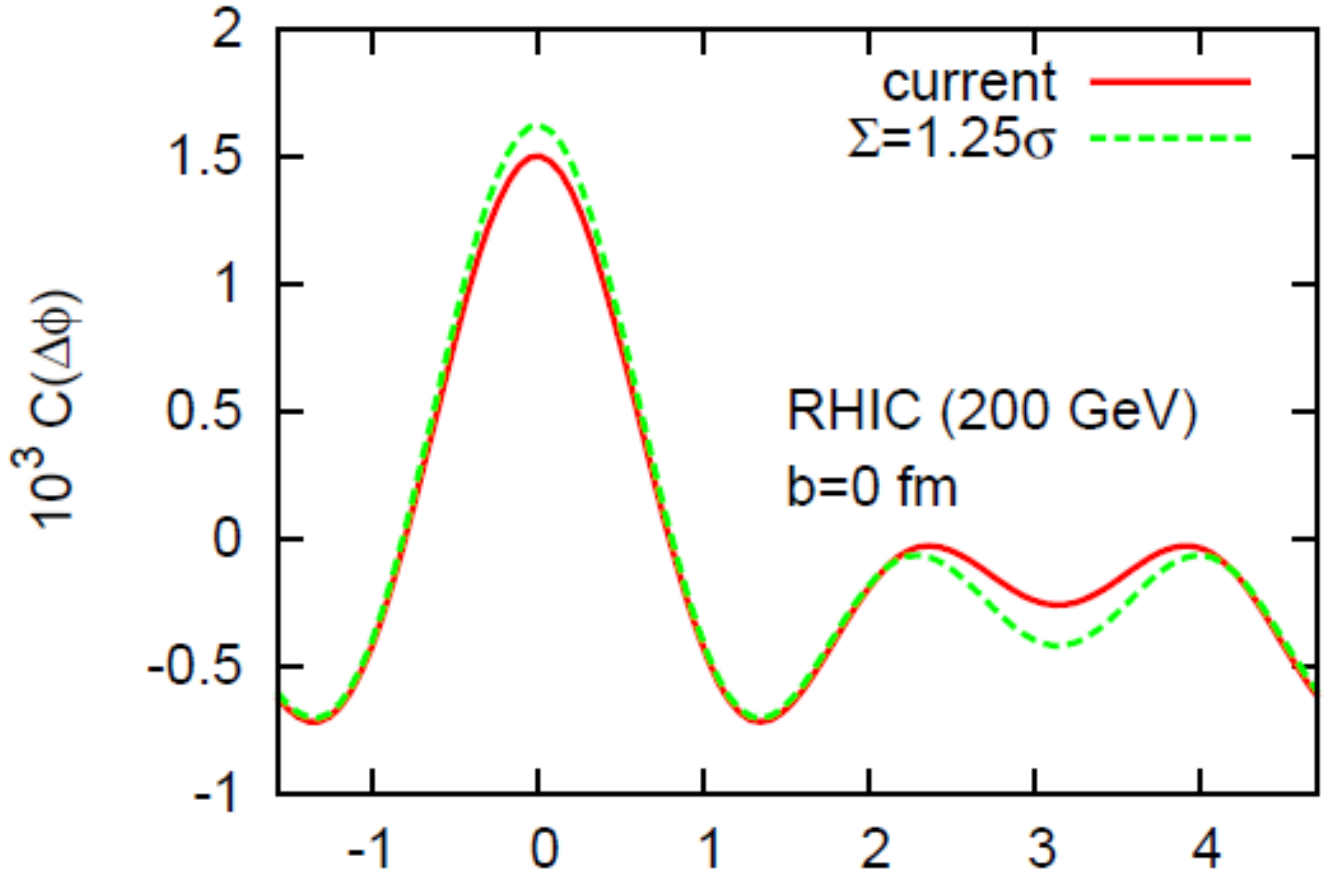

$$\frac{dN^s}{d\phi^s} \sim 1 + 2\sum_n \nu_n^s \cos[n(\phi^s - \psi_n^S)] \ ,$$

$$\frac{dN^h}{d\phi^h} \sim 1 + 2\sum_m \nu_m^h \cos[m(\phi^h - \psi_m^J)]$$

$$< \frac{dN^{hard}}{dyd\phi_1} \frac{dN^{soft}}{dyd\phi_2} > \sim 1 + \sum_{n=1,2,3,\ldots} 2 < v_n^h v_n^s > \cos(n\Delta\phi)$$

*X.Z. and J. Liao, PLB **713**, 35 (2012).*

Hard-soft Correlation

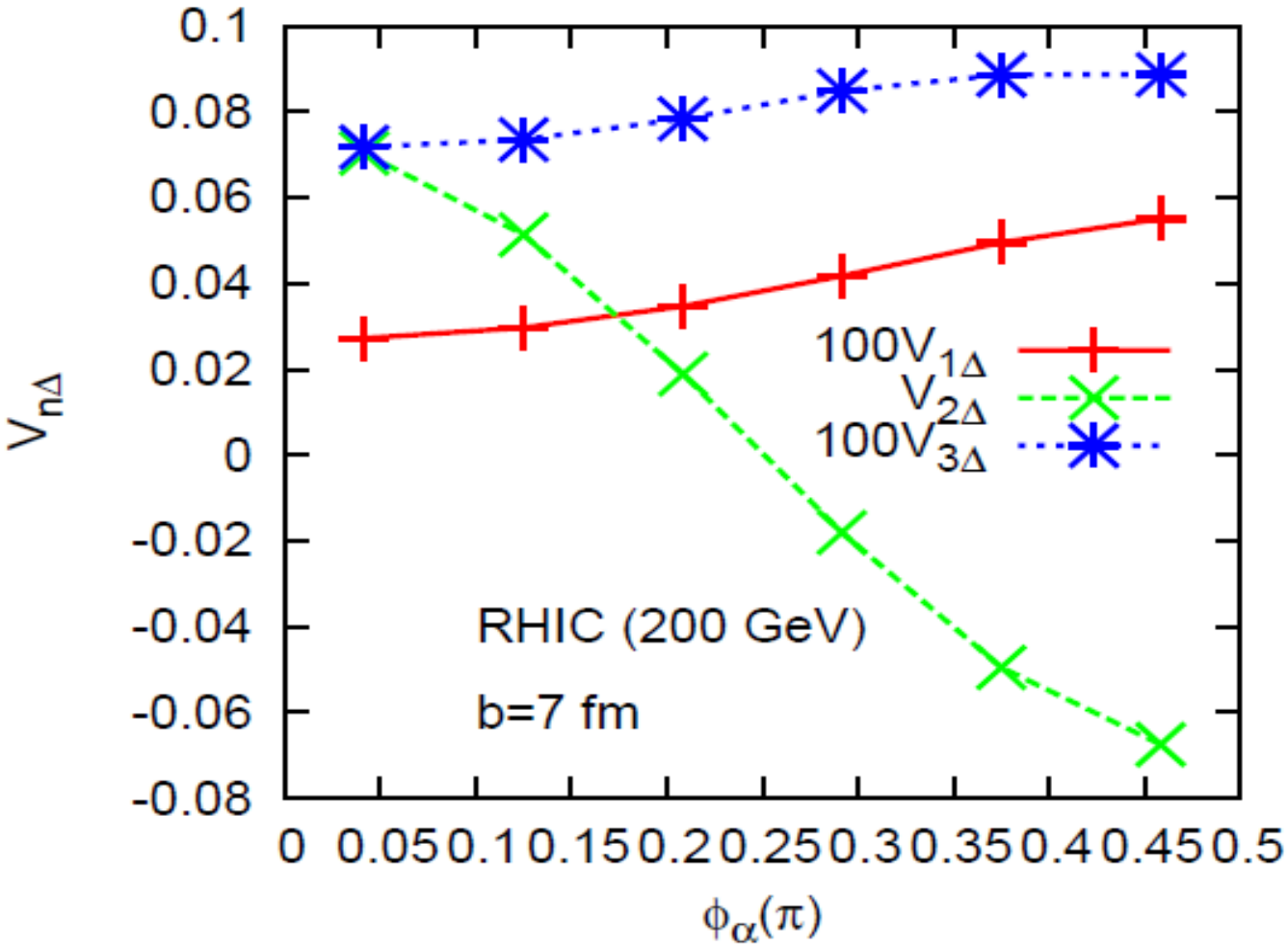

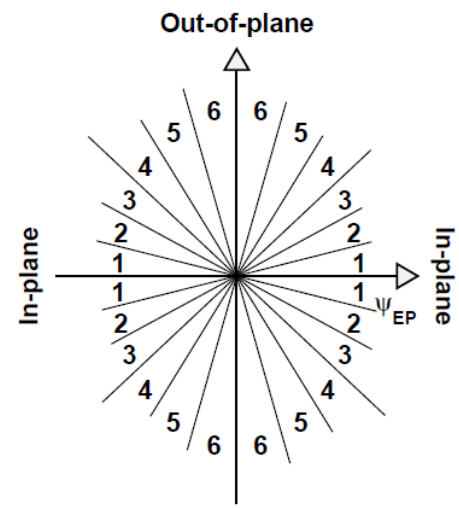

RHIC, arXiv:1010.0690
*M. Luzum, **PLB** 696, 499 (2011)*

$$C(\Delta\phi) \equiv 2 \times \left[\sum_n V_{n\Delta} \cos(n\Delta\phi) \right]$$

X.Z. and J. Liao, arXiv:1210.1245

P-Pb case (5.02 TeV): a try

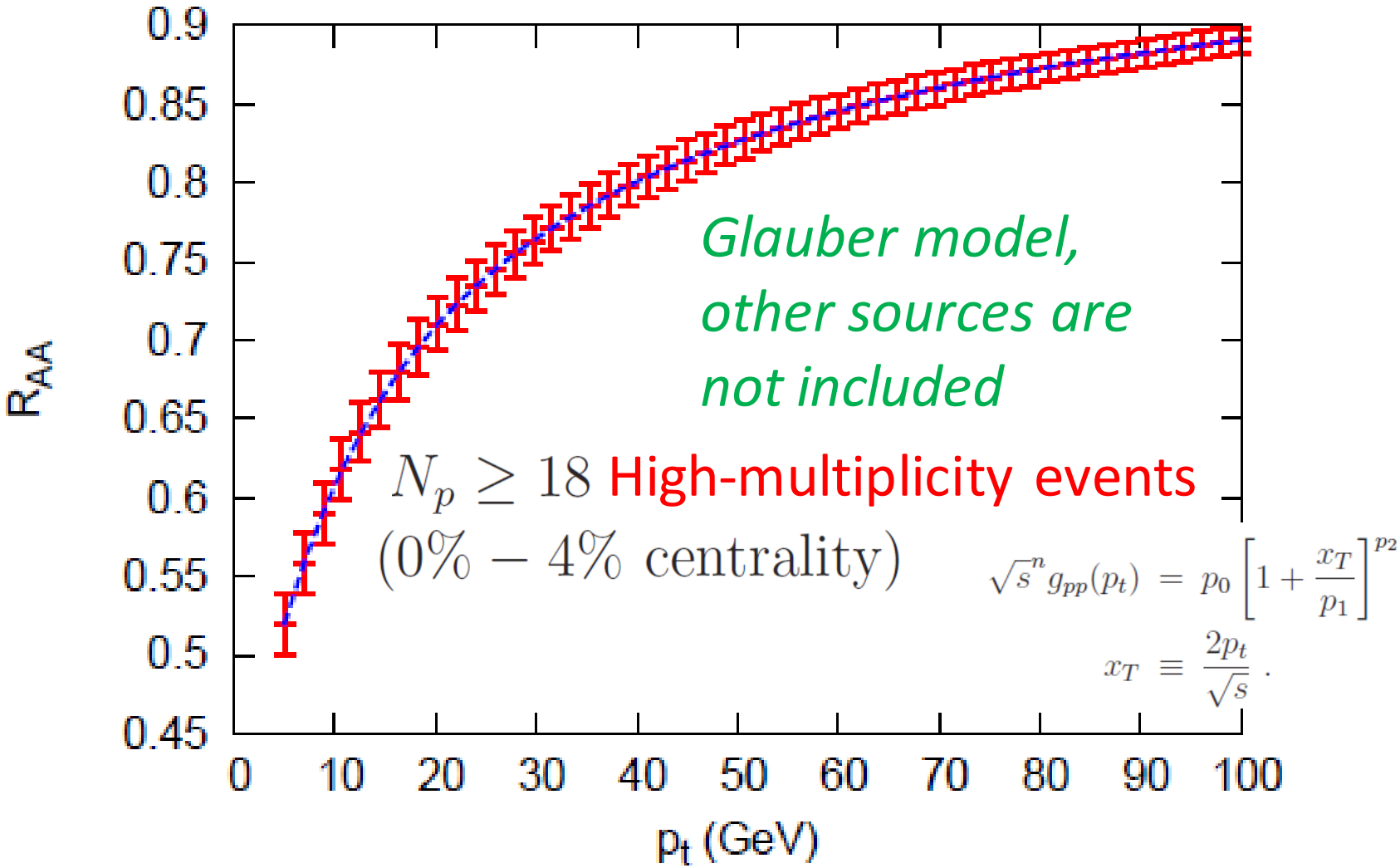

*Piotr Bozek, PRC **85**, 014911 (2012).*

P-Pb case (5.02 TeV): a try

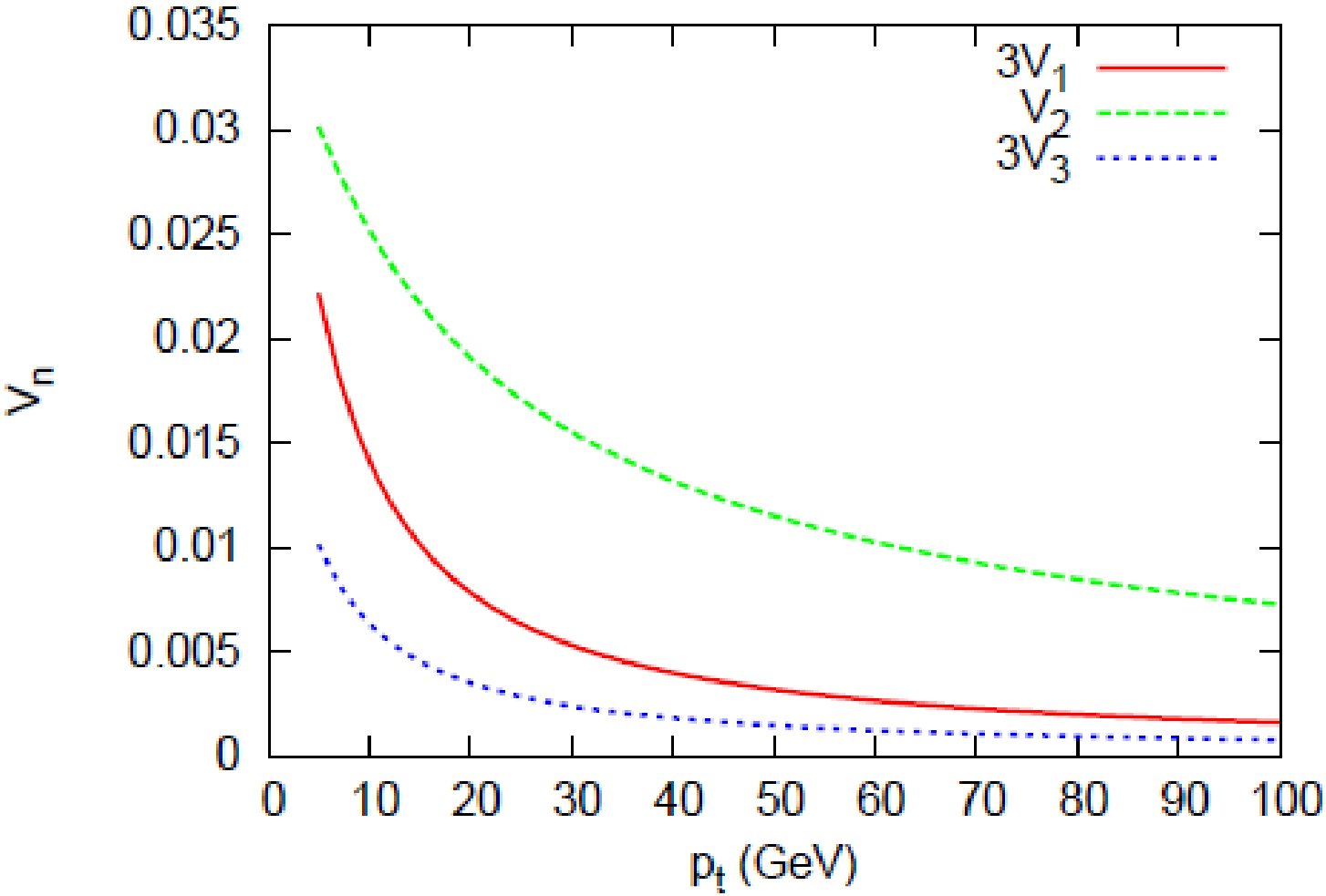

Final state interaction?

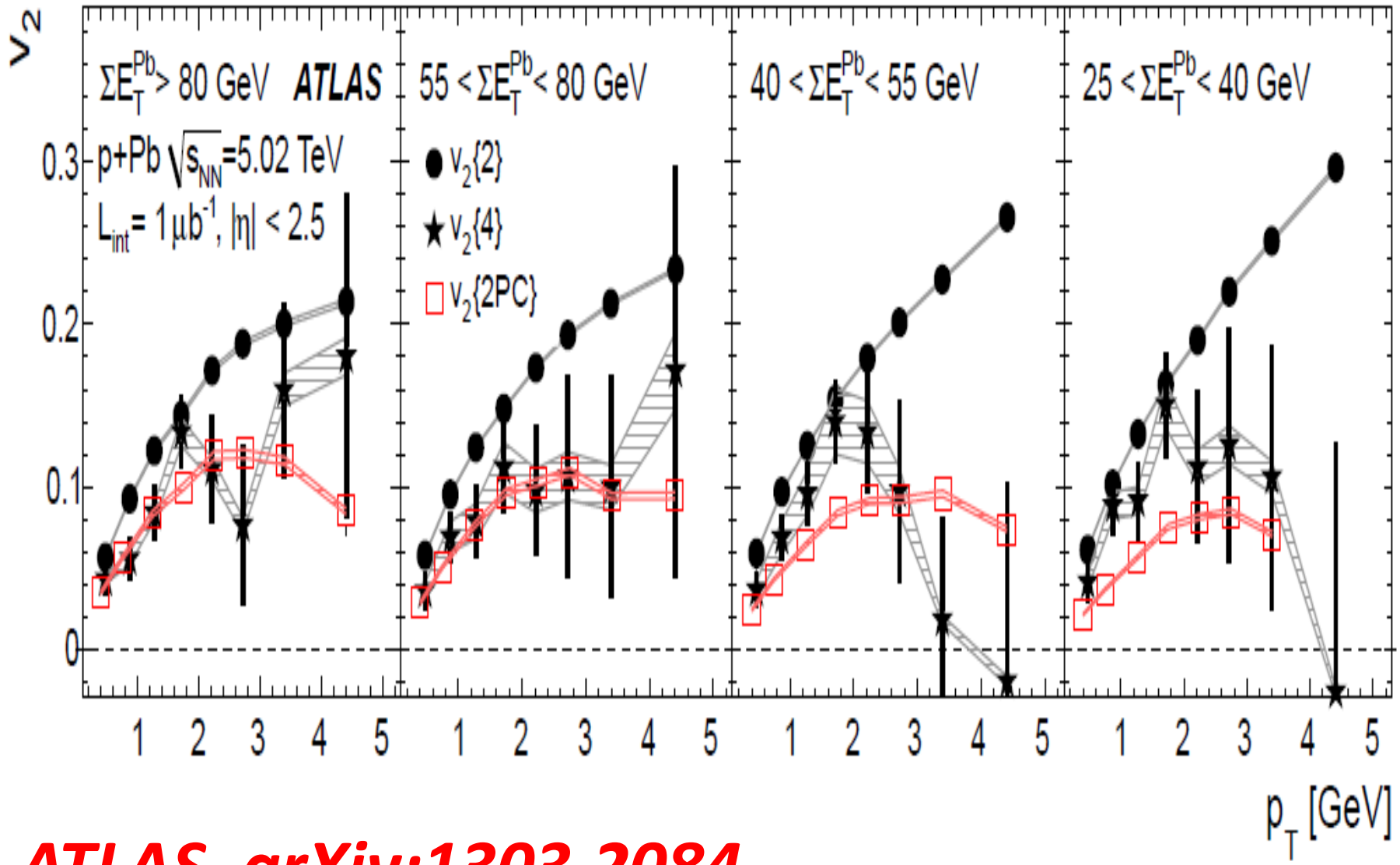

ATLAS, arXiv:1303.2084

P-Pb case (5.02 TeV): a try

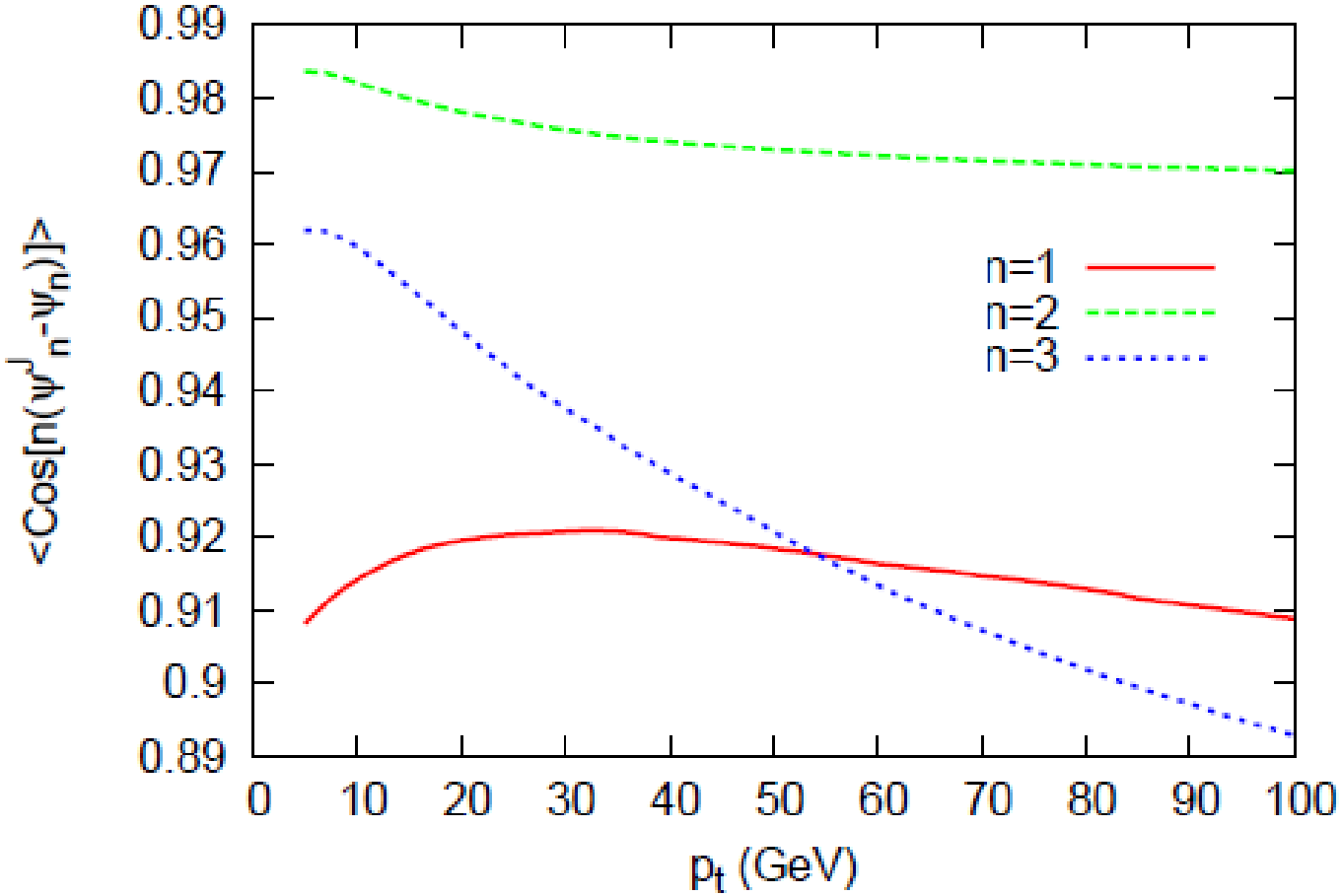

Angle dispersion

Conclusion and outlook

- NTcE explains well the **centrality-dependence** of high-pt V2 from RHIC 200 GeV to LHC 2.76 TeV (Vn?)
- Need more and better data on high-pt Vn
- Vn contribute to hard-soft correlation
- High-pt Raa and anisotropy are explored for high multiplicity P-Pb events, data are needed
- Realistic matter evolution is needed (in progress)
- Connection between NTcE and QCD needs to be explored

Back up

Jet response at b=0 fm

Simple estimate

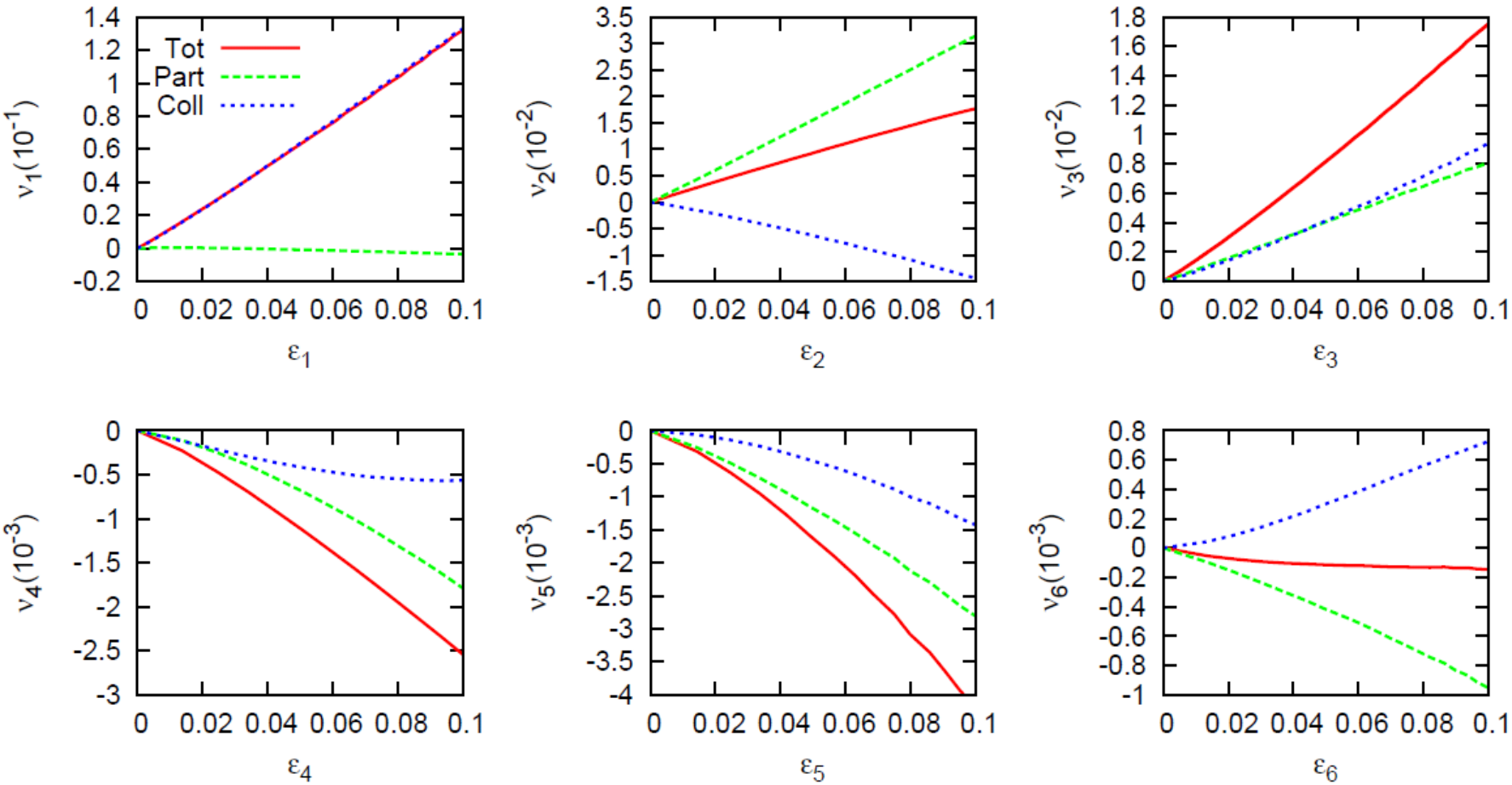

X.Z. and J. Liao, 2012

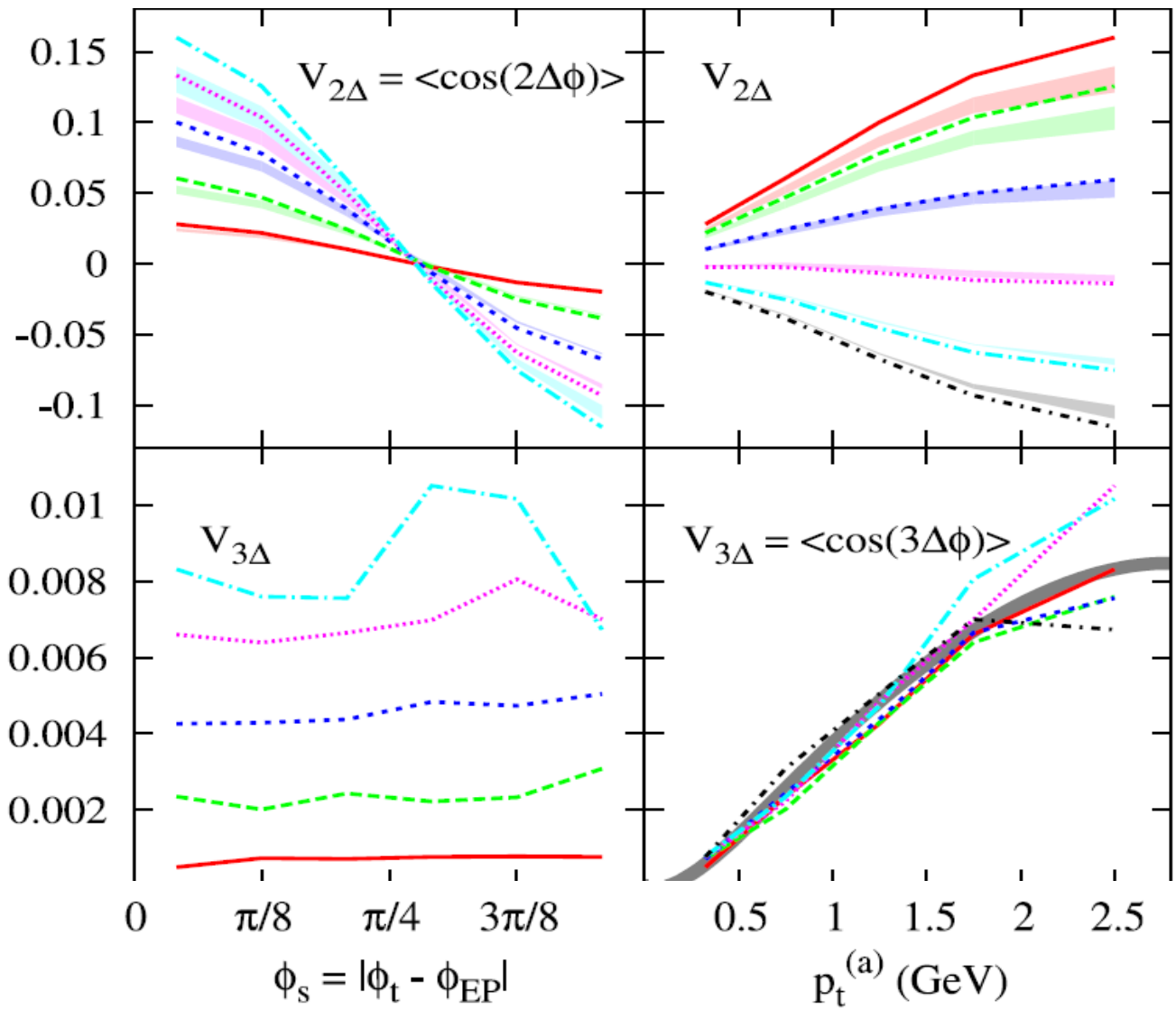

M. Luzum, ***PLB*** *696, 499 (2011)*

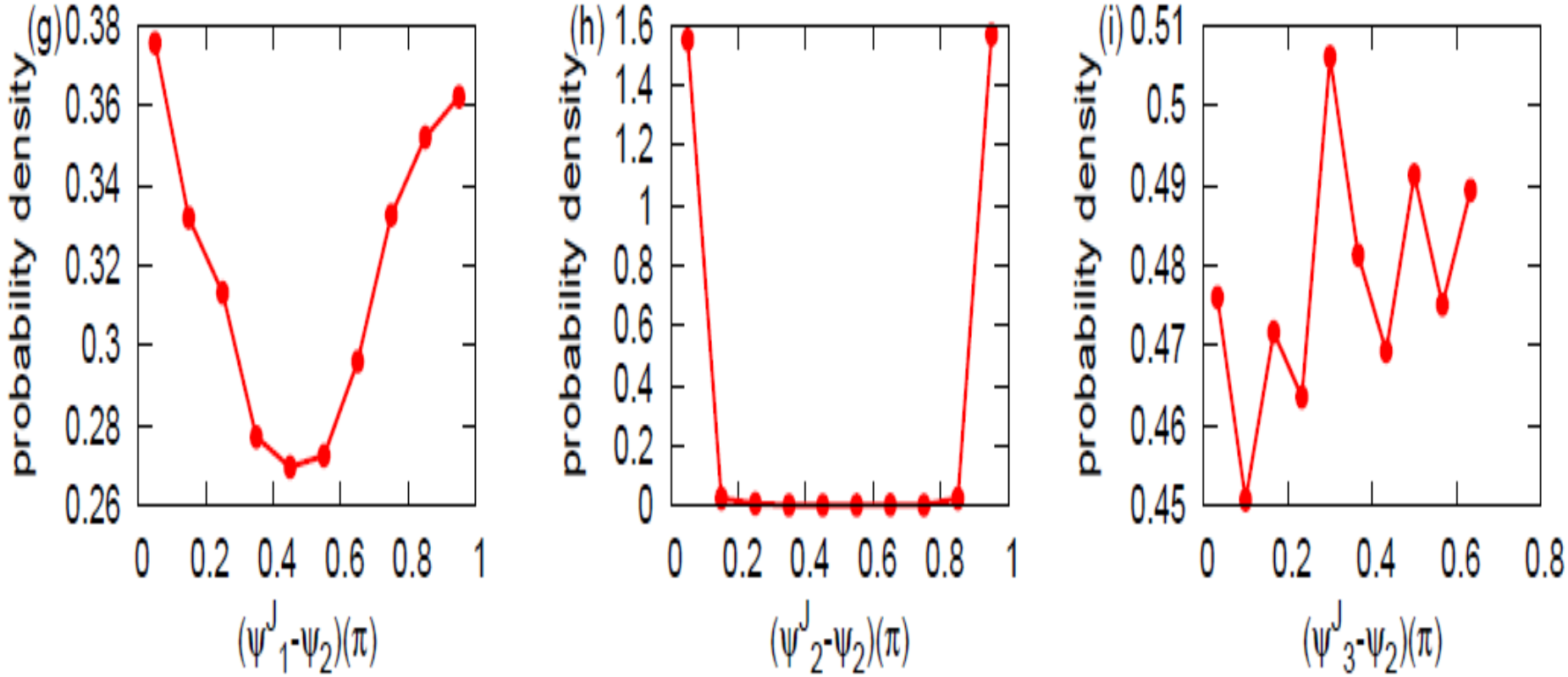

RHIC (200 GeV), b=7 fm

Weak-coupling pQCD (Baier et al.):

$$\hat{q}_{pQCD} = \frac{8\varsigma(3)}{\pi}\alpha_S^2 N_{color}^2 T^3 \sim 0.94\frac{GeV^2}{fm} \text{ at } T = 300 \text{ MeV}$$

Strong-coupling *N*=4 SYM (Liu, Rajagopal and Wiedemann):

$$\hat{q}_{AdS/CFT} = \frac{\pi^{\frac{3}{2}}\Gamma\left(\frac{3}{4}\right)}{\Gamma\left(\frac{5}{4}\right)}\sqrt{\alpha_{SYM} N_{color}}\, T^3 \sim 4.5\frac{GeV^2}{fm} \text{ at } T = 300 \text{ MeV}$$

From P. Jacob's NNPSS2011 lecture

Jet tomography: pt dependence

$$dE = -E^{\delta}\,\kappa[s(l)]\,l^{m}\,dl$$

P-P effective spectrum index is energy dependent.

*W. A. Horowitz and M. Gyulassy, NPA **872**, 265 (2011).*

Two para. fitted to central Raa

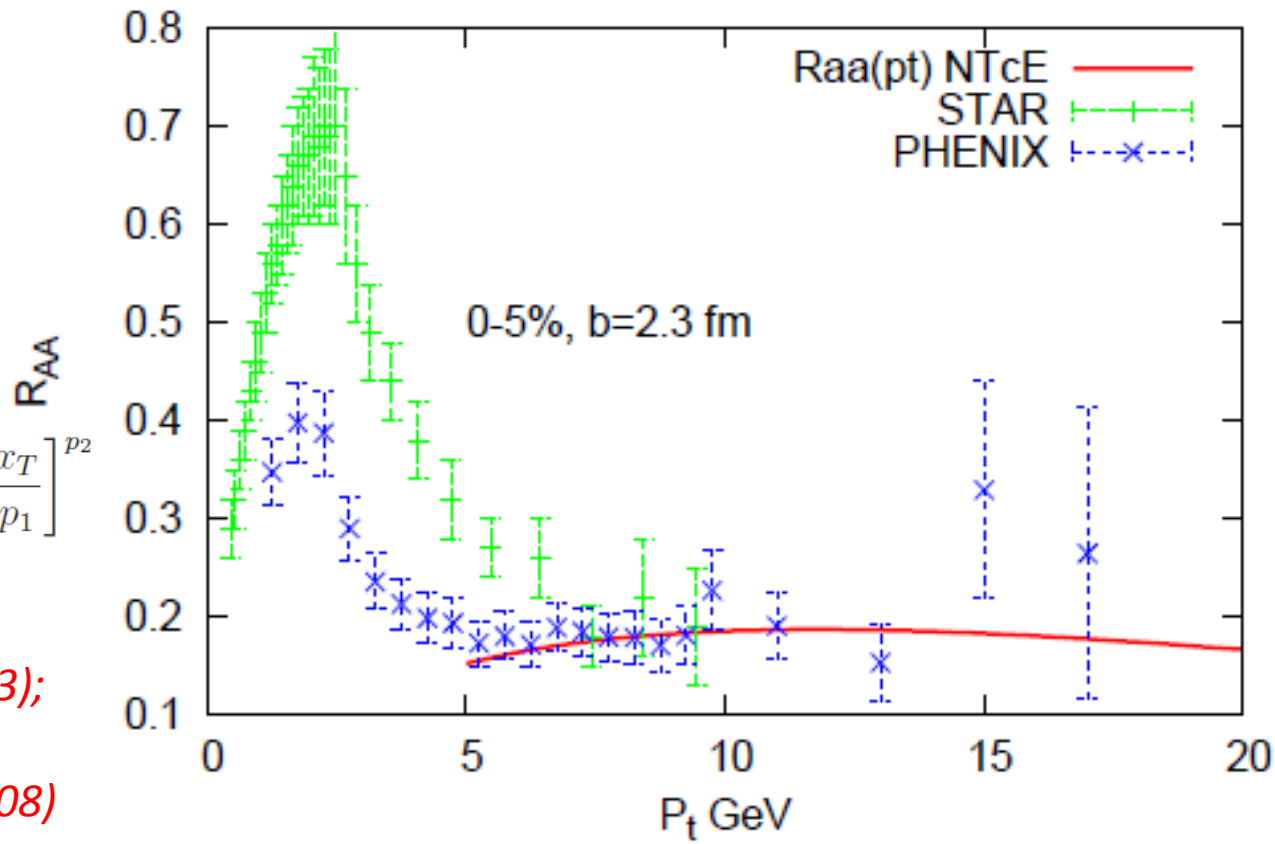

$$\sqrt{s}^{\,n}\,g_{pp}(p_t) = p_0\left[1+\frac{x_T}{p_1}\right]^{p_2}$$

$$x_T \equiv \frac{2p_t}{\sqrt{s}}\,.$$

STAR, PRL 91, 172302 (2003); PHENIX, PRL 101, 232301 (2008)

Jet tomography: pt dependence

P-P spectrum: QCD scaling formula.

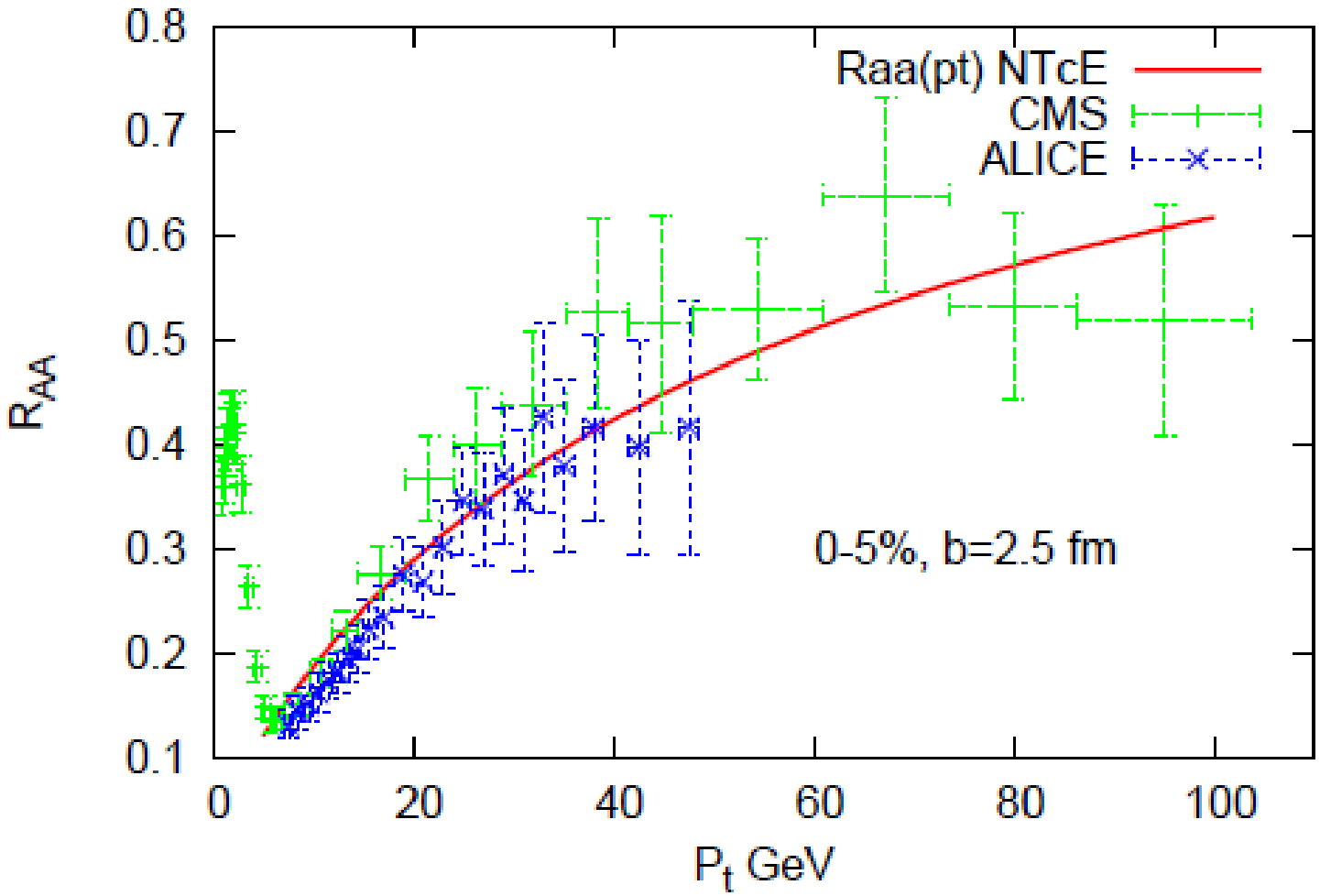

*CMS, Eur. Phys. J. C **72**, 1945 (2012); ALICE, arXiv:1208.2711*

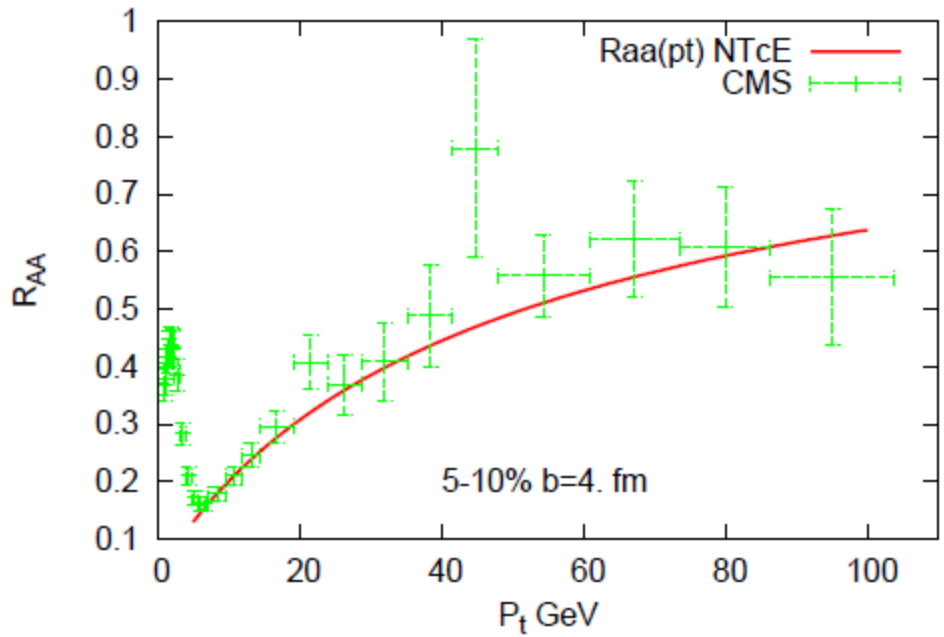
Raa(pt) NTcE
CMS
5-10% b=4. fm
R_{AA}
P_t GeV
1
0.9
0.8
0.7
0.6
0.5
0.4
0.3
0.2
0.1
0
20
40
60
80
100

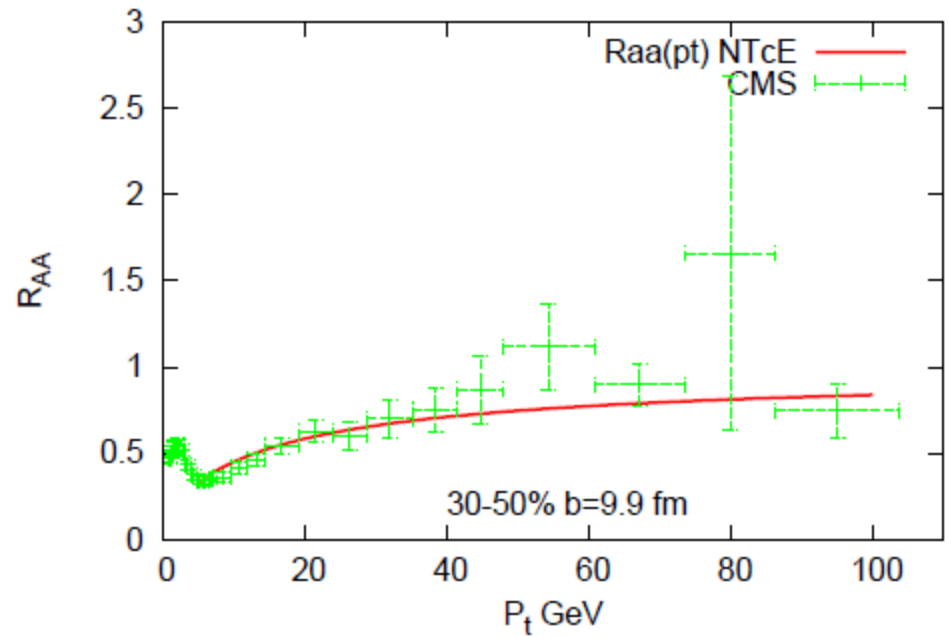
Raa(pt) NTcE
CMS
30-50% b=9.9 fm
R_{AA}
P_t GeV
3
2.5
2
1.5
1
0.5
0
20
40
60
80
100

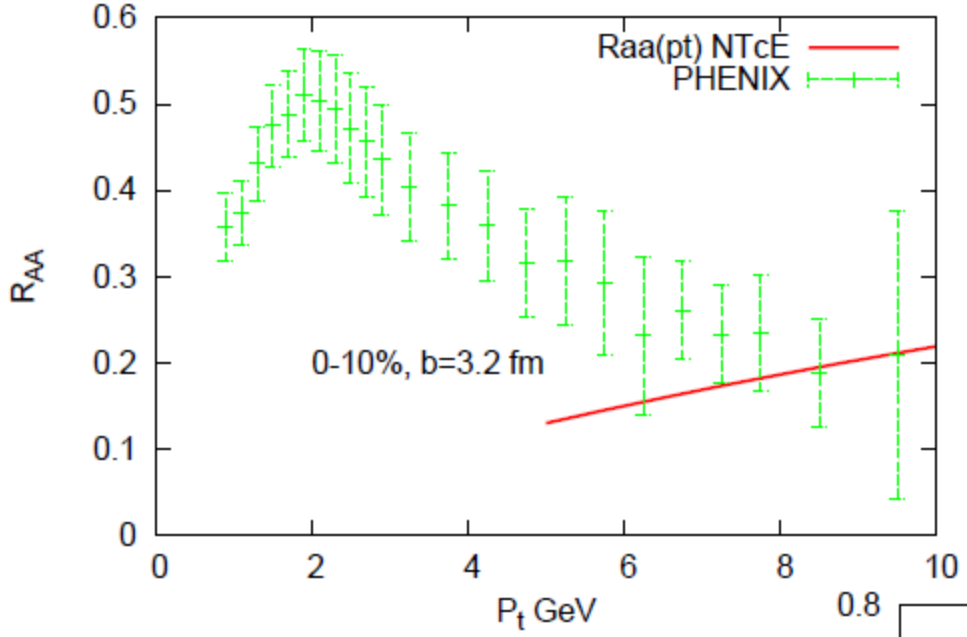
Raa(pt) NTcE
PHENIX
0-10%, b=3.2 fm
R_{AA}
P_t GeV
0
0.1
0.2
0.3
0.4
0.5
0.6
0
2
4
6
8
10

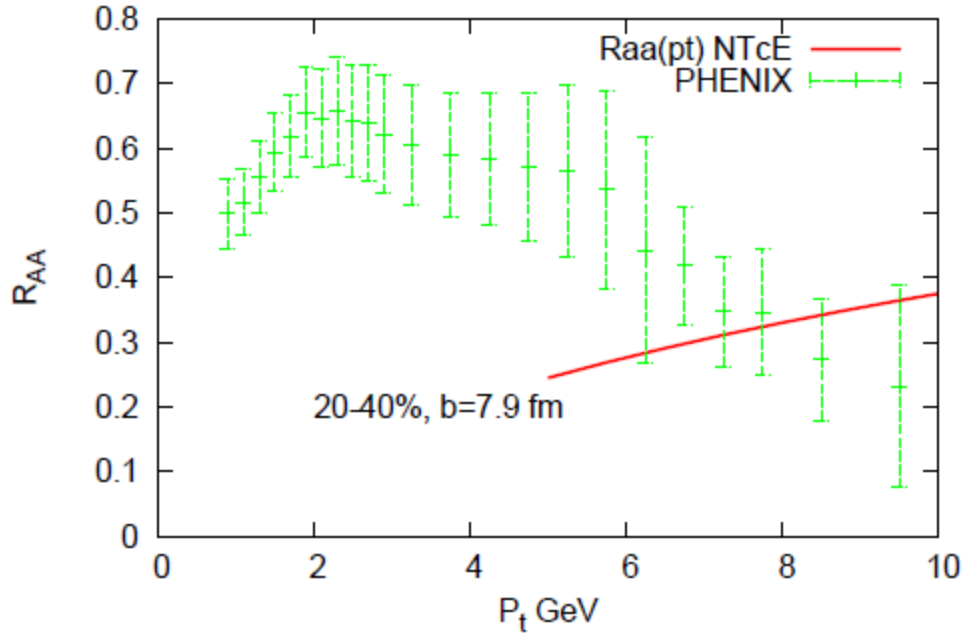
Raa(pt) NTcE
PHENIX
20-40%, b=7.9 fm
R_{AA}
P_t GeV
0
0.1
0.2
0.3
0.4
0.5
0.6
0.7
0.8
0
2
4
6
8
10

Jet tomography: pt dependence

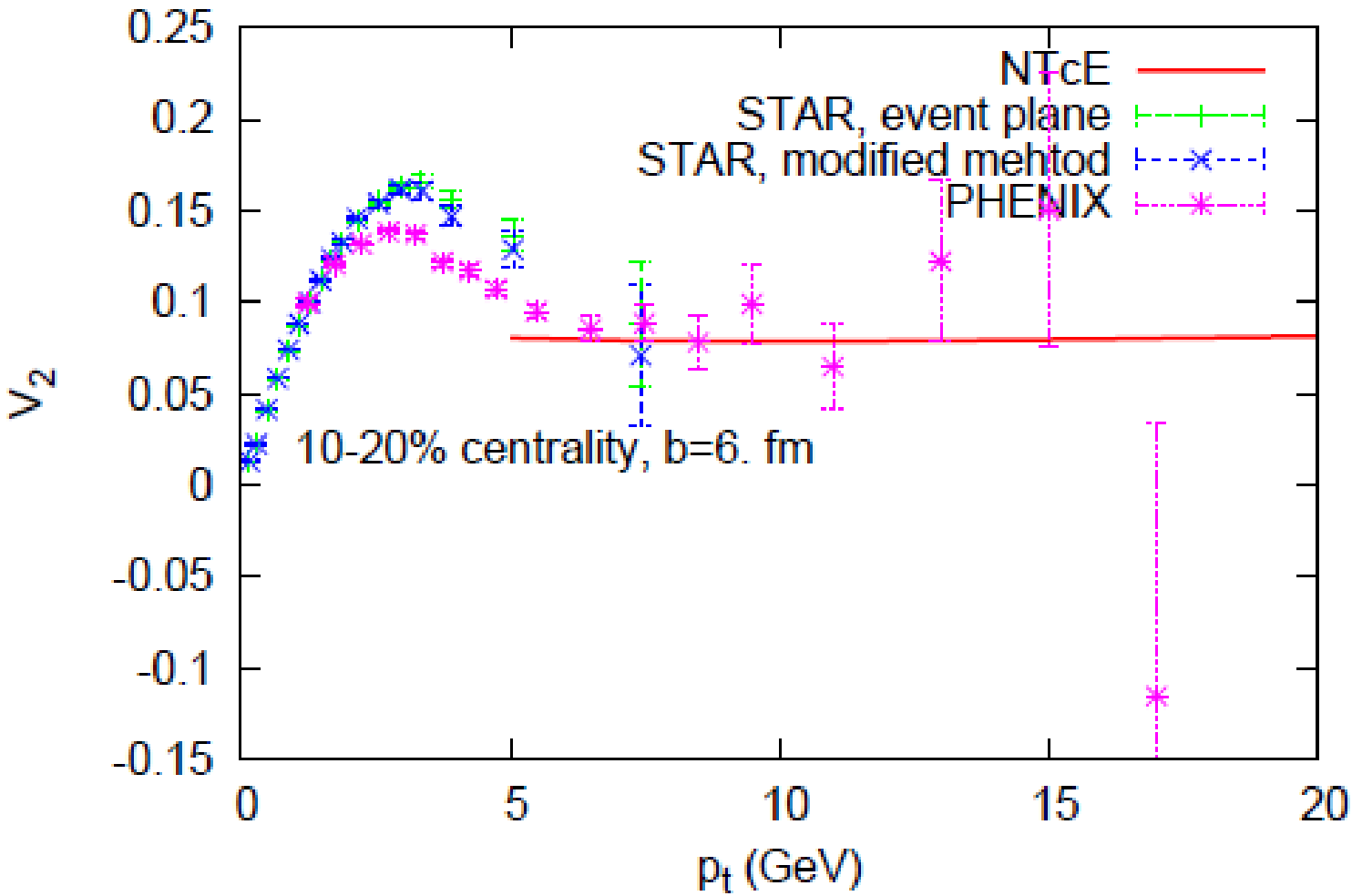

*STAR, PRC **72**, 014904 (2005); PHENIX, PRL **105**, 142301 (2010).*

Jet tomography: pt dependence

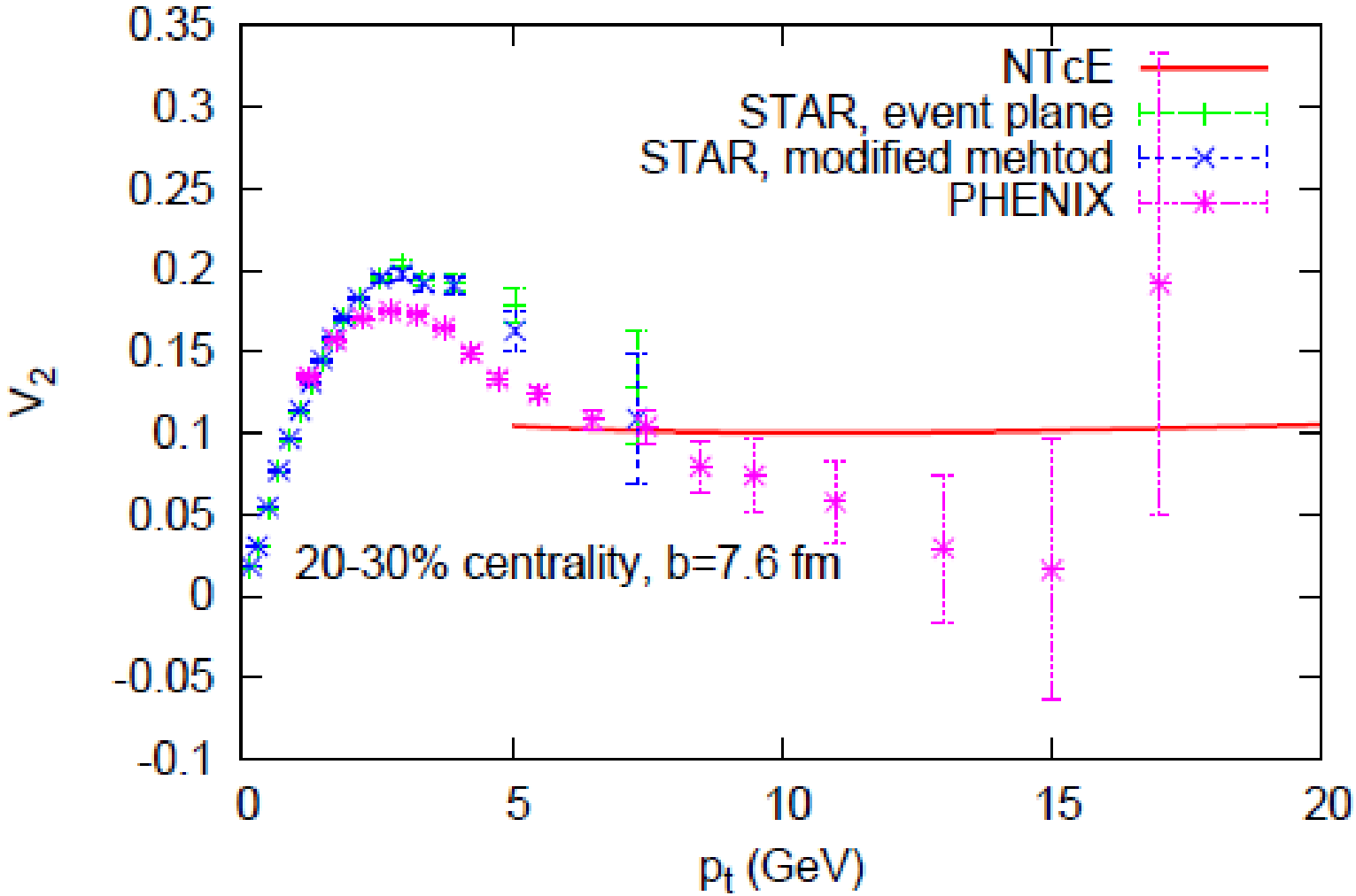

Jet tomography: pt dependence

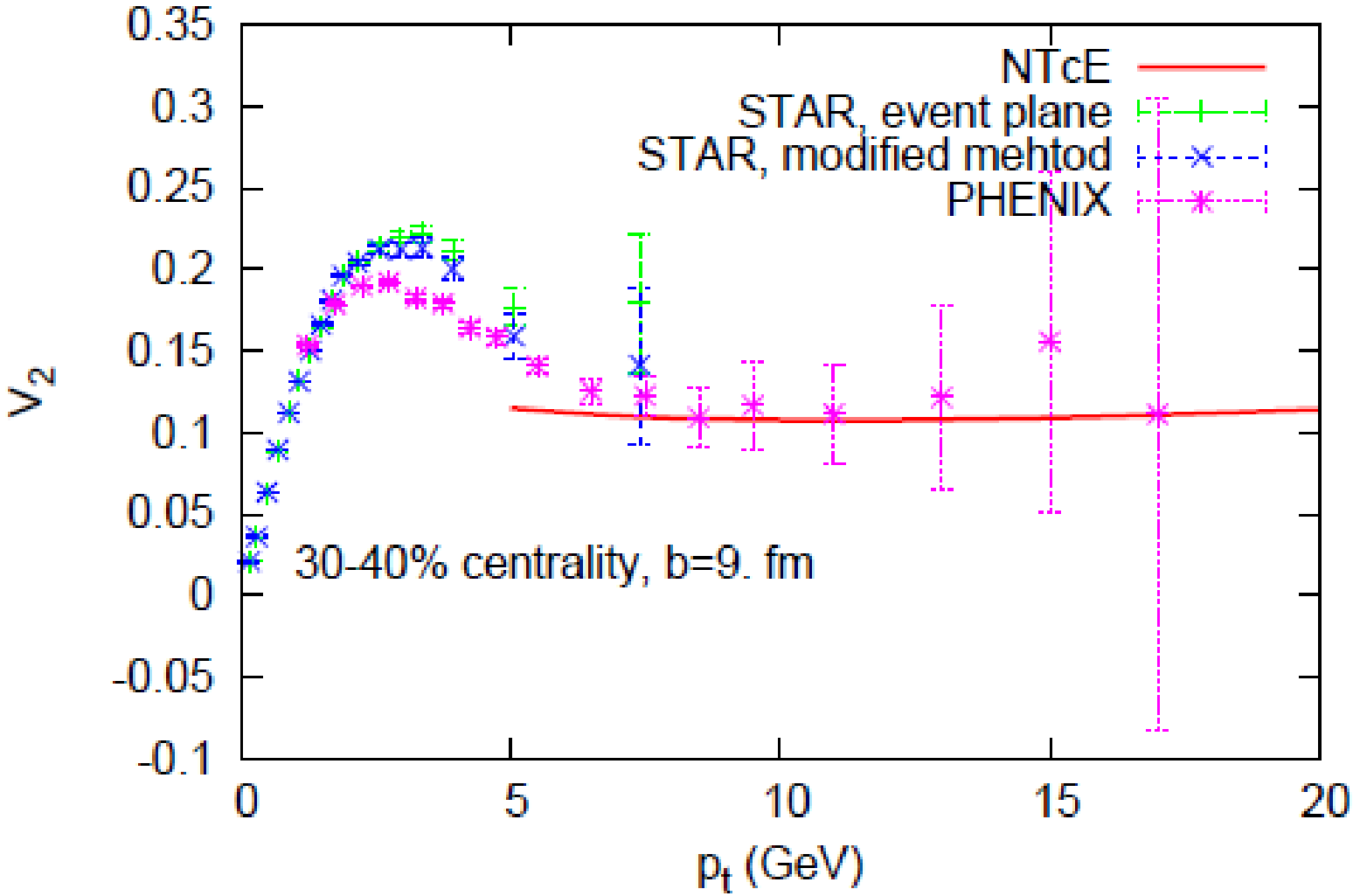

Jet tomography: pt dependence

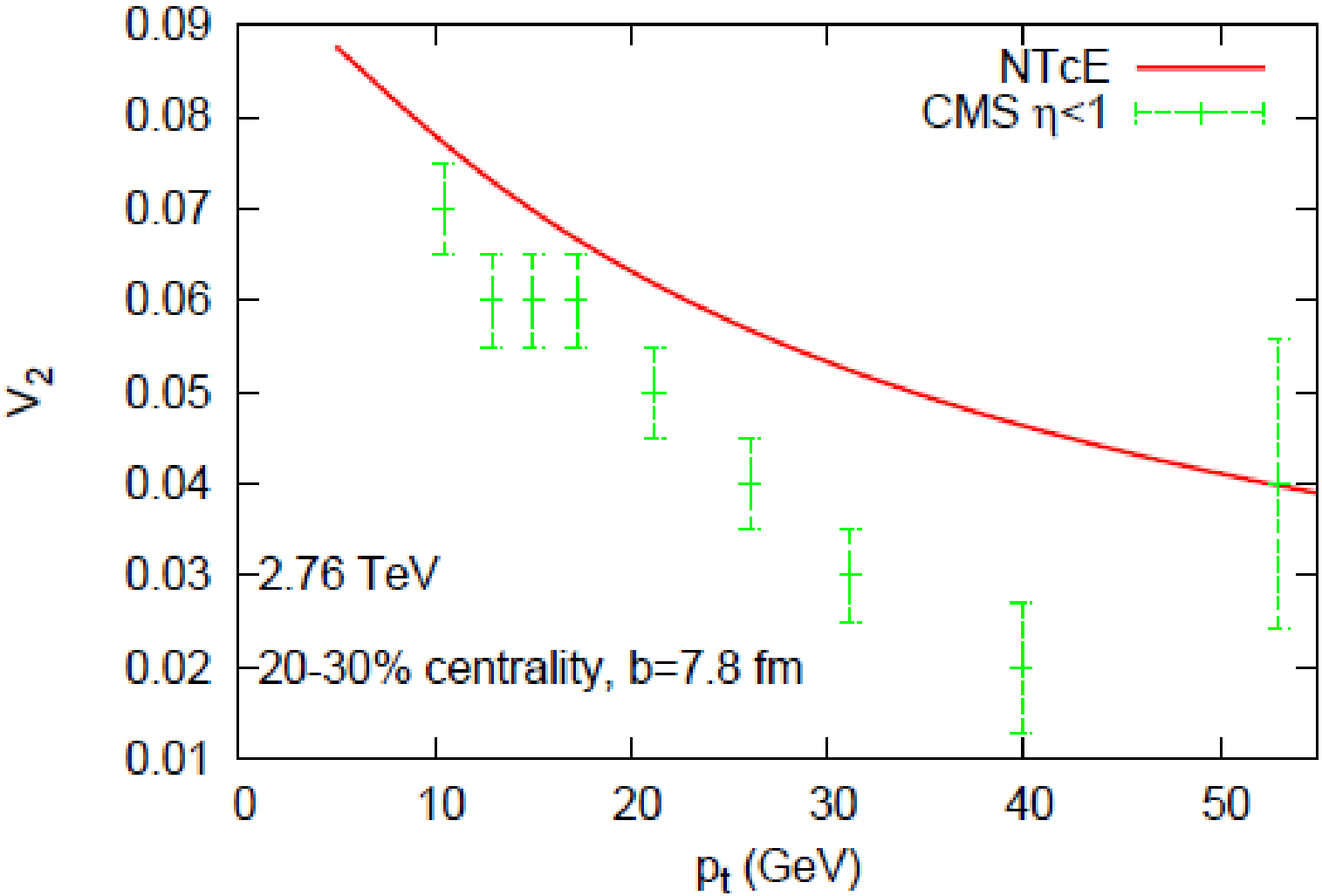

CMS, arXiv:1204.1850

Jet tomography: pt dependence

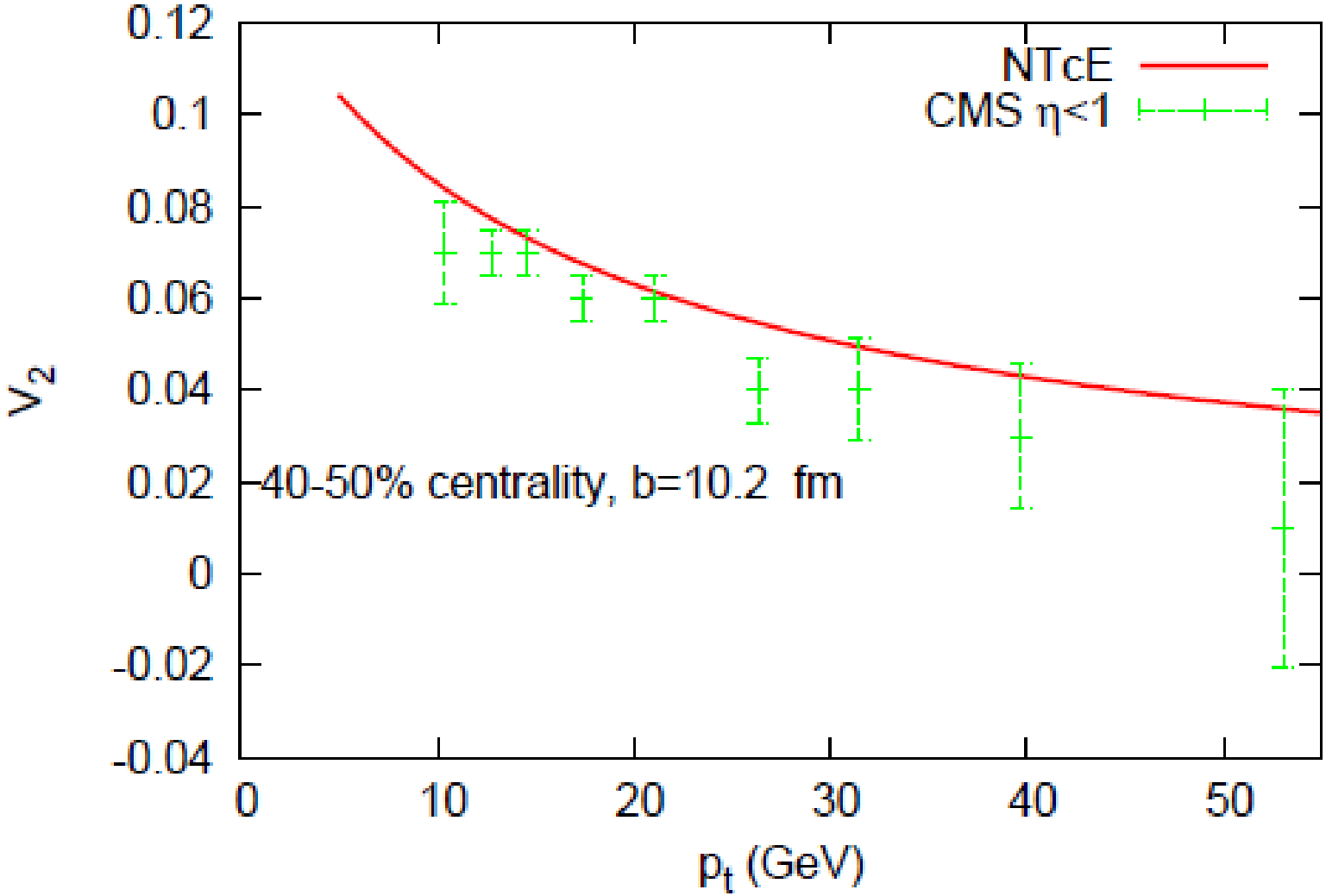

Jet tomography: pt dependence

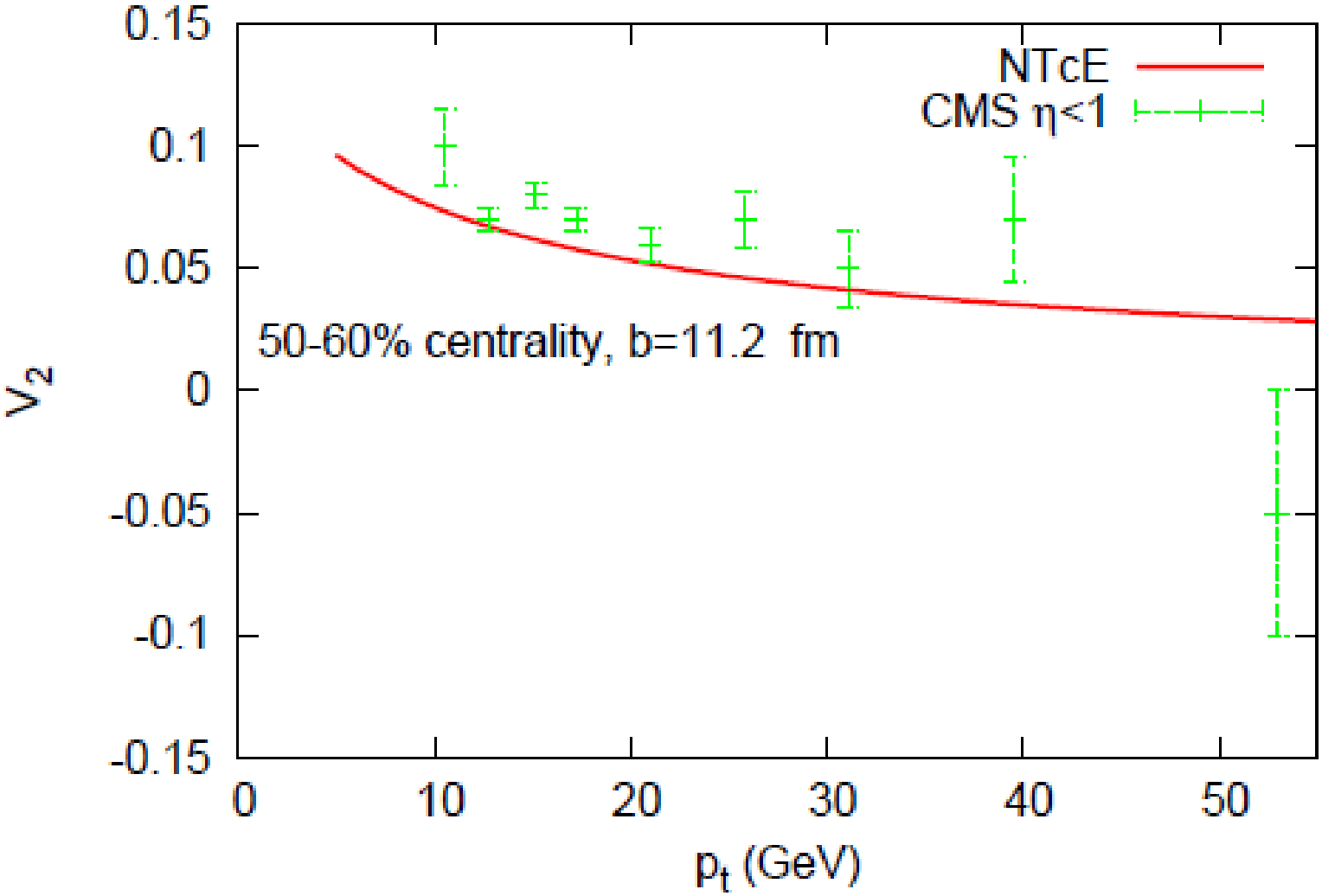

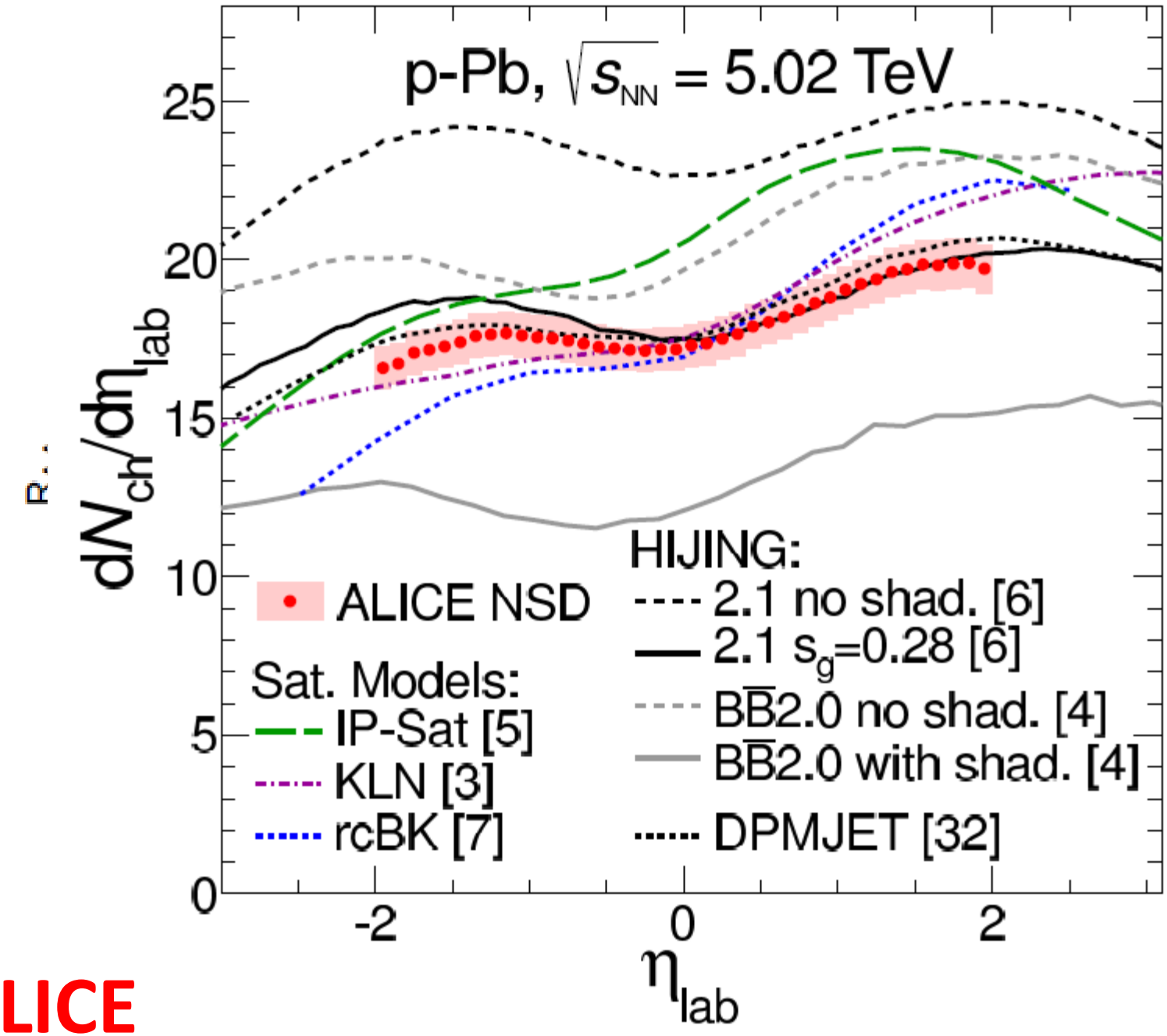
p-Pb, $\sqrt{s_{NN}}$ = 5.02 TeV
$dN_{ch}/d\eta_{lab}$
η_{lab}
ALICE NSD
Sat. Models:
IP-Sat [5]
KLN [3]
rcBK [7]
HIJING:
2.1 no shad. [6]
2.1 s_g=0.28 [6]
BB̄2.0 no shad. [4]
BB̄2.0 with shad. [4]
DPMJET [32]

ALICE

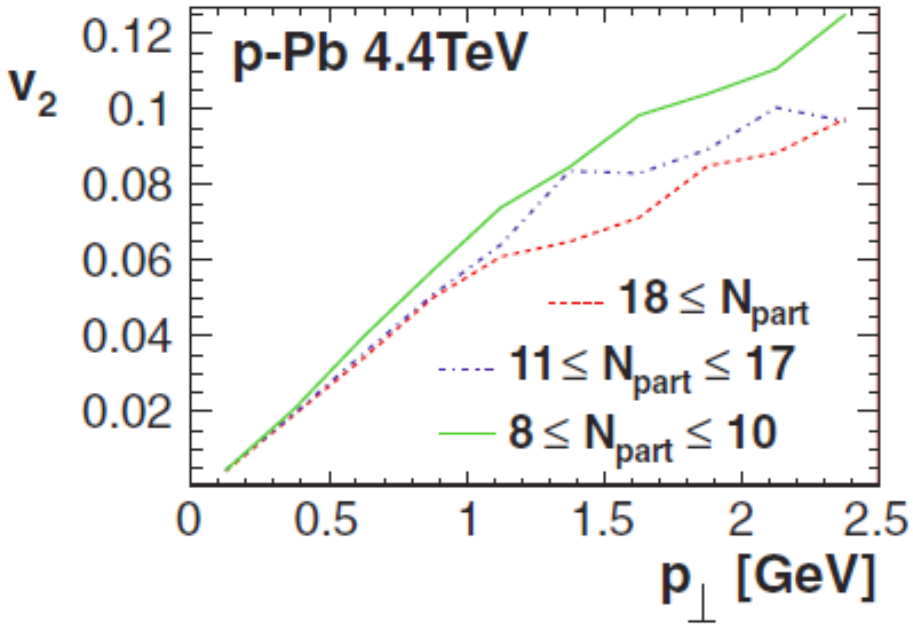
p-Pb 4.4TeV
v_2
0.12
0.1
0.08
0.06
0.04
0.02
0
0.5
1
1.5
2
2.5
$p_\perp$ [GeV]
$18 \leq N_{part}$
$11 \leq N_{part} \leq 17$
$8 \leq N_{part} \leq 10$

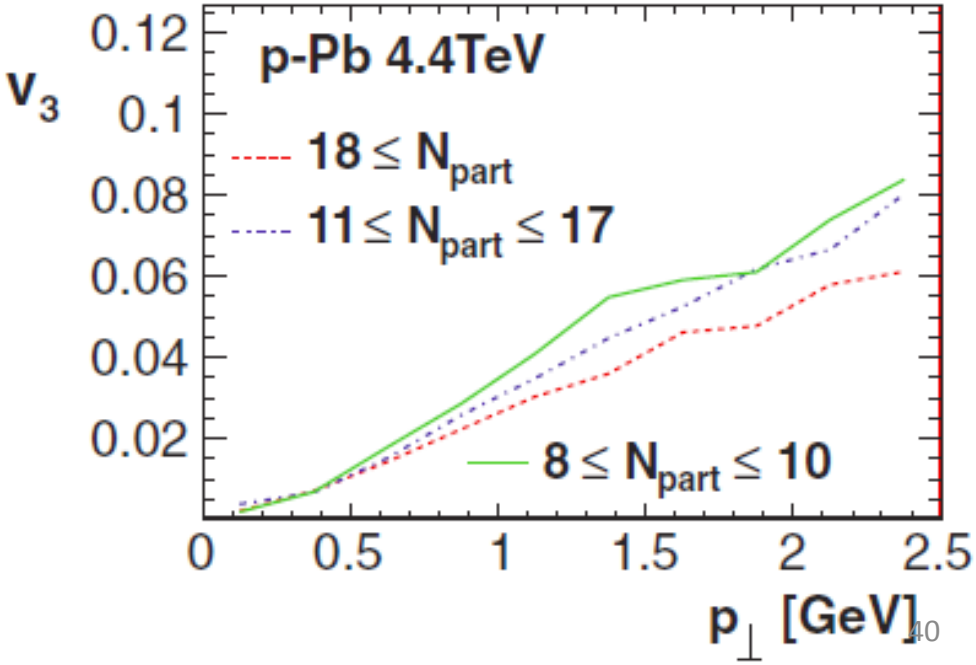
p-Pb 4.4TeV
v_3
0.12
0.1
0.08
0.06
0.04
0.02
0
0.5
1
1.5
2
2.5
$p_\perp$ [GeV]
$18 \leq N_{part}$
$11 \leq N_{part} \leq 17$
$8 \leq N_{part} \leq 10$

Smaller profile

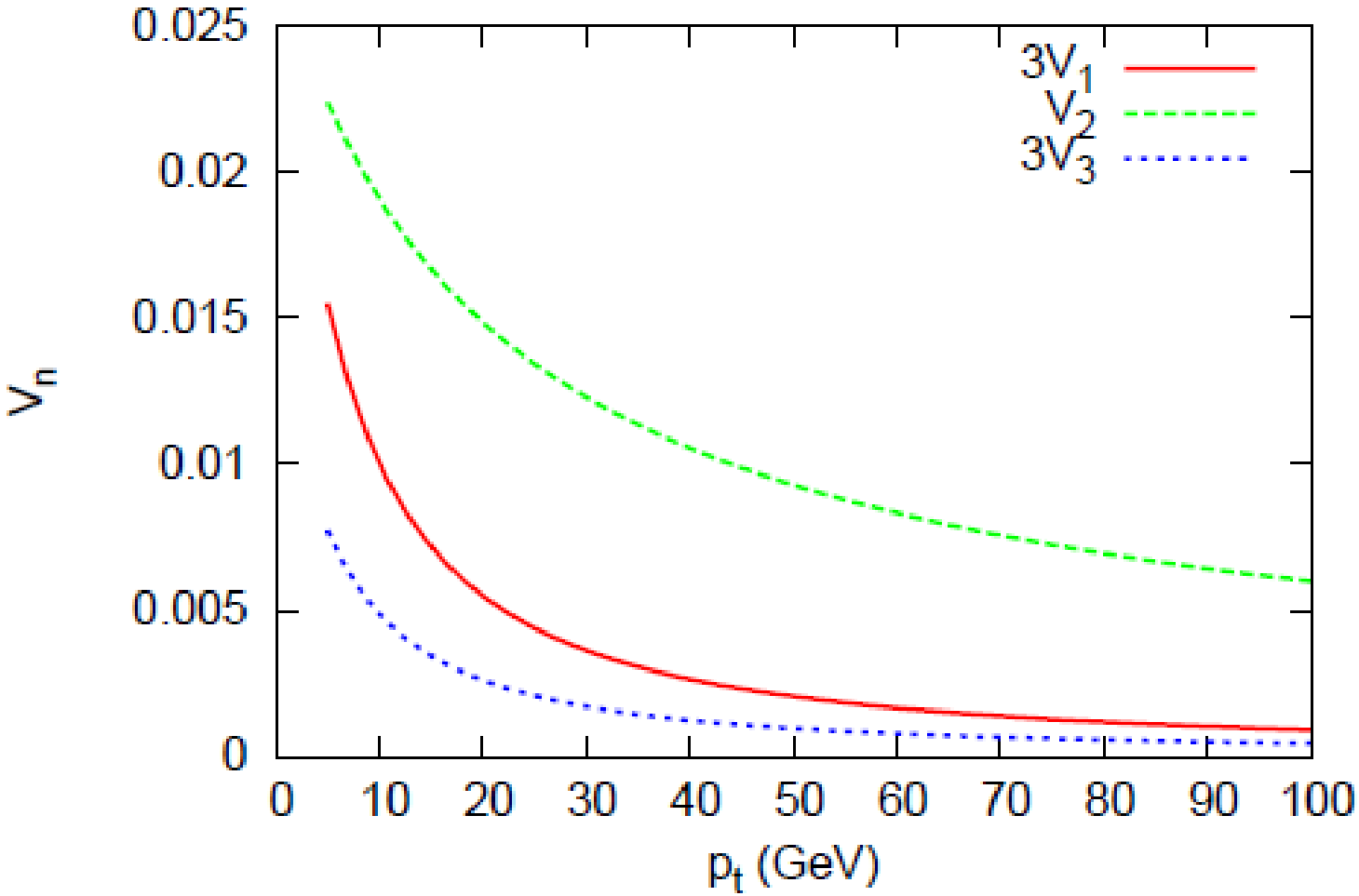

Smaller profile

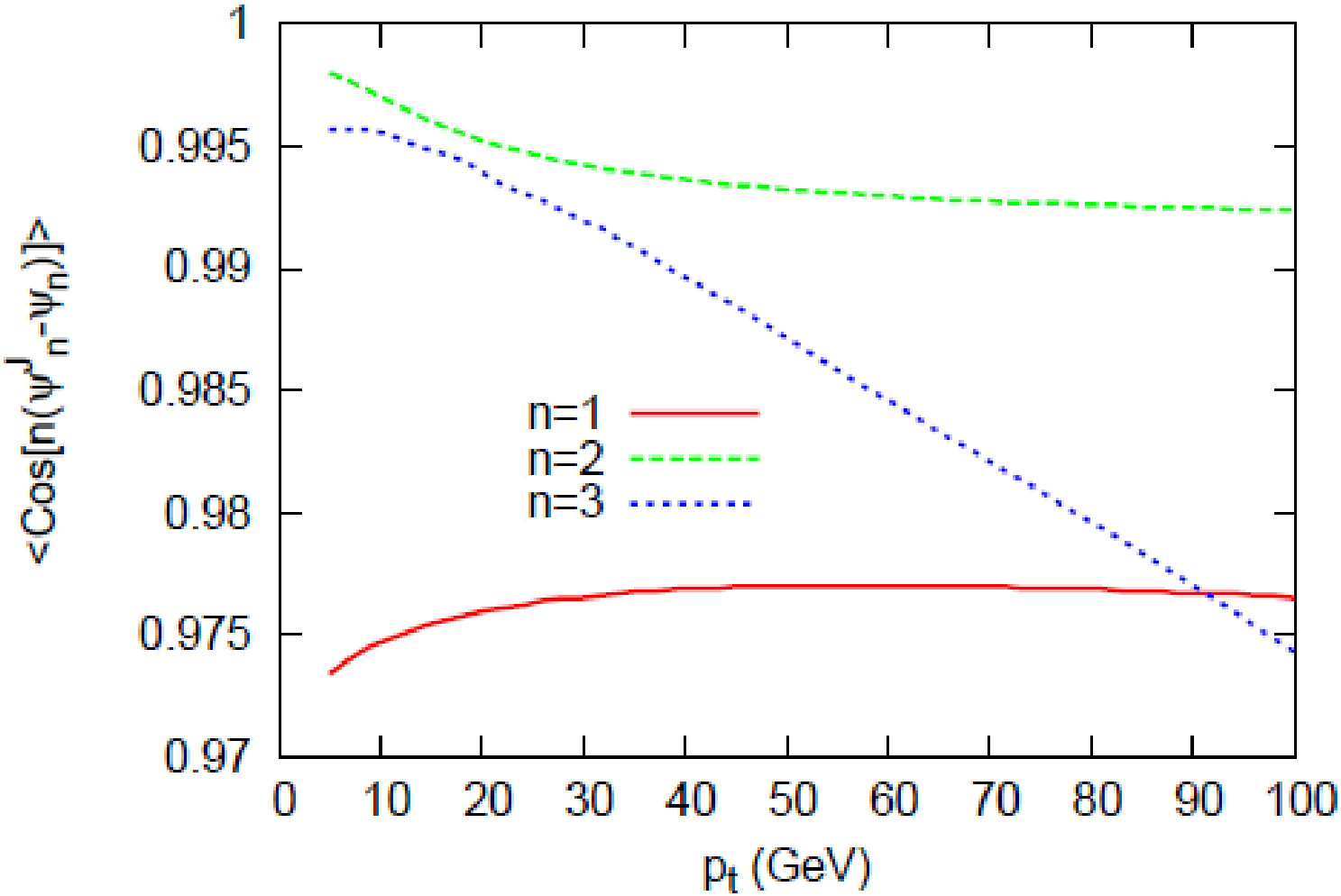

Event activity

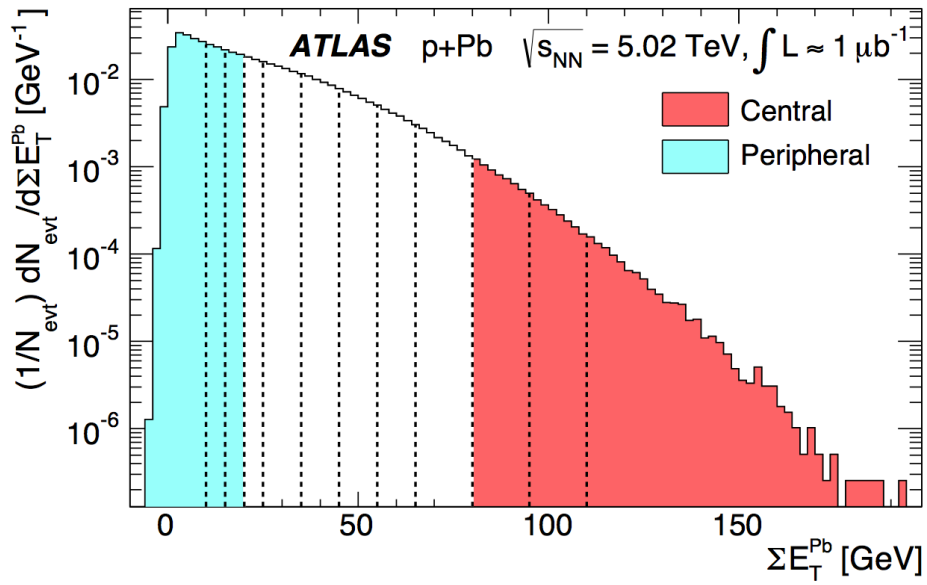

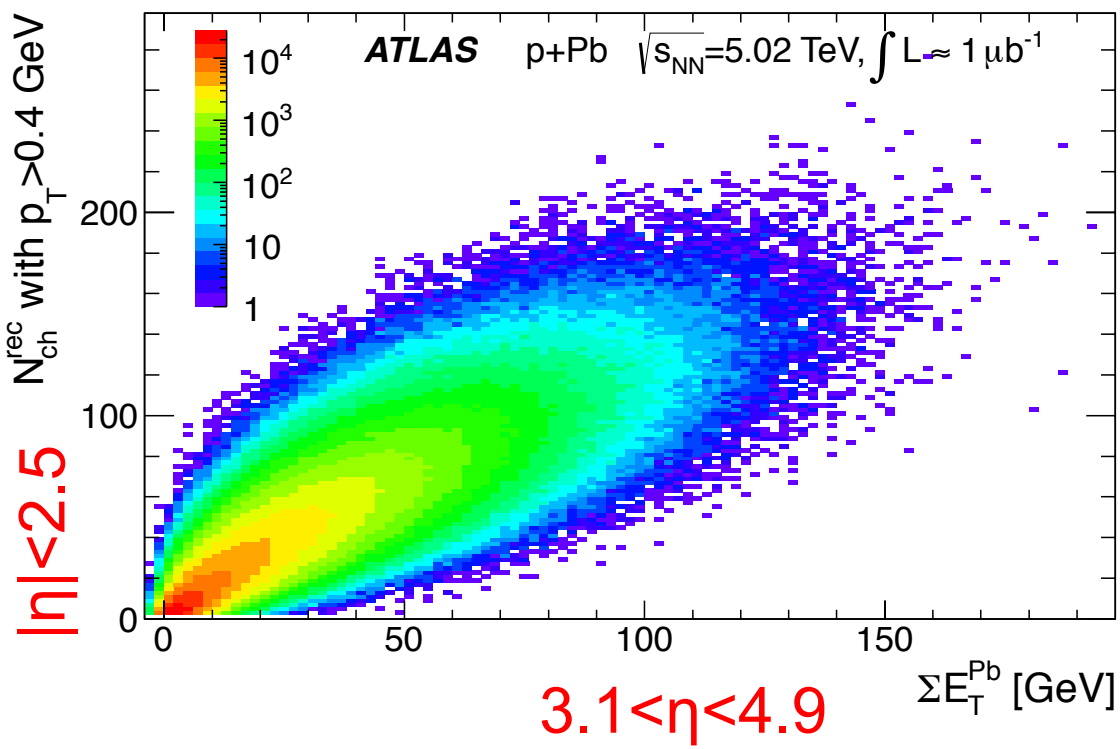

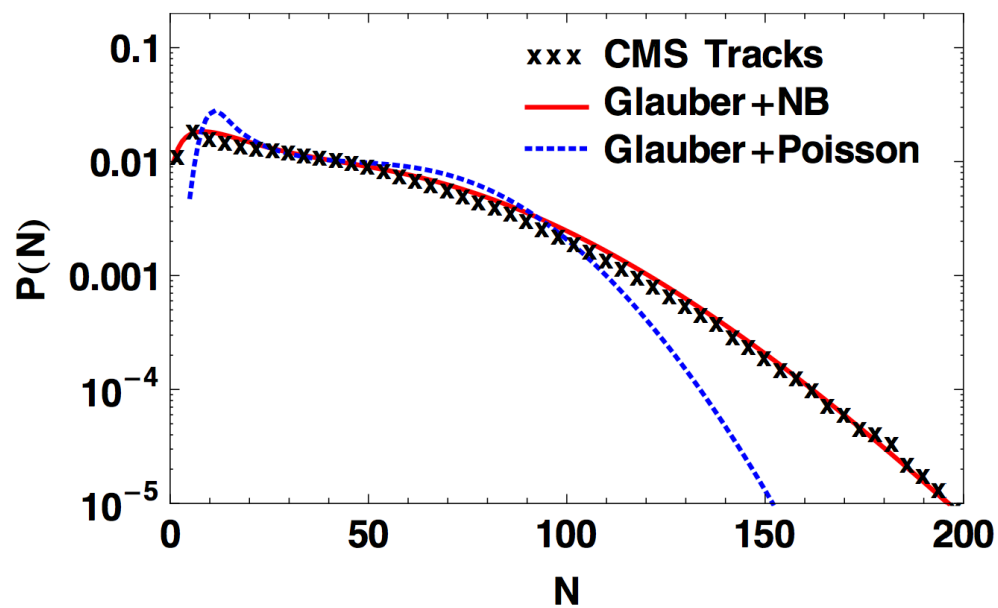

Auto-correlation bias

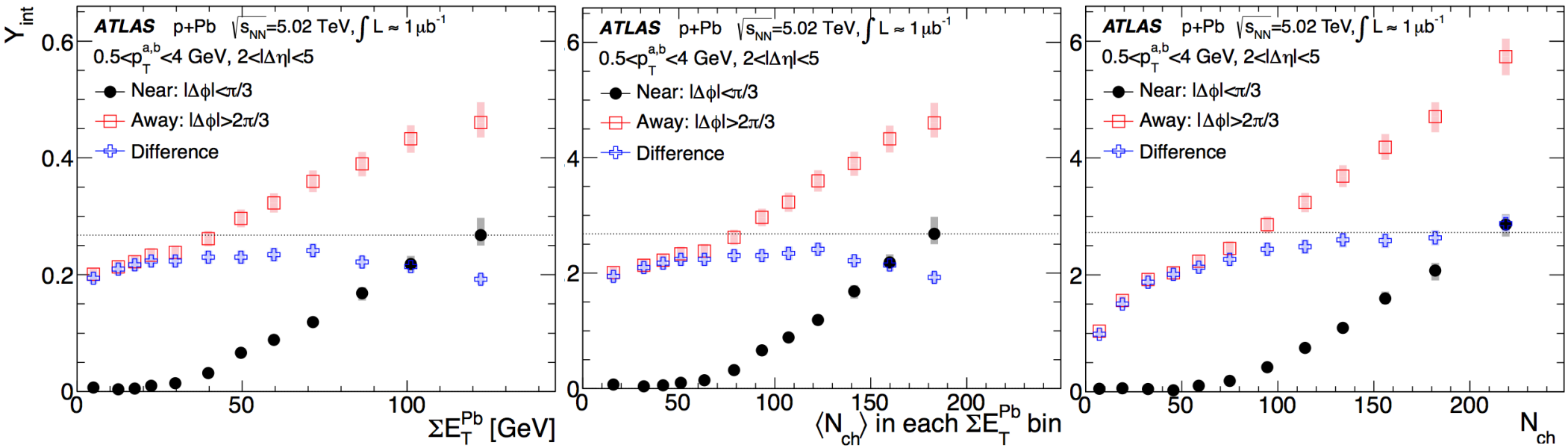

- No bias for long-range global correlations: i.e. the near-side ridge yield.
- Strong auto-correlations between Nch and short range correlation signal.

Illustrate bias with HIJING simulation

- Hijing has no ridge, mostly short range correlations.

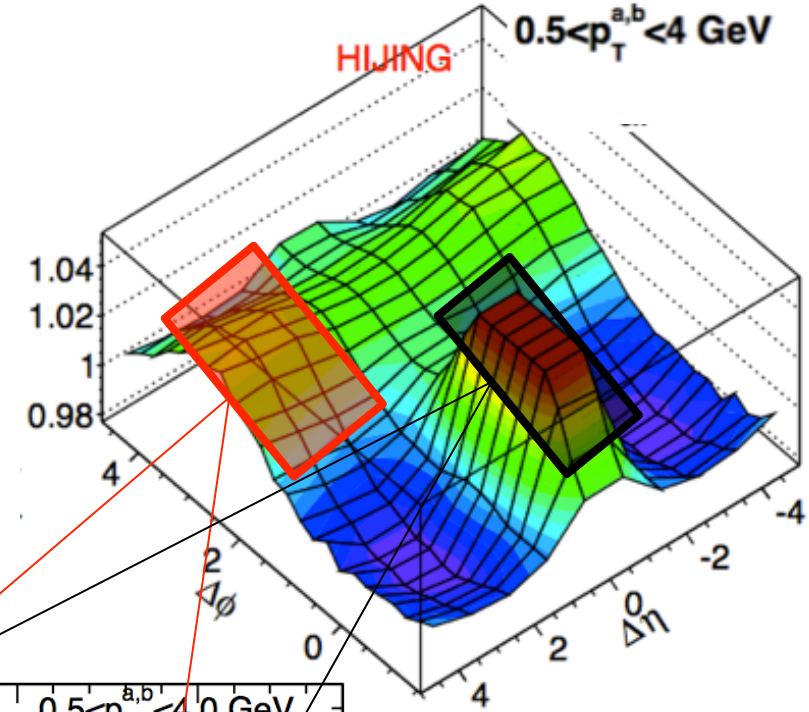

Clear bias effects in N_{ch} based selections

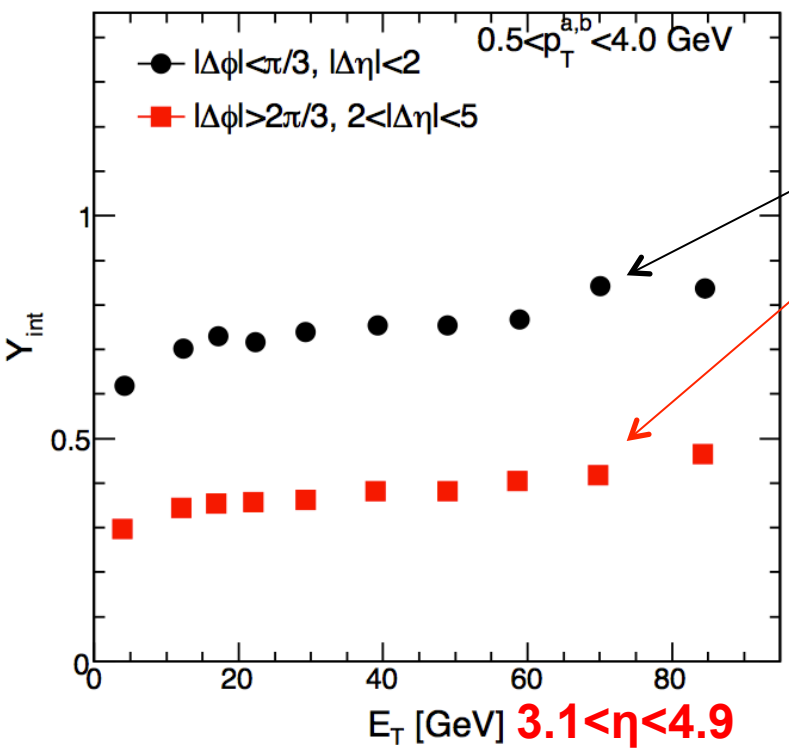

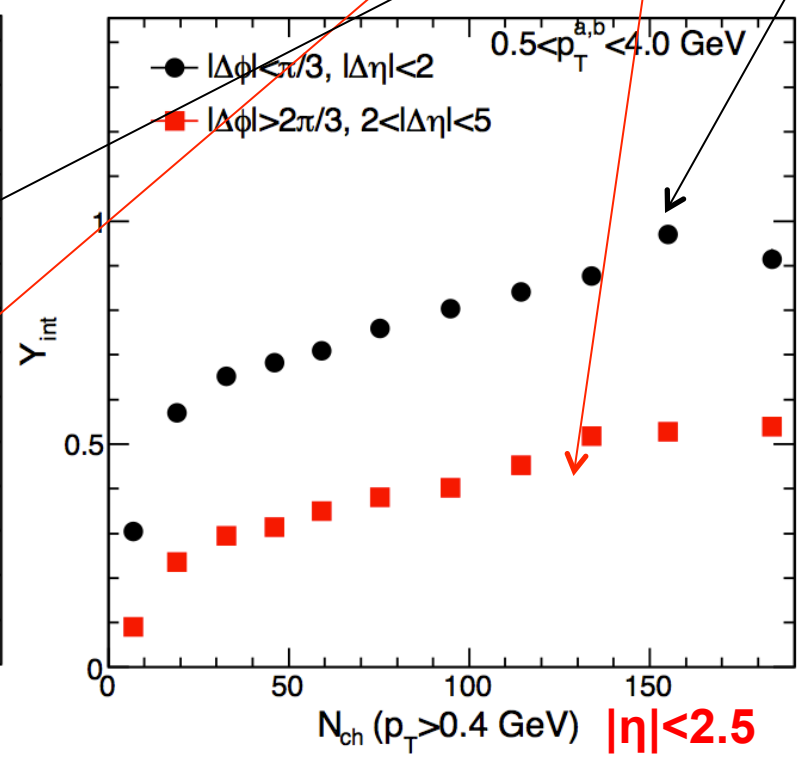

2PC in Δϕ: peripheral

- Define 1-D correlation function over the region $2<|\Delta\eta|<5$
  - normalized to have mean value of 1

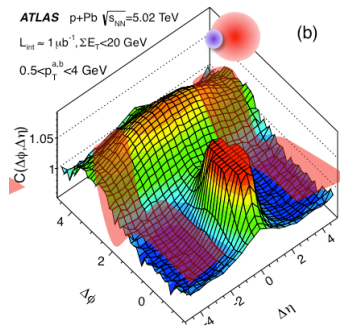

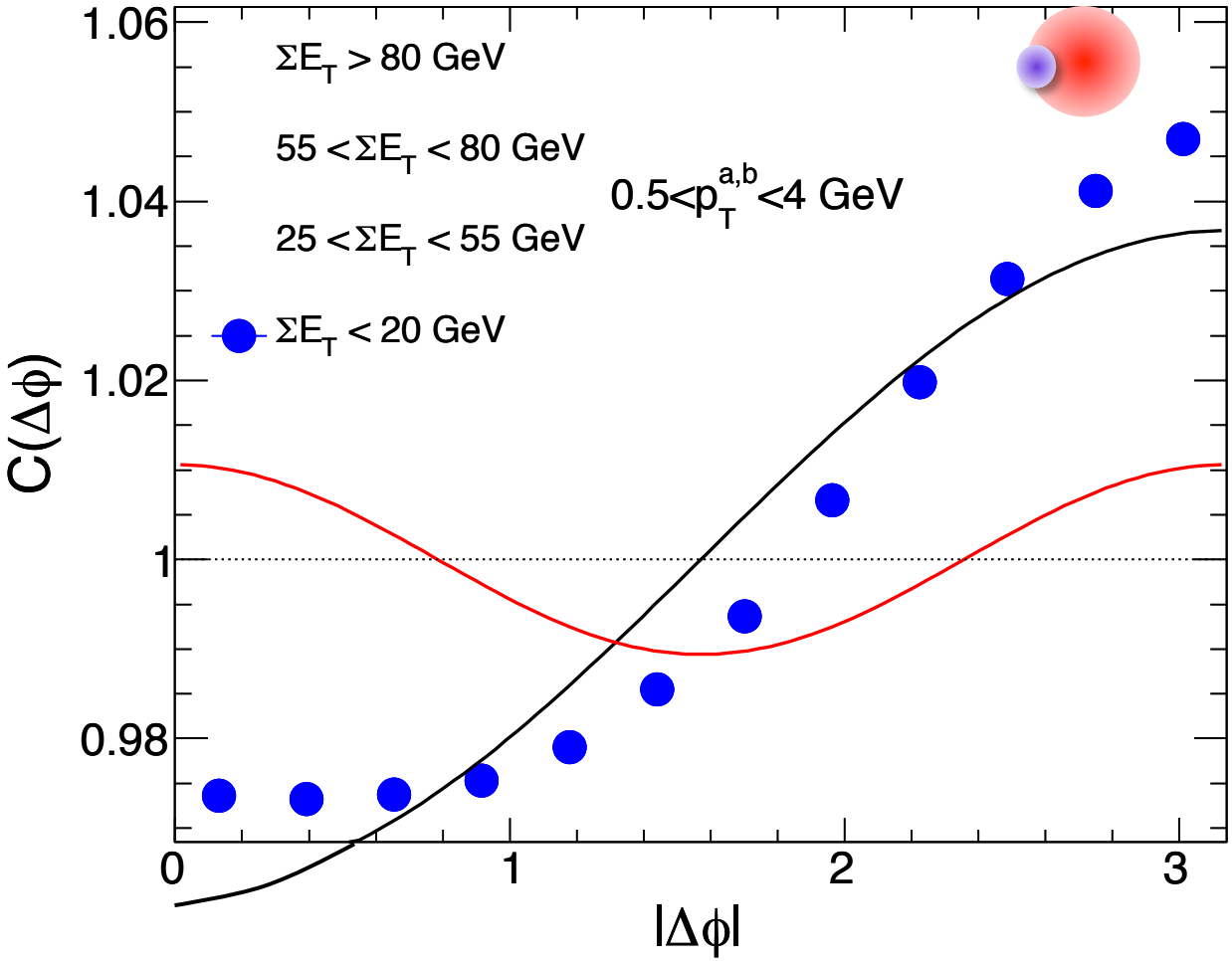

Dominated by a recoil contribution: $\propto -\frac{p_T^a p_T^b \cos\Delta\phi}{N_b}$ N. Borghini 2000

Recoil can also has a small fake v_2 component (about 20% of the yield)

2PC in Δϕ: central

- Define 1-D correlation function over the region $2<|\Delta\eta|<5$
  - normalized to have mean value of 1

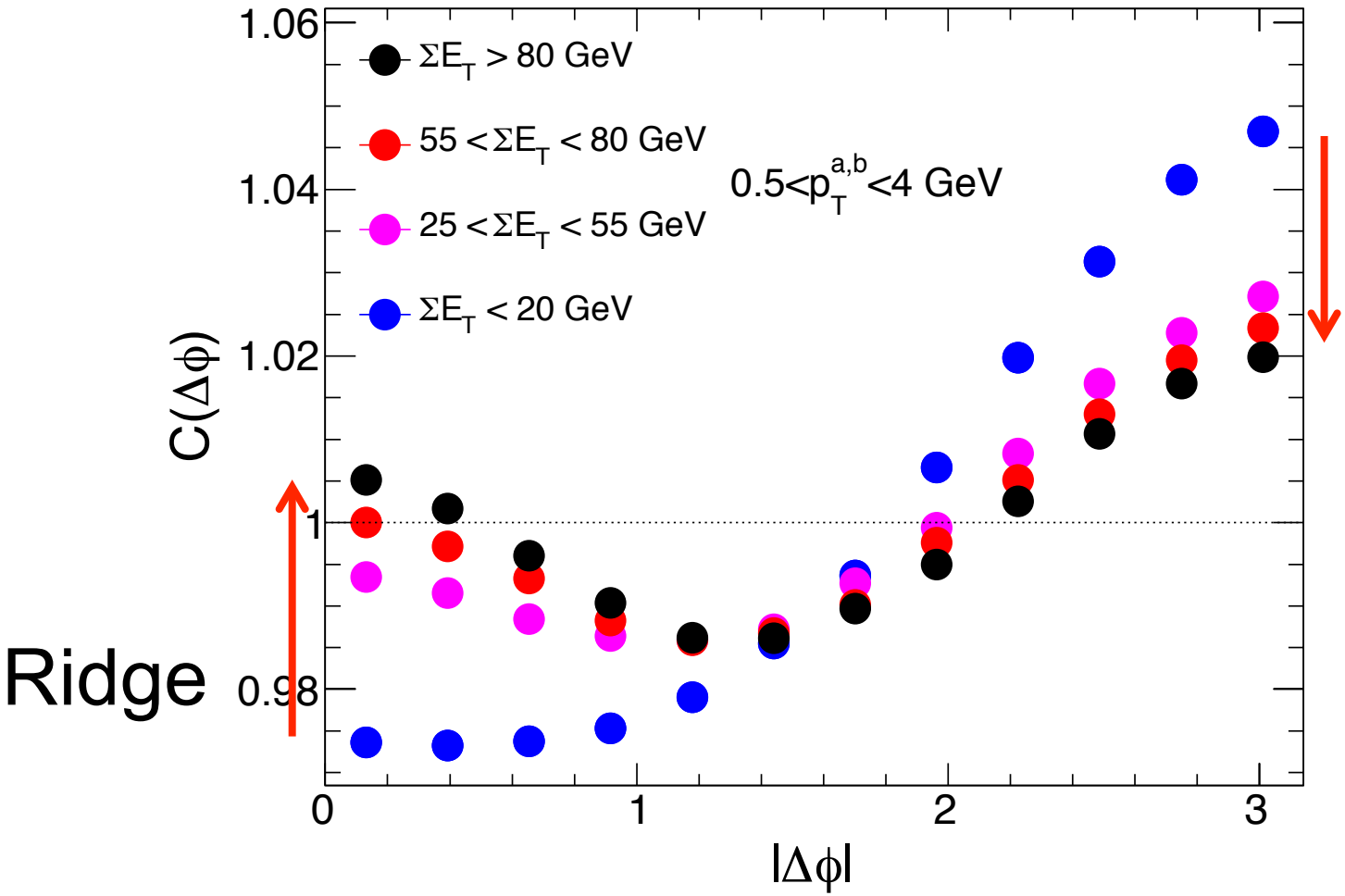

Recoil+Ridge?

$$\text{recoil} \propto -\frac{p_T^a p_T^b \cos\Delta\phi}{N_b}$$

N. Borghini 2000

Need to quantify the recoil to the trigger→ per-trigger yield

$$\text{Corr.} \times N_b = \frac{N_{pairs}}{N_a N_b} \times N_b = \frac{N_{pairs}}{N_a}$$

→recoil is ~ constant

Some personal opinions

Jiangyong Jia

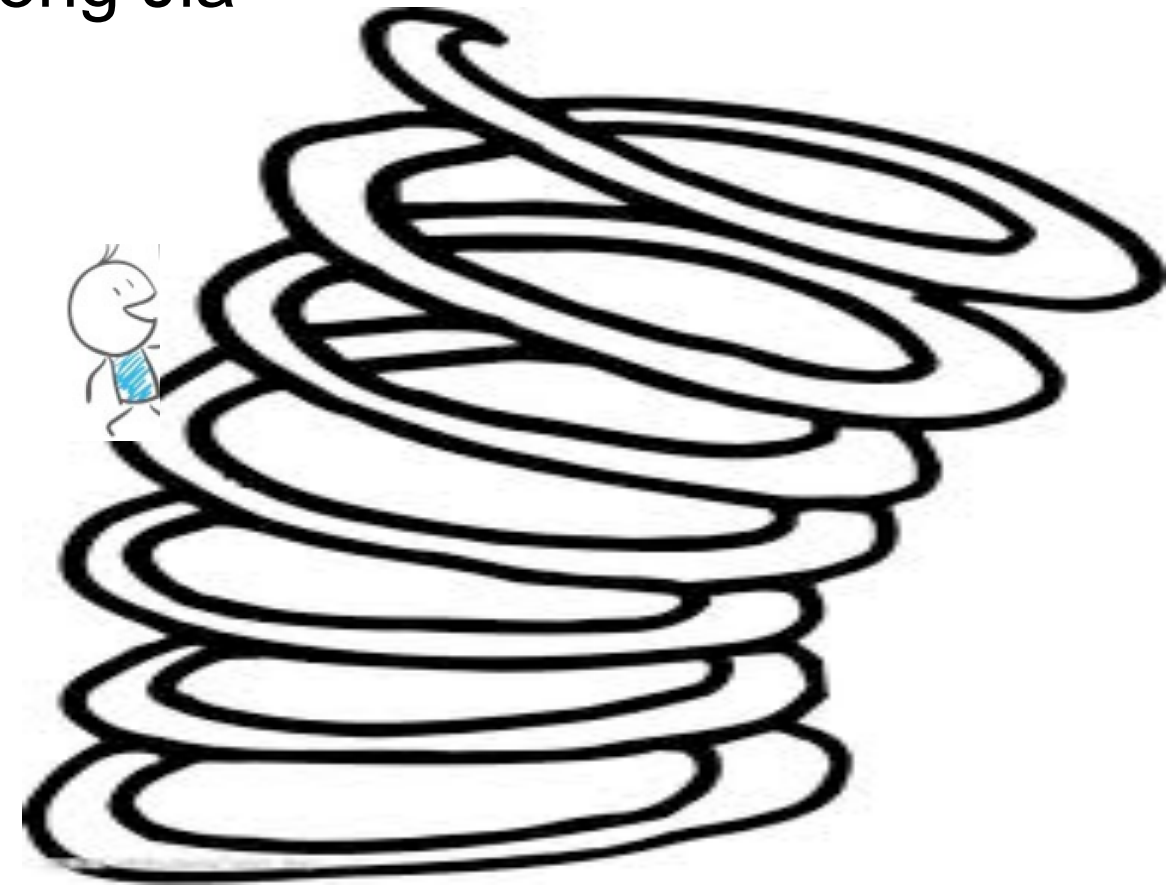

State of affair 2003

CGC

Jet quenching

Hydro

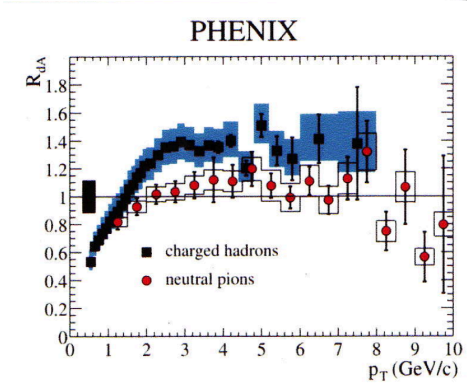

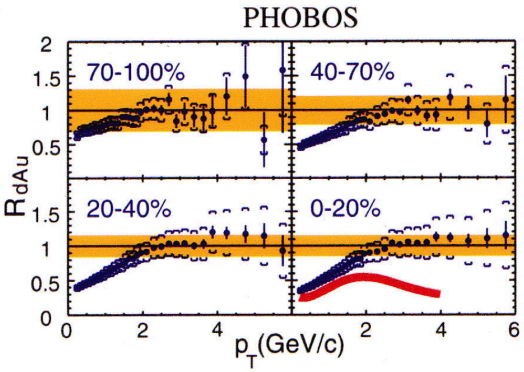

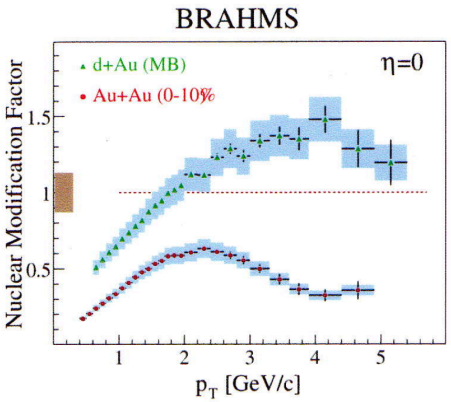

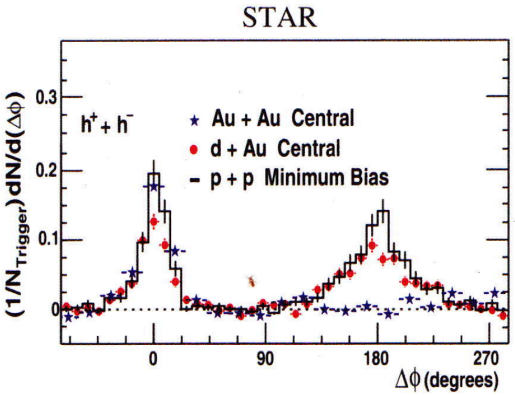

State of affair 2013

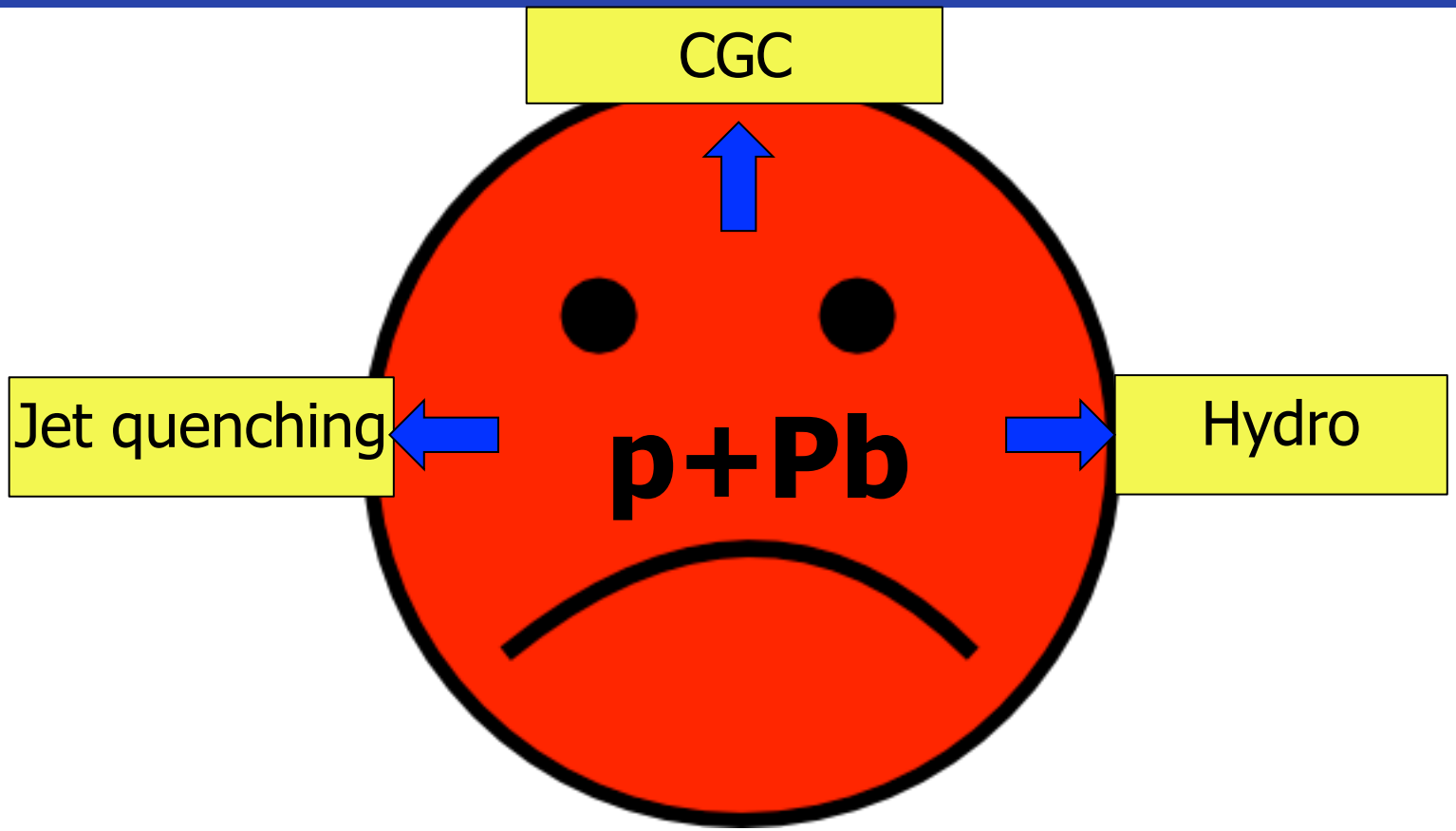

State of affair 2013

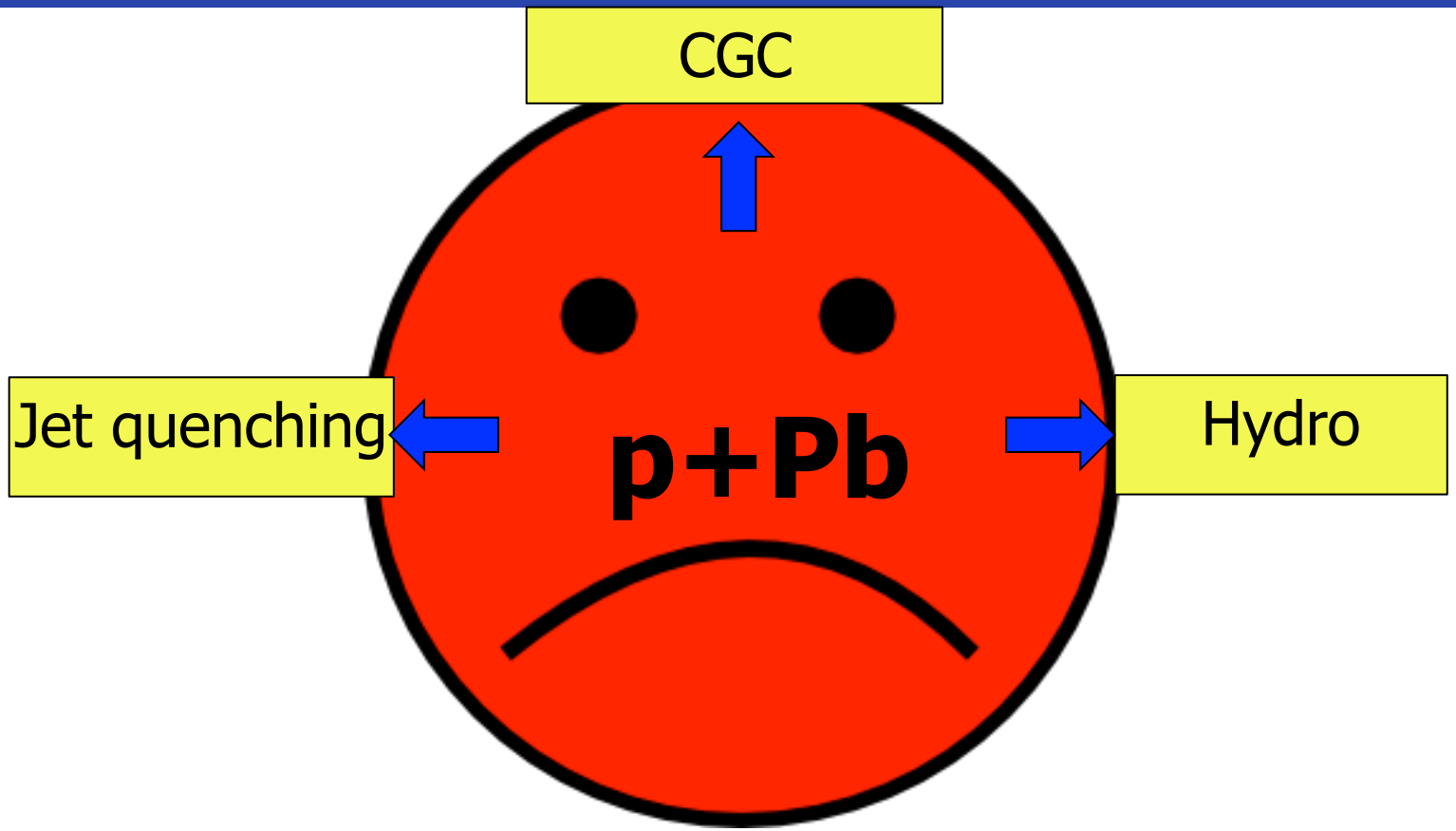

Miklos: My personal perspective is that instead of converging on a solid basis of null controls, we reached a **maximal entropy state both theoretically and experimentally**

- Theory : Indeed…
- Experiment : undigested information ≠ more entropy

What is the effective picture/theory of QCD in high-density system??

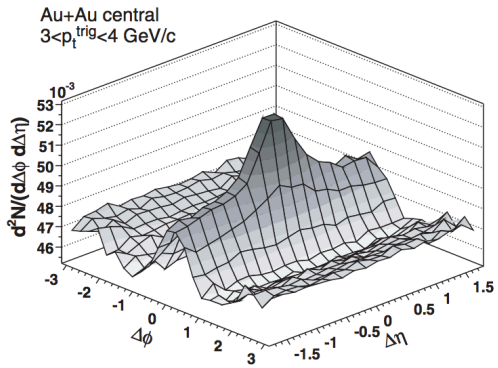

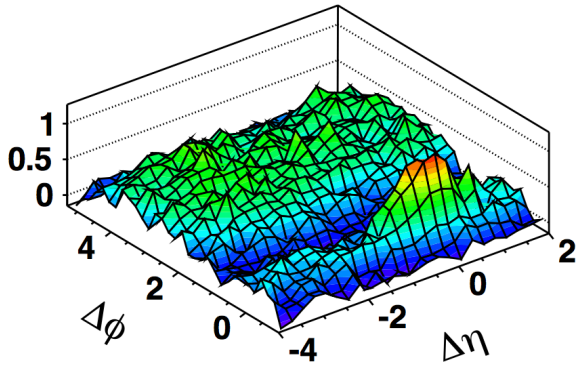

(b) Au+Au 0%-30% (PHOBOS)

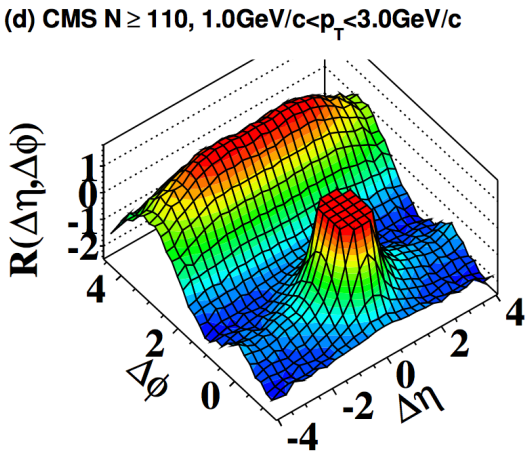

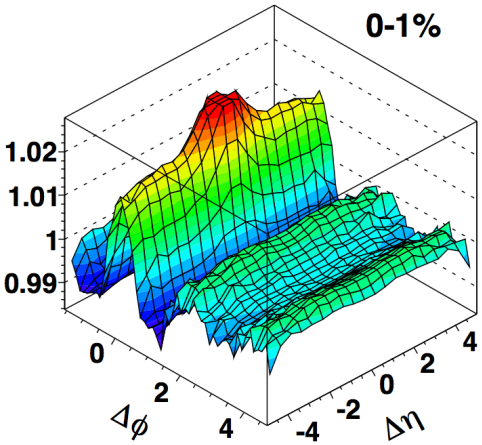

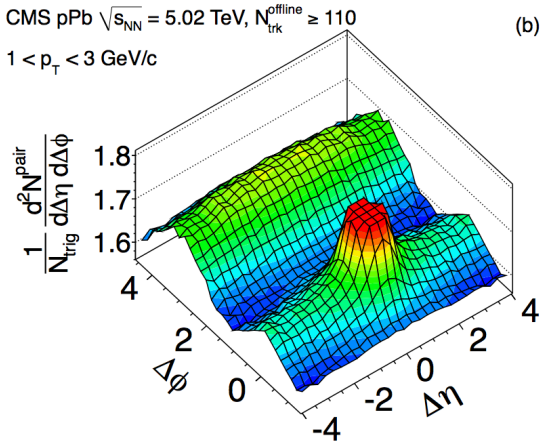

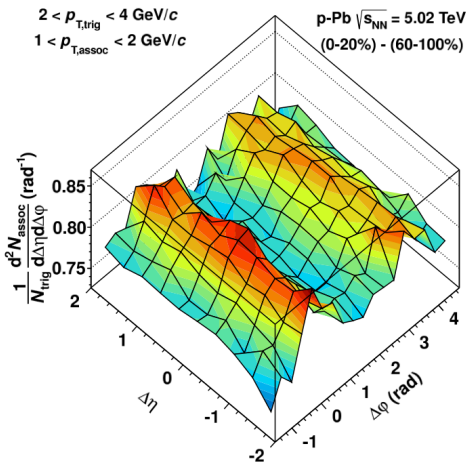

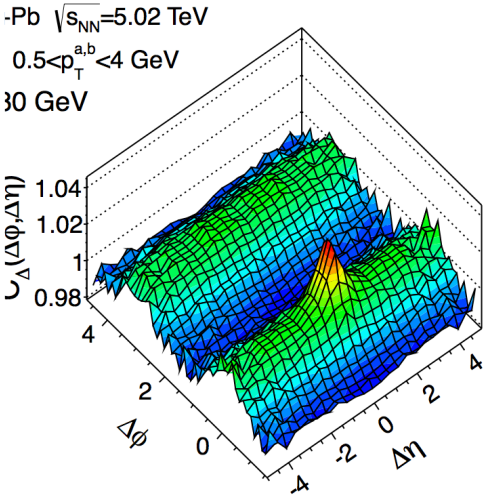

PROJECT

THE RIDGE AT RHIC & THE LHC

leveraging RHIC/LHC differences

initial entropy densitiy

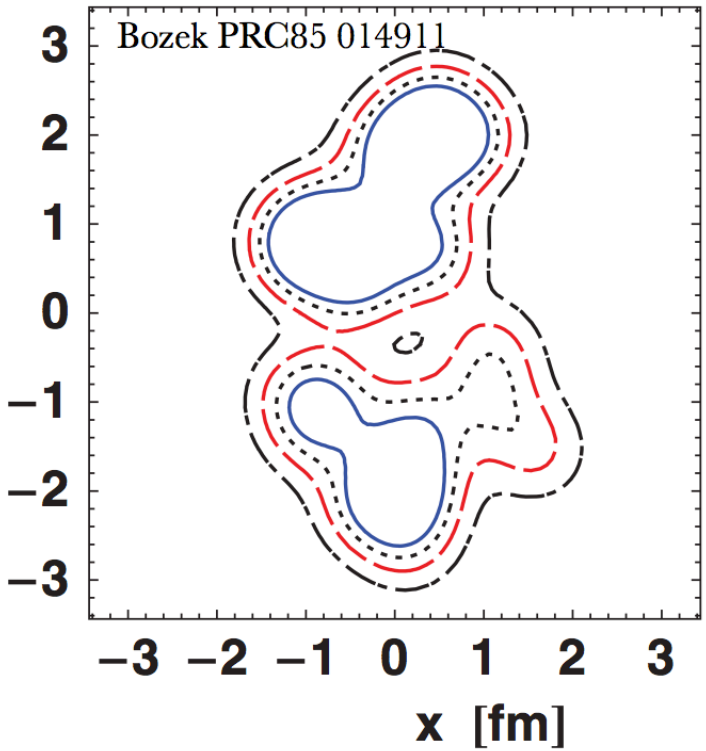

1303.1794

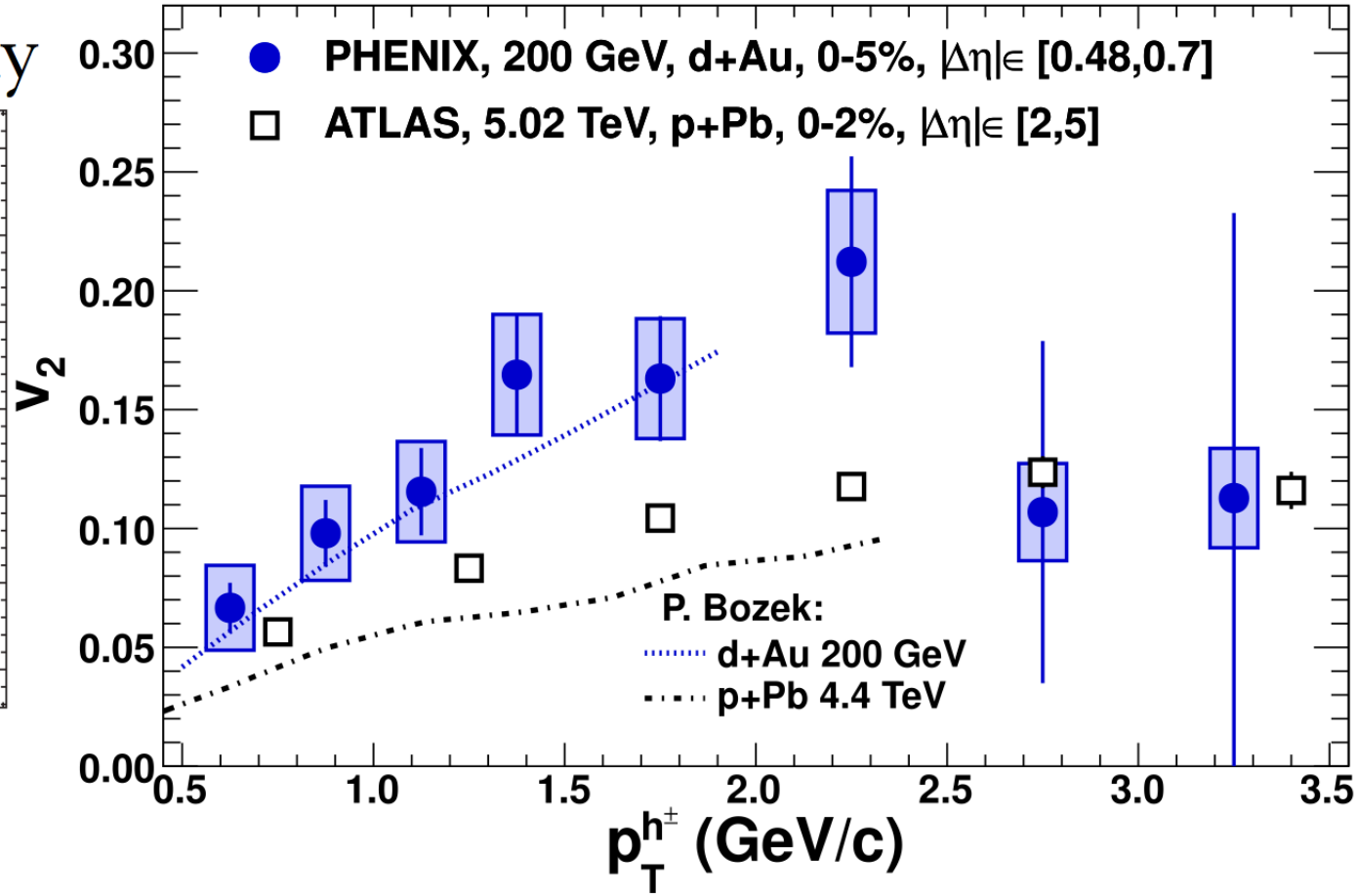

- changing both the collision energy and the shape of the initial system as compared to the ridge seen in pPb

leveraging RHIC/LHC differences

initial entropy densitiy

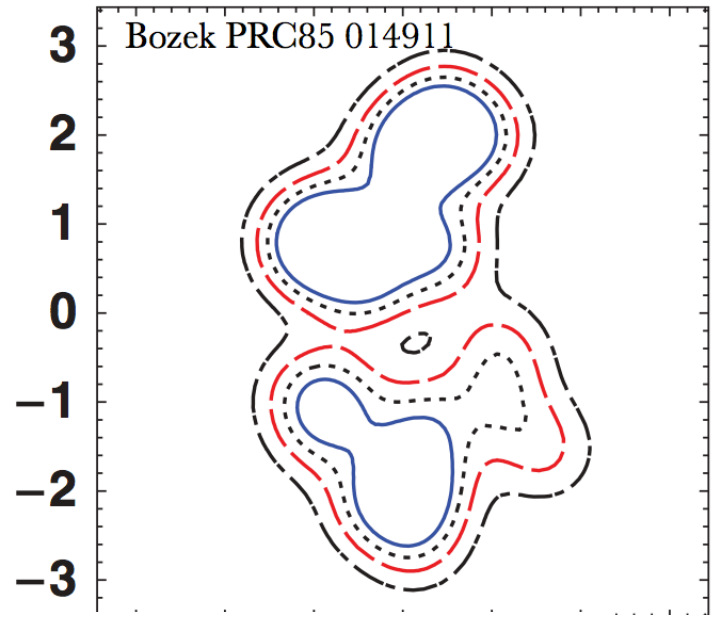

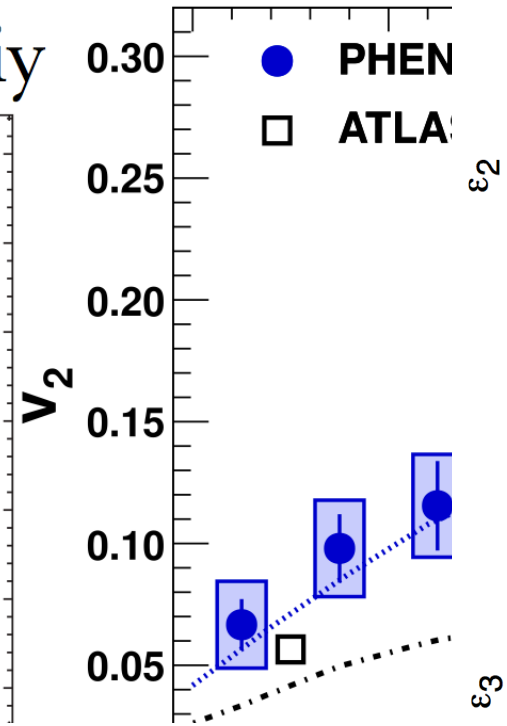

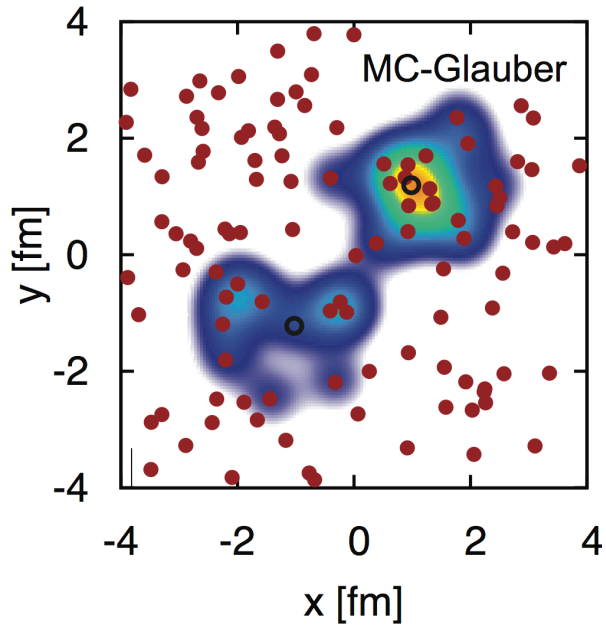

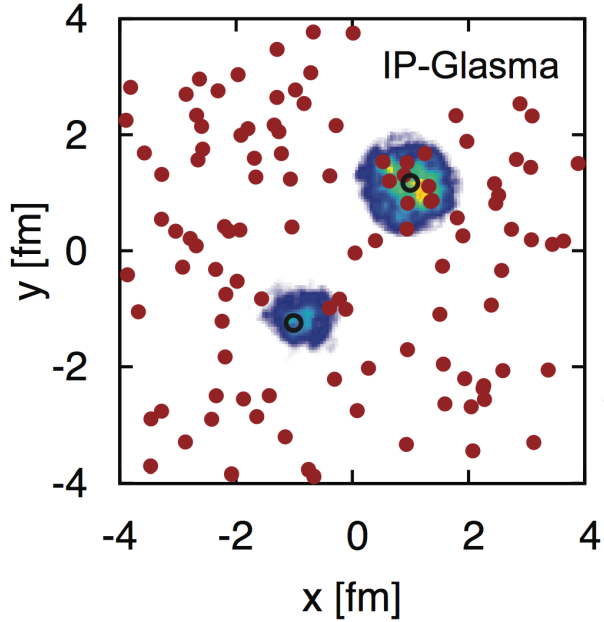

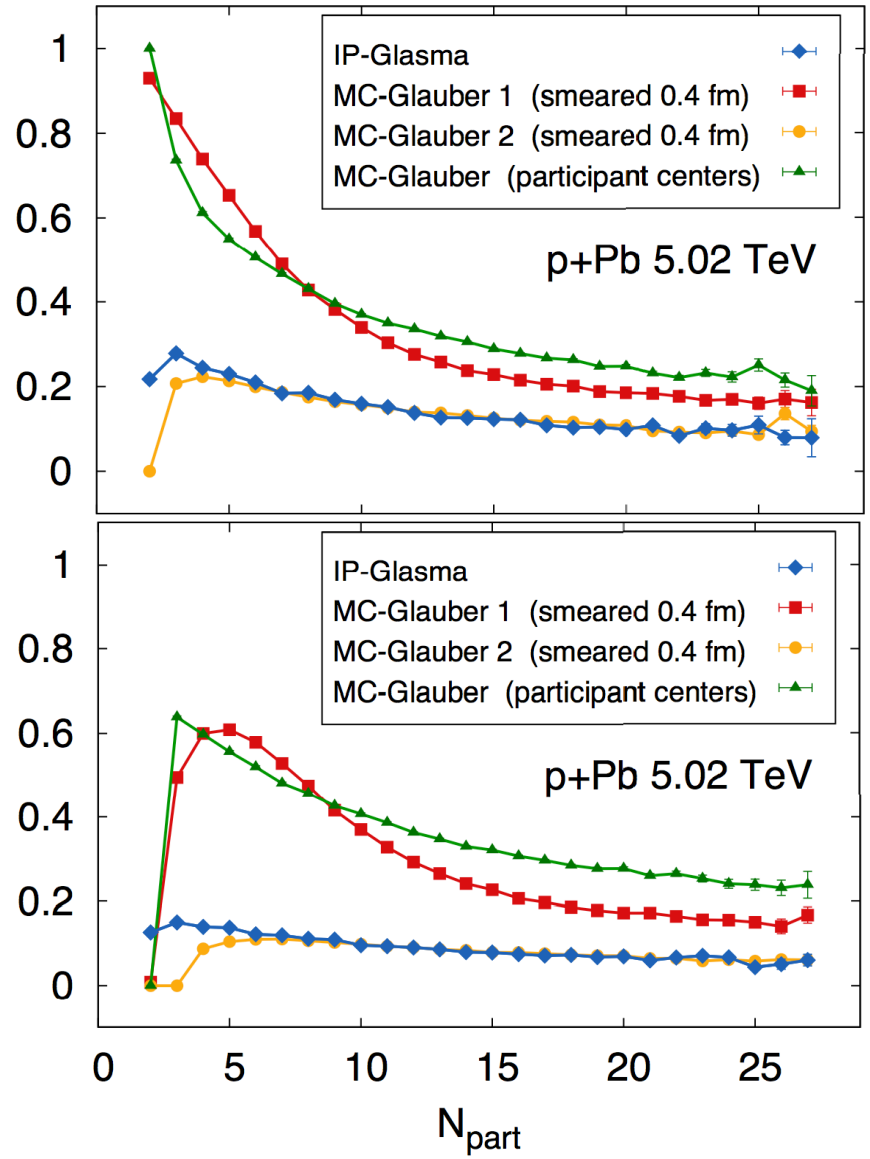

the shape of the initial system

Bzdak et.al. 1304.3403

Hydrodynamics in small system?

- Flow depends on shape and size/gradient

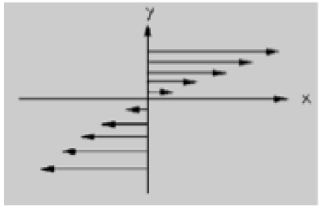

$$\frac{F_x}{A} = -\eta \frac{\partial v_x}{\partial y}$$

- HM pp and pA have larger density (η/s) but much larger gradient!

$$\rho(\phi, r)$$

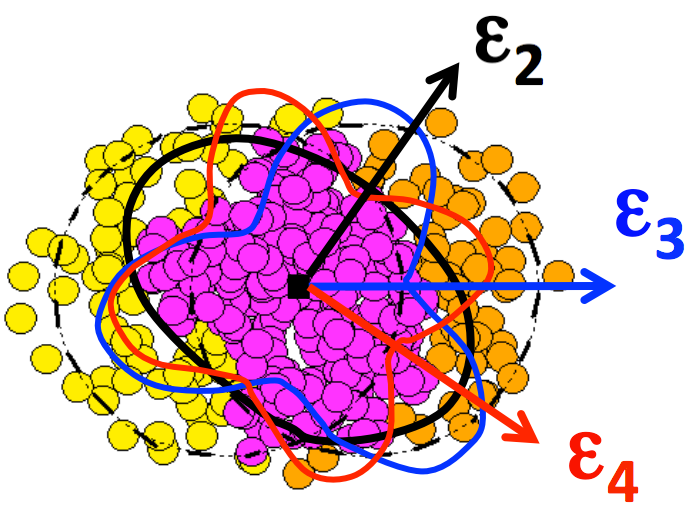

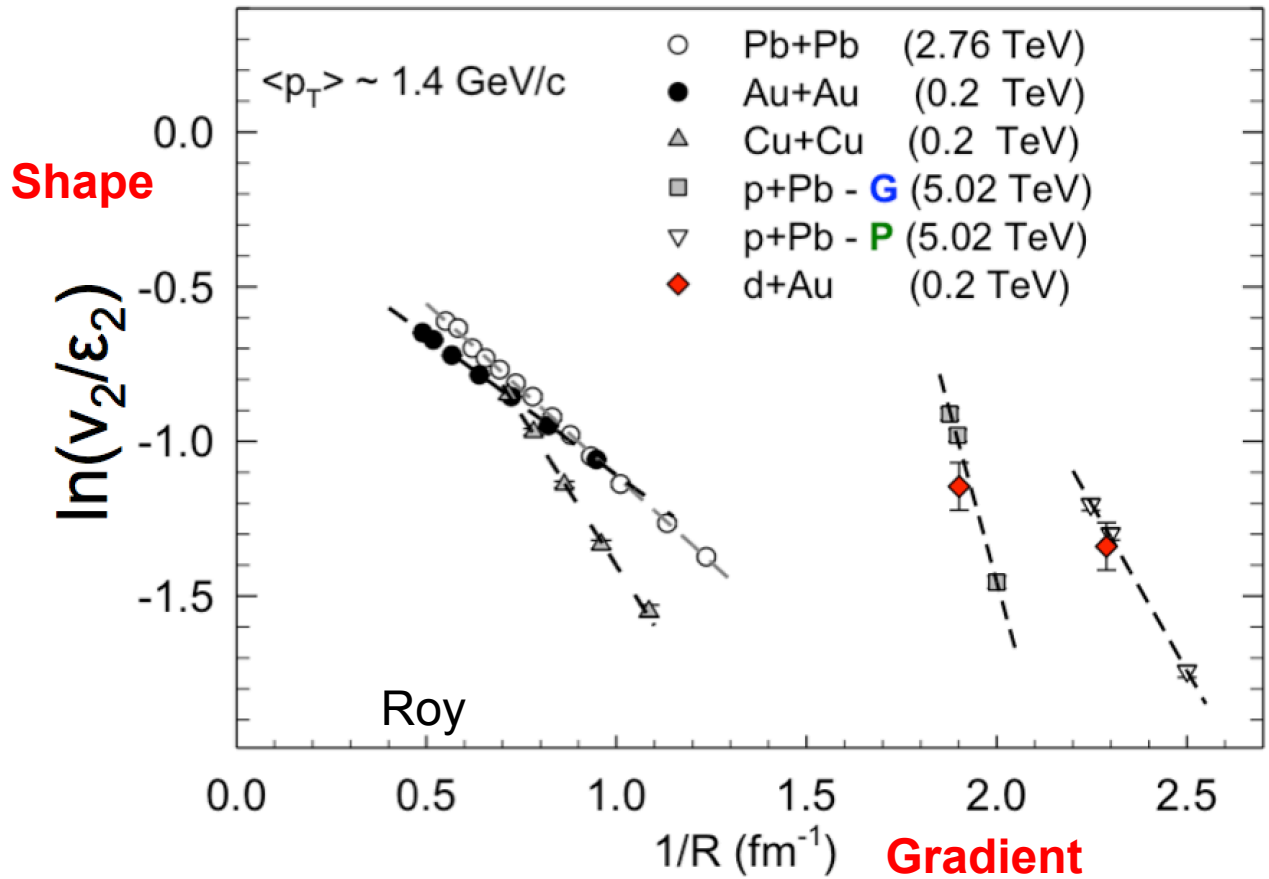

v_3 in pPb and PbPb

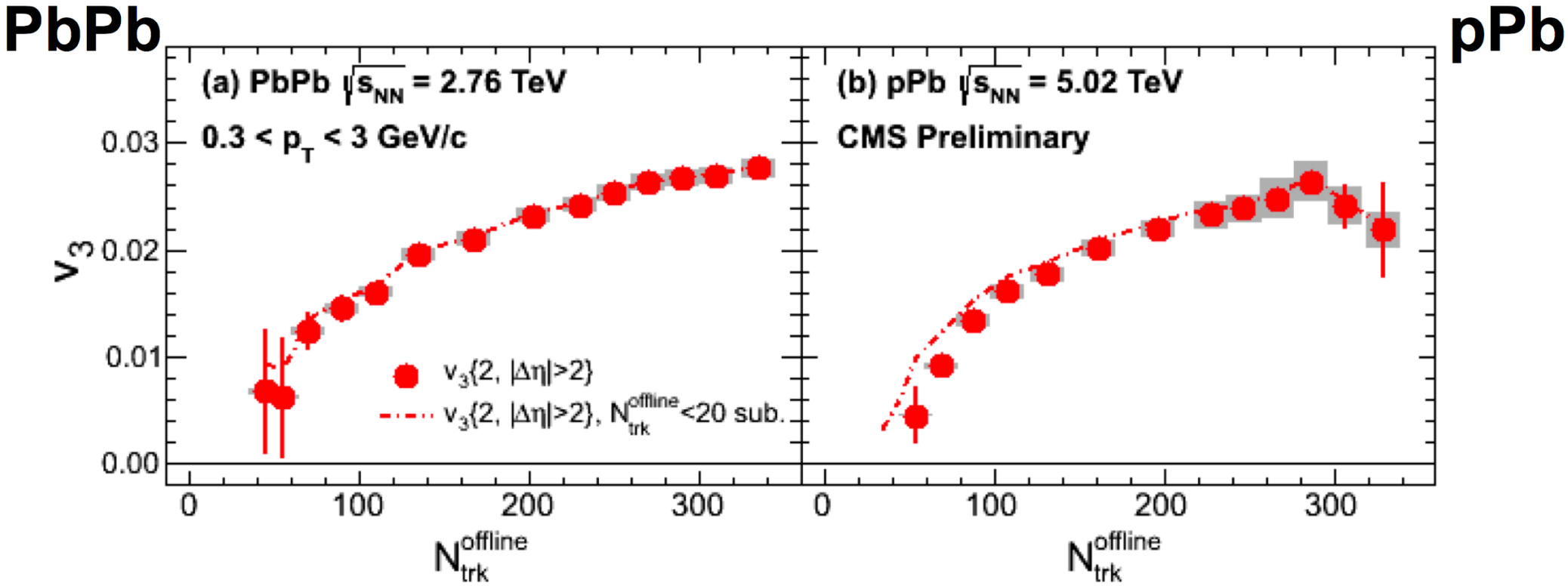

v_3 shows similar shape in pPb and PbPb; magnitude comparable

"Peripheral subtraction" makes essentially no difference

v_2 in pPb and PbPb

PbPb

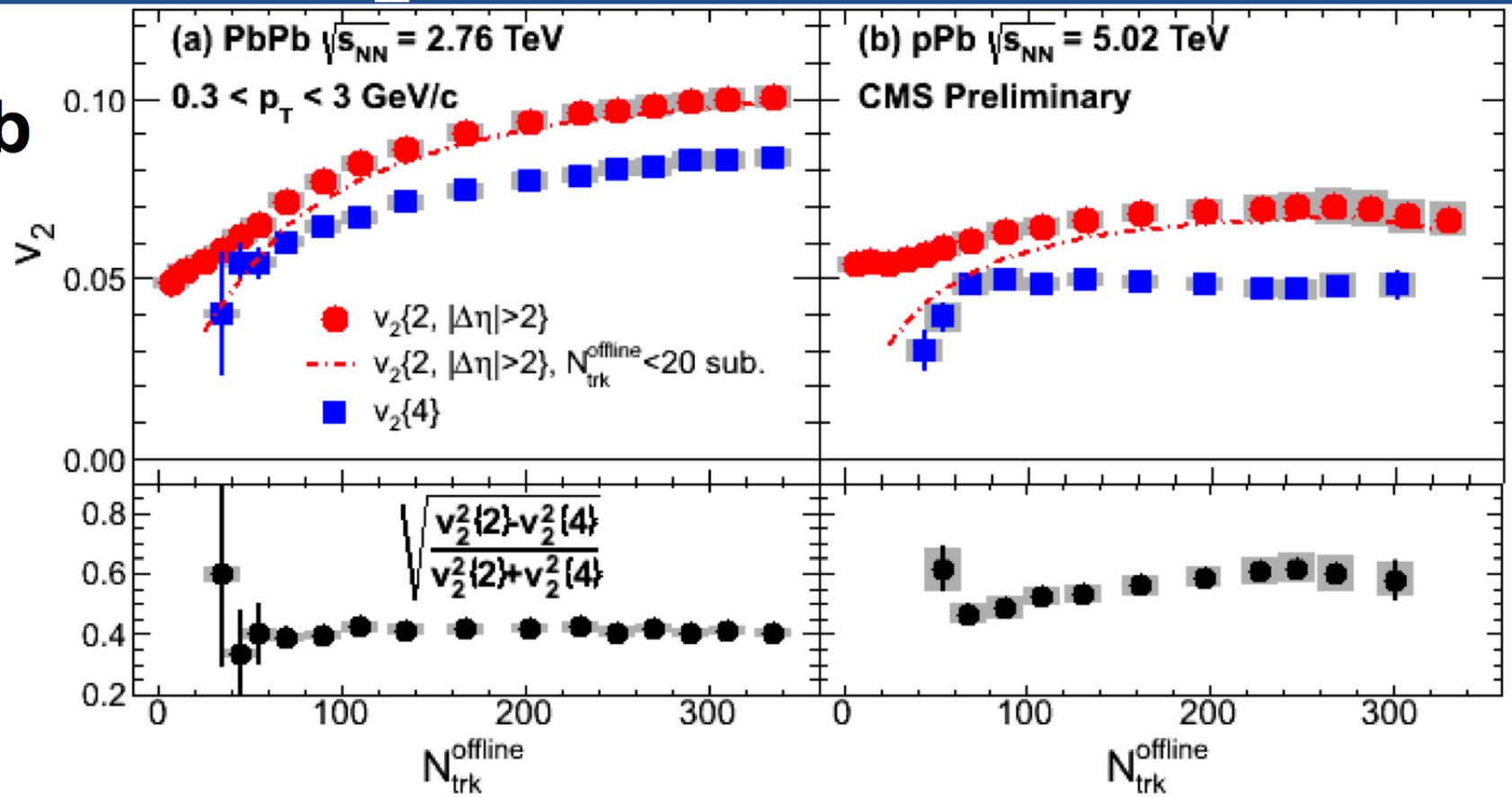

pPb

$$v_2\{2\} = \sqrt{< v_2 >^2 + \sigma_{v_2}^2}$$
$$v_2\{4\} = \sqrt{< v_2 >^2 - \sigma_{v_2}^2},$$

$$\frac{\sigma_{v_2}}{v_2} = \sqrt{\frac{v_2^2\{2\} - v_2^2\{4\}}{v_2^2\{2\} + v_2^2\{4\}}}.$$

"Fluctuations" larger in pPb, with moderate multiplicity dependence

Flow fluctuation & $v_n\{4\}$

- Bessel-Gaussian

$$p(\vec{v}_n) \propto \exp\left(\frac{-(\vec{v}_n - \vec{\bar{v}}_n)^2}{2\delta_n^2}\right)$$

$$p(v_n) \propto v_n \exp\left(\frac{-(v_n^2 + (\bar{v}_n)^2}{2\delta_n^2}\right) I_0\left(\frac{v_n \bar{v}_n}{\delta_n^2}\right) \quad I_0(x) \approx e^{\frac{x^2}{4}}\left[1 - \frac{x^4}{64}\right]$$

For pure fluctuations $\bar{v}_n = 0 \Rightarrow \quad p(v_n) \propto v_n \exp\left(\frac{-(v_n^2)}{2\delta_n^2}\right)$

- When $\alpha = \frac{\bar{v}_n}{\delta_n} <\approx 1$ distribution is very close to pure Gaussian with a redefinition of δ

$$\begin{pmatrix} \delta_n^2 \\ v_n^{RP} \end{pmatrix} \rightarrow \begin{pmatrix} \delta_n^{2'} = \delta_n^2 + \left(\bar{v}_n\right)^2/2 \\ \bar{v}_n{}' = 0 \end{pmatrix}$$

Valid when $\frac{v_n \bar{v}_n}{\delta_n^2} << 64^{1/4} = 2.8$ or $v_n << 2.8\delta_n\alpha$

Flow fluctuation & $v_n\{4\}$

- Bessel-Gaussian

$$p(\vec{v}_n) \propto \exp\left(\frac{-(\vec{v}_n - \vec{\bar{v}}_n)^2}{2\delta_n^2}\right)$$

$$p(v_n) \propto v_n \exp\left(\frac{-(v_n^2 + (\bar{v}_n)^2}{2\delta_n^2}\right) I_0\left(\frac{v_n \bar{v}_n}{\delta_n^2}\right) \quad I_0(x) \approx e^{\frac{x^2}{4}}\left[1 - \frac{x^4}{64}\right]$$

For pure fluctuations $\bar{v}_n = 0 \Rightarrow \quad p(v_n) \propto v_n \exp\left(\frac{-(v_n^2)}{2\delta_n^2}\right)$

- When $\alpha = \frac{\bar{v}_n}{\delta_n} <\approx 1$ distribution is very close to pure Gaussian with a redefinition of δ

$$\begin{pmatrix} \delta_n^2 \\ v_n^{RP} \end{pmatrix} \rightarrow \begin{pmatrix} \delta_n^{2'} = \delta_n^2 + \left(\bar{v}_n\right)^2/2 \\ \bar{v}_n' = 0 \end{pmatrix}$$

Valid when $\frac{v_n \bar{v}_n}{\delta_n^2} << 64^{1/4} = 2.8$ or $v_n << 2.8\delta_n\alpha$

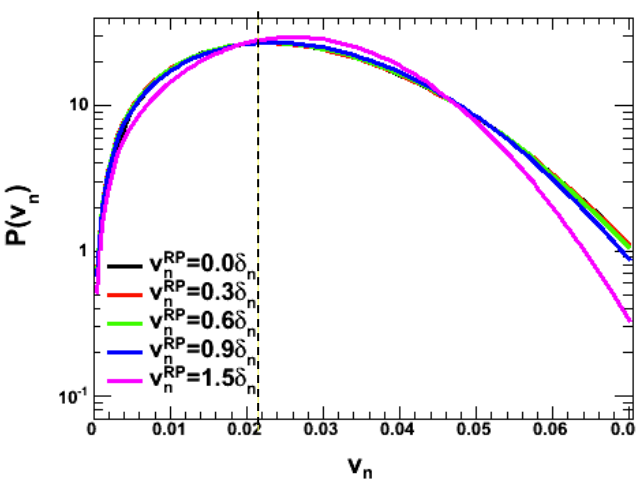

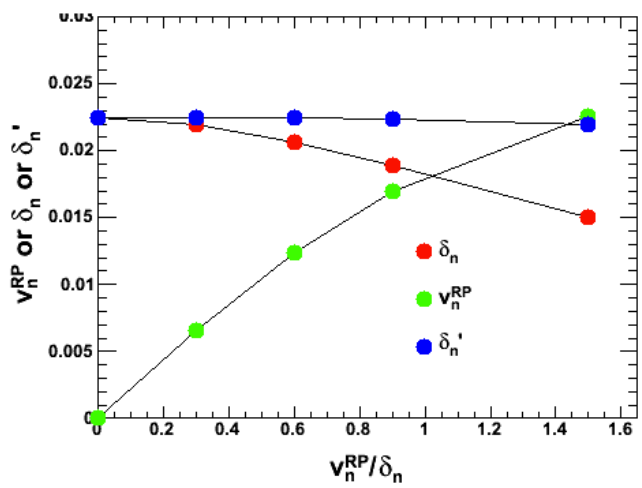

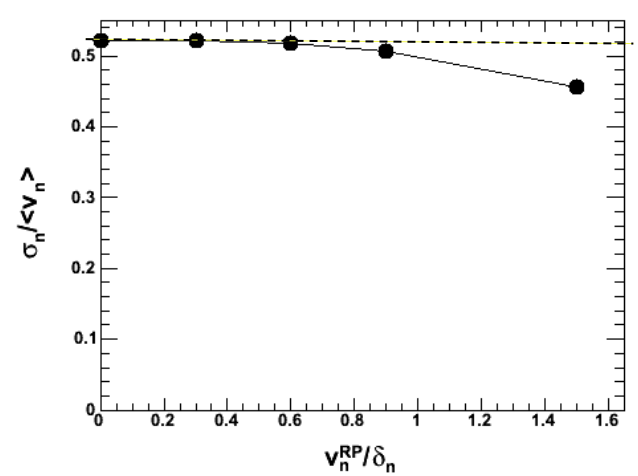

Flow fluctuation & $v_n\{4\}$

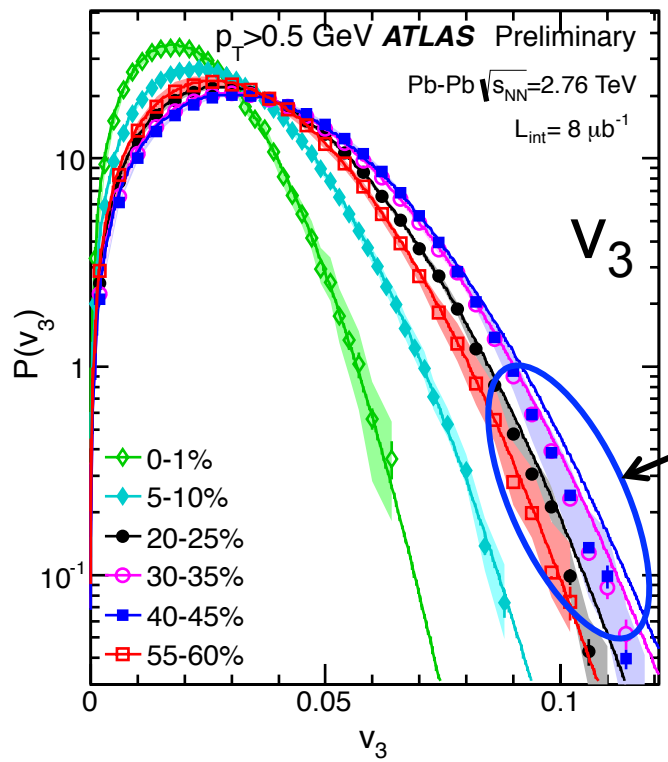

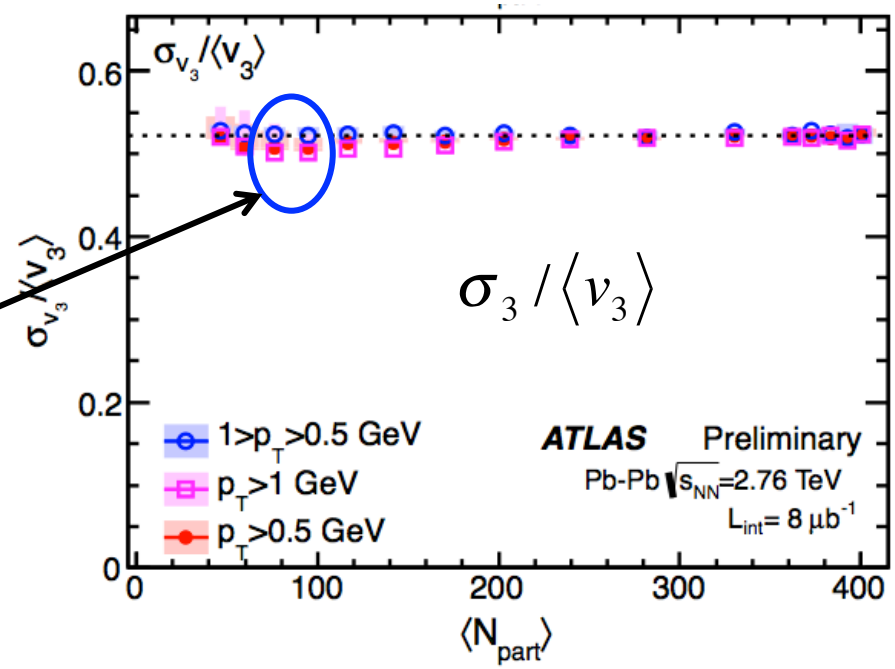

- Even a small deviation will give a large v_n^{RP} or large $v_n\{4\}$

$$v_n\{4\} = \left[2\left\langle v_n^2\right\rangle^2 - \left\langle v_n^4\right\rangle\right]^{1/4}$$

a 4% difference gives a $v_n\{4\}$ value of about 45% of $v_n\{2\}$

Flow fluctuation & $v_n\{4\}$

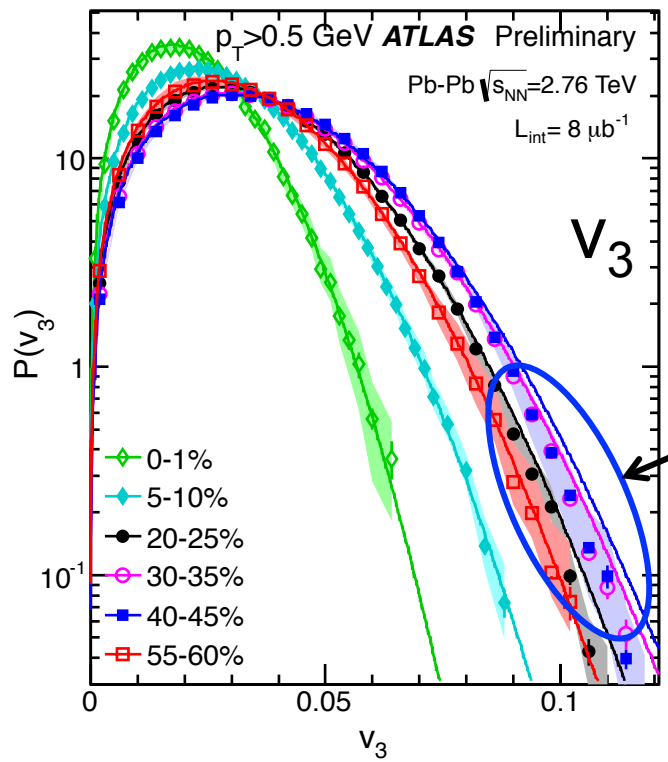

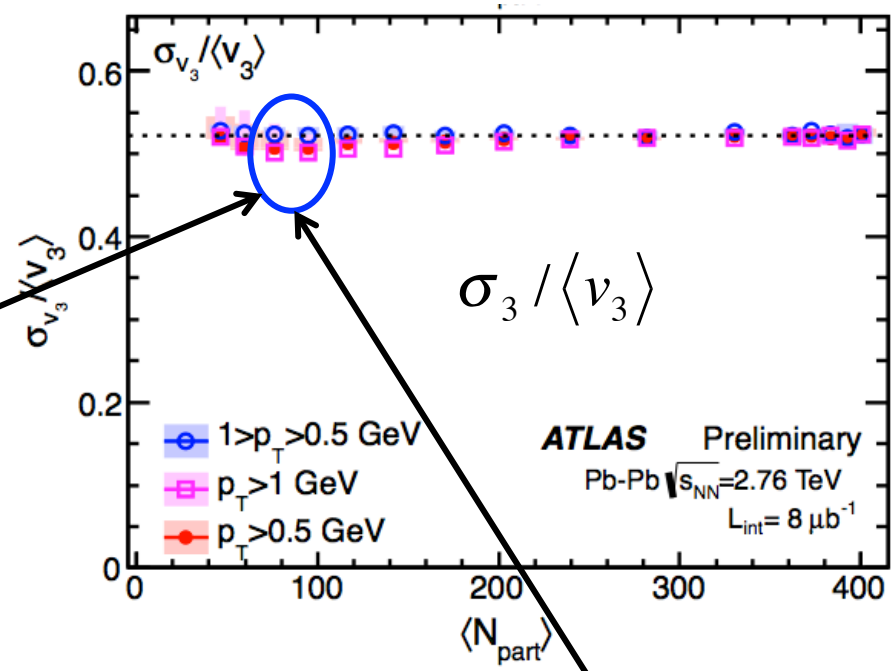

- Even a small deviation will give a large v_n^{RP} or large $v_n\{4\}$

$$v_n\{4\} = \left[2\left\langle v_n^2\right\rangle^2 - \left\langle v_n^4\right\rangle\right]^{1/4}$$

a 4% difference gives a $v_n\{4\}$ value of about 45% of $v_n\{2\}$

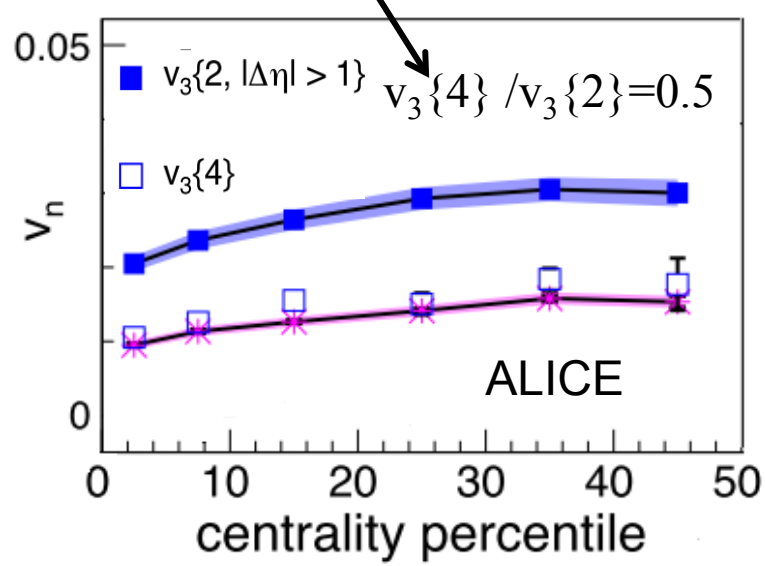

$v_2\{4\}$ in p+Pb

- Just need a small deviation from Gaussian
  - Small N_{part}, or Negative binomial fluctuation (Bozek)
  - Fluctuation of M and v_n aren't de-coupled

$$\frac{dN}{d\phi} = M\left[1 + \sum_n 2v_n \cos n\left(\phi - \Phi_n\right)\right]$$

ATLAS, arXiv:1303.2084 (2013)

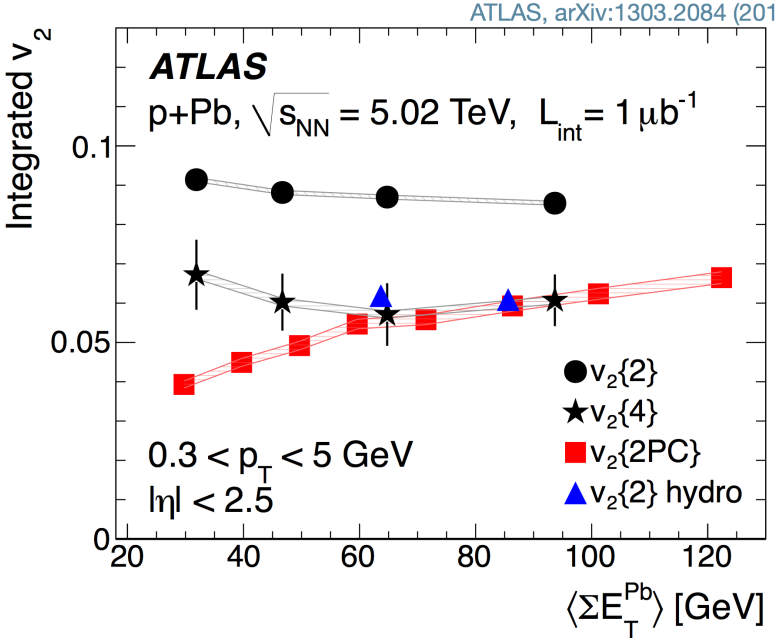

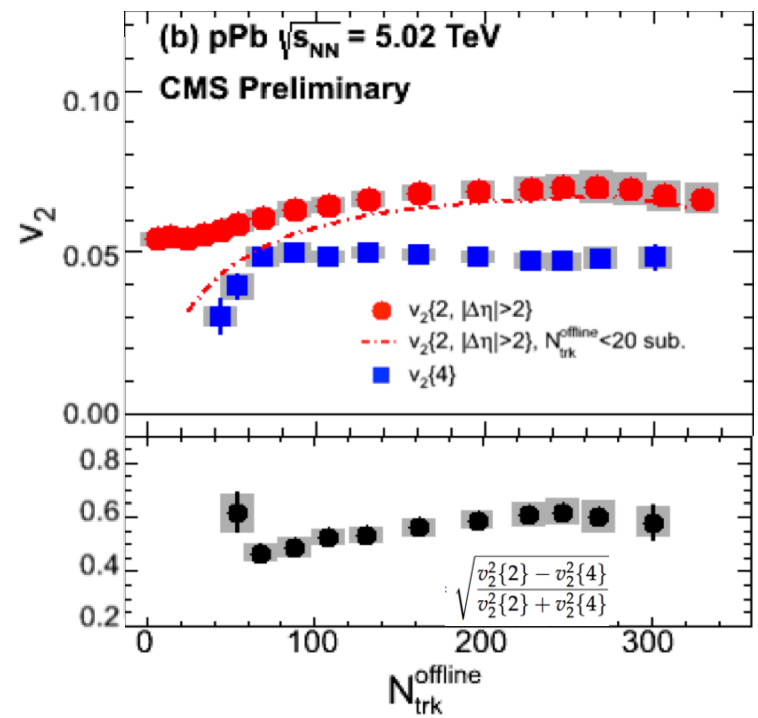

$v_2\{4\}$ in p+Pb

- Just need a small deviation from Gaussian
  - Small N_{part}, or Negative binomial fluctuation (Bozek)
  - Fluctuation of M and v_n aren't de-coupled

$$\frac{dN}{d\phi} = M\left[1 + \sum_n 2v_n \cos n\left(\phi - \Phi_n\right)\right]$$

ATLAS, arXiv:1303.2084 (2013)

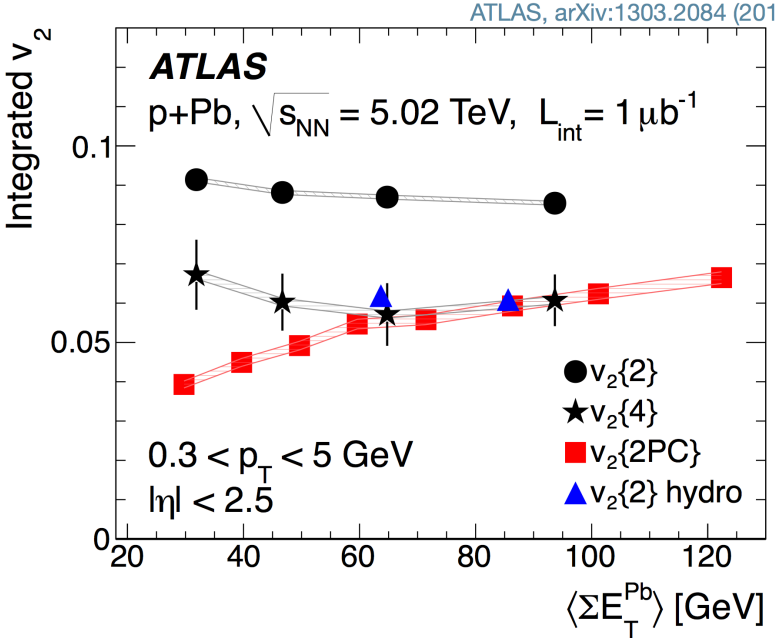

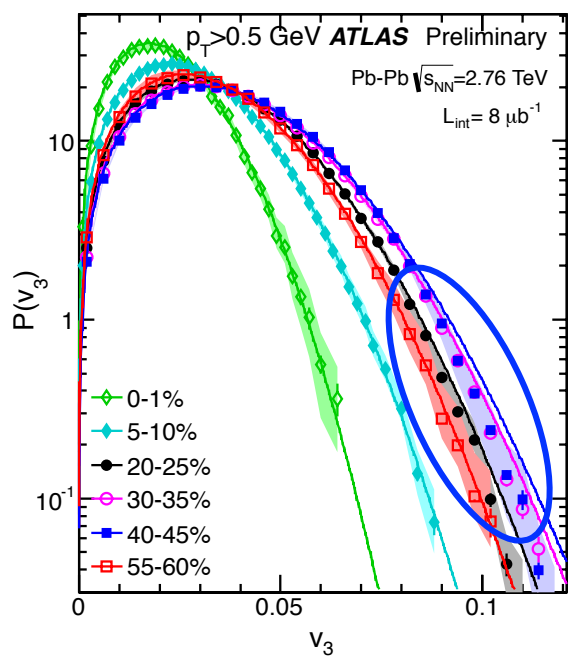

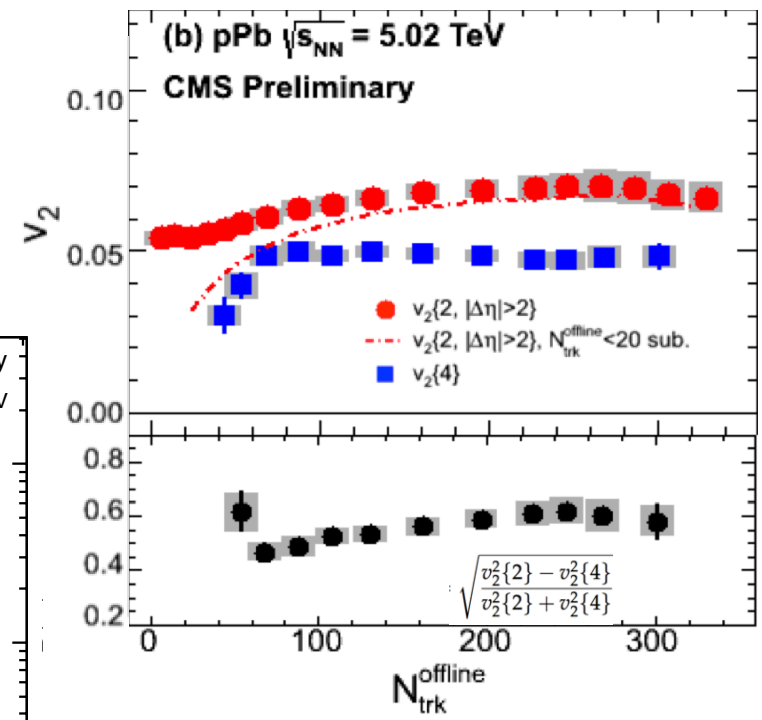

Power spectrum

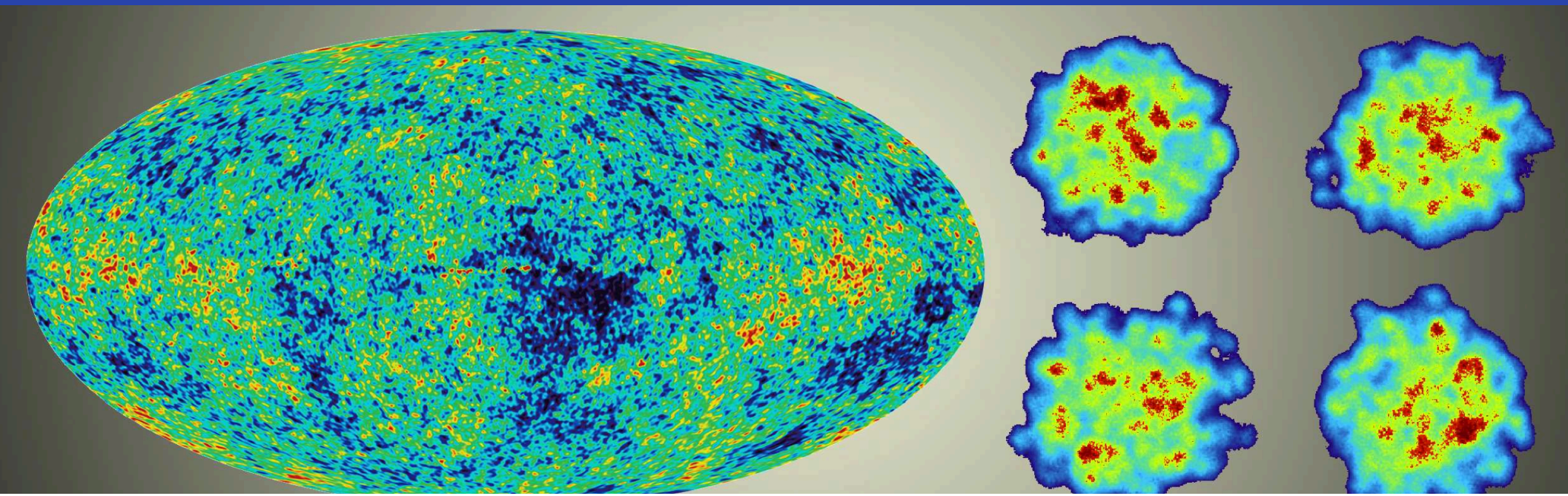

Planck 2013 CMB temperature power spectrum

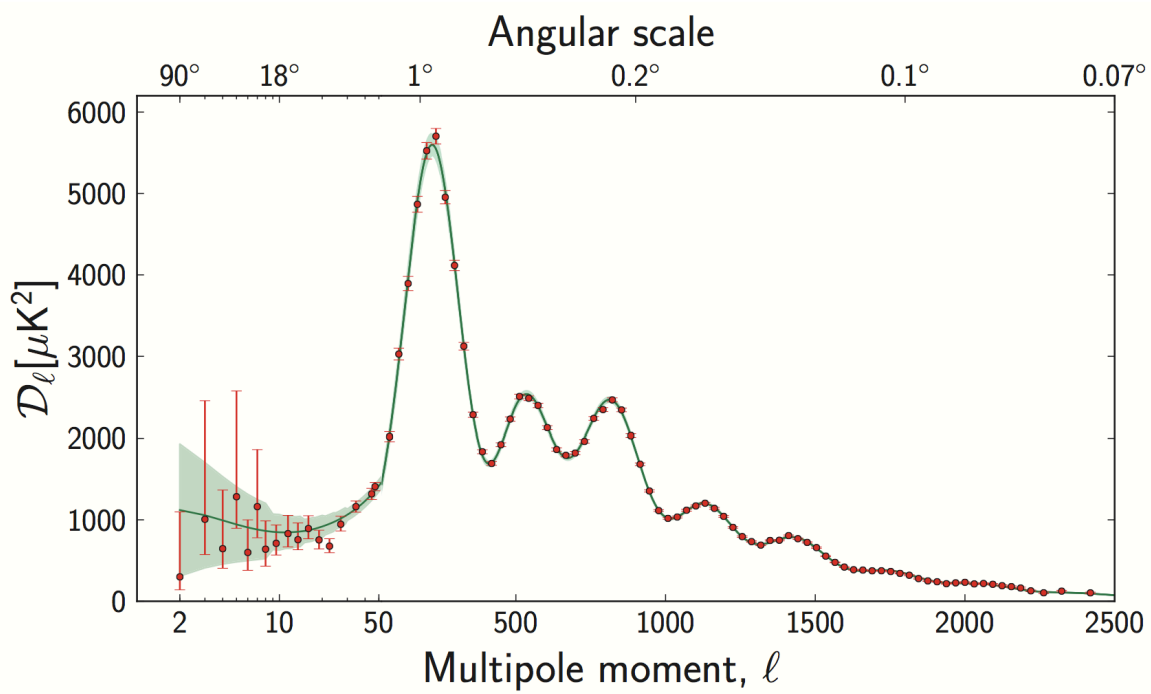

Little Bang density power spectra 2013

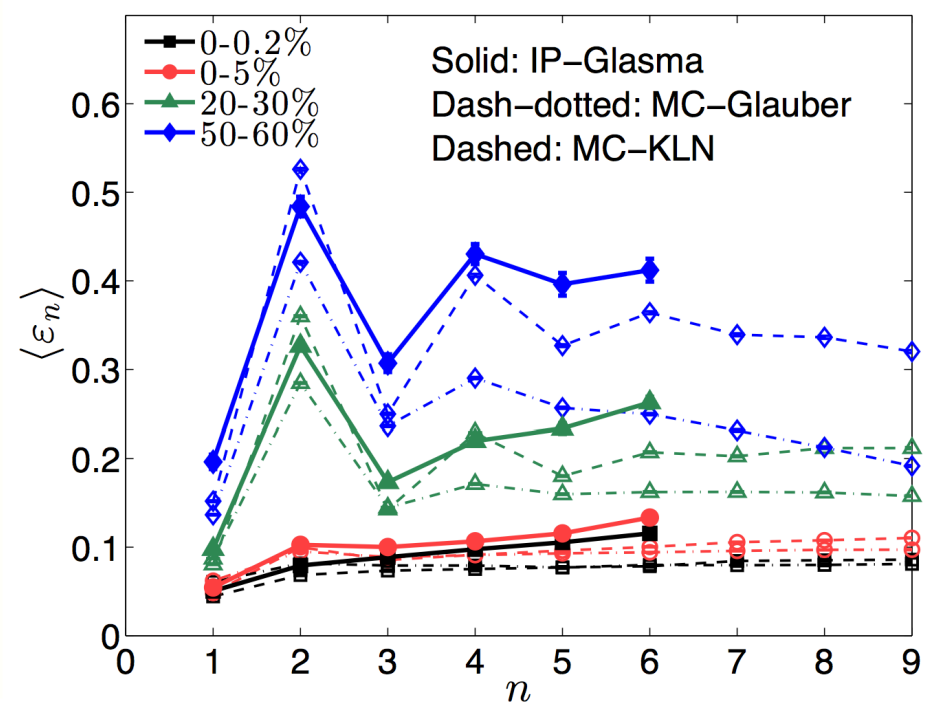

Ripples of "little-bangs"

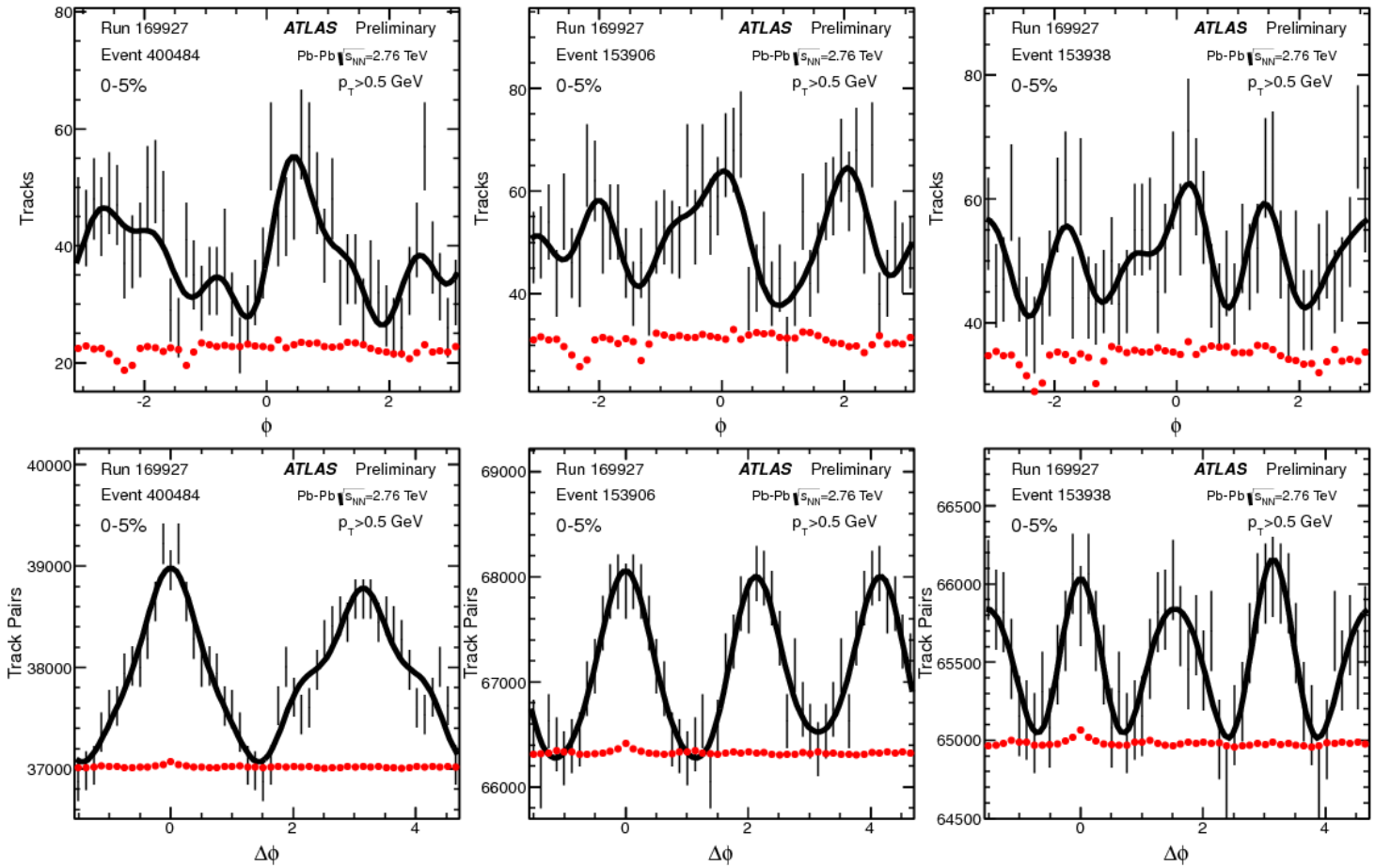

- Data-driven unfolding the key:

Sub-event "A" – Sub-event "B" =
- **Signal : cancelled**
- **Fluctuations+short-range corr. : √2 larger**

$$(\vec{v}_n^{\,\mathrm{obs}})^{\mathrm{a}} - (\vec{v}_n^{\,\mathrm{obs}})^{\mathrm{b}} = \mathrm{nonflow} + \mathrm{noise}$$

$$(\vec{v}_n^{\,\mathrm{obs}})^{\mathrm{a}} + (\vec{v}_n^{\,\mathrm{obs}})^{\mathrm{b}} = 2\vec{v}_n$$

J.Jia, S. Mohapatra: arxiv:1304.1471

Azimuthal power spectrum in hijing: (non-flow)

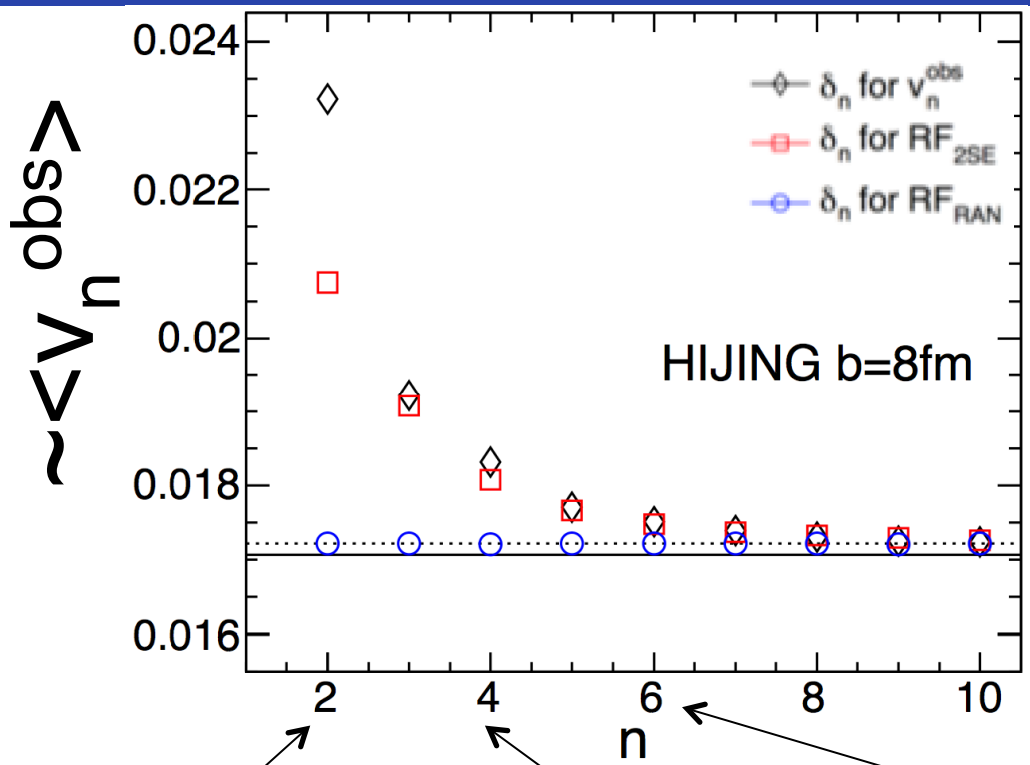

- Unfolding method allow extraction of EbE distribution of short-range and long-range correlations
  - Well-defined noise limit

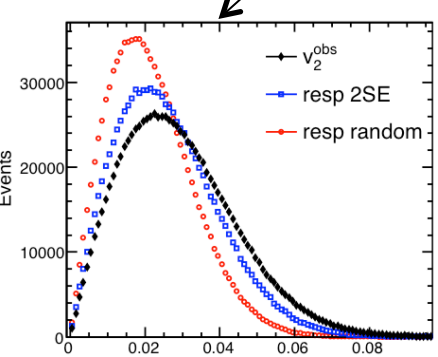

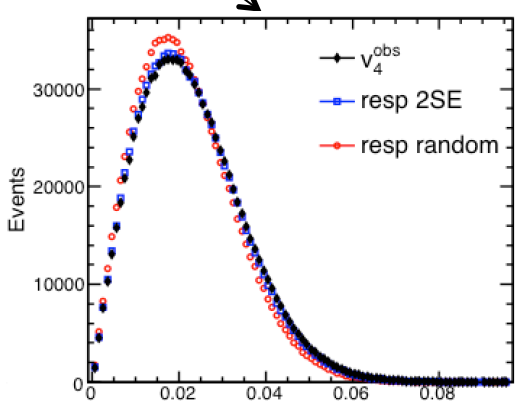

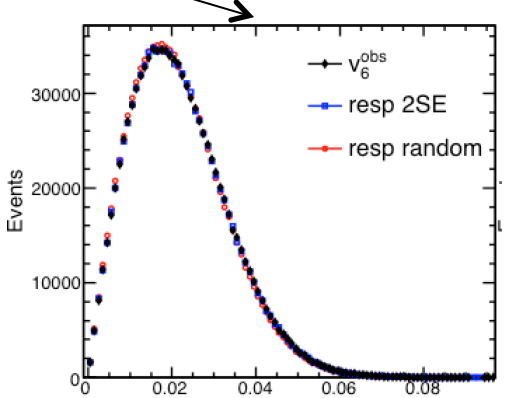

J.Jia, S. Mohapatra: arxiv:1304.1471

Azimuthal power spectrum in hijing: (non-flow)

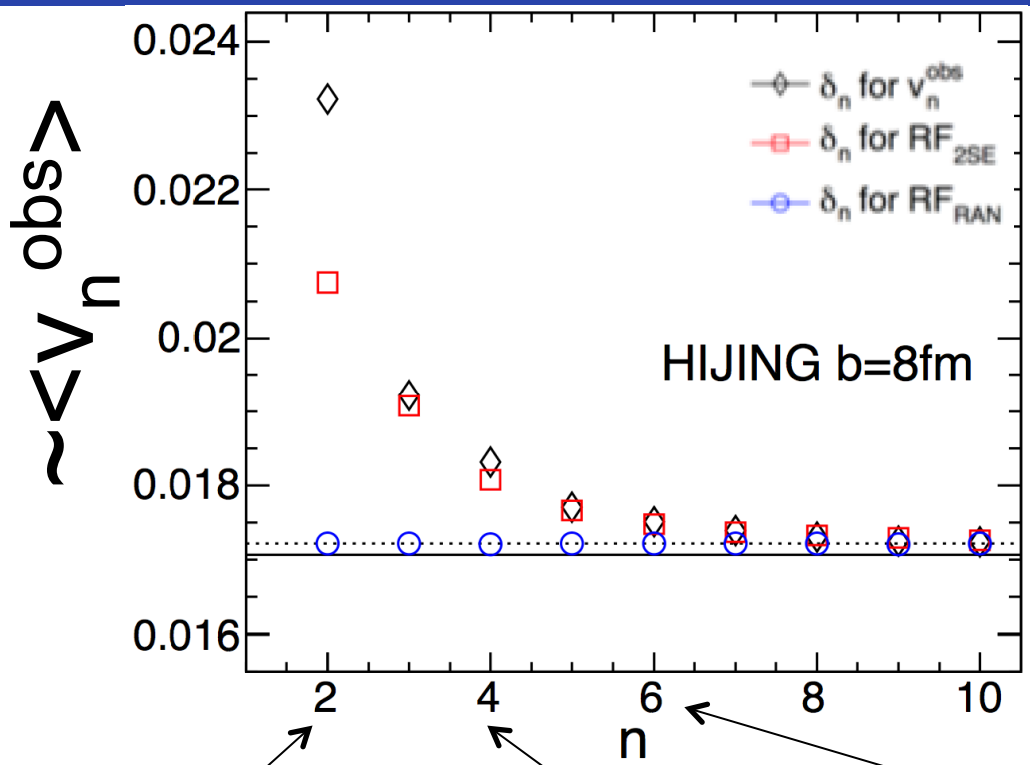

- Unfolding method allow extraction of EbE distribution of short-range and long-range correlations
  - Well-defined noise limit

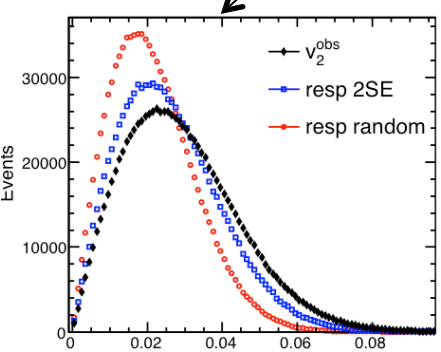

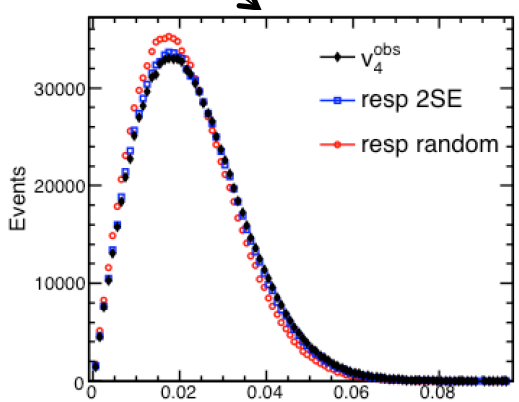

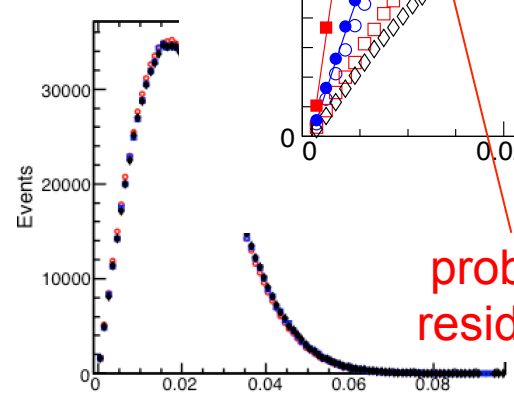

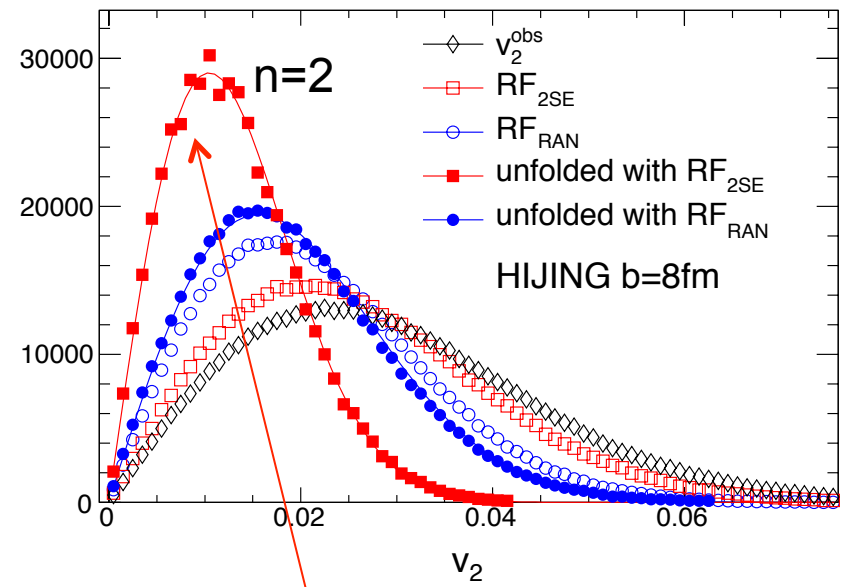

probability distribution of residual non-flow!!!

Azimuthal power spectrum in AMPT: (flow+non-flow)

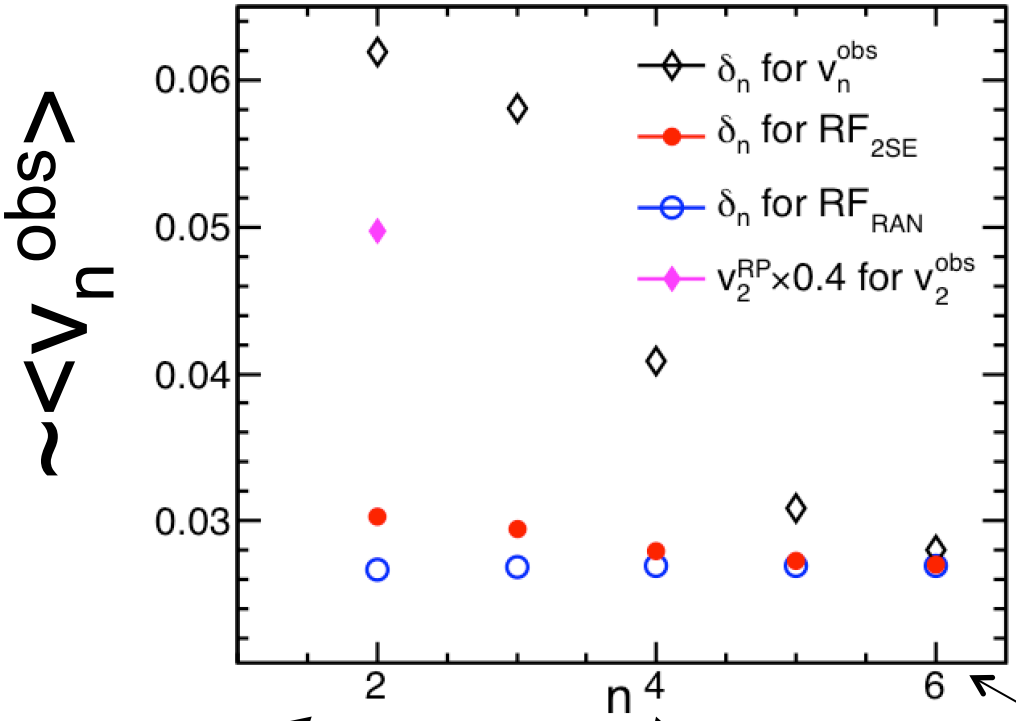

- Unfolding method allow extraction of EbE distribution of short-range and long-range correlations
  - Well-defined noise limit

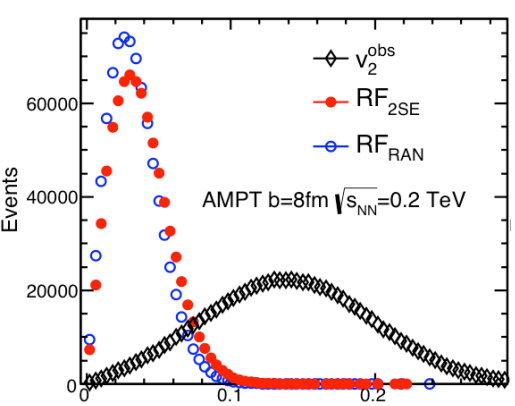

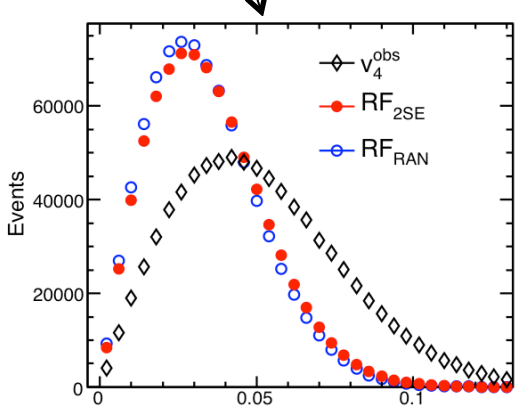

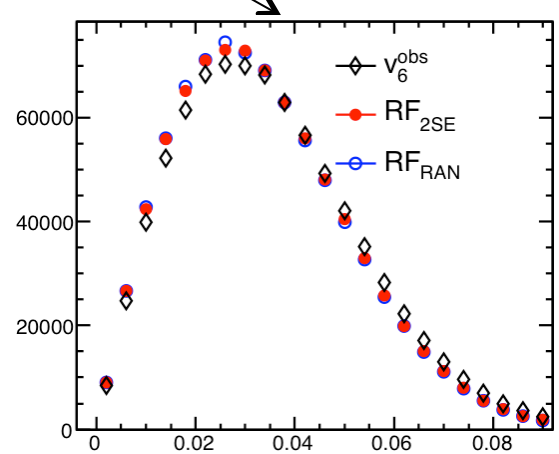

AMPT unfolded distributions

- Unfolded distribution scales well.

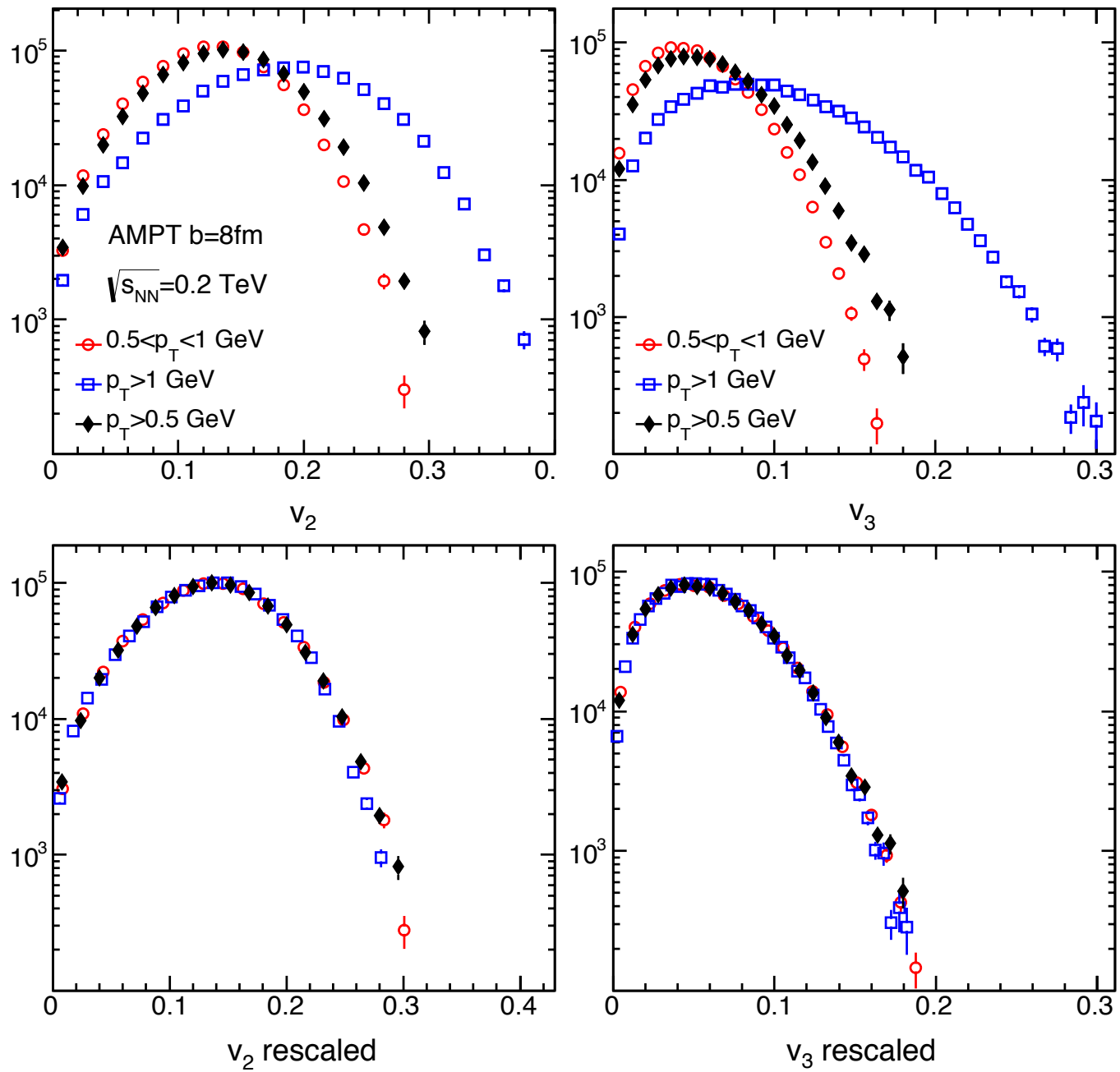

It was a memorable workshop

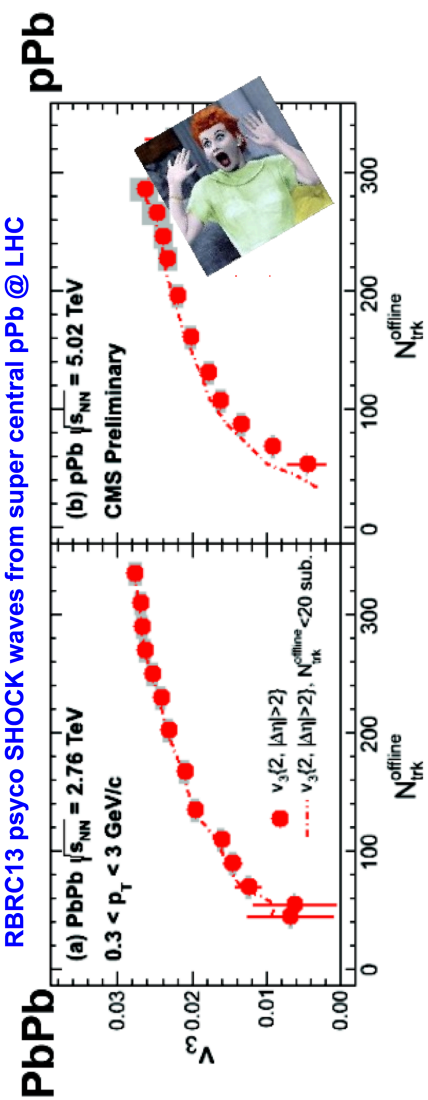

Decrease $\sqrt{s}$: Saturation turns off ($Q_s(x) \sim \Lambda_{QCD}$), hydro phase shorter ($T_{initial}$ decreases, τ_0 increases), maybe jumps with ($c_s, \eta/s$ at deconfinement), Knudsen number $\sim (TR)^{-1}$ higher, chemical composition different ($\tau, Kn \sim \mu_B$?)

Increase rapidity: Saturation effects larger, hydro phase shorter (as above)

Decrease system size Slightly less saturation,$T_0(\sim N_{part}^{1/3})$, bigger R_0^{-1} Knudsen number
(pA : Higher y and smaller size!)

Increase p_T first role of flow is increased, then tomographic regime

Abundance of experimental data makes "toy models" useful

Low p_T harmonics the experimental situation

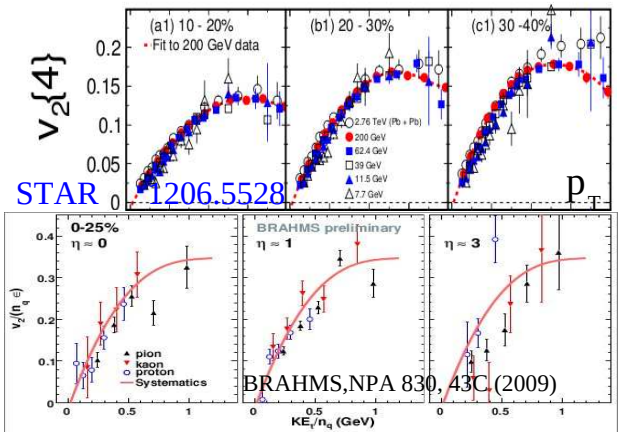

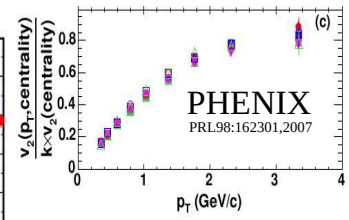

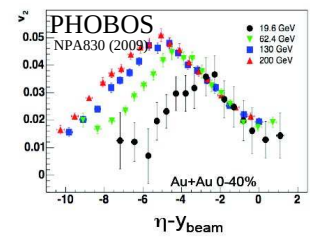

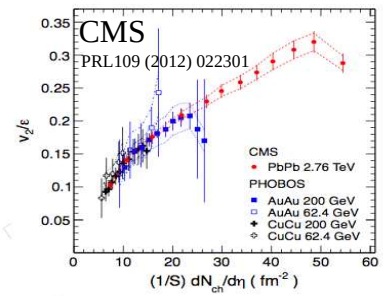

Here is what we know experimentally

$$v_2 \simeq \epsilon(b,A)F(p_T) \quad , \quad \langle v2 \rangle \simeq \int dp_T F(p_T) f\left(p_T, \langle p_T \rangle_{y,A,b,\sqrt{s}}\right)$$

$F(p_T)$ universal for all energies , $f(p_T)$ tracks mean momentum, $\sim \frac{1}{S}\frac{dN}{dy}$

This is an experimental statement, as good as the error bars

$$\frac{v_n}{\epsilon_n} \sim c_s f \underbrace{\left(\frac{1}{T_f^3 \tau_0 R^2} \frac{dN}{dy}\right)}_{\sim \tanh(\ldots)} \left(1 - \mathcal{O}(1) \frac{\eta}{s} \quad \underbrace{\frac{1}{TR}}_{no \quad scaling}\right)$$

No change in any of these termsobserved, from SPS to RHIC!

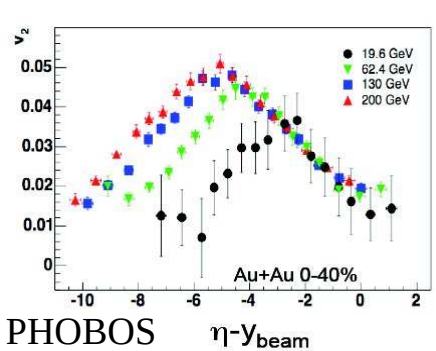

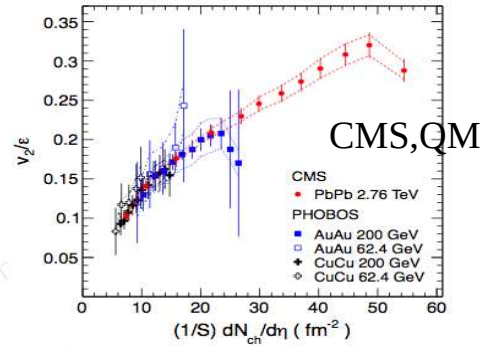

No sign of Knudsen number. v_3 of pA,AA amazing , as $\epsilon_3^{pA} \simeq \epsilon_3^{AA}$, but Kn $\mathcal{O}(10)$ bigger. Also no $\tau_0(\sqrt{s})$ seen.

Low energy scan, STAR 1206.5528

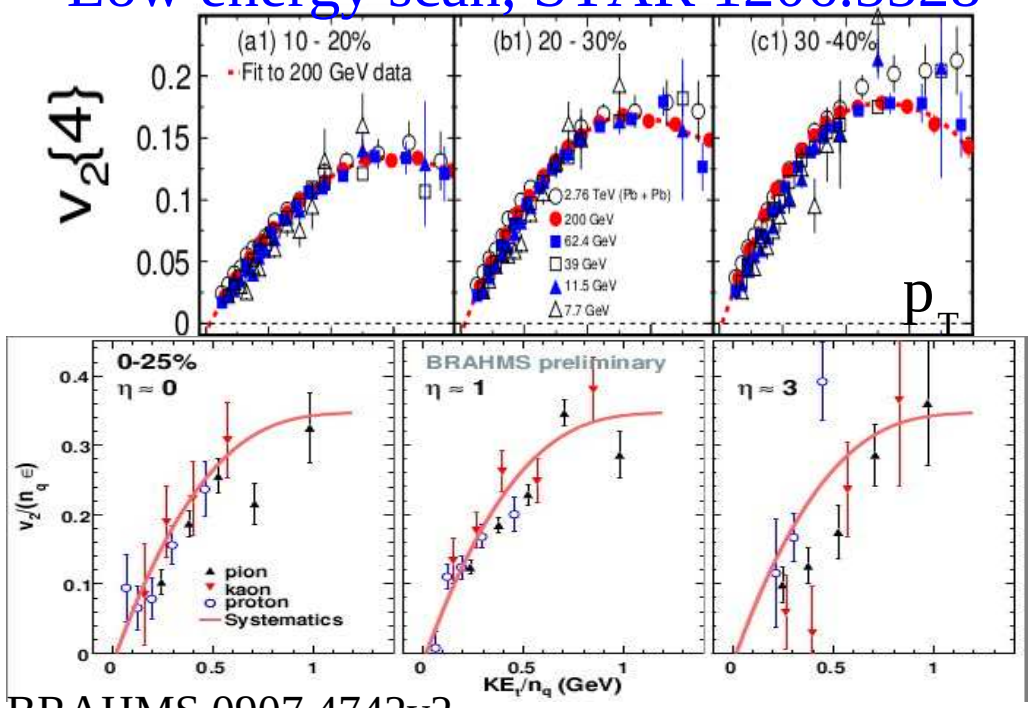

BRAHMS,0907.4742v2

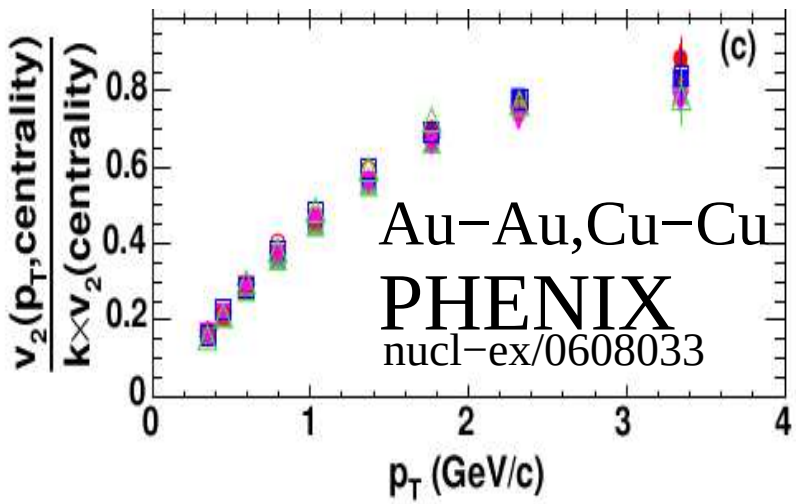

Puzzle2: Why is $v_2(p_T)$ <u>constant</u> (at least at high p_T)?

NB: this means $v_2(p_T)/\langle v_2\rangle$ <u>independent</u> of $N_{part}, y, \sqrt{s}$

Cooper-Frye

$$v_2(p_T) = \int d\phi \cos(2\phi) \left(E - p_T \left(\frac{dt}{dr} + \Delta \frac{dt}{dr}(\phi) \right) \right) e^{\left(-\frac{\gamma(E - p_T(u_T + \delta u_T(\phi)))}{T} \right)}$$

$$\simeq \int d\phi \cos^2(2\phi) \left[\underbrace{e^{-\frac{\gamma(E - p_T u_T)}{T}}}_{=0} - \underbrace{p_T \Delta \frac{dt}{dr}}_{\epsilon p_T} + \underbrace{\frac{\gamma \delta u_T(\phi) p_T}{T}}_{\sim \frac{\delta v_T}{T} p_T \sim \epsilon p_T / T} + \mathcal{O}\left(\epsilon^2\right) + \mathcal{O}\left(Kn\right) \right]$$

As long as $\frac{\delta v_T}{T} \sim \epsilon s^0$ (close to saturation of ϵ_p), $v_2(p_T)$ independent of $\sqrt{s}$

.

In ideal <u>and long-lived limit</u> $\frac{\eta}{sT} \ll R$ in $v_2(p_T) \sim \epsilon \tanh\left(\epsilon \frac{p_T}{T_f}\right) \underbrace{\rightarrow}_{p_T \gg T} p_T^0$

NB: deviations $\sim p_T$, more prominent at @high p_T

U.Heinz C.Shen,1202.6620

viscous hydro

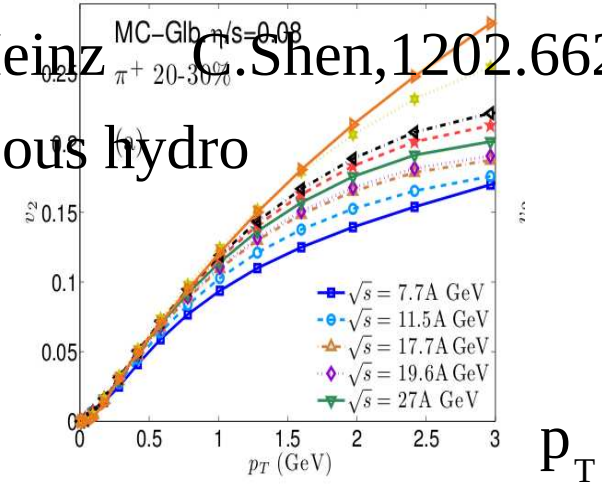

p_T

Solanki,Sorensen et al1210.0512

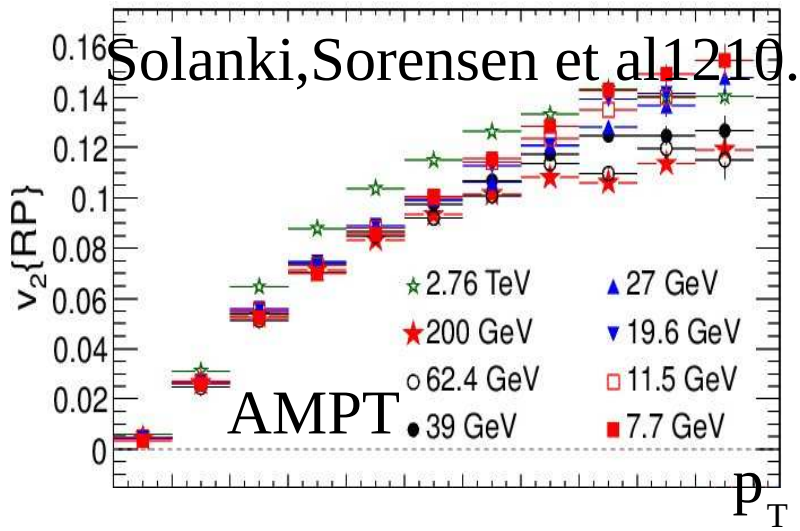

p_T

This is why all hydro and transport models generally give a systematic shift of $v_2(p_T)$ going up with p_T , as long as $p_T \sim \mathcal{O}(1)\langle p_T\rangle$. Thus this data-model disagreement not likely to go away!

Go to high p_T: At $Kn(pT - T) \geq 1$ tomographic regime
Tomographic v_n,unlike hydrodynamic v_n, depends on size as well as density

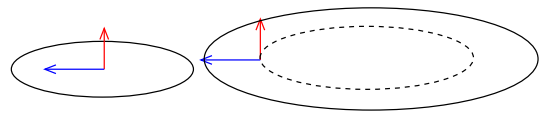

Take, as an initial condition, an elliptical distribution of matter at a given ϵ_n , run jets through it and calculate v_n . Now increase R with constant ϵ_n .

$$\left.\frac{v_n}{\epsilon_n}\right|_{tomo} \rightarrow \frac{Surface}{Volume} \rightarrow 0 \quad , \quad \left.\frac{v_n}{\epsilon_n}\right|_{hydro} \rightarrow \text{constant}$$

Role of "size" different in tomo vs hydro regime (M.Gyulassy,B.Betz,GT).
$\frac{dE}{d\tau} \sim \kappa E^a T^b \tau^c \Rightarrow \Delta E \sim \langle E^x \rangle \langle T^y \rangle \langle R \rangle^z \neq f\left(\frac{1}{S}\frac{dN}{dy}\right)$
Volcanoes and waterfalls can only make this worse, as $\epsilon_n(T \sim T_c) \neq \epsilon_n^{total}$

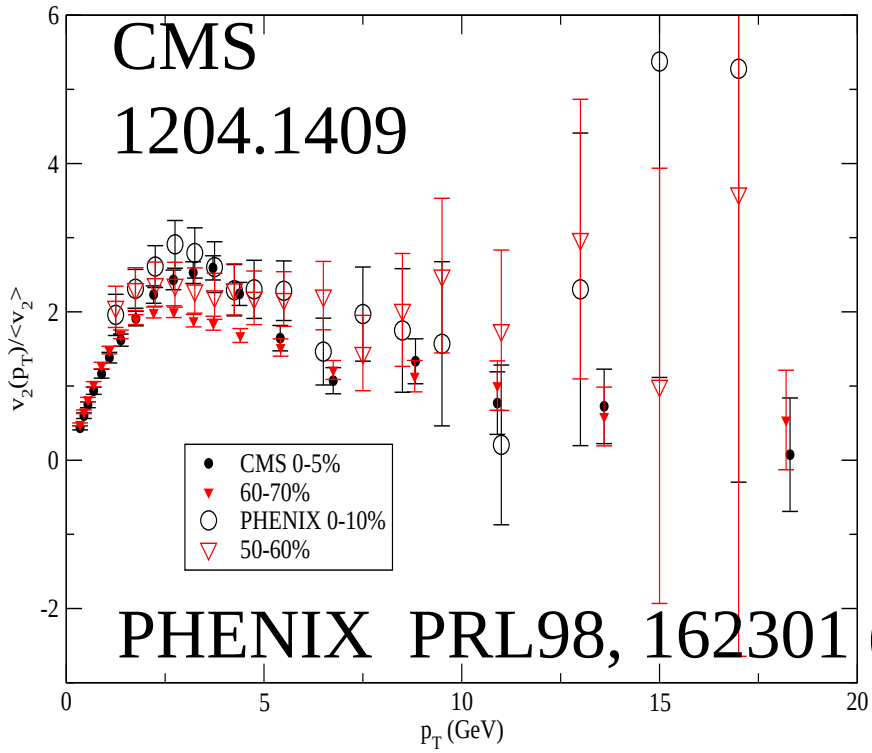

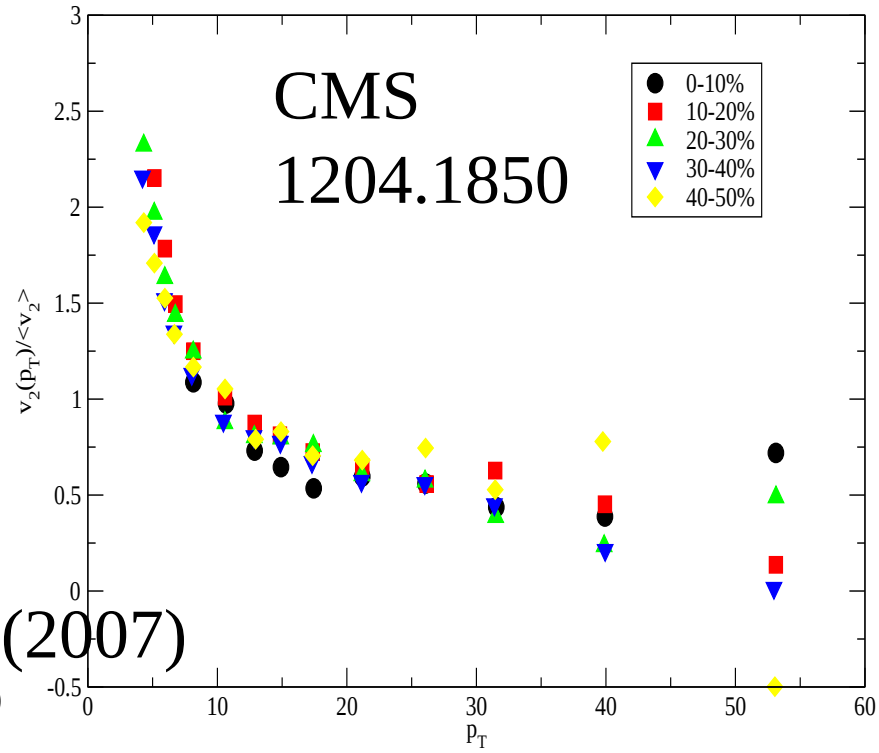

But , it seems no scaling break up to $p_T \sim 3.5$ GeV, maybe til 20 GeV. Split@intermediate p_T , reunification (?) higher (but big errors!). If no scaling violation for all momenta, puzzle for tomography

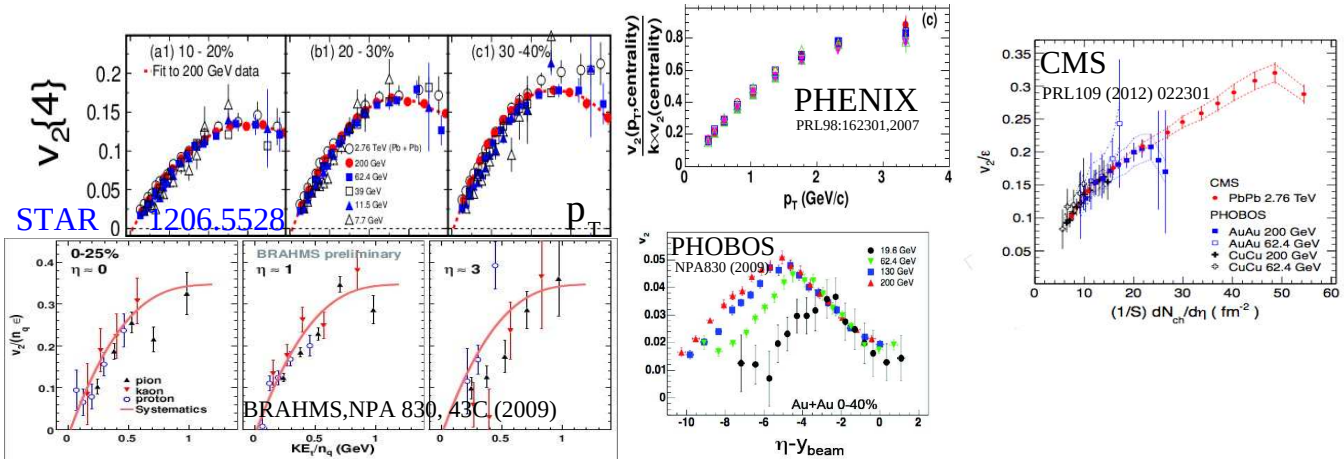

Anti-conclusion: Scalings puzzling for all popular models

Unless scalings break (Experimentalists?) model constrains on scalings more useful than "my model with 10 parameters fits this data at this $\sqrt{s}$".

Remember Bjorken scaling/partons. QCD a descendant of a scaling non-trivial with bootstrap/Smatrix/...

More info: arXiv:1208.5996, arXiv:0911.4775 (PRC), nucl-th/0702013 (PRC) , extensive calculation with ABC model using TITAN supercomputer in progress!

d+Au ridge at RHIC?

Fuqiang Wang
For the STAR Collaboration

2D correlation functions
(mixed-event vertex-matched acceptance corrected)

$0.15 < p_T^{trig} < 3$ GeV/c
$1 < p_T^{assoc} < 2$ GeV/c

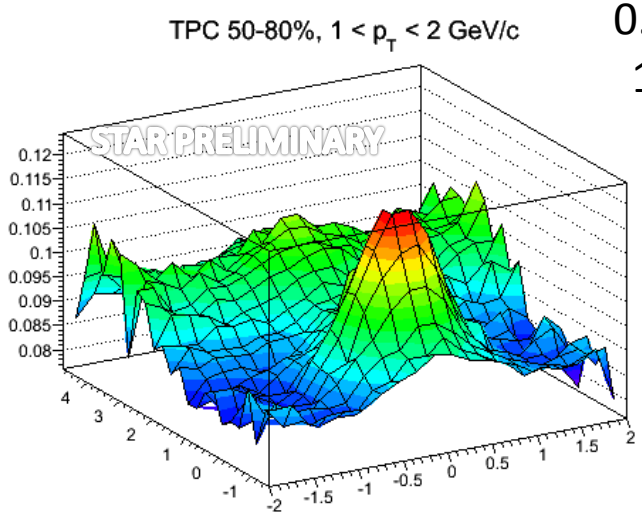

TPC mult.
$|\eta|<1$
as centrality

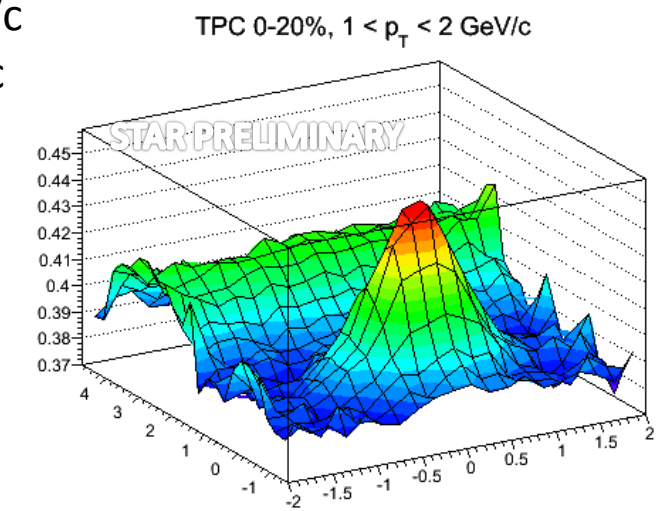

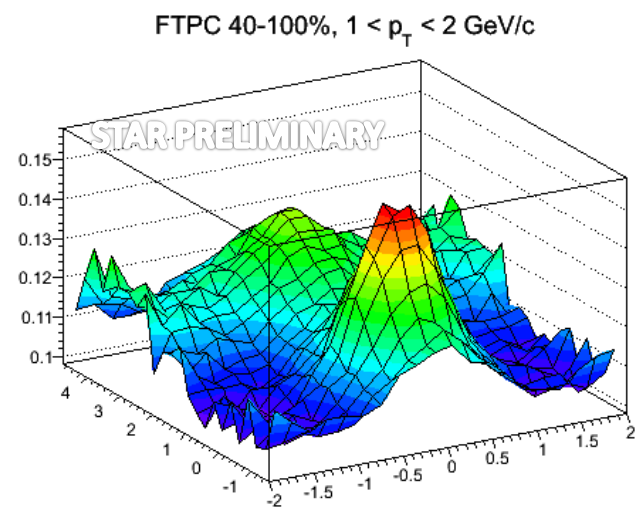

FTPC mult.
$-3.8<\eta<-2.8$
as centrality

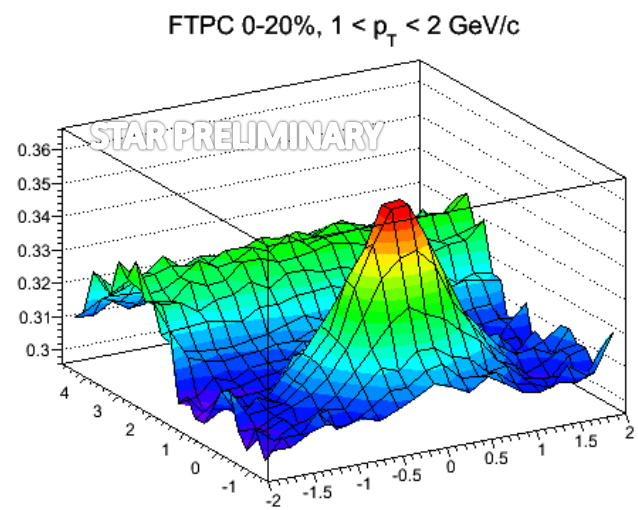

$\Delta\phi$ projections in different $\Delta\eta$ (TPC mult. $|\eta|<1$ as centrality)

$0.15 < p_T^{trig} < 3$ GeV/c, $1 < p_T^{assoc} < 2$ GeV/c

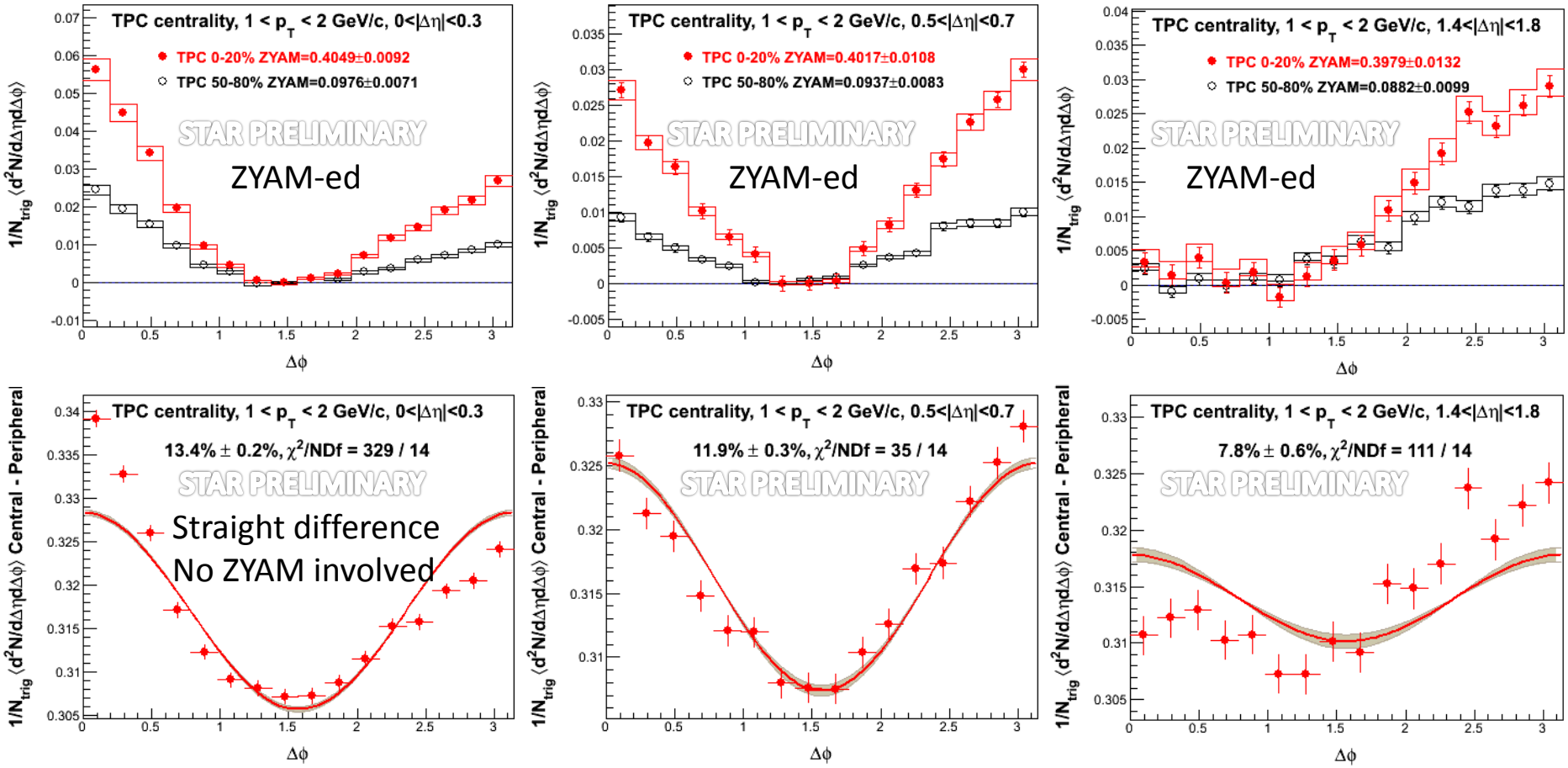

- ZYAM syst. error from different sizes of $\Delta\phi$ region for ZYAM.
- Efficiency corrected: 85 ± 5% .

$\Delta\phi$ projections in different $\Delta\eta$ (FTPC mult. $-3.8<\eta<-2.8$ as centrality)

$0.15 < p_T^{trig} < 3$ GeV/c, $1 < p_T^{assoc} < 2$ GeV/c

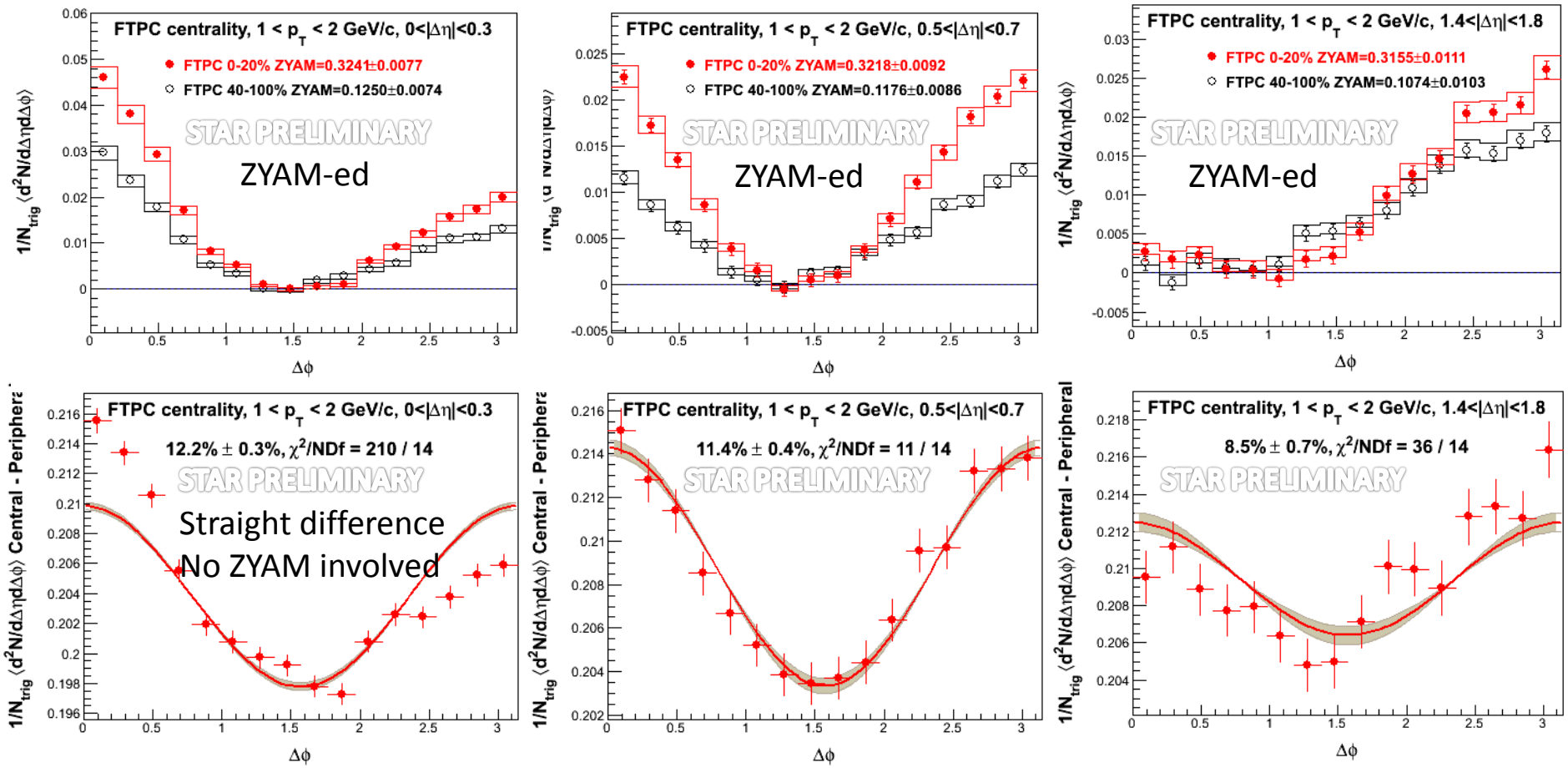

- ZYAM syst. error from different sizes of $\Delta\phi$ region for ZYAM.
- Efficiency corrected: 85 ± 5% .

$\Delta\eta$ projections in different $\Delta\phi$ (TPC mult. $|\eta|<1$ as centrality)

$0.15 < p_T^{trig} < 3$ GeV/c
$1 < p_T^{assoc} < 2$ GeV/c

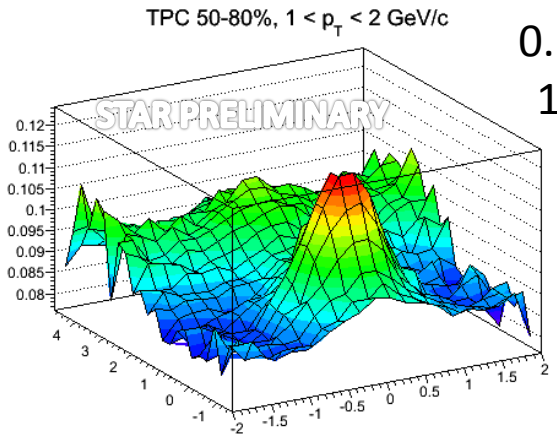

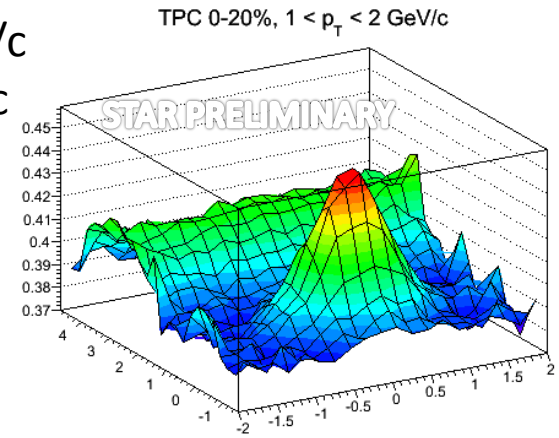

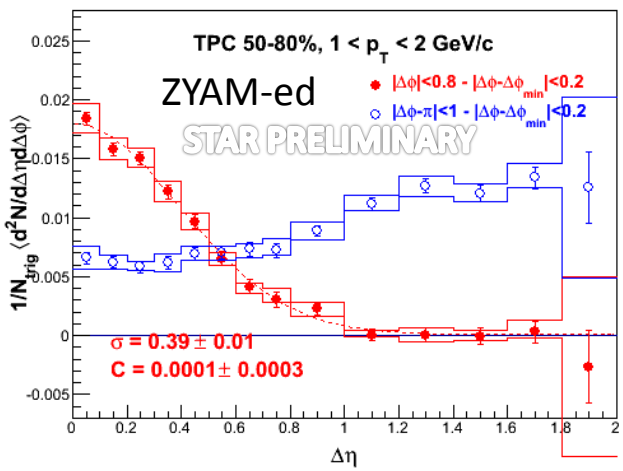

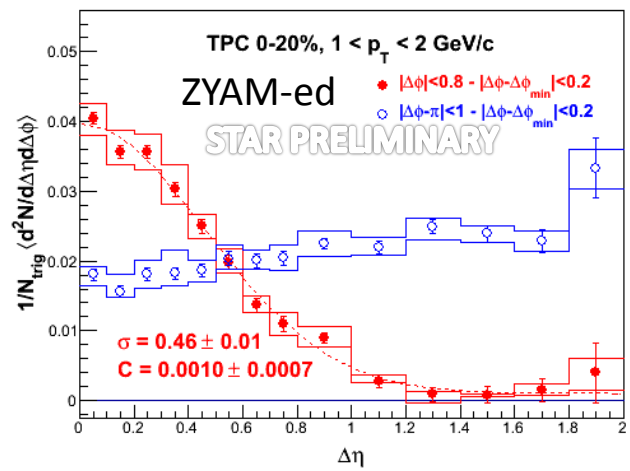

- ZYAM syst. error from different sizes of $\Delta\phi$ region for ZYAM.
- Efficiency corrected: 85 ± 5% .

$\Delta\eta$ projections in different $\Delta\phi$ (FTPC mult. $-3.8<\eta<-2.8$ as centrality)

$0.15 < p_T^{trig} < 3$ GeV/c

$1 < p_T^{assoc} < 2$ GeV/c

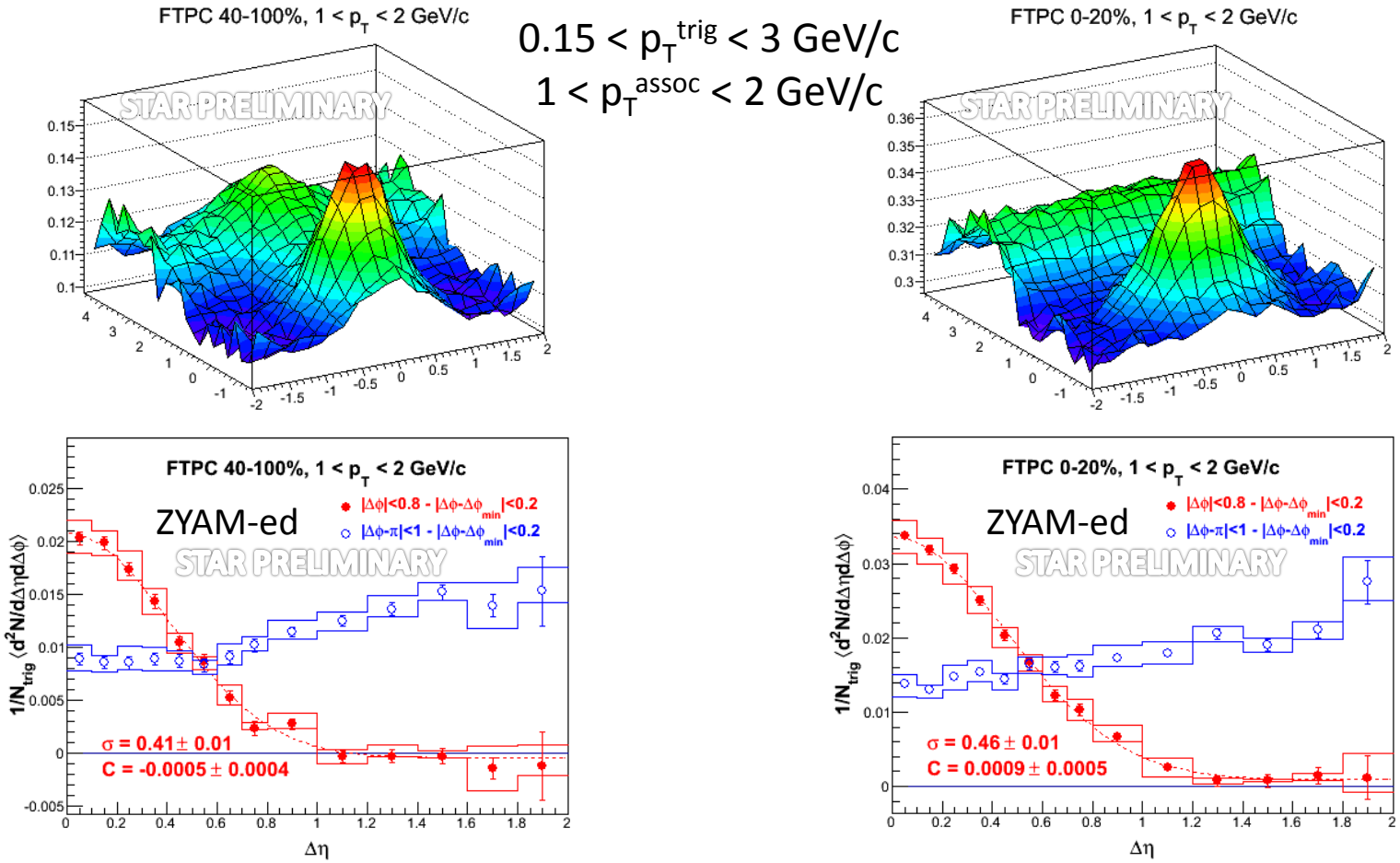

- ZYAM syst. error from different sizes of $\Delta\phi$ region for ZYAM.
- Efficiency corrected: 85 ± 5% .

Central – Peripheral

$0.15 < p_T^{trig} < 3$ GeV/c, $1 < p_T^{assoc} < 2$ GeV/c

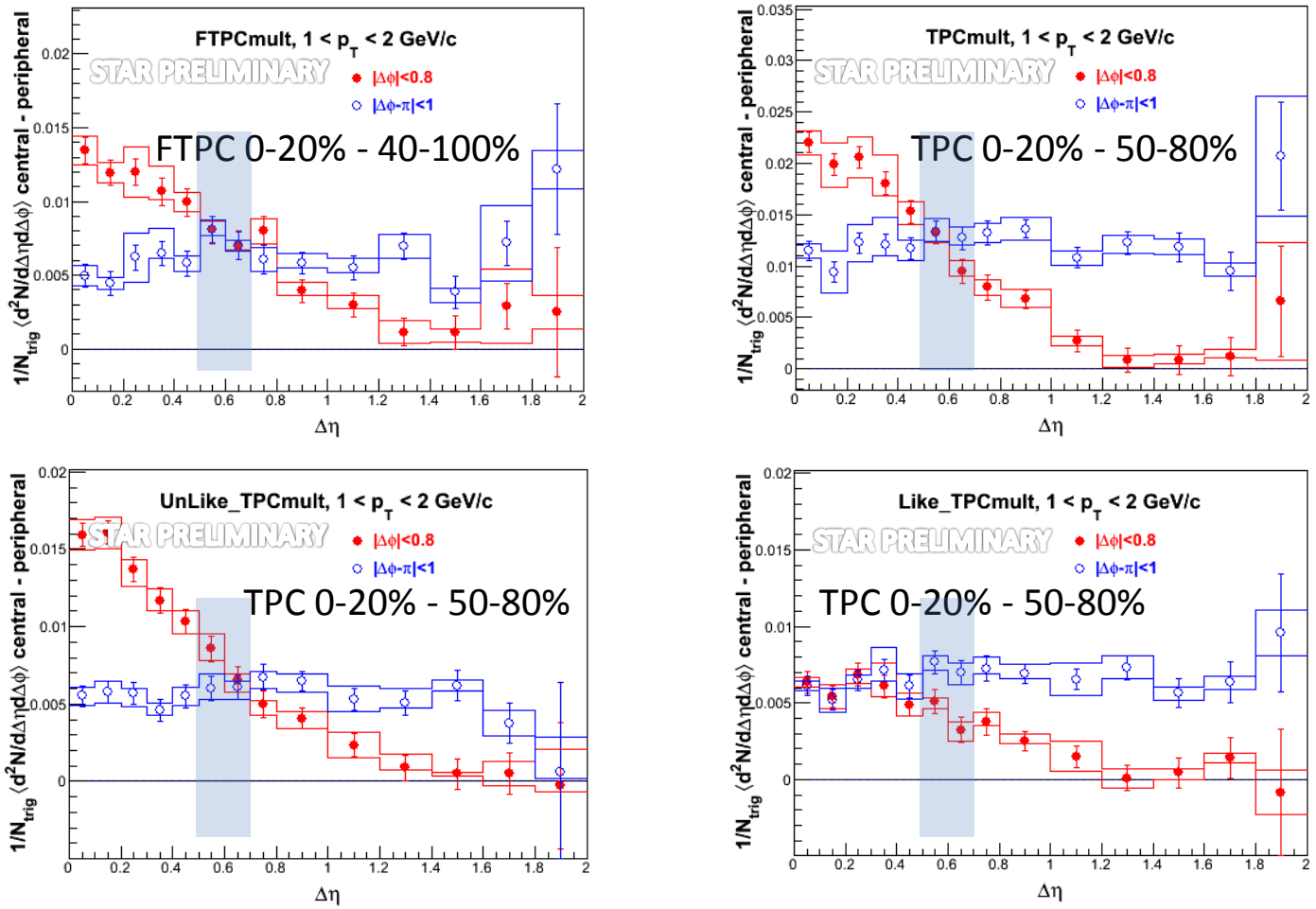

- ZYAM syst. error from different sizes of $\Delta\phi$ region for ZYAM.
- Efficiency corrected: 85 ± 5% .

Conditional yield vs multiplicity

$0.15 < p_T^{trig} < 3$ GeV/c, $1 < p_T^{assoc} < 2$ GeV/c

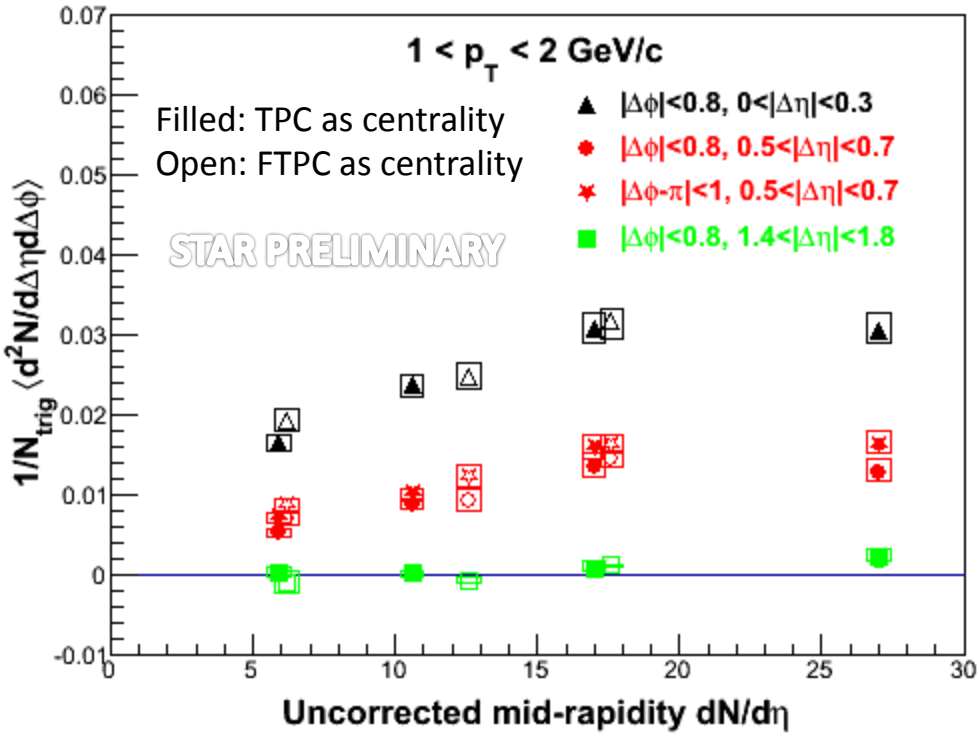

Summary

- Near-side Gaussian peak in $\Delta\eta$.
  Away-side approximately flat.
- Near-side large-$\Delta\eta$ yield consistent with zero.
- Central – peripheral excess resembles near- and away-side shapes and charge ordering.

- d+Au data consistent with jet phenomenology.
  Large multiplicity events → larger-energy jets?

Jet Quenching at RHIC vs LHC in Light of Recent dAu vs pPb Controls

April 15-17, 2013
Large Seminar Room, Physics, Bldg. 510

~ ~

MONDAY, April 15

08:30-12:30 *Session I. dAu/pPb Results, Ridge & Interpretations*
Chairperson: Jiangyong Jia

08:30-09:00		Registration
09:00-09:10	Nicholas Samios	Welcome
09:10-09:40	Wit Busza	History of pA from 1970 to 2013
09:40-10:20	Constantin Loizides	Recent LHC pPb results
10:20-11:00	Peter Steinberg	The Ridge in pp/pA/AA at LHC
11:00-11:30	***COFFEE BREAK***	
11:30-12:00	Raju Venugopalan	Ridge correlations: CGC perspective
12:00-12:30	Piotr Bozek	Ridge correlations: hydro perspective

14:00-18:20 *Session II. dAu/pPb Results, Ridge & Interpretations*
Chairperson: Dmitri Kharzeev

14:00-14:30	Gabor David	Updates/puzzles of dAu at RHIC
14:30-15:00	Wolfram Fischer	Future pA: RHIC machine perspective
15:00-15:30	Gergely Barnafoldi	Cronin & shadowing in pA
15:30-16:00	Boris Kopeliovich	Nuclear suppression in pA
16:00-16:30	***COFFEE BREAK***	
16:30-17:00	Adrian Dumitru	CGC predictions for pp, pA, and AA
17:00-17:30	Alex Kovner	Critical assessment of CGC
17:30-18:20	Dmitri Kharzeev	Brief introduction and moderated discussions

Back to Contents

TUESDAY, April 16

09:00-12:00 *Session III. Jet Quenching at LHC & Opaqueness Evolution*

Chairperson: Andrea Dainese

09:00-09:30	Gunther Roland	LHC jet quenching I
09:30-10:00	Brian Cole	LHC jet quenching II
10:00-10:30	Abhijit Majumder	Higher-twist predictions for pA and AA at LHC
10:30-11:00	***COFFEE BREAK***	
11:00-11:30	Jinfeng Liao	Opaqueness evolution from color liberation
11:30-12:00	Vladimir Skokov	Jet energy loss at Tc
12:00-12:30	Denes Molnar	Hard and soft responses from parton transport

14:00-17:40 *Session IV. RHIC/LHC Complementarity & RHIC Future*

Chairperson: Peter Jacobs

14:00-14:30	Anne Sickles	RHIC jet quenching: present & future
14:30-15:00	Joern Putschke	RHIC/LHC complementarity
15:00-15:30	Fuqiang Wang	Particle correlations at RHIC: present & future
15:30-15:50	***COFFEE BREAK***	
15:50-16:20	Roy Lacey	Combined analysis of RHIC to LHC suppression & geometry
16:20-16:50	Soumya Mohapatra	Event-by-event flow & initial geometry from LHC
16:50-17:20	Frasher Loshaj	Jet quenching & fragmentation from RHIC to LHC
17:20-18:10	Peter Jacobs	Brief introduction and moderated discussions

Workshop Dinner: 18:30-20:00 @ Brookhaven Center, South Room

Back to Contents

WEDNESDAY, April 17

09:00-12:30 Session V. Initial Conditions for Hard/Soft Observables

Chairperson: Rob Pisarski

09:00-09:30	Ulrich Heinz	Hydro with fluctuating initial condition & temperature dependent viscosity
09:30-10:00	Bjorn Schenke	Initial conditions: IP-glasma vs KLN vs Glauber
10:00-10:30	Barbara Betz	Raa and high p_t azimuthal anisotropy
10:30-11:00	Xilin Zhang	Harmonic jet tomography at RHIC+LHC
11:00-11:30	***COFFEE BREAK***	
11:30-12:00	Edward Shuryak	Possible collective behavior & hadron correlations from pp to AA
12:00-12:30	Yuri Kovchegov	Long range rapidity correlations in heavy ion collisions

14:00-17:30 Session VI. Flavor & BES & Closing Remarks

Chairperson: Raju Venugopalan

14:00-14:30	Alessandro Buzzatti	Flavor tomography
14:30-15:00	Andrea Dainesee	Experimental status of flavor tomography
15:00-15:30	Helen Caines	Jet quenching & initial geometry from RHIC BES
15:30-16:00	Elke Aschenauer	eRHIC as the future
16:00-16:30	***COFFEE BREAK***	
16:30-17:00	Jean Paul Blaizot	In-medium QCD cascade: democratic branching and wave turbulence
17:00-17:30	Miklos Gyulassy	Closing remarks

Back to Contents

Jet Quenching at RHIC vs LHC in Light of Recent dAu vs pPb Controls

April 15-17, 2013

List of Registered Participants

Name	Affiliation
Salvatore Aiola	Lawrence Berkeley National Laboratory
Elke Aschenauer	Brookhaven National Laboratory
Gergely Barnafoldi	Wigner RCP of the Hungarian Academy of Sciences
Gokce Basar	Stony Brook University
Jean-Paul Blaizot	CNRS
Piotr Bozek	IFJ PAN / AGH Krakow Poland
Wit Busza	Massachusetts Institute of Technology
Alessandro Buzzatti	Lawrence Berkeley National Laboratory
Adam Bzdak	Brookhaven National Laboratory
Helen Caines	Yale University
Chin-Hao Chen	Brookhaven National Laboratory
William Christie	Brookhaven National Laboratory
Brian Cole	Columbia University
Megan Connors	Yale University
Andrea Dainese	INFN - Padova
Gabor David	Brookhaven National Laboratory
L. Chanaka De Silva	University of Houston
Abhay Deshpande	Stony Brook University
Adrian Dumitru	Baruch College (CUNY) & RIKEN BNL Research Center
James Dunlop	Brookhaven National Laboratory
Andrej Ficnar	Columbia University
Wolfram Fischer	Brookhaven National Laboratory
Miklos Gyulassy	Columbia University
Ulrich Heinz	The Ohio State University
Martin Hentschinski	Brookhaven National Laboratory
Xu-Guang Huang	Indiana University
Peter Jacobs	Lawrence Berkeley National Laboratory
Jiangyong Jia	Brookhaven National Laboratory
Kurt Jung	Purdue University
Dmitri Kharzeev	Brookhaven National Laboratory & Stony Brook University
Boris Kopeliovich	UTFSM, Valparaiso, Chile
Yuri Kovchegov	The Ohio State University
Alex Kovner	University of Connecticut
Roy Lacey	Stony Brook University
Xuan Li	Temple University

Back to Contents

Jinfeng Liao	Indiana University & RIKEN BNL Research Center
Shu Lin	RIKEN BNL Research Center @ Brookhaven National Lab
Tseh Liou	Columbia University
Constantin Loizides	Lawrence Berkeley National Laboratory
Ronald Longacre	Retiree, Brookhaven National Laboratory
Frasher Loshaj	Stony Brook University
Rongrong Ma	Yale University
Abhijit Majumder	Wayne State University
Mohammed Mia	Columbia University
Alice Mignerey	University of Maryland
Soumya Mohapatra	Stony Brook University
Denes Molnar	Purdue University
Mriganka Mouli Mondal	Texas A&M University
Berndt Mueller	Brookhaven National Laboratory
Alice Ohlson	Yale University
Robert Pak	Brookhaven National Laboratory
Annalia Palumbo	Brookhaven National Laboratory
Dennis Perepelitsa	Columbia University
Elena Petreska	Baruch College
Robert Pisarski	Brookhaven National Laboratory
Joern Putschke	Wayne State University
Rosi Reed	Yale University
Gunther Roland	Massachusetts Institute of Technology
Takao Sakaguchi	Brookhaven National Laboratory
Bjoern Schenke	Brookhaven National Laboratory
Edward Shuryak	Stony Brook University
Anne Sickles	Brookhaven National Laboratory
Vladimir Skokov	Brookhaven National Laboratory
Peter Steinberg	Brookhaven National Laboratory
Marco Stratmann	Brookhaven National Laboratory
Deke Sun	Purdue University
Michael Tannenbaum	Brookhaven National Laboratory
Giorgio Torrieri	Columbia University
Raju Venugopalan	Brookhaven National Laboratory
Fuqiang Wang	Purdue University
Bin Wu	IPhT Saclay
Jiechen Xu	Columbia University
Lingshan Xu	CMS
Zhenyu Ye	University of Illinois
Xilin Zhang	Ohio University

Back to Contents

RIKEN BNL Research Center Proceedings

Volume 114 – The The Physics of p↑+A Collisions at RHIC, January 7-9, 2013 – BNL-99107-2013
Volume 113 – Thermal Radiation Workshop, December 5-7, 2012 – BNL-99088-2013
Volume 112 – RBRC Scientific Review Committee Meeting, November 6-8, 2012 – BNL-99621-2013
Volume 111 – Forward Physics at RHIC, July 30-Aug 1, 2012 – BNL-98400-2012
Volume 110 – P- and CP-odd Effects in Hot and Dense Matter, June 25-27, 2012 – BNL-98398-2012
Volume 109 – New Horizons for Lattice Computations with Chiral Fermions, May 14-18, 2012 – BNL-98392-2012
Volume 108 – Hyperon-Hyperon Interactions and Searches for Exotic Di-Hyperons in Nuclear Collisions, February 29 – March 2, 2012 – BNL-97035-2012
Volume 107 – Future Directions in High Energy QCD, October 20-22, 2011 – BNL-98119-2011
Volume 106 – Fluctuations, Correlations and RHIC Low Energy Runs, October 3-5, 2011 – BNL-96514-2011
Volume 105 – Opportunities for Polarized He-3 in RHIC and EIC, September 28-30, 2011 – BNL-96418-2011
Volume 104 – Brookhaven Summer Program on Quarkonium Production in Elementary and Heavy Ion Collisions, June 6-18, 2011 – BNL-96171-2011
Volume 103 – Opportunities for Drell-Yan Physics at RHIC, May 11-13, 2011 – BNL-95236-2011-2011
Volume 102 – Initial State Fluctuations and Final-State Particle Correlations, February 2-4, 2011 – BNL-94704-2011
Volume 101 – RBRC Scientific Review Committee Meeting, October 27-29, 2010 – BNL-94589-2011
Volume 100 – Summer Program on Nucleon Spin Physics, July 14-27, 2010 – BNL-96163-2011
Volume 99 – The Physics of W and Z Bosons, June 24-25, 2010 – BNL-94287-2010
Volume 98 – Saturation, the Color Glass Condensate and the Glasma: What Have we Learned from RHIC? – May 10-12, 2010 – BNL-94271-2010
Volume 97 – RBRC Scientific Review Committee Meeting, October 21-22, 2009 – BNL-90674-2009
Volume 96 – P- and CP-Odd Effects in Hot and Dense Matter, April 26-30, 2010 – BNL-94237-2010
Volume 95 – Progress in High-pT Physics at RHIC, March 17-19, 2010 – BNL-94214-2010
Volume 94 – Summer Program on Nucleon Spin Physics at LBL, June 1-12, 2009
Volume 93 – PHENIX Spinfest School 2009 at BNL - July 1-31, 2009. BNL-90343-2009
Link: PHENIXSpinfestSchool2009@BNL
Volume 92 – PKU-RBRC Workshop on Transverse Spin Physics, June 30 - July 4, 2008, Beijing, China – BNL-81685-2008
Volume 91 – RBRC Scientific Review Committee Meeting, November 17-18, 2008 – BNL-81556-2008
Volume 90 – PHENIX Spinfest School 2008 at BNL, August 4-8, 2008 – BNL-81478-2008
Volume 89 – Understanding QGP through Spectral Functions and Euclidean Correlators, April 23-25, 2008 – BNL-81318-2008
Volume 88 – Hydrodynamics in Heavy Ion Collisions and QCD Equation of State, April 21-22, 2008 – BNL-81307-2008
Volume 87 – RBRC Scientific Review Committee Meeting, November 5-6, 2007 – BNL-79570-2007
Volume 86 – Global Analysis of Polarized Parton Distributions in the RHIC Era, October 8, 2007 – BNL-79457-2007
Volume 85 – Parity-Violating Spin Asymmetries at RHIC-BNL, April 26-27, 2007 – BNL-79146-2007
Volume 84 – Domain Wall Fermions at Ten Years, March 15-17, 2007 – BNL 77857-2007
Volume 83 – QCD in Extreme Conditions, July 31 - August 2, 2006 – BNL-76933-2006
Volume 82 – RHIC Physics in the Context of the Standard Model, June 18-23, 2006 – BNL-76863-2006
Volume 81 – Parton Orbital Angular Momentum (Joint RBRC/University of New Mexico Workshop) February 24-26, 2006 – BNL-75937-2006
Volume 80 – Can We Discover the QCD Critical Point at RHIC?, March 9-10, 2006 – BNL-75692-2006

Back to Contents

Volume 79 – Strangeness in Collisions, February 16-17, 2006 – BNL-79763-2008
Volume 78 – Heavy Flavor Productions and Hot/Dense Quark Matter, December 12-14, 2005 – BNL-76915-2006
Volume 77 – RBRC Scientific Review Committee Meeting, October 10-12, 2005 – BNL-52649-2005
Volume 76 – Odderon Searches at RHIC, September 27-29, 2005 – BNL-75092-2005
Volume 75 – Single Spin Asymmetries, June 1-3, 2005 – BNL-74717-2005
Volume 74 – RBRC QCDOC Computer Dedication and Symposium on RBRC QCDOC, May 26, 2005 – BNL-74813-2005
Volume 73 – Jet Correlations at RHIC, March 10-11, 2005 – BNL-73910-2005
Volume 72 – RHIC Spin Collaboration Meetings XXXI (January 14, 2005), XXXII (February 10, 2005), XXXIII (March 11, 2005) – BNL-73866-2005
Volume 71 – Classical and Quantum Aspects of the Color Glass Condensate – BNL-73793-2005
Volume 70 – Strongly Coupled Plasmas: Electromagnetic, Nuclear & Atomic – BNL-73867-2005
Volume 69 – RBRC Scientific Review Committee – BNL-73546-2004
Volume 68 – Workshop on the Physics Programme of the RBRC and UKQCD QCDOC Machines – BNL-73604-2004
Volume 67 – High Performance Computing with BlueGene/L and QCDOC Architectures
Volume 66 – RHIC Spin Collaboration Meeting XXIX, October 8-9, 2004, Torino Italy – BNL-73534-2004
Volume 65 – RHIC Spin Collaboration Meetings XXVII (July 22, 2004), XXVIII (September 2, 2004), XXX (December 6, 2004) – BNL-73506-2004
Volume 64 – Theory Summer Program on RHIC Physics – BNL-73263-2004
Volume 63 – RHIC Spin Collaboration Meetings XXIV (May 21, 2004), XXV (May 27, 2004), XXVI (June 1, 2004) – BNL-72397-2004
Volume 62 – New Discoveries at RHIC, May 14-15, 2004 – BNL- 72391-2004
Volume 61 – RIKEN-TODAI Mini Workshop on "Topics in Hadron Physics at RHIC", March 23-24, 2004 – BNL-72336-2004
Volume 60 – Lattice QCD at Finite Temperature and Density – BNL–72083-2004
Volume 59 – RHIC Spin Collaboration Meeting XXI (January 22, 2004), XXII (February 27, 2004), XXIII (March 19, 2004)– BNL-72382-2004
Volume 58 – RHIC Spin Collaboration Meeting XX – BNL-71900-2004
Volume 57 – High pt Physics at RHIC, December 2-6, 2003 – BNL-72069-2004
Volume 56 – RBRC Scientific Review Committee Meeting – BNL-71899-2003
Volume 55 – Collective Flow and QGP Properties – BNL-71898-2003
Volume 54 – RHIC Spin Collaboration Meetings XVII, XVIII, XIX – BNL-71751-2003
Volume 53 – Theory Studies for Polarized pp Scattering – BNL-71747-2003
Volume 52 – RIKEN School on QCD "Topics on the Proton" – BNL-71694-2003
Volume 51 – RHIC Spin Collaboration Meetings XV, XVI – BNL-71539-2003
Volume 50 – High Performance Computing with QCDOC and BlueGene – BNL-71147-2003
Volume 49 – RBRC Scientific Review Committee Meeting – BNL-52679
Volume 48 – RHIC Spin Collaboration Meeting XIV – BNL-71300-2003
Volume 47 – RHIC Spin Collaboration Meetings XII, XIII – BNL-71118-2003
Volume 46 – Large-Scale Computations in Nuclear Physics using the QCDOC – BNL-52678
Volume 45 – Summer Program: Current and Future Directions at RHIC – BNL-71035
Volume 44 – RHIC Spin Collaboration Meetings VIII, IX, X, XI – BNL-71117-2003
Volume 43 – RIKEN Winter School – Quark-Gluon Structure of the Nucleon and QCD – BNL-52672
Volume 42 – Baryon Dynamics at RHIC – BNL-52669
Volume 41 – Hadron Structure from Lattice QCD – BNL-52674
Volume 40 – Theory Studies for RHIC-Spin – BNL-52662

Back to Contents

Volume 39 – RHIC Spin Collaboration Meeting VII – BNL-52659
Volume 38 – RBRC Scientific Review Committee Meeting – BNL-52649
Volume 37 – RHIC Spin Collaboration Meeting VI (Part 2) – BNL-52660
Volume 36 – RHIC Spin Collaboration Meeting VI – BNL-52642
Volume 35 – RIKEN Winter School – Quarks, Hadrons and Nuclei – QCD Hard Processes and the Nucleon Spin – BNL-52643
Volume 34 – High Energy QCD: Beyond the Pomeron – BNL-52641
Volume 33 – Spin Physics at RHIC in Year-1 and Beyond – BNL-52635
Volume 32 – RHIC Spin Physics V – BNL-52628
Volume 31 – RHIC Spin Physics III & IV Polarized Partons at High Q^2 Region – BNL-52617
Volume 30 – RBRC Scientific Review Committee Meeting – BNL-52603
Volume 29 – Future Transversity Measurements – BNL-52612
Volume 28 – Equilibrium & Non-Equilibrium Aspects of Hot, Dense QCD – BNL-52613
Volume 27 – Predictions and Uncertainties for RHIC Spin Physics & Event Generator for RHIC Spin Physics III – Towards Precision Spin Physics at RHIC – BNL-52596
Volume 26 – Circum-Pan-Pacific RIKEN Symposium on High Energy Spin Physics – BNL-52588
Volume 25 – RHIC Spin – BNL-52581
Volume 24 – Physics Society of Japan Biannual Meeting Symposium on QCD Physics at RIKEN BNL Research Center – BNL-52578
Volume 23 – Coulomb and Pion-Asymmetry Polarimetry and Hadronic Spin Dependence at RHIC Energies – BNL-52589
Volume 22 – OSCAR II: Predictions for RHIC – BNL-52591
Volume 21 – RBRC Scientific Review Committee Meeting – BNL-52568
Volume 20 – Gauge-Invariant Variables in Gauge Theories – BNL-52590
Volume 19 – Numerical Algorithms at Non-Zero Chemical Potential – BNL-52573
Volume 18 – Event Generator for RHIC Spin Physics – BNL-52571
Volume 17 – Hard Parton Physics in High-Energy Nuclear Collisions – BNL-52574
Volume 16 – RIKEN Winter School - Structure of Hadrons - Introduction to QCD Hard Processes – BNL-52569
Volume 15 – QCD Phase Transitions – BNL-52561
Volume 14 – Quantum Fields In and Out of Equilibrium – BNL-52560
Volume 13 – Physics of the 1 Teraflop RIKEN-BNL-Columbia QCD Project First Anniversary Celebration – BNL-66299
Volume 12 – Quarkonium Production in Relativistic Nuclear Collisions – BNL-52559
Volume 11 – Event Generator for RHIC Spin Physics – BNL-66116
Volume 10 – Physics of Polarimetry at RHIC – BNL-65926
Volume 9 – High Density Matter in AGS, SPS and RHIC Collisions – BNL-65762
Volume 8 – Fermion Frontiers in Vector Lattice Gauge Theories – BNL-65634
Volume 7 – RHIC Spin Physics – BNL-65615
Volume 6 – Quarks and Gluons in the Nucleon – BNL-65234
Volume 5 – Color Superconductivity, Instantons and Parity (Non?)-Conservation at High Baryon Density – BNL-65105
Volume 4 – Inauguration Ceremony and Non-Equilibrium Many Body Dynamics – BNL-64912
Volume 3 – Hadron Spin-Flip at RHIC Energies – BNL-64724
Volume 2 – Perturbative QCD as a Probe of Hadron Structure – BNL-64723
Volume 1 – Open Standards for Cascade Models for RHIC – BNL-64722

Back to Contents

Li Keran

Nuclei as heavy as bulls
Through collision
Generate new states of matter.
T.D. Lee

©CCASTA

Organizers
Miklos Gyulassy (Columbia University)
Jiangyong Jia (BNL)
Jinfeng Liao (IU / RBRC)

RIKEN BNL Research Center
Bldg. 510A, Brookhaven National Laboratory
Upton, NY 11973-5000, USA

April 2013